PROCEEDINGS OF THE FIRST INTERNATIONAL CONGRESS OF RADIATION PROTECTION

IN TWO PARTS

Sponsored by the

INTERNATIONAL RADIATION PROTECTION ASSOCIATION

at

ROME, ITALY

SEPTEMBER 5–10, 1966

EDITED BY

W. S. SNYDER (U.S.A.)

H. H. ABEE (U.S.A.)
L. K. BURTON (U.K.)
R. MAUSHART (Germany)
A. BENCO (Italy)
F. DUHAMEL (France)
B. M. WHEATLEY (U.K.)

PERGAMON PRESS

OXFORD · LONDON · EDINBURGH · NEW YORK
TORONTO · SYDNEY · PARIS · BRAUNSCHWEIG

Pergamon Press Ltd., Headington Hill Hall, Oxford
4 & 5 Fitzroy Square, London W.1.
Pergamon Press (Scotland) Ltd., 2 & 3 Teviot Place, Edinburgh 1
Pergamon Press Inc., 44–01 21st Street, Long Island City, New York 11101
Pergamon of Canada, Ltd., 207 Queen's Quay West, Toronto 1
Pergamon Press (Aust.) Pty. Ltd., Rushcutters Bay, Sydney, N.S.W.
Pergamon Press S.A.R.L., 24 rue des Écoles, Paris 5e
Vieweg & Sohn GmbH, Burgplatz 1, Braunschweig

First edition 1968

Library of Congress Catalog Card No. 67–30114

PRINTED IN GREAT BRITAIN BY A. WHEATON AND CO.,
EXETER AND LONDON
08 003297 4

PROCEEDINGS OF THE FIRST INTERNATIONAL CONGRESS OF RADIATION PROTECTION

PART 1

CONTENTS

PART 1

PLENARY SESSION A

P. CALDIROLA, *Chairman*

SESSION 1

BASIC STUDIES ON RADIATION EFFECTS

B. CH. CHRISTENSEN, *Chairman*

SESSION 2

DOSIMETRY I

P. KAYSER, *Chairman*

SESSION 3

APPLIED RADIATION BIOLOGY I

N. Beken, *Chairman*

SESSION 4

OPERATIONAL HEALTH PHYSICS AND CONTAMINATION OF WORKING AREAS I

Y. NISHIWAKI, *Chairman*

SESSION 5

SPECTROMETRY AND INSTRUMENTATION I

J. SOLANAS, *Chairman*

SESSION 6

RADIOCHEMICAL ANALYSIS

C. TRITREMMEL, *Chairman*

SESSION 7

ENVIRONMENTAL CONTAMINATION, FALLOUT AND FOOD CHAINS I

P. SPAANDER, *Chairman*

SESSION 8

DOSIMETRY II

F. DUHAMEL, *Chairman*

SESSION 9

MEDICAL ASPECTS OF RADIATION PROTECTION I

L. BOZOKY, *Chairman*

SESSION 10

OPERATIONAL HEALTH PHYSICS AND CONTAMINATION OF WORKING AREAS II

C. A. ADAMS, *Chairman*

SESSION 11

PUBLIC HEALTH AND WASTE DISPOSAL

S. HALTER, *Chairman*

SESSION 12

INTERNAL EMITTERS I

E. T. AGARD, *Chairman*

SESSION 13

APPLIED RADIATION BIOLOGY II

H. DIONISI, *Chairman*

PART 2

SESSION 14

DOSIMETRY III

M. VASQUEZ BARETE, *Chairman*

SESSION 15

HAZARD EVALUATION

M. A. CRESPI, *Chairman*

SESSION 16

OPERATIONAL HEALTH PHYSICS AND CONTAMINATION OF WORKING AREAS III

J. ROTNICKI, *Chairman*

SESSION 17

SPECTROMETRY AND INSTRUMENTATION II

G. COWPER, *Chairman*

SESSION 18

ENVIRONMENTAL CONTAMINATION, FALLOUT AND FOOD CHAINS II

G. JOYET, *Chairman*

SESSION 19

OPERATIONAL HEALTH PHYSICS AND CONTAMINATION OF WORKING AREAS IV

V. KLENER, *Chairman*

SESSION 20

INTERNAL EMITTERS II

N. G. GOUSSEV, *Chairman*

PLENARY SESSION B

REPORTS ON A CRITICALITY ACCIDENT

J. R. HORAN, *Chairman*

SESSION 21

MEDICAL ASPECTS OF RADIATION PROTECTION II

Z. DJUKIC, *Chairman*

SESSION 22

ENVIRONMENTAL CONTAMINATION, FALLOUT AND FOOD CHAINS III

Y. FEIGE, *Chairman*

SESSION 23

PERMISSIBLE DOSES AND RADIATION GUIDES

K. KOREN, *Chairman*

SESSION 24

DOSIMETRY IV

M. POWELL, *Chairman*

SESSION 25

MEDICAL ASPECTS OF RADIATION PROTECTION III

F. WACHSMANN, *Chairman*

SESSION 26

OPERATIONAL HEALTH PHYSICS AND CONTAMINATION OF WORKING AREAS V

R. M. FRY, *Chairman*

PREFACE

THE First International Congress of Radiation Protection, sponsored by the newly formed International Radiation Protection Association (IRPA) was held in Rome, September 5–10, 1966. The technical programme was outstanding in quality, thoroughly international in scope, and included papers in every major subject category of radiation protection. The Provisional Council of IRPA decided that the proceedings of the Congress would be a useful repository of the studies reported at the Congress as well as a permanent record of the technical level of the subject area at this time and, therefore, arranged to make them available to Congress registrants and to the general public. The Council is indebted to Pergamon Press for its co-operation and fine performance in realizing this goal.

The papers have been arranged by sessions, thus preserving the continuity established by the Programme Committee. Abstracts of all papers presented orally or read by title are included for each session. If a rapporteur paper was given, it has been included, when available, in the belief that the rapporteur's evaluation and comparisons of the papers he reviewed add considerably to the value of the individual papers. It has not been possible to provide translations of papers or abstracts in all the official languages of the Congress. Thus the arrangements of the papers follows closely that of the Scientific Programme, and these proceedings may serve as a permanent memorial of the excellent organization of this Congress.

The publication of such an extensive body of technical information requires the assistance of many persons, and it is a pleasure for the Editor to acknowledge this indebtedness and express his appreciation to the President of the Congress, Dr. P. Caldirola; to Dr. C. Polvani, Secretary General of the Congress; and to Dr. L. Forti and the members of the Secretariat which she directed for their generous and courteous assistance. In particular, the Secretariat was responsible for collecting manuscripts at the time of the Congress and for the transcription of the discussion. The fine co-operation of W. G. Marley and A. Cigna and of the Programme Committee which they directed was invaluable in planning for the publication of the proceedings. The authors of the papers also deserve thanks for their co-operation; only a few papers could not be obtained for publication. The Editor wishes to acknowledge with gratitude the assistance of the six persons who agreed to serve as Assistant Editors. Each of them had full responsibility for a certain group of papers from their initial delivery to the final reading of the proof, so that, except for some general guidelines, each was, in effect, an editor. Without their assistance, the task would have been unmanageable. It is an especial pleasure to acknowledge the excellent co-operation of Pergamon Press throughout the course of the planning and publication of the proceedings, and the names of E. J. Buckley and Roy E. Strange are recorded here to express my special thanks for their assistance and guidance. Undoubtedly the list of those whose efforts have contributed materially to the work of publishing these proceedings could be extended over several pages of this volume. Many of them are not known to the Editor, and he can only express his general thanks to them.

The Editor believes these proceedings will be a valuable record of the Congress and that all concerned in preparing this material for the press will share his satisfaction in contributing to their publication.

WALTER S. SNYDER
Publications Director, IRPA

DEVELOPMENT OF HEALTH PHYSICS AS A PROFESSION*

KARL Z. MORGAN

Director, Health Physics Division, Oak Ridge National Laboratory, Oak Ridge, Tennessee, U.S.A.

Abstract—A brief history is given of the growth and development of health physics as a scientific profession. It is indicated that scientists and engineers from many disciplines have pooled their interests, combined their efforts and focused their attention on the central objective of providing adequate radiation protection for man and his environment from the harmful effects of ionizing radiation while at the same time enabling him to make better use of the benefits of this great source of energy. These scientists are engaged in education, training, administration, applied activities, engineering and research. Health physics research covers a wide spectrum of problems ranging from the effects of radiation on the living cell and on man to its interaction with matter at the atomic and nuclear levels. Ultimately, the goal of the health physicist is to develop a coherent theory of radiation damage, to assure that he measures and evaluates the proper physical and biological parameters related to the significant forms of potential radiation damage, to establish adequate radiation protection recommendations and measures at the national and international levels and to enforce these in such a manner that the benefits of ionizing radiation far outweigh the damage. Although the Health Physics Society, organized in 1956, was surprisingly successful in developing an international radiation protection organization, it was actually only partly successful in reaching this objective because there were some countries from which there were no members and many persons referred to it as the American society; this led to the formation of the IRPA and the calling of this international congress on radiation protection 10 years after the Health Physics Society was organized. Many old and new problems on a local, national and international level remain to be solved by the health physicist. A few of these problems are given for illustration and are discussed briefly.

RADIATION protection measures were practised rather sporadically from the time of the discovery of X-rays in 1895 until the beginning of World War II when health physics was organized as a profession, a new profession in which experienced and well-trained men with a variety of scientific backgrounds spent full time in activities for the protection of man and his environment from the hazards of ionizing radiation while at the same time encouraging an ever-increasing use of this great source of energy for the benefit of all mankind. This new profession, beginning with only eight health physicists at the University of Chicago in 1942–43, grew very rapidly and spread to all countries in which there were nuclear reactor and high voltage accelerator programs. In 1955 at the University of Ohio, Columbus, Ohio, the Health Physics Society was formed and a year later it was formally organized at the University of Michigan, Ann Arbor, Michigan. Although those organizing this society came from only two countries—the United States and Canada—they deliberately organized what they hoped would become a truly international radiation protection association because as expressed by these founders "problems of radiation protection and their solution, whether in research, education and training or applied activities should not be limited by national boundaries or subordinated to political pressures". By its tenth birthday (1965) the membership of this Society approached the 3000 mark with members in 45 countries and sections in France, the United

* Work sponsored by the U.S. Atomic Energy Commission under contract with the Union Carbide Corporation.

Kingdom, Japan, Central Europe and Israel. Under the presidency of W. T. Ham (1964) it was first officially recognized that the Health Physics Society, although surprisingly successful in fostering an international radiation protection association, was actually only partially successful in attaining this goal of achieving a maximum participation in its programs by qualified individuals of all countries because (1) it had no members from countries such as Argentina, China, Egypt, Hungary, Luxemburg, Peru, Romania, Russia, Uruguay, etc., (2) in Europe, it was referred to frequently as the American Health Physics Society and (3) there were several independent radiation protection societies not affiliated with the Health Physics Society. As a consequence, I was asked to investigate this matter and explore the interest of persons in all parts of the world in forming a single international health physics or radiation protection association. I corresponded on this matter with members of the Health Physics Society and with hundreds of persons outside the Society; altogether I had replies from persons in approximately 70 countries. It was gratifying and very encouraging to find among these an overwhelming desire for the creation of such an organization. This led to the formation of an *ad hoc* committee consisting of 46 persons in 25 countries of the world, a committee to exchange information and pave the way for an international radiation protection association. Table 1 indicates the membership of this *ad hoc* committee.

On February 1, 1964 a small working group of this *ad hoc* committee, consisting of A. Benco (Italy), P. Courvoisier (Switzerland), P. Bonet-Maury, F. Duhamel and H. Jammet (France), W. G. Marley and B. A. J. Lister (United Kingdom), R. Maushart (Germany), S. Halter (Belgium), and W. T. Ham and K. Z. Morgan (United States) was informally assembled in London to discuss the matter. This group decided to proceed with plans to form an international radiation protection association. It agreed unanimously on the basic principles, the

Table 1. *Members of the* ad hoc *Committee to form an International Health Physics or Radiation Protection Organization (January 1964)*

1. A. Alonso, Spain
2. Argeo Benco,* Italy
3. Hanson Blatz,* U.S.
4. Paul Bonet-Maury,* France
5. Robert A. Borthwick, IAEA
6. Louis Bugnard, France
7. J. C. E. Button, Australia
8. R. C. Cavalcanti, Italy
9. N. Chassende-Baroz, France
10. P. Courvoisier,* Switzerland
11. F. P. Cowan, U.S.
12. George Cowper,* Canada
13. Fokke Dijkstra, Holland
14. Francis Duhamel,* France
15. Yehuda Feige,* Israel
16. Jose M. Feola, Argentina
17. Jose A. Ferrer-Monge, Puerto Rico
18. E. H. Graul, Germany
19. S. Halter,* Belgium
20. Jorge Halvas, Mexico
21. H. J. Ham, Australia
22. W. T. Ham,* U.S.
23. H. F. Herr, U.S.
24. Toyohide Ishihara, Japan
25. H. P. Jammet,* France
26. P. Kayser,* Luxembourg
27. Kristian Koren,* Norway
28. B. A. J. Lister,* England
29. W. G. Marley,* England
30. John H. Martin, Scotland
31. R. Maushart,* Germany
32. Joseph S. Mitchell, England
33. Karl Z. Morgan,* U.S.
34. Jan Muller, Czechoslovakia
35. Jung Woo Nam, Korea
36. Hassan Parnianpour, Iran
37. Frank L. Paschal, Jr.,* U.S.
38. C. M. Patterson, U.S.
39. C. Polvani,* Italy
40. Pierre Recht,* Belgium
41. Rolf Sievert, Sweden
42. Joaquin Solanas,* Venezuela
43. F. D. Sowby,* ICRP
44. L. S. Taylor, U.S.
45. F. Yamasaki, Japan
46. J. Zakovsky, Austria

* These persons are listed on the program of the First International Congress of IRPA, Rome, Italy, September 5–10, 1966.

aims and objectives of the organization and drew up articles of agreement as summarized in Table 2.

Following a favorable response from the *ad hoc* committee and the encouraging recommendations from the London meeting, the Board of Directors of the Health Physics Society formed a *pro tempore* Executive Council to further

*Table 2. Articles of Agreement for the formation of an International Health Physics or Radiation Protection Society**

(1) We have clarified to our satisfaction what is the Health Physics Society and the interpretation as used in America has led to a better understanding.
(2) The aims and objectives of an international health physics or radiation protection society shall be:
  (a) to promote international contacts between those engaged in radiation protection work and promote the profession throughout the world,
  (b) to promote and organize international meetings on these matters,
  (c) to support an international journal devoted to radiation protection, and
  (d) to support the work of international bodies concerned with the establishment of radiation protection standards and recommendations for radiation protection.
(3) We are in unanimous agreement that we wish to move toward a single health physics or radiation protection society.

* Drawn up in London, England, February 1, 1964 by a working group of the *ad hoc* Committee to form an International Health Physics or Radiation Protection Organization.

study and expedite these proposals. The first meeting was held at Gatlinburg, Tenn., June 11–12, 1964 and members of the Council attending were H. Jammet (France), R. Maushart (Germany), W. T. Ham and K. Z. Morgan (United States). Proxies were present as follows: P. Bonet-Maury for F. Duhamel (France), R. Maushart for P. Courvoisier (Switzerland), H. J. Dunster for W. G. Marley and B. A. J. Lister (United Kingdom), Y. Nishiwaki for T. Aoki (Japan), M. Izawa for F. Yamasaki (Japan) and P. Recht for S. Halter (Belgium). Members of the Council not represented were A. Benco (Italy), G. A. Zedgenidz (USSR), R. M. Sievert (Sweden), and A. M. Marko (Canada). Other invited attendees were M. Gras, H. Francois, P. Pellerin and J. Pradel (France), and H. H. Abee, J. C. Hart and W. S. Snyder (United States). At this meeting there was unanimous approval on the basic principles and articles of agreement prepared at the London meeting. It was agreed that the name of this organization should be the International Radiation Protection Association (IRPA). With the help of H. H. Abee and the legal guidance of J. C. Hart, this group developed the framework of a constitution.

This constitution called for a rather unique confederated type of association. It stated not more than one organization from each country could be affiliated with IRPA and that individual members of national or regional affiliated societies would automatically become members of IRPA but that membership in IRPA would be possible only through such affiliated societies. The IRPA would be governed by a General Assembly, each member of which was to be elected by members of his affiliated society in accordance with procedures assigned to express the will of the majority of members of his society. The national or regional affiliated societies would have almost complete autonomy in matters of local or national concern. The business of IRPA and particularly that of the General Assembly would be carried on by an Executive Council elected by the General Assembly. The principal objectives and purposes of the International Radiation Protection Association, in addition to those expressed in the London articles of agreement, were summarized in the IRPA constitution: (1) to encourage scientific research and educational opportunities among those scientific disciplines which support the science of radiation protection, and (2) to encourage the establishment of radiation protection societies throughout the world as a means of achieving international cooperation among scientists. There was complete accord of members of the *pro tempore* Executive Council on these recommendations which they then presented a few days later (on June 15, 1964 in Cincinnati, Ohio) to the Board of Directors of the Health Physics Society; the Board in turn approved them unanimously.

At meetings of the *pro tempore* Executive Council in Gatlinburg and in Cincinnati, it was

decided to hold a *pro tempore* General Assembly at a convenient location during the early part of December, 1964. It was later agreed to hold this Assembly in Paris, France, as guests of the French Section of the Health Physics Society. P. Bonet-Maury, past-president of this Section, served as local chairman of arrangements. This now historic meeting of the *pro tempore* General Assembly was held at the Centre de Conferences Internationales, Paris, France, November 30–December 3, 1964. Table 3 is a summary listing those organizations with official delegates at this important Assembly, the number of members reported by each of the organizations, names of attending delegates and others attending but not officially representing specific organizations.

Fifteen societies had official delegates there and, in addition, delegates were present from six other countries. Altogether there was representation from some 4000 health physicists in 50 countries.

The 45 official delegates at this *pro tempore* General Assembly adopted a constitution which states our primary objectives, objectives which are essentially those agreed upon earlier at the

Table 3. Summary of Organizations, Membership reported and Delegates attending the Pro Tempore *General Assembly in Paris, France, November 30–December 3, 1946*

Organization	Members	Delegates
Belgium Radioprotection Association	182	Halter,[A§‡P] Boulenger, Hublet and Recht[A,ζ]
Central European Section of the Health Physics Society (Austria, Germany, Switzerland)	20	Becker [P] and Mehl*
European Society for Radiation Protection	148	Courvoisier[A§‡P] and Maushart[A§‡ζP]
French Health Physics Society (amalgamated)	425	Duhamel,[A§‡P] Jammet,[A§‡ζP] Pellerin,[ζ] Gras,[ζ] Bonet-Maury,[A§ζP] Chassende-Baroz[A]
Health Physics Society (Canada)	29	Marko [‡P]
Health Physics Society (United States)	2302	Andrews, Terrill, Abee,[ζP] Morgan,[A§‡ζP] Ham[A§‡ζP]
Israeli Section of the Health Physics Society	12	Feige[AP] and Donagi
Italian Health Physics Association	125	Argiero, Todisco and Benco[A§‡P]
Japanese Health Physics Society	209	Yamaoka and Nishiwaki[ζP]
Luxembourg	29	Kayser[A] and Rischard
Mexican Society of Radiation Protection and Hospital Physicists	50	Halvas[A]
Netherlands Society for Radiation Hygiene	117	Spaander[P]
Nordic Society for Radiation Protection (Denmark, Finland, Norway, Sweden, Iceland)	201	Sievert,[A‡P] Grande, Salimaki,[A] Koren,[P] Lindell
United Kingdom Section of the Health Physics Society	127	Marley[A§‡P] and Lister[A§‡P]
Yugoslav Health Physics Society	~200	Tasovac

[A] *Ad hoc* Committee Member.
§ Attended London meeting on February 1, 1964.
‡ *Pro tempore* Executive Council Member.
ζ Attended Gatlinburg meeting on June 11-12, 1964.
* Also an IAEA observer.
[P] Elected on December 3, 1964 as a member of the Provisional Executive Council.

National Delegates not Representing Specific Organizations

L. Sklavenitis (Greece)
H. Parnianpour[A] (Iran)
O. Fissore (Monaco)
E. Ramos (Spain)
J. Baarli (Switzerland)
O. Beninson (Argentina)

London and Gatlinburg meetings and summarized above. In particular, the constitution emphasizes our primary purpose and goal of providing a medium whereby international contacts and cooperation may be obtained among those engaged in radiation protection work—both applied and research—in an effort to provide for the protection of man and his environment from the hazards caused by ionizing radiation and thereby to facilitate the exploitation of radiation and atomic energy for the benefit of mankind. I believe it is significant that the constitution of IRPA states the positive as well as the negative purpose of the profession of health physics.

It was decided at the Paris *pro tempore* General Assembly to form a rather large Provisional Executive Council to be responsible for the organization of the International Radiation Protection Association, to prepare for the first International Congress and General Assembly of IRPA and to select and approve appropriate organizations as affiliates in this federation. However, to expedite business matters a smaller executive group of provisional officers was provided. Those elected were P. Caldirola of Italy (Vice-President), thus signifying that the first General Assembly would meet in Italy in 1966, P. Bonet-Maury of France (Secretary), P. Courvoisier of Switzerland (Treasurer), W. S. Snyder of the United States (Publications Director) and myself (Chairman). Other members of the Provisional Executive Council as elected by the *pro tempore* General Assembly were P. Spaander (Netherlands), A. Benco (Italy), Y. Feige (Israel), K. Koren (Norway), K. Becker (Germany), A. M. Marko (Canada), R. M. Sievert with B. Lindell as his alternate (Sweden), S. Halter (Belgium), G. Zedgenidz (USSR), R. Maushart (Germany and also representing Austria and Switzerland), F. Yamasaki (Japan), Y. Nishiwaki (Japan), B. A. J. Lister (England), W. G. Marley (England), F. Duhamel (France), H. Jammet (France), H. H. Abee (United States) and W. T. Ham (United States). In addition the chairman was asked to select one representative from Latin America.

At a meeting of Latin American health physicists in June 1965 in Los Angeles, California, J. Solanas was elected as their representative and the next day at the meeting of the Provisional Executive Council he was appointed as a member of the Council.

The succeeding meetings of the Provisional Executive Council were held in Los Angeles (June 18–19, 1965), Paris (December 16–17, 1965), Sterling Forest (June 18–19, 1966), and finally in Rome (September 3, 1966). Our most important progress at these meetings is indicated in Table 4 by action taken relative to new affiliates of IRPA. Other developments have been made in proposing amendments to the constitution and a set of operating procedures, both of which will be presented for consideration and approval at the General Assembly, Wednesday, September 7.

The Health Physics Society from the beginning has strongly supported efforts for the formation of an international organization in which health physicists in each country would have appropriate representation. The recent presidents, W. T. Ham, H. L. Andrews and M. Eisenbud, have made many personal sacrifices to assure the success of IRPA and the Board of Directors of the Health Physics Society has given strong financial support to these efforts. It has agreed to make available to affiliated members of the International Radiation Protection Association its journal, *Health Physics*, at cost, at present $6.00 per year. One of the principal tasks of W. S. Snyder, the Publications Director, has been to facilitate the availability of *Health Physics* to all members of affiliated organizations and to originate acceptable material for publication in *Health Physics* from you, the members of affiliated societies of the IRPA. The editors of *Health Physics* urge you to submit for publication high-quality papers on all aspects of radiation protection. For example, we welcome papers on such subjects as radiation monitoring and surveys, environmental surveys, waste disposal, transport of radionuclides in air and in water, personnel dosimetry, radiation ecology, internal dose, fallout, contamination control, resuspension of surface contamination, regulations, codes of practice, radiation accidents, instrumentation, basic studies of interaction of radiation with matter at all levels of interaction (atomic, molecular, plasma, crystal, gas, liquid, solid, cell, organism, animal and ecosystem), studies of radiation damage, radiation risks, permissible dose, measurements of

Table 4.

Society name and principal area	Place of action Provisional Executive Council and Date of unqualified acceptance
1. The Central European Section of the Health Physics Society (name changed to Fachverband fur Strahlenschutz)—Germany, Switzerland and Austria.	June 19, 1966, Sterling Forest[1]
2. Association Luxembourgeoise de Radioprotection—Luxembourg	December 17, 1965, Paris[1]
3. Société Française de Radioprotection—France	June 19, 1965, Los Angeles
4. Health Physics Society—U.S. and Canada	June 19, 1965, Los Angeles
5. Nordiska Sallskapet for Stralskyld—Norway, Sweden, Denmark, Finland and Iceland	December 17, 1965, Paris
6. L'Association Belge de Radioprotection—Belgium	December 17, 1965, Paris
7. Japan Health Physics Society—Japan	December 17, 1965, Paris
8. British Radiological Protection Association—United Kingdom (England, Wales, Scotland, and North Ireland)	December 17, 1965, Paris
9. Israel Health Physics Society—Israel	December 17, 1965, Paris
10. Association Italiana di Fisica Sanitaria e di Protezione Contro le Radiazione—Italy	December 17, 1965, Paris
11. Nederlandse Vereneging voor Stralingshygiene—Netherlands	December 17, 1965, Paris
12. Associacion Mexicana de Proteccion Radiologica Y Fisica Medica—Mexico	June 18, 1966, Sterling Forest
13. Argentine Radiation Protection Association—Argentina	June 18, 1966, Sterling Forest
14. Eotvos Lorand Physical Society, Health Physics Section—Hungary	June 18, 1966, Sterling Forest
15. Philippine Radiation Protection Association—Philippines	September 3, 1966, Rome[2]

[1] Provisional acceptance was on June 19, 1965 in Los Angeles, California.
[2] Provisional acceptance was on June 18, 1966 in Sterling Forest, New York.

dose and energy spectra, quality factor, etc. We welcome especially papers from new areas of interest and responsibility of the health physicist, e.g. biological effects and dosimetry of laser radiation, intense magnetic fields, fusion reactors and space radiation.

P. Caldirola of Italy with the assistance of his very able colleagues has had as his principal assignment the arrangements for this, the first meeting of the International Radiation Protection Association in Rome, Italy, September 5–10, 1966. He has had the valuable assistance of his Honorary Committee and Advisory Committee and especially of the Secretary-General C. Polvani, Treasurer of the Conference A. Benco, Scientific Program Chairman W. G. Marley, Local Arrangements Chairman S. Tagliati, Technical Exhibits Chairman L. Argiero and Secretariat L. Forti. Without the untiring efforts and devotion of these individuals to IRPA and the health physics profession, this meeting in Rome could not have been the grand success that it is. I would like to recognize also the strong support IRPA has received from the International Commission on Radiological Protection, the International Commission on Radiological Units, the International Atomic Energy Agency, the World Health Organization and the International Labor Office. They have assisted us by sending observers to meetings of the Provisional Executive Council where they gave us very valuable advice and guidance. We are most grateful also to IAEA, Euratom,

the Health Physics Society, the Société Française de Radioprotection and the Italian Board of Management for giving us very substantial financial assistance without which this meeting would have been impossible and we would not have been able to provide you with published proceedings of this International Congress. I would like to thank also the societies affiliated with IRPA that have made advance contributions of 1966 dues amounting to an extra year of dues in order to assist this fledgling organization. With this kind of voluntary support IRPA is bound to succeed.

It is encouraging that scientists and engineers with many different national, cultural and language backgrounds can sit down together at meetings in London, Gatlinburg, Paris, Los Angeles, Sterling Forest and now in Rome and agree on the formation of a rather unique international organization with such worthwhile scientific and professional objectives and develop a constitution based on such sound, democratic principles—a constitution recognizing the importance of the individual health physicist yet allowing almost complete autonomy of the individual affiliated societies in matters of local and national interest. We have formed an outstanding international organization which is a federation, yet an organization in which the individual is the most important element; he is an entity who expresses rather than impresses his will, both nationally and internationally. Hopefully, this spirit of trust and unanimity may point the way of cooperation not only to other scientists and professions, but to all those seeking a solution to international problems. Although there have been some differences of opinion among members of the Provisional Executive Council, such differences were discussed freely and an understanding was reached; if necessary, satisfactory compromises were attained. Unlike many other international groups, the *pro tempore* General Assembly in Paris and the Provisional Executive Council in its several meetings have met in a spirit of complete harmony and cooperation; this meeting in Rome (September 1966), the first General Assembly of IRPA, is no exception and in fact has set such a high standard and one so close to perfection it is difficult to imagine how future meetings can continue to improve other than by emulating it. We have set a pattern and cultured an environment of cooperation in which we hope to exchange freely all information relating to the protection of man and his environment from radiation damage. With agreement on fundamental issues providing for cooperation of health physicists at the national and international levels and with the adoption of an organizational structure of IRPA that assures a mechanism for free exchange of information, we confidently expect more beneficial uses can be made of ionizing radiation. It is my hope and prayer that through this organization better radiation protection will be provided wherever it is needed—in research establishments, in hospitals, in the doctor's office, in mass X-ray programs, in reactor development and in the space program. Wherever the ratio of benefits to damage from ionizing radiation can be increased with a reasonable amount of effort, the health physicist member of IRPA must recognize a challenge and an opportunity for professional service to man. In education and training each of the societies affiliated with IRPA must be satisfied with nothing but the best because our leaders must be men of stature that can stand shoulder to shoulder with the best scientists. In applied research we must solve the difficult as well as the simple, day-to-day problems, but at the same time we must apply a considerable portion of our research effort to the long-range and more basic studies. We must not be satisfied until we understand the basic mechanisms of radiation damage at all levels of energy exchange following the absorption of ionizing radiation and as the entropy of the system increases. We must continue our research until we have developed a coherent theory of radiation damage that answers our questions regarding permissible dose limits, that indicates the best methods of measuring the proper parameters relating to dose and to biological damage and that permits the prediction of biological consequences of a given exposure which must be carefully weighed against the expected benefits.

In this hour of rejoicing, however, let us not fail to recognize that as yet we have not been completely successful in this first phase of our development since our goal for a truly International Radiation Protection Association will

not be attained until all nations having 20 or more health physicists are affiliated with IRPA. This assembly of health physicists in IRPA has focused attention on the ways in which cooperation is possible rather than stubbornly and blindly argue about and magnify the impossibility of agreement. Perhaps politicians would say such agreements among people of many countries are impossible but maybe we have succeeded because health physicists are a band of scientists that refuse to recognize the impossible. This agreement among health physicists is now an established fact; IRPA is a reality, a going, growing organization and at this meeting in Rome (September 1966) we are proud to announce there are fifteen organizations affiliated in IRPA comprising a total of over 5000 members living in 55 countries of the world. We are moving steadily toward the attainment of our goal for world cooperation among all health physicists in one international organization.

PERMISSIBLE DOSES FOR CRITICAL TISSUES

E. ERIC POCHIN
Medical Research Council Department of Clinical Research, University College Hospital Medical School, London

Abstract—If dose rates regarded as permissible for occupational exposure of different critical organs or body tissues need to be determined less in respect of any likely impairment of organ function at these dose rates than of the risk of neoplastic change or relevant genetic effects, the criteria on which such dose rates are determined ought to be related to any available quantitative information as to the sensitivity of the various human tissues and cell types to such changes. Possible bases for such comparisons are reviewed.

ONE of the most important functions of the International Commission on Radiological Protection, and certainly one of the most difficult, must be its assessment, quantitatively, of the maximum levels of dose or dose rate that can be regarded as permissible, but which should not be exceeded, under various particular circumstances of necessary exposure to ionising radiation. This judgement is of course central to all protection requirements. Yet it is doubly difficult to make if we need to envisage the possibility of occasional radiation damage even at the lowest doses and dose rates, since we must then review, not only the numerical level of risk from various possible injuries at low doses, but also the levels of risk that could be regarded as appropriate for various circumstances of occupational or other exposure. The first is a radiobiological judgement that has to be made in the absence, fortunately, of any direct statistical evidence as to the harmfulness to man of radiation at low doses or dose rates. The second is a sociological judgement as to the right criteria of safety and limitation of hazard, a subject on which the community offers remarkably little direct opinion, at least in the necessary quantitative terms, although it is evident in principle that risks should be minimized, or eliminated if practicable.

I believe that the Commission's recent Publication 9[1] will be of value in helping to keep these difficult and important questions in perspective; and that the report of a Task Group of its Committee 1,[2] on the problems of radiation risk evaluation, will be particularly helpful also for the light it throws on the available quantitative evidence, and on the degree of safety that is implied by particular dose limits. This report is one which appeared in the February number of *Health Physics*—so happily offered by the journal and by the Commission as a tribute to our distinguished colleague and friend, Rolf Sievert.

The necessary translation of recommended limits of dose rate into the corresponding estimates of body burdens, organ burdens or intake—building the bridge from rads to microcuries—has been a heavy and an equally difficult task, for which we all owe much to the President of the Association, Karl Morgan, for his chairmanship of the Commission's Committee on Internal Exposure. This essential task, of making the Commission's recommendations meaningful in terms of monitoring, of organ or body contents, of intakes or excretions, has been the harder because of the sparseness of metabolic data for many nuclides in man, even sometimes in mammals, and a wide field of investigation has to be kept continuously under review to strengthen the bases for the guidance needed on many different elements. The work of special task groups on particular tissues, for example recently on gut and on lung, and currently on bone, is also being of great value in defining the metabolic models which can be used to describe the behaviour

of radioelements in tissues, and to establish criteria for appropriate monitoring.

But all these recommendations on internal dose depend on a basic question which I would like to discuss briefly, since it is also one which requires to be kept under close review in the light of developing knowledge. When individual organs or tissues are exposed singly—owing to selective concentration of particular radionuclides in or near them—what dose rates for each tissue will ensure a degree of safety to the worker equal to that involved when *all* the organs or tissues are equally exposed at 5 rem/year?

This problem again is a difficult one to resolve in the necessary quantitative way. It obviously is less hazardous for the lung only to be exposed at 5 rem per year than for the lung and all other tissues to be exposed at this rate. The dose rate for the lung as critical organ alone should therefore clearly be higher than that for whole body radiation; but how much higher, and what should be the basis for deciding the ratio to be used?

On present criteria, the maximum dose rate for most organs in the body, if irradiated singly, is three times that for whole body irradiation, with the exception of a higher ratio for skin, bone and the thyroid of adults, and a lower one for gonads and red bone marrow. The use in this way of the same limit of dose rate for most organs would seem appropriate, in the absence of better information on the sensitivity of particular tissues, if we are essentially protecting against impairment of organ function, which might well depend on damage to enzyme systems or cell structures that were similar in different tissues; and the very proper present references to the importance of the different organs to the body health reflect the same concern with impairment of function.

It is becoming increasingly clear, however, that, at the low doses and dose rates involved in protection limits, the metabolic function of the organ as a whole will be essentially unimpaired, and the relevant risks to the exposed individual are of the possible occasional induction of malignant change in certain tissues—other changes contributing to life shortening being at present more uncertain in man although probably present. The risks to the individual's progeny will depend on mutations induced by irradiation of germinal tissues. And risks to a foetus would be added in exposure during pregnancy. If these are the hazards, what should be the criteria for setting up permissible doses to different critical organs or tissues?

The following three assumptions might be appropriate as a basis for setting the dose limits for individual body tissues, if irradiated singly, in relation to that adopted for uniform whole body exposure.

Firstly, that the hazard of whole body irradiation is simply the total of the hazards of the radiation of its constituent tissues. This will clearly be untrue at high doses, when the probability of the development of somatic or genetic change in an individual would be affected by the possibility of his earlier death from another somatic effect, or perhaps from effects of radiation on the function of particular tissues or from more subtle effects on endocrine or other forms of co-ordination. At the low doses, and presumably the low probabilities of somatic effects, that apply for permissible dose limits, however, it seems likely to be a reasonable approximation.

Secondly, that within the range of doses or dose rates applicable to permissible dose limits, the frequency of harmful effects is about proportional to the dose or dose rate. This again will not apply for certain (e.g. some chromosomal) changes, or perhaps if high dose limits were postulated for relatively insensitive tissues, or for locally high dose rates associated with non-homogenous dose distributions. It has however been rather widely postulated for protection purposes and might be assumed as an approximation within the range of dose rates involved.

Thirdly, that dose limits for individual tissues, when irradiated singly, or for the whole body, when uniformly irradiated, are set so that the risk from any of these modes of exposure is equal in magnitude. This has never been formally stated as the basis for different tissue dose limits and there are obvious difficulties in assessing the weight to be attached to different risks such as of disease in the exposed individual or in his descendents, fatal and non-fatal disease, or malignancies occurring

after short or long latency. The general aim of an equally high degree of protection for different forms of exposure, however, seems basic.

If these three assumptions are accepted as criteria for reviewing dose limits for critical tissues, I think that the first problem, setting aside for the moment the rather special question of foetal irradiation during a pregnancy, must be to consider the relative total importance of the somatic effects in the individual exposed and the genetic effects in his progeny. To pose a definite question: if a population of a million people of all ages were exposed to one rad of whole body radiation, how would the total of resulting cases of leukaemia, other malignancy or other somatic effect in those exposed compare in importance with the total of all injuries resulting from genetic damage?

This question can of course never be answered by any simple quantitative comparison, between say the number of deaths caused in the exposed individuals and the number of deaths or severe disabilities induced in their descendents. Some opinion must however be expressed, or will be implied, in any attempt to allocate dose rates for different tissues and for the whole body—even though the opinion may simply be that the sum of genetic damage is at present judged likely to be about equal to—or to be several times as important as—the sum of the somatic damage.

Examination of the "Risk Report" indicates that the receipt of one rad by a million people might result in of the order of 50 to 100 fatal malignancies. This number of effects would be increased if non-specific ageing effects were important in man. It would be very much reduced if the dose response relationship in man were quadratic rather than linear.

The same population exposure might result in of the order of 10 seriously defective offspring in the first generation from point mutations, and probably a substantially larger number from chromosomal aberrations. It is indicated that the total number of defects in all generations might reach several hundreds, but should not exceed several thousands even if every point mutation was equivalent to a major defect.

Any comparison of the somatic and genetic impact of radiation is thus beset at present by great quantitative uncertainties, as limiting as those involved in judging the importance of the different types of effect; and either somatic or genetic damage might involve total frequencies of major effects of some hundredths of one per cent per rad. If estimates of the type and frequency of all induced genetic effects led to the opinion that these had an importance equal to that of all induced somatic effects, then strictly the limiting dose rate for the gonads alone should be twice that for whole body radiation: and a gonad dose rate of 10 rem per year would correspond with the whole body rate of 5 rem per year if the hazard from each form of exposure were to be kept to an equally low level. Or if the genetic effects were judged to be more important than the somatic ones, the dose rate for gonads alone should be correspondingly closer to that for whole body radiation.

We may, I think, approach the dose limits for other tissues in a similar way. Suppose for a moment that non-specific ageing effects were unimportant compared with the induction of fatal malignancies, and that leukaemia formed one third of all the latter—again, broadly, on the basis of the Risk Report. If so, and if somatic and genetic effects were held to be equal in importance, the effects of whole body radiation would be due—as to one half to the gonad irradiation, and as to one sixth (one third of the remaining half) to irradiation of the bone marrow, if this is regarded as the critical tissue for induction of leukaemia. If then the whole body rate was 5 rem per year, that for gonads alone should be 10 rem per year and for bone marrow alone 30 rem per year. Clearly one could extend this type of argument with increasing information. If for example the thyroid and the pancreas were each responsible for one third of the remaining malignancies, the dose rates for these tissues, if irradiated alone, should be 45 rem per year—the dose rate for any particular tissue being inversely related to the risk per unit dose for that tissue, at least to levels at which a linearity of dose effect relationship might be assumed.

These values of course are quoted merely as illustrations of the way in which the increasing amounts of quantitative information that are

becoming available on radiation effects will need to be kept in review to ensure that protection criteria are properly related to current knowledge. The next few years are likely to see some clarification of the estimated relative frequencies of genetic and somatic effects; of the relative importance of malignant and other somatic changes; of the greater or less sensitivity of different tissues to malignant change. Already an approximate comparison can be made as to the sensitivity to induction of malignancies in the foetus and in the adult, so that some estimate could be made of relative total risk for different dose rates in the pregnant and non-pregnant individual. When the causes for any non-malignant life-shortening become clearer, we shall be better able to judge of the relative importance of the irradiation of such tissues as muscle or fat in which tumour induction seems likely to be of insignificant probability.

What I have discussed is simply a personal view of emerging information which may in the future alter somewhat, even if perhaps not greatly, the relative importance attached to the irradiation of different tissues—although the present criteria for some tissues may prove to be unduly restrictive. And it is stimulating to see in the scientific programme of this Congress so many papers on subjects which bear upon our advancing knowledge of the types and importance of the hazards with which the Commission is concerned in its protection recommendations and with which we are all involved in our development of protection procedures: the cells which are most sensitive; the dose rates which are of greatest importance; the localization of nuclides within the body, within the tissue or within the cell which are of highest significance; and the techniques of monitoring which can ensure the fullest and most reliable protection. I am sure that there will be the greatest value in this Congress's review of the means of achieving effective radiation protection and of the problems and difficulties which arise in the very varied fields of protection which we will have under discussion.

REFERENCES

1. Recommendations of the International Commission on Radiological Protection (Adopted September 17, 1965). *ICRP Publication* 9. Pergamon Press, 1966.
2. Evaluation of risks of radiation. *Health Physics*, **12**, 239 (1966).

DISCUSSION

M. GIUBILEO (*Euratom*):

1. La ICRP pensa di includere le dosi ricevute per scopi medici nella dosimetria generale dell'individuo?

2. Ritiene attuale considerare il midollo osseo come organo critico per la leucemia in base alle acquisizioni recenti sulla patogenesi periferica della leucemia?

E. E. POCHIN:

1. I believe that one should base one's procedure on the view that, if any radiation exposure may involve some element of risk, the risk should be justified by the need for the exposure. Levels of occupational exposure should correspond to a degree of safety appropriate to good industrial practice, and would not be influenced if a worker additionally required a radiological examination of which the necessity should also justify any risk involved. If the risks of radiation are regarded, at these dose levels, as being additive, the permissible occupational exposure should, on this basis, be no more affected by the need for a radiological examination than, for example, by the need for a surgical operation.

2. I would certainly agree that one cannot exclude the possibility that leukemia might be induced solely by irradiation of the blood, the lymph glands or other tissues, or that irradiation of part of the red bone marrow may be less important than irradiation of all of it. I think that one should, however, regard the red bone marrow as a "critical tissue" for leukemia induction, and that permissible doses for the marrow should be set with this in mind.

ENERGY TRANSFER BY ALPHA-PARTICLES TO BIOLOGICAL ENTITIES OF VERY SMALL SIZE

J. BOOZ
Biology Service, C.C.R. Euratom—Ispra, Italy

Abstract—The energy spectrum of the energy transferred by alpha-particles of ^{239}Pu and ^{210}Po to cylindrical subcellular units has been studied experimentally.

For this purpose a cylindrical proportional counter with tissue equivalent walls of Shonka type and with an internal diameter of 5 mm has been used. The counting gas is tissue equivalent (64·4% CH_4, 32·4% CO_2 and 3·2% N_2) flowing at a rate of 3 ml/min through a vacuum-tight vessel in which the counter is built. The alpha-particles which have an energy of about 5 MeV enter into the counter perpendicular to its axis through a hole 1 mm in diameter, their path length inside of the counter being constant within 1%. By using gas pressures between 1 and 500 torr the biological diameter of the counter has been varied between 70 Å and 3·5 μ of tissue.

The authors discuss the resolution of the counter and present measurements of the mean number of ionization that the alpha-particles produce along a track length of 50 Å.

INTRODUCTION

It is well known that the linear energy transfer (LET) of radiation is in general not a suitable parameter for describing the deposition of radiation energy on the *microscopic* level. This has been shown by Rossi and coworkers, who have measured the energy transferred to small spherical volumes by single events and have developed a new approach for describing the energy deposition by taking into account its quantification.[1-7] This approach has been shown to be very fruitful.[8] However, its practical application is limited by the fact that not all the sub-cellular biological structures that are believed to be significant for a certain biological damage can be approximated by a sphere. For the chromosome, for instance, that might be the significant structure for many observed effects, the infinitely long cylinder is probably a better model.

The purpose of this work was to study the possibility of using a cylindrical proportional counter as a "chromosome counter". The counter used and measurements of its resolution are described below.

INSTRUMENTATION

The proportional counter is shown in Fig. 1. It is cylindrical and has a diameter of 5 mm. Its wall is made from tissue equivalent plastic after Shonka.[9] The tissue equivalent counting gas was that proposed by Rossi and Failla[10] with a composition 64·4% CH_4 + 32·4% CO_2 + 3·2% N_2. When the gas pressure is 0·7 mm Hg, the diameter of the counter corresponds to 50 Å of soft tissue of unit density. This tissue layer that corresponds to the counter diameter at a certain gas pressure we will call from now on the "tissue diameter" d of the counter. The thickness of the counting wire was varied between 40 and 200 μ. For the final measurements the 50 μ wire was used because it gave a better resolution at the higher pressures. At pressures below 10 mm Hg the thickness of the counting wire had no influence on the measured deviation. The total counter was mounted on a BNC-connector passing through a vacuum-flange with which the counter was fastened in a gas tight vessel.

For the measurements of the energy transfer a small pencil beam of alpha-particles

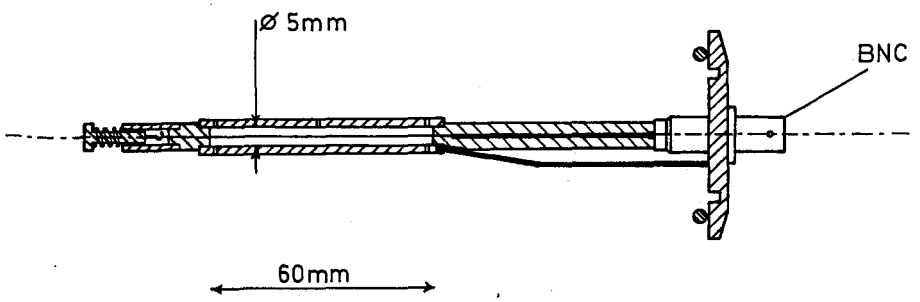

FIG. 1. Side view of the tissue equivalent proportional counter.

from ^{210}Po was used that traversed the counter perpendicular to its axis. The geometrical relation between the counter and the alpha-source is shown in Fig. 2. The alpha-particles passed into the counter through a hole of 1 mm in diameter. In order to prevent scattering at the inner surface of the hole, an aperture of 0·1 mm diameter in an aluminium foil 50 μ thick was put in front of the counter. The source was placed a little to one side of the line between the wire and the aperture, so that the particles could not come into collision with the central wire. The counter length of 60 mm, giving 30 mm at both sides of the pencil beam, is effectively infinitely long when its tissue diameter d is bigger than 400 Å.[11] With smaller sizes the more energetic δ-rays could reach the counter ends. However, this had no influence. Comparative measurements (d > 100 Å) with a similar counter having a length of only 30 mm gave the same results.

Figure 3 shows the instrumentation in form of a block diagram. All measurements were made with a constant gas flow of 3 ml/min passing through a metal gas-tight vessel containing the counter and the source. The pulses had a mean frequency of 10^4 cpm and a rise time of less than 0·2 μsec. The pulses were shaped in the main amplifier first by a differentiating and then by an integrating network, both having a time constant of 0·8 μsec. With this setting the noise level of the electronic system was about 600 electrons at the input of the preamplifier.

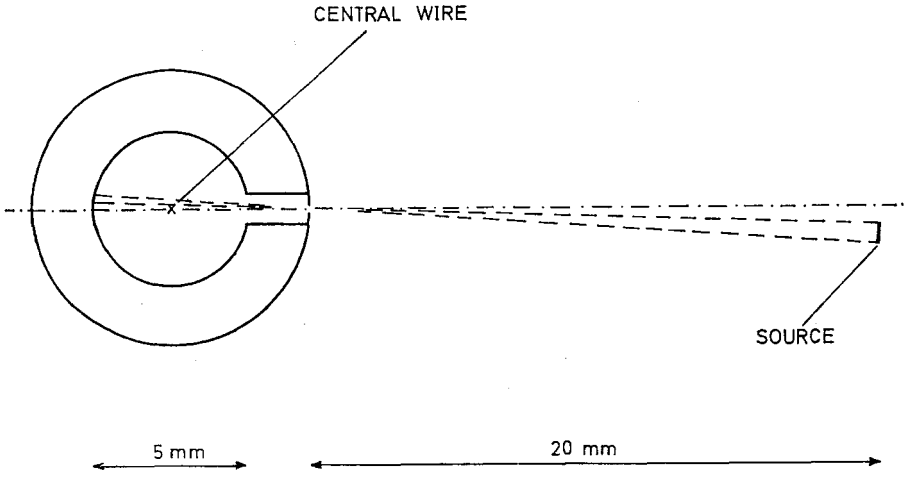

FIG. 2. Geometrical relation between counter and source. The alpha-particles enter through an aperture of 0·1 mm and pass through the counter without coming into collision with the central wire.

MEASUREMENTS

The alpha-source was shielded with 1.05 mg/cm² Al which caused a standard deviation of 1·3% in the particle energy. This deviation, measured with a solid state detector, was regarded as sufficiently small for the present purpose.

The energy transfer to the counter, and its spectral distribution, were measured at tissue diameters between 100 Å and 3·5 μ. At tissue diameters below 100 Å the peak of the energy spectrum began to disappear in the noise. Fig. 4 shows the spectrum measured at 240 Å as an example at low tissue diameters d. It is, like all other spectra measured at $d < 0.3\ \mu$,

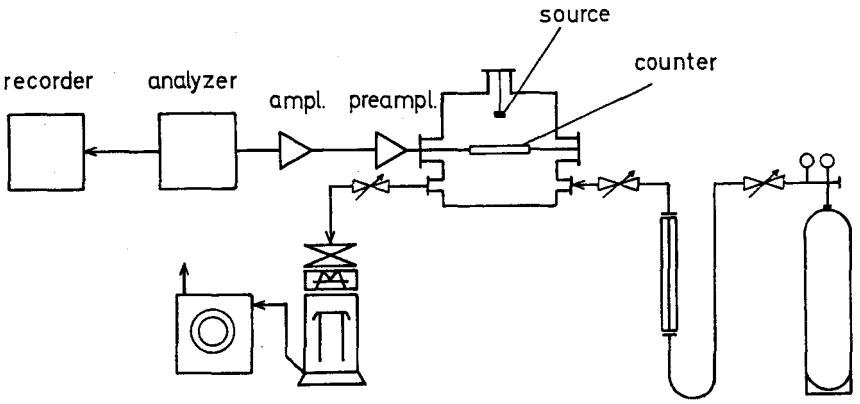

FIG. 3. Block diagram of the total instrumentation.

very close to a Poisson distribution. For the bigger tissue diameters the Gaussian distribution was a better approach. For the analysis of the measured standard deviations, that are shown in Fig. 5, it was assumed that the mean pulse height $\bar{E}$ of any measured pulse height spectrum is equal to the product of the mean values of the different components that contribute to the observed deviation:

$$\bar{E} = \bar{L}\,\bar{N}\,\bar{M}\,\bar{V}\,\bar{A}\,\bar{R}$$

from this follows

$$\frac{\sigma_E^2}{\bar{E}^2} = \frac{\sigma_L^2}{\bar{L}^2} + \ldots + \frac{\sigma_R^2}{\bar{R}^2}$$

The factors influencing the observed deviation are:

1. $\frac{\sigma_L}{\bar{L}}$ is the standard deviation of the mean energy transfer L of the alpha-particles to the counter.

2. N is the number of the ion pairs formed per energy unit.

3. M is the electron multiplication which would occur in an ideal proportional counter in which the region of multiplication at the central wire is infinitely small.

4. The factor V takes into account that the region of multiplication is not infinitely small.

5. A describes the constant deviation that is due to mechanical imperfection of the counter (central wire, counter ends, etc, $\sigma_A/A \approx 2\%$).

6. R is the electric amplification factor

$$\frac{\sigma_R}{\bar{R}} = 5{\cdot}5\% \text{ for } R = 2^{11},$$

$$\frac{\sigma_R}{\bar{R}} \leq 1{\cdot}2\% \text{ for } R \leq 2^9.$$

The standard deviation of the product MVA is the so called counter resolution. In Fig. 5 the measured deviation $\frac{\sigma_E}{\bar{E}}$ is shown.

The standard deviation of V which is calculated in the appendix is also drawn in Fig. 5. The comparison shows that the deviation of the factor V, which takes into account that the region

of multiplication is not infinitely small, is surprisingly low.

It can be concluded, therefore, that the counter has worked like a normal proportional counter.

The contribution of the components L, N, and M to the measured deviation $\sigma_E^2/\bar{E}^2$, unfortunately, cannot be evaluated by experimental methods. However, it can be shown theoretically[12] that the straggling of the energy transfer gives by far the biggest contribution (about 90%), whereas the deviation of N, the so called Fano fluctuation and the deviation that is caused by the multiplication process contribute to $\sigma_E^2/\bar{E}^2$ with about 10% only. Within the limits of accuracy, the measured deviation $\sigma_E/\bar{E}$ is therefore equal to the fluctuation of the energy transferred by alphas of about 5 meV to tissue of thickness d.

AVERAGE ENERGY PER ION PAIR

At tissue diameters between 1 μ and 3·5 μ the counter was used as a pulse ionization chamber to measure the differential average energy per ion pair along small track lengths. The results are shown in Table 1.

The second column gives the mean LET of the alpha-particles in the counter. It is the

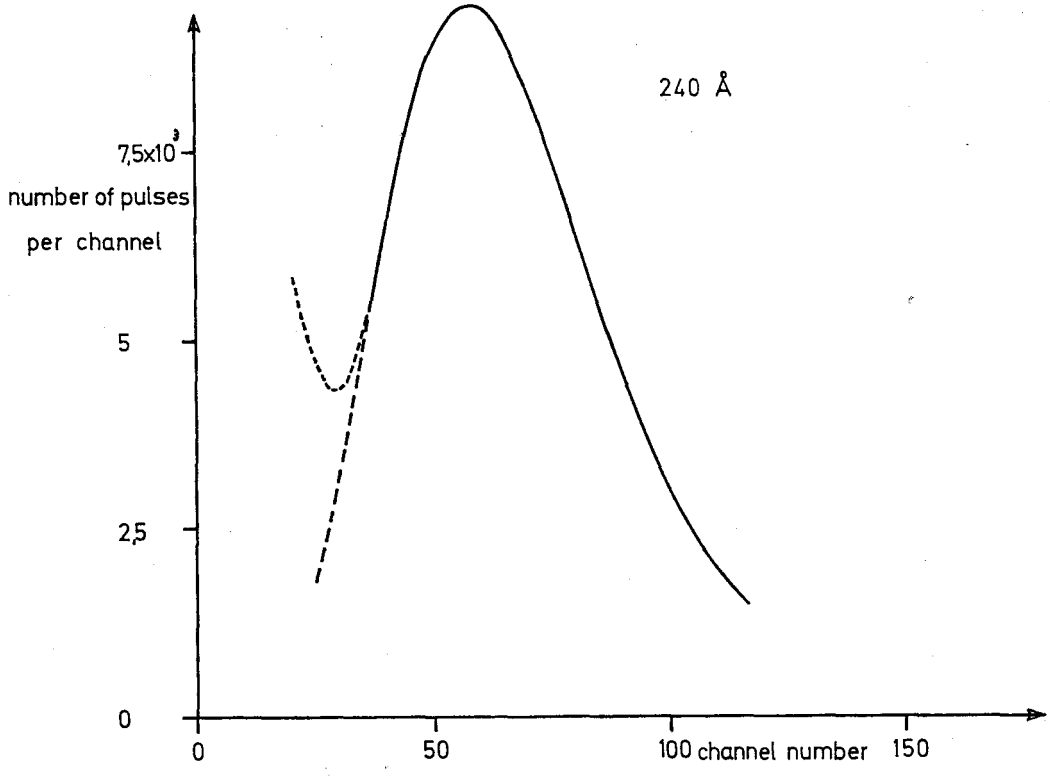

FIG. 4. Energy spectrum measured at a tissue diameter of 240 Å. Channel number 0 is equal to energy zero. The dotted line represents the noise.

TABLE 1.

LET ∞ $\frac{\text{keV}}{\mu}$	N	d $\sim$ μ	w $\sim$ eV
91·5	4·22 × 10³	1·40	30·3 ± 5%
99	1·14 × 10⁴	3·50	30·4 ± 5%
106	4·64 × 10³	1·40	31·2 ± 7%

LET_∞, because the counter is big enough to absorb all δ-rays. The w-values in the last column have been calculated with the following equation:

$$w = \frac{LET_\infty \cdot d}{N}$$

They represent therefore the relation between the energy that have been absorbed in soft tissue along small particle track lengths with a LET_∞ of about 100 keV/μ and the number of produced ion pairs.

SUMMARY

A cylindrical tissue equivalent proportional counter is described, which has been used to measure the fluctuation of the energy transferred by alphas to tissue thicknesses between 100 Å and 3·5 μ. The factors that contribute to the observed standard deviation are analysed and discussed. In addition, measurements of the differential average energy per ion pair along small track lengths of alpha-particles in tissue are described.

ACKNOWLEDGMENTS

We are very much indebted to G. Bertolini and G. Rastelli for the measurements of the spectrum of the alpha source. We also thank Th. Smit for his help during the measurements.

APPENDIX

The multiplication factor for a single electron that is produced at the point r in the counter can be described by:

$$M(r) = C \cdot e^{K\sqrt{r}} = e^{K(\sqrt{r}-\sqrt{a})} \quad (\text{for } a \leqslant r \leqslant r_o)$$

$$M(r) = C \cdot e^{K\sqrt{r_o}} \quad (\text{for } r_o \leqslant r \leqslant b)$$

a is the radius of the central wire,
r_o the radius of the region of electron multiplication, and
b the radius of the counter.

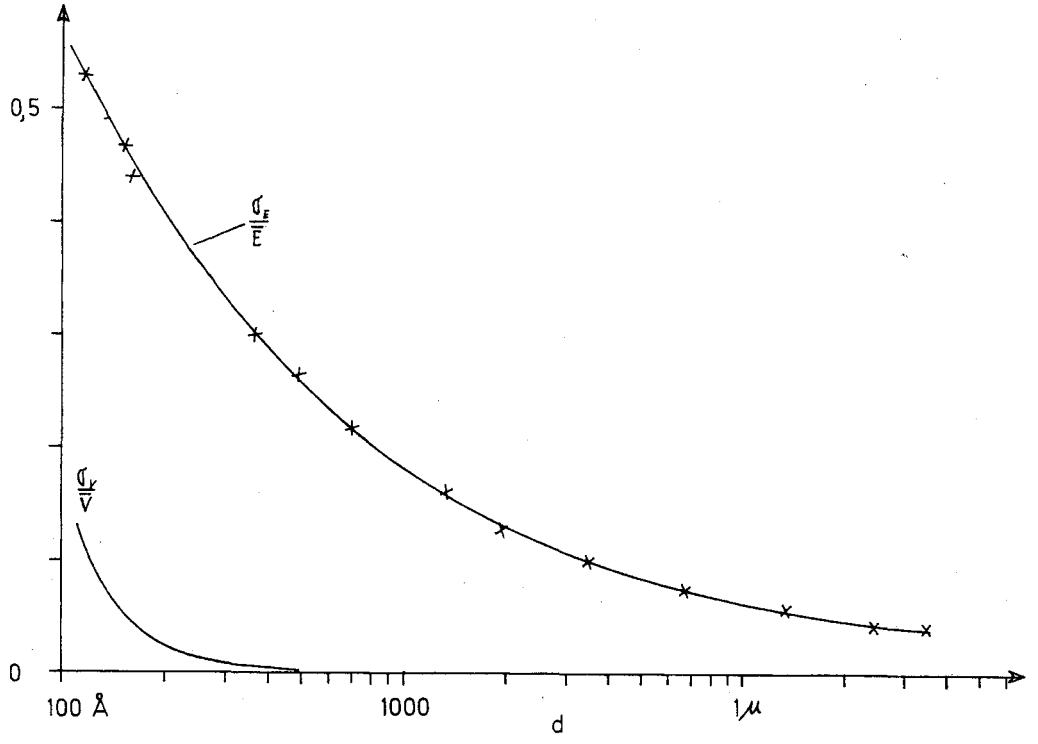

FIG. 5. Measured and calculated standard deviations as a function of the tissue diameter d.

Under the assumption that the ionizations are uniformly distributed in the counter, the distribution function of $M(r)$ is

$$\psi(M)dM = 2\pi r dr = \frac{4\pi}{K^4} \cdot \frac{(\ln M/C)^3}{M} dM$$

From this follows

$$\overline{M(r_0)} = \frac{1}{\pi (b^2 - a^2)}$$

$$\left\{ \int_1^{M(r_0)} M(r) \cdot \psi(M)dM + M(r_0) \cdot \int_{M(r_0)}^{M(b)} \psi(M)dM \right\}$$

$$= \frac{\int_1^{M(r_0)} M(r)\psi(M)dM + M(r_0)\pi(b^2 - r^2_0)}{\pi(b^2 - a^2)}$$

and

$$\overline{M^2(r_0)} = \frac{\int_1^{M(r_0)} M^2(r)\psi(M)dM + M^2(r_0)\pi(b^2 - r^2_0)}{\pi(b^2 - a^2)}$$

The desired mean square deviation of V is finally

$$\frac{\delta^2_v}{\overline{V}^2} = \frac{\overline{M^2}}{\overline{M}^2} - 1.$$

For the evaluation of this formula the radius of the multiplication region r_0 has been defined by

$$I = \int_{r_0}^{r_0 + \Omega} F\,dr = \frac{U}{\ln b/a} \ln\left(1 + \frac{\Omega}{r_0}\right)$$

where I is the mean ionization potential, F the electric field strength and Ω the mean free path of the electrons. It has, therefore, been assumed that the region of electron multiplication begins there, where the electron gains sufficient energy for ionization between two collisions.

REFERENCES

1. H. H. Rossi and W. Rosenzweig. *Radiology* **64,** 404 (1955).
2. H. H. Rossi. *Rad. Res.* **10,** 522 (1959).
3. H. H. Rossi. *Rad. Res.* **12,** 290 (1960).
4. H. H. Rossi, M. H. Biavati and W. Gross. *Rad. Res.* **15,** 431 (1961).
5. H. H. Rossi. *Radiology* **78,** 530 (1962).
6. H. H. Rossi. *Ann. New York Acad. Sci.* **114,** 4 (1964).
7. H. H. Rossi. *Ann. J. Roentgenol. Rad. Ther. Nucl. Med.* **93,** 196 (1965).
8. H. H. Smith and H. H. Rossi. *Rad. Res.* **28,** 302 (1966).
9. F. R. Shonka, J. E. Rose and G. Failla. *Proc. 2nd United Nations Int. Conf. on Peaceful Uses of Atomic Energy*, 21, 148 (1958).
10. H. H. Rossi and G. Failla. *Nucleonics* **14,** No. 2, 32 (1956).
11. D. E. Lea. *Actions of Radiations on Living Cells.* The University Press, Cambridge, 1962.
12. A. M. Kellerer. Private communication.

ÉTUDE DES VARIATIONS DES PARAMÈTRES BIOCHIMIQUES APRÈS IRRADIATION

G. MARBLÉ

Département de la Protection Sanitaire, Commissariat à l'Energie Atomique
Fontenay-aux-Roses (France)

Résumé—Certaines perturbations métaboliques ou fonctionnelles, provoquées par l'irradiation, chez l'homme et les animaux supérieurs, peuvent être mises en évidence par le dosage chimique de catabolites urinaires ou de certains métabolites sanguins.

Dans le but d'évaluer la dose absorbée ou le dommage biologique subi et de pronostiquer les chances de survie de l'irradié, les variations des paramètres biochimiques peuvent être, expérimentalement chez l'animal, suivies

(a) en fonction du temps pour une exposition donnée,
(b) en fonction de l'exposition à un moment donné ou pendant une période de temps déterminée.

Cependant, dans le cas d'irradiation accidentelle humaine, on ne connait que rarement les valeurs des paramètres biochimiques de l'accidenté avant l'irradiation et il est souvent difficile, compte tenu de la dispersion des valeurs individuelles, de relier les résultats trouvés aux valeurs de référence, d'autant plus que celles-ci sont très peu nombreuses. Il peut alors être utile d'étudier la variation relative des valeurs mesurées (sens de la variation, pente de la courbe, amplitude relative, etc.) en fonction du temps.

Des exemples de ces divers modes d'étude sont donnés. Des essais d'interprétation des résultats relatifs à la variation de la glycémie et à l'excrétion urinaire des électrolytes ont été tentés.

INTRODUCTION

L'action des rayonnements sur les structures cellulaires, les systèmes enzymatiques, les glandes à secrétion interne se traduit, sur le plan biochimique, chez l'homme et les animaux supérieurs, par des perturbations métaboliques dont l'amplitude semble liée à la dose absorbée.

Le dosage chimique des catabolites urinaires ou de certains métabolites sanguins permet-il de donner une appréciation quantitative de l'atteinte de l'organisme irradié?

Existe-t-il une relation simple entre la valeur numérique de certains paramètres biochimiques et l'exposition?

La réponse biochimique est-elle suffisamment sensible, précoce, fidèle, précise pour constituer un bon dosimètre biologique?

Ce problème a déjà été très étudié chez l'animal, expérimentalement, beaucoup moins chez l'homme car les irradiations accidentelles, heureusement peu nombreuses, sont les seules possibilités d'étude que nous ayons, les résultats enregistrés à partir des irradiations thérapeutiques étant toujours difficilement interprétables.

NATURE DES PARAMÈTRES BIOCHIMIQUES

Quels sont les paramètres biochimiques qui se prêtent le mieux à l'étude de l'évaluation du dommage radiobiologique?

Les variations sanguines sont, en général, de faible amplitude aux doses subléthales et leur évolution en fonction du temps n'est pas toujours reproductible d'un cas à un autre, ce qui peut, dans une certaine mesure, expliquer certains résultats apparemment contradictoires.

Tous les auteurs sont d'accord sur l'hyperglycémie qui se produit après l'irradiation.[1-7] Nous reviendrons plus loin sur l'étude de la glycémie car elle permet de bien comprendre le problème de la réponse biochimique.

Le cholestérol plasmatique est augmenté. [4, 8-11]

L'hyperlipémie avec hypoliprotéinémie a été également notée par Steadman. [12]

Une hyperbilirubinémie [8, 13, 15] et une hypercréatininémie [8, 16] semblent de règle aussi bien chez l'homme que l'animal.

Les protéines sériques ne sont que peu modifiées, à faible dose. Les protéines totales diminuent [17, 18] et le rapport globulines α/globulines γ augmente. [17, 19, 20]

Il en est de même des composés minéraux, les électrolytes plasmatiques restant, le plus souvent, dans les limites normales. [8]

L'activité des enzymes sériques a paru être un test possible. [21, 22] Augmentation pour les transaminases (SGOT et SGPT), [21-24] les deshydrogénases, [21-26] la phosphatase acide, [27] l'amylase, [28] diminution pour la phosphatase alcaline, [27, 15] la glycérophosphoisomérase, [21] par exemple. Smith et Bates [29] n'ont pas obtenu de résultats nets et pensent que la mesure de la concentration des enzymes sériques est d'une valeur limitée comme index de dommage biologique.

Par contre Rappoport et Fritz [30] ont établi une relation linéaire entre la durée d'inhibition de la nucléoside phosphorylase des érythrocytes et l'exposition.

En ce qui concerne l'excrétion urinaire, les recherches ont surtout été orientées vers le métabolisme des protéines.

L'excrétion de la désoxycytidine, [31, 32, 33] de la thymidine, [32, 33] de la pseudo-uridine, [34] de l'acide xanthurénique, [33] des amines telles que l'histamine, la tryptamine, la sérotonine, [35, 36] et son produit de dégradation l'acide 5-hydroxy-indole acétique [37, 38] ainsi que celle des acides α aminés [9, 24, 39-48] en particulier le glycocolle, l'acide aspartique, le tryptophane, est notablement augmentée. Par contre l'excrétion de sérine libre est diminuée. [9, 39-42, 49] La taurine [40, 50-58] et surtout l'acide β-aminoisobutyrique [40, 54, 59-64] semblent être les meilleurs indicateurs.

L'excrétion d'acide urique, de créatine, [9, 40, 63-68] de certains acides organiques tels que l'acide pyruvique, l'acide α-cétoglutarique, l'acide lactique est également augmentée. [69]

Par contre l'excrétion urinaire des glycuronides [70] ainsi que celle du sodium, du potassium, du chlore est diminuée. [8]

Il faut signaler, également, le dosage des désoxypolyribonucléotides libres, dans la moelle osseuse, effectué par Skalka et Matyasova [71] chez la souris, ce test semble très sensible et très précis.

Dans de nombreux cas, des relations dose-effet ont pu être établies chez l'animal, mais pour l'instant il semble très difficile de pouvoir établir ces mêmes relations chez l'homme.

EXPRESSION DES RÉSULTATS

Les résultats numériques sont, le plus souvent, donnés en fonction du temps, pour une exposition donnée.

Ils sont exprimés soit sous forme de tableaux de valeurs numériques, soit de courbes en coordonnées normales ou plus rarement logarithmiques, soit d'histogrammes lorsqu'il s'agit d'excrétion. Il est préférable, à notre sens, de réserver l'histogramme à l'expression d'une quantité excrétée en fonction du temps, soit

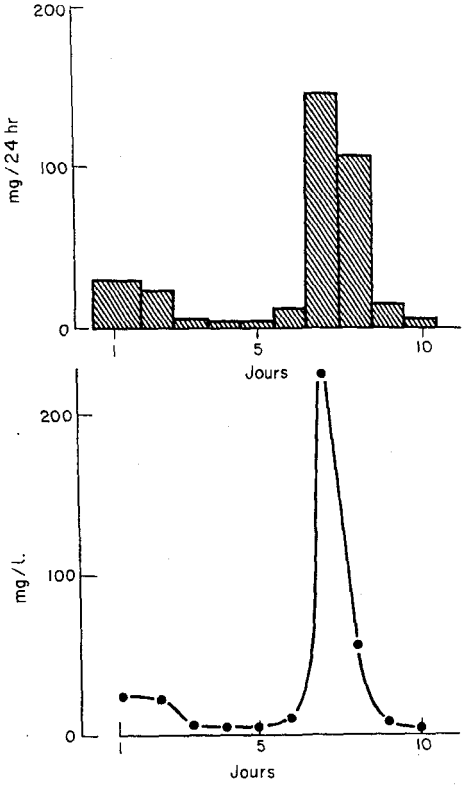

FIG. 1. Excrétion urinaire d'acide aspartique (irradié accidentel).

par exemple (cf. Fig. 1) l'histogramme traduisant l'excrétion urinaire d'un acide aminé: l'acide aspartique, exprimée en milligramme par 24 h, par un homme irradié accidentellement. On conserve alors la courbe pour représenter la variation de la concentration et la superposition sur un même graphique des deux représentations permet, de plus, de voir le rôle de la diurèse.

Les courbes d'excrétions cumulées sont d'un intérêt certain, d'autant plus que lorsque ce sont des droites il est possible de calculer leurs pentes comme l'a fait Hasterlik,[47] pour l'excrétion des acides α aminés par les irradiés de Los Alamos. Cette représentation présente également, en expérimentation animale, l'avantage de donner une image de l'action d'un radioprotecteur chimique ou d'un agent thérapeutique par exemple. L'effet protecteur de l'A.E.T. est ainsi traduit sur les courbes d'excrétion du potassium (cf. Fig. 2) chez des rats non irradiés, irradiés à 750 r, protégés et non protégés. La variation de pente due à l'A.E.T. est très nettement observable.

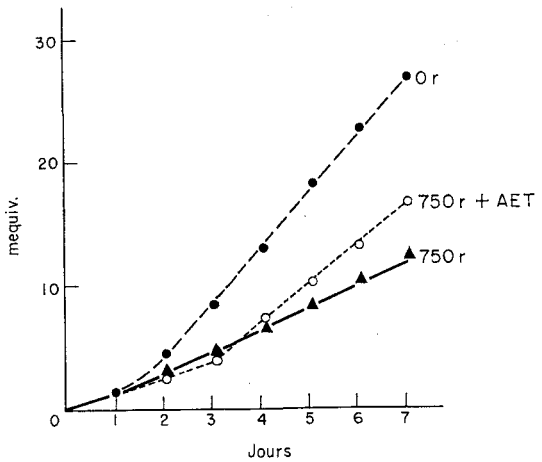

FIG. 2. Excrétions urinaires cumulées de potassium (rats irradiés à 750 r protégés et non protégés par AET).

Le calcul de la quantité moyenne excrétée par unité de temps, pendant une durée déterminée, a la même signification que le calcul de la courbe d'excrétion cumulée. Mechali[72] a employé cette méthode pour établir une relation entre l'exposition et la quantité d'acide β aminoisobutyrique excrétée par les irradiés d'Oak Ridge du troisième au huitième jour après l'irradiation.

La représentation sous forme d'histogramme peut aussi être utilisée lorsque l'on veut montrer l'importance relative de quantités excrétées, en un temps déterminé, de différents composés appartenant à un même groupe, par exemple les différents acides α aminés.

L'expérimentation animale permet d'établir des courbes dans lesquelles les résultats peuvent être exprimés en fonction de l'exposition.

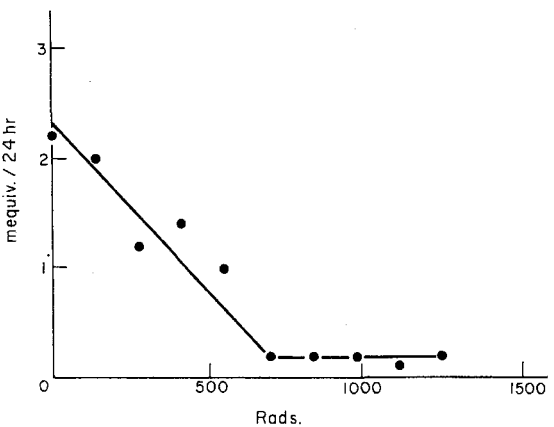

FIG. 3. Excrétion urinaire de sodium (rats) (2° jour après l'irradiation).

Ces courbes peuvent représenter, par exemple, une concentration plasmatique, à un instant donné ou une excrétion journalière comme le montre la courbe (cf. Fig. 3) traduisant l'excrétion urinaire de sodium, pendant le deuxième jour après l'irradiation de rats irradiés à des doses de rayonnement gamma de 0 à 1 250 rads.

La superposition sur un même graphique des courbes d'excrétions cumulées, en fonction de la dose, pour des intervalles de temps successifs permet de vérifier si une variation observée est stable ou transitoire. La courbe d'excrétion urinaire de sodium (cf. Fig. 4) de rats irradiés par les rayons gamma du cobalt met en évidence la diminution de l'excrétion en fonction de l'exposition. La courbe relative à l'excrétion du potassium (cf. Fig. 5) étale les résultats jusqu'au vingtième jour.

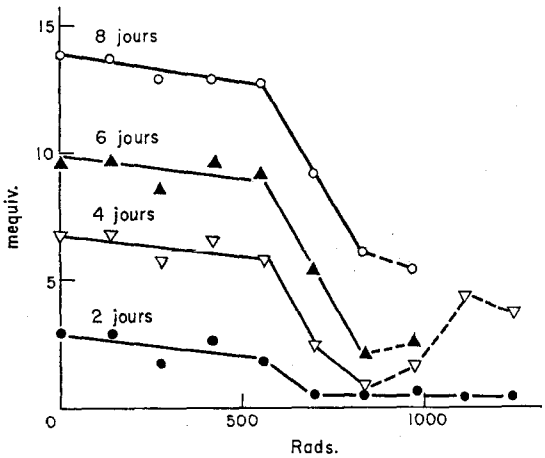

FIG. 4. Excrétions urinaires cumulées de sodium (rats).

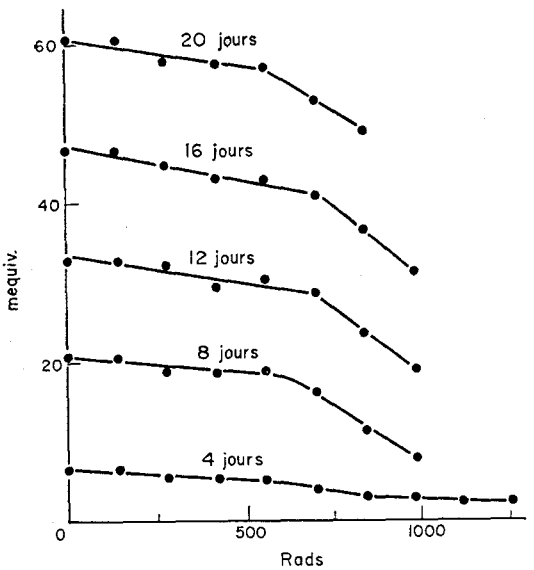

FIG. 5. Excrétions urinaires cumulées de potassium (rats).

INTERPRÉTATION DES RÉSULTATS

Lorsqu'un paramètre biochimique varie, proportionnellement ou en raison inverse, linéairement ou non, mais toujours dans le même sens, en fonction de l'exposition, l'interprétation des résultats numériques est alors facile puisque l'on est ramené dans ce cas à des expositions.

Lorsque la valeur du paramètre varie dans le sens des expositions croissantes on peut admettre que pour une exposition donnée une augmentation exagérée traduit un effet biologique plus grand ou une sensibilité plus grande de l'irradié ce qui, d'ailleurs, revient au même.

Mais il est des cas où les variations du paramètre évoluent, en fonction du temps, de part et d'autre de la normale. L'évolution de la glycémie est un exemple de ce type de variation car à une hyperglycémie précoce succède généralement une hypoglycémie et l'on observe quelquefois plusieurs oscillations. La variation de la glycémie du rat en fonction du temps et de la dose (cf. Fig. 6) illustre ce cas. Des courbes analogues ont été obtenues chez le porc et chez l'homme. La courbe de variation de la glycémie d'un irradié (cf. Fig. 7) semble repré-

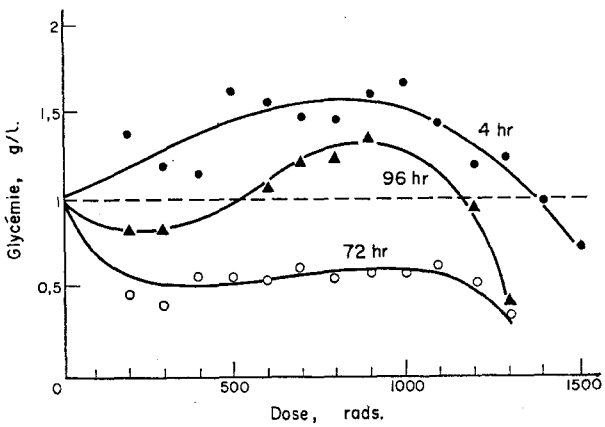

FIG. 6. Variation de la glycémie en fonction de la dose et du temps (rats).

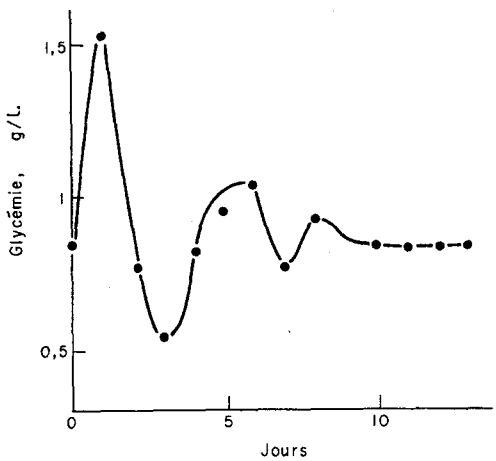

FIG. 7. Variation de la glycémie en fonction du temps (irradié accidentel).

senter les variations d'un mouvement oscillatoire amorti traduisant, en quelque sorte, la réaction du mécanisme physiologique de régulation de la glycémie à la suite de l'exposition au rayonnement. Chez le rat le pronostic est d'autant plus défavorable que l'hyperglycémie est initialement forte et que l'hypoglycémie est ensuite très importante.

Il peut arriver également que les variations de certains paramètres biochimiques ne soient pas, tout au moins directement, liées à la dose mais leur étude peut avoir un intérêt physiopathologique. A titre d'exemple, citons l'excrétion urinaire du sodium et du potassium au cours du développement du syndrome hématologique, chez l'homme; il semblerait y avoir une corrélation entre le rapport sodium/potassium et la variation du nombre de leucocytes (cf. Fig. 8).

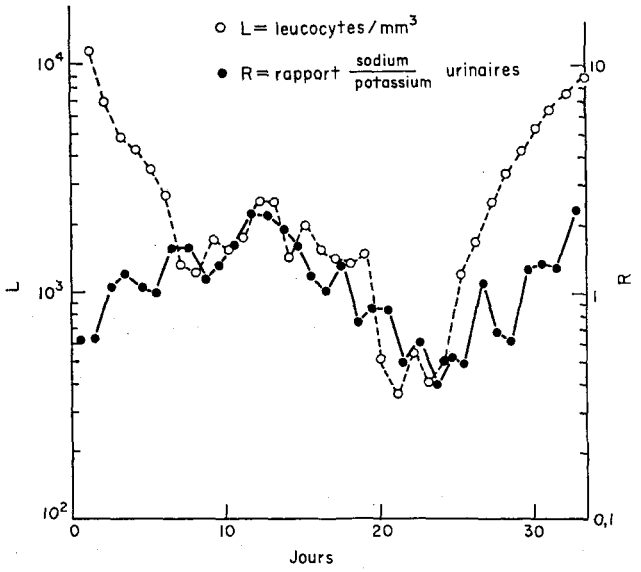

FIG. 8. Rapport sodium urinaire/potassium urinaire et leucocytes.

CONCLUSION

En conclusion, nous pensons que si le dosimètre biochimique n'est pas encore au point, tout au moins dans le cas d'irradiations accidentelles humaines, les résultats obtenus en expérimentation animale permettent d'espérer l'obtention de bons critères dans un proche avenir, mais pour cela il faut absolument que des laboratoires spécialisés puissent pratiquer le plus grand nombre d'examens possible portant en particulier sur l'urine, dans les cas d'irradiations humaines même à très faible dose. Ce n'est que par la compilation de nombreuses données qu'un résultat positif pourra un jour être obtenu.

RÉFÉRENCES

1. G. MARBLÉ, H. FROSSARD, L. BREUIL et R. ENGLER. Evolution de la glycémie chez le rat après irradiation gamma. Rapport C.E.A., R.2922, 1965.
2. A. RAISONNIER. Évolution de la glycémie au cours du syndrome d'irradiation. Thèse Médecine, Paris, 1966. Rapport C.E.A. (à paraître).
3. R. E. KAY et C. ENTENMAN. Hyperglycemia and increase in liver glycogen in rats after X-irradiation. *Proc. Soc. Exptl. Biol. Med.* **6,** 91–143 (1956).
4. H. I. KOHN. Changes in composition of blood plasma of the rat during acute radiation syndrome and their partial mitigation by dibenamine and cortin. *Am. J. Physiol.* **165,** 27–42 (1951).
5. H. I. KOHN, P. LEDFORD, W. J. ROBERTSON et N. SWINGLEY. Changes in plasma of the rat during fasting and influence of genetic factors upon sugar and cholesterol levels. *Am. J. Physiol.* **163,** 410–417 (1950).

6. H. I. KOHN, N. SWINGLEY et W. J. ROBERTSON. Changes in blood plasma of guinea pig during acute radiation syndrome. *Am. J. Physiol.* **162,** 703–708 (1951).
7. D. R. ANDERSON, A. HERNANDEZ DIAZ et F. A. QUINN. Post-irradiation hyperglycemia in the primate. Report S.A.M.-T.D.R. 63–40, U.S.A.F., 1963.
8. G. MARBLÉ. Observations personnelles non publiées.
9. L. H. HEMPELMANN. Evaluation de la gravité des radiolésions aiguës. *Diagnostic et traitement des radiolésions aiguës.* O.M.S. Genève, 1964.
10. W. E. CORNATZER, D. ENGELSTAD et J. P. DAVISON. Effect of whole body X-irradiation on blood constituents. *Am. J. Physiol.* **175,** 153–166 (1953).
11. A. M. KUZIN. *Radiation Biochemistry.* Israel Program for Scientific Translations, Jerusalem, 1964.
12. L. T. STEADMAN et A. J. GRIMALDI. Variation of X-radiation induced lipemia in rabbits with dosage administration of insulin or ammonium chloride and the incidence of tetany. University of Rochester, U.R. 195, 1951.
13. J. LOISELEUR et M. PETIT. Augmentation de la bilirubinémie consécutivement à l'irradiation du rat par les rayons X. *C.R. Soc. Biol.*, 1164–1165, 1963.
14. N. WALD et G. E. THOMA Jr. Radiation accidents: medical aspects of neutron and gamma ray exposures. O.R.N.L. 2748, part B, 1961.
15. D. R. ANDERSON. Le traitement expérimental d'une radiolésion chez des singes. *Diagnostic et traitement des radiolésions aiguës.* O.M.S. Genève, 1964.
16. G. SANNA. Modifications in the ATP creatine system after whole body irradiation. *Riv. Patol. Clin.* **18,** 473–481 (1963).
17. M. TUBIANA, C. M. LALANNE et J. SURMONT. Irradiation totale pour homotransplantation rénale. *Diagnostic et traitement des radiolésions aiguës.* O.M.S. Genève, 1964.
18. J. R. ALLEN, J. L. VAN LANCKER et R. C. WOLF. Pathologic alterations produced by total body X-irradiation in monkeys. *Am. J. Physiol.* **48,** 2, 317–332 (1966).
19. C. WINKLER et G. PASCHKE. Protein content and composition of rat serum as related to amount of whole body X-irradiation. *Rad. Res.* **5,** 156–161 (1956).
20. P. GRABAR, K. P. KASHKIN et J. COURCON. Modifications des constituants du sérum de souris après irradiation létale. *Rev. Franç. Etudes Clin. et Biol.* **8,** 565–569 (1965).
21. L. B. HUGHES. A survey of serum enzymes as a possible index of radiation injury. L.A.S.L. Report LA 2167, 1–61, 1958.
22. H. G. ALBAUM. Serum enzymes following whole body radiation in the rabbit. *Rad. Res.* **12,** 186–194 (1960).
23. F. F. BECKER, R. B. WILLIAMS Jr. et J. L. VOOGD. Effect of X-irradiation in sublethal to supralethal dosage in serum glutamic oxalacetic transaminase. *Rad. Res.* **20,** 221–226 (1963).
24. T. L. SHIPMAN. Cas d'irradiation mortelle par surexposition accidentelle massive à des neutrons et à des rayons gammas. *Diagnostic et traitement des radiolésions aiguës.* O.M.S. Genève, 1964.
25. G. V. DALRYMPLE, I. R. LINDSAY et J. J. GHIDONI. The effect of 2 MeV X-rays on whole body irradiated primates. Report S.A.M.—T.R. 65-9, U.S.A.F. Brooks Air Force, Texas, 1965.
26. G. V. DALRYMPLE, I. R. LINDSAY, C. B. GHIDONI, H. L. KUNDEL et E. T. STILL. The effect of massive doses of 32 MeV protons and ^{60}Co gamma radiation on serum levels of whole body irradiated primates. *J. Nucl. Med.* **6,** 8, 588–593 (1965).
27. N. F. LIPKAN. *Elementy Radiatsionnoi Biologii i Biokhimii*, 45–136. Kiev, 1963.
28. E. D. THOMAS. La transplantation de moelle osseuse chez l'homme. *Diagnostic et traitement des radiolésions aiguës.* O.M.S. Genève, 1964.
29. H. SMITH et T. H. BATES. An assessment of those metabolites considered to be of value in the diagnosis of exposure to radiation. *Personal dosimetry for accidental high level exposure to external and internal radiation,* 199–215. A.I.E.A. Vienna, 1965.
30. D. A. RAPPOPORT et R. D. FRITZ. Influence of total body X-irradiation on nucleoside phosphorylase in rat erythrocytes. *Rad. Res.* **21,** 5–15 (1964).
31. H. K. BERRY, E. L. SAENGER, H. PERRY, B. I. FRIEDMAN, J. G. KEREIAKES et G. SCHEEL. Deoxycytidine in urine of humans after whole body irradiation. *Science,* **142,** 396–398 (1963).
32. J. PRIZEK, M. ARIENT, Z. DIENSTBIER et J. SKODA. The detection of desoxycytidine in urine as an indicator of changes after irradiation. *Proc. 2nd United Nations International Conference on the Peaceful Uses of Atomic Energy.* Report P/2498, vol. 22b, 206–207. Genève, 1958.
33. E. L. SAENGER. Metabolic changes in humans following irradiation. D.A.S.A., 1422, 1963.
34. D. DRAHOVSKY, A. WINKLER et J. SKODA. Increased urinary excretion in rats following irradiation. *Nature,* **201,** 411–412 (1964).
35. F. FRANZEN, H. GROSS et G. FRIEDRICH. Biogene Amine in Urin und Blut von Ratten nach subletale Ganzkörperbestrahlung. *Strahlentherapie,* **122,** 4, 591–594 (1963).
36. F. FRANZEN, H. GROSS et G. TIELICKE. Biogene Amine in Urin und Blut von Ratten nach

subletaler Ganzkörperbestrahlung. *Strahlentherapie*, **120,** 598–610 (1963).
37. Z. Deanovic, Z. Supek et M. Randic. Relationship between the dose of whole body X-irradiation and the urinary excretion of 5-hydroxyindolacetic acid in the rats. *Int. J. Rad. Biol.* **7,** 1–9 (1963).
38. M. Randic et Z. Supek. Urinary excretion of 5-hydroxyindolacetic acid after a single whole body irradiation in normal and adrenalectomized rats. *Int. J. Rad. Biol.* **4,** 2, 151–153 (1961).
39. G. A. Andrews, G. W. Sitterson, A. L. Kretchmar et M. Brucer. Irradiation accidentelle au Centre Y 12. *Diagnostic et traitement des radiolésions aiguës.* O.M.S. Genève, 1964.
40. E. C. Gjessing et S. Warren. Effect of radiation on excretion of some of nitrogenous constituents of urine in man. *Rad. Res.* **15,** 276–289 (1961).
41. H. P. Jammet. Traitement des personnes irradiées lors de l'accident survenu à Vinca avec le réacteur de puissance zéro. *Diagnostic et traitement des radiolésions aiguës.* O.M.S. Genève, 1964.
42. B. Pendic. Accident à Vinca avec le réacteur de puissance zéro. *Diagnostic et traitement des radiolésions aiguës.* O.M.S. Genève, 1964.
43. B. Rodojicic, S. Hadjukovic et M. Antic. Surveillance des personnes irradiées lors de l'accident survenu à Vinca avec le réacteur de puissance zéro. *Diagnostic et traitement des radiolésions aiguës.* O.M.S. Genève, 1964.
44. L. Naftalin. Further observations on amino acid changes in plasma and urine following therapeutic irradiation. *Int. J. Rad. Biol.* **8,** 4, 396 (1965).
45. F. M. Ganis et J. Howland. Observations on amino acid excretion in accidentally irradiated humans. *Int. J. Rad. Biol.* **7,** 1, 107–108 (1964).
46. F. M. Ganis, M. W. Hendrickson et J. W. Holland. Amino acid excretion in human patients accidentally exposed to large doses of partial body ionizing radiation (The Lockport Accident). *Rad. Res.* **24,** 278–291 (1965).
47. R. J. Hasterlik et L. D. Martinelli. Dosimétrie physique et observations cliniques sur quatre êtres humains atteints par les rayonnements à la suite d'une fuite accidentelle dans un ensemble critique. P/478—*Conférence Internationale sur l'utilisation de l'énergie atomique à des fins pacifiques.* Nations Unies, Genève, 1956.
48. J. E. Katz et R. J. Hasterlik. Aminoaciduria following total body irradiation in the human. *J. Nat. Cancer Inst.* **15,** 4, 1085–1107 (1955).
49. A. L. Kretchmar. An alteration in the excretion of free serine in urine from irradiated humans. *Nature*, **133,** 1809–1810 (1959).
50. R. E. Kay et C. Entenman. Free amino acids in the tissues and urine of X-irradiated rat. *Fed. Proc.* **13,** 520 (1954).
51. R. E. Kay, J. C. Early et C. Entenman. Increased urinary excretion of taurine and urea by rats after irradiation. *Rad. Res.* **6,** 98–107 (1957).
52. E. R. Kay et C. Entenman. The effect of multiple exposures and partial body X-irradiation on urinary taurine excretion by the rat. *Rad. Res.* **11,** 357 369 (1959).
53. C. R. Angel et T. R. Noonan. Urinary taurine excretion and the partition of sulfur in four species of mammals after whole body X-irradiation. *Rad. Res.* **15,** 298–306 (1961).
54. E. J. Bigwood et P. Soupart. β-aminoisobutyric acid and taurine excretion and plasma levels after local X-ray irradiation in two cancer patients. *Biological effects of ionizing radiation at the molecular levels.* A.I.E.A., Vienna, 1962.
55. P. L. Boquet et P. Fromageot. Sur l'origine de la taurine excrétée par le rat irradié. B.I.S.T., 93, 7–18. Commissariat à l'Energie Atomique, 1955.
56. M. M. Jovanovic. Influence of repeated ^{60}Co gamma irradiation on urinary excrétion of taurine in rats. *Bull. Boris Kidrich Inst. Nucl. Sc.* **16,** 49–54 (1965).
57. G. M. Watson. The origin of taurine excreted in the urine after whole body irradiation. *Int. J. Rad. Biol.* **5,** 1, 79–83 (1961).
58. D. N. Stern et E. M. Stim. Sources of excess taurine excreted in rats following whole body irradiation. *Proc. Soc. Exptl. Biol. Med.* **101,** 125–158 (1958).
59. F. W. Meichen et A. W. Short. A method for the rapid determination of beta-aminoisobutyrique acid (BAIBA) in urine of irradiated humans. *Int. J. Rad. Biol.* **6,** 5, 495–497 (1963).
60. J. R. Rubini, E. P. Cronkite, V. P. Bond et T. M. Fliedner. Urinary excretion of beta-aminoisobutyric acid (BAIBA) in irradiated human beings. *Proc. Soc. Exptl. Biol. Med.* **100,** 130–133 (1959).
61. H. Lanz et J. R. Rubini. Radiobiological significance of β-aminoisobutyric acid. Report A.E.C. AT 40–1, 2731, 1964.
62. H. Smith, T. H. Bates et C. J. Smith. Excretion of β-aminoisobutyric acid as an index of radiation exposure. *Int. J. Rad. Biol.* **8,** 3, 263–270 (1964).
63. G. B. Gerber. Die Ursachen der Strahlenbedingten Ausscheidung von β aminoisobuttersäure und creatin. Rapport, Euratom, Eur 591d 1964.
64. G. B. Gerber, G. Gerber, S. Kurohara, K. I. Altman et L. H. Hempelmann. Urinary excretion of several metabolites in persons accidentally exposed to ionizing radiation. *Rad. Res.* **15,** 314–318 (1961).

65. G. GERBER, P. GERTLER, K. I. ALTMAN et L. H. HEMPELMANN. Dose dependency of radiation induced creatin excretion in rat urine. *Rad. Res.* **15,** 307–313 (1961).
66. G. B. GERBER, G. GERBER et K. I. ALTMAN. The mechanism of radiation induced creatinuria. *Proc. Soc. Exptl. Biol. Med.* **110**, 797–799 (1962).
67. G. B. GERBER, G. GERBER, T. R. KOSALKA et L. H. HEMPELMANN. Creatine metabolism after X-irradiation. *Rad. Res.* **23**, 648–652 (1964).
68. C. M. WILLIAMS, G. M. KRISE, D. R. ANDERSON et R. M. DOWBEN. Post-irradiation creatinuria in the rat. *Rad. Res.* **7**, 176–183 (1957).
69. H. SCHOEN, F. C. SITZMANN et G. BARTH. Das Verhalten der Brenztraubensäure l(+) milchsäure und alphaketoglutasäure im serum bei therapeutischen Anwendung von Röntgenstrahlen. *Strahlentherapie*, **105**, 585–591 (1958).
70. P. SCOPPA et K. GERBAULET. Escrezione di glucoronidi urinari nel ratto irradiato. Rapport Euratom, Eur 2638i, 1966.
71. M. SKALKA et J. MATYASOVA. The effect of low radiation doses on the release of deoxyribopolynucleotides in haematopoïetic and lymphatic tissues. *Int. J. Rad. Biol.* **7**, 1, 41–44 (1963).
72. D. MECHALI. Méthodes biologiques d'appréciation de la dose reçue au cours d'une irradiation externe. VII. Rassegna Internazionale Elettronica e Nucleare, Rome, 1960.

UTILISATION DES ANALYSES CHROMOSOMIQUES EN TANT QUE DOSIMÉTRIE BIOLOGIQUE*

M. T. BIOLA et R. LE GÔ
Département de la Protection Sanitaire, Commissariat à l'Énergie Atomique
Fontenay-aux-Roses, France

Résumé—L'irradiation *in vitro* de sang prélevé sur un sujet sain, a été faite à l'intérieur d'un fantôme humain, auprès d'un montage critique expérimental. Six échantillons de ce sang ont été inclus en des points divers du fantôme, de façon à ce que chacun reçoive une dose différente de rayonnement mixte gamma + neutrons. Les doses se sont étagées entre 38 rads et 555 rads. Chacun des tubes était par ailleurs environné de nombreux dosimètres de types divers également inclus dans le fantôme.

Vingt-huit cultures de lymphocytes ont été faites à partir de ces échantillons. La technique utilisée a été une micro-méthode, dérivée de celles de Edwards, de Arakaki et Sparkes.

On a étudié les aberrations chromosomiques au niveau de chaque point expérimental, sur deux groupes de cultures: pour le premier groupe, l'arrêt de culture a été fait au bout de 72 h; pour le second groupe, au bout de 96 h.

Les auteurs discutent des relations entre la dose reçue et les aberrations observées, pour chaque point selon le temps de culture et selon les types d'aberrations.

Ils tentent de les relier aux observations faites avant eux sur du sang irradié soit par des rayons X, soit par des rayons γ du ^{60}Co.

Ils discutent de la possibilité de relier ces observations faites sur des irradiations *in vitro*, avec les observations d'anomalies chromosomiques portant sur des sujets humains irradiés.

INTRODUCTION

De nombreux chercheurs ont, depuis que les techniques de culture de sang humain ont permis d'obtenir et d'étudier des images de chromosomes, observé des aberrations de nombre et de structure dans ce matériel biologique.

L'établissement de relation dose-effet a donc été tenté par plusieurs d'entre eux, sur du sang humain, soit *in vivo* à l'occasion d'irradiations accidentelles, soit *in vitro* dans un but expérimental plus précis. C'est ainsi que des courbes ont été établies *in vitro* par:

Bender[1] "Irradiation aux rayons X de 250 keV" aux doses de 0–200 R;

Gooch, Randolph et Bender[2] "Irradiation aux neutrons de 14 MeV" aux doses de 0–200 R;

Kelly et Brown[3] "Irradiation aux rayons X de 200 keV" aux doses de 0–1600 R.

A l'occasion de l'accident d'irradiation humaine survenu à Mol, le 30 décembre 1965, auprès de l'assemblage critique Venus, il nous a semblé intéressant de procéder à de semblables études expérimentales. En effet,

(1°) d'une part, nous avons, sur le sang de cet irradié, effectué des analyses chromosomiques dans un but d'estimation des dommages; les résultats obtenus seront exposés plus particulièrement dans un autre rapport de ce congrès[4] (H. Jammet, R. Gongora, R. Le Gô, G. Marblé et M. Faes);

(2°) d'autre part, au cours d'une reconstitution dosimétrique de l'accident auprès du même assemblage critique, faite sur un fantôme en Mix–D, il nous a semblé intéressant de recouper les données précédentes par une irradiation *in vitro*.

Des tubes contenant des échantillons de sang normal provenant d'un même individu, ont été introduits en divers points

* Ce travail a été effectué avec la collaboration technique de M. Bourguignon, J. Dacher, G. Ducatez et O. Foissac.

dans la profondeur de ce fantôme où ils étaient environnés de dosimètres fournissant des valeurs précises de la dose;

(3°) enfin, nous avons complété les données de cette irradiation *in vitro*—un mélange de $\gamma + 10\%$ neutrons—en effectuant une irradiation aux γ du ^{60}Co, aux doses de 400 et 600 R, toujours sur du sang normal du même sujet.

C'est l'ensemble des résultats obtenus sur ces 3 groupes d'analyses chromosomiques que nous voulons exposer ici.

CONDITIONS TECHNIQUES

I. *Technique des irradiations*

(*a*) *Irradiation accidentelle.* Les conditions de cette irradiation et la dosimétrie à laquelle elle donna lieu, étant exposées par ailleurs de manière extensive au cours de ce congrès, nous nous bornerons à rappeler ici qu'il s'est agi d'une irradiation totale très hétérogène à des doses étagées entre environ 1000 rads et 300 rads pour le tronc et la tête, avec une dose médiane estimée à 500 rads.

Le sang fut prélevé au 4e jour après l'accident.

(*b*) *Irradiation au ^{60}Co.* Nous avons exposé 2 groupes de 3 tubes contenant 3 cc de sang normal aux doses de 400 et 600 R avec un débit de dose de 30 R/min.

(*c*) *Irradiation dans le fantôme* (Fig. 1). Des tubes contenant 5 cc de sang normal ont été disposés de la façon suivante:

1 tube au niveau des coupes 12 et 13 exposées à 40 R,
1 tube au niveau des coupes 24 et 25 exposées à 85 R,
1 tube au niveau des coupes 33 et 34 exposées à 165 R.

En outre, des tubes ont été placés au niveau du membre inférieur, au niveau de la jambe (en profondeur), et au niveau du pied (à sa surface), à des doses respectives de 200 R et 587 R. La durée de l'irradiation ayant été la même pour tous les tubes, soit 150 minutes, le débit de dose a été très faible, et il a varié selon les points d'irradiation de 0,26 R/min. à 4R/min.

II. *Technique des cultures*

Le sang prélevé a été mis en culture immédiatement après, soit le prélèvement, soit l'irradiation expérimentale; dans le cas du fantôme le sang a voyagé, après mise en culture, entre Mol et Paris dans un container isotherme pendant 6 h.

A partir de ces échantillons, nous avons effectué des microcultures selon la technique de Moorhead[5] modifiée par Lejeune.[6] Pour chaque dose nous avons effectué des cultures de 72 h et 96 h. Le contact avec la colchicine a duré 2 heures.

REMARQUE: Il est certain, et nous en sommes conscients, que le temps de culture de 72 h est un facteur technique critiquable: il n'est pas douteux —et nous en donnerons la preuve dans ce qui va suivre—qu'une partie des métaphases observées ont déjà franchi la première mitose. Cependant, comme notre propos était de nous référer par comparaison à des résultats établis précédemment par les auteurs déjà cités, et qui avaient utilisé des cultures de 72 h, il nous a paru préférable de ne pas nous écarter de ces premières conditions expérimentales.

III. *Technique d'analyse*

Toutes les analyses ont été faites après établissement des caryotypes des cellules sélectionnées—sans tenir compte des anomalies chromosomiques—uniquement sur la netteté des centromères et des extrémités des bras.

Seules n'ont pas été montées en caryotypes les cellules polyploïdes, pour lesquelles on a pris en compte les dicentriques et les anneaux qui s'y trouvaient.

Indépendamment des analyses sur caryotypes, nous avons établi, sur 1000 cellules, le pourcentage des polyploïdies et des endoreduplications sur 2 types de cultures de 72 h et 96 h.

RÉSULTATS

Tous nos résultats numériques sont donnés dans le tableau 1.

I. *Comparaison des methodes*

La courbe de relation dose-effet concernant les dicentriques peut être tirée des résultats obtenus respectivement par Bender et Gooch et par Kelly et Brown.

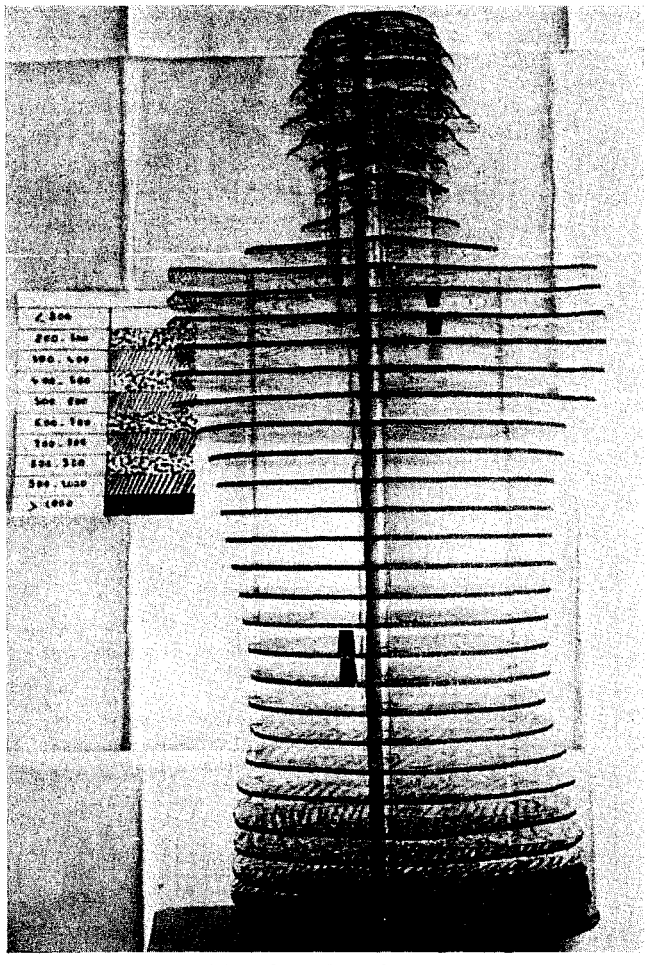

FIG. 1. Répartition des échantillons de sang dans le fantôme au moment de l'irradiation.

Tableau 1. *Évolution des differents types d'anomalies chromosomiques en fonction de la dose, après irradiation de sang humain* in vitro.

Nombre des Aberrations pour 100 Cellules		Gamma + 10% Neutrons					Gamma ^{60}Co	
	DOSE	40	85	165	200	587	400	600 (R)
Dicentriques		1,25	4,5	7,7	12,5	85,0	47,0	85,0
Dicentriques + Anneaux		1,25	4,5	9,2	20,8	97,0	52,7	110,0
Cassures direct^{T} observables		7,5	26,0	48,0	67,0	243,0	192,0	308,0
Cassures totales sur caryotypes		15,0	37,0	61,0	83,0	320,0	231,0	348,0
Cellules anormales		11,3	26,6	41,7	50,0	90,0	83,0	100,0
Nombre de caryotypes étudie's pour chaque dose		80	45	65	24	41	70	26

(*a*) *Culture.* Ces auteurs ont utilisé la macrotechnique originale de Moorhead. Nous avons utilisé, pour notre part, une microtechnique dérivée de façon à limiter le volume total des prélèvements—tant sur l'accidenté—que sur l'unique donneur sain dont le sang a été irradié expérimentalement. Le temps de culture a été de 72 heures pour Bender, de 70 à 96 pour Kelly. Nous avons fait des cultures à 72 et 96 heures en deux séries indépendantes.

Kelly ont porté sur des sangs normaux prélevés sur plusieurs individus sains.

Notre expérience n'a utilisé qu'un seul et même donneur pour toutes les doses, dans les deux séries d'irradiation (n, γ et ^{60}Co).

—*Débits de dose et rayonnements utilisés:* Les expériences de Bender aux rayons X de 250 keV ont été faites aux débits de 60 R/min et 10 R/min.

Les débits de dose employée par Kelly (rayons X de 200 keV) ont varié de 42 à 48 R/min.

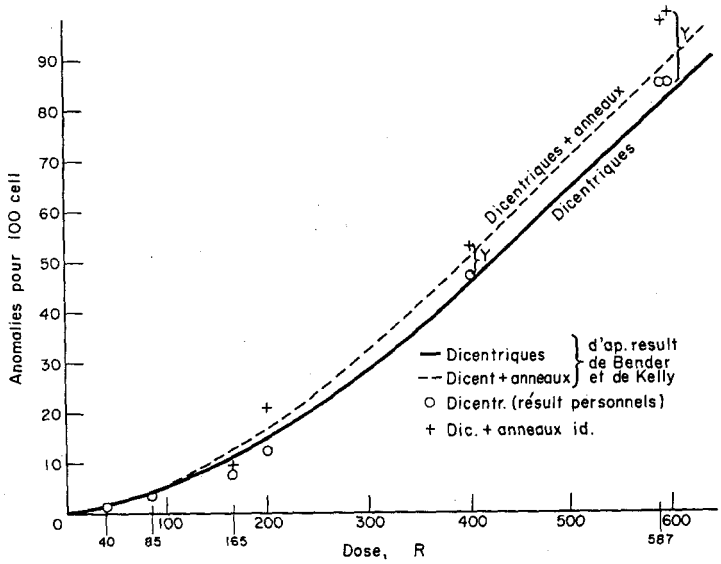

FIG. 2. Évolution du nombre de dicentriques, pour 100 cellules, en fonction de la dose. Analyses chromosomiques Sang Irradié *in vitro*. Comparaison avec les résultats de Bender et de Kelly.

(*b*) *Analyse chromosomique.* Par ailleurs, les auteurs précédents ont fait leurs évaluations par observation microscopique directe ou sur photographies sans montage de caryotypes.

Pour ces techniques, seules ont été prises en considération, par Bender, les anomalies directement constatables: dicentriques, anneaux et les déletions portant sur les paires les plus caractéristiques (1–5), (13–15), (19–22).

Notre travail a comporté, en plus, l'estimation de toutes les translocations et déletions, estimations rendues possibles sur les caryotypes montés.

(*c*) *Irradiation.*

—*Sang:* Les expériences de Bender, de

Dans notre expérience au ^{60}Co, le débit de dose a été de 30 R/min. Dans notre expérience avec le fantôme à Mol, c'est la durée qui a été constante (150 minutes), et les débits de dose ont varié suivant les points entre 0,26 R/min (pour la dose la plus faible 40R) et 4 R/min (pour la plus forte 587 R).

II. *Comparaison des résultats*

(*a*) *Courbe des dicentriques* (Fig. 2). Cette courbe a été tracée en utilisant les points expérimentaux de Bender pour les faibles doses (50–200 R) et ceux de Kelly pour les doses fortes, supérieures à 200 R.

A noter que les points de Bender ont été

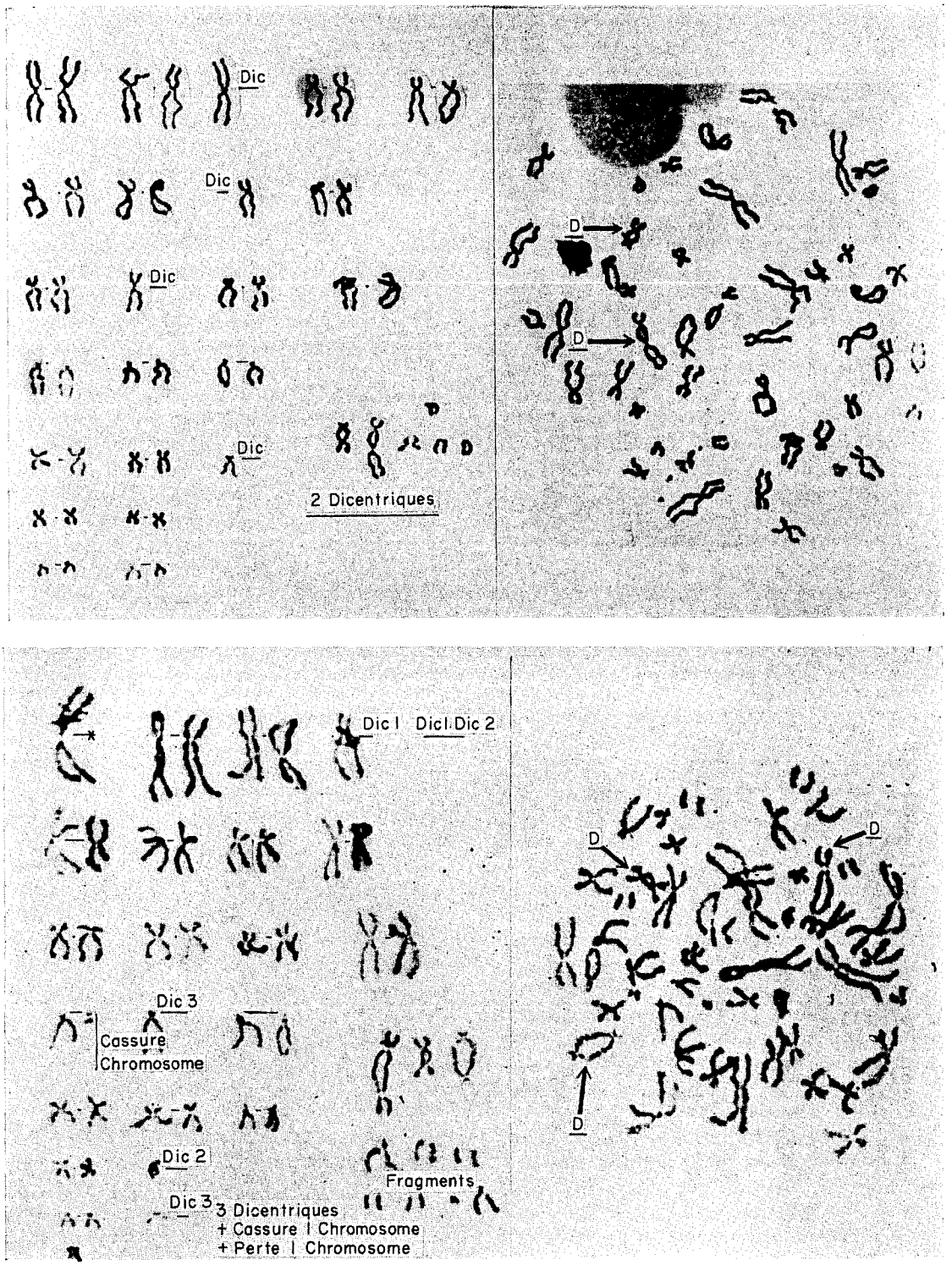

FIGS. 3, 4. Cellules porteuses d'anomalies multiples après irradiation de sang aux doses de 587 R et 600 R.

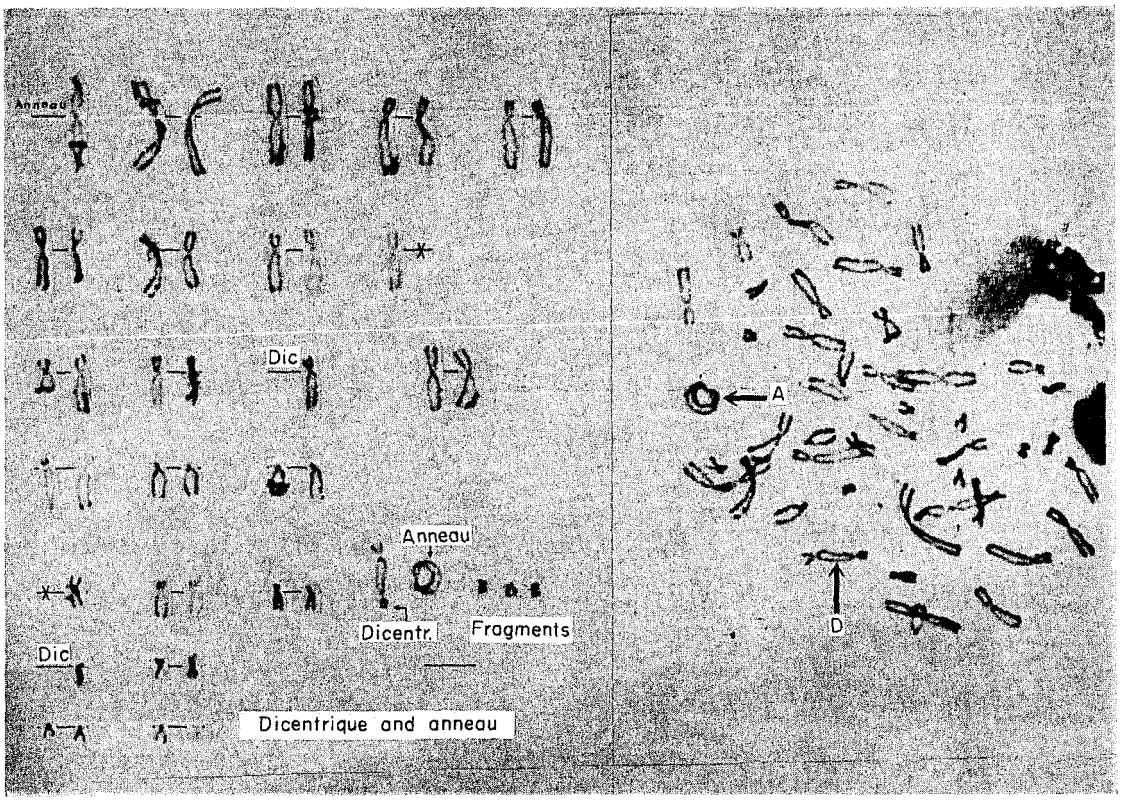

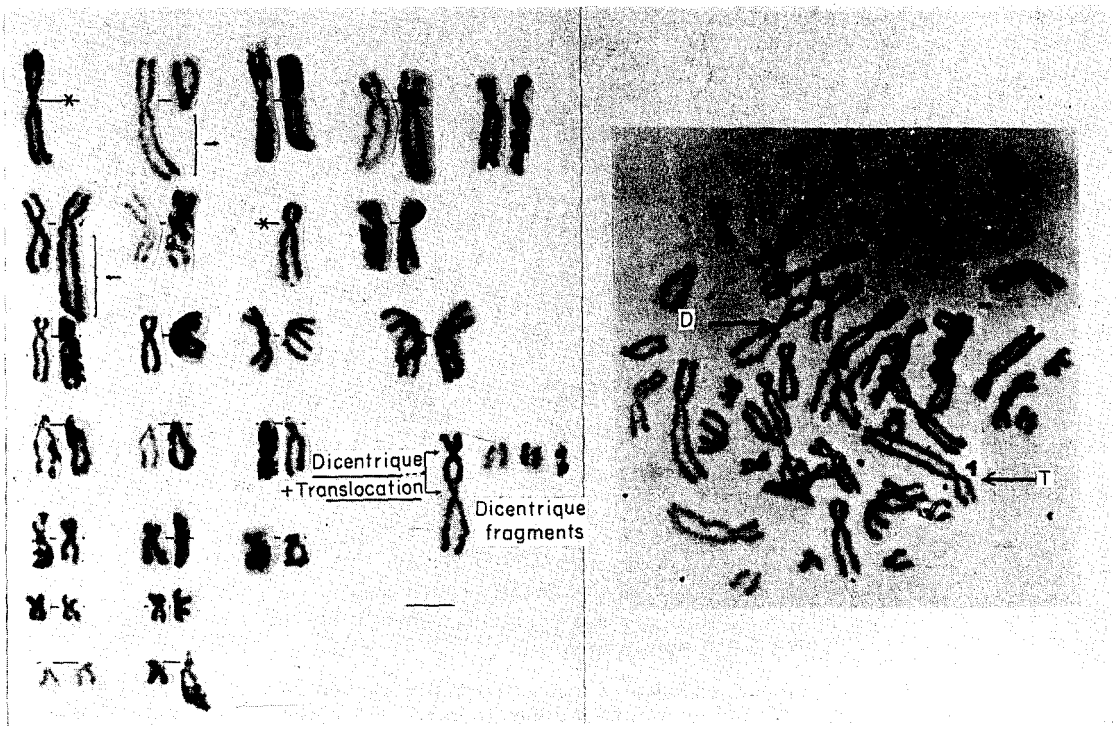

FIGS. 5, 6. Cellules porteuses d'anomalies multiples après irradiation de sang aux doses de 587 R et 600 R.

établis sur 300 à 500 cellules, tandis que ceux de Kelly ne portent que sur un nombre limité de cellules, surtout aux très fortes doses: 59 à 250, 53 à 300, 86 à 400, 10 à 800, 33 à 1600.

La variance sur ces points est donc plus élevée. Une autre raison de variance est le fait que les résultats globaux ont porté sur des temps de culture variables, entre 3 et 4 jours.

Nos points expérimentaux se trouvent cependant en excellente concordance avec cette courbe. *Pour les faibles doses*, jusqu'à 200 R, nos points sont un peu au-dessous de la courbe. Ceci provient probablement de nos débits de dose très faibles. En effet, si l'on compare le point 200 R avec le point. établi par Bender, avec une dose fractionnée de 200 R, on obtient une coïncidence exacte. *Pour les fortes doses*, nos points sont légèrement au-dessus de la courbe. Pour les doses supérieures à 200 R, il semble comme l'a déjà signalé Kelly, que la courbe expérimentale dicentriques + anneaux croisse moins vite que la courbe théorique proposée par Bender selon la formule $y = 0{,}52.10^{-5}\ D^2$ y (nb de D + A/cellule).

Si l'on porte sur ces courbes les résultats obtenus chez l'homme accidenté à Mol, la dose estimée est de 470 R. (Culture de sang prélevé 4 jours après l'accident.)

Il n'a pas été rare d'observer pour les doses très fortes, tant chez l'accidenté qu'*in vitro*, des cellules porteuses de 2 ou 3 dicentriques (Figs. 3, 4) et des cellules porteuses de dicentriques associés avec un anneau ou une translocation (Figs. 5, 6).

(*b*) *Courbe des "cassures"* (Fig. 7). Il est admis que les déletions et fragments proviennent d'un seul impact sur le chromosome, et représentent des lésions à 1 coup;

que les remaniements chromosomiques (dicentriques, anneaux, translocations) sont dus à 2 impacts et doivent être comptés comme lésions à 2 coups.

L'estimation du nombre des "cassures" doit. donc tenir compte du nombre total d'*impacts*, c'est-à-dire:

(nb de déletions + fragments) + 2 × (nb de remaniements : dicentriques + anneaux + translocations).

Les translocations n'étant pas toujours directement observables microscopiquement ou sur photographie, il est nécessaire de les dénombrer sur des caryotypes montés. Notre estimation tient compte de ce fait, qui fournit une relation dose-effet plus précise.

Si nous ne décomptons pas les translocations, ni les déletions sur les paires non reconnaissables sans établissement de caryotypes, nous obtenons des résultats qui sont en parfait accord avec ceux de Bender et ceux de Kelly, sauf aux doses les plus fortes (587 et 600 R) où nos résultats sont inférieurs à ceux de Kelly.

Si nous comptons, au contraire, le nombre total des cassures selon notre technique, c'est-à-dire déletions et translocations comprises, nos points dessinent une courbe qui, pour les doses inférieures à 200 R, est une droite régulière, à telle enseigne que nous pourrions nous en servir comme courbe de référence pour ces faibles doses.

Pour les doses inférieures à 200 R, nous trouvons un coefficient de production de cassures/cellule/R, égal à 0,0032; ce coefficient est en parfait accord avec celui trouvé par Bender [7] sur des leucocytes humains irradiés au cours de la culture lorsque les cellules sont en phase G_2 du cycle mitotique (chromatides déjà dédoublées). L'estimation du nombre total d'anomalies est alors plus simple puisqu'elle ne nécessite pas l'établissement de caryotypes.

Vers 200 R, cette courbe s'infléchit et sa pente augmente; mais au-delà de 400 R, elle passerait au-dessous de la courbe de Kelly (établie sans caryotypes). Leur point de croisement est autour de 400 R.

Nous ne nous croyons pas autorisés à tracer de courbe passant par nos points expérimentaux. Nous nous bornons ici à une simple comparaison.

Par ailleurs, les résultats comparés des deux expériences d'irradiation (γ + n et γ du ^{60}Co) sont sensiblement équivalents; mais rappelons le faible débit de dose dans l'expérience γ, n.

(*c*) *Courbe des "cellules anormales"* (Fig. 8). Nous prenons ici en considération le nombre des cellules porteuses d'une anomalie chromosomique quel qu'en soit le type, exprimé en pourcentage des cellules examinées.

Ces valeurs sont mises en comparaison avec les résultats établis par De Grouchy. [8] Cet auteur a utilisé des rayons X de 200 keV, débit d'exposition de 10–15 R/min, pour

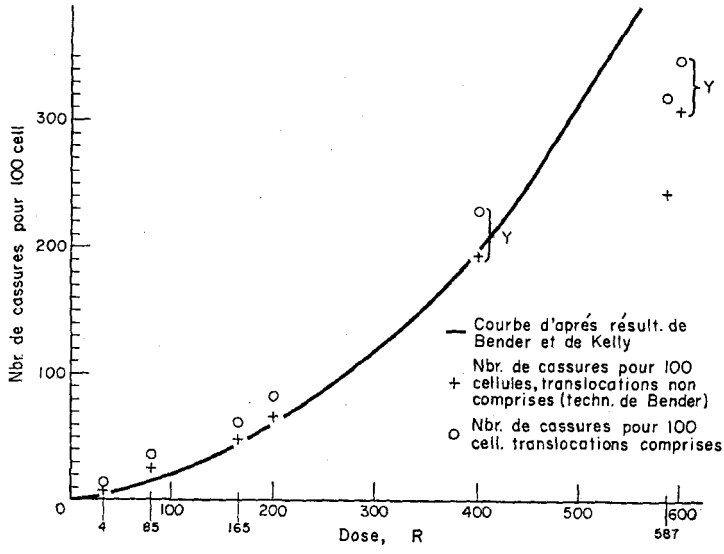

FIG. 7. Evolution du nombre de cassures pour 100 cellules en fonction de la dose.

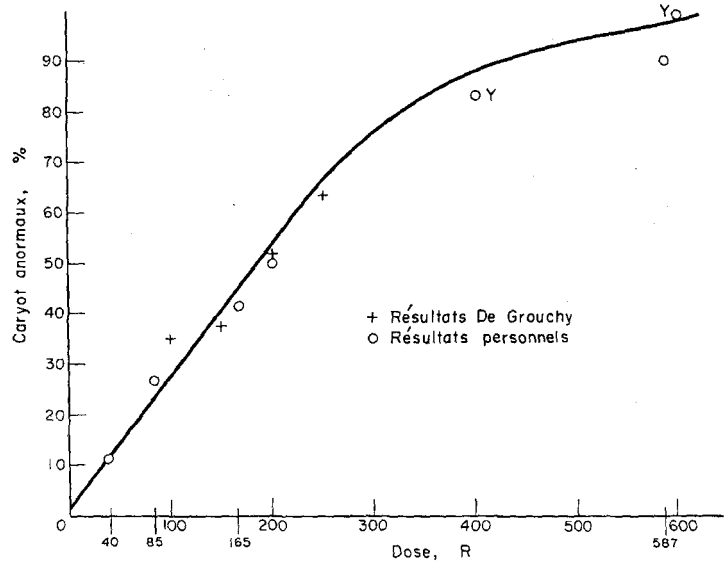

FIG. 8. Evolution du pourcentage de cellules porteuses d'anomalie chromosomique en fonction de la dose.

irradier des cultures de sang venant d'être ensemencées, aux doses de 100 à 300 R. Les résultats portent sur des cultures de 3 jours et 4 jours.

Nous exprimons ici des valeurs obtenues sur cultures de 3 jours uniquement, aux doses déjà indiquées. Nos points sont parfaitement alignés avec la courbe de De Grouchy. Nous obtenons une relation linéaire *jusqu'à 250 R.*

Pour la dose de 200 R, la fréquence de cellules anormales est de 0,5: $y = 0{,}0025$ D. Bender et Kelly ne fournissant pas de données sur le taux constation dont on ne peut tirer d'argument dosimétrique. En effet, il existe un certain pourcentage d'hypoploïdies sur des cellules normales (bruit de fond), et la pente de la courbe obtenue est faible donc imprécise.

L'existence d'un bruit de fond implique vraisemblablement l'intervention d'un facteur technique dépendant de la fragilité du cytoplasme cellulaire. Et ceci ne peut être apprécié quantitativement.

2°/*Polyploïdies–endoreduplications* (tableau 2): Les polyploïdies ont été évaluées sur 1000

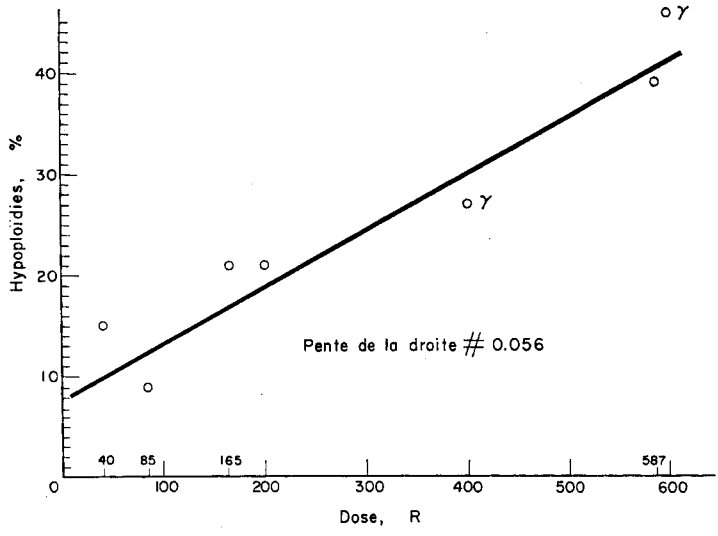

FIG. 9. Évolution du pourcentage de cellules hypoploïdes en fonction de la dose.

de cellules anormales, nous n'avons pas pu faire d'autres comparaisons.

Aux alentours de 300 R, la pente de courbe diminue et tend vers un plateau pour des doses supérieures à celles de nos expériences (600 R).

Ce point de changement de pente (300 R) équivaut approximativement à "1 coup par cellule" estimé sur la courbe des cassures de la figure 7 précédente.

(*d*) *Anomalies modales*

1°/*Hypoploïdies* (Fig. 9): Les hypoploïdies ont été évaluées pour 100 cellules. Nous observons une augmentation régulière avec la dose, selon une loi quasi-linéaire. Ceci est une simple cellules, au cours d'un travail complètement indépendant de l'établissement des caryotypes qui était la base du travail précédent. On a établi en même temps, à cette occasion, le taux des endoreduplications. C'est un type particulier de polyploïdies dans lequel les chromosomes conjoints sont spontanément appariés.

Le taux des polyploïdies s'élève avec la dose sur les deux types de culture, comme le montre le tableau 2.

Cette augmentation linéaire jusqu'à 400 R est assez régulière. Les points obtenus à 600 R avec les γ du ^{60}Co sont également alignés sur cette courbe. Nous avons toutefois obtenu un point extrêmement éloigné pour la dose de

587 R, n, aussi bien sur les cultures de 3 jours que sur celles de 4 jours.

Nous ne formulons aucune conclusion sur cette divergence (EBR des neutrons? Influence du long séjour des cellules dans des tubes en polystyrène précédant leur mise en culture: 8 heures environ avant et durant l'irradiation?).

Du point de vue cytologique, la grande majorité des cellules polyploïdes sont 4 n au 4ème jour. On observe également des cellules 3 n à 10 n (tableau 3).

Les cultures de 3 jours ne montrent pratiquement que des polyploïdies 3 n et 4 n. On en observe même aux doses faibles et dans le témoin.

Les endoreduplications au 3ème jour n'apparaissent pas avant la dose de 400 R. Par contre, sur les cultures de 4 jours, elles apparaissent à partir de 100 R environ (85–112).

Reduplication des "anomalies par remaniement": dans les cellules tétraploïdes prises en compte dans l'établissement des caryotypes, aux doses de 585 R et 600 R, sur des *cultures du 3ème jour*, nous avons observé des reduplications portant sur les "anomalies par remaniement" (dicentriques). Ces dicentriques allant par paire, ont naturellement été comptés pour 2 coups seulement et non 4 coups dans l'estimation des cassures et des dicentriques (Figs. 10, 11).

Cette constatation évoque avec force l'intervention d'une seconde mitose dans de telles cellules. Néanmoins, leur pourcentage est très faible (4 sur 41 = 10% pour 585 R; 1 sur 25 = 4% pour 600 R).

Tableau 2 Évolution de la proportion des cellules polyploïdes en fonction de la dose.

Irr. γ, n Dose (R)	Polyploïdies pour 1000 cellules			
	Cultures de 3 jours		Cultures de 4 jours	
	Nombre total	Endoreduplication	Nombre total	Endoreduplication
Témoin établi (sur 2000 cell.)	1	0	—	—
40	2	0	8	0
85	6	0	12	1
112	—	—	17	1
165	3	0	14	4
200	37	0	32	3
587	188	5	226	46
Irr. γ^{60}Co Dose (R)				
400	45	5	58	12
600	53	1	90	10

Tableau 3. Répartition des polyploïdies dans les cultures de 4 jours, provenant de sang irradié aux différentes doses.

Polyploïdies	3 n	4 n	5 n	6 n	7 n	8 n	9 n	10 n
Cultures de 4 jours	9	103	10	8	3	3	1	1

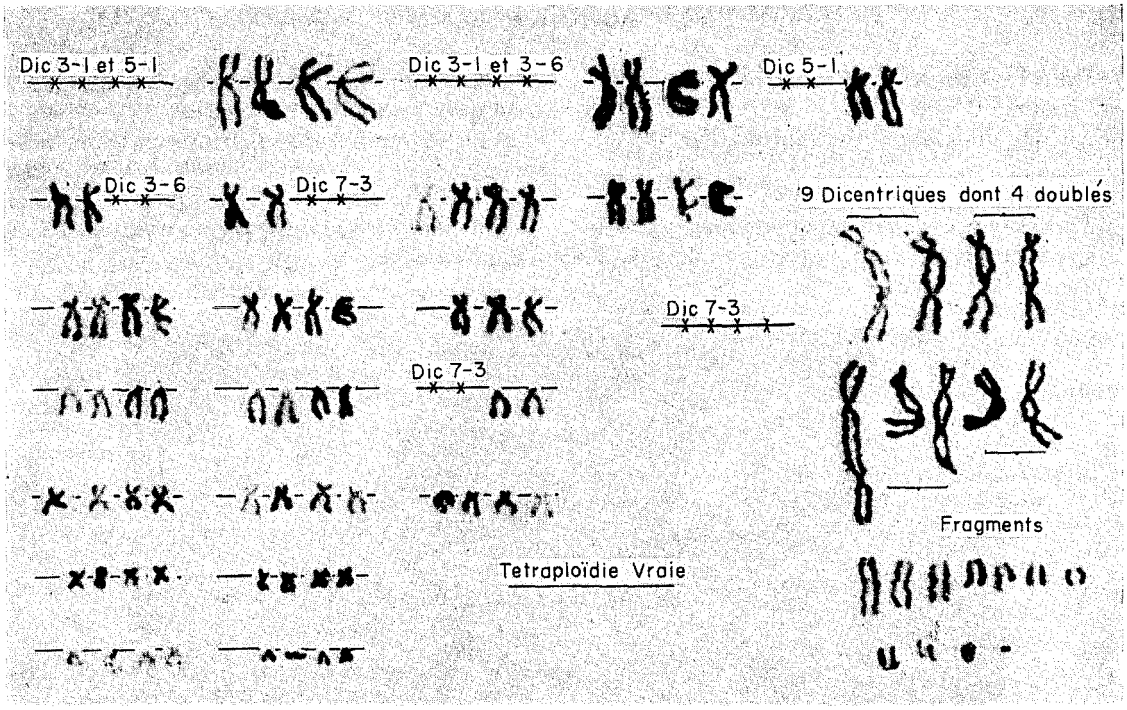

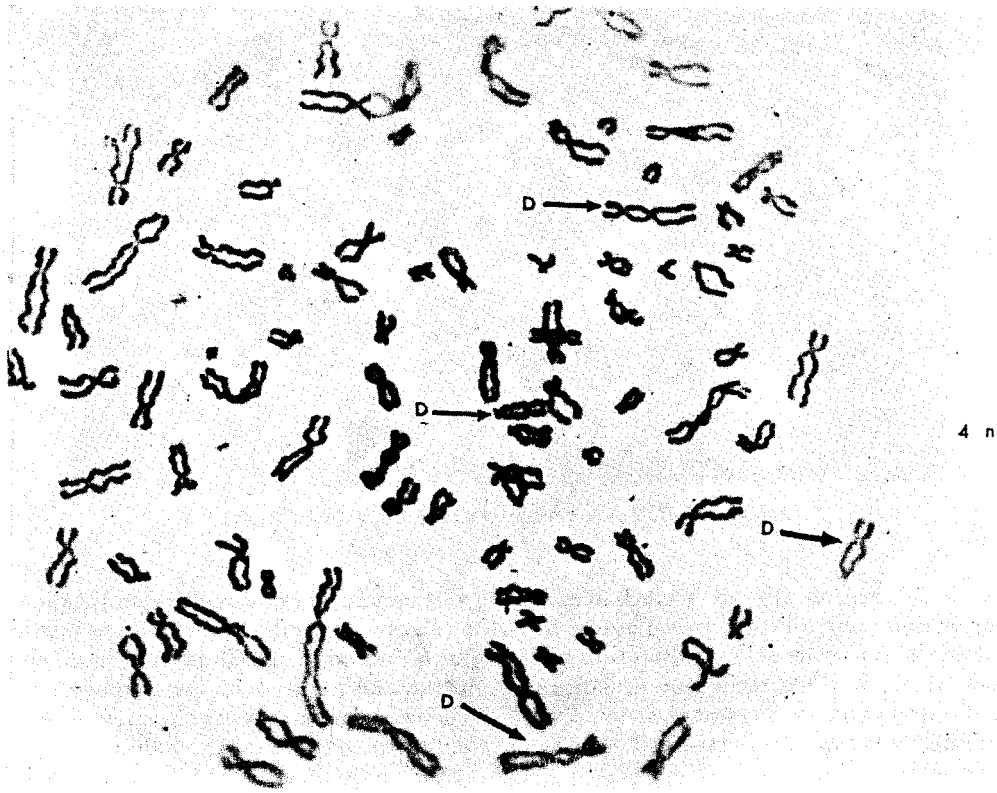

FIGS. 10, 11. Tétraploïdies avec duplication d'anomalies.

Dans les cultures de 4 jours, cette proportion est beaucoup plus forte, et par ailleurs on observe des anomalies trisomiques (Fig. 12).

CONCLUSIONS

1°. Les pourcentages des anomalies chromosomiques observés, dans notre travail, sur des cultures de 72 heures, sont en accord avec les résultats établis, par ailleurs, par d'autres auteurs. Les différences dans le conditions expérimentales (débit de dose, technique de culture, modes d'observation et d'expression des résultats) n'affectent pas, semble-t-il, la concordance des chiffres observés.

Cette constatation permet d'affirmer davantage la valeur des analyses chromosomiques en tant que dosimétrie biologique.

2°. L'estimation dosimétrique pour les doses fortes, supérieures à 200–300 R, peut être faite à partir de courbes de dicentriques + anneaux, ce qui peut être établi par observation directe au microscope.

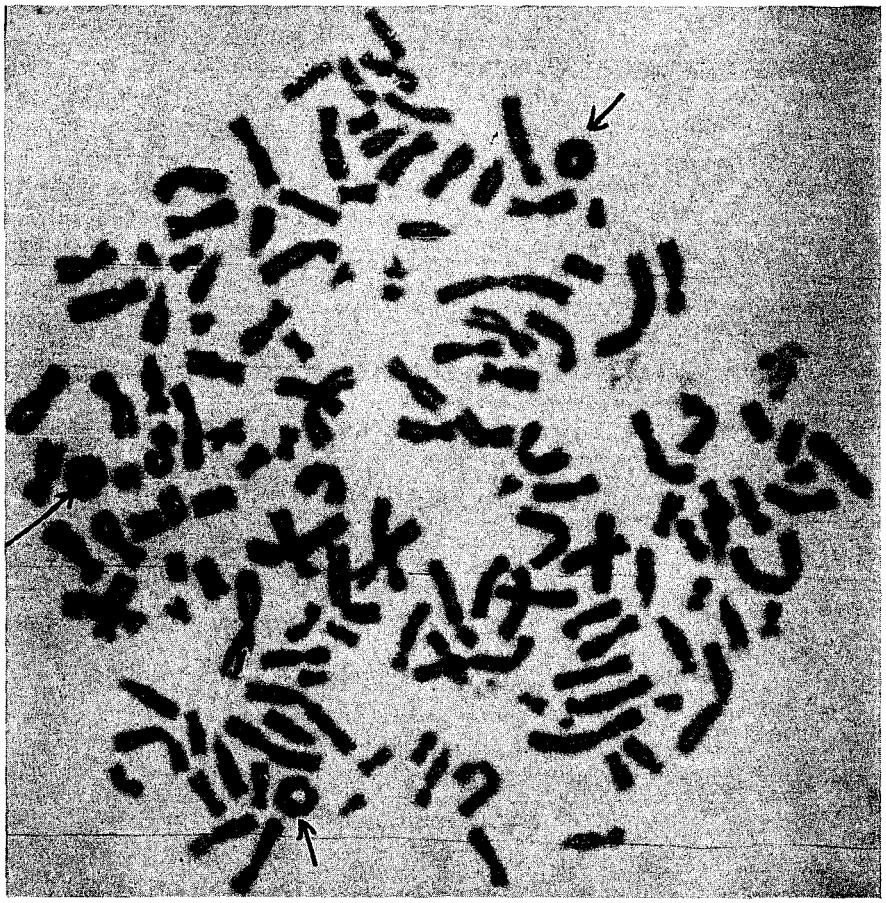

FIG. 12. Cellule hexaploïde porteuse d'anomalie triple.

Cependant, il nous semble que l'établissement de relation dose-effet pour les doses inférieures à 200 R nécessite l'utilisation d'une technique plus raffinée, qui doit avoir recours à l'établissement des caryotypes complets, afin de tenir compte de toutes les anomalies.

3°. Bien qu'il puisse se trouver des cellules en seconde mitose, dans des cultures de 72 heures,

il nous est apparu que le pourcentage de ces secondes mitoses est relativement faible (moins de 10%). A ces doses, l'erreur entre dans le cadre des variances biologiques.

RÉFÉRENCES

1. M. A. BENDER et P. C. GOOCH. Types and rates of X-ray induced chromosome aberrations in human blood irradiated *in vitro*, *Proc. Nat. Acad. Sci.* (*U.S.A.*) **48**, 522–532 (1962).
2. P. C. GOOCH, M. L. RANDOLPH et M. A. BENDER. Chromosome aberrations induced in human somatic cells by neutron, AIEA, Biological effects of neutron and proton irradiation, (Upton) 1963, October 7–11, Vienna AIEA (1964), **1**, 325–342.
3. S. KELLY et C. D. BROWN. Chromosome aberrations as a biological dosimeter, *Am. J. Publ. Health*, **55**, 9, 1419–1429 (1965).
4. H. JAMMET, R. GONGORA, R. LE GÔ et G. MARBLÉ, Observation clinique et traitement d'un cas d'irradiation globale accidentalle—DS: *Radiation Protection*, IRPA Congress, Rome, 5–10 September 1966.
5. P. S. MOORHEAD, P. C. NOWELL, W. J. MELLMAN, D. M. BATIPPS et D. A. HUNGERFORD. Chromosome preparations of leukocytes cultured from human peripheral blood, *Exp. Cell. Res.* **20**, 613–616 (1960).
6. J. LEJEUNE. Techniques d'étude des chromosomes humains, Microtechnique, ds. R. Turpin et J. Lejeune, *Les chromosomes humains*, Ed. Gauthier Villars (1965), 26–29.
7. M. A. BENDER et P. C. GOOCH. Chromatid type aberrations induced by X-rays in human leukocyte cultures, *Cytogenetics*, **2**, 2/3, 107–116 (1963).
8. J. DE GROUCHY, G. VALLÉE et C. NAVA. Analyse chromosomique de cellules cancéreuses et de cellules médullaires et sanguines irradiées *in vitro*, *Annales de Génétique*, **6**, 1, 9–29 (1963).

ABERRATIONS CHROMOSOMIQUES DES LEUCOCYTES DU SANG PÉRIPHÉRIQUE CHEZ DES SUJETS PROFESSIONNELLEMENT SOUMIS AUX RADIATIONS IONISANTES

B. PENDIĆ*

Assistance technique—A. BOGDANOVIĆ

Service de Protection Médicale, Institut des sciences nucléaires "Boris Kidrič"—Vinča, Yougoslavie

Résumé—Ce rapport présente des aberrations chromosomiques observées chez un groupe d'ouvrier de l'Institut "Boris Kidrič" travaillant aux sources de radiations ionisantes et chez un groupe de radiologues. Les doses d'irradiation ne dépassaient pas les doses admissibles. Il est montré par les résultats obtenus que les aberrations chromosomiques sont bien plus accentuées chez les individus professionnellement exposés que chez les témoins.

La corrélation entre les modifications constatées et la dose d'irradiation est discutée dans ce rapport ainsi que l'importance clinique et pronostique des aberrations chromosomiques persistantes.

INTRODUCTION

Il a été montré par de nombreuses études que les radiations ionisantes peuvent influencer les chromosomes humains *in vivo* et *in vitro* provoquant des modifications numériques et structurales.

Des chromosomes de structure modifiée sont révélés même après une exposition à de faibles doses d'irradiation.[1, 2] Quelques unes de ces modifications sont maintenues longtemps après l'exposition chez des sujets professionnellement soumis à l'irradiation,[3-5] ou à titre diagnostique et thérapeutique [6, 7] ainsi que chez des sujets exposés accidentellement à de fortes doses d'irradiation.[8-10]

MATÉRIEL ET MÉTHODE

L'étude des chromosomes a été faite sur les leucocytes du sang selon la méthode de Moorhead,[11] quelque peu modifiée. Les cellules ont été examinées 72 h après avoir été cultivées. Les mitoses sont bloquées par une solution de colchicine à 0,04% pendant une heure. Le choc hypotonique est effectué avec une solution de citrate de soude à 0,95%. Après fixation au Carnoy, les lames sont colorées à l'orceine 2%.

Les groupes expérimentés comprennent quelques ouvriers de l'Institut "Boris Kidrič" et quelques employés de l'Institut Radiologique de la Faculté de médecine à Belgrade. A l'exception de deux sujets de l'Institut Radiologique—deux infirmiers ayant travaillé aux moulages de radium ont présenté des signes remarquables de radiodermite—les autres sujets examinés n'ont pas présenté de signes cliniques perceptibles de dommages dus à l'irradiation. Les données dosimétriques sur l'exposition à l'irradiation sont présentées pour les ouvriers de l'Institut "Boris Kidrič". En ce qui concerne le personnel de l'Institut Radiologique, ces données n'existent pas. C'est pourquoi le tableau présente le nombre d'années que ces individus ont passées aux sources de radiations ionisantes.

Le groupe des témoins comporte 4 sujets qui n'ont pas été soumis aux radiations ionisantes et n'ont pas été atteints de maladies virales, d'hémopathies malignes ou de cancer.

Le plus grand nombre d'analyses des chromosomes a été fait par la méthode générale[9]: constatation du nombre de chromosomes et des modifications morphologiques grossières.

* Adresse actuelle: Hôpital de la Ville 172, rue Baje Sekulića à Belgrade

L'analyse de caryotype ayant été faite sporadiquement devrait être complétée. Les résultats seront donc présentés en supplément.

RÉSULTATS ET DISCUSSION

Les résultats montrent que 289 à 300 cellules analysées chez des témoins présentent un nombre normal de chromosomes, c'est-à-dire 2n = 46. Parmi onze cellules aneuploïdes, il n'y en a qu'une tétraploïde. Les modifications structurales se sont manifestées par des lacunes et cassures chromatidiennes et chromosomiques. Le nombre total des cellules anormales a été 5,7%, ce qui est en accord avec les constatations d'áutres auteurs. [5, 8, 12]

Le taux des aberrations chez des sujets professionnellement soumis à l'irradiation est bien plus significatif que chez des témoins. On observe des chromosomes de propriétés morphologiques différentes de ceux trouvés chez des sujets non exposés: dicentriques (Fig. 1), ronds et extra longs (Fig. 2). Les autres aberrations se rapportent aux lacunes et cassures chromatidiennes et chromosomiques et aux fragments acentriques (Fig. 3).

Les cellules aneuploïdes, surtout les cellules tétraploïdes (Fig. 4) représentent un phénomène plus fréquent chez des sujets exposés. Etant donné que tous les individus exposés avaient plus de 35 ans, on peut supposer que l'âge a eu aussi de l'influence. Il a été constaté par Jacobs *et al.* [13] que les sujets âgés de plus de 35 ans présentent un nombre plus élevé des cellules aneuploïdes que des individus jeunes.

Ces résultats indiquent que l'exposition professionnelle chronique à de faibles doses d'irradiation provoque des modifications *in vivo* chez l'homme. D'après l'opinion de plusieurs auteurs ces modifications sont dues à l'effet direct et indirect de l'irradiation et ne peuvent pas être considérées comme spontanées. [2-4, 6, 7, 10, 14] D'après Mac Kinney *et al.* [15] les cellules du sang se divisant dans la culture sont des lymphocytes.

Puisque la fréquence d'exposition et la dose reçue chez le personnel de l'Institut Radiologique ne sont pas connues, il n'est pas possible de faire une corrélation entre les doses reçues et les lésions observées. Il n'y a pas de différences entre les aberrations chromosomiques chez les ouvriers de l'Institut "Boris Kidrič", bien que la dose soit 3 à 6 fois plus grande chez les

Table 1.

Sujets	Dose	Nombre d'années de travail	Nombre des cellules examinées	Aneuploïdie		Dicentrique	Anneau	Extra long	**	% des anomalies
				Hypodiploïdie	Hyperdiploïdie					
Témoins	0	—	300	8	3	0	0	0	5	5,7
B.I.	12	3	74	2	4	0	0	1	2	12,1
Dj.V.	10	3	50	2	1	1	1	0	3	16,0
T.T.	64	15	56	4	3	0	0	1	2	17,8
M.A.	35	10	57	3	4	1	0	1	2	19,3
R.2	?	12	50	2	3	1	0	0	3	18,0
R.1	?	20	50	2	1	1	0	2	2	16,0
R.6	?	25	41	2	4	0	0	2	2	24,3
R.7	?	25	43	3	2	1	0	2	2	23,6
		Total	421	20	22	5	1	9	18	15,9

** Lacune chromatidienne et chromosomique.
Cassure chromatidienne et chromosomique.
Fragment acentrique.

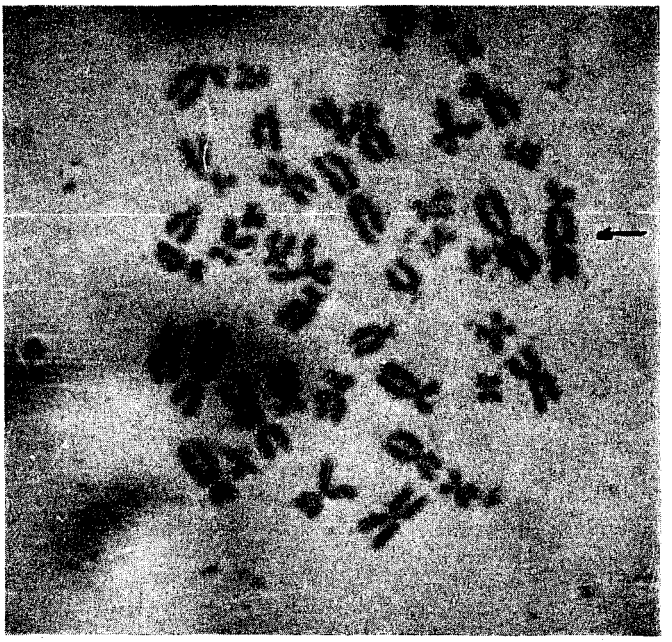

FIG. 1. Chromosome dicentrique.

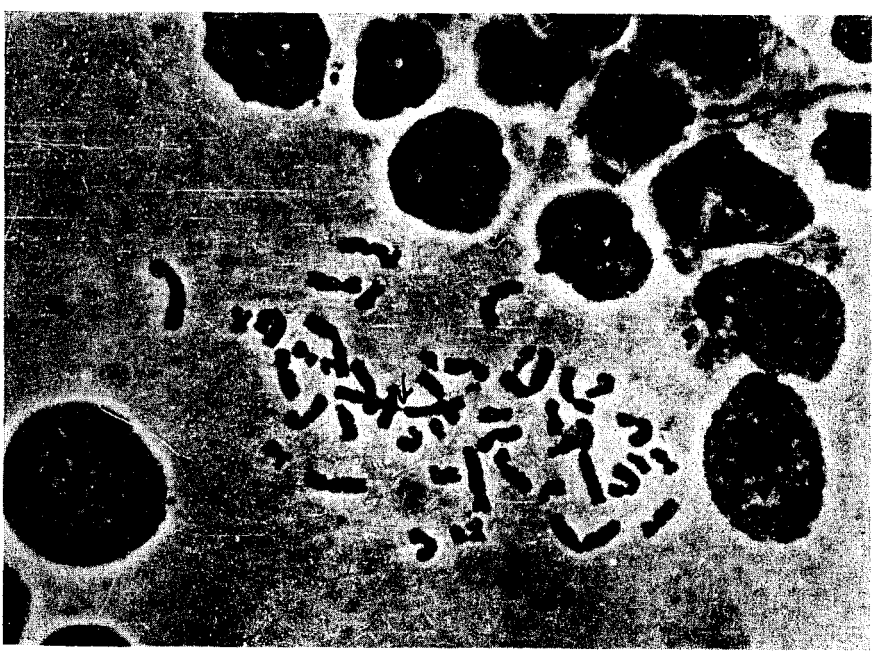

FIG. 2. Chromosome extra long.

FIG. 3. Fragments acentriques.

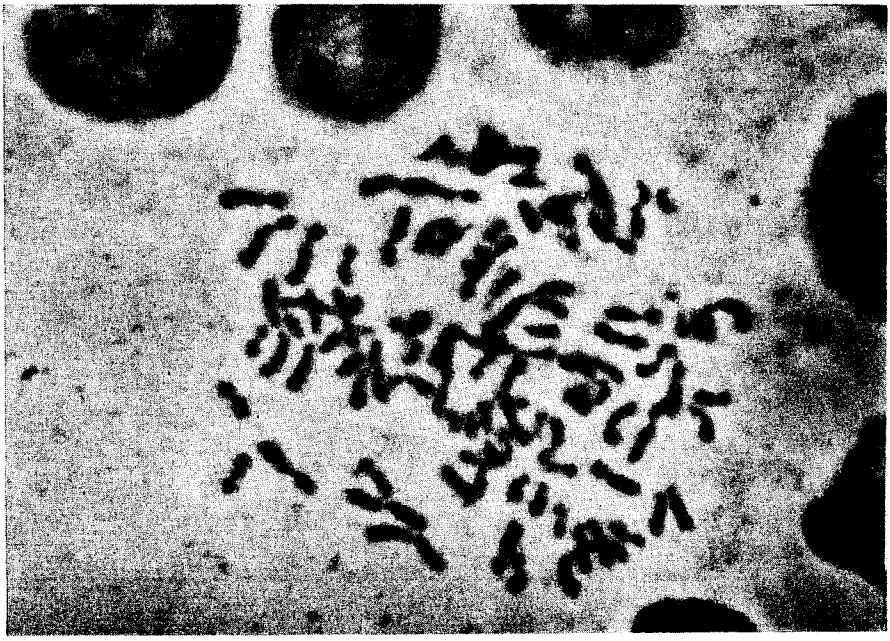

FIG. 4. Tetraploïdie.

troisième et quatrième personnes. Il apparaît, d'après nos résultats, qu'il n'existe pas de liaison entre le temps d'exposition et le nombre des aberrations chromosomiques.

L'importance clinique et pronostique des aberrations persistantes n'est pas tout à fait nette. La plupart des individus ayant des chromosomes modifiés du point de vue clinique ne présentent aucune anomalie. [2, 4, 12]

Buckton *et al.* [16] et Wald [17] soulignent l'importance d'observer des aberrations chromosomiques persistantes afin de pouvoir trouver une corrélation entre ces modifications et des maladies malignes. Cependant, d'après Bender [10] on ne peut pas prouver, pour le moment, une liaison entre ces modifications et les néoplasies éventuelles observées ultérieurement.

CONCLUSION

Les résultats indiquent qu'il existe des modifications numériques et structurales des chromosomes dans les leucocytes du sang chez des sujets soumis aux radiations ionisantes.

On a constaté un nombre élevé des cellules aneuploïdes et des cellules aux chromosomes dicentriques et extra longs par rapport au groupe témoin.

Le taux des cellules présentant des aberrations chromosomiques va de 12,1 à 24,3% chez des sujets professionnellement exposés, tandis qu'il est de 5,7% chez le groupe témoin.

RÉFÉRENCES

1. J. S. Stewart et A. R. Sanderson. *Lancet*, **1**, 978 (1961).
2. A. D. Bloom et J. H. Tjio. *New England J. Med.* **270**, 1341 (1964).
3. M. Sasaki, R. E. Ottoman et A. Norman, *Radiology*, **81**, 652 (1963).
4. C. Mouriquand *et al. C.R. Acad. Sci.* **259**, 3830 (1964).
5. A. Norman, M. Sasaki, R. E. Ottoman et R. C. Veomett, *Rad. Res.* **23**, 282 (1964).
6. K. E. Buckton, P. A. Jacobs, W. M. Court-Brown et R. Doll, *Lancet*, **2**, 676 (1962).
7. A. P. Amarose et D. H. Baxter, *Obst. and Gynecol.* **25**, 828 (1965).
8. M. A. Bender et R. C. Gooch, *Rad. Res.*, **16**, 44 (1962),
9. M. A. Bender et R. C. Gooch, *Rad. Res.* **18**, 389 (1963).
10. M. A. Bender, *Ann. N.Y. Acad. Sci.* **114**, 249 (1964).
11. P. S. Moorhead *et al. Exp. Cell. Res.* **20**, 613 (1960).
12. H. Oishi and C. M. Pomerat. In *Proc. Symp. Intern. Society for Cell Biology*, Vol. 3, Academic Press Inc., New York (1964), p. 137.
13. P. A. Jacobs, W. M. Court-Brown et R. Doll, *Nature*, **191**, 1178 (1961).
14. G. Mathé, J. L. Amiel et L. Schwarzenberg, *L'aplasie myelo-lymphoïde de l'irradiation totale*, Gauthier-Villars, Paris (1965), p. 51.
15. A. A. MacKinney, F. Stohlman et G. Brecher, *Blood*, **19**, 349 (1962).
16. K. E. Buckton *et al.*, *Lancet* **2**, 676 (1962).
17. N. Wald et S. F. Pan, Annual meeting of the Health Physics Society, 15 June 1965, Los Angeles (Reprint).

RICERCHE RADIOBIOLOGICHE IN UNA CENTRALE ELETTRONUCLEARE DELL'ENEL

ANTONIO FARULLA

Cattedra di Radiobiologia dell'Università di Sassari (Italia)

Sommario—Nel presente rapporto sono riferiti i primi risultati di un programma di ricerche indirizzate in particolare allo studio di eventuali modificazioni citogenetiche indotte dall'esposizione prolungata per motivi professionali a piccole dosi di radiazioni ionizzanti.

Lo studio, condotto su dipendenti di una centrale nucleare di potenza, suddivisi in gruppi in rapporto alla destinazione lavorativa ed all'entità dell'esposizione, si é svolto in un primo tempo con la definizione del cariogramma di base e in seguito con periodici controlli effettuati nel corso dell'attività lavorativa.

Allo stato attuale delle indagini é stata osservata una percentuale di piastre aneuploidi del 13% con una netta prevalenza di conte ipomodali su quelle ipermodali; per quanto si riferisce alle anomalie cromatidiche la percentuale riscontrata é stata del 6,7% sul totale delle cellule esaminate.

Nel corso dei successivi controlli non sono state riscontrate significative modificazioni del cariogramma di base.

Valori pressochè analoghi sia per quanto riguarda l'incidenza di cellule aneuploidi che la frequenza di anomalie cromatidiche sono stati osservati in un ampio gruppo di soggètti accuratamente selezionati presi come controllo, con caratteristiche di età, sesso, ecc. sovrapponibili a quelle dei dipendenti della centrale oggetto di studio e in precedenza non esposti a radiazioni per motivi professionali, diagnostici o terapeutici. Da rilevare come le anomalie cromatidiche sinora osservate sia nei controlli che nei dipendenti della centrale sono disposte a caso in tutti gli elementi, e che la frequenza di lacune e rotture a carico di un cromosoma appare in genere proporzionale alla sua lunghezza.

NEGLI ultimi anni l'estensione delle tecniche di cultura delle cellule umane, soprattutto leucociti, e l'accresciuto interesse per gli effetti delle radiazioni sull'uomo hanno stimolato numerose ricerche sulle conseguenze, a livello cromosomico, dell'esposizione a dosi di radiazioni ionizzanti che, rispetto a quelle usate nella pratica sperimentale, sono da considerarsi relativamente basse.

In particolare sono state compiute ripetute osservazioni sulle modificazioni citogenetiche indotte nell'uomo da irradiazioni terapeutiche, e sono state descritte anomalie dei cromosomi anche per effetto di accertamenti radiodiagnostici.

Nell'ambito di questo indirizzo di studi, sono state intraprese una serie di ricerche sulle eventuali modificazioni citogenetiche indotte nel personale di una centrale elettronucleare dalla esposizione prolungata a piccole dosi di radiazioni ionizzanti.

L'interesse di questa ricerca consiste nella possibilità di studiare sistematicamente un campione sufficientemente esteso e relativamente omogeneo, costituito da soggetti sottoposti, per motivi di lavoro, a dosi di radiazioni ionizzanti molto basse e molto diluite nel tempo, ma comunque superiori a quelle cui la popolazione è naturalmente esposta.

Una centrale elettronucleare rappresenta attualmente l'ambiente più idoneo allo studio sistematico e protratto degli effetti che può avere sull'uomo la cronica esposizione a livelli di radioattività lontani da quelli artificialmente elevati propri dell'esperimento, ma indicativi

delle condizioni nelle quali il progresso tecnologico potrà nel futuro condurre parte sempre più larga della popolazione attiva.

Nel presente rapporto vengono riferiti i risultati relativi ad un gruppo di 56 lavoratori della Centrale Elettronucleare ENEL del Garigliano, seguiti con esami citogenetici dal 1964 ad oggi; trattasi di soggetti clinicamente sani, mai sottoposti a trattamenti radioterapici, di sesso maschile, di età compresa come limiti estremi tra 20 e 50 anni (in gran maggioranza tra 25 e 35 anni).

Contemporaneamente vengono riportati anche i dati relativi ad un gruppo di esami eseguiti, con le stesse modalità tecniche, su 30 soggetti di controllo non esposti e con caratteristiche di età e sesso sovrapponibili a quelle dei lavoratori nucleari oggetto di studio. Dall'esame della letteratura e attraverso la nostra diretta esperienza ci siamo infatti resi conto dell'assoluta necessità di riferire i dati riguardanti le eventuali modificazioni cromosomiche degli esposti ad un gruppo di controllo sufficientemente esteso e studiato nelle identiche condizioni. Il fattore tecnico ed i criteri di esame e classificazione più o meno restrittivi sono infatti determinanti, e ciascun gruppo di controllo con i suoi relativi valori "normali" è valido per la serie di osservazioni o di esperienze cui si riferisce.

La tecnica usata è quella, ormai classica, di Moorhead *e coll.* [1, 2]

I preparati, ottenuti dopo 72 ore di cultura, sono stati colorati con blu di Unna o con orceina acetica, ed il loro studio è stato eseguito con un fotomicroscopio Zeiss.

Le fotografie sono state fatte su pellicola Adox Dokuortho e Gevaert Scientia 39 C 56.

Lo studio dei cromosomi, sia dal punto di vista quantitativo (conta degli elementi) che qualitativo (morfologia e identificazione di eventuali anomalie) è stato eseguito sia mediante l'osservazione diretta dei preparati al microscopio che mediante la proiezione per mezzo di un ingranditore del negativo su pellicola di tutte le piastre esaminate. Il doppio esame, che generalmente è stato compiuto da osservatori diversi, assicura un conteggio esatto e permette la correzione degli eventuali errori che si possono compiere all'osservazione diretta.

I cariogrammi relativi a queste piastre sono stati ordinati secondo lo schema di Denver e

Tabella 1.

I° GRUPPO (dosi accumulate in coincidenza del 3° controllo < 1 rem; n. 8 casi)

	N° cell. esamin.	%	con 2 N = 46	%	con 2 N < 46	%	con 2 N > 46	%	con anom. cromat.	%
I controllo	313	100	295	94,25	14	4,47	4	1,28	10	3,19
II controllo	274	100	238	86,86	28	10,22	8	2,92	17	6,20
III controllo	338	100	308	91,12	27	7,99	3	0,89	21	6,21

II° GRUPPO (dosi accumulate in coincidenza del 3° controllo tra 1 e 2 rem; n. 11 casi)

	N° cell. esamin.	%	con 2 N = 46	%	con 2 N < 46	%	con 2 N > 46	%	con anom. cromat.	%
I controllo	369	100	341	92,41	25	6,77	3	0,82	38	10,30
II controllo	401	100	350	87,28	39	9,73	12	2,99	32	7,98
III controllo	504	100	461	91,47	39	7,74	4	0,79	29	5,75

Tabella 2.

III° GRUPPO (dosi accumulate in coincidenza del 3° controllo tra 2 e 3 rem; n. 20 casi)

	N° cell. esamin.	%	con 2 N = 46	%	con 2 N < 46	%	con 2 N > 46	%	con anom. cromat.	%
I controllo	668	100	596	89,22	62	9,28	10	1,50	30	4,49
II controllo	742	100	676	91,10	56	7,55	10	1,35	50	6,74
III controllo	938	100	864	92,11	68	7,25	6	0,64	62	6,61

IV° GRUPPO (dosi accumulate in coincidenza del 3° controllo tra 3 e 4 rem; n. 9 casi)

	N° cell. esamin.	%	con 2 N = 46	%	con 2 N < 46	%	con 2 N > 46	%	con anom. cromat.	%
I controllo	360	100	327	90,83	27	7,50	6	1,67	15	4,17
II controllo	288	100	246	85,42	36	12,50	6	2,08	6	2,08
III controllo	435	100	393	90,34	33	7,59	9	2,07	24	5,52

Tabella 3.

V° GRUPPO (dosi accumulate in coincidenza del 3° controllo tra 4 e 5 rem; n. 4 casi)

	N° cell. esamin.	%	con 2 N = 46	%	con 2 N < 46	%	con 2 N > 46	%	con anom. cromat.	%
I controllo	152	100	140	92,10	12	7,90	—	—	7	4,60
II controllo	112	100	112	100	—	—	—	—	8	7,14
III controllo	216	100	200	92,60	8	3,70	8	3,70	13	6,01

VI° GRUPPO (dosi accumulate in coincidenza del 3° controllo tra 5 e 6 rem; n. 4 casi)

	N° cell. esamin.	%	con 2 N = 46	%	con 2 N < 46	%	con 2 N > 46	%	con anom. cromat.	%
I controllo	156	100	146	93,59	10	6,41	—	—	12	7,69
II controllo	144	100	116	80,56	24	16,66	4	2,78	14	9,72
III controllo	168	100	142	84,52	20	11,91	6	3,57	12	7,14

si è costituito un archivio fotografico, non soggetto al possibile deterioramento dei preparati originali, che permette con grande facilità in ogni momento il riesame dei casi.

La classificazione delle anomalie è stata fatta seguendo i criteri proposti da Buckton *e coll.* [3, 4]

I risultati riportati nelle tabelle 1–3 si riferiscono a 56 dipendenti della Centrale per un totale di 168 culture. Le cellule esaminate e fotografate sono complessivamente 6.568.

I casi studiati sono stati disposti in sei gruppi tenendo conto della dose totale cumulata al momento dell'ultimo prelievo; per ogni gruppo sono indicati il numero delle cellule esaminate, il numero delle cellule euploidi e aneuploidi, la distribuzione delle conte, il numero di cellule con anomalie di tipo cromatidico. Non sono riportate le cellule con altre anomalie (tipo "C" di Buckton) in quanto presenti in numero molto scarso e perciò considerate solo globalmente.

I dati riassuntivi dei gruppi sopra menzionati sono riportati nella tabella 4.

I risultati riportati nella 5 riguardano il gruppo di controllo e si riferiscono a 1001 cellule esaminate e fotografate. Questo materiale è stato ottenuto da 30 soggetti sani in grande maggioranza compresi tra i 25 ed i 35 anni di età, mai sottoposti in precedenza a trattamenti ratioterapici o a prolungati accertamenti radiodiagnostici.

CONSIDERAZIONI

La percentuale di piastre con $2n \neq 46$ osservata nei dipendenti della Centrale è complessivamente del 9,52%, con una netta prevalenza (8,02%) delle piastre con numero di cromosomi inferiore al modale su quelle (1,50%) con 2n superiore a 46. Il rapporto fra conte ipo e ipermodali è perciò 5,4.

Nel gruppo di controllo la percentuale di piastre aneuploidi è del 10,79%, anche qui con una netta prevalenza (9,29%) delle piastre con numero di cromosomi inferiore al modale. Il rapporto fra conte ipo e ipermodali è in questo caso 6,2.

Il confronto fra questi due gruppi di dati non mostra una differenza significativa nella percentuale di cellule aneuploidi tra i lavoratori della centrale e i soggetti normali non esposti.

Premesso ciò restano da fare alcune considerazioni sulle frequenze osservate. Queste per-

Tabella 4.

numero totale delle cellule esaminate	6,578	100%
numero delle cellule con 2 N = 46	5,951	90,48%
numero delle cellule con 2 N ≠ 46	627	9,52%
numero delle cellule con 2 N < 46	528	8,02%
numero delle cellule con 2 N > 46	99	1,50%
numero delle cellule con anomalie di tipo cromatidico	400	6,08%
numero delle cellule con altre anomalie	39	0,60%

Tabella 5.

numero totale delle cellule esaminate	1,001	100%
numero delle cellule con 2 N = 46	893	89,21%
numero delle cellule con 2 N ≠ 46	108	10,79%
numero delle cellule con 2 N < 46	93	9,29%
numero delle cellule con 2 N > 46	15	1,50%
numero delle cellule con anomalie di tipo cromatidico	68	6,79%
numero delle cellule con altre anomalie	5	0,49%

centuali, indubbiamente elevate, sono molto probabilmente dovute a fattori tecnici. L'importanza del fattore tecnico è indicato dal fatto che il contributo di gran lunga maggiore al totale delle piastre non modali è dato da quelle con conte ipomodali, nelle quali si è presumibilmente verificata, durante la preparazione dei vetrini, la perdita di uno o più elementi del normale assetto diploide.

Esse rientrano tuttavia nei limiti della norma; a questa conclusione si giunge esaminando alcuni tra i più recenti lavori di citogenetica umana nei quali siano considerati gruppi di controlli "normali" sufficientemente ampi.

Il criterio seguito nell'esaminare e classificare le anomalie morfologiche osservate nel materiale studiato è quello che, inizialmente proposto da Buckton *e coll.*,[3] è stato successivamente accettato ed impiegato anche da altri ricercatori, e recentemente aggiornato da Buckton e Pike[4]

La classificazione di questi Autori comprende: cellule A—senza nessuna evidente anomalia di struttura; ulteriormente divisibili in: A_1—con un normale numero diploide di cromosomi; A_2—con un numero di cromosomi ipo o ipermodali; cellule B—con sole anomalie di tipo cromatidico; divisibili in: B_1—cellule con una lacuna cromatidica; B_2—cellule con una rottura cromatidica; B_3—cellule con una lacuna isocromatidica; cellule C—con anomalie di tipo cromosomico e comprendenti tutte le modificazioni di struttura diverse da quelle del gruppo precedente; possono essere divise in: C_u—cellule contenenti dicentrici, tricentrici, cromosomi ad anello o frammenti acentrici e che sono considerate instabili perchè destinate a perdersi o a subire ulteriori modificazioni nella successiva divisione cellulare; C_s—cellule che presumibilmente sono stabili alla mitosi, in quanto contengono uno o più cromosomi anormali ma monocentrici.

Per quanto si riferisce alla frequenza delle anomalie cromatidiche in rapporto all'entità dell'esposizione, allo stato attuale non si riscontrano significative differenze tra i singoli gruppi e tra questi e il gruppo controllo.

La percentuale di cellule con anomalie di tipo cromatidico osservata nei dipendenti della centrale è complessivamente del 6,08% (400 su 6.578); la percentuale di cellule con altre anomalie (tipo C della classificazione) è dello 0,60% (39 su 6.578).

Nel gruppo di controllo, su 1001 cellule esaminate, sono state osservate 68 cellule con anomalie di tipo cromatidico (6,79%) e 5 cellule del tipo C (0,49%).

Nessuna differenza esiste tra il materiale ottenuto dai lavoratori della centrale e quello ricavato dal gruppo di controllo anche per quanto riguarda il tipo delle anomalie osservate; si tratta di lacune e rotture cromatidiche e più raramente isocromatidiche, e—tra le cellule di tipo C—soprattutto di frammenti acentrici e di qualche raro dicentrico (Figs. 1–5.)

Importante è la constatazione che sia nei controlli che negli esposti le anomalie più frequenti di tipo cromatidico sono distribuite a caso in tutti gli elementi, e che la frequenza di lacune e rotture a carico di un cromosoma è in rapporto alla sua lunghezza.

La frequenza con cui anomalie morfologiche dei cromosomi possono essere osservate in soggetti normali è molto variabile seguendo i diversi Autori; ciò dipende sia dalle condizioni tecniche, evidentemente diverse in ogni laboratorio, sia dai criteri più o meno restrittivi di valutazione; mentre infatti alcuni considerano tutte le anomalie, comprese le lacune e rotture cromatidiche, altri basano le loro considerazioni esclusivamente sulla presenza di frammenti acentrici o di cromosomi policentrici e ad anello.

Per quanto riguarda la frequenza di anomalie citogenetiche sia morfologiche che numeriche in individui esposti a radiazioni ionizzanti, i dati che è utile ricordare, per un confronto con i nostri risultati, sono quelli—non numerosi che si riferiscono a soggetti sottoposti ad irradiazioni diagnostiche o esposti per motivi di lavoro.[5-33]

Di particolare interesse il confronto con i dati che Court Brown, Buckton e McLean[34, 35] hanno recentemente pubblicato a completamento delle precedenti casistiche sugli aspetti delle irradiazioni terapeutiche.

Si tratta di 42 soggetti esposti professionalmente a radiazioni ionizzanti e divisi in quattro gruppi in base alla dose cumulativa assorbita. Le frequenze di cellule C_u e C_s osservate sono: per il gruppo B, comprendente alcuni individui di cui non è nota con esattezza la dose, 0,6% di C_u e 1,3% di C_s; per il gruppo C (da 1 a 9

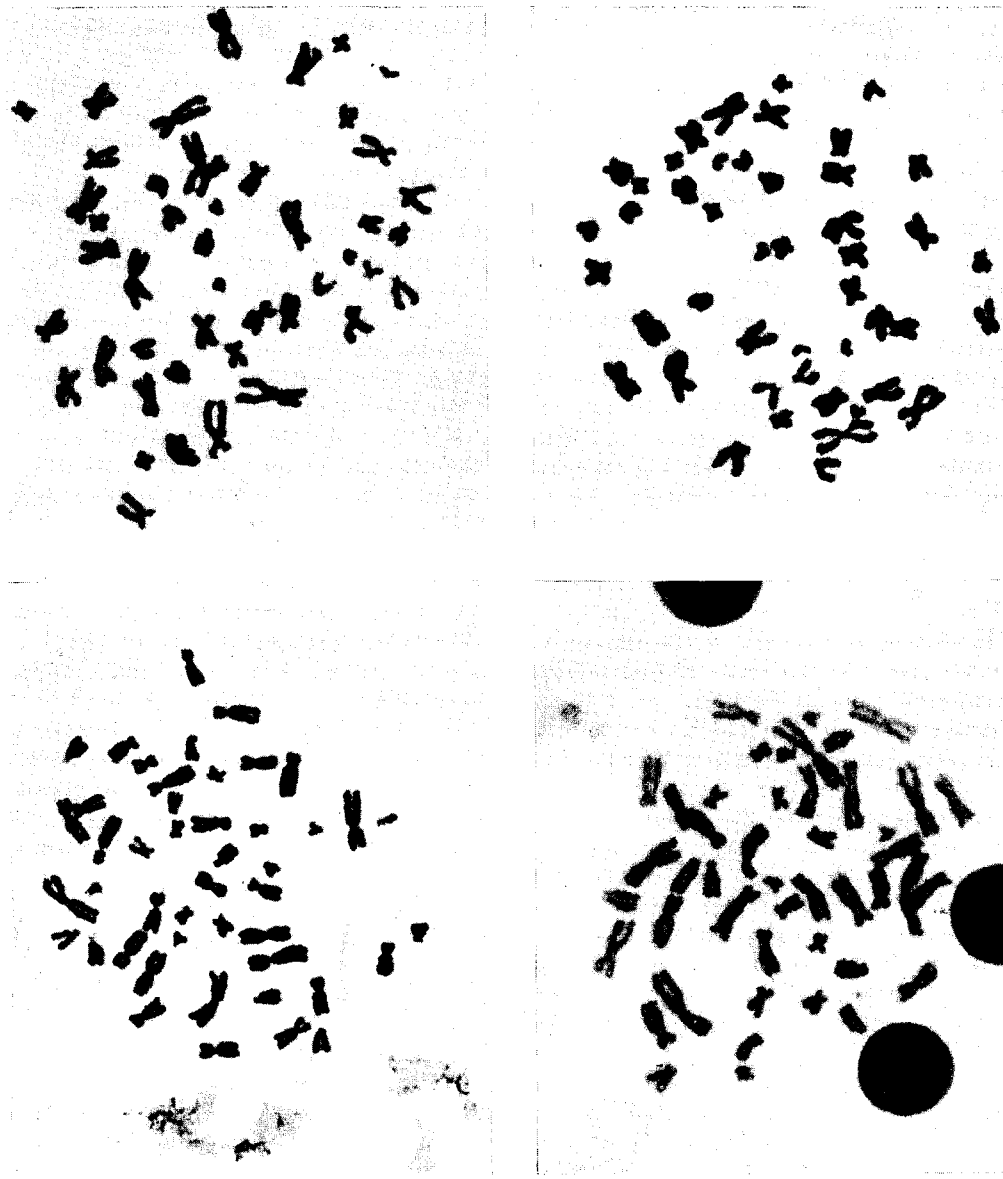

FIG. 1. Cellule normali (di tipo A secondo la classificazione di Buckton e Pike) in soggetti di controllo (fila superiore) e in lavoratori della Centrale (fila inferiore).

rad) 0,9% di C_u e 1,4% di C_s; per il gruppo D (da 23 a 34 rad) 1,8% di C_u e 0,9% di C_s; per il gruppo E (da 76 a 98 rad) 2,2% di C_u e 1,1% di C_s.

Elaborando statisticamente questi dati gli Autori trovano che l'aumento di cellule C_u negli ultimi due gruppi, al di sopra cioè dei 23 rad assorbiti, è significativo; nessuna differenza vi è invece tra questi due gruppi, benché la dose media sia nel primo di 27 e nel secondo di 84 rad. Nessuna significatività sotto i 23 rad, al punto che i valori dei gruppi B e C vengono utilizzati come riferimenti normali, assieme a quelli del gruppo A (non esposti).

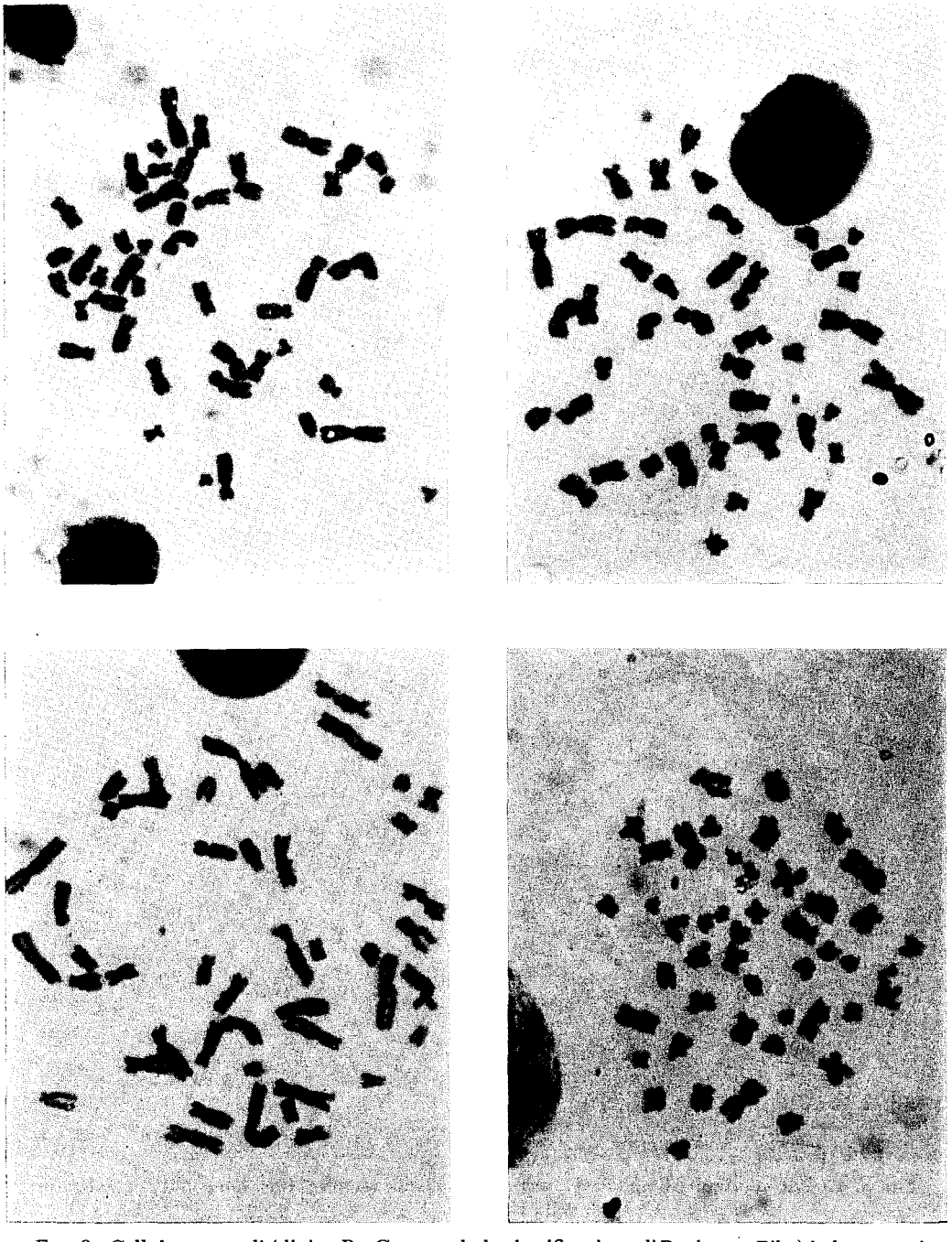

FIG. 2. Cellule anormali (di tipo B e C_u secondo la classificazione di Buckton e Pike) in lavoratori della Centrale.

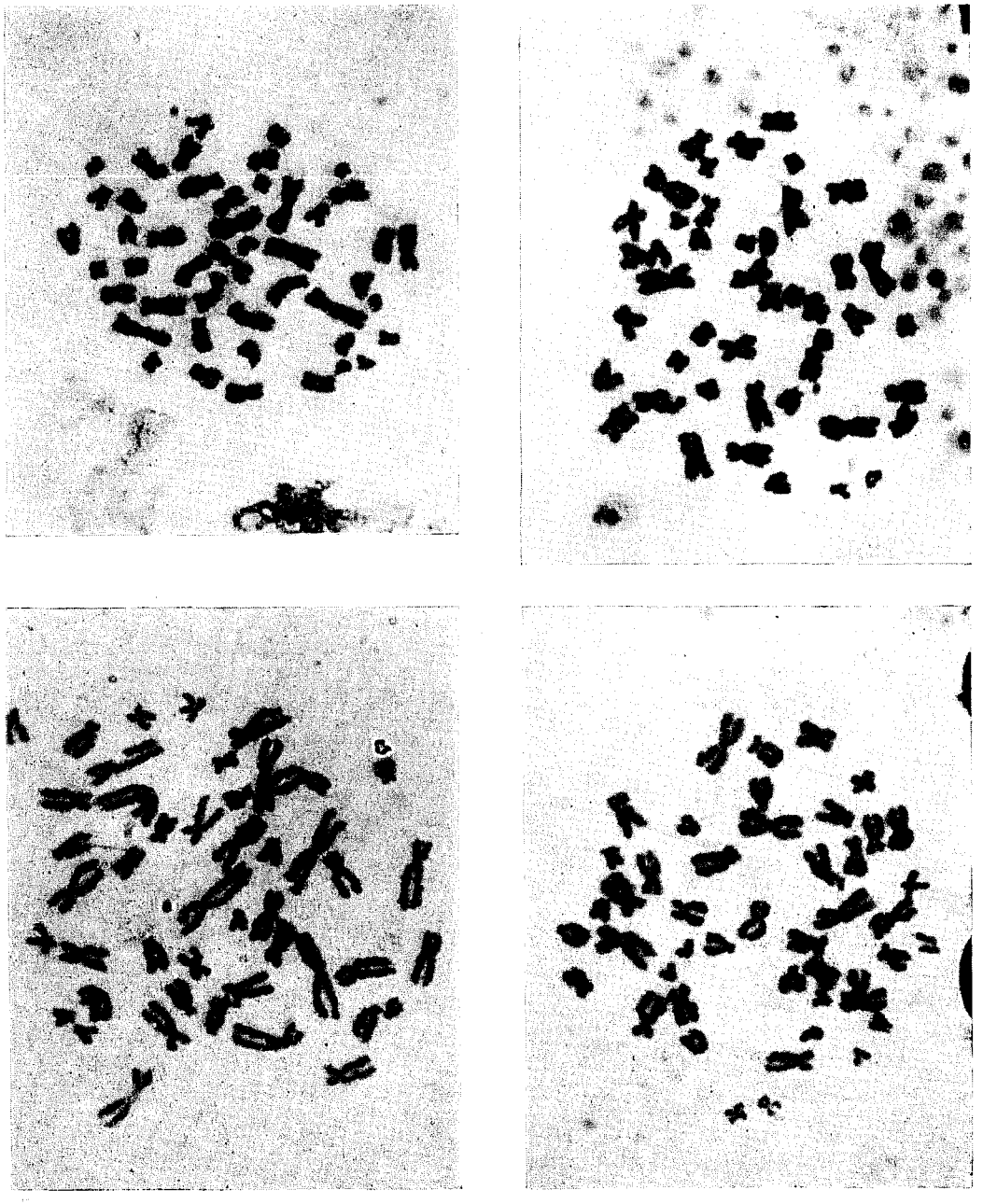

FIG. 3. Cellule anormali (di tipo B e C_u secundo la classificazione di Buckton e Pike) in lavoratori della Centrale.

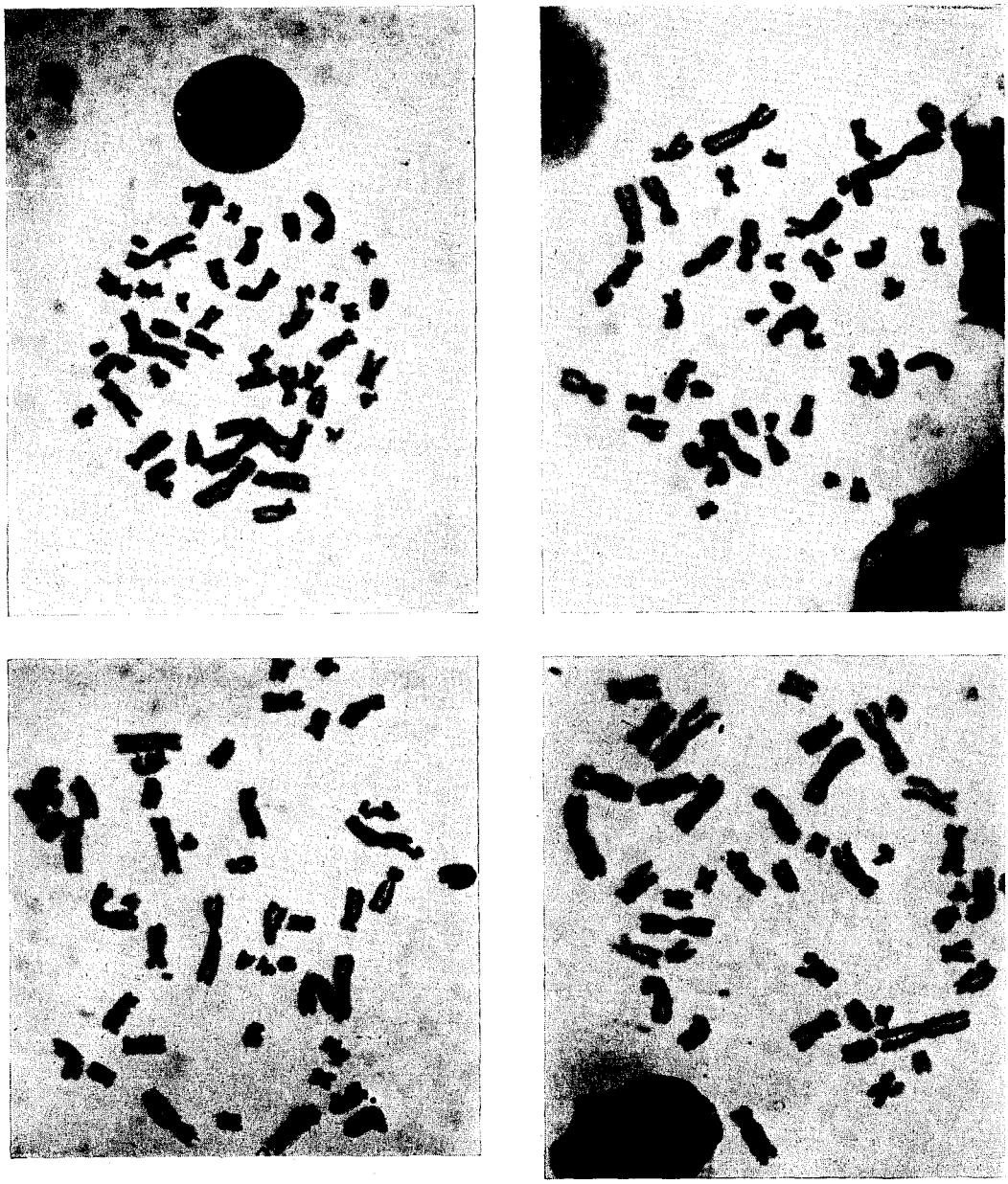

FIG. 4. Cellule anormali (di tipo B e C_u secondo la classificazione di Buckton e Pike) in soggetti di controllo.

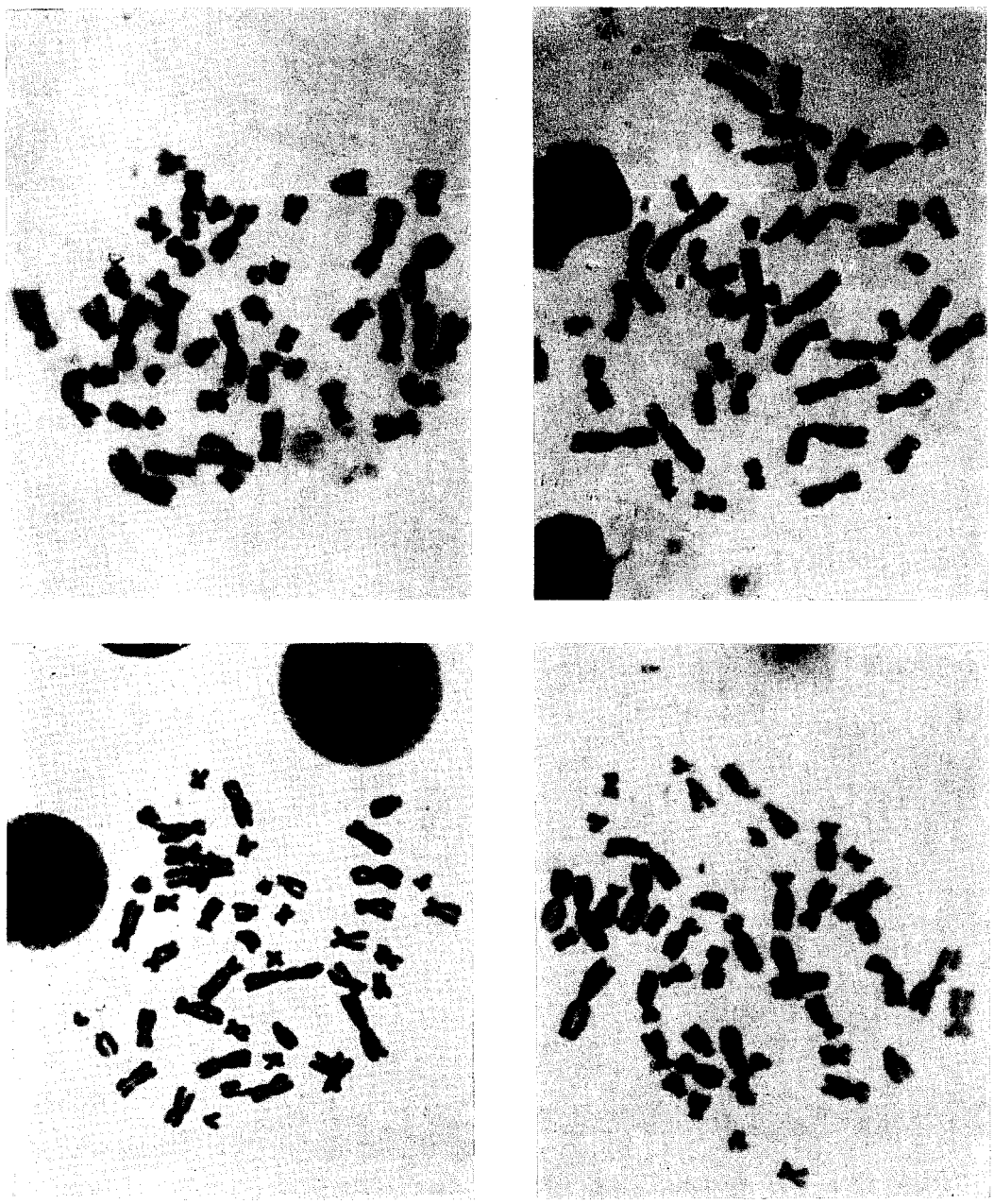

FIG. 5. Cellule anormali (di tipo B e C_u secondo classificazione di Buckton e Pike) in soggetti di controllo.

A conclusione di questo rapporto si può affermare che nel gruppo di 56 dipendenti della Centrale Elettronucleare del Garigliano qui considerati, allo stato attuale non si osservano——a distanza di oltre due anni dall'inizio della cronica esposizione a piccole dosi di radiazioni ionizzanti—particolari modificazioni del quadro citogenetico.

Le percentuali di cellule aneuploidi e di cellule con anomalie morfologiche dei cromosomi trovate, su un totale di 6.578 cellule esaminate, sono simili a quelle trovate in 1001 cellule provenienti da 30 soggetti di controllo non esposti.

Il tipo delle anomalie osservate è lo stesso sia negli esposti che nei controlli, ed è rappresentato in grandissima maggioranza da aberrazioni cromatidiche.

A questa conclusione si può dare naturalmente solo un valore generale provvisorio, perché copre un periodo di esposizione di soli due anni, durante il quale nessuno dei dipendenti esaminati ha accumulato una dose superiore a 6 rem; ne consegue che l'interesse di siffatte ricerche citogenetiche aumenterà in un prossimo futuro con il progressivo incremento delle dosi cumulate dai lavoratori e potrà consentire in eventuali casi di sovra esposizione la ricostruzione della "storia citogenetica" del lavoratore nucleare sin dall'inizio della sua attività lavorativa.

BIBLIOGRAFIA

1. P. S. Moorhead, P. C. Nowell, W. J. Mellman, D. M. Battips e D. A. Hungerford, *Exp. Cell Res.* **20,** 613 (1960).
2. J. J. Yunis, *Human chromosome methodology.* Acad. Press, N.Y. (1965).
3. K. E. Buckton, P. A. Jacobs, W. M. Court Brown e R. Doll, *Lancet* 7258, 676 (1962).
4. K. E. Buckton e M. C. Pike, *Int. J. Rad. Biol.* **8,** 439 (1965).
5. I. M. Tough, K. E. Buckton, A. G. Baikie e W. M. Court Brown, *Lancet* **7155,** 849 (1960).
6. E. Boyd, W. W. Buchanan e B. Lennox, *Lancet* **7184,** 977 (1961).
7. M. N. Macintyre e B. M. Dobyns, *J. Clin. Endocrinol. Metabol.* **22,** 1171 (1962).
8. R. C. Goodlin, *Am. J. Roentgen. Rad. Ther. Nucl. Med.* **87,** 555 (1962).
9. M. A. Bender e P. C. Gooch, *Genetics* **46,** 851 (1961).
10. M. A. Bender e P. C. Gooch, *Cytogenetics* **2,** 107 (1963).
11. M. A. Bender e P. C. Gooch, *Rad. Res.* **18,** 389 (1963).
12. D. S. Newcombe e A. S. Cohen, *Ann. Intern. Med.* **59,** 859 (1963).
13. M. Papiernik-Berkkauer, J. L. Amiel e G. Mathe, *C.R. Acad. Sci.* **256,** 5232 (1963).
14. M. M. Nofal e W. H. Brierwaltes, *J. Nucl. Med.* **5,** 840 (1964).
15. P. C. Nowell, D. A. Hungerford e L. J. Cole, *Ann. N.Y. Acad. Sci.* **114,** 252 (1964).
16. J. G. Moore, J. L. Van Campenhout e W. W. Brandkamp, *Amer. J. Obstetr. Gynecol.* **88,** 985 (1964).
17. J. Visfeldt. *Acta Radiol.* **2,** 95 (1964).
18. A. P. Amarose. *N.Y. State J. Med.* **64,** 2407 (1964).
19. A. P. Amarose e D. H. Baxter. *Obstetr. & Gynecol.* **25,** 828 (1965).
20. S. Warren e L. Meisner. *J.A.M.A.* **193,** 351 (1965).
21. R. E. Millard. *Cytogenetics* **4,** 277 (1965).
22. W. D. Macdiarmid. *Quart. J. Med.* **34,** 133 (1965).
23. J. S. S. Stewart e A. R. Sanderson. *Lancet* **7184,** 978 (1961).
24. P. E. Conen, A. G. Bell e N. Aspin. *Pediatrics* **31,** 72 (1963).
25. A. D. Bloom e J. H. Tijo. *New Engl. J. Med.* **270,** 1341 (1964).
26. R. Schmickel, A. Bloom e C. Cisar. *Rad. Res.* **22,** 232 (1964).
27. M. N. Macintyre, M. A. Stenchever, B. H. Wolf e J. M. Hempel. *Obstetr. & Gynecol.* **25,** 650 (1965).
28. L. Massimo, M. G. Vianello e F. Dagna-Bricarelli. *Acta Gen. Med. Gemell.* **14,** 282 (1965).
29. A. Norman, R. E. Ottoman e R. C. Veomett. *Radiology* **79,** 115 (1962).
30. A. Norman, M. Sasaki, R. E. Ottoman e R. C. Veomett. *Rad. Res.* **23,** 282 (1964).
31. Y. Doida, T. Sugahara e M. Horikawa. *Rad. Res.* **26,** 69 (1965).
32. M. Fraccaro e L. Tiepolo. *Pathol. Biol.* **11,** 1171 (1963).
33. M. Fraccaro. Il fattore tecnico nello studio dei cromosomi umani. *Proc. 11nd Int. Congr. of Hum. Genet.* (1963).
34. W. M. Court Brown, K. E. Buckton e A. S. McLean. *Lancet* **7398,** 1239 (1965).
35. W. M. Court Brown, P. A. Jacobs e M. Brunton. *Lancet* **7412,** 561 (1965).

DISCUSSION

J. Booz (*Euratom*):

Looking at the picture of the phantom used, I had the impression that it had been built out of lucite slides and that between two lucite slides there was another material having a different optical density. I would like to know the composition of the phantom and the influence of possibly different densities of the two materials on the dosimetric measurements.

R. Le Go:

Le fantôme réel qui a été utilisé pour la reconstitution dosimétrique faite à Mol est un fantôme de la firme Alderson, en Mix-D avec squelette inclus.

L'image qui a été projetée montrait une reproduction dans la même géometrie, de ce fantôme, exécutée avec des gabarits en plexiglas, dont la transparence permet de montrer la situation des tubes de sang dans le fantôme réel.

Par ailleurs, ce fantôme transparent nous a servi à dessiner sur chacune des 34 coupes, le tracé des zones isodoses, ce qui donne une représentation spatiale tridimensionnelle de la dosimétrie interne, par la superposition des coupes.

M. Delpla (*France*):

Il serait intéressant de préciser quelques points de l'exposé.

1. Quelle est la valeur numérique la plus faible des doses étudiées? L'auteur a-t-il déterminé les valeurs de l'écart type correspondant? Il va sans dire que ces précisions sont indispensables pour parler de linéarité des courbes.

2. Quel a été le mode d'irradiation: continue ou fractionnée, débit de dose?

3. Les résultats obtenus *in vitro* peuvent-ils être transposés *in vivo*?

R. Le Go:

1. Comme il a été dit dans l'exposé et montré dans le tableau 1, les doses d'exposition se sont situées entre 40 R et 600 R. Le calcul d'un écart type n'a pu être envisagé, puisqu'il s'agit d'une expérience unique, comportant un seul point pour chaque dose. Ce calcul ne pourrait être envisagé que par la répétition d'expériences semblables, aux mêmes points de dose. Ce que l'on peut dire, c'est que la variance est plus faible pour les faibles doses, qui ont permis d'examiner un grand nombre de cellules, et qu'elle est certainement plus élevée aux doses fortes, par exemple pour 600 R, dose à laquelle on n'a pu examiner que 26 cellules.

2. L'irradiation a été continue dans tous les cas de notre expérience. Le débit de dose dans l'expérience au ^{60}Co a été de 30 R/min. Dans l'irradiation à l'intérieur du fantôme, c'est la durée d'irradiation qui a été constante (2 h.30). Le débit de dose a varié selon la distance du tube de sang par rapport à la source, entre 0,26 R/min pour le point le plus distant et 4 R/min pour le point le plus proche de la source. Malgré les grandes différences sur ce paramètre, les points obtenus ne se sont pas montrés aussi aberrants qu'on aurait pu le craindre.

3. En l'absence, fort heureux, de nombreuses irradiations totales homogènes chez des humains, les seules données que l'on peut obtenir sont tirées soit de l'expérimentation animale, soit de l'irradiation *in vitro* de sang *humain normal*. Cependant, le recoupement que nous avons pu faire avec la dosimétrie physique chez l'irradié de Mol, nous a donné des doses estimées (par analyse chromosomique) de 470 rads pour le taux des dicentriques; de 500 rads pour le taux des cassures "totales"—en accord avec les chiffres de la dosimétrie interne dans le fantôme.

RAPPORTEUR PAPER

PERSONAL DOSIMETRY: METHODS OTHER THAN T.L.D.

MARGARETE EHRLICH

Radiation Physics Division, National Bureau of Standards, Washington, D.C., U.S.A.

THIS is a report on eight papers, most of which deal with the old stand-by of personnel monitoring, namely, the photographic film badge. It is quite interesting to go through this collection of papers, some by experienced old-timers, some by people just starting in the field. One becomes aware of how—based on the work of others—the latecomers are making shortcuts and are acquiring competence and sophistication much faster than the earlier workers, and how much the critical eyes of quizzing national and international organizations can contribute toward progress. Also, one notices the latecomers' struggle in the pursuit of the traditional, at the very same time as the young rebels start their shouts for the new and better.

PHOTOGRAPHIC DOSIMETRY: BETA-GAMMA CALIBRATION

M. P. OLIVARES and S. PEREZ-MODREGO (*Spain*)

Most of the papers on photographic dosimetry that were sent to me for review, deal with old, universal questions. Olivares and Modrego tell about their orientation studies in the field of photographic dosimetry and their endeavor to achieve clean, scatterfree calibration conditions. They describe their study of the change in response with developing time, and discuss how they eliminate the influence of processing variations by developing all related samples simultaneously. They also report on studies of some of the basic properties of photographic film exposed to gamma radiation, such as, absence of rate dependence, variation of the characteristic curve with film type, batch-to-batch reproducibility, keeping quality of the developed image, etc. In some instances, their studies do not extend over a large enough range of the particular variable to establish the general characteristics. For instance, they vary developing time from 4 to 5 mins only, a range over which the shape of the characteristic curve does not change appreciably. But, for practical purposes, such a limited study suffices. Also, so far, they only calibrate with Ra^{226} and Co^{60} gamma rays, that is, in a photon energy range in which photographic response varies only slowly with photon energy. But their badge has a lead-covered area and an open window, in anticipation of future work with low-energy x rays and beta radiation.

The authors show characteristic curves for four different types of film, exposed to Co^{60} gamma rays. For the sensitive film of the DuPont-556 packet, they examined samples of two emulsion numbers, and found no difference in response—but, according to DuPont, two emulsion numbers may designate samples from separate coating operations but from the same emulsion batch. For their particular type of processing in a home-mixed metol-hydroquinone developer, the Ilford film seems to be the most sensitive below 1 R. Above, the Mafe film has the steepest slope and highest sensitivity, and also reaches the highest maximum density. The authors did not supply any information on the type of Kodak and Ilford films used, except that they were dental-size personnel monitoring films. This probably means that the Ilford films were of the "P.M." series and the Kodak film was of type KK; all of these film types usually saturate at a density above 5 or 6, rather than at a density of 3, as found by the authors. Also, the sensitivity of Kodak type KK film usually is twice that shown by them for low exposures. The authors concluded that Mafe

film is best suited for personnel monitoring. Yet, possibly, if they had used another developer, they might have arrived at different conclusions.

TRANSPORTABLE CALIBRATION FACILITY FOR FILM DOSIMETRY OF X-RAYS BY MEANS OF RADIOACTIVE SOURCES

V. Paič (*Yugoslavia*)

Paič's main contribution consists in the description of the design and construction of a portable facility for calibrating photographic film badges with radioactive sources, and in a discussion of how to use these calibration sources, in conjunction with energy-dependence data, for personnel-exposure determinations over a wide range of x and gamma rays. She employs Ilford PM3 film in a badge having six copper filters, ranging in thickness from 0.1 to 1 mm. Narrow spectral bands of bremsstrahlung are used to produce effective energies for the x ray calibration between 25 and 156 keV. A radioactive source is used to get a calibration in the region between 0.5 and 1 MeV.

Data are shown for a number of different exposures administered at three different effective x ray energies incident on the film badge. The author points out the disagreement between the effective energies determined from ionization measurements and those determined from the film densities behind the copper filters. This disagreement stems mainly from the use of the narrow-beam absorption coefficients for the photographic determination of effective energy, while the exposures were made under broad-beam conditions. Energy dependence of the film response also is a contributing factor.

The author points out, furthermore, that, in spite of the optical density not being a linear function of exposure, the relation between density and exposure turns out to be strictly exponential. This may be fortuitous. The curvature that one would expect for the thinner copper layers because of a progressive hardening in the beam may be offset by the effect of density saturation for the very high densities under the thin copper layers.

The data also are shown plotted both in the form of density ratios as a function of copper filter thickness, with the parameter effective energy, and density ratio as a function of effective energy, with the parameter copper thickness. From these plots, the effective energy for an unknown exposure can be deduced. This, in turn, enables one to determine the unknown exposure in the usual way, say, by using what is often called the "hardness factors" and one characteristic curve obtained at a convenient energy. To obtain this curve in a simple, reproducible way, the author designed portable calibration assemblies consisting of special lead containers for the sources, and of supports for the film badges.

Photographs are shown of the container and its parts, and of the badges in their reproducible position for exposure. The main body of the container used for Ra^{226} or Cs^{137} is a lead block with a bore through the center. A cylindrical shutter and collimator slides in this bore, and can be positioned so that the source, in its holder, is either shielded or is permitted to radiate through the collimator window. The film-badge supports and the base of the assembly are made of an aluminum alloy. Some badges are positioned quite close to the collimator—but I suppose an inverse-square check was made to show that there is no excessive scatter at this position. The whole assembly weighs about 13 kg, and is easily taken apart. It is being used with either about 4.5 mg of radium or 15 mCi of Cs^{137}.

A simpler lead container is being used with a bremsstrahlung source, consisting of Sr^{90}–I^{90} in aluminum. The source is in a source holder, in the center of the upper surface of a simple lead block, that can be covered with a lead lid. The assembly is designed for use with a bremsstrahlung source containing about 620 mCi Sr^{90}–I^{90}. It weighs about 10 kg.

A NEW CONCEPT IN FILM BADGE DESIGN

J. D. Eastes, M. L. Maurer and F. L. Paschal (*U.S.A.*)

Popular around reactor facilities are film badges which permit inclusion of a number of dosimetric devices other than film. Eastes, Maurer, and Paschal describe the badge which they have been using for the past 1½ years, and which permits an option of dosimeter components and filter systems. It is of molded plastic and has three main components. The recessed central surfaces of the front and rear

components have an open window and accommodate filters in a choice of types, sizes and orientations. The badge incorporates a magnetically released locking mechanism with two stops; one for keeping the badge closed, and one for holding its parts together while it is open for servicing. The front component slides into grooves in the rear component, and allows filters to be mounted opposite to their counterparts in the rear. Also, there is room for a lead identification tape used for radiographic film marking. An identification and work-record card, or some other appropriate credential card of the wearer, slides in at the very front.

The dosimeter holder, which is a separate part of the badge, can accommodate several different monitoring devices. The compartments at the top and bottom ends are for high-range, emergency monitoring devices, which are held in place by small molded packaging components. If one wants to use monitoring devices of different types or shapes, one simply fabricates new packaging components, but the badge as such may remain unchanged. The large center portion of the holder transports and holds in position either one or two film packets, which are confined in their proper places by a frame and thin separators, in a way that enables one to use either one or two film packets. The design also permits essentially automatic removal of either one or two film packets at a time.

The emergency dosimeter components presently in use with this badge are: indium foil, copper, sulfur, and cadmium; they all are used for emergency neutron monitoring. In the near future, LiF will be added for emergency gamma-ray monitoring. The film packets used at present for routine monitoring are the DuPont type 544 x- and gamma-ray monitoring packet and the Kodak type A neutron-monitoring packet.

The filters presently used over the photographic films are made of plastic, aluminum, tin, iron (two thicknesses), and cadmium. The aluminum and the thinner iron are matched for identical attenuation of beta rays from uranium and Sr^{90}, but they attenuate low-energy x rays to a different degree. The tin and cadmium filters are matched in the usual way for identical photon attenuation over the entire energy range of interest. The difference in reading then provides an indication of the amount of thermal neutrons present. Fast-neutron monitoring is done by track counting in a projection microscope, using the area of the neutron-monitoring film that is behind the cadmium filter.

X- and gamma-ray, beta-ray, and thermal-neutron doses are evaluated with the aid of seven simultaneous equations involving the densities in the seven film areas, and suitable calibration data supplying a type of "hardness factor" for photons. The authors call it "energy index factor" and obtain it as the quotient of the sum of the densities behind two of the filters to the sum of the densities behind two others, over the photon energy range from 30 keV to 1.25 MeV. Time does not permit a detailed description of the method; nor is there time to show the results of the performance and reliability studies. The method is fairly elaborate, but the authors feel that it permits a more accurate assessment of the various components of a mixed radiation field than some of the less elaborate photographic methods in use.

A PHOSPHATE GLASS DOSIMETER ADAPTED TO THE REQUIREMENTS OF HEALTH PHYSICS APPLICATION

W. Buttler, R. Maushart and E. Piesch
(*Federal Republic of Germany*)

Whatever the refinements of photographic personnel monitoring, most of us believe that we are about to witness a changeover to different, simpler and maybe more accurate methods. In fact, some are ready to throw out the photographic method right now.

The dosimetry experts in the Karlsruhe and other German reactor centers believe that silver-activated phosphate glasses are *the* personnel dosimeters of the future. In their present paper, Buttler, Maushart and Piesch report on a modification of their previously published system. They are developing a new capsule, which takes care of two problems that, so far, prevented a general acceptance of the spherical version of the low-Z phosphate-glass dosimeter. One objection was the need for periodic, meticulous cleaning of the glass to insure reproducible collection of the luminescence light; the other objection concerned the need

for manipulation of large numbers of glasses during the reading phase, with the possibility of mixups.

The main body of the new capsule is formed by a circular aluminum cylinder. There are two ring-shaped troughs in the cylindrical side wall, and one in the bottom; these are filled with tin, for reduction of the energy dependence of the glass response. The glass is in the shape of a short cylinder, 8 mm in diameter and 9 mm high. An aluminum disc designed to carry the identifying information, remains in contact with the glass at all times, even during readout. While in use, the glass is in total darkness, and, just as important, is hermetically sealed in the capsule. Therefore, it does not have to be cleaned after each use. The hermetic, tamper-proof seal is provided by a steel lid, which can be released magnetically.

The authors show a plot of the response of the new capsule as a function of photon energy for irradiation in a direction perpendicular to the axis of symmetry of the device. The inaccuracy introduced due to the residual energy dependence is about $\pm$ 18% between 50 keV and 1 MeV. Since the instrument has a higher anisotropy than its spherical predecessor, a larger dependence of its response on the direction of photon incidence is to be expected. The authors are now in the process of studying this feature.

Another new development concerns the luminescence reader for the glasses. A semi-automatic instrument is being developed. One of its features is an automatic transfer of the dosimeter identification symbols to the readout record, which eliminates all possibilities of mixups.

Regardless of what the instrument of choice may be, when you see how much time and effort is spent in many countries on improving personnel-monitoring procedure, you start wondering about the justification for the continuing drive toward improvements, and about the returns. Are these returns in terms of a decrease in personnel time spent on routine evaluation procedures? Do the improvements lead to a decrease in personnel exposure, because of the higher accuracy and wider scope of personnel monitoring, or the more efficient method of data processing? You also wonder about where the point of diminishing returns might lie, and, if, in certain instances, it has not been reached now. The following papers touch on some of these questions.

PERSONNEL FILM MONITORING IN POLAND: ORGANIZATION, METHOD, RESULTS

T. Musiałowicz (*Poland*)

I had the opportunity of getting acquainted with personnel monitoring procedure at CLOR through my work at the IAEA, and therefore was very interested in the current progress report by Musiałowicz. CLOR covers all workers in Poland in radioisotope and nuclear establishments; medical departments are covered elsewhere. Currently, they use a film holder having an open window, two plastic and two copper filters of different thicknesses, a combination copper or cadmium and lead filter, a combination tin and lead filter, and a lead filter. They employ a double-emulsion monitoring film made by Foton, with which they are able to cover the exposure range from 60 mR to 1300 R of Co^{60} gamma rays, and from which they also deduce the x-ray, beta-ray, and thermal-neutron exposures. They monitor fast neutrons with the Kodak neutron monitoring film, type A, sealed in a plastic bag, one-half of it covered with cadmium. Calibration, processing, and evaluation is done in the usual way, and will not be further discussed here.

The films are handled in each of the establishments according to CLOR's directions, and are dispatched back to CLOR for processing and evaluation, along with detailed information on the wearer. Personnel cards are kept both at CLOR and at the individual establishments. CLOR investigates all doses exceeding the maximum permissible, and makes the decision on whether or not to take it into account in the cumulative personnel record. The doses from the record cards are summed up every three months. When a dose equivalent of 12 rems or of the usual 5(N–18) rems is exceeded, CLOR recommends withdrawal of the individual from radiation work. The annual totals are published, grouped according to the range of dose equivalent, the type of establishment, and, for dose equivalents exceeding 5 rems, also by sex and age groups. The author reports that, as a

rule, the overexposures are found in the same places, namely, in hospitals using radium applicators, and in industry, where, apparently, Ra^{226} still is used in paints. Also, the exposures in these fields of endeavor depend largely on the individual operators.

The number of persons monitored by CLOR has increased from around 800 in 1959 to around 4500 in 1965. Nevertheless, the percentage of individuals receiving doses above 12 rems per year over this period dropped from 0.3 to 0.06%, while the percentage of workers receiving doses below 0.5 rem per year increased from 72% to 88% over the same period. Since 1961, they also record the percentage of people exceeding 3 rems quarterly, and report that it has dropped from 33% in 1961 to 15% in 1965. They find it disconcerting that most of the doses above 5 rems per year are found in the 18–30 year age group. Nevertheless, the overall record looks fairly impressive.

PRACTICAL PERSONNEL DOSIMETRY OF THERMAL NEUTRONS

D. NACHTIGALL (*Switzerland*) and
E. ROSE (*Federal Republic of Germany*)

In this paper, the question of diminishing returns is raised. Nachtigall and Rose report on the results of calculations of the contribution made by thermal neutrons to personnel dose. The authors made their calculations for a "standard man" phantom, simulating the human thorax. The dimensions were 20 cm × 40 cm × 80 cm, and the thermal neutrons were assumed to be incident perpendicularly to one of the 40 cm × 80 cm bounding surfaces.

The authors set up a computer program for determining the dose contributions due to the (n, γ) reaction on hydrogen, and the (n, p) reaction on nitrogen. For the (n, γ) computations, they started with Snyder's formulation for the decrease of the fluence with depth in the phantom, and then considered that the 2.2 MeV photons produced by the thermal neutrons in any volume element are absorbed partially by other volume elements in the body. Introducing numerical values for the reaction cross section, they obtained an expression for the dose due to gamma rays per unit fluence of thermal neutrons produced at any distance from the point at which the (n, γ) reaction takes place. This equation was then integrated along various directions in the body, and over the body surface. Integration parallel to the long axis of the thorax yielded an essentially constant dose at any one depth up to about 10 cm from the body edge. There, the dose fell to about one-half. The doses at the front and back of the body differed by a factor of ten.

Integrated over the body surface, the equation yielded a dose due to gamma rays that compares very well with the one Heard had obtained from previous data of Snyder, Schalnow and Smith by simple interpolation. But I think that even if the authors had taken one of the values available for the (n, γ) contribution in the other geometries, their subsequent arguments would not have been materially different.

The proton dose distribution due to the (n, p) reaction shows much less of a boundary effect, being essentially constant almost to the body edges, and the calculation for the thorax phantom therefore yielded no new information for this reaction. The authors show plots of the dose distribution per unit fluence as a function of depth along the short central axis of the phantom for the two reactions separately, and also for their sum total. From the dose distribution, they then computed the distribution of the dose equivalent, of which plots are presented also. Here, their approach differed from that of Snyder's. They used the usual quality factor of 1 for the photons, but for the protons they plotted the distributions once for a quality factor of 10, the value recommended by the ICRP for protons of unknown energy, and once for a quality factor of 5, corresponding to the initial proton energy of 0.62 MeV. Snyder and Neufeld, on the other hand, weighted their doses in the integration process with the factor corresponding to the individual proton energies. The curves plotted by the authors for a quality factor of 10 compare fairly well with Snyder's data in the NCRP report to which they make reference. For a quality factor of 10, the total dose equivalent in a depth of 2 cm is shown to be three times the gamma dose equivalent at the surface. At a depth of 6 cm, they are equal. Thus, the authors conclude, that, in a pure neutron field, and for a quality factor of 10, one may determine the total dose

equivalent to deep-seated organs simply by doubling the dose equivalent deduced from the measured gamma-ray dose. For a quality factor of 5, no correction would be required.

The authors then point out that, while these results were deduced for organs lying in the thorax, and in a depth between 2 and 6 cm, the same approach would be acceptable also for the eye and the male gonads. For the eye, the (n, p) reaction plays a smaller role because of the proximity of bone. The (n, γ) reaction is less important both for the eye and the male gonads because the total mass in the proximity of these organs is smaller than for organs in the thorax. This would tend to offset the lack of attenuation by overlying tissue. But, the authors do not consider the eye factor, which, for a quality factor of ten, is three, according to ICRP Report No. 9.*

The authors also discuss the influence of neutron direction on the fraction of the neutron dose measured by the gamma-ray dosimeter on the surface, and it is concluded that, depending on whether mean total-body dose or surface dose is considered, and depending on what quality factor is assumed, the gamma-ray dosimeter on the body surface measures 20 to 100% of the dose equivalent in a pure thermal-neutron field. Since, usually, the contribution to dose equivalent around reactors and accelerators is less than 10%, the authors conclude that, in general, one may dispense with special thermal-neutron personnel monitoring. They strengthen this conclusion by showing the results of gamma-ray and thermal-neutron measurements around thermal columns both at Juelich and Harwell, from which they deduce that even in the vicinity of a thermal column, the fraction of the surface dose that is not registered by a gamma-ray dosimeter or a fast-neutron dosimeter is usually smaller than 20 to 50%; the mean total-body dose even may be overestimated.

* According to the recommendations published in this Report, the maximum permissible level for the eye is 15 rems/year. But, in the case of neutron exposure to the eye, the dose equivalent is computed by multiplying the absorbed dose by two LET-dependent factors, the quality factor and the eye factor. A variation of quality factor between 1 and 10 is to result in a variation of the eye factor between 1 and 3. For quality factors of 10 and above, a constant eye factor of 3 is assumed. Thus, only if the authors chose to use for the eye the same maximum permissible level as for the gonads (5 rems/year), could they ignore the eye factor without introducing an error on the unsafe side. But if they used this lower maximum permissible level, they would needlessly restrict the x- and gamma-ray exposure to the eye to a level lower than the one now recommended. See also the comments of F. D. Sowby in the discussion following his paper.

AUTOMATIC DATA PROCESSING OF A FILM BADGE SERVICE

W. Benari, M. Schatz and G. Ben-David
(*Israel*)

Just as the types of personnel dosimeters and the monitoring procedures are subjected to scrutiny and are undergoing radical changes, so are the methods of keeping personnel monitoring records—a usually very time-consuming, but a vital phase of any personnel dosimetry service. Benari, Schatz and Ben-David report that, at Soreq, completely automatic data processing was introduced about a year ago, for handling all industrial and medical dose records throughout Israel. The badges are assembled in the central service laboratory and are sent to the different organizations together with a dispatch list, a duplicate of which is kept in the central laboratory. The input data for this list, which are stored on an IBM card, consist of the "period" number,* the "run" number, which indicates one of five different groups of organizations, each having a separate section of the magnetic storage tape reserved, and the serial number of the first film in each run. Because of the time lag between the information received for entries in the dispatch list and in the dose reports list, one magnetic tape is prepared for each of the two lists. But the same input cards are used for both, only with a suitable delay, to take care of the lag. Information on each new employee are entered on a different IBM card. Included are: personal identity, full

* Badges are usually changed after a period of two weeks, but, in instances of only intermittent contact of the wearer with radiation, they may be carried six weeks.

name, in terms of suitably coded letters of the alphabet, national registry number, date of birth, badge type and organization identity number.

If an individual transfers from one organization to another, the information on this card is augmented by the new personal identity number and the new organization number. In addition, IBM transfer cards, each carrying information on up to three individuals are prepared. They show the personal identity number, badge-type information, a transfer signal, and the dose accumulated in the other organization. A typical cancellation card contains the personal identity number, badge type, and cancellation signal. Cancellation information on different individuals is entered on the card in the order of the personal identity numbers within each organization.

The input data card for the period-dose report and personal dose record contains information on badge type, personal identity number, period, radiation type, dose (here there is room for dose information from two different types of radiation), and remarks. No record for a returned badge means that no measurable dose was recorded, and is taken to mean a "zero" entry. This scheme reduces the volume of input data considerably. When a badge is not returned or returned late, a remark is entered to this effect. Also, a separate card is made for all individuals or groups with late returns. Dose input data are double-checked against work lists by two operators. The personnel dose records are stored for one year on magnetic tape, from which there is immediate recall of any individual's dose record, if his identity number and the period of interest is known. As a rule, dose-record reports are printed out every three months, separate cards being prepared and mailed to each of the parent organizations.

The authors feel that their computerized record-keeping system is a complete success. Soreq handles several thousand individuals in over two hundred organizations, but has now a record staff of only two people, while, before, they had four. The reduction in errors was even greater, percentagewise. The system is faster and more flexible than a semi-automatic system, and there is never a backlog. The cost of computer time is negligible compared with the other costs of the monitoring service.

EXPÉRIENCE PRATIQUE DE DOSIMÉTRIE COMPARÉE DANS LES SIX PAYS D'EURATOM (PREMIERS RÉSULTATS)

M. COLLET and P. RECHT (*Euratom*)

The best monitoring device and the best record system are useless without the know-how and care necessary for adequate interpretation of the monitor readings in terms of dose and dose equivalent. This is why more and more national and international organizations are trying to develop performance standards and devise performance tests for individual dosimetry laboratories.

Collet and Recht report on performance tests given under the auspices of Euratom and some of its individual member countries over the past two years. X- and gamma-ray exposures were administered by three different central calibration laboratories to over 1700 film badges from many different personnel monitoring services. The services were not given any information about the exposures initially, but had to interpret them as they would interpret unknown exposures for the rest of their clients. Four different calibration centers and three exposure intervals were involved. The centers split the experiment up into four series, sending out batches of exposed films four times, four months apart. The photon energies covered ranged from around 30 keV to 1.25 MeV. Whenever feasible, the calibration stations reported the errors back to the services before the next test series, so that the services could make improvements where necessary between any two successive tests. At the end of the last series, the calibration laboratories were to prepare a report of the complete results, and to reveal radiation quality, exposure, and error to the participating services.

So far, only the 0.1–8-rem exposure interval has been completely evaluated and reported. A comparison in the exposure range below 1 R for one typical service shows considerable improvement between the first and fourth test series. None of the interpretations in the fourth series was off by as much as 50%, while, in the first

equivalent to deep-seated organs simply by doubling the dose equivalent deduced from the measured gamma-ray dose. For a quality factor of 5, no correction would be required.

The authors then point out that, while these results were deduced for organs lying in the thorax, and in a depth between 2 and 6 cm, the same approach would be acceptable also for the eye and the male gonads. For the eye, the (n, p) reaction plays a smaller role because of the proximity of bone. The (n, γ) reaction is less important both for the eye and the male gonads because the total mass in the proximity of these organs is smaller than for organs in the thorax. This would tend to offset the lack of attenuation by overlying tissue. But, the authors do not consider the eye factor, which, for a quality factor of ten, is three, according to ICRP Report No. 9.*

The authors also discuss the influence of neutron direction on the fraction of the neutron dose measured by the gamma-ray dosimeter on the surface, and it is concluded that, depending on whether mean total-body dose or surface dose is considered, and depending on what quality factor is assumed, the gamma-ray dosimeter on the body surface measures 20 to 100% of the dose equivalent in a pure thermal-neutron field. Since, usually, the contribution to dose equivalent around reactors and accelerators is less than 10%, the authors conclude that, in general, one may dispense with special thermal-neutron personnel monitoring. They strengthen this conclusion by showing the results of gamma-ray and thermal-neutron measurements around thermal columns both at Juelich and Harwell, from which they deduce that even in the vicinity of a thermal column, the fraction of the surface dose that is not registered by a gamma-ray dosimeter or a fast-neutron dosimeter is usually smaller than 20 to 50%; the mean total-body dose even may be overestimated.

* According to the recommendations published in this Report, the maximum permissible level for the eye is 15 rems/year. But, in the case of neutron exposure to the eye, the dose equivalent is computed by multiplying the absorbed dose by two LET-dependent factors, the quality factor and the eye factor. A variation of quality factor between 1 and 10 is to result in a variation of the eye factor between 1 and 3. For quality factors of 10 and above, a constant eye factor of 3 is assumed. Thus, only if the authors chose to use for the eye the same maximum permissible level as for the gonads (5 rems/year), could they ignore the eye factor without introducing an error on the unsafe side. But if they used this lower maximum permissible level, they would needlessly restrict the x- and gamma-ray exposure to the eye to a level lower than the one now recommended. See also the comments of F. D. Sowby in the discussion following his paper.

AUTOMATIC DATA PROCESSING OF A FILM BADGE SERVICE

W. Benari, M. Schatz and G. Ben-David
(*Israel*)

Just as the types of personnel dosimeters and the monitoring procedures are subjected to scrutiny and are undergoing radical changes, so are the methods of keeping personnel monitoring records—a usually very time-consuming, but a vital phase of any personnel dosimetry service. Benari, Schatz and Ben-David report that, at Soreq, completely automatic data processing was introduced about a year ago, for handling all industrial and medical dose records throughout Israel. The badges are assembled in the central service laboratory and are sent to the different organizations together with a dispatch list, a duplicate of which is kept in the central laboratory. The input data for this list, which are stored on an IBM card, consist of the "period" number,* the "run" number, which indicates one of five different groups of organizations, each having a separate section of the magnetic storage tape reserved, and the serial number of the first film in each run. Because of the time lag between the information received for entries in the dispatch list and in the dose reports list, one magnetic tape is prepared for each of the two lists. But the same input cards are used for both, only with a suitable delay, to take care of the lag. Information on each new employee are entered on a different IBM card. Included are: personal identity, full

* Badges are usually changed after a period of two weeks, but, in instances of only intermittent contact of the wearer with radiation, they may be carried six weeks.

name, in terms of suitably coded letters of the alphabet, national registry number, date of birth, badge type and organization identity number.

If an individual transfers from one organization to another, the information on this card is augmented by the new personal identity number and the new organization number. In addition, IBM transfer cards, each carrying information on up to three individuals are prepared. They show the personal identity number, badge-type information, a transfer signal, and the dose accumulated in the other organization. A typical cancellation card contains the personal identity number, badge type, and cancellation signal. Cancellation information on different individuals is entered on the card in the order of the personal identity numbers within each organization.

The input data card for the period-dose report and personal dose record contains information on badge type, personal identity number, period, radiation type, dose (here there is room for dose information from two different types of radiation), and remarks. No record for a returned badge means that no measurable dose was recorded, and is taken to mean a "zero" entry. This scheme reduces the volume of input data considerably. When a badge is not returned or returned late, a remark is entered to this effect. Also, a separate card is made for all individuals or groups with late returns. Dose input data are double-checked against work lists by two operators. The personnel dose records are stored for one year on magnetic tape, from which there is immediate recall of any individual's dose record, if his identity number and the period of interest is known. As a rule, dose-record reports are printed out every three months, separate cards being prepared and mailed to each of the parent organizations.

The authors feel that their computerized record-keeping system is a complete success. Soreq handles several thousand individuals in over two hundred organizations, but has now a record staff of only two people, while, before, they had four. The reduction in errors was even greater, percentagewise. The system is faster and more flexible than a semi-automatic system, and there is never a backlog. The cost of computer time is negligible compared with the other costs of the monitoring service.

EXPÉRIENCE PRATIQUE DE DOSIMÉTRIE COMPARÉE DANS LES SIX PAYS D'EURATOM (PREMIERS RÉSULTATS)

M. COLLET and P. RECHT (*Euratom*)

The best monitoring device and the best record system are useless without the know-how and care necessary for adequate interpretation of the monitor readings in terms of dose and dose equivalent. This is why more and more national and international organizations are trying to develop performance standards and devise performance tests for individual dosimetry laboratories.

Collet and Recht report on performance tests given under the auspices of Euratom and some of its individual member countries over the past two years. X- and gamma-ray exposures were administered by three different central calibration laboratories to over 1700 film badges from many different personnel monitoring services. The services were not given any information about the exposures initially, but had to interpret them as they would interpret unknown exposures for the rest of their clients. Four different calibration centers and three exposure intervals were involved. The centers split the experiment up into four series, sending out batches of exposed films four times, four months apart. The photon energies covered ranged from around 30 keV to 1.25 MeV. Whenever feasible, the calibration stations reported the errors back to the services before the next test series, so that the services could make improvements where necessary between any two successive tests. At the end of the last series, the calibration laboratories were to prepare a report of the complete results, and to reveal radiation quality, exposure, and error to the participating services.

So far, only the 0.1–8-rem exposure interval has been completely evaluated and reported. A comparison in the exposure range below 1 R for one typical service shows considerable improvement between the first and fourth test series. None of the interpretations in the fourth series was off by as much as 50%, while, in the first

series, the errors ranged from below 50% to more than 100%. Similar improvements were noted at higher exposures: Between 1 and 4 rems, the same service reduced its errors from 40 to 20%. In the fourth series, errors between 10 and 20% were common among the services for dose interpretations in the 0.1 to 8 rem dose range; for high energies, errors up to 30% were found below 1 rem.

Even at this stage of the evaluation of the results, one gains the impression that the Euratom study has been beneficial. The authors point out in particular that their study has helped the services to obtain better calibration curves without their having to do any high-precision calibrations themselves; it helped them to improve their equipment and procedures, where necessary; and—probably most important—it brought about an interchange of opinions, a sharing of experiences, and a closer contact between Euratom, the four participating calibration centers, and the personnel dosimetry services.

A NEW CONCEPT IN FILM BADGE DESIGN

J. D. EASTES, M. L. MAURER and F. L. PASCHAL
Dynamics Corp., Fort Worth, Texas, U.S.A.

Abstract—Unique concepts are incorporated into a new personnel monitoring badge which include (1) a basic structural design to permit various options in the choice of dosimetric accessories, (2) unusual mechanical features for operational improvements, and (3) a specific film-filter system and an unusual new technique for dealing with the film energy dependence problem.

The basic structure of the badge consists of three molded plastic components which can be assembled or disassembled in a matter of seconds. When assembled the structure is locked together with a tamper-proof locking system. The components are designed to collectively contain two dental size film packets in separated compartments (each opposed by matched filter systems), a system of high range dosimetry devices in two other compartments, and identification and/or security credentials. The high range dosimetry compartments and the areas designated for the filter system are designed to afford numerous options in the choice of components for these systems. Individualized film compartments permit the use of either one or two film packets in the badge and make possible the selective exchange of film packets in a simple manner. A unique locking device serves a dual purpose as a lock when the badge is closed and as a catch which prevents the complete disassembly of the components when the badge is being serviced. The locking system is also unique in that only one magnet is required to open the badge even in automated operations. A specific filter system which consists of five different filters is utilized to accomplish routine dosimetry for beta, gamma, X-, thermal neutron and fast neutron radiations. Dosimetry for beta, gamma, X-, and thermal neutron radiations is accomplished with the same film. The major problem in film dosimetry, energy dependence, is treated in a unique new manner with this filter system, which permits the evaluation of mixed exposures involving photon radiations in the critical energy region with greatly improved accuracy. The technique utilizes an energy index factor which is the ratio of the sum of densities behind two filters to the sum of densities behind two other filters. The photon dose in the critical region is determined from the sum of the excess densities behind three relatively thin filters as compared to a thicker filter, using the apparent energy indicated by the index factor. The density under the thick filter in excess of that predicted for the apparent exposure in the critical energy region is attributed to high energy photons. The filter system and techniques related to those just mentioned permit the evaluation of mixed exposures involving the four types of radiation mentioned previously.

A simple mathematical development of the energy index and low energy dose factors are presented and the film dosimetric capabilities attainable with the system have been verified with appropriate testing; however the test results are not included in this report. The badge has been in use since January 1965 and has proven very satisfactory in routine use and in the evaluation tests. The test results show that the film dosimetry capabilities attainable with the system described greatly exceed proposed standards.

INTRODUCTION

During the past two decades the film badge has continued to be the principal means of (external) personnel monitoring. As a result of ever-increasing requirements, both monitoring and otherwise, the film badge has evolved into a multi-purpose system of credentials and dosimetric devices. Unfortunately this evolution has not resulted in a standard system.

In general, badge structures have been designed to accommodate the particular system of components available at that time, which most nearly satisfied the requirements of the designer. Too often it has been necessary

to design a new badge, or to resort to multiple badges in order to improve personnel monitoring capabilities, or to satisfy new requirements.

In January 1965, the Fort Worth Division of General Dynamics put a new badge design into routine service which continues the evolution of the film badge into a combination monitoring and identification system. The badge represents a significant change in design concept in that the structural components can accommodate a wide variety of choices of paraphernalia for identification and monitoring purposes. Thus, the structure does not limit the system to its current status, but is adaptable to changes which satisfy new requirements, or which improve the state of the art. The badge structure is presently complemented with a diverse array of accessory components which represent current trends, including an unusual approach to the film energy dependence problem.

This paper describes the badge as equipped for use at the Fort Worth Division of General Dynamics, with occasional reference to unique features and to the features which permit unusual options.

STRUCTURAL COMPONENTS

The structural components of the General Dynamics badge are shown in Fig. 1. The three major components will be referred to as the Rear Component, the Dosimeter Holder and the Front Component. These three components are designed to lock together to form a unit which houses the entire monitoring system. (The assembled badge measures 8.3 cm × 5.3 cm × 1.2 cm and weighs approximately 60 g when fully equipped.)

The *Rear Component* composes the back, the top, and both side portions of the badge. Part of the front side of this component is slightly indented to accommodate the rear array of filters. With the exception of the open window and the plastic filter, this design permits some option as to the choice, size, and orientation of the filter array. A long slender strip of spring steel is mounted at one end in a cavity on the right side of this component. This strip has a 90° bend at its free end which permits a small portion of the spring to emerge through a slot into the space occupied by the dosimeter holder and thus to act as a catch or locking device. A clip, which is free to rotate, is attached to the rear side of this component.

The *Front Component* is designed to slide into a groove in the side and top portions of the rear component and thus compose the front side of the badge structure. An array of filters which match those on the rear component is mounted on the back side of this component

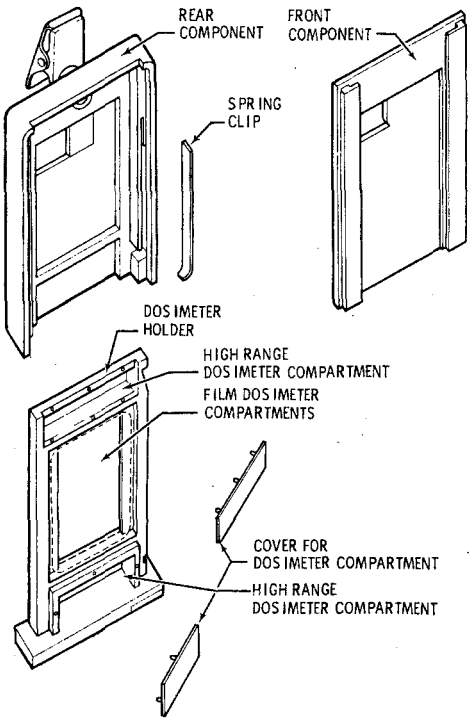

FIG. 1. Structural components of the General Dynamics film badge.

in an indented area which provides the option previously mentioned. The front side of this component also has a slight indentation over the entire film area so that a lead identification tape can be affixed in any desired position and orientation. The front side of this component is designed to accept a 15 column identification-time card or other appropriate credentials. These credentials may be inserted into slots constructed on each side of the front from either the top or bottom when the badge is open.

The credentials can be inserted or removed only from the top when the badge is closed. (With a slight modification of the molds the credentials can be locked in place when the badge is locked.)

The *Dosimeter Holder* is designed to contain the high range monitoring devices and to transport and confine two film packets to their particular location within the badge. This component also composes the bottom of the badge and functions as an integral part of the locking system. The high range dosimetry devices are housed in two rectangular shaped compartments or cavities which are covered with removable clear plastic covers. The compartment at the bottom end of the holder measures 2.70 cm × 1.11 cm × 0.55 cm. The other compartment is located at the top end of the holder and measure s3.49 cm × 0.87 cm × 0.24 cm. The high range dosimetry devices selected for use at the Fort Worth Division are compactly located in these compartments by means of small molded plastic packaging components fabricated to contain each particular device. Any other system of high range devices which are within the size and shape limitations of the compartments can be incorporated into the badge by merely fabricating new packaging components. (This is the second unique option of the design.) The holder is designed to accept either *one* or *two* film packets in the center portion of the unit and to transport and confine the film to its proper location within the badge regardless of whether one or two packets are used. Each packet is confined to its portion of the holder by the walls of a frame-like opening in the center of the holder and by thin separators which protrude from each of the two side walls into the space between the packets. (This is the third unique feature.) The front and rear components serve as the remaining structures which confine the packets when the badge is assembled.

The design features just mentioned make it possible to selectively exchange the packets in a rather simple manner. If the holder is withdrawn from the badge assembly with either *face* directed in the vertical direction the film packet on the opposite side will fall from the holder while the top packet will be retained. (Either packet can thus be removed by this procedure.) When the holder is withdrawn with either *edge* of the badge directed vertically both packets will fall from the badge *but from opposite sides*. Thus, packets can be selectively exchanged, or can be collected separately at exchange time by means of a simple collection system positioned beneath the badge when it is opened.

The right side of the dosimeter holder is designed to function as part of the locking mechanism. There is a small narrow gap across this side near the bottom of the holder and a notched gap near the top. When the structural components are assembled in the closed position the free end of the thin spring which is mounted in the rear component protrudes into the bottom gap; thus, any force which tends to remove the holder results in a shearing force upon the spring. The second (notched) gap serves to retain the holder in the badge while it is being serviced, yet permits the badge to be closed and locked by mechanical action. This two-stop locking feature is designed for use with a single permanent (or electro) magnet. When the right edge of the badge is drawn through a sufficiently strong magnetic field the free end of the spring will be withdrawn from the gap in the holder. As the badge is drawn across the gap of the magnet the field will retain the holder by the attractive force exerted on the soft iron bar which is mounted at the corner of the badge in the bottom of the dosimeter holder. When the body of the badge is drawn far enough to remove the spring from the magnetic field the free end of the spring will ride along the side of the holder until it engages the second catch (i.e. the notch gap). Further movement of the badge in the same direction will remove the iron bar from the magnetic field. The badge can be closed and locked by reversing the direction of motion just described, or by simply pushing the holder into the closed position. The holder may be withdrawn completely from the badge by application of the magnetic field to the spring a second time when the badge is opened. This permits complete disassembly (or assembly without the use of a magnet) of the three structural components in less than ten seconds. All the internal components of the badge and dosimetry system are completely accessible when the badge is disassembled.

ACCESSORY COMPONENTS

Various accessories have been incorporated into the badge structure to fulfill present requirements. These requirements and the applicable components are as follows:

Identification: The identification credentials consist of currently acceptable data printed on colormatch paper and enclosed in a clear plastic envelope. This envelope is located in the front component of the badge structure in grooves at each side which are designed to accept either of the following devices: a 15 column identification-time card; a thick printed form for visitor identification; the credentials just described; any other credential of the appropriate size. The printed form for visitors is retained as part of the personnel monitoring records. X-ray is used to permanently identify the film with a number engraved through a thin lead tape (0.64 cm × 3.02 cm × 0.014 cm) which is affixed to the front component immediately below the filter system. The date can also be X-rayed into the film (below the identification number) with a similar tape appropriately positioned in the X-ray shield.

Routine monitoring accessories: Routine monitoring accessories consist of two film packets, two matching sets of five filters each, one set each bonded to the front and rear components, and the identification tape just described. The two film packets are Dupont's Type 544 X-beta-gamma packet and Kodak's Type A Personal Neutron Monitoring Film packet. The filter materials are aluminum (Al), thin iron (Fe_1), thick iron (Fe_2), tin (Sn), and cadmium (Cd), plus the plastic (Pl) and open window

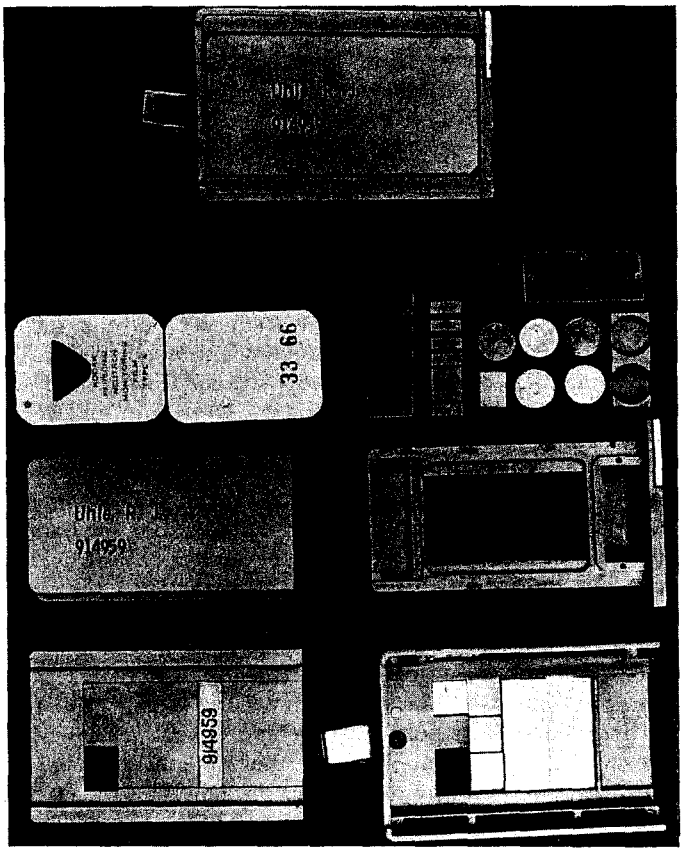

FIG. 2. Front views of the badge; disassembled and assembled.

(OW) which are part of the structural design. The characteristics and location of the filters are given in Fig. 2 and Table 1. The routine monitoring system is designed to render information which may be used for the interpretation and evaluation of beta, gamma, X-ray, thermal-neutron, and fast neutron exposures, whether present concurrently or independently. The position and orientation of the filter system are shown in Fig. 3. There are several reasons for the size and arrangement of the filters. The evaluation of fast neutron exposures is accomplished by the track counting method described by Cheka and others.[1-3] At our facility the track counting is accomplished by means of a projection microscope. The special film holder used during the counting operation will not permit the positioning (or movement) of the microscope objective to the edge of the film. It is also desirable to move the objective in long sweeps across the film during the counting operation rather than a short, bi-directional path. Finally it is highly desirable to provide a Cd shielded area on the neutron film that is large enough to locate easily and to operate within during the reading operation. Thus a large cadmium filter was chosen and positioned near the center of the packet. With the exception of Cd, the filters were chosen large enough to reduce scatter into the center portion of the film behind the particular filter to an acceptable minimum and large enough to be easily positioned in the density reading device (densitometer), yet small enough to fit compactly in the space available in the badge. The filters are mounted close together in a compact array which extends slightly beyond the outer edge of the film packets. This arrangement is an attempt to reduce scattering of radiations into the film behind the filters, a problem of considerable importance.[4]

The Al and Fe_1 filters were experimentally

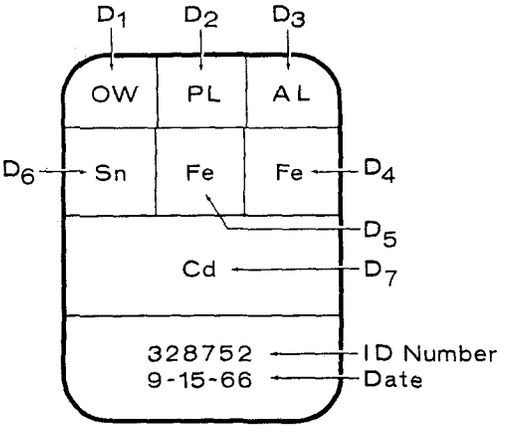

FIG. 3. Position and orientation of the filter system with respect to the film.

matched using both natural Uranium and ^{90}Sr to achieve identical attenuation of beta radiation. High energy photons ($E > 250$ kVe) are also attenuated identically; however, the pair differ significantly in low energy photon attenuation properties. (Henceforth low energy photons will be assumed to be in the $30 < E <$

Table 1. Physical Characteristics of the Filter System

Filter material	Surface dimensions (cm)	Thickness (mm)	Total Mg/Cm² thickness*
Open window	0.953 × 1.27	0	39
Plastic (cycolac)	0.953 × 0.953	2.70	343
Aluminium	0.953 × 0.953	0.84	407
Iron	0.953 × 0.953	0.25	376
Iron	0.953 × 1.03	0.71	728
Tin	0.953 × 1.03	1.14	1013
Cadmium	1.27 × 3.18	0.97	1018

* Includes filter, plastic structure, and identification materials.

250 kVe energy range.) Thus the film response behind these two filters may be conveniently used to detect the presence of low energy photon radiation in an exposure. The Sn and Cd filters were also matched experimentally to produce identical attenuation of high energy gamma radiation. When exposed to thermal neutrons the (N, γ) reaction ($E_{\gamma\text{eff}} = 2.18$ meV) in the Cd filter results in a significant increase in the exposure to the Dupont film behind that filter whereas no appreciable change in exposure will be noted behind the Sn filter. Thus the difference in density behind the matched (Cd: Sn) pair of filters is a measure of the thermal neutron exposure received by the badge. The density produced behind the Cd filter has been reported to be related to the density produced by gamma rays by the ratio $\frac{\text{roentgens }(\gamma)}{\text{rem}(N_{\text{th}})} = \frac{\text{density }(\gamma)}{\text{density }(N_{\text{th}})} = 1.98$;[5] however this ratio may be subject to the cadmium ratio of the neutron spectrum.[6] Tin was chosen as the material to match Cd (1) because its backscatter properties are very similar to those of cadmium and (2) because its absorption edge is below 30 kV. With regard to (1) in the previous statement, it should be noted that if the sensitive component of a film packet is positioned near the surface of a filter system and the badge exposed to photons from the rear rather than the front, the backscatter from dense metal filters such as cadmium, lead, etc., increases the film density in the areas adjacent to them.

The amount of backscatter varies with the filter material and as a result can erroneously indicate a thermal neutron exposure if two filters differ significantly in backscatter properties. Al, Fe, and Sn were all chosen as filter materials because of their low absorption edge, their density, mechanical, and other favorable properties.

High range monitoring components and accessories: The high range monitoring system is patterned after the system which originated at Hanford[7] and consists of a bare indium foil, and a cadium covered indium foil, a sulfur pellet, and a bare copper bar. Provisions have been made for the use of either glass rods or thermoluminescent dosimetry (TLD) materials in addition to the foils and pellets. Recent developments in the TL dosimetry[8] indicate that a TLD system will be a desirable addition to this system. A thick indium tape affixed to the rear component just below the array of filters is also a part of the high range dosimetry system. The physical characteristics of the high range system are exhibited more completely in Tables 2 and 3.

Miscellaneous: The badges are serviced, transported, and stationed for use on racks which are designed to hold 56 badges each (along with 56 pocket dosimeters). The racks are of a step-like construction and are designed to display the entire front of each badge for ease in locating any particular badge. This construction also permits permanent identification of the film in lots of 56 badges each by use of a similarly fashioned lead shield which has

Table 2. Physical Characteristics of the High Range Neutron Dosimetry Components

Dosimetry component	Area (cm × cm)	Thickness (cm)	Weight (g)	Number used	Location and exposure condition
Indium	1.175 × 3.1	0.0381	1.02	1	Rear component below cadmium (film) filter
Indium	1.13 Dia. (disc)	0.0254	0.189	2	Lower cavity—one behind sulfur pellet (bare), one sandwiched between two cadmium discs
Copper	0.92 × 1.1	0.106	0.799	1	Upper cavity—bare
Sulfur	1.116 Dia. (disc)	0.30	0.585	1	Lower cavity—in front of bare indium foil
Cadmium	1.129 Dia. (disc)	0.055	0.468	2	Lower cavity—on either side of an indium foil

windows that are accurately positioned in front of the lead tapes when the shield is placed over a rack.

ROUTINE MONITORING

The evaluation procedure for routine monitoring of X-ray (low energy photons), gamma rays (high energy photons), beta particles, and thermal neutron exposures involves the various densities produced in the Dupont film. The film response (net transmission density versus exposure) to either of these radiations is relatively linear over most of its useful range and thus it is not unreasonable to assume that its response to combinations of these radiations is also approximately linear.

Assuming that the film response is relatively linear to exposures involving individual and multiple radiation types over most of its useful range the following linear equations may be used to represent the densities in the various filter areas:

$D_1 = b_1B + x_1X + g_1G =$ *the net density in the OW area.*

$D_2 = b_2B + x_2X + g_2G =$ *the net density behind the Pl filter.*

$D_3 = b_3B + x_3X + g_3G =$ *the net density behind the Al filter.*

$D_4 = b_4B + x_4X + g_4G =$ *the net density behind the thin Fe filter.*

$D_5 = b_5B + x_5X + g_5G =$ *the net density behind the thick Fe filter.*

$D_6 = b_6B + x_6X + g_6G =$ *the net density behind the Sn filter.*

$D_7 = b_7B + x_7X + g_7G + kN_{th} =$ *the net density behind the Cd filter.*

where b_n, x_n, g_n, and k represent the net density per unit dose of beta, X_{-1} gamma- and thermal neutron radiations respectively, and B, X, G, and N_{th} represent the beta, X-ray, gamma-ray, and thermal neutron dose respectively. The subscript (n) is used to represent the various areas. The filters were chosen such that $b_3 = b_4$, $b_5 \cong b_6 \cong b_7 \cong 0$, and $g_3 \cong g_4 \cong g_5 \cong g_6 \cong g_7$.

Table 3. Analysis of High Range Neutron Exposures

Neutron energy range	Dosimetry component utilized	Cross-section (barns)	Half-life	Method of analysis	Corrections required
0.025 eV to 0.3 eV	In	145	54.3 m	Use activity difference between bare and cadmium covered indium foils.	Backscattering and cadmium absorption.
0.3 eV to 2 eV	In	28,000*	54.3 m	Use activity of cadmium covered indium foil.	None.
2 eV to 1 MeV	Cu	0.09	12.8 hr	Positron annihilation gammas (510 keV) counted. (A 657 keV positron is emitted by 19% of Cu-64).	Thermal and epithermal activation.
1 MeV to 2.9 MeV	In	0.18	4.5 hr	Count cadmium covered indium (either 0.335 MeV gammas or 0.96 MeV betas) for activity produced by inelastic scattering of fast neutrons.	Activity due to fast neutrons of energy above 2.9 MeV
2.9 MeV up	S	0.23	14.5d	Count 1.71 MeV betas from P^{32} produced in the S^{32} (n,p)P^{32} reaction.	None.

* At 1.4 eV resonance.

It should be noted that it is not necessary to utilize all of these equations in a particular analysis and that by a judicious choice of filters the analysis of exposures can be simplified. Therefore, the filter system was chosen such that $b_3 = b_4$ and $b_5 \cong b_6 \cong b_7 \cong 0$ (that is, the filters were chosen for identical beta response behind the Al and thin Fe filters and essentially no beta response behind the other three metal filters) and such that $g_3 \cong g_4 \cong g_5 \cong g_6 \cong g_7$ (that is, essentially equivalent gamma response behind the five metal filters).

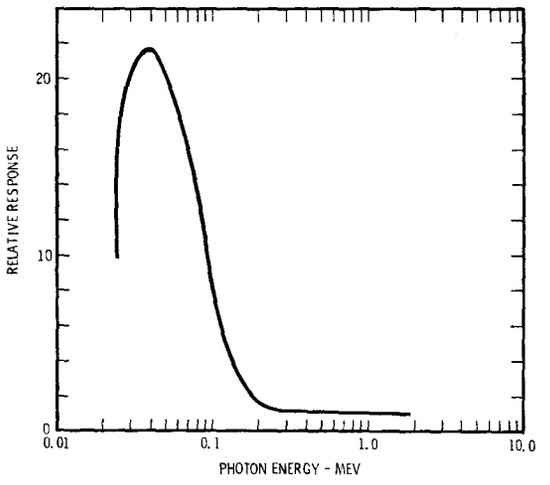

FIG. 4. A typical curve illustrating the energy dependence of film response to photon radiation.

The data represented by the system of equations given above can be used to evaluate exposures involving a single type of radiation or a mixture of radiation types. Since the types of radiation involved in an exposure are not necessarily obvious from the appearance of a processed film it is necessary to proceed from the complicated to the simple in devising a technique for analysis of an exposed film. Fortunately in many cases it is possible to circumvent a lengthy analysis by use of knowledge either of the potential types of exposure or the history of the subject's activities during the period in which the film was exposed. In such cases the appropriate simplified analysis can be applied immediately.

Analysis of exposures involving (X, B, G) radiations: The most important particular problem in film dosimetry is the energy dependence of film response to low energy photons. A typical energy dependence curve for film is shown in Fig. 4. To overcome this problem it is necessary either to ascertain the energy of the photon radiation or to reduce the energy dependence of the film to an acceptable level by attenuation of the incident photon radiation. Either alternative can be used to accomplish a satisfactory analysis procedure; however, the former affords at least two advantages: (1) some information is acquired regarding the photon spectrum (thus the system serves as a simplified spectrometer) and (2) the sensitivity of the detector is preserved. The system described in this report is designed to apply to the former approach to the problem. The first requirement in the analysis of an exposure then is to determine the energy of the low energy component of the incident photon radiation. This determination can be accomplished quite easily by use of the energy index factor, K, which is derived from four of the basic density equations as follows:

Consider the ratio:

$$\frac{D_3 + D_4}{D_5 + D_6} = \frac{(b_3 + b_4)B + (x_3 + x_4)X + (g_3 + g_4)G}{(b_5 + b_6)B + (x_5 + x_6)X + (g_5 + g_6)G}$$

Now $(b_3 + b_4)$ is very small compared to $(x_3 + x_4)$ and for all practical purposes may be neglected. Also b_5 and b_6 are approximately zero and $g_3 \cong g_4 \cong g_5 \cong g_6$ by design, so that the ratio reduces to:

$$\frac{D_3 + D_4}{D_5 + D_6} = \frac{(x_3 + x_4)X + 2\,g_6G}{(x_5 + x_6)X + 2\,g_6G}$$

Now if $G = 0$ (i.e. there is no high energy photon component of exposure) the ratio reduces to:

$$\frac{D_3 + D_4}{D_5 + D_6} = \frac{(x_3 + x_4)X}{(x_5 + x_6)X} = \frac{(x_3 + x_4)}{(x_5 + x_6)} = K$$

where K is a constant which depends only on the low energy photon energy. (It should be noted that K can be used to determine the energy of low energy photons even when $G \neq 0$

provided G is not too great, because $(x_3 + x_4) > > 2g_6$.)

Calibration data at six energies in the 30–215 kVe (kilo-volt-effective) range have been used to produce the smooth curve of K versus energy shown in Fig. 5.

The slope of this curve indicates good resolution of energies up to approximately 150 kVe. It should be noted that K can be used to

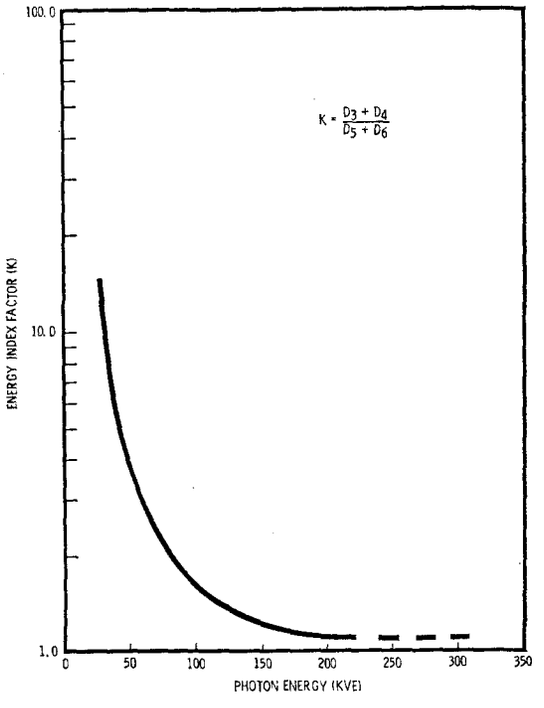

FIG. 5. Calibration curve of the energy index factor (K) as a function of photon energy.

determine the energy of low energy photons even in mixed exposures involving high energy photons (provided G is not too high) because $(x_3 + x_4) > > 2\,g_6$. Experimental evidence to this effect is presented later. Several other energy index factors have been derived from the basic density equations in efforts to improve the energy resolution at higher energies; however, these have generally resulted in curves which give ambiguous results (i.e. the slope becomes positive due to significant scattering contribution to the low densities which occur at the higher energies). Once the effective energy of the low energy photon radiation has been established there still remains the problem of independent determination of the dose contributions by each of the radiations involved in mixed exposures. The normally accepted procedure for determining the high energy and low energy photon contributions to an exposure is to assume that the density behind a thick filter (such as the Sn filter) is due entirely to high energy photons and to use that density (D_6) to determine the high energy photon dose. The high energy dose is then used to predict the "expected" density behind a thin filter (such as the Al) and the difference in the expected and actual densities used to determine the low energy photon dose. The major fallacy in this approach is that it depends upon the assumption that x_6X is zero, that is, that there is no low energy photon contribution to the density behind the thick filter. There is in fact a significant contribution to the density behind the Sn filter because, even though the low energy spectrum is attenuated and hardened by the filter, the emulsion still exhibits a very significant response due to its energy dependence. As a result the high energy component of the exposure (and thus, the total photon exposure) will be greatly exaggerated if such a procedure is used. For example, the density behind Sn for a 200 mr exposure to 120 kVe X-rays is approximately 0.50 net density units. If taken from a ^{60}Co curve this density indicates an exposure of approximately 450 mr. If the normally accepted procedure is used the evaluation would indicate a dose of 450 mr *plus* whatever low energy dose the procedure yields, and thus the result would be a gross over evaluation of the exposure.

This problem can be circumvented by reversing the procedure, that is, by determining the low energy dose first and then determining the high energy dose. The low energy dose can be determined relatively independent of the contribution of the other components of the exposure by use of a low energy dose factor, D_L, which is derived from three of the basic density equations as follows:

Consider the sum of density differences:

$$(D_3 - D_6) + (D_4 - D_6) + (D_5 - D_6) = (D_3 + D_4 + D_5) - 3D_6$$

By substitution of the original density equations and collection of terms this becomes:

$$(b_3B + x_3X + g_3G) + (b_4B + x_4X + g_4G) + (b_5B + x_5X + g_5G) - 3(b_6B + x_6X + g_6G) = (b_3 + b_4 + b_5 - 3b_6)B + (x_3 + x_4 + x_5 - 3x_6)X + (g_3 + g_4 + g_5 - 3g_6)G.$$

For all practical purposes $b_5 \cong b_6 \cong 0$ and $b_3 \mid b_4$ is very small compared to the coefficients of the X term; thus the first term (involving B) may be neglected. Also since $g_3 \cong g_4 \cong g_5 \cong g_6$ the coefficient of the term involving G is approximately zero and the equation reduces to: $(D_3 + D_4 + D_5 - 3\,D_6) = (x_3 + x_4 + x_5 - 3\,x_6)X = AxX$ (where Ax is a constant), which shows that the sum of densities originally stated is a measure of the low energy photon dose. Thus we have a low energy dose factor which we shall designate as D_L, where

$$D_L = (D_3 + D_4 + D_5 - 3\,D_6)$$

The nature of D_L is more apparent in Fig. 6 where D_L versus exposure is shown for six X-ray energies. A comparison of these curves with a set of curves (density versus exposure) produced for any *one* of the basic density equations (with $G = B = 0$) reveals two significant differences: (1) the range of density values for D_L is over three times as great as either of the basic density ranges and (2) the curves for the various energies are more widely separated with some apparent improvement in resolution of points about the individual curves (probably due to the counter-balancing effect of multiple density readings on errors inherent in individual density readings which are attributable to non-uniformity of the film, scatter effects, reader errors, etc.). Once the energy and dose due to the low energy photon radiations have been determined the expected Sn density can be determined from curves similar to those shown in Fig. 6. The high energy photon dose, G, can be determined from the (Sn — Sn$_e$) density difference. Finally, the beta dose, B, may be roughly

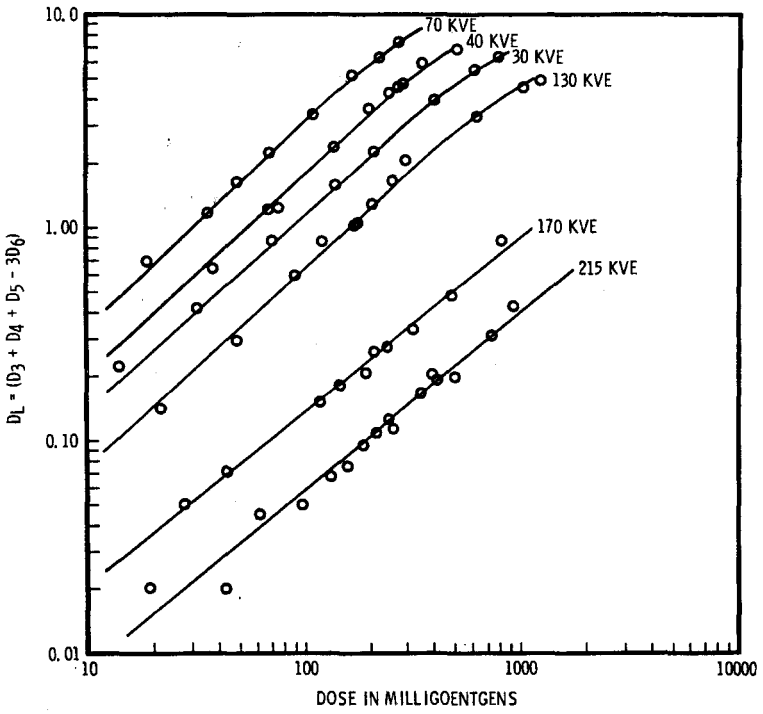

FIG. 6. Typical calibration curves for the low energy dose factor (D_L).

estimated from the difference between the OW or Pl (D_1 or D_2) density and the sum of the expected densities due to the X and G exposures; however, the cautions presented later regarding such an interpretation should be noted. Evaluation of exposures involving only one or two of the three types of radiation may be summarized as follows: $(X + G)$—evaluate as previously described, but eliminate the B evaluation procedure; $(G + B)$—evaluate G from the Sn density (D_7), predict the expected OW density (OW_e) from appropriate curves, then use the ($OW-OW_e$) density difference to determine the B exposure; $(X + B)$—evaluate the X energy, and the X dose, predict OW_e due to the X dose, then evaluate B from the ($OW-OW_e$) density difference; (X only)—same as $(X + G)$ procedure, sum the apparent exposures; (G only)—under normal circumstances evaluate G by use of the OW, (D_1) or a thin filter density (D_3 or D_4); (B only)—evaluate the B exposure by use of the OW density.

Analysis of exposures involving thermal or fast neutrons: Thermal neutron exposures may be evaluated by use of appropriate measures of the responses of either the Dupont or the Kodak film components. Use of the Dupont film response is preferable because of the relative ease, simplicity, and reliability of the measures required. The Dupont film (Cd—Sn) density difference is a measure of the thermal neutron exposure and is independent of the presence of other types of radiation in the exposure, that is: $(D_6-D_5) = kN_{th}$, a result which follows from the fact that b_5 and b_6 are approximately zero and $g_5 = g_6$ by design. Although this measure is independent of the presence of the other types of radiation, the useful range of the measure is governed to some extent by the presence of other radiations. This dependence may be explained as follows: most thermal neutron calibration exposures and actual exposures are accompanied by a gamma exposure and as a result the net Cd and Sn density

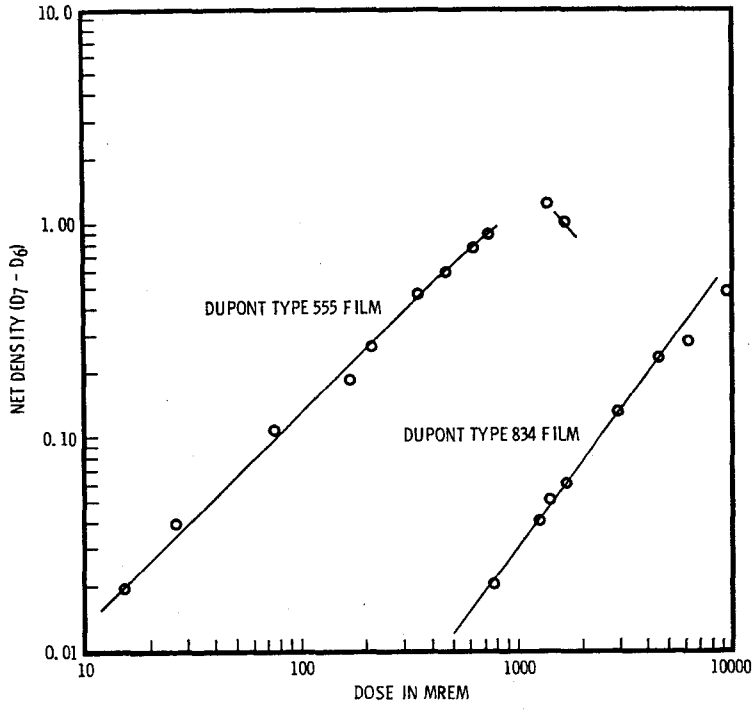

FIG. 7. Typical thermal neutron calibration curves for Dupont type 555 and type 834 films.

curves compose a pattern similar to a hysteresis curve. For such a pattern the density difference in question (Cd—Sn) maximizes at a certain density and continues to decline as the total exposure to the film is increased. Therefore, the use of the density difference must be governed by the gross density under the Cd filter if the possibility of ambiguous results is to be avoided. The gross density behind the Cd is dependent particularly upon the presence of radiations other than N_{th} and to some extent affects the useful range of the film for thermal neutron dosimetry. Figure 7 illustrates how this density maximizes for PuBe neutrons thermalized in paraffin. If a particular result has to be rejected because the gross Cd density is too high the data from a more insensitive film can be used to produce the desired result.

Fast neutron exposures are monitored with the Kodak film which are evaluated by the track counting technique. The track count is determined in the Cd filter area of the film by means of a projection microscope. A scanning technique is used to examine an area equivalent to at least 50 fields of view (6.125 mm^2). If this preliminary scan indicates that the film is exposed, enough individual fields are examined to produce a counting result with acceptable counting statistics ($\pm$ 20% at 95% confidence level). The required number of fields can be determined by use of the data gained from the first few fields counted. The dose is interpreted from an appropriate calibration curve. (It may be of passing interest that the average track production efficiency of PuBe neutrons in Kodak Type A film as determined by several observers with a microprojector using this technique is 6.0×10^{-4} tracks/nf.)

EMERGENCY MONITORING

The badge is presently equipped with a high range monitoring system (Tables 2 and 3) for neutrons which is patterned after the system used in the Hanford Badge.[7] This system extends the capabilities for evaluation of neutron exposures to cover the range which would be of concern should a serious radiation event occur. Although the present emergency system provides only for an extension of neutron monitoring capabilities, provisions are now being made to incorporate a high range gamma monitoring capability. It is anticipated that this system will consist of as many as three separate monitoring units, each containing at least 20 mg of Li-7 enriched LiF, and having a useful range of from 20 mr to 10^5 R. These units are to be contained in the reserve space in the top cavity of the dosimeter holder.

PERFORMANCE OF THE ROUTINE MONITORING SYSTEM

The routine monitoring performance of the badge described in this report has been investigated for a variety of exposures to X-rays, gamma-rays, beta particles, thermal neutrons, and various mixtures of these radiations, using the analysis techniques described earlier. The results of these analyses indicate that the routine monitoring performance of this system easily exceeds the applicable National Sanitation Foundation Film Badge Performance Control Limits.[11] A detailed description of the performance testing is not included in this report; however, the data is included in a separate report which can be obtained upon request from the authors.[12]

CONCLUSIONS

The film badge described in this report has been in service for over 18 months and has performed very satisfactorily. Although the badge is possibly the most extensive design in existence, analyses of the monitoring capabilities attainable with it in conjunction with the techniques and appropriate discretions presented in this report show that these capabilities easily meet and significantly exceed the performance requirements which have been set forth for film badge services.

REFERENCES

1. J. S. Cheka. *Neutron Monitoring by Means of Nuclear Track Film* (NTA), ORNL-547 (Jan. 1950).
2. J. S. Cheka. Recent developments in film monitoring of fast neutrons, *Nucleonics*, **12,** 6, 40–43 (1954).
3. E. C. Watson. *Fast Neutron Monitoring of Personnel*, HW-21552 (Aug. 1952).
4. E. Storm and S. Shlaer. Development of energy-independent film badge with multi-element filters, *Health Physics*, **2,** 11, 1127 (Nov. 1965).

5. L. T. CARUTHERS and E. J. STORY. Capture gammas for neutron dosimetry with a film badge, *Health Physics*, **10,** 667–672 (Sept. 1964).
6. S. BLOCK. The effects of cadmium ratio on film badge neutron dosimetry by capture gammas, *Health Physics*, **3,** 8, 785 (Aug. 1965).
7. L. F. KOCHER, *et al. The New Hanford Film Badge Dosimeter*, HW-76944 (March 1963).
8. F. H. ATTIX. *Present Status of Dosimetry by Radiophotoluminescence and Thermoluminescence Methods.* NRL Report 6145 (Sept. 1964).
9. C. W. TUTTLE. Slow neutron detection by foils. I and II. *Nucleonics*, **8,** 6 (June 1951) and **9,** 1 (July 1951).
10. *Measurement of Neutron Flux and Spectra for Physical and Biological Applications*, U.S. Dept. of Commerce, National Bureau of Standards, Handbook 72 (July 15, 1960).
11. *Film Badges Services.* National Sanitation Foundation, Standard No. 16 (Effective March 1, 1966).
12. J. D. EASTES, M. L. MAURER, and F. L. PASCHAL, JR. *A New Concept in Film Badge Design*, FZM-4699 (August 1966).

AUTOMATIC DATA PROCESSING FOR A NATIONAL FILM DOSIMETRY SERVICE

W. BENARY, M. SCHATZ and G. BEN-DAVID
Israel Atomic Energy Commission, Soreq Nuclear Research Center, Yavne, Israel

Abstract—The operation of a national film dosimetry service involves a considerable amount of documentation, including regular badge dispatch lists, a dosage information bulletin sent to each organization, and full records of individuals and organizations using the service. The smooth operation of the dosimetry service depends on the regular flow of this documentation.

Automatic data processing has been introduced to handle all the documentation of the Soreq Dosimetry Service, which acts as a national scheme for all industrial and medical applications of radiation. This results in a fully flexible system, capable of meeting increased demands without a corresponding increase in the personnel required for documentation. The use of an electronic computer results in considerable saving in manpower and a reduction in errors, and permits convenient storage of all the recorded dosage statistics on magnetic tape.

AUTOMATIC data processing has been applied to the operation of the Soreq Dosimetry Service, to handle all the documentation and data storage. The system is fully flexible and capable of meeting increased demands in documentation, without a corresponding increase in the number of personnel. The use of the electronic computer results in a considerable saving in manpower, a reduction in errors, and convenient storage of all the recorded dosage statistics on magnetic tape.

ORGANIZATION OF THE DOSIMETRY SERVICE

The Soreq Dosimetry Service is a national service covering all personnel working in industrial or medical applications of radiation throughout the country. Interested organizations wishing to join the scheme fill in a special order form giving the personal information required for each worker, i.e. full name, name of father, date of birth, sex, national identity card number, and type or types of film badge required. Each organization is designated by a serial number given by the film service, and this number is used for all operations involving that organization. In addition, each badge wearer is given a personal identification number (not connected with the national registration number). Individuals working for two or more different organizations receive a different identification number in each organization.

The film service at present offers five categories of film badge. Type A, usually worn on the chest, is for measuring the total body dose of beta, gamma, X-rays and thermal neutrons. Types B, C and D are similar to type A, but are worn for measuring hand, foot and head dosage respectively. Type N is used for fast neutron dosage, and is usually worn on the chest. Each badge wearer receives the same personal identity number for all types of badges worn within a given organization.

The badges are usually changed every two weeks (hereafter called the "period"). However, for cases where the film wearer is not regularly in contact with radiation, the change is every six weeks. Badges for new members are delivered at the very first regular dispatch after the order form is received, an improvement in service which has only become possible since the introduction of the computer system. After assembly of the film badges in the film service laboratory, they are sent to the different organizations accompanied by a dispatch list. This list includes the personal identity number

and full name of the badge wearer and the film serial number for that period. A duplicate list is kept as a work list in the laboratory. At the end of the period the badges are returned to the laboratory, where the films are developed under standard conditions and the radiation dose evaluated using film dosimetry techniques. The dose of each film is entered on the work list, which is then used to prepare the input for the computer. The computer prints period dose reports for each organization, and keeps a personal dose record stored on magnetic tape for each badge wearer. Before the introduction of the computer, this documentation was done semi-automatically using business machines.

PREPARATION OF INITIAL DATA FOR THE COMPUTER

For preparing a new service from the start, a full list of organizations and badge wearers is drawn up, using a suitable code to represent the Hebrew letters. Within each organization, the list is ordered according to increasing personal number. One of the main problems in arranging such a list is to keep a continuous check on alterations which occur, even during the preparation of the list. Up-to-date information on changes is therefore added before finally using the programme. Numerical codes are used to describe the badge category, radiation type (X-ray, gamma, beta, thermal neutron or fast neutron), special remarks, and radiation dosage. This saves space in the computer memory. For efficient operation, the organizations are divided into five different groups, each having a separate "run" and using a separate section of the storage magnetic tapes. To minimize errors, several checks are made on the input data, including a check on the correct ordering of personal numbers, a search for faulty numbers, etc. These checks would not of course correct any errors in the actual dosage as recorded by the film laboratory technician.

USE OF THE COMPUTER FOR ROUTINE OPERATION

The full list of badge wearers organizations and addresses, the codes, and other required parameters (including period dates) are recorded on magnetic tape and transferred to the computer memory, one "run" at a time. All changes within this run, including cancellations and additions of new badge wearers, are now brought up to date using IBM cards. For additions, the organization identity number is required. For cancellations only the personal number and a single digit designating cancellation are required. Full details of the input information are shown in Appendix A. It should be emphasized that the present system of adding new badge wearers is considerably simpler than the earlier method, which involved ordering a special address plate with a three weeks delivery time.

Since the period dose report for a particular period is prepared several weeks after its corresponding dispatch list, and meanwhile new dispatch lists have to be prepared which may include changes, two separate magnetic tapes are kept, one for the dispatch and work lists, and one for the period dose reports. The same input data cards are used to introduce changes in both tapes, but with a delay to take into account the extra time needed for the latter tape.

The preparation of dispatch lists and work lists requires input data giving any changes in the badge wearer list for that "run", the period number, the "run", and the serial number of the first film in the whole run. The computer prints this serial number for the whole print out.

The input data required for the period dose reports are entered on IBM cards, according to the organization, keeping strictly to the order of increasing personal number. The code for the particular period and the organization number are given first, then the dose details of badges found to have received a measurable radiation dose. If a badge is not returned, or a special remark is required for the dose report, then this is added here. No entry is required for a badge returned in its proper period and showing no measurable dose; the computer takes the absence of a given personal number as meaning zero dosage. This permits considerable reduction in the input data. In addition, a special code is used for whole groups or subgroups of badges which do not arrive in time for the period development, to permit rapid addition to the input data. The accumulated doses for previous periods are stored on the

period dose storage tape, permitting totals and sub-totals to be given in the dose reports.

The personal dose records are stored for one year on magnetic tape. The dose record of any individual badge wearer can be furnished immediately just by giving his personal identity number and the required periods. Normally such a report is printed every 3 months and sent to the parent organization. The doses received by individuals in more than one organization are printed on separate cards.

The scheme has been running efficiently for over six months and has proved itself excellently over this period. At present the service is operating for several thousand badge wearers in over two hundred organizations. The use of the electronic computer has permitted the documentary staff to be reduced by 2 members (a cut of 50%), with a big reduction in errors. In addition, the very rapid documentation possible with the computer gives a great deal of flexibility to the operation of the whole badge service not possible with semi-automatic documentation, which required many days of preparation. Previously, any backlog in documentation caused by illness or any other reason, could lead to considerable disruption of the whole service. The monthly cost in computer time is only IL.450 ($150), quite insignificant compared with the other costs of the service.

APPENDIX A

I. *Input Data for Dispatch and Work Lists*

This input includes an IBM card giving the period number, the "run" number indicating the organizations included and the serial number of the first film. The main volume of input data here is information on new users, transfer of users from one organization to another, and cancellation of users from the service.

(*a*) *Addition of new badge wearers.* The information on each new user occupies a single IBM card. The following items are included (the number of bits allocated to accommodate each item is shown in brackets): personal identity number (6), full name (16), national registration number (8), date of birth (5), badge type (1), organization identity number (3).

(*b*) *Transfer of badge wearers from one organization to another.* The transfer of badge wearers requires the addition of a card of the type described in (*a*) above, including the former personal identity number and the new organization number. In addition, to permit transfer of partial radiation totals and cancel the position in the former organizations, the following information is required: personal identity number (6), badge type (2), transfer signal (2), radiation dose totals (16). The data for three individuals can be entered in a single IBM card.

(*c*) *Cancellations.* A typical cancellation card contains the following information: personal identity number (6), badge type (2), and cancellation signal (2).

All the above data are entered in order of personal identity number, within each organization.

II. *Input Data for Period Dose Reports and Personal Dose Records*

Each card contains the following information for five badge wearers: badge type (1), personal identity number (5), period (2), radiation type (1)—dose (2) (twice), remarks (2). This permits dose information to be entered about two types of radiation. A film badge returned during the correct period, but not showing any measureable dose, is not included in the input data—its absence being taken to mean zero dose. This considerably reduces the volume of input data. Where a badge has not been returned in the normal period, this is indicated in the "remarks" position and the individual is not included in the period dose report. For a badge returned late from an earlier period, a remark is added to this effect. In addition, a separate card is added for all late films, giving the serial number of the film and the appropriate period number. If a whole group or sub-group is returned late, it is added to the input data with indication of the first and last members of the group and a special remark.

Owing to the extreme importance of accuracy in the dose input data, all the information is double checked against the work lists, by two different operators.

THE USE AND PROCESSING OF FILM BADGE DOSEMETERS AND THE APPLICATION OF AUTOMATIC DATA PROCESSING TECHNIQUES TO ASSESSING, REPORTING AND RECORDING THE DATA

W. N. SAXBY and D. M. WALLACE
Health Physics Branch, AWRE, UKAEA, Aldermaston, Reading, Berks., U.K.

Abstract—In an establishment or occupation where there may be exposure to ionizing radiations it is usually necessary to assess the exposure levels at which people are working. This can be done simply and cheaply by utilizing small integrating dosemeters, of which perhaps the most widely used is the "film badge", with thermoluminescent dosimeters being used increasingly in support of "film badges".

The reasons for issuing film badges as individual personal dosemeters may vary from country to country, from industry to industry and indeed within a single organization or plant. Some of these reasons are explored in the paper.

Where film badges, or other dosemeters, are issued there is a consequent need to identify the badge, its location and period of use, to process the film to establish its radiation exposure, and then to ensure that this radiation exposure is recorded and, where necessary, that the information in the record is assessed and used managerially. A film badge processing technique is described with particular attention being paid to improvements and to special procedures required to maintain a high sensitivity and processing quality. After processing the data on the film are assessed and recorded: in this paper a simple data processing system is described. The system is mainly based on commercially available equipment and is designed to provide an input to commercial accountancy type computers. It is easy to build up the system in stages, utilizing as little or as much of it as may be needed in the local circumstances. The procedure adopted is extremely flexible, and allows for the occurrence of unusual films and other operational problems.

Finally when the film data have been assessed and recorded it may be necessary to transfer all or some of the information to individual's personal radiation records or to other records and reports. The need for such data keeping is discussed and a description given of an established system of maintaining personal radiation records by automatic data processing.

NOTE: This paper was *withdrawn* prior to the Congress.

FILM DOSIMETRY OF X-RAYS BY MEANS OF RADIOACTIVE SOURCES IN A SHIELDED, TRANSPORTABLE CALIBRATION FACILITY*

VALERIJA PAIĆ
Institute of Physics, University of Zagreb, Yugoslavia

Abstract—*I. Evaluation of the effective energy of X-rays to which a film was exposed.*
Ilford PM3 films are used. The film badge has one portion without a filter and six portions with filters of various thicknesses of copper (0·1 to 0·97 mm), on both sides. The optical density under the portion without a filter $D(O)$ and under Cu filters $D(t)$, can be used in three different manners for the evaluation of effective energies of X-rays, namely:

1. By measurements of the half value photographic density layer in the case of effective energies ranging between 25 and 82 keV.
2. By the ratio $D(O)/D(t)$ as a function of the thickness of copper filters in the case of effective energies, ranging between 25 and 135 keV.
3. By the ratio $D(O)/D(0.1$ mm Cu) as a function of effective energies between 25 and 55 keV, or by the ratio $D(O)/D(0.97$ mm Cu) as a function of effective energies between 51 and 156 keV.

II. Use of a ^{226}Ra, ^{137}Cs or $^{90}Sr - ^{90}Y/Al$ source, in a shielded, transportable calibration facility, for the establishment of log $D(O) = f(\log X)$, in the interval 25 keV $\leqslant E_{eff} \leqslant$ 156 keV of X-rays
1. In one set of experiments log $D(O) = f(\log X)$ calibration curves were obtained by X-rays of E_{eff} between 25 and 156 keV.
2. In another set, log $D(O) = f(\log X)$ calibration curves were obtained by means of radioactive sources in a shielded, transportable calibration facility.
   Because of the great difference in photographic sensitivity in the two energy intervals (X-rays : 25 keV $\leqslant E_{eff} \leqslant$ 156 keV; gamma rays : 662 keV to 1·25 MeV mean), it is necessary to give the PM3 films, in the calibration facility with radioactive sources, 6- to 10-fold higher exposures than to the films exposed to X-rays.
3. Using the two sets of measurements, calibration factors were determined.

INTRODUCTION

The energy dependence of the sensitivity of photographic film to X- or gamma-rays especially in the range of approximately 0.02 MeV to 0.3 MeV, is a well-known difficulty in film dosimetry. The knowledge of the effective energy, or energies, to which the film was exposed, as well as the corresponding calibration curves are therefore needed.[1, 2]

If the calibration curves for different energies are given for a certain quality of photographic film, only one more calibration curve, with a known X-ray effective energy, is then necessary for each set of exposure measurements.[3-12]

We considered it worthwhile to replace this single calibration with X-rays by a calibration using a radioactive source. This is placed in a calibration facility which is transportable, protected against radiation hazards, easily operated, having a well-defined and reproducible geometry and radiation. Our experiments were made with Ilford PM3 films for personnel monitoring. We report here the results which make possible the evaluation of the effective energy of X-rays to which such a film was exposed; the photographic density versus exposure curves for different effective energies of

* Research supported by the International Atomic Energy Agency, Vienna.

X-rays; the calibration curves obtained with different radioactive sources in our calibration facility, and the corresponding factors enabling the construction of other calibration curves.

exposure was measured with a Victoreen ionization chamber.

The X-ray source was a Coolidge type, tungsten anode, oil cooled, glass X-ray tube. The

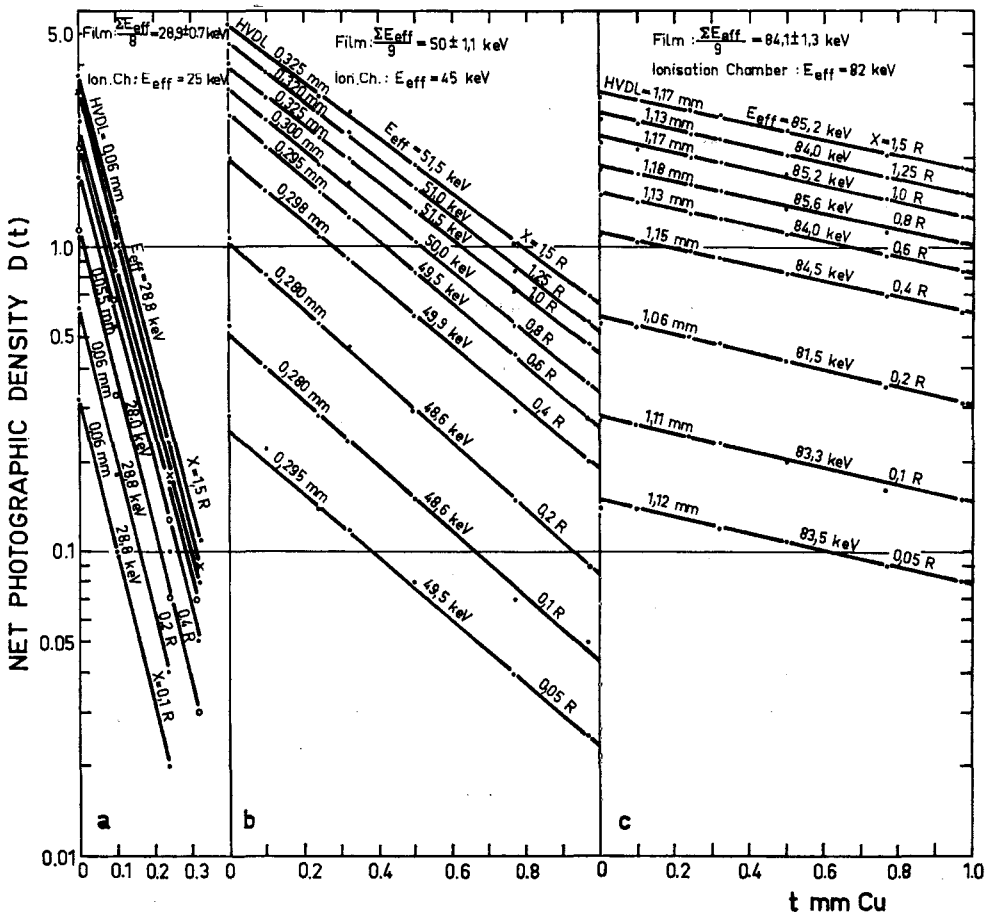

FIG. 1. Determination of effective energies of X-rays by measurements of half value density layers (HVDL) of copper. The results are independent of exposures in the interval from 0·05 to 1·5 R. Three examples for effective energies of (a) 25 keV, (b) 45 keV and (c) 82 keV obtained by measurements of HVL with ion chambers are given.

MATERIAL AND METHODS

A film badge[13] containing an Ilford PM3 film, having an unfiltered portion and six portions filtered back and front by pure copper filters (0.1, 0.24, 0.32, 0.5, 0.77 and 0.97 mm thick, 10 mm long and wide), was exposed to a given narrow energy band of X-rays. The applied voltage was stabilized and had an insignificant ripple. The tube was operated at voltages from 34 to 183 kV and at a constant current of 5 mA. The X-ray beam was filtered through pure copper of 0.047 mm to 15.5 mm thickness. The corresponding effective energies, determined by the half value layer (HVL) of

copper, as described by Johns,[14] using a Victoreen ionization chamber, were in the range of 25 to 156 keV.

The exposed films were developed in Ilford Phen-X developer for 5 min at 20 $\pm$ 0.2°C. The photographic densities were measured with a Baldwin densitometer.

EVALUATION OF THE EFFECTIVE ENERGY TO WHICH A FILM WAS EXPOSED

The nett photographic density $D(t)$, as function of the thickness t of copper filters, and the exposure X is shown (Fig. 1) for three different energies. Two facts merit attention.

1. For a given exposure, log D is a linear function of t. At first sight this is not to be expected when the intensity is measured by means of photographic films. There is no proportionality between the nett photographic density and the exposure.

2. All the effective energies, determined by the half value photographic density layer (HVDL), are fairly independent of the exposure, but are systematically about 11% higher than determined by HVL measured with an ionization chamber.

There is evidently a difference in the two kinds of measurements. The ionization chamber measures only the radiation leaving the filter, whereas the film detects also the radiation backscattered from the back filter.[15] The absorption coefficient therefore appears to be smaller and the effective energy correspondingly greater than in the former case.

The results of the measurements can be presented in two other useful forms:

1. As a family of curves, representing log $D(O)/D(t)$ as function of the thickness t of copper filters for a given effective energy E_{eff} (Fig. 2).

These curves established once for all, enable one to evaluate the unknown energy to which a film was exposed.

2. As curves, representing $D(O)/D(t)$ for a given thickness of copper filters as functions of the effective energy (Fig. 3.)

In fact two such curves, namely for $D(O)/D(0.1$ mm Cu) and $D(O)/D(0.97$ mm Cu) cover the entire range of energies taken into consideration. Knowing the convenient ratio $D(O)/D(t)$ and t, the curves, established once for all, make it possible to find the effective energy to which the film was exposed.

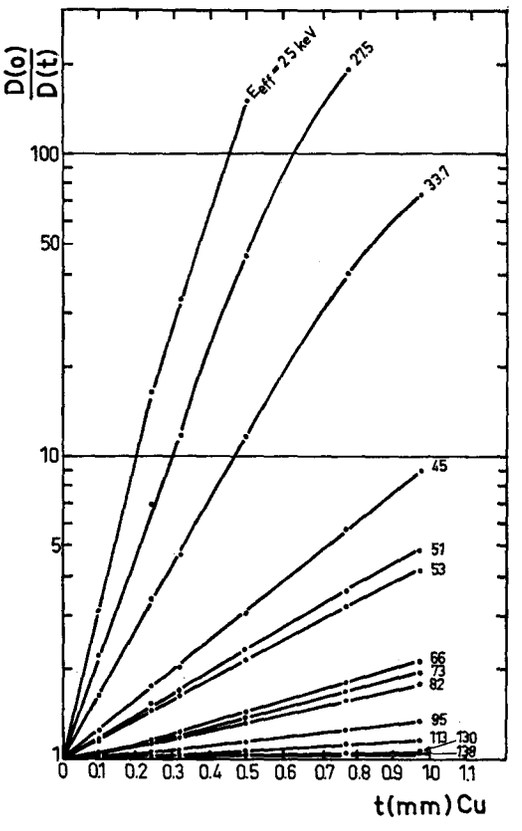

FIG. 2. Ratio of the densities of the unfiltered and filtered portions of the film, $D(O)/D(t)$, as functions of the thickness t of copper filters for various effective X-ray energies. $D(O)$ and $D(t)$ are mean values of densities corresponding to exposures between 0·6 and 1·5 R.

DENSITY–EXPOSURE CURVES FOR X-RAYS OF VARIOUS EFFECTIVE ENERGIES

The experimental data, partially represented in Fig. 1, include the corresponding set of values $D(O)$, X and E_{eff}. This makes it possible to find the relation between $D(O)$ and X for a given E_{eff}.

Ehrlich,[16] Brodsky[17] and Kathreen and Brodsky[18] have shown, for different types of duPont and Kodak Films, exposed to betatron

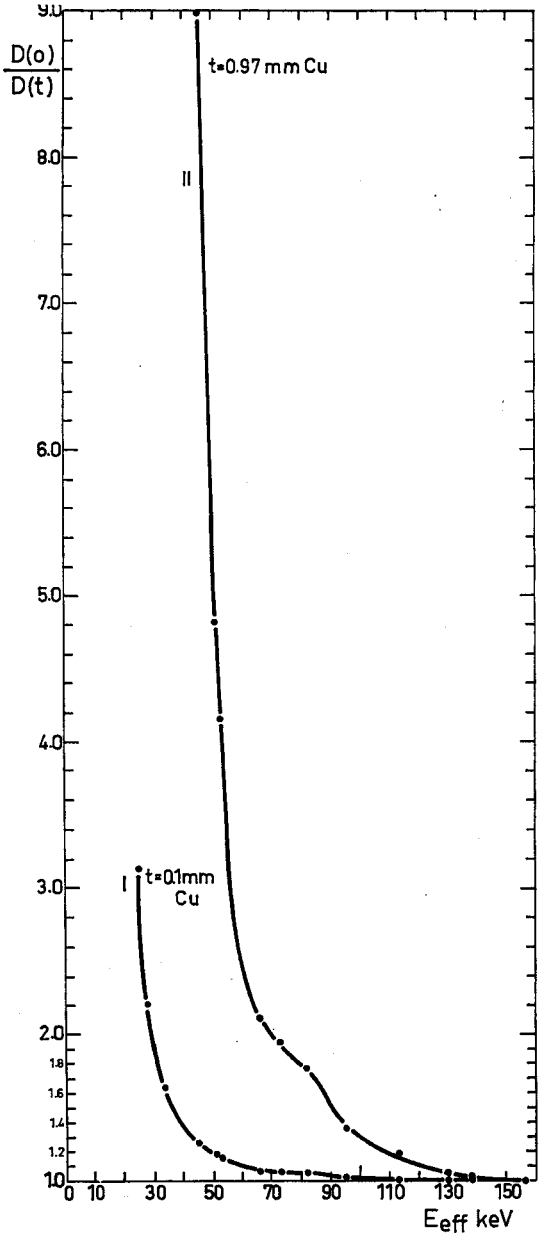

FIG. 3. Curve I: Ratio of densities of unfiltered portions and portions filtered by 0·1 mm Cu $D(O)/D(0{\cdot}1$ mm Cu) as a function of effective X-ray energies between 25 and 55 keV.

Curve II: Ratio $D(O)/D(0{\cdot}97$ mm Cu) as a function of effective X-ray energies between 51 and 156 keV. $D(O)$, $D(0{\cdot}1$ mm Cu) and $D(0{\cdot}97$ mm Cu) are mean values of densities corresponding to exposures between 0·6 and 1·5 R

X-rays, ^{60}Co- or ^{226}Ra-gamma rays, that density–exposure curves can be fitted to a straight line on a log–log plot.

Our results for $D(O)$ and X in this representation fitted to a least square line are given in Figs. 4 and 5. Most of the $\log D(O) = f(\log X)$ relations can be represented by a straight line (Fig. 4), whose corresponding equations are given on the figure.

For some energies a reasonable fit is obtained only if the experimental results are represented by two straight lines, one from 50 mR to about 200 mR, the other from about 200 mR to 1500 mR (Fig. 5).

From Figs. 4 and 5 it is seen that, irrespective of exposure, the maximum sensitivity of the film is about $E_{\text{eff}} = 45$ keV.

DENSITY EXPOSURE CURVES OBTAINED BY MEANS OF RADIOACTIVE SOURCES IN THE SHIELDED, TRANSPORTABLE CALIBRATION FACILITY

1. The calibration facility constructed for ^{226}Ra (4.52 mg, 0.5 mm Pt) and ^{137}Cs (15 mCi, 0.5 mm Pt) (Fig. 6), a modification of a previous device,[9, 10] consists essentially of two units:

(a) A lead block LB, containing a radioactive source RS in a source holder SH, as well as a cylindrical lead shutter and collimator SC, which can slide in the hole H of the lead block LB. By axial translation of SC, the source can be shielded or permitted to radiate through the collimator and the window W.

(b) A film holder FH, with its base BH, made of aluminium alloy, makes it easy to place the films in exactly known positions relatively to the source.

The assembled facility is shown in Fig. 7. Taken to pieces it can be packed into a small volume; it weighs 12.7 kg.

2. For the ^{90}Sr–^{90}Y/Al bremsstrahlung source (620 mCi) a much simpler lead source holder SH was used, as shown in Fig. 8.

The assembled facility is shown in Fig. 9; it weighs 10.2 kg.

If for a set of measurements on personnel monitoring films, the density–exposure curves (Figs. 4 and 5) have to be corrected by comparison with a corresponding curve, obtained by means of a radioactive source, it is necessary that the nett photographic densities of these

curves be in the interval $O \angle D(O) \angle 5.4$ approximately.

Because of the relatively high energies of the radiation spectra of the radioactive sources we have used, and the diminished sensitivity of the PM3 films for these radiations, it is necessary to give the films much greater exposures than when irradiated with X-rays in the energy interval we investigated.

We found that the log $D(O) = f(\log X)$ curves fall in the interesting region if we plot log $D(O)$ vs. log $(X/6)$ for the bremsstrahlung source and vs. log $(X/10)$ for the ^{226}Ra or ^{137}Cs sources. The results fitted to a least square line give linear relations; the corresponding equations are indicated in Fig. 10.

END POINTS FACTORS

Table 1 gives numerical factors by means of which the log $D(O) = f(\log X)$ curves, in the interval 25 keV $\leq E_{eff} \leq$ 156 keV of X-rays can be obtained. If the above relation is a single straight line for a given energy, only two factors F_1 and F_1' are given. If two straight lines are necessary, four factors are indicated. In comparison with the corresponding curves of Fig. 5 it is easy to see which part of each line should be used.

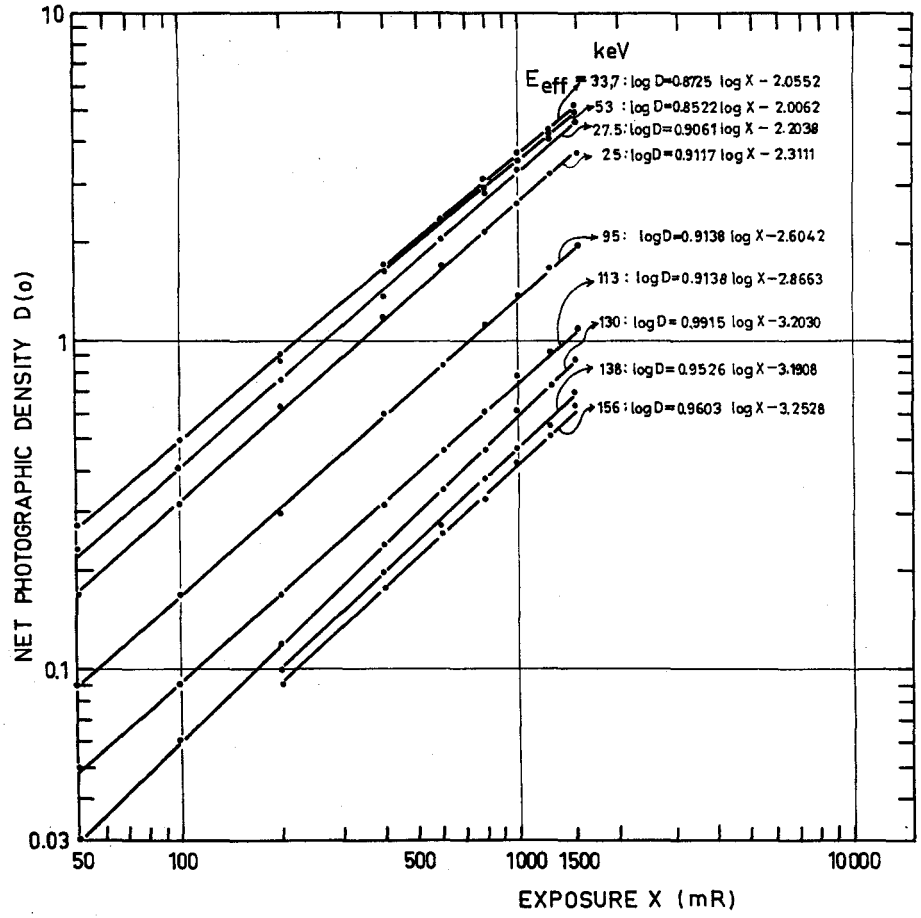

FIG. 4. Density–exposure calibration curves for X-rays of E_{eff}: 33.7; 53; 27.5; 25; 95; 113; 130; 138 and 156 keV. Ilford PM3 films were exposed in the range from 50 to 1500 mR. The densities are those of the unfiltered portions.

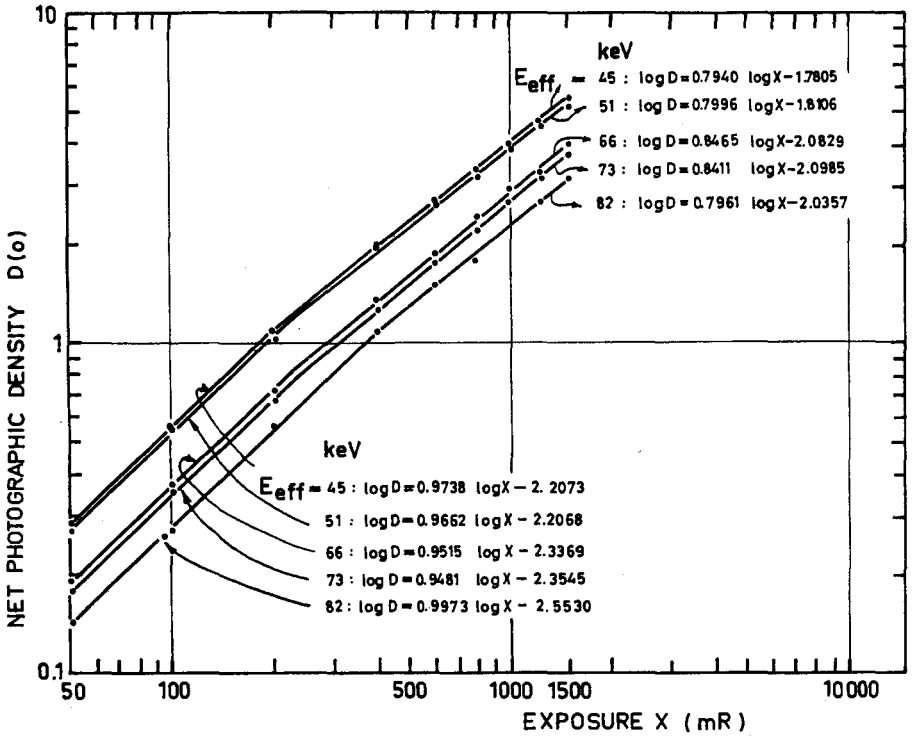

FIG. 5. Density–exposure calibration curves for X-rays of E_{eff}: 45; 51; 66; 73 and 82 keV. Ilford PM3 films were exposed in the range from 50 to 1500 mR. The densities are those of the unfiltered portions.

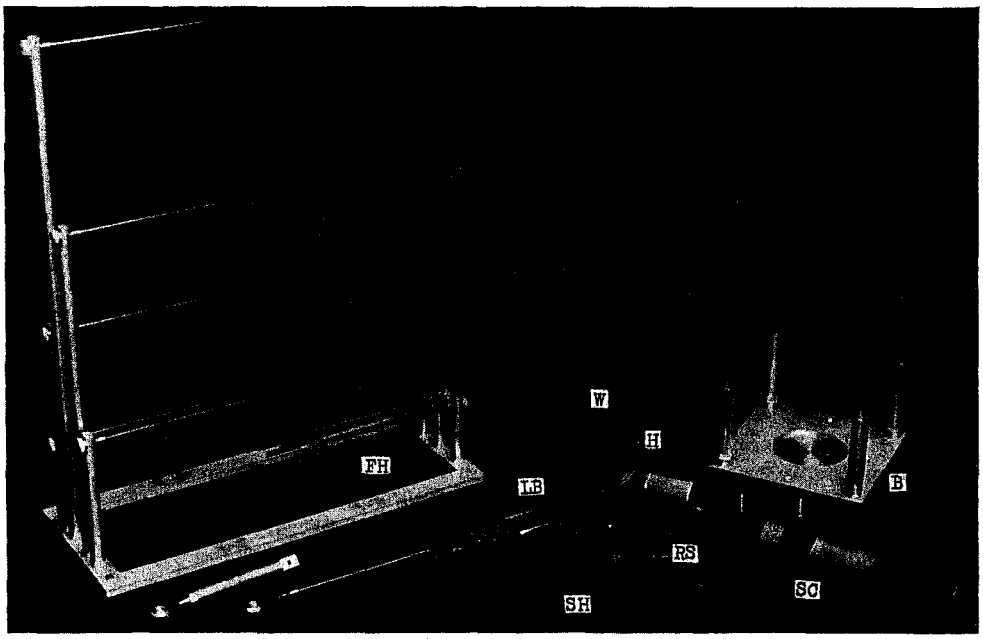

FIG. 6. The shielded, transportable calibration facility constructed for ^{226}Ra (4.52 mg, 0.5 mm Pt) and ^{137}Cs (15 mCi, 0.5 mm Pt). Shutter and collimator, SC. Source holder, SH. Hole, H. Lead Block, LB. Window, W. Radioactive source, RS. Film holder, FH. Base, B.

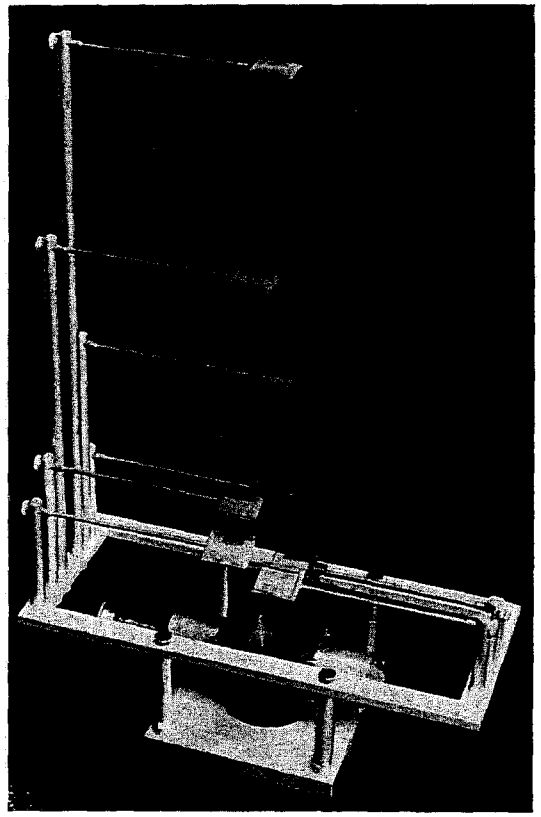

FIG. 7. The assembled facility for ^{226}Ra and ^{137}Cs.

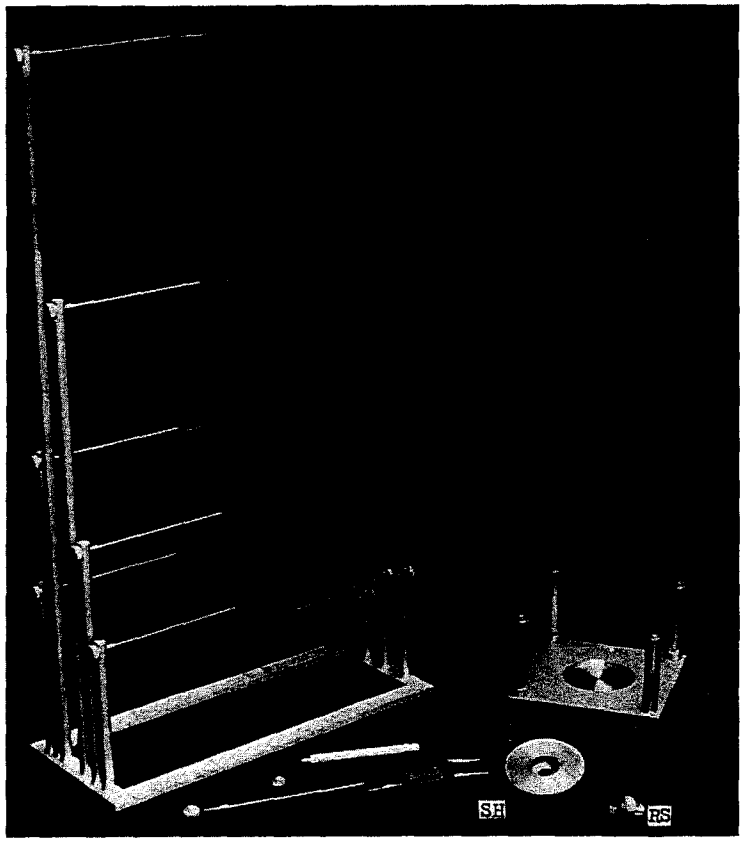

FIG. 8. The shielded, transportable calibration facility for the ^{90}Sr–^{90}Y/Al bremsstrahlung source (620 mCi).

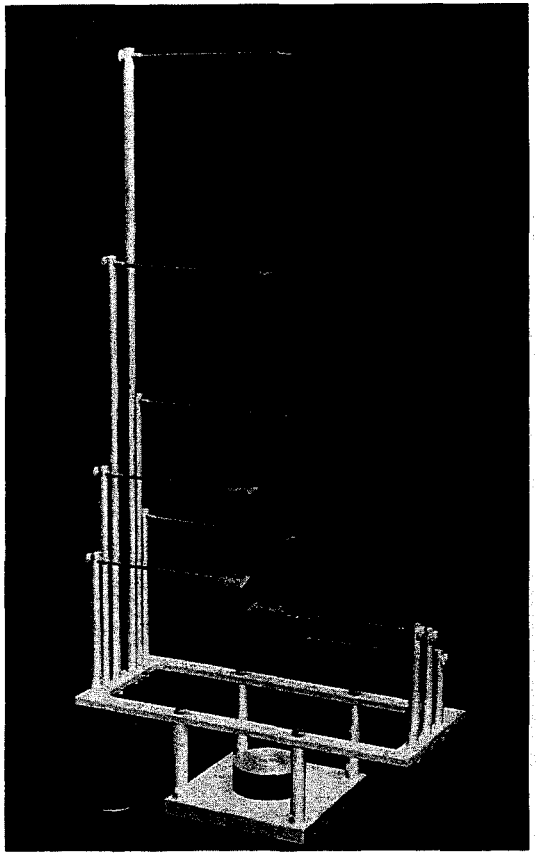

FIG. 9. The assembled facility for the bremsstrahlung source.

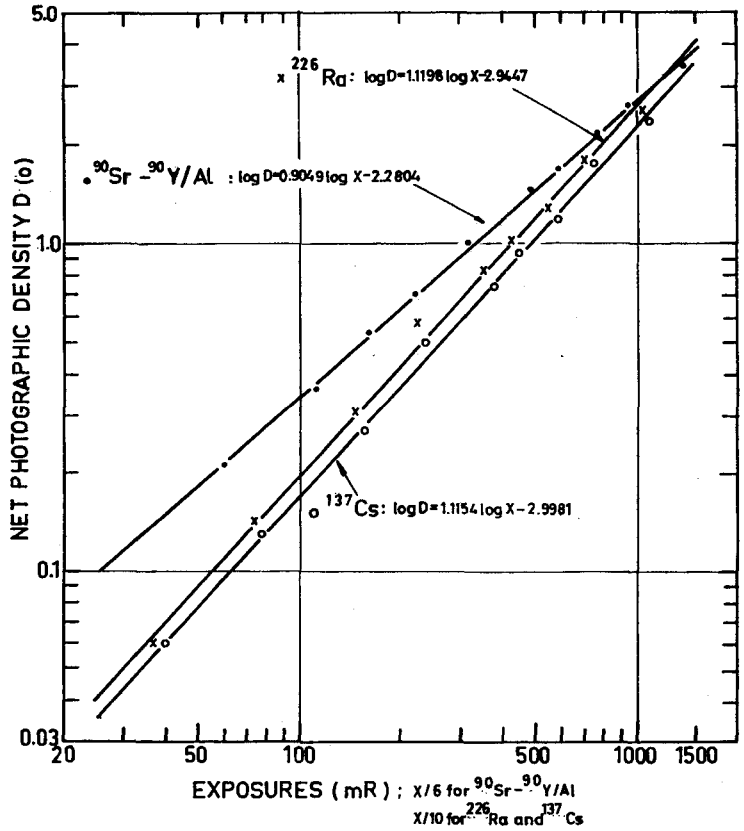

FIG. 10. Density–exposure curves obtained by means of radioactive sources in the shielded, transportable calibration facility.
Three sources were used: 620 mCi ^{90}Sr–^{90}Y/Al bremsstrahlung source, 4.52 mg ^{226}Ra, screened by 0.5 mm Pt, 15 mCi ^{137}Cs, screened by 0.5 mm Pt. The exposures X (mR) indicated correspond to X/6 for the bremsstrahlung source and to X/10 for the ^{226}Ra or ^{137}Cs sources. The densities are those of the unfiltered portions.

Table 1. *Factors for the Determination of End Points of log D = f (log X) Relations.*

E_{eff} keV	F_1	F_1'	F_2	F_2'	F_3	F_3'
25	0.96	0.98	1.91	0.94	2.19	1.10
27.5	1.20	1.20	2.39	1.15	2.75	1.35
33.7	1.48	1.33	2.94	1.27	3.39	1.48
45	1.55	1.96	3.08	1.88	3.55	2.19
	2.05	1.40	4.08	1.35	4.69	1.57
51	1.51	1.85	3.00	1.78	3.45	2.08
	1.96	1.37	3.88	1.31	4.48	1.53
53	1.53	1.28	3.05	1.23	3.50	1.43
66	1.05	1.23	2.10	1.18	2.41	1.38
	1.25	1.03	2.50	0.99	2.87	1.15
73	1.00	1.16	1.99	1.11	2.29	1.29
	1.18	0.95	2.36	0.91	2.71	1.07
82	0.77	1.05	1.53	1.01	1.76	1.17
	1.15	0.79	2.28	0.76	2.63	0.89
95	0.49	0.51	0.98	0.49	1.13	0.57
113	0.27	0.28	0.54	0.27	0.62	0.31
130	0.17	0.23	0.33	0.22	0.38	0.25
138	0.16	0.17	0.32	0.17	0.37	0.19
156	0.13	0.16	0.26	0.15	0.30	0.18

$$F_1 = \left(\frac{D_{x\text{-rays}}}{D_{Sr\text{-}90,Y\text{-}90\,/Al}} \right)_{50\ mR}$$

$$F_1' = \left(\frac{D_{x\text{-rays}}}{D_{Sr\text{-}90,Y\text{-}90\,/Al}} \right)_{1500\ mR}$$

$$F_2 = \left(\frac{D_{x\text{-rays}}}{D_{Ra\text{-}226}} \right)_{50\ mR}$$

$$F_2' = \left(\frac{D_{x\text{-rays}}}{D_{Ra\text{-}226}} \right)_{1500\ mR}$$

$$F_3 = \left(\frac{D_{x\text{-rays}}}{D_{Cs\text{-}137}} \right)_{50\ mR}$$

$$F_3' = \left(\frac{D_{x\text{-rays}}}{D_{Cs\text{-}137}} \right)_{1500\ mR}$$

CONCLUSIONS

1. Using the Ilford PM3 film in a badge provided with six copper filters (0.1 to 0.97 mm thick), it is possible to find the effective energy of X-rays in the interval of 25 to 156 keV.

2. The determination of only one log $D(O) = f(\log X)$ line, by means of the described shielded, transportable calibration facility and a ^{226}Ra, ^{137}Cs or ^{90}Sr–^{90}Y/Al source, enables one to trace other calibration lines, using the given factors for the calculation of the end-points of these lines. Thus the determination of unknown exposures of X-rays, in the above mentioned energy range, is possible.

ACKNOWLEDGEMENTS

The author gratefully acknowledges the advice and helpful comments of Prof. M. Paić. Thanks are also due to V. Petrović for his valuable technical assistance.

REFERENCES

1. M. Ehrlich. Photographic dosimetry of X- and gamma rays. *National Bureau of Standards Handbook* 57 (1954).
2. M. Ehrlich. *The use of film badges for personnel monitoring.* IAEA, Vienna (1962).
3. M. Dorneich and H. Schäfer. *Physik. Zeitschr.* **43,** 390 (1942).
4. H. Langendorff, G. Spiegler and F. Wachsmann. *Fortschr. Röntgenstr.* **77,** 143 (1952).

5. H. DRESEL. *Fortschr. Röntgenstr.* **84,** 214 (1956).
6. E. FUHRMANN and G. SOUDAIN. Dosimétrie photographique des rayons X, CEA/SCRGR/INT/Métrol. (1958).
7. A. M. CHAPUIS and A. JACQUOT. Dosimétre photographique des rayons X de faible énergie, Rapport CEA/SCRGR/INT/BER/Physique (1959).
8. G. SPIEGLER and R. DAVIS. *Brit. J. Radiol.* **32,** 464 (1949).
9. V. PAIĆ. *C.R. Acad. Sci.* **249,** 1951 (1959).
10. V. PAIĆ. *Phys. Med. Biol.* **5,** 119 (1960).
11. S. K. STEPHENSON. *Proc. Symposium on Film Badge Dosimetry*, Harwell, p. 25 (1961).
12. B. E. JONES and T. O. MARSHALL. *J. Photogr. Science* **12,** 319 (1964).
13. V. PAIĆ. *Health Physics* **4,** 180 (1960).
14. H. E. JOHNS. *The Physics of Radiology*, p. 249. Thomas, Springfield, Ill.
15. V. PAIĆ, M. PAIĆ and A. RUBČIĆ. *Phys. Med. Biol.* **11,** 24 (1966).
16. M. EHRLICH. *Health Physics* **4,** 113 (1960).
17. A BRODSKY. *Health Physics* **9,** 463 (1963).
18. R. L. KATHREEN and A. BRODSKY. *Health Physics* **9,** 769 (1963).

DOSIMÉTRIE PHOTOGRAPHIQUE : CALIBRAGE BÊTA-GAMMA

M. P. OLIVARES et S. PÉREZ MODREGO
Division de Radiophysique, Hôpital de San Juan de Dios, Madrid

Abstract—Photographic radiation dosimetry may be defined as the measurement of the dose of a particular electromagnetic or corpuscular radiation by means of establishing a one-to-one correspondence between dose and photographic effect. It is therefore of importance to delineate the terms dose and photographic effect clearly and to understand the difficulties inherent in the measurement of these quantities. The International Commission on Radiation Units recommended that dose be expressed in terms of the quantity of energy absorbed per unit mass of irradiated material at the place of interest. Measurements of the photographic effect are made in terms of diffuse transmission density, representing the logarithm to base 10 of the opacity of a processed photographic film sample. The difficulty in relating dose to photographic density lies in the fact that while the roentgen is a measure of radiation absorbed in air, the photographic action of X- or γ-radiation is essentially the result of ionization in the silver-halide crystals of the photographic emulsion and in the materials surrounding it.

In this paper the fundamentals of photographic dosimetry are set forth, making next a study of the characteristic curve in different types of films exposed to the radiations emitted by radium and cobalt sources of different exposure intensity. Then a study is made on the variation of the characteristic curve with the conditions of processing, the film emulsion, the irradiation rhythm, the energy spectrum of the radioactive source employed, and the different types of films, indicating the most convenient conditions to carry out a good calibration. Similarly, the possibilities of the films studied in individual radiological controls are discussed.

1. INTRODUCTION

Une des premières méthodes connues pour détecter les radiations consiste en une pellicule photographique qui s'impressionne en recevant un faisceau de radiation électromagnétique. Ce procédé a été l'objet d'un grand intérêt ces dernières années étant donné les avantages qu'il offre sous certains aspects si nous le comparons avec les autres méthodes utilisées.

La pellicule photographique est relativement économique et résistante. Par l'effet des radiations, les cristaux d'halogénure d'argent subissent des modifications, permanentes jusqu'à un certain point; avec un calibrage approprié, la densité optique d'une pellicule développée et fixée, peut servir d'indice d'exposition aux radiations. La densité optique ne change pas même si la lecture est faite plusieurs fois ou si le temps de magasinage est prolongé, à condition que celui-ci soit réalisé dans des conditions convenables, les dosimètres photographiques sont le moyen préféré de surveillance dans la plupart des laboratoires bien que la méthode exige une certaine quantité d'appareils pour le calibrage, le traitement et la densitométrie des films.

2. CALIBRAGE BÊTA-GAMMA

Pour utiliser la pellicule photographique comme dosimètre, on a besoin d'établir une relation quantitative entre l'effet photographique et l'irradiation. Pour cela il faut calibrer le film.

La pellicule photographique n'a pas les conditions idéales pour mesurer quantitativement une dose d'irradiation, en surveillance radiologique individuelle. Entre les pellicules et les tissus vivants existe une différence considérable en ce qui concerne la composition chimique. C'est pour cela que la réponse de la pellicule

photographique à l'irradiation est différente de celle des tissus. On peut obtenir une réponse comparable quand l'énergie des radiations est telle que l'épaisseur de la pellicule reste petit en comparaison avec le parcours de la radiation corpusculaire primaire ou secondaire créée par l'effet photographique, car dans ce cas les conditions tissulaires peuvent être simulée en entourant la pellicule d'un matériel équivalent au tissus pour obtenir l'équilibre électronique. De cette manière nous pouvons établir une relation entre la distribution des densités optiques dans une pellicule photographique noircie par l'action d'une irradiation et la distribution de dose aux points antérieurement occupés par le film dans le milieu irradié. Pour étudier cette distribution du point de vue quantitatif nous avons à construire préalablement les courbes de calibrage correspondant à ce type de pellicule et de radiation, en irradiant une série de films avec des expositions connues.

3. CONDITIONS DE DISPERSION DANS LA SALLE DE CALIBRAGE

Afin que les mesures de dose obtenues avec un film soient exactes, il faut que les expositions des pellicules soient parfaitement déterminées. Nous pouvons connaître à chaque instant l'exposition en un point en la mesurant avec une chambre d'ionisation, mais les expositions reçues par une pellicule placée au même point peuvent être différentes de l'exposition mesurée si dans la salle où se réalise l'irradiation existe une réflexion des particules sur les murs car il peut arriver qu'une des particules en changeant sa direction ou son sens tombe sur la pellicule introduisant ainsi un motif d'erreur. Pour cette raison, si nous désirons réaliser un calibrage, il est indispensable que nous verifions préalablement si la piece chosie à cet effect remplit les conditions nécessaires; pour cela il nous suffit de vérifier dans la pièce la loi de variation avec l'inverse du carré de la distance. Si le résultat est affirmatif, il n'y a pas de dispersion et le calibrage peut être réalisé.

Nous avons mesuré des expositions à differentes distances connues avec un condiomètre L-124 de capacité 10 R, nous avons réalisé les lectures dans un appareil de mesure L-64 et nous avons obtenu les résultats donnés dans le tableau 1

Tableau 1. *Dispersion dans la Salle de Calibrage*

Distance (d cm)	Exposition (X R/h)	X_1/X_1	d_1^2/d_1
40 ± 0,1	11,000 ± 0,500	4,007 ± 0,001	4
80 ± 0,1	2,750 ± 0,050	9,01 ± 0,01	9
120 ± 0,1	1,210 ± 0,020	16,01 ± 0,01	16
200 ± 0,1	0,680 ± 0,006		

Les valeurs obtenues vérifient la loi de variation avec l'inverse du carré de la distance et par conséquent il n'y a pas de dispersion dans la salle de calibrage.

4. COURBES CARACTÉRISTIQUES POUR DIFFÉRENTS TYPES DE FILM

Nous avons construit les courbes caractéristiques des types de films suivants: DuPont 556-44; DuPont 556-39; Kodak, Ilford, Mafe en utilisant:

1. Une source de Co-60 d'intensité d'exposition 12 R/h à une distance de 40 cm.

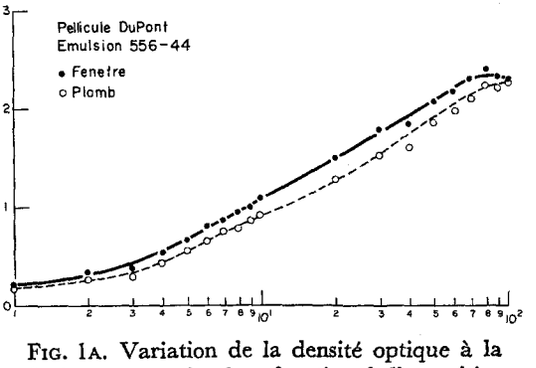

FIG. 1A. Variation de la densité optique à la fenêtre et sous plomb en fonction de l'exposition pour un film DuPont 556–39.

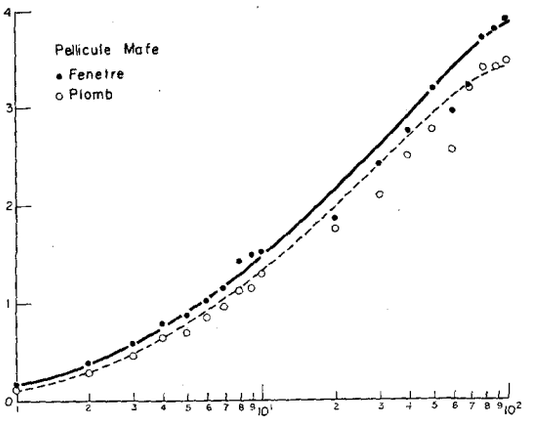

FIG. 1B. Variation de la densité optique à la fenêtre et sous plomb en fonction de l'exposition pour un film Mafe.

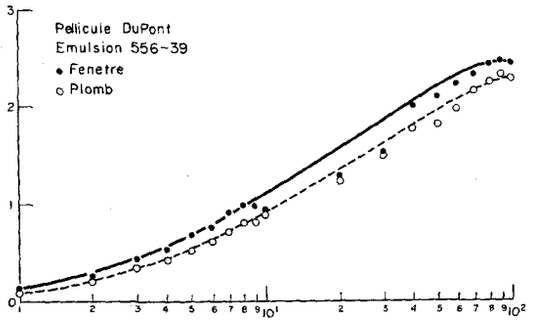

FIG. 1C. Variation de la densité optique à la fenêtre et sous plomb en fonction de l'exposition pour un film DuPont 556–44.

2. Une source de Ra-226 d'intensité d'exposition 50,42 mR/h à une distance de 40 cm.

Les films ont été préalablement marqués pour permettre de les indentifier après. Les pellicules ont été irradiées enfermées dans un cadre de métal, avec un filtre de plomb de 1 mm d'epaisseur et doté d'une fenêtre qui permet aux particules bêta d'atteindre le film.

Toutes les pellicules ont été développées simultanément dans des dispositifs dessinés spécialement à cette fin (Fig. 2) évitant de cette manière des erreurs dues à des variations de temps de développement, de fixation ou de la température des solutions. Le révélateur employé répond à la formule suivante:

Eau tiède: 750 cm^3.
Metol: 5 gr.
Sulfite de sodium anhydre: 60 gr.
Hidroquinone: 7,5 gr.
Carbonate de sodium anhydre: 50 gr.
Bromure de potassium: 4,5 gr.

Les conditions de développement ont été les suivantes:

Température: 20° C.
Temps de développement: 3 mm.
Temps de fixation: 10 m.

Conclusions

En observant le graphique 1 nous avons les conclusions suivantes:

1. La forme de la courbe caractéristique ne change pas de l'un à l'autre type de film, conservant son caractère exponentiel.

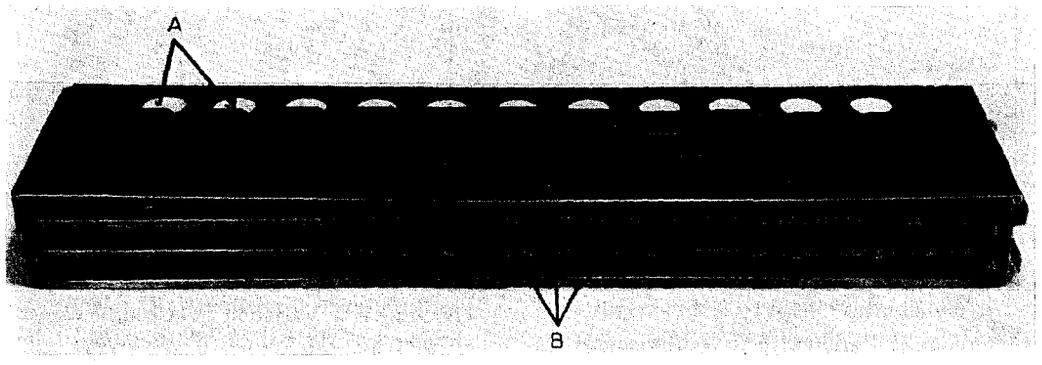

FIG. 2. Dispositif dessiné pour le développement des films.

2. Tous ces types de films peuvent s'employer en contrôle radiologique individuel étant donné qu'avec ces types peuvent se mesurer des expositions allant jusqu'à 5 R (quelques types de films sont capables de mesurer des expositions plus grandes) et que c'est la dose la plus grande qui peut être permise pour être absorbée par un homme dans une année.

3. Les pellicules de sensibilité plus petite sont les DuPont suivies des pellicules Kodak, Ilford, Mafe.

4. La pellicule Mafe est celle qui réunit les meilleures conditions pour le contrôle radiologique individuel étant donné que sa sensibilité est très grande, changeant considérablement de densité optique par petits intervalles d'exposition.

5. La pellicule lente (sensibilité plus petite) DuPont commence à se noircir à partir d'une exposition de 5000 mR, pour cette raison, ce type de film couvre un ample intervalle d'expositions.

5. VARIATION DE LA COURBE CARACTÉRISTIQUE AVEC LE SPECTRE DU FAISCEAU D'IRRADIATION

En comparant les graphiques 1 et 2 correspondant à des courbes caractéristiques obtenues avec des sources différentes d'irradiation nous arrivons aux conclusions suivantes:

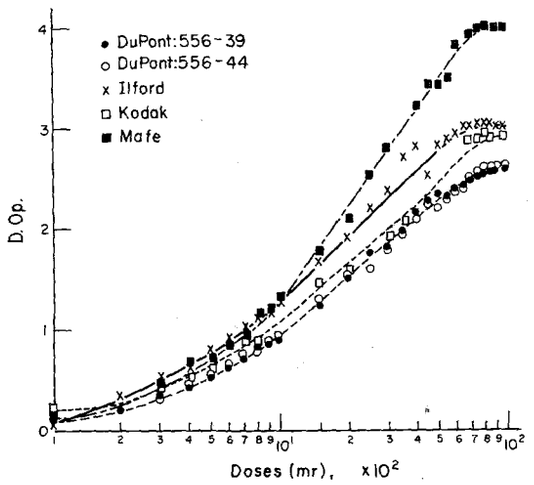

GRAPHIQUE 1. Variation de la courbe caractéristique pour plusieurs films. Nous avons utilisé une source de Cobalt.

1. Le graphique 2 nous permet de ratifier les conclusions 1, 2 et 3 du paragraphe 4.

2. L'effet photographique ne dépend pas du spectre énergétique du faisceau, mais de l'energie cédée (à condition que les énergies soient supérieures à 0,5 MeV).

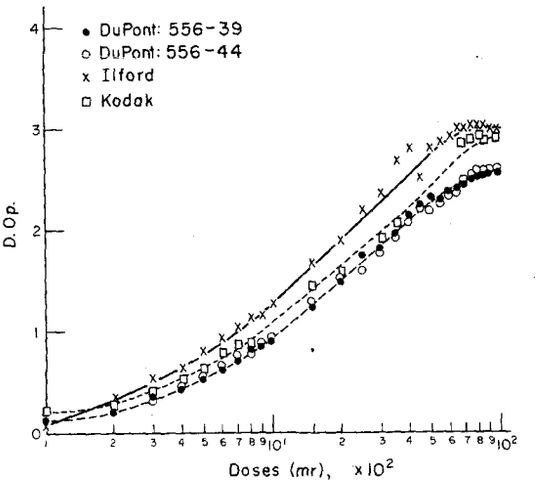

GRAPHIQUE 2. Variation de la courbe caractéristique pour plusieurs films. Nous avons utilisé une source de Radium.

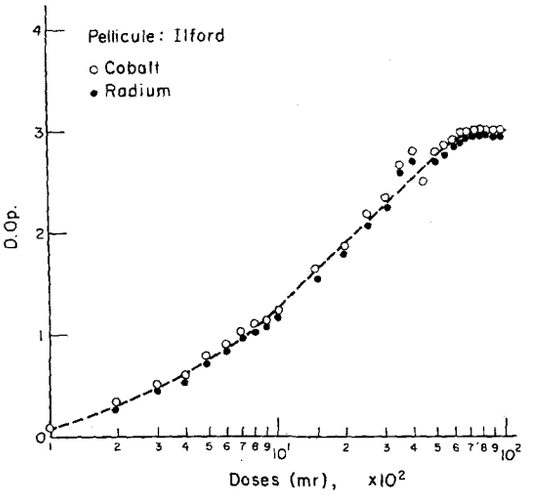

GRAPHIQUE 3. Variation de la courbe caractéristique avec le rythme d'irradiation. Nous avons utilisé des sources de Cobalt (12 R/h) et de Radium (50,42 R/h). Film: Ilford.

6. VARIATION DE LA COURBE CARACTÉRISTIQUE AVEC LE RYTHME D'IRRADIATION

Par comparaison des graphiques 3–7 nous obtenons les conclusions suivantes:

1. l'effet photographique est indépendant de l'intensité d'exposition, dépendant seulement de l'exposition totale reçue.

2. Un de ces films employé comme dosimètre, nous donnera une réponse selon la dose totale absorbée et indépendante du rythme d'irradiation.

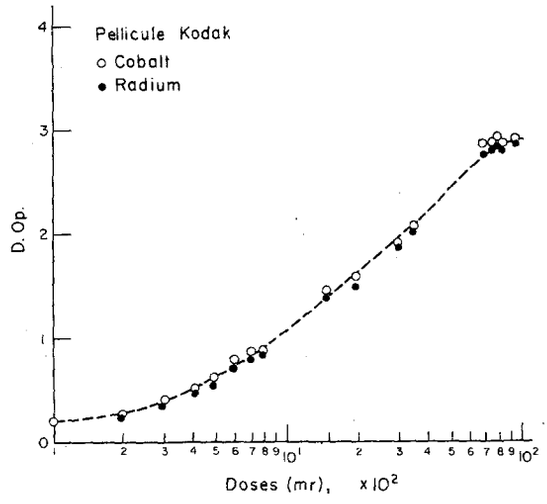

GRAPHIQUE 4. Variation de la courbe caractéristique avec le rythme d'irradiation. Nous avons utilisé des sources de Cobalt (12 R/h) et de Radium (50,42 R/h). Film: Kodak.

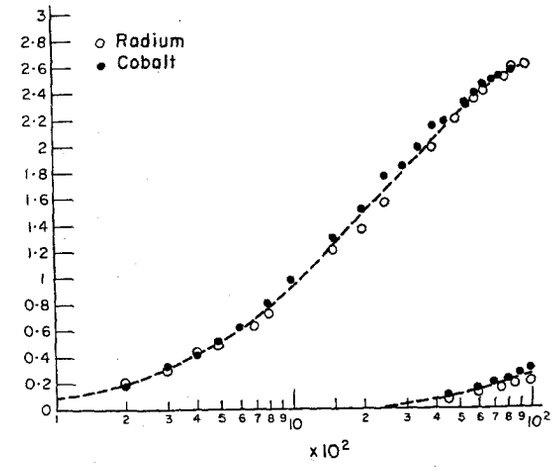

GRAPHIQUE 5. Variation de la courbe caractéristique avec le rythme d'irradiation. Nous avons utilisé des sources de Cobalt (12 R/h) et de Radium (50,42 R/h). Film: DuPont 556–44.

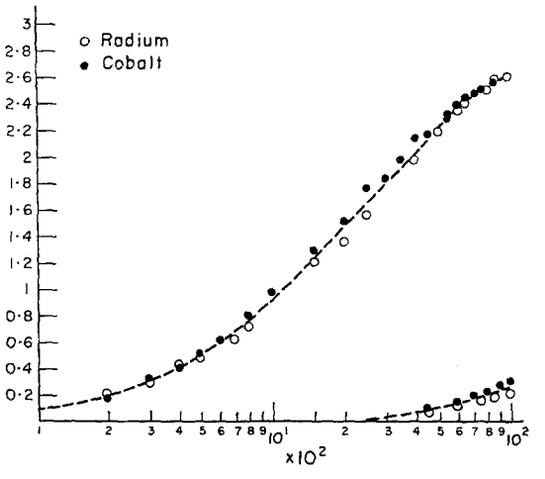

GRAPHIQUE 6. Variation de la courbe caractéristique avec le rythme d'irradiation à la fenêtre. Nous avons utilisé des sources de Cobalt (12 R/h) et de Radium (50,42 R/h). Film: DuPont 556–39.

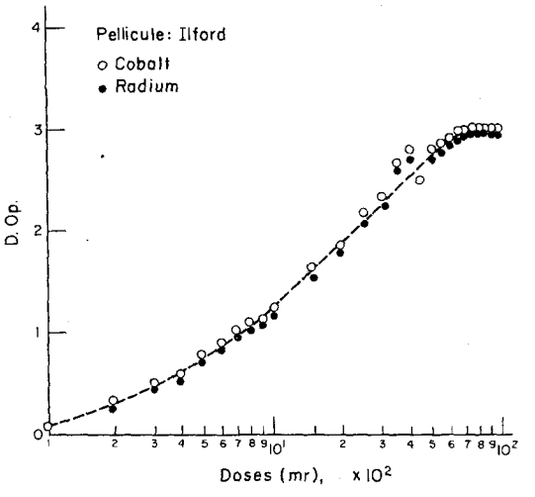

GRAPHIQUE 7. Variation de la courbe caractéristique avec le rythme d'irradiation à la fenêtre. Nous avons utilisé des sources de Cobalt (12 R/h) et de Radium (50,42 R/h). Film: Ilford.

7. VARIATION DE LA COURBE CARACTÉRISTIQUE AVEC LE TEMPS DE DÉVELOPPEMENT

Nous avons irradié des films de type DuPont, avec les caractéristiques indiquées dans le 4ième paragraphe. Les temps de développement ont été de 4 et 5 minutes respectivement et les résultats obtenus, sont représentés dans le graphique 8.

Conclusions

1. La densité optique augmente avec le temps de développement.
2. La courbe caractéristique conserve la même forme.

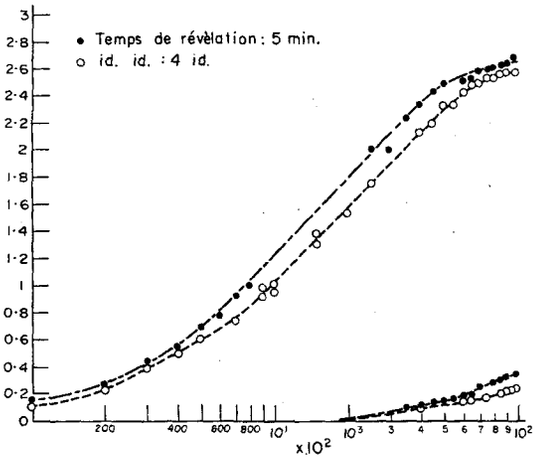

GRAPHIQUE 8. Variation de la courbe caractéristique avec le temps de développement. Film: DuPont 556–44.

8. VARIATION DE LA COURBE CARACTÉRISTIQUE AVEC L'ÉMULSION

Nous avons irradié des films de deux émulsions différentes correspondantes au type DuPont avec des sources de radium et cobalt.

Les résultats sont exposés dans les graphiques 9 et 10. Bien que dans ce cas la réponse du film à l'irradiation ne change pas avec l'émulsion, nous ne devons pas en faire une règle générale étant donné que fréquement la variation de la courbe caractéristique avec le type d'émulsion employé est considérable.

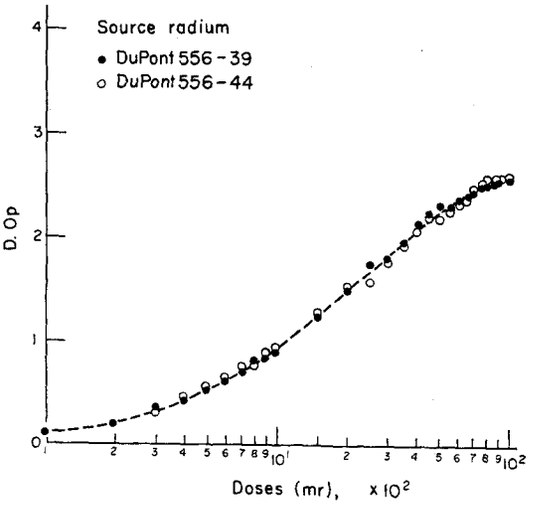

GRAPHIQUE 9. Variation de la courbe caractéristique avec l'émulsion. Source: Radium.

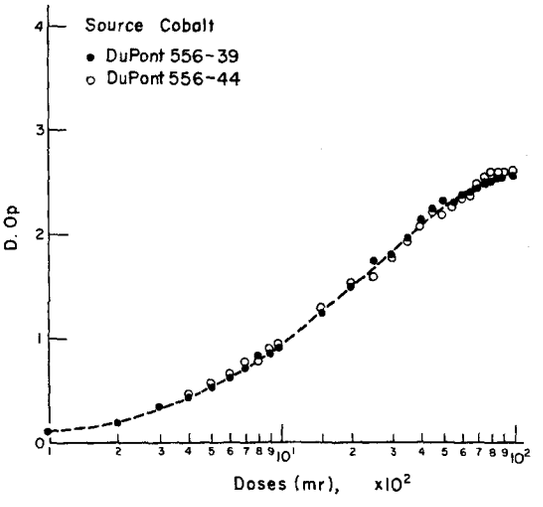

GRAPHIQUE 10. Variation de la courbe caractéristique avec l'émulsion: Source: Cobalt.

9. VARIATION DE LA COURBE CARACTÉRISTIQUE AVEC LE TEMPS DE MAGASINAGE

Tous les films utilisés dans les calibrages antérieurs sont resté emmagasinés pendant trois ans sans aucune précaution, concernant la température, l'humidité etc., et soumis à toutes

les variations atmosphériques. A la fin de ce temps nous avons réalisé une nouvelle densitométrie (graphiques 11–14) donant la conclusion suivante:

1. La courbe caractéristique ne change pas avec le temps de magasinage.
2. Un film convenablement développé devient un document d'exposition aux radiations avec une excellente qualité d'archives.

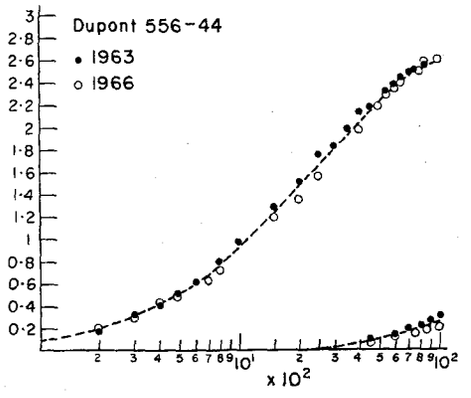

GRAPHIQUE 11. Variation de la courbe caractéristique avec le temps de magasinage. Film: DuPont 556–44.

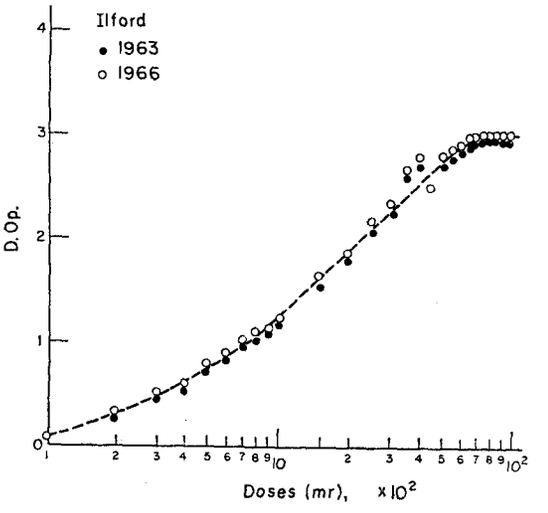

GRAPHIQUE 13. Variation de la courbe caractéristique avec le temps de magasinage. Film: Ilford.

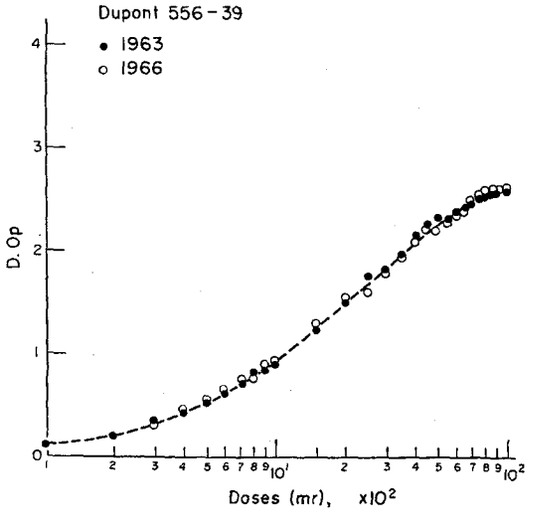

GRAPHIQUE 12. Variation de la courbe caractéristique avec le temps de magasinage. Film: DuPont 556–39.

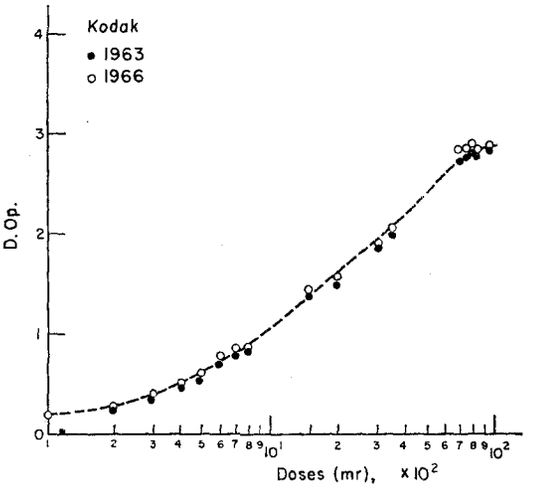

GRAPHIQUE 14. Variation de la courbe caractéristique avec le temps de magasinage. Film: Kodak.

RÉFÉRENCES

AMADESI, P. *et al. Minerva Nucleare*, **3**, 14, 59.

EHRLICH, M. Photographic dosimetry of X- and gamma rays. *National Bureau of Standards Handbook* 57 (1954).

DUDLEY, R. A. *Photographic film Dosimetry in Radiation Dosimetry*. AEREM, 1178, 1963.

GREENINGS, J. R. *Proc. Roy. Soc.*, London, B. 64, 977, 1951.

HEARD and JONES. *A new film holder for personnel monitoring*. IAEA, 1962.

PEREZ MODREGO and PLATA BEDMAR. *Radiaciones Ionizantes*. 1965.

TUBIANA, M. *et al. Bases Physiques de la Radiotherapie et de la Radiobiologie*. 1963.

EXPÉRIENCE DE COMPARAISON DES FILMS DOSIMÉTRIQUES UTILISÉS DANS LES 6 PAYS D'EURATOM (PREMIERS RÉSULTATS)

P. RECHT et M. COLLET

Communauté Européenne de l'Énergie Atomique, Direction de la Protection Sanitaire

Résumé—En 1965, la Commission de l'Euratom—Direction de la Protection Sanitaire—a décidé de procéder, en collaboration avec les Autorités compétentes des Pays membres, à une comparaison des films-dosimètres utilisés dans les divers centres de la Communauté, quant aux informations qu'ils donnent sur les doses reçues.

Cette expérience s'est déroulée de la manière suivante:

(1) l'expérience a porté sur les films dosimétriques X et gamma;

(2) trois gammes d'irradiations ont été choisies entre les limites suivantes: 0–5 R, 4–30 R et 25–400 R;

(3) chaque gamme d'irradiation a été confiée à un seul centre, auquel les établissements de la Communauté ont envoyé leurs films;

(4) les films ont été renvoyés aux centres expéditeurs qui ont procédé aux lectures, sans avoir été précédemment informés des irradiations appliquées;

(5) les résultats des irradiations et des lectures ont été comparés par les soins de la Direction de la Protection Sanitaire;

(6) les expériences d'irradiations ont été répétées à quatre reprises pour chaque gamme au cours d'une année.

Les résultats sont présentés et commentés et permettent d'apprécier le taux de la fidélité des informations fournies pour chaque dose effectivement reçue par les films-dosimètres.

Une vaste expérience d'étalonnage des films individuels a été entreprise au cours des deux dernières années; elle répondait à un désir exprimé conjointement par la Commission de l'Euratom, les responsables des services de dosimétrie individuelle et les Autorités compétentes des Pays membres de la Communauté européenne de l'Energie atomique.

Il s'agissait en fait de procéder aux étalonnages aussi précis que possible des films photographiques dans quelques laboratoires spécialement équipés et travaillant au profit des services dosimétriques de la Communauté intéressés par ce type d'expérience.

Toutefois, pour donner une valeur pratique et réelle aux étalonnages en fonction de l'utilisation des nombreux films utilisés, il a été décidé de faire porter l'expérience:

—sur une assez longue durée,

—sur un nombre important de films,

—sur une gamme d'irradiations aussi étendue que possible.

Pour tenir compte de ces impératifs et parvenir à de bons résultats, la Commission de l'Euratom a mis au point le processus suivant:

Trois centres ont été retenus pour effectuer les irradiations:

—le premier centre, situé dans le cadre du Physikalisch-Technische Bundesanstalt à Braunschweig, a effectué les irradiations de 0 à 8 R,

—le deuxième centre, le Commissariat à l'Energie Atomique français a été chargé d'effectuer les irradiations dans la gamme de 4 à 30 R,

—le troisième centre (Rotterdams Radiotherapeutisch Instituut, Rotterdam et Rijksinstituut voor de Volksgezondheid, Utrecht) effectue les irradiations comprises entre 25 et 400 R.

Au total 1.738 films ont été irradiés, développés, lus et étudiés. Ils ont été adressés par 10 services spécialisés situés sur le territoire des Etats membres.

La plus grande partie de ces films a été soumise à des irradiations gamma, une moins grande partie a été soumise à des rayonnements X. 10% environ des films n'ont pas été irradiés, afin de vérifier si les films, dans leur ensemble, avaient pu subir un noircissement sous l'effet du rayonnement ambiant ou pendant le transport.

Les films étaient tous numérotés et la dose exactement mesurée n'était connue que du seul centre d'irradiation.

L'expérience s'est déroulée en trois phases:

—la première (gamme de 0,1 rem à 8 R) au cours de l'année 1964 et début 1965,

—la deuxième (gamme de 5 à 30 R) au cours de l'année 1965 et début 1966,

—la troisième (gamme de 25 à 400 R) se termine actuellement.

Chacune des phases comportait quatre séries espacées d'environ 3 mois, laissant ainsi une période suffisante pour procéder aux développements, lectures, expéditions et mises au point nécessaires.

CONDITIONS D'IRRADIATIONS

Les sources d'irradiations étaient bien définies et étalonnées au moyen de chambres absolues. La distance source-dosimètre était de plus de 50 cm, les dosimètres étaient éloignés à plus de 1,50 m des parois de la chambre d'irradiation.

L'énergie des rayons X utilisés était supérieure à 20 KeV.

Les sources radioactives n'étaient blindées ni par du plomb, ni par des matériaux lourds.

La durée de l'irradiation était connue ainsi que les conditions de température et d'humidité.

Le contrôle des sources a été effectué par une chambre secondaire directement reliée à une chambre primaire.

La répartition des gammes d'irradiations entre trois centres, telle qu'elle a été étudiée a permis de tester les films sur une très large gamme, le chevauchement des doses gamma délivrées ne laissant apparaître aucune discontinuité.

Dans une première période, s'étendant du printemps 1964 au début de l'année 1965, ont été étudiés 751 films en provenance de 7 services de contrôle dosimétrique. Les doses d'irradiations étaient comprises entre 0 et 8 R. Chacun des services devait faire parvenir au Physikalisch-Technische Bundesanstalt 25 films par trimestre; environ 10% de ces films échappaient à toute irradiation.

La première série d'expérimentations s'est déroulée en mars 1964 et a permis l'étude de 173 films,

la deuxième en janvier 1964 et a porté sur 198 films,

la troisième en septembre 1964 et a porté sur 167 films,

la quatrième en janvier 1965 et a porté sur 213 films.

Les qualités d'irradiations utilisées ont été comprises de 50 à 300 kV pour ce qui concerne les rayons X et de 0,67 à 1,25 MeV pour ce qui concerne les irradiations gamma.

Les films, après irradiation, ont été retournés sur les centres expéditeurs qui en ont assuré, à la fois le développement et la lecture dans les conditions habituelles.

La communication des doses lues a permis aux centres d'irradiations de comparer les doses effectivement délivrées aux films. On a pu ainsi établir, pour chaque centre, les courbes absolues des lectures et déterminer de cette façon les erreurs absolues et relatives par rapport aux irradiations. Les résultats ont été communiqués trimestriellement aux centres et, si possible, avant la mise en oeuvre de l'expérience suivante, ce qui a permis au cours de quatre mises au point successives correspondant aux quatre expériences trimestrielles, d'améliorer les conditions de développement, voire même comme certains centres, de modifier les écrans pour tenir compte de diverses anomalies constatées et tirer au plus vite des conclusions constructives.

En procédant de cette façon, il a été possible de vérifier, à la fois la fidélité des informations et leur reproductibilité.

Dans des conditions analogues, les deux autres périodes d'irradiations ont eu lieu respectivement au Commissariat à l'Energie Atomique à Fontenay-aux-Roses (France), au Rotterdams Radiotherapeutisch Instituut à Rotterdam et au Rijksinstituut voor de Volksgezondheid à Utrecht (Pays-Bas).

Elles ont été également subdivisées chacune

Exemple partiel du tableau récapitulatif

No du film	Qualités de l'irradiation			Dose exacte distribuée	Dose lue	Erreur absolue	Erreur relative
	Rayons X Tension d'accélération	Couche demi-d'absorpt.	Préparation radioactive de la source				
R 01	100	0,83	—	2,81	4,55	1,74	+62%
—							
—							
—							
R 04	—	—	Co 60	0,22	0,26	0,04	+20%
—							
—							
R 14	—	—	—	0	0	—	—

en 4 séries trimestrielles avec la répartition suivante:

Fontenay-aux-Roses: 643 films étudiés dans la gamme de 4 à 30 R
1ère série: 108 films
2ème série: 204 „
3ème série: 190 „
4ème série: 141 „

Rotterdam et Utrecht: 344 films étudiés dans la gamme de 25 à 400 R
1ère série: 87 films
2ème série: 98 „
3ème série: 73 „
4ème série: 86 „

EXPLOITATION DES RÉSULTATS

Après développement et lectures, un relevé général a été effectué indiquant individuellement pour chacun des 751 films, la qualité de l'irradiation subie, la dose délivrée, la dose lue et donnant également après confrontation de ces deux données, l'erreur absolue et l'erreur relative par excès ou par défaut par rapport à la dose d'irradiation délivrée.

Les résultats ont été complètement exploités, pour la première partie de l'expérience générale, c'est-à-dire dans la gamme de 0 à 5 R. Ils sont en cours d'exploitation pour la deuxième partie et le seront très prochainement pour la troisième partie qui se termine actuellement.

En ce qui concerne la première partie, les résultats ont permis de constater une approximation satisfaisante pour le contrôle des rayons X avec des marges d'erreur relative ne dépassant pas 30% par excès ou par défaut.

En ce qui concerne le contrôle du rayonnement gamma, les erreurs relatives ont été un peu plus élevées mais les leçons tirées au cours des premières séries d'irradiations ont permis d'améliorer considérablement la qualité des informations surtout dans les doses inférieures à 1 R. C'est ainsi que pour prendre l'exemple le plus caractéristique, un centre a eu au cours des expérimentations, la répartition suivante:

1ère série < 1 R	*4ème série* < 1 R
> 100% d'erreur par excès 1 film	> 100% d'erreur: 0 film
70 à 100% d'erreur par excès 3 films	70 à 100% d'erreur: 0 film
50 à 70% d'erreur par excès 5 films	50 à 70% d'erreur: 0 film
< 50% d'erreur par excès 5 films	< 50% d'erreur: 12 films

Au delà de 1 R et jusqu'à 4 R, ce centre a également fait baisser ses erreurs relatives de 40 à 20%.

La prise en considération de l'ensemble des résultats du quatrième trimestre de la première partie permet de constater que pour la mesure des rayons X, les erreurs relatives ont été de l'ordre de 10 à 20% jusqu'à 6 R et pour la mesure des rayonnements gamma, les erreurs relatives ont été inférieures à 30% jusqu'à 1 R et inférieures à 20% de 1 à 6 R.

CONCLUSIONS

Une expérience, comme celle qui vient d'être organisée dans les Etats membres de la Communauté européenne de l'Energie atomique sous l'égide d'Euratom, s'est révélée très profitable à plusieurs points de vue.

Elle a permis de faire le point général et à un même moment des principaux types de dosimètres photographiques utilisés dans les Pays de la Communauté.

Elle a libéré les services responsables d'un travail d'étalonnage difficile, fastidieux et long, tout en leur permettant d'effectuer un contrôle général non subjectif.

Elle a favorisé des échanges de vues, des contacts et des mises au point techniques communautaires au cours des réunions de travail qui ont souvent réunis au cours des deux dernières années, les responsables de l'Euratom, des services dosimétriques et des centres d'irradiations participant à l'ensemble des travaux d'étalonnages.

Elle a enfin permis à certains laboratoires de modifier les matériels utilisés pour parvenir à des informations plus fidèles et cela en tenant immédiatement compte des résultats obtenus.

PERSONNEL FILM MONITORING IN POLAND ORGANIZATION, METHOD, RESULTS

TADEUSZ MUSIALOWICZ
Central Laboratory for Radiological Protection, Warsaw, Poland

Abstract—Since 1959 the Central Laboratory for Radiological Protection (CLOR) has been carrying out a centralized personnel monitoring service for radio-isotope laboratories and nuclear installations in Poland.

X-ray laboratories are centrally monitored by the Institute of Labour Medicine.

Films used by CLOR for gamma, beta, thermal-neutron and X-ray radiation measurements are those made by the Polish photochemical factory "Foton". The measurement range for gamma rays of ^{60}Co is between 60 mR and 1300 R.

Kodak PNM films type A have been used for fast neutron dosimetry.

To evaluate the statistics of occupational exposure the results of yearly check-ups are grouped according to:

(i) Dose values:
up to 0·5 rem/yr; 0·5 – 1·5 rem/yr; 1·5 – 5 rem/yr;
5 – 12 rem/yr; 12 – 25 rem/yr; above 25 rem/yr.
(ii) Age groups:
18 – 30 yr; 31 – 40 yr; 41 – 50 yr; over 50 yr of age.
(iii) Type of establishment:
research; industry; medicine; other.

The number of persons monitored by the CLOR ranged from 800 in 1959 to 4500 in 1965. On the average about 80% of the monitored persons received doses below 0·5 rem/yr and about 0·2% received doses over 12 rem/yr.

INTRODUCTION

In Poland a personnel film monitoring service on a large scale was started by the Central Laboratory for Radiological Protection (CLOR) in Warsaw in 1959. According to principles previously established [1] the monitoring service covered all workers directly engaged in radiation work, including those employed in radio-isotope laboratories and nuclear installations. The number of people monitored in 1959 was 800, and in 1965 it was as high as 4500.

Personnel employed at the X-ray departments have only recently been covered by a centralized monitoring service provided by the Institute of Labour Medicine in Łódź. No data as yet have been published from their work and this paper is concerned only with the results of the monitoring service by CLOR.

ORGANIZATION

Film holders, films and other materials for individual dose determinations are dispatched by CLOR to the employer. Depending on the likelihood of being exposed to radiation the monitoring period of one or three months is chosen. Film badges are worn on the outside of the upper pocket of a laboratory coat, or in some cases additionally on the wrist of the right hand.

In each laboratory a special radiological health and safety officer is entrusted with individual dose control according to CLOR instructions. Data concerning personal and working conditions of controlled persons are posted to CLOR at the beginning of each year, changes being transmitted currently during the year.

After the monitoring period is finished, the exposed films together with the control form giving names and film numbers are posted to CLOR. The results of dose estimations are entered on the copy of the form and sent back to the employer.

Each monitored worker has a personal card in his working establishment and in CLOR'S files. If the exposure exceeds the maximum permissible dose according to the values recommended by ICRP [2, 3] CLOR asks the employer to explain the conditions under which the overexposure has taken place. Depending on the explanation received the dose is either entered on the personal record card or is not taken into account, in the latter case the mean value of the last three monitoring periods is entered on the worker's card.

The doses from the record cards are summed every 3 months. When the individual dose exceeds 12 rem or the value determined by the formula $D = 5\ (N–18)$, where N is the age in years of the worker, to limit the subsequent exposure CLOR recommends the employer to withdraw the individual in question partly or even totally from radiation work.

METHOD

Films and Film Holders

Double-emulsion films are used for the measurement of X-rays, gamma, beta and thermal neutron radiation. They are produced by the Polish Photochemical Factory "Foton", their measurement range for gamma-rays of ^{60}Co being between 60 mR and 1300 R. [4]

A new film holder developed according to Dresel, [5] Wachsmann, [6] Heard and Jones [7] and our own experience [8–10] is shown in Fig. 1.

The windows and filters in the holder are designed for the following purposes:

The Window
—to measure beta and low-energy photon radiation, to assist estimation of skin dose,
—to provide data to analyze the photon radiation energy,
—to carry the film number.

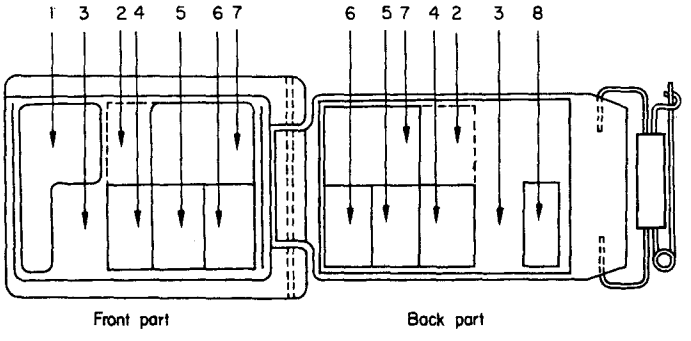

FIG. 1. New CLOR film holder. Filter Types: 1. Window. 2. 50 mg/cm² plastics. 3. 300 mg/cm² plastics. 4. 0.05 mm Cu. 5. 0.5 mm Cu. 6. 1.5 mm Cu or 0.5 mm Cd + 0.3 mm Pb. 7. 0.6 mm Sn + 0.3 mm P6. 8. 1 mm Pb.

Plastic (50 *mg/cm²*)
—to supplement the beta radiation measurements,

Plastic (300 *mg/cm²*)
—to supplement the beta radiation measurements to assist estimation of eye-lens dose,

Copper (0.05 *mm;* 0.5 *mm;* 1.5 *mm*)
—to provide data to analyze the photon radiation energy,

Tin/Lead (0.6 *mm Sn* + 0.3 *mm Pb*)
—to measure the photon radiation at energies above 75 keV,
—to supplement the thermal neutron measurements,

*Cadmium/lead** (0.5 *mm Cd* + 0.3 *mm Pb*)
—to measure thermal neutrons,

Lead (1 *mm*)
—to provide a distinction between beta radiation and the low-energy photon radiation.

For fast neutron measurements Kodak PNM films type A have been used. They are worn in sealed plastic foil bags. To reduce fading, the films together with the bags are dried before sealing at 20°C and 20% relative humidity. To separate the possible effect of thermal neutrons, the film in use is half-covered on both side by a Cd filter.

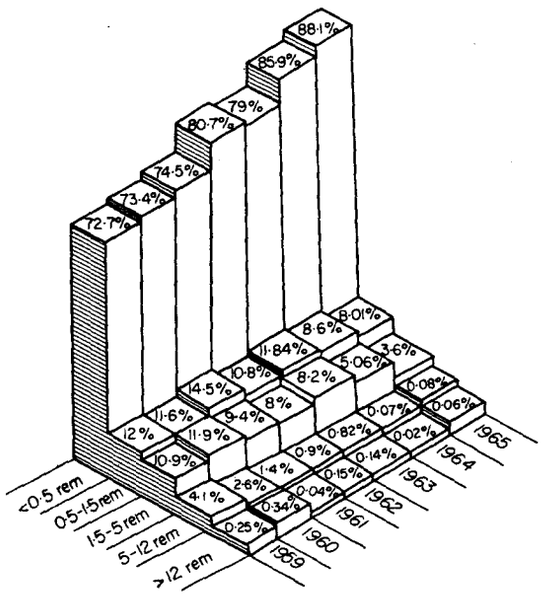

FIG. 2. Yearly doses in percentages of number of persons monitored in 1959–65.

Calibration.

The films are calibrated using the following sources:

Beta radiation
—metallic uranium sheet 80 mm diameter and 3.1 mm thick. The film badge is placed in immediate contact with the surface.

Gamma radiation
—^{226}Ra 28.64 ± 1.5% mCi, filtration 0.5 mm Pt. Exposure is controlled by "Vakutronik" VA-J-15 Dose Rate Meter which has a maximum instrument inaccuracy in energy range 20 keV–1.2 MeV of less than ± 10%.

*X-rays**
—"Siemens—Stabilipan 250" X-ray unit, 50–220 kV filtered to produce "normal radiation".[11] Exposure is controlled by a graphite ionization chamber with inaccuracy less than ± 4%.

Thermal neutrons
—the thermal column of the WWR-S 2 MeV reactor,

Fast neutrons
—a Pu–Be source giving 2.17 × 10^6 n/sec.

Photochemical Processing

The standard calibration films are always developed along with monitoring films. The "Foton" X-ray developer and Kodak D-19 developer are used for "Foton" and Kodak PNM films correspondingly. The developing time is 6 min at 20°C for "Foton" and 5 min at 20°C for Kodak films.

The acid stop-bath is used between developing and fixing baths. After fixing the films are carefully washed in running water and are dried at temperatures up to 30°C.

RESULTS

The results of measurements are summed for each calendar year and are published in CLOR Reports. To facilitate the estimation of occupational radiation hazards in this country, the results are grouped according to:

The dose values
—below 0.5 rem/yr; 0.5–1.5 rem/yr; 1.5–5 rem/yr; 5–12 rem/yr; 12–25 rem/yr; above 25 rem/yr.

* This type filter is only used in holders worn in laboratories where there is a possible hazard from thermal neutrons.

* This calibration is performed by the Polish Bureau of Standards (CUJM).

Type of establishment
—research; industrial; medical; other.

The doses above 5 rem/yr are additionally grouped according to sex and age:

18–30 yr; 31–40 yr; 41–50 yr: above 50 yr.

The percentage of the total number of persons monitored in each dose group between 1959 and 1965 [12, 13] is shown in Fig. 2.

The percentage of workers who received doses below 0.5 rem/yr increased from 72% in 1959 to 88% in 1965, while the percentage of the individuals who received doses above 12 rem/yr dropped from 0.3% to 0.06%. The only disconcerting fact is that most doses above 5 rem/yr are found in the age group between 18 and 30 yr. Since 1961 all doses exceeding 3 rem/3 months have been recorded and filed, their number having decreased from 33 in 1961 to 15 in 1965.

As a rule the cases of overexposure were found in the same places, i.e. in hospitals where radium applicators were used, and in industrial establishments where radioactive paints containing ^{226}Ra were used. Overexposures were not, however, found in all people doing the same kind of work. For Ra applicators the chance of overexposure depended largely on the number of procedures in a given period of time, whereas among workers using radioactive paint it depended mainly on the use of proper safety precautions. Among the latter group cases of false overexposure were reported, usually due to the accidental contact of the film badge with a radiation source. A few cases of wilfully misleading film exposure by the workers themselves were observed.

ACKNOWLEDGEMENTS

The author would like to express his sincere thanks to Miss J. Jasiak, Mr. Z. Szwaj and Mr. J. Wysopolski for their assistance in preparing a part of the data for this paper and for valuable discussions.

REFERENCES

1. T. Musialowicz and J. Wysopolski. Personnel film monitoring service in Poland during the year 1960. Report No. CLOR 8, Warsaw, 1960.
2. Recommendations of the International Commission on Radiological Protection. *ICRP Publication* No. 1. Pergamon Press, 1959.
3. Recommendations of the International Commission on Radiological Protection. *ICRP Publication* No. 6. Pergamon Press, 1964.
4. T. Musialowicz and J. Wysopolski. Ionizing radiation measurements by using wide-range Polish monitoring films. Report CLOR/Foton (in the press).
5. H. Dresel. Filmdosimetrie bei Strahlenschutzmessungen. *Fortschritte auf dem Gebiete der Röntgenstrahlen und der Nuklearmedizin*, **84,** H.2 (1956).
6. F. Wachsmann. The customary method for personnel monitoring by film badges. *Selected Topics in Radiation Dosimetry*. IAEA, Vienna, 1961.
7. M. J. Heard and B. E. Jones. A new film holder for personnel dosimetry. *Proceedings of Symposium on Personnel Dosimetry Techniques*, held at Madrid, April 1963, ENEA, OECD, Paris, 1963.
8. T. Musialowicz and J. Wysopolski. Bestimmung der Personendosis und Energie der Röntgenstrahlung nach der Filmschwärzungsmethode. *Nukleonika* **8,** 191 (1963).
9. T. Musialowicz, J. Wysopolski and B. Fillipiak. The determination of a mixture of thermal-neutron and gamma-ray exposures by film-badges. Report No. CLOR/IBJ-42/D, Warsaw, 1965.
10. T. Musialowicz and J. Wysopolski. Film badges filter combinations for measurement of X and gamma radiation above 75 keV. Report No. CLOR 51/D, Warsaw, 1966.
11. F. Wachsmann and A. Dimotsis. *Kurven für die Strahlentherapie*. Hirzel Verlag, Stuttgart, 1957.
12. T. Musialowicz, S. Dyż and J. Jakubiak. The evaluation of radiological protection conditions in isotope laboratories in Poland, 1958–63. Report No. CLOR 34, Warsaw, 1964.
13. J. Jasiak, T. Musialowicz and J. Wysopolski. Personnel film monitoring in Poland during the years 1963–65 (in the press).

PRAKTISCHE PERSONENDOSIMETRIE THERMISCHER NEUTRONEN

D. NACHTIGALL
Zentralbüro für Kernmessungen, EURATOM, Geel, Belgien
und E. ROSE
Kernforschungsanlage Jülich, Zentralabteilung Strahlenschutz, 517 Jülich, B.R.D.

Zusammenfassung—Für einen Modellthorax aus Standardgewebe mit den Abmessungen 80 cm × 40 cm × 20 cm wurden die Energiedosen und Dosisäquivalente pro Einheitsfluenz thermischer Neutronen und ihr Verlauf entlang verschiedener Achsen mit einer elektronischen Rechenmaschine bestimmt. Die Anteile der (n, γ)-Reaktionen in Wasserstoff und der (n, p)-Reaktionen in Stickstoff wurden besondert berechnet. Die Rechnungen sowie Messungen an Reaktoren, Beschleunigern und thermischen Säulen ergeben, dass im praktischen Strahlenschutz beim Tragen eines γ-Personendosimeters auf ein spezielles Personendosimeter für thermische Neutronen verzichtet werden kann.

1. EINLEITUNG

Bei der Dosimetrie thermischer Neutronen treten u.a. folgende Grössen auf:

1. Flussdichte $\dot{\phi}$ thermischer Neutronen, angegeben in $cm^{-2}s^{-1}$.
2. Fluenz ϕ thermischer Neutronen, angegeben in cm^{-2}.
3. Maximale Energiedosis D(max) bei Bestrahlung des menschlichen Körpers, angegeben in rad.
4. Maximales Dosisäquivalent D_e(max), angegeben in rem.
5. Die entsprechenden Werte für die Oberfläche von Modellgeometrien (unendlicher Halbraum, Scheiben, Quader, meuschlicher Thorax) D(Ob) bzw. D_e(Ob).
6. Die entsprechenden Dosisleistungswerte $\dot{D}$ und $\dot{D}_e$, angegeben in rad/h bzw. rem/h.
7. Die entsprechenden Dosis-Fluenz-Verhältnisse, d.h. die jeweiligen Dosen pro Einheitsfluenz $\delta = \frac{D}{\phi}$ bzw. $\delta_e = \frac{D_e}{\phi}$, angegeben in rad/$cm^{-2}$ und rem/cm^{-2}.

Bei Dosisberechnungen geht man davon aus, dass der bestrahlte Mensch durch einen "Standardmenschen" repräsentiert werden kann, der im wesentlichen aus folgenden vier Elementen besteht[1] (Tabelle 1).

Bei manchen Berechnungen wird auch weiches Gewebe folgender Zusammensetzung zugrundegelegt[2] (Tabelle 2).

Tabelle 1. *Zusammensetzung von Standardgewebe*

Element	Gewicht in g	Gewicht in Prozenten	Atome pro g	Atome in Prozenten
O	45 500	65	$2{,}45 \cdot 10^{22}$	25,7
C	12 600	18	$0{,}903 \cdot 10^{22}$	9,49
H	7 000	10	$5{,}98 \cdot 10^{22}$	62,8
N	2 100	3	$0{,}129 \cdot 10^{22}$	1,36

Tabelle 2. Zusammensetzung von weichem Gewebe

Element	Gewicht in Prozenten
O	73,64
C	12,14
H	10,11
N	4,02

2. ZUSAMMENSETZUNG DER DOSIS THERMISCHER NEUTRONEN IN KÖRPERGEWEBE

Eine Energieabsorption in Körpergewebe durch Einwirkung thermischer Neutronen erfolgt über 2 Reaktionen:

1. $^{1}H(n, \gamma)^{2}H$,
2. $^{14}N(n, p)^{14}C$.

Bei der (n, γ)-Reaktion entsteht das stabile schwere Wasserstoffisotop. Der erzeugte Deuteriumkern strahlt seinen Energieüberschuss in Form von γ-Quanten der Energie 2,2 MeV ab. Wenn thermische Neutronen auf das gesamte Körpervolumen einwirken, strahlt jedes Volumenelement γ-Quanten aus, die in jedem anderen Volumenelement des Körpers zur Dosis beitragen können. Die Energieabsorption in Körpergewebe erfolgt über Photo- und Comptoneffekte.

Bei der (n,p)-Reaktion werden Protonen mit der Energie von 0,62 MeV emittiert. Die Energieabgabe an das Körpergewebe erfolgt über die Protonen, die an die ^{14}C-Kern übertragenen Rückstossenergien brauchen nicht berücksichtigt zu werden. Wegen der kurzen Reichweite der Protonen in Gewebe wird die Protonenenergie lokal absorbiert. Der Anteil der β-Strahlung des ^{14}C ist vernachlässigbar.

Auch die Reaktion $^{14}N(n, \gamma)^{15}N$ mit einer Quantenenergie von 0,73 MeV sowie durch Strahlungseinfang entstehende β-Strahlung von ^{24}Na, ^{32}P und ^{42}K tragen nur unbedeutend zur Dosis bei.

Die makroskopischen Wirkungsquerschnitte für die beiden zu berücksichtigenden Reaktionen sind [3]

$$\Sigma_H = 2{,}11 \cdot 10^{-2}\ \mathrm{cm}^{-1}, \quad (1)$$

$$\Sigma_N = 2{,}18 \cdot 10^{-3}\ \mathrm{cm}^{-1}. \quad 2)$$

3. ABSCHÄTZUNG DES ANTEILS DER (n,γ)—REAKTIONEN ZUR DOSIS THERMISCHER NEUTRONEN

Da die Einfangquanten jedes Volumenelementes des bestrahlten Volumens in jedem anderen Volumenelement zur Dosis beitragen können, ist der (n, γ)-Anteil von der Geometrie des bestrahlten Körpers abhängig.

Es liegen Berechnungen für verschiedene Geometrien vor:

1. Homogener Halbraum aus Standardgewebe: [3]
$$\delta^{\gamma}(\mathrm{Ob}) = 2{,}72 \cdot 10^{-10}\ \mathrm{rad/cm^{-2}} \quad (3)$$
2. 30 cm dicke, seitlich unendlich ausgedehnte Scheibe aus Standardgewebe: [1, 2]
$$\delta^{\gamma}(\mathrm{Ob}) = 2{,}60 \cdot 10^{-10}\ \mathrm{rad/cm^{-2}} \quad (4)$$
3. Kreisscheibe von 30 cm Durchmesser und 20 cm Tiefe aus Standardgewebe: [4]
$$\delta^{\gamma}(\mathrm{Ob}) = 1{,}85 \cdot 10^{-10}\ \mathrm{rad/cm^{-2}} \quad (5)$$

Für die Thoraxoberfläche eines Standardmenschen erhält man durch Interpolation etwa

$$\delta^{\gamma}(\mathrm{Ob}) = 2{,}10 \cdot 10^{-10}\ \mathrm{rad/cm^{-2}} \quad (6)$$

In allen Fällen wird angenommen, dass die thermischen Neutronen in parallelem Bündel senkrecht auf die Oberfläche fallen.

4. BERECHNUNG DES ANTEILS DER (n,γ)—REAKTIONEN ZUR DOSIS THERMISCHER NEUTRONEN

Mit Hilfe einer elektronischen Rechenmaschine haben wir die Dosis und die Dosisverteilung an der Körperoberfläche sowie im Körperinnern berechnet. Der menschliche Thorax wurde dazu durch eine rechteckige Säule aus Standardgewebe mit 80 cm Höhe, 40 cm Breite und 20 cm Tiefe approximiert. Wiederum wurde angenommen, dass ein paralleles Bündel thermischer Neutronen senkrecht auf die Oberfläche trifft. Die in den Körper eindringende Fluenz ϕ der thermischen Neutronen nimmt mit der Körpertiefe x entsprechend einer von Snyder berechneten Beziehung ab:

$$\phi \sim \phi_o \cdot f(x)$$

$$\text{mit } f(x) = 13{,}1 \cdot e^{-0{,}450x} - 5{,}1 \cdot e^{-5{,}17x} \quad (7)$$

$f(x)$ gibt die Zahl der Stösse an, die ein Neutron in der Tiefe x pro cm Weglänge (parallel zur Strahlrichtung) erleidet. Von diesen Stössen

führt der Bruchteil Σ_H/Σ_t (Σ_H = makroskopischer Einfangquerschnitt für Wasserstoff, Σ_t = totaler makroskopischer Wirkungsquerschnitt) zu einer H(n, γ)D-Reaktion. Dadurch entstehen in jedem Volumenelement $dV = dx \cdot dy \cdot dz$ Photonen der Energie E_γ. Diese Photonen werden in der Entfernung r vom Entstehungsort entsprechend dem Abstandsgesetz $e^{-\mu r}/4\pi r^2$

Das ergibt

$$dD^\gamma/\phi_0 = 3{,}12 \cdot 10^{-5} . f(x) . \frac{e^{-\mu r}}{r^2} . dxdydz \quad (\text{MeV/cm}). \quad (9)$$

Umgerechnet in rad erhält man:

$$dD^\gamma/\phi_0 = 5{,}0 \cdot 10^{-13} f(x) . \frac{e^{-\mu r}}{r^2} . dxdydz \, (\text{rad/cm}^{-2}) \quad (10)$$

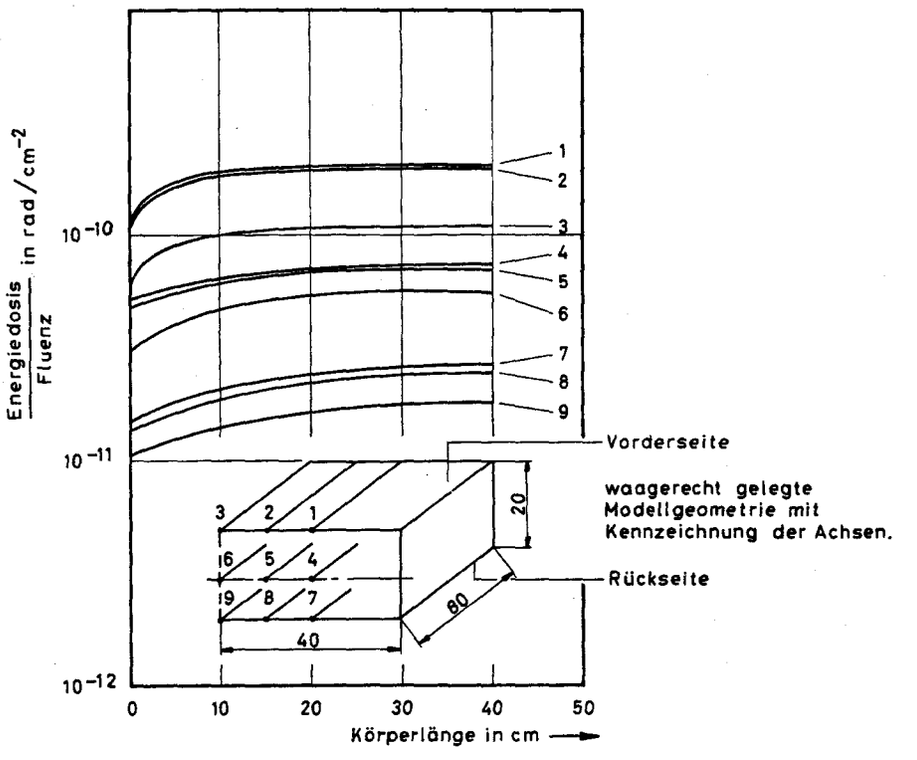

FIG. 1. γ-Dosis pro Einheitsfluenz thermischer Neutronen für verschiedene Längsachsen des Thoraxmodells.

und dem linearen Schwächungskoeffizienten μ für γ-Strahlung absorbiert und verursachen die γ-Dosis dD^γ. Durch Kombination dieser Vorgänge ergibt sich die Beziehung:

$$dD^\gamma = \phi_o \cdot \frac{\Sigma_H}{\Sigma_t} \cdot f(x) . E_\gamma \cdot \mu \cdot \frac{e^{-\mu r}}{4\pi r^2} dxdydz \quad (8)$$

Als Zahlenwerte sind einzusetzen: $\mu = 2{,}5 \cdot 10^{-2}$ cm^{-1}; $\Sigma_H = 2{,}11 \cdot 10^{-2}$ cm^{-1}; $\Sigma_t = 2{,}95$ cm^{-1}; $E_\gamma = 2{,}2$ MeV.

Gleichung (10) ähnelt einer von Schalnow [3] angegebenen Formel, jedoch wird hier die genauere von Snyder berechnete Neutronenverteilung $f(x)$ anstelle der von Schalnow verwendeten einfacheren Verteilung $e^{-0{,}4x}$ benutzt.

Der Verlauf von $\delta^\gamma = \frac{D^r}{\phi}$ in rad/cm^{-2} für das Körperinnere ergibt sich durch Integration der Gleichung (10) über alle Volumenelemente.

Er ist in Fig. 1 für verschiedene Körperachsen parallel zur Längsachse dargestellt. Die Genauigkeit der Integration ist besser als 5%.

Der Dosisverlauf auf der vorderen Körperseite (Kurven 1 und 2) ist über einen grossen Bereich nahezu konstant. Erst in einer Entfernung von weniger als 10 cm von den Aussenkanten beginnt ein starker Abfall bis auf etwa die Hälfte der in der Mitte herrschenden Dosis.

Durch Integration über das ganze Körpervolumen erhält man die mittlere Ganzkörperdosis pro Einheitsfluenz. Sie beträgt

$$\bar{\delta}^{\gamma}\,(\text{Ganzk.}) = 0{,}74 \cdot 10^{-10}\,\text{rad/cm}^{-2} \qquad (12)$$

Die mittlere Dosis pro Einheitsfluenz auf der kurzen Mittelachse, d.h. in den mittleren Körperregionen, erhält man durch Integration über die Kurve 1 der Fig. 2.

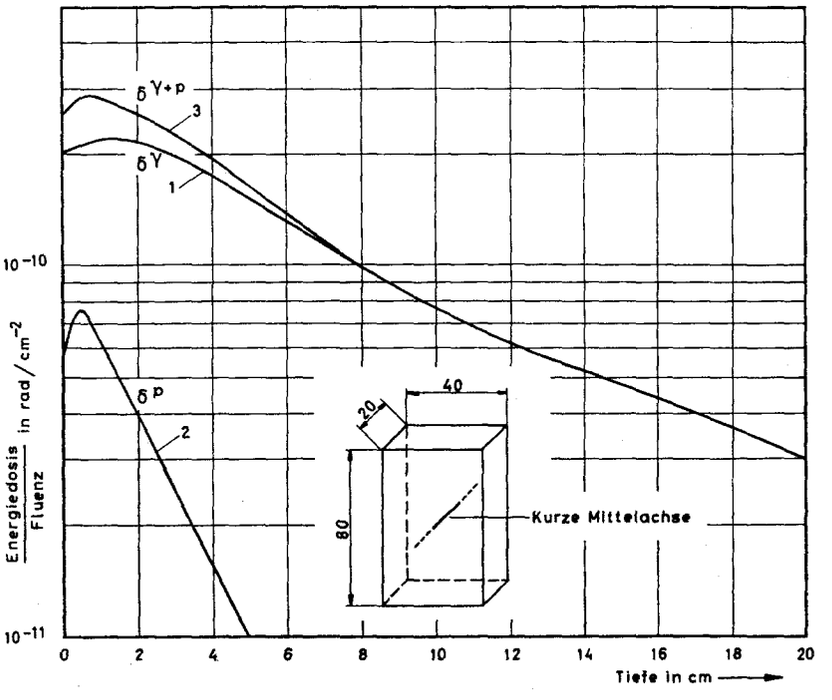

FIG. 2. Energiedosen pro Einheitsfluenz thermischer Neutronen entlang der kurzen Mittelachse senkrecht zur Vorderseite des Thoraxmodells.

Zwischen den Achsen 1 und 9 ergibt sich eine Differenz um den Faktor 10.

Fig. 2 zeigt den Verlauf von δ^{γ} entlang der kurzen Mittelachse senkrecht zur Vorderseite (Kurve 1). Bei etwa 1,5 cm liegt ein Maximum. Danach nimmt δ^{γ} angenähert exponentiell bis zur Thoraxrückseite ab. Für δ^{γ}(Ob) erhielten wir den Wert

$$\delta^{\gamma}(\text{Ob}) = 2{,}09 \cdot 10^{-10}\,\text{rad/cm}^{-2} \qquad (11)$$

Das ist in ausgezeichneter Übereinstimmung mit dem abgeschätzten Wert in Gl. (6).

Sie beträgt

$$\bar{\delta}^{\gamma}\,(\text{Mittelachse}) = 1{,}07 \cdot 10^{-10}\,\text{rad/cm}^{-2} \qquad (13)$$

5. BERECHNUNG DES ANTEILES DER (n,p)—REAKTIONEN ZUR DOSIS THERMISCHER NEUTRONEN

Im Gegensatz zu der γ-Komponente kann die Neutronenfluenz und die damit verbundene Protonendosis in den Ebenen parallel zur vorderen Körperoberfläche nahezu über die ganze Fläche als konstant angesehen werden.

Die Abhängigkeit der Protonendosis von der Eindringtiefe hat daher im ganzen Körper bis nahe an die Seitenkanten angenähert den von Snyder[2] für einen unendlichen Halbraum angegebenen Verlauf.

Es ergibt sich

$$\delta^P = 0{,}0733 \cdot 10^{-10} (13{,}1\, e^{-0{,}45x} - 5{,}1\, e^{-5{,}17x}) \text{rad/cm}^{-2} \quad (14)$$

Der Verlauf dieser Funktion auf der kurzen Mittelachse ist in Fig. 2 als Kurve 2 dargestellt.

Für die Oberfläche ergibt sich

$$\delta^P(\text{Ob}) = 5{,}9 \cdot 10^{-11} \text{ rad/cm}^2 \quad (15)$$

Zur Abschätzung der mittleren Ganzkörperdosis genügt in diesem Falle der Mittelwert auf der kurzen Mittelachse. Durch Integration der Gleichung (14) ergibt sich:

$$\bar{\delta}^P \text{ (Mittelachse)} = \bar{\delta}^P \text{ (Ganzk.)} = 1{,}03 \cdot 10^{-11} \text{ rad/cm}^{-2} \quad (16)$$

Die Addition der mittleren γ- und Protonen-Dosiskomponenten ergibt:

$$\bar{\delta}^{\gamma+P} \text{ (Ganzk.)} = 0{,}84 \cdot 10^{-10} \text{ rad/cm}^{-2} \quad (17)$$

$$\bar{\delta}^{\gamma+P} \text{(Mittelachse)} = 1{,}17 \cdot 10^{-10} \text{ rad/cm}^{-2} \quad (18)$$

Kurve 3 in Fig. 2 zeigt den Verlauf der Gesamtdosis entlang der Mittelachse.

6. BERECHNUNG DER DOSISÄQUIVALENTE

Aus den berechneten Dosen erhält man durch Multiplikation mit dem Qualitätsfaktor Q die entsprechenden Dosisäquivalente. Für die Photonen ist $Q = 1$. Bei der Protonenstrahlung wird im allgemeinen vereinfachend der Pauschalwert $Q = 10$ benutzt. Tabelle 3 enthält die sich daraus ergebenden Dosisäquivalente pro Einheitsfluenz thermischer Neutronen. Mit $Q = 10$ für Protonenstrahlung soll die biologische Wirkung des ganzen Komplexes aller möglichen Protonenenergien in leicht zu handhabender Form erfasst werden. Überdies ist dieser Wert zur sicheren Seite hin aufgerundet. Im Falle der hier vorliegenden Protonenstrahlung handelt es sich aber um eine definierte Strahlung mit bekannter Energie. Es kann daher statt des Pauschalwertes 10 der Q-Wert für 0,62 MeV Protonenstrahlung benutzt werden. Nach[3] ergibt sich

$$Q \text{ (0,62 MeV)} = 5 \quad (19)$$

Die daraus resultierenden Dosisäquivalente sind ebenfalls in Tabelle 3 enthalten. Man sieht, dass mit einem auf der Brust getragenen γ-Dosimeter bei der Wahl von $Q = 10$ für Protonen 26,0% des Oberflächendosisäquivalentes, 100% des mittleren Dosisäquivalentes entlang der Mittelachse und 118% des mittleren Dosisäquivalentes für den Ganzkörper gemessen werden. Bei der Wahl von $Q = 5$ für Protonen erhöhen sich diese Werte auf 41%, 132% und 167%.

Fig. 3 enthält den Dosisäquivalentverlauf für die einzelnen Strahlungskomponenten und für das gesamte Dosisäquivalent entlang der Mittelachse für die Fälle

$Q = 5$ und $Q = 10$ für Protonenstrahlung.

7. DOSISÄQUIVALENTE FÜR KRITISCHE ORGANE

Wir betrachten wieder die beiden Fälle der Annahme von $Q = 10$ bzw. $Q = 5$ für die Protonenstrahlung.

Tabelle 3. Energiedosen und Dosisäquivalente pro Einheitsfluenz thermischer Neutronen

	Energiedosen			Dosisäquivalente	
	γ-Komponente rad/cm^{-2}	p-Komponente rad/cm^{-2}	$\gamma + p$ rad/cm^2	$\gamma + p$ $Q = 10$ für Protonen rem/cm^{-2}	$\gamma + p$ $Q = 5$ für Protonen rem/cm^{-2}
Oberfläche	$2{,}09 \cdot 10^{-10}$	$0{,}59 \cdot 10^{-10}$	$2{,}68 \cdot 10^{-10}$	$7{,}99 \cdot 10^{-10}$	$5{,}09 \cdot 10^{-10}$
Mittelwert, Mittelachse	$1{,}07 \cdot 10^{-10}$	$0{,}10 \cdot 10^{-10}$	$1{,}17 \cdot 10^{-10}$	$2{,}10 \cdot 10^{-10}$	$1{,}58 \cdot 10^{-10}$
Mittelwert, Ganzkörper	$0{,}74 \cdot 10^{-10}$	$0{,}10 \cdot 10^{-10}$	$0{,}84 \cdot 10^{-10}$	$1{,}77 \cdot 10^{-10}$	$1{,}25 \cdot 10^{-10}$

$Q = 10$:

Nach Fig. 3 beträgt das gesamte Dosisäquivalent pro Einheitsfluenz in 2 cm Tiefe auf der Mittelachse das Dreifache des γ-Dosisäquivalentes pro Einheitsfluenz an der Oberfläche. In 6 cm Tiefe sind beide Werte gleich gross. Für die Ermittlung des Dosisäquivalentes für kritische Organe bei reinen thermischen Neutronenfeldern im Bereich von 2 bis 6 cm unterhalb der Körperoberfläche genügt es also, die γ-Dosis an der Oberfläche zu messen und mit dem Korrekturfaktor 2 zu multiplizieren.

$Q = 5$:

Nach Fig. 3 beträgt das gesamte Dosisäquivalent pro Einheitsfluenz in 2 cm Tiefe auf der Mittelachse das Doppelte des γ-Dosisäquivalentes pro Einheitsfluenz an der Oberfläche. In 5 cm Tiefe sind beide Werte gleich gross.

Für die Ermittlung des Dosisäquivalentes in kritischen Organen im Bereich tiefer als 2 cm bei reinen thermischen Neutronenfeldern genügt also die Messung des γ-Dosisäquivalentes an der Oberfläche mit hinreichender Genauigkeit (Korrekturfaktor 1).

Diese Abschätzungen gelten natürlich nicht für die nahe der Oberfläche liegenden Augenlinsen. Jedoch befinden sich diese ausserhalb unserer zugrundegelegten Modellgeometrie. Sie sind daher geringerer γ-Einstrahlung aus der Nachbarschaft ausgesetzt. Sie sind ausserdem in relativ viel Knochenmasse eingebettet, in der H(n,p)D-Reaktionen eine weit geringere

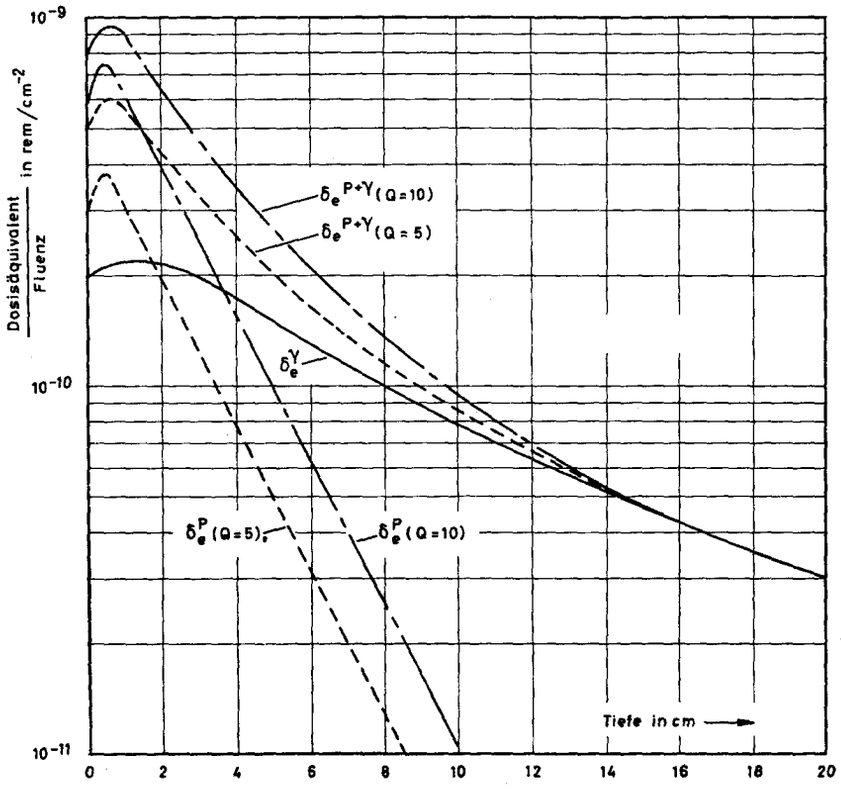

FIG. 3. Dosisäquivalente pro Einheitsfluenz thermischer Neutronen entlang der kurzen Mittelachse senkrecht zur Vorderseite des Thoraxmodells.

Rolle spielen. Ausserdem wird die im Schädelinnern entstehende γ-Strahlung stärker absorbiert als an anderen Körperstellen. Das gesamte Dosisäquivalent pro Einheitsfluenz an den Augen ist daher geringer als an der Thoraxoberfläche. Der relative Unterschied zwischen dem γ-Dosisäquivalent an der Thoraxoberfläche und dem gesamten Dosisäquivalent an den Augen verringert sich deshalb. Im Falle $Q = 10$ für die Protonenstrahlung und reiner thermischer Neutronenfelder genügt auch hier die Multiplikation der gemessenen γ-Dosis mit dem Korrekturfaktor 2. Im Falle $Q = 5$ für Protonenstrahlung genügt der Korrekturfaktor 1.

Die männlichen Gonaden sind durch Kleidung und Gewebe bedeckt. Ihre mittlere Tiefe beträgt etwa 2 cm. In dieser Tiefe ist das gesamte Dosisäquivalent etwa dreimal (bei $Q = 10$) bzw. doppelt (bei $Q = 5$) so gross wie das γ-Dosisäquivalent an der Oberfläche. Ähnlich wie die Augen sind auch sie nicht in dem gleichen Masse wie andere Körperorgane von einer ausgedehnten kompakten Gewebemasse umgeben. Die γ-Einstrahlung aus benachbarten Gewebeteilchen ist deshalb ebenfalls geringer. Für die männlichen Gonaden gelten deshalb die gleichen Korrekturfaktoren wie für die Augen.

8. RICHTUNGSABHÄNGIGKEIT

Die bisherigen Betrachtungen basierten auf der Voraussetzung, dass ein paralleles Bündel thermischer Neutronen senkrecht auf die Oberfläche trifft. Dies ist jedoch nur ein Extremfall. Der entgegengesetzte Extremfall liegt bei Bestrahlung von hinten vor. Normalerweise wird die Strahlung von den verschiedensten Seiten einfallen.

Wie aus den bisherigen Überlegungen hervorgeht, misst ein auf der Brust getragenes γ-Dosimeter an der Oberfläche bei Bestrahlung von vorn etwa 24–42% (je nach Qualitätsfaktor für Protonenstrahlung) des gesamten Dosisäquivalentes an der Oberfläche. Bei Bestrahlung von rückwärts hingegen würde es nach Fig. 2 100% des gesamten Dosisäquivalentes messen, da in diesem Falle die Dosis an der Oberfläche ausschliesslich von der γ-Komponente herrührt. Die wirklich gemessenen Werte werden also zwischen 30 und 100% des gesamten Dosisäquivalentes liegen.

Bezieht man nicht auf das Dosisäquivalent an der Oberfläche, sondern auf das mittlere Dosisäquivalent des Ganzkörpers, so wird bei Bestrahlung von vorn durch ein γ-Dosimeter mehr als das mittlere Dosisäquivalent des Ganzkörpers erfasst (Tabelle 3), bei Bestrahlung von hinten etwa 20% (vgl. Fig. 2). Bei einem Bezug auf das mittlere Dosisäquivalent des Ganzkörpers liegen die Verhältnisse also etwa umgekehrt wie bei einem Bezug auf das Dosisäquivalent an der Oberfläche. Auch hierbei werden die wirklich gemessenen Werte zwischen diesen beiden Extremen liegen.

9. ANTEILE THERMISCHER NEUTRONEN AM TOTALEN DOSISLEISTUNGSÄQUIVALENT

Aus diesen Rechnungen und Überlegungen geht hervor, dass bei einer reinen thermischen Neutronenstrahlung mit einem γ-Dosimeter in der Mitte der Körperoberfläche zwischen 20 und 100% der gesamten von der Neutronenstrahlung verursachten Dosis erfasst werden, wobei der Prozentsatz davon abhängt, ob man auf die Oberflächen oder auf die mittlere Ganzkörperdosis Wert legt und ob $Q = 10$ oder $Q = 5$ für die Protonenstrahlung angesetzt wird.

Erfahrungsgemäss ist jedoch der Anteil thermischer Neutronen am totalen Dosisäquivalent in der Umgebung von Reaktoren und Teilchenbeschleunigern kleiner als 10%.[5-9] Auf ein spezielles Personendosimeter für thermische Neutronen kann also normalerweise verzichtet werden, da der Anteil des Dosisäquivalentes der thermischen Neutronen unterhalb der Fehlergrenzen der Dosismessung liegt, ja in den meisten Fällen wegen des erhöhten γ-Untergrundes überhaupt nicht erkennbar ist.

Nur an thermischen Säulen von Reaktoren kann der Anteil thermischer Neutronen grösser sein.

An der thermischen Säule des FRJ 1 haben wir des γ/n-Verhältnis der Dosisäquivalente gemessen. Die Reaktorleistung war 1 MW. Ein Teil der Abschirmung der thermischen Säule wurde entfernt, so dass in 50 cm Abstand von der äusseren Abschirmungswand ein Messfeld von 60 cm $\times$ 60 cm Grösse entstand, in dem die thermische Neutronenflussdichte sich örtlich um weniger als 5% änderte. Das

Dosisleistungsäquivalent (mit $Q = 10$ für Protonen) war in dieser Fläche 9,1 mrem/h, die γ-Dosisleistung betrug 16,8 mR/h, so dass das γ/n-Verhältnis 1,8 war. Die Abschirmung der γ-Strahlung mit 5 cm Blei ergab das Verhältnis 0,8. Bei gänzlich hochgefahrener Stahl-Betonabschirmung erhielten wir in 1 m Entfernung den Wert 10. Am Reaktor Gleep in Harwell wurde in 2 cm Entfernung von der Graphitaussenwand der Wert 0,37, in 2 m Entfernung jedoch ein Wert > 1 gemessen [10].

Auch wir fanden mit zunehmender Entfernung von der thermischen Säule stets eine Zunahme des γ/n-Verhältnisses. Reine thermische Neutronenfelder ohne γ-Untergrund sind offenbar schwer zu realisieren, da stets Materialien, in denen (n,γ)-Einfänge stattfinden können, in der Nähe sein werden. Je grösser aber der γ-Anteil im Strahlungsfeld der thermischen Säule, desto geringer ist die Rolle, die der von einem γ-Dosimeter nicht gemessene Anteil des Dosisäquivalentes thermischer Neutronen spielt.

10. SCHLUSSFOLGERUNGEN FÜR DEN PRAKTISCHEN STRAHLENSCHUTZ

Bei der Personendosimetrie in der Umgebung von Reaktoren und Teilchenbeschleunigern kann auf ein spezielles Dosimeter für thermische Neutronen verzichtet werden. Selbst im speziellen Fall des Strahlungsfeldes an thermischen Säulen genügt ein auf der Brust getragenes Dosimeter für γ-Strahlung, da der in diesem Falle nicht registrierte Anteil des totalen Dosisäquivalentes an der Körperoberfläche in der Praxis gewöhnlich kleiner als 50%, oft kleiner als 20% sein wird.

Legt man als Dosisbelastung einer bestrahlten Person nicht die Oberflächendosis, sondern die mittlere Ganzkörperdosis zugrunde, so ergibt sich auch an thermischen Säulen mit einem γ-Dosimeter bereits eine Überbestimmung des thermischen Neutronendosisäquivalentes.

LITERATUR

1. *NBS Handbook* 63, Washington, 1957.
2. W. S. Snyder. *Nucleonics* **6,** No. 2, 46 (1950).
3. M. I. Schalnow. *Neutronen-Gewebedosimetrie*, Berlin, 1963.
4. J. W. Smith. Private Mitteilung, 1965.
5. D. Nachtigall. Jül-158-St, 1964.
6. M. J. Heard. *Symposium on Personnel Dosimetry for External Radiation*, Harwell 1965, Diskussionsbeitrag.
7. D. M. Wallace. *Symposium on Personnel Dosimetry for External Radiation*, Harwell 1965, Diskussionsbeitrag.
8. A. E. Souch. *Symposium on Personnel Dosimetry for External Radiation*, Harwell 1965, Diskussionsbeitrag.
9. D. Nachtigall. CERN, ISR-BT/66-18, 1966.
10. H. J. Delafield. Private Mitteilung, 1965.

EIN PHOSPHATGLASDOSIMETER FÜR STRAHLENSCHUTZANWENDUNGEN

W. BUTTLER*, R. MAUSHART† und E. PIESCH‡

Zusammenfassung—Es wird ein neues Dosimeter beschrieben, das aufgrund von Versuchen und Testergebnissen eines kürzlich entwickelten Katastrophendosimetersystems speziell für Strahlenschutzanwendungen geeignet erscheint.

Es enthält ein zylindrisches Phosphatglas von 8 mm Durchmesser, das fest mit einem Teil der Kapselung verbunden ist, welche gleichzeitig die Identifizierungszeichen trägt.

Es gestattet die Bestimmung von γ-Dosen von 50 mR bis zu 1000 R. Das Dosimeter ist luftdicht, feuchtigkeitssicher und zur Erzielung einer geringen Energieund Richtungsabhängigkeit filterkompensiert. Die Ausführung der Filterkapsel ermöglicht eine schnelle und leichte Auswertung, verhindert aber jedes unbefugte Öffnen.

Für die Verwendung von Metaphosphatgläsern als Personendosimeter im Strahlenschutz sind bereits Dosimeterkapselungen entwickelt worden, die eine befriedigende Energie—und Richtungsunabhängigkeit der Dosisanzeige ermöglichen.[1, 2]

Ihre Brauchbarkeit für die routinemäßige Personenüberwachung wurde u.a. durch Vergleichsbestrahlungen erwiesen, bei denen mehrere solcher Glasdosimeter zusammen mit einem Füllhalterdosimeter jeweils von der gleichen Person getragen wurden.[3]

Was jedoch die Eignung der bisherigen Dosimeterkapselung zu einem routinemäßigen Großeinstaz noch einschränkt, ist die technische Manipulierbarkeit bei der Auswertung einer großen Serie solcher Dosimeter. Es war bisher notwendig, das Glas aus dem Dosimeter herauszunehmen und einzeln in das Auswertegerät einzuführen. Mit Sicherheit würde eine Einführung und eine Benutzung der Glasdosimeter als Routine-Personendosimeter wesentlich beschleunigt und erleichtert, wenn man zu einer halb- oder ganz-automatischen Auswertung kommen könnte. Es ist daher in Zusammenarbeit mit einer Firma, welche bereits die in Deutschland für den Zivilschutz entwickelten Glasdosimeterkapselungen[4, 5] mit gekoppelter Erkennungsmarke herstellt, eine neue Dosimeterkapselung konstruiert worden. Diese Kapselung soll im wesentlichen die Eigenschaf-

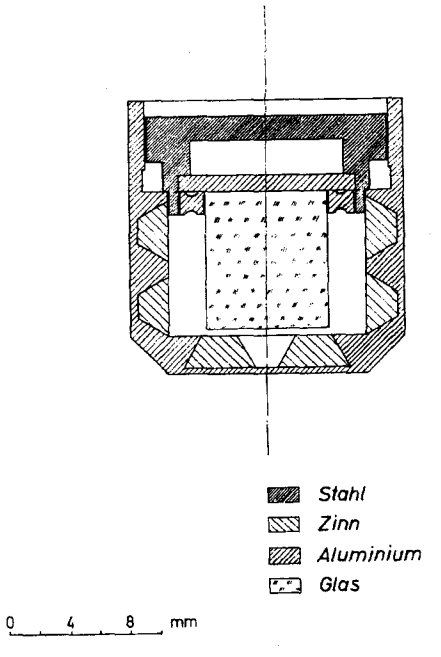

Abb. 1. Schnitt durch die neue Dosimeterkapselung mit zylindrischem Phosphatglas der Abmessung 8 × 9 mm².

* W. Buttler, Fa. Total KG, 6802 Ladenburg, B.R.D.

† R. Maushart, Kernforschungszentrum Karlsruhe, Strahlenmeßdienst 75 Karlsruhe, B.R.D.

‡ E. Piesch, Kernforschungszentrum Karlsruhe, Strahlenmeßdienst, 75 Karlsruhe, B.R.D.

ten der Kugelkapselung, nämlich Energie- und Richtungsunabhängigkeit der Dosimeteranzeige, beibehalten, sich aber durch einige entscheidende technische Vorzüge auszeichnen. Der entscheidenste davon ist, daß das Glas mit einem Teil der Kapsel ständig, auch bei der Auswertung, verbunden bleibt, so daß die Schwierigkeit der Glaskennzeichnung nicht mehr auftritt.

Des weiteren ist die Kapsel völlig licht- und luftdicht abgeschlossen, so daß keine Glasverschmutzung stattfinden kann und der Waschvorgang innerhalb einer routinemäßigen Auswertung normalerweise entfällt. Die Kapsel besitzt einen Vakuum-Magnetverschluß, so daß ein unbeabsichtigtes oder unberechtigtes Öffnen so gut wie ausgeschlossen ist.

Um dies erreichen zu können, wurde von der strengen Kugelform abgegangen und ein zylinderförmiges Glas mit 8 mm Durchmesser und 9 mm Höhe verwendet. Zur Energiekompensation ist ein perforiertes Metallfilter

Tabelle 1. *Verwendete Strahlenqualitäten*

Röhrenspannung kV	Zusatzfilterung mm	angenom. eff. Quantenergie keV
300	2 Al + 5 Cu + 3,5 Pb	240
250	2 Al + 5 Cu + 2 Pb	200
220	2 Al + 5 Cu + 1,2 Pb	170
200	2 Al + 5 Cu + 0,9 Pb	150
180	2 Al + 11 Cu	135
150	2 Al + 7 Cu	110
120	2 Al + 3,5 Cu	87
100	2 Al + 2 Cu	71
80	2 Al + 0,7 Cu	55
70	2 Al + 0,4 Cu	46
60	2 Al + 0,2 Cu	38

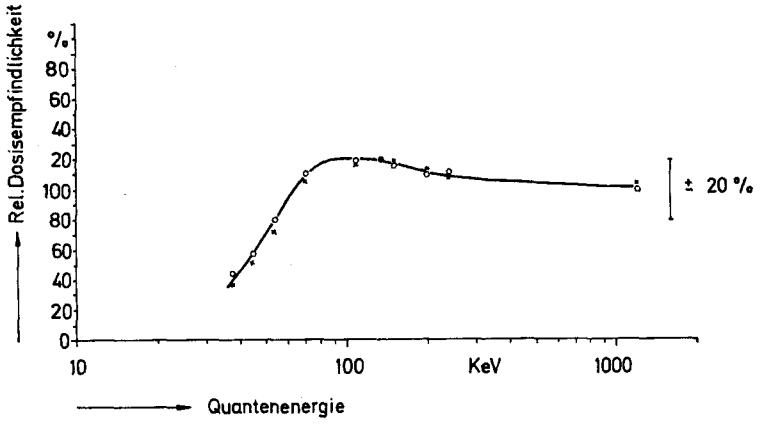

ABB. 2. Die relative Dosimeteranzeige der neuen Dosimeterkapselung mit einem zylindrischen CEC-Phosphatglas (Fa. Carbonisation Entreprise et Céramique, Montrouge, Frankreich) in Abhängigkeit von der Quantenenergie. x-x-x-x Strahlungseinfall längs der Dosimeterachse. o-o-o-o Strahlungseinfall senkrecht zur Dosimeterachse.

erforderlich, welches hier aus rotationssymmetrischen, konischen und teilweise mit Zinn ausgefüllten Ausnehmungen in der Seitenwand und den Stirnböden der zylinderförmigen Kapselung besteht.

Die spezielle Konstruktion der Kapselung (Abb. 1) führt in etwa zu den gleichen Eigenschaften, die mit der Kugelkapselung erreicht werden. Die Energieabhängigkeit der Dosimeteranzeige wurde mit hart gefilterter Röntgenbremsstrahlung bestimmt (Tabelle 1).

Die Werte für die Energieabhängigkeit der Kapselung sind in Abb. 2 für zwei Strahleneinfallsrichtungen dargestellt. Man findet im Energiebereich 50 keV bis 1, 2 MeV Energieunabhängigkeit innerhalb $\pm$ 20%.

Die bisher erzielte energie- und richtungsunabhängige Dosimeteranzeige kann, vor allem was die Dosimeteranzeige bei Strahlungseinfall in Dosimeterachse betrifft, möglicherweise noch verbessert werden.

Für dieses Dosimeter ist ein halbautomatisches Auswertegerät in Konstruktion. Die Automatik sieht vor, auch die Dosimeternummer vom Gerät abzufragen und zusammen mit der Dosis auszudrucken, so daß Verwechselungen, wie sie bei der Einzelauswertung entstehen können, völlig ausgeschlossen sind.

Mit dieser Entwicklung dürfte ein weiterer Schritt zu einer allgemeinen Anwendung von Phosphatglasdosimetern in der Personendosimetrie getan sein.

REFERENZEN

1. E. Piesch. Eine neue Glasdosimeterkapselung zu energie- und richtungsunabhängigen Dosisbestimmung von Quantenstrahlung. *Direct Information*, 17/64.
   R. Maushart und E. Piesch. Photoluminescent personnel dosimeter with spherical case for energy and direction independent dose measurement. FSHPS Symposium, Paris, 1964.
2. R. Maushart und E. Piesch. Phosphate glasses as routine personnel dosimeters. Intern. Conf. on Luminescence Dosimetry, Stanford, 1965.
   R. Maushart und E. Piesch. Eine Glasdosimeterkombination für die Routinedosimetrie von Quantenstrahlung.
   Direct Information, 10/65.
3. E. Piesch. Anforderungen an Personendosimeter für rechtserhebliche Strahlenschutzmessungen. ESG-Tagung Jülich, Juni 1966.
4. H.-J. Hardt. Die Verwendung von Metaphosphatglas in der Individualdosimetrie. *Atompraxis* **12,** S. 135 (1966).
5. W. Buttler. Possibilities in Radiophotoluminescence Dosimetry. Intern. Conf. on Luminescence Dosimetry, Stanford, 1965.

RANGE AND DEPTH DOSE DISTRIBUTION OF LOW ENERGY CHARGED PARTICLES IN DOSIMETER GLASSES

K. BECKER

Health Physics Div., Oak Ridge National Laboratory, Oak Ridge. Tenn.*

Abstract—A new method for the direct determination of particle ranges and depth dose distributions in silver-activated phosphate glasses is based on the successive removal of extremely thin surface layers from the exposed glass by chemical etching ("peeling") and measurement of the residual radiophotoluminescence between successive etchings. Glass composition, etching chemicals and etching speed can be varied within wide limits. The experimental technique, using Yokota-type dosimeter glasses and 28% NaOH at 60°C (etching speed 0·12 μ/min) is briefly described. As an example of the practical application of the method, measurements using several types of radiation sources (aqueous solutions of ^{3}H, ^{63}Ni and ^{35}S, solutions and thin and thick solid sources of ^{239}Pu, ^{237}Np and ^{235}U, monoenergetic protons, deuterons and He^{+} ions in a wide energy range) have been made.

Accuracy, possibilities and limitations of the method are briefly discussed. Possible sources of error are: discoloration of the glass because of very high surface doses; uncertainties in the determination of the etching speed; etching speed along charged particle tracks higher than the bulk etch rate for ions of very high LET.

1. INTRODUCTION

The calculation of the range of low energy electrons and ions in solids is difficult, mainly because charge exchange effects become important and elastic scattering causes an effective range which is smaller than the sum of the total distances measured along the path of the particle. Different theoretical approaches to convert the path length calculated by the Bohr–Nielson equation[1, 2] into the experimentally measured projected range[3, 4] may lead to different results, and the agreement with experimental values has to be proved.[5]

During recent years, several more or less indirect methods for the measurement of average and maximum ranges have been used, for instance by determination of changes in the refraction index of quartz surface layers caused by ion bombardment;[6] by elastic proton scattering at the embedded heavy ions in low Z target materials;[7] by determination of the line-shape of the emitted α particles;[8] and by luminescence excitation[9] or deterioration[10] measurements in thin fluorescent layers.

More direct methods have also been applied, such as the use of stacks of thin metal foils,[11] and the chemical determination of ranges of radioactive ions in some metals (Al, W) by chemical removal of uniform thin surface layers and measurement of the residual radioactivity of the target material.[12-16] In a similar study, the range of ^{134}Cs ions in germanium was determined by etching of the Ge crystal.[17] It was found, however, that approximately 25% of the ^{134}Cs could not be removed by prolonged etching because of either an abnormal range of the ions or non-uniform etching of the crystal.

It would, however, be desirable to apply this relatively simple, fast and direct "peeling" method for range studies without the drawbacks of the earlier methods, in particular:

(*a*) Without restriction to range measurements of radioactive ions. This is, for instance, possible by using irreversible changes in the physical properties of the target material, which are proportional to the energy transferred, localized to

* Work performed during a stay as Scientist-in-Residence at the U.S. Naval Radiological Defense Laboratory, San Francisco/Calif.

the point of energy transfer and can easily be measured.

(*b*) By the use of a target material whose composition can be varied within wide limits.

(*c*) Whose homogenous structure guarantees a uniform etching process.

All these specifications can be met within certain limitations by the use of silver-activated phosphate glasses as target material. Ionizing radiation causes the formation of quasi-permanent luminescence centers (radiophotoluminescence, RPL) in these glasses, which can be detected by simple fluorimetry. It is known that phosphate glasses are etched very uniformly and the glass composition can be varied within certain limits. Glasses containing Ag concentrations between approx. 0.1 and 10% and phosphates of Li, K, Na, Ba, Mg, Al, BeO, B_2O_3, etc., have been described.[18]

2. EXPERIMENTAL PROCEDURE

In general, a range determination by this method consists of the following procedure:

I. The clean dosimeter glass with known background (predose) luminescence is first exposed to the ionizing radiation. In case of monodirectional electrons or positive ions from accelerators, or α or β particles from radioactive planes, glass plates or blocks with a plane surface are most suitable. If the glass is exposed by submersion in a uniform medium, such as an α or β active solution, other shapes, including glass rods or spheres, may also be used.

II. By waiting a prescribed period of time or by heat treating the glass (in most dosimeter glasses about 15 min at 150°C), the optimal stable RPL is obtained,[18] which is measured in a proper glass dosimeter reader (365 mμ excitation, RPL maximum around 620 mμ). The predose effect is subtracted from the reading. The RPL should be intense enough to allow measurements down to at least about 1% of the initial radiation effect. On the other hand, it should not be too intense. Local doses higher than several thousand rads produce a non-linear response because of glass discoloration (for details on this effect, see ref. 19). Discoloration does not affect the results of range measurements, but can cause errors in depth dose determinations.

III. The glass is etched for a known time in a solution of known composition and temperature. Etching conditions depend strongly on the expected range and the glass composition. The thickness of the removed surface layer is determined from earlier calibration data and will depend on the expected range of the ionizing particle and the glass composition.

IV. After rinsing and drying, the RPL measurement is repeated and the predose subtracted. This cycle of etching and reading is repeated until prolonged etching causes no further reduction in the RPL reading.

V. The logarithm of the residual RPL in percent of the original RPL is plotted as a function of the thickness or weight of glass removed by the etching process. The resulting graph then corresponds to the well-known intensity over absorber thickness plots for α, β, and X radiation. In other cases, other graphic representations may have advantages. By differentiation information on the depth dose distribution can be obtained.

There are several methods by which the etching speed can be determined, such as:

(*a*) Measuring the weight reduction of a dosimeter glass block after prolonged etching.

(*b*) Direct measurement of the change in glass thickness by the use of a thickness gauge after prolonged etching.

(*c*) Microscopic methods, either directly, or by measurement of the diameter of etch pits which result after bombardment of the glass with particles of very high LET such as fission fragments, followed by prolonged etching. If an etch pit is large enough, half of the diameter increase per unit of time corresponds within a few percent to the bulk etch speed of the glass surface. If the etching solution is sufficiently agitated, the thickness of the removed glass layer will be proportional to the etch time. Etching during ultrasonic agitation guarantees fast replacement of the exhausted etching agent at the glass surface by a new etching agent.

All chemicals that attack the glass surface at a sufficient speed can be used. In cases of the usual dosimeter glasses this may be inorganic

acids such as HF, bases such as NaOH, or organic complex formers. The etching speed depends mainly on

(*a*) the glass composition,
(*b*) the etching agent,
(*c*) the concentration of the etching chemicals, and
(*d*) the etching temperature.

The etching kinetics of some dosimeter glasses compared with glasses kept at room temperature have been found.

3. RESULTS

As an example for the effect of monoenergetic charged particles, the residual RPL in a glass containing 53.5% O, 33.3% P, 4.6% Al, 4.2% Ag, 3.6% Li and 0.8% B (Toshiba, Tokyo) has been measured as a function of the

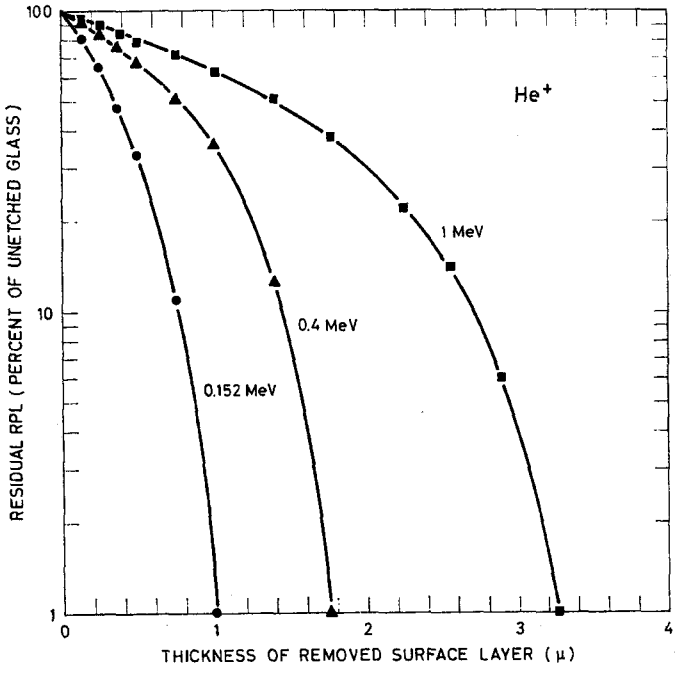

FIG. 1. Residual RPL of a dosimeter glass irradiated with He^+ ions of different energies as a function of the thickness of the removed surface layer, normalized for reading of the unetched glass = 100.

have been described in detail in another publication.[20] Using the Yokota-type dosimeter-glass[21] and 28% NaOH at 60°C, for instance, an etching speed of about 0.12μ/min has been obtained. Even extended etching of unexposed glasses or glasses irradiated with penetrating radiation does not affect the RPL reading. In order to investigate the possible effect of RPL center diffusion in the glass on the measured ranges, glasses have been kept at 200°C for several hours. No differences in the results thickness of the removed surface layer for He^+ ions of 152 keV, 0.4 MeV and 1 MeV. The same glass type has been used in all experiments, the fluorimetric evaluation has been done in a Toshiba FGD-3B reader. Similar results have been obtained with protons and deuterons in the 0.15 to 1.8 MeV range. The obtained ranges were slightly higher than the reported ranges for these particles in aluminium above 1 MeV. The exposures have been made by placing the glass inside the accelerator tube

in the target area of Van de Graaff and Cockroft–Walton type accelerators. Even at very small beam currents, exposure times of less than a second were sufficient. At higher beam currents or exposure times, a yellowish discoloration of the glass surface was visible to the naked eye. In this case the usual slope of the curves (Fig. 1) was changed. Because of the superimposed effects of ultraviolet light absorption in the uppermost discolored layer (absorption maximum around 320 mμ) and the total RPL bremsstrahlung. After exposure to $^{90}Sr/^{90}Y$, as it was expected, no decrease in the RPL intensity has been observed by the removal of more than 20μ.

In glasses exposed to mixed α, β and γ emitters the background may be quite high. But also in such cases an α range determination is possible (Fig. 3). The differences obtained for glasses exposed to a ^{235}U foil of 30μ thickness and a ^{237}Np layer of 0.34μ thickness electrodeposited on steel is caused in part by the

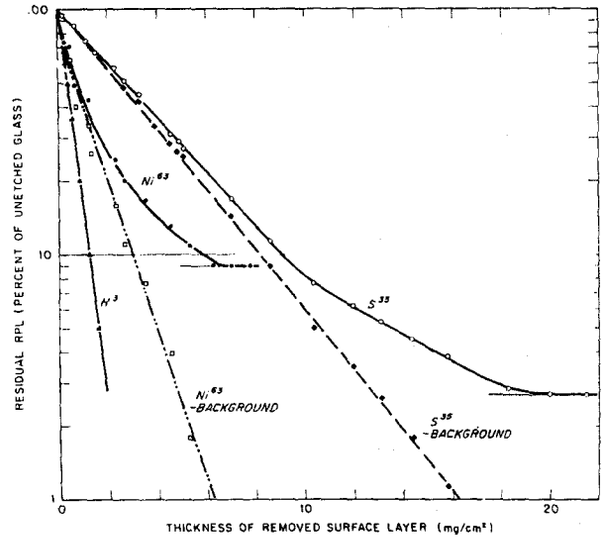

FIG. 2. Residual RPL of a dosimeter glass exposed to solutions of different β emitters as a function of the thickness of the removed surface layer, normalized for reading of the unetched glass = 100.

decrease during etching, the measured RPL decrease was at first slower—in some cases even an increase was observed—and then, close to the maximum range, faster than given in Fig. 1.

In another experiment, glass blocks have been immersed in aqueous solutions of soft β emitters. In Fig. 2, the results for ^{3}H (maximum β energy 18 keV), ^{63}Ni (67 keV) and ^{35}S (167 keV) containing solutions before and after subtraction of the background is given. It can be seen that even in the case of ^{3}H the range can easily be measured. The background may be caused by γ-emitting contaminations and difference in α energies, the ^{237}Np α energies being somewhat higher, in part by the different energy distributions because of different source thickness.

The effect of source geometry can also be seen in Fig. 4, where glasses have been exposed to ^{239}Pu in aqueous solution, in a thin and in a thick solid source. The background effect is higher in the glasses exposed to the solution and the thick source because of the higher contribution of penetrating γ radiation to the glass surface dose. After subtracting the background effect, however, the data for the thin source and the solution agree.

4. DISCUSSION

Also numerous other measurements using the described technique have been made in order to establish the usability of the method. The minimum and maximum ranges measured and the accuracy obtained in the experiments described do not represent its limitations. More accurate determination of the etching speed and more constant etching conditions should, for instance, result in an accuracy and reproducibility of better than $\pm$ 5%.

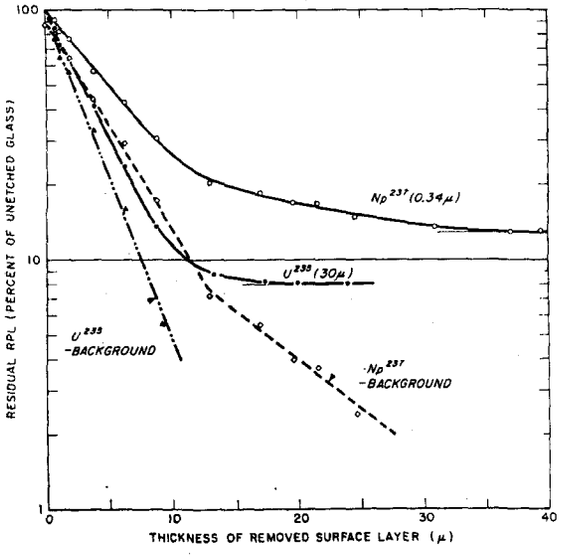

FIG. 3. Residual RPL of a dosimeter glass exposed to a thin ^{237}Np and a thick ^{235}U foil as a function of the thickness of the removed surface layer, normalized for reading of the unetched glass = 100.

The lower limit for range measurements is not given by the etching technique because the thickness of the removed layers can be made extremely small by reduction of etching time and/or concentration and temperature of the etching solution. It will be limited by the fact that the average volume dose of the glass block or plate will become smaller with decreasing range of the particles and discoloration may already occur in a thin surface layer while the total RPL of the glass is still too low for accurate measurements. If stack arrangements of exposed glass plates are used, the limit may be extended because of the increased percentage of the exposed glass volume. For the same reason, glass powders could be submersed in radioactive solutions. There is no upper limit, but at ranges exceeding several tens or hundreds of microns, other even simpler direct methods may be superior.

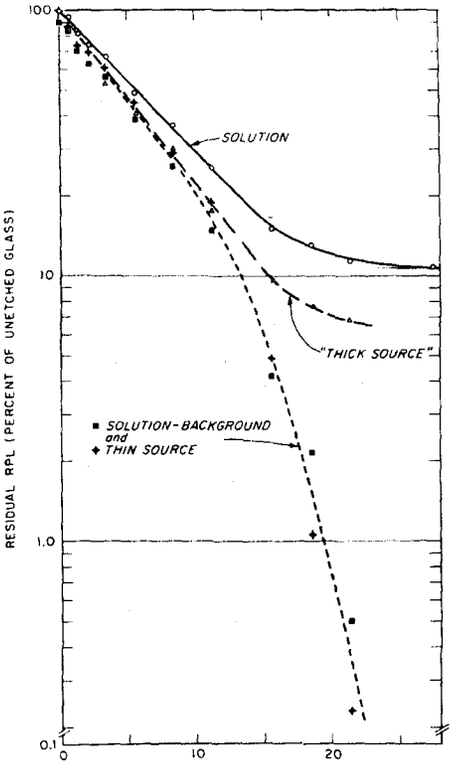

FIG. 4. Residual RPL of a dosimeter glass exposed to a solution, a thin (evaporated solution) and a thick source (metal sheet) of ^{239}Pu as a function of the thickness of the removed surface layer, normalized for reading of the unetched glass = 100.

When the ionization density (LET) along the track of the particle exceeds a critical value, there will be radiation damage produced in the glass. Preferential etching will take place along the particle track. In this case an etch pit is formed which can be seen in an optical microscope and the surface removal method can no longer be applied. The LET limit depends on

glass composition and etching conditions and is not known for the glasses under study, but fission fragments are certainly above and α particles below this limit.

If the decrease in RPL intensity between successive steps of etching is used for depth dose distribution measurements, the LET dependence of the RPL has to be taken into account. It has been demonstrated[22] that the dose response of RPL glasses begins to decrease at about 1 keV/μ, corresponding to a proton energy of 100 MeV, and is at 100 keV/μ ($\sim$200 keV protons) less than 20% of the low LET sensitivity. It is, however, possible to deduct at least approximate depth dose distributions from the experimental data.

ACKNOWLEDGEMENTS

The author thanks his colleagues at NRDL for their assistance in the irradiation work and E. Tochilin for valuable discussions.

REFERENCES

1. N. Bohr. Kgl. *Danske Videnskab. Selskab., Mat.-fys. Medd.* **18,** 8 (1948).
2. K. O. Nielsen. In Electromagnet. *Enrichm. of Isotop. and Mass Spectrometry*, M. L. Smith (ed.), Acad. Press, New York, 1956, p. 68.
3. J. Lindhard and M. Scharf. *Phys. Rev.* **124,** 128 (1961).
4. O. S. Oen, O. K. Holmes and M. T. Robinson. *J. Appl. Phys.* **34,** 302 (1963).
5. L. Morbitzer and A. Scharmann. *Z. Phys.* **185,** 488 (1965).
6. R. L. Hines and R. Arndt. *Phys. Rev.* **119,** 623 and **120,** 1626 (1960).
7. D. Powers and W. Whaling. *Phys. Rev.* **126,** 61 (1962).
8. B. Domeij *et al. Arkiv for Fys.* **24,** 399 (1963).
9. C. Feldmann. *Phys. Rev.* **117,** 455 (1960).
10. L. Morbitzer and A. Scharmann. *Z. Phys.* **177,** 174 and **181,** 67 (1964).
11. O. Selig and R. Sizmann. *Nukleonik* **8,** 303 (1966)
12. V. A. J. Van Lint, R. Schmitt and C. S. Suffredin. *Phys. Rev.* **121,** 1457 (1961).
13. J. A. Davies *et al. Can. J. Chem.* **38,** 1526 and 1535 (1960) and **39,** 601 (1961).
14. J. A. Davies *et al. Arkiv for Fys.* **24,** 377 (1963).
15. I. Bergstrom *et al. Arkiv for Fys.* **24,** 389 (1963).
16. J. Uhler *et al. Arkiv for Fys.* **24,** 413 (1963).
17. M. M. Mredov and M. M. Okuneva. *Dokl. Akad. Nauk SSR,* **113,** 795 (1957).
18. K. Becker. *Symp. on Solid-State and Chemical Dosimetry*, IAEA Vienna, 1966, and IAEA Atomic Energy Rev. **5,** 43 (1967).
19. K. Becker. *Health Phys.* **11,** 523 (1965).
20. K. Becker, USNRDL-Tr 904 (1965) and *Health Phys.* **12,** 769 (1965).
21. R. Yokota, S. Nakajima and E. Sakai. *Health Phys.* **5,** 219 (1961).
22. E. Tochilin *et al.*, Unpublished.

A NEUTRON DOSEMETER WITH SPHERICAL MODERATOR CONTAINING ABSORBERS AND A BF_3 COUNTER

E. ROTONDI* and K. W. GEIGER
Division of Applied Physics, National Research Council, Ottawa, Canada

Abstract—The Bonner moderating sphere, 25–30 cm in diameter, is widely used because of its isotropic and dose equivalent response for neutrons over an energy range from near thermal to about 10 MeV. However, two properties of the instrument limit its convenience: (1) the LiI scintillation counter in its center tends to make it difficult to use the instrument in high γ-fluxes, also response changes of the scintillation counter make frequent recalibrations necessary. (2) The moderating sphere is rather large and heavy for a portable instrument. The use of a BF_3 thermal neutron counter of 5 cm sensitive length and 2.5 cm diameter eliminated all difficulties mentioned under (1). Insertion of cadmium discs at appropriate locations in the polyethylene sphere near the counter ends made the response isotropic for all neutron energies. To improve on (2), neutron absorption studies were made in a slab geometry containing cadmium and polyethylene sheets, so as to obtain the best rem dose response for neutrons from an Am-Be source ($E_{av} = 4.4$ MeV) and from a Sb-Be source ($E_{av} = 40$ keV). On this basis, a compact neutron dosemeter 20 cm in diameter containing an inner cadmium shell of 10 cm diameter was constructed and tested.

INTRODUCTION

To obtain the dose equivalent (DE) at some location of a neutron radiation field, knowledge of the fluence and the neutron energy spectrum is normally required. The measurements are laborious and during the last years use is being made of neutron monitors the response of which is essentially proportional to the DE. Such instruments can then be calibrated in "rem" units. The response, as recommended by the National Committee on Radiation Protection and Measurements[1] is shown in Fig. 1. An approximation to a DE response can for instance be achieved by surrounding a thermal neutron detector with a moderator of appropriate thickness.

Two approaches have been used: the first, consisting of a BF_3 counter surrounded by a cylindrical moderator, was originally realized by De Pangher.[2] The second is a Bonner sphere[3] with a small LiI scintillation detector in the center. Many variations of these basic systems have been reported in the literature.[4-8] Both systems have certain limitations: a cylindrical geometry will not ensure a true isotropic response at all energies and will not respond as a point detector. On the other hand, for the spherical geometry, the γ-rejection rate of a LiI scintillation detector is much less than that of a BF_3 counter which tends to make it difficult to use the spherical dosemeter in high γ-fluxes. Also the smallness of the LiI detector results in reduced neutron sensitivity. For both geometries the moderator has to be rather large and heavy for a truly portable instrument.

It seemed therefore desirable to try to design an instrument which combines the advantages of the two basic systems, by using spherical geometry and a BF_3 counter as detector. To reduce the size of the instrument, neutron absorbing material can be incorporated into the moderator as shown by Andersson and Braun[5] for cylindrical geometry.

* N.R.C. Postdoctorate Fellow from Settore Radiazioni del C.N.E.N., Frascati, Italy.

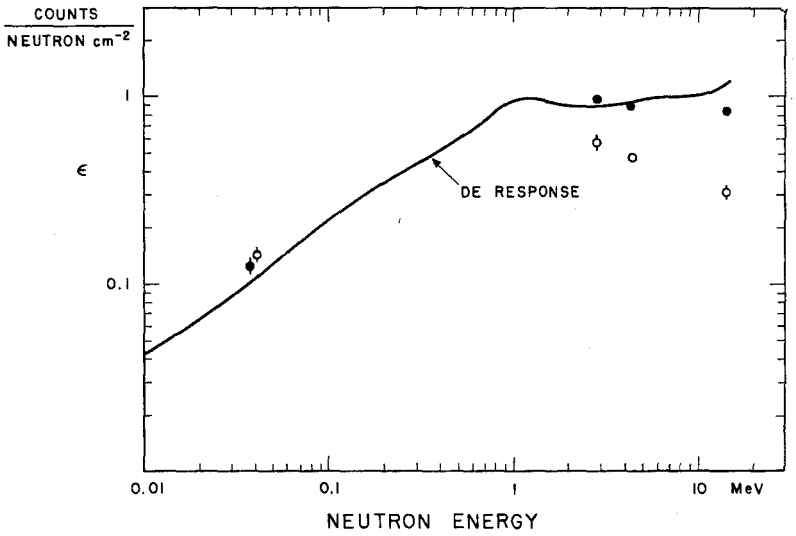

FIG. 1. Closed circles: response of the 30 cm sphere with BF_3 counter in center. Open circles: response of compact dosemeter.

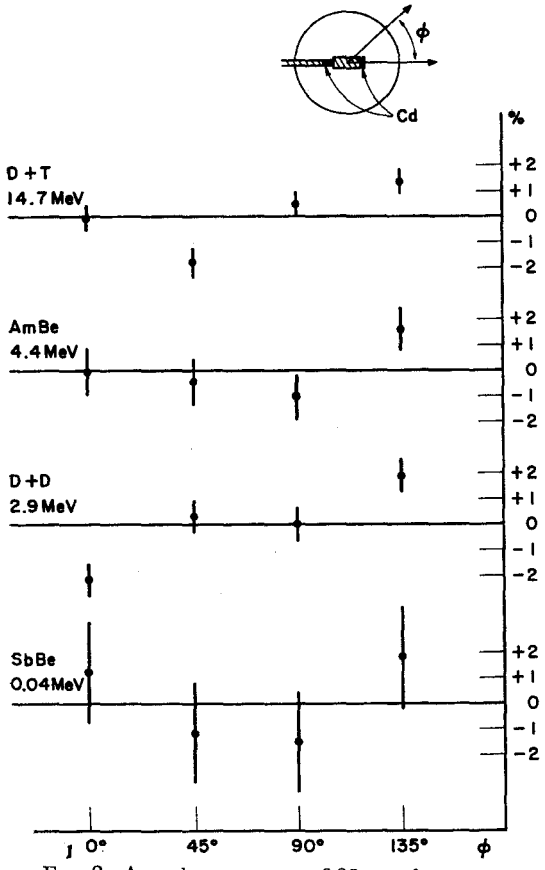

FIG. 2. Angular response of 30 cm dosemeter.

NEUTRON SOURCES

To test the response of the instruments, neutrons from the D + D (2.9 MeV) and D + T (14.7 MeV) reaction were used, as well as from ^{124}Sb-Be(γ,n) and ^{241}Am-Be(α,n) sources. An Sb-Be source emits two neutron groups, one centred around 24 keV, the other around 380 keV with an intensity ratio of 1 : 0.046 respectively,[7] resulting in an average energy of 40 keV. For the Am-Be source a mean energy of 4.4 MeV has been assumed, as derived by Geiger and Hargrove[8] from the measurement of the neutron spectrum.

Neutron emission rates have been determined absolutely with a precision long counter[9] taking into account the change of the effective center with neutron energy. The calibration of the counter was carried out with an Am-Be source, the neutron emission rate of which was measured absolutely in a manganese sulphate bath.[10] The ratio for the emission rate of the Sb-Be source to the emission rate of the Am-Be source as determined with the long counter agreed with the ratio measured in a manganese sulphate bath to within 3%.

POLYETHYLENE SPHERE DOSEMETER, 30 CM DIAMETER

A regular size Bonner sphere, 30 cm in diameter,[3] was equipped with a BF_3 counter of 2.5 cm diameter with its sensitive volume of 5 cm length in the center of the sphere.* The energy response to neutrons conformed to the DE curve of Fig. 1 only when irradiated from a direction at right angles to the BF_3 counter; i.e. the angular response was not uniform. Insertion of a cadmium sleeve at the connector end of the counter and of a cadmium disc at the other end, as indicated on the top of Fig. 2, made the response isotropic for the neutron energies available. The lower part of Fig. 2 shows that the deviations from the mean are less than 2%. The counting efficiency versus energy is shown in Fig. 1 by the closed circles and follows well the dose equivalent curve.

The response of this instrument has also been compared to that of a regular 30 cm polyethylene sphere dosemeter with a 4 × 4 mm ^{6}LiI (Eu) scintillation detector in its center. Within the error of the measurement ($\pm$ 2%) the response agreed with that of the sphere dosemeter containing the BF_3 counter, but the one containing the LiI detector showed its sensitivity reduced by a factor 5.2. Because the high γ-field of the Sb-Be source caused pulse pile-up in the scintillation detector, an Am-Be source, embedded into a 20 cm polyethylene sphere, was used to check the low energy neutron response.

COMPACT NEUTRON DOSEMETER

The 30 cm spherical dosemeter is rather large and heavy for a portable monitor. An attempt was therefore made to reduce its size and still retain approximate DE response by incorporating a cadmium absorber within the moderator. Neutron absorption studies in slab geometry using polyethylene and cadmium sheets were carried out; these measurements led to the design of a 20 cm diameter sphere, containing an inner 0.5 mm cadmium shell, 10 cm in diameter, as shown in Fig. 3. When a cadmium sleeve was added around the connector of the BF_3 counter, an optimized angular response as shown in Fig. 4 was found. The deviations from the mean now reach 6% at low energies which is still acceptable for neutron monitoring. The energy response is shown in Fig. 1 by the open circles. The new design has changed the sensitivity very little but

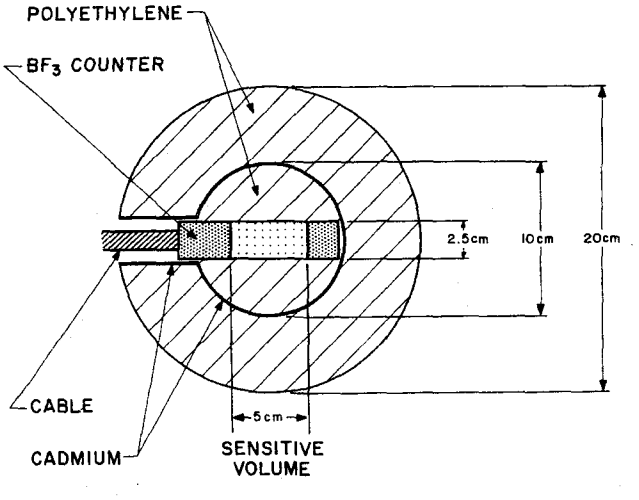

FIG. 3. Compact neutron dosemeter.

* BF_3 counter supplied by Reuter Stokes Inc., Skokie, Ill., filling pressure 70 cm Hg of $^{10}BF_3$, Model No. RSN-40A-M2.

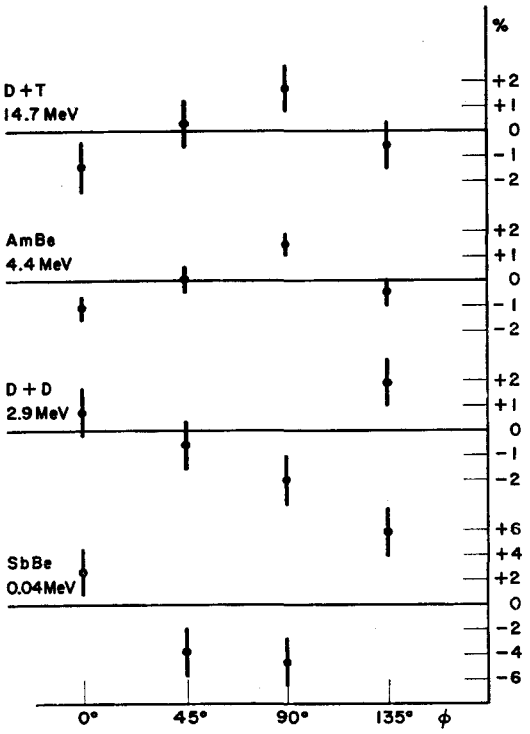

FIG. 4. Angular response of compact neutron dosemeter.

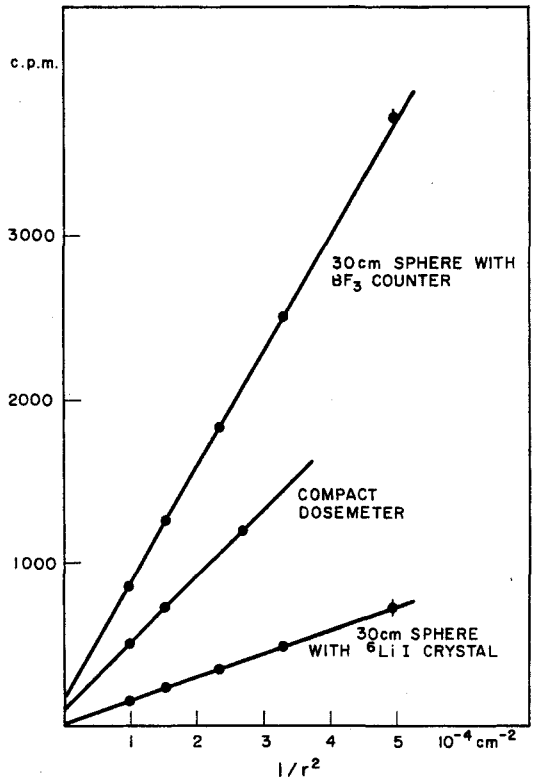

FIG. 5. Counting rate versus inverse square of distance between Am-Be source and center of dosemeter.

deviations from the dose equivalent curve are somewhat larger.

CONCLUSIONS

The use of a BF_3 counter with appropriately located cadmium absorbers instead of a small LiI detector in spherical dosemeters results in a simple to operate and more sensitive instrument with the stable operation inherent to BF_3 counters. By embedding further cadmium into the moderator a truly portable instrument evolved where the weight is reduced from 13.4 kg for the 30 cm sphere to 4.1 kg for the compact dosemeter. The shape of the dose equivalent curve from 0.040 to 5 MeV is still followed to within $\pm$ 30% which can be considered adequate for a radiation protection monitor. Even at higher energies its response follows more closely the DE curve than that of a regular 25 cm diameter polyethylene sphere with a LiI detector,[4] an instrument frequently used at present where weight is a disadvantage. All dosemeters investigated show the properties of a point detector. This is borne out by Fig. 5 showing the dependence of the counting rate on the inverse square of the distance between the center of the sphere and the Am-Be source, resulting in straight lines. The same behaviour is found for the other neutron energies. Room scattered neutrons add a background which is essentially independent of distance. This background is given in Fig. 5 by the intersection of the straight line with the counting rate axis.

The high sensitivity of the instruments containing a BF_3 counter is particularly advantageous for the investigation of radiation shielding effects and protection measurements around accelerator installations. For the 30 cm sphere dosemeter or the compact dosemeter both containing the BF_3 counter of 5 cm sensitive

length, the sensitivity is approximately 20,000 counts per millirem.

REFERENCES

1. National Bureau of Standards, Hdbk. 63. Protection against neutron radiation up to 30 million electron volts (1957).
2. J. De Pangher. *Nucl. Inst. Meth.* **5,** 61 (1959).
3. R. L. Bramblett, R. I. Ewing and T. W. Bonner. *Nucl. Inst. Meth.* **9,** 1 (1960).
4. D. E. Hankins. Determination of the neutron contribution to the rem dose. *Proc. USAEC First Symposium on Accelerator Radiation Dosimetry and Experience,* Brookhaven National Laboratory (1965).
5. I. Ö. Andersson and J. Braun. A neutron rem counter with uniform sensitivity from 0.025 eV to 10 MeV. *Neutron Dosimetry* **2,** 87. International Atomic Energy Agency, Vienna, 1963.
6. J. W. Leake and J. W. Smith. Calibration of a neutron rem counter. Report AERE-R 4524 (1964).
7. H. W. Schmitt and C. W. Cook. *Nuclear Physics* **20,** 202 (1960).
8. K. W. Geiger and C. K. Hargrove. *Nuclear Physics* **53,** 204 (1964).
9. J. De Pangher and L. L. Nichols. A precision long counter for measuring fast neutron flux density. Report BNWL-260 (1966).
10. K. W. Geiger and A. P. Baerg. *Can. J. Phys.* **43,** 373 (1965).

A PRACTICAL METHOD FOR EVALUATING NEUTRON DOSE EQUIVALENT RATE

Y. YOSHIDA, H. TATSUTA, H. RYUFUKU, K. KITANO and S. FUKUDA
Division of Health Physics and Safety, Japan Atomic Energy Research Institute, Tokai-mura, Ibaraki-ken, Japan

Abstract—Measurement of the dose equivalent rate for neutrons is very difficult, when the spectrum is unknown and the energies range from intermediate to fast, such as those leaking from nuclear reactors. A practical method applied to the field monitoring using survey instruments is presented for evaluating the dose equivalent rate for neutrons, the spectrum of which is unknown. The detectors employed include a BF_3 proportional counter, with paraffin moderators 6.5 and 1.0-cm thick sheathed in 0.5-mm thick cadmium, and a scintillation (ZnS + plastic) counter.

The dose equivalent rate D_B (mrem/hr) for neutrons below about 2 MeV is determined as follows. The neutron flux $\phi(E)$ (n/cm^2·sec) is measured by the BF_3 proportional counter covered with a 6.5 cm-thick moderator, uniformly sensitive to neutrons below 2 MeV, and the effective energy E_{eff}(MeV) is determined from the ratio of the counting rate by the BF_3 proportional counter covered with a 1.0 cm-thick moderator, to that covered with a 6.5 cm-thick moderator. Then D_B is determined by means of the equation $D_B = h(E_{\text{eff}})\phi(E_{\text{eff}})$, where $h(E)$ (mrem/hr/n/cm^2·sec) is the conversion factor from the flux density to the dose equivalent rate.

The dose equivalent rate D_S(mrem/hr) for neutrons above about 2 MeV is measured with the scintillation counter, the sensitivity of which is nearly proportional to the dose equivalent rate for neutrons above 2 MeV, calibrated by the proper source in mrem/hr.

Since the neutron energies range in general from epithermal to fast, the total dose equivalent rate D(mrem/hr) is obtained from the equation $D = D_B + D_S$.

The error in evaluating the total dose equivalent rate by the present method was calculated to be a maximum of 60 per cent for typical neutron spectra, in the energy range of epithermal to 10 MeV.

VAN-DE-GRAAFF MESSUNGEN DER REM-EMPFINDLICHKEIT EINES PROTONENRÜCKSTOSSZÄHLROHRS

K. HENNING und U. JANSSEN
Gesellschaft für Kernenergieverwertung in Schiffbau und Schiffahrt m.b.H.,
Geesthacht-Tesperhude (B.R.D.)

Zusammenfassung—Am Van-de-Graaff-Generator der Universität Hamburg wurde die REM-Empfindlichkeit eines ProtonenRückstosszählrohrs für Neutronen in dem Energiebereich von 0,1 bis 6,3 MeV als Funktion der Diskriminatorspannung gemessen. Die über die Neutronen-Energien gemittelte REM-Empfindlichkeit der Zählrohre (vom Typ FN2) nimmt mit wachsender Diskriminatorspannung ab. Es wurde festgestellt, dass bei den verschiedenen Neutronen-Energien die Abweichung von der mittleren REM-Empfindlichkeit bei den gewählten Diskriminatorspannungen zwischen ± 20 und ± 50 Prozentliegt. Da der Einfluss der Diskriminatorspannung auf den mittleren Fehler bei der Ermittlung der REM-Dosis also relativ klein ist, kann für die praktische Neutronen-Dosimetrie im Strahlenschutz auf die vom Hersteller vorgeschriebene genaue Einstellung der Diskriminatorspannung verzichtet werden.

LA DOSIMÉTRIE PRATIQUE DES RAYONNEMENTS ÉLECTROMAGNÉTIQUES ET DES NEUTRONS RAPIDES PAR DES CHAMBRES D'IONISATION À REMPLISSAGES LIQUIDES

D. BLANC, P. CAMINADE, J. MATHIEU et J. P. PATAU

Centre de Physique Nucléaire, Faculté des Sciences, Toulouse; et H. FRANÇOIS et G. SOUDAIN, Service Technique d'Études de Protection, CEA, Centre d'Etudes Nucléaires, Fontenay-aux-Roses (France)

Résumé—Les chambres d'ionisation décrites présentent une géométrie cylindrique; le procédé de remplissage assure une étanchéité et une stabilité parfaites en fonction du temps. L'étude de la sensibilité en fonction du diamètre des électrodes permet de déterminer les dimensions optimales du détecteur.

Pour la dosimétrie des rayons X et rayons γ, le remplissage choisi est un mélange d'hexane normal et de tétrachlorure de carbone, en proportions telles que le rapport du coefficient d'absorption massique en énergie dans ce liquide à celui dans les tissus biologiques mous reste constant de 30 keV jusqu'à 5 MeV. Pour une tension appliquée de 5,000 volts, la sensibilité est de 5×10^{-7} rad sec^{-1} et la réponse est linéaire en fonction du débit de dose, jusqu'à 1 rad sec^{-1}.

Pour la dosimétrie des neutrons rapides, on utilise de l'hexane pur, ou un mélange d'hexane et de benzène présentant la même concentration en hydrogène que le tissu mou. La sensibilité est également de 5×10^{-7} rad sec^{-1}.

Dans un flux constant de particules, un tel dosimètre permet d'évaluer le facteur de qualité du rayonnement incident.

LA DOSIMÉTRIE DES NEUTRONS AU MOYEN DE COMPTEURS DE GEIGER-MÜLLER À CATHODES ACTIVABLES

P. BAYLE, D. BLANC et H. RAKOTONDRAFARA

Centre de Physique Nucléaire, Faculté des Sciences, Toulouse; et M. LEVY et A. VALLÉE, Laboratoire Central de l'Armement, Fort de Montrouge, Arcueil (France)

Résumé—Dans la dosimétrie par activation, le comptage des particules émises par l'échantillon pose des problèmes délicats, liés à la rétrodiffusion des particules, à l'angle de détection, etc. Un procédé simple permettant d'éviter de telles difficultés, consiste à construire un compteur de Geiger–Müller dont la cathode soit activable: l'angle solide de détection est alors voisin de 2π.

Nous avons étudié la réponse à des flux intégrés des neutrons de 14 MeV de diverses cathodes, sélectionnées en fonction de leur travail d'extraction, de leur section efficace d'activation, de la période du radioélément produit. Peuvent convenir l'aluminium, le cuivre, le laiton, l'argent et l'acier inoxydable.

Les compteurs à cathodes d'aluminium, de cuivre ou de laiton permettent de mesurer des doses totales allant de 8 rads à 700 rads, selon le flux des neutrons traversant le détecteur.

Les compteurs à cathodes d'argent ou d'acier inoxydable permettent de mesurer des doses allant de 20 rads à 1900 rads environ.

Le calcul montre que, dans le cas de "flashes" de neutrons d'une durée totale de 0,1 sec on obtiendrait une sensibilité de 10^8 n cm^{-2} sec^{-1} dans le cas de l'aluminium, du cuivre ou de l'argent, et une sensibilité de 10^{10} n cm^{-2} sec^{-1} dans celui de l'acier inoxydable.

Par spectroscopies infrarouges, nous avons également étudié les modifications du remplissage gaseux produites par l'irradiation neutronique.

ABSORBED DOSE DETERMINATION FOR MEGAVOLTAGE X-RAYS AND ELECTRONS

H. MATSUZAWA
National Institute of Radiological Sciences, Chibas, Japan

Abstract—Local absorbed dose in the human body irradiated with megavoltage X-rays or electrons may be determined from ionization measurements at the place of interest by means of the cavity ionization relationship. An air-filled small ionization chamber having a 0.5 mm lucite wall, 0.68 cm^3 volume and 6 mm diameter has been developed to measure the cavity ionization.

Methods for detecting the collected charge through a resistor or a capacitor have been compared with the Townsend balance method. Then, the stem leakage of the chamber has been examined for ^{60}Co γ-rays, 10–29 MeV electrons and 10–29 MV X-rays. The results show that the stem leakage is less than 0.2 per cent of the cavity ionization, and hence the leakage may be neglected in the practical use of the chamber. Subsequently, cavity ionizations in water phantom have been measured by this chamber covered with different thicknesses of lucite caps, and the true cavity ionization without lucite wall has been given by means of extrapolation. It was found that the effect of the wall is negligible for megavoltage radiations, provided the wall is less than 150 mg/cm^2. Absorbed dose in soft tissue relative to the cavity ionization has been estimated on the assumption that water is equivalent to tissue. For example, the values are 0.88–0.82 rads per esu/cm^3 for 10–29 MeV electrons, and 0.98–0.95 rads per esu/cm^3 for 10–29 MV X-rays.

STOPPING POWER AND DOSE EQUIVALENT OF α-PARTICLES IN TISSUE EQUIVALENT GAS

E. ROTONDI
Division of Applied Physics, National Research Council, Ottawa, Canada

Abstract—Biological damage produced by charged particles in tissue depends on the dose delivered and on the linear energy transfer. It appears therefore of fundamental interest to investigate stopping power data for dosimetric purposes. A method has been developed to measure rapidly the range–energy relation and stopping power of α-particles in gases. The apparatus, reported in previous work, consists of a gas absorption cell in which α-particles from ^{210}Po lose their energy, and of a semiconductor detector which measures the residual α-energy. Stopping powers for α-particles have thus been obtained for CH_4, CO_2, O_2 and N_2 over an energy range from 0.1 to 5.3 MeV. Assuming that the stopping power is independent of the state of condensation of the medium and that it follows Bragg's additivity law, stopping powers in tissue (H: 10.1%, C: 12.1%, N: 4.0%, O: 73.6% by weight) have been calculated. The results are higher by as much as 50 per cent at 1 MeV than those given by Neufeld and Snyder. Consequently the dose equivalent for α-particles has, for instance, to be increased by 15 per cent at 1 MeV. Agreement between the present stopping powers and those given in a review by Whaling for $E_\alpha > 2$ MeV has been found.

DISCUSSION

W. N. SAXBY (*U.K.*):

In her excellent seminar of eight papers on widely diverse topics, Dr. Ehrlich made two points which deserve further discussion.

First: She said that in personal dosimetry and record keeping there is perhaps a tendency to be getting insignificant returns for the efforts expended. I believe that this may well be true, and before more effort is used, and certainly before new dosemeter materials are brought into use, operational Health Physicists should critically examine the reasons for carrying out personal dosimetry. Dr. Ehrlich quoted data showing how very few people exceed 1/10th of the annual dose limit, this is also true in England, and of all these it can probably be truly said that they "are most unlikely to exceed 3/10ths of the annual dose limit" and as suggested by ICRP (ICRP Publication No. 9, Pergamon Press, Oxford, 1966) need not therefore be subject to special Health Physics and Medical Surveillance and do not need to have formal personal dose records kept for them. This is not however necessarily to be taken to mean that some form of personal dosemeter will not be issued to this group of people, since in areas handling large and varied research and development programmes, dosemeters worn on the person may well be the only practicable and economic way of checking that the protective measures adopted are keeping the working radiation environment at satisfactory exposure levels. However, any such dosemeters are monitoring the working environment, *not* the person, and the interpretation and record keeping need not be so complicated or so formal as for personal dosemeter data. If we carry out this review carefully and see personal monitoring objectives clearly there is scope for a considerable saving in time, effort and records.

Second: Dr. Ehrlich indicated that there is a strong feeling that the old well established extremely informative, but difficult, film badge should be displaced by some other dosemeter. Such sentiments are too sweeping; at the present time there is no one entirely satisfactory dosemeter and there may never be such a paragon of virtues. *The dosemeter of choice must depend on local circumstances*: on the range of radiations, and types of operations, on national statutory requirements, and on other factors. Thus in a large U.K. nuclear research and radioactive materials development establishment there is a need for a dosemeter which will respond in a known way to all types and energies of radiations, including all gamma energies from say 17 keV to several MeV and will enable processing staff to determine if it has been contaminated and what sorts of energies have been involved, to name just two diagnostic requirements; also the dosemeter should ideally be capable of exposure on the body or on the first finger joints. At the present time the film badge is nearest to doing all of this, helped by LiF thermoluminescent dosemeters; glass cylinders or rods are a long way from meeting these requirements; LiF is expensive, labor consuming and is not yet in a position to be used entirely alone, but current research might make it useable and economical. I hope to hear further discussion on these points during the next few days.

D. NACHTIGALL (*Euratom*):

In ihrem Rapport über unsere Arbeit hat Frau Ehrlich gesagt, dass wir bei unserer Abschätzung über die Augendosis die Empfehlungen der ICRP über die Anwendung modifizierender Faktoren nicht berücksichtigt hätten und dass, wenn wir das getan hätten, unsere Abschätzungen ungünstiger ausgefallen wären. Das ist natürlich richtig. Ich möchte aber hier auf die praktischen Konsequenzen hinweisen, die daraus resultieren würden. Ich möchte zunächst den betreffenden Abschnitt aus den ICRP-Empfehlungen, veröffentlicht in der Publication 9, Seite 4, Pergamon Press, 1966, zitieren: "When the lens of the eye is irradiated, an additional modifying factor may need to be used as well as the QF. The value of the modifying factor should be 3 when the QF is 10 or greater, but should be 1 when the QF is 1. The value of an appropriate modifying factor to be used with values of QF between 1 and 10 may be obtained by interpolation between 1 and 3". Im praktischen Neutronenstrahlenschutz hat man es im allgemeinen mit Streufeldern zu tun. Dabei ist immer mit einer Augenbestrahlung zu rechnen. Der modifizierende Faktor muss also mit in Rechnung gestellt werden. Die Anwendung der genannten ICRP-Empfehlung würde bei schnellen Netronen von 1 MeV zu einem effektiven QF von 30 führen, bei thermischen Neutronen erhielte man den effektiven QF von nahezu 6. Das würde zu einer neuen Dosisäquivalentkurve führen, und man müsste in Zukunft unterscheiden zwischen dem bisher gebräuchlichen Begriff des

Neutronendosisäquivalentes und dem "Augen-Dosisäquivalent" der Neutronen. Ausserdem muss erwähnt werden, dass es im Augenblick kein Survey-Messgerät gibt, dass das "Augen-Dosisäquivalent" misst. Als vorübergehende Kompromisslösung bietet sich an, die mit dem gebräuchlichen rem-counter gemessenen Werte einfach mit dem Faktor 3 zu multiplizieren.

M. EHRLICH:

Well, I agree with Mr. Nachtigall that it is going to be difficult to realize this and I understand that some countries will not go along with ICRP 9. But on the other hand, these recommendations are not made by what is easy to realize but by what is a biological necessity.

K. BECKER (*Germany*):

Offensichtlich ist die Zahl der Filter in Filmdosimetern immer noch im Ansteigen begriffen. Damit wird zwar die Genauigkeit der Energie—und damit der Dosisbestimmung für Photonen unter Laborbedingungen etwas verbessert, gleichzeitig aber die Auswertung kompliziert, Randfehler werden wahrscheinlicher usw. Allgemein bekommt man den Eindruck, dass hier der Aufwand zur Verminderung einer Fehlerquelle dazu führen kann, die Aufmerksamkeit von zahlreichen anderen Fehlerquellen, die nicht weniger bedeutsam sind (Richtungsabhängigkeit, Latenzbildschwund, Verschleierung, Entwicklungs- und Auswertungsfehler, etc.) abzulenken.

Zu völlig falschen Vorstellungen über die mit Filmdosimetern erreichbare Genauigkeit führen Vergleichsmessungen, welche unter idealisierten, d.h. stärker auf die Möglichkeiten der Filmdosimetrie als auf die tatsächlichen Erfordernisse abgestimmten Laborbedingungen (frontale Freiluftbestrahlung mit Quantenstrahlung in einem relative engen Dosis- und Energiebereich unter rückstreuarmen Bedingungen, relativ kurzfristige Lagerung von Kontroll- und Testfilmen unter identischen Bedingungen, ausgesucht sorgfältige Auswertung) immer wieder durchgeführt werden. Wenn die Testbedingungen besser an die tatsächlichen Verhältnisse der Praxis wie z. B. Lagerung für sehr verschiedene Zeiten unter unterschiedlichen Klimabedingungen und verschiedene Einfallrichtungen und Orientierungen zum Phantom angeglichen werden, sind die Ergebnisse ungleich schlechter. Nur in Aussnahmefällen wird dann eine hinreichende Übereinstimmung zwischen Dosimeteranzeige und Ganz- oder Teilkörper- (Organ-) Dosis gefunden.

K. KOREN (*Norway*):

There is one important aspect of personnel dosimetry that must be considered here, namely the cost of distribution from a central institution to users in a whole country. I can not see how solid state dosimeters can make P.M. films obsolete at this stage, because the postage expenses would still be too high for glass and other solid devices. Otherwise I do agree with the remark that one should not overestimate the accuracy of film dosimetry even when a series of filters has been introduced into the filmholder.

G. COWPER (*Canada*):

It has been noted in the discussion that it is difficult to design a film dosimeter whose sensitivity will extend over a very wide range of energies. However, it must be stressed that the objectives of a design should not generally require a great energy dependence characteristic. Only rarely will the primary purpose of a film dosimeter for gamma radiation be to determine the dose to the skin. Most frequently, the principal objective is to assess the dose to the bone marrow, the gonads, or, in an emergency situation, to the GI tract. For such purposes, a dosimeter is required whose sensitivity diminishes below an energy of 100 keV. This is not a particularly difficult task. Multiplicity of filters is only required if spectrometric data of the incident radiation are required. An advantage of a simple system, e.g. an open window, a beta filter and a gamma filter is that it allows a greater area of films for assessment of the dose.

W. N. SAXBY (*U.K.*) (Remarks):

The last gentleman intervening after Dr. Ehrlich suggested that in my comments I had implied a "uniform response from 17 keV to several MeV": this was not so. I said "*a known response*"; I agree with him that what may well be needed in particular circumstances is a dose equivalent in some specific organ or at some point in or on the body, or over a whole organ or body mass—*but* it is still necessary to have a known starting exposure measured by some specified and defined means.

D. NACHTIGALL (*Euratom*):

Ich möchte folgende Frage für diese Diskussion stellen: nach den ICRP Recommendations und Veröffentlichungen, zum Beispiel NBS Handbook 80, ist das Dosisäquivalent gegeben aus dem Produkt Absorbed Dose, also Energiedosis, multipliziert mit dem QF, multipliziert mit dem Distribution Factor oder mit anderen modifizierten Faktoren. Nun haben wir in dem Vortrag des Dr. Rotondi gehört, dass das kugelförmige Dosimeter das Dosisäquivalent entsprechend den ICRP Recommendations misst.

Die Recommendation in der Publication N. 9 empfiehlt, dass der modifying factor 3 für Strahlung, der QF 10 zugeschrieben werden muss, benutzt werden soll; dass heisst als Konsequenz, dass es jetzt nach den ICRP Recommendations 2 verschiedenen Typen von Dosisäquivalenten gibt: ein Typ umfasst nicht den Faktor 3 für schnelle Neutronen und 2 für thermische Neutronen, umfasst also nicht die Bestrahlung der Augenlinsen mit und die andere Definition umfasst diese Bestrahlung mit. Und ich möchte vorschlagen, dass in Zukunft immer dazu gesagt werden soll um welches Dosisäquivalent es sich in diesem Falle handelt: das Dosisäquivalent einschliesslich Augen oder Dosisäquivalent ausschliesslich Augen. Das kompliziert die ganze Sache sehr.

A. RINDI (*Cern*):

Vorrei conoscere quel'è la risposta della vostra camera a dielettrico liquido in funzione del Q.F. per differenti radiazioni (n, gamma di varie energie, campi misti).

D. BLANC:

Les facteurs de qualité des rayonnements sont déduits des points de concours du prolongement des "paliers" sur l'axe des abscisses. Ces points s'échelonnent, dans la partie négative de l'axe, des valeurs du champ électrique moyen de (−10 kV/cm) pour les particules α à (−18 kV/cm) pour les rayons X ou γ. Ces points s'alignent dans l'ordre des facteurs de qualité.

DOSE TO TRABECULAR BONE FROM INTERNAL BETA-EMITTERS

F. W. SPIERS

Medical Research Council, Environmental Radiation Research Unit, Department of Medical Physics, The University of Leeds, Leeds, England

Abstract—Consideration is first given to the general structure of trabecular bone and to the location of tissues within it that are relevant to possible radiation damage, namely (1) active bone marrow, as the blood-forming tissue, and (2) endosteal tissues close to trabecular surfaces.

For dosimetric purposes, data are required on the dimensions of the trabecular cavities and of the over-all dimensions of the trabecular parts and of the cortical thickness in different bones. Investigations are described by which these physical characteristics have been obtained.

Methods of calculation of the mean marrow dose and the mean dose to endosteal surfaces are discussed and results given for individual bones, and for the whole skeleton, for the radioisotopes ^{14}C, ^{45}Ca and ^{90}Sr. The implications of β-particle dosimetry in trabecular bone for the setting of maximum permissible levels of β-emitters in bone are briefly discussed.

1. INTRODUCTION

Bone has for long been recognized as one of the most important organs at risk from the internally-deposited radioisotope, and has been taken as the critical organ for about one-quarter of all isotopes listed in ICRP Publication 2.[1] It is only recently, however, that detailed consideration has been given to the microscopic structure of bone in relation to the dose delivered to particular tissues within it. This is perhaps not surprising in view of the complex nature of bone and the lack of precise information on the relative radiosensitivity of the tissues involved. It is becoming increasingly possible, however, to extend the concept of dose to bone beyond that of the average energy deposited in 7000 g of skeleton, regarded simply as a more-or-less uniform substance, having a greater density and higher atomic number than soft tissue. Work on some aspects of this approach to bone dosimetry will be described in this paper.

2. STRUCTURE OF BONE AND LOCATION OF RELEVANT TISSUES

The section cut through a long bone, the femur, in Fig. 1(a) shows the features which are relevant to the physical aspects of radiation action. The hard bone of the cortex has a thickness of 5 mm or more in the bone shaft but thins out towards the end of the shaft and is very thin at the head of the femur. The bone shaft is filled mainly with connective tissues, yellow marrow and blood vessels, but towards and at the ends of the bone, the bone consists of a network of interlacing thin lamellae of hard bone, forming a system of small cavities which contain the red, blood-forming marrow. This trabecular or spongy bone can be seen in Fig. 1(b) to comprise almost the whole of a vertebral body which furthermore has only a very thin cortex. Trabecular bone is also present in the flat bones of the body such as the hip bone, the scapulae and the ribs (Fig. 1(c)). The cavities in trabecular bone vary considerably in size and shape in any one bone, and different bones, and different parts of the same bone, vary in the range and distribution of cavity sizes. Compare, for example, the large cavities in the femur and the vertebra with the much smaller cavities in the iliac crest.

The thin bone lamellae or trabeculae vary in thickness from place to place but are of the order of 100 μ thick; they contain mature bone

cells, the osteocytes, which receive their nutrients via canaliculi from the plasma of the bone marrow. The photomicrograph in Fig. 2 shows a few such cells in a bone trabecula and shows also other cells, osteoblasts, which lay down the bone matrix, and osteoclasts, which resorb bone, lying close to the trabecular surfaces. The more primitive ancestral cells, or "osteoprogenitor" cells lie somewhat farther away from the trabecular surface. Apart from these layers of endosteal cells, the cavities are filled with cells of the active marrow.

If, as in radiation protection we are concerned with damage to the blood-forming tissues and the avoidance of radiation-induced anaemia, or of leukaemia of the myeloid type, clearly the relevant tissue is the red marrow in the trabecular cavities for there are normally too few active marrow cells in the yellow marrow of the bone shafts to make their consideration significant. If, on the other hand, the risk of radiation-induced bone tumour is to be considered, there is good evidence accumulating, reviewed by Vaughan,[2] that osteogenic tumours in irradiated animals arise in endosteal tissues—presumably in the osteoprogenitor cells from which the osteoblasts develop. This directs attention to the dose to the tissues which lie close to all endosteal bone surfaces but particularly to those in trabecular bone where the extent of these surfaces is so very great. Although it is difficult to define the exact location of the osteoprogenitor cells with respect to the trabecular surface, a zone between 5 μ and 10 μ from the bone surface is thought to be a realistic site for purposes of dose calculation.

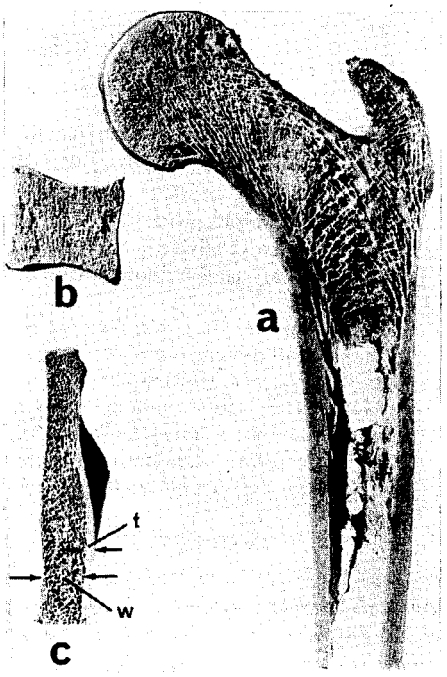

FIG. 1. Sections of human bone: (a) shaft and upper end of femur, (b) lumbar vertebra, (c) part of hip bone sectioned through the iliac crest.

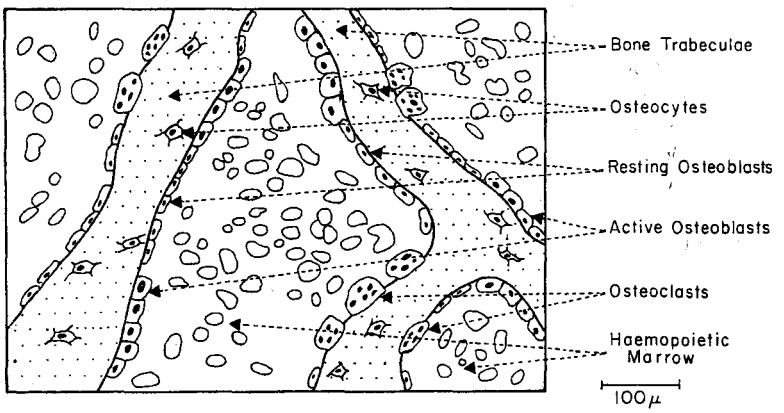

FIG. 2. Photomicrograph of a section through a trabecula showing the associated cells. (By permission of Academic Press, New York.)

3. MENSURATION OF TRABECULAR BONE

Calculations of the endosteal tissue dose and the mean marrow dose require, in the first place, a knowledge of the dimensions of the trabecular cavities. For long range particles, however, the over-all size of the bone may be insufficient to give conditions of particle equilibrium, and in some bones β-particles from isotopes deposited in the cortex can contribute significantly to the trabecular dose. It is necessary, therefore, to specify additionally both the over-all bone dimensions and the thickness of the cortex.

A start on the measurement of cavity dimensions in trabecular bone was made some years ago[3] and mensuration of a limited number of bones in the adult and child has been used as a basis for determining the dose to trabecular bone from $^{90}Sr + {}^{90}Y$.[4] In this work very simplified bone shapes were assumed; flat bones were regarded as made up of a slab of trabecular bone of given average width between two plane sheets of cortical bone; the ends of shafts containing trabecular bone were taken to be cylinders with walls of uniform thickness. Representative average thicknesses and other dimensions were obtained by simple measurement of sections of the bones concerned. The sizes of the cavities in the trabecular parts of the bone were measured on an optical enlargement of a photograph of a section through the trabeculation. The cavity size was taken to be the average linear dimension of the cavity as seen in the section. Such a simple measure of cavity size, however, can be only a rough approximation and it can only be used in a dose calculation by further assuming the cavity to have some simple geometrical shape. With these limitations in mind Fig. 3 depicts the distributions of cavity sizes in the sections of the third lumbar vertebra of an adult and a child; despite the crudity of this approach to the problem there is clearly a very significant difference between the adult and the young bone, a difference which will affect the β-particle dose to the bone marrow.

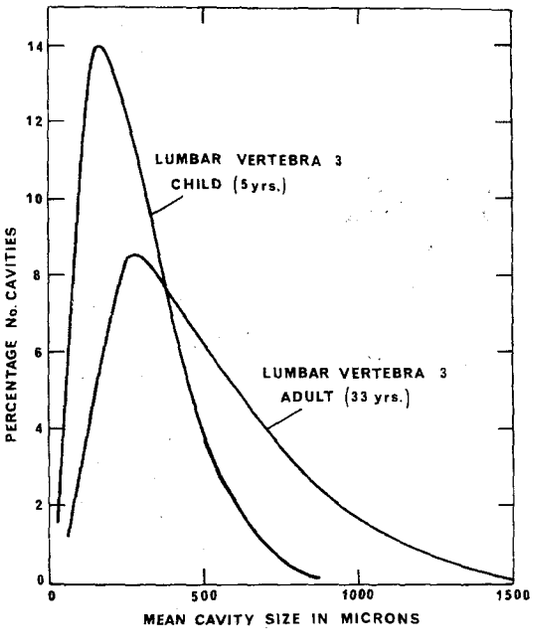

FIG. 3. Distribution of marrow cavity sizes in trabecular bone of the third lumbar vertebra of an adult and a child aged 5 years. (By permission of Academic Press, New York.)

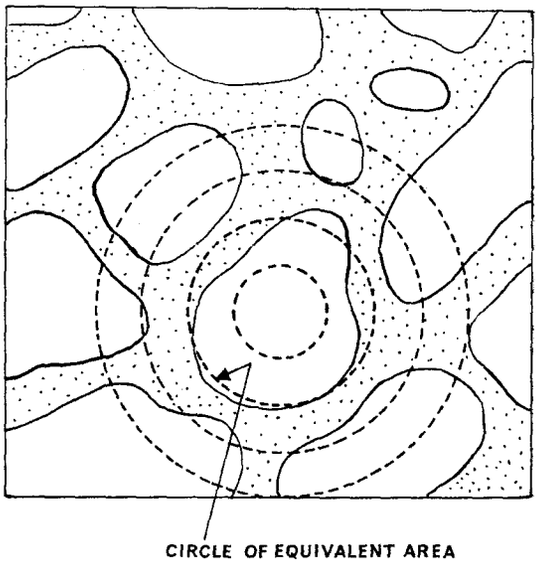

FIG. 4. Equivalent-circle method of determining the mean size of a cavity in trabecular bone.

A convenient and better method of making the measurement of average cavity dimension is illustrated in Fig. 4. A projection microscope is used to view the trabecular bone section and a set of circles on the viewing screen enables

any given cavity to be designated by a circle of "best fit" or equivalent area.

An entirely different method and a new approach to describing the relevant physical dimensions in trabecular bone is shown in Fig. 5. If for the moment we regard the ionizing particles as travelling in straight lines, any given particle will cross one or more cavities with varying path lengths in bone marrow, depending on the cavity size, shape and point of entry. If we had a complete distribution of all possible path lengths (in three dimensions) in a given portion of trabecular bone, we should have a basis on which to calculate the fraction of the particle's energy deposited in the marrow. Although we have only developed this idea so far in relation to what we shall call "single-cavity" calculations, and although we have used only hand-operated, "un-automated" techniques, we have compared the new and the old methods on the same section of an adult lumbar vertebra. The path length distribution has been obtained with the aid of a rectangular grid on the screen of the projection microscope, as shown in Fig. 5, and we have investigated the distributions of path lengths so far in only two mutually perpendicular directions. The results of

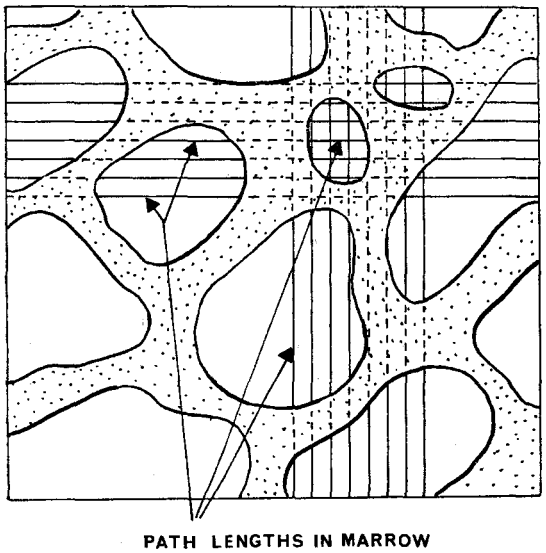

FIG. 5. Method of measuring the distribution of path lengths in marrow cavities in trabecular bone.

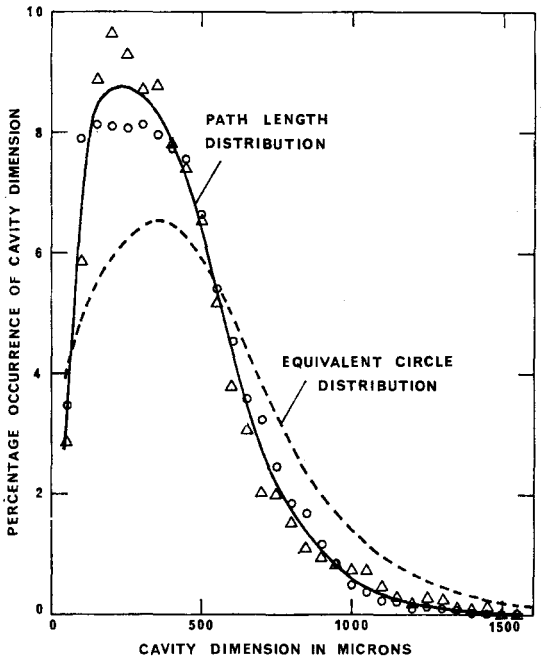

FIG. 6. Equivalent-circle distribution and path-length distribution measured in the same section of a lumbar vertebra. Circles give path-lengths measured in the x-direction and triangles in the y-direction.

the measurements in the two directions are seen to be in reasonable agreement in Fig. 6, where they are also compared with the "equivalent-circle" distributions for the same bone. The important feature of the new method is that it provides a physical description of the cavity dimensions (and, when required, of the dimensions of the trabeculae) which can be used for dosimetry without the necessity for assumptions about the cavity shapes.

4. METHODS OF DOSE CALCULATION AND SOME RESULTS

A number of methods,[5-9] developed in recent years, can be applied to the calculation of dose in trabecular bone; they give the dose inside cylindrical and spherical cavities or in slabs of tissue between plane sheets of bone. If the energy of the β-particle is sufficiently low, its range in bone may be of the same order as

the thickness of the trabeculae and the irradiation of the tissues within a cavity will then arise only from β-particles emitted by its own boundary walls. This is the case for the ^{14}C β-particles ($E_\beta = 0.155$ MeV) and practically so for ^{45}Ca ($E_\beta = 0.25$ MeV), where about 10% of the β-particles have ranges which are greater than the average trabecular thickness, but still insufficient for any significant dose contribution to come from trabeculae other than those immediately around the marrow cavity. Single-cavity calculations of the endosteal surface dose and the mean marrow dose can then be made by assuming spherical cavities and integrating the data of Charlton and Cormack[7] over the ^{14}C and ^{45}Ca β-spectra. The variation of the surface dose ratio D_s/D_o, the mean marrow dose ratio $\bar{D}_m/D_o$ and the ratio $D_s/\bar{D}_m$ with cavity size for these two isotopes is shown in Figs. 7 and 8. The ratio of surface dose to mean marrow dose rises steeply with cavity size and, for a large cavity of 1500 μ diameter, rises to a value of 6 for ^{45}Ca and 13 for ^{14}C. By weighting the values of D_s/D_o or $\bar{D}_m/D_o$ for each cavity size by the relative cavity size distribution (see,

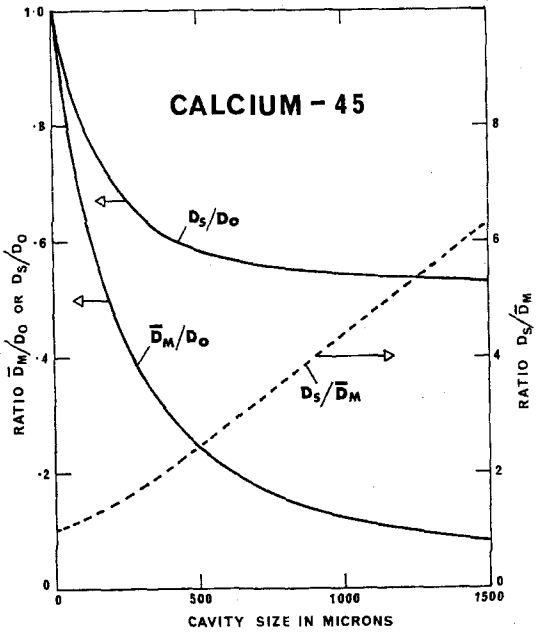

FIG. 8. Variations in $\bar{D}_m/D_o$, D_s/D_o and $D_s/\bar{D}_m$ with cavity size for ^{45}Ca β-particles.

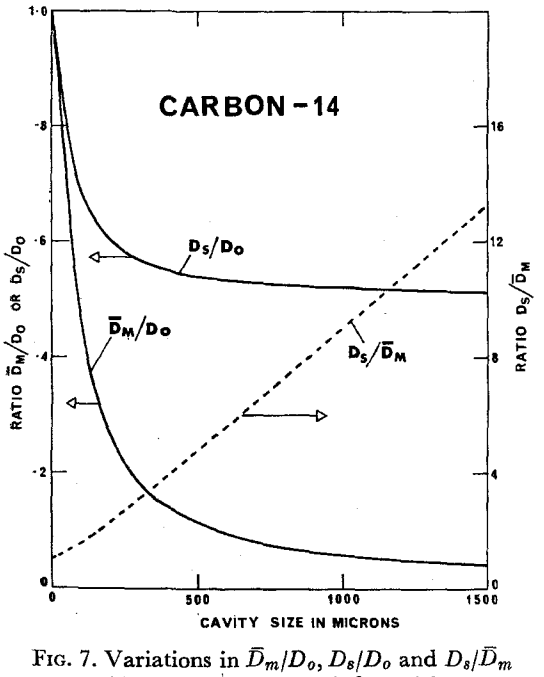

FIG. 7. Variations in $\bar{D}_m/D_o$, D_s/D_o and $D_s/\bar{D}_m$ with cavity size for ^{14}C β-particles.

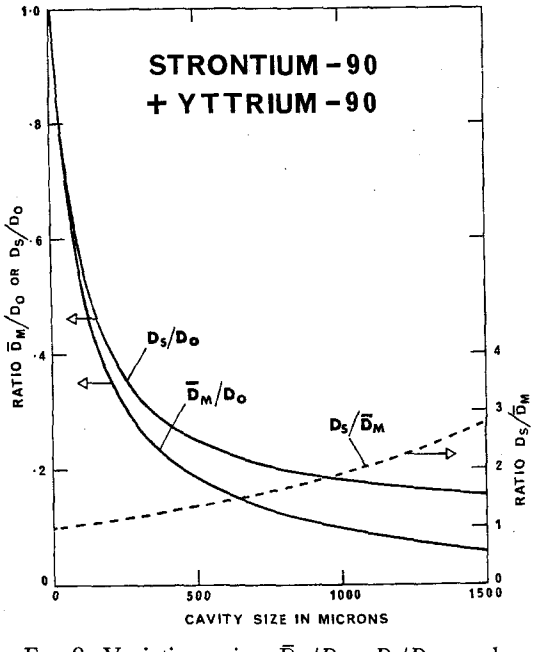

FIG. 9. Variations in $\bar{D}_m/D_o$, D_s/D_o and $D_s/\bar{D}_m$ with cavity size for $^{90}Sr + {}^{90}Y$ β-particles

for example, Figs. 3 or 6), average values for a given bone section can be obtained.

Similar data for $^{90}Sr + ^{90}Y$ are shown in Fig. 9; they are taken from the calculations of Engstrom *et al.*[9] for a sandwich model of trabecular bone, comprising an array of plane lamellae of bone, 70 μ thick, separated by layers of marrow of variable width. These data have been used to obtain dose values for various bones, using measured cavity size distributions and adding an increment of 25% as an estimated allowance for changing from plane to spherical geometry.[4]

Available data on the ratio of the average endosteal dose to the average marrow dose for a number of different bones are listed in Table 1 for the three isotopes so far studied. Estimated values for the whole skeleton are also included. Before considering the implications of the data in Table 1 in relation to the setting of permissible levels of bone-seeking β-emitters, some preliminary results should be given on the application of linear path-length distributions to dosimetry in trabecular bone.

Calculations have been made of the mean dose to bone marrow on the basis of the distributions of cavity dimensions shown in Fig. 6, and for irradiation by mono-energetic X-rays in the energy range 20 to 170 keV. Calculations for X-radiation were made because the mean marrow dose could then be investigated experimentally, using a thermo-luminescence technique in which very fine grain LiF powder is introduced into the actual section of vertebra used for the cavity size measurements.[10] The equivalent-sphere distribution in Fig. 6 was combined with data based on Charlton and Cormack's calculations for the X-ray dose in spherical cavities[7] to give the variation in

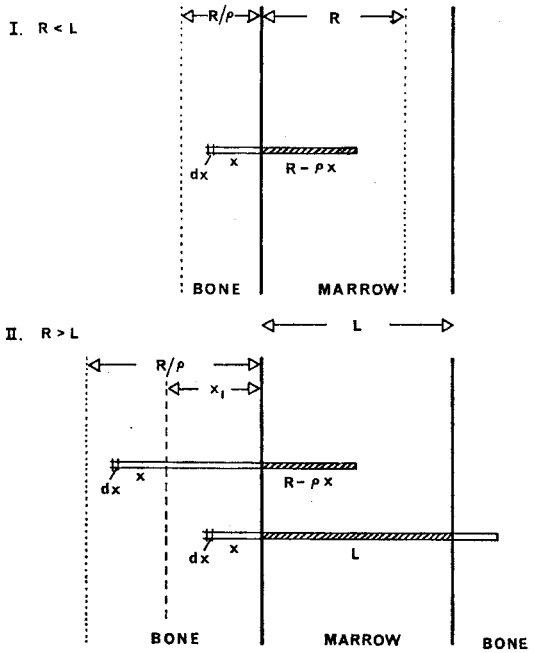

FIG. 10. Diagrams illustrating the method of calculating the energy deposited along a path-length L in marrow by β-particles of range R in tissue and range R/ρ in bone.

Table 1.

Bones	Ratio $D_s/\bar{D}_m$		
$\bar{E}_\beta$(MeV)	^{90}Sr 1.1	^{45}Ca 0.086	^{14}C 0.054
Hip fine	1.5	2.7	5.4
coarse	1.7		
Cranium	1.2		
Rib	1.3	3.4	6.6
Femur head	1.8		
upper shaft	1.6		
Vertebra L.V.3	2.1	4.2	8.4
Whole skeleton	2.0	3.5	7.0

dose with photon energy. The linear path-length distribution was combined with a simple energy-deposition calculation, the principles of which are illustrated in Fig. 10. The formulae for the mean marrow dose can readily be deduced as:

$$\bar{D}_m/D_o = \frac{m}{1+m}\frac{R}{L} \qquad \text{for } R < L$$

$$\text{and } \bar{D}_m/D_o = \frac{m}{1+m}\frac{R}{L}\left[1-\left(1-\frac{L}{R}\right)^{\frac{1}{m}+1}\right] \qquad \text{for } R > L$$

where m is the exponent in the range-energy formula $R = AE^m$ and is taken to be 1.75 for energies up to a few hundred keV, as in the work of Charlton and Cormack[7] and the later evaluations of Howarth.[8]

It can be seen from the results shown in Fig. 11 that the linear path calculations lead to the higher values of $\bar{D}_m/D_o$; the equivalent-sphere calculations are lower partly because there is almost certainly an over-weighting of the low values by the large marrow mass attributed to the larger cavity dimensions as they appear in the section. The experimental results are as yet only very preliminary, but they lie on or above the linear-path curve in Fig. 11. Similar comparisons of calculated and measured mean marrow dose are being made, in collaboration with Dr. M. Goldman of the University of California, on samples of beagle bone containing $^{90}Sr + {}^{90}Y$. One immediately apparent feature of the dog bone, which must greatly affect the level of the mean marrow dose, is the fineness of the trabecular structure compared with the corresponding human bone.

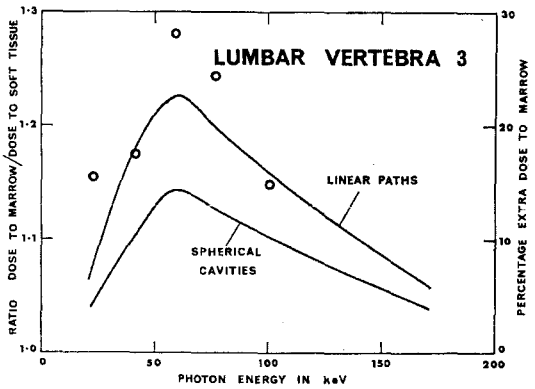

FIG. 11. Calculated values of the dose to marrow in trabecular bone compared with that to soft tissues remote from bone; the right-hand scale gives the percentage extra dose to bone marrow from the photoelectrons released in bone.

Table 2.

Quantity \ Isotope	^{90}Sr	^{45}Ca	^{14}C	Units
1. $\bar{E}_\beta$	1.1	0.086	0.054	MeV
2. D_o*	2.7	0.21	0.13	rem/yr
3. $\bar{D}_m/D_o$	0.21	0.16	0.075	
4. $\bar{D}_s/D_o$	0.42	0.56	0.53	
5. $\bar{D}_m$	0.55	0.034	0.010	rem/yr
6. $\bar{D}_s$	1.10	0.118	0.069	rem/yr
7. Skeletal burden for 5 rems/yr to bone marrow	9	150	500	μCi
8. Skeletal burden for 15 rems/yr to endosteal tissue	13.5	125	220†	μCi

* D_o is dose-rate to bone, taken as 7000 g wet bone without marrow, containing uniform deposit of 1 μCi.

† Dose to body-fat is still the limiting factor in setting mpbb for ^{14}C.

5. PERMISSIBLE LEVELS FOR β-EMITTING BONE-SEEKING ISOTOPES

Although it would be premature, on the basis of this limited data, to put forward new solutions to the difficult problem of setting maximum permissible levels of β-emitters in bone, the dose ratios given in Table 1 suggest that a dosimetric approach is worthy of consideration. Two tissues in bone have been identified as relevant, bone marrow and the endosteal tissues in trabecular bone, and the mean doses to them can be determined at least for some isotopes. In terms of the present maximum permissible annual doses (a) 5 rem to bone marrow and (b) 15 rem to any single internal organ, e.g. to trabecular endosteum, the marrow dose would clearly be the limiting factor in the case of ^{90}Sr. For ^{45}Ca, and for any β-emitter of lower energy, the endosteal dose would set the limit. Some values of the dose-rates produced by a uniform skeletal burden of 1μCi are given in Table 2 to illustrate the order of maximum permissible levels implied by these arguments. Other β-emitters which are deposited in the bone matrix would fall into one or other category according to the ratio of endosteal to mean marrow dose. Provided sufficiently good information is available about their location, even β-emitters which are deposited on bone surfaces, rather than in the matrix, may well be amenable to the type of calculation considered here. If these methods become sufficiently well founded, some of the serious difficulties inherent in the present comparison of low LET β-emitters with the high LET α-radiation of ^{226}Ra may be avoided.

ACKNOWLEDGEMENTS

The author is indebted to Mr. G. D. Zanelli and Mrs. J. McKie for the measurements they have made on the cavity sizes and path lengths shown for the lumbar vertebra in Fig. 6.

REFERENCES

1. Recommendations of the International Commission on Radiological Protection, Report of Committee II on Permissible Doses for Internal Radiation, ICRP Publication No. 2. Pergamon Press, London (1959).
2. J. VAUGHAN. Radiobiology Forum on Radiation Damage to Bone. Medical Research Council, London (1964).
3. N. JACOBS and F. W. SPIERS. In Radiation Effects in Physics, Chemistry and Biology, *Proc. Second International Congress of Radiation Research*, 462 (1963).
4. F. W. SPIERS. *Rad. Res.* **28,** 624 (1966).
5. M. HINDMARSH, M. OWEN, J. VAUGHAN, L. F. LAMERTON and F. W. SPIERS. *Brit. J. Radiol.* **31,** 518 (1958).
6. A. M. KONONENKO. *Biofizika* **2,** No. 1, 94 (1957).
7. D. E. CHARLTON and D. V. CORMACK. *Rad. Res.* **17,** 34 (1962).
8. J. L. HOWARTH. *Rad. Res.* **24**(1), 158 (1965).
9. A. ENGSTROM, R. BJORNERSTEDT, C. J. CLEMEDSON and A. NELSON. *Bone and Radiostrontium*, p. 100, Almqvist and Wiksell, Stockholm (1957).
10. F. W. SPIERS and G. D. ZANELLI, *Proc. XIth International Congress of Radiology, Rome* (1965) (in the press).

MECHANISMS OF PULMONARY CLEARANCE OF INHALED PLUTONIUM DIOXIDE AN AUTORADIOGRAPHIC STUDY AND PARTICLE SIZE ANALYSIS*

L. J. CASARETT† and P. E. MORROW

Dept. of Radiation Biology and Biophysics, University of Rochester Medical Center, Rochester, New York 14620

Abstract—An autoradiographic technique is described for measuring particle size distributions of inhaled $^{239}PuO_2$ in alveoli of dogs and rats at various periods of time after exposure. Additional data are presented for the tracheo-bronchial tree of rats and lymphoid tissue of dogs. In rat alveoli, an early (6 hr) decrease in MMD is followed by a rise (2 days) and a second decrease (7 to 32 days). A similar cyclic change in CMD in dog alveoli is found with a different time sequence (1 to 406 days). The implications of these and other observations are discussed.

INTRODUCTION

The pharmacokinetics and toxicology of plutonium compounds have generated an increasing interest for over twenty years. Of particular interest has been the behavior of insoluble plutonium compounds after inhalation. Earlier studies by Langham, Abrams and others[1-5] have been extended with a view to relating potential human hazard with the properties of the material inhaled, with values for pulmonary deposition and retention and to the pathways and mechanisms of clearance.

In more recent studies in the rat[6-8] and dog, [9-13] one aspect of particular interest has been the relation of particle size to deposition and clearance of alveolar regions. The present report has utilized experimental material from rats in a collaborative study with Boecker[7] and from dogs in a study by Morrow and coworkers.[9-13] Although some pertinent aspects of the autoradiographic findings are included incidentally here, detailed reports of each study will appear separately. This paper deals primarily with the relation of particle size to pulmonary clearance.

Morrow and Casarett[9] reported that in dogs two total respiratory tract deposition patterns were observed, 56% deposition in one group exposed to aerosols with an average CMD of 0.24 μ, σ_g, 1.81 and the second group with an 88% mass deposition following exposure to aerosols with mean characteristics of CMD of 0.7μ, σ_g, 1.77. Studies by Bair *et al.*[10, 12] for three different count median diameters (0.60, 0.43 and 0.86μ) and presumably comparable particle distributions, further extended the relation of alveolar deposition and clearance to inhaled particle size.

To assess possible particle size dependency of rate and route of pulmonary clearance, Morrow and Casarett[9] utilized an autoradiographic estimation of particle size in tissue structures in a preliminary series of four dogs sacrificed from 16 to 125 days after exposure. Among other findings, they reported a more tenacious retention of small particles (0.04–0.12 μ diameter) in alveolar regions and, consequently a relative increase in the percentage of particles of this size found with increasing time after exposure. In an extensive study using nearly the same technique, Bair *et al.*[12] reported

* This work was performed under A.E.C. Contract W-7401-ENG-49.

† Present address: Dept. of Pharmacology, University of Hawaii, Honolulu, Hawaii 96816.

data which, although differing in some details and subject to differences in interpretation, were not markedly unlike that reported previously for equivalent inhaled particle sizes and approximately equivalent times after exposure.

Although the techniques used were reported to be the same in both studies, there were significant differences and both executions were subject to more imprecision than necessary. Neither report included attempts at characterizing the distribution as a continuous function and both used different particle intervals. The study by Bair and co-workers has the advantage of short time intervals after inhalation and, while not strictly comparable to the dog work reported herein and previously, is of considerable value in itself and of particular pertinence in this report in allowing a comparison with rat data for equivalent time periods after inhalation.

A correction for geometry was made in previous studies; Bair *et al*[12] apparently used the same correction of 40% efficiency for all track counts irrespective of the density of radial tracks arising from the particle. Morrow and Casarett[9] used a preliminary sliding scale based on a 30–40% efficiency. The present study employed a refined correction. Figure 1 illustrates the variable ease of detection of tracks. As the density of tracks increases there is a decreasing likelihood of viewing tracks. For example, with small numbers of tracks (A, B), it is relatively easy to detect tracks entering the emulsion at an angle to the horizontal. However, as the number of tracks increases (B, C), fewer of the angular tracks are detectable; thus a smaller fraction of the emissions is counted the larger the number of tracks associated with the autoradiographic manifestation of the particle.

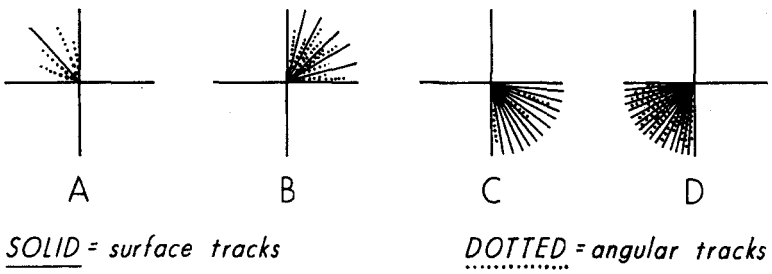

FIG. 1. Schematic representation of alpha track detectability. Relation of sunburst density to detection geometry.

METHODS

Animals were exposed, handled and sacrificed as previously described.[7, 9, 13] Tissues for autoradiography were fixed in 10% neutral buffered formalin, sectioned in paraffin at about 6 μ thickness and sections were floated on NTA* nuclear track plates (20 μ thickness) or covered with NTA nuclear track bulk emulsion (at least 20 μ thickness). Autoradiograms were stored for exposures of 1 day to 1 year and were processed under conditions specified by the manufacturer. Sections were routinely stained in hematoxylin and eosin.

* Eastman Kodak Company, Rochester, New York.

A curve for geometry correction was constructed. It will be noted in Fig. 2 that a measure of efficiency of detection can be taken as the detectability of tracks with the greatest angle of entrance into the emulsion and therefore the shortest apparent lateral length when viewed microscopically. Over 2000 sunbursts ranging from 10 to 285 readily observable tracks were examined for the track with the shortest apparent lateral traversal. As indicated in Fig. 2, the angle θ was calculated from the known length of track ("real") either by direct measurement or by calculation from the Pu energy and the stopping power of the emulsion. The

solid angle of the sphere which is, in fact, all that is really counted, can then be calculated and translated to an efficiency correction.

From autoradiograms of lung from each animal, random fields were viewed microscopically, a minimum of 500 particles was

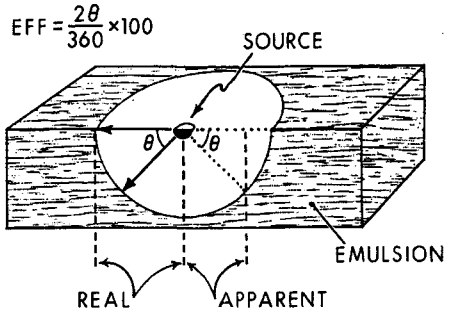

FIG. 2. Diagram illustrating calculation of track count efficiency. Geometry of particle track count.

counted for alveolar regions and the number of tracks for each was registered. Particles viewed in small, medium and large bronchiolar structures and in lymphoid tissue were also recorded. The total number of particles was about evenly divided among three autoradiographic exposures (short, intermediate and long). Each event recorded was corrected for geometry and exposure time and corrected to disintegrations per day. These values in turn were converted to particle size assuming a spherical shape, a density of 11.5 and a specific activity of 5.44×10^{-2} Ci/g PuO_2.

The particle size distribution thus obtained was divided into 15 intervals, interval 1 representing particles less than 0.0584 micron diameter and interval 15 containing all particles greater than 0.298 micron diameter. Data were placed in a program described by O. Raabe,[14] for calculation of the distribution parameters.

RESULTS

The calibration of efficiency of track count is shown in Fig. 3. It is clear that at low track density there is only a slight variation in efficiency, but as the track number density exceeds 100, there is a rapidly declining efficiency of detection (increased correction factor). It will be noted that assumption of a 5 μ depth of field in high density sunbursts, a not unreasonable figure, results in a theoretical efficiency which falls close to the empirically determined curve. It will also be noted that the maximal efficiency (smallest correction) is approximately 40% (2.50), the maximal value used in previous

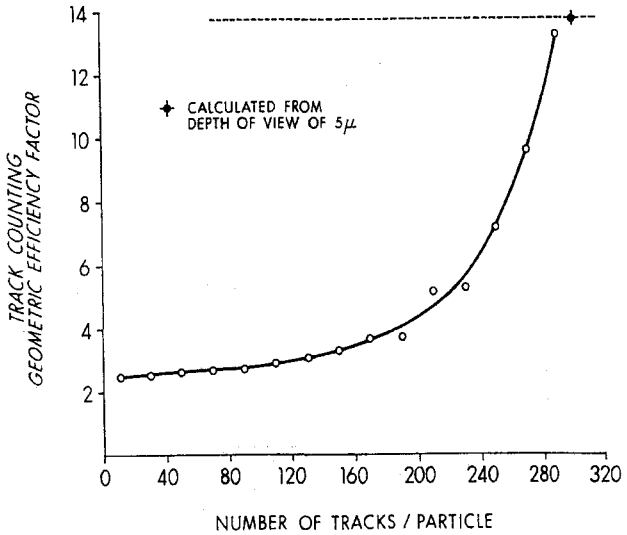

FIG. 3. Calibration curve of track counting efficiency correction.

studies by Morrow and Casarett[9] and Bair *et al.*[12]

Before the computerized data reduction became available, data were plotted and compared graphically. In Fig. 4 is shown an example of the particle size distributions obtained for alveolar regions of some of the rats from one exposure. ("Size" is presented as corrected raw track counts for a single autoradiographic exposure.) It appeared that the distribution first shifted to the left suggesting the clearance of smaller particles. Later the distribution appeared to move to the right of the line designating initially deposited material (immediate sacrifice) indicating the opposite, viz. that smaller particles were being retained preferentially. No significant changes in slopes could be discerned readily.

Although the progression of distribution shifts with time formed a pattern difficult to ignore, there remained a question about whether the distributions could all be considered to be part of the whole population. The more rigorous analysis of data provided several measures

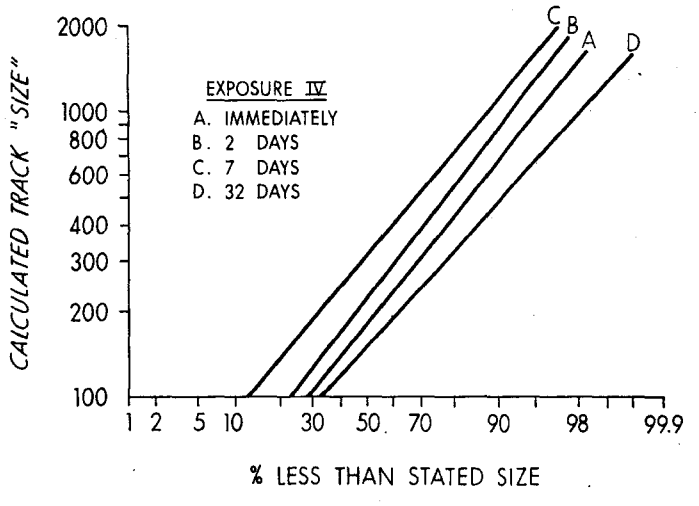

FIG. 4. Example of graphic treatment of particle size distribution of $^{239}PuO_2$ in rat alveolar regions.

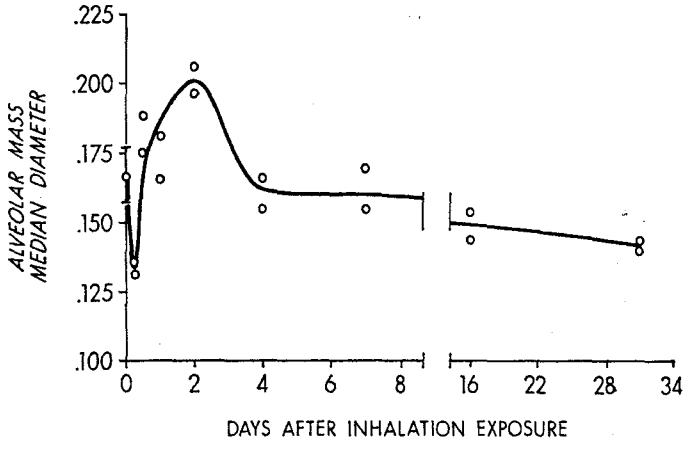

FIG. 5. $^{239}PuO_2$ particle size in alveolar regions of rat lung.

(CMD, MMD, arithmetic mean, etc.), but the most immediately meaningful change was in the CMD and MMD. Figure 5 is a plot of the MMD versus time after inhalation exposure for particles found in alveolar regions.

As suggested by previous graphic analysis, most of the particle distributions were statistically acceptable as log-normal ($p = 0.05$). The mean of counts from rats sacrificed immediately post-exposure is plotted at zero time and the range is indicated. There is apparently an early loss of larger particles as indicated by the fall in MMD at 6 hr, a return to significantly higher levels by 2 days after exposure and a gradual decline to a level below that found on immediate sacrifice at 32 days post-exposure.

Data from the tracheo-bronchial tree were treated similarly; the time change of MMD is presented in Fig. 6. As with the data from alveolar regions there is a marked decrease in median size until 1 day after exposure, an abrupt rise at 2 days and a more gradual decrease beyond 2 days leveling off at about 0.14 μ at 7–32 days post-exposure. Although

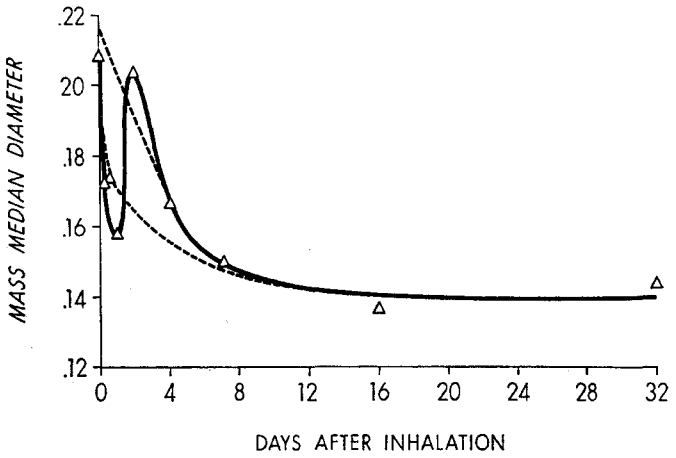

FIG. 6. $^{239}PuO_2$ particle size in tracheobronchial tree of rat lung.

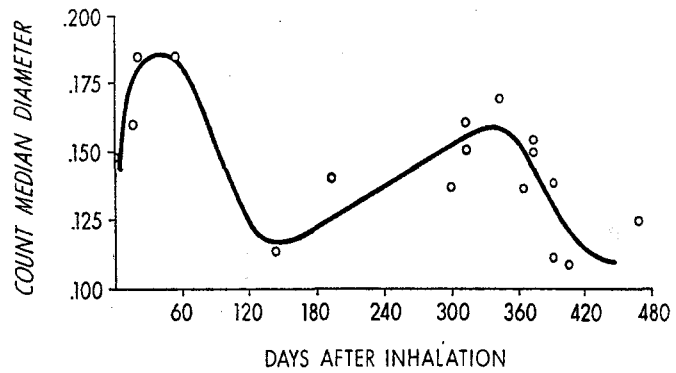

FIG. 7. $^{239}PuO_2$ particle size in alveolar regions of dog lung.

the data at 6 and 12 hr are quite consistent, two extrapolations have been entered (dashed lines) including and excluding these points. In either case the extrapolated value at zero time would be about 0.208–0.216 μ which corresponds to a CMD of approximately 0.16 μ.

Unlike the data from the short post-exposure periods in rats, alveolar particle distributions in dog lung fit log-normal distributions in only about one-fourth of the animals studied. The data are presented in the form of CMD versus days after exposure in Fig. 7. The CMD at early periods after exposure is approximately equivalent to that found for rats. Following an elevation at 22 and 56 days there is a marked fall by 125 days post-exposure. A second, gradual increase in CMD occurs between 125 and 375 days post-exposure followed by a second decrease beyond 375 days. No relation could be identified between the size distribution in alveolar regions and the inhaled aerosol characteristics or the onset or degree of pathologic changes as reported.[13] Insufficient numbers of particles in tracheobronchial areas of the sections prevented similar treatment of the data.

Examination of lymphoid tissue was hampered by sampling variability and comparatively small numbers of particles in the lymphoid tissue in the sections examined. The arithmetic mean particle diameter ranged from 0.084 μ to 0.211 μ with an overall arithmetic mean particle size of 0.160. With minor exception the fraction of particles in the upper intervals of the distribution ($> 0.22\ \mu$ diam.) was considerably smaller than that found in the alveolar particle distribution from the same dog. Additional sections of lymphoid tissue are being prepared to provide sufficient sample size for more meaningful treatment of these data.

DISCUSSION

It is readily apparent that the relation of particle size to rapidity of parenchymal clearance is not a simple one. It is equally apparent, however, that the technique described has a considerable potential for a continued, more refined attack on questions related to particle size and clearance. The material presented here is being extended in several ways. First, additional animals are available for similar treatment to provide data for other periods of time after inhalation exposure. The combination of autoradiographic exposure time is under scrutiny to establish the optimal exposure times and sampling methods to yield realistic results at the ends of the size distribution. Finally the treatment of the distributions as log-normal is convenient and fits most of the rat data and some of the dog data. However, a new program (O. Raabe[15]), tests the distributions against a general function and although more complex, is expected to supply more detailed information on the specific intervals of the distribution.

In the rat, the apparent shift of median diameter with time as viewed graphically (Fig. 4) is borne out qualitatively by the more exacting treatment of the data (Fig. 5). Alveolar deposition can be viewed as having resulted from a deposition of particles having a mean MMD of 0.167 μ and a mean geometric standard deviation of 1.44. This is different from the distribution of particles deposited in the tracheo-bronchial tree, which had a mean MMD of 0.208 μ and a mean σ_g of 1.48. Still higher is the MMD for alveolar deposition in the dog, 0.248, $\sigma_g = 1.51$.

The data obtained from rats point to an early (6 hr) loss of larger particles of the distribution followed by a preferential clearance of the smaller sizes (12 hr to 2 days). Although there are insufficient data to eliminate other pathways, the fact that the tracheo-bronchial clearance follows a pattern similar to alveolar clearance (with a time lag) strongly suggests that the major pathway during this period is the movement to the bronchiolar tree. This conclusion is further supported by the fact that the mass median for both distributions approach the same value of about 0.14 μ. The bicyclic phasing of particle size is similar to the qualitative description of tracheo-bronchial clearance of Po colloid[16] and is corroborative of apparent quantitative two-phase bronchiolar clearance described for Fe_2O_3.[17]

The alveolar clearance in the dog is more difficult to interpret partly because of the relative scarcity of points over long intervals of

time after exposure.* It would appear that there is a preferential clearance of small particles between 1 and 56 days roughly equivalent to that found in the rat at 6 hr to 2 days. Also similar to the rat data, except for the time element, is the decrease of the median to a level of about 0.14 μ at 125 days post-exposure.

For both series of animals, the increase in MMD suggests a possible alternative view, viz. that aggregation of particles occurred. On the basis of observations previously reported,[8,9] if aggregation is a factor during this period, it is most likely to be the result of intracellular incorporation by phagocytic elements. If this is true, it would follow that the fall in size could be related to the mobilization and removal of the phagocytic cells. In the rats the decrease between 2 and 7 days is consonant with the response of alveolar cells reported as a peak mitotic activity at 3 to 5 days after dust inhalation.[18, 19] No equivalent time periods or response data are available for the dog.

The prolonged increase in particle size in the dog from 125 to 343 days might also be considered to be due to aggregation. However, the lymph nodes, although increasing in concentration during this time,[13] show no significant changes in particle size distribution. Thus it is more likely that smaller particles are finding their way to the lymphoid tissue and that the slightly larger range of particles are remaining. There remains, of course, the distinct possibility that some particles are being transported to lymphoid tissue while others of equivalent initial size are more subject to aggregation in alveolar regions with the increased residence time.

The decrease in size occurring at about one year after deposition is also unaccompanied by any significant increase in large particles in lymphoid tissue in the limited data available. Further, although it was expected that changes at this time period might be related to pathologic changes, no clear relationship could be identified. Unless further cycling could be expected, the particle size at the end of the series might be approaching a "steady state" size at very long periods following exposure. It is of some interest that Wurm and Einbrodt[20] using electronmicroscopy, have recently reported CMD's for mineral in miner's lungs below 0.08 μ for periods of 5 to 14 years after exposure. From the dog data a reasonable terminal size is about 0.11 at about 400 days after exposure. These two figures are remarkably similar for having been obtained for different materials in different species and by different methods. Other work[21, 22] suggests that particle size in human lung remains relatively constant over long periods of time at about 0.5 μ as determined by essentially gravimetric methods.

With regard to the implications of particle size in dose distribution, it is essentially immaterial whether aggregation occurs; the fact remains that there is a variation of the size of the sources with time and that it is a complex function, perhaps cyclic for the earlier intervals after exposure. Although the absolute differences in median size are not great, these parameters, translated into total number or mass in the tissue might be expected to be a factor in dose-response relations. Some differences in effects of inhaled PuO_2 have been reported between studies at Hanford[23, 24] and Rochester.[13] Morrow *et al.*[13] have pointed out that these differences might well be related to dose rate differences as calculated from deposition measurements and rates of clearance. It should be added that, at the level of microdistribution of dose, there are also dose rate differences depending upon particle size differences whether in the inhaled atmosphere or, as illustrated here, in the patterns of change occurring in the animals at various time periods after inhalation. The marked lymphopenia observed[13, 24] directs attention to a particular need for the application of this technique to distribution of dose to lymphoid tissue.

ACKNOWLEDGEMENT

The authors are pleased to acknowledge the technical assistance of K. Emilson and F. R. Gibb and are especially grateful to Otto Raabe for his patient aid and advice in the computer program and data processing.

* Additional data are being obtained on dogs sacrificed between 56 and 125 days after inhalation. A collaborative study with Drs. Bair and Park of Battelle Northwest has been initiated for time periods up to about 30 days post-inhalation.

REFERENCES

1. W. H. LANGHAM. Los Alamos Scientific Laboratory Report AECD 1914 (1946).
2. J. CROWLEY, H. LANZ, K. SCOTT and J. G. HAMILTON. University of Chicago Metallurgical Laboratory Report CH-3589 (1946).
3. R. ABRAMS, H. C. SIEBERT, L. FORKER, D. GREENBERG, H. LISCO, L. O. JACOBSEN and E. L. SIMMONS. University of Chicago Metallurgical Laboratory Report CH-3655 (1947).
4. J. CARITT, R. FRYXELL, J. KLEINSCHMIDT, R. KLEINSCHMIDT, W. LANGHAM, A. SAN PIETRO, R. SCHAFFER and B. SCHNAP. *J. Biol. Chem.* **171,** 273 (1947).
5. K. SCOTT, D. J. AXELROD, N. FISHER, J. F. CROWLEY and J. G. HAMILTON. *Arch. Path.* **48,** 31 (1949).
6. W. H. LANGHAM. *Amer. Ind. Hyg. Assoc. Quart.* **17,** 305 (1956).
7. B. B. BOECKER. A study of the deposition and excretion of PuO_2 in rats. M.S. Thesis, University of Rochester (1959).
8. L. J. CASARETT, P. E. MORROW and F. R. GIBB. Abstract, Amer. Ind. Hyg. Assoc., Ind. Health Conf., Chicago, Ill. (1959).
9. P. E. MORROW and L. J. CASARETT. In *Inhaled Particles and Vapours*, p. 167, Pergamon Press (1961).
10. W. J. BAIR, D. H. WILLARD, J. P. HERRING and L. A. GEORGE. *Health Physics* **8,** 639 (1962).
11. W. J. BAIR and D. H. WILLARD. *Health Physics* **9,** 253 (1963).
12. W. J. BAIR, B. C. STUART, J. F. PARK and W. J. CLARKE. In *Radiological Health and Safety in Mining and Milling of Nuclear Materials*, p. 253, *IAEA*, Vienna (1964).
13. P. E. MORROW, F. R. GIBB, H. DAVIES, J. MITOLA, D. WOOD, N. WRAIGHT and H. S. CAMPBELL. *Health Physics*, in press.
14. O. RAABE. Submitted to *Amer. Ind. Hyg. J.*
15. O. RAABE. Personal communication.
16. L. J. CASARETT. *Rad. Res.* Suppl. 5, 187 (1964).
17. L. J. CASARETT and B. EPSTEIN. *Amer. Ind. Hyg. J.*, in press.
18. L. J. CASARETT and P. S. MILLEY. *Health Physics* **10,** 1003 (1964).
19. L. J. CASARETT, G. V. METZGER and M. G. CASARETT. *Proc. Int. Symp. on RES*, Como, Italy (1966).
20. K. WURM and H. J. EINBRODT. *Int. Arch. f. Gewerbepath. μ. Gewerbehyg.* **22,** 149 (1966).
21. H. J. EINBRODT. *2nd Int. Symp. on Particles and Vapours*, p. 399, Pergamon Press (1967).
22. J. CARTWRIGHT and J. W. SKIDMORE. *Ann. Occup. Hyg.* **2,** 151 (1964).
23. W. J. BAIR and D. H. WILLARD. *Rad. Res.* **16,** 811 (1962).
24. J. F. PARK, D. H. WILLARD, S. MARKS, J. E. WEST, G. S. VOGT and W. J. BAIR. *Health Physics* **8,** 651 (1962).

COMPARATIVE DISPOSITION OF FOUR TYPES OF PLUTONIUM DIOXIDES INHALED BY DOGS*

W. J. BAIR and J. F. PARK

Biology Department, Pacific Northwest Laboratory, Battelle Memorial Institute, Richland, Washington, U.S.A.

Abstract—Groups of three dogs were given single inhalation exposures to dry aerosols of one of four different plutonium dioxides to compare retention, translocation, and rates of excretion. Two of the plutonium dioxides were prepared by calcining the oxalate at 350°C and at about 1000°C. Two others were produced by ignition of the stabilized delta metal at 450°C and by slow oxidation of the pure metal at 123°C. The lung retention half-time of the oxalate calcined at 350°C was about one year, half that of the other oxides. This was due to greater accumulation of plutonium in the bronchial lymph nodes rather than greater clearance via the mucus-ciliary pathway or a relatively high rate of solubility. The metal oxidized at 450°C was cleared via the mucus-ciliary route to a lesser extent than the other oxides. This same oxide also showed a selective loss of ^{241}Am, relative to ^{239}Pu, in lung and bronchial lymph node tissue which was not evidenced by the other oxides. The oxalate calcined at 1000°C showed the least translocation to tissues outside the respiratory tract. These results indicate that the physical-chemical state of inhaled plutonium dioxide influences its disposition in the body.

INTRODUCTION

Earlier studies in this laboratory[1-3] indicated that the disposition of inhaled plutonium dioxide in beagle dogs was influenced by the particle size characteristics of the aerosol. Inhalation studies with cerium in dogs showed that oxides prepared by chemical precipitation were more rapidly translocated and excreted in the urine than oxides calcined at approximately 400°C.[4, 5] Therefore, it seemed possible that inhaled plutonium dioxides having different physical and chemical properties, such as those that might occur as a result of the method of formation, could have dissimilar fates in the body. Because of the increasing possibility for human exposures to plutonium dioxides from several different sources and treatments, such as oxidation of the metal in air, high explosive detonation and incineration of nuclear weapons, fallout from nuclear detonations, calcination of oxalates, or as ceramics formed in a very high temperature plasma jet, it is desirable to know whether and how the origin of the plutonium dioxide might influence its disposition in the body and its subsequent biologic effects. In this study the retention, distribution, and excretion rates of four different plutonium dioxides inhaled by dogs were compared. The plutonium dioxides ranged from metal oxidized at 123° to oxalate calcined at about 1000°. In general all oxides, except one which was prepared by calcining the oxalate at 350°, showed similar pulmonary retention, translocation, and excretion rates during the first three months after exposure.

* Work performed under Contract No. AT(45-1)-1830 between the United States Atomic Energy Commission and Pacific Northwest Laboratory, a division of the Battelle Memorial Institute.

METHODS

A. Materials

The experimental protocol is shown in Table 1. The plutonium dioxides prepared by calcining the oxalates were obtained from the Hanford Plant. The oxalate calcined at 350° was an aliquot of that used in most of our previous studies since 1958. Another aliquot was

recalcined at a temperature between 950° and 1000°. The oxides prepared from plutonium metal were obtained from the United Kingdom Atomic Energy Authority through the courtesy of Dr. K. Stewart.† One type was produced by the ignition at 450° of the stabilized delta metal and the other by the slow oxidation of the pure metal at 123°C. In both cases the oxide was the residue remaining after the oxidation of the metal. The oxides were sieved to obtain the fractions with particle size less than 50 μ. According to Dr. Stewart the 123° oxide was very friable, tending to break down into particles of less than 3 μ, and could agglomerate on standing.[6]

laboratory.[8] Training of the dogs eliminated the need for anesthesia or tranquilizers. The aerosol chamber was a 2-ft vertical section of 8-in. (O.D.) lucite pipe. The aerosol was introduced at the top of the chamber, exhausted at the bottom and sampled with membrane filters and a Walkenhorst type thermal precipitator. The respiratory rates and volumes were monitored throughout the 10–20 min exposures with a calibrated respiratory sensor.[9]

The aerosols were produced by directing dry air at a rate of 100 cc/min through a small diameter tube attached as a side arm to a 25 ml flask containing the dry plutonium dioxide dust. The flask was vibrated with an electric

Table 1. *Experimental Protocol*

Group No.	Dog No.	PuO_2 inhaled	Particle size CMD (μ)	Particle size MMD	Percent ultra-filterability
I	1*, 2+, 3*	Oxalate calcined at 1000°	.51	2.8	0.04
II	4△, 5, 6+	Oxalate calcined at 350°	.45	2.8	0.02
III	7+, 8△, 9	Metal oxidized at 450°	.50	4.8	0.006
IV	10△, 11, 12	Metal oxidized at 123°	.46	1.3	0.006

*, +, △ Litter mates.

Female beagle dogs, about three years old, weighing from 8 to 12 kg were used. All dogs were raised in our colony and had complete clinical histories including radiographs. A number of the dogs were litter mates as indicated in Table 1.

B. Aerosol Exposures

For the inhalation exposures the dogs were fitted with masks and required to inhale the aerosol from the chamber through an electronically operated fast-acting three-way respiratory valve[7] by a method previously used in our test tube shaker to keep the dust in motion. The top of the flask was connected to the top opening of the aerosol chamber by flexible tubing. The aerosol concentrations ranged from 10^{-2} to 10^{-3} μCi/cc. These relatively high aerosol concentrations were required to assure that the dogs deposited enough plutonium to excrete detectable levels in the urine. The results of earlier studies indicated that these deposition levels would cause some pathology in the lungs during the three-month period selected for this study, but would not markedly influence the rates of excretion and translocation.

Particle size distributions of the aerosols inhaled by the dogs were determined with the Zeiss Particle Size Analyzer from electron-micrographs of thermal precipitator and mem-

† United Kingdom Atomic Energy Authority, Atomic Weapons Research Establishment, Aldermaston, Berkshire, England.

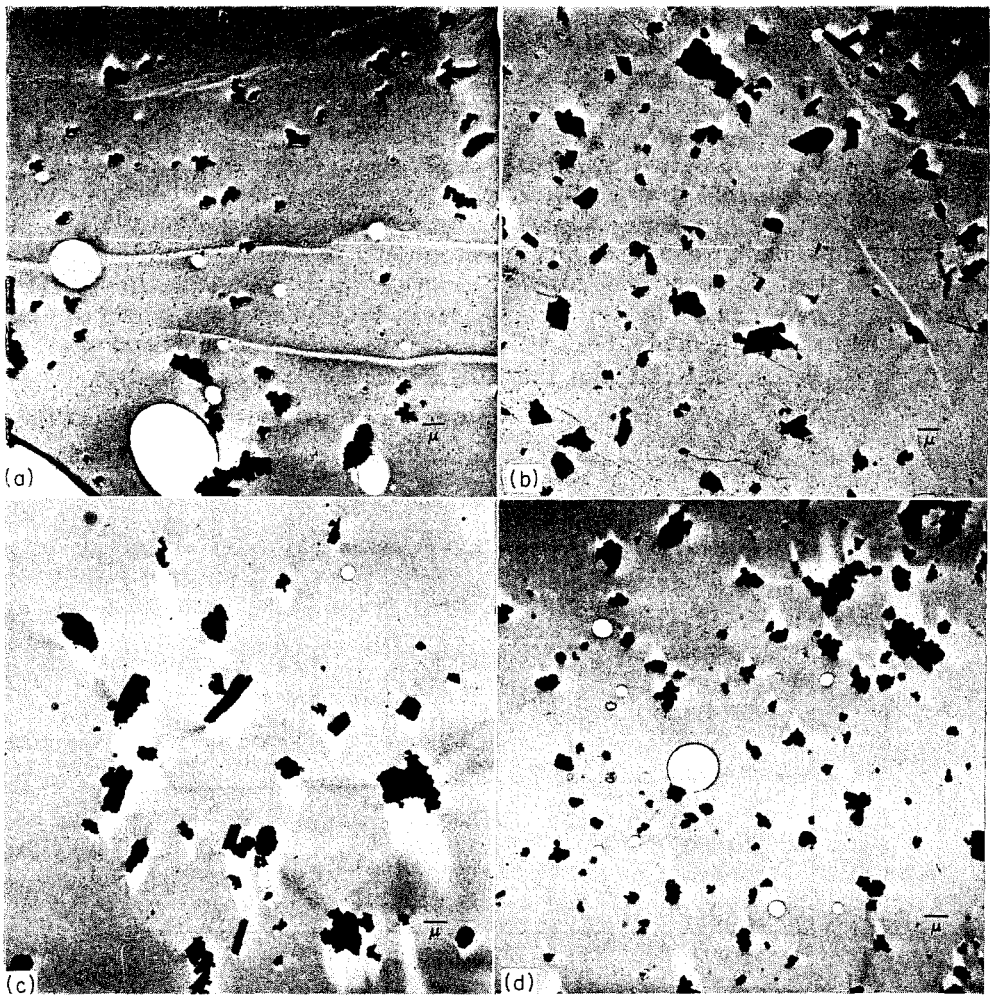

FIG. 1. Electromicrographs of PuO_2 particles (shadowed with chromium at 20°). (a) Plutonium oxalate calcined at 1000°. (b) Plutonium oxalate calcined at 350°. (c) Plutonium metal oxidized at 450°. (d) Plutonium metal oxidized at 123°.

brane filter samples. The values given in Table 1 are means of samples collected from three dog exposures in each group. Unfortunately for the comparative purpose of this study the Mass Median Diameter of the metal oxidized at 450° was greater than, and that of the metal oxidized at 123° was less than the MMD's of the calcined oxalates. The low MMD of the metal oxidized at 123° may reflect the friable nature of the material.

Representative electronmicrographs of the four aerosols are given in Fig. 1. The oxalate calcined at 1000° (Fig. 1(a)) is distinguished by rounded corners and the apparent fusion of several smaller particles. The particles of metal oxidized at 123° (Fig. 1(d)) are all irregular in shape, many of which appear to be aggregates. The oxalate calcined at 350° and the metal oxidized at 450° contain many particles of similar shape and are essentially indistinguishable.

X-ray diffraction analyses of the four plutonium compounds confirmed that all were crystalline PuO_2.

The ultrafilterabilities of the four oxides were determined by the method of Lindenbaum.[10] The results, Table 1, indicate that the calcined oxalates were somewhat more filterable than the oxidized metals.

Immediately following exposure to the aerosols and after 1, 2, 7, and 14 days and 1, 2, and 3 months, blood samples were collected from all dogs for plutonium analyses. Other samples were collected at monthly intervals for hematology. The dogs were maintained in metabolism cages for daily collection of urine and feces for plutonium analyses. After three months all dogs were sacrificed by exsanguination under anesthesia for plutonium analyses and histology of about 40 tissues. Microscopic distributions of plutonium particles in lungs and bronchial lymph nodes were determined from autoradiographs. The dogs also were counted frequently with a multi-detector scintillation counter.[11] The histology, autoradiography, and the results of the whole-body counting study will be reported separately.

RESULTS

A. Retention

The total quantity of plutonium deposited in each dog was determined from the analyses of all urine and feces collected daily and all tissues at necropsy. Whole-body clearance curves were constructed for each dog by subtracting cumulative excretion values from the total quantity of plutonium deposited.[1, 2] An example is given in Fig. 2. Extrapolation of the clearance curve to the ordinate at zero time gives an estimate of the fraction of the deposited plutonium that was deposited below the ciliated epithelium of the terminal bronchioles and was, therefore, unavailable for early clearance by ciliary processes. This fraction was assumed to have been deposited in the alveoli and accounted for the longterm retention of plutonium in the dogs. Since subsequent clearance of the fraction deposited in the alveoli was exponential with time, the expression, $p = Ae^{-bt}$, was evaluated empirically for each dog. Here p is the quantity of plutonium present in the dog at a given time,

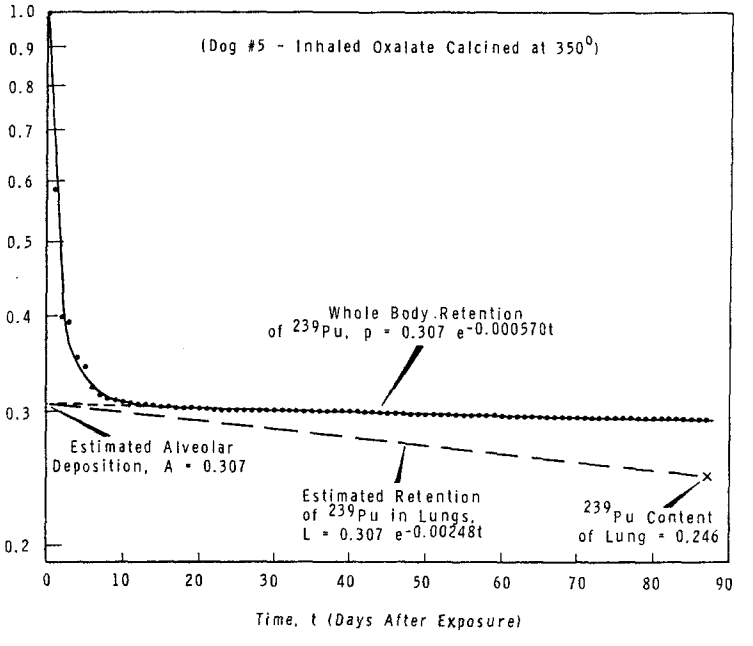

FIG. 2. Whole-body and lung retention of ^{239}Pu.

t, after exposure; A is a constant related to the quantity initially deposited in the alveoli; and b is a constant describing the rate of clearance and excretion in urine and feces of the plutonium deposited in the alveoli.

The amount of plutonium found in the lung at time of sacrifice was expressed as a fraction of the total amount initially deposited. Assuming the clearance of plutonium was exponential with time, an expression for lung retention, $L = Ae^{-b_L t}$, similar to the whole-body retention equation, was obtained for each dog.

Values for the constants in these equations are given in Table 2. The percent of the total deposited plutonium that was deposited in the alveoli varied from 20% to about 45% for all but two dogs which had alveolar depositions less than 10%. Apparently the fractions deposited in the alveoli were independent of the type of PuO_2 inhaled and the total quantity deposited.

The slopes of the whole-body and lung-retention curves are also expressed as retention half-times for convenience of discussion. The whole-body retention half-times ranged from about 1000 days to more than 3400 days, the larger values being observed for the dogs in Group III which inhaled metal oxidized at 450°. The lung retention half-times were in the 600 to 1000 day range for all except the dogs in Group II which inhaled oxalate calcined at 350°. For these dogs the lung retention half-times were about one year, similar to those we observed in previous studies using the same type of PuO_2.[12]

It is to be noted that the lung retention half-times for Group II dogs were about half those for the other groups of dogs although the whole-body retention half-times were not significantly less than those for dogs in Groups I and IV. Also, the lung retention half-times for dogs in Group III were not markedly greater than for dogs in Groups I and IV, although the whole-body retention half-times were generally greater. These differences are reflected in the tissue distribution and excretion data.

Table 2. Whole Body and Lung Retention of Inhaled PuO_2

	PuO_2 inhaled	Dog No.	A (% deposited in alveoli)	Whole body b	Whole body T 1/2 (days) retention half-time	Lung b_L	Lung T 1/2 (days) retention half-time	Total ^{239}Pu deposited (μCi)
I	Oxalate calcined at 1000°	1	24.3	0.000583	1190	0.00095	730	14.1
		2	39.9	0.000463	1500	0.00072	960	4.8
		3	23.6	0.000730	950	0.00109	640	27.4
II	Oxalate calcined at 350°	4	44.6	0.000630	1100	0.00160	430	19.2
		5	30.8	0.000570	1220	0.00248	280	99.4
		6	27.1	0.000406	1710	0.00180	390	75.6
III	Metal oxidized at 450°	7	3.7	0.000333	2080	0.00071	980	29.3
		8	25.7	0.000260	2670	0.00078	890	30.0
		9	20.5	0.000201	3440	0.00109	640	25.4
IV	Metal oxidized at 123°	10	8.1	0.000516	1350	0.00129	540	18.0
		11	26.1	0.000333	2080	0.00107	650	77.5
		12	20.2	0.000510	1360	0.00078	890	37.0

B. Tissue Distribution

Approximately 40 tissues including total skeleton, muscle, and skin from each dog were assayed for ^{239}Pu at necropsy three months after exposure. The ^{239}Pu contents of the tissues having the highest levels are given in Table 3. The dogs in Group II had smaller percentages of the total body burdens in their lungs than the other dogs. This correlates with the difference in lung retention rates shown in Table 2. The low lung values of Group II dogs occurred

Table 3. Tissue Distribution of ^{239}Pu in Dogs 3 Months after Inhalation of PuO_2
(% of total body burden)

PuO_2 inhaled	Dog no.	Lung*	Bronchial lymph nodes†	All other lymph nodes‡	Bone	Muscle	Kidneys	Spleen	Liver	Gall bladder	Heart	G.I. tract	Trachea	Upper nasal passages
I Oxalate	1	96.9	2.76	0.007	0.026	0.033	0.0002	0.0001	0.004	0.0002	0.007	0.014	0.038	0.0002
calcined	2	98.1	1.73	0.007	0.021	0.028	0.0001	0.0002	0.011	0.0003	0.002	0.007	0.026	0.0003
at 1000°	3	96.9	2.88	0.014	0.055	0.040	0.0001	0.0001	0.059	0.0002	0.0002	0.003	0.010	0.0002
II Oxalate	4	91.6	8.00	0.005	0.18	0.036	0.002	0.001	0.083	0.016	0.002	0.004	0.015	0.016
calcined	5	84.2	15.20	0.046	0.11	0.023	0.003	0.016	0.20	0.002	0.019	0.023	0.029	0.002
at 350°	6	88.9	10.50	0.032	0.19	0.049	0.003	0.002	0.19	0.002	0.002	0.015	0.011	0.002
III Metal	7	96.6	2.51	0.27§	0.19	0.070	0.002	0.0007	0.085	0.0001	0.0003	0.025	0.003	0.0001
oxidized	8	95.3	4.45	0.007	0.091	0.058	0.001	0.001	0.047	0.00001	0.001	0.011	0.004	0.00001
at 450°	9	92.3	7.39	0.022	0.094	0.056	0.001	0.001	0.042	0.00001	0.0004	0.014	0.050	0.00001
IV Metal	10	97.3	2.35	0.024	0.15	0.083	0.0008	0.001	0.047	0.00001	0.0001	0.015	0.029	0.00003
oxidized	11	93.7	6.10	0.01	0.038	0.029	0.0006	0.0005	0.032	0.00001	0.002	0.011	0.032	0.00005
at 123°	12	97.6	1.88	0.14§	0.072	0.029	0.0005	0.002	0.031	0.00001	0.0003	0.086	0.020	0.00001

* Total for all lobes of lung.
† Bronchial and mediastinal lymph nodes.
‡ Total of all other lymph nodes in the body which could be dissected.
§ Cervical and mandibular lymph nodes accounted for the high values.

almost entirely as a result of greater translocation to the bronchial and mediastinal lymph nodes rather than translocation to other tissues or excretion from the body. Thus, the whole-body retention of ^{239}Pu was not significantly different from Groups I and IV dogs, Table 2. nodes. Otherwise, translocation in Group III dogs, which showed a tendency toward longer whole-body retention times, did not differ greatly from Groups I and IV dogs with the exception that the kidneys contained a somewhat larger percentage of the body burden.

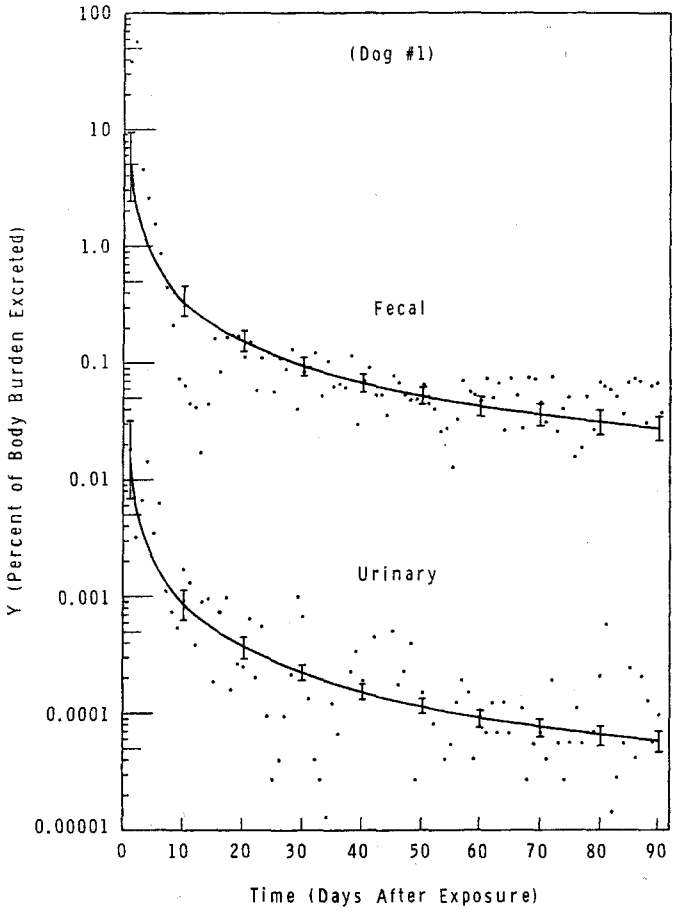

FIG. 3. Daily excretion of ^{239}Pu after inhalation of plutonium oxalate calcined at 1000°.

Translocation of ^{239}Pu to bone and muscle was not significantly greater in Group II dogs than in the other dogs. However, translocation to soft tissues such as kidneys, spleen, liver, heart, etc. was generally highest in Group II dogs. Dog No. 7 in Group III showed a relatively high level of translocation, but this was essentially accounted for by two tissues, the upper nasal passages and the mandibular lymph

C. Excretion

The amount of ^{239}Pu excreted each day in urine and feces was expressed as the percent of the body burden of plutonium at the beginning of the 24-hr period during which the excretion occurred. These data were programmed for curve fitting by least squares analyses using a digital computer. Curves were fitted to each set of data for individual dogs and to daily mean

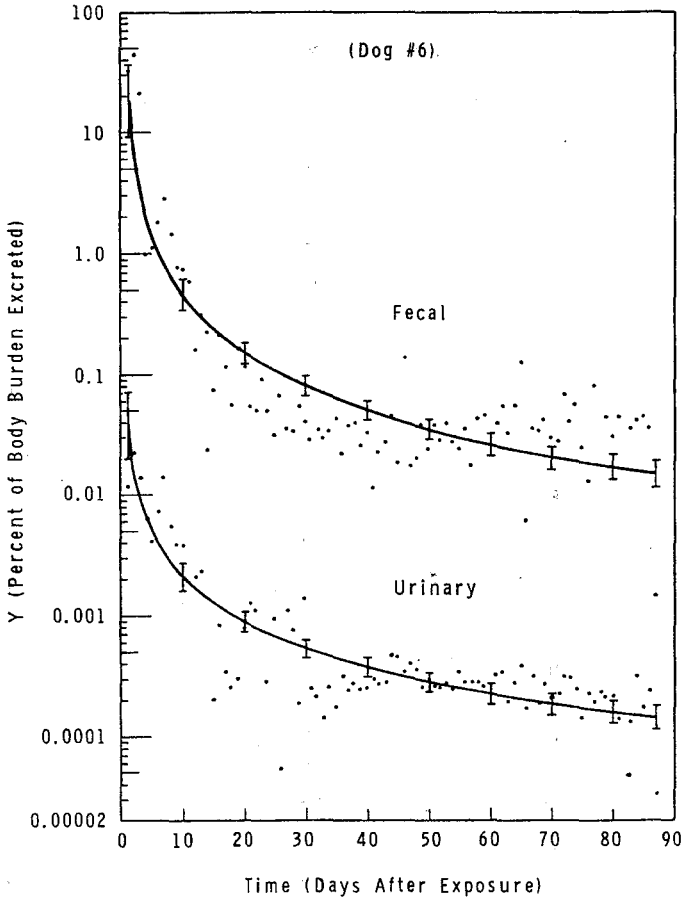

FIG. 4. Daily excretion of ^{239}Pu after inhalation of plutonium oxalate calcined at 350°.

values for the three dogs in each group to obtain equations representing the mean excretion rates for each dog and each group of dogs, respectively. Logarithmic equations of the form $Y = At^b$, where Y is the percentage of plutonium excreted each day in urine or feces, were fitted to all data. Power functions did not always provide the best visual fit, but are probably adequate to compare the four plutonium dioxide aerosols.

Excretion data are shown for representative dogs from each group in Figs. 3–6. Figure 7 is the curves with 95% confidence levels fitted to the mean daily values of all three dogs in each group. The plots of individual excretion values for each of four dogs shows the daily fluctuations in levels of ^{239}Pu in urine and feces. Comparison of these excretion data for representative dogs from the four groups and the constants in Table 4 for the power function equations fitted to the individual and combined excretion data for all of the dogs indicates that there were only minor differences. These differences are more clearly seen in Fig. 7 which shows the curves fitted to the combined data for each group. After the first 20 days the rate of fecal excretion tended to be slightly less for dogs in Group III than for the other dogs. This correlates with the generally longer whole-body retention half-times calculated for these dogs. The rate of excretion of plutonium in urine tended to be greater for Groups II and III dogs than for Groups I and IV dogs.

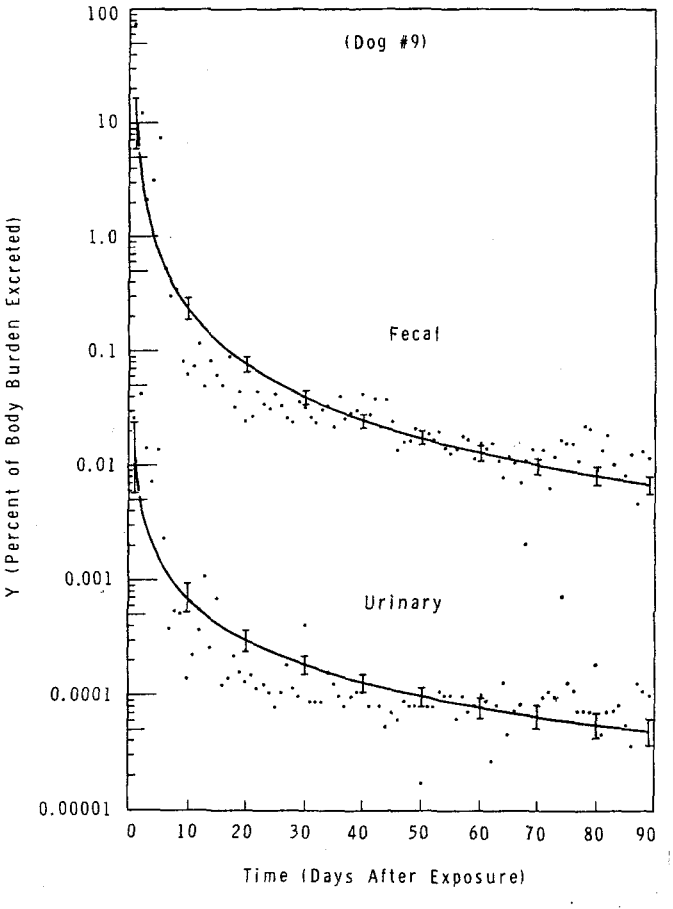

FIG. 5. Daily excretion of ^{239}Pu after inhalation of plutonium metal oxidized at 450°.

D. Disposition of Alveolar Deposited Plutonium

In Table 5 the disposition of ^{239}Pu deposited in the alveoli is shown. Values for amounts deposited in the alveoli of each dog are those shown in Table 2. The fraction of the alveolar deposited ^{239}Pu excreted in urine and feces was estimated by subtracting from the total amount excreted the fraction that was excreted during about the first week after exposure, which brought the body burden down to about the level of the estimated alveolar deposition. In making these calculations certain assumptions were made. For example, since it was found that total blood levels of ^{239}Pu immediately after exposure were considerably less than 0.01% of the total plutonium deposited, it was assumed that the fraction of inhaled plutonium absorbed by the blood immediately after exposure contributed an insignificant amount to the total translocated plutonium found in tissues after three months or excreted in urine during the 1-week to 3-month postexposure period and that practically all of that which was absorbed was excreted in the urine the first few days after exposure. It was also accepted that these calculations might underestimate the clearance and excretion of truly alveolar deposited plutonium since early clearance of some alveolar deposited plutonium probably occurred within the first few days after exposure. However, these calculations probably provide reasonable estimates of the disposition of the fraction of plutonium deposited in the alveoli which was not available for early clearance and which accounted for

*Table 4. Constants for ^{239}Pu Excretion Equations**

PuO_2 inhaled	Dog No.	Urine		Feces	
		A	b	A	b
I Oxalate calcined at 1000°	1	0.015	−1.24	4.7	−1.15
	2	0.035	−1.48	4.9	−1.22
	3	0.0018	−0.86	7.7	−1.143
	Combined†	0.017	−1.27	4.3	−1.11
II Oxalate calcined at 350°	4	0.017	−1.03	4.7	−1.16
	5	0.0037	−0.75	23.0	−1.61
	6	0.038	−1.26	18.0	−1.60
	Combined	0.027	−1.14	16.0	−1.49
III Metal oxidized at 450°	7	0.27	−1.60	22.0	−1.72
	8	0.0034	−0.89	4.5	−1.34
	9	0.012	−1.23	9.9	−1.63
	Combined	0.12	−1.54	16.0	−1.66
IV Metal oxidized at 123°	10	0.036	−1.38	0.15	−0.22
	11	0.0020	−0.85	3.9	−1.23
	12	0.0009	−0.70	2.2	−0.96
	Combined	0.031	−1.43	16.0	−1.47

* With the form $Y = At^b$, where Y is % of body burden excreted on a given day, t, after exposure.
† The arithmetic means for the three dogs in each group were fitted by least square analysis.

Table 5. Disposition of Alveolar Deposited ^{239}Pu 3 Months after Exposure

PuO_2 inhaled	Dog No.	% of alveolar deposited plutonium					
		Excreted		Total body burden	Lung	Bronchial and mediastinal lymph nodes	All other tissues
		Urine	Feces				
I Oxalate calcined at 1000°	1	0.019	5.5	94.5	91.6	2.7	0.18
	2	0.014	4.2	95.8	94.0	1.7	0.12
	3	0.011	6.6	93.4	90.5	2.7	0.18
II Oxalate calcined at 350°	4	0.063	5.0	95.0	87.0	7.6	0.36
	5	0.017	4.7	95.4	80.3	14.5	0.58
	6	0.049	3.5	96.5	85.8	10.1	0.56
III Metal oxodized at 450°	7	0.093	2.9	97.0	93.7	2.4	0.88
	8	0.012	2.5	97.5	93.0	4.3	0.24
	9	0.012	1.7	98.4	90.8	7.3	0.31
IV Metal oxidized at 123°	10	0.023	7.5*	92.4	89.8	2.2	0.36
	11	0.0084	3.0	97.1	91.0	5.9	0.19
	12	0.0083	4.7	95.3	93.0	1.8	0.54

* 3.6% was excreted in last 12 days. (Three other values were excluded because they were several orders of magnitude above the average values, suggesting contamination of the samples.)

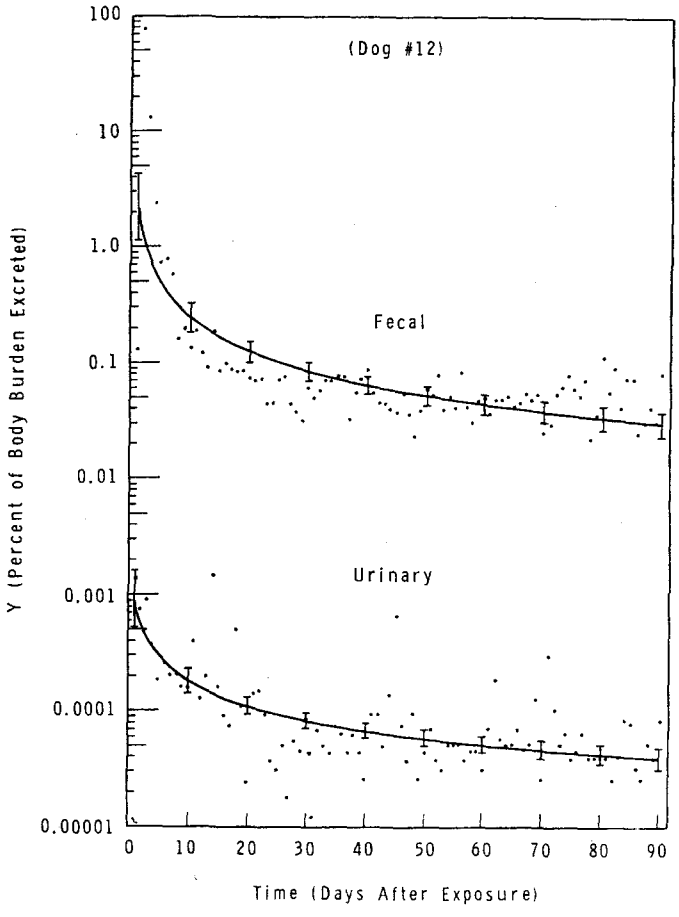

FIG. 6. Daily excretion of ^{239}Pu after inhalation of plutonium metal oxidized at 123°.

the long-term retention and excretion of plutonium.

The values given in Table 5 are generally consistent for the dogs within each group, with the exception of the urine data.

In the case of the fecal data, Group III dogs excreted less than the other dogs suggesting that the mucus-ciliary pathway was least effective for pulmonary clearance of the plutonium metal oxidized at 450°. This assumes that the biliary secretion of plutonium into the gastrointestinal tract was either insignificant or of the same order of magnitude for all dogs.

Three months after exposure greater than 90% of alveolar deposited plutonium was retained in the lungs of all dogs except those that inhaled the oxalate calcined at 350°, Group II. In these dogs, only 80% to 87% was retained and, as indicated above, the difference was in the amount collected in the bronchial and mediastinal lymph nodes.

The fraction of alveolar deposited plutonium translocated to other tissues was apparently less for dogs which inhaled the oxalate calcined at 1000° than for other dogs.

E. ^{239}Pu–^{241}Am Ratios

The dogs were counted with a multi-detector scintillation counter to detect the low energy X-rays and gammas from ^{239}Pu and from the ^{241}Am which is a daughter product of ^{241}Pu, a common contaminant of most ^{239}Pu preparations.

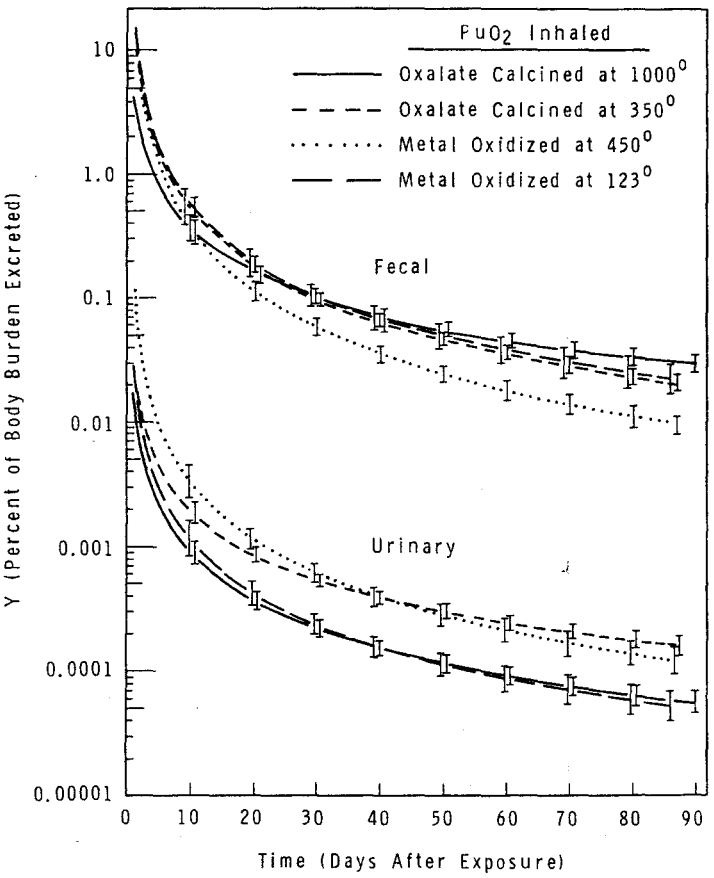

FIG. 7. Comparative excretion of ^{239}Pu following inhalation of four different plutonium dioxides. Curves were fitted to means of daily values for three dogs in each group exposed to one of four different plutonium dioxide aerosols.

Since the whole-body counting data contribute nothing to the comparison of the four different types of PuO_2 in this study, it will not be reported here. However, in evaluating the whole-body counting data it was necessary to determine whether ^{241}Am separated from the ^{239}Pu in the body. Therefore, the ^{239}Pu–^{241}Am ratios in lung and bronchial lymph nodes were examined in respect to the ratios in the material inhaled. Acid dissolved samples of these tissues and the membrane filters used to collect aerosol samples during exposures were counted on platinum disks with a germanium diode alpha detector which had a resolution of 40 keV compared with the 5.15 MeV ^{239}Pu alpha-particles and 5.30 MeV ^{241}Am alphas. The results of these alpha energy analyses are given in Table 6.

The ^{239}Pu–^{241}Am ratios in the inhaled materials were different: the PuO_2 used for Groups I and II dogs was considerably older than the PuO_2 used for Groups III and IV and, thus, contained a greater quantity of ^{241}Am. In Groups I, II, and IV there appeared to be no significant differences between the ratios in the aerosols and the tissues. However, in Group III dogs there was an increased ratio in both lung and lymph nodes. This is interpreted as indicating that there was a selective loss of ^{241}Am relative to the ^{239}Pu, or conversely a selective retention of ^{239}Pu relative to the ^{241}Am, in

the lung and lymph node tissues of the dogs which inhaled the metal oxidized at 450° but not in those dogs which inhaled the other oxides.

F. Biological Effects

To assure adequate levels of plutonium in the excreta and tissues for maximum analytical accuracy, quantities of plutonium were deposited which caused some pathology during the three-month period. In fact, the doses were large enough in most dogs to have caused death within about a year from pulmonary insufficiency as a result of irradiation of the lung tissue.[13] However, previous studies[12] indicated that the levels used in this experiment would not produce changes severe enough to significantly interfere with excretion and translocation of the inhaled plutonium during the three-month duration of this study. Nevertheless, it is important to document the clinical changes seen for the possible bearing they might have on the results observed. Histologic and autoradiographic studies of the tissues collected in this study are in progress and will be reported later.

In other studies in our laboratory it was found that decreasing levels of circulating lymphocytes were the first clinical indications of toxicity following plutonium inhalation.[12-14] This occurred at levels which did not involve major lung pathology. Extensive lung pathology was usually preceded and accompanied by loss of body weight and increasing respiratory rates. In Table 7 are given mean pre-exposure and three-month postexposure lymphocyte counts, body weights and resting respiratory rates and minute volumes. All 12 dogs showed a decreased lymphocyte count, the degree of which was related to the quantity of plutonium in their bodies. However, none of the dogs showed an appreciable weight loss or an increased respiratory rate, with the possible exception of Dog No. 11. Therefore, it is assumed that although some biological damage occurred as a result of the plutonium inhalation, it was not sufficient to markedly alter the disposition of the plutonium and thus invalidate the comparison of the four plutonium dioxides. Further, while the levels of plutonium in the dogs varied from 2 to 29 μCi, there was overlapping of levels among the four groups.

Table 6. ^{239}Pu—^{241}Am Ratios in Aerosols and Dog Tissues

PuO_2 inhaled	Ratio: ^{239}Pu to ^{241}Am		
	Aerosol	Lung	Bronchial lymph nodes
I Oxalate calcined at 1000°	13.8 ± 0.3	13.4 ± 0.3	11.6 ± 0.6
II Oxalate calcined at 350°	12.0 ± 0.2	13.0 ± 1.2	14.2 ± 0.1
III Metal oxidized at 450°	31.0 ± 1.9	37.8 ± 1.5	36.1 ± 1.2
IV Metal oxidized at 123°	31.0 ± 0.6	31.5 ± 1.0	30.0 ± 0.9

DISCUSSION

The results of this study provide further evidence for the relatively long-term pulmonary retention of inhaled PuO_2, its gradual accumulation in bronchial and mediastinal lymph nodes and the accompanying low rate of translocation and urinary excretion of plutonium. Similar findings have been reported from this as well as other laboratories.[1-3, 12-19] None of the four types of plutonium oxides tested in this study showed significant deviations from these earlier studies, although certain differences among them were apparent. Major differences include:

1. The lung retention half-time of the oxalate calcined at 350° was about one year, half of that of the other oxides. This was due to greater accumulation of plutonium in the bronchial and mediastinal lymph nodes rather than greater clearance via

the mucus blanket of the ciliated tracheobronchial pathway or a relatively high rate of solubility.

2. The metal oxidized at 450° appeared to be cleared via the mucus-ciliary route to a lesser extent than the other oxides. This same oxide showed a selective loss of ^{241}Am, relative to ^{239}Pu, in lung and bronchial lymph node tissue which was not evidenced by the other oxides.
3. The oxalate calcined at 1000° showed the least translocation to tissues outside of the lung and bronchial-mediastinal lymph nodes.

These results are of interest to the biologist as well as to the health physicist because biological processes apparently discriminated between the four types of plutonium oxides, all of which were in the crystalline state when inhaled. Their only apparent differences were the Mass Median Diameters of the aerosol particles and the ultrafilterabilities. In considering an explanation for the relatively high accumulation in the bronchial lymph nodes of the oxalate calcined at 350°, none of these observed differences in physical–chemical properties seem to provide a clue. The particle size and ultrafilterability were similar to the oxalate calcined at 1000° and the shapes of the particles closely resembled those of the metal oxidized at 450°. However, there may be a correlation between accumulation of plutonium in bronchial lymph nodes and the total amount of plutonium deposited in the alveoli, Fig. 8. This is especially apparent at the higher alveolar depositions. In an earlier study[2] we found some variation of plutonium lymph node accumulation with the MMD of the inhaled PuO_2 (oxalate calcined at 325°), but there was no positive indication that the fraction of plutonium accumulated in the lymph

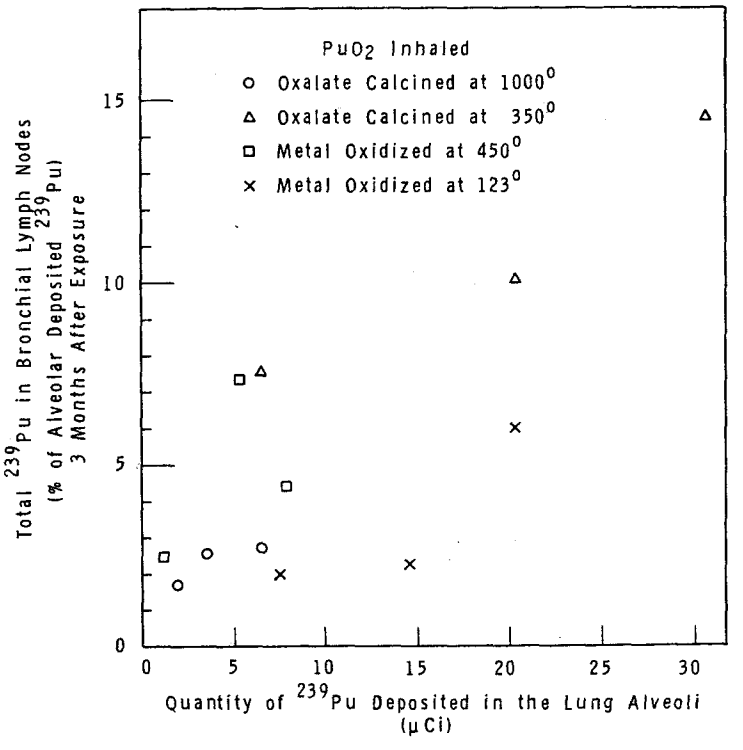

FIG. 8. Relationship between accumulation of ^{239}Pu in bronchial lymph nodes and the total quantity of PuO_2 deposited in the lung alveoli.

Table 7. Clinical Observations

	PuO_2 inhaled	Dog No.	^{239}Pu body burden (μCi)	Body weight (Kg)		Respiratory rate (resp/min)*		Minute volume (L)		Lymphocyte count (10^3 per ml)	
				Initial	Final	Initial	Final	Initial	Final	Initial	Final
I	Oxalate calcined at 1000°	1	3.2	8.4	8.0	20	21	2.8	2.6	2.47	1.15
		2	1.8	11.1	11.0	18	19	2.3	1.9	2.71	1.78
		3	6.0	9.6	10.0	27	25	3.1	2.9	3.30	1.43
II	Oxalate calcined at 350°	4	6.1	9.9	10.8	15	31	4.8	3.6	2.75	1.19
		5	29.0	9.9	11.0	34	32	5.8	5.0	2.50	0.83
		6	20.0	8.5	9.0	22	33	3.4	3.7	3.20	0.73
III	Metal oxidized at 450°	7	1.0	10.0	12.4	27	19	5.2	4.8	2.08	1.77
		8	7.5	12.3	11.6	19	18	4.3	4.1	3.23	1.37
		9	5.1	10.2	9.7	22	21	5.5	3.9	3.62	0.84
IV	Metal oxidized at 123°	10	1.3	12.6	12.6	23	23	6.0	5.6	2.46	1.87
		11	20.0	8.0	7.3	24	53	3.0	2.4	2.75	0.46
		12	7.1	11.0	10.7	38	32	5.4	3.5	3.00	1.53

* Normal values for dogs in our colony range between 15 and 40; the mean is 20 to 25.
† Mean of 2 and 9 week pre-exposure counts.

nodes one month after exposure increased with the amount of PuO_2 deposited in the alveoli. In another study,[18] 39 weeks after two dogs inhaled PuO_2 prepared by calcining the oxalate at 350°, bronchial lymph node levels were about 11% and 50% of the 0.5 and 1.4 μCi, respectively, initially deposited in the alveoli. However, these results are not adequate proof that the fraction of plutonium accumulating in the bronchial lymph nodes was dependent upon the quantity deposited in the alveoli of the dogs in this study.

There does not seem to be any obvious explanation for the lower rate at which metal oxidized at 450° was cleared from the lung by the mucusciliary pathway or the apparent selective loss of ^{241}Am relative to ^{239}Pu in lung and lymph node tissue. Additional alpha energy analyses of tissue and excreta samples from the dogs in the group may show a relationship between these two findings, but none can be identified as yet. The fact that the oxalate calcined at 1000° showed somewhat less translocation from the respiratory tract than the other oxides seems reasonable since the high temperature might be expected to decrease its solubility, yet this material did not show the lowest ultrafilterability. On the other hand it was expected that the metal oxidized at 123° would show the greatest translocation because of its friability and its small mass median diameter. However, this did not occur.

The results of this study have certain radiation protection implications although the differences in behavior of the four types of oxide in the body cannot be considered large. The possible difference in the fraction of plutonium that accumulated in the bronchial lymph nodes can be an important finding. Most animal experimentation with inhaled PuO_2 that has been reported was probably done with oxides prepared by calcining the oxalate at temperatures less than 500°. In the present study the greatest accumulation of ^{239}Pu in the bronchial lymph nodes occurred with this type of PuO_2. In a long-term study[19] with dogs, inhalation of this type of PuO_2 has resulted in a high proportion of animals with primary lung cancer, but despite the heavy accumulation of ^{239}Pu in the bronchial lymph nodes no primary tumors have been identified as originating in this tissue although some metastases to the lymph nodes occurred. If the accumulation of ^{239}Pu in the bronchial lymph node is a desirable phenomenon in respect to the hazard associated with inhaled PuO_2, the inhalation of the types of PuO_2 which show minimal accumulation in the lymph nodes and consequently longer retention times in the lung, where it is known to be carcinogenic, would be more hazardous than inhalation of the low-temperature calcined oxalate. Therefore, it seems that long-term studies of inhaled plutonium metal oxides or high temperature calcined oxalates are required to compare the biological effects with the results of current studies using plutonium oxalate calcined at 350°.[19]

Although the excretion rates of ^{239}Pu in this study suggested some differences among the four types of oxides inhaled, the differences were probably not great enough to cause much concern in interpreting human bioassay data. It is planned to further assess the excretion data collected in this study in terms of the many proposed models.[20-26]

ACKNOWLEDGEMENTS

The authors are indebted to many for the completion of this study. Among these are W. Skinner, M. D. Snyder, and L. R. Richardson for technical assistance; Dr. J. M. Thomas for electronic data processing; R. F. Keough and A. C. Case for plutonium analyses; Dr. J. D. Berlin and R. R. Adee for electronmicroscopy; G. S. Vogt for hematology; T. M. Beasley for alpha energy analyses; and D. E. Skeie for X-ray diffraction analyses.

REFERENCES

1. W. J. Bair and D. H. Willard. *Health Phys.* **9,** 253 (1963).
2. W. J. Bair, D. H. Willard, J. P. Herring and L. A. George, II. *Health Phys.* **8,** 639 (1962).
3. W. J. Bair, B. O. Stuart, J. F. Park, and W. J. Clarke. *Radiological Health and Safety in Mining and Milling of Nuclear Materials* Vol. 1, p. 253. International Atomic Energy Agency, Vienna (1964).
4. E. G. Tombropoulos. Hanford Atomic Products Operation, HW-80500, p. 47 (1964).
5. B. O. Stuart, H. W. Casey and W. J. Bair. *Health Phys.* **10,** 1203 (1964).

6. K. STEWART. Personal communications (1963).
7. B. O. STUART, M. D. SNYDER, W. J. BAIR and N. S. PORTER. Hanford Atomic Products Operation, 1964. Batelle Memorial Institute, Pacific Northwest Laboratory, BNWL-122, p. 29 (1965).
8. W. J. BAIR and J. V. DILLEY. *Proc. Second International Symposium on Inhaled Particles and Vapours*, Pergamon Press, p. 251 (1967).
9. N. S. PORTER. Hanford Atomic Products Operation, HW-81746, p. 5.29 (1964).
10. A. LINDENBAUM and W. WESTFALL, *Int. J. Applied Radiation and Isotopes* **16,** 545 (1965).
11. K. L. SWINTH and B. I. GRIFFIN. Hanford Radiological Science Research and Development Annual Report for 1964. Battelle Memorial Institute, Pacific Northwest Laboratory, BNWL-36 II, p. 2.27 (1965).
12. J. E. WEST and W. J. BAIR. *Rad. Res.* **22,** 489 (1964).
13. W. J. BAIR and D. H. WILLARD. *Rad. Res.* **16,** 811 (1962).
14. J. F. PARK, W. J. CLARKE and W. J. BAIR. *Health Phys.* **10,** 1211 (1964).
15. R. ABRAMS, H. C. SEIBERT, A. M. POTTS, L. L. FORKER, D. GREENBERG, S. POSTEL and W. LOHR. Metallurgy Laboratory, University of Chicago, CH-3655 (1947).
16. P. E. MORROW, F. R. GIBB, H. DAVIES, N. WRAIGHT, J. MITOLA, D. WOOD and C. S. CAMPBELL. *Health Phys.* **12,** 1201 (1966).
17. R. H. WILSON and J. L. TERRY. *Proc. Second International Symposium on Inhaled Particles and Vapours*, Pergamon Press, p. 273 (1967).
18. W. J. BAIR and B. J. MCCLANAHAN. *Arch. Environ. Health* **2,** 648 (1961).
19. W. J. BAIR, J. F. PARK and W. J. CLARKE. Tech. Report AFWL-TR-65-214 (1966).
20. Task Group on Lung Dynamics. *Health Phys.* **12,** 173 (1966).
21. J. D. EAKINS and A. MORGAN. *Assessment of Radioactivity in Man*, Vol. 1, p. 231. International Atomic Energy Agency, Vienna (1964).
22. S. A. BEACH and G. W. DOLPHIN. *Assessment of Radioactivity in Man*, Vol. 2, p. 603. International Atomic Energy Agency, Vienna (1964).
23. G. W. DOLPHIN. *Assessment of Radioactivity in Man*, Vol. 2, p. 589. International Atomic Energy Agency, Vienna (1964).
24. W. S. SNYDER. *Assessment of Radioactivity in Man*, Vol. 2, p. 583. International Atomic Energy Agency, Vienna (1964).
25. J. W. HEALY. *Am. Ind. Hyg. Assoc. Quart.* **18,** 261 (1957).
26. W. H. LANGHAM. *Am. Ind. Hyg. Assoc. Quart.* **17,** 305 (1956).

TRANSFER OF ^{144}Ce VIA PLACENTA AND DURING LACTATION TO OFFSPRING IN MICE

A. NEHARIN and E. LUBIN

Soreq Nuclear Research Center, Israel Atomic Energy Commission, Yavneh, Israel

Abstract—This investigation is a continuation of a similar study on the transfer of $^{152-4}$Eu to the offspring in mice. Our main interest is the case of an acute contamination occurring a long time before the pregnancy. The question is whether the radioisotope, that has already been fixed in the bone, is removed during pregnancy or lactation, and, if so, in what quantities in relation to the time elapsed since contamination.

Four experimental groups, each of 12 female mice, were injected with 3 μCi/0.2 ml of ^{144}Ce–citrate. An additional group was held as control. The groups were mated to untreated males by the harem method.

Group A was mated and the isotope administered on the 18th day of gestation. The animals were sacrificed on the 20th day, the total period of gestation being 21 days and the ^{144}Ce content determined in the whole litters, uterus and placenta, blood (0.5 ml), liver, femur and remaining carcass. These measurements showed the transfer of the contaminant to the fetus through the placenta, very shortly after the contamination has occurred, and also distribution of the isotope in the various organs.

Group B was mated immediately after dose administration. The offspring were whole-body counted for body burden soon after delivery. Thereafter the lactating litter was counted in the same manner twice a week until weaning, after which 3 more counts were taken during the next 5 weeks. From this group mainly the transfer of the contaminant through the milk was determined.

Groups C and *D* were mated 4 and 8 weeks respectively after injection of the isotope. The offspring were counted for body burden as in Group B, to indicate the effect of the time elapsed since contamination on the transfer to the offspring during pregnancy and lactation.

Results

1. The transfer of the contaminant through the placenta, expressed as a percentage of the mother's body burden, at the time of delivery was clearly related to the time elapsed since the date of contamination.
2. The transfer of the contaminant through the milk was considerable. Lactating litters showed a gradually rising body burden which reached a peak on the 11th day and then dropped rapidly till the weaning day. Three more counts taken during the next 5 weeks showed a very small and gradual decrease.
3. The transfer of ^{144}Ce to the lactating litters was higher the closer the gestation period was to the day of the administration of the isotope.
4. The body burden of the contaminant showed a somewhat quicker decrease in the lactating mothers than in the virgin females.
5. The distribution of ^{144}Ce in the offspring was measured in the period of maximal activity and found to be mainly in the digestive tract.

TRANSLOCATION OF ^{90}Sr FROM MATERNAL SKELETON TO PROGENY DURING GESTATION AND LACTATION*

R. J. DELLA ROSA, H. G. WOLF and M. GOLDMAN
Radiobiology Laboratory, University of California, Davis, California 95616, U.S.A.

Abstract—The fractional translocation of ^{90}Sr to progeny during gestation and lactation was determined in five adult Beagles previously fed a diet containing 1.1 or 3.3 μCi ^{90}Sr/g Ca. These proven dams were fed approximately 4 or 12 μCi ^{90}Sr per day for about one year during adulthood, and after 85, 102, 150, and 286 days on non-radioactive food they were re-bred. The body burdens of the dams and/or their litters were determined *in vivo* by monitoring of the (^{90}Sr + ^{90}Y) bremsstrahlung at the time of breeding, whelping, during nursing, and at weaning, at which time the animals were sacrificed and their body burdens radiochemically confirmed. From 10–30% of the maternal skeletal burden of ^{90}Sr was lost by the combined influence of gestation and lactation. The fractional loss of ^{90}Sr appeared to have been dependent primarily on litter size, but may also have been influenced by the length of time from acquisition of the body burden to breeding. At birth the ^{90}Sr content of the litters represented less than 1% of the initial maternal body burdens and increased to more than 10% at weaning. The body burdens of the litters at weaning accounted for nearly 30% of the maternal loss. These data suggest that the evaluation of possible radiation hazards to the newborn from biospheric contamination requires knowledge of the maternal contribution to the body burden of the offspring as well as that from dietary sources.

INTRODUCTION

Theoretical calculations of ^{90}Sr and ^{89}Sr dose in the human fetus and infant have been limited severely by the lack of pertinent experimental data.[1] Of utmost importance is the question of the fractional translocation of the radiostrontium body burden from maternal bone to progeny. Further, the contribution of maternal nursing toward the body burden of the young relative to that acquired during gestation would have to be considered. The study on the effects of continually fed ^{90}Sr in the Beagle, currently under way at the Radiobiology Laboratory, University of California at Davis, provided a unique opportunity to obtain such comparable data in the dog.

METHODS AND MATERIALS

A series of five proven Beagle dams were fed approximately 4 or 12 μCi ^{90}Sr per day for about one year; they were then fed non-radioactive food and kept in outdoor pens. The diet contained one percent calcium with a Ca/P ratio of about 1.5; the average maintenance intake per day was about 400 g food. As the dogs came into estrus they were rebred. Breeding times were at 85, 102, 150, and two at 286 days after acquiring their body burdens.

The respective body burdens of the dams and their litters were determined *in vivo* by total body counting of the (^{90}Sr + ^{90}Y) bremsstrahlung at the time of breeding, whelping, during suckling, and at weaning of the litters. Some of the animals were sacrificed and their body burdens determined radiochemically.

RESULTS AND DISCUSSION

In Table 1 are summarized the losses in maternal body burdens.

From 10–30% of the maternal skeletal burdens of ^{90}Sr was lost by the combined effect of gestation and lactation. In some cases little or no loss in body burden could be detected during

* Supported by U.S. Atomic Energy Commission.

Table 1. Loss of Maternal ^{90}Sr due to Gestation and Lactation

Time to breeding (days)	Body burden (μCi ^{90}Sr)			% body burden lost		
	Initial	Whelping	Weaning	Total	Gestation	Lactation
85	10.8*	9.1	8.0	26	16	10
102	35.5†	32.9	24.6	29	5	24
150	5.4*	5.4	4.5	17	n.d.‡	17
286	31.2†	31.2	26.2	16	n.d.‡	16
286	16.9†	16.0	15.2	10	5	5

* 4 μCi/day.
† 12 μCi/day.
‡ Not detectable.

gestation and it is evident that most of the maternal losses occurred during lactation.

The losses in maternal body burdens should, of course, be corrected for the fraction of the ^{90}Sr which is normally lost by excretion. Since control or non-bred dogs were not available for this study, the data of Goldman, Powell and Young[2] on retention of ^{90}Sr in uniformly labeled Beagles were used to approximate the retention pattern in these dogs. Some of these data, together with the loss in body burdens due to gestation and lactation in this study, are shown in Fig. 1. Thus, if one assumes that the dams' skeletons were essentially uniformly labeled (^{90}Sr/Ca ratios in the different bones of one dam studied did not vary by more than a factor of two), about 6% of the initial body burden would be lost per 100 days—at least for the first year following the end of ^{90}Sr feeding. It is evident from Fig. 1 that during gestation

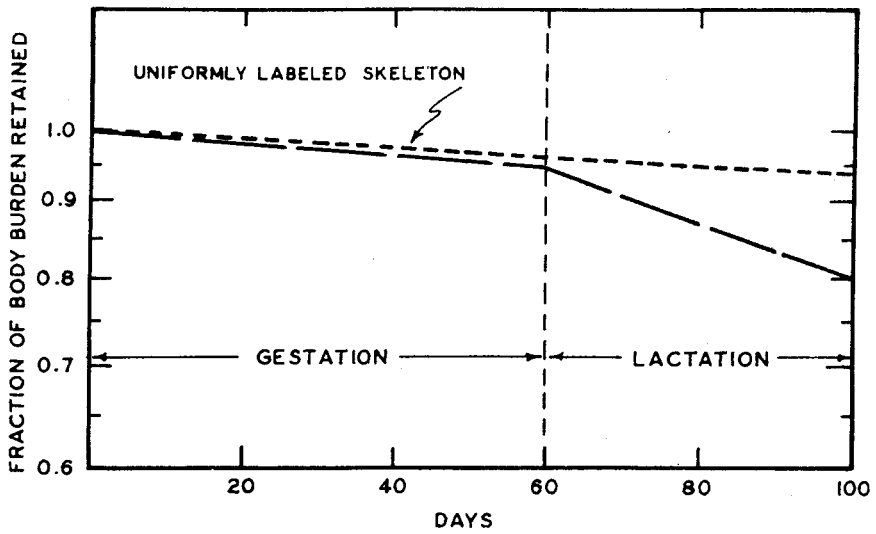

FIG. 1. Whole body retention pattern of ^{90}Sr in uniformly labeled Beagle skeletons, compared to body losses during gestation and lactation.

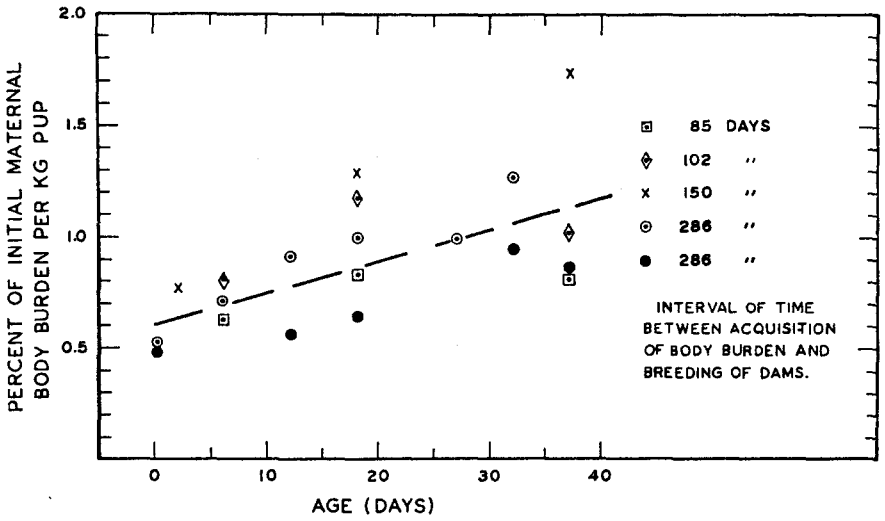

FIG. 2. ^{90}Sr pup body burdens expressed as percent of initial maternal body burden per kilogram of pup body weight.

the slope of the curve did not vary significantly from that of the uniformly labeled bone and that almost all the decrease in body burden was seen during the period of lactation and appears to be primarily a function of litter size.

Table 2 summarizes the accumulation of ^{90}Sr in the litters of pups expressed as percentages of the initial maternal body burdens and of the maternal radiostrontium losses. At birth the ^{90}Sr content of the litters represented about 1% of the initial maternal body burdens, and at weaning the pups had accumulated as much as 13% of the maternal body burdens. The pup

Table 2. Pup Body Burdens from Birth to Weaning

Time to breeding (days)	No. pups born/weaned	μCi ^{90}Sr/litter			% of maternal body burden		
					Initial		Total loss
		0–6 days	18 days	38 days	0–6 days	38 days	38 days
85	6/6	0.1	0.3	0.7	1	6 (~1/pup)*	25
102	7/7	0.8	2.0	3.1	2	9 (~1/pup)	31
150	5/5	0.1	0.3	0.7	2	13 (~3/pup)	80
286	4/3	0.1 (4 pups)	0.5 (3 pups)	1.4 (3 pups)	~0.3	4 (~1/pup)	28
286	5/1	0.1 (5 pups)	0.1 (1 pup)	0.3 (1 pup)	~0.6	2	18

* Expressed as per cent of maternal body burden per pup.

body burdens at weaning accounted for about 30% of the maternal losses. In the dam bred 150 days after acquiring its body burden, the pups contained about 80% of the maternal loss. This may be due in part to the relatively small loss, as well as difficulties of *in vivo* bremsstrahlung measurement on unanesthetized dogs with small body burdens. It is pertinent to mention here that the average body weight of Beagle pups is about 200 g at birth, and at weaning the body weight is about 1–1.5 kg. Total body calcium is about 1 g at birth and 10 g at weaning. As seen from the values in parentheses in Table 2, approximately 1 to 3% of the initial maternal body burden was transferred to each pup at weaning.

Figure 2 shows the data normalized to 1 kg of pup and further indicates this relationship. The line was drawn through the average of all values. Thus, from birth to 38 days there is an approximate increase of 0.01% of the initial maternal body burden per kilogram of pup per day. At birth a litter of 5 pups (about 1 kg) would contain approximately 0.5% of the initial maternal body burden (or about 0.1% per pup); at weaning this value increases to more than 1%, the same tenfold-increased mineralization as noted above.

These data are in essential agreement with the theoretical prediction of Mays[3] that a former ^{90}Sr dial painter of Czechoslovakia, Switzerland or Poland might transfer roughly 0.6% of her body burden to her newborn child.

These limited data reported here on Beagle dogs suggests that the evaluation of possible radiation hazards to newborn pups requires not only knowledge of dietary contamination, but also the extent of maternal transfer via gestation and nursing. Further, in the case of significant contamination of the maternal skeleton the elimination of breast feeding should be considered.

ACKNOWLEDGEMENTS

The assistance of Messrs. L. Young and L. Gilman in whole-body counting of the dogs is gratefully acknowledged.

REFERENCES

1. C. W. Mays and R. D. Lloyd. Federal Radiation Council Protective Action Guides, p. 191. June 1965.
2. M. Goldman, T. J. Powell, and L. G. Young. U.S. AEC Report UCD 472–112: 109 (1965).
3. C. W. Mays. Unpublished manuscript, University of Utah (1965).

ACTION DE LA KALLIKRÉINE SUR LES RADIO-LÉSIONS

S. SIMON
Institut Bordet, Centre Anticancéreux de l'Université de Bruxelles

et J. RODESCH
Euratom

Résumé—Les extraits pancréatiques désinsulinisés (kallikréine ou padutine-dépôt) exercent une action trophique cicatrisante sur les radio-lésions aigües et chroniques.

Une expérimentation sur l'animal montre que les radio-nécroses cicatrisent mieux et plus rapidement. On obtient une guérison après des doses entrainant chez les témoins une ulcération stable.

Chez l'homme, le traitement des radio-lésions accidentelles ou thérapeutiques est étudié sur 127 cas, avec 80% de bons résultats. La diminution marquée ou la disparition des douleurs est rapide. L'extrême diversité des radio-lésions oblige à régler le plan thérapeutique et la durée du traitement pour chaque cas particulier. Des résultats positifs ont été obtenus dans des radio-nécroses cutanées aigües et chroniques, des radio-nécroses du col utérin, de la vessie, des muqueuses, des os, dans des radio-myosites et des retards de cicatrisation.

Quelles que soient les précautions prises et les dispositifs de sécurité adaptés aux appareillages, les risques d'accidents entrainant des radio-lésions restent importants. D'autre part, pour enrayer l'évolution des cancers, les traitements radiothérapiques doivent souvent atteindre des niveaux élevés; ils laissent parfois derrière eux des séquelles indélébiles qui peuvent être fort pénibles et risquent de s'aggraver sous des influences diverses.

Ces radio-lésions sont caractérisées par des troubles trophiques intéressant particulièrement les vaisseaux sanguins dont la lumière s'oblitère, compromettant ainsi la nutrition des tissus voisins. Elles s'accompagnent souvent de douleurs intenses, à type paroxystique. Les thérapeutiques proposées ne sont efficaces que dans un petit nombre de cas; le plus souvent les résultats obtenus sont décevants.

Or depuis les travaux de Vaquez (1931), Benard (1947), Gley (1951), on sait que les extraits pancréatiques désinsulinisés ont une action trophique qui favorise la cicatrisation des plaies atones. Ceci donna l'idée au Dr A. Massart, confronté en 1960 avec une radionécrose aigüe de la main qui se montrait réfractaire aux thérapeutiques classiques et allait conduire à une amputation, à essayer l'action de la padutine-dépôt (connue en France sous le nom de kallikréine); la cicatrisation fut rapide et de qualité spectaculaire. Ce brillant succès a conduit le Dr Massart et nous-même à étudier les applications possibles de ce produit en clinique humaine.

Parallèlement aux essais thérapeutiques et dans le but de pouvoir étudier le mode d'action de ce médicament, une étude expérimentale fut entamée sur différents animaux (rats, lapins, cobayes, porcs).* Cette étude est toujours en cours; elle a confirmée l'efficacité du produit. Le tableau I résume une série d'expériences faites sur le rat: des groupes de 10 animaux adultes, appartenant à une souche homogène, de même âge et de même sexe, sont irradiés à raison d'une dose unique sur une surface de 22 mm², au moyen d'une installation de 50 kV, soit avec un filtre de 0,5 Al (flux 8 000 r/min), soit sans filtre (flux 45 000 r/min); il faut atteindre une dose de 10 000 r pour voir apparaître des ulcérations profondes; mais jusqu'à 30 000 r, la cicatrisation s'effectue spontanément en 12 à

* Travail effectué an laboratoire du Prof. Mandel (Strasbourg).

Tableau 1. *Traitement des Radio-Nécroses par la Padutine Chez Le Rat*

Doses administrées (50 kV)	Durée de cicatrisation	
	Témoins	Animaux traités (2 U.B. tous les 2 jours à partir du 21ème jour.)
10.000 r (filtre 0,5 Al)	7 à 12 semaines	plus rapide
20.000 r (filtre 0,5 Al)	12 semaines	plus rapide
30.000 r (non filtrés)	12 à 13 semaines	environ 6 semaines
50.000 r (non filtrés)	20 semaines ou pas de cicatrisation	12 semaines
60.000 r (non filtrés)	aucune cicatrisation après 20 semaines	6 à 13 semaines
70.000 r (non filtrés)	aucune cicatrisation	6 à 13 semaines
80.000 r (non filtrés)	aucune cicatrisation quelques décès	6 à 13 semaines

13 semaines; après des doses de 60 000 r et 80 000 r, il n'y a plus de cicatrisation spontanée. Après traitement à la padutine, débutant lorsque la radio-lésion est installée, on constate que, pour les doses de 10 000 à 20 000 r, la cicatrisation est plus rapide que chez les témoins; pour 30 000 r, la durée de cicatrisation est réduite de moitié; entre 50 000 et 80 000 r, tous les animaux traités cicatrisent entre 6 et 13 semaines.

En clinique humaine, l'expérimentation systématique n'est pas possible. Nous rencontrons des radio-lésions d'origines très diverses et qui évoluent de façon très variable; elles sont généralement très douloureuses, cicatrisent très lentement et laissent des séquelles pénibles et sujettes aux rechutes.

Nous avons actuellement traité 127 malades, avec un recul suffisant pour pouvoir apprécier

Tableau 2. *Radio-lésions Humaines Traitées par Padutine*

Type de Radio-lésion	Nombre de Cas	Succès	Échecs	Traitement non supporté
Radio-nécroses aigües	3	3		
Radio-nécrose cutanée sur ancienne radio-dermite	12	8	3	1
Radio-nécrose tardive après Ca peau	47	42	3	2
Radio-nécrose lèvre et bouche	10	10		
Radio-dermite chronique du sein	16	13	3	
Radio-nécrose cutanée du sein	9	8		1
Radio-lésions post Ca utérin	9	8	1	
Radio-nécrose vulve, anus, verge, périnée	8	5	3	
Cas O.R.L.	3	1	2	
Cicatrisation trainante	10	8	2	
Total	127	106 (83,5%)	17 (13%)	4 (3,5%)

les résultats obtenus (tableau 2). Nous avons enregistré 4 cas d'intolérance, 17 échecs (soit 13%) et 106 résultats satisfaisants (83,5%).

Le produit commercial utilisé a été la padutine-dépôt. Le traitement d'attaque comporte trois injections intra-musculaires par semaine. En cas de réponse favorable, les douleurs diminuent rapidement; cette réaction subjective—extrêmement importante pour le patient—survient en général avant que l'on observe une modification macroscopique de la lésion. Puis la plaie se déterge, les tissus sous-jacents perdent leur aspect atone et une cicatrice à aspect de tissu presque normal s'élabore. La cicatrisation complète prend un temps très variable, ce qui s'explique par le polymorphisme des lésions: sur les 47 cas de radio-nécrose tardive qui ont guéri, 25 ont cicatrisé en un à deux mois, 10 en trois à six mois, 5 en six à douze mois et 2 en dix huit mois. Nous avons eu quelques cas de séquestres osseux et nous avons eu l'impression que la délimitation du séquestre et son élimination suivie d'une cicatrisation se faisaient en un temps anormalement rapide.

On a intérêt à ne pas arrêter trop tôt le traitement; nous avons en effet observé quelques rechutes qui ont été enrayées par une reprise des injections. Le produit n'étant pas toxique, il est parfois utile de pousuivre une cure d'entretien à raison d'une injection hebdomadaire.

Nos échecs sont souvent imputables à l'importance ou à l'ancienneté de la radio-nécrose. Par principe, nous n'avons éliminé *a priori* aucun cas et certaines réponses ont été spectaculaires.

Nous avons obtenu de très importantes améliorations chez des malades irradiés à doses très élevées pour des cancers profonds et qui conservaient des séquelles pénibles: télangiectasies prurigineuses, sclérodermie, fibrose sous-cutanée, myosite, etc. Dans la majorité des cas, la padutine fait disparaître les douleurs et entraine une régression marquée de la myosite, des troubles circulatoires et des lésions cutanées.

Nous utilisons également la padutine lorsque, après curiethérapie ou radiothérapie de cancers cutanés étendus, il persiste après plusieurs mois une plaie atone, faisant prévoir une cicatrice vicieuse, rétractile, ou une radio-dermite chronique. Chaque fois, la padutine a déclenché un processus de guérison rapide, avec formation d'une cicatrice souple, de bon aloi.

En résumé, les extraits pancréatiques désinsulinisés nous paraissent constituer une thérapeutique de choix pour le traitement de multiples variétés de radio-lésions aigües ou chroniques. Son emploi est facile et il n'y a pas de contre-indication.

Le mécanisme d'action de ces corps n'est pas connu et des recherches de laboratoire sont actuellement en cours en vue d'élucider les problèmes théoriques qui se posent. Mais dès à présent les résultats cliniques obtenus justifient l'emploi de cette médication dans les cas d'accidents radiologiques laissant d'errière eux des séquelles douloureuses ou mutilantes.

REGENERATIONSVORGÄNGE IN THYMUS, MILZ UND KNOCHENMARK DER RATTE NACH RÖNTGEN-GANZKÖRPERBESTRAHLUNG MIT UNTERSCHIEDLICHEN STRAHLENDOSEN

FRIEDRICH BOEGLER
Radiobiologische Abteilung des Heiligenberg-Institutes, 7799 Heiligenberg BRD
und HEINZ KRIEGEL
Gesellschaft für Strahlenforschung, 8042 Neuherberg BRD

Zusammenfassung—Um die reaktiven, reparativen und regenerativen Vorgänge in Thymus, Milz und Knochenmark nach einem Strahleninsult näher zu untersuchen, wurden Ratten mit Strahlendosen zwischen 65 R und 1000 R ganzkörperbestrahlt. Zunächst stündlich, dann in täglichen Abständen bis zu 12 Tagen und mehr nach dem Strahleninsult wurden die Tiere getötet und histologisch untersucht. Blut- und Knochenmarksausstriche wurden angefertigt und von Thymus und Milz Ausstrichpräparate hergestellt unter Anwendung erweiterter Färbemethoden. Außerdem wurden histologische Schnitte von Thymus und Milz gefertigt und über 800 mikrophotographische Bilder von Ausstrichpräparaten aus allen Untersuchungsphasen hergestellt.

Während die bisher bekannten Befunde zu Regenerationsproblemen weitgehend bestätigt werden konnten, führte die Methode der Ausstrichpräparation zur Erkennung weiterer Einzelheiten über die geweblichen Prozesse nach Strahlenbelastung. Dabei zeigte sich, daß nach den dosis- und zeitabhängig auftretenden cytologischen Anomalien gleichzeitig bestimmte Veränderungen der Stützung gefäßgewebsbildenden Funktionseinheiten sowie in den faserbildenden Substanzen der extrazellulären Räume festzustellen sind. Diese Veränderungen sind als direkte Folge der Strahlenschädigung aufzufassen und sind mitbestimmend für den Grad des weiteren Zelluntergangs.

Auch für die Vorgänge der Reparation und Regeneration ist der Schädigungsgrad in den extrazellulären Räumen von Bedeutung. So war es möglich, aus der fortlaufenden Beurteilung der Organausstrichpräparate innerhalb der verschiedenen Dosierungen diese Vorgänge in ihrer morphologischen Vielfalt und ihrem zeitlichen Ablauf zu erkennen. Diese Ergebnisse weisen auf eine übergeordnete Reaktionseinheit hin, die nach allgemein-pathologischen Gesichtspunkten beurteilt, sich als ein typisches Entzündungsphänomen darstellt. Damit ergeben sich wichtige Diskussionspunkte, die für weitere Untersuchungen von Bedeutung sind.

Die Schädigung des Organismus durch ionisierende Strahlen kann letztlich auf zelluläre und biochemische Vorgänge zurückgeführt werden. Untersuchungen über die Strahlenwirkung auf die Zelle liegen bereits in großem Umfange vor.[1-14] Jedoch erscheinen uns die Beschreibungen der zellulären Veränderungen post radiationem, sei es im peripheren Blut, im Knochenmark oder im Gewebe nicht ausreichend, um z.B. Fragen über die Möglichkeiten der Reparation oder Regeneration des Strahlenschadens[15-29] zufriedenstellend zu klären. So sind beispielsweise nicht allein die Degenerationen und die Nekrosen für die Ereignisse der Destruktionsphase kennzeichnend, sondern in weit größerem Ausmaß auch die Vorgänge, die sich neben und zwischen[30] diesen regressiven Strukturanomalien abspielen.

Aus diesem Grunde haben wir in den vorliegenden Experimenten den Versuch unternommen, die extra- und intrazellulären Vorgänge im Gewebe nach Strahlenbelastung mit unterschiedlichen Dosen über die verschiedenen Stufen der Strukturveränderungen in Richtung

Regeneration fortlaufend zu beobachten und in ihrer Vielgestaltigkeit sowie in ihren übergeordneten Zusammenhängen[31] zu erfassen. Als hierfür besonders geeignet erwies sich uns das Organ-Ausstrichpräparat,[32] das besser überschaubar die verschiedenen Organisationsstufen der Grundsubstanz,[33-34] der Faserstrukturen[35-36] und der strahlenresistenteren, mesenchymalen Zellverbände,[37] erkennen läßt.

MATERIAL UND METHODE

Die Untersuchungen wurden an *ca.* 180 g schweren weiblichen Ratten eines institutseigenen Auszuchtstammes vorgenommen. Die Ganzkörperbestrahlung der Versuchstiere erfolgte in Gruppen von je 20 Tieren mit unterschiedlichen Dosen von 65 R, 150 R, 3 × 150 R, 250 R, 500 R, 750 R und 1000 R unter folgenden Bedingungen: 200 kV, 15 mA; 0,52 Cu-Filter; FHA 30 cm; Dosisleistung 160 R/min. In Abständen von 2, 3, 4, 6, 8, 12, 24, 36, 48, 60 Stunden, sowie 3, 4, 5, 6, 8, 10 und 12 Tagen nach Bestrahlungsende wurden die Tiere in Äthernarkose getötet, Blutausstriche angefertigt und Thymus, Milz sowie Knochenmark aus den Femora entnommen. Von Thymus und Milz wurden kleine Gewebsstücke unter Zusatz von physiologischer Kochsalzlösung zerquetscht und wie bei Knochenmarkspräparaten Ausstriche hergestellt. Nach Lufttrocknung erfolgten Färbungen mit Methylblau-Eosin nach Mann, mit Hämalaun nach Mayer, kombinierte May-Grünwald und Giemsa-Färbung nach Pappenheim, Azanfärbung, Sudanfärbung und Feulgens- sowie PAS-Reaktion.

Außerdem wurden in Ergänzung hierzu histologische Schnitte von Thymus und Milz nach Fixierung mit Bouin angefertigt und mit Eisenhämatoxylin gefärbt. Zur Dokumentation und weiteren Beurteilung erwiesen sich die aufgrund charakteristischer histo- und cytologischer Befunde angefertigten 800 Mikrophotographien als sehr wertvoll. Die Auswertung des Versuchsmaterials bei der Durchsicht der histologischen Schnitte und Ausstrichpräparate von Thymus, Milz und Knochenmark erfolgte mit Hilfe eines zur Erfassung der morphologischen Einzelfaktoren besonders gestalteten Schemas. Dieses Schema, das den Ablauf der Veränderungen im Gewebe nach Irritation bis zur Regeneration umfaßt, enthält neben den ergänzenden Einzelfaktoren, die später zur Erläuterung kommen werden, die folgenden Gruppen:

1. Kapillarwand-Permeabilitätsstörungen
2. Grundsubstanz-Entmischung
3. Veränderungen der Faser- und Zellstrukturen
4. Mastzellendegranulierung
5. Fortsetzung der Grundsubstanzveränderungen
6. Proliferationsvorgänge
7. Regenerationsvorgänge

ERGEBNISSE

Wenn wir hier von Regeneration sprechen, so sind nicht die entsprechenden physiologischen Vorgänge innerhalb der verschiedenen Zelltypen der untersuchten Organe für sich allein gemeint. Bei unseren Versuchen handelt es sich vielmehr um das Prinzip der akzidentellen oder reparativen Regeneration[38] nach Strahlenbelastung, das von vornherein in übergeordnetem Zusammenhang die Ereignisse im gesamten Schädigungsbereich der alterierten Gewebe des Gesamtorganismus zum Gegenstand der Betrachtung hat. Demzufolge bleiben die Regenerationsabläufe durch die Phasen Blastembildung, Wachstum und Differenzierung[39] charakterisiert, auch wenn hier die Darstellung auf Thymus, Milz und Knochenmark beschränkt bleiben.

Die Serien von Organ-Ausstrichpräparaten der speziell untersuchten Mausergewebe ergaben in Abhängigkeit von den unterschiedlichen Strahlenbelastungen im gesamten zeitlichen Ablauf recht übereinstimmende, untereinander vergleichbare, geradezu typische Reaktionsphasen, wenn man dabei besonders die Vorgänge in den extrazellulären Räumen der Grundsubstanz zur Beurteilung heranzieht.

Neben Störungen der Permeabilität und des intra- und extra-zellulären Flüssigkeitsaustausches, verbunden mit katabolen Vorgängen des Stoffwechsels aller zelligen und nichtzelligen Strukturen im Schädigungsbereich, neben Grundsubstanzentmischung mit ihren verschiedenen Graden strukturell fassbarer Anomalien, die zusammengefaßt als primäre Acidose angesprochen werden kann, finden sich weiterhin noch Faseraufquellungen, Enzymaktivierung

ortsständiger Bindegewebszellen, RNS-Synthese, Mastzelldegranulierung und Fermenthemmung, als die wesentlichsten Kriterien einer Strahlenschädigung des Gewebes innerhalb der ersten Stunden.

Nach diesem Stand der geweblichen Veränderungen kommt es in den Experimenten nach geringer Strahlenbelastung rasch zum Einsetzen der regenerativen Vorgänge mit Ausbildung von überwiegend Proliferations- und Zellausreifungs-Phasen, während in den Tiergruppen nach mittleren und höheren Dosisbelastungen unter Fortdauer kataboler Erscheinungen im Gewebe die Grundsubstanz-Veränderungen in ihrem Ausmaß noch zunehmen.

Als kennzeichnendes Beispiel hierfür kann ein Thymus-Ausstrichpräparat (Abb. 1) herangezogen werden, das 6 Stunden nach Strahlenbelastung mit 500 R gewonnen wurde. Es finden sich erhebliche Entmischungen der Grundsubstanz mit Zunahme von Quellung und Entquellungsvorgängen, sowie Zerfall zelliger und zwischenzelliger Bindegewebsbestandteile, sowie reichliches Material aus den untergegangenen Thymuszellen.

In Fällen nach letaler Strahlenbelastung kann diese Phase, wie sich übereinstimmend in den Versuchen dieser Tiergruppe gezeigt hat, zum Ausgangspunkt für die kritischen Vorgänge aller irreversiblen Störungen werden.

Erst nach Überwindung dieses wichtigen katabolen Reaktionsabschnittes bei allen mittleren und hohen, aber nicht ausgesprochen letalen Strahlenbelastungen, können auch wieder anabole Teilvorgänge wie Grundsubstanzsynthese, allgemeine Zellproliferation und mesenchymale Reaktionen, sowie Zellreifungsprozesse als erste echte Regenerationsvorgänge beginnen.

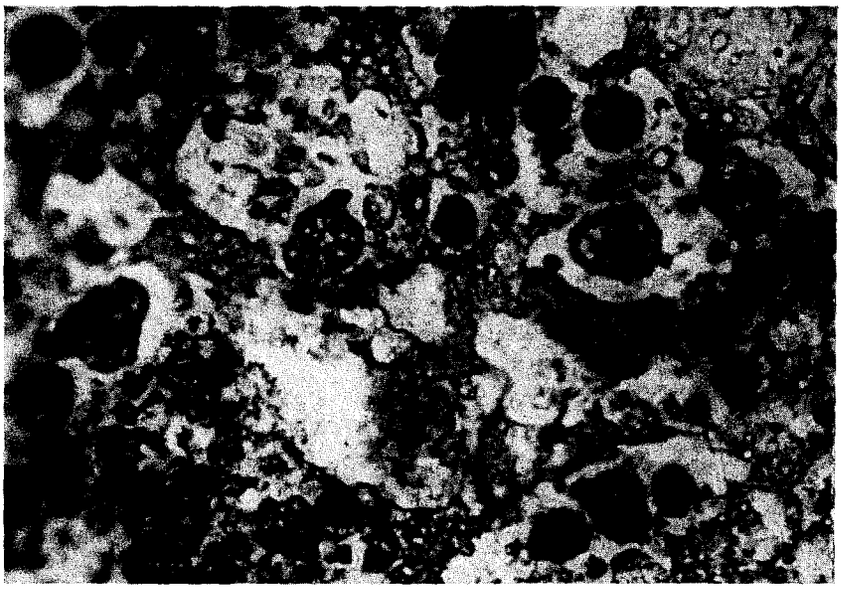

ABB. 1. Ratten-Thymus 6 Stunden nach Ganzkörperbestrahlung mit 500 R. Das Quetschpräparat zeigt Grundsubstanzentmischung, Zerfall zelliger und zwischenzelliger Bindegewebsbestandteile sowie Thymuszelldetritus.

Ein Beispiel dieser Einzelphase stellt ein Thymus-Ausstrichpräparat von der 12. Stunde nach einer Belastung mit 500 R dar (Abb. 2). Kennzeichnend sind hier die Vorgänge der Rückbildung von Grundsubstanz-Entmischungen, sowie mesenchymale Reaktionen mit ersten differenzierten Zellproliferationen und extramedullären Zellneu-sowie Fehlbildungen. Nach Abschluß der Proliferation tritt die eigentliche Regeneration als Regenerationsblastem mit Reifungs-und Rekapillarisierungsvorgängen (Abb. 3) in den Organ-Ausstrichpräparaten der nächsten

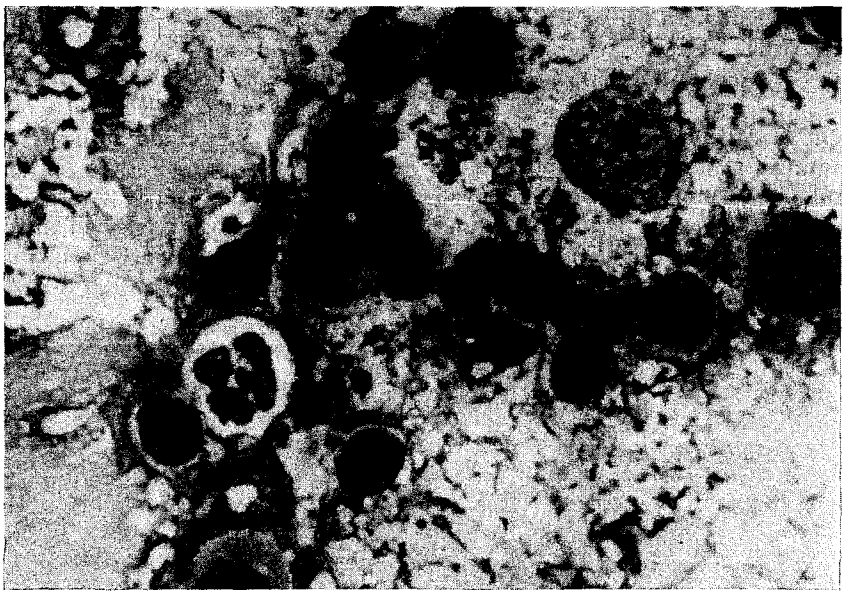

ABB. 2. Ratten-Thymus (Quetschpräparat) 12 Stunden nach Ganzkörperbestrahlung mit 500 R. Kennzeichnend sind Beginn von Grundsubstanzsynthese, mesenchymale Reaktion, Zellproliferationsbeginn und Metaplasie.

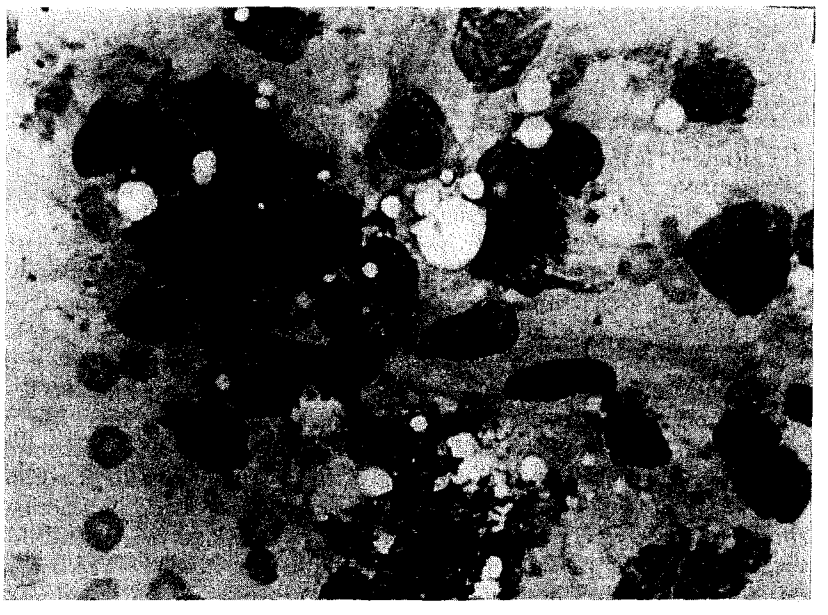

ABB. 3. Ratten-Femurmark 5 Tage nach Ganzkörperbestrahlung mit 750 R. Das Bild läßt deutlich Zellreifungs- und Rekapillarisierungsvorgänge erkennen.

Stunden und Tage deutlich abgegrenzt hervor.

In unseren Versuchen hat sich gezeigt, daß bei Belastungen mit 65 R, 150 R und 250 R die Regenerationsprozesse mit dem 5. Tag im wesentlichen bereits wieder als abgeschlossen betrachtet werden können. Bei 500 R und 750 R dauern die Regenerationsvorgänge noch an oder beginnen erst und bei 1000 R treten sie überhaupt nicht in Erscheinung. Aus diesem Grunde haben wir in einem schematischen Übersichtsbild (Abb. 4) versucht, die Regenerationsvorgänge in Thymus, Milz und Knochenmark nach Strahlenbelastung mit verschiedenen Dosen am 5.Tag vergleichend darzustellen.

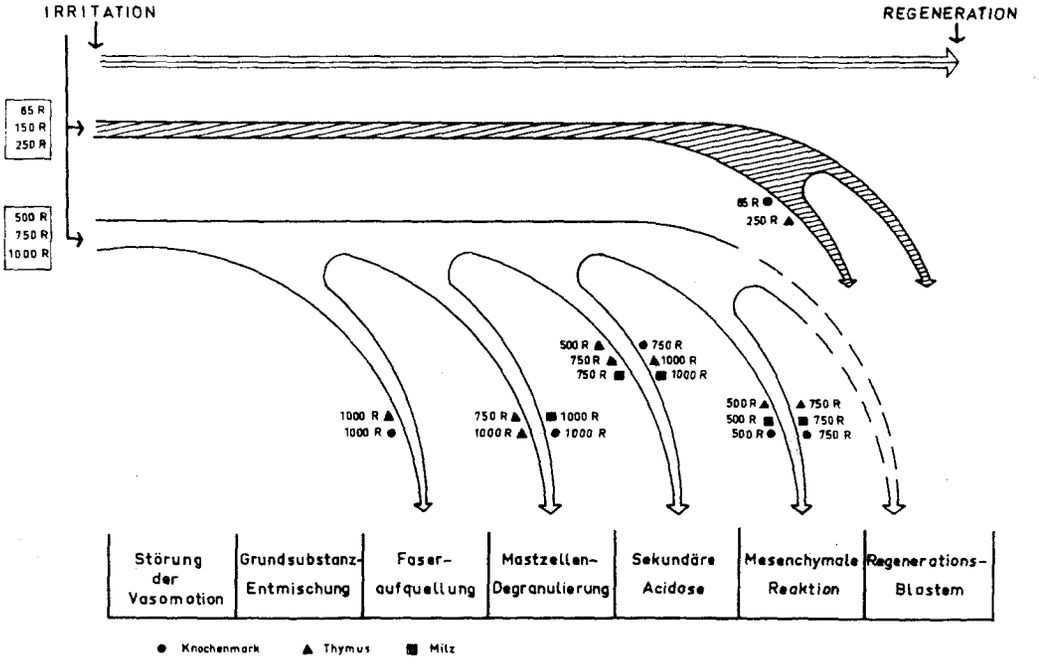

ABB. 4. Schema der Regenerationsvorgänge in Thymus, Milz und Knochenmark am 5. Tage nach Strahlenbelastung mit verschiedenen Dosen.

Wie Abb. 4 zeigt, werden bei den Strahlendosen von 65 R, 150 R und 250 R die verschiedenen Einzelphasen der Regenerationstendenz schrittweise und ohne Retardierung durchlaufen. Lediglich im Knochenmark bestehen bei einer Dosis von 65 R am 5. Tag post radiationem noch mäßig ausgeprägte mesenchymale Reaktionen mit Abbauerscheinungen bei den Erythrozyten, die als gegenläufige Reaktion überschüssiger Proliferation gedeutet weden müssen. Ein ähnlicher Verlauf konnte bei den Versuchsgruppen mit 250 R beobachtet werden, nur mit dem Unterschied, daß hier in der Milz eine mesenchymale Reaktion noch fortbesteht. Insgesamt laufen in den niederen Dosisbereichen die Regenerationsvorgänge bereits in Richtung einer völligen Wiederherstellung ab. So gesehen kann die Regeneration am 5.Tag nach Bestrahlung mit 65 R und 150 R als nahezu abgeschlossen gelten, während bei der mit 250 R bestrahlten Gruppe die Regenerationsvorgänge noch andauern, zumindest in der Milz.

Ganz anders verhalten sich demgegenüber die histologischen Veränderungen nach den mittleren und höheren Strahlendosen. Nach der Manifestation des Strahlenschadens in den beobachteten Organen werden dabei die verschiedenen Reaktionsphasen, die zur Regeneration der Gewebe führen, nicht in allen Teilen

nacheinander durchschritten. In Abhängigkeit von der Strahlendosis wird offenbar das Ingangkommen der Proliferation durch noch fortdauernde Alterationen im Grund- und Zwischengewebe gehemmt, sodaß gleichzeitig die verschiedensten Reaktionsstufen im Gewebe vorhanden sind. Im einzelnen zeigt sich, daß zum Untersuchungszeitpunkt 5.Tag p.r. (siehe Abb. 4) die mit 500 R bestrahlte Tiergruppe den Beginn echter Regenerationsvorgänge erkennen läßt, wohingegen die 750 R-Gruppe noch in der mesenchymalen Reaktionsphase steht. Erwähnenswert bei der 500 R-Gruppe ist das Vorhandensein von geringen mesenchymalen Reaktionen in Milz und Knochenmark und von Veränderungen in der Milz, die der Phase der sekundären Azidose noch zugehören. Bei der 750 R-Gruppe bestehen zum genannten Zeitpunkt neben den mesenchymalen Reaktionen noch Gewebs- und Zellveränderungen, die als Retardierung den vorangehenden Phasen der sekundären Acidose und Mastzellendegranulierung entsprechen. Dieses Erhaltenbleiben von früheren Reaktionsstufen wird besonders deutlich am Beispiel der 1000 R-Gruppe am 5.Tag nach Strahlenbelastung, indem weder die Phase der mesenchymalen Reaktion noch die der Regeneration erreicht wird. Lediglich im Thymus lassen sich bereits Anzeichen einer Grundsubstanzsynthese erkennen, während in Milz und Knochenmark Faseraufquellung, Mastzelldegranulierung und Grundsubstanzentmischung vorherrschend bleiben. Daraus läßt sich entnehmen, daß bei hoher Strahlenbelastung des Organismus die diversen Prozesse, die zum Abbau und zur Regeneration der Gewebe führen, in den einzelnen Organen unterschiedlich ablaufen.

Sieht man von der Vielfalt der Befunde, die sich speziell aus den mikroskopischen Beobachtungen zu den verschiedenen Zeitpunkten nach Bestrahlung mit unterschiedlichen Dosen ergeben haben und die aus Platzgründen hier nicht zur Darstellung kommen können, ab, so lassen sich zusammenfassend folgende Schlüsse ziehen:

1. Die Abhängigkeit der Gewebsveränderungen von der applizierten Strahlendosis zeigt sich an dem zeitlich unterschiedlichen Verlauf der einzelnen Reaktionsphasen.
2. Der Verlauf der Reaktionsprozesse im Gewebe nach Strahlenbelastung ist organspezifisch.
3. Die strahleninduzierten Gewebsveränderungen in den untersuchten Organen und Geweben weisen in ihrem Ablauf Ähnlichkeiten mit den bei Entzündungsprozessen beobachteten Vorgängen auf.

DISKUSSION

Wenn wir aufgrund der zuvor geschilderten Art der fortlaufenden morphologischen Differenzierung einen Überblick über die Gesamtvorgänge in den strahlenbelasteten Organen von Thymus, Milz und Knochenmark geben wollen, so kommen wir zu dem Schluß, daß den verschiedenartigen, aber im Grunde immer gleichen Reaktionsabläufen in unseren Versuchen ein allgemein pathologisches Phaenomen zugrunde liegt, nämlich die Entzündung. Nach Rohr[40] kann die Entzündung in ihrer biologischen Bedeutung als "die Fähigkeit des Organismus zur Abwehr gegen Schädlichkeiten und Einleitung der Regeneration umschrieben werden". Nach Masshoff[41] ist die Entzündung durch ein Zusammenwirken von Faktoren auf einer höheren als der zellulären Ebene gekennzeichnet. Im einzelnen finden wir als physiopathologische Kriterien typische Blutzellwanderungsvorgänge in den eigentlichen Blutzellbildungssystemen sowie Plasmozytose, Mastozytose, gesteigerte Makrophagozytose, Epitheloidzellbildung und Fettzellenwucherung als spezifisch retikulohistiozytäre Reaktion, die zusammen das zelluläre Abwehrsystem des Organismus darstellen.

So ergibt sich aus dem Gesamtbild der morphologischen Reaktionsabläufe in unseren Versuchen eine nahezu völlige Übereinstimmung mit den Ergebnissen anderer Untersucher, wonach es sich bei den Vorgängen in den Geweben nach Strahlenbelastung um den Ablauf eines Entzündungsprozesses handelt.[42] Entsprechend den früher dargestellten physiopathologischen Einzelabläufen des Entzündungsphaenomens treten auch bei unseren Untersuchungen die nachfolgenden Gewebsveränderungen deutlich hervor (Abb. 5):

1. Störungen der Vasomotion mit Änderungen der Kapillarfunktion, Vorgänge der Stase bis zur Diapedese von Serum, Plasma, Leuko-und Erythrozyten;

2. Gewebsveränderungen verschiedenen Grades, wie Aufquellung der Faser- und Membranstrukturen, Aufquellung mesenchymaler Strukturen, Depolymerisierung der MPS-Protein-Komplexe, Hyperosmose und primäre Acidose;
3. Mit den Zellen verbundene Änderungen wie Faseraufquellung, Enzymaktivierung ortsständiger Bindegewebszellen, RNS-Synthese, Zelldemaskierung, Zellreizung, Zellaufquellung, Pino- und Phagozytose;

fiziert. Diese beschriebenen Alterationen können nacheinander, gleich- oder wechselseitig, aber auch einseitig erfolgen. Es zeigt sich, daß geringe gewebliche und cytologische Störungen nach einer kurzzeitigen Noxe innerhalb des 1. Reaktionsstadiums sich schnell ausgleichen und so zu einer raschen restitutio ad integrum oder Ausheilung per primam kommen können.

Anders, wenn die Irritation so groß war, daß das 1. Reaktionsstadium gleichsam nur durchschritten wird, um das 2. Reaktionsstadium zu

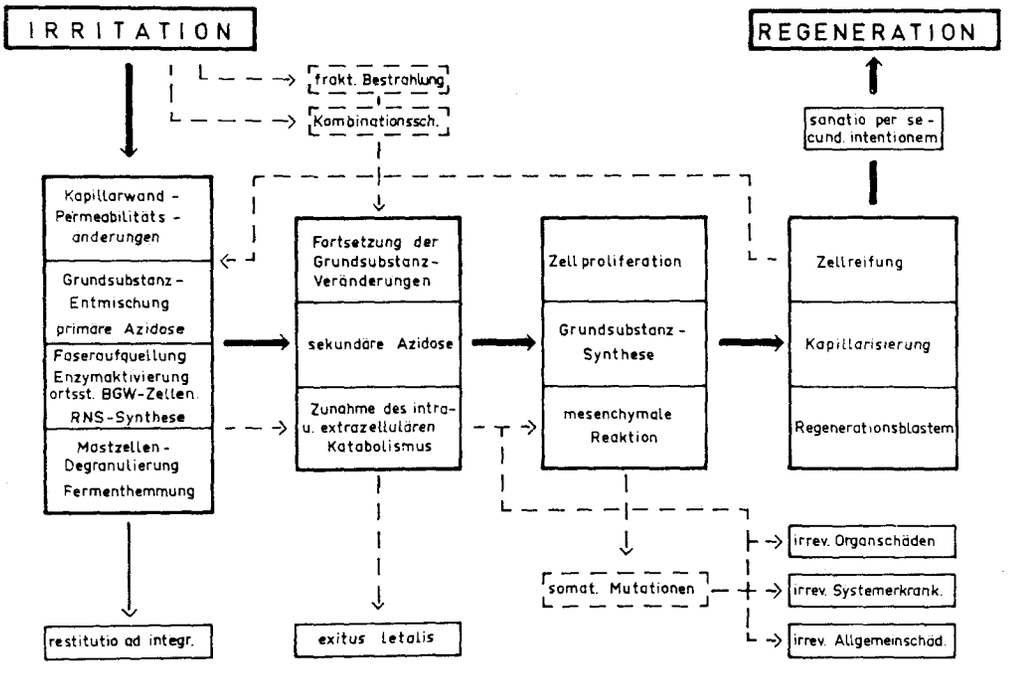

ABB. 5. Schema des Ablaufes entzündlicher Reaktionen nach Strahlenbelastung.

4. Weiterhin Vorgänge, die an die Mastzelldegranulierung und die Freisetzung von Heparin sowie Histamin gebunden sind mit möglichen Änderungen der Thrombozytenbildung und der Gerinnungsvorgänge der Hyaluronsäurewirkung und Fermenthemmung.

Diese verschiedenen Einzelvorgänge, die eng miteinander verknüpft sind und deshalb hier unter dem Begriff des 1. Reaktionsstadiums zusammengefaßt werden sollen, werden durch das Ausmaß einer Strahlenbelastung bestimmt und durch den jeweiligen Gewebsaufbau modi-

erreichen, das als Fortsetzung der Grundsubstanzveränderungen weitere gewebliche und zelluläre, sowie interstitielle Zerfallserscheinungen zeigt. Abbau saurer Mucopolysaccharide, Zunahme gefäßaktiver Abbauprodukte, Denaturierungs- und Degenerationserscheinungen des Kollagens mit Abbau durch unspezifische Proteasen, aber auch Glykolyse, Proteolyse, Lipolyse und Mucolyse sind für das 2. Reaktionsstadium kennzeichnend.

Es ist verständlich, daß nach Eintritt dieses pathologischen Grades von katabolen Gewebs- und Zellzustandsfolgen ein Rücklauf in das 1.

Reaktionsstadium mit dem Ziel eines anabolen Ausgleiches nicht mehr möglich ist. Vielmehr bedingen die gegebenen Gewebsverhältnisse des 2. Reaktionsstadiums weitere progressive und ausgleichende Vorgänge, um über eine mesenchymale Reaktion, über Grundsubstanzsynthese und Zellproliferation noch andere mögliche anabole und damit regenerative Vorgänge in Gang zu setzen, die das 3. Reaktionsstadium bilden. Die Einzelfaktoren dieser Gruppe sind durch Primärfibrillen- und Fibroblastenbildung, Fasersynthese, homogene, galertige Grundsubstanzentstehung, Sprossung von Gefäßwandzellen sowie lymphozytäre und plasmazelluläre Reaktionen gekennzeichnet.

Das 4. Reaktionsstadium der fortlaufenden Gewebsprozesse, das die eigentlichen regenerativen Vorgänge umschließt, wird durch die Ausbildung des Regenerationsblastems, durch Repopulation und Zellreifung aller Systeme sowie Neukapillarisierung markiert. Auch die Mastzellneubildung tritt zu diesem Zeitpunkt wieder hervor. Im Normalfall ist nach Auffüllung der differenzierten und funktionstüchtigen Organzellen, nach Rückbildung der Makro-und Mikrophagentätigkeit, nach abgeschlossener Kapillarisierung, nach Abnahme des entzündlichen Ödems und Zunahme der Eukolloidalität der Grundsubstanz die Wiederherstellung innerhalb physiologischer Grenzen erreicht. Der Entzündungsprozess, der eben diese Regeneration bewirken sollte, darf damit als abgeschlossen gelten.

Nur zum Zwecke der Vervollständigung des Schemas über die Regenerationsvorgänge in ihren positiven und negativen Auswirkungsmöglichkeiten sollen auch die folgenden Möglichkeiten noch erörtert werden:

Der Vorgang einer katabol wirksamen negativen Induktion des 1. Reaktionsstadiums ist dann gegeben und von vornherein anzunehmen, wenn die Strahlenbelastung als protrahierte Dosis verabfolgt oder durch einen Kombinationsschaden[43] groß genug war, um einen längeren Fortbestand der sekundären Azidose mit all ihren Nebenerscheinungen zu bewirken. In diesem Falle akzentuieren und potenzieren sich die verschiedenen Einzelfaktoren des Entzündungsprozesses sowohl im 1. als auch im 2. Reaktionsstadium. Die daraus resultierenden verstärkten Grundsubstanzveränderungen und die länger fortdauernde Azidose sind Faktoren, die einerseits die Regeneration verhindern und andererseits zum Ausgangspunkt des partiellen Gewebsoder Organzusammenbruchs werden können.

Wenn nach geringer fraktionierter Strahlenbelastung oder leichter Kombinationsschädigung[44-45] sich die Stoffwechselanomalien nicht im 2. Reaktionsstadium erschöpfen, sondern Zellproliferationsvorgänge, Grundsubstanzsynthese und mesenchymale Reaktionen, wenn auch nur verzögert und als erste Wiederherstellungsprozesse in Richtung Regeneration, wieder auftreten, so entspricht der Gesamtverlauf dem der chronischen Strahlenbelastung. Anabole und katabole Vorgänge lösen sich in Abhängigkeit der weiteren pathologischen Reizsetzung ab, wobei fortgesetzt die verschiedenen Reaktionsstadien des Entzündungsprozesses durchlaufen werden. Aus Erschöpfungs-, Hyperthrophie- sowie Mutationsvorgängen heraus, wobei letztere nur in Proliferationszentren entstehen könen, sind alsdann jene krankhaften Zustandsänderungen erklärbar, die sich später als irreversible Organ-, System- und Allgemeinkrankheiten manifestieren.

Die Folgerungen, die wir auf Grund unserer Untersuchungen über Regenerationsvorgänge nach Röntgen-Ganzkörperbestrahlung mit unterschiedlichen Strahlendosen ziehen können, sind folgende:

1. Die Vorgänge, die sich nach Strahlenbelastung in den extrazellulären- und zwischenzelligen Räumen, in den mesenchymalen Zellabschnitten sowie in den Reifungszentren der differenzierten Parenchymzellen von Thymus, Milz und Knochenmark abspielen, entsprechen dem Modell eines quasi Entzündungsablaufes.
2. Die Einzelphasen, die jeweils nach einer Actio irritans in Richtung Regeneration durchlaufen werden, sind in ihren Details folgerichtig und konstant; sie werden nur durch die Faktoren einer organspezifischen Reaktionsmöglichkeit und der Dosisabhängigkeit in ihrem zeitlichen Ablauf modifiziert.
3. Die verschiedenen Reaktionsstadien sind durch spezifische histologische Veränderungen charakterisiert und erlauben so Aussagen über Strahlendosis und Zeitpunkt

nach dem Strahleninsult sowie über den jeweiligen Stand der Regenerationssituation.

4. Aus der vergleichenden Beurteilung der histologischen und Organausstrichbefunde unter dem Gesichtspunkt des Entzündungsphänomens, ergeben sich wichtige Diskussionspunkte, die für weitere Untersuchungen von Bedeutung sind.

REFERENZEN

1. W. Lorenz. *Strahlentherapie* **88,** 190 (1952).
2. U. Feine und O. Hug. Allgemeine Zytopathologie der Strahlenwirkung. In B. Rajewsky, *Wiss. Grundl. d. Strahlenschutzes*, 84–88, G. Braun, Karlsruhe (1957).
3. G. Failla und K. Sugiura. *Science* **89,** 438 (1939).
4. K. Rohr. *Das menschliche Knochemark*, 381. G. Thieme, Stuttgart (1960).
5. G. Barth und W. Frick. Strahlenschutzprobleme in ärztlicher Sicht. In *Med. Grundl. Forsch.*, Bd. III, 208–209. G. Thieme, Stuttgart (1960).
6. T. M. Fliedner, E. P. Cronkite und V. P. Bond. *Radiat. Res.* **9,** 114 (1958).
7. K. Miyoshi und T. Kumatori. *Acta Haem. Jap.* **18,** 3794–3806 (1955).
8. H. L. Beleborodov and Y. F. Baranov. In: *The Toxicology of Radioactive Substances*, Vol. I, pp. 185–191. Pergamon Press (1962).
9. Y. Mikamo *u. Mitarb. Clinical and Haematological Studies on Bikini Patients.* Tokyo (1956).
10. A. P. Yegorov und V. V. Bochkarev. *Haemopoiesis and Ionizing Radiation.* Moskau (1954).
11. N. L. Burykin. In *The Toxicology of Radioactive Substances*, Vol. I, 83–102. Pergamon Press (1962).
12. E. E. Reimer. *Wien. med. Wschr.* **108,** 888 (1958).
13. U. Hagen. *Die med. Welt* **18,** 1009–1014 (1962).
14. F. Boegler. Diskussionsbeitrag. In *Strahlenschutz in Forschung und Praxis*, Bd. 4, 146. Rombach, Freiburg (1963).
15. R. Bauer. *Strahlentherapie* **67,** 424 (1940).
16. F. Boegler und H. Kriegel. Leukämoide Reaktion nach 90-Strontium-Inkorporation bei Ratten (im Druck).
17. H. Braun. *Strahlentherapie* **122,** 248–257 (1963).
18. H. Braun. *Strahlentherapie* **126,** 236–245 (1965).
19. J. Comsa. *Strahlentherapie* **126,** 382 (1965).
20. K. E. Fichtelius. On the destination of thymus lymphocytes. In *Haemopoiesis, cell production and its regulation.* Churchill, London, 1960.
21. T. M. Fliedner, E. P. Cronkite und V. P. Bond. *Schweiz. med. Wschr.* **89,** 1061 (1959).
22. E. Frenkel *et al. Radiat. Res.* **19.** 701–716 (1963).
23. U. Hagen. *Med. Welt*, Nr. 18, 1009–1014 (1962).
24. H. Hartweg. *Strahlentherapie* **100,** 21 (1956).
25. F. Hess. *Strahlentherapie* **119,** 161 (1962).
26. H. Langendorff und W. Hagen. *Strahlentherapie* **117,** 321 (1962).
27. R. Pape und A. Pirninger-Kuchinka. *Strahlentherapie* **101,** 523 (1956).
28. H. J. Melching und O. Messerschmidt. *Med. Klinik* **55,** 1831 (1960).
29. G. Ruhenstroth-Bauer, und J. G. Gostomzyk. *Strahlentherapie* **122,** 64–66 (1963).
30. K. F. Bauer und E. Müller. Die Zellenlehre. In *Medizinische Grundlagenforschung.* G. Thieme Verlag, Stuttgart (1959).
31. E. Letterer. Die allergisch-hyperergische Entzündung. *Hdb. allg. Path.* **VII,** 1, 497 (1956).
32. L. Diethelm und W. Lorenz. *Strahlentherapie* **122,** 222–247 (1963).
33. Th. Huzella. *Die zwischenzellige Organisation auf der Grundlage der Interzellulartheorie und der Interzellularpathologie.* Jena, 1941.
34. K. F. Studnicka. *Zschr. mikr.-anat. Forsch.* **52,** 612–657 (1940).
35. D. P. Mertz. *Die extracelluläre Flüssigkeit* 12–17. G. Thieme Verlag, Stuttgart (1962).
36. F. Büchner. Entwicklungslinien und Grenzen der Cellularpathologie. Ref. 98, *Verh. dtsch. Naturforscher u. Ärzte.* Springer Verlag (1955).
37. H. Hartweg. Strahlenwirkung auf Zellen wichtiger Organe. In *Strahlenpathologie der Zelle*, 144. G. Thieme Verlag Stuttgart (1963).
38. W. Masshoff. Die physiologische Regeneration. In *Hdb. allg. Path.* **VI,** 1, 441. Springer Verlag (1955).
39. M. Lüscher. Die Regeneration in der Zoologie. In *Hdb. allg. Path.* **VI,** 1, 406. Springer Verlag (1955).
40. K. Rohr. *Das menschliche Knochenmark* 27. G. Thieme Verlag (1960).
41. W. Masshoff. *Dtsch. med. Wschr.* **90,** 592 (1965)
42. J. Lindner und E. Wilhelmi. Intern. Symposium Grächen, Wallis, 15–17, 1/1965, S. Karger Verlag, Basel.
43. H. Langendorff, O. Messerschmidt und H. J. Melching. *Strahlentherapie* **125,** 332–340 (1964).
44. H. Langendorff, O. Messerschmidt und H. J. Melching. *Strahlentherapie* **126,** 247–252 (1965).
45. O. Messerschmidt, K. Petersen und H. J. Melching. *Strahlentherapie* **129,** 104–111 (1966).

DISCUSSION

J. Booz (*Euratom*):

I have a question about the measurement of path lengths in a cavity. I would like to know what distance has been used between the parallel lines of measurement shown in Fig. 5. Does the evaluated distribution depend on the choice of this distance?

F. W. Spiers:

Measurements were made along parallel lines across the bone section at intervals of 50 microns. Since we required a statistical distribution of path lengths, at random through the trabecular bone, the distribution should not depend too critically on choice of distance between the lines of measurement as a sufficient sampling of the bone is made. There are not many "cavities" below 100 microns and hence 50 microns should be quite adequate; indeed it may be possible to measure at greater intervals.

R. L. Kathren (*U.S.A.*):

On this subject, on the outer flat curve for the dog you should not include the point between 60 and 120 days and attach it to the deepest portion of your slope. I am not sure that this is the bimodal type of distribution. Could you comment, please?

L. J. Casarett:

The comment is a valid one and we have discussed this point briefly in the full text of the paper. The lack of data between 60 and 120 days after inhalation is regrettable but it is due to a change in the experimental procedure from animal sacrifice to an external detection method in following lung loads in this series of dogs. Thus, we didn't have tissues to work with for these intermediate time periods. We do have some points which do not appear in the figure. They are recent values and have not been included because they have been estimated manually and have not been subjected to our computer program analysis. With many thousands of numbers, we felt we should omit them for the present. It appears, however, that they will fall on this curve although the decrease in count median diameter will be more gradual than indicated in the figure. In addition, as I indicated, a collaborative study is planned with Dr. Bair and his colleagues at Battelle Northwest to obtain additional points. In any event, the significance of the curve lies in its documentation of a changing size of the distribution of microscopic radiation sources with time after inhalation, and, with additional data, the shape of the curve can be expected to change somewhat.

G. Tori (*Italy*):

Desidero far notare l'interesse della presentazione dei dati clinici offerti dall'oratrice. Il radiologo si trova spesso in difficoltà non indifferenti per la cura delle radiolesioni; percio ogni acquisizione a tale riguardo ha grande interesse pratico. Chiedo alla relatrice di aggiungere qualche informazione supplementare a quelle già fornite, soprattutto in merito alla posologia della sostanza curativa usata, in particolar modo nei casi di radionecrosi di cancri del collo uterino.

S. Simon:

Le produit que nous utilisons est commercialisé sous le nom de Padutine-dépôt (Bayer), ou kallikréine en France. En présence d'une radio-nécrose, j'appliqué d'abord pendant un mois les traitements classiques (pommades vitaminées, cortisone, infrarouge, etc.). En cas d'échec, je prescris la padutine à raison de 3 injections intra-musculaires par semaine. Le traitement est poursuivi à ce rythme aussi longtemps que nécessaire, d'après l'évolution de la lésion. Lorsque la cicatrisation est obtenue, d'après l'aspect des tissus, j'arrête ou je poursuis à raison de 2 ou d'une injection par semaine. Le traitement doit être individualisé à la demande des lésions: le patient me guide généralement et fort souvent réclame la dose d'entretien, spécialement dans les cas de myosite. En cas de reprise de troubles, j'augmente à nouveau la dose; mais je ne dépasse jamais 3 injections par semaine.

L'ORGANISATION DE LA RADIOPROTECTION À LA CENTRALE NUCLÉAIRE DE CHINON

M. DELPLA
S.G.R.-E.D.F. 73, Bld Haussmann, 75—Paris 8

C. BIGEARD et L. BERTRON
G.R.P.T.O.-S.P.T.-E.D.F. B.P. n° 23, 37—Avoine, France

E. VENTRE
S.P.T.-E.D.F. 3, rue de Messine, 75—Paris 8

Résumé—On trouve sur le site de Chinon les trois premiers réacteurs construits et exploités par Électricité de France (E.D.F.).

Dans toute centrale électrique, au personnel d'exploitation peu nombreux, et où les conséquences d'une négligence peuvent être dramatiques, chaque agent doit respecter rigoureusement les consignes de tous ordres. Nous avons organisé la radioprotection en suivant d'aussi près que possible les consignes relatives à la sécurité conventionnelle, et sur le principe de l'autoprotection.

En exposant comment la radioprotection s'intègre actuellement dans l'exploitation de la centrale nucléaire de Chinon, en précisant la part des responsabilités de chacun (responsabilité hiérarchique et fonctionnelle), les auteurs dressent un tableau des difficultés qui sont apparues à la mise en place de cette organisation, en particulier, pour ce qui concerne la formation du personnel, l'adaptation des travailleurs à un milieu contaminé, les interventions de techniciens étrangers à l'usine.

1. INTRODUCTION

En 1955, Électricité de France (E.D.F.) a établi un programme de construction de centrales de production d'énergie électrique fondé sur l'utilisation d'un type de réacteur déjà étudié par le Commissariat à l'Energie Atomique (C.E.A.) pour le centre plutonigène de Marcoule. Ces réacteurs emploient l'uranium naturel comme combustible, le graphite comme modérateur, l'anhydride carbonique (CO_2) sous pression (environ 25 bars) comme fluide caloporteur.

La centrale nucléaire de Chinon, première réalisation de ce programme, située sur la rive gauche de la Loire, dans la commune d'Avoine, à 45 km en aval de Tours et à 20 km en amont de Saumur, comprend trois tranches comportant chacune un réacteur associé à un ou deux groupes à turbo-alternateur. On trouve également, sur le même site, une installation destinée au stockage et au traitement des effluents radio-actifs et à l'examen de matériaux irradiés, ensemble désigné par le sigle A.M.I. (Ateliers des Matériaux Irradiés).

La figure 1 représente une vue d'ensemble de la centrale de Chinon, et le tableau 1 reproduit les caractéristiques principales des réacteurs (désignés par le sigle E.D.F. suivi du numéro d'ordre) et la date de leur divergence. Nous ne les décrirons pas, cela étant fait ailleurs. [1-3]

L'établissement et la mise en service de cette première centrale nucléaire, longuement étalés, par suite de difficultés techniques, ont permis de traiter sans hâte le problème de l'organisation de l'exploitation et, en particulier, de la radioprotection. Partant de ce que nous savions faire (exploiter une centrale à combustibles fossiles), renseignements pris, essentiellement au C.E.A., et aussi à l'étranger, nous avons tâtonné à la recherche de la meilleure organisation. Nous croyons intéressant, pour ceux d'entre vous qui n'ont encore aucune expérience pratique, de

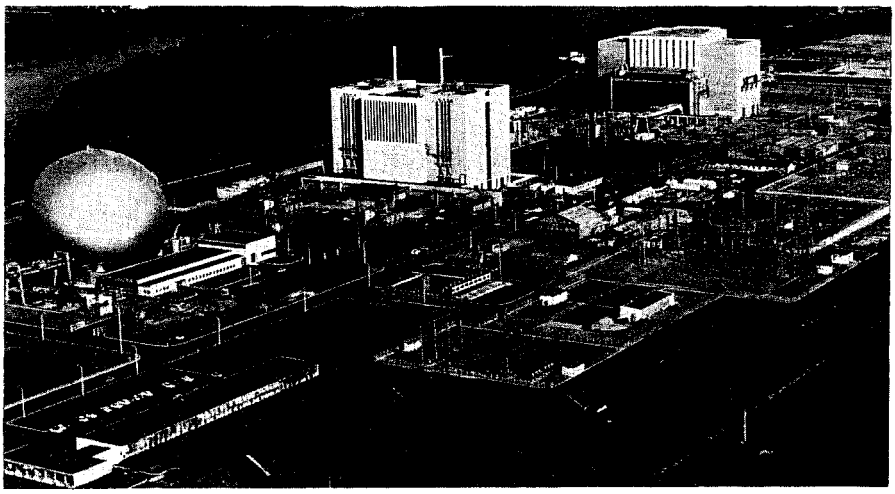

FIG. 1. La centrale nucléaire de Chinon, le 30 octobre 1965. On aperçoit, sensiblement alignés, en allant de gauche à droite: le bâtiment sphérique d'E.D.F. 1, puis le bâtiment parallélépipédique d'E.D.F. 2, surmonté de deux cheminées; puis E.D.F. 3, de dimensions voisines de celles d'E.D.F. 2. Dans la partie supérieure du cliché: la Loire, avec, audessus d'E.D.F. 3, le confluent avec l'Indre. A droite de l'alignement des réacteurs, l'allée centrale traverse le site d'Ouest en Est. Sur le côté Sud de cette allée: au premier plan, dans l'angle inférieur gauche du cliché, les locaux administratifs; plus loin, la piscine d'E.D.F. 1, plus loin encore, les baraquements des entreprises, actuellement en cours de démolition. A l'extrémité de l'allée centrale: Atelier des Matériaux Irradiés (A.M.I.) bâtiments très plats, difficiles à distinguer.—*Vue aérienne Alain Perceval, reproduction autorisée.*

relater les étapes parcourues, et pour ceux qui participent déjà à l'exploitation de centrales nucléaires, de faire le point de la situation actuelle.

2. L'EXPLOITATION D'UNE CENTRALE THERMIQUE CLASSIQUE

Le chef de centrale relève, par l'intermédiaire du chef de groupe (le groupe comprend les centrales thermiques situées dans la même région) de l'autorité du chef du Service de la Production Thermique (S.P.T.), lequel relève de la direction générale de l'E.D.F. par l'intermédiaire du directeur de la production et du transport de l'énergie.

Ce chef de centrale, assisté d'un chef-adjoint de centrale, assure l'exploitation de l'installation avec le concours d'un agent administratif, d'un contremaître de sécurité et de trois services dirigés chacun par un ingénieur.

Cette organisation, en vigueur depuis une dizaine d'années, est caractérisée par une

Tableau 1. *Caractéristiques principales des réacteurs de Chinon*

Réacteur	Parois caisson	Tonnes uranium	Puissance (MW)		Date divergence
			thermique	électrique	
E.D.F. 1	acier	140	300	60	sept. 62
E.D.F. 2	acier	250	850	200	août 64
E.D.F. 3	béton	400	1560	480	mars 66

décomposition fonctionnelle des différentes tâches: conduite, entretien, contrôle technique; par ailleurs, les progrès de l'automation ont permis de réduire sensiblement les effectifs du personnel.

Le service d'exploitation produit l'énergie et surveille les matériels; il assure une présence permanente, par roulement de cinq équipes et trois postes par jour; il doit faire respecter, en toutes circonstances, les règles de sécurité à l'intérieur de la centrale. Dirigée par un chef de quart, une équipe comprend des chefs de bloc et des rondiers.

Le service d'entretien a pour tâche d'assurer la disponibilité maximale de l'installation par un choix judicieux entre l'entretien préventif systématique et l'intervention forcée, sur panne. Il pourvoit à l'approvisionnement et au magasinage des pièces de rechange et des matériaux. Il dispose d'un "bureau des méthodes" pour préparer, organiser et coordonner les interventions.

Le service du contrôle technique procède aux essais périodiques, effectue les mesures nécessaires à la détermination des conditions optimales de fonctionnement des installations de production d'énergie, établit des statistiques. Il dispose d'un laboratoire.

3. LA RADIOPROTECTION DANS UNE CENTRALE NUCLÉAIRE

Pour exploiter une centrale nucléaire, il paraissait logique de compléter l'organigramme par l'adjonction d'un quatrième service, spécialisé en radioprotection. Pour définir les tâches de ce service, lui indiquer ses responsabilités, il fallait situer les risques particuliers à une telle installation.

3.1 *La nature des risques nucléaires*

Aux risques particuliers d'irradiation externe et de contamination interne s'ajoute, dans cette filière de réacteurs, celui de l'inhalation de CO_2; ce dernier ressortit à la sécurité classique.

Une fausse manœuvre qui entraîne une irradiation externe massive peut avoir des conséquences tragiques à bref délai; de ce fait, on peut rapprocher irradiation et électrocution.

Toutefois, dans nos installations, on rencontre le plus souvent des zones dont l'insalubrité provient d'une ambiance de rayonnements, ou de contamination radio-active, de faibles niveaux. Dans de telles conditions, une faute doit être répétée pour entraîner des conséquences graves qui, il faut le souligner, peuvent n'apparaître qu'après de longues années. Cependant, le risque de répétition d'une faute est minime: de telles zones, localisées, sont bien circonscrites; la nature du danger est connue; la situation n'évolue pas brusquement de façon inopinée.

3.2. *L'évaluation des risques*

Par raison de commodité, chaque lieu est qualifié numériquement par un risque exprimé en débit d'équivalent de dose, calculé à l'aide des correspondances rapportées dans le tableau 2.

Lorsqu'un défaut dans la réalisation des écrans de protection laisse passer des faisceaux de neutrons, il est facilement détecté au cours des essais de montée en puissance du réacteur, et corrigé, si bien que le personnel n'est pratiquement pas exposé à des neutrons.

Par contre, au cours d'interventions pour l'entretien du matériel, des agents sont fréquemment appelés à pénétrer dans des zones contaminées. Dans la mesure du possible, il faut décontaminer jusqu'à ce que les frottis n'enlèvent pratiquement plus rien; dans ce cas, nous nous bornons à mesurer l'exposition. Dans

Tableau 2. *Évaluation des risques*

Risque	Équivalent (mrem/h)
1 mR/h	1
10^3 neutron rapide/cm^2. s	100
10^3 neutron thermique/cm^2. s	5
10^{-9} Ci d'aérosol/m^3 d'air	1

le cas contraire, il est commode, pour évaluer le risque, de traduire la contamination surfacique non fixée en contamination volumique potentielle de l'air; nous admettons que:

1 μ Ci/cm^2 équivaut à 10^{-6} Ci d'aérosol/m^3 d'air; ou, exprimé en débit d'équivalent de dose (Tableau 2):

1 μ Ci/cm^2 équivaut à 1 rem/h.

3.3 *Les responsabilités du service de radioprotection*

Le service de radioprotection doit effectuer la détection et la mesure des rayonnements ionisants, non seulement à l'intérieur de l'installation, auprès des travailleurs, mais encore à l'extérieur, à l'attention des populations voisines.

Il doit obtenir de l'ensemble du personnel le respect de consignes qu'il établit en fonction du but à atteindre (limiter l'irradiation des personnes au plus bas niveau possible, compatible avec les conditions de travail) et des résultats de ses mesures.

ORGANISATION INITIALE DE LA RADIOPROTECTION

Suivant l'exemple de l'organisation dans les centres du C.E.A., nous avons créé à la centrale de Chinon un service spécialisé appelé Service Local de Radioprotection (S.L.R.). Pour remplir sa mission, ce service devait être composé de personnel instruit spécialement, disposer de moyens matériels adaptés, et avoir affaire à du personnel averti et respectant les consignes.

4.1. *Composition du S.L.R.*

Dirigé par un ingénieur assisté d'un ingénieur adjoint, le S.L.R. comprenait deux équipes.

Une équipe de quart, chargée de la surveillance auprès des installations, composée de cinq agents par tranche (trois postes par vingt-quatre heures) susceptibles d'être secondés (à toutes fins utiles: nous manquions d'expérience) au démarrage d'E.D.F. 1, par les cinq agents de l'équipe d'E.D.F. 2. Au point de vue hiérarchique, ces agents se situaient au niveau de chef de bloc.

Une équipe de surveillance extérieure, composée de cinq agents présents seulement aux heures ouvrables, mais susceptibles d'être appelés à tout moment. Au point de vue hiérarchique, ces agents se situaient: trois au niveau de chef de bloc, deux à celui de rondier.

4.2. *L'équipement de radioprotection*

Les moyens matériels destinés à la radioprotection ne présentent rien de bien original. Pour ce qui concerne la surveillance à l'intérieur de l'installation, l'accent a été mis d'emblée sur la nécessité de doubler les appareils fixes par des mesures détaillées effectuées durant la montée en puissance du réacteur à l'aide d'appareils portatifs. Pour ce qui concerne la surveillance extérieure, nous avons toujours attaché la plus grande importance à la disponibilité permanente de véhicules garés en dehors du site, près des cités du personnel, équipés de postes radiophoniques émetteurs-récepteurs et d'appareils de mesure portatifs.

L'étalonnage et la vérification du fonctionnement des appareils incombaient au service de radioprotection; leur entretien au service d'entretien.

Dans la centrale, tout agent devait recevoir une instruction adaptée à ses fonctions.

4.3. *L'instruction en radioprotection*

La formation du personnel en radioprotection, très poussée pour les agents spécialisés, se bornait, pour les autres, à une information générale sur les propriétés physiques des rayonnements ionisants et sur leurs effets biologiques, complétée par une instruction précise sur l'emploi des détecteurs de rayonnements et sur la conduite à tenir en présence d'irradiation ou de contamination notables.

Les agents spécialisés suivaient pendant six mois des cours dans une école d'électronique et, pendant trois mois, un stage d'application dans un service de radioprotection du C.E.A.; ils étaient ensuite incorporés dans une équipe du service d'exploitation où ils participaient, avant le démarrage, à l'étude du fonctionnement de l'installation.

4.4. *Répartition hiérarchique des responsabilités en radioprotection*

Le chef de centrale est responsable devant le chef du Service Général de Radioprotection (S.G.R.) pour tout ce qui concerne l'irradiation des personnes, et devant le chef du S.P.T. pour

ce qui relève de la production d'énergie, et aussi de la sécurité conventionnelle. Il y a donc un seul responsable à la direction de la centrale, mais la dualité, nettement posée au-dessus, se retrouvait au-dessous, du fait de la présence d'un service de radioprotection qui, administrativement rattaché à la centrale, relevait hiérarchiquement du S.G.R. sans intermédiaire. Le chef de ce service, localement indépendant, avait autorité pour s'opposer à toute manœuvre jugée dangereuse sous l'angle de la radioprotection (Fig. 2).

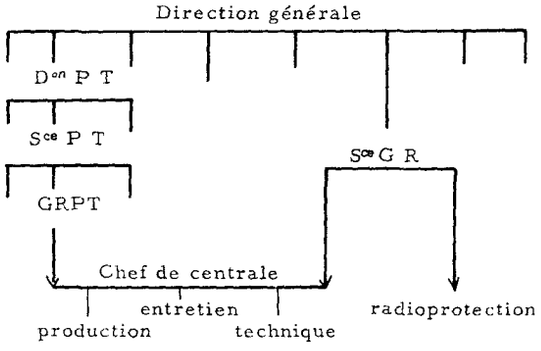

FIG. 2. Conception initiale de l'organisation hiérarchique de l'exploitation et de la radioprotection à la centrale nucléaire de Chinon. Le chef de centrale relève de la direction générale par l'intermédiaire: (1°) du groupe régional de production thermique (G.R.P.T.), du service de la production thermique, de la direction de la production et du transport de l'énergie; (2°) du service général de radioprotection. La centrale comprend trois services: production, entretien et contrôle technique; le service local de radioprotection relève directement de l'autorité du S.G.R.

4.5. *Les inconvénients*

Peu de temps avant la divergence du premier réacteur, nous avions formé une douzaine d'agents destinés à assurer le quart en radioprotection; il en restait deux.

Ces agents, pour la plupart, étaient de jeunes chefs de bloc de centrale thermique conventionnelle; ils venaient à nous, attirés par les prestige d'une technique nouvelle, avides d'apprendre, désireux aussi de promotion sociale.

Après la période de formation, un séjour de quelques mois à la centrale, où ils donnaient toute satisfaction, ils repartaient dans une centrale thermique conventionnelle, certains de ne pas longtemps attendre un poste de chef de quart. Ainsi, nous nous heurtions à une impossibilité: conserver au S.L.R. un effectif suffisant d'agents de qualité.

Par ailleurs, se posait la question de l'opportunité de la dissociation du commandement dans une centrale parce qu'un réacteur nucléaire remplace la chaudière.

4. ORGANISATION ACTUELLE DE LA RADIOPROTECTION

N'étant pas viable tel quel, le S.L.R. fut dispersé et ses attributions réparties sur les autres services. En l'absence de personnel spécialisé, chacun dut prendre des responsabilités adaptées à ses fonctions, et, en conséquence, subir l'instruction correspondante.

5.1. *La répartition des tâches*

La surveillance auprès des installations a été confiée au service d'exploitation: *le chef de quart* a autorité sur la totalité de l'équipe de quart, composée maintenant, outre les rondiers qui n'ont pas de rôle particulier en radioprotection, de trois *chefs de bloc—techniciens de radioprotection.* Ces agents, dont la dénomination compliquée rend compte de la polyvalence, changent de fonction quotidiennement, de façon à ne perdre de vue, ni les problèmes d'exploitation, ni les problèmes de radioprotection.

L'un demeure au pupitre, en salle de commande, ne faisant que de l'exploitation.

Le second effectue les contrôles dans les différentes parties de l'installation, ne faisant que de la radioprotection.

Le troisième prête main forte, suivant les besoins, soit au chef de bloc d'exploitation (par exemple pour le redémarrage), soit au technicien de radioprotection (par exemple en période d'arrêt pour entretien).

Comme dans les centrales classiques, en cas d'intervention, la sécurité des travailleurs repose sur deux personnes:

—le chef de consignation, qui est toujours le chef de quart,
—le chef de travaux, désigné pour la circonstance.

Le chef de consignation fait isoler complètement du reste de l'installation le matériel sur lequel doivent se faire les travaux, fait effectuer les condamnations qu'il juge nécessaires pour éviter le retour intempestif d'un fluide (électrique, liquide, gazeux) ou d'une source de rayonnement (cartouche de combustible irradié, fluide contaminé) et accorde *l'autorisation de travail* qui précise, au besoin:

—la durée de l'intervention,
—l'aménagement des accès,
—les conditions de travail (renforcement de la ventilation, par exemple),
—le détail des tenues vestimentaires,
—la nature, le nombre et l'emplacement des appareils de détection.

Le chef de travaux, technicien responsable de l'exécution des travaux est responsable du respect, par son équipe, des consignes établies par le chef de quart. Toute intervention est précédée par une phase préparatoire au cours de laquelle sont examinées les techniques de démontage, de décontamination, d'usinage, etc. . . . pour prévoir l'outillage, les moyens et les méthodes de manutention en présence de contamination, les pièces de rechange, etc. . . .

Durant la phase préparatoire, le bureau des méthodes dresse le plan d'intervention; au stade de l'exécution, chef de travaux et chef de quart collaborent étroitement; le premier étant particulièrement compétent sur la technique, le second sur la sécurité. Au cours d'une intervention, les risques peuvent évoluer:

—soit pour des causes externes au chantier, liées à l'exploitation du réacteur, le chef de quart doit prendre toutes mesures préventives nécessaires;

—soit pour des causes internes au chantier (ouverture d'une capacité contaminée, manipulation d'un matériel activé par irradiation, etc. . . .); dans le cas où les précautions préventives s'avèreraient—ou mieux, risqueraient de s'avérer—insuffisantes, le chef de travaux doit alerter le chef de quart qui doit adapter ses consignes à la nouvelle situation.

Le chef de travaux appartient souvent au service d'entretien de la centrale; mais il se peut—cas général en période de démarrage—que ce soit un technicien d'une entreprise qui a participé à la construction.

Le service de contrôle technique qui, dans toute centrale, dispose d'un laboratoire, a été complété par l'adjonction d'une section de "mesures nucléaires" de six agents, chargés:

—à l'intérieur des installations, de l'étalonnage des appareils de radioprotection; de la mesure de l'activité volumique du CO_2, avec identification, en cas d'anomalie, des principaux radionucléides; du contrôle des rejets d'effluents gazeux et de la tenue à jour des statistiques correspondantes;

—à l'extérieur des installations, des mesures systématiques de rayonnement gamma et des prélèvements systématiques d'échantillons (aérosols, eaux, lait, fourrage) expédiés au laboratoire du S.G.R. (situé près de Paris et commun à toutes les centrales nucléaires).

En cas d'incident avec rejet inopiné d'effluents radio-actifs à l'atmosphère, alerté par le service d'exploitation (responsable de la conduite à tenir dans la tranche intéressée), le service de contrôle technique doit, en permanence, disposer d'au moins un véhicule susceptible de partir dans la campagne à la recherche de la contamination.

Ainsi, on ne retrouve plus, dans une centrale nucléaire, que les trois services communs à toute centrale thermique, mais adaptés à remplir certaines fonctions particulières. *Le chef de centrale*, toujours responsable de la radioprotection devant le chef du S.G.R., de la production d'énergie et de la sécurité conventionnelle devant le chef du S.P.T., a maintenant autorité sur l'ensemble du personnel (Fig. 3). Comme pour la sécurité conventionnelle, pour toutes les questions relatives à la radioprotection, il délègue son autorité au *chef-adjoint de la centrale*, lequel est assisté d'un ingénieur de radioprotection et de sécurité et d'un ingénieur du S.G.R. détaché à la centrale; le rôle de ces deux derniers est purement fonctionnel: *chaque chef de service assume l'entière responsabilité dans son rayon d'action.* Cette réorganisation, basée sur l'autoprotection à tous les échelons, nous a conduits à reconsidérer l'enseignement de la radioprotection.

5.2. *La formation du personnel en radioprotection*

Tout ingénieur qui se voit confier des responsabilités dans une centrale nucléaire a suivi les cours du génie atomique (une année scolaire

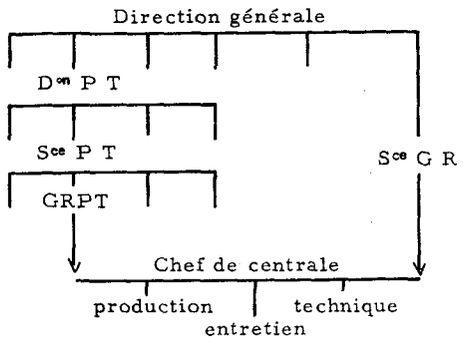

FIG. 3. Conception actuelle de l'organisation hiérarchique de l'exploitation et de la radioprotection dans les centrales nucléaires de l'E.D.F. Par comparaison avec la figure 2, le service local de radioprotection a été supprimé, ses attributions réparties sur les trois services. Le chef de centrale a maintenant autorité directe sur l'ensemble du personnel; il relève toujours de l'autorité de deux services: service de la production thermique, service général de radioprotection.

à temps complet) organisé par le C.E.A. Ensuite, durant quatre semaines, il a subi une formation complémentaire en radioprotection, organisée par le S.G.R., et qui comprend des cours et des travaux pratiques durant quinze jours, puis des stages d'application d'une semaine au centre de Marcoule (C.E.A.), et d'une semaine à la centrale nucléaire de Chinon.

Tout ingénieur chef de service est responsable de la formation de son personnel, pour laquelle il recourt à l'aide des ingénieurs spécialisés présents à la centrale. C'est sur ces deux ingénieurs que repose, pour l'instant, la formation des techniciens d'entreprise habilités à devenir, au besoin, chefs de travaux.

5.3. *Les difficultés*

Vous vous en doutez, le fonctionnement de notre centrale, n'a pas été sans manquements à la radioprotection.

Avec une telle organisation, une fois franchi le bureau du chef de quart, chacun, libre d'aller où son travail l'appelle, se doit de se conformer aux prescriptions des consignes. Les agents d'E.D.F. qui n'ont pas d'habilitation médicale sont refoulés; les agents d'entreprise peuvent être admis jusqu'à concurrence d'un équivalent de dose de 200 mrem (Fig. 4).

En réalité, il nous a paru tout de même prudent de limiter les risques: tout chef de travaux est responsable des membres de son équipe; de plus, pour tout travail dans une zone où le débit d'équivalent de dose dépasse 100 m rem/h, la présence permanente d'un chef de bloc-technicien de radioprotection est obligatoire. En cas de révision de tranche, avec l'ouverture simultanée d'un grand nombre de chantiers fortement contaminés, dans une période qui correspond au minimum de la demande d'énergie électrique sur le réseau, mais aussi aux congés annuels, l'effectif de chefs de bloc s'avère insuffisant. Il fraudra renforcer l'équipe ou modifier les consignes.

Dans l'état actuel de notre expérience en la matière, nous ignorons si nous pourrons nous montrer plus confiants: l'autodiscipline ne peut

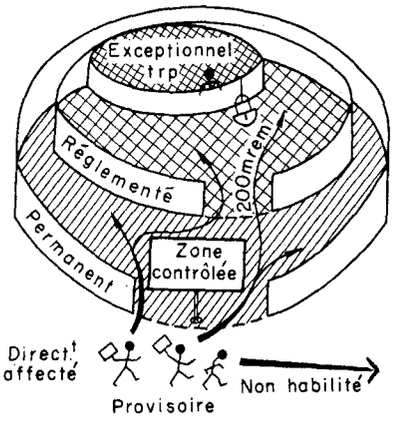

FIG. 4. Une fois franchi le bureau du chef de quart qui délivre l'autorisation de travail, tout sujet, sous la responsabilité du chef de travaux, peut se rendre où son travail l'appelle, sauf dans les zones d'accès exceptionnel. Chacun doit bien connaître les consignes de sécurité et se doit de les respecter. Dans les zones d'accès exceptionnel, la présence d'un chef de bloc—technicien de radioprotection (t.r.p.) est obligatoire. L'autorisation de travail peut être accordée provisoirement aux travailleurs de passage (jusqu'à concurrence de 200 mrem); elle est refusée à tout agent qui, même directement affecté à des travaux sous rayonnement, n'est pas habilité médicalement.

LA CONTAMINATION DU CIRCUIT PRIMAIRE DES RÉACTEURS DE CHINON

J. BARBIER, B. HOUPIN et G. CORDIER
G.R.P.T.O.-S.P.T.-E.D.F., B.P. n° 23, 37—Avoine, France

M. DELPLA
S.G.R.-E.D.F., 73, Bld Haussmann—75-Paris 8°

Résumé—Les auteurs passent en revue les principaux éléments radio-actifs recontrés dans le fluide caloporteur (gaz carbonique) des réacteurs de la centrale nucléaire de Chinon.

Parmi les produits d'activation, certains, imprévus, comme le mercure 203, ont un caractère permanent; d'autres ne se manifestent que transitoirement.

Indépendamment des ruptures de gaine, il y a toujours des produits de fission dans le gaz carbonique. Les auteurs indiquent comment ils mesurent indirectement cette contamination du circuit par le césium 138.

1. INTRODUCTION

Dès l'étude des projets, il convient de connaitre quelle sera la contamination radioactîve du circuit primaire de refroidissement des réacteurs nucléaires, afin de prévoir: d'une part les écrans nécessaires à l'atténuation des rayonnements pénétrants; d'autre part, les moyens à mettre en œuvre pour éviter une concentration excessive de radio-éléments dans l'air susceptible d'être inhalé. Des considérations théoriques, à partir de données parfois incertaines, permettent de prévoir cette contamination: nature et activité volumique des principaux radio-éléments.

Avant d'exposer et de discuter les résultats observés sur nos réacteurs de Chinon, nous donnerons quelques indications sur les installations.

2. LES INSTALLATIONS

Nous allons décrire très sommairement la centrale nucléaire de Chinon et les moyens de mesure de la contamination du fluide caloporteur.

2.1. *La centrale nucléaire de Chinon*

La centrale nucléaire de Chinon comprend trois tranches désignées par le sigle E.D.F. suivi d'un numéro d'ordre allant de 1 à 3. Chaque tranche comporte un réacteur nucléaire et un groupe turbo-alternateur (E.D.F. 1) ou deux (E.D.F. 2 et E.D.F. 3). On emploie l'uranium naturel comme combustible, le graphite comme modérateur, l'anhydride carbonique (CO^2) sous pression (environ 25 bars) comme fluide caloporteur. Les cartouches de combustible, gainé en alliage de magnésium et de zirconium, sont superposées dans des canaux verticaux ménagés dans la masse du graphite. Le nombre de cartouches passe de 17000 à E.D.F. 1 à plus de 40000 à E.D.F. 3, pour une puissance électrique nette allant de 60 à 480 MW. Ce type de réacteur a été décrit en détail dans de nombreuses publications.[1, 2, 3] Le lecteur peut trouver une vue générale de la centrale nucléaire de Chinon dans une communication présentée à ce même congrès.[4]

2.2. *Mesure de la contamination du CO_2*

Plusieurs dispositifs, étudiés et mis au point par le Commissariat à l'énergie atomique (C.E.A.), permettent de suivre l'évolution de la contamination du CO_2; il est en outre possible, dans chacune des tranches, de prélever directement des échantillons dans la veine gazeuse.

Nous nous bornerons à rappeler brièvement le principe de fonctionnement du dispositif de détection de rupture de gaine (D.R.G.) et

être obtenue que si les agents, bien informés des risques, connaissent parfaitement les consignes; elle impose aux cadres un effort constant de formation et d'information du personnel. Le comité d'hygiène et de sécurité de la centrale, dont le médecin du travail, membre de droit, est un membre actif, associé à cet effort, participe à la promotion et au maintien de l'esprit de sécurité. De nombreux moyens sont mis en œuvre: affiches, films, conférences, visites de chantiers.

Si des résultats encourageants ont pu être obtenus avec les agents de la centrale, un problème se pose actuellement avec les agents d'entreprise qui, nombreux, participent à la mise au point du matériel pendant les périodes de démarrage et à l'entretien pendant les périodes de révision: ce personnel, mouvant, ignore le plus souvent les principes de radioprotection les plus élémentaires; son emploi exige, de la part des responsables de la centrale, un effort de formation considérable, d'autant que la plupart des chefs d'entreprise, sans doute effrayés par leur complexité, préfèrent tout ignorer des problèmes de radioprotection.

La présence, sur le site, de l'A.M.I., simplifie l'exploitation de la centrale nucléaire de Chinon, du fait que cette installation indépendante (elle relève aussi du S.P.T.) reçoit les effluents solides (y compris les effets spéciaux après usage) et les effluents liquides, en vue de stockage et, s'il y a lieu, de traitement et de rejet. Si ces opérations devaient être effectuées à la centrale, il faudrait prévoir le personnel et le matériel correspondants. Cela ne créerait sans doute pas de difficultés particulières: les déchets solides vraiment contaminés représentent peu de chose et les effluents liquides contiennent une activité négligeable (57 millicuries rejetés en Loire en 1965).

Par contre, avec ses trois tranches nettement différentes les unes des autres, la centrale de Chinon représente trois étapes importantes dans notre acheminement vers la réalisation d'une centrale nucléaire industrielle. Le franchissement de chaque étape comporte des extrapolations qui, souvent, demandent des corrections; ainsi, nous pensons que l'exploitation des tranches de Chinon deviendra plus facile, et aussi que les tranches à venir poseront moins de problèmes de radioprotection que n'en ont posé celles de Chinon qui, expérimentales, sont encore aujourd'hui en période de mise au point.

6. CONCLUSION

Où sont les limites de la radioprotection dans une centrale nucléaire? Il est classique de dissocier sûreté nucléaire et radioprotection, radioprotection et sécurité. Les problèmes de sûreté nucléaire et de radioprotection doivent être envisagés dès l'étude des projets, aussi le chef de centrale est-il associé dès le début à l'équipe chargée de cette étude dont il suit les progrès, avant de suivre la construction.

Nous n'avons plus à délimiter de frontières: le chef de centrale est responsable de l'ensemble; à ses responsabilités, il associe l'ensemble de son personnel.

En confiant aux travailleurs le soin d'assurer leur propre protection, nous avons misé sur l'avenir: dans chaque centrale nucléaire, du haut en bas de l'échelle, la responsabilité sera assurée par des personnes qui auront été appelées à s'imposer les contraintes dues à la radioprotection à tous les échelons franchis; par exemple, tout chef-adjoint de centrale aura été chef de service et, dans la mesure du possible, représentant local du S.G.R., poste dans lequel la radioprotection et la sûreté nucléaire auront été ses seules préoccupations.

Ce parti pris nous a paru souhaitable: le noyau fissile étant appelé à devenir la principale source d'énergie, il convient que les travailleurs des centrales nucléaires, comme, d'ailleurs, ceux des entreprises qui travaillent à leur mise au point, s'accoutument et s'adaptent à la prévention des risques d'origine nucléaire comme ils l'ont fait pour les autres types de risques, non moins dangereux.

RÉFÉRENCES

1. J. P. Roux et C. Bienvenu. *C.R. 2ème conf. utilisat. pacif. én. at.*, Genève, 1958, Vol. 5, p. 298 (1958).
2. C. Bienvenu, P. Passerieux et P. Bacher. *C.R. 3ème conf. utilisat. pacif. én. at.*, Genève, 1964, Vol. 5, p. 67 (1965).
3. J. P. Roux et C. Bienvenu. *J. Brit. Nuclear En. Sy.* **1,** 235 (1962).

ment au mercure 197, de 65 heures de période; ces deux isotopes n'émettent que des photons, et ces photons sont mous ou très mous. Le mercure 202, de proportion isotopique égale à 30% donne, avec une section efficace de 3,8 barns, du mercure 203, de 45 jours de période; il est intéressant de noter que ce nucléide n'émet que des rayons β très mous et une raie γ à 279 keV.

Il nous est arrivé d'être surpris par l'arrivée d'une contamination importante. Ainsi, peu de temps après la mise en exploitation industrielle du réacteur E.D.F. 1, le circuit primaire de refroidissement a été littéralement envahi par du sodium 24 (période 15h, photons de 1,38 et 2,75 MeV). La charge du dessiccateur, dans le circuit dérivé destiné à assurer l'épuration continue du CO_2, venait d'être changée; le fournisseur confirma l'emploi d'un nouveau produit à base de sodium.

L'origine du radionucléide dont on croit avoir identifié le spectre n'est pas toujours commode à déterminer; il en est ainsi pour l'antimoine 124 et le brome 82, trouvés dans plusieurs échantillons prélevés à E.D.F. 1 et E.D.F. 2.

L'analyse spectrométrique γ donne parfois des pics difficiles à identifier. Par exemple, on trouve, sur certains échantillons, un pic voisin de 560 keV, dont la présence paraît liée à l'introduction accidentelle d'huile dans le circuit de refroidissement; il pourrait bien s'agir d'arsenic 76 ou d'antimoine 122.

Nous nous bornerons à rappeler, pour mémoire, que les réacteurs de cette filière produisent aussi du tritium, trouvé dans l'eau récupérée par dessiccation du CO^2. Les concentrations, faibles, ne posent pas de problèmes de radioprotection.[7]

3.2. *Les produits de fission*

Indépendamment de toute rupture de gaine (événement exceptionnel et promptement détecte par le dispositif de D.R.G.), même lors du premier chargement, le gaz carbonique charrie des produits de fission formés à partir de l'uranium fixé sur les gaines. "La contamination extérieure des gaines peut se mesurer en centimètres carrés d'uranium nu par un détecteur de produits de fission étalonné en surface émissive . . . Un centimètre carré d'uranium métallique nu émet autant de produits de fission que 6, 4 mg d'uranium déposés en couche infiniment mince. . . . La valeur généralement admise pour cette contamination des gaines est de: 10^{-8} g/cm^2. . . ."[5] De ces données et des caractéristiques du chargement,[5, 8] on déduit la surface d'uranium métallique nu équivalente à la contamination des gaines dans chacun des réacteurs. L'ensemble des valeurs numériques est raporté dans le tableau 1.

Il va sans dire que toutes les contaminations mesurées varient d'un réacteur à un autre et, pour un même réacteur, dans le temps.

4. RÉSULTATS ET DISCUSSION

Il importe de connaître l'origine de la contamination du fluide caloporteur, afin de parer à cette contamination à partir du moment où, devenue gênante, elle risque d'arriver à être dangereuse, créant dans les locaux un débit d'exposition excessif par émission γ, ou une contamination notable de l'atmosphère. Par ailleurs, il est possible de mettre à profit certains aspects de cette contamination.

4.1. *Résultats relatifs à l'irradiation*

Le sodium 24 donnait, à plusieurs mètres des filtres du dispositif de D.R.G., un débit

Tableau 1. *Contamination des gaines en uranium* (*Surface équivalente d'uranium métallique*)

Réacteur	E.D.F. 1	E.D.F. 2	E.D.F. 3
Surface gaines/canal (m^2)	5,6	4,8	7,8
Nombre canaux	1150	2500	3264
Surface totale gaines (m^2)	6450	12,000	25,400
Contamination moyenne (g d'U)	0,64	1,20	2,54
Surface équivalente (cm^2 d'U nu)	100	200	400

du dispositif de contrôle continu de l'activité du CO_2 (D.C.C.A.–CO_2).

Le dispositif de D.R.G.[5] met en mémoire l'activité due aux descendants des gaz de fission (rubidiums et césiums) mesurée sur le CO_2 prélevé à la sortie de chaque canal (en moyenne toutes les vingt-quatre minutes) les activités trouvées sont comparées à celles mises en mémoire en l'absence de rupture de gaine, compte tenu, s'il y a lieu, de la variation de la puissance du réacteur et du débit de CO_2. Si l'évolution dépasse un seuil d'alarme, un calculateur numérique donne l'ordre de "passage sur suiveur": l'évolution de l'activité du canal en rupture de gaine est alors suivie de façon continue. Cette évolution est graduée en "surface équivalente d'uranium nu"; par exemple, la D.R.G. de E.D.F. 2 donnerait 1200 impulsions par seconde à la sortie de l'électronique si une surface nue de un centimètre carré d'uranium naturel métallique était placée au centre d'un canal central de la pile fonctionnant en régime nominal.

La D.C.C.A.–CO_2 comprend essentiellement un filtre à haut rendement vu par un compteur Geiger-Muller (G. M.), et suivi d'une chambre d'ionisation à circulation.[6] Il peut ainsi donner une alarme, par le G.-M., en cas de montée brutale de l'activité arrêtée par le filtre, et suivre l'évolution de l'activité β totale due aux gaz mélangés au CO_2 (on laisse à ceux qui ont une courte période, tel l'azote 16, le temps de disparaître dans un volume temporisateur).

Enfin, des échantillons sont prélevés sur le circuit primaire, soit sur filtre, soit, après filtration, en récipient. Sur ces échantillons, on peut procéder, par des mesures globales d'activité, à des études de décroissance, ou chercher à identifier les principaux nucléides par spectrométrie gamma.

3. LES PRINCIPAUX RADIO-ÉLÉMENTS RENCONTRÉS

Tandis que la nature des produits de fission est bien connue, celle des produits d'activation ménage parfois des surprises.

3.1. *Les produits d'activation*

Les éléments activables se trouvent dans les matériaux de structure et dans le fluide caloporteur. Pour l'économie de neutrons, d'intérêt primordial dans cette filière de réacteurs, ces matériaux et ce fluide sont composés d'éléments de très faible section efficace de capture.

Dans le modérateur (graphite), seul le carbone 13 s'active en donnant du carbone 14; toutefois, sa proportion dans le carbone et sa section efficace sont très faibles. L'érosion du métal des gaines des éléments combustibles ne libère que des traces de zirconium 95. En fait, par suite des phénomènes de corrosion et d'érosion, l'acier est un pourvoyeur important: outre du manganèse 56 et du chrome 51, produits en quantités très faibles, on trouve deux isotopes du fer, de nombres de masse 55 et 59; le premier n'émet que des X, par capture électronique, avec une période de 2, 9 ans, le second, des γ assez pénétrants (1, 1 et 1, 3 MeV) avec une période de 45 jours. Les périodes de ces deux isotopes diffèrent grandement; de plus, du fer ayant été irradié à saturation, l'activité du premier est environ cinquante fois plus grande que celle du second. La présence de fer 55 est particulièrement difficile à détecter.

Malgré sa très faible section efficace (20 micro-barns, en moyenne, pour les neutrons rapides) en raison de la masse considérable qui circule au cœur même du réacteur, l'oxygène 16 du CO_2 produit une activité notable d'azote 16, de très courte période (7 s), mais émetteur de rayons γ très pénétrants (6 à 7 MeV).

Enfin le CO_2 charrie des impuretés activables, soit du fait d'épuration incomplète, soit par suite d'introduction, par erreur, de substances étrangères.

L'argon 40 contenu dans l'air mélangé au CO^2 s'active en argon 41 qui, avec une période voisine de 2h, émet un photon de 1,3 MeV. Mentionnons, pour mémoire, la formation de carbone 14 à partir de l'azote 14 et de l'oxygène 17.

Nous avons pris l'habitude de trouver du mercure dans nos réacteurs. Le fait n'est pas surprenant puisque, surtout pendant la période des essais, mais aussi en période d'exploitation, ce liquide est d'un emploi commode pour les mesures de débit du CO_2. Le mercure 196, en faible proportion isotopique (0,15%), présente des sections efficaces de capture considérables pour les neutrons thermiques: avec 420 barns, il conduit au mercure 197 métastable, de courte période (24 h), et avec 880 barns, directe-

d'exposition de 2,5 mR/h. Les sources de cette irradiation étaient très localisées.

A l'inverse des poussières et aérosols qui sont recueillis par les filtres, les gaz radio-actifs diffusent dans l'ensemble du circuit et provoquent l'élévation générale du niveau du rayonnement γ. Les écrans de protection, interposés entre les lieux fréquentés par le personnel et le circuit de CO_2, s'avèrent par endroits nettement insuffisants lors d'un démarrage après vidange lorsque la purge de l'air du circuit n'a pas été assez poussée: l'argon 41 donne plus de 100 mR/h, à E.D.F.1, sur le palier situé à hauteur des réservoirs de stockage du CO_2:

4.2. *Contamination de l'atmosphère, valeur des résultats*

Comme les gaz, les vapeurs se répandent dans l'ensemble du circuit, diffusent à l'extérieur avec le CO_2; de plus, elles sont plus ou moins adsorbées par les surfaces, et elles les contaminent. On peut connaître la contamination de l'air, soit par des mesures directes, soit à partir de mesures effectuées sur le CO_2 du circuit. La première méthode est difficile en raison du faible niveau à atteindre; la seconde peut donner des résultats valables si l'on a une idée du taux de séparation des radio-éléments à travers les orifices de sortie. En première approximation, on peut mesurer la concentration d'un élément à l'intérieur du circuit de CO_2 et en déduire sa concentration dans l'atmosphère en supposant qu'il y a eu simple dilution; cette hypothèse simplificatrice peut conduire à des conclusions tout à fait erronées; elle présente le mérite d'être simple et offre l'avantage, appréciable en radioprotection, d'être prudente.

Pour ce qui concerne les *produits d'activation*, le mercure a particulièrement retenu notre attention. Le mercure 203 l'emporte sur les isotopes de nombre de masse égal à 197: lorsque le mercure est irradié à saturation, l'activité du premier est un peu moindre, mais sa concentration maximale admissible (C.M.A.) dans l'atmosphère est vingt fois plus faible que celle du mercure 197.[9] On sait que le mercure donne des amalgames avec une très grande facilité, toutefois il est difficile de connaître son comportement à travers des orifices; si, par exemple, on fait passer un courant de CO_2 dans un long tube en matière plastique, bourré de charbon activé, l'activité mesurée le long du tube passe par un maximum d'autant plus éloigné de l'entrée que le volume du CO_2 a été plus grand: il y a adsorption, puis élution partielle. On trouve un rapport égal à 10 entre l'activité maximale et la valeur mesurée à l'entrée du tube. Avec la quantité de mercure que nous avons dans nos réacteurs, l'isotope 203 est facile à identifier dans le CO_2 par sa raie γ et grâce à sa période relativement longue, son activité est mesurable en chambre d'ionisation (qui, malheureusement, reste contaminée). A la suite de l'introduction accidentelle de plus d'un kilogramme de mercure, la contamination volumique du CO_2 de E.D.F. 1 en mercure 203 a atteint, au mois de juillet dernier, 3×10^{-4} Ci/m^3. Auparavant, comme à E.D.F. 2, on tournait autour de 10^{-5} Ci/m^3. Signalons que les rayons β du mercure 203 ne sont pas détectés par les sondes que nous utilisions initialement pour la recherche des contaminations de surface.

Malgré la vidange préalable, l'air résiduel contenu dans le circuit lors du remplissage en CO_2 donne, lorsque le réacteur est à sa puissance nominale, une activité volumique qui, ramenée aux conditions ambiantes de température et de pression, dépasse 10^{-2} Ci/m^3; puis décroît au fur et à mesure de l'apport de CO_2 pour compenser les fuites du circuit; cette décroissance, de plus en plus lente, met des semaines pour atteindre la valeur de 10^{-3} Ci/m^3 qui correspond à l'activation de l'argon 40 contenu dans un CO_2 encore chargé d'environ 200 volumes d'air par million (vpm). Le contrat de fourniture prévoit une teneur maximale de 100 vpm.

Pour ce qui concerne les *produits de fission* ou, plus précisément, les radionucléides engendrés par irradiation de l'uranium lui-même, il ne saurait être question de chercher à mesurer directement les plus dangereux, c'est-à-dire ceux qui, comme le strontium 90 ou le plutonium 239, ont les C.M.A. parmi les plus faibles.

Le dispositif de D.R.G. permet de suivre l'évolution d'une rupture de gaine, mais ne donne aucune indication sur la nature des éléments contaminants.

La chambre d'ionisation du D.C.C.A–CO_2 lorsque le réacteur fonctionne à sa puissance

nominale, ne peut déceler les variations de l'activité volumique en gaz et vapeurs, cette activité étant noyée dans celle de l'argon 41.

Le dosage de l'iode dans des filtres à charbon activé s'avère impossible: le pic principal de l'iode 131, situé à 364 keV, est dissimulé par la raie du mercure 203 à 279 keV.

Devant ces difficultés, l'un de nous s'est adressé au *césium* 138.

permet de déduire simplement l'activité volumique a_{op} du xénon 138 dans le circuit de CO_2 de l'activité A_F du césium 138 recueillie sur le filtre et mesurée à partir du pic de 1,44 MeV. Les activités étant exprimées en curies, et le volume du CO_2 ramené aux conditions ambiantes de température et de pression, on peut écrire:

$$a_{op} = 2\,A_F \qquad (1)$$

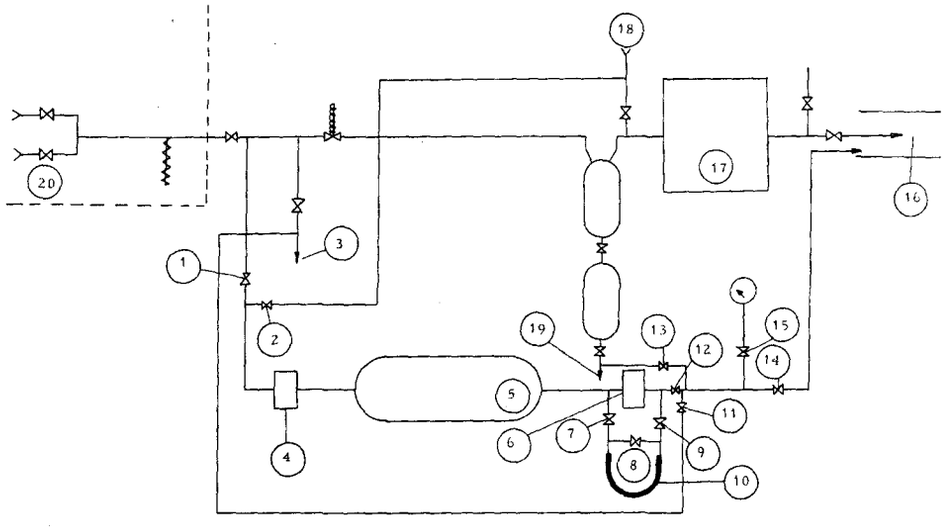

FIG. 1. Dispositif de mesure de la concentration du xénon 138 dans le CO_2 à E.D.F.1. 1, vanne d'isolement (prélèvement). 2, vanne d'isolement (balayage). 3, vers les surpresseurs du dispositif de D.R.G. 4, filtre amont. 5, volume de reconstitution du césium 138. 6, filtre aval. 7, 8, 9, vannes d'isolement du manomètre. 10, manomètre en U. 11, vanne d'isolement (aval). 12, vanne de réglage du débit. 13, vanne de décompression. 14, vanne de mise à l'air libre. 15, vanne d'isolement du manomètre. 16, vers la ventilation. 17, D.C.C.A-CO_2. 18, arrivée du CO_2 de balayage. 19, purge. 20, vers le circuit primaire de CO_2.

Un volume de reconstitution de 20 dm³ a été monté, avec ses accessoires, en dérivation sur le D.C.C.A.-CO_2 de E.D.F.1, conformément au schéma de la figure 1. La circulation est assurée par les surpresseurs du dispositif de D.R.G., sous la même pression que dans le circuit principal (25 bars). La vitesse d'écoulement à travers les filtres (de 4,5 cm de diamètre), voisine de 17 cm/s, correspond à une perte de charge de l'ordre de 70 cm d'eau (valeur satisfaisante) et assure quatorze renouvellements en 17 mm. Avec un temps de collection voisin de deux heures et demie, un tel dispositif

Les détails des calculs qui conduisent à ce résultat sont exposés en annexe (le rendement du filtre a été supposé égal à l'unité).

On trouve ainsi qu'à E.D.F.1 l'activé du xénon 138 oscille autour de 10^{-6} Ci/m³, indépendamment de toute rupture de gaine. Si les teneures de l'atmosphère en iode 131 et en xénon 138 étaient dans le même rapport que leurs rendements cumulatifs de fission, avec 0, 5% de CO_2 contaminé à 10^{-6} Ci/m³ de xénon 138, l'air contiendrait environ 3×10^{-9} Ci/m³ d'iode 131.

Le tableau 2 indique, compte tenu des valeurs trouvées coûramment dans le circuit, quelle

serait la contamination de l'air des locaux contenant 0,5% de CO^2, et quel facteur de dilution serait nécessaire, dans l'atmosphère, pour donner la C.M.A. auprès des personnes du public. On considère trois nucléides parmi les plus importants: mercure 203, argon 41 et iode 131. On suppose qu'il n'y a aucun phénomène de filtration.

On voit qu'il y a lieu de surveiller la contamination de l'air entraînée par celle du CO_2.

4.3. *Mise à profit de la contamination du CO_2*

La contamination radio-active du circuit de refroidissement d'un réacteur nucléaire est un mal inévitable; toutefois, il est possible d'en tirer parti. C'est ainsi que l'activité volumique de l'azote 16 permet de corriger le signal du dispositif de D.R.G., afin de tenir compte des variations de la puissance ou du débit du CO_2. Durant la période de démarrage de E.D.F.1, le dispositif de contrôle de la contamination de l'atmosphère des locaux en gaz radio-actifs a permis, grâce à l'argon 41, de suivre le cheminement du CO_2 de fuites accidentelles, alors que les appareils de mesure directe n'avaient pas encore un fontionnement tout à fait satisfaisant; dans la campagne, les rayons γ de cet argon 41 aident à retrouver le "panache" et à localiser sur le sol la zone de "retombée" maximale. La présence inopinée de sodium 24 dans le circuit de refroidissement de E.D.F.1 a confirmé la défectuosité du branchement, sur ce circuit, de la dérivation où se trouvent les batteries de filtres destinées à l'épuration continue du CO_2. L'huile introduite dans le circuit a débarrassé le CO_2 d'aérosols, ce qui s'avère bénéfique lors d'une fuite brutale de ce gaz dans un local, ou lors de l'ouverture du circuit pour intervention à l'intérieur; en l'absence d'aérosols, nous n'avons pas pu être gênés par les isotopes radio-actifs du fer, et nous n'avons pratiquement pas bénéficié du dispositif d'épuration continue du CO_2 par filtration.

Tableau 2. Conséquence de la contamination du CO_2

Nucléide	203_{Hg}	41_A	131_I
Dans circuit (Ci/m³)	10^{-5}	10^{-3}	5×10^{-7}
Dans locaux (Ci/m³)	5×10^{-8}	5×10^{-6}	3×10^{-9}
C.M.A.[9] (Ci/m³)	6×10^{-8}	2×10^{-6}	6×10^{-9}
Locaux/C.M.A.	≈ 1	2,5	0,5
Dilution public	5000	25,000	2500

5. CONCLUSION

La connaissance de la contamination du circuit primaire de refroidissement de nos réacteurs nous permet de prendre toutes précautions pour éviter une contamination excessive des travailleurs et des personnes du public.

Pour ce qui concerne la contamination par activation, les problèmes les plus importants et les plus difficiles nous sont posés par la présence du mercure: nous allons nous employer à supprimer ces problèmes par suppression du mercure, plutôt que d'avoir à les résoudre.

Pour ce qui concerne les produits de fission, nous nous attachons à en suivre l'évolution dans le CO_2 par une mesure relativement simple. Il reste à déterminer dans quelles proportions les radionucléides les plus abondants et les plus dangereux, tels que l'iode et le mercure, suivent les gaz nobles.

Industriels, nous nous attachons à la recherche des solutions les plus simples et souhaitons la suppression des actes dont nous ne comprenons pas l'intérêt. Nous nous demandons, par exemple, s'il est logique de rechercher systématiquement un radionucléide dans les produits de la chaîne alimentaire alors qu'il n'a pu être détecté dans les circuits primaires de refroidissement des réacteurs.

RÉFÉRENCES

1. J. P. Roux et C. Bienvenu. *C.R. 2ème conf. utilisat. pacif. én. at.* Genève, 1958, Vol. 5, p. 298 (1958).
2. C. Bienvenu, P. Passérieux et P. Bacher. *C.R. 3ème conf. utilisat. pacif. én. at.*, Genève, 1964, Vol. 5, p. 67 (1965).
3. J. P. Roux et C. Bienvenu. *J. Brit. Nuclear En. Sy.* **1**, 235 (1962).
4. M. Delpla, C. Bigeard, L. Bertron et E. Ventre. 1er congrès international de l'association internationale de radioprotection, Rome, 5–10 octobre 1966, à paraître.
5. A. Roguin. Rapport CEA-R 2784 (1965).
6. L. Fitoussi. Rapport CEA-n° 1598 (1960).
7. R. Estournel. Rapport CEA-n° 2205 (1962).
8. Anonyme. Service d'études générales nucléaires, EDF, étude n° EG 58-65 (1965), diffusion interne.
9. Ministre délégué chargé de la recherche scientifique et des questions atomiques et spatiales, décret n° 66-450 du 20 juin 1966 (J.O. du 30 juin 1966).

travers un récipient dans lequel il donne un fils solide, lui-même radio-actif; avant et après le récipient sont disposés deux filtres identiques, de sorte que le père pénètre seul dans le volume de reconstitution et que le second filtre recueille dls noyaux fils formés dans ce volume et non désintégrés (Fig. 2).

Soit V la valeur du volume de reconstitution, P la pression, supposée uniforme, et d le débit du gaz; en mesurant les volumes dans les conditions ambiantes de température et de pression (l'atmosphère étant prise pour unité), le débit D serait:

$$D = Pd.$$

Le temps moyen mis par le gaz pour parcourir le volume de reconstitution s'écrit:

$$t_m = \frac{PV}{D}. \qquad (3)$$

Considérons, dans le volume de reconstitution, une tranche de gaz de volume élémentaire

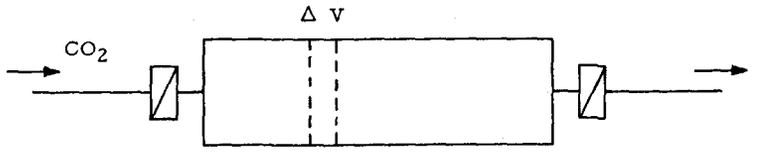

Fig. 2. Principe du dispositif de mesure: volume de reconstitution du césium 138 entre deux filtres traversés par le CO_2 prélevé sur le circuit primaire.

ANNEXE

Mesure de l'activité du Xenon 138 *dans le* CO_2

Soit un récipient rempli d'un gaz radio-actif donnant un fils, lui-même radio-actif.

L'activité du fils, contenue dans le récipient et supposé initialement nulle, est reliée à celle du père par la relation:

$$A_F = A_{0_p} \frac{\lambda_F}{\lambda_F - \lambda_p} (e^{-\lambda_p t} - e^{-\lambda_F t}) \qquad (2)$$

où les notations ont la signification indiquée ci-dessous:

t: temps écoulé depuis l'instant initial;
A_F: activité du fils au temps t;
A_{0p}: activité du père à l'instant initial;
λ_F et λ_p: constantes radio-actives du fils et du père.

Considérons maintenant le père gazeux s'écoulant, mélangé à du gaz carbonique, à ΔV (Fig. 2); dans cette tranche, l'activité du père, à l'entrée s'écrit:

$$A_{0_p} = a_{0_p} P \ \Delta V, \qquad (4)$$

et celle du fils:

$$A_F = a_F P \ \Delta V; \qquad (5)$$

a représente l'activité volumique initiale du père (indices 0 et p), ou du fils dans le récipient (indice F), ou, ci-dessous, du fils à la sortie (indices s et F); ces activités volumiques correspondent aux conditions ambiantes de température et de pression.

La formule (2) ci-dessus devient, d'après (4) et (5), à la sortie du volume de reconstitution:

$$a_{sF} = a_{0_p} \frac{\lambda_F}{\lambda_F - \lambda_p} (e^{-\lambda_F t_m} - e^{-\lambda_p t_m}). \qquad (6)$$

Écrivons que dans chaque unité de temps le nombre de noyaux du fils retenus sur le filtre

est égal aux apports par le gaz carbonique (compte tenu du rendement R de la filtration) corrigés des pertes par désintégration:

$$\frac{dN_F}{dt} = \frac{a_{sF}\, DR}{\lambda_F} - \lambda_F\, N_F,$$

équation dont la solution s'écrit:

$$N_F = \frac{a_{sF}\, DR}{\lambda_F^2}\,(1 - e^{-\lambda_F t});$$

compte tenu de (3) et (6), l'activité recueillie sur le filtre après un temps t de collection peut s'écrire:

$$A_F = a_{0_p} PVR\,(1 - e^{-\lambda_F t})\,\frac{e^{-\lambda_F t_m} - e^{-\lambda_p t_m}}{(\lambda_p - \lambda_F)\,t_m}. \quad (7)$$

L'expression (7) se réduit à une forme approchée:

$$A_F = a_{0_p}\, P\, V\, R \quad (8)$$

à condition que les deux facteurs suivants du second membre de (7) soient suffisamment proches de l'unité.

On aura: $1 - e^{-\lambda_F t} \geqslant 0{,}95$,

pourvu que: $t \geqslant 4{,}3\ T_F$. (9)

Pour le second facteur, on peut sensiblement écrire la condition:

$$e^{-\lambda_p t_m} \geqslant 0{,}95,$$

si, d'après (3):

$$D \geqslant 14\,\frac{PV}{T_p}. \quad (10)$$

D'après la condition (9), la période radioactive du fils ne doit pas être trop longue pour avoir un temps de collection raisonnable; cette période ne doit tout de même pas être trop courte: le résultat du comptage du filtre manquerait de précision.

D'après la condition (10), la période du père ne doit pas être trop courte: le courant gazeux à travers les filtres ne saurait être excessif.

HEALTH PHYSICS EXPERIENCE IN THE OPERATION AND MAINTENANCE ON AN ON-LOAD REFUELLING PROGRAMME ON UNITED KINGDOM CIVIL POWER REACTORS

B. W. EMMERSON and M. DENNETT*

Bradwell Generating Station, Central Electricity Generating Board, Southminster, Essex, England

Abstract—On-load refuelling, an inherent factor in the design of the United Kingdom Civil Power Reactors, was first carried out at Bradwell Power Station in April 1963. Although information regarding dose rates around the charge/discharge machine had been measured during the movement of the active absorber material to and from the core, this did not simulate the effect of the delayed neutron spectrum from freshly withdrawn, irradiated fuel, nor could this effect be calculated with any degree of certainty.

Shielding surveys were made using conventional gamma dose rate measuring instruments, whilst the more complex neutron dose contribution was assessed using BF3 counters, Basson intermediate energy detectors, proton recoil counters, and the Andersson-Braun rem counter. At full power, the dose rate from a fuel element being withdrawn from the reactor was measured and the decay curve plotted. The dose rate due to the delayed neutron fraction was shown to decay almost completely within two minutes of withdrawing the element from the neutron flux.

Although measurements inside the shielding close to the fuel element guide tube indicated peak dose rates up to 10^5 R/h, the results of the on-load fuel handling programme have shown that the delayed neutron contribution, although significant, does not limit access to the reactor pile cap during discharge of fuel at full reactor power.

Occupational exposure associated with on-load fuel handling results mainly from activation of various charge machine components. Experience in limiting the accrued dose to maintenance personnel repairing activated fuel handling grabs is discussed in detail, whilst the use of film and thermoluminescent dosimeters for dose control has allowed work to be undertaken on relatively high dose rate components with confidence. The need for a more accurate beta sensitive monitoring device for this type of work is emphasized.

The Health Physics requirements associated with ancillary fuel handling facilities are discussed together with experience in the recovery of damaged irradiated fuel from a charge machine and subsequent decontamination procedures. The need for an integrated approach to the design of fuel handling plant and the associated reactor ancillary equipment is stressed.

1. INTRODUCTION

There are nine nuclear power stations in the first stage of the United Kingdom Nuclear Power Programme. Each station has two gas cooled, graphite moderated reactors, the fuel being natural uranium canned in magnox. The design is based on operational experience gained at Calder Hall and Chapelcross. Station electrical outputs range from 300 MW to 1200 MW. Each new station commissioned has achieved an appreciable increase in electrical output, whilst a significant reduction has been achieved in physical size and capital cost per kW of installed capacity.

Because of their inherently low operating costs, the civil reactor stations are designed to operate on a "base" or constant load principal. To reduce outage time, the reactors are designed for refuelling whilst at full power. The fuel charge/discharge programme is based on an

* Trawsfynydd Generating Station, Central Electricity Generating Board, Trawsfynydd, Merioneth, Wales.

equilibrium rate which is related to the energy output of the reactors. At Bradwell Power Station it is necessary to recharge an average of two channels of fuel in each 24 hr period to maintain the equilibrium rate and avoid creating a fuelling back log. This assumes a maximum channel average irradiation of 3600 MW days/Tonne and a fuel dwell time within the reactor of six years.

Although a considerable volume of information existed regarding the radiation levels associated with fuel handling on a shutdown reactor, little information was available regarding the dose rate contribution from delayed neutron capture gammas associated with fuel as it was being removed from the core of an operating reactor, nor could this doserate contribution be calculated with any degree of certainty. Hence the performance assessment of the fuel handling equipment was an important aspect of the station commissioning programme. Due to the novel aspect of on-load fuel handling, a detailed health physics investigation was carried out in conjunction with this assessment. These tests were designed to determine the dose rate contribution associated with the delayed neutron spectrum, the effectiveness of charge machine shielding, and the extent of contamination arising from the fuel handling procedures. With on load refuelling now in routine operation, the main Health Physics problems are associated with maintenance of fuel handling components, although a number of non-routine operations such as the recovery of irradiated components from the machine or reactor pressure vessel have provided useful experience in high level radiation and contamination control.

This paper is based mainly on experience gained at the Bradwell and Trawsfynydd Generating Stations, supplemented where necessary with information from other U.K. Civil Nuclear Stations.

2. FUEL HANDLING SYSTEM

Experience described in this paper may be prefaced by a broad outline of the fuel handling system in use at a typical United Kingdom power station such as Bradwell. New fuel is delivered by road from the U.K.A.E.A. Fuel Fabrication Plant at Springfields and stored in an unirradiated fuel store until required for use. From here it is transferred to a fuel preparation room where it is inspected prior to loading into the charge machine.

The charge/discharge equipment consists of a single machine, 9 ft in diameter and 55 ft high, weighing 430 tons, together with a number of auxiliary components for coupling the machine to the reactor vessel and providing adequate shielding during fuel movement. It is designed to provide a shield against radiation and a seal to prevent loss of coolant gas from the reactor during the removal and insertion of components into the reactor vessel. The machine travels along rails on a moveable gantry which spans the reactor pile cap and an enclosed maintenance bay is provided adjacent to this area.

The charge machine consists of a pressure vessel, mounted inside a biological shield. This vessel contains a rotatable inner core or turret extending down through the vessel, fitted with vertical storage and guide tubes, somewhat analogous to the chamber of a revolver, with hoists and turret drives located on the top.

A chute head box is used to form a gas tight connection between the charge machine and any one of the reactor vessel charge standpipes. When connected to the reactor, additional shielding is provided between the pile cap floor and the bottom of the charge machine by means of an annular shield consisting of an upper and lower section, each filled with iron shot concrete. This shield encloses the chute head box, and the upper section is raised telescopically to mate with the base of the charge machine, thus forming a complete biological shield around the base of the charge machine assembly.

The upper sections of the charge machine shielding are of Barytes concrete, whilst the lower sections are of iron shot concrete with additional steel shielding around the base. A slide valve through which all components entering or leaving the machine must pass is fitted in the base of the machine. This valve also acts as a shield and a gas-tight seal when closed, allowing the machine to be disconnected from the reactor while maintained at reactor pressure and containing active components.

After a refuelling cycle, irradiated fuel is lowered from the charge machine through a shielded discharge tube into a skip, positioned in the cooling pond beneath the reactor build-

ing. Facilities are available at this point for selecting and bottling damaged elements. Undamaged fuel is desplittered to remove the magnox splitter fins and braces, after which it is stored in the pond for approximately 100 days. It is then loaded into a shielded transport flask and returned via road and rail to the

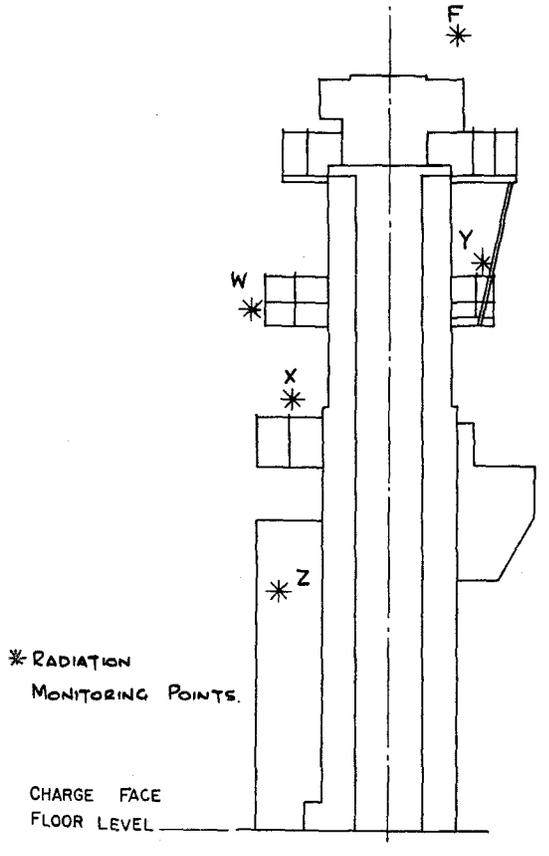

FIG. 1. Charge machine—sectional elevation.

U.K.A.E.A. reprocessing plant at Windscale. Outline diagrams of the charge machine, make-up shielding and interconnections to the reactor are shown in Figs. 1, 2 and 3.

A shielded high level radiation cell equipped with remote control manipulators is provided for maintenance of fuel handling equipment. The charge machine can be used to lower fuel handling components into this facility via a shielded maintenance hole on the reactor pile cap. The entire fuel handling plant is adequately interlocked to ensure safe operation and to prevent any possibility of inadvertent radiation exposure to operating staff.

3. HEALTH PHYSICS MEASUREMENTS DURING CHARGE MACHINE COMMISSIONING

The Health Physics measurements carried out during commissioning of charge machines were aimed at providing the following information:

(i) Basic integrity of the charge machine shielding for storing a full complement of irradiated fuel.

(ii) The extent of neutron and gamma radiation streaming from the core under on load refuelling conditions.

(iii) Decay rates associated with:
  (a) Delayed neutrons.
  (b) Fission product and capture gammas.

(iv) Dose rates on and around the fuelling machines with special reference to radiations referred to in (iii).

(v) The extent of radioactive contamination associated with refuelling operations.

Measurement positions were chosen as shown in Figs. 1 and 2 to provide a comprehensive survey of the radiation levels that would occur during the various stages of an absorber or fuel handling programme. The majority of measurements were made in the normal working areas around the charge machine and associated make-up shielding. Although access into the area below the pile cap floor is not permitted during charge machine operation, there was considerable interest in making measurements in this area due to the absence of shielding around the reactor standpipe. This made it possible to measure with reasonable accuracy the dose rate from items being removed via the standpipe into the charge machine. Measurements were also made of radiation levels associated with operating equipment and components common to both absorber and fuel handling, such as the charge chute and grabs. These latter measurements provided useful information on the radiological conditions

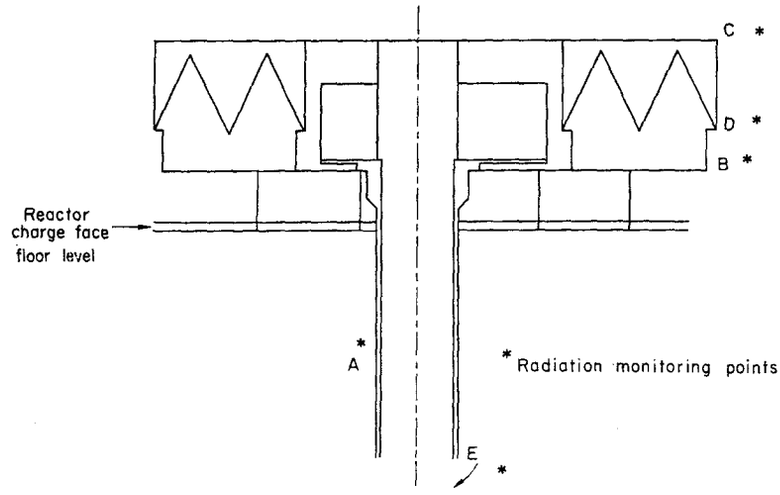

FIG. 2. Make up shielding with control rod sealing sleeve.

associated with the maintenance of charge machine components.

The measurements made and the results obtained are discussed in the following subsections.

3.1. *Charge Machine Shielding*

Radiation measurements were made during various on-load absorber changing operations. The transient dose rate from the non-fissile absorber being discharged, measured at the surface of the standpipe, ranged between 350 R/hr and 1800 R/hr for the discharge of No. 1 and No. 5 absorber respectively, whilst the corresponding maximum radiation levels in the pile-cap working area adjacent to the machine make-up shield were 0·5 mR/hr and 1·5 mR/hr respectively. A time lapse of approximately 2 min occurs between the commencement of withdrawing an absorber (or

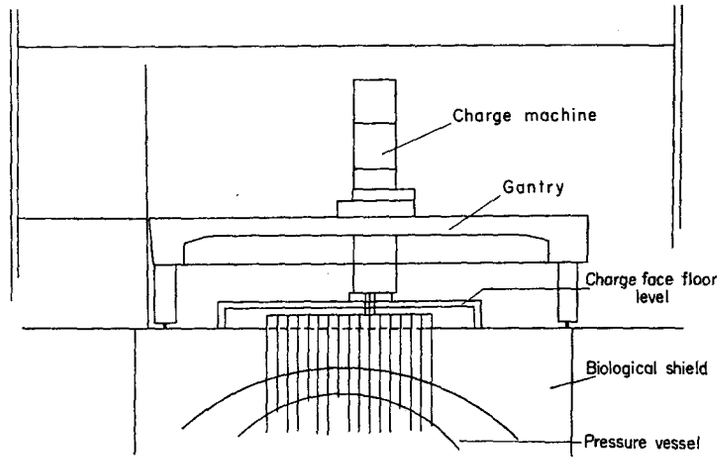

FIG. 3. Charge machine and gantry showing interconnection to reactor pressure vessel.

fuel element) from the reactor core, and its subsequent arrival at pile cap level, prior to entering the charge machine.

^{59}Fe, ^{60}Co and ^{56}Mn are the predominant activities associated with neutron activation of the in-pile fuel handling components such as chutes, grabs, hoist cables and standpipe assemblies. It was estimated that the major dose rate contribution from freshly discharged absorber material would be due to ^{56}Mn. Because of the short half-life (2·58 hr) and relatively high activation cross-section, the manganese will have reached saturation and even a small manganese content, in this case 0·1%, would contribute an estimated gamma dose rate of approximately 1800 R/hr at 1 ft from the surface of the absorber.

Surveys during on load discharge of absorber material and during early off load refuelling exercises showed that there were no major shielding weaknesses in either the charge machine or associated fuel and absorber handling facilities. Particular attention was paid to the storage magazine areas of the machine when loaded with a full complement of irradiated absorbers. A maximum radiation level of 40 mR/hr was measured on top of the machine with the storage magazine empty but with the charging chute stored in the machine. As this area is unoccupied during charge machine operations, these levels do not contribute to a hazard.

3.2. *Core Streaming*

A detailed core streaming survey was carried out on the charge machine between the period of removal of the shield plug and insertion of the fuel chute. The shield plug was held at several chosen positions whilst surveys were carried out with the reactor at power.

The highest levels recorded were of the order of 50 mrem/hr neutron and 50 mR/hr gamma on top of the machine in an area not normally occupied by personnel. These radiation levels existed only with the shield plug removed and with the magazine in a specific orientation.

Radiation levels up to 20 mrem/hr neutron and 1 mR/hr gamma were detected at localized points on the machine at first platform level above the pile cap.

Radiation surveys in working areas adjacent to the machine at pile cap level showed radiation levels only slightly above background.

3.3. *Decay Rates of Delayed Neutrons and Fission Product Plus Capture Gammas*

The decay rates for delayed neutrons and for fission product plus capture gammas were determined by arresting a fuel element in its traverse from the core to the machine and holding it near the base of the machine.

At Bradwell the measurements were made close to the standpipe and were expectedly high. The measurements at Trawsfynydd were made on the pile cap level outside the machine but in a region close to the machine shielding.

The decay curves so determined are shown in Figs. 4 and 5.

Regarding the neutron decay, this shows an initial half-life of approximately ½ min followed by a half-life of almost 1 min after 2 min decay (cf. classically determined delayed neutron half-lives of 22.5 sec and 55.6 sec). The gamma decay curves showed an initial half-life of approximately 1 min.

The major part of the total dose rate (neutron plus gamma) decayed after the first 3 min from withdrawing a fuel element from the core.

3.4. *Dose Rates due to Delayed Neutrons and Fission Products Plus Capture Gammas*

Most of the neutron dose rate measurements made at U.K. civil nuclear power stations are made with the Andersson–Braun rem counter which has a good energy response over the range 0·1 eV to 10 MeV. Using this instrument, comprehensive neutron dose rate surveys were made and transient dose rates determined by extrapolation using the decay curves already determined. These results show:

(a) Negligible transients are experienced at the pile cap operating floor level.
(b) Localized transients as high as 1 rem/hr are experienced above pile cap operating floor level but these are in areas not normally occupied during a refuelling cycle. If access were required for some reason whilst refuelling, then a waiting period of 3–5 min would render radiation levels acceptable. This limitation has not proved embarrassing operationally.

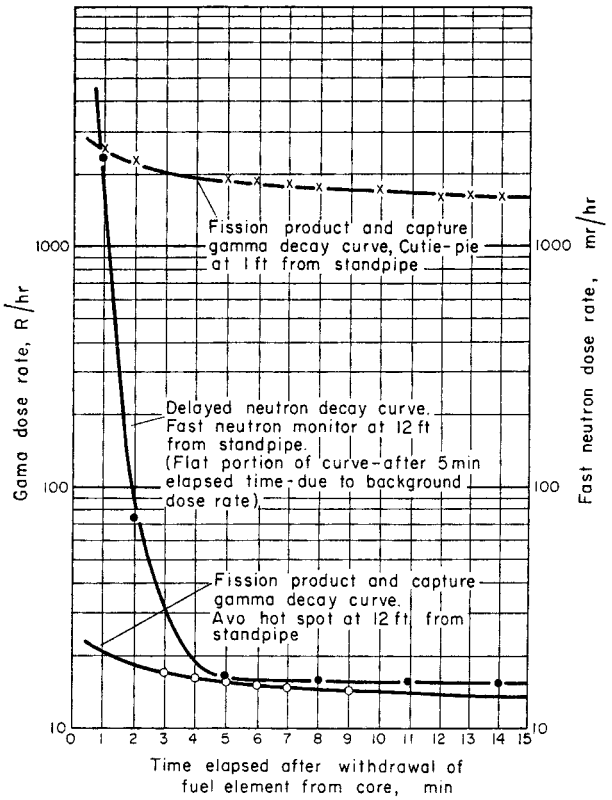

FIG. 4. Capture gamma and delayed neutron decay curves for fuel element withdrawn from reactor whilst at power. Measurements made on Bradwell Reactor No. 1. Reactor power—300 Mw (Thermal). Element Irradiation 1000 MwD/Tonne over 400 days.

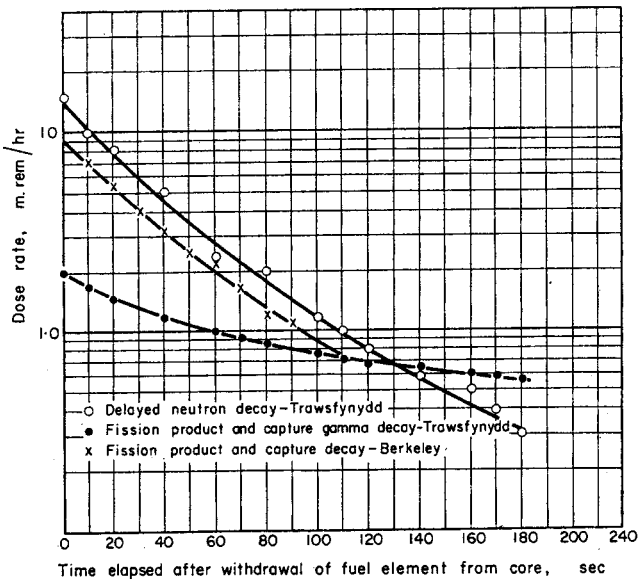

FIG. 5. Capture gamma and delayed neutron decay curves for fuel element withdrawn from reactor whilst at power. Measurements made at Trawsfynydd and Berkeley.

To obtain an estimate of the degree of shielding provided by the charge machine, measurements were made in the vicinity of the unshielded standpipe between the primary and secondary reactor floors whilst fuel was being discharged from the reactor. The dose rate under these conditions, when discharging fuel from the flattened zone at full power, gavc levels up to 50,000 rem/hr (compared with 1800 rem/hr when discharging absorbers). An R.C. 7 ionizing chamber sensitive to both gamma and neutron radiation was used for this measurement, and as there was a considerable fast and thermal neutron contribution in the vicinity of the standpipe (of the order of 5×10^4 neutrons/cm^2) this could lead to an overestimation of the gamma contribution by up to a factor of 10 with this type of detector. Calculations using the Way-Wigner equations show that the surface dose rate from a freshly discharged 3500 MWD/Tonne fuel element is of the order of 3×10^5 rem/hr. This does not include the very short-term fission product decay, and for on-load discharge it is most certainly an underestimate. Thus, the value of 50,000 rem/hr measured at a position approximately 1 ft from the fuel element and shielded by approximately 1 in of steel (with a 90 sec decay after withdrawal from a neutron flux of approximately 10^{13} n/cm^2/sec) would appear to be a realistic value.

The maximum transient radiation level of 13 mrem/hr was measured around the make-up shield during the discharge of elements from the reactor at full power, and the maximum steady radiation level obtained during a comprehensive survey of the machine containing 24 freshly discharged elements was 2·6 mrem/hr opposite the element deflector mechanism, these results being a factor of 10 down on the predicted design radiation levels. Tables 1 and 2 give a summary of the radiation levels obtained when withdrawing irradiated fuel.

Table 1. *Radiation levels measured at various positions beneath the pile-cap floor during on-load fuel discharge from Reactor No.* 1, *Bradwell Nuclear Power Station*

Charge machine operation	Position of measurement (see Fig. 1)	Peak radiation level in rem/hr		
		Fast neutrons at 12 ft. from Point A	γ at 1 ft. from Point A*	Contact at Point A†
Reactor thermal power—300 *MW*				
Discharge—No. 8 Element	A	2	1500	5000
7 ,,	A	2·4	2500	6000
6 ,,	A	3	3200	6000
5 ,,	A	3	3300	8000
4 ,,	A	2·6	2800	7000
3 ,,	A	2·3	2000	6000
2 ,,	A	1·6	1100	5000
1 ,,	A	0·75	500	3000
Reactor thermal power—400 *MW*				
Discharge—No. 8 Element	A	1·5		20,000
7 ,,	A	1·9		30,000
6 ,,	A	1·9		40,000
5 ,,	A	2·3	Instrument	50,000
4 ,,	A	2·4	OFF	50,000
3 ,,	A	2·0	Scale	50,000
2 ,,	A	1·7		20,000
1 ,,	A	0·9		10,000

* Measured with Cutie Pie. † Measured with RC7 ion chamber.

An alternative method of measuring high gamma dose rates adjacent to irradiated fuel has been used at Trawsfynydd. This involved the use of the radiation-induced conductivity of cadmium sulphide crystals to measure dose rates over the range $1–10^6$ R/hr. The ease of placing the detector (no longer than half a cigarette) in awkward positions (e.g. under the charge machine) and the facility to read remotely proved extremely useful. The use of cadmium sulphide crystals for this particular application has been reported by W. H. R. Hudd. [1]

3.5. *Radioactive Contamination Associated with Refuelling Operations*

Contamination of internal surfaces of the fuel handling equipment is bound to occur during fuelling. The charge machine is fitted

Table 2. Integrated gamma doses measured at floor level at various working positions around the Bradwell charge machine during discharge of four fuel channels (32 *Elements*)

Reactor power—400 MW (Thermal)
Total dose integrating time—8·5 hr.

Distance of measurement from edge of charge machine make-up shield	Integrated dose (mr)
2 metres	22
4 metres	2·5
6 metres	4·5

Gamma dose rates due to streaming, measured on the outside face of the charge machine and make-up shielding

No. 4 fuel element held stationary between secondary floor and make-up shield.
Reactor power—300 MW (Thermal)

Position of measurement (see Fig. 1)	Dose rate—mr/hr			
	West face	North face	East face	South face
B	3·0	0·5	10	H 60*
C	5·0	4·5	5	H 12
D	H 20	13	4	0·9

* Decayed to 18 mr/hr after 40 sec.

H, Make-up shield not sitting completely level on pile cap floor. When level, maximum transient dose rate reduced to 13 mr/hr.

Four channels of irradiated fuel stored within charge machine
Reactor power—300 MW (Thermal)

Position of measurement (see Fig. 2)	Dose rate—mr/hr
W	0·35
X	0·12
Y	0·35
Z	2·6

with a gas tight valve which prevents gross contamination reaching the external environment. Nevertheless, the make-up shielding around the base of the machine and the discharge shielding associated with transfer of irradiated fuel elements from the charge machine into the cooling ponds, acquire considerable surface contamination. The maximum level during commissioning was found to be 3×10^{-2} μCi/cm^2 beta/gamma with no evidence of alpha contamination. No abnormal airborne contamination was detected in the vicinity of the charge machine and pile cap during the refuelling operation.

A fairly high proportion of contamination in the main cooling circuit of the reactors has been identified as low energy beta contamination (mainly ^{35}S). Some of the contamination experienced on fuel handling systems is from this source. This low energy activity is not detected by conventional geiger contamination monitors and other types of instruments and measuring systems have been used. The details of this work are outside the scope of this paper.

3.6. *Summary of Measurements*

Results of the on-load fuel handling survey programme proved that despite the high dose rates associated with fuel elements withdrawn on load, the radiation levels in the working area of the pile cap remained sufficiently low to allow unrestricted access during refuelling operations. Localized points of high dose rate occur but access is not required to these areas during normal operations. As would be expected, the radiation levels measured during the commissioning period have remained sensibly constant during the past $3\frac{1}{2}$ years of on-load fuel handling operations.

4. MAINTENANCE OF FUEL HANDLING EQUIPMENT

Ease of maintenance is essential if the on-load fuel handling equipment is to achieve a high load factor. There are two quite distinct health physics aspects. Firstly, maintenance of large plant items such as the internal areas of the charge machine where the major problem is associated with contamination. This will also include work on make-up shielding, test, storage and disposal facilities. Secondly, maintenance on ancillary fuel handling equipment such as grabs, cables, chutes and standpipe assemblies where the items may have received considerable neutron irradiation and for which dose rate will be the controlling factor. Dose rate can also be the controlling factor when dealing with major plant items in the first category if irradiated components or fuel remain stored within these facilities whilst maintenance is being carried out. It is normal procedure to discharge the irradiated fuel from the charge machine before attempting to carry out maintenance work, although certain break-down maintenance may preclude this.

Experience to date has shown that the limiting health physics factor in the maintenance of fuel handling equipment is due to the dose rate from activated components. This in turn depends upon the dwell time within the reactor flux, activation cross-section of the material, and its half-life. Steel is a major component in all inpile equipment and the initial controlling dose rate for handling freshly irradiated components is due mainly to the activation of ^{56}Mn. Small amounts of brazing often associated with electrical contacts can give rise to high localized dose rates due to the use of high activation cross-section brazing materials. The major long term activity build-up in steel components is due to ^{60}Co and it is this isotope which ultimately limits the amount of maintenance which can be carried out on irradiated components.

4.1. *Repair on Fuel Element Grabs*

The fuel element grab is a complex mechanism, and must provide a reliable performance if a satisfactory fuel handling programme is to be achieved. Much of the maintenance on fuel handling equipment has been associated with grab repairs, and considerable emphasis has been placed on the development of repair techniques and measurement of the accrued radiation dose to the repairer. Figure 6 shows a typical decay curve for a fuel handling grab for various irradiation and decay periods. The initial contact dose rate varies between 2000 R/hr for a grab irradiated for 1 hr in a thermal neutron flux of 10^{13} n/cm^2/sec to almost 10,000 R/hr for any irradiation period in excess of 10 hr. The decay curve follows the ^{56}Mn, 2·58 hr half-life, for approximately 2 days, after

which the decay period has a half-life of approximately 30 days. This in turn gives way to a long-term residual activity determined primarily by the decay of ^{60}Co, a typical residual activity value being 7 R/hr per 24 hr period of irradiation.

Due to the mechanical complexity of the fuel handling grab, it is impracticable for any but the simplest repairs to be made using remote handling equipment. However, it has been found advantageous to set up a simple grab handling facility comprising a shielded work bench with a small single arm power manipulator. The more elementary dismantling and assembly operations can be carried out, thus limiting the amount of physical contact time involved. Much of the work, however, involves manual contact with the grab and consequent finger tip radiation exposure. Pre-planning of the repair sequence is an essential feature. Where practical, practice runs are made on a non-irradiated grab to familiarize the operator with the work to be carried out. Working times are established, which in conjunction with measured dose rates taken on the grab to be repaired allow an accurate assessment of the potential exposure.

A typical system for controlling radiation dose to personnel carrying out grab maintenance involves the use of dosimeters as follows:

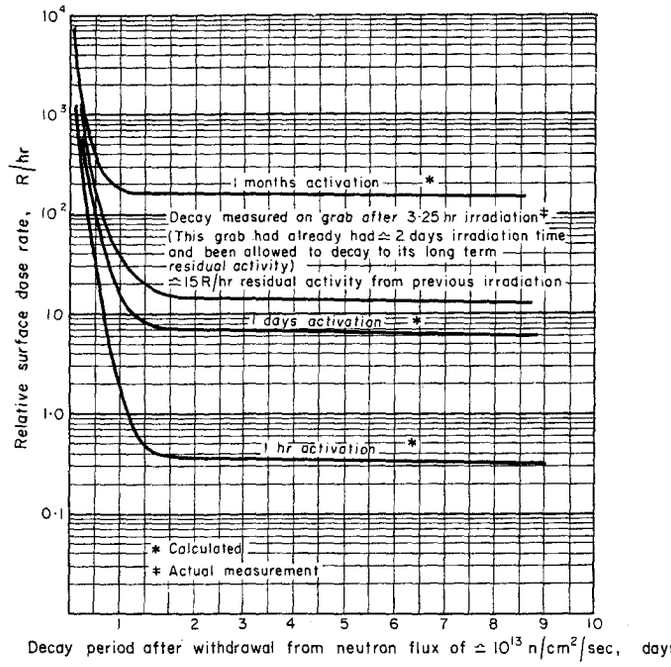

FIG. 6. Comparison of calculated and measured gamma surface dose-rate for Bradwell fuel element grab following various irradiation times.

(a) All personnel involved are issued with a body Q.F.E. (Quartz Fibre Electroscope–Pocket Dosimeter) which together with their monthly film badge measures and controls their whole body dose.
(b) A film badge is attached to each wrist together with a Q.F.E. which can be read by the operator without removal from the wrist.
(c) A lithium fluoride thermoluminescent dosimeter is worn on a finger tip on each hand. These dosimeters consist of

flat sachets of approximately 1 cm^2 in area having a plastic cover of 12 mg/cm^2 (comparable with the dead outer layer of skin on the fingers). The dosimeter is wrapped around the finger and does not interfere with finger sensitivity. This type of dosimeter has a good response to both beta and gamma radiation over a wide energy range and is particularly useful for measuring total dose to finger tips when handling components of this type where the finger dose can be much higher than the wrist or body dose.

Experience has shown that the ratio between the finger tip dose and wrist Q.F.E. dose can vary between 5 and 15 to 1 depending on the item handled. For operational control a ratio of 10 is used and the work is controlled on the basis of dose as shown by the wrist and body Q.F.E.s. A typical permissible figure for a job would be 50 mrem on each Q.F.E. (implying a finger tip dose of not greater than 500 mrem). Using a shielded facility to limit head and body dose, finger-tip dose becomes the controlling factor.

Using the facilities and procedures described above and sharing the work load between operatives, it has been possible to dismantle, repair and reassemble grabs with surface gamma

FIG. 7. Wrist and finger dosimeters used when handling active components. Left-hand picture shows lithium fluoride sachet normally worn under protective gloves (see right-hand picture).

FIG. 8. Use of wrist and finger dosimeters (shown in Fig. 7) when repairing an irradiated fuel element grab.

dose rates in excess of 20 R/hr without accruing a whole body dose greater than 100 mrem or a finger dose greater than 500 mrem.

During the past 2½ years of fuel handling operations, the major dose contribution has been associated with maintaining fuel element grabs. The feed back of this information to the designers has done much to eliminate the use of high activation cross-section, long half-life materials wherever practicable. The simplification of mechanical design has allowed shorter maintenance working times. Where maintenance must be carried out on irradiated components it is essential that the designer and the Health Physicist should be aware of the composition of the materials being used.

4.2. *Non-routine Operation and Maintenance*

There will always be a percentage of non-routine operations due to faults occurring within the normal fuel handling programme. Certain of these will lead to additional Health Physics requirements, either as part of the operation or during any subsequent maintenance work. The following case provides a useful example:

Removal of Fractured Fuel Element from a Charge Machine

During the normal procedure of discharging fuel from the reactor into the charge machine, a fuel element became dislodged from the grab and fell across the rotating section of

the charge machine magazine instead of into a magazine fuel storage tube. With subsequent rotation of the charge machine magazine, the body of the fuel element was severed into two pieces held together by longitudinal splitter vanes which are used to centre the element within the fuel channel. As there is no means of viewing the inside of the charge machine, the degree of damage to the fuel element could not be determined. However, the assumption was made that a fracture had occurred and the appropriate Health Physics precautions were instituted.

Charcoal loaded filter papers were fitted into the charge machine blowdown lines prior to discharging the CO_2 to atmosphere. The machine was blown down to atmosphere in controlled stages, the filter papers being examined at each stage prior to proceeding to further blowdown. The blowdown took place about 3 hr after removing the fuel element from the reactor core, and examination of the filter papers showed no indication of gaseous fission products. With the charge machine at atmospheric pressure it was positioned over the shielded emergency discharge route between pile cap level and the underground fuel element pond. In an attempt to discharge the distorted element into the cooling pond, it became wedged in the upper part of the discharge well shielding. It was still impossible to view the extent of the damage to the fuel element although limited introscope inspection at this stage indicated that it was bent through an angle approximately 30°. The effectiveness of shielding around the discharge well can be appreciated from the following radiation dose rates measured during this operation:

Directly over emergency discharge well 5,000 R/hr
At edge of gap in telescopic shielding 1·5 R/hr
3 ft from gap in shielding (position of operator) 100 mR/hr

The damaged element was eventually freed and lowered down the emergency discharge well, but was prevented from passing into the pond by handling equipment fitted at the bottom of the discharge well tubing. The element was returned into the charge machine whilst entry was made into the discharge area to remove the emergency cropping gear causing the discharge tube restriction. During this period, a number of small particles were found which gave dose rates between 0·1 and 300 R/hr measured at a few inches. A spectrum analysis identified these particles as small flakes of irradiated uranium.

With the discharge tube restriction removed, the element was lowered into the cooling pond. Only at this stage could the degree of damage to the element be assessed. Severance of the element had exposed several square centimetres of uranium metal, and an attempt was made to prevent contamination of the cooling pond water by lowering the element into a dustbin at the bottom of the pond and covering it with a lid. After 4 weeks the water within the dustbin was sampled and the fuel element then returned with other irradiated fuel to the reprocessing plant. The sample of water taken from the dustbin indicated that there had been no significant leaching of fission products from the fractured area of the fuel element during its 4 week storage period. Because of the small pieces of irradiated uranium found in the vicinity of the fuel handling machine, a thorough de-contamination of the internal sections of the machine was carried out. This was important from two aspects. Firstly, due to the potentially high dose rates that could be associated with small particles of this nature, a contamination/radiation hazard could occur whenever the machine was used. Secondly, if these particles of bare uranium were introduced back into the reactor they could give rise to spurious signals on the burst cartridge detector system and could result in considerable embarrassment to subsequent reactor operations. This entire operation was carried out without any of the operators receiving a radiation dose exceeding 100 mrem but did much to emphasize the need for remote viewing equipment to ascertain conditions inside shielded areas.

5. CONCLUSIONS

The results and experiences presented in this paper have summarized some of the more important Health Physics aspects associated with on-load fuel handling in the United Kingdom. Although the initial radiation levels associated with handling freshly irradiated fuel are expectedly high, they have not resulted in a

significant increase in exposure to personnel working within the fuel handling areas. Although there have been several instances where fuel handling components or fuel elements have had to be recovered from the reactor using non-standard routines, there has been no undue radiation exposure to those taking part in these operations. The major dose contribution for personnel has come from maintenance of irradiated fuel handling components and especially from the repair of fuel handling grabs. Care and forethought at the design stage, such as the selection of low activation cross-section materials, and designs, which shorten the time spent on the dismantling and assembly of active components, can do much toward minimizing the radiation exposure of maintenance personnel. When installing expensive and complex fuel handling plant the provision of adequate maintenance facilities, designed to provide the maximum of radiological protection consistent with economic working, should be adopted as a general principle. Finally, as testimony to the success of on-load fuel handling, at Bradwell Power Station over 26,000 fuel elements have been discharged during the past three years without any person receiving a dose in excess of the I.C.R.P. recommendations for occupationally exposed workers.

REFERENCE

1. W. H. R. Hudd. Central Electricity Generating Board, Berkeley Nuclear Laboratories Report RD/B/N567 (1966).

EXTERNAL RADIATION DOSES AT BRITISH CIVIL NUCLEAR POWER STATIONS

G. LEWIS

Berkeley Nuclear Power Station, Central Electricity Generating Board, Berkeley, Glos, U.K.

Abstract—A programme of construction of civil nuclear power stations is being carried out in the United Kingdom by the Central Electricity Generating Board (C.E.G.B.). The first two Stations at Berkeley and Bradwell were brought into operation in 1962 and have been fully operational since then. This paper summarizes experience to date within the C.E.G.B. in the field of external radiation doses received at Nuclear Power Stations.

A description of the various sources of external radiation received by personnel is given. In general activated coolant gas, confined in exposed sections of the coolant circuits, is the most important source of doses received during normal operation by C.E.G.B. employees at the Stations. The situation with regard to this source is entirely satisfactory at the first two Stations; later designs, in particular those using concrete pressure vessels, have improved even on this. Persons living near to the first two Stations do not receive doses greater than those permitted to the general public.

Certain maintenance operations call for the careful control of external radiation dose to C.E.G.B. employees. Maintenance of equipment which becomes activated during refuelling with the reactor critical results in significant doses. Nevertheless it has been possible to carry out sufficient maintenance on such equipment to permit the continuation of on-load fuelling within the dose limits for classified workers. Experience gained at the earlier Stations is likely to contribute to some reduction of doses received in this way at the later Stations.

QUELQUES DISPOSITIFS DE RADIOPROTECTION EN SERVICE AUPRÈS DES PILES PISCINES DU CENTRE D'ÉTUDES NUCLÉAIRES DE GRENOBLE

E. de ROBIEN, H. de CHOUDENS et J. DELPUECH
Centre d'Études Nucléaires de Grenoble, CEA, Grenoble (France)

Résumé—La radioprotection auprès des piles piscines du CEN-G, qui fonctionnent à des puissances relativement élevées et où sont amenés à pénétrer de l'ordre de 500 expérimentateurs ou agents, oblige à réaliser des dispositifs de détection et de contrôle spécialisés.

(a) Le contrôle de la contamination est effectué automatiquement par un portique β-γ et une passerelle pieds, appareils qui possèdent une compensation pour le bruit de fond ambiant.

(b) La surveillance des manipulations et le contrôle de l'irradiation externe des agents peuvent être obtenus par un appareil permettant une mesure précise des doses γ indépendemment de leur énergie par l'emploi d'un scintillateur plastique.

(c) Certains locaux pouvant, dans certains cas, être le siège d'intensités de rayonnements importantes, un dispositif verrouillant automatiquement la porte qui y donne accès lorsqu'un seuil est atteint, a été mis en place.

(d) Enfin le rayonnement au-dessus de la piscine de Siloé étant conditionné par l'existence d'une couche chaude, l'existence de celle-ci est contrôlée par une chambre immergée qui est la seule à commander la chute des barres de sécurité en cas d'incident.

HEALTH PHYSICS ENGINEERING

A. H. EMMONS
Research Reactor Facility, University of Missouri, Columbia, Missouri, U.S.A.

Abstract—The first obligation of the health physicist is the *prevention* of radiation exposures. The earliest opportunity to practice this prevention is in the design and engineering of nuclear installations. The function of health physics engineering is to reduce all accident risks to the lowest level compatible with the economic and technical requirements of the proposed facility.

This paper describes the health physics problems encountered in the design, construction and operation of a ten megawatt university reactor facility. The total facility to be described consists of the highest flux university reactor facility in the United States together with a laboratory complex of 18 radioisotope labs, a 5000 Ci cobalt irradiator, 300 kV X-ray irradiator, hot cell, shops, library, and offices.

The tendency in all fields of science is toward specialization. Health physics is no exception. Each topic within the framework of the discipline is being further differentiated. Health physics engineering must include an integration of all relevant topics (factors) as they influence design and engineering. It is then a systems engineering problem.

The engineer is an applied scientist. He uses the findings, facts and formulas of all sciences in attaining a problem solution. The health physicist must have a diverse background of science from which to withdraw information applicable to the solution of an engineering problem. These inter-relationships and dependencies are defined.

DISCUSSION

B. W. EMMERSON (*U.K.*):

In addition to the contaminants reported, have you made an analysis of the surface contamination for the presence of low energy emitters such as S^{35}? This nuclide represents a considerable proportion of the total surface dose in CO_2 coolant circuits on the U.K. Civil Reactors and is difficult to detect, being a low energy, pure beta emitter.

J. BARBIER:

Oui, nous les avons observés. Nous pensons qu'ils proviennent d'une activation de certaines huiles. Cependant ce n'est pas une préoccupation majeure. Le Hg^{203} nous préoccupe davantage, car il a lui aussi un β mou que l'on ne détecte pas avec les compteurs en verre. Nous sommes dans l'obligation de réequipper les centrales de Chinon avec des compteurs à fenêtre mince.

L. DE FRANCESCHI (*Italy*):

Può l'autore fornire qualche esempio di ambienti nei quali il superamento di un determinato livello di radiazione provoca la chiusura automatica delle porte? In particolare, vi sono persone che lavorano in tali ambienti quando il sistema automatico è innestato con il pericolo conseguente di rimanere chiuse all'interno dell'ambiente stesso?

H. DE CHOUDENS:

Certains locaux tel le local des échangeurs ou la cellule chaude se trouvent automatiquement verrouillés lorsque l'intensité de rayonnement à l'intérieur est trop forte. Les serrures électromagnétiques assurant ce verrouillage par exemple dans le local des échangeurs ont une sécurité qui leur permet d'être toujours ouvertes de l'intérieur pour le cas où justement un agent s'y trouverait enfermé.

D. K. CRAIG (*South Africa*):

Mr. Barbier, would you perhaps like to speculate as to the source of the free uranium which you have routinely observed to be present in the coolant CO_2 gas? It seems to be rather strange that you should observe such uranium, as I would not normally expect there to be any free uranium in the CO_2.

J. BARBIER:

Les produits de fission observés dans le CO_2 proviennent de l'uranium ayant résisté au nettoyage des gaines du combustible. C'est ainsi que pour le 1er chargement de EDFI nous avons estimé la quantité d'U libre à 1 gr pour 17.000 cartouches. C'est une valeur importante qui vaut sensiblement 100 cm^2 d'uranium dégazant sur une épaisseur de 6 microns. Cette épaisseur est celle généralement admise pour la diffusion du Xe et du Kr.

On voit que dans ces conditions une rupture normalement détectée n'apporte que quelques pourcents de plus de Xe et Kr dans le CO_2 (globalement, bien entendu).

G. LEWIS (*U.K.*):

Mr. Chairman, I would like to thank you for this opportunity to say something more about my paper. I am prepared in detail to read the paper, but I will briefly enlarge the details which are given in the abstract. When the stations were designed and before they came into operation, there was a great deal of speculation as to the doses that would be received by the personnel and it was only during the first years of operation that the facts of the situation really became clear. My paper just presents the first three complete years of operation of the stations at Berkeley and Bradwell and gives the actual doses received by classified workers at those two stations. Making recourse to the table of the results given in the paper itself, during the years 1963 to 1965 the percentage of workers at Bradwell and Berkeley receiving not more than 0.5 rem per year lay between the ranges 45% and 87%. I think this is an illustration of the extremely low doses to be received at reactor stations of the type chosen by the Generating Board for power production. Among the people receiving larger doses than this, those receiving for example more than 1.5 rem per year amounted to not more than 4.3% at the biggest. The sources of these radiations are described in the paper and at this point I feel I should make clear what may appear to be a discrepancy between what I have to say and what Mr. Barbier mentioned in his paper to do with N^{16}. He was dealing entirely with a question of contamination of circuits and I am dealing with external radiation doses from the circuits. While N^{16} may not contribute any-

thing to the contamination, it certainly does contribute to the external dose. Gamma spectrometry carried out at various places on the nuclear power stations sites does reveal the rather high energy gammas from N^{16} decay as a prominent part in the external dose received by the personnel. N^{16} certainly is important in the doses to be received during the operations of the stations and another factor which significantly contributes to doses at nuclear stations run by the Generating Board is one mentioned by Mr. Emmerson, namely doses received during maintenance and refuelling operations with material which has been irradiated in the core of a reactor. Here it is generally a question of radiation dose to the extremities, finger-tips or hands which have to carry out the work on irradiated material. A table given in my paper makes it clear that, although a careful control is required in these situations, doses can be kept well within those specified by ICRP, enabling necessary maintenance to be carried out for reactor stations to be kept in good conditions. The conclusions of the paper are that during these first four years of operation of the civil nuclear power stations in the United Kingdom, the operation of the stations has not been embarrassed by external radiation doses received by the personnel. One final point is that experience of the earlier stations fed back to the design departments concerned will certainly lead to reduction of doses at later designed stations.

A. H. EMMONS (*U.S.A.*):

Thank you, Chairman Nishiwaki, for the opportunity of talking for a few moments. There is no doubt in my mind that the health physics people are doing a fine job in radiation monitoring, dosimetry and environmental control. However, I should like to make a plea that we enter the picture in the design stage more frequently and depend less upon feed back of information lately gained. Specifically, let me make the suggestion that there are design problems which should be a basic concern to the health physicist.

D. K. CRAIG (*South Africa*):

I would like to comment upon Dr. Emmons' plea that health physicists be given greater opportunity to participate in the planning of nuclear facilities at the design stage. I agree that it would greatly minimize our subsequent problems in the control of contamination if we were heeded. I have been given the opportunity of participating in the review of building plans, but have frequently found that my requests for the positioning of change rooms, over-shoe barriers, etc., in order to provide for the efficient separation of contamination areas, from areas where contamination should not normally arise, have often been overruled in the interests of economy. Does Dr. Emmons have any solution to offer to this problem?

A. H. EMMONS:

Well, first I should say that you can't be economically careless; secondly, I should suggest that one way is to become the head man in the operation and then you can dictate the facilities to be put in.

L. DE FRANCESCHI (*Italy*):

Con quale metodo viene controllata la contaminazione dell'aria negli ambienti di lavoro? Come vengono fissati gli allarmi per evacuare l'edificio?

A. H. EMMONS:

(a) We monitor by means of scintillation counters located in wells in the off-gas ducts.
(b) These counters (and associated circuitry) initiate alarms.
(c) Personnel are instructed to vacate the labs and reactor by a defined pathway in any instance of an alarm (independent of the identity of the initiating event).

M. DENNET (*U.K.*):

Mr. Bertron mentioned in his paper that operations and maintenance personnel carry out certain Health Physics duties. I should like Mr. Bertron to enlarge on the extent of this work. In addition could Mr. Bertron say something about the number of permanent Health Physics Staff at Chinon. A figure of 40 personnel is typical for U.K. Civil Nuclear Stations.

L. BERTRON:

Tous les agents de la Centrale sont intéressés à la radioprotection. Notre organisation repose cependant sur un certain nombre d'agents ayant des responsabilités particulières dans ce domaine. Ce sont:

—les techniciens de radioprotection—chefs de bloc: grosso modo 1,5 agent par quart et par tranche fait de la radioprotection; il y a 5 équipes de quart en roulement par tranche;

—à l'entretien, les chefs de travaux: pour les 3 tranches de Chinon, environ 80 techniciens ont reçu une formation qui leur permet de conduire des travaux dans des zones à risques nucléaires. Ces techniciens sont responsables d'une équipe d'exécutants. Ils travaillent indifféremment à l'intérieur et à l'extérieur de la zone contrôlée;

—au Service Technique, 6 agents sont plus spécialement chargés des mesures de radioprotection.

Il faut noter que sur le site de la Centrale de Chinon, 50% des travaux de décontamination du matériel, le traitement des effluents liquides et des déchets solides sont entrepris dans un atelier indépendant de la Centrale qui possède ses propres agents de radioprotection.

Le développement des films dosimètres et le contrôle de la chaîne alimentaire ne sont pas effectués à la Centrale.

Y. NISHIWAKI (*Japan*):

Do you have the practice in the United States of comparing the dose rates after the operation of the nuclear installations with those at the original design stage and to re-evaluate the validity of the design? I think such a comparison would be extremely useful for the improvement of the design.

A. H. EMMONS:

To the best of my knowledge no formal comparison technique exists. However, in most instances the designer is also the operator of a facility and then has the opportunity to compare design criteria to actual operational results. I agree that we should more frequently make these comparisons even if they embarrass us!

ENERGIEVERTEILUNG DER GAMMASTRAHLUNG EINER RADIOAKTIVEN WOLKE

A. SCHMIDT und A. WENSEL
Institut für Kernphysik, 6 Frankfurt/M, BRD

Zusammenfassung—Die Energieverteilung der γ-Strahlung einer radioaktiven Wolke wurde mit Monte-Carlo-Methoden berechnet und experimentell bestimmt. Als Streumedium wurde ein homogenes, unendlich ausgedehntes Luft- bzw. Wasservolumen vorausgesetzt. Streuspektren punktförmiger Gammastrahlungsquellen in Abhängigkeit von der Entfernung vom Quellpunkt wurden berechnet. Durch Integration wurden die Streuspektren der γ-Strahlung radioaktiver Wolken verschiedener Geometrien ermittelt und aus diesen wiederum durch weitere Integrationen die entsprechenden Dosisverteilungen gewonnen.

Mit einem zweiten Monte-Carlo-Programm wurden die Streuspektren und Dosisverteilungen der γ-Strahlung einer radioaktiven Wolke direkt berechnet.

Streuspektren der γ-Strahlung radioaktiver Wolken wurden an der Wassertankanlage des Instituts für Kernphysik, Frankfurt/Main, gemessen. Die Wolken wurden durch einen mit radioaktiver Lösung gefüllten Plastiksack, der im Wasser in verschiedener Entfernung vom Detektor angeordnet war, simuliert. Die Energieverteilungen wurden aus den Impulshöhenverteilungen eines NaJ(Tl)- Szintillationszählers mit Matrixinversion bestimmt.

Die gemessenen Werte werden mit den berechneten Spektren und Dosisverteilungen verglichen. Es ergibt sich befriedigende Übereinstimmung, auch mit einigen Dosisangaben aus der Literatur.

Die Ergebnisse wurden im Hinblick auf die Strahlenbelastung der Bevölkerung in der Umgebung von Kernenergieanlagen, bei denen die Abgabe radioaktiver Substanzen möglich ist, diskutiert.

1. EINLEITUNG

Beim Betrieb mancher Kernreaktoren werden radioaktive Gase in die Atmosphäre abgelassen. Dabei bilden sich radioaktive Wolken, die in der Umgebung der Kernenergieanlage eine Gamma-Dosisleistung erzeugen, der die in der Nähe wohnende Bevölkerung ausgesetzt ist. Es ist daher von Interesse, die Strahlenbelastung der Bevölkerung rechnerisch ermitteln zu können.

Radioaktive Wolken entstehen auch bei Unfällen an Kernreaktoren, bei denen radioaktive Substanzen in die Atmosphäre freigesetzt werden. Die Ermittlung der Dosis, die durch diese Wolken verursacht wird, spielt bei der Abschätzung der möglichen Gefährdung der Bevölkerung durch Kernreaktoren eine wesentliche Rolle.

In der vorliegenden Arbeit werden die Energieverteilung und die Dosis der Gammastrahlung radioaktiver Wolken experimentell und theoretisch bestimmt. Die Berechnung der Energieverteilung aus radioaktiven Wolken erfolgt einmal über Integration von Punktquellenspektren und zweitens direkt mit Monte-Carlo-Methoden. Bei der Messung wird die

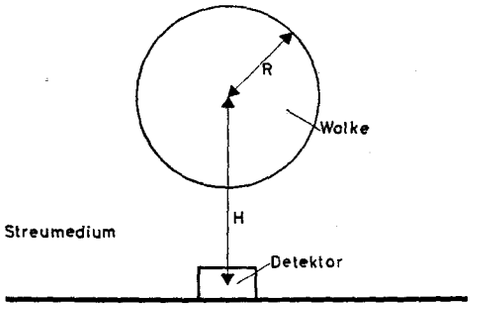

ABB. 1. Skizze der betrachteten Geometrie.

Luft durch Wasser ersetzt und die Wolke durch eine radioaktive Lösung simuliert. Die Dosis wird auf zwei Arten berechnet, durch Integration über das Energiespektrum und mit Hilfe des Build-up Faktors. Zur Vereinfachung des Problems wird angenommen, dass die Wolke kugelförmig sei und sich in einem unendlich ausgedehnten, homogenen und isotropen Medium befinde. Abb. 1 zeigt eine Skizze der betrachteten Geometrie.

2. DIE BERECHNUNG DER ENERGIEVERTEILUNGEN RADIOAKTIVER WOLKEN

2.1. *Allgemeines*

Bei der Berechnung des Transportes von Gammastrahlen in Materie müssen im allgemeinen Fall vereinfachende Voraussetzungen gemacht werden. Der Raum wird als homogen und unendlich ausgedehnt angenommen. Als Gammastrahlenquellen werden in der Literatur,[1, 2] abgesehen von einigen Spezialfällen, punktförmige Quellen, unendlich ausgedehnte Flächenquellen und gleichförmig im ganzen Raum verteilte Quellen behandelt.

Die Gammastrahlungsquellen, die hier betrachtet werden, haben eine endliche Ausdehnung, die bei der Berechnung der Dosis nicht zu vernachlässigen ist.

Mögliche Methoden zur Bestimmung der Energieverteilung der Streustrahlung einer Gammastrahlungsquelle in einem Medium sind die Momentenmethode und die Monte-Carlo-Methode.[3, 4] Die Momentenmethode ist wie alle anderen analytischen Verfahren zur Lösung der Boltzmann'schen Transportgleichung bei der direkten Berechnung der Energieverteilung einer endlich ausgedehnten Volumenquelle nicht brauchbar, da die Randbedingungen nicht oder nur mit grossem Aufwand analytisch dargestellt werden können. Mit der Monte-Carlo-Methode dagegen kann man auch Probleme mit komplizierten Randbedingungen lösen.

2.2. *Die Monte-Carlo-Methode*

Aus den oben erwähnten Gründen wurde die Energieverteilung der Gammastrahlung radioaktiver Wolken mit Hilfe der Monte-Carlo-Methode berechnet. Hierzu wurde ein Rechenprogramm "MCGAMPQ" in FORTRAN II geschrieben. Die Rechnungen wurden auf der elektronischen Rechenanlage IBM 7090 des Deutschen Rechenzentrums, Darmstadt, durchgeführt.* Als Primärenergie der Gammastrahlung wurde 1,53 MeV gewählt.

Bei der Monte-Carlo-Methode muß jedes Randwertproblem getrennt berechnet werden. Um dies zu umgehen, wurde das im folgenden erläuterte Verfahren gewählt.

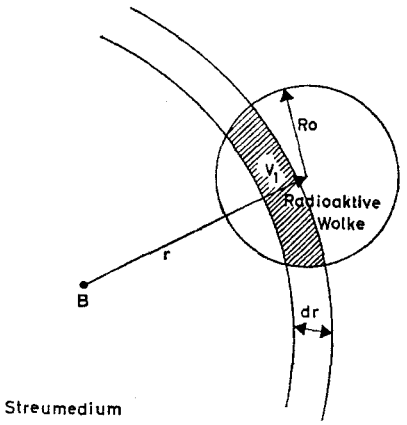

ABB. 2. Zur Ermittlung des Streuspektrums einer radioaktiven Wolke aus den Streuspektren einer punktförmigen Quelle.

2.3. *Integration über Punktquellen*

Die Streuspektren einer punktförmigen Quelle wurden für 56 verschiedene Entfernungen der Quelle vom Beobachtungspunkt berechnet. Da man durch statistische Abschätzung erreichen kann, dass jedes Teilchen bei jedem Stoß zum Fluß in jeder gewählten Entfernung von der Quelle beiträgt, können die Streuspektren einer Punktquelle in vielen Entfernungen in einem Rechengang bestimmt werden. Mit den Streuspektren der punktförmigen Quelle wurden die Streuspektren kugelförmiger Volumenquellen bestimmt. In Abb. 2 ist eine kugelförmige radioaktive Wolke schematisch dargestellt. B ist der Ort, an dem die Dosis bestimmt werden

* Die Arbeiten wurden mit Unterstützung der Deutschen Forschungsgemeinschaft durchgeführt, der wir an dieser Stelle dafür danken möchten.

soll. Man denke sich um B Kugelschalen in äquidistanten Abständen gelegt. Das Volumen V_1, das von der Wolke aus dem Volumen zweier aufeinanderfolgender Kugelschalen herausgeschnitten wird, wird berechnet. Multipliziert man die entfernungsabhängigen Streuspektren der Punktquelle mit V_1 und addiert sie anschliessend, so erhält man das Streuspektrum der Kugelwolke.

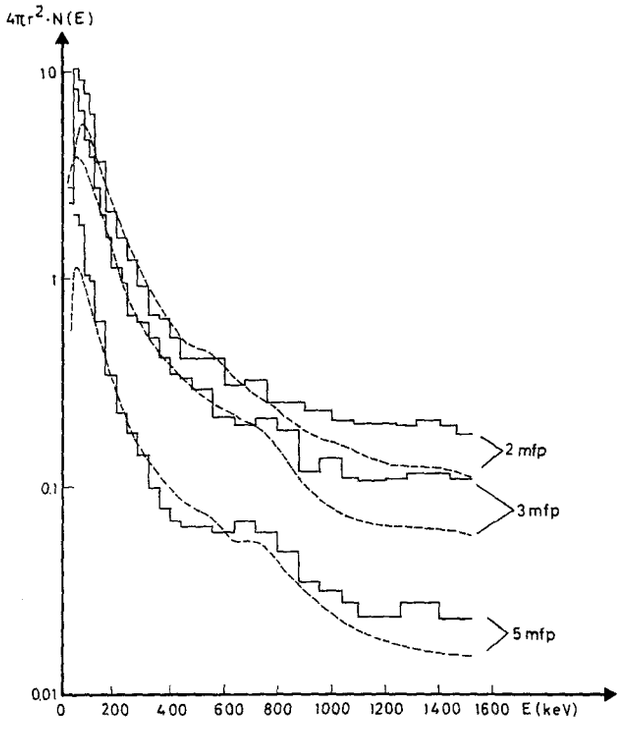

ABB. 3. Spektren einer radioaktiven Wolke für verschiedene Entfernungen. Histogramm: Monte-Carlo-Daten.

Um die Genauigkeit dieses Verfahrens zu prüfen, wurde ein zweites Monte-Carlo-Programm "MCGAMKUG" geschrieben, mit dem das Streuspektrum einer Kugelwolke direkt berechnet werden kann.

Es zeigte sich, dass die auf beide erwähnten Arten ermittelten Spektren innerhalb der statistischen Genauigkeit übereinstimmen.

3. BERECHNUNG DER DOSIS

Die Dosisleistung kann aus dem Streuspektrum durch Integration ermittelt werden. Sie kann auch mit Hilfe des Build-up Faktors berechnet werden,[6] wobei die Kenntnis der Energieverteilung nicht vorausgesetzt wird.

4. MESSUNG

Streuspektren der Gammastrahlung radioaktiver Wolken wurden an der Wassertankanlage des Instituts für Kernphysik, Frankfurt/M., gemessen. Dabei wurden die Wolken durch Plastikbälle simuliert, die mit einer Lösung von K_2CO_3 gefüllt waren, das im Reaktor aktiviert war. ^{42}K ist ein Gammastrahler mit einer Energie von 1,53 MeV. Die Bälle wurden in verschiedenen Entfernungen von einem NaJ-Kristall-Detektor angebracht und die sich ergebenden Impulshöhenverteilungen gemessen. Die Energieverteilungen wurden aus den Impulshöhenverteilungen mit Matrixinversion[5] bestimmt.

5. DISKUSSION DER ERGEBNISSE

5.1. *Vergleiche der Energieverteilungen*

In Abb. 3 werden die Messergebnisse mit berechneten Spektren verglichen. Dabei ist N (E) der Photonenfluß und r die Entfernung des Kugelmittelpunktes vom Beobachtungsort. Wenn man berücksichtigt, daß der Fehler in den gemessenen Spektren bei Energien oberhalb 1,2 MeV wegen des geringen Photonenflusses in diesem Energiebereich und durch die Entfaltung der Impulshöhenverteilung[5] relativ groß ist, so ist die Übereinstimmung zwischen den gemessenen und den berechneten Spektren als gut anzusehen.

5.2. *Vergleich der Dosisleistungen*

In Abb. 4 werden die auf die verschiedenen Arten ermittelten Dosisleistungen miteinander verglichen. Es zeigt sich, daß die gemessenen Werte stets um etwa 15% bis 30% niedriger als die berechneten Werte sind. Dies ist nach den in Abb. 3 gezeigten Ergebnissen zu erwarten.

Die mit Hilfe des Build-up Faktors berechneten Dosisleistungen weichen teilweise sehr stark von den aus den Energiespektren berechneten Werten ab. Aus Abb. 4 kann man erkennen, dass die nach beiden Arten ermittelten Werte umso besser übereinstimmen, je grösser

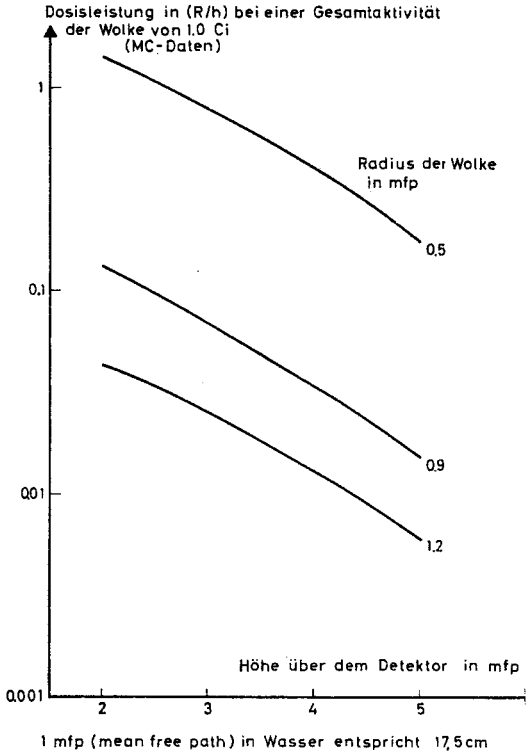

ABB. 5. Vergleich der Dosisleistung verschiedener radioaktiver Wolken.

Radius der Wolke in mfp	Entfernung in mittleren freienWeglängen (mfp)	Dosisleistung in ($10^{-2}\mu$R/h) / (MeV/cm^3 sec)		
		berechnet mit Hilfe des Build-up Faktors	berechnet aus den Energiespektren (Monte Carlo Daten)	gemessen
0.5	2	13.3	7.2	5.1
	3	2.9	4.0	2.9
	4	0.76	1.9	1.4
	5	0.22	0.86	0.75
0.9	2	16.2	4.0	2.7
	3	3.3	2.1	1.65
	4	0.6	1.05	0.83
	5	0.24	0.043	0.036
1.2	2	19.8	2.9	2.05
	3	3.6	1.6	1.25
	4	0.94	0.83	0.70
	5	0.26	0.40	0.34

1 mfp in Wasser entspricht 17.5 cm

ABB. 4. Vergleich der nach verschiedenen Arten ermittelten Dosisleistungen.

die Wolke ist und je weiter sie vom Beobachtungsort entfernt ist. Die Berechnung der Dosisleistung einer grossen Wolke in geringer Entfernung mit Hilfe des Build-up Faktors kann mit relativ grossen Fehlern behaftet sein. Dieses Ergebnis ist insofern bedeutsam, als bei Berechnung von Wolkendosen nach Unfällen bei Kernreaktoren die Dosisleistung im allgemeinen mit Hilfe des Build-up Faktors berechnet wird.

Abb. 5 zeigt in einer graphischen Darstellung einen Vergleich der Dosisleistungen radioaktiver Wolken mit gleicher Gesamtaktivität. Wie zu erwarten, sinkt die Dosisleistung mit zunehmender Wolkengrösse und mit der Höhe über dem Beobachtungsort. Und zwar nimmt die Dosisleistung um einen Faktor von etwa 10 ab, wenn sich der Durchmesser der Wolke verdoppelt.

LITERATUR

1. H. Goldstein und E. Wilkins. NYO 3075 (1954).
2. U. Fano, L. V. Spencer und M. J. Berger. Flügge. *Handbuch der Physik*, Band 38/2 (1959).
3. E. Fessler und M. L. Wohl. NASA TN D-850 (1961).
4. N. R. Baumgardt, A. Trampus und J. MacDonald. XDX 61-5-1 (1961).
5. A. Schmidt. IKF-D-54 (1965), Diplomarbeit.
6. D. S. Duncan. NASA-SR-Memo-4822 (1959).

SOME APPLICATIONS FOR SEMICONDUCTOR DETECTORS IN HEALTH PHYSICS

J. LIPPERT
Risö Research Establishment, Roskilde, Denmark

Abstract—Continuing earlier detector development, a small group in the Health Physics Department started work in the semiconductor detectors field in 1963, with a feeling that these might be valuable for spectrometry as well as low level counting. The present paper will deal with germanium detectors, which is produced in sizes up to 9 cm² at the time of writing (March '66).

An attempt to make a well-type detector is to be done presently and results will be reported.

Some of our detectors are in use in health physics applications, such as fallout measurements (^{57}Co, ^{155}Eu, ^{134}Cs, etc.), identification of components of contaminations and tracer techniques in studies of filter efficiencies. Some examples will be reviewed in the paper.

1. INTRODUCTION

During the last 10 years a small group in the Health Physics Department at Risö Research Establishment has been working on the development of different types of detectors such as low level geiger counters and proportional counters for contamination monitors, etc.[1] As a natural continuation a development program of semiconductor detectors was started some 3 years ago. This work was originally concentrated on silicon detectors in order to investigate their low level characteristics.

The interest, however, shifted to the germanium detectors due to their high resolution capabilities. A number of detectors of different sizes has been produced and some of them used in routine work in the department. After a survey of the more important characteristics of some detectors examples of their use in practical work will be given.

2. Ge(Li) DETECTOR SYSTEMS

For the production of semiconductor detectors of large active volume the method of lithium drifting is used.[2] Typical shapes of detectors are the flat, parallel type having a certain area and sensitive depth, and the so called coaxial type (Fig. 1). The sensitive volume of the flat detector is restricted to 10–12 cm³ at present while the coaxial type is produced up to 53 cm³.[3] A typical size will be 10–30 cm³. Also shown in Fig. 1 is a coaxial type with a drilled hole for use as a "well-type" detector. All types have been produced at our laboratory, the last mentioned only in a single case with not quite satisfactory compensated thickness,

Table 1.

Type	Volume	Size	Sensitive depth	Low energy resolution	Min. distance for source
Flat	2·2 cm³	4·4 cm²	0·5 cm	3·0 keV	0·6 cm
Coaxial	9 cm³	2·3 cm diam.	0·8 cm	2·4 keV	1·6 cm
Well, 16 mm	6 cm³	2·5 cm high	0·4 cm	5·1 keV	0·2 cm

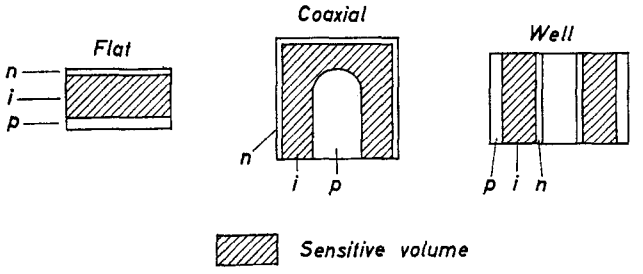

FIG. 1. Types of Ge(Li) detectors.

while the other types have specifications comparable with values from the literature.

Table 1 gives data for the detectors used.

The detectors are mounted, as shown in Fig. 2, in a vacuum chamber on a support cooled by liquid nitrogen through a cold finger.

The amount of nitrogen used is about 1 litre per day. Electrical connection is made to a low noise amplifier system and a 256 channel analyser, this number of channels actually being too low.

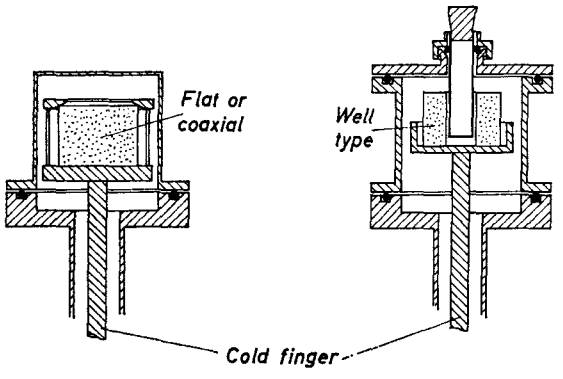

FIG. 2. Mounting of detectors.

A series of calibration measurements was made using a set of standard sources from the IAEA in Vienna. Results are shown in Fig. 3, where the source to detector surface distance was 10 cm. The results for 3 × 3 in. NaI(Tl) crystal is plotted for comparison. At 1 MeV the total number of counts in the photopeak is around 50 times higher in the scintillation detector, but taking into account the much better resolution for the Ge-detector, the height of the peak above a continuous background will be within a factor of 2 as shown by the dotted line. Figure 4 shows results of calibration

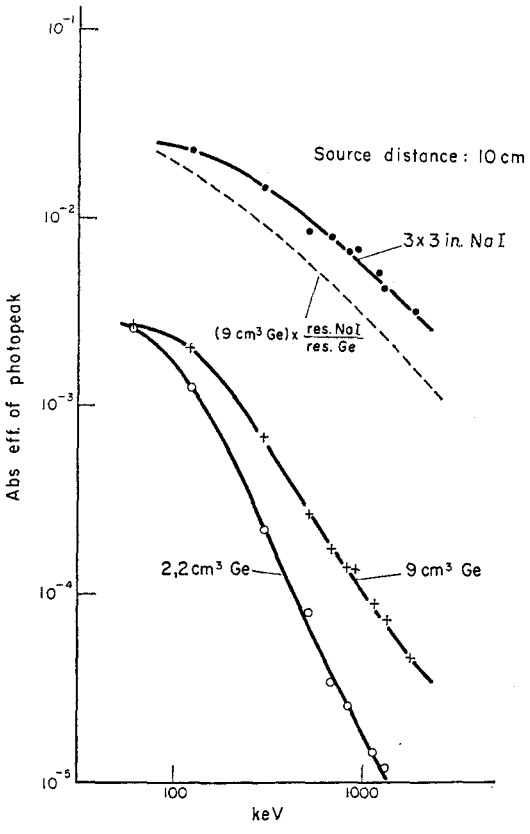

FIG. 3. Efficiency curves for 10 cm source distance.

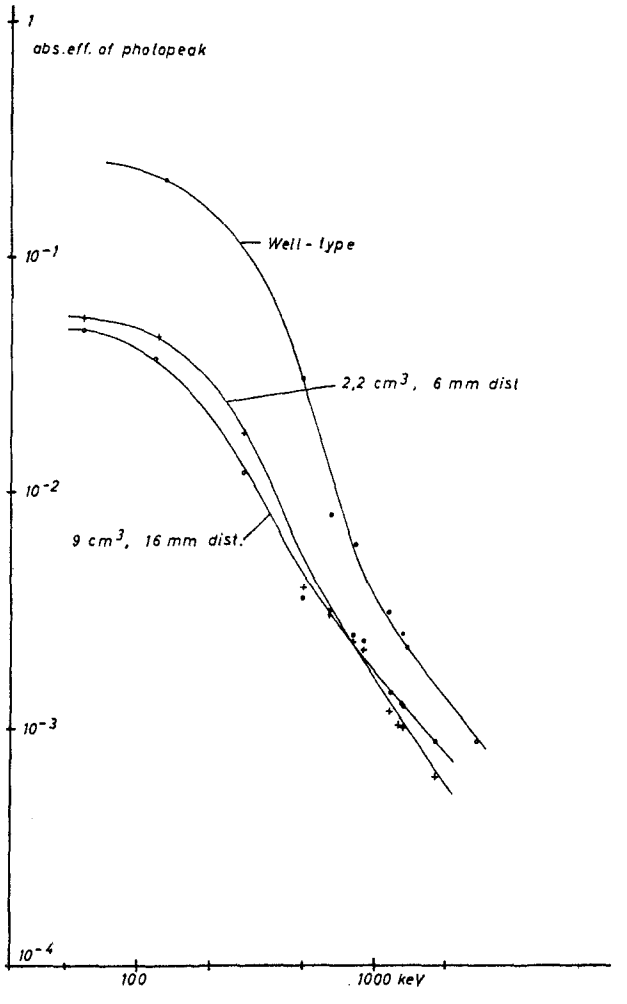

FIG. 4. Efficiency curves for close geometry.

with the sources in close geometry, which for the 9 cm³ crystal should have been closer through a better mounting. Also shown is a curve for the well-type detector using samples of 0·5 ml. It is our hope to construct a similar detector with a thicker sensitive layer and a somewhat better resolution, giving a better high energy performance.

3. LOW LEVEL COUNTING

For this purpose the 2·2 cm³ detector has been used for more than a year. The detector is operated in anticoincidence with a 4 × 3 in. well type NaI(Tl) crystal (see Fig. 5).[4] A ^{137}Cs spectrum obtained with this system is shown in Fig. 6. It is seen that the high energy part of the compton distribution is much reduced and the sharp edge removed giving an advantage in analyzing complicated spectra. The system also gives some reduction of the background due to external sources. Figure 7 gives an example of this type of measurements. The amount of ^{137}Cs in the sample is approximately 25 nCi.

Figure 8 gives a similar example for the 9 cm³ detector. An old air filter sample is measured with this detector and the 3 × 3 in. NaI(Tl)

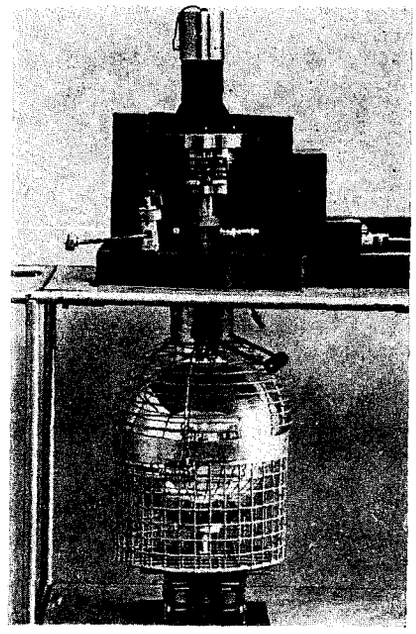

FIG. 5. Detector with anticoincidence system.

detector. It is seen that the following isotopes ^{54}Mn, ^{65}Zn, ^{106}Rh, ^{125}Sb, ^{137}Cs, ^{144}Ce, ^{155}Eu are clearly resolved in the germanium system whereas the ^{57}Co and ^{155}Eu cannot be distinguished from the ^{144}Ce in the scintillation spectrum.

Figure 9 shows a spectrum with the lines of ^{134}Cs and ^{137}Cs measured with the well-type detector. The intention is to use ^{134}Cs as a tracer during a radiochemical treatment of samples in order to concentrate small amounts of ^{137}Cs activity.

Table 2 gives estimated detection limits assuming counting time of 1000 min for samples containing only a single isotope and an accuracy of $\pm$ 20%.

For a NaI(Tl) detector the ^{137}Cs detection limit using the same definition is 5–10 pCi.[1] The figures for the well-type will probably be improved in the future.

4. IDENTIFICATION OF CONTAMINATION

Due to the high energy resolution of the germanium detector, it is an obvious choice for identification purposes. Figure 10 shows a spectrum of a part of a reactor cooling system containing the following activition products: ^{51}Cr, ^{58}Co, ^{59}Fe, ^{60}Co. Experience with this type of measurements shows that the components of mixed radioactivity may be determined faster and more positively than previously.

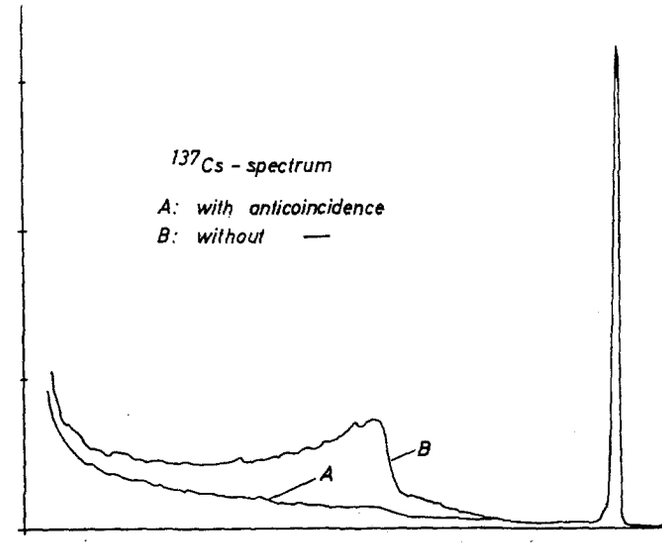

FIG. 6. Spectra with and without anti-coincidence.

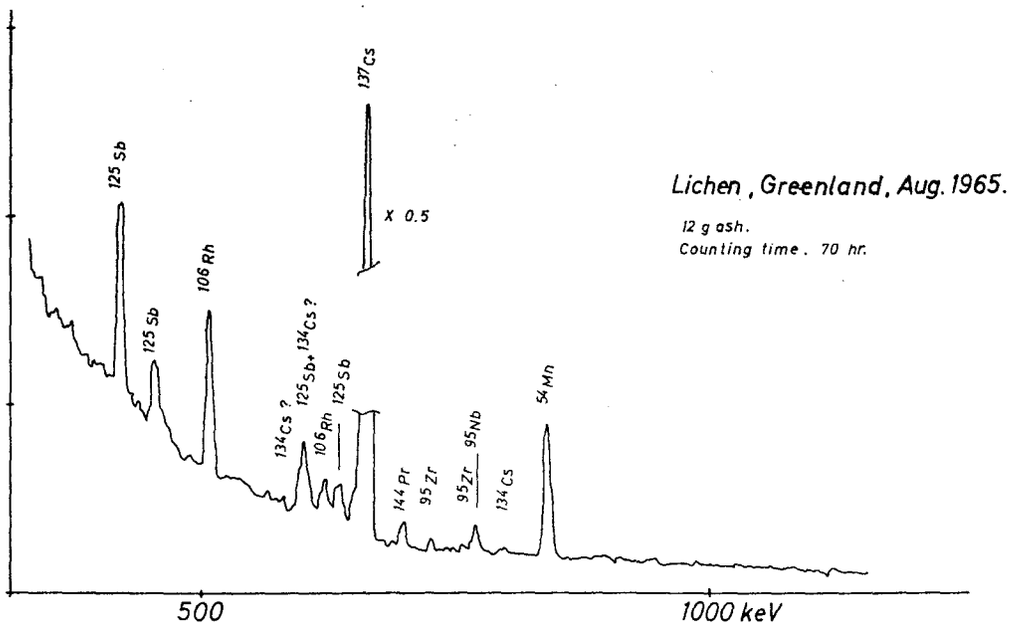

FIG. 7. Sample measured with the anti-coincidence system.

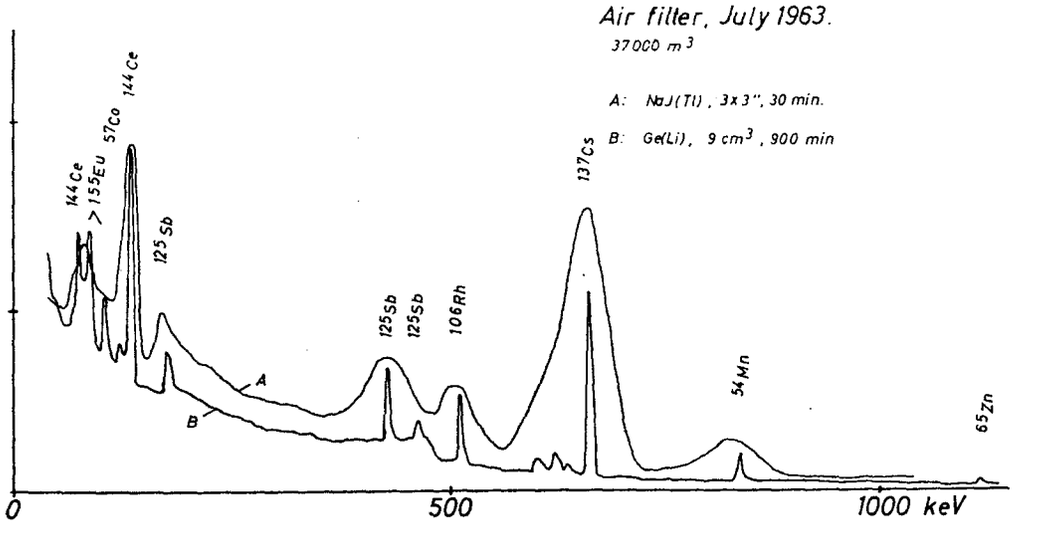

FIG. 8. Sample measured with the 9 cm^3 detector.

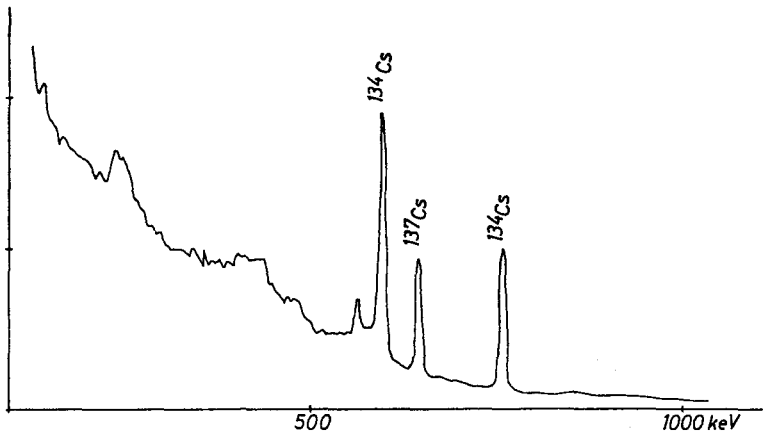

FIG. 9. Well-type detector, ^{134}Cs, ^{137}Cs spectrum.

Table 2. Minimum Detectable Activity

Detector	^{57}Co	^{137}Cs	^{60}Co
2·2 cm³	1–2 pCi	10 pCi	15–20 pCi
Well	10 pCi	10–15 pCi	15–20 pCi

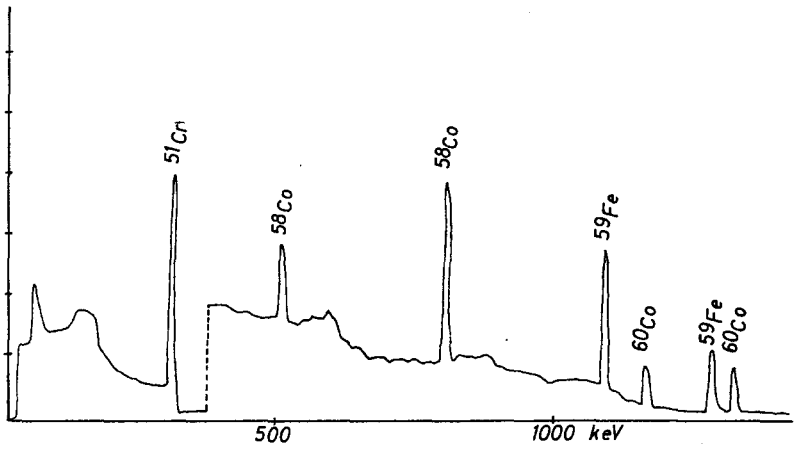

FIG. 10. Activation products from reactor cooling system.

5. CONCLUSION

As shown in the examples given, the use of germanium semiconductor detectors is favoured for most types of measurements involving gamma spectrometry. It is the opinion of the author that it should also be recommended in the field of health physics.

6. ACKNOWLEDGEMENT

The author wishes to thank Mr. K. E. Eriksen for the production of the detectors used.

REFERENCES

1. J. LIPPERT. Low level counting. Risö Report No. 44, 1963.
2. A large number of articles especially in *Nuclear Instruments and Methods* and *IEEE Transactions of Nuclear Science.*
3. H. L. MALM and I. L. FOWLER. Large-volume coaxial germanium gamma-ray spectrometers. AECL-2504.
4. Y. SEVER and J. LIPPERT. *Nuclear Instruments and Methods* **33** (1965).

ENVIRONMENTAL γ-RADIATION SPECTROMETRY AND ISOTOPE IDENTIFICATION

B. S. J. DAVIES
Berkeley Nuclear Laboratories, Central Electricity Generating Board, Berkeley, Glos., U.K.

Abstract—A mobile scintillation spectrometry system is described, which, with the aid of computer analysis, is capable of making high resolution measurements of gamma radiation spectra. Any mixture of line and continuous spectra with photon energies in the range 0·1–10 MeV may be measured provided that the total exposure-rate is less than about 1 mR/hr.

The system has been applied to the problem of the direct measurement of artificially produced radioisotopes on the ground in the presence of naturally occurring radiation. The accuracy and sensitivity of the method for direct measurement of isotopes of interest is discussed.

IN VIVO GAMMA SPECTROMETRY: A MAJOR TOOL FOR LARGE SCALE ROUTINE PERSONNEL MONITORING FOR URANIUM AND THORIUM

C. M. WEST and L. M. SCOTT

Nuclear Division, Union Carbide Corporation, Oak Ridge Y-12 Plant, Oak Ridge, Tennessee, U.S.A.

Abstract—The use of *in vivo* γ-spectrometry over the past five years has proven to be an invaluable tool in the comprehensive assessment of potential internal exposure in some 3,000 employees at the Oak Ridge Y-12 Plant who have worked in uranium and thorium areas.

The purpose of this paper is to report on some of the more interesting aspects and refinements of this unique application of *in vivo* spectrometry.

Improvements in sensitivity. Improvements in minimum sensitivity have been accomplished by the use of multiple crystals. Detection sensitivity was decreased from 130 μg to 80 μg for ^{235}U by the use of back and side detectors.

Detection and avoidance of surface contamination. An effective technique of detecting and avoiding the effects of low level surface contamination on employees has been developed by utilization of the γ-spectrometry data and scintillation detectors positioned over and under the chest. The use of a hair shield and selected hand positioning minimizes the effect of contamination on these portions of the body.

Correction of base spectra. It was found that the base spectra changed with time, apparently as the average cesium burden varies. These base spectra are empirically derived using a statistically computed prediction equation. A continuing control program with an unexposed population is used to evaluate and make the necessary changes to eliminate bias resulting from this change and its attendant adverse effect on the sensitivity and accuracy of the technique.

Optimization of measurement frequency. A method of statistical evaluation of the relative need for *in vivo* measurements was adopted to assure adequate information for employee protection at minimal expense. *In vivo* monitoring experience is summarized.

Major conclusions are: (1) The sensitivity and validity of the technique can be significantly improved by accounting for the effects of surface contamination, the use of additional detectors, and routine assessment of the base spectral prediction equation. (2) *In vivo* monitoring is vital to the evaluation of internal exposures to insoluble thorium and uranium.

DIE SPEKTRALE VERTEILUNG NIEDERENERGETISCHER BREMSSTRAHLUNG

F. PERZL und G. DREXLER

Institut für Strahlenschutz, Gesellschaft für Strahlenforschung, Neuherberg (F.D.R.)

Zusammenfassung—*Einleitung.* Messungen von Bremsstrahlungsspektren über einen weiten Energiebereich sind bisher mit einer erheblichen Messungenauigkeit behaftet. Bei Anwendungen der Röntgenstrahlung vor allem in der Medizin ist eine genaue Kenntnis der spektralen Verteilung sehr wünschenswert. So wurde in letzter Zeit hauptsächlich mit Szintillationsspektrometern mit NaJ-Kristallen die Lösung diese Problems in Angriff genommen. Die neueste Entwicklung in der Spektrometrie der Kernstrahlung—nämlich Silizium- und Germanium-Halbleiterdetektoren—verspricht auch für die Bremsstrahlungsspektrometrie bessere experimentelle Ergebnisse. Germaniumdetektoren besitzen infolge ihrer relativ hohen Ordnungszahl gute Absorptionseigenschaften für nieder-energetische Quantenstrahlung; ihr Energieauflösungsvermögen ist wesentlich besser als das mit NaJ-Kristallen erreichbare. Über die Messung von Bremsstrahlungsspektren bis zu Energien von maximal 150 keV unter Verwendung von Germaniumdetektoren wird im folgenden berichtet.

Experimenteller Teil. Als Bremsstrahlungsquelle wurde eine Hohlanodenröntgenröhre mit Wolframkathode und 1 mm Beryllium als Strahlenaustrittsfenster der Fa. Siemens-Reiniger-Werke AG verwendet. Die Röhrenspannung betrug maximal 150 kV Gleichspannung, der Röhrenstrom war regelbar zwischen 40 μA und 20 mA. Der Detektor in Form eines ungefassten Germaniumkristalls (Grösse 3 × 3 × 3 bzw. 10 × 10 × 10 mm) mit einer Li-gedrifteten Zone von 2 bzw. 8 mm, befand sich in einer Vakuumapparatur und wurde ständig auf −196 °C gekühlt. Der Abstand Röntgenröhre-Germaniumdetektor betrug 2 m. Der elektronische Teil der Apparatur bestand aus einem rauscharmen ladungsempfindlichen Vorverstärker (Typ 105 XL) und einem Linearverstärker (Typ 411) der Fa. Ortec. Die Impulshöhenanalyse wurde mit einem Vielkanalanalysator durchgefürt. Die Strahlung wurde mit einem 1 mm ø Cu-Kollimator durch ein Beryllium-Fenster (1 mm) in den Detektor eingeblendet. Die Energiekalibrierung der Messanordnung wurde mit der charakteristischen K-Strahlung verschiedener Elemente durchgeführt. Die Langzeitkonstanz der Apparatur wurde mit der 122 bzw. 136 keV-Linie des ^{57}Co und mit einem Hg-Pulser überprüft. Das Energieauflösungsvermögen unserer Anordnung betrug 2,5 keV (FWHM) Halbwertsbreite.

Messergebnisse. Die spektrale Verteilung für verschiedene Röhrenspannungen und Filterungen wird gezeigt. Bei Röhrenspannungen über 60 kV sind deutlich die charakteristischen Linien (K_α, K_β, L-Serie) des Antikathodenmaterials dem kontinuierlichen Spektrum überlagert. Die experimentellen Resultate werden nach geeigneten Korrekturen mit den Werten anderer Autoren verglichen.

MEASUREMENT OF TRITIUM IN AIR IN THE PRESENCE OF GAMMA RADIATION

G. COWPER and R. V. OSBORNE

Radiation Dosimetry Branch, Chalk River Nuclear Laboratories, Atomic Energy of Canada Limited

Abstract—A high flux heavy water reactor produces tritium copiously. Since leakage of heavy water from the moderator or the coolant circuit will lead to tritiated water vapour in nearby air in possibly hazardous concentrations, a means for measuring tritium in air is needed. Often such measurements have to be made in places where there are also significant levels of gamma radiation so the detecting device must be capable of distinguishing between the low energy betas from tritium and gamma radiation. The extent of this problem is illustrated by the fact that 1 $(MPC)_a$ of tritium produces only as much ionization in air as a gamma radiation field of 50 microroentgens per hour. Another important aspect of the problem is that the concentration of tritium in air may lie within very wide limits depending upon the particular circumstances of the release.

Several methods have been developed to meet this requirement using large gamma-compensated ionization chambers for installed area monitors, small volume compensated chambers complete with battery operated electrometers for portable use and scintillation detectors which achieve discrimination in favour of tritium by special circuit techniques.

The design of these devices and their application in the Canadian heavy water programme will be discussed.

A BYPRODUCT of the operation of heavy water reactors is tritium which is made in large quantities from deuterium by neutron capture. Since it is also produced in the ternary fission of uranium it may be found in a reactor fuel processing plant. Tritium is also widely used as a tracer for which purpose it is produced by neutron irradiation of lithium.

In the form of water (T_2O, DTO or HTO) it is of particular concern to the health physicist since water may enter the body through the intact skin as well as through the lungs or the digestive tract.[1] Thus, adequate safety of workers is not ensured simply by providing respiratory protection which is enough in the case of most other airborne radioactive materials. To manage radiation protection properly the means must be provided for the measurement of tritium concentrations in air.

In most practical situations, concentrations of tritium in air will be found where there are also moderate to severe levels of background gamma radiation so that the gamma sensitivity of tritium detectors must be minimized. The extent of this problem can be seen in the detection of tritium by measurement of the ionization it produces in air.

The maximum permissible concentration of tritium in air for occupational exposure, $[(MPC)_a]$, is $5 \times 10^{-6} \mu Ci/cm^3$ and this produces as much ionization as a gamma field of $50 \mu R/hr$. However, such a gamma field is only about three times natural background. Thus, a simple ionization chamber containing a filling representative of the atmosphere of interest would be incapable of detecting significant levels of tritium in situations where the external radiation level is quite acceptable even for continuous occupancy.

If gamma sensitivity is reduced fiftyfold, the detector would indicate 1 $(MPC)_a$ in a gamma field of 2.5mR/hr. For the unprotected worker wearing ordinary clothing these levels of tritium concentration in air and external gamma

radiation of the whole body are equivalent hazards and would ultimately produce an annual whole body dose rate of 5 rem/year.

With these considerations tritium detectors have been designed for use as installed and portable air monitors using both ionization chambers and scintillation detectors.

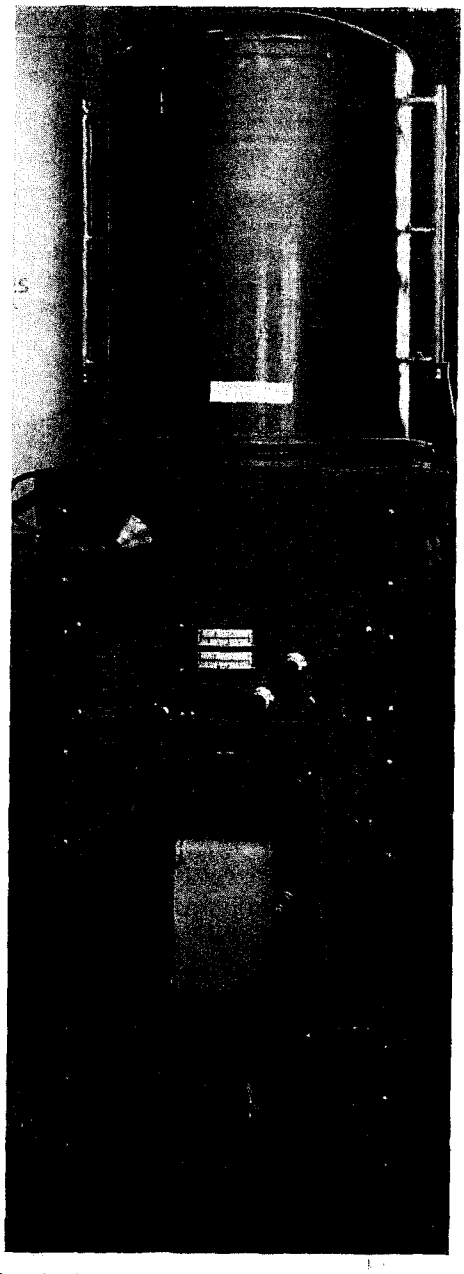

FIG. 1. Area monitor with 40 litre ionization chambers.

The gamma radiation sensitivity of an ion chamber through which tritiated air is flowing may be cancelled by subtracting from the total ionization current the current from a chamber of equal volume which is sealed from the atmosphere. The subtraction is effected conveniently by using a common electrometer and polarizing the chambers in opposition. In practice two widely separated chambers will not be adequate for even with gamma sources located at considerable distances local field irregularities caused, for example, by scattering from nearby solid objects will result in each chamber being exposed to different radiation intensities. An earlier development,[2] in which the two ion chambers consisted of the halves of a cylinder divided along a diametrical plane, was of limited usefulness because of this problem. It is clear that both chambers cannot at the same time occupy the same space but we have found that the requirement is approached by mounting the two chambers coaxially. The inner chamber is sealed and air is circulated through the outer chamber.

Two types of instrument have been designed[3] with coaxial chambers. One, intended for general area monitoring, is line operated and records the tritium concentration on a chart. Its chambers each have a volume of 40 litres. The other used for detailed examination of working areas is battery operated, portable, and presents the tritium concentration on a meter. This type has been made with two sizes of ion chamber (300 cc and 1200 cc) to give different sensitivities for different applications.

A 40 litre assembly is shown in Fig. 1. The ionization chamber stands with its axis vertical on a cabinet holding the electrometer amplifier, its chart recorder and the pump which pulls air through the outer chamber at 36 litres/min. At this flow rate a response time (90% in 2.5 min) is obtained which is adequate for an area monitor. Particles in the air are removed with a glass wool filter. The chamber polarizing voltages are obtained from carbon batteries. Initially mercury batteries were chosen because of their excellent shelf life characteristics but were found to give abrupt changes of potential which,

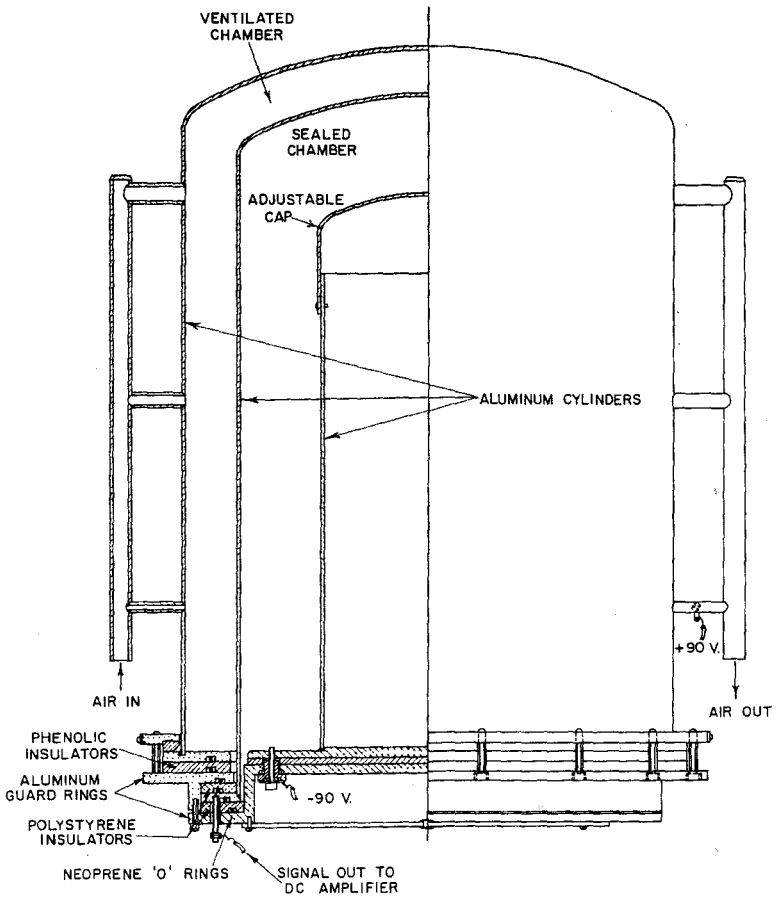

FIG. 2. Details of 40 litre ionization chamber assembly for area monitor.

appearing as spikes on the recorder chart, were frequently large enough to trip alarm circuits. They have however been retained in the portable instruments to be described where the output is not recorded and occasional spikes are unlikely to be noticed by the user.

The electrometer amplifier has a range of switched input resistors as well as a variable meter sensitivity so that a series of scale sensitivities can be obtained. Typically, it is set up to cover the range 0–1.5 $(MPC)_a$ to 0–500 $(MPC)_a$.

The details of the construction of the 40 litre chamber are shown in Fig. 2. The three coaxial cylinders form the two polarizing electrodes and the common collector electrode of the two chambers. The collector electrode is mounted in a guard ring arrangement. With this configuration it is clear that if the volumes of the chambers are equal then the ratio of the radii of the walls of the outer chamber is smaller than the corresponding ratio for the inner chamber. For equal polarizing voltages on the two chambers it follows that the saturation of the outer chamber will be better than that of the inner chamber. This is desirable since the outer chamber must adequately collect the ionization from both tritium and gamma radiation whereas the inner chamber must collect only ionization caused by gamma radiation. It follows that a very high gamma background will not be overcompensated through a differential change

of saturation to give a negative output which could obscure a real concentration of tritium.

The effective volumes of the two chambers are adjusted by moving a sliding cap on the innermost cylinder to the position which gives a minimum output of net ion current. It is important that this adjustment is made in a gamma field from such a direction which gives the greatest response in the compensating chamber. If this is done we avoid the situation where a certain configuration of sources of gamma radiation can give a net negative output when the monitor would again be insensitive to a concentration of tritium in the environment. It is also important to carry out the balancing of the two chambers in a gamma field which is sufficiently small so that there is not a significant difference in ion collection efficiencies. Adjustment carried out in a high field may result in overcompensation in a low field, where ion collection efficiency in the compensating chamber is greater. The monitor would again be insensitive to tritium.

A portable 1200 cc assembly is shown in Fig. 3. In this instrument (and in the 300 cc model) the electronics is adopted from a commercially produced vibrating reed electrometer* developed for an X-ray monitor. The X-ray monitor, with an ionization chamber of about 280 cc volume, gave a maximum full scale sensitivity of 3mR/hr. As a tritium monitor, with a pair of 300 cc chambers, the corresponding full scale sensitivity is $50(MPC)_a$, and with a pair of 1200 cc chambers the sensitivity is $10(MPC)_a$. Both types have a two decade dynamic range. It may be noted that, at the time of the design, the vibrating reed electrometer was an essential component of the development giving a sensitivity an order of magnitude better than might have been obtained with other portable vacuum tube d.c. electrometers. Air is drawn through the outer ionization chamber with a battery operated pump at 3 litres/min.

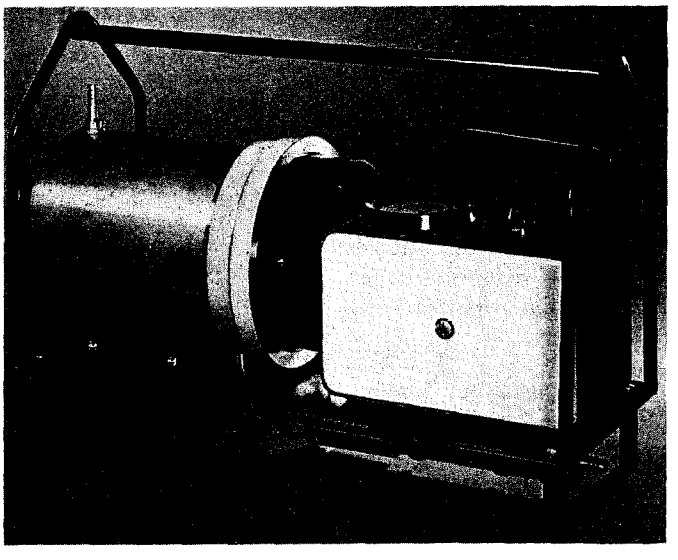

FIG. 3. Portable monitor with 1200 cc ionization chambers.

The details of the construction of the portable chambers are shown in Fig. 4. The cylinders are mounted on a slab of Teflon, the collector is protected with guard rings but only against surface leakage and chamber volumes are adjusted by changing the length of the collector

* Victoreen Model 440.

cylinder. (It is permanently fixed, after adjustment, with a conducting epoxy cement.)

Since it is not possible to entirely eliminate gamma sensitivity by the double chamber technique (and as noted earlier there is a convenience in reducing the gamma sensitivity only by a factor of 50) then at a high enough gamma field a full-scale deflection is obtained on the least sensitive range. At this point the instrument may not detect tritium.

One simple expedient which is useful when the portable units have to be operated in an extremely high gamma field which is interfering with the instrument performance is to switch off the circulating pump in the location of interest and remove the instrument while it still contains a representative sample to a lower gamma background. Often the instrument has to be moved only a few metres to reach a satisfactory field where a reading can be made.

Because the activity is in the form of water vapour, in addition to the time required to replace the enclosed air, the instrument will have a memory which depends on:

(a) The time taken to exchange the tritiated water bound by sundry mechanisms to the interior surface of the ion chamber,

(b) The time taken for tritiated water contained in field free regions (and in draft free regions) such as the joints between insulators and metal surfaces to escape into the main volume of the chamber and be flushed out.

The memory effects are important in the

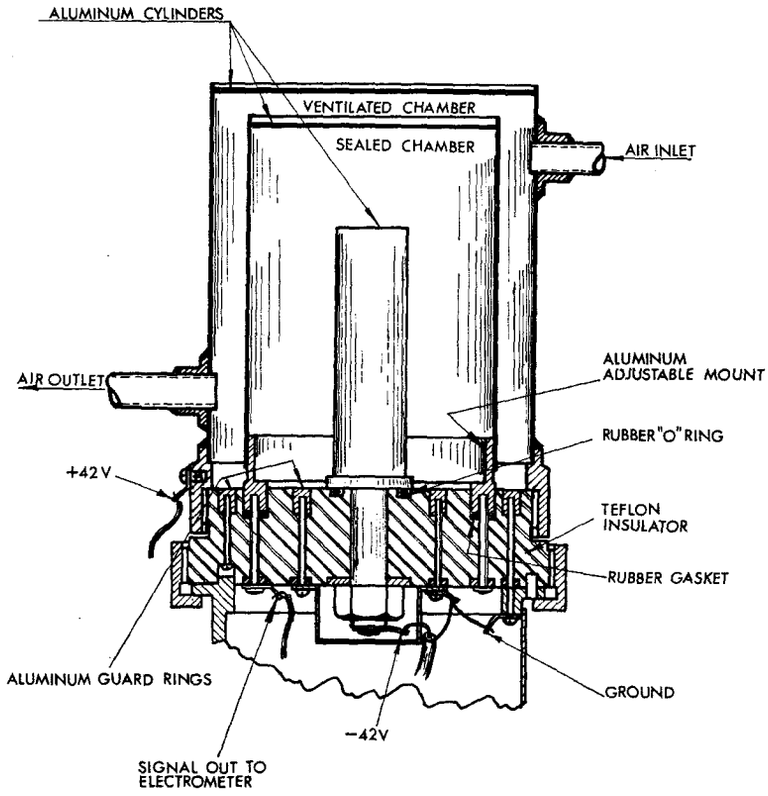

FIG. 4. Details of 1200 or 300 cc ionization chamber assembly.

portable monitors which may be used in quick succession in locations of widely differing tritium concentration.

The response to a pulse of tritiated water is shown in Fig. 5. One way of speeding up the recovery time is to clean out the chamber with humid air. By increasing the water content of the air the reduction of the activity of the bound water on surfaces is accelerated. The recovery obtained when air is passed through a amplifier (Nexus Type SA-1) when driven from a 1200 cc chamber can yield a full scale maximum sensitivity of $3(MPC)_a$. One tenth of this concentration would be measurable. The input resistor had a value of $2 \times 10^{13}\Omega$ and drift of the circuit over one day periods corresponded to a tritium concentration of less than $0.3(MPC)_a$.

Organic scintillators in the form of crystals, liquids, or plastics, are well established as

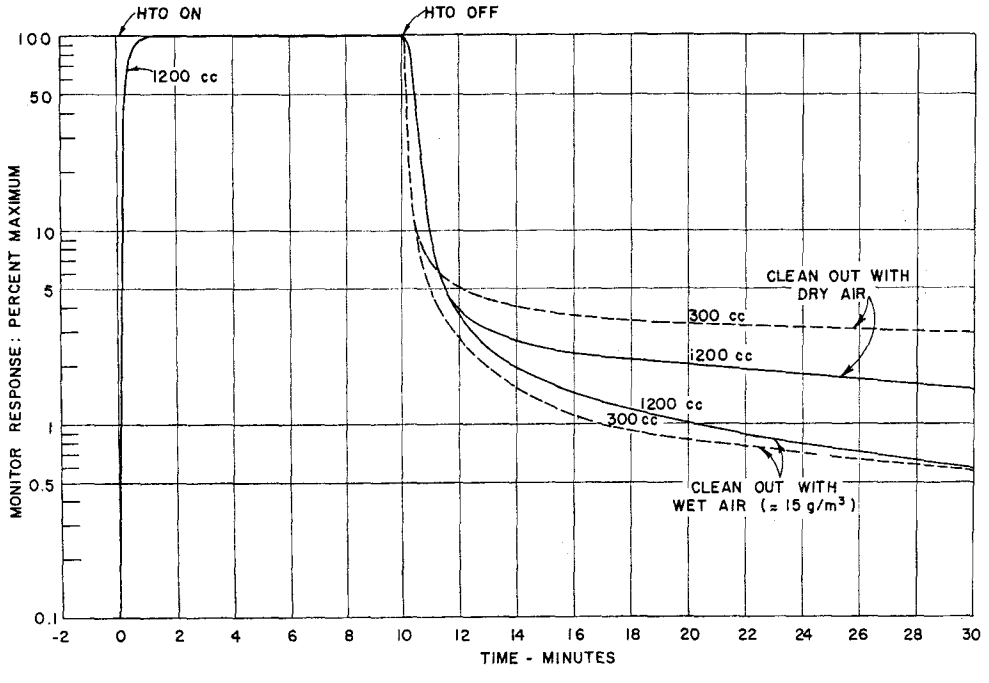

FIG. 5. Response of portable monitors to 10 min pulse of tritium.

water bubbler is also shown in Fig. 5. It is quite a simple matter for the operator of the portable monitor to carry a small water bubbler to be used as needed.

Future developments in ionization chamber methods should be directed towards simplification of the electrometer unit which is expensive. An attractive possibility is the use of a metal oxide semi-conductor field effect transistor in a simple d.c. electrometer circuit. With this device both cost and weight might be significantly reduced. Tests have shown that a 2N3610 transistor feeding an operational detectors of tritium. Because of the low energy of tritium beta particles the resultant pulses from the photomultiplier are comparable to those from thermal noise and the associated electronics has been complex and quite bulky. Tritium assay by scintillation methods has therefore been a technique for the counting room operator rather than the applied health physicist in the field. The development of sensitive discriminators using tunnel diode circuits greatly simplified the pulse amplifier requirements and the simultaneous development of a suitable scintillation detector for tritium in

air has led to a portable air monitor.[4] The detector in its original form consists of a double spiral of plastic scintillator enclosed in a cylinder of about 5 cm dia and 5 cm length (Fig. 6). The double spiral arrangement permits an air flow path over all the surfaces of the scintillator with an entry and exit port on the side of the enclosing cylinder. Photomultipliers are coupled to the end windows of the cylinder and collect light pulses which reach the windows by internal reflection from the scintillator surfaces. The photomultipliers are operated in coincidence and are connected to a pulse height discriminator. The principal design objective is to minimize the total mass of scintillator since only a surface layer a few microns thick is required to absorb the tritium beta rays and any additional thickness only causes unwanted gamma sensitivity. However it is not practical to manipulate plastic scintillators in sheets having a thickness less than about 100μ so gamma compensation is provided electronically. Three pulse height discriminators provide outputs from which a background-free signal is obtained. The lowest discriminator suppresses random coincidences due to thermal noise and inevitably results in a loss of some pulses caused by tritium. The intermediate level discriminator defines the upper level of the tritium channel. A fraction of the count rate above this discriminator is subtracted from the output of the tritium channel and for a monoenergetic background this correction would be sufficient. In general, background is not of constant quality but by adding a fraction of the output above the highest discriminator to the tritium channel an effective compensation is achieved. The constants of these compensating circuits are chosen so that the monitor is insensitive to backgrounds from Cs-137 and Co-60.

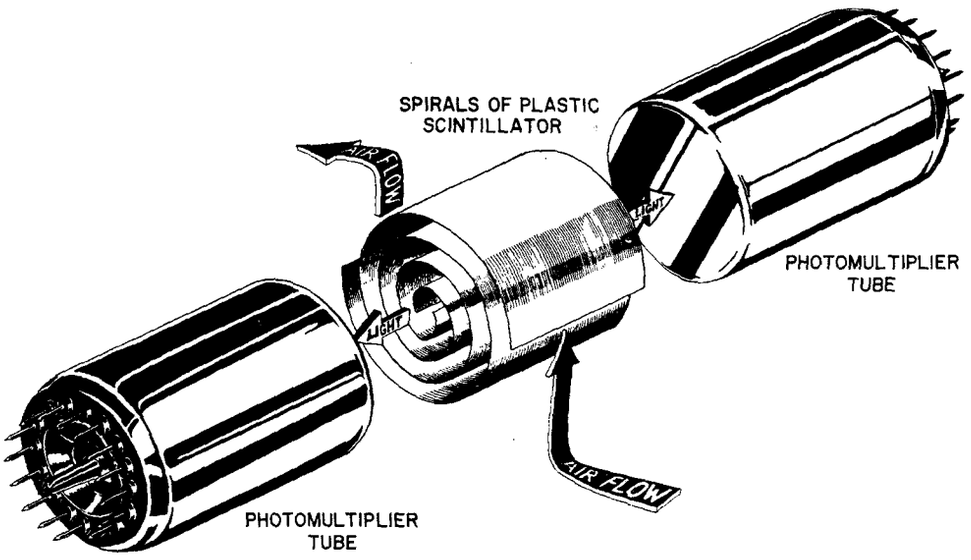

FIG. 6. Spiral-flow tritium detector.

Compensation by electronic techniques is assisted by a small amount of lead shielding around the scintillator unit.

Such an apparatus whose output is a logarithmic rate meter has been operated with a sensitivity extending from $0.2(MPC)_a$ to $10^3(MPC)_a$. In an external gamma field of lmR/hr the monitor reads $0.6(MPC)_a$.

Fabrication of the plastic scintillator spiral has presented certain difficulties and we are developing a labyrinth of flat square sheets of plastic scintillator to replace it.

The problems of memory effects in these devices are similar to those in ion chambers with the additional complication of hairline cracks in glued joints between the scintillator and the windows to the photomultiplier. In addition, rough handling of the scintillator strip while forming it into a spiral shape may cause surface crazing, again providing a reservoir for trapped moisture. A typical recovery characteristic of a spiral unit is shown in Fig. 7.

With all of these methods concentrations of tritium in air can be measured down to the level of about 1(MPC)$_a$. More sensitive techniques are easily conceived but it is questionable whether apparatus with better sensitivity is needed for continuous monitoring. Thus it can be arranged for a cooling device to provide a continuous supply of condensed atmospheric water for assay in an automatic scintillation spectrometer using either liquid scintillator or a bed of organic scintillator crystals.[5] Another approach which avoids a bulky condenser is to use a bed of moist anthracene flakes as an exchanger. We have found that the counting rate from such a system can be made proportional to the total activity in a thirty minute sampling period. The scintillator may then be flushed out with clean water and sampling resumed. However, chronic exposure of workers to fractional (MPC)$_a$'s is quite acceptable and it is sufficient to monitor such a working environment by occasional sampling or integration of total exposure over extended periods such as a whole working day. Such a monitoring facility can be provided by drawing air through a water bubbler and assaying the water for tritium using facilities which exist for other routine functions such as bioassay.

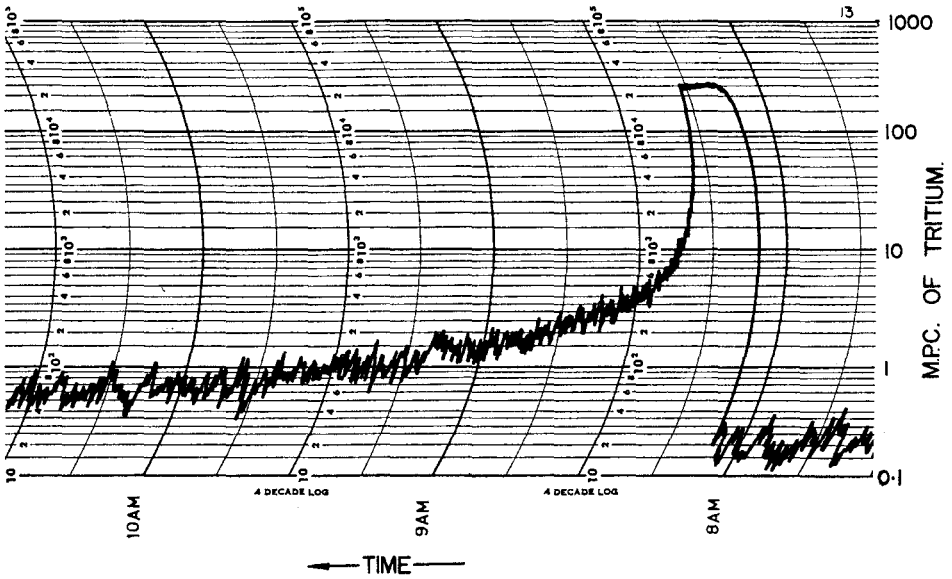

FIG. 7. Response of spiral scintillator detector to tritium pulse.

The integral exposure over a work day of eight hours could be estimated by continuous sampling with the bubbler during this period. A flow rate of 2 litres/min (and a total sampled volume of one cubic metre) would be suitable and would not lead to important losses from the bubbler. Such losses can anyway be estimated by sampling sequentially through two or more bubblers.

A typical liquid scintillation counter will accept a 1 g water sample, count its tritium with an efficiency of 25% and have a background count rate of perhaps 40 counts/min. With such apparatus the background count rate corres-

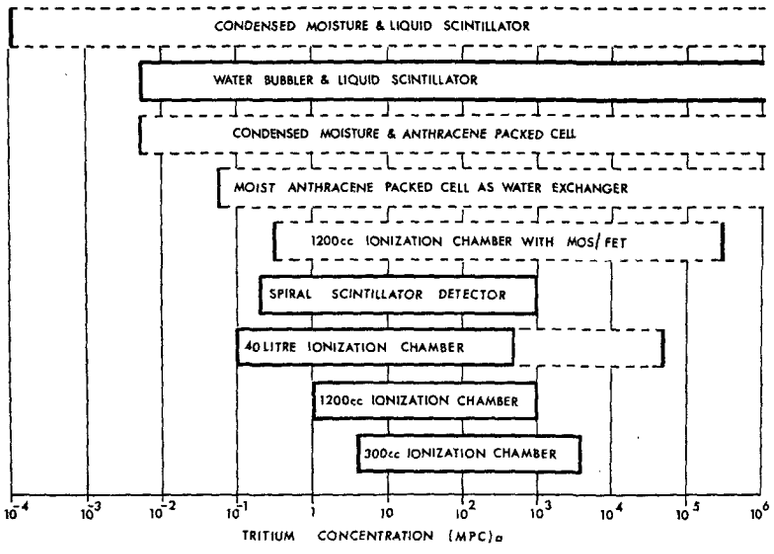

FIG. 8. Comparison of tritium monitoring methods. Complete rectangles indicate methods used routinely. Dotted lines indicate other possibilities. Upper limits are absent in the four cases where the sample may easily be diluted.

ponds to an average tritium concentration in the air passed through the bubbler of 0.005 $(MPC)_a$. Clearly greater sensitivity may be achieved by condensing atmospheric moisture rather than by bubbling and immediately a factor of 20 improvement can be made. In addition the selection of source count rate equal to background count rate is a conservative estimate of the limiting sensitivity of a counter, and a further improvement in performance could be realized. A comparative listing of the sensitivities of several techniques is shown in Fig. 8.

It is important to note however that such sensitivities are far beyond the needs of health physics and properly belong to those interested in such matters as cosmic radiation effects and radioelement dating techniques.

REFERENCES

1. R. V. OSBORNE. Absorption of tritiated water vapour by people. *Health Physics*, 1966, Vol. 12, pp. 1527–1537.
2. G. COWPER and S. D. SIMPSON. A monitor for airborne tritium. AECL 1049, July 1960.
3. R. V. OSBORNE and G. COWPER. The detection of tritium in air with ionization chambers. AECL 2604.
4. F. SANNES and B. BANVILLE. A portable tritium-in-air monitor. AECL 2283, July 1965.
5. J. A. B. GIBSON and A. K. BURT. A method for continuous measurement of tritiated water in air. *J. Nuclear Energy*, Parts A/B, 1966, Vol. 20, p. 185.

A PULSE ANALYSIS SYSTEM AND COMPUTER PROGRAM FOR THE ROSSI LET COUNTER*

ROBERT F. DVORAK
Argonne National Laboratory, Argonne, Illinois, U.S.A.

Abstract—Acceptance of the Rossi LET counter for routine health physics use depends upon the degree to which data collection and analysis can be simplified. This paper describes an electronic system for recording counter events and a computer program prepared for data analysis that contribute toward this end.

In developing this system, we found that spectral stability is significantly affected by voltage and gas purity through the mechanism of varying ion collection time. Circuitry has been developed which delays sampling of the pulse height until full charge collection has been achieved. Operation as a sealed chamber has thereby been achieved over useful periods.

Since the spectra realized are typically exponential in shape, extremely long data collection times are required to achieve statistical significance for the large pulses. To ameliorate this problem, an analog pulse height computer is used to compress the high energy deposition end of the spectrum according to a selectable power function before pulse height analysis is performed.

The data analysis program has been made as flexible as possible to allow further studies in interpretive procedure. The raw data for both radiation field and background (where applicable) are smoothed before determining net counts. The technique used has a minimum of bias as to the spectrum shape. The smoothed spectrum is then analyzed and a probable LET spectrum determined. Since the energy loss spectrum due to mono-LET particles traversing the chamber depends on questionable assumptions, options are included for triangular, exponential, and square stripping functions. From the LET spectrum, the dose and dose equivalent are calculated, and the LET spectrum is smoothed and plotted. Examples are given of the results produced by the system for typical radiation sources.

INTRODUCTION

An instrument capable of measuring the dose equivalent in a radiation field where nothing is known or assumed about the nature of the field would be an extremely valuable tool to the biologist, biophysicist, and health physicist. If this tool is to be useful, it must meet some reasonable requirements involving simplicity and reliability. The Rossi LET chamber,[1] with associated gas supply system, electronics, and calculation techniques as employed today are too complex for routine use in applied Health Physics. This paper describes the work we have done at Argonne National Laboratory to simplify the necessary systems to a point where the Rossi LET chamber can be used reliably and with greater convenience by a health physicist. Utilization of the detector and supporting components must still be restricted to situations where the need for information is sufficiently important as to warrant the cost and time incidental to the use of this instrument.

LET CHAMBER

The Rossi LET chamber is a proportional counter in spherical geometry having a tissue equivalent wall and utilizing a tissue equivalent fill gas. Figure 1 is an X-ray photograph of the 8-in. diameter counter fabricated for us by Dr. H. H. Rossi. In the photograph, the 0.25 in. thick wall of muscle equivalent conductive plastic[2] is seen enclosing a 4100 cc chamber

* Work performed under the auspices of the United States Atomic Energy Commission.

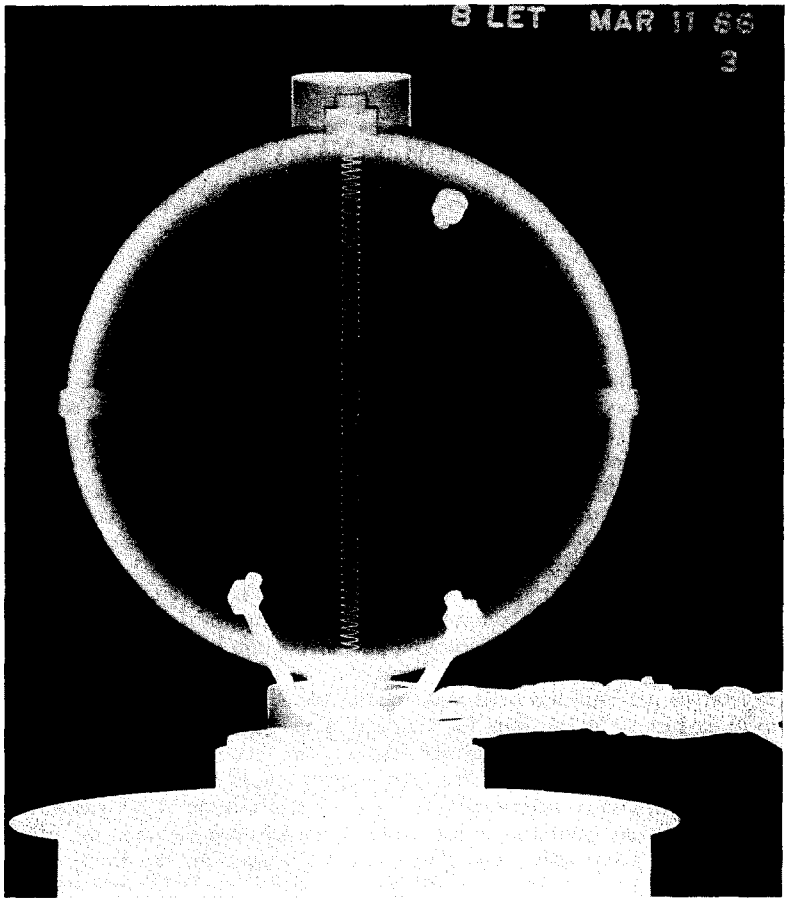

FIG. 1. X-ray photograph of 8-in. diameter LET counter. The opaque object at the upper right is a source holder, objects near bottom are gas inlet and outlet.

cavity. A rather complex sub-assembly penetrating the top and bottom of the sphere supports the 0.25 in. thick diameter grid coil of 0.010 in. diameter stainless steel wire, and accurately locates and supports a concentric 0.0005 in. diameter anode of the same material.

In use, the outer wall is at ground potential, the anode is at a pressure dependent positive potential, and the grid coil is fixed at 50% of the anode potential by a resistive divider. The following sequence of actions occurs in the two regions of the counter. Electrons liberated in the cavity by an ionizing event drift toward the grid under the influence of the electric field. In the region of the grid, the electrons are accelerated toward the anode by the anode field. Proportional multiplication is achieved in a small volume surrounding the anode. The grid serves the dual function of (1) gathering electrons and negative ions and (2) accurately defining the potential gradient in the proportional region of the counter.

The physical analogy simulated by this chamber when it is placed in a radiation field is not entirely clear, but for considerations of radiation equilibrium, the event spectrum should be similar to that at the geometric center of a tissue slab 0.5 in. thick and 8.5 in. in diameter. In setting up the mathematical expressions for the probable cavity path distributions, one must remain with the physical reality (for the chamber described) of a spherical 8 in. diameter cavity that is filled with tissue equivalent gas at low pressure, and is surrounded

by a 0.25 in. thick tissue equivalent wall of approximately tissue density.

Since calibration of energy loss is not direct, but rather is achieved by projecting a collimated beam of alpha particles across a chamber diameter, one is forced to accept the calibration constant

$$K = \frac{\text{LET}_\infty \times \text{chamber diameter}}{\text{pulse height}}$$

as determined with alpha particles to be the same for protons, mesons, electrons, etc. As has been indicated elsewhere,[3] there are a number of additional complications at low particle energies and small effective cavity diameters that can lead to errors in the spectrum, dose, and dose equivalent calculations. However, these errors are probably minor in view of the uncertainties in the LET effect of radiation on biological systems at and below the diameter of a single cell, and the relationship between sub-cellular damage and over-all radiation effect to systems containing a large number of cells.

If one can accept these limitations to accuracy, it is possible to calculate a dose and dose equivalent for the radiation field at the chamber location for the tissue geometry simulated by the chamber.

GAS HANDLING SYSTEM

The Rossi LET chamber is generally used in a continuous gas flow mode to minimize the effects of possible minor leaks, preferential diffusion of fill gas constituents into the plastic wall, and outgassing of detrimental gases and vapors from the wall. The gas system used by Rossi has been illustrated in the literature.[4]

It was decided at the beginning of this development project that the proportional counter would have to be liberated from the gas flow system if any reasonable flexibility of use was to be achieved. When the chamber is used in a periodic-fill mode, the gas handling system is greatly simplified. A schematic of our system is shown in Fig. 2. The transducer for pressure measurement is a simple ionization chamber having the cathode coated with about 500 μc of promethium-147, a fairly low energy beta emitter. Current from the chamber anode is measured by a vibrating reed electrometer. The transducer must be calibrated for the specific fill gas against appropriate mechanical gauges. This method of pressure measurement has no particular advantage over the use of mechanical gauges except in range of measurement, which is from atmospheric down to approximately 0.1 mm. A photograph of the cart-mounted fill station is shown in Fig. 3.

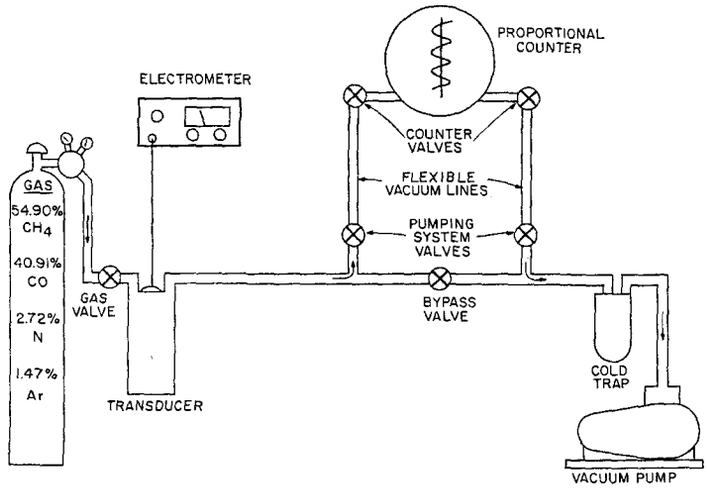

FIG. 2. Schematic of gas handling system for periodic-fill operation.

The fill gas used at present has a composition:

54.90% methane
40.91% carbon monoxide
2.72% nitrogen
1.47% argon

This mixture has an advantage over the more common methane–carbon dioxide–nitrogen mixture[5] in that all components have very similar coefficients of diffusion into the Shonka plastic. It is less than half as expensive as the ethane, ethylene, nitrogen, and neon mixture used by Kastner, Rose, and Shonka,[6] and retains a significant number of oxygen atoms.

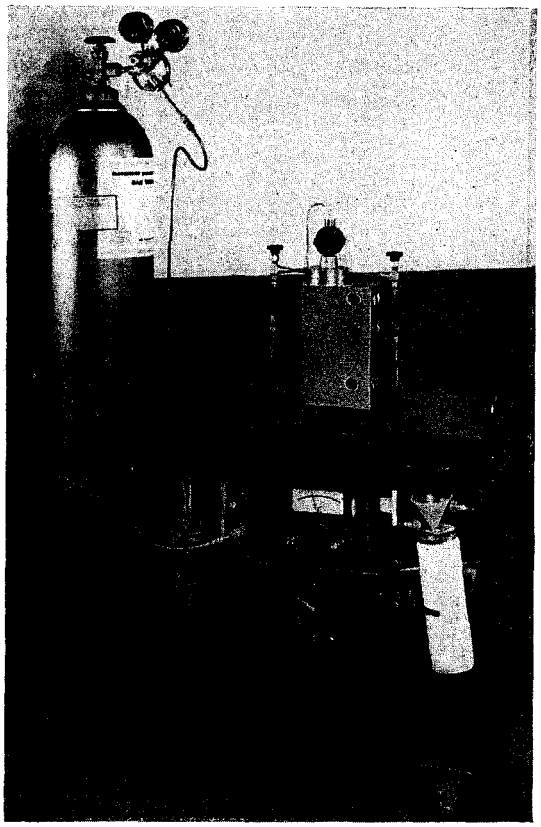

FIG. 3. Cart-mounted gas handling system, showing 2-in. LET chamber and preamplifier in filling position.

When this gas was used under periodic fill conditions, it was found that the multiplication is not completely stable with time, even with extended outgassing prior to filling. The multiplication for the first 8 hr after filling proved to be essentially stable, as shown in Fig. 4. However, an initial aging period of at least 10 min is required during which the multiplication shows a decrease of 1–2%. After 72 hr, the multiplication decreases an additional 6% with no apparent resolution loss. Changes in ambient temperatures appear to be more troublesome, although no quantitative evaluation has yet been achieved.

Under reasonable thermal conditions, the change in proportionality (and hence the calibration constant) is less than 1% in 8 hr. We feel that this does not lead to excessive data error. The data shown here were taken with the 8-in. diameter chamber. With the 2-in. chamber, stability appears to be better.

ELECTRONIC SYSTEM

Several mechanisms have been found which affect the detector pulse shape. First, the time required for full ion collection becomes steadily greater as the gas ages, beginning at 1 or 2 μsec for fresh gas, and eventually exceeding 20 μsec. Second, this collection time is a function of the collection (grid) voltage. Third, at any particular time there will be variations as great as a factor of two in ion collection time, probably depending on location of the ionizing particle track segment within the chamber. Under the described conditions, it is clear that differentiation of the signal pulse cannot be tolerated, and sampling of the pulse height must be delayed until full charge collection is achieved if maximum system stability is to be attained.

This electronic system is designed to take these restrictions into account, and is shown schematically in Fig. 5. The voltage sensitive preamplifier, which serves as a mechanical base for the detector, is a highly modified Oak Ridge design featuring a very low input noise level and very long time constants throughout. The response of the preamplifier to a step function input signal is an output pulse with a rise-time of 80 nsec, and a decay time of 6.8 msec. The gain is 25. In our application, the voltage pulse from the preamplifier is the integral of the charge collected on the input capacitance.

Since, at useful pulse repetition rates, long duration pulses such as these would cause

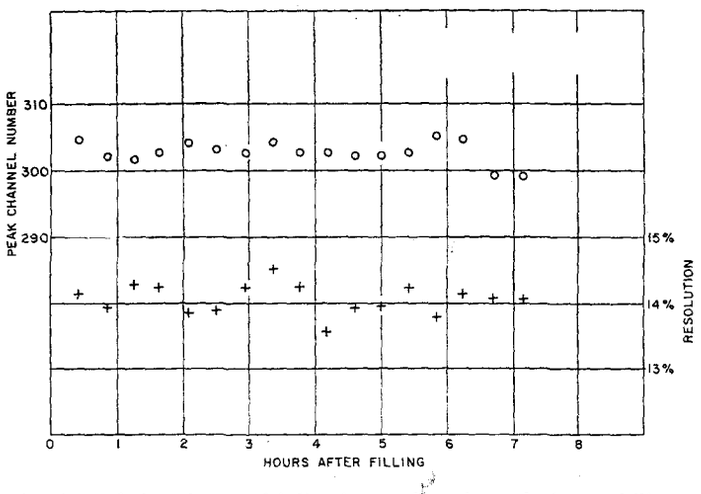

FIG. 4. Determination of chamber multiplication and peak resolution stability. A collimated beam of curium-244 alpha particles projected across a chamber diameter was the source of pulses. The fill pressure was 9 mm.

disturbing bias shifts through pulse pileup, the next circuit element is the Argonne PA 95-B delay line clipper. The pulse may be terminated by reflection at 4, 8, 12, or 16 μsecs, the choice being determined by the conditions under which the measurement is to be made.

Final pulse amplification is performed by the Argonne LPA-5 amplifier. The over-all system response to a step function input signal is an amplifier output pulse with a rise-time of 0.45 μsec and a decay time of 800 μsec that is terminated by the clipper reflection after the selected delay interval. The overall gain of the preamplifier, clipper, and linear amplifier is 1460.

A serious problem with a detector of this type is that the typical pulse height spectrum is roughly exponential in shape. The number of small pulses taxes the memory capacity of the multichannel pulse height analyzer during the time that the number of large pulses per analyzer channel is still statistically very low. It is our feeling that improved statistical accuracy in the number of these high energy loss events is more important than precision in the energy loss determination for each event.

An analog pulse height computer is now

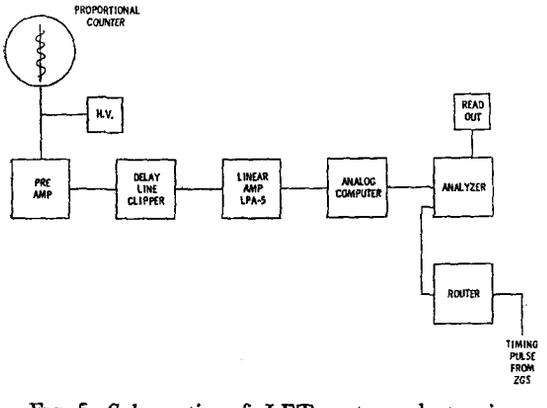

FIG. 5. Schematic of LET system electronic components.

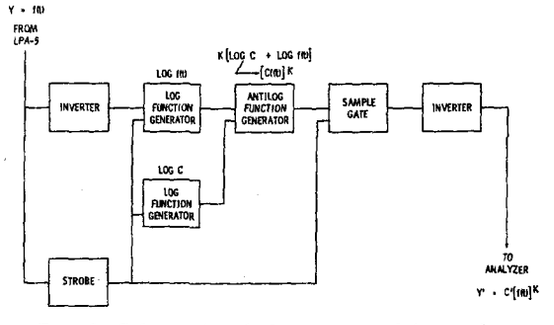

FIG. 6. Schematic of elements used in analog pulse height computer.

available[7] which can perform a spectrum compression that materially aids in this data collection problem. The combination of elements that has been most useful to us is shown schematically in Fig. 6. In our application, the output pulse of the LPA-5 amplifier is analyzed, and a computer output pulse is generated having an amplitude that is a power function of the input pulse height. The pulse shape is square, about 1.5 μsec long, and between zero and + 10 V in height, compatible to almost any pulse height analyzer.

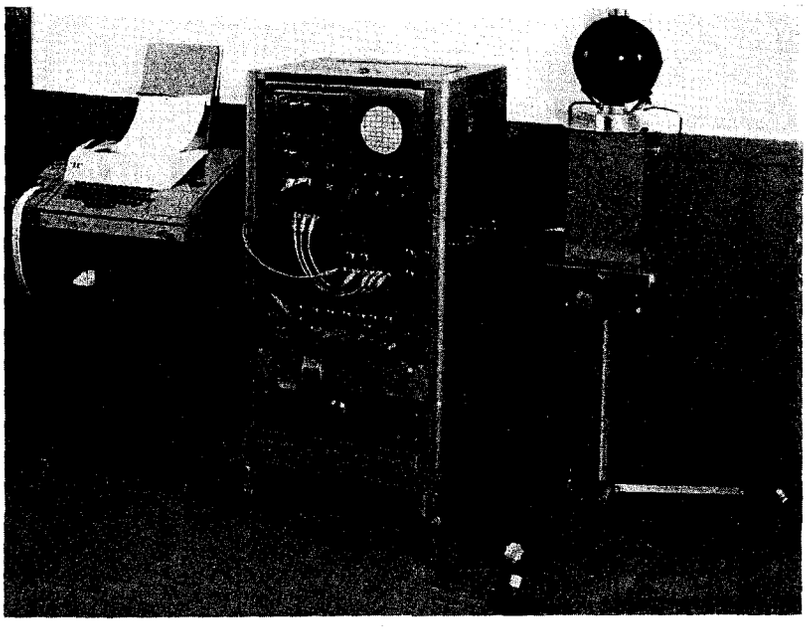

FIG. 7. Component of LET system as used in field measurements. Rack cabinet contains, from top to bottom, the 400 channel pulse height analyzer, the ETC chassis containing amplifier, clipper, router and preamplifier power supply, the analog computer, a high voltage power supply, and a test pulse generator.

The exponent function normally used, 0.5, is near the computer's lower limit of 0.4, and is chosen for simplicity in system calibration. For any exponent less than one, the desired expansion of energy scale for low energy loss pulses and compression of high energy loss pulses is achieved.

The pulses are fed to a 400 channel Victoreen PIP analyzer which has a memory capacity of 10^6 events per channel. In measurements of continuous emission radiation sources, we generally use one quadrant (100 channels) of the memory, and hence can store a total of four separate runs before readout must be made. For measurements of pulsed sources, as at the Argonne Zero Gradient Synchrotron, a routing circuit controls the analyzer. This circuit is triggered by a pulse from the accelerator at the approximate time of proton injection into the ring. The analyzer is gated on and pulses are routed to the first memory quadrant for a preselected interval of time sufficient to cover the entire machine spill period. The analyzer then is held off for a second preselected interval during which routing is changed to the third memory quadrant. Background then is counted for the same length of time as was selected for the machine spill period. The analyzer finally is gated off until the next accelerator timing pulse. In this fashion, the contribution by background events is minimized in the "machine on" memory quadrant and an additional run with accelerator off is not required for background determination. A second pair of runs

can be made in quadrants two and four before readout is required.

The data is delivered in two forms. The total events per channel are simultaneously recorded by tabulated typewriter printout and punched paper tape in ASCII format. The paper tape is then used to prepare the data deck of IBM cards in a format compatible to the computer program. A photograph of the entire system is shown in Fig. 7.

COMPUTER PROGRAM

The most tedious and time-consuming aspect of LET counter utilization is the data analysis. To make application of the counter more attractive to health physics personnel, a computer program was included as part of the instrument development program. A successful program, which requires less than one minute of CDC 3600 computer time has been prepared. In practice, full processed results are available in about 2 hr. The program consists of six steps, of which a number are superfluous to the end point but necessary for careful evaluation of the data.

1. Input data constants are printed out providing run identification, analog computer power function, a channel calibration constant relating channel number to energy loss for the event, keV to ergs conversion constant, fill gas weight, diameter of chamber cavity in terms of equivalent tissue thickness, the exponent for exponential stripping option, the time over which the source data was taken, and the time over which the background data was taken.

2. The raw input data is smoothed using the following technique: To smooth the point K we must consider the sequence of points from $K-2$ to $K+3$. We postulate first that data shall be conserved and that any correction made to K will be compensated in the adjacent channels $K-1$ and $K+1$. We also postulate that no correction will be made unless the necessary compensating correction to K − 1 brings it closer to the average of $K-2$, $K-1$, and K and the correction to $K+1$ bring it closer to average of K, $K+1$, and $K+2$.

The magnitude of the correction is determined by fitting to a cubic curve through construction of a difference table, as indicated in Fig. 8. Setting the fourth differences, $\nabla_4(K)$ and $\nabla_4(K+1)$ equal to zero, one can solve for both β and Δ and the best correction to a cubic curve can be calculated. In the computer program, corrections of only $\frac{\Delta}{20}$ and $\frac{\beta\Delta}{20}$ are applied successively to each K in the spectrum. This smoothing cycle is repeated 100 times.

The raw and smoothed values of both the source and background spectra, as well as the difference between smoothed source and smoothed background spectra are printed out in parallel column format for inspection.

3. The effect of the smoothing program is examined in a rather crude fashion to determine

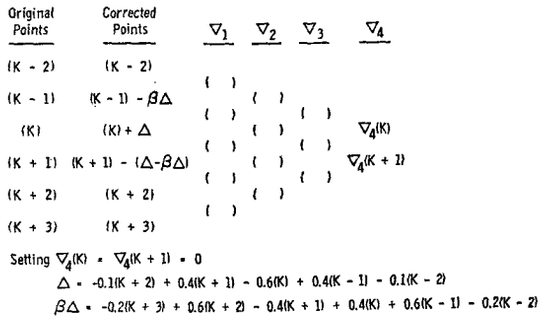

FIG. 8. Conceptual schematic of technique for smoothing a point K. The difference table is indicated and the equations for magnitude of and distribution of the correction are explicitly stated.

where the smoothing has altered a point outside a normal statistical error from the initial data. The first column is the channel number; second column, the square root of the raw event count; third column, the difference between the raw event counts and the smoothed counts; fourth and fifth columns, the same as the second and third except applied to the background counts. In the sixth column, the symbol (1) appears where the difference between smoothed and raw counts exceeds in magnitude the square root of the raw counts for either events or background, and the symbol (2) where the difference is greater than twice the square root of the raw counts.

4. The smoothed data points are normalized

to the proper unit time and analyzed by a subroutine in which the energy loss by events in each energy loss interval is computed and summed. The printout consists of interval number, source counts per unit time, background counts per unit time, energy in keV at the upper limit of the interval, energy in keV at the center of the interval, deposited dose rate for the interval, and cumulative dose rate. The deposited dose rate for the run is the value of cumulative dose rate for the highest K interval.

5. The distribution of events in LET is now determined and from this the dose and dose equivalent distributions in LET are calculated.

Before a calculation can be started, a decision must be made as to the most probable distribution in path lengths for an ionizing particle traversing the chamber. In general, one has no knowledge as to where (in the gas, wall, or exterior environment) a particular event originated and what its actual path length was in the chamber. Rossi and Rosenzweig,[1] and more recently Caswell,[8] have presented arguments leading to a triangular distribution in path lengths for events originating in the cavity wall and traversing the chamber, where the probability per unit path length is directly proportional to the path length. My own feeling is that the assumption of a square spectrum (all path lengths equally probable) also is logically supportable, and that particular cases ranging from square through exponential distributions of the form $A(1 - e^{-\mu})$ to triangular can be demonstrated. In addition, a superimposed

M_{ij} = *Number of Events in LET Interval j Which Traverse the Chamber with an Energy Loss in the Interval i*

$$M_{ij} = \Delta_i\left[\frac{N_j}{\Delta_j} - \frac{N_{j+1}}{\Delta_{j+1}}\right]$$

For Square Path Distribution $\Delta_\ell = E_\ell - E_{\ell-1}$

Triangular Path Distribution $\Delta_\ell = E_\ell^2 - E_{\ell-1}^2$

Exponential Path Distribution $\Delta_\ell = \left[(E_\ell - E_{\ell-1}) - \frac{1}{\beta}\left(e^{-\beta E_{i-1}} - e^{-\beta E_{i-1}}\right)\right]$

Where N_ℓ = Number of Events in Energy Loss Interval ℓ Which Has Upper Bound E_ℓ Lower Bound $E_{\ell-1}$.

FIG. 9. General equation describing the number of events in a given energy deposition interval due to events in a specified LET interval.

$$\text{Events in LET Interval } j = \sum_{i=1}^{i=j} M_{ij}$$

$$\text{Dose in LET Interval } j = \frac{p}{m}\sum_{i=1}^{i=j} \bar{E}_i M_{ij}$$

$$\text{Dose Equiv. in LET Interval } j = g(j)\frac{p}{m}\sum_{i=1}^{i=j} \bar{E}_i M_{ij}$$

where p = constant = 1.60×10^{-9} ERGS/KEV

m = weight of gas in cavity (GM)

$\bar{E}_i$ = average energy of energy loss interval i (KEV)

$g(j)$ = quality factor associated with LET interval j.

FIG. 10. General equations used in calculating the event, dose, and dose equivalent distribution in LET.

and different distribution due to events originating in the cavity gas, is to be expected.[8]

With this uncertainty in mind, the computer program was set up to make the determination using square, triangular, or exponential distribution assumptions, and we routinely calculate all data with both square and triangular assumptions. Techniques for including the noncrossing events are being studied for inclusion in the program.

The computational technique differs somewhat from that of Rossi and Rosenzweig and is similar to spectrum stripping. For an example, let us select the square distribution assumption and no electronic compression. If, in the highest energy loss channel i there are N_i events recorded, then according to the assumptions there are equal numbers of events in each of the lower channels due to particles traversing the chamber on shorter gas paths and having the same LET. Hence, the total number of events of this LET is equal to iN_i. The number N_i is stripped out of each of the i channels, and the process is repeated for the next lower channel. The general equations describing the number of events in a given energy deposition interval due to the events in a given LET interval and the equations for calculating the event, dose, and dose equivalent spectrum are shown in Figs. 9 and 10.

The printout for this step is as follows. The first column is the LET interval, and has direct correspondence to the energy loss interval

in the original data. The second, third, and fourth columns are the number of events, deposited dose, and dose equivalent for the LET interval and the time normalization programmed. The fifth, sixth, and seventh columns are cumulative totals for the same quantities, and the significant cumulative quantities appear in the highest LET interval, being the totals for the run.

6. A third subroutine, primarily for plotting purposes, can be applied selectively to the event, dose, or dose equivalent rate distributions for each of the stripping assumptions programmed. The functions of this subroutine are to determine the average LET for each interval, to normalize the data to unit LET interval, to further smooth from the data some of the irregularities resulting from the stripping program, and to provide various scale information needed by the automatic plotting equipment. A hand-drawn plot of typical output data is in Fig. 11. The case shown is for a 50 channel plutonium–beryllium source spectrum taken with analog computer power funtion of 0.5.

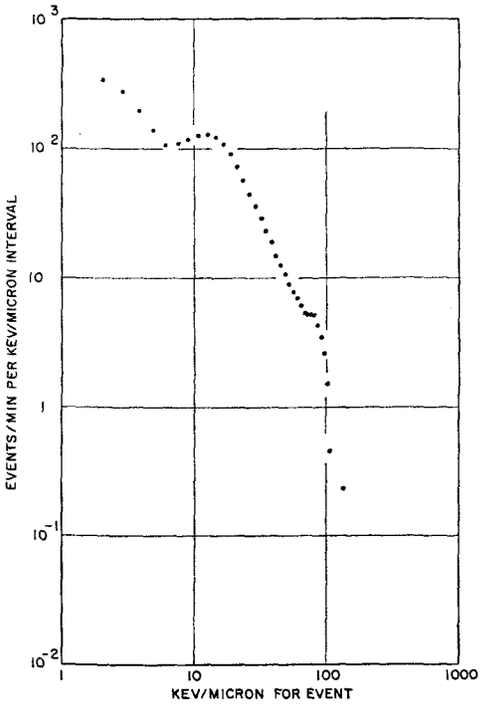

FIG. 11. Plot of output data from computer program. This is the event distribution in LET for a 50 channel spectrum due to Pu-Be neutrons. A total of 130,529 events were analyzed using a square root spectrum compression and assuming a square path length distribution. The typical distribution of data points and degree of smoothing is shown.

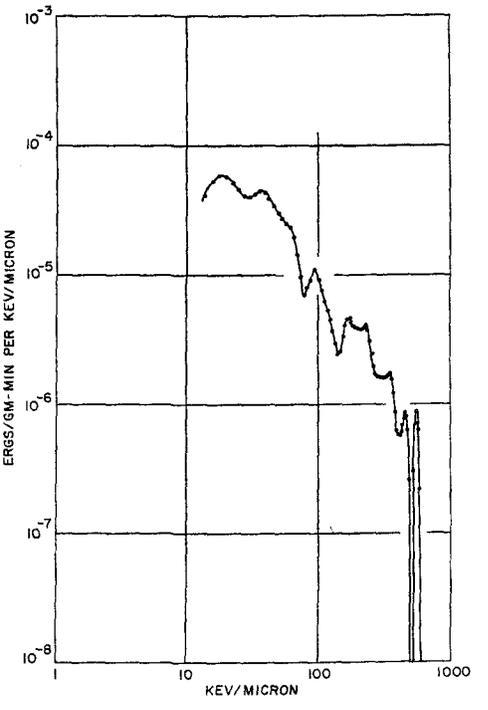

FIG. 12. Dose distribution in LET for plutonium–beryllium neutrons. A total of 107,373 events in 100 channels was analyzed using square root compression, and assuming a square distribution of path lengths.

EXAMPLES OF RESULTS

The following examples of results produced by our system are offered. In each case, the 8-in. diameter chamber was used, the effective cavity diameter was 2.1 microns, and the anode voltage was 660 V.

1. The dose distribution in LET for a plutonium–beryllium source is shown in Fig. 12. The exposure is 80 min at 50 cm from a 4×10^6 n/sec source. The total dose is 2.91 mrad as measured with a tissue equivalent ion chamber of the same dimensions, and a total of 107,373

events were recorded above a 27.2 keV energy loss discriminator level.

2. The dose distribution in LET shown in Fig. 13 is taken under identical conditions to the previous run except that the exposure time was 4 min, resulting in a total dose of 0.145 mrad and a total of 5207 events. As can be seen, the distributions differ only in detail.

3. The dose distribution in LET for a cobalt-60 gamma source is shown in Fig. 14. The exposure is 5.51 mrad for the 40 min run as measured by the ion chamber, resulting in 507,229 events above the 2.0 keV discriminator level. Analysis of the results yields an effective quality factor of 1.09 for this radiation. Since the secondary electrons causing these events do not generally travel in straight line paths across the chamber, the results shown here certainly cannot be accepted at face value.

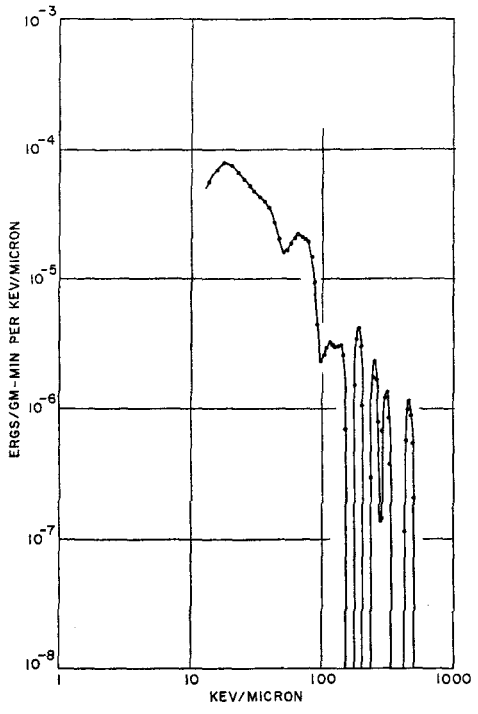

FIG. 13. Dose distribution in LET for plutonium–beryllium neutrons. A total of 5,207 events in 100 channels were analyzed using square root compression and assuming a square distribution of path lengths.

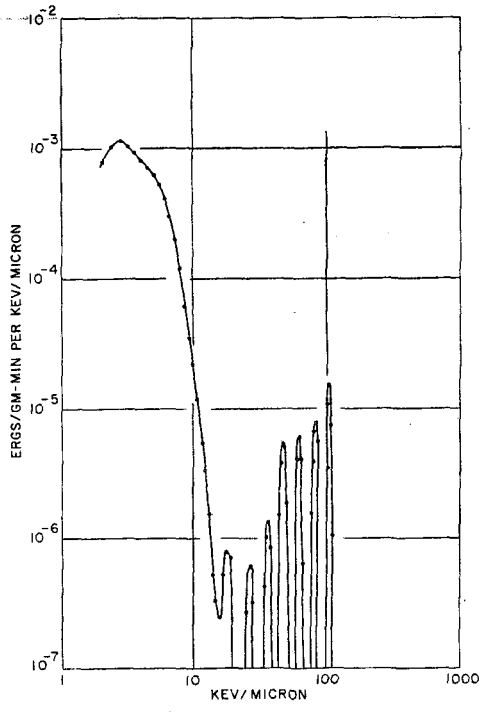

FIG. 14. Dose distribution in LET for cobalt-60 gamma rays. A total of 507,229 events were analyzed using square root compression and assuming a square distribution of path lengths.

4. The dose distribution in LET for a measurement at the Argonne Zero Gradient Synchrotron is shown in Fig. 15. The radiation source was 12.7 BeV protons on a 0.5-in. thick copper target. The detector was placed at a scatter angle of 60° and the shielding at this angle was 5.2 ft of concrete. The detector was located on top of the external proton beam shield. The total dose was 2.25 mrad, measured as before, and resulted in 153,677 events in the 12 min exposure period above a 22.1 keV discriminator level. Analysis of the data indicates an approximate value of 3 for the quality factor.

CONCLUSIONS

An electronic system and computer program has been described which, when utilized with the Rossi LET chamber, produces an assessment of dose, dose equivalent, and quality factor for a radiation field. In addition, distributions in

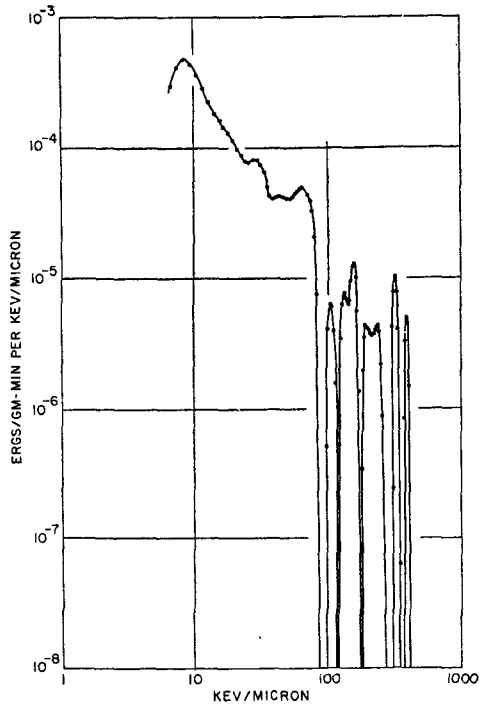

FIG. 15. Dose distribution in LET for radiation from Argonne Zero Gradient Synchrotron. A total of 153,677 events were analyzed using square root compression and assuming a square distribution of path lengths.

LET of the events, dose, and dose equivalent are generated for reasonably small values of dose and consequently short exposure times.

While the system must still be operated by well-trained personnel and the amount of equipment needed to make the measurements is quite impressive, I feel that this system represents a considerable advance in convenience over the currently used systems, and that it attains such improvement without loss in accuracy.

ACKNOWLEDGEMENTS

I would like to express my deepest appreciation to H. R. Sebastian who has assisted in the equipment fabrication, testing, data collection, and preparation of this report. I would also like to thank A. J. Strecok for his assistance in the development of the computer program, and R. W. Fergus for his assistance in design and development in many parts of the electronic circuitry.

REFERENCES

1. H. H. ROSSI and R. ROSENZWEIG. A device for the measurement of dose as a function of specific ionization, *Radiology* **64,** No. 3, 404–410 (March 1955).
2. F. R. SHONKA, J. E. ROSE and G. FAILLA. Conducting plastic equivalent to tissue, air, and polystyrene, *Proc. Second International Conference on Peaceful Uses of Atomic Energy*, Paper 753, Geneva, 1958.
3. Physical aspects of irradiation, *ICRU Handbook* 85, pp. 29–30. National Bureau of Standards, March 1964.
4. Annual Report on Research Project, *NYO*-10050, p. 55. January 1, 1962.
5. H. H. ROSSI and G. FAILLA. Tissue equivalent ionization chambers, *Nucleonics* **14,** No. 2, 32–37 (February 1956).
6. J. KASTNER, J. E. ROSE and F. R. SHONKA. Muscle equivalent environmental radiation meter of extreme sensitivity, *Science* **140,** 1100–1101 (June 7, 1963).
7. M. G. STRAUSS and R. BRENNER. General purpose analog pulse height computer, *Review of Scientific Instruments* **36,** 1857–1876 (December 1965).
8. R. S. CASWELL. Deposition of energy by neutrons in spherical cavities, *Radiation Research* **27,** 92–107 (January 1966).

MEASUREMENTS ON SLOWING DOWN SPECTRA OF SECONDARY ELECTRONS IN ALUMINIUM AND COPPER FROM ^{60}CO γ-RADIATIONS

N. ODA* and J. T. LYMAN

Lawrence Radiation Laboratory, University of California, Berkeley, California, U.S.A.

Abstract—Spectral distributions of the fluxes of secondary electrons produced by a collimated beam of ^{60}Co γ-rays, inside media such as aluminium and copper for five different angles—30, 60, 90, 120, and 150°—relative to the incident direction of γ-rays, were experimentally determined using a lithium-drifted silicon detector.

Targets of the spherical cavity were used, having a circular opening exit on the cavity wall. Secondary electrons inside the cavity were extracted through the exit and absorbed in a silicon crystal. The target wall was of the thickness sufficient to ensure the electron equilibrium inside the cavity.

In order to subtract the background due to various sources, dummy targets were also used, which were of the same weight as the spherical targets and of the doughnut shape, for secondary electrons from the dummy targets not to reach the detector. The target and detector assembly was built in a vacuum chamber and the silicon crystal was cooled by liquid nitrogen.

The spectra were corrected for the spectral distortion due to the backscattering of incident electrons from silicon crystal, by using the back-scattering data obtained with an air core magnetic spectrometer over the energy range measured (25–1100 keV).

The results show that the electron spectra slightly differ between aluminium and copper and remarkably depend on the angles, that is, the higher energy components increase with the decrease of angles. This result is considerably of interest for the reason that the observed spectra are a kind of the black body radiation and was expected to be nearly isotropic.

* Present address : Research Laboratory of Nuclear Reactor, Tokyo Institute of Technology, Ookayama, Tokyo

DISCUSSION

D. BLANC (*France*):

1. Quelle est votre opinion concernant l'emploi possible de détecteurs de silicium à barrière de surface et diffusion de lithium? Ils sont utilisables à la température ambiante et semblent pouvoir donner de bons résultats dans certaines des mesures dont vous avez parlé.

2. Pourrais-je avoir des détails concernant votre technique de fabrication des détecteurs à cavité du type "puits"?

J. LIPPERT:

1. Due to the low photopeak efficiency this will not be advisable except in the low energy range up to about 50 keV. I do not see however any reason to use silicon detectors, as germanium detectors with thin windows will be available in the near future.

2. You will find information on fabrication methods in the literature.

K. J. VOGT (*Germany*):

Für die praktische Anwendung bei der Abschätzung von Gefahren, die in Verbindung mit den Freisetzungen radioaktiver Abluft von Reaktoren in die Atmosphäre entstehen, stellt das Modell der homogenen Kugelquelle eine zu grosse Vereinfachung dar. Hierbei muss die tatsächliche Verteilung der Radioaktivität der Wolke oder Abluftfahne aufgrund der meteorologischen Bedingungen berücksichtigt werden. Es soll in diesem Zusammenhang auf die Arbeiten von Holland und anderen Autoren verwiesen werden, bei denen die Vielfachstreuung über den Aufbaufaktor berücksichtigt wird. Die Bedeutung der vorliegenden Arbeit besteht nach meinem Verständnis darin, die Zulässigkeit dieser Prozedur zu bestätigen.

A. SCHMIDT (*Germany*):

Das Ziel der Arbeit war die Überprüfung der Genauigkeit des Dosiswertes, der mit Hilfe des Build-up-Faktors berechnet wird. Hierbei zeigte sich, dass der mit dem Build-up-Faktor berechnete Dosiswert mit grossen Fehlern behaftet ist, wenn die Entfernung der Wolke vom Beobachtungsort klein ist, d.h. in Luft kleiner als etwa 300 m. In der Literatur wird der Build-up-Faktor auch zur Berechnung der Dosis für Volumenquellen in geringer Entfernung benutzt. Die betrachtete Geometrie ist eine starke Vereinfachung der wirklichen Geometrie. In meiner weiteren Arbeit werde ich vorhandene Grenzen und Grenzschichten zwischen mehreren Medien berücksichtigen.

P. CANDES (*France*):

Quelle est la proportion de la dose due au rayonnement diffusé, par rapport au rayonnement direct, à quelques km de la source?

A. SCHMIDT (*Germany*):

Die durch die direkte Strahlung verursachte Dosisleistung ist sehr viel kleiner als die Dosisleistung der gestreuten Strahlung, falls die Entfernung gross ist. Bei einer Entfernung von 1000 m–2000 m in Luft, d.h. *ca.* 10 mfp bei einer Energie von *ca.* 1,5 meV, ist die Dosisleistung der direkten Strahlung *ca.* 15% der gesamten Dosisleistung.

F. BERTHOLD (*Germany*):

There exists another solution to the problem of continuous tritium monitoring, including gamma-compensation. A flow-through proportional counter may be used, constructed similarly to those used for age determination. An inner sample-counting volume is surrounded concentrically by a multiple-wire guard-counter volume, the two volumes being separated only by a cathode grid. The total volume is 1·3 liters, sample volume about 30%. A 1:1 mixture of the air to be measured and methane is pumped through the detector, and using an anticoincidence circuit only those pulses occurring in the sample counter itself are registered. This ensures that only particles with very short range are measured, and therefore the system is highly selective for tritium, and has very low background (10 cpm behind 1 cm of lead, less than 1 cpm behind 10 cm of lead). This instrument is similar to one described earlier by R. Ehret, H. Kiefer and R. Maushart, in "Direct Information" of the ESG/ESRP/SEPCR, 2/63. With coaxial construction the counting gas consumption is now considerably reduced. In both systems the sample counter "walls" consist only of an array of thin wires, thereby virtually eliminating memory effects, even for HTO. Gamma-compensation is achieved by subtracting from the anticoincidence count-rate a small and adjustable part of the count-rate of the guard-counter in a difference ratemeter.

A theoretically better approach would be to use the rate of coincident pulses for gamma-compensation because in this case one would not also subtract some of the pulses produced by tritium in the guard-counter. However, the performance of this simple gamma-compensation method has been proven to be practically equivalent.

A concentration of 10^{-7} μ Ci/cm^3 can be detected, this being well below the MPC for tritium.

The complete tritium-monitor with detector, gas flow regulation and electronic system (consisting of standard transistorized modules according to the ESONE-system) and recorder is contained in three 19 in. racks, and it is already used successfully in a number of nuclear installations.

J. A. Auxier (*U.S.A.*):

In view of the difference of opinion between experts, relative to whether the pulse height distribution for a given LET should be triangular or square in shape, I wonder if an empirical relationship of pulse height and QF would not only be justified, but desirable from an application point of view.

R. F. Dvorak:

I will answer this in two parts. First, we had studied these spectra using both triangular and square distribution assumptions. The numerical values for dose equivalent turn out surprisingly close, differing by perhaps 30% and depending on the spectrum studied. The LET distributions are also found to be very similar. It would seem that the choice is not crucial.

Second, Dr. Baum at Brookhaven has been working on just this question and mathematically at least there is such a relationship.

J. Booz (*Euratom*):

I have a question on the CO that has been used. What about the electronegativity of this gas? I wonder if you might lose some electrons and what might be the influence on the measured spectrum.

R. F. Dvorak:

Certainly many electrons are lost. All of the better tissue equivalent gases are quite electronegative. For the purpose of achieving stability it seems better to start with the more electronegative gas which is stable rather than a better gas and have rapidly changing multiplication.

N. Oda:

The slowing-down spectra of secondary electrons just inside the medium irradiated by Co^{60} γ-rays were measured for angles 30°, 60°, 90°, 120°, and 150° with Li drifted Si detectors. Specially careful consideration was required to set up the collimators which consist of the lead one and the U^{238} depleted metal. The backscattering effect of the Si detector was corrected for with the use of the data obtained with mono-energetic electrons coming from the air-core magnetic β-spectrometer. The results show that the difference between a copper target and an aluminium one were not remarkable, but the spectra shapes change remarkably with the angle relative to the incident γ-ray. For aluminum, one can see the traces of plural scatterings of the Compton peak electrons for small angles.

ACCURACY CONTROL IN LOW-LEVEL MEASUREMENTS

M. M. FERRARIS and D. MERTEN
International Atomic Energy Agency, Vienna

Abstract—One practical way to determine the accuracy of low-level measurements consists in organizing series of inter-comparison measurements amongst the largest possible number of qualified laboratories. These measurements should be executed on samples possessing the same characteristics as those which are routinely employed, and following the same measurement techniques. The IAEA has been organizing inter-comparison measurements since 1964 and the results of these two years confirm the necessity of this inter-comparison.

The following samples have been analyzed: milk, soil, rice, meat, bone, different kinds of vegetables and a mixture of dried food.

The following radionuclides have been determined: ^{90}Sr, ^{137}Cs, ^{226}Ra, ^{210}Po, and the stable elements calcium, strontium and potassium.

The results obtained cover a wide range. Statistical analysis proves the existence of systematical and accidental errors, the first being easier to identify than the second.

It has been observed that some laboratories which at the beginning of the measurement series gave results which were far from the average, have little by little improved their findings after the results of other laboratories were made known to them.

The participation, except for some items and some radionuclides, has been quite remarkable, about 80 laboratories in 27 countries. It is hoped that the number of laboratories participating in this inter-comparison will still increase, so that all data in relation to the environmental radioactivity may be comparable.

INTRODUCTION

It is well known that laboratories may at times experience difficulties in the determination of the accuracy of their low activity measurements. The use of suitable standards provides means for reducing these difficulties, but the most practical way consists probably in organizing a series of inter-comparison measurements amongst the largest possible number of qualified laboratories, with samples of the same matrix as those which are employed routinely. This method has also the advantage of giving a general picture of the accuracy of such types of measurements, accuracy which is quiet often overestimated.

The IAEA carried out a first small-scale inter-comparison run in 1962/3.[1, 2] The results were so discouraging that it became necessary to carry out the project on a larger scale. Table 1 summarizes the results of inter-comparison runs in 1964/5.[2, 3] It will be seen that a wide range of results was obtained. Unfortunately no questionnaires on the analytical methods and the standards adopted were used for this first inter-comparison run. The reason for possible errors is therefore unknown. The data obtained from this first run indicated that of 70 laboratories which submitted results of analyses of ^{90}Sr, 26 were always correct, 8 gave results containing systematic errors, and 36 with accidental errors. Of 51 laboratories which submitted results of analyses of ^{137}Cs, 24 were always correct, 3 gave results containing systematic errors, and 36 results with accidental errors. Of 51 laboratories which submitted results of analyses of ^{137}Cs, 24 were always correct, 3 gave results containing systematic errors, and 24 results with accidental errors. We come therefore to the conclusion that less than 50% of low-activity measurements are correct within $\pm$ 15% error, and the remaining are doubtful.

On looking at these results it could be argued that the samples submitted for analysis could not

Table 1. *Value in pCi/kg*

Nuclide	Matrix	No. of results	No. of laboratories	General mean (95% C.L.)	Best verified values (95% C.L.)	No. of laboratories giving the best verified value
^{90}Sr	Bone ash	181	31	6450 ± 1600	6560 ± 930	25
	Bone ash	125	26	185,000 ± 66,000	181,000 ± 28,000	18
	Meat dry	159	32	18.9 ± 40	7.6 ± 2.8	17
	Meat ash	177	27	4470 ± 30,000	1620 ± 300	20
	Milk powder	342	56	57 ± 28	53 ± 8	34
	Vegetation	167	34	804 ± 680	837 ± 152	18
	Vegetation	117	23	2333 ± 1700	2522 ± 327	15
	Soil	90	19	254 ± 600	193 ± 41	14
	Rice	98	15	64 ± 17	62 ± 8	10
^{137}Cs	Meat dry	138	30	86 ± 128	51 ± 13	16
	Meat ash	174	28	57,000 ± 19,000	57,000 ± 8000	22
	Milk powder	194	37	2220 ± 1170	2400 ± 400	29
	Vegetation	146	33	800 ± 745	674 ± 145	21
^{226}Ra	Bone ash	40	8	290 ± 1200	114 ± 45	6
	Milk	33	8	193 ± 1000	1.33 ± 45	5
	Vegetation	23	5	140 ± 630	9.7 ± 2.7	3

Table 2. *Value in pCi/kg or g/kg*

Nuclide	Matrix	No. of results	No. of laboratories	General mean (95% C.L.)	Best verified values (95% C.L.)	No. of laboratories giving the best verified value
^{137}Cs	Mixed diet	177	35	355 ± 170	350 ± 36	18
^{90}Sr	Mixed diet	172	31	139 ± 34	136 ± 15	23
^{226}Ra	Mixed diet	37	7	5.16 ± 7.90	2.93 ± 1.06	4
K	Mixed diet	179	34	7.06 ± 2.48	7.26 ± 0.44	21
Ca	Mixed diet	150	31	3.48 ± 1.36	3.58 ± 0.34	18
Sr	Mixed diet	49	12	$(7.7 \pm 15.6) \times 10^{-3}$	$(5.6 \pm 4.8) \times 10^{-3}$	10
^{210}Po	Tobacco	27	5	1257 ± 2100	775 ± 435	3
^{210}Po	Meat	18	4	31 ± 24	—	—
^{210}Po	Bone	19	5	169 ± 285	242 ± 58	4

have been well homogenized. This, however, can reasonably be excluded since of 100 samples submitted 10 were completely analyzed and 30 were controlled by gamma spectrometry in the IAEA laboratory to ensure that the measurements were within $\pm$ 5%. It could also be argued that because the precise weights of the samples distributed were not reported, and the results were required in pCi/kg of original matter, it is possible that differences in the humidity content could have affected the results to a small extent. From now on all samples contain the indication of the original weight. To eliminate this possible source of error, in some cases we also request data concerning other nuclides in the same sample.

Data are elaborated by means of analysis of variances with several criteria of sorting [4,5] nuclide, matrix, methods, etc. In this way data are classified in consistent groups which may be observed in the tables.

RECENT RESULTS

Table 2 contains data obtained after the 1965/6 run (until 5 August 1966). It will be observed that these results are more homogeneous than those of the former run. It must be noted, however, that most of these results come from laboratories which gave already the more homogeneous results in the former run. Only very few results have been received for measurements of ^{226}Ra and ^{210}Po. Unfortunately the percentage of laboratories which submitted the results of their analyses is very low: less than 20% for nuclides such as ^{226}Ra and ^{210}Po, and about 40% for the others.

Figure 1 relates to ^{137}Cs in mixed diet. In this figure, as in all others, the y-axis indicates the number of laboratories and the x-axis the reported specific activities. The plotted step-curve indicates the number of those laboratories which accept as a result, within the standard error limit (95% C.L.), the corresponding specific activity values. This way of presenting data is made so as to give an idea of the frequency of the different values, independent as much as possible of the number of results submitted by each laboratory. Table 3 shows the results after a statistical analysis. As may be observed, apart from two laboratories which have submitted "extreme" results, the others are sufficiently in agreement, even if they could be divided into four distinct groups. Nine analytical methods are adopted by the laboratories, the most common of which are:

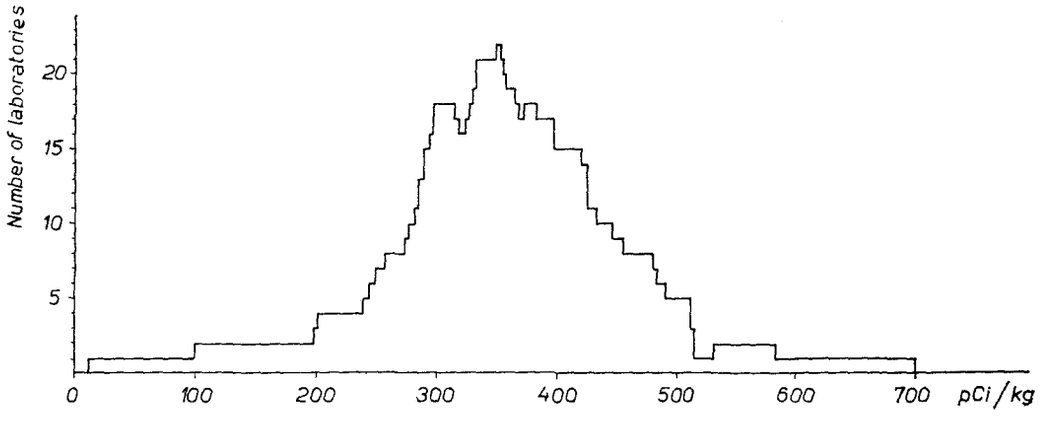

FIG. 1. Distributions of results of the analysis of ^{137}Cs in mixed diet.

(a) ashing of the sample followed by a gamma spectrometry of the ashes, this method is adopted by 11 laboratories, 8 of which are in the range 350 $\pm$ 36;
(b) gamma spectrometry of the original sample, adopted by 8 laboratories, 3 of

Table 3. ^{137}Cs *in Mixed Diet, pCi/kg*

No. of laboratories	No. of countries	No. of results	Mean (95% C.L.)
1	1	5	120 ± 107
4	4	23	270 ± 52
5	4	26	298 ± 35
18	8	97	350 ± 36
8	4	31	414 ± 52
1	1	5	689 ± 157
35	12	177	355 ± 170

which are in the range 350 ± 36 and 4 in the range 414 ± 52;

(c) Cs separation by means of AMP followed by gamma spectrometry adopted by 4 laboratories, 1 of which is in the range 350 ± 36, 2 in the range 414 ± 52, and 1 in the range 298 ± 35;

(d) Cs separation by means of AMP followed by beta counting adopted by 4 laboratories, 3 of which are in the range 350 ± 36 and 1 in the range 689 ± 157 (most probably this last one was still contaminated by K).

The other methods are adopted by one or two laboratories.

As can be seen, no method may be rejected *a priori*. The comparatively high number of laboratories adopting the gamma spectrometry of the original sample giving results slightly over the probable true value is surprising. It could be argued that the other laboratories may have lost some Cs during the ashing, but this is hardly credible. It is more probable that some errors may come from background subtraction or from the geometry of the sample.

Figure 2 relates to ^{90}Sr in mixed diet. The relevant data (after statistical analysis) are summarized in Table 4. It will be observed that the homogeneity of the results is better than for ^{137}Cs. This happened also in the previous inter-comparison run. It is surprising if one thinks that the ^{90}Sr analysis involves generally a higher number of chemical manipulations than ^{137}Cs. Nineteen laboratories

Table 4. ^{90}Sr *in Mixed Diet, pCi/kg*

No. of laboratories	No. of countries	No. of results	Mean (95% C.L.)
1	1	5	93 ± 13
2	2	12	121 ± 13
23	11	125	136 ± 15
5	4	27	158 ± 16
2	2	12	175 ± 55
31	12	172	139 ± 34

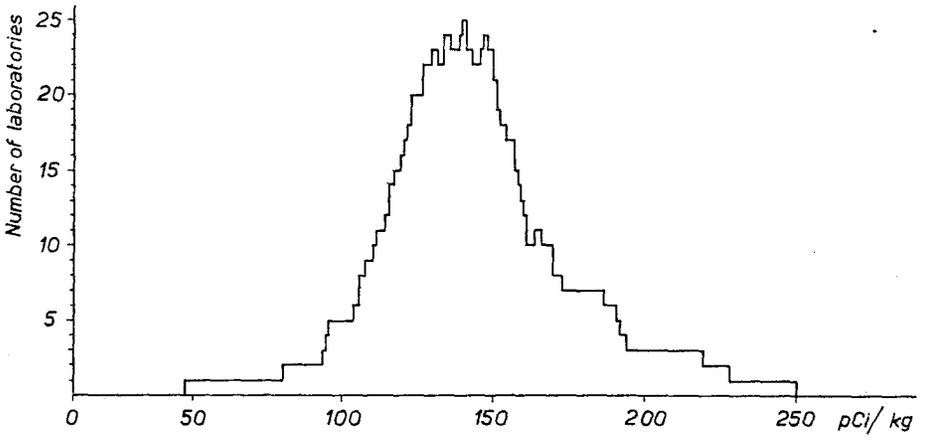

FIG. 2. Distributions of results of the analysis of ^{90}Sr in mixed diet.

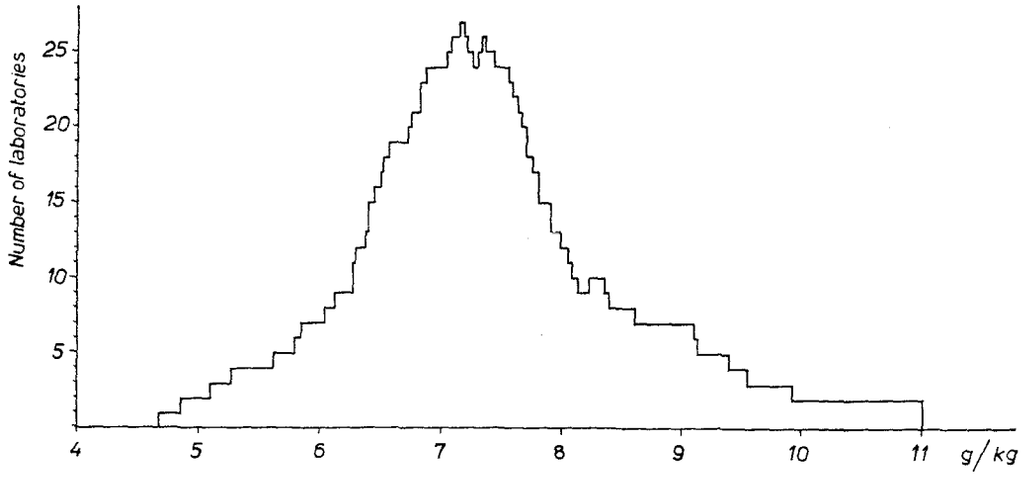

FIG. 3. Distributions of results of the analysis of K in mixed diet.

have adopted the fuming nitric acid separation of Sr followed by Y separation and ^{90}Y beta counting (there are, however, some differences in the determination of chemical yield of Sr separation). Fifteen of these laboratories are in the 136 ± 15 range. Two laboratories have adopted the nitric separation for Sr but do not separate Y and count $^{90}Sr + ^{90}Y$. Both are in the 136 ± 15 range. Two other laboratories used the Sr separation by means of ion exchange, Y separation and beta counting of ^{90}Y. One of these two laboratories is in the range of 136 ± 15 whereas the other is in the 121 ± 13 range. Four laboratories used other methods for Sr separation, three of which are in the 136 ± 15 range. Only two laboratories do not use anticoincidence counting, and both have the results in the 136 ± 15 range. From the foregoing it can be stated that all methods are good.

As regards the measurements of ^{226}Ra in mixed diet (Table 2) it is interesting to compare the results with those shown in Table 1. The range of measurements is reduced and there are no more differences of order of magnitude.

Figure 3 relates to normal potassium in mixed diet. One laboratory gave results in the range of 0.81 ± 0.30, which are not included in the figure. Data (after statistical analysis) are shown in Table 5. As regards the analytical methods used, 18 laboratories employed gamma spectrometry, 15 flame photometry and one used tetraphenylborate. All methods gave equivalent results. Figure 4 concerns normal calcium in mixed diet. One laboratory's results, in the 0.09 ± 0.08 range, are not included in the figure. Table 6 shows the relevant data

Table 5. K in Mixed Diet, g/kg

No. of laboratories	No. of countries	No. of results	Mean (95% C.L.)
1	1	6	0.81 ± 0.30
2	2	10	6.30 ± 0.20
6	4	36	6.65 ± 0.36
21	10	93	7.26 ± 0.44
5	4	27	7.85 ± 0.39
3	3	14	8.38 ± 3.54
34	11	179	7.06 ± 2.48

(after statistical analysis). Also in this case all methods used gave equivalent results. For the measurements of Sr it can be seen from Table 2 that with concentrations in the order of 100 mg/kg the accuracy of the measurements is not better that ± 100%. Only two laboratories gave results out of this range. It is possible to justify this poor result because in all likelihood, the analysis was carried out with small quantities

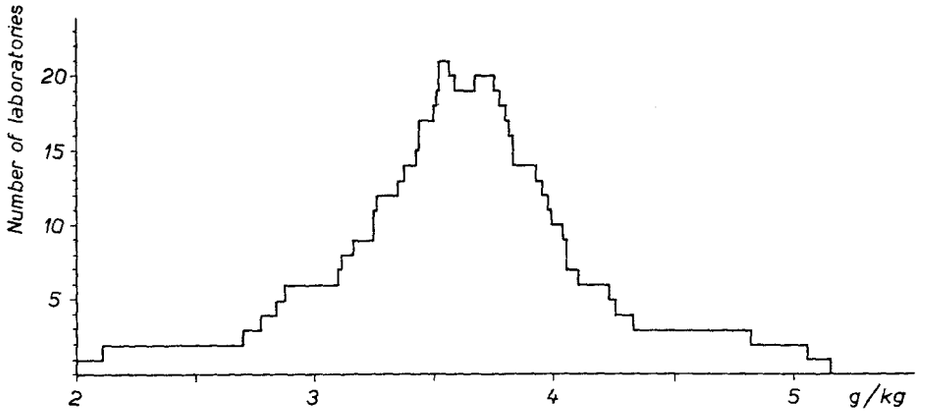

FIG. 4. Distributions of results of the analysis of Ca in mixed diet.

of original matter. It is very surprising that classical analysis like those for potassium and calcium should give results covering so wide a range.

Figures 5 and 6 concern the ratios pCi ^{137}Cs/gK and pCi ^{90}Sr/gCa in mixed diet. Tables 7 and 8 contain the relevant data (after statistical analysis). From these ratios it can be seen that only three laboratories gave results which were affected by errors in the same direction; this is a confirmation of the homogeneity of the samples sent by IAEA.

Unfortunately no conclusion may be drawn from the measurements of ^{210}Po in tobacco, meat and bones. As may be seen from Table 2 the range of measurements is of the order of

Table 6. Ca in Mixed Diet, g/kg

No. of laboratories	No. of countries	No. of results	Mean (95% C.L.)
1	1	6	0.09 ± 0.08
2	1	7	2.97 ± 0.83
5	5	28	3.32 ± 0.23
18	7	85	3.58 ± 0.34
6	4	38	3.88 ± 0.18
2	1	6	4.37 ± 0.95
31	11	150	3.48 ± 1.36

Table 7. pCi ^{137}Cs/g K in Mixed Diet

No. of laboratories	No. of countries	Mean (95% C.L.)
1	1	14.3 ± 32.6
4	4	36.3 ± 6.7
4	4	39.4 ± 6.4
18	7	48·6 ± 5.8
10	5	54.4 ± 4.4
1	1	64.1 ± 9.3
1	1	93.5 ± 34.5
1	1	470 ± 540
34	11	61.4 ± 146

Table 8. pCi ^{90}Sr/g Ca in Mixed Diet

No. of laboratories	No. of countries	Mean (95% C.L.)
1	1	20.4 ± 4.3
9	6	33.5 ± 3.7
17	7	39.8 ± 5.0
5	3	46.1 ± 3.1
1	1	50.3 ± 135
1	1	1922 ± 358
30	11	101.2 ± 690

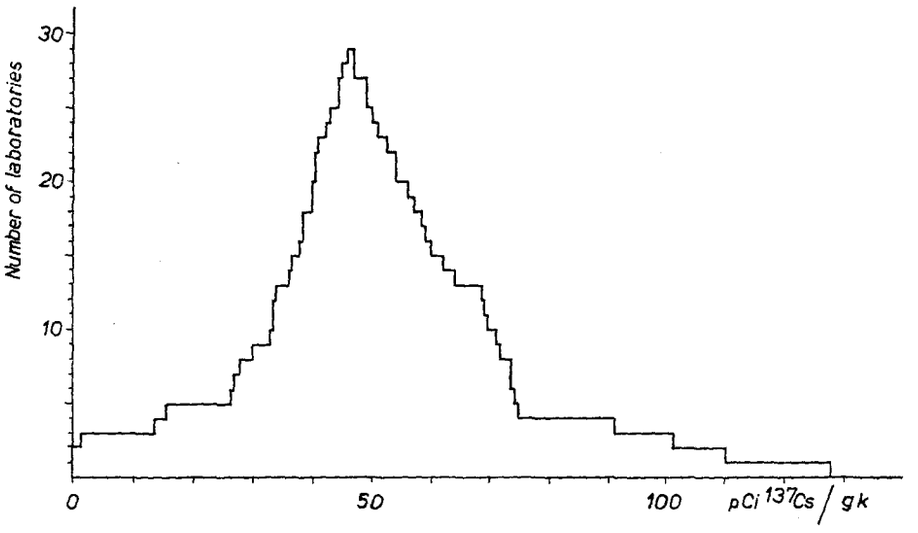

FIG. 5. Distribution of ratio pCi ^{137}Cs/g K in mixed diet.

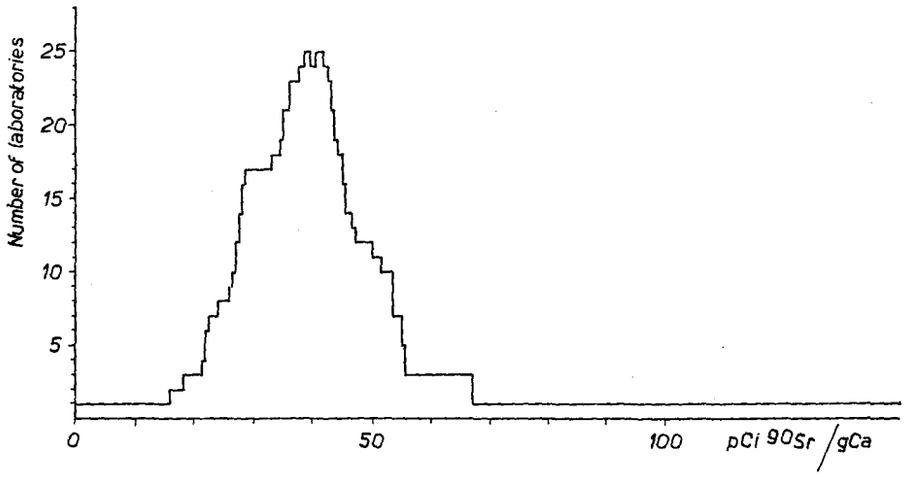

FIG. 6. Distribution of ratio pCi ^{90}Sr/g Ca in mixed diet.

$\pm 100\%$. It cannot be admitted that these differences are due to a different grown-in of ^{210}Po since all samples are older than one year, and the equilibrium between ^{210}Pb and ^{210}Po is attained.

THE PRECISION OF MEASUREMENTS IN VARIOUS LABORATORIES

For ^{137}Cs and ^{90}Sr the average standard deviation is about 4% and 5% respectively. There are two laboratories giving results for ^{137}Cs and one for ^{90}Sr which give a standard deviation of less than 1%. On the other hand there are three laboratories giving results for ^{137}Cs and one for ^{90}Sr which give a standard deviation higher than 15%, and in one case even 33%. The average standard deviation for the analyses of potassium and calcium is about 1.5%. That is a little too optimistic after this intercomparison. There is one laboratory which gives a standard deviation for both elements higher than 15%.

Over 10% of all laboratories made errors in calculation. When we received results far from the normal range of measurements we requested that they check their calculations and often detected errors.

A comparison of the results of the laboratories participating in the inter-comparison run 1964/5 and 1965/6 has shown that seven laboratories are improving the measurements of ^{90}Sr, and two the measurements of ^{137}Cs. The total number of laboratories participating in this inter-comparison is about 80 in 27 countries.[6]

ACKNOWLEDGEMENTS

We wish to thank all the laboratories which have sent to us the results of their analyses. Without their valued co-operation this work would not have been possible. It is hoped that the number of laboratories participating in such inter-comparisons will increase in the future in order to improve the accuracy not only of the low-level measurements, but also of those more classic.

REFERENCES

1. D. MERTEN. Panel on the Standardisation of Low-Level Activity Measurements, Vienna, 28–31 October, 1963.
2. G. BERGERHOFF, M. M. FERRARIS and D. MERTEN. Some critical remarks on environmental radioactivity measurements, *Minerva Fisiconuclear*, in press.
3. G. BERGERHOFF, M. M. FERRARIS and D. MERTEN. Qualitaetskontrolle analytischer Methoden in Internationalen Rahmen, *Zeit. Anal. Chem.*, in press.
4. R. E. SCOSSIROLI. *Manuale di Statistica per Ricercatori*, Olivetti, 1962.
5. G. W. SNEDECOR. *Statistical Methods*. The Iowa University Press, Ames, Iowa, 1956.
6. IAEA Laboratory Activities, Third Report, Technical Report Series No. 55, 1966.

DETERMINATION OF ^{226}Ra IN NATURAL SAMPLES

ELVIRA R. DI FERRANTE*
Euratom

GEORGES KOCH and RENÉ R. BOULENGER
Health Physics Division, Centre d'Étude de l'Énergie Nucléaire, Mol-Donk, Belgium

Abstract—The natural content of ^{226}Ra in environmental samples was determined by the emanation technique. The reliability and sensitivity of the method made measurements possible at a very low level. Analyses of human teeth could, for instance, be performed satisfactorily and the concentrations obtained, ranging from 0.008 to 0.138 pCi/g ash, are in agreement with the literature data. The highest ^{226}Ra contents found are of the order of 1, 2 and 6 pCi per gram of calcined material.

The chemical preparation of the different samples such as milk, bones, teeth and minerals are described. Detailed description of the apparatus with schematic diagram and of the measurement technique is also given. The equation used for the calculation of the activity expressed in pCi ^{226}Ra/g ash or pCi ^{226}Ra/l., is shown.

INTRODUCTION

The natural radiation background may vary greatly from locality to locality. In order to know the differences in population exposure it is, therefore, necessary to monitor as many areas as possible. The aim of the present study is to provide data on levels of radioactivity due to natural radium in human environment. Numerous samples such as water, milk, animal bones and teeth, bovine flesh and soil, were collected for the determination of ^{226}Ra content. When available, human teeth from the monitored areas were also analyzed in order to have an indication of local skeletal burdens. [1]

MATERIAL AND METHODS

1. *Preparation of Samples*

The methods used to prepare the samples for the ^{226}Ra analysis by the emanation technique, varied with the nature of the material collected.

1.1. *Water.* Water samples from fountains, springs and rivers received pre-analysis treatment only by the addition of 2 ml of concentrated HNO_3 to keep the radium in solution and also to avoid the formation of algae. In case of presence of suspended matter, a filtration, followed by a separate analysis of the filter content, was performed. 500 ml were generally used for the measurements. For low activities it was advisable to use larger volumes reduced by evaporation to 500 ml.

1.2. *Milk.* Milk samples were slowly evaporated to dryness in large beakers. The dry residues were then ashed in a muffle at 600°C for 8–10 hr. Amounts ranging from 5 to 10 g of the powdered milk ashes were dissolved in the minimum volume of concentrated HNO_3 in a 50 ml centrifuge tube by using an electric stirrer, and the clear solutions brought to a final volume of 500 ml with 1 N HNO_3.

1.3. *Animal bones and teeth.* A more complex procedure was followed for the preparation of bone and teeth solutions. The samples, sawn into small pieces (2–3 cm of length), were scraped, and cleansed from residues of blood and soft tissue by boiling them several times in ethylene diamine and then in distilled water. After drying in an oven at 120°C the bones were ashed at 600°C, whereas a temperature of

* Present address: c/o Euratom Joint Nuclear Research Center, Biology Dept., Ispra (Varese), Italy.

950°C was required for the ashing of teeth. The ashes, ground in an agate mortar, were dissolved in concentrated HNO_3 and solutions of $\sim$ 500 ml were obtained by diluting with 1 N HNO_3.

1.4. *Bovine flesh.* The ashing of soft tissues is somehow more delicate than for other samples. It was performed in a platinum dish by increasing the temperature of a muffle furnace in steps of $\sim$ 25°C so that the organic matter burned gradually without sudden outburst and consequent loss of substance. The final temperature of 600°C was maintained for about 10 hr. A residue of only 1% of the fresh weight was generally obtained, therefore it was necessary to use considerable amounts of material if a few grams of ashes were desired. The nitric solutions were prepared as for the other samples.

1.5. *Mineral samples.* Suspended matter from water samples, soil, and muds were analyzed not only to obtain information concerning a specific type of environment, but also to establish a suitable routine procedure for the radium determination of ores, silts, river muds and dry food items.

Dissolution of the mineral substances was preferred to leaching with inorganic reagents in order to assure the passage into solution of all the radium. The dry samples, finely ground in a porcelain mortar, were calcined at $\sim$ 600°C for the elimination of any organic matter present. H_2SO_4 and HF (2 : 1) were added, with 50 mg of Ba^{++} as carrier, to a weighed amount (1–5 g) of ashes in a Pt crucible. A slow evaporation on a steam bath was then performed with complete elimination of white fumes of SO_3 until dryness. For material with high silica content the treatment with H_2SO_4 and HF was repeated several times. An extra addition of HF was occasionally necessary. H_3PO_4 was then added to the residue and the crucible heated over a burner. When a clear fused mass was obtained, it was allowed to cool and then dissolved in concentrated HNO_3 and the excess of acid evaporated. A final solution of $\sim$ 500 ml was prepared diluting with 1 N HNO_3. Instead of the acid treatment a fusion of the samples with an alkaline flux followed by a dissolution of the melt in acids[8] may be performed.

Samples of suspended matter from river water received a different treatment. After the filtration the dry filter was burnt in a Pt crucible, HNO_3 and HF (1 : 2) were added to the residue and the crucible heated on a sand bath at 200°C until dryness. The acid treatment was repeated and, after elimination of fumes of HF, a clear nitric solution obtained. Dilution to $\sim$ 500 ml was then performed with 1 N HNO_3. This procedure may be followed for samples of known low silica content.

1.6. *Human teeth.* Because of their low radioactive content human teeth need to be handled with special care to avoid contamination. Pt crucibles and glassware require very thorough cleaning by repeated washing with warm decontaminating solutions or warm diluted HNO_3. The crucibles must previously be cleaned with purified sea sand. Samples having blood residues were boiled, as were bovine teeth, in ethylene diamine and distilled water. Metallic fillings, when present, were removed before the ashing at 950°C. The ground ashes, always 73–75% of the fresh weight, were then dissolved in nitric acid and final solutions of $\sim$ 500 ml were prepared by diluting with 1 N HNO_3.

2. *Technique of radon measurements*

All the solutions prepared by the different procedures described in the previous paragraphs, were transferred into emanation flasks and flushed for about 20 min with nitrogen for complete removal of radon. The flasks were then sealed and the time recorded (t_1, beginning of radon ingrowth). According to the levels of radioactivity the solutions were allowed to stand for a minimum of 5 days to a maximum of 30; at the latter time radium and radon are in equilibrium and no further build-up of the gas takes place. The accumulated Rn was then transferred to a trap containing charcoal and from this to the detector for counting.

The scheme of the emanation technique apparatus* set up for this study is shown in

* Apiezon grease, type M, AEI (Manchester) Ltd., England, is used to connect the spherical joints; type T to seal the flasks. Silicone grease is used for the stopcocks.

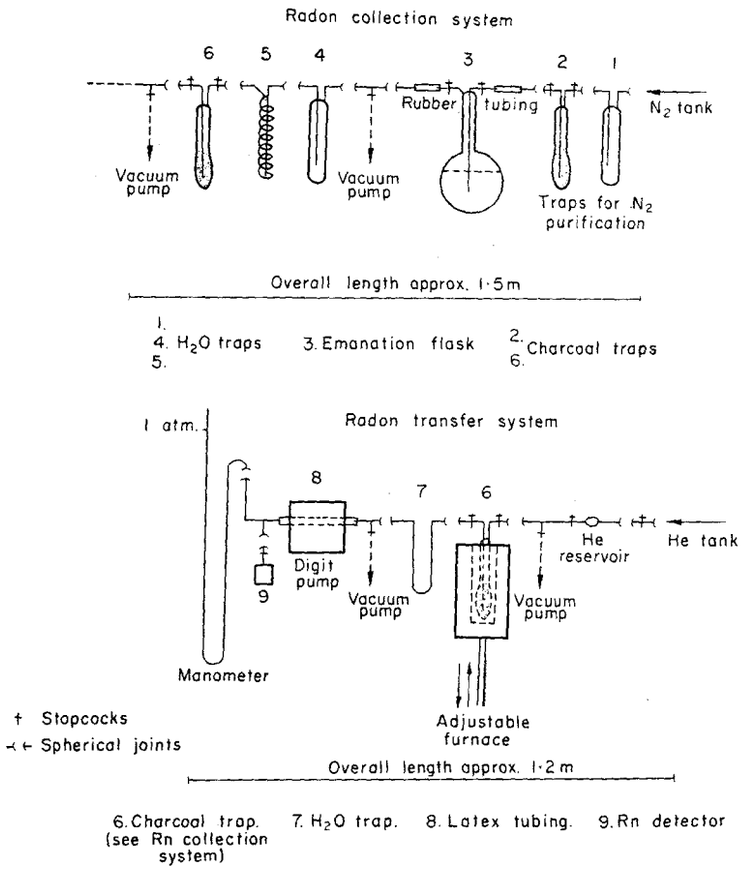

FIG. 1. Apparatus for emanation technique (scheme).

Fig. 1. The nitrogen used for the removal of radon from the flasks during the measurements was dried and purified (radium in the tank steel may cause contamination) by means of a water trap and a charcoal trap cooled to $\sim -80°C$ with dry-ice and acetone and allowed to bubble in the solution contained in the emanation flask (Fig. 2) for 12 min at a flow rate of 45 l/hr. The randon removed by the nitrogen passing through two cooled water traps was absorbed on activated charcoal* also cooled to $\sim -80°C$.

The model of the trap containing a weighed amount (always 7 g) of degassed charcoal, used for the purification of nitrogen and for the absorption of radon, is shown in Fig. 3. When de-emanation was complete the flask was sealed again and the time recorded (t_2, beginning of decay of removed radon and also beginning of a new radon ingrowth in the flask). The charcoal trap on which the gas had been absorbed was evacuated, while still at low temperature, without removing it from the system. The trap placed then in the second section of the apparatus shown in Fig. 1, was heated at 500°C by means of a cylindrical furnace which could be raised and lowered. The Rn liberated from the charcoal, passing through a cooled water trap, was transferred to the detector, a cell with a scintillating layer of ZnS at the interior. Helium was used as carrier gas at a continuous slow flow obtained with two needle

* Activated coconut charcoal. 6–14 mesh. Burrell Corporation, Pittsburgh, U.S.A.

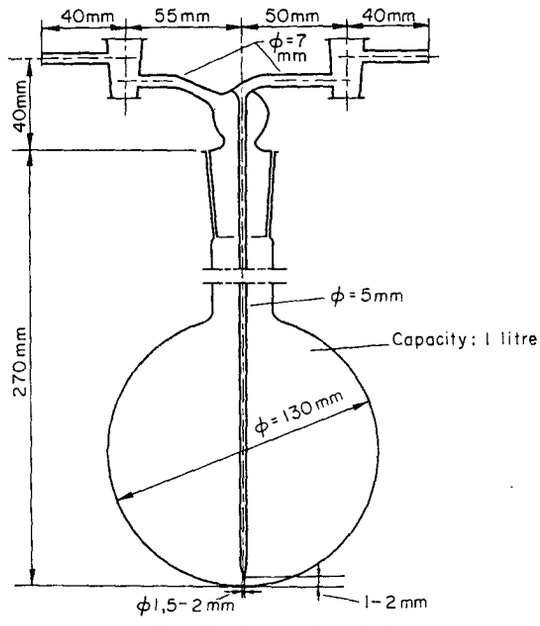

FIG. 2. Emanation flask.

valves* at the exit of the tank. A digit pump† facilitated the filling of the detector until atmospheric pressure was reached, usually in about 8 min. The latex tubing‡ used with the pump (see Fig. 1) was replaced after high counting rate measurements. By means of mechanical pumps the vacuum ($\sim 2 \times 10^{-2}$ Torr) could be obtained in each section of the apparatus, radon collection system and radon transfer system, before the passage of the nitrogen and of the helium, in order to avoid any contamination due to air from the exterior. After the complete transfer of the Rn to the detector the charcoal traps were evacuated, while still heated at 500°C, before using them again. Except when promptly re-used they were evacuated and heated again at the moment of a new analysis. The detectors containing the radon were counted four hours after the end of the de-emanation of the solution, when equilibrium between Rn and its daughters (^{218}Po and ^{214}Po) was reached. Counting times differed according to the radioactivity which had to be detected. For low levels, the samples were usually counted for not less than 16 hr.

Two types of scintillation detectors were used for the present study. One made of stainless steel with quartz window[3] for activities $\geq 10^{-13}$ Ci of ^{226}Ra and one of lucite, which has been described elsewhere,[4] for levels of the order of 10^{-14} Ci. The calibration of the system was performed with the metallic and the plastic detectors measuring the radon from standard solutions of 11.1×10^{-12} and 1.57×10^{-12} Ci of ^{226}Ra. Over-all efficiencies of 80 and 75 $\pm$ 2% were obtained. The decay of the radon emanated from each standard solution was followed observing the counting rates given by the two different detectors during 2 weeks; a half life of 3.8 days was found. Therefore no radon diffusion, suspected especially for the porous lucite, occurred through the detector walls.

CALCULATIONS

The radium content of the samples analyzed was calculated by means of the equation:

$$A\ (^{226}\mathrm{Ra}) = \frac{\frac{N_s}{t_s} - \frac{N_b}{t_b}}{C_1 \times C_2 \times R \times Q \times 3.7 \times 10^{-2} \times 3}$$

pCi/g ash or pCi/l.

where A (^{226}Ra) = activity expressed in picocuries of ^{226}Ra per gram of ash or per liter;

N_s = total counts obtained for the sample;

N_b = total counts obtained for the background;

t_s, t_b = counting times in seconds for samples and for background;

C_1 = radon growth coefficient (fraction of radioactive equilibrium): $1 - e^{\lambda t_g}$; t_g = days elapsed from beginning of radon in growth to de-emanation $(t_2 - t_1)$;

C_2 = radon decay coefficient: $e^{-\lambda t_d}$; t_d = time elapsed from de-emanation to the half of the counting interval;

R = over-all efficiency: 0.80 or 0.75;

* Model Osid; Edward High Vacuum Ltd., England.

† Model T-6S; Sigmamotor, Inc. Middleport, N.Y., U.S.A.

‡ Latex Surgical Tubing 0.5 cm ID., 0.25 cm Wall Amber; Rubber Latex Products, Inc., Cuyahoga Falls, Ohio, U.S.A.

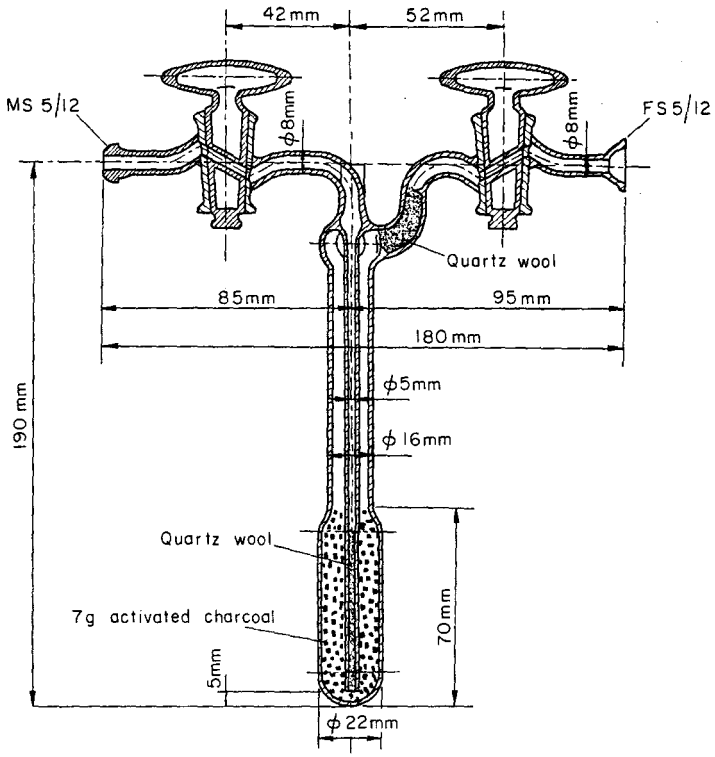

FIG. 3. Charcoal trap.

Q = weight of ashes in grams or volume of sample in liters;
3.7×10^{-2} = conversion factor to picocuries;
3 = correction due to the fact that at equilibrium for each radon disintegration three α-particles are detected, one from Rn, the others from its two daughters ^{218}Po and ^{214}Po.

RESULTS

Tables 1 and 2 show results obtained for water, milk, animal samples and minerals. Since the present paper is concerned mainly with the description of the method of analysis, it was considered unnecessary to list all the numerous samples analyzed and their radium content. The data contained in the tables are sufficient to show the different levels of natural radioactivity due to ^{226}Ra observed in the course of the work, even in samples of the same nature. Radium concentrations of human teeth from normal environments are summarized in Table 3. The values given in the three tables are averages of two analyses on the same solution, in agreement within the statistical counting error which is at maximum $\sim 15\%$. Blank determinations were regularly performed analyzing reagents and distilled water, especially before measurements at very low level. The counting rates obtained, ranging from 0.0015 to 0.0035 counts/sec were always subtracted from the counting rates given by the samples. The high sensitivity of the method permitted the determination of the radium content even of a single human tooth. Nevertheless a pool of teeth of the same origin and same formation time should be made, if possible, for better statistical results.

The analyses of the two bovine mandibles complete with teeth confirmed the results obtained in the course of a previous research.[5] A good agreement exists between the radium

Table 1. *^{226}Ra in Water, Milk and Minerals*

Sample identification and origin	Type of sample	Volume (in l.)	Ash weight (in g)	pCi/l. or pCi/g ash
E 178 Belgium	river water	0.500	—	0.440
E 182 „	„ „	„	—	0.783
A 1 „	drinking water	„	—	1.459
Is 1 Italy	„ „	0.230	—	0.011
Is 2 „	„ „	„	—	0.036
Is 3 „	thermomineral water	0.300	—	0.037
Is 4 „	„	0.600	—	0.345
64 Belgium	milk	0.980	6.539	0.017
65 „	„	1.000	6.635	0.025
22 „	„	1.200	7.356	0.032
69 „	„	1.302	9.377	0.049
21 „	„	1.080	7.572	0.073
14 „	„	1.410	10.080	0.190
R 1 „	mineral	—	1.108	0.763
R 2 „	„	—	1.053	1.088
B 4 „	river mud	—	1.000	2.238
Is 10 Italy	thermal mud*	—	1.288	0.669

Range of estimated error = $\pm 0.015-0.185$ pCi/l. or pCi/g ash.
* Collected near the spring of sample Is 3.

Table 2. *^{226}Ra in Animal Bones and Teeth*

Sample identification and origin	Type of sample	Fresh weight (in g)	Ash weight (in g)	pCi/g ash
65 Belgium	rabbit bone	1.055	0.633	0.154
84 „	„ „	6.829	4.097	6.493
1 B „	cow bone	11.725	7.841	0.184
1 B „	cow tooth I_4*	2.022	1.410	0.177
1 B „	„ „ P_1	2.589	1.961	0.255
1 B „	„ „ P_3	10.799	8.188	0.240
2 B „	cow bone	11.626	7.769	0.318
2 B „	cow tooth I_4	5.088	3.822	0.311
2 B „	„ „ P_1	2.264	1.683	0.265
2 B „	„ „ P_2	7.605	5.772	0.255
2 B „	bovine flesh	144.130	1.423	0.378
2 C† U.S.A.	cow bone	1.502	0.982	0.171
23 C† U.S.A.	„ „	4.790	3.066	2.381

Range of estimated error = $\pm 0.020-0.250$ pCi/g ash.
* I_4 = fourth incisor; P_1, P_2, P_3 = first, second, third premolar.
† Samples analyzed also at ANL (see ref. 5).

Table 3. ^{226}Ra in Human Teeth

Sample identification and origin	Type of sample	Fresh weight (in g)	Ash weight (in g)	pCi/g ash
208 Belgium	2 premolars	1.847	1.681	0.0093
236 „	„	1.514	1.396	0.0098
154 „	3 incisors	2.884	2.535	0.0141
144 „	1 molar	2.331	1.939	0.0142
1 K „	1 incisor	1.051	0.771	0.0153
2 K „	1 „	0.505	0.373	0.0183
153 „	4 premolars	3.767	3.348	0.0187
225 „	2 „	1.863	1.685	0.0198
304 „	3 incisors	3.496	2.483	0.0285
303 „	1 molar	1.786	1.460	0.0451
305 Italy	1 „	1.935	1.560	0.0082
309 „	1 „	2.067	1.630	0.0102
312 „	1 „	1.952	1.520	0.0132
302 „	1 „	0.703	0.614	0.0138
310 „	1 premolar	0.739	0.553	0.0148
307 „	1 molar	1.077	0.779	0.0234
313 „	1 „	1.663	1.335	0.0246
311 „	1 premolar	0.559	0.409	0.0449
308 „	1 molar	1.855	1.340	0.1380

Range of estimated error = $\pm 0.0020 - 0.0150$ pCi/g ash.

concentrations in bone and teeth, especially those with late formation time. This fact justifies again the use of teeth to estimate skeletal burdens when bone samples are not available.

The concentrations found in human teeth, despite their different origin, are very close to those found in teeth or bones from normal environment by several authors and among others by Walton *et al.*,[6] by Lucas,[1] Hursh and Lovaas,[7] Holtzman,[8] Owers and Parker.[9] Hence, since the skeletel radium content is due to the radium ingested with drinking water and food,[1] whenever a systematic abnormal Ra intake is suspected, intensive determinations of body burdens (through analyses of bones and teeth) could be very useful for the study of possible cumulative effects of low level radiations over long periods of time.

ACKNOWLEDGEMENTS

Appreciation is expressed to Mr. F. Verhoeven who skillfully attended to the setting up of the modified radon apparatus and to the construction of the metallic detectors. Thanks are also due to Mr. J. Mermans for his frequent help during the execution of the work and for the preparation of the lucite detectors.

The collection of the samples of milk, animal bones and teeth was due to the interest of Mr. R. Kirchmann (Radiobiology Dept.); of human teeth to the cooperation of Dr. E. Michel of Mol, Dr. C. Hirschhorn of the University of Rome and of several persons who offered their own teeth.

REFERENCES

1. H. F. Lucas. Correlation of the natural radioactivity of the human body to that of its environment. ANL-6297, pp. 55–56 (1960).
2. D. E. Rushing, W. J. Garcia and D. A. Clark. The analysis of effluents and environmental samples from uranium mills and of biological samples for radium, polonium and uranium. *Radiological health and safety in mining and milling of nuclear material.* I.A.E.A., Vol. II, pp. 187–230 (1964).

3. H. F. Lucas. *Rev. Sci. Instr.* **28,** 680 (1957).
4. E. R. di Ferrante, E. Gourski and R. R. Boulenger. Detector for radon measurement at very low level. *The Natural Radiation Environment,* Ed. Adams & Lowder, Chicago Press, pp. 353–357 (1964).
5. E. R. di Ferrante. *Health Physics* **10,** 259 (1964).
6. A. Walton, R. Kologrivov and J. L. Kulp. *Health Physics* **1,** 409 (1959).
7. J. B. Hursh and A. Lovaas. *Nature* **198,** 265 (1963).
8. R. B. Holtzman. *Health Physics* **9,** 385 (1963).
9. M. J. Owers and A. Parker. Radioactivities in human and animal bones. AERE-R 4466 (1964).

RAPID AND SENSITIVE MEASUREMENT OF URANIUM IN URINE (WITHIN 15 MINUTES AND DOWN TO 0.010 μg/l). METHODS AND RESULTS

HUB. WIJKER and M. H. BILLUM
Nuclear Reactor Development Laboratory, N.V. Kema, Arnhem, Netherlands

Abstract—A fluorimetric method is outlined for the determination of the uranium concentration in urine in technical report No. 173 of the World Health Organization (1959). By introducing stringent requirements to apparatus and sample preparations, the sensitivity was largely improved so that concentrations down to 0.010 μg/dm^3 could be determined with an accuracy of about 30 per cent. These requirements will be discussed. The strict standardization of the sample preparation and the rigorous constancy of the operation of the fluorimeter is required because the slope of the calibration curve log i vs. log c (i = indication, c = concentration) is very small in the region below 10 μg/dm^3 (0.077, to be compared with 0.41 for $c > 100$ μg/dm^3).

The worth of measuring very sensitively is twofold:

(*a*) in the KEMA laboratories much of the work is done with a mixture of UO_2 and ThO_2 in a constant ratio of 15 to 85. The Th-inhalation is much more dangerous and difficult to detect than the U-inhalation. In a number of our cases the most sensitive indication of Th-inhalation is the U-excretion, provided very small quantities of the latter can be measured;

(*b*) in many cases the U-excretion appeared to be the most sensitive method to detect incorrect working procedures. Some examples of these will be discussed.

DETERMINAZIONE DI URANIO ARRICCHITO E DI TORIO NATURALE IN CAMPIONI BIOLOGICI MEDIANTE ESTRAZIONE CON OSSIDO DI TRI-N-OTTIL-FOSFINA (TOPO)

A. FRANCESCHINI, C. GANDOLFI e S. TODISCO
Centro Ricerche Nucleari SORIN, Saluggia (Italy)

Sommario—I due metodi illustrati nel presente rapporto per l'analisi di U arricchito e di Th naturale in campioni biologici sono del tutto simili uno all'altro per quanto si riferisce all'isolamento dei metalli, differiscono invece quanto alla tecnica dimisura.

Il campione da analizzare (urina od altro) in entrambi i casi viene mineralizzato con appropriate miscele acide, quindi diluito e parzialmente neutralizzato in modo da raggiungere le condizioni ottime per l'estrazione. L'estrazione viene effettuata mediante una soluzione di TOPO in benzene. Si riestrae poi con HCl nel caso del torio, con HCl + $SnCl_2$ nel caso dell'uranio, che viene così ridotto alla valenza quattro. La successiva evaporazione dell'estratto cloridrico fornisce il campione finale: su di esso nel caso dell'U si conta l'attività alfa, mentre nel caso del Th si effettua la determinazione spettrofotometrica del suo complesso con il toron.

Le rese chimiche dei metodi di analisi descritti sono elevate. Nel caso dell'urina l'analisi in parallelo di U o Th su 5 campioni richiede in totale circa 8 ore, delle quali una buona parte non impegna l'analista. Si riesce a determinare in un campione di 500 cm^3, con una deviazione standard intorno al 50 per cento, 1,5 pCi di U arricchito e 0,5 μg di Th, pari al 10 per cento della concentrazione massima ammissibile nell'urina, se si adottano per essa i valori di 30 pCi/l nel caso dell'U e di 10 μg/l nel caso del Th.

RADIOCHEMICAL ANALYSIS USED AT CEN-MOL FOR THE DETERMINATION OF α-EMITTERS IN BIOLOGICAL MATERIALS

N. M. VALENTIN, C. WEYERS and J. LUYSTERBORG
Centre d'Étude de l'Énergie Nucléaire, Mol, Belgium

Abstract—The radiochemical analysis used at CEN (Mol) for the determination of α-emitters in biological materials are of 2 types: the routine and the incident procedures. Three α-emitters are routinely detected in urine samples. These are uranium, plutonium and americium. The uranium is analyzed by a fluorimetric method using a mixture of NaF–LiF. The sensitivity of the method is 0.6 μg U/24 hr urine. Plutonium and americium are determined by a method involving the following steps: phosphate precipitation, ashing, ion exchange separation, electrode position and counting with a ZnS scintillator. The yield of recovery for each α-emitter is 75 ± 4 per cent (95 per cent confidence) and the sensitivity of the method is 0.06 dpm/24 hr urine. In the case of an accidental contamination, nose blow, feces and urine samples are collected. Uranium, plutonium and americium can be determined in nose blow samples with an efficiency of 85 ± 10 per cent (95 per cent confidence) and a sensitivity of 0.02 dpm. The analysis consisted in a destruction of the organic material with a mixture of acids followed by an electrodeposition of the α-emitter and a counting in a ZnS scintillator. The analytical method used for feces containing plutonium or americium consists in a wet ashing followed by a calcium fluoride precipitation. The insoluble is filtered on a 100 cm^2 Millipore filter paper. The filter is counted in a ZnS scintillator counter. The recovery of the α-emitter is 84 ± 24 per cent (95 per cent confidence) and the sensitivity is 2.0 dpm/24 hr sample. Urine samples collected, following an accidental contamination, are processed for plutonium and americium by the same method as feces samples. However the wet ashing step is replaced by an oxidation of the urine sample. The efficiency of the method is 90 ± 15 per cent (95 per cent confidence) and its sensitivity is 1 dpm/24 hr urine.

DETERMINATION OF ^{137}Cs IN SOIL

ALICE BAUMAN
Institute for Medical Research, Yugoslav Academy of Sciences and Arts, Zagreb, Yugoslavia

Abstract—The method is based on the final precipitation of ^{137}Cs as caesiumtriphenylcyanoborate. Sodiumtriphenylcyanoborate has not been used before as a reagent for determination of radioactive caesium, at least not in the samples of biosphere. Conditions of optimal leaching of ^{137}Cs from various types of soil were found. A 256-channel analyzer was used for sample counting. Conditions of optimal precipitation of caesium were determined.

INTRODUCTION

Most papers on ^{137}Cs in soil deal with the problem of ^{137}Cs fixation[1-5] or uptake by different plant material[6-10] and the evaluation of all possible influences on both.[11-13] Few data are available on chemical methods for the determination of ^{137}Cs in soil.[14-16] Even less data are published on separation of ^{137}Cs from large soil samples as it appears to be necessary in the determination of very low activities due to fall-out. The same applies to the variation of soil types, removal of ^{137}Cs from large amounts of nonradioactive ions obtained by leaching of bulky soil samples, contamination by natural radioactivity and possibility of interference from non-radioactive ions during separation. Starting from the above mentioned papers and published results a method with the following features has been developed:

1. Leaching of ^{137}Cs from soil.
2. Separation from large quantities of nonradioactive ions.
3. Easy to operate for less equipped laboratories.

EXPERIMENTAL

Apparatus and Reagents

Glassware and reagents commonly used in laboratory.

Cesignost: 7% aqueous sodium triphenylcyanoborate solution filtered through a SS 589[3] filter-paper.

^{137}Cs-tracer as CsCl (from the Radiochemical Centre Amersham).

All reagents were of analytical grade.

Gamma-ray spectrometer with NaI crystal and multichannel analyzer.

The Samples

Five soil samples with widely differing characteristics were used for this study. Represented were an acidic, neutral, saline-alkaline and a calcareous soil. Each sample consisted of 10 borings 2 in. deep. All samples were taken from an undisturbed area or from a herbage sampling site. Each sample weighing about 3–4 kg, was air-dried, ground to pass a 2 mm sieve and dried at 110°C.

Method A

Before starting with a large-scale experiment the method has been tested on 5 g samples of soil. Each sample was artificially contaminated after drying at 105°C with 1000 pCi of ^{137}Cs. After ignition at 450°C 10 mg of Cs-carrier and 10 ml of a leaching solution (1 : 1 HCl) were added to each sample, and stirred for 30 min. After digestion over night, the leachate was separated by centrifugation, and the washings (at least 3) joined to the leachate. The leachate was evaporated to dryness and after silica dehydration the hydroxides were precipitated by addition of ammonia (1 : 1) and carbonates by a saturated solution of Na_2CO_3. The pH of the solution was adjusted to 3 by means of 1N H_2SO_4, the solution boiled to expel the excess CO_2, cooled to room temperature, and 5 ml of 7% solution of $Na[(C_6H_5)_3B\ (CN)]$

were added. The resulting solution was left for 15 min, filtered, the filtrate was discarded, and the precipitate containing $Cs[(C_6H_5)_3B(CN)]$ was dried for 30 min at 105°C and weighed. The ^{137}Cs content was measured by gamma spectrometry.[17]

Method B

To an aliquot of 250 g of each soil sample ^{137}Cs tracer was added prior to further treatment.

1. Take 250 g of soil, ignite in a muffle furnace for 2 hr at 450°C (see Note 1).
2. Cool, add 100 mg of Cs-carrier, 500 ml of HCl (1 : 1) stir for 30 min, allow to stand overnight.
3. Filter through a Buchner funnel (Filterpaper SS 589[1])* wash the residue thoroughly with water to neutral reaction.
4. Repeat the leaching twice with 500 ml HCl (2 : 1) and combine all filtrates.
5. Evaporate the whole solution, when nearly dry transfer to a porcelain dish and when completely dry heat for 1 hr.
6. Dissolve the residue in hot 10% HCl and wash the precipitate with hot diluted HCl.
7. Heat the filtrate after silica separation, precipitate the hydroxides by means of a hot fresh 20% NaOH solution.[18, 19] Boil for 2–3 min under gentle stirring, let settle, filter, wash the precipitate with 5% NaOH (containing some Na_2SO_4) (see Note 2).
8. After the separation of the hydroxides, precipitate the carbonates by adding a saturated solution of Na_2CO_3 and heat just below the boiling point. Digest with occasional stirring (see Note 3). Filter after 4 hr.
9. Acidify the filtrate after the separation of the carbonates with 1N H_2SO_4, evaporate to about 200 ml, cool to room temperature, adjust pH to 3 with H_2SO_4, add 50 ml of a 7% Cesignost solution. Filter after 15 min, wash the precipitate with a 1% Cesignost solution, and discard the filtrate.
10. Dissolve the precipitate in a mixture of acetone and water (1 : 1), evaporate the acetone by heating, add 50 ml of water and adjust the pH to 3 with H_2SO_4. Repeat step 9.
11. Dry $Cs[(C_6H_5)_3B(CN)]$ at 105°C for 30 min, weigh and measure by gamma-spectrometry.

Note 1. No losses of ^{137}Cs were observed.

Note 2. If necessary insert between steps 7 and 8 the following separation: Evaporate the filtrate almost to dryness, add 50 mg of Ba-carrier, adjust pH to 5.5 with HCl,[20, 21] add 5 ml of 6 M acetic acid and 10 ml of 6 M ammonium acetate, heat to boiling point, add 5 ml of a 10% Na_2CrO_4 solution, digest under stirring for 15 min, heat until the precipitate starts to settle, cool and centrifuge if possible (dependent on the total volume) or allow to stand for 2 hr. Discard the precipitate.[19]

Note 3. Control the completeness of the precipitation by adding a few drops of Na_2CO_3 solution before filtration.

RESULTS

To control the efficiency of the method the following steps were checked by gamma-spectrometry:

1. Spectrum of soil samples contaminated with ^{137}Cs before chemical treatment and after ignition (for eventual losses due to heating).
2. The residues after leaching.
3. The combined precipitates following each chemical separation for other nuclides that might be present.

The results of these controls are listed in Table 1.

The results show a marked difference in leaching efficiency between large samples, such as are necessary for fall-out determination, and samples used for the development of the method (Table 2). This implies the impossibility of transfering the method from small scale to large scale by simply calculating the amount of necessary solutions. The ratio of count rate versus volume of solution to count rate versus gram of soil is not constant. The results in Table 3 for ^{137}Cs gravimetric and gamma-spectrometric yield in 250 g samples agree within the probable error of the determination.

DISCUSSION

Experiments on 5 g soil samples were made to try the method on samples where no significant natural radioactivity or fall-out radioactivity interfered with the separation. No inter-

* Schleicher & Schuell A. G., Feldmeilen, Switzerland.

Table 1. Percentage of ^{137}Cs Tracer Extracted from 5 g Soil Samples

Sample	Removal per leach 1:1 HCl	Cesignost $Cs[(C_6H_5)_3B(CN)]$ chem. yield
1. Podzol	95·0 ± 0·9	91·0 ± 0·6
2. Rendzina	86·0 ± 1·6	84·0 ± 0·9
3. Alluvial solonetz	80·0 ± 2·3	76·0 ± 1·4
4. Terra Rossa	87·0 ± 1·1	84·0 ± 0·9
5. Mineral carbonate	86·0 ± 1·3	79·0 ± 1·5

The results are an average of 3 values.

ference was found, since all radioactivity present was just under the detection limit of the measuring instrument.

Prior to the chemical analysis all the samples were leached three times. No additional leachings were required, inasmuch as no significant removal of unextracted ^{137}Cs was observed from further treatment of the residue.

The lower leaching efficiency arises from the difficulty of dealing with a large volume of solution and macro amounts of SiO_2, Al_2O_3 and $CaCO_3$ present in samples.

Instead of 9N H_2SO_4 or 8N HNO_3 as proposed by other authors the HCl leaching was adopted according to results published by Shvedov and Zhilkina.[23] To shorten the time for silica elimination attempts have been made to hasten the precipitation by adding 5 g of gelatine in a strongly acidic solution. It proved impossible to obtain the necessary acidity, as no precipitate was formed even after prolonged boiling.

For the hydroxide precipitation, which proved to be satisfactory with ammonia on 5 g soil samples, when dealing with 250 g of soil NaOH had to be used instead of ammonia, since large amounts of ammonia interfere with the Cesignost precipitation. Chromate precipitation has been applied for ^{140}Ba elimination in the case when this happened to be necessary. Cesignost is a less known reagent belonging to the tetraphenylborate group. Until now only Havir studied properties of Cesignost on stable Cs-salt solutions. Cesignost proved to be selective for Cs, forming less soluble salts with cesium than with other alkaline metals. Working with up to 10 mg of ammonia Havir got no precipitate with Cesignost.

There are no interferences in Cs precipitation in the presence of 2–3-valent cations. For that reason NaOH can be applied as a precipitant for hydroxides. Under some circumstances the elimination of ammonia by evaporation can prove to be impractical.

The precipitation of Cs with Cesignost sodium (triphenylcyanoborate) must be performed in sulphuric acid media at temperatures not higher

Table 2. Percentage of ^{137}Cs Tracer Extracted from 250 g Soil Samples

Sample	1. leaching $HCl : H_2O$ (1 : 1)	2. leaching $HCl : H_2O$ (2 : 1)	3. leaching $HCl : H_2O$ (2 : 1)
1. Podzol	65·5	78·2	87·0
2. Rendzina	32·2	56·2	67·4
3. Alluvial solonetz	12·0	32·0	40·0
4. Terra Rossa	53·0	61·7	67·4
5. Mineral carbonate	49·0	54·4	64·6

Table 3. *Yield of* ^{137}Cs *in* 250 *g Soil Samples*

Sample	% chem. yield	% gamma by spectrometry
1. Podzol	66·0	66·0
2. Rendzina	61·0	62·0
3. Alluvial solonetz	45·0	38·0
4. Terra Rossa	64·0	59·0
5. Mineral carbonate	62·0	61·0

than 25°C. At higher temperatures the precipitate partly dissolves. Upon longer standing (several hours) part of potassium present in the solution might coprecipitate with caesium.

Part of the losses in chemical yield may be attributed to sample transfer between beakers.

REFERENCES

1. R. M. Aleksahin. *Radioactive Contamination of Soil and Vegetation* (in Russian). Izdat. Akad. Nauk SSSR, Moscow (1963).
2. H. Nishita, A. J. Steen and K. H. Larson. *Soil Sci.* **98,** 195 (1965).
3. R. K. Schulz. *Health Phys.* **11,** 1137 (1965).
4. E. M. Romney, J. W. Neel and H. Nishita. *Soil Sci.* **83,** 369 (1957).
5. B. W. Nishita and B. W. Kowalevsky. *Soil Sci.* **81,** 317 (1956).
6. A. W. Jackson, D. Craig and H. M. Hugo. *Soil Sci.* **99,** 345 (1965).
7. E. R. Graham. *Soil Sci.* **86,** 91 (1958).
8. F. E. Brikle and J. Letey. *Soil Sci.* **99,** 93 (1965).
9. R. C. Pendleton and R. L. Uhler. *Nature* **185,** 707 (1965).
10. A. Kokotov and R. F. Popova. *Radiochemical Methods for the Determination of Microelements,* p. 76 (in Russian). Zbornik statey Izdat. Akad. Nauk SSSR, Moscow (1965).
11. I. A. Kokotov, R. F. Popova and A. P. Urbanyuk. *Radiokhimiya* **2,** 199 (1961).
12. W. S. Osburn. *Health Phys.* **11,** 1275 (1965).
13. J. Adams. The *Natural Radiation Environment,* p. 513. Univ. of Chicago Press (1964)
14. E. L. Geiger. *Anal. Chem.* **81,** 806 (1959).
15. P. Gaglione, S. Malvicini and L. Vido. *Minerva nucl.* **4,** 156 (1960).
16. B. Kahn. *Anal. Chem.* **28,** 216 (1956).
17. N. A. Vartanov and P. S. Samoylov. *Practical Methods of Scintillation Gamma Spectrometry* (in (Russian). Atomizdat, Moscow (1964).
18. W. F. Hillebrand and G. E. Lundell. *Applied Inorganic Analysis,* J. Wiley, N.Y. (1953).
19. A. P. Kreshkov. *Fundamentals of Analytical Chemistry, Part II.* (in Russian). Izdat. Khimya, Moscow (1965).
20. A. I. Vogel. *Quantitative Inorganic Analysis.* Van Nostrand, N.Y. (1960).
21. J. M. Furman. *Standard Methods of Chemical Analysis.* Van Nostrand, N.Y. (1960).
22. G. A. Fedorov and U. E. Konstantinov. *Problems of Dosimetry and Radiation Protection.* Vol. II, pp. 171–178. Gosatomizdat, Moscow (1963).
23. V. P. Shvedov and M. I. Zhilkina. *Radiochemical Methods for the Determination of Microelements,* p. 171. Zbornik statey. Izdat. Akad. Nauk SSSR, Moscow (1965).
24. S. E. Bresler. *Radioactive Elements.* Gosizd. Techn. Teoret. Lit. Moscow (1957).
25. Heyl *et al.,* Berlin, Cesignost. Personal communication (1961).
26. A. Bauman. Separation of Cs-137. Thesis, Technological Faculty, University of Zagreb (1965).

RAPID FIELD METHOD FOR THE COLLECTION OF RADIONUCLIDES FROM MILK

CHARLES R. PORTER,* MELVIN W. CARTER,* BERND KAHN† and ESTIE W. PEPPER*
National Center for Radiological Health, Public Health Service, U.S. Department of Health, Education and Welfare

Abstract—Surveillance of the radionuclide content of milk is simplified by concentrating the radionuclides on ion-exchange resins. In the field, EDTA added to milk samples complexes calcium ions and prevents loading of the cation-exchange resin by calcium. One-liter samples of milk are then passed consecutively through 40 ml of anion-exchange and 85 ml of cation-exchange resin at a rate as great as 100 ml/min. The resins retain the fission products that enter cows' milk—radioiodine by anion-exchange, and radiostrontium, radiobarium, and radiocesium by cation-exchange. The resin columns are washed with water, sealed, and shipped to the laboratory for analysis.

In the laboratory, iodine-131, barium-140, cesium-137, and naturally occurring potassium-40 are determined by gamma spectral analysis of the resin columns. Radiostrontium and radiobarium are eluted from the cation resin with 4N sodium chloride and radiobarium is separated as the chromate. Radiostrontium is then reprecipitated with strontium carrier as the carbonate, and measured in a low-background beta counter. Strontium-90 is distinguished from strontium-89 by the ingrowth of the yttrium-90 daughter.

Transporting the resin columns from field to laboratory is simpler and more economical than shipping bulk milk samples, and loss of samples in transit is minimized. The columns allow complete analysis of the cited radionuclides in that more than 95% of each is collected on the resin. Sample concentration is rapid, occurring in less than 15 min. By comparison with liquid milk analysis on 3.5-liter samples, gamma spectral analysis is more sensitive than other methods because of increased counting efficiencies resulting from the small volume of the resin, and radiochemical analysis of the radiostrontium is a rapid, simple procedure.

INTRODUCTION

Milk is recognized as one of the most important products for measuring radioactive contamination in man's environment; it is (1) one of the most important components of the diet, (2) available at all seasons of the year in all sections of the country, (3) one of the earliest indicators of the presence of fresh fission products in the environment (the time lapse from vegetation consumption by the cow to milk consumption by man is only a few days), and (4) a major source for the intake of several radionuclides into man. A comprehensive pasteurized milk network was established by the Public Health Service to provide adequate radiological surveillance.[1]

Because the cow discriminates against many radioactive contaminants, only five major fission products are usually found in milk—iodine-131, strontium-89, strontium-90, cesium-137, and barium-140.[2] Due to the low concentrations of these radionuclides and the presence of proteins and salts, a radiochemical analysis requires a large sample volume and extensive separation, and is therefore both difficult and expensive.[3]

Early procedures for the determination of strontium-89 and strontium-90 involved ashing and nitric acid separations[4, 5, 6] or protein precipitation and nitric acid separation.[7] The development of an ion-exchange method for simple determination of strontium-90 and strontium-89 in milk,[8, 9] provided a faster and less expensive procedure. Several other procedures

* Southeastern Radiological Health Laboratory, Montgomery, Alabama.

† Nuclear Engineering Laboratory, 4676 Columbia Parkway, Cincinnati, Ohio.

for analyzing milk for radionuclides were also introduced; e.g. a batch ion-exchange process,[10, 11] rapid methods for estimating fission products,[12] solvent extraction of iodine-131,[13] collection of iodine-131 on anion-exchange resin[14] and silver chloride.[15]

However, the problems of handling and expense in shipping large samples (1-4 liters of milk) were still present. Field methods for the collection and analysis of specific nuclides have been presented for nuclides such as iodine-131[16, 17, 18] and cesium-137.[3]

With the rapid field method presented here, all five significant radionuclides are collected and concentrated for analysis. Provision is made for a complete separation of strontium from calcium for efficient beta counting and yield determination.

In the field, a solution containing disodium ethylenediaminetetraacetate (EDTA), buffer, and strontium and barium carriers, is added to one liter of milk. The milk is passed consecutively through 40 ml of anion-exchange (Cl^-) and 85 ml of cation-exchange (Na^+) resin at a flow rate of approximately 100 ml/min. The radioiodine is retained on the anion resin and the radioactive cations are adsorbed on the cation resins.

In the laboratory, iodine-131, barium-140, cesium-137 and naturally occurring potassium-40 are determined by gamma spectral analysis of the resin columns. Radiostrontium and radiobarium are eluted from the cation resin with 4N sodium chloride and precipitated with their carriers as the carbonates. This precipitate is dissolved and barium is separated as the chromate. Strontium is then reprecipitated and measured in a low-background beta counter.

After a suitable yttrium-90 ingrowth period, the sample is recounted and strontium-89 and strontium-90 activity are determined from ingrowth and decay calculations.[19] Alternatively, after suitable ingrowth, yttrium may be separated as the hydroxide and reprecipitated as yttrium oxalate for beta counting to determine strontium-90 activity.

MATERIALS

Complexing solution (previously prepared in laboratory):

Dissolve 216 g EDTA in 2500 ml distilled water. Add 10 ml each of Sr^{++} (40 mg/ml) and Ba^{++} (40 mg/ml) carrier. Then add 200 ml of ammonium acetate buffer (pH 5.2) and 70 ml 6N ammonium hydroxide to adjust pH to 5.65. Dilute to 3 liters.

3% EDTA:

Dissolve 33.3 g of EDTA in 900 ml distilled water, adjust pH to 5.2 with concentrated ammonium hydroxide and dilute to one liter.

Anion exchange resin, Dowex 2-X8, 20-50 mesh, Cl form:

Wash 40 ml of resin with 150 ml distilled water.

Cation exchange resin, Dowex 50W-X8, 50-100 mesh, Na^+ form:

Wash 85 ml of resin (H^+ form) with 500 ml of 4N sodium chloride followed by 250 ml distilled water, each at a flow rate of 10 ml/min.

Ion-exchange apparatus (Fig. 1):

The ion-exchange apparatus consists of an upper, 2.5-cm diameter column containing 40 ml (wet volume) of anion resin and a lower, 3.2-cm diameter column, containing 85 ml of cation resin. The two columns are joined with a double machine-threaded screw cap. The welded polyethylene disks in the bottoms of the columns contain 0.5-cm diameter holes, and the resin beds are supported by coarse, polyethylene wool. A polyethylene funnel, 1.5-liter capacity, fitted with a screw cap, attaches to the top of the connected columns.

Millipore filter—LS or BC membrane, approximately 5 μ-pore size.

Low-background beta counter.

Multichannel gamma analyzer; 5 × 4 in. NaI (Tl) crystal with $2\frac{1}{2}$ in. deep, $1\frac{3}{16}$ in. diameter well.

PROCEDURE

In the field, add 300 ml of complexing solution to 1 liter of milk and mix well. Remove the screw cap from the top of the anion column and attach the funnel. Pour the sample into the funnel. Remove the screw cap from the bottom of the cation column and let the milk sample pass through at gravity flow ($\approx$ 100 ml/min). Wash the resins with distilled water leaving enough water on the resin to keep it wet. Replace the screw caps on top and bottom of columns and ship to the laboratory for analysis.

In the laboratory, separate the columns; then

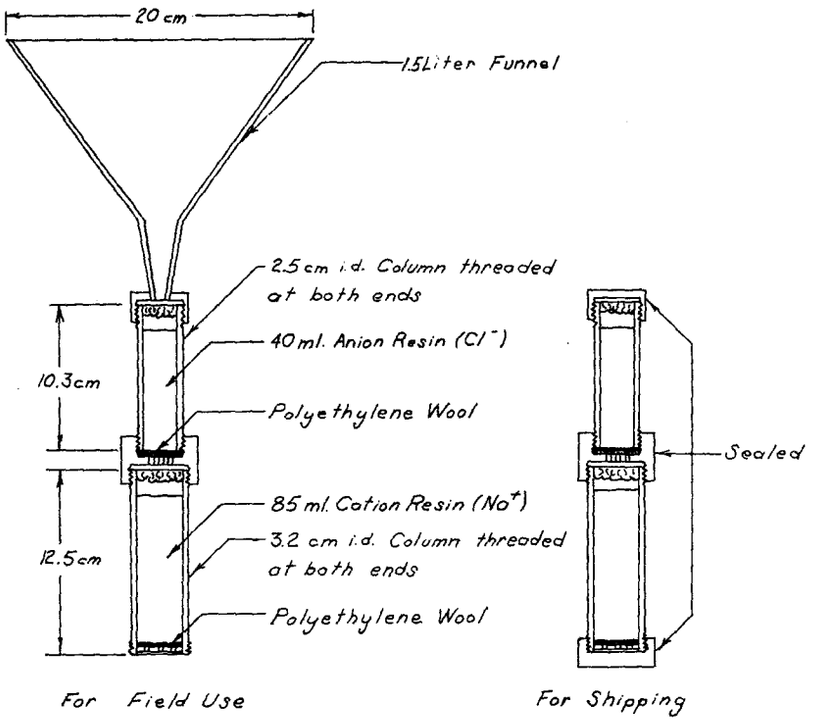

FIG. 1. Ion-exchange apparatus.

invert each and count in a well crystal for gamma activity. Determine iodine-131 activity by gamma spectral analysis of the anion resin and determine cesium-137, barium-140, and potassium-40 from gamma spectral analysis of the cation resin.

Wash the cation resin with distilled water to remove any remaining milk residue. Elute residual calcium retained by the resin with 800 ml of 3% EDTA (pH 5.2) at a flow rate of 20 ml/min followed by 200 ml of distilled water. Record the time of EDTA elution as the beginning of yttrium-90 ingrowth.

Wash absorbed EDTA from the column with 200 ml of 1.5N sodium chloride at 10 ml/min. Place 1000 ml of 4N sodium chloride in a reservoir and let it flow through the column at 20 ml/min. Collect the first 400 ml, which contain strontium and barium. Allow the remaining 600 ml of 4N sodium chloride to pass through to recharge the resin.

Add 1 ml 6N sodium hydroxide to the strontium-barium eluate. Stir and slowly add 10 ml 3N sodium carbonate. Continue stirring with a magnetic stirrer for 30 min. Centrifuge and discard supernatent liquid. Dissolve precipitate with 5 ml 1N nitric acid and add 5 ml of ammonium acetate buffer (pH 5). Heat in a water bath with stirring and slowly add 1 ml of 0.5N sodium chromate. Centrifuge and decant supernatent liquid containing strontium. Add 2 ml concentrated ammonium hydroxide to the supernatent liquid and precipitate strontium carbonate with 2 ml of 3N sodium carbonate. Cool in an ice bath and collect strontium carbonate on a tared membrane filter. Wash with three 10-ml portions each of water, 95% ethanol and diethyl ether. Weigh and count in a low-background beta counter.

RESULTS AND DISCUSSION

Experimental tests with strontium-85, barium-133, cesium-137 and calcium-45 tracers were performed to determine the optimum EDTA

concentration, pH and resin volume. Fresh pasteurized milk, obtained from local dairies, was used in these analyses and contained 1.20–1.24 g Ca/liter and 1.40–1.50 g K/liter. From experience, the levels of calcium and potassium have been found to be fairly constant —1.1–1.3 g Ca/liter and 1.4–1.6 g K/liter. This reasonably constant level helps make the separation of calcium by complexing with EDTA relatively simple.[20] Samples containing higher (1.9 g K/liter and 1.4 g Ca/liter) concentrations were analyzed without adverse effects.

Table 1. *Retention of Radionuclides on the Resins*

Radionuclide	% retention
Anion	
^{131}I	96 ± 3
Cation	
^{133}Ba	99 ± 1
^{85}Sr	99 ± 1
^{137}Cs	98 ± 2
^{40}K	98 ± 2

As shown in Table 1, over 95% of the five radionuclides are retained on the resins by this procedure. The distribution of the nuclides on the resin columns (Table 2) shows that most of the nuclides are contained in the upper portions of the resins. For this reason, the columns are inverted for counting to increase counting efficiency. The concentration of radionuclides in the small volumes allows them to be counted for gamma activity in a well crystal. The spread of cesium on the resin determines the column size and resin volume. If sample quantities greater than 1 liter are to be used, the columns, resins, and reagents must be increased accordingly.

Table 3 indicates that the increased efficiency obtained by gamma spectral analysis of the resin cartridges in a well crystal more than compensates for the smaller sample volume (1 liter) passed through the columns as compared to 3.5 liters when whole milk is gamma counted on the 4 × 4 in. crystal. The analysis of potassium-40 by this procedure provides a check for the volume of milk actually passed over the cartridges as the quantity of potassium-40 in one liter of milk usually lies in the range of 1200–1350 pCi.

The separation of calcium from strontium is shown in Table 4. From 90 to 95% of the calcium is separated in the field in the milk effluent, whereas the residual calcium is removed from the resin by washing with EDTA.

Figure 2 shows good strontium retention with calcium separation occurring below pH 5.3. Less than 0.02% of 1.2 g/l.—that is less than 0.24 mg Ca—is in the strontium precipitate. The pH of 5.2 was selected to provide a safety margin since strontium begins to break through at pH 5.4 and because at lower pH values the milk tended to precipitate as the isoelectric point is approached.

Table 2. *Percentage Distribution of Radionuclides on Resin Columns*

Anion 40 ml Cl^- (20–50 mesh)		Cation 85 ml Na^+ (50–100 mesh)				
Resin volume (ml)	^{131}I	Resin volume (ml)	^{133}Ba	^{85}Sr	^{137}Cs	^{40}K
0–7	51.4	0–14	65.0	62.0	27.0	25.9
8–14	32.1	15–28	23.0	22.0	28.0	34.2
15–21	10.5	29–42	8.0	13.0	22.0	27.7
22–28	4.9	43–56	3.0	2.0	15.0	12.0
29–35	1.0	57–70	1.0	0.6	6.0	<0.1
36–40	<0.1	71–85	<0.1	0.1	2.0	<0.1

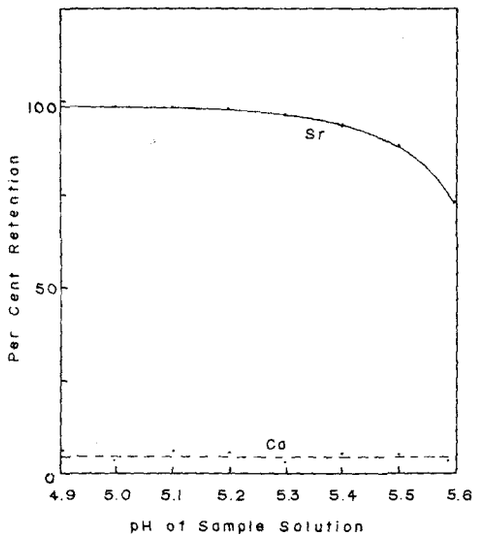

FIG. 2. Effect of pH on strontium-calcium separation on cation resin with 1.5% EDTA solution.

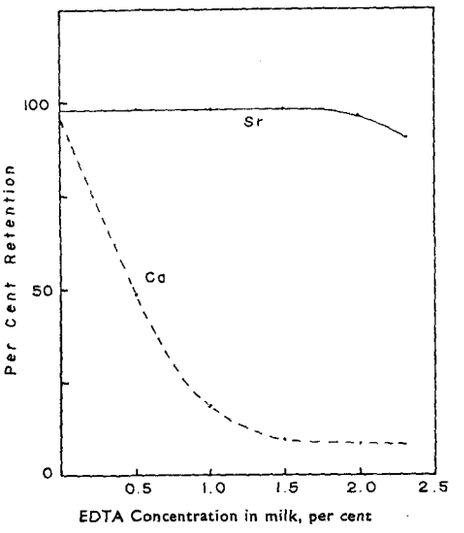

FIG. 3. Effect of EDTA concentration on strontium-calcium separation on cation resin at pH 5.2.

As indicated in Fig. 3, the best EDTA concentration for separating strontium from calcium is 1.5% at pH 5.2. At higher concentrations, EDTA complexes strontium more effectively whereas at lower concentrations calcium is incompletely complexed.

Most of the potassium and cesium together with EDTA that have been adsorbed by the resin[21] are removed from the resin in the 200 ml of 1.5N sodium chloride that is discarded. Barium is separated from the strontium by precipitation of barium chromate.

Strontium recovery is measured gravimetrically and the average yield is 85%. Because 1 liter of cow's milk has been found to contain approximately 1 mg of stable strontium,[22] the milk initially contains 1 mg more than the 40 mg added. Hence the recovery overestimates the yield by approximately 2%.

If fresh fission products are in milk and the

Table 3. Comparison of Counting Efficiencies for Resin Columns and Liquid Milk

Radionuclide	Characteristic peak MeV	Resin column		Liquid milk in Marinelli beaker	
		5 in. × 4 in. crystal, $1\frac{3}{16}$ in. diam. well cpm/pCi	On top of 4 in. × 4 in. crystal cpm/pCi	3.5 liter 4 in. × 4 in. crystal cpm/pCi/l.	1 liter 4 in. × 4 in. crystal cpm/pCi/l.
^{131}I	0.36	1.10	0.28	0.40	0.19
^{137}Cs	0.66	0.43	0.15	0.30	0.14
^{140}Ba	0.49	0.29	0.13	0.25	0.13
^{40}K	1.46	0.029	0.009	0.019	0.009

Table 4. Separation of Calcium from Strontium at Various Steps in the Procedure

Fraction	Volume (ml)	% calcium	% strontium
Sample effluent and water wash	1500	96.0	0.8
3% EDTA and wash	1000	3.2	0.6
1.5N NaCl	200	0.8	3.6
4N NaCl	400	<0.02	90.0
4N NaCl (to recharge)	200		5.0

interval between milking the cow and passing the milk sample through the ion-exchange resin is one hour or longer, appreciable amounts of lanthanum-140 and yttrium-90[8,9] may grow into the sample and be retained on the anion-exchange resin. High concentrations of lanthanum-140, relative to iodine-131, may interfere in the gamma spectral determination of iodine-131. Such interference by lanthanum-140 can be decreased by using one of three alternate procedures:

1. If the presence of lanthanum-140 is expected, *do not* add the complexing solution to the milk, but pass the milk directly through the anion-exchange resin. Then add the complexing solution to this effluent and pass this solution through the cation-exchange resin.

2. Observe the gamma decay in the 0.36 MeV energy range and by use of simultaneous equations distinguish between the 8.1-day half life of iodine-131 and the 1.7-day half life of lanthanum-140.

3. Pass 50 ml of 0.05N silver nitrate solution through the anion-exchange resin. Elute lanthanum-140 from the resin with 300 ml of 2.5N nitric acid. After elution, the resin retains 93% of iodine-131 and only 4% of lanthanum-140.

The average of results from nine replicate samples analyzed by both this procedure and the routine laboratory procedure, a tentative standard method utilizing ion-exchange,[28] agreed within 1.1% as shown in Table 5. Based on the standard deviation, 68% of duplicate values should be within 1 pCi/l. of their average and 95% within 2 pCi/l. Sixty samples of varying origin were analyzed in duplicate by both methods. A comparison shows 97% of the values by the routine procedure and 95% of the values by this procedure were within 1 pCi/l. of their average and 100% of the values by both procedures were within 2 pCi/l. Also 92% of the two sets of values were within 1 pCi/l. of the average of the four measurements and 99% were within 2 pCi/l.

Table 5. Comparison of Strontium 90 Results by this Procedure to Routine Procedure

This procedure pCi/l.	Routine procedure pCi/l.
11.2	9.6
10.4	10.4
10.5	11.0
8.9	9.2
7.9	11.1
10.2	9.0
10.3	8.9
9.8	9.1
9.4	10.9
9.8 ± 1.0*	9.9 ± 0.9*

* Error is expressed as one sigma deviation.

Shipping costs with this procedure are approximately one-sixth that of procedures which require the shipment of large liquid milk samples. Costs are compared in Table 6.

The procedures presented here tend to eliminate or minimize many of the problems previously encountered in the radiological surveillance of milk by providing a system to (1) collect and concentrate all the significant fission

Table 6. Estimated Cost Comparison for Transportation, Present Method Versus Field Method

Field Method

Materials shipped	Destination	Shipping cost (air mail)	
		300–600 mi.	600–1000 mi.
Shipping container, cartridges and complexing solution	Collector	$1.23	$1.34
Shipping container, cartridges and empty complexing solution bottle	Laboratory	.73	.78
Total shipping cost		$1.96	$2.12

Present Method

Materials shipped	Destination	Shipping cost (air mail)	
		300–600 mi.	600–1000 mi.
Shipping container, and empty one gallon bottle	Collector	≈ $4.00	≈ $4.50
Shipping container, and full one gallon bottle	Laboratory	≈ 7.25	≈ 8.25
Total shipping cost		≈ $11.25	≈$12.75

products in milk, (2) eliminate the need for refrigeration and preservative, (3) effectively separate calcium from strontium without using fuming nitric acid, (4) increase gamma counting efficiency by presenting the sample to be counted with improved geometry, (5) provide a rapid, precise, and accurate analysis, and (6) reduce problems and costs in handling and transporting bulk samples.

ACKNOWLEDGEMENTS

The authors thank Mrs. Ann B. Strong for her many comments and suggestions and Mrs. Ursula Moss and Miss Joy Favor for their technical assistance.

REFERENCES

1. *Radiological Health Data* **1,** 7 (1960).
2. J. E. Campbell *et al. American Journal of Public Health* **49,** 225 (1959).
3. A. L. Boni. *Analytical Chemistry* **38,** 89 (1966).
4. G. W. Milton and W. E. Grummit. *Canadian Journal of Chemistry* **35,** 541 (1957).
5. G. K. Murthy and J. E. Campbell. *Journal of Dairy Science* **42,** 1289 (1959).
6. G. K. Murthy, L. P. Jarnagin, and A. S. Goldin. *Journal of Dairy Science* **42,** 1276 (1959).
7. G. K. Murthy, J. E. Coakley, and J. E. Campbell. *Journal of Dairy Science* **43,** 151 (1960).
8. C. R. Porter *et al. Analytical Chemistry* **33,** 1306 (1961).
9. C. R. Porter and B. Kahn. *Analytical Chemistry* **36,** 676 (1964).
10. F. E. Butler. U.S. Atomic Energy Commission Report, DP-473 (1960).
11. C. R. Porter *et al.* Environmental Health Series, Public Health Service Publication, No. 999-RH-10, 1–16 (1965).

12. B. KAHN *et al.* Environmental Health Series, Public Health Service Publication, No. 999-R-2 (1963).
13. Y. OMONO and M. SAIKI. *Radioisotopes* (*Tokyo*) **13,** 304 (1964).
14. B. KAHN. *Journal of Agricultural and Food Chemistry* **13,** 21 (1965).
15. W. D. FAIRMAN and J. SEDLET. *Analytical Chemistry* **38,** 1171 (1966).
16. C. R. PORTER and M. W. CARTER. *Public Health Reports* **80,** 453 (1965).
17. A. L. BONI. *Analyst* **88,** 64 (1963).
18. F. E. BUTLER. *Health Physics* **8,** 273 (1962).
19. R. J. VELTEN. *Nucl. Instr. Methods*, **42**, 169 (1966).
20. C. R. PORTER *et al.* Determination of radiostrontium in food and other environmental samples, Environmental Science and Technology, in press.
21. P. S. DAVIS *Radiobiology*, pp. 183–190, Butterworth, London, 1961.
22. G. L. REHNBERG *et al.* Levels of stable strontium in environmental media (to be published).
23. *Standard Methods for the Examination of Dairy Products* (12th ed.), American Public Health Association, Inc., New York (1966).

Disclaimer

Mention of commercial products does not constitute an endorsement by the Public Health Service.

PREPARATION OF "METAL SALT-ION EXCHANGE RESINS" AND THEIR APPLICATION TO RADIOCHEMICAL ANALYSES

MASAMI IZAWA and KAZUO WATARI
National Institute of Radiological Sciences 9–1, 4-Chome, Anagawa, Chiba, Japan

Abstract—A series of a new type of adsorbents for radionuclides in aqueous solutions has been synthesized consisting of an ion exchange resin and an inorganic salt, and their properties were studied. We named them "metal salt-ion exchange resins". Preparation of the "resins" are simple and easy. For example, "ferric hydroxide-cation exchange resin" can be made by putting a ferric form of a cation resin into a concentrated hydroxide ion solution, and "copper ferrocyanide-anion exchange resin" by putting a ferrocyanide form of an anion resin into a cupric ion solution.

The prepared "resins" have combined adsorption properties of both the metal salt and the exchange resin moieties. They are generally non-hygroscopic and granular, so that they can be stored in dry state.

In principle, the "resins" can be made by any combination of insoluble metal salts and ion exchange resins. By considering adsorption capacity and exchangeability of metal salts and resins, a wide variety of applications of the "resins" can be made for chemical and radiochemical analyses; e.g. "metal hydroxide-resins" for adsorption of zirconium, ruthenium and alkaline earth ions, "metal ferrocyanide-resins" for specific adsorption of cesium and for mutual separation of alkali metals and of fission products (Sr, Zr, Nb, Ru, Cs, Ce). A few examples of applications of "ferrocyanide-resins" are presented.

INTRODUCTION

In radiochemical analyses, co-precipitation with, or adsorption on, insoluble metal salts is often used as the first step for concentrating the desired radionuclides, or as an effective means for scavenging. For example, hydroxides or sulfides have been used for the concentration of nuclides from a large volume of sea water,[1, 2] and ferrocyanides for the collection of cesium from a number of aqueous media.[3] However, experimental techniques of co-precipitation and adsorption are usually rather troublesome and time-consuming. Moreover, synthesis of the adsorbents is difficult and generally not reproducible. Of course, we can use ion exchange resins very effectively, but they have serious limitations for their use: they cannot be used for the analysis of radioactive contamination in solutions of high salt concentration such as sea water.

In the course of our basic study on the behavior of ions in ion exchange resins, we thought that inorganic insoluble salts, which have adsorptive or ion exchange properties, could be formed in resins without impairment of the exchange properties of the resins themselves. Shortcomings of co-precipitation and adsorption methods would largely be overcome by the use of such new adsorbents.

The first use of this type of adsorbents was reported by McIsaac and Voigt[4] in their study of mutual separation of phosphorus and sulfur, and then by Merrill *et al.*[5] for the separation of ^{9}Be from sea water, and by Lal *et al.*[6] for the determination of silica in sea water. All of these authors used iron hydroxide-Dowex 50 combination and the adsorbent was prepared in columns.

We have prepared a number of such type of adsorbents having various combination of metal salts and resins, and proposed the general name of "metal salt-ion exchange resins" for them.

The preparation and the use of "iron hydroxide-cation exchange resin",[7] "metal sulfide-cation and -anion resins"[8] and "copper ferrocyanide-anion resins"[9] have already been reported.

The present report discusses the preparation and the properties of these adsorbents in a more general way, and touches upon some of the applications of "iron ferrocyanide-anion exchange resins".

PREPARATION OF "METAL SALT-ION EXCHANGE RESINS"

In principle, a given "metal salt-ion exchange resin" can be made either from a cation exchanger or from an anion exchanger, although the degree of ease of the preparation varies with the exchangers as well as with the metal salts.

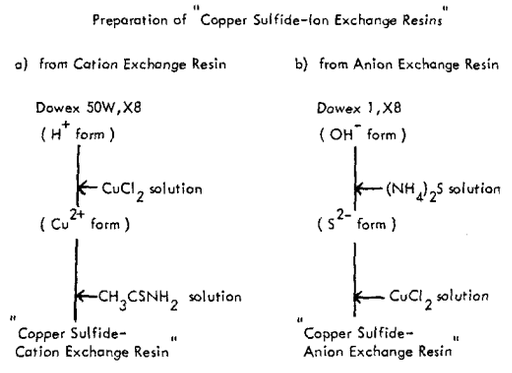

FIG. 1. Preparation of "copper sulphide-ion exchange resins".

The schemes for preparation of "copper sulfide-cation exchange resin" and "copper sulfide-anion exchange resin" are presented in Fig. 1. The hydrogen form of a cation exchange resin, in this case, Dowex 50W, is converted to the copper form by treating the resin with 0.5 M copper chloride solution. After washing the resin with water, thioacetamide solution (5%) is added to the resin suspension, and the suspension is warmed to about 60°C on a water bath. Alternatively, hydrogen sulfide gas may be bubbled into the suspension. The color of the resin changes from light blue to black, showing the formation of copper sulfide in the resin matrix. From the hydroxide form of an anion exchange resin, Dowex 1, the sulfur form is made first by adding concentrated ammonium sulfide solution (1: 1), and then converted to "copper ferrocyanide-Dowex 1" by 1M copper chloride solution.

"Iron ferrocyanide-anion exchange resin" was prepared as follows; Amberlite IRA-904, a macro-reticular resin, is converted to the ferrocyanide form by 0.5 M potassium ferrocyanide solution. After thorough washing, iron ferrocyanide is formed with 1 M ferric chloride solution. The use of a macro-reticular type resin seems to be essential for the preparation of the stable "ferrocyanide-resins", presumably because of the large size of the ferrocyanide anion. "Iron ferrocyanide resin" has higher stability in acid solutions than "copper ferrocyanide-resin" previously reported.[9]

Adsorption of alkali metal ions on the "copper ferrocyanide-resin" was also studied. Distribution coefficients (K_d, as expressed by activity adsorbed on 1 g of the "resin" divided by activity remained in 1 cc of the solution) increased with the increase of the atomic number of the ions, the ratio of K_d for Cs, Rb, K and Na in very dilute ($< 10^{-7}$ M) and acidic solutions being approximately 10^4: 10^3: 10: 1. The effect of cesium carrier on the adsorption of ^{137}Cs is shown in Table 1. Results on the adsorption of ^{137}Cs in sea water showed that other ions, including alkali metals, had no appreciable effect on ^{137}Cs adsorption.

The "metal salt-ion exchange resins" have the same ion exchange capacities as those of the parent resins used as the starting materials. For example, 1.3 g of "copper ferrocyanide-resin" was formed from 1.0 g of the hydroxide form of Amberlite IRA-904, and, by repeating the same treatment, another 0.3 g of ferrocyanide could be incorporated into the resin matrix. If one uses a metal salt other than ferrocyanide for the second treatment, a "mixed metal salt-ion exchange resin" can be made. Such examples are "ferrocyanide-oxalate-resin" and "ferrocyanide-sulfide-resin", and others.

PROPERTIES

"Metal salt-resins" thus prepared retain properties of both the insoluble metal salts and the parent ion exchange resins. As an example,

Table 1. *Effect of Carrier on Distribution Coefficient of Cesium between "Copper Ferrocyanide-Amberlite IRA-904" and Water*

Carrier concentration	Distribution coefficient
carrier free	3.5×10^3
10^{-4} M	2.6×10^3
10^{-3} M	1.5×10^3
10^{-2} M	4.4×10^2
10^{-1} M	6.7
0.5 M	3.0
1.0 M	1.8
5.0 M	5.5×10^{-1}

adsorption of ^{95}Zr on "copper sulfide-resins" from sea water is shown in Fig. 2. Zirconium is adsorbed either on the sodium form of a cation exchanger or on the chloride form of an anion exchanger, as shown in the figure by solid and open triangles, respectively, because zirconium is present as an aggregated form at the pH range of sea water. Adsorption on the "copper sulfide-resins" is distinctly higher than those on the exchangers, as shown by circles in the same figure.

Adsorption of radionuclides on "copper ferrocyanide-Amberlite IRA-904" from acidic solutions is tabulated in Table 2. Cesium is adsorbed on the adsorbent quantitatively, while strontium and cerium is not adsorbed. Adsorptions of zirconium and ruthenium are appreciable, because the nuclides exist in these acidic solutions as complexes and are adsorbed as anions on the exchange residues of the Amberlite IRA-904. In nitric acid solution, the adsorptions are distinctly lower than in hydrochloric acid solution. Adsorption of cesium on "iron ferrocyanide-Amberlite IRA-904" is better than that on "copper ferrocyanide-resin" and quantitative from the solutions of 4 N nitric acid or below (Table 3).

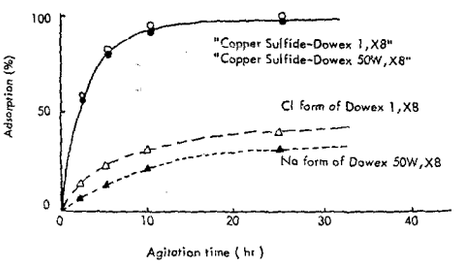

FIG. 2. Adsorption of ^{95}Zr on "copper sulfide-resins" from sea water (Batch experiment: 5 ml solution and 0.5 g resins).

APPLICATIONS

When the properties of the metal salt moiety and those of the original ion exchange resin are duly considered, a variety of applications of

Table 2. *Adsorption of Radionuclides on "Copper Ferrocyanide-Amberlite IRA-904" from Acidic Solution*

(Batch experiment: 5 ml solution and 0.5 g "resin")

Acid concentration \ Nuclide	Adsorption (%) of:				
	^{137}Cs	^{85}Sr	^{144}Ce	^{95}Zr	^{106}Ru
10^{-1} M HCl	99.9 (99.9)	0	0	94.3	54.1
1.0 M HCl	99.7 (96.2)	0	0	78.8	53.6
2.0 M HCl	99.7 (79.1)	0	0	79.6	49.7
4.0 M HCl	99.5 (42.2)	0	0	86.8	59.9
6.0 M HCl	73.9 (19.1)	0	0		
8.0 M HCl	84.2 (8.4)	0	0	93.4	96.8

( ) Adsorption from nitric acid solution.

Table 3. *Adsorption of* ^{137}Cs *on "Iron Ferrocyanide-Amberlite IRA-904" from Nitric Acid Solution*

(Batch experiment: 5 ml solution and 0.5 g "resin")

Agitation time / Acid concentration	Adsorption (%) after:				
	15 min	30 min	1 hr	3 hr	24 hr
10^{-1} M	98.4	98.8	99.4	99.5	99.9
1.0 M	98.7	99.4	99.6	99.8	99.9
2.0 M	99.2	99.5	98.9	99.9	99.9
4.0 M	99.5	99.4	99.6	99.9	99.9
6.0 M	86.6	87.1	91.0	95.8	95.0
8.0 M	66.9	63.3	59.1	77.1	74.7
10.0 M	39.1	36.8	38.1	52.2	46.4

this new type of adsorbents can be anticipated. A few examples of the applications of "ferrocyanide-resins" will be presented below.

Quantitative determination of ^{137}Cs *in sea water*

Quantitative determination of ^{137}Cs in sea water was carried out using "copper ferrocyanide-anion exchange resin". Fifty liters of sea water, collected at a place along the Pacific coast of Japan, was passed through a column filled with 500 g of the "copper ferrocyanide-Amberlite IRA-904" at a flow rate below 1 l./min. Cesium was adsorbed on the column, while strontium and some other nuclides were passed through. Cesium was then eluted from the column with 6 N nitric acid, purified by scavenging with ferric hydroxide, and finally precipitated as cesium chloroplatinate and counted for radiactivity. The radioactive concentration in sea water was found to be 0.47 ± 0.02 $\mu\mu$ Ci/l. For the same batch of sea water, co-precipitation with nickel ferrocyanide and with ammonium molybdophosphate, followed by cesium chloroplatinate precipitation[10] resulted in the radioactive concentration of 0.45 ± 0.02 $\mu\mu$ Ci/l. This is an example of the specific adsorption of cesium on ferrocyanide. The use of the "ferrocyanide-resin" column has advantages over the co-precipitation method in that the former is simpler and less time-consuming than the latter.

Decontamination of ^{137}Cs *from cow's milk*

As another application of "ferrocyanide-resin", decontamination of ^{137}Cs from milk was studied. Data obtained by batch experiment and column operation are shown in Table 4. Here, "nickel ferrocyanide-Amberlite IRA-904" was used, and cesium contamination in milk could be removed with no deterioration of milk properties. Tests performed were: heat coagulation test, alcohol test, pH and calcium content.

Mutual separation of fission products

By using a column of "iron ferrocyanide-Amberlite IRA-904" pre-treated with ammonium oxalate, the successful sequential separation of radionuclides, ^{90}Sr, ^{144}Ce, ^{95}Zr, ^{95}Nb, ^{106}Ru and ^{137}Cs, were done in this order. One cc of carrier-free mixture of the nuclides in 0.5% ammonium chloride solution was first applied to the column, and eluted with water, hydrochloric acid, and nitric acid. The elution curve is shown in Fig. 3. In the same figure, the curve with oxalate form of Dowex 1 X8, by Yajima *et al.*[11] is shown for comparison. Cesium was eluted out first together with strontium, and another column of a cation exchanger must be used for cesium-strontium separation.

Removal of ^{137}Cs *from reprocessing waste*

The use of "iron ferrocyanide-Amberlite IRA-904" for the removal of ^{137}Cs from fuel

Table 4. Adsorption of ^{137}Cs on "Nickel Ferrocyanide-Amberlite IRA-904" from Milk

(Batch experiment: volume of milk, 50 ml)

"Resin" (g)	0.5	0.5	0.5	0.5	0.1	0.05
Agitation time (hr)	1	2	3	14	14	14
Adsorption (%)	98.2	99.0	99.4	99.9	99.4	98.5

Column operation: 7 mm in diamater; 1.5 g "resin"; flow rate, 2 ml/min

Milk (ml)	100	500	1000
Adsorption (%)	99.6	99.3	99.0

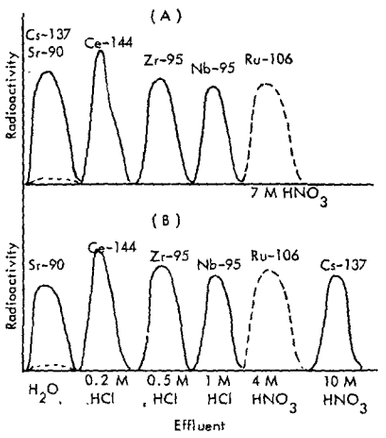

FIG. 3. Mutual separation of fission products by: (a) Anion exchange resin. (b) "Iron ferrocyanide-Amberlite IRA-904".

reprocessing waste solution was expected, because of its high adsorbability of ^{137}Cs in nitric acid solution (see Table 3). A preliminary experiment was carried out by batch method and the results are shown in Table 5. When 2 g of the adsorbent was put into 50 ml of the waste solution, adsorption was above 99% within 1 hr shaking. Composition of the synthetic purex waste solution, after Bruce, is shown in Table 6.

CONCLUSION

"Metal salt-ion exchange resins" are simple and easy to prepare, obtainable in any given particle sizes. They can be used in batch or column operation. As they retain characteristic properties of both the insoluble salt and the ion exchange moieties, a wide range of applications, including those to waste treatment, can be expected. A few examples of applications were presented.

Table 5. Concentration of ^{137}Cs from Synthesized Purex Waste by "Iron Ferrocyanide-Amberlite IRA-904"

(Batch experiment: volume of waste solution, 50 ml)

"Resin" (g)	1	1	1	2	2	2
Agitation time (hr)	0.5	1	3	0.5	1	3
Adsorption (%)	91.1	93.3	95.7	98.0	99.0	99.9

Table 6. *Composition of synthesized purex waste*

Na_3PO_4	0.0004 M/l.
$NaNO_3$	0.0188
$Al(NO_3)_3$	0.004
$Fe(NO_3)_3$	0.01
$Ni(NO_3)_2$	0.0002
$Cr(NO_3)_3$	0.0004
H_2SO_4	0.025
HNO_3	2.337

REFERENCES

1. A. C. WAHL and N. A. BONNER. *Radioactivity Applied to Chemistry*. John Willey & Sons, Inc., New York (1951).
2. V. J. SODD, A. S. GOLDIN and R. J. VELTEN. *Anal. Chem.* **32,** 25 (1960).
3. V. KÔURIM, J. RAIS and B. MILLION. *J. Inorg. Nucl. Chem.* **26,** 1111 (1964).
4. L. D. MCISAAC and D. A. VOIGT. USAEC Document ISC-271 (1952).
5. J. R. MERRILL, E. F. X. LYDEN, M. HONDA and J. R. ARNOLD. *Geochim. Cosmochim. Acta* **18,** 108 (1959).
6. D. LAL, J. R. ARNOLD and B. L. K. SOMAYAJULU. *Geochim. Cosmochim. Acta* **28,** 1111 (1964).
7. KAZUO WATARI, HIROYUKI TSUBOTA, TAKU KOYANAGI and MASAMI IZAWA. *J. At. Energy Soc. Japan* **8,** 130 (1966).
8. KAZUO WATARI, HIROYUKI TSUBOTA, TAKU KOYANAGI and MASAMI IZAWA. *J. At. Energy Soc. Japan* **8,** 182 (1966).
9. KAZUO WATARI and MASAMI IZAWA. *J. Nucl. Sci. Technol.* (*Japan*) **2,** 321 (1965).
10. RYOJI HIGANO, YUTAKA NAGAYA, MASARU SHIOZAKI and YOSHIO SETO. *J. Oceanog. Soc. Japan* **18,** 200 (1963).
11. SEISHI YAJIMA, EIJI SHIKATA and CHIZUKO YAMAGUCHI. *Japan Analyst* **7,** 721 (1958).

L'USO DI COLONNE CROMATOGRAFICHE SELETTIVE PER L'ISOLAMENTO DI ALCUNI RADIONUCLIDI DI PARTICOLARE INTERESSE IN RADIOPROTEZIONE

C. TESTA

Servizio di Medicina e Sanità, Centro Studi Nucleari Casaccia, CNEN, Roma, Italy

Sommario—Vengono presentate diverse applicazioni pratiche di cromatografia in colonna a fasi invertite riguardanti l'isolamento di alcuni radionuclidi di particolare interesse in radiotossicologia, fisica sanitaria e radioattività ambientale.

La tecnica generale si basa sulla possibilità di impregnare irreversibilmente un polimero chimicamente inerte in polvere con un composto liquido (od una soluzione organica di questo) il quale trattenga selettivamente l'elemento da isolare. Tale metodo puó spesso sostituire vantaggiosamente l'uso delle resine a scambio ionico e dell'estrazione con solventi. Usando una colonna di politrifluorocloroetilene (Kel-F) supportante del tri-n-butil fosfato (TBP) è stato possibile separare e determinare l'uranio arricchito (^{233}U, ^{234}U, ^{235}U) nell'urina, precedentemente acidificata con HNO_3. Per l'isolamento del torio naturale dall'urina è stata usata una colonna supportante una soluzione di tri-n-ottil fosfina ossido (TOPO); il ^{239}Pu è stato selettivamente trattenuto dall'urina, 1-2 *M* in HNO_3, con una colonna di Kel-F supportante lo scambiatore anionico liquido tri-n-ottilammina (TNOA). Per la determinazione dell' ^{91}Y nel "fallout" il composto supportato era lo scambiatore cationico liquido: acido di-(2-etil-esil) ortofosforico (HDEHP) il quale separa l'ittrio non solo dai metalli alcalini, alcalino-terrosi, ed altri ioni, ma anche dalla maggior parte della terre rare eventualmente presenti (La, Ce, Pr, Pm, Nd). Il ^{137}Cs è stato separato dai prodotti di fissione trattenendolo selettivamente su una colonna di Kel-F impregnata di tetrafenilborato (TPB) o di dipicrilammina (DPA). Infine lo iodio può essere isolato su una colonna di tetracloruro di carbonio o solfuro di carbonio. I fattori di decontaminazione relativi a queste separazioni sono sull'ordine di 10^2–10^3 e le colonne possono essere rigenerate ed usate per diversi cicli. Anche altri supporti inerti (teflon, politene, p.v.c., ecc) possono essere impiegati con successo.

DETECTION OF FISSIONABLE MATERIALS IN URINE*

J. A. MISKEL
Lawrence Radiation Laboratory, University of California, Livermore, California, U.S.A.

Abstract—A relatively rapid, sensitive method for the determination of uranium or plutonium in urine has been developed. The technique is neutron activation analysis; the reaction involved is (n, fission) and the detection is based on the radiochemical extraction of ^{132}Te. ^{132}Te was chosen since it has a high fission yield, reasonable half-life and cannot be made directly by single neutron capture on any stable tellurium in the sample.

A comparison of the sensitivity of this method with one in which the uranium or plutonium is chemically separated from the urine and α-counted is given in the Table.

Species	Amount (μg)	^{132}Te (count/min)†	α (count/min)
Normal U	2×10^{-2}	5	1.5×10^{-2}
^{235}U	2×10^{-4}	5	1.2×10^{-4}
^{239}Pu	1×10^{-4}	5	7

In practice the standards and unknowns are sealed in polyethylene cones and irradiated. The sample sizes are $\sim$10 ml. After irradiation the cone is opened, tellurium carrier added and a standard radiochemical separation performed. No pre-treatment is given to the specimen. Our irradiation facility allows exposure of six samples simultaneously. Although the method does not distinguish between uranium and plutonium it allows for rapid scanning of a large number of routine samples.

* This work was performed under the auspices of the U.S. Atomic Energy Commission.

† The ^{132}Te data are based on the following conditions: neutron flux: 2×10^{12}/cm^2/sec; irradiation time: 2 hours; chemical yield: 75%; counter efficiency 33%; counter background: 0.5 cpm. The α data assume chemical yield 100%; counter efficiency 50%. Counter backgrounds for alphas are approximately 0.3 cpm.

DISCUSSION

E. Di Ferrante (*Euratom*):

I risultati delle misure di radioattività a basso livello di cui voi determinate il grado di precisione sono sollecitati da voi o inviati spontaneamente dai vari laboratori? Chiedo questo perchè sono io stessa interessata ad analisi di radioelementi naturali, e spesso i campioni analizzati hanno un contenuto piuttosto basso, e potrei in futuro avere bisogno del vostro giudizio.

M. Ferraris (*IAEA*):

La partecipazione a queste misure è del tutto libera. La IAEA invia una lettera di invito con relativo modulo di ordinazione a circa 1000 laboratori. Circa 200 rispondono richiedendo i vari campioni. E' ovvio che la raccolta di indirizzi non potrà mai essere completa per cui si invitano i laboratori a voler fare la più ampia pubblicità alla cosa. Chiunque sia interessato alla cosa puó chiedere di essere incluso nella "mailing list" scrivendo alla IAEA, project LOWRA.

W. J. Meininger (*Netherlands*):

Are calibrations ever made for the adsorbing power of radon on charcoal? Did you calibrate only the radon chambers or did you calibrate other systems as well?

E. Di Ferrante:

The optimum temperature for the maximal adsorption of radon on charcoal is −80° C. We based our calculations on the fact that the calibration of the entire system (and not only of the radon chamber) performed with standard solutions gave an over-all efficiency of about 80% of the α-particles emitted. The calibration was periodically repeated with different charcoal traps and different detectors; the value of the efficiency obtained varied only within 2%.

J. B. Hursh (*U.S.A.*):

1. Do you ever encounter any insoluble residues after preparation by dry and wet ashing? What do you do about these residues?

2. What is the magnitude of the correction you use for the radon originating in the charcoal itself?

I should like to congratulate Dr. Di Ferrante on her very excellent results with what remains a very difficult measurement.

E. Di Ferrante:

1. Muds, ores, food items and all the samples with high silica content may cause some difficulties for their complete dissolution. If a treatment of the ashed samples with H_2SO_4 and HF was not enough, the attack with these acids was repeated several times until a final clear solution was attained. No analysis of solutions having solid residues was performed.

2. During the setting up of the emanation technique apparatus for the preparation of the traps, we tried several types of activated charcoal and the one chosen was found practically with no radium content which could produce some radon. We used anyway always the same exact weight of charcoal for all the traps, so if a correction had to be made, it would always have been the same.

G. Calapaj (*Italy*):

Since 1 pCi of Ra^{226} gives about 7 α-disintegrations per minute on its decay products at equilibrium, and the efficiency of the detector is, as we have heard, about 70%, 1 pCi of Ra^{226} corresponds to about 5 cpm; this means that 1 cpm above the background corresponds to about 0.2 pCi. Since the content of radium exposed in the paper is about 1 pCi per g of ashes (about 0.02 pCi/g) and the weight of the ashes is about 1 g for each sample, I would like to know some more particulars about the procedure illustrated by the Author, including the value of the background and its statistical accuracy.

E. Di Ferrante:

The background is of the order of 0.5 ± 0.1 counts per hour (cph). The lowest samples analysed gave counting rate at least 5 times the background.

A. Franceschini (*Italy*):

1. Quali controlli della tecnica di misura hanno permesso di raggiungere sensibilità di 0,01 μg/l?

2. La media del tenore di U_{nat} in urine di persone non esposte è intorno a qualche μg/l; quale valore medio ha trovato il Dr. Wijker presso il personale del suo centro, e precisamente presso quelle persone che sono poco o per nulla esposte a contaminazione da *U*?

HUB. WIJKER:

1. The great sensitivity of 0.01 μg U/l. urine (= 10 ng/l.) has been achieved by stringent specification of sample preparation and apparatus as described in the detailed abstract issued before the meeting. Sample preparation involves:—(1) using very clean dishes; (2) the way of taking aliquots from the urine samples; (3) very slow drying under a drying bulb; (4) ignition in a flame with a cross section small compared to the dish surface, e.g. in the top of the pilot flame of a Bunsen burner; (5) discarding aliquots with fusion times less than 25 sec or more than 30 sec; (6) cooling without cracking. Apparatus design involves: (1) A.C. supply for UV bulb, D.C. for photomultiplier; (2) separate cooling jackets for photomultiplier and UV bulb; (3) restriction in cooling water inlet to assure constancy of UV bulb temperature; (4) diaphragm and high voltage setting making it possible to fix meter indication for two points according to the calibration curve.

2. The U concentrations in the urine of unexposed people (e.g. children of the employees) were lower than 10 ng/l. The average for the workers with uranium is about 20 ng/l. A value of 30 ng/l is used as a warning level, indicating that there may be something wrong with working procedures or conditions. Examples are given in the detailed abstract.

HUB. WIJKER (*Netherlands*):

How can the speaker relate the amount of thorium to the measured amount of its daughter thoron when the age of the thorium since chemical purification is not known?

A. FRANCESCHINI (*Italy*):

Con la parola "thoron" nel riassunto inglese si definisce un complessante chimico che contiene torio e che in Italia è chiamato "il toron".

M. DE BORTOLI (*Euratom*):

I would like to know the temperature and the duration of the leaching procedure. In our laboratory we perform quantitative extraction of ^{137}Cs from sandy soils and sandy loams by leaching overnight with hot hydrochloric acid under reflux conditions.

A. BAUMANN:

After addition of the leaching solution the sample was mechanically stirred for 30 min and left overnight without heating.

A. FRANCESCHINI (*Italy*):

1. La cinetica dello scambio ionico è alterata dal trattamento subito dallo scambiatore?

2. Si hanno buoni risultati, con questo tipo di materiale, nel caso dei complessi di nitrosil-rutenio?

M. IZAWA:

1. We have not studied in detail the possible changes of the kinetics of exchange. However, as I explained, it appears that the exchange capacity of the exchanger remains unchanged by the treatment.

2. The chemical form used in this experiment was nitrosylruthenium. The behaviours of other forms of ruthenium on the "resin" must await further experiments.

J. BOUQUIAUX (*Belgium*):

Quelle est la stabilité des résines obtenues et quel en est le mode de régénération?

C. TESTA (*Italy*):

Le colonne in questione possono essere rigenerate da 10 a 15 cicli consecutivi; ciò dipende dalla costante dielettrica del composto supportato ed il numero di cicli è inversamente proporzionale ad essa. Le colonne si rigenerano lavandole con una soluzione avente le stesse caratteristiche chimiche del liquido che dovrà essere percolato attraverso la colonna.

J. BOUQUIAUX (*Belgium*):

Quelle est la source qui a servi à l'irradiation? Quel est le temps d'irradiation?

R. L. KATHREN (substituting for Dr. J. A. MISKEL):

Irradiation took place in the Livermore Pool Type Reactor, a 2-MW research facility. A two-hour irradiation time was utilized along with a thermal flux of 2×10^{12} n/cm²/sec.

PLUTONIUM-239 AND 238, STRONTIUM-90 AND CESIUM-137 IN SURFACE AIR FROM MID 1961 THROUGH 1965

M. DE BORTOLI,* P. GAGLIONE,† A. MALVICINI and E. VAN DER STRICHT‡

Abstract—Monthly air concentration values, at ground level, of some longlived radionuclides (strontium-90, cesium-137, plutonium-239 and plutonium-238) from world-wide fallout have been measured at Ispra, from mid 1961 through 1965.

Samples of atmospheric debris were collected by filtering 6 to 8 thousand cubic meters of air through paper filters. The single radionuclides were determined by analytical procedures, which are briefly described in the paper. Particularly, for plutonium a simple and rapid radiochemical method was developed, in order to obtain electrodeposited samples, suitable for alpha spectrometry. This was performed by Frisch-grid ionization chamber and multichannel analyser.

Plutonium-239, strontium-90 and cesium-137 concentrations show, during the five years considered, the well known general trend of fallout, characterized by the spring maxima. Plutonium-238 seems to behave rather particularly and to follow less closely this trend.

Fairly constant values of the ratios $^{137}Cs/^{90}Sr$ and $^{239}Pu/^{90}Sr$ are found, whereas the $^{238}Pu/^{239}Pu$ ratio varies by a factor ten or more and shows two strong fall peaks in 1961 and 1962, i.e. in the periods of heavy nuclear testing in the atmosphere.

The highest concentrations, found during the summer of 1963, attained the values of 1.8×10^{-3} pCi/m³ for plutonium-239, 3.5×10^{-5} pCi/m³ for plutonium-238, 9.6×10^{-2} pCi/m³ for strontium-90 and 0.14 pCi/m³ for cesium-137, respectively.

Some considerations are made about inhalation doses to the population at large. It appears that a significant fraction of the MPC may have been attained, at least for a part of the period considered, particularly for strontium-90 and plutonium-239. Concerning the latter radionuclide, some incertitude stems from the scanty knowledge of the extent to which it is in soluble form. If most of the plutonium-239 present in airborne debris has to be considered soluble, then the maximum concentration observed would represent 0.3% of the MPC for occupational exposure for a 168 hr week.

INTRODUCTION

Among the many fission products originated by the bursts of nuclear devices, the radionuclides which have deserved the greatest attention of the scientists all over the world are strontium-90 and cesium-137. This is due to the long half-life of these nuclides and to their chemical behaviour, which is close to that of biologically important elements, namely calcium and potassium. Another radioactive element spread in the environment by nuclear tests is plutonium, which, like strontium, is a bone-seeker. Most plutonium isotopes have a high radiotoxicity; those of greater concern in fallout are the 239 and 240.*

Plutonium-238 has hitherto represented a small fraction of the activity due to plutonium in fallout, but it is assuming more importance because of the increasing use which is being made of this isotope in the field of power generators. It is well known that one of these devices, the SNAP-9A, with a load of 17kCi of

* Site Survey and Meteorology Branch, Protection Service, Euratom Ispra Establishment.

† Chief, Protection Service, Euratom Ispra Establishment.

‡ Directorate for Health and Safety, Euratom, Brussels.

* Because the energies of the alpha particles emitted by these nuclides are too close as to allow their separation by the technique employed, they are referred to in this paper as plutonium-239.

plutonium-238, launched with a satellite on April 1964, failed to orbit and during re-entry underwent burn up.

As from 1962 these four radionuclides (strontium-90, cesium-137, plutonium-238 and plutonium-239) have been measured in ground level air at Ispra as part of the radiological monitoring program. The analyses have been extended down to mid 1961 in order to know the air contamination levels prior to the resumption of nuclear weapons testing.

EXPERIMENTAL

(a) *Sample collection*

Samples of atmospheric dust are collected routinely at the site survey stations of the ISPRA Euratom Joint Nuclear Research Centre. The air is filtered by suction through 5 cm diam. paper filters (Poelman-Schneider blue), replaced daily. The filtered volume is measured by flow-meters. Pooling the single daily filters of each station, monthly samples are obtained, which are representative of an air volume ranging from 6 to 8 thousand cubic meters.

(b) *Radiochemical procedures*

The filters are submitted to direct gamma spectrometry before ashing, in order to determine (or evaluate) cesium-137, whenever this is permitted by the other gamma activities present in the sample (also by the spectrum-stripping technique). The sample is thoroughly dissolved by fusion and radiochemical determinations of cesium, strontium and plutonium are performed.

Cesium is absorbed by filtration on a thin ammonium phosphomolybdate layer[1] and measured by gamma spectrometry.

Strontium is separated by the fuming nitric acid precipitation and successively purified from calcium through stirring the nitrates with acetone. After hydroxides and chromate precipitations strontium carbonate and yttrium oxalate precipitates are obtained for counting. The chemical recovery of strontium is determined by flame photometric measurement of the added Sr carrier.

Plutonium is separated by an hydroxide precipitation and then purified by a double anion exchange step: plutonium and iron are first absorbed in a strong hydrochloric acid medium and then plutonium only eluted by an hydrochloric–hydrofluoric acids mixture. Finally plutonium is electrodeposited on tantalum discs 3 cm in diam. (the deposit covers an area of about 3 cm^2). The chemical yield is determined through the recovered fraction of the plutonium-236 tracer added. No tracer has been added to the samples processed for the determination of the $^{238}Pu/^{239}Pu$ ratio. Details of the plutonium separation procedure may be found elsewhere.[2]

(c) *Activity measurements*

The strontium-90 activity is determined by counting strontium carbonate just after precipitation and then after build-up of the yttrium-90 daughter. Moreover yttrium-90 is chemically separated as the oxalate and its radiochemical purity tested by control of the decay time. For beta counting anticoincidence plastic phosphor detectors are used, with an area of 20 cm^2 and a background of 1.2 counts/min.

Gamma spectrometry is performed by means

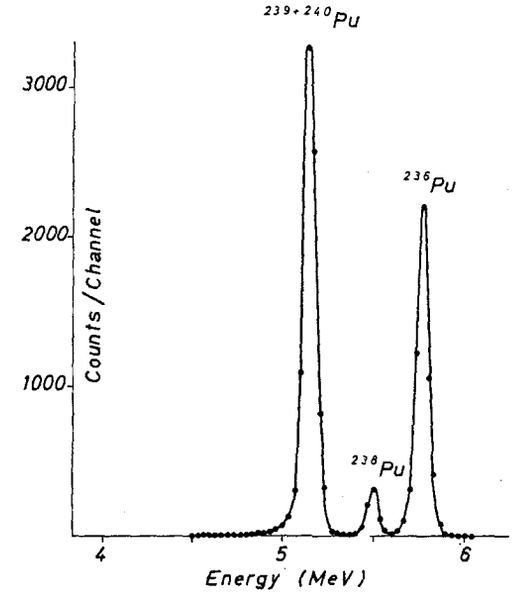

FIG. 1. Alpha spectrum of the plutonium separated from an atmospheric dust sample collected during December 1962. Counting time 63 hr.

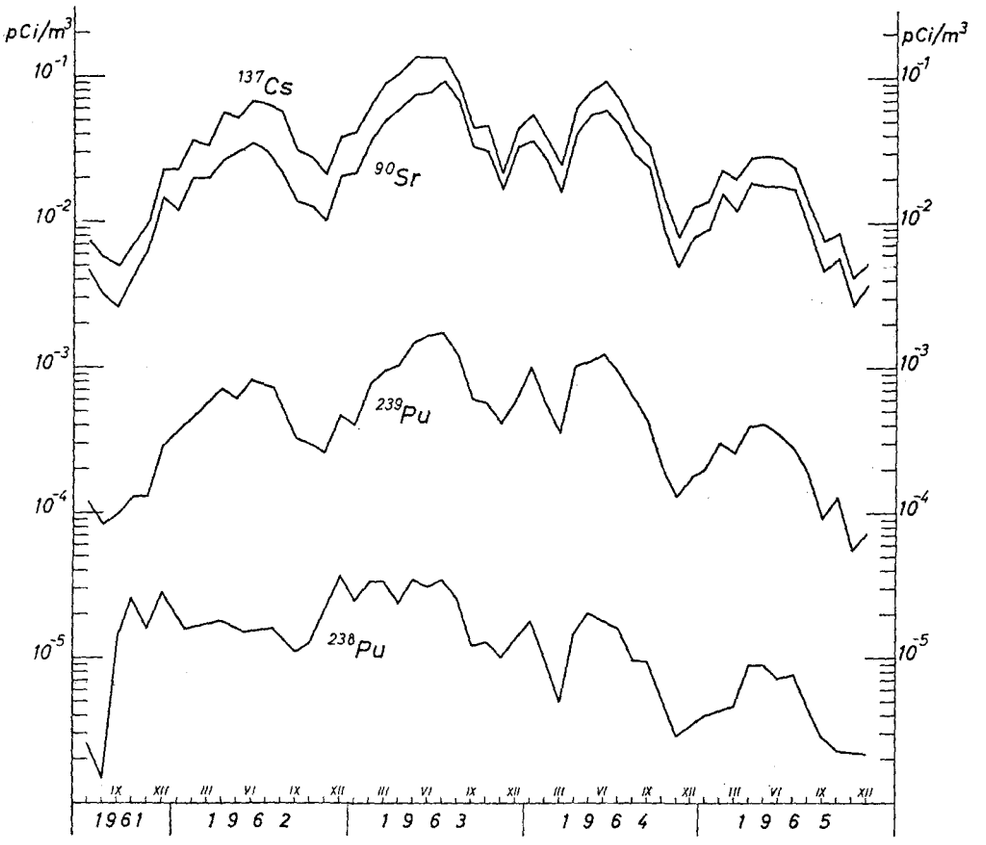

FIG. 2. Plutonium-239, plutonium-238, strontium-90 and cesium-137 concentrations in surface air at Ispra from mid 1961 through 1965.

of a 3 × 3 in. NaI(Tl) integral line detector, connected to a multichannel analyser.

The alpha-spectrometric measurements are performed on the weightless electroplated sources by a pulse ionization chamber. This is a conventional parallel plate Frisch grid system, contained in a cylindrical vessel. The collecting electrode is connected to a low noise preamplifier, mounted directly on the top of the pressure vessel and followed by a usual amplification chain and pulse-height analyser. The chamber is filled with a 98% argon and 2% acetylene mixture at a pressure of 3 kg/cm². After filling, a period of about half an hour is allowed to elapse to obtain stable conditions before counting. With the electrodeposited samples of plutonium-239 alpha-spectra with 50–60 keV half-widths (full width at half the height of a spectral peak) are normally obtained without collimation. A typical alpha-spectrum is represented in Fig. 1. About 0.002 pCi of plutonium-239 double the effective background counting rate in the energy interval considered for the radionuclide (about 200 keV). For the measurement of low level activities, like those of plutonium-238 in air, very long counting times are required, so that stability is of primary importance. The drift observed in our case during measurements as long as 70 hr has been of about 0.5%.

Table 1. *Air Concentrations of* ^{239}Pu, ^{238}Pu, ^{90}Sr *and* ^{137}Cs *from mid* 1961 *through* 1965

Month	Plutonium-239[a] 10^{-16} Ci/m³	Plutonium-238[b] 10^{-17} Ci/m³	Strontium-90[a] 10^{-14} Ci/m³	Cesium-137[a] 10^{-14} Ci/m³
1961				
July	1.2	0.26[c]	0.48	0.75
Aug.	0.83	0.15[c]	0.32	0.58
Sept.	0.98	1.4	0.26	0.50
Oct.	1.3	2.6	0.43	0.70
Nov.	1.3	1.6	0.63	1.0
Dec.	2.9	2.8	1.5	2.3
1962				
Jan.	4.2*	1.6[c]*	1.2	2.3
Feb.			2.0	3.6
Mar.	—	—	2.0	3.3
Apr.	7.1	1.8[c]	2.7	5.6
May	6.2	1.5*	3.0	5.1
June	8.2		3.5	6.9
July	7.4*	1.6[c]*	3.1	6.5
Aug.			2.2	4.8
Sept.	3.3	1.1	1.4	3.1
Oct.	3.0	1.3	1.3	2.8
Nov.	2.6	2.2	1.0	2.1
Dec.	4.7	3.7	2.1	3.9
1963				
Jan.	4.1	2.5	2.2	4.3
Feb.	7.9	3.4	3.7	6.5
Mar.	9.6	3.4	5.1	9.1
Apr.	10.5	2.4	6.1	11
May	14.5	3.5	7.7	14
June	16.5	3.1[c]	7.9	14
July	17.5	3.5	9.6	14
Aug.	12.2	2.6	7.0	9.0
Sept.	6.1	1.2	3.3	4.5
Oct.	5.8	1.3	3.1	4.7
Nov.	4.3	1.0	1.7	2.2
Dec.	6.0	1.4	3.3	4.5
1964				
Jan.	10.1	1.8[c]	3.7	5.6
Feb.	5.7	0.97[c]	2.7	3.8
Mar.	3.6	0.50[c]	1.6	2.5
Apr.	10.7	1.5	4.2	6.3
May	11.2	2.1	5.6	8.1
June	12.2	1.8[c]	6.0	9.5
July	9.3	1.6[c]	4.7	7.0
Aug.	6.1	0.98	2.9	4.4
Sept.	4.3	0.95[c]	2.4	3.4
Oct.	2.0	—	0.90	1.5
Nov.	1.3	0.29	0.50	0.8
Dec.	1.8	—	0.80	1.3

Table 1. *Air Concentrations of* ^{239}Pu, ^{238}Pu, ^{90}Sr *and* ^{137}Cs *from mid* 1961 *through* 1965—Cont.

Month	Plutonium-239[a] 10^{-16} Ci/m³	Plutonium-238[b] 10^{-17} Ci/m³	Strontium-90[a] 10^{-14} Ci/m³	Cesium-137[a] 10^{-14} Ci/m³
1965				
Jan.	2.1	0.40[c]	0.90	1.4
Feb.	3.1	—	1.6	2.3
Mar.	2.6	0.47	1.2	2.0
Apr.	4.0	0.92	1.9	2.8
May	4.1	0.90	1.8	2.9
June	3.5	0.74[c]	1.8	2.8
July	2.8	0.76	1.7	2.4
Aug.	1.9	0.48[c]	0.90	1.3
Sept.	0.93	0.28	0.47	0.75
Oct.	1.3	0.23[c]	0.58	0.85
Nov.	0.55	—	0.27	0.41
Dec.	0.73	0.22	0.37	0.51

Relative standard deviation due to counting only: a < 5%; b between 5 and 10% (except values indicated with c); c between 10 and 20%

— Measurement not performed.

* Values obtained from bi-monthly samples.

RESULTS AND DISCUSSIONS

(a) *General trend of air radioactivity*

The data in Table 1 and the graph in Fig. 2 show the variations of the four radionuclides, air concentrations during the period considered. The variations cover a range of almost two decades and it will be seen that, with few exceptions, the curves follow the well-known general trend of world-wide fallout, with yearly maxima in spring–summer and minima in autumn. Some sharp deviations from this profile are observed to occur for single points corresponding to months with persistent dryness or rainfall.

An interesting and particular behaviour is presented by plutonium-238. A sharp rise of an order of magnitude, in September 1961, of the concentration of this nuclide was followed by a rather slight decrease, ending October 1962, when a new rise occurred to a roughly steady level, higher by a factor about two. The new plateau lasted ten months and then (late 1963) the plutonium-238 concentration started following rather closely those of the other radionuclides.

Although these facts have not been given a full explanation, it seems likely that one or some bursts of devices, affecting mainly the troposphere and yielding an unusually high $^{238}Pu/^{239}Pu$ ratio, have occurred at the beginning of the Russian test series in autumn 1961. This would explain the rise of the plutonium-238 concentration, anticipated with regard to the other nuclides, and its different behaviour. In fact, whereas the concentrations of plutonium-239, strontium-90 and cesium-137 in ground level air have been steadily increasing during the first months of 1962, owing to the deposition of the debris injected into the lower stratosphere, the plutonium-238 concentration has maintained roughly constant or slowly decreasing, because of the smaller content of this isotope in the sinking air. Almost the same seems to have occurred during the second heavy test series (autumn 1962).

(b) *Concentration ratios* $^{137}Cs/^{90}Sr$, $^{239}Pu/^{90}Sr$ *and* $^{238}Pu/^{239}Pu$

A useful term of comparison in the study of air radioactivity is provided by following the concentration ratios between radionuclide pairs. As may be seen in Figs. 3 and 4 respectively, the values of the two ratios $^{137}Cs/^{90}Sr$ and $^{239}Pu/$

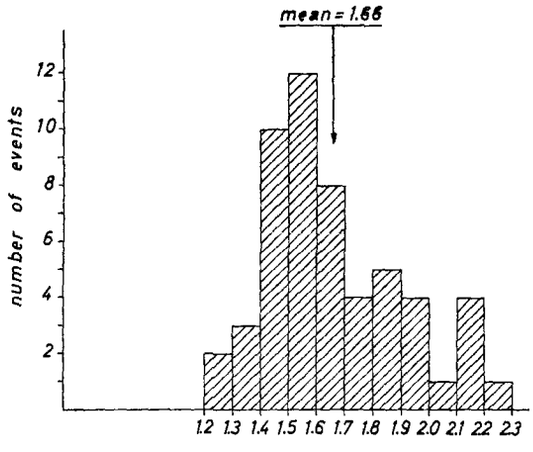

FIG. 3. Distribution of the $^{137}Cs/^{90}Sr$ ratio in surface air from mid 1961 through 1965.

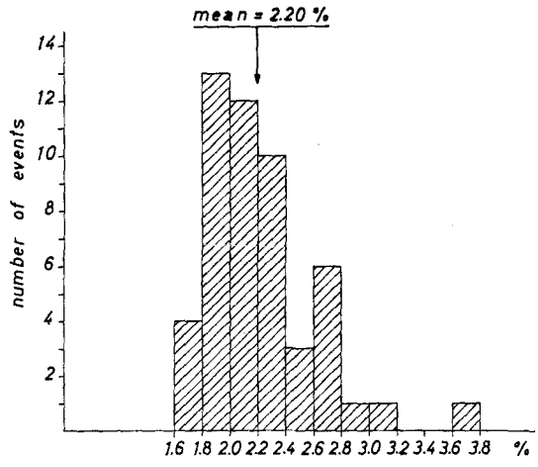

FIG. 4. Distribution of the $^{239}Pu/^{90}Sr$ ratio in surface air from mid 1961 through 1965.

^{90}Sr show a relatively small scatter throughout the five years considered and their mean values are 1.66 (standard deviation of the mean 14.5%) and 2.20% (standard deviation 17.3%), respectively. Because of their relative constancy these ratios have been used to judge the validity of single concentration data.

Unlike the two others, the ratio of plutonium-238 to plutonium-239 shows wide variations (depending on the facts discussed above) prior to April 1963, when it also became fairly constant (see graph in Fig. 5).

A slight upward trend may be noticed in the last portion of the curve in Fig. 5 (late 1965) and this could be attributed to the arrival to ground level of the SNAP-9A debris, mentioned above.[3] The latest measurements, performed on atmospheric dust samples collected by June and July 1966, confirm this hypothesis, yielding for the $^{238}Pu/^{239}Pu$ ratio values as high as 7%, whereas the mean value, obtained averaging the data from April 1963 through March 1965, is 1.94% (standard deviation of the mean 16.4%).

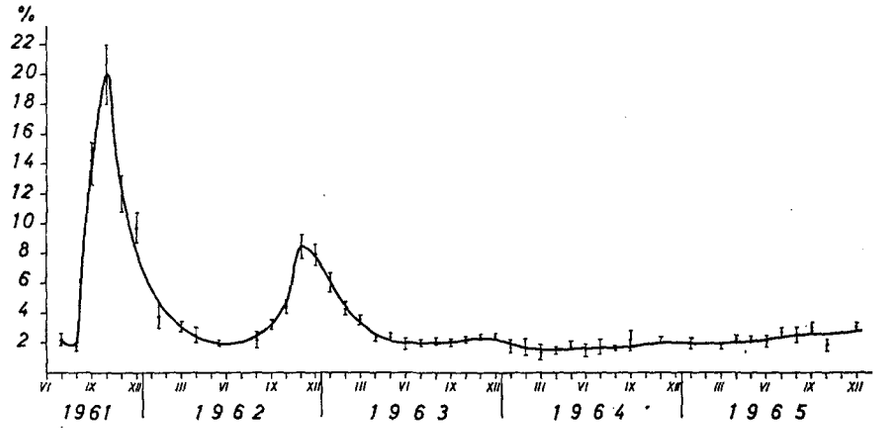

FIG. 5. $^{238}Pu/^{239}Pu$ ratio in surface air at Ispra from mid 1961 through 1965.

(c) *Hazard evaluation*

In order to estimate the inhalation hazards to the population arising from the four radionuclides considered, their air concentrations (averaged over 1963) have been compared with the MPC_a for occupational exposure for a 168 hr week.[4] The following percentages of MPC_a were obtained for the individual nuclides: 0.16 for plutonium-239; 0.0034 for plutonium-238; 0.05 for strontium-90; and 0.0016 for cesium-137. The lowest MPC_a values have been used, owing to the uncertainty about the solubility of radionuclides on airborne particles and consequently the figures obtained represent an upper limit for inhalation exposure.

Because the inhalation dose for strontium-90 and cesium-137 is but a fraction of the total dose delivered by these nuclides, as they are absorbed also via the gastro-intestinal tract, and because plutonium-238 represents a negligibly small fraction of plutonium-239, the interest for the lung burden has been confined to the last radionuclide. For the calculation the following assumptions have been made: (i) exposure period of four years (1962–5); (ii) air concentration of plutonium-239 6×10^{-4} pCi/m^3 (i.e. the mean of the values measured during the period considered); (iii) nuclide in the insoluble form.

According to the ICRP model the calculation yields a lung burden of about 0.7 pCi of plutonium-239.

ACKNOWLEDGEMENTS

The authors gratefully acknowledge the kindness of Dr. John H. Harley, for supplying the plutonium-236 tracer solution.

Thanks are due, moreover, to the personnel of the group and particularly to E. Pecchio, O. Cadario and Miss L. Tortora for the chemical separations, O. Malgarini and E. Lovati for the activity measurements, M. Tramontana for the work in electronics and Miss A. Schieppati for typing this paper.

REFERENCES

1. E. Van der Stricht. *Radiochimica Acta* **3**, 193–199 (1964).
2. M. C. de Bortoli. Radiochemical determination of plutonium in soil and in other environmental samples. *Anal. Chem.* **39**, 375.
3. J. H. Harley. USAEC Report HASL-149 (1964).
4. International Commission on Radiological Protection, Report of Committee II on Permissible Dose for Internal Radiation, Pergamon Press (1959).

PLUTONIUM, TRITIUM AND CARBON-14 IN MAN AND THE BIOSPHERE

J. C. DROBINSKI, Jr., P. J. MAGNO and A. S. GOLDIN

Northeastern Radiological Health Laboratory, Winchester, Massachusetts,
Division of Radiological Health, Public Health Service, U.S. Department of Health, Education, and Welfare, U.S.A.

Abstract—The Division of Radiological Health of the Public Health Service has been aware for some time of the need to extend environmental radionuclide measurements to include plutonium, tritium and carbon-14. In 1963, exploratory measurements were begun in various environmental media. In 1964, a formal network was established for the measurement of tritium in 11 major U.S. rivers; in 1965, another network to measure plutonium, tritium and carbon-14 in total diets became operational.

Data on the plutonium-239 content of air particulates show concentrations from 0.07 to 0.44 fCi/m^3; the content of this same nuclide in precipitation has ranged from 17 to 126 fCi/l. Plutonium concentrations in total diets have ranged from less than 2.0 to 8.5 fCi/kg, but no detectable plutonium has been found in milk. In organs from unexposed humans, the largest concentrations of plutonium were found in liver and in lungs, with no detectable plutonium being observed in bone.

The carbon-14 content of total diets has ranged from 19.0 to 22.5 dpm/g of carbon, which corresponds to an enrichment above natural levels of 35 to 60 per cent. There does not appear to be any consistent geographic trend, nor does the concentration in milk differ markedly from that in the total diet. Levels in human organs do not show any great difference from organ to organ, with the possible exception of a lower value in adult brain.

Concentrations of tritium in river water have ranged up to 20 nCi/l, the highest levels being downstream from a major nuclear installation. Concentrations of tritium in drinking water averaged about 5 nCi/l and data on milk and total diets indicate concentrations of from 1 to 5 nCi/kg. The tritium concentration of the water fractions resulting from the combustion of various human organs was equivalent to 0.3 to 10 pCi/g of wet tissue.

DOSIMETRIC MEASUREMENTS IN BRAZILIAN REGIONS OF HIGH NATURAL RADIOACTIVITY LEADING TO CYTOGENETIC STUDIES*

THOMAS L. CULLEN
Istituto de Física da Pontifícia Universidade Católica Rua M. S. Vicente 263, Rio de Janeiro, Brazil

Abstract—Several Brazilian regions of high natural radioactivity provide excellent opportunities to study effects of chronic exposure to low level radiation and groups from Catholic University, New York University and University of Brazil joined in a cooperative investigation.

In the monazite sand zone external levels are elevated and people live in intimate contact with surface contamination. On beaches levels run as high as 2 mR/hr and in homes up to 0.6 mR/hr. Three sources of exposure are considered: external γ-radiation; internal contamination with long-lived radioisotopes; internal contamination by thoron daughter products.

A survey with lithium fluoride dosimeters showed an average external exposure of 750 mR/yr with a range from 160 to 2500 mR/yr. Measurements of thoron exhaled in breath indicate body burdens of 0.1 to 0.6 nCi of MsTh, although the data is ambiguous. A whole body counter is under construction using sugar as shielding material. Thoron concentration in homes is measured by electrostatic capture on steel cylinders and measurement in ionization chamber.

Using peripheral blood techniques the cytogenetics group has found a much higher frequency of chromosomal aberrations in the exposed than in the control group, although data are still insufficient.

Two sites have been chosen in the region of volcanic intrusives, Môrro do Ferro, near Poços de Caldas, and Araxá.

Môrro do Ferro with levels up to 3.2 mR/hr is a center for studies leading to radioecology. Soil–grass and soil–plant studies show concentrations of ^{226}Ra in grass and plants up to 10^3 pCi/g ash. Rats live in a thoron environment of up to 10^{-8} Ci/l.

In the Araxá farmland soil–food stuff relations are studied. The cytogenetic study will center on the small number of families who subsist mainly on food from the radioactive farms.

THE areas of the world with high natural radioactivity might provide us with valuable information on the long-term effects of chronic exposure to low level radiation. It is the purpose of this paper to discuss one aspect of the work done in the monazite area of Brazil.

Guarapari is a city of 6000 people in the State of Espírito Santo on the Atlantic coast. The interplay of river and ocean currents has built the sand bar on which the town sits. Black sand is found in patches and in layers on the beaches, under the town, and has found its way into construction material. The black sand is composed of ilmenite, rutile, and monazite. Monazite is a combination of rare earth phosphates with 6% thorium and 0.3% uranium impurities. It can give rise to external levels as high as 1.2 mR/hr and abrupt gradients.

The geological origins of the monazite sand [1] and the early surveys of external radiation levels [2] have been described. Three years ago a coordinated multi-discipline approach to the studies in the several areas was begun by the Institute of Physics, Catholic University,

* Work supported by U.S. A.E.C., Contract AT (30–1)–2577, W.H.O., Brazilian Institute of Sugar and National Steel Co.

the Institute of Biophysics, University of Brazil and the Institute of Environmental Medicine, New York University.[3]

The Institute of Biophysics has been conducting a cytogenetic study of the population of Guarapari and the smaller but similar town of Meaipe. As a control population the town of Anchieta, with similar social and economic conditions, has been chosen.

A cytogenetic study requires meticulous care and time. While the group has not processed a sufficient number of control samples they are able to make the following statement.

"Preliminary findings of our cytogenetics laboratory, however, did indicate a significant increase in the frequency of somatic chromosome aberrations of Guarapari's inhabitants, in comparison with controls. A high incidence of multiple break chromosomal aberrations was found, which is more compatible with the interpretation of being caused by alpha and beta radiation from internal emitters, rather than by gamma radiation."[4]

The Institute of Biophysics has also radiochemically analyzed foodstuffs, teeth and excreta. Local foods constitute only a small part of the diet. The analysis of teeth and excreta has not given conclusive results.

The Catholic University group conducts dosimetric studies along three lines: external levels; thoron in the air; body burdens by breath analysis and whole-body counting.

Social and hygenic conditions of the people set boundaries to the work. Infant mortality is high and would mask any visible effect in a classical epidemiological study, even if the population were large enough. They are simple people who are afraid of a big city and suspicious of complicated looking apparatus.

1. EXTERNAL RADIATION LEVELS— THERMOLUMINESCENT DOSIMETERS

Lithium fluoride dosimeters are used to integrate over a long period of time the dose rate received by selected individuals as they moved through the variable gamma field. The packets consisted of Type N phosphor (Conrad) and were enclosed in a medal hung from the neck.

The cytogenetic study determined the aim and protocol of distribution. The aim was to reconstruct, if possible, the life time dose of an individual once his life history is known. For this reason they were distributed in different sections of the city, to all age brackets and to both sexes.

During the first phase of the study 156 dosimeters were distributed in May 1964 and left with the people for three months. Of these 115 were recovered in good condition.[5] In the end of September 1965 another 384 were given out. This time they were more widely distributed through Guarapari, in the newer suburbs, in another monazite town, Meaipe, and in the control city of Anchieta. After six and seven months, hunt and find expeditions were only able to locate 225 of these dosimeters.

The dosimeters were returned to Conrad for readout services. Two corrections were applied to the data received. O'Brien, Lowder and Solon have calculated the fraction of free air dose rate received from terrestrial sources as a function of the radiation energy and depth in man.[6] At zero depth the fraction ranges from 0.687 at 0.375 MeV to 0.735 at 2.25 MeV. Here the average of 0.70 was used to reduce the data to air equivalent dose rates.

The second correction was a result of calibration experiments. For both years sets of dosimeters were exposed to standard radium sources with doses at the level expected in the field. They were then kept at normal levels together with unexposed dosimeters and sent to Conrad with the full collection. The calibration slope for the first experiment was 0.92 and for the second 0.90. This may have been due to fading in a tropical country. A correction factor of 10% was applied to all data.

The average dose rate for the 317 people measured in the exposed population is 636 mR/yr with a minimum of about 100 mR/yr and a maximum of 3200 mR/yr. The data are presented in Table 1, grouped according to neighborhoods and towns. The neighborhoods of Guarapari are designated by certain street names and are listed in the order of descending external levels. The distribution of dose rates received by the exposed population is given in Table 2.

The first observation that can be made is that the movement of daily life tends to equalize dose rates. The highest external levels are found

Table 1. Average Air Equivalent Dose Rates received by samples of populations of Guarapari, Muquiçaba, Meaipe and Anchieta, Brazil

Town and neighborhood	No. of people	Dose rate (mR/yr)
Guarapari		
Pedro Caetano	85	785
Sizenandro Bourgninon	32	608
Joaquim Lima	31	594
Getulio Vargas	24	549
Henrique Coutinho	24	514
Church Hill	22	393
Muquiçaba and other suburbs	65	562
Meaipe	33	777
Anchieta	23	98

Table 2. Dose Rate Distribution in Radioactive Towns, Brazil

Range (mR/yr)	No. of people
0– 99	0
100– 199	23
200– 299	42
300– 399	47
400– 499	47
500– 599	40
600– 699	26
700– 799	15
800– 899	14
900– 999	10
1000–1099	8
1100–1199	9
1200–1299	4
1300–1399	5
1400–1499	5
1500–1599	2
1600–1699	7
1700–1799	0
1800–1899	2
1900–1999	3
more than 2000	5

in Pedro Caetano, which also happens to have a concentration of people. The doses are lower than one would expect, because people move from home to work or to school The external levels on the Church Hill and in Muquiçaba, on the other extreme, are hardly above normal but these people also move into the town for work, school and medical services.

The individual's annual dose is a function of his home, his age and his work, and the presentation of average data tends to obscure the wide difference existing. One elderly couple on the main street receives annual doses of 199 and 212 mR. Around the corner in another home the individuals received 1560, 1310, 1670 and 1190 mR., the smallest being that of a school girl. On Getulio Vargas Street a doctor and his wife receive 1220 and 1210 mR while a man two doors away receives 215 mR.

In the winter survey of 1964 the people in Pedro Caetano received an average dose of 714 mR while in the summer months of 1965–6 the average dose was 540. This is due not only to the fact that in the heat they tend to remain outdoors but also because several families rent their homes to vacationers and live in another section.

A monazite separation plant, Mibra, was closed down in December 1963 but has maintained a skeleton staff. In 1964 these workers, because of rejected sand left nearby, received an annual dose of 990 mR and in 1965–6 1015 mR. The rejected sand, with levels of 0.25 mR/hr, is used as a football field by youngsters and contributes to the level of the population on Sizenandro Bourgninon Street.

School dropouts receive higher dose rates than children who remain in school, but further grouping of data according to age or sex would fail to show any significance. The aim of the survey was to assess the dose rate received by individuals of different ages and occupations who lived in certain homes. A sufficiently large body of data exists now that reasonable estimates can be made.

The opinion of the cytogenetics group in the Institute of Biophysics however is that the aberrations observed are not due to external radiation.

The people in the control town of Anchieta received approximately normal levels, as was expected.

2. THORON IN THE AIR

An important contribution to the internal dose rate can come from the concentration of thoron in closed bedrooms, with the subsequent deposition of decay products in different body organs. Scintillometer readings of 0.1 to 0.6 mR/hr next to walls in the homes showed the possibility of high thoron concentrations in the air.

Some attempts to measure the concentration have not met with complete success. Staplex filter measurements in the streets show the presence of daughter products of the order of 0.3 pCi/l.

This year an electrostatic deposition method was attempted in closed rooms. Sheets of stainless steel were mounted in a cylindrical frame. A voltage source maintained an inner electrode at a positive potential of 1000 V. The decay products of thoron and thorium A are captured on the inner surface of the metal. The metal is then placed in a 4 liter ionization chamber and the current read with a vibrating reed electrometer.

The apparatus itself gives satisfactory results and thoron is measured. What was not foreseen, however, was the reluctance of some people to permit a strange looking metal object in their rooms at night. A further problem is the impossibility of installing a fan and, without circulation, the readings have no certain meaning. It is estimated that the concentrations are above 1 pCi/l.

A further attempt was made with the apparatus designed by Robert T. Drew of New York University, to measure the high concentrations in rat holes on Morro do Ferro. A sample of air is drawn into a 200 ml flask, coated on the inside with zinc sulfide, and the sample is alpha counted. Eleven measurements made in a rainy period showed negative results. It is estimated that the concentration at that time was less than 4 pCi/l.

3. BODY BURDENS

(a) *Measurements of Thoron in Breath*

Because the cytogenetic data suggested the presence of internal contamination, measurements of thoron in breath were resumed. This is an easy and, at the time, the only available method of testing for the presence of mesothorium in the body.

The method, elaborated by Dudley, relies simply on the fact that a certain fraction of the thoron produced in the body is exhaled. A person is asked to breathe for an hour into a 50 liter soup pot. Through the top is suspended a 1 in. brass disk connected to—8000 V. The recoil nuclei of the decay products of thoron and thorium A are electrostatically

Table 3. *Body Burdens inferred from Thoron-in-breath Measurements, Guarapari*

Subject	Sex	Age	Occupation	Mibra*	^{224}Ra (nCi)
A	F	47	Housewife	—	0.52
B	M	50	Owns bar	25	0.28
C	F	17	Bakery	—	0.23
D	M	46	Owns bar	12	0.20
E	F	38	Housewife	—	0.16
F	M	39	Mibra	25	0.45
G	F	18	Telephone	—	0.31
H	M	43	Mibra	25	0.31
I	M	16	Mechanic	—	0.29
J	M	56	Mibra	25	0.22
K	M	17	Student	—	0.22
L	M	57	Office	—	0.18
M	F	22	Pharmacy	—	0.16

* Mibra: Years of work in monazite separation plant. Plant closed December 1963.

captured. The disk, which has been covered with a layer of zinc sulfide, is placed on a similarly covered phototube. Each disk is alpha counted for several hours and only four can be counted per day.

A large uncertainty remains in the results because of the unknown efficiency of exhalation. If the mesothorium is an old deposit in the skeleton only 0.1% is exhaled. If it is in the liver or spleen 8% is exhaled. The apparatus was tested several years ago with three thorotrast patients and confirmed the figure of 8% exhalation.

The data for 13 subjects from Guarapari are given in Table 3. An exhalation efficiency of 8% is assumed, thereby giving the lowest estimate of body burdens. It is possible that this is wrong by more than an order of magnitude. The decay curves are given in Fig. 1.

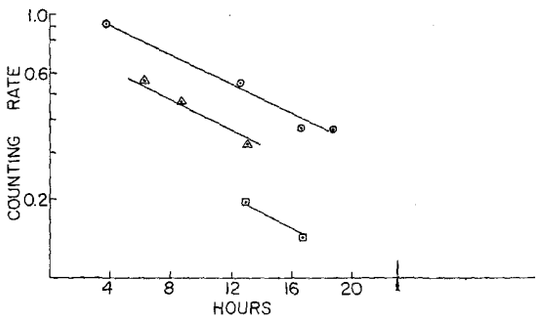

FIG. 1. Typical decay curves for thoron-in-breath measurements.

The choice of subjects centered on families who have lived all their lives in Guarapari, but the definite selection was based on a list of people with chromosomal damage furnished by the Institute of Biophysics. The subjects listed under letters A, H and L are known to have chromosomal aberrations.

(b) *Whole-body Counting "The Sugar Bowl"*

Since the thoron-in-breath measurements indicated a body burden of less than 1 nCi and this could be wrong by more than an order of magnitude, an attempt at whole-body counting was considered justified.

Ten metric tons of sugar were obtained from the Brazilian Institute of Sugar and Alcohol and half a ton of iron from the National Steel Co. as shielding material. The chemical purity of sugar and its low price make it an ideal shield. As shield thickness increases, however, the volume and mass grow disproportionately. A compromise was sought using the principles of the shadow shield.

The 166 sacks of sugar, each 60 kg, were arranged in the form of a bowl to give the equivalent of 6 in. iron shielding below the subject and 4 in. on the sides. Above the cave a shield of 3 × 3 in. iron bars was used together with 2 in.

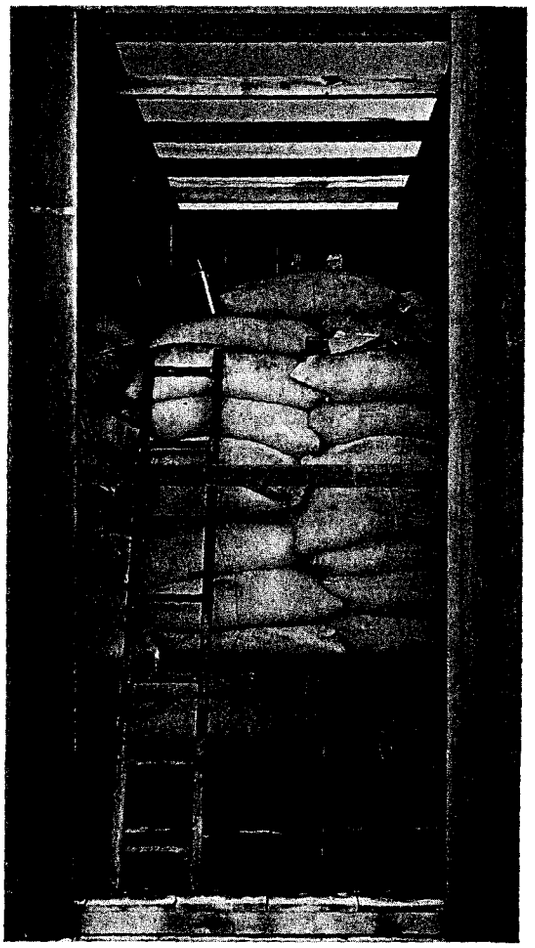

FIG. 2. View of sugar shield for whole-body counter.

Table 4. Body Burdens Measured by Whole-body Counting

Subject	Sex	Age	Occupation	Mibra*	^{224}Ra (nCi)	^{226}Ra (nCi)
A	F	47	Housewife	—	5.5	5.0
B	M	50	Owns bar	25	5.1	N.D.
N	M	39	Fisherman	6	5.1	12.5
O	M	41	Owns Bar	12	3.3	N.D.

* Mibra: Years of work in monazite separation plant. Plant closed December 1963.
Note: Subjects A and B are listed under the same letters in Table 3.

of lead. The shield and detector were housed in a wooden shack in the veranda under the University building. The building added 1.3 m of concrete to the shielding. A picture of the whole-body counter is given in Fig. 2.

A 4 × 4 in. Na (Tl) well-type crystal, integrally mounted to a phototube was used. A small reamplifier sent the pulses through a cable to the fifth floor laboratory where the counts were registered by a Nuclear Data 256 channel analyzer.

The background index, defined here as the total counting rate from 0.4 to 2.0 MeV divided by the volume of the crystal, was found to be 0.92 cpm/cc. This was considered reasonably good for a provisional counter.

The counter was calibrated with standard solutions of ^{226}Ra and ^{228}Ra. The solutions were sandwiched between two 4 in. thick plastic bottles filled with distilled water to represent a phantom of the chest region.

The standard error in the calibration experiments can be used to estimate a lower limit of sensitivity. Defining the Minimum Detectable Amount as twice the standard error, the M.D.A. for ^{224}Ra is 1.2 nCi and for ^{226}Ra 1.8 nCi.

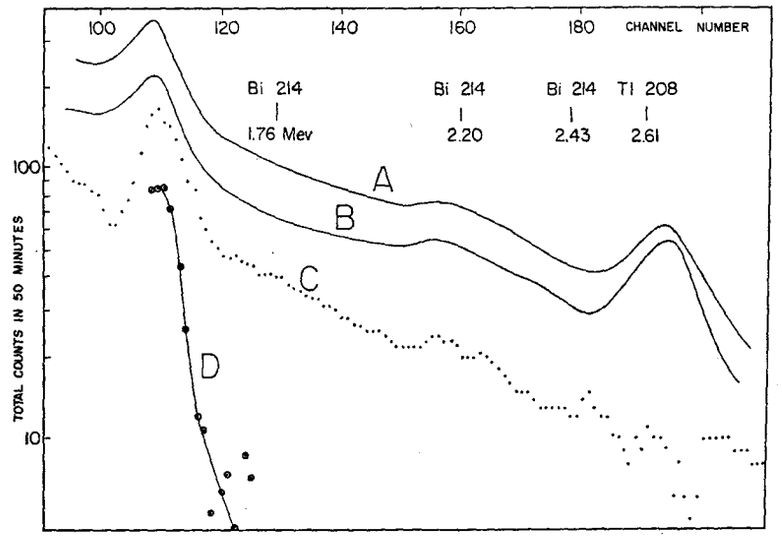

FIG. 3. Whole-body counting spectra. A. Ten Guarapari subjects with background. B. Background. C. Ten Guarapari subjects minus background. D. Ten Rio de Janeiro subjects minus background.

In a provisional set up it is impossible to hold error to a minimum. It is necessary to assess them carefully, especially the systematic errors. Among the smaller errors are temperature change and the subsequent gain shift in the phototube leveling off the peaks of some channels. Another is the variation of the natural background in the well ventillated shack.

Among the two major sources of error is what can be called partial body counting. To lower the background iron bars were closed in tightly about the crystal reducing the cone of sensitivity. Head, shoulders and at least the upper part of the lungs were not within the sensitive cone. The ^{40}K peak was studied to estimate the fraction of the body counted. Assuming normal potassium content, the conclusion is reached that less than a fourth of the body was counted.

The second major source of error was noise captured by the cable. This was studied separately with the phototube voltage off and amounted to approximately 30% of the background in the channels of interest. The error rests in this, that noise is not constant.

Eleven individuals came from Guarapari to be counted. Ten subjects from Rio de Janeiro were also counted. More than a score of background measurements were taken. For each channel in the spectrum the counts from ten subjects from Guarapari were averaged. The same was done with ten backgrounds and ten subjects from Rio de Janeiro. The graph of these averages is given in Fig. 3. The activity of the Guarapari people seemed to be high enough to pass from the idea of population sample to make cautious statements about individuals.

But the sensitivity of a whole-body counter depends less on the background than on the stability of the background. If the ten Rio de Janeiro subjects are accepted as background all the Guarapari subjects have body burdens of ^{224}Ra from 0.5 to 10 nCi. But the noise in the cable varies too much for us to assume that the background of one week is equal to that of another.

Accepting the spectrum with the highest noise level in the three weeks of operation as the background, the body burden for three Guarapari subjects is given in Table 4. The energy regions for ^{214}Bi have been chosen from 1.575 to 1.860 MeV and for the ^{208}Tl peak from 2.575 to 2.730 MeV. The suggestion of peaks in these regions of interest confirms the conclusion of the presence of internal contamination. Four other people appear to have measurable body burdens, but nothing can be said with confidence because they are below the M.D.A.

Nothing is known about the origin of the body burden and, for the present, it is assumed that intimate contact with surface contamination and dust in the air is the source. For this reason the data is given for ^{224}Ra.

One of the subjects mentioned in Table 4, A, is known to have chromosomal aberrations. It is believed that the continuation of this research project can shed light on the biological consequences of chronic exposure to low level radiation.

REFERENCES

1. F. X. Roser, G. Kegel and T. L. Cullen. Radiogeology of some high background areas of Brazil. *Int. Symp. Natural. Radiat. Environment*, Rice University, Houston, 1963.
2. F. X. Roser and T. L. Cullen. External radiation levels in high background areas of Brazil, *Int. Symp. Natural. Radiat. Environment*, Rice University, Houston, 1963.
3. E. Penna Franca *et al. Health Phys.* **11,** 699 (1965).
4. E. Penna Franca *et al. Radiochemical and Radioecological Studies on Brazilian Areas of High Natural Radiation*, Annual Report to U.S. A.E.C. AT (30–1)–2577. Universidade do Brasil, Rio de Janeiro, 1966.
5. T. L. Cullen. *Health Phys.* **12,** 970 (1966).
6. K. O'Brien, W. M. Lowder and L. R. Solon. *Radiat. Res.* **9,** 2 (1958).

PLUTONIUM CONTAMINATION OF LARGE LAND AREAS

WILLIAM S. JOHNSON, Sr.
Eberline Instrument Corporation, Santa Fe, New Mexico, U.S.A.

Abstract—The contamination of large land areas with significant quantities of plutonium has been essentially a situation unique to the non-nuclear detonation of nuclear weapons. However, with the increased use of Pu-239 for non-weapons applications and the availability of Pu-238 in quantity, health physicists need information on the magnitude of the contamination associated with plutonium accidents.

The results of the most extensive field experiments to date, Operation "Roller Coaster" sponsored by the United States and the United Kingdom, provide an insight into the radiological problems of such accidents. As is the case in any true accident involving radioactive material, it is necessary to function and evaluate under conditions entirely different from routine plutonium operations. Special equipment was field tested to enhance plutonium detection by low energy electromagnetic radiations in addition to more conventional alpha monitoring. These techniques may be applied to improve personnel safety and to speed up the collection of radiological measurements where Pu-238, Pu-239, Am-241 and other transuranic elements are involved.

IF THIS were an audience of the general public, a more intriguing title would be "The Two Faces of Plutonium". However, in speaking to this very distinguished group of health physicists, much of the background and historical data on plutonium can be omitted. It is sufficient to comment that the discovery, introduction and use of plutonium have been accompanied by radiological protection measures of unprecedented magnitude. Continuous air monitoring, isolation techniques, protective equipment, special instrumentation and complete bioassay programs have become the acceptable practice wherever plutonium is handled.

Opposed to this is the plutonium contamination of large land areas when essentially all of these control mechanisms are difficult if not impossible to institute. This is a situation unique to the non-nuclear detonation of a nuclear weapon wherein the *chemical* explosive is detonated at some point in handling, storage or transportation. It was thrust into the limelight of international news last January over the southeast coast of Spain during an inflight refueling operation of two aircraft of the U.S. Air Force.

What information is available to the health physicist who may find himself at the scene of a plutonium accident? Fortunately, extensive field experiments, notably Operation "Roller Coaster" conducted jointly by the U.S. and the United Kingdom, provide an insight into some of the problems. In truth, accidents involving plutonium may be categorized as any other radiation accident where the health physicist should:

(a) Have a clear understanding of the problems to be solved and their order of priority.
(b) Reorient himself as to acceptable levels of exposure and contamination.
(c) Be current on measurement techniques for a variety of circumstances.

Taking these categories in order one must first consider the saving of life and property. Or a fire may be involved where precedence is given to extinguishing it. Highly sensitized chemicals which will detonate on contact may be found in the debris. There is the possibility that a small fission contribution may have occurred during the explosion. In this case energetic gamma radiation of 1000 r/hr or more may be encountered. Radiological controls will be governed by this radiation regardless

of the presence or absence of plutonium contamination. Other debris must be approached with caution because it will exist in a twisted and jagged form such that contaminated wounds may occur frequently. Obviously daytime operations are preferable, if not mandatory. Control of access and egress of personnel and equipment must be established regardless of the radiological situation. Non-essential personnel are removed and upwind control points established.

when the site is re-opened to unrestricted traffic.

Just as in the case of the radiation accident involving fission products or energetic gamma sources it is necessary to shift gears mentally in evaluating contamination levels of significance. For example, we concern ourselves daily with the measurement of exposure rates of a few mr/hr or less, while at the accident scene we deal in many multiples of r/hr. To bring the situation under control one has to devote attention to dose rates of this magnitude. Similarly

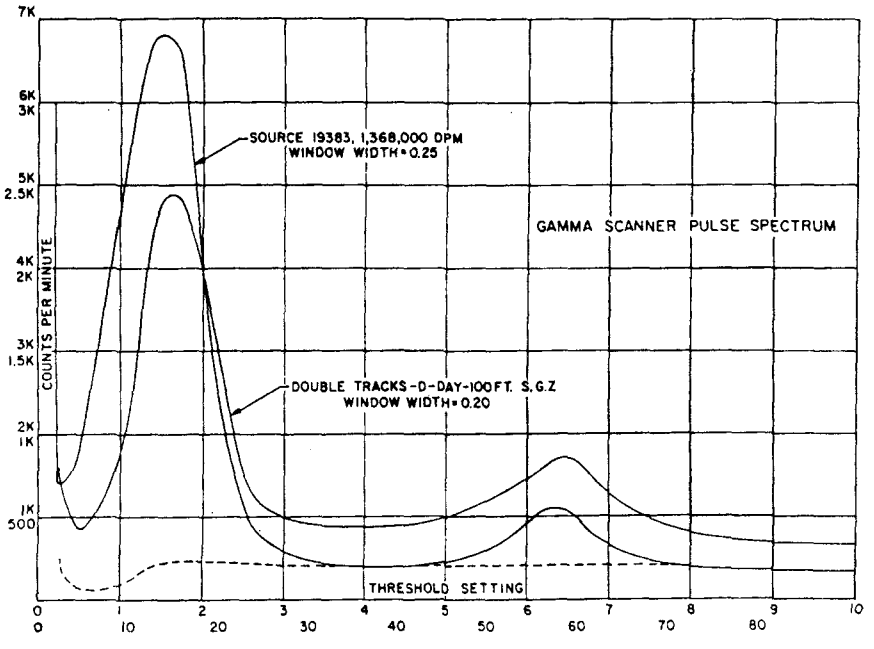

FIG. 1. Electromagnetic radiation spectrum of standard plutonium source (19383) and postdetonation debris (double tracks).

Having progressed to this point, one can begin to think about plutonium contamination, monitoring assignments and other radiological protection measures associated with alpha contamination. As a general rule, it is preferable to isolate the area of immediate concern by moving "in" toward the center and to follow this by moving "out" to the more distant points. These actions will define the magnitude of the area in preparation for the second, or long-term effort, which can be approached in a more leisurely, planned manner and which concludes

where plutonium is involved, one cannot be diverted from the immediate mission by a strict accounting of all places where laboratory tolerances of 100 cpm or 500 cpm or 1000 cpm may occur. To be quite blunt, until a portable alpha counter registers a completely off-scale reading, one has not located the area requiring priority attention.

While we are all prone to relate plutonium contamination monitoring to alpha measurements, it is not a pleasant thought to contemplate this "hands-and-knees" effort over tens

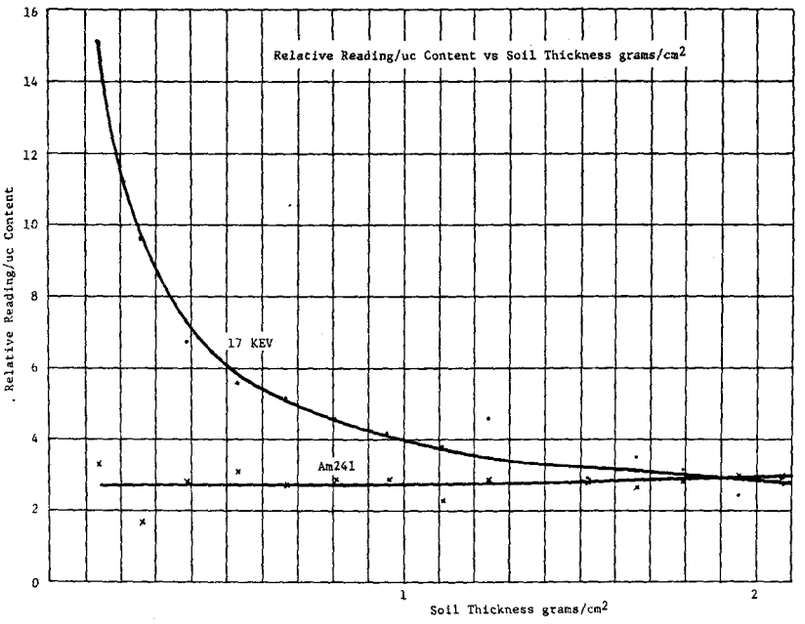

FIG. 2. Shielding effect of soil on 17 and 60 keV electromagnetic radiations.

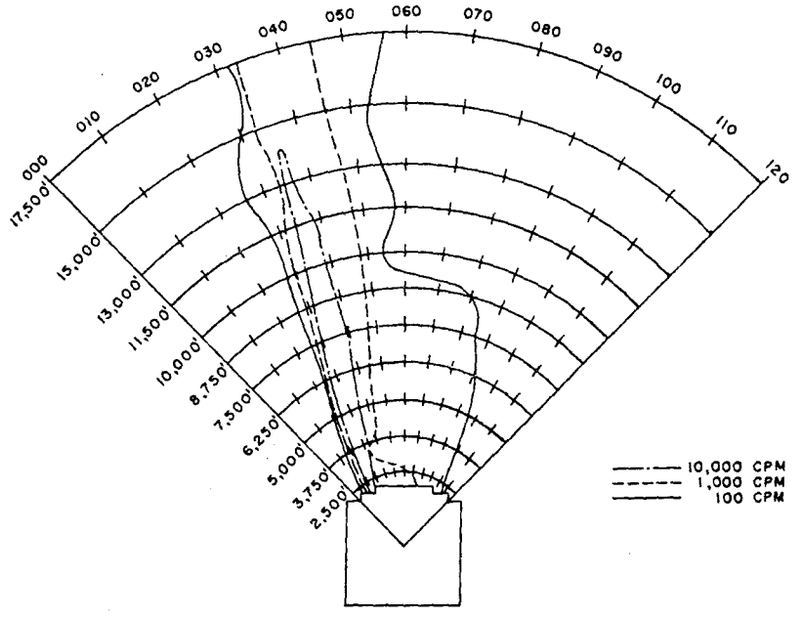

FIG. 3. Downwind alpha contamination plot following field experiment. Distances in feet are measured from detonation point.

of acres, square kilometers or square miles. As a matter of fact, it can exhaust you just thinking about it! So we look for a solution of convenience and try to do what we can with the electromagnetic radiations associated with plutonium. Figure 1 not only shows the expected 17 keV peak but also a second peak representing the Am-241 which occurs in varying minor percentages in all plutonium. Note that the Am: Pu ratio increases from a clean source to deposited fallout indicating the ease with prevailing meteorology. At 2500 feet the maximum contamination level was between 10,000 and 100,000 cpm/60 cm² probe area. This means that the area of immediate concern is relatively confined. As one approaches the centre, however, contamination levels increase rapidly and irregularly being the result of a "debris throwout" phenomenon rather than true fallout. Removal of debris, especially metallic debris, is an effective decontamination measure in the area.

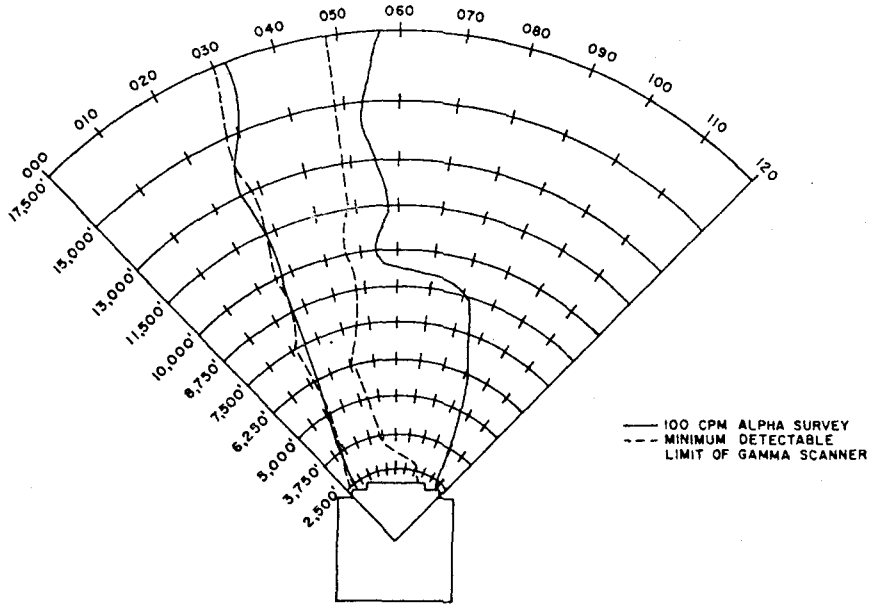

FIG. 4. Portable alpha counter vs mobile low energy gamma scanner (Fig. 5) contamination plots (compare with Fig. 3).

which 17 keV can be effected by environmental conditions. Indeed, soil homogenously mixed with weapons grade plutonium contaminant will mask 17keV at a thickness of about 2g/cm² (Fig. 2). It is well to remember this potential for gamma detection in dealing with Pu-238 which exceeds that of Pu-239 by several orders of magnitude because of its higher specific activity, abundance and energy.

To bring this discussion to practical terms, a fairly typical fallout pattern is shown in Fig. 3. It developed, as would be expected after an explosion, in the downwind pattern of the

The comparative sensitivity with low energy gamma detection is given in Fig. 4. The alpha and gamma contours are most consistent at greater than 1000 cpm alpha. These data were taken with a specially designed vehicle (Fig. 5).

The shielded detector projects in front and the electronics (single channel analyzer) and readout are mounted inside the cab. The bicycle wheel in the rear is synchronized with the recorder chart drive for positional reference. The large appurtenance on top is an air conditioner added for personal and equipment requirements in hot climates. At the sacrifice of one or two

FIG. 5. Mobile low energy gamma scanner.

orders of magnitude in sensitivity, a gamma detection device can be made completely portable at under 10 lb total weight. Developments are presently under way to retain sensitivity in a 20 lb device with microcircuitry though the complete product is some 2–3 years away.

A few personal conclusions on associated problems are in order. First, plutonium depositions on land are quite resistant to resuspension. After the passage of the explosion-formed cloud, the hazard decreases by probably a minimum factor of 100. Further reduction through simple stabilization measures (water spray, etc.) is effective.

Secondly, percolation into soil is extremely limited if a factor at all. The top inch contains nearly 100% of the contaminant even after long weathering. This means that soil decontamination is best accomplished by the removal of a thin layer—thinner than is feasible with large earth moving equipment, unfortunately.

Air concentrations related to operational activities of personnel are difficult to obtain. These activities are not repetitive either in time, location or function. One normally provides respiratory protection in the form of the full face mask without benefit of air concentration information.

The August 1966 Newsletter of the Health Physics Society carried a summary of the report of the Society's Civil Defense Committee. One of the statements in this report encouraged members to become acquainted with the "procedural differences between these [accidents] and the usual peace-time operations". The weapon accident or other plutonium-scattering events, as infrequent as they may be, do require procedural differences. It should be emphasized that they are completely manageable with safety and thoroughness when competent personnel have planned for them.

RAPPORTEUR PAPER
HYDROSPHERIC FOOD CHAINS

J. K. MIETTINEN

THIS session contains papers on factors governing the uptake of radionuclides in the hydrospheric environment, marine or fresh water. In all these papers attempts are made to elucidate general factors, which make possible the prediction of the contamination level of different organisms, especially fish, in given pollution conditions.

The first of these papers is by Dr. Rinnosuke Fukai, from the International Laboratory of Marine Radioactivity, operated at Monaco by the International Atomic Energy Agency. It is titled "Some Biogeochemical Considerations on the Radioactive Contamination of Marine Biota and Environments". In this paper the author points out that if the over-all distribution of a given stable element in sea water and in marine organisms is known, the ultimate level of the radio isotopes of the same element in the same organisms can be predicted.

The author has determined the average concentrations of two stable elements, Co and Cr, in various biogeochemical phases. What the author calls "standard abundance" values (in μg/kg) are presented in his Table 1. As can be seen, considerable concentrations of these trace metals are found in several organisms and sediments, compared with those in sea water.

The author has also compiled from the literature and from his own studies, data on the dry weight as a percentage of the wet weight in representatives of four phylae (Fig. 1). As can be seen, the spread is quite large, in the case of algae, for instance, from less than 5% to 45%. Thus, the average values of "standard abundances" cannot be accurate, as the author himself points out, but they are useful in giving the first rough idea of the concentration of the element in representatives of different trophic levels.

To express the relationships between the concentration of a certain element in marine organisms and that in sea water, the term concentration factor or enrichment factor is in common use. The term is usually defined as the ratio

$$\frac{\text{amount of a nuclide or element in unit mass of a fresh organism}}{\text{amount of the same nuclide or element in unit mass of sea water}}.$$

Thus, for trace elements the ratio is usually expressed

$$\frac{\mu\text{g of element/kg fresh organism}}{\mu\text{g of element/l sea water}}.$$

According to the opinion of the author, the term concentration or enrichment factor implies that in the case of radionuclides the higher concentrations are more hazardous. He points out that this is not so, however, as it is a high specific activity (Ci per g stable element) of the radionuclide which is hazardous, not a high "absolute level" (Ci per g tissue). The author proposes the term "abundance ratio" to be used instead of concentration or enrichment factor, to avoid confusion.

Personally, I am not convinced that the introduction of a third name for this same ratio would decrease or increase the confusion, although it might be preferable from one point of view. The colourful term enrichment factor also has its advantages, at least for accuracy, as it need not be based on an average dry weight of a phylum.

The second paper, by Dr. W. Feldt, from the Isotope Laboratory of the Federal Research Institute of Fischery, in Hamburg, Germany, is titled "Radiation Protection Aspects in the Survey of Fish regarding their Radioactive Contamination". Dr. Feldt looks at the problem not only from the viewpoint of the radiation protection of man, but also that of fish. In addition he studies critically the factors affecting

the contamination levels in fish. The author states that the contamination level of fish in regard to ^{90}Sr is inversely proportional to the Ca concentration in the water and can be calculated from the ^{90}Sr and Ca concentrations in the water by the equation

$$K_F = D_{WF} \cdot \frac{^{90}\text{Sr/l.}}{\text{Ca/l.}}$$

D_{WF} is the discrimination factor water/fish, its value varying from 0.2 to 0.3 in various fish species.

The ^{90}Sr and ^{137}Cs contents of fish from limnologically widely different waters during 1964 are presented in the author's Table 1. As the fish species caught from fresh water and marine environments are different, direct comparison is not possible, but one can see that the radionuclide contents in the fresh water fish are generally 10 to 100 times higher than in the marine fish.

In his Table 2 the author presents the concentration factor for ^{90}Sr and ^{137}Cs in waters having different Ca contents. In each column values for ^{90}Sr are on the left-hand, those for ^{137}Cs on the right-hand side. The concentration factor is defined in the usual way, for ^{90}Sr for instance

$$\frac{\text{pCi } ^{90}\text{Sr per kg fish (fresh wt)}}{\text{pCi } ^{90}\text{Sr per liter water}}$$

For ^{90}Sr the enrichment factor changes from 570 to 1 with increasing Ca content of the water (from 10 to 400 mg Ca/l). For ^{137}Cs the values change from 2000 to 23, with increasing Ca content. We shall see in a later paper of this session that it is really the potassium content of the water which determines the ^{137}Cs level in fish.

Dr. Feldt points out, that in order to evaluate the possible radiation risk to man from consumption of contaminated fish, one can use the specific activity of water and fish assuming that they must not exceed the maximum permissible specific activity (MPSA) in the human body, which has been set to 30 μCi/g Sr by the U.S. National Academy of Sciences National Research Council in its Publication No. 985 (1962), titled "Disposal of Low-Level Radioactive Wastes into Pacific Coastal Waters". Dr. Feldt presents in his Table 3 the specific activities of fish, μCi ^{90}Sr/g Sr. As can be seen, the most radioactive fish, pike from an oligotrophic fresh water lake, have an activity 0.14% of the MPSA, ocean fish having only 0.001% or less.

For ^{137}Cs the specific activity of North Sea fish is about 0.0001% of the MPSA. For freshwater fish it cannot be calculated as their content of inactive caesium is not known well enough.

Dr. Feldt has calculated the gonad doses for fish of two species, the contamination levels of which are presented in Table 4. The first species is typical of the Baltic Sea and the second represents the highest contamination level in the oligotrophic fresh waters. According to rather complicated calculations, the gonad dose of the Baltic Sea fish due to the two artificial nuclides ^{90}Sr and ^{137}Cs amounts to only 2% of the gonad dose caused by the natural radionuclide ^{40}K.

For the fresh water fish the dose from ^{40}K is 0.23 mrem/week and from ^{90}Sr plus ^{137}Cs is practically the same, i.e. 0.29 mrem/week, thus the latter together add about 100% to the natural dose.

The author concludes that the consumption of marine fish as human food does not constitute a radiation risk to man at present. The population of Northern Germany gets only about 5% of its body burden of ^{137}Cs through fish. Only fresh-water fish from the most calcium deficient lakes can play an important role in the dietary intake of ^{137}Cs to some population groups. The author emphasizes the need for increased monitoring of such critical waters. We shall see below that in Finland we have come to exactly similar conclusions in our studies.

The third and fourth papers report results of a research project carried out in our laboratory, The Department of Radiochemistry of the University of Helsinki, using a grant from the U.S. Department of Health, Education and Welfare. The third paper, by Drs. Häsänen, Kolehmainen and myself, is titled "Biological Half-times of ^{137}Cs and ^{22}Na in Different Fish Species, and Their Temperature Dependence". This paper summarizes our results on this subject obtained during the last two years. These studies became of real importance when

we found very high concentrations of ^{137}Cs in fresh water fish in 1962. The highest value observed hitherto is 26 nCi/kg fresh weight in the Finnish perch, measured in 1965. This is more than twice as high as Dr. Feldt's maximum value for the Kolksee pike. Fish flesh is the primary source of ^{137}Cs for Finnish population groups consuming fresh water fish, with the exception of reindeer herding Lapps and others consuming much reindeer or caribou meat, which contains even more ^{137}Cs than fresh water fish. The very laborious half-time determinations became necessary as very few papers have been published on excretion rates of ^{137}Cs in fish and none of these studies was made with species living in Finnish fresh waters.

Our experimental technique has varied slightly, but in most cases we have labelled each fish individually by giving it a precisely known amount of ^{137}Cs—usually 250 or 500 nCi—orally in a tiny gelatine capsule. The capsule has been applied by small forceps through the oesophagus of the fish. Each fish has been marked by clipping different fins and measured alive in the Institute's mobile whole body counter, first daily, later less frequently (Fig. 1). In laboratory experiments the fish were kept alive in thermostated aquaria. In field experiments they were placed in large cages made of Japanese nylon net suspended in an oligotrophic lake. The fish were regularly fed with either commercial inactive fish food, or milled inactive fish. The counting was performed by using a multichannel analyzer and the statistical error was smaller than 3%. Such a statistical error is small compared with the biological variance, which we have found to be 25% for individual fish, and 6% (1σ) for a group of 15 fish of the same species and age after one half-time from the labelling.

The results of a typical experiment are illustrated in Fig. 2. We can see that, as in many mammalia, the excretion rate follows a double-exponential function. A smaller fraction, typically 10 to 20%, shows a short biological half-time marked TB_1, usually varying from a part of a day to a few days (in this case it is 7 days at 15°C). Evidently this fraction mainly represents ^{137}Cs in the extracellular space. The remaining amount shows a biological half-time (TB_2) many times longer, varying from a few days to hundreds of days (in this case 80 days at 15°C). This fraction evidently represents ^{137}Cs in the intracellular space and especially within the muscle cells. In fish and other cold blooded animals the half-time is sharply dependent on temperature. When, in this experiment, at the beginning of October, the water temperature decreased within 2 weeks from 13° to 5°C, the value of the slow component increased to about 230 days.

The other results are summarized in Table 1. After the fish species, the type of experiment is mentioned. In the third column the age of the fish is given since in most species the half-time increases with increasing age of the fish (e.g. see roach). The next column gives the number of fish in the experiment. We attempted to have at least 15 similar fish in each experiment, but it was not always practicable. In the next column is the temperature, which in the field experiments varied more than in the aquaria, which could be thermostated. The last two columns contain figures for the fast and slow components of excretion: the half-times in days and the percentage of the component.

As can be seen, perch have the longest half-time, 200 ± 20 days at 15°C. There may be some increase in the value of the slow component with the ageing of the fish but the change is not definite. In roach the half-time in young fish (57 days) is about half that in the old fish (105 days). The age dependance is also clear in the rainbow trout, also the temperature dependance in all cases when determined. The half-time is about doubled when the water temperature decreases from 15° to 5°C, i.e. by 10 degrees.

The results on ^{22}Na are presented in Table 2. Only the long component is recorded since for sodium the presence of a short component in the excretion curve is not always certain. From perch and roach a small amount ($5 \pm 3\%$) was consistently excreted very rapidly, and from rainbow trout 20% at 6°C, but none was observed at the higher temperature. Temperature dependance seems to be similar to the case of the ^{137}Cs excretion: reduction to about one-half, with a temperature decrease from 15° to 5°C.

Also in this paper there is mentioned all of the similar studies that we have found in the literature. Unfortunately, most

cases are of little interest as a different species was studied and it is not clear whether the fast or slow component is given. Also the age of the fish and the temperature were not mentioned, but in two cases results rather similar to ours are reported. Scott reports for the brook trout (*Salvelinus fontialis*) a half-time of 47 days which corresponds to our 25 to 80 days in rainbow trout (*Salmo iridaeus*) of different ages at 15°C. Kevern, Griffith and Grizzard report for the carp (*Cyprinus carpio*) 98 days at 20°C, and 174 days at 12.5°C, values which are rather similar to those we found for the closely related Crusian carp (*Cyprinus carassius*). It may be mentioned also that Williams and Pickering, and Nelson and Early, in two different studies, report for the blue gills (*Lepomis machrochirus*) a half-time of 40 days for the ^{137}Cs excretion.

It can be concluded from these studies that: (1) the biological half time of ^{137}Cs in different fish species varies greatly, up to 10-fold, being one of the main factors causing different body burdens of this nuclide in different fish species; (2) in winter the half-times are much longer than in summer, for instance in perch well over one year.

The fourth paper, by Drs. Kolehmainen, Häsänen and myself, is titled "^{137}Cs in the Plants, Plankton and Fish of the Finnish Lakes and Factors affecting its Accumulation."

In this paper results from the years 1964 and 1965 are reported of an environmental investigation for 12 lakes of widely different limnological types, varying from eutrophic (rich in nutrients) to oligotrophic (nutrient deficient). Some limnological analyses of these lakes are presented in Table 1. The first lake is nutrient rich, the last ones extremely nutrient deficient. The potassium content in the first lake is 3.5 mg/l., in No. 10 only 0.2 mg/l. As can be seen in the last column the pollution level in these lakes from the global fallout varies very little, only about 2-fold, the extreme difference being 4-fold. This is, of course, one of the factors determining the contamination level of the organisms, but as can be seen, a minor one from the viewpoint of differences in the Finnish lakes.

Our results further show that the ^{137}Cs content of all organisms depends sharply on the potassium concentration of the water, which is the main factor determining the ^{137}Cs level. The contamination of the same organism varies more than 10-fold in different types of lakes as can be seen below.

In Table 2 some plankton analyses are presented, the lakes being in the same order as in the previous table, No. 1 being the most nutrient-rich. As can be seen, the ^{137}Cs content of the plankton varies about 10-fold, in one extreme case even 500-fold. The results represent mainly zooplankton, the percentage of phytoplankton being shown in the last column. Comparison between different years and lakes is difficult as the composition of the samples varies greatly, even from the same lake at different times. The approximate composition of the samples collected in 1965 is shown in Table 3.

The above tendency is also visible in the ^{137}Cs values of the higher plants, especially species rich in minerals like the horsetail (*Equisetum fluviatile*). Values for 2 higher plants are presented in Table 4. As can be seen, there is an approximately 20-fold difference in the ^{137}Cs content of plants grown in eutrophic and oligotrophic lakes. The values of higher plants do not always change regularly, but horsetail seems to be usable as an indicator species.

Relatively few samples of bottom animals have been obtained. Results of three samples are presented in Table 5. The values are practically the same as in plankton from the same lake.

Most clear-cut is the inverse relationship of the ^{137}Cs content of fish and the potassium content of the lake water. It is best illustrated in Fig. 1 of this paper. As can be seen, down to a K content of 1 mg/l. the ^{137}Cs content in pike remains low (< 3 nCi/kg), but with the K content 0.6 mg/l. it reaches the very high value of 21.3 nCi/kg fresh wt. The extreme differences within the same species are 100-fold. The deviating case is a lake polluted by wastes from the cellulose industry, mainly Na and Ca cations. The ^{137}Cs contents of other fish species are shown in Table 6.

A third factor determining the body burden of fish is the ^{137}Cs content of the food of the fish. Our results show that this is a minor factor effecting usually no more than 2- or 3-fold differences.

The fourth factor, and an important one, is

the biological half-time of ^{137}Cs which in the previous paper was shown to vary from 20 to 200 days at 15°C. The biological half-time of ^{137}Cs in perch and pike, for instance, is over a year in natural conditions, the annual mean temperature in the Finnish lakes being 4° to 6°C. This explains also why the ^{137}Cs values in many lakes, especially the oligotrophic ones, were still increasing in 1965.

To summarize, we can state that it is the potassium level of the lake water and the biological half-time of ^{137}Cs in the species which mainly determines the ^{137}Cs-level in the fish at a given pollution level. Especially in oligotrophic lakes, body burdens are fully determined by intake in the food. Our studies show that direct intake of the nuclide by an osmotic mechanism in the gills is negligible. Dr. Feldt's studies show that the ^{90}Sr level in fish is similarly determined by the Ca level in the water, and we can generalize that the contamination of fish in different waters is practically determined by the carrier ion levels in the water at a given pollution level.

SOME BIOGEOCHEMICAL CONSIDERATIONS ON THE RADIOACTIVE CONTAMINATION OF MARINE BIOTA AND ENVIRONMENTS

RINNOSUKE FUKAI
International Laboratory of Marine Radioactivity, IAEA, Monaco

Abstract—The problem of the radioactive contamination of marine biota and environments can be regarded as the successive links of biogeochemical processes in the sea, in view of the transfer of radioisotopes from one geochemical sphere to the other. In the present paper the importance of the accumulation of biogeochemical data concerning the distribution of trace elements in marine biota is emphasized in relation to the prediction of radioactive contamination. The significance of obtaining the "standard abundance" of trace elements for various groups of marine organisms is discussed by presenting some examples. In order to avoid misunderstanding, the significance of the term "concentration factor" or "enrichment factor" is critically reviewed and the use of the term "abundance ratio" is proposed. In aid of the accumulation of comparable data on the trace element distribution in marine biota, remarks are made on the expression and the interpretation of the analytical results and on the computations of the abundance ratio.

INTRODUCTION

Since the radioactive contamination of the sea became the subject of scientific research in the past two decades, valuable scientific information has been supplied from the newly developed studies, not only to the specific field concerned, but also to the general fields of marine science. The ultimate aim of these studies is to clarify the quantitative effect of the radioactive contamination of the oceans on human life, and, thus, to establish a proper scheme of radiation protection for the human being against the potential hazards of contamination. It appears that the goal has been approached from several angles, but in reality, the final goal of these studies, except for some special cases, has not been achieved mainly due to the incompleteness of the scientific understanding of the various phenomena occurring in the sea. The present status of the studies in this field is still essentially in preparation of basic materials for further progress. Each study must be oriented correctly to the final goal, which lies several steps beyond. This paper is concerned with orientation for the purpose of radiation protection.

SIGNIFICANCE OF BIOGEOCHEMICAL DATA

Although the possible effect of radioactive contamination of the sea to human life can be expected through various direct and indirect ways, the most important effect is likely to be caused through the consumption of contaminated marine products as protein sources. For radiation protection, therefore, it becomes very important to predict the level of radioisotopes in marine organisms living in a given condition of the contamination. In order to make this prediction possible, a number of uptake experiments of various radioisotopes by different types of marine organisms have been carried out in laboratory conditions. The results obtained by these experiments are indispensable for understanding the physiological mechanisms of the uptake of radioisotopes, although it is necessary, in general, to make some assumptions in order to apply these results to natural conditions. On the other hand, the transfer of radioisotopes from sea water to marine organisms or from one organism to another can be regarded as successive biogeochemical processes in the sea. The law which governs the distribution of

corresponding stable isotopes in sea water and marine organisms is considered to be valid for the distribution of radioisotopes themselves. In other words, if the over-all distribution of corresponding stable isotopes in each link of biogeochemical cycles is known, the ultimate level of radioisotopes in the links can be predicted. Although the distributions of stable isotopes cannot tell much about the dynamic aspects of the uptake of radioisotopes, these are supposed to be close to the steady state in natural conditions. The hazard estimation of the radioactive contamination will be based on the overall levels of radioisotopes concerned in marine organisms rather than the mechanisms of the uptake of radioisotopes by the organisms. Thus, in this aspect, the significance of a systematic accumulation of data on the biogeochemical distribution of trace elements in sea water and marine biota must be emphasized.

The data obtained to date on the distribution of various trace elements in sea water, and marine organisms, were comprehensively compiled by Riley,[1] and Vinogradov,[2] respectively. Unfortunately, however, these complications cover only a part of the necessary information. Moreover, the majority of the data, especially in the latter, appeared before modern techniques in analytical chemistry became available, so that the accuracy of the results tend to be low, in many cases. For this reason further accumulation of biogeochemical data on the distribution of trace elements in marine organisms has still to be stressed.

STANDARD ABUNDANCE OF TRACE ELEMENTS IN MARINE BIOTA

Since marine biota consists of a large number of species of organisms, complete understanding of the distribution of trace elements in marine biota requires an enormous amount of data. From the view of radiation protection, however, the subject can be restricted to edible species and species which are directly related to edible species in the trophic webs. Although this restriction reduces the number of analyses required, a large amount of labour is still needed to cover the species of marine organisms concerned. Moreover, it is well known that the distribution of trace elements in marine organisms varies, even within one species, depending on various factors, such as stage of growth, part of the body, season, location, etc. For the complete understanding of the distribution pattern of trace elements in marine biota, therefore, the variation of the content of trace elements with the various factors stated above must be clarified. For the practical purpose of radiation protection, however, the time required for complete understanding is certainly too long to wait. For this reason, it seems necessary to compromise between the accuracy of the distribution pattern and the time required for improving the accuracy. In other words, it is necessary to simplify the subject by introducing uncertainty into the conclusion. Based on this idea, an attempt was made by the present author[3, 4] to introduce the concept of "standard abundance" of trace elements for different groups of marine organisms. In Table 1, for example, the set of geochemical data for cobalt and chromium was summarized. The data are supposed to represent the standard abundance of these elements in various biogeochemical phases.

Although these data are only tentative and will be improved when more materials are available, they are useful for the prediction of the levels of corresponding radioisotopes in marine organisms with reservation for the uncertainty implied.

ABUNDANCE RATIO

In order to express the relationships between the concentrations of a certain element in marine organisms and that in sea water, the term "concentration factor" (or "enrichment factor") has been in wide use. This factor is important for the prediction of the levels of radioisotopes as well as trace elements in marine organisms. The term is defined, in general, in the following way:

$$\text{Concentration factor (enrichment factor)} = \frac{C_B}{C_W}$$

where C_B: amount of an element in unit mass of an organism

C_W: amount of the same element in unit mass of sea water.

In this definition wet weight is usually based for expressing the concentration of the element in marine organisms, so that the unit used is microgram of element per gram or kilogram

Table 1. *Distribution of Cobalt and Chromium in Various Marine Geochemical Spheres in the Mediterranean**

Sphere	Sample	Cobalt μg/kg	Chromium μg/kg
Hydrosphere	Sea Water		
	in solution	0.1	Cr^{3+} 0.1, Cr^{6+} 0.3
	in particulate	0.01 >	0.05
Lithosphere	Sediments	5000	25000
Biosphere	Algae	100	200
	Crustacea		
	Copepoda (whole animal)	200	400
	Decapoda (soft parts)	40	60
	Mollusca		
	Lamellibranchia and Gastropoda (soft parts)	100	200
	Fish (flesh)	3	30

* Abundances are given on dry weight basis for sediments, and on wet weight basis for organisms

of wet weight of the organisms. Of course, the unit for sea water is similar. However, this definition of the term has not always been followed by different authors. For example, some of them used dry weight of organisms as the basis[5, 6] and the others extended the definition into the different meanings.[7, 8] Due to these deviations from the definition, there seems to be considerable confusion in the literature. Moreover, the term concentration or enrichment indicates the process, where elements are concentrated or enriched into organisms to a high level, and in turn implies that the higher concentration is more hazardous in the cases of radioisotopes. For the purpose of radiation protection, however, the specific activity of radioisotopes with respect to the corresponding stable isotopes is, in general, more important than the absolute level of radioactivity. If a marine organism has concentrated a trace element to a high level, there will be a higher degree of isotope dilution of the corresponding radioisotopes in the body of the organisms, when the organisms are exposed to contaminated sea water, before the steady state will have been reached. In this case the higher concentration factor does not necessarily indicate the higher potential hazard. For the reasons discussed above, it seems that the simpler term "abundance ratio" can replace the term "concentration factor" in a way to avoid the misunderstanding without introducing any confusion.

PRESENTATION OF BIOGEOCHEMICAL DATA

In the course of the systematic accumulation of data on the content of trace elements in marine organisms, it is important that the data supplied by different authors be comparable. Although the content of trace elements can be expressed on the basis of wet weight, dry weight, ash weight or some special components, it seems most simple and reproducible when dry weight at around 105°C is taken as the basis. For this reason the universal use of dry weight as the basis of the expression of the analytical results may help to increase the comparability

of the data obtained by different authors. Of course, one is free to use any kind of expression depending on the purpose of the studies. However, if the data are referred to the universal basis, beside the special expression of the studies, the usefulness of the data will be doubled.

In order to compute the "abundance ratio" of an element in an organism, the data based on dry weight have to be converted to those based on wet weight. Since the measurements of wet weight of marine organisms are variable depending on the procedures of sample preparation, comparable results are not likely to be obtained. As shown in Fig. 1, however, the percentages of dry weight based on wet weight for some groups of marine organisms seem to have a Gaussian distribution around a certain value. In order to make this figure, more than a hundred results obtained by different authors have been taken as well as those obtained by the present author. The figure indicates the possibility to chose a representative value for each group of marine organisms. By using these representative values the data on a dry basis may be converted to those on a wet basis with reasonable accuracy for obtaining an "abundance ratio".

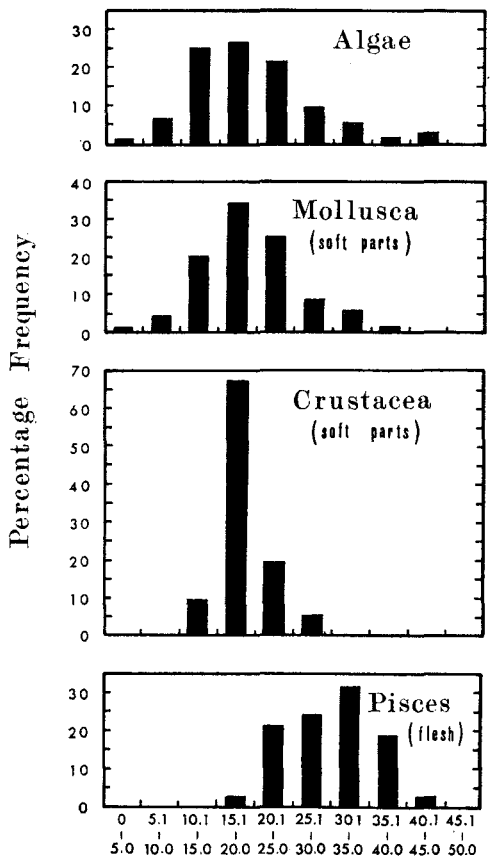

FIG 1. Frequency distribution of percentage of dry weight based on wet weight for the different groups of marine organisms.

Since the data, required in this field for the proper radiation protection, are still far from complete, the effectiveness of data accumulation must be encouraged by choosing a reasonable basis of expressions agreed upon by different workers in this field.

REFERENCES

1. J. P. RILEY. *Chemical Oceanography* (Ed. J. P. Riley and G. Skirrow), Vol. 2, pp. 295–424. Academic Press, London and New York (1965).
2. A. P. VINOGRADOV. *The Elementary Chemical Composition of Marine Organisms* (Translated by J. Efron and J. K. Setlow), Sears Foundation for Marine Research, Yale University, New Haven (1953).
3. R. FUKAI and D. BROQUET. Distribution of chromium in marine organisms. *Bull. Inst. océanogr.* **65,** No. 1336 (1965).
4. R. FUKAI. Distribution of cobalt in marine organisms. *Bull. Inst. océanogr.*, in press.
5. I. NODDACK and W. NODDACK. *Arkiv für zoologi*, **32A,** No. 4, 1 (1939).
6. R. R. BROOKS and M. G. RUMSBY. *Limnol. and Oceanogr.* **10,** 521 (1965).
7. A. F. FEDOROV. Mathematical formulas for concentration coefficient study of radioactive material to sea biota. *Bull. Inst. océanogr.* **63,** No. 1304 (1964).
8. I. HELA. Alternative ways of expressing concentration factors for radioactive substances in aquatic organisms. *Bull. Inst. océanogr.* **61,** No. 1280 (1963).

STRAHLENSCHUTZASPEKTE BEI DER ÜBERWACHUNG DER FISCHE AUF IHRE RADIOAKTIVE KONTAMINATION

W. FELDT

Isotopenlaboratorium der Bundesforschungsanstalt für Fischerei 2 Hamburg BRD

Zusammenfassung—Die Aufgaben der Strahlenschutzüberwachung für die See- und Süßwasserfische werden diskutiert.

Nach einem Überblick über die ökologische Rolle des Strontium und Cäsium werden die gefundenen Kontaminationswerte von Strontium-90 und Cäsium-137 in Fischen mitgeteilt.

Experimentell gewonnene Diskriminierungsfaktoren sowie ein einfaches Rechenmodell gestatten die Berechnung der Fischkontamination aus der Kontamination des Wassers und umgekehrt.

Die Konzentrationsfaktoren einiger Radionuklide in Abhängigkeit vom Salzgehalt des Wassers werden mitgeteilt.

Auf Grund der vorliegenden Ergebnisse wird eine zweckmässige Fischüberwachung diskutiert. Die derzeitige Zufuhr radioaktiver Nuklide über den Fisch zum Menschen wird abgeschätzt.

EINLEITUNG

Eine Strahlenschutzüberwachung der radioaktiven Kontamination von Fischen kann unter folgenden Aspekten geschehen:

(a) Schutz der Bevölkerung vor unzulässig hoch kontaminierten Fischen;
(b) Aufdeckung radioökologischer Zusammenhänge;
(c) Schutz der im Wasser lebenden Tierwelt vor schädigenden Auswirkungen der in das Wasser eingebrachten radioaktiven Abfälle.

Gegenüber der unter (a) genannten Aufgabe, der Aufgabe der Strahlenschutzüberwachung, die einer üblichen Lebensmittelkontrolle gleichzustellen ist, stellt die unter (b) genannte Aufgabe eine Grundlagenforschung für die gesamte Strahlenschutzüberwachung dar. Die Aufdeckung radioökologischer Zusammenhänge vermittelt die Grundkenntnisse, aus denen heraus notwendige vorbeugende Maßnahmen getroffen werden können. Über diese beiden Aufgaben hinaus sollte die Strahlenschutzforschung die unter (c) genannte Fragestellung nicht vernachlässigen, damit wichtige Eiweißreserven der Menschheit vollgültig erhalten bleiben.

Im Folgenden werden anhand von Meßwerten über die radioaktive Kontamination von Fischen aus den verschiedensten Biotopen ökologische Zusammenhänge aufgezeigt, die eine Abschätzung des Transportes von Radionukliden vom Wasser über den Fisch zum Menschen sowie eine Berechnung der derzeitigen Strahlenbelastung der Fische gestattet. Die Betrachtungen werden mit dem Entwurf einer zweckmäßigen Fischüberwachung abgeschlossen.

DIE RADIOAKTIVE KONTAMINATION DER FISCHE

Unter den kontaminierenden radioaktiven Nukliden des Fallouts und der Abfälle der Kerntechnik spielen die Elemente ^{90}Sr und ^{137}Cs eine besondere Rolle, da sie den für das Bestehen des Lebens wichtigen Elementen Ca und K chemisch ähnlich sind.

Inaktives Cs wurde im Meerwasser in einer Konzentration von 0,5–0,05 μg/Liter nachgewiesen. [1] Es ist in allen weichen Gewebeteilen wiederzufinden, in die auch K eingebaut wird. Damit trägt ^{137}Cs auch zur Gonadenbelastung bei.

Tabelle 1. *Die radioaktive Kontamination der Fische* 1964 (*pCi/kg Gesamtfisch*)

Fischart	Herkunft	Analysen-zahl	^{90}Strontium			^{137}Cäsium		
			Minimal-wert	Maximal-wert	Mittel-wert	Minimal-wert	Maximal-wert	Mittel-wert
Scholle (*Pleuronectes platessa*)	Nordsee	3	11	14	12	42	53	49
Hering (*Clupea harengus*)	„	3	0,44	2,0	1,1	35	61	52
Schellfisch (*Melanogrammus aeglefinus*)	„	7	1,5	2,2	1,9	24	30	25
Makrele (*Scomber scombrus*)	„	3	0,60	7,8	3,2	26	54	40
Scholle (*Pleuronectes platessa*)	Ostsee	1	—	—	0,44	—	—	33
Dorsch (*Gadus callarias*)	„	7	4,8	13	7,6	88	160	120
Brachse (*Abramis brama*)	Ratzeburger See i. Norddeutschland	1	—	—	73	—	—	360
Hecht (*Esox lucius*)		1	—	—	76	—	—	1500
Plötze (*Leuciscus rutilus*)	Gr. Plöner See i. Norddeutschland	2	140	170	160	630	700	670
Barsch (*Perca fluviatilis*)	Gr. Plöner See i. Norddeutschland	1	—	—	42	—	—	800
Große Maräne (*Coregonus maraena*)	„	1	—	—	54	—	—	640
Hecht (*Esox lucius*)	Kolksee i. Norddeutschland	6	200	1200	780	2700	9900	5500
Schleie (*Tinca vulgaris*)	„	9	320	2800	1500	3200	11000	6000
Karpfen (*Cyprinus carpis*)	„	2	1200	2200	1700	3500	5400	4500

Inaktives Sr, das überall als Begleitelement des Ca auftritt, ist nach unseren Messungen im Süßwasser in Konzentrationen von 20 μg bis 1mg/Liter vorhanden, während es im Meerwasser in einer Konzentration von 9 mg/Liter vorzufinden ist. ^{90}Sr erscheint in allen Stützgerüsten, die aus Ca aufgebaut sind.

Die Kontamination der Fische in den verschiedenen Biotopen des Meeres und der Binnengewässer ist sehr unterschiedlich. Zur vergleichenden Betrachtung werden im folgenden Meßwerte in einer Tabelle zusammengefaßt, die im Jahre 1964 gewonnen wurden (Tab. 1). Wie die Meßwerte zeigen, ist die radioaktive Kontamination der Süßwasserfische bis zu zwei Größenordnungen höher als die Kontamination der Meeresfische. Die Einstellung der Kernwaffenversuche führte in den Lebensräumen des Meeres und der Binnengewässer bisher nicht zu einer Abnahme der radioaktiven Kontamination.

KONZENTRATIONSFAKTOR UND SPEZIFISCHE AKTIVITÄT

Wie schon in früheren Arbeiten berichtet, ist die Höhe der radioaktiven Kontamination umgekehrt proportional zum Ca-Gehalt der Gewässer.[2, 3] Die radioaktive Kontamination der Fische durch ^{90}Sr in pCi/g Ca läßt sich aus der Kontamination des Wassers berechnen nach der Gleichung

$$K_F = D_{WF} \cdot \frac{^{90}\text{Sr/l.}}{\text{Ca/l.}}$$

D_{WF} ist der Diskriminationsfaktor Wasser/Fisch, der von der Fischart abhängig ist und im Mittel zwischen 0,2 und 0,3 beträgt. Die radioaktive Kontamination durch ^{137}Cs ist ebenfalls abhängig vom Ca- und K-Gehalt der Gewässer.

^{90}Sr und ^{137}Cs werden in Fischen in unterschiedlichen Größenordnungen konzentriert. Tabelle 2 zeigt einige 1964 gewonnene Konzentrationsfaktoren, geordnet nach dem Ca- und K-Gehalt der Gewässer. Der Konzentrationsfaktor für ^{90}Sr liegt im Bereich 1–570 und steigt mit sinkendem Ca-Gehalt des Wassers. Der Konzentrationsfaktor für ^{137}Cs liegt im Bereich 23–2000, ebenfalls ansteigend mit sinkendem K-Gehalt des Wassers.

Um eine Abschätzung über die mögliche Gefährdung des Menschen durch den Verzehr radioaktiv kontaminierter Fische vornehmen zu können, kann man sich der spezifischen Aktivität bedienen, indem man postuliert, daß die spezifische Aktivität im Wasser und in den Fischen nicht die maximal zugelassene spezifische Aktivität im menschlichen Körper überschreiten darf. Im Vergleichsjahr 1964 wurde die spezifische Aktivität an verschiedenen Fischarten in den unterschiedlichen Gewässern bestimmt. Tabelle 3 faßt einige Ergebnisse zusammen. Die maximal zugelassene spezifische Aktivität im menschlichen Körper wird mit 30 μCi/g Sr angenommen.[4]

Die radioaktive Kontamination des Nordseewassers durch ^{137}Cs betrug nach unseren Messungen maximal 1,5 pCi/l. Bei einem Gehalt an inaktivem Cs von 0,5 μg/l. ergibt das eine spezifische Aktivität von 3 μCi/g Cs. Die maximal im Menschen zugelassene spezifische Aktivität von ^{137}Cs wird mit $3{,}1 \cdot 10^6$ μCi/g angenommen, so daß die in der Nordsee vorgefundene spezifische Aktivität 0,001‰ der zulässigen Größe erreicht hat.

Meßwerte über den Gehalt an inaktivem Cs in den Binnengewässern oder in den Organismen der Binnengewässer sind dem Autor leider nicht bekannt, so daß ein Vergleich der spezifischen Aktivität in dem Süßwasserbereich nicht gebracht werden kann.

KONTAMINATION VON FISCHGONADEN

In Tabelle 4 werden einige Meßwerte mitgeteilt, die an den Gonaden von Dorschen und Schleien gewonnen wurden. Aus den Meßwerten kann der Beitrag zur Gonadendosis errechnet werden, der durch die in den Gonaden enthaltenden Radionukliden ^{90}Sr und ^{137}Cs hervorgerufen wird.

Im folgenden wird diese Dosis mit der durch ^{40}K hervorgerufenen Dosis verglichen. Um die Strahlenbelastung durch ^{40}K, ^{90}Sr, ^{90}Y, und ^{137}Cs berechnen zu können, benutzen wir die folgende Gleichung[5]

$$E_{eff} = \sum_{i,k} 0{,}33\, p_{\beta i}\, E_{\beta i} \left(1 - \frac{\sqrt{Z}}{43}\right) \left(1 + \frac{\sqrt{E_{\beta i}}}{4}\right) + p_{\gamma k}\, E_{\gamma k} \left(1 - e^{-\sigma_k R}\right)$$

Hierin bedeuten

Tabelle 2. Konzentrierungsfaktoren für ^{90}Strontium/^{137}Cäsium

Fischart	Calcium-/Kaliumgehalt der Gewässer						
	10/1 mg/l	30/3 mg/l	60/6 mg/l	90/9 mg/l	120/30 mg/l	170/170 mg/l	400/400 mg/l
Scholle (*Pleuronectes platessa*)	—	—	—	—	—	—	11/45
Hering (*Clupea harengus*)	—	—	—	—	—	—	1/47
Schellfisch (*Melanogrammus aeglefinus*)	—	—	—	—	—	—	1,7/23
Makrele (*Scomber scombrus*)	—	—	—	—	—	—	2,9/36
Dorsch (*Gadus callarias*)	—	—	—	—	—	6,9/93	1,7/32
Brachse (*Abramis brama*)	570/690	170/–	–/100	53/–	—	—	—
Hecht (*Esox lucius*)	220/2000	—	26/100	8/–	—	—	—
Schleie (*Tinca vulgaris*)	280/610	96/280	59/140	—	—	—	—
Karpfen (*Cyprinus carpis*)	320/560	120/35	—	—	—	—	—
Barsch (*Perca fluviatilis*)	240/1800	—	—	—	—	—	—
Kaulbarsch (*Acerina cernua*)	—	—	—	29/260	17/180	—	—
Rutte (*Lota vulgaris*)	—	—	—	22/350	—	—	—

Tabelle 3. Spezifische Aktivität ($^{90}Sr/Sr$) in Fischen

Fischart	Herkunft	Spez. Akt. μCi/g Sr	‰ der max. zulässigen spez. Akt.
Hering (*Clupea harengus*)	Nordsee	0,000 051	0,003 3
Dorsch (*Gadus callarias*)	Ostsee	0,000 160	0,01
Hecht (*Esox lucius*)	Gr. Plöner See i. Norddeutschland	0,002 6	0,17
„	Kolksee i. Norddeutschland	0,021	1,4

Tabelle 4. Die radioaktive Kontamination von Fischgonaden

Fischart	Fangort	Fangdatum	^{90}Sr i.d.Gonaden			^{137}Cs i.d.Gonaden		
			pCi/g Asche	pCi/kg Frischgew.	pCi/g Ca	pCi/g Asche	pCi/kg Frischgew.	pCi/g K
Dorsch (*Gadus callarias*)	Ostsee	6.1.66	0,013	0,21	1,5	4,8	81	27
Schleie (*Tinca vulgaris*)	Kolksee i. Norddeutschld.	1.7.65	0,26	5,6	22	160	3 500	1 900

E_{eff}: Die gesamte absorbierte (effektive) Energie in MeV,
$p_{\beta i}$: Emissionswahrscheinlichkeit für das ß-Spektrum der Maximalenergie $E_{\beta i}$,
$p_{\gamma k}$: Emissionswahrscheinlichkeit für γ-Quanten der Energie $E_{\gamma k}$,
σ_k: Linearer Schwächungskoeffizient–Comtonstreukoeffizient (cm^{-1}) von Gewebe für γ-Quanten der Energie $E_{\gamma k}$,
R: Wirksamer Radius des "kritischen Organs" (cm),
Z: Kernladungszahl des Radionuklids.

In der obigen Gleichung wird die pro Zerfallsakt im Gewebe des kritischen Organs im Mittel absorbierte Energie errechnet. Mit den in Tabelle 4 angegebenen Kontaminationswerten errechnen wir für die Dorschgonaden eine Dosis

durch ^{40}K | von 0,36 mrem/Woche
und durch ^{90}Sr u. ^{137}Cs | von 0,006 mrem/Woche.

Das heißt, die durch die radioaktive Kontamination hervorgerufene zusätzliche Belastung der Dorschgonaden beträgt ca 2% der natürlichen Belastung durch ^{40}K.
Für die Schleigonaden ergibt sich eine Dosis, hervorgerufen

durch ^{40}K | von 0,23 mrem/Woche
und durch ^{90}Sr u. ^{137}Cs | von 0,29 mrem/Woche.

Für den Süßwasserfisch wird durch die radioaktive Kontamination eine zusätzliche Gonadenbelastung gegeben, die genau so hoch ist wie die natürliche Strahlenbelastung.

FISCHÜBERWACHUNG

Die hier angeführten Daten zeigen, daß die radioaktive Kontamination der Meeresfische durch ^{90}Sr und ^{137}Cs zur Zeit keine Gefahrenquelle für den Menschen bedeutet. Von den beiden genannten Radionukliden spielt das ^{137}Cs eine gewisse Rolle. Die Zufuhr von ^{137}Cs über die Fische zum Menschen macht für Norddeutschland zur Zeit 5% der Gesamtzufuhr über die Nahrung aus.[3] Zu bedeutenden Zufuhren von Radionukliden kommt es nur bei den Süßwasserfischen aus sehr calciumarmen Gewässern, in denen die Süßwasserfische besonders stark kontaminiert werden können.

Die Fischüberwachung wird sich der Verschiedenheit der Kontaminationsmöglichkeiten anzupassen haben. Eine regelmäßige Kontrolle der Fischanlandungen an den Seefischmärkten kann in großen Zeitabständen erfolgen, um die Entwicklung zu verfolgen. Diese Überwachung muß sogleich verschärft werden, wenn z.B. durch Reaktorunfälle auf See begrenzte Fischweidegebiete sehr stark kontaminiert werden. Die Überwachung der Süßwasserfische sollte häufiger in allen "kritischen Gewässern" durchgeführt werden. Kritische Gewässer sind z.B. Flußgebiete unterhalb eines Reaktors und unterhalb der Abflüsse großer Städte sowie Teichwirtschaften mit besonders ungünstigen Wasserverhältnissen, die außerdem eine hohe Fischproduktion aufweisen.

Bei der Einleitung radioaktiver Abfälle in das Meer und die Binnengewässer sollte nicht die mögliche Gefährdung des Menschen allein Maßstab des Handelns sein. Die im Wasser lebende Tierwelt muß ebenfalls berücksichtigt werden, um nicht durch eine unnötige Belastung einiger Glieder der Nahrungskette ökologische Folgen heraufzubeschwören.

LITERATUR

1. A. A. Smales und L. Salmon. *Analyst* **80,** 37 (1955).
2. W. Feldt. *Proceedings of the Symposium on Nuclear Detonations and Marine Radioactivity*, 105 (1963).
3. W. Feldt. *Proceedings of the IAEA-Symposium Disposal of Radioactive Wastes into Seas, Oceans and Surface Waters* (1966).
4. *Disposal of Low-level Radioactive Waste into Pacific Coastal Waters*, NAS-NRC Publication 985 (1962).
5. B. Rajewsky. *Strahlendosis und Strahlenwirkung.* Herausgegeben vom Georg Thieme Verlag, Stuttgart (1956).

BIOLOGICAL HALF-TIMES OF ^{137}Cs AND ^{22}Na IN DIFFERENT FISH SPECIES AND THEIR TEMPERATURE DEPENDENCE

ERKKI HÄSÄNEN, SEPPO KOLEHMAINEN and J. K. MIETTINEN
Department of Radiochemistry, University of Helsinki, Finland

Abstract—Biological half-times of ^{137}Cs in 5 species of fish were determined by giving *per os* a precisely known dose (usually *ca.* 250 nCi) of ^{137}Cs in a gelatine jelly or in a tiny gelatine capsule and by whole body counting the fish, first daily, then weekly, in the Institute's mobile whole body counter. Experiments were continued for up to 6 months. Twelve experiments were carried out in the field in summer (May–October) and 16 in the laboratory, where it was possible to keep a constant temperature (from 6 to 20°C) in the aquarium.

The excretion of ^{137}Cs from fish follows a two-differential equation: the fast component (usually 5 to 10% but in *Salmo* 25 and in *Cyprinus* 50% of the amount administered) has a half-time of a few days, the slow component is about one order of magnitude longer. At 15°C the long component is for perch (*Perca fluviatilis*) 200 days, roach (*Leuciscus rutilus*) from 100 days (age 11 years) to 57 days (3 years). For the rainbow trout (*Salmo iridaeus*) the long component varies from 20 to 80 days depending on the age of the fish. The value for young fish (1 year, 20 days at 20°C) is increased to 36 days at 7–8°C. Crucian carp (*Cyprinus carassius*) of about 5 years of age has a half-time of 55 days at 20°C, 120 days at 10°C.

The biological half-times of ^{22}Na are much shorter, but the temperature dependence seems to be very similar to that of ^{137}Cs. For perch, half-times of ^{22}Na were 7 days at 20°C, 15 days at 10°C; for roach 7 days at 20°C, 11 days at 10°C; for burbot 30 days at 10°C, for the Crucian carp 10 days at 20°C, 25 days at 10°C.

Knowledge of the body burden and of the biological half-time make possible calculation of the daily intake of ^{137}Cs by fish in natural conditions.

INTRODUCTION

The excretion rate of ^{137}Cs is known for a number of animal species.[1] It usually follows a two-exponential equation: a smaller fraction, typically 10 to 20% shows a short biological half-time (TB_1) varying from part of a day to a few days. Evidently, this fraction mainly represents ^{137}Cs in the extracellular space. The remaining bulk shows a biological half-time (TB_2) many times longer, varying from a few days to one hundred days. This fraction evidently represents ^{137}Cs in the intracellular space and especially within the muscle cells. Knowledge of the biological half-time(s) is necessary for the quantitative treatment of the behaviour of ^{137}Cs (and any other nuclide having an exponential excretion rate) in organisms, which again is necessary for clear understanding of the behaviour of the nuclide in a foodchain.

Except for ^{55}Fe which cannot be measured[2] by ordinary thick crystal gamma spectrometry, ^{137}Cs is the only artificial long-lived nuclide present in easily measurable amounts in the flesh of fish. ^{90}Sr is also present in fish in considerable concentrations but it is mainly located in the bones, which are not eaten by man. The presence of ^{55}Fe has been recently shown independently by Jaakkola[3] in fresh water fish and Palmer[2] in ocean fish. Ocean fish may contain it in high concentration (max. 2 μCi/kg fresh wt. in salmon liver.[2] ^{137}Cs is found in fresh water fish in high concentrations, the highest value was in 1965 in the Finnish perch 26 nCi/kg fresh weight,[4] which is more than in any other food eaten by man except

reindeer meat. Fish flesh is the primary source of ^{137}Cs for population groups consuming fresh water fish, with the exception of reindeer-herding Lapps and other peoples consuming mainly reindeer or caribou meat having 2 to 4 times higher maximal ^{137}Cs contents than the fresh water fish. Even for these peoples fish is usually the second source of ^{137}Cs in importance.[5] ^{137}Cs content of lake fish varies greatly in different waters according to the limnological type of the water,[4] but even in the same water there exist great differences in the ^{137}Cs content between various species of fish. These are partly due to differences in the diets of the fish, but an equally important cause is a different excretion rate of ^{137}Cs in the various fish species, as will be shown in this paper.

EXPERIMENTAL

The experimental technique has varied to some extent. The first experiment was carried out with 150 small perch, 6 months of age, weighing 1–1.5 g each, in an aquarium in the laboratory. In this experiment labelling was given externally by keeping the fish for 1 hr in water (electrolytic conductivity 250 mho, potassium 5 mg/l) containing 860 μCi carrier-free ^{137}Cs in 8 l. Each fish took up 1.8 nCi, 150 fish thus taking 0.27 μCi or 0.03% of the amount given. The concentration factor was 0.012. Then the fish were grown with inactive food in a 200 l. aquarium (conductivity 250 mho, potassium content 5 mg/l.) in slowly changing inactive water. The experiment was continued for 6 months taking samples of 15 to 25 fish for measurement with intervals from 2 days to several weeks.

In most other experiments each fish has been labelled individually by giving it a precisely known amount of ^{137}Cs (usually 250 or 500 nCi) orally in a tiny gelatine capsule (4 × 8 mm). Each fish was then marked by clipping different fins and measured alive in the Institute's mobile whole body counter (Fig. 1), first at one-day intervals, later less frequently.

In field experiments the fish were kept in large cages made of Japanese nylon net and placed in the oligotrophic Suolijärvi lake.[4] They were regularly fed commercial fish food or milled inactive fish. In laboratory experiments they were kept in aquaria of different sizes, up to

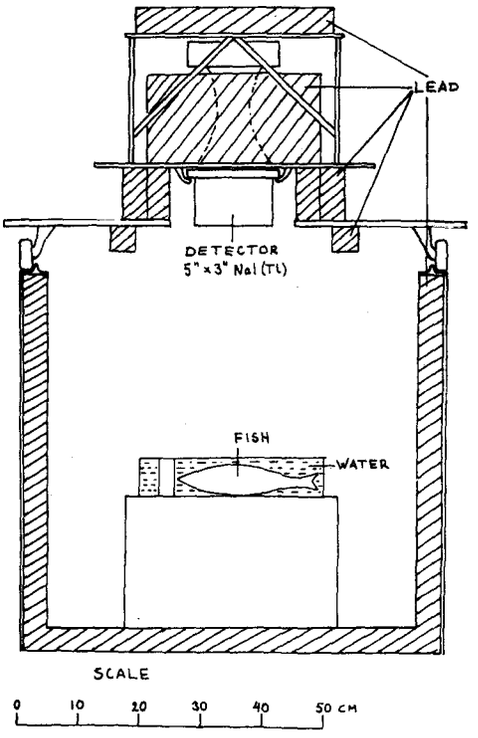

FIG. 1. Arrangement for whole body counting of live fish, initially labelled by an oral dose of 250 nCi ^{137}Cs. This activity gives 1170 cpm net within the ^{137}Cs photopeak channel at a distance of 42 cm. BG is 200 cpm. The lead shield is 4 to 8 cm thick and weighs 1800 kg.

1 m × 2 m × 70 cm (depth). In some experiments, with quite young fish, the isotope was given orally by injecting an aliquot of ^{137}Cs-containing gelatine jelly into the oesophagus. In one experiment the isotope was given by feeding labelled food to the fish.

As the fish in nature get the bulk of their ^{137}Cs in food, oral administration corresponds best to the natural conditions. In addition, a precise determination of the short component requires instantaneous administration of the isotope. Furthermore, the external labelling seems to give a higher percentage of the short component, probably due to partial adsorption on the surface of the fish (Table 1, line 1). Therefore, oral administration has been used in all experiments but the first.

Table 1. Biological Half-time of ^{137}Cs in Five Species of Fresh-water Fish
(F, Field experiment; L, Laboratory experiment)

Fish species	Type of expt.	Age of fish yr.	No of fish in expt.	Temp. °C	Fast comp. (TB_1) days	Fast comp. (TB_1) %	Slow comp. (TB_2) days	Slow comp. (TB_2) %
Perch	L	0.5–1*	150	18 ± 2		17	200	83
(*Perca fluviatilis*)	F	2–3	16	15 ± 5	12	6	175	94
	F	2–3	6	15 ± 5		6	220	94
	F	3–6	12	15 ± 5		4	200	96
	F	6–8	3	15 ± 5		10	220	90
Roach	F	2–3	11	15 ± 5		6	57	94
(*Leuciscus rutilus*)	F	4–6	4	15 ± 5		6	85	94
	F	9–12	3	15 ± 5		10	150	90
	F	2–3	11	5 ± 2			340	
Rainbow trout	L	0.5–1	7	20 ± 0.2			20	94
(*Salmo iridaeus*)	L	0.5–1	11	14 ± 1			19	90
	L	0.5–1	10	7 ± 1	3	26	34	74
	F	0.3–0.5	50	15 ± 5	5	25	25	75
	F	1–2	18	15 ± 5	5	34	55	66
	F	2–3	15	15 ± 5	7	24	80	76
	F	1–2	17	4 ± 1			≃150	
	F	2–3	15	4 ± 1			≃230	
Crusian carp	L	5	29	20 ± 0.2	2	50	55	50
(*Cyprinus carassius*)	L	5	28	8 ± 3	3	55	120	45
Burbot	L	5	1	8 ± 3	8	14	110	86
(*Lota vulgaris*)								

* Labelling given externally.

The *measurement* has been made with a multichannel analyzer at 42 cm distance from the 5 × 3 NaI(Tl) crystal (Fig. 1). With 250 nCi 1170 cpm net are obtained within the ^{137}Cs photopeak channel. With 250 to 500 nCi initial labelling and 2 to 4 min counting time a statistical accuracy (1 σ) better than 3% is obtained throughout the experiment of 2 × TB_2. This statistical error is small compared with the *biological* variance which is for individual fish 25%, and for a group of 15 fish 6% (1 σ) after external labelling and one TB_2 (unpublished). This is mainly due to differences of TB_2 between individuals of the same species.

RESULTS

The results for ^{137}Cs are presented in Table 1. Those for rainbow trout are also illustrated in

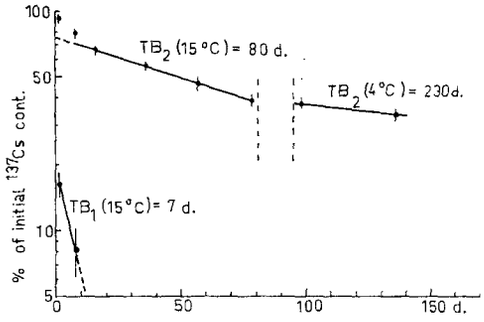

FIG. 2. ^{137}Cs retention in rainbow trout (15 fish) with biological variance (two σ) marked. At least two components are noticeable in the retention at 15°C: a "short" one having a half-time 7 ± 3 days (TB_1), and a "long" one, 80 ± 4 days (TB_2). At 4°C the value of TB_2 is 230 ± 10 days.

Fig. 2. The points for TB_1, the fast component of the biological half-time, have been obtained by subtracting from the total retention the part due to the slow component, TB_2, obtained by extrapolating to zero in the usual way. At the beginning of October the water temperature decreased in 2 weeks from 13°C to 5°C; the value of TB_2 then increased to about 230 days.

As can be seen from Table 1, perch has the longest half-time (TB_2), 200 ± 20 days at 15°C. There may be some increase in the value of TB_2 with the ageing of the fish, but the change is not clear. As the youngest age group (0.5 to 1 year) was labelled externally the results are not strictly comparable with the others.

In roach the half-time (50 days) in young fish is about half of that in old fish (100 days). The age dependence is clear also in rainbow trout as is the temperature dependence in rainbow trout and in the crusian carp. The table is incomplete in many respects due to technical difficulties. In laboratory experiments these include lack of space, presence of impurities in tap water, malfunction of thermostats and occasional infectious diseases. The field experiments have the advantage of more natural conditions, but the disadvantage that the water temperature cannot be kept constant. It was concluded from parallel determinations and parallel experiments that the accuracy of the data presented is better than 10%. Because the biological variance is rather large (see above) it is for most purposes not meaningful to have the average value determined with much higher accuracy; and in any case this would be very cumbersome.

In experiments made with oral labelling of perch and roach the percentage of the short component was 4 to 10%. In rainbow trout it was 25 ± 1% in three experiments, but 34% in one experiment. A large percentage is understandable in salmon which have rapid metabolism and short half-time (TB_2). The high percentage in the crucian carp is exceptional. There was no excretion during the first 24 hr, then about 50% of intake was suddenly excreted during the next 24 hr, and after that a very slow excretion rate (TB_2 55–120 days) was observed.

The results for ^{22}Na are presented in Table 2. The presence of a short component in the excretion curve for sodium is not always clear. From perch and roach a small amount (5 ± 3%) was consistently excreted very rapidly, and from rainbow trout 20% at 6°C but none was observed at the higher temperatures. As the long component was only 2.2 to 2.5 days it would have needed measurements at 1 hr intervals to notice the short one, but these were not made. No signs of a third component were noticed although most of the experiments were continued for several half-times (30 to 40 days).

Table 2. Biological Half-time of ^{22}Na in Five Species of Freshwater Fish

Fish	Age, yr.	No. of fish in expt.	Temp. °C	Biol. half-time of ^{22}Na, days
Perch	1–2	6	20 ± 0.2	7
		5	8 ± 3	15
Roach	1–2	5	20 ± 0.2	7
		5	8 ± 3	11
Rainbow trout	0.5–1	7	20 ± 0.2	2.2
		11	14 ± 1	2.5
		10	7 ± 1	7
Crusian carp	5	30	20 ± 0.2	10
		30	8 ± 3	25
Burbot	5	1	8 ± 3	30

Temperature dependence seems to be similar to ^{137}Cs-excretion: a 10° temperature decrease (from 15 to 5°C) reduces the excretion rate to about one-half.

CONCLUSIONS AND DISCUSSION

It is of interest to compare the above results with those obtained elsewhere, although the species are evidently different in all cases. Dean *et al.*[6] have studied the uptake and excretion of ^{137}Cs in different tissues of another species of rainbow trout, *Salmo gairdneri*. By injecting 10 μCi intravenously into yearling fish they found the "effective half-time" (TB_2) of ^{137}Cs in red muscle 5½ days, in white muscle 13 days. The curves published also suggest the existence of a short component of less than a day in most tissues (heart, gills, blood, liver, kidney). Temperature was not given, but if it was around 20°C and the whole body burden was determined by the white muscle, 13 days corresponds approximately to our value of 19 days at 14°C in *Salmo iridaeus*. Scott[7] reports 47 days for the brook trout (*Salvelinus fontialis*) and Ichikawa[8] 5 to 10 days for salmon (*Salmo salar*). Rudakov[9] has studied Crusian carp (*Cyprinus* sp.) and reports 10 to 15 days, but this value may represent the short component. Our values for TB_2 in the Crusian carp are 55 and 120 days at 20 and 8°C, respectively, but there may be a different species in question. Kevern *et al.*[10] report for the carp (*Cyprinus carpio*) 98 days at 20°C and 174 days at 12.5°C, i.e. about similar temperature dependence as found in this work. From the data of Williams and Pickering[11] we can estimate for very young bluegills (2 g each) the fast component to be about 3 to 4 days, the slow one 40 days. Nelson and Early[12] report the same value, 40 days, for blue gills (*Lepomis macrochirus*). Baptist and Price[13] studied retention of ^{137}Cs in skin, muscle, liver and gonad of the Atlantic croaker fish (*Micropogon undulatus*) finding that each tissue required multiple rate functions involving two or four exponents. Muscle had the longest retention time and it evidently governed the whole body retention. In most of the above studies the age of the fish and the water temperature are not given.

It is evident from the present results, and from those of the earlier workers, that the excretion rate of ^{137}Cs in fish varies greatly, by at least one order of magnitude. For instance, old perch has a two times longer half-time (200 days) than the old roach (100 days). ^{137}Cs body burdens in perch have been in most Finnish lakes 3 to 6 times higher than in roach.[4] Half of this difference is evidently due to different

food activity as perch eats mainly small perch, but roach plankton and bottom animals,[14] half to different half-times. As shown in the above paper by us,[14] if one knows the ^{137}Cs body burden in a fish species at intervals of one to two half-times, and the percentage and value of the long component, one can calculate very accurately the daily intake of ^{137}Cs by the fish. Direct intake of ^{137}Cs through gills is so small that it can be neglected.[4] If, in addition, the activity of the food of the fish is known, one can calculate the food intake by the fish, a factor which is of great interest to fish investigators, and otherwise difficult to determine. Food intake by roach was in this way estimated in 6 lakes and found to vary from 0.8 to 2.3% of the weight of the fish per day. The intake was lowest in eutrophic lakes where a large number of small fish evidently limited the amount of food available. The annual growth of the fish was greater in the oligotrophic lakes where the food intake was greater, too.[14]

These examples show that some benefit may be obtained from the worldwide fallout to ecology and limnology.

ACKNOWLEDGEMENTS

Financial support for this investigation was obtained from the U.S. Department of Health, Education and Welfare (Public Health Service Research Grant No. RH-00307).

We are much indebted to the Kalamiesten keskusliitto organization for allowing us to use in these studies their fish hatchery facilities at Kytäjä.

It is a pleasure to acknowledge skilful technical assistance by Mr. Seppo Takatalo, Cand. Sci., and Mr. I. Vöry.

REFERENCES

1. C. R. Richmond, J. E. Furchner and W. H. Langham. *Health Phys.* **8**, 201 (1962).
2. H. E. Palmer and T. M. Beasley. *Radioecological Concentration Processes*, p. 259. Pergamon Press, London (1967).
3. T. Jaakkola. Ibid., p. 247.
4. S. Kolehmainen, E. Häsänen and J. K. Miettinen. This volume, p. 407.
5. Aili Jokelainen. *Acta Agr. Fenn.* **103,** 1 (1965) (Ph.D. Thesis).
6. J. M. Dean, J. Eapen and R. E. Nakatani. Hanford Biology Research Annual Report for 1964, BNWL-122, 73–4 (1965).
7. D. P. Scott. *J. Fish. Red. Board. Can.* **19,** 194 (1962).
8. R. Ichikawa. *Jap. J. Rad. Res.* **1,** 107 (1965).
9. N. P. Rudakov. *Izv. Oos. Nauchn.—Issled. Inst. Ozern. i Rechn. Rybn. Khoz* **51,** 165 (1961).
10. N. R. Kevern, N. A. Griffith and T. Grizzard. ORNL-3697, 101 (1964).
11. L. G. Williams and Q. Pickering. *Ecology* **42,** 205 (1961).
12. D. J. Nelson and R. C. Early. ORNL-3347, 67 (1962).
13. J. P. Baptist and T. J. Price. *U.S. Fish Wildlife Serv., Fishery Bull.* **62** (206), 177 (1962).
14. S. Kolehmainen, E. Häsänen and J. K. Miettinen. *Radioecological Concentration Processes*, p. 913. Pergamon Press, London (1967).

^{137}Cs IN THE PLANTS, PLANKTON AND FISH OF THE FINNISH LAKES AND FACTORS AFFECTING ITS ACCUMULATION

S. KOLEHMAINEN, E. HÄSÄNEN and J. K. MIETTINEN
Department of Radiochemistry, University of Helsinki, Finland

Abstract—Bioaccumulation of ^{137}Cs in the fresh water organisms was studied during 1964 and 1965 by taking water, plankton, plant, bottom animal, and fish samples from water courses representing widely different limnological types: from eutrophic (rich in nutrients) to oligotrophic (nutrient deficient) lakes.

It was shown that the ^{137}Cs content of all organisms sharply depends on the potassium content of the water. In lakes where this value is less than 1 mg K/l. water, very high values of ^{137}Cs in fish were reached in 1965—max. 26 nCi/kg fresh weight in perch (*Perca fluviatilis* L.).

Quantitative estimations show that the four main factors determining the ^{137}Cs body burdens in the last link of the food-chain, the fish, are:

1. ^{137}Cs content of water—a minor factor as observed differences in the lakes studied have been only about 2- to 3-fold.
2. The limnological type of the lake—this is the main factor effecting 10- to 100-fold differences in the same fish species in different lakes.
3. The quality of food eaten by the fish—a minor factor effecting 2- to 3-fold differences.
4. The biological half-time of ^{137}Cs in fish—an important factor varying from 20 to 200 days at 15°C in different species and effecting up to 10-fold differences in various species in the same water course.

The bulk of the ^{137}Cs intake takes place through food chains. Direct gill absorption plays a minor role only.

INTRODUCTION

It was observed in 1961–62 that the ^{137}Cs content of fish in Finnish lakes was high (1 to 5 nCi/kg fresh wt.)[1] compared with values reported from northern Germany (10 to 100 pCi/kg fresh wt.).[2] This was astonishing insofar as the cumulative fallout in Finland is only from one-half to two-thirds of that in Germany. Great variations in the ^{137}Cs content of the same fish species in lakes of different limnological types were observed, also.[1] This led to a more systematic study, in 1963, of the factors governing the ^{137}Cs uptake in fish. Up to 100-fold differences in the ^{137}Cs content of fish in 12 lakes and 3 rivers of widely different limnological types was found.[3] For instance, in perch (*Perca fluviatilis* L.) the ^{137}Cs content varied from 0.2 to 20 nCi/kg fresh wt., in pike (*Esox lucius* L.) from 0.16 to 16 nCi/kg fresh wt., when the limnological type changed from eutrophic (rich in nutrients) to oligotrophic (nutrient deficient). Simultaneously, the electrolytic conductivity varied from 79 to 11 mho, resp.[3] In a later publication it was shown by us that it is the potassium ion which determines the ^{137}Cs level of the whole fresh water biota.[4] As different fish species in the same water have different ^{137}Cs content, other factors must function in addition. It is the purpose of this paper to discuss the relative importance of four main factors effecting the ^{137}Cs uptake in fish: the ^{137}Cs and potassium content of the water, the kind of food consumed by the fish, and the biological half-time of ^{137}Cs in the fish.

RESULTS

Samples of water, plankton, higher plants, bottom animals and fish have been collected

since 1962 from a total of 23 lakes and 3 rivers representing widely different limnological types. There has been some variation in different years in the lakes studied, but those under study in 1964 and 1965 are presented in Table 1. The limnological type varies from fully eutrophic (No. 1) to dys-oligotrophic (No. 10a). A few of the limnological characteristics determined are presented in Table 1. Other factors determined were color, pH, and the frequency of plant and animal species which were used for characterization of the lake type. The methods and techniques used have been described earlier.[1, 3, 4]

1. *^{137}Cs content of the water* varied in the lakes studied (see Table 1) from 0.3 to 1.2 pCi/l. in 1964, when the highest values were observed in most of these lakes. A larger survey of Finnish surface waters was carried out by the Institute of Radiation Physics, which reports values between 0.2 and 2 pCi/l. in Finnish lakes in general.[5] Thus, variations in the amount of fallout were small compared with up to one-hundred-fold variations observed in the body burdens of fish.

2. *The limnological type of the lake.* This is the main factor affecting great differences in the ^{137}Cs content of the whole biota, as is evident from Tables 2 to 6.

In Table 2 there are presented the ^{137}Cs content of plankton samples from 7 lakes in 1964 and 8 in 1965. Analysis of 8 stable elements in these same samples (1964) as well as in the corresponding waters have been published earlier,[6] together with the frequency of species present. Composition of the samples collected in 1965 is presented in Table 3. Comparison between different years and lakes is made difficult by the fact that the composition of the samples—even from the same lake at different times—varies greatly. In addition, the fat content of some species (*Diaptomus*, *Cyclops*, *Daphnia* and *Bosmina*) varies at different times and one specie (*Holopedium gibberum*) may contain up to 90% of slime, which causes great differences in the percentage of dry matter. If the sample contains diatoms, these increase the ash content. However, the ^{137}Cs content per g of dry wt., and especially per g of potassium, changes rather regularly being lowest in the sample taken from the eutrophic lake 1 and highest in one of the oligotrophic lakes 4 to 9. The difference between the extreme values is 10- to 500-fold.

Table 1. *Limnological Analyses of the Finnish lakes studied during* 1964 *and* 1965.

No.	Lake	Date	Cond. mho 18°C	KMnO cons. mg/l.	Na mg/l.	K mg/l.	Ca mg/l.	^{137}Cs pCi/l.	Limnological lake type
1	Niemenjärvi	9.9.65	85	75	5.2	3.5	8.8		eutrophic
		16.7.64						0.8	
2	Kytäjärvi	8.9.65	72	45	3.0	1.8	7.4		dys-eutrophic
		14.7.64						0.3	
3a	Pyhäjärvi	19.9.65	71	32	3.5	2.4	8.0		eutrophic
3b	Ilmoilanselkä	20.7.65	58	35	2.8	1.7	6.0		eutrophic
3c	Päijänne	2.7.64	47	43	3.8	1.0	4.8	1.2	±eutrophic
3d	Näsijärvi	25.6.64	75	120	5.8	1.0	6.0	1.0	dys-oligotrophic
4	Suolijärvi	11.8.65	44	65	2.2	0.9	4.4		dys-oligotrophic
		14.7.64						0.8	
8	Melkutin	22.6.65	43	6	2.1	1.0	5.8		oligotrophic
		6.9.64						0.5	
9a	Vuohijärvi	3.6.65	31	32	1.8	0.8	3.4		oligotrophic
		14.8.64						1.2	
9b	Keritty	30.7.65	26		1.7	0.6	2.5		dys-oligotrophic
10	Mutkajärvi	23.7.64	16	100	1.3	0.2	1.0		dys-oligotrophic
10a	Akulampi	24.8.65	15		1.3	0.4	1.0		dys-oligotrophic

Table 2. Radiochemical Analyses of Plankton Samples 1964–65

Lake No.	Date	Dry wt. % of fresh wt.	Ash wt. % of dry wt.	^{137}Cs pCi/l.	^{137}Cs pCi/g dry wt.	K mg/g dry wt.	^{137}Cs pCi/mg K	Phyto-plankton, % of plankton
				1964				
1	17.7	2.90	15.6	45	1.51	17.3	0.09	
2	13.7	3.36	15.8	105	3.12	18.8	0.17	
3a	18.9	4.38	13.3	180	4.08	15.2	0.27	5
3d	25.6	2.15	24.8	250	13.2	10.7	1.23	25
4	13.7	7.80	19.5	120	16.0	11.4	1.40	25
8	6.9	5.62	5.0	730	11.9	9.7	1.22	
9a	11.8	3.75	13.5	600	15.9	12.7	1.25	
				1965				
1	9.9	3.17		50	1.48	55.1	0.003	
2	8.9	2.49		110	4.17	8.6	0.48	35
3a	10.9	4.11		90	1.97	20.9	0.09	5
3b	20.7	4.43		260	5.29	28.5	0.19	
3d	16.9	4.35		250	9.25	21.5	0.43	
4	28.7	2.84		440	9.05	23.9	0.38	
8	23.6	0.42		120	27.22	14.5	1.88	
9b	30.7	5.48		360	16.86	19.1	0.88	

This same tendency is usually visible from the ^{137}Cs values of the higher plants, especially species rich in minerals like the Horsetail (*Equisetum fluviatile*). Values for two higher plants, *Equisetum fluviatile* and the Yellow Water Lily (*Nuphar luteum*) from the years 1964 and 1965 are presented in Table 4. Again the ^{137}Cs content is lowest in the eutrophic lakes Nos. 1 to 3, highest in the oligotrophic lakes Nos. 9 and 10. The values of higher plants do not always change regularly, however. One cause of the irregularities may be the algae living on the surface of the plants.

Relatively few samples of bottom animals have been obtained. Even in the eutrophic lakes it is a difficult task to obtain large enough samples of any single species for gamma-spectrometric analysis, and in the oligotrophic lakes it is even more difficult. Results on three samples from the years 1963 and 1964 are presented in Table 5. As can be seen, the value for *Chaoborus* sp. in lake No. 1 in 1964, 1.44 nCi/kg dry wt., is practically the same as that of the simultaneous plankton sample from this lake (1.51 nCi/kg dry wt.). The ^{137}Cs content of the *Trichoptera*-larvae, on fresh weight basis, is about 3.5 times greater, but the potassium content in this lake is only one-third of that in Lake No. 1, as can be seen from Table 1.

Most clear-cut is the inverse relationship of the ^{137}Cs content of fish and the potassium content of the lake water. In an earlier paper [4] this relationship was shown for several fish species. It is also evident from Table 6 and Fig. 1 of this paper. As can be seen in Fig. 1 down to a potassium content of 1 mg/l. the ^{137}Cs content of pike remains low (< 3 nCi/kg), but with the potassium content 0.6 mg/l. it reaches the very high value 21.3 nCi/kg fresh wt. The same regular relationship is visible in other species (Table 6). The larger sized perch have the highest ^{137}Cs content, which in one lake (No. 9b) was 26.2 nCi/kg fresh wt. This is the highest ^{137}Cs content of fish obtained anywhere in natural waters, as far as we know.

3. *^{137}Cs content of the food.* Small perch contain only about one-half of the level in the larger perch, the difference evidently being due to

Table 3. Description of Plankton Samples collected from lakes of Table 2 in 1965.

Lake No.	Lake name	Date	Sample volume ml	Dry weight g	Phytoplankton	Group	%	Zooplankton	Group	%
1	Niemenjärvi	9.9.65						*Eudiaptomus cracilis*	Copepoda	90
								Ceriodaphnia palchella	Cladocera	
								Daphnia cucullata	Cladocera	5
								Cyclops sp.	Copepoda	5
2	Kytäjärvi	8.9.65	96	2490	*Melosira varians*	Diatomae	10	*Bosmina coregonii*	Cladocera	10
					Asterionella formosa	Diatomae	5	*Cyclops* sp.	Copepoda	45
					Melosira islandica	Diatomae	20	*Daphnia cucullata*	Cladocera	10
3a	Pyhäjärvi	10.9.65	190	9211	*Anabaena circinalis*	Cyano-phyta		*Chydorus sphaericus*	Cladocera	30
					Microcystis aeruginosa	„	5	*Eudiaptomus cracilis*	Copepoda	10
								Bosmina coregonii	Cladocera	25
								Cyclops sp.	Copepoda	5
								Daphnia cucullata	Cladocera	25
3b	Ilmoilanselkä	20.7.65	464	22,170				*Bosmina coregonii*	Cladocera	10
								Daphnia cucullata	Cladocera	75
								Mesocyclops hyalinus	Copepoda	15
3d	Näsijärvi	16.9.65	288					*Bosmina obtusirostris*	Cladocera	40
								Daphnia longispina	Cladocera	15
								Eudiaptomus craciloides	Copepoda	10
								Mesocyclops leuckartii	Copepoda	35
4	Suolijärvi	28.7.65	230	11,351				*Bosmina coregonii*	Cladocera	15
								Daphnia cucullata	Cladocera	70
								Mesocyclops hyalinus	Copepoda	15
8	Iso Melkutin	23.6.65	500	2012				*Eudiaptomus cracilis*	Copepoda	40
			490	2202				*Bosmina obtusirostris*	Cladocera	10
								Heterocope borealis	Copepoda	25
								Holopedium gibberum	Cladocera	25
9b	Keritty	29.7.65	500	10,948				*Daphnia cucullata*	Cladocera	40
								Chydorus sphaericus	Cladocera	10
								Diaphtomus brachyurum	Copepoda	40
								Cyclops sp.	Copepoda	10

Table 4. ^{137}Cs Content of Two Water Plants in 1964 and 1965

No.	Lake	1964				1965			
		Horsetail (*Equisetum fluviatile*) ^{137}Cs		Yellow Water Lily (*Nuphar luteum*) ^{137}Cs		Horsetail (*Equisetum fluviatile*) ^{137}Cs		Yellow Water Lily (*Nuphar luteum*) ^{137}Cs	
		nCi/kg d.w.	nCi/ g K	nCi/kg d.w.	nCi/ g K	nCi/kg d.w.	nCi/ g K	nCi/kg d.w.	nCi/ g K
1	Niemenjärvi			0.68	0.03	1.9	0.15	0.67	0.04
2	Kytäjärvi	2.3	0.10			1.1	0.05	0.82	0.03
3a	Pyhäjärvi	3.7	0.16			2.2	0.10		
3b	Ilmoilanselkä					1.9	0.06		
3d	Näsijärvi	8.9	0.43	6.62	0.28	6.7	0.40	7.10	0.26
4	Suolijärvi	4.9	0.17					5.66	0.28
9a	Vuohijärvi	44.8	2.03	12.20	0.66				
9b	Keritty					16.9	0.84	23.3	1.28
10a	Akulampi					92.5	3.40		

Table 5. *^{137}Cs Content in Two Species of Bottom Animals, 1963 and 1964*

Lake No.	Lake name	Date	Specie	^{137}Cs, pCi			K, g per kg dry wt.
				per kg fresh wt.	per kg dry wt.	per g K	
1	Niemenjärvi	11.6.63	*Chaoborus*	70	800	66	1.22
		16.7.64	*Chaoborus*	90	1440	—	—
3c	Päijänne	4.8.64	*Trichoptera*	330	—	122	(2.7 per kg fresh wt.)

variations in the diet. The small perch consumes mainly plankton and bottom animals, the larger ones small fish. However, roach, bream and whitefish also eat plankton, bottom animals and water plants like small perch, but they have lower ^{137}Cs content than the latter. To understand this, however, it is necessary to study the fourth factor affecting the body burdens in fish.

4. *The biological half-time of ^{137}Cs in different fish species.* As shown in another paper in this meeting,[7] the biological half-times of fish (the "slow" component) varies from 20 to 200 days at 15°C. Perch has the longest half-time of those hitherto determined—200 days at 15°C. This is evidently one of the main reasons for its high body burden. At 5°C the excretion of ^{137}Cs is slowed down to about one-half of the value at 15°C. In perch, the half-time of ^{137}Cs does *not* change noticeably in different ages but in roach (*Leuciscus rutilus*) the old fish (9 to 12 years) have about a two times longer half-time (100 days at 15°C) than the young ones (2–3 years old, 57 days at 15°C). In rainbow trout (*Salmo iridaeus*) the change is even greater: 0.5 years: 20 days; 1 to 2 years: 55 days; 2 to 3 years: 80 days, all at 15°C. Pike (*Esox lucius*) also has a relatively long half-time of ^{137}Cs (unpublished) which corresponds well to its high body burden. As the annual mean temperature in the Finnish lakes is low—usually around 4 to 6°C—the average half-times the year round in

Table 6. *^{137}Cs Content of Fish in some Finnish Lakes during summer* 1965

No.	Lake	nCi per kg fresh weight						
		Perch (*Perca fluviatilis*)		Pike (*Esox lucius*)	Burbot (*Lota vulgaris*)	Roach (*Leuciscus rutilus*)	Bream (*Abramis brama*)	Whitefish (*Coregonus* sp.)
		smaller <20 cm	larger >20 cm					
1	Niemenjärvi		0.24	0.25		0.18	0.06	
2	Kytäjärvi	0.52	1.49	0.99	0.63	0.30	0.21	
3a	Pyhäjärvi	0.79		0.60		0.37		
3b	Ilmoilanselkä		2.16	1.38		0.71		
3c	Päijänne	1.10	2.17		3.02	1.18		
3d	Näsijärvi	2.60		2.66	2.87	1.20	0.80	
4	Suolijärvi	3.35	7.92	4.91	2.48	1.14		
8	Melkutin	5.97				2.73		1.75
9a	Vuohijärvi	9.39	13.18	7.07	6.26	4.23		2.78
9b	Keritty		26.25	21.27		6.29		3.55

these predatory fish species must be of the order of one year. This explains also why the ^{137}Cs values in many lakes were still increasing in 1965. This seems to be true especially in the oligotrophic lakes (lake No. 9a; perch 1964 7.9, 1965 13.2 nCi; pike 1964 6.5, 1965 7.1 nCi; burbot 1964 4.3, 1965 6.3 nCi; roach 1964 3.3, 1965 6.3 nCi per kg of fresh wt.).[4] In eutrophic and some oligotrophic lakes a slight decrease has taken place.

CONCLUSIONS AND DISCUSSION

Our results presented above suggest that ^{137}Cs remains in circulation within the biokenosis in the oligotrophic lakes a longer time than the midge larvae (*Chionomus commutatus; Diptera*) 3.5 days.[8] Thus, their activity closely follows the ^{137}Cs level of the water.

Except through food, fish take up ^{137}Cs directly from water by the osmotic mechanisms in the gills. However, this intake is relatively unimportant compared with the intake through food. Preliminary experiments with young rainbow trout in an oligotrophic water show that within one biological half-time (*ca.* 25 days) the fish obtain a specific activity which is about 10 times higher than that of the water. The present ^{137}Cs levels in the Finnish surface waters, about 1 pCi/l., would thus correspond in equilibrium state to a body burden of about 20 pCi/kg

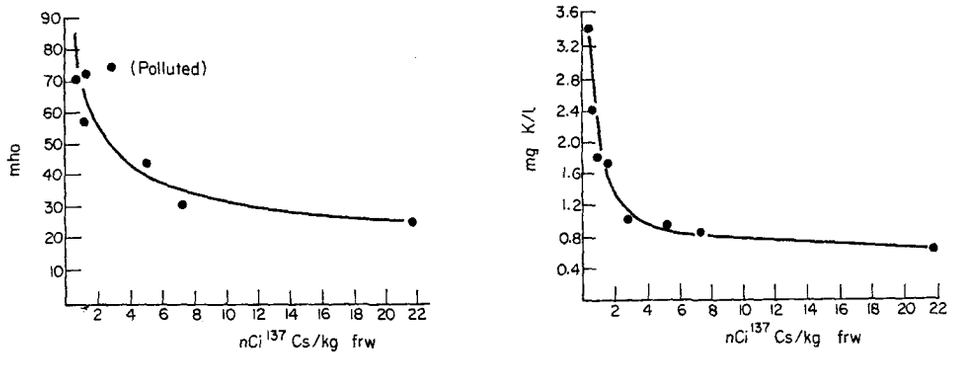

FIG. 1. ^{137}Cs content of pike in different types of lakes in summer 1965 as a function of conductivity (left) and potassium content of the water (right).

in the eutrophic lakes. The reason for this may be a greater content of clay particles, a faster sedimentation, or a slighter depth and a smaller volume of the eutrophic lakes in general. It is evident that the ^{137}Cs contamination of the biota is accentuated in two ways in the oligotrophic waters: the enrichment of ^{137}Cs is increased because of the low potassium level, and it remains high longer. The long half-times in perch and pike, about one year in natural conditions, during the longer pollution times effect continuous increase of the body burdens of fish.

The biological half-times of the lower animals are generally short, a few days or even hours. For instance, in mayfly nymph (*Ephemera varia*; *Ephemerida*) the half-time of ^{137}Cs is 8.3 days, in which is negligible compared with the values observed in oligotrophic lakes. We can come to about the same conclusion by estimating from the data published by Friend *et al.*[9] (their Figs. 3–6).

In reality, a ^{137}Cs content of about 1 pCi/l. effects in oligotrophic lakes in the fish of prey body burdens of 5 to 20 nCi/kg, in other fish about 1 to 5 nCi/kg fresh wt., in eutrophic lakes correspondingly 0.2 to 2 and 0.1 to 1 nCi/kg fresh wt., respectively. The bulk of the body content is thus obtained through food.

The correctness of the above quantitative interpretations was checked in an earlier study[4] by calculation of the intake in diet of ^{137}Cs and of dry matter by perch and roach. The

amount of food intake calculated in this way was found to be reasonable when compared with estimations by other means. In different lakes it was in direct relationship with the growth rate of roach. It is thus evident that the calculations are essentially correct.

Relatively little ^{137}Cs analyses of fresh-water fish have been published elsewhere. In the U.S.A. the fresh water studies have been mainly concentrated to "on-site" areas like the Columbia River and White Oak Creek, where the discharged activity is mixed with fallout-activity and nuclide concentration is rapidly reduced downstream. Although locally important, such studies warrant little generalization. Some results on fish from natural fresh waters have been published from Alaska and the Great Lakes region, however. Watson and Rickard [10] report in whitefish and grayling from two Alaskan lakes during the summer 1962 1.9 and 0.6 to 2 nCi/kg dry wt., respectively, values which are small compared to those from Lapland at the same time—whitefish 7, grayling 5 to 9 nCi/kg dry wt. [1] Gustafson [11,12] reports for fresh water fish purchased during 1965 in food markets in the Chicago area, the following values: northern pike 1.1 to 4.1, lake perch 0.3 to 1.1, and whitefish 0.18 to 2.8 nCi/kg fresh wt., values comparable with our values for corresponding species in eutrophic or slightly oligotrophic lakes.

Lidén, [13] in an oligotrophic lake (K 1 mg/l.) in southern *Sweden* during 1962 and 1963 found in pike 2 to 4 nCi/kg fresh wt., values quite similar to ours. [1] Hannerz [14] reports from the years 1964 and 1965 in the eutrophic lake Mälar, near Stockholm, for pike and pike-perch 0.9, for perch and burbot 0.8, roach 0.4 and bream 0.25 nCi ^{137}Cs/kg fresh wt., values 2 to 4 times higher than those in the same species in the Baltic, and supposes the difference to be due to different potassium concentrations in the water.

Values for *German* fresh water fish and waters are regularly published in the quarterly reports of the Ministry of Science. [15] Pike contained 5.7 to 9.9 nCi, carp (*Cyprinus carpio*) 5.4 nCi and tench (*Tinca vulgaris*) 3.2–11.0 nCi/kg fresh wt. in the lake Kolksee (Ostholstein) having 1.8 mg K and 6.6 pCi ^{137}Cs/l. (ref. 15, I/65, pp. 107–108). Feldt (ref. 15, III/65, pp. 169–183) gives the following relationship for three fresh waters in Germany:

	Kolksee	Gr. Plöner See	Elbe
K content in water, ratios	1	5	10
^{137}Cs/g K in fish, ratios	300	30	1

From *Italy*, values for perch in four lakes are reported from the year 1963. [16] While our values varied from 0.2 to 20.4 nCi/kg, [3] those from the four Italian lakes studied, the Lake Maggiore, Varese, Comabbio and Monate, were in June 1.1, 1.2, 2.8 and 7.4, and in September 1.9, 3.3, 5.2 and 6.3 nCi/kg, respectively. These values are about in the middle of our range, our lakes evidently representing a much wider range of limnological conditions. The unpolluted Alp lakes are usually oligotrophic.

Hannerz [14] reports for plankton (mainly *Limnocalanus* and *Diaptomus*) during summer 1964 in Lake Mälar, Sweden, *ca.* 90 to 130 pCi/l. which corresponds to our plankton value in lake No. 2 (105 pCi/l.); to summer 1965 his values had decreased to about one-half of those in the previous year. For plankton in the Kolksee, Germany, 1.6 nCi/kg dry wt. is reported for April 1964 (ref. 15, I/65, p. 108), which corresponds to our plankton value in the most eutrophic lake No. 1 (1.5 nCi/kg). For horsetail in the same lake 4.0 nCi in stem below water, 9.2 nCi in stem above water per kg dry wt. is reported (ref. 15, II/65, p. 103). This corresponds to our lakes 3 to 4 but is only one-tenth of the horsetail activity in our lake No. 10 (92.5 nCi/kg dry wt. in stem above water).

Several authors who have studied the uptake of ^{137}Cs in lower organisms have observed the negative effect of potassium-ions in the water. Rice [17] observed it while studying algae, Williams [18, 19] while studying *Euglena* and *Chlorella*, and Bryan and Ward [20] while studying ^{137}Cs uptake in crustaceans.

SUMMARY

It can be generalized that uptake of ^{137}Cs in the whole biota of a fresh water lake is sharply accentuated especially if the potassium content of the lake water is below 1 mg/l. The four main factors affecting the ^{137}Cs body burdens in fish are:

1. ^{137}Cs content of water—a minor factor, as observed differences in the lakes studied have been only 2- to 3-fold.

2. Potassium content of the water—a major factor effecting 10- to 100-fold differences and very high ^{137}Cs levels in the whole biota in the most oligotrophic lakes.

3. The quality of food eaten by the fish—a minor factor effecting 2- to 3-fold differences.

4. The biological half-time of ^{137}Cs in fish—a major factor varying from 20 to 200 days at 15°C and effecting up to 10-fold differences in various species in the same water course.

ACKNOWLEDGEMENTS

Financial support for this investigation by the Finnish Atomic Energy Commission and the U.S. Department of Health, Education and Welfare (Public Health Service Research Grant No. RH-00307) is gratefully acknowledged.

It is a pleasure to acknowledge skillful technical assistance by Mr. Seppo Takatalo, Cand. Sci., and Mr. I. Vöry.

REFERENCES

1. E. Häsänen and J. K. Miettinen. *Nature, Lond.* **200,** 1018 (1963).
2. W. Feldt and J. Lange. *Zeitscher. für Lebensmittel-Unters. und Forschung* **117,** 103 (1962).
3. S. Kolehmainen, E. Häsänen and J. K. Miettinen. *Health Physics* **12,** 917 (1966).
4. S. Kolehmainen, E. Häsänen and J. K. Miettinen. *Proc. International Symposium on Radioecological Concentration Processes,* pp. 913–920. Pergamon Press, London (1967).
5. A. Salo. Report SFL-A4 of the Institute of Radiation Physics, Helsinki, April 1966.
6. T. Jaakkola, H. Puumala and J. K. Miettinen. *Proc. International Symposium on Radioecological Concentration Processes,* pp. 341–350. Pergamon Press, London (1967).
7. E. Häsänen, S. Kolehmainen and J. K. Miettinen. This volume.
8. N. R. Kevern, H. A. Griffith and T. Grizzard. ORNL-3697, 101 (1964).
9. A. G. Friend, A. H. Story, C. R. Henderson and K. A. Bush. Behavior of certain radionuclides released into freshwater environments. Annual Report 1959–60. U.S. Department of Health, Education, and Welfare, Public Health Service Publication No. 999–RH-13, Washington, 1965.
10. D. G. Watson and W. H. Rickard. Hanford Biology Research, Annual Report for 1962, HW-76000, p. 244 (1963).
11. P. F. Gustafson. *Radiological Health Data* **6,** 626 (1965).
12. P. F. Gustafson. *Proc. International Symposium on Radioecological Concentration Processes,* pp. 853–858. Pergamon Press, London (1967).
13. K. Lidén. Third Symposium on Radioactivity in Scandinavia. Lund 20–21 May, 1963.
14. L. Hannerz. *Proc. First Nordic Radiation Protection Conference,* Stockholm, 6–9 February 1966.
15. *Umweltradioaktivität und Strahlenbelastung,* Bericht I, II, III und IV/65, Bundesministerium für wissenschaftliche Forschung, Bad Godesberg, 1965.
16. M. De Bortoli, P. Gaglione, A. Malvicini and E. Van Der Stricht. *Environmental Radioactivity,* Ispra, Italy (1963).
17. T. R. Rice. U.S. Public Health Service Publication No. 999-R-3 (1963).
18. L. G. Williams and H. D. Swanson. *Science* **127,** 187 (1958).
19. L. G. Williams. *Limnology and Oceanography,* **3,** 5 (1960).
20. G. W. Bryan and E. Ward. *J. Marn. Biol. Assoc. U.K.* **42,** 199 (1962).

ACCUMULATION, RETENTION AND ELIMINATION OF ^{65}ZN IN FRESH WATER ORGANISMS STUDIED IN POND EXPERIMENTS

L. HANNERZ

National Water Protection Service, Drottningholm, Sweden

Abstract—A pond 82 × 33 × 4 ft was lined with polyethylene sheets which were welded together. Water plants and gravel were introduced and a continuous flow of untreated water from Lake Mälar was arranged.

One hundred small pikes and about 5000 fry of roach and perch were introduced. In all 3·27 mCi ^{65}Zn was gradually dosed into the water to a mean concentration of about 3×10^{-6} μCi/ml.

The activity concentrations were continuously recorded in pond water, sediments, plants, invertebrates and fish.

Considerable concentrations of ^{65}Zn were found in the bottom sediments (concentration factor: about 20,000).

^{65}Zn was taken up in the emergent parts of the water plants to low concentrations. The submersed parts of the plants had much higher concentrations indicating a considerable surface adsorption. Several explanations for this surface absorption are conceivable. The attached microflora and microfauna are believed to play important roles in this connection. Also in invertebrates high concentrations of ^{65}Zn were found. The concentration factor for chironomid larvae was 1700, for snails 590 and for leaches 400.

The mean concentration factor for pike was about 1250. The variation in concentration between individual fishes was, however, considerable. It was found that the ^{65}Zn concentration of the fish was inversely related to its length.

The concentration of ^{65}Zn in the pond water was changed during the experiment. The concentrations in sediments and submerged parts of the plants followed the concentrations of the water rather closely indicating that an exchange equilibrium is rapidly reached for these types of material. The emergent parts of other plants accumulated ^{65}Zn throughout the experiment.

At the end of the experiment about 75 pikes were transferred from the pond to a tank with running water from Lake Mälar and kept there from 27 August to 10 October without being fed. Samples were analysed regularly. No decrease in ^{65}Zn was found.

DISCUSSION

R. B. HOLTZMAN (*U.S.A.*):

Have you measured the ^{224}Ra in urine or other excreta in order to estimate body burden?

T. L. CULLEN:

The Institute of Biophysics has been measuring (1) food contamination: it is innocent, as most of it comes from outside Guarapari; (2) human excreta: with low concentrations. I feel, however, that they have tried to measure Ra^{226}. The Ra^{226} would be found in a ratio of 1: 20 compared with Ra^{228}. This should be measured more carefully.

P. COURVOISIER (*Switzerland*):

Are there any public misapprehensions in the town, such as that a young man from another town should not marry a girl from there because, being irradiated, she may have abnormal children?

T. L. CULLEN:

No; people in Guarapari believe that the sand is health-giving. People bury themselves in the sand to cure arthritis and rheumatism. On the other hand they are afraid of radiation measuring devices and ask if a Geiger counter is harmful. If there are two requirements you need to work in Guarapari they are diplomacy and wit. It would be good to have science too.

P. SPAANDER (*Netherlands*):

I shall be very pleased to be informed about the measurements of Sr^{90} (Feldt) and Cs^{137} (Kolehmainen) in fish. Are they carried out on whole fish, or is any distinction made between bones and muscles? I think this will be of importance, since the muscles are eaten by man, and the bones normally are not eaten.

J. K. MIETTINEN:

I answer regarding the ^{137}Cs values alone. They were measured in whole fish, entrails removed. We know of course that the ^{137}Cs is mainly located in the flesh of the fish. The contents in the flesh alone would be slightly higher. I suggest that Dr. Feldt answers regarding ^{90}Sr.

W. FELDT (*Germany*):

^{90}Sr wurde natürlich in allen Organen gemessen. Da jedoch ^{90}Sr auch im Fleisch auftritt (6–10%), sind in den Tabellen die Kontaminationswerte pro kg Gesamtfisch angegeben. Aus der Kenntnis des Verteilungsmusters lassen sich aus den pCi/kg-Werten alle gewünschten Aussagen erhalten.

RAPPORTEUR PAPER
THERMOLUMINESCENT DOSIMETRY

W. A. LANGMEAD

Radiological Protection Division, Authority Health and Safety Branch, U.K.A.E.A., Harwell, Didcot, Berkshire

INTRODUCTION

Although several groups of workers were interested in the phenomenon of thermoluminescence well before the last war, it is only in recent years that suitable techniques have been developed for applying the thermally released luminescence in suitable crystalline materials to the dosimetry of the exciting radiation. The great interest in this subject of thermoluminescent dosimetry (abbreviated to TLD) was demonstrated conclusively last year at the First International Conference on Luminescence Dosimetry held at Stanford University when 260 people from 17 countries discussed the subject exhaustively for three days. That Conference was stimulating not only for the high quality of the papers presented but also because some attempts were made to explore possibilities for the future development of the subject. One of the main points highlighted in the final discussion was the need for further work to illuminate our understanding of the thermoluminescent mechanism and the parameters on which it depends. A second requirement was for further practical experience of the method in order that TLD could take its rightful place in the armoury of those concerned with dosimetry, including the health physicists.

The six papers which it is my pleasure to review this morning are concerned with one or other of these aspects of the subject. I will start by considering experiments carried out to investigate the mechanism of the TL phenomenon.

REPORT

Dr. Ehrlich from the National Bureau of Standards, Washington, has studied the shape of the response curve of lithium fluoride as a function of radiation *exposure*, *exposure rate* and *photon energy*. ^{60}Co gamma radiation was used at six different exposure rates in the range 100 to 7 million R/hr, as well as X-radiation of half value layer about 5 mm Al at an exposure rate of 7000 R/hr. The range of total exposure studied was 1000 to 20 million R, i.e. that part of the response–exposure curve showing "superlinearity" and also that region of the curve in which the response passes through a maximum. Most of the work was done with Harshaw TLD-100 LiF powder, annealed for 15 min at 400°C prior to exposure and heated for 15 min at 100°C after exposure in order to ensure emptying of shallow traps. The powder was exposed in 1 mm thick polyethylene vials thickened with plastic sleeves to ensure electronic equilibrium when irradiated with ^{60}Co gamma rays. Enough powder was used to allow two read-out values which agreed within 3%.

The results of the irradiations with ^{60}Co gamma-rays at the three highest exposure rates are shown in Ehrlich's Fig. 1. Typical glow curves which are not significantly rate dependent, are shown for three values of exposure. Within the limits of the experimental accuracy (about $\pm$ 15%) no change in the shape of the response curve with exposure rate was found over the whole range of exposure rate or exposures studied. This confirms the work of others, notably Karzmark *et al.*, and Ehrlich suggests that the thermoluminescence of TLD-100 is associated at least mainly with centres other than F-centres, the formation of which are known to be rate dependent.

Ehrlich's Fig. 2 shows the response curves obtained for the two different photon energies. The gamma-ray curve also supplements the previous diagram in showing the negligible effect of exposure rate for the three lower rates. It will be seen that for gamma-rays superlinearity sets in at around 350 rad whereas for soft X-rays not until 2000 rad. The slope of the superlinearity region is steeper for gamma-rays than for X-rays although the curves have the same slope above about 20,000 rad. These results confirm those obtained by Naylor for lower exposures but do not support the findings

of Morehead and Daniels in which considerable difference in curve shape with radiation energy was found at high level exposures. However the importance of the present work is that the possible effect of exposure rate as a parameter has been eliminated, the difference in slope being shown to be due solely to photon energy.

Dr. Ehrlich concludes that the decrease in the slope of the response curve with photon energy supports Cameron's theory that superlinearity is due to the creation of additional electron traps by the radiation.

Turning to new applications in the TLD field, Monsieur Van Espen in his paper, discusses improved systems of operation of the

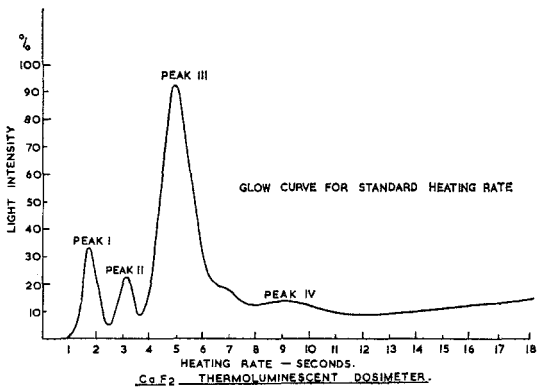

FIG. 1.

calcium fluoride TL dosemeters manufactured by the Belgian firm of M.B.L.E. He points out that erasing the dose effect in the read-out process is a disadvantage of TLD in that it is not possible to recheck a suspect dose-reading or to measure the integrated value of a series of doses if the latter have been read out previously.

Three alternative systems are described to obviate this difficulty. The first consists essentially of two dosemeters in the same glass envelope; by means of twin heating cathodes it is possible to read out doses successively from the two dosemeters, or alternatively to read out individual doses by heating one cathode and to use the other dosemeter as a dose integrating device. These dosemeters are sensitive to doses as low as 100 mR.

The second system depends on a single dosemeter which may be read at two different read-out temperatures. Fig. 1 of this report shows a typical glow curve of M.B.L.E. calcium fluoride. Individual doses are read out by emptying trap II of the glow curve which occurs at about 180°C. Check doses or integrated dose values may be obtained by reading out at a temperature of 375°C which empties traps III', (and III) of the glow curve. The sensitivity of this system allows integrated doses in the range 1–1000 R to be measured.

The third method depends on the use of UV light to transfer a fraction of the energy accumulated in deep traps into shallower traps which are emptied by read-out at normal temperatures. In M.B.L.E. calcium fluoride the main trap (peak III) shown in Fig. 1 is normally emptied at a temperature of 265°C. Electrons trapped at levels corresponding to peak V in the glow curve, which occurs at about 500°C (not shown in the diagram) are not significantly released at 265°C. Hence in a series of irradiations the energy stored in trap V may be used as a measure of the integrated dose level. It is impracticable to tap this energy directly by reading out at 500°C but if the dosemeter is exposed to UV light of wavelength about 3300 Å for 5 min under standard conditions and is then read out at 265°C, about 0.25% of the total dose received by the dosemeter is recorded with an accuracy of 15% or better. The transfer procedure can be repeated a number of times, the results being reproducible within a few per cent, but at present the method is restricted to total doses greater than 20 R.

The measurement of finger and hand doses incurred when radioactive material is handled has always given rise to difficulty particularly when the dose gradient is steep such that ring or wrist dosemeters are of limited value. Drs. Bjarngard and Jones of Controls for Radiation Inc. (Conrad, for short) describe experience with their firm's TL dosemeters consisting of Teflon discs incorporating LiF, which were introduced over a year ago.

The dosemeters, shown in Bjarngard's Fig. 3, are 12.5 mm diameter and 90 mg/cm^2 thick and 28 mg of lithium fluoride is incorporated uniformly throughout the disc. The lightproof

polyethylene pouch is 7 mg/cm² thick. Read-out is conventional and in nitrogen but annealing at 300°C is necessary rather than 400°C since Teflon softens at about 320°C. The response of the disc is a measure of the energy absorbed in it, that is, at effective depths between 7 and 97 mg/cm². Although the biologically important dose is usually taken to be at 7 mg/cm² depth, for the palmar surfaces of the hand and fingers this is usually a gross underestimate, and the average dose to the basal layer is effectively measured by the disc. However, for soft beta radiation a small correction may have to be applied.

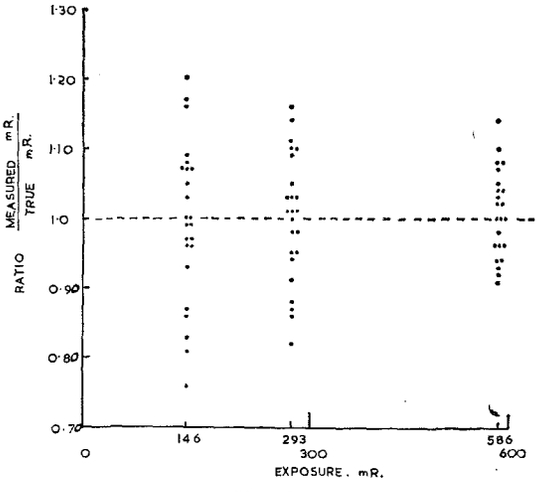

FIG. 2.

Bjarngard's Fig. 4 shows the precision attainable with known doses of ^{60}Co gamma radiation down to 10 mR. At this dose level the standard deviation from the mean of 20 determinations is 20% but decreases to 3% for doses above 3R. It is interesting to compare Bjarngard's results with those obtained by Burton, Foster and Townsend from the U.K. Central Electricity Generating Board. Following similar experiments with Conrad Teflon-LiF discs, these authors found poorer reproducibility, as shown in Fig. 2 of this report, unless the discs were recalibrated after each exposure when similar results to those of Bjarngard and Jones were obtained. However, the British authors underline the need to avoid measurement of the low temperature peak which, on account of its short half-life, can give rise to poor reproducibility of results unless a rigid time schedule is adopted between irradiation and read-out, or the low temperature peak is reduced to insignificance by post-irradiation annealing at say 80°C for several minutes or by delaying 24 hr or so before read-out. Glow curves taken before and after the partial elimination of this peak are shown in Burton's Figs. 4 and 5.

Bjarngard and Jones point out that the background reading associated with unirradiated discs is 1.5 times the net TL signal associated with a dose of 20 mR. This background is made up of the photomultiplier dark current and a component due to what the authors term "spurious thermoluminescence". It has been shown that the latter is not significantly affected by friction or mechanical shocks applied by shaking the discs. The possible effect of visible or ultra-violet light has been investigated and the latter, present in fluorescent laboratory lighting, has been shown to produce definite TL response, as shown in Bjarngard's Fig. 6. It would be interesting to know whether these experiments were undertaken on freshly manufactured discs having no ionising radiation history or whether they had merely been annealed at 300°C following previous irradiation. In the latter case the so-called light excitation may really represent the transfer to shallow traps of stored energy from previous ionising irradiation present in deep traps not emptied in the annealing process, much as in the method employed by Monsieur Van Espen described earlier. However, light excitation is presumably not the cause of the spurious thermoluminescence in the present situation since the discs are used in light-proof pouches. The authors suggest that unirradiated dosemeters should be included for background determination in any measurement series.

There is no doubt that devices of this type have an important place in health physics practice. The next two diagrams show the relative doses received by the hand and fingers in handling a radium needle (Bjarngard, Fig. 1) and a uranium plate (Bjarngard, Fig. 2) and demonstrate the facility with which the system may be used. However, the relatively high cost of these components—25 shillings each ($ 3.50)

—is a limiting factor to their more widespread use—at any rate in the U.K. at present.

Burton, Foster and Townsend have also measured finger-tip doses incurred in the handling of radioactive materials but, instead of Teflon discs, have used LiF powder in PVC sachets. At the same time the total doses to the wrist were measured with wrist film badges, the contributions from gamma, X- and beta radiation being summed. The ratio of the finger-tip dose to wrist dose was found to average about 7 with a maximum value of 22. The types of radiation source are not defined but the large value of the dose ratio clearly arises from the inhomogeneity of the irradiation field.

The remaining papers in this rapporteur session deal with comparative studies of TLD and film badges. Drs. Johnson and Attix of the Naval Research Laboratory, Washington, describe an intercomparison experiment in which 100 NRL personnel wore one or two TL dosemeters in addition to a simple film badge for four one-month collection periods. Quartz fibre pocket dosemeters, specially selected for low electrical insulation leakage, were also worn by some of these staff.

The dosemeters used are shown in Johnson's Fig. 1. The two TL dosemeters, a U.S. Navy experimental prototype (DT-284) and a commercial type designated M, use activated calcium fluoride as phosphor and both incorporate a metal shield which flattens the response per röntgen above 80 keV. The response below 80 keV rapidly falls to insignificance. The film holder is made of stainless steel with a single filter of 1 mm Cd as developed at Oak Ridge. Dual emulsion film packets were used in the holder, the processing and assessment being conventional; the same ^{60}Co source was used to calibrate both film badges and TL dosemeters.

The dosemeters were worn in medium dose-rate areas (although the highest available), only three exposures greater than 100 mR being measured in the monthly periods. Almost all employees wore their film badges on their belts and their TL and quartz fibre dosemeters in their shirt pockets. However, the authors believe that the exposures in the two sites were not significantly different and state that "seldom did any individual wear only part of his complement of dosemeters"! The TL dosemeter readings were corrected for signal fading, shown in Johnson's Fig. 2, and for radiation background, although a large part of the measured background was due to radioactivity present in the dosemeter structures. Johnson's Table 5 summarizes measurements of this radioactivity which contributes some 25 mR/month to the background reading.

Figure 3 of the same paper shows some of the results of the intercomparison in terms of the readings of the DT-284 dosemeter. The points chosen were from among the highest exposures. Considering the low level of the doses being measured, it is surprising that such good agreement was found. In studying this graph it should be borne in mind that the lowest dose measurable with the film badge is 25 mR; smaller doses than this are all recorded as 1 mR on the graph. Further, the authors point out that the largest discrepancies between the film badge results and the TL readings occurred during a failure of the air conditioning system in the NRL Reactor Hall giving rise to temperatures of 27–32°C and relative humidity above 90%; this led the local Health Physicist to disallow the film readings for the purpose of the employees exposure histories. The authors' comment "clearly the film badges were at a disadvantage in these tests", although apparently environmental conditions approaching those described are not atypical of Washington in the summer months. The authors conclude that it is premature to consider replacing film badges by TL dosemeters for personnel monitoring at NRL in the immediate future.

Burton, Foster and Townsend also describe operational trials in which LiF dosemeters are compared with film badges for personal monitoring. These authors used Conrad Type 7 LiF in 45 mg aliquots in PVC sachets; the film badge was the U.K. multi-filter badge. The experiments were performed in two parts. In the first part sachets of LiF powder were *attached to* the film badges which were issued monthly to about 12 members of the staff. In the second part of the experiment the sachets were *not* attached to the film badges, it being left to the operator to wear the sachet as near to the film badge as possible. Burton's Fig. 2 shows the results

obtained with the composite dosemeter. Apart from the dose region up to 50 mrad, which is near the limit of sensitivity of both dosemeters, the correlation is reasonably good despite the fact that the operators were working with varying amounts of gamma, X- and beta radiation. The results of the second part of the comparison (Fig. 3 of this report), unlike the results of Johnson and Attix, show very poor correlation, in most cases attributed to the different positions of the dosemeters on the body.

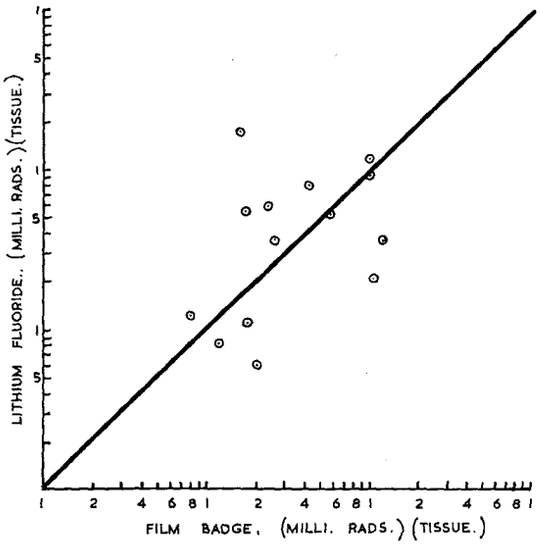

FIG. 3.

The British authors have also irradiated film badges and LiF powder in PVC sachets placed in the front and back surfaces of a man-equivalent thorax using radiation sources of ^{198}Au and ^{60}Co. Very good agreement ($\pm$ 10%) was obtained in the results with ^{60}Co both for the pairs of dosemeters on the front and back surfaces of the phantom, but the film badges consistently gave higher readings amounting to about + 30% with the 0.4 MeV gamma radiation from the ^{198}Au.

The paper by Cameron and Suntharalingam from the University of Wisconsin, describes a laboratory intercomparison experiment using single crystals of LiF (TLD-100) and film badges supplied by commercial companies. The LiF crystals were enclosed in lucite capsules having 4 mm wall thickness and attached to the film holder. The crystals, of mass approximately 20 mg, were cleaved from a single piece of virgin TLD-100 and annealed for 1 hour at 400°C before use in the experiment.

Known exposures of radium and caesium-137 gamma-rays and 140 kVp X-rays, measured with a Victoreen R-meter to an accuracy of $\pm$ 10%, were given to the composite dosemeters. The film badges were returned to the company together with 300 other operationally exposed badges. The company were not informed that a special intercomparison experiment was being undertaken. The LiF crystals were read by the authors using the read-out process described in the literature. In a further similar experiment the irradiations were not made by the authors but by the National Sanitation Foundation Testing Laboratory at Ann Arbor. Twenty composite dosemeters were irradiated with exposures not known to the authors until after they had evaluated the LiF thermoluminescence in their own laboratory. The film badges were evaluated as previously by the commercial company.

Cameron's Fig. 3 shows results of the intercomparison using radium gamma rays. The broken lines represent $\pm$ 20% of the true dose. When mixtures of radium gamma rays and 140 keV X-rays were used the results were still satisfactory (Fig. 4 of same paper) except for dose values of about 20 mR. As the detection threshold for the film badges of one of the companies was stated to be 50 mR, good correlation clearly cannot be expected at these levels. The results of the experiment involving the N.S.F. Testing Laboratory are shown in Cameron's Fig. 7. The LiF results are slightly high and the film readings by and large underestimate the results by a small amount.

The authors claim an overall accuracy of $\pm$ 30% for the single crystal LiF results which can be improved upon if a slight energy correction is applied. The principal disadvantage of these crystals at present is the slow read-out time of 15 min, required because of the need to calibrate each crystal individually.

CONCLUSIONS

In conclusion in view of my earlier restraint perhaps I may use the last minute or two of

THERMOLUMINESCENCE RESPONSE OF LiF TO X- AND GAMMA RAYS; A STUDY OF RATE AND ENERGY DEPENDENCE OVER A WIDE RANGE OF EXPOSURES

MARGARETE EHRLICH
National Bureau of Standards, Washington, D.C.

Abstract—The total thermoluminescence light emission ("response") of LiF (TLD grade) was studied as a function of exposure and exposure rate, and as a function of photon energy. ^{60}Co gamma rays and a broad spectrum of low-energy bremsstrahlung were employed. No rate dependence of the response was detected over the entire range of exposures and exposure rates employed (from about 10^2 R to 2×10^7 R, and from about 10^2 R/h to 7×10^6 R/h, respectively). This represents further evidence that centers other than F centers are involved in the thermoluminescence of LiF (TLD grade).

A comparison of the curves of response versus exposure for the two photon spectra confirms Naylor's findings that the superlinearity region is steeper for ^{60}Co gamma radiation than for low-energy X-rays, and reveals that the effect is indeed dependent on photon energy rather than on exposure rate. These findings are compatible with an explanation of superlinearity as being due to the formation of additional traps by the radiation proper. For exposures above those causing superlinearity, the difference in curve shape again disappears. Also, there is no dependence on energy of the location and height of the response maximum, which suggests that the inhibiting mechanism is independent of photon energy.

INTRODUCTION

Most of the work reported in the literature on the influence of exposure rate (or absorbed-dose rate) and photon energy on the thermoluminescence of LiF (TLD grade) was done over a limited range of total exposure (or dose). Karzmark *et al.*,[1] for example, established the absence of rate dependence over a rate range from about 500 to 2×10^8 rads/sec at three levels of absorbed dose lying between 15,000 and 25,000 rads. More recently, Tochilin and Goldstein[2] employed exposure levels between about 1300 and 5000 R, but not any two of them at the same rate, and found no rate dependence up to 2×10^{11} R/sec. Many authors publishing data on the energy dependence of the thermoluminescence of LiF do not even indicate at what exposure level the data were obtained.[3,4] Frequently, a single exposure level falling in the linear region of the response curve is investigated. A notable exception to this practice is the work of Naylor[5] who studied the shape of the thermoluminescence-response curve* over a total absorbed-dose range from below 50 to around 1000 rads for photons of energies between about 30 keV and 1 MeV. He found that, at the 50-rad level, the response of ConRad "N" LiF powder to bremsstrahlung of an effective energy of 130 keV is more than 110% of that to ^{60}Co gamma radiation, while, at the 800-rad level, it is less than 90% of the ^{60}Co response. He concluded from these findings that, since, in the light of the current theory, superlinearity is due to the formation of new traps, ^{60}Co gamma radiation is considerably more effective in producing new traps in the range from 50 to 800 rads than is 130-keV X-radiation. Naylor found the same effect to exist also in Harshaw TLD-100 powder, but to a lesser degree. No mention is made in his

* Throughout this paper, the terms "thermoluminescence-response curve" and "response curve" are used to designate the curve obtained by plotting the area under the glow curve as a function of exposure.

my time in considering some general issues relating to personnel monitoring policy.

Several papers in this session have been devoted to showing that in many situations TLD produces results as good as or better than film badges. For the measurement of the dose at a point on the surface of the body lithium fluoride certainly takes some beating. However, the film badge does other things besides measuring the dose at a point. It can define the type of radiation giving rise to the dose, whether the radiation is entering or leaving the body at the point of measurement and, when large numbers are involved, the film badge can give results more quickly and more cheaply than lithium fluoride. On the other hand we have seen that for measuring doses to the fingers or the hand the film badge is almost worthless compared with sachets of lithium fluoride or Teflon-LiF discs. A strong case has also been made for using calcium fluoride devices as integrating dosemeters, or as alternatives to quartz fibre dosemeters (although they have not the self-reading facility of the latter); and of course equally strong claims have been made for radio-photoluminescent glass as the basis of a suitable integrating dosemeter. It would seem, therefore, that in view of all these developments in the dosimetry field, the time is not ripe for taking up prepared positions in the defence of either the film badge, TLD, glass or any other system for personnel monitoring. In my view a flexible policy is the correct one in present circumstances—one which allows plenty of opportunity for experimental and operational trials.

Developments I should like to see reported at the second I.R.P.A. Conference would include the following:

(i) Further work on solid TL systems along the lines of the LiF single crystals discussed by Cameron;
(ii) Automation to simplify and speed up the read-out procedures;
(iii) Investigations into other TL materials having fewer idiosyncracies than LiF and cheap enough to throw away after read-out (e.g. lithium borate, which sells at 1*d.* per dosemeter);
(iv) Further work on TL methods for personnel monitoring of fast neutrons;

and, perhaps only obliquely concerned with thermoluminescence,

(v) Consideration by I.C.R.P. of alternative methods of specifying maximum permissible doses for external irradiation, in terms of the dose at the surface of the body. This would resolve the present difficulty whereby personnel dosemeters must also take on the characteristics of a simple spectrometer.

note of the dose rates used in the experiments. If the dose rates were different for the different energies, the observed phenomenon could be due just as well to a variation of curve shape with the rate of energy absorption by the LiF crystal lattice, regardless of photon energy.

The work reported here, which had been conceived before Naylor's note was published, deals with the shape of the LiF (TLD) response curve obtained with photons at different exposure rates and photon energies, with emphasis on the regions of non-linear response. Non-linearity in the response-versus-exposure curve points to either a multiple-stage process or a change in the relative importance of two competing processes. Therefore, shape changes with exposure rate and photon energy are most likely to occur in the non-linear regions of the curve, if at all, i.e. in the "superlinearity" region and the region in which the response curve goes through a maximum.

STATUS OF THEORY

Nature of thermoluminescence centers. Morehead and Daniels exposed LiF crystals to different types of ionizing radiation and studied the resulting thermoluminescence, and the formation and destruction of F centers and their composites.[6] They found the energy required for F-center formation to be different for different types of radiation, and to increase with the total dose delivered. They showed that both the thermal and optical bleaching characteristics of LiF depend on the type of radiation employed, and that, in fact, two LiF crystals exposed to different types of radiation have different types of glow curves, even when they contain the same concentration of F centers. This indicates that, for LiF (TLD grade), a simple F-center theory of thermoluminescence does not suffice. Recently, Claffy reported[7] that the concentration of impurities in the LiF, in particular the concentration of the Mg ions present, determines the shape of the absorption bands of the resulting centers, and also the glow curves. Thus it seems that the thermoluminescence may be due in part to the impurity centers.

The role of lattice damage in the superlinearity region. A further puzzling phenomenon in the thermoluminescence of LiF (TLD grade) is the presence of the "superlinearity" region of the response curve. Cameron *et al.*[8] developed a theory explaining the enhanced thermoluminescence in this region by the assumption that, above a ^{60}Co exposure level of about 2000 R, new electron traps are created by the radiation proper.

A study of the shape of the response curve in the superlinearity region as a function of photon energy could furnish a clue as to whether or not new trap formation is important. Since the probability both for direct lattice-ion displacement by the incident radiation and for the formation of new vacancies at dislocations should decrease with decreasing radiation energy, a decrease in superlinearity with decreasing radiation energy would be compatible with formation of new traps.

Thermoluminescence inhibition. For the segment of the thermoluminescence response curve close to its maximum, Morehead and Daniels[6] obtained information on curve shape as a function of the type of the incident radiation. They found considerable difference in curve shape, as well as a difference in the location and height of the response maximum, the radiation depositing the largest amount of energy for a given interaction producing the highest response maximum. They explained this effect by the greater ability of radiation depositing large amounts of energy per interaction to produce new traps and thus a higher saturation concentration of F centers.

EXPERIMENTAL TECHNIQUE

Sources. A commercial kilocurie ^{60}Co therapy source and two water-shielded kilocurie ^{60}Co sources were used to provide six different exposure rates between about 10^2 and 7×10^6 R/h. Both sources had been calibrated previously with suitable cavity-ionization chambers. Low-energy bremsstrahlung was furnished by a commercial 250 kV constant-potential X-ray machine, modified to provide precision regulation of voltage and current. The X-ray machine was operated at 200 kV constant potential, with inherent filtration only (HVL about 5 mm Al). The exposure rate at the position of the samples was about 7×10^3 R/h. Space did not permit

a variation of X-ray exposure rates over a large enough range to warrant the effort, and variation of rates through adding of filtration was decided against, because of the associated change in spectral shape. A calibrated Victoreen R-meter was used to determine the X-ray exposure rate. All exposures are estimated to have been accurate to within 3%.

Choice and treatment of LiF powder. Most of the experiments were done with Harshaw LiF, TLD-100 powder, of batch DW-48. Some were performed with both TLD-100 and TLD-700 powders. Yet, since the results were qualitatively similar for both types of powder, only the TLD-100 results will be discussed here. All powder was annealed prior to exposure for 15 min at 400°C, and was exposed in hard polyethylene vials of 3 mm i.d. and 1 mm wall thickness. Plastic sleeves were provided around the vials for electronic equilibrium at ^{60}Co photon energies. All powder was stored in the dark in air-conditioned rooms. Before the "readings", the powder samples were heated in their vials for 15 min at 100°C, in order to empty possibly filled shallow traps.

Readout procedure. A commercial powder dispenser, whose operation was found to be reproducible to within 1½% standard deviation, was used to fill the heating cup of a commercial thermoluminescence "reader". Each polyethylene vial contained sufficient powder for two individual reading samples. The particular reader employed permitted simultaneous recording of glow curves and readout of "integral counts". With suitable precautions (such as a sufficient waiting period between readings to bring the temperature of the heating pan down close to room temperature each time), individual readings obtained on simultaneously exposed powder samples with a given photomultiplier setting in any one readout session, could be made to agree to within 3%. Below the region of thermoluminescence inhibition, the number of integral counts proved to be proportional to the height of the glow peaks to within 5%.

In order to cover the required five decades of thermoluminescence intensities, the photomultiplier gain had to be changed during the reading sessions. Since the high exposure range necessitated readout with photomultiplier voltages between only 500 and 1000 V, the weak light source provided with the "reader" as a constancy check could not be used. Instead, gain ratio and gain constancy checks had to be provided by a determination of photomultiplier voltages obtained in the readout of identically exposed powder samples. Whenever possible, inaccuracies due to variations in reader performance were avoided by reading all powder samples belonging to a particular phase of the experiment on the same day. This caused the period between exposure and reading to vary between about one and ten days. No corrections for image fading or growth were made, since the variations of response with time between exposure and reading were within the limits of over-all experimental accuracy. The readings for the various individual phases of the rate-dependence experiment which, in some instances, were obtained weeks apart, were scaled at suitable overlapping tie-in points.

RESULTS OF EXPERIMENTS AND CONCLUSIONS

Rate dependence. Figure 1 is a plot of integral counts as a function of exposure to ^{60}Co gamma rays at the three rates obtained with the water-shielded sources (range from below 5×10^3 to above 7×10^6 R/h). Also shown, at selected exposure levels, are samples of glow curves (total counts versus temperature, not to scale). One curve suffices at any one level, since there is no significant change in curve shape with exposure rate. In order to avoid further scaling and the resulting further inaccuracies, the data obtained with the therapy sources (exposure rate range from about 100 to 2600 R/h) are not shown on this figure, but are included in Fig. 2, where they are compared with the 200-kV data obtained during the same experimental phase. (See the following section on energy dependence for a full discussion of Fig. 2.) It was physically impossible to overlap the rates used with the two types of ^{60}Co sources. Yet, the lowest rate obtained with the water-shielded sources (Fig. 1) is less than a factor of two higher than the highest rate obtained with the ^{60}Co gamma-ray therapy sources (Fig. 2).

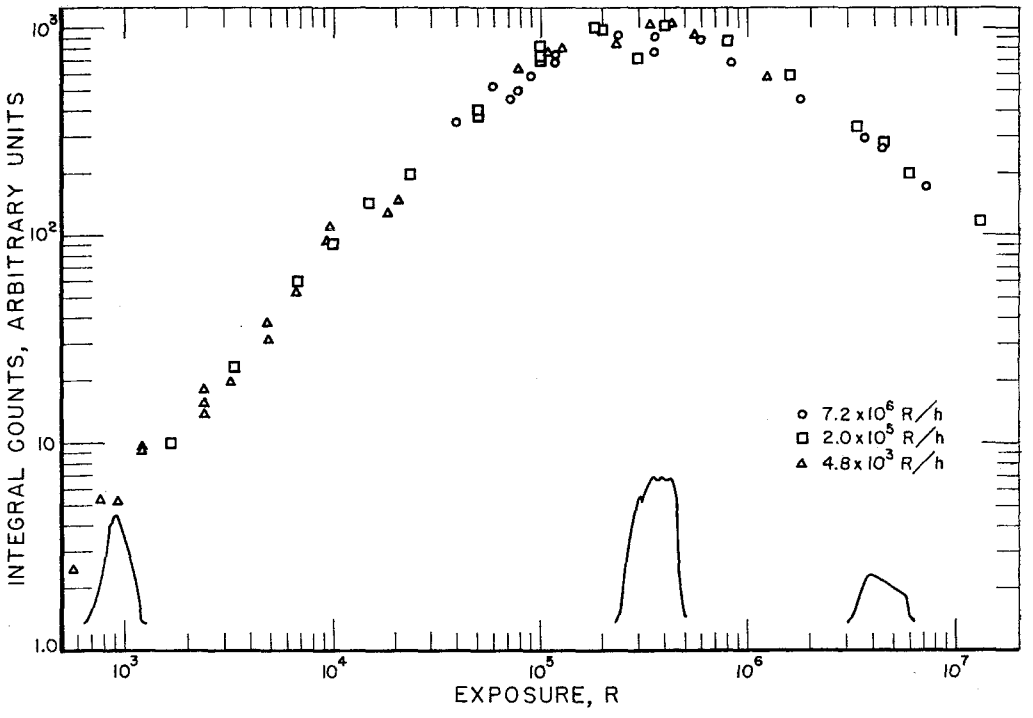

FIG. 1. Rate dependence study with ^{60}Co gamma radiation (water-shielded sources). Circles: 7.2×10^6 R/h. Squares: 2.0×10^5 R/h. Triangles: 4.8×10^3 R/h. At selected exposure levels, samples of glow curves (total counts versus temperature) are included (not to scale).

The continuity provided in this way is considered adequate.

The spread of the individual data points obtained with the water-shielded sources at different reading sessions for any one exposure and exposure rate is seen to be about $\pm 15\%$, even after scaling, at least in the ascending portion and at the maximum of the response curve shown in Fig. 1, and does not seem to vary with exposure level. The spread in the data points is considerably less in Fig. 2, and also in Fig. 1 in the region of decreasing response, for which the data were obtained in a single reading session. Yet, the over-all imprecision probably is still around 10%. Within these rather wide limits of experimental imprecision, no change in the shape of the response curve is detected over the exposure-rate range from about 100 to 7×10^6 R/h for exposures lying between about 10^3 and 2×10^7 R. Inasmuch as Karzmark[1] established the absence of rate dependence at the 20,000 R level within about 5% or better, over a range of exposure rates overlapping the range covered here, and inasmuch as the present data show no trend with rate over the entire response range, there is reason to believe that the thermoluminescence response is, indeed, essentially independent of exposure rate over the entire range covered. This result could be of importance for the theory of thermoluminescence in LiF (TLD grade), since Mitchell *et al.*[9] have shown F-center formation to be dependent on exposure rate, at least in one of the alkalihalides (KCl). It is planned to study the coloration of LiF (TLD grade) as a function of exposure rate over the same range of rates and total exposures over which thermoluminescence has been found to be independent of rate. Rate dependence of the coloration would be conclusive evidence

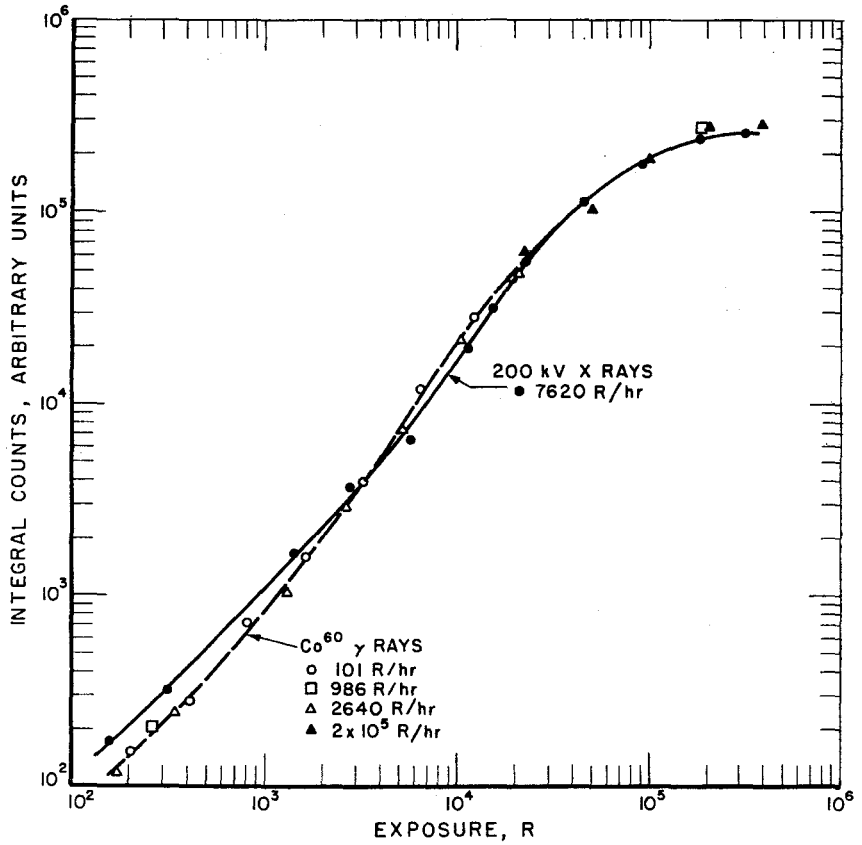

FIG. 2. Energy-dependence study, and rate-dependence study with ^{60}Co gamma radiation (therapy sources). Filled-in circles: 200 kV X-radiation, 7620 R/h. Open circles: ^{60}Co gamma-radiation, 101 R/h. Squares: ^{60}Co gamma radiation, 986 R/h. Open triangles: ^{60}Co gamma-radiation, 2640 R/h. Filled-in triangles: ^{60}Co gamma radiation, 2×10^5 R/h water-shielded source), repeated from Fig. 1, and fitted at about 2×10^4 R.

that F centers do not play an essential role in the thermoluminescence of LiF (TLD grade).

Energy dependence. Figure 2 is a plot of integral counts versus exposure to ^{60}Co gamma-ray photons and to low-energy X-ray photons. The curve shape suggested by the few data points below around 350 R for both photon-energy regions, is consistent with the linear response usually found in this exposure range. Yet, for the ^{60}Co gamma rays, superlinearity sets in above around 350 R, while, for low-energy X-ray exposures, the response remains linear to about 2000 R. The superlinearity region is clearly steeper for ^{60}Co gamma rays than for the low-energy X-radiation.* Above 20,000 R, the curves again have the same slope.

These findings confirm Naylor's results for low exposures[5] and extend them to higher exposure levels. They also reveal that the difference in slope of the response curve to two

* Inasmuch as the relative response to the two different types of radiations depends upon the difference in attenuation for different sample geometries, locations of the two curves obtained with different photon energies (in particular, the fact that they cross) is fortuitous. The only fact of importance is the difference in their slope.

different types of radiation is not due simply to a difference in exposure rate, but truly to a difference in the photon energy, as was assumed by Naylor. In the light of the introductory discussions, the findings are compatible with new trap formation as the cause of superlinearity.

Another interesting result is that the difference in curve slope disappears as the response maximum is approached. In fact, there does not seem to be an appreciable difference in the height and peak of the response maximum for the two types of radiation—a result that is unexpected, particularly considering the findings of Morehead and Daniels.[6] It is planned to extend the study of the region of maximum response to other types of radiation, in order to check these findings over a wider range of energy deposit per interaction.

ACKNOWLEDGEMENT

The author is grateful to Dr. Harold O. Wyckoff for his sustained interest and encouragement, and his helpful suggestions.

REFERENCES

1. C. J. KARZMARK, JOHN WHITE and J. F. FOWLER. *Phys. in Med. and Biol.* **9,** 273 (1964) and private communication.
2. E. TOCHILIN and N. GOLDSTEIN. USNRDL-TR-939, December 1965. N. GOLDSTEIN. Private communication.
3. J. R. CAMERON, F. DANIELS, NOYE JOHNSON and G. KENNEY. *Science* **134,** 334 (1961).
4. B. E. BJÄRNGARD, R. MCCALL and I. A. BERSTEIN. *Proc. First International Conference on Medical Physics*, Harrogate, England, 1965.
5. G. P. NAYLOR. *Phys. in Med. and Biol.* **10,** 564 (1965).
6. F. F. MOREHEAD and F. DANIELS. *J. Chem. Phys.* **27,** 1318 (1957).
7. E. CLAFFY. *Proc. International Conference on Luminescence Dosimetry*, Stanford, California, 1965; U.S.AEC (1967).
8. J. R. CAMERON, D. W. ZIMMERMAN and R. W. BLAND. *Proc. International Conference on Luminescence Dosimetry*, Stanford, California, 1965; U.S.AEC (1967).
9. P. V. MITCHELL, D. S. WIEGAND and R. SMOLUCHOWSKI. *Phys. Rev.* **121,** 484 (1961).

OPERATIONAL TRIALS OF LUMINESCENCE DOSIMETERS

L. K. BURTON, C. J. FOSTER and S. TOWNSEND
Central Electricity Generating Board, Berkeley Nuclear Laboratories, Berkeley, Gloucestershire, England

Abstract—Since the AERE/RPS film holder containing Kodak RM film is the legally accepted method of exposure monitoring in the U.K., comparisons have been made between luminescence dosimeters and film badges over a wide range of conditions. Good correlation was obtained when lithium fluoride samples were attached to film badges, but not when the two were issued together, with instructions that they should be worn close to one another. This indicates that more attention should be given to studying the spatial distribution of dose over the body. A comparison was made between fingertip mounted lithium fluoride samples and film badges worn on the wrist. For operations involving the handling of fission product contaminated material the ratio between the doses measured by the two systems varied between 1 and 20:1. Lithium fluoride in teflon has been used for some measurements. Although this is physically more convenient to use than the powder, some samples produced a low temperature glow peak with a short decay time. This rendered rapid measurements inaccurate.

Dosimeters, readout devices and ancillary equipment are discussed from the operational aspect and disadvantages of present equipment are given, together with suggestions for developments required to produce operationally more acceptable equipment.

1. INTRODUCTION

Thermoluminescence dosimetry is a method of storing and measuring the energy absorbed in a small quantity of relatively inert material. It is an integrating system which complements such devices such as film badges, quartz fibre electrometers and integrating ion chambers. It is at an early stage of development for operational use, but even now it can solve problems hitherto impossible.

Early papers on thermoluminescence dosimetry have dealt mainly with the instrument technology. Angino[1] has published a bibliography which probably contains all references up to the end of 1964. A comprehensive review paper by Spurný[2] has been published, and Langmead[3] has dealt with the health physics applications. In this paper some of the operational problems associated with the use of LiF for thermoluminescence dosimetry are described.

2. THERMOLUMINESCENCE DOSIMETRY

Thermoluminescence is a process in which energy due to an exciting radiation liberates electrons a certain fraction of which become trapped in metastable states a few eV above the ground state. When the material is heated to a temperature of a few hundred degrees C, the thermal energy is sufficient to remove the trapped electrons. When the electrons return to the ground state, light is emitted and can be detected with a photomultiplier. The temperature of emission depends upon the trap depths of the luminescent centres and is highly dependent upon the activators present. Pure lithium fluoride is not suitable for thermoluminescent dosimetry but a commercially available product, which is suitably activated, luminesces at a temperature of about 200°C.

Lithium Fluoride

Lithium fluoride is a white crystalline material which is insoluble, non toxic and inert in ordinary atmospheres. Due to its low atomic number the energy response of lithium fluoride is better than most other unshielded detectors.[4] Before use the powder must be annealed and a standard procedure has been adopted. The powder is heated for 1 hr at 400°C

in a muffle furnace followed by 24 hrs at 80°C in an oven. Cameron[5] has shown that a very similar procedure anneals out all traps and eliminates low temperature glow peaks.

Table 1. *Commercially Available LiF*

Manufacturer	Number	Isotopic composition
Harshaw Chemical Co.	TLD100	Normal
Harshaw Chemical Co.	TLD700	^{7}Li
Con-Rad	Type N	Normal
Con-Rad	Type 7	^{7}Li
Con-Rad	Teflon Disc	Normal

The use of lithium fluoride powder is inconvenient and development of solid systems is urgently required. A method is being developed in which lithium fluoride is embedded in PTFE (teflon). The problem is to find a low atomic number material that will withstand the annealing procedure and also transmit light.

Thermoluminescence Reader

The powder is heated on a metal tray and the light output is measured by a photomultiplier and amplifier system. The tray is normally heated by passing an electric current through it. As the temperature rises the light output passes through a series of peaks corresponding to the energy levels of the trapped electrons. For practical purposes a single peak is desirable and this can be obtained with annealed lithium fluoride. If the glow curve is obtained with an unfiltered photo-multiplier three peaks will be present. As well as the radiation induced peak, a tribothermoluminescence peak and an infra-red peak will be obtained. The tribothermoluminescence peak is thought to be caused by an interaction between oxygen and the crystal surfaces; it can be eliminated by passing nitrogen through the heating chamber. The effect of the infra-red part of the glow curve can be reduced by suitable filters and by stopping the heating cycle at the correct position after the radiation induced peak. It is clear that the heating cycle must be accurately timed but it is also essential that the heating rate is reproducible. This is necessary because the peak position depends upon the heating rate as well as temperature.[6]

In order to obtain a rapid sample turnover rate a fast heating cycle can be used with a measurement of the peak amplitude of the glow curve.

The heating tray can be either fixed or removable. Perry and George[7] have used a fixed system. This has the advantage that sliding contacts are eliminated and a more accurately controlled heating cycle should be possible. The alternative system employs loose trays which are pushed into the heating chamber in a slide. This is satisfactory when new but may lead to contact troubles after repeated use. It is very convenient for loading and unloading the powder. The small tray can be held below the dispenser and can be shaken to evenly distribute the powder. Removal of the used powder is simple compared with the fixed tray systems for which a micro-suction device is necessary. The above arguments apply to loose powder but in the very near future, lithium fluoride may be used in the solid form. For PTFE discs, the disadvantages of the fixed tray no longer apply and this system may become more acceptable because of its inherent reliability.

The d.c. output from the photomultiplier tube can be either amplified as a current or after conversion into pulses. Pulse amplification avoids stability problems associated with d.c. amplification. However, simple stable d.c. systems have been developed in which the photomultiplier current charges a capacitor across which the voltage is measured with a digital voltmeter. In the alternative system a current to pulse converter is used to produce a pulse rate proportional to current. The pulse rate is measured by ratemeter or scaler depending upon the accuracy required.[7] As this system can use standard nucleonic units, it has the advantage over specialized readers that spare units are always available.

3. HEALTH PHYSICS APPLICATIONS

Gamma Dosimetry

The properties of five different integrating dosimeters are listed in Table 2. From this it is clear that lithium fluoride is very good material

for dosimetry, even at this early stage in its development. The question arises whether or not it should replace other methods.

The film badge is at present the legal method of measuring personnel doses in the U.K. Any alternative system must therefore show outstanding advantages in order to replace it. On a strict comparison of properties, lithium fluoride is superior to the film badge for the measurement of energy absorbed at the surface. However, because of its poor energy response the film badge is used with a number of filters and as a result it is possible to obtain an indication of the energy of the incident radiation. This is necessary to determine the organ dose which is required for statutory purposes. The developed film also provides what is considered for legal purposes in the U.K. to be a permanent record of the dose received. For these reasons lithium fluoride is unlikely to replace the film badge during the next few years.

It has been suggested by Langmead[3] that although lithium fluoride is unlikely to replace the film badge in the U.K. within the next few years, it could become a valuable addition to it. Lithium fluoride could become the short term control dosimeter while film badges continue to be the legal dose recording devices. The lithium fluoride could be read as often as necessary while the film badges could be processed at longer intervals than at present unless the lithium fluoride results show good reason for developing the film earlier in order to obtain additional information on beam quality, or to obtain a more accurate reading for the dose register. This would relieve the film badge services of the large load of special badges and would also reduce the frequency of routine badges to be processed. If the individual health physicist still has a method of operational control with on-site lithium fluoride facilities then consideration could be given to regionalization or centralization of film badge services.

The quartz fibre electrometer is still the best method for the individual to control his own exposure. It is unlikely to be replaced by thermoluminescence methods.

Beta Dosimetry

Lithium fluoride has the same response per rad for beta particles as for gamma rays. It can therefore be used without correction factors for measurements of mixed beta plus gamma radiation. When used in a flat container with a PVC cover of the appropriate thickness it can be used to determine the dose to the basal layer of the epidermis. Since the container can be quite small it can be worn on the fingertip, allowing a direct measurement of finger-tip dose. For this sort of $\beta + \gamma$ measurement thermoluminescence dosimetry is the only practical method of direct measurement. Lithium fluoride is also finding wider application for general $\beta + \gamma$ dose measurements due to lack of alternative methods. It is being used in many cases where a beta Q.F.E. would be used if available. If a reliable, robust beta Q.F.E. is developed it would probably be used for operational control of general body exposure in preference to lithium fluoride.

4. OPERATING CHARACTERISTICS OF DOSIMETERS USING LOOSE POWDER

Thermoluminescence dosimeters generally take one of two forms. In the first type the thermoluminescence material is placed in a sealed capsule together with energy correction filters and sometimes heating elements. In this form the amount of thermoluminescence material in the dosimeter is fixed, and it is not necessary to handle the material when evaluating the measured exposure. In the second type of dosimeter a measured amount of thermoluminescence material is dispensed into a suitable container for the measurements being carried out. After exposure the material is removed from the container for evaluation. The most common material used in this type of dosimeter is lithium fluoride. This is a white crystalline solid, and crystals between 80 and 100 mesh Tyler in size have been found to be the most efficient.[5] Dosimeters using loose powder such as lithium fluoride are generally more flexible in their applications than the sealed type, but are not so simple to use.

Advantages to be Gained by the Use of Loose Powder

The main advantage of the loose powder dosimeter is its flexibility of operation. With this system the container used to hold the powder can be specifically designed for the measurements made, e.g. it can be thick walled, rigid

Table 2. Properties of Integrating Dosimeters

	Film badge	Q.F.E.	Condenser ion chambers	Glass*	LiF
Dose range	0–1000 R	0–1000 R	0–6000 R	20 mr–3000 R	10 mr–10^6 R
Energy dependence	High low energy response	High response and cut off at low energy	Very good	High low energy response	Very good
Dose rate dependence	None	Response falls off at very high dose rates	Response falls off at very high dose rates	None	None
Size	Large	Largest	Large	Small	Very small
Robustness	Good	Good	Fragile	Good	Very good
Environment	Spoilt by water	Waterproof	Rapid leakage in damp	Up to 60°C	Up to 100°C
Shelf life	Good in refrigerator	Good	Must be stored in dessicator	Good	Very good
Pre-treatment	None	Charge	Sometimes require high doses to obtain stability. Charge	Measure pre dose. Annealing	Annealing
Readout	Wet chemical treatment. Slow	Instant	Fast	Fast	Fast readout but tedious handling of powder

* Photoluminescence with low Z Toshiba

I.J.R.P. VOL. 1—F*

Table 2 (continued). Properties of Integrating Dosimetres

	Film badge	Q.F.E.	Condenser ion chambers	Glass*	LiF
Readout equipment	Dark room. Bulky equipment and computation time	None Small charger required	Portable charger-reader	Non-portable reader	Non-portable reader
Fading		Leakage rate low when in good condition	Some leak charge very fast	6% year	5% year
Filters	RPS/AERE holder	None	None	Necessary for flat response	None
Reading	Energy absorbed + indication of radiation energy	Ionization	Ionization	Energy absorbed	Energy absorbed
Special advantages	Legal method of personal dosimetry —permanent record—indicates energy—well known	Constant check of dose possible during use	Victoreen condenser ion-chambers very stable—useful for standards	Good dose range, fast readout. Readout does not affect reading	Small, robust wide dose range and rapid readout. Good at high temperatures

* Photoluminescence with low Z Toshiba.

and sensitive to gamma-rays only or thin walled, flexible and sensitive to both beta and gamma radiation. Also the ancillary equipment used is not generally specific to any one thermoluminescence material allowing a choice to be made depending on the qualities of response required. Finally a fairly small stock of powder can be used to service a wide variety of different dosimeters of this type.

sachets used for finger dosimetry, and much less for small polythene phials.

3. The retention of powder in any container is random, it is therefore necessary to weigh each charge of powder before evaluation if an accurate measurement is required. The actual weight of powder recovered from a sachet can be as low as 75% of the initial charge.

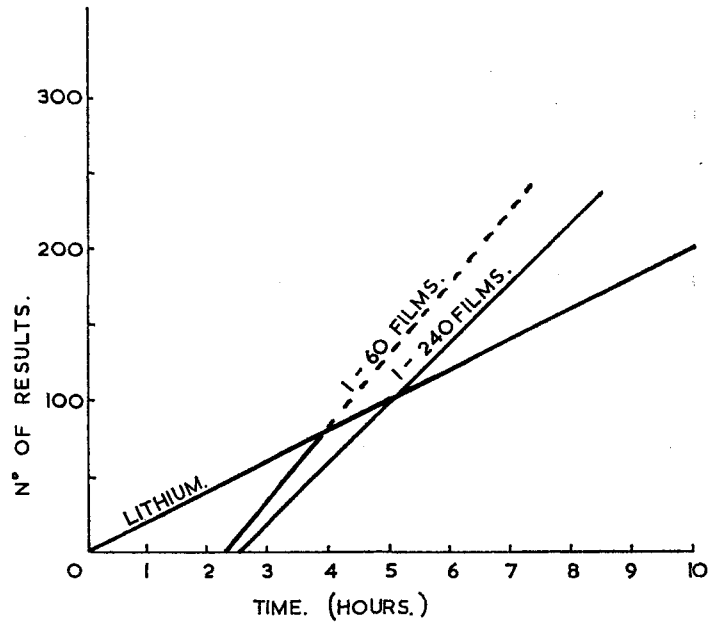

FIG. 1. Processing time for film badges compared with lithium fluoride.

Problems Caused by the Use of Loose Powder

Although a system using loose powder is very flexible, handling the powder causes some operational problems. The following problems are not always apparent from a preliminary appraisal of such a system.

1. Powder is easily spilt by careless handling especially in difficult working conditions. Thus an important measurement or a person's exposure record can easily be lost.
2. Powder losses occur and a 10% loss by weight is not uncommon each time the powder is used. One form of powder loss is due to retention of small amounts in the containers after emptying. The amount varies with the container used, being very high in the

4. Powder size is very critical. If the crystals of lithium fluoride are less than 80 mesh Tyler then their behaviour alters both physically and mechanically. This fine powder has an apparent response one third that of the larger 80–180 mesh size crystals, and is very difficult to handle. It will block a dispenser, and when placed on a heating tray is not easily spread evenly. Due to these difficulties the accuracy of the results obtained with it are low.
5. Due to tribothermoluminescence effects it is necessary to heat the powder in an atmosphere of nitrogen. Errors can be introduced if all samples are not given the same flushing time with nitrogen before reading.

6. The powder has to be bulked, reannealed, and recalibrated after use before it is ready to use again. This means more powder than required must be kept to allow for this procedure to be carried out without interrupting routine work. Variations in response after annealing vary from 3–20%.
7. Different batches of powder also vary in response by as much as 30%, and it is important not to mix dosimeters using different batches of powder unless they are clearly marked.

As a result of the problems listed above the processing and reading of lithium fluoride often takes longer than expected. In fact as shown in Fig. 1 in large numbers exceeding 60 film badges can provide results faster than dosimeters using loose lithium fluoride.

The problems listed above are probably only significant when considering a routine operational service. As a research tool the flexibility of the powder system, added to the tissue equivalence of lithium fluoride far outweigh the problems involved.

The regular operational Health Physics use of lithium fluoride, or any other thermoluminescent powder for both beta- and gamma-ray dosimetry will require improvements in the loose powder technique. Total encapsulation of the thermoluminescent material has to date produced only a gamma-sensitive dosimeter. One technique which may provide a solution however and give both beta and a gamma exposure is the embedding of powder in a flexible high melting point plastic. The results of some work carried out with this type of dosimeter are given below.

Finally the cost of lithium fluoride powder at present (June 1966) is approximately £5 per gram. This is probably due to its limited production by a few manufacturers. However, if increased sales reduced the price to 10/- per gram then it would cost less than the present film badge and would be cheap enough for reprocessing to become uneconomic.

5. EXPERIMENTAL RESULTS

Comparison with Film Badges for Personnel Dosimetry

Measurements have been made to compare the dose recorded by lithium fluoride with the sum of the gamma-, X-, and beta-ray components of the dose recorded on Kodak RM film in an AERE/RPS holder. The lithium fluoride powder was contained in a PVC sachet designed by the U.K.A.E.A. The experiment was divided into two parts. In the first part, sachets containing 45 mg of LiF were attached to the routine film badges issued monthly to 12 personnel likely to receive doses in excess of 30 mrem. The sachets were removed from the film badge holder at the end of the month with the routine monthly film. After weighing, the powder was emptied from the sachet, assessed and the empty sachet reweighed. The results obtained were then corrected to give an estimate of dose based on 45 mg of powder. Calibration was carried out using a similar method of assessment for identically loaded sachets given known exposures to 50 mg of ^{226}Ra. The second part of the experiment involved the issue of sachets of lithium fluoride, prepared and calibrated as in part one, to personnel involved in special operations for which additional film badges were being worn. In this case the lithium was worn separately from the film badges but where possible adjacent to one of the special films. The results of the first part of the experiment showed a reasonable correlation between the doses estimated with lithium fluoride, and with the film badge.

The results in Fig. 2 show considerable scatter in the dose range 0–50 mrad, but this was not unexpected as both systems of measurement were near the limits of their sensitivity in this range. Errors of at least 20% are probable. The correlation obtained was apparently independent of the proportion of the total dose due to gamma-, X-, and beta-radiation.

In the second part of the experiment very little correlation was found between the lithium fluoride and the film badge measurements. In most cases this was attributed to their relative positions. Due to this random positioning of lithium fluoride sachets with respect to the accompanying film badge, when issued loose, this part of the experiment was stopped. However, loose sachets were still issued for wearing on fingers, and these results are reported below. It is clear from the scatter of these results that dose variations over quite small areas of the body make organ doses derived from single surface dose measurements highly inaccurate.

Beta Surface Dosimetry

Using a PVC sachet with a 12 mg/cm² cover it is possible to obtain a direct estimate of skin dose, since lithium fluoride has an almost tissue equivalent response. The dose recorded by the lithium fluoride closely approximate to the $\beta + \gamma$ dose that would be received by the basal layer of the epidermis.

Sachets of lithium fluoride made up and assessed as described above, were issued both with monthly wrist films and for special operations. For monthly issues the sachets were first attached to leather finger-stalls. The wearers were chosen from persons handling active materials regularly, and wore the finger-stall on the forefinger of either hand with their monthly wrist film worn on the wrist of the same hand. For special operations sachets of lithium fluoride were issued both attached to finger-stalls and loose for attaching to the finger. Where possible a special film was also issued to be worn on the wrist of the same hand carrying the lithium fluoride. The results in Table 3 show the discrepancy between the estimates of exposure made with wrist films and those received at the finger-tips. Ratios as high as 20: 1 between wrist films and lithium fluoride finger dosimeters were obtained with an average ratio near 7: 1. Although there may be small differences in the response of film and LiF dosimeters when worn over bony parts of the body, the major part of the discrepancy is clearly due to inhomogeneity of the irradiating field. Thus wrist measurements alone seriously underestimate total hand exposure, and the facilities which LiF offers for finger-tip measurements are unique. The only operational disadvantage noted in the series of measurements was that some operators found difficulty in carrying out fine operations with both the finger-stalls and sachets on their fingers.

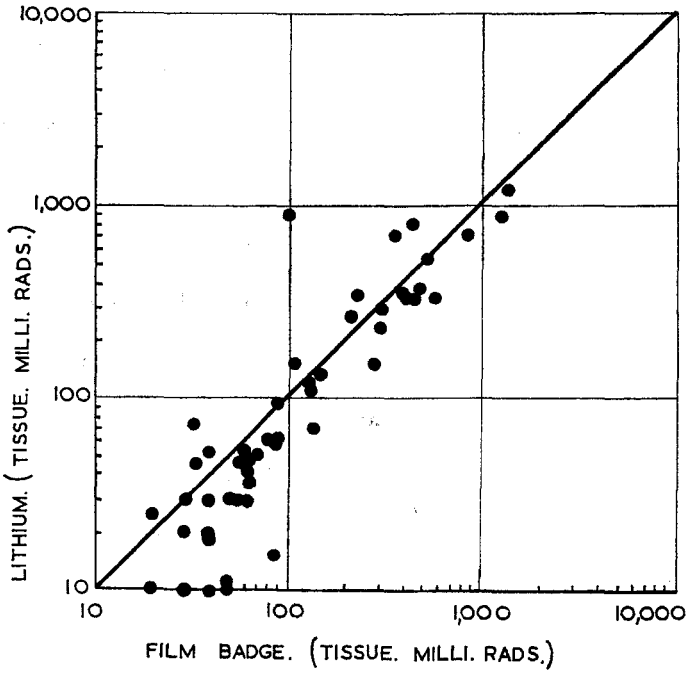

FIG. 2. Comparison between the monthly doses as monitored by film badges and lithium fluoride dosimeters.

Teflon Discs Incorporating Lithium Fluoride

The recent development of rods and discs of PTFE containing 20–30 mg of lithium fluoride offers a possible solution to the problems asso-

Table 3.

A *Total dose recorded by film badges on wrist, rad	B Dose recorded by lithium fluoride on forefinger, rad	Ratio A : B
0·09	0·11	1:1·2
0·81	5·10	1:6·3
0·36	0·94	1:2·6
0·09	0·03	1:0·3
0·15	3·38	1:22·5
0·08	0·89	1:11
0·23	2·27	1:9·9
0·24	0·49	1:2
0·08	1·34	1:16·8
0·20	0·19	1:9·5
0·17	0·94	1:5·5
1·08	2·10	1:2
0·24	0·83	1:3·5
0·70	0·82	1:1·2

*N.B. Total dose consists of the summation of the beta, X, and gamma components of the dose recorded on the film badge.

ciated with handling powder. These dosimeters can be read in a standard reader using a specially designed heating jig. This enables the dosimeter to be heated uniformly throughout its volume. The introduction of these discs and rods simplifying handling procedures, produces a useful reduction in processing time, but they are expensive. Their response is claimed to be identical to the loose powder, but we have not yet confirmed this. The economic advantage of this form of lithium fluoride dosimeter will depend a great deal on the number of times teflon dosimeters can be reused. Our measurements have shown that the repetition of an exposure/reading/annealing cycle up to twelve times has altered the response of 15 mm discs very little. However, the spread in response between individual discs all exposed simultaneously, and assessed at the same time, was as high as 30% of the total exposure. The variation in sensitivity of a given batch of discs, as revealed by the mean reading of six discs, between different cycles was in the order of 20%. This is illustrated in Fig. 3 where the mean, maximum, and minimum readings of the six discs in a batch are shown for twelve consecutive cycles of exposure/reading/annealing. The annealing procedure consisted of a period of 15 min at 300°C followed by 2 hrs at 80°C and was standardized for all cycles except the first shown in Fig. 3. No obvious variation in linearity was indicated between batches exposed to approximately 150 mr, 300 mr and 600 mr. One reason for the variation in response between cycles is thought to be due to a short-lived low temperature peak in the glow curve. This is shown in typical glow curves taken directly after irradiation (Fig. 4). In glow curves taken several days after exposure the low temperature peak is no longer detectable (Fig. 5). The presence of this peak thus introduces a variation in measured exposure dependent upon the time that elapses between the irradiation of the disc and its assessment. This could in part explain the variation in response of the discs between consecutive exposure/reading/annealing cycles. Further investigations will be carried out in order to confirm these findings

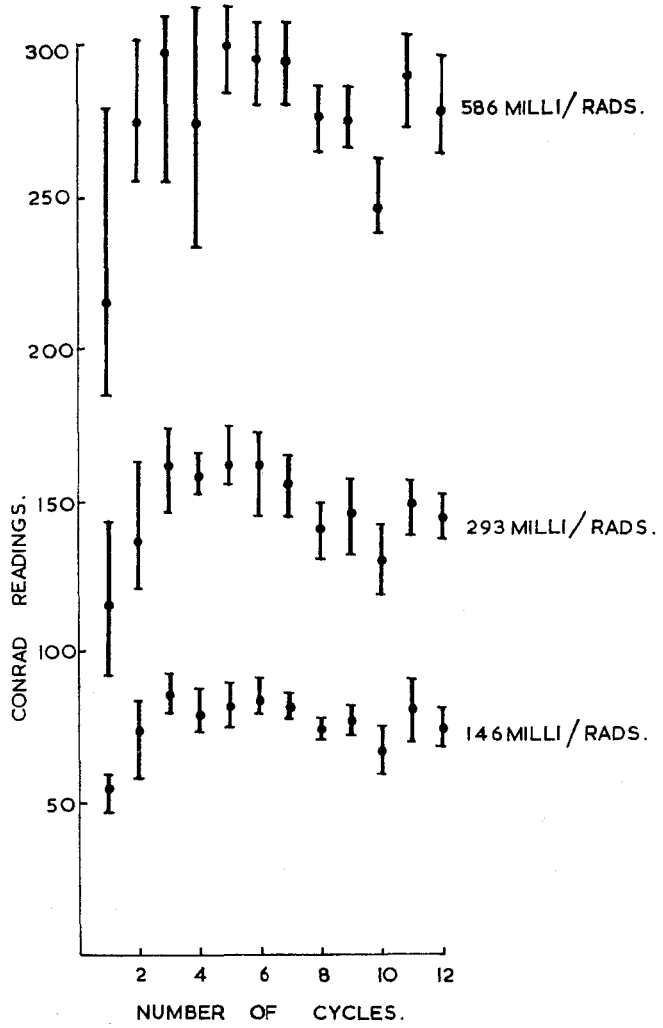

FIG. 3. Variation of teflon disc response with an increased number of exposure/reading/annealing cycles.

which, unless eliminated, could seriously affect the usefulness of the teflon discs for exposure control.

Measurements with a Water Phantom

A standard man equivalent thorax and abdomen consisting of two water filled containers was used. The dosimeters under test were placed in groups on the surface of the thorax facing the source of radiation. AERE/RPS film badges, PVC sachets and polythene phials were used, the latter containing 45 mg of lithium fluoride powder. Two sources of radiation were used, 20 mCi of ^{198}Au and 5 mCi of ^{60}Co. The exposures were carried out with a fixed source to dosimeter distance giving approximately the same exposure rate for all experiments, with the same source. The total exposure was varied by altering the duration of the experiment. The results in Table 4 show the mean value of the fraction measured dose/calculated dose for six dosimeters of each kind. The

calculated dose being that expected at the distance of the dosimeter from the source in the absence of the water phantom.

The results to date show that at 0·4 MeV (^{198}Au) the film badge consistently gives a measured exposure several per cent higher than that obtained with the lithium fluoride dosimeters. The fairly wide spread in the value of measured dose/calculated dose possibly indicates that the degree of accuracy obtained still leaves room for improvement. However, it would appear that the two types of lithium fluoride dosimeters do not vary very significantly in their response to 0·4 MeV gamma radiation.

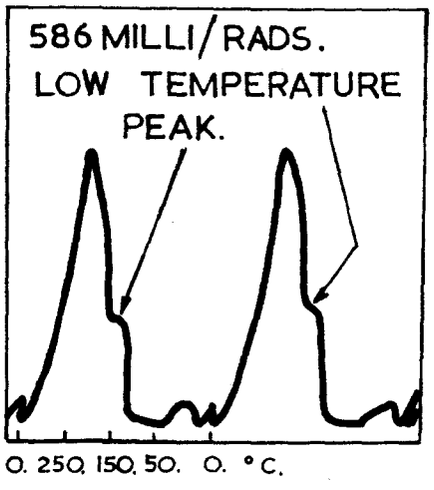

FIG. 4. Teflon disc glow curve read immediately after exposure showing low temperature peak.

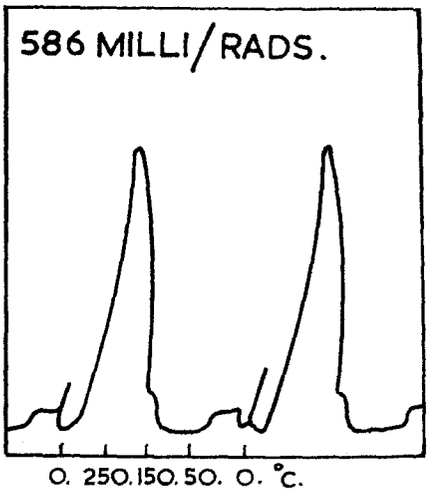

FIG. 5. Teflon disc glow curve read several days after exposure.

The results obtained with the higher energy

Table 4. Mean Values of Measured Dose/Calculated Dose for Groups of Six Dosimeters Exposed on a Water Phantom

Radiation energy	Position	Type of dosimeter	Measured Dose/Calculated Dose			
0·4 MeV ^{198}Au	Front of phantom	Polythene phial	1·12	0·97	1·16	1·14
		PVC sachet	1·07	1·00	1·15	1·19
		Film badge	1·34	1·20	1·52	1·21
1·2 MeV ^{60}Co	Front of phantom	Polythene phial	1·04			
		PVC sachet	1·24			
		Film badge	0·95			
1·2 MeV ^{60}Co	Back of phantom	Polythene phial	0·45			
		PVC sachet	0·50			
		Film badge	0·50			

radiation from ^{60}Co have not been quite so conclusive as at the lower energy. In this case variations in response were caused by the low energy beta-radiation emitted from the capsule containing the ^{60}Co. This had very little effect on the thick walled polythene phials or the film badges but produced an enhancement in the dose measured by the thin walled sachets. This effect was confirmed when sachets were covered with approximately 90 mg/cm^2 of additional PVC giving them a wall thickness of the same order as the polythene phials. Under these conditions the response of the phials and the sachets showed only a 5–6% variation, which is probably within the present accuracy of the methods and equipment. Allowing for the sensitivity of the sachet to the low energy beta-rays present, the results with ^{60}Co show that at this energy there is very little difference in the response of the film badges and the lithium fluoride dosimeters.

Finally one set of measurements were taken with the dosimeters on the phantom surface facing away from the ^{60}Co source. Under these conditions very little variation in response was found between different dosimeters. The degree of attenuation due to the presence of the phantom was about 50% which is in good agreement with the results of H. J. Delafield.[8]

6. CONCLUSIONS

Materials

We have shown that lithium fluoride can be used for some operations hitherto impossible and that comparison between lithium fluoride and film badges shows good correlation except at low doses. However, loose powder is inconvenient for large scale operational use and the widespread introduction of TLD into operational Health Physics will probably be delayed until a satisfactory solid dosimeter has been developed. Lithium fluoride in teflon is a useful development but it has some disadvantages. The ideal dosimeter should be rigid, transparent, large enough to handle easily, be capable of annealing up to 25 times and should have no low temperature peaks in the glow curve. Marking small dosimeters is a difficult problem. We suggest that dosimeters should be made with a piece of inert base material attached for the identification marks. It is worth considering that automatic handling and reading will be required in the future and a system of symbols for automatic identification should be considered. For general personal dosimetry at the present time, low Z glass is operationally more convenient. It must be remembered, however, that glass has many years of development behind it while TLD is still in a very early state of development. The most prudent policy at the present time is to use film, glass and TLD where they are most advantageous, but to defer consideration of complete reliance upon TLD until further development has been carried out.

Readers

Current commercial readers are designed to heat loose powder on a tray. These readers are now being adapted to heat solid dosimeters. Future development should be directed towards producing an alternative heating method to heat solid dosimeters directly. This may lead to a lighter system with a lower power consumption thus providing a more portable reader. Solid dosimeters will avoid nitrogen flushing which will further simplify the equipment.

The complete reader in a box concept is not necessarily the best system for operational use. A more economic system would employ a separate reading head, comprising heating chamber with a photomultiplier together with heating/timing circuits. The output from this unit would preferably be measured using conventional nucleonic modules. Such a system would simplify the supply of spare parts since laboratories using TLD will normally be equipped with conventional nucleonic equipment.

ACKNOWLEDGEMENT

This paper is published by permission of the Central Electricity Generating Board.

REFERENCES

1. E. E. Angino, N. Grogler and R. McCall. T.I.D. 3911 (1965).
2. Z. Spurny. *Atomic Energy Review* **3**, 61–115 (1965).
3. W. A. Langmead; U.K.A.E.A., A.H.S.B. (RP) R61 (1965).

4. J. R. CAMERON, F. DANIELS, N. JOHNSON and G. KENNEY. *Science* **134,** 333–334 (1961).
5. J. R. CAMERON, D. ZIMMERMAN, G. KENNEY, R. BUCH and R. BLAND. *Health Physics* **10,** 25–29 (1964).
6. J. H. SCHULMAN, F. H. ATTIX, E. J. WEST and J. GINTHER. Symposium on Personnel Dosimetry Techniques for External Radiation—Madrid (1963).
7. K. E. G. PERRY and E. GEORGE. U.K.A.E.A., A.E.E.W.—R.411 (1965).
8. H. J. DELAFIELD. *Physics in Medicine and Biology,* II, No. 1, 63–73 (1966).

A COMPARISON OF TLD AND FILM FOR PERSONNEL DOSIMETRY*

JOHN R. CAMERON
and N. SUNTHARALINGAM†
Department of Radiology, University of Wisconsin, Madison, Wisconsin

Abstract—The film badge is today the most widely used personnel monitoring device for want of a more reliable and accurate system. Recent evaluations of the performance of the available commercial film badge services report a wide variation in both the accuracy and consistency of the reported exposures. The best accuracy that one can obtain for X- and gamma-radiation appears to be −50 to +200%. This paper reports the feasibility of using the thermoluminescence of single crystals of LiF (TLD-100)‡ to measure exposure levels of X- and gamma-radiation encountered in the personnel dosimetry range. The use of single crystals greatly reduces the contribution of the non-radiation induced thermoluminescence. The variation in response of individual crystals was taken into account by calibration of the crystal in place at the time of read-out. LiF single crystals in lucite capsules were attached to film badge holders and given known test exposures from X- and gamma-ray sources and mixtures of these radiations. The performance of the TLD system is compared with the measured values reported by the film badge suppliers. No correction was made for the slight energy dependence of LiF at the low keV exposures. The over-all accuracy of the TLD system is about ± 30% for X- and gamma-ray energies above 25 keV effective.

INTRODUCTION

The Federal Radiation Protection Code[1] requires that a monitoring device be worn or carried by an occupationally exposed individual for the purpose of measuring the radiation exposure received. The film badge is the measuring device most widely used for this purpose. Even with its numerous limitations[2-5] the film badge has been called upon to provide accurate dosimetry. Documentation of personnel exposure records have become basic in proving compliance or non-compliance with Federal and State regulations and as such the accuracy and reliability of the available commercial film badge services have been questioned.[6] Two separate evaluations[7, 8] of the performance of the film badge suppliers report a wide variation in both the accuracy and consistency of reporting the exposures received by the film. In one of these studies even the companies that did reasonably well demonstrated an accuracy range of only − 50 to + 200% in reporting gamma and X-radiation exposures with a confidence limit of 90%.[7]

A major advantage of thermoluminescent dosimeters is their wide usable range. The upper limit for LiF (TLD-100) is set by saturation effects that become pronounced at 10^5 R. At the low end of the range, measurements are limited by the presence of a large background part of which is due to the non-radiation induced thermoluminescence from the phosphor. This effect is of the order of 1 R equivalent for a 30 mg sample of TLD-100 when it is used as a loose powder.[9] Single crystals of TLD-100 show a marked decrease (about a factor of 30) in this non-radiation induced thermoluminescence. The feasibility of using the thermoluminescence of single crystals of TLD-100 to measure milliroentgen levels of exposure was investigated

* Part of this paper was presented at the International Conference on Luminescence Dosimetry, Stanford, June 1965. This work was partially supported by AEC Contract No. AT-11-1-1105.

† National Institute of Health pre-doctoral trainee in Radiological Sciences.

‡ Obtained from Harshaw Chemical Co., Cleveland, Ohio.

earlier.[10] This paper reports the results obtained using single crystals of LiF (TLD-100) for monitoring exposures in the personnel dosimetry range in comparison with the film badge evaluation supplied by a commercial company. The advantages of using a TLD system for personnel dosimetry purposes are: (a) relatively good energy independence, (b) linear response with exposure, (c) dose-rate independence, (d) approximate tissue equivalence, (e) negligible decay of stored TL, and (f) unaffected by visible light, moisture, and mechanical vibrations.

METHOD

For the comparative study of personnel dosimetry using LiF single crystals and film badges, the single crystals were placed inside lucite capsules (4 mm wall thickness) and attached to the film badge holders. The single crystals weighing approximately 10–25 mg ($\sim 2 \times 2 \times 3$ mm) were cleaved from a chunk of virgin TLD–100, and annealed for one hour at 400°C before being used in the studies.

Test exposures of known amounts of radium and ^{137}Cs gamma-rays and 140 kVp (~ 3 mm Al hvl) X-rays were given to the LiF crystals and film badges simultaneously. The calibrations for the test exposures were determined using Victoreen R-meters, but, because of the low exposures used, our values are probably accurate to only $\pm$ 10%. These test film badges were sent back together with the ~ 300 routinely used film badges for evaluation by the company. As normal procedure the company is always informed of the type of radiation each badge might have been exposed to, but no indication was given that some badges were being used in a comparative study. The exposed LiF crystals were "read" using a technique which is described in detail elsewhere.[11] All of the readings were done by one of the authors (N.S.), who did not have any prior knowledge of the test exposure values or the quality of the radiation.

In one study, film badges from a second company were also simultaneously exposed and sent back for evaluation.

In a separate experiment, we subscribed to a special testing service offered by the National Sanitation Foundation Testing Laboratory, Ann Arbor, Michigan, and had sent to them twenty badge holders containing both LiF crystals and film. These were exposed to known amounts of ^{137}Cs gamma-rays, 175 keV effective (270 kVp, 4.1 mm Cu hvl) and 24 keV effective (68 kVp, 1.25 mm Al first hvl) X-rays and a mixture of ^{137}Cs and 24 keV-effective radiations, and sent back to us for evaluation. The true exposures were not known to us until the measured values were reported back to the National Sanitation Foundation Testing Laboratory. The LiF crystals were "read" in our laboratory while the films were sent back to the company for evaluation.

RESULTS

The response of the single crystals in the lucite capsules to known exposures of radium γ-rays, ^{137}Cs γ-rays, and 140 kVp X-rays is seen in Fig. 1. The crystals show about a 40% increase in sensitivity for the low energy X-rays.

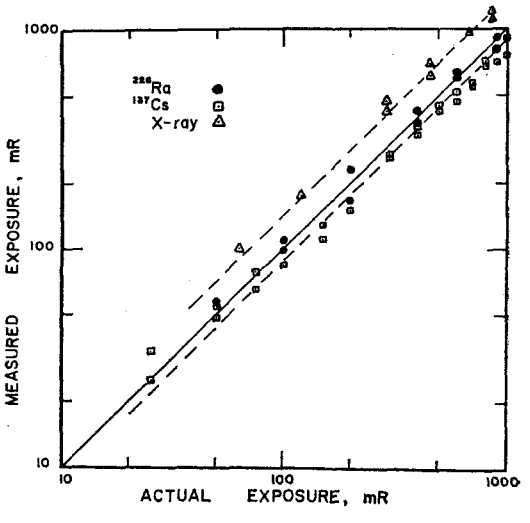

FIG. 1. Response of single crystals to radium and ^{137}Cs gamma-rays and 140 kVp (hvl 3 mm Al) X-rays.

This falls in the range of values previously reported.[9] The ^{137}Cs measurements read about 15% lower than the actual exposures. This was later verified to be an error in the calibration of the source.

Figure 2 shows the results of an experiment

conducted with radium test exposures. The broken lines represent an error of ± 20%. Fourteen of the 15 crystals measured within ± 25% of the actual exposures.

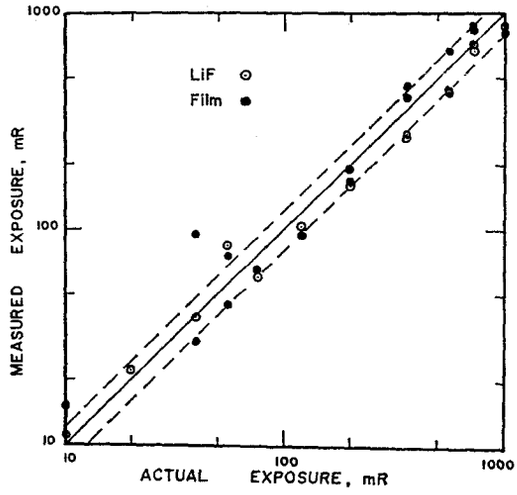

FIG. 2. Exposure readings as measured by LiF single crystals and film. The solid diagonal line represents 100% accuracy. The parallel broken lines indicate an error of ± 20% in the measurements.

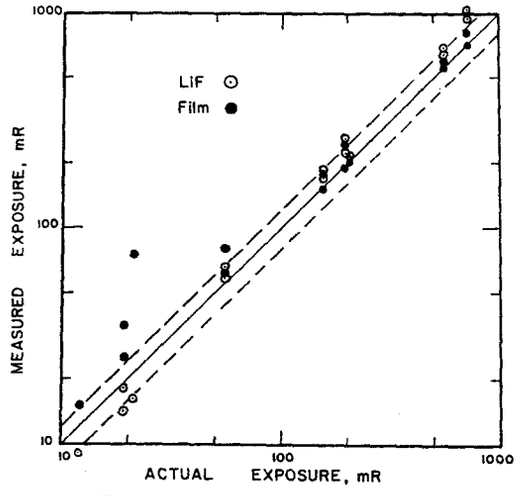

FIG. 3. Exposure readings as measured by LiF single crystals and film. The solid diagonal line represents 100% accuracy. The parallel broken lines indicate an error of ± 20% in the measurements.

Figure 3 shows the results obtained with mixed exposures of radium γ-rays and 140 kVp X-rays. Twelve of the 15 crystals measured within ± 25% of the actual exposures. The measured values using LiF crystals appear to be higher than the actual exposures and this is due to the increase in sensitivity of the LiF to low energy X-rays.

In one experiment film badges from two different companies were exposed simultaneously with the LiF single crystals, to radium γ-rays, ^{137}Cs γ-rays, 140 kVp X-rays and mixtures of these radiations. Figure 4 shows the performance of the LiF single crystals used. Seventeen

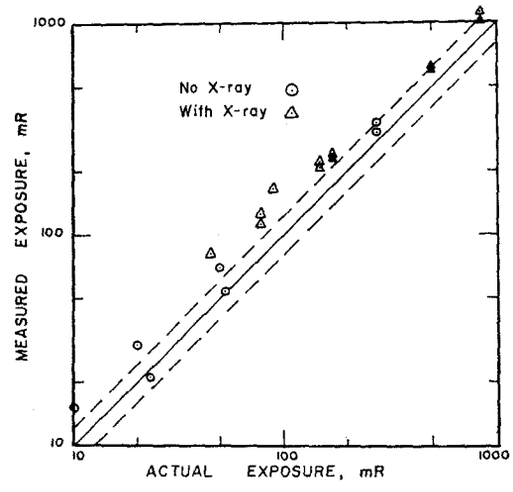

FIG. 4. Exposure readings as measured by LiF single crystals and film. The solid diagonal line represents 100% accuracy. The parallel broken lines indicate an error of ± 20% in the measurements.

of the 20 crystals measured within ± 50% of the actual mixed exposures. Those crystals that had some X-ray exposure are identified separately and these give the higher measured values. No corrections were made for the energy dependence of the LiF. Note, however, the good consistency of measured values on the duplicate sets of crystals given the same exposure.

In Fig. 5 this same performance of the LiF crystals is shown in comparison to the film badge

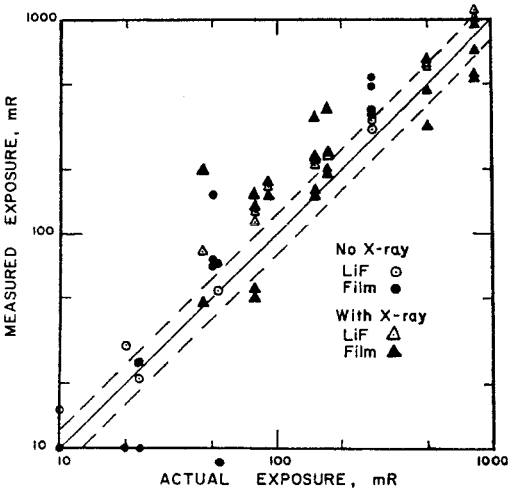

FIG. 5. Exposure readings as measured by LiF single crystals and film. The solid diagonal line represents 100% accuracy. The parallel broken lines indicate an error of ±20% in the measurements.

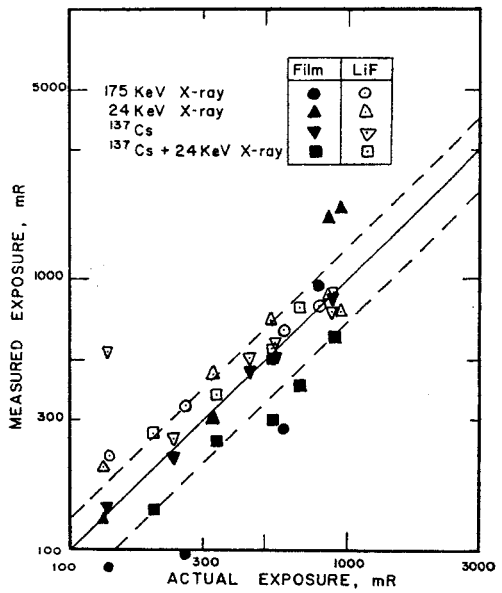

FIG. 6. The results of test exposures given by the National Sanitation Foundation Testing Laboratory, Ann Arbor, Michigan. The parallel broken lines indicate an error of ± 30% in the measurements.

evaluations of the two companies. Note the disagreement between the two companies. One company could not detect anything below 50 mR and reported those badges to have had zero exposure. Also note the poor consistency of some of the duplicate exposures.

The results of the Michigan test exposures are shown in Fig. 6. The measured values using the LiF crystals appear to read high, but within 30%. This is to be expected in the case of the soft X-rays because of the slight energy dependence of the TLD system. No correction has been made for this quality dependence.

CONCLUSION

The film badge continues to be used as the principal personnel monitoring device for want of a better and more accurate and reliable system. This study has clearly demonstrated that the potential exists for the use of LiF single crystals for personnel dosimetry work. The use of single crystals of LiF (TLD-100) in place of the powder is a distinct advantage when measuring milliroentgen levels of exposure. At this lower range the accuracies attainable with the TLD system are somewhat lower than those at higher exposures. The over-all accuracy of ± 30% can be improved upon if one also corrects for the slight quality dependence of the LiF at the lower energies. The TLD system has the advantage that these crystals can be reused over and over again without any loss in sensitivity or accuracy. Also it is possible to monitor each individual with several single crystals, one could be read and replaced at monthly intervals for occupationally exposed personnel and the others used as integrating dosimeters over a longer period of time. Non-occupationally exposed personnel could have their dosimeters read annually or after a suspected exposure. We are undertaking such a program in our institution. The TLD system is inexpensive, rugged and reliable. Suitable single crystals are available in any quantity from the Harshaw Chemical Company. The principal disadvantage at present is the relatively slow read-out (approximately 15 min) because of the need to calibrate each crystal individually. Work is under way to produce single crystals with consistent radiation response to eliminate this calibration step.

We strongly feel that commercial suppliers of film badges should look into the possibility of incorporating a LiF dosimeter in their systems and at least as a beginning monitor the personnel exposures simultaneously with films and the LiF crystals.

REFERENCES

1. Title 10, Code of Federal Regulations. Part 20–101, October 1962.
2. B. E. JONES. *Ann. Occupy. Hyg.* **4,** 104 (1961).
3. M. EHRLICH. *National Bureau of Standards Handbook* 57, Washington, D.C., Government Printing Office, 1954.
4. R. A. DUDLEY. In *Radiation Dosimetry*, edited by G. J. Hine and G. L. Brownell, New York, Academic Press, 1956.
5. B. A. FRIES and D. E. HULL. *Nucleonics* **17,** 116 (1959).
6. USAEC Circular. Notice regarding need for establishment of Film Dosimetry Calibration Laboratory. Washington 25, D.C., July 23, 1963.
7. R. O. GORSON, N. SUNTHARALINGAM and J. W. THOMAS. *Radiology* **84,** 333 (1965).
8. D. F. MENKER and M. DAUER. *Journal of Industrial Medicine & Surgery*, p. 700 (Sept. 1965).
9. J. R. CAMERON, D. ZIMMERMAN, G. KENNEY, R. BUCH, R. BLAND and R. GRANT. *Health Physics* **10,** 25 (1964).
10. D. ZIMMERMAN and J. R. CAMERON. Progress Report, AEC Contract AT-11-1-1105, University of Wisconsin, July 1964.
11. N. SUNTHARALINGAM, D. ZIMMERMAN and G. N. KENNEY. *Proc. International Conference on Luminescence Dosimetry*, Stanford, June 1965.

MEMORY EFFECTS WITH M.B.L.E. CaF_2 THERMOLUMINESCENT DOSIMETERS

ERIC VAN ESPEN

Manufacture Belge de Lampes et de Matériel Electronique S/A, 80, rue des Deux Gares, Bruxelles 7, Belgique

Abstract—The thermoluminescent (TL) dosimetry methods become more and more popular for all applications where personal protection against radiation is needed. For instance, in nuclear installations—civil populations in the case of nuclear accident and military personnel in case of a nuclear conflict. The existing TL systems are very convenient for these applications, as well for low doses as for high doses. However, the principle of TL does not offer theoretically more than one measure of the same dose because of the erasing phenomena caused by the reading process. This erasing characteristic excludes a new reading of the dose in case of an official control or further check.

To fulfil these multireading requirements, we expose three practical methods actually in production giving at the same time with the same dosimeter the total accumulated dose and the reading of the dose received between two measurements. These principles are:

(1) thermal inertia
(2) multipeak reading
(3) light transfer effect in some CaF_2 fluorines.

These three methods are discussed with their respective performances and application field and the conclusion is that they lead from now to a TL dosimeter which combines both properties of photoluminescent and thermoluminescent systems.

INTRODUCTION

Because of the basic principle of thermoluminescence, the reading of a thermoluminescent dosimeter erases the dose information, since it requires emptying the traps. This has the great advantage that it is possible to read any new dose, as low as it may be, without previously recorded doses influencing reading accuracy. On the other hand, in the case of a serious nuclear accident, it may be desirable for medical or legal reasons to check the accidental dose. For this purpose we have created three different types of dosimeters each intended for well defined uses.

1. *Twin-cathode dosimeters with thermal delay memory*

In this system, the cumulated dose may be read above 100 mr. The process is such that the memorized dose is erased. Thus doses can be accumulated with the possibility of reading the total dose; nevertheless once the total dose has been read, the dose and its memory are completely erased. This system is particularly suited to measuring low doses from 100 mR up.

2. *Twin-peak memory dosimeter*

This system is based on the normal reading of dose by emptying trap II of CaF_2 which occurs at about 180°C. The dose accumulation is normally made in peak III which is read at about 375°C. As in the twin-cathode system, the memory is erased by the reading process. The memory facility for this type of dosimeter is designed for doses between 1 and 1000 R.

3. *Memory effect by light transfer*

In this case light is used to transfer a fraction of the energy accumulated in deep traps to traps of lower energy. The memorized doses are read by a normal measurement of these shallow traps after light transfer. The great advantage of this process is that it is possible

to transfer only a very small fraction of the stored energy. Thus the process can be repeated and access to the memory can be made several times with good reproducibility. The process is as follows:

(a) Let us suppose that during its use a dosimeter has received in one or several irradiations, doses totalling more than a score of roentgens, and that has been read and thus erased.

(b) If this dosimeter is exposed to a light source for some time, a new reading made in the usual way gives a dose corresponding to a fraction of the total dose received by the dosimeter.

(c) For constant lighting conditions, the dose read in this way is proportional to this total dose, subject to certain threshold limitations.

It has been proved experimentally that after irradiation and reading, the light transfers charge carriers from traps V and VI to trap III. This phenomenon gives a method for checking repetitively the total dose received by a dosimeter. It is indeed possible, by using appropriate light, to transfer only a very small fraction of the energy stored in peaks V and VI and thus to repeat the measurement a great many times with a good reproducibility. These readings may be repeated ten times with a precision of 15% or better, for total doses exceeding several scores of roentgens. Because of this phenomenon of light transfer the M.B.L.E. CaF_2 thermoluminescent dosimeters have a memory and consequently it is possible to read both partial and total dose.

THE PHYSICAL MODEL OF LIGHT TRANSFER

In a thermoluminescent phosphor, the charge carriers created by ionization at the time of irradiation are trapped in sufficiently deep traps not to be released at ambient temperature. When the phosphor is heated the carriers are released in increasing order of trap depth. They then recombine with light emission. It is the measurement of this light which gives the dose reading. In M.B.L.E. CaF_2, the main trap (peak III) is normally measured at a temperature of 265°C. Nevertheless other traps exist in M.B.L.E. CaF_2, including deeper traps, e.g. peak V, at about 500°C. During manufacturing, all the traps of a new dosimeter are emptied, including those corresponding to peak V. On the other hand, when the dosimeter is used, the reading or erasing heatings do not produce the temperature required to empty peak V traps. Thus traps of peak V fill up progressively at each irradiation, and the amplitude of peak V corresponds to the total dose accumulated by the dosimeter since its manufacture. Because of the high temperatures involved it is difficult to read the amplitude of peak V directly without strongly disturbing the dosimeter characteristics. On the other hand, it is possible to make this measurement indirectly, but with precision, by using the light transfer phenomenon.

OPERATIONAL USE OF LIGHT TRANSFER

The dosimeter is exposed to U.V. light (about 3300 Å) of such an intensity and for such a time (about 5 min) that a new reading of the dosimeter gives a dose exactly equal to 1/400 of the total dose received by the dosimeter. Under these conditions, the measurement may be made ten times with very good reproducibility.

RANGE OF USE AND ACCURACY

At the present stage of development there is a lower limit (about 2R) to the dose which can be read by light transfer. The accuracy of the transfer measurement is 15% of the total dose, and the reproducibility of several transfers is a few per cent.

CONCLUSION

There exist today several possible memory techniques associated with the thermoluminescence phenomenon. The first two processes listed require specially designed dosimeters and permit only one measurement of the memorized dose, while the third process (light transfer) has the great advantage that the total dose can be reread a number of times.

Further research may well reduce the present threshold level of 20 R.

At the present time all M.B.L.E. standard CaF_2 dosimeters can make use of this effect and hence the partial doses can be read by thermoluminescence, and the total dose can be reread as with photoluminescent glass.

PILOT COMPARISON OF TWO THERMOLUMINESCENT DOSIMETRY SYSTEMS WITH FILM BADGES IN ROUTINE PERSONNEL MONITORING

T. L. JOHNSON
Health Physics Staff

F. H. ATTIX
Nuclear Physics Division
Naval Research Laboratory, Washington, D.C.

Abstract—An intercomparison was made of the performance of two thermoluminescent dosimetry (TLD) systems and conventional film badges in a routine γ-ray personnel monitoring operation. Quartz fiber pocket dosimeters were worn in some cases also but were read out more frequently than the monthly interval used for the other systems.

One of the TLD systems consisted of the U.S. Navy experimental prototype Computer–Indicator CP-748 (XN-1)/PD and Detectors DT-284 (XN-1)/PD (respectively the "reader" and "dosimeters"). The other was a commercial model of foreign manufacture which will be referred to here as the "M" system. Both of these types of dosimeters employed calcium fluoride TLD material sealed in a glass envelope with an internal ohmic heater.

The "M" dosimeters were found to agree with the DT-284's within 10% + 6 mR almost without exception and within 10% + 3 mR in three cases out of four. The quartz-fiber dosimeters agreed with the DT-284's within 10% + 6 mR in three fourths of the cases. 20 mR was regarded as the minimum exposure detectable with the film; in the 31 cases where the film exceeded this minimum, it also exceeded the DT-284 reading by 10% + 25 mR in 18 cases, and by 10% + 50 mR in 8 cases.

Both types of TLD's were found to contain radioactive contamination which gave rise to background readings in excess of ambient background by $\approx$ 21–24 mR/mo.

I. INTRODUCTION

In earlier Naval Research Laboratory Test and Evaluation Reports,[1, 2] brief descriptions of the radiation performance of two thermoluminescent dosimetry (TLD) systems were given. The first, a U.S. Navy experimental prototype, consisted of a thermoluminescence reader Computer-Indicator CP-748 (XN-1)/PD and TL dosimeters identified as Detectors DT-284(XN-1)/PD. This system was developed under contract from the Bureau of Ships and was loaned to the Laboratory through the courtesy of Messrs. C. S. Hollander and D. D. Helton, Code 682B of the Bureau of Ships (now NAVELECSYSCOM, Code ELEX 05162). The second TLD system was a foreign commercial one which will be denoted here as the "M" system.

The cited reports[1, 2] indicated that the immediate use of either of these systems for routine personnel-monitoring applications at NRL would be somewhat premature, and it was felt that an intercomparison with typical film badges on a pilot basis in monitoring NRL personnel might indicate further strengths and weaknesses not revealed by the other laboratory tests. Hence, some one hundred NRL personnel were asked to wear simultaneously a DT-284 and/or an "M" thermoluminescent dosimeter, in addition to their regular film badge, for four

one-month collection periods beginning in February 1965. A part of this group also carried a 0–200 mR quartz-fiber pocket dosimeter for day-to-day routine monitoring.

II. THE DOSIMETRY SYSTEMS

A. *Navy Experimental Prototype System (CP-748 (XN-1)/PD Reader and DT-284(XN-1)/PD Dosimeters)*

The DT-284 dosimeters (see Fig. 1) use CaF_2: Mn phosphor of the type developed at NRL by Ginther[3] and are normally enclosed in a shield which flattens the response per roentgen over the γ-ray-energy interval from 80 keV to 1.3 MeV; below 80 keV the response rapidly decreases. The reader covers a range of six decades of exposure, full-scale readings being 0.1, 1, 10, 100, 1000 and 10,000 R. The exposure reading is printed out on paper tape along with the serial number of the dosimeter. The group of DT-284 dosimeters tested showed a standard deviation of $\pm 9\%$ in their γ-ray sensitivity distribution; the reading reproducibility of a single dosimeter repeatedly given the same exposure (near full-scale on the 0–10 R range) had a standard deviation of about $\pm 2\%$. The response of the reader vs. Co^{60} γ-ray exposure was strictly linear on each scale, but the high-exposure scales (> 1 R) read lower than they should by as much as 40% because of incorrect densities of the built-in light filters used for range-changing. This had no bearing on the present tests, however, since all exposures encountered were less than 1 R. A more detailed description of this system may be found in ref. 1.

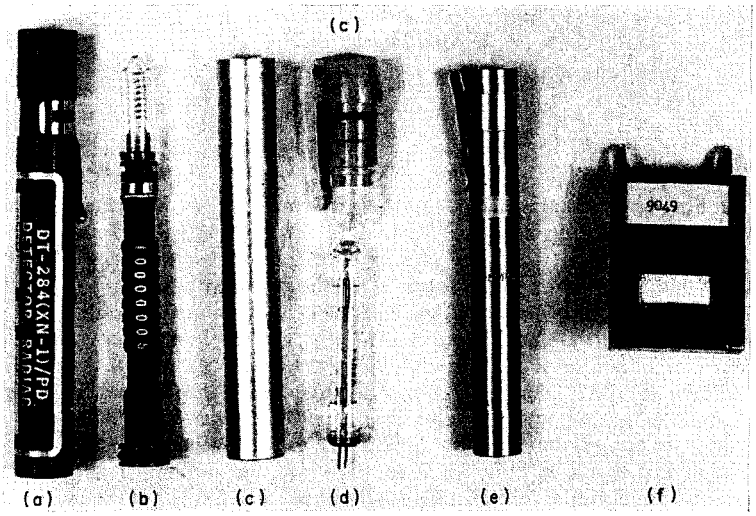

FIG. 1. Principal dosimetry systems involved in the tests: (a) Shielded carrying case for the DT-284 (XN-1)/PD thermoluminescent dosimeter. (b) DT-284 (XN-1)/PD dosimeter. Glass bulb contains CaF_2: Mn phosphor on a Nichrome coil. Numbered cams on attached rod contain identification number information for automatic printout. (c) Carrying case for "M" dosimeter. (d) "M" dosimeter, containing CaF_2:(?) coated on a cylindrical, indirectly heated cathode. (e) 0-200 mR quartz-fiber pocket ion-chamber type dosimeter. (f) NRL film badge.

During the latter part of these tests the Health Physics Staff purchased a commercial TLD reader and a group of dosimeters from the same company that manufactured the Navy prototype, and this commercial system was used in the signal-fading measurements and in some of the radiation background determinations (see Sections IVA and VI). These dosimeters were

similar to the DT-284's except for the elimination of the stem bearing the identification cams.

B. *The "M" System*

These dosimeters contain a type of CaF_2 with an unknown activator (not Mn). The reader displays the γ-ray exposure on a meter having full-scale readings of 0.15, 0.5, 1.5, and 5 R. The proper scale (which need not be chosen before the dosimeter is heated in the reader) is selected by push buttons. The sensitivity variation among the individual dosimeters was found to have a standard deviation of about 5%, the reproducibility of readings of a given dosimeter was about 2% S.D., and the response vs. Co^{60} γ-ray exposure was linear within $\pm$ 2% except on the most sensitive scale, where the response was about 15% too low at exposures less than 25 mR. The detectors (see Fig. 1) were enclosed in shields which made the dosimeters' energy response similar to that of the DT-284. A more detailed description of the "M" system will be found elsewhere (e.g. ref. 2).

C. *Film Badge*

The film badge utilized in these tests (see Fig. 1) was the single-filter (1 mm Cd) stainless-steel type developed at Oak Ridge National Laboratory and identified as AEC Catalog No. PF-4B. The badges were fitted with a conventional dosimetry film packet containing high and low sensitivity component films. All the results in this report refer to the more sensitive film. The films were developed at 20°C for 5 min using X-ray developer, rinsed, fixed for 10 min using X-ray fixer, rinsed for 30 min, dried, and their optical densities measured on a densitometer. A calibration set of twenty films (exposure range 10 to 1000 mR) was developed with every film batch, and a calibration curve determined. The film and the quartz-fiber dosimeters were calibrated using the same Co^{60} source. Intercomparison was made of this source with the Co^{60} source used to calibrate the thermoluminescent dosimeters, to assure consistency.

III. TEST SITUATION

The thermoluminescent dosimeters were worn by four groups of employees during these tests. They were: the Reactor Branch of the Radiation Division, the Reactor Materials Branch of the Metallurgy Division, the Dosimetry Branch of the Nuclear Physics Division, and the Health Physics Staff. Physically these groups were located (and the employees primarily worked) in the following NRL buildings: Reactor Branch, 71R; Reactor Materials Branch, 71M; Dosimetry Branch, 5AB, 28A, and 83; Health Physics Staff, 70E. Employees were identified by employee number and building. These four groups of employees were chosen because previous film exposure records indicated that these were the groups most likely to receive detectable radiation exposures. During the first month of the test, February 1965, only an "M" dosimeter plus the film badge and quartz-fiber dosimeter (if issued) were worn by each employee, since the necessary DT-284 dosimeters had not yet arrived from the manufacturer. Both an "M" and a DT-284 dosimeter, in addition to the regular film badge and quartz-fiber dosimeter, were worn during March and April, and only a DT-284 dosimeter plus the film badge and quartz-fiber dosimeter in May. It was originally planned to have a three-month test of the TLD systems plus the film badge and quartz-fiber dosimeter, but the addition of two thermoluminescent dosimeters to the quartz-fiber dosimeter already worn by the Reactor Branch and Reactor Materials Branch employees proved too much strain on shirt pockets (not to mention inconvenience to personnel) and it was decided to omit the "M" dosimeter during the final month of the test.

During the test almost all employees wore their film badges on their belts and the thermoluminescent and quartz-fiber dosimeters in their shirt pockets. This was not ideal, but trying to keep all the devices constantly side by side did not prove practical. It is very unlikely, for the conditions under which the employees worked, that the exposure to the midsection was significantly different from that at the chest. Because of administrative controls on the wearing of personnel-monitoring devices, it is believed that very seldom did any individual wear only a part of his complement of dosimeters. Racks were provided for overnight storage of all dosimeters, except in Building 83, where they were left on employees' desks. A DT-284, an "M" dosimeter, and a film badge were stored

Table 1A. *March Results*

Employee and Bldg. No.	Gross readings (mR)		Correction factors		Corrected readings (mR)		Corrected readings less bkg. (mR)		Quartz-fiber dosimeter readings (mR) (1)	Film badge readings (mR) (2)
	"M"	DT-284	"M"	DT-284	"M"	DT-284	"M"	DT-284		
0000–71R	27	29	0.91	1.05	26	30	3	2	5	—
0181–71R	29	33	1.01	1.20	29	40	6	12	5	—
0338–71R	37	30	0.88	1.14	33	34	10	6	—	—
0760–71R	32	27	0.88	1.09	28	29	5	1	—	—
1049–71R	27	26	0.94	1.27	25	33	2	5	5	—
1181–71R	27	24	0.90	1.13	24	27	1	−1		—
1233–71R	35	35	0.91	1.14	32	40	9	12	5	—
1511–71R	28	(3)	0.90		25		2		—	—
2127–71R	28	25	0.86	1.24	24	31	1	3	—	—
2130–71R	28	32	0.89	1.05	25	34	2	6	10	—
2155–71R	25	29	1.00	1.08	25	31	2	3	—	—
2160–71R	41	34	0.87	1.18	36	40	13	12	—	—
2170–71R	30	30	1.00	1.21	30	36	7	8	15	—
2347–71R	33	26	0.92	1.41	30	37	7	9	5	—
2471–71R	30	32	0.88	1.13	26	36	3	8	—	—
2692–71R	36	(4)	0.90	1.40	32		9		—	—
3405–71R	27	32	0.93	1.02	25	33	2	5	—	—
3413–71R	27	23	0.94	1.32	25	30	2	2	—	—
3509–71R	28	26	1.01	1.20	28	31	5	3	—	—
3581–71R	72	57	0.92	1.08	66	62	43	34	35	—
3606–71R	97	89	0.87	0.93	84	82	61	54	45	50
3673–71R	32	31	0.88	1.03	28	32	5	4	—	—
3808–71R	28	28	0.90	1.11	25	31	2	3	—	25
3941–71R	110 (8)	52		1.08		56		28	30	—
4596–71R	47	37	0.85	1.18	40	44	17	16	15	60
4768–71R	(5)	(5)							5	—
5012–71R	25	26	0.95	1.23	24	32	1	4	—	—
5055–71R	38	34	0.96	1.08	36	37	13	9	—	—
BKG–71R	30	24	0.86	1.28	26	31	3	3		—

For explanation of references (1)–(8) see page 462.

Table 1A (*continued*)

Employee and Bldg. No.	Gross readings (mR)		Correction factors		Corrected readings (mR)		Corrected readings less bkg. (mR)		Quartz-fiber dosimeter readings (mR) (1)	Film badge readings (mR) (2)
	"M"	DT-284	"M"	DT-284	"M"	DT-284	"M"	DT-284		
0138–71M	34	98	0.93	1.21	125	119	102	91	145	50
0484–71M	26	30	1.05	1.13	27	34	4	6	—	—
0890–71M	26	29	0.95	1.16	25	34	2	6	—	—
1067–71M	(5)	(5)							—	—
1117–71M	33	30	0.94	1.17	31	35	8	7	5	—
1405–71M	112	79	0.88	1.25	99	99	76	71	65	40
1429–71M	27	23	0.89	0.98	24	23	1	−5	15	—
1619–71M	52	42	0.93	1.21	48	51	25	23	30	—
1787–71M	28	28	0.96	1.23	27	34	4	6	20	—
2290–71M	26	29	0.88	1.13	23	33	0	5	—	—
2688–71M	28	29	0.85	1.12	24	32	1	4	—	—
3368–71M	44	37	0.91	1.13	40	42	17	14	10	—
3439–71M	33	62 (6)	0.85		28		5		—	—
3655–71M	28	25	0.86	1.22	24	31	1	3		—
3875–71M	33	31	0.80	0.97	26	30	3	2	—	—
4237–71M	28	28	0.94	1.15	26	32	3	4	—	—
4309–71M	27	25	0.88	1.23	24	31	1	3		—
5125–71M	(5)	(5)								—
BKG–71M	27	25	0.84	1.20	23	30	0	2		—
0114–70E	27	26	0.96	1.13	26	30	3	2		—
0117–70E	34	34	0.91	1.03	31	35	8	7		—
0136–70E	25	(3)	0.89		22		−1			—
0172–70E	52	47	0.93	1.11	48	52	25	24	30	—
0495–70E	71	62	0.85	1.14	60	71	37	43		—
0616–70E	25	(3)	0.83		21		−2			—
0777–70E	27	(3)	0.83		22		−1			—
0894–70E	31	23	0.83	1.13	26	26	3	−2		—
0949–70E	63	(7)	0.90		57		34			—
1330–70E	24	(3)	0.95		24		1			—

Table 1A (*continued*)

Employee and Bldg. No.	Gross readings (mR)		Correction factors		Corrected readings (mR)		Corrected readings less bkg. (mR)		Quartz-fiber dosimeter readings (mR) (1)	Film badge readings (mR) (2)
	"M"	DT-284	"M"	DT-284	"M"	DT-284	"M"	DT-284		
2314–70E	27	25	0.92	1.13	25	28	2	0		—
2527–70E	(5)	(5)								—
3046–71E	33	33	0.81	1.13	27	37	4	9		—
3189–70E	24	(3)	0.93		22		−1			—
3239–70E	(5)	(5)								—
4010–70E	32	31	0.88	1.08	28	33	5	5		—
4631–70E	33	29	0.87	1.07	29	31	6	3		—
BKG–70E	25	25	0.90	1.13	23	28	0	0		—
0893–5AB	28	23	0.91	1.20	25	28	1	−1		—
3873–5AB	27	31	0.92	0.99	25	31	1	3		—
BKG–5AB	28	23	0.93	1.27	26	29	2	1		—
2633–28A	27	23	0.90	1.25	24	29	0	0		—
3637–28A	28	30 (6)	0.92		26		2			—
BKG–28A	29	26	0.89	1.14	26	30	2	2		—
0359–83	32	34	0.93	1.01	30	34	6	5		40
2738–83	27	26	0.89	1.07	24	28	0	−1		—
BKG–83	32	28	0.91	0.98	29	28	5	−1		—

1. Quartz-fiber dosimeter readings are corrected for background and insulation leakage. Dash indicates no detectable reading (>5 mR); blank indicates none issued.
2. Film badge readings are less background in Building 70E. Dash indicates no detectable reading (>20 mR).
3. Dosimeter not issued.
4. Broken dosimeter.
5. Dosimeter not read.
6. Apparent malfunction of reader.
7. Dosimeter dropped during readout.
8. Dosimeter worn two months.

Table 1B. *April Results*

Employee and Bldg. No.	Gross readings (mR)		Correction factors		Corrected readings (mR)		Corrected readings less bkg. (mR)		Quartz-fiber dosimeter readings (mR) (1)	Film badge readings (mR) (2)
	"M"	DT-284	"M"	DT-284	"M"	DT-284	"M"	DT-284		
0000–71R	26	26	0.91	1.05	24	27	3	1	5	20
0181–71R	32	33	1.01	1.20	32	40	11	14	15	35
0338–71R	32	30	0.88	1.14	28	34	7	8	10	—
0760–71R	38	33	0.88	1.09	33	36	12	10	—	75
1049–71R	26	24	0.94	1.27	24	30	3	4	—	25
1181–71R	(3)	(3)								—
1233–71R	33	31	0.91	1.14	30	35	9	9	—	100
1511–71R	27	(4)	0.90		24		3		—	—
2127–71R	28	21	0.86	1.24	24	26	3	0	—	100
2130–71R	27	27	0.89	1.05	24	28	3	2	—	50
2155–71R	23	27	1.00	1.08	23	29	2	3	5	20
2160–71R	40	31	0.87	1.18	35	36	14	10	25	50
2170–71R	59	51	1.00	1.21	59	62	38	36	60	50
2347–71R	28	24	0.92	1.41	26	34	5	8	10	60
2471–71R	28	26	0.88	1.13	25	29	4	3	10	20
2692–71R	28	22	0.90	1.40	25	31	4	5	—	25
3405–71R	26	30	0.93	1.02	24	31	3	5	5	50
3413–71R	26	22	0.94	1.32	24	29	3	3	—	25
3509–71R	31	25	1.01	1.20	31	30	10	4	10	25
3581–71R	68	60	0.92	1.08	63	65	42	39	30	75
3606–71R	71	69	0.87	0.93	62	64	41	38	40	120
3673–71R	32	28	0.88	1.03	28	29	7	3	—	50
3808–71R	26	28	0.90	1.11	23	31	2	5	—	75
3941–71R	51	46	0.91	1.08	46	50	25	24	40	100
4596–71R	37	30	0.85	1.18	31	35	10	9	—	75
4768–71R	77 (5)	64 (5)	1.00	1.29	77	82	56	56	—	35
5012–71R	24	24	0.95	1.23	23	29	2	3	5	20
5055–71R	32	32	0.96	1.08	31	35	10	9	5	60
BKG–71R	28	21	0.86	1.28	24	27	3	1		—

For explanation of references (1)–(8) see page 465.

Table 1B (*continued*)

Employee and Bldg. No.	Gross readings (mR)		Correction factors		Corrected readings (mR)		Corrected readings less bkg. (mR)		Quartz-fiber dosimeter readings (mR) (1)	Film badge readings (mR) (2)
	"M"	DT-284	"M"	DT-284	"M"	DT-284	"M"	DT-284		
0138–71M	76	56	0.93	1.21	71	68	50	42	35	—
0484–71M	24	140	1.05	1.13	25	158	4	132	—	—
0890–71M	23	23	0.95	1.16	22	27	1	1	—	—
1067–71M	87 (6)	50 (5)							20	—
1117–71M	155	70	0.94	1.17	146	82	125	56	60	—
1405–71M	40	29	0.88	1.25	35	36	14	10	15	—
1429–71M	26	(7)	0.89		23		2		—	—
1619–71M	37	31	0.93	1.21	34	37	13	11	30	—
1787–71M	57	47	0.96	1.23	55	58	34	32	45	—
2290–71M	38	41	0.88	1.13	33	46	12	20	25	—
2688–71M	27	22	0.85	1.12	23	25	2	−1	—	—
3368–71M	(3)	(3)							—	—
3439–71M	28	35	0.85	1.07	24	37	3	11	—	—
3655–71M	27	21	0.86	1.22	23	26	2	0		—
3875–71M	28	29	0.80	0.97	22	28	1	2	—	—
4237–71M	23	(7)	0.94	1.15	22		1		—	—
4309–71M	26	21	0.88	1.23	23	26	2	0		—
5125–71M	(3)	(3)								—
BKG–71M	26	23	0.84	1.20	22	28	1	2		—
0114–70E	61	48	0.96	1.13	58	54	37	28		—
0117–70E	27	(3)	0.91		24		3			—
0136–70E	24	(4)	0.89		21		0			—
0172–70E	56	50	0.93	1.11	52	55	31	29	65	75
0495–70E	28	25	0.85	1.14	24	28	3	2		—
0616–70E	26	(4)	0.83		21		0			—
0777–70E	(3)	(4)								—
0894–70E	28	20	0.83	1.13	23	23	2	−3		—
0949–70E	(3)	(3)								—
1330–70E	(3)	(4)								—

Table 1B (*continued*)

Employee and Bldg. No.	Gross readings (mR)		Correction factors		Corrected readings (mR)		Corrected readings less bkg. (mR)		Quartz-fiber dosimeter readings (mR) (1)	Film badge readings (mR) (2)
	"M"	DT-284	"M"	DT-284	"M"	DT-284	"M"	DT-284		
2314–70E	24	22	0.92	1.13	22	25	1	−1		—
2527–70E	55	60	1.00	1.03	55	62	34	36		—
3046–70E	43	37	0.81	1.13	35	42	14	16		—
3189–70E	26	(4)	0.93		24		3			—
3239–70E	(3)	(3)								—
4010–70E	27	21	0.88	1.08	24	23	3	−3		—
4631–70E	(3)	(3)								—
BKG–70E	23	23	0.90	1.13	21	26	0	0		—
0893–5AB	30	31	0.91	1.20	27	37	2	7		—
3873–5AB	27	39	0.92	0.99	25	39	0	9		—
BKG–5AB	27	28	0.93	1.27	25	35	0	5		—
2633–28A	29	26	0.90	1.25	26	32	1	2		—
3637–28A	32	32	0.92	1.12	29	36	4	6		—
BKG–28A	35	30	0.89	1.14	31	34	6	4		—
0359–83	36	38	0.93	1.01	33	38	8	8		—
2738–83	38	41	0.89	1.07	34	44	9	14		—
BKG–83	85	130	0.91	0.98	77	127	52	97		—

1. Quartz-fiber dosimeter readings are corrected for background and insulation leakage. Dash indicates no detectable reading (>5 mR); blank indicates none issued.
2. Film badge readings are less background in Building 70E. Dash indicates no detectable reading (>20 mR).
3. Dosimeter not read.
4. Dosimeter not issued.
5. Dosimeter worn two months.
6. Dosimeter worn three months.
7. Broken dosimeter.

in each building on the dosimeter rack to determine the local background radiation level. The thermoluminescent dosimeters were collected and read on the same night that the film badges were collected, and were returned to the employees the next morning.

IV. INDICATED EXPOSURES

Tables IA and IB show the results of the testing program for March and April, the months during which both the thermoluminescent dosimeters were worn. The numbers shown under "Gross Readings" are the exposures indicated by the thermoluminescence readers. These readings multiplied by the "Correction Factors" give the "Corrected Readings". Included in these factors are corrections for the following:

A. *Fading of the stored thermoluminescence signal.*

Both the DT-284 and "M" dosimeters exhibit some fading of the stored thermoluminescence signal, the effect being greater in the former. This fading is shown graphically in Fig. 2. These data were obtained at NRL* with the exception of two points at 60 hr and 45 days for the "M" dosimeters (shown by "o"s), which were determined by the Belgian Army (private communication). Fading is arbitrarily taken as zero at 6 min after exposure. The fading correction factors used for the monthly thermoluminescent dosimeter readings were 1.02 for the "M" dosimeters and 1.09 for the DT-284 dosimeters.

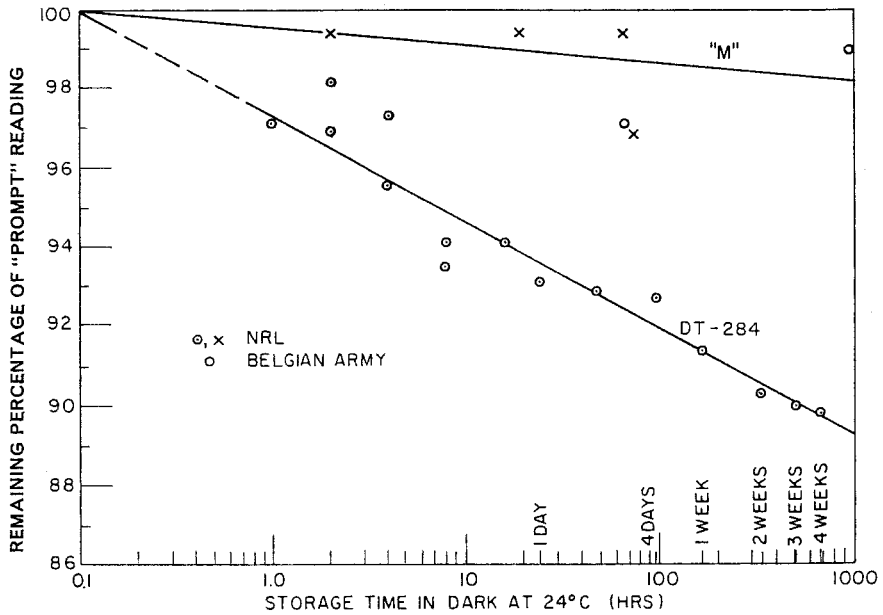

FIG. 2. Percentage of "prompt" (6 min after exposure) reading remaining vs. storage time in dark at 24°C. for thermoluminescent dosimeters. Exposures used for NRL results were 4 R, for the Belgian Army, 60 R.

B. *Difference in Dosimeter Sensitivity*

Each reading was corrected to compensate for the variation in Co^{60} γ-ray sensitivity of each dosimeter from the average of the group.

C. *Reader Calibration Error*

Both the CP-748 and the "M" readers were provided with radioactively-powered light sources

* The authors thank J. A. Pfaff of the NRL Dosimetry Branch for these fading measurements. The commercial TLD system made by the manufacturer of the Navy prototype system was used for these measurements (see Section IIA).

for maintaining constancy of reader sensitivity. In the latter reader the light source was built in. The CP-748 reader was provided with a dummy dosimeter in which the CaF_2: Mn phosphor was caused to radioluminesce continuously by a plating of Ni^{63} on the Nichrome wire filament. When the PM-tube voltage adjustments were set to give the dial readings specified by the manufacturers for the light sources provided, it was found that the thermoluminescence readings obtained with dosimeters of average sensitivity, given known exposures (< 1 R) of Co^{60} γ-rays, were incorrect. Rather than determine a different PM-tube voltage to give correct response, it was decided simply to apply the necessary correction factors: 1.04 for the CP-748 reader, and 0.88 for the "M" reader.

The product of these three component correction factors is the "Correction Factor" in column three of Tables 1A and 1B.

The results given under "Corrected Reading Less Background" are the "Corrected Readings" minus the background readings measured in Building 70E by "M" and DT-284 dosimeters. This building, a wooden structure, has the lowest radiation background of any NRL building, amounting to about 3 mR/month. The "M" and the DT-284 dosimeters read respectively about 21 and 24 mR more than this due to the presence of radioactive contamination in the dosimeter structure, a problem discussed further in Section VI.

The last two columns in Tables 1A and 1B give the quartz-fiber dosimeter readings and the film badge readings, each corrected for Building 70E background (including quartz-fiber dosimeter insulator leakage). The quartz-fiber dosimeter readings were supplied by the Survey and Evaluation Section of the Health Physics Staff, and the film-badge results were taken from the monthly computerized film-badge report prepared by the Health Physics Staff.

V. COMPARISON OF EXPOSURE READINGS

An examination of Tables 1A and 1B shows that very few significantly large exposures were received, most exposures being under 10 mR, as recorded by the TLD systems. Also it is apparent that there is relatively good agreement between the two TLD systems, and with the quartz-fiber dosimeters, but that the film-badge readings are seldom in good agreement with the other dosimeters. The "M" dosimeters agreed with the DT-284's within 10% + 6 mR almost without exception, and within 10% + 3 mR in three cases out of four. The quartz-fiber dosimeters agreed with the DT-284's within 10% + 6 mR in three-quarters of the cases. 20 mR was regarded as the minimum meaningful film reading: below that the reading was assumed to be zero. In the 31 cases where the film read ≥ 20 mR, it exceeded the DT-284 reading by 10% + 25 mR in 18 cases, and by 10% + 50 mR in 8 cases.

These observations are shown more clearly in Tables 2 and 3, and in Figs. 3 and 4. Table 2 summarizes all exposures where either TLD indicated an exposure of 10 mR or greater; Table 3 includes only cases where film readings were ≥ 20 mR. Figure 3 contains a resumé of the data given in Tables 2 and 3, plotted against the DT-284 reading on the abscissa. The histogram in Fig. 4 illustrates how closely the two TLD systems agreed, even in those instances when either dosimeter gave a net reading of $\leq$ 5 mR.

The closeness of agreement between the thermoluminescent dosimeters and the quartz-fiber dosimeters is to some extent fortuitous, considering the very low exposures and the approximate form in which the quartz-fiber dosimeter readings were recorded. It had not been intended originally to include them in this pilot study; therefore no special arrangements were made to optimize the precision of their readings. Normally the function of these dosimeters at NRL is to provide short-term control of exposures between film-badge readings. Twice a week the technician recorded the exposure (corrected for background and insulator leakage) accumulated since the previous reading, rounding the result to the nearest 5 mR. The readings given in the present tables are the sums of the readings so recorded during each month. It is conceivable, although unlikely, that rounding errors could add up to as much as 20 mR/month by this method.

Two of the rows of data given in Table 2 (indicated by arrows; employees No. 0484 and 0117 in Bldg. 71M, Table 1B) are in poorer agreement than the rest. These two employees kept their dosimeters side-by-side in the

Table 2. Summary of the Larger Exposure Readings in Tables 1A *and* 1B *(corrected reading less background* $\geq$ *10 mR on either TLD)*

"M"	DT-284	Q.F. dosimeter	Film badge
6	12	5	—
10	6	—	—
9	12	5	—
13	12	—	—
43	34	35	—
61	54	45	50
17	16	15	60
13	9	—	—
102	91	145	50
76	71	65	40
25	23	30	—
17	14	10	—
25	24		—
37	43	—	—
11	14	15	35
12	10	—	75
14	10	25	50
38	36	60	50
10	4	10	25
42	39	30	75
41	38	40	120
25	24	40	100
10	9	—	75
10	9	5	60
50	42	35	—
→ 4	132	—	—
→125	56	60	—
14	10	15	—
13	11	30	—
34	32	45	—
12	20	25	—
37	28		—
31	29	65	75
34	36		—
14	16		—
9	14		—

Table 3. Summary of Corrected Readings less Background in Tables 1A *and* 1B *for all Detectable Film Badge Readings*

Film badge	"M"	DT-284	Q.F. dosimeter
50	61	54	45
25	2	3	—
60	17	16	15
50	102	91	145
40	76	71	65
40	6	5	
20	3	1	5
35	11	14	15
75	12	10	—
25	3	4	—
100	9	9	—
100	3	0	—
50	3	2	—
20	2	3	5
50	14	10	25
50	38	36	60
60	5	8	10
20	4	3	10
25	4	5	—
50	3	5	5
25	3	3	—
25	10	4	10
75	42	39	30
120	41	38	40
50	7	3	—
75	2	5	—
100	25	24	40
75	10	9	—
20	2	3	5
60	10	9	5
75	31	29	65

dosimeter rack, and it seems possible that they accidentally exchanged "M" dosimeters. However in that case the 4 mR reading of the "M" dosimeter seems to be much too low.

Although the film-badge readings are not closely correlated with the TLD readings, the film badges did indicate some exposure in every case where either of the TLD systems indicated an exposure in excess of 50 mR. As noted before, the film badge readings generally were higher than the TLD readings in those cases where the film indicated $\geq$ 20 mR. This becomes very apparent on examination of Table 3; in a number of cases the film badge alone seems to be indicating significantly large exposures which were not detected by any of the other systems, and presumably therefore did not exist. Most of the film badge exposures occurring where the TLD systems showed no exposure were obtained in the NRL Reactor building during a period when a failure of the air con-

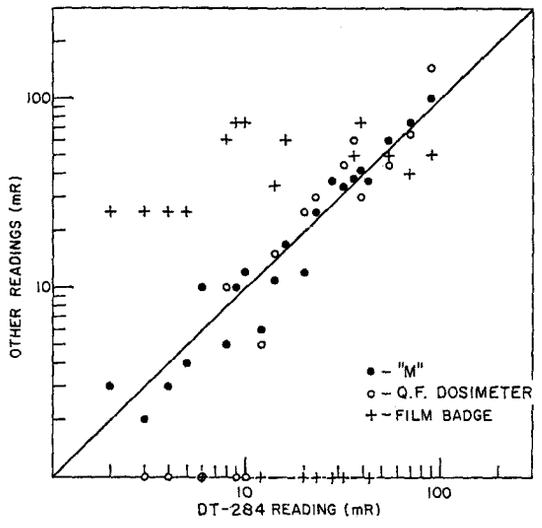

FIG. 3. Resumé of the data in Tables 2 and 3, plotted vs. the DT-284 readings. To avoid crowdings of points, only the first occurrence of each integral value of DT-284 readings is plotted.

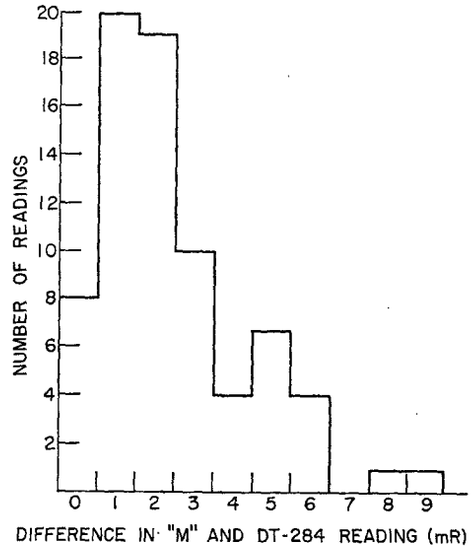

FIG. 4. Histogram of the absolute difference in corrected DT-284 and "M" readings (less background) in Tables 1A and 1B, for those cases where either value was ≤ 5 mR.

ditioning system caused temperatures to rise to 27–32°C, accompanied by high relative humidities. Clearly the film badges were at a disadvantage in these tests because of the adverse environmental conditions, which had no effect on the sealed-glass-bulb type thermoluminescent dosimeters. Better agreement with the TLD results might be expected under more moderate conditions of temperature and humidity, or by using hermetically-sealed film packs. Nevertheless, these tests reveal the extent of the errors which can occur with ordinary film badges in unfavorable environments.

VI. BUILT-IN RADIOACTIVITY OF DOSIMETERS

As can be noted in Tables 1A and 1B, background readings of the TLDs are on the order of 22–25 mR per month. This is primarily due to radioactive materials unintentionally built into the dosimeters. In an effort to determine the amount of this built-in background, dosimeters were stored in a low-background room at the Naval Medical Research Institute, Bethesda, Maryland. The background in this shielded room is negligible compared to ambient background. Dosimeters were stored singly and in groups of five for 135 days (6/18/65 –11/1/65) and read out promptly thereafter. The results of this test are shown in Table 4. All readings have been corrected for variations in individual γ-ray sensitivity of the dosimeters, reader error, and fading. Fading correction factors of 1.02 and 1.12 respectively were used for the "M" and DT-284 dosimeters. The results thus obtained for built-in background exposure agree with others previously determined in the low-background room for a one-month storage period, where fading correction factors of 1.02 and 1.09, respectively, were used. Note that the "M" dosimeters showed the lowest internal-source reading (21 mR/mo) followed by the DT-284 (24 mR/mo) and the commercial equivalent of the DT-284 (27 mR/mo).

In an attempt to identify the radioactive materials in the dosimeters, several dosimeters were taken apart and the glass and phosphor from a single dosimeter granulated and counted separately on a Geiger-Müller and a windowless gas-flow counter. The results of this test are

Table 4. Readings of Dosimeters Stored in Low-Background Room for 137 Days (6/18/65-11/1/65)

Type	Dosimeter number	Corrected reading	Exposure rate
		(mR)	(mR/mo)
"M"	7612 (Single)	87	19
	7605	100	22
	7607	91	20
	7602	94	21
	7624	95	21
	Average	93	21
DT-284	(Single not read)		
	A40	103	23
	A43	105	23
	A24	111	24
	A12	110	24
	Average	107	24
Commercial (Similar to DT-284)	B815 (Single)	131	29
	576	125	27
	A711	125	27
	C43	125	27
	B637	125	27
	Average	126	27

shown in Table 5; they indicate that both the DT-284 phosphor (+ binder) and glass are definitely contaminated. The binder used to hold the CaF_2: Mn on the filament in the DT-284 is potassium silicate; thus the K^{40} is probably responsible for the contamination in that case. The similar commercial model dosimeter is slightly more contaminated than the DT-284, in agreement with the low-background-room readings. The "M" phosphor (+ binder) shows only slight if any contamination, but the glass envelope indicates almost twice as much beta contamination as does the DT-284 glass.

The nuisance of having a relatively large background due to built-in contamination is alleviated somewhat, at least in the case of the DT-284 dosimeters*, by the fact that they respond individually to this contamination approximately in proportion to their response to external γ-radiation. Consequently the built-in background reading accumulated per unit time need not be determined for individual dosimeters. This was demonstrated by comparing the readings obtained after storing 50 DT-284 dosimeters for three months, with those resulting from an 80-mR γ-ray exposure. Figure 5 shows the results of this test. The distribution of the dosimeters' background readings (unshaded histogram) shows a standard deviation of 9.6% which is in agreement with the standard deviation (9.4%) of the 80-mR external γ-ray exposure readings. When the background readings were individually divided by the corresponding external radiation readings, the resulting distribution was reduced to 4.3% S.D. (see shaded histogram, Fig. 5). The readings of an individual dosimeter repeatedly exposed to

* The "M" dosimeters were not given this test because of termination of the loan period of that system.

Table 5. Built-in Radioactivity of Thermoluminescent Dosimeters

Sample	Net count rate (c.p.m.)	
	Geiger counter	Gas flow counter
DT-284 Phosphor + Binder	0.4 ± 0.5	3.3 ± 1
Commercial Model Phosphor + Binder (similar to DT-284)	1.2 ± 0.5	4.3 ± 1
"M" Phosphor + Binder	0.0 ± 0.5	1.3 ± 1
DT-284 Glass Envelope	1.8 ± 0.5	16 ± 2
Commercial Glass Envelope (similar to DT-284)	2.5 ± 0.5	17 ± 2
"M" Glass Envelope	2.8 ± 0.5	31 ± 2

80 mR of γ-rays show a standard deviation of 2.8%, which would probably be the same for repeated background exposures to 80 mR, if such a measurement were feasible. The theory of propagation of errors predicts a distribution with a standard deviation of 4.0% for the ratio of background to γ-ray readings, in good agreement with the 4.3% value obtained. This verifies that the individual DT-284 dosimeters give readings due to built-in radioactivity which are nearly proportional to their γ-ray sensitivities.

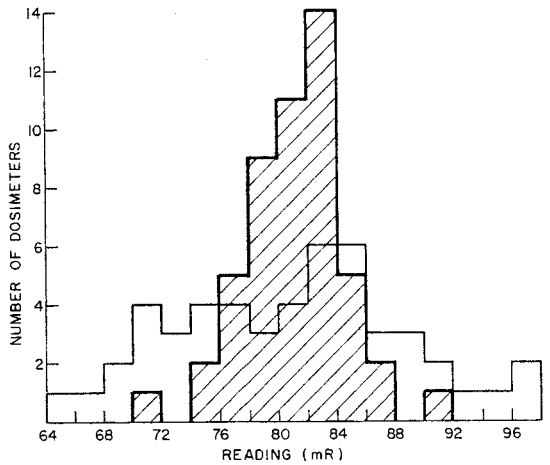

FIG. 5. Histogram (unshaded) of the background distribution of 50 DT-284 dosimeters stored for three months, and (shaded) the distribution of the ratio of background reading to that resulting from an 80 mR Co^{60} γ-ray exposure, multiplied by 80 mR for scale normalization. The standard deviations of the two distributions are 9.6% and 4.3% respectively.

Thus, for purposes of data processing, the built-in background can be treated the same as if it were natural ambient background.

VII. MECHANICAL OPERATION OF THE TLD SYSTEMS

What has been said about the two systems previously [1, 2] was in general confirmed during this test. The "M" system functioned without mechanical failure except for a broken clip on one dosimeter. No "M" dosimeters were broken during the test, and it was possible to obtain a reading for every dosimeter. Difficulty in opening the dosimeters was the most bothersome aspect of the "M" system. There was no detectable change in the response of the "M" dosimeters for the duration of the experiment.

Three DT-284 dosimeters could not be read because of broken bulbs, and two readings were questionable because of apparent malfunction of the reader. In addition, two dosimeter cases were broken by the wearers, and one had to be destroyed in order to remove the jammed detector. At the end of the test, several dosimeters showed apparent flaking of the phosphor from the heating coil, but not enough to cause a detectable change in calibration.

VIII. CONCLUSIONS

The fact that the two independent thermoluminescent dosimetry systems (when properly corrected) agreed so closely with one another, and generally with the quartz-fiber dosimeter results as well, seems to indicate that they were measuring the true exposures with greater accuracy than were the film badges. The latter were operating under the considerable handicap that they were not hermetically sealed against a warm, high-humidity environment, but conditions approaching this are not atypical of Washington in the summer months.

Further comparative testing is underway with the commercial model (made by the manufacturer of the DT-284 and CP-748 system) which is more reliable mechanically inasmuch as it does not contain the auto-identification feature, and uses electronic rather than mechanical range-changing. The results of these tests will be reported later.

The problem of built-in radioactivity in the thermoluminescent dosimeters, which is probably the limitation on minimum detectable exposure at present, can certainly be eliminated in later models. For example, hot-pressed pellets of CaF_2: Mn containing no binder have recently been developed and are now commercially available. The use of one of these in place of the present coil-type element, properly mounted in a non-radioactive glass envelope, should eliminate both the built-in background and the phosphor-chipping problem. Extruded rods and hot-pressed wafers of LiF (TLD-100) have also recently become available, so that the

advantage of having the phosphor in a bulk, solid form will not be limited to CaF_2: Mn.

In conclusion one can say that although the thermoluminescent dosimeters used in the present tests out-performed the film badges, it nevertheless seems premature to replace the film badges for NRL personnel monitoring at this time. Current developments in the packaging of thermoluminescent phosphors indicate that considerable additional improvements in their performance may be expected in the immediate future. Moreover some composite dosimeter, perhaps incorporating both high and low-Z phosphors, may be necessary to retain the capability of estimating the γ-ray effective energy,[4] especially for monitoring at an establishment like NRL, which has such a wide variety of radiation sources. Alternatively a single thermoluminescent dosimeter, designed to have a response vs. energy which is proportional to the absorbed dose in specific critical organs, might suffice in some cases.[5]

REFERENCES

1. S. G. Gorbics and F. H. Attix. Brief evaluation of the U.S. Navy prototype thermoluminescent dosimeter system: Computer Indicator, Radiac, CP-748 (XN-1)/PD and Detector, Radiac, DT-284 (XN-1)/PD. NRL Test and Evaluation Report No. 37, 1964.
2. T. L. Johnson and S. G. Gorbics. NRL Test and Evaluation Report No. 58, 1965.
3. R. J. Ginther and R. D. Kirk. Thermoluminescence of CaF_2: Mn and its application to dosimetry. Report of NRL Progress, Sept. 1956, p. 12.
4. W. A. Langmead (1967). The place of luminescence dosimetry in the control of occupational hazards of ionizing radiation. *Proc. International Conference on Luminescence Dosimetry*, U.S.A.E.C., CONF-650637.
5. F. H. Attix. Must personnel dosimeters also serve as γ-ray energy spectrometers? *Health Physics 13*, 219 (1967).

EXPERIENCE WITH A NEW THERMOLUMINESCENCE METHOD FOR FINGER AND HAND DOSIMETRY EMPLOYING LITHIUM FLUORIDE-TEFLON DOSIMETERS

BENGT E. BJÄRNGARD and DOUGLAS JONES
Radiation Physics Division, Controls for Radiation, Inc., Cambridge, Massachusetts, U.S.A.

Abstract—A new type of finger and hand dosimeter has been designed which consists of a solid, flexible disc of thermoluminescent LiF incorporated in polytetrafluoroethylene (Teflon) enclosed in black polyethylene covering (7 mg/cm² thickness) which is attached to an adhesive tape. The thickness of the polyethylene has been selected to simulate the radiation insensitive layer of the skin. Precision of the dosimeters has been evaluated for gamma and beta irradiation. Ten millirads can be measured with a standard deviation of better than ±20% without individual calibration of the dosimeters. Effects contributing to background such as light sensitivity, mechanical shock and friction have been studied. It is concluded that these dosimeters offer the prospect of reliable routine finger and hand dosimetry with results that can be directly related to the biologically significant dose.

FINGER and hand dose measurements have presented a serious and largely unsolved problem in routine personnel dosimetry. The particular difficulty is that the maximum dose to the finger and hand has to be estimated in an unpredictable radiation field with perhaps very steep dose gradients, and that this estimate must be based on a measurement technique which does not interfere with the monitored persons ability to perform delicate manipulations.

To illustrate the type of dose patterns that can occur, doses at several points on the fingers, palm, and wrist of a person holding a radium needle inside a plastic tube have been measured using LiF-Teflon thermoluminescent dosimeters. As shown in Fig. 1, the maximum dose was 560 mrad on the thumb, while ring and wrist dosimeters showed less than 2% of this. In a similar experiment, illustrated in Fig. 2, a plate of natural uranium was placed on a water-filled glove, simulating a hand. The tips of the fingers in immediate contact with the plate received almost 100% of the dose measured on the surface of the plate, while the ring dosimeters showed less than 0.2%.

It is evident from these experiments that a realistic estimate of the maximum dose to the hand in similar situations can seldom be made unless measurements are actually made where the maximum exposure can be expected, usually on the finger tips.

Consequently the conventional technique for finger and hand dosimetry, i.e. to use photographic film as ring or wrist dosimeters, is of little or no value. As a new approach, Johns[1] used loose thermoluminescent LiF phosphor in plastic sachets, which were fixed to the fingertips. Recently, Portal[2] assessed existing finger dosimetry techniques and also advocated the use of LiF thermoluminescence for this purpose. Both authors based their judgement mainly upon the properties of LiF, being essentially energy independent for X- and gamma-radiation, the wide range of measurable doses with some tens of mrads as the smallest detectable dose, the ease and speed with which the dosimeters can be read out, and the flexibility of a practical system in routine as well as emergency situations.

Our work has been directed toward maximizing the usefulness and technical capability of the TLD technique in finger and hand dosimetry. The objectives of our work, which is

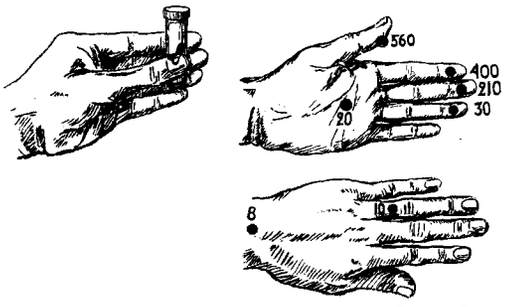

FIG. 1. Doses in mrad at various points after holding a 1 mg radium needle, as shown, for 5 min.

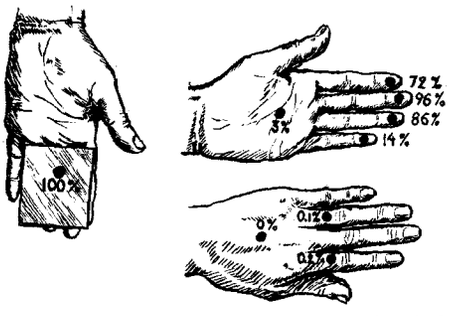

FIG. 2. Doses recorded on the hand after holding a plate of natural uranium as shown. The doses are expressed as a % of the dose at the surface of the uranium plate.

still in progress, have been to design a convenient, technically reliable dosimeter and to evaluate its operational value.

The dosimeters which were developed are illustrated in Fig. 3. The radiation sensing component is a disc, 12.5 mm diameter by 0.4 mm thick, consisting of 28 mg of thermoluminescent LiF uniformly incorporated in polytetrafluoroethylene (Teflon).[3] This disc is contained in a light-proof polyethylene pouch, 7 mg/cm² thick. The pouch is, in turn, fastened to a strip of adhesive tape for attachment to the skin. In situations where low energy photon or beta radiation is encountered, a minimum cover over the disc is essential, and the adhesive tape is fastened only to the ends of the pouch, resulting in a covering thickness of 7 mg/cm². When a thicker cover can be tolerated, the adhesive tape, 30 mg/cm² thick, can be allowed to extend over the pouch.

After exposure the LiF-Teflon discs were measured in a standard Controls for Radiation, Inc. readout instrument, in which the thermoluminescence light is integrated during a 15 sec readout cycle. Nitrogen flush has been employed during readout.[4, 5]

The LiF-Teflon disc responds to the energy deposited by the ionizing radiation within its volume. If the disc is covered with 7 mg/cm² and since it is itself 90 mg/cm² thick, the response of the disc is a measure of the energy absorbed in a layer at a depth between 7 and 97 mg/cm². The biologically important dose is usually taken to be that to the thin basal layer at 7–10 mg/cm² depth. As long as there is no significant dose gradient between 7 and 97 mg/cm² depth, the measured value in the LiF-Teflon disc will correspond to the dose to the basal layer. This is usually the case for X- and gamma-radiation. Insufficient electron equilibrium may in certain cases complicate interpretation of measured data, but otherwise the close tissue equivalence of the composition of LiF-Teflon ensures a simple relation between the dosimeter response and the dose to the basal layer.

The energy dependence of LiF has been calculated[6, 3] and to some extent also studied with monoenergetic radiation.[7] The two methods agree reasonably well. However,

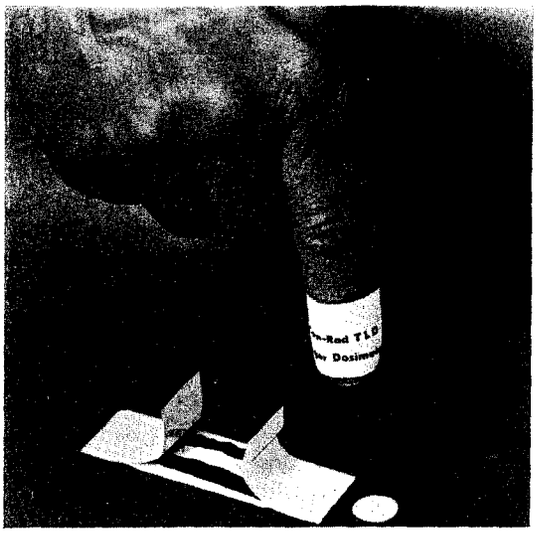

FIG. 3. The Con-Rad Finger Dosimeters.

Naylor[8] has reported an anomalous energy dependence for LiF. He attributes this effect to the relative efficiency of various photon energies in creating traps. We have not observed this effect for exposures below 100 R. Above this dose the effect is significant but small.

For beta and electron radiation, the thickness of the discs is not negligible. 7 mg/cm^2, the thickness of the radiation insensitive surface layer of the skin as well as of the plastic pouch, corresponds to the maximum range of an electron of about 60 keV energy. Electrons of less energy are therefore hardly of interest. 300 keV electrons have a maximum range corresponding to the thickness of the disc. In the region between these energies, the interpretation of measured values will be difficult and the average dose measured by the discs will be less than the dose to the basal layer. Further calculations are needed to clarify these conditions, as for example, were made by Casnati and Breuer for skin contamination.[9]

For still higher electron energies, the response becomes easier to interpret. In the very important case of natural uranium, the average dose in the discs is about 80% of the dose to the basal layer as estimated from previously published data.[3]

The precision of dose measurements with these dosimeters without individual calibration has been measured by exposing a number of dosimeters to known doses of ^{60}Co radiation. The results presented in Fig. 4 show that measurements down to 10 mR are possible. At this exposure the standard deviation in the set of 20 data was less than $\pm$ 20%. The standard deviation decreases with increasing dose. Our experience from production control is that the standard deviation of the sensitivity in a production batch approaches $\pm$ 3% for exposures above 3 R.

These experiments were conducted in the laboratory under controlled conditions. At 20 mR, the signal due to the irradiation is 40%

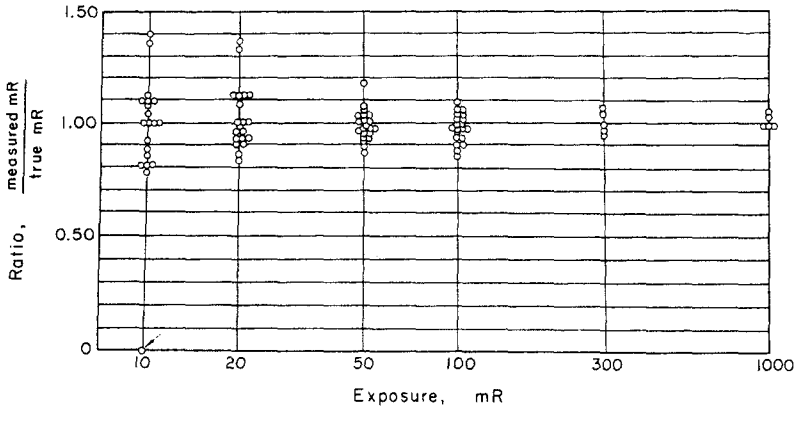

FIG. 4. The precision of dose measurements using LiF-Teflon discs 12.5 mm diameter by 0.4 mm thick.

of the gross value. The background consists of the photomultiplier dark current which is about 40%, and a component which we have called "spurious thermoluminescence" which is the remaining 20%. This latter component is also present in unirradiated dosimeters and is responsible for almost 80% of the *variation* in a set of measurements of 20 mR. The results of an investigation of some possible causes for this effect are described below.

The sensitivity of the dosimeters to mechanical shock was studied by dropping a hammer onto the LiF-Teflon discs. A signal equivalent to about 10 mR was induced after a dosimeter had been hit 300 times by a hammer dropped through 3 cm. Clearly, the dosimeters are

practically insensitive even under these extreme conditions. The possibility that friction could produce tribo-thermoluminescence was investigated by violently agitating dosimeters in a black plastic box on a shaking machine. The results obtained show a slight response to shaking. Here a signal equivalent to about 5 mR was induced after the box had been shaken about 5000 times and 20 mR after shaking 30,000 times. The conclusion must be that mechanical disturbance plays only a small role in the practical use of these dosimeters.

following the annealing. The reason for this is not known at present.

The conclusion of these experiments is that unirradiated dosimeters should be included in any measurement series for background determination.

In conclusion, these dosimeters fulfill practically all the requirements for finger and hand dosimetry. The most serious drawback is associated with the inherent problems in any measurement of beta and electron dose to a very thin layer. Compared to photographic film dosimeters, the dosimeters have the

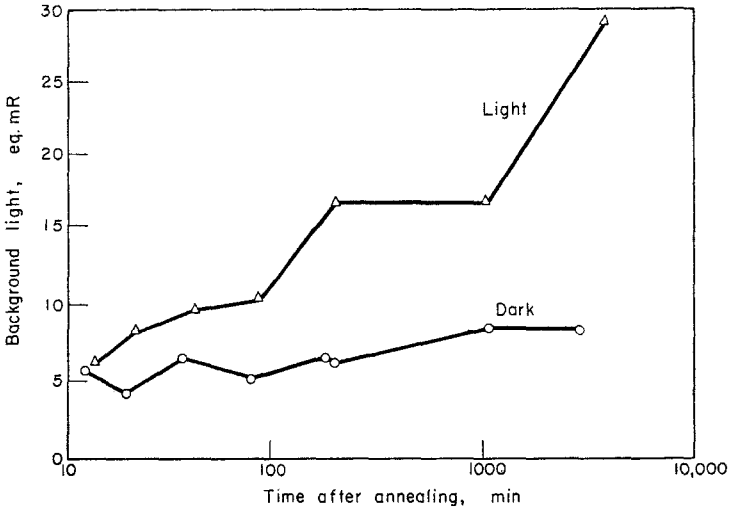

FIG. 5. The appearance of thermoluminescence following annealing in LiF-Teflon discs which have been kept in darkness or exposed to normal laboratory fluorescent light.

Another possible cause for the spurious thermoluminescence is excitation by light, which has been reported previously for LiF.[3, 10] Dosimeters exposed to normal fluorescent laboratory light exhibit a definite light sensitivity as shown in Fig. 5. Experience with ultraviolet radiation suggests that it is this component of the light that is responsible for the excitation. Light is, however, efficiently excluded by the use of the light-proof pouches into which the LiF-Teflon discs are packed in subdued light. The data in Fig. 5 indicate a slight increase in the signal from dosimeters stored in the dark

advantages of being capable of at least the same precision, of having a vastly superior energy dependence for X- and gamma-radiation which leads to better accuracy, and of allowing the monitored person to comfortably and conveniently wear dosimeters where meaningful doses will be recorded, i.e. on the finger tips, without interfering with his work. The ease and speed of readout result in a versatile and adaptable monitoring procedure, a condition that must be fulfilled before finger and hand dosimetry assumes the place in health physics which its importance justifies.

REFERENCES

1. T. F. JOHNS. AEEW-R408 (1964).
2. G. PORTAL. Bague dosimetre au fluorure de lithium thermoluminescent. Presented at Congress International sur la Radioprotection dans l'Utilisation Industrielle des Radioelements, Paris, 1965.
3. B. E. BJÄRNGARD, R. C. MCCALL and I. A. BERSTEIN. Lithium fluoride-Teflon thermoluminescence dosimeters. *Proc. Int. Conf. Luminescence Dosimetry*, p. 308, USAEC CONF-650637 (1967).
4. R. C. FIX and R. C. MCCALL. A sensitive LiF dosimeter for routine beta and gamma personnel monitoring. Presented at Health Physics Society Annual Meeting, Cincinnati, 1964.
5. V. SVARCER and J. F. FOWLER. Spurious thermoluminescence and tribothermoluminescence in lithium fluoride dosimetry powder. *Proc. Int. Conf. Luminescence Dosimetry*, p. 227, USAEC CONF-650637 (1967).
6. B. C. CLARK and J. F. JANNI. X-ray absorption in dose-equated material. WL-TR-64-134 (1965).
7. R. W. HARDIE and G. W. R. ENDRES. Hanford Status Report HW-84398 Oct. (1964).
8. G. P. NAYLOR. *Phys. Med. Biol.* **10,** 564 (1965).
9. E. CASNATI and F. BREUER. *Proc. IAEA Symp. Personnel Dosimetry For Radiation Accidents*, p. 525, Vienna, 1965.
10. J. LIPPERT and V. MEJDAHL. Thermoluminescence readout instrument for measurement of small doses. *Proc. Int. Conf. Luminescence Dosimetry*, p. 204, USAEC CONF-650637 (1967).

A METHOD OF ASSESSMENT OF WHOLE BODY INTEGRAL DOSE FOLLOWING ACCIDENTAL RADIATION EXPOSURE FROM AN EXTERNAL MOVING SOURCE

W. A. LANGMEAD
Radiological Protection Division, Authority Health and Safety Branch,
U.K.A.E.A., Harwell, Didcot, Berkshire

and

S. M. B. HILL
Health and Safety Division, Dounreay Experimental Reactor Establishment,
Thurso, Caithness, Scotland

Abstract—The dosimetry requirements following an accidental exposure of personnel to external radiation at an establishment of the U.K. Atomic Energy Authority are reviewed; in general the required information falls into two categories involving two distinct operations separated in time.

There is an immediate need for dose data which will enable decisions to be taken regarding the appropriate medical treatment, if any, to be given to the exposed persons. Such dose data is usually obtained from the processing and evaluation of personnel films which were worn on the exposed person's body. At a later stage more refined determinations of absorbed doses received by critical organs of the body are required for record purposes and for medico-legal reasons.

An important dose parameter which may be considered in this latter category is the integral dose to the whole body, defined as:

$$\text{Integral dose} = \int_{M} D.dm$$

where D is the absorbed dose in rads received by a mass element, dm, of the body, the product $(D.dm)$ being integrated over the whole mass, M, of the body. The reasons for the importance of this function are discussed and a method for its determination is described, employing the so-called "reciprocity dose theorem" and taking as example a case of an accidental exposure at one of the Authority's establishments.

The report concludes with an assessment of the accuracy of the determination and a discussion of the limitations of the method.

1. INTRODUCTION

Whenever a person is accidentally exposed to external radiation such that there is a possibility that the maximum permissible doses recommended by I.C.R.P.,[1] or their national equivalents, have been exceeded, there is a requirement for dose information which falls into two categories. Two distinct operations, separated in time, are usually necessary for the determination of these two categories of information.

There is an immediate need for dose data which will assist in making decisions regarding the appropriate medical treatment, if any, to be given to the exposed person. Such data may usually be obtained from the processing and evaluation of films and/or other dosimetric devices worn on the exposed person's body. If fast neutron irradiation has occurred, the measurement of activation products in the body, such as blood–^{24}Na or ^{35}S in the hair, or in

articles carried upon the person, such as ^{64}Cu or ^{58}Co in coins,[2] may result in sufficiently precise estimates of dose to assist with the early planning of medical care.

At a later stage, however, more refined determinations of the absorbed doses received by critical organs of the body are required for record purposes and for medico-legal reasons. These determinations may involve measurements in body phantoms in sometimes elaborate reconstructions of the circumstances of the accident.[3, 4] The experimental dosimetry procedures undertaken will be determined by the nature of the accidental exposure and the critical organs involved. An important dose parameter which may be required is the integral dose to the whole body defined in equation (1):

$$\text{Integral dose to whole body} = \int^{M} D.dm \text{ gram-rad} \quad (1)$$

where D is the absorbed dose in rads received by a mass element, dm, of the body, the product $(D.dm)$ being integrated over the whole mass, M, of the body.

It is the purpose of this paper to indicate briefly the relevance of this quantity and the associated concept of "average" dose to the body, and to describe a method for their experimental determination which has been applied with success in the Atomic Energy Authority in a gamma-radiation exposure of two men who accidentally handled an irradiated reactor fuel element.

2. WHOLE BODY EXPOSURE AND "AVERAGE" DOSE TO THE BODY

In the Report of the International Commission on Radiological Protection,[1] a distinction is drawn between the more or less uniform irradiation of the whole body and irradiation which is limited to portions of the body. In the former case the critical tissues are the red bone marrow and the gonads, but where only parts of the body are irradiated, the critical tissue must be assessed from a consideration of where permanent damage is most likely to arise.

It is therefore of importance to determine in the case of an over-exposure whether substantially uniform whole body irradiation has taken place or whether the irradiation is significantly non-uniform. The information provided by a single detector such as a film badge can be highly misleading in this regard and, whilst rough estimates of the dose inhomogeneity may be made from a consideration of the geometrical relationship of the radiation source and the irradiated person's body, it is suggested that a more revealing parameter, when related to the surface skin dose, is the "average" dose to the body defined as:

$$\text{"Average" dose} = \frac{1}{M} \times \text{integral dose} \quad (2)$$

Recently it has been suggested that certain aberrations in the structure of the chromosomes of circulating blood cells are related to the radiation absorbed doses received by the cells.[5, 6] Such a biological indicator of absorbed dose would be helpful in the dosimetry of over-exposed persons and, in the absence of information as to the individual doses to the affected cells, the parameter most likely to correlate with the observed chromosome damage would be the average dose to the body.

For these reasons the average doses to the bodies of the two men who had been accidentally irradiated were determined using the "reciprocal dose" relationship.

3. THE RECIPROCAL DOSE THEOREM

It has been pointed out by Mayneord[7] that theorems relating to reciprocity between radiation from a point and a finite volume have been given over fifty years ago by King[8] and are well known in meteorology.[9] A more general treatment in which both radiation source and absorbing medium are finite may be applied in the determination of average and integral dose to the body.

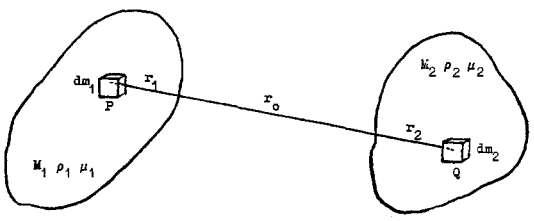

Consider a body of mass M_1 being irradiated by another body of mass M_2 filled with gamma radiating material having specific activity, ρ_2 mCi/g of material. Let the effective linear absorption coefficients of the materials of M_1 and

M_2 be μ_1 and μ_2 respectively for the radiation and geometry considered. Then d_p, the dose rate at P due to radiation emanating from the mass element dm_2, may be written:

$$d_p = \Gamma . \frac{\rho_2 . dm_2}{(r_1 + r_0 + r_2)^2} \exp [- (\mu_1 r_1 + \mu_2 r_2)]$$

where Γ is the specific gamma-ray constant for the radiation.

The dose rate at P due to the total activity in M_2 is given by:

$$D_p = \Gamma . \rho^2 \int^{M_2} \frac{\exp [- (\mu_1 r_1 + \mu_2 r_2)]}{(r_1 + r_0 + r_2)^2} dm_2 \quad (3)$$

From equation (1), the integral dose rate, I_1 in M_1 is

$$I_1 = \int^{M_1} D_p . dm_1 = M_1 . \bar{D}_1 \quad (4)$$

where $\bar{D}_1$ is the average dose rate in M_1.

Hence:

$$I_1 = \int^{M_1} \Gamma . \rho_2 \int^{M_2} \frac{\exp [- (\mu_1 r_1 + \mu_2 r_2)]}{(r_1 + r_0 + r_2)^2} dm_2 . dm_1$$
$$= M_1 . \bar{D}_1 \quad (5)$$

If it is now supposed that M_2 is irradiated by M_1 filled with the same type of radiating material of specific activity, ρ_1 mCi/g of material, then by a similar argument, provided that μ_1 and μ_2 can be assumed to have the same values as previously, the integral dose rate I_2 in M_2 is:

$$I_2 = \int^{M_2} \Gamma . \rho_1 \int^{M_1} \frac{\exp [- (\mu_1 r_1 + \mu_2 r_2)]}{(r_1 + r_0 + r_2)^2} dm_1 . dm_2$$
$$= M_2 . \bar{D}_2 \quad (6)$$

Hence:

$$\bar{D}_1 . M_1 . \rho_1 = \bar{D}_2 . M_2 . \rho_2 \quad (7)$$

or

$$\bar{D}_1 . A_1 = \bar{D}_2 . A_2 \quad (8)$$

where A_1 and A_2 are respectively the total activities of the radiating material in M_1 and M_2.

4. METHOD OF APPLICATION OF RECIPROCAL DOSE THEOREM

The accident used to illustrate the application in practice of the reciprocal dose theorem, involved the removal from behind shielding of an irradiated reactor fuel element and its subsequent handling by two men in the belief that the element was unirradiated. For the purposes of this paper attention will be focussed on subject A who first handled the element. In its motion vertically upwards from its shielding, the element moved parallel to A's body, and for most of the time of his involvement which was less than three seconds, the axis of the element was no more than 5 cm from the surface of his body. A's film badge, which was worn on the left breast of his overalls, showed on assessment a dose of 27 rad of penetrating gamma radiation.

The experimental procedures described below have been used to determine the average dose to A's body from its irradiation by the fission product source. This has been achieved by interchanging the source and absorbing body and determining instead the average dose at positions occupied by the fuel element source from a radiation source of similar size and shape to A's body. The procedure may be summarized as follows:

(i) the motion of the fuel element relative to A is represented by a number of stationary positions of the element each with an appropriate irradiation time;

(ii) measurements of dose rates around the fuel element fission product source enable a number of unshielded ^{137}Cs point sources in a certain linear arrangement to be specified which give a dose rate distribution in air similar to that measured for the fission product source;

(iii) measurements of dose rates around a hollow man phantom filled with a ^{137}Cs solution enable dose rates to be interpolated at each of the ^{137}Cs source points referred to in (ii) for each of the stationary positions of the transformed fuel element referred to in (i);

(iv) by multiplying the dose rates so determined by the appropriate irradiation times and summing the resulting doses, a value is obtained from which the average dose to A's body may be calculated as shown in Section 5.

Thus, four separate but inter-related studies were made:

(a) the taking of a cine film to enable a reconstruction of the incident in time and space;

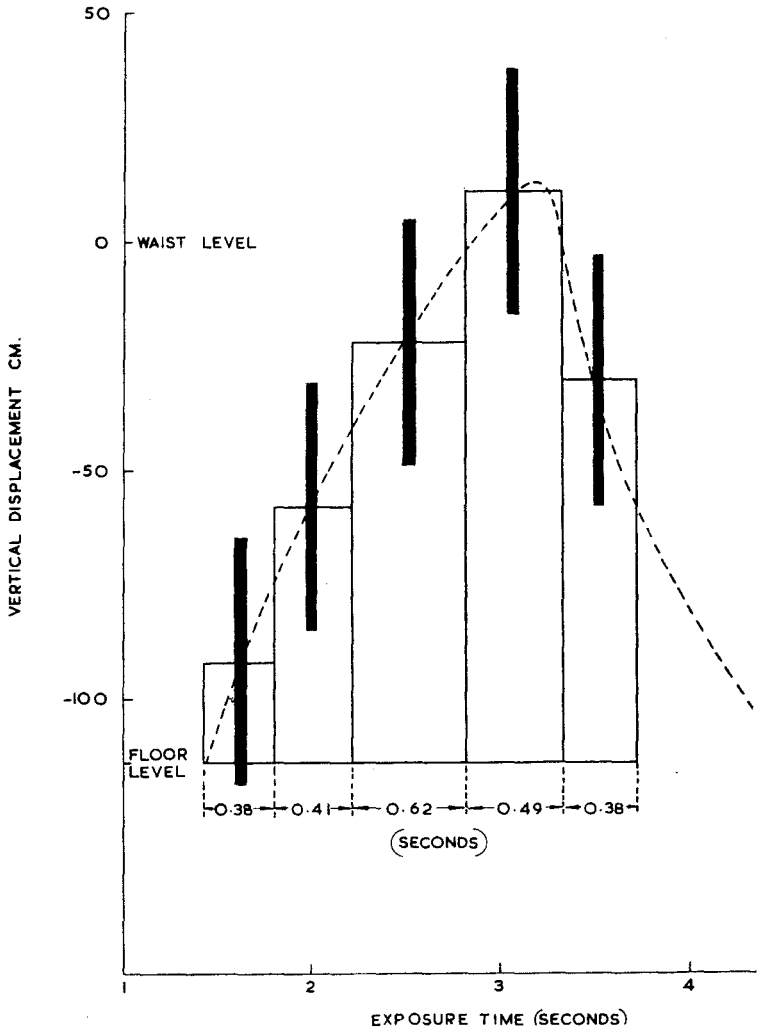

FIG. 1. Vertical displacement of fuel element as a function of exposure time.

(b) the measurement of dose rates in air around an identical reactor fuel element having closely similar irradiation history and cooling time, and the determination of isodose lines;

(c) the calculation of the number of ^{137}Cs point sources, their activities and their relative positions to give a similar isodose distribution as the fuel element;

(d) the measurement of dose rates around a hollow man phantom filled with 100 mCi $^{137}CsCl_2$ solution.

4.1. *Cine film study*

The two men involved in the accident were filmed in the process of handling an inactive fuel element as nearly as possible in the same manner as previously used in handling the irradiated element. A number of runs of the episode were filmed and from a study of the rate of change of position of the fuel element relative to subject *A*'s body, it was possible to define five representative positions in which the element could be considered stationary for certain fractions of the total exposure time. In

this way the irradiation of *A*'s body by the moving source was broken down into the sum of the irradiations from five stationary sources.

Figure 1 shows the vertical displacement of the element as a function of time during the period when significant irradiation of *A*'s body was taking place. The positions of the five stationary sources and the method of determining the fractions of the total irradiation time from the step-function which most closely fits the observed displacement-time curve is also shown in Fig. 1. The five source positions relative to *A*'s body are shown schematically in Fig. 2.

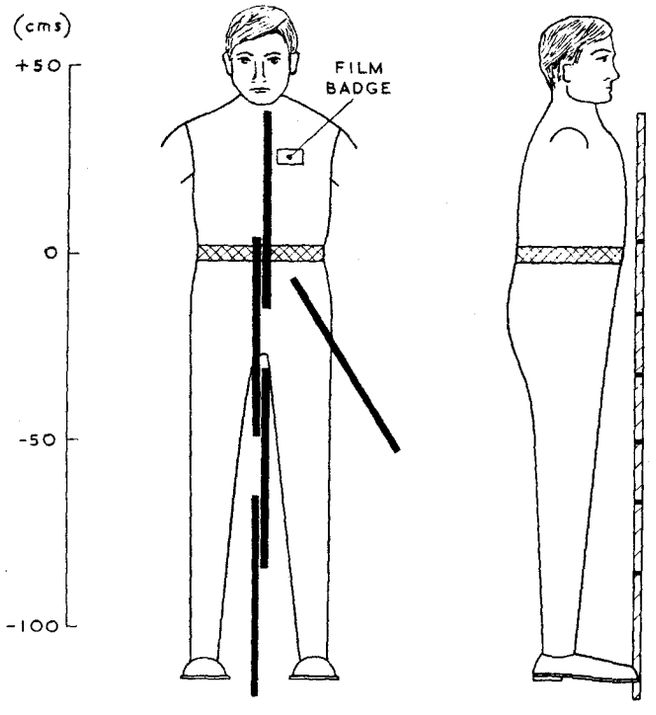

FIG. 2. Positions of fuel element relative to operator.

4.2. *Dose rate distribution around irradiated fuel element*

Dose rate measurements were made at a large number of points around a fuel element having the same irradiation history and cooling time as the element which had been concerned in the accident. Owing to the very high dose rates involved, all measurements were made inside a shielded cell, the Baldwin "Ionex" dosemeter probe being moved relative to the fuel element by means of a remotely operated, powered manipulator. Figure 3 shows the general arrangement inside the cell. The fuel element was clamped vertically and a reference grid, shown in close-up in Fig. 4, used to assist in the accurate positioning of the small ion chamber at known distances from the surface of the element can.

By interpolation between dose rates measured at intersections of the grid, isodose lines were drawn in a plane containing the axis of the fuel element. Figure 5 shows such a set of isodoses. A noticeable feature of the distribution is the rapid fall-off in dose rate beyond the end of the uranium fuel element within its steel can.

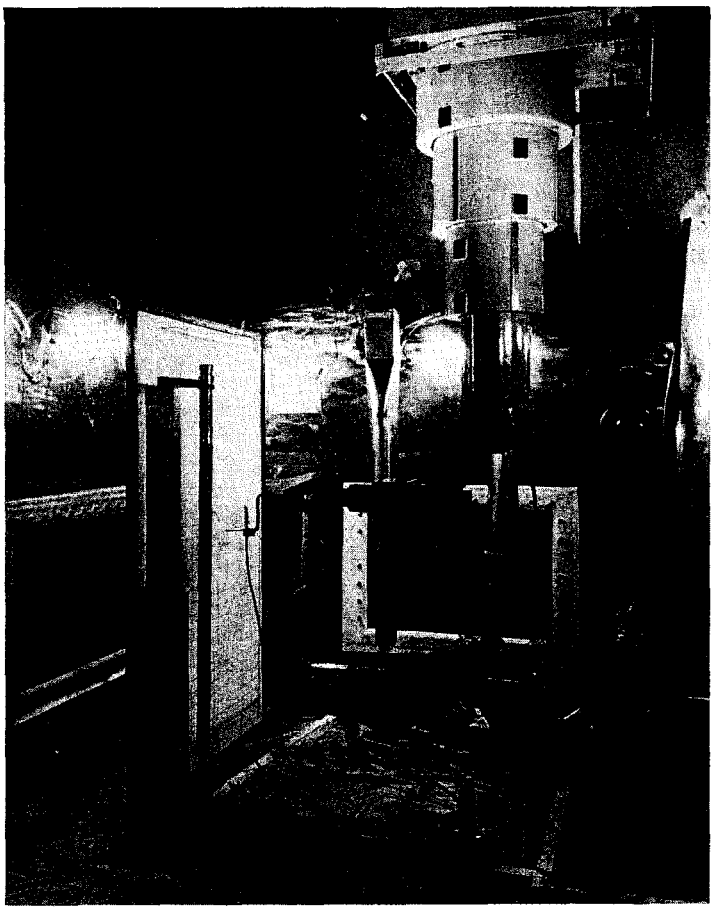

FIG. 3. Experimental arrangement showing fuel element can in vertical position with the Baldwin-Ionex probe held in power manipulator traversing reference grid.

4.3. *Equivalent ^{137}Cs fuel element*

In order to remove the complications inherent in applying the reciprocal dose theorem to a self-absorbing mixed fission product source, it was convenient to assume a small number of unscreened point sources of a suitable gamma emitting nuclide which would be equivalent to the fuel element in respect of its dose rate distribution. Although a match of the distribution in air was attempted, the energy of the gamma radiation from the point sources must be similar to the effective gamma energy of the fission product source in order that the two radiation distributions in the body tissues should also be similar.

The gamma radiation from ^{137}Cs is very suitable for this purpose, its predominant gamma energy of 662 keV being little different from the weighted mean gamma energy from the self-absorbing fission product source. Since the percentage depth dose in tissue is a slowly varying function of gamma energy in this range of energies, no appreciable error is introduced by the substitution.

From consideration of Fig. 5 it is seen that the dose rate distribution is symmetrical about a perpendicular to the axis of the fuel element through its mid-point. By a process of trial and error it was found that four point sources, symmetrically placed in relation to the mid-point

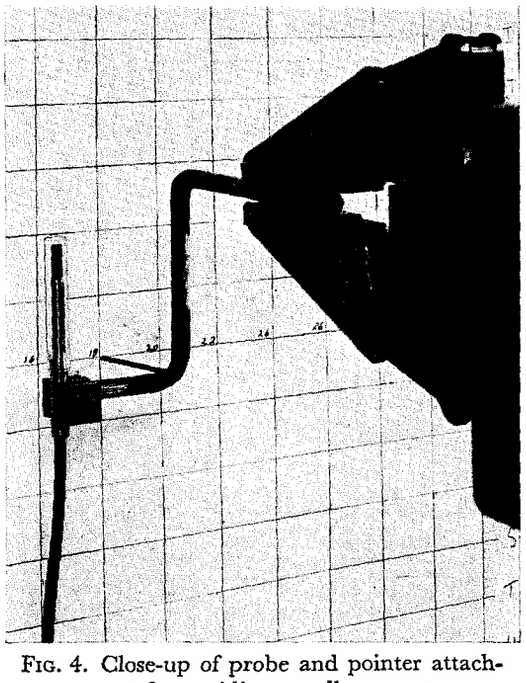

FIG. 4. Close-up of probe and pointer attachment for avoiding parallax errors.

along the axis of the fuel element, were adequate to achieve a satisfactory match of the dose-rate distribution. Two of these sources, each of 10,000 Ci, were 10.7 cm from the mid-point and the other two, each of 1,000 Ci but of *negative* sign, were 64 cm from the mid-point.

4.4. *Dose rate distribution around radiating man phantom*

The required radiating man was constructed using a standard commercial hollow phantom made of polythene to the dimensions suggested by Bush.[10] The dimensions and volumes of the various parts of the phantom are listed in Table 1. The phantom was filled with a solution of caesium chloride containing 100 mCi ^{137}Cs, the activity concentration of the solution being 1·74 $\mu Ci/cm^3$.

The phantom was arranged on a wooden table 78 cm above the floor in the centre of a large room. Measurements of dose rates were made in several planes parallel to the surface of the table, using AERE Type 1120 air-equivalent ionisation chambers (i.e. Type BD 11

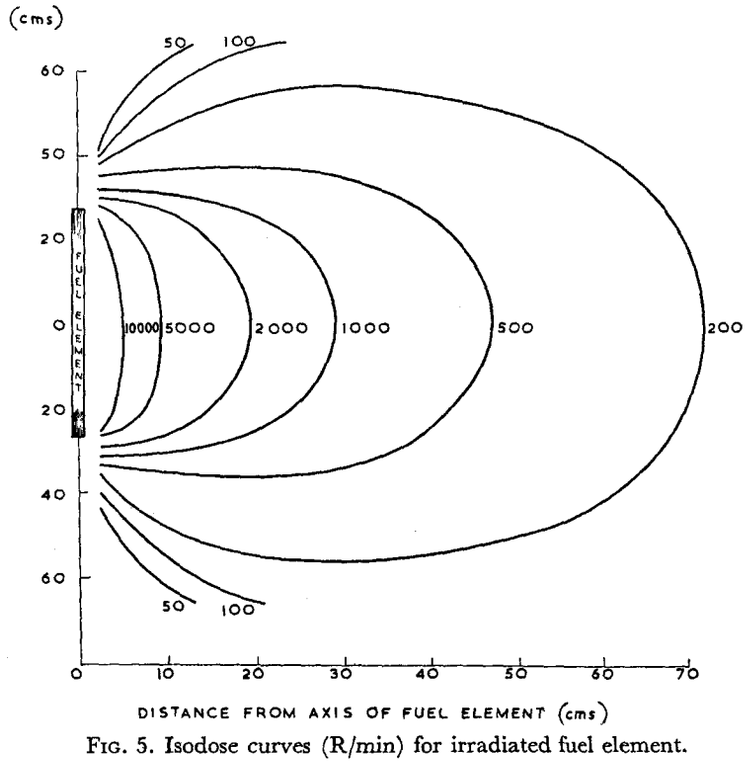

FIG. 5. Isodose curves (R/min) for irradiated fuel element.

Table 1. Dimensions of Parts of Hollow Man Phantom

Part of phantom	Shape	Major axis or diameter (cm)	Minor axis (cm)	Length (cm)	Volume (litres)
Head	eliptical cylinder	18·5	14	19·9	3·43
Chest	eliptical cylinder	29·5	20	39·5	16·95
Abdomen	eliptical cylinder	35·5	20·4	19·9	9·48
Neck	circular cylinder	13	—	10	0·97
Thighs	circular cylinders	14·6	—	40·3	(1) 5·91 (2) 5·89
Legs	circular cylinders	12	—	40	(1) 3·58 (2) 3·66
Arms	circular cylinders	10·1	—	60·3	(1) 3·85 (2) 3·82

Total volume of phantom = 57·54 litres

chambers but with polytetrafluoroethylene insulators) in conjunction with a Baldwin-Farmer electrometer. A large number of chambers were exposed in one plane simultaneously by attaching them to the under surface of a 6 mm thick sheet of Perspex supported above the phantom by a framework of aluminium rods. The Perspex sheet complete with chambers could be removed and replaced quickly at the end and beginning of each exposure. The chambers were calibrated using a small radium source under virtually scatter-free conditions.

From the matrix of dose rates so obtained, graphs were plotted enabling determination of values between measurement points by interpolation.

5. CALCULATION OF AVERAGE AND INTEGRAL DOSES TO A's BODY

Table 2 lists the various parameters required for the calculations. For each stationary fuel element position with its appropriate exposure time are listed the dose rates, interpolated from the BD 11 data, at the four ^{137}Cs source points. The sum of these dose rates, suitably weighted in proportion to the source activities, is given in column IV of Table 2 and the dose value appropriate to each fuel element position is given in the last column of the table.

From equation (8) we have:

$$\bar{D}_1.A_1 = \bar{D}_2.A_2$$

Hence:

$$\bar{D}_1 = \bar{D}_2.\frac{A_2}{A_1}$$

where

$$\bar{D}_2 = \frac{7632 \times 10^{-3}}{3600} \text{ rad}$$

where

$$A_2 = 10^4 \text{ curies}$$

where

$$A_1 = 1{\cdot}0 \text{ curie}$$

i.e.

$$\bar{D}_1 = \frac{7632 \times 10^{-3}}{3600} \times \frac{10^4}{1{\cdot}0} \text{ rad}$$

$$= 21 \text{ rad}$$

The integral dose to A's body is given by the product $M_1 \cdot \bar{D}_1$. A's mass (M_1) was 75 kg so the integral dose, I, is:

$$I = 75 \times 21 \text{ kg rad}$$

$$= 1{\cdot}58 \text{ Mg rad}$$

6. CORRECTION OF RESULTS AND ACCURACY ATTAINABLE

An indication of the order of accuracy attainable in the use of part of the method may be obtained by deriving the expected dose received

Table 2. Parameters required for Calculation of Average and Integral Dose

Fuel element position	I Effective exposure time (sec)	II Dose rate at four point source positions (mrad/hr)	III Point source strength (kCi)	IV (II × III)	V I×IV (mrad × 3600)
1 (lowest position)	0·38	19	−1·0	−19	
		79	10	790	
		106	10	1060	
		204	−1·0	−204	618
				Σ=1627	
2	0·41	54	−1·0	−54	
		131	10	1310	
		170	10	1700	
		280	−1·0	−280	1097
				Σ=2676	
3	0·62	102	−1·0	−102	
		196	10	1960	
		241	10	2410	
		182	−1·0	−182	2533
				Σ=4086	
4	0·49	158	−1·0	−158	
		265	10	2650	
		276	10	2760	
		86	−1·0	−86	2531
				Σ=5166	
5 (oblique position)	0·38	21	−1·0	−21	
		94	10	940	
		148	10	1480	
		155	−1·0	−155	853
				Σ=2244	
				TOTAL	7632

by *A*'s film badge from the assumptions made in the reconstruction.

In Table 3 is calculated the film badge exposure arising from the sum of the exposures from the five stationary fuel element positions. When allowance for backscatter is made the reconstructed dose is 35 rad compared with the measured 27 rad. This difference may arise from one or a combination of several causes. If the difference is due solely to an error in the total exposure time assumed in the reconstruction, then a correction factor of 27/35 = 0·77 must be applied to the values of average and integral doses calculated in Section 5. If, however, the discrepancy is due mainly to a slight difference in the assumed geometrical relationship of the fuel element and *A*'s body compared with that which obtained during the incident, then the correction factor may be very little different from unity. Only a very small change in the assumed source-skin distance of 5 cm is required to account for the difference between

Table 3. Assessment of Exposure at Position of A's Film Badge

Position of badge {25 cm above waist (belt)
7 cm to left of centre of trunk

Axis of fuel element is 5 cm from front surface of trunk (parallel to vertical centre line of trunk) for first 4 positions (see Fig. 2)

Fuel element position	Weighting time (sec)	Distance from centre of fuel element to film badge (cm)		Dose rate from fuel element (rad/min)	Dose (rad)
		parallel to vertical axis	perpendicular to vertical axis		
1 (lowest position)	0·38	125	9	(7)	(0·05)
2	0·41	90	9	(18)	(0·1)
3	0·62	55	9	94	1·0
4	0·49	22	9	3800	31·0
5 (oblique position)	0·38	56	14	143	0·9
				TOTAL	33

Figures in brackets are extrapolated values

Dose with backscatter = 33 × 1·05
= 34·7 rad

the observed and reconstructed film badge doses, whereas such a small change in geometrical relationship would have a negligible effect on the values of average and integral doses. Although the latter explanation of the difference is more likely, a mean correction factor of 0·89 (= (0·77 + 1·0)/2) was assumed.

A small inaccuracy arises on account of the mass and size of the radiating phantom being different from the mass and stature of *A*. The heights of the man and the phantom were very nearly the same but the mass of *A* was 75 kg compared with 57 kg of radiating fluid. It is difficult to make a satisfactory correction to the average dose to take account of this difference since so much depends on where the difference in girth occurs. No significant correction need be applied to the integral dose value since this was calculated using the true mass of *A*.

It is estimated that the measurements of dose rate described in Sections 4.2 and 4.4 gave results having errors no greater than ± 10%. The assumptions made in Section 4.1 have been shown, by means of the estimate of dose to the film badge, to introduce an error of + 11%, and the simulation of the fission product source by means of ^{137}Cs point sources may introduce an error of about 10%.

Taking all the above sources of inaccuracy into account, the expected error in the value of the average dose and integral dose is no more than ± 25%.

7. DISCUSSION OF RESULTS

The most interesting implication of the results is the very great effect of the source-skin distance in determining the ratio of the average dose to the surface dose to *A*'s body. Despite the estimated maximum skin dose to the abdomen of 120 rad, the corrected "average" dose to the body was about 19 rad.

From depth dose measurements determined

in another experiment it has been found that the true absorption in the thickness of *A*'s trunk is about 30% of the incident radiation. However, due to the small source-skin distance of 5 cm in this particular case, the inverse square law accounts mainly for the measured apparent absorption of about 88% of the incident radiation.

ACKNOWLEDGEMENTS

We should like to thank members of the Health and Safety Division at D.E.R.E. for carrying out the experimental work described in this paper; in particular Dr. J. Brown and Messrs. B. Holliday and G. Tyler who undertook the dosimetry measurements. We are also grateful to the Photographic Department at D.E.R.E. who made the cine film, and to the Metallurgy Division for use of their shielded cells.

We also thank Mr. N. Adams of the Authority Health and Safety Branch at Harwell who undertook most of the calculations involved in the determination of average dose.

REFERENCES

1. Recommendations of the International Commission on Radiological Protection (*ICRP Publication* 9). Pergamon Press, Oxford (1966).
2. J. A. DENNIS. Dosimetry in criticality accidents. Report AERE-R4365, U.K.A.E.A. (1964).
3. F. S. PATTON *et al.* Accidental radiation excursion at the Y-12 plant. Report Y-1234, Union Carbide Nuclear Company, Oak Ridge, Tenn. (1958).
4. G. S. HURST, R. H. RITCHIE *et al.* Dosimetric investigation of the radiation accident, Vinca, Yugoslavia. TO/HS/22, IAEA (1960).
5. M. A. BENDER and P. C. GOOCH. *Proc. Natl. Acad. Sci., U.S.* **48,** 522–532 (1962).
6. K. E. BUCKTON, P. A. JACOBS, W. M. COURT-BROWN and R. DOLL. *Lancet* **2,** No. 7258, 676–682 (1962).
7. W. V. MAYNEORD. *Brit. J. Radiol.* **18,** 12–19 (1945).
8. L. V. KING. *Phil. Mag.* **23,** 242 (1912).
9. W. E. ELSASSER. In *Heat transfer by Infra-red Radiation in the Atmosphere,* Harvard University (1942).
10. F. BUSH, *Brit. J. Radiol.* **22,** 96–105 (1949).

A STANDARDIZED METHOD FOR MAKING NEUTRON FLUENCE MEASUREMENTS BY FISSION FRAGMENT TRACKS IN PLASTICS. A SUGGESTION FOR AN EMERGENCY NEUTRON DOSIMETER WITH RAD-RESPONSE

S. PRÊTRE,* E. TOCHILIN and N. GOLDSTEIN
U.S. Naval Radiological Defense Laboratory, San Francisco, California 94135

Abstract—A neutron detector is described which consists of a fission foil (^{232}Th, ^{235}U, ^{238}U, ^{237}Np or ^{239}Pu) in contact with a plastic track detector. These detectors were exposed to reactor neutrons and to monoenergetic neutrons with energies between 1.0–18 MeV. Fission fragment tracks registered in the plastic were selectively etched by a hydroxide and counted in an optical microscope. For thick foils of fissionable metals the sensitivity of the system was found to be $(1.16 \pm 3\%) \times 10^{-5}$ $\frac{\text{fission fragment tracks}}{\text{neutron} \cdot \text{barn}}$ which is in good agreement with theoretical calculations. This sensitivity is independent of the fissionable element used, independent of the neutron energy, fairly independent of the material chosen for tracks registration (plastics, glass, mica) and of etching conditions. Since the (n,f) cross-sections are accurately known for most neutron energies, the above constant can be used for standardized measurements of neutron fluences. An application to emergency neutron dosimetry is suggested. The fissionable material must be readily available and have low specific activity while the (n,f) reaction cross section should follow the $\frac{\text{rad}}{\text{n/cm}^2}$ curve for tissue. As first compromise, natural thorium is suggested to measure the "proton-part" of the neutron dose (above 1 MeV). The second compromise is an alloy made of natural thorium and 0.5% (by weight) of natural uranium. Using the technique of track counting, these dosimeters have a practical range between 5 rad and 30,000 rad. To avoid track counting, a direct read-out method using thin Mylar film was investigated. This plastic is opaque in the deep ultra-violet (below 3000Å), and the etching of fission fragment tracks in this plastic film produces holes. Neutron dose is determined by the amount of UV light passing through the etched film.

A. Measurements of Neutron Fluence

INTRODUCTION

A method by which tracks from heavy nuclear particles can be observed visually in materials such as mica, certain glasses and plastics has been described by Fleischer, Price and Walker.[1-5] These solid state nuclear track detectors have already found wide application in many fields including neutron dosimetry. The neutron detector consists of a fission foil in contact with a nuclear track detector. Fission fragments produced by neutron interactions penetrate the detector producing trails of radiation damage. The trails can be chemically etched in a reagent which selectively creates hollow channels or tracks along the damaged regions. The number of tracks per unit area can be counted in an optical microscope and correlated with neutron fluence.[6-8]

Earlier measurements at this Laboratory indicated that, for thick fission foils, the track

* Permanent address: Federal Institute for Reactor Research, Health Physics Division (SU), 5303 Würenlingen, Switzerland.

density produced in mica, certain plastics and glasses could be equated to neutron fluence by a constant, weighted by the fission cross section of the foil material. This suggested that a standardized method for measuring neutron fluence could be developed. The present study investigates over what limits and to what accuracy such measurements can be made.

EXPERIMENTAL MEASUREMENTS

Fission foils thicker than the maximum range of fission fragments in fission materials (about 13 microns) were used primarily in the neutron detector. The thick fission foils consisted of 0.01 in. ^{232}Th, ^{235}U and ^{238}U. The relative sensitivities of thin fission foils and a Mg-Th alloy containing 4 percent ^{232}Th by weight were also established. The thin fission foils of ^{235}U, ^{238}U and ^{237}Np were of mass thickness of about one mg/cm^2 of isotope deposited on a nickel backing over a $\frac{3}{4}$ in. diameter circle. Alpha particle autoradiographs established that the material was uniformly deposited over the active area. Six ^{239}Pu foils weighing approximately 0.02 mg and deposited over a $\frac{1}{2}$ in. diameter circle were found to be highly non-uniform. Small areas of uniform activity were found on three of the plaques. An aperture covering all but the uniform region allowed the ^{239}Pu foils to be used in some experiments.

Two plastic foils, Lexan* and Mylar,† were used as nuclear track detectors. Most of the track counting measurements discussed in this section were obtained with Lexan mainly because of its clear background and the easy discrimination between tracks and non-tracks. Whenever thin detector material was required (see Section B), Mylar films were used. Tracks of good quality were obtained with a solution of potassium hydroxide (KOH) at a concentration of 28% and a temperature of 60°C. Sodium hydroxide which has often been used with Lexan was found to produce less controllable etching along with some undesirable background effects. A typical fission fragment track etched with KOH is represented in Fig. 1. Selective etching is seen to take place along the trail of radiation damage. In both Lexan and Mylar the directional etching proceeds at a rate of approximately 0.55 μ/min. At the same time the surface is being removed at a rate of about 0.05 μ/min. The ratio of track to surface etching speed (eleven for the two plastics) provides a method of expressing the selectivity of this etching process.[9] Figure 2 depicts the formation of a track as a function of developing time while Fig. 3 describes the etching of fission fragment tracks as a function of etching time.

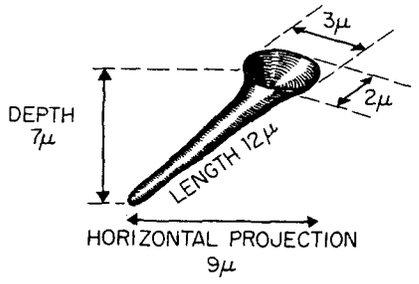

FIG. 1. Typical fission fragment track in plastic etched with KOH.

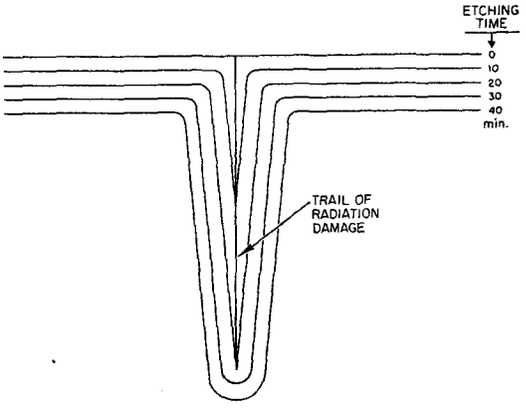

FIG. 2. Cross-sectional view of a typical track after different etching times. In this example, the best etching time is 20 min. With longer etching, the track will no longer increase in length, but only in width.

A regular optical microscope at a magnification of 430 power was used for track counting whenever the track density ranged from 10^4 to 10^6 tracks/cm^2. Optimum etching time was found to be dependent on track density as shown

* General Electric Company, Pittsfield, Mass.
† E. I. duPont de Nemours and Company, Wilmington, Del.

in Fig. 4. For track densities less than 10^4 tracks/cm^2 maximum etching time was used which produced thick tracks that could be readily identified at lower microscope magnifications. For an upper limit it was possible to count as many as 10^7 tracks/cm^2 where minimum etching times and higher microscope magnifications are required for positive track identification. Figure 5 shows the difference in track structure produced when Lexan with a heavy track density is etched for 5 min compared to a lower track density etched for 40 min.

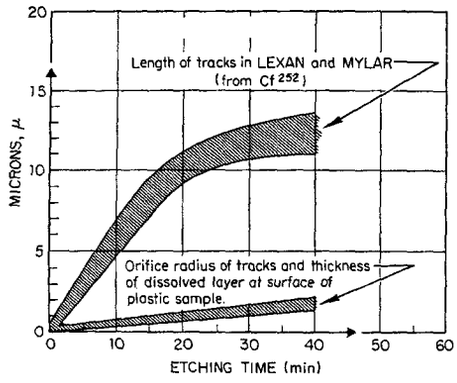

FIG. 3. Etching kinetics of fission fragment tracks in KOH at a concentration of 28% and a temperature of 60°C. In Lexan and Mylar, directional etching speed along the trail of radiation damage is approximately eleven times faster than the volume dissolution speed.

Selective etching with a faster rate at high track density is observed in Lexan. This is particularly noticeable when tracks begin to overlap as in Fig. 5(A). Only a small fraction of all tracks will be seen when Lexan with low track density is etched for 5 min as compared to almost complete track recognition above 10^6 tracks/cm^2. This effect did not occur with any of the other track detectors investigated during this study.

Optimum etching time for Lexan will vary over wide limits whenever track counting is used to determine fast neutron fluence. However if track counting is replaced by other detecting methods in which track length or track width become critical (i.e. densitometry, photometry, etc.) then etching conditions must be more rigidly controlled. Use of the photometric technique described in Section B required several refinements to the simple etching apparatus

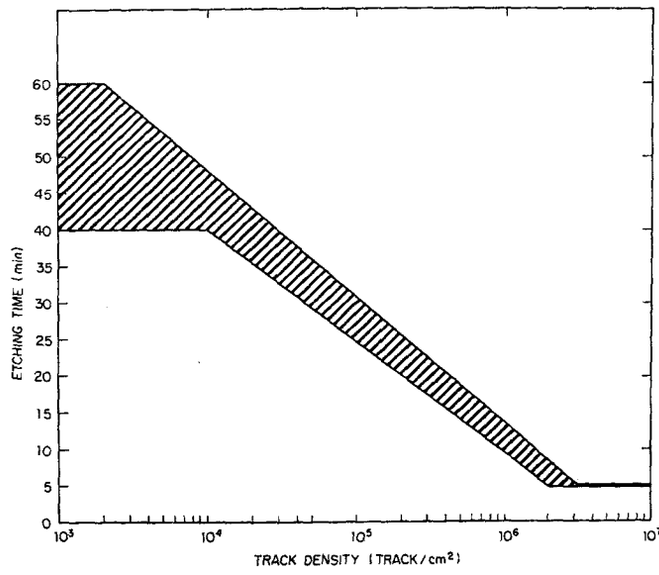

FIG. 4. Optimal etching time for track counting in Lexan. The solution is KOH 28% concentration at 60°C. Recommended etching procedure: etch 5 min to determine approximate track density; continue etching up to the optimal etching time.

used for track counting. The refinements are given as recommendations for others who may have similar requirements:

1. The volume of etching solution should be large in order to minimize changes in concentration during the etching process.

FIG. 5. Fission fragment tracks in Lexan. (A) High track density ($\sim 4 \times 10^6$ cm^{-2}) and short etching time (5 min). (B) Lower track density ($\sim 10^5$ cm^{-2}) and longer etching time (40 min).

2. The concentration of etching solution should be monitored to insure that changes do not occur either because of evaporation or contamination.

3. A cover should be placed over the etching bath to keep down evaporation. For some types of plastics the cold etching technique described by Benton and Collver[10] could be used. (This method was found to improve track definition in cellulose nitrate.)

4. The etching solution should be continuously agitated in order to avoid the formation of density and temperature gradients. Ultrasonic agitation is recommended over other methods.

5. Samples should be placed vertically rather than horizontally in the solution to avoid the formation of small bubbles at the lower surface which may interfere with track formation.

Neutron exposures were made at the USNRDL 2 MeV Van de Graaff accelerator, the Fast Burst Reactor, White Sands Missile Range, New Mexico (WSMR reactor) and the Aerojet-General Nucleonics Industrial Reactor, San Ramon, California (AGNIR reactor). Monoenergetic neutrons were obtained at the accelerator ranging from 1.9 to 5.2 MeV from the D$(d,n)^3$He reaction and from 12 to 18 MeV from the T$(d,n)^4$He reaction; exposures were also made with 1.0 MeV neutrons from the T$(p,n)^3$He reaction. A calibrated long counter was used to measure neutron fluence up to energies of 5 MeV while a sulfur threshold detector was used at energies of 12 MeV and above. The sulfur (n,p) cross section as well as the (n,f) cross-sections for the different foils was taken from the summary cross section data tabulated by Barrall and McElroy.[11] Measurements at the accelerator, made over a wide range of energies, determined the relative efficiency with which Lexan will detect fission fragments at different bombarding neutron energies.

The WSMR reactor has been calibrated with a fission foil technique developed by Hurst *et al.*[12] where the residual gamma ray fission product activity is counted. ^{239}Pu, ^{237}Np and ^{238}U fission detectors are placed in a spherical shell of ^{10}B and together with ^{32}S are exposed to fission neutrons. In this case an intercomparison study (Table 3) was made with the Hurst system and our fission foil-Lexan detectors. A similar intercomparison has recently been described by Kerr and Strickler.[13]

RESULTS AND DISCUSSION

Our preliminary experiments using nuclear track detectors of mica, plastics, microscope glass slides and silver-activated phosphate glass indicated a sensitivity for thick fission foils approximately 10^{-5} fission fragment tracks/

Table 1. *Measured Sensitivity of Thick Fission Foils in the Neutron Energy Range from* 1.0–16 MeV

Fission foil	Neutron energy [MeV]	Sensitivity fission fragment tracks/ neutron · barn
^{232}Th	2.6	1.15×10^{-5}
	3.8	1.19
	5.0	1.14
^{235}U	1.0	1.17×10^{-5}
	2.0	1.23
	5.2	1.13
^{238}U	1.9	1.12×10^{-5}
	2.0	1.14
	2.6	1.07
	3.8	1.20
	5.0	1.11
	5.2	1.19
	12–16 (8 points)	1.17 ± 4.5%
Weighted average		1.16×10^{-5}

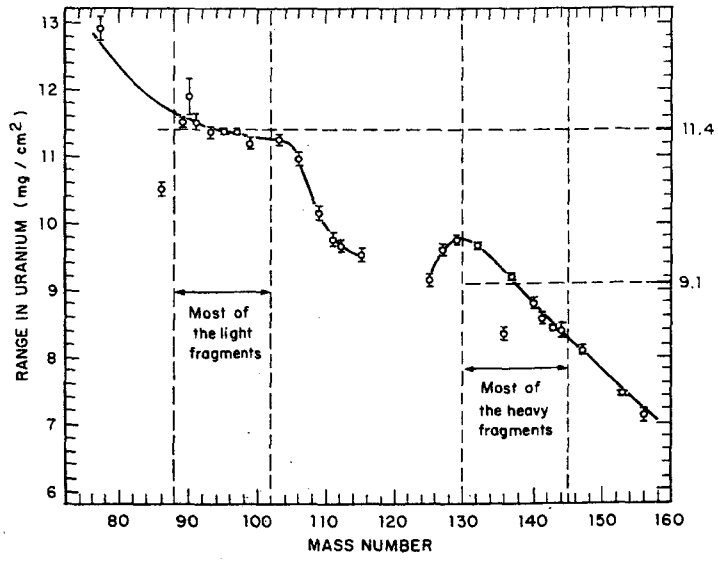

FIG. 6. Integral ranges of fission products of ^{235}U measured in uranium metal (Niday[14]).

neutron·barn independent of neutron energy. Becker's more systematic investigation of fission track detection in silver-activated phosphate glass gave a value of 1.3×10^{-5} fission fragment tracks/neutron·barn with an accuracy of $\pm$ 10%.[8] One objective of the present report was to determine this value for Lexan with sufficient accuracy to allow its use as a direct method for measuring thermal and fast neutron fluence.

A summary of measurements with monoenergetic neutrons from the Van de Graaff accelerator is found in Table 1. Given are the neutron energy, type of foil material and the measured sensitivity in fission fragment tracks/neutron·barn. A weighted average of 1.16×10^{-5} fission fragment tracks/neutron·barn with standard error of 3% was obtained.

Thermal neutron measurements were made at the thermal neutron column of the AGNIR reactor with two groups of uranium foils, one containing 378 ppm ^{235}U and the other 3600 ppm ^{235}U. A cadmium ratio of greater than 100 was obtained at the point of exposure. Measurements made in a Cd shield established that 4% of the tracks from the 378 ppm ^{235}U foil was from fast neutron contamination in the thermal column. With this correction the thermal neutron fluence obtained with the two sets of foils agreed within experimental error. Simultaneous measurements made with gold foil monitors gave values 10% higher than indicated by the ^{235}U fission foils. This difference is within the limits of accuracy of the two measurements.

Measurements by Niday[14] giving the ranges of fission products in uranium metal have been reproduced in Fig. 6.[15] From this data it is possible to calculate the neutron sensitivity of thick fission foils. Consider a uranium target of 1 cm² area and a thickness R equal to the range of fission fragments. This target has $\frac{NR}{A}$ atoms/cm². Thus the number of induced fissions will be:

$$\frac{N}{A} \cdot \frac{R_L + R_H}{2} \cdot r = 2.6 \times 10^{-5} \frac{\text{fissions}}{\text{neutrons} \times \text{barn}}$$

where R_L is the range of light fission fragments in uranium (11.4×10^{-3} g/cm²); R_H is the range of heavy fission fragments in uranium (9.1×10^{-3} g/cm²); N is Avogadro's number (6.025×10^{23} atoms/mole); A is the atomic weight of uranium metal (238.1 g/mole); r is a conversion factor (10^{-24} cm²/barn).

Referring to Fig. 7, if one fission occurs at

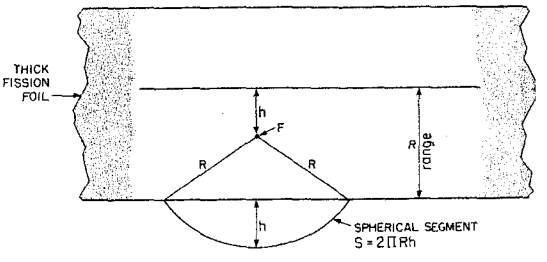

FIG. 7. Geometry factor for thick foils. One fourth of all fission fragments produced within the thickness R, will emerge at the surface.

point F (producing two fission fragments) the probability that one fission fragment will emerge at the lower surface is:

$$\frac{2\pi Rh}{4\pi R^2}$$

Assuming a uniform distribution of the fission events within this foil, the total geometry factor is

$$\frac{\int_0^R 2\pi Rh \cdot dh}{\int_0^R 4\pi R^2 \cdot dh} = \frac{1}{4}$$

The number of fission fragments which will emerge out of this thick fission foil is:

$$\frac{N}{A} \cdot \frac{R_L + R_H}{4} \cdot r = 1.3 \times 10^{-5} \frac{\textit{emerging fission fragments}}{\textit{neutron} \times \textit{barn}}$$

However, not all emerging fission fragments will produce observable tracks. Assuming that the etching process dissolves approximately 1μ of the plastic surface (see Fig. 3) and that the tracks

must be at least 1μ in depth to be observed, we see that, in order to produce an observable track, the emerging fission fragments must have enough energy to penetrate at least 2μ deep in the plastic.

It can be shown that some 90% of the emerging fission fragments will fulfill this requirement. Thus the sensitivity of a thick fission foil can be approximated as:

$$1.17 \times 10^{-5} \frac{\textit{fission fragment tracks}}{\textit{neutron} \times \textit{barn}}$$

Excellent agreement is seen to exist between the experimental and calculated values. Since the (n,f) cross-sections are accurately known for most neutron energies the above constant can be used for standardized measurements of neutron fluences. The advantages offered by using a thick foil are that this constant can be directly applied independent of fission material (^{235}U, ^{238}U and ^{232}Th), independent of neutron energy (no difference was observed between slow fission processes and fast fission processes) and reasonably independent of the track registration material (assuming that the fission fragment registration efficiency is 100%). This was found to be the case for both Lexan and Mylar.

Figure 8 gives the range of neutron fluence over which the different foils were found usable. The solid bars indicate the optimum counting region for each detector while the dashed regions to the right and left indicate the range of upper and lower limits over which track counting to an accuracy of $\pm$ 5% can still be obtained. One could of course identify tracks below the arbitrarily assigned lower limit of 1000 tracks/cm^2 but the times required to obtain good counting statistics tend to become excessively long. The upper counting limit will be that point where overlapping tracks begin to make positive track identification difficult.

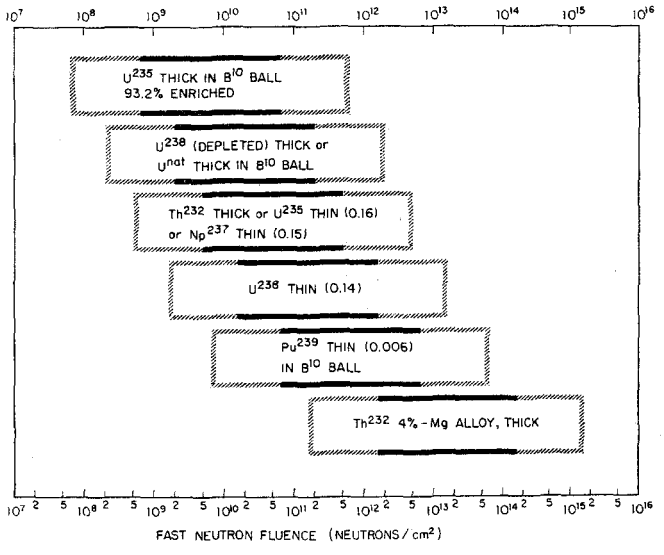

FIG. 8. Range of fast neutron fluence measured with fission foils. The lower limit of measurable track density is given as 10^3 cm^{-2} while the upper limit is 10^7 cm^{-2}. The number given in parenthesis for thin foils is the thickness factor as defined in the text.

A "thickness factor" was determined for the fission foils less thick than the maximum range of the fission fragments and has been included, where applicable, in Fig. 8. The relative counting sensitivity of the thin fission foils was established for the monoenergetic neutrons from the NRDL Van de Graaff and compared to the value obtained for thick fission foils. The ratio of the two values is the "thickness factor" and when

Table 2. Calculated Average (n,f) Cross-Sections for Neutron Energy Intervals Measured with Threshold Detectors

Element and corresponding (n,f) average cross-section (barns)	Energy interval (MeV)			
	(ϕPu–ϕNp) 0.01 to 0.60	(ϕNp–ϕU) 0.60 to 1.5	(ϕU–ϕS) 1.5 to 3.0	(ϕS) >3.0
^{235}U	1.5	1.2	1.3	1.2
^{239}Pu	1.7	1.75	2.0	1.9
^{237}Np	0.2	1.2	1.6	1.5
^{238}U	0	0.08	0.5	0.57
^{232}Th	0	0.005	0.11	0.14

combined with the sensitivity factor for thick foils gives a relative sensitivity factor for the thin foil.

The fission foil detectors were also used in an intercomparison study at the WSMR reactor with the standard threshold detector system.[16] Fast neutron fluences were measured by the White Sands group within the four energy regions indicated in Table 2. We have calculated the average fission cross-section of five fission foils in each energy region.[11] These cross-sections were then used to evaluate the neutron fluence above 0.6 MeV with ^{237}Np-Lexan detector and above 1.5 MeV with a ^{232}Th-Lexan detector. Since the thorium foil was exposed bare the sensitivity factor previously determined for thick foils could be directly applied. Additional corrections required for the ^{237}Np foil included a "thickness factor" and a ^{10}B attenuation factor. Results of the intercomparison check is given in Table 3. In both cases the neutron fluence above 3 MeV was independently determined with a ^{32}S(n,p) ^{32}P threshold detector with an assigned effective cross-section of 0.30 barns.[17] Depleted ^{238}U fission foils were exposed together with thorium, but the associated thermal neutron fluence complicated their interpretation.

In any calibrated neutron facility where neutron flux and spectrum have been determined, the sensitivity constant for thick fission foils can also be used for direct measurements of the (n,f) cross-section. An example of such measurements is given in Fig. 9, where the (n,f) cross-section for ^{232}Th was determined between 12 and 18 MeV.[18] Earlier cross-section measurements by Pankratov,[19] over the same energy interval are included for comparison along with the curve drawn through the data points.

Table 3. Intercomparison of Neutron Measurements at the White Sands Missile Range Fast Burst Reactor

Neutron energy	Measured neutron fluence (n/cm^2)			
	WSMR		NRDL	
	61 in.	150 in.	61 in.	150 in.
>0.6 MeV	3.16×10^{11}	1.43×10^{11}	3.18×10^{11}	1.48×10^{11}
>1.5 MeV	0.63×10^{11}	0.26×10^{11}	0.59×10^{11}	0.26×10^{11}

B. A Suggestion for an Emergency Dosimeter with Rad-response

INTRODUCTION

The purpose of an emergency dosimeter is to permit an estimate of any significant radiation exposure which may produce acute biological effects. In most neutron experiments with large animals the midline tissue dose has been used as the reference dose. Bond *et al.*[20] exposed dogs to neutrons of 9 MeV average energy and found an RBE (or QF) of 0.95. Alpen *et al.*[21] made similar exposures with simulated fission neutrons and found a quality factor of 0.9. In both cases the biological effects were compared to that of 250 kVp X-rays. These studies indicate that a dosimeter measuring total midline tissue dose in rads can be directly related to biological effects. One should further note that this is not the case with a detector that records only first collision dose unless additional information on neutron energy is available.

The two major processes by which the body absorbs neutrons is by elastic scattering (the (n,p) reaction) and by thermal neutron capture in hydrogen leading to the $^1H(n,\gamma)D$ reaction. We can thus speak of a "proton-part" and a "gamma part" of the neutron dose. Depth dose curves in tissue giving the neutron and gamma-ray contributions have been calculated by Snyder[22] for neutron energies from thermal to 10 MeV. The absorbed dose in a 30 cm phantom at a depth of zero to 4 cm and at 10 cm is plotted in Fig. 10. If we consider the absorbed dose within this range to be the most significant we see that for neutron energies above 1 MeV the proton dose is predominant while for neutron energies below 0.1 MeV the gamma dose is predominant. Between these energy intervals both components are important.

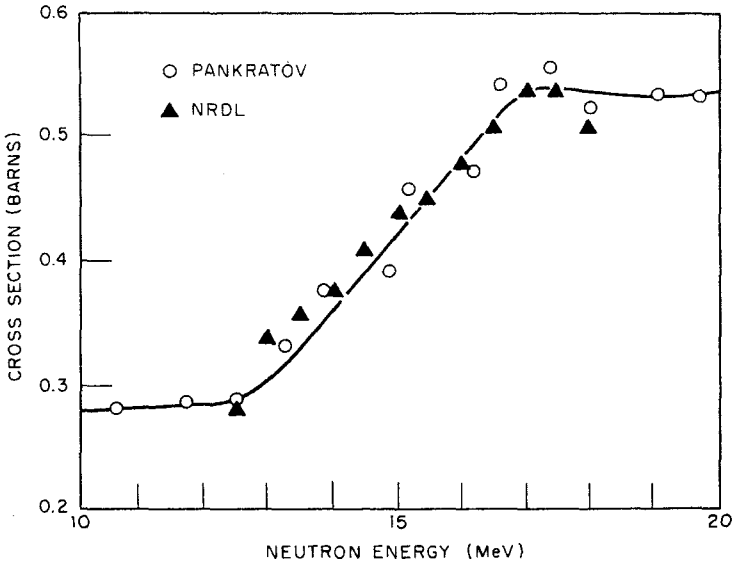

FIG. 9. Fission cross-section of ^{232}Th for neutrons from 12.5–18 MeV measured with Lexan. Earlier measurements by Pankratov[19] are also shown.

The emergency neutron dosimeter considered here is intended primarily for use in the event of a reactor accident or a nuclear explosion. Since it is based on a system of fission foils it is important to know the probable spectrum to be encountered and how the neutron dose is distributed over this spectrum. Braun and Nilsson[23] have examined several representative spectra from infinite homogeneous reactors with different moderators and from a fission plate in a graphite moderator. Ritchie and Eldridge[24] described methods for calculating

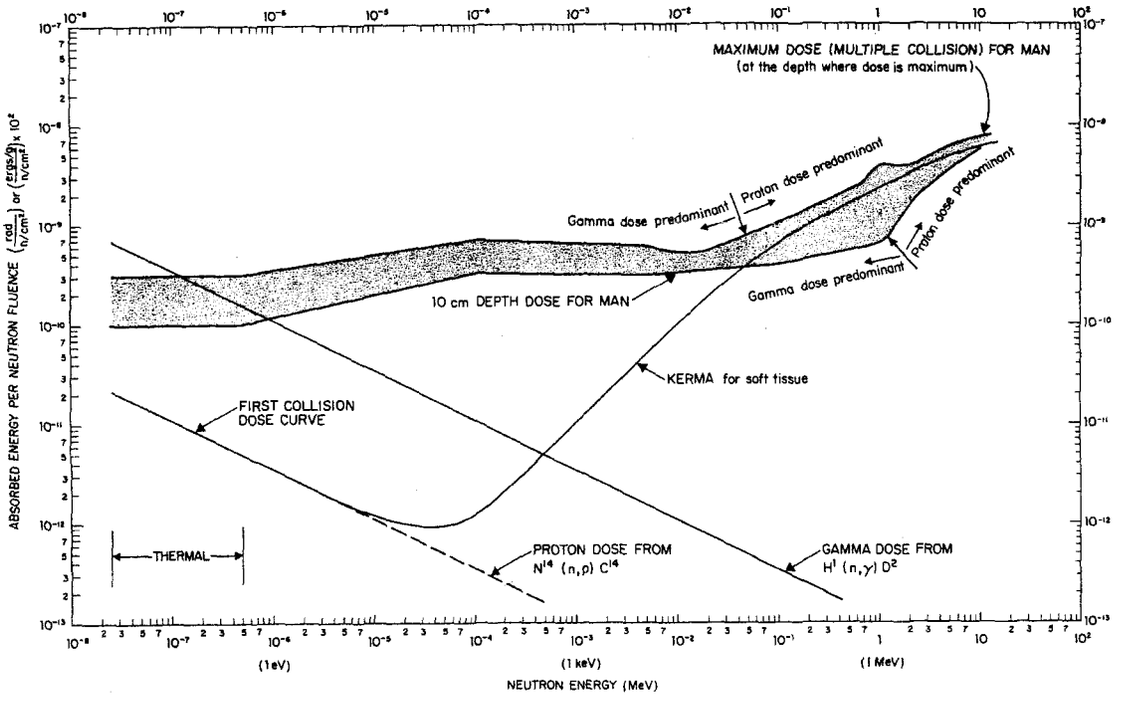

FIG. 10. Absorbed dose in tissue irradiated by neutrons. The depth at which dose is a maximum may be considered to be 4 cm except in the energy region between 0.1–2 MeV. In this region the 4 cm depth dose will be approximately 2/3 the maximum dose. The first collision dose curve is shown for comparison.

neutrons from critical assemblies while Yampolskiy[25] described the probable distribution of neutron dose from fission weapons. While no typical spectrum can be assumed it is possible to say that, except where large masses of non-hydrogenous moderator could exist (> 30 g/cm^2), most of the neutron dose will be from neutrons in the energy range above 0.1 MeV. About 90% of the dose comes from energies less than 4 MeV, 40–60% from energies less than 1 MeV and only about 20% for energies below 0.1 MeV. Under these conditions most of the neutron dose will be in the energy range from 0.1 to 2 MeV.

It should be noted that for a typical fission neutron spectrum approximately half the total midline dose received by the human body will be from capture gamma-rays. Since gamma-ray dosimeters worn on the body will detect this component one already has the capability for recording the gamma portion of the total neutron dose (at the same time there is no way of separating primary gamma dose from neutron produced gamma-rays). The neutron dosimeter should therefore reflect as close as possible the biologically significant radiation dose without remeasuring the gamma contribution and having it registered twice. On the other hand if one could measure the region below 0.1 MeV by matching fission foil response to the midline dose it would be possible to evaluate this gamma-ray contribution and subtract it from the total gamma dose registered by a dosimeter worn on the body.

FISSION TRACK EMERGENCY NEUTRON DOSIMETER

Fission foils in combination with a fission track detector possess many desirable properties to recommend their use as personnel neutron dosimeters. They can be made small and light weight and are completely unaffected by gam-

ma-rays, by environmental conditions or by storage time. Neutron dose can be measured over many orders of magnitude. Where thick foils are used the measured track density can be directly related to neutron fluence. Fission tracks striking the detector leave a permanent record of radiation damage which can be processed at any later time by simple chemical techniques.

While many of the transuranic elements can be used as fission foils practical considerations restrict the choice to readily available materials. This automatically limits present usage to either thorium or natural uranium. However, the fission cross sections of these materials are such that they can be satisfactorily used as emergency neutron dosimeters.

Rad-response of Natural Thorium

In this case we will restrict ourselves to the measurement of the proton part of the neutron dose above the threshold energy of ^{232}Th. To obtain a neutron dosimeter with rad response we require the tracks/cm^2·rad ratio to be constant for all neutron energies. It means that the product of rad·cm^2/n and neutrons/track be independent of neutron energy. In other words, the following three quantities must be proportional: rad·cm^2/n, tracks/neutron and cross-section (barns). Thus a neutron dosimeter will have a rad response if we can match the rad·cm^2/n curve (Fig. 10) with the (n,f) cross-section curve. Assuming that we are only interested in the proton portion of the neutron dose, we see from Fig. 11 that above 1.3 MeV we can match the thorium (n,f) cross-section curve with the rad·cm^2/n curve using a response factor of

$$3 \times 10^{-8} \frac{\text{rad}}{(\text{n/cm}^2)\cdot\text{barn}}.$$

Using the sensitivity obtained in Section A we can rewrite this response factor as

$$390 \frac{\text{tracks/cm}^2}{\text{rad}}.$$

Our minimum and maximum counting criteria of 10^3 and 10^7 tracks/cm^2 give us a practical detection range between 3 and 30,000 rad.

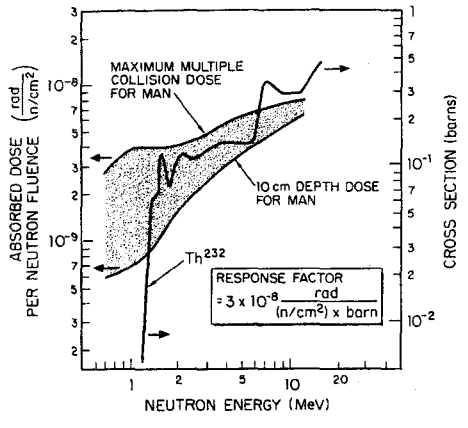

FIG. 11. Response of thorium as an absorbed dose detector. It is assumed that the gamma part of the neutron dose would be detected by usual gamma-ray dosimeters.

Rad-response of a Thorium–Uranium Alloy

If it is important to measure the total absorbed dose from neutrons then we need a fission material having a cross-section curve that will match the rad·cm^2/n curve over all neutron energies.

As a compromise we suggest a thorium alloy containing 0.5% (by weight) of natural uranium (0.5% by weight = 0.3% by atoms). The ratio of ^{235}U atoms to ^{232}Th atoms is thus 1/46000. The (n,f) cross-section for the thorium alloy is plotted in Fig. 12 in a way to best match the midline tissue dose response. One sees that this dosimeter has very low sensitivity in the region 0.1 MeV to 1 MeV which is an important region for fission neutrons. In order to compensate for this deficiency we have given the dosimeter a higher sensitivity above 1 MeV. We assume that $\sim 40\%$ of the fast neutron dose is due to neutrons with $E_n > 1$ MeV, and thus we raise the cross-section curve by a factor 2.5. The response factor becomes:

$$7.5 \times 10^{-8} \frac{\text{rad}}{(\text{n/cm}^2)\cdot\text{barn}}$$

and our sensitivity for the thorium–uranium alloy becomes

$$155 \frac{\text{tracks/cm}^2}{\text{rad}}$$

giving a practical detection range between 6 and 60,000 rad.

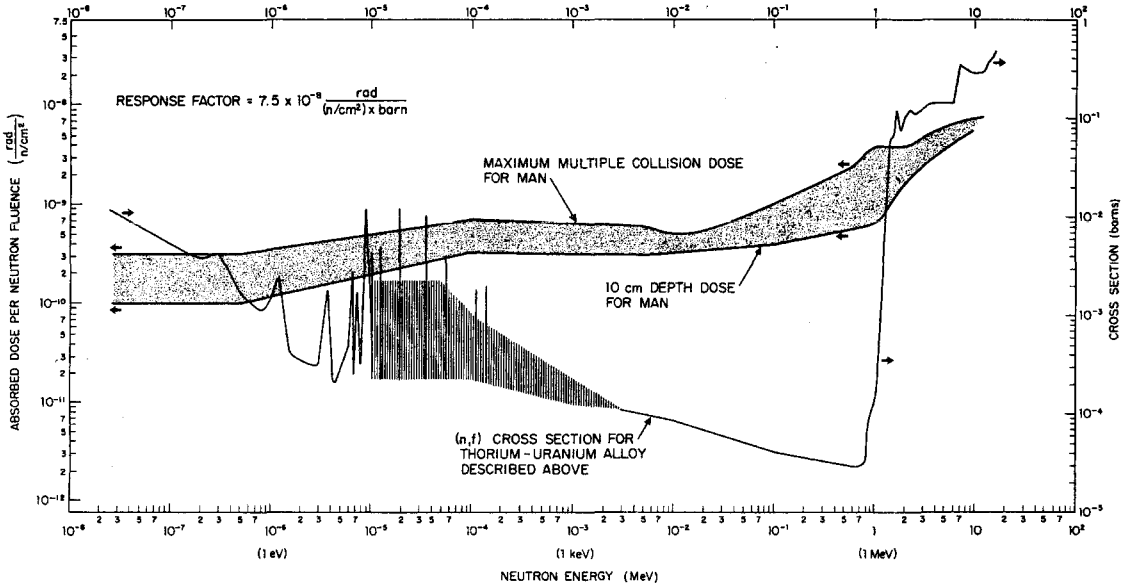

FIG. 12. Response of thorium–uranium alloy as an absorbed dose detector. The (n,f) cross-section for thorium alloy containing 0.5% by weight of uranium is compared to the multiple collision dose curve for neutrons energies from 10^{-8}–10^{2} MeV.

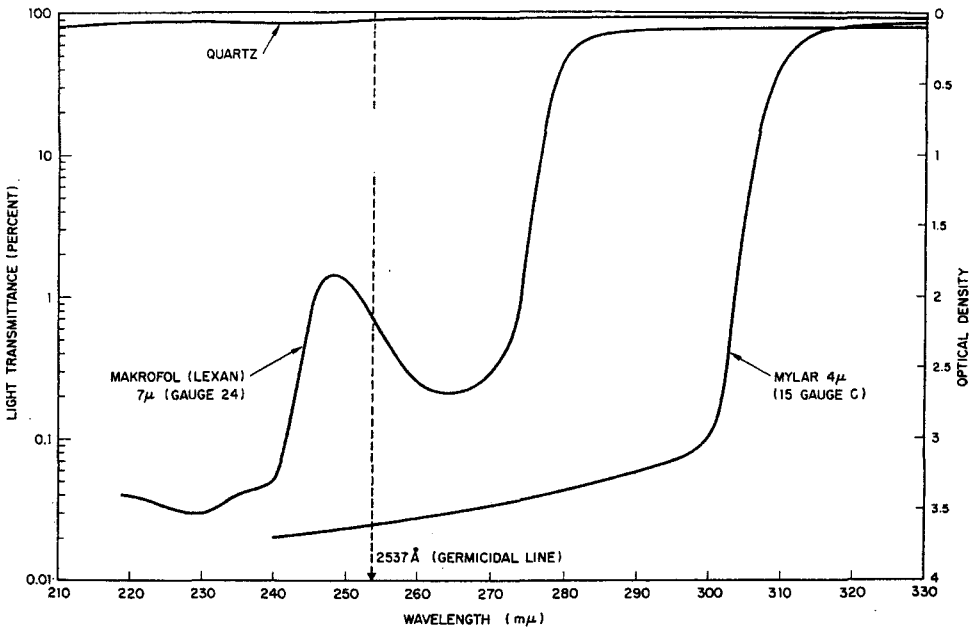

FIG. 13. Transparency of thin plastic foils to ultra-violet light. Measurements were made with a Beckman DU spectrophotometer.

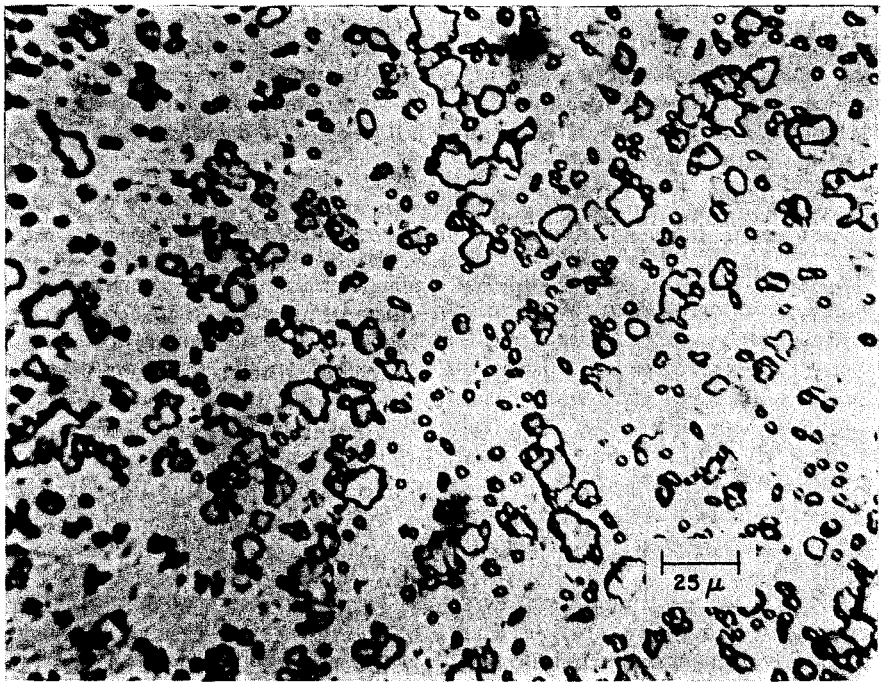

FIG. 14. Holes etched in thin Mylar film. The fission track density was approximately 10^6 cm^{-2} and the etching time was 30 min. in standard KOH solution.

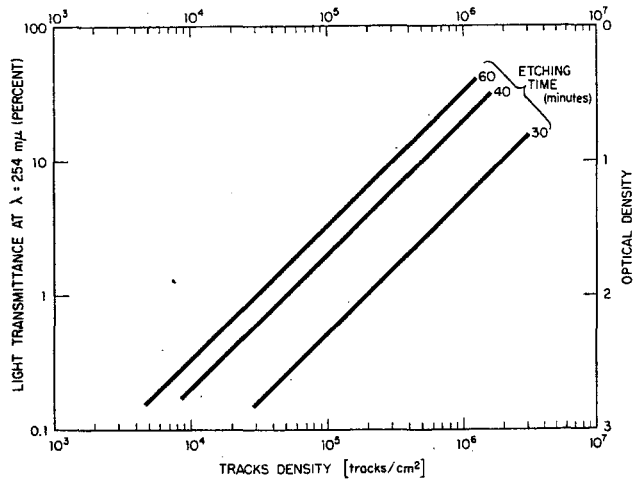

FIG. 15. Transmittance of ultra-violet light (254mμ) through Mylar film exposed to fission fragments and etched in standard KOH solution. The light transmittance is directly proportional to the track density, therefore also proportional to the neutron dose.

NEUTRON DETECTION BY LIGHT TRANSMISSION

Despite the many obvious merits of track counting the process is slow and somewhat tedious. Methods to replace track counting by simpler and more direct measurements have already been described.[6, 8, 26] Another such method is to use a thin opaque plastic film so that the etched tracks will produce holes in the material. The amount of light passing through the film should be proportional to the number of holes. Unfortunately, almost every plastic in very thin layers (4μ–12μ) is transparent to visible light. We discovered only one plastic which was simultaneously thin and opaque (0.5 mil black Tedlar PVF film*) but we could not produce the selective etching in it.

However, plastics such as Mylar, Lexan and Makrofol† are opaque to deep ultra-violet light, even in very thin layers.

Observing Fig. 13, we see that Mylar, even in the thinnest gauge, is more opaque than Makrofol. Mylar is also easier to handle and available in a large variety of thicknesses. We used 15C Mylar 4 microns thick and a working wave length of 2537Å (254mμ) which is called the "germicidal line". The choice of this wave length is based on the easy availability of ultra-violet sources giving most of their energy in that particular wavelength (germicidal lamps).

Etched tracks in thin Mylar (4μ) become holes as illustrated by Fig. 14. Using our standard etching conditions we have found that the light transmittance at 254 mμ is directly proportional to the track density. Figure 15 shows that light transmittance measurements can replace track counting between 5×10^3 and 3×10^6 tracks/cm^2. This track range corresponds to a midline dose between $\sim$ 25 and 10,000 rad. It is thus possible to measure the track density without counting the number of tracks. Unlike track counting, this method requires precise control of etching conditions.

Handling of very thin Mylar film is still a problem. We used concentric rings to mount the Mylar film. Unfortunately preferential etching occurs at the places where the plastic is under strain, and even a relatively short etching time can split the Mylar where it is held between the rings. This difficulty could be eliminated by mounting the plastic film with adhesive on a backing of quartz (see Fig. 13).

* E.I. duPont De Nemours and Co., Wilmington, Delaware.

† Bayer Co., Germany.

CONCLUSIONS

The suggested emergency dosimeter would consist of a fission foil in juxtaposition with a plastic foil. Either thorium or a thorium–uranium alloy could be used as the fission foil. Lexan or any other appropriate detector could be used for track counting while Mylar is recommended for transmitted light measurements. A "germicidal" lamp with an optical filter to eliminate all lines other than 2537Å was found to be a suitable light source.

REFERENCES

1. P. B. Price and R. M. Walker. Chemical etching of charge-particle tracks in solids, *J. Appl. Phys.* **33,** 3407 (1962).
2. P. B. Price and R. M. Walker. A new track detector for heavy particle studies, *Phys. Rev. Letters* **3,** 313 (1962).
3. R. L. Fleischer and P. B. Price. Tracks of charged particles in high polymers, *Science* **140,** 1221 (1963).
4. R. L. Fleischer, P. B. Price and R. M. Walker. Neutron flux measurement by fission tracks in solids, *Nuclear Science and Engineering* **22,** 153 (1965).
5. R. M. Walker, P. B. Price and R. L. Fleischer. A versatile disposable dosimeter for slow and fast neutrons, *Appl. Phys. Letters* **3,** 28 (1963).
6. M. Debeauvais, M. Maurette, J. Mory and R. Walker. Registration of fission fragment tracks in several substances and their use in neutron detection, *Int. J. Appl. Rad. & Isotopes* **15,** 289 (1964).
7. P. R. Prevo, R. E. Dahl and H. H. Yoshikawa. Thermal and fast neutron detection by fission—tracks production in mica, *J. Appl. Phys.* **35,** 2636 (1964).
8. K. Becker. Nuclear track registration in dosimeter glasses for neutron dosimetry in mixed radiation fields, *Health Physics* **12,** 769 (1966).
9. M. M. Collver, E. V. Benton and R. P. Henke. Charged particle tracks in polymers: Number 1—Delineation and measurement of sub-surface tracks. USNRDL-TR-917 (1965).
10. E. V. Benton and M. M. Collver. Charged particle tracks in polymers: Number 2—Registration of heavy ions during the flight of Gemini VI, USNRDL-TR-1037 (1966).

11. R. C. Barrall and W. N. McElroy. Neutron flux spectra determination by foil activation, Vol. II, Experimental and Evaluated Cross Section. AFWL-TR-65-34 (1965) Air Force Weapons Laboratory, Kirtland Air Force Base, New Mexico.
12. G. S. Hurst, T. A. Harter, P. N. Hensley, W. A. Mills, M. Slater and P. W. Reinhardt. Techniques of measuring neutron spectra with threshold detectors; tissue dose determination, *Rev. Sci. Instr.* **27,** 153 (1956).
13. G. D. Kerr and T. D. Strickler. The application of solid-state nuclear track detectors to the Hurst threshold detector system, *Health Physics* **12,** 1141 (1966).
14. T. Niday. Radiochemical study of the ranges in metallic uranium of the fragments from thermal neutron fission, *Phys. Rev.* **121,** 1471 (1961).
15. E. K. Hyde. A revised version of a review of nuclear fission. UCRL-9036-Rev (1962).
16. K. Humphreys, W. Quam, C. Rainbolt, R. Durkee and T. Dahlstrom. Nuclear radiation dosimetry measurements of the White Sands missile range fast burst reactor. EG and G Report No. S-262-R, Santa Barbara, California.
17. ASTM Tentative Procedure D-2365-65T. Tentative Method of Calculation of Neutron Dose to Polymetric Materials and Application of Threshold-Foil Measurements, Am. Soc. for Testing and Materials Publication, Philadelphia, Pa. (1965).
18. P. Rago and N. Goldstein. Thorium fission cross section for neutrons between 12.5 and 18 MeV using fission fragment damage tracks in Lexan, *Health Physics* **13,** 654 (1967).
19. V. M. Pankratov. Fission cross-sections of ^{232}Th, ^{233}U, ^{235}U, ^{237}U, ^{238}U for 5–37 MeV neutrons. *Atom. Energ.* **14,** 177 (1963).
20. V. P. Bond, R. E. Carter, J. S. Robertson, P. H. Seymour and H. H. Hechter. The effects of total-body fast neutron irradiations in dogs, *Rad. Res.* **4,** 139 (1956).
21. E. L. Alpen, O. S. Shill and E. Tochilin. The effects of total body irradiations of dogs with simulated fission neutrons, *Rad. Res.* **12,** 237 (1960).
22. W. S. Snyder. Protection against neutron radiation up to 30 MeV, *NBS Handbook* 63, Appendix 1 (1957).
23. J. Braun and R. Nilsson. An emergency dosimeter for neutrons, *Proc. Symp. Selected Topics in Radiation Dosimetry*, Vienna, 1960, 623, IAEA, Vienna (1961).
24. R. H. Ritchie and H. B. Eldridge. Calculation of the radiation yield from fission assemblies and comparison with experiments, *Proc. Symp. Selected Topics in Radiation Dosimetry*, Vienna, 1961, 657, IAEA Vienna (1961).
25. P. A. Yampolskiy. *Neutrons from an Atomic Explosion.* U.S.S.R., English translation: JPRS 11873 (1962).
26. J. W. N. Tuyn. On the use of solid state nuclear track detectors in reactor physics experiments. Institute for Atomenergi, Norway, NORA Memo No. 123 (1966).

DISCUSSION

E. VAN ESPEN (*Belgium*):

The CaF_2 used by MBLE is different from the one commonly called Mn-activated CaF_2.

B. BJARNGARD (*U.S.A.*):

In answer to Dr. Langmead's (rapporteur) question of the light-sensitivity reported by us, the dosimeters had been used before but had not received an accumulated exposure in excess of IR. My opinion is, therefore, that it is a true excitation by light and not a rearrangement of trapped electrons. Similar experiences have been reported in other investigations of LiF. With regard to the different precision attained by us and the British group with LiF-Teflon discs, no influence of the low temperature glow peak is present in our results. This glow peak was minimized in the preirradiation annealing, using 80°C for 2 hr after 300°C for 15 min. Besides, the dosimeters were read out immediately after irradiation. In any case, postirradiation annealing as used by Dr. Ehrlich in one of the papers reported by Dr. Langmead, is the most efficient way to eliminate the low temperature glow peak. I would appreciate it if this point was commented upon by the authors of the other paper concerned.

L. K. BURTON (*U.K.*):

No elimination of the low temperature glow peak was attempted for the measurements recorded. There is some indication that the low temperature glow peak develops only after several irradiation-annealing cycles.

R. L. KATHREN (*U.S.A.*):

Dr. Langmead's comments with respect to not advocating one or another system for personnel dosimetry are well taken. We should endeavour to study both the accuracy and sources of error of all currently used and promising systems. Since untoward effects of environment on film dosimeters have been reported, I would like to inquire of those who reported on comparison studies between film and thermoluminescence systems whether the films used were given appropriate protection from adverse environment. (Apparently those used by Johnson and Attix were not since a faulty air conditioner in their building was stated to be responsible for some spurious effects on film.) A comparison study at our Laboratory indicated reasonably good agreement between film and thermoluminescence dosimeters. However, in a few cases, the TLD read very much higher than the film. This effect, viz. apparently inexplicably high TLD readings, has occasionally been noted in TLD used for other experimental purposes. And, with respect to TLD impregnated in Teflon, studies at our Laboratory also indicated a pronounced reduction in light output per unit dose upon reuse.

J. CAMERON (*U.S.A.*):

I want to comment briefly on several points raised earlier. One of them is the matter of testing or comparing two systems: it is nice to use a new system in practice, but it is almost impossible to make a true test of it, because you are comparing a system, for example thermoluminescence, to film and film has a rather wide inaccuracy in practical use, and the only way you can make a practical test is to do a blind test and to have somebody exposed with the film *and* the new system and to read these out. In the work reported by Dr. Langmead and performed in our laboratory, all of the exposures were unknown. The exposures were made by our health physicist and read out by Suntharalingam. The matter of variability from one laboratory to another can depend upon factors such as the batch of material; this is somewhat variable. The annealing effect is another large variability, for example at the reading of Teflon dosimeters, if you anneal them at 300° for 1 hour, and then anneal them at 80° for about one day, the original response is essentially restored. I think these are the main comments.

G. COWPER (*Canada*):

When Teflon-LiF is used as a finger dosimeter it is required to lie on an approximately cylindrical surface. To be read accurately, it must however lie on a flat surface and must therefore itself be flat to give good heat transfer. Would the authors care to comment on the problem of achieving results which are not subject to error because of this effect?

B. BJARNGARD (*U.S.A.*):

The possible deformation of the discs, as pointed out by Dr. Cowper, is certainly to be taken into consideration when reading them out. Our heating element for the discs has a perforated metal screen attached to a Nichrome planchet, in which the heat is generated. The disc is inserted between the screen and the planchet. Provided the screen is not deformed, it presses the disc to the hot support. No special difficulties result from deformation of the discs if this technique is used.

G. TORI (*Italy*):

Come radioterapista, ho apprezzato molto il valore delle informazioni rese note dai vari sperimentatori. Queste nuove possibilità di accertamento dosimetrico offrono prospettive assai interessanti anche per le applicazioni pratiche sui pazienti in cura e sul personale. Chiedo se, nell'ambito delle determinazioni di confronto fra i differenti sistemi dosimetrici, sono state effettuate prove tra i dosimetri a termoluminescenza (LiF) e quelli a fotoluminescenza, ossia quelli basati sull'impiego di metafosfati misti di Al, Na, ecc., il cui elemento sensibile è rappresentato dall'argento.

K. BECKER (*Germany*):

Es sind sowohl Vergleiche zwischen Film- und Thermolumineszenz-Dosimetern wie auch Vergleiche zwischen Film- und Glasdosimetern durchgeführt worden. Bei letzteren zeigte sich eine gute Übereinstimmung der Glasdosimeteranzeige mit der von Ionisationskammer-Stabdosimetern, dagegen eine schlechte Übereinstimmung mit der Filmdosis. Vergleiche zwischen Glas- und Thermolumineszenzdosimetern sind u. W. in der Praxis noch nicht durchgeführt worden. Aufgrund der dosimetrischen Eigenschaften dieser Systeme wäre jedoch dabei sicherlich mit einer guten Übereinstimmung beider Systeme zu rechnen.

J. BOOZ (*Euratom*):

I want to make a remark on the described comparisons of dose response curves of LiF-dosimeters that had been irradiated with radiations of different energy. I wonder, what might be the influence of the material surrounding the dosimeters during irradiation? The secondary electrons produced by ^{60}Co γ radiation, for instance, are sufficiently energetic to partly penetrate the dosimeters and to contribute to the measured dose, which might be not the case for low energy X-radiation. Therefore, I would like to know what was the surrounding matter that has been used for the measurement shown in Fig. 2.

M. EHRLICH (*U.S.A.*):

At both energies, an electronic-equilibrium layer of polyethylene or an equivalent plastic surrounded the LiF. However, this fact is of no importance to the results shown in Fig. 2, concerned with the change in the shape of the response vs. log exposure curves. A change in the surrounding material would simply cause a shift of the curves parallel to the exposure axis.

W. N. SAXBY (*U.K.*):

Mr. Langmead has given two excellent presentations this morning. I am sure that we all greatly admire this *tour de force*. In his own paper he described how to determine the average dose absorbed by the body, this being the integrated dose over the body volume divided by the body mass.

He did not say why this is a "revealing dose" and in particular he did not say why the integrated dose was chosen. This particular choice needs further justification both from a dosimetric and radiobiological viewpoint and from an ICRP and regulating viewpoint. I would like to have the views of the author and of any radiobiologists or ICRP members who may be present.

W. A. LANGMEAD:

The question is why we wished to know the "average" dose to the body. Recently it has been suggested that certain chromosome aberrations in circulating blood cells are related to the absorbed doses received by the cells. Such a biological indicator of absorbed dose would be helpful in the dosimetry of over-exposed persons and, in the absence of information as to the doses received by the affected cells, the dose value most likely to correlate with the observed chromosome damage is the "average" dose to the body. In the U.K. Atomic Energy Authority, chromosome investigations of this kind are undertaken and hence the need to know the "average" dose to the body of this irradiated person.

K. BECKER (*Germany*):

Einige Autoren haben gefunden, dass die Spaltfragmentregistrierung in Gläsern mit einer geringeren Ausbeute erfolgt als in Kunststoffen. Die ausgezeichnete Übereinstimmung der Empfindlichkeit von $1,2 \times 10^{-5}$ Spuren/Neutron/barn, die Herr Prêtre mit Kunststoffen gefunden hat, mit dem Wert von Unruh et al. für Kunststoffe und dem von uns für Phosphatgläser gefundenen Wert bestätigt unser Ergebnis, dass unter optimierten Ätzbedingungen die Empfindlichkeit für Gläser und Kunststoffe nahe bei 100% liegt.

SOINS MÉDICAUX AUX TRAVAILLEURS SOUMIS AUX RADIATIONS IONISANTES

H. P. JAMMET

Commissariat à l'Énergie Atomique, Département de la Protection Sanitaire, Fontenay-aux-Roses, France

Résumé—La protection radiologique repose essentiellement sur la prévention et le contrôle des nuisances radiologiques par les procédés technologiques et les méthodes dosimétriques appropriés.

L'action médicale a pour but de contrôler l'état de santé des travailleurs soumis aux radiations ionisantes et d'assurer les soins nécessaires aux irradiés et contaminés éventuels.

Le contrôle médical de l'état de santé des travailleurs n'est pas compétitif, mais complémentaire du contrôle physique des radiations ionisantes. Il vise d'abord à déterminer l'aptitude médicale au poste de travail considéré, ensuite à vérifier la conservation d'un état sanitaire satisfaisant au cours de l'exercice de la profession, enfin à prendre les décisions qui s'imposent soit en cas de surexposition aux radiations, soit en cas de déficience de l'état de santé. Il met en œuvre des méthodes classiques d'investigation pour l'examen clinique général et des méthodes spéciales pour les examens particuliers des organes et des fonctions les plus sensibles aux nuisances radiologiques: système hématopoïétique, peau, œil, etc.

Les soins médicaux à dispenser aux irradiés ou aux contaminés au cours d'accidents radiologiques nécessitent une triple action dans les domaines complémentaires de la dosimétrie, du diagnostic et du traitement.

La première tâche consiste dans la collecte de toutes les informations utiles sur les circonstances précises de l'accident, la nature et l'importance de l'irradiation ou de la contamination; elle impose l'évaluation des doses externes reçues ou des contaminations internes incorporées; elle nécessite souvent la reconstitution de l'accident pour mieux préciser ces données.

La seconde tâche vise à recueillir tous les renseignements relatifs aux effets biologiques de l'irradiation ou de la contamination; les investigations portent sur les dommages aux organes et aux fonctions les plus exposés qui sont, selon les cas, la peau, la moelle osseuse, l'intestin, les poumons, le foie et les reins; le diagnostic doit, si possible, être non seulement qualitatif, mais quantitatif et corrélé aux données de la dosimétrie.

La troisième tâche consiste à mettre en œuvre les traitements appropriés, sur la base des indications thérapeutiques établies à partir des informations dosimétriques et cliniques: dans le cas d'irradiations externes partielles ou globales elle nécessite la mise en œuvre des procédés de lutte contre l'infection, l'hémorragie, la dégradation tissulaire; dans le cas de contamination, elle entraîne l'utilisation des méthodes de décontamination externe ou interne.

Ces actions médicales ne peuvent être accomplies de façon correcte et efficace que par une organisation adéquate; sur les lieux même de travail, les médecins du travail doivent disposer d'infirmeries permettant d'effectuer les investigations indispensables et d'assurer les premiers soins; dans les hôpitaux, seules des équipes spécialisées, rassemblant l'éventail complet des compétences et disposant des moyens convenables d'isolement et de décontamination, peuvent offrir une efficacité certaine pour la prise en charge et le traitement des irradiés et des contaminés.

INTRODUCTION

La Protection Radiologique repose essentiellement sur la prévention et le contrôle des nuisances radiologiques par les procédés technologiques et les méthodes dosimétriques appropriés.

L'action médicale a pour but de contrôler l'état de santé des travailleurs soumis aux radiations ionisantes et d'assurer les soins nécessaires aux irradiés et contaminés éventuels.

Le contrôle médical de l'état de santé des travailleurs n'est pas compétitif, mais complémentaire du contrôle physique des radiations ionisantes. Il vise d'abord à déterminer l'aptitude médicale au poste de travail considéré, ensuite à vérifier la conservation d'un état sanitaire satisfaisant au cours de l'exercice de la profession, enfin à prendre les décisions qui s'imposent soit en cas de surexposition aux radiations, soit en cas de déficience de l'état de santé. Il met en œuvre des méthodes classiques d'investigation pour l'examen clinique général et des méthodes spéciales pour les examens particuliers des organes et des fonctions les plus sensibles aux nuisances radiologiques.

La surveillance médicale bien organisée est complétée par l'enregistrement de toutes les données relatives aux travailleurs dans des dossiers sanitaires. Le service médical doit donc connaître de façon précise les nuisances radiologiques auxquelles sont exposés les travailleurs, participer à l'élaboration des moyens de prévention mis en place pour limiter l'irradiation professionnelle à des niveaux admissibles, contribuer à l'éducation des travailleurs en matière de protection radiologique.

I. CONTRÔLE MÉDICAL AVANT L'EMPLOI

Avant l'emploi de tout travailleur exposé aux radiations ionisantes, il convient d'établir un bilan qui a un double but: il sert d'abord à déterminer dans quelle mesure les antécédents et l'état actuel du travailleur permettent de le juger apte ou non au travail auquel il est destiné; ensuite en cas d'aptitude à un tel travail, il sert de point de comparaison pour toutes les modifications ultérieures qui pourraient survenir du fait des risques liés au travail.

L'interrogatoire précisera les antécédents héréditaires, personnels et professionnels. Il est particulièrement important de noter les irradiations subies antérieurement en distinguant celles qui sont d'origine professionnelle et celles qui sont dues à des examens ou à des traitements radiologiques. En effet, on devra tenir compte des premières pour fixer les limites maximales admissibles à ne pas dépasser. Par contre, les secondes doivent être simplement notées sans être forcément incompatibles avec une exposition professionnelle aux radiations ionisantes.

Un examen médical complet doit être effectué avant l'emploi, en principe dans les deux mois qui précèdent l'embauche, comportant des investigations générales permettant de juger de l'aptitude banale au travail, et des investigations spéciales testant l'aptitude particulière aux travaux avec risques d'irradiation externe ou de contamination radio-active. C'est ainsi qu'en cas d'irradiation de l'organisme entier, il convient de pratiquer un examen hématologique, en cas d'exposition à des rayonnements β peu pénétrants, un examen dermatologique, en cas d'exposition à des rayonnements neutroniques, un examen ophtalmologique, en cas de pollution radio-active de l'atmosphère, un examen pulmonaire.

Les antécédents et les résultats des examens généraux et spéciaux doivent aboutir à des décisions d'aptitude. Celles-ci sont fondées sur un certain nombre de critères dont les valeurs n'ont pas été établies de façon définitive. Ainsi les chiffres retenus pour les formules et numérations sanguines varient d'un pays à l'autre et dépendent des techniques utilisées. En règle générale, les candidats sont répartis en trois catégories: aptes, provisoirement inaptes, définitivement inaptes à des travaux avec risque d'irradiation ou de contamination radio-active. Ceux placés dans la deuxième catégorie devraient être mis en observation, subir de nouveaux examens et n'être déclarés définitivement inaptes qu'après plusieurs résultats se confirmant.

II. CONTRÔLE MÉDICAL PENDANT L'EMPLOI

Pendant l'emploi, les travailleurs exposés aux radiations ionisantes doivent être soumis régulièrement à des examens médicaux. Des irradiations ou contaminations anormales peuvent passer inaperçues, et il faut en déceler les effets éventuels. Des changements peuvent survenir dans l'état sanitaire du travailleur,

contre indiquant son maintien à un poste de travail sous radiations.

La nature des examens médicaux à pratiquer dépend des nuisances radiologiques auxquelles le travailleur est exposé. En plus des examens cliniques généraux, des examens spéciaux sont à mettre en œuvre pour tester les organes et les fonctions les plus sensibles à l'irradiation externe ou à la contamination radio-active.

La fréquence des examens médicaux est à fixer en fonction de deux critères. D'une part, on doit tenir compte de la nature et de l'importance des risques d'irradiation ou de contamination. D'autre part, on doit faire intervenir l'état de santé du travailleur notamment les troubles morphologiques ou fonctionnels qu'il peut présenter.

En cas d'exposition globale à des rayonnements pénétrants ou de contamination par des radio-éléments à métabolisme général, l'irradiation de l'ensemble des tissus hématopoïétiques conduit à pratiquer des examens hématologiques. Les hémogrammes doivent indiquer le nombre, par millimètre cube, d'érythrocytes, de réticulocytes, de granulocytes, de lymphocytes et de thrombocytes. Ils doivent en outre comporter un dépistage des modifications morphologiques ou fonctionnelles des cellules sanguines: anisocytose érythrocytaire, anomalies cytoplasmiques granulocytaires, noyaux bilobés lymphocytaires.

En cas de contamination par des poussières radio-actives, des examens pulmonaires sont indispensables. Les investigations doivent renseigner sur l'état morphologique et fonctionnel de l'appareil respiratoire, soit par les méthodes radiologiques soit par les épreuves spirométriques.

Les examens ophtalmologiques, portant essentiellement sur le cristallin, sont indiqués en cas d'exposition à des rayonnements de transfert linéaire d'énergie élevé. Les examens dermatologiques sont utiles en cas de manipulation de sources de rayonnements β ou de substances radio-actives contaminantes. Les examens biochimiques n'ont pas tant pour but de déceler des altérations métaboliques, que de tester l'état fonctionnel des émonctoires hépatique et rénal, sollicités en cas de contamination radio-active.

Les résultats de ces examens médicaux servent de base aux décisions de maintien au poste de travail ou d'exclusion temporaire ou définitive.

III. CONTRÔLE MÉDICAL APRÈS L'EMPLOI

Les effets des rayonnements ionisants se manifestent toujours après une certaine période de latence, pouvant aller de quelques heures ou quelques jours, à plusieurs mois, plusieurs années. Il est donc indispensable d'exercer une surveillance des travailleurs après la cessation de l'emploi en vue de déceler des maladies professionnelles tardives.

Cette surveillance n'incombe pas au service médical de l'entreprise. Mais celui-ci doit pouvoir assurer les relations avec les médecins traitants qui pourraient dépister dans l'avenir une affection imputable aux radiations ionisantes.

Parmi ces affections, l'attention des médecins traitants devrait être attirée sur l'apparition d'altérations cutanées, oculaires ou sanguines et sur le dépistage des néoplasies. Il va sans dire que l'établissement d'une corrélation entre l'irradiation professionnelle et ces manifestations tardives est très difficile, surtout en ce qui concerne les affections malignes.

IV. CONTRÔLE MÉDICAL EN CAS D'ACCIDENT

En cas d'accident, des examens particuliers doivent être mis en œuvre afin de déceler les premiers troubles éventuels et d'établir, dans la mesure du possible, les corrélations entre l'irradiation ou la contamination et les manifestations cliniques.

Lorsqu'une surexposition globale est à redouter, il convient de pratiquer d'urgence un certain nombre d'examens. L'interrogatoire doit enregistrer les premières manifestations de déséquilibre neuro-végétatif: nausées, vomissements, diarrhée. Les numérations lymphocytaires, granulocytaires et réticulocytaires présentent à la fois un intérêt diagnostique et pronostique. L'étude des altérations cytologiques, bilobation nucléaire des lymphocytes, anomalies chromosomiques des cellules sanguines, offre un intérêt tout particulier. Les myélogrammes comportant numération et formule sont un appoint essentiel. L'étude de la spermatogénèse chez l'homme permet de tester l'une des fonctions les plus radiosensibles. Les examens biochimiques sont à recommander dès le premier jour, en vue d'évaluer la crise catabolique initiale, concernant notamment certains acides aminés tels que l'acide amino-isobutyrique et

la taurine. Lorsqu'une surexposition partielle est à envisager, notamment au niveau de la face et des mains, l'examen immédiat de l'état cutané et oculaire s'impose. Il fournira la base de référence pour juger de l'évolution ultérieure des lésions dermatologiques ou ophtalmologiques.

Lorsqu'une contamination notable par des substances radio-actives s'est produite, ce ne sont pas tant les investigations cliniques qui s'imposent dans l'immédiat, mais les premiers soins à pratiquer d'urgence. Le plus rapidement possible, doivent être mises en œuvre les différentes méthodes de décontamination radioactive: nettoyage cutané, parage des plaies, évacuation du contenu gastrique, selon les circonstances accidentelles. En outre, l'utilisation précoce de complexants, tels que l'acide diéthylène triaminepentacétique, s'impose dans les cas de contamination de la peau, de plaies ou des poumons par des radio-éléments de valence élevée.

V. TENUE DES ARCHIVES MÉDICALES

Un contrôle médical bien organisé est inconcevable sans un enregistrement systématique et fidèle de toutes les informations utiles pour juger de l'état sanitaire des travailleurs exposés aux radiations ionisantes. Ces données constituent le dossier médical individuel, qui doit être conservé conformément aux conditions qui régissent, dans chaque pays, le secret médical. Ce dossier doit comprendre les fiches d'affectation et de nuisance, les résultats des mesures physiques et des examens médicaux, le relevé des accidents du travail et des maladies professionnelles.

Les fiches d'affectation et de nuisance permettent de déterminer, pour chaque travailleur, les conditions de travail et les risques d'irradiation et de contamination. La fiche d'affectation est établie à l'embauche et doit indiquer toutes les mutations de poste qui interviennent par la suite. La fiche de nuisance renseigne sur les risques d'irradiation externe et de contamination radio-active liés à chaque activité.

Les résultats des mesures physiques et des examens médicaux sont indispensables pour préciser les conditions réelles d'exposition aux radiations ionisantes et pour apprécier l'état de santé du travailleur. Les mesures physiques doivent porter sur tous les éléments utiles pour l'évaluation des doses reçues, avant l'emploi du fait des irradiations professionnelles antérieures, pendant l'emploi du fait de l'irradiation externe et de la contamination radio-active auxquelles est exposé le travailleur chaque trimestre, après l'emploi en récapitulation cumulative. Les examens médicaux doivent apporter toutes les données relatives à l'état de santé du travailleur, avant l'emploi pour les décisions d'aptitude, pendant l'emploi pour les observations d'anomalies ou de troubles des organes ou fonctions radiosensibles, après l'emploi pour l'établissement du bilan sanitaire.

Les relevés des accidents du travail et des maladies professionnelles méritent d'être groupés dans des archives spéciales. Il y a lieu d'enregistrer tous les cas de surexposition ou de contamination dépassant les limites trimestrielles, ainsi que les constatations médicales faites à cette occasion. Il y a également lieu de noter les maladies professionnelles vraies ou présumées, ainsi que les corrélations physiques établies à leur sujet.

VI. PRINCIPES D'ORGANISATION DU CONTRÔLE MÉDICAL

Les principes d'organisation du contrôle médical sont à considérer aussi bien en ce qui concerne les circonstances normales que les circonstances accidentelles.

Dans les circonstances normales, la médecine du travail doit être organisée de façon telle qu'elle puisse tenir d'une façon correcte les archives médicales sus-mentionnées. Par ailleurs, compte doit être tenu des dispositions légales ou des habitudes professionnelles existant dans les différents pays.

De toute façon, le service médical doit pouvoir apprécier l'état de santé du travailleur avant et pendant l'emploi. Il doit collecter toutes les informations concernant l'exposition aux radiations ionisantes ou les contaminations radioactives. C'est, compte tenu des informations relatives aux conditions de travail et des informations relatives à l'état sanitaire des travailleurs que pourront être prises les décisions d'aptitude ou d'inaptitude au poste d'affectation.

En ce qui concerne les circonstances accidentelles, les soins médicaux à dispenser nécessitent une double action dans les domaines complémentaires de la dosimétrie, du diagnostic et du traitement.

La première tâche consiste dans la collecte de toutes les informations utiles sur les circonstances précises de l'accident, la nature et l'importance de l'irradiation ou de la contamination; elle impose l'évaluation des doses externes reçues ou des contaminations internes incorporées; elle nécessite souvent la reconstitution de l'accident pour mieux préciser ces données.

La seconde tâche vise à recueillir tous les renseignements relatifs aux effets biologiques de l'irradiation ou de la contamination; les investigations portent sur les dommages aux organes et aux fonctions les plus exposés qui sont, selon les cas, la peau, la moelle osseuse, l'intestin, les poumons, le foie et les reins; le diagnostic doit, si possible, être non seulement qualitatif, mais quantitatif et corrélé aux données de la dosimétrie.

La troisième tâche consiste à mettre en œuvre les traitements appropriés, sur la base des indications thérapeutiques établies à partir des informations dosimétriques et cliniques; dans le cas d'irradiations externes partielles ou globales elle nécessite la mise en œuvre des procédés de lutte contre l'infection, l'hémorragie, la dégradation tissulaire; dans le cas de contamination, elle entraîne l'utilisation des méthodes de décontamination externe ou interne.

Il convient de bien noter que la distinction entre l'exécution des diverses mesures et examens dans des circonstances normales ou accidentelles et l'interprétation des résultats en vue des décisions médicales à prendre.

En effet, les services médicaux ne sont pas forcément chargés d'exécuter les diverses tâches physiques et biologiques. Celles-ci peuvent être accomplies soit par d'autres organismes de l'entreprise: Service de Protection Radiologique, Service de Chimie Analytique, Service de Sécurité, soit par des services extérieurs à l'entreprise: Laboratoires d'hématologie, Laboratoires de biochimie, Médecine spécialisée. Par contre, la collecte des informations, leur interprétation et la prise des décisions médicales consécutives doivent relever du service de médecine du travail.

VII. MOYENS NÉCESSAIRES DANS LES ÉTABLISSEMENTS INDUSTRIELS

Compte tenu des principes d'organisation précédents, le Service de Médecine du Travail doit pouvoir disposer, à l'intérieur des établissements industriels, de moyens appropriés. Mais ces moyens peuvent être extrêmement variés en fonction de la répartition des tâches d'exécutions par exemple, alors que dans certains grands établissements le service de médecine du travail exécute lui-même les examens biologiques spécialisés en hématologie ou en biochimie, dans les petits établissements en général, ce sont des laboratoires extérieurs qui exécutent ces mêmes examens.

Un autre exemple est celui des investigations radio-toxicologiques sur prélèvements biologiques qui, dans certains pays, sont effectuées dans les services médicaux et dans d'autres, par les services de protection ou par un service de chimie analytique. Un dernier exemple est celui des investigations et des soins d'urgence à donner aux accidentés radiologiques; alors que dans certains grands établissements, le service médical dispose des moyens nécessaires à une action propre, dans les plus petits, il faudra faire appel à des organismes spécialisés extérieurs. De toute façon, il est un minimum de moyens indispensables qui constituent le fond commun nécessaire: salle de réception pour l'interrogatoire, salle d'examens cliniques, salle de pansements, salle de décontamination, etc.

VIII. MOYENS NÉCESSAIRES DANS LES ÉTABLISSEMENTS HOSPITALIERS

Comme nous venons de le voir précédemment, il se peut que, soit dans des circonstances normales, soit dans des circonstances accidentelles, des services de Médecine du Travail fassent appel à des Services Hospitaliers. Il peut s'agir de l'exécution d'un certain nombre d'examens médicaux ou d'examens de laboratoires spécialisés, utiles dans les circonstances normales; dans les circonstances accidentelles, d'une façon générale, il est fait appel aux services hospitaliers pour prendre en charge les accidentés radiologiques après les traitements d'urgence qui ont pu être effectués. A ce propos, il convient de signaler que n'importe quel service hospitalier n'est pas forcément compétent pour le diagnostic ou le traitement des affections radiopathologiques. L'efficacité des soins donnés dépend, en grande partie, de l'éventail des compétences et de l'entraînement préalable des équipes hospitalières. Dès qu'il s'agit d'accident grave d'irradiation globale ou partielle ou

de contamination interne, il est préférable de s'adresser à des équipes hospitalières susceptibles d'effectuer les études dosimétriques, les examens diagnostiques et les actes thérapeutiques. De telles équipes doivent pouvoir disposer:

—dans le domaine dosimétrique: des laboratoires de dosimétrie radiologique, d'analyse radio-active, de spectrométrie γ, de scintigraphie γ, de mesure radio-active *in vivo*.
—dans le domaine diagnostique: des laboratoires d'hématologie, de cytogénétique, de biochimie, de toxicologie radio-active, de métabolisme radio-actif, d'électrophysiologie.
—d'une unité de traitement médical avec possibilité d'isolement et de télésurveillance et d'une unité de traitement chirurgical avec salle d'opération spécialisée pour le traitement de contaminés.

Les rôles respectifs des services médicaux de l'établissement et de l'hôpital doivent être complémentaires. Une coordination est indispensable pour aboutir à des conceptions identiques, une confiance réciproque et des consignes préétablies.

CONCLUSION

Le contrôle médical des travailleurs exposés aux radiations ionisantes exige la mise en œuvre de moyens appropriés, tant en ce qui concerne la compétence des médecins du travail que l'équipement matériel dont ils doivent disposer. Il ne peut s'accomplir efficacement qu'en collaboration étroite avec les services chargés du contrôle physique des rayonnements. Il exige des liaisons régulières avec la hiérarchie et la direction de l'établissement. Il nécessite enfin des relations confiantes avec le personnel et ses délégués.

Enfin, il doit être complété par la prise en charge éventuelle des accidentés radiologiques par une équipe hospitalière compétente.

IMPORTANCE DE L'AUGMENTATION DU NOMBRE DES LYMPHOCYTES BINUCLÉÉS POUR LA BIODÉTECTION DES FAIBLES DOSES DE RADIATIONS IONISANTES

B. PENDIĆ* et V. TOMIN

Service de Protection Médicale. Institut des sciences nucléaires "Boris Kidrič"—Vinča, Yougoslavie

Résumé—On présente les résultats obtenus lors de l'observation des lymphocytes binucléés (BnL) dans le sang périphérique chez quatre groupes d'individus exposés à de faibles doses de radiations ionisantes.

Chez les individus du premier groupe, où la dose de radiation gamma prise par le corps entier, lors de l'irradiation unique, était de l'ordre du rad, on a constaté une augmentation statistiquement significative de BnL au cours de la deuxième semaine après l'irradiation.

Dans le deuxième groupe, où l'exposition professionnelle en continu aux doses de radiations ionisantes restait dans les limites tolérables, on a constaté aussi l'augmentation de BnL par rapport au groupe témoin.

Dans le troisième et le quatrième groupes, où l'irradiation partielle du corps provenait de la radioscopie diagnostique du poumonet où le rayonnement X mesuré dans l'air au niveau de la peau était 2 R et 6 R, l'augmentation de BnL n'a pas été constatée.

On a discuté dans ce rapport le caractère de certitude de ce test hématologique pour la biodétection des faibles doses de radiations ionisantes.

INTRODUCTION

Les modifications hématologiques représentent souvent la première indication des effets biologiques dues aux radiations ionisantes.[1] Elles peuvent être classées en deux groupes: modifications quantitatives du nombre et du rapport numérique des éléments du sang périphérique et de la moelle osseuse et modifications qualitatives morphologiques des cellules sanguines.

Dans le cas d'une exposition à de faibles doses d'irradiation, ne dépassant pas les doses tolérables, les modifications quantitatives apparaissent d'habitude au bout de plusieurs années. C'est alors que ces individus présentent, comme le dit Lacassagne,[2] "l'image sanguine d'un radiologue", manifestée par une anémie modérée de type macrocytaire, par la leucopénie avec une lymphocytose relative et une trombocytose. Les tests quantitatifs très intéressants pour l'étude des groupes particuliers, peuvent être difficilement appliqués au contrôle individuel, étant donné les variations physiologiques importantes.

Modifications qualitatives: 1. modifications de la structure du noyau de la souche leucocytaire du sang périphérique et des cellules médullaires; 2. apparition des cellules jeunes de la souche monocytaire avec une monocytose modérée; 3. apparition des lymphocytes binucléés et bilobés, des lymphocytes avec des fragments du noyau; 4. apparition des cellules mononucléées basophiles; 5. apparition des cellules de la souche érythrocytaire avec le noyau dans le sang périphérique et 6. aberrations chromosomiques des cellules sanguines. Tous ces phénomènes peuvent servir comme indicateurs dans la biodétection de faibles doses d'irradiation.[3]

L'observation du phénomène des lymphocytes binucléés (BnL) dans le sang périphérique et des aberrations chromosomiques dans les leucocytes du sang et des cellules médullaires est très intéressante pour l'étude des effets biologiques.

L'accroissement du nombre de BnL dans le

* Hôpital de la Ville, 172 rue Baje Sekulica, Belgrade.

sang périphérique chez des individus soumis à de faibles doses de radiations ionisantes, révélé d'abord par Ingram,[4-6] a été confirmé aussi par d'autres auteurs.[3, 7-11] Nous avons observé le même phénomène dans nos travaux précédents.[12] La croissance de BnL a lieu chez des individus chroniquement soumis à de faibles doses d'irradiation.[7, 8] Après avoir examiné les sujets professionnellement exposés de 0,017–0,079 R par semaine au cours de trois ans, Blazekova[11] a aussi constaté une croissance de BnL statistiquement significative. L'exposition unique du corps total aux doses de l'ordre de 1 R provoque l'accroissement transitoire de BnL, le plus important au cours de la deuxième semaine après l'irradiation.[7, 12] Les expériences effectuées sur des animaux ont donné des résultats qui sont en bon accord avec ceux obtenus sur des humains.

Il est à souligner que le nombre de BnL accru n'est pas dû seulement à l'irradiation, mais aussi, dans certains cas, à quelques maladies virales, à la leucémie lymphatique et lors du traitement à de fortes doses de cortisone et d'antibiotiques.

MATÉRIEL ET MÉTHODE

Ce rapport présente les résultats de l'étude relatifs au phénomène de BnL observé chez quatre groupes des individus exposés à l'irradiation.

1er groupe, exposition unique du corps total aux rayonnements gamma de 1 à 3 R, reçus lors des travaux de maintenance au réacteur RA de notre Institut.

2ème groupe. Ce groupe comprend les sujets ayant été professionnellement soumis en continu à de faibles doses d'irradiation. Le temps d'exposition a été de 1 à 10 ans, et la dose moyenne par an pour tout le groupe 2,268 R.

3ème et 4ème groupes, exposition partielle aux rayons X, lors de la radioscopie du poumon à titre diagnostique. Les individus examinés n'ont pas été soumis aux radiations ionisantes au cours de la dernière année. La radioscopie du poumon a été faite à l'appareil de type "Morava". Les conditions de l'exposition ont été les suivantes: 65 kV, 3 mA, temps d'exposition pour le troisième groupe—20 secondes, et pour le quatrième—1 minute. La dose d'exposition a été mesurée dans l'air au niveau de la peau au milieu du thorax au moyen de la chambre d'ionisation Victorin. Elle est de l'ordre de 2 R et 6 R respectivement. Les mesures ont été effectuées par le Service de Protection contre les Radiations de notre Institut.

Le groupe témoin comprend 10 hommes et 10 femmes. Tous ces individus ont été en état de santé satisfaisant, n'ayant pas été atteints de maladies virales ou de maladies aiguës pendant la période de contrôle. Ils n'ont subi aucune irradiation au cours de la dernière année.

Les échantillons de sang des 1er, 3ème et 4ème groupes ont été prélevés tous les trois jours après l'irradiation au cours d'un mois. Les frottis ont été préparés par la méthode habituelle et colorés selon Papenheim. On a compté pour chaque date au moins 10.000 lymphocytes. Pour choisir les BnL le critérium suivant est adopté: le lymphocyte binucléé est une cellule un peu plus grande que celle du jeune lymphocyte, contenant deux noyaux de même taille, lesquels ressemblent au noyau des lymphocytes normaux. Ces deux masses nucléaires sont complètement séparées (Figs. 1 et 2). On n'a pris en considération que les BnL qui correspondent à cette description.

RÉSULTATS ET DISCUSSION

Chez le groupe témoin, tableau 1, le taux moyen est 0,90 ± 0,32 BnL à 10.000 lymphocytes, ce qui est en accord avec les résultats de Dobson,[15] qui a aussi fait la différentiation des

Tableau 1.

GROUPE TÉMOIN
BnL à 10.000 Ly

hommes	femmes
0,40	0,96
0,70	0,97
0,77	0,74
0,73	1,40
1,11	0,92
1,02	0,60
1,00	1,00
1,00	1,02
1,58	0,00
1,00	1,00

M = 0,90
SD = ± 0,32

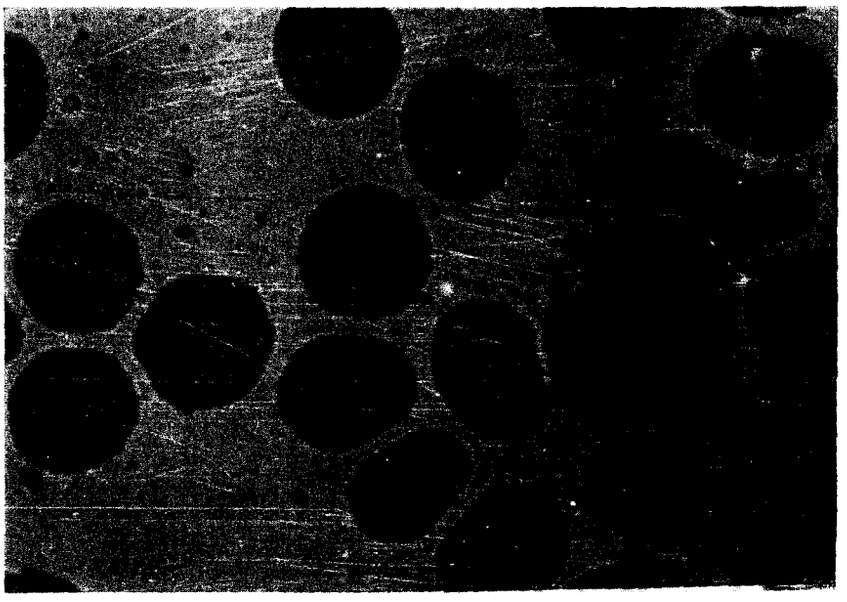

FIG. 1.

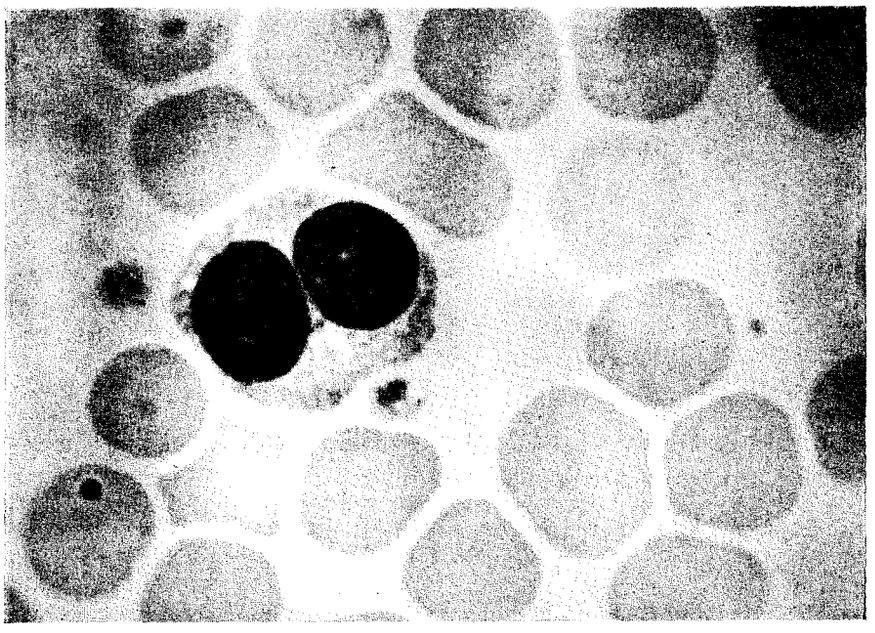

FIG. 2.

préparations natives. Ingram et Taranger [8, 16] ont révélé un taux élevé sur les frottis enrichis des sujets non exposés. Nous n'avons pas expérimenté avec des frottis des leucocytes enrichis, parce que nous avons constaté dans les travaux précédents que les méthodes utilisant la centrifugation changent le pourcentage des leucocytes dans la formule leucocytaire, car les petits lymphocytes mûrs étant perdus dans le sédiment. Nous n'avons pas constaté d'influence du sexe sur le nombre de BnL, comme il a été remarqué par Taranger et Davydoff. [16] L'âge des sujets examinés n'influence pas non plus le nombre de BnL dans le sang.

Tableau 2.

GROUPE 1er

BnL à 10.000 Ly

	Dose en R	Semaines après irradiation		
		I semaine	II semaines	III et IV semaines
1.	1 à 3	1,50	4.50	2,00
2.		1,50	3,23	0,75
3.		0,96	2,76	1,84
4.		2,00	3,65	1,02
5.		1,66	3,63	1,84
6.		0,60	3,03	0,60
7.		0,60	2,42	0,60
8.		1,05	1,09	1,11
9.		0.50	0,60	0,25
		M = 1,15	M = 2,77	M = 1,11
		SD = ± 0,50	SD = ± 1,13	SD = ± 0,59
		P 0,10	P 0,002	P 0,10

Le tableau 2 présente les résultats obtenus lors de l'observation du phénomène de BnL chez le premier groupe des individus examinés dont la dose d'irradiation était de 1 à 3 R. Une croissance remarquable est constatée au cours de la deuxième semaine après l'irradiation, comme il a été déjà révélé par d'autres auteurs aussi [7, 8, 13] Cette croissance est à peu près quatre fois plus grande chez les premiers 7 individus que celle des témoins. Les deux derniers individus n'ont présenté aucune réaction de BnL et le nombre, de ceux-ci au cours de l'examen, ne différait guère de celui qui a été constaté chez les témoins. Bien que la croissance de BnL soit statistiquement significative pour le groupe entier, on ne peut pas affirmer que la dose inférieure à 1 R, lors de l'irradiation unique, puisse déclencher la croissance de BnL compte tenu d'une distribution non uniforme. La dose seuil de cette réaction, d'après nos expériences, est certainement supérieure à 1 R. Les différences constatées plaident en faveur d'une réaction individuelle dont il faut tenir compte lors de l'évaluation des effets biologiques.

Le tableau 3 présente les résultats des sujets professionnellement soumis aux radiations ionisantes. On y constate une croissance statistiquement significative de BnL, ce qui est en accord avec les observations d'Ingram [6] et de Blazekova. [11]

Les tableaux 4 et 5 présentent les résultats des troisième et quatrième groupes des individus examinés. L'irradiation partielle du corps, radioscopie du poumon, où la dose des rayons X varie de 2 et 6 R, n'a pas provoqué la croissance de BnL dans le sang périphérique.

L'apparition de BnL due à d'autres effets nocifs, outre l'irradiation, indique qu'il s'agit peut-être de la réaction stress du tissu lymphoïde à l'irradiation. Examinant la teneur de BnL en

Tableau 3.
GROUPE 2ème

	Dose en R Moyenne annuelle	BnL à 10.000 Ly	Temps d'exposition en années
1.	4,320	4,91	1
2.	1,185	2,15	2
3.	2,207	4,76	3
4.	2,050	2,68	3
5.	1,850	3,64	3
6.	1,566	6,11	3
7.	2,420	1,95	3
8.	2,941	6,45	3
9.	1,880	2,87	3
10.	1,770	3,85	3
11.	3,475	6,57	10
12.	2,110	1,86	3
13.	2,000	2,60	3
14.	2,000	2,00	3
	M = 2,268	M = 3,74 SD = ± 1,66 P 0.001	

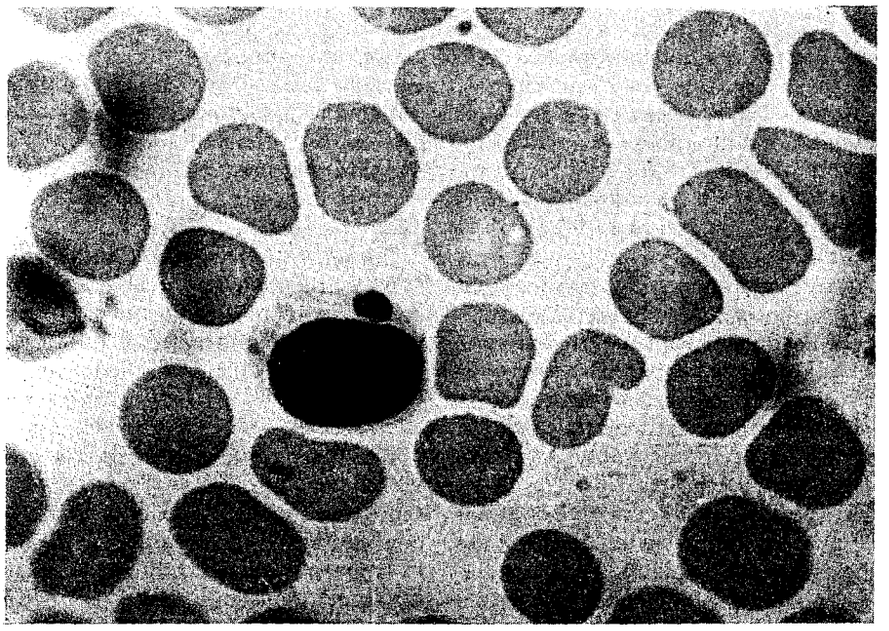

FIG. 3.

Tableau 4.
GROUPE 3ème
BnL à 10.000 Ly

	Dose en R	Semaines après irradiation		
		I semaine	II semaines	III et IV semaines
1.	2	1,00	1,00	0,50
2.		1,49	1,63	1,00
3.		0,50	1,66	0,50
4.		0,84	0,97	0,91
5.		1,29	1,97	1,93
6.		0,00	0,66	0,00
7.		0,33	1,64	1,50
8.		0,97	0,00	0,49
9.		0,00	0,00	0,50
		M = 0,71	M = 1,06	M = 0,81
		SD = ± 0,48	SD = ± 0,65	SD = ± 0,53
		P 0,10	P 0,10	P 0,10

ADN, Dobson[15] suggère qu'il s'agit probablement de la teneur lymphatique normale de BnL en ADN. Il traite les BnL comme des cellules dyploïdes, ce qui plaide en faveur de la division amytotique du noyau. Il considère que leur apparition est la conséquence de la réaction stress. Compte tenu des données insuffisantes, on ne peut pas considérer cette constatation comme définitive. Dans le cas de faibles doses, nous avons tendance à interpréter le phénomène d'apparition de BnL comme un effet direct de l'irradiation sur l'appareil mytotique de la cellule. D'après Schrek,[17] Policard,[18] Mathé[19] aussi les modifications des lymphocytes sont provoquées par l'irradiation. Pour le moment on ne peut pas encore déterminer si le phénomène de BnL est directement provoqué par l'effet de l'irradiation sur l'appareil mytotique—effet génétique, ou s'il est la conséquence de la réaction stress. En étudiant parallèlement le phénomène de BnL et des aberrations chromosomiques dans les leucocytes du sang périphérique (il s'agit en réalité des aberrations chromosomiques des lymphocytes[20]) chez des mêmes sujets, nous avons observé une corrélation assez nette entre ces deux phénomènes.

Bien qu'on sache d'après la radiobiologie que les effets de l'irradiation à dose égale sont bien plus importants dans le cas de l'exposition totale que lors d'une exposition partielle, on n'est pas à même d'expliquer de façon satisfaisante les différences du nombre de BnL, observées lors de l'exposition totale ou partielle à doses pratiquement égales.

Lors du comptage différentiel des éléments sanguins on a observé aussi d'autres modifications morphologiques, telles que: apparition d'un nombre élevé de lymphocytes bilobés et de lymphocytes avec fragments de noyau (Fig. 3) et apparition d'un grande nombre de cellules mononucléées basophiles.

Ingram[8] a souligné l'importance de BnL non seulement en tant que biodétecteur de faibles doses d'irradiation, mais aussi en tant que pronostic d'un nombre élevé de BnL sur l'effet latent d'irradiation—effet leucémogène.

CONCLUSION

Bien que l'apparition de BnL ne soit pas caractéristique pour l'irradiation,—à l'exception de toutes les autres influences possibles, ce qui était le cas dans notre rapport—l'observation de la croissance de leur nombre dans le sang périphérique peut être utilisé comme indicateur assez sensible de l'exposition du corps total à de faibles doses d'irradiation lors de l'exposition

DETECTION OF RADIATION EXPOSURE BY FLUORESCENT MICROSCOPY OF HUMAN BLOOD CELLS

E. VIDER, A. YAARI,* D. SHAFIR and E. RIKLIS
Atomic Energy Commission, Negev Nuclear Research Center, Beer-Sheba, Israel

Abstract—Changes in blood and bone marrow cells involving effects of irradiation on nucleic acids can be detected by fluorescence microscopy much prior to any morphological changes. When blood smears are stained with acridine orange, the leucocytes appear mostly as doubly coloured in a fluorescence microscope, the nucleus being green and the cytoplasm red, yellow or orange. The ratio of doubly coloured cells (DCC) to red coloured cells is fixed for each subject but decreases following X-irradiation, as found in the following experiments. Persons exposed to X-ray routine radiography of chest, as well as hospital personnel were taken as subjects. X-ray doses were measured with a Victoreen Condenser R-Meter and Victoreen Ionization chambers, as skin doses, and exposure time was 0.05 to 0.1 sec. Blood samples were taken from a finger tip before exposure and at fixed intervals after exposure. Blood smears were prepared and stained with acridine orange in phosphate buffer (5 mg/50 ml or 10 mg%, pH 6.85). Two hundred cells were counted and classified according to colour. In all cases the number of doubly coloured cells (green and red) before irradiation was above 68%. Following exposure, in most cases the number of DCC decreased while the number of red coloured cells increased. The observed changes began 6 hr after exposure, reached a maximum 24 to 48 hr after irradiation and then began to subside. The extent of the effect increased with dose, giving noticeable results already at a dose of 18 milliroentgen. There was a uniform response among persons exposed in the chest, but a smaller change in persons exposed in other organs. Blood smears of technicians and clerks not directly involved in work near the X-ray unit showed no changes in the ratio of DCC to red coloured cells. Physicians after fluoroscopy, however, showed a drop in percent of doubly coloured cells. Further development of these investigations might lead to a simple method of internal dosimetry for small doses of X-rays.

1. INTRODUCTION

The need for better biological methods of measuring the extent of radiation exposure on humans is evident. Lately some progress was made in the field of biological dosimetry[1] and the evaluation of radiation effects on chromosomes.[2]

Blood cells, and leucocytes in particular, are known to be very sensitive to ionizing radiations. Changes in blood and bone marrow cells involving effects of radiation on nucleic acids and nucleoproteins are found much prior to any morphological changes. It is well established that desoxyribonucleic acids (DNA) are the cell component most sensitive to both ultraviolet[3] and ionizing irradiation.

* Blood Morphology and Cytology Laboratory, Kaplan Hospital, Rehovot, Israel

The use of fluorescent microscopy for observing early radiobiological effects of irradiation on cells is described in a number of publications.[4-9]

Adsorption of dyes on DNA and RNA is apparently affected by their sensitivity to irradiation. When blood cells are stained with acridine-orange and leucocytes are observed in a fluorescence microscope—the nucleus is coloured green, and the cytoplasm red, yellow or orange.

Leucocytes appear as doubly coloured—green and red under a fluorescence microscope. The ratio of doubly coloured cells to red cells is apparently fixed for each subject. This ratio changes, however, after irradiation. Meisel and Kondrateva,[6] using cell cultures of spontaneous mammary gland cancer of mice, showed

Table 1. *Results of Counts of Fluorescing Blood Cells of Persons exposed to X-ray Chest Radiography. Dose was* 18 *mR. Microscopy performed on Zeiss or Reichert fluorescence microscopes*

	Fluorescence of leucocytes after chest X-ray											
	0 h		3 h		6 h		24 h		48 h		72 h	
Subject	DCC	RCC	DCC	RCC	DCC	RCC	DCC	RCC	DCC	RCC	DCC	RCC
1.	69	27	48	40	40	54	—	—	48	50	67	26
2.	89	5	75	21	—	—	37	67	58	38	69	24
3.	72	24	—	—	—	—	24	72	69	28	80	17
4.	73	21	72	21	—	—	69	27	85	10	—	—
5.	78	17	78	19	—	—	68	24	83	13	62	32
6.	89	10	—	—	—	—	71	6	94	4	—	—
7.	84	13	—	—	—	—	71	23	49	40	81	16
8.	92	7	—	—	—	—	83	1	85	11	—	—
9.	84	13	—	—	—	—	81	16	90	8	—	—
10.	84	14	—	—	—	—	62	26	62	36	88	10
11.	86	12	—	—	—	—	71	8	94	5	—	—
12.	72	25	45	51	28	69	66	27	—	—	—	—
13.	87	11	81	16	—	—	62	33	85	10	—	—
14.	88	8	73	25	—	—	56	38	66	29	84	14
15.	66	30	50	45	38	55	62	29	76	16	—	—
16.	83	15	82	16	—	—	49	50	61	32	63	33
17.	86	12	—	—	66	22	10	86	23	25	80	17
18.	93	6	83	14	73	22	81	18	69	29	90	8
19.	82	17	82	11	—	—	47	45	66	28	72	25
20.	70	29	74	22	66	30	66	31	63	30	81	16
21.	79	17	—	—	—	—	73	21	53	31	75	22
22.	80	18	74	3	51	44	30	56	59	36	68	27
Average	81	15	70	23	51	40	59	33	68	24	75	20

changes by exposure to X-irradiation ranging from 25,000 to 500,000 R.

Kafafova [9] found a similar change with small doses (1 R, partial body irradiation). Kolesar [10] applied the latter method for observing late effects of irradiation on humans, when he observed in radiation workers, that after several years of chronic exposure to low levels of irradiation, the % of green nuclei decreases by about 5%.

2. METHODS AND MATERIALS

Subjects: Persons exposed to X-irradiation of chest at routine X-ray radiography, and hospital personnel, involved and not involved in radiation work.

2.1. *Dosimetry*

An ionization chamber was placed in the exact position of the exposed part of the person's body and was irradiated at the same conditions of electron current, photon energy and exposure time.

The dose was measured with a Victoreen Condenser R-Meter 570 A. The ionization chambers were Victoreen chambers models 188, having a range of 0–0.025 R; models 130 and 576, having a range of 0–0.25 R; model 227 having a range of 0–1 R; and model 633 having a range of 0–2.5 R. All models have a rated accuracy of ± 10%. The readings were corrected by the T factor. Exposure time was $\frac{1}{20}$–$\frac{1}{10}$ sec. All doses are skin doses.

2.2. *Sampling*

Blood samples were taken from a finger tip before and after exposure at fixed intervals and were stained with acridine orange solution prepared in phosphate buffer $\frac{M}{15}$ (5 mg/50ml., pH 6.85), by mixing in a leucocyte pipette for 30 min.

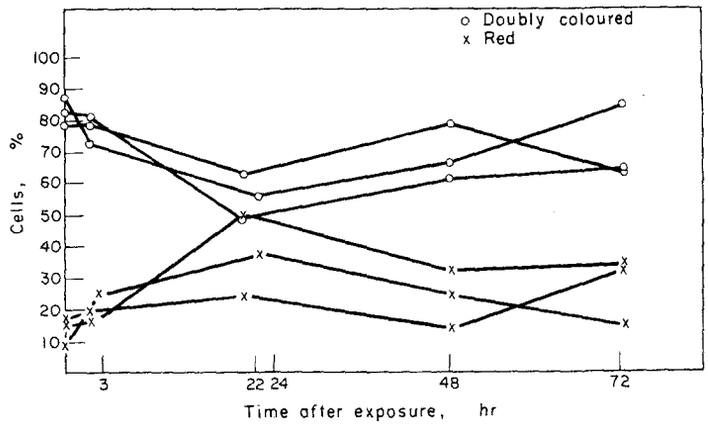

FIG. 1. Graphical description of three cases out of those summarized in Table 1.

Blood smears were prepared and counted in a UV fluorescent microscope.

3. RESULTS AND DISCUSSION

Over 50 cases were included in this investigation. It has been first established that in all cases the number of doubly coloured cells before irradiation is always above 68%.

In the first type of experiment patients were examined before and after X-irradiation of the chest. Peripheral blood smears were prepared and 200 cells were counted and classified by colour.

Table 1 summarizes results of several such counts.

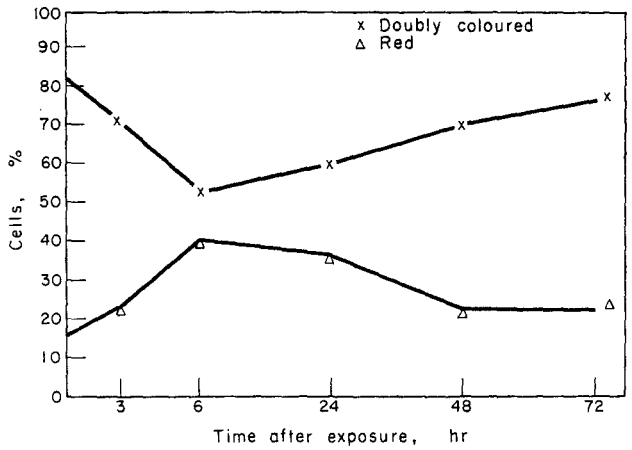

FIG. 2. Average results of 50 cases exposed to chest X-radiography at a dose of 18 mR, and analyzed as described in test.

Pre-irradiated human blood samples showed always over 68% of green–red coloured cells.

Following exposure, the number of DCC decreased while the number of red cells increased.

The changes observed began about 6 hr after irradiation, and usually reached a maximum at a deflection point 24 to 48 hr after irradiation, after which a reversed effect began. Figure 1 shows examples of these results for three cases.

The blood picture returned to the normal percentage of green and red cells after about 96 hr. Figure 2 shows average results of 50 cases.

Two groups of people could be classified as follows:

1. Persons of similar age, sex and weight, exposed on chest.
2. Hospital workers, physicians, technicians and clerks in the vicinity of the exposure area.

Persons of group 1 showed usually a significant drop in ratio of doubly coloured cells.

Blood smears of technicians and clerks, not directly involved in work near the X-ray machine, showed no changes in the ratio of DCC to RC.

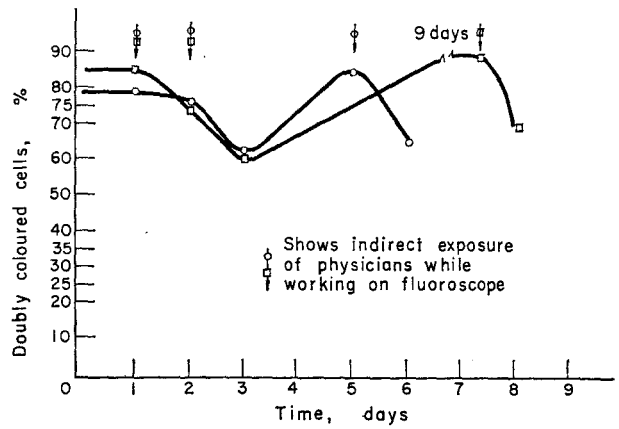

FIG. 3. Results of count of fluorescing blood cells taken from radiologists performing X-ray fluoroscopies. Arrows indicate day of work whereby indirect exposure occurred.

Physicians after performing fluoroscopy showed a significant drop in percent of doubly coloured cells (Fig. 3).

It is rather early to present an explanation of the observed effect. A logical assumption can be made that the radiation damage, whether direct or indirect, is affecting stem cells in such a way that their DNA and RNA content does not stain normally. The affected cells appear in circulation from 6 to 24 hr after irradiation and then are gradually removed from circulation and the blood picture becomes normal again.

4. CONCLUSION

Through a simple procedure, changes affected by small doses of X-irradiation on blood cells can be followed.

Development of this investigation might lead to an internal dosimetry method. The problem of variations in determination of ratios of green to red to doubly coloured cells is yet to be analyzed and the counts given by different observers should be checked independently to overcome subjectiveness.

ACKNOWLEDGEMENTS

We wish to thank Professor P. Ephrati, Dr. M. Ronen, Dr. Fishel, Dr. Yoel and Mr. J. Gal for helpful discussions and assistance. M. E. Gartzansky is thanked for able technical assistance. Mr. A. Epstein is thanked for help in dosimetry. Mr. M. Rosen is thanked for translations from Russian.

REFERENCES

1. J. F. Whitfield, S. Kellerer, H. Brohee and T. Youdall. The feasibility of a new procedure for biological dosimetry. Eur—2.505 e (1965).
2. S. Warren and L. Meisner. Chromosomal changes in leucocytes of patients receiving irradiation therapy. *JAMA* **193,** 5, 351 (1965).
3. E. Riklis. *Can. J. Biochem.* **43,** 1207 (1965).
4. S. P. Jarmonenco. Fluorescent microscopy of bone marrow after the action of radioisotopes, *Radiologica Medicini,* No. 3 (in Russian) (1953).
5. M. N. Meisel and V. A. Sandir. *Dokl. A.N. SSSR* **105** (6), 1221 (1955).
6. M. N. Meisel and T. M. Kondrateva. Early changes in tissue culture cells under the influence of X-rays (1956). *Problems of Radiation Biology* (translated from Russian by Pobedinskii and Kiselev, Eds., 1962). *Israel Program for Scientific Translation,* Vol. 1, p. 268.
7. O. S. Sergel and A. A. Climenco. The fluorescent technique in blood and bone marrow research of radiation sickness. *Vestnik Radiologia and Rentgenelogia* No. 5 (in Russian) (1957).
8. M. I. Hodas. Fluorescent microscopy of peripheral blood after X-irradiation. *Radiologica Medicini,* No. 3 (in Russian) (1959).
9. D. D. Kafafova. The changes of hemopotesis in patients with thyrotoxicosis treated with radioiodine. *Problems of Hematology and Transfusions,* No. 8 (in Russian) (1959).
10. D. Kolesar, O. Ballog and J. Krizko. Application of fluorescent microscopy in prevention of damage by ionizing radiation. Klin. Chor. 2, Povolania Kat. Lek., Biochem. Lek. Fak. U.K. Bratislava, Pracov. Lek., 1964, 16/10, 443–7 (in Czech.).

HÉMATOLOGIE DU SUJET NORMAL: VARIATIONS PHYSIOLOGIQUES

M. DELPLA, J. CHINARDET et D. MOULIN

Service Général de Radioprotection, Électricité de France, Paris, France

Résumé—Devant l'intérêt qu'il y a à ne pas attribuer des variations physiologiques à l'effet d'une irradiation, il convient de les étudier systématiquement.

Dans ce but, les auteurs suivent, depuis maintenant six mois, un petit groupe de sujets volontaires par quatre prélèvements capillaires étalés dans le courant d'une journée normale de travail, effectués toujours dans les mêmes conditions (d'heure en particulier), au rythme de deux par mois.

On peut déjà signaler l'ampleur de quelques variations:

sur les G.R., un sujet stable varie de ± 6 pour cent (chaque résultat est la moyenne de quatre comptages mécaniques),

sur les G.B., avec une moyenne de 9000, un sujet oscille de 4500 à 15 000 (chaque résultat est la moyenne de deux numérations indépendantes),

sur les granulocytes totaux, dans la même journée, un sujet passe de 54 à 79 pour cent, un autre de 42 à 60 pour cent (chaque résultat est la moyenne des lectures d'environ 250 éléments sur deux lames différentes).

REAL VALUE OF THE CONVENTIONAL HEMATOLOGICAL EXAMINATION IN THE MEDICAL SUPERVISION OF PROFESSIONALLY EXPOSED WORKERS

H. LETARD

Service Général de Médecine de Travail, Electricité de France, Paris (France)

Abstract—It is universally admitted that professionally exposed workers should undergo, at least once a year, a hematological examination which comprises a globular numeration, a leucocytal formula and determination of Duke's test and coagulation.

Such an examination is justified when hiring personnel in order to divert risk from any subjects suffering from hematological complaints. It is necessary to state the value which should be given to it in practice in the systematic examinations of periodical supervision.

In fact, various statistical studies have shown that the normality to 95 per cent of the population represented a very extended zone of variability.

On the other hand, individual physiological changes are also important. Lastly, microbial infections and especially viral infections are able to bring durable and important alterations in the blood formula. On the other hand, the absorption of certain medicaments can also lead to changes.

It is therefore necessary that professionally exposed persons, as well as the Medical Officers entrusted with their supervision, should be well aware of the orientation and practical value of the hematological examination to which it is very difficult and rather hazardous to give a standard of efficiency value.

On the other hand, the establishment and the periodical control of the hematological formula can obviously have its usefulness as basic medical reference in case of accident from acute exposure.

STANDARDS HÉMATOLOGIQUES DANS LE CONTRÔLE MÉDICAL DU PERSONNEL TRAVAILLANT AUPRÈS DE SOURCES DE RADIATIONS IONISANTES

D. VELJKOVIĆ et Z. DJUKIĆ

Service de Protection Médicale, Institut des Sciences Nucléaires B. Kidrič, Vinča (Yugoslavia)

Résumé—Des examens hématologiques sont généralement adoptés en tant que mesures obligatoires entreprises afin de protéger la santé des gens professionnellement exposés à l'effet des radiations ionisantes. Ils comprennent les valeurs numériques des leucocytes, érythrocytes, trombocytes ainsi que la concentration de l'hémoglobine. Les valeurs physiologiques standards de ces éléments dans le sang périphérique pour notre population sont déterminées par un règlement de la part du Secrétariat Fédéral de la Santé Nationale. En appliquant ce règlement il s'est présenté qu'un grand nombre d'individus sains ont les valeurs de la formule sanguine qui ne sont pas incluses dans les standards fixés. C'est pourquoi nous nous sommes proposé de faire des formules sanguines de notre population appartenant à différentes régions. Ces examens sont en cours.

Le présent rapport contient les résultats hématologiques obtenus pour un groupe de jeunes gens qui sont des candidats potentiels pour s'embaucher dans les centres nucléaires ou dans différentes institutions utilisant des sources de radiations ionisantes. On a donné parallèlement les résultats hématologiques pour un groupe des collaborateurs de l'Institut Boris Kidrič. Ces résultats sont obtenus lors du premier examen et au bout de quatre ans. Au cours de cette période ce personnel a été professionnellement exposé aux faibles doses de radiations.

Les résultats obtenus ont montré que, d'après les standards nationaux valables, un grand nombre de personnes saines seraient atteintes de la leucopénie ou de la lymphocytose, ce qui ne leur permettrait pas de s'embaucher et de travailler auprès des sources de radiations ionisantes. Le changement du nombre des éléments dans le sang périphérique, constaté chez un individu chroniquement exposé aux faibles doses de radiations ne pourrait pas indiquer à temps et avec certitude des dommages précoces de l'organisme dus aux radiations ionisantes. Mais ces examens pourraient servir comme un indicateur très important de la santé générale et de l'état du système hématopoïétique, ce qui est d'un grand intérêt pour le contrôle de la santé des individus qui travaillent ou qui travailleront auprès des sources des radiations ionisantes.

DISCUSSION

S. LIN (*Italy*):

Desidererei fare alcune domande al Dr. Jammet: la prima riguarda la presenza in diversi soggetti normali di opacità centrali o periferiche del cristallino. Può dirmi il Dr. Jammet quali di tali opacità hanno importanza nel giudizio di idoneità al lavoro con radiazioni ionizzanti?

La seconda si riferisce a soggetti portatori di nevi con notevole contenuto di melanina e, pertanto, notevolmente influenzabili dall'azione di agenti fisici. Qual'è in questo caso il criterio da seguire nel giudizio di idoneità?

L'ultima richiesta è collegata all'osservazione, da noi ripetutamente fatta, che nei soggetti esposti anche a basse dosi di radiazioni si osserva un notevole aumento dei grossi linfociti a scapito dei piccoli linfociti e si nota una linfocitosi relativa. Tale osservazione, già descritta da Shields alcuni anni or sono nel British Journal of Radiology, quale importanza ha, secondo il Dr. Jammet, nel guidizio di danno da irraggiamento?

H. JAMMET:

Les examens du cristallin ont un double intérêt: d'une part pour connaître le moment d'apparition d'une cataracte, qui peut être physiologique ou pathologique; d'autre part pour apprécier le degré d'incapacité visuelle.

Pour ce qui concerne la pigmentation mélanique et l'exposition aux irradiations, il faut noter les pigmentations et en fonction de leur évolution ou de leur stabilité on peut juger de l'aptitude au travail sous radiations.

L'interprétation des variations lymphocitaires est difficile, compte tenu des connaissances imparfaites sur la nature et la physiologie des mononucléaires.

G. COWPER (*Canada*):

The requirement of a medical examination two months prior to employment must present a formidable obstacle to successful recruiting. Perhaps Dr. Jammet would indicate what fraction of candidates are rejected for medical reasons?

H. JAMMET:

Le pourcentage d'éliminés à l'embauche, pour toutes les raisons possibles et non seulement celles liées aux radiations, est, au Commissariat à l'Énergie Atomique Français, compris entre 10 et 20%.

M. GIUBILEO (*Euratom*):

Il relatore ha accennato alla opportunità di affidare le cure delle malattie tardive dovute alle irradiazioni professionali ai medici curanti.

Chiedo: (1) se al CEA è stata messa a punto una modalità particolare per permettere ai medici curanti un giudizio sull'importanza delle dosi di radiazioni ricevute dal paziente; (2) quale relazione può esistere fra questa pratica e le norma Euratom che prescrive il controllo medico delle vittime di incidenti nucleari.

H. JAMMET:

La responsabilité des examens médicaux après emploi incombe à la médecine courante. La médecine du travail n'a qu'à conserver les archives médicales, en vue de fournir des informations éventuellement utiles en cas de maladie professionnelle.

E. STRAMBI (*Italy*):

1. Quale ritiene l'oratore, secondo la propria esperienza, il limite inferiore di sensibilità di questo metodo di indagine in caso di esposizione acuta dell'intero corpo a radiazioni penetranti?

2. E' stata effettuata una analisi citochimica a sostegno delle osservazioni morfologiche?

3. Le indagini sono state eseguite con tecniche di arricchimento (leucoconcentrazione) o secondo l'abituale tecnica degli strisci di sangue periferico?

B. PENDIĆ:

1. La dose seuil, d'après nos expériences, se trouve autour de 1 R.

2. Nous n'avons pas fait l'identification biochimique des cellules observées.

3. Nous n'avons pas expérimenté avec les frottis enrichis, parce que dans les travaux précédents nous avons constaté que les méthodes utilisant la centrifugation changent le pourcentage des leucocytes dans la formule leucocytaire.

PH. BOURDEAU (*Euratom*):

As a cytological and biochemical explanation for the fluorescence staining differences you have

observed, have you considered the phenomenon of nuclear homogenization described by Whitfield, Scaife *et al.*? The intensity of this phenomenon in thymocytes and lymphocytes is well related to exposure dose, at least for the laboratory rat.

E. RIKLIS:

This could be one possible explanation. The nuclear homogenization is explained as a result of dissociation of histones from nucleoproteins. The fact that green fluorescence is from DNA and red fluorescence from RNA has been established by employing the action of the corresponding enzymes, DNAase and RNAase which breakdown these polymers respectively resulting in disappearance of the corresponding fluorescence colours.

It is also known that DNA stranding is very sensitive to radiation and single stranded DNA gives a different fluorescence than double stranded DNA—this could also be happening here. I would not like to come out with a theory of what the cause for this effect is. There is a lot more to be done. Firstly, we have to carry out dose-response curves and this will tell whether the phenomenon could become a biological dosimeter. We have to turn from the fixed dose of X-ray radiography to changing diagnostic and treatment doses. We plan to try *in vitro* work and isolate the effects on DNA and RNA. The surprising thing in this phenomenon is the response to such low doses (18 mR).

S. A. KHAN RANA (*Pakistan*):

While pointing out the importance of various medical aspects of radioprotection, I am afraid we are neglecting an equally valuable test, i.e. urine activity measurement which deserves to be done as a routine and at periodical intervals on account of its simplicity and greater sensitivity. We must not forget that most of the radioisotope laboratories in the world to-day, utilize unsealed radionuclides and hence the danger of internal contamination by ingestion or absorption through skin is very likely accidental, owing to neglect or lack of necessary equipment. Measurement of urine samples, especially when smaller activities are involved, would reveal an internal contamination otherwise undetected by other routine procedures. Mr. G. H. C. Dancer of Amersham has reported two such cases where urine alone indicated an internal contamination. The importance of this procedure was also remarked upon at the last meeting of the Radioprotection Association of Belgium. Besides, being quite informative, it is useful to see that internationally prescribed measures are being observed in a laboratory. It is better not to wait till an appreciable dose exposure or contamination be shown by a dosimeter or change of blood picture and then proceed on measuring urine activity. Why must we not nip the evil in the bud?

M. DELPLA:

Pour être bref, je me bornerai à vous présenter trois graphiques qui montrent les variations de la numération leucocytaire dans le temps.

Chaque jour ouvrable, à tour de rôle, l'un des sujets d'un petit groupe (formé de six hommes et cinq femmes, tous volontaires, tous en bonne santé) est appelé à subir des prélèvements de sang capillaire à heures régulières: 9 h, 11 h 30, 14 h et 16 h 30; pour cela, il cesse son travail qu'il reprend aussitôt après. Cette expérimentation a été commencée il y a un an. Chacun des points représente la moyenne de deux prélèvements effectués à la même heure; chaque numération porte sur la totalité des leucocytes contenus dans deux hématimètres de Malassez, soit 2/10 mm^3 de sang. Chaque sujet en expérience est suivi par le même laborantin.

Le sujet le plus stable du groupe oscille entre 5.000 et 8.000 globules/mm^3, avec trois pointes inférieures à 4.500 et deux supérieures à 10.000 et 11.000.

Voici un sujet instable: il oscille entre 6.000 et 12.000, avec deux pointes à 5.000 et deux pointes à 14.500.

Ce dernier sujet simule les réactions d'un irradié; le premier jour, on a trouvé, en milliers de globules/mm^3: 15, 17, 12 et 9; les examens successifs ont montré, après une décroissance initialement rapide, une stabilisation entre 7.000 et 9.000, avec une pointe à 4.500.

Je regrette de ne pouvoir résumer nos résultats sur les différentes variétés de cellules et leur interprétation statistique; je ne saurais abuser de votre temps, si précieux.

MAJOR HEALTH PHYSICS EXPERIENCES DURING 15 YEARS OF REACTOR TESTING

J. R. HORAN
United States Atomic Energy Commission Health, and Safety Division,
Idaho Falls, Idaho, United States of America

Abstract—The case histories of the major incidents involving the uncontrolled release of radioactive materials and radiation exposure to personnel will be reviewed. The most serious incidents in the 15-year operating history of the National Reactor Testing Station will be presented in an ascending order of seriousness using the following categories:

1. Property damage.
2. In-plant contamination.
3. Environmental contamination.
4. Inhalation exposure.
5. External total body exposure.
6. Radiation injury.
7. Maximum credible accident.

THE National Reactor Testing Station (NRTS) of the United States Atomic Energy Commission is a complex of facilities for nuclear reactor development extending over 900 square miles of public land in the north-western part of the United States. Since establishment of the NRTS in 1949, hundreds of millions of dollars and man-hours have been devoted to its primary mission to develop economic nuclear power and other peacetime uses of atomic energy. More experimental reactors of more advanced and different types have been built at this desert location than in any other equivalent area—a total of 42 to date.

The long-promised day of economic nuclear power is at hand. In the past year, we achieved the economic breakthrough of using large-scale reactors for commercial electrical power. As a result of rapid progress in research, technology, and operating experience, the United States today is years ahead of its planned nuclear power program. As of January 1, 1966, 22 nuclear power plants were operating or under construction with a total capacity in excess of 5000 MWe. During the first half of this year, orders were placed by various utilities for constructing 21 new nuclear power plants with a capacity in excess of 14,000 MWe. This means that more than 50% of the new electrical generating capacity in the United States has been assigned to nuclear power plants.

This new technology, now being applied in the United States and a few other nations, will be available to the world. Already European utilities are on the verge of placing an outburst of nuclear plant orders comparable to that experienced in the United States. A recent forecast of the nuclear power market abroad for the next 20 years provides the following consensus forecast of installed nuclear capacity. The free world in the next decade from 1970 to 1980 is expected to see nuclear power grow from approximately 22 millions of electrical kilowatts to approximately 200 millions of kilowatts and reaching approximately 400 millions of kilowatts by 1985. In the words of the late Dr. H. J. Bhabha of India at the Third International Conference on the Peaceful Uses of Atomic Energy, "There is no form of power as expensive as *no power*, i.e. doing without power altogether. . . . We know now that atomic power has come to stay." Because of the widespread concern about radiation due to the military birth of the atom, it is worthwhile to consider the experience at the National Reactor Testing Station where new concepts and new ideas

for nuclear power have been developed. I am quite confident that a review of this experience will result in an overwhelming vote of confidence in the safety of design and the meticulous care which is taken in the construction and operation of nuclear facilities. The many barriers which are used to protect people against injury and equipment against damage provide evidence that serious accidents are quite improbable. But if a serious accident does occur, the engineered safeguards are adequate to protect personnel outside the radiation control zones.

Safety is the first law of nature. By nature every organism tends to conserve life and the faculties with which it is endowed. The character and magnitude of the hazards which could arise with the improper use of nuclear energy required that a framework of safety protection be established from the beginning. This philosophy was new to industry, which was to see every phase of the research, development, and operation of the peaceful development of uses of the atom tempered by a judicious concern for occupational and public safety. Experience shows that any quantity of radioactive materials can be handled safely. The safety experience record has been phenomenal.

The emergence of nuclear power as an important factor in the world's economy has brought both public interest and concern—interest in the economic benefits and concern about safety. The lack of basic knowledge, particularly lack of understanding of the essence and the extent of the danger, breeds fear. Unfortunately, this fear can deter the continued development of nuclear energy despite the promise it holds for mankind.

The health physics profession is committed to the prevention of injury from radiation and reducing the impact of damage which may result from any radiation incident. While we can be proud of the past record, we realize that our skill and our best efforts cannot be sufficient to prevent all accidents. Therefore, let us study the accident experience at a major establishment where all phases of reactor design, construction, maintenance, modification, and operation have been performed in research and testing of practically all types of reactors.

The case histories of all the incidents and accidents involving radioactive material or its release to the working environment or radiation exposure to personnel suggest the following general categories of incidents in an ascending order of seriousness:

1. Property damage.
2. In-plant contamination.
3. Environmental contamination.
4. Inhalation exposure.
5. External total body exposure.
6. Radiation injury.
7. Maximum credible accident.

As a health physicist, I have followed the innate pessimism of my profession by selecting the most serious incident of each type for analysis. While a number of the incidents may qualify for several of the categories listed, each will be reviewed under the most serious category for which it may qualify. Most of this detailed information has not appeared previously in the open literature.

1. PROPERTY DAMAGE (JULY 23, 1957)

A railroad flatcar was being used to transfer a spent air-cooled reactor core from a hot cell to a storage area. While a 25-ton capacity crane was moving the highly radioactive core from the flatcar to the storage pit, the boom started to lower causing the load radius to increase excessively. As the operator attempted to arrest this motion, the crane over-balanced and turned over on its side. The 13.5-ton core struck the ground with a swinging motion bending the flanges, and the core subassembly struck the ground on its side. The impact broke the core supports from the plug. No fuel was involved; the core was not reuseable. Although much of the material was salvable, the damage was estimated at $105,000. Except for superficial cuts sustained by the crane operator, there were no injuries. The estimated radiation exposure to three personnel directly involved in salvage work was less than 300 mr. The maximum radiation level from the core was 5 R/hr at 2 m. Contributing causes to the accident were the following:

The crane was being operated near its maximum capacity with a boom radius of about 4 m and an angle of approximately 63 degrees. The crane was being operated blindly with

hydraulic controls. Because of the high radiation fields, the front window of the cab was covered with a sheet of lead and about a ton of lead brick had been added to shield the operator who was guided by a rigger. Finally, the operator had failed to lock the boom in position.

2. IN-PLANT CONTAMINATION (OCTOBER 5, 1957)

During the testing of an experimental air-cooled fuel sample, a fire of undetermined origin occurred in the charcoal filter in the off-gas line. The heat caused a gasket to fail at a flange, releasing burning charcoal dust which spread radioactively contaminated air throughout the reactor building. Air monitors alarmed; the reactor was scrammed; and personnel were evacuated. High levels of air activity persisted for approximately 30 min and then gradually decreased in intensity. The flames in the charcoal filter subsided when airflow to the experiment was shut off and the fire was extinguished with carbon dioxide. It is believed that the fire was caused by the spontaneous ignition of oil which had leaked into the charcoal bed during nonoperating periods.

The total loss chargeable to the fire was $22,000, of which $400 was due to the direct fire damage to the filter, $2400 for decontamination, and $19,600 chargeable to the downtime of the reactor. Although 11 employees, at one location in the reactor building, were without respiratory protection during the early phase of the incident, there was no significant exposure either from radioactive materials or other toxic materials.

It is interesting to note that the total fire loss in the 17 years of NRTS operations to date has been approximately $68,000. The current valuation of the facilities is in excess of a half-billion dollars.

3. ENVIRONMENTAL CONTAMINATION (NOVEMBER 18, 1958)

During the startup of the HTRE-III experimental air-cooled reactor, faulty instrumentation resulted in a power burst which seriously damaged a number of fuel elements. An estimated 15,000 curies of fresh fission products were discharged through a 60-m stack under inversion conditions, contaminating approximately 600 hectares of desert land. There was no contamination to the farming areas beyond the Testing Station since the winds were from the northeast and the nearest off-site boundary in the downwind direction is more than 50 km away. Ground surveys indicated maximum readings of 0.15 mr/hr 1 m above the surface. Assuming that iodine-133 was the primary contaminant, this would be approximately 20 μCi/m^2. The estimated maximum infinity dose from inhalation due to cloud passage would be approximately 5 mr. The financial loss as a result of property damage was estimated at $1,100,000.

4. INHALATION EXPOSURE (MARCH 20, 1958)

A criticality incident occurred in a chemical processing plant during the transfer of a waste solution to permanent storage. Earlier chemical separations had been performed in a hot cell on a fresh fuel element. During cleanup of the process equipment, a momentary pressure surge caused vapor to be released through partially opened valves in the solution addition lines. These lines had not been used for six months. The associated valves were stuck in a partially opened position which was not detected by manual checks. Interestingly enough, at least five similar operations had been performed previously without incident despite the same existing conditions. Evidently, the precise process circumstances for the radioactive release did not exist during the prior transfers.

Approximately 1 curie of iodine-131 was released into the operating corridor. Originally, it was believed that iodine inhalation exposures would be insignificant, and the early urine samples supported this evaluation. However, the following day it became evident that at least two individuals had received high inhalation exposures. At approximately 20 hr post incident, stable iodine was administered, reducing the total dose to the thyroid by a maximum of 10%. Eleven individuals received thyroid inhalation exposures ranging from 12 to 220 rad. Six individuals exceeded the maximum permissible dose of 30 rad per year, with the two highest exposures being 200 and 220 rad, respectively. Iodine-131 uptake in the thyroid

varied from 2 to 40 μCi. As a precautionary measure, all 11 individuals were placed on work restrictions, varying from two weeks to eight months. The highest external radiation exposure, as a result of submersion in the radioactive cloud, was approximately 1 R.

5. EXTERNAL TOTAL BODY EXPOSURE (OCTOBER 16, 1959)

A criticality incident occurred in the process equipment waste collection tank of a chemical processing plant used for recovering highly enriched uranium. The incident resulted from accidental transfer of about 200 liters of uranyl nitrate solution containing about 34 kg of enriched uranium (91% U-235) from critically safe process storage tanks to a geometrically unsafe tank through a line normally used for waste transfers. Although no specific instances of maloperation were discovered, several unsafe conditions were found which contributed substantially to the incident. An estimated 4×10^{19} fissions occurred in a waste tank located 17 m below grade and shielded by $1\frac{1}{3}$ m of concrete. Of the 21 persons directly involved in the incident, seven received external exposure to radiation as a result of the passage of a radioactive cloud through drains and vents into the inhabited areas; but none received whole-body exposure to penetrating radiation in excess of the annual permissible dose of 12 r. However, two individuals received skin doses from soft radiation of 50 and 32 rem, respectively. No medical treatment was required for any of the exposed individuals.

Although this was the first criticality incident at the NRTS, it was the twelfth such event in the United States. It is of interest to note this was the first such incident where personnel were wearing film badges. Another interesting aspect is that two days prior to the incident, personnel neutron threshold detectors had been installed in 95% of the badges for the 400 employees working in the Chemical Processing Plant. Ironically, only four of the personnel involved in the incident were equipped with this new monitoring device.

There was no significant property damage as a result of the excursion. The total loss chargeable to the incident was approximately $60,000 to recover the contaminated uranium solution.

Approximately two years later, on January 25, 1961, a second criticality incident occurred at the same facility. The lessons learned during the earlier incident proved very profitable. The maximum exposure was less than 55 mrem, or less than the daily exposure guide.

6. RADIATION INJURY (JULY 27, 1955)

Following shutdown of a prototype propulsion reactor, maintenance personnel entered an equipment compartment to grind open the access ports to the heat exchanger for visual inspection. To reduce radiation exposure from corrosion and fission products within the exchangers, the units had been partially filled with water and pressurized. On grinding through the last weld, a mild blast of air was released from one of the contaminated heat exchangers impinging on a laborer. About a week later, this employee reported to the dispensary with a draining ear and was treated for an ear infection. Three days later upon the completion of another work assignment in a contaminated area, the same employee received a routine contamination check with a Geiger counter. This survey revealed radiation levels of from 2 to 20 mr/hr on the left side of his head. Examination and treatment at the dispensary resulted in the removal of a 70-micron particle with a radiation field of approximately 1 r/hr at 3 cm. This intense radiation field had damaged tissue in a local area sufficient to perforate the eardrum. Following the removal of the radioactive particle, the employee was hospitalized for observation.

The extremely minute particle had a gamma ray spectrum which indicated aged fission products which resulted in a beta-ray exposure in the thousands of roentgens to an extremely limited area of the ear. The injury resulted in 12 days of lost time; however, the individual has fully recovered except for a 10% loss of hearing in the one ear and is still employed at the project. The person involved was a new employee who had received routine indoctrination in basic radiation protection. Among the items which contributed to the injury were the following: failure to wear protective covering of the head, failure to shower and monitor following work in a highly contaminated area, and the lack of portal monitors at the exits to

the plant. Those items which contributed to the incident were subsequently corrected.

During the seventeen years of NRTS operation, over 140,000,000 manhours of work have been performed with 275 lost-time injuries experienced. Only one of these—described above—was caused by radiation. Almost 300 times as many injuries resulted from gravity than from radiation.

7. MAXIMUM CREDIBLE ACCIDENT (JANUARY 3, 1961)

A 3 MW electrical prototype reactor known as the SL-1 underwent a nuclear excursion during a maintenance shutdown. The excursion destroyed the reactor, fatally injured three operators, and resulted in property damage estimated at $4,400,000. The accident was caused by a single event which covered a time interval of only 30 sec. An experienced military technician, knowing the hazards involved, deliberately withdrew the 39 kg central control rod to a height of 51 cm instead of making a 6 mm adjustment as dictated by the standard operating procedure. The reactor was capable of reaching criticality with this one rod withdrawn approximately 40 cm. A total nuclear energy release of 130 ± 10 MW-sec occurred. Five percent of the fuel in the center 16 fuel elements attained vaporization temperature of 2060°C. Altogether approximately 20% of the reactor core was destroyed.

The rapid formation of 34 atm of steam in the pressure vessel accelerated a 2 m column of water above the core and slammed it into the thick top head of the pressure vessel at an approximate velocity of 50 m/sec, producing a phenomenon known as a "water hammer". The impact of the compressed water produced a peak pressure of about 680 atm and transferred momentum to the pressure vessel itself which sheared the connecting piping and lifted the vessel approximately 3 m into the air. About 3 sec after the initiating event, the incident was over, and the vessel had fallen back onto its support cylinder. Based upon the best available data, approximately 5% of the gross fission products (estimated at 5×10^5 Ci) was ejected from the pressure vessel.

Large amounts of radioactive particles were released inside the reactor building. The cylindrical reactor building was made of steel plate, most of which had a thickness of 6.4 mm. The building was 13 m in diameter with an overall height of 16 m. Access to the building was provided by ordinary doors. The building was not a pressure-type containment shell, as would have been used for a reactor located in populated areas. Nevertheless, the building did contain almost all of the radioactive particles released by the explosion. Essentially all of the released material, with the exception of iodine-131 and the noble gases, fell out within the 1.2-hectare plot which contained the reactor and its support buildings. It was estimated that $\frac{1}{2}$ Ci of cesium-137 and $\frac{1}{10}$ Ci of strontium-90 were released from the building. In fact, more contamination was spread in the vicinity of the reactor by human and vehicular traffic during the subsequent rescue operations than by the accident itself. Air and vegetation sampling indicated that approximately 10 Ci of iodine-131 were released during the first 16 hr and approximately 70 Ci over the remaining 30-day period. Continuous air samples during this period indicated that the infinity thyroid dose for an adult at the nearest populated center 7 km was approximately 35 mrad which was slightly greater than 1% of the radiation protection guide value for off-site population which was in effect at that time.

Of interest is the fact that four of the health physicists involved in the early rescue operation became the first members of the profession to be decorated for heroism. Along with three other individuals, these men were presented with bronze medals by the Carnegie Hero Fund Commission for their attempt to rescue the three casualties after the accident. Rescue operations which involved short-term exposures in radiation fields up to 800 R/hr resulted in an integrated gamma exposure of 375 R to a total of 263 personnel of which 14 individuals received total body radiation exposures in excess of 5 R with the highest exposure being 27 R. The highest infinity thyroid dose from iodine-131 was 5.5 rad.

During operations over the following three-week period, all activities were performed under rigid exposure control procedures which involved an additional 300 individuals. During this interval, there were no injuries nor did a single individual exceed the guide value of 3 R per quarter.

The decision was made to demolish the reactor building and to restore the general area to a useable condition. It may be of interest that in the reactor room only one light bulb had been broken, despite the pressure shock and the number of missiles which peppered the area. The site cleanup resulted in removal of approximately 2500 m^3 of shielding gravel, contaminated equipment, and decontamination materials to a special burial ground. This material contained an estimated 22,000 Ci of fission products.

In speculating on the impact which the SL-1 accident could have had upon the public if the reactor had been located in a populated area, it would have been unlikely that any person would have unavoidably received a radiation exposure greater than that allowed on an annual basis. However, control measures would most likely have been necessary in a milk-producing area as a protective action to prevent ingestion exposure via the milk-chain.

SUMMARY

These examples of the most serious incidents over the years at the National Reactor Testing Station have been presented to support the thesis that even the most serious accidents experienced at a major testing establishment have not produced exposure or injury to personnel outside the immediate radiation control zone. It has been demonstrated that man can work with and control the hazards resulting from the use of any quantity of radioactive materials.

As the world enters the nuclear power era, the health physicist has been the first to accept the challenge given by the late President Kennedy, "Regardless of the scope of modern research and development, safety is the primary purpose and most important product of today's scientists."

REFERENCES

1. W. L. GINKEL *et al.* Nuclear incident at the Idaho Chemical Processing Plant. IDO-10035, 2-15-60.
2. J. W. LATCHUM *et al.* Nuclear incident at the Idaho Chemical Processing Plant. 1-25-61, La-54-61A.
3. Final Report of SL-1 Recovery Operation, May 1961 through July 1962. IDO-19311, July 27, 1962.
4. Statements to the SL-1 Board of Investigation by Combustion Engineering Incorporated and Argonne National Laboratory on the SL-1 Accident. IDO-19312, dated August 21, 1962.
5. J. R. HORAN and W. P. GAMMILL. The health physics aspects of the SL-1 accident, *Health Physics* **9,** 177–186 (1963).

THE HEALTH PHYSICS ASPECTS OF THE FAILURE OF A PLUTONIUM-BERYLLIUM START-UP SOURCE IN THE SAFARI 1 REACTOR

D. K. CRAIG, B. C. WINKLER and J. R. COLLEY

National Nuclear Research Centre, Pelindaba, South Africa

Abstract—A neutron start-up source, containing 160 grams of plutonium, was supplied by the subcontractors for the Safari 1 reactor. During the start-up and commissioning period, for which the reactor was under the control of the subcontractors, the container for this source ruptured.

This allowed some of the plutonium and its fission products to escape into the various reactor systems.

The resulting increased levels of radioactivity were first indicated definitely on April 22, and after extensive investigations, the rupture of the source container was discovered on April 26, 1965. After removing the source from the reactor vessel and taking such other steps as were practical to control the increased radiation and contamination hazards, the reactor was brought back to power on April 28 and was operated at full power for seven consecutive days.

The events leading up to and surrounding the incident are described. The health physics aspects of the incident are presented and the consequences are discussed. It is shown that, while greatly increased radiation and contamination hazards arose, no personnel suffered injury, ingested radioactive material or received radiation exposures in excess of internationally recommended maximum permissible limits. Furthermore, no danger to the general public arose in any way as a consequence of the incident.

I. INTRODUCTION

It has become customary in the atomic energy industry to report reactor incidents in the open literature. This has been done in the hope that by revealing personnel errors, procedural inadequacies and instrumental failures, and by analysing the incidents and describing the methods used to combat them and prevent recurrences, others involved in this new and rapidly developing field might benefit. Examples of such reports are given in refs. 1 through 14. It is with this in mind that the present report is presented.

Safari 1 is a 90% enriched uranium fuelled, light-water cooled and moderated, tank-type research and materials testing reactor based on the ORR facility at Oak Ridge. It is located at the National Nuclear Research Centre at Pelindaba in South Africa. A general outline of the facility has been given by Roux,[15] and a more detailed description will be found in the "Engineering Design and Safeguards Report on the Safari 1 Research Reactor".[16]

II. BACKGROUND

On March 15, 1965, a 10 Ci Pu-Be start-up source (Fig. 1) was placed in the bottom of an aluminium basket 1.875 in. i.d. and inserted into a 2.00 in. i.d. hollow beryllium reflector element in the reactor core. Fuel element loading commenced next day and the reactor went critical with nine fuel elements and four control rods during the evening of March 18. Following control rod calibration, the source was moved to core location F7 (Fig. 2) on March 23, and on the following day, after loading more elements, the full operating core, as shown in Fig. 2, was attained. On March 25 the source was moved to reactor location E1 to increase the counting rate in the start-up channel, and low power runs were made up to

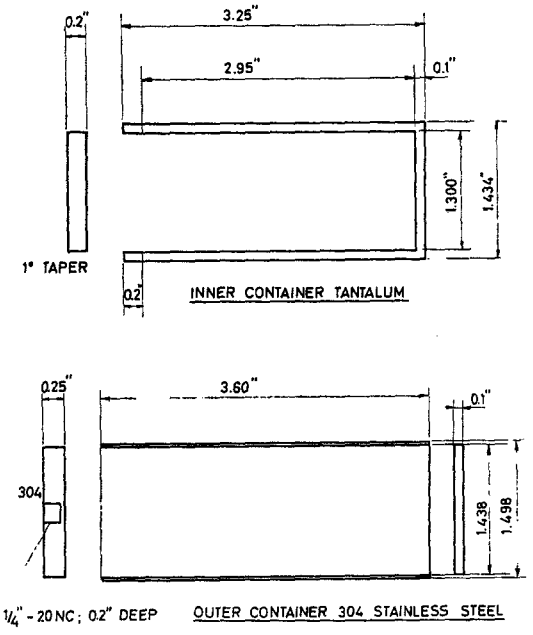

FIG. 1. Container of plutonium-beryllium source.

April 9 when the power was increased to 2.2 MW. At this time the reactor was run continuously, and power was brought up to the design maximum of 6.7 MW in the early morning hours of April 10, and maintained at this level through April 13. After this two days were spent performing Xenon build-up and decay tests at 60 W, and then all plant, including the ventilation system, was shut down for the Easter holidays, April 16–19 inclusive. When the ventilation system was started up on the morning of April 20 the stack particulate monitor readings increased by two orders of magnitude and returned to normal values of about 6×10^2 counts/min. Previously, increases by factors of up to five had been regularly observed under nocturnal inversion conditions, and as the much larger rise could be attributed to the build up of radon and thoron decay products, it had no disturbing effect upon the reactor operators.

III. THE INCIDENT

The reactor was started on April 21 but was shut down after a few hours due to an instrument fault. Some 10 hr after shutdown the reactor hall ventilation duct monitor, which was set at 30% above normal background, tripped the ventilation system from a 30,000 cfm unfiltered system to a 2000 cfm filtered system with stack discharge. The ventilation trips were reset and the reactor was started up again reaching full power at 00:43 hr on April 22.

During the rise to power the stack particulate monitor readings rose steadily (Fig. 3) and by 02:00 hr the shift health physicist had to change the range from 10^4 to 10^6 counts/min. Neither the rate of increase of this reading nor that of the

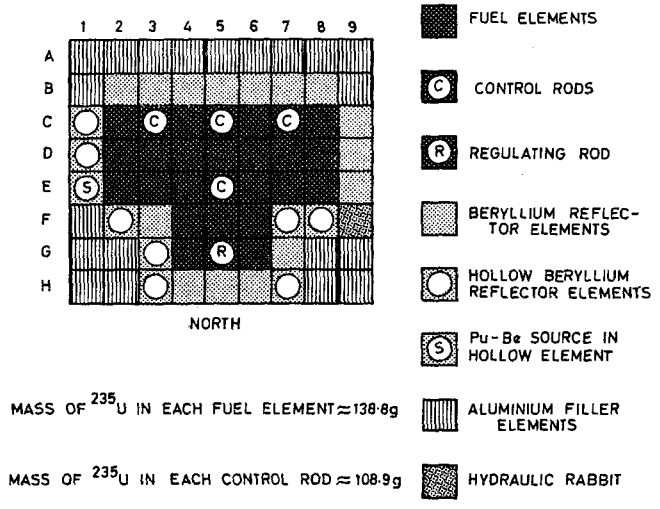

FIG. 2. Safari 1 core configuration at time of incident.

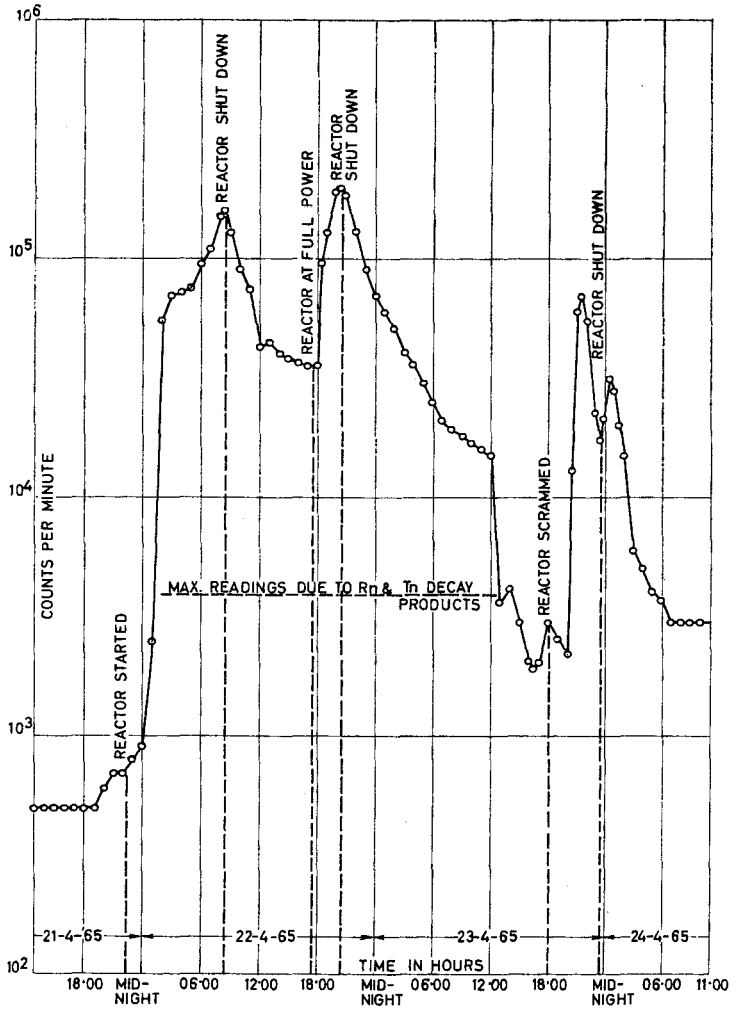

FIG. 3. Stack particulate monitor readings from 14:00 hr 21.4.65 to 09:00 hr on 24.4.65.

stack gaseous monitor reading (Fig. 4) was recognized as a serious abnormal condition. At 03:30 hr the duct monitor tripped the reactor hall ventilation system again and, although previous peaks in the duct monitor has been observed (Fig. 5), these were attributed to instrument behaviour. Routine smear tests and air samples taken at this time throughout the reactor area showed no increases above normal background. However, at 04:19 hr the secondary water monitor showed abnormally high readings, not due to contamination from the secondary water but to direct radiation from other equipment. Following high readings from the reactor fission products monitor at 05:10 hr a special survey was started. At 06:00 hr several areas of high exposure rate were identified (50 R hr^{-1} at the surface of the primary water demineraliser filter, 25 mR hr^{-1} at the entrance to the degasifier room) and at 07:54 hr the sub-pile room monitor tripped its alarm (Fig. 6). A few minutes later the senior health physicist arrived to take over the shift and on his advice the reactor was shut down at 08:34.

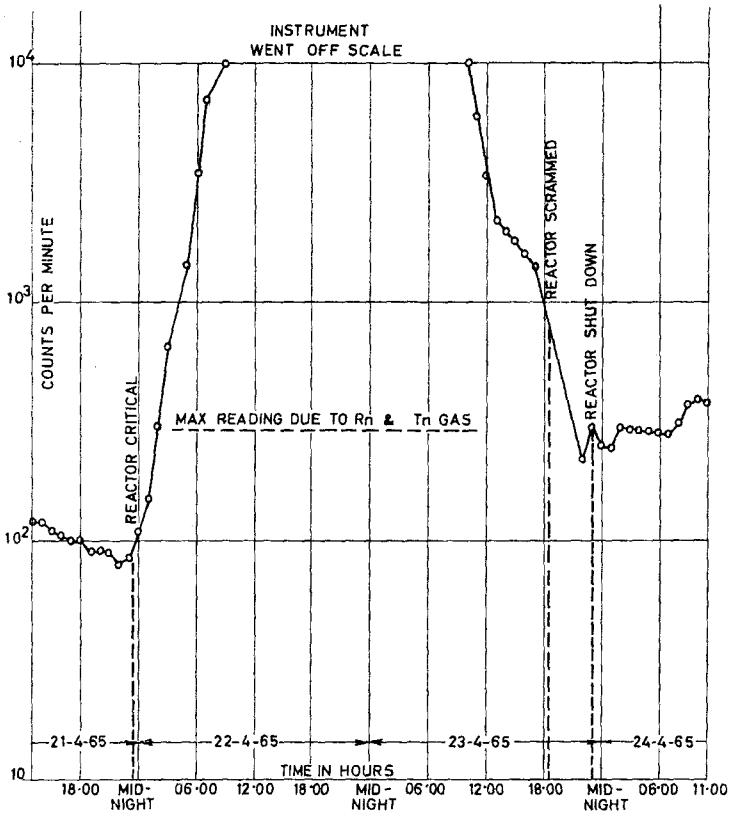

FIG. 4. Stack gaseous monitor readings from 14:00 hr on 21.4.65 to 09:00 hr on 24.4.65.

IV. INVESTIGATIONS AND SUBSEQUENT ACTION

Investigation into the cause of the high readings was commenced immediately, but fission products could not be identified in samples of primary water, or any filters. The fission product monitor filter contained a considerable quantity of ion exchange resin known to have been released from the demineralizer at an earlier date, and some consideration was given to the possibility that the high radiation levels were due to the accumulation of activated resin at obstructions in the primary water circuit. This did not explain high stack readings and therefore the reactor was brought up to full power between 17:02 and 17:40 hr in order to obtain further data (Figs. 3, 5, 6). Within five minutes the duct ventilation monitor tripped due to direct radiation. At 18:22 hr the pool water monitor gave a high level alarm, and at 20:54 hr the reactor was shut down because exposure rates around the primary coolant circuit were high and increasing. While the reactor was operating a gas sample was taken from the off-gas ventilation system, and by 08:30 hr on the following morning (April 23) it was confirmed that this contained fission products. The water level in the pool was lowered to just above the surface of the vessel, and a gas sample from the vessel showed a high Xenon content. The vessel access hatch was removed, and the water level lowered slightly to permit water sampling from each fuel channel. Initial results were indefinite, so sampling continued with the reactor operating at 5 kW, having refilled the pool and with all process systems shut off.

A Victoreen VMS-5/830 C continuous monitor responding to particulates in air was installed above the pool and after it had sounded an alarm at the 168 hr MPC level for radon all

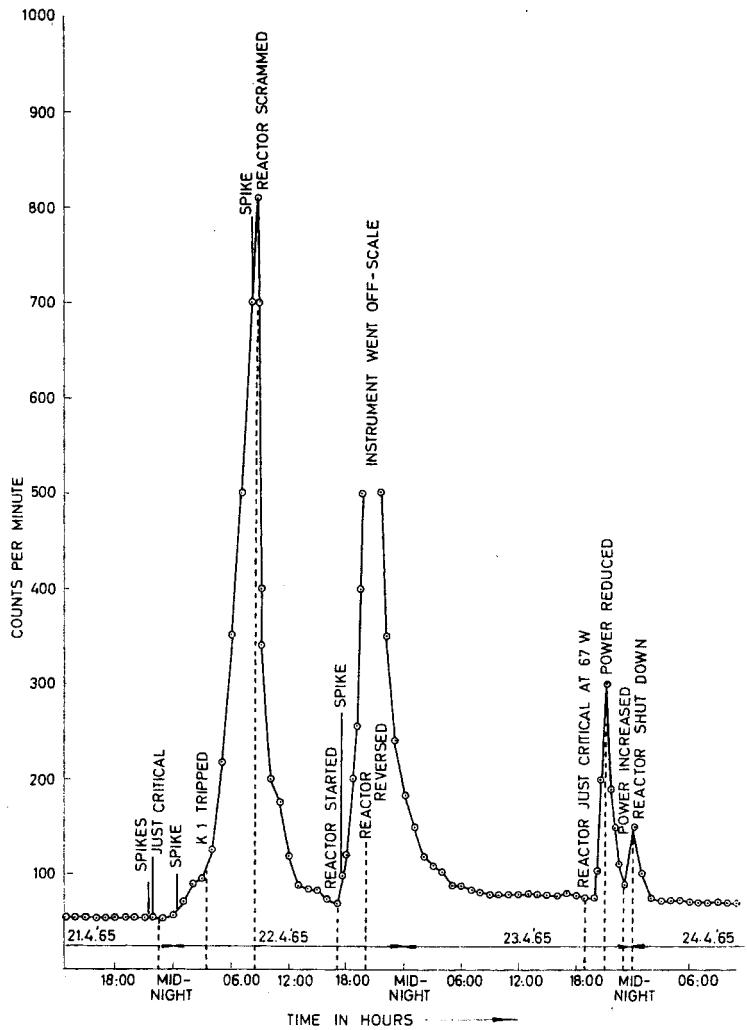

FIG. 5. Reactor hall ventilation duct (K1) monitor readings from 14:00 hr on 21.4.65 to 09:00 hr on 24.4.65.

personnel in the area wore full-face or half-face respirators. A 5 ml water sample from core location E2 (Fig. 2) gave over 90,000 counts/min compared with 6000–10,000 counts/min for similar samples from adjacent channels. This differential was confirmed during a short run at 50 kW and the reactor was shut down just before midnight in the belief that the high readings may have been due to a faulty fuel element. At 01:16 hr on the next morning (April 24) a new fuel element was fitted. On April 26 it was suggested that the Pu-Be might also be considered as a possible source of contamination. The ratio $^{140}La/^{140}Ba$ to $^{103}Ru/^{103}Rh$ in the spectrum of water from channel E2 was more consistent with a fission product release from ^{235}U than from ^{239}Pu. The reactor was therefore started up at 15:00 hr and operated at 30 kW to gather more data. Access to the reactor hall was, of course, restricted to essential personnel and respirators were worn. Even with the new fuel element in place water

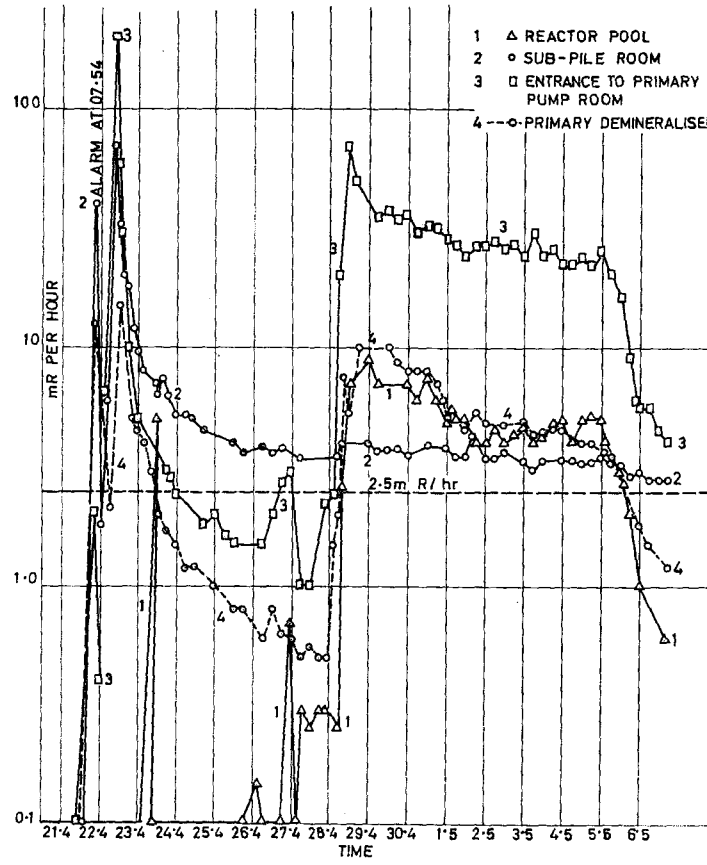

FIG. 6. Some area radiation monitor readings for the period April 21 through May 6, 1965.

samples from location E2 still showed very high readings and it was decided to remove the basket containing the source and nine beryllium plugs for visual examination. The source was removed with considerable difficulty late on April 26, and was seen to have split longitudinally (Fig. 7). Discoloration of the steel case indicated that very high temperatures had been reached. On the following morning activity and irradiation levels were seen to be decreasing, and the alpha activity in the pool water was about 5×10^{-6} μCi/ml. Two days were spent in cleaning up the reactor area and consideration was given to the safety of starting up the reactor again. Although some chips of the Pu-Be source were probably in the reactor vessel, primary coolant circuit and pool, and would release further fission products on start up, it was decided that these could best be disposed of by operating the plant and allowing the primary circuit and pool filters to remove the plutonium and fission products. With a close watch on activity and radiation levels the reactor was run up to 2.2 MW without a source in the afternoon of April 28 and kept steady for two hours during observations. At 18:00 hr power was increased to 4.4 MW, and the main source of stack activity was shown to be the degasifier. By 19:12 hrs the reactor was at full power and all monitor readings began to level off. Full power was maintained during a warranty run which lasted for the next 7 days. After this the reactor was shut down with the reactor and pool water purification systems still running continuously to clean up as much activity as possible.

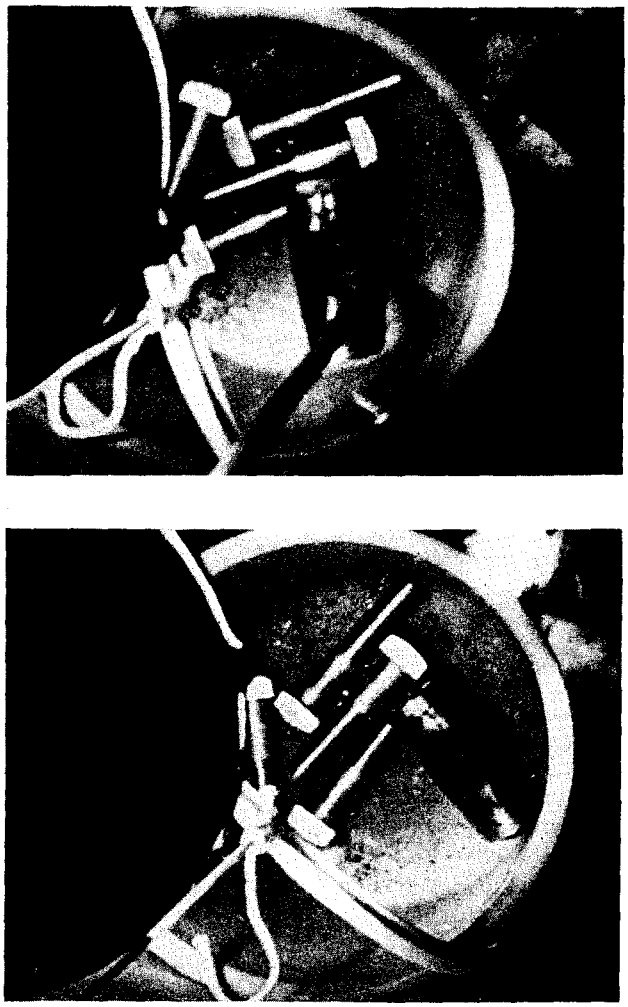

FIG. 7. Photographs of ruptured source container. These photographs were taken with the source in a plastic bucket, located under about 12 ft of water. The upper photograph shows the longitudinal rupture along the top of the container. The lower photograph was taken with the container rotated through 90°.

V. HEALTH PHYSICS ASPECTS OF THE INCIDENT

Table 1 shows the results of personal dosimeters worn by all people involved in the incident and who received more than 10 mR exposure. It will be noted that all results are well within ICRP Recommendations. Five people were selected for special examination, including whole body counting, urine analysis, and a complete medical examination. All tests showed that no person had suffered any injury whatever as a result of the incident.

VI. RELEASE OF AIRBORNE RADIOACTIVITY TO THE ENVIRONMENT

Figures 3 and 4 show that airborne radioactivity was released from the stack whenever the reactor was operated. The analysis of gas samples showed that the gaseous activity was almost entirely due to ^{133}Xe and ^{135}Xe, which

Table 1. *Integrated β–γ Exposure received by Personnel involved in Incident*

Person	Function	Total exposure in mR	
		Film badge 19.4.65–14.5.65	Pocket dosimeter 22.4.65–9.5.65
K.T.B.	Reactor operator	30	48
D.F.C.	Reactor engineer	35	75
J.R.C.	Reactor engineer	55	41
D.K.C.	Health physicist	565	603
G.P.D.	Health physicist	385	361
A.D.	Operations manager	293	326
T.E.	Reactor operator	160	91
D.J.F.	Plant engineer	30	48
R.D.G.	Electrician	10	21
N.G.	Chem. operations ass.	30	66
R.H.J.	Reactor operator	17	45
P.J.J.	Plant engineer	160	184
E.L.	Fitter	14	33
J.M.	Reactor operator	80	88
C.M.	Reactor supervisor	150	172
W.M.	Reactor operator	35	46
C.W.P.	Ass. operations manager	30	145
A.S.	Health physicist	80	78
A.M.V.	Reactor operator	10	28
R.V.	Reactor analyst	10	25
J.D.V.	Reactor analyst	200	185
D.J.W.	Health physicist	635	535
B.C.W.	Health physicist	260	231

Table 2. *Airborne Particulate Activity in the Stack at Various Times during and Subsequent to the Incident*

Date	Time	Reactor power	μCi/cc	
			α $\times 10^{10}$	β–γ $\times 10^{10}$
22.4.65	18:00–20:00	6.67 MW	0.8	780
24.4.65	23:01	Off	0.5	1.8
29.4.65	00:20	6.67 MW	1.9	410
29.4.65	22:38	6.67 MW	1.4	16
29.4.65	23:43	6.67 MW	1.4	40
30.4.65	04:30–06:30	6.67 MW	2.0	300
16.2.66	11:41	6.67 MW	1.2	21
23.2.66	10:54	Off	0.7	1.6
25.2.66	11:45	Off	0.2	0.3

Note: All measurements were made after allowing 30 min for decay.

of course passes unimpeded through the filtration banks. ^{88}Rb and ^{138}Cs, with half-lives of 18 and 32 min, were identified in the airborne particulate samples. These are the decay products of the fission product noble gases ^{88}Kr and ^{138}Xe. It is assumed that the decay nuclides rapidly attached themselves to the surfaces of dust particles,[17] which in turn were collected by the filter paper of the various monitors and samplers. The isotopes ^{88}Rb and ^{138}Cs are not listed in the report of Committee 2 of the I.C.R.P.[18] An $(MPC)_a$ value of 1×10^{-6} $\mu Ci/cm^3$ has been calculated[19] for ^{88}Rb for a 40 hr week, i.e. approximately 2×10^{-7} $\mu Ci/cm^3$ for a 168-hr week. Table 2 gives airborne particulate activity concentrations obtained from samples taken on GF/A filter paper from the stack, both at the time of the incident and more recently. The highest β-γ value observed was 7.8×10^{-8} $\mu Ci/cm^3$, well below the $(MPC)_a$ value for the isotopes identified.

It is estimated that, for the period April 21 through May 7, a total of 2.5 Ci of particulate-borne activity (mainly ^{88}Rb and ^{138}Cs) and of the order of 650 Ci of gaseous activity was discharged from the stack. On the basis of relative toxicities, this is equivalent to about 10 Ci of ^{131}I, which is within our accepted monthly release.

VII. DISCHARGE OF ACTIVE EFFLUENT ONTO THE SITE

During water sampling procedures on April 23 the active waste tanks became full due to normal drainage from the building. At this time the effluent treatment plant was incomplete and no other transfer tank was available. Approximately 1000 gallons of water with an activity of 0.14 $\mu Ci/ml$ were pumped out onto the ground resulting in a contaminated area about 60×30 yd which was fenced off. No contamination of any dam, river, or water supply resulted from this, and by May 11 the activity of the soil was normal for alpha activity (50 pCi/g) and only six times background for beta activity.

VIII. ENVIRONMENTAL SURVEY RESULTS

The normal levels of airborne activity around the plant were already well established before the incident.[20] These data enabled the high levels during the incident to be interpreted, and it appeared that the only observable fission product escape was of the noble gases Krypton and Xenon. Gamma surveys over a 500 yd radius on April 22 and over a 5 mile radius on April 29 showed no increase above normal levels.

IX. HEALTH PHYSICS COVERAGE OF OPERATIONS

The Reactor H.P. personnel consisted of two health physicists and three H.P. technicians, two of them untrained at the time of the incident. This was considered sufficient for normal reactor operation for one shift a day, five days a week. Prior to fuel loading operations, the building had been classified into zones on the basis of expected radiation and contamination hazards. Regulations governing entry to and exit from the zones had been issued. A comprehensive pre-start up survey of background radiation, air and surface contamination was conducted. This was repeated at various power levels.

Few of the operations personnel had previously had experience of working in high radiation fields and areas of gross contamination. Previously simple routine jobs now involved considerable risk of spreading contamination, of ingesting or inhaling radioactive material, and of receiving an excessive external radiation dose. All available H.P. personnel on the site were employed in providing 24-hr coverage of the numerous jobs that had to be performed in high radiation and/or contamination areas. This involved the demarcation of such areas by conducting radiation and smear surveys and taking air samples, controlling the access of personnel to the areas, deciding what protective clothing and respiratory equipment should be worn, etc.

The most serious problems that arose were:

(a) A shortage of trained health physics personnel, particularly those with sufficient knowledge and experience to make value judgements; and

(b) communications between operations personnel and health physicists. On several occasions, unnecessary exposure occurred or contamination was spread due to operations being carried out without first contacting health physics.

Table 3. *Airborne Particulate Activity Levels under Normal Operating Conditions and at Various Times during Incident*
(*Readings after* 30 *min decay, except those followed by asterisk, which were after* 5 *min decay*)

Date	Times	Reactor power MW	Overpool μCi/cc		Control room μCi/cc		Basement μCi/cc		Process wing μCi/cc	
			$\alpha \times 10^{10}$	$\beta\gamma \times 10^{10}$	$\alpha \times 10^{10}$	$\beta\gamma \times 10^{10}$	$\alpha \times 10^{10}$	$\beta\gamma \times 10^{10}$	$\alpha \times 10^{10}$	$\beta\gamma \times 10^{10}$
	Normal	0	0.6 to 2	3 to 8	0.9 to 3	4 to 20	0.8 to 2	4 to 7	0.3 to 2	2 to 8
	Normal	6.7	0.8 to 2	3 to 7	2 to 3	6 to 10	2 to 3	6 to 10	0.7 to 2	3 to 7
22.4	18:00–20:00	6.7	1	40	—	—	2	4	0.6	4
23.4	21:30	5.4 kW	—	700	—	—	—	—	—	—
	22:00	5.4 kW	—	100	—	20	—	—	—	—
24.4	00:21	Off	—	1000*	—	—	—	—	—	—
25.4	01:05	Off	—	200*	—	—	—	—	—	—
	09:00–10:30	Off	—	10*	0.4	20	—	—	—	—
28.4	12:00–15:30	Off	1	4	1	9	—	—	0.6	2
	20:22	6.7	1	300	—	—	—	—	—	—
	23:24	6.7	3	600	—	—	—	—	—	—
29.4	03:00–03:30	6.7	—	—	4	20	5	60	3	10
	15:20–18:00	6.7	—	900	2	10	—	—	—	—
	22:05	6.7	2	100	—	—	—	—	—	—
30.4	04:30–06:30	6.7	4	400	3	20	4	40	3	10
	22:17	6.7	—	200	—	—	—	—	—	—
1.5	02:00–05:00	6.7	6	300	5	20	5	30	4	10
	12:15	6.7	300†	5000†	—	—	—	—	—	—
2.5	01:00–02:30	6.7	5	400	—	—	4	40	3	20
	19:35	6.7	0.7	200	—	—	0.9	10	0.3	20

† Very large sample. After 5 hr decay, readings were 0.8 and 20 for α and β, respectively.

Table 3 gives some typical airborne concentrations of β-γ particulate activity observed during the period under discussion. The high β-γ value observed at 21:30 hr on April 23 occurred while water samples were being drawn from each fuel element in turn in the search for the source of the fission products in the primary cooling system.

Table 4 presents the results obtained from some of the numerous smear samples taken during the incident in the search for abnormal surface contamination. The major cause for concern in the results shown in Tables 3 and 4 was the long-lived alpha values. All smear tests before the incident had yielded zero values for alpha contamination, so the positive results were presumably due to plutonium. The fact that the contamination was transferable indicated the possibility that it could become airborne.

The 40-hr week $(MPC)_a$ for ^{239}Pu is 2×10^{-12} $\mu Ci/cm^3 = 4.44$ d.p.m./m^3 of air. The last value in Table 4, 1.4×10^{-5} $\mu Ci/cm^2$, is equal to 3108 d.p.m./100 cm^2. The dispersion of just 2% of this activity into the air would be sufficient to give an $(MPC)_a$ value for 14m^3 of air. For the above reasons, all areas where transferable surface contamination was found to be present were carefully decontaminated as soon as possible.

Table 4. Some Typical Smear Sample Results obtained during Incident

Date	Location of smear	$\mu Ci/cm^2$	
		α $\times 10^5$	β $\times 10^4$
27.4	Upper portion of pool gate: West side	—	11.2
	Upper portion of pool gate: North side	6.6	5.6
	Upper portion of pool gate: South (partly washed)	—	6.5
28.4	Entrance to overpool area, west	—	0.03
	Floor in front of elevator entrance, overpool level	—	0.17
	Elevator floor	—	0.03
	Gallery floor, in front of steps	—	0.26
	Beam port floor, in front of steps	0.124	0.51
	Handling tool storage floor	7.72	18.1
29.4	Overpool floor, blue side of change room	—	0.06
	Overpool floor, red side of change room	—	0.38
	Overpool level, north wall above crane	0.001	0.001
	Beam port floor, door out of reactor hall to main entrance	0.007	0.018
	Beam port floor, south of handling tool storage	0.20	2.8
1.5	Overpool floor, east, next to steel stairs	0.082	0.68
	Overpool floor, south-west corner of storage rack	0.245	0.12
	Overpool floor, between storage rack and pool	0.015	0.12
	Overpool floor, between storage rack and pool	1.4	1.10

Note: The maximum values for blue contamination zones are
1×10^{-5} $\mu Ci/cm^2 = 2220$ dis/min/100 cm^2 for alphas and
1×10^{-4} $\mu Ci/cm^2 = 22200$ dis/min/100 cm^2 for betas.

Table 5. Radiation Levels at Various Points inside the Process Wing

Date	Time	Reactor MW	Shut down pump pipe	Primary pump pipe	Primary heat exchanger	Primary strainer		Primary demin. filters		Primary degasifier tank	Off-gas line	Pool system filters	
						On tank	On pipe	East	West			Full flow	Demineralizer
			mR/hr	mR/hr	R/hr	mR/hr	mR/hr	R/hr	R/hr	mR/hr	mR/hr	mR/hr	mR/hr
Before incident		6.7	3.2	8.2	4.4×10^{-3}	4.1	—	0.170	0.170	8.0	—	0.8	0.8
22.4	08:00	6.7	2000	2000–3000	5.0	—	—	—	150	—	—	—	—
22.4	20:49	6.5	5500	5000	16.0	—	—	16.0	—	—	—	—	—
23.4	10:15	Off	68	110	4.0	—	—	3.7	—	130	12.5	—	—
24.4	12:15	Off	28	42	2.3	—	—	21	12	35	2.6	—	—
25.4	12:10	Off	17	27	1.4	—	—	17	—	11	1.3	—	—
26.4	19:20	Off	12.5	20	1.6	40	45	15	8.5	8.0	0.9	—	—
28.4	16:15	Off	70	12	1.9	25	47	16	8.0	7.0	1.0	60	200
28.4	16:35	Started	60	10	1.4	20	35	15	6.0	4.3	0.7	56	135
28.4	17:15	0.277	70	36	1.4	60	57	15	6.0	11.0	1.3	85	150
28.4	17:35	2.2	160	230	1.5	350	220	16.5	6.2	60	6.0	110	160
28.4	18:25	4.4	430	750	1.65	1000	620	21	6.6	300	27	175	175
28.4	19:40	6.7	680	1200	2.15	1300	950	26	7.3	410	45	300	180
29.4	18:30	6.48	450	720	2.2	800	550	26	7.0	380	33	900	270
1.5	15:30	6.53	360	500	1.9	600	390	23.5	5.2	250	21	780	195
3.5	20:50	6.48	340	460	2.0	510	375	21.0	6.0	260	21	900	185
5.5	16:29	6.5	255	350	1.6	—	—	18.0	—	200	—	750	160
6.5	19:45	0.020	110	42	1.5	50	68	15.0	4.0	19	1.8	500	100
End of year		6.7	95	200	0.170	—	—	8.0	—	200	—	60	48
Similar reactor after 6 days at		20	—	400	0.180	—	—	0.5	—	—	—	—	10

Note: The west primary demin. filter was on line at the time of the incident. The east one was placed on line during the day of 22.4.65.

No method for the biological monitoring of ingested or inhaled plutonium was available at this time. A method for analysing the amount of plutonium excreted in the urine was subsequently developed and none has been detected in the urine of operations personnel since tested.

Apart from the known presence of plutonium and fission product contamination in the reactor water systems, a major concern was the high radiation levels in the process wing, particularly on the primary filters. Table 5 gives a selection of radiation readings, during and after the incident. Some comparable data from a similar reactor are also given.

Table 5 shows how dramatically the radiation dose rates rose when the Pu-Be source was ruptured and, also, the effect of subsequent reactor operation on the levels. In most cases the year-end values, while considerably lower than at the height of the incident, were still very significantly higher than those obtained prior to the rupture.

The effect has been to demand much stricter health physics control over maintenance work in the process wing, particularly when such work involved breaking into the primary or pool water systems. It was nevertheless possible to prevent any of the operations personnel from acquiring any radioactive body burden or from receiving greater than the permissible quarterly radiation dose of 3 rem.

X. DISCUSSION AND CONCLUSION

Calculations that were carried out subsequent to the rupture indicate that the cooling for the source, in the core location chosen, was probably inadequate for operation at 6.7 MW.

The incident emphasised the following essential requirements for the construction and operation of a reactor:

(i) checking of design, materials and construction of every part of the reactor system;
(ii) checking of all reactor operations;
(iii) planning for accident conditions;
(iv) provision of adequate H.P. coverage;
(v) provision of sufficient protective clothing;
(vi) provision of adequate waste disposal facilities;
(vii) provision of a radiological training programme for all radiation workers.

Although the resources of the reactor health physics group have been taxed to the limit, a great deal of invaluable experience has been gained in a fairly short period.

XI. ACKNOWLEDGEMENTS

Thanks are due to Mr. D. van As who, with his colleagues, provided the data for sections VII and VIII. The paper is published by permission of the South African Atomic Energy Board.

REFERENCES

1. W. B. Lewis. The accident to the NRX reactor on December 12, 1952. Report DR-32, AECL 232 (1953).
2. D. G. Hurst. The accident to the NRX reactor Part II. Report GPI-14, AECL 233 (1953).
3. M.W. Kellogg Co. radiation incident on March 13, 1957, *Nucleonics* **15,** 42 (1957).
4. Accident at Windscale No. 1 Pile on October 10, 1957, *Nucleonics* **15,** 43 (1957).
5. Oak Ridge Y-12 accidental excursion, June 16, 1958, *Nucleonics* **16,** 138 (1958).
6. D. Callihan and J. T. Thomas. Accidental radiation excursion at the Oak Ridge Y-12 Plant. I. Description and physics of the accident, *Health Physics* **1,** 363 (1959).
7. J. D. McLendon. Accidental radiation excursion at the Oak Ridge Y-12 Plant. II. Health physics aspects of the accident, *Health Physics* **2,** 21 (1959).
8. G. S. Hurst, R. H. Ritchie and L. C. Emerson. Accidental radiation excursion at the Oak Ridge Y-12 Plant. III. Determination of radiation doses, *Health Physics* **2,** 121 (1960).
9. G. A. Andrews, B. W. Sitterson, A. L. Kretchmar and M. Brucer. Accidental radiation excursion at the Oak Ridge Y-12 Plant. IV. Preliminary report on clinical and laboratory effects in the irradiated employees, *Health Physics* **2,** 134 (1960).
10. Yugoslavian criticality accident, October 15, 1958, *Nucleonics* **17,** 106 (1959).
11. H. C. Paxton, R. D. Baker, W. J. Maraman and R. Reider. Los Alamos criticality accident, December 30, 1958, *Nucleonics* **17,** 107 (1959).
12. E. C. Hughes and J. W. Greenwood. Contamination and cleanup of NRU, *Nucleonics* **18,** 76 (1960).
13. J. R. Horan and W. P. Gammill. The health physics aspects of the SL-1 accident, *Health Physics* **9,** 177 (1963).
14. W. L. Marter. Radioiodine release incident at the Savannah River Plant, *Health Physics* **9,** 1105 (1963).

15. A. J. A. Roux. The first reactor installation of the Republic of South Africa, *S. Afr. Mech. Engr.* **12,** 29 (1962).
16. D. F. Carroll, J. R. Colley, C. Möller and P. J. Joubert. Engineering design and safeguards report on the Safari I Research Reactor. Report PEL 75 (Pelindaba, Dec. 1965).
17. D. K. Craig. An investigation of the interactions that occur between I_2 radionuclides and an iron oxide aerosol in the respirable size range, *Health Physics* **12,** 1047 (1966).
18. Report of ICRP Committee II on permissible dose for internal radiation (1959), with Bibliography for Biological, Mathematical and Physical Data, *Health Physics* **3** (June 1960).
19. A. Diaz. Personal communication.
20. D. Van As. Omgewingsradioaktiwiteit te Pelindaba. Halfjaarverslag: Januarie–Junie 1965. Report PEL 105 (Mar. 1966).

CONSÉQUENCES DU POINT DE VUE DE LA RADIOPROTECTION D'UN INCIDENT DE CONTAMINATION ÉTENDUE À LA PILE EL.3 DU CENTRE D'ÉTUDES NUCLÉAIRES DE SACLAY

L. FITOUSSI et P. LEBOULEUX

Commissariat à l'Énergie Atomique, Centre d'Études Nucléaires de Saclay*

Résumé—Un incident mécanique sur une cellule présentant une rupture de gaine a eu comme conséquence un incident radio-actif. Cet incident s'est produit pendant le transfert de cette cellule de la cuve de la pile, à la cuve de stockage. Il en est résulté une émission de produits de fission qui s'est prolongée pendant plusieurs jours, et une contamination étendue des aires de travail et des parois du bâtiment de stockage.

Après avoir indiqué les résultats des mesures de contamination effectuées dans les fluides de refroidissement de la pile, dans l'air, sur les surfaces et à la cheminée de l'installation, les auteurs présentent leurs observations sur l'émission des produits de fission et leur comportement dans les conditions de l'incident.

D'autre part, les auteurs présentent les conséquences de l'incident du point de vue de la radioprotection.

I. INTRODUCTION

L'objet de cette communication est de présenter quelques observations sur les conséquences d'un incident survenu à la pile EL.3 du Centre d'Études Nucléaires de Saclay. Il s'agit d'un incident de rupture de gaine d'un élément de combustible qui a conduit à une contamination radio-active très étendue parce qu'il s'est conjugué avec un incident mécanique survenu au cours des déplacements de la cellule incriminée.

Cet incident est caractéristique parce qu'il est la conséquence d'une suite de deux circonstances dont les probabilités d'occurrence sont relativement faibles.

II. CIRCONSTANCES DE L'INCIDENT

2.1. *Présentation de la pile EL.3* (Fig. 1)

La pile EL.3 est une pile à eau lourde. Sa puissance nominale est de 15 MW pour un flux thermique maximal de 10^{14} neutron/cm^2 . s. Cette pile sert en particulier à tester les combustibles nucléaires et son chargement comprend 15 à 20% de cellules expérimentales. C'est sur une cellule de ce type qu'est survenue la rupture de gaine.

La mise en place et l'extraction des cellules s'effectue pile à l'arrêt, avec une hotte blindée. Cette hotte est munie d'un dispositif autonome de refroidissement des cellules (Fig. 2).

Les cellules extraites sont transportées dans le bâtiment de stockage adjacent au bâtiment de la pile. Avant stockage, les cellules sont examinées aux rayons X, en particulier, celles présentant une rupture de gaine (Figs. 3 et 4).

2.2. *Description de l'incident*

L'incident s'est produit au cours d'un examen radioscopique d'une cellule ayant un taux de combustion de 3 650 MWj/t et présentant une rupture de gaine (cf. annexe I). La cellule, dont le dispositif d'accrochage s'est détérioré, est tombée dans le puits du sas d'observation et s'est coincée entre le sas d'observation et la hotte blindée.

La partie supérieure de la cellule (sans uranium) est restée engagée dans la hotte blindée.

* B.P. No. 2, gif S. Yvette 91, France.

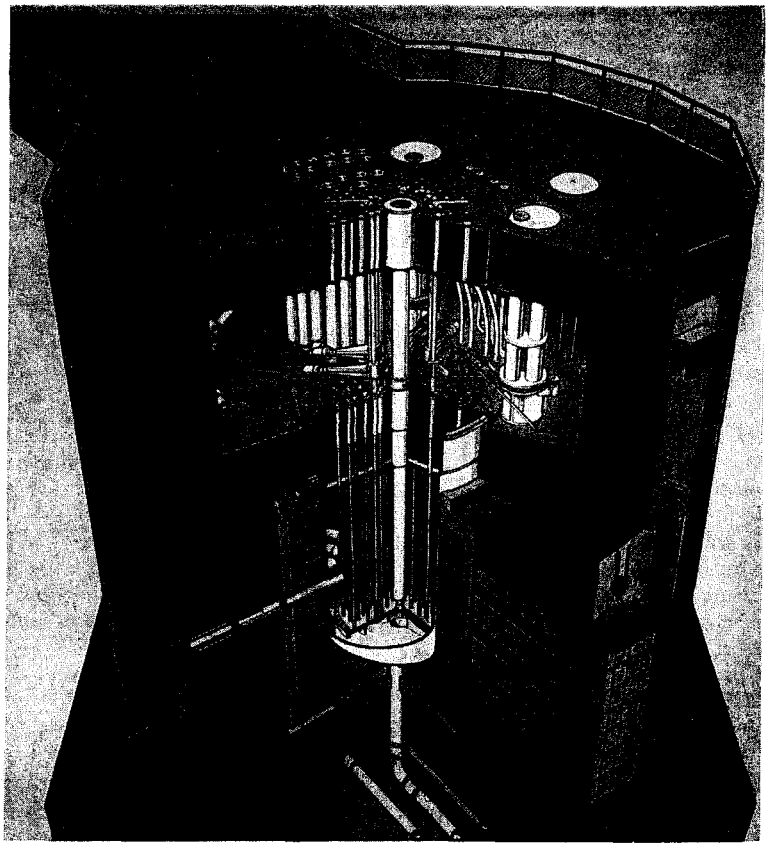

FIG. 1. Vue éclatée du bloc pile.

L'échauffement du combustible, qui ne peut être refroidi dans cette position, a provoqué une contamination atmosphérique due à un dégagement important de produits de fission qui a cessé lorsque le puits du sas d'observation a été rempli d'eau.

La cellule est transférée successivement dans deux alvéoles de la cuve de stockage, pour cellules avariées, car la première alvéole de stockage s'est avérée non étanche et insuffisamment refroidie (Fig. 5).

C'est au cours de ces opérations que le bâtiment de stockage, isolé fort heureusement du hall de la pile, a été presque entièrement contaminé.

III. CONTRÔLES DE RADIOPROTECTION

3.1. *Contamination atmosphérique*

Pendant toute la durée des opérations, la contamination atmosphérique a été contrôlée par des prélèvements effectués sur papier filtre et charbons actifs. Les résultats obtenus sont portés sur la courbe de la Fig. 6.

A partir de ces résultats, l'activité totale de l'iode 131 libérée dans l'atmosphère du bâtiment a été évaluée à environ 0,1 à 0,2 Ci. Cette valeur a été corroborée par les mesures effectuées dans l'air rejeté par la cheminée de la pile qui ont donné 0,17 Ci. Ces dernières mesures ont montré que l'activité des produits de fission solides rejetée dans l'atmosphère était inférieure à 2.10^{-4} Ci en raison de l'efficacité des filtres du circuit d'extraction d'air. [1]

Néanmoins, des contrôles par prélèvements d'herbe ont été effectués autour du Centre d'Études Nucléaires de Saclay, dans la direction des vents dominants. Comme prévu, ces prélèvements n'ont pas permis de déceler la présence de produits de fission. Par contre, des

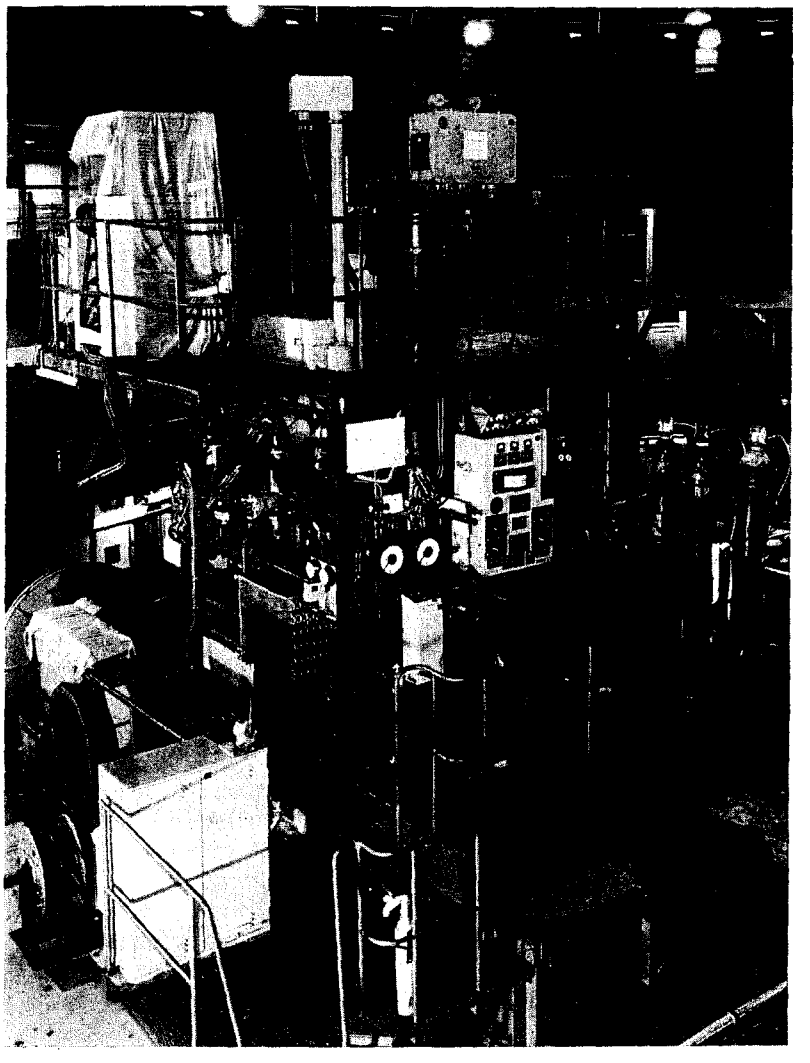

FIG. 2. Hotte de défournement.

prélèvements de thyroïde de bovins ont donné des résultats positifs (jusqu'à 48 pCi/g). Toutefois, rien ne permet de conclure actuellement que cette contamination ait été liée aux rejets d'iode à partir de EL.3.

REMARQUE: Du fait du taux de combustion relativement élevé de l'uranium, la quantité des isotopes du plutonium formé dans le combustible était importante: de l'ordre de 1 mg par gramme d'uranium. En admettant un taux d'émission du plutonium de l'ordre de 1% de la quantité formée, on calcule un risque potentiel de contamination par le plutonium de l'ordre de 2 à 10% du risque potentiel dû à l'iode 131. Cependant, dans les mesures faites a posteriori sur les prélèvements, il ne nous a pas été possible de mettre en évidence le plutonium.

3.2. *Contamination des surfaces*

Par suite de l'émission importante des produits de fission, de fortes contaminations des surfaces de travail, des parois et du plafond du bâtiment ont été observées (tableau 1). Les

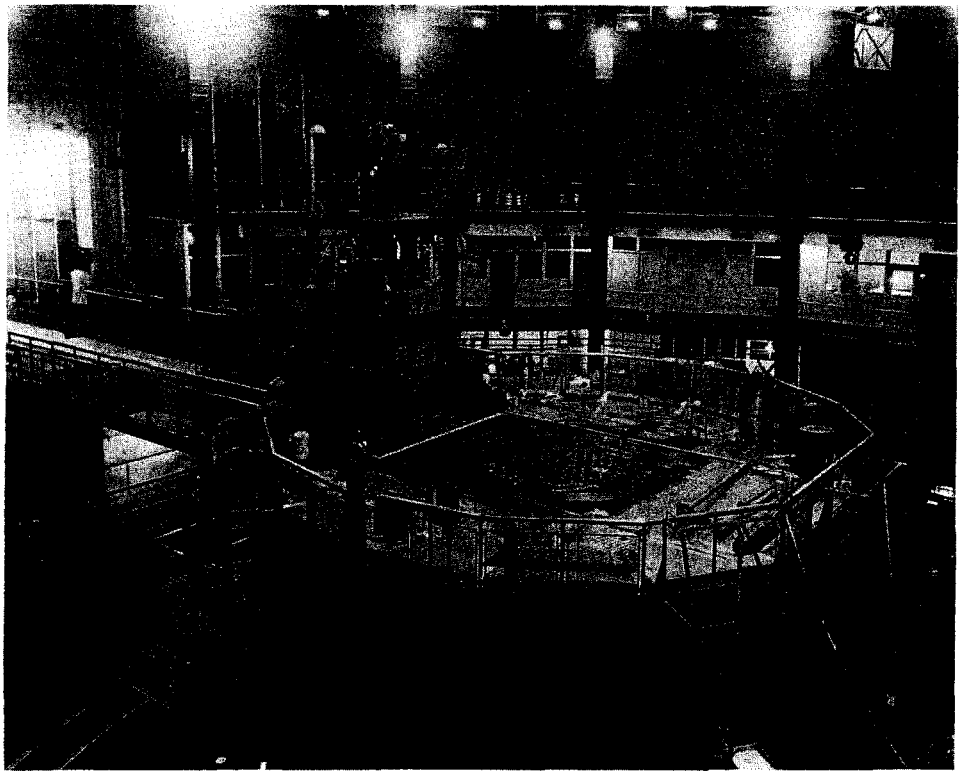

FIG. 3. Hotte de défournement sur le toit de la pile.

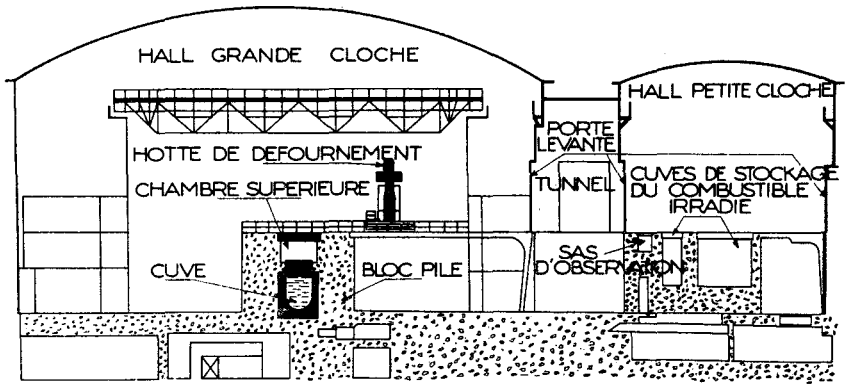

FIG. 4. Coupe schématique du bâtiment de la pile et du bâtiment de stockage.

FIG. 5. Alvéoles des cuves pour éléments irradiés du bâtiment de stockage.

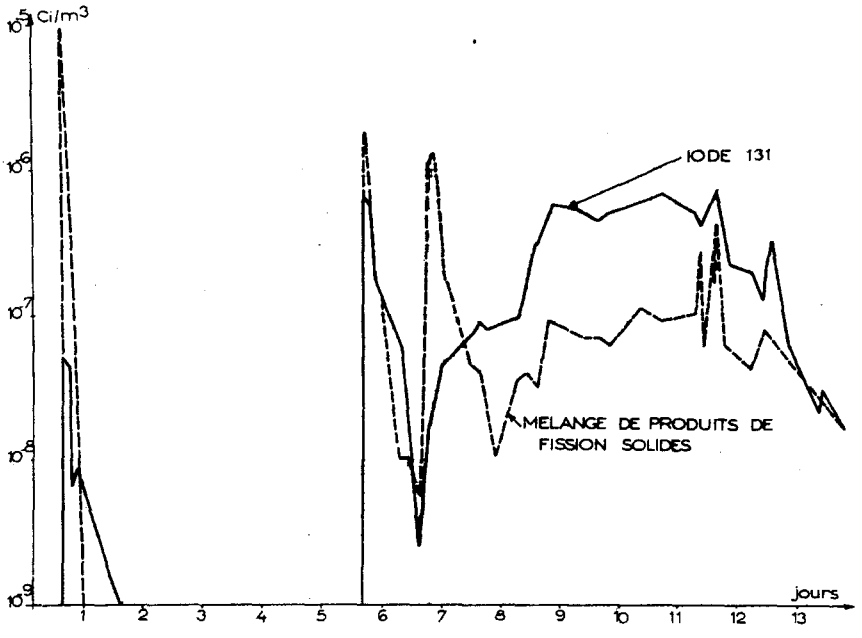

FIG. 6. Évolution de la contamination atmosphérique dans le bâtiment de stockage.

contaminations les plus importantes ont été mesurées sur les aires de travail (10^{-5} à 10^{-3} Ci/dm^2) et sur la hotte blindée de défournement des cellules. À l'intérieur de cette hotte dans le logement de la cellule, la pollution était telle que l'on a mesuré une intensité d'irradiation de l'ordre de 100 rad/h.

IV. ÉTUDES DES RÉSULTATS DES MESURES DE LA CONTAMINATION

Les résultats des mesures effectuées sur les prélèvements atmosphériques et de surfaces nous ont conduits à formuler quelques observations sur le comportement des produits de fission.

Pour pousser plus à fond nos investigations concernant l'évolution de l'incident, nous avons été conduits à effectuer des prélèvements dans les circuits d'eau lourde et d'hélium de la pile EL.3, ainsi que dans le puits du sas d'observation et la première alvéole de stockage de la cellule.

4.1. *Émission des produits de fission dans les circuits de la pile*

À partir des résultats de ces prélèvements donnés au tableau 2 et d'hypothèses simples, nous avons calculé la quantité d'uranium mise en jeu au fur et à mesure de l'évolution de l'incident et les pourcentages des produits de fission émis dans l'eau lourde.

La quantité d'uranium impliquée dans la rupture de gaine a été tout d'abord calculée en supposant un taux d'émission de 100% des gaz de fission et le passage de l'activité totale de ces gaz dans l'atmosphère en hélium de la cuve.[3–5,8] Avec ces hypothèses, la masse d'uranium calculée est de 10 grammes. On en a déduit les activités des autres produits de fission formés.[2]

En fait, une rupture de gaine n'entraîne pas obligatoirement la fusion de l'uranium. Il en résulte que le taux d'émission réel des gaz de fission est inférieur à 100%. En admettant un taux d'émission compris entre 20 et 70%[9, 10] la quantité d'uranium touchée par la rupture de gaine est comprise entre 15 et 50 g.

Les pourcentages d'émission des produits de fission dans l'eau lourde au moment de la rupture de gaine peuvent être compris entre les deux valeurs mentionnées dans le tableau 2.

Mis à part le taux d'émission du ^{137}Cs qui peut paraître élevé, ces résultats semblent en assez bon accord avec les valeurs généralement admises.

4.2. *Comportement des produits de fission libérés dans le bâtiment*

4.2.1. Les résultats concernant ^{131}I et ^{137}Cs des analyses effectuées sur les prélèvements d'eau du puits du sas d'observation et de la première alvéole de stockage ont montré que les activités de ces deux radio-éléments libérées successivement dans ces deux volumes étaient 5, puis 40 fois, supérieures à celles libérées dans l'eau lourde.

Ces résultats ont donc confirmé l'aggravation progressive de l'incident en raison du mauvais refroidissement de l'uranium dû aux mauvaises conditions de stockage. Les quantités d'uranium mises en jeu évaluées à partir de ces deux radio-éléments, comparativement aux résultats obtenus dans l'eau lourde sont respectivement de l'ordre de 10^2 et de 10^3 grammes. La valeur maximale calculée de 2,3 kg a été confirmée par les examens visuels et radiographiques qui ont été effectués ultérieurement.

4.2.2. Les constatations les plus marquantes du comportement des produits de fission libérés dans le bâtiment sont les suivantes:

—Mis à part l'iode 131, nous avons trouvé, dans l'atmosphère et sur les surfaces, les mêmes produits de fission dans les mêmes proportions relatives moyennes.

Ces proportions relatives moyennes, en prenant le couple ^{140}Ba-La comme unité, sont les suivantes:

^{95}Zr–^{95}Nb	1,2
^{103}Ru	0,5
^{140}Ba–^{140}La	1
^{141}Ce	0,5

—L'iode 131 dont la présence dans l'atmosphère a été mise en évidence et suivie régulièrement n'a pu être décelé sur les surfaces contaminées. Les raisons évoquées pour rendre compte de ce résultat sont d'une part, la faible vitesse de dépôt[6, 7] et, d'autre part, la difficulté de le prélever sur des surfaces par simple frottis.

—Les Césium 134 et 137 n'ont pas été mis en évidence dans l'atmosphère du bâtiment,

bien que les activités mesurées dans l'eau lourde, les eaux du puits du sas d'observation et de la première alvéole de stockage sont relativement importantes.

V. CONSÉQUENCES DE L'INCIDENT DU POINT DE VUE DE LA RADIOPROTECTION

5.1. *Irradiation externe et interne du personnel*

Les différentes opérations de transfert et de stockage de la cellule défectueuse ont nécessité l'intervention de 49 personnes. Une réglementation stricte des conditions de travail a conduit à des irradiations externes relativement faibles puisque pour la durée des opérations (environ 10 jours de travail) 47 personnes ont subi une irradiation inférieure à 300 mrem et deux personnes ont subi respectivement 315 et 550 mrem* (cf. annexe II).

Les contaminations internes ont également été faibles. En général, elles ont été subies le premier jour au cours de la brusque émission de produits de fission, alors que le personnel ne portait qu'un appareil respiratoire filtrant. Les contaminations internes mesurées par le Service Médical ont été inférieures à 50 CMA.h et le plus souvent de l'ordre de 1 CMA.h.†

5.2. *Enseignements acquis à la suite de l'incident*

Des enseignements utiles ont été acquis à la suite de cet incident. Ces enseignements concernent l'équipement des locaux, l'équipement du personnel, les matériels et les méthodes de mesure en radioprotection (cf. annexe III).

Quoique cet incident n'ai eu que des conséquences très limitées concernant les irradiations externes et internes du personnel, il a pris une ampleur inhabituelle par sa durée, les taux de contamination atteints, l'importance des surfaces contaminées et le nombre des personnes impliquées.

Il convient donc d'être extrêmement vigilant en cas d'incident même apparamment mineur, survenant sur des matériaux présentant des risques radio-actifs importants.

Une fois de plus, nous constatons, que des vérifications minutieuses et systématiques, tant sur les projets d'appareillage que sur les méthodes de travail, peuvent dans certains cas économiser beaucoup de temps et d'argent même si à la longue, elles peuvent apparaître fastidieuses et inutiles.

ANNEXE I

Caracteristiques de la cellule

Combustible: Uranium enrichi à 1,6% allié à du molybdène (0,22%), du fer (0,03%) et du chrome (0,11%)

Poids de combustible: 12,4 kg (soit environ 3,1 kg par cartouche)

Taux de combustion: 3 650 MWj/t

La rupture de gaine a été signalée le 28 Octobre 1965 à 9h 25 par le dispositif de détection de rupture de gaine, alors que la pile fonctionnait à 4 MW depuis 9h 07. Cette alarme a provoqué l'arrêt de la pile par chute des barres de sécurité.

Auparavant, la pile était à l'arrêt depuis le 21 Octobre 1965 à 18h.

ANNEXE II

Conditions de travail pendant les interventions dans le bâtiment de stockage

1. Les conditions de travail dans le bâtiment de stockage ont été réglementées pour limiter l'irradiation externe et la contamination des équipes d'intervention.
2. Les équipes d'intervention étaient constituées de 3 agents du Service d'exploitation de la pile et d'un agent du Service de protection contre les radiations.
3. Le temps de travail par équipe était de l'ordre de ¼ d'heure d'une part, pour limiter l'irradiation externe et, d'autre part, en raison de l'autonomie de 20 minutes conférée par

---

* Les niveaux d'irradiation mesurés, dus à la présence des gaz de fission, à la contamination des surfaces et des fuites de rayonnement, étaient généralement inférieurs à 40 mrad/h. Une seule intervention de très courte durée n'intéressant que les mains et les avant-bras, a dû être effectuée dans une intensité d'irradiation de 70 rad/h.

† La CMA pour l'iode 131 est de $4{,}5.10^{-9}$ Ci/m³ (réglementation EURATOM) 1 CMA.h correspond à une quantité inhalée de $5{,}6.10^{-9}$ Ci.

Tableau 1. *Contamination des Surfaces Dans le Batiment de Stockage*

Zone contaminée	Surface intéressée m^2	Taux de contamination Ci/dm^2 (2)
Niveau + 7 m (1)	130	10^{-5} à 10^{-3}
Niveau 0	200	10^{-6} à 10^{-5}
Niveau—6 m	200	10^{-7} à 10^{-6}
Pont roulant	30	10^{-6} à 10^{-4}
Plafond (+ 22 m)	400	10^{-6}
Parois verticales	1 500	10^{-7}

(1) Niveau où les travaux étaient effectués.
(2) Radioéléments identifiés ^{95}Zr–^{95}Nb–^{103}Ru–^{140}Ba–^{140}La–^{141}Ce

Tableau 2. *Émission des Produits de Fission dans les Circuits de la Pile El.*3 *Lors de la Rupture de Gaine*

Radio éléments	Activité volumique Ci/m^3		Pourcentage d'émission dans D_2O	
	Circuit He	Circuit D_2O	I	II
^{133}Xe	$2{,}8.10^{-1}$			
^{135}Xe	$2{,}3.10^{-2}$			
^{85m}Kr	$2{,}9.10^{-3}$			
^{88}Kr–^{88}Rb	$1{,}5.10^{-3}$			
^{95}Zr–^{95}Nb		6.10^{-2}	5	1–3
^{97}Zr–^{97}Nb		9.10^{-3}	10	2–6
^{103}Ru		$4.7.10^{-2}$	10	2–8
^{131}I		$5{,}8.10^{-2}$	20	4–13
^{137}Cs		7.10^{-3}	50	10–35
^{140}Ba–^{140}La		$3{,}1.10^{-2}$	2	0,5–1,5
^{141}Ce		$4{,}2.10^{-2}$	5	1–4

I. En supposant un taux d'émission des gaz rares de 100% (fusion uranium)
II. En supposant un taux d'émission des gaz rares de 20 à 70%. (9, 10)

les bouteilles d'air des appareils respiratoires.

4. Pour les interventions effectuées sur la cellule avariée, l'emploi d'un scaphandre en matière plastique recouvrant les vêtements de travail et l'appareil respiratoire isolant était indispensable pour limiter la contamination radio-active du personnel (Fig. 7). Cependant, ce scaphandre n'était pas revêtu pour les travaux de préparation sans intervention sur la cellule, afin d'augmenter le rendement du personnel.

ANNEXE III

Mesures envisagées consécutives aux enseignements acquis à la suite de l'incident

Équipement des locaux.

—Aménagement de vestiaires spéciaux pour le bâtiment de stockage
—Mise en place d'un dispositif de ventilation autonome à efficacité élevée dans le bâtiment de stockage
—Nécessité d'une possibilité d'isolement des zones de travail dans les bâtiments de pile

pour éviter la généralisation de la contamination à la suite d'incident de ce type.

Équipement du personnel. Un risque grave d'asphyxie est apparu dans l'utilisation de l'appareil respiratoire isolant porté à l'intérieur du scaphandre. Il a été décidé, d'une part, de revoir le dispositif de sécurité de l'appareil isolant signalant l'épuisement de la réserve d'air, et,

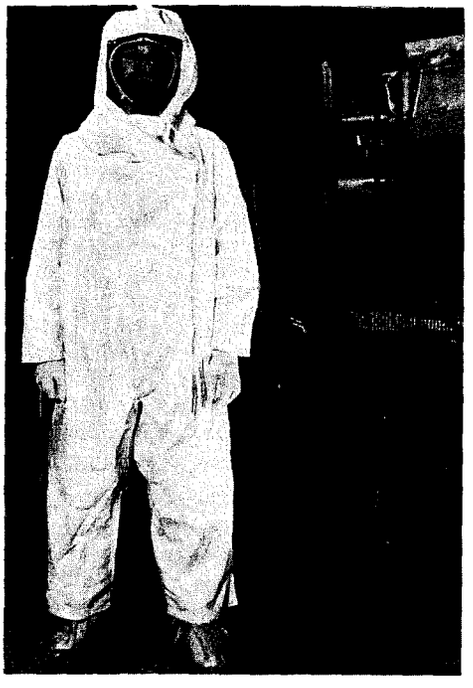

FIG. 7. Scaphandre utilisé pendant les interventions dans le bâtiment de stockage.

d'autre part, d'utiliser un autre type de scaphandre (fig. 8).

Matériels et méthodes de mesure en radioprotection.

—Nécessité d'une réserve importante de matériel de radioprotection à stocker dans des armoires facilement accessibles et protégées contre la contamination radioactive.

—Mise en évidence des risques potentiels des isotopes du plutonium dans le cas des cellules de combustibles présentent des taux de combustion élevés.

—Mesure des contaminations déposées sur les surfaces à l'aide de prélèvements effectués sur papier gommé (méthode analogue à celle utilisée pour les retombées des explosions nucléaires) et par mesure directe par spectrométrie γ.

RÉFÉRENCES

1. L. FITOUSSI et P. LEBOULEUX. Étude de la radioactivité rejetée par les piles EL.2 à EL.3 du CEN.S—Colloque International sur la pollution radio-active des milieux gazeux. Saclay 1963.
2. J. O. BLOMEKE et M. F. TODD. Uranium 235 fission product production as a function of thermal neutron flux, irradiation time, and decay time. ORNL 2127.
3. J. M. LAVIE et A. DOURY. Évaluation des risques radio-actifs liés au fonctionnement d'une installation nucléaire. Rapport CEA n° 1724 (1960).

FIG. 8. Type de scaphandre dont l'emploi a été retenu pour les interventions ultérieures.

4. F. T. BINFORD. Étude de quelques problèmes liés au dégagement accidentel de produits de fission provenant d'un réacteur nucléaire. Colloque International sur la pollution radio-active des milieux gazeux. Saclay 1963.
5. J. R. BEATTIE. An assessment of environmental hazards from fission products releases. UKAEA AHSB(S)—R 64 (1961).
6. J. F. CROFT et R. S. ILES. Experimental release of radio-Iodine in the Zenith Reactor containment. AEEW R 172 (1962).
7. J. F. CROFT, R. S. ILES et R. E. DAVIS. Experiments on the surface deposition of airborne iodine of high concentration. AEEW R 265 (1963).
8. Theoretical possibilities and consequences of major accidents in large nuclear power plants. USAEC report Wash. 740 (1957).
9. J. DADILLON. Étude de la contamination libérée par la fusion de combustible dans le cœur d'une pile piscine—Experiences I et II à Cabri. Report interne. SESR/EDC 66–15.
10. F. R. FARMER. The evaluation of power reactor sites. VII° Congresso Internazionale Nucleare. Roma 11/17/6/62.

COMPARISON OF FISSION PRODUCT RELEASES FROM THE DESTRUCTIVE TESTS OF TWO SNAP 10A/2 REACTORS*

O. L. CORDES
Phillips Petroleum Co., Atomic Energy Division, Idaho Falls, Idaho

Abstract—Retention of fission products by the water environment surrounding a water-moderated reactor has long been considered an effective measure for reducing the radiological consequences of a reactor accident. Little credit has been taken for this factor in reactor safety analyses, however, because experimental evidence as to the degree of this reduction has been lacking.

An unusual opportunity to study the retention effect of the water environment upon the fraction and type of fission products released during a reactor accident was provided as part of an experimental program in aerospace safety conducted by Phillips Petroleum Company for the United States Atomic Energy Commission. In separate experiments two modified SNAP 10A/2 flight system reactors containing fuel made of an alloy of uranium and zirconium-hydride were intentionally destroyed. One of these reactors was tested while immersed in water and the other was tested in air to determine the consequence of an uncontrolled self-limiting excursion in each of these environments.

This paper compares the fission product release information obtained from these experiments and evaluates the fission product retention effect of the water environment. The major conclusions reached regarding the retention effect of the water environment are that:

1. The water cooling effect on the hot fuel, which limited the destruction of the fuel and caused the fission products to remain trapped in the fuel matrix, is an important mechanism in suppressing the release of fission products.
2. The release fraction of noble gas fission products is greatly reduced by a water environment. Only 4% of the total noble gas fission products were released from the water-immersion test.
3. Halogen and "solid" fission products from an underwater destruction excursion are completely retained, provided the water environment exists following the excursion.

1. INTRODUCTION

In the safety analysis of many water-cooled reactors the coolant has been assumed to supply an additional barrier to the release of fission products. However, little credit has been taken for this factor because experimental evidence as to its effectiveness has been lacking. In the past, information concerning the effectiveness of such a barrier was studied by subjecting small, fueled capsule experiments to conditions simulating a reactor accident and observing the effect of an added water barrier upon the fraction of fission products released. [1] This approach has certain limitations since it is necessary to scale the results from the capsule experiments to full-scale integral-core reactors. Because the conditions in a full-scale reactor core vary from point to point and cannot be uniquely represented by a small isolated sample, the methods for scaling are approximate and not well known. This uncertainty in scaling generally results in an over-conservative estimate when applied to fission product releases.

An ideal experiment for determining the extent a water environment reduces the release of fission products from a reactor accident would consist of two full-scale reactor destructive tests,

* Work performed under the auspices of the U.S. Atomic Energy Commission (Contract AT(10-1)-205).

with one reactor immersed in water and the other in air. This use of full-scale integral-core reactors would eliminate the necessity of scaling the results of smaller capsule-type experiments to actual reactor accident conditions.

An approximation to this ideal experiment occurred as part of an experimental program in aerospace safety conducted by Phillips Petroleum Company for the United States Atomic Energy Commission at the National Reactor Testing Station in Idaho. In this experiment, designated the SNAPTRAN program, two modified SNAP 10A/2 flight system reactors were intentionally subjected to severe reactivity insertions which resulted in their destruction. The first of these was an underwater test designed to determine the radiological consequences of an accidental immersion of one of these reactors in water, such as could occur from the aborting of an attempted launch of the reactor into orbit around the earth. The second test was conducted in an air atmosphere to gain information on reactor kinetics as well as to demonstrate the radiological consequences of an uncontrolled self-limiting excursion in an air environment.

The purpose of this paper is to compare the fission product release data from these two destructive tests in order to evaluate the extent to which the water environment reduced the release of fission products to the atmosphere. In addition, radiological instruments and sampling techniques are briefly described.

2. REACTOR DESCRIPTION

The two reactors used in the SNAPTRAN destructive tests were SNAP 10A/2 flight system reactors with modified control systems to provide for rapid insertion of reactivity. Each of the identical reactor cores contained thirty-seven fuel rods in a thin, cylindrical, stainless-steel vessel approximately 23 cm in diameter and 31 cm in height. The fuel rods were made from a homogeneous alloy of zirconium-hydride and uranium and were clad with Hastelloy-N. With this arrangement, each reactor contained 4.75 kg of U-235 and 464 g-moles of hydrogen. For normal flight system operation, an external, fixed beryllium reflector was placed around the core to provide sufficient neutron reflection for reactor operation and the interstitial spaces in the core were filled with a sodium-potassium (NaK) liquid-metal coolant.

For the water-immersion test, the reactor was located in a concrete environmental tank which had an internal diameter of 4.25 m and a depth of 3.1 m. When filled, the water depth above the reactor was approximately 1 m. The size of the tank was selected to simulate a large body of water yet remain small enough to facilitate pressure measurements and evaluation of other phenomena. Because it had been shown that the normal beryllium reflector would be stripped from the reactor during entry into water following a launch abort, the beryllium reflector was not used in the water-immersion test. Instead, the water environment provided the necessary neutron reflection to achieve criticality, and the axial position of a 0.64-cm-thick, neutron-absorbing, boron-aluminum sleeve controlled the reactor. The NaK coolant was used, however, to provide for the possibility of an additional energy release through a NaK-water reaction. To initiate the test the boron-aluminum sleeve was rapidly withdrawn from around the reactor by a pyrotechnic actuator.

For the open-air destructive test, the reactor was mounted in the normal beryllium reflector assembly to simulate the space reactor package. Reactor control was accomplished by the position of beryllium drums which were rotated into rounded slots 90 degrees apart in the fixed beryllium reflector (Fig. 1). Rapid reactivity insertion was achieved by rapidly rotating the steel drive shafts of the beryllium drums with a rack-and-pinion gear train connected to a pneumatically driven cylinder and piston.

To facilitate movement from the test area to the assembly and examination area, both test reactor packages were mounted on railroad dollies. Reactor control and initiation of the destructive tests were accomplished from an underground shielded equipment and control building adjacent to the reactor test pad. The shielded roadway tunnel shown in Fig. 2 gave access to the underground area. The test cell building, also mounted on railroad-type wheels and steel tracks, was pulled back from the test pad prior to the initiation of both tests, leaving the test package essentially open to the environment.

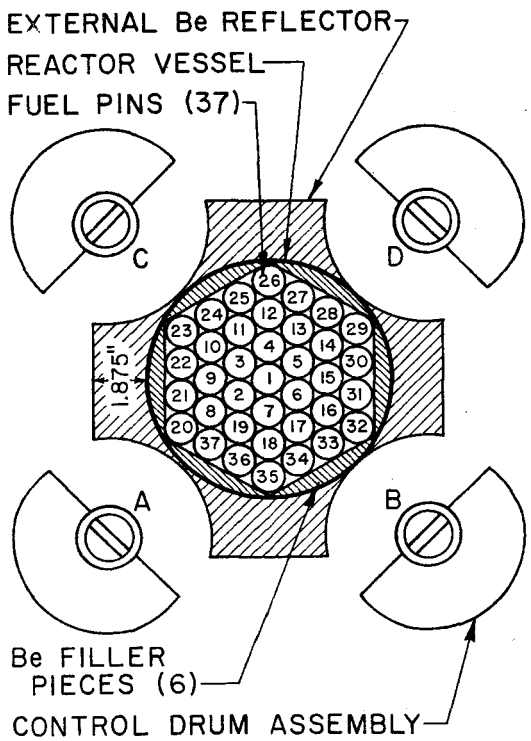

FIG. 1. Typical SNAP 10A/2 reactor and beryllium reflector cross-section.

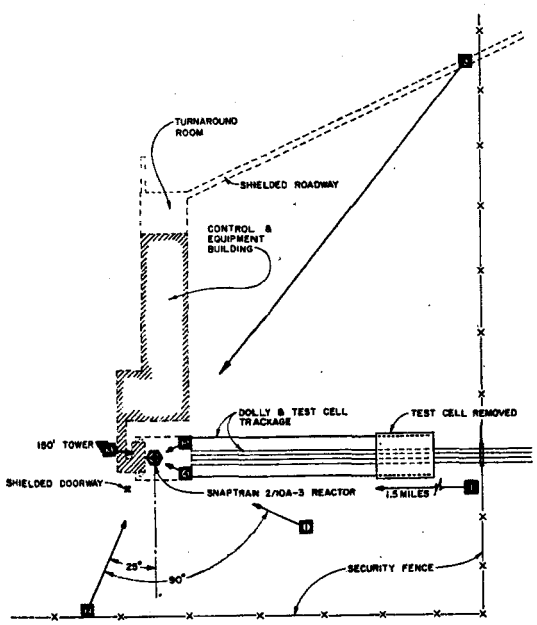

FIG. 2. Test pad layout.

3. TEST DESCRIPTION

The two destructive tests were conducted under similar weather conditions. The first test, which was the water-immersion test, was conducted on April 1, 1964, with a 10 meter per second wind speed and a slightly unstable vertical temperature profile (Pasquill class C). The second, or beryllium-reflected test, was conducted on January 11, 1966, with a 5 meter per second wind speed and a neutral (Pasquill class D) vertical temperature profile. Each test produced a single radioactive cloud which traveled downwind over an instrumented radiological grid.

The radioactive cloud from the water-immersion test seemed to be delayed for several seconds following the excursion, during which time the initial column of water and steam collapsed back into the environmental tank. Following the collapse of the water, the visible vapor-filled cloud moved downwind over the radiological grid. The short delay in release of the cloud was confirmed by a measured shift in the isotopic ratio of the daughters of krypton gases. For example, measured ratios agree with the theoretical ratios if a delayed release time of 3 sec is postulated.

Figure 3 shows the twin flashes from the pyrotechnic actuator which removed the control sleeve and initiated the water-immersion destructive test. In the next picture (Fig. 4) the reactor is at peak power, and the entire environmental tank is illuminated by the Cerenkov glow. The development of the water and steam cloud at 200 msec and 550 msec after peak power is shown in Figs. 5 and 6, respectively. Figure 7 shows the nearly collapsed water and steam cloud at 2.6 sec after peak power. Immediately following this, the visible cloud arose and moved downwind.

The beryllium-reflected test was somewhat more spectacular in that the entire test pad (some 20 m across) was covered with burning hydrogen and fuel. A visible cloud arose from this test without delay and continued to rise, reaching a height of approximately 50 m before leveling off at a distance of 100 m downwind. Some of the fuel pieces continued to burn for several seconds following the test and undoubtedly continued to evolve fission products. Measurements made with samplers located at

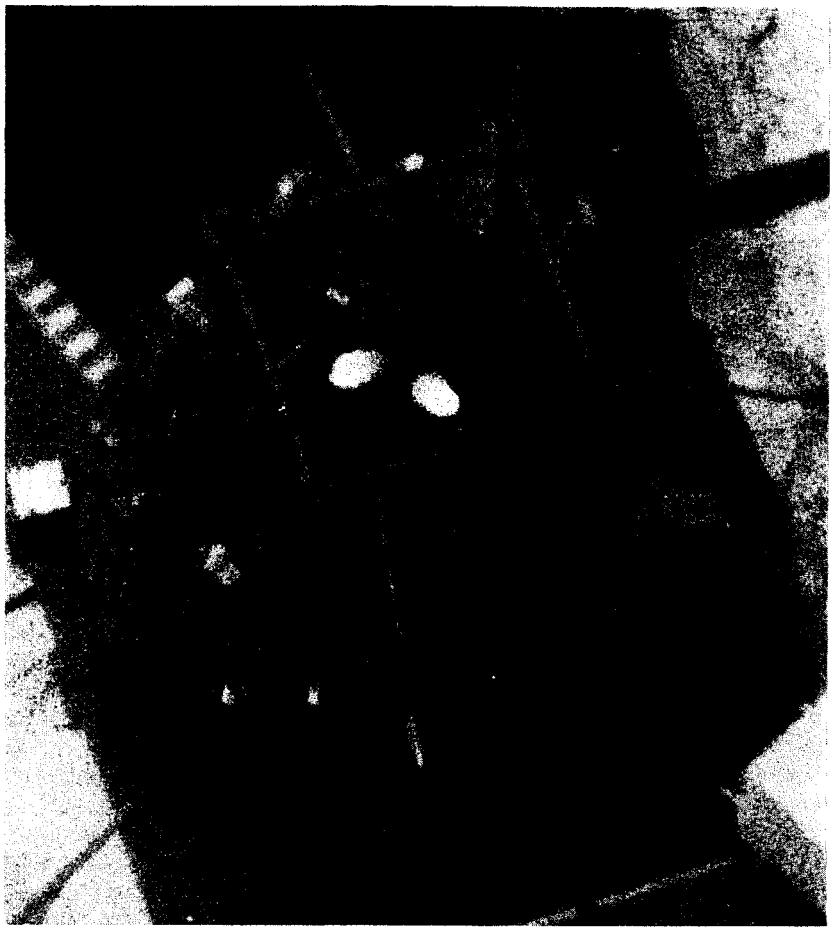

FIG. 3. Overhead view of the water-immersion test initiation.

intervals on a 46-m-high tower indicate that the amount of activity released by the burning fuel was small compared to that which followed the path of the visible cloud. Figure 8 shows the beryllium-reflected reactor on the test pad immediately prior to the test. The beginning and rise of the visible cloud are shown in Figs. 9 and 10 taken at 1.10 sec and 2.35 sec, respectively, after peak power.

4. RADIOLOGICAL MONITORING AND INSTRUMENTS

Both destructive tests were monitored to obtain radiological data from which the magnitude of the fission product releases and radiological hazards could be determined. This monitoring was accomplished by a radiological monitoring grid located on a series of concentric arcs surrounding the reactor test pad. In a 60-degree sector centered on a line 30 degrees east of true north, which coincided with the movement of the prevailing wind, sampling stations were located out to a distance of 5 miles to provide downwind monitoring. The placement of the samplers used on the monitoring grid is shown in Figs. 11, 12, and 13. Figure 14 shows a typical grid station with a high volume air sampler, a fallout plate, a direct radiation monitor, and a balloon-type fission gas sampler. In addition to the downwind ground-level grid samplers, several sets of samplers were located

FIG. 4. Overhead view of the water-immersion test at peak power.

above the reactor test pad on a 46-m-high exhaust stack and a 46-m-high tower. These samplers provided information on the effective height of the radioactive releases and obtained samples through a vertical section of the radioactive cloud.

Figure 15 shows the primary sampler used on the grid. The sampler consisted of a Staplex high-volume air pump modified to hold a 4-in. diameter by 1-in. deep charcoal bed in series with a 4 in. diameter particulate filter (Microsorban). Noble gases were sampled using the balloon-type sampler shown in Fig. 16. The amount of noble gas drawn into the balloon through a one-way valve is determined by counting the radioactive daughters formed during a measured decay interval. Particle sizing of the debris from the destructive tests was attempted using the six-stage Anderson impactor samplers. Several Unico four-stage cascade impactors were also used during the water-immersion test. Horizontal fallout plates containing sticky paper sampled the deposition of radioactive debris. During the water-immersion test, water catch trays and cans were also used. Direct radiation measurements were made using film badge dosimeters, ionization chambers, and thermoluminescent dosimeters. For a more complete description of the reactors and the radiological sampling grid, the reader is referred to United States Atomic Energy Commission reports IDO 17019, IDO 17083, and IDO 17194.[2-4]

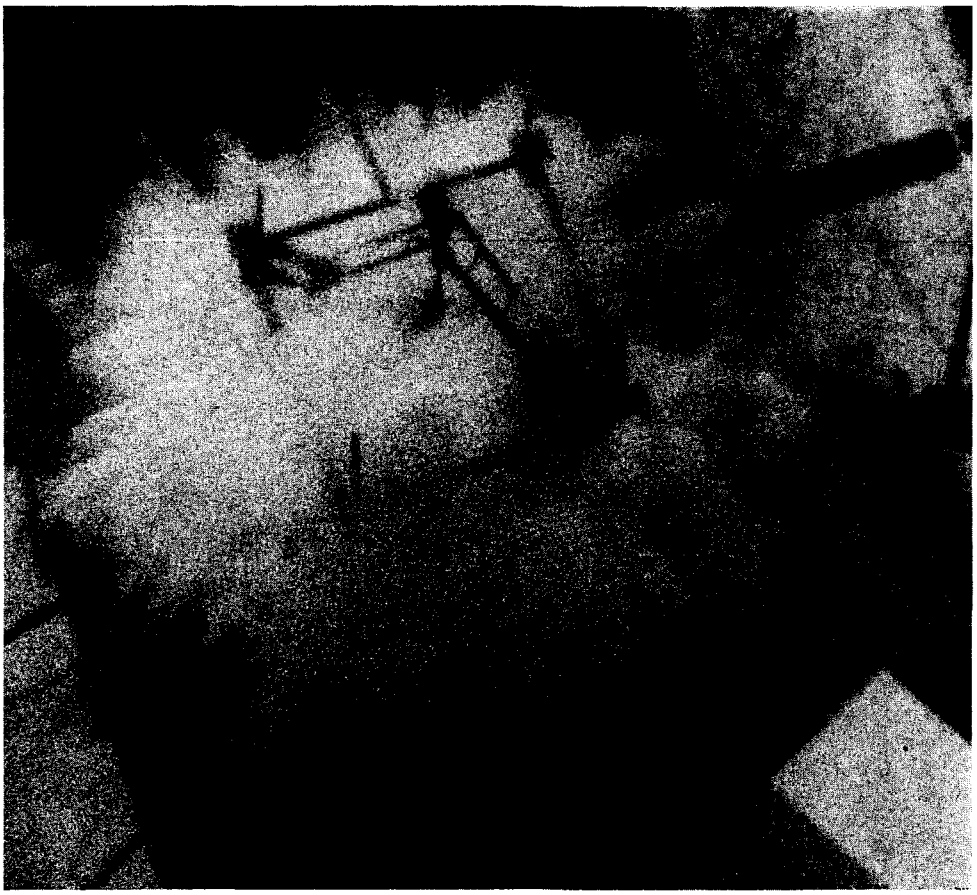

FIG. 5. Overhead view of the developing cloud from the water-immersion test 200 msec after peak power.

5. DATA AND ANALYSIS

Since the magnitude of the nuclear energy release from each of the two tests was similar (45 MW-sec for the water-immersion test and 54 MW-sec for the beryllium-reflected test) the quantity of fission products available for release from each test was of the same order of magnitude. The quantity or fraction of the fission products actually released to the atmosphere differed between the two tests, however, indicating that the release of fission products from a reactor accident is a function of the immediate environment of the reactor.

Data from the radiological grid indicated that the only fission products released from the water-immersion test were noble gases. There were no indications of halogen or "solid" fission products outside the water of the environmental tank other than those which were also the daughters of the short-lived radioactive gases. Only daughters of 3-sec Kr-92, 10-sec Kr-91, 16-sec Xe-140, and 41-sec Xe-139 were detected on the filters of the high-volume air samplers. In addition, the cesium daughter of 17-min Xe-138 was detected in the fission-gas sampler.

Because of this surprising lack of fission products, several lines of investigation were undertaken to verify and establish an upper limit for release fractions of the noble gases and the iodines.

Four independent methods were used to determine the release fraction for the noble gases. The first method, based on a generalized Gaussian dispersion formula[6] in which a source

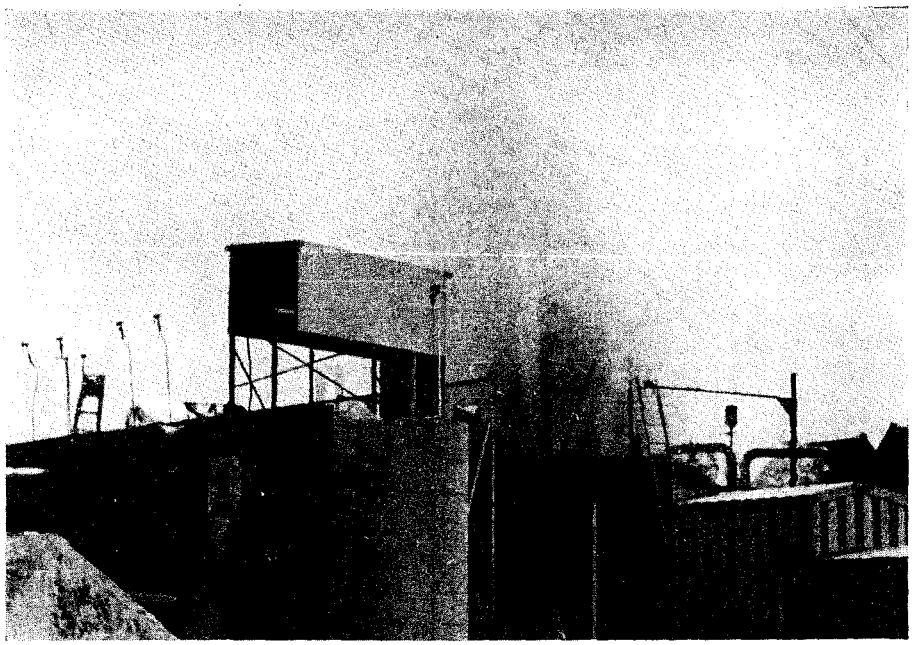

FIG. 6. Elevation view of the developing cloud from the water-immersion test 550 msec after peak power.

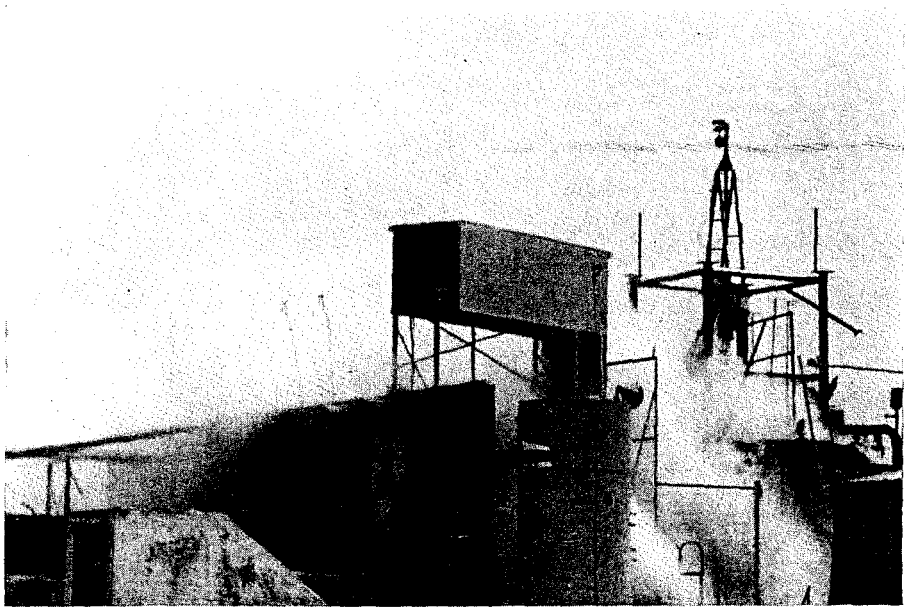

FIG. 7. Elevation view of the nearly collapsed cloud from the water-immersion test 2.6 sec after peak power.

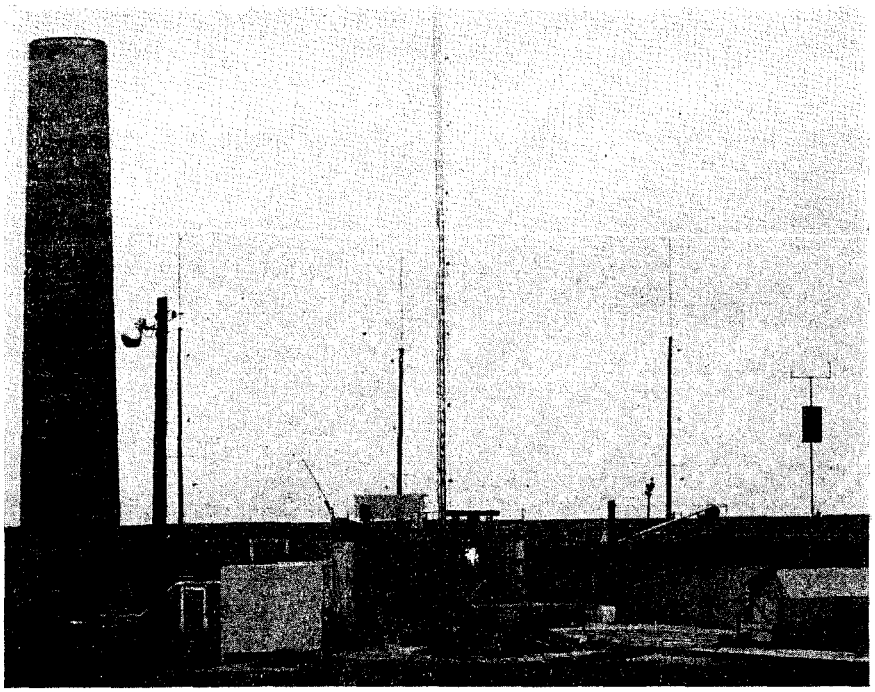

FIG. 8. Elevation view of the beryllium reflected test at 50 msec prior to reactor destruction.

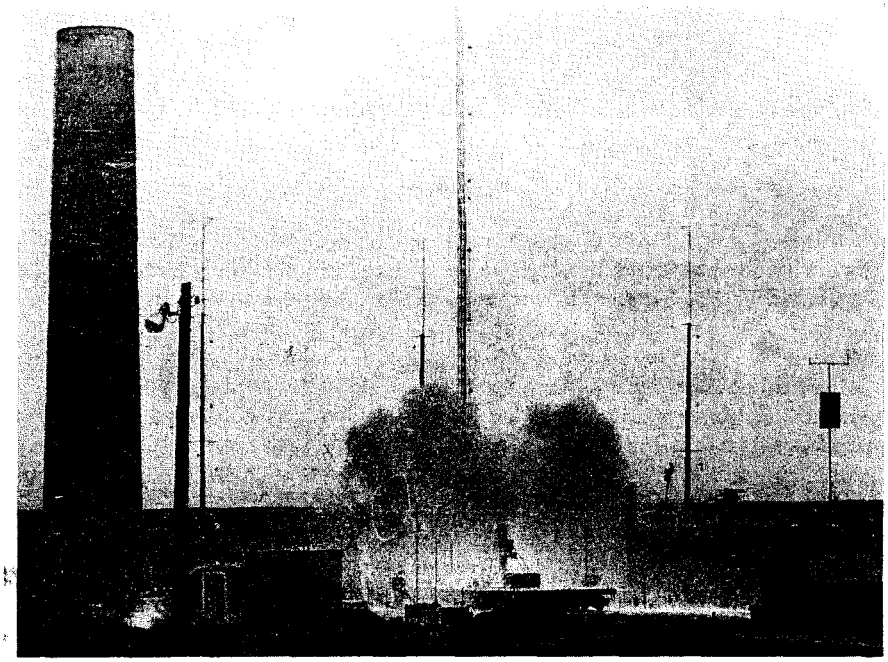

FIG. 9. Elevation view of the developing cloud from the beryllium-reflected test 1.10 sec after peak power.

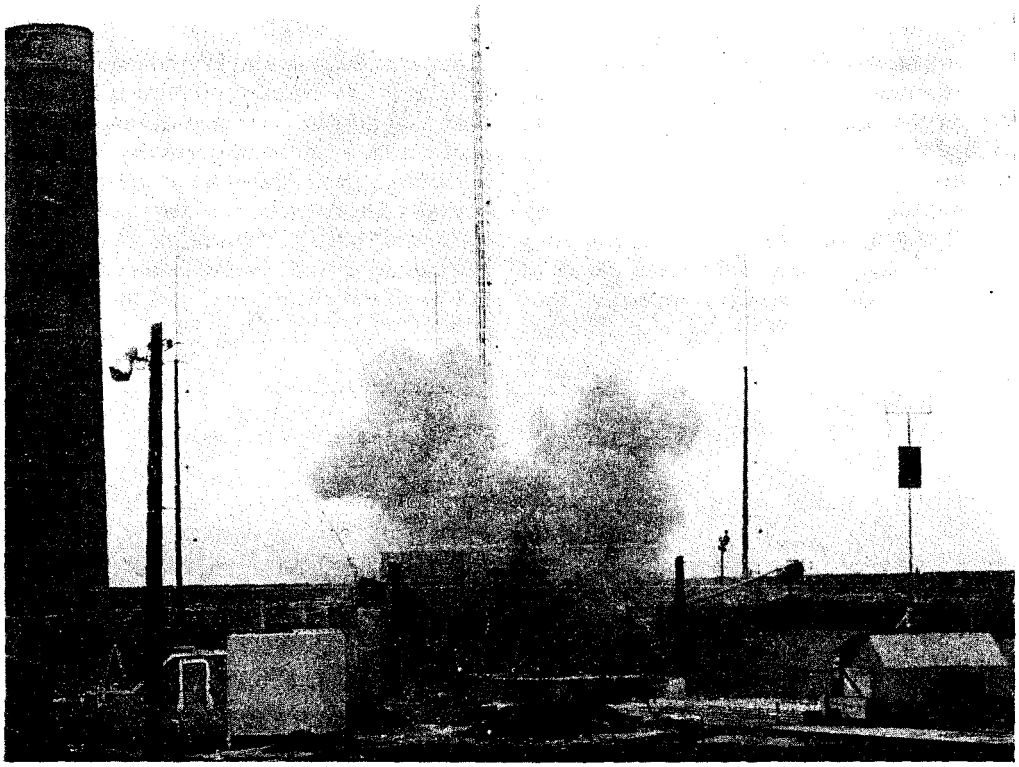

FIG. 10. Elevation view of the developing cloud from the beryllium-reflected test 2.35 sec after peak power.

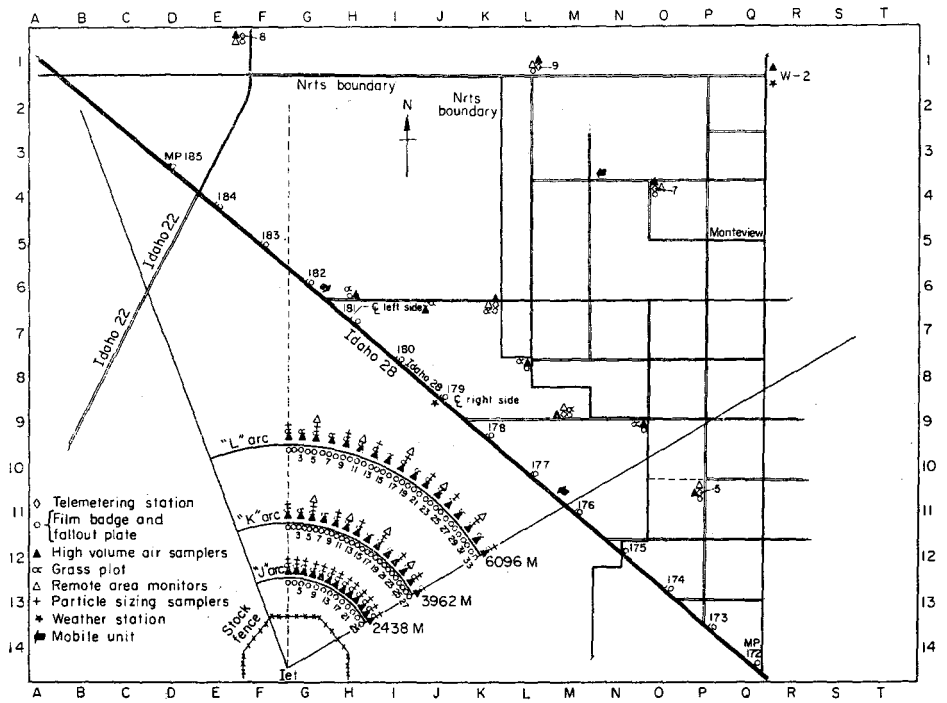

FIG. 11. Radiological monitoring grid beyond 1600 m.

term is calculated from field measurements, led to estimated releases of 4% for Kr-91, 3% for Kr-92, and 3% for Xe-139. In the second method, a physical estimate of the cloud volume was made from photographs and radiation measurements. This volume was assumed to be uniformly filled with the maximum concentration of Xe-138 detected in the cloud to estimate the total quantity released. This method indicated a release of 2% for Xe-138. In the third method, all (99%) of the recovered reactor fuel was dissolved and sampled for Cs-137, the daughter of I-137 and Xe-137. The difference between the calculated quantity produced in the reactor core and the measured amount would be that which was released as I-137 or Xe-137. This method indicated that 0% of the Xe-137 chain was released. The fourth method consisted of measuring the amount of Kr-85 remaining in a small piece of fuel and extrapolating this measured concentration to the entire core. This method indicated that 80% of the krypton remained in the fuel. It is felt that this amount is somewhat less than that actually retained during the excursion partly because of the opportunity for the krypton to diffuse from the fuel during the interval between the destructive test and the analysis time and partly because of the difficulty in extrapolating the results from one small piece of fuel to the entire core. All four independent methods indicate a very small release percentage of the noble gases. On the basis of these measurements and the assumption that all noble gases behave essentially the same as those measured, the estimate of 4% is taken to represent a reasonable upper limit of the noble gas release from the water-immersion test.

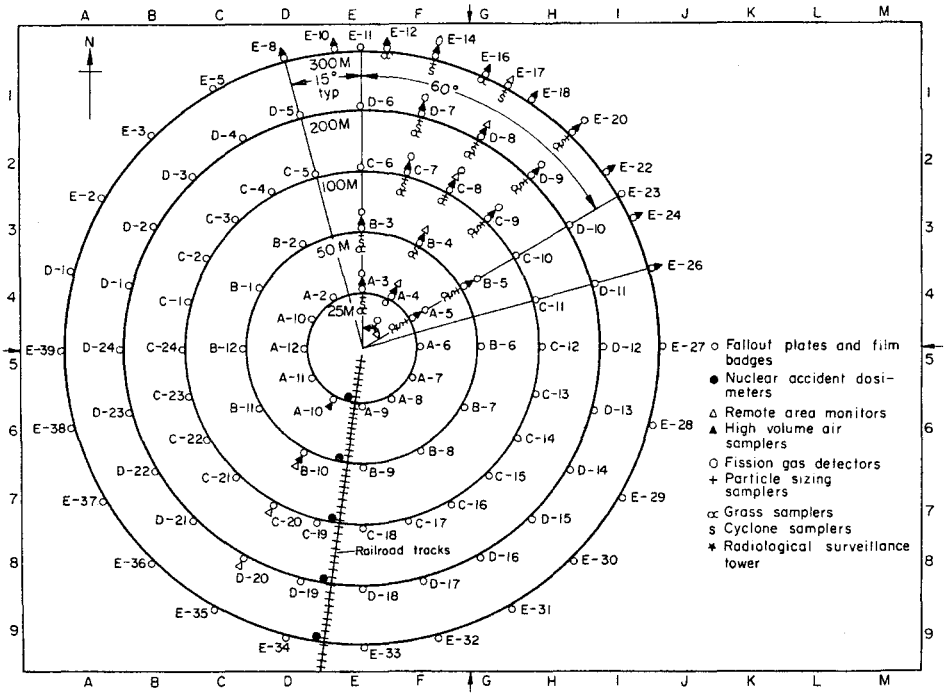

FIG. 12. Radiological monitoring grid to a radius of 300 m.

The lack of detectable quantities of iodine on the downwind grid samplers (specifically designed to be highly sensitive to airborne radioiodine) implied that the halogen fission products were completely retained in the fuel or in the water environment during the water-immersion

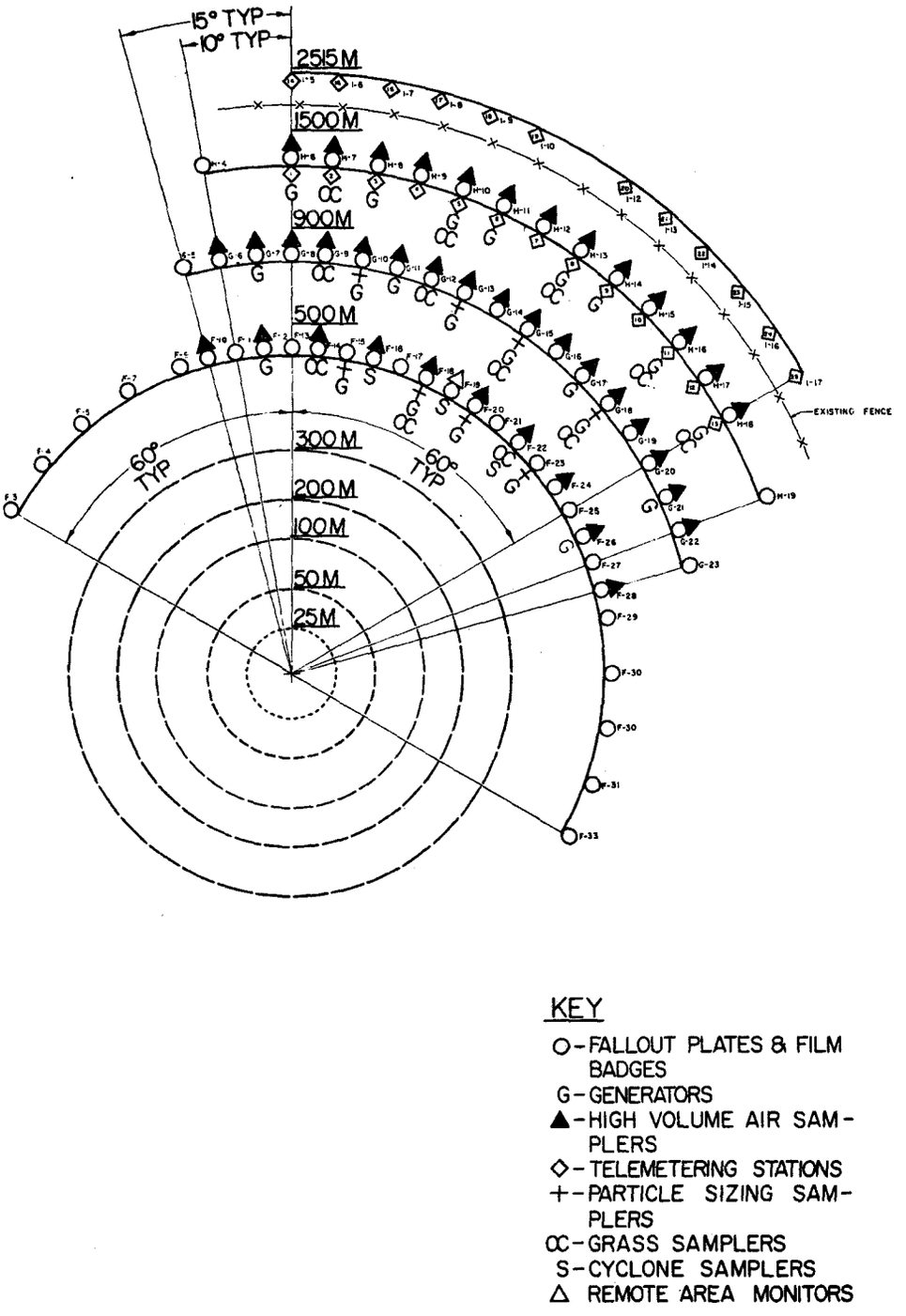

FIG. 13. Radiological monitoring grid to a radius of 2500 m.

test. To substantiate the downwind grid measurements, samples of the environmental tank water and the reactor fuel were analyzed for iodines. Significant quantities of I-131 and I-133 were detected in the samples of the environmental water taken several days after the test (after the water had been drained to a holding tank) indicating that iodines had been held up in the water. A quantitative balance was not possible because there was no way to distinguish between iodine produced directly by fission and that produced indirectly by tellurium decay. Tellurium strongly tends to plate out on piping and cold surfaces, thus reducing by some unknown quantity the total amount of iodine reaching the sampling point. In addition, the fuel analysis indicated that a significant amount of iodine had been retained in the fuel matrix. Radiochemical analysis of the fuel showed that approximately 87% of the expected I-131 was in the fuel at the time of analysis. This was anticipated because essentially all I-131 comes from telluriums with half-lives longer than 20 min, and tellurium would be expected to remain with the fuel material during the quick cooldown following the excursion. While a quantitative iodine balance was not achieved, the detection of significant quantities of iodine in the water and fuel tends to confirm the positive downwind measurement that halogens were not released to the atmosphere from the water-immersion test.

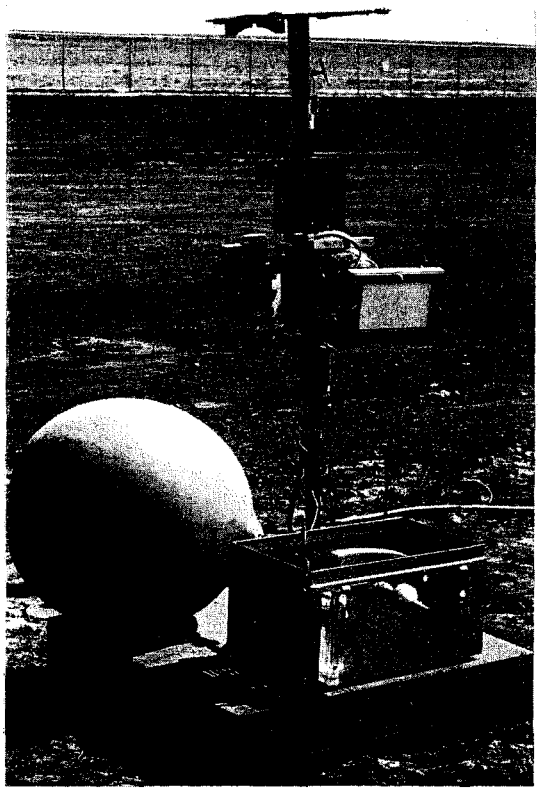

FIG. 14. Typical grid station consisting of a fallout plate, a film dosimeter, a high volume air sampler, and a balloon fission gas sampler.

The test data from the beryllium-reflected test differed significantly from water-immersion test data with respect to the release of fission products. Large quantities of the noble gases, iodines, and telluriums were detected on the downwind radiological grid. In addition, small fuel particles were recovered as far as 200 m downwind, and significant quantities of the "solid" fission products were detected in the radioactive cloud.

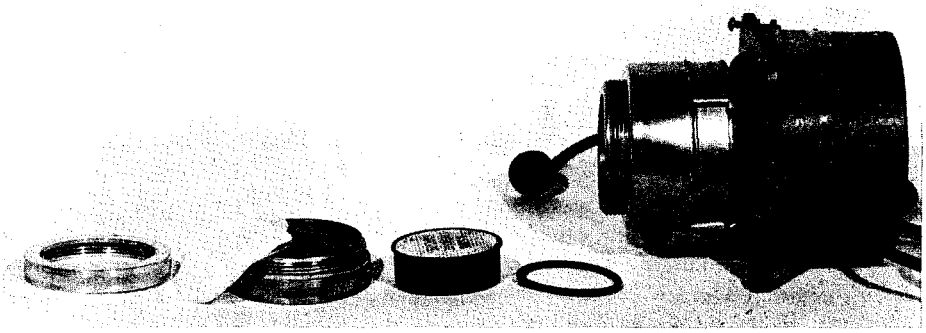

FIG. 15. High volume air sampler with charcoal and dust filter.

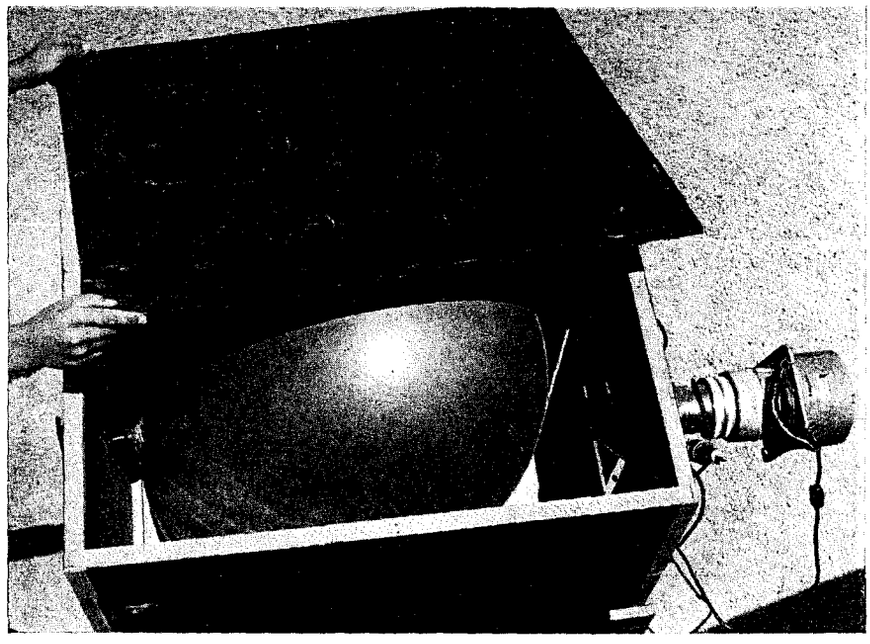

FIG. 16. Balloon fission gas sampler.

The radioactive cloud from the beryllium-reflected test rose considerably higher than did the cloud from the water-immersion test and as a result could not be adequately sampled by the close-in ground-level samplers. This circumstance, plus the interference from the small fuel fragments, limited the release analysis to samples collected beyond 500 m downwind. Accordingly, all release estimates were made on the basis of dispersion calculations[6] in which a source term, developed from measured data, was compared with the calculated quantity available in the reactor.

Analysis of the activities of tellurium-132 and molybdenum- and technetium-99 collected directly by the samplers indicated that 45% of the tellurium-132 and 5% of the molybdenum- and technetium-99 had been released. These three isotopes were the only fission products other than halogens and daughters of noble gases detected on the grid. By assuming that the isotopes which are also daughters of noble gases were released with the same percentage as molybdenum, the activity on the samplers from the noble gas daughters could be calculated and the release percentage of the noble gases could be determined. With this assumption the release values from the Kr-91, Kr-92, Xe-139, and Xe-140 chains indicated a release of 75%.

The iodine and tellurium release fractions were determined by solving simultaneous equations of the form:

$$D_n = F_0 D_{no} + \sum_{i=1}^{n} F_i D_{ni}$$

where D_n = detected activity of the nth isotope in a decay chain (corrected for diffusion);

D_{ni} = computed activity of the nth isotope from decay of the ith precursor;
D_{no} = computed activity of the nth isotope available for release;
F_i = fraction of the ith precursor released;
F_0 = fraction of the nth isotope of the decay chain released.

By comparing data from any two of the 131, 132, 133, and 135 decay chains and assuming all iodine detected on the grid was from either direct yield iodine or tellurium decay and that the samplers were 100% efficient, release fractions for both iodine and tellurium were obtained. This technique, when applied to all

Table 1. *Summary of SNAPTRAN Destructive Test Data*

	Water-immersion test	Beryllium-reflected test
Noble gas release (%)	4	75
Iodine release (%)	0	70
Tellurium release (%)	0	45
Solid release (%)	0	5
Total inventory release (%)	<1	20
Maximum reactivity inserted ($)	3.8	5.1
Minimum period (msec)	0.64	0.20
Maximum power (GW)	18	75
Maximum energy release (MW-sec)	45	54
Maximum fuel temp. (°F)	2400	3000
	2000	2400
Highest avg. core temp. (°F)	1900 at Disassembly	1400 at Disassembly

available data from each of the decay chains, gave an estimated release of 70% for the iodines and 45% for the telluriums. The 45% release of tellurium agrees with the 45% release value determined from direct measurement of tellurium-132 collected on grid samplers.

Table 1 summarizes the fission product release data from the two tests and lists some of the reactor physics data as well.

From Table 1 it can be seen that the water environment was extremely effective in reducing the quantity of fission products released to the environs beyond the water. Ninety-six percent of the noble gases and essentially 100% of the halogen and "solid" fission products were retained in the fuel and in the water barrier. The reactor physics data indicates that there were differences between the two tests, especially in the amount of reactivity inserted and in the peak power attained; however, the total energy release and thus the quantity of fission products available for release were nearly the same. This similarity between the two tests indicates that the difference in fission product release to the environment was almost entirely due to the water environment.

6. DISCUSSION

Most surprising of the observed phenomena was the unexpectedly small release of noble gases from the water-immersion test. Since noble gases do not react with or absorb in water to any appreciable extent, it appears that the retention of the noble gases resulted from the rapid cooling action of the water on the disrupted fuel. The quickly cooled fuel apparently regained sufficient integrity to hold the gases within the fuel matrix. A comparison of the composite photographs of the core remains from both reactors shows that the cooling action of the water was effective in reducing the amount of fuel disruption. A significant portion of the thirty-seven fuel pins was identified and recovered from the water-immersion test (Fig. 17). However, in the beryllium-reflected test (Fig. 18) most of the fuel pins were completely shattered into small unidentifiable fragments.

The absence of the release of iodines from the water-immersion test was not unexpected, and the test served to confirm predicted results. In an excursion-type accident, iodine is produced in two ways: directly by fission and indirectly by tellurium decay. If the energy release is such that a water-environment exists over the core following a destructive excursion, the iodine produced from the tellurium which escaped from the fuel would be expected to form slowly enough to insure 100% absorption in the water. The iodine produced from tellurium remaining in the fuel would also be expected to remain trapped in the fuel. The direct-yield iodine which was available for

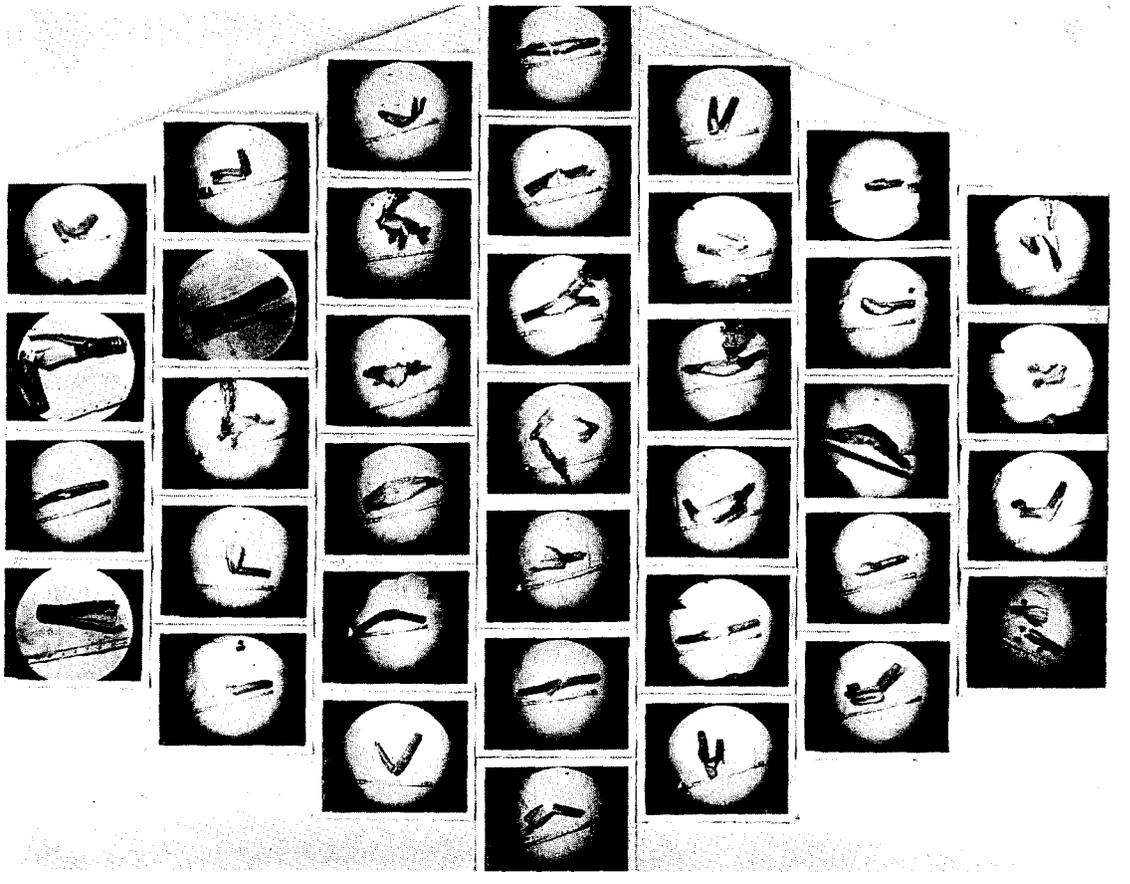

FIG. 17. Fuel rod remains from the water-immersion test arranged according to original core layout.

instantaneous release would have a high probability of reacting with and remaining in the environmental water since most forms of iodine readily dissolve in water, and the vigorous mixing of the fuel and water during the excursion should provide ample contact. In addition, the fuel from these particular reactors contained copious quantities of hydrogen which would be expected to dissociate from the zirconium-hydride lattice. The immediately available direct yield iodine could be expected to react with the hydrogen to form highly soluble hydrogen iodide,[7] once again keeping the iodine confined to the water environment. Also it is likely that the NaK coolant used during the water immersion test had some retention effect upon the iodines released from the fuel. The SNAPTRAN test did not demonstrate which mechanism was responsible for the retention of the direct yield iodine, only that the combination of the mechanisms was completely effective. Further experimentation with smaller capsule experiments could probably determine if the hydrogen and/or NaK were required for the observed iodine retention.

The release of a large fraction of the tellurium fission products from the beryllium-reflected test was another surprising result of these tests. While both tellurium and the other "solid" fission products were completely retained in the water-immersion test, 45% of the tellurium and 5% of the other "solid" fission products were released from the beryllium-reflected test. In most reactor safety analysis work, the telluriums

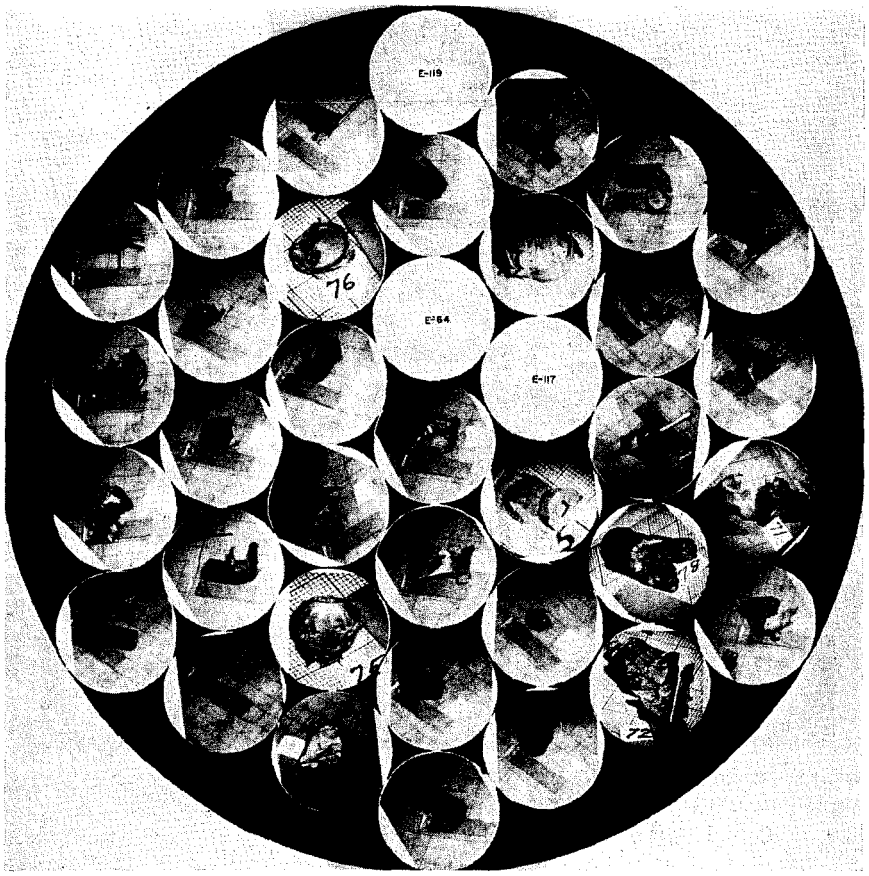

FIG. 18. Fuel rod remains from the beryllium-reflected test arranged according to origina core layout.

are grouped with the "solid" portion of the fission products. These SNAPTRAN tests indicate that this method of grouping is valid only for the water-immersed-type accident and that significantly larger release fractions of tellurium must be considered for reactor excursion accidents not immersed in water.

7. CONCLUSION

The use of full-scale integral-core reactors in these SNAPTRAN tests has demonstrated the effectiveness of a water environment in suppressing the release of fission products in a manner which is free of approximate and conservative scaling methods inherent with small scale experiments. Experimental results show that 96% of the noble gases and 100% of the halogens, tellurium, and remaining "solids" were retained during the water-immersion test while only 25% of the noble gases, 30% of the halogens, 55% of the tellurium and 95% of the "solids" were retained during the beryllium-reflected test.

The extraordinarily high retention of the noble gases during the water-immersion test was apparently due to the quick cooling action of the water on the fuel, causing the individual gas atoms to be trapped into the remaining fuel matrix. The complete retention of iodine by the water-immersion test confirmed predictions that iodine produced from tellurium decay would be released sufficiently slow to insure complete absorption by the water, while iodine produced by direct yield would either combine

with free hydrogen or NaK and be absorbed in the water or would dissolve in the water directly. Further work is required, however, to determine if the large amount of hydrogen available during these tests is required to obtain the observed retention of iodine.

The surprisingly high release fraction of tellurium (45%) from the waterless beryllium-reflected test when compared with the 5% release fraction for "solids" demonstrates that tellurium can be classed as a "solid" only when the reactor is immersed in water. For the safety analysis reviews of reactors without a water environment, fission product release inventories will have to consider a higher release of the tellurium.

In summary, these SNAPTRAN tests, although conducted for different purposes, have successfully demonstrated some of the suspected conservatism in the assumptions used in our standard analytical models for performing safety analysis reviews and suggest that the full-scale, integral-core-type tests are the most effective way of obtaining the integrated effects of reactor accidents.

ACKNOWLEDGEMENTS

The author wishes to acknowledge the cooperation of the STEP project of Phillips Petroleum Company and the Health and Safety Division of the Idaho Operation Office of the USAEC in the preparation of this paper. In particular the cooperation of Mr. D. F. Bunch in obtaining field data and the editorial efforts of Mrs. Gail A. Cordes, G. A. Dinneen, J. R. Fielding, P. E. Ruhter, W. E. Kessler, and D. R. Wenzel are acknowledged.

REFERENCES

1. G. W. Parker, R. A. Lorenz and J. G. Wilhelm. Simulated Transient Accidents in TREAT, pp. 39–67. Nuclear Safety Program Semiannual Progress Report, USAEC Report ORNL-3843 (1965).
2. W. E. Kessler, O. L. Cordes, G. A. Dinneen, R. D. Fletcher and G. F. Brockett. SNAPTRAN 2/10A-3 Destructive Test Results. USAEC Report IDO-17019 (January 1965).
3. O. L. Cordes, R. P. Bird, G. A. Dineen and J. R. Fielding. Radiological Aspects of SNAPTRAN 2/10A-3 Destructive Test. USAEC Report IDO-17038 (January 1965).
4. W. E. Kessler *et al.* SNAPTRAN-2 Destructive Test Results. USAEC Report IDO-17194 (January 1967).
5. G. R. Yanskey, E. H. Markee Jr. and A. P. Richter. Climatology of the National Reactor Testing Station. USAEC Report IDO-12048 (January 1966).
6. Ibid.
7. A. W. Castleman, Jr., and F. L. Salzamo. Current Studies of Fission Product Behavior at BNL. USAEC Report BNL-7423 (September 1963).

RADIOLOGICAL ASPECTS OF A REACTOR DESTRUCTIVE TEST

D. F. BUNCH and W. P. GAMMILL*
U.S. Atomic Energy Commission, Idaho Operations Office, Health and Safety Division,
P.O. Box 2108, Idaho Falls, Idaho 83401

Abstract—This paper describes the radiological considerations connected with planning and conducting reactor destructive tests at the National Reactor Testing Station in Idaho. There have been, in recent years, five reactor destructive tests, including one on January 11, 1966. In the last test a modified SNAP 2/10A reactor was intentionally disassembled as a result of a nuclear excursion designed to simulate the "maximum accident" for this system. The primary radiological objectives of these tests were to determine the magnitude of the fission product release and to assess the radiation exposures resulting from the test.

This paper presents information on planning prior to the tests and a summary of the radiation exposures resulting from the releases, with special emphasis given to the SNAPTRAN-2 Destructive Test. It is shown that, by using a properly designed environmental sampling system and the statistical approach of atmospheric dispersion, one can quickly and accurately estimate the magnitude of a release. An equation is shown which is amenable to hand or computer solution and will allow estimates of the fractionation of the fission products. Many of the considerations in this paper are applicable to any test involving the release to the atmosphere of significant quantities of fission products.

INTRODUCTION

The National Reactor Testing Station (NRTS) was established in 1949 as a site where the U.S. Atomic Energy Commission could build, test and operate various types of reactors and allied plants with maximum safety. The Health and Safety Division of the Idaho Operations Office has been responsible for all environmental monitoring outside the areas specifically assigned to the operating contractors. A continuing objective of this division has been to study the behavior of fission products in the environment whenever the opportunity presents itself. Thus, it is to be expected that any discussion of the radiological aspects of reactor destructive tests at the NRTS will include a detailed description of the environmental monitoring considerations.

Due to the very nature of the NRTS, there have been numerous opportunities to study the behavior of fission products that have been released to the atmosphere as a result of both planned and unplanned events. Notable among the planned releases are the reactor destructive tests, which included the BORAX-I, three SPERT-I cores and SNAPTRAN-2 and 3. In addition there have been the direct cycle Aircraft Nuclear Propulsion reactor tests (BOOT, FEET, LIME and SUBLIME), the radioactive lanthanum (RALA) recovery process at the Idaho Chemical Processing Plant which involved the dissolution of 2–3-day-old Materials Testing Reactor fuel assemblies, operation of the Fluidized Bed Waste Calcination Facilities, and the present Controlled Environmental Radioiodine Test program (CERT). In general, the accidental releases, which include the SL-1 accident and the two criticality incidents at the ICPP, have not resulted in the release of large enough quantities of fission products to justify major research efforts.

In monitoring these fission product releases,

* Now with Division of Reactor Development and Technology, U.S. Atomic Energy Commission, Washington, D.C.

many different techniques have been employed in the collection, analysis and interpretation of data. A general monitoring plan has evolved out of these efforts incorporating all of the techniques which over the years have proved of greatest value. This plan places emphasis on obtaining the maximum amount of *useful* information at a minimal cost. It is unlikely that others interested in this field of study will be able to employ the system used at the NRTS without some modification. Nevertheless, it is hoped that they will be able to utilize some of the described techniques to advantage in their research programs.

Many of the techniques used in assessing the consequences of a reactor destructive test are applicable to other types of planned or accidental releases. However, this discussion will be restricted to the considerations which go into the planning, assessment of risks, and evaluation of the consequences of a reactor destructive test resulting in a short term or "puff" release of fission products to the atmosphere.

PLANNING CONSIDERATIONS

In recent years there have been a number of tests at the National Reactor Testing Station where reactor cores have been intentionally subjected to extreme conditions, leading to partial or total destruction of the core and concommitant releases of fission products to the atmosphere. As in any field test where the quantity and quality of fission products that will be released is not known, it is vitally important that the safe conduct of these "destructive tests" be assured. This assurance can be gained by careful preplanning and by adequate test-time sampling. In those cases where environmental samples must also provide a source of information for reasons other than for safety, analytical techniques must be derived to fully utilize the gathered data.

There are two major factors that must be considered in monitoring a reactor destructive test: samples needed to determine the actual consequences of the test and the radiological test objectives. Normally, several months prior to the accomplishment of a particular test, a hazards evaluation will give a computation of the maximum as well as the expected releases. This information, with knowledge of the appropriate dose criteria, can be used to establish meteorological conditions that should be met. Sampling stations can then be placed at selected downwind locations to determine test consequences. The radiological objectives, on the other hand, determine the kind, number and location of additional samples to be taken.

On January 11, 1966, a modified SNAP 2/10A Flight-System reactor was disassembled as a result of an intentional excursion designed to simulate the "maximum accident" for this system. The radiological planning considerations in this test were typical of those for previous destructive tests. First, a safety analysis report was prepared [1] and reviewed. It was determined that there were three major objectives that influenced the type and degree of radiological monitoring: (1) to estimate the magnitude of the fission product release so that the results could be extrapolated to any situation, (2) to assess the environmental hazards resulting from the test and (3) to gather data on the behavior of fission products in the environment. On the basis of these objectives certain meteorological requirements were established in order to minimize the environmental hazards. As shown in Fig. 1, favorable meteorological diffusion conditions resulted from the combination of distance factors (distance to nearest populated area) and dose criteria (dose limits of occupational and non-occupational personnel). In addition to the general stipulation of diffusion, it was also required that winds be greater than 3 m/sec to ensure persistent directional travel and that there be no precipitation in the predicted trajectory—to ensure proper operation of sampling equipment. On the basis of the other objectives (1 and 3), only two of the sectors were preferred, allowing a single grid arrangement to be established so that optimum data recovery was possible. In these tests primary reliance was placed on the initial determination of potential radiation exposures.

If safety is the only concern, a number of monitoring stations placed at selected populated locations, plus sampling performed by mobile monitoring units who may be directed into the cloud path, will provide estimates of concentrations of fission products and thus estimates of exposures to people. If, however, estimates of the magnitude of the release and

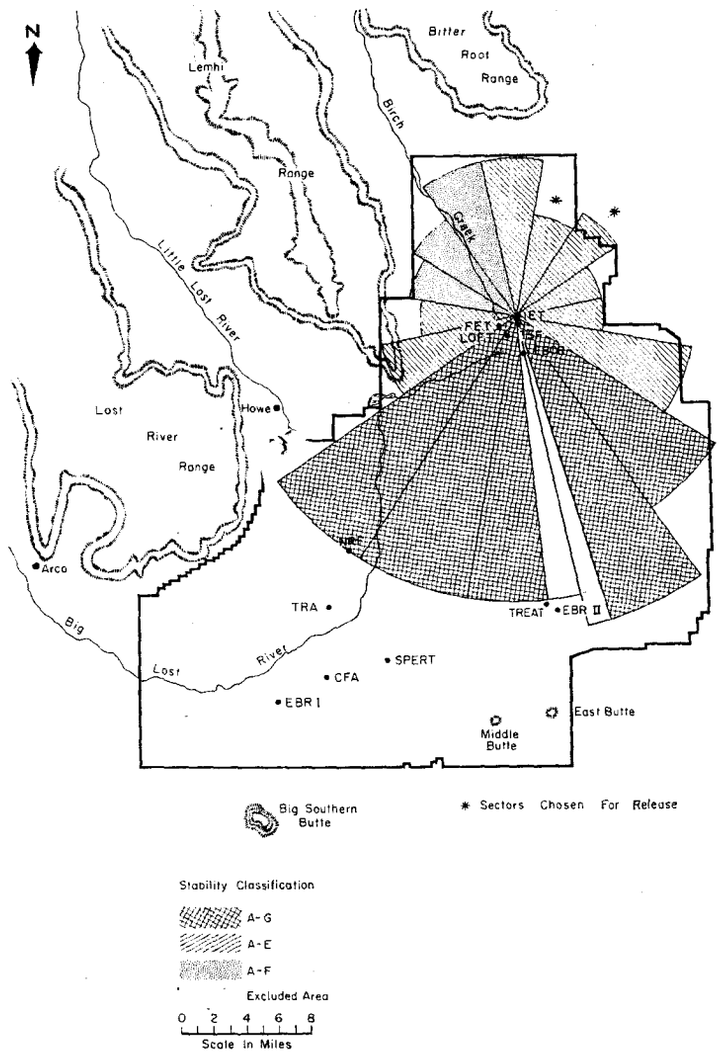

FIG. 1. Minimum meteorological requirements for the SNAPTRAN-2 destructive test, by sector.

data for research studies are desired, the sampling array must define the characteristics of the cloud.

The design of a monitoring program is to a large extent dependent upon the nature and expected consequences of the destructive test. Two different monitoring approaches will be discussed in this section. The first is the standard approach of a fully instrumented fixed monitoring grid (Figs. 2 and 3) and the second is a flexible plan which places a strong emphasis on mobility (Figs. 2 and 4). The latter approach proved extremely successful during the SNAPTRAN-2 destructive test early this year.*

Regardless of the monitoring scheme chosen,

* Monitoring for the SNAPTRAN destructive tests was a joint effort of Phillips Petroleum Company's Health and Safety Branch and the Idaho Operations Office, Health and Safety Division.

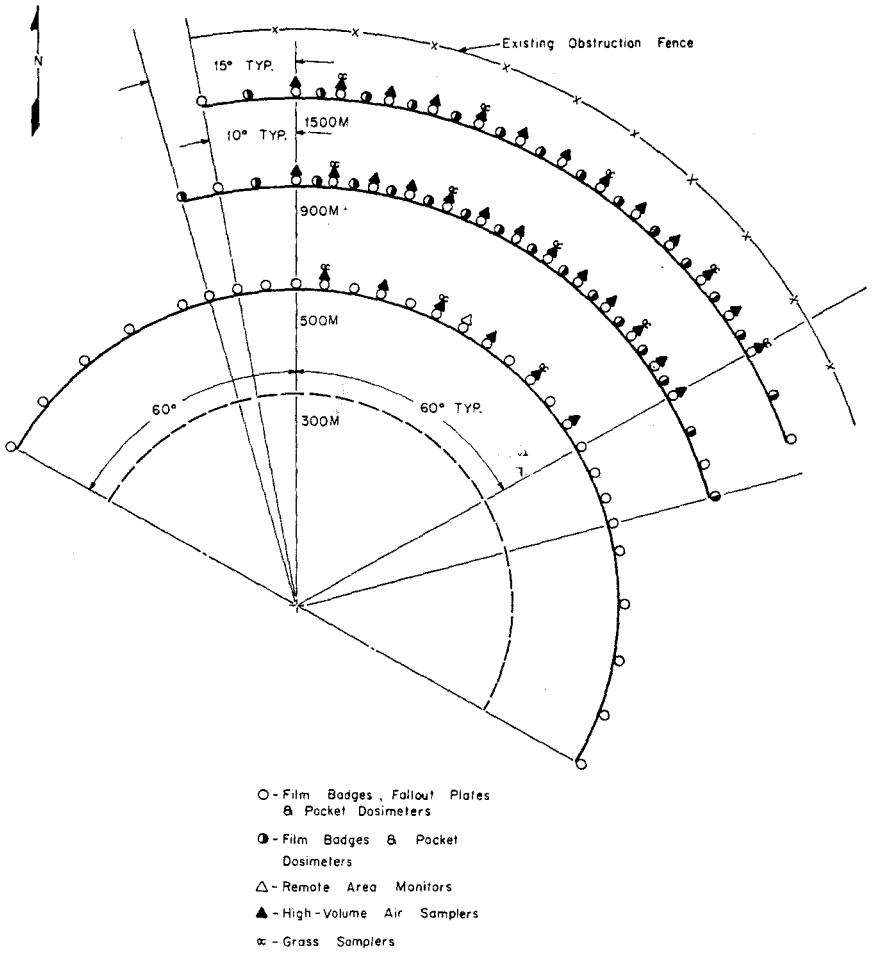

FIG. 2. Typical inner arc monitoring for the SNAPTRAN destructive tests.

there are certain features and requirements that are common to both approaches. The full support of a competent meteorological group is required to provide comprehensive weather forecasts and to monitor the weather conditions at the time of the test. In addition, this group may provide important after-the-fact information on diffusion characteristics of the atmosphere at the time of the test to aid in the analysis of fission product behavior. At the NRTS this support is provided by the Institute for Atmospheric Sciences (IAS), ESSA, which was formerly a Division of the U.S. Weather Bureau. This group has done a substantial amount of research on the meteorology of the NRTS. Also, IAS has developed a technique for tracking constant density balloons (Tetroons) by RADAR which has proved quite useful in determining the trajectories of radioactive clouds following reactor destructive tests.

Aerial monitoring is a technique that has gained wide acceptance in monitoring planned and accidental atmospheric releases of this type. Though aerial monitoring is normally not considered a test requirement at the NRTS, it has become a valuable means of obtaining early information with respect to the magnitude of the fission product release and the cloud trajectory. The instrumentation used at the NRTS is a sensitive transistorized single channel

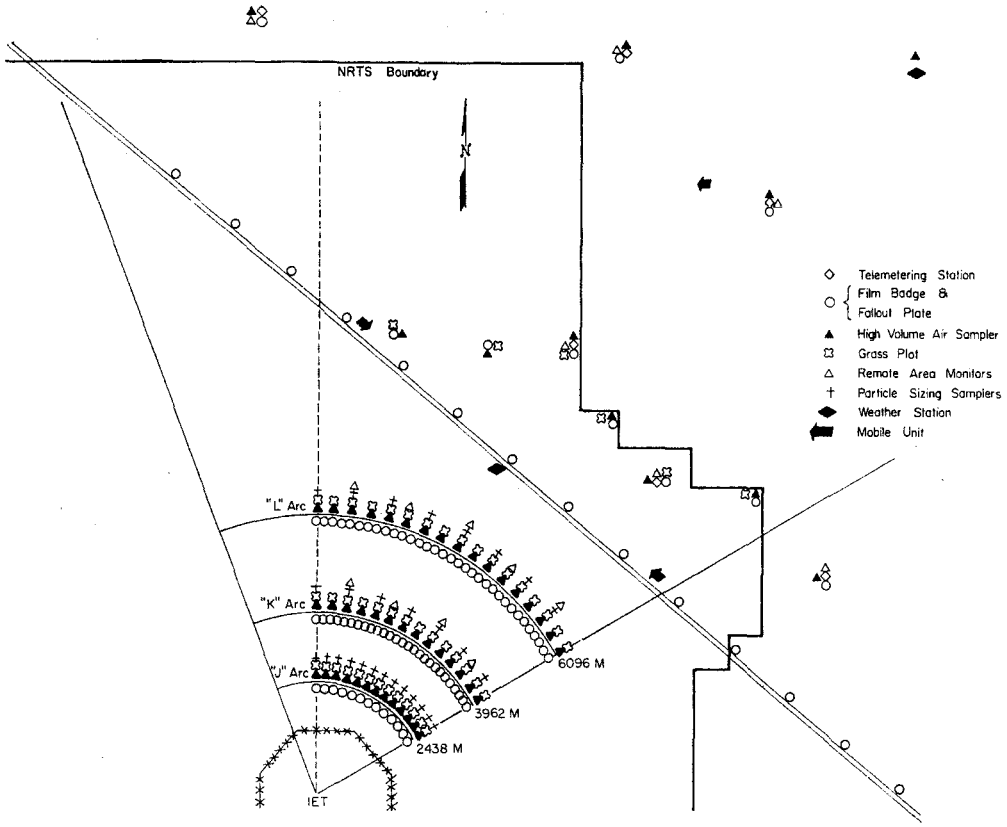

FIG. 3. Remote monitoring for the SNAPTRAN-3 destructive test.

gamma spectrometer with a strip chart recorder. However, a simple gamma scintillation survey instrument is usually adequate for monitoring releases of this type. A light single-engine aircraft with a cruising speed of 160 km/hr or more has been found to be best suited for this type of monitoring. Costs can be minimized by renting an airplane from a local flying service, as is done at the NRTS.

The off-site radiological surveillance program is normally not affected by the large research oriented on-site monitoring plan. The routine NRTS Radiation Monitoring Telemetry System forms the backbone of the off-site surveillance program, though it might be supplemented by the addition of a few stations in populated areas that are expected to be in the path of the radioactive cloud. This system is capable of measuring cloud gamma dose rate, airborne particulate activity, and airborne halogen activity. All measurements are transmitted to and recorded by the master station in the Idaho Operations Office Health and Safety Laboratory.

In designing the on-site surveillance program, the primary objective is to assure that the system will provide all of the information necessary for an early evaluation of any radiological hazards associated with the test. The required information can generally be obtained from minimal monitoring efforts within approximately 2 km of the reactor site. The most rapid means of evaluating the magnitude of the release is to measure the maximum gamma dose rate or integrated dose which can then be compared with predicted values. These measurements are normally obtained by means of one or two monitoring vehicles which are positioned in the path of the cloud. These monitoring personnel wear appropriate protective clothing and respiratory equipment. In addition to the

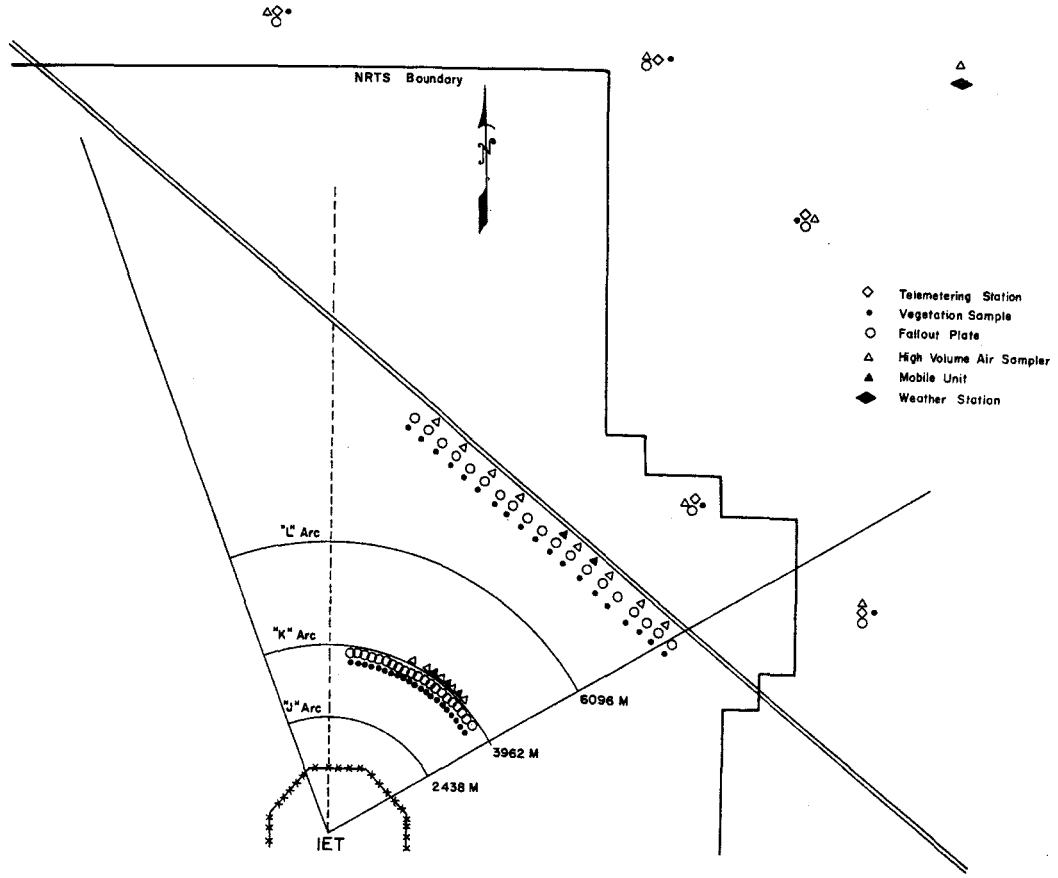

FIG. 4. Remote monitoring for the SNAPTRAN-2 destructive test.

dose measurements, these personnel are responsible for collecting the air samples which provide the earliest information on identity of the released fission products. Once the required "safety monitoring" is established, the remaining portion of the monitoring program is all related directly to the investigation of fission product behavior. Following is a list of important considerations relevant to the planning of such a monitoring system:

1. Meteorological restrictions on test
2. Types of samples required
3. Critical sampling distances
4. Desired number of sampling points in the cloud path at each distance of interest
5. Analytical support availability
6. Amount of lead time expected to be available to establish a monitoring network
7. Availability of monitoring vehicles (with and without two-way radios), and portable two-way radios
8. Inventory of portable and mobile electrical power generators
9. Availability of access roads in the area of interest
10. Terrain of the monitoring area.

Meteorological restrictions on the test generally determine the feasibility of establishing a fixed monitoring grid. If the acceptable wind direction is limited to a sector of less than 90°, a common approach has been to completely instrument three to five arcs across the entire sector. Since the area of interest may extend out ten to twenty kilometers, this becomes an extremely expensive system requiring a large quantity of monitoring equipment. A major

disadvantage of this approach, other than expense, is the amount of time and effort required to instrument such a grid. The greatest amount of time is required to establish the electrical system necessary to power the air samplers. This may involve the use of 100–150 mobile or portable generators, which would have to be positioned on the grid and routinely serviced.

The alternate system to be discussed is capable of providing the same information as may be obtained from a standard monitoring grid. This approach emphasizes mobility and close coordination between the monitoring control point, meteorological forecasting group, the aerial monitoring team and the monitoring personnel in the field. A reliable radio communications system is an absolute requirement for the successful use of this technique. Though this system can be used in place of a monitoring grid, it is particularly useful when the wind restrictions are so broad that a grid is not feasible or for distances more remote from the release point (> 2 km).

In essence, the objective of this technique is to reduce to about three hours the amount of time required to establish the monitoring network. This is done by eliminating essentially all of the air sampling and associated equipment which will not lie in the path of the cloud and is accomplished in the following manner. At test time minus three hours, a fairly accurate forecast of wind direction can be expected. Once this forecast has been received, all efforts are directed toward positioning four to five generators and air samplers on each preselected downwind arc or road in the predicted cloud path. Two or three monitoring vehicles are placed on standby on each arc as soon as the air sampling stations have been positioned. The spacing between these fixed sampling stations should be $\frac{1}{3}$ to $\frac{1}{2}$ the predicted cloud width at that particular distance. During the last few minutes prior to the test the wind direction should be firmly established and each monitoring vehicle can be moved into a gap between two of the fixed stations. This will provide a minimum of three samplers in the cloud at each distance. In the event the early wind direction forecast is incorrect, all of the monitoring vehicles can be moved to one side or the other of the fixed stations. Any wind shift after initiation of the test can be detected by the monitoring aircraft which will allow the downwind monitoring vehicles to make position corrections.

The lateral spread of the cloud can be accurately assessed by extensive vegetation sampling or by the liberal use of gummed paper or carbon coated gummed paper fallout plates if sufficient vegetation is not available. Once the ratio of airborne to deposited activity has been established at the air sampling locations, the entire lateral profile of the cloud can be inferred. The advantages of this technique include:

1. More rapid evaluation of possible hazards.
2. Minimum cost.
3. Maximum versatility.
4. Minimum impact on the analytical support laboratory.

ESTIMATING THE MAGNITUDE OF THE RELEASE

In any evaluation of the consequences of a release of fission products to the atmosphere there are two measurable parameters of value, the identity of fission products in the atmosphere and the concentration of fission products. A detailed knowledge of either of these, as a function of time and distance, must depend on an adequate estimate of the magnitude of the release.

In many cases, as with the SNAPTRAN-2 Destructive Test, there is no direct method whereby this information may be obtained. However, accurate determinations are possible from downwind air samplers.

To simplify somewhat, there are several major steps involved in estimating the total magnitude of the release:

1. Collection of samples of airborne materials.
2. Counting of samples and conversion of data to time integrated concentrations ($Ci\text{-}sec/m^3$).
3. Correcting of all concentrations to a common time.
4. Estimating the lateral spread of the cloud and the peak concentrations—at any distance.
5. Estimating the vertical dispersion and wind speed.
6. Correcting for the initial size of the cloud.

7. Correcting for materials that were not collected by the air samplers.
8. Estimating corrected peak concentrations as a function of distance to obtain the effective source at the corrected time.
9. Correcting the source to the time of the release.

Our technique of estimating the magnitude of the release stems from the use of the statistical theory of atmospheric dispersion[2] in order to account for the mass dilution of airborne material as a function of the stability of the atmosphere and the travel of this material to the point of interest. This dilution may be expressed as:

$$(1) \qquad \chi = \frac{Q}{\pi \bar{u}(\sigma_y^2 + \sigma_{yI}^2)^{\frac{1}{2}}(\sigma_z^2 + \sigma_{zI}^2)^{\frac{1}{2}}} \exp\left[-\tfrac{1}{2}\frac{h^2}{(\sigma_z^2 + \sigma_{zI}^2)}\right]$$

where $\bar{u}$ = the mean wind speed (m/sec),
σ_y = the lateral dispersion (m),
σ_z = the vertical dispersion (m),
σ_{yI} = the initial lateral dispersion (m),
σ_{zI} = the initial vertical dispersion (m),
h = the effective height of the release,
Q = the source (Ci),
χ = the time-integrated concentration at any distance of interest (Ci-sec/m^3).

If this equation is used, Q—the source term—may be determined from knowledge of the other parameters.

In actual practice, the most difficult steps in the analysis are to correct counted activity to a common time and to accurately account for materials that were not collected by the air samplers.

As indicated in a report[3] on the radiological results of the SNAPTRAN-3 (water immersion) test, a reactor transient produces large quantities of short-lived noble gases. Only the daughters of these gases are collected by the normal air samplers. This is an important consideration when estimates of cloud concentrations must be determined from collected activity for samples at small distances (< 2000 m).

The calculation of cloud activity may be computed from the following equations:

(2) *First Isotope*

$$N_1(t) = N_1(0) \exp[-\lambda_1 t]$$

(3) *Second Isotope*

$$N_2(t) = \frac{N_1(0)\,\lambda_1}{(\lambda_1-\lambda_2)}\left[\exp[-\lambda_2 t] - \exp[-\lambda_1 t]\right] + N_2(0)\exp[-\lambda_2 t]$$

(4) *Third Isotope*

$$N(t) = \frac{N_1(0)\,\lambda_1\lambda_2}{(\lambda_1-\lambda_2)(\lambda_1-\lambda_3)(\lambda_2-\lambda_3)}\left[(\lambda_2-\lambda_3)\exp[-\lambda_1 t] - (\lambda_1-\lambda_3)\exp[-\lambda_2 t] + (\lambda_1-\lambda_2)\exp[-\lambda_3 t]\right] + N_2(0)\frac{\lambda_2}{(\lambda_2-\lambda_3)}\left[\exp[-\lambda_3 t] - \exp[-\lambda_2 t]\right] + N_3(0)\exp[-\lambda_3 t]$$

where $N_i(t)$ = number of atoms of ith isotope at time t after excursion,
λ_i = radioactive decay constant of ith isotope,
$N_i(0)$ = initial atoms produced of ith isotope.

As this cloud passes by an air sampler at time T (and assuming the noble gas is the precursor to the chain), the equations must be modified to calculate collected activity, as shown in the next examples.

(5) *First Isotope*

$$N_1'(t) = 0 \qquad t \geq T$$

(6) *Second Isotope*

$$N_2'(t) = N_2(T)\exp[-\lambda_2(t-T)]$$

(7) *Third Isotope*

$$N_3'(t) = N_2(T)\frac{\lambda_2}{(\lambda_2-\lambda_3)}\left[\exp[-\lambda_3(t-T)] - \exp[-\lambda_2(t-T)]\right] + N_3(T)\exp[-\lambda_3(t-T)]$$

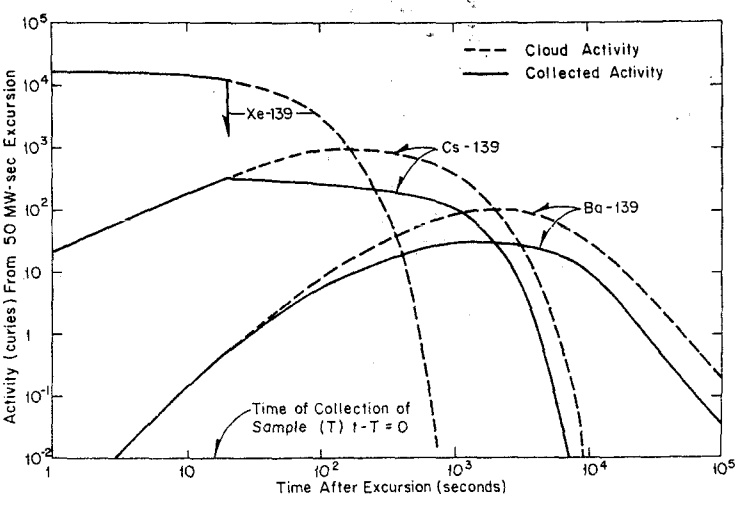

FIG. 5. Comparison of cloud activity and collected activity when the precursor of a decay chain is not collected.

Thus the correction factors may be obtained from $N_i(t)/N_i^1(t)$. The importance of this correction is shown in Fig. 5. In this example an estimate of released Xe-139 based on counted Ba-139 would underestimate the true value by a factor of seven.

Before estimates of peak concentrations can be attempted, the counted activities must be corrected to a common time. This may be accomplished by two methods. If sequential counts are taken from representative samples at each distance, the peak concentrations at each distance may be easily estimated, by fitting a Gaussian distribution to the corrected data points (Fig. 6). The lateral diffusion, σ_y, is that strong-wind distance where the concentration is 0.6 that at centerline. With values of $\bar{u}$ and σ_z from meteorological data, the source term at the count time may then be determined. This can be compared to the amount produced to estimate fractional release.

Alternately, all samples can be corrected to the same count time, once corrections for the non-collection of nobles have been made. This was done in analyzing the results of the SNAPTRAN-2 Destructive Test. With that data a curve of peak concentrations as a function of

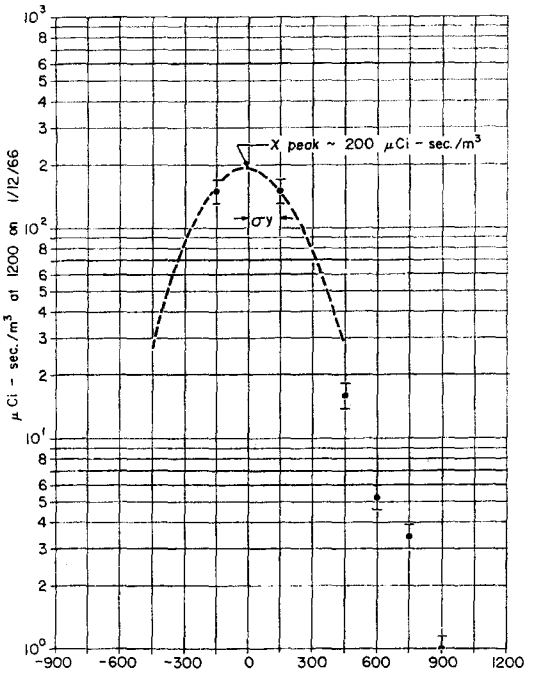

FIG. 6. Derivation of peak concentrations from measured crosswind concentrations.

distance can be derived to find both the magnitude of the release and the initial height and size of the release. As shown in Fig. 7, the estimates using this approach compare very favorably with observed results. In this case, estimates of Q can be obtained from values of the other factors at any point of interest. From the equation and parameters listed in Fig. 7, a release fraction of 25% of that produced is indicated for the SNAPTRAN-2 Test.

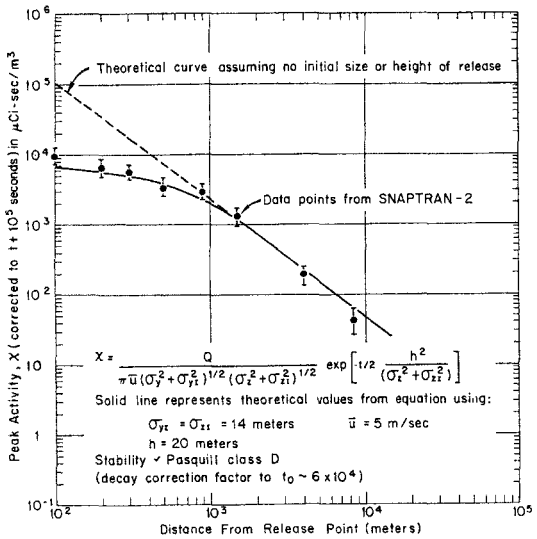

FIG. 7. Comparison of actual and predicted peak concentrations.

Before the consequences of the release can be adequately assessed, knowledge of the release of each chain or of groups of chains (e.g. nobles, halogens) must be obtained. This can be obtained from isotopic analysis of the collected activity—such as by gamma spectrometric analyses. The actual fractionation can be solved by a series of simultaneous equations:

(8) *Fractionation of the Parent*

$$F_1 A_{11} = A^*_1$$

(9) *Fractionation of Two-membered Chains*

$$F_1 A_{21} + F_2 A_{22} = A^*_2$$
$$F_2 B_{22} + F_2 B_{22} = B^*_2$$

(10) *Fractionation of Three-membered Chains*

$$F_1 A_{31} + F_2 A_{32} + F_3 A_{33} = A^*_3$$
$$F_1 B_{31} + F_2 B_{32} + F_3 B_{33} = B^*_3$$
$$F_1 C_{31} + F_2 C_{32} + F_3 C_{33} = C^*_3$$

(11) *Fractionation of Four-membered Chains*

$$F_1 A_{41} + F_2 A_{42} + F_3 A_{43} + F_4 A_{44} = A^*_4$$
$$F_1 B_{41} + F_2 B_{42} + F_3 B_{43} + F_4 B_{44} = B^*_4$$
$$F_1 C_{41} + F_2 C_{42} + F_3 C_{43} + F_4 C_{44} = C^*_4$$
$$F_1 D_{41} + F_2 D_{42} + F_3 D_{43} + F_4 D_{44} = D^*_4$$

where A, B, C, D refer to 4 chains that are expected to behave similarly (I-131, I-132, I-133, I-135),

F_j is the fraction released of each isotope in the chain (F_1—fraction released of parent) and assumes no isotopic differences in fractionation; $F_{I\text{-}132} - F_{I\text{-}132}$,

A_{ij} indicates the expected activity of the ith isotope from the amount of the jth isotope that was initially produced,

A^*_i is the counted activity of the ith isotope *corrected for diffusion.*

As can be seen this determination may be simply described as:

(12) $$A^*_i = \Sigma F_j A_{ij}$$

or taking the data from the point of concentration

(13) $$A^*_i = \chi_i \pi \bar{u} (\sigma_y^2 + \sigma_{y_1}^2)^{\frac{1}{2}} (\sigma_z^2 + \sigma_{zI}^2)^{\frac{1}{2}} \exp\left[\frac{1}{2} \frac{h^2}{(\sigma_z^2+\sigma_{zI}^2)}\right] \Sigma F_j A_{ij}$$

where χ_i is the time integrated concentration of the ith isotope at the point of interest.

Equation (13) can be solved either by hand calculations or by computer techniques using tabulated values of inventories.[4,5] Use of key equations (1) and (13) allows rapid and accurate evaluations of the magnitude and kind of release to the atmosphere. These can be used to provide rapid estimates based on initial results or to provide more accurate estimates when all data has been analyzed.

By the use of the techniques shown earlier the magnitude and fractionation of fission product releases in five recent reactor destructive

Table 1. *Release Estimates*

	SPERT-I			SNAPTRAN-3	SNAPTRAN-2
	Test I	Test II	Test III		
Total release (Ci)	1.8×10^4	4×10^2	1×10^3	3.2×10^4	2×10^6
% release	0.36	1.5×10^{-3}	3.9×10^{-3}	0.4	20
% nobles	3.6	1.5×10^{-2}	3.8×10^{-2}	4	75
% iodines	$< 5 \times 10^{-3}$	$< 1 \times 10^{-2}$	$< 1 \times 10^{-2}$	$< 2 \times 10^{-2}$	70
% tellurium	—	—	—	—	45
% others	$< 5 \times 10^{-4}$	$< 1 \times 10^{-3}$	$< 1 \times 10^{-3}$	$< 2 \times 10^{-2}$	5

Table 2 indicates significant factors in the test that have importance in evaluating this release data.

tests including SNAPTRAN-2, have been estimated. The results are shown in Table 1, which also gives information on the percent of the core inventory that was released.

All the tests, except SNAPTRAN-2, were conducted with the reactor immersed in water at ambient temperature and pressure. Also, all tests were conducted with no significant inventory previous to the transient.

There are two factors of immediate interest, the scrubbing effect of water and the fractionation of fission products. These scrubbing factors appear to be of the order of 10^3 for iodines and 10^4 for solids. The fractionation of SNAPTRAN-2 seems, as expected, to follow the relative volatility of the fission products.

With data on releases and fractionation it is possible to extrapolate the actual consequences of the tests to any given set of meteorological conditions or to any location where samples were not taken.

EVALUATION OF ENVIRONMENTAL HAZARDS

There are essentially three phases of hazards evaluation: (1) Pretest evaluations to determine the feasibility of test operations and to define the desired meteorological conditions; (2) Early estimates of test consequences based on initial results; and (3) Final estimates based on a detailed knowledge of the release.

Since the results of a destructive test cannot be completely guaranteed prior to its initiation, it is important that data gathered soon after a release be evaluated to define the actual consequences to off-site areas.

A rough estimate of the total magnitude of the release can be obtained from an estimate of the peak concentration at any given distance (as shown in Fig. 7) and an estimate of the diffusion to that distance for a stability category representative of test-time conditions (as, for example, from ref. 6). This can normally be obtained

Table 2. *Reactor Test Data*

	SPERT-I			SNAPTRAN-3	SNAPTRAN-2
	Test I	Test II	Test III		
Fuel type	U-Al alloy	UO_2	UO_2	Zirconium-hydride 10 weight % U	Zirconium-hydride 10 weight % U
	Plate	Pin	Pin	Pin	Pin
Clad	Al	SS	SS	Hastelloy-N	Hastelloy-N
Enrichment (%)	93.5	4	4	Fully enriched	Fully enriched
Mw-sec	30.7	155	165	45	54

Table 3. Summary of Off-site Doses from the SNAPTRAN-2 Destructive Test (rem)

	Criteria[1]	Pretest estimates[2]	Early estimates	Actual
Thyroid — Ingestion	5×10^{-1}	4.4×10^{-2}	10^{-1}	3×10^{-2}[3]
Inhalation		1.3×10^{-3}	3×10^{-4}	10^{-4}
Whole body	1.7×10^{-1}	6.6×10^{-4}	3×10^{-4}	3×10^{-4}
Bone	5×10^{-1}	1.1×10^{-4}	—	$< 10^{-4}$

[1] From ref. 10.
[2] From ref. 1.
[3] Potential dose—no cows known to be grazing.
All calculations except thyroid ingestion based on ICRP[7] standard man.

within a few hours after the release. With gamma spectrometric analyses of a few samples, a fairly good approximation of off-site concentrations of airborne materials can be obtained. Milk and vegetation samples provide a continuous check on possible ingestion dose.

After the data have been more completely analyzed, accurate estimates of test consequences can be made. Comparisons of the three phases of dose estimates for SNAPTRAN-2 with relevant criteria are shown in Table 3.

SUMMARY AND CONCLUSIONS

By use of an environmental sampling system which provides values of peak concentrations as function of distance, and by proper analytical techniques, it is possible to obtain reliable and accurate estimates of the total magnitude of a release to the atmosphere and a detailed knowledge of the isotopic concentrations of airborne materials. These results can then be extrapolated to any point of interest or for any given set of meteorological conditions. These techniques have been of value in evaluating the results of five destructive tests at the National Reactor Testing Station and may be applied to any similar situation where estimates of fission product releases are desired.

ACKNOWLEDGEMENTS

The authors wish to acknowledge the individuals responsible for the analysis of the recent destructive tests, much of which has been reported in refs. 3, 8 and 9.

REFERENCES

1. W. J. Neal (ed.). Safety Analysis Report, SNAPTRAN 2/10A-1 and 2, Safety Tests Revision 2, IDO-17076, October 1965.
2. W. F. Hilsmeir and F. A. Gifford. Graphs for estimating atmospheric dispersion. ORO-545, 1962.
3. O. L. Cordes *et al.* Radiological Results of SNAPTRAN 2/10A-3, Destructive Test, IDO-17038, January 1965.
4. D. B. Kochendorfer. Calculated activities of U-235 fission products for very short nuclear reactor operation. USNRDL-TR-757 Volumes I and II, June 1964.
5. R. L. Coates and N. R. Horton. RSAC-A Radiological Safety Analysis Computer Program, IDO-17151, May 1966.
6. G. R. Yanskey *et al.* Climatography of the national reactor testing station. IDO-12048, January 1966.
7. International Commission on Radiological Protection, *Radiation Protection*, Recommendations of the International Commission on Radiological Protection, ICRP-2. Report of Committee II on Permissible Dose for Internal Radiation. New York, Pergamon Press, 1959.
8. D. F. Bunch. Spert I Destructive Test Series. Environmental Monitoring and Research Studies, IDO-12039, January 1965.
9. O. L. Cordes *et al.* Radiological Aspects of the SNAPTRAN-2 Destructive Test, IDO-17203. February 1967.
10. U.S. Atomic Energy Commission Manual, Chapter 0524, "Standards for Radiation Protection", 1963.

RADIOLOGICAL ASPECTS OF THE DEACTIVATION OF HANFORD PRODUCTION REACTORS

L. R. WALLIS
Radiation Protection, Atomic Power Equipment Department, General Electric Company

and

C. D. CORBIT
RL Health and Safety Division, United States Atomic Energy Commission

Abstract—Deactivation of three of Hanford's eight large plutonium production reactors at Richland, Washington, brought to light radiological problems which had not been encountered before in the nuclear industry. Large volumes of activation and fission products were generated during the 15 years of operations. Much of this material had been retained in storage and retention basins and some was charged into the ground at designated burial locations. In addition, a small portion of these products had accumulated in open work areas.

The basic procedures used to ensure short-term radiological control of deactivated Hanford production reactors consisted of essentially reducing the radioactive contamination in the open areas to a nominal level and sealing off those locations and systems where decontamination was deemed impractical. Long-term radiological control will be maintained with minimum surveillance during the postdeactivation period by ensuring that traffic in the open areas is kept to a minimum and that sealed-off systems are not disturbed. The proposed paper will describe, with the aid of slides, radiological conditions of the various zones before decontamination work was started and will summarize the techniques used in the decontamination and containment program.

Control programs were also established for numerous underground radiation zones such as the reactor effluent systems and miscellaneous burial grounds. Open retention basins containing up to 300 tons of radiocontaminated silt and sand required implementation of unique containment techniques. The proposed paper, in conjunction with slides, will also describe the techniques used to deactivate these zones.

Approximately 1 year has elapsed since deactivation work was completed on the reactors and their associated facilities. The adequacy of the confinement and decontamination activities is supported by the fact that no contamination spreads have occurred. Within the next 5 years, the major portion of the activation products will be eliminated through natural decay. The remaining activity will largely be attributable to the longer-lived fission products, but these are thought not to be prohibitive in reclaiming much of the land for more purposeful future activities.

I. PLANT DESCRIPTION

The Hanford Plant of the U.S. Atomic Energy Commission is a complex of production, research, development and supporting facilities distributed over a 575 sq miles area of southeastern Washington (Fig. 1). The Plant is under the direction of the USAEC Richland Operations Office (RL). Its mission as a production site has been the production of plutonium weapons parts, and the performance of other atomic energy related activities as required by the Commission. To accomplish these assignments, a physical plant has been constructed at an initial capital cost in excess of $1 billion. The principal process facilities are two fuels fabrication plants; nine large nuclear reactors, three of which are now shut down; two large chemical separations plants; and a final

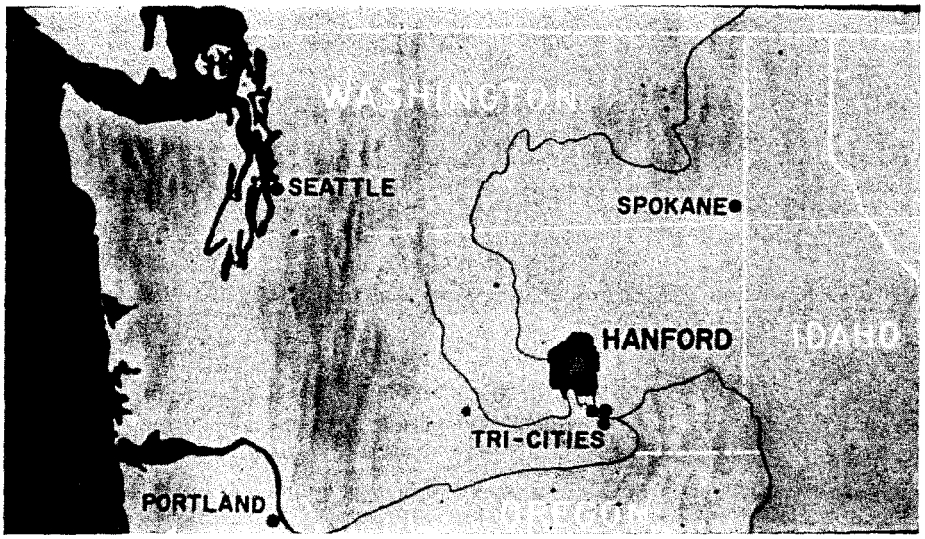

FIG. 1. Location of the Hanford plant.

plutonium processing and fabrication facility. These are supplemented by hundreds of satellite and supporting buildings and facilities.

Until November of 1965, the General Electric Company (G.E.) was responsible for operating the nine production reactors. Since that date, Douglas United Nuclear, Inc., has taken over the "older" reactor operations, and G.E. continues to operate the new dual-purpose reactor. The RL Hanford reservation is also a major research and development center of the Atomic Energy Commission and has an annual Research and Development budget in excess of $30 million. About one-third of this Research and Development effort is in support of Hanford production operations, and the remainder is directed toward a variety of peaceful applications of atomic energy. About three-fourths of this work is conducted within the Laboratories organization and the remainder by research and engineering groups directly attached to production organizations. The nearest city is Richland, Washington (shown in Figs. 2 and 3).

A. *Topography*

The general topography of the Hanford reservation is shown by Fig. 4. The terrain, typical of much of eastern Washington and Oregon, is generally treeless, covered with bunchgrass and sagebrush, and varies from plains to gently rolling hills. A long, high ridge (Rattlesnake Mountain, 3500 ft elevation) bounds the area on the southwest, while the Columbia River is along the north and east boundary. The river shore on the reservation side is gently sloping. The eastern shore from 300 Area north to about 100-H Area consists of high bluffs; river elevation at Richland is about 350 ft.

B. *Geology*

Three major rock formations comprise the geology of reactor sites along the Columbia River. The Columbia River Basalt series forms the bedrock of the region, and current estimates place its thickness at 14,000 to 15,000 ft. The Ringold Formation overlies basalt at a depth of about 500 ft. The late Pleistocene to recent fluviatile and glaciofluviatile sediments overlie the irregularly eroded surface of the Ringold Formation sediments, so that in places they grade into and are almost indistinguishable from the older sediments. Elsewhere, they consist of poorly sorted, but generally coarse-grained sand to pebble and cobble gravel and boulders, largely derived from the basalt plateau to the north.

No damaging earthquake has ever been recorded in the immediate vicinity of the RL

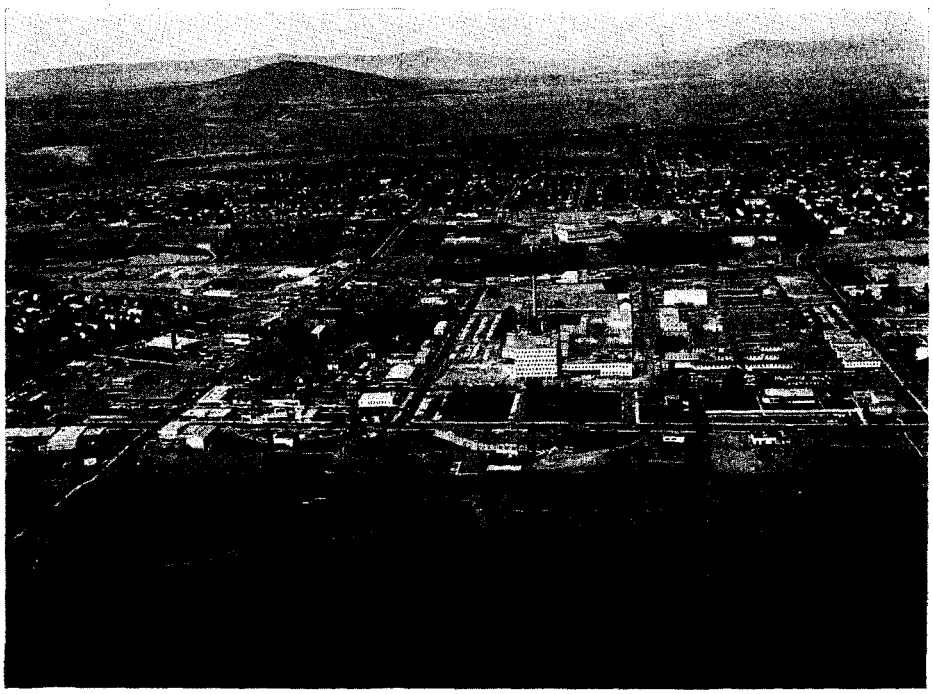

FIG. 2. View of Richland, Washington.

FIG. 3. View of Richland, Washington, and the Columbia River.

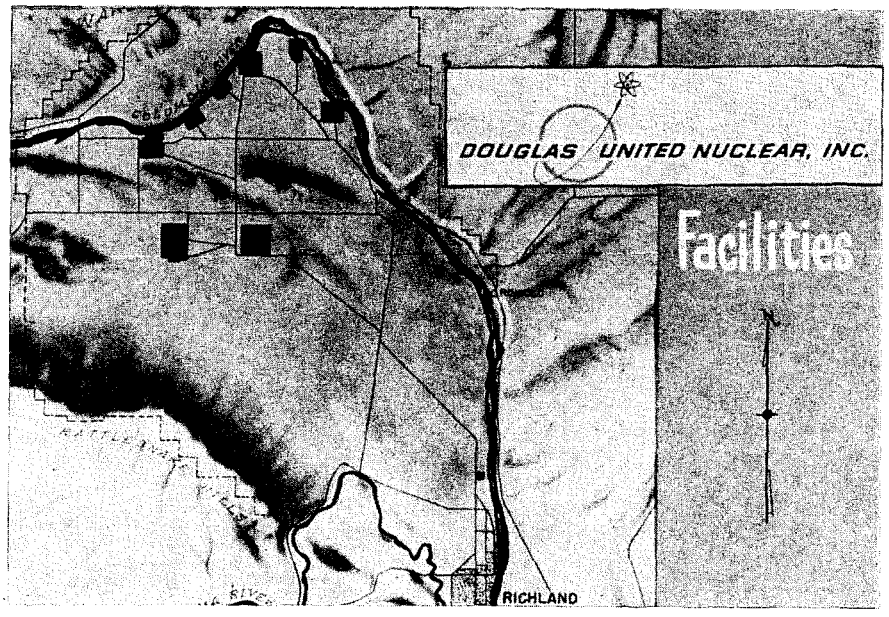

FIG. 4. Douglas United Nuclear, Inc., facilities.

Plant, although the area lies in a region susceptible to earthquake damage from the active seismic zones of western Washington and from the active seismic zone that includes the Walla Walla area. For comparison, the expected probability of earthquake damage at the National Reactor Test Site (NRTS) at Idaho is about the same as RL, but both areas are actually quite low in probability. For building code purposes, the entire area east of the Cascades is in Zone 2 of the Seismic Probability Map. (Pacific Coast Building Officials Conference, Uniform Building Code, 1959 Edition).

C. *Climate*

The Hanford reservation has a semiarid climate of warm summers and mild winters. Daytime temperatures above 90°F are common during July and August. Nights are invariably cool throughout the entire spring and summer. Even in the hottest month (July), the average night-time minimum is 60°F.

Subfreezing temperatures are frequent during the short winter with occasional temperatures below zero. The average minimums for January and February are 24°F and 30°F, respectively. Average highs are 40.5°F in January and 48.8°F in February.

Precipitation is light, averaging about 8 in./year. Most of this falls from November through February. Snowfall usually is confined to January and February and normally comprises about 25% of the annual precipitation. The amount of snow, which may accumulate, is insignificant and generally ranges from a trace to 4 in.

Occasional early-morning fog appears near the river lowlands during the winter months; however, smog is unknown. The climate and physical features necessary for smog formation and continuance are absent and visibility is seldom less than 10 miles. The average annual wind velocity is 7 mph.

D. *Water Supply*

The basic water supply for the Hanford reservation is the Columbia River with average annual flow rates of 394,000 ft^3/sec, 59,000 ft^3/sec minimum, and 127,000 ft^3/sec average. Water from the Columbia River is pumped to the Hanford reactor areas. It is treated and then filtered for use as coolant in the reactors.

E. *Radioactive Waste Disposal*

Conditions at the RL site are particularly favorable for solid, gaseous, and liquid waste disposal, probably more so than at any other major AEC site. Subsurface lateral water flow is very slight, rainfall is low and penetrates to only a shallow depth that is well above the water table. Ion exchange characteristics are good. Thus, if needed, large quantities of low-level liquid and solid wastes can be charged into the ground to decay.

Thermally hot reactor cooling water discharged to the Columbia River contains radionuclides produced mainly by neutron activation of impurities. The impurities originate as corrosion products, chemical additives, and trace elements that are not removed in water treatment processes. Most of these are short-lived radioisotopes which effectively disappear within 24 hr. Nevertheless, reactor effluents are ordinarily retained for short periods in large open basins to allow:

The short-lived activation products to decay.
Particulate radioactive materials to settle.
Cooling time for effluent prior to discharge into the river.

Even though additional direct discharge of once-through reactor coolant to the Columbia River from new facilities is not allowed, activity and contamination levels found in the river are much below the imposed AEC limits.

Small amounts of contaminated reactor ventilation air can be safely discharged to the atmosphere through tall stacks; however, to guard against significant contamination of the environs outside the reservation boundaries, fog-spray equipment, backed by high efficiency filters, has been installed in reactor production facilities. RL reactors are presently confined rather than contained (with the exception of the Plutonium Recycle Test Reactor, which is located near a residential area).

Contaminated solid wastes from the manufacturing and laboratory facilities are buried in permanently marked trenches above the level of the regional ground water. The low rainfall in the area results in moisture penetrating the soil to a depth of only a few feet; hence, leaching of radioactive materials from the solids is negligible.

All radioactive waste streams, gaseous and liquid, are sampled and, in many instances, continuously monitored prior to discharge to assure that established RL-AEC waste disposal limits are not exceeded.

II. REACTOR DESCRIPTION

A. *General*

The deactivated Hanford reactors are graphite moderated, light-water cooled, and fueled with uranium metal. Each of the deactivated reactors consists of a near cubical stack of graphite (the core) which approximates 30 ft on an edge. Each core is traversed from front to rear by about 2000 channels containing aluminum process tubes. These tubes hold fuel elements and provide passage for the "once through" cooling water entering at the front face and leaving at the rear face. The control rods, consisting of neutron absorbing material, enter the reactor from one side and are positioned remotely by controlled motor drives. The "scram" systems (safety rods, etc.) for emergency shutdown are operated from the top of the reactor. The reactor core is surrounded by a graphite "reflector", to conserve neutrons, and by a heavy neutron and radiation absorbing shield. Figure 5 shows a cut-away view of a typical Hanford reactor.

B. *Water Flow*

Water that passes through the reactors is pumped from the Columbia River, into water treatment basins for flocculation and pH treatment, through anthracite filters, and into large storage tanks. The treated water is then pumped into large risers on both sides of the reactor's front face. Horizontal cross connections between the risers (crossheaders) carry the water to jumpers from the crossheaders and thus into the aluminum tubes. The jumpers are called "pigtails"; descriptive of their particular shape. The water flows through the tube, out the rear and into a similar plumbing system on the rear, through downcomers, and out through a discharge line into large retention basins. The retention basins provide both decay time for short-lived radionuclides and time for cooling of the water by way of evaporation prior to discharges back into the river. Figure 6 shows the water flow through a typical reactor area.

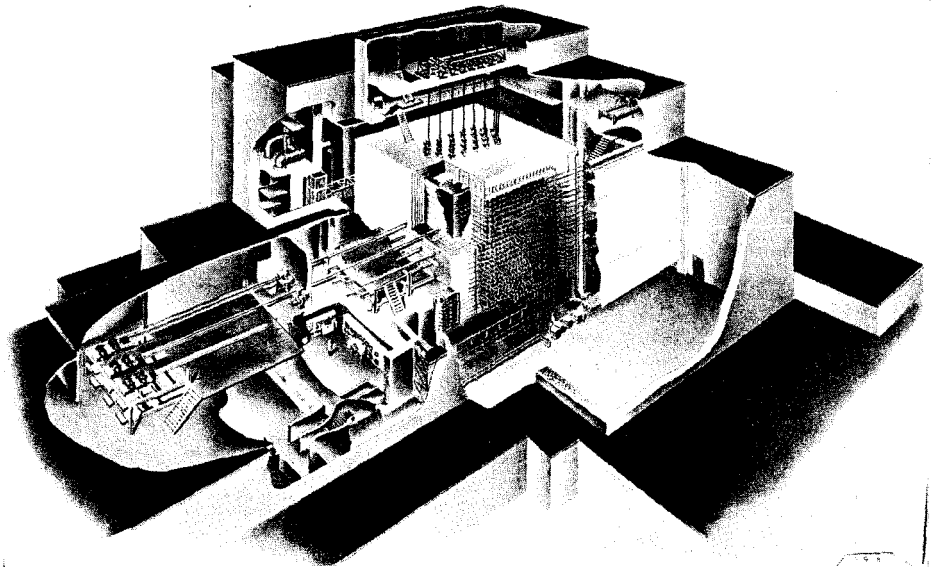

FIG. 5. Cut-away of a typical Hanford reactor.

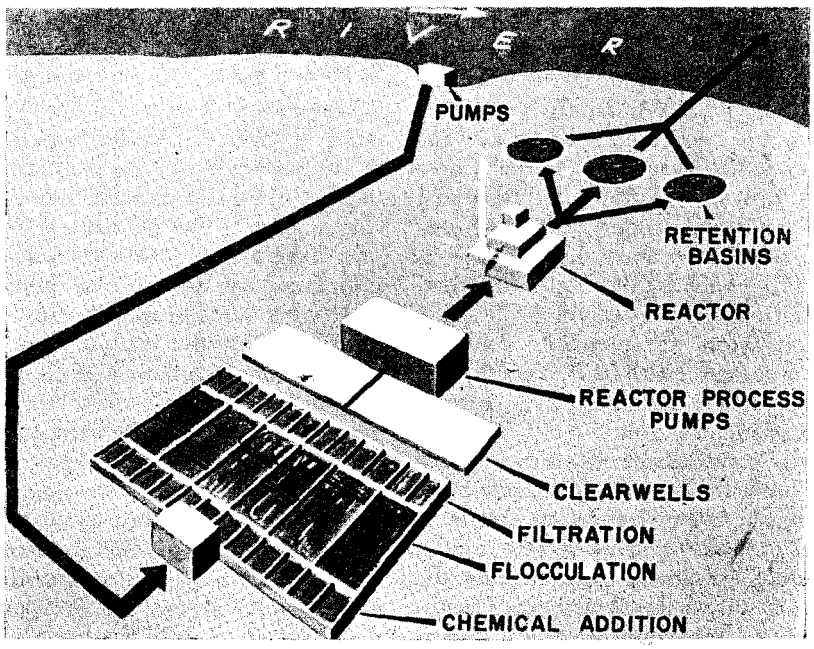

FIG. 6. Water flow through a typical reactor.

C. *Fuel Handling*

Fuel elements (uranium) are transported from the 300 Area Production Fuels plant in special semitrailer trucks. Pallets of "elements" are transferred from the trucks to the reactor metal storage room. During refueling of the reactor, the metal fuel elements are moved from the shipping pallets to charge boxes. The boxes are loaded with fuel, "dummies" (perforated aluminium spacers), and mixers in the appropriate order. The fuel elements are also visually inspected during the charge-makeup operation, and made-up charges are placed on "Tea Carts" for subsequent transfer via the metal elevator to a work platform and the charging machines. The contents of the charge box are unloaded onto the front face charging machine in proper sequence so the fuel will be located, as previously planned, in the process tube. A strict piece count of all fuel is maintained.

After rear-face discharge of irradiated fuel elements, the spent fuel is sorted, picked up, counted, weighed, and sorted in buckets under several feet of water in a large basin. After a specified cooling period, fuel is shipped in special railroad cars to the Chemical Processing plants for separation work.

Irradiated dummies and mixers are also collected in buckets in the water-filled basin, and many are decontaminated for future use. Some of the dummies (those next to the fuel elements) have radiation intensities too high for immediate decontamination, and are charged into large ground pits for radioactive decay.

III. REACTOR DEACTIVATION

A. *Administration*

A deactivation "unit" was specially formed as shown in Fig. 7. This unit was established to coordinate activities for deactivation of DR, H and F Reactors. The guides established by this group were written into a manual covering DR Reactor and later modified for use in deactivating H Reactor and finally F Reactor. The manual contains specific items to be performed during deactivation activities.

Although each deactivation procedure includes appropriate references and suggestions relative to safety, the deactivation unit has no direct safety responsibility. Such responsibility continued under the direction of the area manager who redelegates safety considerations to the various managers of Maintenance, Processing and Power. The supervisors reporting to these managers are considered to be the "mainstays" in the organization, for they assume the direct contact responsibilities with the operating personnel in their respective areas.

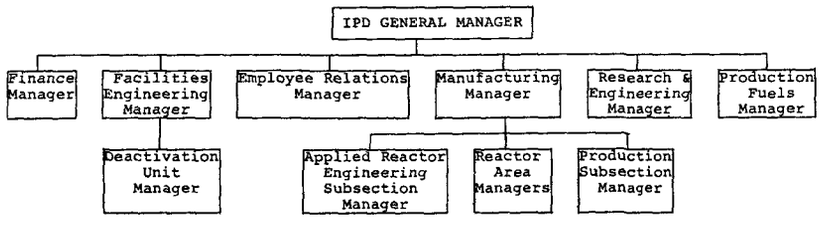

FIG. 7. Organization chart—Personnel Affecting Reactor and Radiation Safety Plus Deactivation Personnel.

The only special procedures required in the operation prior to shutdown of the reactors are those used in physics experiments designed to measure certain nuclear safety parameters. To assure accurate results and safe conditions, a scheduling chart was set up prior to beginning the tests. This chart is shown in Fig. 8. The date is shown along the top with the test listed in the columns staggered to the right indicating the amount of time each test would take. Some of the tests include:

Local control strength
Vertical safety rod calibration
Spline worth
Discharge to minimum critical slab
Cold reactivity—exposure dependence
Supercell

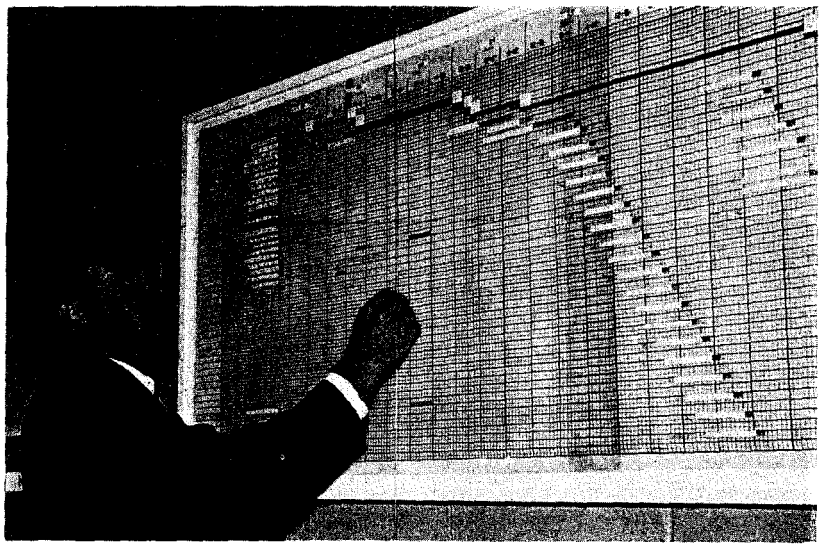

FIG. 8. Scheduling chart.

FIG. 9. Physics test equipment.

Since some of the data obtained have not been fully analyzed, and since much of the material is classified, the results will not be discussed (see Fig. 9 for physics test equipment).

B. *Standard Procedures*

Standard procedures were used to shut the reactors down and to discharge the fuel elements.

C. *Deactivation Procedures*

Procedures were written for:

Decontamination activities
Physical safeguards (e.g. locks, tag)
Posting radiation areas
Transfer of waste to burial grounds and "ultimate posting"
Periodic surveillance after deactivation

These procedures were reviewed by appropriate General Electric Company and AEC personnel for adequacy both in coverage and "safeness".

IV. REACTOR LAYAWAY

General

The deactivation unit mentioned earlier was formed for the specific purpose of closing the reactors known as DR, H and F. DR was shut down in December 1964 and put on a standby status. Since the deactivation of H and F were similar to DR, the deactivation plans for DR were issued in the form of a manual. The manual contained specific items and tasks that were to be performed as part of the deactivation program. All tasks outlined in the deactivation manual were planned and scheduled with safety in mind, whether it was nuclear, industrial or radiological. A special column was included on each instruction sheet pointing out any safety-connected items that should be considered in the performance of work.

Decontamination of the reactors began as soon as the fuel had been discharged. Storage basins, retention basins, and associated effluent piping were given necessary treatment after the irradiated fuel had been shipped. Decontamination, in general, was based on conventional cleanliness and good house-keeping practices prevalent to the nuclear industry. Included were vacuum cleaning, hose-down, wipe-up and disposal of contaminated items. Chemical decontamination was used in specific locations where it had proven to be effective in the past in the removal of rust and encrusted water salts. Materials with a high radiation dose rate were left in locations where there was adequate shielding. These areas were then posted with radiation identification markers and barricaded as required. Equipment and locations not having economic justification for complete decontamination were either isolated, or the contamination was fixed to prevent an inadvertent spread. They were then properly marked, fenced, or barricaded and posted with information on the nature and level of contamination. Contaminated items valued at less than $5000 were either buried or used in the operating reactor areas. Expendable contaminated materials and equipment were removed and either utilized or buried, if this was less costly than decontaminating the items. Interior contaminated surfaces of piping systems and equipment not contributing to radiation dose in general required no treatment other than sealing to contain the contamination. Posting of appropriate warning signs was then initiated to maintain the integrity of the system; the effluent water piping is one example. All parts of the facility, equipment and grounds received a complete radiation survey, and the radiological status was documented and made a part of the layaway information package.

1. *Cleaning Methods.* Low-level loose contamination in such locations as corridors and main traffic areas was removed by water washing, sponging, and mopping. High level loose contamination in other corridor areas that could be contained and removed with a minimum probability of spreading was collected with vacuum cleaning equipment. This was followed by water washing. Contamination that was fixed or had penetrated into porous surfaces required the use of additional cleansing agents in the water, such as detergents and commercial chemical cleaning agents. In stubborn cases, detergent was applied with steam cleaning equipment.

Commercial chemical cleaning agents were used on reactor hardware where past experience indicated no detrimental effects. These agents

were used freely on iron and concrete surfaces where rust, scale, and water salts trapped and concentrated contamination. With this technique, the contamination carriers were, in effect, put into the solution and washed away. Extra caution and additional controls were exercised in the application of these chemical cleansing agents so that they did not inadvertently contact materials and equipment that could be damaged. Some mechanical equipment and almost all the electrical equipment and instrumentation could not be cleaned with water or chemical agents. Therefore, vacuum cleaning and careful wiping with suitable solvents, rags, and swabs were used on this type of equipment. In general, where equipment was not subject to damage and floor drains were present, water washing, sponging and mopping were used prior to the application of chemicals. In other locations, vacuum cleaning was used exclusively. Vacuum cleaners were equipped with traps to collect contaminated dust and dirt and were designed for the easy removal and disposal of the collected dirt.

2. *Shielding and Fixing Methods.* Conventional shield materials were used as required. Radioactive materials not readily removed by normal cleaning methods were fixed in place with either paint or a sprayable plastic. Even high-level contamination was fixed without using concrete or asphalt coatings. Where economically justified, lead brick and lead sheet of appropriate thickness were selected for gamma shielding. However, significant quantities of lead brick were not needed after reactor shutdown. Some locations, which involved large areas and where subsequent removal was a consideration, were shielded with earth fill.

3. *Radiological Criteria.* The Hanford Radiation Control Standards and Procedures (HW-45674) were used where applicable and were consulted as a guide for problems peculiar to the task of reactor plant layaway. The sections in the standard on radioactive waste disposal, shipment of radioactive materials, release from radiation zone status, and radiation markers, plus other sections, were directly applied in the Plant deactivation program.

The following radioactive contamination activity and radiation dose-rate levels were used as a guide in decontamination and cleaning of the plants and appurtenances.

(*a*) *Nonradiation zones.* Working surfaces, doors, tables, work benches, and control panels were to be decontaminated to less than 100 counts per minute (cpm)* as determined by the standard smear technique and to less than 1 mR/hr.

(*b*) *Radiation zones requiring posting.* In general, porous floor surfaces and equipment surfaces were to have less than 3000 cpm of smearable contamination and a dose rate less than 3 mR/hr measured at 1 ft from the surface. The common traffic areas within controlled radiation zones were to be cleaned to less than 1000 cpm by smears. The external surfaces of the reactor, except the rear face, were to be decontaminated to less than 3000 cpm of smearable contamination and less than 3 mR/hr measured at 6 in. from the surface. The rear face and rear discharge area of the reactor were to be cleaned to approximately 10 mR/hr measured at 1 ft from the surface.

(*c*) *Significant contamination zones.* Barricades, warning signs, and/or fixation of contamination were used as safeguards for equipment, material, or locations where:

Significant contamination spread could occur, or

Dose rates exceeded 10 mR/hr.

Included in this classification, for example, were the reactor interior, downcomer and effluent system interior, gas dryer beds, and irradiated metal storage basin.

When a reasonable amount of time and effort had been expended in cleaning any location or piece of equipment without attaining the above goals, the work was to be stopped and the condition reevaluated. An alternate treatment was to be used such as fixing the contamination, shielding, and disposal, accompanied with appropriate posting of warning signs and barricades. All loose contamination was to be removed even though the activity level was below the recommended levels.

4. *Application.* A systematic program was developed and followed during the decontamination of radiation zones within the deactivated

* A standard GM was used for measurements in cpm.

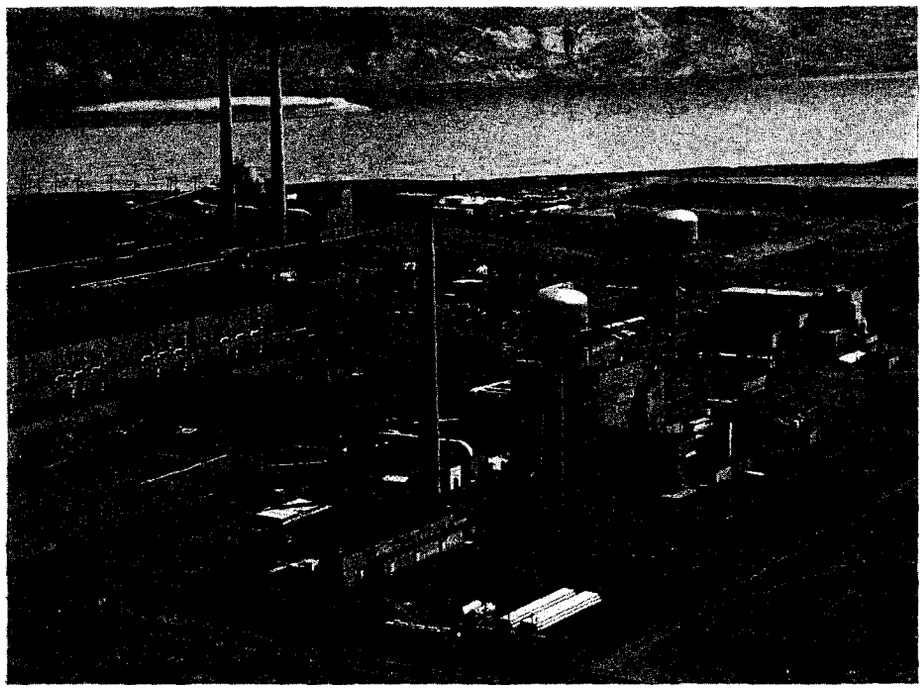

FIG. 10. Aerial view of a typical reactor area.

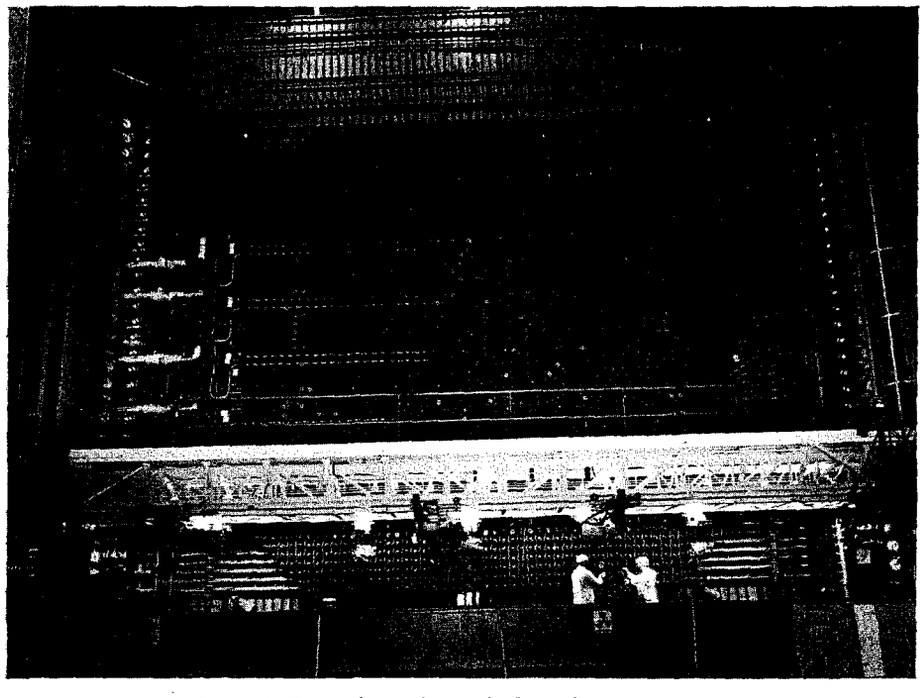

FIG. 11. Front face of a typical production reactor.

reactor facilities. An aerial view of F-Area buildings is shown in Fig. 10. Initial efforts consisted of removing equipment, tools and materials that were not intended for storage in the reactor buildings. This was followed by the implementation of a general "housekeeping" effort and an eventual survey of each radiation zone. In many cases, the radiation surveys indicated that no additional decontamination effort was required to satisfy the postdeactivation radiological control measures mentioned earlier. Figure 11 shows the front face of one of the Hanford reactors and is typical of the type of area that had to be decontaminated. The reactor building contained numerous radiation zones, some of which contained smearable contamination as high as 50,000 cpm. The general flow of decontamination work was from top to bottom and from the right side to the left.

The radioactive contamination in the open areas was, however, readily reduced to a nominal level of less than 3000 cpm. There were several locations where a spread of contamination could occur or which involved dose rates above 10 mR/hr; these locations were either sprayed with a sealant or barricaded and posted with tags describing their status. In each case, the amount of effort expended on decontamination of a specific location was based to some extent on previous decontamination experience.

Approximately 70 locations were surveyed for contamination in each reactor. An average of 43 were previously established radiation zones. Some 25 zones required decontamination with detergent solutions or chemicals to satisfy the decontamination criteria as discussed above.

(*a*) *Reactor pile and discharge basin.* The reactor was sealed; Fig. 12 shows a schematic of a typical reactor pile and the associated discharge basin. Reactor tubing and hardware were also sealed. The discharge and storage area shown in Figs. 13 and 14 did pose special problems. The reactor discharge basin contained a considerable inventory of radionuclides deposited during discharge activities. These radionuclides originated in three ways:

Loss of fission products from irradiated, ruptured metal fuel elements

Neutron activated stable elements (from cooling water) that had collected on fuel elements, dummies, mixers, and tube walls

Activated elements in structural materials in the reactor pile

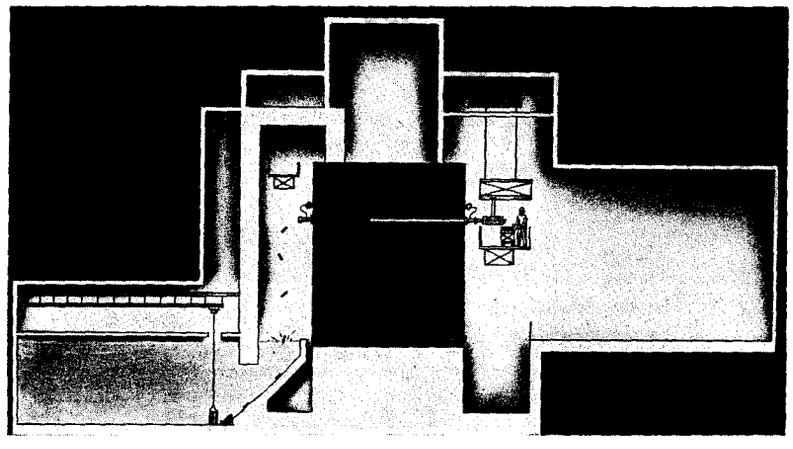

FIG. 12. Schematic of a typical reactor.

The quantity of materials deposited in the basin precluded economical removal. Therefore, each reactor storage basin was left in a partially water-filled condition.

All loose contamination was secured and irradiated material was removed or shielded to reduce radiation levels below 3 mR/hr at 1 ft. Equipment and foreign objects that could be

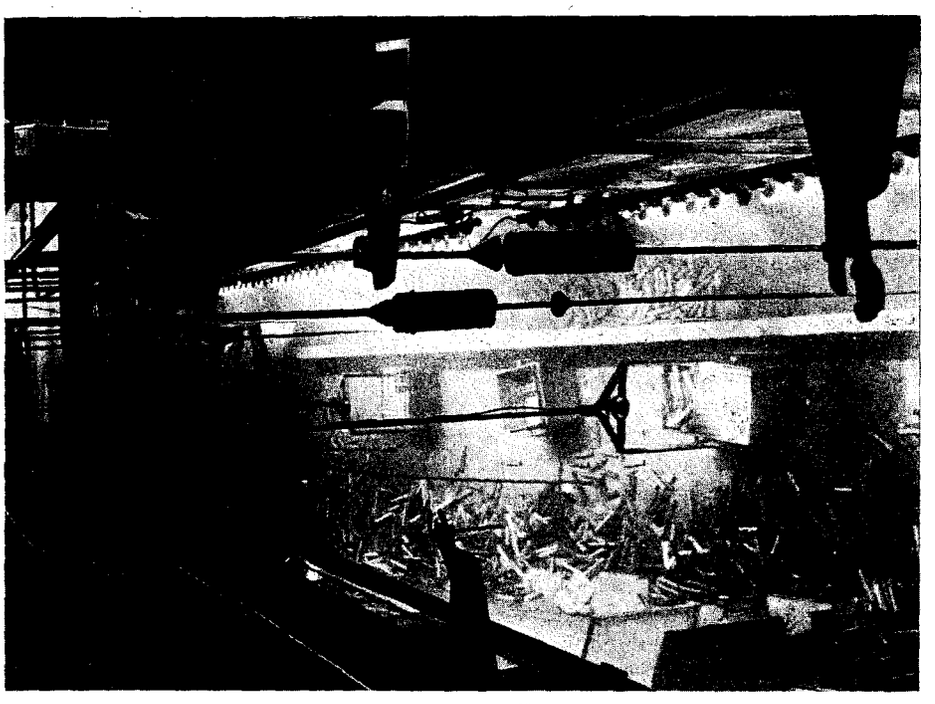

FIG. 13. Reactor discharge area.

FIG. 14. Reactor storage area.

readily picked up were removed from the basin. The water level was gradually lowered and the basin walls were hosed down and scrubbed with commercial detergents and chemical cleansing agents. The radioactive sludge on the bottom of the basin was left in place. The basin was then posted and barricaded as required by existing radiation protection standards.

A radiological analysis was made at one of the deactivated reactors. The basin water level was lowered from 17 ft 7 in. to 4 ft. Dose-rate measurements taken at the top of the basin did not exceed 7 mR/hr and no smearable contamination was detected on the basin walls. The analysis demonstrated that radiation dose rates and contamination could be controlled by keeping an appropriate level of water in the basins. An alternate method for radiological control would be to dump a nominal amount of earth or cinder into the basins. To date, it has proven to be less expensive, however, to keep water in the basins instead of filling them with earth or cinder.

(*b*) *Ventilation system.* The reactor ventilation supply system did not require decontamination. A borderline exception was the internal portions of the DR and F Reactor rear face supply ducts that required stabilization of loose contamination. All dry and wet filters were left in place.

Except for the 105-H rear face exhaust duct, the ventilation exhaust ducts did not require decontamination. Access covers were left in place to prevent contamination spread, and radiation warning signs were then posted at appropriate locations.

On completion of decontamination work on a given reactor, a ventilation test was then conducted. All supply and exhaust fans were shut off for a continuous period of 16 hr. In effect, this left the reactor building ventilation system in a deactivated status. In conjunction with the test, all outside doors were closed, and the exhaust ducts to the reactor building stack were left in the open position. At the conclusion of the test, a complete radioactive contamination survey was made in the building to determine if any radioactive contamination had migrated from the various radiation zones to "clean" areas; the results were negative.

(*c*) *Water plant piping and equipment.* As can

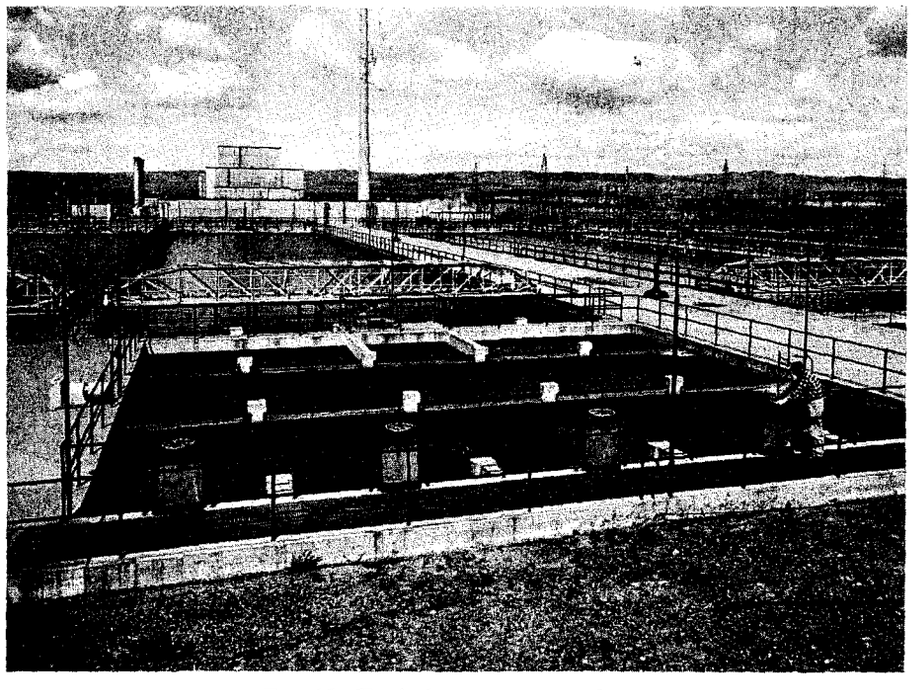

FIG. 15. Typical reactor water plant.

be seen in Fig. 15, the three water plants supporting the reactors were large and complex. Since all three deactivated reactors were immediately down river from other operating reactors, "low-level" activity, from neutron activation of stable elements in the cooling water used for the upstream reactors, had plated out on the equipment used in the water plants. The 183 settling basins (Fig. 16) were cleaned of loose foreign material and hosed down. The rest of each water plant was hosed down and left in a standby condition. After a short period of time, contamination levels were low enough for transfer of the equipment to other water plants.

Because the coolant effluent systems are still contaminated with very low levels of radioactivity, control measures are necessary. The

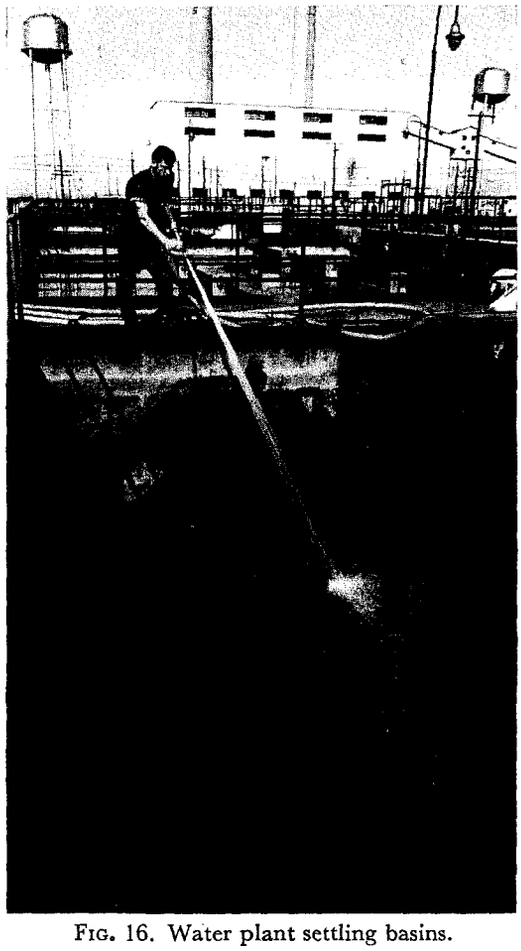

FIG. 16. Water plant settling basins.

radionuclide of greatest concern is ^{65}Zn with a 245-day half-life. The control procedures established for the water plants will preclude the spread of contamination, and will prevent personnel contact for a period of 5 years. After the 5-year period, no further control will be necessary because the activity will decay to an insignificant level.

(*d*) *Reactor retention basins.* Perhaps the reactor retention basins presented the biggest radiological problems. Original plans called for complete removal of baffle plates and the separating center wall (see Figs. 17, 18, 19 and 20). A demolishing crane was used to knock down the baffle plates (baffle plates insure water mixing) to the floor of the basin. Jackhammer operators tried to weaken the center concrete partition, so that the demolishing crane could knock it over to the floor of the basin, too. Jackhammer operators were required to wear full protective apparel and respiratory protection.

All wrecking attempts proved ineffective because of the reinforcement steel within the center wall. Originally, the activity in the bottom of the basin was to be stabilized with 4 ft of earth fill, which would slope upwards and cover the sides, subsequently creating a large earthen "bowl".

The amount of dirt necessary to fill the retention basin soon proved to be costly. To eliminate the additional cubic ft of dirt fill required for sloping the sides, an asphalt spray was used to fix contamination on the center, side, and end walls. The resultant savings in manpower and equipment were significant. The end result was probably more effective using asphalt, since high winds could move sloped earth shoulders and cause a spread of "low-level" contamination.

Prior to deactivation of the retention basins, representative samples were taken to ascertain levels of contamination in the 500 tons (total F and H Reactor basins) of sludge on the basin floor. These representative samples revealed accumulations of:

$\sim$ 800 Ci of ^{152}Eu ($\sim$ 13-year half-life).
$\sim$ 400 Ci of ^{65}Zn ($\sim$ 245-day half-life).
$\sim$ 40 Ci of ^{60}Co ($\sim$ 5-year half-life).
$\sim$ 30 Ci of total β emitters (e.g. ^{147}Pm, $^{89\text{-}90}Sr$, ^{99}Te).

Since these radionuclides were uniformly mixed in the 500 tons of sand and silt, dose rates from

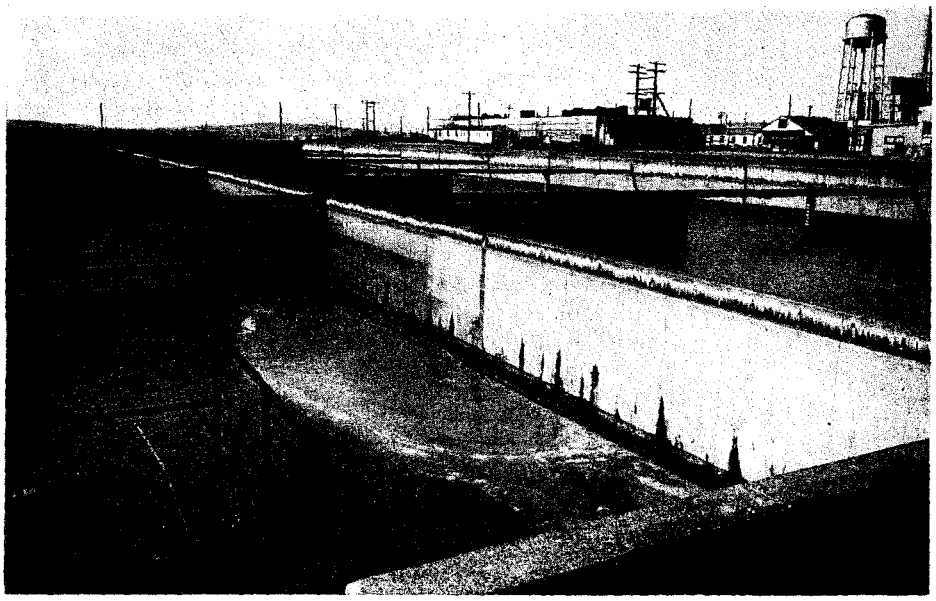

FIG. 17. Retention basin and waffle plater.

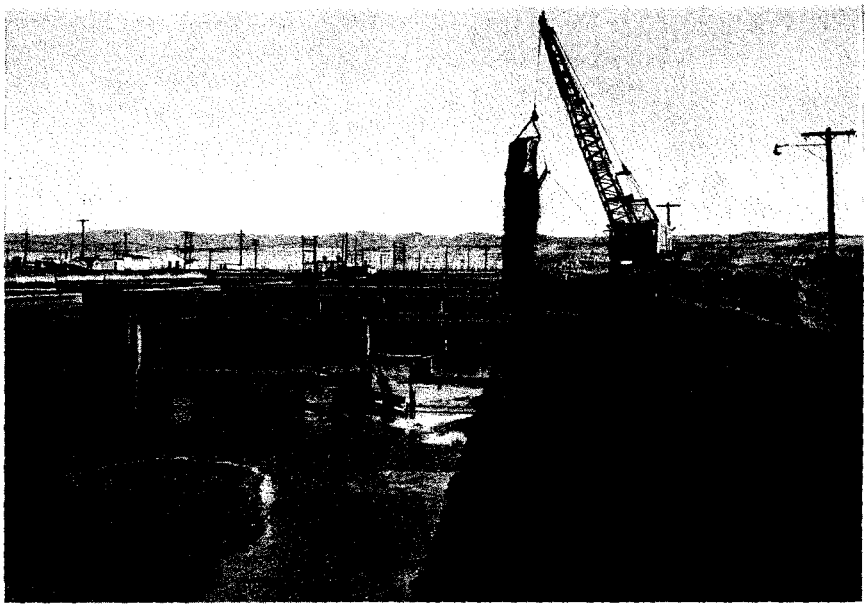

FIG. 18. Initial filling operation.

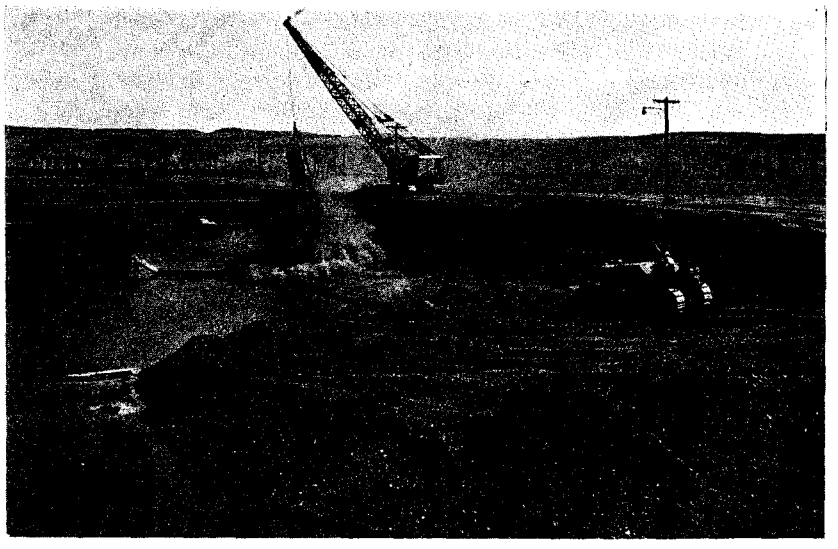

FIG. 19. View of basin center cavity.

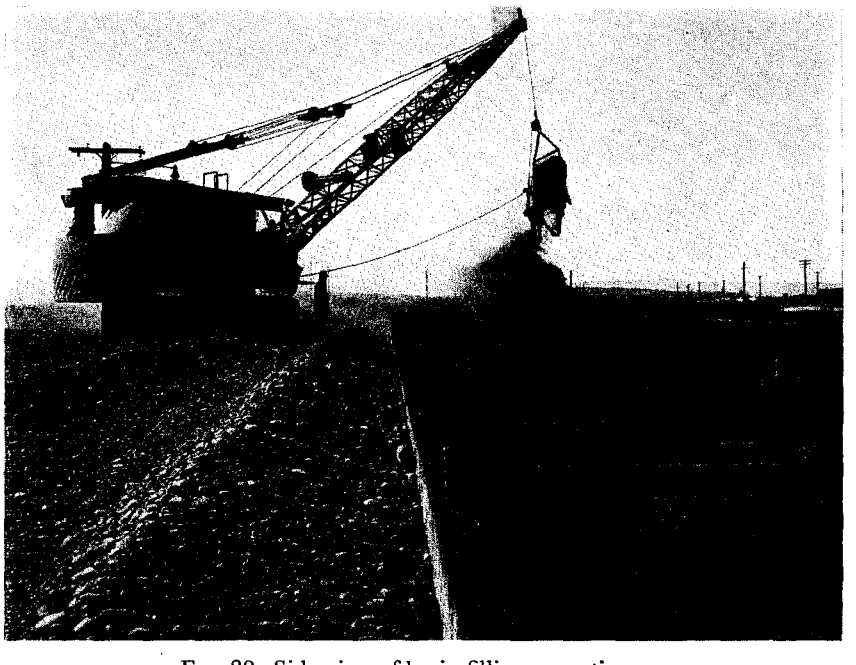

FIG. 20. Side view of basin filling operation.

the wet sludge were nominal. Modest safeguards and controls would be required if use for the land was mandatory within the next 5 years.

FIG. 21. Low-level burial site.

Estimates show that in 10 years, dose rates will be low enough to reclaim the area encompassed by the basin walls with little exposure to workers. After 50 years, radionuclides will not be significant even though ^{152}Eu will theoretically have a calculable value.

Radiation symbols were posed after deactivation activities were complete.

(*e*) *External radiation zones.* There were several locations in each reactor area that contained underground radioactive materials. Only two of the deactivated reactor areas will be discussed, since one plant is located in a dual area with an operating reactor.

At one of the reactor areas there are 13 underground radiation zones; the other area has 16. Five of these locations, encompassing a perimeter of 6000 ft, have been permanently terminated as burial sites. Figure 21 shows a typical "low-level" burial site. The permanently posted burial grounds contain two general types of radioactive waste: neutron activated reactor components and surface contaminated material and equipment. The activated components consist almost entirely of steel and aluminum. Figure 22 shows the boron-steel balls used for emergency reactor control being removed from a deactivated reactor. The boron-steel balls are typical of the type of activated material placed in the permanent burial grounds. The

FIG. 22. Boron steel balls being removed from a reactor facility.

most significant radionuclide contained in this type of material is ^{60}Co which has a half-life of 5 years. Other types of neutron activated materials placed in the burial grounds are aluminum tubes, reactor hardware, and thermocouple wires. Bundles of process tubing have dose rates as high as 5 R/hr at 6 ft. The surface contaminates are primarily corrosion and activation products from the reactor cooling water. The most significant long half-life radioisotope for this type of material is ^{65}Zn which has a half-life of 245 days.

All abandoned burial trenches and pits were backfilled to normal grade, which provided at least 4 ft of cover and limited the radiation intensity level to less then 1 mR/hr.

Table 1. Typical Decay Rates

Zone	March 5, 1965		March 21, 1966	
	Direct	Smears	Direct	Smears
Winch	3 mR/hr	1000 cpm	1 mR/hr	500 cpm
Top of unit	3 mR/hr	1000 cpm	1 mR/hr	500 cpm
Ball collection	300 mR/hr	1000 cpm	3 mR/hr	500 cpm
X-2 level	3 mR/hr	1000 cpm	1 mR/hr	100 cpm
X-1 level	3 mR/hr	1000 cpm	1 mR/hr	100 cpm
Vacuum system	50 mR/hr	1000 cpm	40 mR/hr	500 cpm
Rear face	40–70 mR/hr		20 mR/hr	
Charge face	4–6 mR/hr		3 mR/hr	

The burial grounds were then posted in accord with existing RL-AEC standards; the concrete posts conform to the standard established by the state of Washington for highway marking.

Some of the other underground radiation zones were liquid waste disposal sites not requiring permanent markers. Concrete posts were not installed in these areas, since it was predicted that radiological control measures will not be necessary for any use of the land 5 years after reactor deactivation.

(*f*) *Personnel exposure.* Whole-body radiation exposure received by workers during deactivation work was considerably less than that received during normal maintenance and discharge work. To be specific, an exposure accountability program showed that:

DR Reactor craftsmen received 12 R of whole-body exposure; 2 R to monitors, 7 R to operators, 2 R to maintenance craftsmen and 1 R to others.

H Reactor craftsmen received 11 R of whole-body exposure; 1 R to monitors, 5 R to operators, 1 R to maintenance craftsmen and 4 R to others.

F Reactor craftsmen received 14 R of whole-body exposure; 3 R to monitors, 7 R to operators, 2 R to maintenance craftsmen and 2 R to others.

The 37 R received by workers during the deactivation activities for the three reactors represents approximately one-fifth of the total exposure required to operate a Hanford production reactor for 1 year.

V. CONCLUSION

Approximately 1 year has elapsed since deactivation work was completed on the reactors and their associated facilities. During this period, routine monitoring and control programs have continued in force. Some of the deactivation procedures have been casually mentioned in the body of this paper.

The total surveillance program, however, has been much more sophisticated than these notations would imply. For example, complete

annual survey programs have been completed for each of the reactor buildings. Typical data on decay rates for specific locations within a reactor building are given in Table 1.

To assure continued control throughout the year, surveys on frequently travelled locations were made. Experience to date has adequately shown that the radiological criteria adhered to during the deactivation of the three reactors were sufficiently restrictive. The periodic radiation and contamination surveillance program (as described above) for the reactors has proven to be adequate. The decay rates for the remaining radioactive materials apparently have decayed with a half-life considerably below the predicted value of 5 years.

Deactivation experience gained to date at Hanford has demonstrated that:

Economical deactivation of large single pass reactor production facilities can be accomplished safely and effectively.

Relatively large quantities of activated elements decay rapidly and will not limit future renovation activities.

Considerable thought and preplanning is required to achieve continued radiological control.

Remaining activity in Hanford facilities will be largely attributable to the longer-lived fission products, but these will not be prohibitive in reclaiming much of the land for more purposeful future activities.

DISCUSSION

J. POMAROLA (*France*):

J'ai apprecié la très remarquable concordance des films et des dosimètres de poche. M. Craig peut-il nous donner des précisions sur les films et les dosimètres?

D. K. CRAIG:

The film badges were the standard AERE film badges as used by the U.K. Radiological Protection Service and the pocket dosimeters were Stephen self-reading quartz fibre dosimeters.

D. C. LAWRENCE (*U.S.A.*):

What was the total amount of Pu^{239} involved and what percent was released?

D. K. CRAIG:

The source contained 160 g of plutonium, i.e. 10 Ci. We estimate that about 30% of this was released into the primary and pool water systems. The ruptured source is still, at this stage, in double containment at the bottom of the pool. An attempt will be made to measure the amount of Pu released by extracting and measuring the amount of Pu left as soon as our hot cell facilities are completed.

O. L. CORDES (*U.S.A.*):

What was the estimated cause of source failure?

D. K. CRAIG:

Quite frankly, stupidity. No one had, prior to the incident, calculated the heat transfer from and heat generation of the source. Subsequent calculations showed that, at a reactor power of 6–7 MW, the cooling of the source was inadequate in the core location chosen. Hazard evaluations of the reactor had omitted to consider possible hazards arising from the source.

L. DE FRANCESCHI (*Italy*):

Due domande per il Dr. Craig:

1. Nel reattore Safari non si usa allontanare la sorgente di neutroni dal core non appena raggiunta la criticità?

2. Che cosa significavano, nelle figure che sono state mostrate, i "massimi livelli di attività" raggiunti?

D. K. CRAIG:

1. The reactor was at the time of the incident still under the control of the nuclear sub-contractor. It had been suggested to him prior to the start of the acceptance test that the Pu-Be source be removed. The Operations Manager declined to do so as he thought the source would be all right.

2. The "maximum activity levels" prior to the incident indicated in Figs. 2 and 3 referred to the maximum readings that had been obtained with the reactor at a power of 6–7 MW and all ventilation systems operating normally.

J. POMAROLA (*France*):

Je désire demander une précision à M. Fitoussi. Il nous a parlé d'une contamination par les produits de fission. Mais dans le cas d'une rupture de gaine survenant sur une telle cellule, n'y a-t-il pas eu aussi une contamination par le Pu^{239}?

L. FITOUSSI:

La question de M. Pomarola est importante. En effet dans le cas d'éléments de combustible présentant des taux de combustion élevés, la concentration des isotopes du plutonium peut être élevée. Dans le cas de la cellule qui a donné lieu à l'incident décrit dans ce rapport, le taux de combustion a été évalué à 3650 MWj/t, ce qui correspond pour cette cellule à une concentration de 1 mg de plutonium par gramme d'uranium. En supposant un taux d'émission de l'ordre de 1% (comme pour les produits de fission solides) on calcule un risque potentiel de l'ordre de 10% relativement à celui de l'iode-131. Toutefois, comme il est dit dans le rapport, nous n'avons pas pu mettre en évidence a posteriori la présence du plutonium dans les prélèvements atmosphériques et de surface.

B. W. EMMERSON (*U.K.*):

1. At what fuel temperature was I^{131} still being released from the fuel element?

2. Was the gaseous effluent released via an I^{131} extraction filter?

L. FITOUSSI:

1. Pour répondre à la première question je dois donner une précision complémentaire concernant la

pile EL3 qui présente une puissance spécifique de l'ordre de 40 MW/t. La puissance dégagée par les produits de fission est donc importante et nécessite un refroidissement efficace car 12 heures après le défournement la température de l'uranium peut dépasser 600°C.

2. Le circuit d'extraction d'air de la pile EL3 comporte un dispositif de filtres de secours comprenant entre autres un piège à iode à charbons actifs. Ce dispositif n'est mis en service qu'en cas d'accident important car il nécessite l'arrêt de la pile.

Or pendant ces opérations, la pile était en fonctionnement et l'activité rejetée ne présentait pas de risque important. C'est pourquoi le dispositif de secours n'a pas été mis en service.

E. W. Jackson (*U.K.*):

In the results of downwind concentration of I^{131} given by Gammill and Bunch for several release experiments, and claimed to be capable of being used to predict the amount in curies emitted by the reactor, there is no mention whatever in the tables shown of the deposition of material from the clouds in transit. I cannot see what it is possible to calculate from the results on this basis.

D. F. Bunch:

Although not indicated in the presentation, depletion of the cloud by deposition was considered. For the stated meteorological conditions, depletion of airborne activity by deposition was found to be insignificant in these tests.

B. W. Emmerson (*U.K.*):

1. How was contamination, as collected on surface smears, examined for isotopic and energy distribution?

2. What degree of protective clothing was required whilst decontaminating large surfaces, as exampled in Fig. 9?

L. Wallis:

1. We have no data bearing on this question.

2. Airborne contamination was not a problem. Therefore, no protective clothing was worn.

THE APPLICATION OF A PERSONNEL MONITORING SYSTEM TO POPULATION DOSIMETRY OF BACKGROUND RADIATION*

JACOB SHAPIRO, ASCHER SEGALL and JANE WORCESTER
Departments of Industrial Hygiene, Epidemiology, and Biostatistics, Harvard School of Public Health, Boston, Massachusetts

Abstract—A field study was undertaken to evaluate the use of pocket ion chamber dosimeters for measuring population dose to background radiation. The chambers were charged to a low voltage to minimize leakage and read after exposure with a pulse-reading method. The method had a sensitivity reported to be 1 mr ± 0.2 mr.

Special tests were devised for selection of stable and reproducible ion chambers. The dosimeters were worn by individuals for a week at a time over a five-week period and calibrated and standardized after each week of use. Results of an analysis of variance on the standardization data obtained with 41 dosimeters over the period of use are presented. The tests showed that after field use, the system, including reader plus dosimeters, showed increased variability over the variability at the beginning of the tests. The leakage of the dosimeters was also apparently increased in field use over that found in laboratory experiments. The study showed the need of frequent testing in the field of any system used for population dosimetry at the low levels characteristic of background radiation.

The design of a study of population exposure to background radiation with personnel monitoring devices is discussed. Formulas are presented for determining the total number of dosimeters to use and the number of dosimeters to assign per individual, based on initial pilot studies.

The test data obtained in this survey should be useful for comparison with test data on other dosimeter systems, such as the thermoluminescent type in evaluating the performance of detection systems for the measurement of low-level population exposure.

INTRODUCTION

Interest in the measurement of background radiation for epidemiologic studies has, in recent years, stimulated efforts to develop methods that are capable of detecting differences in low-level gamma radiation and that are, at the same time, suitable for use in large-scale population studies. Such methods should be sufficiently sensitive to monitor the low dose rates characteristic of background radiation with a high degree of reliability. In addition, the dosimetric system should exhibit minimal energy dependence within the range of energies likely to be encountered in studies of natural background radiation and should be relatively dose-rate independent. The instruments should also be portable and sufficiently stable to ensure reliable operation under a variety of field conditions.

Of particular concern to epidemiologic investigations is the dose received by members of the population during the course of their normal activities. This may be estimated from spot measurements of the potential exposure in the environment as recorded by a pressurized ionization chamber or a geiger or scintillation detector. If a detailed mapping of the environment is made over the time period of interest and knowledge of the time spent by the subjects in areas of different exposure rates is obtained, the personnel dose may be calculated.

Environmental measurements provide a satisfactory method of determining population dose, and estimates based on their use have been

* Aided by research grant GMO7615–03 from the National Institutes of Health.

presented in several studies.[1] Where the main information desired is the exposure of a selected group of individuals, or the difference in exposure of individuals in different areas, personnel monitoring devices provide an attractive alternative approach to background measurements, since they measure personnel exposure directly.

Personnel monitoring devices may also be particularly useful when the background levels, which are affected by rainfall, fallout, and barometric pressure, change significantly over the period of time of interest.

The two detection devices which have been used most extensively to date for monitoring of individuals occupationally exposed to radiation are pencil condenser ionization chambers and personnel monitoring film. Because of their widespread use and commercial development, both types of detectors are available at sufficiently low unit cost to enable their use by large numbers of individuals. However, the usual methods of using these detectors for radiation protection purposes are not sufficiently sensitive to enable their direct application to the low levels generally accumulated in population exposure studies.

The sensitivity of the personnel monitor film can be improved vastly by surrounding it with scintillation material, and the performance of this unit has been studied in detail by Henson.[2] It turns out that the film is highly dose-rate and temperature dependent when the exposure is produced by light from the scintillator rather than by background radiation directly.

The sensitivity of pencil ionization chambers may also be greatly increased by the use of a special read-out system designed in 1958 by Roesch, McCall and Rising.[3] In this method, a precision, stable voltage supply is used to charge the ion chambers. After exposure, the chamber is recharged to the same voltage through a resistor. A voltage pulse is produced across the resistor proportional to the differences in voltage between the ion chamber and charging voltage and, therefore, proportional to the measured dose. According to McCall, this system has several advantages as compared to the conventional method of reading condenser ion chambers.[4]

First, the method is a differential one; and the difficulties of measuring a small difference between two large numbers is avoided. Second, the method uses pulse measurements rather than direct current, and it becomes much simpler to obtain high sensitivity and stability. Selected single pencil dosimeters can measure 1 mr levels with an accuracy of ± 0.2 mr in 95% of the trials. The pencils are mechanically stable and undergo little change due to thermal cycling.

The characteristics of this system suggest that it may be adaptable for use in epidemiologic studies of background radiation. The present study was designed to assess this possibility.

INSTRUMENTATION

Specially selected Victoreen Model 36 Z pocket ion chamber dosimeters and a commercial reader were used. The reader is of the type described by Roesch *et al.*[3] and was supplied by Controls for Radiation, Cambridge, Massachusetts. A photograph of the reader is given in Fig. 1. It consists essentially of three parts—input circuit, amplifier, and peak-reading voltmeter. The input circuit is a high-impedance cathode follower using an electrometer tube. Long time constants are used to minimize the effect of electrical noise caused by the insertion of the ion chamber. The amplifier is a low-gain circuit with a choice of attenuators to provide high and low ranges. The peak-reading voltmeter converts the pulse into a very long high-current pulse whose amplitude can be displayed on a meter. The rest of the circuitry includes a highly stable power supply for charging the ion chambers and a system for simulating various doses on the ion chambers. This latter system makes it possible to check quickly the calibration and linearity of the reader.

Since a broad spectrum of gamma rays is encountered in the measurement of background radiation, it is desirable to have detectors as nearly energy-independent as possible. The Victoreen pencil dosimeters used were reported by their manufacturer to have a dose response which varied only a few percent with energy between 0.1 MeV and 1 MeV.

A seven-day period was chosen as a convenient time interval for measuring exposure. Readings of approximately 2–4 mr were expected for this period. The reader had two ranges and was adjusted so that the lower range was 0–5,

and the meter read directly in mr. The high range of 0–50 mr was not used in this study. To avoid excessive leakage, the chambers were charged to only 20 V. At this voltage, saturation is obtained up to dose rates of at least 50 mr/hr, and this saturation continues down to about ten volts. Leakage was reported to increase the reading by about 1 mr/month at 20 V.[3, 5]

SELECTION OF DOSIMETERS

The use of pencil chambers for measurement in the 1 mr range required special care in their selection. Residual mechanical strains in the insulators, loose connections, and excess dust or moisture may produce erratic and nonreproducible readings. It was therefore necessary to establish criteria for screening dosimeters prior to field evaluation.

During the course of initial screening, it was noted that even those dosimeters which appeared to be functioning in a reliable manner would occasionally give readings which differed appreciably from the average, e.g. as much as 0.5 mr when the average was 1.1 mr. Consequently, selection criteria were based on the average results of several readings rather than on a single reading. After several preliminary trials, the following empirical criteria for acceptance of dosimeters for field use were adopted.

1. Dosimeters were tested as a set, and the whole set was accepted or rejected depending on their meeting the prescribed conditions.

2. All the dosimeters were given a constant exposure of approximately 1 mr, and the exposure time was 5 min. The value chosen for the reference exposure was the average of all the readings of the dosimeters suitable for field use.

3. Each set of dosimeters was exposed for five times in succession. At least 90% of the readings had to be within 0.3 mr of the average reading, and each dosimeter had to read within 0.3 mr of the average in three out of five trials.

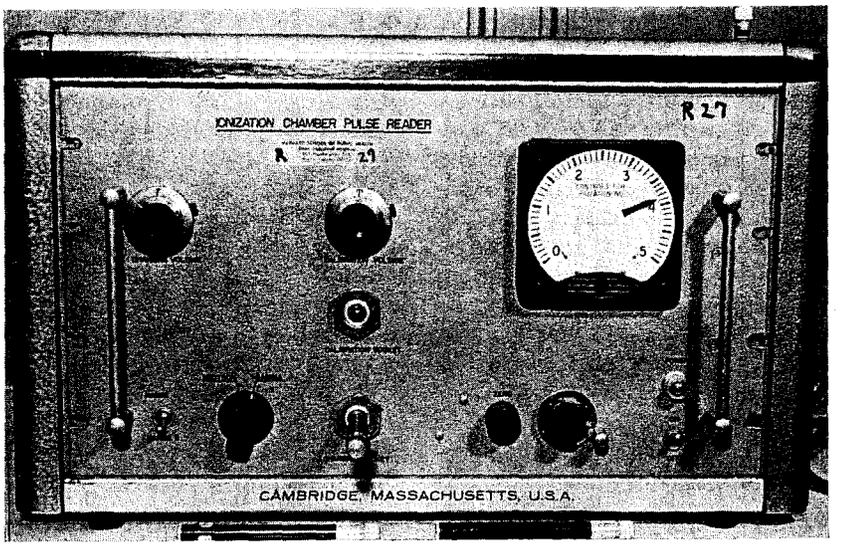

FIG. 1. Ionization chamber pulse reader.

The initial set of dosimeters tested could not meet these criteria. Another set of 50 dosimeters which was tested gave a mean reading of 1.03 mr, and the numbers of dosimeters giving all five, four, and three readings within the prescribed range were 39, 8, and 3 respectively. These readings represented 92% of the total taken. A third set gave a mean value of 1.24 mr and was rejected. Some dosimeters which gave erratic results because of induced charges on the insulator were improved and found suitable for use after exposure to 100r of X-radiation.

Table 1. *Screening of Dosimeters Prior to Field Use*

Instrument number	Trial 1 (mr)	Trial 2 (mr)	Trial 3 (mr)	Trial 4 (mr)	Trial 5 (mr)	Mean (mr)
14,508	1.10	1.20	1.10	1.00	1.10	1.10
14,532	1.10	1.10	1.20	1.00	0.95	1.07
14,544	1.00	1.00	1.10	1.00	0.90	1.00
14,743	1.00	1.10	0.80	1.00	0.60	0.90
14,817	1.10	1.10	0.80	0.90	1.20	1.02
14,897	1.00	0.90	0.70	0.80	1.00	0.88
14,946	1.00	0.70	0.90	1.10	0.90	0.92
14,961	1.05	1.00	1.10	1.00	1.20	1.07
15,175	0.80*	0.70	0.80	0.90	0.80	0.80
15,208	0.80	0.60	0.10	1.70	0.80	0.80
15,338	1.30	0.90	0.10	1.00	1.10	1.08
15,605	0.90	1.30	1.00	1.00	0.90	1.02
15,639	1.20	1.00	0.60	1.00	1.20	1.00
15,688	1.20	1.20	1.00	1.20	1.00	1.12
15,704	1.00	1.20	0.80	1.30	1.10	1.08
15,734	0.95	1.00	1.00	1.10	0.90	0.99
15,805	0.95	1.00	0.70	0.70	0.90	0.85
15,903	0.90	1.20	1.10	1.20	1.00	1.08
15,918	1.20	1.10	0.90	1.00	0.95	1.03
15,946	1.10	0.90	1.00	1.20	1.20	1.08
16,023	1.00	1.30	0.80	1.10	1.00	1.04
16,059	1.20	0.60	0.80	0.90	0.85	0.87
16,310	1.00	0.80	0.80	0.80	1.00	0.88
16,337	1.50	1.00	0.90	1.00	1.10	1.10
16,368	1.10	1.00	1.00	1.20	1.10	1.08
16,397	1.50	1.10	1.00	1.20	1.10	1.18
16,478	1.20	1.30	1.10	1.50	1.00	1.22
16,629	0.90	0.90	1.00	0.70	0.70	0.84
16,662	0.90	0.80	0.90	0.80	0.90	0.86
16,705	0.85	0.80	1.00	0.90	1.00	0.91
16,842	0.90	0.70	0.90	0.80	1.00	0.86
16,868	0.90	1.00	0.80	0.90	0.90	0.90
16,959	1.00	1.10	0.90	1.00	1.00	1.00
17,046	1.10	1.30	1.10	0.90	1.10	1.10
17,127	1.20	1.10	0.90	1.00	1.30	1.10
17,169	1.10	0.90	1.10	0.70	1.00	0.96
17,173	1.10	1.10	0.90	1.20	1.00	1.06
17,185	0.80	0.90	0.60	1.00	0.70	0.80
17,291	1.20	1.80	1.10	1.40	1.20	1.34
17,303	1.10	1.00	0.80	1.10	1.00	1.00
17,404	1.00	0.83*	0.83*	0.90	0.60	0.83

* Instrument mean substituted for missing reading.

PERFORMANCE TESTS DURING FIELD USE

Test results obtained with one set of dosimeters that was selected for field use are given in Table 1. This group consisted of 41 dosimeters. The mean reading of the exposure was 1.00 mr. Thirty-one of the dosimeters read between 0.7 and 1.3 mr; 9 dosimeters gave readings in this range in four out of five trials; and only 1 dosimeter exceeded these readings in two of five trials. Ninety-five percent of the readings were within the prescribed range.

Table 1 provides an indication of the extent to which the response characteristics of the 41 dosimeters varied, both within a single instrument and between instruments, when the instruments were exposed to a reference source under standard conditions. An analysis of variance based on the observations in Table 1 is shown in Table 2(a). The detailed methods for calculating the mean squares can be found in standard statistical textbooks.[6]

The mean square 0.0222 represents the error variance associated with reading and timing as well as those factors inherent in the nature of the individual instruments. The variability between instruments was significantly greater than the variability within instruments.

The dosimeters were worn by individuals for a week at a time over a five-week period to measure exposure from background radiation. The results of this study have been published elsewhere.[7, 8] Following each weekly read-out, the pencil chambers were exposed to two calibration trials with the same reference source and using the same technique employed prior to the field studies. The results of these calibration trials are shown in Table 2(b) and indicate a significant variation between the means of the five weeks.

The variation may have been caused by difficulties in accurate adjustment of the read-out system over an extended time period, as well as by possible changes in average dosimeter performance. As before, the variation between dosimeters was also significant. The interaction between weeks and dosimeters was not significant. Also worth noting is the fact that the error variance 0.0407 during field use is significantly larger than the error variance 0.0222 in the laboratory selection tests shown in Table 1. This may be due, in part, to the mechanical trauma to which the dosimeters were subjected when worn over a period of five weeks and to variations in leakage of the individual dosimeters.

Following the population survey, the dosimeters were returned to the laboratory where they were again exposed to four calibration trials. Table 2(c) gives the analysis of variance for the same set of 41 dosimeters following field use. The variation between dosimeters is no longer significant. However, the error variance has increased greatly. This increase was due presumably not only to the effect of handling

Table 2. Analysis of Variance

	Source of variation	Degrees of freedom	Mean square	F
(a)	*Before field use*			
	Between dosimeters	40	0.0770	3.45 $P < 0.01$
	Within dosimeters	164	0.0222	
(b)	*During field use*			
	Weeks	4	0.189	4.65 $P < 0.01$
	Dosimeters	40	0.157	3.84 $P < 0.01$
	Interaction	160	0.0415	1.02 not significant
	Within dosimeters	205	0.0407	
(c)	*After field use*			
	Between dosimeters	40	0.2604	1.37
	Within dosimeters	164	0.1893	

during field use on the dosimeters, but also to an unexpected difficulty encountered with respect to the read-out unit. This suggests the necessity of frequent testing of the entire system under actual survey conditions.

Experience acquired in repeated tests of the dosimeters indicated that the variance in dosimeter readings was significantly influenced by the method of handling the dosimeters and the method of inserting the dosimeters into the reader, and a proper technique had to be developed to give minimum variance in the readings. Apparently, as the limit of sensitivity of this system was approached, as much art as science was required in getting the best performance possible.

During the time the dosimeters were used to measure personnel exposure, a concurrent independent study of background radiation in the area was conducted by Lowder and Condon with the use of high-pressure argon ionization chambers and a gamma spectrometer system. [8]

The dosimeters averaged 1.1 mr/week higher than the personnel exposure calculated by Lowder and Condon in all areas. The higher exposure values obtained with the dosimeters indicated a systematic error which was attributed by Lowder and Condon to be due to leakage of the dosimeters in the field which was considerably higher than the expected value used to correct the readings. The expected value based on laboratory tests had indicated a leakage correction of 0.2 mr/week, so the average total leakage for pencil chambers when worn by individuals was of the order of 1.3 mr/week.*

Because the purpose of the dosimeters was primarily to measure a difference in levels between two areas, the leakage produced only a second order error in the desired results. This may be seen by comparing the differences in the weekly exposure for two regions as derived by Lowder and Condon based on ionization chamber and dosimeter readings. The two sets of results are presented in Table 3.

* A leakage rate of approximately 1 mr/week was also observed in tests at Harvard of dosimeters used as area monitors.

Table 3. Comparison of Differences in Weekly Exposures for two Regions as Determined from Pressurized Ionization Chamber and Pencil Dosimeter Measurements

Regions compared*	Difference in mr/week	
	Ionization chambers	Pencil dosimeters (average of 100 readings per area, 2 dosimeters/individual)
8–4	0.82	0.97
8–1	0.76	0.70
8–2	0.69	0.81
8–3	0.67	0.66
8–5	0.61	0.57
8–6	0.52	0.70
7–4	0.44	0.49
8–7	0.38	0.49
7–1	0.36	0.24
7–2	0.31	0.35
6–4	0.30	0.27
7–3	0.29	0.20
7–5	0.23	0.08
6–1	0.22	0.00
5–4	0.21	0.43

* Regions 1 through 8 were classified on the basis of underlying bedrock. The equivalent uranium bedrock concentration ranged from a minimum in region 1 progressively up to a maximum in region 8.

The results in Table 3 indicate good agreement between differences in exposure in different areas as determined from pencil chamber and pressurized ionization chamber measurements for differences greater than 0.3 mr. Lowder and Condon report a high degree of correlation between the two methods with a line of slope equal to one fitting very well a plot of dosimeter measurements versus ionization chamber measurements. It is not possible to determine to what extent the differences in results for the two methods reflect true differences in exposure or errors in the methods.

DETERMINATION OF SAMPLE SIZE

In planning a survey to measure differences in the population exposure between two regions it is necessary to determine the number of persons to be included in the sample as well as the number of dosimeters to be worn by each individual. For this purpose it is advisable to conduct a pilot study in order to obtain estimates of the magnitude of the variation between dosimeters worn by the same individual (inter-dosimeter variability) and of the variation between individuals within a region (interindividual variability).

Table 4, based on data obtained during a survey in northern New England, indicates the type of information which should be collected in a pilot study, preferably but not necessarily, in the two regions. In this case 20 individuals, 5 from the urban and rural parts of each region, wore 2 dosimeters each for a week. This period of exposure is such that readings were, for the most part, between 2 mr and 4 mr. Since the top scale reading is 5 mr, it is necessary to keep the exposure under this level.

The information of particular importance from the pilot survey is the within areas sources of variation. Dosimeters, when worn by individuals, show greater variation (0.3978) than they did when exposed to a constant source. Variations between individuals, (0.9248) is significantly greater than variation between dosimeters. Consequently, if the between areas mean squares are to be tested for significance, it must be against the between individuals' mean square rather than against that for dosimeters.

The general formula for the determination of sample size is:[10]

$$n = \frac{2s^2(t_\alpha + t_\beta)^2}{\Delta^2}$$

where n is the number of observations in each of the two groups, s^2 is the estimate of variance, Δ is the difference to be established, t_α is the t-value associated with the level of significance and t_β is the t-value associated with power. t_α, t_β and Δ are chosen by the investigator. The value of s^2 is determined from the pilot survey.

Table 4. Readings on Dosimeters Worn by Individuals in Pilot Study

Region A	Urban			Rural		
Individual	1	3.5	3.4	6	4.3	4.8
	2	4.2	4.6	7	5.0	4.4
	3	4.0	4.8	8	3.7	2.1
	4	5.0	5.0	9	5.0	4.2
	5	3.4	2.7	10	5.0	4.8
Region B						
Individual	11	2.6	2.6	16	2.1	1.8
	12	2.5	2.2	17	3.3	2.2
	13	3.3	3.3	18	3.0	2.8
	14	2.8	2.8	19	2.6	2.5
	15	2.8	2.6	20	2.5	5.0

The analysis of variance on these 40 observations is shown in Table 5.

Table 5. Analysis of Variance from the Pilot Survey

Source of variation	Degrees of freedom	Mean square
Between Areas	3	6.5396
Regions	1	19.1822
Urban–Rural	1	0.0562
Interaction	1	0.3802
Within Areas	36	
Between individuals	16	0.9248
Between dosimeters within individuals	20	0.3978

From the within areas mean squares, it is possible to determine the components of variance σ_D^2 and σ_I^2 associated with dosimeters and individuals. In general, the between individuals mean square is $\sigma_D^2 + D\sigma_I^2$ where D is the number of dosimeters worn by an individual. The between dosimeters mean square is σ_D^2. In this case

$$\sigma_D^2 + 2\sigma_I^2 = 0.9248, \sigma_D^2 = 0.3978$$

This gives $\sigma_I^2 = 0.2635$.

The variance s^2 in the sample size formula is the variance between individuals, $\sigma_D^2 + D\sigma_I^2$, which becomes $0.3978 + 0.2635D$. The number of observations per group is ID where I is the number of individuals in each area.

The formula for the determination of sample size becomes

$$ID = \frac{2(t_\alpha + t_\beta)^2}{\Delta^2} (\sigma_D^2 + D\sigma_I^2)$$

Putting in the values from the pilot survey, this becomes

$$I = \frac{2(t_\alpha + t_\beta)^2}{\Delta^2} \left(\frac{0.3978}{D} + 0.2635\right)$$

As an illustration of the use of the formula, let us assume the investigator considers the establishment of differences, Δ, of 0.55 and 0.30, to be significant at the 5% level and that he wishes to be 90% sure of establishing such a difference if it exists. Under large sample theory $t_{0.05} = 1.96$ and $t_{0.10}$ (one tail) $= 1.28$.

CONCLUSIONS

Field experience with a pencil ionization chamber type of personnel monitoring system for measuring weekly exposures to background radiation produced results with considerably greater variability and additional systematic errors than were expected on the basis of laboratory studies.

Table 6. Number of Dosimeters Required to Establish Differences of 0.55 and 0.3 mr between two Areas, based on Results of Pilot Survey

	$\Delta = 0.55$ mr			$\Delta = 0.3$ mr		
Dosimeters per individual, D	1	2	3	1	2	3
Individuals required in each area, I	46	32	27	154	108	91
Observations per group in each area, ID	46	64	81	154	216	273

The main source of error in field application of the pencil chambers was excessive leakage, which probably precludes the application of the pencils for absolute measurements at their limits of sensitivity. However, the pencil chambers were effective in measuring differences in exposure because the effects of leakage were to a large extent cancelled out.

The procedures employed in the field study were able to detect differences of greater than 0.3 mr/week when 100 observations were made at each point.

The evaluation data presented in this paper for pencil dosimeters should be useful to investigators interested in using this method at the limit of its sensitivity. The statistical and experimental methods of testing these dosimeters as outlined in this paper are indicative of the type of information which should be obtained with other systems for personnel dosimetry at radiation background levels if useful evaluations and comparisons of their performance are to be made.

REFERENCES

1. J. A. S. Adams and W. M. Lowder, ed. *The Natural Radiation Environment*, University of Chicago Press, 1964.
2. P. W. Henson. A photographic dosimeter for the measurement of personal doses of environmental radiation, *Phys. Med. Biol.* **8,** No. 4, 423–438 (1963).
3. W. C. Roesch, R. C. McCall and F. L. Rising. A pulse reading method for condenser ion chambers, *Health Physics* **1,** 340–344 (1958).
4. R. C. McCall. Personal communication. Controls for Radiation, Inc., Cambridge, 1962.
5. F. L. Rising. Experience with the ionization chamber pulse reader at Hanford. Paper presented at Health Physics Society, Las Vegas, June 1961, unpublished.
6. W. J. Dixon and F. J. Massey, Jr. *Introduction to Statistical Analysis.* McGraw-Hill, 1957.
7. A. Segall. Radiogeology and population exposure to background radiation in northern New England, *Science* **140,** 1337, 1963.
8. W. M. Lowder and W. J. Condon. Measurement of the exposure of human populations to environmental radiation. *Nature* **206,** 658–662, May 15, 1965.
9. A. Segall and R. Reed. Human exposure to external background radiation, *Archives of Environmental Health* **9,** 492–499, 1964.
10. J. Worcester. The statistical method, *New England Journal of Medicine* 274, No. 1, January 6, 1966.

SOME PROBLEMS OF ORGANIZING A SUPERVISION SYSTEM FOR RADIATION PRODUCING MACHINES IN A SMALL COUNTRY (ISRAEL)

A. DONAGI

Tel-Hashomer Hospital, Israel Ministry of Health, Tel-Hashomer, Israel

Abstract—Israel has more than two thousand radiation producing machines. Some of these machines are quite ancient. They emit excessive amounts of radiation and endanger both operators and patients. Despite this, there was no law regulating the supervision and inspection of such machines until a year ago. Recently, an ordinance in this regard was passed and a centralized system of supervision was installed, based on a special laboratory, organized and equipped for this purpose.

The paper presents a variety of administrative and technical problems involved in the organization of a supervision system within a short time in a small country where previous data was scarce or non-existent. Special problems arising from the fact that Israel is an immigration country and, as a result, contains many makes and models of machines, are presented.

It is hoped that the experience gained and the techniques used may be of assistance to small countries facing similar problems.

ANALYSE ET BILAN DES RISQUES ASSOCIÉS À LA GESTION DES DÉCHETS RADIO-ACTIFS

F. DUHAMEL
Commissariat à l'Énergie Atomique, Paris

Résumé—Les dangers que présentent les déchets radio-actifs sous le rapport de la santé publique ne se situent pas aisément dans le cadre des hypothèses qui ont été faites par la Commission Internationale de Protection Radiologique pour en définir les ordres de grandeur. La considération de la toxicité radiologique ainsi définie ne permet pas, dans ce cas particulier, de donner une idée, même sommaire, du danger réel.

En reprenant l'analyse de ce problème on peut montrer qu'il existe un certain nombre de cas, tous différents, dans lesquels les dangers doivent être considérés d'une manière spéciale, amenant la toxicité biologique à ne plus jouer qu'un rôle secondaire en regard de certaines caractéristiques physiques.

La communication a pour but, d'une part, de rechercher quels sont les paramètres essentiels, facteurs de danger, sur lesquels doit principalement porter notre attention, d'autre part, d'essayer d'évaluer l'importance de ces dangers afin d'en tirer des conclusions sur les moyens propres à les réduire.

L'homme devant un danger réagit d'instinct comme s'il en était lui-même directement menacé. Une telle réaction est intimement liée à la notion même du danger car c'est elle qui inspire chez lui le sentiment de crainte qui est inséparable de cette notion. Cependant, nous cherchons à dominer le danger et pour cela nous devons apprécier dans quelle mesure la menace pèse réellement sur nous-mêmes; or, si la science a pu montrer que certains dangers étaient purement imaginaires, elle a aussi révélé l'existence ou la possibilité de dangers que nous n'imaginions pas, et il faut que nous déterminions si ces nouveaux dangers correspondent bien à des menaces qui nous sont réellement destinées.

Dans ce but, il nous faut faire de chaque danger une évaluation quantitative, bien que cette notion puisse nous sembler, à première vue, difficile à enfermer dans l'expression d'une quantité. Une telle expression doit en effet dépendre d'un très grand nombre de paramètres dont nous devons faire une exploration très détaillée afin de découvrir ceux qui, dans chaque cas particulier, commandent le phénomène principal. Nous pouvons ainsi simplifier l'étude par une première estimation qui bénéficie à la fois de l'expérience et de l'imagination.

A *priori*, les paramètres les plus importants sont ceux qui définissent le "véhicule" du danger mais il n'est pas certain qu'il faille nécessairement les étudier à fond. Par exemple, si on veut tracer une route dans une région escarpée, l'un des dangers proviendra des chutes de pierres; il faudra donc s'en protéger et ceci aura des conséquences appréciables sur le tracé de la route. On ne cherchera toutefois pas à définir le danger spécifique à chaque type de pierre selon sa grosseur, sa densité et sa hauteur de chute: et pourtant, on a tendance à opérer de cette manière dans le domaine de la contamination radio-active. Il est certes nécessaire de définir quelle part de danger recèle chaque radio-élément; sa toxicité radio-active en exprime en quelque sorte le danger spécifique et permet de le comparer aux autres radio-éléments ou même à certains toxiques chimiques; mais, par contre, cette expression quantitative ne permet pas à elle seule une évaluation réaliste du danger. N'a-t-on pas admis, parfois, faute de renseignements suffisants, les normes

de potabilité comme limites de contamination des eaux de mer et des eaux d'égout?

Il est au contraire indispensable d'analyser les divers processus par lesquels les dangers de contamination peuvent se manifester lors des différentes étapes de la gestion des déchets radio-actifs. Certes, il ne peut être question de détailler ici méthodiquement et rigoureusement cette analyse mais seulement d'en rechercher les grandes lignes.

Deux grandes catégories de contaminations doivent, a priori, être considérées séparément: d'une part les contaminations qui résultent des rejets intéressant les masses d'eau océaniques, *où la diffusion peut théoriquement s'étendre à toute la masse*, d'autre part celles qui n'intéressent aucunement ces masses d'eaux car elles sont liées à des rejets au sol ou dans le sol loin des côtes et, dans ce cas, la diffusion reste nécessairement limitée à une zone beaucoup plus restreinte. Entre ces deux catégories existent des frontières multiples, principalement les contaminations de l'atmosphère, des estuaires et des régions côtières.

La contamination des sols ou des océans ne produit pas de contamination significative de l'atmosphère. D'une part, on sait que l'eau de pluie ne contient pas plus de 10^{-4} fois la concentration de l'eau de mer en ses produits contenus, d'autre part divers travaux ont montré que la remise en suspension dans l'atmosphère de contaminants du sol ne jouait qu'un rôle très minime dans la contamination atmosphérique.[1] Par contre, *la contamination de l'atmosphère produit une contamination du sol et des océans dont l'étude est extrêmement instructive.* Quant aux contaminations des estuaires et des côtes, leur étude doit être jointe à celle de la contamination des océans avec laquelle elles sont en étroitet relation.

Dans l'atmosphère, les rejets sont nombreux mais leurs effets sont masqués par deux phénomènes principaux: la contamination radio-active naturelle et la contamination artificielle par les retombées des explosions nucléaires. Il est intéressant d'examiner les effets de ces différentes contaminations. Tandis que l'homme est soumis, du fait de la radio-activité naturelle, à une irradiation externe d'environ 100 à 200 mrem par an, il reçoit environ 40 mrem par an du fait des diverses sources artificielles de rayonnement[2] et il a reçu au maximum 50 mrem par an par le rayonnement direct des retombées radio-actives provenant des explosions nucléaires antérieures; la dose qu'il va maintenant recevoir chaque année de ce même fait sera inférieure à 10 mrem par an.[3] Au regard de cette irradiation externe, celle que peut produire un rejet dans l'atmosphère lors du fonctionnement normal d'installations nucléaires reste négligeable, à l'exception toutefois des irradiations par les panaches contaminés par l'Argon 41 qui, lorsqu'ils ne concernent qu'une zone étroite peuvent atteindre le niveau de l'irradiation naturelle.

L'aspect le plus intéressant de la contamination radio-active atmosphérique par les retombées réside dans la contamination consécutive de la surface de la terre et de la biosphère. L'étude de cette contamination permet de suivre les processus de diffusion des différents radio-éléments. Elle permet en même temps de guider l'analyse des dangers liés aux rejets de déchets radio-actifs car on y trouve les mêmes radio-éléments bien qu'ils se présentent sous des formes chimiques souvent fort différentes. On arrive à ce résultat que l'inhalation des poussières joue un rôle secondaire dans l'effet global d'une contamination générale tandis que la diffusion de certains radio-éléments, notamment Carbone 14, Strontium 90 et 89, Césium 137 et Iode 131 dans les chaînes alimentaires produit des effets significatifs.[4, 5] Il résulte d'ailleurs de ces études que *la contamination interne produite par les retombées radio-actives produit une irradiation du même ordre que l'irradiation externe produite directement par ces mêmes retombées* c'est-à-dire doit rester inférieure à 10 mrem par an. On peut s'inspirer des méthodes et des résultats de ces études pour rechercher les conséquences éventuelles des rejets de déchets dans les sols et les océans.

Les rejets de liquides dans les masses océaniques donnent lieu à une diffusion mécanique dont il faut étudier les lois dans chaque cas particulier; elle aboutit fréquemment à diluer la concentration des rejets par un facteur 10^8 à 10^{10} sans requérir des délais considérables.

Les phénomènes importants sont ensuite l'absorption et l'élution sur les différents constituants hétérogènes du milieu: suspensions, sédiments, alluvions et enfin chaînes alimentaires aboutissant à l'homme. Parmi tous les circuits

possibles qui, théoriquement, aboutissent à l'homme, beaucoup peuvent être laissés de côté grâce à une analyse soignée des processus. En outre, si tous les radio-éléments doivent être suspectés a priori, seul, un petit nombre apporte une contribution non négligeable à l'irradiation totale de l'homme. Enfin, il faut évaluer, pour chaque manière dont l'irradiation de l'homme est possible, le taux approximatif de cette irradiation.

Par exemple, dans une zone de pêche artisanale, on trouvera que l'irradiation directe externe venant de la mer est négligeable par rapport à l'irradiation provenant de la manutention des engins de pêche. Près d'une plage, on trouvera que l'irradiation des baigneurs dans l'eau de mer est faible par rapport à l'irradiation qu'apporte un séjour prolongé sur la plage. Après avoir étudié l'alimentation des populations voisines, on comparera comme précédemment l'irradiation par contamination interne à l'irradiation externe. (Il faut noter que les produits de la mer peuvent être consommés directement mais peuvent aussi servir à la fertilisation des sols, à l'alimentation du bétail ou encore peuvent être incorporés dans des produits d'origine agricole.) On a à tenir compte de facteurs de reconcentration pouvant atteindre 10^4 ou même 10^5 mais comme, en même temps, les produits se dispersent parmi d'autres, l'effet final reste très petit.

On peut ainsi calculer que, pour une masse d'eau océanique, brassée mais non rapidement déplacée, présentant des conditions moyennes de turbidité, et pour un rejet continu de 30 Ci/jour de produits de fission au voisinage des côtes, donnant en quelques jours une zone contaminée de plusieurs centaines de km^2, on obtient une irradiation individuelle totale inférieure à 1 mrem/an.

En respectant certaines limites, d'ailleurs bien larges, eu égard aux besoins, on peut donc utiliser aux rejets d'effluents les masses d'eaux océaniques tout en évitant d'irradier l'homme à un niveau qui ne serait pas négligeable par rapport au niveau de l'irradiation naturelle.

Le cas des estuaires a fait l'objet de nombreuses études et on peut conclure que les conditions d'absorption et d'élution successives des radio-éléments entre l'eau douce et l'eau de mer ne sont pas défavorables aux rejets.[6] Les facteurs de reconcentration trouvés ne dépassent pas 10^2 et le phénomène n'est pas entièrement reversible.[7] *L'influence de la contamination des fleuves sur celle de la mer est, en définitive, négligeable.*

Une grande partie des études physico-chimiques effectuées en laboratoire ou dans les océans peut servir indifféremment à l'évaluation de la contamination des sols ou des océans; cependant, les caractéristiques hydrogéologiques des sites restent les paramètres fondamentaux permettant d'évaluer le devenir des radio-éléments et les risques de contamination lors des rejets au sol ou dans le sol. On a acquis dans ce domaine une grande expérience pratique du fait de l'exploitation, dans certains sites privilégiés, de méthodes empiriques de stockage et de rejet dans le sol.[8] Beaucoup d'études ont été faites pour extrapoler les résultats des expériences pratiques et évaluer les capacités de stockage des sites terrestres.[9] Ceci a permis d'appliquer à des sites particuliers ne présentant pas a priori les caractéristiques les meilleures sous ce rapport, des méthodes plus perfectionnées qui se sont révélées à la fois économiques et sûres.[10]

De cette somme considérable de résultats on peut déduire que les méthodes de stockage et de rejet dans le sol sont excellentes à la double condition, d'une part qu'il soit procédé à une étude suffisamment précise du sol, aux résultats de laquelle la méthode choisie doit être adaptée, d'autre part, que le contrôle consécutif aux rejets soit organisé: la vitesse d'élution des radio-éléments est très variable selon certains paramètres physico-chimiques et doit être mesurée, les points de résurgence, où la consommation est possible, doivent être connus et surveillés, le front de contamination doit être suivi. Si les points de résurgence sont situés à plusieurs centaines de mètres du point de stockage et que le terrain n'est pas fissuré, le stockage est sûr dans une limite de capacité qui peut être évaluée en fonction de la nature et du conditionnement des déchets. *Des dizaines de milliers de curies peuvent ainsi être stockés sans qu'aucune irradiation appréciable ne puisse atteindre un élément quelconque de la population avoisinante.* Les radio-éléments les plus importants à surveiller sont le Tritium, le Strontium, le Ruthénium et le Cobalt.

On peut s'intéresser à titre d'exemple à l'irradiation qui résulterait du rejet dans un étang

ou dans une rivière comme cas particuliers dans lesquels le rejet au sol se présente dans les conditions a priori les moins favorables. Un rejet d'environ 10 Ci par an de Ruthénium 106 dans un étang peu drainé, situé dans une région tempérée, produirait sur les berges une irradiation de l'ordre du millirem/heure; une telle méthode est donc peu favorable. Par contre, dans une rivière bien brassée on peut rejeter par an autant de curies de produits de fission qu'il ne s'écoule de m^3 par seconde, sans que l'irradiation totale consécutive à l'alimentation directe par la rivière ne dépasse 10 mrem/an, et en pratique, dans le cas le moins favorable, l'irradiation réelle serait très probablement 10 à 100 fois plus faible encore. On a cherché à utiliser des régions réellement désertiques mais, si les rejets peuvent y être faits en toute sécurité, malheureusement les conditions économiques sont très défavorables.

On peut dire, en résumé, que, dans l'ensemble, moyennant certaines précautions, il est possible de rejeter et de stocker au sol et dans le sol, des quantités considérables de radio-éléments sans rechercher un éloignement exagéré des populations.

D'une manière générale les migrations des radio-éléments à l'intérieur et à l'extérieur des sites de stockage ou de rejet sont la cause principale des dangers de contamination, mais les conditions de ces migrations peuvent être méthodiquement étudiées. [12]

Les résultats des nombreuses études ainsi entreprises dans le monde montrent que les irradiations moyennes concernant les populations voisines des sites de rejet ou de stockage sont réellement négligeables. Avant de conclure, à l'inocuité de rejets, il faut cependant examiner l'éventualité d'une contamination isolée par de grosses particules. On fait en effet souvent l'hypothèse implicite que la contamination est répartie de manière uniforme et on évalue des irradiations moyennes. Il est nécessaire d'examiner quelle serait la conséquence d'une répartition très hétérogène et discontinue qui se traduirait par l'existence de "points chauds", c'est-à-dire d'amas de substances radio-actives. Dans ce cas, l'évènement à redouter serait l'absorption en une seule fois, par un individu unique, d'une substance dangereuse. On sait que le calcul du danger biologique peut être ramener à celui du danger résultant d'une contamination continue. [13] C'est ainsi qu'on peut admettre qu'un individu absorbe en une fois la quantité de radio-activité qu'il pourrait normalement absorber en un an. Pour que cela soit effectivement réalisé, il faut supposer qu'une telle activité a échappé au contrôle: la probabilité d'un tel évènement dépend donc de la manière dont le contrôle est organisé. En l'absence d'un contrôle continu et représentatif, le danger est réel car, si les prélèvements sont de 1 litre, il faut qu'un litre d'eau ayant échappé au contrôle contienne environ 1.000 fois plus d'activité que la moyenne pour que la dose annuelle soit dépassée, tandis que si les grains de substance radio-active passent de 0, 1 micron à 0,1 millimètre, la radio-activité en est multipliée par 10^9. *Lors d'un rejet dans une masse d'eau, des conditions doivent donc être imposées à la turbidité des eaux au point de rejet, avant et après leur mélange, afin d'éviter des anomalies de granulométrie.*

Pour la même raison, le rejet de déchets solides dans les eaux n'est admissible que pour des blocs monolithiques qui ne peuvent être ni désagrégés ni entamés et qui ne risquent pas de foisonner par corrosion. Par contre, dans un sol non fissuré, le transport de radio-éléments ne peut se faire que par élutions successives, donc avec homogénéité et continuité. C'est là un avantage considérable propre au stockage dans le sol.

Pour conclure, il nous faut confronter les résultats actuels des études sur la sûreté des rejets et des stockages avec les taux de production futurs des déchets radio-actifs. Selon les estimations les plus valables on peut penser que, du fait des applications pacifiques de l'énergie atomique, la quantité totale de produits de fission dans le monde est maintenant de l'ordre de 10^{10} Ci et qu'elle sera d'environ 10^{12} Ci en l'an 2.000. Dans cette dernière quantité il faut comprendre environ 10^{10} Ci de Strontium 90. [14] Cette radio-activité restera stockée au sol car, seule, une petite partie sera diffusée par rejet ou élution. Actuellement, seule une fraction de l'ordre de 10^{-5}, soit 10^5 Ci environ, en est rejetée annuellement en sorte qu'elle s'échappe des sites de production. La situation deviendrait préoccupante si l'augmentation de la production correspondait, non pas à une multiplication des points de rejets mais seulement à un développe-

ment des sites anciens. On pourrait alors être gêné par la saturation de leurs capacités de rejet. Dans ce cas, il est clair que les méthodes de rétention devraient être perfectionnées; mais ceci est possible car on peut observer que la part du coût des traitements dans le prix de revient de l'énergie est actuellement inférieure à 1%:[14] des améliorations sont certainement possibles. On dispose donc de deux facteurs de sécurité: la multiplication des points de rejet et l'amélioration des traitements, et ceci, à partir d'une situation qui n'est nullement inquiétante.

En résumé, actuellement, le rejet des déchets radio-actifs demande, dans chaque cas particulier, des précautions sérieuses, notamment l'évaluation scientifique des capacités de réception des sites et l'organisation de contrôles techniques bien adaptés au but poursuivi.[15] Cependant on peut tenir pour acquis que, si ces précautions sont prises, aucun individu parmi les populations avoisinantes ne peut recevoir plus de quelques pour cent de la dose d'irradiation naturelle. Enfin on est en droit de penser que, dans l'avenir, il suffira d'assurer aux études de traitement ainsi qu'aux études et contrôles de site un développement parallèle à celui de l'énergie atomique pour être certain de ne pas dépasser le très faible taux d'irradiation obtenu jusqu'à présent.

RÉFÉRENCES

1. K. Stewart. The resuspension of particulate material from surfaces. International Symposium on Surface, ORNL, 1964.
2. W. Seelentag. L'irradiation des hommes de notre temps par les sources naturelles et artificielles de rayonnement, niveaux, signification et conséquences. *Gesellschaft für Kernforschung, Bundesgesundheitsamt,* Institut für Strahlenschutzkunde, K 20, Berlin 1963.
3. Y. Nishiwaki *et al.* Global contamination due to radioactive fallout. Article à paraître dans *Progress in Nuclear Energy*, Série XII, Volume 2, Pergamon Press, Oxford.
4. United Nations Scientific Committee on the effects of atomic radiation, General Assembly, XIXth Session, New York, 1964.
5. C. L. Comar. Movement of fallout radionuclides through the biosphere and man. *Ann. Rev. Nucl. Sci.* **15,** 175–206 (1965).
6. T. D. Reynolds et E. F. Gloyna. Radioactivity transport in water. Technical Report to the AEC-1963-TID 19559, Washington, D.C.
7. Proceedings of a Symposium held in Savannah. Studies of the fate of certain radionuclides in estuary and other environments. Public Health Service Publication n° 999 R 3, Washington D.C., May 1963.
8. C. A. Mawson. *Management of Radioactive Wastes.* Van Nostrand Co. Inc., Toronto, 1965.
9. Colloque International sur la rétention et la migration des ions radio-actifs dans les sols. Presses Universitaires de France, Paris, 1962.
10. L. Baetslé *et al.* Migration de radio-éléments dans le sol. Rapport Euratom, Bruxelles, 1966.
11. Proceedings of the Hanford Symposium on radiation and terrestrial ecosystems, Richland, Wash. 3–5 May 1965. *Health Physics,* Vol. II, No. 12, Pergamon Press, December 1965.
12. N. V. Timofeyev-Resovskiy. Contamination radio-active de la biosphère et mesures permettant de lutter contre cette contamination. Akad. Nauk. URSS. Uralskiy filial, *Trudy Instituta Biologii* No. 22, 1962.
13. F. Duhamel et J. M. Lavie. Comment établir des règles pratiques pour éviter la contamination. Symposium de Risø, mai 1959, OECE-Paris.
14. W. G. Belter. U.S. Operational experience in radioactive waste management (1958–1963) et Advances in radioactive waste management technology—Its effect on the future US nuclear power industry Conf. 28 P 868 et 869. Conférenec de Genève 1964.
15. F. Duhamel. Le problème de rejet et stockage de produits radio-actifs et ses répercussions sur le choix des sites nucléaires. Symposium de Bombay, 1963, pp. 149–165. IAEA, Vienna.

ÉVALUATION EXPÉRIMENTALE DES POSSIBILITÉS DE DIFFUSION DES EFFLUENTS GAZEUX D'UNE CENTRALE NUCLÉAIRE

J. J. MARTIN, R. ROCHE et J. KIEFFER
Electricité de France 73 Bd Haussmann, 75 Paris 8e

Résumé—Cette conférence analyse les résultats des mesures de diffusion effectuées sur le site de la centrale des Ardennes de mai à octobre 1964. On a évalué, avec une approximation jugée suffisante pour les besoins de la radioprotection, la répartition de la contamination volumique et surfacique consécutive à des rejets expérimentaux.

Les résultats des mesures météorologiques menées sur le site de 1960 à 1965 sont brièvement présentés.

L'étude expérimentale permet le calcul des valeurs de consigne applicables aux rejets d'effluents radio-actifs à l'atmosphère, en vue de respecter les normes de protection sanitaire.

1. INTRODUCTION

Une centrale nucléaire est susceptible de rejeter des effluents gazeux radio-actifs dans l'atmosphère. Les rejets peuvent être normaux ou accidentels; ils provoquent une contamination de l'atmosphère à un niveau variable avec le débit de rejet de l'installation.

1.1. *Rejets normaux*

Dans le cas de rejets normaux, la contamination de l'air inhalé doit être inférieure en moyenne à la contamination maximale admissible pour la population.

Dans la période expérimentale actuelle, il nous est demandé que la contamination ne dépasse pas, en valeur instantanée, dix fois la contamination maximale admissible.

Pour satisfaire à ces critères, l'exploitant de l'installation nucléaire doit choisir le débit de rejet approprié, lequel est fonction des conditions météorologiques de diffusion des effluents. Dans le but de simplifier l'exploitation, il nous a paru préférable de fixer un débit admissible pour les rejets permanents en choisissant des conditions météorologiques moyennes, tout en permettant des rejets temporaires lors des conditions plus favorables que les conditions moyennes.

1.2. *Rejets accidentels*

Dans le cas des rejets accidentels, il est souhaitable d'évaluer a priori:

—d'une part, les niveaux de contamination possibles dans le cas de l'accident maximal hypothétique;

—d'autre part, les niveaux d'alarme à partir desquels il conviendra de déclencher des dispositifs de sauvegarde.

Dans le premier cas, il s'agit, dès la mise en exploitation de l'installation, de donner des informations aux organismes officiels en vue de la préparation de dispositifs de sauvegarde adaptés au risque c'est à dire qui ne soient pas exagérément sous-évalués, ou surévalués. Les niveaux de contamination possible seront donc calculés avec des hypothèses de conditions météorologiques défavorables, ayant un risque faible, connu et accepté, d'être dépassées.

Dans le deuxième cas, il s'agit, au moment de l'accident, de choisir le dispositif de sauvegarde approprié en fonction du débit ou de la quantité d'effluents rejetés; il n'est pas nécessaire en effet de mettre en œuvre l'ensemble du dispositif si cela ne se justifie pas. Bien que l'on puisse disposer, dans ces circonstances, de la connaissance des conditions météorologiques réelles, il semble préférable d'adopter les mêmes

hypothèses que dans le cas précédent. Il ne paraît pas souhaitable de compliquer la tâche des responsables en cas d'accident; par contre, il est très certainement plus judicieux de corriger les dispositions prises "a priori" en fonction des mesures de contamination effectivement réalisées sur le terrain.

1.3. *Évaluation des débits-seuils*

Pour évaluer les débits-seuils d'activité des effluents gazeux, il nous faut déterminer le rapport existant entre la contamination atmosphérique observée au sol et le débit d'activité, ce rapport pouvant être défini comme le coefficient de diffusion atmosphérique.

Le coefficient de diffusion atmosphérique a été représenté par des formules dont les paramètres ont été ajustés par différents expérimentateurs opérant sur des terrains plans. Il nous paraît utile actuellement de mesurer ce coefficient "in situ", pour tenir compte de l'influence des bâtiments avoisinant le point d'émission et du relief irrégulier de certains sites.

Nous essayons de déterminer le coefficient de diffusion en fonction des conditions météorologiques: vitesse et direction du vent, état de stabilité thermique ou dynamique de l'atmosphère. Parallèlement, nous déterminons la probabilité des différents types de conditions météorologiques.

Cette conférence analyse les enseignements tirés de campagnes de mesures menées sur le site de la centrale des Ardennes, que nous avons choisi pour nos premières expérimentations en raison de son relief accusé.

L'étude météorologique a été conduite de 1960 à 1965 et traitée par un programme de calcul mis au point à notre demande par la Direction des études et recherches d'Électricité de France.

L'étude de la diffusion atmosphérique a fait l'objet de dix semaines d'expérimentation sur le site; pendant cette période, 40 émissions ont été effectuées depuis un point aussi voisin que possible du point d'émission prévu pour les effluents; on a réuni ainsi environ 2500 observations de contamination atmosphérique et 5000 observations de contamination du sol.

Ces résultats ont été obtenus avec la participation d'organismes français et belges, que nous tenons à remercier pour leur collaboration.

2. DESCRIPTION DU SITE

La centrale des Ardennes se situe dans la pointe dessinée par la frontière franco-belge autour de la petite ville de Givet (fig. 1). La centrale est située dans la partie méridionale d'une boucle de la Meuse, sur la commune de Chooz. Le relief à l'intérieur de la boucle ne dépasse guère 150 m NGF*, la cote de la Meuse s'établissant vers 100 à 105m. L'extérieur de la boucle est constitué par un plateau boisé dont la cote moyenne est de l'ordre de 300m. Ce plateau est creusé par l'étroite vallée de la Houille, affluent de la Meuse. Au nord-ouest de la vallée de la Meuse, le relief s'établit à la cote 220m environ.

La partie nucléaire de la centrale est souterraine. Le rejet des effluents gazeux est fait à partir d'une cheminée dont la base est à la cote 300 environ. Sa hauteur n'était pas définie à l'époque des mesures. Celles-ci ont été réalisées en supposant la source d'effluent à une hauteur de 50 ou 25 m, avec l'intention de préciser la hauteur optimale d'émission en fonction des résultats d'expérience.

La pente du terrain au nord de la cheminée, entre cheminée et Meuse, est voisine de 100%.

On conçoit que, dans ces conditions de relief, l'on ait craint d'appliquer un formulaire standard. En particulier, on pouvait se demander si la hauteur d'émission devait être considérée comme identique lors des rejets vers le sud (sol à la cote 300) ou vers le nord (sol à la cote 150).

3. MATÉRIELS ET MÉTHODES

3.1. *Mesures météorologiques*

Les mesures météorologiques ont été mises en service sur le site fin 1959 pour les premières (précipitations, humidité, température), courant 1963 pour les dernières (mesure de vent des stations provisoires et mesure de température sur la pente). Leur emplacement est repéré sur la figure 1.

Le tableau 1 donne la liste de ces mesures avec leurs caractéristiques.

Les emplacements de mesure ont été choisis:

—pour les mesures de vent, de façon à avoir une idée de la trajectoire moyenne des effluents

* NGF: nivellement général de la France.

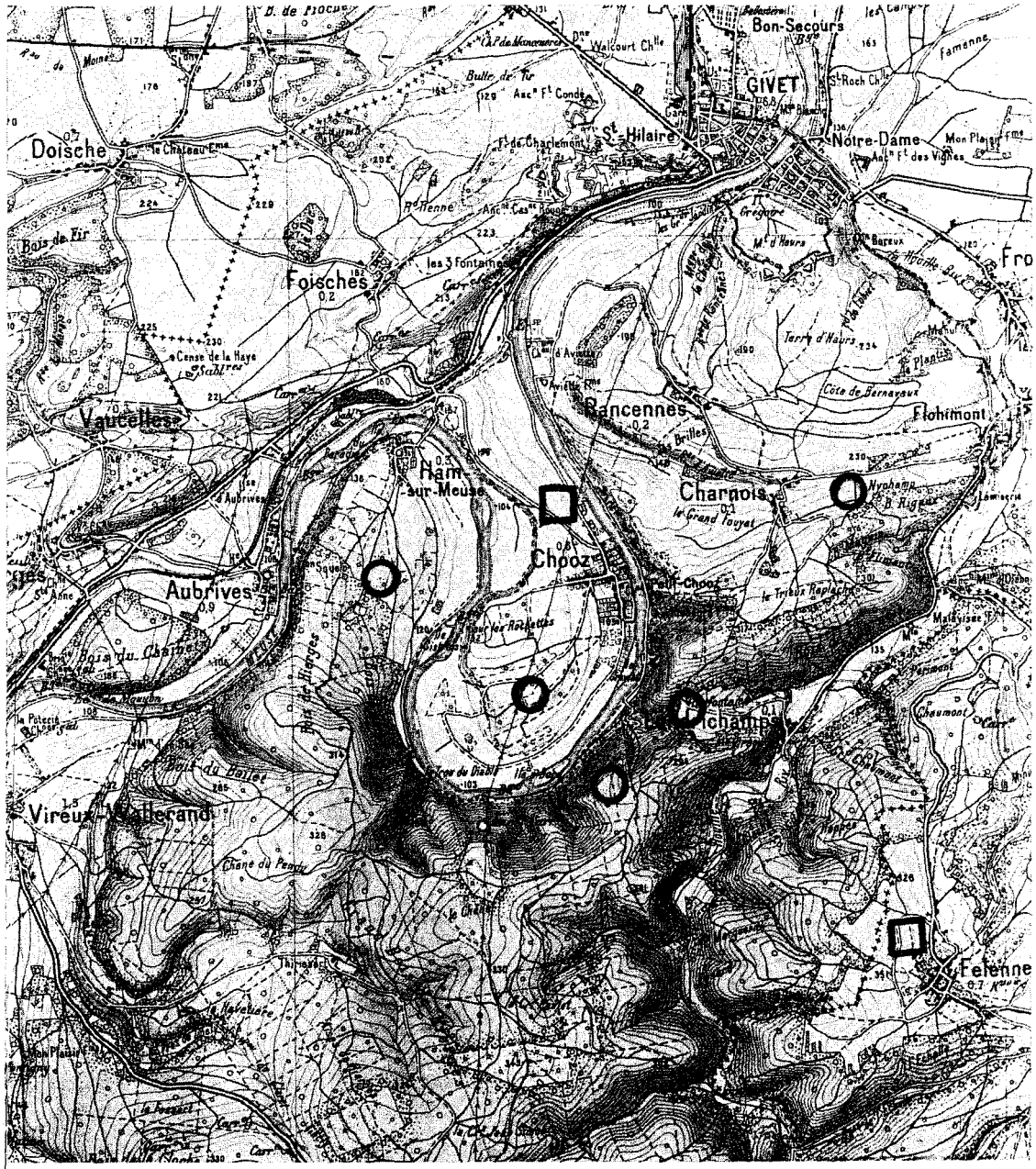

FIG. 1. Carte du site des Ardennes. Les cercles indiquent les emplacements des mesures météorologiques, les carrés ceux des stations de contrôle radiologique où sont effectuées des mesures météorologiques.

Tableau 1. *Mesures météorologiques*

Grandeur	Lieu-dit	Caractéristique du lieu
Vitesse et direction du vent	Cote 350	Pylône de 50 m proche de la cheminée
,,	Cote 325	À mi-hauteur du pylône de 50 m
,,	Cote 135	À l'intérieur de la boucle
,,	Chooz	Station de radio-protection en bord de Meuse
,,	Felenne	Station de radio-protection sur une hauteur
,,	Charnois	Station provisoire à un col entre Meuse et Houilles
,,	Ham	Station provisoire à l'ouest de la boucle
,,	Landrichamps	Station provisoire à un col entre Meuse et Houilles
Température, Humidité, Précipitation	Chooz, Felenne	Mesures débutées sur le site de 1959 à 1962
Température	Cote 300	Mesures par thermographes répartis entre la base du pylône et la Meuse
	Cote 235	
	Cote 170	
	Cote 105	

et de la stabilité dynamique de l'atmosphère;

—pour les mesures de température, le long de la pente, dans l'espoir de pouvoir caractériser l'état de stabilité thermique de l'atmosphère.*

Le programme de calcul élaboré pour le traitement de ces mesures permet, outre le traitement individuel de chaque mesure, de rechercher des liaisons entre différentes grandeurs:

—recherche de la direction du vent en un point d'observation quelconque en fonction de la direction simultanée en un point repère qui a été choisi à la cote 350, ce choix devant intervenir dès le début du traitement; ceci permet de définir des trajectoires moyennes;

—calcul des gradients de température à partir des températures échelonnées en latitude;

—calcul du coefficient de stabilité à partir de la vitesse du vent mesurée à des hauteurs différentes;†

—comparaison du gradient de température et du coefficient de stabilité;

—recherche de la direction et de la vitesse du vent la plus probable en fonction du gradient de température;

—calcul de la probabilité de conserver en fonction du temps, la direction du vent ou le gradient de température dans un intervalle de valeurs donné.

À l'occasion des mesures de diffusion, des mesures météorologiques complémentaires ont été effectuées:

—mesure du gradient de température par

* Pour évaluer cet état de stabilité d'une façon plus satisfaisante, il eut fallu disposer d'un pylône de 300 m implanté dans la vallée.

† Le coefficient de stabilité n est déduit de la formule

$$\frac{V}{V^1} = \left(\frac{h}{h^1}\right)^{\frac{n}{2-n}}$$

où V et V^1 sont les vitesses de vent mesurées au même instant aux hauteurs h et h^1.

thermocouples sur le pylône principal entre les cotes 302 et 350;

—sondage par ballon captif emportant une sonde photographique et donnant la température en fonction de l'altitude jusqu'à 500 m environ;

Ces mesures ont été complétées par des sondages de vents en altitude établis avec des ballons libres emportant une radiosonde; ces mesures ont permis de disposer de données sur la température et le vent en altitude jusqu'à des hauteurs importantes.

3.2. *Mesures de diffusion atmosphérique*—

La méthode a déjà été décrite par R. le Quinio et J. Hugon.[1] On utilise un traceur, constitué par un aérosol de fluoresceine, qui est émis d'un emplacement représentant la cheminée et que l'on recueille sous le vent de l'émission par aspiration sur filtre ou par dépôt sur des surfaces. La mesure est ensuite faite par fluorescence.

3.2. 1. *L'émission* (fig. 2) a été réalisée à partir du pylône proche de l'emplacement prévu pour la cheminée, successivement aux cotes 350 et 325. La durée de chaque émission est de 70 à 90 mn.

La solution de fluorescéine à 100 g/l est montée par mise en pression dans une cuve, jusqu'au

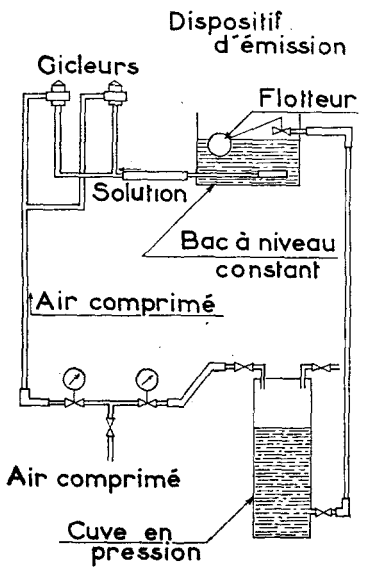

FIG. 2. Dispositif d'émission.

niveau d'émission. Une rampe de gicleurs est alimentée en air comprimé; par effet de trompe, les gicleurs assurent la pulvérisation de la solution.

La granulométrie des aérosols obtenus est satisfaisante. Des agglomérats de cristaux de diamètre supérieur à 10 μ ne sont observés qu'au voisinage immédiat de l'émission. Nous avons considéré que cet aérosol est représentatif des aérosols ou des produits volatils qui peuvent être émis par une installation nucléaire.

3.2. 2. *Les prélèvements* portent sur les aérosols en suspension dans l'air et sur les aérosols déposés.

Les aérosols en suspension sont captés sur des filtres en fibres synthétiques. Une trompe à air utilisant une bouteille, de volume 6 litres, d'air comprimé à 200 bars, permet de filtrer 6,5 m³ d'air ambiant en 45 mn à travers un filtre de 120 mm de diamètre. Après correction en fonction de la pression réelle de la bouteille, qui est lue au début de l'aspiration, l'erreur sur le volume d'air aspiré est inférieure à 10%.

Les aérosols déposés sont recueillis sur des boîtes de Petri de 80 mm de diamètre et en matière plastique pour les distances proches, de 165 mm de diamètre et en verre pyrex pour les grandes distances. Ces boîtes de Petri sont disposées sur un socle à une dizaine de centimètres du sol. Il est souhaitable qu'elles soient déposées sur un terrain aussi homogène que possible, une étendue d'herbe par exemple, pour que les résultats soient reproductibles.

Les dispositifs de prélèvement sont placés sur le terrain par des équipes constituées chacune par deux agents disposant d'un véhicule; chaque équipe a la charge de 10 prélèvements atmosphériques et de 20 prélèvements de surface. Il a été formé jusqu'à 8 équipes lors des opérations dans les Ardennes.

À chaque équipe est affecté un itinéraire choisi en fonction de la direction prévue du vent pendant l'émission. L'heure de début d'aspiration est fixée en fonction de l'heure d'émission et de la vitesse de propagation prévue pour le panache. On essaie de centrer la période d'aspiration par rapport à la période de passage du panache. Des corrections sont ensuite apportées éventuellement en fonction de la vitesse de propagation effectivement observée pendant l'émission.

Une attention particulière doit être portée à la protection du matériel contre une contamination en fluorescéine. On utilise des enveloppes ou des sachets ou des boîtes de protection. Une contamination de 10^{-8} g de fluoresceine sur un support, filtre ou boîte de Petri, conduit en effet à une mesure significative.

3.2. 3. *La mesure* est faite par lavage du filtre ou de la boîte de Petri avec une quantité connue d'eau permutée. Cette eau est ensuite analysée avec un fluorophotomètre. Les réglages de cet appareil permettent d'avoir une lecture directe en contamination volumique de la solution entre 10^{-6} et 10^{-3} g/l. Pour des contaminations supérieures, qui ne sont obtenues que pour les points de prélèvement proches, il y a lieu de diluer la solution pour effectuer la mesure.

Le tarage de l'appareil est effectué périodiquement à partir d'une solution étalon préparée au laboratoire. Les corrections sont pratiquement nulles si l'on a soin de laisser l'appareil chauffer pendant une heure avant d'effectuer tout tarage.

L'appareil peut effectuer une mesure sur une solution à 2.10^{-7} g/l, ce qui correspond au "bruit de fond" de l'eau distillée ou bi-permutée. Dans le cas d'un filtre, lorsque celui-ci est lavé avec 20 cm³ d'eau permutée (volume utilisé habituellement), la mesure sur un filtre vierge peut atteindre 10^{-6} g/l avec le filtre utilisé, 10^{-5} avec des filtres plus courants.

Il importe de s'assurer que le rendement de lavage des filtres ou des boites de Pétri est constant. Il est fait périodiquement des évaluations de ce rendement en opérant deux lavages successifs sur un même prélèvement. Le rendement moyen de lavage se tient autour de 85% pour les filtres, de 95% pour les boîtes de Petri.

3.2. 4. Pour évaluer la précision, nous avons comparé les mesures sur des filtres obtenus par deux équipes différentes, en des points proches, lors d'une même émission. Certains de ces prélèvements étaient même analysés par des postes de mesure différents.

Pour les couples de mesure retenus,* la différence relative (rapport de la différence des mesures à leur valeur moyenne) a toujours été inférieure à 25%.

Cette précision parait très suffisante; elle englobe toutes les erreurs de prélèvement et de mesure.

4. RÉSULTATS DES MESURES DE DIFFUSION ATMOSPHÉRIQUE

Les résultats bruts des mesures sur les filtres et les boîtes de Petri ont été traités de façon à obtenir des lois de variation de la contamination atmosphérique ou surfacique en fonction de la distance et des conditions météorologiques. [2]

4.1. *Première representation des résultats*

Les contaminations atmosphérique et surfacique ont été rapportées respectivement au débit de fluorescéine à l'émission et à la quantité globale rejetée. On obtient ainsi des valeurs comparables d'une émission à l'autre.

Ces valeurs sont reportées sur une carte à l'emplacement de mesure et servent à tracer des courbes d'isocontamination. On obtient ainsi la trace au sol du panache. On observe des panaches multilobés (fig. 3) ou monolobés (fig. 4). L'un et l'autre cas peuvent se rencontrer par vent fort, mais selon la direction principale du vent, le relief peut provoquer un renforcement du panache (cas de la fig. 4 où le panache suit la vallée de la Meuse) ou induire un panache

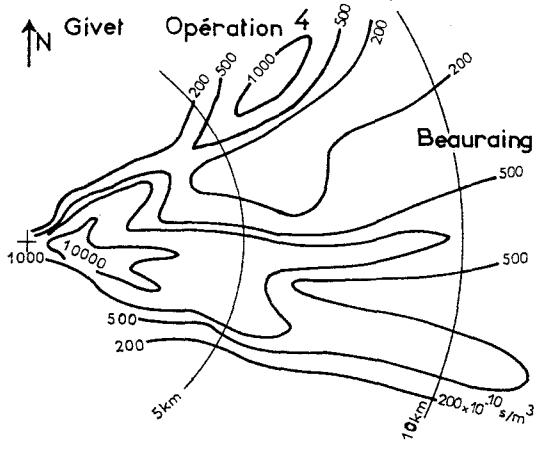

FIG. 3. Contamination atmosphérique observée pendant la 4ème opération.

* Les mesures ont été retenues à condition de dépasser le double du bruit de fond et de correspondre à des points de prélèvement de deux équipes différentes, opérant à moins de 500 m. de distance, mais à l'écart de l'axe de panache.

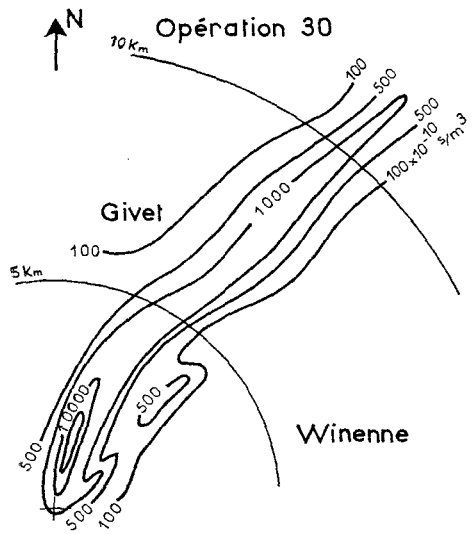

FIG. 4. Contamination atmosphérique observée pendant la 30ème opération.

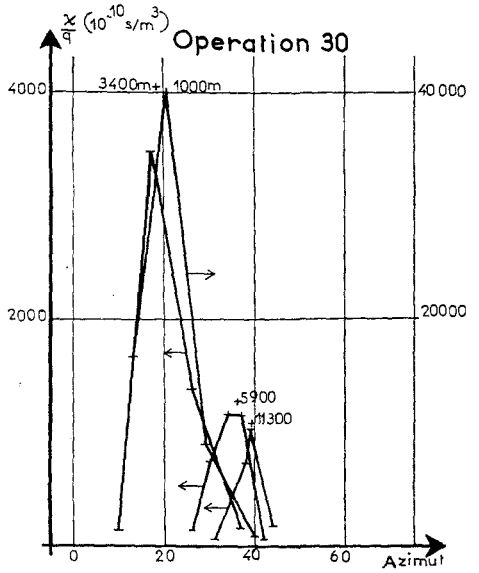

FIG. 5. Coupes transversales du panache durant l'opération 30.

secondaire (cas de la fig. 3 où le panache septentrional s'est formé dans la vallée de la Houille alors que le vent était d'ouest nord-ouest.)

Dans le cas des vents faibles sans direction préférentielle, il est apparu difficile, sinon impossible, de déterminer des panaches; tous les secteurs sont alors soumis au panache pendant un temps plus ou moins long et l'on obtient une contamination homogène sans maximum marqué.

On conçoit dès à présent que, pour une même quantité émise, la contamination maximale observée est d'autant plus faible que le nombre de panaches obtenus est grand. Ce nombre est fonction de la fluctuation en direction du vent et d'un facteur non météorologique, le relief, qui varie suivant chaque direction.

4.2. *Détermination des contaminations maximales*

À partir des courbes d'isocontamination, on détermine les coupes intéressantes des panaches sur lesquelles on trouve les valeurs maximales (fig. 5).

Les points d'observation ne sont qu'exceptionnellement placés sur l'axe de panache. Les valeurs maximales observées ne sont donc pas les valeurs maximales réelles.

Il est possible d'effectuer une correction sur les valeurs maximales observées. Pour ce faire, à chaque coupe valable a été superposée une courbe de Gauss; ceci a permis de déterminer une valeur maximale extrapolée et l'écart-type de la courbe de Gauss appropriée (ce qui revient à définir une "largeur" du panache; la contamination est réduite à 1% de la contamination maximale à une distance de l'axe égale à trois fois l'écart-type).

Par cette méthode, on a réduit considérablement la dispersion des valeurs maximales. Celles-ci ont été multipliées par la vitesse du vent observé pendant l émission pour obtenir des valeurs maximales comparables entre elles (fig. 6).

On a entouré les points d'observation par deux droites parallèles enfermant entre elles 95% des points. Le rapport entre les valeurs maximale et minimale pour une abscisse déterminée définit la largeur de la bande. Alors que cette largeur est égale à 70 pour les valeurs observées, elle n'est que de 20 pour les valeurs extrapolées.

Les valeurs observées étant des valeurs maximales connues par défaut, il faut choisir comme loi de variation une enveloppe maximale difficile à préciser. Par contre, dans le cas des valeurs

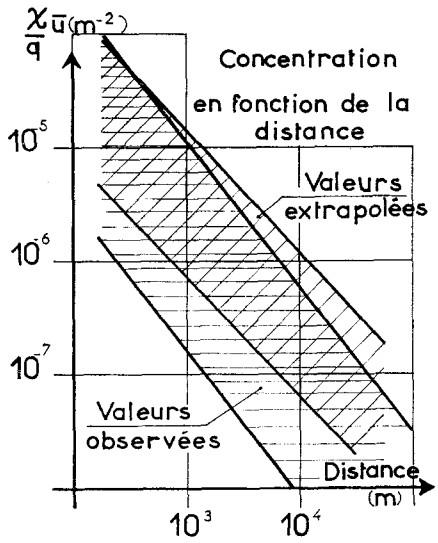

FIG. 6. Concentration en fonction de la distance: valeurs observées et extrapolées.

extrapolées qui sont des valeurs maximales connues par excès ou par défaut, il est possible de choisir une moyenne.

Parmi les valeurs extrapolées, il est donc possible de tracer une droite moyenne* sachant que 95% des valeurs réelles seront dans une bande de largeur connue.

4.3. *Étude de l'influence des paramètres météorologiques ou autres*

La représentation précédente a utilisé toutes les observations quelles que soient les caractéristiques du point d'observation ou des conditions météorologiques.

Il est apparu que différents facteurs pouvaient provoquer une dispersion des observations. Notons que l'on a supposé avoir tenu compte du facteur vitesse du vent en multipliant les contaminations relatives par ce facteur.

Pour souligner l'influence de ces facteurs les valeurs extrapolées ont progressivement été réparties en différentes classes:

a—deux classes suivant la hauteur d'émission H (cotes 350 et 325).

b—pour chacune de ces classes H, trois classes suivant la stabilité S caractérisées par le gradient vertical de température observé soit sur le pylône et la pente, soit, également, par le moyen des sondages d'altitude; ces classes ont été cotées I (gradient vertical inférieur à—1°C/100 m), II (gradient entre—1 et 0° C/100 m) et III (gradient vertical positif);

c—pour chacune des classes (H, S) trois classes suivant la "cote relative" h; il est apparu en effet que selon la position du point d'observation, la différence de cote, appelée ici cote relative, entre le point d'émission et le point d'observation pouvait varier de—50 à + 250 m; cette cote relative peut être assimilée à une hauteur d'émission; ces différentes classes h avaient les limites suivantes: h_1 pour $h \leqslant 50$, h_2 pour $50 < h \leqslant 150$, h_3 pour $150 < h \leqslant 250$.

Il est apparu dès le début que la contamination n'était pas liée de façon significative à la cote relative: tout se passe comme si la turbulence atmosphérique due au relief annihilait le relief en replaçant tous les points d'observation à un même niveau.

À partir des groupes d'observations, réparties dans les classes (H, S), on a tracé les droites moyennes et les bandes à 95% pour chacune des classes (les bandes à 95% ne sont plus tracées ici à vue, mais à partir de l'écart type de la distribution des observations sur différentes abcisses).

Les droites moyennes sont ainsi tracées:

—sur la figure 7, pour la contamination atmosphérique multipliée par la vitesse du vent;

—sur la figure 8, pour l'écart-type de la distribution de la contamination atmosphérique perpendiculairement à l'axe du panache.

On a comparé les pentes des droites et évalué la surface de recouvrement des bandes entre elles.

Il est ainsi apparu que toutes les bandes ont une proportion de recouvrement supérieure à 60%, sauf la bande tracée à partir des contaminations atmosphériques, dans le cas d'émission à 325 m, en période de stabilité III et de vent faible, qui ne présente aucun recouvrement avec ses voisines. Il a paru utile de créer cette

* Les formules théoriques donnent des courbes asymptotes à une droite au-delà d'une certaine distance (en coordonnées logarithmiques). L'approximation par une droite permet sa détermination par la méthode des moindres carrés et le traitement statistique ultérieur.

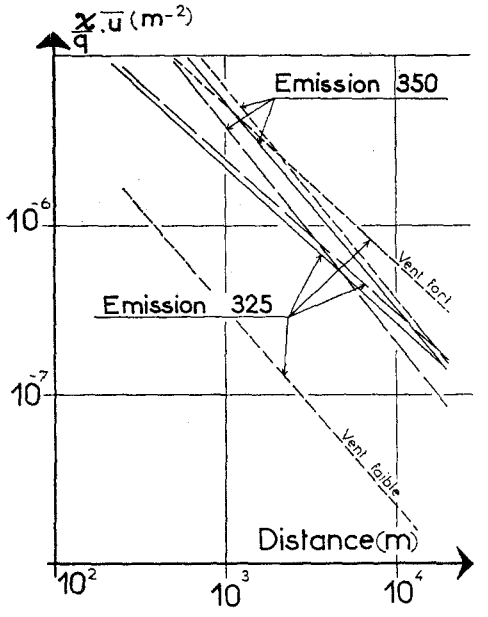

FIG. 7. Concentration $\frac{\chi}{q}\bar{u}$ en fonction de la distance.

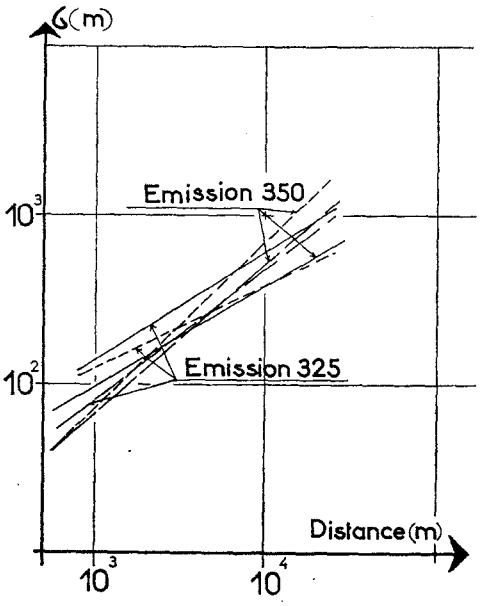

FIG. 8. Écart-type σ en fonction de la distance.

sub-division entre vent faible (inférieur à 2 m/s) et fort (supérieur à 4 m/s) dans ce cas particulier.*

Les pentes des droites moyennes ne sont pas significativement différentes:

—dans les différents cas d'écart-type σ;

—pour une cote d'émission donnée (350 et 325), dans les différents cas de stabilité de la contamination atmosphérique.

Par contre, il apparaît une différence, significative au risque 1%, entre les pentes des droites de contamination atmosphérique des émissions à 350 et 325 m.

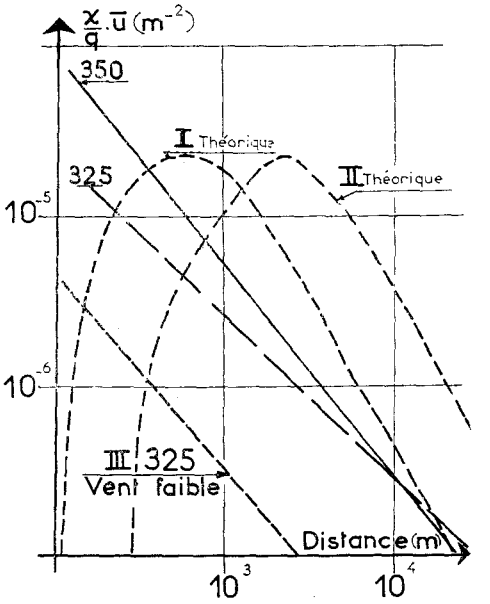

FIG. 9. Résultats de contamination atmosphérique comparés à la théorie.

4.4. *Conclusions de l'étude de diffusion*

4.4. 1. *La contamination atmosphérique* moyenne peut être représentée en fonction de la distance par une droite (en coordonnées logarithmiques) différente selon la cote d'émission et valable pour des distances supérieures à 300 m (fig. 9).

Les facteurs météorologiques ou orographiques ne semblent pas avoir un effet déterminant sur la contamination. Cependant, dans les cas de

* Il n'y a pas eu d'émission dans le cas III pour des vitesses de vent intermédiaires.

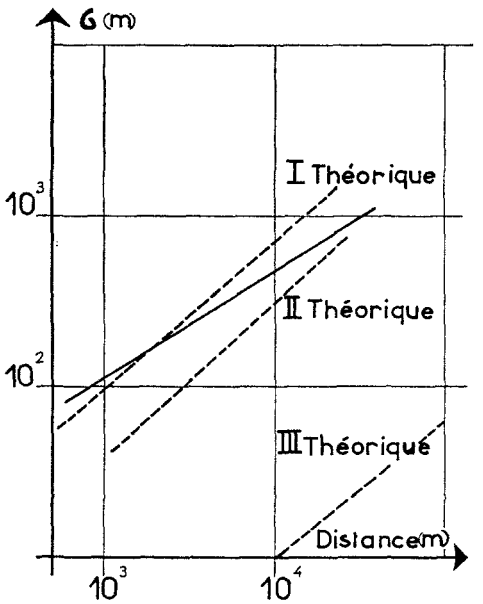

FIG. 10. Résultats d'écart-type comparés à la théorie.

grande stabilité où, par vent faible, la turbulence dynamique et thermique est nulle, la contamination est nettement plus faible que dans les autres cas. Dans ce cas le panache subit une grande diffusion latérale et une faible diffusion verticale, ce qui tend à réduire la contamination au niveau du sol.

La contamination atmosphérique est plus faible pour une émission à la cote 325 que pour une émission à 350 m jusqu'à des distances importantes. Ceci peut être dû à l'absorption de l'effluent par la forêt avoisinant le point d'émission, absorption plus importante pour une émission d'une hauteur plus faible. On peut supposer que cette rétention est également valable pour les effluents radio-actifs. En conséquence, on a admis d'élever une cheminée d'une hauteur de 18 m qui, compte tenu de la vitesse ascensionnelle des gaz à la sortie, permet d'admettre la valeur de 325 m comme cote effective de rejet.

Compte tenu de la largeur des bandes à 95%, on a une estimation de la valeur maximale observable, avec un risque 2,5% de voir cette valeur dépassée, en multipliant par 3 la valeur moyenne déduite de la droite.

4.4. 2. *L'écart-type* de la distribution de la contamination atmosphérique perpendiculairement à l'axe du panache peut être traduit par une représentation linéaire en fonction de la distance et en coordonnées logarithmiques (fig. 10).

4.4. 3. Un traitement analogue a été fait pour la *contamination surfacique observée en l'absence de pluie.* Les contaminations observées sont assez peu différentes, mais, néanmoins, en progression croissante du cas I au cas III de stabilité (fig. 11).

En règle pratique, la contamination surfacique Ω divisée par l'activité rejetée Q peut être déduite de la contamination atmosphérique en appliquant un coefficient 10^{-2} à la contamination atmosphérique corrigée du débit d'activité et de la vitesse du vent.

$$\frac{\Omega}{Q} \simeq 10^{-2} \cdot \frac{\chi}{q} \cdot u$$

Ce coefficient 10^{-2} est prudent. La valeur trouvée est $(6{,}2 \pm 4{,}6)\ 10^{-3}$. Elle ne varie pas de façon significative avec la distance.

4.4. 4. L'étude de la *contamination surfacique par temps de pluie* s'est soldée par un échec: le résultats obtenus, très hétérogènes, ne permettent pas de déterminer une loi de variation.

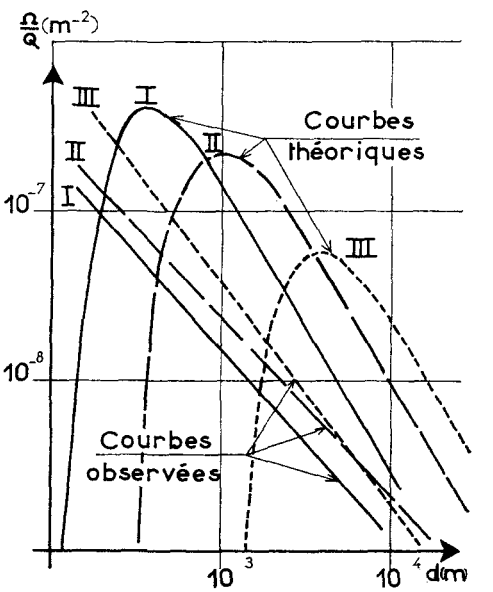

FIG. 11. Résultats de contamination surfacique comparés à la théorie.

En accord avec des considérations théoriques, il semble pratique d'adopter une valeur dix fois supérieure à celle de la contamination en l'absence de pluie.

4.5. *Comparaison des résultats trouvés avec les valeurs théoriques*

On a représenté (figs. 9, 10 et 11) sur les mêmes graphiques, les courbes expérimentales et les courbes théoriques tracées à partir de la formule de Sutton pour une hauteur d'émission supposée à 50 m.

On constate que les contaminations expérimentales maximales sont plus faibles que les contaminations théoriques, alors que l'écart-type σ observé est généralement plus grand que l'écart-type théorique.

Ces constatations sont le résultat d'un même phénomène: la diffusion latérale du panache est beaucoup plus grande que ne le prévoit la théorie, essentiellement parce que la direction du vent est susceptible de variations, ce que ne prévoit pas la théorie, et parce que ces variations sont d'autant plus grandes que le temps de mesure est long. Il semble qu'un temps d'expérimentation voisin de l'heure soit bien adapté à nos besoins.

Les variations en direction du vent se marquent par un écart-type plus grand à courte distance, mais dès que les différents panaches sont établis, aidés en cela par le relief par exemple, leur écart-type devient relativement plus faible. L'écart-type à courte distance est, en fait, un écart-type apparent sur plusieurs panaches juxtaposés.

Il apparaît donc qu'il est un caractère météorologique qui a été négligé au cours de ces expérimentations: les fluctuations en direction du vent qui pourraient être traduites par l'écart-type de la distribution en direction du vent autour d'une valeur moyenne pendant l'émission. Ce paramètre pourrait être déduit d'un enregistrement continu du vent, mais il faut reconnaitre que pour passer ensuite à des règles d'exploitation, il ne peut être un critère pratique. Il n'a pas paru regrettable dans notre cas particulier, de perdre un peu en précision au bénéfice de la simplicité.

On peut remarquer accessoirement que les courbes observées ne rendent pas compte des faibles valeurs théoriques de la contamination aux courtes distances. Nous avons bien observé cependant des valeurs faibles en amont des valeurs maximales et sous le vent de l'émission. Si des maximums ont été isolés à des distances de plusieurs kilomètres de l'émission, nous avons considéré que ceci était dû au relief. En fait, notre méthode de recherche statistique nous a obligé à considérer que la courbe moyenne était une droite en coordonnées logarithmiques. Nous avons admis cette loi de variation en acceptant de surestimer la contamination pour les courtes distances et de ne la considérer comme valable qu'à partir de 300 m environ du point d'émission.

5. RÉSULTATS DES MESURES METEOROLOGIQUES

Les résultats essentiels pour le problème de diffusion sont seuls rapportés ici.

5.1. *Vitesse du vent*

La vitesse moyenne générale ressort à 5,3 m/s à la cote 350, 4,6 m/s à la cote 325.

La vitesse la plus fréquente est de 5 m/s en général, 7 m/s par temps de pluie.

La fréquence des vents inférieurs à 5 m/s est de l'ordre de 30% par temps de pluie, 50% par temps sec. La fréquence des vents inférieurs à 1 m/s est de 3% par temps de pluie, 5% à la cote 350, 7% à la cote 325 par temps sec.

La fréquence des vents supérieurs à 10 m/s a été variable au cours des années d'observation:

—2 à 20% en cas de pluie à la cote 350

—1 à 10% dans le cas général.

5.2. *Direction du vent* (figs. 12 et 13)

La direction la plus fréquente se situe généralement dans le secteur sud (sud-sud-est à sud-ouest) avec une fréquence variable de 10 à 15%, atteignant 20% pour les cas de pluie en 1963 et 1964.

La direction la moins fréquente est généralement l'est-sud-est mais a été quelquefois du secteur nord-ouest, la fréquence variant de 1 à 3%.

Dans le cas des vents faibles (vitesse de 1 et 2 m/s), on observe une différence significative de la répartition de la direction avec le cas général. La direction la plus fréquente se situe dans le secteur nord; dans ce cas, les effluents sont rejetés vers la forêt, les premières

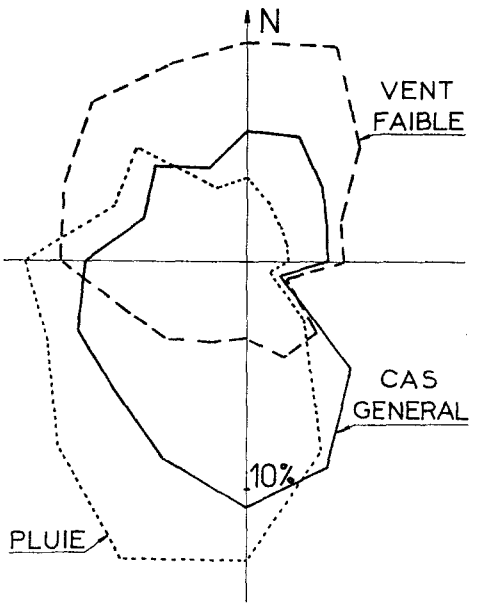

FIG. 12. Direction du vent à la cote 350.

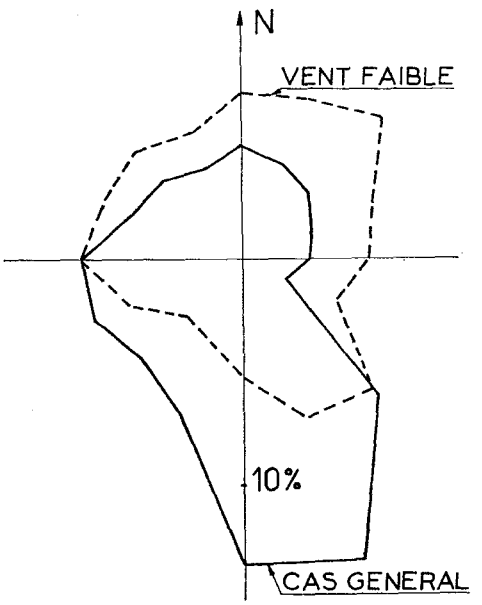

FIG. 13. Direction du vent à la cote 325.

agglomérations se situent alors à une distance de 6 à 7 km.

La permanence de la direction a été recherchée en déterminant le nombre d'observations successives pour lesquelles la direction a conservé une valeur fixée dans un secteur de 90 degrés (sans annulation de la vitesse); on sélectionne ainsi des séquences d'observation. Les séquences sont classées par saison en groupant différentes années. La séquence observée la plus longue est supérieure à 300 observations horaires (chiffre maximal admis au programme de calcul). La saison présentant le maximum de permanence est l'hiver; la direction la plus permanente est le sud-ouest.

On a observé, dans ce secteur sud-ouest, au cours de deux années consécutives, que 2 à 4% des séquences, groupant au maximum 9% du temps, ont une durée supérieure ou égale à 60 h et 7 à 9% (au maximum 14% du temps) une durée supérieure ou égale à 30 h.

5.3. *Stabilité de l'atmosphère*

Le gradient vertical de température observé sur la pente présente une dominance nettement négative (tableau 2).

Seule, la première classe de gradient présente une certaine permanence: 3 séquences en deux ans d'une durée supérieure à 200 h et 30 d'une durée supérieure à 30 h. Il n'a pas été observé de séquence supérieure à 30 h pour les autres classes.

Le coefficient de stabilité n (voir page 646) a été classé en fonction du gradient observé simultanément. La valeur moyenne de n ressort à 0,3 ou 0,4 quelle que soit la classe (fig. 14); théoriquement elle devrait varier de 0,1 à 0,6 sensiblement, lorsque le gradient varie de -3 à $+5°$ C/100 m (ce qui a été trouvé sur d'autres sites plus plats).

Le coefficient de stabilité subit une variation diurne de grande amplitude en été, de faible amplitude en hiver (fig. 15). Par contre, le gradient mesuré ne présente pas de variation diurne significative.

Ceci montre que le gradient observé le long de la pente n'est pas présentatif de l'état de stabilité de l'atmosphère, qui est mieux représenté par la valeur calculée n. Cette anomalie est très certainement due au relief. Lorsque le vent n'est pas faible, l'absence de stabilité ther-

Tableau 2. *Gradient observé entre les cotes* 300 *et* 105

Valeur du gradient (°C/100 m)	Fréquence %	Classe
inférieur à–1	58	I
entre–1 et 0	26	II
entre 0 et + 3	15	III
supérieur à + 3	1	III

(nombre total d'observations: 15975)

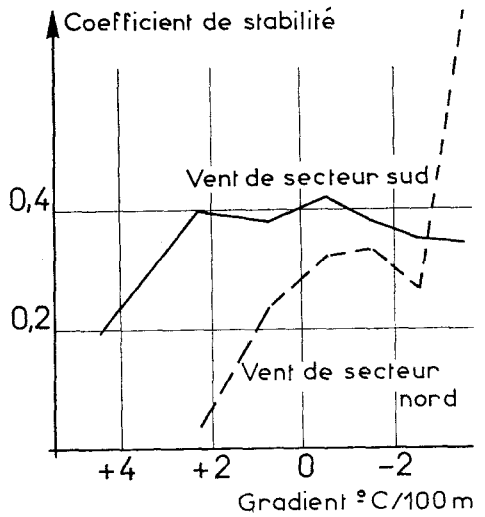

FIG. 14. Coefficient de stabilité en fonction du gradient.

mique est compensée par l'instabilité dynamique due au relief.

5.4. *Vitesse et direction en fonction du gradient*

Les vitesses faibles ou moyennes sont aussi fréquentes quel que soit le gradient. Par contre, les vitesses élevées sont plus fréquentes lorsque le gradient est négatif que lorsque le gradient est positif.

Si on met à part les gradients fortement positifs, dont la fréquence est très faible, les autres classes de gradient présentent la même probabilité que dans le cas général lorsque le vent provient du demi-horizon est. Par contre, lorsque le vent souffle du demi-horizon ouest, la fréquence du gradient diminue quand le gradient devient positif. Ainsi, à titre d'exemple, les fréquences pour le vent d'ouest sont les suivantes:

79% pour les gradients inférieurs à $-1°$ C/100 m

18% pour les gradients compris entre -1 et 0

3% pour les gradients compris entre 0 et $+3$ moins de 0,1% pour les gradients supérieurs à $+3°$C/100 m.

Ces fréquences montrent une disproportion encore plus marquée que dans le cas général.

En fait, dans le cas particulier de la centrale des Ardennes, ces conclusions n'ont pas de répercussion sur la façon de traiter le problème des effluents gazeux, puisque les résultats de l'étude de diffusion n'ont pas permis de mettre en évidence l'influence du gradient.

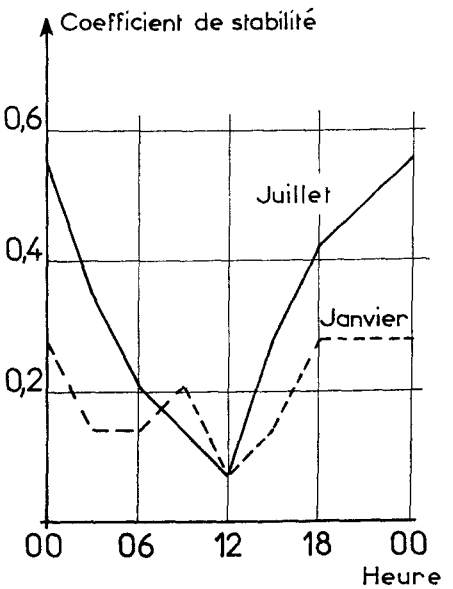

FIG. 15. Coefficient de stabilité en fonction de l'heure.

6. RÉGLES DE REJET

À la suite de cette étude, il parait possible de définir des règles pratiques concernant:

—les rejets admissibles en exploitation normale

—des niveaux d'intervention en cas d'accident.

6.1. *Rejets normaux*

Dans le cas de rejets normaux, les règlements sanitaires nationaux demandent que la contamination atmosphérique résultant de ces rejets soit inférieure à la concentration maximale admissible pour la population (CMAP) en valeur moyenne trimestrielle, sans que la contamination instantanée n'excède 10 CMAP.

Il convient d'abord de se demander où doit être respectée cette convention. Les effluents étant le plus fréquemment dirigés vers le nord, on peut adopter comme point critique les premières habitations situées dans ce secteur, celles de la commune de Chooz situées à la distance de 1500 m.

Pour évaluer le débit admissible de rejet q, on peut faire intervenir trois facteurs:

—le facteur "diffusion" $\left(\frac{\chi}{q}\bar{u}\right)$ déduit des essais de diffusion (on peut prendre une valeur moyenne ou une valeur maximale selon le cas).

—le facteur "vitesse" $\bar{u}$,

—le facteur "direction" d, qui tient compte du fait que le vent n'est pas toujours dirigé vers le point critique. Le débit est ainsi évalué par

$$q = \frac{\bar{u}}{d}\,\frac{\chi}{\left(\frac{\chi}{q}\bar{u}\right)}$$

χ étant la contamination maximale admissible que l'on désignera par χ_0 (1 CMAP) pour la valeur moyenne admissible et $10\chi_0$ pour la valeur maximale admissible.

En fait de valeur maximale admissible, il s'agit plus exactement d'une valeur maximale pour laquelle on admet un dépassement dans un nombre limité de cas.

Le débit maximal admissible (q max) conduisant à la contamination $10\chi_0$, a été évalué (tableau 3) pour différentes valeurs des facteurs. À partir des études précédentes, on a déterminé les probabilités de voir ces facteurs augmenter la contamination atmosphérique. On a calculé dans chaque cas la contamination moyenne résultant de l'adoption de ce débit maximal admissible en supposant que ce soit le débit permanent.

On pourrait choisir comme débit maximal admissible un débit intermédiaire entre les cas 1 et 2, tel que la contamination moyenne serait χ_0. La probabilité de dépasser dix fois la CMAP serait alors comprise entre 0,025 et 0,25, ce qui peut sembler excessif.

En fait le débit permanent de rejet d'une centrale est en général faible, et il peut être utile de conserver quelques possibilités de rejet pour des cas d'exploitation particuliers.

Tableau 3.

	cas moyen	cas défavorables					
		cas 1	proba.	cas 2	proba.	cas 3	proba.
$\frac{\chi}{q}\bar{u}(m^{-2})$	2×10^{-6}	2×10^{-6}	0,5	2×10^{-6}	0,5	6×10^{-6}	0,025
$\bar{u}$(m/s)	5	5	0,5	1	0,05	1	0,05
d	0,2	1	1	1	1	1	1
q max Ci/s		$2{,}5 \times 10^{7}.\chi_0$	0,25	$5 \times 10^{6}.\chi_0$	0,025	$1{,}7 \times 10^{6}.\chi_0$	0,00125
χmoyen, Ci/m³		$2\chi_0$		$0{,}4\chi_0$		$0{,}14\chi_0$	

On peut ainsi choisir le débit maximal admissible du cas 2 pour lequel la probabilité de dépasser 10 CMAP est inférieure à 2,5%, si ce débit est le débit permanent. Cette solution donne une certaine latitude de rejet et permet d'effectuer des rejets temporaires à des débits plus élevés en profitant des circonstances plus favorables. Si, en particulier, durant la période de rejet concerté, la direction du vent est du secteur nord, la vitesse étant supérieure à 5 m/s, le débit maximal peut être 20 fois supérieur au débit maximal précédent sans que la contamination ne dépasse 10 CMAP en un endroit habité.

6.2. *Rejets accidentels*

Les niveaux d'intervention en cas d'accident sont généralement donnés en termes de contaminations atmosphérique ou surfacique intégrées (Ci-s/m^3 ou Ci/m^2). Soient A ou S ces contaminations.

La mesure au rejet de l'installation peut porter sur le débit d'activité ou sur l'activité totale rejetée Q. Il est toujours possible de se ramener à la connaissance de cette grandeur.

Il nous faut donc calculer les rapports Q/A et Q/S. Ce calcul doit être effectué "a priori" donc indépendamment des conditions météorologiques qui pourraient exister au moment de l'accident. Il faut cependant tenir compte des conditions météorologiques par leur probabilité d'occurence. On peut accepter, en prévoyant les dispositifs de sauvegarde, que ceux-ci soient insuffisants dans un pourcentage minime de cas.

En choisissant les conditions météorologiques du cas 2, du paragraphe précédent, on détermine les coefficients suivants:

$Q/A = 5 \times 10^5$ (m^3/s)
$Q/S = 5 \times 10^6$ (m^2) par temps de pluie,
$Q/S = 5 \times 10^7$ (m^2) par temps sec.

Ces coefficients peuvent être inférieurs aux valeurs précédentes dans 2,5% des cas.

Ces coefficients peuvent être multipliés par quatre pour l'adaptation des dispositifs de sauvegarde au sud de la centrale, en raison de l'éloignement des agglomérations.

Notons encore que la probabilité de précipitations est de 15% durant le mois le plus pluvieux, la probabilité de conserver une direction de vent pendant plus de 60 h étant inférieure à 10%.

7. CONCLUSION

Les mesures de diffusion atmosphérique et les mesures météorologiques ont permis de définir des niveaux maximaux admissibles et des niveaux d'intervention. De plus, on a précisé la probabilité de voir ces niveaux conduire à des contaminations supérieures à celles qui sont prévues.

On a pu penser que la dispersion des résultats, observée lors des mesures de diffusion, était importante. En fait, en multipliant la contamination moyenne par un facteur 3, on est assuré d'avoir une surestimation de la contamination dans 97,5% des cas. Ceci semble un résultat d'une précision suffisante pour nos besoins.

Ces mesures ont été réalisées sur un terrain particulièrement accidenté. Nous étudions actuellement les conditions de diffusion sur d'autres terrains plus proches de l'état plan théorique. Nous pensons obtenir une connaissance des conditions de diffusion assez précise pour ne pas devoir répéter cette expérimentation sur chacun de nos sites.

8. REMERCIEMENTS

Nous tenons à remercier les différents organismes qui ont participé à ces mesures, en particulier:

—l'équipe de mesure de diffusion du service de contrôle des rayonnements et de génie radioactif du Commissariat à l'Énergie Atomique et tout particulièrement Mr. le Quinio qui a bien voulu prendre la direction des premières opérations;

—l'équipe de prélèvement, dirigée par Mr. Bultynck, du département "mesures et contrôle des radiations" du centre d'études nucléaires de MOL (Belgique);

—la section météorologique de l'armée belge, dont l'aide est dûe à l'intervention aimable de Mr. de Maere de MOL.

—les différents services d'Électricité de France, en particulier le laboratoire de pollution atmosphérique du service de la production thermique.

—enfin notre hôte, la Société franco-belge d'Énergie Nucléaire des Ardennes qui a marqué un vif intérêt pour nos études dès le début de la construction de la centrale.

RÉFÉRENCES

1. R. Le Quinio et J. Hugon. Expériences de diffusion atmosphérique en vraie grandeur, compte rendu du colloque international sur la pollution radio-active des milieux gazeux, Saclay, 13–16 novembre 1963.
2. Service général de radioprotection, Diffusion des effluents atmosphériques de la centrale des Ardennes, rapport SGR, DE.SES No. 10 (1966).
3. Service général de radioprotection—Résultat des mesures météorologiques effectuées sur le site de la centrale nucléaire des Ardennes, rapport SGR, DE.SES No. 13 (en préparation).

ENVIRONMENTAL MONITORING OF ^{131}I AS A VERIFICATION OF METEOROLOGICAL CALCULATIONS OF DISPERSION FROM A 100 METER STACK*

A. P. HULL and M. E. SMITH
Instrumentation and Health Physics Department, Brookhaven National Laboratory, Upton, New York

Abstract—A number of similar methods for estimating long term ground-level concentrations of the effluent from a continuous elevated point source have been developed by meteorologists. Although these are generally accepted and applied, relatively few verifications of them have been conducted. This can be attributed to the difficulties of securing sufficiently accurate continuous measurements of the source, and of mean ground level concentrations to produce significant data.

In 1964 a project was established at Brookhaven National Laboratory to utilize ^{131}I emitted from a 100 m stack as an atmospheric tracer. Stack effluent samples indicate that during 1965 the routine emission by the Brookhaven Graphite Research Reactor (BGRR)-Hot Laboratory complex from this stack was about 10 mCi/day. On March 1, 1965 an overheated sample resulted in the additional release of 100 mCi of ^{131}I and about 1.0 Ci of ^{133}I over the next few days.

This project is a joint effort of the Laboratory's Meteorology and Health Physics Environmental Monitoring Groups. The former employs a nearby tower to obtain continuous measurements of both ground-level and stack elevation temperatures and winds. Using meteorological parameters determined from these measurements, and the known emission from the stack, estimates of mean ground-level concentrations are made.

The Environmental Monitoring Group has developed techniques for sampling and evaluating the minute concentrations of ^{131}I encountered, in the order of 0.0001–0.0010 pCi/m^3. During 1965, monitoring stations were added at 0.7 km and 1.3 km in prevailing downwind directions, supplementing the existing stations at about 2.5 km from the stack. The measurements obtained from these sets of stations provide a unique opportunity for the verification of the estimated concentrations for periods from days to years.

An examination of the data obtained during the March 1 release indicated that the field measurements at several downwind sampling distances were generally consistent with regard to particulate to charcoal filter and $^{133}I/^{131}I$ ratios, but that those at the close-in stations were much lower in concentrations then initially estimated. As a result, assumptions about the rise of the plume above the stack were revised. The short term data from the March 1 release verify the adjusted meteorological estimates to within the error of measurement.

The long term data show far more variation in comparison with the meteorological estimates, as would be expected with field dosages close to the threshold of measurement. The data reveal, however, important features of the behavior of the BGRR plume and of dispersion patterns at this site.

---

* Research carried out at Brookhaven National Laboratory under contract with the U.S. Atomic Energy Commission.

INTRODUCTION

Most environmental monitoring programs are conducted to document the ambient types and levels of radioactivity resulting from effluent releases from a facility. At Brookhaven National Laboratory we have also sought ways to broaden the scope of our program to include obtaining useful scientific information by utilizing the isotopes present in our effluents as tracers to investigate natural phenomena. This paper describes one such effort.

A number of similar methods for estimating long term ground level concentrations from an elevated point source have been developed by meteorologists, but relatively few verifications have been conducted owing to the difficulties in securing sufficiently accurate continuous measurements of the source, of meteorological conditions and of mean ground level concentrations. The use of the ^{41}Ar in the effluent cooling air of the Brookhaven Graphite Research Reactor (BGRR) as a tracer to make such a verification was one of our first multi-purpose programs. It was a joint effort of the Health Physics Division and the Meteorological Group at the Laboratory. The data indicated that the prediction system was substantially accurate, although conservative [1] in that it tended to overestimate the ground level dosages. The monitoring equipment detected the ^{41}Ar 1.29 MeV gamma, as well as some portion of its beta radiation. The former's long mean free path in air made the ground level measurements relatively insensitive to small variations in the concentration pattern aloft and, therefore, made it difficult to use this tracer source to verify details of the dispersion model.

During the early 1960's the BNL Environmental Monitoring Group initiated a program of the identification and measurement of levels of fallout isotopes, especially ^{131}I, in various environmental samples. [2] As fallout levels declined after 1962, interest shifted to the possibility of evaluating the minute ground level concentrations of ^{131}I resulting from the routine emission of about 10 mCi/day from the 100-m stack serving the BGRR-Hot Laboratory complex.

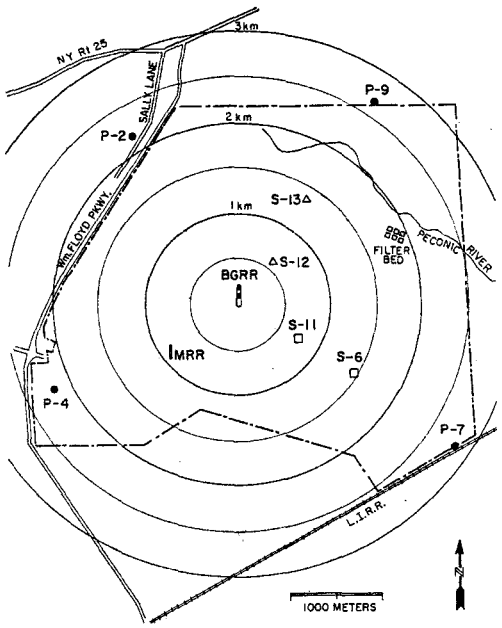

FIG. 1. Environmental monitoring stations at Brookhaven National Laboratory.

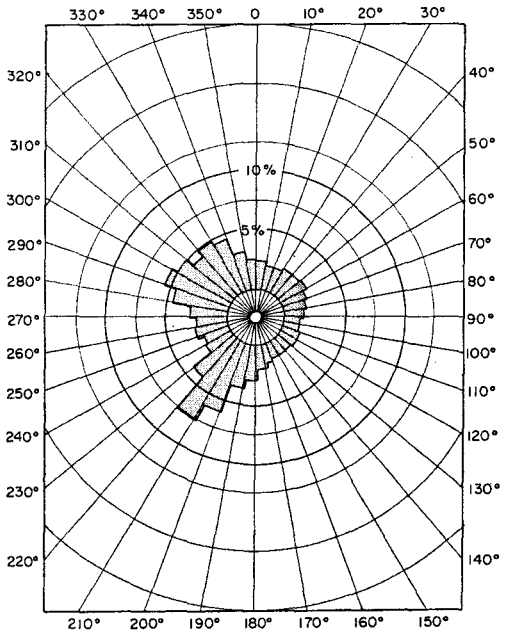

FIG. 2. Annual percentage frequency of wind directions at 100 m, 1961–3.

SAMPLING AND MEASUREMENT TECHNIQUES

By 1964, routine measurements were being made of average ^{131}I air concentrations as small as 0.001 pCi/m^3. The improved techniques for sampling and evaluating these minute concentrations have been reported in detail elsewhere [3] and will, therefore, be reviewed only briefly. High volume positive displacement pumps capable of continuously drawing over 500 l./min of air through a 10-cm diameter particulate filter and 2.5-cm thick charcoal canister in series were utilized. The usual sampling periods were two weeks.

During 1964 these samplers were operated at the four perimeter stations shown on Fig. 1. An annual distribution of the observed wind directions at the stack height elevation is shown in Fig. 2. The large southwesterly component reflects the summer time prevailing winds and the more variable northwesterly component the winter situation. To obtain more information about the pattern of ground concentrations closer to the stack, during 1965 the additional on-site stations also shown in Fig. 1 were installed. These are in line with the downwind perimeter stations in the two most prevailing directions. They were operated on a seasonal basis, those at 217° from the stack during the warmer months and those at 300° during the cold half of the year.

Utilizing two opposed 10 × 5-cm NaI crystals and a multi-channel analyzer, a 5 hr gamma spectrum of both the particulate filter and charcoal cannister was obtained two or three days after collection. The charcoal cannisters were then recounted after several ^{131}I half-lives had elapsed and the residual ^{214}Bi (RaC) interference in the ^{131}I 0.36 MeV photopeak region was subtracted from the original spectrum to determine the amount of ^{131}I on the filter at the end of the collection period.

At the stack, about 1% of the effluent ^{131}I is filterable on a two-day particulate sample [4] and the balance is collected on an in-line charcoal cartridge. The interference from other isotopes in routine field particulate samples made it impossible to determine the ^{131}I particulate fraction in these samples, so it was initially assumed that it was comparable to that observed in the stack sample. On the average, about one-third of the total concentrations of ^{131}I observed after recent weapons tests has been collected on field particulate filters. By comparing particulate filter collections from stations downwind from the stack with others obtained during the immediate post-weapons test sampling periods we have now established that the field particulate fraction of the routine stack effluent is less than 5%.

On March 1, 1965 an overheated fuel sample containing 1.0 g of ^{235}U resulted in the emission of about 100 mCi of ^{131}I and 1.0 Ci of ^{133}I (about 50% of these radio-iodines present in the sample) during the next few days. The release rate of both isotopes began at a fairly high level, 34.4 mCi/hr of ^{131}I and 365 mCi/hr of ^{133}I. The 21-hr ^{133}I was detectable in the field for only a few days, but the 8-day ^{131}I was found in above normally encountered concentrations for a full two weeks. The stack sample data did not indicate an unusually large particulate fraction of these radio-iodines. This fraction in field samples during the first day after the initial release was close to 50%; a day later it was 40%; from the second to fifth day samples 30%; and from the fifth to fifteenth day the particulate fraction was 20% of the total collection.

METEOROLOGICAL ESTIMATION OF GROUND LEVEL CONCENTRATIONS

After it became apparent that the ambient field concentrations of stack effluent ^{131}I could be measured with some degree of accuracy, the Meteorology Group and the Health Physics Division instituted another joint project that has revealed important aspects of the actual behavior of the plume. The meteorological contribution has been the calculation of ground level concentrations. The Health Physicists have supplied information about the stack output as well as the field concentrations. The calculation method itself is not unique to Brookhaven, but includes the same series of steps that most such estimates entail.

The first one is the determination of appropriate dispersion parameters. These have been well defined [5] from studies of oil fog test plumes and other tracers at Brookhaven and instruments on the 125-m tower erected for these early experiments continue to supply meteorological data needed for current calculations.

The second step is the estimation of the effective stack height of the plume. This is the sum of the actual height and additional rise associated with buoyancy and momentum effects of the plume itself as well as the wind speed and the stability of the atmosphere. The effective stack height of the BGRR plume has not been accurately determined, since its principal constituent, ^{41}Ar, is a rather unsuitable tracer for this purpose. It is known that the plume rises well above the top of the 100-m stack, since 115 m^3/sec of air is released at 50° C above ambient temperature and with a vertical speed of 6 m/sec. Estimation of plume rise is an uncertain aspect of air pollution evaluations and this study sheds some light on the problem.

A Gaussian plume model of the following form is used as a representation of the dispersion process:

$$X(x,y,z) = \frac{Q}{\pi\sigma_y\sigma_z\bar{u}} \exp - [h^2/2\sigma_z^2 + y^2/2\sigma_y^2] \quad (1)$$

where X = concentration (units/m^3) or dosage (units-sec/m^3),
Q = release rate (units/sec) or total release (units),
$\sigma_y\sigma_z$ = crosswind and vertical plume standard deviations (m),
$\bar{u}$ = mean wind speed (m/sec),
h = initial source height (m),
x, y, z = downwind, crosswind and vertical distance (m)

For short periods (1–24 hr) it is practicable to establish for each hour the mean wind direction and values of $\bar{u}$, σ_y, σ_z and h from which a ground level concentration pattern is established as shown in Fig. 3. A given sampling point will occupy an x, y position (or series of positions) in relation to such patterns.

For longer periods, such as a week or a month, it is more convenient to apply a simplified model of the dispersion equation. This involves determining a concentration pattern that would be present if the wind direction were distributed uniformly throughout a given angular sector and if a single dispersion parameter persisted unchanged for the entire period. Mathematically this consists of integrating equation (1) in the y-direction and dividing it by the circumference of the circle at the distance (radius) of interest. The equation is then of the form:

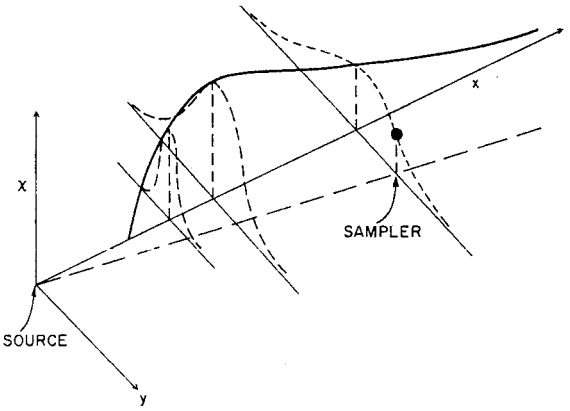

FIG. 3. Precise estimate of receptor concentration.

$$X = \frac{360\,Q}{\theta\,\pi^{3/2}\,2^{1/2}\,\sigma_z\bar{u}x} \exp - h^2/2\sigma_z^2 \quad (2)$$

where θ is the angular width of the sector.

A plot of a typical concentration distribution is shown in Fig. 4. In this case, the lateral position of the sampler within the sector is not important and the concentration depends only on the dispersion condition, the effective stack height, the distance from the source and the average wind velocity. In applying this model it is assumed that whenever the wind direction is such as to include a sampler within a sector width (30° in these studies), it will be affected by the concentration specified by equation (2).

Several non-meteorological corrections and adjustments are required in this evaluation to

Table 1. *Dispersion Parameters Used in the Study*

Gustiness class	σ_y	σ_z
	(m)	(m)
B_2	$0.40\,x^{0.91}$	$0.41\,x^{0.91}$
B_1	$0.36\,x^{0.86}$	$0.33\,x^{0.86}$
C	$0.32\,x^{0.78}$	$0.22\,x^{0.78}$
D	$0.31\,x^{0.71}$	$0.06\,x^{0.71}$

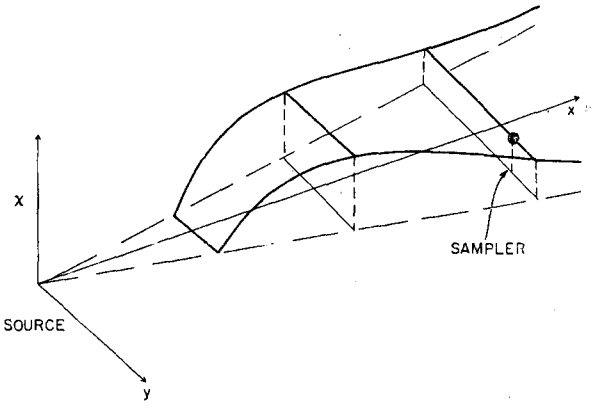

FIG. 4. Sector estimate of receptor concentration.

account for variations in output rate, sampler operation and radioactive decay.

It is the practice at Brookhaven[5] to classify all hours in terms of four dispersion conditions, determined from the wind direction trace at the 110-m level on the meteorological tower. The associated dispersion parameters are given in Table 1. In practice, hours having D gustiness (inversions) type are discarded since studies of tracer plume[6] in this area have shown that during these conditions there are no ground level concentrations within the radius of the sampling stations.

COMPARISONS OF CALCULATED AND OBSERVED CONCENTRATIONS

The 1964 comparisons of calculated and observed concentrations of ^{131}I at the Lab perimeter already reported[3] were made using sector calculations based on 1958-63 average meteorological conditions. There was agreement within the estimated error of measurement, except at the north-east station where the observed average concentration was almost twice that calculated. The 1965 comparisons for the same perimeter stations reported in Table 2, indicate that all the observed concentrations were uniformly greater than those calculated from past average conditions. It was therefore decided to refine all the 1965 calculations by employing the observed meteorological data for each sampling period. Since the prevailing concentrations are less than 0.01 pCi/m^3, several orders of magnitude below established radiation protection standards, the calculations were simplified by comparing the amount of ^{131}I collected by field samplers with the amount which should have been collected.

The first such comparisons using calculations based on observed meteorological data were made in connection with the unusual release during the first half of March 1965. The samples

Table 2. Calculated and Measured Annual Concentrations of ^{131}I at the BNL Perimeter January–December 1965

Station	From stack		Calculated	Measured
	Distance (km)	Direction	($\times 10^{-15}$ μCi/cm^3)	($\times 10^{-15}$ μCi/cm^3)
E-2 (NW)	1.8	140°	0.7	1.2
E-4 (SW)	2.2	65°	0.6	1.0
E-7 (SE)	2.5	321°	1.9	3.2
E-9 (NE)	2.75	217°	2.3	3.7

were obtained over periods ranging from initial ones as short as 1 hr to as long as 10 days as the release rate declined. Most of the dispersion conditions bringing material to the samplers were of the B_1 (typical daytime) type. Both dispersion equations (1) and (2) were employed, the selection depending primarily on the length of the sampling period.

It is obvious from Table 3, which summarizes only ^{131}I data, that the calculated/observed ratios tend to be large close to the stack and to decrease to values close to the ideal 1.0 between 2 and 3 km. This tendency must almost certainly be associated with an error in the estimation of the effective stack height (h), since this appears to be the only way of obtaining a grossly erroneous estimate close to the source and reasonable values at greater distances. This is illustrated in Fig. 5, in which the discrepancy between the concentration curves can be seen to be large in the region from 0.5 to 1.0 km and diminishing at larger distances where the effect of the initial source height assumption becomes small.

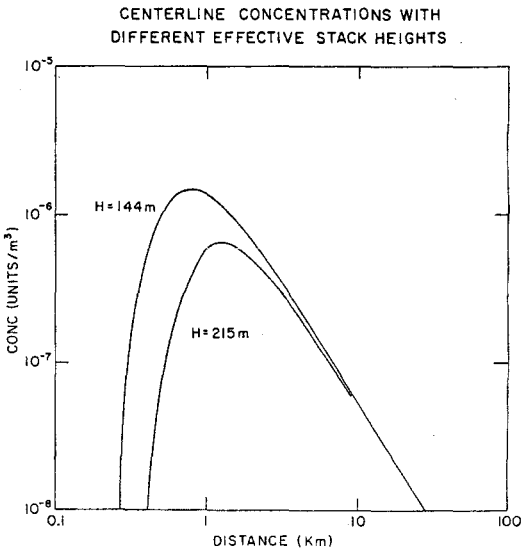

FIG. 5. Centerline concentrations with different effective stack heights.

The calculated sample amounts in Table 2 were based on the Bosanquet equation.[7] Recent independent study of hot puff behavior[8] suggests that the buoyancy effect of the warm gas emission might be more significant than allowed for by the Bosanquet equation, and the entire series of data were recomputed on the basis of the Central Electric plume rise equation.[9] Comparison of the calculated effective stack heights for these two equations are shown in Fig. 6, from which it can be seen that the C.E.

Table 3. Comparison of Observed and Calculated Samples, March 1965 Series Bosanquet Δh Equation

Station	Distance (m)	^{131}I (pCi)		
		Obs.	Calc.	C/O
E-11	700	35	250	7.1
		43	260	6.0
		35	65	1.8
		13	22	2.8
		14	46	3.3
Igloo	1750	100	300	3.0
E-4	2200	6	6	1.0
E-7	2550	36	22	0.6
		75	140	1.8
		47	54	1.1
		20	32	1.6
E-9	2750	10	5	0.5
		12	5	0.4

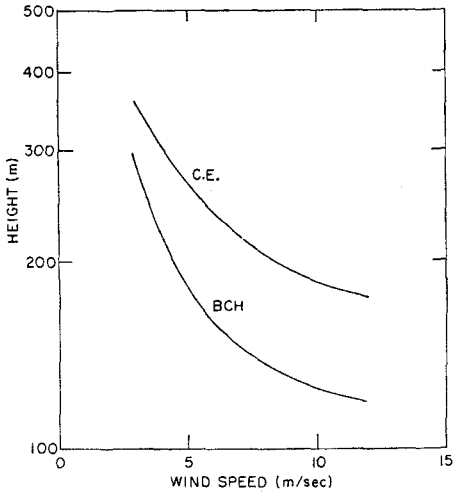

FIG. 6. Comparison of effective stack heights.

estimates are higher by more than 50 m at typical wind speeds.

The lefthand ^{131}I portion of Table 4 is identical to Table 3, except that the calculations are based on the C.E. estimate for effective stack height. There is still a tendency for the C/O ratios to be higher close to the stack, but they have been greatly reduced without seriously affecting the C/O ratios at 3.0 km and beyond. The consistency between the ^{131}I and ^{133}I data support the reliability of the measured collections.

With the encouragement of the agreement of the revised data shown in Table 4, the entire set of routine ^{131}I samples obtained at approximately two-week intervals during 1965 was evaluated. The C.E. plume rise estimates were employed. Several sampling periods had to be eliminated owing to interference during June from the second Chinese weapons test and a lower level interference during November of ^{131}I from some unreported off-site source.

The method of calculation was similar to that used for the intensive evaluation of the March data, except that an overall mean wind speed was assumed to be associated with a given dispersion condition. Adjustments for half-life were also made, but a uniform emission rate throughout each sampling period was assumed unless marked changes were known to have occurred. In all, 17 sampling periods were examined and these data were combined with the March series.

Many samples contained so little ^{131}I that they obviously strained the capability of the measurement system, and it is equally true that the assumptions of the simplified calculation method may not have been satisfied when a sampling station was downwind for only a few hours during a two-week period. The first

Table 4. Comparison of Observed and Calculated Samples, March 1965 Series Central Electric Δh Equation

Station	Distance (m)	^{131}I (pCi)			^{133}I (pCi)		
		Obs.	Calc.	C/O	Obs.	Calc.	C/O
E-11	700	35	50	1.4	380	520	1.4
		43	52	1.2	380	520	1.4
		35	17	0.5	150	115	0.8
		12	9	0.7	50	32	0.6
		14	8	0.6	—	—	—
Igloo	1750	100	220	2.2	700	2440	3.5
E-4	2200	6	3	0.5	—	—	—
E-7	2550	36	19	0.5	380	198	0.5
		75	115	1.5	740	1150	1.5
		47	45	1.0	48	78	1.6
		20	26	1.3	—	—	—
E-9	2750	10	4	0.4	20	14	0.7
		12	4	0.3	—	—	—

examination of the data was made with a view toward identifying the reliable, meaningful cases. From Table 5 it is apparent that the scatter of the C/O ratios is large when the observed amount is less than 10 pCi and becomes more orderly when it is more than 10 pCi. Based on this and a knowledge of the variability of the meteorological factors, it was decided to confine the comparison to samples containing more than 10 pCi and estimated exposures of at least eight hours.

Table 5. Distribution of Samples by C/O Ratios and Amount Collected

C/O ratio	No. of samples with	
	0.1 to 10 pCi	> 10 pCi
0.0–0.2	7	23
0.3–0.5	9	21
0.6–1.0	5	16
1.1–2.0	7	3
2.0–5.0	3	1
5.0–10.0	2	
> 10	3	

These data were then classified according to distance from the source and Table 6 shows such a breakdown. Although there are differences in the mean values of the C/O ratios and considerable scatter among individual cases, there is no obvious distance related trend. It therefore appears that the Central Electric equation gave an accurate estimate of effective stack height.

That the geometric mean of all C/O ratios is 0.61 suggests a persistent tendency for the calculation methods to underestimate the observed values. Two possible reasons for this are currently being examined as the 1966 data become available.

Table 6. Calculated/Observed Ratios as a Function of Distance

	Distance from source				
	500–999 m	1000–1499 m	1500–2200 m	2500–3000 m	
	0.4	0.6	0.1	0.2	
	0.6	0.4	0.6	0.4	
	1.4	1.0	0.5	0.4	
	1.2	0.8	0.9	0.3	
	0.5	0.7	0.4	0.7	
	0.7		5.5	0.9	
	0.6		7.1	0.2	
	0.5			0.3	
	5.2			0.4	
	0.3			0.5	
	0.2			5.7	
	0.1			0.4	
	0.2			0.2	
	0.4			0.8	
	0.3			0.5	
	0.2			1.5	
	0.4			1.0	
	0.5			1.3	
	1.4			1.8	
	0.7			1.2	
				0.5	All data
Mean	0.49	0.66	0.90	0.60	0.61
No. ⩾ 1.0	4	1	2	6	13
No. < 1.0	16	4	5	15	40

The wind speed, $\bar{u}$, appearing in the denominator of both equations (1) and (2) applies to a medium having a uniform flow throughout, whereas the atmosphere usually showed an increase with height. Selection of $\bar{u}$ is therefore a somewhat arbitrary process. The wind speeds used in all calculations have been those at stack height, this selection being justified from the oil fog tracer tests. It may be argued that the mean wind speed in the layer between the source and the ground is lower than that at stack height. Following this line of reasoning, one would have to use the wind speed at 50 ft elevation to achieve a mean C/O ratio of 1.00. Typical daytime (B_1) conditions prevail in these test cases, for which change of wind with height is described by a $\frac{1}{4}$ power law.

It is also possible that, at much lower emission rates than those prevailing during the March release, there is a systematic underestimate in the output rate, Q, or overestimate of the amounts of ^{131}I collected by the ground level samplers. Comparison of the two groups does show that the 13 samples of early March had a mean C/O of 0.80 while the 41 useful cases obtained during the rest of the year had a mean of only 0.56, but the authors can visualize no mechanisms which can satisfactorily explain this discrepancy.

The discussion of the long term results has indicated obvious and suspected flaws in both the methods of calculation and in the evaluation system. Nevertheless, the project has revealed important features of the BGRR plume and of dispersion patterns at this site. The environmental monitoring data have verified that the method of calculation is a useful means of estimating long term dispersion of the reactor plume, probably more accurately than engineering estimates (as opposed to measurements) of pollutant emission rates, and therefore adequate for general use.

REFERENCES

1. I. A. Singer. A comparison of computed and measured dose rates from radioargon emitted by the Brookhaven Reactor Stack. BNL-292 (1954).
2. A. P. Hull. Vegetation retention and vegetation-milk ratios of fallout ^{131}I, *Health Physics* **9,** 1173–77 (1963).
3. A. P. Hull. Environmental monitoring of ^{131}I in small concentrations and some comparisons with meteorological predictions, *Health Physics* **12,** 1317–25 (1966).
4. C. F. Foelix and A. P. Hull. Monitoring the cooling air effluent from the Brookhaven Graphite Research Reactor at the point of release and in the environment. *Int. Coll. on the Radioactive Pollution of Gaseous Media*, Saclay, France, November 1963, Vol. II, p. 449 (1964).
5. I. A. Singer and M. E. Smith. Atmospheric dispersion at Brookhaven National Laboratory, *Int. J. of Air and Water Poll.* **10,** 125–35 (1966).
6. M. E. Smith. The variation of effluent concentrations from an elevated point source, *AMA Arch. Ind. Health* **14,** 56–69 (1956).
7. G. H. Bosanquet, W. F. Carey and E. M. Halton. Dust deposition from chimney stacks, *J. Mech. Eng.* 355–67 (1950).
8. J. A. Frizzola, I. A. Singer and M. E. Smith. Measurements of the rise of buoyant clouds, submitted *J. AGU* (1966).
9. D. H. Lucas, D. J. Moore and G. Sporr. The rise of hot plumes from chimneys, *Int. J. of Air and Water Poll.* **7,** 473–500 (1963).

QUÈLQUES PROBLÈMES DU REJET DES EFFLUENTS RADIO-ACTIFS DANS LES FLEUVES INTERNATIONAUX

P. S. BOJOVIĆ

Institut des Sciences Nucléaires "Boris Kidrič", Vinča, Service de Protection contre les Radiations, Yougoslavie

Résumé—On expose dans ce rapport certaines difficultés rencontrées lors du rejet des effluents radio-actifs dans les fleuves internationaux. Ce problème est devenu actuel, étant donné qu'un assez grand nombre de centres nucléaires dans le monde entier sont situés auprès des fleuves internationaux ou de leurs affluents.

En posant ce problème on considère l'influence des valeurs des CMA (concentration maximale admissible) de l'eau, l'influence de l'apport national au débit total d'un fleuve international, ainsi que l'influence de quelques autres facteurs. Afin de contribuer à la solution de ce problème on propose une formule destinée à déterminer l'activité de seffluents radio-actifs qui pourraient être rejetés dans les fleuves internationaux.

INTRODUCTION

Le rejet d'effluents radio-actifs liquides dans les fleuves date de plusieurs années dans beaucoup de pays en Europe et hors d'Europe. Une dilution significative des effluents dans le fleuve diminue leur teneur en isotopes radio-actifs au dessous de la CMA. Cette manière d'élimination par dilution des effluents radio-actifs est pratiquement inévitable à présent.

Quand il s'agit d'un pays où l'on rejette des effluents dans des fleuves nationaux, les problèmes de CMA, de débit du fleuve, des conditions et de la dynamique du rejet, sont faciles à résoudre. Tout cela peut être réglementé par un protocole national. Il n'en est pas de même pour les pays rejetant des effluents dans des fleuves internationaux. Beaucoup de difficultés y sont rencontrées, comme il est exposé dans plusieurs communications et rapports. [1-3]

Nous nous sommes proposés de contribuer par ce rapport à la solution des problèmes cités ci-dessus, utilisant les principes connus et les expériences acquises lors du rejet d'effluents radio-actifs dans les fleuves nationaux.

MANIÈRE DE POSER LE PROBLÈME

Un problème bien posé, dit-on, est un problème presque résolu. Cependant, de nombreuses difficultés rencontrées lors du rejet des effluents radio-actifs dans les fleuves internationaux rendent difficiles la solution d'un ensemble de problèmes aigus.

Dans un livre récemment publié: "Management of radioactive wastes", par C. A. Mawson [3] l'auteur traite ce problème de façon nette et convaincante:

"Quand les effluents sont rejetés dans les fleuves, lacs ou mers internationaux, ce sont les populations ne faisant aucun contrôle des effluents qui peuvent être exposées à un effet nocif. Tel niveau de contamination, admissible pour un pays, ne le serait pas du tout pour un autre. Un pays situé en amont d'un fleuve serait prêt à développer une industrie nucléaire, même au prix de tolérer de fortes doses d'irradiation, tandis qu'un autre pays, situé en aval, qui s'intéresse surtout à l'agriculture, utilisant de l'eau courante uniquement pour l'irrigation et comme boisson, ne consentirait à tolérer aucune contamination".

Le passage cité est absolument juste et représente la situation actuelle. Cependant, prenant comme base un des principes législatifs fondamentaux "Sic utere tuo ut alienum non laedas", d'après lequel on n'oserait pas profiter d'un droit aux dépens des autres, et tenant compte d'une expérience acquise au cours de longues années, relative au rejet des effluents dans les fleuves nationaux, il est certainement possible de trouver une solution acceptable

pour tous les pays rejetant des effluents dans un fleuve international.

La formule de rejet des effluents apparaît comme le premier problème, d'ailleurs facile à résoudre d'après un principe bien connu.[1, 4, 5] Le débit des fleuves, la CMA et la dynamique du rejet posent des problèmes très importants, mais difficiles à résoudre. Le contrôle de l'activité d'un fleuve international, bien qu'il exige l'engagement de nombreux experts dans ce domaine, peut être résolu de manière satisfaisante. Les problèmes d'ordre administratif et législatif seront résolus à condition que les autres problèmes fondamentaux soient posés et définis de façon à être acceptables par tous les pays intéressés rejetant des effluents dans un fleuve international.

PROPOSITION DE FORMULE DE REJET DES EFFLUENTS RADIO-ACTIFS DANS LES FLEUVES INTERNATIONAUX ET DISCUSSION

Le rejet dans la Tamise des effluents du Centre Nucléaire de Harwell (Angleterre) s'effectue selon la formule suivante:

$$(\mathrm{Ra} \times 2.500) + (\text{autres émetteurs } \alpha \times 420) + (\mathrm{Sr} \times 50) + + (\text{autres émetteurs } \beta) \leqslant 20\ C_i$$

pour un mois dans laquelle Ra, autres émetteurs α, etc. représentent l'activité en curies pour un mois.

Le rejet dans le Rhône des effluents radioactifs est réglementé suivant le même principe par un protocole conclu entre le CEA et le Ministère de la Santé Publique. La formule de rejet est la suivante:

$$\frac{\alpha}{2.10^{-7}} + \frac{\beta}{6.10^{-6}} + \frac{\mathrm{Pu}}{3.10^{-7}} + \frac{\mathrm{Sr}}{8.10^{-8}} \leqslant D$$

dans laquelle α, β, Pu et Sr sont les curies rejetés par jour, D étant le débit du Rhône par jour (m^3). Les valeurs des dénominateurs représentent les CMA correspondantes.

La formule recommandée par l'Agence Internationale de l'Énergie Atomique de Vienne,[1] est basée sur le même principe.

Tenant compte de ce principe lors du rejet des effluents dans les fleuves internationaux, la formule suivante serait acceptable pour calculer le niveau de l'activité tolérable:

$$\sum_{i=1}^{n} \frac{A_i \times e^{-\lambda_i t}}{CMA_i} \leqslant \frac{D_n}{F_c}$$

où D_n est l'apport national au débit du fleuve international. Si $D_{\text{d'entrée}}$ désigne le débit du fleuve international lors de son entrée sur le territoire national et $D_{\text{de sortie}}$ le débit du fleuve au point où quitte le territoire national, l'apport national au débit du fleuve international est défini par l'équation suivante:

$$D_n = D_{\text{de sortie}} - D_{\text{d'entrée}}$$

Les autres symboles de la formule sont:

- A_i — activité d'un isotope en curies,
- λ_i — constante de désintégration d'un isotope,
- t — temps passé depuis le rejet des effluents jusqu'au moment où les effluents quittent le territoire national,
- CMA_i — concentration maximale admissible des isotopes radio-actifs dans l'eau,
- F_c — facteur commun pour tous les pays traversés par des fleuves internationaux.

Pour que cette formule puisse être appliquée en pratique il faudrait que tous les pays soient d'accord au sujet de CMA et F_c. La valeur D_n n'est pas en principe discutable, parce qu'il s'agit d'une valeur connue qu'il ne faudrait que vérifier. Le facteur $e^{\lambda t}$ est important pour chaque pays particulier. Il tient compte de la désintégration des isotopes sur le trajet depuis le rejet jusqu'au point où le fleuve quitte le territoire national. D'après ce facteur même le rejet d'une activité élevée des isotopes à courte période serait admis s'il ne s'opposait pas aux règlements nationaux. Ce facteur peut avoir de l'influence sur le choix de l'endroit de rejet des effluents et de l'emplacement des centres nucléaires.

Tout en respectant les recommandations de l'ICRP, les pays de l'Europe et hors de l'Europe ne sont pas tout à fait d'accord au sujet des CMA. En tout cas, les recommendations de l'ICRP pourraient être prises comme base pour les CMA dans les fleuves internationaux. Nous estimons que les CMA devraient être uniformes pour tous les pays, car l'irradiation ne fait

aucune différence entre les pays, les peuples et les races.

Le facteur F_c représente une valeur qui diminue fictivement le débit du fleuve D_n, c'est-à-dire une fraction des CMA. Il peut être, par exemple, 10, 100, etc. Dépendant de la flore et de la faune, de l'utilisation de l'eau, du peuplement des rives et de beaucoup d'autres circonstances, ce facteur diffère d'un pays à l'autre. L'adoption des valeurs de F_c est d'autant plus difficile que les caractéristiques d'un fleuve international ne sont pas identiques pour tous les pays intéressés. Pour cette raison et pour d'autres la détermination des valeurs de F_c est un travail délicat et de responsabilité. Le facteur F_c devant être commun à tous les pays situés le long d'un même fleuve international, la solution consisterait à adopter une valeur expérimentale variant avec le temps en fonction des résultats du contrôle de l'activité du fleuve et des environs.

Nécessitant les mesures d'un grand nombre d'isotopes de faible activité, ce qui représente un inconvénient de ce procédé, la formule proposée ne serait peut-être pas convenable pour tous les pays. C'est pourquoi il faudrait prendre en considération aussi un autre type de formule, par exemple:

$$\frac{a}{CMA_a} + \frac{\beta}{CMA_\alpha} \leqslant \frac{D_n}{F_c}$$

où ne figurent que l'activité totale a et l'activité totale β. Le débit et F_c ont la même signification que ceux de la première formule. La formule du deuxième type est plus simple que la précédente, mais en raison des toxicités différentes des isotopes radio-actifs, elle donne des résultats moins corrects.

CONCLUSION

Pour appliquer les formules proposées, il faudrait effectuer des expériences préliminaires, déterminer la distance minimale entre le point de rejet des effluents et l'endroit où le fleuve international quitte le territoire national, il faudrait adopter des méthodes uniformes de contrôle de l'activité, élaborer des programmes de recherche communs afin de pouvoir suivre le sort des isotopes radio-actifs rejetés dans le fleuve et assurer l'échange des informations et des résultats. C'est l'Agence Internationale de l'Énergie Atomique de Vienne qui devrait en prendre l'initiative. C'est à elle d'encourager aussi les travaux concernant la vérification de D_n, l'adoption d'une valeur F_c et la solution des problèmes d'ordre législatif et administratif. Dans ce but l'Agence se mettrait en contact avec les pays traversés par les fleuves internationaux ou avec les organismes chargés de réglementer l'utilisation des fleuves en question.

RÉFÉRENCES

1. Disposal of Radioactive Wastes in Fresh Water, Safety Series No. 10. IAEA, Vienna, 1963.
2. *Proc. Conference on Water Pollution Problems in Europe.* United Nations, Geneva, 1961.
3. C. A. MAWSON. *Management of Radioactive Wastes,* Van Nostrand, Princeton, N. J. (1965).
4. R. H. BURNS. Radioactive waste control at the United Kingdom Atomic Energy Establishment, Harwell. *Proc. Monaco Conference on the Disposal of Radioactive Waste,* IAEA, Vienna, 1960.
5. J. RODIER *et al.* Étude de la dilution dans le Rhône des effluents radio-actifs du Centre de Marcoule. Rapport CEA No. 2003 (1961).
6. International Commission on Radiological Protection, Report of Committee II, Pergamon Press, New York (1959).

AN EVALUATION OF HAZARDS FROM IMMERSION OF PLUTONIUM IN THE MARINE ENVIRONMENT

J. D. TERESI*
U.S. Naval Radiological Defense Laboratory, San Francisco, California 94135

and

C. L. NEWCOMBE
San Francisco State College, San Francisco, California

Abstract—The potential hazard due to a single immersion and subsequent release of plutonium was evaluated on the basis of its possible incorporation in the marine food chains including the alga, *Porphyra*, and the seaweed products agar and alginic acid. The hazards were estimated by comparing the recommended permissible body burdens for large populations (1/10th occupational permissible body burden) with the expected body burden calculated on the basis of very conservative assumptions. The concentration of plutonium from a single release in the sea that would lead to the permissible body burden through the fish food chain was calculated on the basis of published concentration factors. The value of the concentration of plutonium to give this body burden was found to be 6.4×10^{-2} μCi/ml assuming a single intake of 200 gms of fish per individual. The expected body burdens from *Porphyra*, agar, and alginic acid were then calculated on the basis of the calculated plutonium concentration and the published concentration factor for seaweed. Calculations were also made of various diffusion parameters using six published diffusion models to obtain areas of contamination with time and the duration of a hazardous concentration.

INTRODUCTION

The objective of this study was to evaluate the potential hazards from the contamination of the California inshore ocean environment with plutonium following an instantaneous release upon immersion. The analysis considered the ocean environment at those distances from shore at which the ocean depth was about 10 m. At depths greater than this, one would expect the extent of the hazard to be less than that calculated for the 10 m case.

DESCRIPTION OF SOURCES OF HAZARD

Hazards from the existence of plutonium in the marine environment depend upon the physical and chemical properties of its compounds. Equally important are the relative amounts of contaminant in the several parts of the physicochemical and biological environments that may represent avenues of transport of the radioactivity to man.

Released plutonium in direct contact with water, or with naturally occurring suspended particulates of sea water (colloidal particles, sediments, and microscopic organisms), or with sea-bottom materials may result in a wide variety of interactions, most of which are poorly understood. Attention here is limited to those interactions that directly or indirectly affect the availability of plutonium to man.

In California, principal commercial sources of chemically processed marine algae are the phycocolloids agar and algin. Agar is a gelatinous substance produced on the Pacific Coast of the United States from the red alga, *Gelidium cartilagineum*. It is used by the baking industry, in icings, as a stabilizer in pies, as a moisture

* The opinions or assertions contained in this article are the private ones of the writer and are not to be considered as official or reflecting the views of the Navy Department or the Naval Service at large.

regulator in fruit cakes, in cream cheese, in jelly desserts and in puddings. Little is known about the extent to which chemical compounds of plutonium may be adsorbed or absorbed by *Gelidium*.

Algin is a term referring to the polyuronic acid, alginic acid $(C_6H_8O_6)_n$ and its derivatives. Algin occurs in large quantities in many seaweeds. Sodium alginate solutions may be transposed by solutions of salts of a large number of metals, including uranium; e.g. $U(SO_4)_2 \cdot 4H_2O$, to form insoluble alginates.

A dozen or more of the larger algae along the coast of California and lower California, such as the giant kelp, *Macrocystis pyrifera*, are used for the manufacture of algin. Annually, thousands of tons are collected south of Point Conception. The principal uses of algin are in pharmaceuticals, dairy products, soda-fountain drinks, cosmetics, drugs, salad dressings, candy, jelly, and chocolate milk. Algin is also used in stock feed and chicken feed. Although little is known of the extent of uptake of radionuclides by kelp, the potential plutonium body burden in man was estimated by using gross assumptions and available data (see hazard estimates below).

Edible algae, although poor sources of energy because of their indigestibility, possess an important vitamin and mineral content. Irish moss is harvested on the Atlantic Coast in considerable quantities but the amount of commercial utilization for food on the Pacific Coast of the United States is small. *Porphyra* is the only alga utilized directly for food in any quantity in California. In 1929 about 300,000 lb were harvested in Central and Southern California by American Chinese for distribution to Chinese stores or for exporting to the Orient. The potential hazard to the California Chinese is estimated in the section on estimate of the hazards.

Local spawning areas of pelagic fishes near the coast of California and centers of commercial fishing and sportfishing in shallow waters may, due to accidental situations, become centers for the origination of radioactive contamination that reaches man. The release of plutonium in a partially enclosed or restricted local area, as projected in this report, could result in a small-scale dispersal of the plutonium and in a correspondingly localized contamination of the food web of a local area. The scale of the resultant hazard from plutonium would depend in large part on the solubility of the radionuclide in sea water, the rate of diffusion, and the extent of uptake and transport of the contaminant through the food web to man. The scarcity of experimental data necessitates the use of conservative assumptions to make adequate estimates of the likely presence or absence of hazards due to plutonium in water.

ESTIMATE OF THE HAZARDS

The potential hazard due to immersion in seawater and subsequent release of the radionuclide is evaluated on the basis of its possible incorporation in the marine food chains including the alga *Porphyra* and the seaweed products agar and alginic acid.

The hazards from these various sources are estimated by comparing the recommended permissible body-burden for large populations (1/10th the occupational permissible body burden) with the expected body burden calculated on the basis of conservative assumptions.

Estimation of the Hazard Due to the Ingestion of Plutonium Through the Fish Food Chain

Desired information for a detailed description of the hazard has proved, in most instances, to be lacking. However, for present purposes, hazards to man from projected releases of plutonium can be satisfactorily evaluated by utilizing established knowledge of the marine environment and by resorting to necessary assumptions customarily utilized in analytical techniques for the evaluation of hazards. Many of the customarily used mathematical models and useful dosage concepts regarding levels of absorption and tolerance assume an organ-organ system equilibrium and/or an organism-environment equilibrium. Because of the relatively rapid dispersion of radioactivity (see the Appendix) throughout the environment and the consequent decrease with time of the concentration levels, the organism-environment equilibrium referred to above is in fact not likely to be reached in the situations under consideration. Thus the cylindrical-dispersion model is very conservative. Also, due to the behavior patterns of pelagic fish—their schooling habits and mi-

gratory movements—the probability of their remaining in a seriously contaminated area long enough to permit an equilibrium state is expected to be low. Hence, the likelihood of netting a sizeable number of contaminated fish is low. Furthermore, the total commercial catches per boat are proportionately large and, to this extent, the likelihood that a processing plant will turn out consecutive batches of this hypothetically contaminated product is correspondingly remote. Therefore it is reasonable to anticipate a single exposure by the consumer rather than a continuous exposure.

The maximum permissible body burden (MPBB) for the general population is usually assumed to be 1/10 that of the occupational value. In the case of ^{239}Pu the value chosen for the general population is, therefore, 0.004 μCi.

The body burden can be calculated in the following manner (neglecting decay and biological elimination):

$$q = f_w \cdot f_c \cdot I \cdot S \qquad (1)$$

where q = body burden in microcuries,
f_w = retention factor (fraction of total ingested that is retained in the body),
f_c = concentration factor (total concentration through all fish food chains),
I = food intake (g),
S = plutonium concentration in seawater (μCi/cm^3).

The value of f_w used here [1] is 2.4×10^{-5}. The value for f_c is 1 according to Dunster [2] and 13 according to Aten. [3]

The average daily intake of fish food has been estimated to be about 200 g, [4] assuming all protein food is obtained from marine sources.

If q is set at the maximum permissible value of 0.004 μCi and f_c is assumed to be 13, then the value of S will be 6.4×10^{-2} μCi/cm^3. The following expression for S results if we assume an instantaneous plutonium release (C), in curies, with immediate mixing throughout a cylinder of water of depth (D), in meters, and a surface area given by (A). (Other diffusion models are treated in the Appendix.)

$$S = \frac{C}{AD} \ (\mu\text{Ci/cm}^3) \qquad (2)$$

where A = area (m^2).

Substituting for S the value of the concentration that would result in the maximum permissible body burden and 10 for D and transposing, equation 3 results:

$$A = \frac{C}{10 \times 6.4 \times 10^{-2}} = 1.56\,C \ (\text{m}^2). \qquad (3)$$

For any given total release of plutonium the area of the sea containing the concentration 6.4×10^{-2} μCi/cm^3 can be calculated. The radius of the equivalent circular area can then be determined. Examples of contaminated areas for various total amounts of plutonium released to a depth of 10 m are shown in Table 1.

Table 1. *Radii* (r) *of Cross-sectional Areas* (A) *of Contaminated Cylindrical Volumes as a Function of Total Plutonium* (C) *Released to a Depth of* 10 *meters*

C (curies)	A (meters^2)	r (meters)
10^2	1.56×10^2	7
10^3	1.56×10^3	22
10^4	1.56×10^4	70
10^5	1.56×10^5	220
10^6	1.56×10^6	700

The sample results shown in Table 1 can be used to indicate the volume and the areas of offshore water involved under assumptions of instantaneous releases of plutonium in amounts of 10^2 to 10^6 Ci. The calculations based on a concentration factor of 13, indicate that 200 g of fish obtained from these areas during a short period of time while the plutonium concentration is at the level of 6.4×10^{-2} μCi/cm^3 would have to be eaten by each individual of a large population to result in the general population MPBB of 0.004 μCi. This type of estimate of the hazard is a conservative one since it implies that fish concentrate plutonium to the equilibrium value during their stay in the body of water involved. It also assumes that a large population will obtain enough to supply it with food for one day's consumption of 200 g per individual.

Estimation of the Hazard Resulting from the Ingestion of Agar

The value of the plutonium body burden from ingestion of agar processed from seaweed is a function of the concentration factor for seaweed, the yield of agar, and the amount of plutonium carried with the agar.

Agar is prepared from a filtrate obtained from a hot-water treatment under pressure and therefore would probably not contain plutonium. Since there are no data available on this point, it has been assumed that the plutonium of the seaweed will follow the agar in a proportional manner.

According to Tseng,[5] the 650,000 lb of agar used annually in the United States were distributed approximately as shown in Table 2. As can be seen, only about $\frac{1}{2}$ of the total is ingested. Of this total amount used, only 52,000 lb, or 8%, is produced in the United States (Southern California) and, therefore, the amount of the Southern California produced agar ingested is 26,000 lb per year.

Table 2. Annual Distribution of Agar in the United States

Utilization	Amount (lb)
Laxatives	100,000
Microbiological culture	100,000
Bakery	100,000
Confectionery	100,000
Dental impression mold	75,000
Meat packing	50,000
Emulsifier	50,000
Cosmetics	25,000
Miscellaneous	50,000

The total area from which this much agar is produced constitutes about 100 mi^2[6] (2.59×10^8 m^2). As shown in Table 1, the area of concern relative to a plutonium contamination of 6.4×10^{-2} $\mu Ci/cm^3$ is 1.56 m^2 per curie of plutonium released for a cylindrical instantaneous dispersion model. Therefore, the amount of plutonium which could just contaminate this 100/mi^2 area to the above concentration is 1.66×10^8 Ci, and thus the amount of contaminated agar that would be ingested is about 7.1×10^{-2} g/Ci of released plutonium.

If we assume a population of about 10^8 then the *per capita* ingestion of the contaminated agar would be 7.1×10^{-10} g/Ci released. The concentration factor for seaweed is assumed to be 500, which is only a guess given by Dunster,[2] probably based on soluble plutonium compounds.

To calculate the body burden from agar ingestion the following expression is used:

$$q = I_{ag} S f_c f_w$$

where:

q = body burden (μCi),
I_{ag} = intake of agar (g),
S = plutonium concentration in seawater ($\mu Ci/cm^3$),
f_c = concentration factor for seaweed,
f_w = body retention factor.

Substituting 500 for f_c, 2.4×10^{-5} for f_w, 6.4×10^{-2} for S and 7.1×10^{-10}/Ci for I_{ag}, $q = 5.5 \times 10^{-13}$ μCi/Ci of released plutonium.

Thus, on the basis of the conservative assumptions used in the calculations, a release of about 7×10^9 Ci of plutonium would be required to result in an average body burden due to agar ingestion equal to the MPBB of 0.004 μCi.

Estimation of the Hazard Resulting from the Ingestion of Algin

The value of the plutonium body burden from ingestion of algin from seaweed is a function of the concentration factor for seaweed, the yield of algin, the plutonium content of seawater, the amount of plutonium carried with the algin, and the body retention factor for plutonium. According to Tseng,[8] fresh kelp, *Macrocystis pyrifera*, is digested with soda, which reacts with alginic acid in the kelp to form soluble sodium alginate. After filtration, the filtrate is acidified, precipitating the alginic acid.

Since alginic acid is prepared by an alkaline treatment of kelp, the plutonium would probably be in an insoluble form and, therefore, the amount of plutonium contamination in the alginic acid should be negligible. However, since the amount of contamination actually expected is not known, the calculation of the body burden is based on the assumption that plutonium

is not precipitated out in the production and purification of alginic acid.

According to Tseng, [9] the annual production of algin in the United States is estimated at two to three million pounds. More than 70% of the total algin produced comes from Southern California.

As in the case of agar, the total area from which this much algin is produced constitutes about 100 mi^2 (2.59×10^8 m^2). The amount of contaminated algin that would be ingested assuming a 3-million-pound total production and an area of concern, shown in Table 1, of 1.56 m^2 per curie released, relative to a seawater plutonium concentration of 6.4×10^{-2}, is 1.8×10^{-2} lb/Ci released (8.2 g/Ci released). Based on a population of 10^8, the *per capita* ingestion of contaminated algin would be 8.2×10^{-8} g/Ci released.

The following expression is used to calculate the body burden expected from ingestion of algin:

$$q = I_{al} \cdot S \cdot f_e \cdot f_w$$

where

I_{al} = intake of algin (g).

After substituting the values of S, f_e, f_w as above for the agar calculations and the value of 8.2×10^{-8} g/Ci released for I_{al},

$q = 6.3 \times 10^{-11}$ μCi/Ci of released plutonium.

Thus, on the basis of the conservative assumptions used in the calculations, a release of about 6.3×10^7 Ci of plutonium would be required to result in a body burden due to algin ingestion equal to the MPBB of 0.004 μCi.

Estimation of the Hazard Resulting from the Ingestion of Porphyra

About 300,000 lb of *Porphyra* [8] are harvested annually from an area of about 100 mi^2. Since the contaminated area as shown above would be about 1.56 m^2 per curie of plutonium released, the amount of *Porphyra* harvested from the area of possible contamination would be 1.8×10^{-3} lb/Ci released (0.82 g/Ci released).

If one assumes that this amount is distributed to the 94,000 California Chinese only, then the *per capita* ingestion of contaminated alga would be 8.7×10^{-6} g/Ci released.

The body burden can be calculated from the following equation:

$$q = I_p \cdot S \cdot f_e \cdot f_w$$

where I_p = intake of *Porphyra* (g).

By substituting the values S, f_e, f_w given above and the value of 8.7×10^{-6} g/Ci of released plutonium for I_p, the value for the body burden q per curie of plutonium released is 6.7×10^{-9} μCi.

It is seen then that a release of about 6×10^5 Ci of plutonium would be required to result

Table 3. Summary of Calculated Body Burdens obtained for Values of Parameters shown

Concentration factor fish food web		13*
Concentration in seawater to give body burden of 0.004 μCi (fish food)		6.4×10^{-2} μCi/cm^3
Area of 10 m depth containing 6.4×10^{-2} μCi/cm^3		1.56 m^2/Ci released
Calculated body burden from ingestion of:		
	Agar	5.5×10^{-13} μCi/Ci released
	Algin	6.3×10^{-11} μCi/Ci released
	Porphyra†	6.7×10^{-9} μCi/Ci released

* This is a conservative factor since it was obtained with soluble nuclide under equilibrium conditions. The actual exposure time of the fish food web is a matter of minutes or, at most, a few hours (see Appendix).

† The evaluation of the body burden from *Porphyra* is conservative since it is based on the assumption that the *Porpyhra* harvested is consumed by 94,000 Californians.

in a body burden of 0.004 μCi in 94,000 Chinese due to the ingestion of *Porphyra.*

SUMMARY

Table 3 presents a summary of information used and values obtained in the analyses presented above.

APPENDIX

Calculation of Dispersal and Concentration of Substances Released into the Ocean

Equations to describe the change with time of the concentration of a diffusing substance have been described by Okubo.[9] These are presented below and may be applied to the release of plutonium.

1. *Joseph and Sendner Solution:*

$$\frac{\partial S}{\partial t} = \frac{1}{r}\frac{\partial}{\partial r}\left(Pr^2\frac{\partial S}{\partial r}\right) \qquad \text{(A1)}$$

From this was obtained

$$S(r, t) = \frac{nM}{2\pi D(Pt)^2}\, e^{-\frac{r}{Pt}} \qquad \text{(A2)}$$

where $n = 360°/\theta_n$

θ_n = the angle of the sector to which diffusion is restricted (180° for uniform coastline and 360° for open ocean),

S = concentration in Ci/m^3,

r = distance from origin in meters,

D = thickness of the contaminated layer in meters,

P = "diffusion velocity"* (m/hr) = 54 m/hr,

M = amount of radioactivity released in curies.

The maximum concentration is at the center of the diffusing volume and is given by

$$S_o(t) = \frac{nM}{2\pi D(Pt)^2} \qquad \text{(A3)}$$

2. *Modified Ozmidov Solution:*

$$S(r, t) = \frac{M}{6\pi\gamma^3 t^3 D}\, e^{-\frac{r^{2/3}}{\gamma t}} \qquad \text{(A4)}$$

where γ = "energy-dissipation parameter" (m$^{2/3}$/hr)
$= 1.17$ m$^{2/3}$/hr

$$S_o(t) = \frac{M}{6\pi\gamma^3 t^3 D} \qquad \text{(A5)}$$

3. *Modified Okubo and Pritchard Solution:*

$$S(r, t) = \frac{M}{\pi W^2 t^2 D}\, e^{-\frac{r^2}{W^2 t^2}} \qquad \text{(A6)}$$

where W = "diffusion velocity" (m/hr)
$= 86.4$ m/hr

$$S_o(t) = \frac{M}{\pi W^2 t^2 D} \qquad \text{(A7)}$$

4. *Okubo Solution:*

$$S(r, t) = \frac{4M}{3\pi^{3/2}\bar{\alpha}^3 t^3 D}\, e^{-\frac{r^{4/3}}{\bar{\alpha}^2 t^2}} \qquad \text{(A8)}$$

where $\bar{\alpha}$ = "energy-dissipation parameter" in m$^{2/3}$/hr
$= 1.67$ m$^{2/3}$/hr

$$S_o(t) = \frac{4M}{3\pi^{3/2}\bar{\alpha}^3 t^3 D} \qquad \text{(A9)}$$

5. *Obukhov Solution:*

$$S(r, t) = \frac{M}{\pi\beta^3 t^3 D}\, e^{-\frac{r^2}{\beta^3 t^3}} \qquad \text{(A10)}$$

where β = "energy-dissipation parameter" (m$^{2/3}$/hr)
$= 2$m$^{2/3}$/hr

$$S_o(t) = \frac{M}{\pi\beta^3 t^3 D} \qquad \text{(A11)}$$

6. *Schonfeld Solution:*

$$S(r, t) = \frac{M\omega t}{2\pi D(\omega^2 t^2 + r^2)^{3/2}} \qquad \text{(A12)}$$

* The values for "diffusion velocity" and "energy dissipation parameter" used in the various solutions were taken from a table of data on diffusion of radioactivity reported in ref. 9.

where ω = the "diffusion velocity" (m/hr) = 68.4 m/hr

$$S_0(t) = \frac{M}{2\pi D\omega^2 t^2} \quad \text{(A13)}$$

Expressions for the time, t_m, required to reach the maximum distance, r_m, for a given concentration, S, were obtained by differentiation with respect to t and setting dr/dt equal to zero in each of the diffusion equations. The resulting expressions are given below.

1. *Joseph and Sendner Solution* $(n=1)$:

$$t_m = K_1 e^{-1} \quad \text{(A14)}$$

where $K_1 = \left(\frac{M}{2\pi DP^2S}\right)^{1/2}$

$$r_m = 2Pt_m = \sqrt{2}\left(\frac{M}{\pi DS}\right)^{1/2} e^{-1} \quad \text{(A15)}$$

2. *Modified Ozmidov Solution:*

$$t_m = K_2 e^{-1} \quad \text{(A16)}$$

where $K_2 = \left(\frac{M}{6\pi\gamma^3 DS}\right)^{1/3}$

$$r_m = (3\gamma t_m)^{3/2} = \frac{3}{\sqrt{2}}\left(\frac{M}{\pi DS}\right)^{1/2} e^{-3/2} \quad \text{(A17)}$$

3. *Modified Okubo and Pritchard Solution:*

$$t_m = K_3 e^{-1/2} \quad \text{(A18)}$$

where $K_3 = \left(\frac{M}{\pi W^2 DS}\right)^{1/2}$

$$r_m = Wt_m = \left(\frac{M}{\pi DS}\right)^{1/2} e^{-1/2} \quad \text{(A19)}$$

4. *Okubo Solution:*

$$t_m = K_4 e^{-1/2} \quad \text{(A20)}$$

where $K_4 = \left(\frac{4M}{3\pi^{3/2}\bar{a}^3 DS}\right)^{1/3}$

$$r_m = \left(3/2\bar{a}^2 t^2_m\right)^{3/4} = \left(\frac{6}{\pi}\right)^{1/4}\left(\frac{M}{\pi DS}\right)^{1/2} e^{-3/4} \quad \text{(A21)}$$

5. *Obukhov Solution:*

$$t_m = K_5 e^{-1/3} \quad \text{(A22)}$$

where $K_5 = \left(\frac{M}{\pi\beta^3 DS}\right)^{1/3}$

$$r_m = \left(\beta^3 t^3_m\right)^{1/2} = \left(\frac{M}{\pi DS}\right)^{1/2} e^{-1/2} \quad \text{(A23)}$$

Table A1. *Values, as a Function of Diffusion Model, of the time, t_m, required for the concentration to reach a value of* 6.4×10^{-2} *μCi/cm^3 at a maximum distance, r_m, and the time, t_o, required for the center of contamination (release point) to reach* 6.4×10^{-2} *μCi/cm^3*

Model	$M = 10^4$ Ci			$M = 10^8$ Ci		
	r_m (meters)	t_m (hr)	t_o (hr)	r_m (meters)	t_m (hr)	t_o (hr)
Joseph & Sendner ($n = 1$)	36	0.34	0.92	3600	33.8	92
Ozmidov	33	2.9	8	3300	63	172
Okubo & Pritchard	43	0.49	0.8	4300	49	81
Okubo	38	5.6	9.2	3800	121	199
Obukhov	43	6.1	8.5	4300	131	183
Schonfeld	31	0.32	0.72	3100	28.6	72.4

6. *Schonfeld Solution:*

$$t_m = K_6 \left(1/3\right)^{3/4} \tag{A24}$$

where $$K_6 = \left(\frac{M}{2\pi DS\omega^2}\right)^{1/2}$$

$$r_m = \sqrt{2}\omega t_m = \left(1/3\right)^{3/4} \left(\frac{M}{\pi DS}\right)^{1/2} \tag{A25}$$

Values of the maximum distance at which the concentration of 6.4×10^{-2} μCi/cm^3 will be found can be calculated from the summary equations presented above. The time required for this maximum distance to be reached can also be calculated. The time, t_0, required for the center of the contaminated area (release point) to reach the concentration of 6.4×10^{-2} μCi/cm^3 can also be calculated from the equations for S_0. These values are shown in Table A1 for two values of the amount of plutonium released (M).

REFERENCES

1. ICRP Committee II. Permissible dose for internal radiation, *Health Physics* **3,** 1 (1960).
2. H. J. DUNSTER. *Proc. International Conference on the Peaceful Uses of Atomic Energy, Reactor Technology and Chemical Processing* **9,** 712 (1956).
3. A. H. W. ATEN, JR. *Health Physics*, **6,** 114 (1961).
4. Committee on the Effects of Atomic Radiation on Oceanography and Fisheries, Radioactive Waste Disposal from Nuclear Powered Ships, NAS-NRC 658 (1959).
5. C. K. TSENG. *Sci. Monthly* **58,** 25 (1944).
6. P. BONNOT. *California Fish and Game* **17,** 40 (1931).
7. C. K. TSENG. *Sci. Monthly* **59,** 37 (1944).
8. C. K. TSENG. *Econ. Bot.* **1,** 69 (1947).
9. A. OKUBO. Chesapeake Bay Institute Technical Report 30, Reference 62–20 (1962).

STUDIES ON THE RELEASE OF RADIOACTIVITIES FROM THE ION EXCHANGE RESINS INTO THE SEA WATER

YASUSHI NISHIWAKI
Tokyo Institute of Technology

YOSHIHIDE HONDA, HIROSHI KAWAI, TAKEO HARADA, YUICHIRO KIMURA, HIROSHIGE MORISHIMA and TAEKO KOGA
Atomic Energy Research Institute, Kinki University

Abstract—For the purpose of estimating the release of radioactivities from ion exchange resins disposed into sea water, we have conducted a series of experiments in a water bath containing natural sea water, using such radioactive nuclides as ^{51}Cr, ^{55}Fe, ^{60}Co, ^{89}Sr and fission products by changing the weight ratio of ion exchange resin to the sea water and the amount of nuclide initially adsorbed on the ion exchange resin under static and turbulent conditions. The results are summarized as follows:

1. The radioactivities were rapidly released from the ion exchange resin particles (Dowex 50 and Dowex 1, 50–100 mesh) on contact with the sea water. However, some differences were observed in the degree of release depending on the different nuclides. Such nuclides as ^{60}Co and ^{89}Sr were easily released, while ^{51}Cr and ^{55}Fe not so easily.
2. The released activity was observed to increase with the decreasing weight ratio of the ion exchange resin to the sea water, but with the weight ratio below 10^{-4} of the ion exchange resin to the sea water no remarkable difference was observed.
3. The results of fractionation of suspended matter in sea water containing ^{55}Fe, ^{60}Co and ^{89}Sr will be discussed also.

1. INTRODUCTION

It is considered to be an important problem to investigate the behaviour and distribution of radioactivities in the eco-system in the ocean, when radioactive contamination and its effects due to radioactive waste disposal into sea water are studied.[1-6] If by any chance high-level activities of spent ion exchange resins were disposed into the sea, the possible effect on man who might consume the marine products contaminated with radioactivity should be adequately assessed. To consider the effects, it is necessary as a first step to investigate the percentage of the release of radioactivities adsorbed on the ion exchange resin and to investigate the behaviour and distribution of released radioactivities in the sea water. In order to estimate the release of radioactivities from the ion exchange resins disposed into sea water and to estimate the behaviour and distribution of radioactivities released into sea water, we have conducted a series of experiments in a water bath containing natural sea water, using several radioactive nuclides.

Further, the behaviour and distribution of radioactive nuclides in suspended matter in sea water were also studied experimentally by fractional filtration.

2. MATERIALS AND APPARATUSES

2.1. *Sea Water*

Natural surface sea water was sampled at about 50 m distance from the Misaki beach of Osaka-Bay. The total sodium content was estimated at 9500 ppm, the chlorinity 17.7 ‰ and pH 8.0–8.2.

2.2. *Ion exchange resins*

H-types of cation exchange resin, Dowex 50-X8 (50–100 mesh), were used. Their exchange capacity was estimated to be 4.44 meq

for Na^+ per 1 g of dry resin, 3.37 meq for Sr^{++} and 3.49 meq for Co^{++}. Cl-types of anion exchange resin, Dowex 1-X8 (50–100 mesh), were also used. Their exchange capacity was estimated to be 1.91 meq for Cl^- per 1 g of dry resin.

2.3. *Radioactivities*

^{51}Cr ($CrCl_3$, HCl solution), specific activity 13.3 mCi/mg, 2.8 mCi/ml.
(Commissariat à l'Energie Atomique)

$^{55, 59}Fe$ ($FeCl_3$, HCl solution) carrier free, 26.8 mCi/ml.
(Nuclear Science and Engineering Co.)

^{60}Co ($CoCl_2$, HCl solution) Co 0.44 mg/ml, specific activity 55 mCi/mg, 24.2 mCi/ml.
(Oak Ridge National Laboratory)

^{89}Sr ($SrCl_2$, HCl solution) carrier free 1.7 mCi/ml.
(The Radiochemical Centre)

Each radioactive chemical was diluted, and about 10 or 100 μCi was adsorbed on ion exchange resin for one experiment.

2.4. For measuring β-radioactivities of samples a G-M counting system and a low-background gas-flow type counting system were used. A scintillation counter was used for counting γ-radioactivities.

2.5. A spectro-photometer was used to determine the quantities of cobalt and strontium carriers. Sodium content of sea water was measured with a flame-photometer, pH of sea water was measured with a pH-meter with glass electrodes.

2.6. Water baths used for experiments were made of acryl-plastics. The size was 1000 mm (length) × 500 mm (width) × 1000 mm (height). Cylindrical water baths made of glass and those of polyethylene were also used, the sizes of which were 113 mmϕ × 145 mm (height) and 300 mmϕ × 430 mm (height), respectively.

2.7. Sea water in the acryl plastic water bath was stirred with compressed air which was led into the center of the water bath through a vinyl chloride pipe (inner diameter 13 mm) connected to a blower-pump with a flow-rate of 1 l./sec (Fig. 1). A glass water bath and a stirrer with a stainless steel propeller (about 200 r.p.m.) were also used.

2.8. Suspended matter in the sea water was filtered successively with Toyo-filter paper No. 5A (mean pore size 18 μ), milli-pore filter OS type (mean pore size 10 μ), SM type (mean pore size 5 μ), RA type (mean pore size 1 μ), and HA type (mean pore size 0.5 μ).

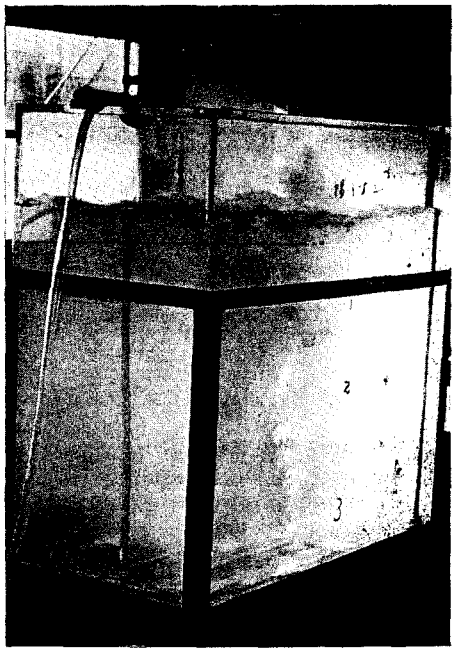

FIG. 1. Experimental water bath.

3. EXPERIMENTAL PROCEDURES

3.1. *Weight ratios of ion exchange resins to sea water*

Keeping the volume of sea water in the water bath constant, the weight of ion exchange resins mixed with the sea water was changed for the range of weight ratio from 10^{-3} to 10^{-7}.

3.2. *Initial carrier quantities in ion exchange resins*

The quantities of stable carriers adsorbed on the cation exchange resins were changed, keeping the radioactivity previously adsorbed on the resins constant.

3.3. *Released radioactivity from ion exchange resins*

In performing these experiments, ion exchange resins on which radioactive nuclides were adsorbed were placed in the sea water

contained in the water bath. An aliquot of the water (1 ml) was sampled with definite time interval at each of the 5–9 points indicated in Fig. 2 in order to determine the spacial distribution of the radioactivity in the sea water.

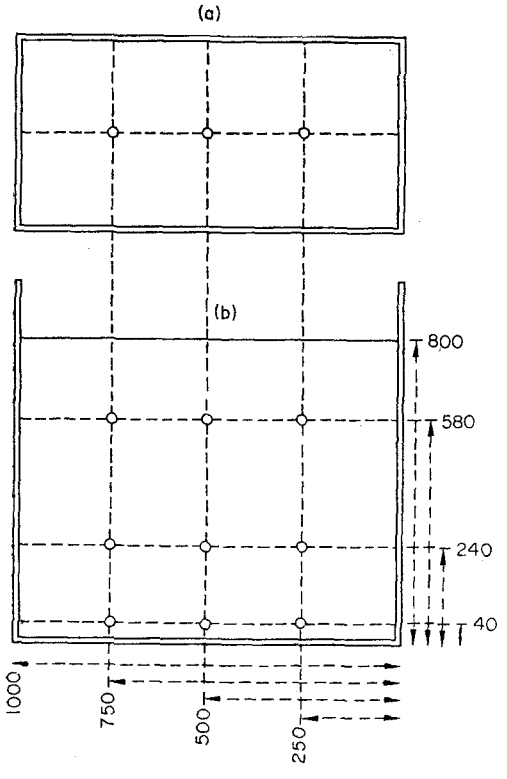

FIG. 2. Experimental water bath and sampling position.

After equilibrium, the percentage of released radioactivity was estimated from the residual radioactivity in the resins.

3.4. *Measurement of suspended matter in the sea water*

3.4. 1. *Fractionation of suspended matter.* At definite times an aliquot of sea water (1.5 l.) was sampled and filtered successively through five different types of filters, as listed in Table 1, in the order of pore sizes, to fractionate suspended matter in the sea water by suction with rotary vacuum pump. Each fraction was rinsed with distilled water. The chloride in the filtrate was tested with silver nitrate and the ammonium with Nessler's reagent.

3.4. 2. *Measurement of dry weight of suspended matter in sea water.* Fractionated suspended matter was dried in a desiccator until the weight became constant, and weighed.

3.4. 3. *Measurement of organic suspended matter.* Total nitrogen of dry samples was determined by the microkjeldahl method. The quantities of nitrogen were used as index of organic suspended matter. The amount of total organic matter was estimated by multiplying the nitrogen quantities by 17 according to D. L. Fox *et al.* [7]

3.5. *Concentration factor and accumulation fraction of radioactive nuclides in suspended matter in sea water*

Concentration factor is defined as the ratio of radioactivity (cpm/g) of each fraction of

Table 1. *Properties of Filters*

Filter	Material	Color	Thickness microns	Flow rate* ml/min. cm²	Mean pore size microns
TR-No. 5A	Cotton	White	200	—	18
MF-OS	Cellulose plastic	White	280	500	10
MF-SM	Cellulose plastic	White	170	560	5
MF-RA	Cellulose plastic	White	150	300	1
MF-HA	Cellulose plastic	White	150	65	0.5

TR: Toyo Roshi (Toyo Filter Paper), Japan.
MF: Millipore filter, U.S.A.
* Flow rate of water at 25°C with a pressure 70 cm Hg.

suspended matter in the sea water per dry weight to the radioactivity concentration (cpm/ml) of final filtered sea water (sea water filtered with HA type filter).

$$\text{Concentration factor} = \frac{\text{Radioactivity of each fraction per dry weight (cpm/g)}}{\text{Radioactivity concentration of final filtered sea water (cpm/ml)}}$$

At equilibrium state, the accumulation fractions of radioactive nuclides in each fraction were calculated by the following formula.

$$\text{Accumulation fraction} = \frac{\text{Accumulated radioactivity in each fraction of suspended matter per liter of sea water containing suspended matter (cpm/l.)}}{\text{Total radioactivity per liter of sea water containing suspended matter (cpm/l.)}}$$

This final filtered sea water was again filtered through five other new filters of the same types used above. In each case residual activities on these filters were subtracted from the above values as backgrounds.

3.6. *Autoradiography of accumulation of radionuclides in suspended matter*

The autoradiograms of each fraction of suspended matter in the sea water were taken by the contact method. Fuji medical X-ray films (PX type) were used.

3.7. *Temperature*

All experiments were conducted at room temperature.

4. EXPERIMENTAL RESULTS

4.1. *Release of Radioactivities from the Ion Exchange Resins into the Sea Water*

4.1. 1. *Effects of weight ratios of ion exchange resin to sea water on release of radioactivities.* The percentages of activities of ^{60}Co, ^{89}Sr and fission products released from the cation exchange resins into the sea water were measured under static and turbulent conditions for different weight ratios (about 10^{-4}, 10^{-5}, 10^{-6}, 10^{-7}) of ion exchange resin to sea water. The final percentages of released activities after the equilibrium state was reached are shown in Table 2.

As can be seen in this table, the ^{60}Co and ^{89}Sr were observed to be released nearly 100% and no marked differences in the release percentages were observed for the weight ratio 10^{-5} to 10^{-7}. A similar tendency was observed with the fission product mixture. However, since the relative percentages of the different

Table 2. Effects of the Weight Ratio of Cation Exchange Resin to Sea Water on the Release of the Radioactivities, under the Static and Turbulent Conditions

Weight ratio resin: sea water	Release of activity (%)			Condition of release
	^{60}Co	Fission products	^{89}Sr	
10^{-4}	99.25	89.85*	98.80	Turbulent
10^{-4}	—	—	98.50	Static
10^{-5}	99.92	96.26*	99.95	Turbulent
10^{-5}	—	—	99.94	Static
10^{-6}	99.97	98.30*	99.99	Turbulent
10^{-6}	—	—	99.96	Static
10^{-7}	—	—	99.97	Static

* The gross beta activity.

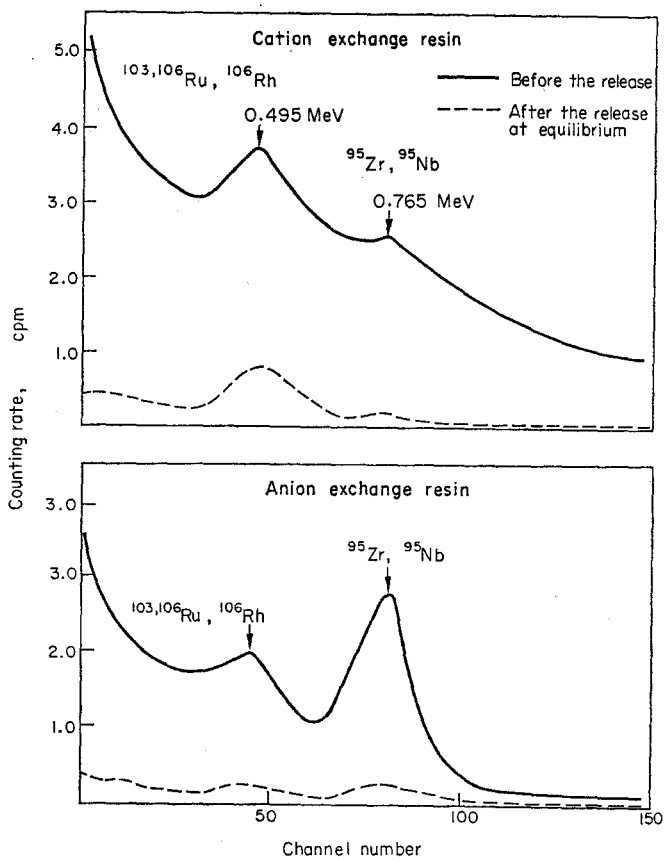

FIG. 3. Gamma-ray spectra of fission products before and after the release. (The weight ratio of resin: sea water = 10^{-3}).

Table 3. Final Percentages of the Released Activities of Various Nuclides, after the Equilibrium State or about 50 hours elapsed, under the Static and Turbulent Conditions (the weight ratio of resin: sea water = 10^{-6})

Radioactive nuclides	Ion exchange resin	Release of activity (%)	
		Static condition	Turbulent condition
^{89}Sr	Cation exchange resin	99.96	99.99
^{51}Cr	Cation exchange resin	44.0	47.0
^{55}Fe	Cation exchange resin	19.0	36.6
^{60}Co	Cation exchange resin	99.79	99.97
F.P.	Cation exchange resin	75.0*	98.3*
F.P.	Anion exchange resin	80.0*	97.4*

* The gross beta activity.

nuclides included in the fission product mixture may change according to age, the percentage of release as measured with the gross activity may also change.

4.1. 2. *The percentages of the release of activities of different nuclides.* The percentages of the release of activities of different nuclides were measured under static and turbulent conditions for the fixed weight ratio 10^{-6} of the ion exchange resin to the sea water. The results are shown in Table 3.

As can be seen in this table, such nuclides as ^{60}Co and ^{89}Sr were easily released, while ^{51}Cr and ^{55}Fe not so easily.

In the case of the fission product mixture, the release experiment was conducted not only with the cation exchange resins but also with the anion exchange resins. The gamma ray spectrum of the fission product mixture on the ion exchange resins was measured before and after the release.

The results are shown in Fig. 3.

The photo-peaks corresponding to ^{103}Ru, ^{106}Ru (^{106}Rh) and ^{95}Zr, ^{95}Nb were observed. Because of the marked lowering of the corresponding peaks after the release, it may be estimated that the corresponding nuclides might have been released.

4.1. 3. *The effects of the amounts of nuclide initially adsorbed on the ion exchange resins on the release of activities.* Prior to the release experiment, different amounts of non-radioactive carriers of Co and Sr (varying from nearly zero to about maximum exchange capacity of the resins) were adsorbed on the ion exchange resins together with fixed activities of ^{60}Co and ^{89}Sr.

The release experiment was conducted for the fixed weight ratio 10^{-3} of the ion exchange resins to the sea water.

The residual activity and the residual amount of carrier nuclide in the resins at equilibrium state are shown in Fig. 4.

The percentages of released activities are given in Table 4.

The specific activities in the ion exchange resins before and after the release of the activities are shown in Fig. 5.

According to the results of the experiments, the residual percentages of activities in the ion exchange resins were observed to remain the same in spite of the large differences in the initial amount of carriers. In other words, the residual percentages of the carriers in the ion exchange resins were observed to increase

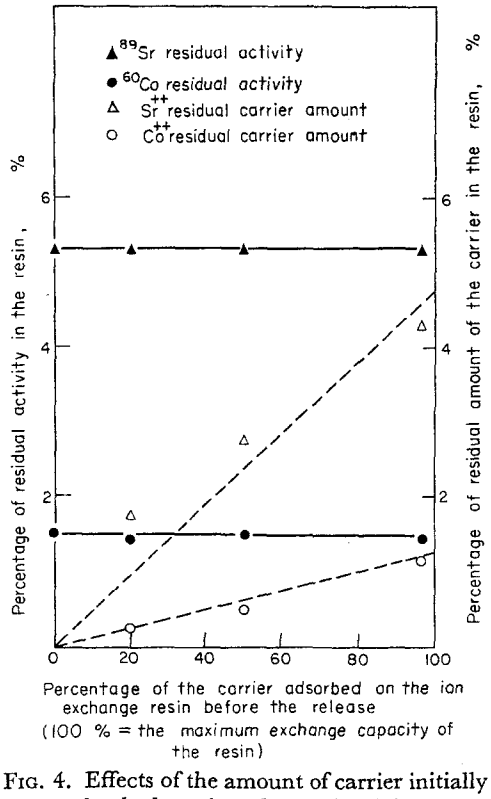

FIG. 4. Effects of the amount of carrier initially adsorbed on the release of activity.

Table 4. Effects of the Initial Amount of Carrier in the Resin on the Released Activity, under the Turbulent Condition (the weight ratio of resin: sea water = 10^{-4})

Amount of carrier in the resin before the release* %	Release of activity	
	^{60}Co %	^{89}Sr %
20	98.55	95.75
50	98.50	94.82
100	98.52	94.48

* 100% = The maximum exchange capacity of the resin.

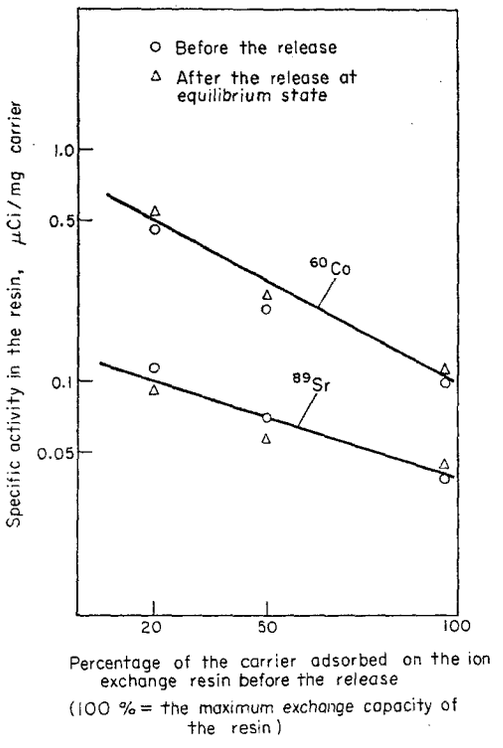

FIG. 5. Specific activity in the cation exchange resins before and after the release.

linearly with the increase of the initial amount of the carriers expressed as percentage of the saturation capacity of the ion exchange resins. From these results it was confirmed that the mass action law holds in the exchange reactions under the condition of the experiments.

The specific activities in the ion exchange resins before and after the release remained unchanged in each experiment within the limit of error in these experiments. The behaviour of the non-radioactive carrier nuclides was the same as that of the radioactive and therefore the use of the carrier was justified in this case.

4.1. 4. *The distribution of concentration of the released activities.* Vertical and horizontal distributions of the activities released from the ion exchange resins into the sea water have been measured under static and turbulent conditions in the experimental bath. The results are shown in Figs. 6–16 as a function of time.

In the case of ^{89}Sr (Fig. 6), the distribution was observed to be almost uniform after a few hours. However, in the case of ^{51}Cr (Fig. 11) the distribution was observed to be quite irregular with respect to time as well as with respect to location. Such a difference in the distribution pattern might be ascribed to the difference in the physico-chemical state of the nuclide in the sea water.

4.2. *Fractionation of suspended matter in sea water and accumulation of radioactive nuclides in each fraction*

In Table 5 the analytical data of each fraction of suspended matter in sea water and the concentration factors of radionuclides per dry weight of suspended matter are given. It can be seen that the quantity of organic matter was relatively less than that of inorganic matter and that the greatest concentration factors and accumulation fractions of radionuclides were obtained in the fraction of large particle sizes recovered by Toyo Filter Paper Type No. 5A (mean pore size 18 μ), rather than in the fractions of relatively small particle sizes.

The concentration factors of radionuclides in each fraction of suspended matter as a function of elapsed time are shown in Fig. 17.

The accumulation of radioactive nuclides in suspended matter was observed to reach an equilibrium in about 7–10 days. The accumulation fraction of radioactivity in each fraction of suspended matter is shown in Fig. 18. It can be seen that the majority of radioactivity was not retained on any of the filters used in this experiment.

4.3. *The distribution of radioactive nuclides in each fraction of suspended matter*

The distribution of radionuclides in each fraction indicated the tendency for a higher activity of ^{60}Co to be present in the fraction containing the larger particles, while the activity of ^{55}Fe was greater in the fraction containing the smaller particles (Table 5, Fig. 18).

The ratio of the specific activity per dry weight of suspended matter in each fraction to the average activity per dry weight of the total suspended matter is shown in Fig. 19. A higher activity for ^{55}Fe was also observed in the fraction containing the smaller particles.

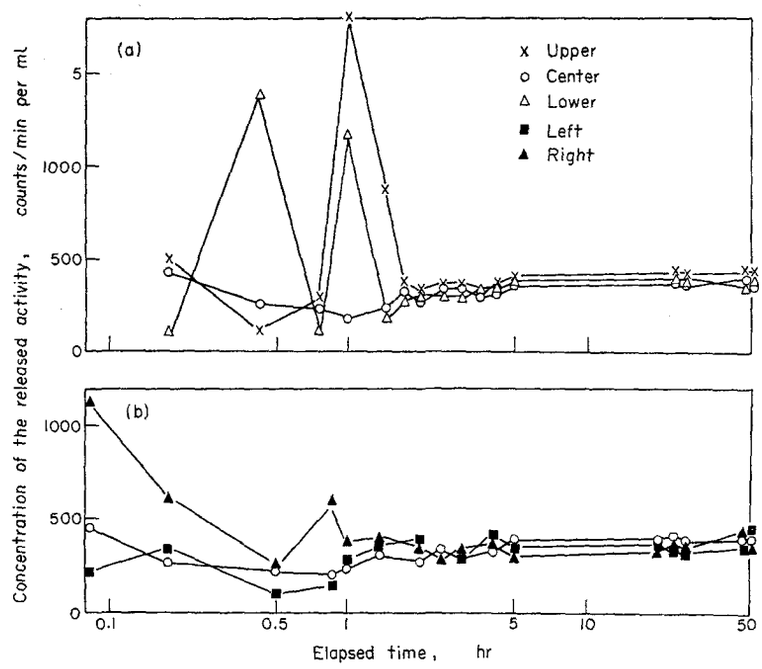

FIG. 6. Distributions of concentrations of the released activity of ^{89}Sr adsorbed on cation exchange resin under the static condition.

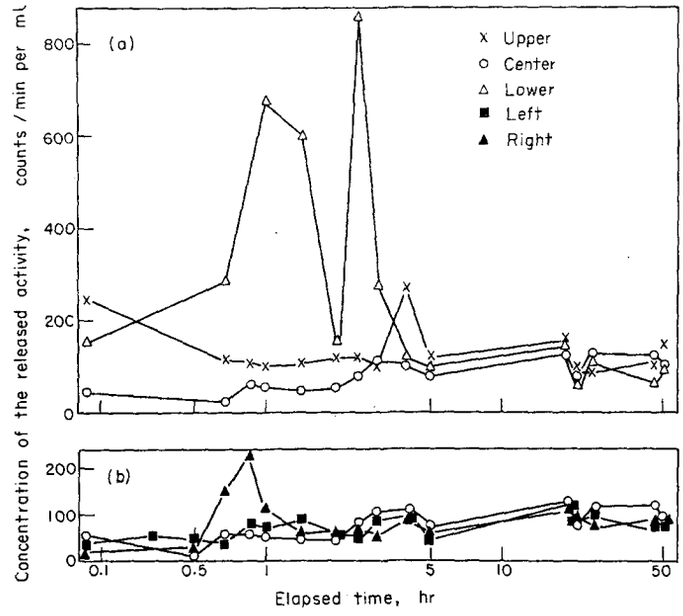

FIG. 7. Distributions of concentrations of the released activity of ^{60}Co adsorbed on cation exchange resin, under the static condition.

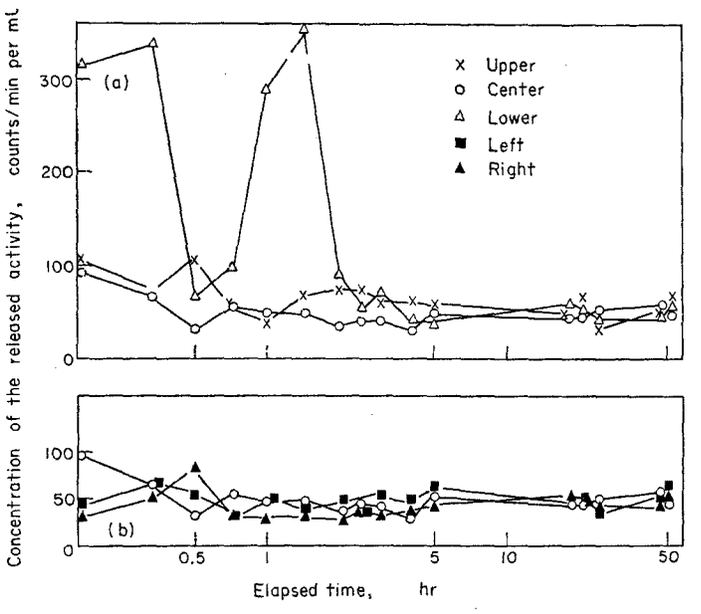

FIG. 8. Distributions of concentrations of the released activity of fission products adsorbed on cation exchange resin, under the static condition.

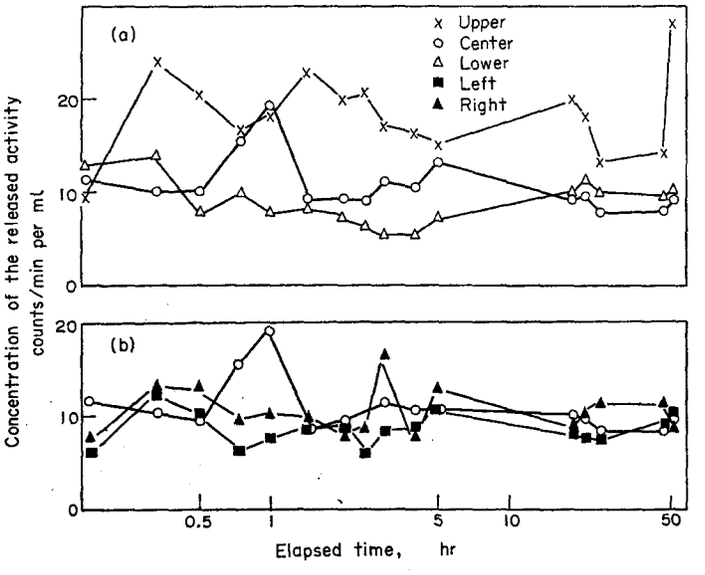

FIG. 9. Distributions of concentrations of the released activity of fission products adsorbed on anion exchange resin, under the static condition.

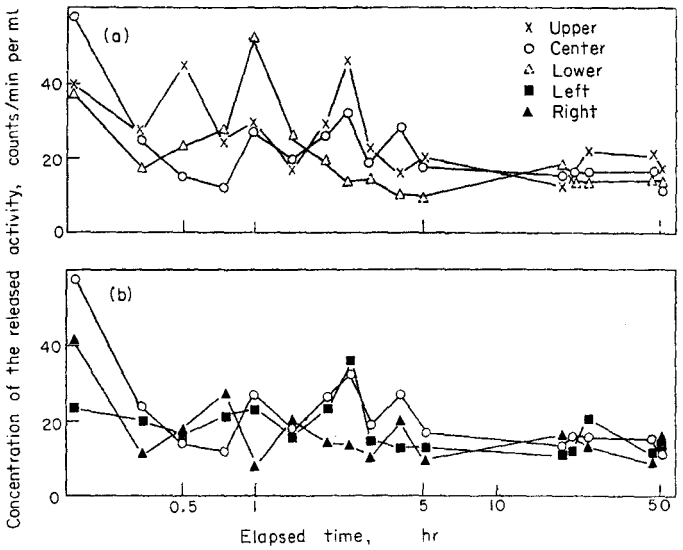

FIG. 10. Distributions of concentrations of the released activity of ^{55}Fe adsorbed on cation exchange resin, under the static condition.

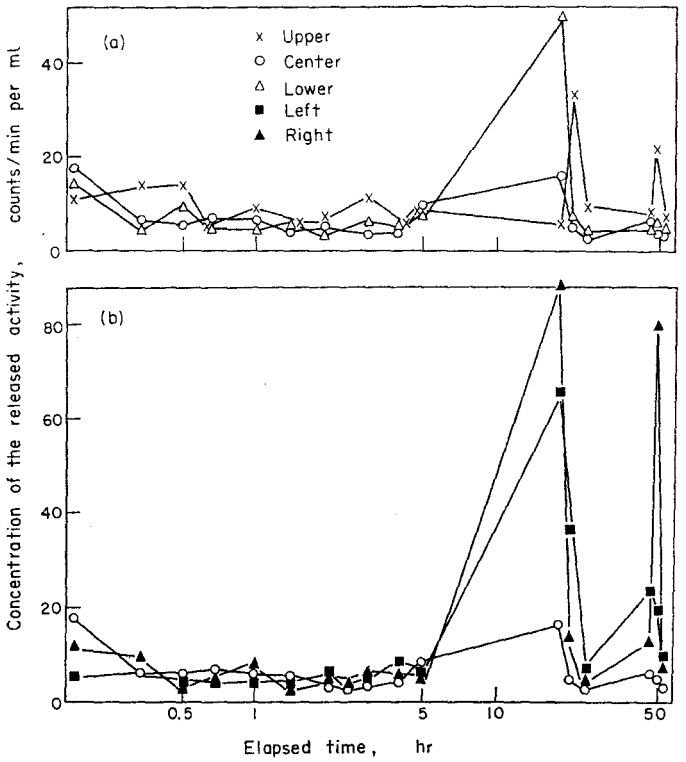

FIG. 11. Distributions of concentrations of the released activity of ^{51}Cr adsorbed on cation exchange resin, under the static condition.

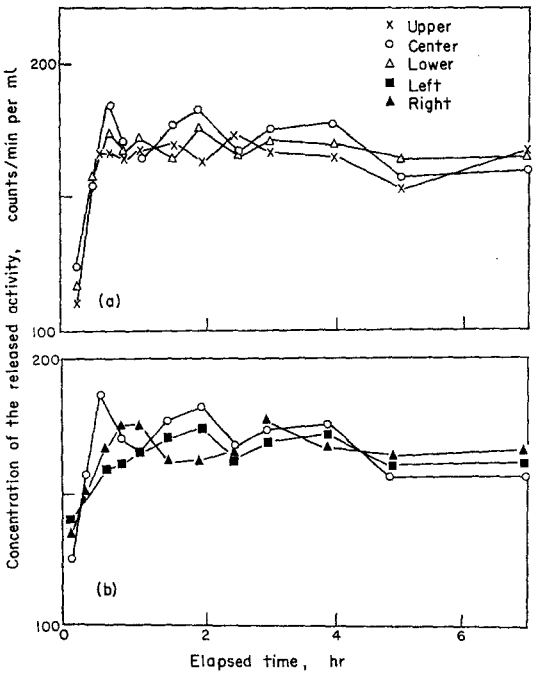

FIG. 12. Distributions of concentrations of the released activity of ^{89}Sr adsorbed on cation exchange resin, under the turbulent condition.

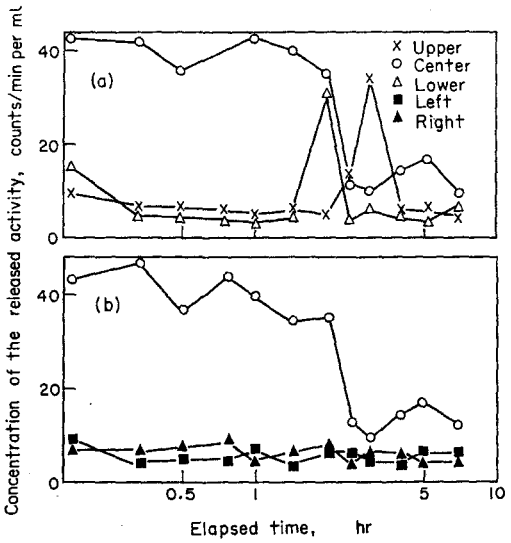

FIG. 13. Distributions of concentrations of the released activity of ^{51}Cr adsorbed on cation exchange resin, under the turbulent condition.

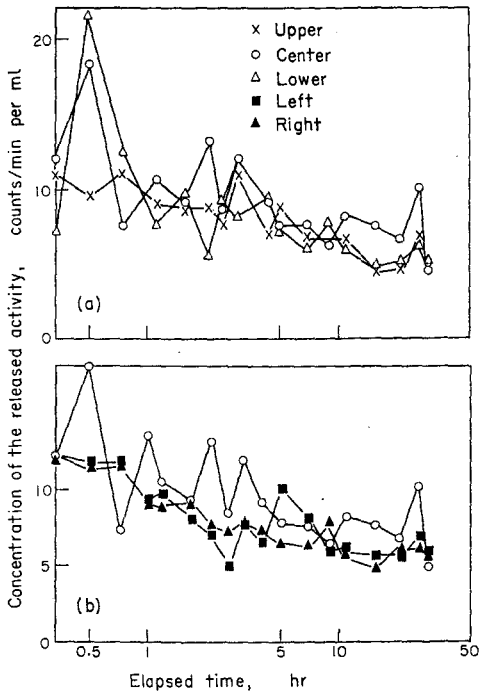

FIG. 14. Distributions of concentrations of the released activity of ^{55}Fe adsorbed on cation exchange resin, under the turbulent condition.

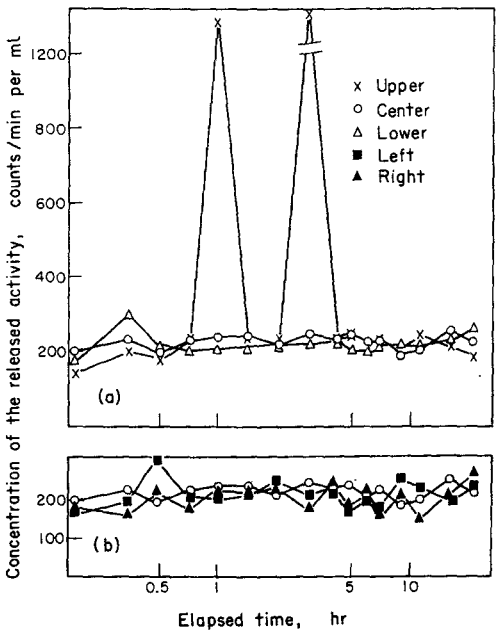

FIG. 15. Distributions of concentrations of the released activity of ^{60}Co adsorbed on cation exchange resin, under the turbulent condition.

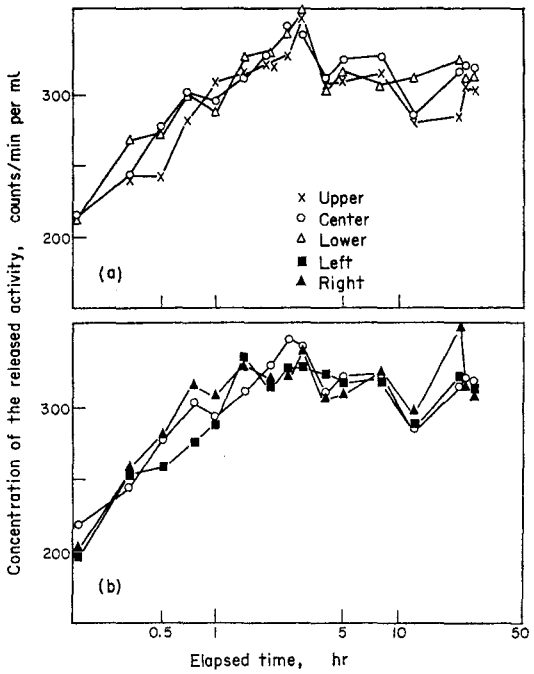

FIG. 16. Distributions of concentrations of the released activity of fission products adsorbed on cation exchange resin, under the turbulent condition.

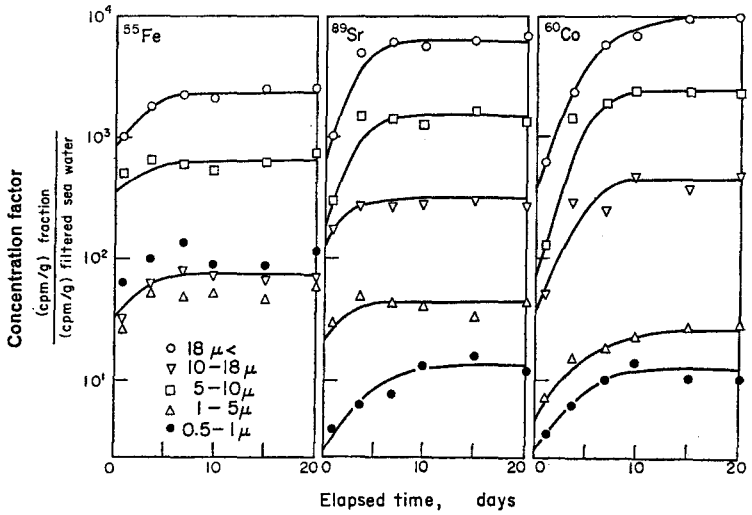

FIG. 17. Uptake of radioactivity in each fraction of suspended matter (per dry weight).

Table 5. Fractionation of the Suspended Matter and Accumulation of Radioactive Nuclides (initial radioactive concentration in the sea water was about 10^{-4} μCi/ml)

Size range of suspended matter micron	Dry weight mg/ml	Organic N mg/ml	Organic matter* mg/ml	Inorganic matter by difference mg/ml	Concentration factor per dry weight			Accumulation fraction		
					^{55}Fe —	^{60}Co —	^{89}Sr —	^{55}Fe —	^{60}Co —	^{89}Sr —
18	4.19	0.06	1.02	3.17	23.0×10^2	93.0×10^2	52.0×10^2	5.2×10^{-2}	56.1×10^{-2}	2.0×10^{-4}
10–18	0.94	0.02	0.34	0.60	0.6×10^2	4.2×10^2	2.6×10^2	0.8×10^{-2}	7.8×10^{-2}	0.4×10^{-4}
5–10	2.74	0.01	0.17	2.61	8.0×10^2	24.0×10^2	14.0×10^2	2.9×10^{-2}	10.2×10^{-2}	0.8×10^{-4}
1–5	4.05	0.03	0.51	3.54	0.6×10^2	0.27×10^2	0.4×10^2	0.7×10^{-2}	1.3×10^{-2}	0.5×10^{-4}
0.5–1	3.90	0.04	0.68	3.22	0.6×10^2	0.11×10^2	0.4×10^2	0.5×10^{-2}	0.7×10^{-2}	0.4×10^{-4}

* Organic matter (mg/ml) = Organic nitrogen (mg/ml) × 17.

$$\text{Concentration factor} = \frac{\text{Activity of fraction (cpm/g)}}{\text{Activity of filtered sea water (cpm/ml)}}$$

$$\text{Accumulation fraction} = \frac{\text{Activity of fraction per liter of sea water (cpm/ml)}}{\text{Activity of sea water containing suspended matter (cpm/l)}}$$

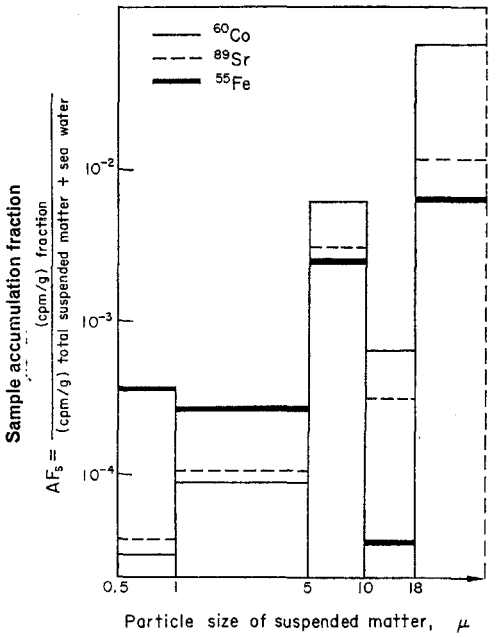

FIG. 18. Sample accumulation fraction of nuclides in each fraction of suspended matter.

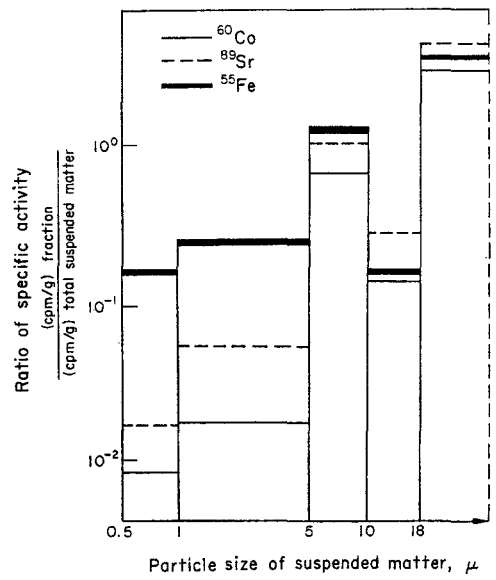

FIG. 19. Ratio of the specific activity in each fraction to the average specific activity of the total suspended matter (per dry weight).

4.4. *Autoradiography of radioactive nuclides in the suspended matter*

The autoradiograms of ^{59}Fe, ^{60}Co and ^{89}Sr in the fraction ($> 18\,\mu$) recovered by Toyo Filter Paper Type No. 5A are shown in Fig. 20. It can be seen that the radioactivity was accumulated in relatively large particulates. On the other hand, the autoradiograms of radionuclides in the fractions (5–10 μ) recovered by Millipore Filter Type SM, do not show any large exposed spots as shown in Fig. 20.

5. DISCUSSION

The exchange reactions of ion exchange resins have been investigated by many authors not only from the basic viewpoint but also from the viewpoint of applications.

In the present report, the percentage of released radioactivities was determined by adding the ion exchange resins containing adsorbed radioactive nuclides to the sea water. This system may be considered a heterogeneous one consisting of salt solution and particles. The processes by which these adsorbed radionuclides would be released from the resin into the sea water and how they would distribute in the medium have been discussed.

From these experiments, it was observed that the adsorbed radioactive nuclides were released as soon as the resin particles came in contact with the sea water, and that the released nuclides formed a water mass with locally concentrated radioactivities by the diffusion process and then diffused gradually through the sea water finally to reach a macroscopically homogeneous equilibrium. In such release experiments, it was found that some nuclides such as ^{60}Co and ^{89}Sr were easily released, while others as ^{51}Cr and ^{55}Fe not so easily. The percentage of the release of activities increases with the decrease of weight ratios of ion exchange resins to the sea water, and no marked differences in the release were observed for the weight ratio between 10^{-5} to 10^{-7}. The distribution patterns of radioactivity concentration in the sea water after the release seem to depend on the physical-chemical state of the nuclides in the sea water. In the experiments with a fixed weight ratio of ion exchange resins to sea water, it was observed as a tendency that the more the initial amounts of adsorbed activities on the

resins, the less, although not so remarkably, the activities released from resins into sea water.

From the abovementioned results the mechanisms of releasing adsorbed activities from resins into sea water were considered to depend exclusively on the ion exchange reaction, although some other reactions might also occur.

Studies of suspended matter in sea water have been conducted in the past by many other authors [6-15] from the viewpoint of oceanography and fishery. However, in order to estimate the behaviour and distribution of radioactive nuclides in suspended matter in sea water, the method of fractional filtration was employed. It was observed that the accumulation of each radionuclide reached equilibrium in 7–10 days and that the maximum concentration factor, expressed as a ratio of the activity in the suspended matter per dry weight to that in the sea water per milli-liter, of each radionuclide was found in the fraction of larger particles recovered by Toyo Filter Paper Type No. 5A (mean pore size 18 μ).

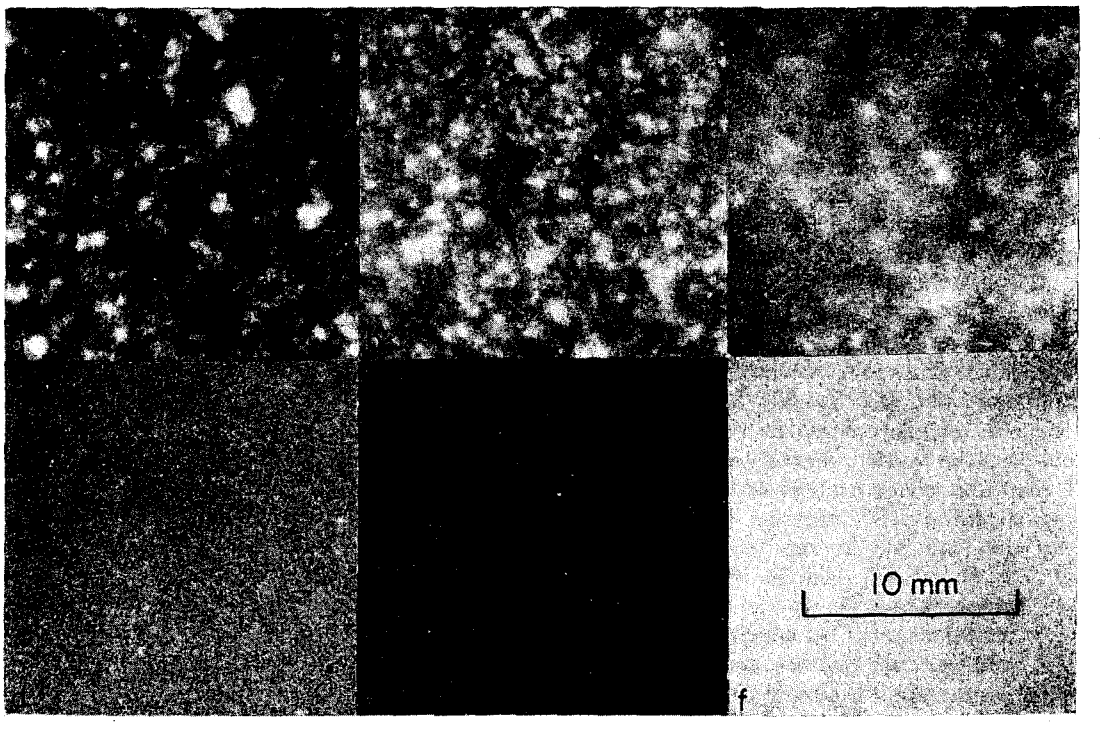

FIG. 20. *The autoradiograms of nuclides in the fraction of suspended matter.*

Plate	Nuclide	Range of particle sizes (μ)	Exposure (hr)
a	^{59}Fe	> 18	43
b	^{60}Co	> 18	60
c	^{89}Sr	> 18	40
d	^{59}Fe	5–10	43
e	^{60}Co	5–10	60
f	^{89}Sr	5–10	60

It might be expected as a general rule that the smaller the particles, i.e. the larger the surface area per unit weight, the larger the amount of radioactivity which could be

accumulated per unit weight. In these experiments, on the contrary, the accumulation of radioactivity in the fraction with larger particles was greater. Judging from these results, it may be inferred that not all particulate fractions obtained by fractional filtration from natural sea water have the same composition, and that the organic and inorganic matter of particulates accumulating nuclides in each fraction would be different in quality and quantity. The distribution of radioactive nuclides in each fraction indicated the tendency for a higher activity of ^{60}Co to be present in the fraction containing the larger particles, while the activity of ^{55}Fe was greater in the fraction containing the small particle sizes. In order to interpret such a tendency more adequately, further studies might be necessary.

In assessing the possible effects due to the disposal of radioactive nuclides in the environmental hydrosphere, the so-called concentration factor as defined in the beginning of this paper has been used. Oftentimes, the expected average concentration of activity in a water medium is estimated by simply dividing the total activity of the waste present by the estimated total volume of the environmental water medium, and then the concentration of activity in the biological sample is estimated by just multiplying the expected average concentration of activity in the water medium by the so-called concentration factor. If the concentration factor is really the factor by which the biological sample may concentrate the activity from the environmental water medium, or if the so-called concentration factor is the one obtained under the equilibrium condition which could simulate the actual situation of the waste disposal, and if the sample fraction or the concentration of sample in the medium is sufficiently small, the estimation of the final concentration of activity in the biological sample by the above procedure may be approximately justifiable.

However, if a highly contaminated fish at the highly contaminated part of the sea water medium swims out into the surrounding low contaminated water, and if the so-called concentration factor is estimated as the ratio of the concentration of activity of the highly contaminated fish sample to that of the low contaminated water medium where the fish was caught, an unusually high concentration factor may result. In this case, the concentration factor is merely a ratio of the concentration of the sample to that of the medium at the place where the sample was caught, but it does not represent the factor by which the sample may concentrate the activity from the environmental water medium. If such a high concentration factor were used evaluating the possible hazard to man at the time of the radioactive waste disposal into the environmental hydrosphere, a much too conservative result may be indicated for the permissible level of waste disposal, giving the people an erroneous impression. Therefore, in the case of the hazard analysis of the waste disposal into hydrosphere, the use of the sample accumulation fraction (AF_S) or the sample concentration factor (CF_S), as defined below, seems to be more reasonable. In the following, some of the relationships and interrelationships between some of the parameters which may be useful in the analysis of problems of contamination are introduced.

* * *

Notation:

(Medium + Sample) = MS, Medium = M, Sample = S

$A_{(M)}$ = activity of medium

$A_{(S)}$ = activity of sample

$A_{(MS)} = A_{(M)} + A_{(S)}$

A/kg = concentration of activity per kg of material concerned

$A_{(S)}/kg_{(S)}$ = concentration of activity per kg of sample

$A_{(M)}/kg_{(M)}$ = concentration of activity per kg of medium

$A_{(S)}/kg_{(MS)}$ = activity of the sample included in kg of medium plus sample

$A_{(M)}/kg_{(MS)}$ = activity of the medium included in kg of medium plus sample

In the following relations, the activity per unit mass is used instead of the activity per unit volume because strictly speaking the volume may be dependent on the temperature. However, even if we replace the activity per unit mass with the activity per unit volume, it is obvious that similar relations should hold.

(1) *Sample to Medium Concentration Ratio:* $CR_{(S-M)}$

$$CR_{(S-M)} = \frac{A_{(S)}/kg_{(S)}}{A_{(M)}/kg_{(M)}}$$

This is the so-called concentration factor which is the ratio of the concentration of the activity of the sample to that of the medium.

(2) *Medium to Sample Concentration Ratio:* $CR_{(M-S)}$

$$CR_{(M-S)} = \frac{A_{(M)}/kg_{(M)}}{A_{(S)}/kg_{(S)}} = \frac{1}{CR_{(S-M)}}$$

This relation may be important when the medium is more useful than the sample itself, for instance, when decontaminating a water medium by the biological sample in it.

(3) *Sample Accumulation Fraction:* AF_S

$$AF_S = \frac{A_{(S)}/kg_{(MS)}}{A_{(MS)}/kg_{(MS)}} = \frac{A_{(S)}}{A_{(MS)}} \leqq 1$$

(4) *Medium Accumulation Fraction:* AF_M

$$AF_M = \frac{A_{(M)}/kg_{(MS)}}{A_{(MS)}/kg_{(MS)}} = \frac{A_{(M)}}{A_{(MS)}} \leqq 1$$

(5) *Sample Concentration Factor:* CF_S

$$CF_S = \frac{A_{(S)}/kg_{(S)}}{A_{(MS)}/kg_{(MS)}}$$

(6) *Medium Concentration Factor:* CF_M

$$CF_M = \frac{A_{(M)}/kg_{(M)}}{A_{(MS)}/kg_{(MS)}}$$

(7) *Sample to Medium Ratio:* $R_{(S-M)}$

$$R_{(S-M)} = \frac{kg_{(S)}}{kg_{(MS)}}$$

(8) *Medium to Sample Ratio:* $R_{(M-S)}$

$$R_{(M-S)} = \frac{kg_{(M)}}{kg_{(S)}} = \frac{1}{R_{(S-M)}}$$

(9) *Sample Fraction:* F_S

$$F_S = \frac{kg_{(S)}}{kg_{(MS)}}$$

Fraction of the sample per $kg_{(MS)}$.

(10) *Medium Fraction:* F_M

$$F_M = \frac{kg_{(M)}}{kg_{(MS)}}$$

Fraction of the medium per $kg_{(MS)}$.

(11) *Some of the Important Interrelationships.*

$$(CF_S)(F_S) = (AF_S) \leqq 1$$
$$(CF_M)(F_M) = (AF_M) \leqq 1$$

From these relationships and interrelationships, it is clear, for instance, that if the sample concentration factor (CF_S) is 10^5, the sample fraction (F_S) or the concentration of sample in the aqueous medium must be smaller than 10^{-5}. In the case of hazard analysis of waste disposal into the hydrosphere, the expected average initial concentration of activity ($\bar{C}$) per unit volume or mass of the water medium is usually estimated by dividing the total activity of the waste present by the estimated total volume or mass of the environmental water medium which may include the sample in question, regardless of the sample fraction in the medium. In this case, the final concentration of the activity in the biological sample ($A_{(S)}/kg_{(S)}$) may be estimated by using the sample concentration factor (CF_S) defined in (5) above from the following relation:

$$A_{(S)}/kg_{(S)} = (\bar{C})(CF_S)$$

where $\bar{C}$ is the average concentration of the activity per $kg_{(MS)}$ and may be considered to be equivalent to the overall average concentration $A_{(MS)}/kg_{(MS)}$ in the above notation.

Similarly, the final total activity transferred to and accumulated in the sample per kg of medium plus sample ($A_{(S)}/kg_{(MS)}$) may be estimated by using the sample accumulation fraction (AF_S) defined in (3) above from the following relation:

$$A_{(S)}/kg_{(MS)} = (\bar{C})(AF_S)$$

If the concentration of the sample in the medium, the sample fraction (F_S) or the medium fraction (F_M) is known, the factors involved in the above estimation could be checked, whether they are grossly in error or not, by using the interrelation indicated in (11) above.

From these points of view, the effective volume or mass of the medium associated with the sample or the average volume or mass of the medium that could be effectively utilized by a biological sample in question seems to be an important factor also.

6. SUMMARY

The release of radioactivities from ion exchange resins into sea water was studied in a water bath containing natural surface sea water sampled at Osaka Bay, using several radionuclides for the different weight ratios of ion exchange resins to sea water and the amount of nuclide initially adsorbed on the ion exchange resins under the static and turbulent conditions. The behaviour and distribution of radionuclides in suspended matter in sea water was also studied experimentally by fractional filtration using several types of filters with different pore sizes. The results are summarized as follows:

1. The radioactivities were rapidly released from the ion exchange resin particles on contact with the sea water. However, some differences were observed in the degree of release depending on the different nuclides. Such nuclides as ^{60}Co and ^{89}Sr were easily released, while ^{51}Cr and ^{55}Fe not so easily.

2. The released activity was observed to increase with the decreasing weight ratio of ion exchange resins to sea water, but with the weight ratio below 10^{-4} of ion exchange resin to sea water no remarkable difference was observed.

3. With the weight ratio below 10^{-3} of the ion exchange resin to the sea water, the initial adsorbed amount on the ion exchange resin gave no remarkable effects on the release of radioactivities.

4. The accumulation of the radioactive nuclides in suspended matter was observed to reach an equilibrium in about 7–10 days.

5. The greatest accumulation and concentration of radioactivity per dry weight of suspended matter in the sea water were observed in the fraction containing the larger particles recovered by Toyo Filter Paper Type No. 5A (mean pore size 18 μ), rather than in the fractions containing relatively smaller particles.

6. The distribution of radionuclides in each fraction indicated a tendency for a higher activity of ^{60}Co to be present in the fraction containing the larger particles, while the activity of ^{55}Fe was greater in the fraction containing the smaller particles.

7. Finally, after discussing the so-called concentration factor, it is pointed out that the ratio of the concentration of activity of the sample to that of the medium may not necessarily represent the real factor by which the biological sample may concentrate the activity from the environmental water medium. The use of the sample concentration factor, which is the ratio of the concentration of activity of the sample to the average concentration of medium plus sample, is proposed for the estimation of the final concentration of the biological sample for the purpose of hazard analysis due to radioactive waste disposal into the environmental hydrosphere.

ACKNOWLEDGEMENTS

Most experimental results in this paper are based on work conducted under the Atomic Energy Contract No. 1030 (1964) and No. 1142 (1965) between Kinki University Atomic Energy Research Institute and the Science and Technology Agency of the Japanese Government on the Peaceful Uses of Atomic Energy in Japan. The authors gratefully acknowledge the grant and encouragement by the Atomic Energy Bureau, Science and Technology Agency of the Japanese Government.

REFERENCES

1. Radioactive Waste Disposal from Nuclear-Powered Ships, National Academy of Science. National Research Council, Pub. No. 658, Washington, D.C. (1959).
2. Radioactive Waste Disposal into the Sea. IAEA Safety Series No. 5, IAEA Vienna (1961).
3. The Effects of Atomic Radiation on Oceanography and Fisheries, National Academy of Science. National Research Council, Pub. No. 551, Washington, D.C. (1959).
4. D. W. Pritchard. *Health Physics* **6,** 103 (1961).
5. Y. Miyake and Y. Hiyama, *Kagaku* (*Science*) **33,** 492 (1963).
6. Y. Nishiwaki, H. Kawai, Y. Honda, Y. Kimura, H. Morishima, T. Koga and R. Ono. *Radioisotopes* **14,** 368 (1965).
7. D. L. Fox, J. D. Isaacs and E. F. Corcoran. *J. Mar. Res.* **11,** 29 (1952).

8. E. D. GOLDBERG, M. BAKER and D. L. FOX. *J. Mar. Res.* **11,** 194 (1952).
9. D. L. FOX, C. H. OPPENHEIMER and J. S. KITTREDGE. *J. Mar. Res.* **12,** 232 (1953).
10. W. V. BURT. *J. Mar. Res.* **14,** 47 (1955).
11. T. HANAOKA, A. FURUKAWA and K. NOGAMI. *Bull. Japanese Soc. Sci. Fisheries* **22,** 213 (1956).
12. A. FURUKAWA, Y. OGASAWARA, M. HISAOKA and K. NOGAMI. *Bull. Japanese Soc. Sci. Fisheries* **22,** 220 (1956).
13. A. FURUKAWA. *Bull. Japanese Soc. Sci. Fisheries* **23,** 124 (1957).
14. T. TSUJITA. *J. Oceanographical Soc. Japan* **18,** 234 (1963).
15. F. A. J. ARMSTRONG. *J. Mar. Res.* **17,** 23 (1958).

DISPOSAL OF RADIOACTIVE WASTES IN GEOLOGIC FORMATIONS*

W. J. BOEGLY, Jr., F. L. PARKER and E. G. STRUXNESS
Health Physics Division, Oak Ridge National Laboratory, Oak Ridge, Tennessee

Abstract—The ultimate disposal of radioactive wastes into geologic formations has received increasing attention during the past 10 years. Due to the varying heat-generation rates of the different categories of wastes and the allowable costs, no single formation is capable of handling the entire spectrum of wastes produced. Therefore, three different methods of disposal have been investigated to handle the high-, intermediate-, and low-level wastes generated. High-level, small-volume wastes would be converted to solids and stored in a dry impermeable underground formation such as salt; intermediate-level, intermediate-volume wastes would be slurried with cement and additives and injected into slightly permeable formations using the hydrofracturing technique; and low-level, large-volume wastes would be injected into deep porous formations. The engineering-scale demonstration of the hydrofracturing concept has been completed, and a demonstration of the disposal of radioactive solids in a salt mine is underway.

A total of seven injections at depths from 800 to 1000 ft have been made at the Oak Ridge National Laboratory using the hydrofracturing technique. These injections have shown that horizontal conformable fractures are possible and have contributed valuable operating experience. In addition, a number of mixes have been developed and tested and are capable of satisfactorily retaining fission product waste.

Project SALT VAULT is a demonstration of the disposal of solidified high-level wastes in an out-of-service mine in Lyons, Kansas. In November 1965, fourteen Engineering Test Reactor fuel assemblies, containing 1,000,000 Ci of fission products, were placed in the mine floor. During the course of the 2-year test, four sets of fuel assemblies will be used to achieve a peak dose to the salt of about 8×10^8 rad and to obtain experience with the waste-handling equipment. The operation has proceeded smoothly, and most of the experimental objectives have been already achieved.

Laboratory studies on the flow path of radionuclides through a sandstone block have been carried out. However, it appears that a field scale demonstration of the deep well technique is some years away.

INTRODUCTION

In September 1955, the Atomic Energy Commission requested the Earth Sciences Division of the National Academy of Sciences, National Research Council to organize a meeting of geologists and engineers to discuss the possibilities of permanent disposal of radioactive wastes in geologic formations. At this meeting,[1] the disposal of high-level wastes in salt was recommended as having the greatest present potential. Disposal of diluted high-level wastes into deep porous formations was suggested as a possible method for the future. In subsequent discussions with representatives of the petroleum industry, it was agreed that it might be possible to dispose of radioactive wastes by pumping them into formations using hydraulic fracturing techniques. Research and development, leading up to demonstration experiments using radioactive materials, have been carried out on the disposal of high-level radioactive solids in salt formations and the disposal of intermediate-level liquid wastes by hydraulic fracturing. To date, no field demonstration has been performed

* Research sponsored by the U.S. Atomic Energy Commission under contract with the Union Carbide Corporation.

on injection of low-level liquid wastes into deep permeable formations.

DISPOSAL IN SALT FORMATIONS

Salt was suggested as a possible medium for high-level waste disposal because of its availability, geographic distribution, thermal conductivity, plasticity, impermeability, and low cost of mining.[2-5] Initially, studies on the direct disposal of liquid radioactive wastes in salt were performed, but in 1961 the liquid waste studies were terminated and solid waste studies were initiated. The solid waste to be stored in salt are those produced by the solidification or calcination of first-cycle wastes from reactor fuel reprocessing. In the United States a Waste Solidification Pilot Plant is currently under construction to demonstrate the potential methods for achieving the desired solidification. The solids produced are highly radioactive and generate significant amounts of heat.

There are two ways in which the waste containers can be stored in the mine; above the mine floor in racks, or below the floor in drilled holes. For storage above the mine floor, cooling can be obtained by convection but all handling operations would have to be performed remotely. Storage in the mine floor allows access to the rooms for transfer operations, but requires drilling of individual holes for each waste container. After detailed study, storage in the mine floor with heat dissipation by conduction through the salt adjacent to the containers was deemed most suitable. A computer program was written to determine the optimum spacing of waste containers to dissipate the heat in the salt and prevent overheating of the waste cans or the salt.[6] The computer results were checked by field experiments using electrical heaters and the calculated results agreed favorably with the experimental observations.

Allowable salt temperature rises are limited by the shattering of the salt due to increased vapor pressure in small bubbles containing brine ("negative crystals") located within the salt, and by an increased rate of plastic flow of the salt. Laboratory and field studies have shown that the problems of salt shattering and plastic flow can be minimized if the salt temperature is not allowed to exceed 200°C.

As a result of the theoretical calculations and experimental studies it appeared that it would be possible to dispose of high-level solid wastes in a salt mine. In order to determine the equipment and handling operations necessary in an actual disposal operation and the most economical design of the disposal facility, a full-scale field demonstration was needed. This demonstration, called Project Salt Vault, is currently in operation in a salt mine in Lyons, Kansas.[7]

The engineering and scientific objectives of Project Salt Vault are: (1) demonstration of waste-handling equipment and operating techniques; (2) determination of the possible production and release of radiolytically produced chlorine; (3) determination of the possible gross effects of radiation (up to 10^9 rad) on the uplift and salt-shattering temperatures in an area where salt temperatures are in the range of 100–200°C; and (4) collection of information on creep and plastic flow of salt at elevated temperatures which can be used later in the design of actual disposal facilities.

The Lyons mine was operated for a number of years before it was placed in an inactive status in 1948. In the existing mine space the marketable salt has been mined leaving the more impure salt in the floor and ceiling. Since the impure salt remaining in the mined out areas contains significant moisture bearing shale impurities, it was necessary to mine a new experimental area above the existing mine floor such that the fuel assemply canisters would be located in pure salt. Excavation of the new experimental area involved the mining of 19,000 tons of salt. The new mine level, which is about 14 ft above the old mine floor, is connected by a ramp having a 10% grade.

A schematic cross section of Project Salt Vault is shown in Fig. 1. The waste solids, after canning in Idaho, are loaded into a carrier and shipped on a specially designed truck trailer to Lyons, Kansas. At Lyons the carrier is removed from the trailer and placed vertically over a steel-cased charging shaft which extends from the surface to the mine level, approximately 1000 ft below. The waste canisters are lowered, one at a time down the shaft into a shielded container mounted on a mobile vehicle. This vehicle (Fig. 2) moves from the fuel assembly charging shaft to the experimental area where

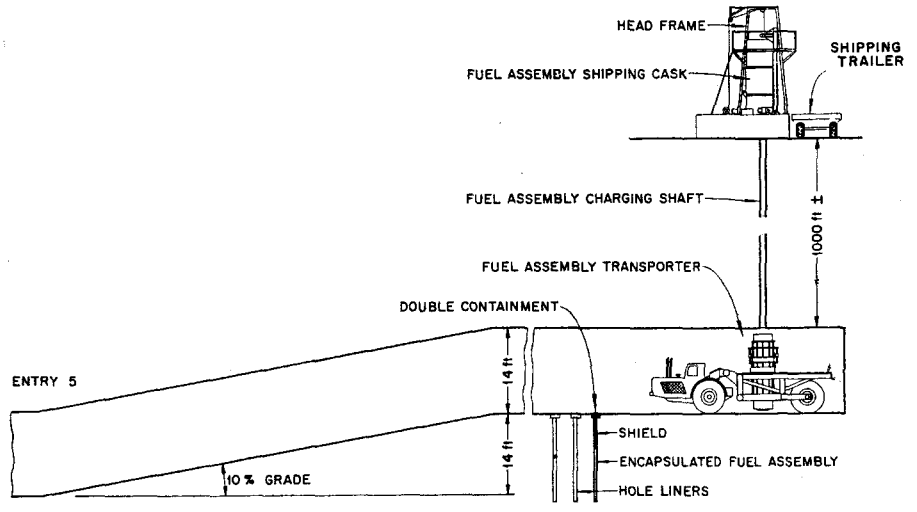

FIG. 1. Schematic cross-section of Project Salt Vault.

the canisters are to be lowered into the storage holes.[8]

Since high-level packaged solids were not in production at the time the demonstration was proposed, irradiated fuel assemblies from the Engineering Test Reactor (ETR) were used as the heat and radiation sources. In order to achieve a peak dose to the salt of about 10^9 rad, it is necessary to replace the fuel assemblies every six months with freshly irradiated assemblies. Each shipment from the Idaho Chemical Processing Plant (ICPP) consists of 14 ETR fuel assemblies contained in seven stainless steel canisters. The canisters supply the secondary containment system and are about 5 in. in diameter by $7\frac{1}{2}$ ft long. A depleted uranium shield plug is located at the upper end of the canister and thermocouples are installed to monitor fuel assembly temperatures during the experiment. When Project Salt Vault has been completed all canisters will be returned to Idaho for recovery of the fuel assemblies.

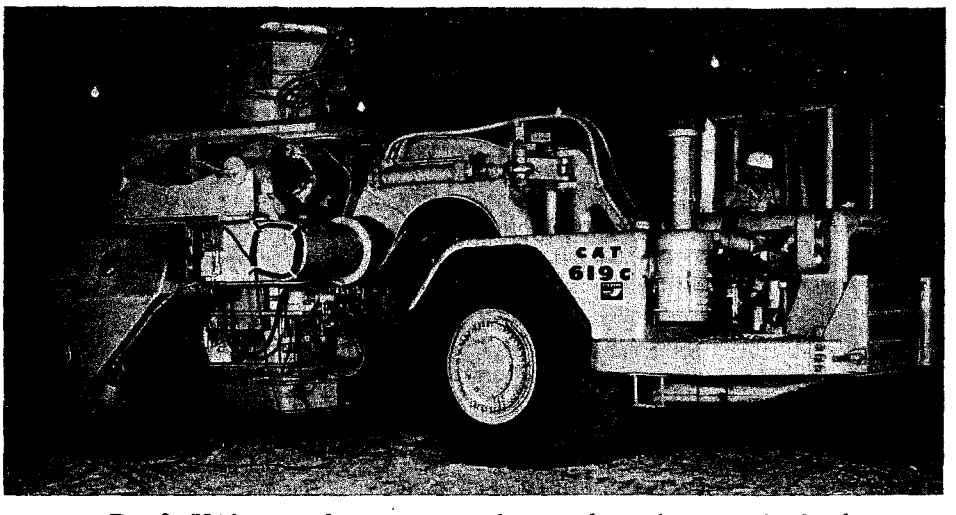

FIG. 2. Underground transporter used to transfer canisters at mine level.

Project Salt Vault is composed of four experiments: (1) an array of seven fuel assembly canisters located in pure salt in the newly mined area; (2) a non-radioactive control array using electrical heaters to study the effects of radiation on plastic flow and chlorine release; (3) a heated pillar experiment for plastic flow and mine stability studies; and (4) an array of seven canisters in the old mine floor to determine operational problems related to the use of abandoned mines for radioactive waste disposal. Their location in the mine is shown in Fig. 3.

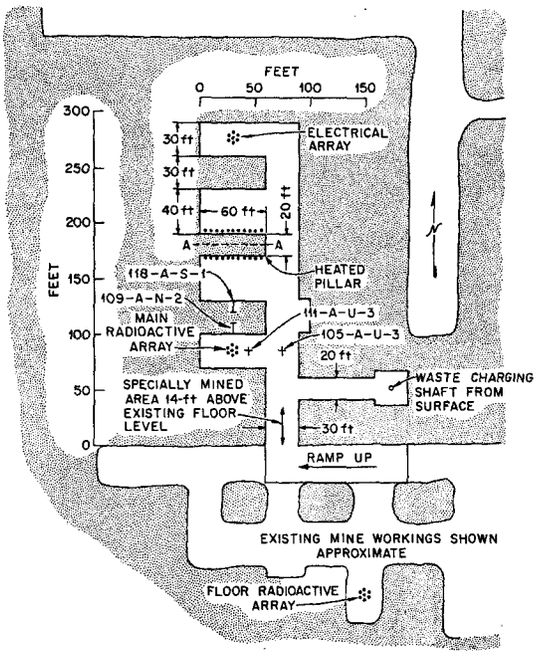

FIG. 3. Plan of experimental area.

The first transfer of fuel assemblies to Project Salt Vault occurred on November 17–19, 1965. Seven canisters were lowered into the mine and placed in the main radioactive array. The fuel assemblies were about 105 days out of reactor and contained approximately one million curies. The maximum radiation dosage received by the operating personnel during the transfer operation was 200 mr.[9]

Transfer of the seven canisters from the main radioactive array to the array in the existing mine floor, followed by the insertion of seven new canisters in the main array, took place on June 13-15, 1966. The seven new canisters contained assemblies that were 105 days out of the reactor. The second set of assemblies received higher irradiation in the ETR and their heat generation rate was 800 W initially and they contained about 1½ million curies. As in the case of the initial loading operation, no handling problems were encountered, and radiation exposures of operating personnel were minimal.

Temperatures in both the electrical and radioactive arrays are reasonably close to those predicted by the theoretical calculations. Figure 4 shows the temperature rises in the salt 1½ ft from the center line of the center holes in the arrays along with the calculated temperature rises. It can be seen that most of the temperatures are somewhat lower than the calculated values. This is due in part to heat loss from the salt to the mine room. The peak fuel element temperatures reached about 300°C soon after placement in the mine.

In Fig. 5(a) is shown the uplift profiles for room 1 (radioactive array), along the north–south and east–west axes of the room. It is apparent that thermal expansion of the material in the floor extends to 40 or 50 ft from the center of the array. The north–south uplift profile shows the restraining effect produced by the presence of the adjacent pillars.

Vertical thermal expansion of the floor in the center of the arrays had reached nearly an inch by the end of December 1965. The floor uplift (measured in feet) as a function of time for each array at the center and 10 ft from the center is shown in Fig. 5(b). It may be observed that the rate of rise in and near the array is slowing down. This is due to the fact that the rate of rise of the salt temperature is also slowing down. The total vertical expansion had reached about 1¼ in. in May 1966.

Project Salt Vault will continue, with fuel assembly changeouts every six months, until about November 1967. Following completion of the demonstration essentially all basic data necessary for the design of an actual disposal facility will have been obtained.

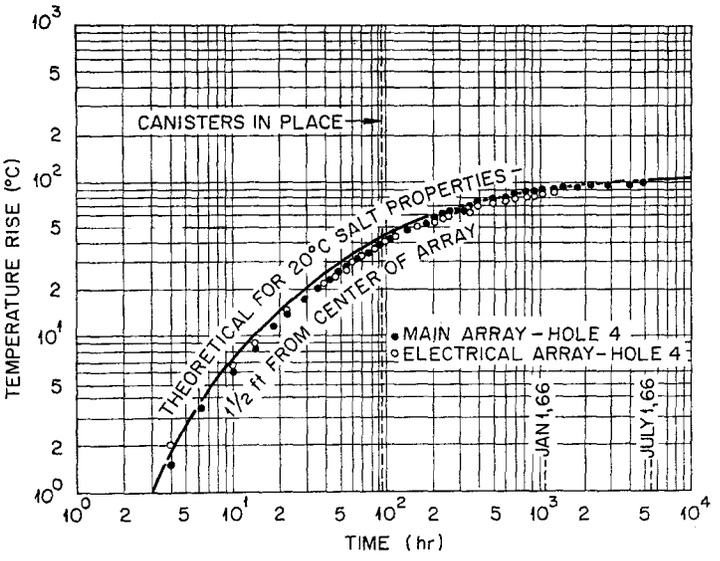

FIG. 4. Comparison of actual and theoretical temperature rises in radioactive and electrical arrays.

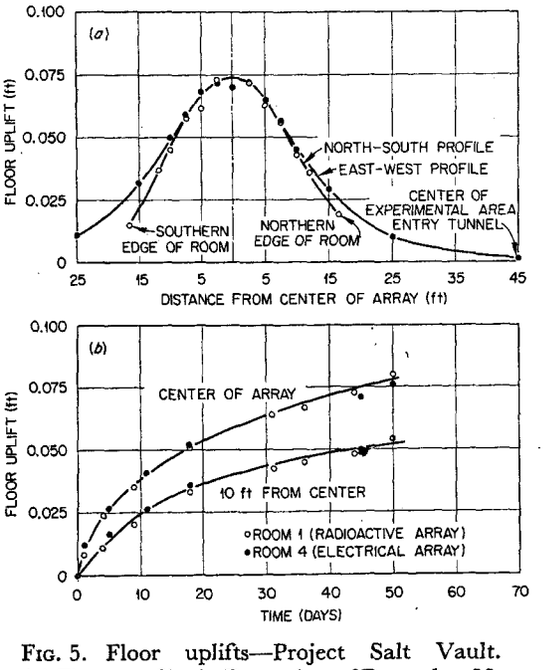

FIG. 5. Floor uplifts—Project Salt Vault. (a) Floor profiles in Room 1 as of December 30, 1965. (b) Floor uplift in array rooms.

DISPOSAL BY HYDRAULIC FRACTURING

Hydraulic fracturing has been used for many years in the petroleum industry to increase production from oil wells. Normally, a mixture of sand and water or sand and oil is forced out into a hydraulically produced crack in the formation where the sand is deposited, allowing the oil to drain into the sand layer and then out into the well. In the case of radioactive waste disposal, however, the problem is not one of increased oil production but rather one of pumping the material requiring disposal into the fracture.

The disposal well is possibly the most critical part of the disposal facility. The well must be drilled into the formation selected for disposal operation, cased, and cemented to prevent ground water from entering the well. When an injection is to be performed, this casing is slotted and water is pumped into the well until the pressure builds up producing a fracture or crack in the formation (see Fig. 6). The waste-cement mixture is then injected into this fracture. In the case of radioactive waste disposal, solid ingredients (such as cement, clay, and a retarder are mixed with the waste to produce a

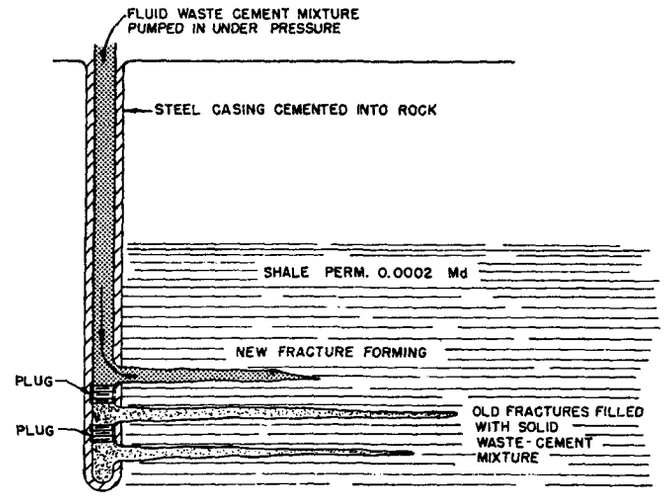

FIG. 6. Schematic cross-section of hydraulic fracturing operations for radioactive waste disposal.

slurry which will harden in the fracture and retain the fission products.

An essential prerequisite in the use of hydraulic fracturing for radioactive waste disposal is the need for producing horizontal fractures in the formation. Considerable controversy exists in the petroleum industry over the conditions necessary to produce horizontal rather than vertical fractures. Since experience in the petroleum industry is mainly with permeable formations and not the relatively impermeable formations proposed for radioactive waste injections it was decided to perform a series of test injections in the shale at Oak Ridge. The first experimental injection was made at a depth of 290 ft and consisted of 27,000 gal of a mixture of water, cement, and diatomaceous earth tagged with 35 Ci of ^{137}Cs. Subsequent coring and gamma-ray logging verified that the grout sheet had followed the bedding planes and that the fracture was essentially horizontal (see Fig. 7). The second experiment included two injections at greater depths. The final injection was made at a depth of 934 ft and consisted of

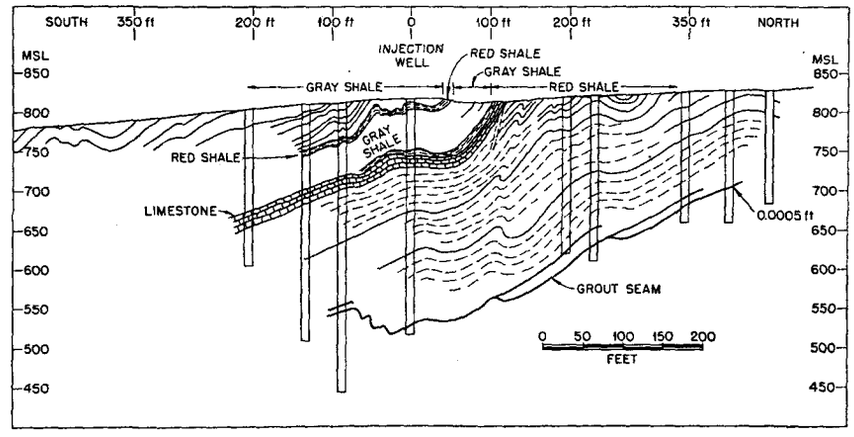

FIG. 7. Location of grout sheet—First experiment.

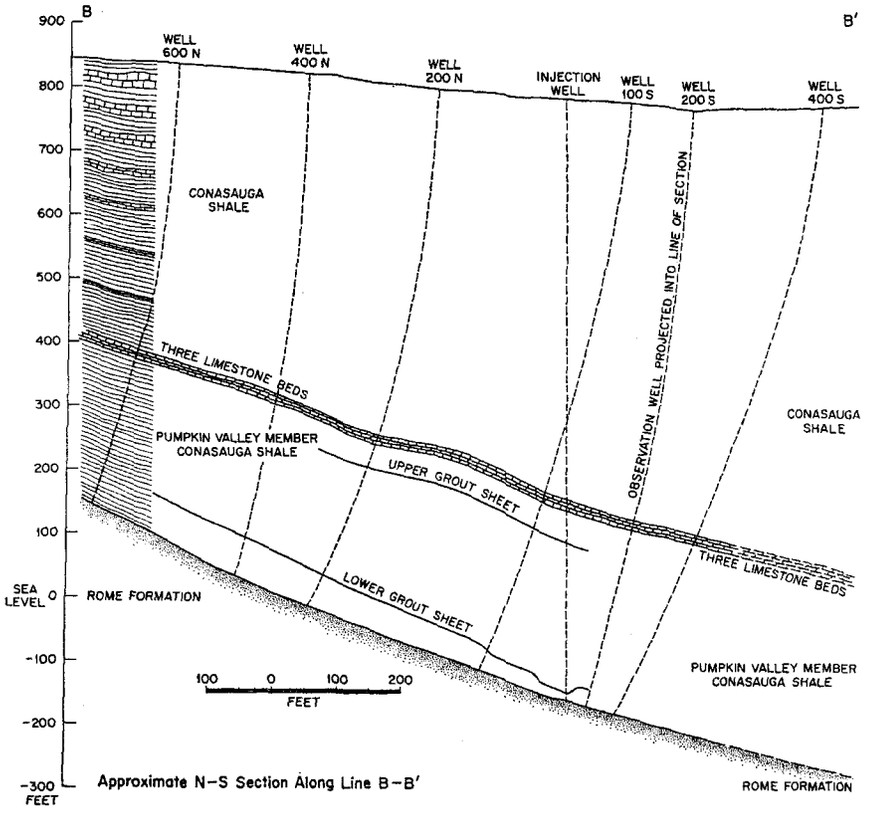

FIG. 8. Location of grout sheet—Second experiment.

91,500 gal of water, cement, and bentonite, tagged with 25 Ci of ^{137}Cs. Several days later a second injection was made in the same well at a depth of 700 ft. Core drilling and logging again verified that the grout sheets followed the bedding planes in the formation (see Fig. 8). During the course of these experimental injections, measurements were made on surface uplift and wellhead and observation well pressures in order to develop an understanding of the mechanics of fracture formation.[10, 11]

Desirable characteristics of a waste-cement slurry for the disposal of radioactive waste by hydraulic fracturing are: (1) low viscosity for the period of time the waste is injected; (2) sorption and retention of the radioactive liquid after the slurry sets; and (3) a mixture that is relatively cheap. Studies of the waste-cement slurries for use with ORNL intermediate-level waste have shown that it is possible to develop mixtures with these properties. For long pumping times a "retarder" such as calcium lignosulfonate (CLS) must be added; if the cement content is reduced a "suspender" such as attapulgite is required. For improved retention of radiocesium a clay material such as illite must be added. From the studies completed to date it is apparent that mixes can be designed having any range of physical properties and cost for any composition of radioactive waste.[12]

Based on the results obtained in the experimental injections, an experimental plant has been built at ORNL to dispose of intermediate-level wastes and evaporator concentrates. A view of the Fracturing Plant is shown in Fig. 9. The four large bins contain the mixture of solids used in the slurry. The solids are transferred pneumatically to the mixing cell in the

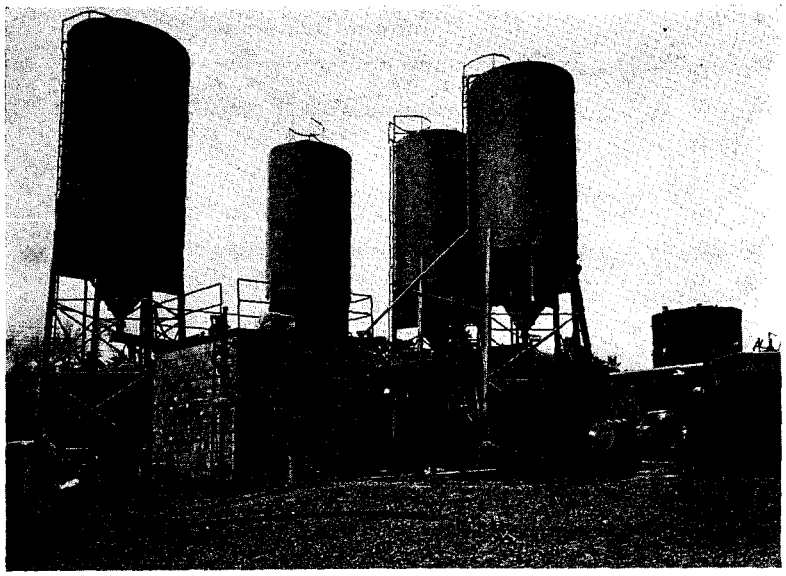

FIG. 9. View of facilities at fracturing plant.

concrete block structure where they are mixed with the liquid waste and the resulting slurry is pumped into the well by the high pressure pump shown in the foreground. In order to provide radiation protection, it is necessary to enclose the waste pump, mixer, wellhead, and injection pump in concrete cells.[13]

Geologic conditions at the site are shown in Fig. 10. Shale formations exist at several depths that are believed to be suitable for waste disposal injections. Economic considerations suggested the use of the shale located at a depth of 720 to 950 ft. All the formations are well below the deepest known water bearing formation (about 200 ft).

Experimental operation of the plant during the past two years has resulted in the safe disposal of approximately 430,000 gal of waste containing 11,500 Ci. A total of seven experimental injections ranging in size from 40,000 to 148,000 gal have been made. During these injections it has been shown that it is possible to halt the injection, clear the well and equipment, make repairs, and resume operation without undue hazard to the operating personnel. Core drilling has shown that the grout sheets from the first five experimental injections conformed to the bedding planes of the shale.

Cost estimates have shown that the cost of injecting 400,000 gal per year of radioactive waste would be $0.13 per gallon including solid ingredients, depreciation, and operating costs.[14] The estimated costs are based on one injection of 100,000 gal per slot and a well life of 10 years.

The major unknown in hydraulic fracturing is that of well life. As successive injections are performed and layers of the waste are built up in the formation, the earth's surface is slowly pushed up and stresses build up in the overlying formations. Exactly how many injections can be made until the stresses in the rock will produce failure in the system (vertical fractures) is currently under study.

At the present time the plant used at ORNL for experimental hydraulic fracturing is being upgraded to an operating facility for injecting intermediate-level wastes and evaporator concentrates on a routine basis. Routine operation of this facility is scheduled to begin this fall.

INJECTION INTO POROUS FORMATIONS

For a number of years the petroleum industry has used deep well injection as a means of disposal of waste brines. In the East Texas field alone, 7×10^9 gal of brine were injected in 1958, and the total volume of brine injected

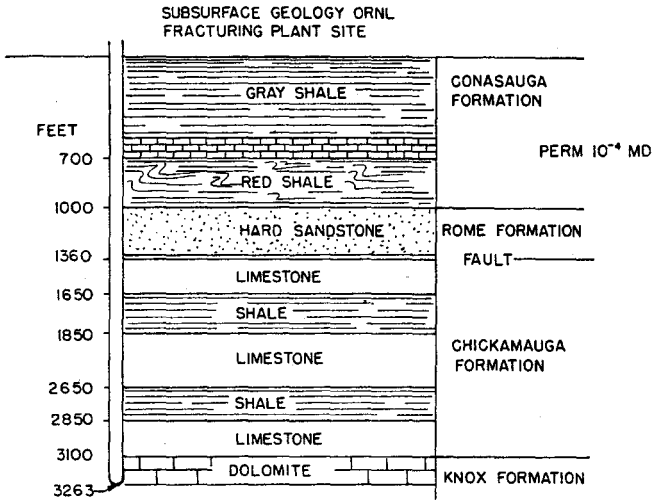

FIG. 10. Geology of shale fracturing site.

since operations were initiated in 1935 was 1×10^{11} gal.[15] At the present time, a number of companies are also using deep well disposal methods for their industrial wastes.[16, 17]

Before using deep well injection for radioactive wastes there must be an adequate disposal site and the waste must be compatible with the formation and its fluid.[18] An ideal site would be one in which a brine saturated permeable formation is bounded above and below by impermeable strata. The original concept was to store the wastes in the interstices of the formation, but the current philosophy allows injection into flowing formations since the normal flow is usually very slow; sufficient decay time should be available to reduce the radionuclide concentrations to safe levels. Radionuclides have been found to move much slower in the formation than the liquid due to ion-exchange and adsorption. However, nonhomogeneities in the formation could produce higher velocities in given areas and this may prove to be limiting.

In 1959 the American Association of Petroleum Geologists (AAPG) was requested to make a survey of potential sites where deep well injection could be performed. Their report[19] describes six basins which apparently would supply the necessary permeable formations. Three of the basins selected also contain shale reservoirs and salt deposits which might be used for intermediate- and high-level waste disposal.

The movement of the liquid and radionuclides

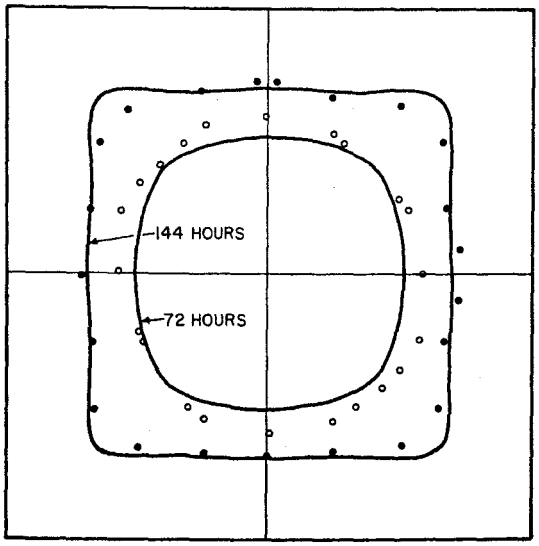

FIG. 11. Contours of mean ^{85}Sr movement in sandstone block as a function of time.

in homogeneous isotropic formations can be calculated.[20] Laboratory studies using a Berea sandstone block have verified the calculations.[21] Figure 11 shows the rate of movement of ^{85}Sr from a single injection well. It can be seen that the measured distribution agrees quite well with the predicted behavior.

Experience in the deep well injection of brines and other wastes has shown that unless the waste is compatible with the formation and its fluid the well will eventually plug. Plugging can also be caused by suspended solids or by bacterial growth. If the well were to plug by these mechanisms it might be possible to remove the plugged area by acid treatment, but the resulting waste containing radionuclides washed from the formation would present an additional disposal problem. It would appear simpler to pretreat the waste and filter prior to injection. The type and degree of pretreatment would be dependent on the characteristics of the waste and the injection formation and would have to be determined for each specific site.

At the present time there are no firm plans for a field scale demonstration of deep well injection. This is due, in part, to the large volumes of waste required to carry out a meaningful field study. It would also require a considerable period of time to complete a field study of any significant size. The results of a single field study could not necessarily be extrapolated to other sites due to local geologic peculiarities because the imperfections or non-homogeneities of the formation would probably control the degree of leakage.

CONCLUSION

Field scale demonstrations have shown that it is possible to safely and economically store high-level solidified wastes in salt formations and intermediate-level wastes in the slightly permeable shales at Oak Ridge. Disposal of low-level liquid wastes in permeable formation has not yet been demonstrated in field scale plants but the concept has been proven on laboratory scale models.

ACKNOWLEDGEMENTS

The authors would like to acknowledge the contributions by the following individuals to the work described in this paper: R. L. Bradshaw, W. de Laguna, F. M. Empson, D. G. Jacobs, H. Kubota, W. C. McClain, W. F. Schaffer, Jr., R. C. Sexton, T. Tamura, and H. O. Weeren.

REFERENCES

1. Committee on Waste Disposal, Division of Earth Sciences, *Disposal of Radioactive Waste on Land*, National Academy of Sciences, National Research Council Publication 519, April 1957, p. 6.
2. *Mineral Resources of the United States*, p. 180. Public Affairs Press (1958).
3. F. Birch and H. Clark. The thermal conductivity of rocks and its dependence on temperature and composition, *Amer. J. Sciences*, **238,** 529–558, 613–635 (1940).
4. R. L. Bradshaw, F. M. Empson, W. J. Boegly, Jr., H. Kubota, F. L. Parker and E. G. Struxness. Properties of salt important in radioactive waste disposal, *Proc. International Conference on Saline Deposits*, Houston, Texas, November 12–17, 1962 (1967).
5. A. E. Inman. *Salt, an Industrial Potential for Kansas*, p. 22. University of Kansas Research Foundation (1951).
6. W. J. Boegly, Jr. *et al.* Disposal in salt formations, *Health Physics Division Annual Progress Report for Period Ending July* 31, 1962, pp. 10–20.
7. W. J. Boegly, Jr. *et al.* Project salt vault: a demonstration disposal of high-level radioactive solids in Lyons, Kansas, Salt Mine, *Health Physics* **12,** 417–424 (1966).
8. W. F. Schaffer, Jr. *et al.* Project salt vault: design and demonstration of equipment, *Proc. International Symposium on the Solidification and Long-term Storage of Highly Radioactive Wastes*, Richland, Washington, February 14–18, 1966 (in press).
9. *Health Physics Division Annual Progress Report for Period Ending July* 31, 1966 (in Press).
10. W. de Laguna. Disposal of radioactive wastes by hydraulic fracturing. Part I. General concept and first field experiments, *Nucl. Eng. Design* **3,** 338 (1966).
11. W. de Laguna. Disposal of radioactive wastes by hydraulic fracturing. Part II. Mechanics of fracture formation and design of observation and monitoring wells, *Nucl. Eng. Design* **3,** 432 (1966).
12. T. Tamura. Disposal of radioactive wastes by hydraulic fracturing. Part IV. Chemical development of waste cement mixes, *Nucl. Eng. Design* **3** (1966).
13. H. O. Weeren and J. O. Blomeke. Disposal of radioactive wastes by hydraulic fracturing, *Nucl. Eng. and Design* **4,** 108–117 (1966).

14. H. O. WEEREN. Cost estimates for hydrofracture facilities. Letter to E. G. Struxness dated June 21, 1963.
15. W. S. MORRIS. Sub-surface disposal of salt water from oil wells, *J. Water Pollution Control Federation,* **32,** 41–51 (1960).
16. R. F. SELM and B. T. HULSE. Deep well disposal of industrial wastes, *Chem. Engrg. Progr.* **56,** No. 5, 138–144 (1960).
17. R. S. STEWART. Proposed underground disposal of industrial wastes in the Northeast U.S., *Proc. 12th Industrial Waste Conf.*, Purdue Univ. Engrg. Extn. Ser. No. 94, 1957, pp. 494–501.
18. T. V. MOORE *et al.* Problems in the disposal of radioactive wastes in deep wells. Report of Subcommittee on Disposal of Radioactive Waste, Central Committee on Drilling and Production Practice, Division of Production, American Petroleum Institute, Dallas, Tex. (1958).
19. American Association of Petroleum Geologists, Inc. *Radioactive Waste-Disposal Potentials in Selected Geologic Basins*, SAN-413-2 (1964).
20. D. G. JACOBS. Ion exchange in the deep-well disposal of radioactive wastes, *International Colloquium on Retention and Migration of Radioactive Ions in Soils*, October 16–18, 1962, Center d'Études Nucléaires de Saclay, France (1963).
21. D. G. JACOBS and M. U. SHAIKH. Liquid injection into deep permeable formations, *Health Division Annual Report for Period Ending July* 31, 1964. ORNL-3697, pp. 3–10 (1964).

STOCKAGE DE DÉCHETS RADIO-ACTIFS SUR LE SITE DE BAUZOT

J. PRADEL, F. BILLARD et A. GRANIER

Service d'Études Techniques de Protection, CEA, Centre d'Études Nucléaires, Fontenay-aux-Roses (France)

Résumé—Des déchets radio-actifs en provenance de différentes usines sont stockés depuis 1958 sur le carreau d'une ancienne exploitation d'uranium à Bauzot (Saône-et-Loire).

Ces résidus sont logés dans des futs métalliques de 100–200 l. deposés par couches horizontales et recouverts par 50–70 cm de stériles de la mine.

Une étude hydrogéologique a montré que les eaux qui traversent la zone de stockage s'infiltrent vers une nappe qui alimente un puits situé en contrebas. Des contrôles de la radioactivité des eaux de ce puits permettent de suivre l'évolution de la contamination éventuelle de la nappe phréatique.

Après sept années d'exploitation le site de Bauzot donne toutes garanties de sécurité pour les populations avoisinantes.

DISCUSSION

A. LAFONTAINE (*Belgium*):

Lors d'essais tels qu'ils ont été décrits, il se produit des retombées très locales aux abords même de la cheminée. Il est utile de connaître l'ampleur de tels phénomènes.

J. J. MARTIN:

La pollution locale du lieu d'émission est due à la capture du traceur par les membrures du pylône et à un refoulement de la solution à la fin de l'émission. On peut estimer la perte de solution à moins de quelques %, les éléments du pylône présentant un faible obstacle au panache.

X. DE MAERE (*Belgium*):

M. Martin pourrait-il fournir des informations concernant les différences éventuelles observées entre les gradients de température mesurés suivant une verticale dans la vallée et le long des pentes de celle-ci?

J. J. MARTIN:

Nous n'avons pas fait de comparaison statistique entre les gradients observés par différents moyens. En étudiant successivement les diverses émissions, on constate une bonne concordance, mis à part le gradient observé au voisinage immédiat de la Meuse, entre le gradient le long de la pente et le gradient mesuré dans la vallée à la même altitude.

D. BLANC (*France*):

La mesure à diverses altitudes des concentrations en radon et en thoron de l'air atmosphérique permet de mesurer le coefficient vertical de diffusion turbulente. Je voudrais savoir si M. Martin a effectué des mesures de ce genre.

J. J. MARTIN:

Nous n'avons pas fait de mesure de diffusion verticale à partir du thoron émis par le sol, mais seulement des mesures de gradient vertical de température.

E. W. JACKSON (*U.K.*):

Can Mr. Martin tell me whether the results in this most interesting paper can be used to predict the downwind concentrations when the flow is over a simple obstruction, such as a low hill, assuming that the meteorological conditions at the time are low wind speed and strong inversion? On the basis of your experimental results would it be permissible for example to take the flow pattern for a plane, which can be determined theoretically, and "bend" it appropriately?

J. J. MARTIN:

Notre expérimentation a porté sur un site de relief très marqué. Nous n'avons pas dépouillé complètement les expérimentations faites sur un autre site plan. It est possible que nous y obtenions une dispersion de résultats plus faible que sur le site des Ardennes.

La méthode est applicable sur n'importe quel site. Sur le site des Ardennes, la différence de niveau entre le point de mesure et le point d'émission n'a pas d'influence significative sur la contamination. Tout se passe comme si tous les points d'observation étaient ramenés à un même niveau.

HUB. WIJKER (*Netherlands*):

It is not my purpose to put a question to the speaker but more to make a communication in connection with Mr. Jackson's question.

We performed a number of wind tunnel experiments and found no influence of ditches on stream lines of smoke from the model stack, especially not at low wind speeds.

A. FRANCESCHINI (*Italy*):

Furono eseguite misure della velocità di deposizione dello I^{131}?

A. P. HULL:

If I understand the question correctly, you are asking if we have looked for ground deposition of the I^{131} in our stack effluent. Unfortunately, for our purposes, our reactor is too well behaved a machine. We would need about two orders of magnitude greater emission to have measurable deposition.

B. W. EMMERSON (*U.K.*)

With reference to the earlier studies made at Brookhaven, what was the A^{41} emission rate from the stack, and at what distance from the site did the lower limits of plume detection occur?

A. P. HULL:

The A^{41} studies were made at Brookhaven prior to my employment there and at a time when the emission rate was 7000 Ci/day. It is presently 20,000 Ci/day in a concentration of 2×10^{-3} μCi/cm^3. The original studies were conducted from as close in as the plume could be determined to be at ground level, which is somewhat difficult with equipment which is gamma sensitive, to a distance of about 60 mi. The latter was by airplane flight during inversion conditions when the plume is rather well confined at great distances.

C. A. ADAMS (*U.K.*):

Is allowance made in the calculation of effective stack height for the entrainment effects which can be caused by neighbouring buildings if they are of comparable height?

A. P. HULL:

The stack is at least five times higher than any surrounding structures, so we have no perturbations of this sort to contend with.

A. LAFONTAINE (*Belgium*):

La formule proposée par notre collègue yougoslave est certainement intéressante et constitue une approche pour attirer l'attention sur le problème des fleuves internationaux. Elle ne serait pourtant acceptable que pour les produits solubles, car pour les isotopes insolubles, une série d'autres paramètres doivent être pris en considération (écologie, évolution des sédiments, etc.).

P. S. BOJOVIĆ:

Si j'ai bien compris la question, vous avez l'impression que la formule proposée n'est pas entièrement correcte. C'est peut-être la vérité car, cette formule n'a pas la prétention d'être définitive. En tous cas le rejet des effluents radio-actifs dans un fleuve international existe comme un problème actuel, et la communication que j'ai exposée ici est un apport à la solution de ce problème.

En ce qui concerne une précipitation favorisée, dont M. Lafontaine a parlé avec juste raison, c'est le facteur commun *Fc* qui tient compte de ce phénomène.

R. FUKAI (*IAEA*):

1. What was the chemical form of chromium-51 used in the experiments?

2. Was the suspended matter which the speaker referred to in his experiments the natural suspended matter or that which is produced in the experiments?

In connection with the first question, I wanted to stress the importance of the chemical forms of radionuclides in discussing the problem. For example, in the case of chromium, the behaviour of chromium in sea water is completely different between trivalent and hexavalent forms, and accordingly, the concentration factors of chromium by marine organisms are different.

Y. NISHIWAKI:

1. Cr^{51} used for this experiment is originally in the form of $CrCl_3$ in HCl solution with specific activity 13.3 mCi/mg and 2.8 mCi/ml. This solution was diluted to 100 μCi/400 l. in natural sea water. It may change into the chromate in natural sea water.

2. The suspended matter studied in the experiment is the natural one contained in the natural sea water sample at Osaka bay in Japan.

I quite agree with your remarks. Thank you very much for your kind attention.

P. GIULIANI (*Italy*):

1. Is there any indication of the behaviour of salt formations when subjected to seismic disturbances?

2. What is the maximum concentration of radioactivity which can be tolerated in liquid wastes to be injected in deep wells?

W. J. BOEGLY:

1. There is no evidence of any reported damage to salt mines by earthquakes. Because very old mines still exist the probability of damage must be low.

2. There has been considerable controversy on the activity level of wastes used for deep well injection. Originally it was proposed that high-level wastes be injected but currently only low-level wastes are under consideration. Probably the main limiting factor would be the chemical composition of the waste.

INGESTED RADON AS A SOURCE OF HUMAN RADIATION EXPOSURE

BO LINDELL
National Institute of Radiation Protection, Stockholm 60, Sweden

Abstract—^{222}Rn is usually mentioned as a source of radiation exposure of man in connection with inhalation rather than ingestion. However, since radon is a natural contaminant of ground water, it is of interest to study also the doses caused by intake with water. For ingestion of water containing radon, the stomach is the critical organ. The radon retention in the body is mainly determined by the transport from stomach to blood, since radon is rapidly eliminated from blood. After 4 hr only a few per cent of the ingested amount remains in the body, but is then likely to be eliminated at a lower rate, probably because of the high solubility in adipose tissues. The dose equivalent per 1 μCi radon ingested is estimated at 200 mrem, corresponding to $(MPC)_w = 10^{-4}$ μCi/ml (100 nCi/l.). Concentrations of up to 5000 nCi/l. have been reported in the literature. A frequent value for tap water from ground water supplies is 1 nCi/l. in many countries, while waters from deep bored wells frequently show concentrations of the order of 10 nCi/l. It is interesting to note that radon concentrations of up to 1 nCi/l. have been observed in some dairy milk.

INTRODUCTION

Although there are numerous reports on the content of ^{222}Rn in drinking waters (distributed in time from 1904, when one paper was published by Mme Curie[1] up to the present no value for the maximum permissible concentration of this nuclide has been proposed until recently (Bernard,[2] Andersson and Nilsson,[3] von Döbeln and Lindell,[4] and Hursh *et al.*[5]), with the exception of a value given in 1953 by the United States National Committee on Radiation Protection in NBS Handbook 52[6] but not repeated in later NCRP reports. The International Commission on Radiological Protection does not recommend any value for $(MPC)_w$.

There are several obvious reasons for this, one being that radon in water rarely constitutes an occupational risk since it is usually naturally occurring. Another reason is that the radon does not remain in the water very long, and that it stays an even shorter time in the body once ingested. Already in the 1910's the apparent mean residence time was found to be less than one hour, and in the 1930's detailed studies of the radon retention was published, e.g. by Stefen Meyer[7] and by Fernau and Smereker.[8]

With the present attitude towards radiation protection, however, even radon in water has become of some interest from the radiation protection point of view. Protection efforts are not only directed towards the radiation worker; ICRP has given "dose limits" also for the general public, "intended to provide standards for the design and operation of radiation sources so that it is unlikely that individuals in the public will receive more than a specified dose".

These dose limits have not been designed to apply to naturally occurring radiation sources or, in fact, to any *occurring* situation. For such situations it is countermeasures rather than planning that are required. However, the $(MPC)_w$-values are based also upon the doses per unit intake of activity, and the results of such calculations are also needed in the assessment of the possible risk from a given source. Therefore, the doses due to intake of radon with drinking water justify some investigation. The doses may not always be entirely insignificant: it has been shown that there exist in nature drinking waters that may give local tissue doses as high as 1 rem/day at a water consumption of 1 l./day, i.e. 1 rem per liter consumed.

LEVELS OF ^{222}Rn IN WATER

A number of relatively recent reviews (Federov and Baranov,[9] Hursh *et al.*,[5] Muth *et al.*,[10] Kiefer and Maushart,[11] Turner *et al.*,[12] Smith *et al.*,[13] von Döbeln and Lindell[4]) and old reports (Sahlbom,[14] Stephan,[15] Engelmann,[16] Ludewig,[17,18] Genser[19,20]), mostly on spa waters, relatively portray the frequency of various ^{222}Rn levels in ground water.

Sahlbom found already in 1915 that typical Swedish values for the radon concentration in ground water in sedimentary rocks ranged between 0.7 and 1.1 nCi/l., while wells in igneous rocks usually covered the range 2–20 nCi/l. Kiefer and Maushart found levels between 0.1 and 2.5 nCi/l. in tap waters from a number of German towns which use ground water or springs. Surface waters usually show less than 0.05 nCi/l. Turner *et al.* found an average of 1.1 nCi/l. in Cornish waters, while they assumed that the average for the whole of Britain is only 0.002 nCi/l. Smith *et al.* found average concentrations of 16 and 30 nCi/l. in wells in Maine and New Hampshire, respectively, with maximum values as high as 200 nCi/l. The highest levels found in Sweden are near the same level (Armands[21]).

Spa waters in Oberschlema in Germany have been reported by Kuroda[22] and by Genser[20] to hold activities ranging from 100 to 5000 nCi/l.

The radon content of the drinking water has been suggested by Allen-Price[23] as a possible cause of an alleged higher than normal cancer frequency in certain parts of West Devon, but these levels as reported by Abbatt *et al.*[24], were not found to be higher than 13 nCi/l.

THE FATE OF THE INGESTED RADON

In 1933, Fernau and Smereker[8] gave an exponential expression for the radon expiration rate after ingestion with water. Their expression contained two exponential terms and represented a rapid increase, with a time constant $k_A = 0.149\ \text{min}^{-1}$, followed by a more slow decrease, corresponding to a time constant $k_B = 0.023\ \text{min}^{-1}$. Fernau and Smereker correlated the time constants to the elimination from the gastrointestinal tract and the blood, i.e. from two compartments. A more general multi-compartment analysis will be needed to illustrate the phenomenon over a longer time period. The general circuit graph of a five compartment system would be as follows

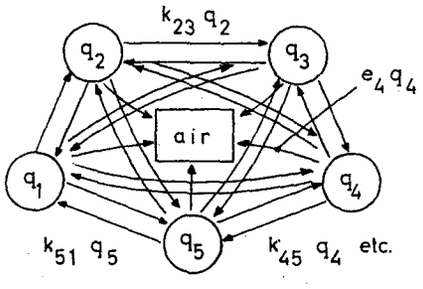

The *amount* of radon transferred from compartment (m) to compartment (n) per unit time can be written as

$$R_{mn} = k_{mn}q_m - k_{nm}q_n$$

where the q's denote the quantity of radon in the various compartments.

The radon transport will be governed by five differential equations, namely

$$\frac{dq_1}{dt} = -(k_{12} + k_{13} + k_{14} + k_{15} + e_1)q_1 + k_{21}q_2 + k_{31}q_3 + k_{41}q_4 + k_{51}q_5;$$

$$\frac{dq_2}{dt} = +k_{12}q_1 - (k_{21} + k_{23} + k_{24} + k_{25} + e_2)q_2 + k_{32}q_3 + k_{42}q_4 + k_{52}q_5;$$

. . . etc.

where the e's denote elimination constants. A detailed analysis of this system has been reported by von Döbeln and Lindell.[4] A rough approximation of the circuit graph can be made as follows:

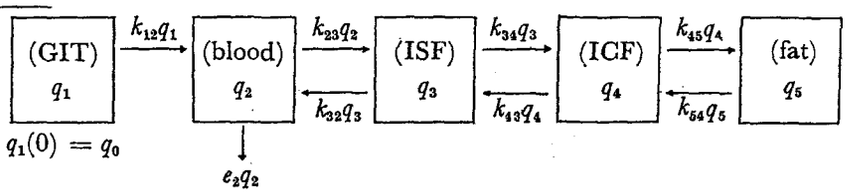

The analysis yields curves of the type shown in Fig. 1. In addition to the total retention curve, the retention is also shown in the following five compartments: blood (B), stomach (S), extracellular fluids (ECF), intracellular fluids (ICF) and fat (F). The broken curve represents the retention in fat calculated on the basis of experimental data presented by Hursh *et al.*[5] and Harley *et al.*[25] The long-term retention is entirely governed by the fat content.

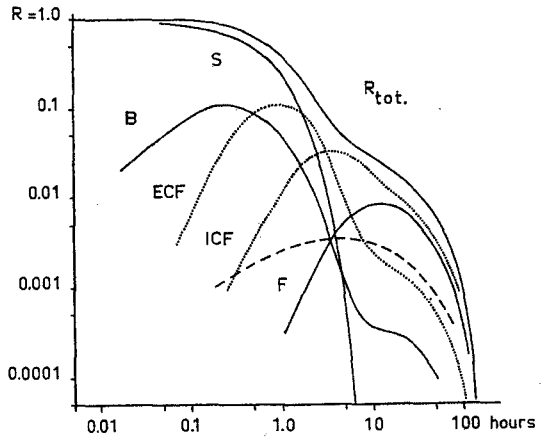

FIG. 1.

The mathematical model, used here only for illustrational purposes, reflects facts that were reported and well understood already by Meyer in 1937.[7] The radon is transferred from the stomach to the blood at a rate which varies depending upon whether the water was ingested on a full or on an empty stomach. Fat in the stomach will decrease the rate of transfer because radon is more soluble in the fat which is also more slowly absorbed than the water. An equilibrium between the radon in the fat and in the intestinal fluids will probably not be attained until the fat is in emulsion after the influence of bile and other intestinal fluids.

Once the radon has reached the blood, it is eliminated very rapidly through the lungs, with an effective half-time of only about one minute. While in the blood, the radon is retained possibly by adsorption and absorption processes.

After four hours, only a few per cent of the ingested amount remains in the body. The remaining radon is mainly located in the adipose tissues, because of the higher solubility in fat. This has been demonstrated on the rat by Nussbaum and Hursh,[26] in a study of the distribution between different organs under equilibrium conditions.

Figure 2 shows some examples of retention curves for ^{222}Rn after a single ingestion, as suggested by various authors. Curve 1 represents a single exponential function assumed by Andersson and Nilsson.[3] Curve 2 illustrates the double exponential expression suggested by Fernau and Smereker.[8] Curves 3 and 4 correspond to data obtained by Hursh *et al.*[5] for an empty and a full stomach respectively. Curve 5 can be obtained from the compartment analysis discussed above, on the basis of experimental data presented by Harley *et al.*[25]

Retention measurements by von Döbeln and Lindell[4] on subjects who had ingested radon with water on an empty stomach yielded the data shown in Fig. 3. The technique did not permit measurements for more than about five hours. The diagram actually shows the body content of the daughter product ^{214}Bi (RaC) as measured by whole-body counting. The full

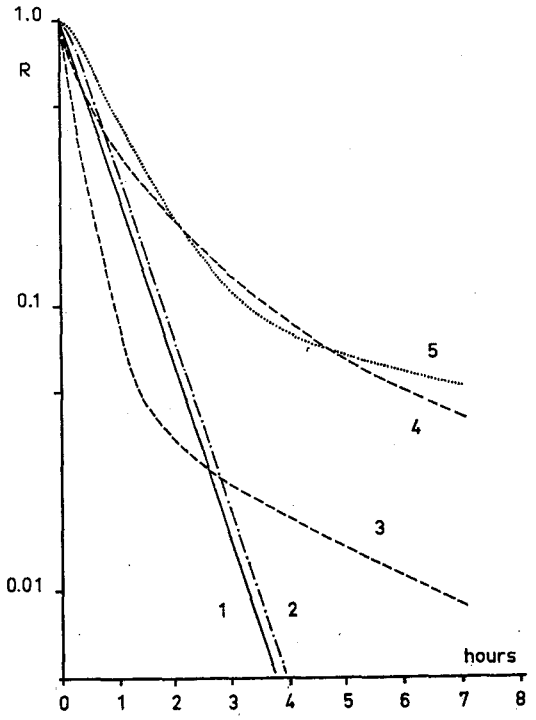

FIG. 2.

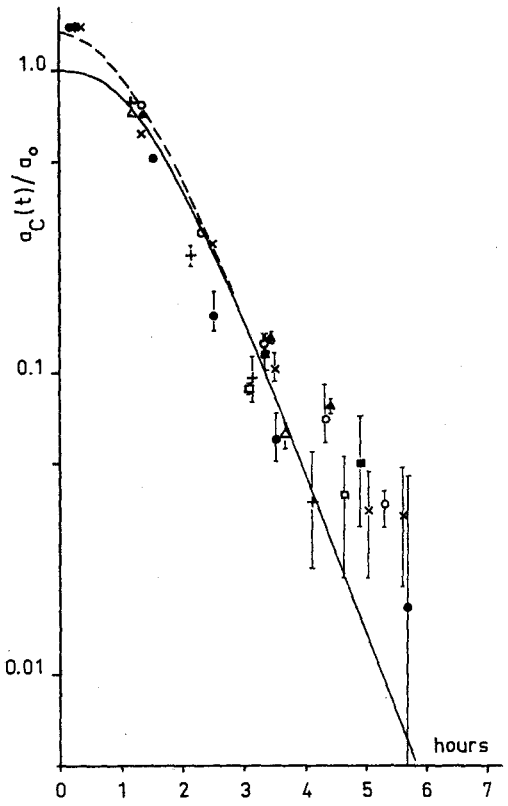

FIG. 3.

curve represents the body content of ^{214}Bi calculated on the assumption of a single exponential retention of ^{222}Rn ingested in initial equilibrium with ^{214}Bi, while the broken curve is based upon the assumption that 25% of the radon gas is lost initially. The experimental points have been normalized to make the average retention between 3 and 4 hr fall upon the calculated curve.

The long-term retention is only vaguely indicated by these data, but experiments aimed at measuring the retention at more than five hours after ingestion will be carried out.

MAXIMUM PERMISSIBLE CONCENTRATIONS

On the basis of the information referred to above, the radiation doses to various organs and hence also values for $(MPC)_w$ can be calculated. The results derived by von Döbeln and Lindell are shown in Table 1:

Table 1. *Suggested* $(MPC)_w$ *Values for* Rn^{222}

Organ of reference	Dose equivalent per 1 μCi radon ingested (mrem)	$(MPC)_w$ (μCi/ml)
Critical organ		
GIT (stomach)	200	10^{-4}
Other organs		
Liver	7	3.10^{-3}
Fat	6	3.10^{-3}
Whole body	2	3.10^{-3}
Lung	2	10^{-2}
Kidney	1	2.10^{-2}

The stomach is the critical organ with a dose equivalent to the stomach wall of 200 mrem per μCi radon ingested and $(MPC)_w = 10^{-4}\mu$Ci/ml. This value of $(MPC)_w$ is 50 times as high as the value once suggested in NBS Handbook 52, but it is in accordance with the estimate by Hursh *et al.*[5] It is 1/5 of the value proposed by Bernard[2] who, however, suggested fat as critical organ, and 1/9 of the value proposed by Andersson and Nilsson.[3] Both the latter values seem to have been derived on the unrealistic assumption that all energy delivered within the body is dissipated in living tissues. In fact, 50–75% of the energy is delivered in the stomach content and in the mucus, even if the energy from the α-emitting daughters which fail to penetrate the mucus is completely neglected.

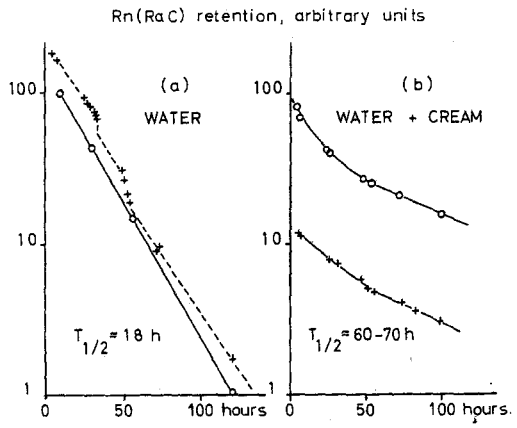

FIG. 4. Rn(RaC) retention, arbitary units.

Table 2. Bunsen and Ostwald Solubility Coefficients for Inert Gases in Water and Olive Oil at 37°C (*Ref. Lawrence et al.*, 1946; *last entry: Nussbaum*, 1957.)[39]

Gas	Molecular weight	Water	Olive oil	Oil/Water ratio
		Bunsen absorption coefficients (α)		
Helium	4	0.0085	0.015	1.7
Neon	20.2	0.0097	—	—
Nitrogen	28	0.013	0.067	5.2
Argon	39.9	0.026	0.14	5.3
Krypton	83.7	0.045	0.43	9.6
Xenon	131.3	0.085	1.7	20.0
Radon	222	0.15	19.0	125.0
		Ostwald absorption coefficients (α_1)		
Radon (from above):		0.17	21	125
Radon (Nussbaum):		0.165	6.25	$\approx$40

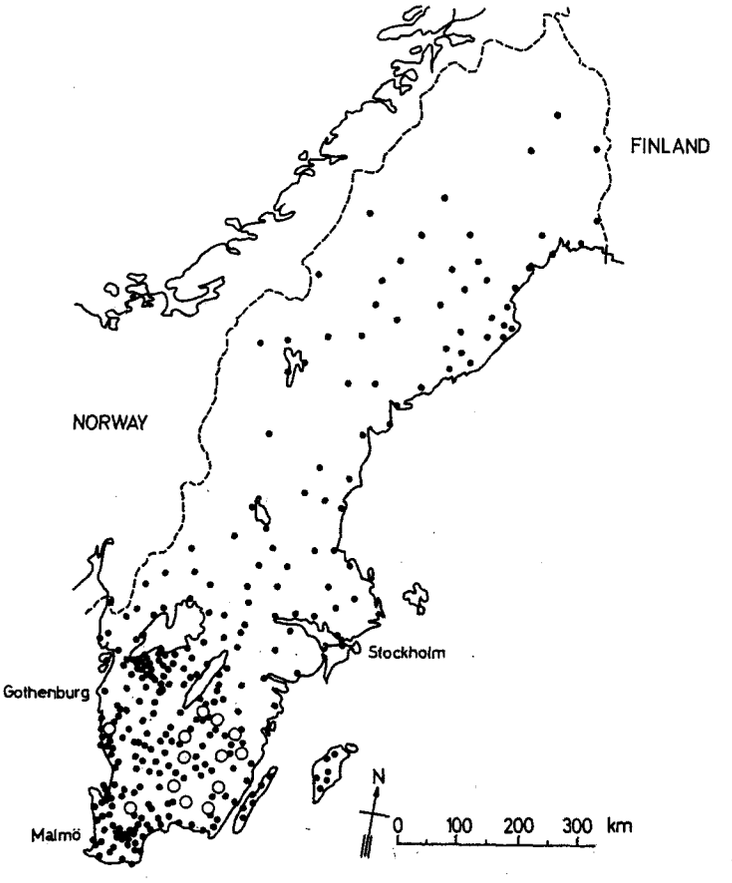

FIG. 5.

On the basis of $(MPC)_w = 10^{-4}$ μCi/ml, or 100 nCi/l., some natural waters exceed the maximum permissible occupational levels. In risk assessments, however, it must be borne in mind that the ICRP method of calculating $(MPC)_w$ is based on the assumption that the total water intake is ingested as drinking water and, furthermore, that radon is likely to disappear from the water unless it is ingested immediately after tapping.

RADON IN MILK

If water containing radon is kept in an open container of normal shape, the radon is eliminated with an apparent half-time of about 20 hr (cf. Fig. 4(a)). If the water is stirred the loss is greater, and if the water is poured from one container to another, about 10–15% of the radon is lost each time (the broken curve in Fig. 4(a)). If some cream is added to the water, the retention time will increase (Fig. 4(b)) and approach the physical life of ^{222}Rn (91.8 hr half-life). Again, the explanation is the higher solubility in fat, which is also illustrated by the Ostwald solubility coefficients for inert gases in water and oil as shown in Table 2.

Because of its higher solubility in fat, radon is also retained in milk. This has been shown to have some interesting consequences. It has been demonstrated by von Döbeln and Lindell [4] that ^{222}Rn can be found in cow's milk if the animals have had access to radon-rich water. The ratio of the concentrations (nCi/l.) found in milk and in water at the same farm was less than 0.04, with 0.025 as a representative value. This means that if milk is found to contain ^{222}Rn, the water supply is likely to hold the 40-fold concentration. This opens a possibility to trace high radon concentrations in ground water through milk.

Magi and Lindell [27] have recently reported on a survey (for ^{137}Cs) covering milk from all Swedish dairies (about 300), which revealed the presence of radon in samples from 13 dairies located in a relatively limited part of Sweden, mostly in Småland. The location of the dairies is indicated in Fig. 5, where the dairies with radon are represented by circles.

The highest concentration was 0.6 nCi/l. which would suggest that the *average* concentration for about 400 farms delivering milk to this dairy would be at least 25 nCi/l., or that a few farms have water supplies with much higher concentrations. This is being further investigated.

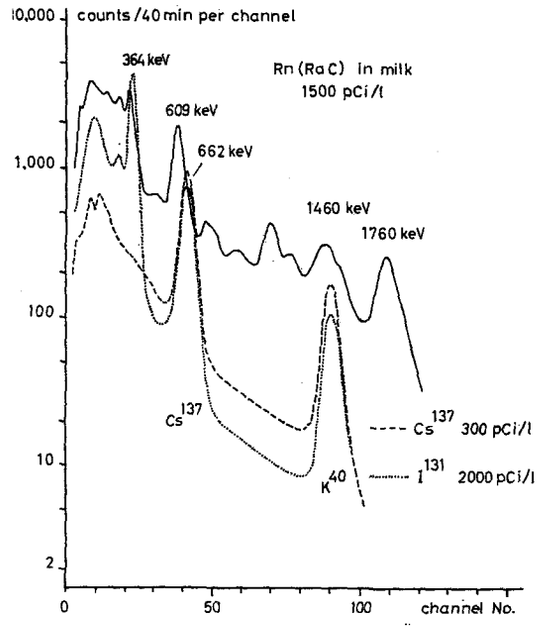

FIG. 6. γ-spectra illustrating some of the most active milk samples found in the Swedish sampling programme of 1962; cf. discussion in the text.

Even though the concentrations of ^{222}Rn in milk are much lower than in water, they are sometimes sufficiently high to dominate the γ-spectrum completely, even at relatively high levels of artificial contamination, as can be seen from Fig. 6. Not even the highest ^{131}I concentration measured in Swedish milk (in 1962) did give such a high counting rate as the highest ^{222}Rn concentration found in milk. The naturally occurring contamination can, indeed, be as intriguing as the far more investigated contamination caused by nuclear debris.

REFERENCES

1. P. CURIE and E. LABORDE. Sur la réactivité des gas qui se degagent de l'eau des sources thermales. *Compt. rend. Acad. d. Sc. Paris* **138,** 1150–1153 (1904).

2. S. R. BERNARD. An $(MPC)_w$ for Rn^{222}. Paper presented at the Eighth Annual Meeting of the Health Physics Society, New York, 1963.
3. I. O. ANDERSSON and I. NILSSON. Exposure following ingestion of water containing radon-222. Paper presented at the (IAEA) Symposium on Assessment of Radioactive Body Burdens in Man, Heidelberg, 1964.
4. W. VON DÖBELN and B. LINDELL. Some aspects of radon contamination following ingestion. *Arkiv för fysik (Stockholm)* **27,** 531–572 (1965).
5. J. B. HURSH, D. A. MORKEN, TH. DAVIS and A. LOVAAS. The fate of radon ingested by man. Univ. of Rochester Atomic Energy Project Report No. UR-648 (1964), also *Health Physics* **11,** 463–476 (1965).
6. National Committee on Radiation Protection (U.S.), Maximum permissible amounts of radioisotopes in the human body and maximum permissible concentrations in air and water. National Bureau of Standards, Handbook 52. Washington, 1953.
7. S. MEYER. Physikalische Grundlagen von Emanationskuren. Strahlentherapie **58,** 656–663 (1937).
8. A. FERNAU and H. SMEREKER. Über des Verbleiben radioaktiver Substanz im Organismus bei Radium-Emanationstrinkkuren. *Strahlentherapie* **46,** 365–373 (1933).
9. E. K. FEDEROV and V. I. BARANOV. Content of natural radioactive substances in the atmosphere and in natural waters in the territory of the USSR. Academy of Sciences, Moscow (1956).
10. H. MUTH *et al.* The normal radium content and the Ra^{226}/Ca ratio of various foods, drinking water and different organs and tissues of the human body. *Health Physics* **2,** 239–245 (1960).
11. H. KIEFER and R. MAUSHART. Die natürliche Radioaktivität im Wasser. *Nukleonik* **1,** 22–27 (1958).
12. R. C. TURNER, J. M. RADLEY and W. V. MAYNEORD. Naturally occurring alpha-activity of drinking water. *Nature* **189,** 348–352 (1961).
13. B. M. SMITH, W. N. GRUNE, F. B. HIGGINS and J. G. TERRILL. Natural radioactivity in ground water supplies in Maine and New Hampshire. *Journal Am. Water Works Ass.* **53,** 75 (1961).
14. NAIMA SAHLBOM. Om radioaktiviteten hos svenska källvatten och dess samband med de geologiska förhållandena. *Arkiv för Kemi, Mineralogi och Geologi (Stockholm)* **6,** No. 3, 1–52 (1915).
15. I. STEPHAN. Der Emanationsgehalt ausserdeutscher radioaktiver Quellen nach französischen und amerikanischen Messungen aus den Jahren 1918–1923. *Strahlentherapie* **16,** 560–574 (1923).
16. W. ENGELMANN. Die Radioaktivität der Heilquellen im deutschen Sprachgebiet und ihr Anteil am deren therapeutischer Wirkung, Strahlentherapie **18,** 686–709 (1924).
17. P. LUDEWIG. Der Emanationsgehalt der radioaktiven Quellen in Brambach und Oberschlema. *Strahlentherapie* **18,** 718–720 (1924).
18. P. LUDEWIG. Der Emanationsgehalt der Quellen in den wichtigsten radioaktiven Quellengebieten. *Strahlentherapie* **19,** 170–171 (1925).
19. C. GENSER. Über die Entstchung und die Natur radioaktiver Quellen. *Geologische Rundschau* **23,** 188–238 (1932).
20. C. GENSER. Radioaktive Heilquellen in Deutschland. *Z. der Deutschen Geologischen Gesellschaft* **85,** 482–495 (1934).
21. G. ARMANDS. Geochemical prospecting of a uraniferous bog deposit at Masugnsbyn, Northern Sweden. Swedish Atomic Energy Company Report AE-36, Stockholm (1961).
22. P. K. KURODA. Radioactivity tables of some natural waters. University of Arkansas (1953).
23. E. D. ALLEN-PRICE. Uneven distribution of cancer in West Devon. *Lancet* **II,** 1235–1238 (1960).
24. J. D. ABBATT, J. R. A. LAKEY and D. J. MATHIAS. Natural radioactivity in West Devon water supplies. *Lancet* **II,** 1272–1274 (1960).
25. J. H. HARLEY, E. JETTER and N. NELSON. Elimination of radon from the body. New York's Operations Office Report No. 3, United States Atomic Energy Commission (1951).
26. E. NUSSBAUM and J. B. HURSH. Radon solubility in rat tissues. *Science* **125,** 552–553 (1957).
27. A. MAGI and B. LINDELL. Rn^{222} in milk. *Proc. International Symposium on Radioecological Concentration Process*, Stockholm, 25–29 April 1966. Pergamon Press, London.
28. J. H. LAWRENCE *et al.* Preliminary observations on the narcotic effect of xenon with a review of values for solubility of gases in water and oils. *J. Physiol.* **105,** 197–204 (1946).
29. E. NUSSBAUM. Radon solubility in body tissues and in fatty acids. Univ. of Rochester Atomic Energy Project Report No. UR-503 (1957).

THE METABOLIC AND DOSIMETRIC SIGNIFICANCE OF ^{210}Pb TO ^{226}Ra RATIOS IN THE BONE OF RADIUM DIAL PAINTERS*†

HENRY G. PETROW

New York University, Institute for Environmental Medicine, New York, New York

Abstract—The concentration of ^{210}Pb and ^{226}Ra was measured at 89 different sites in the skeletons of two deceased radium dial painters. Using an exponential model for both ^{210}Pb and ^{226}Ra clearance from the skeleton, the data indicate:

1. ^{210}Pb and ^{226}Ra have equal biological half-lives.
2. Variation in the ratios of ^{210}Pb to ^{226}Ra in individual long bones follows a distinct and reproducible pattern. The value of the ratio is lowest in the end pieces of long bones, and highest in the shaft. The ratio is high in rib and low in vertebra. These variations have been interpreted as arising from differences in the ^{222}Rn retention factors at the sites analyzed. These retention factors have been calculated, and vary from 0.20 to 0.57 compared to the skeletal average of 0.33. It is felt that the variations in the ^{222}Rn retention factors reflect fundamental differences in bone structure, namely crystal size, mineral density, and amorphous mineral content.
3. For a ^{226}Ra burden carried 50 years, it is estimated that 5–6% of the average alpha dose delivered to the skeleton results from ^{210}Pb decay.
4. The vertebra would appear to be the bone of choice to be used in estimating total body burden of ^{226}Ra.
5. In a given dial painter, ^{226}Ra concentrations with respect to ash content, varied by a factor of 15 between the highest and lowest values.

THE longest lived daughter of ^{226}Ra is 21.4 year ^{210}Pb. An important intermediate daughter product is the noble gas, 3.83 day ^{222}Rn. In an individual, such as a radium dial painter, who has carried an elevated skeletal burden of ^{226}Ra for many years, the average skeletal ratio of ^{210}Pb to ^{226}Ra is a function of several variables. These include the ^{222}Rn retention factor, the biological half-lives of ^{210}Pb and ^{226}Ra, the physical half-life of ^{210}Pb, and the time elapsed since exposure. These factors which control the average skeletal ratio of ^{210}Pb to ^{226}Ra, likewise control the ratio at specific skeletal sites. However, it does not necessarily follow that specific sites in the skeleton will have the same values for biological parameters that are found for the total skeleton.

In the evaluation of the data to be presented, long time clearance of radium from the skeleton is assumed to be exponential. The bases for this assumption are recent studies which indicate that long term clearance of radium from the skeleton can be described by a single exponential function, and that the average biological half-life of radium is 15–20 years.[1, 2] Schroeder and Balassa have made a compilation of existing data concerning the distribution of stable lead in human tissue, including bone.[3] Analysis of the data for bone, wherein the concentration of lead was measured as a function of age for 79 different individuals, indicates that

---

* This study is part of the thesis submitted in partial fulfillment of the requirements for the degree of Doctor of Philosophy, New York University, 1966.

† This investigation was supported by a project grant from the U.S. Atomic Energy Commission, Division of Biology and Medicine, Contract AT(30-1) 3086, and is part of a core program supported by the U.S. Public Health Service, Bureau of State Services grant ES 00014 and the National Cancer Institute grant CA 06989.

the concentration of lead in bone increases exponentially with age, the half period being approximately 20 years. Therefore, it is also assumed that skeletal elimination of lead can be approximated by an exponential function.

As regards the retention of ^{222}Rn by the skeleton, it has been shown by many workers that the average skeletal retention factor for ^{222}Rn is 0.33,[4] the remainder being expired via the lungs. The rate at which specific skeletal sites lose radon is not known, however, and since the structure of bone is not uniform, it is possible that the ^{222}Rn retention factor is not constant and equal to 0.33 at all skeletal sites, but is dependent upon the locus of ^{226}Ra deposition. If the retention of radon is dependent upon the locus of formation, there are two important consequences. First, the dose delivered by a given amount of deposited ^{226}Ra is a function of the fraction of ^{222}Rn retained. Secondly, it has been postulated by Rowland *et al.*[5] and Mays *et al.*[6] that the fraction of ^{222}Rn retained by bone is controlled by the size of the bone crystals and the mineral density in the region of the ^{226}Ra deposit. Hence, variability of the ^{222}Rn retention factor from site to site within the skeleton, if such is the case, would reflect variability in the fundamental structure of bone.

It was, then, the purpose of the study to be described to measure the ratio of ^{210}Pb to ^{226}Ra at as many skeletal sites as possible in individuals having old, elevated burdens of ^{226}Ra with the expectation that the data would yield information concerning variability within the skeleton of ^{222}Rn retention factors and the relative biological half-lives of ^{210}Pb and ^{226}Ra. This information, in turn, would permit more refined dose calculations to be made, and hopefully lead to qualitative estimates of the variations in the fundamental structure of bone.

BRIEF CASE HISTORIES OF THE INDIVIDUALS STUDIED

The ratio of ^{210}Pb to ^{226}Ra has been measured at 89 different sites in the skeleton of two deceased female radium dial painters. The first case, New Jersey Department of Health No. 5281, was born in 1898. She was continuously exposed as a dial painter from 1914 to 1917.[7] In 1956, her right leg was amputated as a result of an osteogenic sarcoma of the femur. Her body burden of ^{226}Ra, as measured by whole body counting in 1962, was estimated to be 0.54 μCi.[8] She died in 1964 of an acute coronary occlusion. At autopsy, bone specimens were obtained, and thirty-two bone sites taken from eleven different bones, representing about 11% of the total skeleton, were analyzed for ^{210}Pb and ^{226}Ra.

The second case, New Jersey Department of Health No. 5278, was born in 1893. She was continuously exposed as a dial painter in 1917.[7] Her burden of ^{226}Ra was estimated in 1961, by whole body counting, to be 0.046 μCi.[8] She died in 1965 of diffuse metastatic carcinoma. A total of fifty-seven different bone specimens, taken at autopsy from fifteen different bones, were analyzed for ^{210}Pb and ^{226}Ra. Approximately 20% of the skeleton was analyzed.

ANALYTICAL METHODS

All bone samples analyzed were kept frozen and sealed in polyethylene bags prior to analysis.

Each bone section was weighed, ashed for 16 hr at 600°C, and the resulting ash weighed. From these data, the percent ash of each sample was computed. Temperatures in excess of 600°C were avoided less lead be lost by volatilization.

The weighed ash was dissolved in hydrobromic acid, lead carrier added, and ^{210}Pb determined according to the procedure of Petrow and Cover.[9] After the separation of lead, the ash solution was treated with nitric acid to remove bromide ion, the bulk of the free nitric acid removed by evaporation, and radium coprecipitated with lead sulfate after the addition of lead and sulfuric acid. The ^{226}Ra content of the sample was then determined according to the procedure of Petrow *et al.*[10, 11]

ASSUMPTIONS TO BE CONSIDERED

In the introduction, it was pointed out that the ^{222}Rn retention factor and the biological half-lives of ^{210}Pb and ^{226}Ra can affect the value of the ^{210}Pb and ^{226}Ra ratio at any given skeletal site, and in the total skeleton. There are also other factors, including time of bone storage after death and the ^{222}Rn loss rate

during storage, and the ^{210}Pb content of ingested dial paints.

For the first case, 5281, the samples were stored, frozen and sealed in polyethylene for one year between autopsy and analysis. The loss of ^{222}Rn during this year of storage must be considered. Compared to the approximately 67% average ^{222}Rn loss assumed during life, there can be two extremes for the storage period, 100% loss, or zero loss. It has been assumed, for purposes of this study, that ^{222}Rn loss during storage was zero, or very nearly so. This is not a purely arbitrary choice, since the samples were stored, frozen and sealed, and Mays has shown that ^{222}Rn loss from frozen bones is very low.[12] Since the samples were stored for only one year, any error that would arise in the calculations due to a 10% to 20% ^{222}Rn loss during storage would be small. Therefore, for Case 5281, all calculations are based upon a radium burden carried for 49 years to death, during which an average ^{222}Rn loss rate of 67% is assumed. Finally, a zero ^{222}Rn loss rate during the year of storage is assumed.

For Case 5278, the storage period was only 3 months, and hence, any storage error is even less than for Case 5281. The exposure is assumed to have occurred in mid-1917, so 48 years elapsed between exposure and death. All calculations are based on a burden carried for 48 years during which the average ^{222}Rn loss rate was 67%, and 3 months of storage at zero ^{222}Rn loss.

A second factor to be considered is the ^{210}Pb content of the ingested dial paints, for if there were substantial amounts of ^{210}Pb in the paints, then there would be a source of skeletal ^{210}Pb other than ingrowth from ^{226}Ra deposited in the skeleton. The fraction of ingested ^{210}Pb that would be deposited in the skeleton is not known. As will be shown, the data for both cases analyzed indicate that ^{226}Ra and ^{210}Pb formed from ^{226}Ra decay are cleared from the skeleton at equal rates, and this is confirmed by excreta analysis of ^{210}Pb and ^{226}Ra for Case 5281.[13] These data will also be considered later. Therefore, the assumption will be made, in the absence of actual data on the fate of ingested ^{210}Pb, that equal fractions of ingested ^{210}Pb and ^{226}Ra are fixed in the skeleton. The question, then, is what is the likely ^{210}Pb content of a ^{226}Ra preparation used in the period 1914–17, and what effect would this amount of ^{210}Pb have on the results.

The source of ^{210}Pb in the earth is from the decay of ^{238}U. The half-life of ^{238}U is 4.5×10^9 years. The age of the earth is estimated to be about 3.5×10^9 years. That is, about 40% of the uranium present at creation has decayed to ^{206}Pb. Were all the lead formed still present in the mineral, from an original one gram of uranium, there would be remaining 0.6 g of uranium and 0.35 g of lead. Associated with this 0.6 g of uranium would be 0.18 μCi of ^{226}Ra. Hence, in the mineral, one would expect a lead-to-radium mass ratio of 2×10^6. In the analysis of many uranium minerals for lead and uranium, the author has found that the stable lead-to-uranium ratio can vary from about 0.15 to as high as 10. This is the result of many factors, including leaching, recrystallization, and the incorporation of stable lead in the mineral of origin other than uranium decay. However, it is safe to say that the ratio of stable lead to radium is always greater than 10^5. Therefore, in order to prepare ^{226}Ra of high specific activity, as is needed for dial paint formulation, well over 99% of any lead present would have to be separated from the radium. Hence, freshly prepared ^{226}Ra would be very nearly free of ^{210}Pb, since chemical separation processes do not make isotopic distinctions.

The second consideration is how long the radium was stored between purification and use. The period of exposure for the two cases analyzed was 1914–17 and 1917. Radium was discovered in 1898. The maximum age, then, was 16–19 years for the radium used in the paints. In fact, however, during World War I, demand for radium was so great that the material was used almost immediately after preparation,[14] and hence, there was very little time for ^{210}Pb ingrowth. Since ^{210}Pb ingrowth in one year is only 3% of the ^{226}Ra content, and probably less due to ^{222}Rn leakage, it is safe to assume that the ^{210}Pb content of the paints was less than 3% of the ^{226}Ra content, which is negligible.

BASIS FOR THE CALCULATIONS

If one accepts the qualifying assumptions made above concerning sample storage and the

^{210}Pb content of ingested radium paints, there remain two possible causes which can significantly affect the value of the ^{210}Pb to ^{226}Ra ratio at any given skeletal site: the biological half-lives of ^{226}Ra and ^{210}Pb, and the ^{222}Rn retention factor.

The effect of the biological half-lives of ^{210}Pb and ^{226}Ra on the value of the ^{210}Pb to ^{226}Ra ratio at any given skeletal site can be massive. If the relative difference between the biological half-lives of the two radionuclides is large, this alone can influence the value of their ratio to an extent that dwarfs all other factors. If the biological half-life of ^{210}Pb is very long relative to that of ^{226}Ra at a given site, the ratio will be large. If, on the other hand, ^{210}Pb is cleared much more rapidly than ^{226}Ra, the ratio will be small. Therefore, the effect of the ^{210}Pb and ^{226}Ra biological half-lives on the value of the ratio should be considered for three different situations: where the ^{210}Pb biological half-life is greater than, less than, or equal to that of ^{226}Ra.

The Bateman expression for the ratio of ^{210}Pb to ^{226}Ra activity in bone at some time t after the deposition of ^{226}Ra can be expressed as follows:

$$\frac{^{210}\text{Pb}}{^{226}\text{Ra}} = \frac{A^0_{\text{Ra}} \cdot R \cdot \lambda^P_{\text{Pb}}}{\lambda^P_{\text{Pb}} + \lambda^B_{\text{Pb}} - \lambda^P_{\text{Ra}} - \lambda^B_{\text{Ra}}} \cdot \frac{\left[\exp\left[-\left(\lambda^P_{\text{Ra}}+\lambda^B_{\text{Ra}}\right)t\right] - \exp\left[-\left(\lambda^P_{\text{Pb}}+\lambda^B_{\text{Pb}}\right)t\right]\right]}{A^0_{\text{Ra}} \exp\left[-\left(\lambda^P_{\text{Ra}} + \lambda^B_{\text{Ra}}\right)\right]}$$

A^0_{Ra} = initial ^{226}Ra concentration,
t = years elapsed since exposure,
R = ^{222}Rn retention factor,
λ^P_{Pb} = physical decay constant for ^{210}Pb, years $^{-1}$,
λ^P_{Ra} = physical decay constant for ^{226}Ra, years $^{-1}$,
λ^B_{Pb} = biological decay constant for ^{210}Pb, years $^{-1}$,
λ^B_{Ra} = biological decay constant for ^{226}Ra, years $^{-1}$.

Since there is no way of knowing the values of λ^B_{Ra} and λ^B_{Pb} at a given skeletal site, the equation, as written cannot be solved. However for the special case where $\lambda^B_{\text{Pb}} = \lambda^B_{\text{Ra}}$, the equation simplifies to

$$\frac{^{210}\text{Pb}}{^{226}\text{Ra}} = \frac{R \cdot \lambda^P_{\text{Pb}}}{\lambda^P_{\text{Pb}} - \lambda^P_{\text{Ra}}}\left[1 - \exp[-(\lambda^P_{\text{Pb}} - \lambda^P_{\text{Ra}})t]\right]$$

Therefore, when ^{210}Pb and ^{226}Ra have equal biological half-lives, the value of the ratio is independent of their magnitude, regardless of their value. Since the value of R for the total skeleton is known, and is equal to 0.33, one can calculate the value of the ratio when t is known, and when $\lambda^B_{\text{Pb}} = \lambda^B_{\text{Ra}}$. Furthermore, if the average skeletal ratio is greater than that calculated for the special case of equality of ^{210}Pb and ^{226}Ra biological half-lives, it can be said that ^{210}Pb has a longer biological half-life than ^{226}Ra, and conversely, if the average skeletal ratio is less than that calculated for the special case of equality, ^{210}Pb has a shorter biological half-life than ^{226}Ra. Despite the handicaps of a surplus of unknowns, the value of the skeletal ratio permits one to say whether ^{210}Pb is eliminated faster, slower, or at the same rate as ^{226}Ra, to the limits of certainty permissible in our knowledge of R and t.

THE SIGNIFICANCE OF THE MEASURED AVERAGE SKELETAL RATIOS

For Case 5281, with an assumed ^{222}Rn retention factor of 0.33, a 49-year post-exposure history, and one year of bone storage at a zero ^{222}Rn loss rate, the ratio of ^{210}Pb to ^{226}Ra can be calculated for the special case of equal lead

and radium biological half-lives, using the following expression:

$$\frac{^{210}Pb}{^{226}Ra} = \frac{0.33 \times 0.0324}{0.0324 - 0.0004}\left[1 - e^{-0.0320 \times 48}\right] e^{-0.0324 \times 1} + 1 - e^{-0.0324 \times 1} = 0.286$$

which is simply the Bateman expression for the ratio already presented corrected for ^{210}Pb ingrowth and decay during one year of sample storage.

From this it follows that for an average ^{222}Rn retention factor of 0.33, a ratio greater than 0.286 is the result of lead being cleared more slowly than radium, and a ratio less than 0.286 is the result of lead being cleared more rapidly than radium.

In Table 1 are presented the data, for the analysis of 32 bone sites taken at autopsy, from 11 different bones, for Case 5281. The total weight of ash analyzed was 259 g. If we consider her post-amputation ash content to have been 2300 g, it can be seen that 11% of the total skeleton was analyzed. Considering the quantity of ash analyzed and the number of bones and bone sites involved, the total sample is very likely representative, and the average ^{210}Pb and ^{226}Ra concentrations determined are equal, or very nearly equal, to her skeletal concentration of these two radionuclides. This is confirmed by the average ^{226}Ra concentration in the 259 g analyzed, 259 pCi/g ash. Her post-amputation body burden was 0.54 μCi. For an estimated skeletal ash weight of 2300 g remaining after amputation, an average ^{226}Ra concentration of 235 pCi/g ash would be expected. Allowing for the uncertainty in the estimate of her skeletal ash content, the agreement is good and the sample, therefore, is very likely representative.

The average skeletal ^{210}Pb to ^{226}Ra ratio, as determined radiochemically, is 0.266. This is very nearly equal to the value of 0.286 to be expected when the ^{222}Rn retention factor is 0.33 and ^{210}Pb and ^{226}Ra have equal biological half-lives. The data suggest that on the average, lead and radium are cleared from the skeleton at equal or very nearly equal rates. The fact that ^{210}Pb and ^{226}Ra are cleared at equal rates is confirmed by excreta analyses performed at the Argonne National Laboratory on a one-week feces and urine collection obtained from Case 5281 before her death.[13] The ratio of ^{210}Pb to ^{226}Ra found in the excreta was 0.255. The ratio in the skeleton found in this study, corrected for the ratio change during one year storage, is 0.243, nearly perfect agreement with the Argonne excreta data.

The data for the second case, 5278, are given in Table 2. Based upon a single whole body count, this individual had a ^{226}Ra burden of 0.046 μCi. A total of 57 different bone sites, taken at autopsy from 15 different bones, were analyzed. The total ash weight analyzed was 607 g, or 22% of an assumed total skeletal ash content of 2800 g. For a body burden of 0.046 μCi, an average ^{226}Ra concentration of 16.4 pCi/g ash would be expected. The average ^{226}Ra concentration found was 15.4 pCi/g ash, indicating that the sample was representative.

For a ^{222}Rn retention factor of 0.33, the ^{210}Pb to ^{226}Ra biological half-lives can be calculated, as before,

$$\frac{^{210}Pb}{^{226}Ra} = \frac{0.33 \times 0.0324}{0.0324 - 0.0004}\left[1 - e^{-0.0320 \times 48} \times e^{-0.0324 \times 0.25}\right] + 1 - e^{-0.0324 \times 0.25} = 0.266$$

The average skeletal ratio, as determined from the analysis of bone, is 0.284, once again very close to that predicted for equal ^{210}Pb and ^{226}Ra biological half-lives.

It would appear, then, that the average skeletal ratio of ^{210}Pb to ^{226}Ra, as determined radiochemically, is consistent with equal biological half-lives for ^{210}Pb and ^{226}Ra, provided one assumes that the clearance of both nuclides is exponential, and the ^{222}Rn retention factor is 0.33. Equal clearance rates of ^{210}Pb and ^{226}Ra from the skeleton for Case 5281 are confirmed by the very close agreement between the ^{210}Pb to ^{226}Ra ratios in the skeleton and in the excreta. Furthermore, Holtzman[15] has calculated a biological half-life of stable lead in the skeleton of 17.4 years, and the data in ref. 3 indicate a half-life of 20 years, both in close agreement with the average biological half-life of radium determined in refs. 1, 2, about 15-20 years.

Table 1. *Analysis of Case* 5281 *Bone for* ^{210}Pb *and* ^{226}Ra

Sample	Bone	g ash	% ash	^{210}Pb pCi/g ash	^{226}Ra pCi/g ash	$^{210}Pb/^{226}Ra$
2786	L. Tibia	12.15	30.0	29.4 ± 1.47	118 ± 5.90	0.249 ± 0.017
2787	,,	6.61	38.5	23.3 ± 1.16	88.0 ± 4.40	0.266 ± 0.019
2794	,,	10.20	24.2	148 ± 7.40	691 ± 34.6	0.214 ± 0.015
2795	,,	4.27	14.6	93.4 ± 4.67	415 ± 20.8	0.225 ± 0.016
* Weighted Average		33.23		72.6 ± 2.42	326 ± 10.9	0.222 ± 0.010
2847	L. Ribs, 6 & 7	2.61	14.8	92.1 ± 4.60	279 ± 14.0	0.330 ± 0.023
2849	,,	3.20	16.5	82.4 ± 4.12	236 ± 11.8	0.349 ± 0.024
2850	,,	2.60	18.9	68.4 ± 3.42	196 ± 9.8	0.349 ± 0.024
2851	,,	2.48	13.6	116 ± 5.80	331 ± 16.6	0.349 ± 0.024
2852	,,	2.48	10.8	102 ± 5.10	309 ± 15.5	0.330 ± 0.023
Weighted Average		15.37		92.9 ± 1.82	268 ± 5.25	0.346 ± 0.010
2716	L. Humerus	3.96	25.9	58.8 ± 2.94	210 ± 10.5	0.280 ± 0.020
2720	,,	3.95	26.3	126 ± 6.30	424 ± 21.2	0.295 ± 0.021
2725	,,	12.50	33.9	26.1 ± 1.30	86.7 ± 4.34	0.301 ± 0.021
2730	,,	8.14	42.4	21.0 ± 1.05	69.9 ± 3.49	0.301 ± 0.021
Weighted Average		28.55		43.4 ± 1.16	146 ± 3.90	0.297 ± 0.011
2697	L. Radius	3.21	33.8	26.1 ± 1.30	84.0 ± 4.20	0.310 ± 0.022
2700	,,	1.20	15.4	148 ± 7.40	628 ± 31.4	0.235 ± 0.016
2704	,,	4.20	21.0	233 ± 11.7	1030 ± 51.5	0.227 ± 0.016
Weighted Average		8.61		144 ± 4.66	621 ± 20.1	0.232 ± 0.011
2811	Sternum	8.87	8.70	70.7 ± 3.53	186 ± 9.40	0.380 ± 0.027
2813	,,	3.88	7.09	69.6 ± 3.48	220 ± 11.0	0.316 ± 0.022
Weighted Average		12.75		70.4 ± 2.68	196 ± 7.47	0.359 ± 0.019
2752	Mandible	3.77	13.6	139 ± 6.95	467 ± 23.4	0.298 ± 0.021
2764	,,	2.11	13.5	151 ± 7.55	521 ± 26.1	0.291 ± 0.020
Weighted Average		5.88		143 ± 5.20	486 ± 18.1	0.294 ± 0.015
2766	Vertebra, Thor.	14.9	14.4	64.5 ± 3.22	291 ± 14.6	0.222 ± 0.016
2863	Vertebra, Cerv.	25.0	15.4	74.4 ± 3.72	296 ± 14.8	0.252 ± 0.018
Weighted Average		39.9		71.0 ± 2.62	295 ± 10.9	0.240 ± 0.012
2842	L. Fibula	3.99	17.1	110 ± 5.50	476 ± 23.8	0.231 ± 0.016
2844	,,	3.51	16.1	19.8 ± 0.99	67.0 ± 3.35	0.294 ± 0.021
Weighted Average		7.50		68.0 ± 2.96	284 ± 12.4	0.240 ± 0.015
2816	L. Ulna	8.23	28.6	92.1 ± 4.60	358 ± 18.0	0.256 ± 0.018
2822	,,	1.96	14.4	88.8 ± 4.44	411 ± 20.6	0.215 ± 0.015
Weighted Average		10.19		91.0 ± 3.81	368 ± 15.4	0.247 ± 0.015

Table 1. *Analysis of Case* 5281 *Bone for* ^{210}Pb *and* ^{226}Ra*—Cont.*

Sample	Bone	g ash	% ash	^{210}Pb pCi/g ash	^{226}Ra pCi/g ash	$^{210}Pb/^{226}Ra$
3088	Calvaria	34.85	50.0	26.1 ± 1.30	108 ± 5.40	0.242 ± 0.017
2871	L. Femur	20.96	31.8	23.5 ± 1.18	66.6 ± 3.33	0.354 ± 0.025
2877	,,	11.35	44.2	55.5 ± 2.78	197 ± 9.85	0.283 ± 0.020
2884	,,	9.16	28.6	77.6 ± 3.88	264 ± 13.2	0.294 ± 0.021
2891	,,	8.21	30.9	152 ± 7.60	542 ± 27.1	0.280 ± 0.020
2896	,,	12.52	16.7	82.6 ± 4.13	322 ± 16.1	0.256 ± 0.018
Weighted Average		62.20		66.1 ± 1.56	234 ± 5.52	0.282 ± 0.009
Total Skeletal Average		259		68.6 ± 0.75	259 ± 2.82	0.266 ± 0.004

* Weighted average $= \dfrac{\Sigma \text{sample weight} \times \text{nuclide concentration}}{\Sigma \text{sample weight}}$.

The assumption concerning the ^{222}Rn retention factor as being 0.33 can be questioned, in that various laboratories use values ranging from 0.3 to 0.4.[16] However, Vennart *et al.*,[4] in a survey of the published work of many laboratories making *in-vivo* ^{226}Ra measurements, concludes that the ^{222}Rn retention factor is equal to 0.33. At any rate, were the retention factor either 0.3 or 0.4, the conclusion concerning the equal biological half-lives of ^{226}Ra and ^{210}Pb would not be greatly changed. Considering the data for Case 5281, if the ^{222}Rn retention factor was taken as 0.4 and the biological half-life of ^{226}Ra as 16 years, the calculated biological half-life for ^{210}Pb is 13.3 years. On the other hand, were the retention factor 0.3, the biological half-life of ^{210}Pb calculates to be 17.7 years. The range of the biological half-life of ^{210}Pb is 13.3 to 17.7 years relative to ^{226}Ra taken as 16 years. This is not an enormous range. However, there are other factors, both chemical and physical, that suggest that equality of biological half-lives for ^{226}Ra and ^{210}Pb formed from ^{226}Ra decay is not only reasonable, but likely. When ^{210}Pb is formed, it is formed very close to the parent ^{226}Ra deposit, probably in the same crystal or an adjacent crystal. Both ions are bivalent. Both ions have similar ionic radii. The chemistry of lead and radium is similar in a large number of reactions. Therefore, while the biological half-life of ^{210}Pb could be somewhat smaller or larger than that of ^{226}Ra, it is the author's belief that they are equal based upon the arguments presented.

It should be pointed out that the proposed equality is only for ^{210}Pb formed from ^{226}Ra decay since in this case a constraint is imposed upon the system in that the birth place of ^{210}Pb is controlled by the locus of radium deposition. It by no means proves that if lead and radium were deposited independently in the skeleton, the equality would hold. However, data already cited concerning the biological half-life of stable lead[3,15] indicate that independently deposited lead has a half-life similar to that of ^{210}Pb formed from ^{226}Ra decay.

The conclusion that ^{210}Pb and ^{226}Ra have equal biological half-lives is in disagreement with that of Holtzman.[15] Analyzing about 10 pieces of bone taken from five different individuals, he concluded that ^{210}Pb is cleared more slowly than ^{226}Ra. However, this work suffers from several weaknesses. First, the samples were stored for as much as 10 years before being analyzed, thereby magnifying possible errors arising from the unknown ^{222}Rn retention factor during storage. Only a few pieces of bone were analyzed for each case. Finally, it was assumed that the ^{222}Rn retention factor is invariant at every site in the skeleton, an assumption which,

Table 2. Analysis of Case 5278 Bone for ^{210}Pb and ^{226}Ra

Sample	Bone	g ash	% ash	^{210}Pb pCi/g ash	^{226}Ra pCi/g ash	$^{210}Pb/^{226}Ra$
3719	L. Tibia	19.74	17.9	12.6 ± 0.63	51.4 ± 2.57	0.246 ± 0.017
3721	,,	9.68	23.2	6.55 ± 0.33	23.0 ± 1.15	0.284 ± 0.020
3723	,,	9.65	32.6	4.24 ± 0.21	14.0 ± 0.70	0.302 ± 0.021
3737	,,	18.79	48.1	1.81 ± 0.09	5.40 ± 0.27	0.335 ± 0.023
3731	,,	25.03	29.6	6.31 ± 0.32	21.7 ± 1.08	0.294 ± 0.020
Weighted Average		82.89		6.60 ± 0.18	24.3 ± 0.68	0.272 ± 0.011
3760	L. Rib, 7	3.36	13.9	3.60 ± 0.18	9.91 ± 0.50	0.362 ± 0.025
3762	,,	2.16	11.7	3.87 ± 0.19	9.70 ± 0.48	0.400 ± 0.028
Weighted Average		5.52		3.71 ± 0.13	9.84 ± 0.35	0.378 ± 0.019
3588	L. Femur	14.54	43.5	2.93 ± 0.15	8.40 ± 0.42	0.350 ± 0.025
3592	,,	16.34	47.2	2.46 ± 0.12	6.45 ± 0.32	0.380 ± 0.027
3598	,,	11.22	43.0	2.80 ± 0.14	8.56 ± 0.43	0.327 ± 0.023
3604	,,	6.83	33.4	5.50 ± 0.28	21.2 ± 1.06	0.260 ± 0.018
3605	,,	19.77	22.1	9.42 ± 0.47	37.1 ± 1.85	0.255 ± 0.018
3611	,,	13.73	34.7	2.11 ± 0.10	5.42 ± 0.27	0.389 ± 0.027
3612	,,	13.43	26.4	4.73 ± 0.24	17.6 ± 0.88	0.267 ± 0.019
3614	,,	19.95	21.0	4.64 ± 0.23	17.3 ± 0.86	0.267 ± 0.019
Weighted Average		115.81		4.52 ± 0.10	16.1 ± 0.36	0.282 ± 0.009
3750	L. Metatarsal	2.48	19.6	4.90 ± 0.24	16.3 ± 0.81	0.301 ± 0.021
3752	,,	3.21	24.8	10.3 ± 0.51	37.1 ± 1.85	0.278 ± 0.020
Weighted Average		5.69		7.95 ± 0.31	28.1 ± 1.09	0.284 ± 0.016
3636	L. Clavicle	4.02	19.1	3.30 ± 0.16	9.34 ± 0.46	0.352 ± 0.025
3641	,,	3.75	20.8	2.37 ± 0.11	6.56 ± 0.32	0.362 ± 0.025
Weighted Average		7.77		2.84 ± 0.10	8.00 ± 0.29	0.356 ± 0.018
3772	L. Rib	1.31	11.2	3.76 ± 0.18	7.70 ± 0.38	0.480 ± 0.034
3774	,,	4.63	14.7	3.49 ± 0.17	9.00 ± 0.45	0.386 ± 0.027
Weighted Average		5.94		3.54 ± 0.14	8.72 ± 0.35	0.406 ± 0.023
3732	L. Fibula	4.93	22.8	8.71 ± 0.43	46.7 ± 2.33	0.186 ± 0.013
3736	,,	7.23	37.4	2.72 ± 0.13	8.88 ± 0.44	0.306 ± 0.021
3738	,,	6.80	19.8	7.52 ± 0.35	43.2 ± 2.16	0.174 ± 0.012
Weighted Average		18.96		5.98 ± 0.29	31.1 ± 1.52	0.192 ± 0.013
3713	Vertebra	23.06	11.9	2.99 ± 0.15	14.7 ± 0.74	0.206 ± 0.014
3708	Calvaria	53.79	53.2	2.75 ± 0.13	11.7 ± 0.58	0.235 ± 0.016
3712	,,	64.59	52.6	2.02 ± 0.10	6.57 ± 0.33	0.308 ± 0.022
Weighted Average		118.38		2.36 ± 0.08	9.00 ± 0.32	0.262 ± 0.013

Table 2. Analysis of Case 5278 Bone for ^{210}Pb and ^{226}Ra—Cont.

Sample	Bone	g ash	% ash	^{210}Pb pCi/g ash	^{226}Ra pCi/g ash	$^{210}Pb/^{226}Ra$
3753	R. Rib, 6	1.00	5.8	4.66 ± 0.23	12.7 ± 0.64	0.367 ± 0.026
3757	,,	1.69	14.8	4.60 ± 0.23	12.1 ± 0.60	0.381 ± 0.027
3759	,,	2.07	22.0	2.34 ± 0.11	5.41 ± 0.27	0.430 ± 0.030
Weighted Average		4.76		3.63 ± 0.11	9.32 ± 0.28	0.389 ± 0.016
3627	L. Ulna	10.80	25.5	4.86 ± 0.24	13.9 ± 0.70	0.350 ± 0.025
3633	,,	4.60	44.7	3.69 ± 0.18	11.5 ± 0.58	0.321 ± 0.023
3635	,,	4.35	25.6	4.92 ± 0.24	14.1 ± 0.70	0.350 ± 0.025
Weighted Average		19.75		4.60 ± 0.15	13.4 ± 0.44	0.344 ± 0.016
3671	L. Humerus	3.47	32.9	2.41 ± 0.12	6.04 ± 0.30	0.399 ± 0.028
3673	,,	4.33	36.6	2.94 ± 0.14	8.00 ± 0.40	0.368 ± 0.026
3675	,,	5.18	46.3	2.74 ± 0.13	7.70 ± 0.38	0.355 ± 0.025
3677	,,	6.70	44.4	2.56 ± 0.12	7.16 ± 0.36	0.359 ± 0.025
3681	,,	2.77	37.9	2.74 ± 0.13	7.70 ± 0.38	0.355 ± 0.025
3684	,,	3.16	25.7	2.78 ± 0.13	7.80 ± 0.39	0.356 ± 0.025
3687	,,	4.52	22.4	9.05 ± 0.45	31.2 ± 1.56	0.290 ± 0.020
3690	,,	3.68	32.2	4.58 ± 0.27	18.0 ± 0.90	0.310 ± 0.022
3694	,,	4.90	12.0	4.91 ± 0.24	14.7 ± 0.74	0.336 ± 0.024
Weighted Average		44.79		3.74 ± 0.07	11.2 ± 0.20	0.333 ± 0.008
3765	R. Rib, 7	1.71	7.6	3.58 ± 0.17	10.9 ± 0.54	0.327 ± 0.023
3769	,,	2.83	20.2	2.37 ± 0.11	7.65 ± 0.38	0.310 ± 0.022
Weighted Average		4.54		2.84 ± 0.10	8.86 ± 0.31	0.320 ± 0.016
3615	L. Radius	2.83	24.0	6.89 ± 0.34	29.4 ± 1.47	0.234 ± 0.016
3618	,,	6.52	43.3	2.24 ± 0.11	6.90 ± 0.34	0.325 ± 0.023
3621	,,	4.29	47.5	2.50 ± 0.12	7.02 ± 0.35	0.357 ± 0.025
3626	,,	3.53	28.9	6.41 ± 0.32	23.6 ± 1.18	0.271 ± 0.019
Weighted Average		17.17		3.93 ± 0.10	14.1 ± 0.36	0.278 ± 0.010
3643	R. Femur	15.87	45.2	3.04 ± 0.15	8.31 ± 0.42	0.366 ± 0.026
3645	,,	10.94	47.7	2.75 ± 0.14	7.56 ± 0.38	0.364 ± 0.026
3649	,,	12.62	48.5	2.96 ± 0.15	7.44 ± 0.37	0.399 ± 0.028
3654	,,	10.55	43.0	3.90 ± 0.20	12.0 ± 0.60	0.323 ± 0.023
3658	,,	7.75	36.5	4.92 ± 0.25	14.7 ± 0.74	0.335 ± 0.023
3659	,,	18.19	24.6	9.40 ± 0.47	35.9 ± 1.80	0.262 ± 0.018
3661	,,	28.76	23.9	7.95 ± 0.40	26.8 ± 1.34	0.296 ± 0.021
3665	,,	24.24	26.5	3.00 ± 0.15	7.74 ± 0.39	0.387 ± 0.027
3669	,,	8.00	23.8	7.37 ± 0.37	24.2 ± 1.21	0.304 ± 0.021
Weighted Average		140.92		5.16 ± 0.11	16.6 ± 0.36	0.311 ± 0.010
Total Skeletal Average		606.95		4.38 ± 0.46	15.4 ± 0.16	0.284 ± 0.004

as will be shown later, is highly questionable.

There is, therefore, very little reason to doubt that ^{210}Pb and ^{226}Ra are eliminated from the skeleton at very nearly equal rates, and that the two rates, if not exactly equal, are sufficiently similar to justify the use of the simplified Bateman expression that results when the two rates are equal. This has several important consequences. First, since long-term measurements of ^{226}Ra elimination rates can be made by whole body counting, the ^{226}Ra data can be used to estimate stable lead elimination rates as well, provided radiogenic and indigenous lead are eliminated similarly. Secondly, for individuals whose radium exposure occurred at some unknown time, excreta analyses for ^{210}Pb and ^{226}Ra can be used to establish the ratio of ^{210}Pb to ^{226}Ra in the skeleton, and hence, the date of exposure can be calculated, assuming a ^{222}Rn retention factor of 0.33. Third, the whole body skeletal dose due to ^{210}Pb, ^{210}Bi, and ^{210}Po can be more accurately calculated.

CONSIDERATION OF THE VARIABILITY IN INDIVIDUAL RATIOS

Far more difficult to interpret than the value of the average skeletal ratio of ^{210}Pb to ^{226}Ra are the variations in the ratio values found for the different skeletal sites. For Case 5281, the ratios varied from 0.214 to 0.380, and for Case 5278, from 0.174 to 0.480. The variability in the ratios is not random in nature. As will be noted from the data in Tables 1 and 2, there is a distinct pattern in long bone, with regard to ratio and radium concentration. In general, for a given long bone, the greater the ^{226}Ra concentration, the lower the ratio. The striking correlation between the ^{226}Ra concentration in a bone and the ratio value can be seen in Table 3. Equally striking is the fact that each bone is an independent entity with respect to this correlation. For neither case does the correlation exist for all the long bones taken as a single group. However, as can be seen from Case 5278, where both femurs were analyzed, they are very similar. In general, however, ratio values for tibia, fibula and radius tend to be considerably lower than for humerus and femur. There is also a striking correlation between the ratio value and the locus of radium deposition. For a given long bone, high radium concentration and low ratios are found in the end pieces of the bone, with the shaft having high ratios and low radium concentrations. This is particularly true, for both cases, in the fibula, tibia, and radius, where the end pieces have ratios lower than the skeletal average, while the shaft values are equal to or higher than the skeletal average. Humerus and femur, on the other hand, while showing the same pattern as regards ratio, radium concentration, and locus of deposition, have, for both cases, nearly every ratio higher than the average skeletal ratio.

All ratios found in rib, again for both cases, are higher than the average skeletal ratio, whereas vertebra have ratios much lower than the average. Therefore, bone characteristics are, without question, exerting an influence on the value of the ratio.

There are two mechanisms which could result in the observed ratio variations, each quite different:

1. While the average skeletal elimination of ^{210}Pb and ^{226}Ra occurs with equal biological half-lives, non-equality of these rates at discrete skeletal sites might account for the observed differences in ratio values.
2. Variation in the ^{222}Rn retention factors from site to site in the skeleton is a possible cause.

It is difficult to believe that differences in the clearance rates of lead and radium at discrete skeletal sites is the decisive factor controlling ratio variation. If one assumes the ^{226}Ra biological half-life to be constant throughout the skeleton and equal to 16 years, and that the ^{222}Rn retention factor is constant and equal to 0.33, then to account for the ratio variations noted, the biological half-life of ^{210}Pb would have to vary from 5 years to 50 years, depending upon the site analyzed. This wide range of ^{210}Pb biological half-lives, from one-third to three times that of ^{226}Ra, is difficult to accept, especially when one considers the added constraint that despite the wide range of possible differences, the average biological half-lives of both radionuclides are equal. For this reason, differences in metabolic clearance rates are not considered to be a likely cause of the observed differences in ratio.

Table 3. A Comparison of ^{210}Pb to ^{226}Ra Ratios and ^{226}Ra Concentrations in Long Bone

Bone and Case	^{226}Ra pCi/g ash	^{210}Pb/^{226}Ra
L. Tibia, 5278	51.4	0.246
,,	23.0	0.284
,,	21.7	0.294
,,	14.0	0.302
,,	5.40	0.335
L. Tibia, 5281	691	0.214
,,	415	0.225
,,	118	0.249
,,	88.0	0.266
L. Radius, 5281	1030	0.227
,,	628	0.235
,,	84	0.310
L. Radius, 5278	29.4	0.234
,,	23.6	0.271
,,	7.02	0.357
,,	6.90	0.325
L. Fibula, 5281	476	0.231
,,	67.0	0.294
L. Fibula, 5278	46.7	0.186
,,	43.7	0.174
,,	8.88	0.306
L. Humerus, 5281	424	0.295
,,	210	0.280
,,	86.7	0.301
,,	69.9	0.301
L. Humerus, 5278	31.2	0.290
,,	18.0	0.310
,,	14.7	0.336
,,	8.00	0.368
,,	7.80	0.356
,,	7.70	0.355
,,	7.70	0.355
,,	7.16	0.359
,,	6.04	0.399
L. Ulna, 5281	411	0.215
,,	358	0.256
L. Ulna, 5278	14.1	0.350
,,	13.9	0.350
,,	11.5	0.321
L. Femur, 5281	542	0.280
,,	322	0.256
,,	264	0.294
,,	197	0.283
,,	66.6	0.354
L. Femur, 5278	37.1	0.255
,,	21.2	0.260
,,	17.6	0.267
L. Femur, 5278—*cont.*	17.3	0.267
,,	8.56	0.327
,,	8.40	0.350
,,	6.45	0.380
,,	5.42	0.389
R. Femur, 5278	35.9	0.262
,,	26.8	0.296
,,	24.2	0.304
,,	14.7	0.335
,,	12.0	0.323
,,	8.31	0.366
,,	7.74	0.387
,,	7.56	0.364
,,	7.44	0.399

Next, we come to the question of whether variation in ^{222}Rn retention factors can be regarded as the cause of ratio variations. Of all the possible causes of ratio variation, differences in ^{222}Rn retention factors have, by far, the greatest dosimetric significance, and it is important to establish whether ^{222}Rn retention is variable. First, however, it would be helpful to consider the presently accepted theory of ^{222}Rn loss from the skeleton.

Rowland *et al.*[5] have postulated a ^{222}Rn recoil hypothesis to explain the loss of this radionuclide from the skeleton. Mays *et al.*[6] have proposed a similar mechanism. The essence of their postulate is that if a recoiling ^{222}Rn atom, which at birth has 86 keV of kinetic energy, and a mean range in bone of about 200–300 Å,[5] comes to rest within a bone crystal, it will very likely decay within that crystal, since diffusion rates of gases in a crystal are slow, relative to the half-life of ^{222}Rn, 3.83 days. If the recoiling atom comes to rest within the organic bone matrix, where there is a constant flow of fluids, then ^{222}Rn will escape due to the ease of gaseous diffusion in liquids as compared to crystalline solids. The escape path is diffusion into the circulation, followed by exhalation.

Whether the recoiling ^{222}Rn atom comes to rest within a crystal or the organic matrix is controlled by several variables. The size of the crystal is, of course, very important. The larger the crystal, the higher the probability that the ^{222}Rn atom will lose its kinetic energy before escaping from the crystal. It is currently believed that bone crystals are tablet shaped, being 200–300 Å long and 50 Å thick.[17] However, it is believed that in long bones, crystals are larger in the shaft than in the ends.[17]

Mineral density in the region of a recoiling ^{222}Rn atom can affect the ^{222}Rn retention factor. Mineral density can be defined as the fraction of the total density in the recoil volume that is mineral. The greater the mineral density, the greater should be the ^{222}Rn retention factor, since mineral density simply reflects the probability of a recoiling ^{222}Rn atom coming to rest in the crystalline mineral portion of bone. Ash content of a bone is an index, although not an exact measure of mineral density. The greater the ash content, the greater the mineral density. In long bones, the shafts have a considerably higher ash content than the end pieces, and hence, one would expect a higher mineral density in the shafts and a greater retention factor.

A third factor, and one very difficult to evaluate, is the recent discovery[18] that a portion of the mineral content of bone is amorphous. Gaseous diffusion rates in an amorphous solid are much greater than in a crystal. Many early workers noted that if radium is co-precipitated with barium sulfate, ^{222}Rn retention is nearly quantitative, while, on the other hand, amorphous solids such as ferric hydroxide or silica gel lose radon almost quantitatively. Commercial sources of ^{220}Rn (thoron), which consist of ^{228}Th co-precipitated with ferric hydroxide, are available. These release a large portion of ^{220}Rn, despite the fact that the half-life of ^{220}Rn is only 55 sec. Therefore, the greater the fraction of mineral bone that is amorphous, the greater should be the ^{222}Rn loss rate. The work cited[18] indicates that for long bone, the amorphous mineral fraction is lower in the shaft than in the ends.

In long bones, crystal size is greatest in the shaft, the ash content, and hence, the mineral density is highest in the shaft, and the shaft contains relatively less amorphous mineral than the end pieces. All three factors would favor higher ^{222}Rn retention in the shaft relative to the bone ends, and, therefore, higher ^{210}Pb to ^{226}Ra ratios in the shafts. This is precisely the effect noted for long bones, higher ratios in the shaft relative to the ends. Therefore, what we know about crystal size, mineral density, and amorphous mineral content of long bones supports the hypothesis that variable ^{222}Rn retention factors are the cause of the observed differences in the ratio of ^{210}Pb to ^{226}Ra.

As was mentioned earlier, ratios in rib are high, and ratios in vertebra are low. Both vertebra and rib have a low ash content. Therefore, if ^{222}Rn retention controls ratio values, ash content is not the dominant factor. Crystal size and/or the amorphous mineral content must override mineral density. It is for such reasons that it is so important to establish the true cause of ratio variations. If ratio variations are due to differences in ^{222}Rn retention factors, then we have a potential tool for studying bone structure.

As a result of the fact that ^{210}Pb and ^{226}Ra have equal biological half-lives, it is a simple matter to calculate what the ^{222}Rn retention factor was at a site where the ^{210}Pb to ^{226}Ra ratio is known. For both Case 5281 and 5278, were there no ^{222}Rn loss, the ^{210}Pb to ^{226}Ra ratio would be 0.850, as calculated from the Bateman expression already presented. Therefore, the retention factor at any given site is the quotient of the determined ratio and 0.850. For the range of ratios found for the two cases, 0.170 to 0.480, the retention factors must vary from 20% to 57%. The dosimetric significance of this will be considered later.

It can be argued that translocation of ^{210}Pb and ^{226}Ra could produce the variations in the ratio observed. As lead and radium are cleared from bone and enter the blood stream, a portion of both radionuclides is resorbed by the skeleton. This process of elimination followed by resorption can, of course, alter the value of the ratio at any given skeletal site. However, in order for this mechanism of translocation to account for the observed ratio variation, the process would have to occur with the same pattern as has been observed for the ratios themselves. That is, ^{210}Pb would have to be preferentially

resorbed at certain skeletal sites, namely the shafts of long bones and in rib, at the expense of resorption in vertebra and the ends of long bones, where low ratios have been observed. In order to determine whether such a preferential deposition of lead occurs within the skeleton, the distribution of stable lead in the skeleton has been studied. The rationale behind this approach is that resorbed ^{210}Pb should deposit in the skeleton in an identical manner to stable lead entering the blood stream via the gut or the lungs.

Bone samples from an individual who died at the age of 62 were analyzed for stable lead. The data are presented in Table 4.

The pattern of stable lead deposition is not consistent with an hypothesis of preferential deposition of ^{210}Pb via resorption. In fact, if anything, the opposite pattern is indicated.

Table 4. Analysis of Human Bone for Stable Lead

Sample	μg/g ash
Radius, Shaft	87
Tibia, Shaft Piece 1	97
Tibia, Shaft Piece 2	92
Femur, Shaft	77
Femur, End Piece 1	106
Femur, End Piece 2	131
Femur, End Piece 3	154
Vertebra	132
Rib	120
Calvarium	88

For the femur, the lead concentration is lowest in the shaft, and highest in the end pieces, precisely opposite to the pattern noted for the ratios in the femur of the two dial painters. The vertebra has a high lead concentration, whereas the ratio in vertebra was found to be low for both dial painters. For the dial painters, the highest ratios were found in rib. This is not the case as regards the concentration of stable lead. From these data, it is inferred that translocation is not the cause of the observed variations in ratio. In the writer's opinion, differences in ^{222}Rn retention factors are the dominant cause of the variations in ratio.

ESTIMATION OF BODY BURDEN FROM THE ANALYSIS OF A SINGLE BONE

As the data in Tables 1 and 2 indicate, there is a wide range of ^{226}Ra concentrations in the skeleton of an exposed individual. For Case 5281, the range of ^{226}Ra concentrations found was 67–1030 pCi/g of ash, with the average being 259 pCi/g of ash. If one attempted to measure the body burden of an individual by analysis of a single piece of bone, it would be difficult to do so with any degree of accuracy whatsoever, but for one exception, the vertebra. For Case 5281, the two pieces of vertebra analyzed had ^{226}Ra concentrations of 291 and 296 pCi/g of ash, as compared to the average value of 259 pCi/g of ash. For Case 5278, the single piece of vertebra analyzed gave a result of 14.7 pCi/g of ash as compared to the average of 15.4 pCi/g of ash found as the average. Based upon a sampling far too small to be conclusive, it would appear that vertebra would be the most reliable index of body burden.

DOSIMETRIC CONSIDERATIONS

Using an exponential model for ^{210}Pb and ^{226}Ra clearance from the skeleton, with both radionuclides having equal bilogical half-lives and an average skeletal ^{222}Rn retention factor of 0.33, it has been possible to predict the actual average ^{210}Pb to ^{226}Ra ratio in the skeleton of two radium dial painters. This suggests that the model is valid and, therefore, applicable to the calculation of the average skeletal alpha dose. Only the alpha dose will be considered since there is little reason to doubt that bone is the critical organ, and the bulk of the dose to bone is from alpha radiation.

For Case 5281, the terminal burden of ^{226}Ra is known, 0.54 μCi. Were it not for the amputation of her right leg, her terminal burden of ^{226}Ra would have been approximately 0.66 μCi. In calculating dose, it is this value that will be used, since she carried her leg most of her life. Four whole body measurements, taken over a period of 3 years, indicate that her radium biological half-life was 20 years.[1] The author, however, through measurement of ^{228}Th to ^{228}Ra ratios in her skeleton, calculated her radium biological half-life to be 10.4 years.[19] Both values will be used in calculating the average skeletal alpha dose. It is assumed that the

skeletal mass was 10,000 grams, and the average ^{222}Rn retention factor equal to 0.33. It is also assumed that all ^{210}Po formed *in vivo* decayed *in vivo*. The time elapsed since exposure was 49 years.

Taking 10.4 years as the biological half-life of ^{226}Ra (and of ^{210}Po), her initial burden of ^{226}Ra was 17.1 μCi. Up to the time of death, approximately 16.4 μCi of ^{226}Ra were removed from the skeleton. Of this total, 0.105 μCi of ^{226}Ra actually decayed in her skeleton. The dose delivered by the decay of this much ^{226}Ra and one-third that amount of ^{222}Rn, ^{218}Po, and ^{214}Po is 5160 rad. The dose due to ^{210}Po was calculated as being derived from the total number of ^{210}Pb atoms that decayed *in vivo*. This calculated to be 2.93×10^{13} atoms, and the associated dose, 258 rad. Hence, the total dose was 5418 rad, of which 4.8% results from ^{210}Po.

Assuming a biological half-life of 20 years for radium, the initial burden of ^{226}Ra was 3.97 μCi. A total of 3.31 μCi was removed from the skeleton, of which 0.039 μCi ^{226}Ra disappeared via decay. The resulting dose from ^{226}Ra, ^{222}Rn, ^{218}Po, and ^{214}Po was 1920 rad. The ^{210}Po dose was 120 rad, and 5.9% of the total dose resulted from ^{210}Po decay.

It can be seen that the fraction of the total dose derived from ^{210}Po decay is rather insensitive with regard to the magnitude of the biological half-lives of ^{226}Ra and ^{210}Pb, and it is safe to say that for long periods of exposure, the ^{210}Po dose is approximately 5–6% of the total alpha dose.

Calculations based upon data presented elsewhere,[19] indicate that the total dose arising from the ^{226}Ra decay chain was approximately 5200 rad, assuming a 10.4 year biological half-life for radium. Therefore, it would appear that her total radium dose was 10,000 rad, or less, depending upon the biological half-life of radium used in the calculation. Since it is unlikely that the radium biological half-life is less than 10.4 years, the figure of 10,000 rad is the upper dose limit. It might seem inconsistent, at first, that smaller doses are associated with longer biological half-lives of radium. This arises from the fact that the initial radium burden is calculated from a known terminal burden, and becomes smaller as the radium biological half-life increases.

Considering the individual sections of the skeleton, the average ^{222}Rn factors calculated for these sections, the ^{226}Ra concentration in each section, and a biological half-life of radium of 10.4 years, the highest dose calculated due to the ^{226}Ra decay chain is 13,000 rad, and the lowest dose, 840 rad, as compared to the skeletal average of 5418 rad.

For Case 5278, whole body counting indicated her biological half-life for radium to be about 10 years. Using this figure, her average skeletal dose from ^{226}Ra was calculated to be 390 rad, with a range of 110 rad to 840 rad for the individual bone sections.

ACKNOWLEDGEMENTS

The author wishes to thank the members of the Radium Research Project, New Jersey Department of Health, who provided the bone samples, and without whose cooperation the study could not have been done.

REFERENCES

1. H. W. Berk, G. R. Laurer, R. H. Schneider, L. Block, R. T. Drew, N. Cohen and M. Eisenbud. Annual Report, U.S.A.E.C. Contract AT (30–1) 3086. New York University Medical Center, September 1, 1965.
2. E. C. Miller and A. J. Finkel. Radiation Research Society Annual Meeting, Vol. 25, p. 48, May 1965.
3. H. A. Schroeder and J. J. Balassa. *J. Chronic Diseases* **14,** 408 (1961).
4. J. Vennart, G. Maycock, B. E. Godfrey and B. L. Davies. *Assessment of Radioactivity in Man*, Vol. II, pp. 277–290. IAEA, Vienna, 1964.
5. R. E. Rowland, J. Jowsey and J. H. Marshall. *Rad. Res.* **8,** 298 (1958).
6. C. W. Mays, M. A. Van Dilla, R. L. Floyd and J. S. Arnold. *Rad. Res.* **8,** 480 (1958).
7. Ann Johnson. Personal communication.
8. Gerard R. Laurer. Personal communication.
9. H. G. Petrow and A. Cover. *Anal. Chem.* **37,** 1600 (1965).
10. H. G. Petrow, O. A. Nietzel and M. A. DeSesa. *Anal. Chem.* **32,** 926 (1960).
11. H. G. Petrow and R. Lindstrom. *Anal. Chem.* **33,** 313 (1961).
12. C. W. Mays. U.S.A.E.C. Report, COO-216. University of Utah, March 1958.
13. R. B. Holtzman and H. G. Lucas, Jr. Personal communication, 1966.

14. CARROLL CLAYTON. Personal communication. U.S. Radium Corp., 1966.
15. R. B. HOLTZMAN. *Health Physics* **8,** 315 (1962).
16. C. J. MALETSKOS, A. G. BRAUN, M. M. SHANAHAN and R. D. EVANS. *Assessment of Radioactivity in Man*, Vol. II, pp. 225–252. IAEA.
17. R. A. ROBINSON and M. L. WATSON. *Annals N.Y. Acad. Sci.* **60**.
18. J. D. TERMINE, A. POSNER and I. PULLMAN. Tenth Annual Meeting of the Biophysical Society, Feb. 23–25, 1966, Boston, Mass.
19. H. G. PETROW. U.S.A.E.C. Report NYO-3086-5 New York University (in Press).

INFLUENCE OF THE PHYSICO-CHEMICAL BOUND OF ^{226}RA IN THE FOOD, ON BODY BURDEN AND DISTRIBUTION IN GUINEA-PIGS (CAVIAE)

O. VAN DER BORGHT

Département de Radiobiologie, Centre d'Etude de l'Energie Nucléaire, Mol

L. BUGYAKI

Institut d'Hygiène et d'Epidémiologie, Ministère de la Santé Publique, Bruxelles

R. KIRCHMANN, S. VAN PUYMBROEK

Département de Radiobiologie, Centre d'Etude de l'Energie Nucléaire, Mol (Belgium).

Abstract—Analysing the extractability of ^{226}Ra from *in vivo* contaminated roots and leaves of pea plants showed that the ^{226}Ra in leaves was about twice as soluble in water as the ^{226}Ra present in the roots. No significant difference was found between the quantity of ^{226}Ra extracted by $NaNO_3$, CH_3COOH or HCl from food pellets made with powdered carrots and *in vivo* contaminated pea leaves, compared with similar pellets contaminated *in vitro* by addition of a $RaCl_2$-solution.

The enhanced quantity of the water-extractable ^{226}Ra in food pellets prepared from contaminated leaves or from *in vitro* contaminated pellets, as compared with pellets prepared from contaminated roots, had no significant influence on the body burden in guinea-pigs. This could be explained by the anyhow low percentage of water soluble ^{226}Ra (about 5–12% of the total Ra-content) in the food.

When fasting animals were given an aqueous $RaCl_2$-solution, the body burden reached a level twice as high as when the Ra was given together with food pellets (resp. 5% and 2% of administered dose).

Contamination by intubation of a $RaCl_2$-solution or together with food on which ^{226}Ra could partly be adsorbed in the gastro-intestinal tract, did not result in a different distribution of radioactivity between the organs. When the radioactivity/g fresh muscle is taken as unity, a level of 6×10^2 is obtained in the femur, of 4×10^2 in the eye and of 2×10^1 in kidneys and intestinal walls. The very high Ra-content of the eye is particularly interesting, as it is known that also Ca and Ba, but not Sr, are concentrated to a considerable extent in this organ.

In Vivo MEASUREMENT OF LUNG BURDENS OF NUCLIDES EMITTING SOFT, PENETRATING RADIATIONS

G. R. LAURER

Institute of Environmental Medicine, New York University Medical Center, New York, N.Y., U.S.A.

Abstract—The objective of this study is the design and calibration of a whole body counter crystal detection system for the *in vivo* measurement of lung burdens of the nuclides ^{90}Sr, ^{239}Pu and uranium (natural and enriched) at levels of fractions of the MPC. The study is divided into two parts, (1) the design, construction and performance of the crystal detection system, and (2) calibration of the system for the three nuclides using appropriate lung phantoms.

A major problem in the measurement of small amounts of these low energy photon emitters (^{90}Sr-bremsstrahlung, ^{239}Pu-17 keV X-ray, uranium-90 keV and 186 keV γ-rays, is the reduction of background in the low energy region of the spectrum. Accordingly, the first part of the experiment involved the reduction of low energy background by optimization of crystal thickness for detection of photons in this energy region and by use of anti-coincidence methods for reduction of the Compton continuum.

Experiments performed on several thicknesses of a 4.5 in. dia. CsI crystal, utilizing S^2/B as a figure of merit, show that a thickness of 1 mm is very close to optimum for all three nuclides. To further reduce the background, an experiment was performed using a 3 in. dia. $\times$ 1 mm. thick CsI crystal optically coupled to a 3 in. dia. $\times$ 1 in. thick NaI crystal, the crystal pair being viewed by a single multiplier phototube. The principle of rise-time discrimination was used to attenuate the low energy background due to Compton events in the CsI crystal. The results of the experiment show a reduction of 40 per cent at the Compton edge and 70 per cent in the low energy region for a point source of ^{137}Cs. Overall background reduction was 75 per cent from approximately 30 keV to 750 keV.

The second part of the study, now in progress, involves the calibration of an 8 in. dia. $\times$ 1 mm thick CsI crystal optically coupled to an 8 in. dia. $\times$ 4 in. thick NaI crystal for the *in vivo* measurement of the three nuclides. This part of the experiment, utilizing appropriate lung phantoms, will define the lower limit of detectability for the anti-coincidence system, and the variance in the measurement between the two probable extremes of source configuration in the lung, i.e. a point source and a distributed source.

ACCUMULATION OF ^{90}Sr IN HUMAN PERMANENT TEETH IN THE UNITED KINGDOM. ROYAL NAVY SURVEY 1959–1965

W. E. STARKEY
Royal Naval Medical School, Alverstoke, Hampshire, U.K.

Abstract—A continuing survey of ^{90}Sr accumulating in human permanent teeth has been conducted by the Royal Navy since 1959. The investigation is confined to perfect teeth, viz. premolars from persons 9–13 years old and third molars from persons 17–21 years old. Roots and crowns are divided, bulked according to age group and analysed separately. Continuous results are available up to the end of 1965 respecting over 11,000 teeth collected from all parts of the United Kingdom. The findings have reflected the rising nuclear yields. ^{90}Sr is accumulated in the teeth by irreversible deposition and the obtained values (estimated in pCi/g Ca) steadily increased with the passage of time. At any given point they were highest in the teeth of the youngest groups since these were obtained in an active state of mineralization during a period when dietary levels were rising. Similarly, in any given age group, concentrations were higher in the roots than in the crowns since the roots were affected by recent uptake whereas the crowns (which are the first to form) had mineralized when dietary levels were relatively lower. Since the crowns related to previous uptake, it was possible to deduce the probable activity of ^{90}Sr during mineralization for the years 1956/1959. The overall relationships corresponded closely with the results of the bone survey reported by the Medical Research Council in respect of deceased subjects age 5–19 years. This suggests that selective tooth sampling could provide useful information about the level of ^{90}Sr in the bones of living subjects.

INTERNAL DOSIMETRY OF ^{75}Se-METHIONINE

R. E. JOHNSTON, J. R. MATHER and A. B. BRILL

Division of Nuclear Medicine and Biophysics, Vanderbilt University School of Medicine, Nashville, Tennessee, U.S.A.

Abstract—^{75}Se-methionine is in limited use for radioisotopic visualization of the pancreas and parathyroid glands. Also, ^{75}Se in the form of sodium selenate is a promising means for estimating the extracellular fluid volume. Some dosimetry studies have been reported, but present estimates of the pertinent radiologic dosimetric factors show discrepancies. It is thus important to determine more accurately the radiation hazard of ^{75}Se in order to assist in the evaluation of its usefulness in medical diagnostic procedures.

A detailed determination of the γ-coefficient and average β-energy per disintegration has been carried out using experimental data whenever possible, and theoretical values where experimental data are unavailable. The γ-coefficient was calculated to be 1.925 r/mCi hr at 1 cm; the average energy from electrons and β-type radiation ($\bar{E}\beta$), was calculated to be 12.8 keV/dis.

Some biological distribution studies in animals limited to short time periods (<24 hr) have been reported. We have made a long term investigation (70 days) of ^{75}Se-methionine metabolism in rats. These investigations show a disproportionality high amount of ^{75}Se in the gonads which only becomes apparent after about 15 days. Since the gonadal deposition of this radioactive element could be a function of the stage of reproductive ability of the organism, experiments have been conducted to evaluate the gonadal uptake and retention as a function of age of the organism.

Results of these experiments and the relation to radiation dose in humans will be presented.

PROBLEMI DI DOSIMETRIA E DI PROTEZIONE NELL'IMPIEGO DI DIURETICI MERCURIALI MARCATI NELLA SCINTIGRAFIA CEREBRALE

G. TORI *e coll.*
Istitutodi Radioterapia, Ospedale Civile, Verona (Italy)

Sommario—Questi problemi si pongono in differenti termini in rapporto al tipo del radionuclide usato per la scintigrafia cerebrale.

L'uso di un diuretico marcato con ^{203}Hg comporta l'assorbimento di una dose totale corporea che è di modesta entità mentre invece la dose assorbita dai reni può raggiungere valori di 40–60 rad.

Tali dosi non rappresentano un serio rischio, ma possono dar luogo a qualche perplessità soprattutto nei riguardi dell'impiego dello ^{203}Hg nei bambini e nelle donne giovani.

La ripetizione della scintigrafia in diversi periodi di tempo, pone inoltre il problema della fissazione del radiomercurio a livello delle cellule tubulari renali.

E' questo un problema oggetto di particolare studio, e noi stiamo conducendo delle ricerche allo scopo di:

1. ridurre la captazione renale del radionuclide;
2. accertare l'esistenza di eventuali alterazioni provocate dal radionuclide nei tubuli renali.

Nell'intento di ridurre la dose-rene, noi usiamo somministrare due ore prima dell'iniezione del radionuclide, 1 ml di mercuhydrin non radioattivo, il quale è in grado di saturare parzialmente le cellule tubulari e di ridurre le loro capacità di captazione.

Nel tentativo di studiare le alterazioni renali in pazienti sottoposti a ripetute scintigrafie con radiomercurio ^{203}Hg, noi abbiamo eseguito biopsie renali a differenti periodi di tempo dalla iniezione del radionuclide.

Le suddette cause di perplessità nei riguardi della dose-rene non hanno ragione di esistere se si impiega il radiomercurio ^{197}Hg. Questa sostanza consente infatti di ridurre grandemente la dose-rene, in pratica a circa il 3 per cento della dose-rene corrispondente all'impiego del ^{203}Hg.

AN ESTIMATE OF DOSE TO VARIOUS BODY ORGANS FROM ADMINISTRATION OF NEOHYDRIN LABELED WITH ^{203}Hg

M. R. FORD and W. S. SNYDER

Health Physics Division, Oak Ridge National Laboratory, Oak Ridge, Tennessee, U.S.A.

Abstract—Neohydrin tagged with ^{203}Hg is a useful agent for brain tumor localization. However, its use in routine scanning has been questioned because it is known to deliver a relatively high radiation dose to the kidneys. Also, the question of the dose it delivers to the gonads has been posed.

Immediately following intake, the ^{203}Hg will be distributed generally throughout the body. Thereafter it will be present largely in the kidneys, in the bladder, and in the ureters where its residence times will vary considerably in individual cases. For this reason, the doses to body organs, particularly to the cortex and medulla of the kidneys and to gonads, are calculated for 1 mCi·hr of source in each of the organs where the ^{203}Hg resides. In this form the results may be adjusted to provide an estimate of dose in an individual case. The organs are simulated by simple geometrical configurations within a man-like tissue phantom, and they have approximately the location, dimensions, and masses of "standard man". The β-dose is computed by conventional methods, but the doses from γ-rays and X-rays are estimated by use of a Monte Carlo-type computer code.

Estimates using biological data from several patients indicate that the doses to the cortex, medulla and ovaries might be roughly in the ratio 15:1:0.1. Frequently 10 μCi/kg is administered, and at this level the dose to the ovaries in typical cases might be of the order of 0.5 rad. Data obtained by analysis of blood and urine specimens can be used to adjust the above estimates in individual cases.

DISCUSSION

J. B. HURSH (*U.S.A.*):

I should like to ask Dr. Lindell if the radon found in the cow's milk derives, in his opinion, entirely from the ingested water or if respired radon is an appreciable supplemental source.

B. LINDELL:

We first found Rn^{222} in cow's milk from two farms which were investigated for Cs^{137} in milk. We visited the farms and were able to prove that the radon originated in the water that was used by the cows and which was taken from deep bored wells which held about 40 nCi/l.

W. S. SNYDER (*U.S.A.*):

Did your calculations take into account the retention of Pb^{210} in the body?

B. LINDELL:

We have not made any measurements of lead-210, as yet.

R. B. HOLTZMAN (*U.S.A.*):

Are you familiar with the Rn emanation bones which show emanation values *in vitro* bone about equal to the measured wholebody emanation?

H. G. PETROW:

Yes, I am familiar with the data of Rowland *et al.* and Mays *et al.* pertaining to the loss of radon from *dead* bone, both human and beagle. I submit first, that human bone that is living, is not the same as dead bone, whether human or dog. Secondly, Mays *et al.* have shown that in young beagle bone, radon retention is less in the ends of long bone, than in the shaft.

W. E. STARKEY:

The concentration of Sr^{90} in the roots relates to recent dietary levels while the mean concentration in the crowns seems to relate to dietary levels prevailing about 4 years previously. By extrapolation, curves can be constructed to express the uptake of Sr^{90} throughout the period of development of the tooth. When this is done they correspond closely with the bone values obtained from similar age-groups.

Since the tooth burdens are permanent and the bone levels are labile this suggests that the teeth could be used to estimate levels that had previously prevailed in bone, many years after they had been modified by changing dietary conditions.

R. J. DELLA ROSA (*U.S.A.*):

Sr^{90} in teeth of beagle dogs, relative to bone, represents the maximum concentration in teeth relative to Sr^{90} concentration of diet at time teeth are formed. Unlike bone which has a discrete turnover of mineral, that of teeth is very small, and thus can be considered representative of diet and the deposition of dietary Sr^{90} in hard tissue at any time after the formation of permanent teeth. These observations are in essential agreement with those made by Dr. Starkey.

R. E. JOHNSTON (*U.S.A.*):

In the paper on Se^{75} dosimetry, I should like to point out a correction. With more recent experimental data for the decay scheme of Se^{75}, and in more proper units, the gamma factor is equal to 1.93 roentgens per mCi-hr at 1 cm, and the average β-energy is 12.8 keV/dis.

In our biological studies we found an increased concentration of selenomethionine in pre-pubertal rat organs, as compared to the post-pubertal organs. In addition we also note a peak concentration in the gonads between 10 to 15 days, as compared to 6 to 24 hr for other organs. We thus feel that it is important to consider the stage of development of the animal when investigating the biological distribution of radionuclides for dosimetric purposes.

G. TORI (*Italy*):

Pongo due domande:

1. Se gli autori hanno calcolato il rapporto di accumulo della Se^{75}-metionina nei ratti tra fegato e gonadi.

2. Se gli autori possono precisare l'entità dell'accumulo del radionuclide nelle gonadi nei ratti giovani ed in quelli di età adulta ed avanzata.

R. E. JOHNSTON:

1. We attempted to relate the integral concentrations in the organ to the organ retention, the total body mass, and organ mass. We found the ratio of organ retention for pre-pubertal to organ retention for post-pubertal for the gonads to be 0.88 or approximately 1, which implies an independence of age for organ retention for the gonads. The same ratio for the kidneys was found to be 0.5.

2. We found a difference of 2½ times greater concentrations in all pre-pubertal organs in general, i.e. livers, kidneys, and gonads.

G. TORI:

Il problema della dosimetria beta, gamma del Hg^{203} a livello renale è tuttora aperto. I dati della letteratura sono piuttosto discordanti. Noi saremmo lieti di avere al riguardo qualche suggerimento da parte di esperti qui presenti. Presentemente stiamo controllando, mediante biopsie renali nell'uomo, se l'entità delle dosi assorbite dai reni è stata in grado di determinare lesioni apprezzabili. Finora però, il periodo trascorso dalle osservazioni effettuate non è sufficientemente lungo per trarre conclusioni definitive.

M. R. FORD (*U.S.A.*):

I should like to add that the dose value we have estimated for a typical treatment is within the range of values reported by Dr. Tori in his paper.

THE VARIATION WITH AGE OF ELEMENTAL CONCENTRATIONS IN HUMAN TISSUE*

ISABEL H. TIPTON, JUDY C. JOHNS and MONICA BOYD
Oak Ridge National Laboratory, Oak Ridge, Tennessee

Abstract—To determine MPC values for various segments of the population it is desirable to take into account the possible variation with age of the concentration of an element in a tissue. Studies carried out on data for 173 subjects from the United States indicate a significant ($p \leqslant 0.001$) correlation with age of: aluminum in lung; calcium in aorta, rib, kidney, and testis; copper in cartilage and liver; magnesium in aorta, rib and vertebra; manganese in rib; phosphorus in aorta and testis; tin in lung. Since the values for the concentrations of these elements are found to be distributed log-normally (except those for calcium in rib which were normally distributed), equations for regression lines of the log of concentration on age (concentrations on age for calcium in rib) have been determined and lines drawn with a 95% confidence interval. The concentrations of calcium, magnesium, and manganese in bone, and copper and manganese in liver are found to decrease; and the concentrations of calcium, magnesium, and phosphorus in aorta, calcium in kidney, and aluminum and tin in lung to increase with age.

To determine whether or not the concentrations of elements in human tissue vary with age, studies of the correlation between age and elemental concentration have been carried out using the data on 150 adult subjects[1-4] plus 23 children[5] from the United States. Rank correlation coefficients have been computed for each element in each tissue and the difference from zero tested as described previously.[6]

To take age dependence into consideration when attempting to determine MPC values for various segments of the population it is desirable to estimate the quantitative relation between age and concentration. It is useful to calculate intercept and slope of a regression line relating age and concentration and to make a plot of the line for quick visual reference.

Before a meaningful regression line can be plotted, it is necessary to establish the fact that the quantities can be expected to have a linear relation. If, for every fixed value of the independent variable (in this case age), the values for the dependent variable (in this case concentration) show a normal statistical distribution about a mean value, then the regression line may be determined by the method of least squares and confidence intervals determined by ordinary statistical procedures. However, in this study most of the values for concentration of a trace element in human tissue prove not to be distributed normally. Therefore before plotting regression lines for an element, the data have been tested for normality and for log normality.[7, 8]. Since calcium in bone showed a normal distribution, a regression line of concentration on age has been plotted for calcium; for all other elements the log of the concentration has been used instead of concentration in calculating and plotting the regression line.

Table 1 includes those correlation coefficients of magnitude 0.32 and above and significantly ($p \leqslant 0.001$) different from zero for elements which were observed in concentrations above the limit of detection in 90% of the samples of a tissue. In this table the column "Number of Individuals" shows the number of samples for which both a value for the concentration of the element in wet tissue and the age of the individual were known. The last column in this table contains the equation of the regression line of concentration or log concentration on age.

* This work was supported by subcontract 2351 under W7405 eng 26 between Union Carbide Nuclear Corporation and The University of Tennessee.

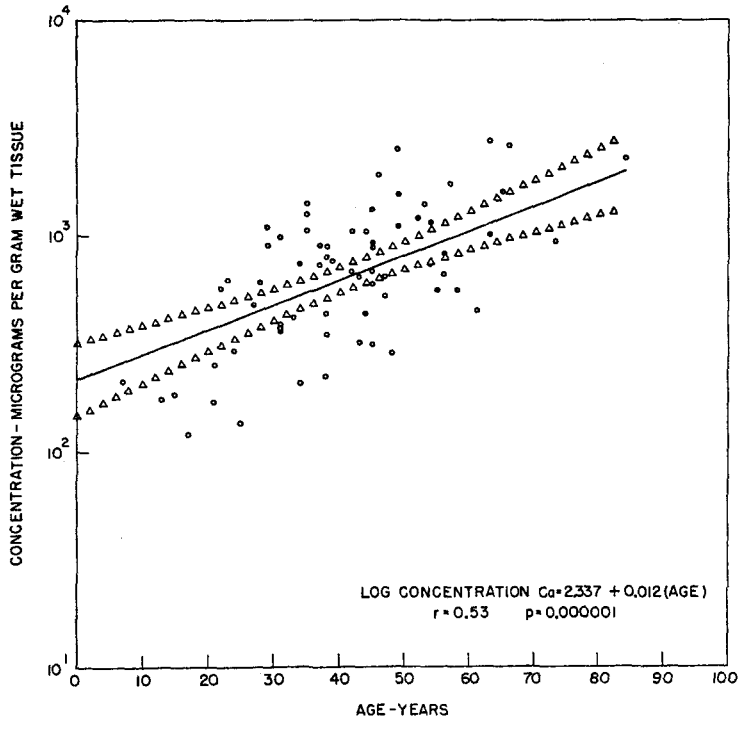

FIG. 1a. Variation with age of calcium in aorta. The circles are actual data points. The triangles define the 95% confidence interval of the regression line.

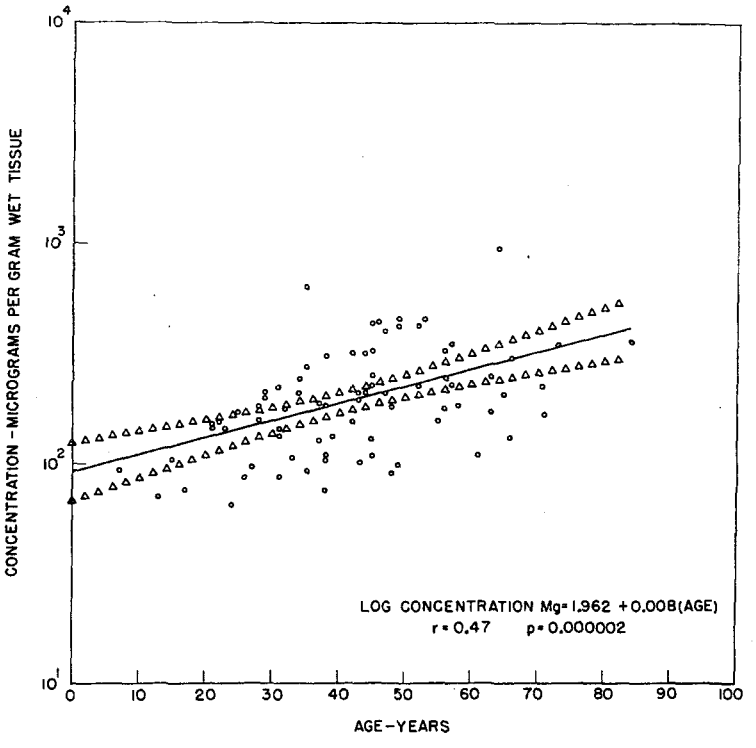

FIG. 1b. Variation with age of magnesium in aorta. The circles are actual data points. The triangles define the 95% confidence interval of the regression line.

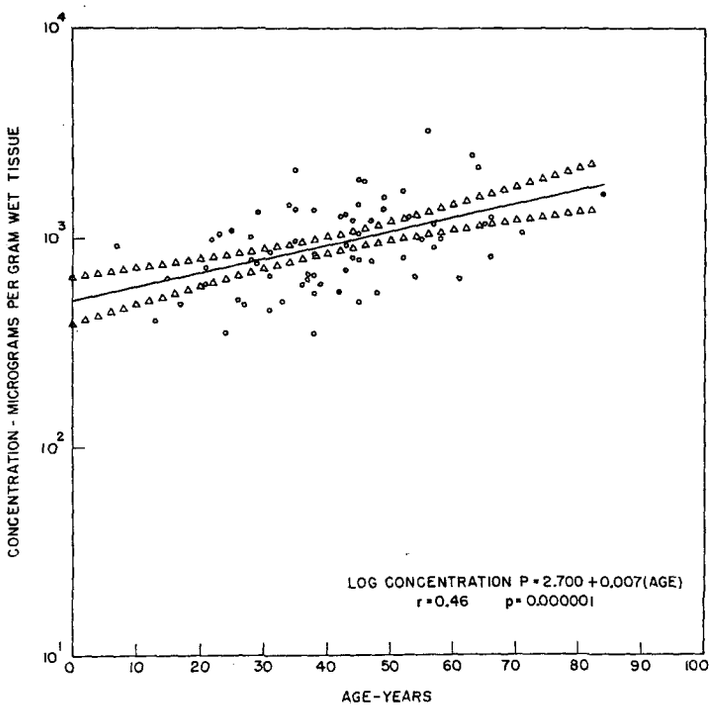

FIG. 1c. Variation with age of phosphorus in aorta. The circles are actual data points. The triangles define the 95% confidence interval of the regression line.

In the figures age is plotted as abscissa, and concentration or log of concentration of an element in wet tissue is plotted as ordinate. The equation of the line, the value of the correlation coefficient and the probability that the value could have occurred by chance are included within the outline of the figure. Individual values are indicated as small circles. The 95% confidence interval is indicated by triangular points on each side of the regression line. This interval is not bounded by straight lines, because there were different variabilities and different numbers of observations for different age groups.

The increase in aorta of the concentrations of calcium (Fig. 1a), magnesium (Fig. 1b), and phosphorus (Fig. 1c) reflects the commonly observed changes in blood vessels with age.

The analyses which provided the values for the elements in bone (rib) were made on ashed samples of wet rib from which the marrow had not been removed. The ash fraction of wet weight of these samples decreased significantly, whereas the dry fraction of wet did not change significantly with age. The decrease in the concentration of calcium (Fig. 2a), magnesium (Fig. 2b), and manganese (Fig. 2c) in the wet sample (concentration in wet = concentration in ash × ash fraction of wet) is thus a reflection not only of the actual decrease of the inorganic matrix of the bone with age but also of an increase of the low-ashing fat component of marrow.

Calcification accompanying pathologic lesions in the kidney apparently has no specific correlation with age.[9] Since the kidneys which were analyzed for the present study were taken from grossly normal individuals, the increase in the concentration of calcium in kidney (Fig. 3) probably reflects an increase with age in the deposition of plaques in the blood vessels within the kidney rather than an increase in the concentration of calcium in the tissue of the kidney itself. The increase of calcium in testis can

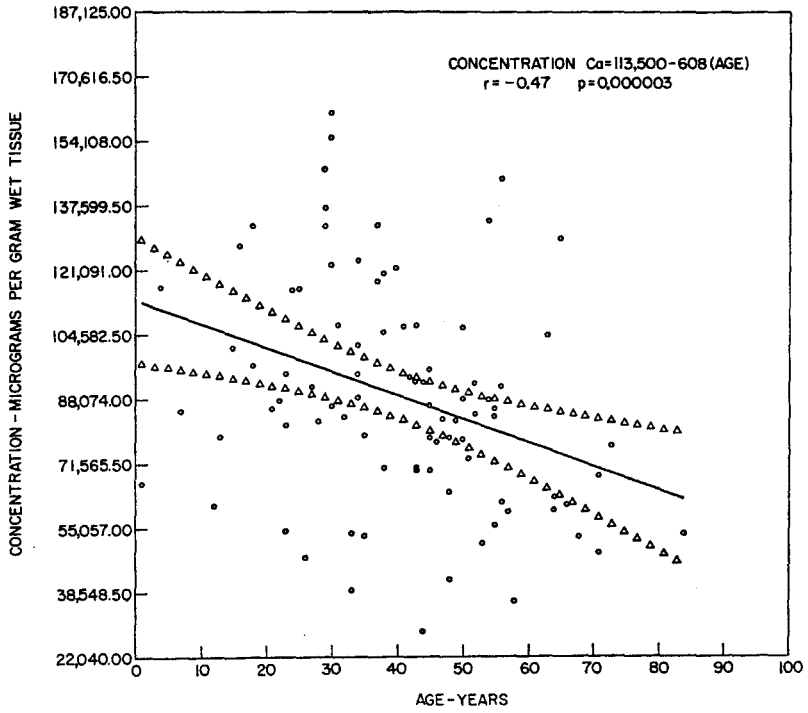

FIG. 2a. Variation with age of calcium in bone (rib). The circles are actual data points. The triangles define the 95% confidence interval of the regression line.

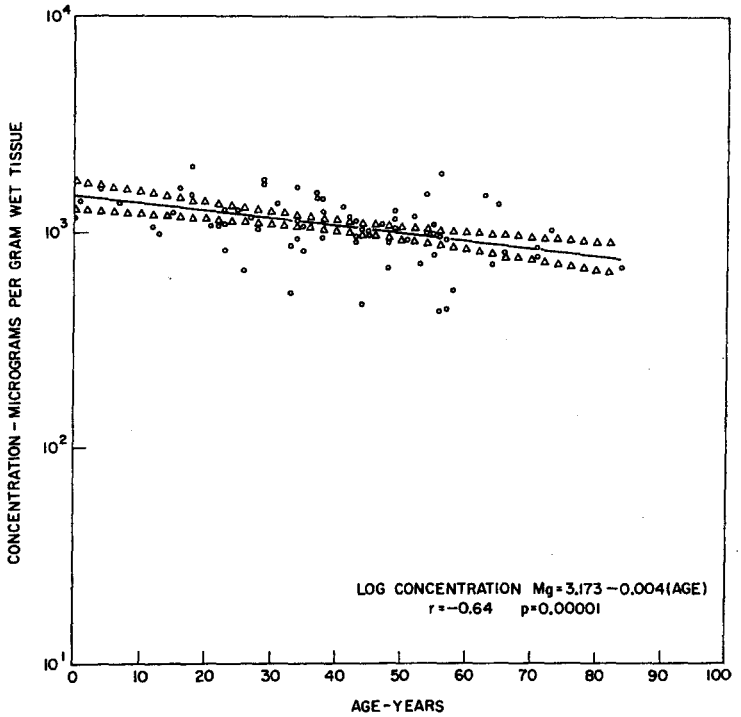

FIG. 2b. Variation with age of magnesium in bone (rib). The circles are actual data points. The triangles define the 95% confidence interval of the regression line.

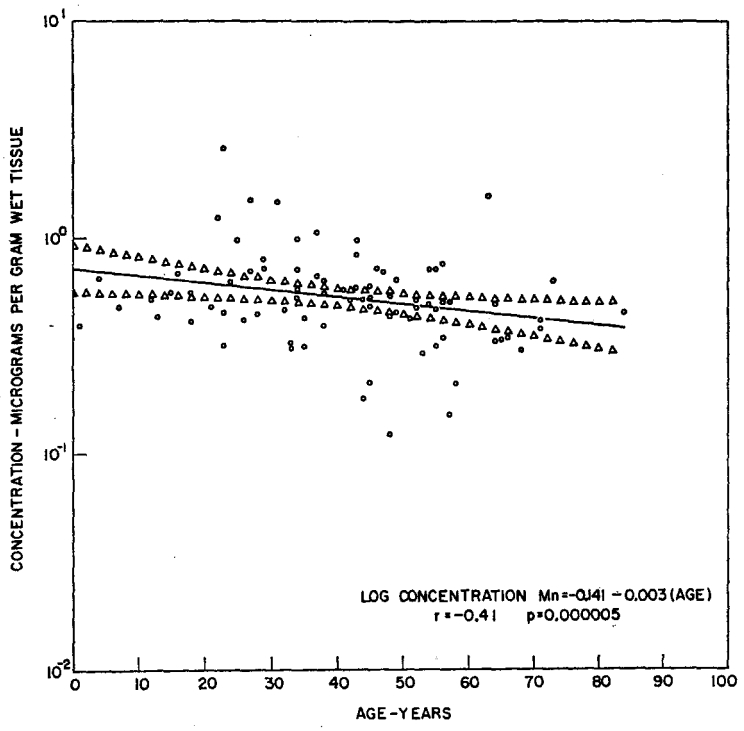

FIG. 2c. Variation with age of manganese in bone (rib). The circles are actual data points. The triangles define the 95% confidence interval of the regression line.

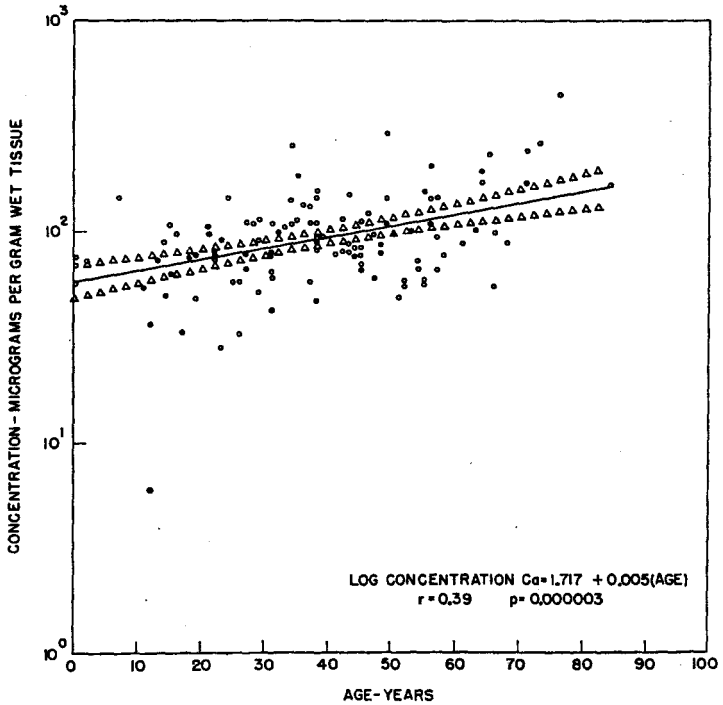

FIG. 3. Variation with age of calcium in kidney. The circles are actual data points. The triangles define the 95% confidence interval of the regression line.

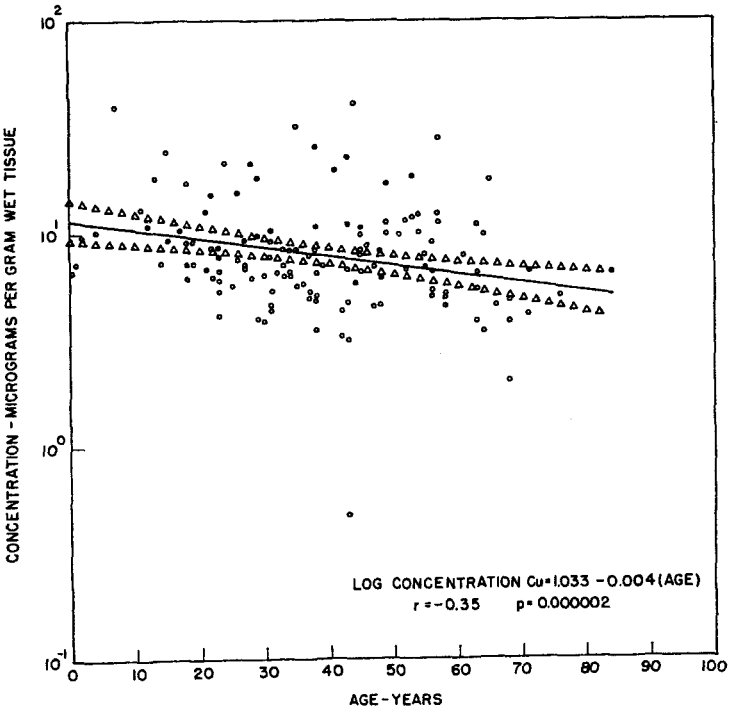

FIG. 4a. Variation with age of copper in liver. The circles are actual data points. The triangles define the 95% confidence interval of the regression line.

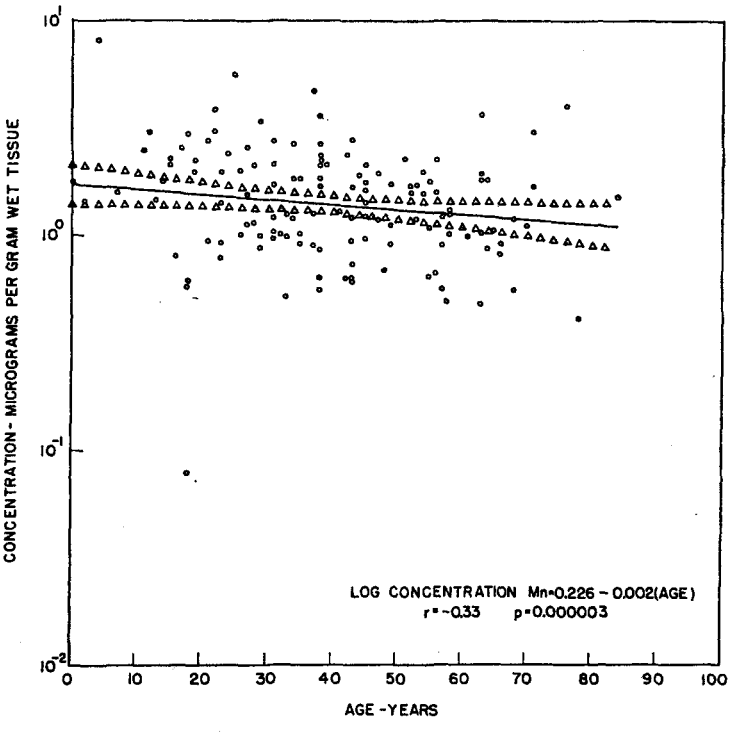

FIG. 4b. Variation with age of manganese in liver. The circles are actual data points. The triangles define the 95% confidence interval of the regression line.

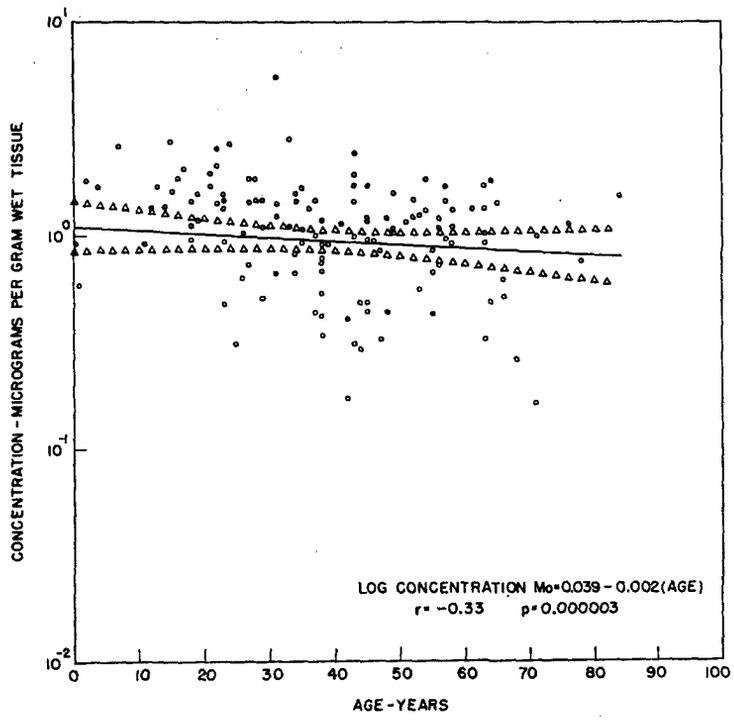

FIG. 4c. Variation with age of molybdenum in liver. The circles are actual data points. The triangles define the 95% confidence interval of the regression line.

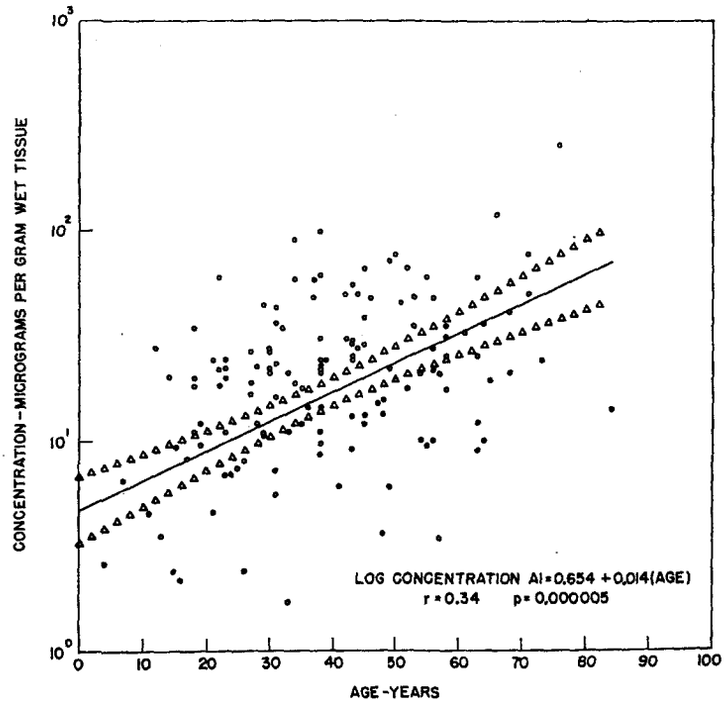

FIG. 5a. Variation with age of aluminum in lung. The circles are actual data points. The triangles define the 95% confidence interval of the regression line.

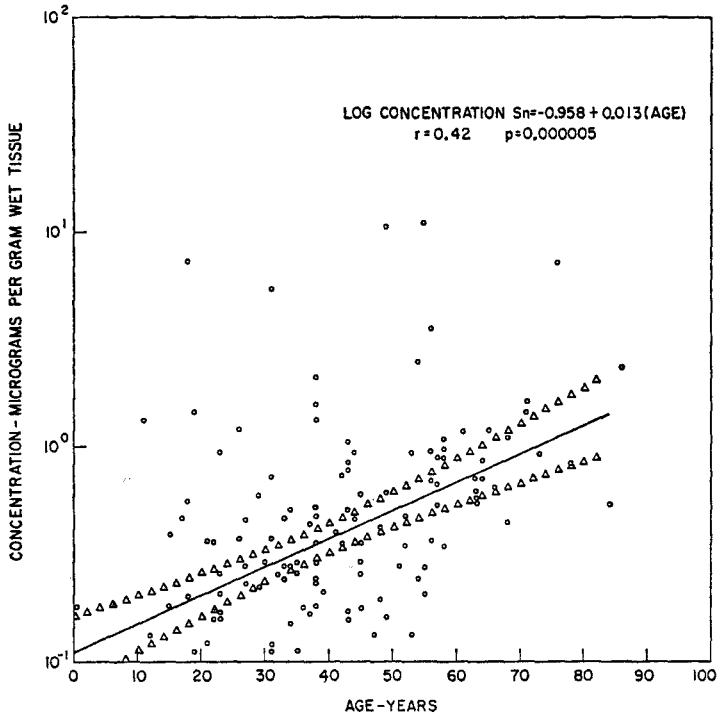

FIG. 5b. Variation with age of tin in lung. The circles are actual data points. The triangles define the 95% confidence interval of the regression line.

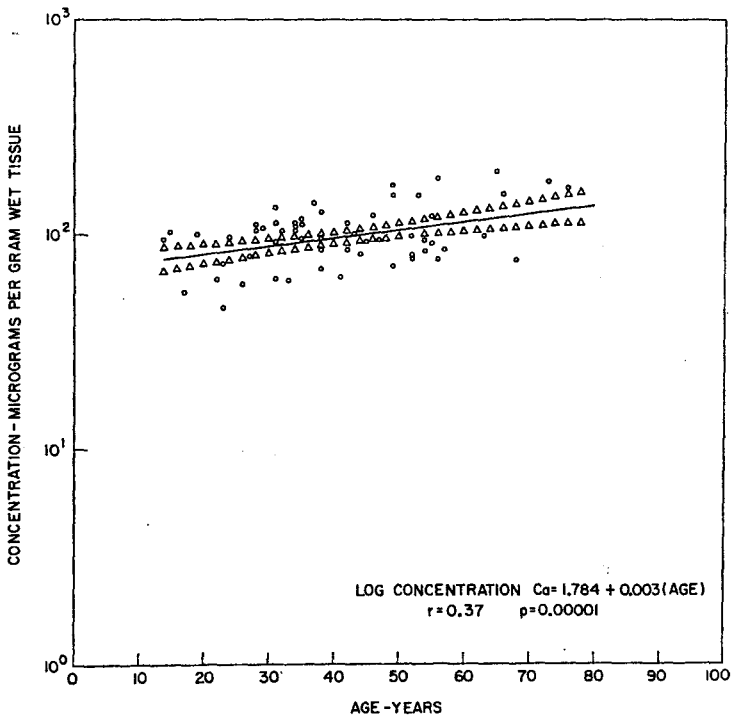

FIG. 6. Variation with age of calcium in testis. The circles are actual data points. The triangles define the 95% confidence interval of the regression line.

Table 1. *Correlation of Concentration of Trace Element in Wet Tissue with Age*
(Correlation coefficients different from zero $p \leq 0.001$*)*
(Concentrations in micrograms per gram of wet tissue)

Element	Tissue	Number of individuals	Correlation coefficient	Equation of regression line
Aluminum	Lung	153	0.34	log conc Al = 0.654 + 0.014 (Age)
Calcium	Aorta	94	0.53	log conc Ca = 2.337 + 0.012 (Age)
	Bone (rib)	91	−0.47	conc Ca = 113,500 − 608 (Age)
	Kidney	129	0.39	log conc Ca = 1.717 + 0.005 (Age)
	Testis	71	0.37	log conc Ca = 1.784 + 0.003 (Age)
Copper	Liver	157	−0.35	log conc Cu = 1.033 − 0.004 (Age)
Magnesium	Aorta	94	0.47	log conc Mg = 1.962 + 0.008 (Age)
	Bone (rib)	92	−0.64	log conc Mg = 3.173 − 0.004 (Age)
Manganese	Bone (rib)	92	−0.41	log conc Mn = −0.141 − 0.003 (Age)
	Liver	157	−0.33	log conc Mn = 0.226 − 0.002 (Age)
Molybdenum	Liver	157	−0.33	log conc Mo = 0.039 − 0.002 (Age)
Phosphorus	Aorta	91	0.46	log conc P = 2.700 + 0.007 (Age)
Tin	Lung	152	0.42	log conc Sn = −0.958 + 0.013 (Age)

probably be attributed to the same cause (Fig. 6).

The decrease of copper (Fig. 4a), manganese (Fig. 4b), and molybdenum (Fig. 4c) in liver is slight but significant.

The individual variation of aluminum (Fig. 5a) and tin (Fig. 5b) in lung is wide but the general increase from birth to old age is more than tenfold. The compounds of these elements which enter the lung by inhalation as dust are for the most part insoluble and so are not absorbed.

REFERENCES

1. I. H. Tipton, M. J. Cook, R. L. Steiner, H. M. Perry Jr., and H. A. Schroeder. *Health Physics* **9,** 89 (1963).
2. I. H. Tipton and M. J. Cook. *Health Physics* **9,** 103 (1963).
3. S. R. Koirtyohann and C. Feldman. *Health Physics Annual Report* ORNL-3492, p. 178 (1963).
4. I. H. Tipton and J. J. Shafer. *Health Physics Annual Report,* ORNL-3697, p. 179 (1964).
5. Unpublished data.
6. I. H. Tipton and J. J. Shafer. *Archives of Environmental Health* **8,** 58 (1964).
7. "Tests of Non-Normality". Memorandum from D. A. Gardiner to W. S. Snyder, June 20, 1963.
8. Biometrika Tables for Statisticians, ed. by E. S. Pearson and H. O. Hartley, Cambridge Press (1954).
9. J. O. Salik and B. S. Abeshouse. Radium therapy and nuclear medicine, *Am. J. Roentgenology* **88,** 125 (1962).

CALCULATION OF SPECIFIC ACTIVITY–TIME CURVES IN RELATIVELY INACCESSIBLE COMPARTMENTS OF A THREE COMPARTMENT KINETIC STEADY STATE MODEL

MORIS L. SHORE and RICHARD K. FRED

Department of Health, Education, and Welfare, Public Health Service,
Division of Radiological Health, Rockville, Maryland, U.S.A.

Abstract—When a radioactive tracer is administered intravenously to a living organism one can follow with relative ease the specific activity–time curve of the compound in the circulation. However, it is difficult to establish the specific activity–time curve of the compound in the various tissues of the organism. The nearest approach that can be made at the present time is the measurement of activity in the total organism using whole body counting techniques, or external and possible internal scanning procedures to obtain information on the specific accumulation of the radioactive tracer in a given tissue. The present study is designed to make use of the information available in the specific activity curve obtained from the plasma in conjunction with a single specific activity value obtained from a tissue to permit the calculation of the actual specific activity–time curve of the compound in the tissue. This approach has been tested in a three compartment model which has been simulated with a digital computer.

INTRODUCTION

Radioactive tracers have been used extensively to elucidate dynamic biological processes.[1-4] Their use has provided considerable insight into the turnover of elements and compounds of biological significance in the plasma and tissues of living organisms. Such studies are often complicated by the existence of compartments of limited access. Thus, a radioactive element or labeled compound can be injected intravenously, and its specific activity followed closely through repeated sampling of the plasma compartment. However, generally it is not possible to sample a tissue compartment repeatedly. Any attempt to effect such tissue sampling might result in perturbation of the system being examined.

Tissue specific activity–time curves may be helpful in the estimation of rates of synthesis and breakdown of the compound within tissue compartments.[1, 5, 6] Additionally, in experiments where a radionuclide is administered to a living organism, it might be desirable to determine the total concentration–time curve of the radioisotope, within a given tissue, during the course of the experiment. Such curves might make possible a reasonable estimate of the radiation dose delivered to the tissue by the internal emitter.[7]

Ginsburg and Wilde,[8] in a previous investigation of the distribution kinetics of intravenously administered ^{42}K, described the plasma specific activity disappearance curve for ^{42}K in the rat as the sum of five exponential terms. These workers considered their data to be consistent with a six compartment mammillary model composed of a central compartment and five peripheral compartments. In their experiments, they attempted to calculate the tissue specific activity–time curves that might be predicted on a mathematical basis. Their predicted curves were not in good agreement with composite experimental tissue specific activity–time curves.

In the present study, experiments were performed using a computer simulated model of a three compartment open mammillary system. Experimental specific activity–time curves were

obtained from each of the compartments of the model after simulated introduction of a radioactive tracer into the central ("plasma") compartment. Using data obtained from an independent analysis of the time curve of specific activity in the "plasma" compartment, and a single data point from each of the two peripheral ("tissue") compartments, it was possible to calculate the specific activity–time curves for each of the peripheral "tissue" compartments. Each experimentally obtained "tissue" curve was in good agreement with its respective calculated "tissue" curve.

METHODS

Two models having the configurations shown in Figs. 1 and 3 were simulated using the digital–analogue simulation techniques. Programs developed for the IBM Models 1620 [9] and 7094 [10] computers were employed.

Programs were developed in our laboratory for the generation of multiexponential functions, and for their resolution into exponential components. The latter was accomplished by a programmed tail–subtraction method which was helpful in eliminating subjectivity from such analysis.

RESULTS AND DISCUSSION

Tracer kinetics in the two compartment open model in the steady state have been previously examined.[6, 11, 12] In such a system (Fig. 1), it can be demonstrated that following initial introduction of label into one compartment, the specific activity–time curves of each of the compartments can be described by the following equations:

$$y/V_y = C_1e^{\alpha t} + C_2e^{\beta t}, \quad (1)$$

and

$$x/V_x = C_3e^{\alpha t} + C_4e^{\beta t}. \quad (2)$$

If the initial specific activity $(y/V_y)_{t=0} = 0$, then $C_1 = -C_2$, then equation (1) reduces to:

$$y/V_y = -C_2e^{\alpha t} + C_2e^{\beta t}, \quad (3)$$

and equation (2) will remain unchanged. Similarly, if the specific activity $(x/V_x)_{t=0} = 0$, then $C_3 = -C_4$, equation (2) will reduce to:

$$x/V_x = -C_4e^{\alpha t} + C_4e^{\beta t}, \quad (4)$$

and equation (1) will remain unchanged. Given: (a) conditions described in either (3) or (4), (b) the specific activity–time curve in the compartment into which tracer is initially introduced and (c) a single specific activity point in the second compartment of the system, one has sufficient data for the calculation of the specific activity curve of the second compartment.[4] Such an approach is feasible for the relatively simple 2 compartment open system, as has been demonstrated theoretically and can be illustrated practically with the use of data obtained from a well-defined model system (Fig. 2).

While the kinetics of a number of substances have been described in terms of two compartment systems,[3, 12] such simple models may have limited application to the study of substances administered intravenously to normal organisms. Models of considerably greater complexity have been proposed to describe, among others, the kinetics of carbonate, iodine, iron, sodium, potassium, and calcium.[3, 4]

The following discussion relates to a specific well-defined 3 compartment open mammillary model in the steady state (Fig. 3), consisting of a central compartment representing the "plasma", and two finite peripheral "tissue" compartments. A fourth, infinite compartment, is implied in this model and represents the pathway of loss of label and compound from the system, i.e. excretion. Ginsburg and Wilde used a number of animals to determine composite specific activity–time curves with only one time-point contributed by each animal. For the purpose of critical analysis, our study was

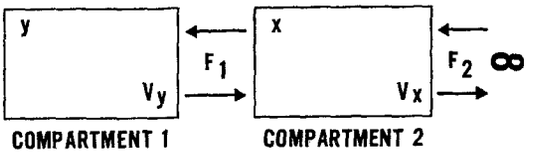

FIG. 1. The two-compartment open dynamic model. y, x, amount of labeled compound in compartments 1 and 2. V_y, V_x, amount of total compound (labeled and unlabeled) in compartments 1 and 2. F_1, rate of exchange of compound between compartments 1 and 2. F_2, rate of synthesis and breakdown of compound.

confined to a computer simulated model, whose characteristics and parameters were clearly defined. This provided data relatively free of experimental error and biological variation.

If the model system in Fig. 3 is initially unlabeled, and labeled compound is introduced into the central compartment, the time curves of specific activity in the various compartments can be described by the following

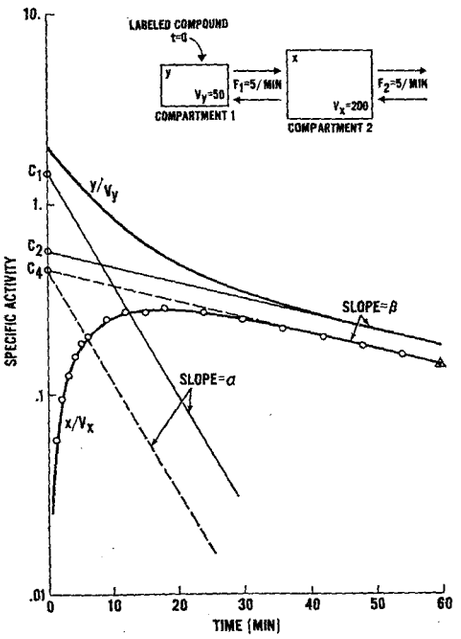

FIG. 2. Calculation of specific activity–time curve in compartment 2, using data obtained from compartment 1 and the single terminal point (△) in compartment 2. The two compartment open model was simulated using a digital computer. "Labeled compound" was introduced into compartment 1 and specific activity –time curves were obtained in compartments 1 and 2 as shown by the solid lines. Using graphical analysis y/V_y was resolved into its two components and α and β were determined. Through the terminal point obtained from compartment 2 (△) a line was drawn with slope $= \beta$ to zero time. Through the zero time intercept (C_4), a line was drawn with slope $= \alpha$. $C_4e^{\beta t} - C_4e^{\alpha t}$ was computed, giving the points (○) of the calculated curve for x/V_x.

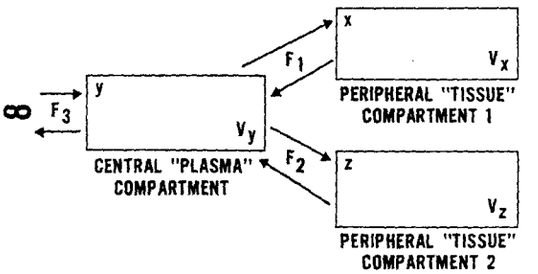

FIG. 3. The three compartment open mamillary model. y, x, z = amount of labeled compound. V_y, V_x, V_z, amount of total (labeled and unlabeled) compound. F_1, F_2, rates of exchange between "plasma" and "tissue" compartments. F_3, rate of exchange between "plasma" compartment and an external infinitely large compartment.

equations (F_1, F_2, F_3, V_x, V_y, and V_z are constants):

$$y/V_y = C_1e^{\alpha t} + C_2e^{\beta t} + C_3e^{\gamma t} \quad (5)$$

$$x/V_x = C_4e^{\alpha t} + C_5e^{\beta t} + C_6e^{\gamma t} \quad (6)$$

$$z/V_z = C_7e^{\alpha t} + C_8e^{\beta t} + C_9e^{\gamma t} \quad (7)$$

By definition, the specific activity of the implied infinitely large compartment is always equal to zero.

The values of α, β, and γ are negative and it is assumed for the purposes of this discussion $|\alpha| > |\beta| > |\gamma|$. Thus, if we consider that y/V_y represents the specific activity in the central or accessible compartment, γ represents the final slope of the specific activity curve that will be obtained from that compartment. Gamma (γ) has the same significance relative to each of the two "tissue" compartments.

If the system is initially unlabeled, and labeled compound is introduced into the "plasma" compartment, then at $t = 0$ the specific activities in the "tissue" compartment $(x/V_x)_{t=0}$ and $(z/V_z)_{t=0}$ will be equal to zero and the following relationships exist:

$$C_4 = -(C_5 + C_6), \quad (8)$$

and

$$C_7 = -(C_8 + C_9). \quad (9)$$

The exponents α, β, γ may be obtained by resolution of the components of the "plasma"

specific activity–time curve. The coefficients of the exponential terms, viz. C_3, C_6, and C_9, are the zero time extrapolates of the final (γ) component of each curve. With this information, it appears theoretically possible to get values for the other coefficients (C_4, C_5, C_7, and C_8) by the simultaneous solution of a system of algebraic equations. Such an approach, however, is in fact not feasible: at the time when the final slope (γ) is established for each of the "tissue" compartments, the more rapidly "decaying" exponential components of the "tissue" specific activity curves can no longer be used to obtain information on the parameters of the rapidly decreasing exponential components (i.e. those with slopes α and β). Therefore, another item of independent information is required before a solution can be effected.

If one examines the relationships between the "tissue" and the "plasma" compartments, it can be seen that in each instance labeled compound in the "plasma" compartment is the immediate and only precursor of label in the "tissue" compartment. In accordance with the compound–precursor relationship described by Zilversmit *et al.*,[13] this imposes a constraint on the specific activity curves that will be obtained from the compartments of this model when label is introduced into the "plasma" compartment of the system: namely, when "tissue" specific activities achieve their maxima, the "tissue" specific activities will in each case be equal to the specific activity of compound in the "plasma" compartment at that time. This is illustrated in Fig. 4. Thus, if labeled compound is initially introduced into the "plasma" compartment (Fig. 3), at time T1 the specific activity in peripheral "tissue" compartment 1 will reach its maximum and the following relationship will hold:

$$C_1e^{\alpha T1} + C_2e^{\beta T1} + C_3e^{\gamma T1} = C_5(e^{\beta T1} - e^{\alpha T1}) + C_6(e^{\gamma T1} - e^{\alpha T1}). \quad (10)$$

Since the specific activity in the "tissue" compartment 1 goes through its maximum at T1 the following can be written:

$$\frac{d(x/V_x)}{dt} = 0$$

$$= C_5(\beta e^{\beta T1} - \alpha e^{\alpha T1}) + C_6(\gamma e^{\gamma T1} - \alpha e^{\alpha T1}) \quad (11)$$

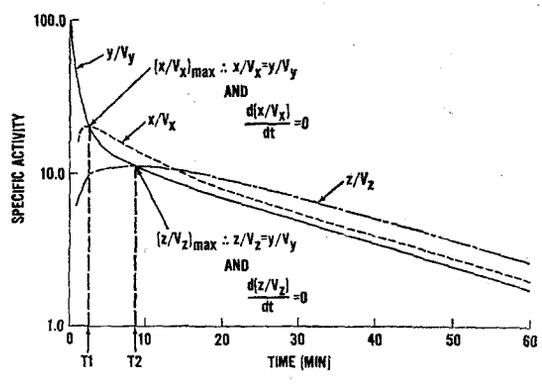

FIG. 4. Constraints imposed upon specific activity–time curves obtained in the various compartments of the three compartment model (Fig. 3), when labeled compound is introduced into the central "plasma" compartment, and is the immediate and only precursor of label in the "tissue" compartments.

It follows that:

$$-C_5 = C_6\left[\frac{\gamma e^{\gamma T1} - \alpha e^{\alpha T1}}{\beta e^{\beta T1} - \alpha e^{\alpha T1}}\right] \quad (12)$$

Substituting equation (12) into equation (10) we now have:

$$C_1e^{\alpha T1} + C_2e^{\beta T1} + C_3e^{\gamma T1} = C_6\left[\frac{(\gamma e^{\gamma T1} - \alpha e^{\alpha T1})\,(e^{\beta T1} - e^{\alpha T1})}{(\alpha e^{\alpha T1} - \beta e^{\beta T1})} + (e^{\gamma T1} - e^{\alpha T1})\right] \quad (13)$$

Numerical solution of equation (13) provides the value of T1 which can be substituted into equation (12) to yield the value of C_5. From equation (8) the value of C_4 can now be obtained. With the values of α, β, and γ obtained by resolution of the "plasma" specific activity curve we can now calculate the specific activity curve for peripheral "tissue" compartment 1. A similar algorithm can be used to obtain the specific activity curve for peripheral "tissue" compartment 2.

It is important to appreciate the significance of the early portion of the "plasma" specific

activity curve, particularly during the time when it is undergoing transition from the early rapid disappearance, near t = 0, to the final tail portion of the curve (with the slope = γ). This transitional portion of the curve contains the crucial information necessary to accurately resolve the more rapidly decreasing components of the disappearance curve. Unless a sufficient number of values is obtained experimentally in this region, any attempt to resolve the multiexponential curve into its exponential components may yield invalid results. One of the disadvantages of the tail subtraction method values obtained from the two peripheral "tissue" compartments are presented. Using a programmed tail subtraction technique, the "plasma" curve was resolved into its exponential components, and the slopes α, β, and γ were determined. Through each of the 60 min terminal values obtained in the peripheral "tissue" compartments, extrapolations were made to time = 0 with slope equal to γ. These zero time extrapolates are the values of C_8 and C_9. Using the computer, a numerical solution was obtained for T1 (equation 13); and similarly, T2. T2 is the time at which peripheral

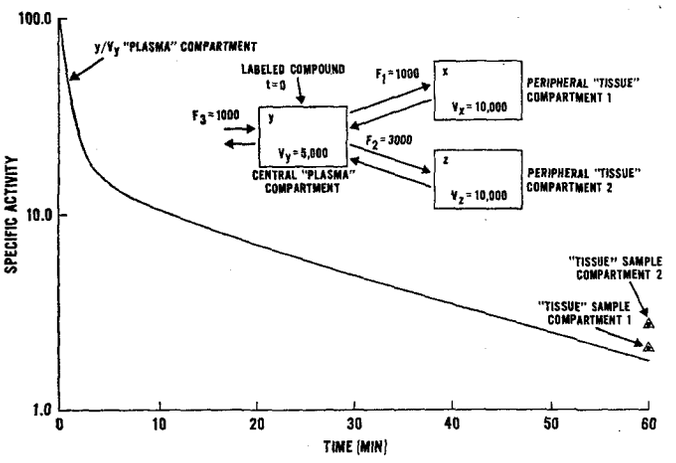

FIG. 5. "Tracer experiment" performed using the three compartment open model shown in the insert. The values of V_y, V_x and V_z are in arbitrary units. The values of F_1, F_2, and F_3 are in arbitrary units per minute. The experimentally obtained "plasma" specific activity–time curves and single specific–activity values from the "tissue" compartments are plotted.

is the compounding of error as successive exponentials are "peeled off" from the multiexponential curve. Given sufficient data of high accuracy, the difficulties of analyzing multiexponential curves containing even three components are considerable. Given insufficient data or data with a high degree of variability, and particularly with curves that contain more than three exponential components, the problems may become insurmountable.

Figure 5 presents an experiment performed with the computer simulated model. At time = 0 a dose of "radioactively labeled compound" was introduced in the "plasma" compartment. The "plasma" curve and each of the terminal "tissue" compartment 2 goes through its maximum. The value for C_5 was obtained from equation (12); and similarly, C_8, C_4, and C_7 were obtained by substitution of the proper values into equations (8) and (9). It was then possible to generate the curves for peripheral "tissue" compartments 1 and 2 using equations (6) and (7). The calculated curves and the experimentally obtained curves are presented simultaneously in Fig. 6. It can be seen that good agreement was obtained between the calculated and the experimentally obtained curves. Thus, with the three compartment open mammillary model it is not only theoretically, but also practically possible to perform an

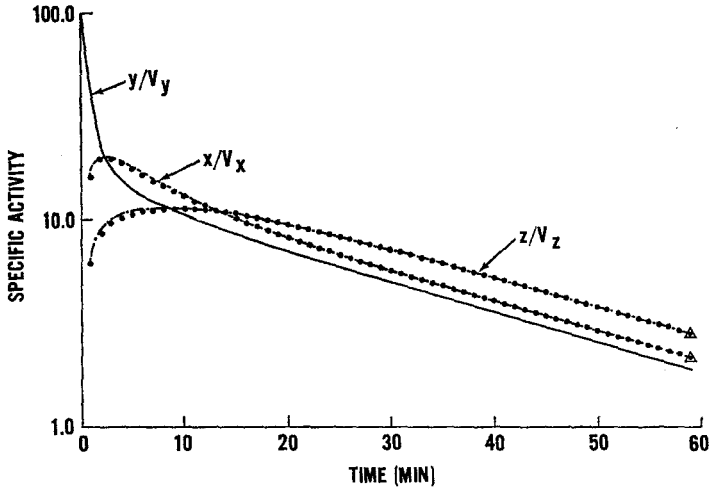

FIG. 6. Comparison between calculated (●) and "experimentally" obtained specific activity curves in peripheral "tissue" compartment 1 (x/V_x) and compartment 2 (z/V_z) (represented by solid lines). The terminal measured values for specific activity in each of the "tissue" compartments are indicated (△). Experimental parameters are given in Fig. 5. Details involved in the calculation of the "tissue" specific activity curves are given in the text.

experiment in which specific activity curves in relatively inaccessible compartments can be calculated using information available from the "plasma" compartment of the system, and a single point from each of the peripheral "tissue" compartments.

REFERENCES

1. G. HEVESY. *Radioactive Indicators*, Interscience Publishers, Inc., New York (1948).
2. J. SACKS. *Isotopic Tracers in Biochemistry and Physiology*, McGraw-Hill (1953).
3. J. S. ROBERTSON. *Physiol. Rev.* **37,** 133 (1957).
4. C. W. SHEPPARD. *Basic Principles of the Tracer Method*, John Wiley and Sons, Inc., New York (1962).
5. D. B. ZILVERSMIT, C. ENTENMAN, M. C. FISHLER and I. L. CHAIKOFF. *J. Gen. Physiol.* **26,** 333 (1943).
6. M. L. SHORE. *J. Appl. Physiol.* **16,** 771 (1961).
7. R. LOEVINGER, J. G. HOLT and G. J. HINE. Internally administered radioisotopes. *In Radiation Dosimetry*, ed. G. S. Hine and G. L. Brownell, Academic Press, N.Y. 801 (1956).
8. J. M. GINSBURG and W. S. WILDE. *Am. J. Physiol.* **179,** 63 (1954).
9. R. D. BRENNAN and H. SANO. AFIPS Conference Proc. 26, 299 (1964).
10. R. T. HARNETT, F. J. SANSOM and L. M. WARSHAWSKY. Wright-Patterson Air Force Base SEG-TDR-64-1 (1964).
11. D. B. ZILVERSMIT and M. L. SHORE. *Nucleonics*, **10,** 32 (1952).
12. M. L. SHORE and R. CALLAHAN. *Ann. N.Y. Acad. Sci.* **108,** 147 (1963).
13. D. B. ZILVERSMIT, C. ENTENMAN and M. C. FISHLER. *J. Gen. Physiol.* **26,** 325 (1943).

RADIATION EXPOSURE FROM RADIOPHARMACEUTICALS IN CHILDREN*

J. G. KEREIAKES, H. N. WELLMAN and E. L. SAENGER
Department of Radiology and Radioisotope Laboratory, University of Cincinnati, College of Medicine, Cincinnati, Ohio

Abstract—The average radiation doses to whole body and to certain organs were calculated for a selected population of children administered radio-pharmaceuticals for diagnostic purposes. The thyroid uptake studies and dose calculations, collated with the findings of other investigators, suggest that thyroid tests for suspected disease in newborns, e.g. cretinism and inborn errors of thyroid metabolism, be made at least 1–2 weeks following birth unless the diagnosis becomes a life-saving procedure. The observations concerning other radionuclides indicate that both whole body and organ doses do not exceed those expected and that these labelled pharmaceuticals can be used in their accustomed doses safely in children. The findings are part of a continuing program for obtaining metabolic data in children to allow modifications of the dose calculations presented here and in previous reports and provide more accurate and complete estimates of radiation exposure.

INTRODUCTION

The increasing use of radionuclides in medical diagnosis and research together with continuing environmental contamination from fallout and from industrial operations requires that we have accurate knowledge of the radiation exposure from the procedures of nuclear medicine. Although this information is frequently available for adults,[1-3] only occasional reference is found to doses received by children,[4] a group in whom there is more concern about radiation exposure. Furthermore, many of the available data are based upon experience with the inorganic form of the radionuclide whereas today many radionuclides are incorporated into other molecules. These "tagged" substances are metabolized differently than the inorganic forms, resulting in an altered radiation exposure.

In recent communications we reported the average doses received by normal persons of varying ages from diagnostic tests employing several radionuclides.[5-7] Doses were calculated for "normal children" based in many instances on metabolic values reported for adults. Because of differences of the physiological response between adults and children, studies were initiated to obtain information on the metabolic fate of several radiopharmaceuticals in infants and children who were referred for various illnesses or because of diagnostic problems.

The average dose from an internally deposited radionuclide varies with the radionuclide, its chemical form, and its route of administration. Average doses calculated for medical use of radionuclides in standard man were calculated using standard beta-gamma formulae described by Loevinger *et al.*[8] The application of these formulae to infants and children required careful consideration of certain parameters, particularly the following: (1) $\bar{g}$, the average geometrical factor, which would be smaller in younger individuals because of their smaller size; and (2) T_b, the biological half-life, which may be different in younger individuals because of a different metabolism.

Whole body values of $\bar{g}$ in children were calculated using the procedure of Bush.[9] Average heights for infants and children were obtained from tables given by Stuart and Stevenson.[10]

* Supported in part by Public Health Service Training Grant 4TIRH36-04 from the Division of Radiological Health; Public Health Service Training Grant 1TIGM-1247 from the National Institute of General Medical Sciences; and by the Albertine O. Schoepf Research Fund of the College of Medicine, University of Cincinnati.

Table 1. *Body Weights, Organ Weights and Calculated Geometrical Factors for Various Ages*

		Newborn	1 year	5 years	10 years	15 years	Standard man
Whole body	wt(g)	3540	12,100	20,300	33,500	55,000	70,000
	ht (cm)	50	75	108	139	166	170
	$\bar{g}$ (cm)	64	89	94	102	112	126
Thyroid	wt (g)	1.9	2.5	6.1	8.7	15.8	20.0
	$\bar{g}$ (cm)	7.0	8.0	11.0	12.0	14.0	15.0
	g_p (cm)	71.0	99.0	104.0	113.0	124.0	140.0
Kidney	wt (g)	23	72	112	187	247	300
	$\bar{g}$ (cm)	16	22	25	30	33	35
	g_p (cm)	92	127	134	146	160	180
Liver	wt (g)	136	333	591	918	1289	1700
	$\bar{g}$ (cm)	27	36	44	50	55	59
	g_p (cm)	92	127	134	146	160	180
Spleen	wt (g)	9.4	31	54	101	138	150
	$\bar{g}$ (cm)	12	17	20	25	28	29
	g_p (cm)	92	127	134	146	160	180
Liver-spleen	wt (g)	145	364	645	1019	1427	1850
	$\bar{g}$ (cm)	28	37	45	51	56	61
	g_p (cm)	92	127	134	146	160	180

Values of $\bar{g}$ for whole body and various organs are shown in Table 1. The calculations of the average geometrical factors for organs account for tissue absorption. Spherical shapes were assumed for the organs (with elongation ratios assumed for certain organs as kidney, spleen and liver). As noted, independent calculations of the average geometrical factor for each age group[7] are essential since extrapolation of values for standard man on the basis of some parameter as weight alone would result in underestimation of the $\bar{g}$ for younger individuals, as noted by the log–log relationship shown in Fig. 1. Values of $\bar{g}$ for any child of specific height and weight can be derived by use of the detailed method of Bush.[9]

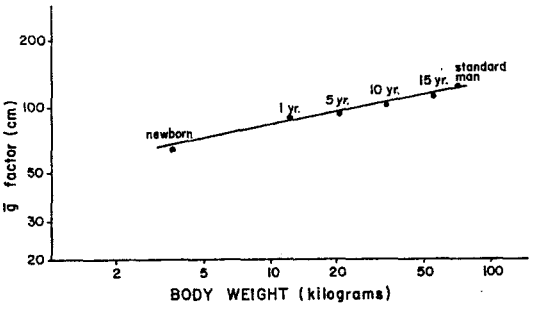

FIG. 1. Calculated whole body average geometrical factors, $\bar{g}$, for various age groups as a function of body weight.

The metabolic fate of the various radionuclides has not been widely studied, a circumstance which is responsible for some of the assumptions made in dose calculations. If biological half-lives are not well known for adults, e.g. ^{137}Cs,[11] the situation is even more complex for children because of the reluctance of investigators to administer radionuclides to children in order to study their normal physiological processes.

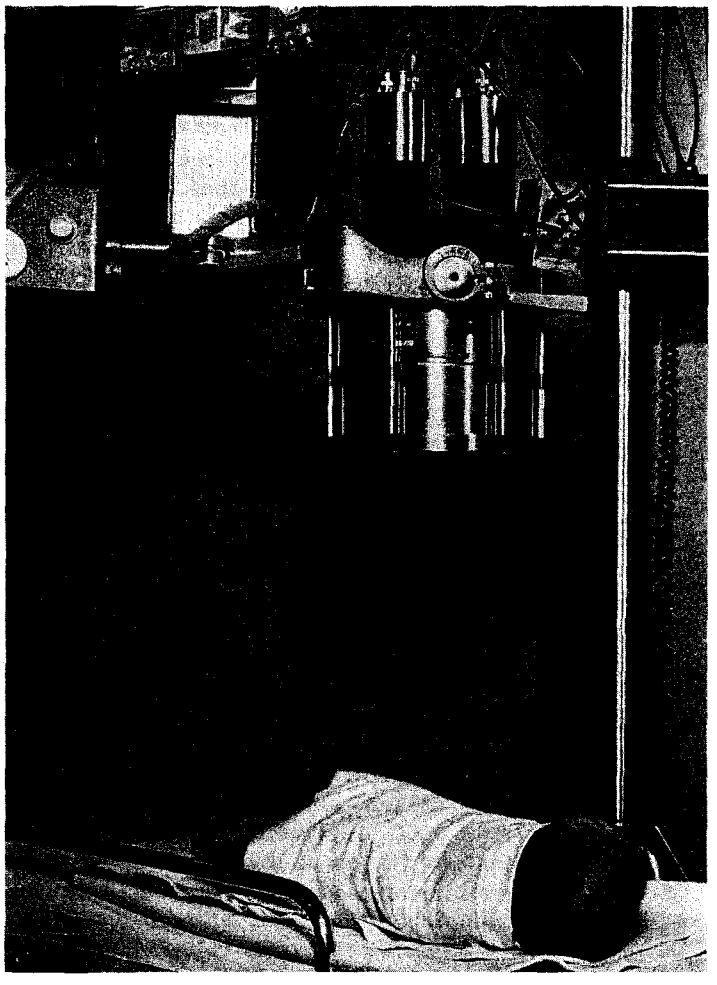

FIG. 2. Whole body counting arrangement for children.

METHOD

In this study, infants and children were followed for extended periods of time in a whole body counter following the administration of radiopharmaceuticals for diagnostic purposes. The whole body counter, shown in Fig. 2, has inside dimensions of 8 × 8 × 8 ft high with 8 in. thick steel walls. One counting arrangement utilized an 8 in. diameter by 4 in. thick sodium iodide (Tl) crystal with the subject either in the standard chair position (59 cm and/or 80 cm distances to apex of the chair) or in a 59 cm supine position as shown in Fig. 2. Most of the whole body counting data reported here result from the measurements made at the 59 cm supine position.

A sensitive thyroidal-uptake system was utilized for most of the thyroid studies, consisting of two 3 in. diameter by 1½ in. thick sodium iodide (Tl) crystals each coupled to a 3 in. photomultiplier tube (Fig. 3). These crystals are suspended from a yoke which fixes their position with one another with a central axis at 90° in the same plane. The crystals and lower portions of the phototubes are shielded by a quarter inch of lead. This same crystal arrangement is also used for extra-thyroidal tissue (thigh) measurements. The outputs of these two

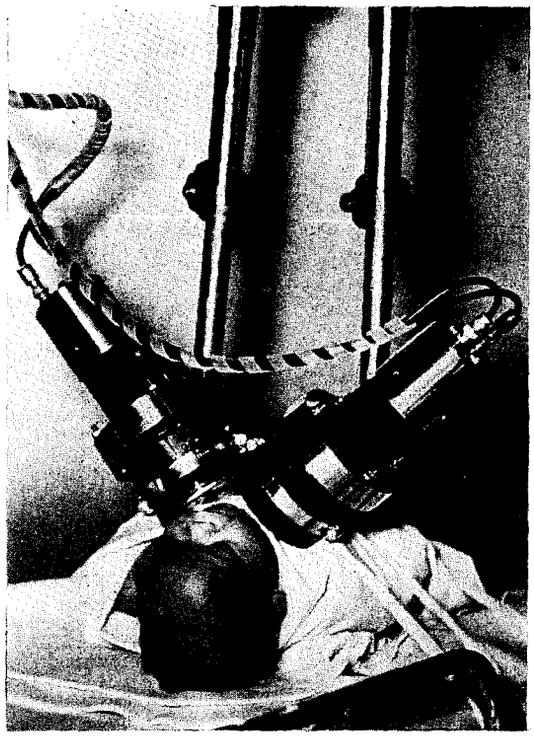

FIG. 3. Thyroid counting arrangement.

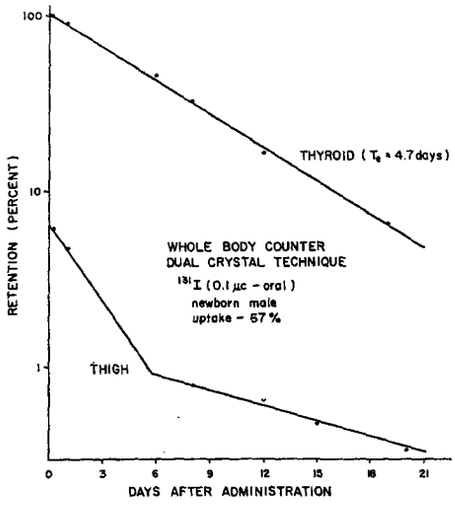

FIG. 4. ^{131}Iodine retention in newborn.

detectors are summed and processed by a multichannel analyzer with standard punch tape and typewriter output.

RESULTS AND COMMENTS

^{131}I (*Sodium iodide.*) Typical retention curves for the dual crystal counting technique used in this study are given in Fig. 4. An effective half-life of 4.7 days was determined for a newborn male having a normal uptake of 67%. The uptake was determined as given in some previous work.[12] It consists primarily of using the Compton to photo peak ratio to obtain a corrected patient photo peak that takes into consideration the effective thyroid gland depth. Single exponentials were always found for the thyroid retention, whereas the extra-thyroidal (thigh) measurements showed at least two compartments.

As shown in Table 2, the uptake for the newborn was measured as 67%; whereas the thyroid uptakes for the other children studied ranged from 10 to 22%. The thyroid uptake values reported in the literature for children vary to a great extent, see review by Eisenbud *et al.*[13] Elevated 24 hr ^{131}I uptake measurements in newborns (1-3 days) have been reported. A number of investigators observed the uptake to be elevated early in the neonatal period, attaining maximal values of 62% within the first 48 hr and the returning to normal on the fifth day of age.[14-17] Kearns *et al.*[18] showed increased values for the thyroid uptake in infants soon after birth. On the other hand, Martmer *et al.*[19] and Ogborn *et al.*[20] reported values of 30% and 23%, respectively, in normal newborn infants. Oliner *et al.*[21] measured 24 hr and 48 hr uptake values ranging from 17–50% in children (2½ months to 18 years). Van Dilla and Fulwyler[22] found the percentage of dose present in the thyroid at 24 hr similar for both children and adults. In eight apparently normal children, ranging in age from 4–10 years, the average retention of radioiodine was 20% (range of 10 to 29%). In three adolescent children 12–14 years of age, the 24 hr thyroid uptake was 15–16%. The biological half-lives for children in Van Dilla's study averaged 84 days with a considerable range of 59 to 163 days. The biological half-lives for the three adolescent children ranged from 73 to 142 days. In this

Table 2. Thyroid Doses from ^{131}I(Sodium Iodide) in Children

Age	Uptake %	Effective half-life days	Thyroid dose	
			Observed rad/μCi	Calculated* rad/μCi
2 day	67	4.7	23.8	32
1 month	10	7.0	5.0	32–10
3 month	20	5.0	7.2	32–10
2 year	10	5.2	2.5	6.2–2.6
4 year	21	6.3	3.9	6.2–2.6
6 year	22	5.8	2.9	2.6–1.8

* Standard child groups.[5]

study, the biological half-lives (calculated from effective half-life values given in Table 2) averaged 23.2 days with a range of 11.2 to 51.5 days. Doses to the thyroid per microcurie of ^{131}I were found to be somewhat below those previously calculated by us[5] as shown in Table 2. These values were found in patients whose levels of thyroid function were determined by ^{131}I uptake, PBI and/or thyroxine levels, serum cholesterol values and clinical observation. Since it is now possible to do uptake studies with 0.1 μCi of ^{131}I or less, radiation doses can be lowered significantly. When possible ^{125}I or other isotopes of iodine may reduce radiation dosage without interfering with diagnostic accuracy. Since after the first week or so of life, there is a reduction in iodine uptake in the thyroid, isotopic tests should be deferred for this period unless the diagnostic procedures are required for a life threatening situation.

Other ^{131}I-labelled pharmaceuticals. Effective half-lives measured and doses calculated for other ^{131}I-labelled radiopharmaceuticals are given in Table 3. For the triolein dose calculations, absorption was considered to be complete and instantaneous. Ten percent of the administered dose was assumed to be distributed over the total body and not excreted. The remainder

Table 3. Radiation Doses from ^{131}I Pharmaceuticals in Children

Age	Weight kg	Effective half-lives days		Whole body doses	
		T_{e_1}	T_{e_2}	Observed mrad/μCi	Calculated† mrad/μCi
^{131}I (*triolein*)					
3 month	3.18	—	6.4	7.2	10–3.3
2 year	9.55	0.4	6.0	2.5	3.3–2
^{131}I (*serum albumin*)					
2 year	7.50	4.7	—	12.3	8.9–5.4
^{131}I (*rose bengal*)*					
4 year	15.45	1.3	—	1.7	1.5–.92

* Calculated dose to organ (liver) was 2.6 mrad/μCi.
† Standard child groups.[6]

Table 4. Radiation Doses from Radiopharmaceuticals in Children

Age	Weight kg	Effective half-lives days		Calculated doses	
		T_{e_1}	T_{e_2}	Whole body mrad/μCi	Organ mrad/μCi
^{51}Cr (*sodium chromate*)					
4 month	8.18	15.0	—	1.6	—
^{197}Hg (*chlormerodrin*)					
3 year	14.55	0.8	2.6	0.16	68.1 (kidney)
12 year	47.28	0.9	2.6	0.07	39.0 (kidney)
^{47}Ca (*calcium chloride*)					
7 year	25.00	0.7	4.6	2.8	4.5 (bone)
^{85}Sr (*strontium nitrate*)					
4 year	15.47	3.5	58.0	16.3	68.3 (bone)
12 year	40.00	1.4	53.0	8.6	32.8 (bone)

was considered to be distributed over the total body with biological half-lives of 0.5 day (with 86% of the dose in the compartment) and 26 days (14% of the dose in the compartment). In consideration of the whole body dose for ^{131}I-tagged rose bengal, the dose to the whole body is the sum delivered by the circulating tagged rose bengal, circulating iodine (5% of the administered dose), the tagged rose bengal in the liver, and the tagged rose bengal in the gastrointestinal tract. For the latter, it was assumed that 95% of the administered activity is present in the gastro-intestinal tract with a biological half-life of 1.5 days. The reciprocal dose theorem was used, with g_p taken for the abdomen. The liver dose was calculated assuming a biological half-life of 90 min.[23]

^{51}Cr (*sodium chromate*). In the calculation of the whole body dose for chromium-51 (sodium chromate), see Table 4, all the radioactive chromium administered was considered to have a total body distribution with a biological half-life of 33 days. The value agrees with that reported for the average biological half-life of 33 days for chromium-51 in the circulation of the normal adult.[24, 25] This value reflects both red-cell destruction and mere elution of the tag *in vivo*. The released chromium is in the chromic state and is not reincorporated into new erythrocytes.[26]

^{197}Hg *chlormerodrin*. For chlormerodrin (neohydrin) labelled with mercury-197, the whole body dose is delivered by the beta-equivalent and gamma radiation from the circulating radioactivity (biological half-life of 21 min) and gamma radiation from radioactivity within the urinary tract (g_p taken from the mid-abdomen) with biological half-times characterized by two phases, 1.4 days (with 75% of dose in the compartment) and 70 days (25% of dose in the compartment). In the calculation of the renal dose, it is assumed that the material is deposited in the kidneys and released in the two-component manner described above.

^{85}Sr (*strontium nitrate*) *and* ^{47}Ca (*calcium chloride*) Strontium-85 retention was followed in two children with metastatic neoplasm for an extended period of time using the 8 × 4 in. sodium iodide ($T1$) crystal and the 59 cm supine position. These data, shown in Fig. 5, show at least two compartments having effective half lives of 3.5 and 58 days for a 4-year-old male and 1.4 and 53 days for a 12-year-old female. Associated compartment concentrations are also given in Fig. 5. For the ^{85}Sr dose calculations (see Table 4) one compartment comprises the bone and the other compartment the soft tissue. The weight of bone includes the marrow component and is taken as 14.3% of the body weight.[27] The average whole body dose is

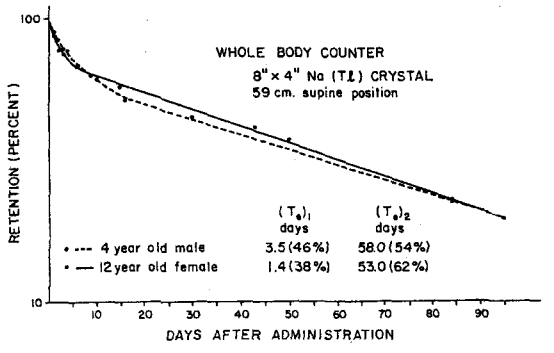

FIG. 5. ^{85}Strontium retention in children.

taken as a weighted average of that to each compartment. The long-life component (54% and 62% for the 4-year and 12-year-old, respectively) contributes to the calculated bone dose.

The ^{47}Ca measurements were made on a 7-year-old girl with hypoparathyroidism. The same weighted average was used for the whole body dose calculations for ^{47}Ca. Calcium was assumed to be lost from both compartments with a biological half-life of 20 hr. The long-life compartment concentration for ^{47}Ca was only 4%. This child is the only one at present for whom data is available.

Both the whole body dose and organ (bone) dose calculated for ^{85}Sr were higher than for ^{47}Ca.

REFERENCES

1. Report of Committee II of the International Commission on Radiological Protection on Permissible Dose for Internal Radiation (1959). *Health Physics* **3,** 192 (1960).
2. N. VEALL and H. VETTER. *Radioisotope Techniques in Clinical Research and Diagnosis*, p. 143. Butterworth, London (1958).
3. J. VENNART and M. MINSKI. *Brit. J. Radiol.* **35,** 372 (1962).
4. E. B. LEWIS. *Proc. Nat. Acad. Sci. U.S.A.* **45,** 894 (1959).
5. R. A. SELTZER, J. G. KEREIAKES, E. L. SAENGER and D. H. MYERS. *Radiology* **82,** 486 (1964).
6. R. A. SELTZER, J. G. KEREIAKES, and E. L. SAENGER. *New Eng. J. Med.* **271,** 84 (1964).
7. J. G. KEREIAKES, R. A. SELTZER, B. BLACKBURN and E. L. SAENGER. *Health Physics* **11,** 999 (1965).
8. R. LOEVINGER, E. M. JAPHA and G. L. BROWNELL. *Radiation Dosimetry* (edited by G. J. Hine and G. L. Brownell), Chap. 17, p. 718. Academic Press, New York (1956).
9. F. BUSH. *Brit. J. Radiol.* **22,** 96 (1949).
10. H. C. STUART and S. S. STEVENSON. General factors in the care and evaluation of children. Physical growth and development. *Textbook of Pediatrics* (7th ed.) (edited by W. E. Nelson), p. 12. Saunders, Philadelphia (1959).
11. Report of the United Nations Scientific Committee on the Effects of Atomic Radiation. Nineteenth Session, Supplement No. 14 (A/5814), United Nations, New York, 59 (1964).
12. H. N. WELLMAN, T. B. YEAGER, G. J. KARCHES and J. G. KEREIAKES. A sensitive technique for measuring thyroidal uptake of iodine-131. Presented at Meeting of the Society of Nuclear Medicine, Philadelphia, Pennsylvania, 1966.
13. M. EISENBUD, B. PASTERNACK, G. LAURER, Y. MOCHIZUKI, M. E. WRENN, L. BLOCK and R. MOWAFY. In *Biology of Radioiodine*, pp. 201–9. Proceedings of the Hanford Symposium, Richland, Washington, Pergamon Press, New York (1964).
14. L. VAN MIDDLESWORTH. *Amer. J. Dis. Child.* **88,** 439 (1954).
15. G. GOMIRATO-SANDRUCCI and P. NICOLA. *Minerva Pediat.* **10,** 767 (1958).
16. D. A. FISHER, T. H. ODDIE and J. C. BURROUGHS. *Amer. J. Dis. Child.* **103,** 738 (1962).
17. R. T. MORRISON, J. A. BIRKBECK, T. C. EVANS and J. I. ROUTH. *J. Nucl. Med.* **4,** 162 (1963).
18. J. E. KEARNS and H. F. PHILIPSBORN. *Quart. Bull. Northw. Univ. Med. Sch.* **36,** 47 (1962).
19. E. E. MARTMER, K. E. CORRIGAN, H. E. CHARBENEAU and A. SOSIN. *Pediatrics* **17,** 503 (1956).
20. R. E. OGBORN, R. E. WAGGENER and E. VANHOVE. *Pediatrics* **26,** 771 (1960).
21. L. OLINER, R. M. KOHLENBRENER, T. FIELDS and R. H. KUNSTADER. *J. Clin. Endocrine* **17,** 61 (1957).
22. M. A. VAN DILLA and M. J. FULWYLER. *Science* **144,** 178 (1964).
23. J. M. LOWENSTEIN. *Clin. Res. Proc.* **5,** 39 (1957).
24. I. M. WEINSTEIN, C. L. SPURLING, H. KLEIN and T. F. NECHELES. *Blood* **9,** 1155 (1954).
25. J. H. JANDL, M. S. GREENBERG, R. H. YONEMOTO and W. B. CASTLE. *J. Clin. Investigation* **35,** 842 (1956).
26. F. G. EBAUGH, C. P. EMERSON and J. F. ROSS. *J. Clin. Investigation* **32,** 1260 (1953).
27. Recommendations of International Commission on Radiological Protection. In National Bureau of Standards Handbook, No. 47, 1950.

EFFECT OF AGE AND DIET ON EXCRETION OF STRONTIUM AND CALCIUM BY RATS*

ROY C. THOMPSON and RAY F. PALMER

Biology Department, Battelle Memorial Institute, Pacific Northwest Laboratory, Richland, Washington, U.S.A.

Abstract—Mature (8-month-old) and growing (26-day-old) rats, maintained on diets varying in calcium content from 0.03 to 2.0% were given a single injection of ^{90}Sr and ^{45}Ca and subsequent excretion of these radionuclides, in urine and feces, was measured over a period of 60 days. Similarities and differences in their patterns of excretion are discussed in relation to the probable mechanisms responsible for the behavior noted. Of particular interest was the decrease in ratio of urinary to fecal excretion of both ^{90}Sr and ^{45}Ca as a function of time following injection. This change was more evident for strontium than for calcium, was more evident in the adult than in the growing rat, and was most marked on a high calcium diet. To explain this variation it is hypothesized that strontium and calcium released from firm binding sites in bone may exist in the blood in a different form than strontium and calcium in equilibrium with freely exchangeable sites on bone surfaces.

PREVIOUS publications from our laboratory described the deposition and retention of ^{90}Sr and ^{45}Ca in the bone of mature [1] and growing [2] rats. These studies involved both single administration and continuous feeding of the radionuclides and were designed particularly to elucidate the effect of dietary calcium intake on the interrelated behavior of strontium and calcium. Whereas these earlier studies were concerned primarily with radionuclide retention, as measured in serially sacrificed groups of rats, we have attempted in the presently reported experiments to approach the problem by analysis of daily urinary and fecal excretion following single doses of ^{90}Sr and ^{45}Ca. Studies are reported in both mature and growing animals and at several levels of dietary calcium intake.

METHODS

Rats employed were females of the Sprague-Dawley strain. Studies were performed with mature animals, 7 months of age at start of experiment, and with weanling animals, 22 days of age at start of experiment. The mature animals were conditioned for 28 days to 0.03, 0.1, 0.5, and 2.0% calcium diets. All diets contained 0.5% phosphorus. The further composition of the diets is described in detail in an earlier publication. [1] Three animals were maintained on each of the diets. After the 28-day conditioning period, each rat received a single intraperitoneal injection of 30 μCi ^{45}Ca and 15 μCi ^{90}Sr. The rats were kept in individual metabolism cages and urine and feces were separately collected, daily, for 14 days following radionuclide injection. Thereafter, collections were made on each of 2 consecutive days out of each week, with the final collection made at 60 days postinjection.

The experiment with growing animals was similarly performed except that 5 animals were included in each dietary group, the conditioning period was reduced to 4 days, the radionuclide injection was reduced to 4 μCi ^{45}Ca and 2 μCi ^{90}Sr, the 0.03% calcium diet group was eliminated, and daily urine and feces collections were continued through only the first 9 days postinjection, with twice weekly collections thereafter. The animals within each dietary group were kept in a single metabolism cage and pooled excreta samples obtained.

* This paper is based on work performed under United States Atomic Energy Commission Contract AT(45-1)-1830.

Table 1. *Summarized Excretion Data* (% *of injected dose*)

	Mature rats				Growing rats			
	^{90}Sr		^{45}Ca		^{90}Sr		^{45}Ca	
	Urine	Feces	Urine	Feces	Urine	Feces	Urine	Feces
0.03% *Ca Diet*								
Day 1	22	7.0	0.09	4.3				
Day 2	5.0	8.7	0.17	6.5				
Days 5–9 (Avg/d)	0.80	0.66	0.06	0.92				
Days 40–60 (Avg/d)	0.07	0.17	0.02	0.28				
Days 1–60 (Total)	42	33	1.8	35				
0.1% *Ca Diet*								
Day 1	30	3.6	0.90	2.6	4.9	4.3		0.45
Day 2	5.2	10.8	0.71	9.0	0.93	1.3	0.09	0.10
Days 5–9 (Avg/d)	0.82	0.74	0.18	1.3	0.60	0.54	0.01	0.03
Days 40–60 (Avg/d)	0.06	0.17	0.03	0.28	0.11	0.21		0.07
Days 1–60 (Total)	49	31	5.2	40	23	23	<1.0	3.1
0.5% *Ca Diet*								
Day 1	34	5.6	5.7	5.3	4.5	5.5		2.7
Day 2	6.2	8.4	1.4	10.	0.88	1.8		0.69
Days 5–9 (Avg/d)	0.80	0.62	0.30	1.5	0.50	0.54		0.16
Days 40–60 (Avg/d)	0.05	0.15	0.02	0.30	0.14	0.16	0.06	0.14
Days 1–60 (Total)	54	29	12	45	21	27	<5.0	15
2.0% *Ca Diet*								
Day 1	57	4.8	25	4.7	20	3.1	10	2.5
Day 2	5.5	8.1	4.2	9.6	1.4	2.8	0.66	2.3
Days 5–9 (Avg/d)	0.54	0.27	0.50	0.58	0.96	0.42	0.64	0.36
Days 40–60 (Avg/d)	0.02	0.08	0.02	0.14	0.17	0.10	0.17	0.12
Days 1–60 (Total)	72	20	38	29	45	20	31	19

Urine and feces samples were dry ashed at 600°C, the residue dissolved in nitric acid and aliquots assayed for ^{90}Sr and ^{45}Ca by a differential beta-particle absorption technique. Counting of samples was delayed for 2 weeks to ensure establishment of ^{90}Sr–^{90}Y equilibrium. All counting rate data were corrected for radioactive decay.

RESULTS

A summary of certain features of the excretion data, from both the mature- and growing-rat experiments, is given in Table 1. The average daily excretion of ^{90}Sr and ^{45}Ca in urine and feces is shown for the first and second days post-injection, for the period of 5–9 days, and for the period of 40–60 days. Cumulative figures are given for the total 60-day period. The first and second days' excretions of ^{90}Sr and ^{45}Ca were uniquely high, the second days' fecal excretion usually being higher than the first, due to holdup in the intestine. The 5–9 day period was one during which daily collections were made; it was beyond the early period of rapidly falling excretion rates; and it was a period of relatively stable urinary/fecal (U/F) excretion ratios. Data for the 40–60-day periods represent the average of six collections made during the final 3 weeks of the experiment. In several instances urinary ^{45}Ca data were unavailable from the growing animals, due to the smaller injection levels employed with these animals, and due to limitations of the differential beta particle absorption technique which make it difficult to quantitate small

amounts of ^{45}Ca in the presence of large amounts of ^{90}Sr.

There was a considerable scatter in day-to-day excretion values. This is illustrated in Fig. 1, where there are plotted daily average total ^{90}Sr excretion values for the growing animals on all three diets, and ^{45}Ca total excretion values for the growing animals on the 2.0% calcium diet.

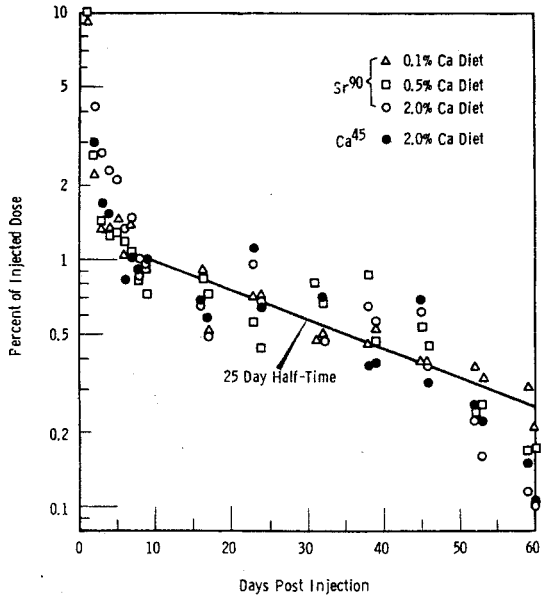

FIG. 1. Daily average total excretion of ^{90}Sr and ^{45}Ca injected intraperitoneally at age 26 days.

While fluctuations by as much as a factor of 2, from day to day, or even from week to week, were common, the general trend of change in excretion rate was clearly evident.

Strontium-90 and ^{45}Ca retention curves for the animals on each dietary regimen were constructed by subtracting each days total excretion from the initial injected dose. These curves are shown in Fig. 2 (mature rats) and Fig. 3 (growing rats). During the latter portion of the experiment, when excreta collections were not made daily, the daily excretion increment employed in the construction of the retention curves was read from an eye-fitted smooth curve drawn through the experimental excretion data. The line drawn in Fig. 1 is an example of such an interpolation curve.

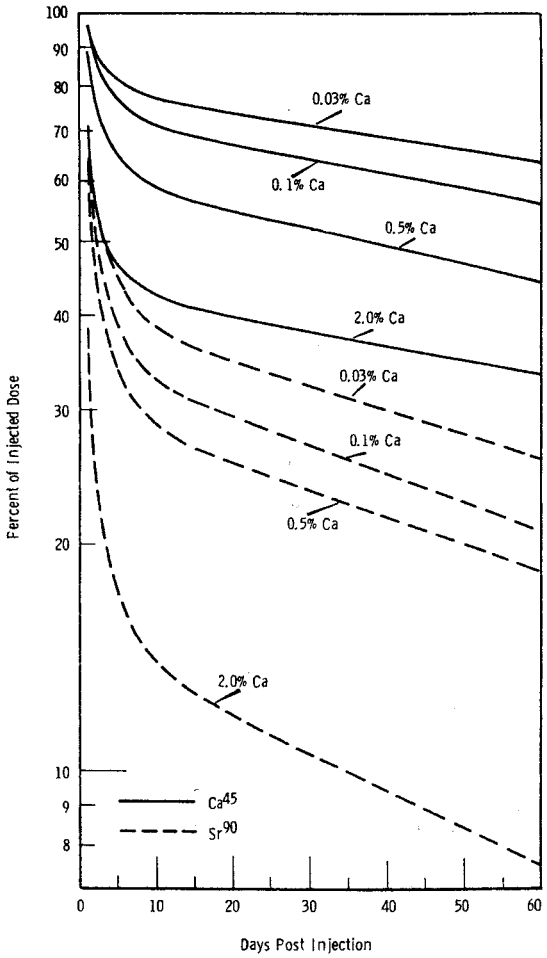

FIG. 2. Effect of dietary calcium level on the retention of ^{90}Sr and ^{45}Ca injected intraperitoneally at age 8 months.

An interesting feature of the experimental results was the variation in the U/F ratio of both ^{90}Sr and ^{45}Ca, between animals on different calcium intakes, and with time following radionuclide administration. This is shown in Fig. 4 (mature rats) and Fig. 5 (growing rats) where curves are drawn to indicate the change in U/F as a function of time postinjection. Because of the retention of feces in the intestine, U/F ratios, during the early period of daily collections, were calculated using a given day's urine value and the succeeding day's fecal value. The first day's urine value was compared with the sum of the

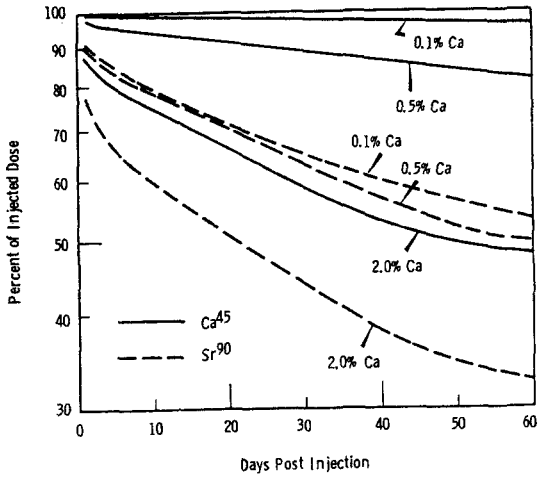

FIG. 3. Effect of dietary calcium level on the retention of ^{90}Sr and ^{45}Ca injected intraperitoneally at age 26 days.

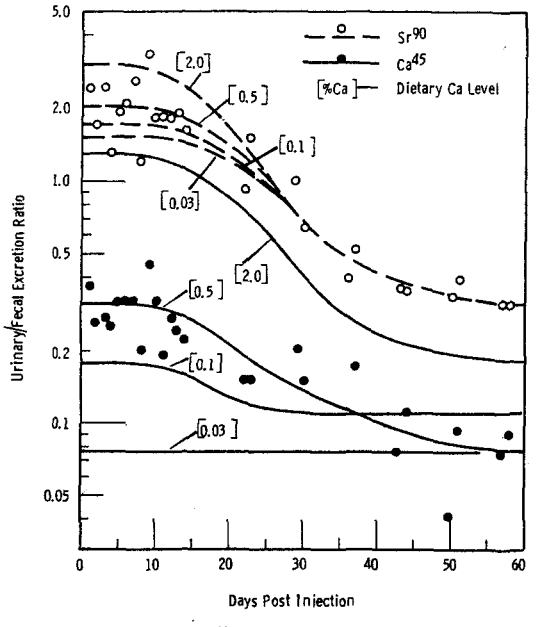

FIG. 4. Effect of dietary calcium level on the urinary/fecal excretion ratio of ^{90}Sr and ^{45}Ca injected intraperitoneally at age 8 months. Data points for daily average U/F ratios are shown for only the 0.5% calcium diet.

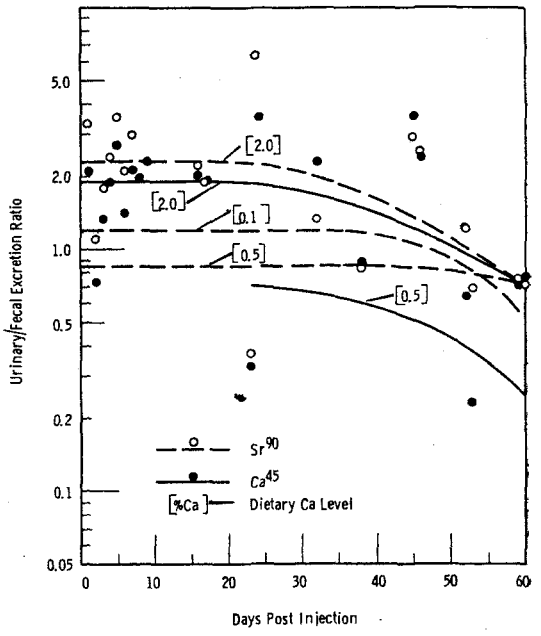

FIG. 5. Effect of dietary calcium level on the urinary/fecal excretion ratio of ^{90}Sr and ^{45}Ca injected intraperitoneally at age 26 days. Data points for daily average U/F ratios are shown for only the 2.0% calcium diet.

first and second day's fecal value. As one might anticipate, U/F ratios showed a considerable day-to-day variation. Individual data points (daily averages) are shown for two of the curves in Fig. 4 and Fig. 5 as an indication of the variability observed. The exact shape of the curves drawn are clearly not defined, and small differences between curves are of no significance. Certain of the curves, however, are clearly distinct from others.

DISCUSSION

The three diets employed markedly affected the general growth and skeletal development of the growing rats as indicated by the data obtained at sacrifice which is summarized in Table 2. More extensive data on the behavior of growing rats on these diets were obtained in earlier studies and are discussed in detail in a previous publication.[2] The 0.1% calcium diet was clearly inadequate for normal skeletal mineralization. The slight growth retardation on the 2.0% calcium diet was due to self-limited food

Table 2. Effect of Diet on Growth and Skeletal Development (Average values from five rats at sacrifice)*

	Calcium content of diet (%)		
	0.1	0.5	2.0
Animal wt. (g)	142	181	161
Femur, wet wt. (g)	0.33	0.51	0.44
Femur ash wt. (g)	0.094	0.22	0.19
Femur ash (% wet wt)	28	44	44

*Animals sacrificed at age 86 days, after 64 days on indicated diets.

intake. These discrepancies must be borne in mind in interpreting the ^{90}Sr and ^{45}Ca behavior in the growing rats.

Grossly, there was no indication of effect of diet on general appearance or weight maintenance of the mature rats. In earlier studies on the same diets, with somewhat younger animals (3 months old), there was a slight, but statistically significant increase in femur weight and ash content on the 2.0% calcium diet.[1] The possibility of significant radiation effects from these diets was discussed in connection with the previous studies,[1] and seems quite unlikely.

Retention in mature rats. The retention curves for ^{90}Sr and ^{45}Ca in the mature rats (Fig. 2) are qualitatively similar to those which have been described by many other investigators, working with a variety of mammalian species, including man.[1, 3-6] These retention curves were resolved into exponential components as detailed in Table 3. In all cases the retention subsequent to about 15 days postadministration was closely approximated by a single exponential expression involving a half-retention time of from 60 to 180 days. Subtraction of this long-lived component left a component, or components, with half-times of 2 days or less. It is important to note that there is no indication, in any diet group, of more than a single component of half-time longer than 2 days. Considering the manner in which these curves were constructed, and the relatively short duration of the experiment, the possibility of components of intermediate, or of very long half-time cannot be ruled out; however, it seems quite certain that

Table 3. Resolution of Retention Curves for Mature Rats

Diet group (% Ca)	^{90}Sr components		^{45}Ca components	
	Half-time (days)	% of injected dose	Half-time (days)	% of injected dose
0.03	90	40	180	80
	$\lesssim 2$	60	$\lesssim 2$	20
0.1	80	35	150	73
	$\lesssim 2$	65	$\lesssim 2$	27
0.5	80	30	120	61
	$\lesssim 2$	70	$\lesssim 2$	39
2.0	60	15	160	44
	$\lesssim 2$	85	$\lesssim 2$	56

any such components would constitute a small fraction of the total ^{90}Sr or ^{45}Ca. This conclusion is supported by the fact that the half-time for decrease in daily excretion rate, subsequent to about 15 days postadministration, was, in all groups, essentially the same as the retention half-time.

Within each diet group the retention of ^{90}Sr, as compared with the retention of ^{45}Ca, is characterized by the presence of a greater fraction of the total dose in the short-lived components, and by shorter long-lived components. In general, about twice as much ^{90}Sr is present in the short-lived components, and the half-time of the long-lived ^{90}Sr component is about half that of the long-lived ^{45}Ca component. The differences between adjacent diet groups are usually small and, in most cases, of questionable significance. There is an obvious trend, however, for larger short-lived components, and shorter long-lived components with increasing calcium intake.

Retention in growing rats. The retention curves for ^{90}Sr and ^{45}Ca in the growing rats (Fig. 3) are distinctly different from those obtained in the mature animals. As one might expect, ^{45}Ca is tenaciously retained on the 0.1% and 0.5% calcium diets. A single exponential component accounts for essentially all of the ^{45}Ca, with a biological half-time of approximately 1,000 days on the 0.1% calcium diet, and 200 days on the 0.5% calcium diet. A quite different pattern of retention is seen for ^{45}Ca in animals on the 2.0% calcium diet, and for ^{90}Sr on all diets. These are obviously multicomponent curves, consisting of a short-lived component (or components), an intermediate component (or components) which determines the greater portion of the available curve, and a long-lived component (or components) which is only suggested by the "tailing off" during the final 20 days of the experimental period. More positive evidence for the existence of a long-lived component may be deduced from the excretion curves. These are shown for ^{90}Sr on all diets and for ^{45}Ca on the 2.0% calcium diet, in Fig. 1. For the period from 10–60 days postinjection all of these data are reasonably fitted by an exponential function corresponding to a half-time of 25 days. The retention curves over this same time period, however, show a much slower rate of decrease, indicating that some substantial fraction of the ^{90}Sr and ^{45}Ca must be retained with a half-time much longer than 25 days.

Resolution of the retention curves for ^{90}Sr and ^{45}Ca in the growing rats is detailed in Table 4. The listed components must be considered quite approximate because of the very limited information which the retention curves provide concerning the long-lived components. The existence of an approximately 25-day half-time component for ^{90}Sr on all diets and for ^{45}Ca on the 2.0% calcium diet is established by the excretion data (Fig. 1) and these 25-day components were taken as a starting point in the graphic resolution of the retention curves. The

Table 4. Resolution of Retention Curves for Growing Rats

Diet	^{90}Sr components		^{45}Ca components	
Group (% Ca)	Half-time (days)	% of injected dose	Half-time (days)	% of injected dose
0.1	> > 25	50	1000	100
	25	40		
	< 2	10		
0.5	> > 25	45	200	97
	25	45		
	< 2	10		
2.0	> > 25	20	> > 25	35
	25	50	25	50
	< 2	30	< 2	15

long-lived components were assumed to have an infinite half-time. The curves were resolved into that combination of a 25-day half-time component and an infinite half-time component which best fit the retention data beyond about 7 days postinjection. Subtraction of these components left a short component of less than 2 days half-time. The long-lived component does not, of course, have an infinite half-time, but the data of this experiment provide no estimate of its true value, beyond the fact that it is evidently much longer than 25 days. Over the 60-day period of these retention curves, the choice between an infinite half-time or a 200-day half-time for the long-lived component would have little influence on the resolution of the remainder of the curve.

In comparing the behavior of calcium in growing and mature rats it seems clear that growing animals on an inadequate (0.1%) or marginally adequate (0.5%) calcium intake constitute a special case. The excretion of ^{45}Ca in both urine and feces of the growing rats on the 0.1% and 0.5% calcium diets was sharply reduced, as compared to the case of mature rats on the same diets (Table 1). These growing rats required essentially all of the calcium available and quite efficiently utilized their limited supply.

The behavior in growing rats of calcium supplied in excess (2.0% calcium diet), and of strontium under all dietary calcium conditions, are remarkably similar, and differ from the situation in mature rats in one major respect. The early rapid elimination observed in mature animals is greatly reduced in the growing animals, and the excess of retained calcium and strontium is lost gradually, with a half-time of about 25 days—such a 25-day half-time component is notably absent in the retention curves of the mature rats. Thus, on the 2.0% calcium diet, which provides perhaps a fourfold excess of calcium for the growing rat, total elimination of ^{45}Ca by urine and feces during the first 2 days postinjection amounts to about 15% of the injected dose—in mature animals on the same diet total elimination of ^{45}Ca during the same 2-day period amounted to nearly 45% of the injected dose (Table 1). Excretion during later time periods, however, was as high, or higher, in growing rats than in mature rats. This contrasting behavior of growing and mature rats might reasonably be explained by the much greater availability in growing rats of sites of new bone growth which tie up the injected ^{90}Sr and ^{45}Ca, preventing its rapid excretion. The processes of bone growth, however, involve continual resorption of old bone and deposition of new bone, so that the turnover of a substantial proportion of firmly deposited strontium and calcium occurs more rapidly in the growing rat than it does in the mature rat.

Mechanisms of strontium-calcium discrimination. In the mature rats the faster rate of ^{90}Sr excretion, as compared with ^{45}Ca excretion, is due principally to differences in urinary excretion (Table 1). The total fecal excretion of ^{45}Ca, on a percent of injected dose basis, is actually somewhat greater than that of ^{90}Sr. If allowance is made for the high urinary excretion of ^{90}Sr on the first day postinjection, the fecal excretion of ^{90}Sr and ^{45}Ca, on a retained dose basis, is very similar. This is true not only within a given diet group but is quite similar when comparisons are made between all dietary groups. This discrimination between strontium and calcium in renal clearance, and lack of discrimination in fecal excretion, has been noted in several studies in man. [7, 8, 9] As dietary calcium intake increases, the renal discrimination between strontium and calcium decreases, as is clearly evident in Table 1, and as has been indicated in studies with man reported by Samachson and Spencer-Laszlo. [10]

This effect of dietary calcium level on renal discrimination in the mature rat is also evident from a consideration of the urinary/fecal excretion ratios as presented in Fig. 4. On the 0.03% calcium diet, where retention of ^{45}Ca is at a maximum, the U/F ratio for ^{45}Ca is less than 0.1, excretion occurring predominantly via the intestinal route. With an increase in dietary calcium level, the initial U/F ratio increases to a maximum value of about 1.3 for ^{45}Ca on the 2.0% calcium diet. The initial U/F ratios for ^{90}Sr are all higher than those for ^{45}Ca, increasing as a function of calcium intake by only a factor of 2. In an earlier paper [1] we suggested that this type of behavior might be explained on "the assumption of a common threshold mechanism for the excretion of calcium and calcium-like elements. When the threshold

is not exceeded, excretion would be determined by the efficiency for each element of the reabsorption mechanisms operating. When the threshold is exceeded, there would be total and indiscriminate excretion of all calcium-like elements in excess of the threshold level. Thus, exceeding the threshold by only a small percentage could result in a markedly increased [percentagewise] excretion of the otherwise efficiently retained calcium, while having a quite negligible effect on the excretion of the always less efficiently retained strontium." Evidence indicating a maximum renal tubular transport of calcium has been presented by Copp, McPherson and McIntosh.[11] This simple hypothesis will not, however, explain the change in U/F ratios with time following radioisotope injection, which is a prominent feature of the data shown in Fig. 4, and which will be further considered in subsequent discussion.

In growing rats (Fig. 5) the initial U/F ratios for ^{45}Ca are much higher than was the case with mature rats, and very similar to those for ^{90}Sr on the same diet. These high U/F ratios are due to the very low excretion of ^{45}Ca, and to a lesser extent, ^{90}Sr, in the feces of growing rats. It would seem quite plausible that this lowered fecal excretion is due, not to a decreased secretion into the intestine, but to a more efficient reabsorption of the secreted ^{45}Ca and ^{90}Sr from the intestine. Intestinal absorption of calcium and strontium is known to be much more efficient in the young, than in the mature rat, and more responsive to dietary calcium intake.[12, 13] Direct comparisons of the numerical values of U/F ratios in growing and mature rats therefore have little meaning. Were it possible to correct the U/F values of the growing rats for enhanced reabsorption of intestinally secreted ^{90}Sr and ^{45}Ca, it is quite likely that they would fall below the U/F values for mature animals. What is more significant than the absolute numerical values is the close grouping of U/F values for both ^{90}Sr and ^{45}Ca on all diets. This is certainly indicative of a more similar treatment of strontium and calcium by the young rat. This fact was also evident in our earlier retention studies where young growing rats were observed to discriminate against strontium, relative to calcium, to a significantly lesser degree than the mature animals.[2] Studies in pigs,[14] dogs,[15] and humans[16, 17] have indicated a similarly lessened discrimination in the very young.

Evidence for differently excreted forms of ^{45}Ca and ^{90}Sr. The marked change in U/F ratios of both ^{45}Ca and ^{90}Sr, in mature rats, as a function of time following injection (Fig. 4) is an observation of particular interest. These animals (in any given group) were on a constant calcium intake dating from a month prior to ^{90}Sr and ^{45}Ca injection, and any change in the metabolic handling of these elements can hardly be attributed to a change in the physiological status of the animal. It seems necessary to postulate the existence of at least two different forms of calcium and strontium in the blood, which differ in their relative ease of excretion via renal and intestinal routes. The form preferentially excreted via the kidney is present in highest proportion immediately following injection, this proportion decreasing with time. The initial proportion of this form decreases with decreasing level of calcium intake.

The present experiment, with its lack of data on blood ^{90}Sr and ^{45}Ca, is of little help in further characterizing these forms. One may speculate that calcium or strontium released at long times following injection, from a site of "firm" deposition in bone, is present in some complexed form which is different from that released from "freely exchangeable" sites. It is tempting to equate the form of strontium and calcium exhibiting high U/F ratios with the short-lived component of the retention curves, and the form exhibiting low U/F ratios with the long-lived component. While qualitatively attractive, such a hypothesis does not appear to be quantitatively in accord with the data, since the high initial U/F ratios are maintained for longer periods than would be consistent with the 2 day or shorter half-lives of the rapidly lost components.

The relative constancy of U/F ratios in the growing rats might be taken to indicate a predominance, throughout the experimental period, of a single form of ^{90}Sr and ^{45}Ca, or, less plausibly, of a constant proportion of different forms. If the major proportion of the ^{90}Sr and ^{45}Ca injected into young growing rats is incorporated into the firmly-bound component of bone, as indicated by the small proportion lost

with a half-time of less than 25 days (Table 4), then nearly all of the ^{90}Sr and ^{45}Ca present in the blood and available for excretion must have been derived from stable bone, and be in the form which is characterized in mature rats by low U/F ratios. In other words, U/F ratios in growing rats do not decrease markedly with time because the ^{45}Ca and ^{90}Sr in the blood of growing rats is, essentially from the start, in the form which predominates in mature rats only after a period of several weeks.

Clearly, the further elucidation of this problem requires a more complete characterization of the physico-chemical state of calcium and strontium in the blood, in relation to excretion patterns, and as a function of the duration of retention of these elements in bone.

ACKNOWLEDGEMENT

The authors gratefully acknowledge the capable technical assistance of Mrs. Joan O. Hess.

REFERENCES

1. R. C. Thompson and R. F. Palmer. *Am. J. Physiol.* **199,** 94 (1960).
2. R. F. Palmer and R. C. Thompson. *Am. J. Physiol.* **207,** 561 (1964).
3. M. Bishop, G. E. Harrison, W. H. A. Raymond, A. Sutton and J. Rundo. *Intl. J. Radiat. Biol.* **2,** 125 (1960).
4. S. H. Cohn, H. Spencer, J. Samachson and J. S. Robertson. *Radiat. Res.* **17,** 173 (1962).
5. M. Fujita, A. Yabe, K. Ueno, M. Oshino and N. Okuyama. *Health Phys.* **9,** 407 (1963).
6. L. M. Van Putten. *Intl. J. Radiat. Biol.* **5,** 477 (1962).
7. F. Bronner, J. P. Aubert, L. J. Richelle, P. D. Saville, J. A. Nicholas and J. R. Cobb. *J. Clin. Invest.* **42,** 1095 (1963).
8. E. C. Dow and J. B. Stanbury. *J. Clin. Invest.* **39,** 885 (1960).
9. H. Spencer, M. Li, J. Samachson and D. Laszlo. *Metabolism* **9,** 916 (1960).
10. J. Samachson and H. Spencer-Laszlo. *J. Appl. Physiol.* **17,** 525 (1962).
11. D. H. Copp, G. D. McPherson, and H. W. McIntosh. *Metabolism* **9,** 680 (1960).
12. D. V. Kimberg, D. Schachter and H. Schenker. *Am. J. Physiol.* **200,** 1256 (1961).
13. D. M. Taylor, P. H. Bligh and M. H. Duggan. *Biochem. J.* **83,** 25 (1962).
14. R. O. McClellan. *Nature* **202,** 104 (1964).
15. R. J. DellaRosa, M. Goldman, and A. C. Andersen. *Radiat. Res.* **16,** 582 (1962).
16. F. J. Bryant and J. F. Loutit. *Proc. Roy. Soc. B.* **159,** 449 (1964).
17. S. A. Lough, J. Rivera and C. L. Comar. *Proc. Soc. Expt'l Biol. & Med.* **112,** 631 (1963).

^{90}Sr AND CALCIUM EXCRETION IN URINE OF MAN

W. CZOSNOWSKA

Central Laboratory for Radiological Protection, Warsaw, Poland

Abstract—The calcium and ^{90}Sr intake and excretion was studied under hospital conditions in 10 adult patients over a period of 2 weeks. The patients were divided into two subgroups according to composition of the diet and intake of calcium which on the average amounted to 1.3 and 0.79 g per day, respectively. The average dietary intake of ^{90}Sr in the two subgroups was 28.8 and 16.7 pCi/day, respectively.

The excretion of ^{90}Sr and of calcium, when expressed as a percentage of intake varied in the two subgroups; however, the observed ratio (O.R.) $= \frac{^{90}Sr/Ca \text{ urine}}{^{90}Sr/Ca \text{ food}}$ was relatively constant (about 0.75). On the other hand, in individuals the $O.R._{urine\text{-}food}$ varied systematically with the calcium excretion rate in urine. On the basis of our data and of those of other authors a more general relationship between the $O.R._{urine\text{-}food}$ and the Ca-excretion in urine was established.

RAPPORTI TRA LIVELLI DI UNITÀ CESIO E DI UNITÀ STRONZIO NELLA DIETA E NELLE URINE DI GRUPPI DI POPOLAZIONE INFANTILE DI DIFFERENTE ETÀ

A. FERRO-LUZZI, A. MARIANI, M. A. SPADONI e G. TOMASSI

Istituto Nazionale della Nutrizione, Roma, Italy

Sommario—Negli anni 1963–1965, in gruppi di bambini di ambo i sessi di differente età (5–7 e 8–10 anni rispettivamente) sono stati mensilmente studiati, per oltre un anno in ciascun gruppo di età, i rapporti fra livelli di unità cesio e unità stronzio nella dieta e nelle urine.

Ad intervalli irregolari è stato anche studiato il comportamento dei rapporti tra unità cesio e unità stronzio nella dieta e nelle feci degli stessi soggetti.

I risultati dimostrano che, indipendentemente dal sesso, nei bambini di 5–7 anni i valori del rapporto dieta/urina sono inferiori all'unità sia per il ^{137}Cs che per lo ^{90}Sr (il che significherebbe una eliminazione preferenziale del ^{137}Cs e dello ^{90}Sr nei confronti, rispettivamente, del K e del Ca); mentre in quelli di 8–10 anni, particolarmente nel caso dello ^{90}Sr, i valori del rapporto si presentano superiori all'unità. Le misure effettuate sulle feci indicano l'esistenza di un rapporto con la dieta pressocché costante e superiore all'unità per il ^{137}Cs nei due gruppi di età, mentre per lo ^{90}Sr si hanno valori inferiori ad 1 e leggermente più bassi nei bambini di 5–7 anni rispetto a quelli di 8–10. I risultati sembrano indicare l'esistenza di una correlazione tra fase di sviluppo e capacità di discriminazione dell'organismo dei suddetti radionuclidi nei confronti degli elementi stabili affini. Ulteriori ricerche sono in corso su ragazzi di 14–16 anni e su giovani adulti di 20–22 anni.

STRONTIUM AND CALCIUM METABOLISM IN CHILDREN OF VARIOUS AGES

H. N. WELLMAN, B. KAHN, A. SALEM and P. J. ROBBINS

Nuclear Medicine Section, Radiological Health Research Activities, Robert A. Taft Sanitary Engineering Center, Cincinnati, Ohio, Division of Radiological Health, Public Health Service, U.S. Department of Health, Education and Welfare (U.S.A.)

Abstract—As part of a study to determine the effect of age on ^{90}Sr retention by children, metabolic balance studies were performed with 3 children aged 6 years and 3 children aged 9 years. The children were selected as being normal on the basis of clinical history, physical examination, serum calcium, phosphorus, and alkaline phosphatase, routine laboratory tests and bone-age radiographs. The children were maintained in a metabolic ward for the 15-day balance period and were fed commercially available foods. A balanced diet, recommended by the National Research Council, provided normal intakes of all dietary components. The diet was consumed quantitatively during the balance period and for one month prior to the period. Diet, urine and feces were analyzed for calcium, phosphorus, stable strontium, and ^{90}Sr content.

The average daily intake of the 6-year-old children contained 1.34 g calcium, 1.36 phosphorus, 1.01 mg strontium, and 24 pCi ^{90}Sr; that of the 9-year-olds, 1.49 g calcium, 1.54 g phosphorus, 1.31 mg strontium, and 29 pCi ^{90}Sr.

There was a marked difference in the dietary components which contribute stable strontium and ^{90}Sr, with dairy products responsible for 70 per cent of ^{90}Sr, but only 40 per cent of stable strontium. Urine specific activities (pCi ^{90}Sr/mg Sr) in the children were approximately one-half that in the diet. In previously studied infants, for comparison, the ratio of urine specific activity to dietary specific activities was about 0.7. These specific activities would suggest either that ^{90}Sr was not as available from the diet as stable strontium, or that the skeleton was not yet in equilibrium with ^{90}Sr in comparison to stable strontium.

Mean observed ratios (O.R.) in infants have been found to be about 0.6. Mean O.R.s were 0.4 in 6-year-olds and 0.3 in 9-year-olds. This may indicate a trend downward toward the O.R. of 0.25 which has been found in most adult studies.

DISCUSSION

C. A. ADAMS (*U.K.*):

The solution in the form of the sum of three exponentials implies that the transfer between one compartment and the next is proportional to the amount of substance available in the first compartment. It is possible that other assumptions could give the same solution as an approximation. It would be of interest to know what assumptions were made.

A further question arises in connection with the dependence of the transfer rates on the amount of the available substance, if this amount is very greatly increased. Where blocking action is possible the implication is that the transfer rates can be reduced. It would be interesting to know if the authors have undertaken this analysis which I have carried out for a particular three compartment model. The solution is, however, dependent on the range of numerical values of some of the constants.

M. L. SHORE:

The model investigated represents a steady state system which follows first order kinetics relative to the tracer substance or radionuclide. The amount of tracer moving out of a compartment is determined by the constant amount of unlabeled compound moving out of the compartment per unit time, and constitutes a constant percentage of the total amount of compartmental radionuclide per unit time. In the strictest sense the triexponential equations presented apply only to the steady state systems. More practically, however, they can be used in those instances where systems approximate the steady state. Where very gross deviations from steady state occur, non-steady state kinetic equations must be derived. These are considerably more complex and may present a formidable problem to the mathematician. In the experiments described above it is assumed that a negligible amount of compound is injected as the radioactive tracer. Thus no alterations occur in the normal steady state metabolic dynamics of the system.

G. JOYET (*Switzerland*):

1. Je voudrais souligner l'importance considérable que représente pour le diagnostic l'adoption d'un schéma de compartiments, à la condition toutefois, que celui-ci soit adéquat. L'établissement du schéma et son contrôle expérimental demandent un travail préliminaire considérable. Mais quand le schéma est bien établi, le nombre des mesures peut être considérablement réduit.

2. Il faut remarquer que la loi de proportionnalité du passage d'un compartiment à l'autre ne s'applique plus au cas de certains compartiments tissulaires comme la thyroïde pour l'iode et la masse osseuse pour les os.

A. LAFONTAINE (*Belgium*):

J'ai été particulièrement intéressé par l'excellente communication de M. Thompson. Je me permet de lui poser deux questions tout en étant convaincu que la réponse apparaitra dans le texte intégral.

1. Sous quelle forme le Ca et le Sr ont ils été administrés et par quelle voie?

2. A-t-il été tenu compte des ions P et Mg dans le régime?

R. C. THOMPSON:

The details concerning which Dr. Lafontaine questioned will appear in the published version. Sr^{90} and Ca^{45} were injected intraperitoneally as the chlorides at approximately physiological pH. Phosphorus was present in all diets at a level of 0.5%, therefore the Ca/P ratio varied between diets. Mg was present at a constant level in all diets.

H. N. WELLMAN (*U.S.A.*):

I was wondering about the second component in the Sr curves; I don't believe it will resolve itself in such a clear exponential if you followed them much longer. At least in the children and the adults we are following, this is the case, and this has been previously reported by Cohn, also, and he had made a curve specifically. Anyway, after that first exponential it seems to be a constantly changing curve to which one could relate a single exponential, as it could be seen in our children and in our dogs. The second point I would like to comment on, the Ca curves clearly have different exponentials than the Sr curves, which is very interesting. I would like also to comment that our Ca curves versus Sr curves, in patients in which we have done both Ca^{47} and Sr^{85} studies simultaneously, are similar. There seem to be three, sometimes four, clearly visible exponentials for the Ca curves vs.

the one early exponential in the Sr curve and they are constantly changing their curves thereafter.

R. B. HOLTZMAN (*U.S.A.*):

Would Drs. Thompson and Wellman care to comment on the possibility of the power function fitting the data and the significance thereof? There is some evidence and a school of thought that the power function does have a significance similar to that of the exponential which represents a first order reaction kinetics. The power function represents n-th order kinetics. Other explanations of the significance of the power function are possible. [*Note added*: The power function is particularly useful in health physics in that if retention does fit this function it is easier from a measurement at a certain time to estimate the initial and subsequent dose rates. Unless a single exponential applies or the exacting details of the multiple exponential representation are known, retention estimates are more difficult than with a single power function.]

R. C. THOMPSON:

In response to the question concerning the use of "power function" vs. "exponential function" to describe data, I think it is important to keep in mind that the data represent neither a power function nor an exponential function, but, rather, a biological function. How we may choose to represent this biological function mathematically is purely a matter of expediency. For some purposes an exponential function may serve best; for other purposes a power function may be preferable. In this report I was not concerned with precise representation of the data, but rather with pointing out the marked differences between the observations on mature and growing animals, and this was more effectively accomplished by an exponential approach.

H. N. WELLMAN (*U.S.A.*):

I think I have to say much the same. I think that the power function is just a description of the curve; it really does not tell us anything biological. It is not a mathematical construction like the exponential which helps us in the kinetical analysis. It is just a mathematical description of the curve. I don't think it can help us.

R. C. THOMPSON:

What I want to say is that there are a few, perhaps, good ideas about what the power function does mean. It does have some significance which is close to that of the exponential, that is, an exponential represents a first order chemical kinetic reaction, while a power function represents one possibility of a changing order of a chemical kinetic reaction. All of this is rather a wild thing with respect to this particular system.

[*Note*: The discussion is interrupted by the Chairman, who invites the speakers to continue their discussion during the interval.]

H. N. WELLMAN (*U.S.A.*):

The abstract we presented represents the work on six children; we subsequently had data on nine more children and this is a continuing study and we will try to get at least ten children of various ages.

If anyone would like to look at detailed data, I have them with me.

R. J. DELLA ROSA (*U.S.A.*):

The work on beagles (University of California, Davis, California) following long term ingestion of Sr^{90} starting *in utero* suggests that at 3 years—following acquisition of body burden—both the power function model or a series of exponential functions can be used to describe the whole body (skeletal) retention of Sr^{90}. Continued follow-up in these animals (years) may shed further light on which of these two mathematical models can better describe the biology.

STRAHLENSCHUTZ-DOSIMETERSYSTEME ZUR VERBESSERTEN MESSUNG VON ENERGIEDOSEN

R. MAUSHART und E. PIESCH
Kernforschungszentrum Karlsruhe, Strahlenmeßdienst
75 Karlsruhe, BRD.

Zusammenfassung—Es werden Dosimetersysteme für die Dosisbestimmung von Quantenstrahlung beschrieben. Die Dosimeter unterscheiden sich von den bisherigen insofern als ihre Anzeige direkt proportional zur absorbierten Dosis ist. Die unterschiedliche Kalibrierung der Personendosimeter am Phantom und der Ortsdosimeter in Freiluftbestrahlung gestattet den Vergleich der Messwerte von Personen- und Ortsdosimetern.

Zur Anwendung im Strahlenschutz werden Dosimetersysteme beschrieben, die sich durch eine geringe Energie- und Richtungsabhängigkeit der Dosisanzeige auszeichnen. Die Verfasser zeigen, wie diese Dosimeter mit Hilfe von neuen Detektoranordnungen so ausgelegt werden können, dass sie die in einem bestimmten kritischen Organ absorbierte Energie-dosis anzeigen. Die spezielle Methode der Kalibrierung vermag die Einflüsse der Körperrückstreuung und der Körperorientierung in gewissen Grenzen herabzusetzen.

Die Beispiele von Dosimetersystemen zeigen, dass Strahlenschutzmessungen der absorbierten Energiedosis damit weitgehend realisiert werden können.

1. DAS MESSTECHNISCHE GRUNDPROBLEM DER STRAHLENSCHUTZDOSIMETRIE ÄUSSERER γ-STRAHLUNG

Die Strahlengefährdung einer Person wird letztlich durch die im jeweiligen kritischen Organ absorbierte Dosis (Organdosis in rad) beschrieben. Dosismeßgeräte zeigen jedoch nach den heute üblichen Meß- und Kalibriermethoden eine Bestrahlungsdosis (in Röntgen) an,—die Ortsdosimeter eine Freiluft-Bestrahlungsdosis, die Personendosimeter eine Bestrahlungsdosis an der Körper- oder Phantomoberfläche. Dies führt dazu, daß nicht nur der jeweilige Meßwert des Dosimeters auf die Organdosis umgerechnet werden muß, wozu im allgemeinen die Kenntnis der Energieverteilung der einfallenden Strahlung Voraussetzung ist, sondern daß auch die Anzeigen von Ortsdosimeter und Personendosimeter im gleichen Strahlungsfeld verschieden ausfallen.

Bei einer Bestrahlung des Körpers von außen gibt es nur einige wenige Organe, die als kritisch gelten. Das sind für kleine Strahlendosen und Langzeit-Strahleneinwirkung die Gonaden, für Kurzzeitbestrahlung und hohe Strahlenbelastung (Unfall) die blutbildenden Organe (Knochenmark). Bei Teilkörperbestrahlungen oder bei sehr energiearmer Quantenstrahlung können die Haut oder die Augen kritisches Organ sein.

Es ist das grundlegende Problem der Strahlenschutzdosimetrie, das für die jeweiligen Bestrahlungsbedingungen gültige kritische Organ —nämlich dasjenige, welches mit der größten Wahrscheinlichkeit am stärksten geschädigt wird—anzugeben und aus dem Dosimetermeßwert die im kritischen Organ absorbierte Dosis zu bestimmen.

2. MÖGLICHKEITEN ZUR BESTIMMUNG DER IM KRITISCHEN ORGAN ABSORBIERTEN DOSIS

Da die im Organ absorbierte Dosis allenfalls bei medizinischen Bestrahlungen, nicht aber im praktischen Strahlenschutz durch ein eingepflanztes Dosimeter direkt ermittelt werden kann, ist ihre Bestimmung aus den Messungen des äußeren Strahlungsfeldes immer nur mit mehr oder weniger guter Annäherung möglich. Es gibt dazu zwei verschiedene Wege. Der eine besteht in der Berechnung der Organdosis. Er ist im Prinzip immer gangbar, wenn die notwendigen Daten bekannt sind. Man braucht dazu außer der Energieverteilung der einfallenden Strahlung (und evtl. ihrer Einfallsrichtung zum Körper bzw. Dosimeter) die Energieabhängigkeit der Dosimeteranzeige und natürlich den ebenfalls energieabhängigen Umrechnungsfaktor der Freiluft-Bestrahlungsdosis auf die absorbierte Organdosis, der mittels Phantommessungen ermittelt werden kann. Die Zuverlässigkeit dieser Methode steht und fällt daher mit der Genauigkeit, mit der man die Energieverteilung kennt. Es ist andererseits ihr großer, unbestreitbarer Vorteil, daß sie allen vorkommenden Fällen angepaßt werden kann und auch die Dosen in verschiedenen Organen aus dem gleichen Meßwert gewonnen werden können.

Der andere Weg zur Bestimmung der Organdosen ist rein meßtechnischer Art. Er darin, daß durch geschickte konstrukt staltung des Dosimeters und durch Kalil sowohl des Orts- wie des Personendo auf Energie-statt auf Bestrahlungsdosen c meteranzeige über einen möglichst große giebereich direkt proportional der in vorgegebenen Organ absorbierten Dosis g wird. Die Kenntnis der Energieverteil Bestimmung der Organdosis wird dar nötig.

Die technische Ausführung solcher Do wird im folgenden am Beispiel eines Or eines Personendosimeters beschrieben. kann auch gezeigt werden, daß die Meßanordnung durch einfachen Wech Dosimeter-Hülle die absorbierte Dosis i schiedenen Organen jeweils energiepropo wiederzugeben vermag.

Orts- und Personendosimeter untersc sich insofern, als das erstere die Freilu das letztere die Oberflächendosis am I oder Phantom mißt, die bis zu 60% als die Freiluftdosis sein kann (siehe Abb. 1 Auch wenn man den Meßwert nicht a bestimmtes Organ beziehen will, ersche sinnvoll, diesen Einfluß des Körper das Personendosimeter auf alle Fälle Kalibrierung am Phantom so gut wie m mit zu berücksichtigen. Die Vorteile neuen Konzeption einer Strahlenschut

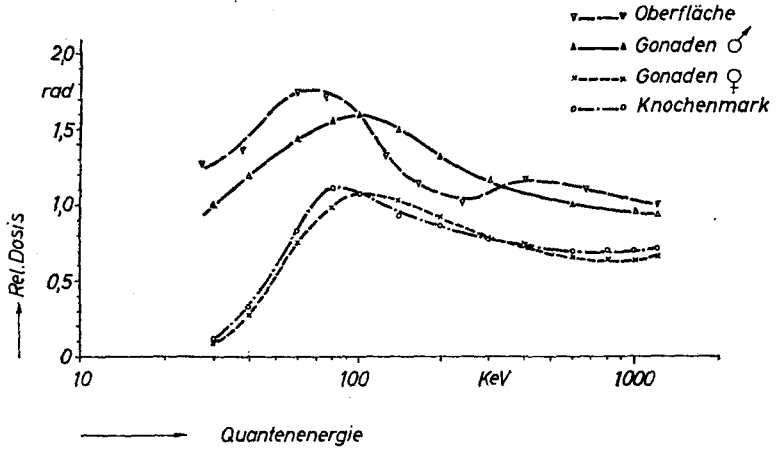

ABB. 1. Die Energiedosis in verschiedenen Organen eines Mensch-Phantoms bezogen auf die Bestrahlungsdosis 1 R in Abhängigkeit von der Quantenenergie nach (1,2).

metrie sind von einem der Autoren bereits mehrfach dargelegt worden.[3, 4]

Die in diesem Vortrag angegebenen Versuche und Meßwerte beschränken sich auf Einstrahlungen aus dem vorderen Halbraum des Körpers. In Fortsetzung der hier begonnenen Arbeiten werden jedoch auch von der Einfallsrichtung unabhängige Dosimetersysteme entwickelt.

3. DETEKTOREN UND BESTRAHLUNGSBEDINGUNGEN

Im folgenden wird am Beispiel eines Ortsdosisleistungs-Meßgerätes und am Beispiel verschiedener Phosphatglas-Personendosimeter gezeigt, in welchem Maße die Dosimeteranzeige, unabhängig von der Energieverteilung der einfallenden Strahlung, der Energiedosis im vorgegebenen kritischen Organ entsprechen kann.

Als Ortsdosismeßgerät wurde ein Proportionalzählrohr (Typ Tol D) mit Aluminiumwandung benutzt, dessen Energieabhängigkeit durch verschiedene Metallfilterkombinationen im gewünschten Maß verändert wurde. Als Personendosimeter wurden Yokota-Gläser der Abmessungen $8 \times 8 \times 4,7\ mm^3$[5] sowohl in einer Kugelkapselung mit konischen Öffnungen[6] untersucht, wie sie bereits als Routine-Personendosimeter eingesetzt werden[9] (Phosphatglasdosimeter I), als auch in einer Kugelkapselung mit gegenüber der Routinekugelkapselung veränderter Metallfilterung (Phosphatglasdosimeter II).

Für die Energieabhängigkeit der in den kritischen Organen absorbierten Dosis wurden die von Jones[1, 2] an einem Menschphantom mit LiF-Dosimetern bestimmten Meßwerte bei Vordereinstrahlung (Ausnahme beim Knochenmark, Rückwärtseinstrahlung) zugrundegelegt (siehe Abb. 1).

Auch die folgenden Untersuchungen wurden an einem Alderson-Menschphantom durchgeführt. Die Bestrahlungen erfolgten mit hartgefilterter Röntgenstrahlung bzw. γ-Strahlung verschiedener Energien (Tab. 1). Die Dosiswerte wurden mit zwei Sekundärstandards bestimmt, deren Anzeige von der Physikalisch-Technischen Bundesanstalt in Braunschweig auf eine Bestrahlungsdosis kalibriert worden war (Philips Ionisationskammer Nr. 37486 in Verbindung mit Universal-Dosimetern, sowie Proportionalzählrohr Tol D).

4. DOSISLEISTUNGSMESSGERÄT ZUR ENERGIEUNABHÄNGIGEN BESTIMMUNG DER ABSORBIERTEN DOSIS

Die Anzeige des verwendeten Proportionalzählrohres mit Aluminiumwandung weist zunächst eine ausgeprägte Energieabhängigkeit auf. Es wurden aber verschiedene Filterkombinationen experimentell ermittelt, welche wahlweise über das Zählrohr geschoben werden können und welche durch selektive Schwächung der Quantenstrahlung eine jeweils einer anderen Energiedosis proportionale Anzeige ergeben.

Die Filterhülle I (0,8 mm Zinn mit 80% Flächenbelegung) erzielt beispielsweise eine energieunabhängige Dosisleistungsanzeige der Bestrahlungsdosis im Energiebereich 25 keV bis 1,2 MeV innerhalb $\pm$ 12% (Abb. 2).

Die Verwendung der Filterkombination II (0,4 mm Zinn mit 80% Flächenbelegung) gestattet hingegen die annähernd energieunabhängige Dosisleistungsmessung einer Gonaden- oder einer Oberflächendosis (Abb. 3). Die Anzeige der Gonadendosis ist hierbei oberhalb 25 keV innerhalb $\pm$ 7%, die Anziege der Oberflächendosis oberhalb 30 keV innerhalb $\pm$ 16% energieunabhängig. Durch andere Filterkombinationen kann auch die annähernd energieunabhängige Anzeige der Knochenmarksdosis erreicht werden.

Das benutzte Dosisleistungsgerät (Handgerät in transistorisierter Ausführung, Meßbereich 10 μR/h bis 100 mR/h bzw. durch Nachkalibrierung bis 100 R/h) gestattet folglich durch Auswechseln von Zählrohrhüllen die wahlweise Bestimmung einer Freiluft-Bestrahlungsdosis oder einer gewünschten absorbierten Dosis im Organ. Für routinemäßige Strahlenschutzmessungen sollte vor allem die Gonadendosis von Interesse sein.

5. PERSONENDOSIMETER ZUR ENERGIEUNABHÄNGIGEN BESTIMMUNG DER ABSORBIERTEN DOSIS

Ein in der praktischen Routinedosimetrie verwendetes Phosphatglasdosimeter mit Kugelkapselung (Phosphatglasdosimeter I) erzielt bei Freiluftbestrahlung im Energiebereich von 45 keV bis 1,2 MeV eine Energieunabhängigkeit

Tabelle 1. *Verwendete Strahlenqualitäten*

Röhrenspannung (kV)	Filterkombination I: Zusatzfilterung (mm)	Filterkombination I: angenommene, eff. Quantenenergie (keV)
Co-60		1200
Cs-137		660
300	2 Al + 5 Cu + 10,5 Pb	270
200	2 Al + 5 Cu + 4 Sn + 2 Pb	185
130	2 Al + 7,5 Cu + 2 Sn	108
100	2 Al + 2 Cu + 1,5 Pb	80
78	2 Al + 3,5 Cu	65
56	2 Al + 1,2 Cu	50
45	2 Al + 1,35 Cu	40
35	2 Al + 0,5 Cu	30
25	2 Al + 0,15 Cu	20
15	0,2 Al + 0,1 Cu	10

Röhrenspannung (kV)	Filterkombination II: Zusatzfilterung (mm)	Filterkombination II: angenommene, eff. Quantenenergie (keV)
300	2 Al + 5 Cu + 3,5 Pb	240
250	2 Al + 5 Cu + 2 Pb	200
220	2 Al + 5 Cu + 1,2 Pb	170
200	2 Al + 5 Cu + 0.9 Pb	150
180	2 Al + 11 Cu	135
150	2 Al + 7 Cu	110
120	2 Al + 3,5 Cu	87
100	2 Al + 2 Cu	71
80	2 Al + 0,7 Cu	55
70	2 Al + 0,4 Cu	46
60	2 Al + 0,2 Cu	38

* Die Kalibrierung der Dosisleistungsmeßgeräte erfolgte mit Filterkombination I, der Personendosimeter mit Filterkombination II.

bis auf ± 8%.[6] Die Anzeige des an der Person getragenen Dosimeters wird jedoch im Vergleich zur Freiluftbestrahlung durch den Einfluß der Körperrückstreuung verändert. Das Dosimeter wurde daher an der Oberfläche des Menschphantoms mit verschiedenen Strahlungsenergien bestrahlt. Abb. 4 gibt die relative Anzeige des Kugeldosimeters am Phantom in Abhängigkeit von der Quantenenergie wieder. Die Anzeige der Bestrahlungsdosis ist demnach oberhal keV auch am Phantom innerhalb ± 14% gieunabhängig. Bei Ionisationskammern auch bei gewissen Filmdosimetern wird dings ein größerer Einfluß des Phantoms au Dosisanzeige festgestellt.

Die Personendosisbestimmung mit dem I phatglasdosimeter I würde somit—abges vom unterschiedlichen Körpereinfluß bei

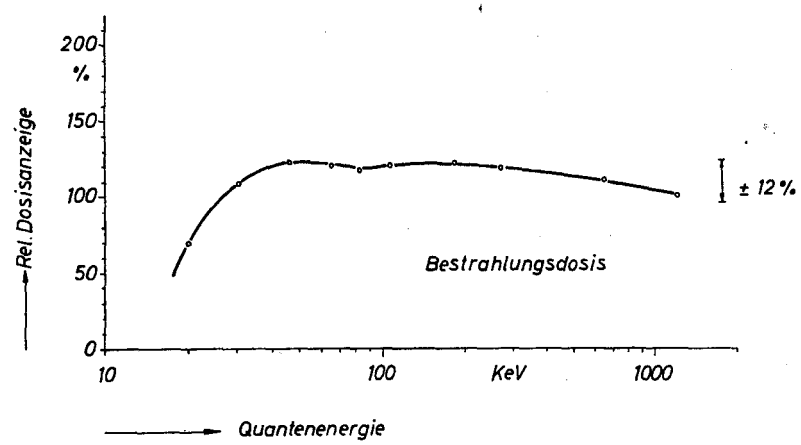

ABB. 2. Die relative Dosisempfindlichkeit des Proportionalzählers I mit Al-Wand und einer Filterkombination aus 0,8 mm Sn bei 80% Flächenbelegung bezogen auf die Bestrahlungsdosis 1 R in Abhängigkeit von der Quantenenergie.

schiedenen Personen oder bei rückwärtiger Strahleneinfallsrichtung—am Phantom annähernd dieselbe Dosis anzeigen wie ein am gleichen Ort in Abwesenheit des Phantoms exponiertes Ortsdosimeter. Abb. 5 zeigt nun die Änderung der relativen Dosisanzeige des Phosphatglasdosimeters I, wenn der Meßwert anstelle einer Bestrahlungsdosis auf eine absorbierte Gonadendosis oder Knochenmarksdosis bezogen wird. Für die Anzeige der Gonadendosis wird hierbei oberhalb 45 keV innerhalb ± 18% Energieunabhängigkeit erzielt; das Dosimeter eignet sich demnach gleichermaßen zur Bestimmung der Gonadendosis.

Durch Änderung der Kugelkapselung (neue Kapselung bestehend aus 1,2 mm Zinn mit 85% Flächenbelegung) erhält man eine relative Anzeige, die in Abb. 6 für Freiluftbestrahlung und für Phantombestrahlung in Abhängigkeit von der Quantenenergie wiedergegeben ist. Ein

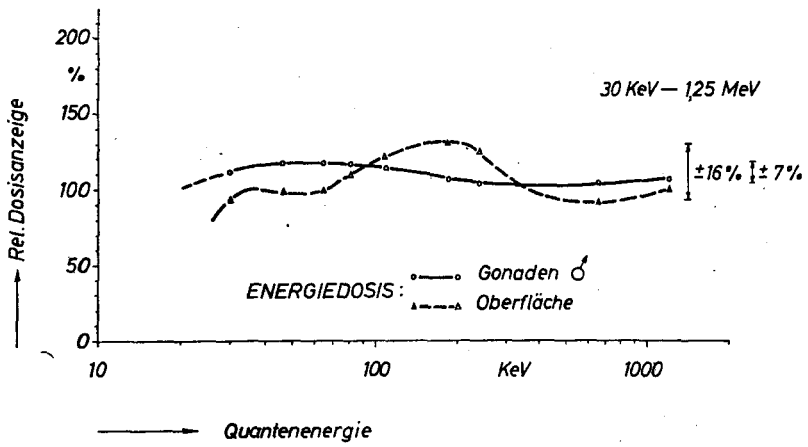

ABB. 3. Die relative Dosisempfindlichkeit des Proportionalzählers II mit Al-Wand und einer Filterkombination aus 0,4 mm Sn mit 80% Flächenbelegung bezogen auf die Energiedosis 1 rad in Abhängigkeit von der Quantenenergie. o–o–o Energiedosis in den Gonaden ♂. △–△–△ Energiedosis an der Oberfläche.

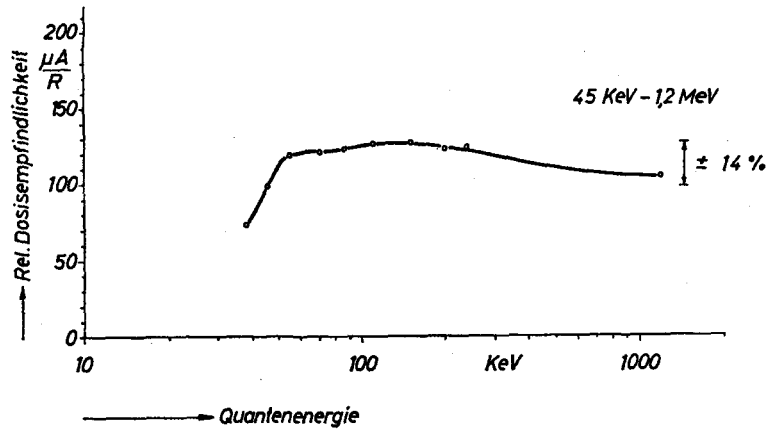

ABB. 4. Die relative Dosisempfindlichkeit des Phosphatglasdosimeters I (Phosphatglas in Kugelkapselung) [6] an der Oberfläche eines Mensch-Phantoms bezogen auf die Bestrahlungsdosis 1 R in Abhängigkeit von der Quantenenergie.

solcher Personendosimeter zeigt bei einer Phantombestrahlung nicht mehr proportional der Bestrahlungsdosis an. Wird die Anzeige des Dosimeters jedoch auf die Energiedosis in den Gonaden bzw. im Knochenmark bezogen, dann erhält man in beiden Fällen eine annähernd energieunabhängige Energiedosisanzeige des am Phantom getragenen Personendosimeters.

Wenn das Dosimeter für die Anzeige der Energiedosis in den Gonaden kalibriert wird, dann kann aus dem so gewonnenen Meßwert die Energiedosis im Knochenmark durch Berücksichtigung eines für alle Strahlungsenergien einheitlichen Korrekturfaktors (Faktor 1,6) erhalten werden. Da auch die in den Eierstöcken absorbierte Dosis etwa dieselbe Energieabhängigkeit zeigt wie die Energiedosis im Knochenmark, kann auf gleiche Weise die Energiedosis in den Eierstöcken bestimmt werden (es gilt somit: Dosismeßwert = Energiedosis in den

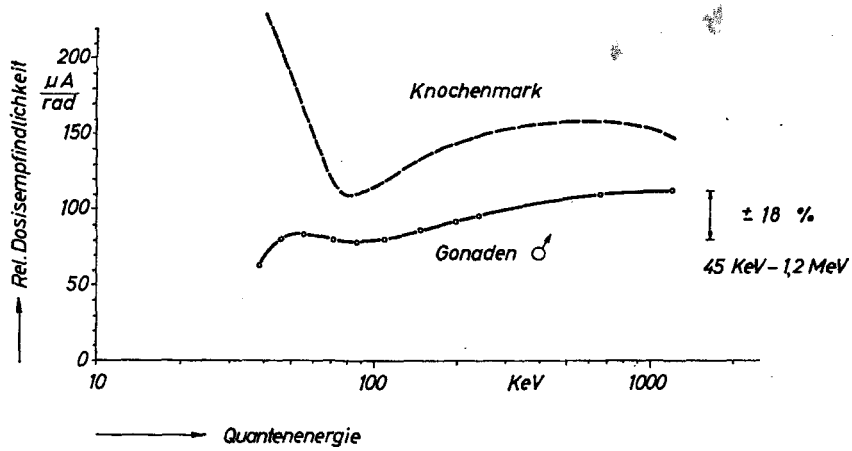

ABB. 5. Die relative Dosisempfindlichkeit des Phosphatglasdosimeters I (Phosphatglas in Kugelkapselung) [6] an der Oberfläche eines Mensch-Phantoms bezogen auf die Energiedosis 1 rad im Knochenmark und in den Gonaden ♂ in Abhängigkeit von der Quantenenergie.

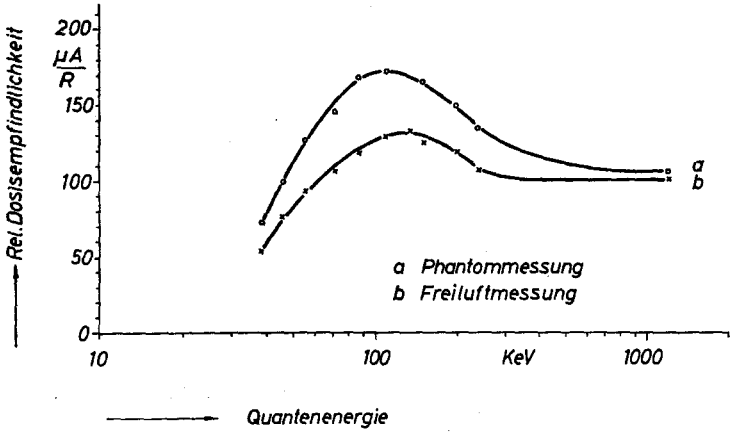

ABB. 6. Die relative Dosisanzeige des Phosphatglasdosimeters II bezogen auf die Bestrahlungsdosis 1 R in Abhängigkeit von der Quantenenergie. x–x–x Freiluftmessung. o–o–o Phantommessung.

Gonaden (Hoden) = 1,6 × Energiedosis im Knochenmark ≈ 1,6 × Energiedosis in den Gonaden (Eierstöcke)).

Alle Energiedosismessungen sind oberhalb 45 keV bzw. 50 keV innerhalb ± 15% energieunabhängig (Abb. 7 und 8). Aus den Meßwerten des Personendosimeters kann damit wahlweise ohne Kenntnis der Quantenenergie im Energiebereich 45 keV bis 1,2 MeV die gewünschte Energiedosis ausreichend genau ermittelt werden.

Damit werden mit einem einzigen, nur ein Meßelement enthaltendes Dosimeter (Einfach-Dosimeter) in dem für die Kerntechnik hauptsächlich interessierenden Energiebereich die Energiedosen in allen wichtigen kritischen

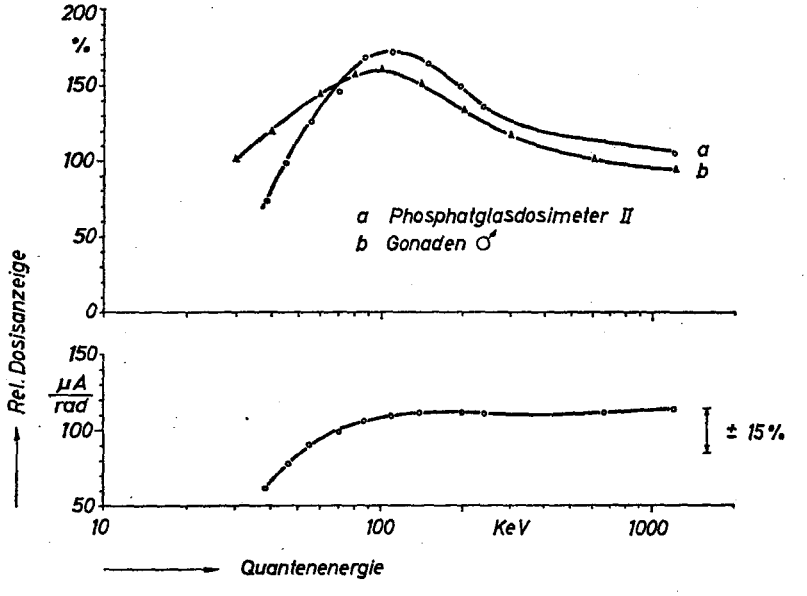

ABB. 7. Die relative Dosisanzeige des Phosphatglasdosimeters II an der Oberfläche eines Mensch-Phantoms bezogen auf die Bestrahlungsdosis 1 R bzw. auf die Energiedosis in den Gonaden 1 rad in Abhängigkeit von der Quantenenergie.

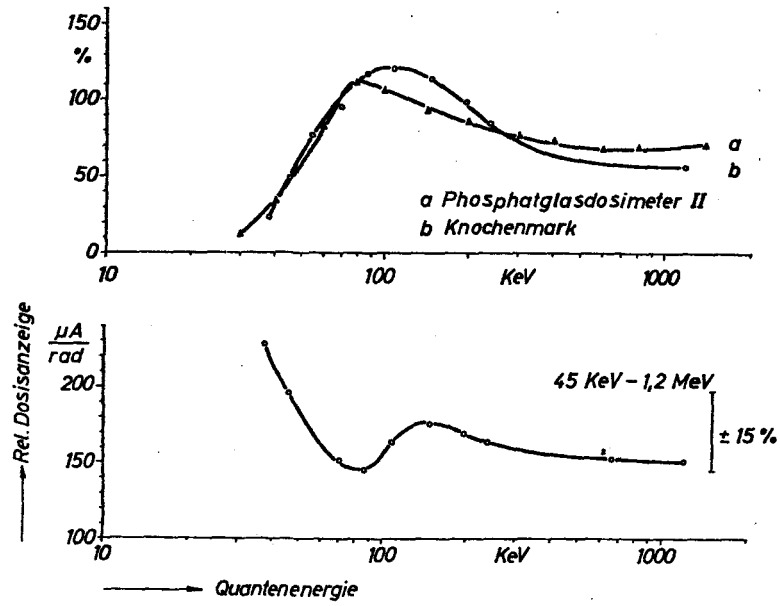

ABB. 8. Die relative Dosisanzeige des Phosphatglasdosimeters II an der Oberfläche eines Mensch-Phantoms bezogen auf die Bestrahlungsdosis 1 R bzw. auf die Energiedosis 1 rad im Knochenmark in Abhängigkeit von der Quantenenergie.

Organen ohne rechnerische Ermittlung direkt gemessen. Der Meßwert und die Zuordnung zur Energiedosis ist allerdings bisher nur für eine frontale Strahleneinfallsrichtung gültig.

6. FOLGERUNGEN FÜR DIE STRAHLENSCHUTZDOSIMETRIE

Am Beispiel des Phosphatglas-Kugeldosimeters wurde gezeigt, daß die von uns angestrebte Übereinstimmung der Meßwerte von Personendosimeter und Ortsdosimeter mit befriedigender Genauigkeit erreicht werden kann. Das beschriebene Glasdosimeter mißt auch bei Verwendung als Personendosimeter an der Oberfläche des Trägers die Freiluftbestrahlungsdosis. In genügend guter Näherung entspricht der Meßwert auch der Energiedosis in den Gonaden (Hoden). Das vorliegende Dosimeter eignet sich demnach für die Routineüberwachung der Personendosis, wenn und solange wie die Angabe der Bestrahlungsdosis für die Ortsdosimetrie bindend ist.

Es scheint uns jedoch aus den zu Beginn angeführten Gründen immer noch der Vorschlag erwägenswert, Ortsdosismessungen statt auf eine Freiluftbestrahlungsdosis auf eine Organdosis zu beziehen. Bei kleineren Dosisleistungen (Umgebungsüberwachung, Arbeitsplatzüberwachung, Abgrenzung von Kontrollbereichen) ist für strahlenexponierte Personen vor allem die genetische Schädigung von Interesse. Es wurde hier erstmalig gezeigt, daß mit geeigneten Dosisleistungsmeßgeräten durch Austausch der Filterkombination anstelle einer Bestrahlungsdosis unabhängig von der Energie die Energiedosis in den Gonaden bestimmt werden kann. Weiterhin kann mit den bisher in der Routinedosimetrie verwendeten Kugeldosimetern direkt am Dosimeterträger ebenfalls die Gonadendosis mit ausreichender Genauigkeit angezeigt werden. Veränderte Kapselungen bieten darüberhinaus die Möglichkeit, außer der Gonadendosis der Hoden auch die der Eierstöcke oder die Knochenmarksdosis energieunabhängig anzuzeigen. Dasselbe Dosimeter könnte damit bei der Routineüberwachung die Gonadendosis und bei einem möglichen Unfall die Dosis in den blutbildenden Organen anzeigen.

Wenn der Anzeigewert in beiden Fällen auf Energiedosis in den Gonaden bezogen wird, ist

damit für Energien oberhalb 45 keV die Übereinstimmung zwischen Personen- und Ortsdosismessung erreicht und zugleich der wirklich interessierende Meßwert "Gonadendosis" ohne Umrechnung unmittelbar zugänglich.

Allerdings wird die Realisierung unseres Vorschlages erst sinnvoll, wenn gesichert ist, daß die Gesamtgenauigkeit und Zuverlässigkeit der Personendosismessung besser oder zumindest vergleichbar ist in bezug auf die Fehlergrenzen, innerhalb derer sich die Abweichungen von Bestrahlungs- und Organdosen bewegen.

Bei der Verwendung der bisherigen konventionellen Personendosimeter (Filmdosimeter) war es letzten Endes unwesentlich, welche Dosisgröße zugrundegelegt wurde und in welchem Maße die Personendosis mit der Ortsdosis übereinstimmte. Filmdosimeter zeigten selbst bei definierten Bestrahlungen in Deutschland in über 50% der Fälle Abweichungen $> \pm 10\%$ und in fast 20% der Fälle Abweichungen von $> \pm 25\%$,[7] in den Vereinigten Staaten wurden bei einzelnen Auswertestellen in 50% der Fälle Abweichungen von $> \pm 50\%$ festgestellt.[8] Demgegenüber zeigten Glasdosimeter auch im Routineeinsatz nur in 25% der Fälle Abweichungen $> \pm 10\%$ und in 12% der Fälle Abweichungen von $> \pm 15\%$.[9] Die besseren physikalischen Eigenschaften der Phosphatgläser, vor allem aber die erwiesenermaßen höhere Meßgenauigkeit auch bei routinemäßigem Einstaz, lassen es diskutierenswert erscheinen, ob nicht auch diese geringen, aber jetzt deutlicher als bisher bei der Strahlenschutzüberwachung in Erscheinung tretenden Unstimmigkeiten zwischen Personendosimetrie und Ortsdosimetrie durch das vorgeschlagene Konzept ausgeschlossen werden sollten.

LITERATUR

1. A. R. Jones. FSHPS Symposium, Paris, 1964.
2. A. R. Jones. Proposed calibration factors for various dosimeters at different energies. *Health Physics* **12,** 663 (1966).
3. E. Piesch. A concept of Health Physics dosimetry for quantum radiation, *Health Physics* **13,** 759 (1967).
4. E. Piesch. Das Konzept einer Ganzkörperdosis für Quantenstrahlung und ihre meßtechnische Verwirklichung in der Personendosimetrie. Bericht an den Arbeitskreis IV/2 der Deutschen Atomkommission, unveröffentl.
5. R. Yokota und S. Nakajima. High sensitivity silver-activated phosphate glasses for the simultaneous measurement of thermal neutrons, γ- and/or β-rays. *Health Physics* **5,** 219 (1961).
   R. Yokota und S. Nakajima. Improved fluoroglass dosimeters as personnel monitoring dosimeter and microdosimeter. *Health Physics* **11,** 241 (1965).
6. E. Piesch. Eine neue Glasdosimeterkapselung zur energie- und richtungsunabhängigen Dosisbestimmung von Quantenstrahlung. *Direct Information* 17/1964.
   R. Maushart und E. Piesch. Photoluminescent personnel dosimeter with spherical case for energy and direction-independent dose measurement. FSHPS Symposium, Paris, 1964.
   R. Maushart und E. Piesch. Phosphate glasses as routine personnel dosimeters. Int. Conference on Luminescence Dosimetry, Stanford, 1965.
7. F. Wachsmann und G. Drexler. Ergebnisse der Auswertung der von der PTB in den Jahren 1961–1964 für die Erlanger *Auswertestelle* bestrahlten Kontrollfilme. *Atompraxis* **11,** 2, 93 (1965).
8. R. O. Gorson, N. Suntharalingam und J. W. Thomas. Results of a film-badge reliability study. *Radiology* **84,** 333 (1965).
9. E. Piesch. Intercomparison of results for film, glass, and ionisation chamber dosimeters in routine personnel monitoring. *Radiation Dose Measurements,* Paris, 1967, p. 151.

MÉTHODES DE MESURE SIMULTANÉE D'ÉQUIVALENT DE DOSE *(DE)* ET DE COEFFICIENT DE QUALITÉ *(QF)* DE RAYONNEMENTS MIXTES

S. PSZONA, M. ZIELCZYŃSKI et K. ŻARNOWIECKI

Service de Protection Contre les Radiations, Institut des Recherches Nucléaires, Otwock, Świerk, Pologne

Résumé—Pour mesurer directement *DE* et *QF* on peut utiliser des détecteurs dont la sensibilité depend du *TEL*. On a mis au point une chambre differentielle à recombinaison permettant de mesurer l'équivalent de dose de n'importe quelle radiation mixte directement en rem/heure. Pour les mesures simultanées de *DE* et *QF* on utilise une chambre double et deux électromètres.

Le compteur à scintillation permet aussi de mesurer *DE* et *QF* pour un rayonnement mixte.

POUR établir l'équivalent de dose (*DE*), le paramètre le plus fondamental de la protection contre les radiations, il faut connaître la valeur de la dose absorbée par le tissu (*D*) et le coefficient de qualité (*QF*) du rayonnement, lequel est fonction du transfert d'énergie linéique (*TEL*). Ce n'est qu'en certains cas exceptionnels que la grandeur de *QF* est constante et connue, ou même égale à l'unité. Le plus souvent on rencontre plusieurs types ou énergies de radiation, de *QF* différent. En particulier, des rayonnements mixtes sont produits pendant le fonctionnement des accélérateurs, dont le rayonnement primaire provoque de nombreuses réactions nucléaires et pendant le fonctionnement des réacteurs, lesquels émettent des radiations gamma et neutronique ayant un large spectre d'énergie. À ce type appartient aussi le rayonnement cosmique primaire et secondaire dont la composition depend de l'altitude et dont les effets biologiques ne sont pas encore suffisamment etudiés. Jusqu'à présent, il n'existait pas d'appareil de mesure gradué en rem permettant facilement de déterminer l'équivalent de dose d'un rayonnement de nature quelconque. Dans plusieurs laboratoires on mesure encore les doses absorbées par les flux de rayonnements de types divers successivement, avec differents appareils et ensuite on calcule l'équivalent de dose grâce à des valeurs de *QF* théoriques adoptés a priori.

Au Service de Protection Contre les Radiations de l'Institut des Recherches Nucléaires en Pologne les études de méthodes de mesure directe de *QF* et *DE* sont poursuivies depuis quelques années.*

On a la possibilité d'utiliser diverses sortes de détecteurs dont la sensibilité dépend du *TEL*. L'analyse théorique effectuée[1] prouve que la quantité de détecteurs indispensables à la mesure de *QF* dépend du caractère de la relation entre la réponse et le *TEL*. Actuellement la méthode de recombinaison colonnaire[2-4] est la plus developpée et la meilleure pour les mesures en physique de santé appliquèe.

Grâce à cette méthode nous avons mis au point un dispositif transportable composé d'un électromètre et d'une chambre d'ionisation différentielle d'équivalence tissulaire. Ce dispositif permet de mesurer directement l'intensité de l'équivalent de dose en rem/heure de n'importe quelle radiation mixte traversant les parois de la chambre. La chambre est du type multicellulaire à électrodes plates. Une moitié de cette chambre double est une chambre ordinaire à mesurer la dose absorbée. La seconde partie, de construction semblable, est alimentée en tension plus basse.

En conséquence son courant peut être diminué par la recombinaison colonnaire. Cet effet

* Actuellement sous contrat de l'AIEA.

devient plus fort si la densité de l'ionisation le long des traces de particules augmente. Si on choisit une certaine tension particulière on peut obtenir une relation linéaire entre l'efficacité de collection d'ions et QF. Dans ce cas le courant différentiel sera proportionnel à la dose D et à QF. Il est alors aussi proportionnel au DE:

$$DE = D \cdot QF = ai \qquad (1)$$

où: i = courant de la chambre différentielle,
a = coefficient constant de la chambre.

La sensibilité de l'appareil est de 1 mrem/heure environ. La limite supérieure de la mesure depend du QF du rayonnement et va de 10 rem/h pour $QF = 1$ jusqu'à plus de 200 rem/h pour $QF = 10$. Si l'intensité du rayonnement est très grande, outre la recombinaison colonnaire apparaît aussi la recombinaison de volume et l'efficassité de collection d'ions est trop petite. Les traveaux sur l'application de la méthode aux intensités plus élevées sont en cours. Comme suite à nos études, la réalisation d'un appareil portatif à chambre differentielle est prévue. La développement d'un dosimètre individuel est en projet.

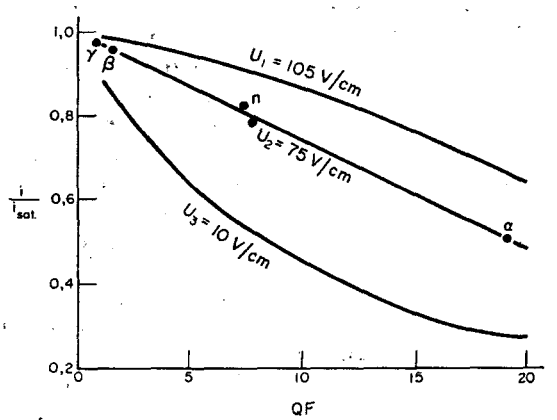

FIG. 1. Relation entre la sensibilité de la chambre à recombinaison et QF de diverses radiations.
i, courant de la chambre. i_{sat}, courant de saturation. U, tension entre les électrodes. Les points d'étalonage correspondent aux radiations: gamma (^{60}Co), beta (^{3}H), neutronique (Po-Be et Po-B) et alpha (^{235}U).

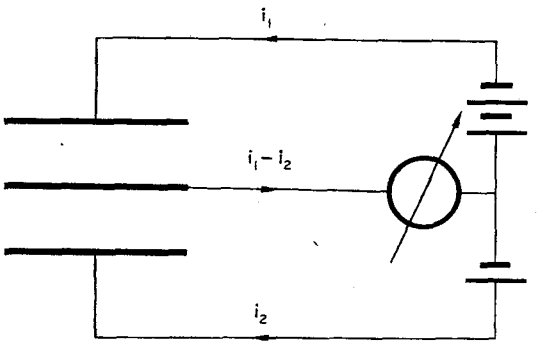

FIG. 2. Principe de la mesure de DE avec une chambre differentielle à recombinaison.

Dans le cas où il est important de connaître non seulement DE, mais aussi QF, on utilise une chambre semblable mais munie de deux électromètres, un pour chaque moitié de chambre. Les relations entre les deux courants et les grandeurs mesurées sont tout à fait simples

$$D = \frac{a}{b} i_1 \qquad (2)$$

$$QF = b\left(1 - \frac{i_2}{i_1}\right) \qquad (3)$$

$$DE = a\,(i_1 - i_2) \qquad (4)$$

où: i_1 = courant de saturation,
i_2 = courant de la chambre de recombinaison,
a, b = coefficients constants de la chambre.

Après avoir comparé les résultats des mesures effectuées, grâce à la méthode développée, aux valeurs de QF généralement fixées[5] nous estimons que la précision de la méthode est de 25% environ. Cette précision semble tout à fait suffisante à cause de la relation peu certaine entre QF et les effets biologiques des irradiations par les rayonnements de TEL divers. En utilisant la méthode de recombinaison nous avons mesuré les QF des radiations suivantes:

—rayonnement secondaire d'un faisceau de protons entre 3 et 10 GeV d'un synchrotron;[6]

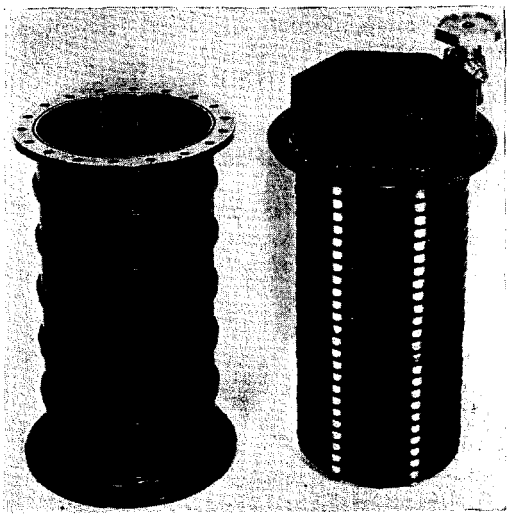

FIG. 3. Une des chambres differentielles à recombinaison (démontée).

—protons de 680 MeV d'un synchrocyclotron;[6]
—protons entre 150 et 660 MeV dans un fantôme;[7]
—neutrons de 660 MeV dans un fantôme;[8]
—neutrons de 14 MeV;[7]
—neutrons d'une source Po-Be dans un fantôme;[3]
—radiation mixte d'un réacteur.[9]

La première chambre à recombinaison fut construite par M. Zielczyński en 1960 durant son séjour à l'Institut Reuni à Dubna[2, 3] et elle est en service dans le laboratoire des énergies élevées. Indépendamment, un peu plus tard, une autre méthode, dérivée aussi du principe de recombinaison colonnaire, fut développée au CERN. Les mesures et le traitement des résultats sont dans cette méthode assez compliqués et prennent beaucoup de temps. C'est pourquoi l'application de cette méthode est limitée. Surtout il est impossible de l'appliquer dans le cas ou le rayonnement est variable.

Outre la méthode de recombinaison, les travaux sur la méthode de mesure de *QF* au moyen d'un compteur à scintillation ont été poursuivis. Le courant de ce compteur est une fonction approximativement linéaire du *QF* des radiations gamma et neutronique. En conséquence le compteur à courant, muni d'un scintillateur organique bien choisi, couplé à un détecteur mesurant la dose absorbée (p.e. une chambre d'ionisation) permet de mesurer *DE* et *QF* des radiations gamma et neutronique. Á partir des neutrons d'une source Po-Be et de 14 MeV on a obtenu respectivement $7{,}2 \pm 0{,}7$ et $6{,}9 \pm 0{,}4$. Ces résultats sont tout à fait compatibles avec les valeurs généralement fixées.[5]

Dans une autre méthode étudiée on utilise le fait que le rapport de la composante rapide par la composante lente de scintillation du stilbène dépend du *TEL*. On a constaté que la composante lente est proportionelle à l'énergie de la particule absorbée par le scintillateur. Le rapport de la composante rapide à la composante lente est une fonction décroissante du *TEL*. Cette méthode permettra d'étudier les distributions de *DE* en fonction de *QF* pour les radiations mixtes gamma et neutronique.

L'utilisation des méthodes par scintillation en physique de santé appliquée exige encore certainement de nombreux travaux.

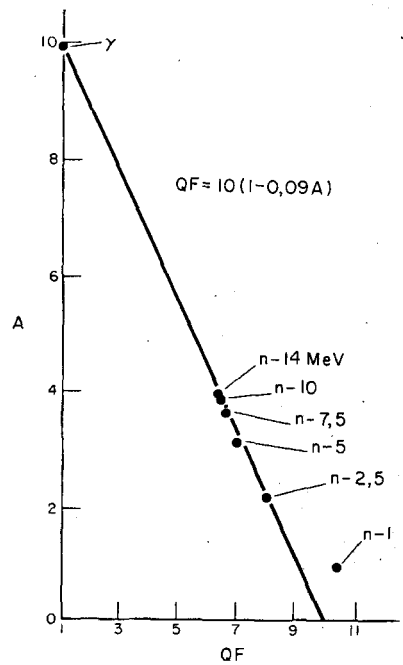

FIG. 4. Relation entre la reponse du compteur à scintillation et les *QF* de radiations gamma et neutronique.

RÉFÉRENCES

1. M. Zielczyński. International Symposium on Neutron Monitoring for Radiological Protection, Vienna, 29 août—2 septembre 1966. Communication SM-76/39.
2. M. Zielczyński. *Nukleonika* **7,** No. 3, 175 (1962).
3. M. Zielczyński. *Neutron Dosimetry,* Vol. II, 397. IAEA, Vienna, 1963.
4. M. Zielczyński et K. Żarnowiecki. International Symposium on Neutron Monitoring for Radiological Protection. Vienna, 29 août—2 septembre 1966. Communication SM-76/40. Le même—Rapport IBJ No. 739/XIX/D.
5. RBE Committee of ICRP and ICRU. *Health Phys.* **9,** 357 (1963).
6. V. N. Lebedev, M. Zielczyński et M. J. Salatskaya. *Atomnaya Energia* **20,** No. 5, 392 (1966).
7. Non encore publié.
8. M. Zielczyński. *Nukleonika* **10,** No. 2, 77 (1965).
9. B. Filipiak, R. Siwicki, M. Zielczyński et K. Żarnowiecki. *Nukleonika* **11,** No. 3, 193 (1966).

DEPTH DOSE DISTRIBUTION IN A BEAGLE PHANTOM WITHIN A MIXED FIELD OF NEUTRONS AND GAMMA-RAYS

R. E. SIMPSON

Walter Reed Army Institute of Research, Walter Reed Army Medical Center, Washington, D.C., U.S.A.

J. A. SAYEG and A. C. LUCAS

Edgerton, Germeshausen & Grier, Inc., Santa Barbara Division, Goleta, California, U.S.A.

Abstract—As a result of the recommendations adopted by the International Commission on Radiological Units and Measurements (ICRU) for Class B irradiations (cases where the irradiation is not uniform because of absorption) a series of investigations for the evaluation of depth dose has been initiated in order to more accurately describe the absorbed dose at all points of interest for different size phantoms.

The work to be reported here includes studies with two phantoms the approximate size of a beagle. These include a homogeneous tissue equivalent liquid phantom and an Alderson beagle phantom constructed of tissue equivalent plastic containing a skeleton.

The incident radiation field being studied is the mixed field of neutrons plus gamma-rays within a fast neutron exposure volume of the Walter Reed Research Reactor, a homogeneous L-54 type designed by Atomics International.

The detectors being used in this study are miniature tissue equivalent condenser ionization chambers to measure the total dose (neutron plus gamma), Li^7F (TLD-700) for measuring the gamma dose within the mixed field and the threshold detectors of Pu^{239}, Np^{237}, and U^{238} (shielded with B^{10}) and S^{32} to obtain the neutron dose.

Dose variations with respect to depth are currently being obtained and evaluated for both phantoms. The linear energy transfer (LET) distribution of dose with respect to depth is also being evaluated using the threshold detector technique of Hurst. Results from these evaluations are being compared with those obtained by use of a modified Rossi tissue equivalent LET proportional counter. The results of the neutron and gamma depth dose variations and distribution of neutron LET will be discussed with respect to the techniques employed and input parameters used.

I. INTRODUCTION

Recently the International Commission on Radiological Units and Measurements (ICRU) has recommended that absorbed dose values of Class B irradiations (cases where the radiation is not uniform because of absorption*) be based on a nominal value which may best be chosen at the midline or center of the volume of interest.[1] In addition they have recommended that this information be supplemented by at least the entrance and exit dose values, and preferably by a depth dose relation in a phantom that represents the experimental conditions. This investigation was performed to supplement the available information for depth dose patterns in a small phantom placed in a reactor (fission neutron) environment as well as to compare different phantom types. The work to be reported here includes a description of the techniques used for the determination of these patterns and results which clearly show the need for the evaluation of these dose distributions if biological effects are to be correlated with the absorbed dose at the region of interest.

* The ICRU has defined Class B irradiation where the ratio of entrance dose to exit dose is > 1.15.

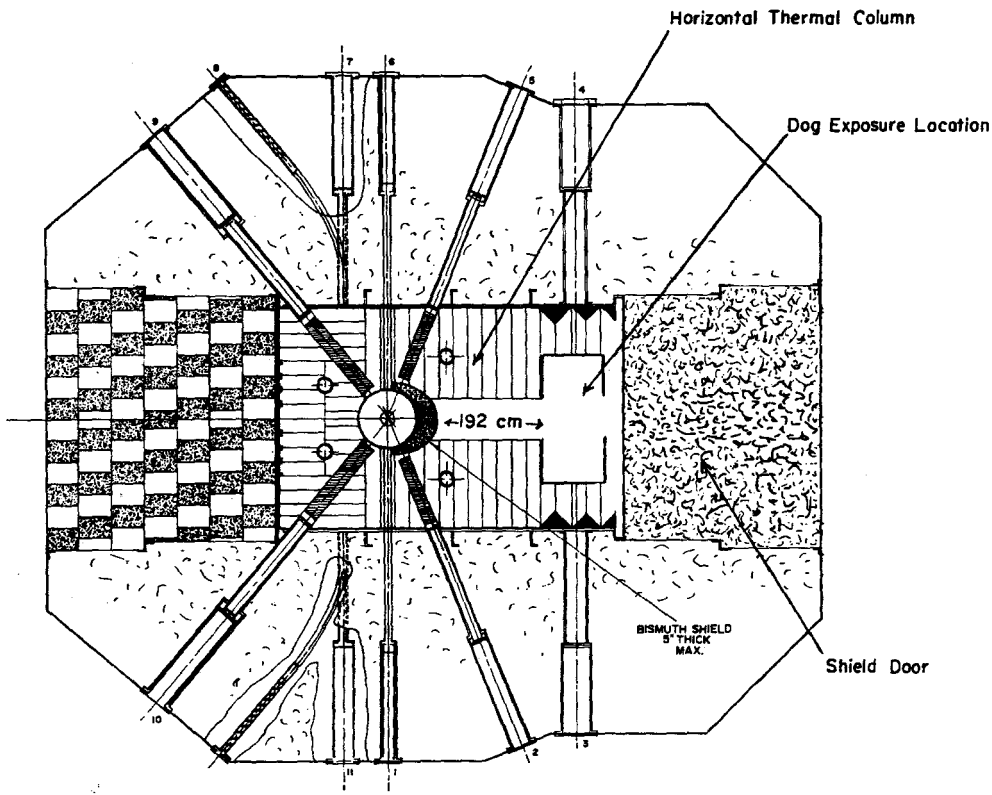

FIG. 1. Horizontal section of reactor and experimental animal exposure volume.

II. MATERIALS AND METHODS

A. *Reactor Description and Exposure Environment*

The Walter Reed Research Reactor (WRRR), illustrated in Fig. 1, is a 50 kW, graphite reflected, homogeneous steady-state reactor.* The core contains a 26.5 l. aqueous solution of uranyl sulfate (93% U^{235}) within a stainless steel sphere $15\frac{3}{4}$ in. in diameter. The sphere is surrounded by a semi-annular bismuth shield which reduces the gamma flux density in the thermal column exposure environment. In addition, eleven exposure ports are available which provide beams of neutrons with different characteristics.

To provide a broad beam of fission neutrons for exposing animals as large as a dog, two sets of graphite stringers were removed from the mid-section of the horizontal thermal column. This provided a port 1 ft square. An additional 36 × 36 × 48 in. volume was removed from the outer face of the thermal column to accommodate the animal exposure support assembly which permitted closing of the shield door. Dogs the size of a beagle could then be positioned across the 12 × 12 in. port face for abdominal exposures to the mixed radiation field of neutrons and gamma-rays at a distance of 192 cm from the reactor core.

* Constructed and designated as L-54 by Atomics International.

B. *Description of Phantoms*

Two types of phantoms were used to evaluate the depth dose characteristics of the mixed radiation field passing through a tissue-like volume. A beagle phantom designed by Alderson,[2] containing a skeleton in a tissue equivalent plastic ("Plastinaut" 8.9% H, 3.2% N, 64.8% C, 22.8% O, percentages by weight)

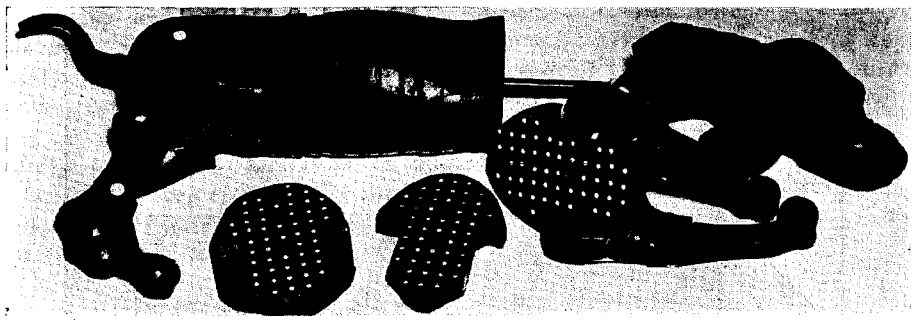

FIG. 2. Inhomogeneous Alderson beagle phantom.

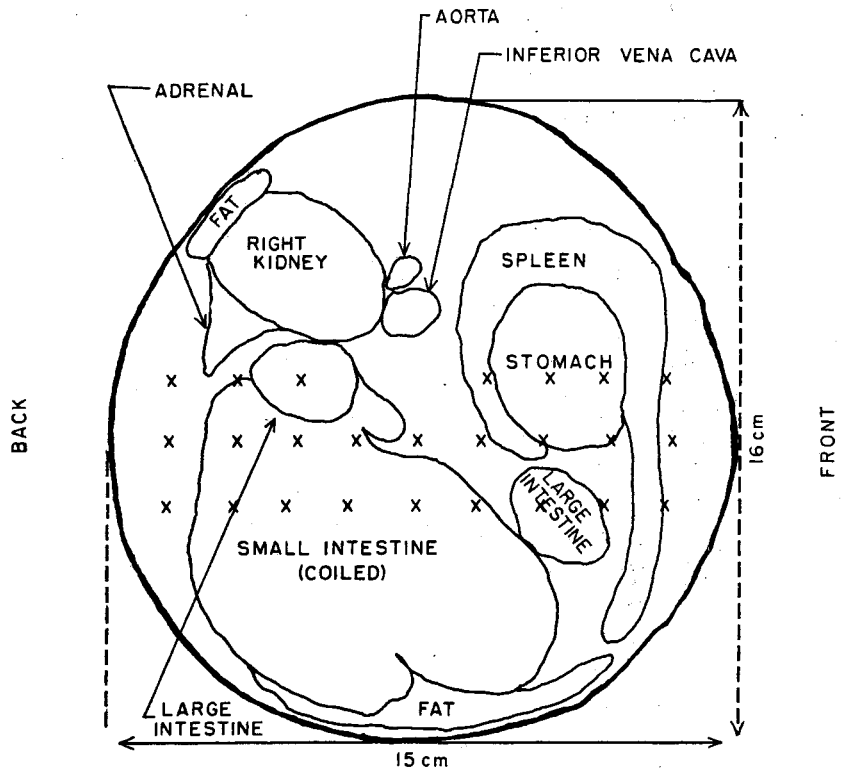

FIG. 3. Abdominal cross-section of organs that would be exposed in a beagle.

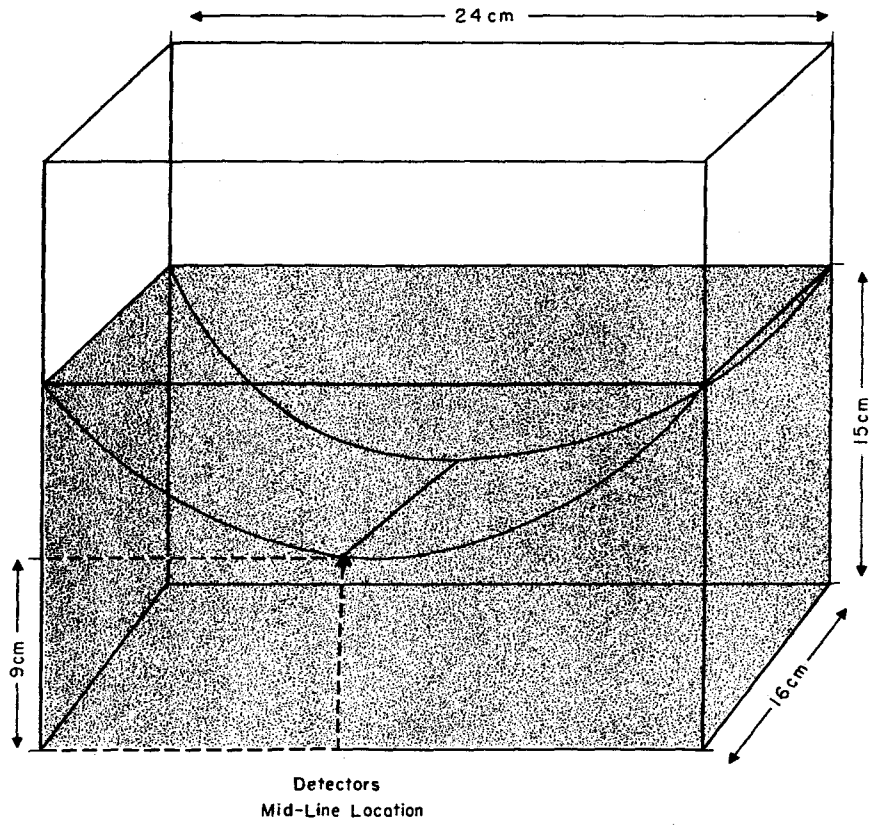

FIG. 4. Lucite container for homogeneous tissue equivalent liquid phantom.

which is shown in Fig. 2, was used to represent the inhomogeneous case. This phantom contained holes 5 mm in diameter by 20 mm deep evenly distributed throughout its volume. Hence, only small detectors could be placed in these holes which were filled with tissue equivalent plugs when not in use. Exposures were made with detectors placed in depth through the mid-abdominal section of the phantom as illustrated in Fig. 3.

For larger detectors such as fission foils and their B^{10} shields, a second phantom consisting of a lucite container 16 cm thick was constructed as indicated in Fig. 4. This container was filled with a solution of 7.1% sucrose, 7.6% urea, 28.4% glycerol and 56.9% water (9.8% H; 15.6% C; 61.0% O; 3.5% N by wt) which was considered to be tissue equivalent,[3] $(C_5H_{40}O_{18}N)n$, and representative of the homogeneous case. Detectors were positioned in depth within this phantom on a mid-line plane parallel with the radiation beam.

C. *Detectors and Ancillary Equipment*

The following detector systems were used to measure the components of the mixed radiation field:

1. *Total (neutron plus gamma) tissue dose—miniature condenser ionization chambers of the Sievert type*[4] *constructed of conducting tissue equivalent plastic.*[5] These chambers are 5 mm in diameter and 20 mm in length with a sensitive volume of approximately 30 mm^3. The chambers were charged to 600 V and read with a precision of 3% on a specially designed reader by Lucas.[6] These chambers were used with air at atmospheric pressure, as the cavity gas in view of the previous experimental evidence by Simpson *et*

al.[7] which indicated no significant difference in response between air and tissue equivalent gas.

2. *Gamma exposure and tissue dose—Li^7F (TLD-700) thermoluminescent powder.* An aliquot of approximately 50 mg of Li^7F powder was contained in teflon capsules 5 mm in diameter and 20 mm long, which was shielded by 1/16 in. thick Li^6 metal to eliminate any response due to thermal neutrons. After exposure the thermoluminescence of the powder was evaluated by means of a commercial readout system* with a precision of 5%.

The response of the Li^7F was considered to be approximately tissue equivalent and hence no energy discrimination shield was necessary.

3. *Fast neutron fluence tissue dose and LET distribution of dose.* The threshold detector system included foils of 0.05 g Pu^{239}, 0.028 g Np^{237} and 0.6 g U^{238} surrounded by shields of 30 mil thick cadmium and 1.65 g/cm^2 B^{10}. These foils were encapsulated with pure copper 5 mils thick with a diameter of 0.37 in. The overall diameter of the outer B^{10} shield was $1\frac{1}{4}$ in. These foils were used to measure the neutron fluence distribution from 10 keV to 3 MeV. Bare S^{32} foils, 1 in. in diameter and 1/8 in. thick, were used to evaluate neutron fluence values greater than 3 MeV. The induced activity of the fission threshold detectors were measured with two opposing 3 in. diameter, 3 in. thick NaI (Tl) crystals housed in a "Tobor" lead shield.† The overall design was similar to that described by Reinhardt and Davis.[8] This system was calibrated using the equivalent foil technique proposed by Hurst and Ritchie.[9]

4. *Thermal neutron fluence and dose—bare and cadmium covered Au^{198} foils.* The foils were 1 cm in diameter and 2.5 mils thick. The cadmium shields were 30 mils thick.

5. *LET distribution of tissue dose—A LET proportional counter initially designed by Rossi*[10] *and modified by Lucas.*[11] This detector was a spherical counter, 2 in. in diameter, with a wall thickness of 0.25 in. and fabricated from conducting tissue equivalent plastic.[5] The central electrode consisted of a 0.005 in. stainless steel wire which was coaxial to a 0.005 in. helix grid. The counter was filled with tissue equivalent gas (3.1% nitrogen, 32.5% carbon dioxide, and 64.4% methane, percentages by partial pressures) at a reduced pressure of approximately 30 mm of Hg. The ionization pulses produced by recoil protons (and heavy recoils) were measured using a 100 channel analyzer. The LET spectra were obtained from the pulse height values using a computer program devcloped by Lucas.[11]

D. *Method*

1. *Neutron and gamma tissue dose evaluations from tissue equivalent ionization chambers and Li^7F (TLD-700) detectors.** By use of two simultaneous equations shown below it was possible to evaluate both the neutron and gamma tissue dose components of the mixed radiation field.[12] That is

$$T = aN + b\gamma \qquad (1)$$

$$L = kN + b\gamma$$

where T = the response in roentgens of the tissue equivalent (T.E.) ionization chambers in terms of hard X- or gamma-ray calibration,†
a = efficiency of tissue dose evaluation by the tissue equivalent ionization chamber in units of roentgens per rad of tissue dose ($a = 1.00$ for tissue equivalence),
N = neutron tissue dose in rad,
b = the rad to roentgen conversion factor for hard gamma-rays ($b = 1.04$ r/rad),
γ = gamma tissue dose in rad,
L = response in roentgens of the Li^7F detectors in the mixed neutron and gamma field in terms of hard X- or gamma-ray calibration,

* Controls for Radiation Inc., Cambridge, Mass.
† Nuclear Chicago Inc.

* The overall precision of the data collected for three separate exposures under free field and phantom conditions was: *Ionization Chambers*, $\pm 4.7\%$ σ for eleven positions in depth of field and nine pieces of data per position; *Li^7F*, $\pm 5\%$ σ for nine positions in depth of field and twelve pieces of data per position.

† The tissue equivalent ionization chambers and the Li^7F thermoluminescent dosimeters were calibrated with a Co^{60} gamma teletherapy unit (Walter Reed Medical Center).

K = response of the Li^7F detectors in roentgens when exposed to a neutron radiation field that delivers 1 rad to tissue (units = r/rad).

From the simultaneous solution of equations (1) and (2)

$$N = \frac{T - L}{a - k} \tag{3}$$

and

$$\gamma = \frac{L - kN}{1.04} \tag{4}$$

From the fast neutron response studies of Li^7F as reported by Wingate *et al.*[13] $K = 0.005$ such that $(a - k) = 0.995$. Within the $\pm 5\%$ precision of our TLD system the low response of Li^7F to fast neutrons may be neglected. Then equations (3) and (4) reduce simply to

$$N = T - L \tag{5}$$

and

$$\gamma = L/1.04 \tag{6}$$

Simpson[14] had previously found that the response of Li^7F to thermal neutrons was approximately 0.7 rad per 10^{10} n/cm^2 and could not be ignored. Therefore, due to the high thermal neutron environment of our exposure location, it was necessary to shield the Li^7F capsules with a 1/16 in. thickness of Li^6 metal.

2. *Neutron fluence, tissue dose, and LET distribution of dose by means of the threshold detectors* Pu^{239}, Np^{237}, U^{238} (*surrounded by* B^{10}) *and bare* S^{32}. Neutron fluence values were computed from the method originally proposed by Hurst[1] and modified by recommendations made by the Dosimetry Task Group D9/D20 of the American Society for Testing and Materials (ASTM).[16] The cross-sections and threshold energy values used in these evaluations are shown in Table 1 and are considered to be best fit values for a variety of spectra since the actual spectrum in the determination is unknown.

Table 1. Threshold Energies and Cross-sections used in Fluence Evaluations by Threshold Foils

Reaction	Effective threshold energy, MeV	Effective cross-section σ_{eff}, barns
$Pu^{239}(n,f)F,P$	0.01	1.7
$Np^{237}(n,f)F,P$	0.60	1.6
$U^{238}(n,f)F,P$	1.5	0.54
$S^{32}(n,p)P^{32}$	3.0	0.30

The fast neutron tissue dose was calculated from the equation

$$D = [a(\emptyset_{Pu} - \emptyset_{Np}) + b\,(\emptyset_{Np} - \emptyset_{U}) + c(\emptyset_{U} - \emptyset_{S}) + d\emptyset_{S}] \times 10^{-9} \text{ rad}^*$$

where the coefficients before the parentheses represent the fluence to dose conversion factors for the spectrum under consideration and $\emptyset$ represents the fluence values.

Since the resolution of the spectral determinations by this method is poor, it seemed necessary to investigate limiting spectra in the tissue dose evaluations. The limiting spectra considered in this investigation were the dE/E and Godiva variations. Fluence to dose conversion factors based on these spectra are shown in Table 2. The coefficients differ only in the region 0.01–0.60 MeV. The values in the other energy regions are not considered to be significantly different.

The fractional values of dose distribution obtained from the threshold detector method were used to calculate the LET distribution of dose according to the procedure given by Hurst *et al.*[15] The LET distribution for monoenergetic neutrons as first derived by Boag[17] and later by Hurst[15] and Biavati *et al.*[18] were weighted by the fractional component of dose in each energy interval. Monoenergetic LET distributions for 0.3, 1.0, 2.0, and 4.5 MeV were considered adequate to approximate the LET distribution for the energy interval under consideration.

3. *Tissue dose vs LET distribution measurements with a proportional counter.* Measurements of the distribution of dose as a function of LET were

* Actually it is the kerma that is calculated; however, under conditions of secondary charged particle equilibrium which is assumed in the above case, the kerma is equal to the absorbed dose.

Table 2. Fluence to Dose Conversion Factors for Different Spectra

Spectrum	Fluence to dose conversion factor $\frac{\text{rad}}{\text{n/cm}^2} \times 10^{-9}$ rad			
	0.01–0.6 MeV	0.6–1.5 MeV	1.5–3.0 MeV	>3.0 MeV
Godiva	1.29	2.33	3.08	4.06
dE/E	0.63	2.23	3.07	4.04

made by means of spherical proportional counter first devised by Rossi[10] and later modified by Lucas.[11] The analysis was similar to that of Rossi and his co-workers. The equation used for the LET distribution was

$$D(L) = \frac{1.6 \times 10^{-4}}{100 \times 2\pi r^2} \times h^2 \left[Q(h) - Q(h + \Delta h) + \frac{Q(h + \Delta h)}{h + \Delta h} \right] \frac{1}{\Delta h^2} \quad (7)$$

which for the 2-in. counter used in this investigation reduced to

$$D(L) = 3.14 \times 10^{-9} h^2 \left[\frac{\Delta Q(h)}{\Delta h} + \frac{Q(h + \Delta h)}{h + \Delta h} \right] \frac{1}{\Delta h} \quad (8)$$

where h = the channel number,
r = radius of the sphere in cm,
$Q(h)$ = number of particles with pulse height h.

Details of these derivations and description of the counter have been given in an earlier paper by Lucas and Simpson.[19]

4. *Thermal neutron dose calculation.* The thermal neutron dose was computed from the neutron fluence values by considering a small piece of tissue placed at the point of interest. The equation relating dose to fluence can be written as

$$\frac{D}{\phi} = 1.60 \times 10^{-8} \sum_t N_i \sigma_i f_i E_p \quad (9)$$

where D = absorbed dose in rad,
ϕ = neutron fluence (neutrons/cm^2),
N_i = number of atoms of the ith element per gram of tissue,
σ_i = cross-section (10^{-24} cm^2) for the ith element,
f_i = fractional energy absorption per interaction,
E_p = energy of the resultant particle responsible for energy deposition,
1.6×10^{-8} = conversion factor from MeV/g to rad.

The main reactions which occur when thermal neutrons interact with tissue are ${}_1H^1(n,\gamma){}_1H^2$ and ${}_7N^{14}(n,p){}_6C^{14}$. For a small tissue mass (e.g. radius approximately 0.2 cm) under "free field" conditions the dose due to the ${}_1H^1(n,\gamma){}_1H^2$ reaction may be neglected. In the depth dose measurements the gamma detector (Li^7F in this case) should respond to all gamma-rays, regardless of their source, including the gamma dose due to the ${}_1H^1(n,\gamma){}_1H^2$ reaction. Hence, the only thermal neutron dose component that should be considered in our additivity test (when the thermal neutron fluence to dose conversion is made) is that due to the ${}_7N^{14}(n,p){}_6C^{14}$ reaction. Therefore, for the homogeneous phantom, substitution of $\sigma = 1.7$ barns, $N_i = 1.8 \times 10^{21}$ atoms/g (3.5% nitrogen by weight), $f = 1$, and $E_p = 0.62$ MeV yields the value $(\frac{D}{\phi})_{\text{proton}} = 2.66 \times 10^{-11}$ rad/n/cm^2. In the case of the Alderson inhomogeneous phantom[2] $N_i = 1.36 \times 10^{21}$ atoms/g (3.2% nitrogen by weight) and $\frac{D}{\phi} = 2.43 \times 10^{-11}$ rad/n/cm^2.

III. RESULTS AND DISCUSSION

A. *Response of detectors*

To determine whether the responses of the various detectors were additive dose, evaluations were made under free field conditions and subjected to the following test criterion.

$$D(N+\gamma)_{TE} = D(N)_{\text{fast}} + D(N)_{\text{thermal}} + D(\gamma)_{Li^7} \quad (10)$$

where $D(N+\gamma)_{TE}$ = total dose as indicated by the tissue equivalent ionization chamber,

$D(N)_{\text{fast}}$ = fast neutron dose calculated from the threshold detector data,

$D(N)_{\text{thermal}}$ = proton component of thermal neutron dose inferred from bare and cadmium covered gold foil activation, and

$D(\gamma)_{Li^7}$ = gamma dose as indicated by the Li^7F thermoluminescent detectors.

Tables 3 and 4 summarize the fluence and dose values obtained for free field conditions by the various methods. Table 4 also includes the correlation analysis of additivity. It can be seen from Table 4 that the fast neutron dose evaluated by use of the dE/E fluence to dose conversion coefficients appears to give a better correlation than the Godiva coefficients. This conclusion had been previously confirmed by comparison of the threshold detectors with the Hurst proportional counter[11] and a LET proportional counter (see note at bottom of Table 4). The difference in our neutron tissue dose evaluations using the dE/E and Godiva fluence to dose conversion coefficients was a factor of 1.3, the Godiva coefficients indicating the higher value. This difference was due to the relatively large percentage of fast neutrons in the region 0.01–0.60 MeV (approximately 70%) and the large difference of the fluence to dose conversion factor in this interval. The difference from complete additivity (using the dE/E coefficients) was less than 20% (see column 12 of Table 4).

B. *Neutron fluence and depth dose measurements in different phantoms*

Tables 5 and 6 show the neutron fluence and neutron and gamma dose values as a function of depth for the homogeneous tissue-equivalent liquid phantom and the inhomogeneous Alderson beagle phantom.* Although the surface dose for both phantoms was approximately the same, the homogeneous phantom exhibited a greater degree of neutron attenuation while the gamma attenuation appeared to be the same. Figures 5 and 6 illustrate these variations with comparison to the free field case.

The fast neutron depth dose relations shown in Fig. 6 were derived from: (a) Tissue equivalent ionization chamber total dose values by subtraction of the gamma dose (as evaluated by the Li^7F thermoluminescent dosimeters) and the proton component of the thermal neutron tissue dose (as inferred from the thermal neutron fluence); and (b) Threshold detector fluence values greater than 10 keV. The derived values from (a) and (b) were corrected for free field attenuation to obtain patterns due to absorption only. The difference in patterns between the tissue equivalent ionization chamber and threshold detector techniques (approximately 40% at a depth of 2.0 cm and 60% at distances greater than 5.0 cm) in the homogeneous phantom can possibly be explained by the epithermal neutron response of the ionization chambers, a component not taken into consideration in the threshold detector evaluations. This interpretation is also reflected into the additivity of dose components shown in Table 7. The difference in fast neutron dose between the

* Due to the aforementioned limitations of the Alderson phantom only miniature ionization chambers and small foils would fit in the holes at 2 cm intervals in depth. To accommodate the Li^7F detectors and their Li^6 shields a modified section of tissue equivalent plastic designed by the Armed Forces Radiobiological Research Institute [2] was substituted in the phantom. This section contained cavities 2 cm in diameter located at 3 cm depth, mid-line and 14 cm depth. In addition to these locations shielded Li^7F detectors were placed on the front and back surfaces of the phantom. Therefore the gamma dose data of Table 6 are interpolated values used to compute the neutron depth dose for this phantom.

Table 3. Neutron Fluence and Tissue Dose Distributions for Free Field Conditions

Distance from reactor core, cm	Fluence >10 keV $n/cm^2 \times 10^6$ / watt-min	Tissue dose >10 keV rad $\times 10^{-2}$ / watt-min		Percentage in energy interval										
				0.01–0.60 MeV			0.60–1.5 MeV			1.5–3.0 MeV			>3.0 MeV		
				Fluence	Dose		Fluence	Dose		Fluence	Dose		Fluence	Dose	
		E^{-1}	G		E^{-1}	G		E^{-1}	G		E^{-1}	G		E^{-1}	G
192 (0)*	12.7	1.44	2.10	75.0	41.9	58.5	14.5	27.9	20.5	7.82	21.1	14.7	2.54	9.1	6.3
200.9	9.50	1.17	1.63	69.7	35.7	52.6	18.7	33.7	25.4	8.54	21.3	15.3	2.85	9.3	6.7
207.3	7.26	0.924	1.27	69.3	34.3	50.7	18.5	32.5	24.8	10.3	24.3	18.0	2.80	8.9	6.5
213.0	5.87	0.753	1.04	67.2	33.0	49.2	18.9	31.4	25.1	10.5	26.3	19.0	2.97	9.3	6.7
220.5	5.06	0.632	0.087	69.0	34.9	51.3	18.8	33.5	25.0	9.77	23.9	17.7	2.62	7.7	6.0

* Distance to phantom surface.

$E^{-1} = dE/E$ fluence to dose conversion coefficients.

G = Godiva fluence to dose conversion coefficients.

Table 4. Free Field Correlation of Dose using Tissue Equivalent Ion Chamber and Li^7F *with Threshold Foils for* E^{-1} *and Godiva Coefficients*

Free field depth cm	(rad/watt-min × 10^{-2}) E^{-1} coefficients						Godiva coefficients				Ratio $ff T + Li^7$ to TE	
	TE $(N+\gamma)$	Li^7 (γ)	ff (N)	$ff + Li^7$ $(N+\gamma)$	ffT (N)	$ffT + Li^7$ $(N+\gamma)$	ff (N)	$ff + Li^7$ $(N+\gamma)$	ffT (N)	$ffT + Li^7$ $(N+\gamma)$	E^{-1}	Godiva
0	1.962	0.222	1.455	1.677	1.820	2.042	2.105	2.237	2.450	2.672	1.035	1.36
2	1.957	0.222	1.395	1.617	1.725	1.947	1.975	2.197	2.320	2.542	0.995	1.30
4	1.922	0.222	1.315	1.537	1.630	1.852	1.860	2.082	2.180	2.402	0.965	1.25
6	1.877	0.222	1.245	1.467	1.540	1.762	1.750	1.972	2.060	2.282	0.940	1.22
8	1.822	0.217	1.170	1.387	1.450	1.667	1.640	1.857	1.940	2.157	0.913	1.18
10	1.757	0.212	1.110	1.322	1.370	1.582	1.530	1.742	1.820	2.032	0.905	1.16
12	1.687	0.212	1.030	1.242	1.290	1.454	1.430	1.642	1.710	1.922	0.870	1.14
14	1.612	0.207	0.965	1.172	1.220	1.427	1.340	1.547	1.600	1.807	0.885	0.96
16	1.533	0.203	0.905	1.108	1.145	1.348	1.250	1.453	1.500	1.703	0.890	0.95

TE = Total dose by tissue equivalent ionization chamber = $D(N+\gamma)TE$.
Li^7 = Gamma dose by Li^7F = $D(\gamma)Li^7$.
ff = Threshold foil dose, $E_n > 0.01$ MeV = $D(N)$ fast.
ffT = Threshold foil dose plus thermal neutron dose = $D(N)$ fast + $D(N)$ thermal.

192 cm LET-free field (LET proportional counter)	Rad/watt-min		
	10–120 keV/μ	120–400 keV/μ	Total
	0.0116	0.00115	0.01275

Table 5. Fast Neutron Fluence and Depth Dose Distributions within a Homogeneous Tissue Equivalent Liquid Phantom (16 cm thickness)

Distance from phantom surface, cm	Fluence > 10 keV $n/cm^2 \times 10^6$ / watt-min	Tissue dose > 10 keV rad $\times 10^{-2}$ / watt-min		Percentage in energy interval									
				0.01–0.60 MeV			0.60–1.5 MeV			1.5–3.0 MeV		> 3.0 MeV	
				Fluence	Dose		Fluence	Dose		Fluence	Dose	Fluence	Dose
		E^{-1}	G		E^{-1}	G		E^{-1}	G		E^{-1}	G		E^{-1}	G		E^{-1}	G
−2.0	11.5	1.29	1.88	76.4	43.1	60.0	12.8	25.6	18.3	8.23	22.6	15.5	2.45	8.70	6.2
+2.0	5.33	0.715	0.957	65.5	31.4	47.8	18.1	29.8	23.3	10.3	23.4	17.6	5.07	15.4	11.3
5.0	2.04	0.359	0.432	49.5	17.8	30.1	22.4	28.1	24.5	18.1	31.2	26.2	9.95	22.9	19.2
8.0	1.40	0.227	0.280	57.7	22.4	37.1	18.0	26.0	27.0	14.6	27.3	22.5	9.67	24.3	19.7
14.0	0.59	0.095	0.119	59.4	23.2	37.8	15.1	21.1	17.7	14.9	28.4	22.7	10.8	27.3	21.8
16.0	0.47	0.078	0.096	55.3	21.8	35.5	22.1	29.5	25.0	12.9	24.4	19.7	9.90	24.3	19.8

$E^{-1} = dE/E$ fluence to dose conversion coefficients.
G = Godiva fluence to dose conversion coefficients.

Table 6. Neutron and Gamma Depth Dose in an Inhomogeneous Beagle Phantom

Distance from phantom surface, cm	Total dose (*TE* ion chamber) rad × 10^{-2} / watt-min	Gamma dose (Li^7 fluoride) rad × 10^{-2} / watt-min	Fast + thermal* neutron dose rad × 10^{-2} / watt-min
−0.5	3.09	0.70	2.39
0.0	3.12	0.73	2.39
0.5	3.13	0.75	2.38
2.0	3.09	0.79	2.30
4.0	2.83	0.84	1.99
6.0	2.30	0.79	1.51
8.0	1.99	0.68	1.31
10.0	1.75	0.59	1.16
12.0	1.49	0.47	1.02
14.0	1.30	0.40	0.90
16.0	1.19	0.40	0.79

*(Fast + thermal) neutron dose = *TE* − Li^7 (γ).

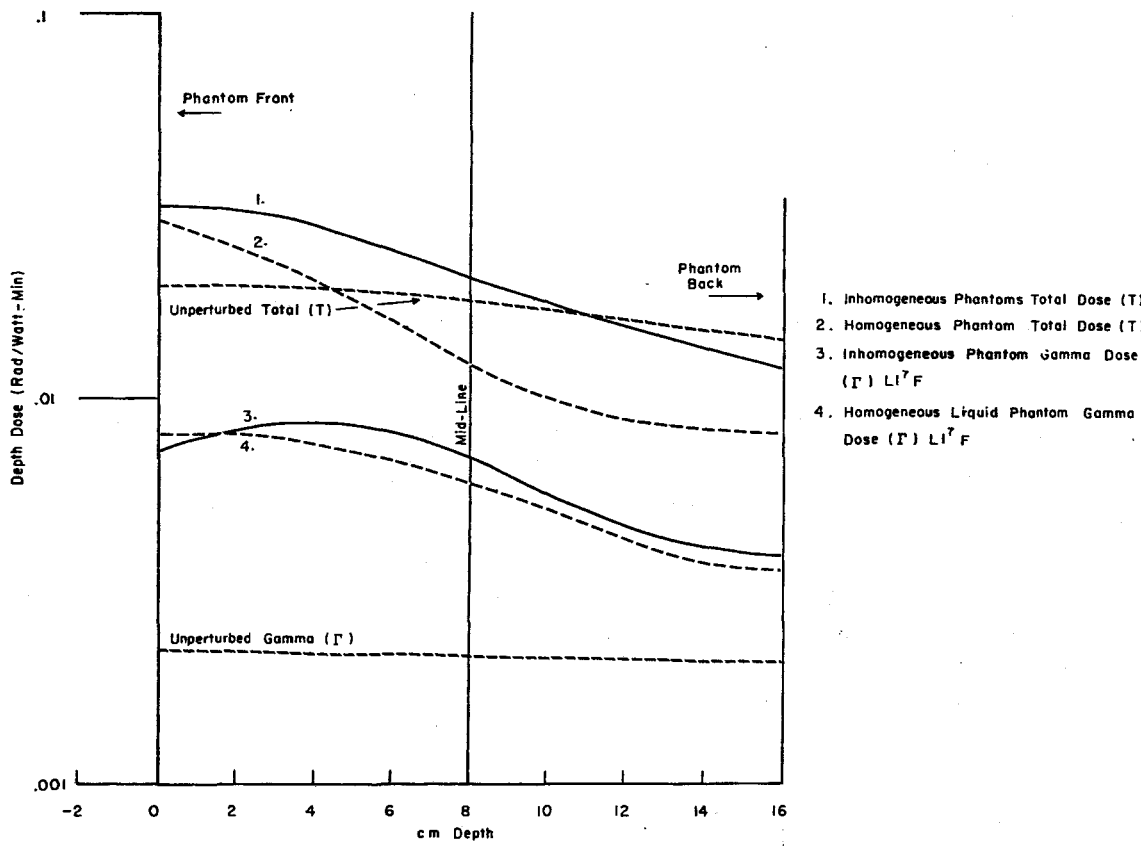

FIG. 5. Comparative depth dose between the inhomogeneous and homogeneous phantoms and free field conditions.

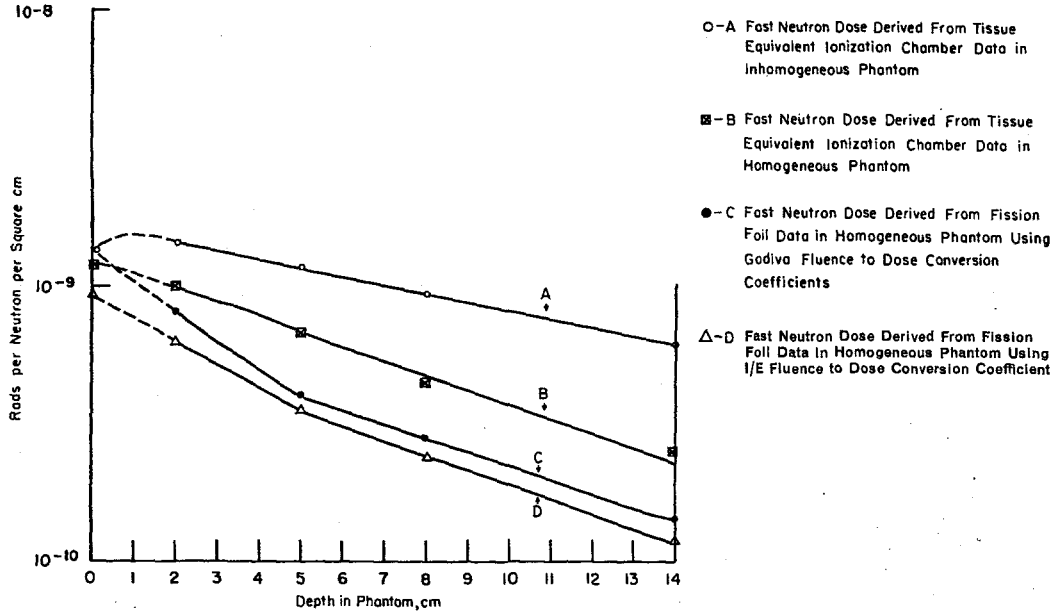

FIG. 6. Experimental neutron depth dose variations employing different phantoms and detectors.

homogeneous and inhomogeneous phantoms as evaluated by the tissue equivalent ionization chambers, etc., can only be attributed to differences in the hydrogen composition and density of the homogeneous phantom. The differences in surface dose values in the case of the two phantoms are within the precision of the methods employed. The fast neutron dose variations shown can be approximated by the mathematical relations obtained from the tissue equivalent ionization chambers:

Inhomogeneous Phantom

$$D = 1.70 \times 10^{-9}\, e^{-d/13.6} \quad (d > 1.0 \text{ cm}) \qquad (11)$$

Homogeneous Phantom

$$D = 1.25 \times 10^{-9} e^{-d/8.2} \ \frac{\text{rad}}{\text{n/cm}^2} \qquad (12)$$

Threshold detectors using Godiva fluence to dose conversion coefficients:

$$D = [0.80\, e^{-d/1.7} + 0.70\, e^{-d/8.5}] \times 10^{-9} \frac{\text{rad}}{\text{n/cm}^2} \qquad (13)$$

Threshold detectors using $1/E$ fluence to dose conversion coefficients:

$$D = [0.31\, e^{-d/2.0} + 0.65\, e^{-d/8.0}] \times 10^{-9} \frac{\text{rad}}{\text{n/cm}^2} \qquad (14)$$

where D = fast neutron tissue dose in rads per incident n/cm^2,

d = distance from surface of phantom to point of interest in centimeters.

C. *Free field, surface, midline and exit dose comparisons for the different phantoms*

Table 8 lists the free field (at the phantom midline), surface, midline, and exit dose values for the two phantoms tested. The dose ratios

Table 7. Total Neutron and Gamma Depth Dose Values for a Homogeneous Tissue Equivalent Phantom

Distance from phantom surface, cm	Thermal neutron fluence $\frac{n/cm^2 \times 10^8}{watt\text{-}min}$	Thermal neutron dose $\frac{rad \times 10^{-2}}{watt\text{-}min}$	Fast + thermal neutron dose $\frac{rad \times 10^{-2}}{watt\text{-}min}$		Gamma dose $\frac{rad \times 10^{-2}}{watt\text{-}min}$	Fast + thermal + gamma (total dose) $\frac{rad \times 10^{-2}}{watt\text{-}min}$		Total dose TE ionization chamber $\frac{rad \times 10^{-2}}{watt\text{-}min}$
			E^{-1} *fast*	*G-fast*		*E*$^{-1}$ *fast*	*G-fast*	
+2.0	1.73	0.46	1.18	1.417	0.810	1.99	2.23	2.60
+5.0	1.02	0.27	0.624	0.700	0.740	1.36	1.44	1.95
8.0	0.53	0.14	0.362	0.420	0.550	0.92	0.97	1.33
14.0	0.22	0.06	0.155	0.179	0.370	0.53	0.55	0.83
16.0	0.18	0.05	0.128	0.146	0.290	0.41	0.44	0.80

*Table 8. Free Field, Surface, Midline, and Exit Dose Ratios for Different Phantoms**

Phantom	Dose $\frac{rad \times 10^{-2}}{watt\text{-}min}$								Dose ratio					
	Free field at midline of phantom		Phantom surface		Phantom midline		Phantom exit		Phantom midline / free field		Phantom midline / surface		Phantom exit / surface	
	N	*γ*	*N*	*γ*	*N*	*γ*	*N*	*γ*	*N*	*γ*	*N*	*γ*	*N*	*γ*
Homogeneous tissue equivalent liquid	1.56	0.218	2.10	0.80	0.60	0.60	0.50	0.32	0.38	2.8	0.28	0.75	0.24	0.40
Inhomogeneous Alderson Beagle	1.56	0.218	2.38	0.72	1.35	0.70	0.96	0.39	0.86	3.2	0.57	0.97	0.40	0.54

*Interpolated values from figure 5.
N = fast + thermal neutron tissue dose.
γ = gamma tissue dose.

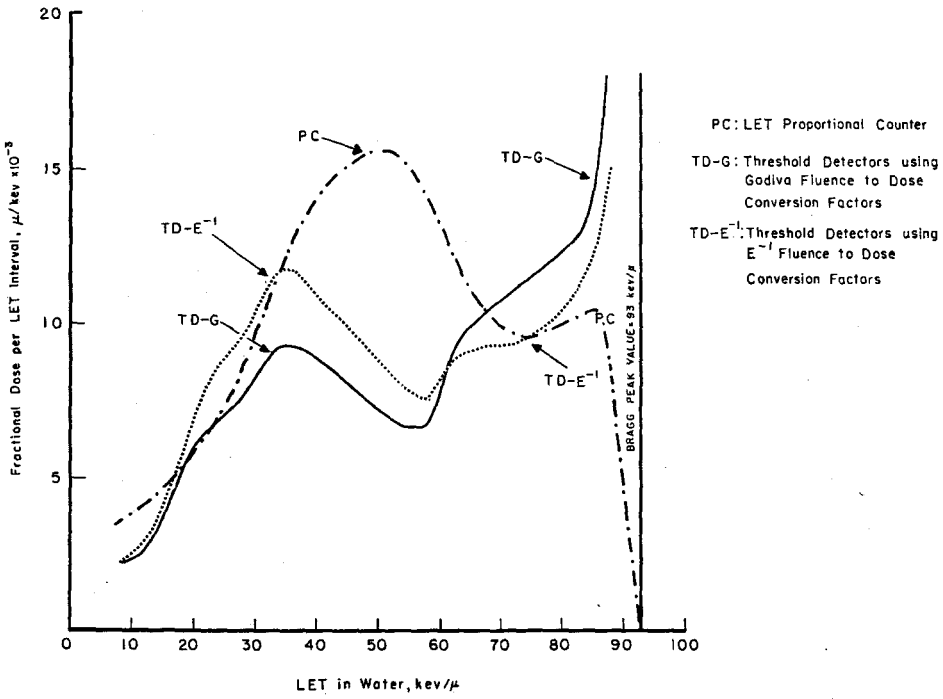

FIG. 7. LET distribution of the proton component of neutron tissue dose for free field conditions.

are also shown. These data clearly show the importance of assigning a dose to the region of interest for the correlation of biological effects. In the case of the homogeneous phantom the midline and free field (at the phantom midline) neutron values differ by a factor of 2.6 whereas the total dose $(N+\gamma)$ would differ by a factor of 1.5. In the inhomogeneous case the difference is a factor 1.2 for the neutrons alone and 0.9 for the total dose.*

D. *Distribution of neutron dose with LET*

The LET distribution of dose as calculated by the method of Hurst *et al.*[20] is shown in Fig. 7 for free field conditions. Also shown is the LET spectrum as measured with a tissue equivalent LET proportional counter. In Fig. 8 are shown the LET distributions for the surface of the phantom and for those calculated in depth for an average value of neutron spectrum throughout the phantom. The LET distributions (Fig. 7 and 8) were calculated using both the dE/E and Godiva fluence to dose conversion coefficients and were normalized to an area of 0.9 to compensate for the fraction of total dose contained in the heavy recoil region. An analysis of the LET distributions for the monoenergetic neutrons used in our calculations indicated that the 0.3 MeV distribution contained approximately 65% of the dose to 90 keV/μ, whereas the other distributions contained a fraction nearly equal to 1. It has previously been indicated by Boag[17] and Biavati *et al.*[18] that low energy neutrons may contain a significant fraction of the dose near the Bragg peak. In our summations of the LET distribution for the cases under consideration it was observed that approximately 15% of the total proton recoil dose is contained in the LET region near the Bragg peak.

An examination of Fig. 7 indicates that the LET spectrum obtained by the LET proportional counter differs markedly in the region

* Total dose at midline of phantom is greater than the free field value.

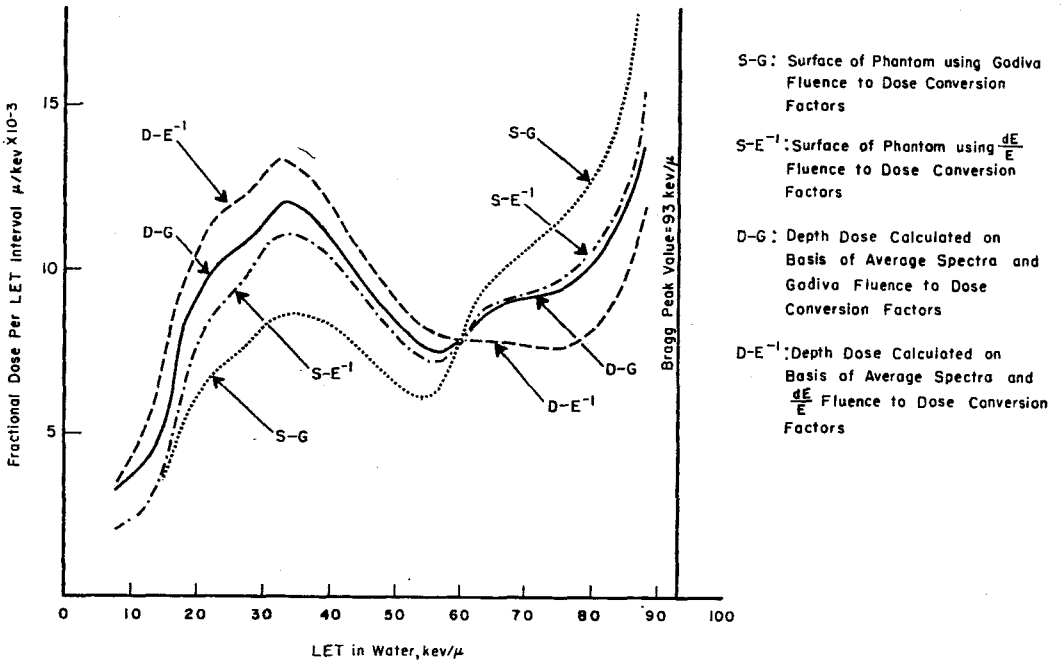

FIG. 8. LET distribution of the proton component of neutron depth dose in a homogeneous tissue equivalent beagle phantom.

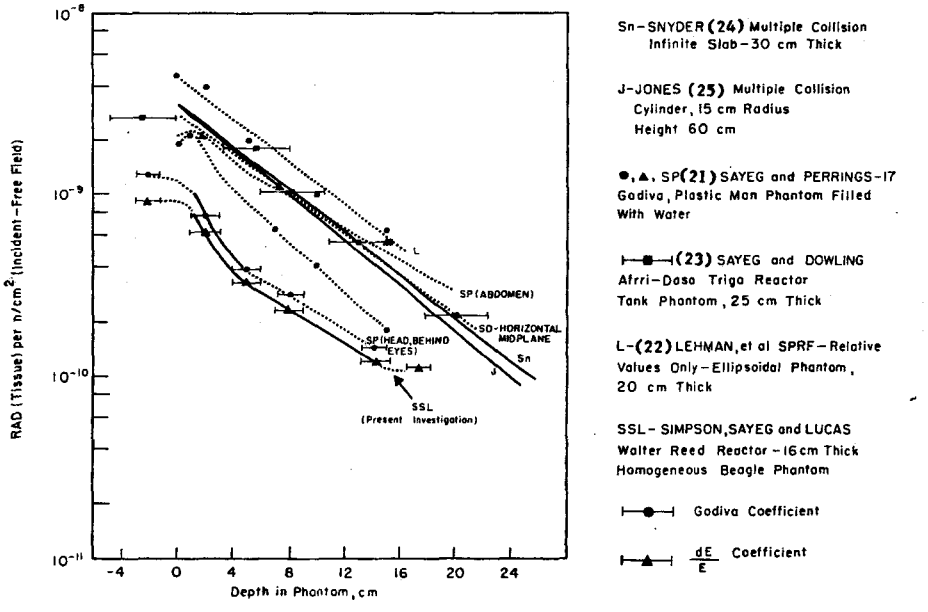

FIG. 9. Experimental depth dose relations obtained by different investigators with comparison to the present investigation. Horizontal bars represent the size of the B^{-10} sphere-shield used with threshold detectors.

greater than 40 keV/μ. The difference is attributed to the protons produced by thermal neutrons as a result of the $N^{14}(n,p)C^{14}$ reaction in tissue, again, a LET component not taken into consideration in the calculations with the threshold detectors. This interpretation was partially confirmed by obtaining the response of the counter in radiation fields containing a different proportion of fast to thermal neutrons and observing a decrease in this component as the number of thermal neutrons relative to the fast neutrons decreased.[11] As a second difference, the proportional counter distribution did not exhibit the large fraction of dose near the Bragg peak as theoretical calculations have indicated.

E. *Comparison with other depth dose studies with fission neutrons*

The results of the present investigation have been compared with other studies carried out with fission neutrons. Figure 9 illustrates experimental depth dose relations (normalized to incident free field fluence) obtained at the Godiva II critical assembly (Los Alamos),[21] the Sandia Pulse Reactor facility (SPRF)[22] and the AFRRI-DASA Triga Reactor at the Armed Forces Radiobiology Research Institute (AFRRI).[23] In addition, the results of theoretical studies based upon the work of Snyder[24] and Jones[25] with a 30 cm thick infinite tissue equivalent slab and finite cylinder 30 cm in diameter are included. The experimental studies were carried out with homogeneous tissue equivalent, chest-type phantoms, except for the Godiva studies of Sayeg and Perrings[21] in which an Alderson phantom containing a skeleton was used. The recent investigation of Sayeg and Dowling[23] shows closer agreement with the theoretical studies and both indicate that the proton and heavy recoil components of the fast neutron dose, from a Godiva-type spectrum, can be approximated by the relation:

$$D = 3.20 \times 10^{-9} e^{-d/7.5} \frac{\text{rad}}{\text{n/cm}^2 \text{ (incident)}} \quad (15)$$

where d is the depth in the phantom in centimeters, 3.20×10^{-9} rad/n/cm^2 is the surface fluence to dose conversion factor, and 7.5 is the mean free path in centimeters (absorption coefficient $\mu = \frac{1}{7.5} = 0.13$/cm). Sayeg and Dowling were also able to support Lehaman and Fekula's[22] observations that in a Godiva-type radiation environment the fast neutron spectrum through a homogeneous phantom did not change markedly and closely resembled the emission spectrum of the source. The results of the present investigation, however, did not exhibit such simple interpretations as indicated in a previous discussion (see Section III, B). The depth fluence* to dose conversion factor appeared to increase from a value of 1.1×10^{-9} rad/n/cm^2 (based on dE/E coefficients) at the surface to a value of 1.7×10^{-9} rad/n/cm^2 at a depth of 5 cm, where it appeared to have reached an equilibrium value to the back surface of the phantom. These values of fluence to dose conversion factors can be compared to the Godiva spectrum value of 2.4×10^{-9} rad/n/cm^2. This difference can be understood in terms of the percentage of neutrons in the energy range 0.01–0.60 MeV (50–70% in the present study vs. 34% for the Godiva spectrum).

ACKNOWLEDGEMENTS

The authors deeply appreciate the cooperation of Cmdr. J. H. Dowling (USN), Lt. Col. J. E. Kuritzky, and Maj. W. P. Pfeiffer (USAF) of the Armed Forces Research Institute Radiobiology for the use of their Alderson Phantom. Also the assistance of Messrs. J. B. Smathers and W. B. Bass of the reactor and electronics staffs of the Walter Reed Army Institute of Research (WRAIR) were invaluable to the success of this study.

REFERENCES

1. Radiobiological Dosimetry. ICRU Report 10e. National Bureau of Standards Handbook 88 (1963).
2. AFRRI. Standard Beagle Phantom, Alderson Research Laboratories, Inc., Long Island 1, New York.
3. H. H. Rossi. Neutrons and mixed radiation, pp. 680–682. *Radiation Dosimetry*, Hine and Brownell, Academic Press, New York, New York, 2nd printing 1958.

* This is the fluence measured in the phantom at the point of interest. It should be noted, however, that the previous mathematical formulations refer to incident fluence.

4. H. SKOLDFORM. On the design, physical properties and practical application of small condenser ionization chambers. Supplement 187 to *Acta Radiologica* (1959).
5. F. R. SHONKA, J. R. ROSE and G. FAILLA. Conducting plastic equivalent to tissue, air and polystyrene, *Progress in Nuclear Energy*, Series XII.
6. A. C. LUCAS. Development of a reader for condensor ionization chambers. AFRRI, CR-65-7 (1965).
7. R. E. SIMPSON, E. TOCHILIN and N. GOLDSTEIN. Neutron and gamma-ray dosimetry in an animal exposure at a pulsed TRIGA reactor, *Health Physics* **9,** 1021–1030 (1963).
8. P. W. REINHARDT and F. J. DAVIS. Improvements in the threshold detector method of fast neutron dosimetry. *Health Physics* **1,** 169 (1958).
9. G. S. HURST and R. H. RITCHIE (eds.) Radiation accidents: dosimetric aspects of neutron and gamma-ray exposures. ORNL-2748, Part A (1959).
10. H. H. ROSSI and W. R. ROSENZWEIG. Measurement of neutron dose as a function of linear energy transfer. *Rad. Res.* **2,** 417 (1955).
11. A. C. LUCAS, J. A. SAYEG and W. M. QUAM. Neutron and gamma dosimetry measurements at Walter Reed Army Institute of Research. Tech. Report No. 5-324-R (1966), Edgerton, Germeshausen & Grier, Inc., Santa Barbara Div.
12. Physical Aspects of Irradiation (ICRU NBS Handbook 85: Methods of fast-neutron and mixed-field dosimetry, 26–30).
13. C. L. WINGATE, E. TOCHILIN and N. GOLDSTEIN. Response of LiF to neutrons and charged particles. USNRDL-TR-909 (1965).
14. R. E. SIMPSON. The response of lithium fluoride to reactor neutrons, *Proc. International Conference on Luminescence Dosimetry*, Stanford University, California (1965).
15. G. S. HURST, W. A. MILLS, F. P. CONTE and A. C. UPTON. Principles and techniques of mixed radiation dosimetry—application to acute lethality studies of mice with the cyclotron. *Rad. Res.* **4,** 49 (1956).
16. K. C. HUMPHREYS. Some neutron dosimetry standardization efforts of the American Society for Testing and Materials, *Proc. Selected Topics of Radiation Dosimetry*, P-337. International Atomic Energy Agency (IAEA), Vienna (1961).
17. J. W. BOAG. The distribution of linear energy transfer or ion density for fast neutrons in water, *Rad. Res.* **1,** 323 (1954).
18. M. H. BIAVATI, W. ROSENZWEIG, H. H. ROSSI and I. MIYANAGA. The dependence of RBE on the energy of fast neutrons. III. Evaluations of radiation quality, *Rad. Res.* **19,** 512 (1963).
19. A. C. LUCAS and R. E. SIMPSON. The measurement of the L.E.T. distribution in a reactor environment. Paper presented before the Health Physics Meeting, Houston, Texas (1966).
20. G. S. HURST, J. A. HARTER, P. N. HENSLEY, W. A. MILLS, M. SLATER and P. W. REINHARDT. Techniques of measuring neutron spectra with threshold detectors—tissue dose determination. *Rev. Sci. Instrum.* **27,** 153 (1956).
21. J. A. SAYEG and J. D. PERRINGS. Preliminary data on neutron and gamma depth dose relations with fission neutrons using a plastic man phantom. Los Alamos Scientific Laboratory Report LAMS 2627, pp. 127–136 (1961).
22. R. M. LEHAMAN and O. M. FEKULA. Neutron spectra measurements inside human phantoms, IAEA-WHO Symposium on Nuclear Accident Dosimetry, Vienna (March 8–12, 1965).
23. J. A. SAYEG and J. H. DOWLING. Experimental evaluation of absorbed dose and LET distribution of dose in a nuclear accident—depth dose considerations. Presented at the 1966 Annual Meeting of the Health Physics Society, June 27–30, 1966, Houston, Texas.
24. National Bureau of Standards Handbook 63. Protection against neutron radiation up to 30 million electron volts. U.S. Department of Commerce (1957).
25. T. D. JONES. Distribution of dose and dose equivalent in a cylindrical tissue phantom from fission of neutrons. Oak Ridge National Laboratory Report No. ORNL-P-655 (Nov. 13, 1964).

DOSIMÉTRIE DE L'IRRADIATION PAR DES PROTONS DE HAUTE ÉNERGIE PAR MESURE DU BÉRYLLIUM–7

G. LEGEAY,* L. JEANMAIRE, M. L. DABURON, N. DE BOTTON et S. BERTRAND

Département de la Protection Sanitaire
Commissariat à l'Énergie Atomique, Fontenay-aux-Roses, France

et

PH. TARDY-JOUBERT, H. DE KERVILLER

Service de Protection contre les Radiations
Commissariat à l'Énergie Atomique, Saclay, France

Résumé—L'utilisation des accélérateurs de particules à de très hautes énergies pose des problèmes de dosimétrie en cas d'irradiation accidentelle.

Au Symposium sur la "Dosimétrie Personnelle en cas d'exposition accidentelle" organisé par l'Agence Internationale de l'Énergie Atomique en 1965 à Vienne, une méthode originale de mesure de la dose absorbée lors d'irradiation aux protons de haute énergie a été proposée.

L'analyse par spectrométrie γ met en évidence, aussitôt après l'irradiation, des radio-éléments de périodes très courtes, émetteurs β^+, donnant des photons d'annihilation de 511 KeV. Après 36 heures, un pic apparaît et persiste au niveau de 479 KeV. Il traduit l'émission des gamma du béryllium-7 dont la période est de 53,6 jours.

Ce béryllium-7 est produit par des réactions de spallation provoquées par les protons de très haute énergie sur les noyaux des tissus.

L'activité rapportée au jour de l'irradiation en utilisant la période physique du ^{7}Be, est reliée à la dose absorbée par un coefficient de proportionnalité indépendant de l'énergie des protons utilisés dans l'intervalle 600 MeV–2,8 GeV et égal à 0,023 $\pm$ 0,003 pCi/g.rad, en tenant compte de la valeur la plus récente du rapport de branchement des γ du ^{7}Be.

La sensibilité de la méthode par spectrométrie gamma est suffisante pour que cette dosimétrie biologique soit utilisable en cas d'irradiation accidentelle partielle ou totale.

Une série d'expérimentations a été réalisée pour vérifier les possibilités de cette méthode dont l'application pratique présente des difficultés inhérentes à la répartition de la dose absorbée dans l'organisme et à la diffusion du ^{7}Be formé.

INTRODUCTION

L'irradiation de rats avec des protons de 600 MeV du Synchrocyclotron du CERN à Genève et avec les protons de 2,8 GeV du Synchrotron Saturne du CEN-Saclay, nous a permis d'établir le coefficient reliant l'activité correspondant au béryllium-7 formé dans les tissus à la dose absorbée.

On sait en effet que les interactions des protons de haute énergie avec les tissus sont de deux types:

—des collisions avec les électrons atomiques se traduisant par une ionisation directe:

—des interactions nucléaires de spallation qui conduisent à un éclatement du noyau en fragments de basse énergie, après émission d'un ou plusieurs nucléons de haute énergie et de mésons.

Le nombre d'éléments radio-actifs qui peuvent être formés dans le second cas est très limité pour les noyaux légers constituant les tissus vivants. L'un d'eux est le béryllium-7.

Nous rappellerons brièvement les conditions dans lesquelles nous avons établi cette relation activité-dose que nous avons exposée dans une communication à l'Agence Internationale de l'Énergie Atomique à Vienne en 1965.[1]

Nous comparerons ensuite les résultats expérimentaux à ceux prévisibles à partir des données

* Détaché par le Service Biologique et Vétérinaire des Armées.

physiques. Nous exposerons enfin les résultats d'un certain nombre d'expérimentations entreprises pour explorer les possibilités de cette méthode dans le cas d'une exposition accidentelle de l'homme aux protons de haute énergie.

I. ÉTABLISSEMENT DE LA RELATION EXPERIMENTALE ACTIVITÉ-DOSE POUR LES RATS IRRADIÉS "IN TOTO"

I. 1. *Dosimétrie*

Les difficultés inhérentes à la mesure de la dose absorbée lors d'une irradiation par les protons de haute énergie exigent des précisions sur la dosimétrie.

Pour les protons de 600 *MeV*, BAARLI plaçait des chambres d'ionisation Baldwin de 0,6 cm^3 au centre des fantômes en polyéthylène, dans lesquels une variation de $\pm$ 4% de la dose a été notée entre 1 et 11 g/cm^2 de profondeur. Il intégrait dans une capacité un courant proportionnel au courant d'ionisation produit dans la chambre par les protons. Le dispositif était étalonné avec une chambre en matériau équivalent au tissu de ROSSI et FAILLA et la quantité d'électricité intégrée dans la capacité correspondait à la dose en rads.

Pour les protons de 2,8 *GeV*, une chambre de 0,6 cm^3 identique à celle utilisée à 600 MeV servait à mesurer la dose absorbée dans l'air devant l'animal irradié. Le rapport des pouvoirs d'arrêt respectifs de l'air et des tissus pour ces protons étant de 0,89, une dose de 1 rad dans une épaisseur mince de tissu correspondait à 0,89 rad mesuré dans l'air.

Ces résultats étaient comparés à ceux obtenus par activation grâce aux réactions ^{12}C (p, pn) ^{11}C et ^{27}Al (p, 3pn) ^{24}Na de sections efficaces respectives 27 mb et 9,1 mb à 2,8 GeV. Sachant qu'une fluence de $3{,}05.10^7$ p/cm^2 correspond à 1 rad dans un échantillon mince, nous avons pu vérifier que l'écart entre la dose calculée à partir des fluences et la dose mesurée n'excédait pas 8%.

Le bon accord entre les résultats obtenus a permis de limiter l'erreur sur la mesure à l'erreur statistique sur l'une ou l'autre des méthodes de mesure, soit environ 10%.

I. 2. *Spectrométrie γ et résultats*

Les spectres d'activité recherchés sur les rats

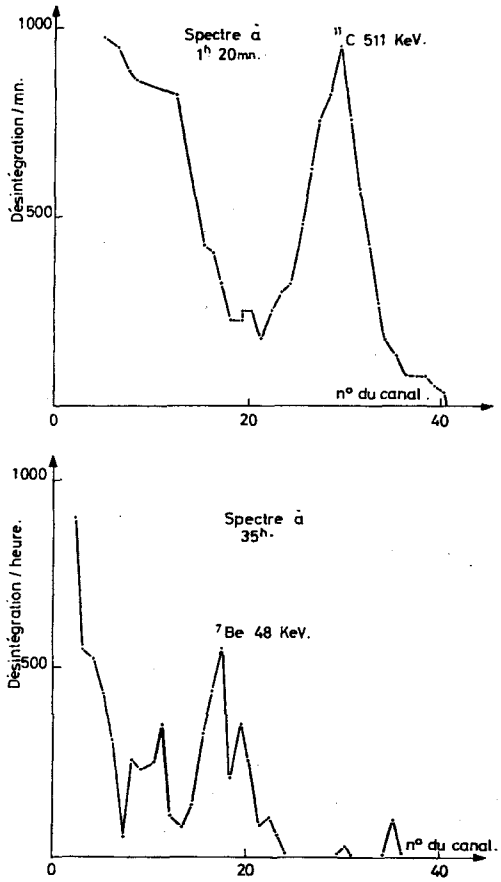

FIG. 1. Spectres de l'activité gamma, d'un rat irradié "in toto" par des protons de 2,8 GeV. Dose 1000 rads.

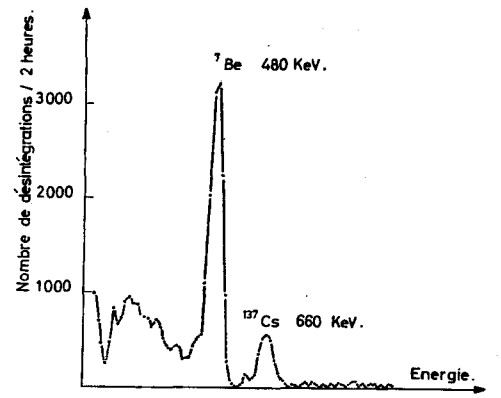

FIG. 2. Spectre de l'activité gamma de 2 rats au 5ème jour, après l'irradiation aux protons de 600 MeV. Dose 800 rads. (Cristal 4′ × 4′.)

vivants évoluent de la manière suivante en fonction du temps (figures 1 et 2).

—celui effectué 1 h 20 après l'irradiation montre l'existence d'un pic à 511 KeV. Celui-ci correspond aux gammas d'annihilation des trois émetteurs β^+ identifiés comme étant le ^{11}C, le ^{13}N et le ^{15}O.

—celui effectué 35 h après l'irradiation montre que le pic précédent a diminué considérablement. Par contre on observe un pic à 479 KeV correspondant à des gamma de transition du ^{7}Be dont le rapport de branchement est de 10,3% si l'on se réfère aux derniers documents publiés. [2]*

Des traces d'autres radioéléments apparaissent, notamment le ^{24}Na.

—celui effectué le 5ème jour après l'irradiation montre essentiellement un pic de ^{7}Be; celui-ci peut être observé assez longtemps en raison de sa période physique de 53,6 jours.

Les mesures de l'activite γ du ^{7}Be furent effectuées sur les cendres de rats irradiés par des protons de 600 MeV et de 2,8 GeV à des doses de 200 à 1000 rads. Le Laboratoire de Mesures des Radio-éléments du CEN-Saclay a effectué la mesure absolue à 7% près d'un étalon d'eau bérylliée, obtenu par irradiation d'eau distillée avec des protons de 2,8 GeV.

L'activité rapportée au jour de l'irradiation en utilisant la période physique du ^{7}Be est reliée à la dose absorbée par un coefficient de proportionnalité indépendant de l'énergie des protons utilisés et égal à 0,023 ± 0,003 pCi/g. rad (tableau 2). Ce coefficient expérimental et le coefficient calculé à partir des données figurant dans la littérature ont fait l'objet de recherches dont nous allons maintenant exposer les résultats.

* Cette valeur de 10,3% a été utilisée dans l'évaluation théorique (cf. II.1) et les comparaisons sont ainsi indépendantes de cette valeur.

II. CALCULS DES VALEURS THÉORIQUES D'ACTIVATION

II. 1. *Relation activité-dose dans un échantillon mince de tissu*

La dose expérimentale de 0,023 ± 0,003 pCi/g pour une dose absorbée au milieu du rat égale à un rad ayant été confirmée, nous avons été conduit à préciser les prévisions théoriques.

Dans notre communication à l'A.I.E.A., notre interprétation théorique de la production

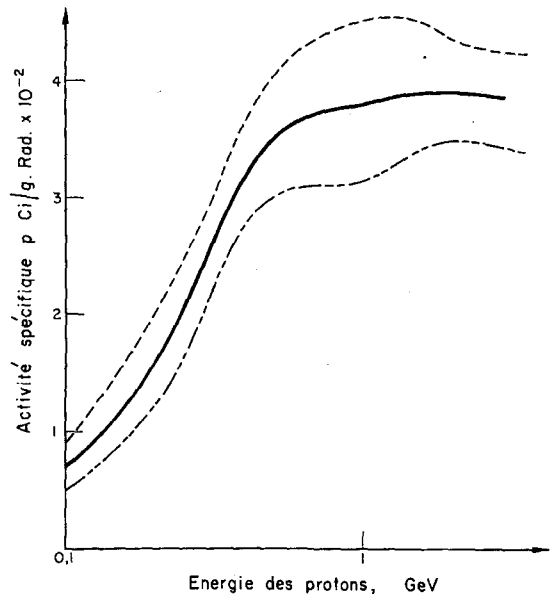

FIG. 3. Création de Be^7 par des protons de haute énergie dans un échantillon mince de tissu biologique.

Tableau 1. *Données sur les réactions prévisibles*

Élément	Concentration en %	Nombre d'atome-gramme par g. de tissu.	Réaction	Sections efficaces en mb.	
				Ep = 0,6 GeV	Ep = 2,8 GeV
C	12,3	$1{,}02.10^{-2}$	^{12}C (p, 3p, 3n) ^{7}Be	11,2 ± 1,1	10 ± 1
N	3,5	$0{,}25.10^{-2}$	^{14}N (p, 4p, 4n) ^{7}Be	10,4 ± 2	9,9 ± 2
O	72,9	$4{,}55.10^{-2}$	^{16}O (p, 5p, 5n) ^{7}Be	10,4 ± 2	8,7 ± 1

Tableau 2. *Comparaison des mesures in toto et sur cendres chez le rat.*
(*Dose absorbée:* 665 *rads.*)

Date de sacrification	Activité mesurée sur les cendres* en pCi/g	Activité mesurée in toto* en pCi/g	Coefficient de proportionnalité activité-dose† en pCi/g × rad
J + 6	15,4	10,2	0,25
J + 8	15,3	9,4	0,25
J + 9	15,7	7,1	0,26
J + 12	14,6	7,6	0,25
J + 13	14,6	7,1	0,25
J + 15	11,3	7,3	0,20

* Activité rapportée au gramme de poids de l'animal sacrifié, ramenée au jour de l'irradiation, en tenant compte de la période physique du ^{7}Be.
† Corrigé en tenant compte de la période biologique $T_b = 70$ J.

de ^{7}Be, à partir d'une dose absorbée par les tissus, se fondait sur des valeurs de sections efficaces connues à 20 ou 30% près. Des mesures plus récentes ont apporté des rectifications sur les trois constituants principaux (O, N, C).

Le tableau 1 donne les sections efficaces de production de ^{7}Be pour le carbone, l'oxygène et l'azote; la contribution des autres éléments des tissus est négligeable en raison de leur faible concentration, mais les sections efficaces de formation du ^{7}Be sur ces éléments sont très voisines.

Ceci nous conduit aux équivalences suivantes: 12,8 $\pm$ 1,8 pCi/g pour 10^{10} proton/cm^2 de 3 GeV correspondant à 0,039 $\pm$ 0,005 pCi/g. rad. Sur la figure 3 est représentée la courbe de variation de cette activité en fonction de l'énergie entre 0,1 et 3 GeV, avec les limites extrêmes de précision des calculs.

L'activité ainsi calculée correspond à une dose absorbée dans un échantillon mince de tissu placé dans l'air.

II. 2. *Variation de la dose et de l'activité en fonction de la profondeur*

Dans toutes les expériences précédentes, la dose absorbée est mesurée dans la partie médiane ("midline dose") d'un fantôme de rat en Mix D.

Au cours de nos expériences sur les protons de haute énergie, nous avons montré que la dose absorbée varie en fonction de la profondeur.[3] Pour le rat, nous avons déterminé le rapport entre la dose absorbée au milieu de l'animal et la dose dans un échantillon mince de tissu: la valeur moyenne déterminée à la suite de plusieurs expériences est égale à 1,4 avec un écart quadratique moyen de 0,1. La formation de ^{7}Be est due non seulement aux interactions produites par les protons primaires, mais aussi aux particules secondaires d'énergies supérieures au seuil de production.

Cette formation du ^{7}Be en fonction de la profondeur a été étudiée dans les deux expériences suivantes:

—une dose de 10.000 rads fut administrée à un cylindre de tissu mou de 30 cm de longueur sur 9 cm de diamètre dans le faisceau de protons. Fractionné de 5 cm en 5 cm, chaque morceau fut minéralisé et son activité mesurée. Celle-ci demeure sensiblement constante dans une épaisseur de 25 cm (tableau 3)

—un cylindre de Mix-D de 22,4 cm de longueur sur 6,5 cm de diamètre, constitué de 16 disques identiques, fut irradié dans les mêmes conditions. Nous avons constaté une légère augmentation de la quantité de ^{7}Be formée, de l'ordre de 5% pour une traversée de 14 cm de Mix-D.

En ce qui concerne la formation de ^{7}Be et pour les profondeurs qui nous intéressent, il semble donc qu'il se produit une compensation entre la disparition des particules primaires

Tableau 3. *Activité en ^{7}Be en fonction de la profondeur dans les tissus mous*

Profondeur cm	Activité en pCi/g frais
0–5	208
5–10	212
10–15	207
15–20	194
20–25	199
25–30	144

avec un libre parcours moyen de 60 $g.cm^{-2}$ et la création de particules secondaires d'énergies supérieures au seuil de création du radionuclide.

II. 3. *Relation activité-dose au milieu du rat*

La dose absorbée au milieu du rat étant de 40% supérieure à la dose absorbée dans un échantillon mince, la valeur calculée en II. 1. peut être corrigée pour la rapporter à la dose mesurée au milieu de l'animal, ce qui donne alors 0,028 pCi/g. rad à $\pm$ 15% près.

On observe donc un bon accord entre les valeurs expérimentales et les prévisions théoriques.

III. VÉRIFICATIONS DES DONNÉES EXPÉRIMENTALES

III. 1. *Contrôle des pertes de ^{7}Be au cours de la minéralisation*

La différence constatée entre les prévisions théoriques et les résultats expérimentaux pourrait être imputable à ces pertes car nous ignorons la nature des composés du béryllium qui se forment dans les tissus.

Le composé le plus probable est l'oxyde de béryllium dont le point d'ébullition est voisin de 4.000°C sous une pression normale. La minéralisation à 800° ne doit donc pas le volatiliser. Nous l'avons vérifié en injectant 300 cm^3 d'eau distillée irradiée possédant une activité de $4{,}4.10^{-4}$ $\mu Ci/cm^3$ dans une masse de viande de 2,5 kg que nous avons ensuite minéralisée. 95% du béryllium injecté fut retrouvé dans les cendres ce qui permet—aux erreurs expérimentales près—de considérer qu'il n'y a pas de pertes.

L'existence possible de composés plus volatils du béryllium nous a conduit à réaliser l'expérience suivante. Un rat irradié fut entièrement réduit en une pâte à l'aide d'un broyeur. L'homogénéité de celle-ci fut vérifiée sur plusieurs échantillons. Deux échantillons furent ensuite mesurés, l'un frais, l'autre minéralisé sous une géométrie identique. Le rapport des activités fut de 5,42 pour un rapport de poids de 5,56. La différence des rapports n'étant pas significative, nous devons donc admettre que la méthode de minéralisation mise en œuvre pour déterminer le coefficient reliant l'activité à la dose n'était pas une cause d'erreur.

III. 2. *Mesure de l'activité γ du ^{7}Be sur le rat "in toto"*

Nous avons effectué une comparaison entre les mesures d'activité "in toto" sur les rats, préalablement sacrifiés, et celles sur leurs cendres.

La géométrie des mesures sur les cendres correspondait à un disque de 50 millimètres de diamètre et de 10 à 12 mm d'épaisseur. Pour les mesures in toto, le rat fut placé dans une boîte cylindrique de 10 centimètres de hauteur et de 6,5 centimètres de diamètre. L'étalonnage était effectué avec une boîte analogue contenant de la gélatine irradiée avec les protons, elle-même étalonnée avec notre étalon habituel (voir I. 2.)

Les résultats de cette comparaison (tableau 2) montrent que le rendement de la mesure in toto par rapport à la mesure des cendres est de 75%. L'erreur de comptage avec la géométrie des cendres n'excède pas 5% si on admet que tout le ^{7}Be s'y retrouve. Elle est beaucoup plus élevée pour un comptage in toto, ce qui nécessite des corrections pour appliquer la relation activité-dose.

III. 3. *Mesure de l'activité sur un singe in toto*

Les caractéristiques du faisceau de protons de 2,8 GeV nous ont permis une irradiation globale d'un singe de 1,8 kg à la dose de 200 rads. Les comptages effectués 20 jours après l'irradiation avec un cristal de 20 cm de diamètre et 10 cm de hauteur ont montré que les mesures d'activité en ^{7}Be étaient encore possibles.

IV. DIFFUSION ET ÉLIMINATION DU ^{7}BE DANS L'ORGANISME

L'irradiation locale entrainant une formation de ^{7}Be tant dans les cellules que dans les milieux extra-cellulaires, il nous a semblé nécessaire d'effectuer un certain nombre d'expérimentations concernant sa diffusion. Celle-ci comporte un transfert au cours de l'irradiation par la voie sanguine, puis des échanges entre les espaces intra- et extra-cellulaires. Par ailleurs, comme tout radio-élément introduit ou formé dans l'organisme, le ^{7}Be est soumis aux processus d'élimination biologique et de décroissance physique qui aboutissent à la notion de période effective.

IV. 1. *Diffusion du ^{7}Be de la tête vers le corps après une irradiation céphalique du lapin*

L'irradiation locale étant la plus probable lors d'un accident auprès d'un accélérateur, une mesure localisée ne pourrait qu'accroître la sensibilité de la méthode. Mais, auparavant, il faut s'assurer de l'importance de la diffusion dans le temps du béryllium formé.

Compte tenu de la section du faisceau de protons dont nous disposions, la tête du lapin se prêtait le mieux à une irradiation locale.

Une première série de lapins reçut des doses allant de 900 rads à 9000 rads. La mort par hémorragies méningées qui se produisit du 2ème au 10ème jour limita nos observations. Elles montrèrent cependant une diffusion non négligeable du ^{7}Be formé dans la tête vers le reste du corps.

Une deuxième série de lapins fut irradiée à des doses de 600 rads dans une section de faisceau à bordure nette permettant une limitation exacte de l'irradiation de la tête du lapin. Le tableau 4, colonne 1, montre le protocole suivi.

Cas des animaux irradiés morts. Sur les trois animaux de ce lot, le corps présentait une activité totale égale à 30% de celle de la tête. L'étude du faisceau par autoradiographie a permis de mettre en évidence l'existence d'un halo de particules autour du faisceau principal entraînant une irradiation de l'ensemble du corps à une dose moyenne égale à 3% de celle reçue

Tableau 4. Évolution de l'activité dans la tête et dans le corps en fonction du temps après irradiation

Date de sacrification	Tête		Corps		Rapport des activités/g Tête/Corps (moyenne)
	Poids en g à la sacrification	Activité $\bar{m}$ en pCi/g	Poids en g à la sacrification	Activité $\bar{m}$ en pCi/g	
Avant l'irradiation	190	15,6	1890	0.59	
	190	13,0 } 14,5	1740	0.32 } 0.49	29,6
	185	15,0	1710	0.55	
Après l'irradiation	210	10,6	1670	0.69	
	215	11,6 } 9.8	1985	0.68 } 0.60	16,3
	260	7,2	2490	0.44	
	290	9,3	2855	0.67	
J + 0,5	230	10 } 9,8	2310	0.80 } 0.69	14,2
	190	10,3	2080	0.60	
	300	11,2	2820	1.00	
J + 1	250	9,3 } 9,8	2430	0.62 } 0.74	13,2
	275	9,1	2395	0.61	
J + 2	260	10,4	2550	0.46	22,6
J + 5	250	9,3	2540	0.85	10,9
J + 11	250	7,8	2130	0.56	14
J + 15	280	7,8	2860	0.64	12,3

par la tête. Ceci a permis d'expliquer une activité du corps qui ne pouvait résulter d'une diffusion biologique.

L'activité due au ^{7}Be formé dans la tête de ces lapins (tableau 4) peut être reliée à la dose grâce au coefficient déterminé expérimentalement sur le rat, ce qui s'explique du fait que les géométries d'irradiations étaient voisines.

Cas des animaux sacrifiés après l'irradiation. L'activité spécifique de la tête des lapins sacrifiés immédiatement après l'irradiation est inférieure de 30% à celle des lapins irradiés morts.

Cette décroissance rapide traduit le transfert par voie sanguine du ^{7}Be formé dans les espaces extra-cellulaires durant l'irradiation.

Pour les lapins sacrifiés après l'irradiation, la loi de décroissance de l'activité spécifique de la tête en fonction du temps séparant l'irradiation de la sacrification (figure 4)-en corrigeant la mesure avec la période physique du ^{7}Be en vue de rapporter tous les résultats au même instant —est de caractère exponentiel, la période de diffusion biologique est $T = 32 \pm 3$ jours.

Nous avons vérifié par ailleurs, pour des doses absorbées proportionnelles entre elles, que le même processus se produit au facteur de proportionnalité près.

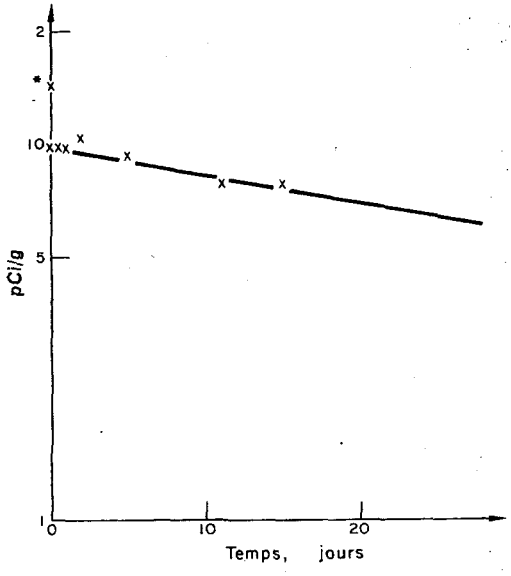

FIG. 4. Activité de la tête en ^{7}Be en fonction du temps après sacrification. Recherche de la periode biologique. Les activités sont ramenées au jour de l'irradiation (correction de la période physique).

* animal sacrifié avant irradiation.

IV. 2. *Période effective du ^{7}Be pour le rat irradié in toto*

La valeur 0,024 pCi/g. rad a constamment été retrouvée sur les mesures faites les premiers jours suivant l'irradiation. Pour effectuer des corrections exactes sur des mesures faites ensuite, il est nécessaire de connaître la période effective du ^{7}Be.

La Commission Internationale de Protection Radiologique[4] indique, pour l'homme, une période effective de 41 jours, la période biologique étant de 180 jours.

Nous avons recherché, grâce aux mesures in vivo sur le rat et le singe après irradiations globales, les valeurs correspondantes.

Sur 16 rats irradiés à 400 rads, la période effective est de 30 ± 5 jours. Ceci correspond à une période biologique de 70 jours environ compte tenu de la dispersion des résultats. Utilisant cette valeur moyenne nous avons effectué sur le tableau 2 les corrections de période biologique ce qui nous a permis de retrouver le coefficient de proportionnalité de $0,025 \pm 0,003$ pCi/g. rad absorbé au jour de l'irradiation.

Pour l'unique singe irradié à 200 rads, nous avons trouvé une période effective de 35 jours, soit une période biologique de 100 jours: cette valeur est donnée à titre indicatif.

V. DISCUSSION

Nul n'ignore les difficultés que pose la détermination de la dose absorbée par un individu lors d'un accident. La dosimétrie physique est trop souvent imprécise du seul fait que le dosimètre ne se trouve pas toujours placé en indicateur de dose en surface sur le sujet irradié par rapport à la source de rayonnements.

La dosimétrie biologique par activation offre a priori l'avantage de fournir directement la dose absorbée. Celle que nous proposons pour les protons de haute énergie n'est pas sans analogie avec la méthode de dosimétrie des neutrons par activation du sodium que nous avons d'ailleurs relevé également dans nos spectres.

Le ^{7}Be peut se former dans tous les tissus, aussi bien dans les espaces intercellulaires que

dans les cellules. Sa période effective permet d'effectuer des mesures d'activité avec toute la liberté de temps désirable.

Nous avons déterminé le coefficient de proportionnalité entre l'activité et la dose. Il est indépendant de l'énergie des protons incidents dans l'intervalle exploré (600 MeV – 2,8 GeV) et pour les conditions de géométrie dans lesquelles nous avons expérimenté. Nous avons enfin mis en évidence une période de diffusion dans le cas d'une irradiation locale particulière.

Les possibilités actuelles de la spectrométrie permettent de détecter les photons gamma émis à des niveaux d'activité suffisants pour être d'un intérêt réel en cas d'accident.

La mesure de l'activité in toto sur un singe irradié à 200 rads permet d'estimer que sur un individu standard, absorbant une dose de 5 rads uniformément distribuée dans l'organisme, l'activité correspondante de l'ordre de 10^{-2} μCi serait décelable.

Mais nous connaissons les difficultés que présente la mise en œuvre d'une dosimétrie biologique par activation. Pour établir l'activité en ^{7}Be formé dans l'organisme, nous pensons qu'il est indispensable d'effectuer, parallélement aux mesures locales et in toto sur l'individu irradié, des mesures analogues sur fantômes contenant des taux d'activité en ^{7}Be connus.

La possibilité de produire celui-ci par irradiation de l'eau permet de résoudre aisément le problème de l'étalonnage. Signalons au passage la nécessité de saturer l'eau à irradier de béryllium stable afin d'éviter une concentration par adsorption du ^{7}Be sur les parois des récipients.

Nous estimons, par ailleurs, que si des mesures locales—notamment celles sur les gammas d'annihilation des émetteurs β^{+} à vies très courtes—ont permis de préciser la région de l'organisme irradié, il peut être utile de réaliser un modèle en tissu mou de la zone atteinte. Son activation par irradiation, son utilisation pour des mesures locales et in toto dans le fantôme précédent ainsi que la détermination exacte de son activité permettraient de compléter les bases d'information.

Les corrections à l'aide de la période effective pour le sujet irradié, de la période physique pour les mesures du fantôme, l'introduction du facteur de diffusion qu'il est possible de préciser par des mesures d'activité relatives locales, doivent permettre d'établir la dose absorbée avec une approximation relativement bonne.

CONCLUSION

L'irradiation de la matière vivante par les protons de haute énergie offre donc la possibilité de réaliser une dosimétrie biologique.

Celle-ci est possible pendant un temps relativement long du fait de la période effective du ^{7}Be; la relation entre l'activité et la dose est simple dans l'intervalle 0,6–2,8 GeV; la sensibilité de la méthode par spectrométrie gamma est suffisante pour que cette dosimétrie biologique soit utilisable en cas d'irradiation accidentelle partielle ou totale.

Comme pour toutes les méthodes de dosimétrie biologique, l'application pratique présente des difficultés inhérentes à la répartition de la dose absorbée dans l'organisme et à la diffusion du ^{7}Be formé. Ce sont ces difficultés que nous avons explorées dans cette étude.

REMERCIEMENTS

Nous tenons à remercier Messieurs Guenet, Tulasne, Dupin, Desaivre du Groupe de Radiopathologie Générale et Messieurs Quéchon, Pagès et Brochen du Groupe de Radioprotection de Saturne pour l'aide qu'ils nous ont apportée au cours de nos expérimentations auprès du Synchrotron Saturne.

RÉFÉRENCES

1. G. Legeay, L. Court, L. Prat, L. Jeanmaire, M. L. Daburon, H. de Kerviller et Ph. Tardy-Joubert. Personnel dosimetry for radiation accidents. IAEA (Vienne), pp. 507–523 (1965).
2. J. B. Cumming. *Ann. Rev. Nucl. Sci.* **13,** 261 (1965).
3. G. Legeay, Ph. Tardy-Joubert et N. de Botton. Congrès Health Physics, Houston (Juin 1966).
4. I.C.R.P. Publication 2 (1959).

THE DOSIMETRY OF ^{55}Fe*

McDONALD E. WRENN

Institute of Environmental Medicine, New York University Medical Center
New York, New York, U.S.A.

Abstract—Recent detection in human blood of radioactive ^{55}Fe produced in nuclear weapon tests has led to a re-evaluation of the dosimetry for this radionuclide which decays exclusively by electron capture. The revised dosimetric estimates for blood are approximately twice those previously calculated. Approximately 3/4 of the decay energy capable of producing ionization is emitted in the form of Auger electrons which have a range of 0.3μ in water. In blood the dose from these Auger electrons is delivered primarily to the erythrocytes which contain relatively large concentrations of stable iron uniformly distributed as hemoglobin. The dose to the erythrocytes is approximately twice that previously calculated for whole blood.

As a consequence of the concentration of ^{55}Fe within the erythrocytes, the short range of the characteristic Auger electrons emitted, and the frequency of Auger electron emission relative to X-ray emission, the dose to the erythrocytes is 10 times the dose to the rest of the blood, so that this form of exposure is primarily intracellular.

A specific activity of 1 pCi of ^{55}Fe per mg of stable iron results in a dose rate of 2 μrad/week to the erythrocytes. This same specific activity in iron rich aggregates of ferritin molecules may deliver local dose rates up to 800 μrad/week.

Although estimates of the amounts of iron in the erythrocyte precursor cells are not sufficiently quantitative to permit accurate dosimetric calculations, the presence of significant concentrations of iron in cells from all stages of erythropoiesis has been reported for rat bone marrow indicating that irradiation of the more sensitive erythrocyte precursors may be significant.

INTRODUCTION

^{55}Fe produced in nuclear testing has been reported in the environment since 1959[1] and has since been reported in human blood from United States residents on the East and West coasts[2] and in Finnish samples.[3] In the groups reported by Wrenn and Cohen in 1965, women generally had higher concentrations of ^{55}Fe than men.[4]

A group of fish eaters has been identified in the East coast U.S.A. study having significantly higher burdens of ^{55}Fe in blood than non-fish eaters. Subsequently, samples of tuna meat were found to have a much higher specific activity than terrestrially based food items.[2,4]

In view of the widespread presence of ^{55}Fe in humans and in view of the possibility that fish eating populations may have significantly higher burdens than other groups it was felt that the dosimetry should be critically examined.

This paper reports several aspects of this dosimetry of this nuclide which have not been adequately appreciated before. Only the distribution of absorbed energy will be dealt with here. The biological implications are presently under investigation in our laboratories.

PROPERTIES OF THE DECAY OF ^{55}Fe

^{55}Fe decays exclusively by electron capture since the total energy difference between initial and final states, 0.214 MeV, makes positron decay energetically impossible. Most of the energy is carried off by a monoenergetic neu-

* This investigation was supported by a project grant from the United States Atomic Energy Commission Contract AT(30–1) 3086, and is part of a core program supported by the United States Public Health Service, Bureau of State Services grant ES 00014 and the National Cancer Institute grant CA 06989.

trino, but the resulting excited state of ^{55}Mn which usually has a vacancy in the K shell has 6.5 keV residual energy of excitation, an amount equal to the binding energy of a K shell electron of Mn. About 10% of the disintegrations of ^{55}Fe proceed by L capture rather than K, resulting in ^{55}Mn atoms with one vacancy in the L shell. In this case the excitation energy of the resulting Mn atom is 0.65 keV, the highest ionization energy for an L shell electron.[5-7]

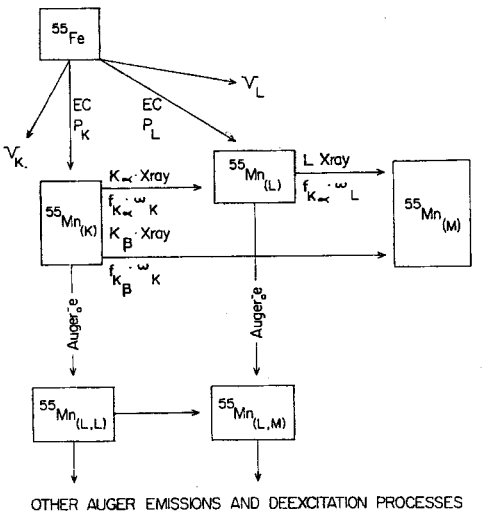

FIG. 1. Simplified de-excitation scheme for ^{55}Fe–^{55}Mn.

A very small portion of the capture processes are accompanied by the emission of internal bremsstrahlung which occurs with a probability of 0.8×10^{-5} per disintegration.[8] The whole process can be summarized as:

$$M_{Fe} - M_{Mn} = E(K, L) + E_\nu + E_\gamma \quad (1)$$

where M_{Mn}, M_{Fe} is the energy equivalent of the atomic mass of ^{55}Mn and of ^{55}Fe,
E_γ is the energy of the internal bremsstrahlung emitted,
E_ν is the energy of the neutrino emitted,
$E(K, L)$ is the binding energy in Mn of the appropriate K or L shell electron, depending on the capture process.

After electron capture the atom is left in an excited state. The process of de-excitation must be considered in detail in order to arrive at the proper formulation of the dosimetry for electron capture nuclides. Figure 1 diagrams decay and de-excitation processes followed by ^{55}Fe and ^{55}Mn. Each rectangle represents a different state of the atom and letters in parentheses represent holes in the shell of that designation.

On this diagram vertical transitions represent changes in the electron configuration without the emission of an X-ray whereas horizontal transitions represent a change in the orbital electron configuration accompanied by X-ray emission. Table 1 summarizes the data on the relative frequencies of the most important de-excitation modes and also the energies involved in the various stages of de-excitation.

The total energy per disintegration available for deposition in surrounding material includes all forms of energy except that carried away by neutrinos. The average energy per disintegration which is available for absorption in tissue (E_A) is given by:

$$E_A = P_K E(K) + P_L E(L) + P_b \bar{E}_b + P_{b-c} E_{b-c} \quad (2)$$

where: E_A is the average energy of de-excitation of an excited daughter atom initially formed by electron capture,
E_b is the average energy emitted in the form of bremsstrahlung,
E_{b-c} is the average energy of orbital electrons "converted" as an alternate to bremsstrahlung emission,
P_b is the probability of bremsstrahlung emission per disintegration,
P_{b-c} is the probability of orbital electron ejection in the process of electron capture.

Since $P_{b-c} < P_b$ and P_b is negligibly small, the two terms of equation (2) on the far right can be neglected. Then the energy of de-excitation available for deposition (E_A) which results from either K or L capture can be closely approximated by:

$$E_A = P_K E(K) + P_L E(L) \quad (3)$$

Table 1. Physical Constants Pertinent to the Dosimetry of ^{55}Fe

Term	Symbol	Value	Source
K fluorescence yield (Mn)	ω_K	0.251	Burhop, 1952[9]
L fluorescence yield (Mn)	ω_L	0.006	Burhop, 1952
Ratio of probabilities of L to K capture (Fe)	P_L/P_K	0.107	Manduchi and Fannoni, 1962[10] Scobie *et al.*, 1959[11] Fink, 1961[12]
K binding energy (Mn)	$E_Z(K)$	6.54 keV	Fine and Hendee, 1955[7]
L binding energy (Mn)	$E_Z(L)$	0.650 keV	,,
M binding energy (Mn)	$E_Z(M)$	0.052 keV	,,
L binding energy (Fe)	$E_{Z+1}(L)$	0.849 keV	,,
prob. of emission of $K\alpha$ X-ray (Mn)	$f_{K\alpha}$	0.872	,,
prob. of emission of $K\beta$ X-ray (Mn)	$f_{K\beta}$	0.128	,,
prob. of bremsstrahlung emission per disintegration	P_b	0.8×10^{-5}	Biavati, 1964[8]

In the case of ^{55}Fe, E_A is equal to 5.97 keV. The ICRP conservatively overestimates the effective energy as 6.5 keV.[13] Other investigators have used the energy of the K X-ray as the effective energy.[14-16] Although conceptually incorrect, the K X-ray has an energy of 5.9 keV which is numerically close to the value of the available energy derived above.

The energy available from de-excitation must be considered in two parts, that resulting in "short range" emissions and that resulting in "longer range" emissions. In this case, short range refers to all the de-excitation processes except the emission of the K X-rays. Then referring to Fig. 1 the fraction, F, of the available energy of de-excitation emitted by the K X-rays is:

$$F = \frac{P_K\omega_K[\{E(K)-E(L)\}f_{K_\alpha}+\{E(K)-E(M)\}f_{K_\beta}]}{P_KE(K)+P_LE(L)}$$

Substituting numerical values from Table 1 leads to $F = 0.226$. The fraction of the total energy emitted in short range emissions is $1 - F$, so that 0.774 of the de-excitation energy is deposited by short range emissions. Now let us examine the range of the short ranged emissions. The highest energy Auger electron emitted will have an energy giver by:[9]

$$E_{\text{Auger (Max)}} = E(K) - E(L, L) \qquad (4)$$

Removing one electron from the L shell requires an energy of $E_Z(L)$. The removal of a second electron requires approximately $E_{Z+1}(L)$ because one less electron is present to shield the total nuclear charge. The maximum kinetic energy an Auger electron can have occurs when an L shell electron is emitted following K capture. In this case the energy is given by:

$$E_{\text{Auger (Max)}} = E_Z(K) - E_Z(L) - E_{Z+1}(L) \qquad (5)$$

Using the data from Table 1 the highest energy Auger electron emitted has an energy of 5.04 keV.

CALCULATION OF THE PATH LENGTH OF ELECTRONS IN BODY TISSUE

The range of low energy electrons has been measured in several gases.[17] The range (R) may be loosely defined as the thickness of an absorber which the electron can penetrate.

The total path length (S) which electrons traverse in going through an absorber is of course longer than the range because the electrons

will change direction when scattering. S is nevertheless proportional to R.[18] For 19.6 keV electrons in oxygen the average range, R, which one-half of the electrons will exceed is $\frac{1}{2}$ the average mean path length, S. In this case only 3% of these electrons have sufficiently straight paths to penetrate an absorber thickness equal to the mean path length.

The range rather than the path length is a more appropriate index of the distance within which most of the energy will be deposited, and therefore is the more appropriate quantity to use for dosimetric purposes.

The range of the Auger electrons from ^{55}Fe in tissue has not been studied experimentally, but it can be inferred from both theoretical and other experimental data. The average path length of monoenergetic electrons in oxygen and hydrogen has been measured by Williams[17] and values are abstracted in Table 2.

The path lengths at different energies can be inferred from the Thompson–Whiddington Law:[18]

$$S = \frac{k E^2}{N Z} \qquad (6)$$

where: N = atoms/cc,
Z = atomic number,
k = a constant,
E = kinetic energy of the electron.

By applying this relationship to the data in Table 2 the path lengths of 5.04 keV Auger electrons in hydrogen and oxygen at standard temperature and pressure are found to be 0.05 and 0.4 cm respectively.

If the gas under consideration were a mixture of hydrogen and oxygen in the ratios found in water then the effective average path can be found using equation (6) and noting that the inverse of the average path length is proportional to the electron density. Then adding electron densities and inverting leads to an expression for the effective path length:

$$\bar{S}_{\text{eff}} = \frac{S_H}{1 + \frac{N_O Z_O}{N_H Z_H}} \qquad (7)$$

where the subscript H refers to the element hydrogen and the subscript O to the element oxygen.

Then for a gaseous combination of H_2 and O_2 in the molecular ratio of 2 to 1 as found in water at 0°C and a pressure of 76 cm Hg, $\bar{S}_{\text{eff}} =$ 0.0754 cm. Since the density of this gas is 0.804×10^{-3} g/cc, conversion to unit density leads to an average path length of 0.62 microns in water and an average range of 0.3 micron. This important result is consistent with other data on electron ranges. Lea using theoretical expression for electron collisions developed by Bethe estimates the path length of a 5 keV electron in water is 0.74μ,[19] and recent experimental determinations of energy loss by electrons in thin films gives results consistent with the estimate made here.[20] For purposes of this paper the range derived from experimental data in gases will be used.

Since the number of L X-rays emitted are negligible ($\omega_L = 0.006$) in terms of energy transport we may safely assume that all short range emissions of ^{55}Fe have ranges less than 0.3μ in water or tissue.

DOSIMETRY OF ^{55}Fe IN MAN

Iron in humans is found in greatest concentrations in the blood. The particular loci of iron are the red blood cells (erythrocytes) and consequently in the dosimetry of radioiron we

Table 2. Average Path Length, S, for Electrons in Gases at 0° and 76 cm Hg[17]

Gas	Initial energy (keV)	Average path length (cm)
Oxygen	7.56	0.117
Hydrogen	7.56	0.72
Hydrogen	4.80	0.35

may consider that the iron is distributed in the blood only inside the erythrocytes. Effectively the erythrocytes are floating concentrations of iron in a fluid, the plasma, itself relatively devoid of iron.

Normal erythrocytes are biconcave discs with a mean diameter of 7.5 microns. Most cells have diameters between 6.9 and 8.1 microns in adult humans. The mean thickness ranges from 1.84 to 2.05 microns. The mean corpuscular volume in adults is 86 cubic microns with an experimentally determined range (2 σ) from 78 to 96 cubic microns.[21, 22]

These dimensions have interesting dosimetric consequences. Since the range of the Auger electrons emitted are all small compared with normal cell dimensions, most of the energy from any one decay is deposited in the same cell in which the decay occurs. In short, the dose is primarily delivered intracellularly to the erythrocytes.

The appropriate mass for dosimetric calculations in blood for ^{55}Fe is the red cell mass for that fraction of the energy liberated in short range emissions and the whole blood for the longer ranged X-ray emissions. Previously the mass of the whole blood has been used for dosimetric calculations.[14-16]

The dose to whole blood from ^{55}Fe is delivered by that part of the decay energy emitted in the form of K X-rays. Since the mean free path of a K X-ray in tissue is approximately 1 mm[23] we can assume that most of the K X-rays will be absorbed in the blood and can neglect the deposition of energy in tissues adjacent to the blood. In the capillaries, however, this will overestimate the dose to the whole blood. Assuming a specific activity of iron of 1 pCi/mg of stable iron the dose rate of the whole blood from the X-rays can be calculated as follows:

$$1\ \frac{\text{pCi}}{\text{mg}} \times \frac{0.503\text{mg}^{*}\ (\text{Fe})}{\text{ml (blood)}} \times \frac{0.95\ \text{ml}}{\text{g}}\ (\text{blood})$$

$$\times\ 2.22\ \frac{\text{dpm}}{\text{pCi}} \times \frac{10^{4}\ \text{min}}{\text{week}} \times 5.97$$

$$\times\ 10^{3}\ \frac{\text{eV}}{K\ \text{X-ray}} \times 0.226\ \frac{E\ \text{X-ray}}{E_{A}} \times 1.61$$

$$\times\ 10^{-12}\ \frac{\text{erg}}{\text{eV}} \times \frac{1\ \text{rad-g}}{100\ \text{erg}} \times 10^{6}\ \frac{\mu\text{rad}}{\text{rad}}$$

$$= 0.23\ \mu\text{rad/week}$$

The dose rate to the red cells can be calculated as follows:—

$$D_{\text{red cells}} = (K\ \text{X-ray dose rate}) + \text{Auger dose rate}$$

$$\text{Auger dose rate} = (K\ \text{X-ray dose rate}) \times \frac{(E\ \text{of short range emissions/dis})}{(E\ \text{of X-ray emissions/dis})} \times \frac{(\text{blood mass})}{(\text{red cell mass})}$$

$$= 1.77\ \mu\text{rad/week/pCi/mg (Fe)}$$

Adding the dose to the erythrocytes from the Auger electrons and X-rays gives:

$$D_{\text{red cells}} = 0.23 + 1.77$$

$$= 2.00\ \mu\text{rad/week/pCi/mg (Fe)}$$

The erythrocytes may be relatively radioinsensitive, since they will not undergo any more divisions. For this reason other tissues may in fact be more important and with this in mind the marrow, therefore, becomes the next tissue of concern. Although studies of the uptake of iron by marrow in humans have not been made in sufficient detail to permit good, quantitative calculations of the dose, uptake has been studied in rats. Although the intracellular synthesis of hemoglobin does not start when the stem cell precursors of the red cells are dividing, nevertheless iron enters into the immature cell precursors and is present in most of the earliest stages of erythropoiesis in the rat.[25] For this reason it is apparent that radioiron uniformly distributed in the body pools of stable iron will irradiate the blood forming cells. Although the presence of iron in fairly large amounts has been verified in the pre-erythrocytic cells, accurate, quantitative estimates of

* 0.503 mg arises from the means of the average adult male and female values.[24]

the concentrations of iron present are not available.

Since the details of each stage of erythropoiesis such as cell volume, intracellular iron concentration, and time and number of divisions are not well known, the dose calculation for the bone marrow cannot be performed as accurately as that for red cells. Bothwell and Finch[16] estimate that the stable iron concentration in marrow is 1/3 that in whole blood. Assuming the ratio of intracellular to extracellular mass is the same in marrow and blood the dose calculations for marrow cells lead to values approximately 1/3 those for the erythrocytes. For ^{55}Fe uniformly distributed in the body pools the dose rate to marrow is continuous at approximately 0.7 μrad/week/pCi/mg (Fe).

The highest local concentrations of iron and also the highest dose rates are found in aggregates of ferritin molecules present in liver, spleen, and even within reticulocytes. The ferritin molecule consists of a core, probably containing 6 micelles of iron, surrounded by a protein shell. The iron comprises 20% of the ferritin although some variation is found due to inhomogeneity of the iron and protein moities.[12] For ferritin aggregates infinite in extent the dose rate from 1 pCi/mg of stable iron can be calculated as follows:

$$5.9 \times 10^{-3} \frac{\text{MeV}}{\text{dis}} \times \frac{2.22 \text{ dis}}{\text{pCi - min}} \times \frac{1 \text{ pCi}}{\text{mg}}$$

$$\times \frac{200 \text{ mg(Fe)}}{\text{g (tissue)}} \times 1.6 \times 10^{-6} \frac{\text{erg}}{\text{MeV}} \times 1.01$$

$$\times 10^{4} \frac{\text{min}}{\text{week}} \times \frac{1}{100 \text{ ergs/rad-g}}$$

$$= 0.44 \text{ mrad/week/pCi/mg}$$

Assuming no biological turnover leads to a mean life of 203 weeks and dose to infinity of

$$D = 90 \text{ mrad/pCi/mg}$$

This represents an upper limit to the true dose to ferritin aggregates, due to their limited sizes. Since only 77% of the energy is deposited by short range emissions and since the short range Auger electrons will deposit some of their energy outside of the aggregate, the dose from 1 pCi/mg(Fe) to an aggregate of finite size would be:

$$90 \text{ mrad} \times .77 \times f$$

where f is the fraction of short range energy deposited inside the aggregate.

Of course f depends on the geometry, and should be evaluated in detail for pertinent geometries, suggested by the observed biological distributions of stable iron. The problem of finding the fraction of energy deposited as a fraction of size and shape of the aggregate is presently under investigation.

The dose calculations presented here for blood are compared to those of other authors in Table 3. The details of the dose calculations are given in the Appendix. Note that the highest dose is delivered to ferritin aggregates. The integral doses are all approximately equivalent. Which of the formulations is radiobiologically most significant, is still a controversial subject, but it is clear that ^{55}Fe offers a tool for such an investigation.

^{55}Fe DOSES TO ADULTS IN NEW YORK AREA IN 1965

The dose commitment to a population of twelve New York residents which has been reported elsewhere[4] is summarized in Table 4. The dose to all regions of interest is small compared with that from several years of background radiation with the exception of that to ferritin which roughly equals that from two years of background.

SUMMARY

For ^{55}Fe the energy available for deposition in biological systems averages 5.97 keV per disintegration, and not 6.5 keV which is conservatively used by the ICRP.[9] The energy is emitted either as X-rays or as short ranged Auger electrons. The short range emissions account for 77% of the available energy, so that for cells containing high concentrations of iron the irradiation from ^{55}Fe is primarily intracellular.

The dose to the erythrocytes calculated by

Table 3. Dose Calculations by Several Investigators—^{55}Fe Infinity Dose to Various Organs and Tissues in Man

Organ of reference mass (g)	Dose mrad/pCi/mg	Integral dose rad-g/pCi/mg	Source
Whole body (70,000)	0.0236	1.65	Seltzer *et al.*, 1964 [26]
Blood (5000)	0.197	1.00	Peacock *et al.*, 1946 [14]
Blood (5000)	0.214	1.08	Bothwell and Finch, 1962 [16] Quimby *et al.*, 1958 [15]
Red blood cells (2500)	0.406	1.02	This paper
Red marrow (1500)	0.135	0.202	This paper
Ferritin (2)	69.3	0.180	This paper

Assumptions: 1. No biological elimination of iron. 2. Radioiron uniformly mixed in the iron pools of the body. 3. Ferritin content of the body is 2 g, containing 400 mg of stable iron.

taking the short range of the Auger electrons into consideration is approximately twice that previously reported. However, the integral dose remains the same. Because of the short range of the Auger electrons the highest dose in humans is delivered to ferritin aggregates. The dose to ferritin aggregates is two orders of magnitude greater than that to erythrocytes, but the integral dose to ferritin aggregates is less than that to erythrocytes.

ACKNOWLEDGEMENTS

The author wishes to express his thanks to Professor Merril Eisenbud for his guidance and support; to Dr. Richard Heimbach for a number of stimulating discussions; and to Mr. Norman Cohen for aid in the experimental work which led to this paper, helpful discussions, reading of the manuscript, and suggestions.

APPENDIX

^{55}Fe Dosimetry Calculations

Whole Body

Source: Quimby *et al.*, 1958

$D_\beta = 73.8\ \bar{E}_\beta\ C_0\ T$

where: $\bar{E}_\beta$ is average β energy in MeV,
C_0 is concentration of the radionuclides in tissue in μCi/g,
T is half-life in days,
D_β is the infinity dose in rad.

Source: Seltzer *et al.*, 1964
5.9 mrad/microcurie

Source: Standard Man; ICRP II, 1959
4 g stable Fe

$$\frac{5.9\ \text{mrad}}{10^6\ \text{pCi}} \times 4000\ \text{mg}$$

$$= 0.0236\ \text{mrad/pCi/mg}$$

Table 4. Infinity Dose to Various Biological Loci from the Average 3.4 pCi-mg Concentrations of ^{55}Fe in Blood of New York Residents, August 1965*

Biological Locus	(g)	Dose (mrad)	Integral dose (rad-g)
Erythrocytes	2500	1.4	3.5
Red marrow	1500	0.46	0.69
Ferritin†	2	235	0.60

* Assumes no biological elimination of iron.

† Ferritin aggregates assumed much larger than 0.3μ in all dimensions.

Whole Blood

Source: Quimby *et al.*, 1958; Bothwell and Finch, 1962

Assume: concentration of 1 pCi/mg stable iron:

Specific activity:

$$\frac{1\ \text{pCi}}{\text{mg}} \times \frac{0.5\ \text{mg}}{\text{g (blood)}} \times \frac{10^{-6}\ \mu\text{Ci}}{\text{pCi}}$$

$$= 0.5 \times 10^{-6} \frac{\mu\text{Ci}}{\text{g}}$$

$$D_{ec} = 73.8 \times 0.0059 \times 0.5 \times 10^{-6} \times 985 = 0.214\ \text{mrad/pCi/mg}$$

Source: Peacock *et al.*, 1946

40,000 dpm/ml is equivalent to 0.04 r/week, where 1 r in tissue is equivalent to 84 ergs.

$$\frac{0.04\ \text{r}}{\text{week}} \times \frac{84\ \text{rad}}{100\ \text{r}} \times \frac{1}{40{,}000\ \text{dpm/ml}} \times \frac{1}{0.95\ \text{ml}} \times \frac{2.22\ \text{dpm}}{\text{pCi}} \times \frac{0.5\ \text{mg}}{\text{g}}$$

$$= 0.197\ \text{mrad/pCi/mg}$$

*Red Marrow**

Source: Marrow composition from Bothwell and Finch, 1962

$$(0.406\ \text{mrad/pCi/mg})_{RBC} \times \frac{200\ \text{mg}}{1500\ \text{ml}}(\text{marrow}) \times \frac{5000\ \text{ml}}{2000\ \text{mg}}(\text{blood})$$

$$= 0.135\ \text{mrad/pCi/mg}$$

* This assumes the ratio of intracellular to extracellular fluid in marrow and blood is constant.

REFERENCES

1. M. Koide Rama and E. D. Goldberg. *Nature* **191,** 162 (1962).
2. H. E. Palmer and T. M. Beasley. *Science* **149,** 431–432 (1965).
3. T. Jaakkala. University of Helsinki, Department of radiochemistry annual report for 1965–66.
4. M. E. Wrenn and N. Cohen. Presented at the Eleventh Annual Meeting of the Health Physics Society, June 27–30, 1966, Houston, Texas (to be published).
5. D. Strominger, J. M. Hollander and G. T. Seaborg. *Review of Modern Physics* **30** (2), 585–904 (1958).
6. Hill, Church and Mihelick. *Review of Scientific Instruments* **23,** 523 (1952).
7. S. Fine and C. F. Hendee. *Nucleonics* **13,** 36 (1955).
8. M. H. Biavati, S. J. Nassiff and C. S. Wu. *Physical Review* **125,** 1364–1372 (1962).
9. E. H. S. Burhop. *The Auger Effect and Other Radiationless Transitions.* Cambridge University Press, Cambridge (1952).
10. C. Manduchi and J. G. Fannoni. *Nuclear Physics* **36,** 497–504 (1962).
11. J. Scobie, R. B. Moler and R. W. Fink. *Physical Review* **36,** 657–660 (1959).
12. R. W. Fink. Radiochemical studies of decay properties of radioactive nuclei. NP-10070 (1961).
13. Recommendations of the ICRP "Report of Committee II on Permissible Dose for Internal Radiation", Pergamon Press (1959).
14. W. C. Peacock, R. D. Evans, J. W. Irvin, Jr., W. M. Good, A. F. Kip, S. Weiss and J. G. Gibson. *Journal of Clinical Investigations* **25,** 605 (1946).
15. E. H. Quimby, S. Feitelberg and S. Silver. *Radioactive Isotopes in Clinical Practice.* Philadelphia: Lea and Febiger (1958).
16. T. H. Bothwell and C. A. Finch. *Iron Metabolism.* Little, Brown and Co., Boston, Mass. (1962).
17. E. J. Williams. *Proceedings of Roy. Society* (London) **A130,** 310 (1931).
18. R. D. Evans. *The Atomic Nucleus.* McGraw-Hill Book Co., Inc., New York (1955).
19. D. E. Lea. *Actions of Radiation on Living Cells.* Cambridge University Press, Cambridge (1955).
20. A. M. Rauth and J. A. Simpson. The energy loss of electrons in solids. *Radiation Research* **22,** 643–661 (1964).
21. "*Documenta Geigy*" *Scientific Tables.* Sixth edition. Ed. K. Diem (1962).
22. M. M. Wintrobe. *Clinical Hematology.* Fifth edition, Lea and Febiger, Philadelphia (1961).
23. L. H. Griffin. *K* capture absorption analysis: instrumentation and techniques. In *Encyclopedia of X-Rays and Gamma-Rays.* Ed. G. C. Clark. Reinhold Publishing Corp., New York, p. 539 (1963).
24. P. C. Altman. *Blood and Other Body Fluids.* Federation of American Societies for Experimental Biology, Washington, D.C. (1961).
25. M. E. Austoni. *Proceedings of the Society for Experimental Biology and Medicine* **85** (1954).
26. R. A. Seltzer, J. G. Keriakes and E. M. Saenger. *New England Journal of Medicine* **271,** 84 (1964).

EFFECTIVE ENERGY AND ENERGY SPECTRUM OF γ-RADIATION BEHIND THICK SHIELDS

P. F. SAUERMANN and K. SCHNEIDER

Zentralabteilung Strahlenschutz, Kernforschungsanlage, Jülich, F.D.R.

Abstract—The dose rate caused by the γ-radiation of a monoenergetic γ-source behind a shield can be divided into two parts:

1. The γ-radiation of the original energy E_0 (primary radiation) penetrating the shield is given by the basic equation for the absorption of γ-radiation in matter

$$I_{\gamma_a} = I_{\gamma_0} \cdot \exp(-\mu x)$$

and

2. The scattered radiation arising in the shield by Compton scattering, given by the equation

$$I_{\gamma_0} = I_{\gamma_a} (B - 1)$$

The dose rate of the scattered radiation behind thick shields can amount to many times the dose rate of the primary radiation as the above equation makes evident. The dose rate, for instance, caused by the primary radiation of a ^{60}Co-source with an activity of 10^4 Ci behind a 100 cm shield of normal concrete is 8 mR/hr, while the dose rate of the scattered radiation amounts to 195 mR/hr.

The attenuation of the dose rate of this source to the permissible dose rate of 2.5 mR/hr requires about 136.5 cm of normal concrete according to the attenuation equation

$$I_\gamma = I_{\gamma_0} \cdot B \cdot \exp(-\mu x)$$

It is possible to reduce considerably the costs of shielding by using a material of high density (lead for instance) for the attenuation of the scattered radiation of low energy behind a concrete shield of high thickness (>10 relaxation lengths). To calculate the thickness of this second shield of high density material it is necessary to get information about the energy of the scattered radiation.

The energy spectrum of the scattered radiation is comprised of γ-energies from several keV to the original energy E_0, but it is possible to determine an effective energy of this radiation allowing the thickness of the shield to be calculated with sufficient accuracy.

This paper gives a report on the measurement of the effective energy and the energy spectrum of the scattered radiation behind concrete shields of various thicknesses.

NEUTRON CROSS-SECTIONS AND REACTION PRODUCTS FOR H, C, N, AND O FOR THE ENERGY RANGE FROM THERMAL TO 15 MEV*

J. A. AUXIER and M. D. BROWN

Health Physics Division, Oak Ridge National Laboratory, Oak Ridge, Tennessee

Abstract—The accurate calculation of neutron dose must be based on definitive cross-sections and a precise knowledge of the reaction products in tissue. Although there are still several uncertainties in these parameters, a compilation has been made of the most detailed cross-section data available and reaction products for the four major elements in tissue (i.e. H, C, N, and O). The compilation is for neutron energies below 15 MeV, but the energy interval requiring the most study and analysis was that from 2.5 to 15 MeV. Particular attention was directed to the non-elastic reactions [e.g. the $C(n,n^1)3\alpha$ reaction]. Average values for the energies of the various charged particles as a function of the energy of the incident neutron have been computed. These values were compiled to provide a basis for revision of the dose-distribution functions for neutron exposures of man and of animals used in radiobiological studies. An analysis of the results of various measurements are compared with calculated values based on these cross-sections and with the values listed in NBS Handbook 63.

ANY absolute measurement of neutron fluence or any calculation of "dose" from fluence requires a knowledge of neutron cross-sections for the materials of interest. For some applications, only an activation cross section is required, and in some instances only elastic cross-sections are needed. However, the health physicist must have available the best cross-sections for many types of reactions because his interests and activities are so broad. Of particular interest are the cross-sections of the principal elements in tissue: hydrogen, carbon, nitrogen, and oxygen, for neutrons. The values for the thermal neutron cross-sections for these materials have not changed greatly during the past ten years, and those for the region below 2.5 MeV have changed in a few instances only. For higher energies the changes have been greater, for the neutron energy span from about 6 to 14 MeV, many uncertainties have been encountered and many changes made in recent years and until the present. This has resulted in frequent changes in accepted values at most laboratories. Similarly, there have been considerable uncertainties in the reaction products, both in terms of particle or quantum types[1] and in values for the energy released by the specific reaction products; Q values[2] have been known generally for about a decade. The formation of nuclear data information centers such as those at Oak Ridge National Laboratory and at Brookhaven National Laboratory has made the compilations easier; in the future, they may provide most of the information in the form needed. However, due to the special nature of the dosimetry requirements, the information presented here was taken from many sources and averages and interpolations made as required for a computation of absorbed dose in the energy range below 15 MeV. For neutron energies of 2.5 to 15 MeV, a smooth curve based on extrapolation between the available data points is generally a good approximation of the cross-section curves for dosimetry applications. Figure 1 shows the elastic scattering cross-section[3] of the four principal elements in tissue for the energy range below 14 MeV. The relative macroscopic cross-section

* Research sponsored by the U.S. Atomic Energy Commission under contract with the Union Carbide Corporation.

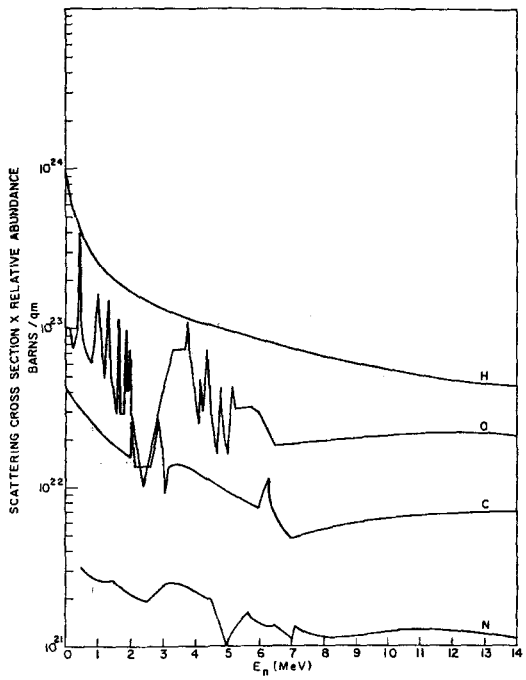

FIG. 1. Macroscopic elastic scattering cross-sections for the H, O, C, and N in tissue for the neutron energy range from thermal to 14 MeV.

has the advantage here that the relative number of interactions with each element can be seen readily. The relative contribution of the C, N, and O recoils to dose equivalent is greater than for absorbed dose because of the higher average values of LET (i.e. greater QF's). The elastic cross-sections are generally decreasing functions of neutron energy to 15 MeV.

Two of the cross-sections for neutrons of thermal and near-thermal energies are shown in Fig. 2.[3] These cross-sections, decreasing with neutron energy as $1/V$, have been accepted generally for some time. The only important reactions are the ${}_1^1\mathrm{H}(n,\gamma){}_1^2\mathrm{H}$ and the ${}_7^{14}\mathrm{N}(n,p){}_6^{14}\mathrm{C}$ reactions [e.g. all other (n,γ) reactions total about 0.5% of the ${}_1^1\mathrm{H}(n,\gamma){}_1^2$ reaction].

All significant nonelastic cross-sections for neutrons incident on tissue are shown in Fig. 3.[3] These are relative macroscopic values with all proton-producing reactions, all alpha-producing reactions, etc., summed. These threshold reactions are generally increasing functions

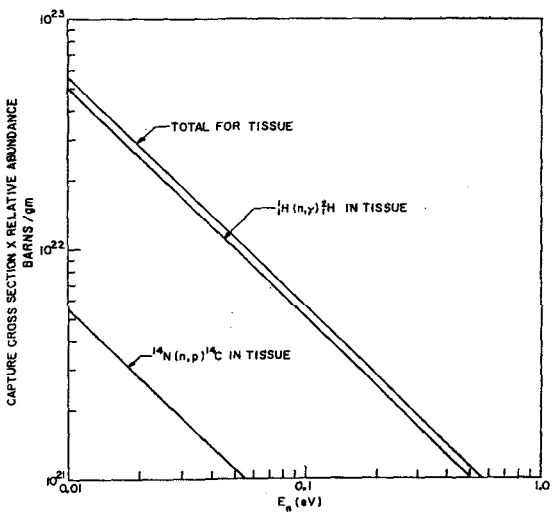

FIG. 2. Macroscopic capture cross-sections for the H and N in tissue for the thermal and near-thermal neutron energy range.

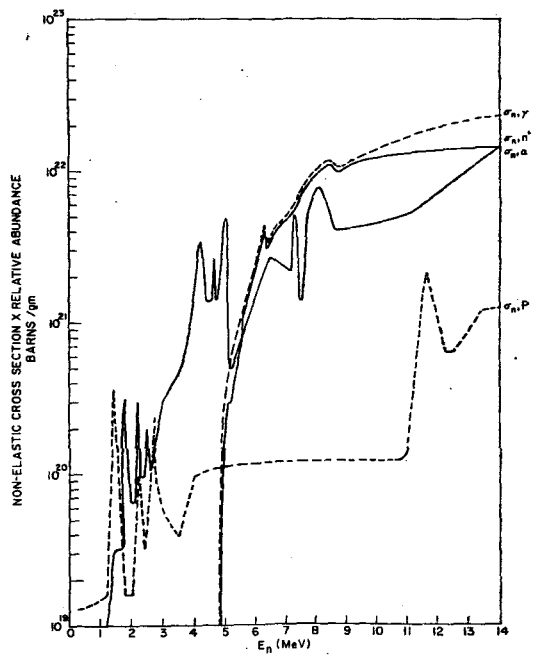

FIG. 3. Total macroscopic nonelastic cross-sections for tissue for the energy range from thermal to 14 MeV.

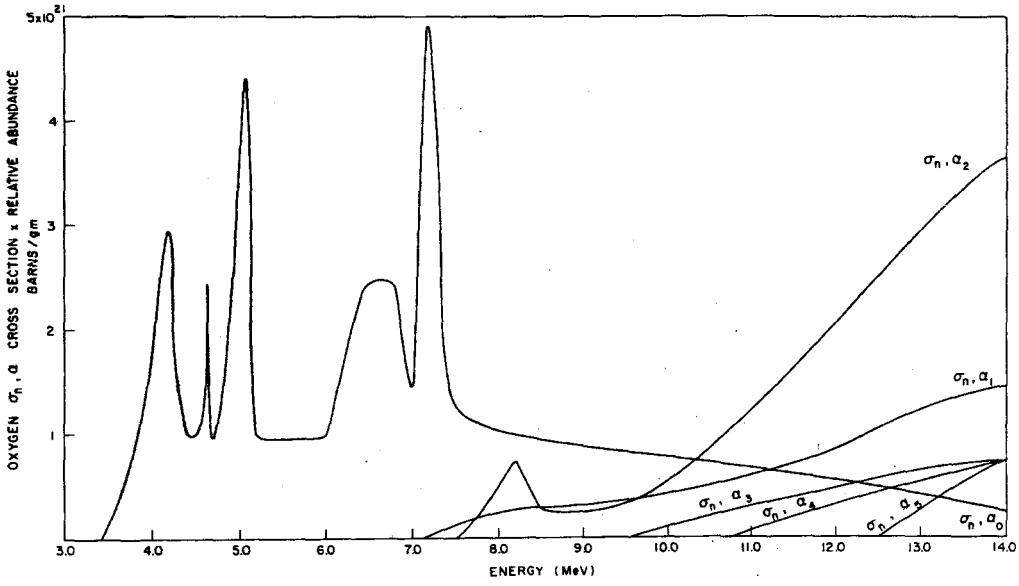

FIG. 4. Total oxygen cross-sections for alpha-producing reactions in tissue for the neutron energy range from 3 MeV (below the lowest threshold) to 14 MeV.

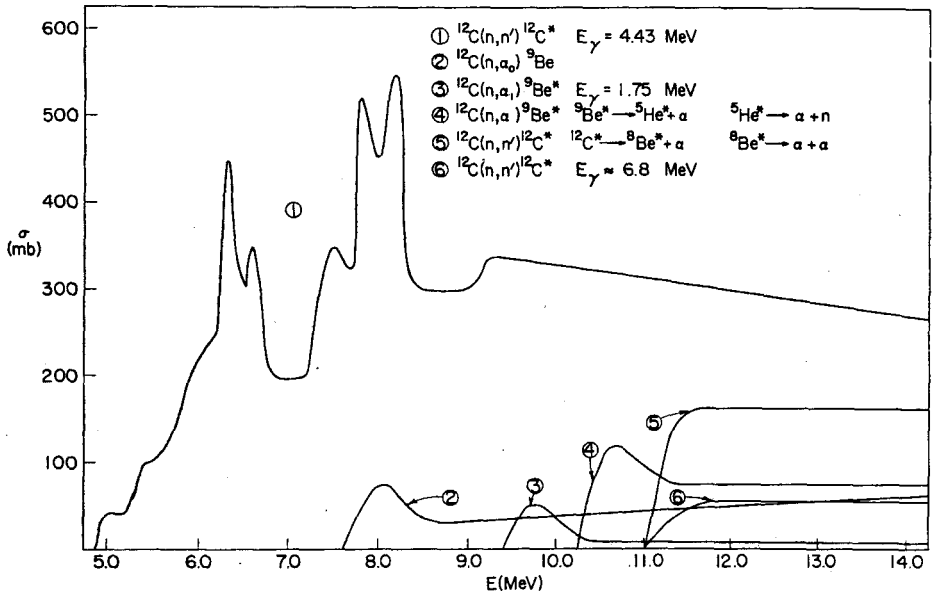

FIG. 5. Microscopic cross-sections for inelastic and nonelastic reactions in ^{12}C for the neutron energy range from 5 MeV to 14 MeV.

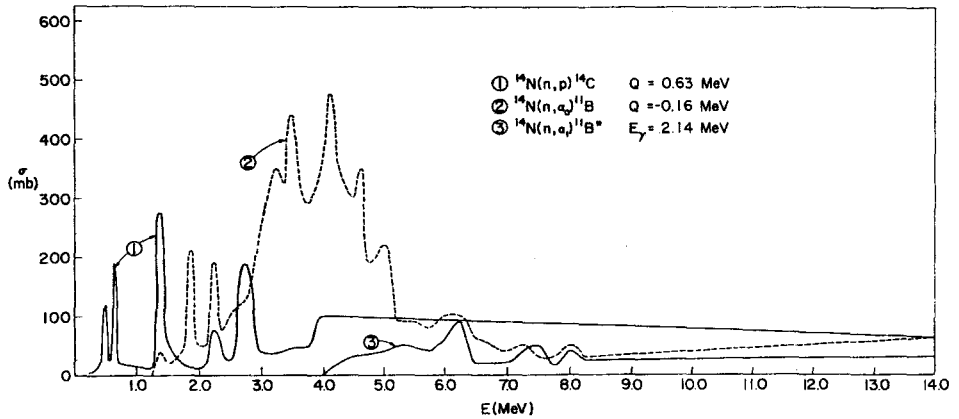

FIG. 6. Microscopic cross-sections for the three reactions, $^{14}N(n,p)^{14}C$, $^{14}N(n,\alpha_0)^{11}B$, and $^{14}N(n,\alpha_1)^{11}B^*$, for the energy range from thermal to 14 MeV.

of energy to 15 MeV. The sum of the macroscopic (n,γ) reaction cross-sections is shown as a separate curve; the sum includes the cross-sections of charged particle reactions which yield de-excitation gamma-rays [e.g. $^{12}C(n,n')^{12}C^*$]. This curve is not the sum of the other curves because some charged particle reactions do not yield gamma-rays [e.g. the $^{12}C(n,n')3\alpha$]. Some of the reactions [e.g. $^{14}N(n,p)^{14}C$] yield greater energy for local deposition than the incident neutron (i.e. they have positive values of Q).

Cross-sections for reactions which cause alpha-particle emission from oxygen nuclei are shown in Fig. 4.[3-13] Although these general values are convenient for estimating dose or

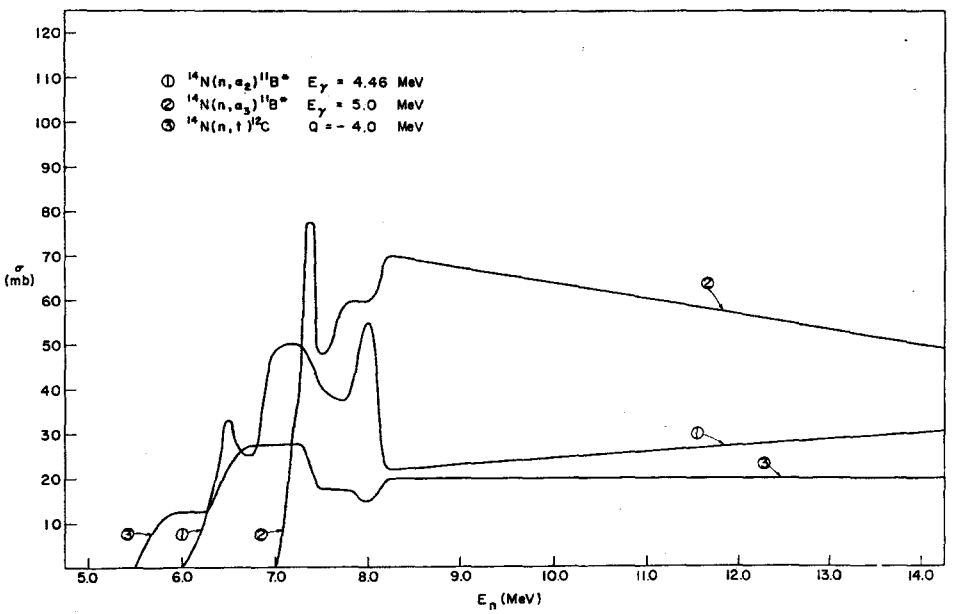

FIG. 7. Microscopic nonelastic cross-sections for the three reactions, $^{14}N(n,\alpha_2)^{11}B^*$, $^{14}N(n,\alpha_3)^{11}B^*$, and $^{14}N(n,t)^{12}C$, for the neutron energy range from 5 MeV to 14 MeV.

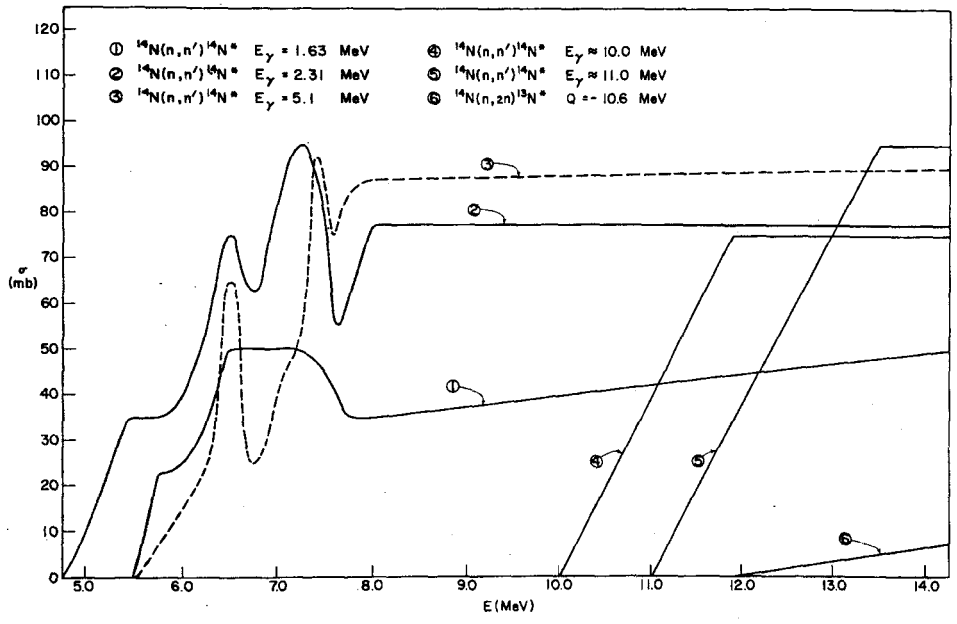

FIG. 8. Microscopic inelastic cross-sections for five (n,n') and one $(n,2n)$ reactions in ^{14}N for the energy range from 4.75 MeV to 14 MeV.

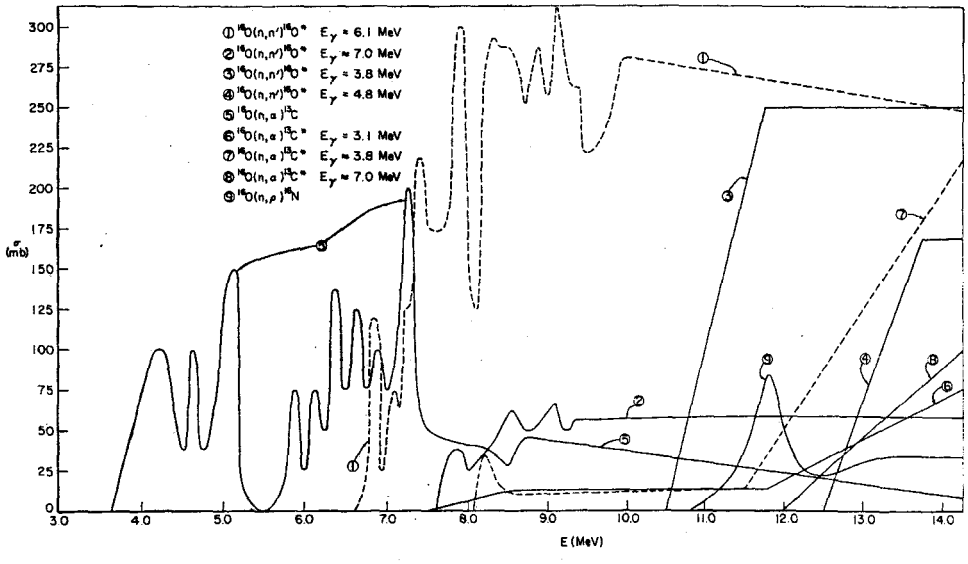

FIG. 9. Microscopic inelastic and nonelastic cross-sections for ^{16}O for the neutron energy range from 3 MeV to 14 MeV.

Reaction	Q Value (MeV)	E_n = 14 MeV		EI = 7 MeV	
		E_{max} (MeV)	R_{max} (cm)	E_{max} (MeV)	R_{max} (cm)
$^{12}C(n, \alpha)^{9}Be$	−5.70	7.89	6.5×10^{-3}	1.28	3.8×10^{24}
$^{14}N(n, p)^{14}C$	0.63	14.6	2.23×10^{-1}	7.62	6.90×10^{-2}
$^{14}N(n, t)^{12}C$	−4.01	9.67	4.5×10^{-2}	2.98	6.3×10^{-3}
$^{14}N(n, \alpha)^{11}B$	−0.16	12.8	1.5×10^{-2}	6.30	4.5×10^{-3}
$^{16}O(n, p)^{16}N$	−9.63	4.19	2.38×10^{-2}	0	0
$^{16}O(n, d)^{15}N$	−9.90	4.03	1.34×10^{-2}	0	0
$^{16}O(n, \alpha)^{13}C$	−2.21	11.04	1.17×10^{-2}	4.57	2.6×10^{-3}

FIG. 10. Charged particle reactions in tissue with maximum ranges for 14 MeV and 7 MeV neutrons.

dose equivalent, an extensive set of cross-sections are required for detailed calculations; the detailed non-elastic and inelastic cross sections are given in Figs. 5 through 9.[3-13] Figure 10 shows a list of the most important charged particle reactions by neutrons in tissue. The maximum ranges for the charged particles for 7 and 14 MeV neutrons are shown as are the accepted Q values. The equation used to compute the average energy deposited by a charged particle is given below. This equation is based on an assumed particle emission with equally probable energies between zero and maximum.

$$E_2 = \frac{2 M_1 M_2 E_1}{(M_2 + M_3)^2} + \frac{M_3 Q + E_1 (M_3 - M_1)}{M_2 + M_3}$$

where: M_1 = mass of incident particle,
M_2 = mass of reaction product with energy E_2,
M_3 = mass of reaction product with energy $E_3 = E_1 + Q - E_2$,
Q = Q value of reaction,
E_1 = energy of incident particle, and
E_2 = average energy of reaction product with mass M_2.

A more comprehensive presentation and analysis of the calculational results will be presented in a paper by Jones *et al.*[14]

REFERENCES

1. F. AJZENBERG-SELOVE and T. LAURITSEN. *Nucl. Phys.* **11,** 1 (1959).
2. F. EVERLING *et al. 1960 Nuclear Data Tables,* Parts 1 and 2, Nuclear Data Project, NAS-NRC (Edited by K. Way) (1961).
3. D. J. HUGHES and R. B. SCHWARTZ. *Neutron Cross-Sections.* Brookhaven National Laboratory Report BNL-325, 2nd edition (1958).
4. D. J. HUGHES, B. A. MAGURNO, and M. K. BRUSSEL. *Neutron Cross Sections.* Brookhaven National Laboratory Report BNL-325, 2nd edition, Supplement 1 (1960).
5. J. R. STEHN *et al. Neutron Cross Sections.* Brookhaven National Laboratory Report BNL-325, 2nd edition, Supplement 2, volume 1 (1964).
6. J. R. SMITH. *Phys. Rev.* **95,** 730 (1954).
7. A. B. LILLIE. *Phys. Rev.* **87,** 716 (1952).
8. W. J. MCDONALD *et al. Nucl. Phys.* **75,** 353 (1966).
9. V. V. NEFEDOV *et al. Soviet Progress in Neutron Physics* (Edited by P. A. KRUPCHITSKII), pp. 241–247 (1961).
10. R. A. AL-KITAL and R. A. PECK, JR. *Phys. Rev.* **130,** 1500 (1963).
11. V. E. SCHERRER, R. B. THEUS, and W. R. FAUST. *Phys. Rev.* **91,** 1476 (1953).
12. J. P. CONNER. *Phys. Rev.* **89,** 712 (1953).
13. J. B. SINGLETARY and D. E. WOOD. *Phys. Rev.* **114,** 1595 (1959).
14. T. D. JONES *et al.* Dose distribution functions for neutrons and gamma rays in anthropomorphous and radiobiological phantoms (see first article of Session 24 of these Proceedings).

DISCUSSION

G. JOYET (*Switzerland*):

Ich möchte fragen ob Sie mit den gleichen Koeffizienten die Gonadendosis für den Mann und für die Frau bestimmen können und wo Sie ihr Dosimeter anbringen.

E. PIESCH (*Germany*):

Das beschriebene Phosphatglasdosimeter II zeigt an der Phantom-Oberfläche einen in gleicher Weise zur Energiedosis in den Gonaden (Hoden) und zur Energiedosis im Knochenmark proportionalen Messwert an. Nach Messungen von Jones erhält man für die weiblichen Gonaden (Eierstöcke) dieselbe Energieabhängigkeit der Energiedosis wie für das Knochenmark. Der Messwert des Personendosimeters entspricht daher den Energiedosen in den männlichen und weiblichen Gonaden sowie der Energiedosis im Knochenmark. Die Phantombestrahlungen wurden im Strahlungsfeld einer hartgefilterten Röntgenbremsstrahlung durchgeführt. Das Personendosimeter wurde hierbei auf der Phantomvorderseite in Brusthöhe aufgehängt. Die Messwerte beziehen sich nur auf eine frontale Strahleneinfallsrichtung.

D. NACHTIGALL (*Euratom*):

Können Sie noch einige Angaben zum transportablen Gerät machen: wie ist das Gewicht, der Gasdruck und die Richtungsabhängigkeit? Welche mittleren QF sind in der Umgebung von Hochenergiebeschleunigern gemessen worden?

H. ŻARNOWIECKI (*Poland*):

1. Bis heute ist nur ein Prototyp konstruiert. Das Gewicht des Gerätes wird 3–4 kg sein: Der Gasdruck hängt von dem Modell ab. Der mittlere Gasdruck ist 6 Atü. Die Richtungsabhängigkeit ist Funktion des Modells. Es kann nach Wunsch fast isotropisch sein. Mehrere Messungen sind am Phantom gemacht worden.

2. Die QF wurden in der Umgebung von Hochenergiebeschleunigern gemessen und sind publiziert. Ich kann Ihnen die Literatur dazu angeben.

D. BLANC (*France*):

Je voudrais faire un commentaire. Les chambres d'ionisation à remplissage de diélectriques liquides constituent, à mon avis, d'excellents détecteurs à recombinaison. Les points de concours des paliers s'alignent, sur l'axe des abscisses, dans l'ordre des transferts linéaires d'énergie, qu'il s'agisse de rayonnements purs ou mixtes. Nous avons réalisé, en liaison avec le Commissariat à l'Énergie Atomique, des détecteurs cylindriques, parfaitement stables en fonction du temps, dont nous avons d'ailleurs parlé lors de notre communication à ce Congrès. Je pense qu'il y a là une voie de recherche très fructueuse.

G. COWPER (*Canada*):

What is the upper limit of dose rate which may be detected without ambiguity of LET and rate effects?

K. ŻARNOWIECKI:

The upper limit of dose when volume recombination does not exist depends on QF and ranges from 10 to more than 200 rem/hr.

J. A. AUXIER (*U.S.A.*):

Did you use the threshold detector system complete with boron ball? (*Answer*: Yes.)

Due to the relatively large size of the boron ball compared to the phantom, I would expect the type divergence you observed due to the highly different composition and consequent shift of the effective center of detection.

R. E. SIMPSON:

The center of detection, in this small phantom, of the threshold foils shifts with depth. This is significant when compared with the small center of mass of the ion chamber. Therefore a divergence in depth dose measurement would be expected. The threshold foil system is not the most satisfactory system for depth dose measurements of neutrons.

M. E. WRENN (*U.S.A.*):

Have you looked at the long term retention of Be^7? Workers in the 40's found tenacious retention in bone, which may show a longer half-time than that in the whole body. Have you followed the body burden for a longer period to see if the retention curve might show two compartments?

G. LEGEAY:

Notre étude ne concernant que la formation du Be^7 en vue d'une investigation dosimétrique après accident, nous n'avons envisagé son devenir que pendant un temps relativement court. Une étude du métabolisme du Béryllium *in vivo* après irradiation protonique est envisagée.

HEALTH PHYSICS ASPECTS OF SUPERSONIC TRANSPORT*

WALTER S. SNYDER

Health Physics Division, Oak Ridge National Laboratory, Oak Ridge, Tennessee, U.S.A.

Abstract—Passengers and crew of a supersonic transport (SST) will be exposed to more intense fields of cosmic radiation than are usually encountered in commercial flights at the present time. The assessment of the radiation hazard posed by this new development must take into account the intensity of the radiation fields in the cruising altitude of the SST (60,000–80,000 ft), the quality factors appropriate for these radiations, and the many factors which determine the frequency and duration of exposure and the age distribution of the exposed as members of the population.

Using presently available data on the relevant radiation fields, the dose rate and dose equivalent rate to occupants of the SST are estimated separately for solar cosmic radiation and for galactic cosmic radiation. These dose rates would be considerably higher in the case of planes flying a polar route than for those following a route at lower latitudes. Unusually high dose rates may occur during periods of a major solar flare, and it seems possible, in very exceptional cases, some change in flight plans might be desirable to reduce the dose from solar cosmic radiation.

The cumulative exposure of a crew member who is constantly flying on polar routes might well be in the range of the present recommended levels for occupational exposure. The dose for the vast majority of passengers would be expected to be well within the permissible limits on population exposure. Extrapolating present data on passenger miles flown per year, it appears that the total contribution to the genetic dose would be well below 1% of the recommended limit of 5 rem per generation.

INTRODUCTION

The supersonic transport aircraft, hereafter referred to as the SST, is being designed to cruise at altitudes of 60,000 to 80,000 ft. At these heights, passengers and crew will be exposed to somewhat higher levels of cosmic radiation because the overlying absorption thickness (g/cm^2) of air is less than half what it is at 30,000 or 40,000 ft, the heights used by many present commercial aircraft. Undoubtedly, the problem of solar flares, which produce radiation fields with intensity much above the average levels, has served to call attention to the general problem of radiation exposure entailed by the use of the SST. Consequently, there have been a number of studies of the problem (for example, refs. 1–5), including one by an ICRP Task Group,[6] and this paper is, in a sense, a summary of these reports and an updating with what new information has been found during the last year.

The British and French governments are cooperating to produce an SST which is termed the Concorde. Several U.S. firms are also actively at work on design, but it appears the American planes may not be ready for commercial use as soon as the Concorde which is tentatively scheduled for service in 1971. The Concorde is designed to fly from New York to Paris, for example, in 3 hr and 15 min, or from London to Sydney in 13 hr and 20 min, and will carry from 110 to 130 passengers. Nine airlines have already placed orders for 45 of these planes, and the interest in the American version is comparable. An artist's representation of the Concorde is shown in Fig. 1.

The primary spectrum of cosmic radiation is fairly well documented. There is considerable

* Research sponsored by the U.S. Atomic Energy Commission under contract with Union Carbide Corporation.

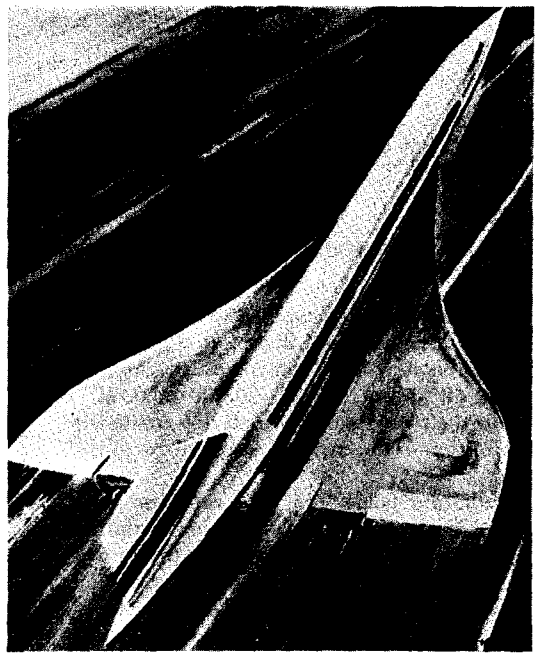

FIG. 1. The SST (Concorde).

absorption due to the 30 to 70 g/cm² of air above these altitudes so that this primary spectrum is considerably altered, and there have not been many direct measurements of the radiation fields within this belt. Thus the radiation fields encountered between 60,000 and 80,000 ft are not as well determined as those at lower altitudes or those at higher altitudes. It is convenient to consider these radiation fields under two separate categories: (1) galactic radiation, which originates outside the solar system, and (2) solar radiation originating with the sun, the latter including solar flares which are, in fact, only more intense and limited periods of solar radiation.

Galactic radiation consists primarily of energetic protons, alpha particles, and to a lesser extent heavier nuclei, and it is relatively constant in intensity except for effects due to magnetic fields associated with sun spot activity and solar flares. In Fig. 2, which is taken from ref. 1, the change of the composition of the cosmic ray beam with altitude is shown. The height of 60,000 ft is just beyond the region where the "transition effect" occurs and the particle fluxes begin to decrease. At lower elevations the dose will be primarily due to radiation of low LET, i.e. electrons and mesons, but at altitudes of 60,000 to 80,000 ft, the flux of nucleons increases and makes a very significant contribution to the dose and even more to the dose equivalent.

In the upper atmosphere, the total ionization increases from the earth's equator toward the poles owing to the magnetic field of the earth which deflects low-energy particles. Because of this screening effect, the number of high-energy primary particles reaching a given height above the earth increases with latitude, being minimal at the equator. This screening effect is less at lower altitudes and is hardly significant at sea level. Fowler and Perkins[3] have estimated this latitude effect for a height of 70,000 ft, and their estimate is shown in Fig. 3. It is seen

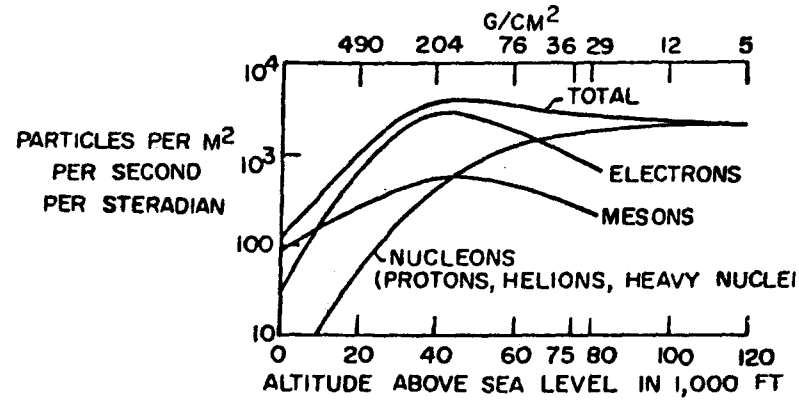

FIG. 2. Altitude profile of particle transition of cosmic ray beam in the atmosphere (from H. J. Schaefer).

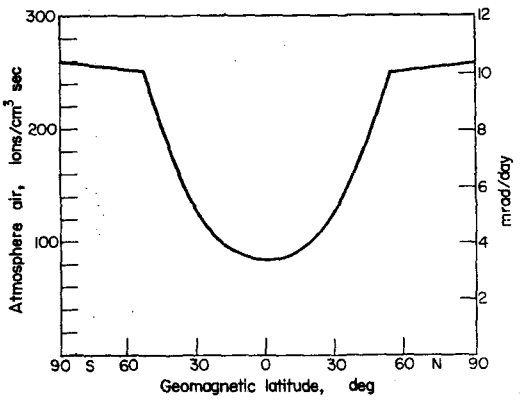

FIG. 3. Intensity of ionization at maximum of ionization depth curve (~50 g/cm²) for June–December 1965 (Neher and Anderson (1962))

that at 60° or more of north latitude the intensity of ionization is about three times greater than at the equator. Many of the most traveled routes pass through these high latitudes, and if it appears desirable to reduce dose to passengers or crew, one might achieve a substantial reduction by following routes that lie in lower latitudes so far as practicable. Crew members might be rotated so that the same individual did not fly predominantly on the routes through high latitudes. However, while these are possibilities, it is not at all clear that such practices will be required to meet current standards limiting exposure of either passengers or crew.

In years of high solar activity such as 1958–9, an interplanetary magnetic field is superimposed on the earth's magnetic field. This effect is represented in Fig. 4 which shows this effect for 1954, a year of low solar activity, and for 1937, a year of high solar activity. In the region of 60,000 to 80,000 ft, this effect is only a difference of 20–30%. The similar data for 1954 are, however, practically a factor of 3 higher than for 1958 in northern latitudes and at an elevation of ~90,000 ft according to Neher and Anderson.[7] Thus, this effect can account for a very substantial increase or decrease in the total dose received from galactic radiation.

Fowler and Perkins[3] have summarized and evaluated the dose and dose equivalent using the ICRP recommendations to obtain the quality factor (QF) from the linear energy transfer (LET). A significant fraction of the total ionization is produced by protons and heavier nuclei, but they have rather high energies so that the QF only averages 1.5 according to their estimate.[3] This estimate neglects the dose due to neutrons which undoubtedly increases the value of QF. The ICRP Task Group, using data of Haymes,[8] evaluated the dose from neutrons separately. Using a QF of 8 for this dose, the QF for all dose from galactic radiation averages about 2. However, it must be recognized that the measured values on which this estimate is based only include neutrons of energy above 1 MeV, and, while allowance has been

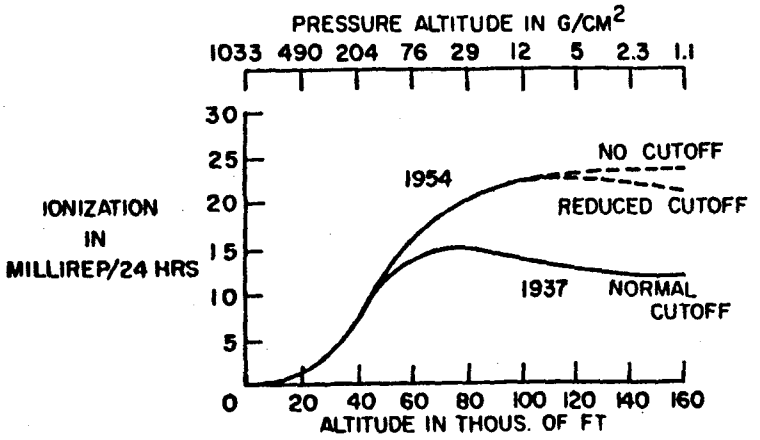

FIG. 4. Altitude profile of the total ionization in a year of high (1937) and low (1954) solar activity (from H. J. Schaefer).

made for the neutrons of lower energies, there is some uncertainty in the estimate, perhaps as much as a factor of 2. Watt *et al.*[9] give a higher dose estimate based on somewhat different assumptions concerning the neutron energy spectrum and the effect of isotropic incidence on the depth dose curve. The ICRP Task Group estimates a dose rate of 1.3 to 1.9 mrem/hr at heights of 60,000 to 80,000 ft, respectively, for polar latitudes and for years of a quiet sun. Thus these dose rates are "conservative" so far as latitude and solar effects are concerned.

Using the spectrum estimated by Fowler and Perkins,[8] one finds that about 5–10% of the dose is due to nuclei with mass greater than that of an alpha particle, and some of these have sufficient energy to produce a broad path, perhaps 10 μ in diameter, extending over many cell diameters. Schaefer has calculated the number of these "thin-down" hits per day/cm^3,[1] and they have been measured by Yagoda.[10] The variations of these hits with altitude during years of a "quiet" sun and of an "active" sun are shown in Fig. 5. The ICRP Task Group recognized the unique problems posed by this type of radiation as have other investigators. Referring to these "thin-downs", the report notes that "Such tracks of affected cells have been observed experimentally in the skin of mice exposed to cosmic radiation in the upper atmosphere and, although of little functional importance in the skin, might be of much greater importance in the embryo or in vital organs such as the brain. Attempts to study this question with microbeam irradiation suggest that the observed changes per exposed cell are smaller than for the same number of ions per cell delivered to a larger volume of tissue; however, no RBE value can be cited for an effect that is produced by high-LET radiation but not by low-LET radiation under the conditions of interest. Some other means will have to be found, therefore, if such effects are to be taken into account in calculation of the dose equivalent. Apart from this special case, the risk-limiting somatic effects from high-energy radiations are not different from those ordinarily considered in protection work."

The dose rate from solar radiation averages somewhat less than that from galactic radiation, as is indicated on Fig. 6 which is due to Fowler and Perkins. The solar radiation is composed largely of fast protons, but as these penetrate to a depth of 60,000 to 80,000 ft in the atmosphere, a spectrum of secondaries is produced so

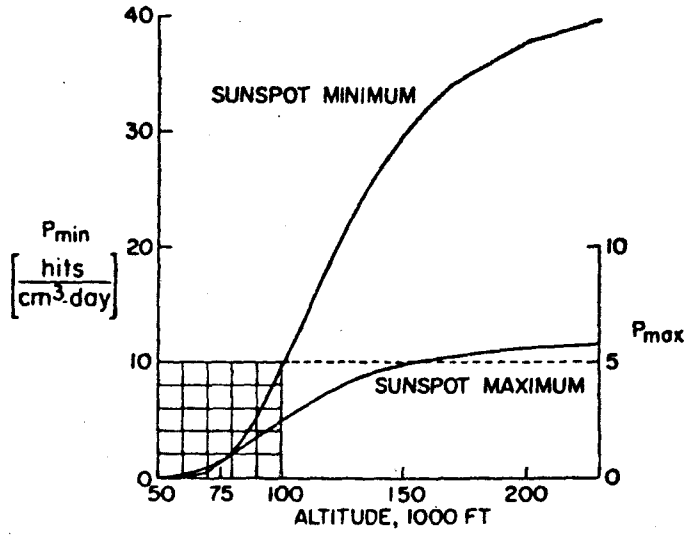

FIG. 5. Variation of thin-down intensity with altitude for seasons of maximum and minimum sunspot activity (from H. Yagoda)

that the radiation field has much of the same complexity as does galactic radiation at these depths. As will be noted from Fig. 6, the average intensity does not constitute a severe problem as compared with the galactic radiation field. However, solar radiation varies greatly in intensity, the activity being closely correlated with sun-spot activity which follows a rather regular cycle of intense and depressed activity, one cycle representing about 10–11 years and the intensity of a particular burst or "flare" may vary over as much as 6 orders of magnitude. There have been seven giant flares that have occurred during the last two solar cycles, that is, in the last 20 years, that have carried substantial fluxes of photons of 1 GeV or higher energies. These flares have produced geophysical phenomena which could be used as a basis for detection soon enough for the SST to descend to a lower altitude and have the benefit of the shielding of more of the atmosphere. The giant flare of 23 February 1956 is by far the largest observed to date and is estimated to have produced doses ranging from 2–20 rad during the first hour of the event at the 60,000- and 80,000-ft altitudes and over the polar regions. The range of values, as estimated by Fowler and Perkins, is shown in Fig. 7. The intensity at SST altitudes depends not only on the protons ejected by the sun but also is markedly influenced by the state of the magnetic fields existing between the sun and earth which may serve

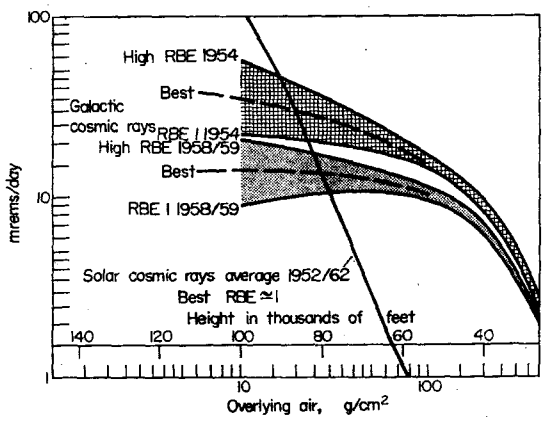

FIG. 6. Radiation intensity in rems for galactic and solar cosmic rays as computed for this report.

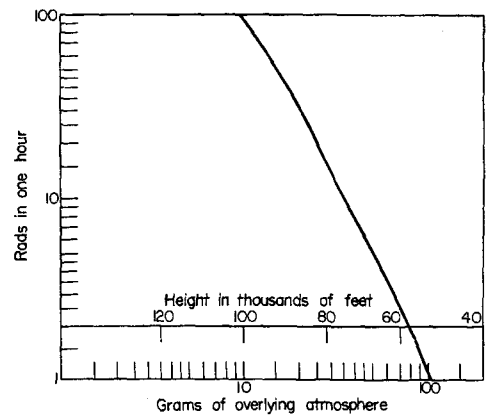

FIG. 7. Estimated dose from the most severe solo cosmic ray outburst 0345–0445 23 Feb 1956. The radiation dose for the one hour period 0345–0445 UT 23 February 1956 as a fraction of height or depth in the atmosphere for $\lambda \geq 60°$. The rest of the outburst produced a further irradiation of about 50% of that produced during the first hour.

to deflect much of the radiation or to facilitate its passage to the earth. It must be recognized that there is considerable uncertainty in this estimate, because there was no useful balloon flight until 20 hr after the event, and the dose estimates depend upon extrapolated data on the actual intensities and spectra at SST altitudes.

As Fowler and Perkins[3] state, "We must now ask the question as to whether the sample over the last sunspot maximum is likely to have been representative. We estimate that the outburst of 23 February 1956 was responsible for approximately one half of all the solar particles of energy > 100 MeV that have arrived since 1950, and greater fractions of particles of higher energy. Are such outbursts to be expected more or less often than once in 10 years—or could we expect even more severe outbursts—say 10 or 100 times as great?

"We mentioned earlier that the 53 outbursts in the last solar cycle were spread over an estimated range of 10^5 in intensity, and that this huge range was due to propagation conditions between the sunspot and Earth as well as to the intrinsic intensity of the solar flare. . . . So

it seems likely that the probability of experiencing another solar event comparable to that of 23 February 1956, or an even more intense one during the course of any 11 year sunspot period is rather high."

The question of taking evasive action, i.e. descending to lower altitudes or, in periods of intense activity, flying over routes which lie closer to the equator, has been proposed and often arouses quite divergent opinions. It is

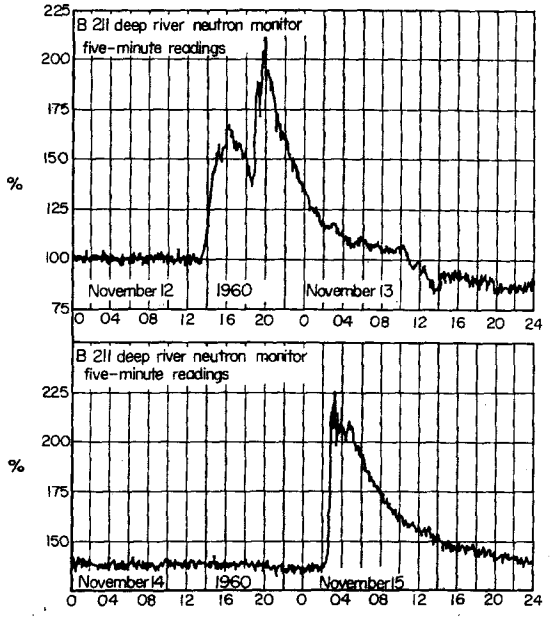

FIG. 8. Cosmic ray indices (pressure corrected hourly totals). Record of neutron monitor readings for the solar outbursts at Deep River, Ontario, for 12–15 November 1960 taken from ref. 4 or 5.

estimated that an SST in flight might have some 10–15 min warning before the arrival of the really intense build-up of the field which may reach peak intensity in a matter of minutes. The time course of neutron monitor readings, as observed at Deep River, Ontario, in November 1960, are shown in Fig. 8.[3] The sharp rise in intensity shown here, followed by the gradual decline in intensity extending over hours is fairly typical. In the giant flare of 23 February 1956, Fowler and Perkins estimate that the total dose during the entire day was only 50% higher than the dose during the first hour. Thus any evasive action must be rather prompt.

It has been questioned whether a very prompt change in course might not entail other hazards for the occupants of the SST[11] which would be more severe than the hazard posed by the radiation fields. Certainly, those who propose that such action be taken are not envisioning actions which would involve any appreciable probability of wrecking the plane or causing severe physical distress to the occupants. Those designing the SST are well aware of the problem of radiation exposure and are investigating the desirability and means of taking evasive action. Of course, this is not a definite commitment to such a policy, but some of the working reports discuss in detail the type of monitoring instruments to be carried on the plane; and, in one case, a "safe" range up to 5 mrem/hr, an "alert" or "warning" range up to 50 mrem/hr, and an "action" range above 50 mrem/hr have tentatively been selected. None of the working papers the author has seen mention or discuss any hazard that might be involved in descending to lower altitudes. Many airlines are distributing advance publicity concerning the SST in the material they offer to passengers in the seat pockets on current flights. A survey of this literature reveals that several airlines are already educating the public as to the presence of these radiation fields and reassuring them that adequate measures are being taken to meet the problem. Several of these brochures mention the possibility of evasive action, and all indicate that in the years before commercial flights begin, there will be considerable study of the problem, and during the year or more of extensive testing of the craft, there will be much more data on the problem than we now have.

In summary, the average levels of galactic and solar radiation do not pose any great problems. The ICRP Task Group report estimates, conservatively, that the average dose rate on a polar route and at 60,000 to 80,000 ft might be as much as 3 mrem/hr. For the great bulk of travelers who make only a few flights a year, this is well within the limits on exposure of individuals of the population recommended by the ICRP. For the crew, or the courrier who

is continually making such trips, it is another matter, and they may have to be classed as radiation workers. For example, a schedule of 40 hr/mo of time in actual flight over high latitudes might entail about 1.5 rem/yr as an average, although it must be remembered these are generally conservative estimates. As mentioned above, some of the present plans provide for monitoring instruments on board, and these will provide better estimates as flying experience accumulates. Also, taking account of the fraction of the population likely to be involved and of time factors, the contribution to the total genetic load is small as noted by the report of the ICRP Task Group.

REFERENCES

1. H. J. SCHAEFER. Radiation and man in space. *Advances in Space Science*, Vol. 1, p. 267. Frederick I. Ordway III, ed. (Academic Press, Inc., New York, 1959).
2. T. FOELSCHE and E. H. GRAUL. Radiation exposure in supersonic transports, *Atompraxis* **8,** 365 (1962).
3. P. H. FOWLER and D. H. PERKINS. Cosmic Radiation and Solar Particles at Aircraft Altitudes —Background Note, Air Registration Board, Supersonic Aeroplane Airworthiness Committee, SAAC/20 (1962).
4. E. J. FLAMM and R. E. LINGENFELTER. *Science* **144,** 1566 (1964).
5. M. LEIMDORFER, R. G. ALSMILLER, JR. and R. T. BOUGHNER. Calculations of the radiation hazard due to exposure of supersonic aircraft to solar flare protons. In press.
6. Radiobiological aspects of the supersonic transport (a report of the ICRP Task Group on the Biological Effects of High-Energy Radiations), *Health Phys.* **12**(2), 209 (1966).
7. H. V. NEHER and H. R. ANDERSON. *J. Geophys. Res.* **67,** 1309 (1962).
8. R. C. HAYMES. *J. Geophys. Res.* **69,** 841 (1964).
9. D. E. WATT, D. M. CLARE and A. R. B. GORDON. *Tissue Dose-Equivalent Rates (i) From Cosmic Ray Neutrons. (ii) In the Low Level Environment of Chapelcross Nuclear Power Station.* PG Report 734 (CC), United Kingdom Atomic Energy Authority (1966).
10. H. YAGODA. Cosmic-ray monitoring of the manned stratolab, balloon flights, *Geophys. Research Directorate Notes*, No. 43 (1960).
11. H. W. PATTERSON. Hazards of flight in the supersonic transport, *Health Phys.* **12**(8), 1151 (1966).

RESULTS OF A SPACE DOSIMETRY EXPERIMENT TO ASSESS RADIATION PROTECTION CALCULATIONS FOR MANNED SPACE FLIGHT

M. C. CHAPMAN* and R. E. FORTNEY
Northrop Space Laboratories, Hawthorne, California, U.S.A.

and

F. E. HOLLY and R. STOVALL
Air Force Weapons Laboratory, Kirtland AFB, New Mexico, U.S.A.

Abstract—On October 5,1965, a dosimetry satellite was placed in a rectrograde earth orbit with an inclination of 144°. Apogee and perigee were 3460 km and 411 km respectively. This orbit was such that virtually all of the inner Van Allen zone was covered. The instrumentation package consisted of seven separate electron and proton spectrometers (0.56 to 5 MeV for electrons—10 to 120 MeV for protons), a proton depth-dosimeter measuring absorbed energy at three depths in an aluminum shield, an X-ray or bremsstrahlung spectrometer measuring secondary dose behind an aluminum shield, and two tissue equivalent ionization chambers. Thus proton and electron tissue dose and bremsstrahlung production were measured simultaneously with both uni- and omni-directional radiation environment data. The material distribution of the satellite was experimentally determined and a magnetometer was used to relate spacecraft geometry to particle distributions in space. Therefore, a controlled experiment was performed to investigate the importance of simplifying assumptions in the calculation of proton and electron doses as well as a measurement of the spatial dose and particle distributions. Utilizing this data, representative doses are calculated and compared with the results of the on-board dosimetry.

I. INTRODUCTION

With the advent of manned space flight it became apparent that space radiations would play a significant role in man's ability to successfully negotiate space. Radiations trapped in the magnetosphere (Van Allen Regions), Galactic Cosmic Rays, and Solar Flare Radiation could presumably limit the duration of any space mission.[1]

Many computer programs have been developed which use various theoretical models of the space radiation environment. Ideally, when all relevant factors are known to a high degree of precision, only a single computer program will be required. Such a program would require only two inputs—the shielding configuration of the vehicle and its proposed spatial path; the radiation environment being contained within the program. Programs such as this have been developed for the Air Force by the Boeing Corporation[2] and Northrop Space Laboratories[3] and are represented by the flow chart in Fig. 1. In any program where information is accumulated step by step, the error in the end result is cumulative. Therefore, the accuracy of the end result can be no better than the accuracy of a single input or step, and each of the eight inputs or blocks of Fig. 1 must be known to a high degree of precision. Extensive experimental programs are under way to test the ability of these computer programs to predict dosages received by space-crew members during an arbitrary space mission. It is the purpose of this paper to describe one such experiment which has been performed.

Assuming that dose can be measured in biologically relevant terms, one experiment would

* Now at TRW Systems Laboratories, Redondo Beach, California, USA.

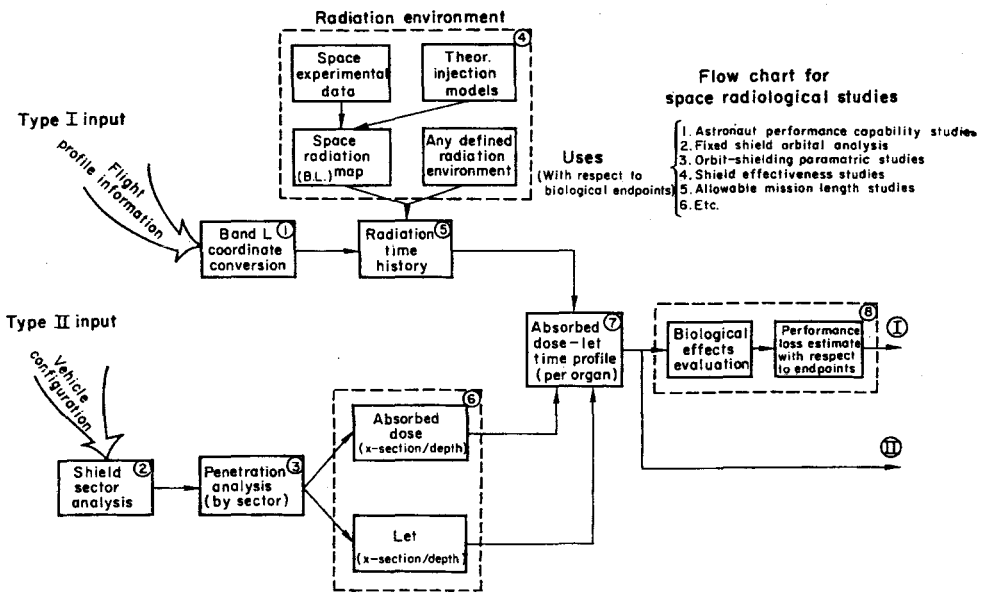

FIG. 1. Flow chart for space radiological studies.

be simply to measure the dose at some arbitrary spatial location and compare this measurement with calculated results. This implies a strong reliance on previously gathered environmental data (Block 4, Fig. 1). Since the environment may change slowly with time and rapidly with spatial position, difficulties may arise in comparing a computed dose for a point or points in space with an actual measurement. The experiment described herein obviates the necessity for reliance on past environmental data by adopting the philosophy of simultaneous measurement of the radiation environment and absorbed dosage. This allows the following goals to be accomplished:

1. Provide extra measurements of the radiation environment for further updating of the computer program.
2. Provide measurements of absorbed dosages throughout space.
3. Provide valid checks on the shielding analysis, radiation transport, and dosage computation portions of the computer program by elimination of the environmental portion of the program.

II. EXPERIMENTAL TECHNIQUE

A. *Instrumentation*

Our experiment was designed with a single philosophical ground-rule—that of providing simultaneous measurement of the radiation environment and absorbed dose in such a manner that the results may be used to check theoretical calculations.

To this end, a satellite was instrumented with seven separate electron and proton spectrometers for the complete measurement of the entire radiation environment and four instruments to measure absorbed dosage. Brief descriptions of these instruments are contained in Tables 1 and 2.

The flux, energy spectra, and angular distributions of electrons and protons were measured by four directional spectrometers employing scintillation techniques and multichannel analyzers. Three instruments, provided by Aerospace Corporation, measured the omnidirectional flux and energy spectra of electrons and protons and employed solid state ionization techniques.[4] The above instruments utilize well-known techniques and will not be described in further detail. They provided measurements of the radiation environment over the energy ranges of 0.56 to 5 MeV for electrons and 6 to 160 MeV for protons. These instruments were well calibrated utilizing Sr^{90} and Cs^{137} beta sources and the 50 MeV proton accelerator facility at the University of California at Los Angeles.

For the measurement of absorbed dose, four

Table 1. *Environmental Instrumentation*

Instrument	Number used	Detector	Type of measurement	Dynamic range
Electron spectrometer	1	CsI—plastic phoswich with pulse height analysis	Electron flux energy spectra, angular distribution	0.5 to 10^4 counts/sec. 0.5 to 5.0 MeV in eight channels
Proton spectrometer	1	Same as above with plastic absorber	Proton flux, energy spectrum, angular distribution	0.5 to 10^3 counts/sec. 49 to 120 MeV in four channels
Delta E proton spectrometers	2	Thin plastic scintillators with threshold detection	Integral proton flux between limits, angular distribution	Delta E_1: 5×10^{-1} to 5×10^3 counts/sec. (10 MeV $< E <$ 20 MeV) Delta E_2: 5×10^{-1} to 5×10^3 counts/sec. (20 MeV $< E <$ 49 MeV)
Omni-directional* proton-electron spectrometers	3	Solid state detector with threshold	Integral proton flux between limits	Protons: 6–20, 40–80, 100–160, and < 100 MeV
			Integral electron flux above threshold	Electrons: 0.3 and 4.5 MeV

* Provided by Aerospace Corporation, El Segundo, California.

Table 2. *Dosimetric Instrumentation*

Instrument	Number used	Detector	Type of measurement	Dynamic range
Proton dosimeter	1	Solid state detectors imbedded in Al sphere at depths of 0, 4, and 16 g/cm^2	Energy deposition at known depths in simple geometry	0.5 to 2×10^4 MeV/sec (each detector)
X-ray or bremsstrahlung dosimeter	1	Thin CsI crystal behind known aluminum shield	Energy deposition per unit time caused by bremsstrahlung from electrons striking known shield	1.62×10^3 to 1.62×10^6 MeV/sec.
Tissue-equivalent	2	Small ionization chamber constructed of Shonka Muscle-equivalent plastic	Absorbed dose in rad/hr at depth of 0.17., 3.2 and 8 g/cm^2	0.2 to 200 rad/hr

instruments of three types were utilized. They are as follows:

1. Tissue Equivalent Ionization Chambers (T.E.I.C.). Two instruments of this type were utilized and imbedded in a tissue-equivalent material (lucite) at depths of 0.17 and 3.2 g/cm^2. Anisotrophy of shielding provided another apparent depth of 8.0 g/cm^2 in certain instances. Basically these chambers are constructed of Shonka muscle-equivalent plastic and are described in the literature in numerous places.[5, 6] A thorough calibration was performed utilizing Sr^{90} and Cs^{137} beta sources as well as the proton accelerator facilities at Oak Ridge National Laboratory and Harvard University.

2. Proton Dosimeter Sphere. The proton dosimeter is designed to measure, primarily, proton dose rates penetrating various degrees of shielding material in a simple geometry. This measurement is achieved by using solid state detectors placed at three different depths in an aluminum sphere: 0, 4 and 16 g/cm^2. To obtain a wide dynamic range with good accuracy, the instrument alternates between two overlapping sensitivity ranges. The solid state detectors produce a signal proportional to the energy deposited by an intercepted proton in the semiconductor material. This signal is amplified by a charge-sensitive solid state preamplifier and fed to a pulse height discriminator which rejects noise and signals below a predetermined level. The pulse-height discriminator passes signals above this level to the pulse-height to pulse-width converter, where each pulse is converted to a constant amplitude pulse whose width is proportional to its height. These pulses are then fed to a log-integrator which integrates the signal for a variable-known time. The sensitivity of the proton dosimeter is controlled by alternately increasing and decreasing the integrating period.

The three solid state detectors were calibrated so that the output in volts may be related directly to rate of energy deposition in the detectors. The parameters which had to be determined included detector sensitive area and thickness and the relation between detector pulse height and energy deposited.

The Ph/PW converters for all three channels have a nominal 20 μsec/V conversion factor. To establish accurately the integrating time versus particle energy, the gain is adjusted using a radioactive calibration source to obtain pulse widths corresponding to each channel's sensitivity. A monoenergetic 5.30 MeV alpha source and Cs^{137} and Sr^{90} beta sources were used as calibration sources to accurately adjust gains and to establish the acceptance threshold level of the pulse height discriminator at 0.5 MeV.

Having set the gains of the preamps and electronic thresholds, it was desirable to calibrate the system at various dose rates, simulating as closely as possible the nuclear environment (random rates and pulse heights). It was possible to approximate this condition by generating a random pulse-rate of constant amplitude pulses that closely simulated the pulse shape from the detectors. The rate and amplitude were varied and recorded, along with the dosimeter output.

In addition to the calibration of the various electronic assemblies mentioned previously, four of the solid-state detectors were calibrated at the University of Southern California 30 MeV Proton Accelerator. Calibration consisted of a set of identical experiments to determine detector thickness for all four detectors.

Energy loss in the detector (which is proportional to the pulse-height output from the charge sensitive preamplifier) is a linear function of the energy of the incident particle as long as this energy is sufficiently low that it is completely absorbed in the detector. If all energy is not absorbed in the detector, the energy loss in the detector decreases as the incident energy increases. The thickness corresponding to total absorption may be uniquely determined.

The final calibration of each detector within the system consisted of placing the dosimeter in a flight configuration and exposing each detector to Sr^{90} beta particles. The output (in volts) of the dosimeter was noted, and the output analyzed. The data collected from the multichannel analyzer can be integrated to yield the MeV/sec exceeding the known (0.5 MeV) threshold and this measured total dose compared with the dosimeter output. The agreement among measurements using this technique was found to be excellent.

3. X-Ray Bremsstrahlung Dosimeter. The X-ray dosimeter is designed to measure the energy per unit time which bremsstrahlun

from electrons striking a known shielding will produce in a thin CsI crystal. This allows the assessment of results of calculations of bremsstrahlung within shielding media. The sensor consists of a small CsI crystal (0.25 in. in diameter by 0.020 in. thick) cemented to a photomultiplier tube. The output current from the anode of the photomultiplier tube is converted into a voltage which is proportional to the logarithm of the current.

Calibration of this instrument was accomplished in the following manner. The energy flux striking the CsI crystal was calculated for peak flux in the inner Van Allen belt. This was estimated as $\sim 1.08 \times 10^5$ MeV/sec. The photomultiplier tube saturates near 100 μA; thus the maximum current calculated for the peak flux was limited to 20 μA, to provide a factor of 5 for safety. The calibration factor to be derived was then

$$F_{calc} = \frac{1.08 \times 10^5}{20} \frac{\text{MeV}}{\mu\text{A} \cdot \text{sec}} = 5400 \frac{\text{MeV}}{\mu\text{A} \cdot \text{sec}}$$

The calibration procedure was to irradiate the detector with a 1 mCi Cs^{137} source (the crystal is shielded by 5 g/cm^2 aluminum). Only the Cs^{137} gamma and bremsstrahlung would be present inside the shield. A multi-channel analysis was made of the anode pulses from the photomultiplier tube, and the anode current was monitored. The energy calibration per channel was done by identifying the 662 keV Cs^{137} gamma peak (3.28 keV/channel) and calculating the area under the spectrum (1.02×10^8 counts $\times$ number of channels). Therefore the total energy flux seen by the crystal was, for a time of 600 seconds, $E_T = 557.5$ MeV/sec. The anode current measured was 0.102 μA, so that

$$F_{meas} = \frac{E_T}{I_a} = 5483 \text{ MeV}/\mu\text{A} \cdot \text{sec}$$

The run was then taken at a high voltage value of 820 V. If the measured F did not equal the calculated F, the high voltage could be adjusted to yield the correct measured F. This is done by constructing a curve of anode current versus high voltage. The ratio of F_{meas} to F_{calc} determines the I_a required to yield the correct factor, and the high voltage is adjusted to yield this current.

The anode current is converted to a d.c. voltage output by the appropriate electronics.

B. *Satellite System*

The above-described instrumentation was integrated into an OV1-2 Satellite built by General Dynamics Corporation for the Air Force.

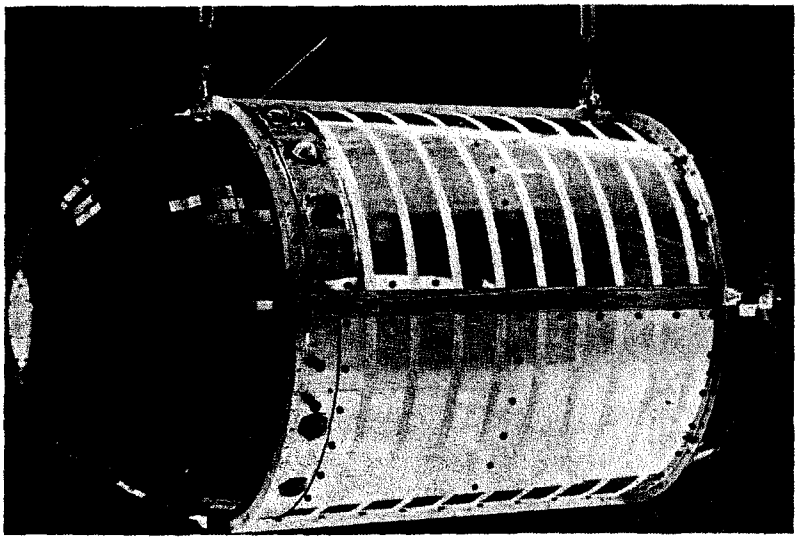

FIG. 2. OV1-2 Satellite (1965 78A)

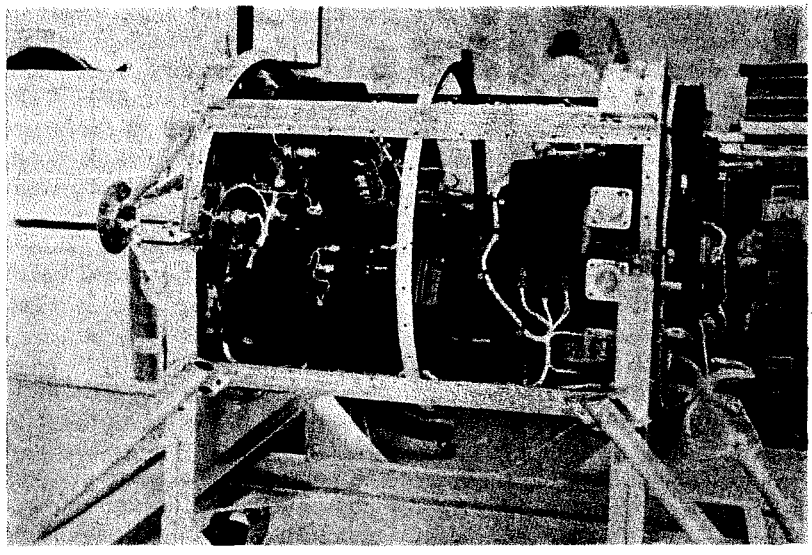

FIG. 3. Layout of instruments.

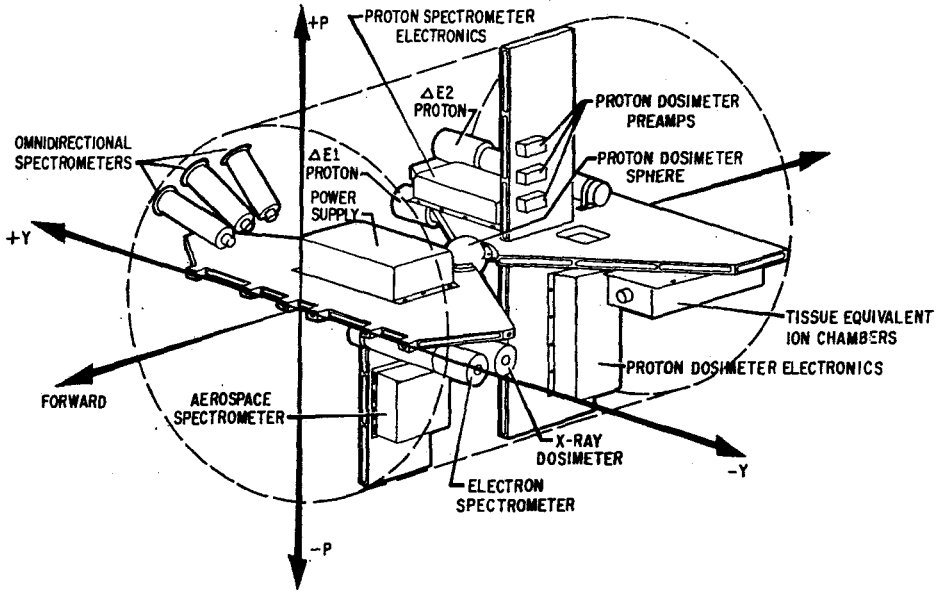

FIG. 4. Layout of instruments (OV1–2).

This satellite is shown in Fig. 2. and the instrument layout is shown in Figs. 3 and 4.

An additional instrument, a three axis magnetometer, was provided as an integral part of the satellite system. This provided information regarding the orientation of satellite axes with respect to the magnetic field line. This allows the measurement of any particle angular distribution which may be present. The ability to independently command each instrument on and off was also provided.

The instrument outputs could be stored on tape for 120 min and read out on command, allowing the accumulation of entire orbits of data. A separate command bypassed the tape recorder and allowed the instruments to be read out in real time.

C. *Spacecraft Material Distribution*

The purpose of the space flight experiment was the correlation of dosimetry and radiation environment measurements; hence, the material distribution surrounding the various dosimeters had to be well known in order to calculate dosimeter response. Even for the simple spherical geometry where the proton dosimeter is located at the geometric center of the spacecraft (Figs. 3 and 4), shielding by other instruments, spacecraft structure, etc., introduce perturbations which must be considered.

Since protons and electrons lose energy mainly through collisions with atomic electrons (to a first order approximation), it will be sufficient to specify the areal density of electrons as a function of solid angle about the point of interest. In general, neither the collision stopping power of primary charged particles or photon attenuation, in the Compton region, is a strong function of attenuator atomic number. It is evident that if the photon attenuation throughout the vehicle geometry is determined the areal electron density may be easily calculated. Aluminum is extensively used in space vehicle construction, and since aluminum is a representative low Z material, the areal density may be expressed in g/cm^2 of aluminum, or the aluminum equivalent electron/cm^2 of path length.

A 1.0 μCi Co^{60} source was positioned at the center of the aluminum sphere (proton dosimeter) in the satellite vehicle. The vehicle could be positioned accurately through three degrees of freedom. A 2 $\times$ 2 in. NaI crystal was located at a distance where it subtended a 1° half-angle from the source. The remainder of the experimental apparatus is shown in Fig. 5. At these (Co^{60}) energies Compton Scattering is the dominant loss mechanism (98%). Thus a measurement of the unscattered to scattered photons yields the areal density through the following relation:

$$I = I_0 e^{-tx}$$

where I = unscattered photons,
I_0 = total photons before absorption,
t = mass absorption coefficient, cm^2/g,
x = absorber path length, g/cm^2.

Using the above technique over 800 solid angles were scanned and translated into equivalent aluminum thickness or areal density.

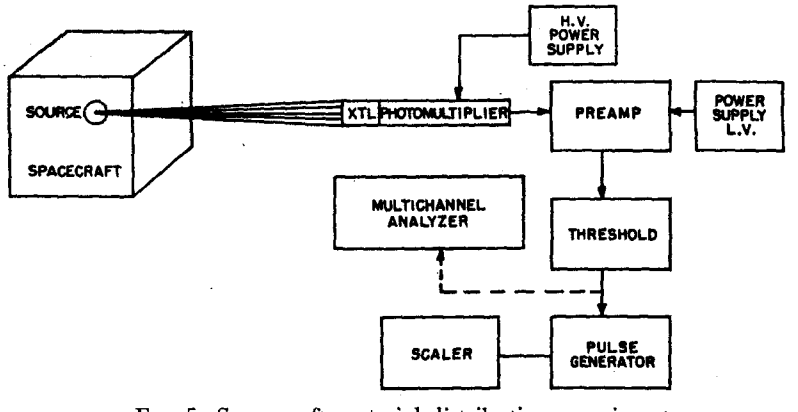

FIG. 5. Spacecraft material distribution experiment.

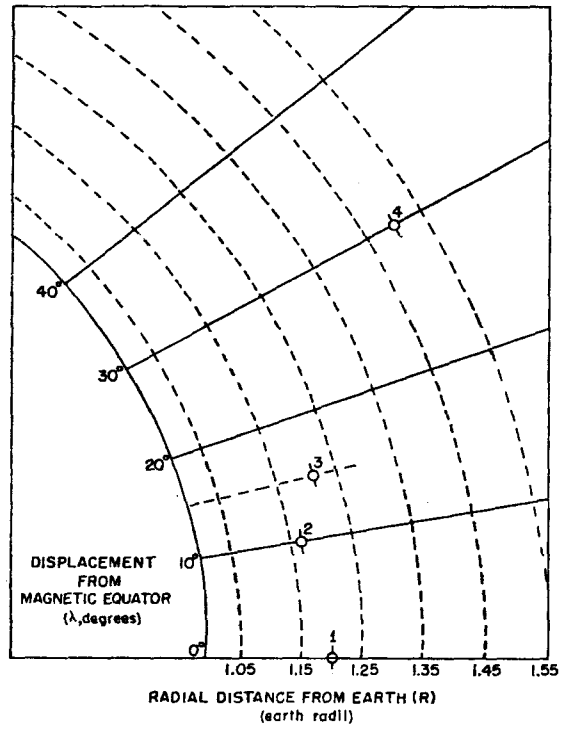

FIG. 6. Spatial location of data points.

A technique was also developed for utilizing this data to specify the material distributions about all dosimeter locations.

III. EXPERIMENTAL RESULTS

This experiment was placed in orbit aboard the OV1-2 Satellite on October 5, 1965. A retrograde orbit with an 1865 n-mi apogee, a perigee of 222 n-mi, and an inclination of 144° were achieved. This orbit was such that nearly all of the Inner Van Allen Zone is swept out by succeeding orbits.

The data reduction has been fully automated and computerized. The instrument calibrations, temperature calibrations, and tape recorder nonlinearities, etc., are removed and the data is printed out as raw count rates, dose rates, etc., as a function of time and spatial position. For convenience in handling, as well as standardization, the spatial position is given in terms of the four parameters R, λ, B, and L. R is the radial geocentric distance to the point, λ is the angular displacement from the magnetic equator, B is the magnetic field strength, and L is the "McIllwain Parameter" [7] which corresponds to the radial, geocentric distance at the equator of the magnetic field line which passes through the point.

Four points in space were arbitrarily selected for this paper. These points are shown in Fig. 6. This figure also depicts the general limits of the satellite coverage. Table 3 gives the pertinent information regarding the selected points.

A. *Electron Spectra*

The outputs of each electron spectrometer channel were plotted as a function of time, and the peak fluxes were selected. These peak fluxes correspond to the instrument aperture being aligned at 90° to the magnetic field line (i.e. at the maxima of the angular distribution). The Greenwich Mean Time of the exact point in space was determined, and the data for a four-minute interval of time around the point was reduced.

Figure 7 shows such data for two spectrometer channels. The modulation is caused as

Table 3. Points Selected for Analysis

Point	R (Earth radii)	B (gauss)	L (Earth radii)	λ (degrees)	Date/Orbit
1	1.20	0.178	1.20	0	9 Oct/29 14 Oct/100
2	1.17	0.200	1.20	9.5	12 Oct/75
3	1.23	0.199	1.30	16	9 Oct/42
4	1.51	0.120	2.00	30	6 Oct/10

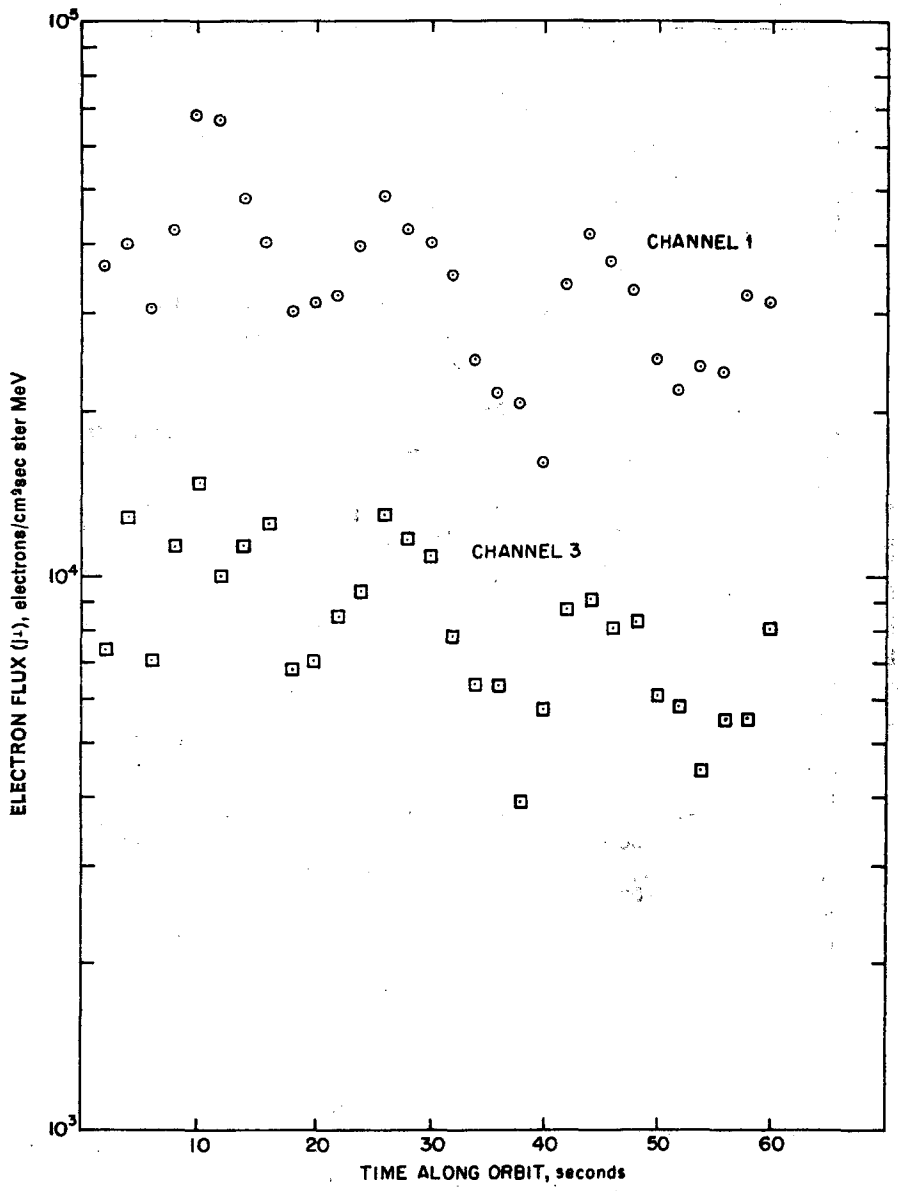

FIG. 7. Electron spectrometer channels 1 and 3, $L = 1.20$, $\lambda = 0°$.

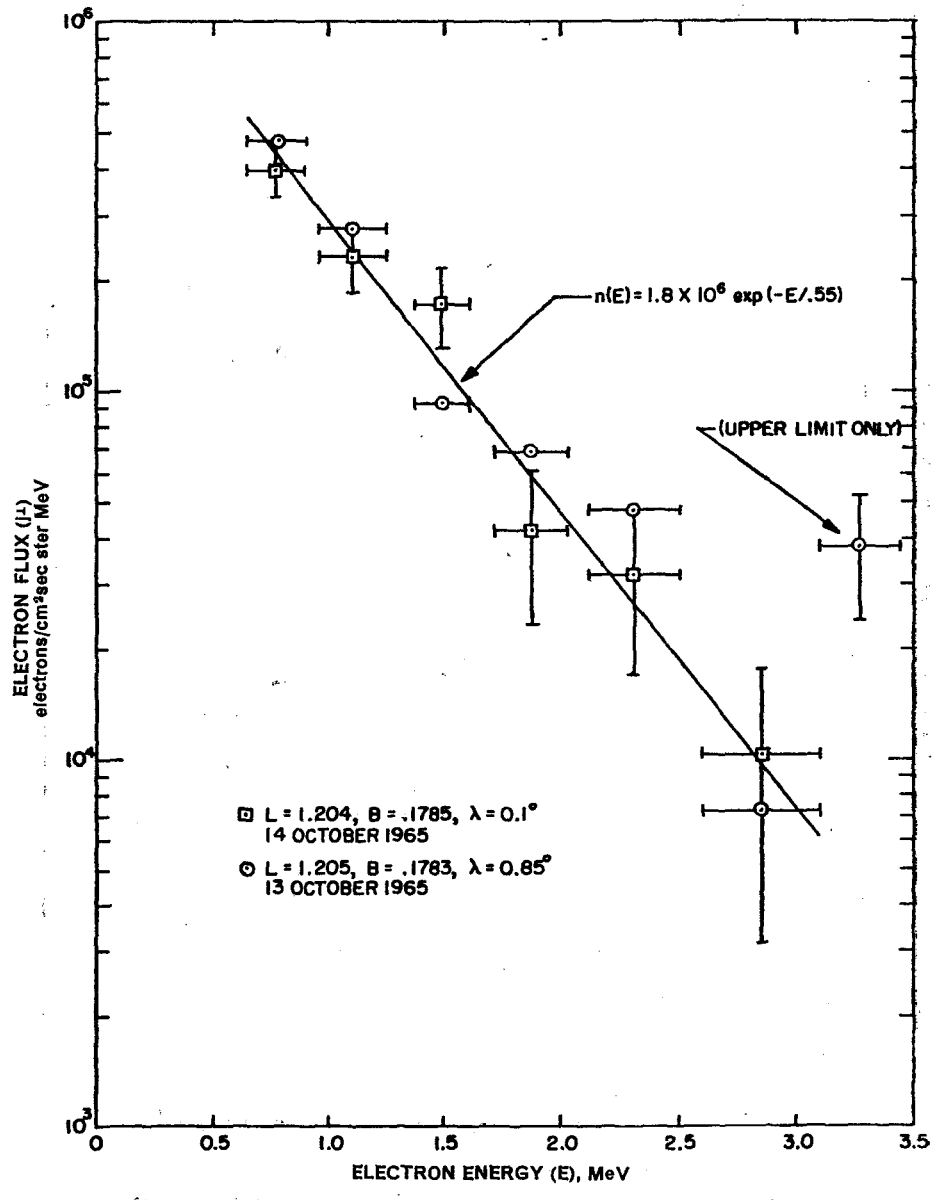

FIG. 8. Differential electron spectrum, October 13–14, 1965.

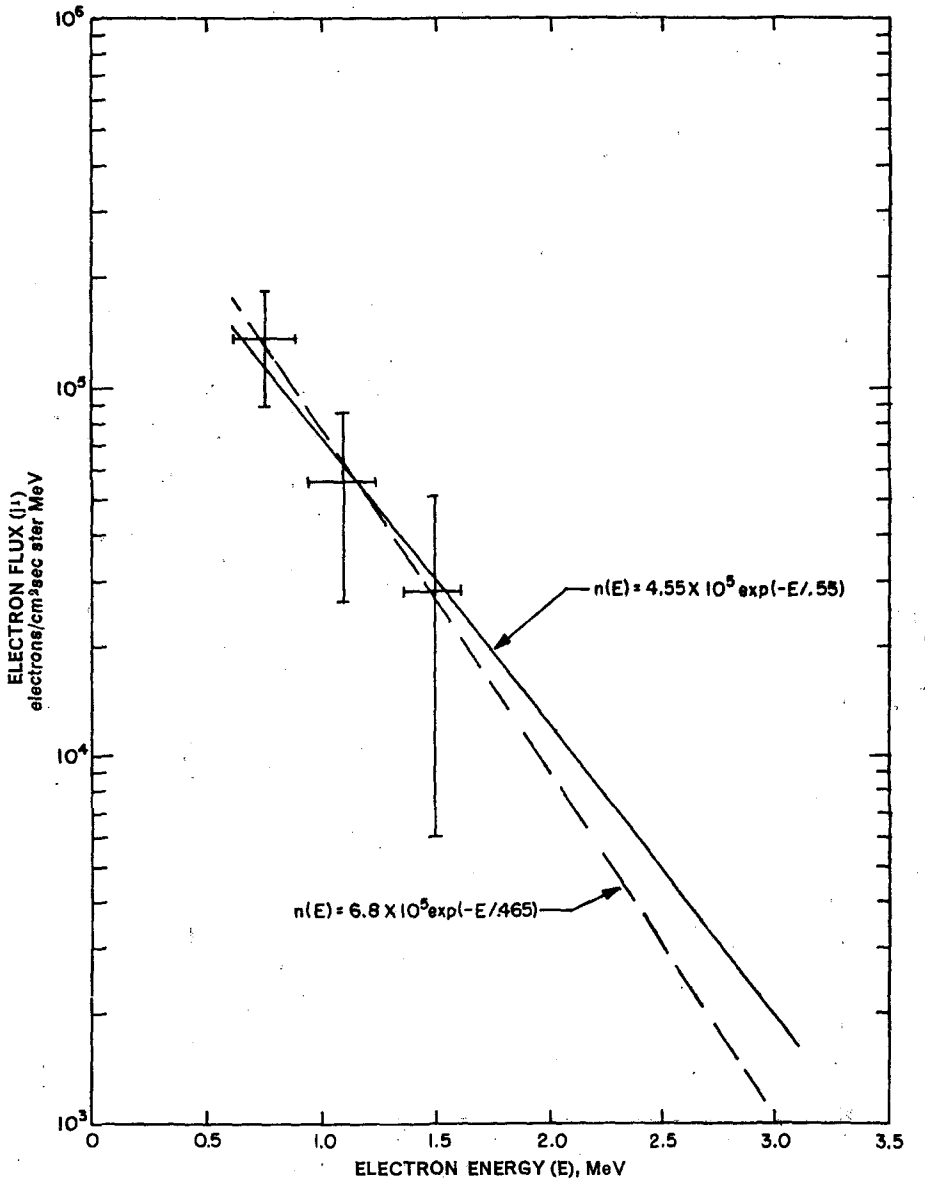

FIG. 9. Differential electron spectrum, October 12, 1965, $L = 1.207$, $B = 0.200$, $\lambda = 9.46°$.

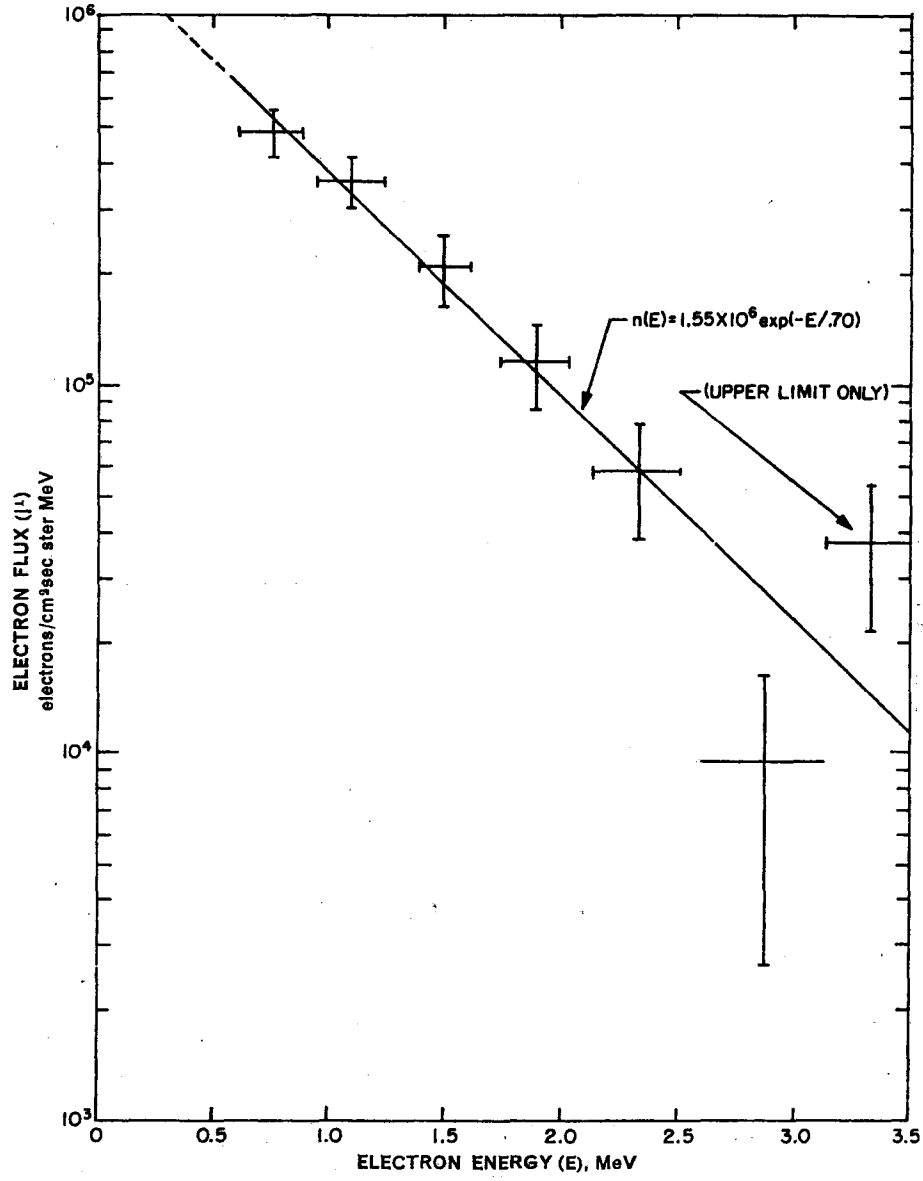

FIG. 10. Differential electron spectrum, October 9, 1965, $L = 1.30$, $B = 0.1993$, $\lambda = 16°$.

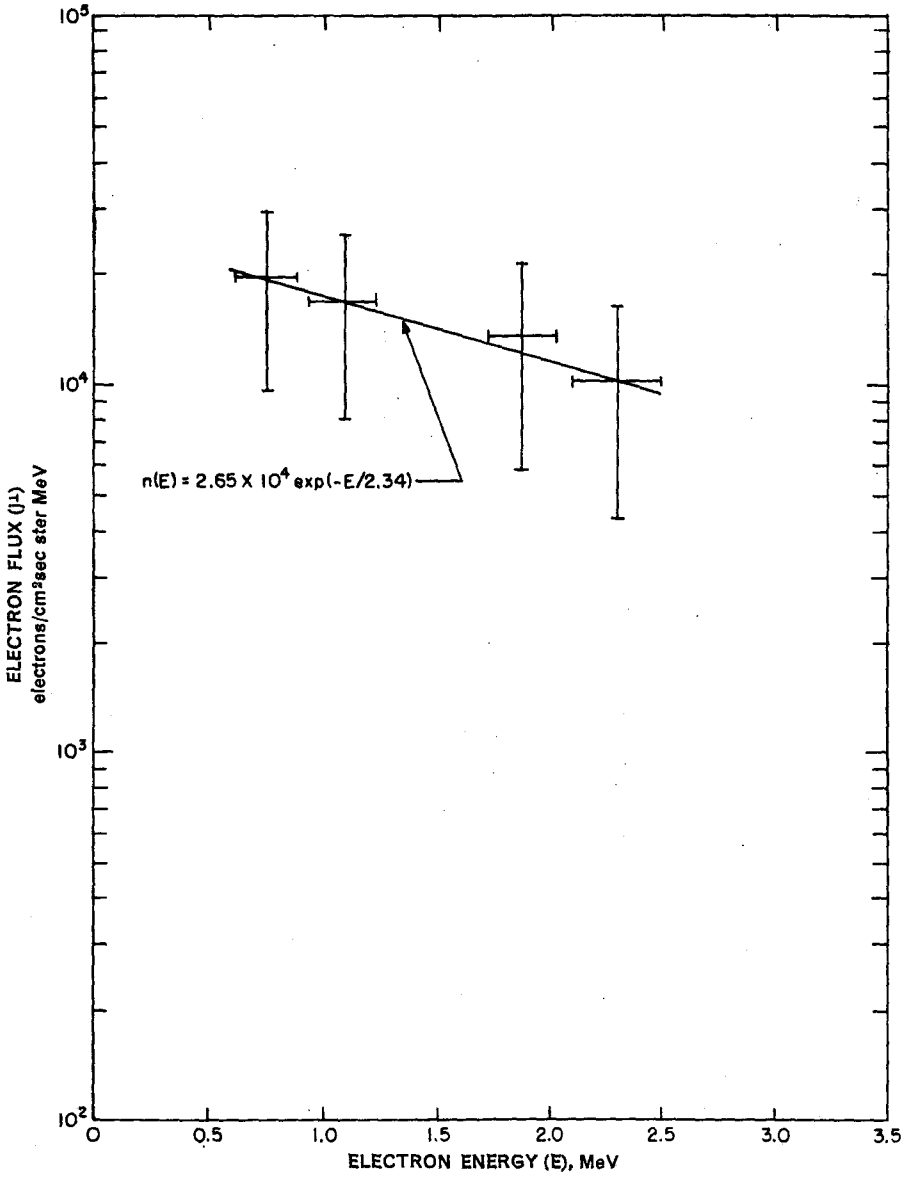

FIG. 11. Differential electron spectrum, October 6, 1965, $L = 2.00$, $B = 0.120$, $\lambda = 29.8°$.

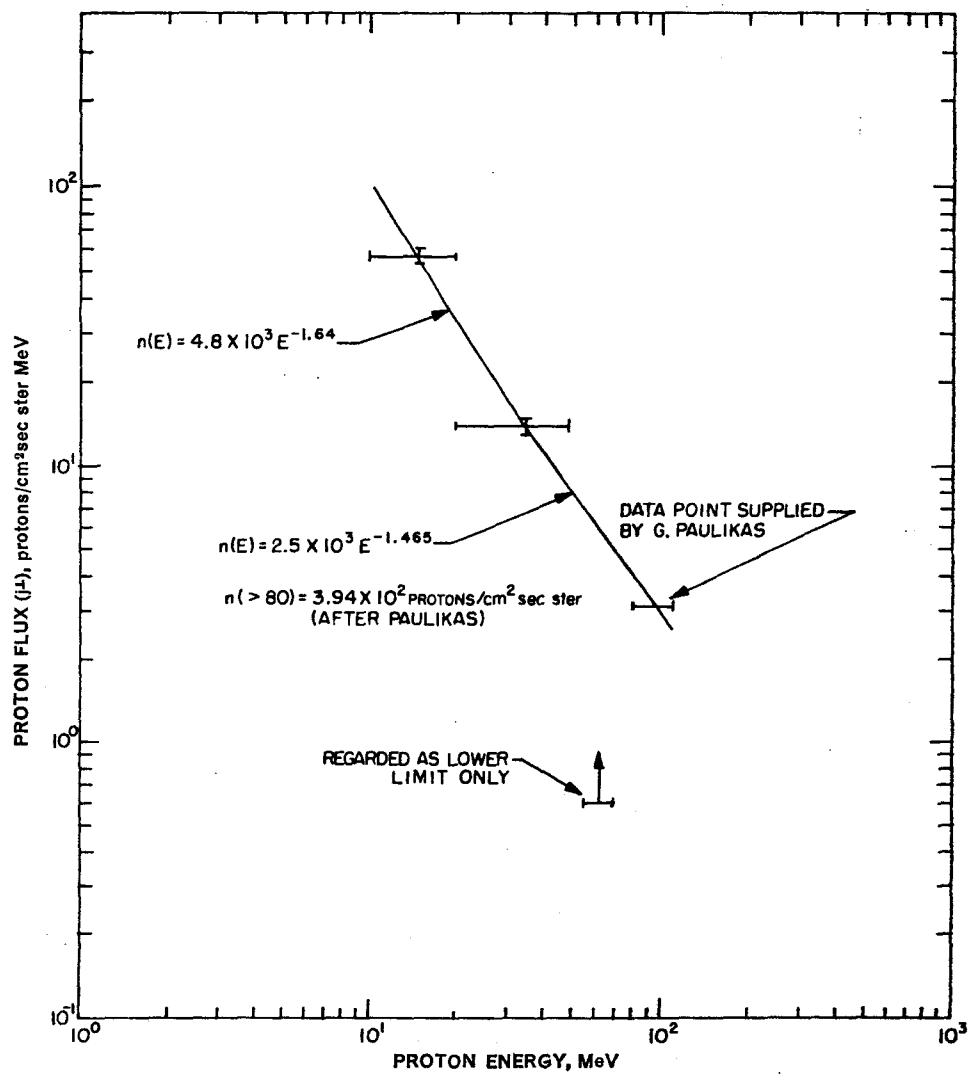

FIG. 12. Differential proton spectrum, October 1965, $L = 1.20$, $B = 0.178$, $\lambda = 0°$.

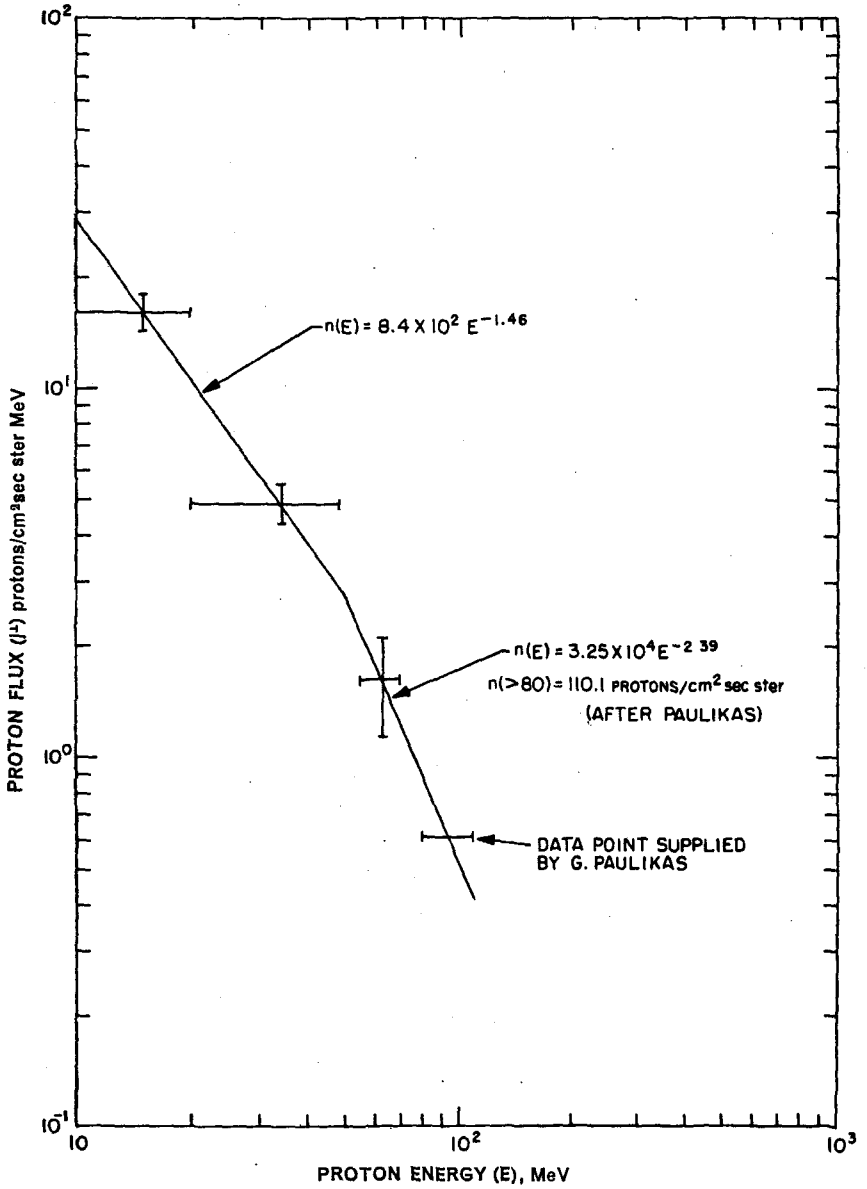

FIG. 13. Differential proton spectrum, October 12, 1965, $L = 1.207$, $B = 0.200$, $\lambda = 9.46°$.

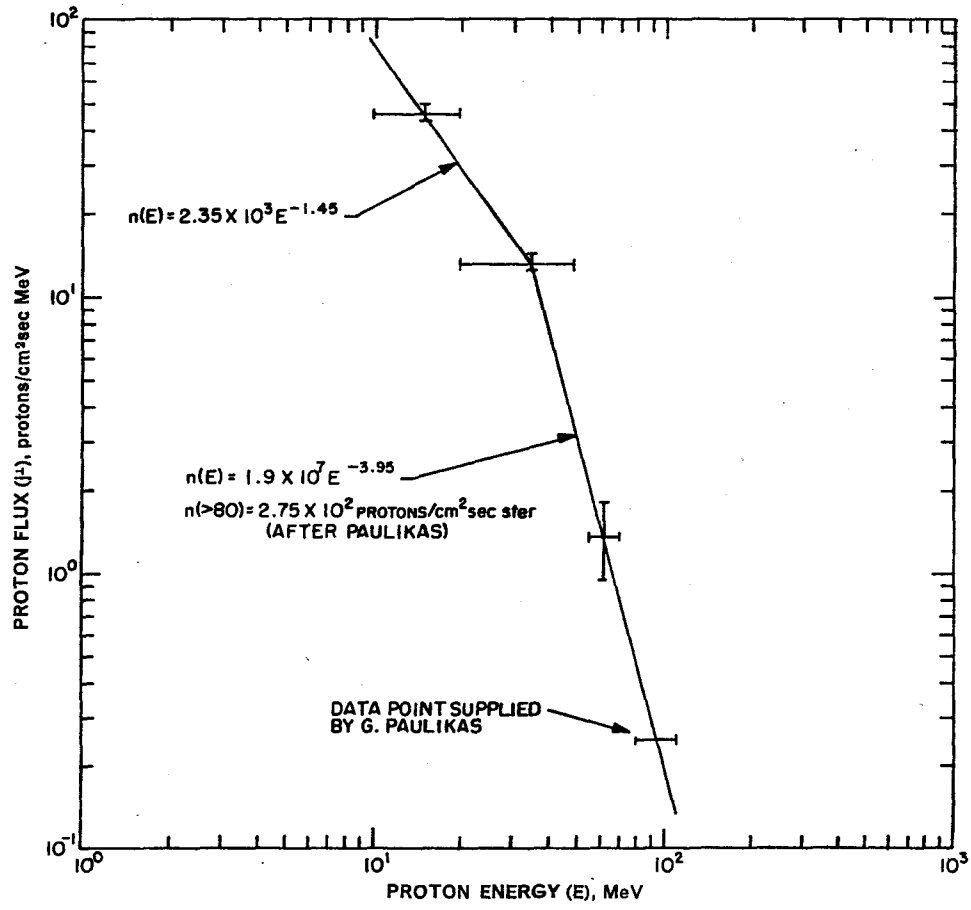

FIG. 14. Differential proton spectrum, October 9, 1965, $L = 1.30$, $B = 0.1993$, $\lambda = 16°$.

the vehicle tumbles in space and the directional aperture passes in and out of the plane of maximum intensity. This modulation is typical for all directional instruments.

Figures 8, 9, 10, and 11 show the spectra determined for each of the four points. Following earlier experimenters, the data have been fitted with analytical expressions of the form $N(E) = A \exp(-E/E_0)$. These expressions as found for the four points are as follows:

Point 1: $N(E) = 1.8 \times 10^6 \exp(-E/0.55)$

Point 2: $N(E) = 6.8 \times 10^5 \exp(-E/0.46)$ or $4.55 \times 10^5 \exp(-E/0.55)$

Point 3: $N(E) = 1.55 \times 10^6 \exp(-E/0.70)$

Point 4: $N(E) = 2.65 \times 10^4 \exp(-E/2.34)$

There has been postulation by many experimenters, with some verification, that the electron spectral slope does not change with B (or λ) along points of constant L. It should be observed that while the best fits are not identical, both points 1 and 2 ($L = 1.20$) may be fitted with the same analytical expression within experimental error. The difference in spectral shape and/or flux with other spatial positions should be noted.

B. *Proton Spectra*

To construct proton spectra the data from the two Delta E Spectrometers, the Proton Spectrometer, and one of the Aerospace Omnidirectional Spectrometers ($80 < E < 110$ MeV) [8] were used. The data from the Proton

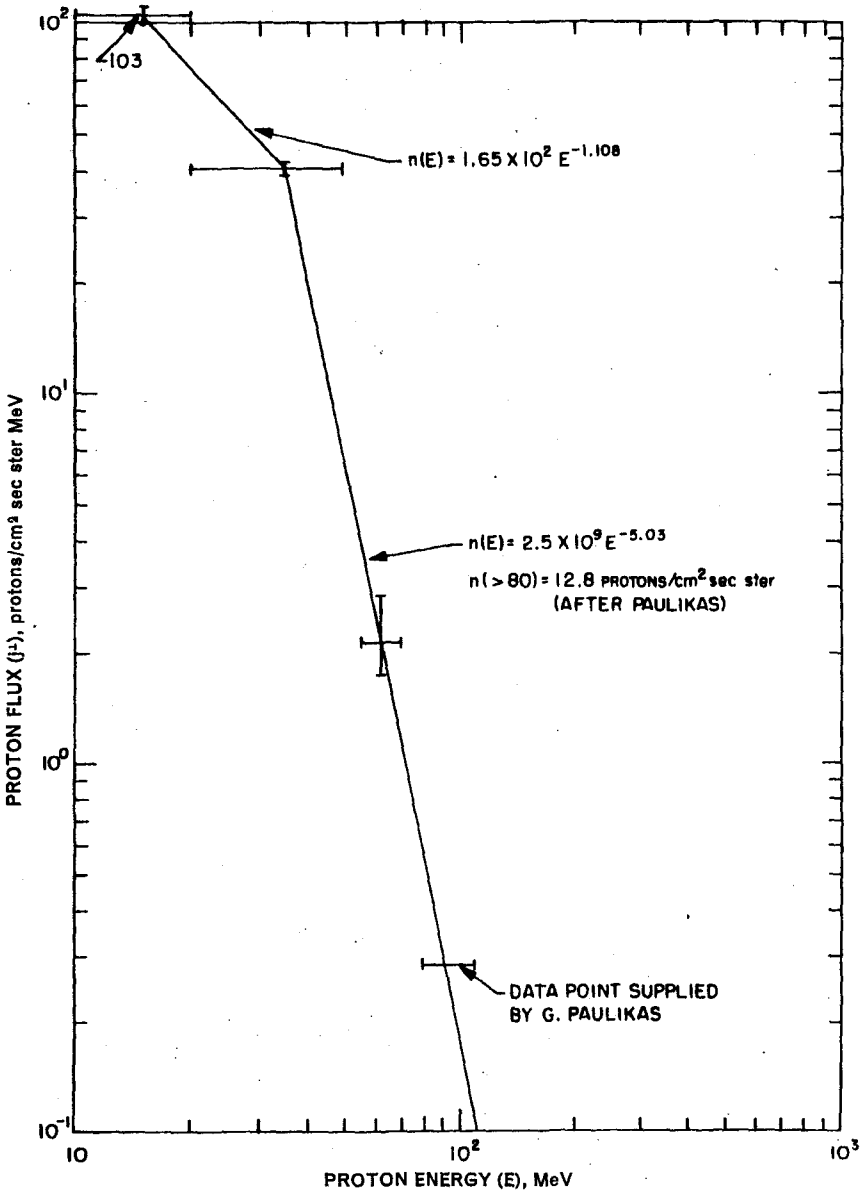

FIG. 15. Differential proton spectrum, October 6, 1965, $L = 2.00$, $B = 0.12$, $\lambda = 29.8°$.

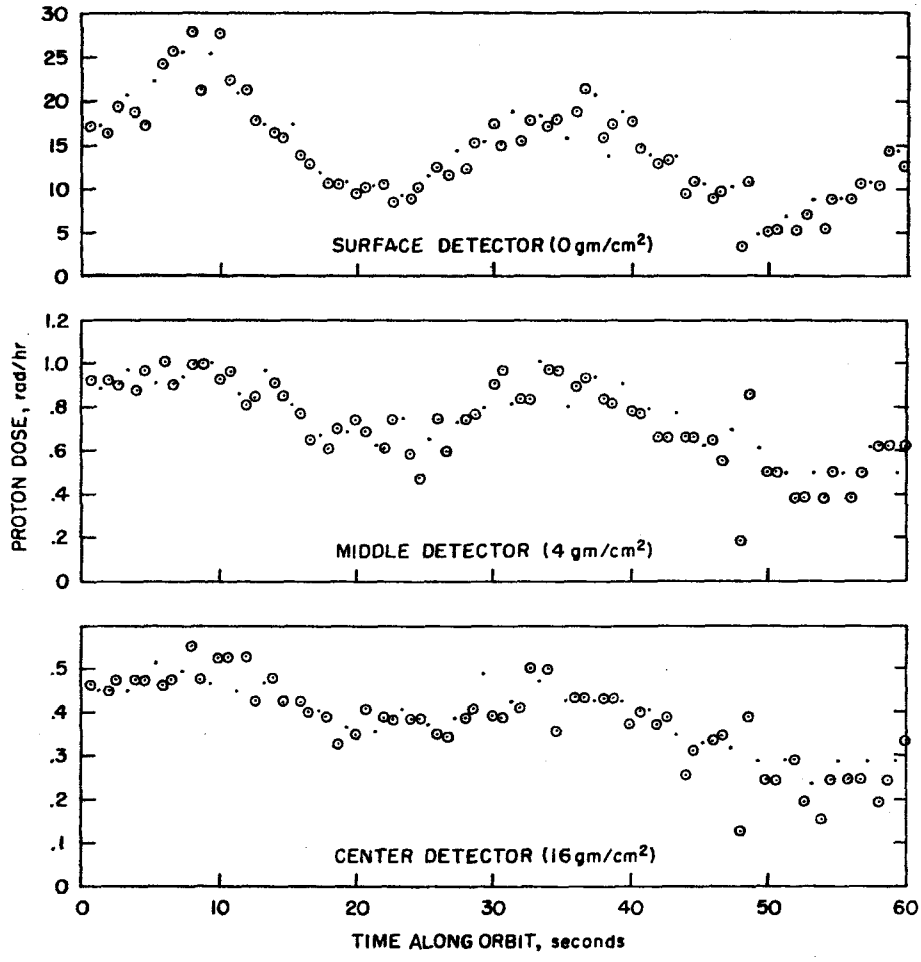

FIG. 16. Proton dosimeter data-revolution 10, October 6, 1965.

Spectrometer was sometimes difficult to interpret due to saturation and at these points the data were considered as lower units only. The data furnished by Aerospace described the omni-directional flux whereas our spectra are in terms of uni-directional fluxes. To convert omni-directional fluxes to uni-directional fluxes a program developed by Dr. Thomas Farley of UCLA was used. The spectrums thus derived are shown in the Figs. 12, 13, 14, and 15. Again following the lead of earlier experimenters, the spectrums were fitted with two power law analytical expressions, of the form $N(E) = AE^{-\gamma}$ over separate energy ranges. These are given for the four points as follows:

Point 1: $N(E) = 4.8 \times 10^3 E^{-1.64}$ $10 < E < 35$ MeV

$N(E) = 2.5 \times 10^3 E^{-1.46}$ $35 < E < 110$ MeV

Point 2: $N(E) = 8.4 \times 10^2 E^{-1.46}$ $10 < E < 50$ MeV

$N(E) = 3.25 \times 10^4 E^{-2.30}$ $50 < E < 110$ MeV

Point 3: $N(E) = 2.35 \times 10^3 E^{-1.45}$ $10 < E < 35$ MeV

$N(E) = 1.9 \times 10^7 E^{-3.95}$ $35 < E < 110$ MeV

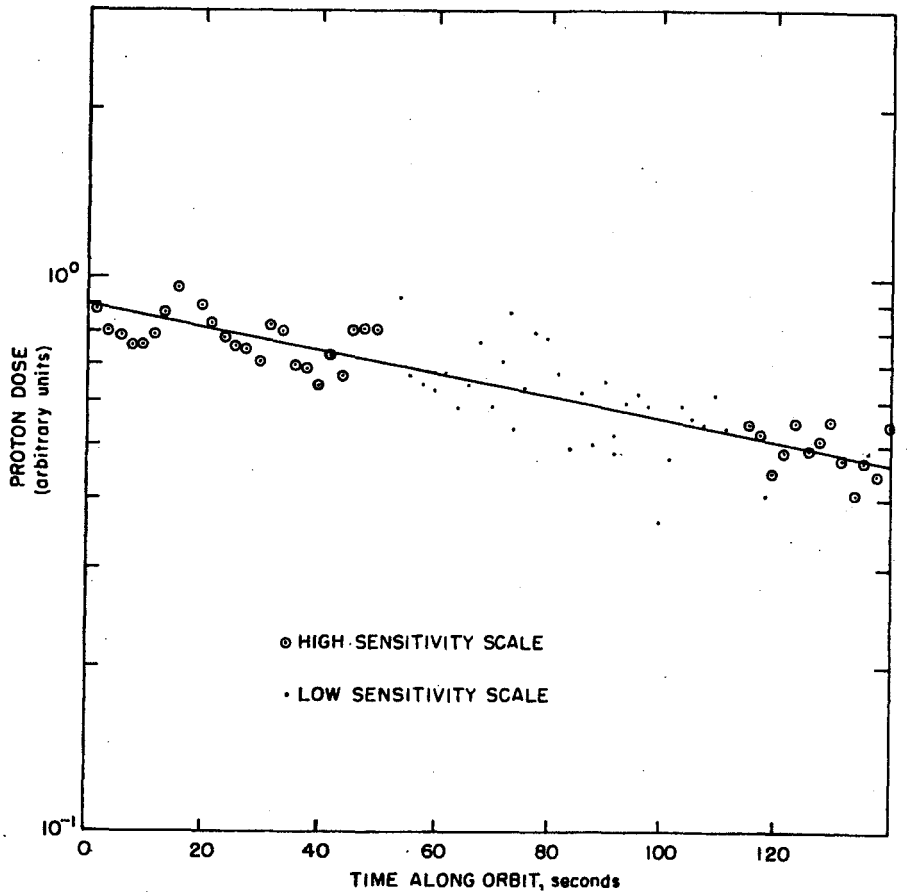

FIG. 17. Proton dosimeter middle detector, method of dose determination.

$$\text{Point 4: } N(E) = 1.65 \times 10^2 E^{-1.74} \quad 10 < E < 35 \text{ MeV}$$
$$N(E) = 2.5 \times 10^9 E^{-5.02} \quad 35 < E < 110 \text{ MeV}$$

As with the electron spectrums, the change in flux intensity and spectral shape with spatial position should be noted.

C. *Dose Rate Measurements*

The experimental radiation dose rates at the four chosen positions in space were obtained for the same time that the spectral determinations were made. Six experimental doses were obtained at each point in space from: three solid-state proton dosimeters, one X-ray detector, and two tissue-equivalent ionization chambers. The radiation dose rate determinations, the general dose rate variation with time, and the experimental dose rate variation are discussed for the various instruments in the following paragraphs.

1. Proton Dosimeters. The proton dosimeters are sampled every two-thirds of a second. A typical output for 1 min is illustrated in Fig. 16. This shows the roll-modulated output, the range switching, and the general fluctuation in the experimental data. The dose rate for the desired time, corresponding to the desired point, was determined by plotting the average of three dose rates for two plus minutes and then drawing a line through the data. (An example of this technique is shown in Fig. 17) The proton dosimeter changes scale approximately every

Table 4. Proton Dosimeter Doses for the Four Selected Locations in Space

Detector	Point in space	Dose rate (rad/hr)	Rate of change (rad/hr/min)	% Variation	
				Positive	Negative
Surface (0 g/cm²)	1	6.9	5.5	41	41
	2	1.7	2.1	37	41
	3	9.4	1.0	35	25
	4	2.8	0.47	26	48
Middle (4 g/cm²)	1	0.64	0.19	33	35
	2	0.21	0.11	22	18
	3	0.46	0.08	22	18
	4	0.066	0.014	71	29
Center (16 g/cm²)	1	0.49	0.12	32	22
	2	0.16	0.08	39	32
	3	0.34	0.06	20	13
	4	0.15*	—	—	—

* Indicates an upper limit only.

Table 5. X-ray Detector Doses for the Four Selected Locations

Point in space	Dose rate (rad/hr)	Rate of change (rad/hr/min)	% Variation	
			Positive	Negative
1	0.80	0.26	10	10
2	0.25	0.11	26	22
3	0.50	0.08	23	14
4	0.099	0.03	35	23

Table 6. T.E.I.C. Doses for the Four Locations

Point in space	Dose rate—T.E.I.C. No. 1 (rad/hr)			Dose rate—T.E.I.C. No. 2 (rad/hr)		
	Peak	Minimum	Average	Peak	Minimum	Average
1	4.8 ± 0.9	2.1 ± 0.5	3.6 ± 0.8	3.0 ± 1.0	3.6 ± 0.6	4.2 ± 0.8
2	1.6 ± 0.6	0.7 ± 0.2	1.2 ± 0.3	1.5 ± 0.3	1.2 ± 0.3	1.4 ± 0.3
3	6.6 ± 1.2	1.9 ± 0.6	4.7 ± 0.6	3.6 ± 0.6	2.5 ± 0.5	3.1 ± 0.5
4	0.7 ± 0.3	0.3 ± 0.1	0.5 ± 0.2			0.3 ± 0.1

minute and may be "off-scale" for one minute but may be providing good data both before and after that minute. Plotting more than 2 min centered about the off-scale data provides useful dose rate versus time information. The dose rate is then determined at the desired time (point), the time variation is determined, and the percentage variation (roll modulation) of dose rate is noted.

The results for the proton dosimeters are listed in Table 4. The center (16 g/cm^2) dosimeter was always below its minimum sensitivity at $L = 2.0$, $B = 0.122$ and only an upper limit of 0.015 rad/hr could be determined.

2. X-Ray Detector. The X-ray detector was sampled once every two seconds. This data was plotted against time. As with the proton dosimeter data, a line was drawn through the data. The dose rate was then determined at the desired time, the time variation determined, and the experimental variation noted. Results for the four positions are tabulated in Table 5.

3. Tissue-equivalent Ionization Chambers (T.E.I.C.). The data from the two tissue-equivalent ionization chambers were reduced in a manner similar to that from the other dose rate instruments except that the peak rates as well as an average over a roll modulation were determined. This was done in an effort to further evaluate the effect of the material distribution of the satellite. The results are shown in Table 6. T.E.I.C. No. 1 is shielded by 0.17 g/cm^2 and T.E.I.C. No. 2 by 3.2 g/cm^2.

IV. COMPARISON OF EXPERIMENTAL AND CALCULATED RESULTS

In the previous sections, an experiment has been described the results of which may be used to assess the validity of certain assumptions basic to computer programs used in predicting dose rates which may be encountered in space. In addition, the strengths and weaknesses of many of the sub-routines, such as radiation transport and dose conversions, may be determined.

Preliminary dose calculations have been performed, for certain cases, to provide a general comparison of calculated and experimental dose at three of the points discussed in the previous sections. These calculations have been performed only for two detectors of the Proton Spectrometer (0.0 g/cm^2 and 4.0 g/cm^2) and the most thinly shielded ionization chamber (0.17 g/cm^2).

For the case of the ionization chambers two of the available computer programs (Boeing[2]

Table 7. Comparison of T.E.I.C. No. 1 Dose Rate Calculations to Measurements

Point in space	Type of dose rate*	Dose rates in rad/hr	
		AFWL-Boeing	AMRL-Northrop
1	Electron	3.2	3.6
	Proton	1.6	2.8
	Total	4.8	6.4
	Expt.	3.6 ± 0.8	3.6 ± 0.8
2	Electron	1.4	0.8
	Proton	0.8	0.3
	Total	2.2	1.1
	Expt.	1.2 ± 0.3	1.2 ± 0.3
3	Electron	3.2	7.9
	Proton	0.8	1.6
	Total	4.0	9.5
	Expt.	4.7 ± 0.9	4.7 ± 0.9

* The photon dose rate was negligible in all cases when compared to primary dose rate.

Table 8. Comparison of Proton Dosimeter Dose Rate Calculations to Measurements (AMRL-Northrop method only)

Point in space	Type of dose rate	Dose rates in rad/hr	
		Surface detector (0 g/cm²)	Middle detector (4 g/cm²)
1	Electron	4.6	–0–
	Proton	3.2	0.4
	Total	7.8	0.4
	Expt.	6.9	0.6
2	Electron	1.1	–0–
	Proton	0.3	0.1
	Total	1.4	0.1
	Expt.	1.7	0.2
3	Electron	9.6	–0–
	Proton	2.0	0.03
	Total	11.6	0.03
	Expt.	9.4	0.46

and Northrop[3]) were utilized in making calculations. Only the Northrop program was utilized in calculations concerning the Proton Spectrometer.

The results of the above calculations and comparisons with the experimental data are presented in Tables 7 and 8. These data should be viewed as preliminary serving only as an example of the results which may be expected from such a technique. No effort was expended to improve or modify the existing calculational procedures other than to further simplify the computational methods.

For a detailed discussion of the calculational methods involved, the reader is referred to refs. 2 and 3.

Three components of the dose were calculated utilizing the particle spectrum obtained by this experiment at the spatial locations involved. These were: (1) dose due to primary protons; (2) dose due directly to electrons; and (3) dose due to photons produced by the slowing down of electrons. Each dose component has assumptions peculiar to the calculations which yield the dose rate for primary particles versus the material thickness for that dose component. The material thickness about the dose points was calculated from the results of the gamma mapping experiment. The material distribution was obtained directly for the Proton dosimeter sphere and approximated for the ionization chambers assuming a right circular geometry for the satellite experimental bay. Once calculated, each material distribution was grouped according to thicknesses to determine the amount of solid angle having the specified ranges of thickness. For each dose point, this was then plotted as a histogram of solid angle per thickness versus thickness and a smooth curve plotted. The dose rates for proton, electron and photon dose components were then calculated by integrating the product of dose rate and material distribution range. In one case (Northrop), the measured spectra were extrapolated beyond the experimental values (using the shape factors present) before they were input to the calculations. In the second case (Boeing) no such extrapolations were made.

In general, fair agreement was obtained (in spite of the simplifications) at points of thin external shielding. This agreement progressively worsened as the shielding thickness increased; however, the discrepancies may be explained to a large degree by the manner in which the material distribution was handled and to a lesser degree by the spectral extrapolations.

In summary, the radiation transport and dose-conversion portions of the computer techniques seen are verified with the environmental and material distribution inputs being the most critically sensitive. In fact, a separate study of the importance of material heterogeneity in the calculation of radiation doses has shown that the dose rate is underestimated when constant mean thicknesses are used for solid angles which don't really have constant thicknesses. The calculated dose rate can vary a factor of four or more depending on the spectrum, the material thickness, and the degree of heterogeneity, if one first assumes a constant thickness and then takes into account heterogeneities.

REFERENCES

1. W. H. LANGHAM *et al. Aerospace Med.* **36,** Sec. 11. Special Report (Ed. by Langham), Feb. 1965.
2. Air Force Weapons Laboratory. Technical Documentary Report Number WL-TDR-64-71. *Computer Codes for Space Radiation Environment and Shields*, Vol. I, Aug. 1964.
3. R. E. FORTNEY. USAF Aeromedical Research Laboratory Technical Documentary Report Number AMRL-TDR-64-11, *Computer Analysis of Radiation Shielding*, Feb. 1964.
4. S. C. FREDEN and G. A. PAULIKAS. *J. Geophys. Res.* **69,** 1259–1269 (1964).
5. B. C. CLARK. *Life Sciences and Space Research* III (Ed. by M. Flarkin), 29–47. North Holland Pub. Co., 1965.
6. M. C. SCHNEIDER. Air Force Weapons Laboratory. Technical Documentary Report Number WL-TDR-64-96, *Advanced Spaceborne Dosimetry Instrumentation*, Dec. 1965.
7. C. E. MCILLWAIN. *J. Geophys. Res.* **66,** 3681–3691 (1961).
8. G. A. PAULIKAS. Private communication, July 1966.
9. T. A. FARLEY. Private communication, Feb. 1966.

AN EXPERIMENT TO MEASURE THE TISSUE-EQUIVALENT ABSORBED DOSE (LET) AND DEPTH-DOSE DISTRIBUTIONS PRODUCED BY RADIATIONS IN SPACE

M. C. CHAPMAN*
Northrop Space Laboratories, Hawthorne, California, U.S.A.

and

F. E. HOLLY
Air Force Weapons Laboratory, Albuquerque, New Mexico, U.S.A.

Abstract—An experiment to measure the absorbed dose distribution and depth-dose distribution in tissue-equivalent material is described. The experiment uses cellular-sized spheres of plastic scintillator to detect the dose deposition, and a pulse-height analysis is performed on the signals.

The sensor consists of a number of 100 micron spheres of plastic scintillator bonded to a lucite light-pipe. The lucite is cemented to a photomultiplier tube, and the output signal is processed by digital pulse height analyzers. This technique has many advantages over present ion chamber systems, including:

(1) measurements of absorbed dose with a detector approaching the cellular level,
(2) negligible dose gradient through the detector and minimum perturbation of the tissue-equivalent sample, and
(3) excellent resolution and gain stability.

It appears feasible to measure the absorbed dose distribution spectrum from 0.4 keV/micron to > 300 keV/micron with a single sensor. By utilizing multiple sensors with varying amounts of tissue-equivalent pre-filtering, a depth-dose distribution can be obtained. By integrating the absorbed dose spectrum, a measure of the total absorbed dose is obtained. In addition, the experiment provides data on cell hit frequency.

The removal of particle type-dependent response and geometrical considerations are discussed. One specific application of this technique involving an astronaut-manipulated space experiment is described.

INTRODUCTION

It has been well established that radiation poses a hazard to manned space flight, either through early acute effects or longer somatic effects. It is essential that dosimetric parameters such as the spectrum of radiation energy deposition and total absorbed dose be measured for small regions of tissue samples. In addition, the radiation depth-dose distribution would be important data. The experiment described in this paper utilizes very small ($\leq$ 100 micron) plastic scintillators as tissue-equivalent dosimeters, and yields measurements of absorbed dose distribution, total absorbed dose, depth-dose distribution, and cell hit frequency data not possible with present space dosimeters. The concept is based on unique application of state-of-the-art techniques of scintillation spectroscopy, and obtains data which is radiobiologically more meaningful than present "LET" devices. The dosimeter has a wide dynamic range, and can

*Now at TRW Systems Laboratories, Bedondo Beach, California, U.S.A.

perform satisfactorily in a variety of space radiation environments and missions. It is believed that this program represents a very significant scientific contribution to the knowledge of radiobiological hazards to manned space flight.

The experiment is particularly suited for missions operating within the radiation zones. The experiment will perform satisfactorily for low altitude (typically 200 n. mi.) missions or lunar flights. While it is desirable to utilize astronaut capability to modify the instrument in space, the experiment is not seriously compromised if utilized on an unmanned mission.

SCIENTIFIC BACKGROUND

The problems involved in investigating radiation hazards to living organisms in space are very complex. However, specification of the "LET" or absorbed dose spectrum, total absorbed dose, and depth-dose distribution will enable many meaningful conclusions to be drawn, using laboratory radiobiological results. No rigorous attempt will be made in this paper to scientifically justify the measurement of absorbed dose distributions or the other parameters yielded by the technique under discussion; instead, a brief summary of "LET" importance is presented.

Experiments have clearly established that the biological effectiveness of radiation depends not only on the amount of energy absorbed but also on spatial distribution of the energy deposition. Since the energy is deposited in or near the tracks of charged particles, it has been convenient to express this energy deposition in terms of the linear density of energy transfer along these tracks, or linear energy transfer. The linear energy transfer (LET) is defined as the linear rate of loss of energy ("locally absorbed") by an ionizing particle traversing a material medium. While this quantity is expressed in kiloelectron volts per micron (keV/μ), it is more rigorously a function of energy deposited per unit volume surrounding a track. The stopping power or ionization loss is a similar quantity which is defined as the loss of energy per unit path length by an ionizing particle traversing a material medium. LET emphasizes the process of energy transfer, while the stopping power emphasizes the energy lost by the particle. In the case of stopping power all energy losses resulting in the production of secondary charged particles are commonly included, while in the case of LET such losses are included only if they are absorbed in some arbitrary vicinity of the primary charged particle track.

On the basis of the physics of the energy transfer processes, estimates of LET can be made. Thus the quality of radiation can be expressed by specifying the fraction of the dose deposited in each LET interval. The LET has some utility for characterizing the ionizing track and this parameter has been found in general to correlate well with the biological effectiveness of the radiation.

While theoretically it is possible to calculate a LET distribution spectrum in a given material exposed to some specified radiation field, such calculations are quite laborious and require detailed knowledge of the flux and energy spectra of the primary radiation, and particularly the secondary particles and the material distribution around the sample. For much of the radiation encountered in space, detailed calculations are not possible since many high energy interaction cross sections are not well known. These uncertainties introduce serious errors in estimating radiation hazards since some secondaries are very heavily ionizing and generate high LET tracks.

In an environment such as a space vehicle cabin, it is currently very difficult to predict the local radiation spectra with sufficient accuracy for manned space missions. Uncertainties in the primary radiation fields, the complicated distribution of secondary particles and scattered radiation and material heterogeneity indicate that experimental determinations of LET spectra are desirable. The effect of the dose delivered in space can be approximated in the laboratory by using a combination of laboratory radiation sources to deliver a LET spectrum simulating that measured in the spacecraft.

The radiation encountered in space due to trapped radiation (VAB), solar flares (SCR), and galactic cosmic rays (GCR) will consist mainly of electrons, protons, photons, and heavier nuclei. For trapped radiation very near the earth, the electrons will produce the greatest dose for lightly shielded tissue. As shielding

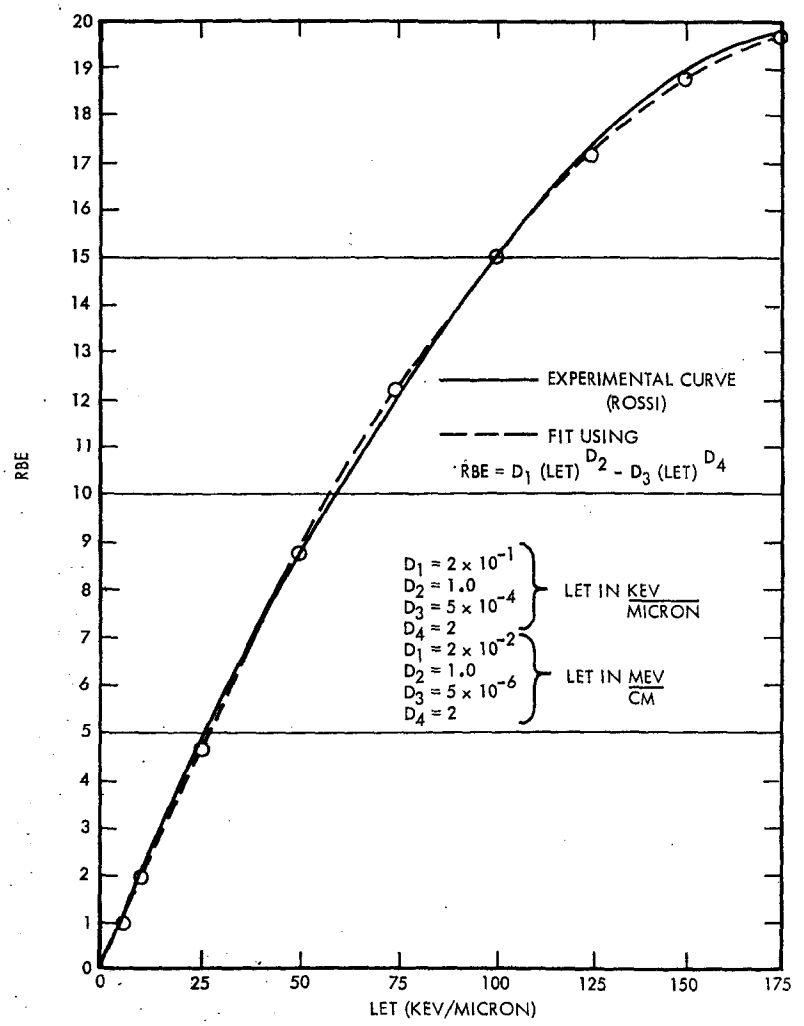

FIG. 1. RBE–LET relationship of Rossi.

increases, the proton and photon components become important. When the protons have been stopped, the photon component remains with a neutron component. Consider first the case where electrons and protons are important. Due to the steep energy spectra observed in the radiation zones, the dose gradient due to electrons and protons will be quite steep through a tissue sample. This gradient is also very important when solar flare radiation is present, since the alpha particle component is quickly attenuated in the first tissue layers.

Schaefer[1] points out that the fraction of high LET events to total dose of the alpha component of solar flares is substantially larger than the fraction of proton-induced high LET events to dose to tissue depths in excess of 10 g/cm^2. The alpha dose is especially important at small thicknesses of less than 2 g/cm^2. Schaefer recommends separate determinations of the high LET alpha and lower LET proton doses, and points out that insufficient data exists on incident spectra to permit calculation of the alpha doses under small thicknesses.

Thus, radiobiologically, it is important to determine the LET or absorbed dose distribution

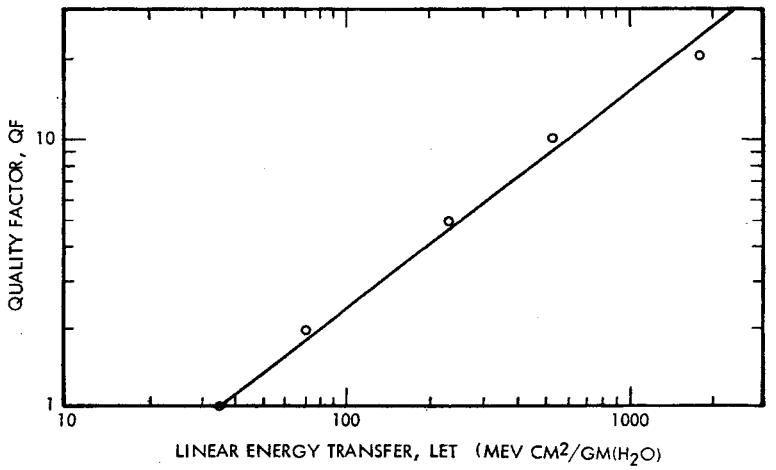

FIG. 2. The monoenergetic quality factor versus the linear energy transfer.

for both low values of LET and for high values of LET.

The importance of LET to description of radiobiological effects has been known for some time. The relative biological effectiveness (RBE) and radiation quality factor (QF)[2] both depend upon knowledge of the LET spectrum. Rossi has obtained a reasonably satisfactory relation for the dependence of RBE on LET as shown by Fig. 1[3] (after Haffner, 1964). The quality factor, LET, and dose relationship have been discussed by Madey and Stephenson,[4] where they present the LET/QF relationship shown in Fig. 2 and Table 1. The usefulness of RBE and QF is that they consider the effectiveness of the radiations in producing a biological effect for a total absorbed dose. For some biological effects, an absorbed dose (in rads) of alpha particles may be many times more damaging than the same rad dose of photons. The ratio of radiation effectiveness is expressed by RBE or QF.

Table 1. *Relationship between Linear Energy Transfer (LET) and Quality Factor (QF)*

LET∞		QF
MeV cm²/gm (H_2O)	(keV/μ in water)	
35 or less	3.5 or less	1
35–70	3.5–7.0	1–2
70–230	7.0–23	2–5
230–530	23–53	5–10
530–1750	53–175	10–20

LET∞ is the same as the "stopping power".

Curtis, Dye, and Sheldon[5] have approached the problem of radiation damage by considering the fractional number of cells of an organ killed, or inactivated, as a function of LET. They calculate a fractional cell lethality (FCL), using inactivation cross-sections shown in Fig. 3. Their results for the November 12, 1960 solar flare are shown as Figs. 4, 5, and 6, expressing the inactivation hits per cell per unit time-integrated particle flux. The abscissa value (P_0) is a measure of the momentum of the solar flare protons. Some of the inactivation cross-sections are those reported by Todd,[6] who determined the cross-sections for various types of tissue (including human kidney) under different conditions. His results are shown in Fig. 7, with the human kidney data shown in greater detail in Fig. 8. It is evident from these data that the high LET region is of great interest, in spite of the low flux of particles in space capable of producing these LET values.

It would also be desirable to measure the depth-dose distribution, since the dose generally exhibits a steep gradient with tissue depth. Figure 9 shows the depth-dose variation through the midline of an astronaut in the Apollo

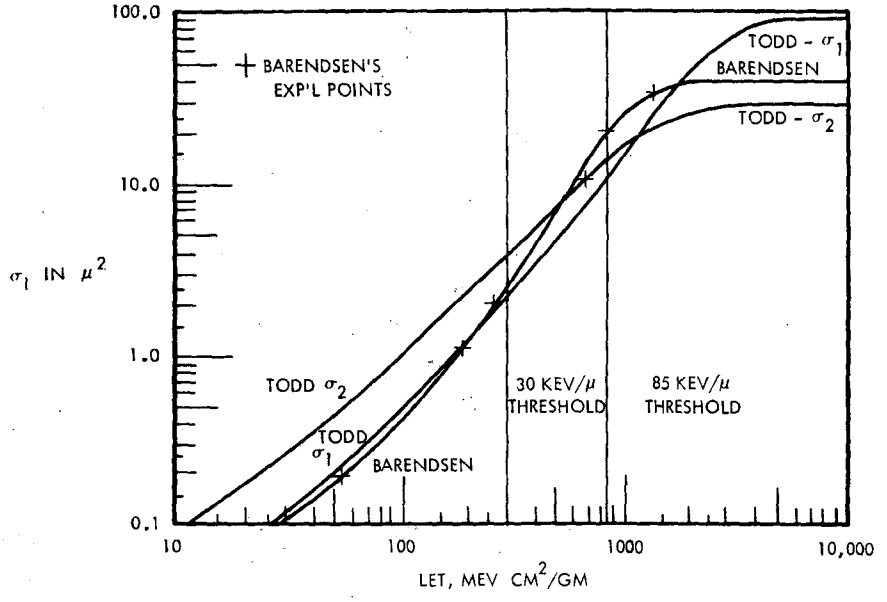

FIG. 3. Inactivation cross-sections.

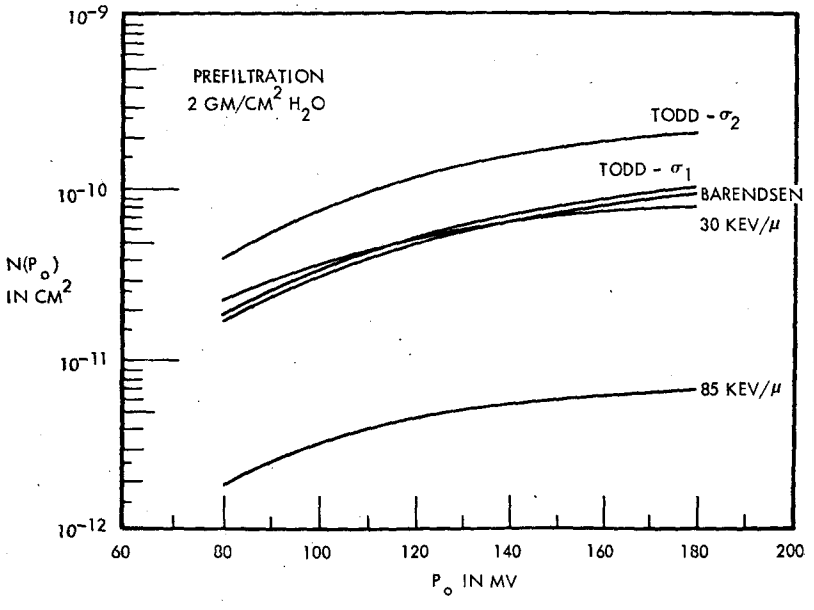

FIG. 4. Inactivation hits per cell per incident proton/cm^2.

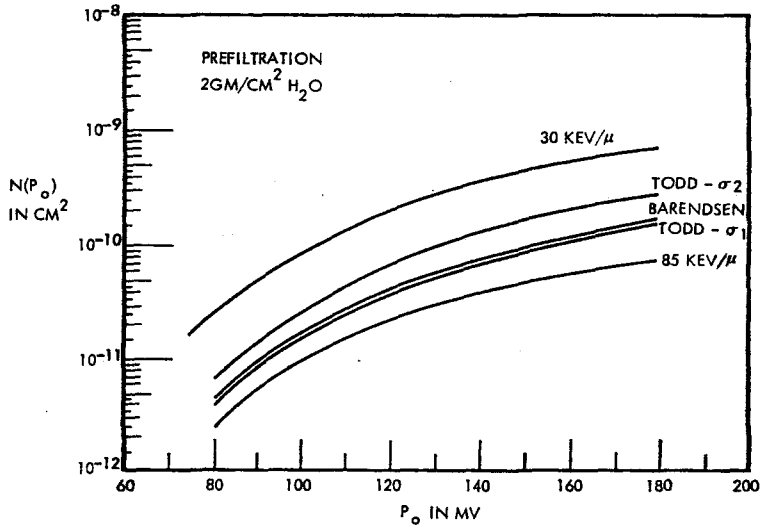

FIG. 5. Inactivation hits per cell per incident alpha/cm².

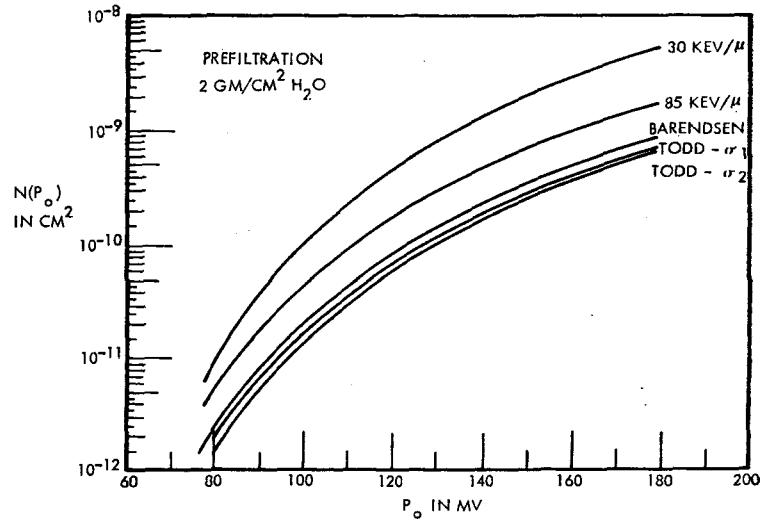

FIG. 6. Inactivation hits per cell per incident m-particle/cm².

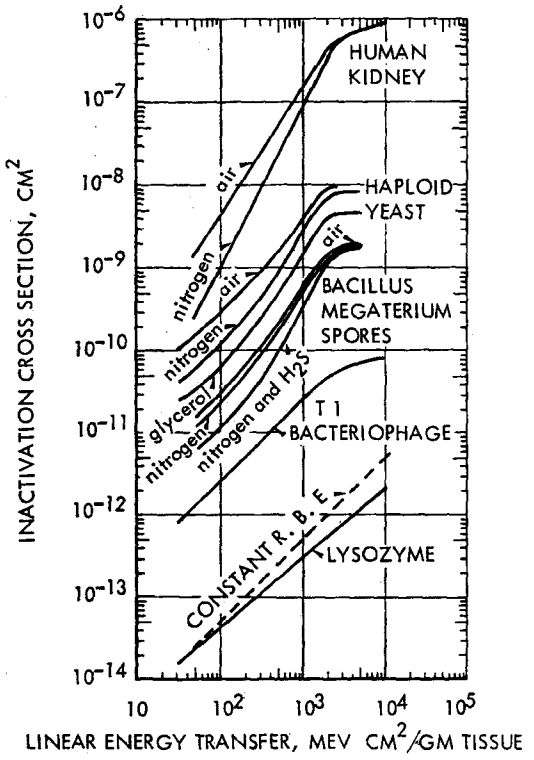

FIG. 7. Inactivation cross-sections of biological test objects obtained from experiments using the Berkeley HILAC

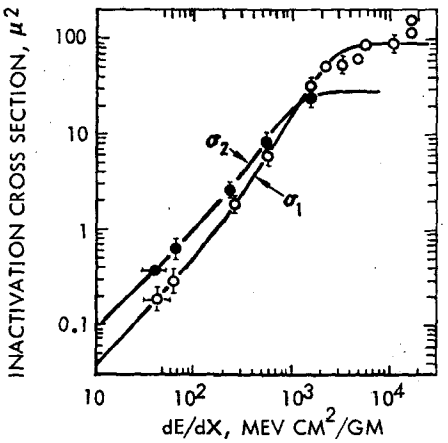

FIG. 8. Log-log plots of the inactivations cross-sections of human kidney (T1) cells *in vivo*; the probability of irreversible inactivation is expressed by σ_1, the initial slope of the "sigmoid" inactivation curves, and the probability of reversible inactivation (in which cells recover between fractionated doses) is expressed by σ_2, determined from the final slope of the inactivation curves.

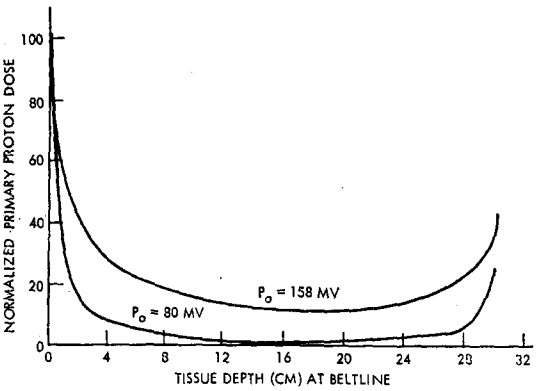

9. Depth dose variation for astronaut in Apollo command module.

command module, calculated for two solar flare spectra. It can be seen that, while a single depth point measurement is very valuable, a sampling of depth points would greatly enhance hazard evaluation.

To summarize, it is of great importance to determine the LET (absorbed dose distribution) spectra, total absorbed dose, and depth-dose distribution in space. To make a meaningful measurement, one must not introduce a detector so large that a dose gradient will exist within it. Present LET devices utilize large ion chambers which perturb the dose in the region being considered (in addition to many other defects of the ion chamber technique). It is felt that a much smaller device must be used, and be constructed of a tissue-like material, both in composition and density.

It is also desirable to know what percent of a population of cells are struck by the particles as they penetrate a tissue sample. Then, for these cells, one would like to know the distribution of energy losses in the cells. To complete the picture on a macroscopic scale, one would like the total absorbed dose rate and depth-dose distribution at several depths of tissue. These data then enable intelligent extensions to be made from laboratory experiments to conditions in space, and vice-versa.

SCIENTIFIC APPROACH

The concept of linear energy transfer (LET), although in use for some time, is difficult to place on a rigorous basis. LET refers to the energy transfer per unit length of the track of a charged particle traversing a medium. Since the energy deposition is a volume effect, this "linear" transfer is ambiguous; the transfer is certainly volume and geometry dependent. Limitations in this concept have recently been discussed by Rossi,[7] where he advocates use of a standard geometry (spherical), and reports distributions normalized to the diameter of the sphere. The proposed concept of a scintillator absorbed dose distribution (SADD) spectrometer is based on measurements of Rossi-type distributions in small spherical plastic scintillators the size of large cells.

The SADD system is a much improved technique for making absorbed dose distribution measurements. Its advantages over present ion-chamber systems are:

measurements with a detector the size of a cell

small size, resulting in negligible dose gradient through the detector

much better characteristics with regard to resolution and gain stability.

The reasons why scintillators have not been used previously are:

ion-chambers have been used extensively in radiobiological research in the past

widespread use of plastic scintillators has only recently occurred

new developments in photomultiplier tubes have resulted in much more precise and smaller systems than previously available

plastic scintillators exhibit different (non-linear) response for different types of particles (Fig. 10).

A close examination of the physics of the non-linear response of plastic scintillators to charged particles has resulted in a technique for solving the non-linear response problem for the SADD concept. It should be noted that the technique for folding in the path length distribution for the detector, a necessary method for interpreting data, is essentially the same as used in unfolding ion-chamber data.[8] It is believed that the SADD technique offers many advantages in absorbed dose distribution measurements over present systems.

As mentioned previously, devices presently used to measure LET are ion-chambers constructed of a "tissue-equivalent" wall, and filled with a "tissue-equivalent" gas. These detectors are large (2 in. dia.), and exhibit instability of gain and resolution. Consider now the new technique for LET measurement based on organic scintillation spectroscopy.

Organic scintillators have been used for some time. Of the many varieties, the plastic scintillator (a loaded polyvinyltoluene) has been chosen as being the best compromise for space use. Typical manufacturers are Nuclear Enterprises (NE-102) and Pilot Chemical (Pilot-B). The response of all organic scintillators to charged particles is quite similar, and varies according to particle type and energy. A typical response curve for an organic scintillator is shown as Fig. 10.[9]

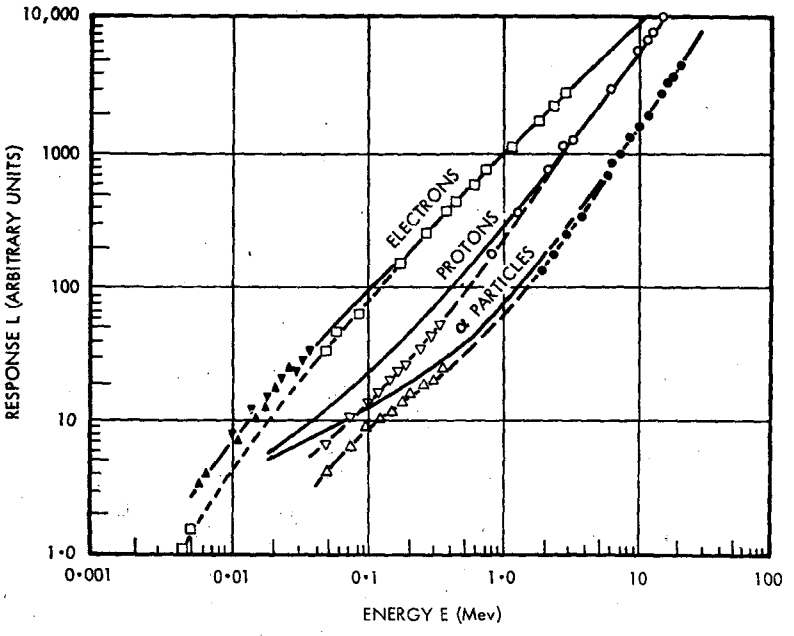

FIG. 10. Anthracene crystals: scintillation response to electronics, protons, and alpha particles (Brooks, 1956).

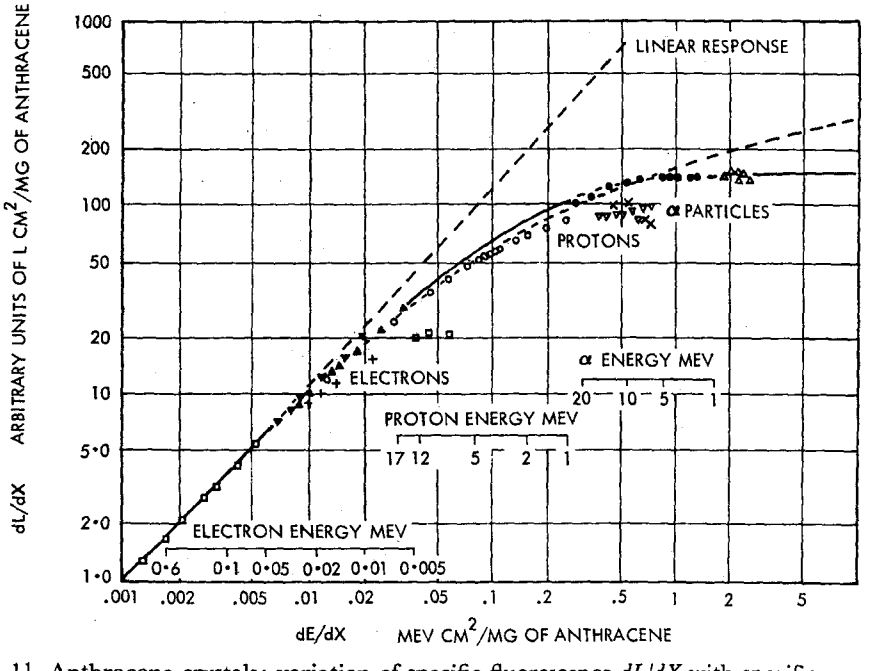

FIG. 11. Anthracene crystals: variation of specific fluorescence dL/dX with specific energy loss dE/dX (Brooks, 1956).

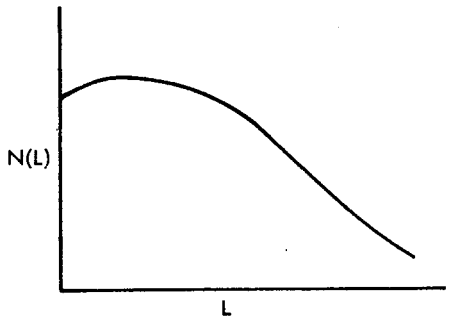

FIG. 12. Spectrum of particles incident on a plastic scintillator.

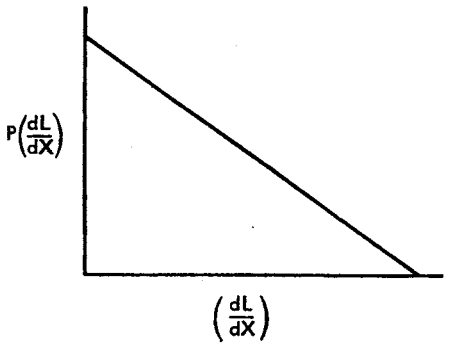

FIG. 14. Probability distribution of dL/dX.

However, if one considers the physics of this phenomenon, it is seen that the nonlinear response is related to the quenching of the primary excitation by the high local density of ionized and excited molecules. Birks[9] expresses this effect as

$$\frac{dL}{dX} = \frac{S\,(dE/dX)}{1 + k\,B(dE/dX)}$$

where L is light output, S is absolute scintillation efficiency, kB is a quenching constant, (dL/dX) is light output per unit path length, and (dE/dX) is energy loss per unit path length.

If one plots (dL/dX) vs. (dE/dX), a curve as shown in Fig. 11[9] is obtained. This result is very important, since the (dL/dX) spectrum is what the scintillator produces, and the spectrum of (dE/dX) is the desired end result. There is a one to one correspondence between $\frac{dL}{dX}$ and $\frac{dE}{dX}$ irrespective of the type of charged particle.

Suppose one measures, experimentally in space, the output spectrum for particles incident on a plastic scintillator, Fig. 12, where L is the light output from the scintillator. Assume also that the path length distribution in the detector is known, shown for a sphere in Fig. 13. Then, under the constraint that

$$L = \left(\frac{dL}{dX}\right) X \text{ or } \frac{dL}{dX} = \frac{L}{X},$$

i.e. dL/dX does not change appreciably in passing through the detector, one calculates, for each measured L point in the spectrum of $N(L)$ vs. L, the probability $P(L)$ that a given L was produced by a value of (dL/dX). The distributions for each L at specific values of (dL/dX) are summed and $N(L)$ vs. L has been transformed to $P\left(\frac{dL}{dX}\right)$ vs. (dL/dX), Fig. 14.

Using the relation of Birks between (dL/dX) and (dE/dX) as shown in Fig. 11, the probability

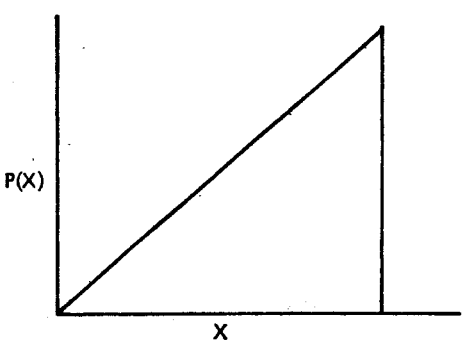

FIG. 13. Detector path length distribution.

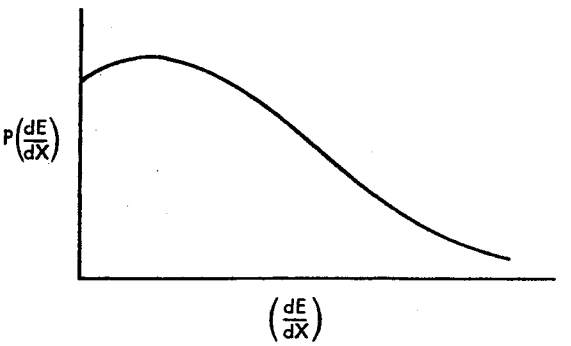

FIG. 15. Probability distribution of dE/dX.

distribution of (dE/dX) is calculated, Fig. 15. Note that by carrying the light output parameter (dL/dX) it is not necessary to know whether a particle producing the response is a proton, electron, or heavier particle. When transformation from (dL/dX) to (dE/dX) is made, again it is independent of the type of particle. Thus the problem of particle type-dependent response (e.g. Fig. 10) is removed.

Consider now the error introduced by particles stopped in the scintillator or in any detector (violation of the $L = \left(\frac{dL}{dX}\right) X$ assumption). If a particle is stopped one does not know and it is regarded as a lower dE/dX event than it actually is. Thus in the energy loss (dE/dX) spectrum, one shifts stopped particles from high to low LET, due to the self-shielding in the scintillator sphere.

The ambiguity in specifying dE/dX when a particle is stopped in the detector is reduced by making the detectors small. A 100 micron-path length (sphere diameter) stops approximately 2 meV protons and 80 keV electrons. Using the above method of converting the energy deposited to a (dE/dX), one would specify the particles to have had (dE/dX) of 20 keV/μ and 0.8 keV/μ respectively. The pulses generally fall in the low pulse-height channels (LOADD) and can be set aside for special data processing techniques. All other higher pulse heights must have been particles of high dE/dX passing through the detector, and fall into high pulse height channels (HIADD). There is a very small possibility of a galactic cosmic ray star event sending two or more highly ionizing particles through a sphere or spheres. This pulse would be counted as a single particle. Minimum ionizing particles ($dE/dX \approx 2$ meV cm^2/g) will leave approximately 20 keV pulse heights; these will be near, or below, the threshold of LOADD channel 1. Nominally, the threshold of LOADD channel 1 will be 40 keV (i.e. 0.4 keV/μ). The threshold perhaps could be lowered to 20 keV to include minimum ionizing particles, if it is deemed desirable. The sixteen channels will nominally be distributed from 0.4 keV/μ to $>$ 300 keV/μ (energy losses in the spheres from 4 meV cm^2/g to 3000 meV cm^2/g).

INSTRUMENTATION

Sensor Design

The sensor consists of spheres of NE 102 plastic scintillator surrounded by a specified depth of tissue equivalent material. The spheres approach the size of large cells, are approximately 100 microns or less in diameter, and are bonded to a lucite light pipe by an organic material such as solithane. The light pipe serves to couple the scintillators to the photomultiplier tube, and also provides a tissue-like backstop between the spheres and the quartz face of the photomultiplier tube, thus reducing the probability of back-scatter radiation from a non-tissue like material. Therefore, the scintillators experience an unperturbed dose field, closely approximating the ideal case of a tissue sample. There will be no appreciable air spaces or dissimilar materials near the detectors.

It is feasible to use spheres of 100 micron diameter or smaller. To obtain reasonable count rates for cosmic ray studies as well as for low energy–high flux background doses, it is necessary to expose a relatively large surface area to the ambient flux. This is accomplished by using many spheres, loosely spaced to reduce the probability of a single particle traversing more than one sphere. If one restricts the maximum count rate to 10^4 counts/sec, then approximately 1300 spheres would produce this rate in an omnidirectional flux of 10^5 particles/cm^2 sec. The same number of spheres would produce a count rate of 12.6 counts/min in a galactic cosmic ray flux of 2 particles/cm^2 sec.

The spheres, if closed-packed, would require being spread over an area of 0.02 in.^{2} (the area of a 0.14 in. dia. circle). Therefore it is feasible to achieve adequate loose spacing by using a 0.5 in. diameter circular base. This permits use of a small photomultiplier tube such as the ruggedized RCA 4460. A full-size sketch of the unit is shown as Fig. 16 for a tissue depth of 2 cm (no material pre-filtering).

A scintillator unit has been fabricated and is being used to examine the limitations of the technique. Sample NE-102 plastic spheres 100 +5/−9 microns have been obtained from Nuclear Enterprises, Ltd., of Canada, and the spheres have proved to be generally of uniform contour and free of bubbles. A uniform layer of spheres was cemented to a $\frac{1}{4}$ in. diameter by

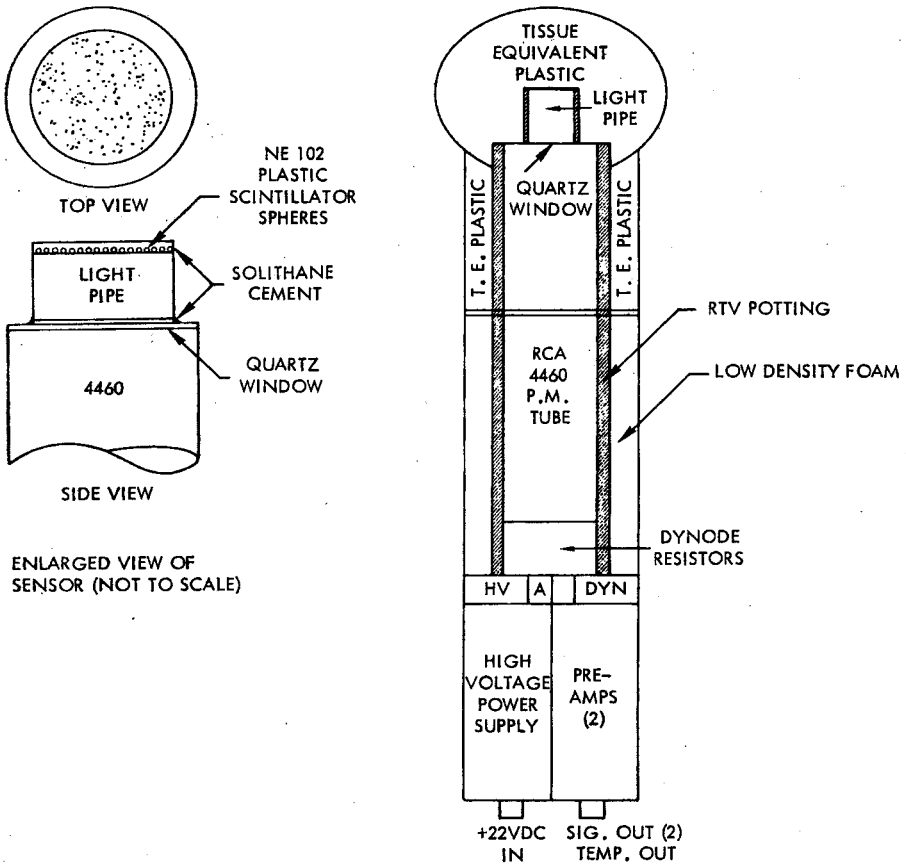

FIG. 16. Typical SADD sensor with 2 cm pre-filtering.

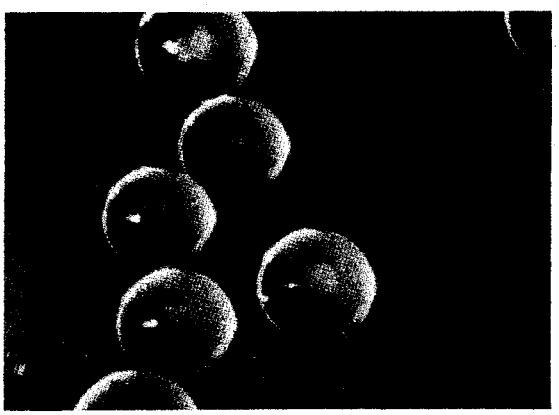

FIG. 17. 100 micron diameter spheres of NE-102 plastic scintillator.

$\frac{1}{4}$ in. thick lucite light pipe with a soft epoxy (solithane); Fig. 17 shows some of these spheres.

Two factors which limit the analysis of small pulses from the scintillators are the noise spectrums of the photomultiplier tube and self-scintillation of the lucite light pipe. These factors were investigated using an RCA 7767 photomultiplier tube (a typical tube not selected for low noise) and a lucite light pipe. The photomultiplier noise spectrum is shown in Fig. 18; no change was noted when the photomultiplier tube was irradiated with 0.1 millicurie of ^{137}Cs, or when the tube plus a $\frac{1}{2}$ in. diameter by $\frac{1}{2}$ in. thick piece of lucite were irradiated. The photomultiplier was then used with the lucite and the 100 micron spheres; the resulting pulse height spectrum is shown as Fig. 19. These tests indicate that analysis of

pulse heights down to 40 keV are certainly feasible; lower pulse heights may be analyzed if the system is optimized with respect to photomultiplier tube high voltage, temperature, selection for low noise, etc.

Signal Processing

The signals from the photomultiplier are processed by two preamplifiers, two eight channel differential pulse height analyzers, and two fifteen-bit binary storage registers. The dynamic range of each preamplifier-analyzer combination is approximately 30: 1. Thus, to accomplish analysis from 0.4 keV/μ to 300 keV/μ we propose to use two preamplifier analyzer combinations, one for low pulse heights (LOADD) and one for high pulse heights (HIADD) (it may be possible that no preamplifier is needed for the high pulse heights). If the preamplifier is connected in parallel, the low pulse height preamplifier must be nonoverloading at the high pulse heights. Each analyzer consists of a single channel analyzer, which shifts among eight attenuators to effectively yield eight channels of analysis. Note that the analysis proceeds sequentially in time, not simultaneously. The output is fed to a fifteen bit binary storage register. The sixteen channels of analysis will be distributed approximately logarithmically over the absorbed dose distribution range from 0.4 keV/μ to $>$ 300 keV/μ as Table 2.

A block diagram is shown as Fig. 20. Characteristics of one of the proposed preamplifiers and pulse height analyzers are shown as Fig. 21.[10]

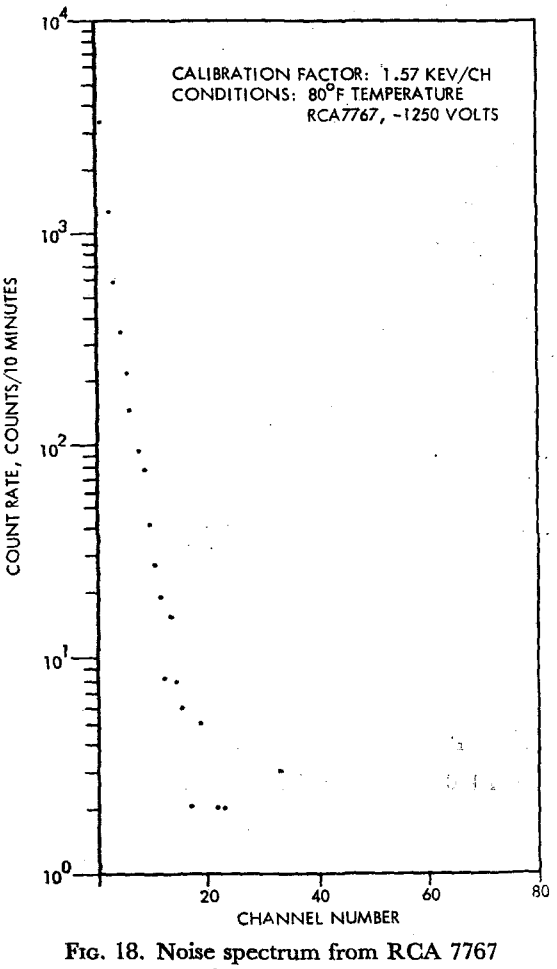

FIG. 18. Noise spectrum from RCA 7767 photomultiplier.

Table 2. Channel Distribution of Absorbed Doses

LOADD	HIADD
Channel 1: $0.4 < S < 0.6$ keV/μ	$12 < S < 20$
Channel 2: $0.6 < S < 1.0$ keV/μ	$20 < S < 30$
Channel 3: $1.0 < S < 2.0$ keV/μ	$30 < S < 50$
Channel 4: $2.0 < S < 3.0$ keV/μ	$50 < S < 75$
Channel 5: $3.0 < S < 5.0$ keV/μ	$75 < S < 100$
Channel 6: $5.0 < S < 7.5$ keV/μ	$100 < S < 200$
Channel 7: $7.5 < S < 10$ keV/μ	$200 < S < 300$
Channel 8: $10 < S < 12$ keV/μ	$S > 300$

The division of a pulse height spectrum into eight logarithmically distributed channels by the analyzer is shown in Fig. 21. This data was taken, not with a pulse generator, but with actual random pulses from a photomultiplier tube. The output from the flight pulse height analyzer was used to gate the same pulses into a 512 channel laboratory analyzer. This calibration technique allows one to determine exactly which pulses are counted in each flight analyzer channel with random pulses at various average counting rates. Some of the indicated variation in the threshold of the lowest channel is due to this calibration technique, which places pulses corresponding to this threshold in a very low channel number in the laboratory analyzer.

Data shown here were taken at an average

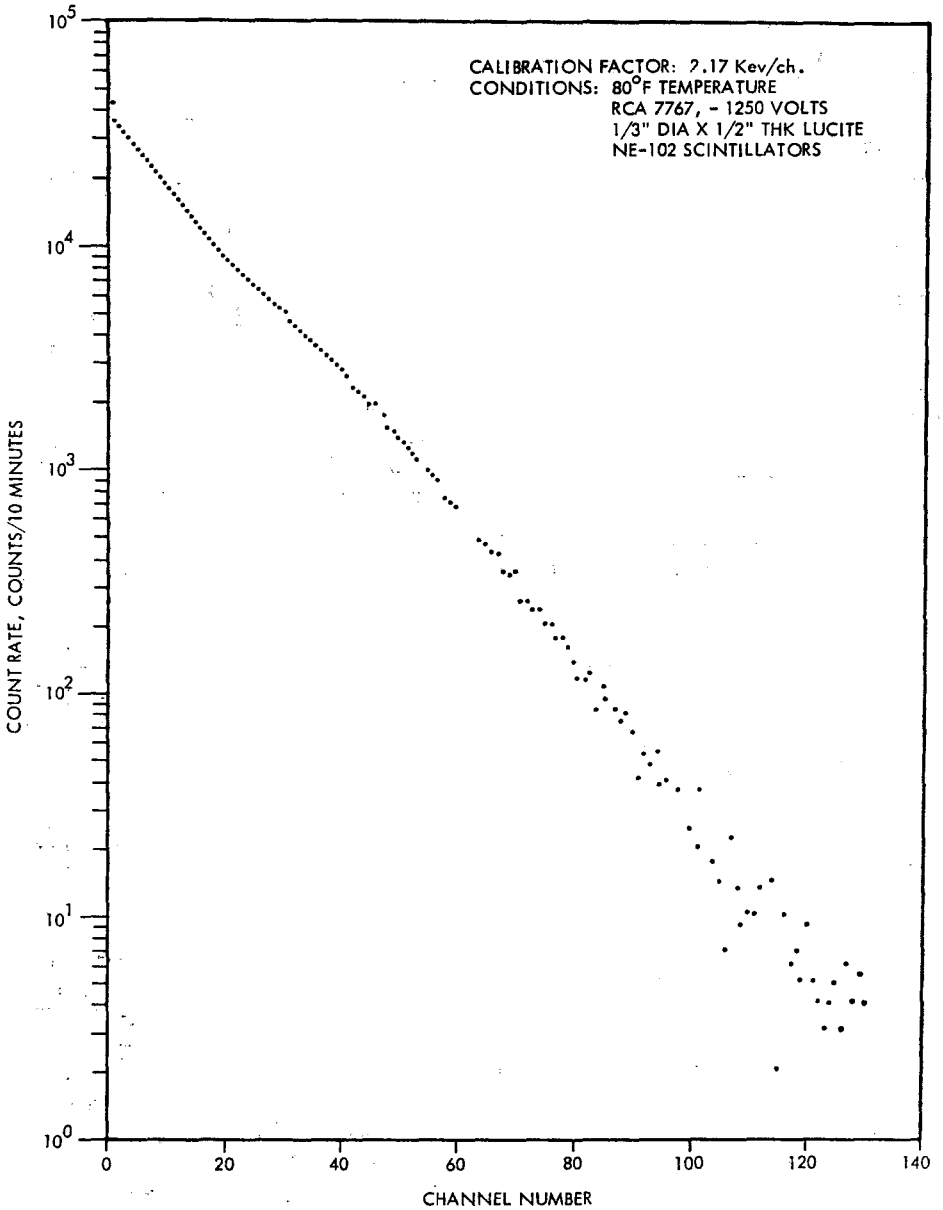

FIG. 19. Absorbed dose spectrum from 100 micron NE-102 spheres.

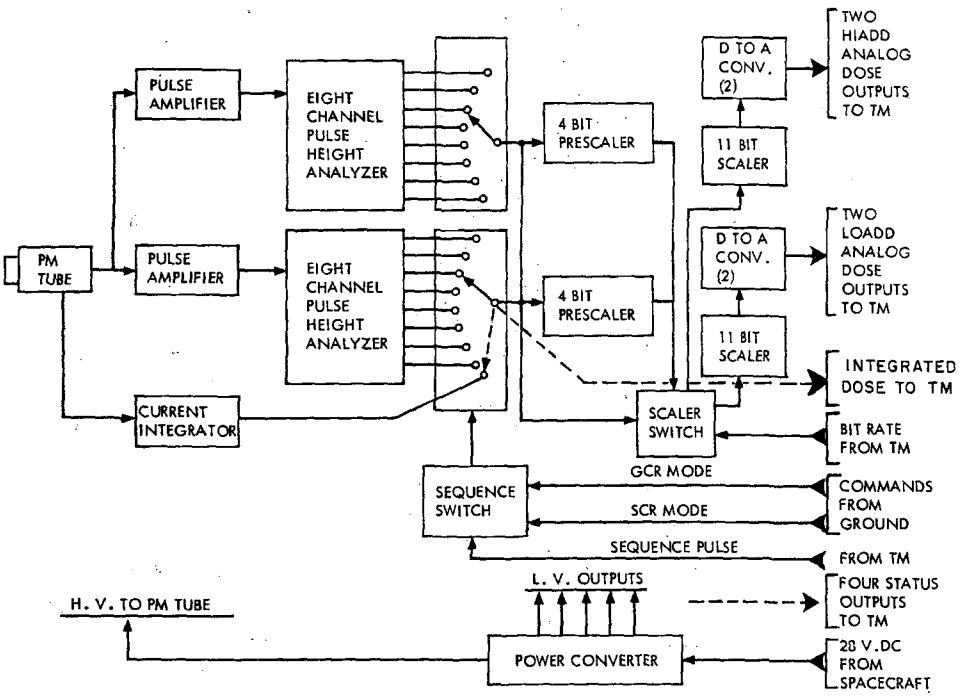

FIG. 20. Block diagram of electronics.

rate of 3000 pulses/sec. Significant shifts in the pulse height channels do not occur at rates up to 100,000 pulses/sec. Pulse pair resolution is about 400 nsecs. The temperature performance curves were taken with both the preamplifier and pulse height analyzer within the temperature chamber. Diagonal lines indicate gaps between channels, which occur at low temperatures. Some small overlap occurs at high temperatures, and is indicated by solid black areas. These gaps and overlaps are taken care of by calibration.

Each storage register contains an 8-bit D to A converter whose output is presented to the telemetry system. If PAM/FM telemetry is used, each storage register will feed two 6-bit D to A converters, and thus will require two data words on the commutator instead of one. The output from each channel will be sequentially read out. Note that for a PAM system the anode current (total absorbed dose) is not processed by the digital registers, but is presented directly to the telemetry in analog form from a readout circuit covering a dynamic range of four decades.

To operate satisfactorily in a quiet galactic cosmic ray (GCR) flux, a solar flare (SCR) event, or in a low energy, high-intensity electron background, different dose accumulation times will be used. In the low (GCR) mode, the registers will accumulate over 1 min, whereas in the high flux (SCR) mode, all channels will sum over 2 sec time periods. Normal operation will be 10 min in the GCR mode and 2 min in the SCR mode. Two ground commands are required to lock the instrument in either the SCR or GCR mode, to be used if one of the modes show marked superiority over the other.

The high voltage power supply produces regulated voltage for the photo-multiplier tube. The temperature dependence of the photomultiplier tube is compensated with a thermistor on the ninth dynode of the photomultiplier tube, which allows tube gain stabilization over a large temperature range. The low voltage power supply produces regulated voltages from an unregulated (28 V $\pm$ 5 V) input.

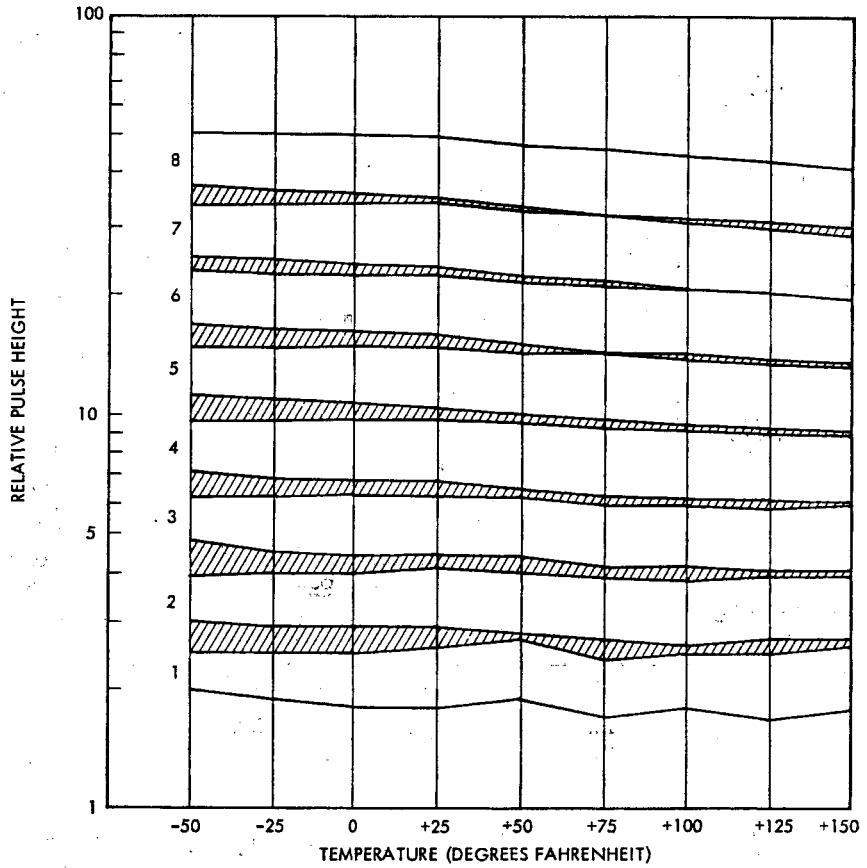

FIG. 21. Performance of preamplifier-pulse height analyzer combination.

Configuration

Design considerations divide the instrument into two packages. The first includes the photomultiplier assembly, high voltage power supply, and preamplifiers. The second package contains the remainder of the signal processing equipment, including the low voltage power supply. This flexible mounting arrangement enables the sensor to be placed in an optimum position for sampling the dose.

If the instrument is used on a manned spacecraft, the astronaut can change the tissue surrounding the detector, and thus obtain depth-dose measurements using one sensor. If the instrument is used on unmanned spacecraft, the depth-dose information is obtained by using several sensors with various amounts of tissue pre-filtering. The sensors can time-share the same electronics, or duplicate electronics can be used with attendant weight, power, volume, and telemetry penalties.

The technique is certainly applicable to ground-based laboratory use as well as for space flight measurements. The flexibility and sophistication of laboratory equipment permit much more precise measurements to be made.

Instrument specifications are detailed in Table 3.

CONCLUSION

The technique described in this paper makes possible a measurement of certain dosimetric parameters in a physically significant configuration. The actual detectors are of the density of tissue, and closely approximate the radiation-stopping powers of tissue. The size of the detectors approaches that of large cells (≤ 100

Table 3. Instrument Specifications

1. Power	2.0 W
2. Weight	4.0 lb
3. Volume	120 in^3 (electronics 4 × 5 × 5; sensor 1.5 × 1.5 × 7 in.)
4. Telemetry	Three analog words on main data commutator in SCR mode, i.e. three words read out at 2 sec intervals, and three words on subcommutator in GCR mode, i.e. three words read out at 1 min intervals. Four additional status words on subcommutator irrespective of mode. Note that PAM telemetry requires use of 6, 6, and 4 words.
5. Duty cycle	Continuous operation is desired, but reduced operation is acceptable.
6. Commands	4: ON, OFF, GCR mode, SCR mode.
7. Mounting requirements	To be determined.
8. Other desirable measurements	Trapped electrons and protons, solar flare protons and alpha particles, glactic cosmic rays, photons interior to vehicle, vehicle orientation, and vehicle location in position and time.
9. Temperature range	−50°F to +150°F survival operating; 0°F to +100°F

microns), and therefore measures energy depositions in a physically significant volume.

A pulse-height analysis of the signals from the sensor provides an absorbed dose distribution, while a measurement of the anode current from the photomultiplier tube is proportional to the total absorbed dose. Assignment of a weighting factor (such as a quality factor) to each channel of the absorbed dose distribution would lead to a direct readout of a biological dose, as compared with a physical dose (rads/hour). In addition, changing the tissue prefilter surrounding the 100 micron detectors can yield depth-dose distribution. Since the total number of spheres is known, and each pulse represents a bit of one sphere, information on the cell hit frequency is directly obtainable.

The technique can be applied using many instrument configurations. The limitations of the concept are currently being investigated both in the laboratory and in space; the first space flight of an instrument using this technique is scheduled for spring of 1967. It is believed by the authors that this technique has many advantages over present ion-chamber techniques, the more important being the physical characteristics of the dosimeters and the calibration stability of the instrument.

REFERENCES

1. H. J. SCHAEFER. Local dose from proton and alpha particle enders behind complex shield systems. *Proc. Second Symposium on Protection against Radiation in Space*, Gatlinburg, Tennessee, 1964.
2. National Bureau of Standards. U.S. Department of Commerce. Report of the International Commission on Radiological Units and Measurements (ICRU) 1959, Handbook No. 78, U.S. Government Printing Office, Washington, D.C., 1961.
3. J. W. HAFFNER. RBE of protons and alpha particles. *Proc. Second Symposium on Protection against Radiation in Space*, Gatlinburg, Tennessee, 1964.
4. R. MADEY and T. E. STEPHENSON. Quality factors for degraded proton spectra, Ibid.
5. S. B. CURTIS, D. L. DYE and W. R. SHELDON. Fractional cell lethality approach to space radiation hazards.
6. P. TODD. Biological effects of heavy ions. Ibid.
7. H. H. ROSSI. Specification of radiation quality. *Rad. Res.* **10,** 522 (1959).
8. H. H. ROSSI and M. S. ROSENZWEIG. A device for the measurement of dose as a function of specific ionization. *Radiology* **64,** 404 (1955).
9. J. B. BIRKS. *The Theory and Practice of Scintillation Counting*, Pergamon Press, New York, 1964.
10. T. A. FARLEY. Institute of Geophysics, University of California at Los Angeles, private communication, 1965.

ALCUNI PROBLEMI DI METEOROLOGIA NUCLEARE NELLA VALUTAZIONE DI UN SITO DAL PUNTO DI VISTA DEL RISCHIO NUCLEARE

L. SANTOMAURO
Reparto di Meteorologia e Geofisica dell'Osservatorio Astronomico di Brera
Milano, Italy

Sommario—La scelta di un sito per impianto nucleare rappresenta una delle fasi maggiormente impegnative del meteorologo nucleare, in quanto egli, il più delle volte, deve basarsi sulla sua esperienza professionale e solo in alcuni casi, purtroppo non frequenti, può disporre di validi elementi di giudizio. A tale scopo, dopo una breve rassegna critica delle esperienze già effettuate in materia, si espongono alcuni criteri generali di analisi anche riguardo al tipo di impianto nucleare.

Nella seconda parte del lavoro, invece, vengono esposti i limiti geometrici della porzione di atmosfera che si ritiene utile analizzare e controllare, sia nella fase di costruzione sia in quella di esercizio degli impianti nucleari, alla luce delle attuali ricerche sullo strato e substrato limite dell'atmosfera, ai fini dell'altezza effettiva delle sorgenti di emissione degli effluenti gassosi radioattivi nonchè del loro trasporto e dispersione.

PREMESSA

Come è noto, il continuo e crescente sviluppo della energia nucleare ha dato vita a due nuove specialità della fisica dei bassi strati dell'atmosfera: la micrometeorologia e la microclimatologia nucleare, le quali si occupano di tutte le questioni, principali e derivate, relative alla diffusione atmosferica dei prodotti volatili provenienti da qualsiasi tipo di impianto nucleare. Entrambe le specialità devono affrontare dei problemi di estrema delicatezza quali, ad esempio, quelli dell'analisi preventiva e della valutazione del sito per i quali ancora oggi non esistono specifici criteri generali informativi.

Difatti, si è constatato che mentre in alcuni Rapporti di rischio nucleare, la parte meteorologica è svolta in maniera addirittura magistrale, in altri, invece, essa si limita ad una nuda esposizione di dati che denunciano una indagine più statica che dinamica. Di conseguenza, in questi ultimi, l'ambiente atmosferico locale non diventa una parte integrante del Rapporto e quindi lo scopo per cui si richiede l'analisi e la valutazione meteorologica non sempre viene completamente raggiunto.

Probabilmente, queste diversità sono dovute alla mancanza di adatti criteri generali, e quindi molte indagini sulla meteorologia e climatologia della diffusione, portano, nelle loro strutture, un'impronta fin troppo personale e specialistica, mettendo, a volta, in difficoltà coloro ai quali è devoluta la responsabilità del giudizio finale di scelta.

La necessità di questa uniformazione è stata già sentita da alcune organizzazioni internazionali. Difatti, l'International Standard Organization (ISO) già da qualche anno ha messo sul tappeto la standardizzazione delle misure nel campo dell'energia nucleare; inoltre, l'International Atomic Energy Agency (IAEA) ha organizzato un Simposio (Bombay—11–15 marzo 1963) sui criteri generali informativi per la scelta del sito a seconda del tipo di impianto nucleare. Poichè tale simposio, oltre al suo scopo principale, aveva anche quello, non meno importante, di assicurare l'opinione pubblica che un sito fosse scelto soltanto dopo una accurata valutazione scientifica del bilancio dei vantaggi e di tutte le conseguenze prevedibili,[1] si concluse con una discussione a

Panel. In esso, tra l'altro, venne anche dibattuto il principio che la valutazione meteorologica del sito venisse effettuata secondo determinati criteri generali.

Già precedentemente alla riunione di Bombay, l'Italia si era fatta promotrice presso l'IAEA di un Panel dedicato esclusivamente alla meteorologia dei siti nucleari, presentando un programma di argomenti di discussione. Benchè il programma fosse stato accettato dell, Agenzia e fosse stato fissato anche il periodo per la riunione questa venne rinviata per un succedersi di avvenimenti indipendenti dalla volontà dell'Agenzia stessa e del Governo Italiano. Tuttavia, si ritiene doveroso annunciare che è in corso di avanzata redazione un documento di lavoro ad hoc e si auspica che questa riunione non debba essere ulteriormente rimandata.

Scopo di questa nota è quello di esporre due dei problemi che si ritiene siano di maggiore interesse e che potrebbero essere in linea di massima normalizzati; cioè, i criteri che si potrebbero adottare nell'analisi e nella valutazione meteorologica, e nella determinazione dei limiti geometrici della porzione di atmosfera che deve essere considerata ai fini del controllo nella fase di costruzione e di operazione di un impianto nucleare.

1. CRITERI DI ANALISI E DI VALUTAZIONE METEOROLOGICA

1.1. *Generalità*

La scelta del sito per un impianto nucleare sì basa su considerazioni di ordine politico, tecnico, economico, ambientale, logistico, ecc. che, prese nel loro insieme, il più delle volte, sfociano in un compromesso discriminatorio costituito da elementi contrastanti. A questo, che è il punto di arrivo, si giunge attraverso un processo di analisi e di valutazione. In entrambi, ovviamente, vi sono delle considerazioni così dette ambientali, tra le quali un posto di primo piano è occupato da quelle di ordine meteorologico. Queste vanno intese come accertamento sia del potere diluente dell'atmosfera, nei confronti dei prodotti volatili provenienti dall'impianto nucleare (*analisi*), sia della diffuzione, in termini tridimensionali (spazio-tempo-concentrazione), degli stessi prodotti volatili (*valutazione*).

Sia l'analisi, sia la valutazione meteorologica hanno lo scopo di fornire una base possibile e probabile allo scopo finale che è quello della valutazione del rischio nucleare, cui, potenzialmente, sono sottoposte le aree intorno agli impianti nucleari. Le suddette ricerche devono essere compiute in due momenti diversi del programma nucleare; cioè, l'analisi meteorologica deve fornire degli elementi discriminatori del sito, e quindi va fatta in sede preventiva, mentre la valutazione meteorologica deve essere fatta per il sito già scelto e prima che l'impianto diventi operativo.

1.2. *Criteri generali per l'analisi*

Il quesito che viene posto al meteorologo può essere pressappoco il seguente: *dato un certo numero di siti programmati, determinare tra questi quello (o quelli) in cui il potere diluente dell'atmosfera, o potere autodepurativo, sia tale da rendere minimo il rischio nucleare.*

Una simile risposta comporterebbe una serie di indagini e di informazioni preliminari che non è possibile espletare ed ottenere dato che il tempo a disposizione è sempre molto limitato. Di conseguenza è necessario che le analisi e le valutazioni siano spedite ed abbiano carattere qualitativo.

Tuttavia, e qui è il punto più delicato della questione, il risultato dell'analisi, sebbene ottenuto in via preventiva, non può essere notevolmente diverso da quello che si otterrà quando, una volta che il sito sia stato scelto, si potranno effettuare indagini regolari e sistematiche. Anzi, proprio per una norma di etica professionale, il risultato quantitativo dovrà confermare e completare quello qualitativo ottenuto in un primo tempo.

Premesso quanto sopra, si ritiene che per raggiungere lo scopo che ci si propone l'analisi meteorologica preventiva deve essere sviluppata secondo una metodica semplice ma efficace. Ciò perchè essa possa rimanere entro i confini della reale applicabilità per chi dovrà poi emettere il giudizio di idoneità finale del sito alla recezione di quel tipo di impianto nucleare.

Il problema meteorologico dell'analisi dei siti programmati consiste, come è stato già accennato, nel determinare l'andamento e l'evoluzione di quegli elementi atmosferici che concorrono nella diffusione trasporto e diluizione

degli effluenti radioattivi, provenienti dall'impianto nucleare progettato.

Questa analisi può essere realizzata per appossimazioni successive; cioè, partendo da alcuni dati di progetto per poi arrivare all'analisi delle diverse zone in programma.

1.2. 1. *Calcolo teorico delle variabili spazio-tempo-concentrazione.* Il primo passo dell'analisi è quello di determinare il raggio della zona da prendere in considerazione. Questo può essere compiuto conoscendo i dati di progetto (volume e composizione degli scarichi radioattivi nell'atmosfera, operativi e di emergenza, nonchè dell'altezza prevista sul suolo delle sorgenti di emissione) e tenendo presente le raccomandazioni della Commissione Internazionale per le Protezioni Radiologiche [2] e le direttive e raccomandazioni della Comunità Europea dell'Energia Atomica in materia di protezione dalle radiazioni ionizzanti. [3]

Poichè si tratta di un calcolo teorico, occorre necessariamente presupporre che:

(a) la durata e l'intensità degli scarichi radioattivi sia la massima accettabile secondo il progetto;
(b) la distribuzione degli scarichi radioattivi nell'atmosfera sia isotropica e omogenea;
(c) il potere diluente dell'atmosfera sia scarso (fumigazione);
(d) il terreno sia uniforme e pianeggiante.

In questo modo si possono ottenere una o più rose spazio-tempo-concentrazione, le quali essendo calcolate su dati previsti dal progetto dell'impianto e su presupposti ambientali teorici, possono ritenersi valide per qualsiasi località compresa nel programma di scelta del sito.

Questa prima fase del processo di analisi può essere abbastanza rapida, specie se si fa uso degli appositi regoli calcolatori, adattabili a vari tipi di modelli matematici di diffusione. [4]

1.2. 2. *Analisi topografica.* Conclusa questa fase, il secondo passo è quello di procedere all'analisi topografica per ciascuna località. Ciò allo scopo di determinare l'influenza della configurazione del terreno sul comportamento atmosferico degli scarichi in aria calma (e ad equilibrio neutrale). Tutto questo per prevedere sia l'effetto riduttivo delle eventuali barriere naturali, sia quello esaltante delle eventuali zone di canalizzazione.

In altri termini, questa procedura che può essere seguita mediante similitudini idrodinamiche, servendosi di modelli [5] o di carte topografiche a rilievo, permette di stabilire, in seconda approssimazione, le deformazioni che subisce la rosa teorica degli scarichi per effetto della topografia locale. Si tratta perciò di stabilire l'orizzonte della diffusione non tenendo ancora conto di quelle che possono essere le condizioni micro- e meso-meteorologiche medie o prevalenti.

Con questa seconda fase dell'analisi, si ha già una prima discriminazione sul numero delle località programmate, specialmente se essa viene integrata con quella demografica ed ecologica condotta da chi di dovere.

Stabilito in questo modo il numero delle zone da esaminare si può passare all'analisi meteorologica preventiva vera e propria.

1.2. 3. *Analisi meteorologica.* Questa è la fase più delicata in quanto, nella quasi totalità dei casi, non si dispone di tutti i dati necessari all'analisi, e il più delle volte il meteorologo deve affidarsi alla sua sensibilità personale nel rischio nucleare e alla sua esperienza professionale nel campo dell'analisi.

Premesso che il problema del comportamento atmosferico degli scarichi radioattivi si basa principalmente sulle condizioni anemologiche e su quelle di equilibrio dei bassi strati atmosferici, l'analisi meteorologica deve, ovviamente, imperniarsi sulla valutazione di questi due elementi.

Ora si possono presentare tre casi per i siti programmati:

(a) che vi siano già dei posti di osservazione della rete meteorologica nazionale, le cui serie siano sufficientemente lunghe per ottenere delle informazioni valide;
(b) che vi siano dei posti di osservazione le cui serie non siano abbastanza lunghe ma nelle vicinanze esistano altri posti di osservazione meteorologicamente rappresentativi, le cui serie possono essere usate come riferimento; oppure, che non esistano informazioni dirette ma si dispone invece di altri posti di osservazione, meteorologicamente rappresentativi;
(c) che non esistano informazioni nè dirette nè di referimento, o, pur esistendo queste

ultime non è possibile effettuare una "triangolazione" delle osservazioni a causa della situazione topografica e orografica.

Il caso (a) è naturalmente il più fortunato e su di esso è superfluo soffermarsi. Esso permette di fornire nel rapporto di rischio dati numerici, che, una volta elaborati secondo i normali criteri di climatologia dinamica, possono anche permettere, oltre all'analisi, la valutazione meteorologica. Purtroppo però i siti destinati ad ospitare grossi impianti nucleari raramente si trovano in queste condizioni.

Il caso (b) è il più frequente. In esso è possibile adottare i criteri di triangolazione climatica di Helmert o di Abbe [6] e, per quanto riguarda il vento, quello di Rosini. [7] Tali criteri non hanno bisogno di essere illustrati in quanto sono usati nella prassi normale per stabilire l'andamento di alcuni elementi meteorologici di una località o di una zona della quale la serie di osservazioni dirette non è sufficiente a definire l'andamento o, caso limite, quando non si dispone di nessuna osservazione diretta. In entrambi i casi, ma specie nell'ultimo, la procedura della triangolazione viene adottata solo quando la serie di osservazioni è omogenea e si riferisce a posti meteorologicamente rappresentativi, sia tra loro sia con la località in esame.

Nei due casi esposti, ma particolarmente nel secondo, è necessario fare alcune considerazioni di carattere generale circa l'uso dei dati della rete nazionale.

Premesso che la valutazione meteorologica dei siti viene fatta da un punto di vista relativo soltanto agli scarichi radioattivi, i dati provenienti dalle Stazioni Meteorologiche della rete nazionale vanno opportunamente interpretati e vagliati a questo scopo. Ciò perchè le Stazioni della rete nazionale sono ubicate secondo criteri di rappresentatività su una scala (macroscala) molto diversa da quella usata in meteorologia nucleare (mesoscala e microscala).

Quindi una certa cautela va presa nella determinazione dei dati del vento, in quanto essi, nelle Stazioni della rete nazionale, vengono normalmente prelevati ad un'altezza standard di 10 metri (vento al suolo) mentre per la diffusione degli scarichi radioattivi si ha necessità di conoscere l'andamento del vento in uno spessore verticale almeno dieci volte maggiore. Ora, se si è su un terreno pianeggiante e non molto distanti (20 Km) da una stazione di radiosondaggi, il caso può essere risolto con una analisi del vento ad una altezza pari a 900 millibar di pressione; applicando poi una opportuna relazione matematica [8] è possibile calcolare il profilo teorico del vento in base anche a diverse categorie di equilibrio atmosferico. Qualora ciò non fosse possibile bisogna ricorrere ad una analisi combinata topografica-anemologica, per quanto riguarda la direzione di provenienza del vento, e ai profili teorici, per ciò che concerne la velocità.

Eguale cautela va adottata per la determinazione della frequenza delle inversioni termiche qualora si è in prossimità di stazioni di radiosondaggi ma non si dispone del sondaggio delle ore 6 (T.U.). In questo caso, sul diagramma termodinamico relativo alle ore 0 (T.U.) si riporta la temperatura minima rilevata al suolo e seguendo poi l'adiabatica fino ad incontrare la curva della temperatura di stato si calcola lo spessore dello strato di inversione. E' questa una prassi molto comune in meteorologia. Qualora ciò non fosse possibile vi è sempre la risorsa della consultazione dei diagrammi termoigrometrici.

Però, occorre attirare l'attenzione sul fatto che, qualora il sito o i siti programmati rientrano nel caso (b), l'analisi preventiva non può essere compiuta celermente.

Da qualche anno a questa parte, per un primo orientamento della scelta delle località che devono entrare nella rosa delle valutazioni, si forniscono dei dati sotto forma tabulare o grafica sulla frequenza delle inversioni nei bassi strati atmosferici [9] o sulla distribuzione degli spessori di massimo mescolamento diurno dovuto all'insolazione. [10]

Questi lavori affrontano però soltanto un lato del problema preventivo perchè non prendono in esame l'altro punto che è quello del vento, come invece fa il Pasquill [11] nello stabilire le varie categorie di equilibrio atmosferico e che sono servite per compilare una tabella di frequenza per alcune località della Gran Bretagna. [12]

Queste rappresentazioni pur avendo una limitazione geografica dipendente dal grado di omogeneità del terreno possono essere di grande

aiuto in una analisi preventiva e sta naturalmente al meteorologo stabilirne i criteri di validità.

Il caso (c), cioè quello in cui non si posseggono informazioni nè dirette e nè indirette, è naturalmente quello che offre maggiori difficoltà nella soluzione.

Si è dell'opinione però che riconosciuto il principio della correlazione, o corrispondenza, tra condizioni topografiche e situazioni mesometeorologiche e tra queste e quelle macrometeorologiche, la prima valutazione possa essere fatta in base all'analisi delle situazioni meteorologiche che interessano mediamente la zona. Alcuni Servizi Meteorologici dispongono addirittura delle carte di frequenza delle situazioni medie, con relativa rappresentazione grafica, che evitano al meteorologo nucleare di selezionare e classificare migliaia di carte del tempo.

Tale metodo è stato recentemente adottato da chi scrive [13] nell'analisi dell'area del C.C.R. di Ispra (Varese) dell'Euratom quando si è dovuto compilare la climatologia della diffusione. Poichè, per la zona di Ispra si possedeva già un abbondante numero di dati osservati, questi sono serviti da controprova alle deduzioni qualitative. Difatti, mentre l'analisi delle situazioni forniva una frequenza anticiclonica media annuale di circa l'80%, l'analisi anemologica diretta forniva una frequenza media del 76% circa per i venti di intensità eguale o inferiore a 2 metri al secondo.

Un altro sistema può essere quello dei campioni e cioè scegliere le situazioni meteorologiche tipiche per la diffusione rielaborandole per le regioni che interessano con i normali criteri di mesoanalisi.

Sia l'uno o l'altro sistema permettono al meteorologo di procedere, mediante una similitudine idrodinamica, teorica o sperimentale, alla valutazione qualitativa del comportamento micrometeorologico della zona.

E' doveroso il richiamare l'attenzione sul fatto che in questo caso l'analisi meteorologica può essere soltanto qualitativa in quanto non è possibile suffragarla con entità fisiche; logicamente la bontà delle conclusioni dipende in maniera decisiva e determinante dalla obiettiva ed equilibrata sensibilità che il meteorologo ha nei riguardi del rischio nucleare.

1.3. *Criteri generali per la valutazione*

La valutazione di un sito è, in linea di massima, la condizione combinata dell'analisi del sito con i dati specifici dell'impianto nucleare. [14]

Di conseguenza la valutazione meteorologica che è, come si è detto, l'accertamento della diffusione in termini tridimensionali dei prodotti radioattivi consiste, in ultima ratio, nello sviluppo del problema della diffusione sulla base dell'analisi meteorologica effettuata per la protezione radiologica dei lavoratori e delle popolazioni, nonchè per la salvaguardia del ciclo alimentare.

La valutazione meteorologica, che è l'apporto vivo della meteorologia alla fisica sanitaria nucleare, può essere compiuta perciò soltanto dopo che il sito sia stato riconosciuto idoneo, in sede di analisi, a ricevere quel determinato impianto nucleare. Ciò perchè è indispensabile che sul sito vengano effettuate quelle misure ed osservazioni adatte a stabilire i parametri, e quindi i modelli micrometeorologici, della diffusione.

A tale proposito corre l'obbligo di denunciare una certa prevenzione, specie in micrometeorologia, sull'uso dei modelli. Una tale presa di posizione contro tale tipo di rappresentazione sembra che sia ingiustificata; bisogna, innanzi tutto, considerare i modelli non come delle leggi di natura e poi di saper valutare i loro risultati. [15] Inoltre, si ritiene utile, se non indispensabile, stabilire dei modelli di diffusione in quanto essi servono oltre che a sviluppare e a meglio comprendere il problema fisico e le tecniche delle misure anche ad essere efficacemente usati per prevedere il comportamento delle variabili del problema della diffusione.

Affinchè tali modelli possano essere veramente efficaci è indispensabile che non vengano usati come un comune formulario matematico e che essi, oltre ad essere provati sperimentalmente, siano continuamente aggiornati con i dati osservati; ciò allo scopo di una efficace utilizzazione, al momento opportuno, da parte dei Servizi di Protezione e Sicurezza del Centro Nucleare.

Ma il criterio meteorologico di valutazione di un sito, dal punto di vista del rischio nucleare, deve essere anche quello di contribuire a definire l'area di esclusione del sito. Questo contributo

può essere dato soltanto dopo un certo periodo di ricerche e di correlazioni parziali, tra gli elementi atmosferici e gli scarichi degli impianti nucleari, per non incorrere in errori di eccesso o di difetto.

1.4. *Valutazione meteorologica in relazione al tipo di impianto nucleare*

Come consequenza di quanto esposto nel paragrafo precedente, si ritiene che la valutazione meteorologica di un sito sul quale verrà installato un reattore di potenza non può essere eguale a quella del sito che ospita un reattore di ricerca o un impianto radiochimico.

Il CNEN, già da qualche anno, ha redatto un documento informativo [16] relativo ai dati meteorologici da raccogliere prima dell'avviamento di un reattore. In esso, riconosciuto il principio che l'ampiezza dei mezzi da impiegare per la ricerca e la portata stessa delle indagini sono funzioni del grado di sicurezza dell'impianto, i reattori sono stati divisi in due classi:

Classe I. Reattori che (a) durante il normale esercizio rispettano le raccomandazioni per la protezione radiologica dei gruppi circostanti di popolazione, anche senza tener conto della diluizione degli effluenti dovuta alla diffusione atmosferica tra il punto di emissione e le zone abitate; (b) nella eventualità di un incidente, anche grave, qualunque siano le condizioni meteorologiche, rispettano ancora le raccomandazioni che valgono per i casi di emergenza.

Classe II. Ogni reattore che non soddisfi ad una o ad entrambe le condizioni precedenti.

Per i reattori compresi nella prima delle due classi, l'indagine degli elementi meteorologici e dei fattori climatologici deve tendere alla valutazione del contributo alla dose-popolazione. A questo scopo il documento raccomanda di raccogliere informazioni relative al regime anemologico completo (direzione, velocità e struttura del vento), al regime termoigrometrico (per dedurre informazioni indirette sulle condizioni di stabilità dei bassi strati atmosferici in assenza di informazioni dirette relative al gradiente termico verticale) e al regime pluviometrico.

Per i reattori della classe II, invece, il documento lascia ampia libertà di stabilire il programma di ricerca richiamandosi, e giustamente, alle future esigenze operative dell'impianto (che sono funzione del tipo, della potenza e dell'impiego del reattore) e alle caratteristiche geografiche e topografiche della zona di ubicazione. Per quanto riguarda le esigenze operative dell'impiego, il predetto documento, pone tre ordini di problemi relativi agli scarichi continui, a quelli occasionali preordinati e, infine, a quelli di emergenza, riassunti come segue:

(a) determinazione della quantità massima ammissibile dei singoli radioisotopi, o loro miscele, che può essere immessa per tempo unitario con continuità nell'atmosfera dal camino, dalle bocche di ventilazione, ecc;
(b) determinazione dei valori statistici relativi alla frequenza e alla durata delle situazioni meteorologiche che consentono l'immissione nell'atmosfera di quantità prefissate di singoli radioisotopi, o loro miscele, per tempo unitario;
(c) determinazione dei metodi per stabilire tempestivamente, in funzione delle osservazioni meteorologiche del momento, la quantità massima ammissibile di effluenti radioattivi che può essere scaricata nell'atmosfera in tempi relativamente brevi ed eventualmente per individuare le località ove debbano prendersi provvedimenti di emergenza.

Ora si è dell'opinione che in questo documento vi siano le basi per un ulteriore approfondimento delle operazioni meteorologiche da effettuare per la valutazione del sito nei confronti del rischio nucleare; operazioni da stabilirsi, come è stato già accennato, soltanto in base alle caratteristiche geografiche e topografiche della zona di ubicazione.

2. LO STRATO LIMITE SUPERFICIALE DELL'ATMOSFERA

Di solito, l'analisi meteorologica viene estesa per una determinata estensione orizzontale della superficie terrestre contenente il sito nucleare; mentre per quanto riguarda la dimensione verticale vengono richiesti dati in quota, fino ad altezze spesse volte esagerate.

Pur non escludendo la possibilità che i

prodotti volatili comunque provenienti da un impianto nucleare possano interessare anche gli strati superiori della troposfera terrestre, qualora siano in atto dei moti convettivi al momento del rilascio o lungo il percorso degli effluenti, tuttavia, l'accumulo dei prodotti radioattivi è più facile negli strati più bassi dell'atmosfera. Questo è indicato come "strato limite di superficie dell'atmosfera terrestre", ed è uno spessore d'aria in cui gli elementi meteorologici hanno un particolare andamento verticale; logicamente la struttura, termica e dinamica, di questo strato limite differisce da quella del resto della troposfera terrestre; inoltre, questo strato ha anche una sua specifica geometria dipendente, oltre che dalla situazione meteorologica generale, anche dall'aspetto e dalla natura della superficie sottostante.[17]

Sullo spessore verticale dello strato limite vi è un principio statistico,[18] che lo considera di 50–100 metri, nel quale la struttura del vento è determinata dalla natura della superficie e dal gradiente verticale termico, sul quale scorre una regione di transizione di 500–1000 metri, nella quale la struttura del vento è influenzata dall'attrito di superficie ed è controllata dal gradiente di densità e dalla forza di deviazione terrestre (forza di Coriolis). L'insieme di questi due strati determina lo strato limite planetario. Per contro, vi sono due altri principi, uno dinamico[19] ed uno termodinamico,[20] che considerano invece lo strato limite come una entità oscillante. Difatti, secondo quest'ultimo, lo spessore dello strato limite è funzione della capacità della diffusività termica del mezzo e del periodo di oscillazione delle variazioni della radiazione solare incidente sulla superficie terrestre e della variazione nella velocità e direzione del vento.

Poichè i profili termici e dinamici nello strato limite non hanno un andamento costante per tutto il suo spessore, a causa dell'influenza del suolo, si ha, nella parte inferiore di esso, un substrato. Questo è caratterizzato da valori molto accentuati nei gradienti verticali degli elementi meteorologici. Benchè i processi che si verificano nel substrato limite sono in stretta interazione con i fenomeni dell'itnero strato limite, lo stabilire le relazioni interne soltanto fra gli elementi meteorologici nel substrato superficiale è spesso sufficiente per la soluzione di importanti problemi, primo fra tutti quello della diffusione atmosferica degli effluenti provenienti da impianti nucleari.

L'andamento caratteristico dello strato limite è dato dai profili verticali degli elementi meteorologici, che sono reciprocamente dipendenti, e singolarmente determinati dal gradiente orizzontale della pressione, dall'influenza della radiazione solare, dai parametri termici e fisici del suolo, dalle irregolarità della superficie ed anche dalla temperatura ed umidità all'esterno dello strato limite. E' evidente che la variazione di ognuno di questi fattori esterni determina delle variazioni di tutte le caratteristiche dello strato limite.

Lo spessore dello strato e del substrato limite presentano una variazione media annuale dovuta alle oscillazioni del bilancio termico e delle condizioni dinamiche ed alla persistenza delle varie situazioni meteorologiche.

A Milano, dove si stanno perseguendo da parte di chi scrive tali ricerche, è stato trovato che lo strato limite superficiale va da un minimo di 100 metri, in gennaio, ad un massimo di 1200 metri, in luglio, e il substrato limite oscilla tra i 20 metri in dicembre e i 200 metri in maggio. La correlazione per il solo semestre freddo (cioè quello in cui è in atto il riscaldamento domestico) tra concentrazioni di SO_2 e variazioni dello strato limite ha dato un risultato più soddisfacente di quello ottenuto dalle correlazioni parziali tra concentrazioni di SO_2 e gradiente termico verticale e intensità del vento, rispettivamente misurati, nei primi 100 metri e a 120 metri dal suolo.

E' evidente che la migliore conoscenza delle vicende spazio-tempo dello strato limite possa permettere una maggiore puntualizzazione di quelli che sono i meccanismi difensivi naturali nel campo della diffusione degli effluenti e cioè il potere diluente dell'atmosfera e, per contro, la sua capacità a generare delle barriere protettive che ostacolano o deviano il trasporto degli effluenti stessi. Non solo, ma nella particolarità dei rapporti nucleari di rischio si verrebbero ad immettere dei dati fisici che rispecchiano l'effettivo stato di quello spessore di atmosfera più soggetto all'inquinamento radioattivo.

BIBLIOGRAFIA

1. I.A.E.A. *Proc. Symp. on Siting of Reactors and Nuclear Research Centres*, Bombay, March 11–15 1963. Vienna, 1963.
2. I.C.R.P. *Recommendations of the International Commission on Radiological Protection.* Pergamon Press, London, 1959.
3. Comunità Europea. *Gazz. Uff. delle Comunità Europee.* 20 febbraio 1959.
4. C. E. WALLINGTON. *An Atmospheric Diffusion Slide-rule.* Met. Off., London. Sci. Paper No. 24, 1966.
5. L. FACY, C. PERRIN DE BRICHAMBAUT, A. DOURY e R. LE QUINIO. *L'utilisation des maquettes aériennes et hydrauliques pour l'étude de la pollution atmospherique.* La met., S.M.F., Paris, janvier 1963.
6. V. CONRAD e L. W. POLLAK. *Methods in Climatology.* Harvard Univ. Press, Cambridge, Mass., 1950.
7. E. ROSINI. Studio delle variazioni del vento fra due o più punti con metodo statistico. *VI Rass. Elettron. e Nucl., Roma,* Vol. II, 1959.
8. J. FINDLATER, T. N. S. HARROVER, G. A. HOWKINS e H. L. WRIGHT. *Surface and* 900 *mb Wind Relationship.* Met. Off., London, Sci. Paper No. 24, 1966.
9. C. R. HOSLER. Low-level inversion frequency in the contiguous United States. *Mo.We.Re.* **89,** 319–339 (1961).
10. G. C. HOLZWORTH. Estimates of mean maximum mixing depths in the contiguous United States. *Mo.We.Re.* **92,** 235–242 (1964).
11. F. PASQUILL. The estimation of the dispersion of windborne. *Met. Mag.* **90,** 33–49 (1961).
12. J. K. BANNON, L. DODS e P. J. MEADE. *Frequencies of Various Stabilities in the Surface Layer.* Met. Off. Mem. No. 88, 1962.
13. L. SANTOMAURO. *Report about Climatology of Diffusion at Ispra.* Milano, Oss. di Brera, 1965.
14. J. A. LIEBERMAN, D. A. PACK e E. S. SIMPSON. Environmental aspects of nuclear facility site selection. A.I.E.A. *Proc. Symp. Sit. of Reactors and Nucl. Res. Cen.* Vienna, 1963.
15. R. E. MUNN. *Descriptive Micrometeorology.* Academic Press, London, 1966.
16. G. FEA, D. REDELE, B. PAVESI, A. PERSANO, E. ROSINI, L. SANTOMAURO, C. SENNIS e S. TAGLIATI. Le informazioni meteorologiche da raccogliere prima dell'avviamento di un reattore. *Notiz. del CNEN* No. 2, 1962.
17. L. SANTOMAURO. Il comportamento atmosferico degli effluenti civili e industriali. *Atti del Conv. Aspetti giuridici Igienici degli inquinamenti atmosf. Italedi. Roma,* pp. 83–106, 1965.
18. O. G. SUTTON. *Micrometeorology.* McGraw-Hill, New York, 1953.
19. J. L. LUMLEY e H. A. PANOFSKY. *The Structure of Atmospheric Turbulence.* John Wiley, London, 1964.
20. D. L. LAIKTHAM. *Physics of the Boundary Layer of the Atmosphere.* Israel Progr. Sc. Transl., 1964.

UMWELTKONTAMINATION UND STRAHLENBELASTUNG BEI FREISETZUNG RADIOAKTIVER STOFFE IN DIE ATMOSPHÄRE

K. J. VOGT

Kernforschungsanlage Jülich, Zentralabteilung Strahlenschutz, 517 Jülich BRD

Zusammenfassung—Nach der Theorie der turbulenten Diffusion wurde die Ausbreitung radioaktiver Stoffe in der Atmosphäre behandelt. Unter Verwendung der von Pasquill empfohlenen meteorologischen Parameter wurden die Verteilung der Aktivitätskonzentration in der Atmosphäre, die Ablagerung der Luftkontaminationen am Boden und die Abnahme der Aktivität der Abluftwolke durch Fallout, Washout und radioaktiven Zerfall berechnet, aus denen sich die Inhalations- und Ingestionsgefährdung herleiten läßt.

Während bei Emissionen radioaktiver Aerosole die Inkorporation durch Atmung und Nahrungsaufnahme die kritische Belastungsart darstellt, muß bei Freisetzung radioaktiver Gase die äußere Bestrahlung ermittelt werden. Dabei kann die Strahlenbelastung durch β-Strahlung wegen ihrer geringen Reichweite aus der Aktivitätskonzentration am Ort der exponierten Person berechnet werden. Die Submersionsdosis für γ-Strahlung ergibt sich durch Integration über die Bestrahlungsbeiträge der Volumenelemente des Halbyraums. In die Rechnung gehen neben der dreidimensionalen Verteilungsfunktion u. a. die Energie, die Halbwertszeit und die Dosiskonstante des freigesetzten Nuklids sowie die Absorption und Streuung der γ-Strahlung in Luft ein. Die Submersionsdosis wurde für ^{41}Ar und für Spaltgasgemische berechnet. Die Verteilungsfunktionen der ausgewerteten Größen wurden in Abhängigkeit von der Quelldistanz in Kurvenscharen und Nomogrammen dargestellt. Eingangsparameter sind Schornsteinhöhe, Diffusionskategorie, Windgeschwindigkeit und die Ablagerungskonstanten für Fallout und Washout. Die graphischen Auswertehilfen erlauben bei Zwischenfällen mit Freisetzung radioaktiver Stoffe in die Atmosphäre schnelle Prognosen über die Ausbreitung der Abluftfahne und die dadurch bedingten Umweltbelastungen.

Bei der Standortwahl kerntechnischer Anlagen, bei der Planung von Schornsteinhöhen und Filtereinrichtungen für Emittenten radioaktiver Abluft, bei der Umgebungsüberwachung unter normalen Betriebsbedingungen und besonders nach Aktivitätsfreisetzungen infolge von Zwischenfällen ist die Kenntnis des Ausbreitungsverhaltens von Abluftfahnen in der Atmosphäre erforderlich.

Auf der Grundlage der Theorie der turbulenten Diffusion[1, 2] wurden daher die Kontamination und Strahlenbelastung in der Umgebung von Emissionsquellen berechnet. Die Ergebnisse wurden in Kurvenscharen und Nomogrammen zusammengestellt, die als Unterlagen für Schornsteingutachten und Sicherheitsberichte dienen und vor allem in Unfallsituationen schnelle Analysen und Prognosen ermöglichen sollen. Ausgehend von der Verteilungsfunktion der Luftaktivität bei Gaussförmiger Ausbreitung momentaner Emissionen (Puffs)

$$C(x,y,z,t) = \frac{Q}{(2\pi)^{3/2}\sigma_x\sigma_y\sigma_z} e^{-(x-ut)^2/2\sigma_x^2} \cdot e^{-y^2/2\sigma_y^2} \cdot \left(e^{-(z-H)^2/2\sigma_z^2} + e^{-(z+H)^2/2\sigma_z^2}\right) \quad (1)$$

(Ci/m³)

Q(Ci) = Aktivität der Abluftwolke,
H(m) = Emissionshöhe (z-Richtung),
u(m/s) = Windgeschwindigkeit (x-Richtung),

$t(s)$ = Transportzeit,
$\sigma_x, \sigma_y, \sigma_z$(m) = von der Quelldistanz x abhängige Ausbreitungsparameter,

wurden die Hauptbeiträge zur Strahlenbelastung berechnet,[3] nämlich

1. Die durch die Kontamination der bodennahen Luft mit radioaktiven Aerosolen bedingte Inhalationsbelastung unter der Ausbreitungsachse

$$I(x, 0, 0) = \frac{Q}{\pi\sigma_y\sigma_z u} e^{-H^2/2\,\sigma_z^2} \quad (\text{Ci s/m}^3), \quad (2)$$

aus der sich durch Multiplikation mit dem Inhalationsdosisfaktor g (rem m³/Ci s) die Dosisbelastung des kritischen Organs ergibt.

2. Die Ingestionsbelastung, die auf Nahrungsmittelkontaminationen infolge Ablagerungen radioaktiver Stoffe auf dem Boden durch trockenen Fallout

$$F(x, 0) = v_g\, I(x, 0, 0) \quad (\text{Ci/m}^2) \quad (3)$$

und durch niederschlagsbedingten Washout

$$W(x, 0) = \Lambda Q/\sqrt{2\pi}\,\sigma_y u \quad (\text{Ci/m}^2) \quad (4)$$

beruht, wobei v_g (m/s) die Falloutkonstante und Λ(s^{-1}) die Washoutkonstante bedeuten.

3. Die äußere Strahlenbelastung durch β-Strahlung aus der unmittelbaren Umgebung der exponierten Person

$$D_\beta\,(x, 0, 0) = 0{,}27\, E_\beta\, I(x, 0, 0)\ (\text{rem}), \quad (5)$$

wobei E_β (MeV) die mittlere β-Energie pro Zerfall ist.

4. Die äußere Strahlenbelastung durch γ-Strahlung aus dem Halbraum

$$D_\gamma\,(d, 0, 0) = I_\gamma \iiint B \frac{e^{-\mu r}}{r^2} C(x, y, z, t)\, dx\, dy\, dz\, dt\ (\text{R}) \quad (6)$$

mit I_γ (R m²/Ci s) = Dosisleistungskonstante,
μ (m^{-1}) = Absorptionskoeffizient von Luft,
$r = [(d-x)^2 + y^2 + z^2]^{1/2}$ (m) = Abstand des Aufpunkts $(d, 0, 0)$ vom Quellelement (x, y, z),
B = Aufbaufaktor.

Beim Einsetzen von Q ist zu berücksichtigen, daß die Wolkenaktivität infolge von radioaktivem Zerfall, Washout- und Falloutеffekten nach der Transportzeit $t = x/u$ auf den Bruchteil

$$Q/Q_0 = e^{-\lambda\frac{x}{u}} \cdot e^{-\Lambda\frac{x}{u}} \cdot e^{-\frac{v_g}{u}\sqrt{\frac{2}{\pi}}\int_0^x \frac{1}{\sigma_z} e^{-H^2/2\sigma_z^2}\, dx} \quad (7)$$

der Quellstärke Q_0 zurückgegangen ist.

Hinsichtlich der theoretischen Herleitung dieser die Strahlenbelastungsbeiträge beschreibenden Berechnungen aus den grundlegenden Modellvorstellungen muß auf die Literatur verwiesen werden.[4, 5] Die numerische Auswertung der Gleichungen (2) bis (7) erfolgte unter Verwendung der von Pasquill[6] empfohlenen Ausbreitungsparameter σ_y und σ_z unter Variation der Parameter Quelldistanz, Emissionshöhe, Diffusionskategorie sowie Fallout- und Washoutkonstante. Als Beispiele für die Auswertungsergebnisse werden nachfolgend einige Kurvenscharen und Nomogramme gezeigt.

In Abb. 1 sind die normierten Ausbreitungsfunktionen bei einer Emissionshöhe von 100 m für die verschiedenen Diffusionskategorien A bis F, die durch zunehmende Stabilität der Schichtung charakterisiert sind, dargestellt. Dividiert durch die Windgeschwindigkeit und multipliziert mit der differentiellen oder integralen Quellstärke (Ci/s bzw. Ci) erhält man daraus die Aktivitätskonzentration der bodennahen Luft unter der Ausbreitungsachse (Ci/m³) oder die Inhalationsbelastung (Ci s/m³). Aus der Abbildung ist ersichtlich, daß die Entfernung des Aktivitätsmaximums und in geringerem Maße seine Größe von der Stabilität der Schichtung abhängen. Die Abhängigkeit der Aktivitätskonzentration von der Emissionshöhe bei mäßig stabiler Schichtung (Diffusionskategorie E) ist in Abb. 2 veranschaulicht.

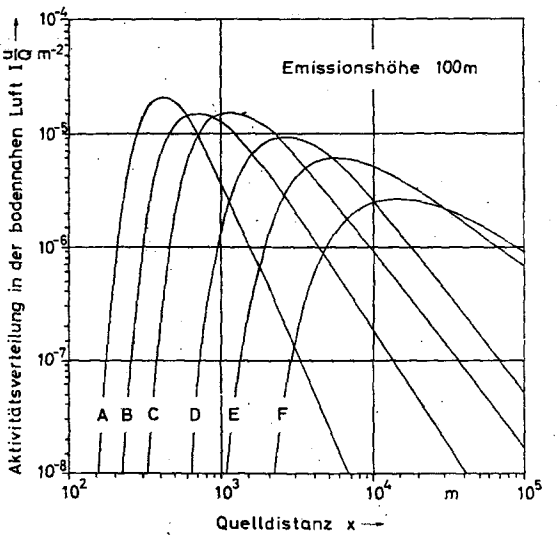

ABB. 1. Auf die Einheit der Emissionsstärke und der Windgeschwindigkeit bezogene Aktivitätskonzentration der bodennahen Luft unter der Ausbreitungsachse in Abhängigkeit von Quelldistanz und Diffusionskategorie bei einer Emissionshöhe von 50 m.

Für einige Nuklide, wie z.B. Radiojod, stellt unter Umständen nicht die Inhalationsbelastung, sondern, bei Ablagerung auf landwirtschaftlich genutzten Flächen, die Ingestionsbelastung als Folge der Kontamination der Nahrungskette die überwiegende Gefährdung dar. Die Ablagerung durch trockenen Fallout ergibt sich durch Multiplikation der bodennahen Aktivitätskonzentration mit der Falloutkonstanten (Werte für v_g werden in der Literatur angegeben [7, 8]). Die Ablagerung durch Niederschläge läßt sich dem in Abb. 3 gezeigten Nomogramm entnehmen. Sie ist nach dem zugrundeliegenden Modell von der Emissionshöhe unabhängig und ergibt sich, ausgehend von der Quelldistanz über die durch die Diffusionskategorie und den Quotienten aus Washoutkonstante und Windgeschwindigkeit gegebenen Hilfslinien. Wenn die von der Niederschlagsintensität, der Tropfengröße und der Partikelgröße des radioaktiven Aerosols abhängige Washoutkonstante [7, 9] nicht genauer bekannt ist, kann näherungsweise der Wert $2{,}5 \cdot 10^{-4}$ s^{-1}, multipliziert mit der Maßzahl der in mm/h gemessenen Niederschlagsintensität verwendet werden. Bei Kenntnis der abgelagerten Nuklide können die vom Boden ausgehende β- und γ-Strahlung und, zusammen mit anderen Parametern, die Nahrungsmittelkontamination und die Ingestionsbelastung abgeschätzt werden.

Die Abnahme der Wolkenaktivität durch Washout und radioaktiven Zerfall während der Transportzeit läßt sich durch einfache Exponentialfunktionen berücksichtigen. Der Korrekturfaktor für das Falloutdefizit wurde aus der letzten Exponentialfunktion in Gl. (7) durch numerische Integration bestimmt. Am Beispiel einer Wetterlage mit mäßig stabiler Schichtung

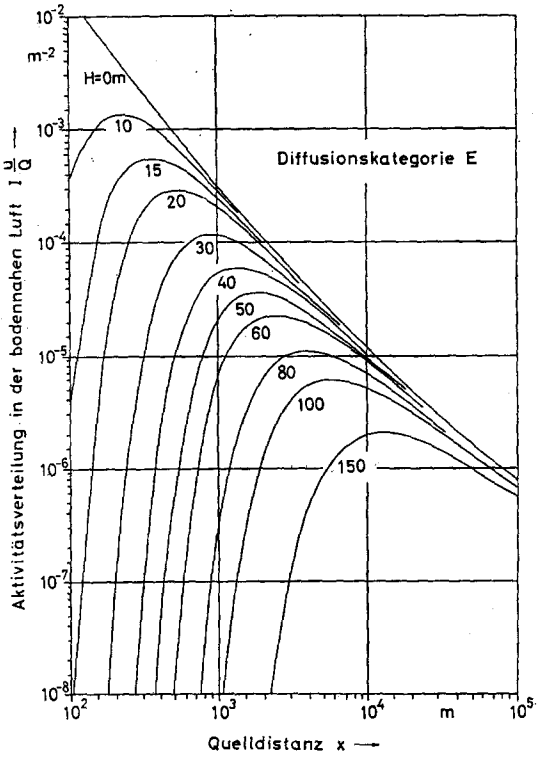

ABB. 2. Auf die Einheit der Emissionsstärke und der Windgeschwindigkeit bezogene Aktivitätskonzentration der bodennahen Luft unter der Ausbreitungsachse in Abhängigkeit von Quelldistanz und Emissionshöhe bei mäßig stabiler Schichtung (Diffusionskategorie *E*).

(Diffusionskategorie E) sind die Ergebnisse in Abb. 4 dargestellt. Ausgehend von der Quelldistanz läßt sich aus dem Nomogramm durch "Spiegelung" an der Emissionshöhe und dem Verhältnis von Falloutkonstante und Windgeschwindigkeit die Aktivitätsabnahme der Wolke ermitteln.

Während die Inkorporationsbelastung durch Inhalation und Ingestion von Radionukliden im allgemeinen bei Aerosolen sowie bei Radiojod überwiegen, spielt die Submersionsdosis durch äußere β- und γ-Strahlung vor allem bei der Emission radioaktiver Edelgase eine Rolle.

Die β-Dosis, der Haut und Augen ausgesetzt sind, ist nach Gl. (5) der Aktivitätskonzentration am Ort der exponierten Person proportional. Von Nukliden mit sehr geringer γ-Emissionswahrscheinlichkeit wie ^{85}Kr abgesehen, kann sie im allgemeinen gegenüber der γ-Dosis vernachlässigt werden.

Bei der Berechnung der γ-Dosis ist nach Gl. (6) über die räumliche Verteilung der Wolkenaktivität unter Berücksichtigung von Absorption, Vielfachstreuung und radioaktivem Zerfall zu integrieren. Im Vergleich zu früheren Autoren [10-13], die vielfach von isotroper Ausbreitung ausgehen und die Ausbreitungsformel von Sutton benutzen, oder Absorption und Aufbaufaktor vernachlässigen, oder sich auf bodennahe Emissionen bzw. bestimmte Energien beschränken (z.B. 0,7 MeV für Spaltproduktgemische), oder relativ grobe Mitteilungen der Verteilungsfunktion zugrunde legen, haben wir die Berechnung im wesentlichen ohne derartige Vernachlässigungen vorgenommen. Allerdings wurde die dreidimensionale numerische Integration nur im mittleren Entfernungsbereich durchgeführt. Für kleine Entfernungen konnte die Verteilung durch eine Linienquelle und für große Entfernungen durch eine homogene Ver-

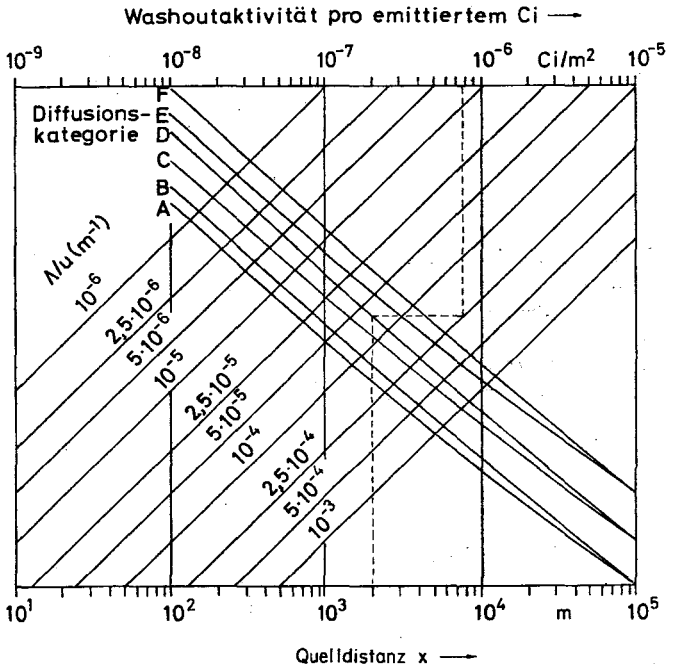

ABB. 3. Auf die Einheit der emittierten Aktivität bezogene Bodenkontamination durch Washout in Abhängigkeit von Quelldistanz, Windgeschwindigkeit, Diffusionskategorie und Washoutkonstante.

teilung angenähert und dadurch die Rechnung vereinfacht werden).*

Entsprechend den wichtigsten Anwendungen wurde die γ-Dosis für ^{41}Ar und für Spaltgas-Emissionshöhe 50 m für verschiedene Diffusionskategorien, die jeweils mit ihrer charakteristischen Windgeschwindigkeit angesetzt wurden, dargestellt.

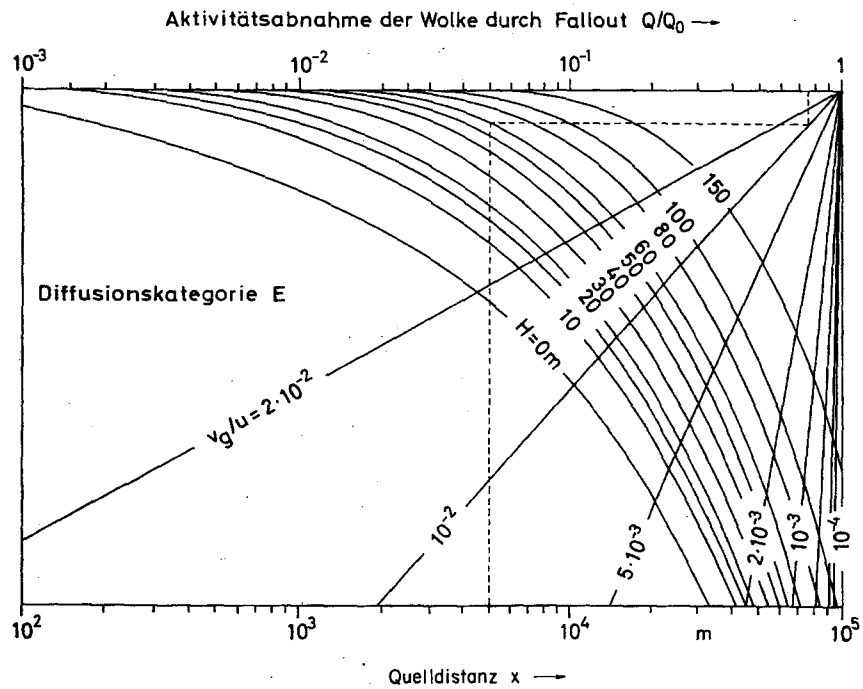

ABB. 4. Abnahme der Wolkenaktivität durch Fallout in Abhängigkeit von Quelldistanz. Windgeschwindigkeit, Emissionshöhe und Falloutkonstante bei mäßig stabiler Schichtung (Diffusionskategorie *E*).

gemische†) berechnet. Als Beispiel zeigt Abb. 5 die γ-Dosis, der eine Person aus der über sie hinwegziehenden Abluftfahne bei einer Emission von 1 Ci ^{41}Ar exponiert wird, in Abhängigkeit von der Emissionshöhe bei neutraler Schichtung (Diffusionskategorie *D*). In Abb. 6 ist, ebenfalls für ^{41}Ar, die γ-Dosis bei der

Außerdem haben wir die Abhängigkeit der γ-Dosis von der Energie zwischen 0,25 und 2 MeV untersucht. Es ergab sich etwas überraschend, daß die auf die Einheit der Dosisleistungskonstante normierte γ-Dosis, trotz der starken Energieabhängigkeit der Absorption und des Aufbaufaktors, nur sehr wenig von der Energie abhängt. Bei der Berechnung der γ-Dosis kann man also für alle Energien von den gleichen Kurvenscharen ausgehen, wobei die Werte nur noch mit der Dosisleistungskonstanten zu multiplizieren sind. Die γ-Dosis hängt damit im wesentlichen in gleicher Weise von der Energie ab wie die Dosisleistungskonstante, d. h., im betrachteten Energiebereich ist die

* Die numerische Auswertung wurde mit einer elektronischen Datenverarbeitungsmaschine vom Typ IBM 7090 beim Deutschen Rechenzentrum Darmstadt durchgeführt. Für die Aufstellung des Programms bin ich meinem Kollegen F. Rohloff zu Dank verpflichtet.

† Es wurde Gleichgewicht der Spaltgase (außer ^{85}Kr) nach längerer Reaktorbetriebszeit angenommen.

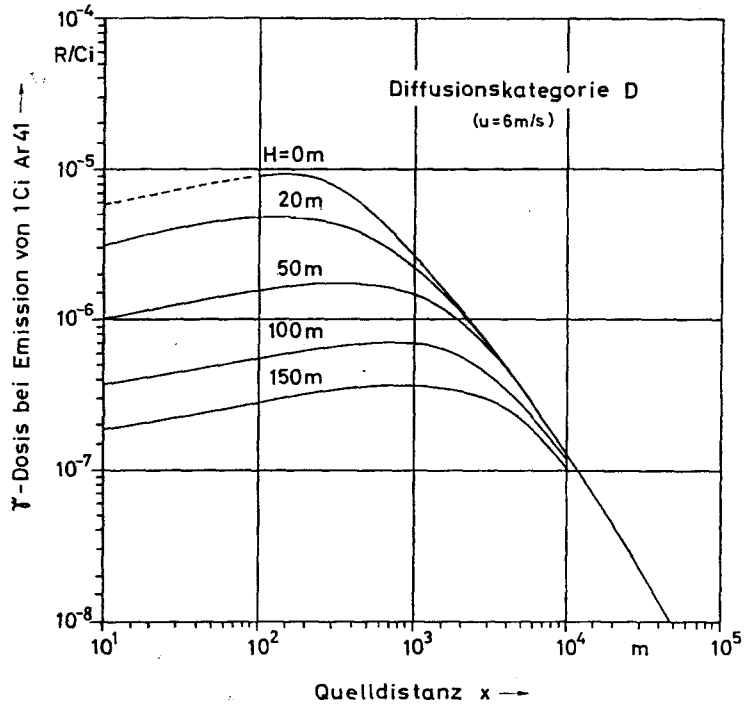

ABB. 5. Auf die Einheit der emittierten Aktivität bezogene Submersions-γ-Dosis bei der Freisetzung von ^{41}Ar in Abhängigkeit von Quelldistanz und Emissionshöhe bei neutraler Schichtung (Diffusionskategorie *D*) und einer Windgeschwindigkeit von 6 m/s.

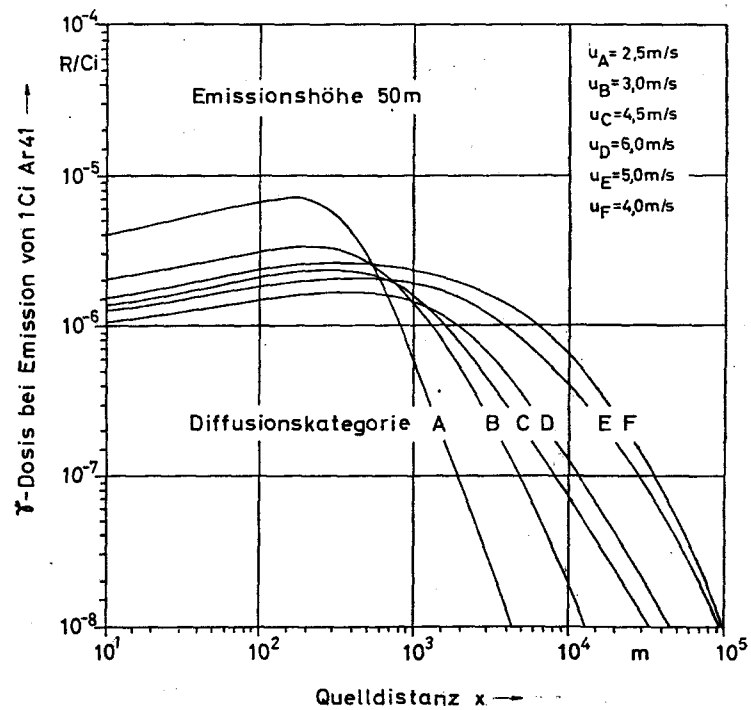

ABB. 6. Auf die Einheit der emittierten Aktivität bezogene Submersions-γ-Dosis bei der Freisetzung von ^{41}Ar in Abhängigkeit von Quelldistanz und Diffusionskategorie bei einer Emissionshöhe von 50 m. (Für jede Diffusionskategorie wurde mit einer charakteristischen Windgeschwindigkeit gerechnet.

γ-Dosis für Nuklide mit gleicher γ-Emissionswahrscheinlichkeit näherungsweise der Energie proportional.

Hinsichtlich näherer Angaben über die physikalischen und meteorologischen Aspekte der Ausbreitung (effektive Schornsteinhöhe,[14] Bestimmung der Diffusionskategorie[15] usw.) sowie über Voraussetzungen und Grenzen bei der Anwendung der Ausbreitungsformeln sei auf die einschlägige Literatur verwiesen.

REFERENZEN

1. O. G. Sutton. *Micrometeorology*, McGraw-Hill, New York, 1953.
2. F. Pasquill. *Atmospheric Diffusion.* Van Nostrand, London, 1962.
3. K. J. Vogt. *Kerntechnik* **8,** 453 (1966).
4. Meteorology and Atomic Energy. AECU (1955).
5. G. Blässer und K. Wirtz. *Nukleonik* **3,** 210 (1961).
6. F. Pasquill. *Met. Mag.* **90,** 33 (1961).
7. A. C. Chamberlain. AERE HP/R 1261 (1953).
8. J. R. Beattie. AHSB (S) R 64 (1963).
9. F. G. May. *Quart. J. Roy. Met. Soc.* **84,** 451 (1958).
10. P. H. Lowry. BNL-81 (1950).
11. I. A. Singer. BNL-292 (1954).
12. J. Z. Holland. *Proc. Internat. Conf. Peaceful uses Atomic Energy* P/572 (1955).
13. M. Tsunokawa und T. Aoki. *J. Atom. Energy Soc. Japan* **5,** 110 (1963).
14. H. Moses, G. H. Strom und J. E. Carson. *Nucl. Saf.* **6,** 1 (1964).
15. G. Polster. *Kerntechnik* **8,** 409 (1966).

RELATIVE HAZARDS OF FISSION PRODUCTS IN THE ENVIRONMENTAL HAZARDS EVALUATION OF NUCLEAR REACTORS

J. TADMOR and H. GALRON

Soreq Nuclear Research Centre, Israel Atomic Energy Commission,
Yavneh, Israel

Abstract—The fission products and their decay products which accumulate in the fuel during the operation of a nuclear reactor consist of about 300 isotopes of different physical, chemical and biological properties. However, only a relatively small number of these isotopes contribute significantly to the hazard to the population, in the event of an accidental release of fission products into the environment.

The relative hazard of the fission products in the environmental hazards evaluation of nuclear reactors was calculated in order to ascertain which fission products must be taken into account. Consideration was given to (1) the various ways in which the population might be subjected to irradiation (external cloud radiation, external radiation from contaminated land, and internal irradiation due to inhalation); (2) the properties of the fission products (fission yield, percentage of release from the fuel in an accident, energy of radiation, physical and biological half-life, velocity of deposition); and (3) the critical organ in the human body in which the fission product concentrates.

Although several studies deal with the relative hazards of various radioisotopes in general and of fission products in particular, no comprehensive study has been made so far concerning the specific aspect of environmental hazards evaluation of nuclear reactors.

In our study, the relative hazards of the fission products were calculated for external cloud radiation, external radiation from contaminated land and internal radiation from inhalation, assuming a reactor power of 1 MW (th) and an accident occurring after 3 years of operation. The hazards were calculated for different times after the occurrence of the accident and for different distances from the point of release of the fission product.

The importance of using the individual γ-energies rather than the average energy of all the fission products is shown and the contribution of the fission product daughters formed during the travel of the cloud is also evaluated. The study summarizes the sequence of importance of the different fission products in the framework of the hazards evaluation of nuclear reactors.

PESSIMAL HEIGHT OF RELEASE AND THE RADIATION DOSES FROM A RADIOACTIVE CLOUD AND FROM DEPOSITION OF FISSION PRODUCTS

J. TADMOR, Y. MILMAN, H. GALRON and Y. GILAAD
Soreq Nuclear Research Centre, Israel Atomic Energy Commission,
Yavneh, Israel

Abstract—In the evaluation of the hazards to the environment resulting from a release of radioactive materials from a nuclear reactor, it is generally considered that an increase in the height of release would be advantageous in minimizing the concentrations in the environment and that inversion atmospheric conditions and deposition of the radioactive material by rain represent the most hazardous atmospheric condition.

In the present study it is shown that when the depletion of the cloud by deposition during its travel from the release point to the distance of interest is taken into account, a different picture is obtained: (1) an increase in the height of release, within certain limits, may cause an increase in the ground concentration at a given distance from the source, and (2) for certain distances from the release point, at which highly populated centres may exist, consideration of the hazards during inversion and rainout conditions only may result in an underestimation of the environmental hazards.

The computation of the integrated radiation doses from the fission products released from a ground source following a reactor accident and deposited during dry or rainout conditions shows that at relatively short distances from the source the doses are greater if deposition occurs during dry conditions; at greater distances the doses are greater if deposition occurs during rain conditions. The distance from the release point to the point of intersection between the radiation doses from dry and rainout depositions decreases with time since deposition, the time factor reflecting the more rapid decay of the iodines.

The Total Integrated Cloud Concentration (TIC) of the iodines computed for lapse and inversion atmospheric conditions, considering the depletion of the cloud by deposition, reveals the following: due to the relatively high deposition of the iodines and to the greater deposition during inversion conditions, the TIC during lapse conditions will be greater, from a certain distance on, than during inversion conditions. Higher wind velocities during inversion conditions and lower wind velocities during lapse conditions cause the approach to the point of release of the intersection point between the TIC for inversion and for lapse conditions.

LASER RADIATION PROTECTION*

WILLIAM T. HAM, JR., W. J. GEERAETS, R. C. WILLIAMS, D. GUERRY, III, and HAROLD A. MUELLER

Medical College of Virginia, Richmond, Virginia

Abstract—Although most health physicists and others in the field of radiation protection have confined their efforts primarily to the hazards from the so-called ionizing radiations (X-rays, gamma-rays, neutrons, high energy particles, etc.), an increasing number of workers in this field are being called upon to protect personnel from laser radiation. The phenomenal development of laser technology during the past three years has introduced new hazards for industry, for governmental agencies, particularly the military and space agencies, and for universities and medical schools.

The necessity for such criteria will be examined. Since the eye is the most vulnerable organ of man to laser radiation, the effects of wavelength, pulse duration, intensity of irradiation (power density), energy density, and other factors on the eye will be given. Current data from several laboratories will be reviewed briefly. Finally, protective practices and equipment in current use in the United States will be discussed.

HISTORICAL BACKGROUND

Man lives in a natural radiation environment. He is exposed daily to the electromagnetic radiation spectrum from a nuclear fireball—the sun—to natural radioactivity both within and surrounding his body, and to cosmic rays coming from intergalactic space. Were this his integral radiation exposure there would be no need for radiation protection and health physics. Although solar radiation may produce thermal injury to the skin (sunburn) and to the eyes (retinal burns), not to mention the painful inflammation of the cornea resulting from ultraviolet (UV) rays, nonetheless, experience through the ages has taught man how to protect himself from the natural radiation background. Not content with the radiations provided naturally, man has extended and broadened the electromagnetic spectrum to include wavelengths which have increased the hazards to his health. Maxwell's theory and the production of electromagnetic waves by Hertz led to the modern development of radio, radar, and television with a consequent increase in the hazards from microwaves. At the other end of the electromagnetic spectrum, Röntgen produced X-rays, opening the "floodgates" to the biological effects of ionizing radiation. Becquerel and the Curies completed the spectrum by discovering radioactivity, thus providing both the particulate alpha- and beta-rays and the very short wavelength gamma-rays. All of this took place before the beginning of the 20th century. The study of atomic and nuclear structure by Rutherford, Bohr, and many others led inevitably to the production of giant accelerators to study the nucleus and the interactions between the elementary particles of physics. By the late 1930's man had increased his arsenal of radiations to include neutrons, positrons, and mesons, to mention but a few. Then came the discovery of fission at the beginning of World War II. By the end of the war the world had been introduced to the nuclear age. Man had created a new radiation environment which had tremendous potentialities for good and evil. The knowledge of how to handle, manipulate, and dispose of large quantities of radioactive materials grew out of the Manhattan project. The peaceful applications of nuclear

* Support for this research was provided by Contract DA 49 193 MD 2241, U.S. Army, MRDC, Office of the Surgeon General and Contract DA 49 146 XZ 416 Defense Atomic Support Agency, DOD, Washington, D.C.

energy to modern civilization are now well advanced, but over mankind still hangs the spectre of nuclear war with the possibility of world-wide radioactive contamination on a scale that might threaten the survival of mammalian life. In this atmosphere of hope and fear, the Health Physics Society was founded in 1955. The Society is dedicated to radiation protection with a special emphasis on "ionizing radiation".

Meanwhile, the first operating optical maser was described by Gordon, Zeiger, and Townes [1] in 1954 at a time when active efforts were under way to form the Health Physics Society. Townes had suggested as early as 1951 that it should be theoretically possible to obtain amplification by using a molecular generator at a specific frequency inherent to the molecule. He and his colleagues used a beam of ammonia gas passing through a microwave cavity tuned to approximately 24,000 Mc/s, a frequency corresponding to a natural resonance in NH_3. Townes coined the acronym maser—*m*icrowave *a*mplification by the *s*timulated *e*mission of *r*adiation. When, in 1958, Schawlow and Townes [2] demonstrated the feasibility of extending the maser principle to the optical region of the electromagnetic spectrum by employing solid state devices, the term "optical maser" was suggested. It was Maiman, [3] however, in 1959, who first operated a solid state maser by producing stimulated emission from a ruby crystal. Since this was radiation in the visible or optical region of the spectrum (694.3 nanometers, nm), laser rather than maser came into use to denote *l*ight instead of *m*icrowave. The term laser has been adopted by most workers in this field and is used generally to denote the emission of stimulated light from all sources and under all operating conditions. Javan, Bennett, and Herriott [4] made a notable contribution in 1961 when they succeeded in producing the first continuous wave (CW) gas laser from a mixture of helium and neon. The production of "giant pulses" of laser radiation by utilizing a "Q-spoiling" technique was announced by McClung and Hellwarth [5] in 1963 and represented another notable advance in laser technology.

Technical advances in the production and application of laser beams have been extremely rapid during the past 3 years. Parallel beams of intense radiation which are plane polarized, monochromatic, and coherent both in space and time, are available throughout the electromagnetic spectrum from the far infrared (IR) to the near ultraviolet. There is even the possibility of producing laser sources in the far ultraviolet and the X-ray region, and some consideration has been given to a gamma-ray laser. Sources involve gaseous, liquid, and solid state lasers and power levels range from milliwatts to gigawatts. Lasers may be operated continuously to produce CW radiation or pulsed to produce multiple spikes of radiation or single giant pulses which last for only a few nanoseconds. Power densities can reach the gigawatt/cm^2 level, and even optical materials like quartz are broken down by the intense electric field strengths generated by a focused laser beam. When focused in air a "fireball" is produced, rising to temperatures high enough to produce a plasma, so that multiple ionization and even X-rays are observed. [6] High power densities in solids and liquids have produced many so-called non-linear effects such as frequency doubling, multiple photon absorption, intensified Raman and Brillouin scattering, and self-focusing in certain media. Theoretical optics and optical physics have received new impetus from the rapidly developing field of laser technology. Quantum theory and the classical theory of the electromagnetic field meet in a bewildering variety of phenomena which has stimulated much interest among both theoreticians and experimental physicists.

In view of the above it is not surprising to learn that the effects and applications of laser radiation are being studied throughout the industrial complex of the country, in the military establishments, and in the universities and research institutions, both private and public. Range finding, memory devices for computers, holography, communications, weapons, light coagulation of the eye, and welding devices are some of the many applications being developed. The escalation in laser research has produced a growing radiation hazard which demands the best efforts available for radiation protection. Many health physicists in industrial, governmental, and university positions are being "saddled" with this new responsibility in radiation

protection, and there is a growing clamor from industrial and governmental agencies for an organized effort to establish safety criteria for this "new-yet-old" type of radiation. As yet, no specific agency or society or group has stepped forward to assume responsibility, though there are several movements afoot to cope with the problem.

PHYSICAL ASPECTS OF LASER ACTION

A brief and rudimentary description of the physics of laser action is in order before discussing the radiation hazards. The ruby laser is chosen as typical and a former paper by the authors [7] will be used for this purpose.

The primary element of a ruby laser consists of a crystal of sapphire (Al_2O_3) doped with chromium ion (Cr^{3+}) usually to about 0.05% by weight, giving approximately 1.6×10^{19} chromium atoms per cm^3. Each ion in the sapphire crystal is bonded to 8 oxygen atoms. The energy levels of the chromium ion determine laser action, the sapphire serving only as a crystal matrix to fix the foreign ions. Ruby crystals are usually in the form of cylinders, varying in diameter from 0.25 to 0.625 in. and having lengths of from 3 to 6 in. It is essential that the ends of the ruby cylinder be parallel and optically flat to a high degree of precision. Most ruby crystals are cut with the optic axis at 60 or 90 degrees to the axis of the cylinder so that plane polarized light is emitted during laser action.

Irradiation of a ruby crystal with white light shows two strong absorption bands in the green and yellow portions of the spectrum. A characteristic feature of ruby is the large fluorescent quantum efficiency which is defined as the ratio of the number of fluorescent photons emitted to the number of exciting photons absorbed. Maiman found this to be 70% in ruby. This means that a large percentage of the photons absorbed in the green and yellow bands undergo a relatively fast radiationless transition to a metastable doublet state before having time to return to the ground state. This metastable doublet state has a half-life of approximately 3.5 msec before returning to the ground state with the spontaneous emission of two monochromatic lines at wavelengths of 694.3 and 692.9 nm respectively. This is why, of course, ruby exhibits its characteristic red color. Under ordinary conditions of irradiation with white light, the number of chromium atoms in the ground state greatly exceeds the number in the excited state. But by using an intense source of white light to optically "pump" chromium atoms into the excited state, Maiman was able to achieve a population inversion; that is, the number of chromium atoms in the excited state exceeded the number in the ground state, violating Boltzmann statistics and creating a so-called "negative temperature". The optical pump consisted of a xenon flash tube wound in the form of a helix with the ruby cylinder placed along the central axis of the helix. A highly reflecting sheath of polished aluminum surrounded the xenon helix. A condenser bank charged to a high voltage was discharged suddenly through the xenon flash tube, thereby irradiating or pumping the ruby crystal with an intense source of white light.

Under normal conditions the number of photons/cm^2/sec of wavelength 694.3 nm incident normally on an end face of the ruby cylinder would exceed the number of photons/cm^2/sec leaving the opposite end face by an amount determined by the linear absorption coefficient for the ruby wavelength according to the well known law of Beer. However, under the conditions of population inversion, the absorption coefficient changes sign. This means that the number of photons/cm^2/sec leaving an exit face exceeds the flux entering the opposite face of the ruby crystal, i.e. amplification by the stimulated emission of radiation has taken place. Photons of the proper wavelength, 694.3 nm, stimulate the excited atoms of chromium to return to the ground state with the emission of additional photons. Moreover, the stimulated photons are in phase with the photons producing the stimulation as would be predicted from the classical theory of dipole radiation.

High fluorescent quantum efficiency and broad band absorption are necessary conditions in any solid state substance before amplification by stimulated emission of radiation can take place. However, something more is needed before laser action can be attained. Some method must be devised for increasing the effective path length of the stimulating photons in the crystal. Photons which by chance are emitted parallel to the crystal axis will be reflected back

normally into the crystal, while those inclined at an appreciable angle to the crystal axis will escape. Thus, an avalanche of highly directional and phase coherent photons is built up suddenly. If one of the reflectors is partially transparent, an intense beam of parallel light which is plane polarized, coherent in time and space, and monochromatic is emitted. By placing an optical shutter between the ruby rod and one of the reflectors, Q-spoiling can be accomplished. The shutter is closed normally when the pumping light irradiates the ruby rod. After a time of the order of a few hundred microseconds, a sufficient number of excited chromium atoms have been accumulated to accomplish population inversion but laser action is withheld because the light path to the reflector is blocked. If now, this light block is removed suddenly, a giant pulse of radiation is emitted. This is the principle of the so-called Q-switch. The shutter employed by McClung and Hellwarth was an electro-optical Kerr cell, but rotating mirrors and substances which lose their opaqueness when irradiated have also been employed successfully to produce Q-switched pulses lasting for only a few nanoseconds. Another and equally valid way of presenting laser action is to consider the laser rod with its highly reflecting mirrors as a high Q cavity which can oscillate in any one or several of a number of modes appropriate to the frequency to which the cavity is tuned. The higher the Q, the less the pumping energy needed to attain laser action. Light waves traveling along the axis of the crystal and bouncing back and forth through an amplifying medium between the mirrors set up a coherent standing wave of light. Waves traveling off normal soon miss the mirrors and are lost. In essence, this is a "Fabry-Perot" type of structure which serves as a resonant cavity for oscillations. Obviously, in Q-switching, the cavity Q is raised suddenly to a very high value, thereby allowing a giant pulse to be emitted from the system.

The rudimentary principles of pulsed laser action as elucidated above are appropriate to all pulsed laser systems. Normal pulsed laser action produces multiple spikes in which the overall duration of the pulse may extend from a few hundred microseconds to several milliseconds, depending upon the system involved. Q-spoiling generally produces single spikes or pulses lasting from 5 to 100 nsecs. Neodymium-doped glass lasers and ruby lasers are the two solid state systems most prevalent among the pulsed systems. Their wavelengths, 1060 nm and 694.3 nm respectively, together with their frequency doubling wavelengths, 530 nm and 347 nm, constitute the principal hazards from pulsed laser systems at the present time. Among the CW systems which constitute a hazard are the gas lasers, CO_2 at 10.6 microns, He-NE 632.8 nm, and the argon laser at several wavelengths in the region of 480–500 nm. All of these sources are capable of emitting electromagnetic radiations which are hazardous to man.

THE RADIATION HAZARD

Since the mammalian eye is acknowledged to be the most sensitive organ to laser radiation, this discussion will be confined to ocular hazards. This is permissible since it is highly unlikely that other types of deleterious effects can take place at distances and at laser intensities where ocular effects are negligible. Verhoeff and Bell[8] in a classic paper published in 1916 demonstrated that the pathological effects of radiant energy on the eye could be explained in terms of thermal injury resulting from the absorption of radiation in the pigment epithelium (PE) and in the choroid. In considering the ocular hazards from lasers it is fortunate that a large body of knowledge on retinal burns has been accumulated over the past two decades. Some of the data most pertinent to laser hazards has been collected in recent publications by the authors.[9]

Solon, Aronson, and Gould[10] have discussed the physical principles of image formation by the human eye when exposed to laser beams in the near and the far field. Laser sources emit highly directional beams of radiation with angular divergences ranging from fractions of a milliradian to about 10 mrad. For nearfield illumination the entire cone of radiation may enter the eye depending on the beam diameter relative to the diameter of the pupil. Under these conditions the diameter of the image focussed on the retina will be given by the product of the angle of divergence and the equivalent focal length of the human eye, usually taken as

17 mm. For angles of divergence exceeding 1 mrad the image diameter may exceed the minimum size as determined by diffraction in the human eye. There is no general agreement among authorities as to what constitutes the diffraction limited size of the image on the human retina but most estimates place it as being between 10 and 20 microns. In the far field from a laser source the cone of radiation illuminates the entire eye with almost parallel light, resulting in a diffraction limited image on the retina (10–20 microns). Thus, unless optical instrumentation is employed laser beams produce small images on the retina, varying from perhaps 170 microns to 10 or 20 microns in diameter. For purposes of comparison the image of the sun on the human retina is approximately 160 microns.

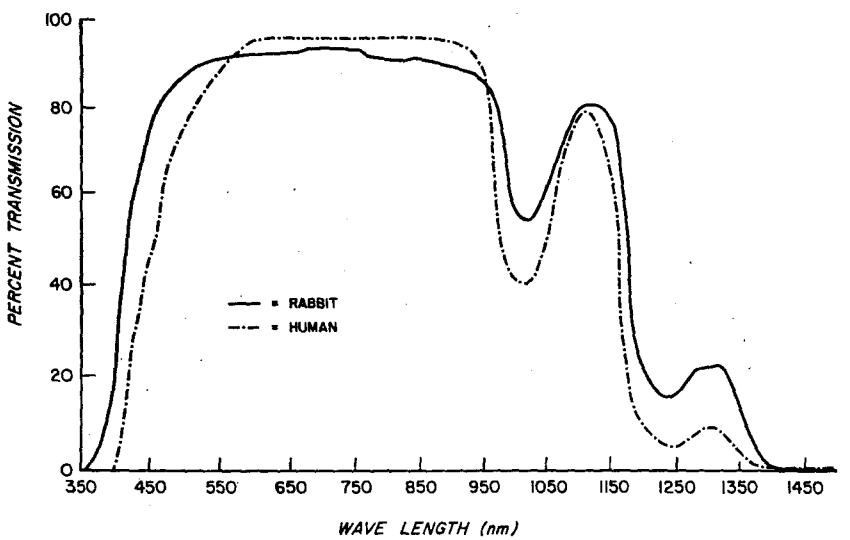

FIG. 1. Percent transmission through the ocular media vs. wavelength for light of uniform intensity incident on the cornea; comparison between man and rabbit.

Transmission of light through the ocular media (OM) of the human and rabbit eye has been measured by the authors[11] and is illustrated in Fig. 1; it extends from approximately 350 nm to 1450 nm, exceeding 0.80 in the range 500–950 nm. There are two peaks in the near IR, a large one at 1100 nm and a much smaller one (0.10) at 1300 nm. As might be expected the transmission through the human OM is similar to that of water. Wavelengths shorter than 400 nm are absorbed primarily in the outer layers of the cornea producing an acute inflammation similar to snowblindness. Thus, laser sources producing radiation beams in the UV will produce corneal damage rather than retinal damage. Wavelengths beyond 1400 nm do not penetrate the OM to produce retinal images. The CO^2 laser which produces a strong beam of CW radiation at 10.6 microns would be dangerous to the cornea since the half-value layer in water for this wavelength is about 10 microns. In the far infrared the hazard becomes that which has been observed for microwaves, usually heat damage to the proteins of the crystalline lens resulting in a type of cataract commonly designated as infrared cataract. In the range of wavelengths 350–1450 nm the human eye can focus an image on the retina. The hazard here is thermal injury or retinal burns for CW lasers producing enough power to raise the temperature of the retina to levels above ambient where denaturation of proteins can occur. Some proteins are damaged irreversibly at temperatures as low as 45°C if

maintained at this temperature for considerable periods of time. Time-temperature history must be considered in any evaluation of thermal injury to biological substances. The authors have shown that an irradiance of 6 W/cm^2 on the rabbit retina for a period of 3 min produced a mild retinal burn which appeared first at the center of the retinal spot which was about 800 microns in diameter. It is estimated from theoretical calculations that the temperature of the retinal tissues was maintained at approximately 17°C above ambient during the exposure. The source of radiation was a high pressure xenon lamp producing white light. Wavelengths beyond 900 nm were removed by a filter. Considerations of heat conduction indicate that the temperature attained at equilibrium and the time taken to reach equilibrium temperature are strong functions of the image size. The smaller the image size the lower the equilibrium temperature and the shorter the time taken to attain it. Equilibrium is reached in a matter of milliseconds. Thus, the small images produced by CW lasers having small angular divergences should withstand irradiances well above 6 W/cm^2 before attaining temperatures comparable to those produced on the retina by the xenon lamp. On the other hand, 17°C above ambient is certainly too high a temperature for sensitive retinal tissue. It is recommended that CW retinal irradiances be kept well below 1 W/cm^2 regardless of image size until more definitive data are available. The safety criteria for exposure to CW lasers in the spectral range 350–1450 nm should be based ideally on retinal irradiances which produce equilibrium temperatures which will not cause irreversible damage to retinal tissues, even over long periods of time. Such temperatures may be only a few °C above ambient.

A major portion of the radiation impinging on the retina is absorbed in the PE and the choroid. The authors have investigated absorption vs. wavelength in these elements for 24 human eyes.[11] In Fig. 2 it can be seen that maximum and minimum absorption in the PE at the ruby wavelength (694.3 nm) is 0.40 and 0.15 respectively; for neodymium doped glass at wavelength 1060 nm the coefficients are 0.15 and 0.05 respectively. Peak absorption in the PE for light incident on the cornea occurs between 500–550 nm. The first harmonic for neodymium doped glass at 530 nm and the green lines in the argon CW laser are in the region of maximum absorption by the PE. Actually, for light incident on the cornea, the absorption in the PE and in the choroid is approximately equal for the 24 eyes studied. However, the PE is roughly 10 microns in thickness, whereas the choroid is about 100–150 microns in thickness. Therefore, the energy absorbed per unit volume (joules/cm^3) in the PE will exceed that in the choroid by a large factor. It is not surprising, under these circumstances, to learn that for mild lesions of the retina produced by laser pulses of relatively short time duration (0.2 msec–2.0 msec) damage is observed histologically to occur in the PE and in the strata of the retina immediately adjacent to the PE rather than in the choroid.

The authors have investigated the production of mild lesions in the rabbit retina by pulsed ruby lasers, both in the multiple spiked mode involving exposure times of 10, 50, 100 and 200 μsecs and in the Q-switched mode, exposure time 30 nsecs. Fig. 3 is a schematic diagram of the optical system used to produce these lesions and Fig. 4 illustrates the modified ophthalmoscope used in conjunction with the system. Mild lesions are defined as being just visible ophthalmoscopically within 5 min after exposure. These lesions are not considered to be threshold burns since irreversible damage has been demonstrated at lower levels of irradiance by more refined techniques such as histochemistry, electroretinography, and electron microscopy. Figure 5 is a log–log plot of watts/cm^2 vs. exposure time in seconds for minimal lesions of 800 microns diameter in the rabbit retina. Irradiances in the range 2–3 kw/cm^2 for exposure times of 200–300 μsec produce very mild lesions on the rabbit retina. The lesions are thermal in nature and correspond rather closely to those produced by a white light source. The irradiance required to produce these lesions is reasonably independent of image size. No damage has been detected in the rabbit retina when these irradiances are reduced by a factor of two.

In the Q-switched mode, irradiances of from 3–5 MW/cm^2 delivered in 30 nsec produce mild lesions as defined above. These lesions

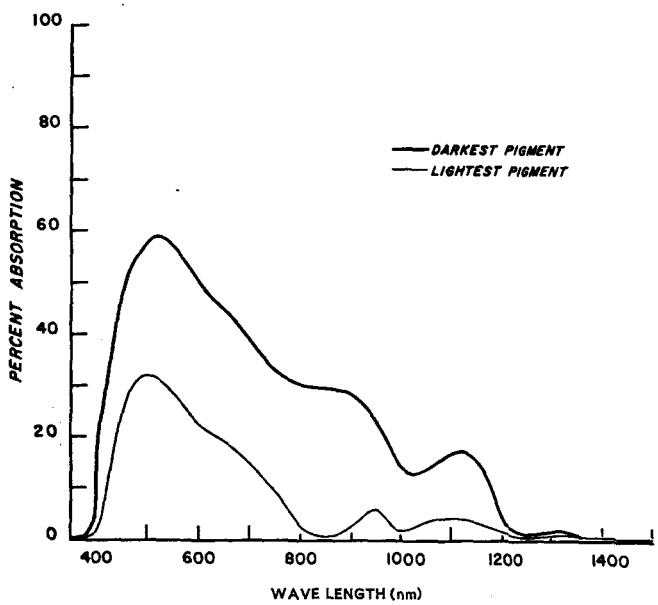

FIG. 2. Graph of percent absorption in human pigment epithelium vs. wavelength for light of uniform intensity incident on the cornea; plots are for the lightest and darkest pigmented eyes studied.

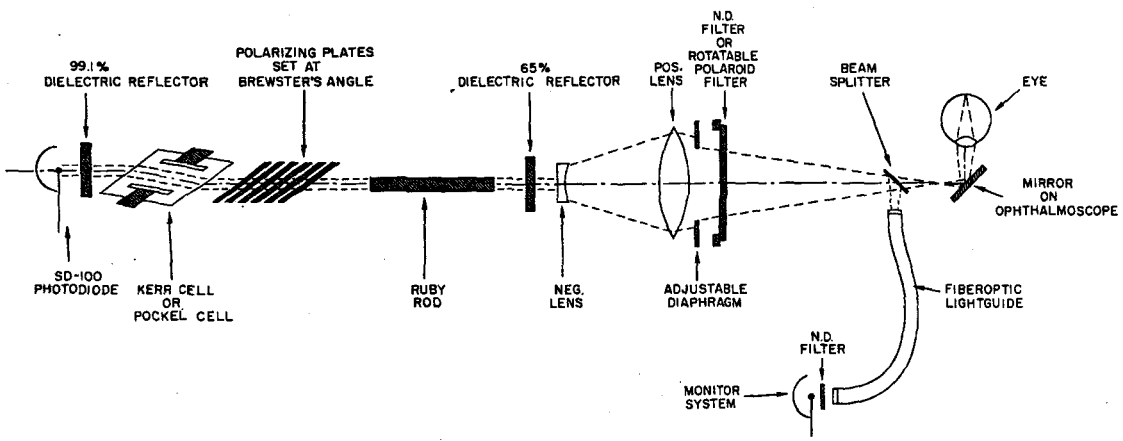

FIG. 3. Schematic diagram of laser optical system used to produce experimental lesions in the rabbit eye.

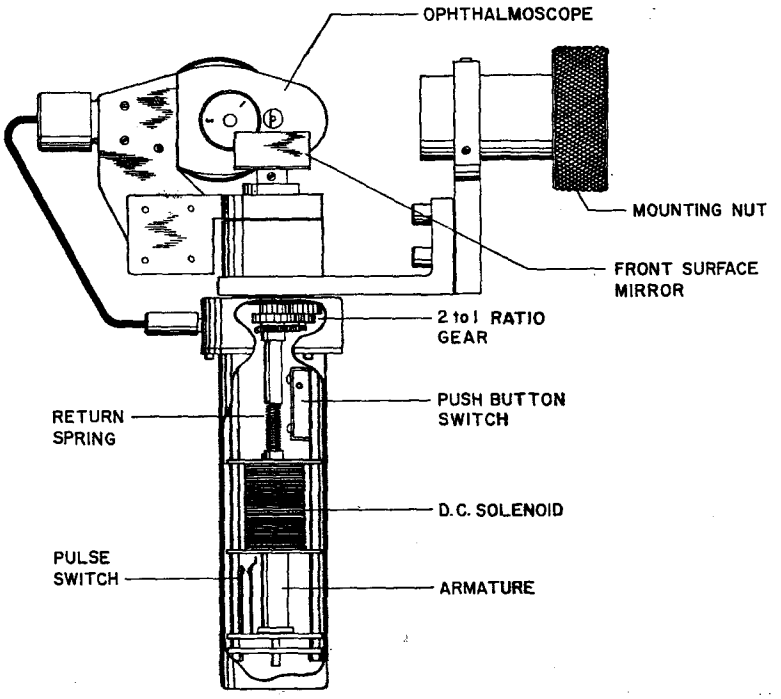

FIG. 4. Schematic drawing of modified ophthalmoscope used in conjunction with the laser optical system for producing and observing lesions in the experimental animal eye.

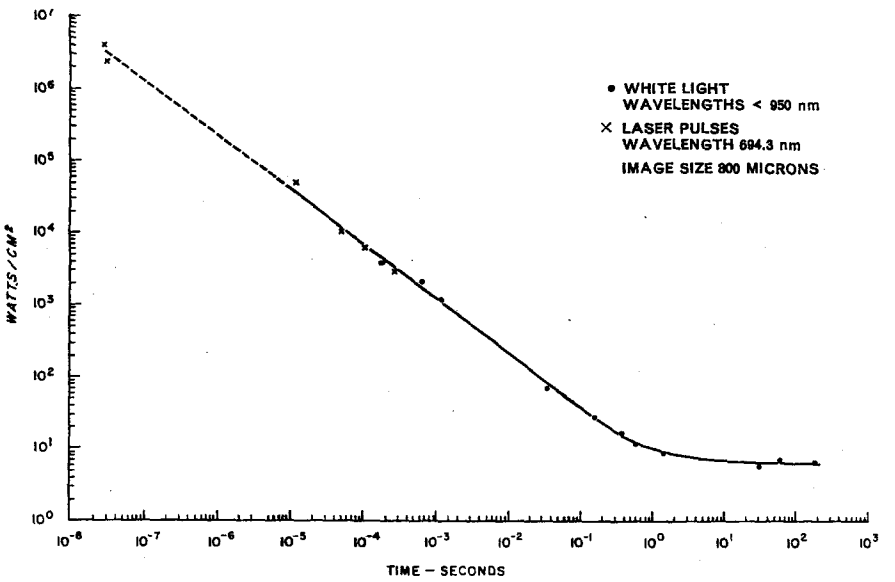

FIG. 5. Log–log plot of watts/cm² vs. time in seconds for minimal lesions observed within 5 min after exposure; image diameter, 800 microns. The data include both white light (wavelength <850 nm) and ruby laser exposures.

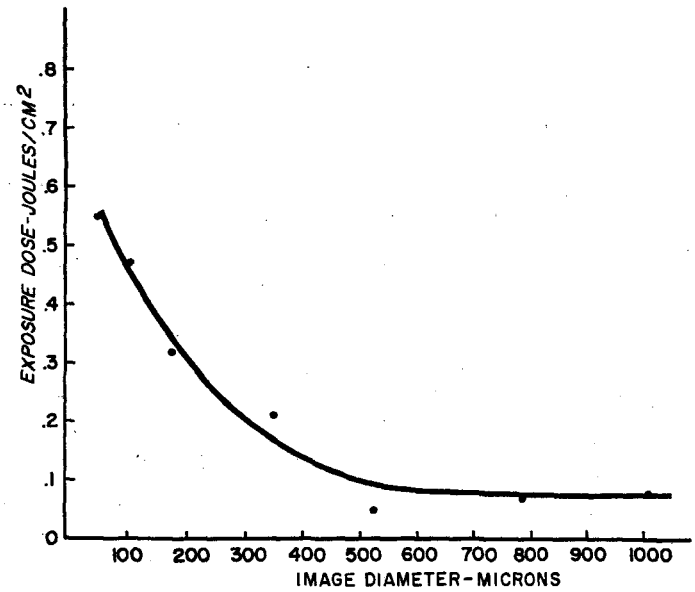

FIG. 6. Exposure dose. J/cm² vs. image diameter, microns, for minimal lesions observed with the ophthalmoscope immediately after exposure to 30 nsec Q-switched ruby laser.

may not be entirely similar to those produced at lower power densities. There is the possibility that non-linear effects may play a role in producing these lesions and the authors are unwilling to call them thermal burns until further investigations have been made. In addition to the Q-switched data shown in Fig. 5 for lesions of 800 microns diameter, the authors have investigated the energy density needed to produce minimal lesions at much smaller image diameters. Figure 6 is a graph of energy density in joules/cm² vs. image diameter in microns for minimal lesions in the rabbit retina as produced by the Q-switched ruby laser. These data, in fair agreement with recent findings by Tengroth and Bergqvist,[12] seem to indicate that larger energy densities are needed to produce minimal damage as the image diameter is reduced. However, both the authors and Tengroth *et al.* are inclined to believe that this may be an artifact resulting from the difficulty of observing damage at the smaller image sizes. When irradiances are raised to 25–50 MW/cm², material is extruded into the vitreous, hemorrhaging occurs, and there is evidence to suggest that shock waves may be partially responsible for the damage.

CURRENT STATUS OF RADIATION PROTECTION FROM LASERS

The purpose of the above outline of ocular damage is to illustrate that data are available to make an intelligent estimate of safe exposure levels to laser radiation under various conditions of operation. The question arises naturally as to what can be done to protect the public from the hazards of laser radiation and who should propose these measures and see that they are enforced. The answer to the first question is relatively simple. Protective devices and certain operational procedures are known and practiced by many reputable firms and organizations. For example, goggles specifically designed to protect against laser radiation are manufactured by several optical companies in America and in Europe.[13] Several designs

for a protective symbol against lasers have been proposed.

In answer to the second question, no single group, society, agency or organization has stepped forth as yet to establish basic criteria for radiation protection and permissible levels of exposure to laser radiation. This is not because the large and growing group of scientists, military personnel, and technicians involved in laser research and development are unaware of the hazards involved or because they wish to be left alone to cope with their own problems. On the contrary there is a genuine concern about radiation protection from lasers. Many health physicists, often without adequate background or information, have been saddled with company or organizational responsibility for laser safety. In recent months the Martin Marietta Corporation has developed a "laser hazard" slide rule and published a company brochure on "Determination of Laser Hazards".[14] This is typical of the concern over laser hazards in American industry. Several companies have established their own rules and procedures for laser safety. The Hughes Aircraft Company has published a report on laser eye damage levels.[15] Quite recently, a draft of guidelines for safe operation of laser systems was prepared by the Commission on Environmental Hygiene of the U.S. Armed Forces Epidemiological Board.[16] A conference on laser safety was held in May 1966 in Orlando, Florida. More than 150 participants from all over the United States attended this conference. The proceedings were published in 1966 by the Martin Company, Orlando Division.[17] The National Academy of Sciences National Research Council has formed a laser committee to consider the hazards of laser radiation. This committee reported informally on its findings at the second Gordon Conference on lasers in medicine and biology, held at Andover, N.H., in July 1966. Symposia on the biological effects of laser radiation have been held by the Optical Society of America[18] and by the Armed Forces Institute of Pathology.[19] A safety group on optical masers has been organized by interested groups in the Department of Defense and in university circles. The NCRP has been approached informally as to what its attitude might be regarding radiation protection from lasers.

Despite the efforts listed above no centralized agency comparable to IRPA or its member societies has volunteered to establish safety criteria and permissible levels of exposure to laser radiation. Whether IRPA and its member societies should attempt to amalgamate current efforts into a responsible organization with official status comparable to that enjoyed by the NCRP, the ICRP, and the American Board of Health Physics is a question which should be presented to this first International Congress on Radiation Protection.

REFERENCES

1. J. P. Gordon, H. J. Zeiger and C. H. Townes. *Phys. Rev.* **95,** 282 (1954).
2. A. L. Schawlow and C. H. Townes. *Phys. Rev.* **112,** 1940 (1958).
3. T. H. Maiman. *Nature* **187,** 493 (1959).
4. A. Javan, W. R. Bennett and D. R. Herriott. *Phys. Rev. Letters* **66,** 106 (1961).
5. F. J. McClung and R. W. Hellwarth. *Proc. I.E.E.E.* **51,** 46 (1963).
6. C. S. Naiman, J. Schwartz, M. Y. DeWolf and I. Goldblatt. Abs., 7A-6, 1966 International Quantum Electronics Conference, Phoenix, Arizona (April 12–15, 1966).
7. W. T. Ham, Jr., R. C. Williams, W. J. Geeraets, R. S. Ruffin and H. A. Mueller. *Acta Ophthalmologica,* Suppl. **76,** 60 (1963).
8. F. H. Verhoeff and L. Bell. *Proc. Am. Acad. Arts & Sci.* **51,** 630 (1916).
9. Reference 7 and W. T. Ham, Jr., R. C. Williams, H. A. Mueller, D. Guerry, A. M. Clarke and W. J. Geeraets, *Trans. N.Y. Acad. Sci.,* Feb. 1966.
10. L. R. Solon, R. Aronson and G. Gould. *Science* **134,** 1506 (1961).
11. W. J. Geeraets, R. C. Williams, G. Chan, W. T. Ham, Jr., D. Guerry, III, and F. H. Schmidt. *A.M.A. Arch Ophth.* **64,** 606–615 (1960). Also: ibid. *Invest. Ophth.* **1,** 340–347 (1962).
12. Bergqvist, Tore, Kleman, Bengt and Tengroth, Bjorn. Retinal Lesions Produced by Q-switched Lasers. Personal communication to the authors; submitted for publication to *Acta Ophthalmologica.*
13. J. C. Kaufman. *Microwaves.* April 1966, pp. 38–45.
14. G. W. Flint. Martin Marietta Corp., OR 8336 (May 1966).
15. T. Lubensky. Ref: 2720. 01/02, Hughes Aircraft Co. (August 1965).

16. W. E. FROEMMING. Personal communication to the authors. Guidelines for Safe Operation of Laser Systems (June 1966).
17. *Proceedings of the First Conference on Laser Safety*, sponsored by Martin Company, in cooperation with the U.S. Army, Surgeon General's Office, Orlando, Florida, 19–20 May 1966.
18. Symposium on Physiological Effects and Hazards of Laser Radiation, J.O.S.A. 1964 Spring Meeting Program, WI1–WI16, 1 April 1964, Washington, D.C.
19. *Federation Proceedings* **24,** No. 1, Part III, Suppl. No. 14, Jan.–Feb. 1965.

DISCUSSION

J. E. McLaughlin (*U.S.A.*):

I notice your proton spectra fall rapidly with energy and were quite smooth. Could you comment on:

1. The effect of local radiations from the space vehicle on these results.

2. The effect of energy resolution of the spectrometer on the spectra.

M. C. Chapman:

The proton spectral data were taken using phaswich scintillation detectors. These detectors use CsI as the energy detector, and plastic scintillators as a guard counter. Thus all spacecraft-produced protons are rejected by the guard counter. Four channel analysis, with 12% energy resolution, is performed on all acceptable events.

The smooth spectral shape is consistent with data obtained by other experimenters, and is consistent with our three or four energy determinations.

R. E. Simpson (*U.S.A.*):

Have you made comparative measurements between your scintillator (plastic) and an LET proportional counter? If so, what kind of agreement?

M. C. Chapman:

Concerning the comparison of Rossi-type ion chambers and the scintillator dosimeter, tests of this type are planned and will be accomplished shortly. Results should begin to be available in a month or several weeks.

D. Nachtigall (*Euratom*):

In den Wänden von gewebeäquivalenten Ionisationskammern ist normalerweise O durch C ersetzt. Wie weit sind die Wirkungsquerschnitte hochenergetischer Partikel für O und C bekannt, so dass man sagen kann, dass diese Kammern auch im hochenergetischen Bereich tatsächlich gewebeäquivalent sind?

Die Rückstossprotonen, die von Neutronen mit Energien kleiner als 20 keV in gewebeäquivalenten Kammern ausgelöst werden, ionisieren nicht mehr und werden deshalb nicht mehr nachgewiesen. Wie gross schätzen Sie den Fehler ein, der dadurch bei den gegebenen Spektren entsteht?

F. E. Holly:

We use two separate types of ion chambers, both constructed of shonka tissue-equivalent plastic and the types, mixtures, and proportions of gases varies depending upon the purpose. A report exists, which I can give you, describing their use, calibration, and tissue equivalency. About the neutron sensitivity and the error estimate, we have both neutron and neutron-insensitive chambers. These are described in the paper previously referred to.

C. A. Adams (*U.K.*):

Dr. Vogt's emphasis on hazards did not appear to correspond with their order of importance in the releases which could occur from nuclear reactors. In general our analysis shows that inhalation is the dominating hazard. In particular I understood him to say that ^{131}I could give an ingestion risk greater than the inhalation risk. This would be understandable if there were an area of crops, with no individual present on the land or its neighbourhood. However, if an individual is present I should like to know the circumstances in which deposition could give a risk to him greater than that to which he would be subjected by inhalation of the cloud. Could Dr. Vogt give an example of the circumstances he had in mind?

J. K. Vogt (*Germany*):

Bei der Freisetzung von ^{131}I kann tatsächlich die Strahlenbelastung durch Ingestion die Inhalationsbelastung erheblich überwiegen, wenn es zu Ablagerungen aus der radioaktiven Wolke über landwirtschaftlich genutzten Flächen und damit zu einer Kontamination der Nahrungskette kommt. Im Einzelfall hängt die Gefährdung durch Ingestion natürlich von den Ernährungsgewohnheiten ab. Bei einem Milchkonsum von 1 Liter pro Tag kann die Ingestionsbelastung durch ^{131}I zwei bis drei Zehnerpotenzen über der Inhalationsbelastung liegen, wenn der gesamte Bedarf an Milch und Milchprodukten aus dem Aufkommen gedeckt wird, das auf kontaminierten Weideflächen erzeugt wurde.

B. W. Emmerson (*U.K.*):

Under actual accident conditions I consider that the nomograms presented by the speaker would

require considerable time in estimating the actual hazard from the release plume. Has any attempt been made to produce simplified nomograms in terms of the two major release hazards, namely, inhalation and deposition. At Bradwell nuclear power station we have produced simple nomograms on which the minimum evacuation time for various levels of airborne activity, and the degree and types of agricultural foodstuff banning for given levels of deposited activity, can be read directly from two main nomogram charts.

K. J. VOGT (*Germany*):

Ausser den hier anhand von Beispielen gezeigten allgemeinen Unterlagen für die Abschätzung der Umgebungsbeeinflussung bei Freisetzung radioaktiver Abluft haben wir für einzelne Emittenten wie die Reaktoren spezielle Unfallanalysen erarbeitet. Dabei wurden für bestimmte hypothetische Unfälle in Karten die Bereiche eingetragen, in denen die äussere Bestrahlungsdosis und die durch Inhalation und Ingestion von ^{131}I sich ergebende Schilddrüsendosis für Erwachsen bzw. Kinder die zulässigen Unfallbelastungen überschreiten können, so dass Evakuierungen und Lebensmittelrestriktionen erwogen werden müssen. Die zur Verfügung stehenden Aktionszeiten können aus Kurven abgelesen werden.

A. P. HULL (*U.S.A.*):

This sort of analysis is quite commendable and useful for hazards analysis, but I wonder if this degree of sophistication is applicable to the accident situation in which one seldom has a very accurate estimate of either source term or of prevailing meteorology.

K. J. VOGT (*Germany*):

In aktuellen Unfallsituationen wird es tatsächlich oft schwierig sein, einigermassen sichere Angaben über die Quellstärke zu erhalten. Dagegen entstehen bei der Bestimmung der meteorologischen Bedingungen keine Probleme, wenn die Anlage über eine meteorologische Beobachtungsstation verfügt. In der Kernforschungsanlage Jülich werden die für die Bestimmung der Diffusionskategorie erforderlichen Beobachtungen des Temperaturgradienten und des Windgeschwindigkeitsprofils, sowie der Windrichtungsschwankungen und der Strahlungsbilanz an einem 120 m hohen Turm durchgeführt.

E. W. JACKSON (*U.K.*):

I am a little doubtful about the policy of including data on downwind concentrations following the release of a radioactive cloud. In my view the data obtained by calculating on the basis of a release at ground level should suffice in practice. If the release in fact occurred above ground level the information obtained in this way would be pessimistic which would perhaps not be a disadvantage.

G. COWPER (*Canada*):

Would Prof. Ham tell us what has been the incidence of permanent or temporary damage from lasers?

W. T. HAM:

I cannot give any real statistics on injury today from lasers, but I can assure you that at least in the United States there has been a considerable amount of damage in this field. As you can well understand the various companies which are doing the laser radiation and making applications from laser research have had accidents on numerous occasions, but these involve legal matters and do not often see the light.

Dr. Milton Zaret, an ophthalmologist in New York City, is a consultant to many of these companies and Dr. Zaret has come in contact with a good many cases of damage due to laser radiation. I cannot give you any exact figures as to how great this hazard is at the present time, but damage which is caused is of course permanent; the type of damage I am speaking about is an irreversible damage to the retina and does not heal. Does this answer your question?

RADIATION PROTECTION REQUIREMENTS FOR FABRICATING RECYCLED PLUTONIUM REACTOR FUEL*

T. A. STEELE, A. B. SHUCK and P. K. DOHERTY†
Argonne National Laboratory,
Argonne, Illinois

Abstract—A computer program was developed that calculated the dose rates from plutonium as a function of source weight, geometry, isotopic composition, age, and shielding composition and thickness. Dose rates from plutonium sources were measured and compared with the calculated values. Personnel radiation exposures were monitored during the fabrication of fuel elements containing varying isotopic compositions of plutonium. The information derived from the calculations, radiation measurements, and radiation exposures were applied to glovebox procedures for the fabrication of reactivity coefficient fuel elements. Radiation protection criteria for the fabrication of recycled plutonium are discussed.

INTRODUCTION

Plutonium is fabricated into fuel elements and specimens for reactor research at the Argonne National Laboratory Plutonium Fuel Fabrication Facility. This facility was constructed in the late 1950's to meet Argonne's requirements for plutonium to be used in experimental reactors. Maximum fabrication flexibility, the safety of operating personnel, and the protection of the surrounding environment were concerns of prime importance.

The probability of operating personnel sustaining internal radiation exposures from plutonium at the facility was minimized by enclosing all of the process equipment in a leak-proof helium atmosphere, glovebox system,[1, 2] as illustrated in Fig. 1. To date, this system has proved effective in preventing any significant internal insult of plutonium to workers at the facility. It also has prevented any significant release of plutonium to the environment.

Commercial utilization of plutonium in power reactor fuel cycles depends on a developed capability to safely and economically process, fabricate, and use fuel elements that contain large proportions of ^{238}Pu, ^{240}Pu, ^{241}Pu, and ^{242}Pu. X, gamma, and neutron radiations from these isotopes and their daughter products, particularly ^{241}Am and ^{237}U, present an external radiation hazard during fabrication. Early plutonium contained less than 10 w/o of these isotopes, but recycled power reactor plutonium will contain 20 to 60 w/o of them.

The external radiation hazard to personnel fabricating recycled plutonium in a glovebox was evaluated by the following three steps. A computer program was developed to calculate dose rates from typical isotopic mixtures of plutonium. Details of the sources and shields encountered in a fuel plate fabrication process were formulated and dose rates were calculated. Next, dose rate calculations were checked by measurements of X, gamma, and neutron radiations from sources of known isotopic composition and age. Finally, the dose rates found from the calculations and radiation measurements were used to establish fuel plate fabrication procedures. Personnel radiation exposures were examined, and radiation protection considerations for recycle plutonium fuel plate fabrication were made.

DEVELOPMENT OF A COMPUTER PROGRAM

A computer program was developed for the calculation of neutron and gamma ray dose rates encountered in the fabrication of plutonium

* Work performed under the auspices of the United States Atomic Energy Commission.

† AMU-ANL Summer Engineering Practice School Student from Purdue University, Lafayette, Indiana.

reactor fuel inside a glovebox system. Surface and shielded dose rates were calculated as a function of the weight, geometry, and isotopic composition of the source, the composition and thickness of the shielding, and the elapsed time after chemical purification of the plutonium.

The program first calculated source strengths using the Bateman equations,[3] standard decay formulae, gamma-ray energy and yield data,[4] and spontaneous fission data.[5]

The source geometry was considered next. Typical sources encountered in the fabrication process were represented by a spherical or disc shape. For each model, the dimensions of the source were calculated from weight and density of the plutonium or plutonium alloy. The distance from the source to the dose point was varied.

Next, the self-shielding factors, which allow for self-absorption of X- and gamma rays by the source, were computed for the source material.[6] Attenuation of the X and gamma flux by the shield material was calculated using expressions derived by Rockwell.[7] The X- and gamma-ray attenuations were found for 14 representative gamma-ray energies. Attenuation coefficients were taken from the data of Grodstein and Storm *et al.*[8,9] Plane monodirectional and isotropic point source build-up factors, which account for scattered gamma rays, were used for the disc and spherical sources. Build-up factors for each energy were fitted to the form

$$B = 1 + \alpha \mu t \tag{1}$$

All of the build-up factor data were taken from Goldstein and Wilkins' work.[10]

FIG. 1. A view of the ANL fuel fabrication facility glovebox system.

The surface X- or gamma-ray dose rate, D, from a disc source was derived via

$$D = \frac{SB_1F_{s_2}}{A_2C} \tag{2}$$

where S = X- and gamma-ray source strength, photons/sec,
$B_1 = \frac{1}{2}$ surface area of disc source excluding edges,
F_{s_2} = source build-up factor,
A_2 = self-shielding factor,
C = conversion of gamma-ray flux to dose rate.[7]

The dose rate for a disc source through attenuating media was derived via

$$D = \frac{SB_1B_2F_{s2}}{A_2C}\left[E_1(x) - E_1(x \sec\theta)\right] \quad (3)$$

where B_2 = shield build-up factor,

$$x = \sum_{i=1}^{n} \mu_i t_i, \text{ for } n \text{ shield layers,}$$

μ = attenuation coefficient,
t = thickness,

$$E_1(x) = \int_x^\infty \frac{e^{-t}}{t} dt$$

θ = angle formed by the center line of the source and a line from an elemental area of the source to the dose point.

Similar expressions are used for spherical sources. Dose rates were calculated for each of the fourteen energy groups and summed. The spontaneous fission rate was calculated using data from Steindler.[5]

The source strength of neutrons produced by the (α, n) reaction with the light elements such as aluminum was calculated from data given by Arnold.[12] Birchall suggests a factor of 1.5 for neutron multiplication in a 1 kg sphere of plutonium;[13] however, no factor was used in this calculation. Neutron intensity was assumed to be attenuated by distance alone. The total surface and distance attenuated neutron dose rate was computed using a quality factor of 10. The neutron and gamma dose rates at the surface and at a dose point were printed out for each source-shield configuration.

SHIELDING REFERENCE DATA

The composition and densities of the shielding materials had to be known before X- and gamma-ray attenuation coefficients could be determined.

The alpha phase density of plutonium, 19.86 g/cm³, was used. Type 304L stainless steel, composed of 69% Fe, 19% Cr, 10% Ni, 1.5% Mn and less than 1% Si, has a density of 7.92 g/cm³. Helium was assumed to be a pure gas at atmospheric pressure and room temperature and having a density of 2.32×10^{-4} g/cm³. The hoodline windows were composed of a material commercially designated CR-39. This material is chiefly allyl diglycol carbonate with a density of 1.31 g/cm³.[15] The neoprene used in the hoodline gloves has a density of 1.28 g/cm³.[14] Leaded gloves are specified in equivalent lead thickness. Lightly leaded gloves have a 0.1 mm equivalent lead thickness with a density of 1.52 g/cm³. Leaded glass has attenuation characteristics similar to tantalum and a density of 6.2 g/cm³.[16]

FABRICATION OF REACTIVITY COEFFICIENT ELEMENTS

Several hundred plate-type plutonium fuel elements are being fabricated at Argonne National Laboratory to determine the effects of increasing amounts of ^{240}Pu, ^{241}Pu, and ^{242}Pu on reactor kinetics.[17, 18] The elements required are of the type shown in Fig. 2. They consist of Pu-1.1 w/o Al alloy plates that are sealed in tight-fitting stainless steel jackets. The flow diagram of the process for manufacturing these fuel elements is shown by Fig. 3. The purified, highly irradiated plutonium is received in the form of reduction buttons that weigh

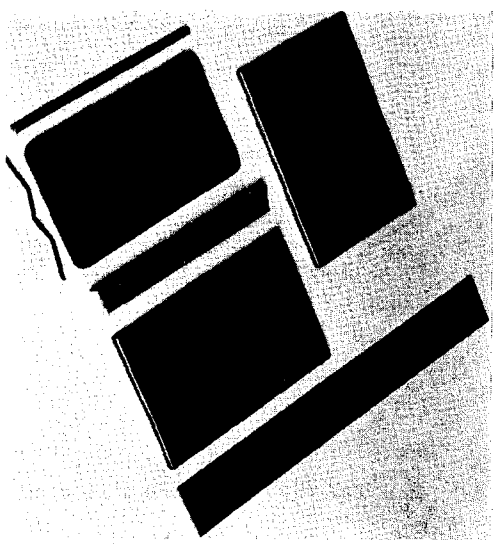

FIG. 2. Plutonium reactivity coefficient fuel element.

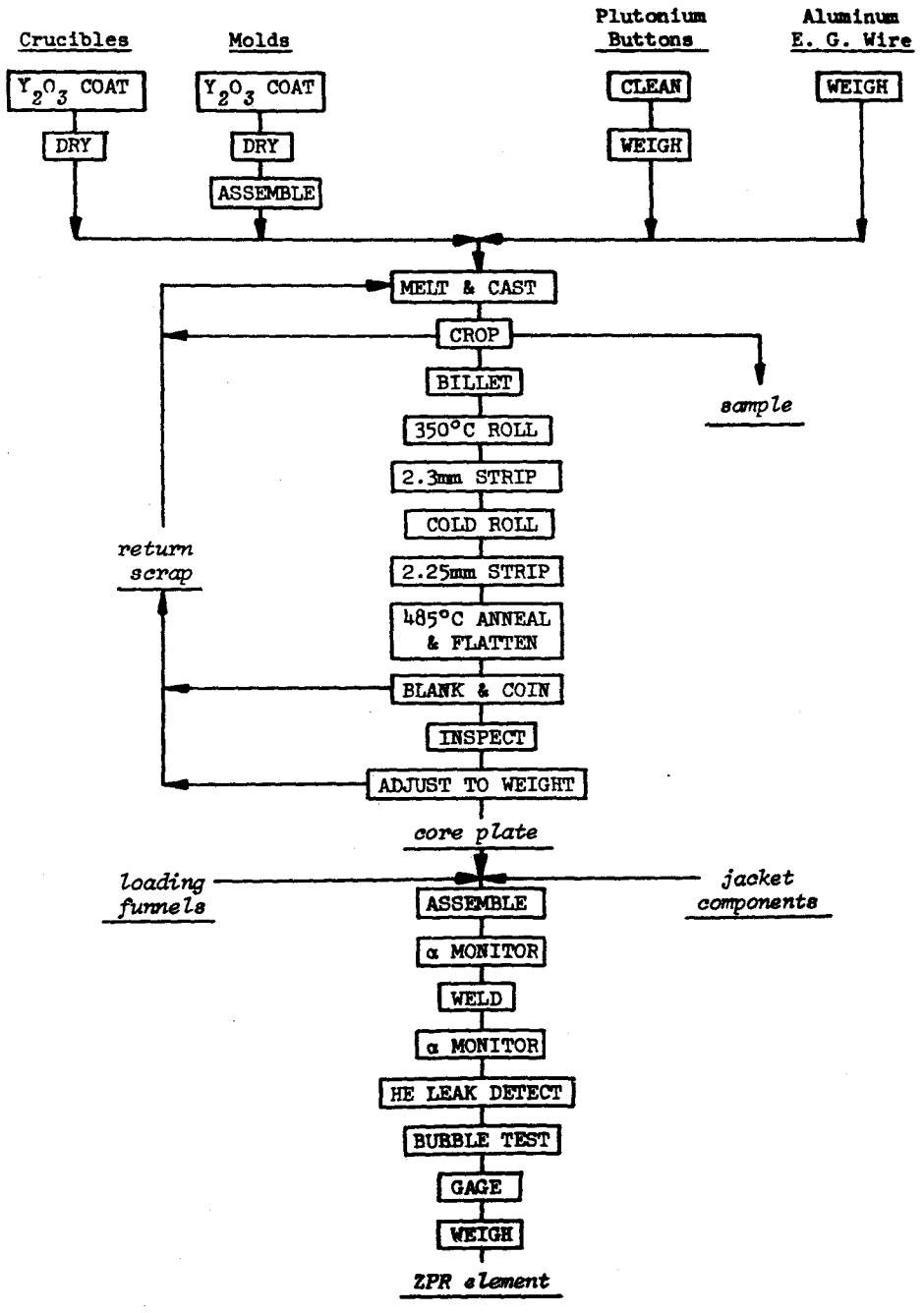

FIG. 3. Flow diagram of process for manufacturing reactivity coefficient elements.

about 2 kg each. The plates are fabricated in a helium atmosphere glovebox system, but without shielding other than that provided by the equipment.

The Pu-Al alloy is made in a vacuum induction furnace. Electrical-grade aluminum wire is placed in the bottom of an yttria-coated carbon crucible, and a broken plutonium button is placed on top of the wire. The charge is melted and heated to 950°C. It is bottom-poured into an yttria-coated carbon billet mold. After the casting cools, the furnace is opened and the billet is removed and carefully cleaned. The top is sawed off to produce a rolling billet that measures approximately 16 mm × 50 mm × 125 mm.

The billet is heated to 350°C and hot rolled from 16 mm to 2.30 mm thickness. Reductions are 15% per rolling pass between 125 mm diameter × 200 mm two-high rolls that are electrically heated to 250°C. The 2.30 mm strip is cold finished to 2.25 mm thickness. It then is annealed by heating to 485°C and flattened by pressing between steel flats.

Three sizes of core plates (measuring 2.25 mm × 45.0 mm × 23.9 mm, 2.25 mm × 45.0 mm × 49.3 mm, and 2.25 mm × 45.0 mm × 74.7 mm) are blanked and coined from strip by a combination die in a 200-tonne press. Coining pressures of 4 tonnes/cm² are used. The core plates are cleaned, adjusted to within ± 0.5 g of a nominal weight by punching holes in the plates, and inspected.

The inspected core plates are assembled in 0.3 mm thick stainless steel jackets. A spring in each jacket holds the core plate against one end. An aluminum foil funnel is used during loading of the core to protect the jacket lip from being contaminated by plutonium. The funnel is removed and the end plug is inserted. Welding is done by means of a tungsten-electrode d.c. arc process in copper chills that completely enclose the element except at the edges being joined. One-third to one-half of a standard atmosphere pressure of 85v/o He-15v/o A gas is used in the welding chamber to reduce the internal jacket pressure. The completed reactivity coefficient elements are monitored for alpha contamination, leak-detected, gaged, weighed, inspected, and packed for shipment to the reactor experimental groups.

Table 1 lists personnel exposure times associated with the fabrication of 2 kg of plutonium into reactivity coefficient elements.

EXPOSURE CONDITION CALCULATIONS

The dose rates to the extremities were considered both in contact with the source material and at varying distances. Dose rates to the whole body were considered at varying distances. Table 2 illustrates the source-shield configurations considered.

The dose rate for each of these cases was calculated for 3 months, 6 months, 1 year, 2 years, and 5 years after plutonium separation. Table 3 gives the plutonium compositions investigated.

Table 1. Exposure Times Associated with Fabrication Operations

Fabrication operation	Exposure time
Transfer plutonium from storage vault to glovebox system	5 min
Weigh plutonium	20 min
Break plutonium into pieces and weigh	30 min
Transfer to furnace glovebox	5 min
Alloy plutonium in furnace	15 min
Cast plutonium in graphite mold	15 min
Open mold and break off sprue	1 hr
Roll ingot into plates	6 hr
Cut and machine core plates	4 hr
Clean and weigh core plates	4 hr
Jacket and weld fuel element	2 hr
Inspect fuel element	1 hr

Table 2. Source Shield Configurations

Source	Source geometry	Shield
2.0 kg plutonium	Spherical	44.8 cm He, 0.95 cm CR-39
2.5 kg plutonium	Spherical	30.4 cm He, 0.076 cm neoprene
2.5 kg plutonium	Spherical	29.5 cm He, 0.95 cm 6.2 g/cm^3 lead glass
2.53 kg plutonium-1.25 w/o aluminum	Slab	44.8 cm He, 0.95 cm CR-39
2.53 kg plutonium-1.25 w/o aluminum	Slab	43.8 cm He, 0.95 cm CR-39, 0.95 cm 6.2 g/cm^3 lead glass
71.66 g plutonium-1.25 w/o aluminum	Slab	12.6 cm He, 0.076 cm neoprene
71.66 g plutonium-1.25 w/o aluminum	Slab	12.6 cm He, 0.076 cm lightly leaded glove
71.66 g plutonium-1.25 w/o aluminum	Slab	12.6 cm He, 0.076 cm neoprene, 0.03 cm 304L-SS
71.66 g plutonium-1.25 w/o aluminum	Slab	12.6 cm He, 0.076 cm lightly leaded glove, 0.03 cm 304L-SS

*Table 3. Plutonium Isotopic Compositions Studied**

Source	^{238}Pu	^{239}Pu	^{240}Pu	^{241}Pu	^{242}Pu
A	0.00001	95.01	4.51	0.47	0.01
B	0.0001	91.15	8.00	0.80	0.05
C	0.002	80.91	16.69	2.15	0.267
D	0.020	76.68	20.00	3.00	0.3
E	0.030	72.55	22.16	4.60	0.666
F	1.000	64.00	20.00	12.00	3.00
G	0.040	62.76	30.00	6.00	1.20
H	2.000	40.00	30.00	18.00	10.00
I	0.100	34.90	35.00	10.00	20.00
J	0.200	4.80	25.00	10.00	60.00
K	0.300	0.70	2.00	1.00	96.00

* All in weight %.

Sources D, E, F, G, and H are representative isotopic compositions of recycled plutonium fuel from power reactors. Sources having isotopic compositions I, J, and K represent specially separated material to be used for physics experiments in zero power reactors.

CALCULATED RESULTS

The computed slab surface dose rates from X- and gamma rays are illustrated in Fig. 4. The calculated neutron surface dose rates were less than 15% of the 3-month X- and gamma-ray dose rates, except for source composition K which was 22% of the 3-month dose rate.

Figure 4 shows that the surface X- and gamma-ray dose rates for plutonium more than 1 year old were primarily from the ^{241}Am and, therefore, a function of the ^{241}Pu content. Examples of calculated dose rates as a function of source geometry, weight, isotopic composition, age, source-to-dose-point distance, shielding material, and shielding thickness are illustrated in Figs. 5 through 8. Figure 5 gives the calculated total neutron and gamma dose rates at 30.5 cm through the hoodline window from a 2.5 kg plutonium sphere. The distance was established as an average exposure distance of the fabrication worker. The dose rates through the neoprene gloves from this source were nearly the same. Replacing the 0.95 cm CR-39 with 0.95 cm of 6.2 g/cm³ density leaded glass reduced the calculated 3-month dose rates by factors of 2.6 to 3.3 for isotopic compositions A, B, C, D, E, G, and I, factors of 8.5 and 9.4 for isotopic compositions F and H, and factors of 1.5 and 2.1 for isotopic compositions J and K. The important consideration in this calculation was that with the leaded glass there is no significant build-up in calculated dose rates with time after separation. The absence of build-up was due to the absorption of the low energy decay products by the leaded glass. Figures 6, 7, and 8 illustrate the dose rates to the hands from a single plutonium fuel plate under various shield configurations. Calculations indicate that no increased attenuation was gained with the use

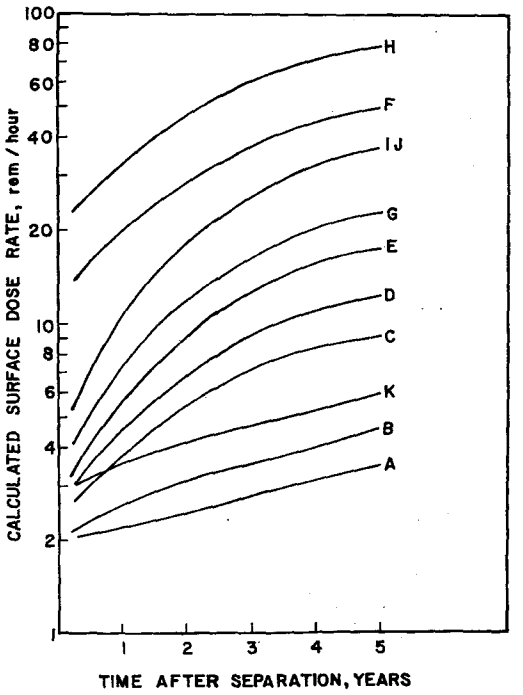

FIG. 4. Calculated X- and gamma-ray surface dose rate from a slab for various plutonium isotopic compositions.

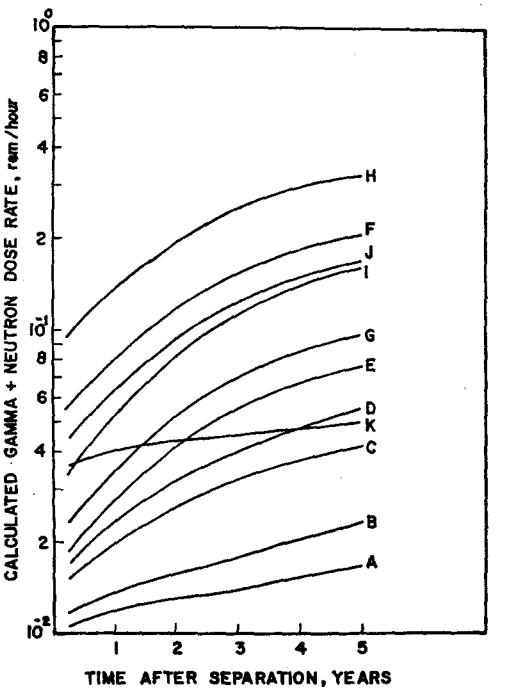

FIG. 5. Calculated total dose rate at 30.5 cm from a 2.5 kg plutonium sphere shielded by 0.95 cm CR-39.

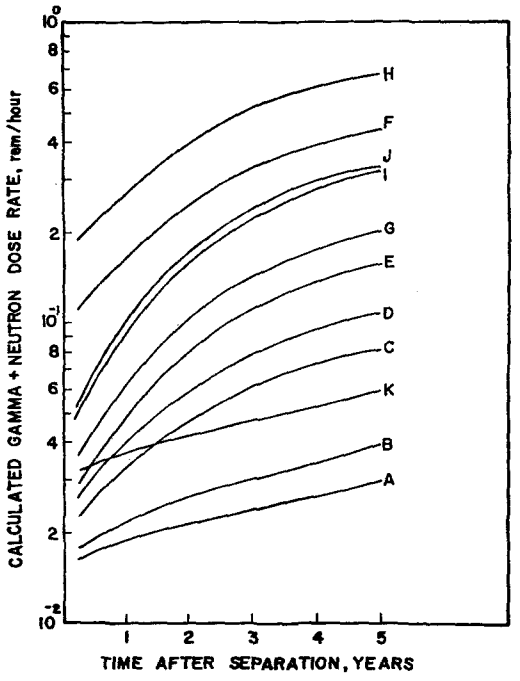

FIG. 6. Calculated total dose rate at 12.7 cm from a 71.66 g plutonium core plate shielded by 0.76 mm neoprene glove.

of lightly leaded gloves during handling of jacketed fuel elements.

CONFIRMATION OF CALCULATED DOSE RATES

Preparation of Samples

Specimens of plutonium used for surface exposure rate measurements were prepared by casting 25 mm × 32 mm × 3.18 mm and 25 mm × 32 mm × 1.59 mm plates. These plates were pure plutonium with less than 1% impurities. Samples of plutonium for the shielded dose rate measurements were of two basic geometries: (1) a disc source approximately 10 cm in diameter and 2.5 cm thick, and (2) a fuel core plate 4.5 cm × 4.9 cm × 0.32 cm. These sources were typical of the ones encountered during fuel element fabrication.

The surface dose-rate samples were placed in a 63 mg/cm² vinyl container before insertion in the extrapolation chamber.

Surface Exposure Rate Measurements

Surface exposure rates were measured with an ANL-developed extrapolation chamber.[19] This instrument is very similar to the devices described in refs. 20–21. The extrapolation chamber is a parallel-plate ionization chamber having a volume that can be varied. The area of the collecting electrode is 0.724 cm². The depth of the chamber can be varied from 0.04 cm to 0.25 cm. A vibrating reed electrometer measures the current generated in a predetermined volume. After determining and taking into account the vinyl attenuation, the current reading was converted to roentgens/hour using an electronic calibration. This calibration is checked frequently with a standard uranium source which consistently yields 0.240 ± 0.015 R/hr through a 6 mg/cm² aluminum alpha absorber.

Measurements of the surface exposure rates of the plutonium specimens were made, and the build-up in intensity was observed as a function of time after plutonium separation.

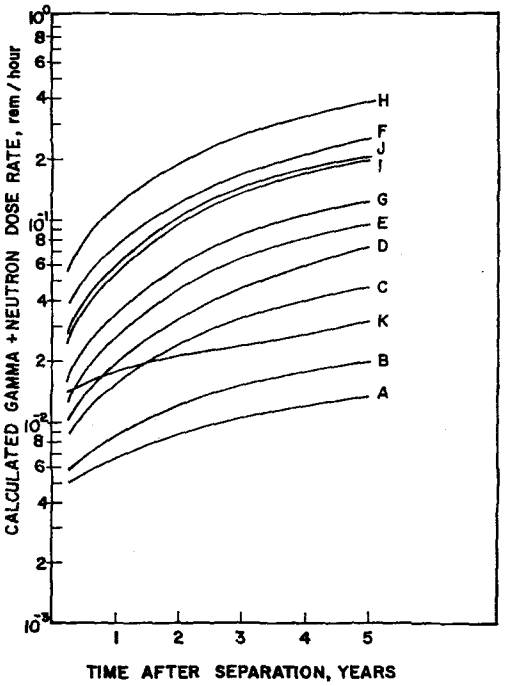

FIG. 7. Calculated total dose rate at 12.7 cm from a 71.66 g plutonium core plate shielded by 0.76 mm lightly leaded neoprene glove.

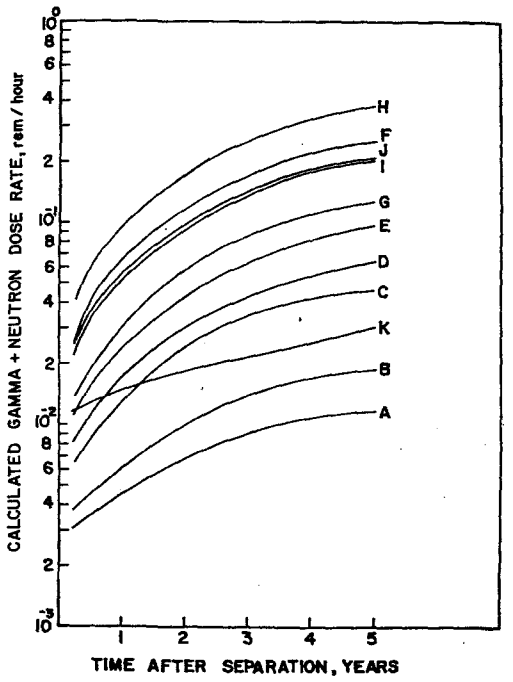

FIG. 8. Calculated total dose rate at 12.7 cm from a 71.66 g plutonium core plate jacketed by 0.3 mm stainless steel and shielded by 0.76 mm neoprene gloves.

Comparison of the measured exposure rates from specimens having compositions C and E yielded X- and gamma-ray surface exposure rates ± 25% of the calculated values. Table 4 illustrates typical measurements made with the extrapolation chamber.

Shielded Radiation Measurements

Measured exposure rates from the disc and plate sources in various shielding configurations were made. The X- and gamma-ray measurements were made with National Bureau of Standards calibrated R-meters, standard ion chamber instruments, and personnel dosimeters which were calibrated to the radiation field produced by the plutonium in the glovebox system. Neutron dose rate measurements were made with a 25 cm diameter, tissue equivalent, polyethylene, neutron dosimeter calibrated in mrem/hr. Measured neutron dose rates from the small single plate were within ± 25% agreement with the calculated dose rates for the isotopic compositions A, C, and E. The X- and gamma-ray exposure rates from the small plate also were in agreement with the calculated values ± 30%. Radiation measurements from the 2.5 kg disc source with isotopic composition E one year after separation was 50 mR/hr X and gamma and 5 mrem neutron at 30.5 cm through CR-39. This measurement can be compared to the calculation for the spherical source. The variations in dose rates can be attributed to differences in the geometry of the compared sources and self-shielding.

Table 4. Extrapolation Chamber Measurements

Source isotopic weight %					Source weight grams	Time after purification (approx.)	Surface exposure rate R/hr
^{238}Pu	^{239}Pu	^{240}Pu	^{241}Pu	^{242}Pu			
0.02	80.91	16.67	2.15	0.27	30.2	8 months	2.92 ± 0.17
						9 months	3.34 ± 0.2
						11 months	3.7 ± 0.22
						1 year	3.81 ± 0.23
0.034	72.55	22.16	4.62	0.67	21.6	10 months	4.5 ± 0.27
						11 months	5.0 ± 0.3
0.034	72.55	22.16	4.62	0.67	40.9	8 months	4.1 ± 0.25
						9 months	4.55 ± 0.27
						10 months	4.95 ± 0.3
						11 months	5.44 ± 0.33

WHOLE BODY AND EXTREMITY RADIATION EXPOSURE EXPERIENCED DURING PLUTONIUM FABRICATION

Past experience has indicated that whole-body radiation exposure is the limiting consideration during plutonium fabrication at the ANL Plutonium Fuel Fabrication Facility. The whole body of the fabrication worker is monitored with a film badge with aluminum, silver, and cadmium filters containing a Dupont 558 film packet and a Kodak NTA neutron film. A secondary device, the Shonka tissue-equivalent dosimeter, is used in conjunction with the film badge for day-to-day and comparison measurements of the fabrication worker's exposure. The neutron film in the badge is not a good indicator of neutron exposure due to the low intensity and energy of the Plutonium Fabrication Facility's neutron background.[23] Neutron exposures are assigned as a function of the worker's activities and the associated neutron backgrounds.

Hand exposures, previous to this year, were monitored by wrist badges only. Correlation of wrist/hand exposures have been made, and a 1/3 ratio was found.[24] A method of using thermoluminescent dosimeters to determine hand exposures has been developed.[25, 26] The dosimeters are worn on the fingers of operating personnel, and the hand exposures are determined through calibration of the dosimeters with the plutonium handled at the time of the exposures. Results from these dosimeters compared to wrist badges indicate that the 1/3 wrist/hand ratio is conservative.

Personnel exposures are the greatest when fabrication workers are handling plutonium sources that have large surface areas and weigh more than 1 kilogram. The highest radiation exposures encountered during the fuel fabrication process are those received during the casting and weighing operations. The amount of plutonium fabricated at ANL each year and its isotopic compositions are given in Table 5. Whole body and hand exposures during the casting operation are listed. Hand exposures listed as beta are considered to be nonpenetrating scattered X-rays with energies below 12 keV. Administrative guidelines on radiation exposure are 5 rem/year for the whole body, 75 rem/year to the extremities, and 30 rem/year to the skin of the whole body.

Table 5. Total Radiation Exposure Experienced by Personnel During Plutonium Casting Operation

Year	Kilograms plutonium fabricated	Isotopic composition weight % Pu				Personnel exposure	
		^{239}Pu	^{240}Pu	^{241}Pu	^{242}Pu	Whole body	Hand
1963	37	95	4.5	0.4	0.01	1 rem (1 individual)	14 rad β 2.5 rem X, γ
1964	23	91	8	0.8	0.05	3 rem (1 individual)	11 rad β 5 rem X, γ
1965	21	91	8	0.8	0.05	3 rem (1 individual)	4 rad β 1.5 rem X, γ
	3.1	88	10	1.4	0.03		
	1	73	22	4.6	0.7		
1966 (6 months)	25	91	8	0.8	0.05	5 rem (2 individuals)	10 rad β 2.7 rem X, γ
	8.5	90	9	1.1	0.05		
	5.3	88	10	1.4	0.05		
	23	73	22	4.6	0.7		

RADIATION PROTECTION CONSIDERATIONS FOR GLOVEBOX FABRICATION OF RECYCLED PLUTONIUM

From Table 5, it can be seen that the present problem is the whole body exposure. Hand exposures are less than 25% of the maximum guides. These exposures were all through the CR-39 windows and nonleaded gloves.

Comparing Fig. 5, which are the calculated dose rates from a spherical 2.5 kg plutonium source through CR-39, with the computed dose rates through 0.95 cm of 6.2 g/cm^3 lead glass, the calculated lead glass shielded dose rates from isotopic compositions B through H are reduced to levels below that from composition A through CR-39. In addition, there is no dose rate build-up with increasing source age. Neutrons then become the predominant source of radiation exposure. This shielding configuration centers attention on the dose rates through the lightly leaded gloves, which increases with source age.

Lightly leaded gloves generally reduce the X- and gamma-ray dose rates by a factor of 2. Heavy leaded gloves are 3.5 times as effective in reducing the exposure rates; however, they are too cumbersome and restrict manipulation with the fingers. Direct contact exposure to the hands through lightly leaded gloves for plutonium sources with compositions F and H must be limited. Direct hand contact with plutonium sources having compositions D through J would have to be limited if processed 5 years or more after separation. Processing at intermediate times after separation would have to be done under carefully established guidelines to keep extremity exposures below radiation protection exposure limits.

Fabrication of large amounts, greater than 100 kg/year, of recycled plutonium fuel in a glovebox system will require shielding and close surveillance of personnel exposures. Fabrication of small amounts, less than 10 kg/year, of material with compositions E, F, G, H, I, and J would be possible in a partially shielded glovebox system.

Close surveillance of personnel exposures will be required for rotation of personnel to tasks calculated to keep their radiation exposures within prescribed limits. The fabrication of large amounts of recycled plutonium per year will require many personnel available for rotation, and glovebox fabrication may not be economically feasible due to the number of personnel required. Under those circumstances, a remote fabrication process would have to be developed.

CONCLUSION

Radiation exposures of personnel who fabricate plutonium fuels in an unshielded glovebox system are not a serious radiation protection problem when the plutonium contains less than 5 w/o of ^{240}Pu, ^{241}Pu, and ^{242}Pu. Some radiation exposure difficulty is encountered during glovebox fabrication in the 5 to 10 w/o range. Increasing difficulty in minimizing radiation exposures is encountered during glovebox fabrication of plutonium containing greater than 10 w/o of the higher isotopes.

Exposure of personnel to radiation from recycled plutonium fuel can be minimized during glovebox fabrication by the following measures:

1. Early fabrication after chemical separation.
2. Shielding applied to equipment within the gloveboxes and the glovebox surfaces.
3. Use of leaded glass for the glovebox windows.
4. Immediate removal of plutonium residues from the glovebox system.
5. Use of lightly leaded gloves and mechanical techniques for handling the plutonium.
6. Monitoring of extremity and whole body exposures to enable rotation of personnel for tasks having high exposure rates.
7. Planning fabrication procedures to reduce exposure times to a minimum.
8. Use of shielded temporary storage areas in the glovebox system.
9. Knowledge of plutonium isotopic compositions, light element analysis, and time after plutonium separation.

Some of those precautions may be neither practical nor economical for extensive and continuing fuel fabrication operations. In such cases, it will be necessary to minimize exposures of personnel to radiation by automated fabrication and inspection techniques.

ACKNOWLEDGEMENTS

The authors wish to acknowledge the assistance of K. O. Jordan, who made many of the radiation measurements, J. R. Novak, G. T. Lonergan, W. D. Dillow, and R. J. Sullivan, who made valuable comments, the following Plutonium Fabrication Facility Staff Members J. E. Ayer, N. J. Carson, Jr., H. F. Jelinek, and A. G. Hins, whose assistance was invaluable, and also R. C. Frank, W. G. Karafiat, Marjorie Bobysud, and Doris Pinneo, who assisted in the report preparation.

REFERENCES

1. A. B. Shuck and R. M. Mayfield. The Process Equipment and Protective Enclosures Designed for the Fuel Fabrication Facility No. 350. ANL-5499, Argonne National Laboratory (1956).
2. R. M. Mayfield, W. G. Tope and A. B. Shuck. The Facility 350 Helium-Atmosphere System. ANL-6489, Argonne National Laboratory (1962).
3. H. Bateman. *Proc. Cambridge Phil. Soc.* **15,** 423 (1910).
4. L. G. Merker, L. G. Faust and W. J. Bailey. Battelle-Northwest Fuel Fabrication Experience with High-Exposure Plutonium. BNWL-27, Battelle Northwest (1965).
5. M. J. Steindler. Radiation Problems Associated with the Handling of the Actinide Elements. ANL-6540, Argonne National Laboratory (1962).
6. M. L. Storm, H. Hurwitz and G. M. Roe. Gamma-Ray Absorption Distribution for Plane, Spherical and Cylindrical Geometries. KAPL-783, Knolls Atomic Power Laboratory (1952).
7. T. Rockwell, III. *Reactor Shielding Design Manual.* D. Van Nostrand Company, Inc., Princeton, New Jersey (1956).
8. G. W. Grodstein. X-ray Attenuation Coefficients from 10 keV to 100 MeV. NBS-583 National Bureau of Standards (1957).
9. E. Storm, E. Gilbert and H. Israel. Gamma-Ray Absorption Coefficients for Elements 1 through 100 Derived from the Theoretical Values of the National Bureau of Standards. LA-2237, Los Alamos Scientific Laboratory (1958).
10. H. Goldstein and J. E. Wilkins. Calculations of the Penetration of Gamma Rays. NYO-3075, Nuclear Development Associates, Inc. (1954).
11. H. Goldstein. *Fundamental Aspects of Reactor Shielding.* Addison-Wesley Publishing Company, Inc., Reading, Massachusetts (1959).
12. E. D. Arnold. Radiation Limitations on Recycle of Power Reactor Fuels. Paper 1838 Second United Nations International Conference on the Peaceful Uses of Atomic Energy, Vol. 13, pp. 237–250, Geneva (1958).
13. I. Birchall. Radiation Dose Rates for Plutonium Isotopes. AHSB(s) R10, United Kingdom Atomic Energy Authority, Authority Health and Safety Branch, Risley (1960).
14. J. E. Ayer. Private communication.
15. A. F. Avery *et al.* Methods of Calculation for Use in the Design of Shields for Power Reactors. AERE-R-3216, United Kingdom Atomic Energy Authority, Research Group (1960).
16. Technical Glass Bulletin No. 103. Absorption Coefficients and Buildup Factors of Nuclear Shielding Glasses. Pittsburgh Plate Glass Company (1963).
17. A. B. Shuck *et al.* Development of a Process for Manufacturing ZPR-III U-Pu-Mo Test Fuel Elements. ANL-6955, Argonne National Laboratory (1965).
18. A. B. Shuck, A. L. Lotts and K. Drumheller. The Remote Fabrication of Reactor Fuels. USAEC Report TID-8541, 71–147 (1966).
19. P. C. Gray. An Extrapolation Chamber for Measurement of Surface Exposure Rates. Unpublished report, Argonne National Laboratory (1963).
20. G. Failla. The measurement of tissue dose in terms of the same unit for all ionizing radiations. *Radiology* **29** (2), 202–215 (1937).
21. G. Failla *et al.* The Measurement of Tissue Dose of Ionizing Radiation. AECD-2142, Argonne National Laboratory (1947).
22. Robert Loevinger. Extrapolation chamber for the measurement of Beta sources. *Review of Scientific Instruments* **24** (10), 907–914 (1953).
23. T. A. Steele. Use of Personal Monitoring Neutron Film Near the 50 MeV Injector of the ZGS. CONF-651109, Accelerator Radiation Dosimetry and Experience (1965).
24. W. E. Bleiler and W. B. Grant. A study of the Correlation Between Hand and Wrist Exposures. ANL-6765, Argonne National Laboratory (1963).
25. T. F. Johns. Measurement and Assessment of Radiation Doses from the Handling of Reactor Fuels. AEEW-R 408, Winfrith (1964).
26. W. M. Trenholme and J. H. Pingel. A versatile Readout System for Thermoluminescent Dosimeter Studies. Argonne National Laboratory (to be published).

THE DETECTION AND MEASUREMENT OF PLUTONIUM AIRBORNE CONTAMINATION IN MAJOR PLUTONIUM FACILITIES

R. T. BRUNSKILL and S. T. HERMISTON
Health and Safety Department, Windscale and Calder Works, U.K.A.E.A.
Production Group

Abstract—A review is presented of air sampling experience in three kinds of plutonium facilities, viz. a laboratory containing lines of glove boxes, a manufacturing facility employing a sealed face to separate operating and maintenance areas, and a workshop used for the cleaning of safety equipment contaminated with plutonium.

The level of airborne contamination as measured on fixed, installed air samplers in these areas is shown to be critically dependent on the type of work being carried out, the position of the sampler and the nature of the ventilation system. Personal air samplers invariably indicate higher levels of airborne contamination than these installed samplers. Over periods of months in the areas under examination, it is generally safe to assume that the integrated exposure measured using personal air samplers will not be more than ten times the exposure measured with the installed samplers. Under incident conditions, however, the installed sampler might underestimate inhalation exposures by several orders of magnitude. The distribution of air sampling data shows a deviation from log normal where incidents occur producing abnormally high airborne contamination.

It is concluded from these observations that there is a requirement in certain plutonium areas to use personal air samplers for the measurement of inhalation exposures. In addition, a personal air sampler with an audible alarm has been developed for the early detection of airborne contamination in operating areas.

Particle size distributions on air samples have been studied, and their significance is discussed in relation to the assessment of the plutonium inhalation hazard.

1. INTRODUCTION

The potential inhalation hazard from plutonium airborne contamination is a major risk on any plutonium manufacturing facility. It is a feature of many plutonium plants, particularly those employing extensive use of glove boxes, that plutonium tends to be released over extremely small time intervals, with long, quiescent periods when no contamination is produced in the working areas. This makes plutonium operational control difficult. Measurement of plutonium intakes by biological methods is a laborious procedure and is post event, also because of the limited sensitivity of these techniques, and the fact that interpretation of results is a lengthy process extending over periods of months, they cannot by themselves provide adequate control of plutonium exposures.

As Dunster has pointed out, [1] although organ doses from long-lived isotopes will only exceed I.C.R.P. recommendations when the maximum permissible organ burden is exceeded, it is sound practice to attempt to limit all intakes to those appropriate to a 13-week period. Because of the intrinsic difficulties in measuring and controlling plutonium intakes, the designer of a plutonium facility must do his utmost to provide absolute containment. This ideal is in practice never achieved and the difficulties of measurement and control of plutonium intakes by inhalation must be faced.

This report considers how detection and measurement techniques for plutonium airborne

contamination have developed with a continuing experience of handling plutonium, and also discusses future developments. Observations and measurements made on facilities at Windscale are also discussed.

2. HISTORICAL DEVELOPMENT

2.1. The earliest type of air sampling programme employed portable air samplers to collect samples over a short duration of sampling (say ½ hr) in all operating areas of plutonium plants and laboratories. Provided that these tests were carried out regularly, it was considered that leakages of activity due to weaknesses in design of operating procedures would be detected. A practical reason for this approach was the lack of air sampling devices which could operate continuously over long periods of time.

It is now well established that under many conditions air contamination levels in operating areas of plutonium plants follow a log normal distribution. With this form of distribution the mode (the value most likely to be observed) may only be one-sixth or less of the mean concentration. It follows, therefore, that "spot sampling" may seriously underestimate the true concentration. Another disadvantage of the short term sample is the lengthy counting period required to give results with reasonable statistical accuracy for an element such as plutonium with its low M.P.C. in air.

2.2. In certain operating areas it was soon realised that a potential airborne hazard did exist and that it might be necessary to limit the time spent by individuals in these areas. To improve the methods of control, more frequent, in fact almost continuous, half-hourly samples were taken with a view to obtaining early information on the levels of airborne contamination. With this information available, breathing apparatus was prescribed if it was estimated that air concentrations were greater than one M.P.C.

This system certainly provided a higher degree of protection for the operators than the earlier approach depending on intermittent air sampling. Also, the accuracy of information about average air contamination levels in an area, derived by counting the filter papers after a time lag sufficient to allow daughter products of radon and thoron to decay, was improved by the introduction of a higher frequency of sampling. A practical disadvantage of this system, however, is the scale of effort that must be mounted (in men and equipment) to assess samples obtained. This is a consequence of the large numbers of samples to assay, and the lengthy counting periods required to produce results of reasonable accuracy because of the small volumes of air sampled. Furthermore, because data accruing from this type of sampling is retrospective, it is not possible to guarantee that releases of plutonium will always be detected early enough to prevent significant personal exposure.

2.3. Because of these defects, the whole philosophy of air sampling in plutonium areas was reviewed. In the first place, equipment was developed to allow continuous sampling in all areas where plutonium was handled. Eventually, within the U.K.A.E.A. a monitoring system was developed, based on continuous sampling through a fixed filter paper which is presented to a scintillation detector with associated counting equipment. Because of the interference from alpha active decay products of radon and thoron, the instrument has a minimum alarm level in the conditions obtaining on the Windscale plants, of about 120 d.p.m./m³ hr.* To provide increased sensitivity, the latest development is a sampler employing a solid state detector and alpha energy discrimination against naturally occurring alpha emitters. By this means an alarm can be given on detection of an exposure of less than 30 d.p.m./m³ hr.

2.4. So far, air sampling had been confined to static samplers, i.e. high volume air samplers installed in a fixed position in the working area. As more data became available, however, it was obvious that the levels of airborne activity measured by these samplers was critically dependent on their exact location within a laboratory or other operating area. Large variations in measured airborne concentrations could be

* 120 d.p.m./m³ hr represents the integrated level of air contamination occurring as a result of an air concentration of 120 d.p.m./m³ of plutonium lasting for 1 hr, or 12 d.p.m./m³ for 10 hr, etc.

obtained over a distance of a few feet, the pattern of results being influenced by the type of operations being carried out and the nature of the ventilation system.

These results suggested that the use of static samplers for measuring environmental plutonium airborne contamination could give very misleading results. To investigate this more closely Sherwood and Greenhalgh[2] developed the "personal" air sampler capable of measuring concentrations in the workers' breathing zones. The use of this sampling device on the Windscale Plants during the past two years has confirmed that the static sampler invariably underestimates the airborne concentrations at the point where activity is released to the operating area, which is normally close to the operator who causes the release. The results of these surveys have necessitated a further review of the principles to be applied in the detection and measurement of plutonium air contamination.

3. MEASUREMENTS OF AIRBORNE ACTIVITIES ON WINDSCALE PLANTS

The historical review in the preceding paragraph has been given to present a broad outline of the experiences which have influenced developments leading to present-day practices. However, the techniques employed in this field are still in a state of some flux and further developments are certain to take place. In order to gain a proper appreciation of the "state of the art" now, and likely developments in the future, a survey is given of the data accrued recently from the use of static and personal air samplers.

Three areas were selected for investigation, these are as follows:

A. A facility employing interconnected "free-standing" or "island" glove boxes in an open laboratory, and used for the manufacture of plutonium oxide/uranium oxide ceramic fuel for reactors.

B. A section of a plutonium manufacturing plant, used for the preparation of plutonium metal and oxide via the oxalate precipitation and fluorination route. On this plant the interconnected line of glove boxes in which the process is carried out is sited in a "maintenance area", separated from the operating area by a "sealed face". The maintenance and operating areas are separately ventilated and there are no ambidextrous gloves in the sealed face; movements of plutonium in trays through the line are effected by push–pull rod operation from the operating face. Respiratory protection is always provided for workers in the maintenance area. A block plan of this facility is shown in Fig. 1.

C. A decontamination facility, used for the cleaning of safety equipment (mainly respirators and pressurised suits which have been contaminated with plutonium) and health physics survey instruments.

Areas A and B both handle plutonium on the kilogram scale. In Area C, of course, only microgram quantities are encountered. Thus these three facilities differ considerably from each other in functions, but are each representative of conditions in other areas where measurements have also been made.

3.1. *Static Air Samplers*

Area A. At five positions in the laboratory, at 2 to 3 ft above floor level air is drawn continuously through glass fibre filter papers, at a sampling rate of approximately 5 m^3/hr. The samples are changed at the end of each working period, i.e. at 8-hr intervals. Table 1 shows the mean air contamination levels measured over several months' operations.

In this laboratory the ventilation system is arranged so that clean air is injected into the room through a false roof and is extracted at floor level at a number of positions distributed throughout the laboratory. Contamination released near one particular air sampler should therefore be extracted without seriously affecting the remaining samplers. It would be expected that the relative levels recorded at the sampling positions should reflect the magnitudes of the activity released during operations in their immediate vicinity.

Results on single days in fact showed much wider variations in levels measured at the five

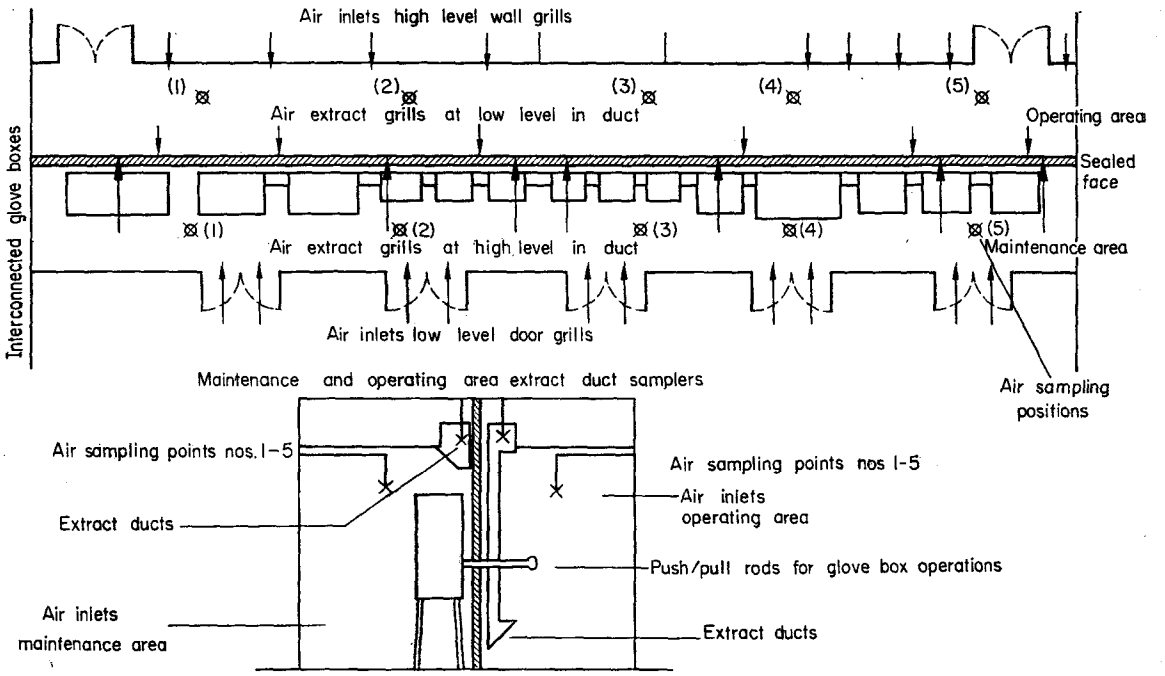

FIG. 1. Layout of Area A showing airflows and locations of air samplers.

sampling positions than is apparent from the mean values shown in Table 1. The ratio of the activities collected by the samplers showing the highest and lowest values over the same working periods varied from 2 to 400, with a mean ratio of 30.

Area B. Air sampling data for both operating and maintenance areas have been examined.

In the maintenance area there are five air sampling locations spaced at intervals of 15 ft down the line at heights of 6 ft 6 in. above floor level. The mean values of air contamination obtained over a period of one year are shown in Table 2. (Samples were collected over 8 or 12 hr periods.)

The situation in this area is that a sampler at one end of the line (position 1) shows much higher levels than the remaining samplers. Those situated in the central positions indicate very similar average air contamination levels, whilst the remaining sampler at the opposite end of the line indicates markedly lower levels than at any other position.

The ventilation system for this area is shown in Fig. 1. Clean air is injected into the line at ground level through grills in the cubicle doors and is discharged to the active extract line in ducts at ceiling level. The air flow across the line is about 1000 linear ft/min, the system being deliberately arranged so that there is a 20%

Table 1. *Mean Air Contamination Levels (d.p.m./m³) Measured at Fixed Positions in the Operating Area of Area A*

Position 1	Position 2	Position 3	Position 4	Position 5
1.29	0.97	0.63	1.68	1.03

Table 2. Mean Air Contamination Levels (d.p.m./m³) Measured at Fixed Positions in the Maintenance Area of Area B

Position 1	Position 2	Position 3	Position 4	Position 5
122	67	76	68	9

higher flow at the centre of the line than at the ends.

With this arrangement, it would be expected that each air sampler would be affected mainly by the air contamination generated in the vicinity of the sampler, although those samplers in the central part of the line would tend to be influenced as well by operations carried out at the extremities of the area. The air sample results confirm this assessment. Position 5 is at the "clean" end of the line where the plutonium metal or oxide is canned and the glove boxes are only contaminated to relatively low levels. Most of the direct handling of dry plutonium as oxide or fluoride is done in the middle of the line and the majority of maintenance work involving breakage of the containment is carried out close to position 1.

In the operating area, clean air is injected through grills almost at ceiling height in the wall at the back of the operator and is extracted at floor level at five separate points into an extract air duct. There are five air sampling locations in the area, the sampling heads being spaced at equal intervals of distance down the line and positioned 6 ft 6 in. above floor level. In addition, continuous samples are taken from the final, common air extract duct from the area. The results of a sampling programme carried out over a period of two months are shown in Table 3 below.

The low levels of air contamination in this area demonstrate the effectiveness of the sealed face concept. The similarity of the measurements at each sampling location, with no large day-to-day variations, probably indicates that the air contamination in this area has its origin in very low levels of surface contamination on surfaces and clothing and that little or no direct transfer of activity occurs between the maintenance and operating areas.

Area C. There are only two static air samplers in this area, one situated centrally and one close to the point where respirator facepieces are monitored after decontamination. Over a sampling period of six months, the mean air contamination levels measured at the two sampling positions were 4.2 and 1 d.p.m./m³ respectively, the sampler immediate to the working position giving the higher result.

The ventilation provided in this room consists of an extract from a central position in the room producing a modest eight air changes/hr. Thus the air is fairly static and variations in air contamination levels throughout the area are the consequence of a gradual dispersion of activity from the point of release. Under these conditions the difference between the value of air contamination measured at the two sampling positions is perhaps somewhat greater than might have been expected.

Comment

The pattern of results illustrated above is one of considerable variations in the levels of air contamination measured in working areas at

Table 3. Mean Air Contamination Levels (d.p.m./m³) Measured at Fixed Positions in the Operating Area of Area B

Extract Duct	Position 1	Position 2	Position 3	Position 4	Position 5
0.2	0.11	0.23	0.2	0.17	0.23

sampling positions a few feet from each other. These variations are caused by local ventilation conditions and the nature of the work being carried out in the vicinity of the samplers.

Averaged over long periods (of several months' duration) static samplers distributed within a particular laboratory generally produce results which do not differ from each other by more than one order of magnitude and agreement is often much closer. On the other hand, several orders of magnitude difference occasionally appear over single (8 hr) sampling periods under incident conditions. This suggests that air contamination can be highly localised, in which event a static sampler might measure air contamination which is unrelated to the level of air contamination to which the workers are exposed.

3.2. *Personal Air Samplers*

The doubts raised by the above evidence as to the adequacy of static air samplers for measuring environmental air contamination led to the development of a personal air sampler.

The sampler consists essentially of a small diaphragm air pump which samples the atmosphere at about 2 l./min through a 1 in. diameter glass fibre filter paper contained in a sampling head. The sampling orifice is adjusted in size such that the linear velocity of sampling is equivalent to the mean air velocity during breathing.

In the last two years a comprehensive experimental programme, utilising this personal air sampler, has been carried through at Windscale Works. The investigations have been made in a wide variety of working areas and laboratories. However, the results obtained in the three areas chosen to illustrate the significance of static air sampler results are used here because they typify the data obtained in this programme.

Area A

During the same period for which static air sampler data were obtained, twenty operatives wore personal air samplers. Taken over the whole period, the mean exposures incurred by the operatives ranged from 12 to 320 d.p.m./m^3 hr, per 8 hr "shift", giving a ratio of about 25 between the exposures recorded for the highest and least exposed individuals. (In this paper, the term "exposure" refers to the integrated level of air contamination as indicated by measurements with personal or static air samplers.) It should be noted, however, that results in the high exposure range were strongly influenced by one or two very high results. For instance, the most highly exposed individual received 80% of his exposure in a single working period, the remaining 20% being spread over 19 similar periods.

The personal air samplers invariably gave results significantly higher than the installed, static air samplers. Using the mean data from the five static samplers, the ratio of the integrated air contamination levels (P.A.S./S.A.S.) measured in units of d.p.m./m^3 × hours, varied between 2 and 27 with a mean value of 11.

The ratios for single working periods, however, were spread over a much wider range of values; using the data from the personal air samplers and static air samplers giving the highest results during each working period, the ratio $\frac{\text{P.A.S.}}{\text{S.A.S.}}$ varied from less than 1 to 500, with a mean value of 12.

Another feature of these results is that the ratio $\frac{\text{P.A.S.}}{\text{S.A.S.}}$ shows a tendency to increase as

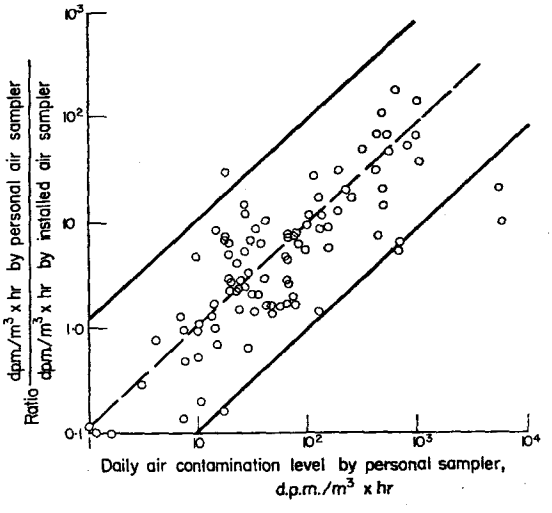

FIG. 2. Daily air contamination level by personal sampler d.p.m./m^3 × hours. Highest values of personal and corresponding installed samplers in a plutonium laboratory.

the P.A.S. activity increases and this trend can be seen in Fig. 2. Here there is a wide scatter about a line showing the ratio $\frac{\text{P.A.S.}}{\text{S.A.S.}}$ increasing from 1 to 100, as the personal air sampler results increase from 10 to 1000 d.p.m./m³ × hours. This relationship demonstrates clearly that even static samplers in close proximity to the source of release of plutonium to the operating area are much less sensitive to changes in conditions than personal air samplers. Although not reported here there are similar results for Areas B and C, the only difference lying in the absolute values of the $\frac{\text{P.A.S.}}{\text{S.A.S.}}$ ratio. This ratio is likely to be influenced by a number of factors, including the nature of the work, normal chronic background level of air contamination, proximity of static sampler to the source of release etc.

Area B

Personal air samplers were worn over a two month period by personnel operating the plant from the "clean" side of the sealed face. The mean level of air contamination as measured by these samplers was 0.8 d.p.m./m³ as compared with 0.2 d.p.m./m³ measured on the static samplers, i.e. a $\frac{\text{P.A.S.}}{\text{S.A.S.}}$ mean ratio of 4.

Area C

Three workers engaged in check monitoring of safety equipment and monitoring instruments after a decontamination process, wore respirators over periods of 2 to 3 months.

Analysis of this data is difficult because the workers were not all engaged on this work at the same time. Also the work was of an intermittent nature; often the three workers were only employed for one or two hours each day in the area. It is thus impossible to compare accurately the personal and static air sampler results.

However, a number of deductions are possible from the data available. Even though these workers were employed on identical work, the mean air contamination levels as recorded by their personal air samplers varied by factors of two or three. In each case the personal air samplers indicated higher levels of air contamination than the static samplers; the mean ratio of personal to static air sample activities expressed in d.p.m./m³ hr, was 5. The use of personal air samplers in fact demonstrated that conditions in this area were not satisfactory and led to the introduction of improved local ventilation.

Discussion

The most important fact which emerges from these measurements is that personal air samplers invariably indicate higher levels of air contamination than static air samplers. The explanation for this would appear to be that air contamination in operating areas is nearly always associated with the actions of individual workers, as opposed to unexpected malfunctioning of plant or equipment. Because of the nature of the work carried out on plutonium facilities, particularly during glove box operations, this means that the contamination will initially be generated close to the worker, before being dispersed by the ventilation system. Hence, the personal air sampler, with its sampling head in close proximity to the operator's breathing zone should collect samples which are representative of the air contamination to which the worker is exposed.

The inference to be drawn is that in some areas the measurement of environmental air contamination by static air samplers is an unreliable technique. In Area A, for example, about 50% of personal air sampler results at the 1000 d.p.m./m³ × hours level coincided with static air sampler results not significantly different from the normal background level of air contamination in the laboratory. Most of these exposures would have remained undetected if personal air samplers had not been worn, since there were no obvious causes for the exposures and the incidents did not reveal themselves by producing abnormal surface or personal contamination.

On the other hand, there is some evidence from this area that for exposures of the order of 5000 d.p.m./m³ × hours on personal air samplers there are likely to be significant increases in static air sampler results. Also, in Area B operating area the results obtained with static air samplers, suitably corrected by a factor

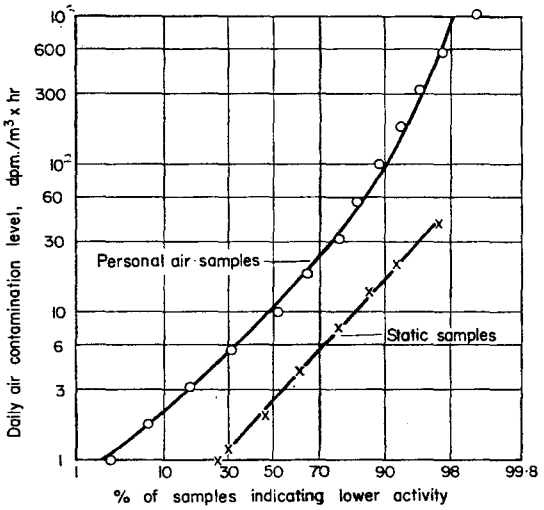

FIG. 3. Air sample measurements in a plutonium laboratory.

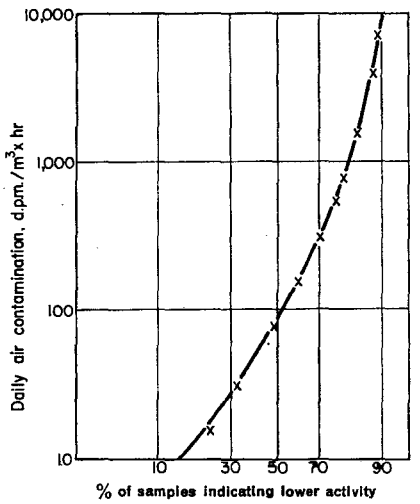

FIG. 5. Static air sample measurements in a maintenance area of a plutonium manufacturing plant.

of about 4 give reasonably reliable estimates of the exposure of workers in this area. The results obtained from the routine use of personal air samplers in areas such as this would add little information to that obtained from static samplers. The personal air sampler results for this area supplement the evidence from static air samplers in justifying the use of a sealed face, on major plutonium facilities, to isolate the operating area from the main plant.

Both the static and personal air sample data are plotted on log probability paper in Figs. 3 to 6 inclusive. In Area B operating area and in Area C the observations lie on a straight line. demonstrating a true log normal distribution, The personal air samples from Area A, and the static air sample results for the maintenance area of Area B, however, show a deviation from a log normal distribution caused by a larger number of high values than would be expected from a log normal distribution of data.

It is suggested that where the spread of air-

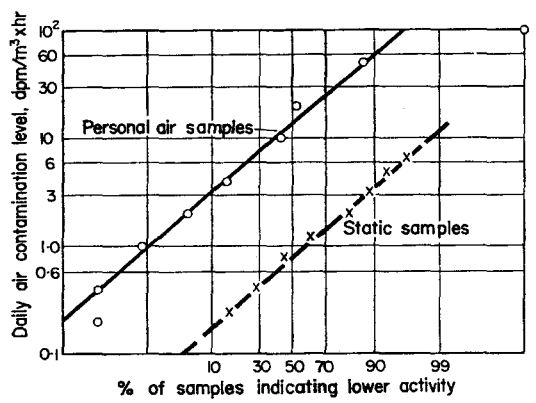

FIG. 4. Air sample measurements in a plutonium manufacturing plant.

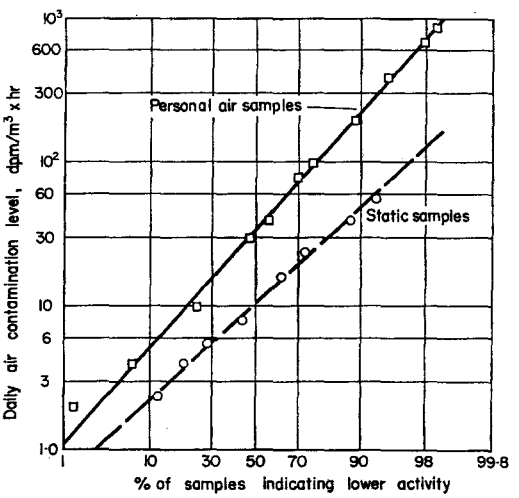

FIG. 6. Air sample measurements in a decontamination centre.

borne contamination is due only to abrasion of activity from contaminated surfaces, the observations are more likely to follow a log normal distribution. Such are the conditions in Area B operating area and Area C. In the other two areas, however, the chronic air contamination pattern will be modified by infrequent incidents due to accident or mal-operation, in which more significant quantities of activity will become airborne. Most incidents of this nature are caused by glove failures. The deviation of the data from log normal will be dependent on the frequency and magnitude of the "incidents" in each area.

4. PARTICLE SIZE ANALYSIS

4.1. Measurements of total air contamination in the breathing zone are not necessarily an accurate indication of the hazard to individuals. This is dependent on a number of other factors, notably particle size and solubility in tissue fluids of the material inhaled. Investigations made to ascertain the size spectra of plutonium aerosols in operating areas at Windscale are described below.

4.2. *Method*

The activity size distributions of plutonium particles collected on filter samples were determined using the autoradiographic technique described by Carter.[3] In this method the alpha particle energy is converted to visible light by means of a zinc sulphide screen and the light output is recorded on a photographic plate. The zinc sulphide is spread over vinyl backed sellotape and placed in contact with the sample. A photographic plate is placed under pressure in contact with the screen and, after a suitable exposure time, developed and fixed. Plutonium particles on the sample produce black spots on the plate, the diameter of a given spot being indicative of the associated particle activity. Individual particles of known activity are used to calibrate the system. By using an enlarger to view the plate, the minimum detectable activity size for an exposure of 10^4 min is about 0.01 d.p.m. The size spectrum of particles in a given area was determined by assuming that all particles assessed autoradiographically were of pure plutonium dioxide of density 11·4 g/ml.

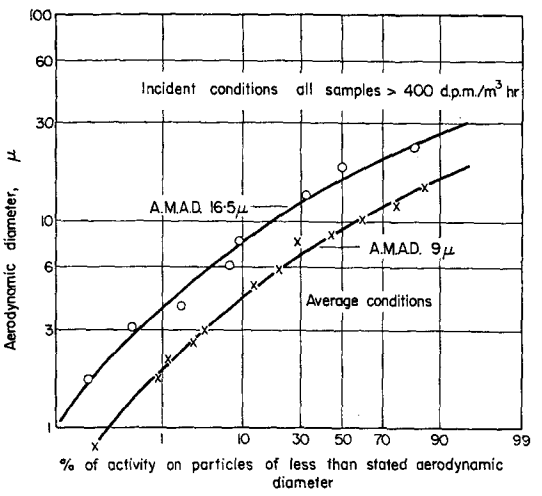

FIG. 7. Plutonium particle activity size measurements in a laboratory area.

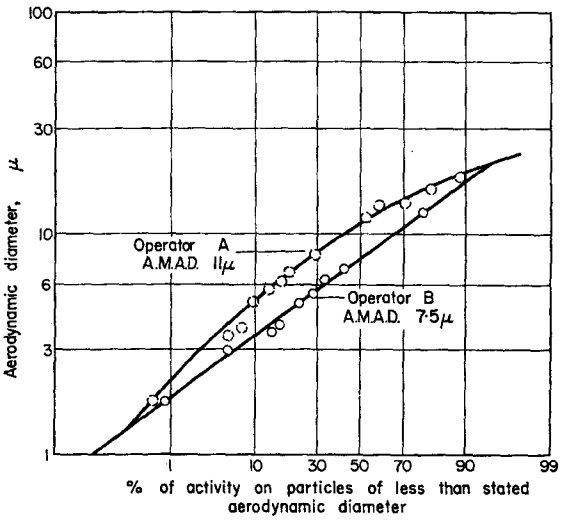

FIG. 8. Plutonium particle activity size measurements in a decontamination centre. Operator A—Decontamination of respirators. Operator B—Monitoring of respirators.

4.3. Personal air samples from Areas A and B have been analysed autoradiographically. Samples were taken in Area A during the manufacture of 25% PuO_2/75% UO_2 pellets. All personal air samples taken over a prescribed period were analysed and the results for samples indicating an integrated air contamination in

excess of 400 d.p.m./m³ × hours were analysed as a separate group.

In the decontamination centre (Area C) the personal air samples associated with the operators responsible for (a) the decontamination of respirator facepieces and (b) the monitoring of facepieces after decontamination, were analysed as two separate groups. The duties of both these operators were carried out in the same room.

The results of these analyses can be seen graphically in Figs. 7 and 8. Median particle diameters have been converted to equivalent aerodynamic diameters by using a multiplying factor $\rho^{\frac{1}{2}}$ assuming a density of 11·4 g/ml.

4.4. *Discussion*

The particle size spectrum in both areas closely approximates to log normal. There is, however, some variation in the activity median aerodynamic diameter (A.M.A.D.) for each distribution. Analysis of the most active personal air samples in Area A indicates an A.M.A.D. of 16–17 μ. The A.M.A.D. based on analysis of all the personal air samples is 9 μ, thus indicating that high air contamination is generally associated with the presence of larger particles, rather than a general increase in the numbers of those normally present. However, it should be noted that incident conditions are infrequent, and contributed only 7% of the total air contamination over the period of interest.

In Area C the A.M.A.D. for the activity on samples associated with the operator carrying out the decontamination of respirator facepieces is about 11 μ and, not unnaturally, somewhat greater than the A.M.A.D. which is associated with the duties of monitoring decontaminated facepieces (7·5 μ).

The interpretation of these results in terms of relative hazard requires a knowledge of the deposition and translocation of particulate matter in the respiratory tract. The currently adopted maximum permissible concentration for insoluble plutonium in air (4×10^{-11} μc/cc or 88 d.p.m./m³) is based on an assumed 12½% retention of inhaled activity in the lung and a biological half life of one year. A task group appointed by the International Commission on Radiological Protection (I.C.R.P.) has recently proposed a new lung model defining the deposition and translocation of particulate matter in the respiratory tract.[4] The model assumes a log-normal distribution of particle diameters and a knowledge of the A.M.A.D. and the nature of the activity is all that is required to define the M.P.C. in air for a particular distribution. For average conditions in Area A for example (A.M.A.D. : 9 μ) the derived M.P.C. for plutonium dioxide in air is about 250 d.p.m./m³. Under "incident" conditions (A.M.A.D. : 16–17 μ) the M.P.C. rises to about 350 d.p.m./³. In Area C the M.P.C.'s associated with the decontamination and monitoring of respirator facepieces are respectively 270 and 220 d.p.m./m³.

Some caution is required, however, before applying the data in this manner. As has been remarked earlier, the technique of particle size analysis used in these investigations only measures the diameter of the radioactive component of the sample. Inert dust adhering to active particles is not detected, nor is uranium because of its low specific activity. Therefore unless pure plutonium oxide is collected, particle sizes are likely to be underestimated.

On the other hand, particle activities of less than 0·01 disintegrations/min (equivalent to pure PuO_2 particles of 0·25 μ diameter, or 0·85 μ aerodynamic diameter) were not detected, mainly because of the limited exposure time of the sample papers (1 week). This will introduce an error leading to an overestimate of the A.M.A.D.'s. The error is unlikely to be serious, because of the large numbers of small particles required to make any significant difference to the A.M.A.D.'s. However, particle size investigations are now in hand, using longer exposure periods to reduce significantly the threshold detection level.

5. CONCLUSIONS

For each type of facility considered in this paper it has been demonstrated that static air samplers invariably underestimate air contamination levels in the vicinity of plutonium workers, as measured by personal air samplers. This is particularly true under "incident" conditions; our experience shows that individual exposures of at least 1000 d.p.m./m³ × hours might easily escape detection by static air

samplers sited in the operating area. There is limited evidence which suggests a much higher probability of detecting exposures greater than 5000 d.p.m./m³ hr. Static samplers will give more representative results the nearer they are sited to possible releases. Unfortunately, it is often impossible to guarantee optimum siting of these samplers because of the numbers of individuals at work and their movements around the plant. In these circumstances, a routine air sampling programme involving the use of static air samplers in the working area is of doubtful value.

On all plutonium plants there is a requirement for a monitoring system to give immediate warning of abnormal air contamination. It has been shown that static air samplers sited in the general working area cannot be relied on to fulfil this function. This requirement can best be met at the present time by sampling the air in the ducts which extract air from operating and maintenance areas. The use of a fixed air sampler for this purpose is illustrated in Fig. 9.

Since an instrument of this type samples on a continuous basis, all the air extracted from the area being monitored, it can also be used to establish trends in air contamination conditions in the area.

To establish an accurate picture of the plutonium air contamination levels it is necessary to use personal air samplers. Particle size analysis of a selection of the filter papers used in the personal air samplers can be carried out to determine how these measurements should be modified to give a true picture of the inhalation hazard. A study of particle sizes on two plutonium facilities at Windscale, has indicated that measurements of total air contamination in these areas using personal air samplers are likely to overestimate the inhalation hazard.

If the assessed concentrations of "respirable" activity are below the maximum permissible

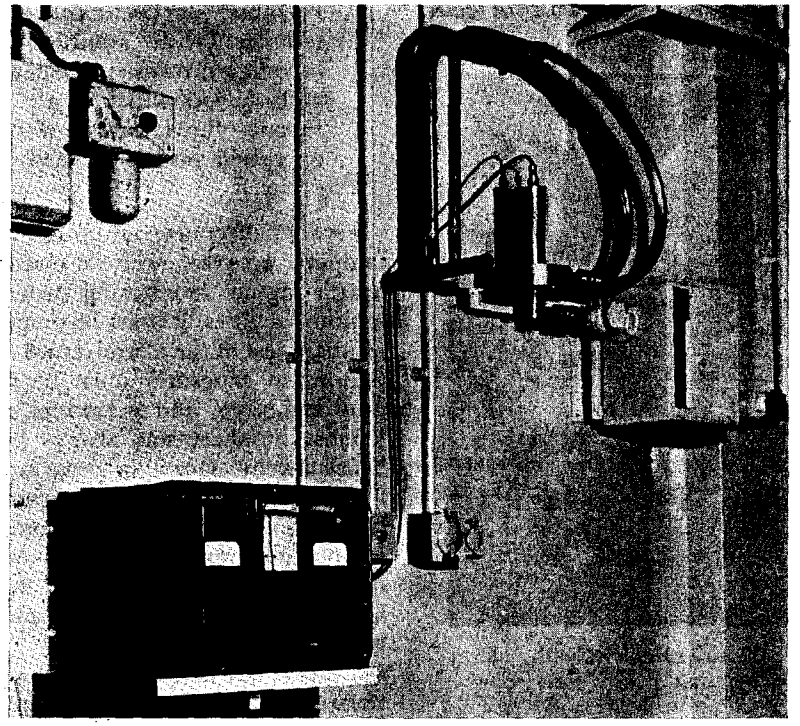

FIG. 9. Extract duct air samples.

concentration, it may be possible to dispense with the use of personal air samplers unless the duct samplers suggest a deterioration in working conditions. The use of personal air samplers is recommended during the commissioning of new plant as an aid to detecting weaknesses in design or operation which lead to the release of plutonium to the working area. To enhance their usefulness in this respect, it would be advantageous if an audible alarm system could be incorporated in their design. Such a device, employing a semi-conductor detector

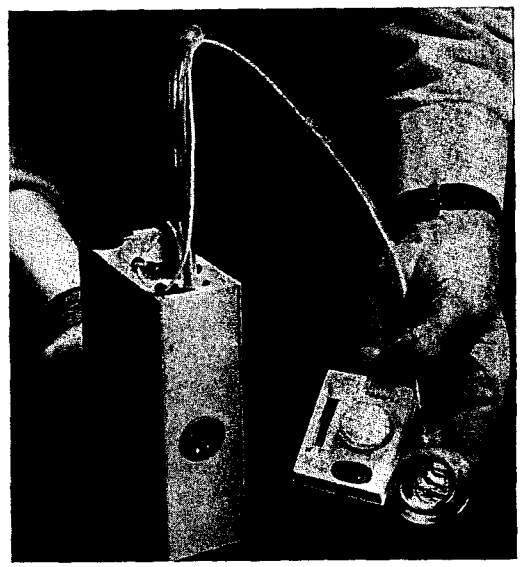

FIG. 10. Personal air sampler, with alarm unit.

mounted in front of the filter paper feeding a transistorised amplifier circuit activating a whistle alarm, is being developed at Windscale (see Fig. 10). This prototype instrument has been designed to alarm at an exposure greater than 400 d.p.m./m^3 hr.

Summarising, therefore, the evidence presented in this paper suggests the following basic principles for an air sampling programme on plutonium facilities:

1. Continuous sampling in extract ducts for the purpose of triggering alarm systems in the event of abnormally high air contamination, and for *detecting* trends in air contamination levels in working areas.
2. Personal air samplers to be used for *measurement* of total air contamination in the breathing zone, in areas where static air sampling has been shown to give unreliable or ambiguous results. They may also be used in the collection of samples for particle size analysis and other operational investigations.
3. Portable, or preferably "personal", air samplers with audible alarm level to investigate transient releases of activity—such devices will indicate the time of the release, the location of release and the operation which caused the release to occur.

Finally, of course, although an effective air sampling programme is an essential part of the health physics monitoring programme on plutonium facilities, it must be emphasised that the ultimate test of the effectiveness of the control of plutonium exposures must be made by biological sampling, and personnel monitoring. At Windscale, there has always been a comprehensive urine sampling programme backed up by faecal sampling where significant intakes have been suspected, and in common with other radiological protection groups we are developing techniques, using our whole body monitoring facility, for measurement of plutonium in the lungs.

Despite the discrepancies that have been reported in this paper, between static and personal samplers, this biological monitoring has demonstrated that the design of our plutonium facilities and operational procedures have been effective in controlling plutonium intakes to acceptable levels. The continuous development of improved air sampling techniques will reduce still further the possibility of individual plutonium exposures.

ACKNOWLEDGEMENTS

The authors wish to thank B. Tagg and D. Laidlow who carried out the particle size analysis and who, with R. Smith, helped to collect and assemble the data used in this paper.

REFERENCES

1. H. J. DUNSTER. Some problems in the application of I.C.R.P. maximum permissible levels for occupational exposure. *Health Physics* **12,** No. 1 (1966).
2. R. J. SHERWOOD and D. M. S. GREENHALGH. A personal air sampler. *Am. Occup. Hyg.* **2,** 127–132 (1960).
3. R. F. CARTER. An autoradiographic method for particle size estimation of plutonium dioxide. A.W.R.E. Report, unpublished.
4. Task group on lung dynamics, Deposition and retention models for internal dosimetry of the human respiratory tract. *Health Physics* **12,** No. 2 (1966).

EXPÉRIENCE EN MATIÈRE DE RADIOPROTECTION TIRÉE DE 8 ANS DE FONCTIONNEMENT D'UN CENTRE DE PRODUCTION DU PLUTONIUM

J. RODIER, J. P. CHASSANY, H. PEYRESBLANQUES, R. ESTOURNEL et R. COURT
Centre de Marcoule, Service de Protection contre les Radiations

Résumé—Protéger le personnel et assurer la sécurité de la production sans l'entraver, telle est la tâche d'un Service de Radioprotection. Dans le Centre de Production de Plutonium, les activités du Service de Protection contre les Radiations ont commencé avec la divergence de la Pile G.1. Le développement progressif du Centre a vu la mise en place d'équipes de contrôle dont le rôle est précisé. Des consignes de travail en milieu radio-actif ont été élaborées. Un programme d'éducation du personnel au moyen de conférences et d'affiches a été mis sur pied.

Les résultats atteints (répartition des doses d'irradiation externe, cas de contamination corporelle . . .) sont discutés. Ils montrent que l'exploitation d'un Centre Nucléaire peut se faire sans que la sécurité des travailleurs soit affectée.

Lors de la création du Centre de Marcoule un des problèmes qui s'est posé aux responsables du Commissariat à l'Énergie Atomique fut celui de la radioprotection du personnel. Ce problème était particulièrement important en raison des quantités considérables de matières radioactives qui devaient être mises en jeu, et de l'inexpérience des agents qui, pour la plupart, avaient à travailler pour la première fois en milieu radioactif. Par ailleurs, la vocation industrielle du Centre imposait que la solution retenue ne crée pas une entrave à l'exploitation des installations. Enfin, Marcoule étant le premier centre industriel français de ce type, aucune expérience antérieure ne permettait d'évaluer les risques d'irradiation ou de contamination auxquels serait exposé le personnel.

Ces risques sont d'ailleurs différents suivant les installations: piles plutonigènes ou usine de traitement du combustible irradié.

À proximité des piles, qui furent les premières installations françaises de la filière graphite-gaz, c'est le risque d'irradiation qui est prédominant. Par contre, dans l'usine de traitement du combustible irradié ou transitent journellement sous forme de liquides et de précipités des quantités de radioactivité dépassant le million de curies, c'est la contamination qui constitue le risque principal.

Devant l'ampleur du problème posé par la radioprotection du personnel, le choix a été fait à Marcoule de confier celle-ci à un Service de Protection contre les Radiations indépendant des services d'exploitation. Cette solution a été retenue, car en confiant la surveillance radiologique à des agents spécialisés disposant de moyens adaptés, elle décharge les équipes d'exploitation de la lourde tâche que représente les contrôles tant du personnel, que des lieux de travail et du matériel. En outre, la séparation des équipes de radioprotection et d'exploitation évite que l'idée "production avant tout" ne prenne le pas sur la sécurité.

MOYENS MIS EN ŒUVRE POUR ASSURER LA RADIOPROTECTION DU PERSONNEL

Les premières solutions au problème de la radioprotection ont été apportées lors de la construction des réacteurs et de l'usine. Des protections importantes destinées à isoler les parties les plus actives des installations des lieux de travail habituels ont été mises en place, tout

en laissant des possibilités d'intervention à distance. Les constructeurs ont également attaché une importance toute particulière à la sûreté des installations. Tout accident peut, en effet, modifier la sécurité des travailleurs et avoir des répercussions sur la continuité de la production.

Les moyens d'action du Service de Protection contre les Radiations ont été mis en œuvre progressivement au fur et à mesure de l'entrée en production des Ensembles Industriels. Les agents de ce Service sont chargés, en particulier, de l'évaluation des différents risques radioactifs présentés par les installations et du contrôle de l'irradiation et de la contamination éventuelles du personnel à la fin du travail. Cette surveillance est facilitée par la classification des lieux de travail. Les conditions d'accès dans chacun d'eux étant définies de façon stricte, l'exposition des travailleurs peut ainsi être parfaitement contrôlée. Les doses intégrées par les agents sont par ailleurs surveillées grâce aux détecteurs individuels, films ou stylos dont ils sont porteurs. L'utilisation généralisée de moyens de protection individuels (vêtements, masques, etc. . . .), adaptés aux différents risques permet une lutte efficace contre la contamination.

Un autre élément contribuant à réduire le danger d'irradiation et surtout de contamination du personnel, est l'élimination des sources inutiles. Ce travail, confié à la Section des Opérations Radio-actives appartenant au Service de Protection contre les Radiations, consiste essentiellement à décontaminer les locaux, le matériel ou les vêtements et à évacuer les résidus radio-actifs. Effectué par un personnel spécialisé disposant de moyens adaptés, il permet un confinement très efficace de la radioactivité dans les parties les plus actives des installations.

Par ailleurs, la prévention technique a été complétée par une prévention psychologique. Le personnel qui dans sa grande majorité travaillait pour la première fois en milieu radioactif était partagé entre la crainte et l'inconscience. Son éducation par des moyens audiovisuels (conférences, films, affiches, recueils de consignes) lui a permis de prendre conscience des risques réels que présente l'industrie nucléaire. L'expérience montre que la sécurité en a largement bénéficié.

CONDITIONS NORMALES DE TRAVAIL

À Marcoule, dans les Ensembles Industriels où sont manipulés des produits radio-actifs, tous les lieux de travail ont été classés en fonction des risques réels ou potentiels auxquels est exposé le personnel qui y séjourne. Cette classification a été établie en fonction des résultats des mesures effectuées par les agents de radioprotection.

Les 480 lieux définis et caractérisés faisant l'objet d'une surveillance permanente se répartissent de la façon suivante:

—10 lieux de classe 1 où les débits de dose dus à l'irradiation externe ou à la contamination restent inférieurs à 0,75 mrems/h.

—310 lieux de classe 2 où les débits de dose sont compris entre 0,75 et 2,5 mrems/h.

—160 lieux de classe 3 où les débits de dose sont supérieurs à 2,5 mrems/h.

Les lieux de classe 2 et 3 sont eux mêmes divisés en 3 sous classes a, b et c, en fonction de la nature du risque, irradiation ou contamination. Les conditions de travail et les mesures individuelles à appliquer à l'intérieur de chacun de ces lieux sont strictement règlementées, elles sont rappelées aux agents à l'aide d'affiches. Il est à noter qu'à la suite de toute variation du risque d'irradiation externe ou de contamination, chaque lieu de travail peut être déclassé par les agents du Service de Protection contre les Radiations.

L'expérience montre que ce sont dans les lieux de classe 1 et 2 que sont situés les principaux postes de travail c'est-à-dire ceux qui exigent le temps de présence du personnel le plus long. Il s'agit en particulier des ateliers, des pupîtres de commande ou de surveillance, des lieux de passage, des nefs piles, des laboratoires, etc. . . . Dans ces lieux, les débits de dose sont suffisamment faibles pour que, sans limitation des temps de séjour, les doses intégrées restent inférieures aux valeurs permises.

Les risques de contamination sont également très faibles en raison de la politique adoptée qui vise à éliminer toutes les sources inutiles et à décontaminer systématiquement le matériel et les locaux. Les dispositifs de ventilation, le cloisonnement des lieux de travail, les multiples contrôles effectués sur le personnel, l'utilisation de sas étanches fixes ou mobiles à la sortie des zones contaminées limitent la

propagation des produits radio-actifs. Le port d'un vêtement de travail particulier, appelé tenue universelle, peut être complété par des survêtements; il évite la pollution des effets personnels et la contamination corporelle des agents. L'utilisation des appareils de protection respiratoire est relativement peu fréquente car les contaminations atmosphériques découlant d'accidents sont elles-mêmes très rares.

Ainsi, les conditions normales de travail dans les installations sont telles qu'il en résulte un risque très faible. Pratiquement elles diffèrent peu de celles rencontrées dans d'autres industries.

CONDITIONS DE TRAVAIL EXCEPTIONNELLES

Tous les travaux nécessaires à l'exploitation des Ensembles Industriels du Centre de Marcoule ne peuvent cependant pas être effectués dans des conditions aussi favorables. En effet, les installations ayant été conçues selon le principe de l'intervention directe: les opérations d'entretien, de modification ou de remplacement des appareils situés dans les parties actives des réacteurs ou de l'usine ne sont pas effectué automatiquement. L'exposition de certains agents à des risques d'irradiation externe ou de contamination plus élevés est donc inévitable.

Toutefois, ces expositions exceptionnelles n'ont jamais entraîné, à Marcoule, de dépassement des normes de radioprotection en vigueur. Ces résultats ont pu être obtenus par plusieurs moyens. D'une façon générale, les installations ont été prévues pour que les interventions dans les enceintes fortement radio-actives puissent être effectuées dans les meilleures conditions. La mise en place des dispositifs d'observation (hublots, périscopes, télévision) ainsi que d'appareils de détection, permet une appréciation plus poussée du risque radio-actif et des travaux à exécuter. Le danger peut généralement être ramené à un niveau acceptable grâce à la décontamination préalable des circuits: les injections de vapeur et de réactifs sont couramment utilisées. L'isolement des appareillages par des blindages individualisés facilite les interventions. Ainsi, dans l'usine, la séparation est réalisée au moyen de cellules indépendantes en béton dont un des côtés est constitué par des briques amovibles en béton baryté.

Enfin, ces opérations étant étudiées à l'avance, des mesures sont prises pour que les doses intégrées ou les contaminations corporelles restent inférieures aux normes en vigueur. Elles consistent essentiellement à mettre en place des protections supplémentaires, à limiter le temps de travail, à rendre obligatoire le port de vêtements spéciaux ou d'appareils de protection respiratoire.

À Marcoule, les travaux qui entraînent une exposition du personnel à un débit de dose supérieur à 7,5 mrem/h, sont considérés comme des travaux à caractère exceptionnel. Ils sont règlementés de façon très stricte et ne peuvent être réalisés qu'après accord d'une autorité responsable. Les conditions de travail sont, dans chaque cas, examinées par le Service de Protection contre les Radiations; ceci en liaison étroite avec les exploitants pour que les risques restent aussi faibles que possible.

Les travaux effectués dans ces conditions exceptionnelles sont de natures extrêmement diverses et leurs causes sont très variées. Certains d'entre eux, tels que prises d'échantillons particuliers, surveillance d'appareillages situés dans les parties actives des installations, font partie de l'exploitation des ensembles industriels. Ils sont toutefois peu fréquents et n'entraînent que l'exposition d'un nombre réduit d'agents. Cependant, la grande majorité des travaux effectués dans des conditions exceptionnelles est constituée par des opérations d'entretien, de remise en état ou de modification des parties actives des installations ou dans des lieux devenus radio-actifs après un incident. Leur durée est généralement plus importante et peut atteindre plusieurs mois.

Parmi les travaux de cette nature, on peut relever quelques exemples:

—Une intervention à l'intérieur du caisson de la pile G.2 a été effectuée après quelques mois de fonctionnement à pleine puissance. Elle devait permettre une modification de la répartition du gaz caloporteur devenue nécessaire après la mise en évidence d'un point chaud dans le béton. Ce travail, très particulier, a duré 17 jours pendant lesquels 881 entrées dans le caisson ont été enregistrées. Les doses intégrées sont restées faibles. Pour les 7 agents les plus exposés, elles étaient comprises entre 750 et 1 500 mrems. Aucune contamination interne n'a été à déplorer.

—Les modifications réalisées sur les échangeurs des piles G.2 et G.3 constituent également un exemple typique des travaux effectués dans des conditions exceptionnelles. L'exiguïté et l'encombrement des lieux rendaient les conditions de travail particulièrement pénibles. Le port d'un équipement vestimentaire complet était imposé par les risques de contamination importants. À l'intérieur des échangeurs, la contamination des surfaces était de l'ordre de 5.10^{-2} μCi/cm^2. L'efficacité des survêtements en toile a été telle qu'aucune contamination des tenues universelles n'a été décelée, sauf lorsque des liquides contaminés (huile) avaient souillé les vêtements aux coudes et aux genoux. Les seules contaminations corporelles observées ont concerné les mains, elles ont cédé à de simples lavages.

—À la suite d'un échauffement accidentel du canal W. 19 E du réacteur G.2, les cartouches d'uranium, dont certaines étaient détériorées n'ont pu être déchargées par la voie normale et ont dû être évacuées par la face avant de la pile. Les barreaux d'uranium et les débris de gaine étant très actifs, les risques d'irradiation étaient élevés. La mise en place à l'extrémité du canal d'un conteneur blindé et l'évacuation rapide de tous les résidus a permis au personnel d'effectuer cette intervention dans une ambiance généralement inférieure à 7,5 mrems/h. L'intervention a duré 1 mois et demi: les doses intégrées n'ont pas dépassé 800 mrems, et 80% d'entre elles ont été inférieures à 150 mrems. La lutte contre la contamination a été menée avec une extrême vigueur. De ce fait, pendant toute la durée des opérations, les enregistreurs d'aérosols radio-actifs n'ont jamais accusé une contamination atmosphérique supérieure à la C.M.A.

—À l'Usine d'Extraction du Plutonium, une intervention a été effectuée sur un dissolveur présentant une fuite au raccordement d'un tuyau. Les mesures d'irradiation au contact du dissolveur indiquaient des valeurs allant de 1000 rads/h à 23,000 rads/h. Une décontamination interne par rinçages acides et basiques alternés, suivis d'une décontamination externe du dissolveur, permirent de ramener les niveaux d'irradiation de 2 à 10 rads/h. Toutefois, ces débits de dose ayant été jugés encore trop élevés, des protections de plomb furent mises en place avant l'intervention. Le débit de dose auquel ont été finalement soumis les opérateurs a été au maximum de 200 mrems/h. Une trentaine d'agents ont participé à cette intervention, aucun d'eux n'a reçu plus de 360 mrems.

—Un autre exemple peut être trouvé dans une fuite peu importante sur une batterie d'extraction présentant cependant une forte contamination α et en même temps des débits de dose atteignant 8 rads/h. Grâce à la mise en place d'écrans de protection constitués par de l'eau et du plomb, l'irradiation a pu être ramenée à un maximum de 700 mrads/h. Par ailleurs, les soudeurs s'exercèrent préalablement sur une pièce inactive identique de façon à accroître la précision et la rapidité de leurs gestes. Dans ces conditions, les doses intégrées sont restées inférieures à 50 mrems.

Un grand nombre de travaux de décontamination destinés au maintien de la salubrité des lieux de travail sont également effectués dans des conditions exceptionnelles. Cependant, les équipes qui en sont chargées étant constituées par du personnel entraîné au travail en actif et disposant de moyens adaptés, les doses intégrées sont faibles et les contaminations corporelles rares.

—Il peut être cité comme opération typique le démontage d'une installation de purification de plutonium désaffectée qui nécessita l'enlèvement du matériel en place (boîtes à gants, cuves, tuyauteries) et l'assainissement complet des locaux. Les travaux ont duré environ sept mois, et à leur terme, une nouvelle installation pouvait être implantée dans les salles exemptes de toute pollution. Initialement la contamination de certaines surfaces était de l'ordre de 10^{-2} μCi/cm^2 avec des valeurs beaucoup plus élevées dans les circuits. Malgré les découpages, le personnel a rarement travaillé dans une atmosphère contaminée à plus de 10^{-2} Ci/m^3 de plutonium. L'organisation rationnelle du chantier et le port d'appareils respiratoires bien adaptés, ont permis le déroulement des opérations sans qu'aucun incident individuel de contamination ne soit enregistré.

Dans l'ensemble, les manipulations à caractère exceptionnel autorisées, pour un débit de dose supérieur à 7,5 mrems/h, sont relativement nombreuses, mais la plupart d'entre elles sont de courte durée.

Tableau 1. *Travaux à Caractère Exceptionnel*

	Autorisations accordées pour une exposition du personnel à un débit de dose	
	compris entre 7,5 et 75 mrem/h	compris entre 75 et 750 mrem/h
1959	196	67
1960	583	19
1961	1729	111
1962	2445	6
1963	2791	11
1964	3773	12
1965	3319	0

Le nombre des autorisations accordées depuis 1959 pour les travaux entraînant une exposition du personnel à des débits de dose compris entre 7,5 et 750 mrems/h. est donnée par le tableau 1.

Ainsi, le Centre de Marcoule a été exploité pendant 7 ans sans qu'il ait été nécessaire d'exposer un seul agent à un débit de dose supérieur à 750 mrems/h. Ce résultat a pu être atteint bien que toutes les installations soient du type à entretien direct. Les autorisations accordées pour des débits de dose compris entre 75 et 750 mrems/h, relativement fréquentes en 1959, ont diminué considérablement grâce à l'expérience acquise dans la conduite des interventions. Les 3319 autorisations accordées en 1965 correspondent à un temps de travail total de 42.000 heures, ce qui représente environ le travail à plein temps de 20 agents, c'est à dire de moins de 1% du personnel du Centre. En fait, un nombre d'agents bien plus élevé y participe mais pendant des temps relativement courts. Il en résulte que chacun d'eux est exposé à un risque faible. Par ailleurs, les débits de dose pour lesquels sont autorisées ces opérations, ne se rencontrent qu'en des points bien précis des chantiers. Les agents n'y sont pas exposés de façon permanente au cours de l'intervention. Les résultats dosimétriques montrent que les agents qui ont participé en 1965 à ces opérations ont reçu des doses individuelles correspondant à un débit de dose moyen de 6 mrems/h.

Les agents exposés à un risque d'irradiation externe, c'est à dire tous ceux qui travaillent à proximité des installations où sont manipulés des produits radio-actifs, portent en permanence un film dosimètre. La lecture mensuelle de ces détecteurs individuels permet donc une comptabilisation des doses intégrées au cours des travaux effectués dans des conditions normales et dans des conditions exceptionnelles. Jusqu'en 1961, les doses moyennes annuelles ont constamment augmenté, pour atteindre à cette date la valeur d'environ 250 mrems. Depuis, elles se sont maintenues à ce niveau, en accusant cependant quelques légères variations dues à l'importance et à la nature des grands travaux effectués. Le graphique en annexe indique la répartition des doses mensuelles intégrées par les agents en 1965. Celles qui correspondent à des films ne présentant pas de noircissement

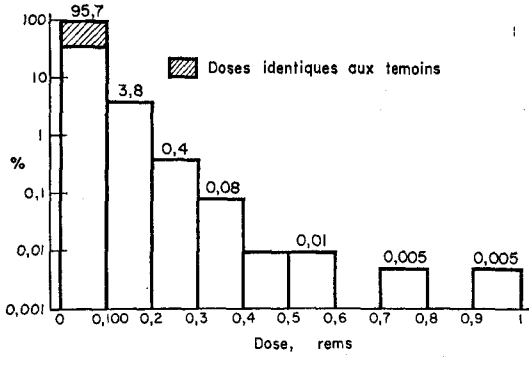

FIG. 1. Repartition des doses mensuelles rélevée en 1965.

apparent représentent 60% du total, 0,1% d'entre elles sont supérieures à 0,3 rem, aucune ne dépasse 1 rem.

Le tableau 2 indique les doses moyennes annuelles qui ont été calculées à partir des résultats de lecture des films depuis 1956.

Tableau 2. Évolution des Doses Moyennes Integrées (Irradiation en profondeur)

Année	Dose en mrems
1956	96
1957	30
1958	143
1959	176
1960	120
1961	271
1962	251
1963	269
1964	302
1965	243

CONDITIONS DE TRAVAIL ACCIDENTELLES

Parmi tous les accidents ou incidents qui peuvent survenir dans des installations nucléaires, certains n'affectent que le fonctionnement des appareillages. D'autres, par contre, entraînent également une élévation brutale et imprévue de la radio-activité des lieux de travail. Dans ces deux cas, la remise en état de fonctionnement du matériel fait généralement l'objet de travaux effectués dans des conditions exceptionnelles telles que celles decrites précédemment. Du point de vue de la radioprotection, les accidents les plus importants sont ceux qui créent des risques radio-actifs nouveaux. En effet, ils peuvent entraîner une exposition externe ou une contamination. Cette exposition inopinée découlant de circonstances incontrôlées peut avoir des conséquences graves.

Les accidents qui ont été enregistrés à Marcoule, depuis la mise en service des installations, n'ont jamais entraîné une irradiation ou une contamination du personnel supérieure aux normes en vigueur. Malgré cela, leur analyse, l'étude de leurs causes et de leurs conséquences, ont permis d'améliorer leur prévention et de mieux connaître le risque lié à l'exploitation d'un centre nucléaire.

Les réacteurs G.2 et G.3 en service à Marcoule, sont refroidis par du CO^2 sous pression. Ce gaz est contaminé par des produits d'activation dont la dispersion en cas ce fuite peut provoquer un accident de pollution atmosphérique auquel s'ajoute celui dû à la toxicité propre du CO^2. La détection de ces fuites, particulièrement dans les points bas des installations et dans les locaux mal ventilés, fait l'objet d'une surveillance permanente basée sur la mesure de la contamination radio-active et de la teneur en CO^2 de l'atmosphère.

Parmi les accidents dus à une fuite de CO^2, les plus fréquents ont été causés par la mauvaise étanchéité de soudures, de vannes ou de joints. Le plus important est survenu à l'occasion du chargement du combustible d'un réacteur. L'appareil utilisé pour introduire les cartouches d'uranium dans la pile ne s'étant pas verrouillé, le CO^2 a fui par l'orifice d'un canal. À proximité du lieu de l'incident, la contamination atmosphérique a atteint des valeurs variant de 5 à 60 CMA. La contamination du sol est restée inférieure à 5.10^{-2} $\mu Ci/cm^2$. L'évacuation du personnel ayant été immédiate, aucune contamination individuelle n'a été enregistrée.

Lors du démarrage des réacteurs, le transfert des cartouches irradiées s'effectue par gravité dans des conduits métalliques qui les acheminent jusqu'à l'appareil assurant leur mise en conteneurs. Ces installations sont situées dans des enceintes dont l'accès est habituellement interdit. Cependant lorsqu'une cartouche se trouve coincée à la sortie du canal, une intervention directe est nécessaire. Bien que les manœuvres de déchargement soit alors interrompues, et malgré l'existence de dispositifs de sécurité, la chute inopinée de cette cartouche entraîne une irradiation exceptionnelle du personnel. Le temps d'exposition est très court car la chute de la cartouche est rapide. Dans un cas de ce type, la dose intégrée par l'agent exposé au débit de dose le plus élevé (150 rems/h environ) a été de 450 mrems. Chacun des autres agents exposés a reçu une dose de 50 mrems.

Dans l'Usine d'Extraction du Plutonium et ses annexes, laboratoires et Station de Traitement des Effluents, transitent journellement des liquides et des boues dont la radiotoxicité très élevée est due à des produits de fission et à du plutonium. Malgré les moyens efficaces et

coûteux destinés à confiner ces produits dans les parties les plus actives des installations, leur dispersion au hasard d'interventions ou en cours d'exploitation peut être à l'origine d'accidents. En particulier, leur acidité provoque des phénomènes de corrosion qui s'ajoutent aux causes habituelles des fuites: joints défectueux, vannes non étanches, débordements, etc. . . . Les éjecteurs à vapeur fréquemment utilisés sont, dans certaines circonstances, à l'origine d'une dispersion de la radio-activité.

À l'occasion d'opérations de transfert par siphonnage ou de mise en dépression pour effectuer des prises d'échantillons, des remontées d'activité dans les circuits de vide peuvent se produire malgré l'existence de pots de garde et de filtres. La contamination de ces circuits pour lesquels une protection n'a généralement pas été prévue peut être à l'origine d'accidents d'irradiation. Un accident de ce type a été enregistré à l'atelier de concentration des produits de fission. Cependant, malgré les débits de dose élevés (jusqu'à 720 rems/h), il n'y a pas eu d'incident d'irradiation car on se trouvait dans une zone de travail occasionnel bien délimitée.

Une dispersion des produits radio-actifs peut également se produire à l'occasion d'opérations de démontage des circuits. Un tel accident a été enregistré lors du découpage d'une tuyauterie contenant de l'oxalate de plutonium. Il a entraîné une contamination atmosphérique importante de plusieurs locaux qui a atteint en certains points la valeur de 4000 CMA. La décontamination des surfaces a exigé 2 mois de travail. Grâce à l'évacuation immédiate des personnes présentes sur les lieux et au port du masque, cet incident n'a pas eu de conséquences pour le personnel.

L'établissement d'une liste exhaustive de tous les accidents qui peuvent survenir dans des installations nucléaires est très difficile. Les causes pouvant provoquer la dispersion de produits radio-actifs ou l'exposition du personnel à une irradiation élevée sont en effet très nombreuses et variées. On peut citer à titre d'exemple les accidents mineurs consécutifs au renversement de flacons, à la rupture de dispositifs d'isolement ou d'emballages d'objets contaminés, à l'incendie de sas en vinyle. . . .

Les accidents dus à des défaillances du matériel ou des dispositifs de sécurité sont les plus fréquents. L'importance des quantités de produits radio-actifs mises en jeu, l'utilisation de CO^2 sous pression dans les réacteurs, l'acidité des liquides manipulés à l'Usine d'Extraction du Plutonium constituent autant de facteurs d'accroissement des risques. Cependant le nombre des incidents a pu être réduit d'année en année grâce à une constante recherche de l'amélioration de la sécurité des installations. D'une façon générale, un soin particulier a été apporté au choix du matériel de manière à avoir des installations robustes, d'une surveillance aisée et de réparation facile. Pour lutter contre les phénomènes de corrosion, des aciers inoxydables particulièrement résistants ont été adoptés pour la construction des appareils les plus délicats. Les soudures réalisées avec le plus grand soin font l'objet de contrôles radiographiques systématiques. Enfin, toutes les précautions prises lors de la conception des installations sont complétées par de fréquentes vérifications de l'état du matériel et par la mise en place de dispositifs de sécurité et d'alerte.

Mais les accidents ne sont pas tous dus à des facteurs techniques. La défaillance du matériel ou d'une méthode trouve: souvent son origine dans le comportement des individus et les conséquences d'un incident peuvent être considérablement modifiées par des initiatives heureuses ou malheureuses. Dans l'industrie nucléaire les facteurs humains pouvant être à l'origine d'accidents ne sont pas différents de ceux mis en évidence par les spécialistes de la sécurité du travail classique. C'est pour cette raison qu'à Marcoule, la prévention technique a été complétée par une prévention psychologique. Grâce à la mise en œuvre généralisée de moyens audio-visuels (conférences, films, affiches), la grande masse des travailleurs a pris conscience des risques réels que présente l'industrie nucléaire. Cette prévention psychologique est renforcée par la présence constante des agents de radioprotection parmi les travailleurs.

L'expérience montre que la sécurité a largement bénéficié de tous les efforts dépensés pour améliorer la prévention. En analysant les résultats obtenus après 8 ans de fonctionnement, il apparaît que c'est une erreur de croire que le travail dans l'industrie nucléaire est particulièrement dangereux. Les incidents survenus à

Marcoule n'ont jamais eu de conséquences graves pour le personnel tant du point de vue d'irradiation externe que du point de vue contamination individuelle. Ainsi l'habitude est prise de développer immédiatement le film dosimètre chaque fois qu'un agent est supposé avoir été victime d'une irradiation accidentelle. Pour une centaine de lectures effectuées chaque année dans ces conditions 85 n'ont donné aucun résultat significatif. Pour les 15 autres les doses lues, généralement de quelques mrems, n'ont jamais dépassé 3 rems.

Les cas de contamination corporelle sont plus nombreux. Ils ont des causes très diverses. Les ingestions ou inhalation de produits radio-actifs sont généralement consécutifs à un accident de contamination atmosphérique ayant entraîné l'exposition d'agents non équipés de masques. Les blessures et les brûlures de tous types peuvent aussi être à l'origine de contamination interne. En particulier des piqûres avec des aiguilles de prise d'échantillons ont été enregistrées à plusieurs reprises.

Les contaminations externes sont dues, dans la plupart des cas, soit au manque de précautions des agents lorsqu'ils se débarrassent de leurs vêtements, soit à des déchirures de gants. Il y a lieu de signaler ici que les vêtements de toile dont l'utilisation a été généralisée constituent une protection particulièrement efficace contre la contamination corporelle. Ils absorbent très bien des projections de liquides contaminés et leur port ne constitue pas une gêne pour le personnel.

En cas de contamination individuelle, détectée ou suspectée par les agents de radioprotection, les travailleurs sont dirigés vers le bloc de décontamination du Service Médical qui est équipé pour appliquer des traitements efficaces et pour effectuer des contrôles précis. Ainsi, les contrôles exceptionnels s'ajoutent aux contrôles systématiques et périodiques de l'ensemble du personnel du Centre. Jusqu'à maintenant aucune contamination interne supérieure aux Quantités Maximales Admissibles n'a été enregistrée, la plupart d'entre elles étant de l'ordre de la centième de Q.M.A.

CONCLUSION

Malgré les quantités énormes de radio-activité manipulées, le Centre de Marcoule a pu être exploité en restant largement au-dessous des limites fixées par les normes d'irradiation et il n'y a pas eu d'accident ayant entraîné des conséquences graves pour le personnel.

Ces résultats sont peut-être dus au facteur chance, mais aussi beaucoup à l'organisation de la radioprotection. La stricte définition des lieux et des conditions de travail, la règlementation sévère des manipulations considérées comme exceptionnelles dès que le débit de dose dépasse 7,5 mrems/h, la préparation des chantiers, l'éducation du personnel constituent autant d'éléments favorables.

Comme toute chose, la sécurité se paie. Elle est toujours le résultat d'une somme d'efforts patients et elle exige une infrastructure et du personnel. Il devrait être évident pour tous que son prix est moins élevé que la réparation des accidents qu'elle évite. Cependant les installations de contrôle sont parfois jugées chères et les effectifs indispensables pour la surveillance sont souvent trouvés trop importants. Dans l'ensemble du Centre, nous avons de nuit, dimanches et fêtes 24 agents de radioprotection présents en permanence, ce qui conduit, par le jeu de la relève des équipes, à un effectif de 140 agents encadrés par 4 ingénieurs. Il est possible de discuter de la nécessité de ce personnel qui paraît ne pas participer directement à la production. Les agents de radioprotection sont toutefois intimement mêlés à la vie des ensembles industriels et leur influence est inséparable de l'expérience acquise pendant ces dernières années. Quels auraient été les résultats en l'absence d'un système de radioprotection bien structuré? Il est évidemment difficile de répondre à cette question; cependant quelques remarques peuvent être faites. Lorsqu'on parle d'évolution de la radioprotection, il est souvent fait appel à la notion de "protection individuelle" ou d'"autoprotection". Pratiquement ceci revient à confier des responsabilités plus ou moins grandes au personnel d'exploitation. Cela suppose que l'on accorde une certaine confiance à la compréhension et à l'esprit de discipline des individus. Les résultats obtenus ne peuvent que dépendre du bon usage que les agents feront de leur liberté.

En fait pour pratiquer sans contrainte ce qui leur est recommandé par les consignes, les travailleurs doivent avoir bien assimilé les

risques radio-actifs et être solidement éduqués. Mais ce n'est pas seulement un problème d'éducation, c'est aussi une question d'individu. Ainsi, il semble qu'il soit plus facile de faire respecter les consignes en pays anglo-saxon qu'en pays latin. Il est bien évident qu'une législation réglementant la circulation routière mais sans organisme de contrôle pour la faire respecter, tomberait inévitablement en désuétude. En radioprotection, l'évolution ne pourrait être qu'identique; si l'on peut envisager de diminuer ces contrôles, il n'est pas possible de les supprimer dans leur totalité. En ce qui nous concerne, environ le 1/6 du travail de nos équipes de radioprotection est constitué par la surveillance du bon respect des consignes. Certes, la suppression de ces contrôles pourrait conduire à une économie. Il ne nous est malheureusement pas possible de préciser quelles en seraient les conséquences sur le niveau de la sécurité.

CONCEPTION ET EXPLOITATION DU TABLEAU DE CONTRÔLE DES RADIATIONS DU LABORATOIRE D'EXAMEN DES COMBUSTIBLES IRRADIÉS DU CENTRE D'ÉTUDES NUCLÉAIRES DE SACLAY

J. BERTRAND, Y. MARQUE et F. MATHERN
Service de Protection contre les Radiations, CEA, Centre d'Études Nucléaires, Saclay, France

Résumé—La mise en place et l'exploitation des dispositifs fixes de contrôle des radiations auprès du Laboratoire d'Examen des Combustibles Irradiés de Saclay ont été effectuées dans un double but:

1. Évaluer avec toute la précision possible les niveaux de radiation et rassembler le maximum de renseignements concernant le fonctionnement des installations de sécurité du laboratoire de façon à assurer la sécurité du personnel et des installations.
2. En fonction des renseignements recueillis, être en mesure de définir rapidement les conditions de travail pour les manipulations proposées par les utilisateurs, de façon à limiter au mieux les sujétions imposées par les impératifs de radioprotection, ne pas ralentir les cadences de travail du laboratoire, et par là même accroître le rendement.

Les contrôles automatiques et continus effectués sont de nature diverse:

Contrôles de rayonnement (irradiation ambiante, contamination atmosphérique, contamination du personnel à la sortie des zones actives).

Contrôle des accès aux zones actives.

Contrôle des réseaux de ventilation.

Contrôle des mouvements des convoyeurs d'éléments combustibles dans les cellules $\beta\gamma$.

Détection des incendies éventuels dans les points importants du laboratoire (ligne $\alpha\beta\gamma$, ligne $\beta\gamma$, ventilations, tableau de contôle).

Contrôle du niveau des effluents dans les cuves actives.

L'ensemble de ces dispositifs de contrôle et de commande est regroupé dans la salle de Contrôle des Radiations du bâtiment. Un tableau de contrôle abrite la totalité des chaînes électroniques de mesure et les appareillages d'enregistrement. Un tableau synoptique permet à tout moment d'avoir une vue d'ensemble sur les niveaux de radio-activité et sur la totalité des sécurités du laboratoire.

Une caméra de télévision, implantée dans la zone à accès réglementé, et télécommandée depuis la salle de contrôle, permet de suivre avec efficacité les manipulations d'introduction et d'extraction dans les cellules.

ÉVALUATION DU RISQUE INDIVIDUEL LORS DE CONTAMINATIONS ATMOSPHÉRIQUES PAR LE PLUTONIUM

J. POMAROLA, A. RISSELIN et P. FELIERS

Section de Protection contre les Radiations, CEA, Centre d'Études Nucléaires, Fontenay-aux-Roses, France

Résumé—Le contrôle de la contamination atmosphérique dans un laboratoire vise généralement trois objectifs distincts:

1. Obtenir une alarme en cas d'incident de contamination atmosphérique.
2. Obtenir des prélèvements représentatifs pour évaluer le risque encouru par chaque agent présent.
3. Suivre l'évolution de la contamination au cours du temps.

Le plus souvent, il n'est pas possible d'atteindre ces trois objectifs au moyen d'un appareillage unique, c'est pourquoi nous avons fait réaliser d'une part deux installations pilotes destinées à l'alarme et à la mesure continue, d'autre part deux installations pilotes destinées à l'évaluation du risque individuel.

Après avoir indiqué les avantages et les inconvénients des appareils généralement utilisés au CEA pour évaluer l'exposition du personnel, cette communication se propose de décrire l'une des installations pilotes réalisées dans ce but et de faire le bilan des résultats obtenus, après une année d'exploitation dans un laboratoire de Métallurgie du Plutonium.

Grace à cette installation, nous avons pu mettre en évidence l'hétérogénéité de la contamination lors de plusieurs incidents. À cause de cette hétérogénéité, le niveau du risque encouru, par le personnel, à différents postes de travail peut varier d'un facteur 200, ce qui nécessite de disposer, dans le laboratoire, de nombreux points de prélèvement. Cette multiplicité des points de prélèvement permet en outre, éventuellement de confirmer ou de localiser l'origine de l'incident.

Le coût de cette installation a été très inférieur à celui de l'équipement, en appareils traditionnels, qui aurait été nécessaire, pour obtenir des résultats comparables.

Enfin une telle installation, peu bruyante et d'entretien aisé, est mieux acceptée par les utilisateurs que les appareils traditionnels.

Pour toutes ces raisons, nous avons décidé d'équiper entièrement, selon cette conception de prélèvement, un nouveau bâtiment de Métallurgie du Plutonium en cours d'aménagement.

VENTILATION SYSTEM FOR A RADIOMETALLURGICAL BUILDING. DESIGN, COMMISSIONING AND OPERATING INSTRUCTIONS

M. A. CRESPI GONZALEZ

División de Ingenieria, Junta de Energia Nuclear, Ministerio de Industria, Madrid, Spain

Abstract—The ventilation system of a radiometallurgical building, belonging to the Junta de Energia Nuclear of Spain, is described. The building is located at the Centro Nacional de Energia Nuclear Juan Vigón of the Junta de Energia Nuclear in Madrid and is destined to house a 1000 Ci (1 MeV) β-γ metallurgical cell. This cell will be operated by the Metallurgy Division for dismantling experimental loops, handling irradiated materials, disassembling irradiated fuel elements and other operations. The hot cell will be mainly used for handling materials irradiated in the adjacent JEN-1 pool reactor.

Design criteria of the ventilation system are shown in the first part of the paper. Zoning of the building according to the contamination probability is indicated. A brief outline is given of the ventilation system design, with indication of the selected equipment to obtain these conditions.

The cell filtration system is described in detail because of its importance in preventing outleakage of contaminated dusts that may follow a failure of the ventilation system.

The air flow control system and monitoring and warning equipment used are described. Finally the commissioning procedure and operating instructions are presented.

DISCUSSION

W. N. SAXBY (*U.K.*):

From his experience and measurements does Mr. Steele consider that it would be practicable to handle long irradiated plutonium in quantity by using a combination of (a) local shielding, both against neutrons and X/γ radiations around apparatus within the glove-box and (b) distant handling by the use of long manual handling tools. This if practicable would give flexibility and be less expensive than the complicated automatic handling systems.

I would also like to ask what instruments Mr. Steele used for measuring the neutron dose rates in arriving at his personal exposures.

T. A. STEELE:

Fabrication of small amounts (<10 kg/year) of recycled plutonium would be possible under local shielding conditions using careful planning. Fabrication of large amounts (>100 kg/year) of recycled plutonium having an isotopic composition of 0.1 w/o Pu^{238}, 34.9 w/o Pu^{239}, 35 w/o Pu^{240}, 10 w/o Pu^{241} and 20 w/o Pu^{242} would require automated fabrication and inspection techniques.

As for the method we use for neutron personal monitoring, at Argonne the Kodak NTA neutron film is used; however, in the plutonium facility the energy and intensity of the neutron background are not sufficient to make the film useful. At the plutonium facility, neutron exposures are assigned as a function of the neutron backgrounds, working times and the gamma radiation exposures.

D. K. CRAIG (*South Africa*):

It seems to me that very little airborne plutonium has any chance of reaching the functional areas of the lung. Do you not think that it would be more appropriate to use a respirable fraction sampling device (a size selection sampler) for your personal air sampler?

What is the source of the relatively high levels of airborne Pu that you have reported, apart of course from glove fractures and other breaks in the seals of your glove-boxes or contaminants? Finally, have you attempted to make any correlation between the results obtained n the personal air samplers and the results of analyses for the plutonium content of urine samples and, if so, what are the results?

S. T. HERMISTON:

1. The particle diameters that I referred to in my talk were the activity median aerodynamic diameters (A.M.A.D.). This is the most appropriate unit of measurement if we are interested in the amount of deposition in the lung. For instance, the ICRP Task Group on Lung Dynamics has proposed a lung model, which allows deposition patterns to be assessed from a knowledge of the A.M.A.D.'s. For comparison with our own results, this Task Group suggests a A.M.A.D. of 1μ to be used, if the actual A.M.A.D.'s have not been determined by practical measurements.

2. It would seem to me that a size selection sampling device might well be used, particularly if air contamination levels are approaching maximum permissible concentrations. We are looking into this: our difficulty at the present time is that I am unaware of any size selection device which closely matches current lung deposition models. In many areas where air contamination levels are well below the maximum permissible concentration, measurements of total air contamination will be sufficient to demonstrate that working conditions are satisfactory.

3. The main source of plutonium air contamination in working areas, is leakage of activity through gloves. For this reason, on our major plutonium production facilities we have eliminated the use of gloves, by the use of a "sealed face", and provide completely separate ventilation for maintenance and operating areas.

4. We have not yet attempted to correlate the results obtained with personal air samplers, with plutonium in urine measurements. When "insoluble" plutonium is being handled, faecal measurements made during the first four days following a possible exposure are the most profitable to make. However, due to the difficulties of collecting much samples, we have no detailed results to report. Mr. Johns, from Winfrith, has carried out such sampling programme, and may wish to comment.

T. F. JOHNS (*U.K.*):

We have considerable information on the relationship between the readings of personal air samplers and subsequent excretion in urine and faeces. We have, at Winfrith, an area in which large (tonne),

quantities of PuO_2/UO_2 fuel elements are manufactured in a large number of free-standing glove-boxes. Our experience is that there is no chronic contamination of the air; the exposure of individuals arises from a small number of discrete incidents, in most of which PuO_2 is released to the air as the result of damage to one of the gloves. The airborne contamination is very localised in both space and time, and usually only the individual working at that particular glove-box is significantly exposed. In most of these incidents we find good agreement between the estimate of personal exposure made from the personal air sampler, on one hand, and from faeces measurements on the succeeding five days, on the other. This confirms that the personal air sampler does give a good measure of the amount of plutonium inhaled. On the other hand we have found little or no plutonium in the urine of such individuals, and this urine data strongly suggests that only a small proportion of the PuO_2 initially taken into the body is retained in the lungs. This confirms Dr. Craig's suggestion that these gross measurements of intake lead to an over-estimate of the hazard (because of the large particle size of much of the aerosol).

There is one other point to which I would draw your attention. Although our experience shows that normal installed air samplers usually lead to a gross underestimate of the exposure of individuals, we are hopeful that a new air sampling system which we have recently installed will obviate the need for many personal air samplers. This system, which is demonstrated outside this hall, provides an air sampling point near the operating face of each glove-box, and gives an alarm in case of unusually high airborne levels.

D. C. LAWRENCE (*U.S.A.*):

1. What type of filter media are used and how are they counted?

2. How do they propose to solve the Radon–Thoron problem for their personal-alarm type air sampler?

3. Why do they use glass filter paper?

S. T. HERMISTON:

1. We use glass fibre papers. The detector in the personal sampler with alarm is a semi-conductor. However, for accurate assessment of the filter papers from the sampler we allow 72 hr to elapse from the end of sampling to allow daughter products of radon and thoron to decay. We then assay the papers using scintillation counters.

2. Whether we need be concerned about interference from natural activity on the P.A.S. with alarm, depends on the alarm setting. When the contamination is "insoluble" plutonium oxide, with a relatively high MPC in air, this interference is not important. On the other hand, if the contaminant is soluble plutonium with an MPC in air only 1/20 of that for insoluble plutonium, then it is possible that alpha energy discrimination might be used to achieve a desired sensitivity.

3. The glass fibre paper that we use has a very good efficiency over all particle sizes of interest. I will be pleased to supply you with the specification for this paper, if you wish.

M. GIUBILEO (*Euratom*):

Vorrei sapere se i dati di dosimetria esterna esposti nella tabella si riferiscono a dosi alfa oppure alle comuni dosi beta-gamma globali.

J. CHASSANY:

Les doses intégrées citées sont des doses "en profondeur" indiquées par les films dosimètres.

HUB. WJIKER (*Netherlands*):

In Fig. 2 I noticed the following sequence in the colours used when going from a less dangerous to a more dangerous zone: white, blue, green, yellow, red. My question is: why has green been taken for a more dangerous zone than blue and not the other way round? We are accustomed to the use of green for safety, e.g. in traffic.

J. CHASSANY:

Les zones de travail sont définies dans le *Dictionnaire des Sciences et Techniques Nucléaires*, 1963.

C. O. WIDELL (*Sweden*):

I would like to answer your question about the colour code. This is a code adopted by ISO and almost adopted by the Committee ISO/TC 85/SC 2, Radiation Protection. Green for safety and red for danger.

S. A. KHAN RANA (*Pakistan*):

The speaker has pointed out that there were no cases of internal contamination. Could I ask him the criteria on the basis of which this conclusion was arrived at and which particular group of workers was subjected to the examinations?

J. CHASSANY:

Le personnel affecté aux Ensembles Industriels est contrôlé systématiquement par le Service Médical. Ces contrôles consistent en des examens spectrométriques pour le dépistage des contaminations β γ et

concernent l'ensemble du personnel. Les contrôles de la contamination interne α sont pratiqués sur les travailleurs de l'Usine d'Extraction de Pu et comprennent des prélèvements d'urine. Par ailleurs le Service de Protection contre les Radiations a la possibilité de détecter une contamination dès son origine dans tous les lieux fréquentés par le personnel. Si, à la suite de ses contrôles, il estime qu'un agent a pu être exposé il le dirige immédiatement vers le Service Médical qui procède alors à des examens particuliers.

R. BAZIRE (*France*):

Dans quelle mesure les appareils de prélèvement tiennent-ils compte de la granulométrie du Plutonium?

J. POMAROLA:

Nous avons deux types de circuits dans l'installation en vue du contrôle de la contamination du Pu^{239}:

1. Ceux qui permettent d'obtenir une alarme et une mesure en continu de la contamination.

2. Ceux qui permettent d'obtenir une évaluation de la dose reçue au poste de travail, par des prélèvements continus sur filtre. Dans les deux cas nous tenons compte de la granulométrie:

1. Les appareils d'alarme par impacteur ou sur filtre.

2. Les filtres utilisés sont des filtres en papier alpha et fibre de verre dits "absolus" dont l'efficacité est de 99,98% pour des aérosols de 0,3 μ, en moyenne, mais qui peuvent arrêter aussi des poussières de 0,1 μ.

M. GIUBILEO (*Euratom*):

A proposito delle determinazioni granulometriche sull'aria contaminabile da plutonio, vorrei conoscere se ritiene sufficiente per il controllo del personale l'efficienza dei filtri fino a 0,3 micron di diametro. Tenendo conto che generalmente le particelle più fini di 0,5 micron costituiscono la metà della quantità totale, esse sono le più interessanti dal punto di vista tossicologico, anche per la possibilità di una solubilizzazione nei liquidi biologici e di un passaggio nelle vie linfatiche.

J. POMAROLA:

Je ne crois pas que nous puissions répondre de manière complète à la question qui vient d'être posée, parce que cela nous entraînerait dans un débat extrêmement long. Ce que je peux dire c'est ceci: lorsque je dis que les poussières, les aérosols retenus, ont une dimension de 0,3 micron, il s'agit d'une dimension moyenne. Les filtres sont capables d'arrêter des poussières jusqu'à 0,1 micron, mais ils sont presque totalement efficaces pour les poussières de 0,3 micron, tandis que le pourcentage des poussières de 0,1 micron arrêtées est beaucoup plus faible. On peut admettre que 99% des poussières de 0,3 μ sont arrêtées mais non pas celles de 0,1 μ. Nous avons fait des expérimentations à la fois sur des aérosols liquides et sur des aérosols solides par émission dans des installations et cela nous a permis de déterminer quel type de filtres il fallait adopter pour les prélèvements et quel type d'appareillage pour les alarmes. Nous nous sommes arrêtés, pour les installations de radiométallurgie, aux impacteurs, puisque là nous nous trouvions exclusivement en présence de poussières solides d'une certaine granulométrie. Pour les autres laboratoires, en particulier les laboratoires de radiochimie nous utilisons des filtres absolus.

D. K. CRAIG (*South Africa*):

If I understand correctly, Mr. Pomarola said that his particles had a mean size of 0.3 μ physical diameter. I would like to emphasize that it makes little sense to talk of an 0.3 μ diameter plutonium particle in terms of its inhalation hazard to man, as this is equivalent to an aerodynamic equivalent sphere of about 6 microns, which has little chance of reaching the functional areas of the lung or of staying in the body for a long enough time to present a hazard. I think that it is very important to attempt, in our air sampling, to determine the respirable fraction of the aerosol of interest by using some sort of size selection sampler.

EXPERIENCE WITH THE USE OF A CONTINUOUS ALPHA AIR MONITOR, USING LARGE AREA PROPORTIONAL COUNTERS AND AN IMPROVED PSEUDO COINCIDENCE CIRCUITRY

J. P. VAANE and E. M. M. DE RAS
European Transuranium Institute (Euratom), Karlsruhe

Abstract—The construction of a continuous alpha particulate air monitor is described and experience during one year of sampling air from active glove boxes is discussed.

The detection of alpha contamination in the presence of natural radioactivity uses the principle of counting pseudo-coincidences between the beta-disintegrations from RaC (or ThC) and the alpha disintegrations from RaC′ (or ThC′).

Compared with earlier instruments, a second pseudo-coincidence circuit has been introduced, in which the alpha-pulses arrive 350 μsec later than in the first one.

Thus the chance coincidences can be subtracted from the total coincidences, making the instrument very insensitive to changes in the equilibrium between the various radioactive natural daughter products, as well as to a background of beta radiation.

A sensitivity of 6×10^{-12} Ci hr m^{-3} (3 mpc hr) has been obtained under normal conditions of ventilation.

1. DETECTION PRINCIPLE

The use of pseudo-coincidence counting to measure alpha contamination in the presence of natural radioactive daughter products of radon and thoron in the air of nuclear installations is of course not new.[1] The method depends upon the following facts:

(a) In the decay chain of radon daughter products (Fig. 1) an alpha disintegration from RaC′ (^{214}Po) follows the beta disintegration of RaC (^{214}Bi) within 160 μsec, with a probability of 50%. A similar sequence of events exists in the thoron series (^{212}Bi$\rightarrow^{212}$Po; $T_{1/2} = 0{\cdot}3$ μsec).

Because of the very short time interval between these beta and alpha disintegrations, the events are called pseudo-coincidences.

(b) When the "total alpha count rate" (α_{tot}) and the "pseudo-coincidence alpha count rate" (α_{psco}) are determined from filters containing dust sampled from air

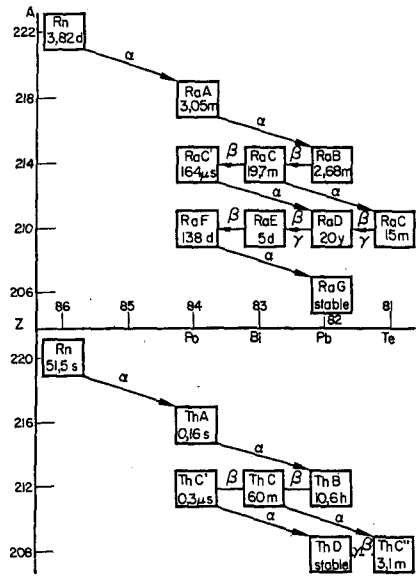

FIG. 1. Daughter products of radon and thoron.

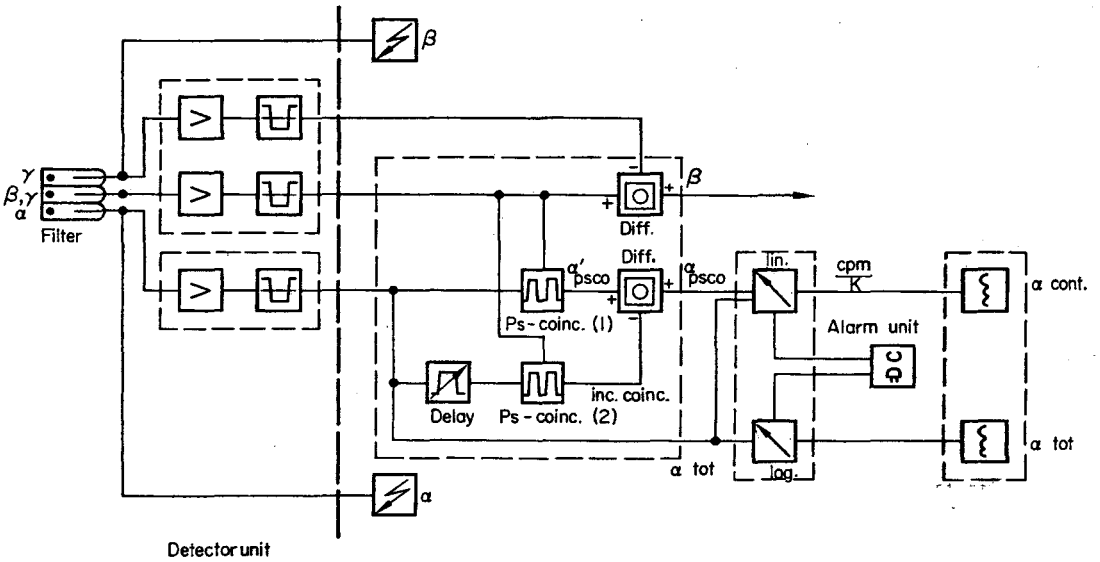

FIG. 2. Block diagram of the instrument.

which is free from radioactive contamination, the fraction

$$K = \frac{\alpha_{tot}}{\alpha_{psco}}$$

does not vary much under the usual circumstances of ventilation in a nuclear installation.

Therefore, taking an average value of K, the alpha count rate from contamination can be derived from

$$\alpha_{cont} = \alpha_{tot} - K \cdot \alpha_{psco}.$$

2. DETECTION SYSTEM

A diagram of the detection system is shown in Fig. 2.

2.1. *The detector unit* consists of a sandwich of 3 proportional counters of which only two, the α- and the β,γ-detector, are used for our purpose. The counting gas is a mixture of 90% argon + 10% methane; window size 25 × 25 cm, thickness 0·9 mg/cm^{-2}.

A 20 cm Ø glass fibre filter is positioned a few mm from the window of the alpha detector.

A second window of 10 mg cm^{-2} separates the α-detector from the β,γ-detector.

The preamplifiers, and the filter housing, are contained in this same unit (Fig. 3).

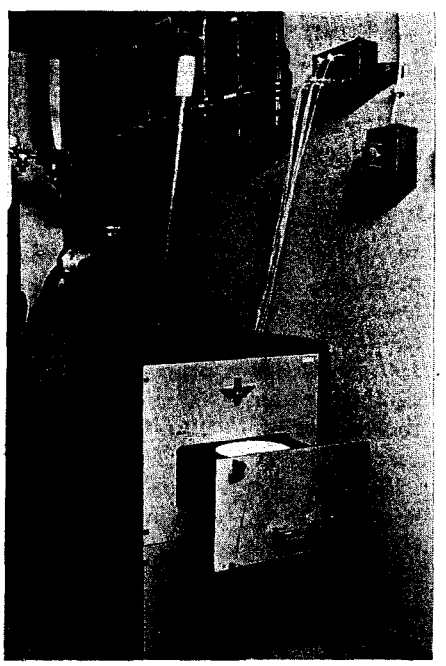

FIG. 3. The detector unit with the 20 cm Ø filter shown in the position ready to be changed.

An important advantage compared with instruments using scintillators is the fact that, in our case, both detectors are situated on the same side of the filter. This simplifies the solution of the problem of obtaining a homogeneous distribution of dust on the filter.

2.2. *The electronic system* contains a conventional pseudo-coincidence unit [psco (1)], in which every beta pulse opens an electronic gate for 300 μsec.

All the alpha pulses are fed into this unit which only passes those which arrive within the 300 μsec opening period. All air monitors described in the literature use the pseudo-coincidence principle to derive the factor K, and thus the α_{cont} from α_{psco}.

However, the number of counts, α_{psco} (total), through the gate of psco (1) consist of two categories:

(a) the real α_{psco},
(b) the chance coincidences (α_i), consisting of alphas not originating from ^{214}Po (or ^{212}Po), but incidentally arriving at the gate during the opening period.

The number of these coincidences depends on the α and β count rates and the opening time of the gate.

It is obvious that the presence of α_i results in an underestimation of possible contamination.

To avoid this, a second pseudo-coincidence unit [psco (2)] parallel to the first has been introduced in this instrument. Every alpha pulse fed into [psco (1)] is also fed into this second unit, but after a delay time of 350 μsec. Thus, the alphas which pass this second 300 μsec gate are (statistically) only chance coincidences. They are, therefore, subtracted from α_{psco} (total) in a differential unit.

The resulting α_{psco} count rate is fed into the unit marked "lin" into which α_{tot} is also fed. In this unit the following equation is computed:

$$\frac{\alpha_{tot}}{K} - \alpha_{psco} = \frac{\alpha_{cont}}{K}$$

The factor K can be chosen by varying a potentiometer.

The result is shown on a count rate meter and α_{tot} and $\frac{\alpha_{cont}}{K}$ are registered on a recorder. Alarm can be given at a preset count rate of $\frac{\alpha_{cont}}{K}$.

The electronic equipment with the registration unit (Fig. 4) has been placed in a second rack, which is situated in a central control room.

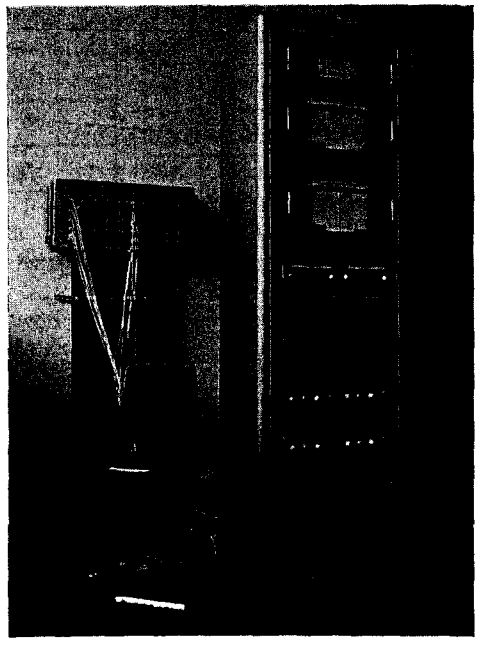

FIG. 4. Cabinet containing, from top to bottom: (a) Alarm indicator unit. (b) Registration units. (c) Ratemeters. (d) High voltage supply units.

3. RESULTS

A monitor of this type has been used for one year to monitor the air coming from 150 contaminated glove boxes before it enters the final absolute filters in the ventilation stack. The air from every box passes through 2 absolute filters before it reaches the sampling point. The sampling rate is 25 m^3 hr^{-1}. Figure 5 shows a plot of α_{tot} (on the right) and $\frac{\alpha_{cont}}{K}$. The value of K was obtained from the measurement of α_{tot} and α_{psco} and set to a fixed value of 3.8. The glove box ventilation rate was reduced to half the normal rate of 10 changes per hour, for the period shown on the diagram. It is clear that

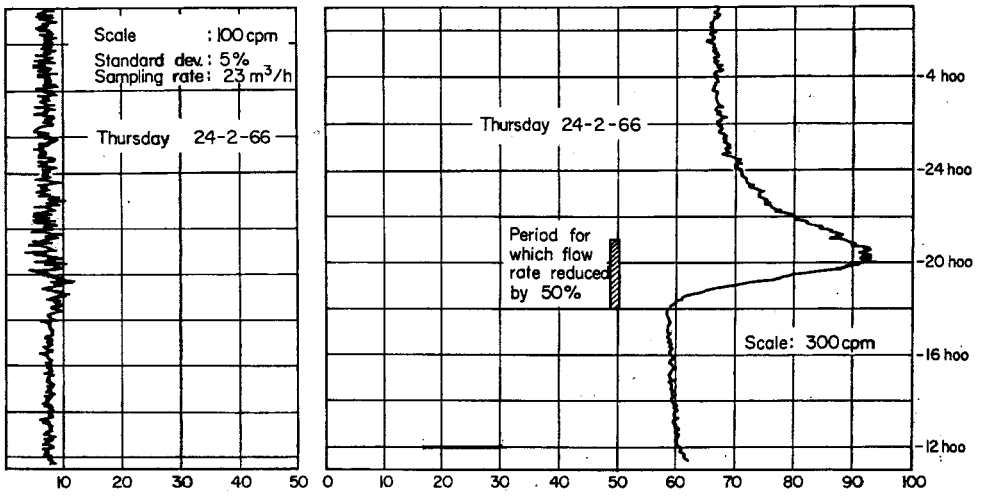

FIG. 5. Recorder traces showing how $\frac{\alpha_{cont}}{K}$ (left) remains constant when the ventilation rate is reduced to 50% which causes the α_{tot} count rate to increase from 180 cpm to 300 cpm.

this has practically no influence on the average value of $\frac{\alpha_{cont}}{K}$.

Calculation shows that with normal ventilation, assuming $\alpha_{tot} = 160$ cpm and $\alpha_{psco} = 40$, then a change in K from 4 to 4·4 gives a simulated α_{cont} of 16 cpm.

4. SENSITIVITY

The sensitivity of the instrument, which is approximately 3 mpc hr (1 mpc $= 2 \times 10^{-12}$ Ci m^{-3}) can be calculated from the following data:

(a) An alarm setting of $\frac{\alpha_{cont}}{K} = 16$ cpm, and

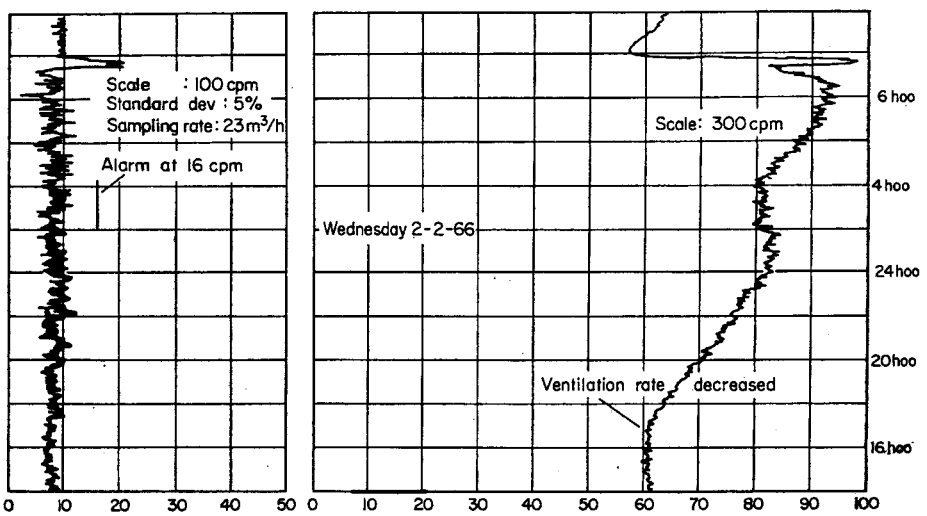

FIG. 6. Recorder traces, showing contamination of the sampled air coinciding with an increase of α_{tot}, the latter being due to a decreased ventilation rate.

an RC-time constant (τ) of 2 min, have been chosen for practical reasons (no false alarms, reasonable statistics).

(b) Counting efficiency = 20%.

(c) Air sampling rate 25 $m^3\ hr^{-1}$.

(d) $K = 3{\cdot}8$.

Substituting the corresponding values in the formula

$$\frac{[\text{cpm}]_{\alpha_{\text{cont}}}}{\frac{[\text{cpm}]}{[\text{dpm}]} \times \frac{[\text{dpm}]}{[\ \text{Ci}\ ]} \times \frac{[\text{Ci}] \cdot [\text{m}^3]^{-1}}{[\text{mpc}]} \times \frac{[\text{m}^3]}{[\text{hr}]}},$$

we obtain a sensitivity of 2.8 mpc hr.

With a $\tau = 2$ min, $\frac{\alpha_{\text{cont}}}{K}$ reaches 99·9% of its final value in 14 min. Thus 14 min is the limiting time period in which an alarm can be obtained for a contamination of 2.8 mpc hr. This corresponds to 12 times the mpc during this period.

The fact that the contamination usually consists of several small particles, which will not be deposited simultaneously on this filter is not taken into account in this calculation. In reality therefore the sensitivity may be slightly less than 2.8 mpc hr. Figure 6 shows the recorder traces taken after a small leak had occurred in one of the glove box filters. The diagram shows clearly that α_{tot} cannot be used with sufficient sensitivity for alarm purposes. (The increase in α_{tot} is due to a decrease in ventilation rate during this period.)

Measurement of the filter (after 8 days) showed an alpha count rate of 120 cpm (5 mpc hr).

ACKNOWLEDGEMENTS

We thank Mr. Gebauer[2] of Frieseke & Hoepfner in Erlangen and his colleagues for their co-operation in the planning stage and for the development of the instrument.

REFERENCES

1. C. Jehanno, A. Blanc, C. Lallemant and G. Roux. Appareils récents et méthodes nouvelles pour la mesure de la concentration des produits radioactifs dans l'atmosphère. *Proc. IInd Int. Conf. on the Peaceful Uses of Atomic Energy*, 15/P/329.
2. H. Gebauer. A method to compensate the natural air-radioactivity by means of beta-alpha pseudo-coincidences. *Kerntechnik, Isotopentechnik und -Chemie*, **7**, Jg. 1965, Heft 7, S. 322–325.

A TRIAL PRODUCTION OF PLUTONIUM CONTAMINATED WOUND COUNTERS

Y. YAMAOKA, H. KURODA and H. TATSUTA

Division of Health Physics and Safety, Japan Atomic Energy Research Institute, Tokai-mura, Naka-gun, Ibaraki-ken, Japan

Abstract—A rapid increase of the amount of plutonium to be handled in our Institute has accelerated the need for preparation of wound counters capable of detecting at least a fraction of MPBB (40 nCi) in a plutonium contaminated wound.

Two kinds of wound counters, a xenon gas-filled proportional counter and a cesium iodide crystal scintillation counter, were constructed and their characteristics were examined. The minimum detectable amount for the former was 5.5 nCi and that for the latter was 0.83 nCi when the plutonium was imbedded 6 mm under tissue and the window of the detector was positioned at 3 mm above the skin surface. In order to determine the location of plutonium, a 0.1-mm-thick lead plate and a lead-impregnated flexible material were prepared.

The method of determination of the effective depth of contaminants is discussed below mainly for the cases of pure plutonium and plutonium with an unknown content of americium in the wound. Furthermore, we have shown that the depth distribution of the contaminants can be obtained in fairly good agreement with the actual distribution by the method of expansion of source distribution using the orthonormal function series method. This method will be valid provided the contaminant lies continuously in the wound.

1. INTRODUCTION

Following the rapid increase of the amount of plutonium handled in the plutonium laboratory in our Institute, the preparation of wound counters has become an urgent necessity in order to determine the location, the depth and the amount of plutonium in wounds when such an accident occurs and surgical excision of skin and tissue is required. It is necessary to detect at least a fraction of the maximum permissible body burden (MPBB = 40 nCi) in a plutonium contaminated wound, without cutting or probing, in order to aid the decontamination operation and the medical treatment of personnel who sustain such injuries. Similar counters, especially the scintillation types, were already developed in several other countries.[1-4] But, considering the cases of pure plutonium or unknown content of americium in plutonium to be handled, a xenon gas-filled proportional counter was examined to determine the effective depth of contaminants in wounds using the photopeak ratio of L_α–X and L_β–X rays emitted from plutonium. A cesium iodide crystal scintillation counter was also examined to determine the effective depth using L–X and γ-radiation. Other characteristics of these two counters were compared.

In order to determine the location of contaminants, a 0.1-mm-thick lead plate or a lead-impregnated flexible material were prepared to perform grid surveys. A transparent material is preferable.

Furthermore, the development of a code for computing the depth distribution of contaminants in a wound was carried out by means of an expansion of the source distribution using the orthonormal function series method.[5]

2. EXPERIMENTAL ARRANGEMENTS

A proportional type detector, Aloka PC-101 Xe tube filled with xenon gas containing 10 per cent methane gas under a pressure of 32 cm Hg and having a 1.8 mg/cm^2 mica window, was used. The mica window was covered by an aluminium foil with sufficient thickness to

cut off α-rays emitted by plutonium. The sensitive volume of the counter is 24 mm (diameter) $\times$ 100 mm.

The scintillation type detector probe assembly contains a cesium iodide scintillation crystal, 1 in. in diameter and 1 mm in its thickness, with an aluminium foil having sufficient thickness to cut off α-rays. The crystal was mounted on a Toshiba 7696 photo-multiplier tube.

These detectors were used together with a TMC 400 channel pulse height analyzer.

In both cases L–X rays produced by the internal conversion of 37- and 51-keV gamma radiation associated with the alpha decay of plutonium-239, the energy ranging from 13.6- to 20.5-keV and having an emission rate of 3.8% against alpha decay, were used because the 51-keV gamma-ray was difficult to detect.

Acryl acid resin plates having various thicknesses and with specific gravity in the range 1.16–1.2 were used as tissue equivalent material instead of human tissue to measure the absorption curves of the X-rays and thus assess an effective depth of plutonium in tissue.

The standard source of plutonium-239 made in the Radiochemical Centre (RCC) in England having activity equal to $(8.897 \pm 0.01) \times 10^{-2}$ μCi and distributed on a platinum plate for about 3 mm in diameter, and a standard source of americium-241 made in the radiochemical laboratory in JAERI having the activity of 0.5 μCi in alpha decay were used.

3. RESULTS AND DISCUSSIONS

3.1. *Proportional Counter Method*

A plateau curve and a background counting rate of the xenon gas-filled proportional counter were measured using an americium-241 standard source in order to obtain an adequate working high voltage with background counting as low as possible, as shown in Fig. 1. From Fig. 1, the working high voltage of 1600 V was selected, the background counting rate for the whole energy range being about 54 cpm.

Figure 2 shows the relationship between the channel number of the multichannel pulse height analyzer and the X-ray energy when the xenon gas-filled proportional counter was operated under the high voltage of 1600 V. Standard sources of barium-133 and selenium-75 were used to plot the curve.

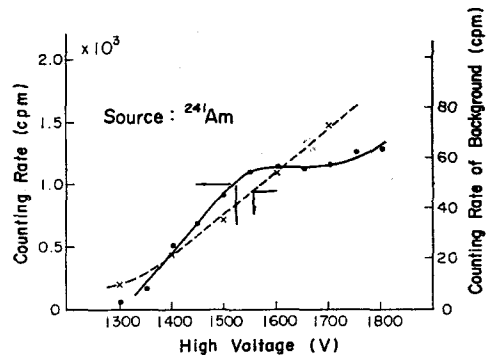

FIG. 1. Plateau and background curves of Xe gas-filled proportional counter.

Figure 3 shows the X-ray spectrum of plutonium-239 obtained by the proportional counter. The second and the third photopeaks are considered as L_α– and L_β–X rays emitted by the plutonium-239 source, respectively, on the basis of the channel number to the pulse height–energy dependence curve in Fig. 2. The distance between the source and the window of the proportional counter was 3 mm. The first peak lying at the energy of about 6 keV was investigated by comparing the spectra with and without absorber as shown in Fig. 4. The lead plate having 0.1 mm thickness was used as an absorber and inserted between the americium-241 source and the window of the counter. It is obvious from the figure that the occurrence of the first peak is not due to emission from the source because, in spite of the disappearance of the peaks of the L_α– and

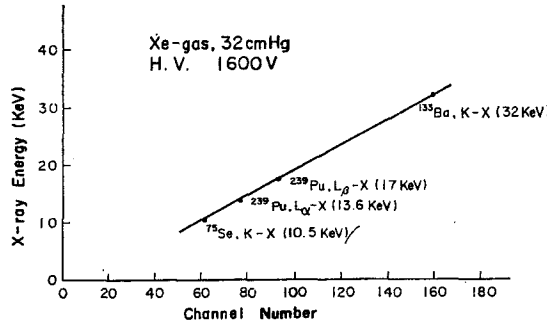

FIG. 2. Relation between pulse height and energy of Xe gas-filled proportional counter.

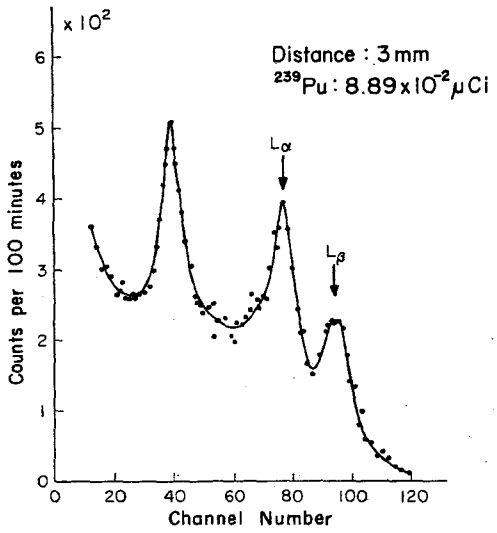

FIG. 3. X-ray spectrum of ^{239}Pu measured by Xe gas-filled proportional counter.

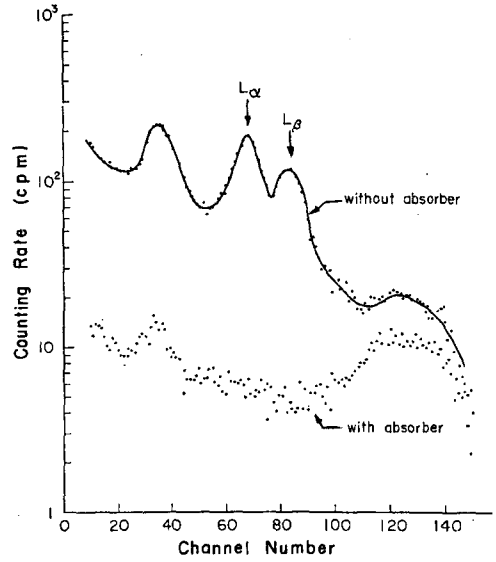

FIG. 4. X-ray spectra of ^{241}Am with and without absorber of 0.1 mm thick Pb.

L_β–X rays with absorber present, the first peak with lower energy remained almost unchanged.

The attenuation coefficients of L_α– and L_β–X rays in tissue differ according to their energy as shown in Fig. 5, for example. In this case, a 3.1 mm thick acryl acid resin plate was inserted between the americium-241 source and the window of the counter. Curves (a) and (b) in Fig. 5 show the spectra of the americium-241 source without and with the 3.1 mm thick acryl acid resin plate, respectively.

It is easy to calculate the depth of contaminants in tissue in the case of a point source by using results obtained for the arrangements shown in Fig. 6 (a) and (b). Fig. 6 (a) shows the case when the contaminants were imbedded at the depth x under the skin surface and the end of detector was positioned at the distance t from the skin surface. The counting rates and the attenuation coefficients of X-rays are designated by N_α and μ_α for the L_α–X ray and by N_β and μ_β for the L_β–X ray, respectively. If the tissue in Fig. 6 (a) was removed, the counting rates will be designated $N_{\alpha o}$ for the L_α–X ray and by $N_{\beta o}$ for the L_β–X ray, and the attenuation coefficient for air is nearly equal to unity, as indicated in Fig. 6 (b). In both cases the geometry remains the same. The following relationships hold with these notations:

$$\left.\begin{aligned} N_\alpha &= N_{\alpha o} e^{-(\mu_\alpha)x} \\ N_\beta &= N_{\beta o} e^{-(\mu_\beta)x} \end{aligned}\right\} \qquad (1)$$

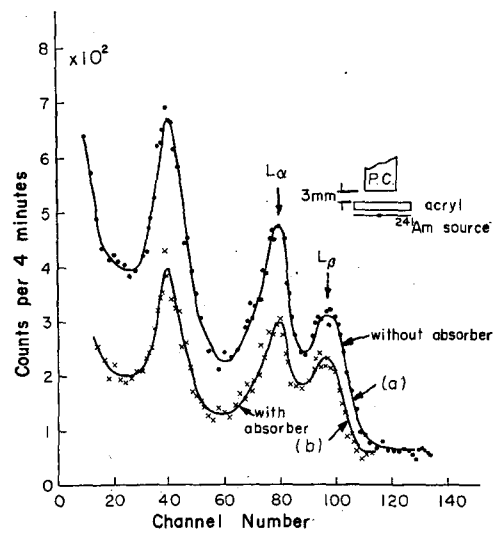

FIG. 5. X-ray spectra of ^{241}Am without and with absorber of acryl (3.1 mm).

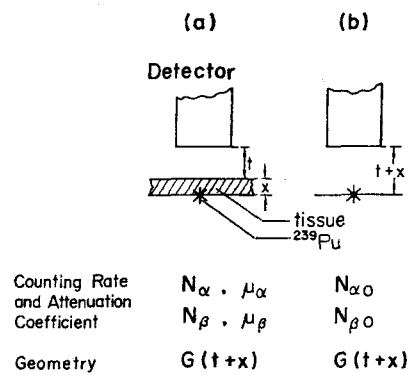

FIG. 6. Schematic arrangement of detector and source.

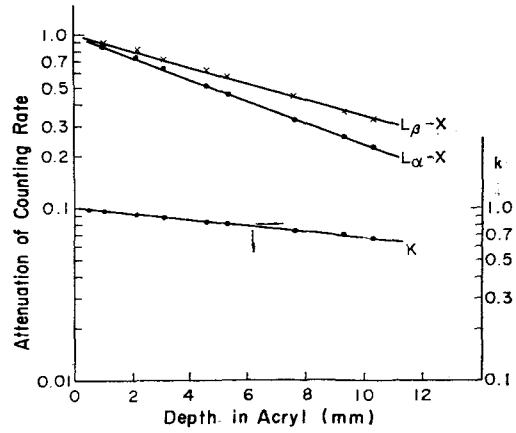

FIG. 7. X-ray attenuation curves in acryl measured by Xe gas-filled proportional counter.

If we put,

$$K = (N_\alpha/N_\beta)/(N_{\alpha o}/N_{\beta o}) = (N_\alpha/N_{\alpha o})/(N_\beta/N_{\beta o}) \quad (2)$$

then,

$$\ln K = -(\mu_\alpha - \mu_\beta)\, x. \quad (3)$$

If we consider that the values μ_α and μ_β for the tissue are constant, the depth x can be calculated from equation (3) when the value K is known. In Fig. 7, the straight lines L_α–X and L_β–X show the values $N_\alpha/N_{\alpha o}$ and $N_\beta/N_{\beta o}$ of equation (2), respectively, when the thickness of the acryl acid resin plates is changed, and the straight line K shows the change of the ratio $(N_\alpha/N_{\alpha o})/(N_\beta/N_{\beta o})$ with the increase of the thickness of the plate. In practice, N_α and N_β can be obtained easily from measured values for the contaminated wound with the proportional counter, and the value K by dividing the ratio N_α/N_β by the value $N_{\alpha o}/N_{\beta o}$ measured beforehand. Then the depth of the point source contaminant x can be obtained from the straight line K in Fig. 7, and the amount of contaminant in the wound can also be obtained from the peak value of the spectrum. At the same time the location of the contaminant can easily be determined by a grid survey method using a 0.1-mm-thick lead plate or a lead-impregnated material.

But, it is not practical to consider that the contaminants always lie in the wound in such a single point source. It is rather usual that the contaminants are distributed in several points in the wound in the case of insoluble contaminants, and distributed continuously in the case of soluble contaminants. In such cases, the estimated value of the depth x will become an effective depth of the whole contaminants. It is desirable to know the exact depth distribution of contaminants quickly, if possible, in order to perform an effective surgical excision of skin or tissue. Consequently, the development of a code for computing the depth distribution of contaminants in a wound was carried out theoretically.

Let us consider that contaminants having unit activity are imbedded in tissue at various depths x and the spectra having n peaks were measured from outside the skin surface. Furthermore, let us put $g_i(x)$ for the counting rates of the ith peak for various x's. Then, it is possible to obtain an orthonormal function set $\{\phi_i(x)\}$ from the response group $\{g_i(x)\}$ by applying the Gram-Schmidt process. The relationship can be represented by a matrix G as follows:

$$G = B \cdot \psi \quad (4)$$

where G is an n-column matrix having $\{g_i(x)\}$ as the elements, B is a conversion matrix $(n \times n)$, and ψ is also an n-column matrix having $\{\phi_i(x)\}$ as the elements.

Now, let us represent the distribution function of the contaminants along the depth x of the wound by $s(x)$. Assuming that the function $s(x)$ can be expanded by the orthonormal function set $\{\phi_i(x)\}$, we have again the following matrix equation;

$$s(x) \cong A \cdot \psi \tag{5}$$

where A is an unknown conversion matrix. If we denote the measured value of the ith peak of the spectrum by n_i, it follows that

$$n_i = \int g_i(x) \cdot s(x)dx.$$

Therefore,

$$N \cong B \cdot \int \psi \cdot \psi^T dx \cdot A^T$$
$$= B \cdot W \cdot A^T \tag{6}$$

where N is a column matrix having $\{n_i\}$ as the elements, and W is $\int \psi \cdot \psi^T dx$. From equation (6), we have

$$A \cong (W^{-1} \cdot B \cdot N)^T. \tag{7}$$

Substituting from equations (4) and (7) into equation (5), we have

$$s(x) \cong N^T \cdot (B^{-1})^T \cdot (W^{-1})^T \cdot B^{-1} \cdot G. \tag{8}$$

It is obvious from equation (8) that the approximate distribution of contaminants can be obtained by the combination of the response function G weighted by the counting rate N.

In order to confirm the theoretical results experimentally, a 0.5 μCi americium source was used to obtain the spectra for americium imbedded at various depths under tissue. The $g_i(x)$'s for the counting rates of L_α–, L_β– and L_γ–X rays of the spectra were plotted as shown in Fig. 8. Using these $g_i(x)$'s, two different kinds of depth distributions $s(x)$'s which were assumed as the solid lines in Fig. 9, were calculated by IBM computer. The calculated $s(x)$'s are shown by the dotted lines in the same figure. It is obvious from the figure that the calculated distributions agree fairly well with the assumed

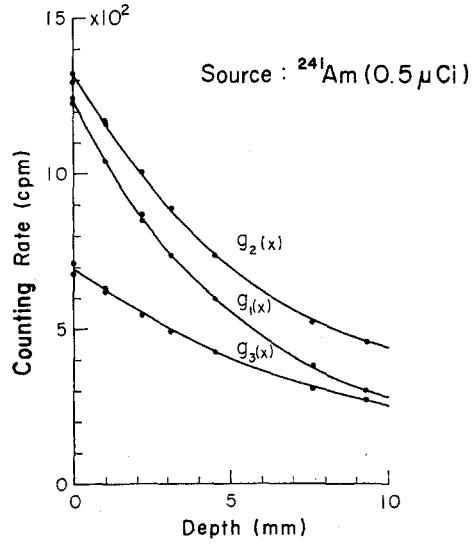

FIG. 8. Depth dependence curves of counting rate for L_α–, L_β– and L_γ–X rays.

distributions of contaminant in the case of a continuous distribution, but presumably it is difficult to obtain such a successful agreement in the case of discontinuous distribution.

3.2. *Scintillation Counter Method*

Another experiment using a thin cesium iodide scintillation crystal was carried out in order to compare with the results obtained

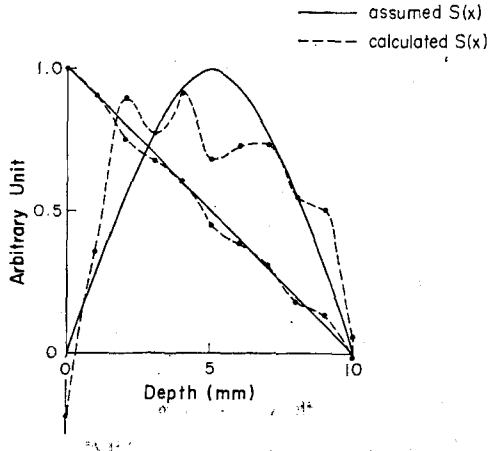

FIG. 9. Assumed and calculated depth distributions of contaminants (^{241}Am).

with the xenon gas-filled proportional counter. Figure 10 shows the X- and γ-rays spectra of americium-241 and plutonium-239 obtained by the cesium iodide scintillation crystal, 1 in. in diameter and 1 mm thick. It is obvious from the figure that the plutonium-239 source has a small content of americium-241.

Here again we have examined the sensitivity for determining the depth of contaminants using

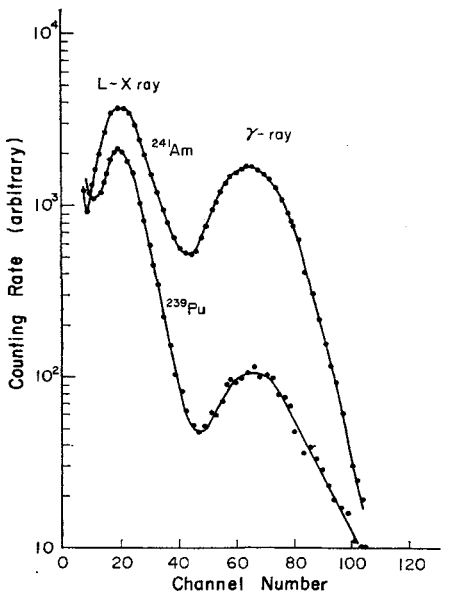

FIG. 10. X- and γ-ray spectra of ^{241}Am and ^{239}Pu measured by CsI(Tl) crystal.

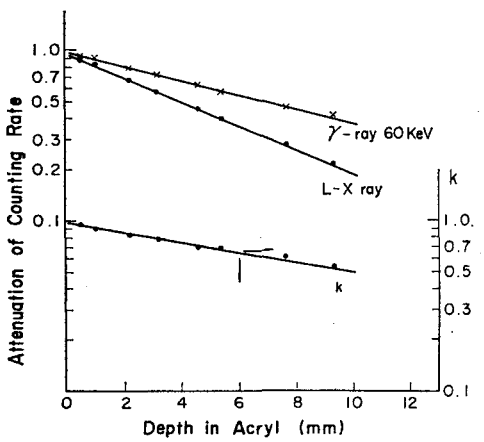

FIG. 11. X- and γ-ray attenuation curves in acryl measured by CsI (Tl) crystal.

L–X and γ-rays (60 keV) emitted from the americium-241 source and acryl acid resin plates having various thicknesses for absorber, as shown in Fig. 11. By comparing Figs. 7 and 11, it is clear that the sensitivity for determining the depth of contaminants is greater for the scintillation counter than for the proportional counter owing to the utilization of the higher energy 60 keV γ-radiation. The minimum detectable amounts for the proportional counter and for the scintillation counter were 2.5×10^{-3} and 3×10^{-4} μCi, respectively, when the contaminants were on the skin surface and 5.5×10^{-3} and 8.3×10^{-4} μCi, respectively, when the contaminants were at the depth of 6 mm in the tissue equivalent acryl acid resin plate, for a measuring time of 10 min with a confidence limit of 95% if the window of the detector were positioned at 3 mm above the skin surface, as shown in Table 1. From these results, a scintillation counter appears to be more effective than a proportional counter, but the proportional counter is useful when the orthonormal function series method is used to obtain the depth distribution of contaminants in a wound, especially in the case of a contaminant composed of pure plutonium.

4. CONCLUSION

Because of the urgent need for wound counters in order to determine the location, the depth and the amount of plutonium in wounds as an aid in determining the need for surgical excision of skin and tissue, a xenon gas-filled proportional counter was examined as a means of making effective depth estimation when the wounds were contaminated by pure plutonium. A thin cesium iodide crystal type scintillation counter was also examined to compare its sensitivity for determining the effective depth and the minimum detectable amount of contaminants in a wound with the comparable results using the proportional counter when the wounds were contaminated both by plutonium and americium.

In the case of a contaminant including both plutonium and americium, the sensitivity for effective depth determination and the minimum detectable amount were better for the scintillation counter than for the proportional coun-

Table 1. *Characteristics of detectors.*
(^{239}Pu source: 8.89×10^{-2} μCi)

Detector	Proportional counter	CsI (Tl) crystal 1 in. dia × 1 mm thick
Distance to source (mm)	3	3
Energy range of L-X ray (keV)	10.5–22	10.5–22
Net counting rate (cpm)	106	2482
Background (cpm)	9	67
M.D.A.* (μCi)		
Skin surface	2.5×10^{-3}	3×10^{-4}
Under tissue (6 mm)	5.5×10^{-3}	8.3×10^{-4}

* Measuring time, 10 min.
Limit of confidence, 95%.

ter, but the effective depth estimation was only possible by use of the proportional counter when the contaminant includes only pure plutonium.

Furthermore, the development of a code for computing the depth distribution of contaminants in a wound was carried out, theoretically, by means of an expansion of results obtained by the counters, using the orthonormal function series method. For this purpose, the high resolution of the proportional counter is needed to make it successful. A verification of this method was performed using measured $\{g_i(x)\}$ values, and has shown that the two calculated distribution curves of the contaminants agree fairly well with the assumed distribution curves.

ACKNOWLEDGEMENTS

The authors wish to thank Mr. H. Ryufuku for coding the IBM computer and for his helpful discussion. Thanks also to Dr. N. Makino and others who indirectly supported the project.

REFERENCES

1. E. A. Putzier, J. R. Mann and V. P. Johnson. *Am. Ind. Hyg. Assoc. J.* **19,** 384 (1958).
2. R. G. Maras. Dow Chemical Co., Rocky Flats Division, Golden, Colorado, 3 (1960), unpublished data.
3. W. C. Roesch and J. W. Baum. *Proc. 2nd U.N. Intern. Conf. Peaceful Uses Atomic Energy*, P/756. (United Nations, Geneva, 1958) Vol. 23, p. 142.
4. G. H. Gruber. TID-4500 (1960).
5. H. Ryufuku. *JJAP*, I, II and III (to be published).

DÉTECTEUR DE PARTICULES IONISANTES ET DE NEUTRONS RAPIDES PAR SCINTILLATION DANS L'HÉLIUM OU L'ARGON SOUS FORTE PRESSION

DANIEL BLANC, JACQUES GALY et JEAN-LOUIS TEYSSIER
Centre de Physique Atomique et Nucléaire, Faculté des Sciences de Toulouse, France

Résumé—Pour détecter des neutrons rapides à l'aide d'un scintillateur gazeux, il est nécessaire de faire des remplissages sous des pressions de plusieurs dizaines d'atmosphères. C'est dans ce but qu'on étudie ce type de détecteur.

On emploie l'hélium ou l'argon contenant respectivement 5 et 10 ppm (partie pour million) d'azote, 5 et 3 ppm d'oxygène, 5 et 1 ppm de vapeur d'eau. L'intensité de la fluorescence de l'hélium irradié par les particules α du ^{210}Po décroit lorsque la pression passe de 6 à 40 atmosphères. L'addition d'azote en quantité contrôlée (concentration maximale: 10%) montre que cette diminution ne dépend pas de la quantité d'azote introduite. Ceci justifie la diminution observée, lorsque les impuretés sont présentes à l'état de traces. Un phénomène identique se produit dans l'argon.

Pour recueillir suffisamment de lumière avec un remplissage sous pression élevée, on fait appel à un convertisseur de longueurs d'onde, le salicylate de sodium en l'occurrence. Celui-ci dégaze peu et la réponse du détecteur est stable dans le temps. Dans ces conditions, l'intensité de la fluorescence de l'argon reste constante entre 2 et 7 atmosphères. Dès qu'on ajoute de l'azote, tant dans l'hélium que dans l'argon, l'intensité de la lumière émise diminue. Lorsqu'on augmente la pression, les courbes obtenues pour des concentrations différentes, sont parallèles, comme précédemment.

Pour les neutrons de 14 MeV, obtenus par réaction (d, t), l'hélium sert à la fois de cible et de scintillateur. Ceux-ci sont détectés à l'aide des noyaux de recul d'hélium produits par diffusion élastique. On trace les spectres en énergie des noyaux de recul. On apporte à ces spectres expérimentaux les corrections d'effet de bord et de résolution en énergie, ce qui est nécessaire pour obtenir les valeurs de la section efficace différentielle de diffusion élastique.

INTRODUCTION

Les scintillateurs gazeux ne sont pas couramment utilisés en physique nucléaire, car ils sont d'un emploi peu commode: si l'on augmente le rendement lumineux grâce à un convertisseur de longueurs d'onde, la réponse n'est pas stable en fonction du temps. On peut pallier cet inconvénient en assurant une purification continue du gaz de remplissage, mais le dispositif est très complexe et ne peut être facilement déplacé.

Pourtant, ces scintillateurs présentent l'avantage de ne pas être sensibles au rayonnement gamma qui accompagne toujours l'émission de neutrons. C'est ce qui nous a incité à les employer pour détecter les neutrons rapides de 14 MeV produits par la réaction $(d-t)$ à l'aide de l'accélérateur électrostatique Sames que possède notre Centre. Austin,[1] Jenkin,[2] Pasma[3] et Czmider[4] ont fait appel au mélange contenant 90% d'hélium et 10% de xénon, qui délivre la même quantité de lumière que le xénon pur. Nous avons choisi non plus un mélange, mais un seul gaz, l'hélium en l'occurrence, qui sert à la fois de cible et de scintillateur. À pression égale, l'efficacité de détection se trouve améliorée.

Il est indispensable, pour obtenir une efficacité convenable, de faire des remplissages sous des pressions élevées. C'est pourquoi, nous

avons d'abord étudié le comportement des scintillateurs gazeux aux fortes pressions, dans le cas de l'argon et de l'hélium.

I. LE DISPOSITIF EXPÉRIMENTAL

L'emploi de gaz sous des pressions élevées pose des problèmes techniques difficiles à résoudre. Le boîtier doit satisfaire à deux exigences contradictoires: il doit être étanche pour un vide de l'ordre de 10^{-6} torr, vide limite de l'installation de pompage; il doit pouvoir supporter des pressions voisines de 50 atmosphères, ce qui est nécessaire pour la détection des neutrons. L'ensemble de détection est représenté sur la figure 1.

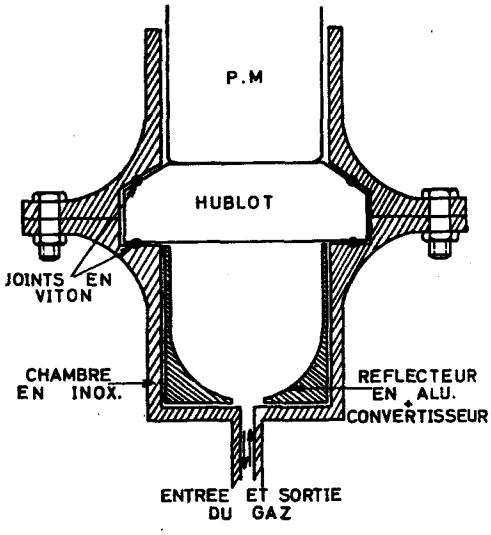

FIG. 1. Le détecteur.

La chambre est en acier inoxydable, matériau qui dégaze peu, et qui ne s'active pas lorsqu'il est irradié par des neutrons.

Sa forme est cylindrique (diamètre 6 cm, hauteur 6 cm), les parois ont 5 mm d'épaisseur; un hublot en silice fondue isole le photomultiplicateur du remplissage gazeux; son épaisseur de 3 cm, permet de supporter une pression de 50 atmosphères. Un joint torique en viton assure l'étanchéité au vide. Les gaz de remplissage sont l'hélium et l'argon qui contiennent respectivement comme impuretés: 5 et 10 ppm d'azote, 5 et 3 ppm d'oxygène, 5 et 1 ppm de vapeur d'eau (ppm: parties pour million).

Pour avoir un rendement lumineux convenable, nous avons été obligés d'employer un convertisseur de longueurs d'onde, malgré tous les inconvénients que cela entraîne.[5]

Le salicylate de sodium a l'avantage de posséder un rendement quantique constant entre 850 et 2500 Å. Appliqué en solution dans le méthanol, il se dépose en couche homogène, après évaporation du solvant. Le quaterphényl donne de meilleurs résultats: l'intensité de la lumière recueillie est 7 fois plus grande. La difficulté provient du fait qu'il doit être déposé sous vide et qu'il existe une épaisseur optimale, de l'ordre de 75 g/cm^2.[5] Compte-tenu des dimensions de la chambre, il est difficile d'obtenir des dépôts uniformes dont l'épaisseur soit connue avec précision.

Avec ces deux convertisseurs de longueurs d'onde, la réponse du détecteur varie en fonction du temps: à la température ambiante, l'amplitude des impulsions délivrées par le P.M. diminue d'environ 8% par heure. Nous avons amélioré les choses, en étuvant la chambre sous un vide de 5.10^{-6} torr pendant 48 heures à la température de 80°C. Au bout de 12 heures, la diminution n'est que de 8%. Compte-tenu de la durée moyenne de nos expériences, le dégazage n'est alors pas gênant.

On augmente encore le rendement lumineux du dispositif en recouvrant les parois de la chambre d'une substance réflectrice pour les rayons ultraviolets. Avec le salicylate de sodium, nous employons l'aluminium; avec le quaterphényl, la combinaison oxyde de magnésium et aluminium.

Nous avons choisi le photomultiplicateur 56 UVP Radiotechnique qui a une très grande rapidité de réponse et un gain très élevé.

II. COMPORTEMENT DES SCINTILLATEURS GAZEUX AUX FORTES PRESSIONS

II. 1. *Influence de la pression sur l'intensité de la luminescence*

Nous avons placé à l'intérieur du détecteur, à 2,6 cm de la face interne du hublot, une source non collimatée de particules α (^{210}Po). Cette distance est égale au rayon intérieur de la chambre. Ainsi, pour toute pression supérieure à p_0, si p_0 est la pression du gaz correspondant à un parcours des particules α de 2,6 cm, les particules émises dans l'angle solide 2π perdent

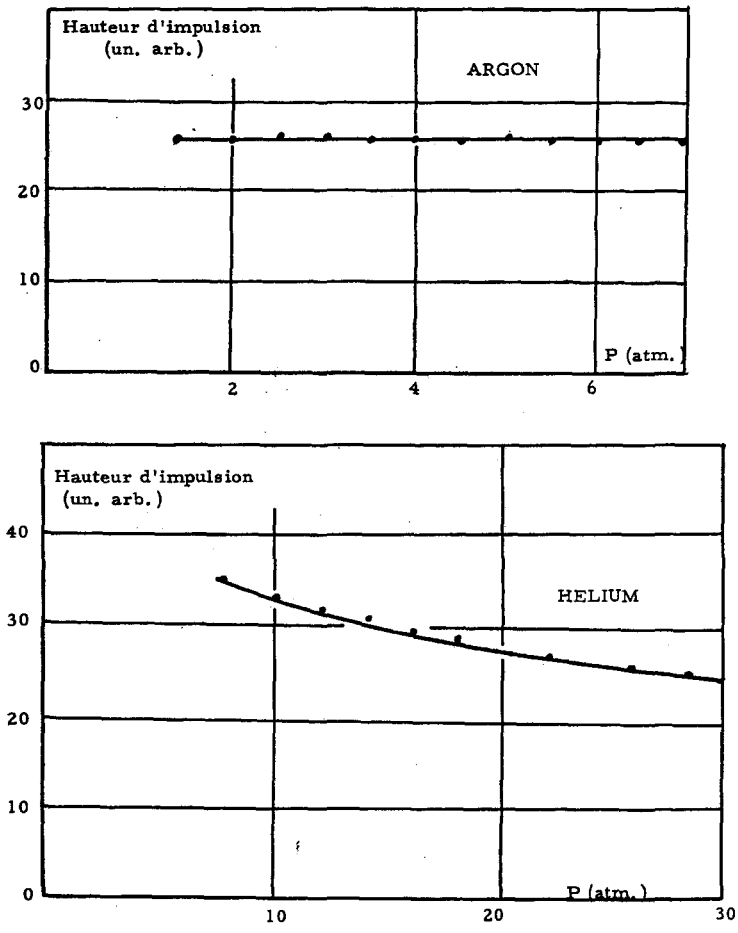

FIG. 2. Variation de l'amplitude des impulsions alpha en fonction de la pression pour l'hélium et l'argon.

la totalité de leur énergie dans le gaz. Dans l'argon $p_0 = 1{,}6$ atmosphère et dans l'hélium $p_0 = 8$ atmosphères. p_0 fixe la limite inférieure du domaine des pressions étudiées. Le convertisseur de longueurs d'onde est le salicylate de sodium.

La figure 2 montre la variation de l'amplitude des impulsions alpha en fonction de la pression P du gaz.

Si les résultats obtenus pour l'argon sont conformes à ceux de Perrin[6] et de Sayres et Wu,[7] pour l'hélium par contre, le désaccord est plus net. Esterling[8] et Rubbia[9] trouvent que la hauteur d'impulsion reste constante ou augmente légèrement entre 20 et 100 atmosphères; Baldin[10] observe une augmentation d'un facteur 2 environ, lorsque la pression passe de 20 à 70 atmosphères.

Ces désaccords tiennent aux effets d'ordre géométrique dans les chambres à scintillations employées et à l'état de pureté des gaz. Nous allons examiner ces deux questions.

II. 2. *Les effets d'ordre géométrique*

Lorsque la pression de remplissage augmente, le parcours des particles α diminue. Deux phénomènes qui ont des effets opposés se manifestant:

(a) La source lumineuse est plus ponctuelle. Le nombre de photons susceptibles d'être

Tableau 1. *Influence du convertisseur de longueurs d'onde et du réflecteur sur l'intensité de la lumière recueillie*

Conditions expérimentales Hélium	hauteur d'impulsion (p = 8atm) (un. arb.)	résolution en % (p = 8 atm)	Diminution de la hauteur d'impulsion entre 8 et 12 atm en %
(I) Chambre sans réflecteur, ni convertisseur	1	80	23
(II) Avec Aluminium, sans convertisseur	3	45	16
(III) Avec Aluminium et salicylate de sodium déposé sur les parois	7	36	11
(IV) Avec oxyde de magnésium déposé sur l'aluminium, et quaterphényl déposé sous vide sur les parois et la face interne du hublot.	42	20	7,5

collectés directement par le photomultiplicateur augmente par rapport au nombre de photons réfléchis.

(b) La source lumineuse est plus éloignée du photomultiplicateur. On collecte moins de photons, car l'angle solide sous lequel le PM voit la source diminue.

Ce que l'on observe représente la résultante des deux phénomènes. Ainsi, la variation de l'intensité de la lumière recueillie en fonction de la pression dépend étroitement des paramètres d'ordre géométrique.

Le tableau 1 en donne la confirmation: la loi de variation change selon les conditions de l'expérience. Une comparaison entre les résultats trouvés par les différents auteurs n'a pas de valeur significative.

La présence d'un convertisseur de longueurs d'onde et d'un réflecteur est intéressante car elle améliore le rendement lumineux du détecteur. De plus, le nombre de photons recueillis après conversion et réflexion sur les parois de la chambre augmente par rapport au nombre de photons collectés directement. Les effets d'ordre géométrique s'en trouvent atténués d'autant. Ainsi, sous une pression de 30 atmosphères d'hélium, lorsque la distance d qui sépare la source de la fenêtre passe de 10 à 50 mm, la quantité de lumière recueillie dans les conditions (I) diminue de 90%. Par contre, dans les conditions IV, lorsque d augmente de 13 à 40 mm, on observe une augmentation de 32%.

II. 3. *Rôle des impuretés*

Nous nous sommes intéressés au cas de l'azote qui est l'impureté présente en concentration la plus élevée dans les gaz de remplissage. Nous nous sommes placés dans les conditions III du tableau I. Les concentrations en volume d'azote sont comprises entre 0,12 et 7% pour l'argon, entre 0,06 et 0,84% pour l'hélium.

Dès que l'on introduit de l'azote dans l'argon, la luminescence diminue constamment, lorsque la pression croît (figure 3). Ces courbes normalisées pour une pression de 1,6 atmosphère sont superposables (figure 4). Ceci signifie que le mécanisme de la scintillation des mélanges d'argon et d'azote est inchangé pour les teneurs en azote considérées.

On observe dans l'hélium des phénomènes similaires, comme le montre la figure 5. Dans les mélanges d'argon ou d'hélium avec l'azote, le mécanisme de l'émission lumineuse est donc le même, pour les concentrations considérées. Il s'agit vraisemblablement de la destruction d'états métastables. Enfin, il apparaît que

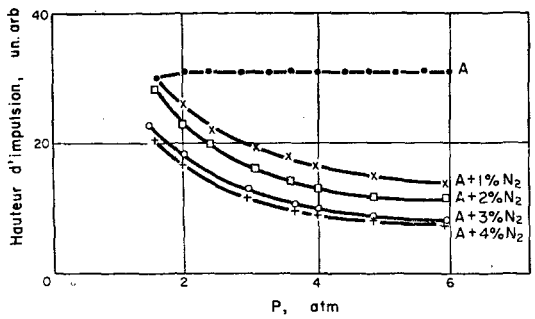

FIG. 3. Variation de l'amplitude des impulsions alpha en fonction de la pression pour l'argon et les mélanges (A-N_2).

pour les fortes pressions, la quantité de lumière recueillie est d'autant plus faible que la concentration en azote est plus grande.

III. DÉTECTION DES NEUTRONS DE 14 MeV

Nous avons utilisé le détecteur précédent rempli d'hélium sous une pression de 40 atmosphères. Nous avons opéré successivement dans les conditions III et IV du tableau I.

III. 1. *La méthode expérimentale*

Au cours de la réaction $(d-t)$, la cible de tritium se charge progressivement en deutérium; il apparaît des réactions parasites telles que $d(d, n)He^3$ et $d(d, p)t$. C'est une des raisons pour lesquelles nous avons employé la méthode de la particule associée, appelée ainsi, car on met en coïncidence le neutron et la particule α créés en même temps par la réaction (d, t).

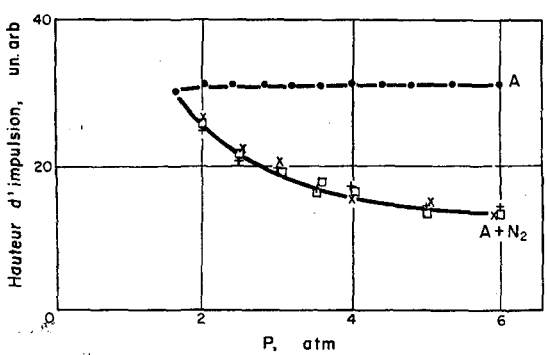

FIG. 4. Courbes normalisées de variation de l'amplitude des impulsions alpha en fonction de la pression pour l'argon et les mélanges (A-N_2).

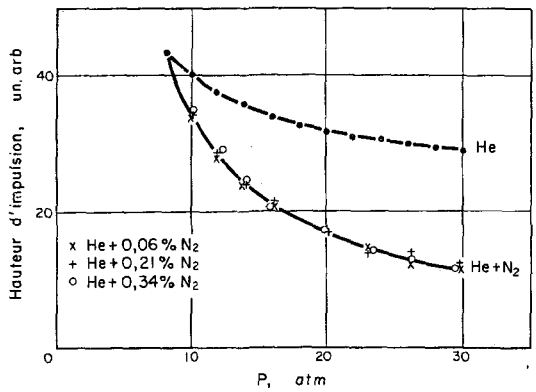

FIG. 5. Courbes normalisées de variation de l'amplitude des impulsions alpha en fonction de la pression pour l'hélium et les mélanges (He–N_2).

(a) *Méthode de la particule associée.* Si l'on place deux détecteurs, l'un sur la "voie alpha", l'autre sur la "voie neutron", il est possible de compter les neutrons, après mise en coïncidence des 2 voies (figure 6).

"Voie alpha"

Nous détectons les particules α émises perpendiculairement à la direction du faisceau incident, à l'aide d'un scintillateur plastique de

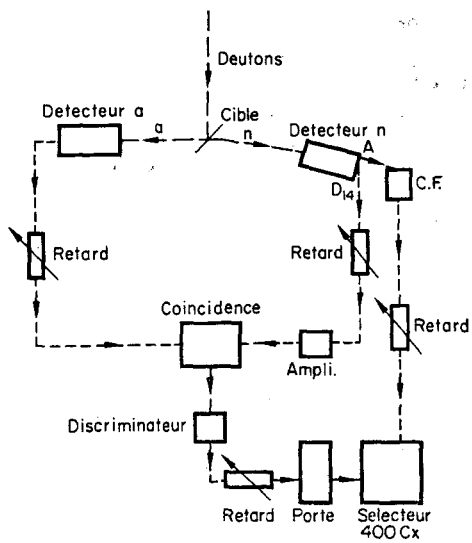

FIG. 6. Schéma du montage expérimental.

0,1 mm d'épaisseur placé devant un photomultiplicateur (en abrégé PM) Radiotechnique 56 AVP. L'angle solide délimité par le scintillateur est de $5{,}65.10^{-3}$ stéradian.

"Voie neutron"

Le détecteur est constitué par le remplissage d'hélium sous 40 atmosphères.

—Circuits d'électronique

Le principal élément est le circuit de coïncidences (SAIP, type TNC 2–3), dont le temps de résolution est fixé par le seuil d'un discriminateur d'amplitude placé à la sortie. Le temps de résolution choisi est de 6.10^{-9} s.

Nous avons procédé aux réglages habituels:

—Retard entre les 2 voies; position optimale du détecteur par rapport à la cible (5° par rapport à la direction des particules α),

—Réglage de l'ouverture de la porte du sélecteur d'analyse à 400 canaux.

(b) *Mesure de flux de neutrons.* Les neutrons sont détectés à l'aide d'un scintillateur d'anthracène associé à un P.M. 53 AVP. Les impulsions dues aux protons de recul sont décomptées après passage dans un sélecteur d'amplitude monocanal. Comme l'on connaît l'efficacité de ce détecteur, on peut déterminer la valeur du flux de neutrons.

III. 2. *Résultats expérimentaux*

(a) *Spectres des neutrons.* Les figures 7 et 8 donnent la répartition en énergie des noyaux de recul, dans le cas où l'on utilise comme convertisseurs de longueurs d'onde le salicylate de sodium puis le quaterphényl.

Ces spectres expérimentaux sont entachés de distorsions d'origines très diverses: effets de bord, pouvoir de résolution non nul du détecteur. Dans ce qui suit, nous allons étudier le rôle de ces différents facteurs.

(b) *Efficacité de détection.* La mesure du flux de neutrons permet de connaître le nombre de neutrons qui arrivent sur le détecteur; l'intégrale du spectre expérimental fournit le nombre de noyaux de recul créés, donc le nombre de neutrons détectés. On peut déterminer la valeur expérimentale de l'efficacité qui est de $4{,}5.10^{-4}$.

Il est difficile de recouper ce résultat par la théorie, car le calcul rigoureux de l'efficacité est compliqué, mais on peut avoir un ordre de grandeur par un calcul approché. On peut supposer [11] que pour un scintillateur de longueur L composé d'atomes de même nature, placé

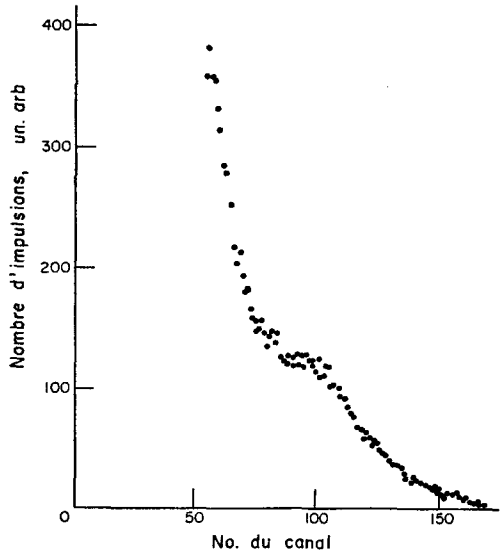

FIG. 7. Spectre des noyaux de recul obtenu avec l'hélium et le salicylate.

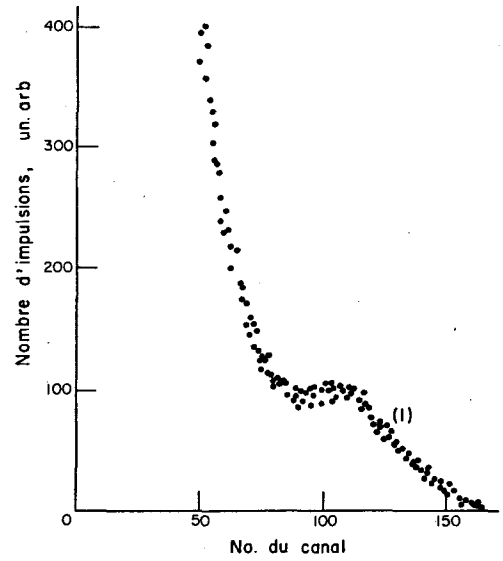

FIG. 8. Spectre des noyaux de recul obtenu avec l'hélium et le quaterphényl.

dans un flux de neutrons monoénergétiques, l'efficacité e s'écrit:

$$e = 1 - \exp(-aL)$$

où $a = n\sigma$; n = nombre d'atomes de la cible/cm³; σ = section efficace de diffusion pour l'énergie considérée. Si $aL \ll 1$

$$e \not= aL$$

dans les conditions de l'expérience (hélium sous 40 atmosphères), $n = 0{,}106.10^{22}$ atomes/cm³. La section efficace totale de diffusion des neutrons de 14 MeV dans l'hélium 4 est de 1,02 barns (cf par exemple: Austin[1]). On trouve que:

$$e \not= 6.10^{-4}$$

III. 3. *Corrections des spectres expérimentaux*

(a) *Effets de bord.* Un noyau de recul qui est créé à une distance des parois inférieure à son parcours, ne cède pas toute son énergie au milieu gazeux; la hauteur d'impulsion correspondante est plus petite qu'en l'absence des effets de bord.

Le détecteur était placé à 50 centimètres de la cible et son axe de symétrie était dirigé selon la direction des neutrons incidents. Comme le faisceau des neutrons associé aux particules α détectées délimite un angle solide très faible, les effets de bord sur la paroi cylindrique de la chambre n'interviennent pas; seuls se manifestent les effets sur la face terminale (figure 9).

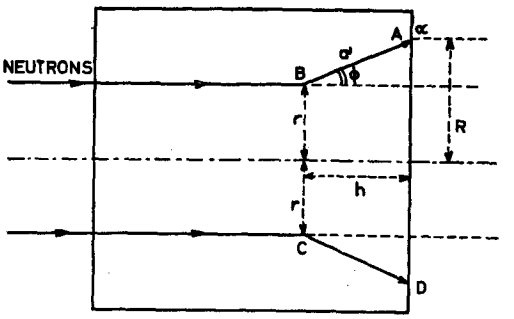

FIG. 9. Effets de bord sur la face terminale du détecteur.

Le faisceau de neutrons a une ouverture très faible. Pour le calcul, on peut supposer qu'on a affaire à un faisceau cylindrique; le rayon r du cylindre est égal à celui du cercle intersection du cône des neutrons incidents avec la face terminale du détecteur.

La fraction des noyaux de recul d'une énergie donnée affectés par les effets de bord est égale au rapport du volume $ABCD$ et du volume du détecteur. Le tronc de cône $ABCD$ a pour hauteur:

$$h = a' \cos \Phi$$

et pour rayons: r et $R = r + a' \sin \Phi$, où Φ est l'angle de diffusion des noyaux d'énergie E dans le système du laboratoire.

Les calculs montrent que la fraction de noyaux de recul d'énergie maximale affectés par les effets de bord atteint 20% (cf tableau 2). La

Tableau 2. Quelques valeurs du pourcentage de noyaux de recul affectés par les effets de bord

Énergie des noyaux de recul (en MeV)	Pourcentage des noyaux affectés par les effets de bord
1	0,204
2	0,90
3	2,19
4	4,11
5	56,75
6	10,1
7	14,06
8	18,28
8,96 (E_{max})	20,76

distorsion correspondante ne peut être négligée et l'on voit qu'il est indispensable de faire des remplissages sous des pressions très élevées.

Pour faire les corrections, nous supposons que les impulsions a d'énergie E effectées par les effets de bord se répartissent uniformément depuis l'énergie zéro jusqu'à $E - \epsilon'$ ($\epsilon' \to 0$). Cependant, il faut connaître la position dans le spectre du point d'énergie maximale. Ce problème est abordé plus loin.

(b) *Pouvoir de résolution en énergie.* Vedrenne[12] a évalué l'importance de la distorsion introduite par le pouvoir de résolution non nul des détecteurs. Nous utilisons cette méthode de correction dans le cas d'un scintillateur gazeux. Rappelons-en brièvement le principe:

Un scintillateur irradié par des particules ionisantes monoénergétiques délivre des impulsions qui se répartissent autour d'une valeur moyenne, selon une loi de Gauss. La répartition en énergie correspondante autour de la valeur E' est donc de la forme:

$$f(E, E') = \frac{1}{a\sqrt{\pi}} \exp - \left(\frac{E - E'}{a}\right)^2$$

la ½ largeur a de la courbe, prise à $1/e$ du maximum, fixe la résolution du détecteur. a est bien sûr fonction de E'.

Lorsque le scintillateur est soumis à un flux de particules dont les énergies sont comprises entre 0 et E'_{max} selon une loi de distribution $\rho\ (E')$, la transformée $N\ (E)$ du spectre théorique est de la forme:

$$N(E) = \frac{1}{\sqrt{\pi}} \int_0^{E'_{max}} \frac{\rho\ (E') \exp - \left(\frac{E - E'}{a}\right)^2}{a}\, dE'$$

Dans ces conditions, a est de la forme:

$$a = (\epsilon E)^P$$

à 14 MeV, pour les diffusions (n, p), (n, d) et (n, t), la valeur de P est égale à 0,5.[12] C'est celle qui a été adoptée. D'autre part, à condition de considérer que seules les ondes S et P sont responsables de la diffusion élastique,[13] $\rho\ (E')$ peut se représenter par une forme parabolique.

La figure 10 représente $\rho\ (E')$ et ses transformées $N\ (E)$ pour différentes valeurs du paramètre ϵ. Le spectre théorique est, on le voit, très déformé.

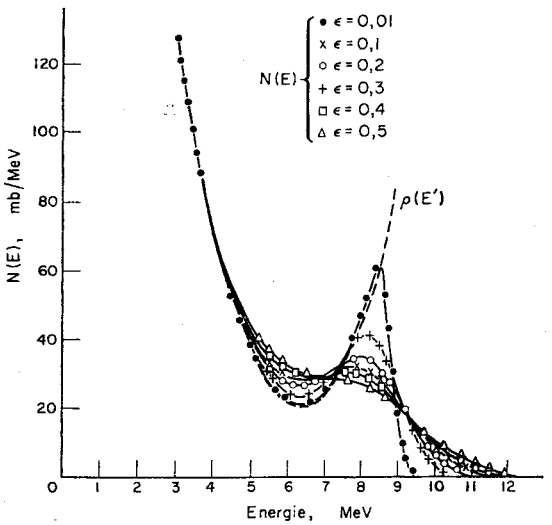

FIG. 10. Transformées $N(E)$ de la distribution théorique $\rho\ (E')$ pour différentes valeurs de ϵ.

Pour déterminer le point d'énergie maximale, nous procédons de la manière suivante: on déforme les spectres théoriques obtenus pour différentes valeurs de ϵ, en tenant compte des effets de bord. On détermine la relation qui lie la résolution théorique $2\sqrt{\epsilon/E'}$ à la résolution expérimentale (rapport de deux fois la demi-largeur à mi-hauteur et de l'abscisse du maximum), et la valeur R du rapport entre l'ordonnée du maximum et celle du point d'énergie maximale. La valeur de ϵ choisie correspond à une résolution expérimentale égale à celle du spectre expérimental (spectre 1 de la figure 8, dans le cas du quaterphényl). On connaît alors la valeur de R, et on peut déterminer la position du point d'énergie maximale sur le spectre expérimental.

Les résultats obtenus avec le salicylate de sodium confirment bien les considérations

théoriques précédentes. D'après les calculs, le spectre ne présente pas de maximum, lorsque la résolution expérimentale pour les particles α de 5,3 MeV est supérieure à 60%. Effectivement, en plaçant dans la chambre une source α de ^{210}Po, nous avons trouvé un pouvoir de résolution au moins égal à 70%.

L'emploi de quaterphényl s'est donc révélé indispensable. Lorsqu'on fait les corrections indiquées plus haut, il faut adopter pour R, 1,4 et pour ϵ 0,3; le pouvoir de résolution correspondant pour les particules α de 5,3 MeV est de 48%. Si l'on corrige le spectre 1 des effets de bord, ce qui est possible puisqu'on connaît la position du point d'énergie maximale, on obtient le spectre 2 de la figure 11 qui donne la répartition des noyaux de recul dans le système du laboratoire, avec un détecteur dont on connaît exactement le pouvoir de résolution en énergie.

Il faut ensuite corriger le spectre 2 des effets de la résolution pour obtenir la distribution expérimentale $\rho'(E')$. Ceci est théoriquement possible puisqu'on connait ϵ. En fait, la méthode directe est difficile car une déformation locale

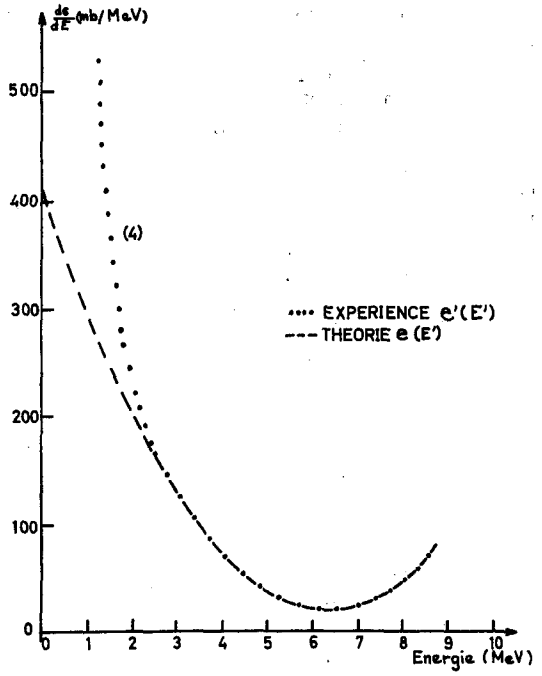

FIG. 12. Comparaison de la distribution théorique $\rho(E')$ et de la distribution expérimentale $\rho'(E')$.

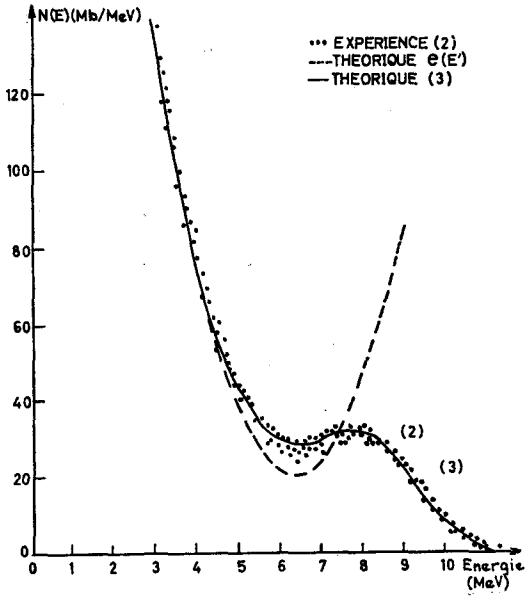

FIG. 11. Comparaison entre le spectre expérimental corrigé des effets de bord et le spectre théorique correspondant à $\epsilon = 0{,}3$.

du spectre expérimental peut entraîner une oscillation dans le spectre corrigé. Nous avons pu lever cette difficulté de la manière suivante: on constate que la transformation $\rho(E') \rightarrow N(E)$ pour $\epsilon = 0{,}3$ ne modifie pas le spectre jusqu'à 4,5 MeV (figure 10); de plus, les spectres 2 et 3 (3 représente la transformée $N(E)$ pour $\epsilon = 0{,}3$) coïncident pour des énergies supérieures à 2,6 M'V (figure 11). L'obtention de $\rho'(E')$ est immédiate:

—de 0 à 2,6 MeV $\rho'(E')$ est représenté par la partie correspondante du spectre 2;

—au delà de 2,6 MeV $\rho'(E') \equiv \rho(E)$.

Nous constatons que le spectre 4 qui représente $\rho'(E')$ (figure 12) ne coïncide pas avec $\rho(E')$ au-dessous de 2,6 MeV. Effectivement, si l'on intègre $\rho'(E')$, la valeur de la section efficace obtenue est supérieure à 1,02 barns.

Ce désaccord tient à plusieurs raisons. En voici deux, parmi les plus importantes:

(a) On ne peut éliminer totalement les coïncidences fortuites. Ceci tient en particulier à la durée trop importante de l'impulsion de

commande de la "porte" de l'analyseur d'amplitude.

(b) Seagrave[14], qui constate le même désaccord que nous, pense que celui-ci provient essentiellement des neutrons diffusés inélastiquement dans l'enveloppe métallique du détecteur. Comme la section efficace de ce processus croît lorsque l'énergie diminue en $E^{-1/2}$, les neutrons doivent produire un nombre élevé d'interactions lorsqu'ils ont des énergies faibles. Malheureusement, on ne connaît pas le nombre de neutrons qui induisent cette réaction, et toute correction est impossible.

CONCLUSION

Jusqu'à présent, seuls Austin et ses collaborateurs[1] ont étudié d'une manière systématique la diffusion élastique (n–α) à l'aide d'un scintillateur gazeux, pour différentes énergies des neutrons. Comme nous l'avons indiqué, le gaz de remplissage était un mélange d'hélium et de xénon. A pression égale, l'efficacité est moins bonne que dans notre cas, mais le pouvoir de résolution en énergie doit être plus élevé, et les effets de bord sont moins importants, puisque le pouvoir d'arrêt du mélange est plus grand.

Cependant, ces auteurs présentent pour les neutrons de 14 MeV un spectre expérimental corrigé des effets de bord qui ne correspond à aucune transformée $N(E)$. En fait, pour étalonner l'échelle des ordonnées en unité de section efficace différentielle, Austin et ses collaborateurs ont admis que l'intégrale du spectre expérimental était de 1,02 barns. La méthode est rigoureuse, mais elle introduit dans la pratique une erreur importante: comme l'expérience ne portait pas sur la totalité des angles de diffusion, ils ont dû extrapoler la courbe obtenue; le spectre expérimental est situé au-dessous du spectre théorique et ne le recoupe pas. En opérant de la même façon, nous avons fait une constatation analogue. C'est pourquoi, nous avons préféré normaliser le spectre expérimental et la courbe $N(E)$ au point d'énergie maximale; nous avons pu ainsi graduer l'échelle des ordonnées. Le bon accord obtenu pour les autres énergies confirme la validité du procédé.

RÉFÉRENCES

1. S. M. Austin, H. H. Barschall et R. E. Shamu. *Phys. Rev.* **126,** 1532 (1962).
2. J. G. Jenkin et R. E. Shamu. *Nucl. Instr. and Methods* **34,** 116 (1965).
3. P. J. Pasma. *Nucl. Phys.* **6,** 141 (1958).
4. J. Czmider et J. Szymakowski. Rapport 266, Inst. Nucl. Phys. Cracow 1963.
5. J. L. Teyssier, D. Blanc et A. Godeau. *J. Phys. Rad.* **24,** 55 (1963).
6. A. Perrin. Thèse Doctorat de 3° cycle, 1959, no. 15, Lyon.
7. A. Sayres et C. S. Wu. *Rev. Sc. Instr.* **28,** 758 (1957).
8. R. J. Esterling et N. H. Lipman. *Rev. Sc. Instr.* **36,** 493 (1965).
9. C. Rubbia et M. Toller. *Nuovo Cimento*, **10,** 410 (1958).
10. S. A. Baldin, V. V. Gavrilovski et F. E. Chukreev. *Atom. Energya* **28,** 1092 (1957).
11. C. D. Swartz et G. E. Owen. *Fast Neutron Physics*, Part I. Interscience Publishers, New York, 1960.
12. G. Vedrenne. Thèse Doctorat ès-Sciences, 1966, n°. 254, Toulouse.
13. J. Galy. Thèse Doctorat de 3° cycle, 1966, no. 425, Toulouse.
14. J. D. Seagrave. *Phys. Rev.* **92,** 1222 (1953).

A WIDE-RANGE GAMMA-RAY DOSE-RATE METER

D. SRDOČ
Institute "Ruđer Bošković", Zagreb, P.O.B. 171, Yugoslavia

Abstract—Properties of gas-filled detectors have been discussed in connection with their use in portable dose-rate meters. It has been pointed out that the relatively long dead time of a G.M. counter causes a serious limitation to high dose-rate measurements. Since G.M. counters offer some advantages in comparison with ionization chambers (substantially higher current output per unit dose-rate) an attempt has been made to obtain a wide range dose-rate meter by using a newly developed G.M. counter tube. A substantially shorter dead time of the order of a microsecond has been obtained. The new counter tube does not saturate until 10^3 r/hr in the Geiger region. Several tubes have been tested up to 5×10^5 r/hr in the proportional region without observing saturation phenomena or radiation damage after prolonged exposure. Schematic diagrams of a portable dose-rate meter and a monitoring system for a kilocurie ^{60}Co source using the newly developed tubes have been presented.

INTRODUCTION

It is desirable to combine the wide measuring range and the spectral insensitivity of a properly designed ionization chamber with the fast response, acoustic indication and high sensitivity of a G.M. counter. An approach to such a device might be attained by using a halogen G.M. tube, measuring the pulse-rate at low dose-rates and the average current in the high dose-rate region. A G.M. tube has a current amplification of 10^4 to 10^6, which allows substantial simplification of the electronic circuitry. However, the phenomenon of high internal amplification of a G.M. tube is accompanied by a long "dead time" which causes saturation at a relatively moderate dose-rate, thus limiting the use of G.M. counters in dose-rate meters. A halogen counter, such as a Philips 18504 tube, covers about two decades before reaching saturation. There exists a possibility—at least in principle—of combining a set of counters, each of them being of a different size and having overlapping radiation vs. current characteristics. Such an arrangement has the serious drawback from the practical point of view that counters of different sizes usually have different working voltages, pulse amplitudes and dead times. This may lead to a cumbersome design of radiation detection instrument. An attempt has been made to overcome these difficulties by using a parallel plate halogen filled G.M. counter [1] which has some outstanding properties, such as fast response to ionizing particles, short dead time and high charge per pulse.

PARALLEL PLATE COUNTER

Several authors have pointed out [2, 3] that parallel plate geometry should give rise to a faster response to an ionization event. This is because in a cylindrical counter, electron multiplication only occurs in a small region of high potential gradient around the anode. Electrons produced outside this region are in an area of relatively low potential gradient through which they slowly drift without multiplication until they reach the area around the anode where multiplication can occur. In a parallel plate counter there is no time lag due to this electron transit before multiplication. If such a fast rise time is followed by a short recovery time then a substantial increase in counting rate may be achieved allowing the counter to be used at higher dose-rates. Earlier attempts [2, 3] were unsuccessful in obtaining the short recovery time; a very fast pulse rise time of the order of a few tens of nanoseconds was followed by a recovery time of a few milliseconds. However, our experiments with halogen quenching

mixtures showed that the recovery time might be reduced to a fraction of a microsecond by proper counter design and by the use of an optimum gas mixture.

The counter geometry is very simple, consisting of two stainless steel plates, separated by a glass ring. Measurements of the counter characteristics showed an optimal gap around 0.3 cm at 100 mm of neon plus 1.0 mm of bromine. Departures from these values are permissible if a shorter operating range may be tolerated. The plate diameter is not critical up to several cm. However, further increase leads to a capacitance which may be large enough to affect the discharge mechanism, leading to a self-sustained streamer.

The mechanism responsible for discharge propagation in our counter is photoionization in the gas. This is a very fast process, requiring about 10^{-8} sec to complete the avalanche at a high overvoltage. At lower overvoltages near the Geiger threshold a very slow buildup of the pulse is observed indicating another mechanism, probably the production of metastable states and their slow diffusion and de-excitation. This region should be avoided, because the slow pulse build-up takes several micro-seconds. The time necessary for the completion of a discharge includes the time for the transit and neutralization of positive ions. Because of the high potential gradient extending across the whole counter, positive ions will cross a parallel plate counter faster than a cylindrical counter with its large region of relatively low electric field near the cathode. Thus a transit time of a fraction of a microsecond can be obtained. Taking the drift velocity of positive ions to be approximately 1–2 cm/μsec at the E/p value of $\approx$ 20 V/cm mm Hg (the exact values for gas mixtures under consideration are not known), the time necessary for an ion to cross the gap is $\approx$ 0.15—0.3 μsec. The oscilloscope measurement shown in Fig. 1 confirms these assumptions, giving for the discharge development a rise time of $\approx$ 20 nsec and an ion transit time of $\approx$ 150 nsec. Thus the discharge is completed

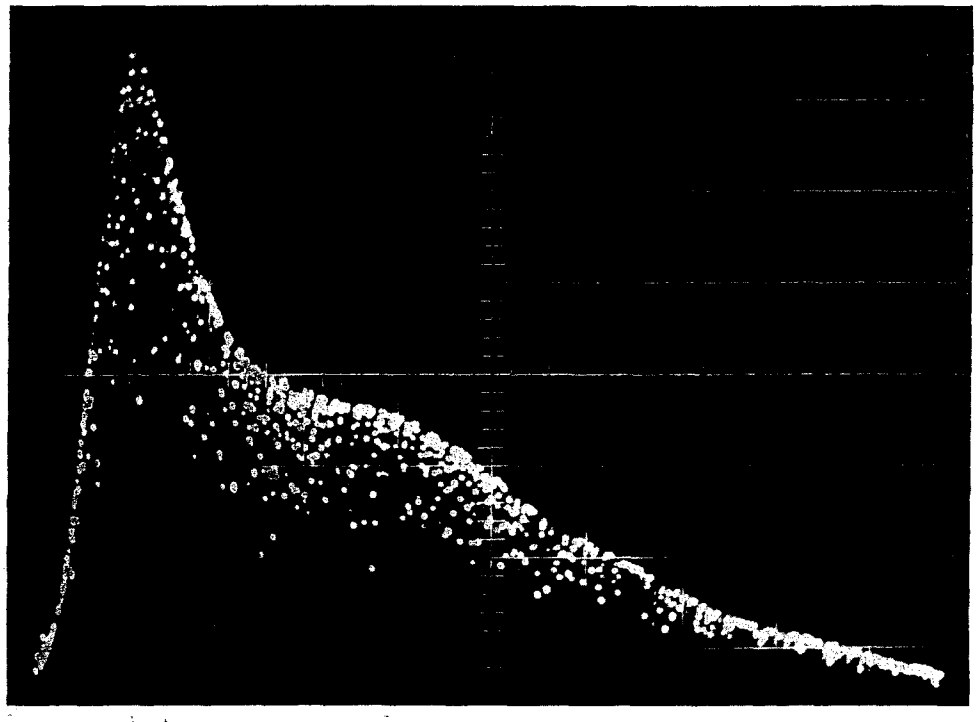

FIG. 1. Parallel plate counter pulse. Time: 20 nsec per larger division. Vertical scale: 4.6 mA per larger division.

in less than 200 nsec, which is shorter than typical values for conventional G.M. counters by several orders of magnitude. In order to exploit fully the very short dead time of a parallel plate counter it should be emphasized that the RC constant (R = series resistance, C = total capacitance of the electrode system) should be kept reasonably low. This is not always possible, because too low a series resistance causes poor counter characteristics. A simple transistorized circuit is under development by means of which it will be possible to take full advantage of the fast completion of the discharge.

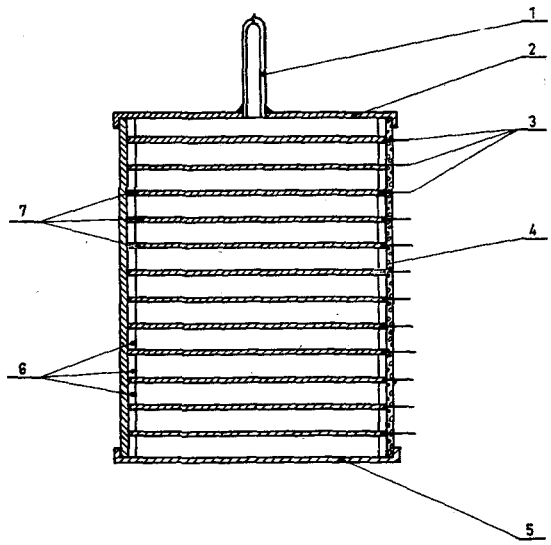

FIG. 2. Multiple counter. Schematic diagram and exploded view. 1, filling tube; 2, 5, top and bottom caps, glass matching alloy; 3, leads; 4, powdered glass seal; 6, glass or ceramic spacers; 7, stainless steel discs.

For practical purposes it is convenient to use a stack of parallel plate counters, thus increasing the pulse rate or the average current for a given radiation intensity. Figure 2 shows an assembly of parallel plate counters. The construction and preparation of a counter is relatively simple, using prefabricated parts. Every cell consists of two metal discs separated by a glass ring. The thermal coefficient of linear expansion of glass and metal should match closely in order to avoid stresses. A glass to metal vacuum-tight seal is obtained using low melting point powdered glass, the whole assembly being heated up to the melting point of the powdered glass in an inert gas atmosphere.

The properties of a parallel plate counter are compared with those of a conventional G.M. counter of the same dimensions in Fig. 3. For the parallel plate counter the average current for a given radiation intensity is 5–10 times larger, depending on the radiation intensity; furthermore, the conventional G.M. tube saturates at 10^2 mr/hr, while the parallel plate counter only reaches 90% of its saturation current at 10^5 mr/hr.

A further extension of the counting range towards high dose-rates is observed when the tube operates at a few volts below the Geiger threshold. No saturation phenomenon occurs at 10^6 r/hr, the maximum dose-rate available is our experimental set-up. The pulse amplitude spectra observed on the oscilloscope show that the detector is working as a typical proportional counter. The amplification factor is estimated to be 10^4. No radiation damage is observed after $\approx$ 1 Mrad, the estimated absorbed dose during experiments.

DOSE-RATE METER AND MONITORING SYSTEM

The use of a parallel plate counter in portable dose-rate meters makes a substantial simplification of the electronic circuitry possible. The block diagram of a portable dose-rate meter is shown in Fig. 4. The main parts consist of a stabilized high voltage supply, a linear D.C. amplifier and a 50 μA meter. The instrument is provided with a ^{90}Sr calibration source. The calibration is performed by opening the ^{90}Sr source and adjusting the EHT voltage until the counter current reaches a defined value.

Fig. 5 shows a detailed electronic circuit diagram, and Fig. 6 is a photograph of the portable survey meter using the newly developed tube.

A high current output, ranging about 50 μA, and excellent resistance to radiation damage make the parallel plate counter suitable for monitoring the area close to radiation sources and for positioning them. A schematic diagram in Fig. 7 shows such an arrangement applied

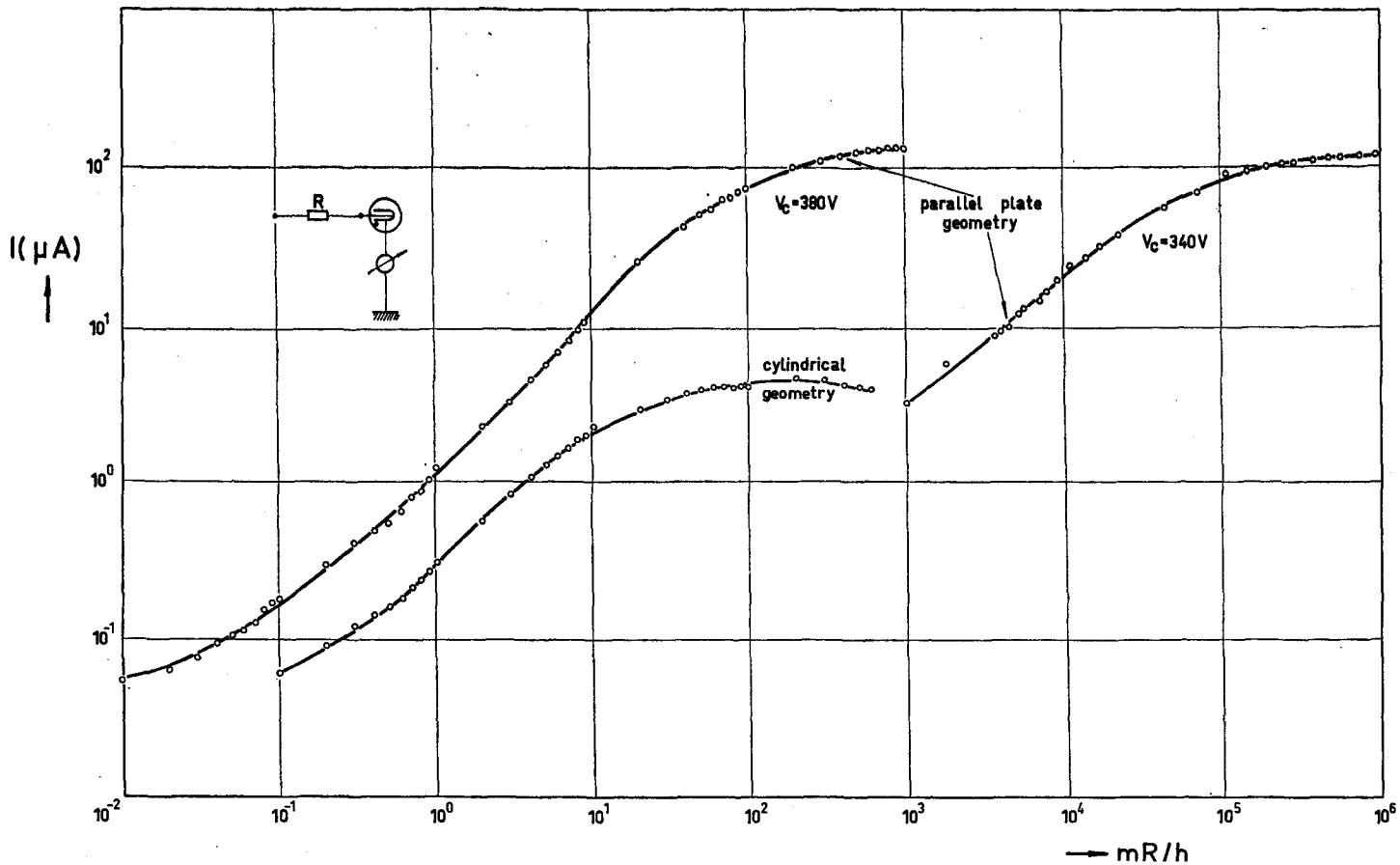

FIG. 3. Counter current vs. dose-rate plot. Comparison between the parallel plate and the cylindric counters.

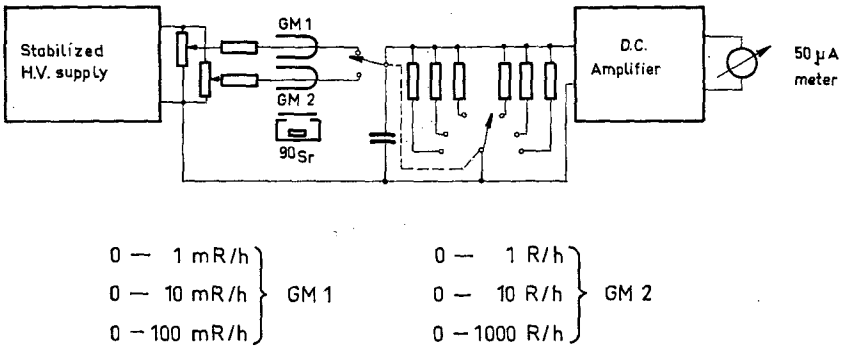

FIG. 4. Block diagram of a portable dose-rate meter based on the parallel plate counter.

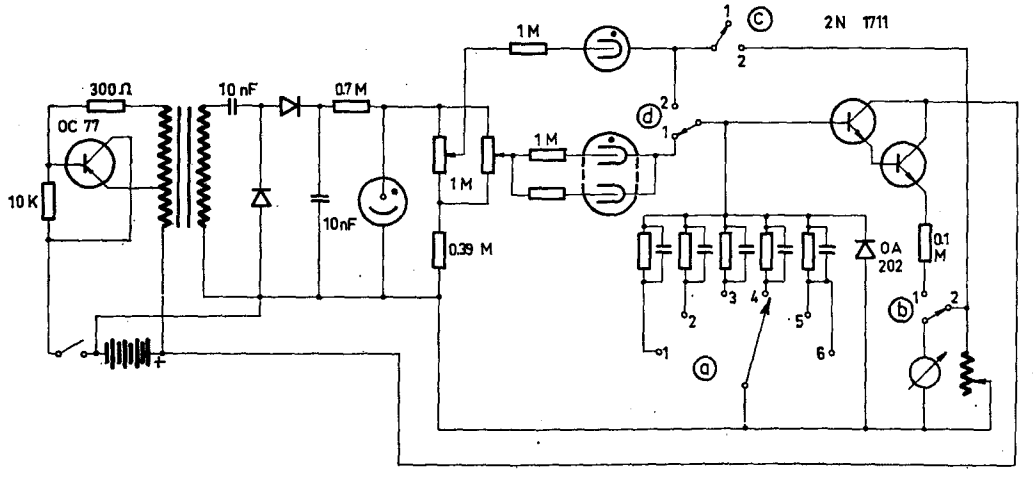

Positions	a	b	c	d
0-1 mR/h	1	2	3	4
0-10mR/h	2	1	1	1
0 100mR/h	3	1	1	1
0 - 1 R/h	4	1	1	2
0-10 R/h	5	1	1	2
0 1000 R/h	6	2	2	2

FIG. 5. Circuit diagram of a portable dose-rate meter based on the parallel plate counter.

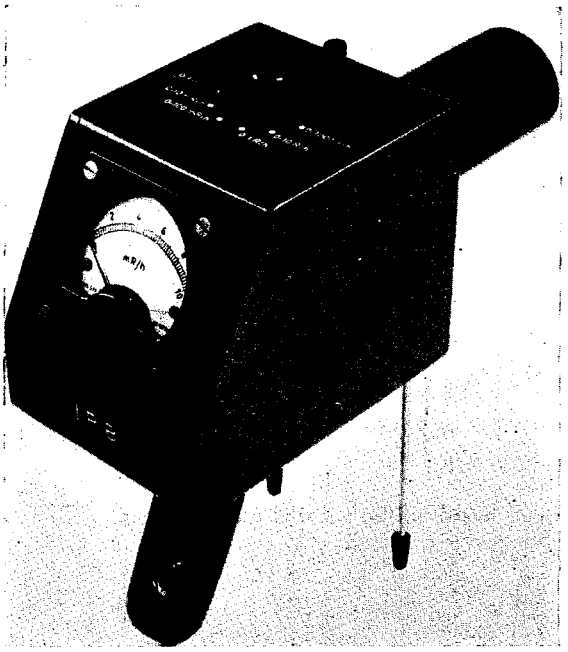

FIG. 6. Portable wide-range dose-rate meter.

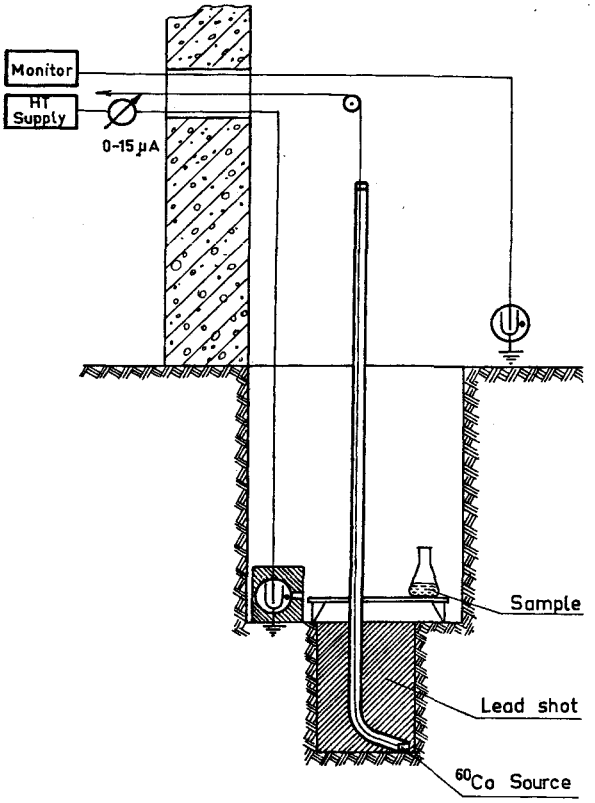

FIG. 7. Schematic diagram of a monitoring and positioning system using a parallel plate counter.

to a ^{60}Co gamma irradiation unit. During operation of the system it was observed that the electrical cables suffered from radiation damage, the leakage current through the cable insulation amounting to several microamperes when irradiated. Using teflon instead of polyethylene insulated cables reduced the leakage current below values which would affect the monitoring system.

CONCLUSIONS

The properties of the parallel plate counter offer the possibility of widening the dose rate range and of substantial simplification of dose-rate meter design.

The use of tissue-equivalent materials for counter walls is not possible because of the present technology of halogen counter production. Therefore, correction of the spectral sensitivity of the multiple counter could only be achieved by using filters. Another feature of this instrument is its directional sensitivity. This depends on the plate material, thickness, and diameter, so there is a possibility of minimizing the errors due to counter orientation. In the case of the multiple counter shown in Fig. 2, when the incident radiation was parallel with the counter axis the output current was 12% higher than for a beam perpendicular to the axis.

REFERENCES

1. D. SRDOČ. *Nuclear Instrum. Methods* **21,** 243 (1963).
2. J. W. KEUFFEL. *Rev. Sci. Instrum.* **20,** 202 (1949).
3. J. CHRISTIANSEN. *Z. angew. Phys.* **4,** 326 (1952).

DOSAGE SÉLECTIF DE TRACES D'URANIUM PAR FLUORIMÉTRIE

E. MUSYCK
Centre d'Études de l'Energie Nucléaire, Mol, Belgium

Résumé—Après extinction de la lumière excitatrice u.v., les sels d'uranyle présentent une décroissance de la luminescence avec une constante de quelques dizaines de μsec.

L'appareil décrit met à profit cette particularité pour augmenter la sélectivité d'un fluorimètre destiné au dosage de traces d'uranium.

Il se compose d'une source de lumière ultraviolette pulsée à extinction rapide, et d'un circuit de mesure commandé par un circuit-porte retardé.

En utilisant la relation quasi logarithmique du gain du photomultiplicateur en fonction de la tension, on a constitué un dispostif à lecture directe s'étendant sur quelques décades.

ZUR MESSUNG DER UMGEBUNGSSTRAHLUNG MIT PLASTISCHEN SZINTILLATOREN

R. BERNARD und A. WENSEL
Institut für Kernphysik der Universität, Frankfurt/Main, F.D.R.

Zusammenfassung—Ein transistorisiertes Gerät für die Messung geringer γ-Dosisleistungen zur Verwendung in Messwagen wird beschrieben. Als Detektor dient ein Szintillationszähler mit einem grossvolumigen Plastik-Szintillator (17,5 cm Ø × 15,5 cm). Die Pulsrate ist kein energieunabhängiges Mass für die Dosisleistung. Eine energieunabhängige Messung ist jedoch möglich, wenn die Pulse ihrer Höhe nach bewertet werden. Das geschieht in einem sogenannten "Impulsintegrator", der aus mehreren Diskriminatoren mit dualen Zählstufen besteht.

Die Schwellen der Diskriminatoren liegen in einem Bereich von etwa 20:1. Es ist daher möglich, Dosisleistungen von γ-Strahlung mit Energien von etwa 150 keV bis 3 MeV energieunabhängig zu messen. Dieser Energiebereich liefert im allgemeinen den wichtigsten Beitrag zur gesamten Dosisleistung. Das Gerät ist empfindlich genug, um die natürliche Umgebungsstrahlung zu messen und geringe zusätzliche, z.B. durch Kernenergieanlagen verursachte Strahlenbelastungen festzustellen. Durch die Verwendung von Tunnel-Dioden in den Diskriminatoren und von integrierten Schaltkreisen als Untersetzer wird gute Stabilität, grosse Zuverlässigkeit und ein Minimum an Raumbedarf und Gewicht erreicht. Die Ausgangsimpulse des Integrators können einen Zähler ansteuern oder über ein Ratemeter registriert werden. Wegen der hohen Empfindlichkeit können im Ratemeter kurze Zeitkonstanten verwendet werden, so dass Messungen im fahrenden Wagen durchgeführt werden können.

Die Überwachung von relativ grossen Gebieten ist deshalb in kurzer Zeit möglich. In der Umgebung des Forschungsreaktors Frankfurt wurde mit einem Messwagen die Dosisleistung der γ-Strahlung ermittelt. Die Ergebnisse werden diskutiert.

DISCUSSION

K. Żarnowiecki (*Poland*):

Qu'arrive-t-il si, après 250 μsec l'émission α qui est comptée en coïncidence décroit brutalement?

J. P. Vaane:

Even if this was the case, the effect of the second circuit would be the same, because essentially the same alpha particles which pass the first gate, arrive at the second gate at the moment that this gate is closed. Therefore, the length of the delay period does not affect the number of α_{psco} passed and does not affect the correction applied by this second circuit.

A. Rindi (*Cern*):

Qual'è la sensibilità ai n di 14 MeV del rivelatore da lei presentato?

D. Blanc:

La valeur *expérimentale* de l'efficacité est de $4{,}5.10^{-4}$ pour les neutrons de 14 MeV. La valeur *calculée* est de $6{,}0.10^{-4}$ mais avec une erreur possible de 30% et les deux valeurs me paraissent en bon accord.

D. Blanc (*France*):

J'ai été très intéressé par votre détecteur. Dans le cas d'une géométrie cylindrique, Van Zoonen a montré que le temps de latence subit des fluctuations très grandes. Avez-vous observé un phénomène analogue? D'autre part, quelle est la longueur du palier de comptage? Quelle est sa pente? Quelle est la tension de fonctionnement utilisée?

D. Srdoc:

The first part of your question was about the mechanism and the scattering at the beginning of the passage of a particle. Yes, it was possible to observe at a low over voltage a time lag of several microseconds between the passage of a particle and the pulse on the oscilloscope. A standard arrangement was used for such measurements consisting of the experimental counters and a very fast crystal, which will trigger the time based on the oscilloscope immediately. At a higher voltage, say about a hundred volts above the threshold, it was not possible to observe any delay between the response of the crystal and this type of counter. This means that instead of a classical discharge we believe there is photo-ionization which is a very fast phenomenon.

The second part of your question was about this pulse. The pulse amplitude was 200 V, the rise time 20 nsec, and the total length about 200 nsec. I think that's all.

F. Berthold (*Germany*):

The detector described seems to operate similarly to a spark chamber, which is also characterized by fast rise-times of less than 10 ns and pulse heights well over 100 V. But spark chambers need long recovery times of about 10 msec because the electrodes seem to be left in an excited state, and therefore a long dead-time has to be provided before the chamber can be triggered again.

Could the speaker point out what time-resolution is obtained with this detector if it is used as a pulse counter?

D. Srdoc:

The geometry and the mechanism of the detector are very similar to those of a spark chamber and I have had discussions with people working with spark chambers at Brookhaven. We decided that the difference is due to the filling gas. In our counter we use a mixture of neon and bromine which is responsible for the gas discharge mechanism; in the spark chamber there is a different gas mixture. It seems that the small percentage of quenching mixture allows the very fast recovery of time, which is of the order of 1 or even less microseconds. There is no secondary effect after 1 μsec. Regarding the slope of this counter, perhaps this is the main drawback of this design because it is very steep and the supply voltage must be very well stabilized compared with standard conventional cylindrical geometry. But when measuring the average current, there was need for stabilization in either case. Have you a flat or a steep plateau?

G. Cowper (*Canada*):

I think that, in common with many people, Mr. Srdoc has found that if you start to play games with Geiger counters, you'll finish with a device which does not have a plateau or at least it has a plateau with a slope, which is a contradiction. I think maybe, what we need is another name for this kind of device: it is not a G.M. counter.

CONCEPTION ET RÉALISATION D'UN CONTRÔLE DE LA POLLUTION RADIO-ACTIVE DE LA CHAÎNE ALIMENTAIRE

R. COULON

Département de la Protection Sanitaire, Commissariat à l'Energie Atomique
Fontenay-aux-roses, France

Résumé—L'utilisation de l'énergie nucléaire étant appelée inéluctablement à prendre une part de plus en plus importante dans tous les domaines, il importe de l'entourer du maximum de garanties quant aux conséquences proches ou lointaines de ses effets sur la santé des populations: il s'agit essentiellement de contrôler le respect des niveaux fixés et de parfaire nos connaissances sur les mécanismes de transfert et d'introduction chez l'homme, afin d'être en mesure d'effectuer des prévisions.

Ainsi, outre la surveillance particulière de certaines zones critiques, une surveillance générale, portant sur le milieu et les principaux vecteurs alimentaires, a été organisée par le Département de la Protection Sanitaire avec l'aide du Ministère de l'Agriculture. Les efforts portent essentiellement sur le lait, les céréales, les fruits et légumes et s'étendront à d'autres produits (viande, poisson, etc.).

Le contrôle est basé sur un échantillonnage rationnel des denrées au stade de la production, et ceci selon une localisation qui permet de superposer les résultats des mesures faites au niveau de l'atmosphère, des retombées, et des différentes productions animales ou végétales et de les interpréter en fonction des caractères climatiques, pédologiques, agronomiques et zootechniques locaux.

Ce contrôle de type vertical est complété par l'implantation de "stations d'observations" où la meilleure connaissance des conditions citées ci-dessus et l'individualité des prélèvements autorisent des interprétations plus fines et à caractère plus scientifique.

En France, comme dans la plupart des autres nations, il est indiscutable que l'avenir verra l'utilisation intensive de cette nouvelle source d'énergie qu'est l'énergie nucléaire. Il a donc paru essentiel, pour pouvoir progresser en ce domaine, de s'entourer de toutes les garanties possibles et de disposer d'un ensemble d'études et d'observations qui permettraient d'en prévoir valablement les conséquences d'ordre sanitaire.

Dans le même temps, et du fait que déjà des pollutions radio-actives apparaissaient à la surface du globe, il était urgent de mettre en place une large structure destinée à contrôler le bien-fondé de ces prévisions et à mettre en évidence toute manifestation jugée suspecte.

Il s'agit là d'un ensemble très vaste, où rien ne peut être fait isolément, et qui utilise les compétences les plus diverses: biologistes, physiciens, mathématiciens, météorologistes, hygiénistes, chimistes, agronomes, etc.

Notre propos est d'en extraire ce qui concerne la mise en place des programmes de contrôle, tant sur le plan de la conception que sur celui de la réalisation et de l'exploitation.

On verra que les réalisations citées sont fondées sur un certain nombre de principes dont quelques-uns ont un caractère purement national et par conséquent ne sont pas toujours extrapolables: mais peut-être, et nous le souhaitons, certaines des idées exprimées pourront-elles apporter quelque chose au patrimoine commun.

CONCEPTION DU CONTRÔLE

Nous ne parlerons pas ici de la surveillance particulière qu'il y a lieu d'exercer dans les secteurs où un risque potentiel est à considérer

(environnement d'un site nucléaire, zone de rejet). Les problèmes posés par ce type de contrôle sont généralement assez aisément résolus en raison des dimensions restreintes de la zone à contrôler et de la bonne connaissance que l'on peut en avoir.

Le problème de la surveillance générale est plus délicat à aborder car il englobe à la fois l'ensemble du pays, avec toute sa diversité géographique, climatique, pédologique, agronomique ou zootechnique, et l'ensemble de la population si hétérogène dans ses habitudes alimentaires.

Il importe donc au départ de définir clairement les objectifs à atteindre.

Sur le plan strictement sanitaire, il s'agit d'être en mesure d'évaluer l'ingestion de radioactivité (et partant, les risques encourus) soit pour l'individu moyen de l'ensemble de la population, soit pour les individus des groupes que l'on peut considérer comme critiques en raison de leur régime alimentaire particulier ou de leur situation géographique.

À ceci s'ajoute ce qui relève stricto sensu de la notion de "contrôle", à savoir la connaissance du niveau de contamination des différents produits selon l'origine et selon la date.

Enfin, compte tenu des lacunes qui subsistent encore dans la connaissance des mécanismes de pollution et des processus de transfert, il semble intéressant de chercher à utiliser les résultats du contrôle pour en tirer des enseignements en cette matière.

Comment atteindre ces objectifs?

Pour ce faire, il se présente deux solutions:

—la première consiste à faire porter l'échantillonnage sur l'alimentation de la population et des groupes d'individus choisis comme les plus exposés. Il est alors nécessaire, pour respecter les buts fixés, d'échantillonner les différents produits en connaissant leur origine et leur date de production;

—la deuxième solution est inverse. Elle revient à échantillonner les différents produits selon leur origine et en fonction du temps, puis à calculer la contamination ingérée par la population et les groupes dits "critiques", ce qui se fait aisément si l'on connaît les régimes alimentaires.

Nous ne nous étendrons pas sur les avantages et les inconvénients de chacune des deux méthodes. Après avoir pesé soigneusement les uns et les autres, nous avons jugé que, dans le cas de la France, la deuxième méthode était sans conteste la mieux adaptée et la plus facile à réaliser.

En effet, on peut considérer que, en matière de produits agricoles, la production nationale couvre en quasi-totalité la consommation. Sans contrôles complémentaires, la connaissance de la contamination des denrées produites sur le territoire permettra d'évaluer la contamination ingérée.

Il faut ajouter que ce principe du contrôle à la production offre d'autres avantages non négligeables:

le contrôle est effectué au plus tôt et éventuellement des mesures locales ou générales pourraient être prises avant consommation;
les échantillons restent entourés de tout le contexte "milieu" et des relations utiles peuvent être établies entre leur contamination et les facteurs naturels;
enfin, comme on le verra plus loin, le nombre des échantillons à analyser peut se trouver avantageusement réduit.

RÉALISATION DU CONTROLE

Principes—Si l'on considère la pollution générale au niveau d'une nation, on peut penser que les conditions essentielles de la contamination des produits agricoles sont d'ordre climatique, géographique, pédologique, agronomique et zootechnique.

Ainsi, lorsque au sein d'une région, se manifeste une certaine homogénéité pour chacun de ces facteurs, il y a tout lieu de croire qu'il en sera de même pour la pollution d'un produit agricole issu de cette région, et que les variations qui apparaissent n'ont aucun caractère systématique.

En conséquence, il sera possible de définir la pollution moyenne de ce produit en analysant un seul échantillon, si toutefois on prend la précaution de le constituer d'un nombre de sous-échantillons suffisant pour éliminer les fluctuations aléatoires.

Le critère homogénéité est une base de départ: il est toujours possible de vérifier ultérieurement son bien-fondé.

Le choix des sous-échantillons peut s'effectuer par des prélèvements faits soit au hasard, soit rationnellement, par exemple un système calqué sur la production de la denrée envisagée. Nous avons opté pour le second mode, qui permet d'avoir un plan d'échantillonnage mieux structuré et plus limité.

Schéma de base—Si l'on veut connaître la contamination d'un produit agricole *P*, on sera amené, par ce système, à effectuer les opérations suivantes:

1. Etudier la production de *P* sur l'ensemble du territoire: volume, répartition dans le lieu et le temps, ainsi que toute caractéristique locale susceptible d'influer sur le résultat final.
2. Sur ces bases, complétées par des données géographiques, climatiques et agricoles, chercher à répartir les lieux ou la production de *P* n'est pas négligeable en un certain nombre de régions présentant les caractères d'homogénéité précédemment définis. L'expérience montre que l'on peut résoudre le problème sans dépasser une quinzaine de régions.
3. Dans chacune de ces régions, déterminer les principales zones de production *P*, ainsi que le volume produit en chacune.
4. Dans chaque zone, choisir le lieu de prélèvement, de préférence un centre de groupement pour *P* (coopératives de producteurs, lieux de stockage, etc.)
5. Enfin, établir pour la région et pour *P* un plan de pondération tenant compte du volume de l'échantillon composite final et de l'importance de la production en chaque zone initiale.

Réalisation pratique—Celle-ci est bien évidemment fonction de la structure économique et administrative de la nation.

Pour nous, nous avons pu la mener à bien grâce au Ministère de l'Agriculture, qui est concerné par ces problèmes, et qui a apporté l'aide de ses divers services extérieurs. Un avantage évident provient du fait que les interventions auprès des producteurs ou organismes fournissant les échantillons sont faites par des personnes bien connues d'eux et au titre du Ministère de l'Agriculture; certaines difficultés d'ordre psychologique sont ainsi évitées.

Ainsi, poursuivant dans le sens de la définition d'unités à caractère régional, nous avons pu réaliser une décentralisation parfaite. Au sein de chaque région, des responsables locaux surveillent les opérations de collecte et résolvent les problèmes matériels et financiers tandis qu'un laboratoire centralise les prélèvements, éventuellement effectue les premiers traitements (dessiccation, minéralisation) et même, dans une nouvelle étape actuellement en cours, effectue des mesures d'activité totale, de façon à obtenir des informations rapides sur le niveau de contamination des échantillons.

L'ensemble de ces opérations est coordonné à l'échelon central.

État actuel de l'organisation

Le premier problème abordé a été celui du lait. Le réseau qui est en place concerne environ 150 points de prélèvements (industries ou coopératives laitières) répartis dans 13 régions. Ainsi sont représentés 44 départements, qui produisent 70 à 75% du lait destiné à la consommation humaine en France.

Les prélèvements sont effectués quotidiennement et constitués en un échantillon mensuel.

Le contrôle de la contamination des céréales a été résolu dans le même temps. Il porte sur 52 départements, répartis en 10 régions et produisant environ 90% du blé tendre d'hiver.

Les prélèvements sont effectués annuellement en 150 points, qui sont des silos coopératifs. Ils concernent le grain, et les analyses sont effectuées sur la farine après les habituelles opérations de mouture.

Enfin, le problème du contrôle de la pollution des fruits et légumes, beaucoup plus difficile à réaliser, a été abordé de façon analogue. Il s'exerce sur 39 départements, qui fournissent entre 60 et 90% (selon la denrée) de la production nationale. Les 39 départements sont groupés en 13 régions: 7 fournissent actuellement les échantillons, les 6 autres seront mises en place prochainement. Il y aura ainsi une centaine de points de prélèvements, ceux-ci étant effectués deux fois par mois.

Le contrôle sera également étendu prochainement à la viande.

Exploitation

Comme il a été indiqué plus haut, l'ensemble de cette organisation permet:

1. De connaître le niveau de pollution des principaux vecteurs alimentaires selon leur origine géographique et d'en suivre l'évolution dans le temps.
2. De calculer l'ingestion moyenne de radio-activité pour l'ensemble de la population, ceci à l'aide des enquêtes alimentaires disponibles.
3. De calculer l'ingestion de radio-activité pour la population des différentes régions et pour celle des grandes agglomérations, en utilisant les enquêtes alimentaires régionales et en connaissant l'origine des produits consommés.
4. De calculer l'ingestion de radio-activité pour ceux des groupes qui, par suite de leur régime alimentaire particulier, peuvent être considérés comme critiques (cas des jeunes enfants par exemple).
5. D'établir toute corrélation entre la contamination des différents produits et celle des vecteurs initiaux (air, précipitations) pour lesquels un réseau de contrôle existe déjà.
6. D'étudier localement l'influence des facteurs naturels sur le niveau de la pollution.

Pour parfaire cette exploitation, et pour éviter de ne travailler que sur des valeurs moyennes, nous cherchons à implanter dans quelques grandes régions, des stations dites "d'observation" où ces mêmes prélèvements seront effectués à l'échelon d'une seule exploitation agricole, considérée comme caractéristique de la région qu'elle représente. Tout résultat sera alors entouré de renseignements précis quant au milieu et aux conditions de production. Il sera également possible de s'intéresser aux étapes intermédiaires (sol, alimentation animale, etc.).

CONCLUSION

L'organisation d'un tel réseau de surveillance des produits alimentaires a été conçue selon trois principes de base, qui sont:

—obtenir les seules données nécessaires aux hygiénistes chargés de leur interprétation,

—réduire au maximum le nombre des échantillons à analyser et ceci en accordant à chacun d'eux un caractère représentatif plus grand,

—atteindre du même coup un objectif plus scientifique qui aiderait à une meilleure connaissance des mécanismes de pollution.

Ces objectifs sont pratiquement atteints. Les méthodes utilisées sont certes perfectibles. Des améliorations sont encore apportées dans le détail, mais il est important de chercher à obtenir un certain automatisme qui seul permettra une grande continuité avec un minimum de difficulté.

CONTAMINATION OF AIR AND THE RESULTING CONTAMINATION OF GRASS

P. COURVOISIER
Sektion für Sicherheitsfragen von Atomanlagen, Würenlingen, Switzerland

and E. NAGEL
Eidg. Institut für Reaktorforschung, Würenlingen, Switzerland

Abstract—Since the summer of 1963 a lawn was mown every second week during the growing season. The β-activity of the consecutive grass samples collected was considered to have been produced by fallout throughout the two week period of regrowth of the grass. It was compared with the activity of the air due to fission products during the same period. In this way an overall deposition velocity was obtained, covering both dry deposition and deposition by rain. This deposition velocity shows considerable scatter and increases during the period of observation. The increase is larger than can be explained by the influence of soil contamination.

In addition, the activity found on the grass samples was compared with the activity found on other fallout collectors. Here, too, the ratios increased with time, whereas the ratios between physical samplers stayed constant.

GRASS SAMPLING

Deposition of fallout on grass has been observed by different authors. However, the present authors are not aware of any longer series of consecutive samples taken to study the variation over a longer period of the deposition on to grass of fallout present in the lower atmosphere.

Since the summer of 1963, therefore, a lawn (96 m^2) at the Eidg. Institut für Reaktorforschung was mown every two weeks during the growing season. The same mowing machine was always used in order to mow the grass at the same height above ground. The mown grass was collected as completely as possible by a brushing machine.

The samples were analysed for gross β-activity which was expressed in units of pCi per m^2 of ground harvested. It may be assumed that a grass sample obtained this way is contaminated exclusively by fallout from the atmosphere during the two week period, together with a contribution from older fallout isotopes entering into the plants by the growth process and stemming from root uptake or uptake into parts of the grass below the height of mowing. This assumption may be not quite correct, as grass grows not only by producing new leaves but also by stem growth; accordingly, some direct contamination of the grass sample may be due to fallout in periods preceeding a period in question. However, this possible contribution of fallout was neglected.

It is well known that deposition of fallout on samplers or on vegetation can be described by a deposition velocity, which is usually given in units of cm per sec, or as a ratio to the wind velocity. This indicates that deposition is considered as an instantaneous process rather than as the result of processes acting over a considerable length of time. For a sampling programme such as the one outlined above it would be impractical, however, to take samples at short intervals. One week is the shortest feasible interval for sampling over the whole season in which grass grows and samples of reasonable size can be obtained. In our climate, this minimum period of one week is not short enough to permit with a reasonable probability any useful discrimination between periods of exclusively dry deposition and periods of mixed dry

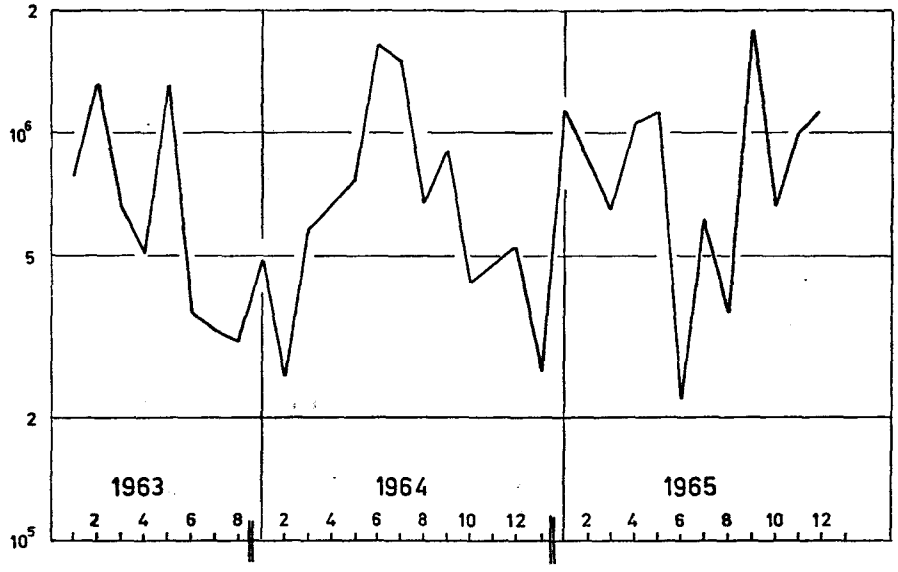

FIG. 1. Ratio of concentrations of radioactivity in rain and in air, both in pCi/cm³.

and wet deposition.* A period of two weeks was therefore considered acceptable, especially in view of decreasing fallout concentrations after the weapons test ban of 1962. The comparison of fallout on grass to fallout in air or rain can, therefore, only produce an averaged deposition velocity $\bar{v}_g$, where:

$$\bar{v}_g = \frac{\mathrm{Act}_{\mathrm{grass}}}{\int_0^T \bar{v}_g \, \mathrm{Act}_{\mathrm{air}} dt} = \frac{\mathrm{Act}_{\mathrm{grass}}}{T \cdot \overline{\mathrm{Act}_{\mathrm{air}}}} \qquad (1)$$

in which formula it is assumed that

$$\mathrm{Act}_{\mathrm{rain}} \text{ is proportional to } \mathrm{Act}_{\mathrm{air}}.$$

Accordingly, data on $\bar{v}_g$ are quoted in m/day only, in order to eliminate confusion with short period observations.

PHYSICAL SAMPLERS

The following samples were collected by physical samplers over the same period as the grass samples.

(*A*) Air samples taken by moving filter bands, ashed at the end of the period and counted after decay of natural activity.

(*R*) Rain samples, collected in a large rain sampler rinsed every day to remove dry fallout as far as possible.

(*T*) Samples of fallout deposited on to an open water surface (Totalisator: plastic tray kept filled with water, rain water collected by the tray flowing via over-flow to a plastic bottle).

(*V*) Samples of fallout deposited on to a flat and level plate of plexiglass covered by vaseline and placed on a short pole. By a long series of special observations we have shown that fallout trapped by the vaseline is not lost by subsequent weathering (at least for periods of up to three months), and that dry fallout is trapped as well as by a tray full of water.

RESULTS OF PHYSICAL SAMPLERS

The data of the three physical samplers (*R*), (*T*) and (*V*) agree reasonably well. The ratio of the average activity in rain (*R*) to the average activity in air (*A*) yields a mean of $7 \cdot 72 \pm 0 \cdot 74) \times 10^5$, if concentrations in pCi/cm³ are compared; the data presented in Fig. 1 shows the

* In the following data only the periods 6 and 7 for 1964 and period 13 for 1965 were generally dry, rainfall being less than 10 l./m² in 14 days.

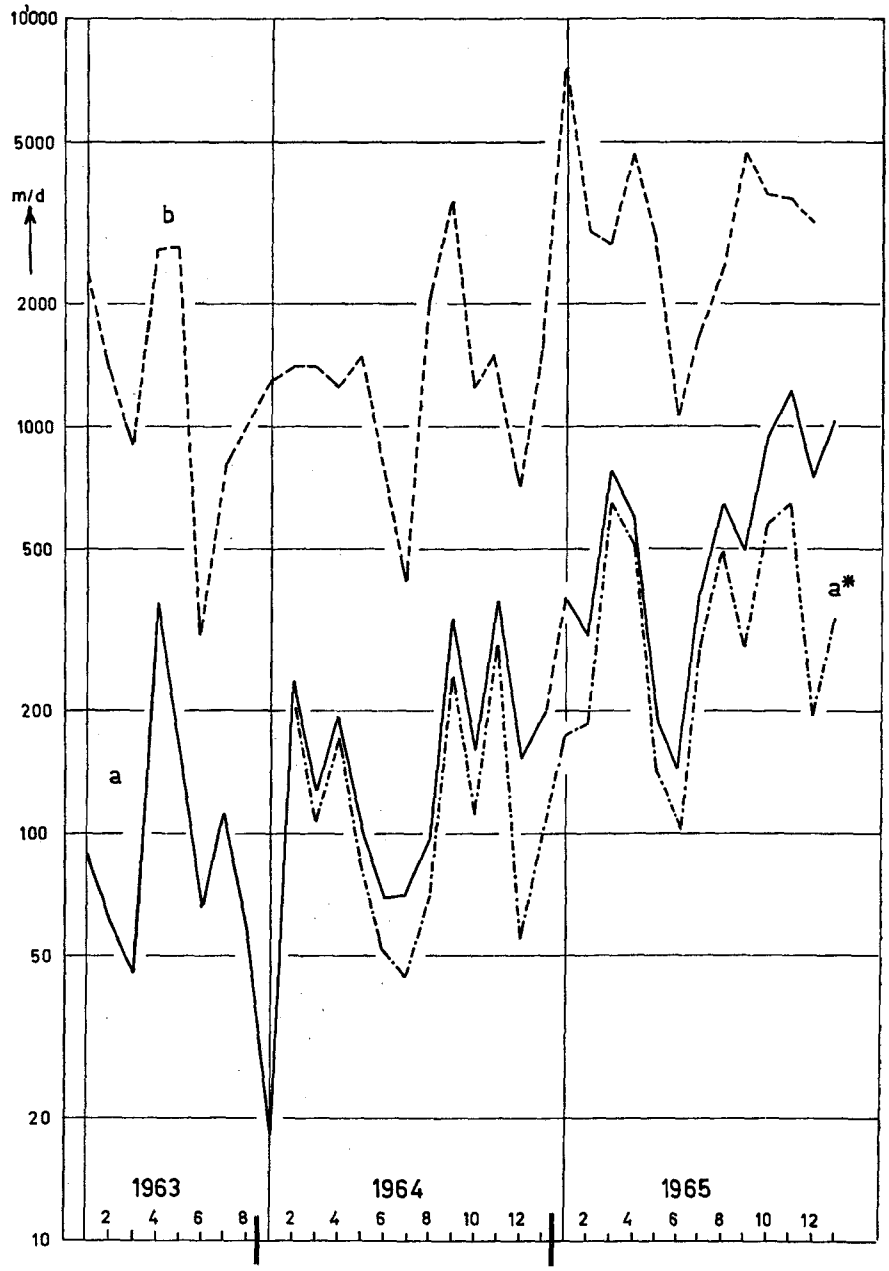

FIG. 2. (a) Ratio of average concentration of radioactivity on grass, in pCi/m² day, and in air, in pCi/m³. (a*) Values of curve a, minus ground contribution to the total radioactivity on grass. (b) Ratio of concentration of radioactivity deposited by rain, in pCi/m² day, and average concentration in air, in pCi/m³.

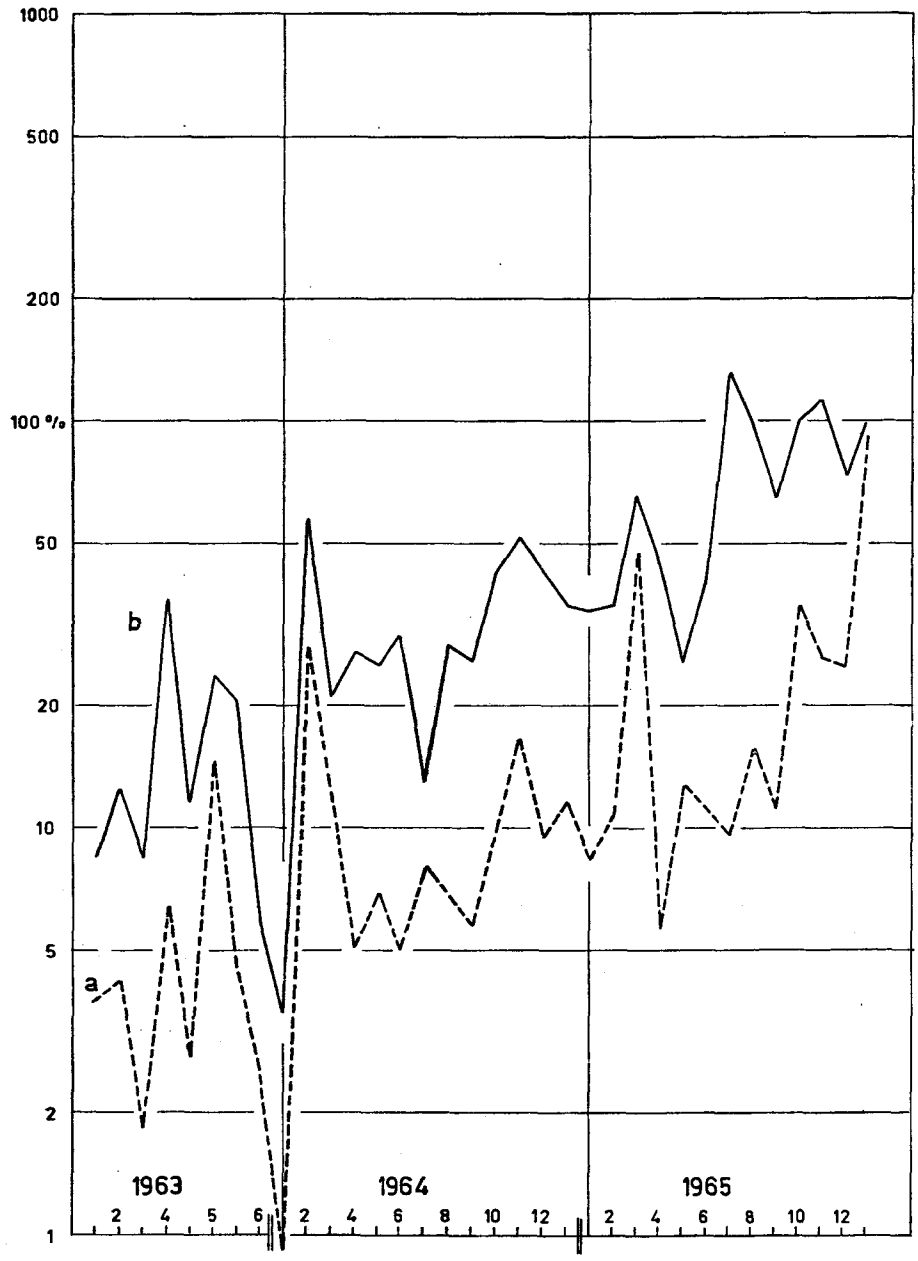

FIG. 3. (a) Ratio of concentration of radioactivity on grass and in totalisator, both in pCi/m².
(b) Ratio of concentration of radioactivity on grass and on vaseline-sampler, both in pCi/m².

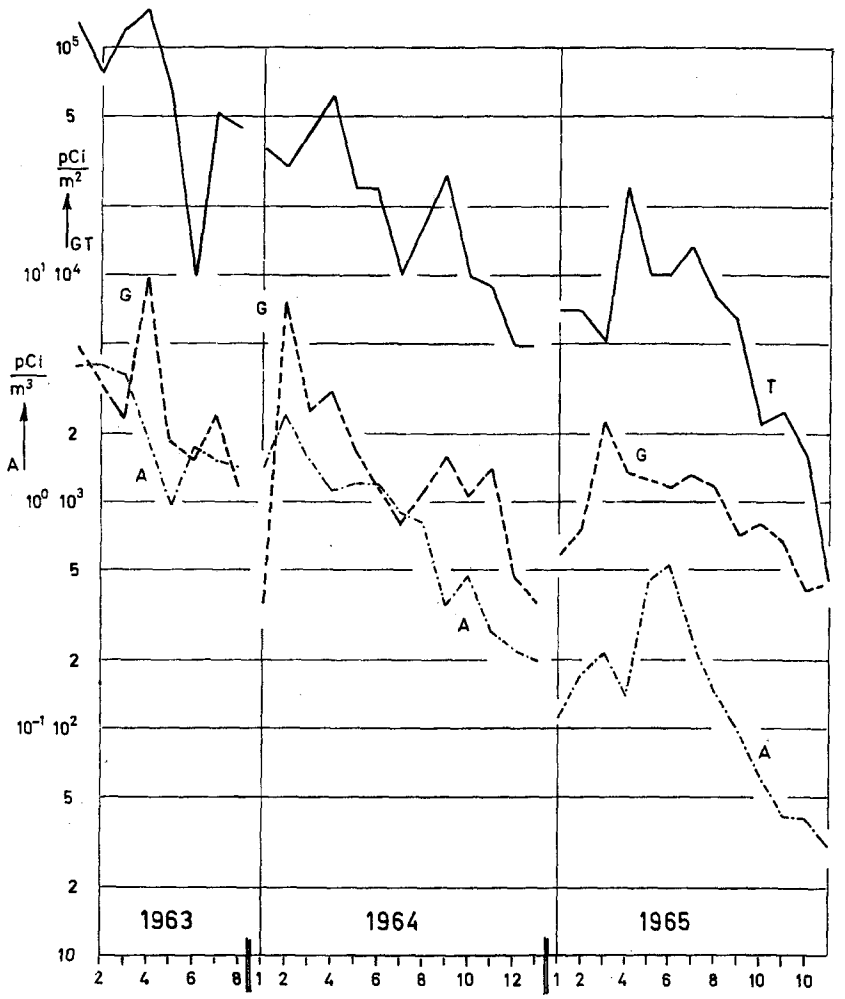

FIG. 4. (T) Gross β-radioactivity in totalisator, in pCi/m^2. (G) Gross β-radioactivity, minus ^{40}K on grass, in pCi/m^2. (A) Gross β-radioactivity in air, in pCi/m^3.

ratio to be fairly constant in spite of possible changes of particle size with age of fallout.

Figure 2 (curve b) shows the ratio of (R) in pCi/m^2 and per day to average (A) in pCi/ m^3. This ratio of (R) to (A) is expressed as a velocity of (wet) deposition, but this is not strictly correct as rain is not falling constantly. The data (curve b) shows somewhat more scatter than the ratio of the concentrations per unit volume and the values for 1965 are markedly increased, presumably due to the higher rainfall during that summer.

The deposition velocities calculated from (T) or (V) and (A) according to formulae like (1) show fairly constant values in spite of a reduction of activities by a factor of about 100 over the three summers of observation. The averages are 2980 $\pm$ 420 m/day for (T) and 740 $\pm$ 60 m/day for (V).

We have determined the coefficients in the regression formula $(V) = r.\ (R) + \bar{v}_g\ (A)$ for our continuous series of two weekly periods from 1959 through 1965 to be $r = 27 \pm 2{\cdot}3\%$ (r = efficiency of collection of wet fallout by

vaseline) and $\bar{v}_g = 237 \pm 32$ m/day (corresponding to 0·27 cm/sec) as deposition velocity of dry fallout on to vaseline.

RESULTS OF GRASS SAMPLES

The deposition velocity on grass, as calculated according to formula (1) and without any correction for ground contamination, is given in Fig. 2 by curve a. It is seen that again there is considerable scatter and that the velocity increases with time. This increase is also seen in the efficiencies of deposition on grass as compared to deposition on the physical samplers (Fig. 3). Both curves show an increase with time which is similar to the increase in curve a, Fig. 2.

THE EFFECT OF GROUND CONTAMINATION

At the end of 1964 this trend in the data on grass activity had not been fully recognized, being rather veiled by the scatter. A correction for the effect of ground contamination seemed, therefore, to be unimportant. This was further supported by the result of comparisons between two series of grass samples grown during 1964 in parallel over three week periods, in part open and in part permanently covered by plastic hoods. The 1 m² areas under the plastic hoods were watered using tap water with a negligible activity content. Some air circulation through the hoods had to be tolerated in order not to over-heat the plants but contamination from this way was shown to be negligible (vaseline-sampler under one of the hoods). Hence, the contamination found in the covered samples was considered to be derived from the existing contamination of the soil only. For the purpose of comparison between both series of grass samples, a correction for the somewhat different yields in dry-weight/m² had to be made. The ground contribution to the total activity found in the open grass samples, averaged over the summer for six different fallout isotopes (γ-emitters), was 27% (ranging between 22 and 32% for the different isotopes). The average for all the isotopes increased somewhat during the summer, due to the decreasing air activity. ^{40}K could be used as a control for the above mentioned correction, yielding a ground contribution of practically unity, as would be expected for this isotope.

Soil activity was determined by gamma spectroscopy and ^{90}Sr analysis. The contamination of soil was practically the same in 1965 as it was in 1964, whereas the fallout intensities decreased further, as shown in Fig. 4. If, accordingly, a constant value of the ground contribution deduced from the 1964 data on open and covered samples is deducted from the grass activities in 1964 and 1965, the corrected curve a* in Fig. 2 results. However, this correction does not remove the trend which shows in the uncorrected curve a.

DISCUSSION AND CONCLUSIONS

The trend which remains in curve a* may be due in part to the somewhat increased rainfall during 1965, as shown by curve b in Fig. 2 and mentioned above, but a representation of the deposition velocity on to grass as a function of the amount of rainfall showed no clear correlation.

Further explanation of the rest of this trend is difficult. It may be due to a general change in particle size of fallout which will influence the deposition effects that are basically due to the movement of particles in boundary layers around the sampler.

In conclusion it may be stated (using mainly the data for 1963 and 1964) that deposition of fallout on to short grass is of the order of 150 m/day if averaged over periods of two weeks with mixed dry and wet deposition. There is considerable scatter and single periods may differ from an average by as much as a factor of 5. The efficiency of grass as a sampler is 10% or less if compared to an open water surface. It is 20 to 30% if compared to a level surface covered with vaseline.

ABSORPTION DU ^{226}Ra PAR LES PLANTES CULTIVÉES

R. KIRCHMANN, R. BOULENGER
Centre d'Étude de l'Énergie Nucléaire, Mol, Belgique

et A. LAFONTAINE
Institut d'Hygiène et d'Épidémiologie, Bruxelles, Belgique

Résumé—L'absorption de ^{226}Ra par plusieurs plantes cultivées (Ray-grass, trèfle violet, chou, carotte, pomme de terre, orge et betterave) a été examinée à travers les expériences effectuées en champs d'essais et en serre. La spectrométrie gamma a été utilisée pour la mesure des teneurs en ^{226}Ra des divers échantillons. Pendant les expériences effectuées en serre, on a examiné l'influence sur l'absorption de ^{226}Ra par les plantes des apports de Ca sous les formes hydroxydes et chlorures. Des comparaisons de l'absorption de ^{226}Ra par ray-grass de cinq divers sols, à deux niveaux de contamination ont été effectuées; les résultats ont montré qu'il y a une corrélation inverse entre le ^{226}Ra de la plante et la quantité de matériel sorptif du sol. Les résultats des expériences en champs d'essais realisées durant trois années consécutives, dans un sol sablonneux dont la couche supérieure a été antérieurement soumise a la contamination artificielle aux différents niveaux par ^{226}Ra, sont donnés. Ces résultats ont révélé qu'il y a quelques différences entre l'absorption de ^{226}Ra parmi les espèces végétales etudiées; parailleurs, la distribution de ^{226}Ra dans les plantes n'est pas uniforme. En général les valeurs O.R. ((^{226}Ra/Ca) plante/(^{226}Ra/Ca) sol = O.R.) montrent la présence d'une discrimination très forte contre ^{226}Ra dans le transfert entre le sol et la plante.

INTRODUCTION

La contamination, par les isotopes du radium, des aliments de l'homme, notamment des végétaux, est mentionnée dans la littérature.[1-5] Cependant il y a peu de données sur l'absorption de ^{226}Ra par des végétaux cultivés dans des conditions identiques, ainsi que sur les facteurs susceptibles d'influencer l'absorption de ce radionuclide par la plante.[6]

Le présent mémoire décrit des expériences, effectuées en champs d'essais et en serre, sur l'absorption de ^{226}Ra par divers végétaux cultivés des régions tempérées; l'influence de l'apport de calcium au sol, ainsi que l'influence du type de sol sont également examinées.

MATÉRIEL ET MÉTHODES

A. *Expériences en serres*

1. *Étude de l'influence de l'apport de calcium au sol.* Les espèces végétales suivantes ont été mises en expériences: pomme de terre, carotte, betterave, chou, ray-grass, trèfle violet et orge. La culture a été effectuée en pot contenant du sable tourbeux, sol de même nature que celui des champs d'essais contaminés. Le niveau de contamination du sol utilisé pour les expériences en serre était de 100 μCi ^{226}Ra/kg de sol sec.

Le traitement appliqué consistait en apport de diverses doses de calcium (0 à 62,5 me Ca/100 g de sol). Deux formes chimiques ont été employées dans une étude parallèle: hydroxyde et chlorure. Chaque essai a été réalisé en répétition triple.

2. *Étude de l'influence du type de sol.* Nous avons employé comme plante-test le ray-grass, cultivé dans des pots contenant 1 kg de divers types de sols belges. Trois des caractéristiques de ces substrats sont données dans le tableau 1.

Tableau 1.

Type de sol	Matériel sorptif *	Ca total (%) (mg/100 g sol)	pH (H_2O)
Sablonneux I	29,0	160	6,0
Sablonneux II	22,0	190	6,75
Sol brun acide	69,2	410	6,55
Sol brun sur limon lœssique	51,5	500	7,20
Sol podzolique sur sable	10,0	83	6,4

* Teneur en matériel sorptif égale au pourcentage de la fraction 0–20 μ, plus deux fois le pourcentage d'humus.

Deux niveaux de contamination des sols étudiés ont été appliqués; ces niveaux étaient respectivement de 0,5 et de 5 μCi ^{226}Ra/kg de sol sec.

B. *Expériences en champs d'essais*

—Principe de l'expérimentation: Nous avons appliqué la méthode dite du "carré latin" pour la disposition des parcelles. Le nombre total de parcelles était de 49 (7 végétaux $\times$ 7 répétitions); chacune de ces parcelles avait une surface utile de 4 m^2.

Des plantes présentant un intérêt économique ont été choisies. Les espèces végétales étudiées sont les mêmes que celles utilisées pour l'expérience 1 en serre.

Dans chacune des parcelles, la zone de bordure et la zone médiane ont été récoltées séparément; seule cette dernière a été analysée car les plantes qui y ont poussé se sont trouvées dans des conditions de milieu comparables pour chacune d'elles. Les différentes organes à analyser sont séparées au moment de la récolte et constituent des échantillons distincts. Des échantillons de sol (sable tourbeux) ont aussi été prélevés sur chacune des parcelles.

C. *Technique de mesures*

La spectrométrie gamma a été utilisée pour la mesure des teneurs en ^{226}Ra des divers échantillons. Le pic gamma de 610 KeV du ^{214}Bi, descendant du ^{226}Ra, a été choisi pour effectuer la mesure. Comme, dans la chaîne de désintégration, un déséquilibre apparaît toujours au niveau du radon-222 qui est gazeux et diffuse hors de l'échantillon, nous avons été amenés à sceller les flacons afin de rétablir l'équilibre de la chaîne radio-active jusqu'au niveau du ^{214}Bi. L'activité en ^{214}Bi est déterminée par planimétrie du pic, mesuré après un délai de 20 jours assurant une activité égale à plus de 97% de celle atteinte à l'équilibre, en comparaison avec celui d'un étalon pris dans les mêmes conditions.

RÉSULTATS ET DISCUSSION

A. *Expériences en serre*

1. *Étude de l'influence de l'apport de calcium au sol.* Les teneurs en ^{226}Ra des organes végétaux observés pour des apports de calcium sous les formes hydroxydes et chlorures sont données dans le tableau 2.

L'analyse statistique, effectuée sur des séries de résultats dont l'examen permet d'envisager une influence éventuelle de l'apport de calcium, a montré que le traitement n'a pas eu d'influence significative ($P = 0{,}05$) sur la teneur en ^{226}Ra de la matière sèche, tant du feuillage que des racines. Les valeurs du critère F* sont données dans le tableau 3.

Nos résultats sont en accord avec ceux obtenus par K. B. Mistry[6] d'après ses expériences sur divers végétaux, en aquiculture; selon cet au-

* Test de Fisher et Snedecor.

Tableau 2. Teneurs en ^{226}Ra des organes de diverses espèces végétales cultivées sur sol contaminé, amendé par différentes doses de Ca

Traitement me/100 g sol	Concentration en ^{226}Ra (cpm/g matière sèche)												
	Trèfle violet		Ray-grass		Orge		Betterave		Carotte		Pomme de terre		
	R	PA	R	PA	R	PA	R	PA	R	PA	R	PA	Tuber
$CaCl_2$													
0	3844*	2538	4804	5490	5208	964	6902	11983	9450	19272	5506	3473	301
12,5	(†)	—	—	2995	4595	616	6398	10290	14414	9003	4375	2061	337
37,5	—	—	4597	2629	4639	788	4461	11079	5598	14044	3816	978	256
62,5	—	—	4310	2570	2156	1028	7643	13026	8548	6227	4277	1354	335
$Ca(OH)_2$													
0	2300	3279	3616	2735	3651	759	2731	9086	5097	9903			
12,5	1297	583	4448	1906	3129	342	2378	4444	2722	2979			
37,5	1006	799	4766	1325	4179	455	2436	3003	3963	1770			
62,5	2501	942	5192	922	3914	254	4666	1929	2989	1800			

* Valeur moyenne $\bar{x}$ pour 3 répétitions ($n = 3$). La probabilité P que la valeur vraie soit extérieure à l'intervalle $\bar{x} \pm t_p s_{\bar{x}}$ est de 0,05; t_p est le fractile de la loi de Student ($t_p = 4{,}303$ pour $P = 0{,}05$) avec $2DL$ (nombre de dégrés de liberté $= n$-1).

† Plantes mortes, toxicité due au chlorure.

R = Racine.

PA = Partie aérienne (tige + feuille).

Tableau 3. Valeurs du critère F relatives à l'apport de calcium au sol

Traitement	Plante	Organe	F (calculé)	F (tables) pour	
				$P = 0{,}05$	$P = 0{,}01$
$Ca(OH)_2$	Trèfle violet	Partie aérienne	4,6	5,99	13,74
	Ray-grass	id.	1,10	id.	id.
	Orge	id.	< 0	id.	id.
	Betterave	id.	3,21	id.	id.
$CaCl_2$	Pomme de terre	id.	0,20	id.	id.

teur, bien que l'absorption du radium soit déprimée par l'addition de calcium à la solution nutritive, il n'y a pas de relation étroite entre les deux ions. D'autre part cet auteur a observé que l'absorption de ^{226}Ra est quelque peu réduite lorsque le pH passe de 4 à 6.

L'examen du tableau 2 montre une diminution de teneurs en ^{226}Ra des organes des plantes cultivées sur sol traité par $Ca(OH)_2$; cependant, cette diminution est statistiquement non significative ($P = 0,05$) (voir tableau 3). Cette tendance à la diminution pourrait être rapprochée de l'élévation du pH consécutive à l'apport de calcium sous forme hydroxyde, ainsi que le montre le tableau 4.

Tableau 4. Effet de l'apport de calcium sur le pH du sol

Forme chimique	Traitement me Ca/100 g sol	pH
$CaCl_2$	0	5,95
	12,5	5,80
	37,5	5,25
	62,5	5,10
$Ca(OH)_2$	0	5,90
	12,5	7,20
	37,5	8,25
	62,5	8,55

A. J. Andersen[7] a étudié l'influence de l'apport de $CaCO_3$ (2 me/100 g sol) sur l'absorption de ^{89}Sr par le ray-grass et le trèfle violet; il n'a pas constaté, pour la plupart des types de sol utilisés, de réduction significative d'absorption consécutive à cet apport. Cependant, si l'apport augmente, une réduction de ^{89}Sr dans la plante est constatée. Cet auteur a aussi observé une baisse considérable de rendement lorsque la forme chlorure est employée, le trèfle violet étant plus sensible à cet effet toxique que le ray-grass. Une constatation similaire a été faite au cours de nos essais.

2. *Étude de l'influence du type de sol.* Quelques caractéristiques des cinq sols utilisés sont mentionnées dans le tableau 1.

Les rendements en matière sèche et les teneurs en ^{226}Ra des organes du ray-grass, employé comme plante-test, figurent dans le tableau 5.

Une corrélation inverse entre les teneurs en ^{226}Ra des organes végétaux et la quantité de matériel sorptif du sol est observée. Les valeurs des coefficients de régression, calculées à partir des résultats du tableau 5, sont respectivement de: $-0,014 \pm 0,003$ et $-0,005 \pm 0,003$ ($P < 0,01$) pour les parties aérienne et radiculaire du ray-grass.

Lors d'une étude[8] sur la contamination de certains sols par ^{226}Ra, la détermination des coefficients de distribution a indiqué que la tourbe avait une capacité de sorption dix fois plus forte que le sable environnant (Tourbe: Kd variant de 1500 à 3000; Sable: Kd variant de 150 à 200).

3. *Facteurs de concentration observés.* Les expériences sur substrats uniformément contaminés (sol et aquiculture) permettent le calcul des facteurs de concentration donnés par la relation

$$F\,C = \frac{^{226}Ra/g \text{ matière sèche végétale}}{^{226}Ra/g \text{ substrat (sol ou solution nutritive)}}$$

Les valeurs calculées pour les diverses espèces végétales étudiées sont données dans le tableau 6.

L'examen du tableau 6 montre que, dans le cas de culture sur sol, les facteurs de concentration sont du même ordre de grandeur (unité ou inférieur). Quelques valeurs F C intéressantes sont à noter: de très faibles valeurs pour les tubercules de pomme de terre et les épis d'orge; les valeurs les plus élevées sont observées pour le feuillage des betteraves, pommes de terre et carottes; la valeur relativement élevée pour la gousse du pois est également à souligner.

La culture sur solution nutritive donne des valeurs F C beaucoup plus élevées pour les racines, de deux ordres de grandeur par rapport au feuillage. Une constatation analogue a été faite par K. B. Mistry[6] pour l'orge, le pois, le maïs et la tomate.

Cette différence dans le niveau de contamination des organes végétaux selon le substrat de culture est probablement due au degré élevé de rétention du radium sur les surfaces

Tableau 5. *Rendement et teneurs en ^{226}Ra du ray-grass cultivé sur divers types de sol*

Sols (Type)	Apport de ^{226}Ra (μCi/kg sol)	Répét.	Racine		Partie aérienne (2ème coupe)	
			Rendem. g ms/pot	^{226}Ra (pCi/g ms)	Rendem. g ms/pot	^{226}Ra (pCi/g ms)
Sablonneux I	0	1	4,13	3,6	1,02	65
		2	3,07	3,2	0,45	<20
	0,5	1	4,36	252	0,63	175
		2	5,83	171	0,64	119
	5	1	5,80	4135	0,87	1374
		2	4,57	3285	0,83	915
Sablonneux II	0	1	7,37	1,5	1,24	± 10
		2	7,87	1,5	1,24	± 12
	0,5	1	12,37	178	1,25	136
		2	8,55	152	1,35	88
	5	1	12,12	2558	1,58	1010
		2	10,77	1858	1,85	1299
Brun acide	0	1	11,16	2	4,34	$\leqslant 2,5$
		2	6,76	4	2,79	$<3,5$
	0,5	1	9,70	—	3,83	29
		2	8,94	93	3,18	28
	5	1	8,37	1195	3,05	361
		2	8,53	1407	3,89	334
Brun sur limon lœssique	0	1	3,98	10	1,43	14
		2	4,26	5	0,90	18
	0,5	1	4,14	186	0,90	61
		2	3,78	167	1,02	48
	5	1	5,59	2685	1,34	576
		2	3,87	2586	1,00	700
Podzolique sur sable	0	1	2,54	12	0,51	<2
		2	2,59	6	0,31	<3
	0,5	1	2,64	268	0,34	133
		2	1,81	287	0,39	253
	5	1	2,72	3642	0,30	2479
		2	3,33	3906	0,53	3018

du sol. Ce qui a pour conséquence, comme le souligne K. B. Mistry,[6] que dans les sols la disponibilité du radium pour les plantes est considérablement plus faible que celle du strontium et du calcium.

B. *Expériences en champs d'essais*

Les résultats de ces expériences, réalisées durant trois années consécutives, nous ont permis de calculer les facteurs de concentration ainsi que le rapport observé (O.R.). Pour ces calculs, le sol pris en considération est la couche explorée par les racines.

Le tableau 7 permet de comparer l'absorption du ^{226}Ra par différentes espèces végétales placées dans les mêmes conditions de milieu; les valeurs F C moyennes, minimales et maximales observées sont indiquées.

Ce tableau, qui donne les valeurs de l'O.R. (organe/sol) permet aussi de comparer le trans-

Tableau 6. Facteurs de concentration (F.C.) pour ^{226}Ra chez des plantes cultivées sur substrat contaminé d'une façon homogène

Espèces	Organe	F.C.	
		Culture sur sol	Solution nutrit.
Ray-grass	Racine	0,63	2190
	Feuillage: 1ère coupe	0,71	67
	2ème coupe	0,53	67
Trèfle violet	Racine	0,54	—
	Feuillage: 1ère coupe	0,48	68
	2ème coupe	0,32	—
Orge	Racine	0,32	35
	Paille	0,83	0,31
	Épi	0,07	0,16
Chou	Racine	0,39	—
	Tige	0,31	—
	Feuille	0,75	—
Carotte	Racine	0,29	—
	Feuillage	1,02	—
Betterave	Racine	0,21	—
	Feuillage	1,38	—
Pomme de terre	Racine	0,57	—
	Feuillage	1,07	—
	Tubercule	0,024	—
Pois	Racine	1,8	2750
	Feuillage	0,60	30
	Gousse	3,1	88
Haricot	Racine	—	710
	Feuillage	0,36	22
	Gousse	$<0,1$	2,3

fert du radium et du calcium, du substrat au sein du végétal.

On remarque qu'il y a une forte discrimination contre le ^{226}Ra dans le transfert du sol à la plante. Nos expériences en aquiculture [9] et celles de K. B. Mistry [6] ont permis de faire la même constatation en ce qui concerne la partie aérienne des végétaux étudiés.

L'O.R. varie selon les espèces et selon les organes.

L'analyse statistique des résultats des trois années de culture a montré notamment que:

(1) Le teneur en ^{226}Ra du feuillage du ray-grass est significativement plus élevée ($P = 0,05$) que celle du feuillage du chou et de l'orge.

(2) Le rapport des concentrations en ^{226}Ra dans l'épi d'orge et la paille est de $0,41 \pm 0,13$ ($P = 0,05$).

(3) La valeur du facteur de concentration pour le ^{226}Ra dans le tubercule de pomme de terre est de $0,016 \pm 0,0024$ ($P = 0,05$).

REMERCIEMENTS

Les auteurs remercient Messieurs L. Schotsmans et O. Van der Borght pour l'aide appréciée apportée dans l'analyse statistique des

Tableau 7. Facteurs de concentration (F.C.) et rapport observé (O.R.) pour Ra-226 chez des plantes cultivées en champs d'essais contaminés superficiellement (1961)

Espèce	Organe	F.C.			O.R. (Ra/Ca) organe (Ra/Ca) sol
		Moyen	Minim.	Maxim.	
Ray-grass	Racine	0,58	0,34	1,01	—
	Feuillage	0,08	0,02	0,19	0,051
Trèfle	Racine	—	—	—	—
violet	Feuillage	0,27	0,08	0,44	0,046
Orge	Racine	0,63	0,39	0,88	
	Paille	0,05	0,01	0,15	0,028
	Épi	0,015	0,005	0,03	—
Chou	Racine	0,28	0,14	0,55	0,015
moëllier	Tige	0.57	0,02	0,99	0,06
	Feuille	0,40	0,03	1,00	0,03
Carotte	Racine	0,09	0,07	0,10	0,12
	Feuillage	0,09	0,08	0,10	—
Betterave	Racine	0,045	0,04	0,05	—
	Feuillage	0,09	0,03	0,16	—
Pomme de	Racine	0,55	0,25	0,85	—
terre	Feuillage	0,25	0,08	0,57	—
	Tubercule	0,016	0,011	0,038	—

résultats. Leurs remerciements vont également à Monsieur J. Colard et à ses collaborateurs qui ont effectué les mesures spectrométriques des échantillons.

RÉFÉRENCES

1. United Nations Scientific Committee on the Effects of Atomic Radiation. Rept. Gen. Assembly, United Nations, New York (1962).
2. W. V. Mayneord et C. R. Hill. *Nature* **184,** 667–669 (1959).
3. F. X. Roser. *Annals. Acad. Brasil. Ciencias* **30,** 24–25 (1958).
4. M. Eisenbud, H. Petrow, R. T. Drew F. X. Roser, G. Kegel et T. L. Cullen. *The Natural Radiation Environment.* A. S. Adams and W. M. Cowder, Editors, Univ. Chicago Press, Chicago, Ill., 837–854 (1964).
5. R. C. Turner, J. M. Radley et W. V. Mayneord. *Health Phys.* **1,** 268–273 (1958).
6. K. B. Mistry. ARCRL 10, 86–89. H.M. Stationery Office, London (1963).
7. A. J. Andersen. *Soil Science* **95,** 52–59 (1963).
8. L. Baetsle. Communication personnelle.
9. R. Kirchmann, R. Roncucci et J. M. Mousny. Isotopes and radiation in soil plant nutrition studies, 277–300, Seminar I.A.E.A., Vienna (1965).

FIVE YEARS EXPERIENCE OF ^{90}Sr AND ^{137}Cs HERBAGE TO MILK TRANSFER UNDER FIELD CONDITIONS

M. de BORTOLI, P. GAGLIONE, A. MALVICINI
Protection Service, Euratom Ispra Establishment

and E. VAN DER STRICHT
Directorate for Health and Safety, Euratom, Brussels

Abstract—Routine radioactivity measurements on grass and milk are performed as part of the radiological monitoring programme of the Euratom Ispra Establishment. Herbage samples are collected monthly from May to October in six stations; milk is sampled weekly in four small dairies and the pooled monthly samples analysed. The ^{90}Sr and ^{137}Cs contamination found hitherto is due to the world-wide fallout, whose rate has changed considerably during the period 1961 to 1965. This fact has enabled the study of the transfer of the two radionuclides from grass to milk, under conditions of both direct and indirect prevailing contamination.

Particular consideration has been given to the ^{90}Sr milk-herbage observed ratio

$$\left(\frac{\text{pCi } ^{90}\text{Sr/g Ca milk}}{\text{pCi } ^{90}\text{Sr/g Ca herbage}}\right),$$

which has been found rather constant from year to year at a value of about 0.16. The same does not hold for the ^{137}Cs observed ratio

$$\left(\frac{\text{pCi } ^{137}\text{Cs/g K milk}}{\text{pCi } ^{137}\text{Cs/g K herbage}}\right),$$

which ranges from 0.9 to 1.7.

The $^{137}Cs/^{90}Sr$ ratio in herbage shows relatively large variations, if compared to the same ratio in fallout. These variations, however, reflect the different behaviour of the two nuclides in the transition fallout/herbage, yielding high values of the ratio during periods of high fallout rate (direct contamination predominant) and low values in the periods of low fallout rate (uptake from the soil prevailing). The same trend is observed in milk.

INTRODUCTION

This paper describes the results obtained from the measurements of milk and herbage radioactivity, performed during five years in the environs of the Ispra Establishment of the Euratom Joint Nuclear Research Centre.

The Establishment is located near lake Maggiore in a moderately hilly zone, about 1/5 covered with woods and a roughly equivalent area of permanent meadows. The radiological survey of herbage and milk is performed in an area within a radius of about 5 km from the Establishment on a monthly basis, the herbage collection being limited to the growing season.

In the area considered, there are roughly 200 dairy cows, spread over a number of small farms. Except for a few weeks in autumn during which cattle graze out of doors, the animals are always kept in sheds and fed with herbage cut three times a year in May, July and September. The hay yield normally decreases from the first to the last cutting and, on the average, the whole seasons yield may be estimated as 1 kg (dry matter)/m^2.*

* Except when otherwise stated all the herbage values referred to hereafter are concerning dry matter.

Additional feeds, giving a minor contribution to the diet, are provided by green vegetables during the summer months and mill products during the entire year.

The milk produced on the farms is taken to dairies in the villages, where it is sold. Samples for monitoring purposes are collected in the dairies of three villages (Brebbia, Ispra and Osmate) and in the largest farm of the village nearest to the Establishment (Barza). The milk monitored in this way may be regarded as representative of that produced and consumed in the zone under control.

The data reported in this paper have been obtained from measurements conceived to fulfil radiological monitoring requirements only. None the less attempts were made to work out some relationships between fallout and the subsequent contamination of the various links in the food chain and at the same time, to check the variations which might occur when the contributions of direct and indirect contamination change. In this respect the pattern followed by the world wide fallout due to nuclear weapons testing during the past few years has been particularly favourable.

This report summarizes the results of the period 1961 to 1965 and follows two previous papers[1, 2] covering shorter periods.

EXPERIMENTAL

Dry and wet deposition samples are collected monthly in four stainless steel pots (area 1 m^2) and the dry residue obtained after evaporation is analysed.

The herbage samples are built up from small amounts taken randomly in the meadows. Each sample amounts to 2 kg fresh weight. As from 1963 sampling is performed monthly from May to October, whereas during the two preceding years collection was limited to May, July and August, with the addition of September in 1962.

One liter of milk is collected twice a week and these sub-samples are pooled to give monthly samples for analyses.

^{137}Cs and ^{40}K are determined by gamma spectrometry measurements performed on the dried samples (employing the spectrum stripping

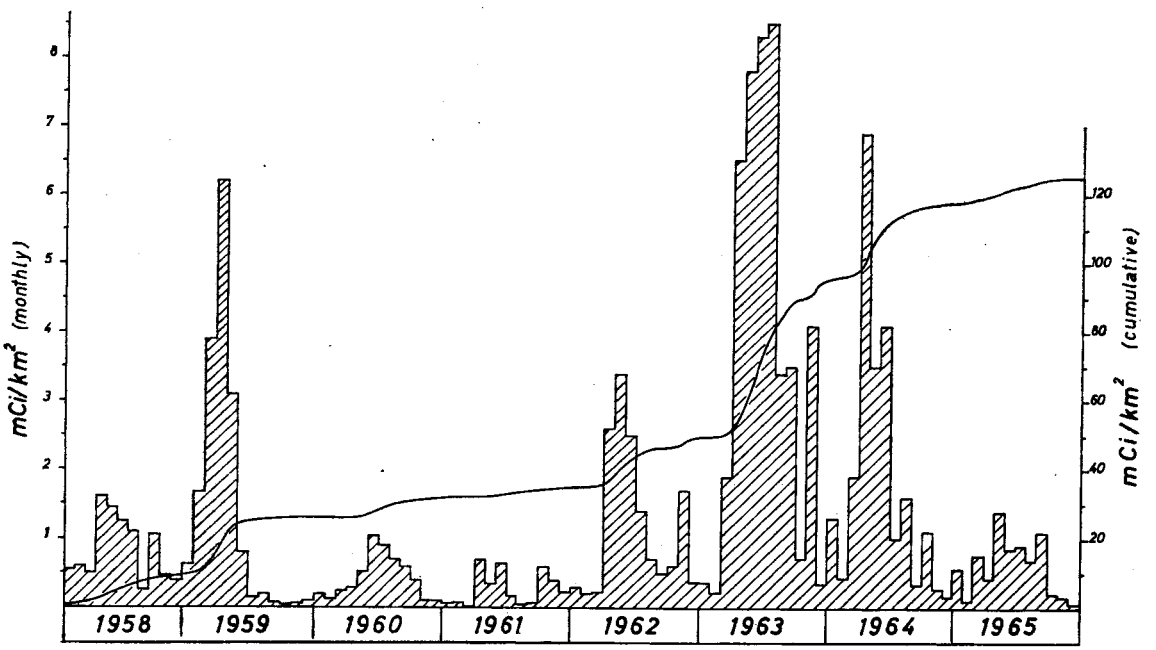

FIG. 1. ^{90}Sr monthly deposition and cumulative deposit (not corrected for radioactive decay) at Ispra from 1958 to 1965.

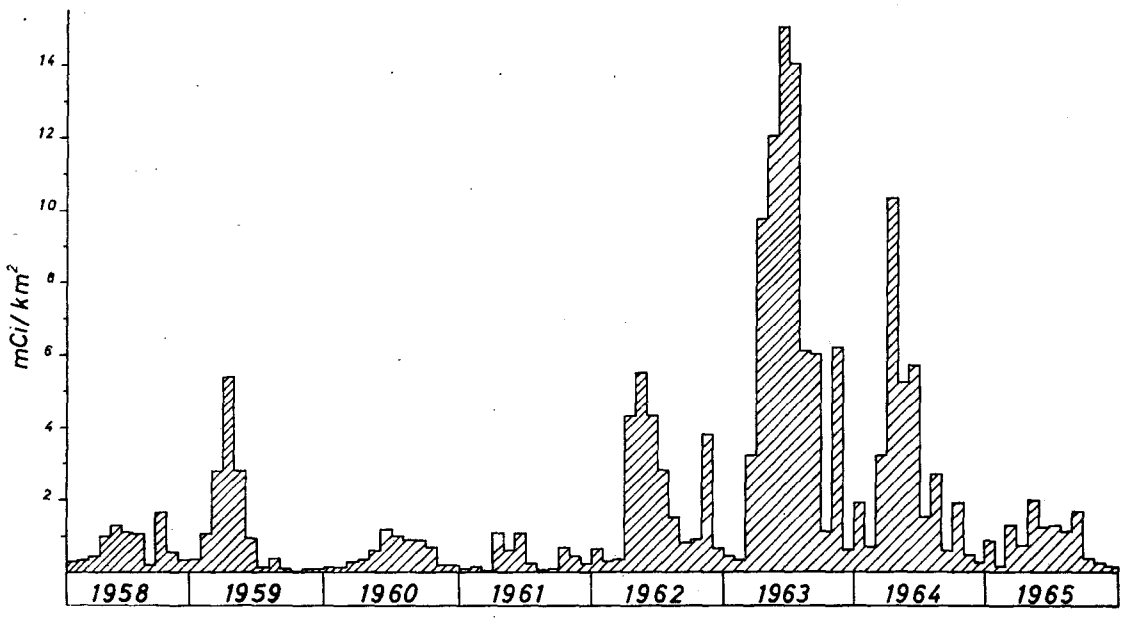

FIG. 2. ^{137}Cs monthly deposition at Ispra from 1958 to 1965.

technique whenever necessary). ^{137}Cs is also determined radiochemically using thin layers of ammonium phosphomolybdate (AMP) [3] which are measured by gamma spectrometry.

^{90}Sr is determined in ashed sample aliquots by the fuming nitric acid procedure. The activity of the final strontium carbonate precipitate as well as that of yttrium oxalate is determined by low level anticoincidence plastic phosphor detectors.

Each year 48 milk samples (12 months, 4 sites) and 36 herbage samples (6 months, 6 sites) were analysed, except in 1961 and 1962 when the number of herbage samples was 18 and 24 respectively.

RESULTS AND DISCUSSION

The monthly amounts of ^{90}Sr and ^{137}Cs deposited at Ispra from 1958 to 1965 and the cumulative ^{90}Sr are represented in Figs. 1 and 2. Figures 3 and 4 illustrate the contamination due to the two radionuclides in herbage and milk, respectively, for the five years considered. Because of the feeding habits of the cattle, described above, milk data have been averaged over annual periods ending in April of each year, instead of the calendar years. The annual values of fallout deposition and of the concentrations in herbage and milk for ^{90}Sr and ^{137}Cs, are reported in Tables 1 and 2, respectively.

(a) *Relationship between the radioactivity in fallout and in herbage*

An attempt has been made to find a correlation between the amounts of ^{90}Sr deposited and its concentration in herbage. The plot in Fig. 5 shows the relationship found by plotting the yearly average values of the ^{90}Sr concentration in herbage (pCi/g) versus the values of the cumulative deposit* (mCi/km^2), both divided by the amount of the nuclide (mCi/km^2) deposited during the growing season (April to September). This was done with the aim of

* Because deposition data for Ispra are available as from 1958 only, it has been assumed from ref. 4 that 10 mCi/km^2 of ^{90}Sr have deposited in the preceding years. This value has been used for the calculations of the cumulative deposit figures.

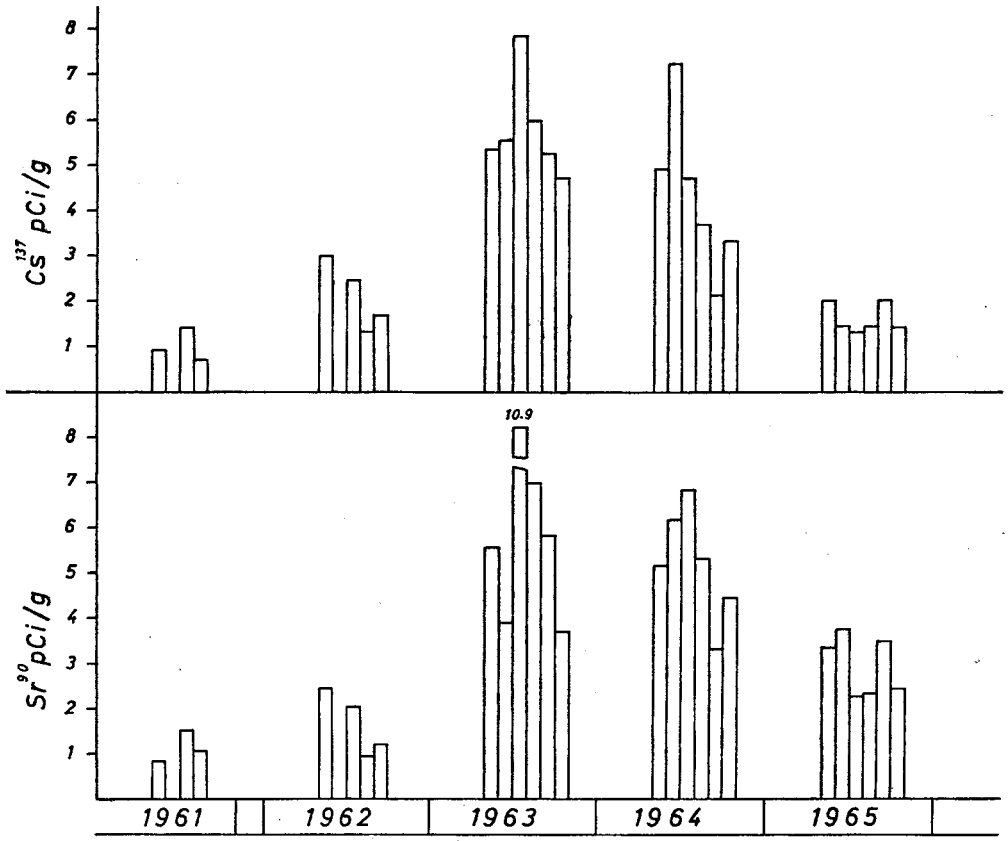

FIG. 3. ^{90}Sr and ^{137}Cs average concentrations in the herbage of the zone around Ispra from 1961 to 1965.

normalizing the values of the variables to the fallout rate of the year. A linear regression (significant at the 0.01 confidence level) fits the data points and the least squares line has the following equation:

$$Y = 0.129 + 0.0191\,X \qquad (1)$$

No similar relationship was found for ^{137}Cs.

The intercept 0.129 represents the average transfer coefficient from fallout deposition to herbage, in absence of indirect contamination. As the yearly herbage production of the zone is estimated to be roughly 1000 g/m^2 the coefficient does also represent the average fraction retained by herbage of the ^{90}Sr deposited from April to September.

The coefficient can be also used to calculate the fraction of herbage contamination which is due to direct deposition. This is done by multiplying the amounts of ^{90}Sr deposited during the growing season (April to September) by 0.129 and the resulting figures are given in the third and fourth columns of Table 3 as absolute and relative values respectively.

From these data it appears that 1962 and 1963 were years of prevailing direct contamination as expected. On the contrary during 1961 and 1965 the main mechanism of herbage contamination was indirect uptake. An intermediate situation characterizes 1964.

When the fraction of the ^{90}Sr concentration in herbage, which remains after subtraction from the total of the amount due to direct contamination (third column Table 3), is divided

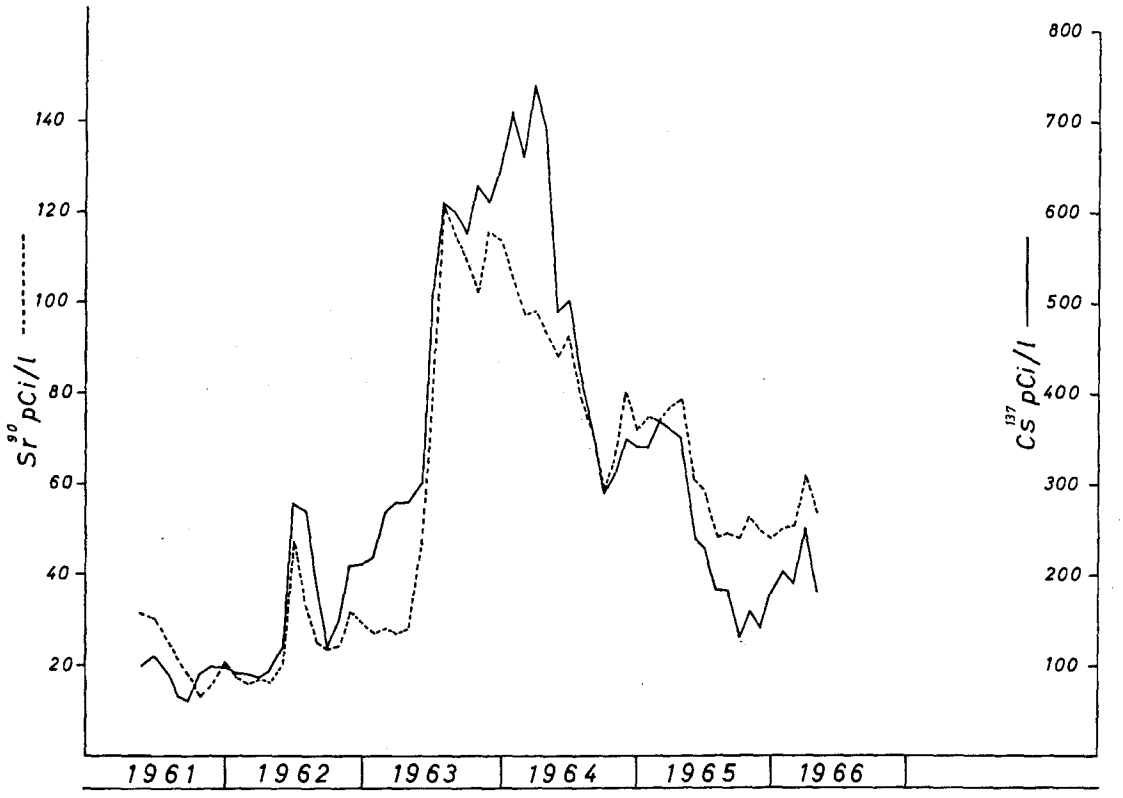

FIG. 4. ^{90}Sr and ^{137}Cs average concentrations in the milk of the zone around Ispra from May 1961 to April 1966.

by the ^{90}Sr cumulative deposit, the data reported in Table 4 are obtained

These figures represent the number of pCi/g taken up by herbage per mCi/km^2 deposited on the soil. If the figure for 1962, which is very low, is excluded, the other values are rather constant around 0.02 pCi/g per mCi/km^2, while the average inclusive of the low value is represented by the regression coefficient (0.0191) of equation (1). As the average calcium content of herbage is roughly 12 mg/g, it may be inferred that 1 mCi/km^2 cumulative deposit yields about 1.6 pCi/g Ca of ^{90}Sr in herbage.

The variations shown by the coefficient in the different years could be caused by the fact that ^{90}Sr becomes progressively less available to plants, owing to ageing of the deposit and because of penetration into deeper soil layers.

The figures of ^{90}Sr deposition are used throughout the discussion instead of those obtained by soil measurements, because the latter are only available from 1964. These values of the ^{90}Sr concentration in the soil are consistent with the figures of the cumulative deposit.

(b) *Relationships between radioactivity in herbage and in milk*

Table 5 shows yearly averages of the ratios between the concentrations in milk and herbage for both ^{90}Sr and ^{137}Cs, also the observed ratio of the milk to herbage activities for strontium-calcium and for cesium-potassium (O.R.).

The ratios were fairly constant throughout the five years considered which suggests a linear correlation between the concentrations in milk

Table 1. *^{90}Sr—Yearly Average Values of Deposition and Concentrations in Herbage and Milk.*

Year	Fallout—Deposition		Herbage			Milk		
	mCi/km² Year	mCi/km² April–Sept.	pCi/g (1)	Ca mg/g (1)	pCi/g Ca (2)	pCi/l. (3)	Ca g/l. (3)	pCi/g Ca (2) (3)
1961	3.4	2.0	1.14	10.83	111	20.1	1.200	16.8
1962	14.5	11.1	1.66	10.70	185	28.7	1.223	23.6
1963	45.6	38.0	6.08	11.65	536	99.3	1.167	85.4
1964	22.6	17.4	5.20	13.75	427	76.0	1.197	63.6
1965	7.3	5.4	2.91	12.95	235	52.7	1.183	44.8

(1) These values are averaged over the period May–October.
(2) These values are obtained averaging the single values of the ratios and not by division of the average figures of ^{90}Sr by those of calcium.
(3) These values are averaged over the annual periods ending April of next year.

Table 2. *^{137}Cs—Yearly Average Values of Deposition and Concentrations in Herbage and Milk.*

Year	Fallout—Deposition		Herbage			Milk		
	mCi/km² Year	mCi/km² April–Sept.	pCi/g (1)	K mg/g (1)	pCi/g K (2)	pCi/l. (3)	K g/l. (3)	pCi/g K (2) (3)
1961	4.9	3.3	1.01	20.47	62.3	88.8	1.576	57.5
1962	25.8	19.2	2.10	28.75	79.8	217	1.604	137
1963	74.8	62.8	5.77	28.92	223	605	1.661	366
1964	34.4	26.0	4.33	19.50	251	371	1.676	223
1965	11.1	8.0	1.59	21.73	104	189	1.611	118

(1) These values are averaged over the period May–October.
(2) These values are obtained averaging the single values of the ratios and not by division of the average figures of ^{137}Cs by those of potassium.
(3) These values are averaged over the annual periods ending April of next year.

Table 3.

Year	^{90}Sr deposition mCi/km²	^{90}Sr herbage contamination by direct deposition	
		pCi/g	% of total
1961	2.0	0.26	23
1962	11.1	1.43	86
1963	38.0	4.90	81
1964	17.4	2.24	43
1965	5.4	0.70	24

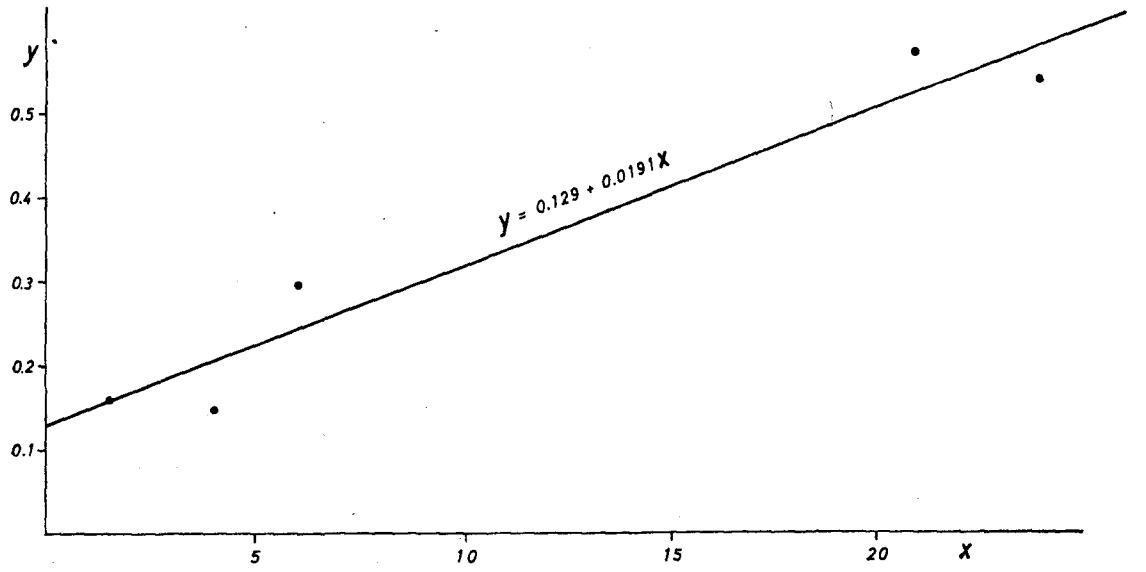

$$y = \frac{Sr^{90}(pCi/g)\ Herbage}{Sr^{90}(mCi/km^2)\ Fallout\ deposition\ (April - September)}$$

$$X = \frac{Sr^{90}(mCi/km^2)\ Fallout\ cumulative\ deposit}{Sr^{90}(mCi/km^2)\ Fallout\ deposition\ (April - September)}$$

FIG. 5. Relationship between ^{90}Sr deposition and its concentration in herbage.

and in herbage. A statistical analysis of the data has shown that this correlation exists and is significant at the 0.01 confidence level. The least square lines obtained have been compared with the lines through the origin and no significant difference has been found. The latter have therefore been drawn through the experimental points and their equations are the following:

^{90}Sr

$$Y\ (\text{pCi/l. milk}) = 16.0\ X\ (\text{pCi/g herbage}) \quad (2)$$

$$Y\ (\text{pCi/g Ca milk}) = 0.157\ X\ (\text{pCi/g Ca herbage}) \quad (3)$$

^{137}Cs

$$Y\ (\text{pCi/l. milk}) = 99.1\ X\ (\text{pCi/g herbage}) \quad (4)$$

$$Y\ (\text{pCi/g K milk}) = 1.23\ X\ (\text{pCi/g K herbage}) \quad (5)$$

These lines are plotted in the graphs of Figures 6 and 7.

The coefficients of equations (3) and (5) represent the herbage to milk "observed ratios" for ^{90}Sr and ^{137}Cs, respectively. Whereas the

Table 4.

Year	1961	1962	1963	1964	1965
pCi/g herbage (uptake) / mCi/km² (Cu/m. deposit)	0.022	0.004	0.020	0.028	0.017

Table 5. Concentration Ratios and Observed Ratios (O.R.) for ^{90}Sr and ^{137}Cs between Milk and Herbage (1)

Year	^{90}Sr		^{137}Cs	
	$\frac{\text{pCi/l. milk}}{\text{pCi/g herbage}}$	O.R. $= \frac{\text{pCi/g Ca milk}}{\text{pCi/g Ca herbage}}$	$\frac{\text{pCi/l. milk}}{\text{pCi/g herbage}}$	O.R. $= \frac{\text{pCi/g K milk}}{\text{pCi/g K herbage}}$
1961	17.6	0.151	88	0.92
1962	17.3	0.128	103	1.7
1963	16.3	0.159	105	1.6
1964	14.6	0.149	86	0.89
1965	18.1	0.191	119	1.1

(1) See notes to Tables 1 and 2 for the periods over which averages are calculated.

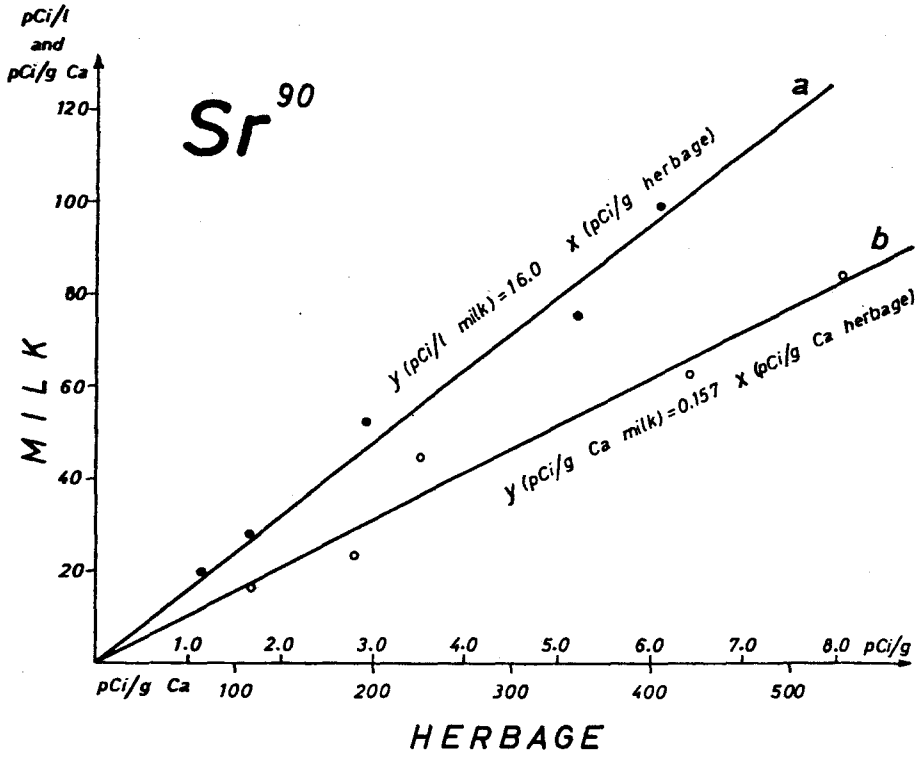

FIG. 6. Relationships between the concentrations of ^{90}Sr in herbage and in milk.

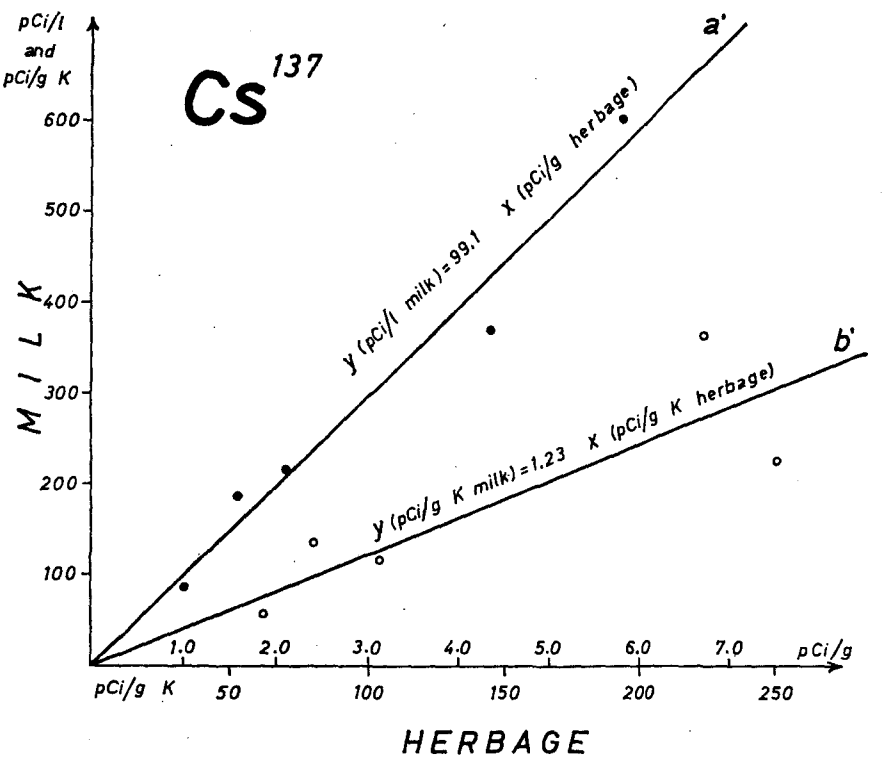

FIG. 7. Relationships between the concentrations of cesium-137 in herbage and in milk.

value for ^{137}Cs looks somewhat lower than those found elsewhere[5, 6] the value for ^{90}Sr is among the highest reported in the literature.[7]

To estimate the value of the O.R. milk-diet through measurements on herbage samples one must know the extent to which these represent the diet actually consumed by the cattle. This is not easily attained under field conditions.

Two main factors may exert an influence upon the O.R. values in this case. They act in the opposite senses.

(i) The yearly averages of the ^{90}Sr concentration in herbage (pCi/g Ca), used in the calculation of the O.R., are merely the means of the single values found in the different months of the growing season. If only the data of the months in which herbage is cut by the farmers are considered and these values are averaged, weighting for the different herbage yields, then higher values are found for the ^{90}Sr concentration in herbage and the difference may be 20%.

(ii) From an inquiry on the management practices in the farms of the area considered, we find that about 80% by weight of the cattle diet consists of hay, the remaining 20% being made up of various feeds (particularly mill products). Some measurements performed on these additional foods have shown that their calcium content is similar to that of herbage, whereas ^{90}Sr is much lower.

An accurate evaluation of these two factors is not easy but it is clear that the former will decrease and the latter increase the O.R. value and it is likely that they may balance each other.

The regression coefficients of equations (2) and (4) are the proportionality factors for the transfer of radioactivity from herbage to milk. Using these coefficients and the daily intake of

Table 6.

	X	Y	C measured	C calculated
	mCi/km²		pCi/g Ca	
1961	2.0	41.5	16.8	16.0
1962	11.1	44.8	23.6	33.4
1963	38.0	59.3	85.4	86.2
1964	17.4	105.0	63.6	62.8
1965	5.4	128.2	44.8	48.2

herbage, which for a lactating cow is estimated as 15 kg, one can calculate the fraction found per liter of milk of the total ingested radioactivity. The values obtained are 0.11% for ^{90}Sr and 0.07% for ^{137}Cs.

(c) *Relationships between fallout and milk radioactivity*

For a given area, the relationship between the cumulative deposit of ^{90}Sr and the rate of fallout which occurred during the growing season on one side, and the concentration of ^{90}Sr in milk (expressed as pCi/g Ca) on the other side is a rather complex one. An attempt has been made, however, for prediction purposes in the monitored area, to test a simple equation of the type:

$$C = aX + bY \qquad (6)$$

where C = average annual concentration of ^{90}Sr in milk (pCi ^{90}Sr/g Ca);
X = amount of ^{90}Sr deposited (mCi/km²) during the growing season (April–September) of the current year;
Y = cumulative ^{90}Sr (mCi/km²) deposited during previous years.

The coefficients a and b have been calculated by considering the annual values of the ^{90}Sr concentration in milk (C) composed of a "direct" fraction and an "indirect" one. These have been given the numerical values found for herbage. The two partial concentrations obtained for each year, divided by the amounts of ^{90}Sr deposited during the growing season and cumulated, respectively, yielded the single annual values of the coefficients. Averaging these values, which are pretty constant, except that of the "indirect" coefficient for 1962, discarded because very low, the following figures are obtained

$$a = 1.8 \qquad b = 0.3$$

In Table 6 the values of C, both calculated from equation (6) and measured are reported together with values of X and Y as defined above.

With the exception of 1962, which appears anomalous, the calculated values agree within $\pm$ 10% with those observed.

Table 7. *Yearly Averages of the Ratio $^{137}Cs/^{90}Sr$ in Fallout, Herbage and Milk*

Year	Fallout Year	Herbage May–October	Milk May–April next year
1961	1.44	0.89	4.4
1962	1.78	1.3	7.6
1963	1.64	0.95	6.1
1964	1.52	0.83	4.9
1965	1.52	0.55	3.6

(d) *^{137}Cs/^{90}Sr ratio*

Another interesting feature of milk contamination is presented by the ratio of ^{137}Cs to ^{90}Sr. This ratio, which is relatively constant in fallout, shows wide variations in herbage reflecting the changing pattern of fallout. The trend of the ratio in milk is closely related to that in herbage, as can be seen from the data reported in Table 7.

According to the well known model of direct and indirect contamination of herbage, lower values of the ratio are found during periods of fallout rate, depending upon proportionately higher uptake from the soil of ^{90}Sr than ^{137}Cs.

REFERENCES

1. M. De Bortoli, P. Gaglione, A. Malvicini and E. Van Der Stricht. Strontium-90 and cesium-137 in milk at Ispra, Italy, during 1960–1962. *Nature* **201,** 1175–1177 (1964).
2. M. De Bortoli, P. Gaglione, A. Malvicini and E. Van Der Stricht. Correlazione fra le attività dello stronzio-90 e del cesio-137 nelle ricadute, nell'erba e nel latte della zona di Ispra durante il periodo 1962–1963. *Minerva Nucleare* **9,** 76–78 (1965).
3. E. Van Der Stricht. Détermination rapide du cesium-137 des retombées radioactives au moyen de phosphomolybdate d'ammonium. *Radiochimica Acta* **3,** 193–199 (1964).
4. R. S. Cambray, Miss E. M. R. Fisher, W. L. Brooks, A. Hughes and G. S. Spicer. Radioactive fallout in air and rain—Results to middle 1965. AERE-R 4997 (1965).
5. F. W. Lengemann and C. L. Comar. The metabolism of some fission products by farm animals. Seminar on Agricultural and Public Health Aspects of Radioactive Contamination in Normal and Emergency Situations. Scheveningen, Netherlands, 11–15 December 1961.
6. R. H. Wassermann, C. L. Comar and A. R. Twardock. *Intern. J. Radiation Biol.* **4,** 299–310 (1962).
7. C. L. Comar. Transfer of strontium-90 into animal produce. *Radioactivity and Human Diet.* Edited by R. S. Russell, Pergamon Press, Oxford, 1966.

ON THE VARIATION OF THE LEVELS OF ^{90}Sr AND OTHER FALLOUT NUCLIDES IN THE GRAIN OF RYE, BARLEY, WHEAT AND OATS

A. AARKROG

Health Physics Department, Danish Atomic Energy Commission,
Risö, Roskilde, Denmark

Abstract—The predominant influence of cereal grains as a ^{90}Sr donor (and a ^{137}Cs and ^{54}Mn donor as well, in certain years) in total Danish diet has stimulated the present investigation. A country wide collection of grain samples has been carried out in the years 1959–64 at a number of selected state experimental farms. Along with the grain sampling, data on ^{90}Sr in air, soil and precipitation have been collected.

Analysis of variance shows that rye contained more ^{90}Sr, ^{137}Cs and ^{54}Mn than barley or wheat or oats. It is demonstrated that awns and, to some degree, grain size play an important role in the direct contamination of grain. The variation between locations, as regards ^{90}Sr levels in grain, depended upon the amounts of precipitation and, to some degree, on the calcium level and the stable strontium to calcium ratio of the soil. The variation between years followed the ^{90}Sr activity in air in August and the amount of precipitation in this month. Winter and spring varieties of rye and wheat did not differ significantly in ^{90}Sr and ^{137}Cs contents. The uptake of ^{54}Mn in cereals related to the fallout rate rather than to the accumulated fallout.

By multiple regression analysis it is shown that the pCi ^{90}Sr/g Ca level for the years 1959–64 in the different species of Danish grain considered separately can be described by equations of the type:

$$\text{pCi } ^{90}\text{Sr/g Ca} = k_0 \cdot A^{k_1} \cdot B^{k_2} \cdot C^{k_3}$$

where A, B and C respectively represent mm precipitation in August, pCi $^{90}Sr/m^2$ air in August and accumulated mCi $^{90}Sr/km^2$ in soil by September; k_1, k_2 and k_3 are the respective partial regression coefficients.

INTRODUCTION

In most countries in Europe, North America and Oceania dairy produce is the predominant source of radiostrontium in the human diet.[1] However, in countries where the consumption of wholemeal bread is common, as, for example, in Poland and Denmark, the contribution from grain products to the total ^{90}Sr intake with the diet might be greater than that from dairy products.[2] In the years 1959–65 grain products have on the average contributed approx. half of the daily ^{90}Sr intake in Denmark.

As regards the other important long-lived fission product from worldwide fallout ^{137}Cs, it appears that cereals in the period 1962–5 contributed approx. one third of the total ^{137}Cs intake from Danish diet.

In December 1963 and June 1964 the daily mean intakes of ^{54}Mn with total Danish diet were 134 and 83 pCi respectively. More than 80% of this radiomanganese originated from bread.[3]

The purpose of the present investigation is to elucidate the variations existing in the Danish environment between the contents of various fallout nuclides in grains of rye, barley, wheat and oats, and to demonstrate the relations between ^{90}Sr in cereal grain and the levels of nuclear debris found in air, precipitation and soil.

MATERIAL AND METHODS

The samples used have been obtained from 10 Danish state experimental farms. As indicated in Fig. 1, locations Tl, S, and J have sandy soils, the other farms predominantly clayey soils. Figure 2 shows the relative annual mean precipitation for the years 1953–64 (the period of global fallout). Location S shows a maximum (814 mm per year) and farms Ts a minimum (524 mm/year). The overall mean for the 10 stations was 658 mm/year, i.e. nearly equal to the area weighted country mean: 682 mm/year (in 1953–64).

Samples of rye, barley, wheat and oats have, as far as possible, been collected from each farm since 1959. In 1960 the samples from locations Tl and Ab were lost, and location Ø was first included in the programme in 1961. Wheat has never been obtained from location Tl and seldom from S. Since 1962 samples of spring varieties of wheat and rye have been obtained in several cases along with the more common winter varieties of these species.

The cereal grain in Denmark is harvested in August–September. The mean harvest date for the years 1962–4 in this study was August 27 (interval August 4–September 25). Barley is on the average harvested 10 days before the other species. The samples were received for analyses 2–3 months after harvest. Each sample consisted of 1–2 kg grain. Approximately 1 kg of grain was counted in a 1.6 l. can fitting over a 3 × 3 in. NaI (Tl) crystal (hat geometry). The pulses were analysed in a 256 channel TMC pulse height analyser. From this measurement the ^{137}Cs and ^{54}Mn contents were determined. After γ-counting, the grain was ashed at 500–550°C in silica dishes and radiostrontium analyses were carried out according to the classical method using fuming nitric acid.[4] Finally the levels of calcium and stable strontium were determined according to Webb *et al.*[5] Since 1961 most of the strontium analyses of grain have been carried out as double determinations. The estimated overall relative standard deviation (S.D.) of the ^{90}Sr analyses was 10–15%, somewhat higher in the first years than in the last due to higher levels since harvest 1962, and to increasing analytical experience throughout the years. The relative S.D.'s of the γ-measurements were approx. 15%.

The data on ^{90}Sr in air, precipitation and soil

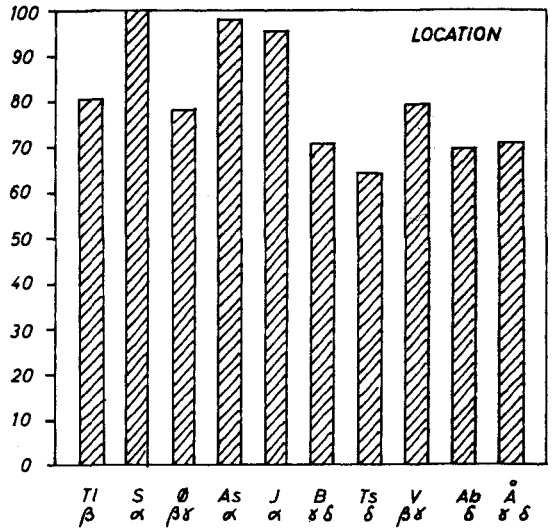

FIG. 2. Relative mean amounts of annual precipitation at the state experimental farms in the period 1953–64.

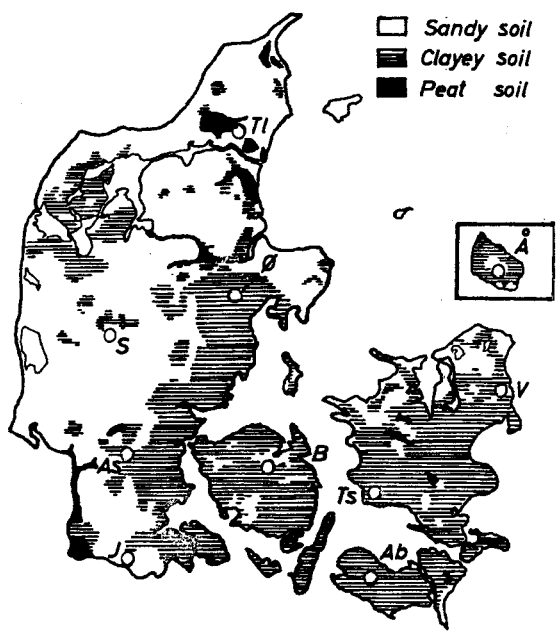

FIG. 1. State experimental farms in Denmark and soil types. Scale: 1:4,400,000.

used in the multiple regression analysis were obtained from ref. 3. Missing soil figures for the years 1959–60 were estimated from U.K. data.[6] The amounts of precipitation at the different stations were obtained from the Meteorological Institute in Copenhagen.[7]

The statistical methods used in the treatment of the results are given in the statistical literature.[8, 9] Multiple regression analysis and analysis of variance have been calculated on a Gier computer.[10, 11] The programme used for analysis of variance[11] has been especially useful because this programme makes it possible to accomplish the analysis, even when several figures are missing, which is inevitable in a field-study such as this.

In the significance tests the following symbols will be used:

x: probably significant	(confidence level: 0.05)
xx: significant	(confidence level: 0.01)
xxx: highly significant	(confidence level: 0.001)

Columns with identical greek letters in the diagrams do not differ significantly by the *t*-test, but they might, in some cases, be probably significantly different.

RESULTS

Tables 1–5 show the results of the measurements of pCi ^{90}Sr/g Ca (S.U.), g Ca/kg, mg stable Sr/g Ca, ^{137}Cs and ^{54}Mn respectively in Danish cereal grain collected in the period 1959–64. It appears from Table 6 that the variation between species of the levels of S.U., pCi ^{137}Cs/kg and pCi ^{54}Mn/kg were all significant.

^{90}Sr

Figure 3 shows that rye displayed a significantly higher pCi ^{90}Sr/g Ca ratio than barley and oats. As regards the pCi ^{90}Sr/kg level (Fig. 4), it was found that the activity in rye was higher than in the other three species, which, as a whole, did not differ significantly. The low S.U. level in oats is a result of the relatively high Ca level in this cereal (Fig. 5).

As regards locations (Fig. 3) the highest levels were found at S, J and Tl, which showed pCi ^{90}Sr/g Ca ratios nearly a factor of two higher than those found at Ab, B and Ts.

If the S.U. mean levels for the period 1959–64 are considered (Fig. 3), it appears that 1963 showed a pronounced peak, which was ten times higher than the minima measured in 1960 and 1961.

^{137}Cs

The relative mean contents of ^{137}Cs in grain collected in 1962–4 appear in Fig. 6. Rye contained significantly more ^{137}Cs than the other cereals. The differences between locations were less pronounced than for ^{90}Sr. The ^{137}Cs level in 1963 was approximately twice as high as in 1962 and 1964.

^{54}Mn

^{54}Mn in cereal grain (Fig. 7), which was determined only in 1963 and 1964 (the 1962 levels were not measurable), showed a picture similar to that of ^{90}Sr and ^{137}Cs, i.e. rye displayed a higher ^{54}Mn level than the other species. The *t*-test could, however, only prove that the activity in the rye was higher than for wheat.

When comparing the years, it should be noticed that the ^{54}Mn 1964 level was corrected for decay ($t^{1/2} = 310$ days) back to the 1963 harvest dates. The corrected 1964 level was approx. 45% of the 1963 level, i.e. nearly equal to the percentage found for ^{90}Sr (43%), but lower than that for ^{137}Cs (55%).

Table 1. *pCi* $^{90}Sr/g$ *Ca in Danish Grain,* 1959–64

Location		Tl	S	Ø	As	J	B	Ts	V	Ab	Å
Year	Sort										
1959	Rye	108	135	—	173	188	—	125	129	93	184
	Barley	116	88	—	67	44	63	81	68	65	130
	Wheat	—	—	—	89	—	88	81	61	68	213
	Oats	13	66	—	23	47	57	36	38	24	111
1960	Rye	—	118	—	105	166	77	90	79	—	103
	Barley	—	112	—	66	72	63	56	58	—	60
	Wheat	—	96	—	76	251	82	58	81	—	115
	Oats	—	78	—	71	60	31	35	39	—	45
1961	Rye	116	51	36	123	103	114	98	80	—	92
	Barley	81	106	67	84	208	45	54	87	57	80
	Wheat	—	—	93	76	—	60	61	86	49	118
	Oats	64	74	29	31	64	32	20	45	41	44
1962	Rye	470	418	470	425	627	193	319	297	—	371
	Barley	336	374	231	483	479	171	92	237	229	328
	Wheat	—	—	433	347	548	334	297	—	139	283
	Oats	147	243	175	179	300	93	162	—	109	215
1963	Rye	1781	1168	1500	1870	1077	1286	994	830	—	703
	Barley	1125	1353	559	1293	669	662	439	680	484	443
	Wheat	—	—	1300	903	931	910	878	—	538	831
	Oats	472	466	439	674	290	380	318	453	147	362
1964	Rye	760	733	508	565	535	261	253	425	—	325
	Barley	631	868	398	544	471	107	238	302	209	219
	Wheat	—	—	438	691	—	295	290	413	150	224
	Oats	242	352	189	190	251	106	102	174	91	76

Table 2. g Ca/kg Danish Grain, 1959–64

Location		Tl	S	Ø	As	J	B	Ts	V	Ab	Å
Year	Sort										
1959	Rye	0.35	0.38	—	0.38	0.40	—	0.35	0.45	0.48	0.35
	Barley	0.27	0.44	—	0.39	1.02	0.32	0.37	0.54	0.41	0.48
	Wheat	—	—	—	0.36	—	0.30	0.40	0.52	0.28	0.42
	Oats	0.69	0.98	—	0.85	0.81	0.71	0.79	0.83	0.76	0.55
1960	Rye	—	0.41	—	0.32	0.32	0.51	0.46	0.36	—	0.35
	Barley	—	0.43	—	0.41	0.37	0.40	0.37	0.41	—	0.62
	Wheat	—	0.45	—	0.35	0.30	0.33	0.38	0.32	—	0.35
	Oats	—	0.96	—	0.68	1.02	0.96	0.78	1.20	—	0.85
1961	Rye	0.42	0.30	0.42	0.38	0.22	0.28	0.30	0.26	—	0.65
	Barley	0.47	0.49	0.49	0.41	0.35	0.45	0.43	0.49	0.46	0.49
	Wheat	—	—	0.32	0.43	—	0.42	0.28	0.35	0.47	0.30
	Oats	0.62	0.51	1.48	1.10	0.89	0.87	0.65	0.74	0.89	0.74
1962	Rye	0.33	0.55	0.46	0.42	0.37	0.51	0.50	0.56	—	0.43
	Barley	0.44	0.41	0.65	0.55	0.43	0.55	1.02	0.54	0.50	0.43
	Wheat	—	—	0.43	0.30	0.43	0.39	0.32	—	0.62	0.36
	Oats	0.78	0.71	0.85	0.74	0.68	0.87	0.74	—	1.29	0.69
1963	Rye	0.37	0.41	0.32	0.51	0.40	0.54	0.62	0.50	—	0.44
	Barley	0.66	0.43	0.59	0.62	0.39	0.63	0.38	0.58	0.42	0.60
	Wheat	—	—	0.32	0.59	0.43	0.38	0.42	—	0.46	0.32
	Oats	0.93	0.63	0.79	0.81	0.85	0.83	0.85	0.98	0.98	0.87
1964	Rye	0.65	0.55	0.44	0.41	0.42	0.40	0.39	0.50	—	0.35
	Barley	0.48	0.36	0.54	0.59	0.43	0.98	0.47	0.46	0.48	0.35
	Wheat	—	—	0.39	0.36	—	0.40	0.36	0.35	0.45	0.41
	Oats	0.81	0.56	0.76	0.81	0.85	0.65	0.83	1.12	0.98	0.74

Table 3. mg stable Sr/g Ca in Danish Grain, 1959, 1962–4

Location		Tl	S	Ø	As	J	B	Ts	V	Ab	Å
Year	Sort										
1959	Rye	2.8	3.2	—	1.1	2.2	—	1.6	1.8	3.4	1.9
	Barley	1.4	3.5	—	2.2	1.4	2.0	1.6	3.2	2.3	2.6
	Wheat	—	—	—	2.2	—	3.0	2.0	0.9	2.7	1.9
	Oats	2.8	2.4	—	0.7	2.1	1.3	1.7	1.9	2.3	1.6
1962	Rye	1.9	2.4	3.6	3.7	2.1	1.5	2.3	1.5	—	2.6
	Barley	2.4	6.9	2.8	3.7	3.0	1.7	2.3	2.5	2.1	3.2
	Wheat	—	—	5.4	8.9	2.4	2.5	5.1	—	2.3	3.7
	Oats	2.3	3.2	2.6	2.8	2.8	1.9	1.9	1.6	1.0	1.3
1963	Rye	3.5	2.0	2.6	5.3	1.9	1.4	1.8	2.8	—	1.8
	Barley	3.0	3.9	1.9	4.5	3.2	1.0	1.7	2.1	3.5	1.6
	Wheat	—	—	4.5	4.3	3.2	2.3	1.7	—	2.6	2.1
	Oats	1.1	3.0	1.9	1.7	1.5	1.7	1.7	2.1	1.4	1.8
1964	Rye	1.3	2.7	1.7	1.2	2.7	2.0	1.1	1.7	—	1.7
	Barley	2.2	4.9	4.1	1.2	1.4	2.3	2.8	4.2	4.2	2.1
	Wheat	—	—	5.1	3.2	—	2.4	3.3	2.4	3.7	2.8
	Oats	1.3	2.7	1.9	0.6	1.7	1.3	0.8	1.2	1.2	0.9

Table 4. ^{137}Cs in Danish Grain, 1962–4

Location		Tl	S	Ø	As	J	B	Ts	V	Ab	Å
Year	Sort	pCi ^{137}Cs/g K									
1962	Rye	159	186	218	110	—	80	116	110	—	145
	Barley	148	148	88	123	135	79	81	90	84	122
	Wheat	—	—	124	100	252	108	62	—	70	71
	Oats	92	143	74	—	232	70	117	—	—	42
1963	Rye	264	371	202	537	299	274	325	243	—	183
	Barley	179	264	200	372	214	448	218	148	308	139
	Wheat	—	—	245	608	206	202	152	—	222	226
	Oats	296	183	206	380	168	169	258	174	248	191
1964	Rye	232	248	181	274	252	133	125	125	—	140
	Barley	111	159	92	170	163	63	92	74	71	86
	Wheat	—	—	132	153	—	79	96	92	69	84
	Oats	140	161	101	126	123	70	91	120	59	88
		pCi ^{137}Cs/kg grain									
1962	Rye	570	553	734	446	—	374	486	442	—	610
	Barley	326	385	480	480	500	393	318	354	390	534
	Wheat	—	—	445	415	690	278	238	—	278	342
	Oats	164	166	420	—	805	224	366	—	—	248
1963	Rye	985	1130	775	2300	1200	1060	1910	1225	—	715
	Barley	930	1080	905	1220	898	2120	785	620	1430	530
	Wheat	—	—	812	1780	725	715	533	—	670	685
	Oats	1265	552	760	1520	562	466	1068	758	955	582
1964	Rye	1080	1040	777	1070	944	579	575	405	—	662
	Barley	485	643	434	715	872	408	475	282	360	415
	Wheat	—	—	475	654	—	360	334	344	268	344
	Oats	497	700	309	614	491	297	410	394	294	384

Table 5. pCi ^{54}Mn/kg Danish Grain, 1963–4

Location		Tl	S	Ø	As	J	B	Ts	V	Ab	Å
Year	Sort										
1963	Rye	1785	3290	1495	3640	2880	1630	1810	1330	—	955
	Barley	1290	3130	1775	2320	1080	2545	1320	2000	1210	945
	Wheat	—	—	1885	1080	1260	1350	1085	—	1100	1040
	Oats	2760	1530	1780	1425	1850	1310	1130	1425	1215	1020
1964	Rye	500	753	340	482	189	294	334	242	—	219
	Barley	458	671	435	682	268	249	364	204	373	246
	Wheat	—	—	253	256	—	192	173	172	198	190
	Oats	424	426	339	288	496	133	286	268	305	226

Table 6. Summary of the Significance Test from the Analysis of Variance derived from the Logarithm of the Figures in Tables 1–5

Effect	Source	pCi ^{90}Sr/g Ca (cf. Table 1)	g Ca/kg (cf. Table 2)	mg Sr/g Ca (cf. Table 3)	pCi ^{137}Cs/kg (cf. Table 4)	pCi ^{54}Mn/kg (cf. Table 5)
Main	Sort	xxx	xxx	xxx	xxx	xx
	Location	xxx	—	xxx	xxx	xxx
	Year	xxx	x	x	xxx	xxx
2-factor interaction	Sort · Loc.	xxx	—	—	—	—
	Loc. · Year	xxx	—	xxx	xxx	—
	Year · Sort	xx	—	x	—	—
Coefficient of variation (3-factor interaction and residual error)		0.25	0.22	0.30	0.26*	0.26
Degrees of freedom		202	103	63	41	22

*The errors for ^{137}Cs were not homogeneous for the three years considered; this does, however, not invalidate the significance of the main effects.

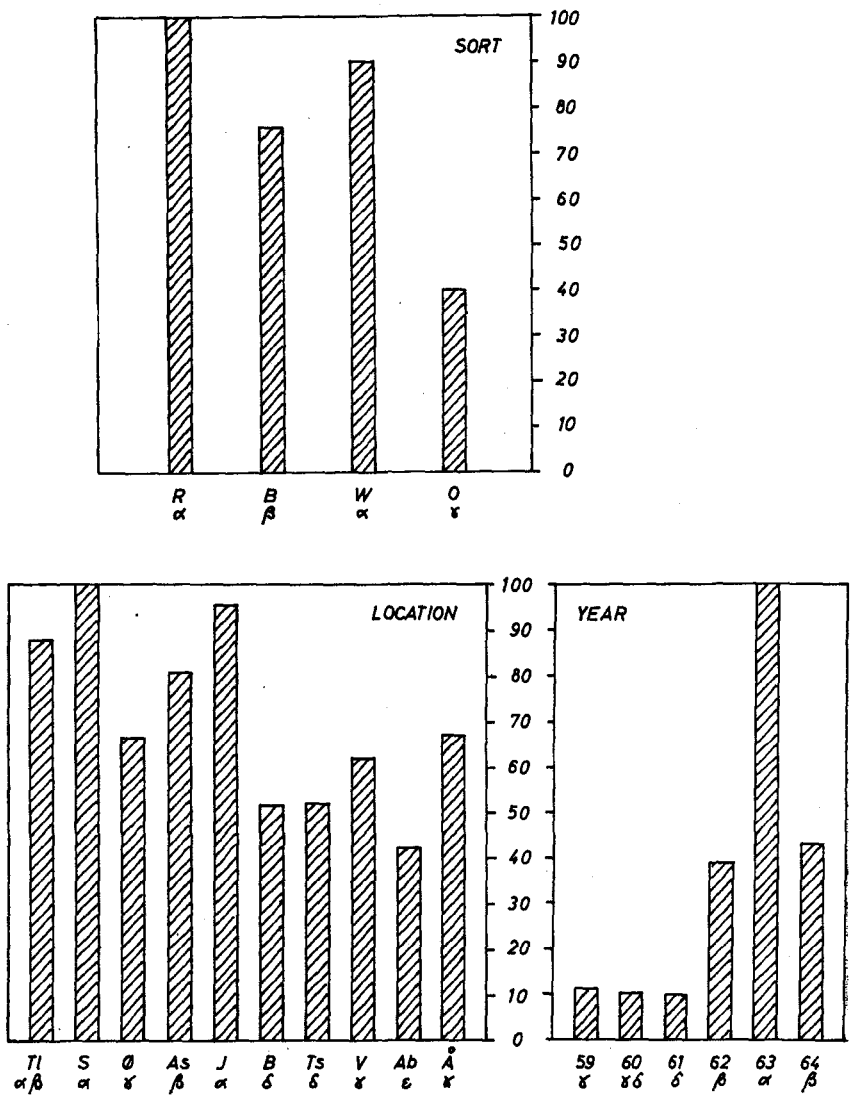

FIG. 3. Relative pCi ^{90}Sr/g Ca ratios in Danish cereal grain, 1959–64.

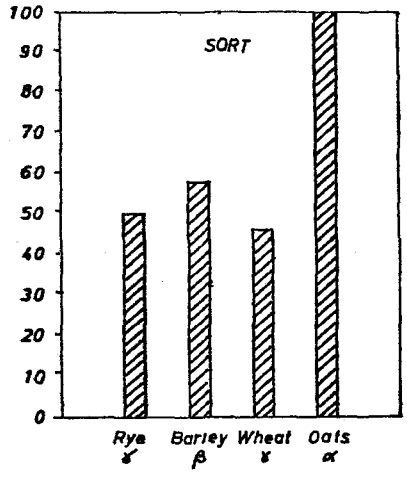

FIG. 4. Relative pCi ^{90}Sr/kg grain, 1959–64.

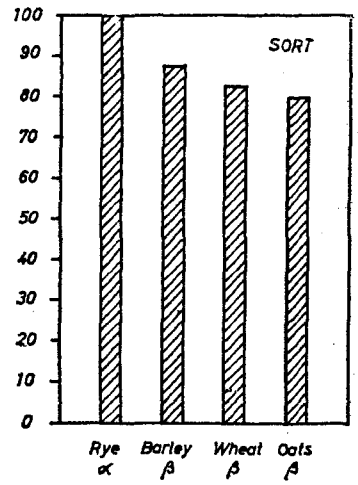

FIG. 5. Relative g Ca/kg grain, 1959–64.

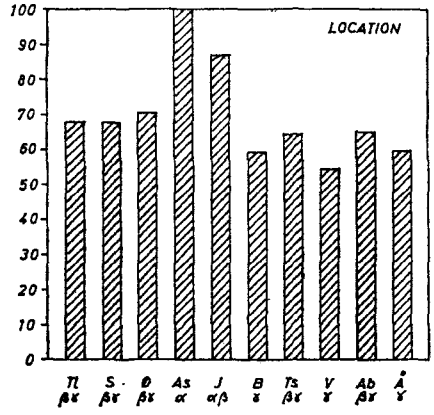

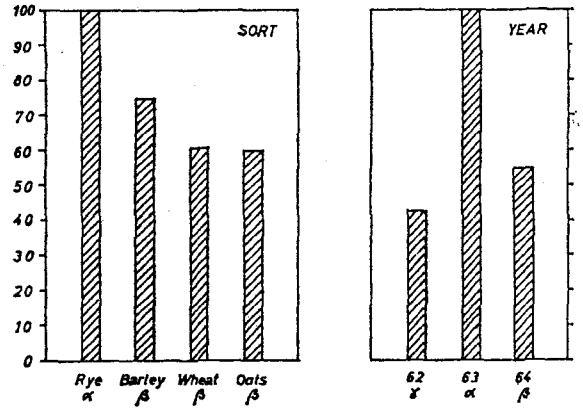

FIG. 6. Relative pCi ^{137}Cs/kg grain, 1962–4.

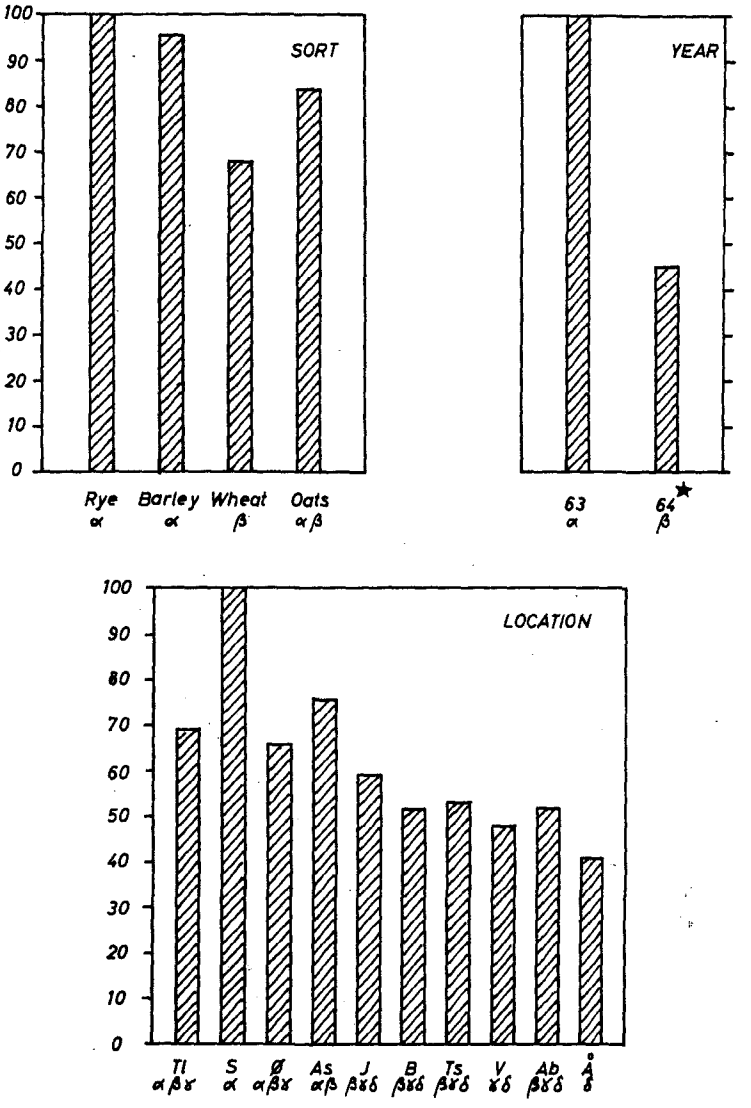

FIG. 7. Relative pCi ^{54}Mn/kg grain, 1963–4. *Corrected for decay back to the 1963 harvest.

DISCUSSION

Variation between species

Experiments with artificial application of activity carried out by Milbourn *et al.*[12] and Middleton *et al.*[13, 14] have shown that the radiostrontium from nuclear weapons tests has entered cereal grain mainly through direct absorption of the debris after the ears have emerged (floral absorption) and only to a minor degree through uptake from the soil. The direct contamination of cereal grain with ^{137}Cs in addition occurs to a significant degree before the emergence of the ears, because ^{137}Cs is easily translocated in the plants.[13, 14] As regards root uptake, this is normally even less for ^{137}Cs than for ^{90}Sr.[15]

An attempt can obviously be made to explain the higher levels of nuclear debris in rye than in wheat by the particular morphological and physiological conditions which make rye more sensitive than the other species of grain to floral contamination. The ears of rye are furnished with awns, and it seems reasonable to imagine that these awns would display some adsorptive effect on the direct fallout.

To test this hypothesis, ^{137}Cs was measured in samples of wheat with awns and without awns,* grown in the same field in 1965. The ^{137}Cs content in the wheat with awns was 50% higher than in the wheat without awns.

Another possible explanation for the high rye levels could be that rye has a relatively small grain size compared with the other species. According to Pedersen[16] the 1000 grain weight of rye is 25 g, whereas the corresponding weights of wheat, barley and oats are 40, 40 and 35 g respectively. Rye thus displays a greater surface-to-weight ratio than the other cereals and might consequently be more susceptible to direct contamination (Andersen[17]).

To examine this theory, fractions (separated according to grain size) of rye and wheat grown in the same area in 1964 were analysed. The S.U. level in small rye grains (15 g/1000 grains) was 18% higher than in large rye grains (37 g/1000 grains). Wheat showed a 26% higher S.U. level in a (25 g/1000) fraction than in a (42 g/1000) fraction. If, however, rye and wheat of similar grain size were compared, the S.U. level in rye was 20% higher than in wheat.

The conclusion of these experiments is that both awns and small grain size will increase the floral absorption of fallout nuclides in cereals, the presence of awns probably playing a more significant role than grain size.

The awns of barley are longer and thicker than those found in rye, but the activity levels in barley are lower than in rye. The difference in grain size between rye and barley (cf. above) would undoubtedly explain some of this difference in activity levels. It should, however, also be recalled that the period from the emergence of the ears to harvest is two or three weeks shorter for barley than for the other Danish grain species.[16] Barley is thus exposed to floral contamination for a shorter period than the other cereals. Hence it seems reasonable that barley shows lower levels than rye for this reason. That the awns on barley on the other hand play an important role for the direct contamination is indicated by the fact that the activity levels in barley in most cases exceeded those found in wheat and oats (Figs. 4, 6 and 7).

While the method of direct contamination of cereal grain with ^{90}Sr and ^{137}Cs is fairly well known,[13, 14] no experimental data has yet been available regarding ^{54}Mn. Recently Sutton and Kelly[18] have found in field surveys that the ratio of pCi ^{54}Mn to mg stable manganese is fairly constant in U.S. wheat grown during 1963, and that this ratio was nearly constant in the different milling fractions of a Kansas wheat sample. They concluded that uptake of ^{54}Mn in wheat had taken place through the root of the plants rather than as a result of the physical adhesion of inert radiomanganese.

From measurements of ^{90}Sr in precipitation and air and of ^{54}Mn in air,[2] it was estimated that the accumulated ^{54}Mn levels by May–August 1963 and 1964 were nearly equal in Denmark, whereas the ^{54}Mn fallout rates in these periods were approx. 10 times greater in 1963 than in 1964. The concentrations of ^{54}Mn in grain (Table 5) were on the average 5 times higher in 1963 than in 1964. To estimate the uptake of fallout nuclides deposited in the soil, barley was grown in 1964 in a greenhouse placed on a field contaminated during 1963 with ^{54}Mn fallout. It was not possible to detect

* Danish wheat normally has no awns.

any ^{54}Mn in the barley grain from the greenhouse, whereas barley grown outside the house, and thus exposed to the 1964 ^{54}Mn fallout, contained 390 pCi ^{54}Mn/kg grain. When these observations are compared with Sutton and Kelly one reaches the conclusion that if ^{54}Mn is taken up through the root system, it must in Denmark have been during a rather short time after the deposition of the ^{54}Mn, that is, probably before the radiomanganese had been fixed to the soil and thus been made unavailable to the cereal plants. Hence the contamination of Danish grain products with ^{54}Mn from nuclear debris depends upon the fallout rate rather than the accumulated fallout.

Variation between locations

A comparison of Fig. 2 with Fig. 3 shows that there exists a correlation between S.U. in grain and the yearly mean amounts of precipitation at the different locations. The locations S, As, J, and Tl show higher levels than Ts, Ab, B, and Å, both as regards S.U. and mm precipitation. However, the variation between pCi ^{90}Sr/g Ca seems to be greater than the variation between amounts of precipitation. The greater difference between S.U. values might be a result of the fact that the soil in the western part of the country is more sandy than the soil in East Denmark (Fig. 1), and that the sandy soil contains less Ca and probably shows a greater mg Sr/g Ca ratio than the clayey soil, and thus favours the root uptake of strontium.

To examine this phenomenon two sets of soil samples were collected, one in Jutland at location S, and one in Funen at B. The samples were collected as double samples and taken in five 25 cm long cores down to a depth of 125 cm. Calcium and stable strontium were determined in the 20 cores by HCl extraction.

The total Ca mean content of the B soil (down to 125 cm depth) was 33 g/kg and in the S soil the level was 0.45 g Ca/kg. The top soil (0–25 cm) at B contained 6 g Ca/kg, and at S 1.3 g Ca/kg soil. As regards mg Sr/g Ca it was also possible to prove significant variation between locations. The soil from S contained 4.4 mg Sr/g Ca and the soil from B 53% of this value, i.e. 2.3 mg Sr/g Ca.

In Fig. 8 the relative amounts of mg Sr/g Ca in grain are plotted. At location B the ratio is 51% of the ratio found at S, i.e. essentially the same as found for the soil samples. Hence it seems reasonable to expect that the S.U. level in grain, at least to some degree, depends upon the stable strontium-to-calcium ratio in the soil.

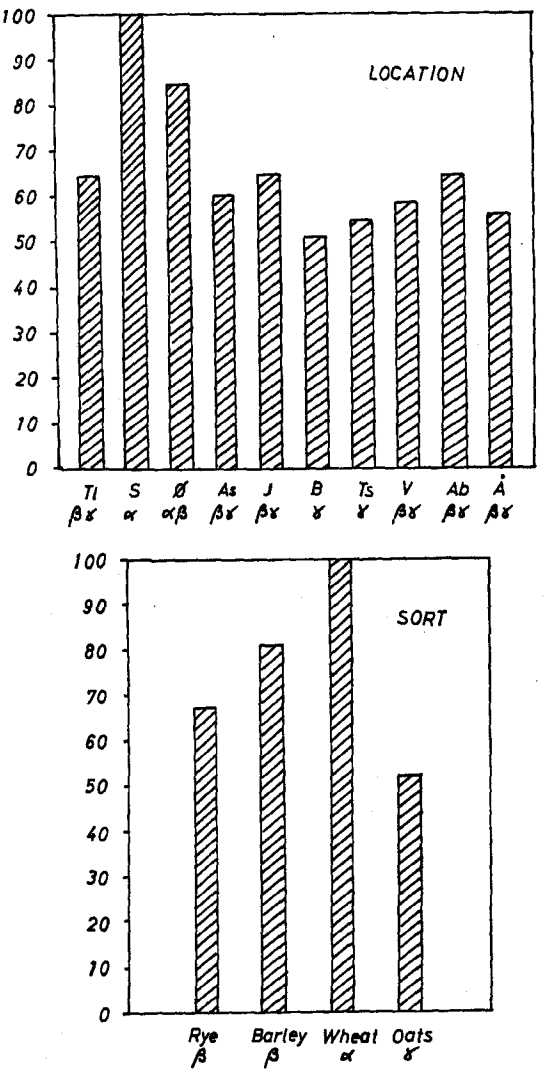

FIG. 8. Relative mg stable Sr/g Ca in Danish grain, 1959, 1962–4.

Figure 8 shows further that the mg Sr/g Ca ratio in the four species of grain differs significantly. Wheat appears to have the highest

ratio, oats the lowest. Rye and barley were only probably significantly different.

Variation between years

A comparison of Fig. 9 and Fig. 3 shows that there is a pronounced correlation between air activity in August and the S.U. level in cereals.

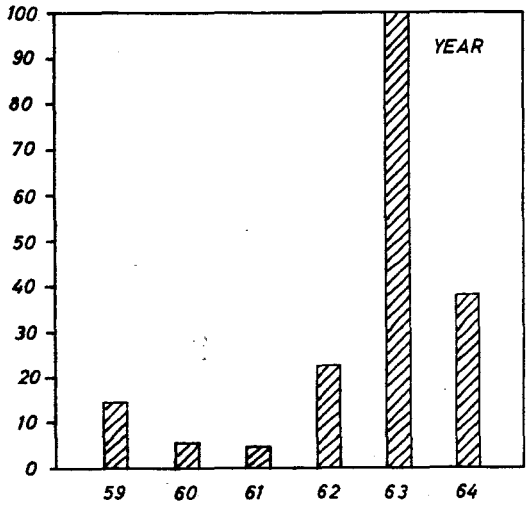

FIG. 9. Relative pCi $^{90}Sr/m^3$ air in August at Risö, 1959–64.

The grain activity, however, is to some degree also dependent on the amount of precipitation in August. This explains why the grain levels in 1959, as compared with 1960 and 1961, were relatively low, and why the 1962 S.U. level was nearly equal to the 1964 level (the amount of precipitation in August 1959, as well as in August 1964, were rather low).

Variation between spring and winter varieties

Wheat and rye grown in Denmark are normally winter varieties, i.e. they are sown in September and harvested in August–September the following year. To a certain extent, however, spring varieties of rye, as well as of wheat, are also grown. These varieties are sown in the early spring, at the same time as barley and oats, and harvested a little later than the winter varieties. It was thus of interest to investigate whether the different growing periods of the two varieties were detectable through their respective activity levels.

Table 7 shows the levels of ^{90}Sr and ^{137}Cs in spring varieties of wheat and rye collected in 1962–4. If these figures are compared by a *t*-test with the corresponding figures in Tables 1 and 4 for winter varieties, it is not possible to

Table 7. ^{90}Sr and ^{137}Cs in Spring Varieties of Rye and Wheat, 1962–4

Year	Sort	Location	pCi ^{90}Sr/g Ca	pCi ^{137}Cs/g K
1962	Wheat	Ts	251	—
	,,	Ab	215	—
1963	Rye	As	745	485
	Wheat	As	839	386
	,,	Ts	870	200
	,,	Ab	459	236
1964	Rye	S	789	407
	,,	As	831	242
	,,	J	685	312
	Wheat	Ø	419	92
	,,	As	549	195
	,,	Ts	293	84
	,,	V	251	115
	,,	Ab	158	67
	,,	Å	169	72

show a significant difference between winter and spring varieties.

Several authors [19, 20] have, in greenhouse experiments, found that significant differences exist in the root uptake of radiostrontium in grain among a wide range of genotypes in wheat, barley and oats. A field survey [21] carried out on six varieties of hard red winter wheat showed significant differences between the varieties, the upper levels being approx. 25% higher than the lower.

In the present study no attempts have yet been made to investigate the variation in activity content in grain with genotype. If, however, the variance of the ratios: S.U. spring var./S.U. winter var. from the different locations and years are compared by a F-test with the variance of the double determination of the samples, the two sets of variances were not found to be significantly different. Considering that the ratio: S.U. spring/S.U. winter not only includes the analytical error, but also the error from sampling, and differences arising from displaced growing periods and from dissimilarity in genotype, it does not seem likely that the latter are important for the activity contents in the present study. This is, however, probably valid only as long as the direct contamination of the crops is several times the contamination from root uptake, as was the case in 1962–4.

MULTIPLE REGRESSION ANALYSES OF THE S.U. FIGURES

Rivera [22] has calculated a formula for S.U. in the U.S.A. wheat grain collected in the period 1958–62:

$$V = 0.49\,S + 246\,R$$

where V is the production-weighted S.U. ratio in wheat grown in the United States during a given year, S is the estimated ^{90}Sr content of the soil on which the wheat was grown in mCi/km^2 for the middle of the crop year, and R is the fallout rate in mCi/km^2 deposited in June of the crop year. Another formula has been proposed by UNSCEAR [1] mainly based on wheat:

$$C = 0.5\,F_d + 20\,F_r$$

where C is pCi ^{90}Sr/g in the grain, F_d is accumulated deposition of ^{90}Sr (mCi/km^2) and F_r is the current rate of deposition (mCi/^{90}Sr/km^2/year).

The two equations are nearly identical, provided the fallout throughout the year is assumed to be twelve times that measured in June. This is clearly an overestimate of the annual fallout, and consequently it would be expected that the latter equation yields lower results than the former. It is thus not surprising that the UNSCEAR formula estimated the Danish S.U. levels in wheat to be approximately a factor of two lower on the average than those actually measured in 1962–5.

In the present study it has been found that the S.U. levels in grain seem to be lognormally rather than normally distributed. Further it has been found feasible to use air activity (pCi ^{90}Sr/m^3) and mm precipitation instead of directly measuring the value mCi ^{90}Sr/km^2, because the two first-mentioned variables gave a better fit to the grain data than the latter, when tested for the period 1962–4. As the variation in monthly mean air activity has been shown to be rather constant within an area as small as Denmark (44,000 km^2) (cf. e.g. U.K. air measurements [6]), it is only necessary to measure the air activity at one location. To determine the accumulated fallout, the mean value for the ten state experimental farms from the annual sampling in September has been used instead of individual values. This is because the contribution from the soil uptake in the period considered has been rather low, and because factors other than the accumulated fallout in the soil influence the root uptake (e.g. Ca-content of the soil and mg Sr/g Ca ratio), factors which probably conceal the effect of varying ^{90}Sr levels in the soil.

An equation of the following form was used:

$$\text{S.U.} = k_0\,A^{k_1} \cdot B^{k_2} \cdot C^{k_3}$$

or

$$\log \text{S.U.} = k_1 \cdot \log A + k_2 \cdot \log B + k_3 \cdot \log C + \log k_0$$

where S.U. is pCi ^{90}Sr/g Ca in the cereal grain, A is the mm precipitation in certain months (Table 8) near the harvest, B is pCi

$^{90}Sr/m^3$ in air during the same months, measured at one location (Risö), C is mCi $^{90}Sr/km^2$ accummulated in the soil by September of the crop year, calculated as the mean of the accumulated fallout at the ten state experimental farms. k_0 is a constant, and k_1, k_2 and k_3 are the partial regression coefficients.

Table 8 shows the partial regression coefficients, k_0, and the multiple correlation coefficients r, for the four grain species calculated for three different periods by multiple regression analysis using the data in Table 1 and ref. 3 and 7.

It is to be expected that Danish cereals would be exposed to direct contamination with ^{90}Sr predominantly during the period June–August (cf. Middleton[13, 14] and Pedersen[16]). In 1962, where fresh fallout began to appear in Denmark in August[23] the increase in the $^{89}Sr/^{90}Sr$ ratio took place during the Danish harvest period. From a greenhouse experiment it was found that approx. 10% of the ^{90}Sr in the grain of that year's harvest was due to root uptake. Hence it was possible from measurements of the $^{89}Sr/^{90}Sr$ ratio in the grain samples to estimate the age of the florally absorbed ^{90}Sr in the grain, and it appeared that the following equation fitted the data:

$$y = 100\ e^{-t}$$

where y was the accumulated percentage of total ^{90}Sr at harvest time in the grain from direct contamination at a time t-fortnights before the date of harvest. The equation indicates that the contribution of ^{90}Sr from fallout prior to one month (two fortnights) before harvest was less than 15% of the total direct contamination with ^{90}Sr. As the harvest for most Danish grain species normally occurs in the period August 15–September 15, the three contamination periods shown in Table 8 were selected for examination. It appears from the table that it is reasonable to regard August as the only month of significance for the direct contamination of Danish grain with radiostrontium in the period 1959–64. In this connection it should be emphasized that the regression equations indicated throughout Table 8 are valid only for the period and area considered.

The partial regression coefficients (k_2) in Table 8 were all significant, indicating that the

Table 8. Values and Significance (by t-test) of the Partial Regression Coefficients and the Multiple Correlation Coefficients for the Equation:

$$\log Y = \log k_0 + k_1 \log A + k_2 \log B + k_3 \log C$$

Period of direct contamination	Sort	Partial regression coefficients			log k_0	Multiple correlation coefficient
		k_1	k_2	k_3		
July–Aug.	Rye	0.3937	0.6677^{xxx}	0.3720	2.5182	0.94^{xxx}
	Barley	0.4764^{x}	0.4152^{x}	0.9150^{xx}	0.9289	0.91^{xxx}
	Wheat	0.5204	0.5375^{xx}	0.5582	1.6994	0.94^{xxx}
	Oats	0.5931^{x}	0.4202^{xxx}	0.7373	0.6889	0.90^{xxx}
Aug.	Rye	0.3710	0.6560^{xxx}	0.4402	2.4768	0.95^{xxx}
	Barley	0.4628	0.4048^{xx}	0.9636^{xx}	0.8865	0.92^{xxx}
	Wheat	0.5028	0.5241^{xx}	0.6211	1.6447	0.95^{xxx}
	Oats	0.5809^{x}	0.4019^{xx}	0.8121^{xx}	0.6042	0.91^{xxx}
Aug.–Sept.	Rye	0.3323	0.8431^{xxx}	−0.0306	3.6185	0.94^{xxx}
	Barley	0.4876	0.6229^{xxx}	0.3805	2.0825	0.92^{xxx}
	Wheat	0.5337	0.7620^{xxx}	−0.0167	2.9507	0.95^{xxx}
	Oats	0.5930	0.6706^{xxx}	0.0991	2.0986	0.91^{xxx}

Table 9. *S.U. in Danish Grain in* 1965.

	Rye	Barley	Wheat	Oats
Calculated	258 ± 13	278 ± 18	256 ± 18	120 ± 10
Measured	238 ± 32	166 ± 26	227 ± 31	102 ± 12

The error term is the S.E. of the mean of the 10 locations.

air activity, in the period around harvest-time, plays an important role for the ^{90}Sr content of the grain. Accumulated fallout (k_3) seemed only to be of significance for the S.U. levels in barley and oats. It is, however, to be expected that the S.U. levels in grain in the coming years, provided the test-ban continues, will for all species depend increasingly on the accumulated fallout.

Although the equations are valid only for the period 1959–64, the 1965 S.U. levels were estimated from the August regression coefficients in Table 8. Table 9 shows the calculated results compared with those actually measured.

All calculated figures except barley agreed fairly well with the measured levels.

ACKNOWLEDGEMENTS

I thank Mr. Arna Andersen and Mr. Heinz Hansen for valuable discussions and proposals and the staffs of the state experimental farms for their never failing co-operation.

REFERENCES

1. Report of the United Nations Scientific Committee on the Effects of Atomic Radiation (U.N. New York, 1962).
2. Report of the United Nations Scientific Committee on the Effects of Atomic Radiation (U.N. New York, 1964).
3. A. Aarkrog and J. Lippert. Risö Reports Nos. 14, 23, 41, 63, 85 and 107 (1960–5).
4. F. J. Bryant, A. Morgan and G. S. Spicer. AERE-R-3030 (1959).
5. R. S. Webb and P. C. Wildy. AERE-AM-23 (1959).
6. R. S. Cambray, E. M. R. Fisher, W. L. Brooks, A. Hughes and G. S. Spicer. AERE-R-4997 (1965).
7. Meteorologisk Institut. Ugeberetning om Nedbør m.m. Copenhagen (1953–64).
8. A. Hald. *Statistical Theory with Engineering Applications.* John Wiley and Sons, Inc., New York, 1955.
9. C. L. Davids. *The Design and Analysis of Industrial Experiments.* Oliver and Boyd, London, 1956.
10. P. Timmermann. Multilin, AEK program 101. Risö, 1963.
11. J. Vestergaard. GIER system Library No. 211, A/S Regnecentralen. Copenhagen, 1964.
12. G. M. Milbourn, F. B. Ellis and R. Scott Russel. *J. Nucl. Energy, Part A. Reactor Science* **10,** 116–132 (1959).
13. L. J. Middleton. *Int. J. Rad. Biol.* **4,** 387–402 (1959).
14. L. J. Middleton and Helen M. Squire. *Int. J. Rad. Biol.* **6,** 549–558 (1963).
15. I. V. Gulyakin and E. V. Yudintseva. *Proc. 2nd U.N. Intern. Conf. on the Peaceful Uses of Atomic Energy.* A/Conf. 15/P/2311, vol. 18, pp. 476–485 (1958).
16. Axel Pedersen. Landbrugets Plantekultur II. Den kgl. Veterinær-og Landbohøjskole, København, 1963.
17. Arna Andersen. Personal communication (1964).
18. D. C. Sutton and J. J. Kelly. *Nature* **209,** 1081–83 (1966).
19. D. C. Rasmusson, L. H. Smith and W. M. Mayar. *Crop Sci.* **3,** 34–37 (1963).
20. C. C. Lee and F. W. Sosulski. *Canad. J. Plant Sci.* **45,** 13–17 (1965).
21. R. A. Anderson and V. F. Pfeifer. *Radiological Health Data* **6,** 438–440 (1965).
22. J. Rivera. HASL-140, 276–279 (1963).
23. A. Aarkrog, J. Lippert and J. Petersen. Risö Report No. 63 (1963).

^{22}Na IN FALLOUT AND FOODS IN ITALY

A. A. CIGNA and F. G. GIORCELLI

Laboratorio per lo Studio della Radioattività Ambientale, Centro Studi Nucleari Casaccia, CNEN, Casaccia Roma, Italy

Abstract—The concentration of ^{22}Na and its ratio with ^{137}Cs were measured in fallout and in some foods (milk, meat, etc.) in the period 1961–1965. The samples of milk were collected in 15 areas scattered all over the country and may be considered representative of 80 per cent of the whole Italian production. Other samples of foods were collected in General Wholesale Markets and may also be considered representative of wide areas. Fallout was collected at the Casaccia Nuclear Centre, Rome.

The gamma ray spectra of the food chain samples obtained in previous years by a low background spectrometer (NaI(Tl) crystal 5 cm × 5 cm and 400 channel analyzer) were analyzed by an IBM 7094 computer. A linear least-squares fitting program including a gain-shift routine (R. G. HELMER *et al.*, IDO-17015), slightly modified in order to meet the requirements of the present research was utilized. In such a way the concentrations of ^{22}Na, ^{137}Cs and natural K were determined.

A random check of the computer results was made by determining directly ^{22}Na in a certain number of samples by gamma-gamma sum coincidence spectrometry. A good agreement was obtained between the values obtained by the two methods described.

The measurements of ^{22}Na in fallout samples were obtained by gamma–gamma sum coincidence spectrometry, while ^{137}Cs was determined by a stripping technique on gamma ray spectra.

This paper was withdrawn and it will be published probably not before Spring 1968.

^{90}Sr IN FALLOUT AND FOODSTUFFS IN YUGOSLAVIA

S. V. POPOVIC
Department of Environmental Radioactivity, Institute for Medical Research,
Zagreb, Yugoslavia

Abstract—Analysis of ^{90}Sr in foodstuffs shows that in the period from 1961 to 1965 ^{90}Sr concentration was gradually increasing in almost all foodstuffs. Since 1965 a lower concentration has been observed. At the same time, up to 1964, ^{90}Sr concentration in fallout was also increasing, but in 1964, there followed a slow, and in 1965 a very rapid, decrease of concentration.

In the literature numerous attempts have been recorded aiming at determining factors governing the ecological cycle. We too have tried to find out adequate parameters (constants). Using data about average ^{90}Sr concentration in milk and fallout during the 1962–1966 period we have calculated from the equation $C_m = a_m(Fd + 1/2\,fd) + b_M fd^*$, turning it into

$$Fd = \frac{C_M - 1/2\,fda_M - b_M fd}{a_M},$$

which should be the amount of ^{90}Sr in soil expressed in mCi/km^2. The results obtained indicate that only exceptionally is it possible to use the same constants (in this case a_M and b_M) because ^{90}Sr entry into various foodstuffs is conditioned by several factors. The same was observed when data from other countries were used for same calculations.

This is illustrated by figures presenting data about ^{90}Sr content in milk and fallout. It is clearly noticeable that the average ^{90}Sr concentration in milk in the years 1963, 1964 and 1965 remained almost the same, while the concentration of ^{90}Sr in fallout showed considerable changes.

We have also tried to apply the discrimination factor for the plant/milk, but it varied to such a degree (in some of our calculations it has been even higher than 0.4) that there would have occurred an enormous error were it used for calculating ^{90}Sr concentration in milk only on the basis of ^{90}Sr concentration in plants.

^{226}Ra AND THE NATURAL AIRBORNE NUCLIDES ^{210}Pb AND ^{210}Po IN ARCTIC BIOTA*

RICHARD B. HOLTZMAN
Radiological Physics Division, Argonne National Laboratory

Abstract—In order to better determine the characteristics and effects on humans of arctic biota with high concentrations of ^{210}Pb and ^{210}Po, these nuclides, along with their long-lived predecessor, ^{226}Ra, were measured in lichens, in bone and muscle of caribou and other arctic animals, and in Eskimo placenta. ^{226}Ra with concentrations 1/3 to 1/50 those of the other nuclides, cannot be the direct source of the other nuclides. In caribou bone the ^{210}Po was in radioactive equilibrium with the ^{210}Pb and averaged about 11.7 pCi/g ash, twice the ^{210}Pb in reindeer bone. The ^{210}Pb content of muscle of both species was 10 pCi/kg (wet). By contrast, the ^{210}Po content was much greater, about 200 pCi/kg. A definite seasonal decrease was noted in the ^{210}Pb in muscle during the second half of the year. Similar variations were indicated for ^{210}Po in muscle and for ^{210}Pb in bone. The high levels in caribou are attributed to the high fallout levels of these nuclides in lichens, their winter forage, which contain (in dry weight) 6 pCi ^{210}Pb/g and 12 pCi ^{210}Po/g. The other animals exhibited appreciably lower concentrations in bone and muscle. Wolf, which consumes large quantities of caribou, exhibited activities in bone of 1 pCi/g ash, about that observed in some Eskimo bone by Hill. The ^{210}Po content of wolf muscle was about the same as that of caribou, 200 pCi/kg, but the ^{210}Pb was only about 1 pCi/kg. Similar, but less dramatic, differences were observed in Eskimo placenta.

Estimates of uptake show that Eskimos could acquire sufficient of the long-lived ^{210}Pb to double the total skeletal radiation dose (rad) over that of Midwesterners. However, despite the high concentrations of the ^{210}Po in meat, direct intake accounts for only a relatively small increase in total dose.

BECAUSE of their ubiquity and contribution to the total radiation dose to man and animals, the naturally occurring nuclides ^{226}Ra, ^{210}Pb, and ^{210}Po have been studied extensively in man and his environment. The latter nuclides appear to enter the environment to a large extent through natural fallout, analogous to that of nuclear bomb fallout which yields nuclides such as ^{137}Cs [1-3] and ^{90}Sr. [4] In the natural case, as shown in the decay scheme of Fig. 1, ^{226}Ra in the soil decays to the inert gas, ^{222}Rn, some of which emanates into the atmosphere and decays therein through a series of short-lived species to the 21.4-year ^{210}Pb. This nuclide then decays further to the 5.0-day ^{210}Bi and to the 138-day ^{210}Po.

In Arctic biota, although relatively small concentrations of ^{226}Ra have been found, [5, 6] the concentrations of the ^{210}Pb and ^{210}Po have been found to be higher than those in analogous biota of the temperate zone. [5-9] These fallout nuclides tend to accumulate on the sedges and lichens, which because of their slow growth acquire high specific activities. This vegetation forms a substantial portion of the diet of caribou and reindeer which, in turn, constitute a substantial fraction of the diets of predators and of man in these regions. The long-lived precursor of the series, ^{226}Ra, is also of interest in the animal, both for its contribution to the dose and as a possible direct source of the ^{210}Pb series.

In order to establish the origin of the ^{210}Pb series and to determine the effects on the food chain, the possible accumulations in man,

* This work was performed under the auspices of the U.S. Atomic Energy Commission.

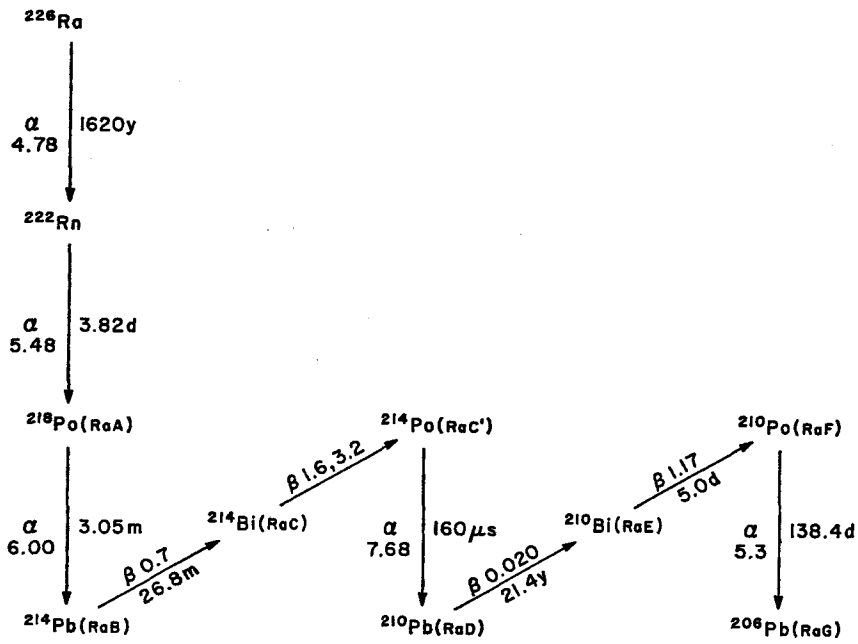

FIG. 1. Radioactive decay scheme of ^{226}Ra series.

radiation effects, and methods of reducing the accumulation of these nuclides, various studies have been made.

The winter food base, lichens, has been shown to contain relatively large amounts of both the ^{210}Pb and ^{210}Po compared to fresh grasses.[6,7] Animals consuming these plants, reindeer and caribou, have been shown to accumulate relatively large amounts of these nuclides. Reindeer muscle, kidney, liver, and spleen exhibit a high concentration of the daughter nuclide, ^{210}Po[8], which, like that of ^{137}Cs in man and caribou, is seasonally variable.[10, 11] The ^{210}Pb concentrations in reindeer and Alaskan caribou[6] account for a large fraction of the excess amounts observed in the tissues of humans whose diets consist of meat from these animals. Some bones from a group of Canadian Eskimos, measured by Hill, contained ^{210}Pb concentrations substantially higher than in others of the same group.[7, 8] Placental tissues from Alaskan Eskimos appeared to contain more ^{210}Pb and ^{210}Po than tissues of non-Arctic residents,[6] and in some groups of Canadian Eskimos the concentrations of the daughter were substantially greater than in other Canadians.[12]

Presented here are the results of further analyses of these three nuclides in Alaskan animals of various types, comparison of the ^{210}Po–^{210}Pb ratios, and a discussion of the seasonal variations of the ^{210}Pb activities in caribou and reindeer bone and muscle.

Except for these previously described samples (Tables 1–3), 62–2, 3 and 61–1, 2, from Finland and College, Alaska,[6] and all the lichens except samples 65–13, 14, 15, these samples were collected near Anatukvuk Pass in northern Alaska by W. C. Hanson of Battelle-Northwest Laboratories. The caribou muscle was taken from the hind quarter and the bone from the shaft of the rear femur of the animal. Most of these specimens had been dry-ashed at about 450°C (for ^{137}Cs analysis).

The ^{210}Po and ^{210}Pb concentrations were determined as previously described.[13] To ensure complete dissolution, the samples, even though previously dry-ashed, were wet-ashed

in nitric and perchloric acids. The solution was then converted to 0.5 N hydrochloric acid and the ^{210}Po plated onto a silver disk which was counted for alpha particles. The ^{210}Pb was determined by replating the solution after allowing the ^{210}Po to grow in for at least 3 months. The actual activities of the ^{210}Po and ^{210}Pb and the statistical errors were determined and calculated for the time of collection from the parent-daughter relationships of the Bateman equations. The calculated errors are based on counting statistics only. The ^{226}Ra was determined by the ^{222}Rn emanation method of Lucas.[14]

Along with the dates of collection, the specific activities of the various nuclides in the muscle and bone specimens of caribou are presented in Table 1. Similar data and average values for each group of other animals, reindeer, moose, willow ptarmigan, seal, fish and wolf, are given in Table 2, and for lichens in Table 3. ^{210}Po activities are presented only for samples dried at no higher than 110°C and measured within a few months of collection.

The ^{210}Pb levels in animal bone are of significance in determining the radiation levels in the animal and, in terms of human intake, as representative of average intake levels. Also because of the relatively high specific activities, the ^{210}Pb content is easier to determine in bone than in muscle. As shown in Fig. 2 the ^{210}Pb specific activities in caribou bone are nearly twice those in reindeer, which in general are more than twice those in other animals. This confirms earlier suggestions[5, 6] that, although reindeer are closely related to caribou, their dietary habits are different, even though in this case as contrasted to the previous one, the reindeer live in the same region as the caribou, i.e. the reindeer appear to run in herds and consume forage with growth more rapid than that of lichens (the specific activities of ^{210}Pb are lower), while the caribou feed more widely and probably consume more lichens. The ^{210}Pb in the bones of other animals is quite a bit lower; moose is similar to U.S. cattle;[15] and the amount of ^{210}Pb in seal and fish is still lower and similar to that in human bone from residents of the midwestern United States.[13] The high levels observed in wolf bone indicate that a large fraction of the diet of wolves is caribou meat and they attain levels similar to those of the human Eskimo bones of Hill.[8] The willow ptarmigan shows a relatively high average, mainly because one of three specimens was high, possibly because of consumption of older plants (lichens?) and a high respiratory rate.

Because muscle is probably the major tissue consumed by the man, the ^{210}Pb activity in this tissue is the most significant one in the animal. In this case, as shown in Fig. 2, the concentrations in caribou and reindeer are about the same (averaging all the samples at hand) and much higher than those of the other animals and humans. In most animals the ratio of this nuclide in bone to that in muscle is 2000 or greater, while in caribou and reindeer it is one half this ratio, even if the higher level of "winter" for caribou is taken.

The seasonal variations of the ^{210}Pb in caribou can be seen in Figs. 3 and 4 in which the concentrations in muscle and bone are plotted seasonally, regardless of year of collection. Figure 5 shows the quarterly averages with standard errors. Seasonal variations in bone are apparent and confirmed by Student's *t*-test in that the specific activity of 8.3 pCi/g ash in the fourth quarter of the year is probably significantly different than the 11.6 pCi/g ash in the other quarters ($P < 0.05$). The concentrations in these quarters are not significantly different from each other.

In muscle the seasonal variations of the ^{210}Pb are more striking (Fig. 5), and here the concentration of 9.7 pCi/kg (wet) during the first half of the year is significantly different than the 4.1 pCi/kg in the last half ($P < 0.005$). The two quarters within each half are not significantly different from each other.

These seasonal variations probably are caused by caribou feeding on vegetation high in ^{210}Pb (lichens), principally when no other vegetation is available, i.e. during the winter. Thus, as seen in muscle, a minimum would be expected during the summer or third quarter and then a rise in the last one. In bone, however, the slower rate of turnover causes a time delay which produces a minimum in the fourth quarter and also reduces the magnitude of the variations. The correlation between the ^{210}Pb in

Table 1. *^{210}Pb, ^{210}Po and ^{226}Ra in Caribou Bone and Muscle*

Sample No.	Date of collection	BONE			MUSCLE		
		^{210}Pb pCi/g ash	^{210}Po pCi/g ash	^{226}Ra pCi/g ash	^{210}Pb pCi/kg (wet)	^{210}Po pCi/kg (wet)	^{226}Ra pCi/kg (wet)
62–1	8–28–62	16.0 ± 0.2	—	0.532 ± 0.025	4.3 ± 0.6	—	1.97 ± 0.12
62–2	12–6–62	11.0 ± 0.2	15.5 ± 0.7	—	6.1 ± 0.6	222 ± 4	—
62–3	12–6–62	11.1 ± 0.2	14.6 ± 0.7	—	8.3 ± 0.6	163 ± 4	—
63–1	6–6–63	9.86 ± 0.15	—	—	4.8 ± 0.5	—	—
63–2	7–22–63	10.9 ± 0.18	—	—	1.3 ± 0.4	—	—
63–3	7–28–63	8.46 ± 0.14	—	—	3.9 ± 0.9	—	—
63–4	10–19–63	—	—	—	4.6 ± 1.3	—	—
63–5	11–25–63	5.54 ± 0.12	—	—	7.4 ± 1.1	—	—
63–6	11–25–63	5.65 ± 0.12	—	—	3.6 ± 1.3	—	0.3 ± 0.3
64–1	1–10–64	14.8 ± 0.2	—	—	12.7 ± 1.9	—	6.3 ± 1.0
64–2	1–14–64	12.4 ± 0.2	—	—	9.4 ± 1.4	—	—
64–3	2–22–64	8.95 ± 0.20	—	—	13.3 ± 1.6	—	—
64–4	2–22–64	13.4 ± 0.2	—	—	5.7 ± 0.9	—	—
64–5	3–2–64	13.2 ± 0.2	—	0.421 ± 0.020	15.8 ± 1.7	—	3.5 ± 0.6
64–6	3–16–64	12.4 ± 0.2	—	—	9.8 ± 1.4	—	—
64–7	3–16–64	7.95 ± 0.15	—	—	12.8 ± 1.7	—	—
64–8	3–17–64	7.00 ± 0.13	—	—	10.4 ± 1.6	—	—
64–9	3–17–64	10.2 ± 0.2	—	—	12.0 ± 1.7	—	—
64–10	3–26–64	14.0 ± 0.2	—	—	16.1 ± 1.6	—	—
64–11	5–9–64	9.27 ± 0.14	—	—	15.6 ± 1.7	—	—
64–12	5–24–64	11.0 ± 0.15	—	0.429 ± 0.022	10.2 ± 1.2	—	3.4 ± 0.4
64–13	5–24–64	9.88 ± 0.14	—	—	9.3 ± 1.4	—	—
64–14	6–2–64	9.81 ± 0.14	—	0.380 ± 0.020	7.8 ± 1.4	—	0.9 ± 0.3
64–15	6–4–64	12.0 ± 0.16	—	—	9.6 ± 1.6	—	—
65–1	3–21–65	20.3 ± 0.2	—	0.591 ± 0.033	4.0 ± 1.3	360 ± 7	0.3 ± 0.2
65–2	3–21–65	12.33 ± 0.16	11.8 ± 0.3	—	5.5 ± 0.7	—	—
65–3	4–24–65	17.35 ± 0.15	15.33 ± 0.26	—	11.0 ± 0.7	—	—
65–4	4–24–65	5.23 ± 0.08	4.86 ± 0.15	0.442 ± 0.015	3.1 ± 0.9	—	0.0 ± 0.2
65–5	5–28–65	9.44 ± 0.09	7.98 ± 0.12	0.466 ± 0.016	6.2 ± 0.5	—	0.09 ± 0.07
65–6	5–31–65	15.40 ± 0.14	11.18 ± 0.18	—	9.9 ± 0.7	—	—
65–7	8–18–65	18.79 ± 0.39	17.07 ± 0.59	0.698 ± 0.040	6.0 ± 1.6	72 ± 3	0.57 ± 0.019
65–8	8–18–65	17.13 ± 0.39	11.89 ± 0.34	0.554 ± 0.032	3.3 ± 1.3	87 ± 4	0.17 ± 0.15
65–9	8–24–65	11.72 ± 0.38	12.62 ± 0.12	0.488 ± 0.031	1.1 ± 1.0	97 ± 3	0.13 ± 0.13

Table 2. ^{210}Pb, ^{210}Po and ^{226}Ra in Reindeer, Moose, Ptarmigan, Wolf, Seal and Fish

Sample No.	Date of collection	BONE			MUSCLE		
		^{210}Pb pCi/g ash	^{210}Po pCi/g ash	^{226}Ra pCi/g ash	^{210}Pb pCi/kg (wet)	^{210}Po pCi/kg (wet)	^{226}Ra pCi/kg (wet)
Reindeer							
61–1	3–14–61	5.00 ± 0.11	6.33 ± 0.23	1.84 ± 0.022	15 ± 2	575 ± 36	0.3
62–4	11–1–62	8.21 ± 0.13	—	0.396 ± 0.015	3.7 ± 1.1	—	—
62–5	11–15–62	9.67 ± 0.11	—	—	6.2 ± 1.2	—	—
63–7	8–8–63	—	—	—	1.3 ± 0.6	—	—
63–8	8–8–63	6.13 ± 0.12	—	—	1.4 ± 0.7	—	—
63–9	8–8–63	4.73 ± 0.09	—	0.197 ± 0.011	1.7 ± 0.7	—	—
Average ± S.D.		6.75 ± 2.12	—	0.81 ± 0.90	4.9 ± 5.3	—	0.3 ± 0.3
Moose							
63–10	8–1–63	0.716 ± 0.042	—	—	1.5 ± 1.1	—	—
63–11	8–1–63	0.689 ± 0.042	—	0.195 ± 0.014	1.6 ± 0.7	—	0.4 ± 0.2
Average ± S.D.		0.702 ± 0.059	—	0.195	1.6 ± 1.3	—	0.4
Willow Ptarmigan							
63–12	7–27–63	6.94 ± 0.11	—	—	27.3 ± 1.9	—	—
63–13	7–27–63	1.84 ± 0.05	—	—	4.2 ± 1.3	—	11.7 ± 0.7
63–14	7–28–63	1.60 ± 0.05	—	0.031 ± 0.005	3.3 ± 0.9	—	—
Average		3.46	—	0.031	11.6	—	11.7
Wolf							
65–10	3–15–65	1.385 ± 0.034	1.315 ± 0.011	0.103 ± 0.006	1.3 ± 0.3	257 ± 5	0.12 ± 0.11
65–11	3–16–65	0.631 ± 0.022	0.634 ± 0.048	0.099 ± 0.006	2.6 ± 0.6	205 ± 5	0.23 ± 0.15
Average ± S.D.		1.018 ± 0.53	0.974 ± 0.48	0.101 ± 0.003	2.0 ± 0.9	231 ± 37	0.17 ± 0.18
Seal							
63–15	7–18–63	0.0487 ± 0.007	—	0.074 ± 0.006	2.0 ± 0.7	—	—
63–16	7–25–63	0.074 ± 0.010	—	—	2.6 ± 1.3	—	—
63–17	7–25–63	0.068 ± 0.010	—	0.064 ± 0.007	5.1 ± 1.3	—	—
Average ± S.D.		0.063 ± 0.015	—	0.054 ± 0.009	3.2 ± 1.6	—	—
Fish							
63–18	7–1–63	—	—	—	0.27 ± 0.20	—	—
63–19	8–1–63	0.289 ± 0.024	—	0.024 ± 0.006	0.76 ± 0.24	—	2.41 ± 0.13
63–20	8–24–63	0.047 ± 0.020	—	0.026 ± 0.010	1.50 ± 0.40	—	—
Average ± S.D.		0.168	—	0.025 ± 0.012	0.84 ± 0.63	—	2.41

Table 3. Lichens

	Sample No. (Old)*	Sample No. (New)	Date of collection	^{210}Pb pCi/g dry	^{210}Po pCi/g dry	^{226}Ra pCi/g dry
	Finland	61–2	3–61	4.54 ± 0.07	12.98 ± 0.12	0.035 ± 0.0010
AL	Lichens III	61–3	6–61	26.0	—	0.40 ± 0.02
AL	Lichens II	61–4	6–61	69.6	—	0.415 ± 0.017
AL	Lichens I	61–5	6–61	11.5	—	0.101 ± 0.005
AL	Rumen I	62–6	12–6–62	7.48 ± 0.06	14.28 ± 0.20	—
AL	Rumen II	62–7	12–6–62	4.96 ± 0.06	16.52 ± 0.26	—
N.H.	Lichens IV	65–12	7–10–65	7.61	7.32	—
		65–13	7–25–65	5.08 ± 0.20	7.83 ± 0.29	0.0527 ± 0.0095
		65–14	7–26–65	7.26 ± 0.23	9.77 ± 0.34	0.0318 ± 0.0082
		65–15	7–30–65	9.98 ± 0.28	17.44 ± 0.47	0.0412 ± 0.0093

* Data from first 7 specimens taken from Reference 6.

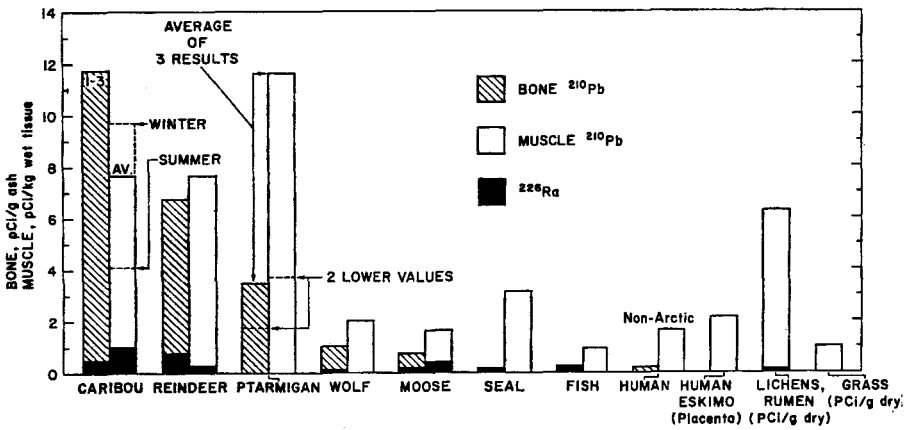

FIG. 2. ^{210}Pb and ^{226}Ra in muscle, bone and vegetation in Arctic biota and man.

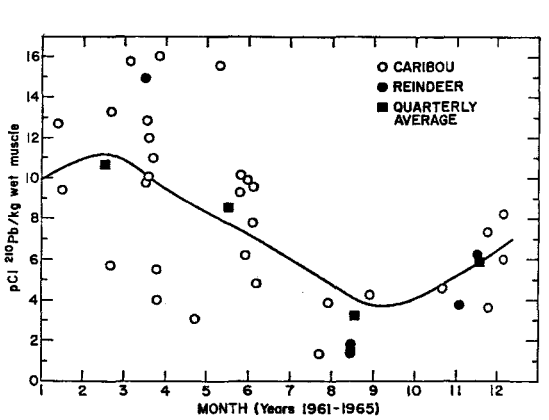

FIG. 3. ^{210}Pb in caribou and reindeer muscle.

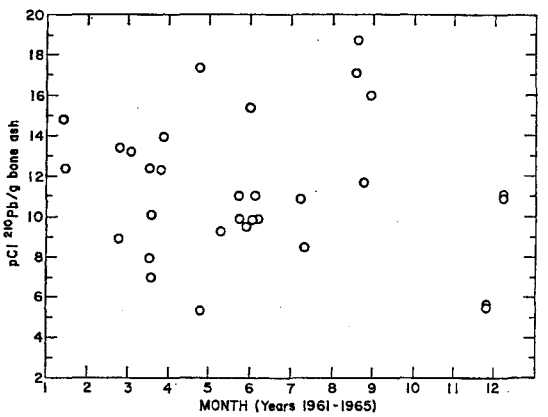

FIG. 4. ^{210}Pb in caribou bone.

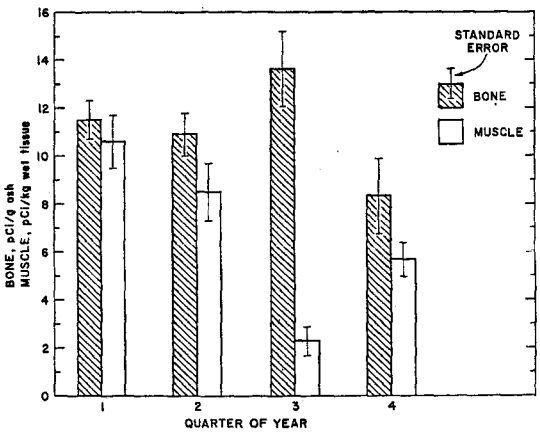

FIG. 5. Quarterly averages of ^{210}Pb in caribou muscle and bone.

muscle and that in bone from the same animal is $r = -0.36$, a value probably significantly different from zero ($P < 0.05$). This negative correlation is probably produced by a combination of the out-of-phase seasonal variations between bone and muscle and accentuated by sampling artifacts.

Although the ^{210}Po data are few, they do exhibit certain definite characteristics. In caribou bone this nuclide is in radioactive equilibrium with its parent and the seasonal variation is weak. Thus in seven specimens the ^{210}Po/^{210}Pb ratio $= 0.88 \pm 0.12$ (s.d.) and the coefficient of correlation $r = 0.91$. There is an indication of a higher ratio in the specimens collected in December. The wolf bone also exhibited radioactive equilibrium with a ratio of 0.98 (see Fig. 6).

Muscle of winter-killed caribou had more than three times the ^{210}Po concentration of summer-killed animals, but a variation less than the factor of 10 observed by Hill on Canadian reindeer.[8] The actual levels for the winter-killed animals reported here and by Hill are quite comparable while the summer-killed reindeer (15.5 pCi/kg) are significantly lower than these caribou, again probably because of the relatively lower lichen content of the reindeer summer diet.

Wolf muscle is remarkable in that the concentrations of ^{210}Pb observed here, about 200 pCi/kg, are about equal to those of caribou muscle. This effect thus suggests that other organs of the caribou supply a major fraction of the food for the wolf, i.e. liver, kidney, spleen and marrow, organs which appear to preferentially concentrate ^{210}Po by a factor of 10.[8, 9] This excess may also arise from bone consumption, rib, etc.; however, the relatively low concentrations of ^{210}Pb mitigate against this, unless this nuclide is preferentially and rapidly removed from the soft tissues.

In most, but not all cases, specific activity of the ^{226}Ra was lower than that of the ^{210}Pb and thus, the parent nuclide in the animal could not be the primary source of ^{210}Pb. Moreover, because the ages of the animals were probably less than 10 years and 70% of the ^{222}Rn would emanate anyway (by analogy to human and other bone data),[16] the ^{210}Pb could have attained only a small fraction of radioactive equilibrium.

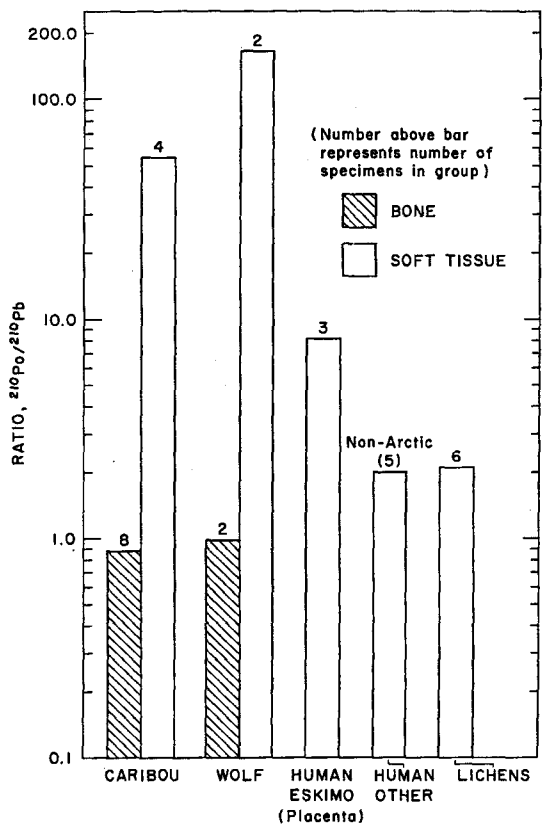

FIG. 6. ^{210}Po–^{210}Pb ratios in biota and man.

As shown in Table 1 and Fig. 2, the concentration of ^{226}Ra, 0.500 $\pm$ 0.095 (s.d.) pCi/g ash of caribou bone, was fairly consistent and about equal to that observed in bovine [17] and sheep bone, [6] a value expected on a diet of grass. Similar concentrations were observed in reindeer and moose, and levels comparable to the low ^{226}Ra levels in humans were found in ptarmigan, fish and seal. The combination of high ^{210}Pb and low ^{226}Ra levels in ptarmigan indicates a diet high in fallout products and low in ash content, such as lichens.

The wolf was somewhat higher again, indicating a relatively large ingestion of ^{226}Ra, possible either from a consumption of vegetation or herbivore bone. In the case of this nuclide, since caribou muscle and other soft tissues do not concentrate it (Table 1), these tissues would appear to be unlikely sources of excess ^{226}Ra.

The source of this nuclide in caribou and other animals appears to be vegetation other than lichens, since as seen in Table 3 most of these contain little ^{226}Ra. The high correlation of ^{226}Ra content in the lichens with fraction of ash content suggests the ash to be mainly dust contamination, so that the true digestible level of this nuclide is that in the Finnish sample which also had a low ash content. [6]

Seasonal variations in lichens are not accessible from these data. However, they confirm the previous conclusion [6] that the specific activity of the ^{210}Po may be greater than that of its parent ^{210}Pb. Because the atmospheric concentrations of ^{210}Po are lower than those of ^{210}Pb and there is no reason to expect great differential retention of the ^{210}Po over its parent from air, this result implies either greater uptake of ^{210}Po from soil or greater leaching of the parent from the plant.

The specific activities of ^{210}Pb and ^{210}Po measured in caribou muscle reported here are quite a bit higher than the concentrations in human placenta, which in wet tissue for ^{210}Pb are 1 to 5 pCi/kg and for ^{210}Pb are 9 to 30 pCi/kg. [6] These values are higher than in non-Arctic soft tissues and about equal to those found in the muscles of animals other than caribou. Hill, on the other hand, found some placentae with even higher ^{210}Po concentrations, 30 to 100 times these. [12]

These data allow some estimation of the size of the sources of the nuclides available to the groups of humans consuming caribou meat and confirm the conclusions of an earlier paper [6] that Eskimos may ingest daily 4 or more times the ^{210}Pb of non-Arctic residents. On the other hand, Beasley and Palmer's data for ^{210}Pb in caribou meat of 30 pCi/kg imply the levels of ^{210}Pb intake in some cases may be another factor of 3 or more times that estimated here. [9] Muscle tissue from the other animals, except ptarmigan, would not appear to contribute much of this nuclide to the diet.

The average contribution of the daughter, ^{210}Po, to the diet is probably somewhat smaller than previously estimated since seasonal variations are present and radioactive decay during storage further reduces the concentrations. Thus, we estimate, from the exponential model of nuclide metabolism below, [18] that with intakes of 50 to 90 pCi/day, the soft tissue concentrations relative to those in non-Arctic residents would be doubled,

$$T_{ef}\frac{mC}{I} = \frac{T_{ef}}{0.693}$$

where m is the mass of the body,* C is the concentration of the nuclide, I is the daily intake, T_e is the half-life of the nuclide in the body,* and f is the fraction of the nuclide entering the body.* It should be noted, however, that the ^{210}Po derived from direct ingestion would then constitute an even smaller fraction of the ^{210}Po present since most of it is derived from the much higher ^{210}Pb body content in Arctic residents. [19]

The ^{226}Ra contribution to the human diet from the caribou is fairly low being about 1 pCi/day from 900 g of meat, a value comparable to the 2 pCi/day in non-Arctic residents. [14] Again most other animals would contribute even less, except in the case of fish where this value might be doubled. Fish may also contribute substantially more since to a large extent the bone may be consumed. Unless some other sources of ^{226}Ra are present in the Eskimo diet, the body content of this nuclide would be

* Organ or tissue of interest may be substituted for "body".

expected to be about the same as that for other unexposed population groups.

The dose rates to caribou could be quite appreciable, as shown by Beasley and Palmer,[9] as high as 0.45 rad/yr to the liver. However, over the whole year the average dose might be only half of this. In bone on the other hand with little seasonal variation, the average dose is about 0.4 rad/yr, which, with the dose from other natural sources, would produce a dose about 3 times that to the "average cow" of Lucas and Di Ferrante.[15] If one assumed an RBE of 10, the skeletal dose would be about 4 rem/yr. The dose levels in reindeer would be about one half these.

The dose to human populations dependent on caribou meat may possibly be inferred from those observed in wolf in which the ^{210}Po–^{210}Pb skeletal concentrations are about 1 pCi/g ash. The specific activity of each nuclide in non-Arctic humans is about 0.145 pCi/g ash,[13] which with an RBE of 10, is equivalent to a dose rate of about 50 mrem/year from a total skeletal dose rate of 185 mrem/year. Thus, a concentration of 1 pCi/g ash is equivalent to a total dose of 500 mrem, 2.7 times the non-Arctic dose. However, if the effective dose is that delivered to the 10-μ layer of surface cells of bone,[20] the increase in dose would be about 100 mrem/yr, an increase in total dose rate of about 60%.

Although the levels of ^{210}Po are apparently greatly increased in human placenta, the actual increase in dose would be only about 10%. On the other hand if the levels are comparable to those in wolf muscle (200 pCi/kg) and some of Hill's specimens of placenta,[12] this would double the dose. These numbers, although small compared to the dose in bone, may be of relatively greater significance because the radiation effects to soft tissue may be greater than in bone.

The very high levels of these nuclides observed in wolf and in the human bone and placental specimens of Hill[8, 12] suggest that the assumed sources of these nuclides bear further investigation since it appears unlikely that these sources, caribou and reindeer muscle, can supply the large concentrations observed by Hill. Thus, the following things bear closer examination: the possibility of systematic errors of measurement; that these measurements are representative of diets and other exposure of these high-level subjects; and that the exponential model of nuclide metabolism describes these nuclides with any degree of accuracy.

The available information indicates that the measurements are probably reasonably reliable in that results from different laboratories and by different methods are reasonably consistent.[6-10] The metabolic model, which is accepted primarily for lack of a better model, could be in substantial error.[18] However, even less is known about the high level subjects. Precise studies of these people, their work, dietary and smoking habits, and health could be valuable; and although epidemiological studies might be unprofitable because of the small population receiving high dose rates, intensive studies of metabolic balance, that is, actual intake, excretion and body content of these nuclides, might be valuable in establishing the various parameters and theoretical considerations.

ACKNOWLEDGEMENTS

I gratefully acknowledge the help with this project, particularly to W. C. Hanson, D. G. Watson and F. P. Hungate of Battelle–Northwest Laboratories for collecting and sending the samples, to F. H. Ilcewicz for the analyses, and to L. D. Marinelli for helpful discussion and encouragement.

REFERENCES

1. K. Liden. *Acta Radiol.* **56,** 237 (1961).
2. H. E. Palmer, W. Hanson, B. I. Griffin and W. C. Roesch. *Radioactivity in Man,* Meneely and Linde, eds. (Charles C. Thomas, Springfield, Ill., 1965), p. 527.
3. J. K. Miettinen, Aili Jokelainen, P. Roine, K. Liden, Y. Naversten, G. Bengtsson, E. Häsanen and R. C. McCall. *Annales Academiae Scientiarum Fennicae Series A. II. Chemica* **120** (1963).
4. A. R. Schulert. *Science* **136,** 146 (1962).
5. Richard B. Holtzman. Argonne National Laboratory, Radiological Physics Division Summary Report, ANL-6769, p. 59 (1963).
6. Richard B. Holtzman. *Nature* **210,** 1094 (1966).
7. C. R. Hill. Pb^{210} A naturally occurring component of "fallout". Symposium on Radioactivity in Scandinavia, Denmark, October 1964.
8. C. R. Hill. *Nature* **208,** 423 (1965).

9. THOMAS M. BEASLEY and HARVEY E. PALMER. *Science* **152,** 1062 (1966).
10. GÖRAN K. SVENSSON and KURT LIDEN. *Health Physics* **11,** 1393 (1965).
11. W. C. HANSON and H. E. PALMER. *Health Physics* **11,** 1401 (1965).
12. C. R. HILL. *Science* **152,** 1261 (1966).
13. RICHARD B. HOLTZMAN. *Health Physics* **9,** 385 (1963).
14. H. F. LUCAS, JR. Argonne National Laboratory, Radiological Physics Division Semiannual Report ANL-6297, p. 55 (1961).
15. HENRY F. LUCAS, JR. and ELVIRA R. DI FERRANTE. *Radiation Research* **27,** 718 (1966).
16. W. P. NORRIS, T. W. SPECKMAN and P. F. GUSTAFSON. *American Journal of Roentgenology* **73,** 785 (1955).
17. ELVIRA R. DI FERRANTE. *Health Physics* **10,** 259 (1964).
18. International Commission on Radiological Protection, Committee II on Permissible Dose for Internal Radiation (1959). *Health Physics* **3,** 1 (1960).
19. R. B. HOLTZMAN. *Health Physics* **10,** 763 (1964).
20. Report of the United Nations Scientific Committee on the Effects of Atomic Radiation: Supplement 16 (A5216), p. 418 (Total dose to bone and to bone cells), and Robert E. Rowland, Argonne National Laboratory, Radiological Physics Division Annual Report ANL-7060, p. 64 (1965).

POLONIUM-210 IN ITALIAN TOBACCO

N. CARFÌ and R. DUGNANI LONATI
Laboratori CISE, Segrate, Milano

Abstract—It is known that ^{210}Po contained in tobacco is volatile at the temperature of a burning cigarette. Hence a radiation hazard from ^{210}Po may arise for a smoker's bronchial epithelium.

Hence measurements of ^{210}Po were started in most popular Italian cigarettes. A later stage of the work will consider the tobacco from some Italian regions. Polonium was extracted from tobacco samples by a wet ashing procedure and plated on nickel discs. The discs were mounted on ZnS phosphors and the alpha activity was counted. The polonium alpha spectrum was measured by an ionization chamber. The method can be simply carried out, but difficulty arises from the low-background alpha counting necessary for determining accurately the minute quantities of ^{210}Po (of the order of 10^{-2} pCi).

INTRODUCTION

Some authors [6, 8, 9] have suggested that ^{210}Po is a factor in the genesis of bronchial cancer in smokers. This nuclide—decay product of ^{210}Pb, having a 19.4 year half-life—is an alpha emitter with a 138 day half-life. The principal modes of introduction into the human body are (1) through almost all foods (vegetables, fruits, water, etc.); (2) as natural fall-out due to radon disintegration products escaping into the atmosphere from the soil; (3) as contamination in smoke from tobacco.

Considering tobacco, it is well-known that polonium is volatile at the temperature of a burning cigarette and can therefore be absorbed with smoke. Neglecting, for the time being, any consideration of how natural radioactivity enters the lungs through smoke and therefore on the dose to the organ, the ^{210}Po concentration is being measured in tobacco grown in Italy. In order to analyse in more detail the absorption of this nuclide in the plant, we also intend to examine:

(a) how it is distributed in leaves, roots and bark;
(b) what is the degree of radioactive equilibrium between the ^{210}Po and its parent ^{210}Pb;
(c) whether it is absorbed by plants directly from the soil or through deposition on leaves of natural fall-out contained in the atmosphere or by a combination of both.

A number of tobacco plants were therefore chosen in various plantations of an Italian region. The leaves are treated in the laboratory, some of them being fresh and the others being cured. Later a determination will be performed of the radioactive content of the soil in which they have been growing. Finally to investigate the absorption mechanism from leaves and roots a series of plants has been grown with hydroponic culture in a glasshouse. Some of these will be exposed to an atmosphere rich in radon, others will be nourished with ^{210}Pb and ^{210}Po solutions. The oldest tobacco samples to be found in Italy will also be studied.

The first part of the work was concerned with the ^{210}Po content in the most popular Italian cigarettes, that is Alfa, Nazionali, Nazionali Esportazione and Nazionali Super. Preference was given to types that are cured with Italian tobacco blends.

ANALYTICAL METHODS

1–2 g of tobacco previously dried at 105°C are digested in 70 ml of cold concentrated

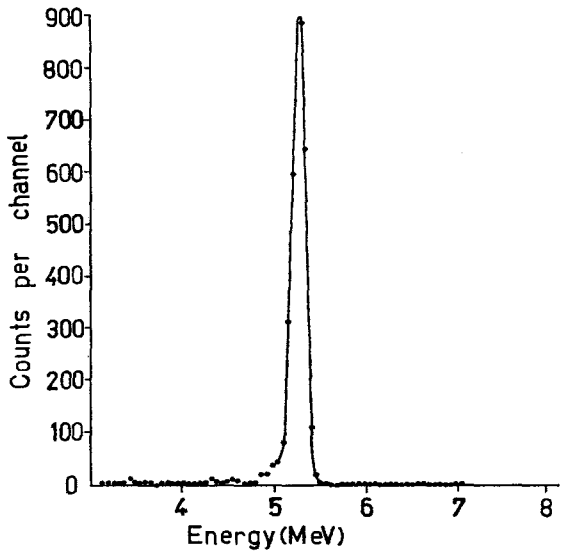

FIG. 1. α-spectrum of a sample of 2 g of tobacco, using an ionization chamber. Counting duration was 25 hr.

HNO_3. This is then heated in a water bath for about 4 hr and subsequently in a sandbath until 10–20 ml remains. 20 ml of 70%$HClO_4$ are added and the solution is heated again in the sandbath until fuming. It is then cooled and cautiously diluted with distilled water until the solution is 20–30 ml. It is neutralized with 18 N NaOH and is re-acidified with 0.1 N HCl to dissolve possible metallic hydroxides. It is filtered and washed with 0.1 N HCl adjusting the volume to 200 ml. 200 mg of ascorbic acid are then added to eliminate possible interference due to trivalent cations present in the solution (i.e. Fe). The solution is then poured into the plating cell which is placed in a thermostatic bath at 90°C. ^{210}Po plating is carried out on Ni discs (previously pickled with heptane, acetone and then dried) by stirring the solution at 250 rpm. The deposition time was 4 hrs. Calibration tests showed that the deposition recovery is of the order of 90%.

The deposition cell consists of a commonly used commercial baby nursing bottle with the bottom removed. The Ni disc diameter is 36 mm.

The deposits were measured by means of ZnS(Ag) scintillation counters with an extremely low background equal to 0.36 ± 0.05 counts/hr. The ZnS(Ag) layers were 50 mm in diameter. The mean of several reagent blank determinations was 1.1 ± 0.1 counts/hr. The counting efficiency of 45% was determined with electrolytically plated ^{239}Pu calibrated sources.

Alpha particle spectroscopy was performed on several samples using an ionization chamber. This confirmed that only ^{210}Po was present.

The results obtained are reported in pCi/g of dry tobacco in Table 1 below. These results have been corrected for the yield of the chemical separation and counting efficiency, taking into account the activity due to the ^{210}Po collected on the filter during the chemical processing.

Table 1. ^{210}Po content of Popular Italian Cigarettes

Type of cigarette	^{210}Po pCi/g of tobacco (mean value)
Alfa	0.37 ± 0.03
Nazionali	0.48 ± 0.03
Nazionali Esportazione	0.53 ± 0.03
Nazionali Esport. Super	0.42 ± 0.04

REFERENCES

1. F. A. SMITH, R. J. DELLA ROSA and L. J. CASARETT UR-305 (1955).
2. S. C. BLACK. UR-463 (1956).
3. R. B. HOLTZMAN. Some determinations of the RaD and RaF concentrations in human bone. ANL-6199 (1960).
4. S. C. BLACK. *Health Physics* **7,** 87 (1961).
5. E. P. RADFORD, JR., V. R. HUNT and D. SHERRY. *Radiation Research* **19,** 298 (1963).
6. E. P. RADFORD JR. and V. R. HUNT. *Science* **143,** 247 (1964).
7. T. C. TSO, N. A. HALLDEN and L. T. ALEXANDER. *Science* **146,** 1043 (1964).
8. E. P. RADFORD, JR. and V. R. HUNT. *Science* **144,** 366 (1964).
9. E. P. RADFORD, JR. and V. R. HUNT. *Science* **146,** 87 (1964).
10. L. P. GREGORY. *Science* **150,** 74 (1965).
11. I. YAVIN, G. DE PASQUALI and P. BARON. *Nature* **205,** 899 (1965).
12. R. L. BLANCHARD. *Anal. Chem.* **38,** 189 (1966).

CONTAMINATION WITH POLONIUM-226, URANIUM AND RADIUM-226 DUE TO SMOKING

M. KILIBARDA, D. PETROVIĆ, D. PANOV and D. DJURIĆ
Institute of Occupational Health, Dept. of Radiological Protection,
Beograd, Pasterova 14/II, Yugoslavia

Abstract—The content of ^{210}Po, ^{226}Ra and uranium has been examined in well-known Yugoslavian cigarettes and in tobaccos from regions of Yugoslavia where the best tobacco is produced. Simultaneous measurements were made of the content of these nuclides in the urine of smokers and non-smokers.

The distribution of ^{210}Po in smoke, ash and cigarette stubs as a function of combustion temperature was studied. Values of ^{210}Po in cigarettes ranged from 0.4–0.6 pCi/g, ^{226}Ra below 10^{-12} Ci/g and uranium was less than 5γ/g of cigarette.

Analysis of the distribution of ^{210}Po has shown that about 40% is found in smoke. The urinary ^{210}Po values in smokers and non-smokers are different, but there is no significant statistical difference between them.

So far more than 270 organic substances and 15 elements have been identified in cigarette smoke. These could be divided into four main groups from the toxicological point of view:

(1) nicotine and similar alkaloids,
(2) irritants like aldehydes,
(3) substances binding on blood pigments like carbon monoxide (1), cyanides (2), etc.,
(4) carcinogenic substances like radionuclides, arsenic, chromium, nickel, etc.

Recently more and more attention has been paid to the radionuclide content of tobacco and cigarettes. Turner and Radley[3] and Mulvaney[4] observed high radioactivity in cigarette ash. Mulvaney[4] ascribed this radioactivity to the presence of ^{40}K, and later to ^{87}Rb. He discussed the hazard to the respiratory tract due to smoking. Spiers and Passey[5] consider that the specific radioactivity of ^{40}K is very low and could not represent a real hazard. On the other hand Ash[6] calculated that the radioactivity of ^{40}K in the smoke could cause carcinogenic effects. Runeckless[7] studied the radioactivity of the whole cigarette, the stub and smoke. This author established that 90% of the total radioactivity was in the ash and only 1% is inhaled.

Turner and Radley[3] paid attention to the alpha-radioactivity of the smoke. They showed low alpha-activity due to radon and thoron, the relative quantity being 1% of the total activity. Radford and Hunt[8] studied the ^{210}Po content in the cigarette, stub and smoke. The quantity of ^{210}Po in one cigarette is within the limits 0·39–0·48 pCi and about half of this quantity is inhaled by smoking. These authors calculated that by smoking two packs of cigarettes daily a dose of about 5 rem could be reached in 25 years of smoking. If the distribution is not uniform, local doses could reach 165 rem in 25 years. These doses could cause carcinogenic effects. Skrable *et al.*[9] pointed out that the lung model used by Radford and Hunt is not identical with the lung model proposed by ICRP and concluded that the real doses are lower.

Gregory[10] determined ^{210}Po in tobacco leaves from four countries. Tobacco from New Zealand had a mean value of 0·15 pCi of ^{210}Po per gram; from the U.S.A. and South Africa about 0·49 pCi/g and in Rhodesian tobacco even more. Russian authors[11] established that

tobacco contains 0·43 pCi ^{210}Po per gram and that filter tips could contain 10% of ^{210}Po from the smoke. Brown and Jarvis[12] analyzed the ^{90}Sr content of Canadian tobacco, concluding that this radionuclide does not represent a carcinogenic hazard. Kelly[13] studied ^{210}Po in the inhaled cigarette smoke and established values between 0·029 to 0·044 pCi per type of cigarette. Yavir *et al.*[14] performed spectroscopic analysis of the ^{210}Po content of cigarettes and found quantities similar to Radford and Hunt. Chaterjee *et al.*[15] analyzed the radium content in tobacco ash and found about 0·5 pCi per cigarette.

Some time ago we started to study various sources of radioactive contamination of uranium miners[16-19] and therefore we wished to establish the content of ^{210}Po uranium and radium in Yugoslavian tobacco and cigarettes.

METHOD

Tobacco was digested in the following way: to one gram of tobacco (content of one cigarette) 1 ml of distilled water and 2 ml of fuming HNO_3 was added and slowly digested for 2 hr. Another 5 ml of distilled water and 1 ml of conc. H_2O_2 was added and heated to dryness. Some drops of perchloric acid were then added to digest organic substances and the standard procedure was followed for the determination of ^{210}Po by deposition on silver foils.[20] Determination of polonium in the urine of smokers and non-smokers was performed by the same method.

Uranium was determined using a fluorimetric method[21] and radium indirectly by the determination of radon.[22]

RESULTS AND DISCUSSION

We studied the content of ^{210}Po, uranium and radium in the four most popular kinds of cigarettes and tobaccos from the most important region in Yugoslavia. We paid special attention to tobaccos from the region around uranium mines.

We also studied the distribution of ^{210}Po in the cigarette, smoke and butt and the smoking habits of 25 smokers.

We also analyzed the uranium and radium content of cigarettes and tobaccos. The results obtained were very low and so unreliable that statistical evaluation was impossible.

In Table 1 the results of ^{210}Po determinations of four popular kinds of Yugoslavian cigarettes are presented. It is obvious that some differences exist in the ^{210}Po content. The mean value of ^{210}Po in cigarettes is 0·38 pCi/g. These results are in accordance with those of Radford and Hunt,[8] and very similar to American[10] and Russian[11] results.

It is very interesting to correlate the absorption of ^{210}Po during smoking with excretion of ^{210}Po in the urine of smokers and non-smokers.

To study this correlation we had to establish the smoking habits of Yugoslavian smokers. We measured the temperature of the glowing part of Yugoslavian cigarettes and established that the temperature is 600–650°C. It is known[23] that ^{210}Po is volatilized at this temperature but we checked this fact by adding standard concentrations of ^{210}Po to cigarettes. The ratio of ^{210}Po in the smoke and butt was equal to the ratio between the mass of the whole cigarette and the butt (4: 1).

Table 1. *Activity of* ^{210}*Po in Yugoslavian Cigarettes*

Kind of cigarette	Number of samples	Mean value in pCi/g
"Morava"	5	0·36 ± 0·30
"Ibar"	10	0·20 ± 0·14
"Drava"	9	0·36 ± 0·10
"Zeta"	10	0·60 ± 0·08

Total mean value = 0·38 ± 0·13 pCi/g.
1 cigarette = 1 g.

Table 2. Activity of ^{210}Po in the Urine of Smokers and Non-smokers

	Number of samples	Mean value in pCi/litre	Standard error	*T*-test	
Smokers	20	0·60	±0·05	2·70	0·05
Non-smokers	9	0·37	±0·07		

We examined the smoking habits of 25 Yugoslavian smokers and established that in smoking a cigarette, the smoker:

inhales	30%
combusts	45%
leaves in the butt	25%

Because of ^{210}Po volatilization the same proportions are applicable for this substance. We conclude that smokers inhale about 30% of ^{210}Po present in the cigarette. Therefore, smokers are exposed to a higher quantity of ^{210}Po than non-smokers. In this case a higher excretion of ^{210}Po in the urine of smokers is to be expected.

Urine of 20 smokers and 9 non-smokers was analyzed for ^{210}Po and the results are presented in Table 2. After statistical evaluation of the results it was established that a significantly higher concentration exists in the urine of smokers. This increase is caused by the smoking of cigarettes.

We also wished to establish if differences exist in the ^{210}Po content of tobaccos from various regions of Yugoslavia. From the Institute of Tobacco Research in Beograd, we obtained representative samples of tobaccos from the most important producing areas of Yugoslavia. The results of these determinations are presented in Table 3. We established that statistically significant differences between these tobaccos are not evident. The mean value of these tobaccos was 0·405 pCi of ^{210}Po per gram and we presume that this value represents a mean value for Yugoslavian tobaccos.

We wished to compare this value with ^{210}Po content of tobaccos from some regions around uranium mines. We analyzed tobaccos grown around the uranium mine of Kalna and the uranium field at Pirot and these results are presented in Table 4. In only one case (Inovo at Kalna) we found a significant difference from the Yugoslavian mean value, presented in Table 5.

SUMMARY

We have established that the ^{210}Po content in Yugoslavian tobaccos is about 0·405 pCi/g and for cigarettes 0·38 pCi/g. If a man smokes 20 cigarettes per day containing 7·6 pCi of ^{210}Po he will inhale 30% which is 2·3 pCi per day.

In the urine of smokers we found an increase of 0·23 pCi of ^{210}Po compared with the

Table 3. Activity of ^{210}Po in Tobaccos from Most Important Yugoslavian Areas

	Area	Number of samples	Mean value in pCi/g	Standard error
1	Hercegovina, Stolac	4	0·36	±0·05
2	Vojvodina, Novi Sad	6	0·76	±0·12
3	Makedonija, Prilep	10	0·52	±0·08
4	Srbija, Knjaževac	11	0·36	±0·04
5	Srbija, Pirot	4	0·40	±0·04

Total mean value (excluding No. 2 sample): 0·405 ± 0·153 pCi/g.

Table 4.

	Area	Number of samples	Mean value in pCi/g	Standard error
1	Knjaževac, Trgoviste	11	0·36	0·09
2	Kalna, Inovo	6	0·84	0·09
3	Pirot, Cerova	4	0·40	0·04
4	Pirot, Sugrin	2	0·40	Small number
5	Pirot, Ragadeš	2	0·60	Small number
6	Pirot	2	0·52	Small number

Table 5. *Statistical Evaluation of Results obtained near Oil Field and Uranium Mine with Mean Value for Yugoslavian Tobaccos*

Number of samples	Area	Mean value	Standard error	*T*-test	*P*
35	Yugoslavian tobaccos	0·405	±0·153	4·73	0·01
6	Novi Sad (oil field)	0·76	±0·12		
6	Kalna, Inovo (uranium mines)	0·84	±0·09	6·12	0·01

excretion of non-smokers. Knowing that normal diuresis is 1–1·5 l. of urine per day, we would conclude that of the inhaled ^{210}Po about 10–15% is absorbed and excreted.

The polonium content in various tobaccos and cigarettes does not vary very much over various regions of the country. We obtained an increase in only one place in the vicinity of a uranium mine (Inovo at Kalna) and also in one case at Novi Sad (No. 2 in Table 3) where the oil fields are located.

It would be of interest to continue this study by analyzing the polonium content in plants, soils and waters in the vicinity of oil fields and uranium mines.

REFERENCES

1. F. Valić and D. Djurić. *Arh. hig. rada* **5,** 49 (1954).
2. D. Djurić, P. Raičević and I. Konstantinović. *Arch. Environm. Health* **5,** 12 (1962).
3. R. C. Turner and M. M. Radley. *Lancet* **i,** 1197 (1950).
4. D. K. Mulvaney. *Lancet* **i,** 205 (1953).
5. F. W. Spiers and R. D. Passey. *Lancet* **ii,** 1259 (1953).
6. M. Ash. Cit. Runeckless, ref. 7.
7. V. C. Runeckless. *Nature* **191,** 322 (1961).
8. E. P. Radford and V. R. Hunt. *Science* **143,** 247 (1964).
9. W. K. Skrable, F. J. Haughey and E. L. Alexander. *Science* **143** (1964).
10. L. P. Gregory. *Science* **150,** 74 (1965).
11. A. P. Ermalieva, L. A. Percov and D. K. Popov. IV Naučno praktičerska konferencija po radiacionoj gigieni. Leningrad, 15–20 mart 1965.
12. J. Brown and A. Jarvis. *Med. Service J. Canada* **20,** 613 (1964).
13. Kelly. *Science* **149,** 537 (1965).
14. I. A. Yavir, G. De Pasquali and P. Baron. *Nature* **205,** 899 (1965).
15. R. K. Chaterjee, P. Banerji, N. N. Ghosh and S. D. Chaterjee. *Science and Culture* **31,** 188 (1965).
16. D. Djurić, D. Panov, M. Kilibarda, Lj. Novak and M. Vukotić. *Radiological Health and Safety in Mining and Milling of Nuclear Materials*, Vol. II, p. 431, IAEA, Vienna 1964.

17. D. KARAJOVIĆ, M. KILIBARDA, D. PANOV, D. DJURIĆ, M. MEDJEDOVIĆ, P. RAIĆEVIĆ and V. DELIĆ. *Ibid.* p. 443.
18. R. DAJLEVIĆ, D. DJURIĆ, H. FRANCOIS, D. ROCHE-DAJLEVIĆ, D. PANOV and P. SIGLI. *Compte Rendu du Colloque Franco-Yougoslave*, Herceg-Novi, 24–27 September 1963, Vol. I.
19. D. DJURIĆ, M. KILIBARDA, LJ. NOVAK, D. PANOV and M. VUKOTIĆ. *Health Physics* **10,** 1059 (1964).
20. J. B. HURSH. Redactor: Chemical methods for routine bioassay. AECU-4024.
21. L. WÓDKICWICZ. Fluorometric determination of uranium in urine. Polish Academy of Sciences Report No. 234/VIII, Warsaw, 1961.
22. J. PRADEL and E. FUHRMAN-BENCIX. *Bull. d'Information Scient. et Techn. Franc.* No. 2, 1956, p. 12.
23. A. SMITH, J. DELLA ROSA and L. CASARETT. University of Rochester. UR-305.

WILD DEER AS A SOURCE OF RADIONUCLIDE INTAKE BY HUMANS AND AS INDICATORS OF FALLOUT HAZARDS*

F. W. WHICKER, G. C. FARRIS AND A. H. DAHL
Department of Radiology and Radiation Biology, Colorado State University,
Fort Collins, Colorado

Abstract—Concentrations of various fallout radionuclides were measured in native forage and in tissues of wild mule deer over a five-year period in north-central Colorado. Concentrations of ^{137}Cs in deer flesh were 5 to 13 times higher than concentrations reported in beef and in pork. The data indicated that consumption of deer flesh could result in a ^{137}Cs intake which could possibly exceed the intake of the nuclide from all other items of the total diet combined. Consumption of deer liver would result in the ingestion of ^{144}Ce, ^{137}Cs, ^{54}Mn, and ^{106}Ru. The data indicated that deer tissues can be useful and in some cases, unusually sensitive indicators of environmental contamination by ^{144}Ce, ^{137}Cs, ^{131}I, ^{54}Mn, ^{106}Ru, and ^{90}Sr. Relationships between forage and deer tissue for ^{137}Cs, ^{131}I, and ^{90}Sr were investigated. During 1963, the radiation dose to the skeleton of yearling deer from ^{90}Sr averaged 330 mrad, which was generally higher than the total dose from natural background and other sources combined. During the same period, the ^{90}Sr concentrations in deer bone were higher by a factor of 35 than reported bone levels in humans. During the study, dose rates to deer thyroid, liver, and muscle reached 20, 0.014, and 0.012 rad/year, respectively.

INTRODUCTION

Studies on radionuclide levels in tissues of wild mule deer (*Odocoileus hemionus hemionus*) during the past four years demonstrated that this animal accumulated measurable concentrations of ^{137}Cs, ^{144}Ce, ^{131}I, ^{54}Mn, ^{106}Ru, and ^{90}Sr. Nuclide concentrations measured were usually considerably higher than those measured in domestic meat products during the same periods. Since flesh of deer and other wild game is consumed by some segments of the human population, it was of interest to study this particular food item.

In addition, because deer accumulate measurable concentrations of fallout, they can be convenient and sensitive indicators of environmental contamination. Deer are harvested in large numbers in many areas of the world through sport, commercial, and control hunting. Samples can also be obtained through mortality from automobiles, disease, starvation, and predators.

Radionuclide levels and calculated dose estimates for deer were much higher than for most humans. Thus, assuming similar radiosensitivities between the species, one could possibly observe radiation effects from fallout in deer populations at considerably lower levels of environmental contamination than would be necessary to produce effects in the bulk of the human population. It therefore seems that we should be concerned about potential indirect effects of radiation on man through damage to the native plants and animals upon which man ultimately depends. In general ecological terms, it is difficult to assess the importance of deer to the well-being of mankind. It is obvious that reindeer and caribou are essential to the Lapps and Eskimos of the arctic regions, but the importance of this family of animals to most Americans for example, is likely more subtle. In economic terms, however, it was estimated that during 1964 in the state of Colorado alone, 168,319 hunters spent over $30 million [1]

* Work supported by Contract No. AT(11-1)-1156 between the U.S. Atomic Energy Commission and Colorado State University.

in pursuit of deer, killing approximately 118,840 animals.[2]

METHODS

All sampling was done within the Cache la Poudre drainage west of Fort Collins, Colorado. The area comprises about 580 square miles and ranges between 5200 and 13,000 feet in elevation. Deer were collected weekly from February 1962 to January 1965 from a uniform distribution of locations within the study area by personnel of the Colorado Department of Game, Fish and Parks. Certain deer tissues were also obtained in larger numbers from hunters during October and November of 1961 and 1962.

Quantitative assay for gamma emitters was accomplished by gamma-ray spectrometry. The counting system included a solid 4 in. thick × 8 in. diameter NaI (Tl) crystal which was mounted over three matched photomultiplier tubes and surrounded by 5 in. steel shielding. Electrical pulses were stored in a transistorized 400 channel pulse height analyzer. Gamma-ray spectra were resolved by matrix inversion using an IBM 1620 computer. Samples were counted in bulk form under uniform conditions of geometry. Standards were prepared by contaminating water contained in the same geometrical configurations as the samples in question, with known quantities of each radionuclide requiring consideration.

Strontium-90 was assayed by counting beta particles from the ^{90}Y daughter after chemical separation and preparation. Ground and ashed bone samples were dissolved in nitric acid and the strontium was separated and purified by a series of precipitations with fuming nitric acid. The purified strontium solution was allowed to stand until secular equilibrium of ^{90}Y was established. Yttrium was separated from the ^{90}Sr solution as the hydroxide and converted to the oxalate which was mounted on a plastic disc for counting with a Sharp laboratories low background flow-gas beta counter.

RESULTS AND DISCUSSION

Radionuclide Intake by Humans

From the standpoint of radionuclide transfer to humans from deer, ^{137}Cs is probably the most important. During our studies, deer flesh contained considerably higher mean concentrations of ^{137}Cs than beef and other meats (Table 1). For example, from July 1962 through April 1963, deer flesh contained higher mean ^{137}Cs concentrations than United States beef and pork[3] by factors of approximately 13 and 11, respectively. Comparisons with beef from the Fort Collins, Colorado area[4] during 1962 and 1963 indicated that deer flesh ^{137}Cs concentrations averaged higher than stall-fed and pasture cows by a factor of at least 5. Data indicate that this difference could be explained by normally higher fallout levels in deer forage and possibly by a higher transfer coefficient (flesh/feed ratio) in deer. The percentage of the daily ^{137}Cs intake per kg meat averages less than 4% in cattle (J. E. Johnson, unpublished data) while we have calculated possible values of 15 to 30% in deer.

Comparisons were also made between possible intake of ^{137}Cs from deer flesh and from the total diet (Table 2). In October, November, and December of 1962, the average dietary intake rate of ^{137}Cs in Chicago, New York, and San Francisco was approximately 51 pCi/day.[5] During the same period, deer flesh averaged 575 pCi ^{137}Cs/kg and if one consumed the average U.S. human meat intake of 200 g/day,[5] the intake rate from this source alone would amount to approximately 115 pCi/day. In a similar comparison, the total dietary intake rate of ^{137}Cs in Denver, Colorado institutions during 1964 was 150 pCi/day.[6] The mean ^{137}Cs concentration in deer flesh during 1964 was 872 pCi/kg[7] which could yield a possible intake rate of about 175 pCi/day from deer meat alone. Individual deer collected in 1963 contained as much as 3300 pCi ^{137}Cs/kg of flesh which could lead to an intake rate by humans of 660 pCi/day.

It must be stressed that past and current fallout levels have not been sufficiently high to make deer flesh hazardous for human consumption. Based on present knowledge, the levels of ^{137}Cs would have to be increased by several orders of magnitude to produce somatic effects in deer or in humans.

Since deer liver is considered a choice food item by most hunters, samples collected from May 1963 to August 1964 were assayed for gamma-ray emitting fallout radionuclides.[8] It

Table 1. Comparison of ^{137}Cs Concentrations in Flesh of Colorado Deer with Beef and Pork

Period	Mean ^{137}Cs concentrations in pCi/kg		
	Deer	Beef	Pork
July 1962–April 1963	698(40)	55(52)*	
July 1963–Oct. 1963	1526(16)		133(52)*
April 1962–Nov. 1963	1213(76)	226(20)†	

Sample sizes given in parentheses.
* United States averages.[3]
† Pasture and feedlot cattle from Colorado.[4]

Table 2. Comparison of Possible ^{137}Cs Intake from Colorado Deer Flesh with Intake from the Total Diet

Period	Probable ^{137}Cs intake in pCi/day		
	Deer flesh alone*	Total diet, Tri-cities[5]	Total diet, Denver Institutions[6]
Oct.–Dec. 1962	115	51	
Jan.–Dec. 1964	175		150

* Based upon the average US daily meat intake of 200 g/day.[5]

Table 3. Summary of data on Gamma-ray Emitting Fallout Radionuclides Measured in 43 Colorado Mule Deer Livers from May 1963 to August 1964[8]

Nuclide	Nuclide levels in pc/Kg		Probable amount ingested by humans during period in pCi/liver*
	Means	Std. Dev.	
^{144}Ce	1420	1060	2420
^{137}Cs	440	290	750
^{54}Mn	230	160	390
^{106}Ru	460	370	780

* The adult deer liver weighs approximately 1.7 kg.[9]

was found that ^{144}Ce, ^{137}Cs, ^{54}Mn, and ^{106}Ru were present in liver in readily measurable concentrations. A summary of these data is given in Table 3. It appears that the probable amounts of fallout radionuclides ingested by humans from deer liver during 1963 and 1964 were relatively small. Nevertheless, liver tissue may be a relatively unique but likely insignificant vector for human consumption of ^{144}Ce, ^{54}Mn, and ^{106}Ru.

The chance of ^{131}I being transferred to humans from deer thyroid appears to be very small because of the short half-life of ^{131}I and because this gland is not ordinarily consumed by humans.

Deer are probably not important ^{90}Sr vehicles to humans because we have found that at least 97% of the total body burden of strontium is located in bone which is not ordinarily consumed by humans.

Deer as Indicators of Fallout Levels

Estimation of fallout levels in a given environs is difficult to accomplish with precision because of the normally large sampling variations. Under certain conditions, it may be helpful to sample a free-roaming native animal population, rather than air, soil, or vegetation, because each individual would carry radionuclide burdens which would be more or less representative of an integrated sample of forage from a certain area for some period of time. Also, the concentrations of certain radionuclides in animal tissues may exceed considerably the concentrations in forage or air and in these instances, animal tissues would be simpler to assay with precision. Of course, the problems of sampling variability would still exist for the animal population and an appropriate sample size and sampling design would still need to be determined. Once this was accomplished, the relationship between plant and animal for instance, must be established and this relationship may be subject to rather large uncertainties. We have investigated some radionuclide relationships between deer and native forage.

The correlation coefficient of 0.90 between mean ^{137}Cs levels in deer flesh and in native forage plants which we previously reported,[7] indicates that levels of environmental contamination with this nuclide could be estimated using deer samples. We have found an accumulation of about 0·24 pCi ^{137}Cs/g deer flesh per pCi ^{137}Cs/g air dry vegetation (assuming equilibrium conditions). Of course, the concentrations of ^{137}Cs in deer flesh would reflect levels of the nuclide in the plants consumed by deer and not necessarily the other types of plants which may be preferred by domestic grazing animals.

Earlier communications[10-13] have demonstrated the high sensitivity of deer thyroids for estimating levels of environmental contamination with ^{131}I. More recent data indicate that ^{131}I can be detected in deer thyroids during periods when it is below the detection limit in milk,[13] forage samples,* or in rabbit thyroids. Deer thyroids appear to have concentrations of ^{131}I similar to rabbit thyroids but the deer thyroid usually contains approximately 25–50 times more tissue which greatly facilitates ^{131}I detection and measurement.

Schultz and Longhurst[16] have measured fallout ^{90}Sr in jaw bones of California deer and we have previously discussed factors affecting ^{90}Sr accumulation in Colorado deer.[17, 18] We have found that in 4–5-month-old deer, the skeleton accumulates about 9 pCi ^{90}Sr/g bone ash per pCi ^{90}Sr/g air dry plant material. This simple linear relationship would not hold true for older deer, however, because equilibrium of ^{90}Sr is not reached rapidly as in the case of ^{137}Cs and the bone levels would be slow to respond to rapid changes in forage levels.

* The estimated equilibrium relationship between ^{131}I in deer thyroid and forage indicates that the thyroid concentration could exceed the forage concentration by at least 1000-fold:

$$\frac{\text{thyroid } ^{131}I \text{ conc.}}{\text{forage } ^{131}I \text{ conc.}} = \frac{(1500 \text{ g forage/day})\ (0.3 \text{ ingested to thyroid}^{(14)})\ (7.6 \text{ days}^{(14)})}{(0.693)\ (4 \text{ g/thyroid})} = 1{,}235$$

This calculation is in reasonable agreement with experimental work on continual ingestion of ^{131}I by sheep.[15]

Table 4. Estimates of Radiation Dose Rates to the Skeleton of Yearling Colorado Mule Deer from Various Sources during 1963

Source	mrad/yr
^{90}Sr in bone	330*
Natural background and terrestrial fallout	250–350†
^{137}Ce in muscle	12

* Calculated from mean concentrations of ^{90}Sr in yearling deer bones by a method described elsewhere.[21]

† Based on measurements taken in the Cache la Poudre drainage, Colorado with a calibrated portable scintillation counter.

Schultz has also discussed advantages and disadvantages in using deer antlers for monitoring ^{90}Sr.[19]

Since deer liver accumulates isotopes such as ^{144}Ce, ^{54}Mn, and ^{106}Ru which seldom can be measured in other organs and tissues commonly assayed, the liver may be useful for estimating environmental concentrations of these particular nuclides.[8].

Fallout Hazards to Deer

Although radiation doses to deer from fallout radionuclides during this study have been orders of magnitude lower than those required to produce somatic damage in other mammals, the estimated doses to certain tissues have been higher than natural background levels. Furthermore, the doses received by deer from fallout materials have been considerably higher than doses received by the general human population. It should be pointed out, however, that Lapps[20] and Eskimos received doses from ^{137}Cs which were probably higher than the ^{137}Cs doses received by Colorado deer.

From the standpoint of potential harm to deer from fallout, ^{90}Sr is probably the most important radionuclide to consider. For example, in 1963, it was estimated that the dose to the skeleton of yearling deer was probably greater from ^{90}Sr than from all other sources combined. Estimates of these sources and their relative importance are given in Table 4. It was also found that during 1963, ^{90}Sr concentrations and radiation doses in bone of yearling deer were higher by a factor of about 35 than in 0–20-year-old humans from New York, Chicago, and San Francisco.[22]

Doses to deer thyroids have been low in comparison to a dose required to produce adenomas. However, during the one-year period from April 1962 to April 1963 these deer received a thyroid dose of about 20 rad,[11] which approaches the maximum permissible annual thyroid dose of 30 rad for radiation workers.

Doses to deer liver tissue from fallout radionuclides were estimated to approach 110 mrad/lifetime or approximately 14 mrad/year during this study.[8]

ACKNOWLEDGEMENTS

The authors wish to thank A. E. Anderson and D. E. Medin, Colorado Department of Game, Fish and Parks for providing deer samples and other supplementary data. R. A. Walters, Colorado State University, collaborated on the assay of liver samples and J. E. Johnson, V. Schultz, and G. M. Ward made helpful suggestions during preparation of the manuscript.

REFERENCES

1. Anonymous. The economic value of hunting and fishing to the people of the state of Colorado, 1964. Colorado Department of Game, Fish and Parks, Denver, Colo., 2 p. mimeo. (1965).
2. Colorado Department of Game, Fish and Parks. 1964 *Annual Report*, p. 27 (1965).

3. L. R. SETTER, D. SMITH and M. SPECTOR. *Radiol. Health Data* **7,** 145 (1966).
4. G. M. WARD and J. E. JOHNSON. *Health Phys.* **11,** 95 (1965).
5. J. RIVERA and J. J. KELLY. *Radiol. Health Data* **5,** 434 (1964).
6. Public Health Service. *Radiol. Health Data* **6,** 371 (1965).
7. F. W. WHICKER, G. C. FARRIS, E. E. REMMENGA and A. H. DAHL. *Health Phys.* **11,** 1407 (1965).
8. F. W. WHICKER, R. A. WALTERS and A. H. DAHL. *Nature, Lond.* **214,** 511 (1967).
9. A. E. ANDERSON and D. E. MEDIN. Colorado Department of Game, Fish and Parks. Unpublished data (1966).
10. W. C. HANSON, F. W. WHICKER and A. H. DAHL. *Science* **140,** 801 (1963).
11. W. C. HANSON, A. H. DAHL, F. W. WHICKER, W. M. LONGHURST, V. FLYGER, S. P. DAVEY and K. R. GREER. *Health Phys.* **9,** 1235 (1963).
12. F. W. WHICKER, E. E. REMMENGA and A. H. DAHL. *Health Phys.* **11,** 293 (1965).
13. F. W. WHICKER, G. C. FARRIS and A. H. DAHL. *J. Wildl. Mgmt.* **30,** 781 (1966).
14. International Commission on Radiological Protection. *Health Phys.* **3,** 193 (1960).
15. L. K. BUSTAD, L. A. GEORGE, JR., S. MARKS, D. E. WARNER, C. M. BARNES, K. E. HERDE and H. A. KORNBERG. *Rad. Res.* **6,** 380 (1957).
16. V. SCHULTZ and W. M. LONGHURST. *Radioecology.* Edited by V. Schultz and A. W. Klement, Jr., p. 73, Reinhold Publ. Corp., New York (1963).
17. F. W. WHICKER, G. C. FARRIS and A. H. DAHL. *Radioecological Concentration Processes.* Edited by B. Aberg and F. P. Hungate, p. 621, Pergamon Press, New York (1967).
18. G. C. FARRIS, F. W. WHICKER and A. H. DAHL. *Strontium Metabolism.* Edited by J. M. A. Lenihan, J. F. Loutit and J. H. Martin p. 93, Academic Press, New York (1967).
19. V. SCHULTZ. *J. Wildl. Mgmt.* **29,** 33 (1965).
20. K. LIDEN and Y. NAVERSTEN. *Assessment of Radioactivity in Man,* Vol. II, p. 167. International Atomic Energy Agency, Vienna (1964).
21. National Bureau of Standards. *NBS Handbook* 52, U.S. Dept. of Commerce, p. 31 (1953).
22. J. RIVERA and J. H. HARLEY. U.S. Atomic Energy Commission, Health and Safety Laboratory, HASL-163, p. 8 (1965).

PRE-OPERATIONAL SEARCH FOR BASELINE RADIOACTIVITY, CRITICAL FOOD AND POPULATION GROUP AT THE TARAPUR ATOMIC POWER STATION SITE

P. R. KAMATH, I. S. BHAT, A. A. KHAN and A. K. GANGULY
Preoperational Environmental Survey Laboratory, Tarapur
Health Physics Division, Atomic Energy Establishment, Trombay,
Bombay 74, India

Abstract—Two reactors each of 200 MWe are under construction at Tarapur, 100 km north of Bombay on the west coast. A pre-operational environmental survey laboratory was set up in 1964 to carry out environmental investigations and research.

In the first phase of the pre-operational programme 45 monitoring stations were established in the 0–32 km region from the station and nearly 1200 environmental samples were examined for natural and fallout radioactivity and trace element content. Information on social habits of people, land utilization and dietary habits were collected during the survey trips. In the near zone (0–8 km) of the reactors detailed information on dietary items and food consumption were collected from 100 families belonging to different professions and socio-economic groups.

Applying the data obtained from assays of environmental samples and demographic surveys, an attempt is made to predict the possible critical food and critical group of population in the region.

In the Indian diet most of the fallout contamination is obtained from cereals (predominantly from rice). Exposure from activation products is likely through intake of fish harvested from shore waters. $^{90}Sr/Ca$ ratios in Tarapur and New York diets are surprisingly in close agreement. However, Ca in N.Y. diet comes from milk, fish and meat whereas in Tarapur diet it comes from cereals and vegetables. The same observation applies to the availability of P in the two diets.

It is observed that the fishing population in the area could be the critical group in the environment under normal operating conditions.

THE Tarapur Atomic Power Project (TAPP) site is on the west coast of India nearly 100 km north of Bombay. Two power reactors each of 200 MWe are under construction to go into operation in 1968.

Figure 1 gives the location of the TAPP site, monitoring stations and gamma radiation levels in the environment. The site gets heavy rains (up to 250 cm) from S.W. monsoons during the months of June–September, which constitute the principal source of fresh water. The land is flat up to about 16 km from the coastline and is used for farming. There is considerable export of fruits and hay from the area to adjacent towns and Bombay. A hold-up water reservoir is being built at Sakharepada beyond the 16 km zone for a supply of water to the power station, housing colony and for agricultural use. The project housing colony is beyond the 8 km range.

Being a coastal site with a headland jutting out of the coastline, the land spreads in a 170° arc behind the site. The coastal region is a popular fishing ground and fishermen live close to the site at Ghivali, Pophran and Dandepada. Between 4.8 km and 8 km from the reactors there are creeks where oysters and clams seasonally exist along with a luxuriant growth of sea weeds. There is an oyster farm at Uchali, 5 km away and a larger farm at Kelwa within 20 km. Dahanu in the north and Sathpathi in the south, both within 16 km from the station,

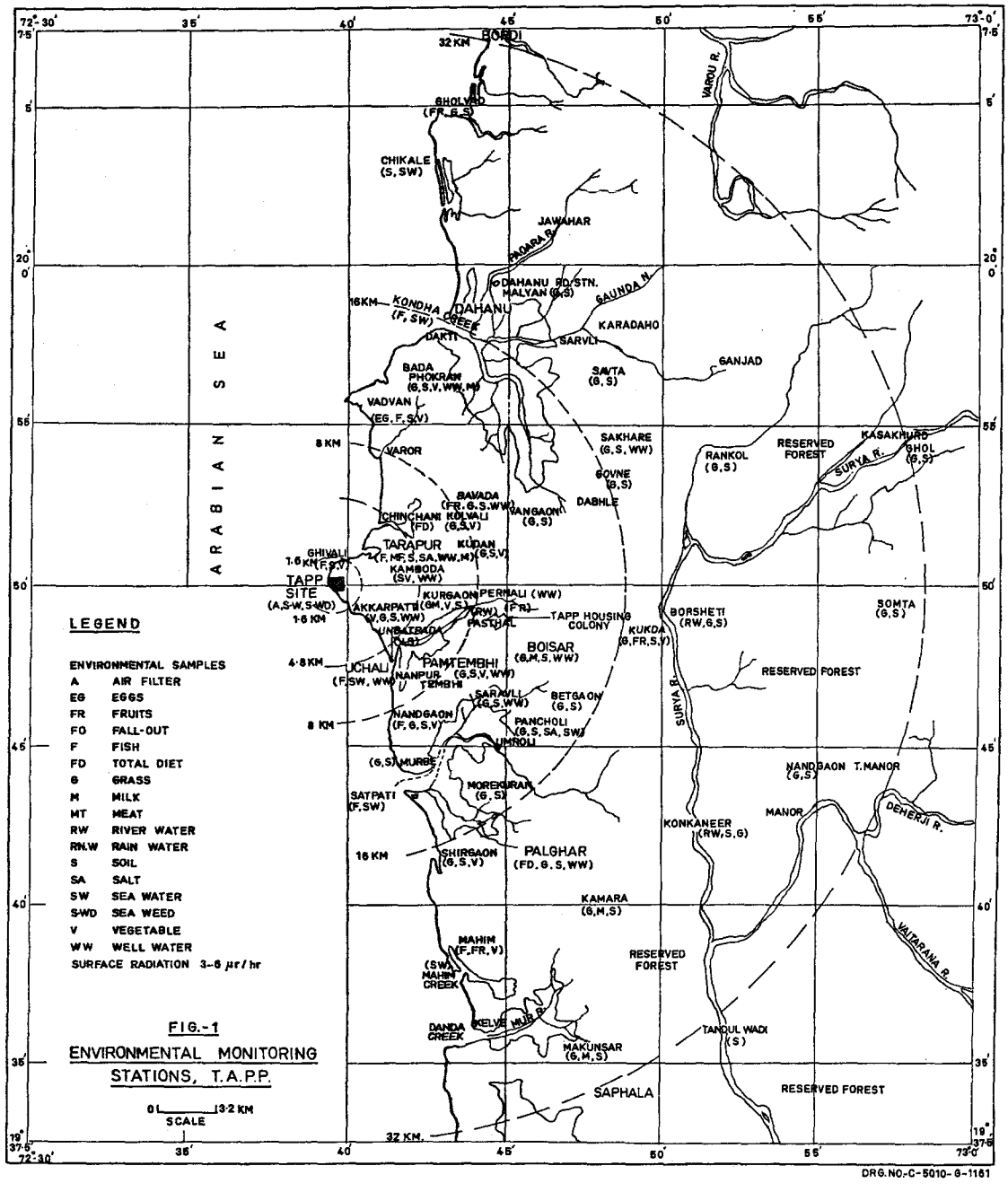

FIG. 1. Environmental monitoring stations, TAPP

are important fish landing centres. Large catches of pomfrets (*Pampus argenteus*) and Bombay duck (*Harpondon neherus*) are seasonally landed in these centres.

Table 1 gives the population and area under cultivation in the region up to 8 km from site. The principal population (1961 census) centres and occupations of the people in the 0–8 km zone are:

Ghivali (Pop. 2083)	Fishing.
Tarapur (Pop. 4232)	Agriculture, fishing, poultry farming and sea salt production.
Chinchani (Pop. 8446)	Agriculture, fishing, business and poultry farming.
Dandepada (Pop. 800)	Fishing.
Kudan (Pop. 1045)	Agriculture.
Kolvali, Bavada (Pop. 1097)	Vegetables and fruits farming, agriculture.
Akkarpatti, Pophran (Pop. 1950)	Fishing, agriculture.
Kurgaon (Pop. 492)	Cattle fodder cultivation, agriculture.
Pamtembhi (Pop. 2000)	Agriculture, hay production.
Uchali, Nawapur (Pop. 2890)	Fishing, oysters and poultry farming.

A pre-operational environmental survey laboratory was set up at the project site in December 1964 for environmental investigations and research. The paper presents:

1. Baseline radioactivity levels in the 0–8 km region of the TAPP site environment.
2. Distribution of significant elements and radionuclides in the different components of food and in the total diet.
3. Then attempts to identify the group in the population which would receive the highest exposure from environmental contamination.

BASELINE DATA

Survey programmes were drawn up first to monitor land and land produce, sea water, sea food, drinking water supplies and air in the 0–32 km region from the site. 1200 dietary and environmental samples were analysed for radioactivity and stable elements (Bhat *et al.*[1]). The results obtained for ^{90}Sr, ^{137}Cs, ^{226}Ra and stable elements like Ca, K, P, Sr, Mn and Zn are summarized in this paper.

Table 2 gives the values of particulate fallout activity in air at the site, ground deposited activity and rainfall between April 1965–March 1966. The air activity reported is the sum of weekly continuous air samples and fallout contamination on a roof top (16 m above ground), collected in polythene lined trays for dry deposition and plastic buckets during precipitation. The air activity was observed to be a maximum during pre-monsoon periods of April, May and early June and during these months the dust load in the atmosphere was also observed to be high. Air activity was a minimum during monsoon periods of June, July and August and ground deposition was maximum during these months.

The results of radionuclides and trace element determinations in soil, grass, water and foods are given in Tables 3–10.

Table 1. *Population and Land Under Cultivation within* 8 *km zone*

Zone from site km	Area in 170° arc (land) km²	Farming area km²	Total population (1961 census)
0–1.6	3.8	—	500
1.6–4.8	30.7	9.4	10,257
4.8–8.0	61.5	24.4	17,020

Table 2. Fallout Activity in Air and Ground Deposition (April 1965–March 1966)

Months	Air activity		Ground deposition		Rainfall mm
	^{90}Sr $\times 10^{-3}$ pCi/m^3	^{137}Cs $\times 10^{-3}$ pCi/m^3	^{90}Sr $\times 10^{-2}$ mCi/km^2	^{137}Cs $\times 10^{-2}$ mCi/km^2	
April 1965	36.0	74.0	5.7	8.5	—
May 1965	45.0	65.0	6.1	7.0	—
June 1965	21.2	26.4	73.0	85.0	475.7
July 1965	2.5	11.3	96.0	108.0	871.4
August 1965	3.7	4.2	29.0	31.0	239.8
Sept. 1965	4.5	6.4	16.7	25.0	1.8
Oct. 1965	3.8	5.2	4.1	7.1	—
Nov. 1965	3.6	7.3	No sample		—
Dec. 1965	2.6	4.9	1.7	2.5	—
Jan. 1966	6.3	9.3	0.8	1.2	—
Feb. 1966	11.6	15.5	0.9	1.4	—
March 1966	10.4	21.6	0.7	1.0	—

Table 3. Radioactivity and Stable Elements in Surface Soils

S. No.	Location	g/kg		pCi/kg		
		Ca	K	^{90}Sr	^{137}Cs	Ra (α)
1	Ghivali	2.06	0.64	45.0	135.0	1.8×10^3
2	Akkarpatti	11.70	8.00	35.0	47.0	2.94×10^3
3	Bavada	7.48	2.50	91.0	146.0	0.52×10^3
4	Kamara	10.10	1.36	84.1	126.0	0.37×10^3
5	Wangaon	—	6.90	138.0	224.0	0.83×10^3
6	Chinchani	9.58	2.19	24.0	54.0	1.8×10^3

Table 4. Fallout Radioactivity in Grass

S. No.	Location	Description (Local names)	nCi/kg of dry (110°C) grass	
			^{90}Sr	^{137}Cs
1	Kurgaon	Root and mat grass	0.88	1.81
2	Boisar	Root and mat	0.98	0.92
3	Badaphokran	Root and mat	0.45	1.09
4	Betegaon	Para grass	0.14	0.38
5	Palghar	Para grass	0.03	0.36
6	Kamara	Ber grass	0.11	0.64
7	Morekuran	Grass from cattle grazing land	0.23	1.09
8	Kamara	Kolum paddy grass	1.07	2.35
9	Vadhvan	Kudruk paddy grass	0.72	1.33
10	Kolvali	Dangi paddy grass	0.27	0.75
11	Umroli	Jirbhotty paddy grass	0.20	0.32
12	Murbe	Patni paddy grass	0.95	1.86
13	Akkarpatti	Berseem grass	0.14	1.47
14	Wangaon	Moosa grass	0.03	0.53
15	Betegaon	Gajraj grass	0.14	0.53

Table 5. Stable Elements and Radioactivity in Freshwater Samples

Location	Description	ppm					^{90}Sr pCi/l.	^{137}Cs pCi/l.	$^{226}Ra \times 10^{-6}$ pCi/ml
		Ca	K	Sr	Mn	Zn			
Sakhare-pada	Drinking water from the pond	58.0	0.005	—	0.013	0.08	**	**	6.30
Parnali	Drinking water from well	29.5	0.005	0.52	0.004	0.08	**	**	*
Tarapur	Well water	106.7	0.005	—	0.006	0.16	**	**	11.70
Borsheti	Surya river water	27.2	0.005	0.22	0.005	0.15	**	**	7.50
Pasthal	Banganga river water	25.0	0.005	—	0.003	0.02	**	**	0.20

* Below detection limit for 2 litre sample.
** Below detection limit for 10 litre sample.

Table 6. Stable Elements and Radioactivity in Fruits

Fruits	g/kg (wet wt.)		mg/kg (wet wt.)			pCi/kg (wet wt.)		
	Ca	K	Sr	Mn	Zn	^{90}Sr	^{137}Cs	^{226}Ra
Chikkoo (*Achras sapota*)	1.15	2.36	5.25	1.58	1.10	4.24	12.40	—
Banana (*Musa paradisiaca*)	0.13	3.60	4.10	1.13	0.82	Nil	10.80	—
Papaya (*Carica papaya*)	0.32	0.80	1.08	0.19	0.31	1.04	5.04	1.35
Jamboo (*Cugenia jambos*)	0.28	0.84	1.02	0.53	0.29	1.89	8.44	0.48
Peru (guava) (*Psidium guyava*)	0.19	2.16	1.60	1.68	1.12	3.54	22.50	2.06
Mangoes (*Mangifera indica*)	—	—	—	—	—	8.80	24.18	1.05
Palmtree fruit (*Borassus fabellifer*)	0.23	0.78	0.51	0.92	0.65	—	10.30	—

Table 7. Stable Elements and Fallout Activity in Milk

S. No.	Location	g/litre		mg/litre			pCi/litre	
		Ca	K	Sr	Mn	Zn	^{90}Sr	^{137}Cs
1	Kurgaon	1.41	0.88	1.55	0.14	2.88	11.45	21.0
2	Kamara	1.16	0.98	1.16	0.14	2.15	8.38	22.2
3	Makunsar	1.63	0.96	0.83	0.15	—	12.50	25.9
4	Gholvad	1.45	1.13	—	—	—	4.00	15.0
5	Badaphokran	1.41	1.12	—	—	—	10.80	25.9
6	Boisar	1.29	1.50	—	—	—	13.90	32.4

Table 8. Stable Elements and Radioactivity in Typical Vegetables and Condiments

S. No.	Vegetable	g/kg (wet wt.)		mg/kg (wet wt.)			pCi/kg (wet wt.)		
		Ca	K	Sr	Mn	Zn	^{90}Sr	^{137}Cs	Ra (α)
1	Radish root	0.37	2.96	1.90	1.03	2.20	10.90	6.65	3.30
2	Radish leaves	2.80	1.30	14.00	4.75	1.04	6.30	18.80	7.38
3	Brinjals	0.27	0.91	0.70	1.25	1.35	4.37	6.84	1.78
4	Spinach	0.47	10.00	—	—	—	5.24	2.90	12.90
5	Tomato	—	2.14	—	—	—	—	13.50	—
6	Okra (*Bendhi*)	0.59	0.89	—	—	—	15.40	19.70	3.34
7	Gowar (*Cyanopsis psoraliodes*)	1.30	2.40	—	3.80	1.90	19.10	60.40	11.70
8	Onion (bulb)	0.51	1.68	4.05	2.00	1.35	11.90	6.00	2.26
9	Onion (leaves)	1.06	2.12	5.40	3.20	1.30	3.10	5.30	2.30
10	Tondli (*Coccinia indica*)	0.28	1.25	—	—	—	1.40	9.36	1.98
11	Chillies (*Capsicum*)	0.14	0.90	—	—	—	12.40	45.70	—
12	Cabbage	0.50	1.60	—	—	—	2.36	8.50	—
13	Pumpkin (*Cucuribita*)	0.08	0.25	1.25	0.15	0.22	4.25	3.76	0.26
14	Coconut kernel	0.18	—	2.84	3.46	2.80	**	0.90	0.21
15	Coconut water	0.28	0.24	15.10	1.17	1.24	**	0.76	0.07
16	Tamarind (*Tamarindus indica*)	0.32	1.28	3.96	1.24	2.14	10.70	23.30	0.62
17	Betel leaves (*Piper betel*)	0.58	5.25	15.30	14.60	1.85	87.00	191.00	21.80
18	Plantain leaves	1.94	7.50	—	—	—	83.00	99.00	13.4

** Below detection limit.

Table 9. Stable Elements and Fallout Activity in Soft Tissues of Sea Food

S. No.	Sea food	g/kg			mg/kg			pCi/kg	
		Ca	K	P	Sr	Mn	Zn	^{90}Sr	^{137}Cs
1	Pomfret	1.90	2.64	0.79	1.62	1.85	3.20	1.4	2.50
2	Bombay duck (*Harpodon nehereus*)	1.70	1.60	0.64	8.90	0.53	1.53	*	4.95
3	Prawns	1.34	1.25	1.12	10.90	0.67	3.40	*	13.40
4	Shrimps	0.57	1.04	0.83	—	1.70	3.04	*	9.25
5	Oysters	0.79	1.34	0.56	3.20	4.35	5.30	4.1	8.90

* Below detection limit.

Table 10. *Stable Elements and Radioactivity in Local Rice Samples*

Local varieties of rice	g/kg		mg/kg			pCi/kg		
	Ca	K	Sr	Mn	Zn	^{90}Sr	^{137}Cs	^{226}Ra
Dangi	0.12	2.01	2.85	11.86	11.60	11.10	49.00	1.50
Jirbhotty	0.13	2.36	2.12	14.75	13.50	12.30	29.78	2.86
Kolum	0.22	1.61	—	—	—	4.44	29.10	—
Kudruk	0.10	2.34	—	—	—	10.10	31.20	—
Patni	0.21	2.53	2.23	15.10	11.05	10.24	10.10	—

DIETARY SURVEY

Dietary surveys have been carried out in India by the Indian Council of Medical Research and other national bodies periodically and statistical data have been compiled to prepare the *Diet Atlas of India.*[3] Such national data are of somewhat limited applicability when one considers the special conditions of a small region in a large country. For example, in a preliminary demographic survey, it was observed that the *per capita* fish consumption by the fishing community in the region of interest is about an order of magnitude higher than the *per capita* consumption in the state. Thus critical food evaluation required detailed study in the small area of the reactor environment, where sections of people falling in the category of special groups have to be defined on the basis of variations in dietary composition and daily intakes of minerals.

Table 9 gives the distribution of adults, children and occupation of the 100 families surveyed.

The first dietary survey was undertaken to cover 100 families to obtain a daily *per capita* food consumption. The families were chosen to cover the wide range of professional types: farmer, fisherman, businessmen, teachers, etc. (cf. Table 11).

Data on food habits of the families were compiled by checking weekly purchases and consumption for a month.

Table 12 gives the daily *per capita* intake of food by the three major groups in the population. Each person above 12 years of age was taken as one unit and each child (2–12 years) as a half unit; infants below 2 years were not considered for the computation.

In classifying the dietary information the following preliminary observations are made:

(i) Of the 100 families, only 10 indicated that they did not consume any fish, meat or eggs. Even amongst the declared non-vegetarians, diet principally (80%–90%) consists of rice, pulses and vegetables.

(ii) The cereals in the diet consist besides rice of small quantities of wheat, millets and jowar.

DISCUSSIONS ON INTAKE OF ELEMENTS AND RADIONUCLIDES

Daily intakes of significant elements and radioactivity were calculated from the diet components for two major groups of the local population within 2.4 km from the sea shore. Tables 14 and 15 give the daily intake data for farmers and fishermen. ^{226}Ra activity in the tables was calculated from ^{226}Ra activity reported by Chhabra[4] for the food stuffs obtained in Bombay.

Elemental intake from meals (2 meals a day) served in hotels (cf. Table 13) in the area agree reasonably well (except for K) with the intakes computed for farmers and fishermen from individual diet components. This agreement also demonstrates the consistency of elemental intakes by different groups of people in the environment.

Ca, ^{90}Sr AND Sr

Ca intake and pCi ^{90}Sr/g Ca ratios in New

Table 11. *Occupational Distribution of Families in the Diet Survey*

Occupation	Distance from sea shore km	No. of families surveyed	Members in the family		
			Adults and children > 12 yr	Children (12–2 yr)	Infants (< 2 yr)
Farming	(a) 0–2.4	25	171	61	15
	(b) > 2.4	27	207	71	11
Fishing	(a) 0–2.4	11	62	24	9
	(b) > 2.4	—	—	—	—
Business	(a) 0–2.4	4	12	9	1
	(b) > 2.4	7	50	12	7
Teaching and clerical trades	(a) 0–2.4	7	41	9	4
	(b) > 2.4	3	17	8	2
Miscellaneous (carpenters, mechanics, diemakers, electricians)	(a) 0–2.4	10	63	23	3
	(b) > 2.4	6	21	13	3
Total		100	644	230	55

Table 12. *Per Capita Dietary Data of Major Population Groups around TAPP*
(*Results of survey of* 100 *families*)

Dietary item	Farmers near the sea coast*	Farmers in the interior†	Fishermen	Average for Tarapur	Average for Maharashtra
	(Consumption per day in grams)				
Rice	575.0	465.0	490.0		
Wheat	49.5	29.4	81.3	552.7	444.0‡
Pulses	50.6	46.3	22.1	133.0	55.0
Vegetables	129.0	103.0	66.0	54.6	105.0
Fruits	10.0	10.0	5.0	10.2	18.0
Milk	97.0	110.0	38.0	115.0	113.0
Fish	65.0	41.5	170.0	74.3	14.0
Mutton	17.8	22.2	10.0	16.3	
Chicken	4.7	6.2	2.4	3.9	14.0
Eggs (No.)	(0.14)	(0.16)	(0.04)	(0.13)	
Salt	18.4	11.2	19.6	15.8	15.0
Sugar	29.2	26.2	30.6	22.6	38.0
Jaggery	27.6	19.7	24.0	20.8	
Fats	31.4	30.0	32.4	25.9	31.0
Chillies	7.1	6.7	8.1	7.0	NA
Tamarind	13.3	7.8	14.9	10.5	NA
Total	1125.6	935.2	1014.4	1072.4	
Water (litres)	(3–5)	(3–5)	(3–5)	(3–5)	(3–5)

* Within 2.4 km from coast.
† Beyond 2.4 km from coast.
‡ Includes millets, wheat and other cereals (rice 108 g) (*Diet Atlas of India*, 1964).

Table 13. *Stable Elements and Radioactivity in Meals served in Hotels*

Location	Description	Ca g/meal	K g/meal	Sr mg/meal	Mn mg/meal	Zn mg/meal	P g/meal	^{90}Sr pCi/meal	^{137}Cs pCi/meal	Ra α pCi/meal
Tarapur	Rice plate	0.26	0.65	1.69	2.89	2.62	0.368	4.56	20.32	1.26
Chinchani	Vegetarian meal	0.28	0.29	2.60	2.20	1.50	—	5.80	7.80	—
Palghar	Vegetarian meal	0.27	0.29	0.81	3.50	—	—	7.10	20.30	—
Palghar	Vegetarian meal	0.14	0.52	1.40	1.90	1.81	0.217	5.58	11.46	1.18
Palghar	Non-vegetarian meal	0.47	0.50	2.95	4.29	4.76	0.216	—	—	—
Dahanu	Vegetarian meal	0.23	1.79	3.04	7.54	5.24	0.639	—	—	—

Table 14. *Daily Intake of Some Significant Elements and Radionuclides by Farmers*

Food material	Farmers near the coast								
	Ca g	K g	mg			μg	pCi		
			Sr	Mn	Zn	I	^{90}Sr	^{137}Cs	^{226}Ra
Rice	0.082	1.213	1.380	7.820	6.850	29.40	6.00	22.20	0.360
Wheat	0.028	0.197	0.443	1.470	0.560		1.12	1.53	0.046
Pulses	0.023	0.525	0.121	0.645	1.111	1.50	1.38	5.05	0.036
Vegetables	0.080	0.214	0.316	0.238	0.156	3.74	3.88	5.65	0.036
Milk	0.166	0.111	0.112	0.013	0.232	4.55	1.18	2.28	0.015
Fish	0.068	0.106	0.575	0.093	0.156	54.00	—	0.41	
Mutton	0.032	0.034	0.070	0.012	0.140	—	0.53	1.02	0.050
Chicken	0.006	0.008	0.019	0.007	—	1.12	0.06	0.12	—
Salt	0.036	0.039	0.446	—	—	1.55	1.12	0.26	—
Jaggery	0.022	0.264	—	0.125	0.305	—	—	—	—
Tamarind	0.004	0.024	0.028	0.017	0.029	—	0.32	0.32	—
Total	0.547	2.735	3.510	10.440	10.539	95.86	15.41	38.84	0.543

Table 15. *Daily Intake of Some Significant Elements and Radionuclides by Fishermen*

Food material	Fishermen								
	Ca g	K g	mg			μg	pCi		
			Sr	Mn	Zn	I	^{90}Sr	^{137}Cs	^{226}Ra
Rice	0.069	1.028	1.170	6.450	5.650		5.10	19.50	0.308
Wheat	0.046	0.324	0.727	2.420	0.920	27.00	1.84	2.52	0.075
Pulses	0.011	0.228	0.054	0.288	0.490	0.66	0.61	2.29	0.015
Vegetables	0.041	0.110	0.164	0.126	0.067	1.92	1.98	2.38	0.015
Milk	0.066	0.044	0.044	0.005	0.071	1.80	0.46	1.12	0.006
Fish	0.178	0.278	1.515	0.251	0.428	141.00	—	1.05	—
Mutton	0.018	0.019	0.039	0.006	0.065	0.62	0.29	0.57	0.107
Chicken	0.003	0.004	0.009	0.003	—	—	0.03	0.06	—
Salt	0.025	0.034	0.475	—	—	1.65	0.11	0.22	—
Jaggery	0.18	0.230	—	0.109	0.266	—	—	—	—
Tamarind	0.004	0.026	0.029	0.018	0.032	—	0.16	0.35	—
Total	0.479	2.325	4.226	9.676	7.987	174.65	10.58	30.06	0.528

Table 16. *Ca Intake from and* $^{90}Sr/Ca$ *Ratios in Different Food Groups of New York* (1965) *and Tarapur Diet*

Food groups	New York		Tarapur			
			Farmer		Fisherman	
	Ca % of total	$^{90}Sr/Ca$ pCi/g	Ca % of total	$^{90}Sr/Ca$ pCi/g	Ca % of total	$^{90}Sr/Ca$ pCi/g
Cereals and pulses	15.7	52.5	24.3	64.0	26.3	60.0
Vegetables	8.1	59.0	14.6	48.5	8.6	48.5
Milk and milk-products	61.3	19.3	30.3	7.1	13.8	7.1
Fish and meat	10.6	11.1	18.3	5.6	41.6	1.6
Total diet	—	28.3	—	28.0	—	22.0

York[5] and Tarapur diets are compared in Table 16. The *per capita* daily intakes of Ca and Sr in Tarapur are ~ 500 mg and ~ 4 mg respectively and the corresponding intakes in the Western diet[6] are ~ 1000 mg and ~ 1.3 mg.

In New York diet[5] ~ 50% of ^{90}Sr intake is accounted for by milk and milk products, and 30% is accounted for by cereals and pulses. In Tarapur diet, milk and milk products account for less than 10% of the intake, cereals and pulses account for ~ 70% of intake by fishermen and ~ 50% by farmer. The ratios of $^{90}Sr/Ca$ for the total intake in the two areas are very similar, viz. New York diet 28.3, Tarapur farmer's diet 28, and Tarapur fisherman's diet 22. Average intake of ^{90}Sr from New York diet is about twice that obtained in Tarapur diet. Major contribution of ^{90}Sr in the Tarapur diet comes from rice (~ 50% of total) and vegetables rank next in significance (~ 20%).

About 80% of total intake of stable Sr comes from cereals and pulses, and fish in farmer's and fisherman's diets. In the cereals and pulses group, rice is the major contributor to Sr intake (~ 70%). Intake of ^{90}Sr is highest through cereals because of higher ^{90}Sr activity and larger consumption of cereals. Fall-out activity in rice is relatively high because of this being a rain crop (cf. Grummitt and Robertson[7]).

^{226}Ra

For the intake of ^{226}Ra, cereals and pulses account for 81% in farmers' diet and 75% in fisherman's diet, rice alone contributes 80% of the intake by farmers and 75% by fishermen from this food group.

^{137}Cs AND K

Approximately 70% of the total intake of ^{137}Cs and also of K is contributed by cereals and pulses (Table 17) of which rice contributed ~ 80% of the intake from this group. The K intake of 2.3–2.7 g/day in Tarapur diet compares with 2.3–3.4 g/day in U.S. diet.[5] In U.S. ~ 70% of ^{137}Cs intake is obtained from milk, fish and meat in contrast with Tarapur, where these groups contribute only about 10% to the daily intake of ^{137}Cs.

Total ^{137}Cs intake from New York diet[5] is three times that from Tarapur diet. ^{137}Cs intake in Tarapur would be approximately proportional to ^{137}Cs activity in cereals and pulses and in view of the fact that the bulk of the food is comprised of this group, the ^{137}Cs body burden in the population is largely determined by ^{137}Cs content in this food group; vegetables are next in significance.

An examination of four persons from the area showed that on an average they have a body burden of 1.9 nCi ^{137}Cs for an average body

Table 17. Contribution to Daily Intake from Major Food Group in Diet of Farmer and Fisherman

Food groups / % of daily intake of	Cereals and pulses		Vegetable		Milk		Fish	
	Farmer	Fisherman	Farmer	Fisherman	Farmer	Fisherman	Farmer	Fisherman
Foodstuff	60.0	58.5	11.5	6.5	8.6	3.80	7.8	18.0
Ca	24.3	26.3	14.6	8.6	30.3	13.80	18.3	41.6
K	71.0	67.8	7.8	4.7	4.1	1.90	5.4	12.9
Sr	55.4	54.5	9.0	3.3	3.2	0.90	18.9	31.2
Mn	95.0	95.0	2.3	1.3	0.1	0.05	1.1	2.7
Zn	80.0	89.0	1.5	0.8	2.2	0.88	1.2	6.2
I	30.6	15.7	3.9	2.3	4.7	1.06	58.0	81.5
^{90}Sr	55.0	72.0	25.0	18.6	7.7	4.40	3.8	3.2
^{137}Cs	76.0	74.0	12.0	7.9	6.0	3.70	4.2	5.6
^{226}Ra	81.2	75.5	6.7	2.8	2.8	1.10	9.3	20.5

weight of 55 kg and 84 g body potassium.[1] These studies are being extended and will be useful in identifying build-up of body burden from sources other than fallout in the region.

Mn AND Zn

Trace elements like Mn and Zn are present in high concentrations in cereals (11–30 mg/kg) and again rice alone contributes about 70% of the total intake. Betel leaves (*Piper betel*) and radish leaves (*Raphanus sativus*) show high concentration of Mn. Gowar (*Cyanopsis psoraliodes*), onion and coconut kernel show somewhat high concentrations of Mn and Zn (cf. Table 8). There is significant concentration of Mn and Zn in fruits (cf. Table 7), but the daily intake of fruits is very small.

Oysters (cf. Table 9) are likely to be the significant carriers for radioactive Mn and Zn from station effluents as they are found near the shore and show high concentrations of the stable isotopes. The total intake of oyster meat in the diet, however, is small and most of the oysters harvested are exported to cities. Oysters having the highest cumulative concentration of Mn and Zn in soft tissue, among sea foods examined, would serve as a useful single indicator for build-up of induced ^{54}Mn and ^{65}Zn radioactivity in the shore waters of Tarapur.

PHOSPHORUS

Fishermen take on an average about 170 g of fish a day, i.e. 18% of the total diet. Survey data indicate that there are families of fishermen consuming as much as 250–300 g of fish a day. Among the poorer section of fishermen the fish intake is often 25–30% by weight of a day's total food intake.

High accumulation factors for ^{32}P coupled with high percentage intake of fish by a fisherman indicate that ^{32}P can contribute a high exposure, particularly when the diet abounds in sea foods like shrimps, fingerlings and intertidal organisms. If the bulk of P in the diet comes from cereals and vegetables which are rich in phytin phosphorus,[8, 9] then isotopic dilution of ^{32}P from fish will be reduced. It has been observed by other workers that Indian meals comparable to Tarapur diet, have a phytin P content as high as 42%[10] of the total P. It would therefore be necessary in assessing the significance of this element to characterise the source of supply and not judge only by the concentrations present in the dietary intakes.

IODINE

The environmental monitoring programme includes sampling of sea weeds and sheep thyroids for measurement of radioiodine contamination.

Monitoring of bovine thyroid under field conditions has shown that it is a sensitive method [13] for detection of environmental ^{131}I. Sheep thyroids under identical conditions of exposure have been reported to accumulate five times [14] more ^{131}I than bovine thyroids. [11]

For exposures resulting from the ingestion of radioiodine, milk has often been regarded as the most important source. [11] The British Medical Research Council, in setting up the acceptable level for ^{131}I contamination has considered exposure of a child's thyroid as critical. In rural Indian conditions [12] infants are mostly breast fed and are weaned only on medical grounds. Sometimes animal milk of some kind is given to supplement breast milk—the quantity rarely exceeding 200 ml/day. The supplementary foods for the infants are usually prepared from cereals, particularly rice.

Because of low intake, milk is not likely to be the critical food around Tarapur though there may be small groups of individual families (rich farmers), who may receive a higher exposure through consumption of milk.

The iodine content in food components given in Tables 14 and 15 has been calculated from reported iodine values for dietary components. [15, 16] The highest intake of iodine in Tarapur diet is from marine fish. Of the two population groups examined, iodine intake by fishermen is twice that by farmers. Approx. 80% of total iodine intake by fisherman and $\sim 60\%$ by farmer is obtained from fish. Therefore restriction on milk consumption in emergency circumstances does not much affect the net intake of iodine. Under the circumstances, it is possible that the population would receive most of the ^{131}I exposure from fish consumption and fishermen would receive the highest.

Radioiodine intake through fish has been reported to be unimportant because of the short half-life of ^{131}I and delays involved in the uptake chains. [17] For most short lived activities, this point requires to be investigated in detail and particularly with reference to amounts of release and types of fingerlings and juveniles caught in the shore waters.

CRITICAL GROUP IN THE TARAPUR ENVIRONMENT

It is possible to predict from the information presented, the population group which will receive high radiation exposures through living in the vicinity of the power station and by eating food produced near the site.

Fishermen living in the near vicinity at Ghivali and Pophran ply their fishing gear in the coastal waters that would be receiving reactor effluents, and consume fish caught in these waters. The average intake of fish is 170 g per day by fishermen while that for farmers living in the interior it is only 40 g (cf. Table 12). Contamination of the land environment is not expected to be significant in normal operation and the exposure of farmers and fishermen from this source are expected to be very close to one another and as such the fish growing close to the shore and caught by fishermen may be the critical component in the diet. Oysters and shrimps grown in the area are likely to accumulate activation products and could be monitored as indicator organisms to follow any build-up of activation products from reactor effluents. Bombay duck (*Harpodon nehereus*) and shrimps are abundant and cheap and are consumed by local fishermen in large quantities. *Therefore the fishing population in the area could probably be the Critical Group in the environment.*

SOME SAMPLES FOR TERRESTRIAL MONITORING

High concentrations of Mn, Zn and P and relatively large ratios of $^{90}Sr/Ca$, $^{137}Cs/K$ in rice show that rice is a useful environmental sample to indicate terrestrial contamination. As a seasonal crop, its usefulness for round the year monitoring is limited. However, it contributes significantly to the body intake of trace elements and fallout contamination. Table 8 has shown that some vegetables (leafy ones because of high foliar absorption) are more selective than others to accumulate fallout contamination. None of them however, is likely to be a critical food because of small intake.

An interesting sample listed in Table 8 is the betel leaves, reputedly known as the "Indian Pan". Samples of betel leaves have consistently shown high concentrations of trace elements and radioactivity. Of the leafy vegetation examined, the betel and plantain leaves promise to be good indicators for terrestrial contamination.

COMMENTS IN CONCLUSION

In this study contributions from drinking water are not discussed, as contamination of main drinking water supply is most unlikely.

The search for the critical food through dietary surveys has shown that ^{90}Sr and ^{137}Cs contamination in the Tarapur diet is obtained from cereals and pulses (predominantly from rice) and the activation products are likely to be obtained through sea food harvested from the shore waters.

The ratios referred to in Table 16 for $^{90}Sr/Ca$ for Tarapur and New York diet (28.3 and 28.0) should be treated with caution since the bulk of Ca in the New York diet comes from milk and milk products, fish and meat and therefore largely available [8] while only 40% comes from these sources in the Tarapur farmer's diet. Cereals and vegetables in the Tarapur diet contain large amounts of phytin phosphorus which reduces considerably [8, 9] the availability of Ca.

This survey has brought out the typical features of the rural Indian diet in contrast to Western types of diet. Though it was anticipated in the beginning of the survey that possibly there would be a wide divergence in the dietary intakes of the different population groups in the area, because of different socio-economic conditions, the survey indicated that the general types of diets are very similar excepting for a small variation in the most easily available food stuffs for the group-like cereals and vegetables for the farmers and fish for the fishermen. These small variations and professional activities ultimately feature in the final selection of the possible critical group in the area.

ACKNOWLEDGEMENTS

The authors are indebted to TAPP Organization for providing laboratory and field work facilities. The assistance received from Ss. B. U. Kothari, K. A. R. Nair, C. A. Chowdhari, K. G. Pimple and M. S. Patil in carrying out analysis of samples and collection of environmental and dietary data is gratefully acknowledged.

REFERENCES

1. I. S. Bhat, A. A. Khan and P. R. Kamath. Progress Report. AEET-242 (1965). Atomic Energy Establishment, Trombay, India.
2. K. Venkataraman, S. Somasundaram and S. D. Soman. An evaluation of radiation protection standards for Indian conditions. *Health Physics* **9,** 647–652 (1963).
3. *Diet Atlas of India.* Indian Council of Medical Research. Special Report Series No. 48. India, 1964.
4. A. S. Chhabra. Radium-226 in food in man in Bombay and Kerala State. *Br. J. Radiol.* **39,** 141–146 (1966).
5. *Radiological Health Data* **6,** No. 9, 503–505 (1965). U.S. Public Health Service.
6. C. L. Comar and F. Bronner. *Mineral Metabolism* **II,** Part A, 364–365 (1962).
7. W. E. Grummitt and R. Robertson. Strontium-90 and cesium-137 in Canadian wheat (1957–9). AECL Publication CRER-1000 (1960).
8. C. L. Comar and F. Bronner. *Mineral Metabolism* **II,** Part A, 251 (1962).
9. J. T. Irving. *Calcium Metabolism,* pp. 21–28. Methuen, London, 1957.
10. K. Mitra. The results of diet surveys in India (1935–48), ICMR Special Report No. 25 (1953).
11. *Hazards to Man of Nuclear and Allied Radiations—a Second Report to the Medical Research Council.* H.M.S.O. London, 1960.
12. Annual Report (1955–1956). Field Investigations: Protein malnutrition surveys in S. India. ICMR, 1956.
13. H. J. Baratta *et al* I-131 in bovine thyroids. *Radiological Health Data,* p. 575. U.S.P.H.S **6,** No. 10 (1965).
14. A. H. Wolff. Fallout and uptake of I-131. *Fallout from Nuclear Weapons Tests. Congressional Hearings.* U.S. Govt. Publ. Vol. 2, p. 1311. Washington, 1959.
15. J. McClendon. *Iodine and Incidence of Goiter.* University of Minesota Press, Minneapolis, 1939.
16. D. D. Sabu. *Determination of Iodine in Sea Water, Fresh Water and Marine Salt.* Indian Science Congress, 1963.
17. M. Eisenbud and M. E. Wrenn. Biological disposition of radioiodine—a review. *Health Physics* **9,** 1133 (1963.)

DISCUSSION

M. DELPLA (*France*):

Je ferai deux remarques: la première de caractère général: la seconde, relative à un point très particulier.

1. M. Coulon étudie le contrôle de la pollution radio-active de la chaîne alimentaire en hygiéniste; il se place sur le plan de la santé publique et embrasse un vaste territoire, le pays tout entier. Il est aussi possible de considérer, à l'opposé, ce qui se passe à proximité d'une installation nucléaire, et utiliser la radio-analyse des produits de la chaîne alimentaire à la mesure de la contamination du milieu par cette installation. C'est suivant ces principes que nous surveillons nos sites nucléaires. Nous nous proposions de vous faire part de notre méthode—originale—et de nos résultats; nous ne pouvons que regretter qu'aucun des rapports que nous proposions sur ce sujet n'ait pu être retenu. Veuillez m'excuser, Monsieur le Président, d'avoir été aussi long.

2. M. Coulon cite à plusieurs reprises le ministère de l'agriculture. Bien d'autres ministères s'intéressent aussi, en France, à la pollution de la chaîne alimentaire. Il me paraît difficile, en cette matière, si l'on cite un ministère, de ne pas mentionner les efforts accomplis en cela par celui des affaires sociales (santé publique).

E. DI FERRANTE (*Euratom*):

Les pH 5,9; 7,2; 8,25; 8,55 du sol mentionnés dans le mémoire sont-ils des valeurs naturelles, c'est-à-dire, trouvées dans les différents sols étudiés, ou bien les auteurs ont-ils corrigé le pH d'un même type de sol?

R. KIRCHMANN:

Ces différentes valeurs du pH ont été observées lors des expériences en serre, après apport d'hydroxyde de calcium à un même type de sol. En conditions naturelles la valeur $(pH)_{eau}$ du sol étudié est environ de 5,9.

T. L. CULLEN (*Brazil*):

Have the authors considered any other soil parameters in their studies? For example there are 35 or 40 parameters used by the agronomer: particle size, pH in water, pH in KCl, oxides of metals, exchangeable cations. There are trace elements like Barium whose presence or absence is important.

It is proper in a laboratory to control all but one or two variables and let them vary. But in nature there are so many variables that influence uptake of the natural radioisotopes.

R. KIRCHMANN:

En ce qui concerne le facteur sol, nos expériences ont été limitées à la comparaison des niveaux de contamination, par Ra^{226}, d'une graminée cultivée sur quelques types de sols belges que nous connaissons bien grâce à nos travaux sur le comportement de Sr^{90} dans ces sols. Nous n'avons pas considéré séparément chacun des nombreux paramètres pouvant éventuellement influencer le taux de transfert du Ra^{226} du sol au végétal. Nous avons d'abord recherché si le type de sol jouait un rôle et ensuite, en examinant les caractéristiques différenciant les sols étudiés, nous avons constaté que la teneur en matériel sorptif donnait la meilleure corrélation avec les teneurs en Ra^{226} observées dans le végétal. Pour l'étude de l'interaction ionique, nous estimons que l'agriculture se prête le mieux à des tels travaux.

G. JOYET (*Switzerland*):

Je désire moi-même faire remarquer que ces auteurs ont trouvé une corrélation entre l'activité des herbages et l'activité du lait, corrélation qui paraît être assez sûre et que d'autres auteurs n'ont pas trouvée.

E. VAN DER STRICHT:

Les conclusions diamétralement opposées des rapports présentés par M. Popović et par M. de Bortoli et al. peuvent à mon avis s'expliquer par l'étendue géographique très différente des zones surveillées.

M. DELPLA (*France*):

Comme vous même, M. le Président, j'avais remarqué l'opposition des conclusions des deux rapports de MM. Popović et de Bortoli. Je signalerai que, de notre côté, nous ne trouvons pas de corrélation entre les activités, dans l'herbe et dans le lait, mesurées sur les éléments alcalino-terreux. En fait, l'établissement d'une telle corrélation n'est pas possible en raison de la variabilité des résultats obtenus sur l'herbe, variabilité due, sans doute, aux

conditions expérimentales, en particulier, au fauchage successif de pièces juxtaposées délimitées dans une prairie naturelle.

R. B. HOLTZMAN (*U.S.A.*):

I would like to ask these authors of the papers on ^{210}Po in tobacco why the ^{210}Po appears to be lower than that in the United States? Could it be due to differences in the curing process? I would also like to ask the Yugoslav authors how they treated their urine samples; that is were they wet-ashed?

D. PANOV:

La première question concerne la concentration de polonium dans l'urine. Nous avons attaqué l'urine par HNO_3 et l'acide perchlorique; on a fait ensuite une déposition sur une plaque d'argent et le comptage par alpha.

La deuxième question est sur les résultats qui sont les mêmes à peu près dans le tabac et dans la cigarette: nous n'avons pas trouvé non plus de différences selon les différentes sortes de cigarette.

W. KOLB (*Germany*):

Im Auftrag der deutschen Zigarettenindustrie haben wir ebenfalls Messungen an Tabaken und Rauchkondensaten vorgenommen. Die spezifische ^{210}Po-Aktivität der Rauchkondensate (main stream smoke) lag zwischen 1,22 und 1,45 pCi/g ± 17%. Signifikante Unterschiede zeigten sich bei 12 verschiedenen Rohtabaksorten. Die ^{210}Po-Aktivität lag zwischen 0,30 und 0,71 pCi/g und unterschied sich damit extremal um den Faktor 2.

G. JOYET (*Switzerland*):

Je voudrais faire moi-même une remarque. Dans ce travail on a mesuré des totalités d'activité de césium de l'ordre de 1,9, c'est-à-dire environ 2 nanocuries par individu. J'ai vu les publications présentées par l'auteur à ce sujet et je voudrais signaler qu'en Suisse par exemple nous trouvons des activités pour l'homme et pour le sujet masculin de 20 ans qui sont exactement dix fois plus élevées. La valeur pour la femme est de 19 nanocuries pour le césium-137, et de 9,5 nanocuries pour la femme de 20 ans. Ces valeurs sont valables pour le printemps de cette année. Elles coïncident à peu près avec certaines valeurs américaines qui ont été trouvé à diverses periodes au Brookhaven National Laboratory. Je voulais signaler ces différences car je pense qu'ici il y a avant tout un effet de latitude.

SOME RECENT DEVELOPMENTS IN TECHNIQUE FOR MONITORING HIGH-ENERGY ACCELERATOR RADIATION*

JOSEPH B. McCASLIN, H. WADE PATTERSON, ALAN R. SMITH and LLOYD D. STEPHENS
Lawrence Radiation Laboratory, University of California, Berkeley, California

Abstract—In order to accurately evaluate the exposures received by individuals working near high-energy accelerators it is necessary to measure the separate components in the radiation field and to determine their energy spectrum. Since no single instrument or detector will do this, a variety of different detectors and instruments must be used. Three recent developments in technique for monitoring particulate radiation above 20 MeV use nuclear emulsion, elemental mercury, and Be^7 production in light elements; below 20 MeV, the use of moderated foils of In, Au, and Co has been extended to include Ta.

When emulsion is used, the number of stars formed by high-energy inelastic collisions is counted, together with the number of gray prongs. The ratio of gray prongs per star was previously found to be linearly related to the energy of the neutron which formed the star, over the energy range 20 to 300 MeV. This technique is used to measure average neutron energy and to estimate spectrum shape for neutron energies above 20 MeV. A second technique makes use of the spallation of Hg to Tb^{149}, an alpha-emitter of 4.12-hr half-life. The threshold for this reaction is near 500 MeV, and it therefore extends the use of threshold detectors for the estimation of spectrum shape to a higher energy domain and gives additional confidence in previous estimates of spectrum shape made with Bi fission, $C^{12}(n, 2n)C^{11}$, and $Al^{27}(n, a)Na^{24}$. Thirdly, production of Be^7 from C^{12}, N^{14}, and O^{16} has been studied; it offers a method of high-energy neutron threshold detection with practical thresholds extending from 30 to 40 MeV for carbon to 45 to 55 MeV for oxygen. The practical sensitivity can be arbitrarily high without making the extraction process either too lengthy or unwieldy. Another recent development involves the inclusion of Ta in the class of detectors which use a thermal-neutron-sensitive activation element inclosed in a Cd-clad hydrogenous moderator to allow an integration period of a few months and a sensitivity considerably greater than with Co. Finally, recent improvements in the performance of our large parallel-plate Bi fission chamber are discussed.

RADIATION MEASUREMENTS AT LRL

Application to Personnel Safety and Shielding Evaluation

The instruments and methods described here should be viewed in the light of the type of problems we encounter and our approach to their solutions. In addition to evaluating extraneous radiation fields of high-energy accelerators so that adequate personnel protection is assured, we are also called upon to determine shielding requirements both for personnel safety and for experimental equipment. In the course of this work we develop instruments and techniques appropriate to the task.

Radiation fields are measured in physical terms, using the tools and techniques of the experimental physicist. We strive to identify the various components of the radiation field and to determine their energy distribution. Extensive use is made of threshold detectors to yield both flux density and spectral information. This information is directly applicable to shielding problems, and, in conjunction with National Bureau of Standards Handbook No. 63 and ICRP recommendations, the dose

* Work done under auspices of the U.S. Atomic Energy Commission.

delivered by the radiation field can be computed.[1] Direct measurements of accelerator radiation in rad or rem units are not generally made because of their limited usefulness in situations which require a quantitative evaluation of shielding.

INSTRUMENTS AND TECHNIQUES

The threshold detector systems we use can be grouped into two categories.[2] The first category (activation elements) consists of those detectors which can be used with a γ-ray spectrometer system along with a digital computer program to provide great spectral detail over a limited energy range of about 2 to 30 MeV (Table 1). Data analysis with this system can be time-consuming. Gamma-ray spectra are often quite complex, and lack of neutron cross section data for energies greater than about 15 MeV, and production of activities of interest by reactions other than (n, p), (n, α), and $(n, 2n)$, are problems that require careful consideration.

Detectors which fall in the second category (mixed activation elements and pulse counters) include pulse counters such as BF_3, polyethylene-lined gas proportional counters, and Bi fission counters. Other detectors in this category are moderated thermal-neutron-sensitive foils, aluminum disks, and plastic scintillators for carbon activation. These detectors can be used to determine the broad spectral features of a neutron field while embracing a wide range of neutron energies from about 0.02 MeV up to the highest energy of the primary particle. A digital computer program produces a neutron spectrum by comparison of the observed detector response to trial neutron spectra. We also determine neutron spectra by measurement of proton recoil track length in Ilford L.4 600-μ emulsions.

The use of 4π detectors is favored because quite often the radiation fields we encounter are nearly isotropic, and particle spectrometers that depend on knowing the direction of the incident particle can not be used.

RECENT DEVELOPMENTS

In addition to the instruments and techniques just described, we have added the following items.

1. *Neutron Spectroscopy Using Stars in Emulsions*

The average number of gray prongs per star in nuclear emulsion is found to be proportional to the average incident neutron energy.[3] This

Table 1. *Threshold Detectors**

Reaction	Theoretical threshold† (MeV)	Effective threshold† (MeV)	Half-life of residual nucleus	Form of detector
Ni^{58} (n, p) Co^{58}	−0.4	1.2	71 days	4-in. metal disk
Al^{27} (n, p) Mg^{27}	1.8	2.7	9.5 min	4-in. metal disk
Co^{59} (n, α) Mn^{56}	−0.3	5.3	2.58 hr	4-in. metal disk
Fe^{56} (n, p) Mn^{56}	2.9	5.0	2.58 hr	4-in. metal disk
Ti^{48} (n, p) Sc^{48}	3.2	5.2	44.0 hr	4-in. metal disk
Mg^{24} (n, p) Na^{24}	4.7	6.1	15.0 hr	4-in. metal disk
Al^{27} (n, α) Na^{24}	3.1	5.9	15.0 hr	4-in. metal disk
I^{127} $(n, 2n)$ I^{126}	9.3	9.4	13.2 days	Boxed crystals
Co^{59} $(n, 2n)$ Co^{58}	10.2	10.8	71 days	4-in. metal disk
Ni^{58} $(n, 2n)$ Ni^{57}	11.8	12.5	36 hr	4-in. metal disk

* From Alan R. Smith, Threshold detector applications to neutron spectroscopy at the Berkeley accelerators, Lawrence Radiation Laboratory Report UCRL-16312, Nov. 19, 1965.

† The theoretical threshold is calculated as $-Q \times (1 + M)/M$, where Q is the Q value for the reaction and M is the mass number of the target nucleus. The effective threshold is the energy at which the cross section is 1/100 of its peak value.

has been investigated for neutron energies from 20 to 300 MeV. Two advantages to this system over measurement of proton recoil track length are clearly seen. Because the kinetic energy of a proton from a nuclear star is less than that of a recoil proton, the range in the emulsion is considerably less. Recoil proton tracks, on the other hand, seldom have both beginning and end in the same emulsion. Also, the direction of the incident neutron need not be known for counting prongs from nuclear stars.

Neutrons of 20 to 260 MeV from stripped deuterons were used to irradiate six Ilford K.5 emulsions (3 × 1 in., 600 μ). The neutrons were considered to be monoenergetic, with a peak energy of one-half the deuteron energy. There is, of course, a symmetrical spectrum of energies about the peak with a full width at half-maximum energy given by

$$E_{1/2} = 4.18\, E_D.$$

Neutrons of 300 MeV_{peak} were obtained by bombarding Be with 360-MeV protons.

Over the energy region from 20 to 300 MeV the ratio gray prongs/star increased by a factor of 50 from ≈ 0.01 at 20 MeV to ≈ 0.5 at 300 MeV (Fig. 1). Between 500 and 1400 stars were scanned for each energy region. Figure 2 defines the classes of prongs.

The rigor involved in track selection and identification is recognized as being an important aspect of work of this nature, and a certain amount of subjectivity could influence the results. A comparison, between the gray-prong method and an independent determination using threshold detector methods was made by Patterson and Omberg.[4] They found substantial agreement between these two methods for flux shapes derived from cosmic rays and for radiation fields at the Bevatron.

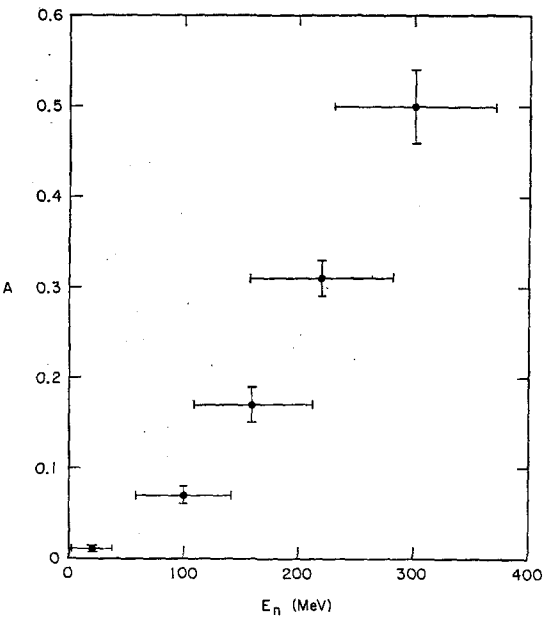

FIG. 1. Average number of gray prongs per star A versus incident neutron average energy E_n. Errors shown in A are statistical errors due to counting. Errors shown in E_n are values of $\triangle E_{1/2}$. (From René Remy, Neutron spectroscopy by the use of nuclear stars from 20 to 300 MeV. Lawrence Radiation Laboratory Report UCRL-16325, Aug. 1965.)

2. *Hg Spallation at 500 MeV as a Sensitive Flux Detector*

The high-energy spallation reaction in Au has been previously reported along with cross-sections for the α-emitting branch ($\approx 10^{-27}$ cm^2), α energy (3.95 MeV), and half life (4.12 hr) of the reaction product, Tb^{149}.[5] Use of Hg instead of Au for this reaction allows us to effectively and easily concentrate the Tb in a form suitable for counting.[6] The task of removing Tb from $\frac{1}{2}$ kg quantities of Hg proved less formidable a problem than might be expected because Tb slowly rises toward the top of the irradiated Hg pool. We simply accelerate this process by centrifuging the Hg, and remove a large portion of the Tb from the top of the Hg pool with a cellulose acetate pressure-sensitive adhesive tape. The ultimate sensitivity of this system for measuring Tb^{149} relative to a thin gold foil depends on the amount of Hg used and the ability of the centrifuge to process it. However, a modest centrifuge which can accommodate 500-g samples will allow one to achieve an α-counting rate $> 10^4$ times as high as with a 10-mg gold foil. It then becomes possible to measure flux densities of about 10 n/cm^2-sec. And with larger volumes of Hg the sensitivity improves proportionally.

The threshold for this reaction in Hg was

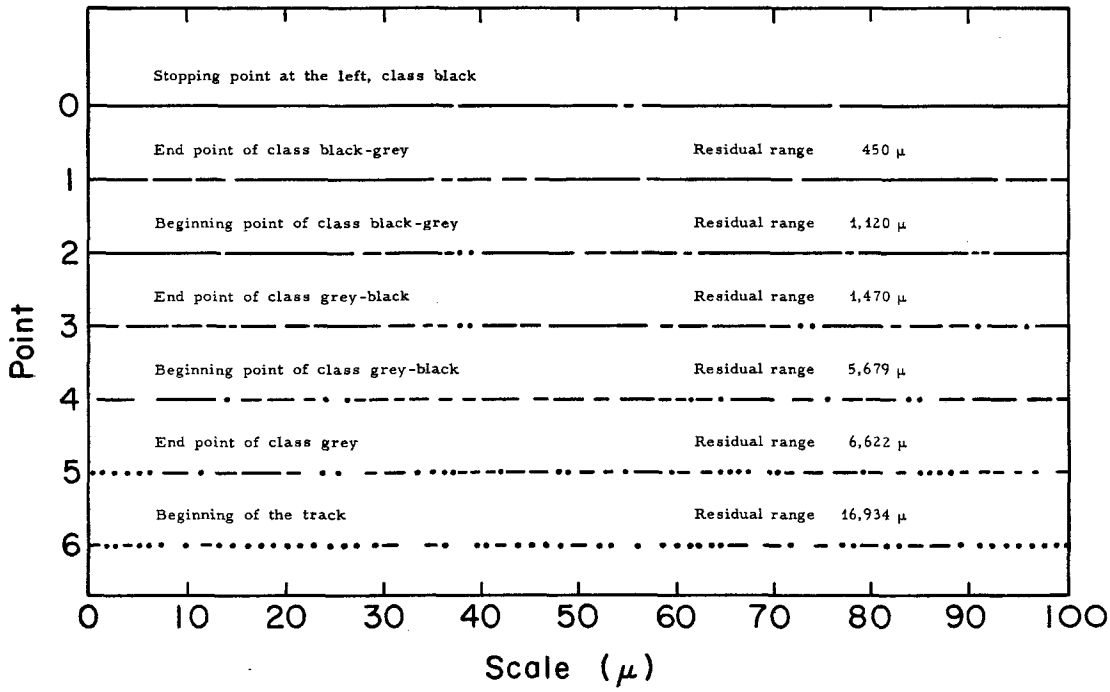

FIG. 2. Calibration track (recoil proton with 70-MeV kinetic energy).

Class	Criteria
Black	< 10 gaps in the field of view (100 microns)*
Black-gray	10 to 20 gaps in the field of view
Gray-black	21 to 50 gaps in the field of view
Gray	> 50 gaps in the field of view

* The number of gaps were counted in the field of view (100 microns of projected length) so that the error made in counting gaps in tracks having a great dip angle is more or less compensated for.

bracketed between 300 and 700 MeV (values in between will be determined at a later date) by irradiating samples of HgF and Au in the internal proton beam at the 184-in. cyclotron. Pending completion of the threshold studies, it is reasonable to assign the same activation threshold value to Hg as is used for Au.

Although it is easy to count α particles directly from the surface of the centrifuged Hg, the vagaries involved in unavoidable mechanical and convective mixing, relaxation of the Tb concentration gradient at the surface, etc., were considered to be too difficult a problem for our initial studies. Instead, we have found a practical and effective method of Tb concentration and extraction. We centrifuge the Hg at about 1700 g for the somewhat arbitrarily determined time of 1 hr, with the tape on top of the Hg and a 2.5-g Al disk on top of the tape. The tape is then removed for counting which is started between 100 and about 1500 min after the end of the irradiation so as to

avoid α particles with shorter or longer half-lives. This process, when repeated several times on the same Hg sample, shows that the activity on the first tape is about 58% of the total activity in the Hg. Each successive tape sample removes about half of the remaining Tb. Four tapes remove about 91%, appropriate corrections being made for decay during the 5-hr extraction time. Comparison of Tb^{149} α activity in a 400-g Hg sample with Tb^{149} α activity in a thin (1.6 mg/cm^2) Au foil irradiated simultaneously in the external 6.2-GeV proton beam at the Bevatron showed that the Hg-Tb activity was greater than the Au-Tb activity by the ratio of their respective numbers of target atoms. And the activity in the Hg was exactly what would be expected by calculation that uses a 1-mb cross section and the proton flux density indicated by the thin Au foil activity. Activity in the 400-g Hg sample is 1.1×10^{-3} disintegrations/min/g at zero time when irradiated to saturation in a field of 1 p^+/cm^2-sec above the threshold.

A windowless α counter of 50% of 4π geometry, and a 90-min processing time following irradiation to saturation at 12 p^+/cm^2-sec and a 50% extraction, would yield an initial counting rate of 0.2 count/min. This can be compared to an easily attainable counter background of 0.2 count/min.

It is assumed that the reaction cross section for Tb^{149} production for neutrons bears a close resemblance to that for protons.

3. *Be^7 Production from C^{12}, N^{14}, and O^{16} with Near 100% Extraction Efficiency*

It would be advantageous for some purposes to have a high-sensitivity reaction which has an energy threshold as high as C^{11} or Bi fission without either the short half-life of C^{11} (20.4 min), which limits both integration time and the number of simultaneous measurements, or the low sensitivity and unwieldiness of the large Bi-fission counter.

Production of 53-day Be^7 from light nuclei would seem to be a useful reaction, but the difficulty in detecting the 0.478-MeV γ-ray (12% of all disintegrations) from large volumes of target material has until now been a sizeable obstacle. However, a simple, reproducible, and rapid separation process for extracting Be^7 from large volumes of liquid target material has been found.[7] Be^7 from irradiated water (O), benzene (C), or liquid nitrogen is deposited on filter paper when the liquid flows through the filter. Reproducible and nearly complete separation is achieved from an arbitrarily large volume of liquid with a series of four or five separate filters. Each filter (Whatman No. 541) extracts about 50% of the Be^7 in the carrier.

Be^7 does not adhere to the walls of polyethylene containers as it does to glass.

The reaction threshold for Be^7 production should increase from carbon to nitrogen to oxygen with $C^{12} \rightarrow Be^7$ at 30 to 40 MeV and $O^{16} \rightarrow Be^7$ at about 45 to 55 MeV, depending somewhat on the reaction paths. Good cross-section information exists only for the proton-induced reaction in C. Neutron cross-sections are not known for any of these reactions. Calculation of sensitivities, assuming a cross-section of 10 mb in all cases, is as follows.

(a) *Benzene* (*C*). One liter irradiated to saturation in a field of 1 neutron/cm^2-sec would yield a count rate of 0.88 count/min in the Be^7 peak. NaI(Tl) background in this spectral interval is 12 counts/min.

(b) *Water* (*O*) would yield 0.72 count/min under the above conditions. Background is 12 counts/min. It has been found that the distilled water should have a pH of 4.5 to 6.5 for proper extraction.

(c) *Liquid nitrogen* (*N*). Comparable to benzene and water.

4. *Moderated Ta as a Fast-neutron Flux Integrator*

This detector is an extension of our use of thermal neutron-activated elements encased in Cd-clad hydrogenous moderators.[8] Six-in.-diameter moderators have been shown to exhibit a response characteristic nearly independent of incident neutron energy in the range 0.2 to 20 MeV. In, Au, and Co have been extensively used in this manner[9, 10] in a number of laboratories.

Integration time for Ta, with a 115-day half-life for Ta^{182}, extends to several months. In and Au integrate over periods of minutes or hours, respectively, and Co is used for integration periods of at least 1 year.

By using a 4-in. diam by 2-in. NaI(Tl)

crystal, a flux integral of 10^7 n/cm^2 produces 1.8 counts/min in the selected energy band for a Co disk 2 in. in diam by 1/8 in., while the background is 10.1 counts/min. A Ta integrator of the same size produces 9.46 counts/min with a background of 8.01 counts/min.

In foils (1 in. diam by 0.005 in.) and Au foils (1 in. diam by 0.002 in.) are counted in a methane gas-flow proportional counter. Nominal initial count rates at saturation in a field of 1 neutron/cm^2-sec and zero time is 10 counts/min-gram and 3 counts/min-gram respectively.

5. *Bi-Fission Counter Improvements*

Advantage has been taken of recent improvements in the noise characteristics and transconductance of *p-n* junction field-effect transistors to upgrade the performance of our large parallel-plate Bi-fission counter. This has resulted in a simplification of the arrangement of the parallel plates and a substantial improvement in the signal-to-noise ratio.

Previously, delay line coupling of the plates was essential to proper performance in order that an event on one set of plates not be adversely affected by the full capacitance of all of the plates ($\approx$ 8000 pF).[11] By using a recently available high-trans-conductance *p-n* junction FET as the preamplifier input stage, we are able to remove the delay line from the chamber and, with all plates in parallel, achieve an overall increase in performance as shown in Figs. 3 and 4. Figure 5 shows the simplicity of the FET input stage.

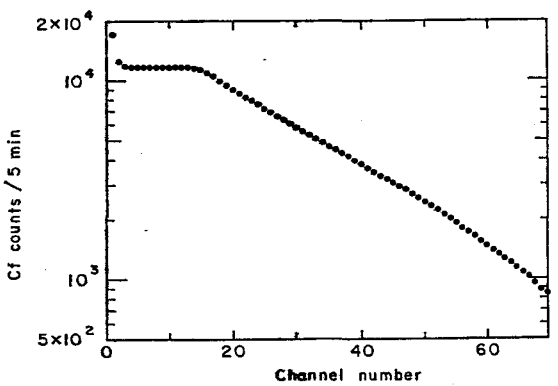

FIG. 3. Discriminator curve for Bi fission counter with delay line and Cf^{252} spontaneous fission source.

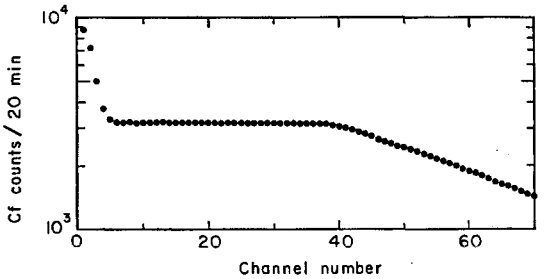

FIG. 4. Discriminator curve for Cf^{252} source with plates stacked in parallel and with FET preamplifier.

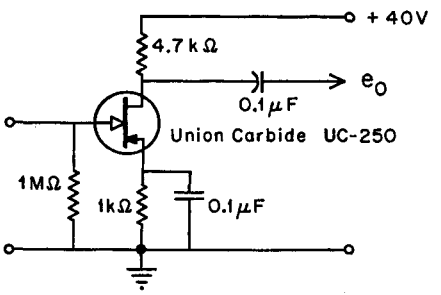

FIG. 5. FET preamplifier stage.

REFERENCES

1. H. WADE PATTERSON. Accelerator radiation monitoring and shielding at Lawrence Radiation Laboratory, Berkeley. In *Proceedings of the USAEC First Symposium on Accelerator Radiation Dosimetry and Experience*, held at Brookhaven National Laboratory, Nov. 3–5, 1965. CONF-651109 Health and Safety.
2. ALAN R. SMITH. Threshold detector applications to neutron spectrometry at the Berkeley Accelerators. In *Proceedings* (as in Ref. 1).
3. RENÉ REMY. Neutron spectroscopy by the use of nuclear stars from 20 to 300 MeV (M.S. thesis). Lawrence Radiation Laboratory Report UCRL-16325 Nov. 19, 1965.
4. H. WADE PATTERSON and RONALD OMBERG. Application of the stars produced in a nuclear emulsion to the determination of a high neutron energy spectrum. UCRL-17063 (in preparation).
5. E. M. FRANZ and G. FRIEDLANDER. Cross-sections for production of Tb^{149} from gold by high-energy protons. Brookhaven National Laboratory Report BNL-9454.

6. JOSEPH B. MCCASLIN and LLOYD D. STEPHENS. High-sensitivity neutron and proton flux detector with a practical threshold near 500 MeV, Hg (Spallation) Tb^{149}. Lawrence Radiation Laboratory Report UCRL-17505, 1966 (in preparation).
7. ALAN R. SMITH and FRANCIS M. MILLER. High-sensitivity method for using Be^{7} production from C^{12}, N^{14}, and O^{16} in high-energy threshold detector applications. Lawrence Radiation Laboratory Report UCRL-16652, 1966 (in preparation).
8. ALAN R. SMITH. A tantalum fast neutron flux integrator. Lawrence Radiation Laboratory Report UCRL-17051, 1966 (in preparation).
9. LLOYD D. STEPHENS and ALAN R. SMITH. Fast neutron surveys using in-foil activation. Lawrence Radiation Laboratory Report UCRL-8418, Aug. 1958.
10. ALAN R. SMITH. A cobalt neutron flux integrator. *Health Physics* **7,** 40–47 (1961).
11. WILMOT N. HESS, H. WADE PATTERSON and ROGER WALLACE. Delay-line chamber has large area, low capacitance. *Nucleonics* **15,** [3], 74–79 (1957).

PERSONNEL MONITORING AROUND THE CERN HIGH-ENERGY ACCELERATORS

J. DUTRANNOIS and J. BAARLI
CERN, Geneva, Switzerland

Abstract—The present methods of personnel monitoring applied near the CERN high-energy accelerators are reviewed. This includes the technical as well as the administrative procedures in use. Results of statistical analyses of the data are presented, discussed and compared with data obtained from radiation survey measurements. The apparent limits of validity of the system are deduced and discussed with a view of possible improvements.

INTRODUCTION

Sources of radiation of all kinds exist in the CERN site. Some are classical, such as radioactive isotopes used to calibrate and check detectors and others arise from the induced radio-activity in the accelerators. In addition, there is the stray radiation resulting from the operation of the accelerators. This either emerges through the main shielding or comes from experimental areas when primary or secondary beams are used for experiments.

The radiation hazard at the various places is estimated by frequent and extensive radiation survey measurements.[1] According to the results obtained it is possible to divide the CERN site into two main regions as shown in Fig. 1. However the greater part of the Laboratory is not considered as a radiation area and this explains why about half of CERN staff are not classified as radiation workers and therefore are not subject to regular personal monitoring.[2]

The CERN radiation workers are defined in accordance with the Recommendations of the ICRP, that is, those people working in an area where a dose-rate exists that could give to an individual a yearly dose exceeding 1.5 rem.[3] Due to the existence of very high local dose-rates in some of these areas, people occasionally carrying out special work in these areas are also considered as radiation workers.[4]

Before a newcomer or a CERN staff member is classified as a radiation worker, he has to go through a medical examination including haematology tests, the results of which are used for a medical clearance for the radiation worker. Routine medical examinations are made at regular intervals in order to avoid confusion as to the origin of an eventual future illness.

All newcomers when arriving at CERN visit the Health Physics Group where information is given about the radiation hazard at CERN and the relevant precautions to be taken. The previous radiation history of the new staff is investigated and information collected from previous employers. The Health Physics Group also decides whether or not a person should be considered as a radiation worker depending on the proposed nature of the work and his location within the Laboratory.

THE RADIATION AREAS AT CERN AND THE PERSONNEL MONITORING

The radiation encountered at CERN varies in nature and energy as well as in distribution from one place to another.[5] It also varies with the mode of operation of the accelerators. Figure 2 gives an overall picture of dose-rates and Quality Factors (QF) at various places during the operation of the proton-synchrotron. The composition of the radiation and the ratio of the different components also vary from one place to another.

Figures 3 and 4 show typical dose-rates due to the induced radioactivity inside the machine

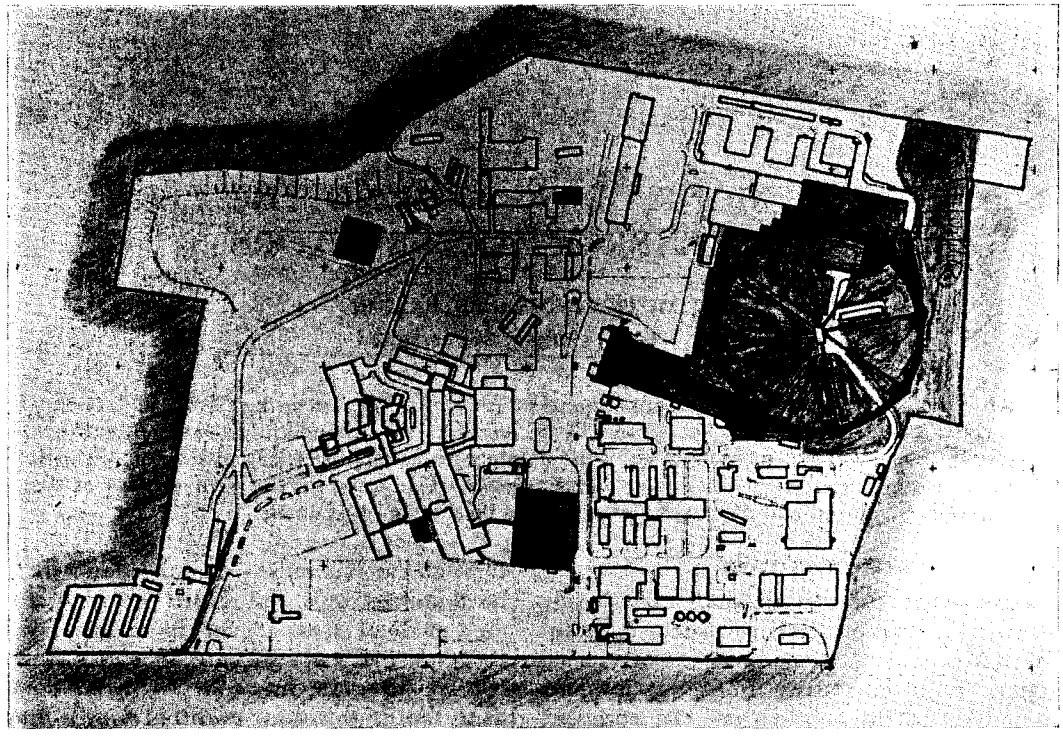

FIG. 1. CERN site and radiation areas.

halls and inside the machines themselves. In certain areas where most of the maintenance and repair or modification work has to be carried out, radiation levels are often of the order of several rem/hour.

To monitor people working in such areas the classical method of film-badges is applied. The β-γ sensitive film used is the Kodak RM. This film has been adopted because it has a good sensitivity, a large recordable dose range due to the two different emulsions and it has also acceptable variations in the fog. To extract the maximum information about the greatly degraded γ-rays near the accelerators and also about the β doses, a film holder with seven different areas corresponding to seven filters has been adopted. This is shown in Fig. 5.

The γ film records the dose due to γ and to the ionization of charged particles of any energy and also to slow neutrons by the use of a cadmium filter. The neutron film, NTA type B, records fast neutrons and also, to a certain extent, the spallation effects of high-energy particles through the observation of nuclear stars.[6] About half of the CERN radiation workers are issued with a neutron film. For this reason a film holder has been designed which can accept both types of films simultaneously, or the neutron film is replaced by a cardboard phantom. We have observed no unacceptable directional sensitivity changes resulting from this arrangement.

CALIBRATION AND READING OF FILM-BADGES

Calibration of film-badges is performed with reference to a standard radium source and a calibrated PuBe fast neutron source. The response of the γ film under the various filters has been studied for energies ranging from 40 keV up to 2 MeV. The practical limits of sensitivity are 10 mrem for the γ film, and twice the background for our neutron film. The calibration factor for the neutron films is expressed in mrem/track/standard area. The reading is made with a semi-automatic projection microscope, using a magnification of about 500. The doses are expressed with a

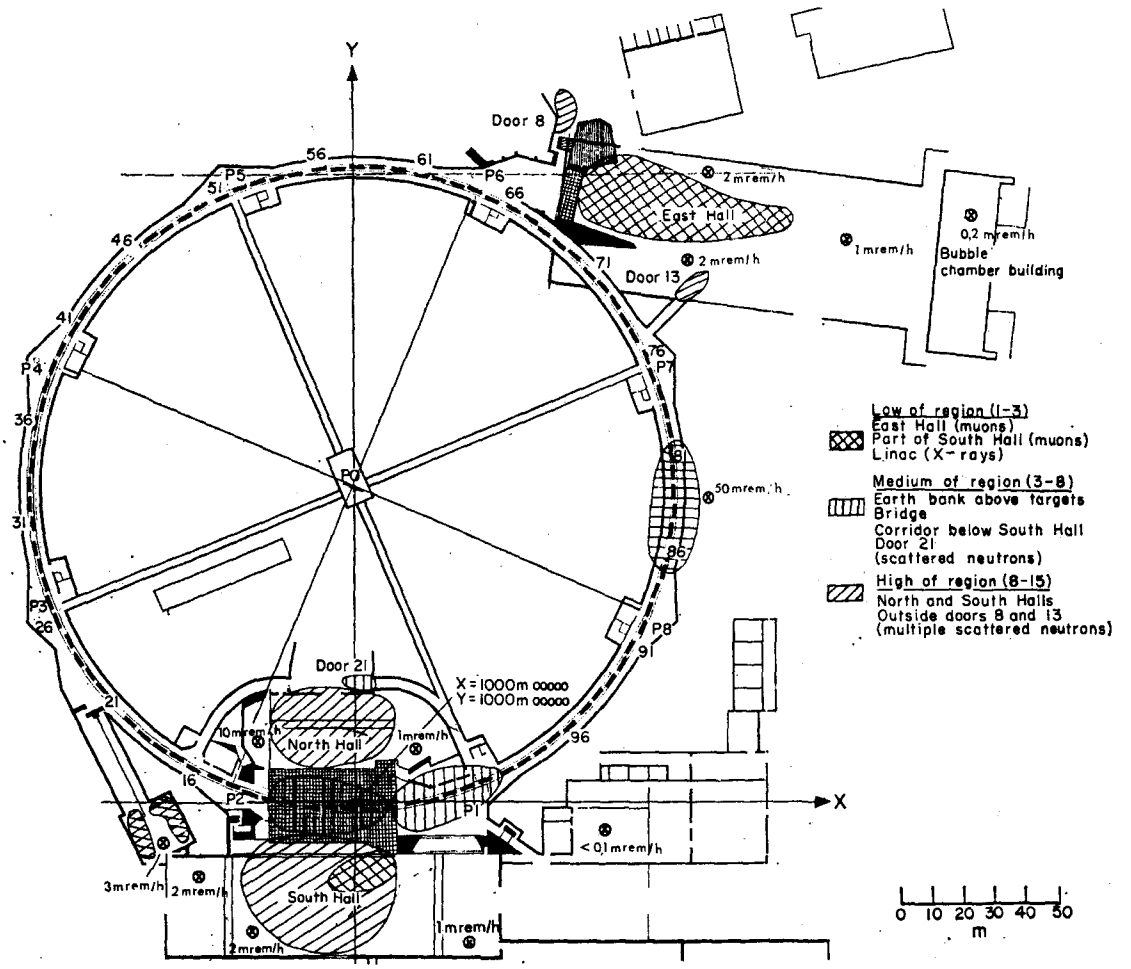

FIG. 2. Typical quality factors and dose-rates (expressed in mrem/hr) in experimental areas of the proton-synchrotron.

Quality Factor corresponding to that of the PuBe source.

The standard method used for the treatment of the exposed films, including the calibrated and background films, ensures the reproducibility of the results. The different areas of the γ films are read with a special densitometer using the optical transmission of light. The output is in BCD and translated in the form of punched cards. The identification code is still manual.

Due to the radiation encountered near high-energy accelerators all neutron films have to be scanned. Frequently no dose is recorded on the γ film while a substantial fast neutron dose exists. Among people wearing neutron films more than one third have a neutron dose higher than the dose recorded by the gamma films, and 10% have a neutron dose without detectable gamma dose.

ORGANIZATION AND DATA ON PERSONNEL MONITORING AT CERN

The administration of the film-badge service has been set up following the structural organization of the CERN staff. The staff is divided

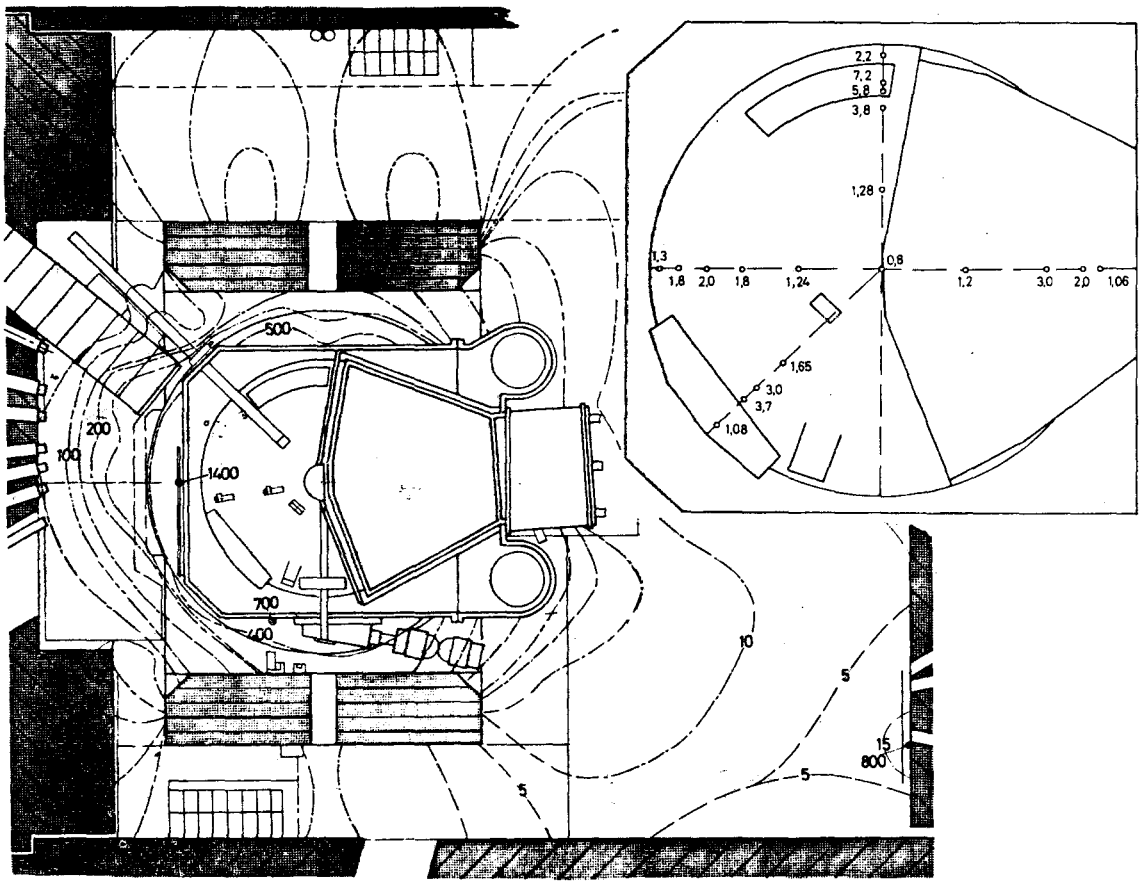

FIG. 3. Dose-rates inside the synchro-cyclotron hall during shutdown (dose-rates expressed in mrad/hr). Inside view of the vacuum chamber with dose-rates expressed in rad/hr, 14 days after machine stop.

into divisions and each division into groups or working teams. Identification of the films is facilitated by this system and requires only four figures, plus the code for the related period. The distribution and exchange of films is made by the internal mail, through the responsible person of each group or working team. Newcomers and people leaving as well as transferred personnel are treated automatically, as they have to report to the Health Physics group. Visitors may be incorporated into a standard CERN group or into special groups that can be set up, depending on the anticipated period of the project at CERN.

The information is recorded automatically on punched cards for gamma films and manually for neutron films. This is then treated by our CDC 6600 computer as shown in the block diagram (Fig. 6). The programme has been made as flexible as possible to facilitate introduction of new numbers, transfers or extractions. The calibration and other basic data are easily changed if necessary. To ensure accuracy, a number of tests are made during the process and any eventual errors introduced with cards are ignored and messages are duly recorded concerning these errors. This procedure is adopted to protect previous data retained by the memory tape.

The routine output presents lists per division, per group and per individual including information about the doses recorded during the

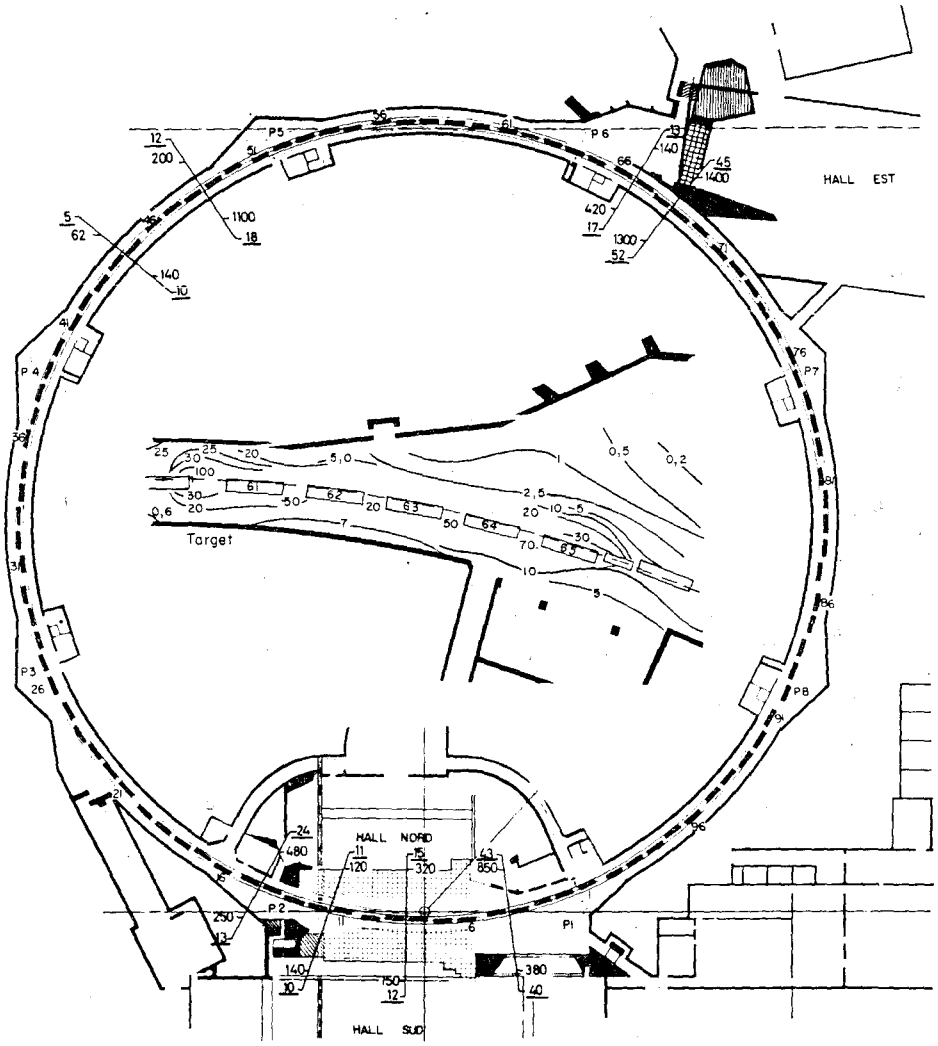

FIG. 4. Dose-rates inside the proton-synchrotron tunnel during shutdown. The underlined values correspond to measurements at 1 m from the vacuum chamber, the other values correspond to measurements at 10 cm from the vacuum chamber.

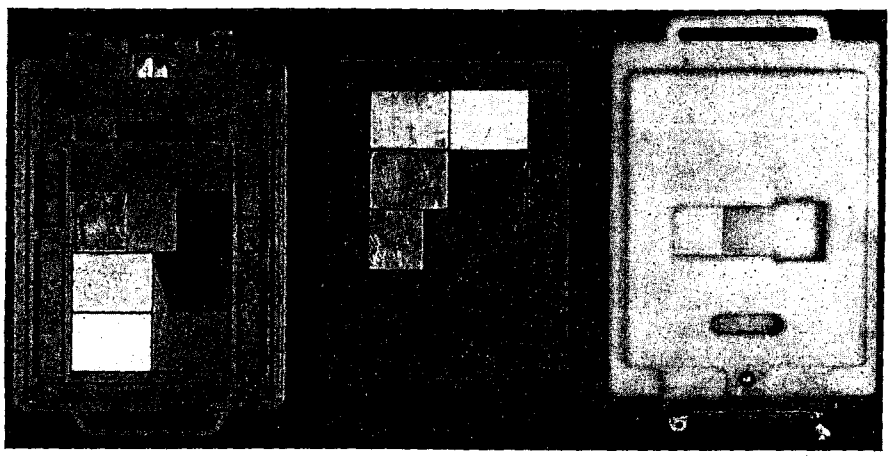

FIG. 5. New film holder.

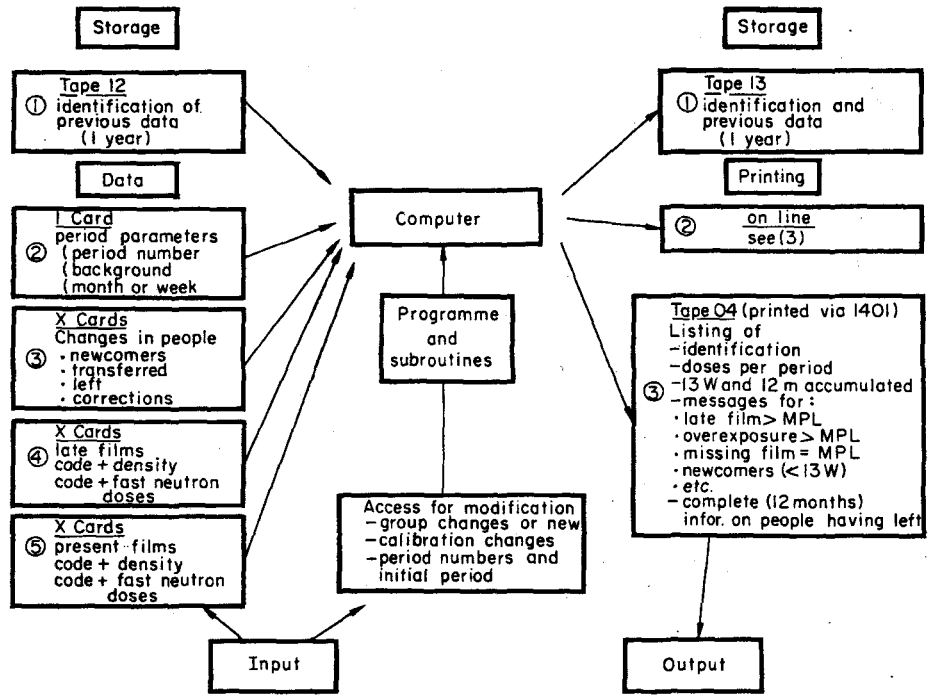

FIG. 6. Block diagram of the film-badge results processed by the Computer.

current period (β, γ, slow neutrons, fast neutrons and total dose in mrem, and in addition the accumulated total doses for the previous 13 weeks and 12 months). Films that are not returned are assigned the average maximum permissible dose for the period in question, but this value is corrected if the films are subsequently returned. Other messages, such as overexposure, etc., are also printed out.

The information for a complete year is memorized on a tape. It is then an easy task to work out relevant statistics or to extract at any time any useful data. The copies of the results are filed with the Health Physics group, as a whole and per group. A copy of the result is sent to each group or team leader for information on his own staff. The responsible Health Physics technician for a radiation area also receives a copy in order to know the radiation received by the workers. This information is used for issuing access permits to radiation restricted zones and also for the control of individual exposures on the spot.

RESULTS AND DISCUSSION

The number of people at CERN under routine personnel radiation control is increasing from year to year. This can be seen from Table 1. With the exception of about 10% of the radiation workers whose film-badges are changed weekly, all film-badges are changed every month.

In 1965, more than 20,000 gamma films and 6000 neutron films were processed and read. The percentage of lost films was the same for the last two years and amounted to 3.1%.

Any dose exceeding the recommended average maximum dose for any one period (400 mrem/month or 100 mrem/week), is considered as an overexposure: 228 such cases occurred in 1965. This is understandable since these overexposures (almost exclusively due to gamma radiation) were received by people carrying out repair and maintenance work of the accelerators. Access to the accelerators for this kind of work is limited to only one to two days in

Table 1. Distribution of doses

Dose (rem/year)	Number of persons			
	1962	1963	1964	1965
0–1	687	871	1058	1220
1–2	42	45	105	36
2–3	11	18	22	21
3–4	8	12	8	3
4–5	6	2	5	0
5	3	1	1	1
Number of people under routine cont.	757	949	1199	1280

every two-week period, and this explains such overexposures. In some of these cases there were exposures exceeding the ICRP recommended dose value for 3 and 12 month periods.

One of the most important problems in assessing the personnel radiation dose near high-energy accelerators is to what extent the results obtained are valid and reliable. This problem reflects the method of interpretation of the film-badge reading. No attempt is made in this paper to elucidate this problem, but some few remarks can be given in the light of comparison with the results obtained from the rather complicated set of radiation survey instruments used near the CERN accelerators. Such comparison has shown that the film-badges normally overestimate the dose by a factor of about 1.5. In regions with low dose-rates it has been observed that an underestimation of 20% occurs. These figures are sufficiently conservative and at the same time not restrictive for the work to be done. This applies however only to regions outside and far away from the shields. As soon as direct beams exist close to weak shielding, the readings become irregular and might lead to large factors of over-estimation or underestimation of the dose. Such conditions are normally recognized by the existence of special tracks on the neutron film-badges.

REFERENCES

1. J. Baarli and A. H. Sullivan. Radiation dosimetry for protection purposes near high-energy accelerators. *Health Physics* **11,** 353 (1965).
2. J. Baarli. The radiation protection of the CERN Laboratory and its surroundings when operating the CERN accelerators. *Proc. Congrès inter-national sur la Dosimétric des Irradiations dues à des Sources externes.* Paris, 23–27 Nov. 1964, in press.
3. I.C.R.P. Publication 4 Report of Committee IV. Pergamon Press, 1964.
4. J. Baarli, St. Charalambus, J. Dutrannois, K. Goebel, H. H. Hubbell, Jr., T. R. Overton, A. Rindi and A. H. Sullivan. Hazard from induced radioactivity near high-energy accelerators. *Proc. Radiological Protection of the Worker by the Design and Control of his Environment.* Bournemouth 18–22 April, 1966.
5. J. Baarli and A. H. Sullivan. Health physics survey methods for measurements of stray radiation around the CERN accelerators. *Proc. Symp. on Accelerator Radiation Dosimetry and Experience,* Brookhaven, 1965.
6. J. Baarli and J. Dutrannois. The nuclear stars in personnel neutron track films carried at CERN. *Proc. Symp. on Personal Dosimetry Techniques for External Radiation.* Madrid, 1–15 April, 1963.

AIRBORNE RADIOACTIVITY PRODUCED IN THE CERN ACCELERATORS

A. RINDI, S. CHARALAMBUS and J. BAARLI
CERN, Geneva

Abstract—It is of interest in connection with radiation protection of accelerators to evaluate the risk from radioactivity of the air near such installations. This radioactivity is produced in the accelerator as a result of interactions of primary and secondary particles with the atmospheric air. Due to ventilation, radioactive air may also be released to regions outside the main shielding enclosure and should therefore also be considered in this respect.

In order to provide some information about this radioactivity, calculations have been made of possible isotopes and their concentration. These results are compared with measurements made near the CERN high-energy machines. It is found that after 30 minutes of accelerator operation ^{41}A, ^{11}C, ^{13}N and ^{15}O are the isotopes of main importance and measurements show that their total concentration near a target region may reach values up to a few μCi/l of air.

The relative contribution of these isotopes was found to be 14% for ^{41}A, 31% for ^{11}C, 47% for ^{13}N and 8% for ^{15}O. For longer operational time ^{3}H and ^{7}Be may in addition make a contribution to the total radioactivity of the air.

The data obtained are compared to maximum permissible concentrations recommended by the International Commission on Radiological Protection. For those isotopes not stated in the ICRP tables calculated maximum permissible concentrations have been used for comparison. It is concluded that with the present intensities of high-energy beams (10^{11} p/sec) a radiation risk from air activity can be present and should be taken into consideration.

The paper has been published in *Nuclear Instruments and Methods*, 47, 227–232 (1967).

LA RADIOPROTEZIONE INTORNO AGLI ACCELERATORI DI FRASCATI

M. LADU, M. PELLICCIONI e M. ROCCELLA
Gruppo di Dosimetria delle Alte Energie, CNEN, Frascati, Roma (Italy)

Sommario—Vengono dapprima esposti i problemi di radioprotezione intorno agli acceleratori di alta energia. In particolare vengono discussi i seguenti problemi:

(a) schermature;
(b) produzione di gas radioattivi;
(c) produzione di gas tossici;
(d) radioattività residua;
(e) pozzi di spegnimento dei fasci.

Si accenna anche al problema dello "skyshine" e a quello di ventilazione dei locali in rapporto all'espulsione di pulviscolo atmosferico attivato.

Si esamina quindi il caso degli acceleratori di Frascati con particolare riguardo ai monitori fissi e ai vari dispositivi messi in atto per la sicurezza del personale.

Il lavoro termina con un cenno ai problemi di radioprotezione che potranno presentarsi nel prossimo futuro, con l'entrata in funzione di nuovi e sempre più potenti acceleratori di particelle.

REMOVAL OF RADIOACTIVE LUMINOUS PAINT FROM INSTRUMENT DIALS

N. ROSENTAL

Health Physics Department, Soreq Nuclear Research Center, Israel Atomic Energy Commission, Yavneh, Israel

Abstract—The overhaul of radioactive luminous painted dials is a common practice. Usually, the old radioactive paint is mechanically scraped, then the dial is manually reprocessed and then repainted with fresh radioactive luminous paint.

All these operations raise airborne and surface radioactive contaminations, which may result in health hazards to the workers.

The present work describes a safe facility and procedure for the above listed operations which will prevent external and internal radioactive contamination hazards.

The facility consists of a fume hood convertible into a glovebox with a built in system for the removal of old luminous paint and dial decontamination. The conversion of the fume hood into a glovebox is made when the preparation stage is reached for the luminous paint. The process will be described in some detail and experimental decontamination results will be discussed.

AIRBORNE IODINE MONITORING AT THE RADIOISOTOPE TEST PRODUCTION PLANT, JAERI

S. FUKUDA, M. NARITOMI, S. IZAWA and Y. IZUMI
Division of Health Physics and Safety, Japan Atomic Energy Research Institute,
Tokai-mura, Naka-gun, Ibaraki-ken, Japan,

Abstract—During production of iodine-131 from an irradiated telluric acid (H_2TeO_4) by the distillation method, a considerable amount of airborne radioiodine is generated in the cell and its major portion is discharged to the atmosphere through a stack after passing through air cleaning systems, consisting of prefilters, charcoal filters and high efficiency particulate filter. Some minor portion of airborne iodine generated leaks directly out of the cell to the service area and operation area, although a negative pressure is maintained in the cell.

To evaluate the airborne iodine concentration in air and the amount discharged as accurately as possible, extensive radiation monitoring was performed using various kinds of monitoring devices. As one of these devices, an iodine sampler was developed which is composed of three sampling components, i.e. HV-70 filter paper, charcoal-impregnated filter paper and charcoal cartridges.

At several sampling positions of the air cleaning systems, the overall collection efficiency of the sampler was evaluated by taking into account activities collected in cold traps (containing granular charcoal) which are connected to the sampler in series. It was found that the overall collection efficiency ranges from 70% to 100%, highly dependent on whether the samples were taken at upper stream or downstream of the air cleaning systems.

Data obtained from the airborne iodine monitoring at the stack and in the working areas conducted during the iodine-131 test production are presented, and internal exposures of the operating personnel received by inhaling the airborne iodine are described in relation to the air contamination of the working areas.

INTRODUCTION

Many of the papers on methods or techniques of airborne radioiodine sampling are mainly concerned with the characterization and behaviour of airborne iodine under the accidental conditions of a reactor. There are few reports [1-7] concerning a routine sampling of airborne iodine released from a stack during normal operation of a radioiodine production facility or fuel processing plant, and also routine airborne iodine monitoring in working areas.

In general, it is much more difficult to sample efficiently and evaluate the concentration of radioiodine in air during routine operations than during accidental events. The more reactive components of airborne iodine have such properties as to be easily adsorbed and to be generally removed in passing through the filtering media of an air cleaning system. The less reactive components constitute a major portion of the airborne iodine discharged. The behaviour of iodine leaking directly into the working areas from the processing cell, etc., would be rather similar to that in the accidental release.

In the radioisotope test production plant, which was constructed to gain experience for the construction of a large-scale radioisotope production plant, iodine-131, the chemical form of which is NaI in basic sodium sulfite, is produced from a sulfuric acid solution of irradiated telluric acid (H_2TeO_4) by the distillation method. During the processing, a considerable amount of airborne iodine is generated in the cells and its major portion is discharged into the atmosphere after passing through two existing air cleaning systems. Some minor portion of the airborne iodine leaks directly

into the service and operation areas from the cells.

In order to evaluate the iodine concentration in the air and the amounts released, extensive radiation monitoring was performed with various types of air monitoring devices. The present paper describes the airborne iodine monitoring carried out during the iodine-131 test production prior to the routine operation and also the performance of an iodine sampler employed in this monitoring program.

RADIATION MONITORING SYSTEM AND MONITORING DEVICES

Stack monitoring system

A schematic diagram of the air cleaning and monitoring systems for the iodine discharged into the atmosphere is shown in Fig. 1. The airborne iodine generated in the cells, mostly in a distillation cell, is filtered by two air cleaning systems before it is discharged through the stack (17 m high). The first is a cell-ventilation air cleaning system, consisting of a glass wool filter, 4 charcoal filters (670 × 1000 × 57, Barnebey Cheney–10 granular charcoal used) and an absolute filter installed on the top of each cell. The second is an exhaust air cleaning system, consisting of a glass wool filter and a charcoal filter (Model 7 FE filter manufactured by Barnebey Cheney Co., U.S.A.).

In the normal operation, the concentration of airborne iodine discharged increases very rapidly 30 min after start of the distillation, reaches a maximum in about one hour, and then decreases at the end. However, the iodine still continues to be released at low concentration. The variation in the concentration of released airborne iodine amounts to about 2 orders of magnitude during and following the processing.

To cope with such problems as highly filtered exhaust air and the varying concentration,

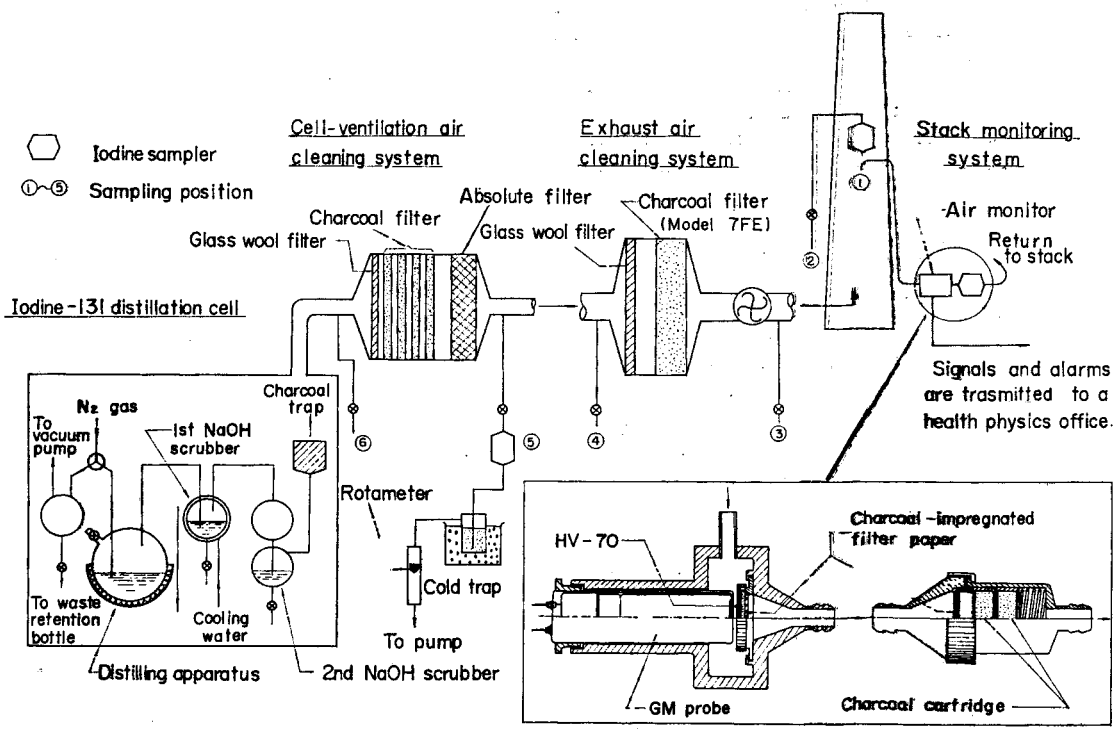

FIG. 1. Schematic diagram of airborne iodine monitoring and air cleaning systems at the radioisotope test production plant.

and to make it possible to evaluate the average concentration or the amount of airborne iodine released from the stack as accurately as possible, the iodine sampler, shown in Fig. 2 and in Table 1, was constructed in trial. The sampler was designed to ensure high overall collection efficiency under various sampling conditions, ease of handling and quick counting after the sampling, and low cost to be applicable to routine work.

FIG. 2. Iodine sampler.

Table 1. *Air Monitoring Devices*

Monitoring devices	Characteristics	Sampling media
Iodine sampler	Air flow rate: 25∼100 l./min External dimension: 70 mmØ, 215 mm or 230 mm long	HV-70 or HE-40 filter paper (50 mmØ, 9 mil thick) 1 Charcoal filter paper* 1 Charcoal cartridge† 2 or 3
Local air sampler‡	Air flow rate: 25 l./min	HV-70 or HE-40 filter paper 1 Charcoal filter paper 2∼3
Stack air monitor	Air flow rate: 50∼150 l./min Detector: end window type GM tube (window thickness 1∼2 mg/cm²) Range: 6 ranges from 0.1 to 10^4 cps	HV-70 or HE-40 filter paper 1 Charcoal filter paper 1∼2 (The iodine sampler is connected in series.)
Laboratory air monitor	Air flow rate: 25∼50 l./min Detector: end window type GM tube or 1 3/4″ × 2″ NaI scintillator Range: 4 ranges from 150 to 1.5×10^5 cpm	HV-70 or HE-40 filter paper 1 Charcoal filter paper 1 Charcoal cartridge 2
Iodine monitor§	Air flow rate: 50∼100 l./min Detector: 1 3/4″Ø × 2″ NaI scintillator Range: 6 ranges from 0.1 to 10^4 cps Single channel pulse height analyzer used	HV-70 or HE-40 filter paper 1 Charcoal filter paper 1 (The iodine sampler may be connected in series.)

* Charcoal-impregnated filter paper, manufactured by Toyo Roshi (Toyo Filter Paper) Co. Ltd., Tokyo, Japan: 50 mmØ × 2 mm thick, average diameter of carbon particles ∼2μ.

† Charcoal cartridge, manufactured by Toyo Roshi Co. Ltd., Tokyo, Japan: 50 mmØ × 20 mm thick (effective thickness 18 mm), 30-mesh coconut shell charcoal used.

‡ Installed to evaluate an air contamination in fixed points of working areas.

§ A sample collected for a preselected interval, during which the sample is counted, is automatically moved and a succeeding filter paper is placed over a detector from a filter paper stocker.

The sampling positions in Fig. 1, except position No. 1, were used for measuring the collection efficiencies of the iodine sampler and the installed charcoal filters. These positions were not used for routine monitoring. A continuous air monitor and the iodine sampler are installed at position No. 1 for routine stack monitoring. The primary purpose of installing the air monitor is to indicate the relative variations of iodine concentration with time by measuring continuously the activity accumulated in the charcoal filter paper and to actuate an alarm immediately if such an abrupt change of the concentration or an unusual release that exceeds a preset level should occur. It would be impossible to calibrate the air monitor for iodine and determine the correct concentration because of the uncertainty of the collection efficiency of each sampling medium for the various forms of airborne iodine. For these reasons, the air monitor is employed together with the iodine sampler to evaluate the correct average concentration or the amount released over a certain period. Characteristics of these monitoring devices are listed in Table 1.

Monitoring system for the working areas

The monitoring system for the working areas is shown in Fig. 3. The local air sampling system was designed for the purpose of examining the correlation between the iodine concentrations in the air and the actual thyroid burdens as determined by a whole body counter. Using these results necessary measures are taken to control the internal exposure by inhalation. The other purpose of this monitoring system is to find the origin of leaks of the airborne iodine and to improve the air-tightness of the cells and their equipment. In addition, a laboratory air monitor was operated to monitor continuously the general air in the service area and to actuate the alarm. The monitoring devices

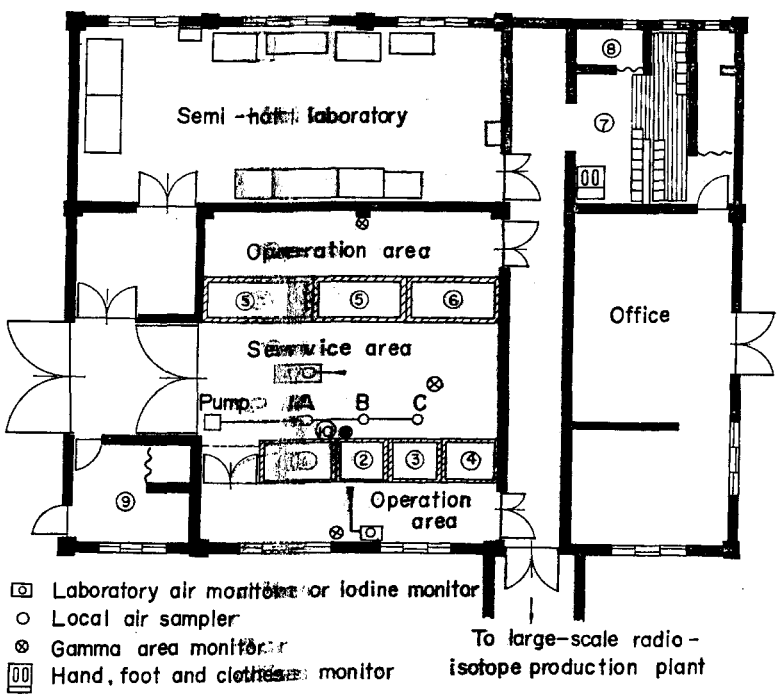

FIG. 3. Radiation monitoring system for working areas. 1–4. Iodine-131 processing cells. 1. Preparation. 2. Distillation. 3. Dispensation. 4. Storage. 5. Phosphor-32 processing cells. 6. Sulfur-35 processing cell. 7. Changing room. 8. Shower room. 9. Decontamination room. ▨ Temporary liquid waste retention bottle.

employed are listed in Table 1 and shown in Fig. 4.

Counting of the samples

The counting method for the charcoal filter paper and charcoal cartridge is somewhat complicated. Two kinds of counting equipment were used: (1) a 400 channel pulse height analyzer with 5 in. × 4 in. NaI(Tl) detector for the measurement of the collection efficiency of the iodine sampler; and (2) a scaler with $1\frac{3}{4}$ in. Ø × 2 in. NaI(Tl) detector for the routine monitoring. The former was calibrated for the charcoal filter paper by counting the 0.364 MeV photopeak of standard iodine-131 sources. In this case, its overall counting efficiency is 17% and the minimum detectable amount is approximately 10^{-5} μCi for 4-min. counting.

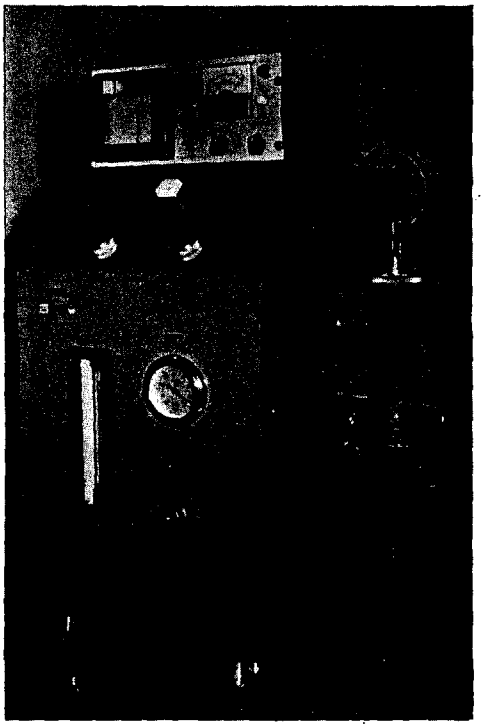

FIG. 4a. Laboratory air monitor.

FIG. 4b. Iodine monitor.

The overall counting efficiency for the charcoal cartridge was determined to be 14%, assuming that the collected iodine was uniformly distributed throughout the cartridge. The efficiency selected was between 14% and 17%, according to the actual distribution of iodine in the cartridge.

The calibration of the scaler with $1\frac{3}{4}$ in. Ø × 2 in. NaI(Tl) detector was also performed, using standard iodine-131 sources by suitably setting the discriminator. The minimum detectable amount is approximately 10^{-4} μCi for 10-min counting.

MONITORING OF AIRBORNE IODINE AT THE VENTILATION DUCT AND STACK

In order to ensure the effectiveness of airborne iodine monitoring at the stack and in the working area, the field test for determining the collection efficiencies of the iodine sampler was carried out (using the airborne iodine produced during the processing) in parallel with the routine stack monitoring, because the results obtained by a laboratory test could not be directly applied to the field monitoring. The details of this test, conducted under the various sampling conditions, will be given in a later paper together with the counting methods for the sampling media. The present paper describes the measuring results relating to the stack monitoring.

The overall collection efficiency of the iodine sampler was determined, using one or two reference cold traps which were connected to the sampler in series and consisted of glass wool and activated granular charcoal (Barnebey Cheney-10, 130 g used) maintained at a temperature of less than −50°C with dry ice immersed in ethanol.

To examine the dependence of the collection efficiency of the iodine sampler on the degree of the filtration by the air cleaning systems, the samplings were carried out at several different positions in the air cleaning systems shown in Fig. 1. In passing through the air cleaning systems, the physical and/or chemical forms of iodine might be changed and the fraction of less reactive components in the discharged iodine would be considerably increased.

Sampling at the inlet of the cell-ventilation air cleaning system

Two types of samplings whose periods are different were adopted as follows: (1) short period sampling (less than 2 hr, in general 30 min), which was employed for the purpose of following the variations of concentration with time and at the same time determining the collection efficiency in this sampling period; and (2) long period sampling (more than 8 hr) for examining the dependence of the collection efficiency on the concentration determined by the short period sampling, which is usually applied to the routine stack sampling. An example of results obtained is shown in Fig. 5.

In the short period sampling the overall collection efficiency was around 100%, while in the long period sampling it varied within the range of from 95% to 100%, depending on the concentrations and atmospheric conditions.

The distributions of the iodine collected in each component of the sampler during and following the processing are shown in Fig. 6 and Table 2 for the short period sampling and the long period sampling, respectively. As seen

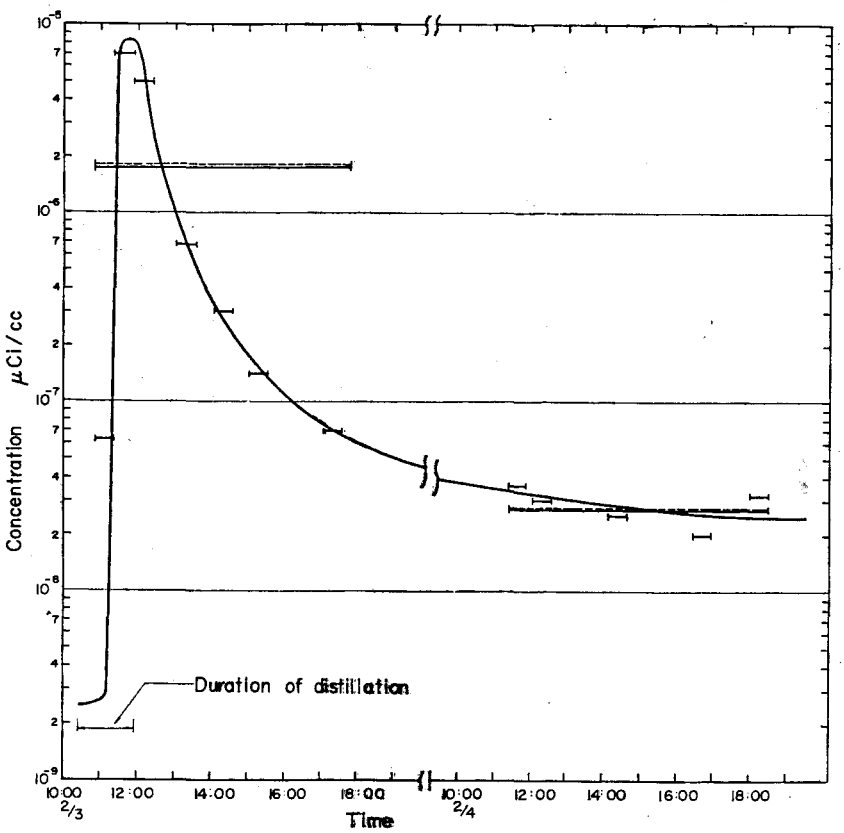

FIG. 5. Variation of concentration of airborne iodine at the inlet of the cell-ventilation air cleaning system during and following the processing.

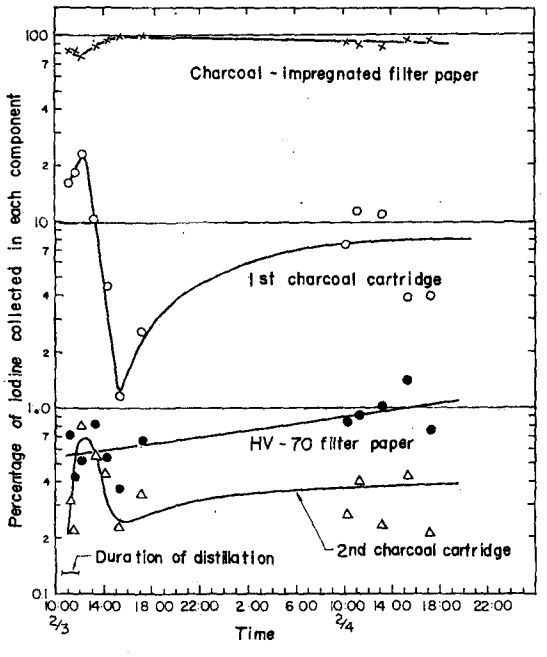

FIG. 6. Distribution of airborne iodine collected in each component of the sampler during a 30-min sampling at the inlet of cell-ventilation air cleaning system. Air flow rate is 45 l./min. Detectable quantity of iodine-131 is not collected in the cold trap.

in Fig. 6, more than 80% of the iodine is collected in a charcoal-impregnated filter paper. The percent of iodine collected in the charcoal filter paper increases up to approximately 100% and then gradually decreases with time after the end of the processing, although the released amount of iodine markedly falls off. The fraction of iodine in the first charcoal cartridge shows a remarkable fluctuation during the processing, in particular within about 3 hr of the start of the distillation. These results indicate that the chemical forms of airborne iodine, probably including I_2, HI, HIO_3 and HIO_4,[8] may well be changed from the initial stage of generation to the end of distillation. In comparing Fig. 6 and Table 2, little difference is found between the distributions of iodine collected in each component of the sampler for the short period and for the long period, although in the long period sampling the fractions collected in the first and second charcoal cartridge were of the same order of magnitude. The increase of the fraction in the second cartridge is caused by the fact that the iodine adsorbed in the activated charcoal during the abrupt change of concentration is desorbed in the course of the long period sampling under the low concentration.

Sampling at the exit of the cell-ventilation air cleaning system

In the sampling at the exit of the cell-ventilation air cleaning system, the distributions of the iodine collected in each component of the sampler is quite different from those collected at the inlet. As shown in Fig. 7 and Table 2, more than 60% of airborne iodine is collected in the first charcoal cartridge, whereas less than 20% of iodine is collected in the charcoal filter paper. This indicates that after passing through the cell-ventilation air cleaning system the fraction of the less reactive components in the residual airborne iodine increases relatively and the collection efficiency of the charcoal filter paper for the filtered iodine is only less than 20%. Despite such great differences between the iodine distributions among the components of the sampler obtained by the exit sampling and those obtained by the inlet sampling, overall collection efficiency of the sampler was still maintained at higher than 90% (94% on the average) in both the short period and the long period sampling.

Sampling at the exit of the exhaust air cleaning system and the stack

The exhaust air cleaning system originally consisted of a glass wool filter and an absolute filter and the discharged amount of the total processed iodine was rather high, ranging from 0.5% to 5%. In addition, the distributions of iodine among the components of the sampler and its overall collection efficiency at the stack or the exhaust air cleaning system, which ranged from 89% to 94% (91% on the average), were almost the same as those obtained at the exit of the cell-ventilation air cleaning system, indicating that the absolute filter was not efficient for removing the airborne iodine.

Based on these results, a charcoal filter (Model 7FE) was installed instead of the absolute filter in the exhaust air cleaning system, in order to

Table 2. Distribution of Iodine-131 Activity Collected in each Component of the Sampler during the Long Period Sampling at Various Positions of the Air Cleaning Systems. Airflow Rate 25 l./min.

Run No.	Sampling position*	Sampling period	Activities collected in each component of the sampler: Total activity collected μCi	HV-70 filter paper μCi	HV-70 filter paper %	Charcoal filter paper μCi	Charcoal filter paper %	1st charcoal cartridge μCi	1st charcoal cartridge %	2nd charcoal cartridge μCi	2nd charcoal cartridge %	Cold trap μCi	Cold trap %	Overall collection efficiency %
[illegible]	[illegible]	2/3 [illegible]	19.6	2.8 × 10^{-3}	0.14	16.3	83.3	1.65	8.4	0.88	4.5	0.73	3.7	96
21	No. 6	2/4 10:20～17:30	0.30	1 × 10^{-3}	0.3	0.28	93.8	1.2 × 10^{-2}	4.0	1.2 × 10^{-3}	0.4	2.5 × 10^{-3}	0.8	99
20	No. 5	12/16 10:00～18:00	0.93	< 10^{-5}	—	0.15	15.5	0.66	71	7.9 × 10^{-2}	8.5	4.6 × 10^{-2}	5.0	95
		12/17 10:00～18:00	2.0 × 10^{-2}	< 10^{-5}	—	2.6 × 10^{-2}	13	0.13	67	2.1 × 10^{-2}	11	1.7 × 10^{-2}	9.0	91
26	No. 3	5/27 14:30～21:30	1.4 × 10^{-2}	1 × 10^{-5}	—	3.4 × 10^{-3}	24	6.8 × 10^{-3}	47	2.0 × 10^{-3}	14	2.2 × 10^{-3}	15	85
		5/30 10:45～17:45	3.6 × 10^{-3}	< 10^{-5}	—	2.5 × 10^{-4}	7	1.8 × 10^{-3}	50	9.7 × 10^{-4}	27	5.8 × 10^{-4}	16	84

* Sampling positions of No. 6 and No. 5 are located at the inlet and exit of the cell-ventilation air cleaning system, respectively and a sampling position of No. 1 is located at the exit of 7 FE charcoal filter in the exhaust air cleaning system, as seen in Fig. 1.

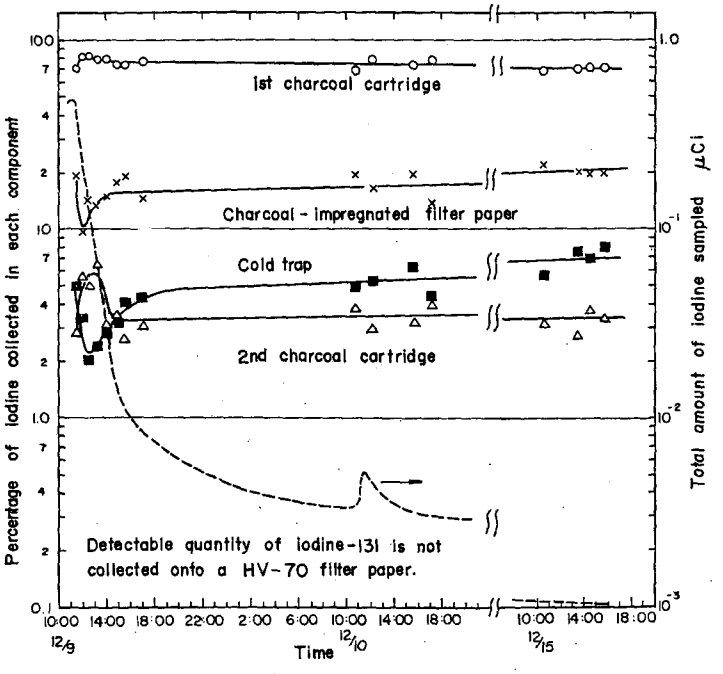

FIG. 7. Distribution of airborne iodine collected in each component of the sampler during a 30-min sampling and variation of concentration at the exit of cell-ventilation air cleaning system. Air flow rate is 45 l./min.

make the filtration much more efficient and to assure the environmental radiological safety. As a result of this change, the percent of the discharged iodine was reduced to less than 0.03%, as seen in Fig. 8. On the other hand, the overall collection efficiency of the sampler decreased down to a minimum of 70% in the long period sampling, showing that the relative amounts of less reactive components in the airborne iodine discharged increased considerably. However, there was not much difference between the distributions of the iodine among the components of the sampler in the samples taken at the exit of the cell-ventilation air cleaning system, and those taken at the exit of the exhaust air cleaning system.

The collection efficiencies of the sampler obtained in each stage of the filtration are summarized in Fig. 9. The overall collection efficiencies ranges from 70% to 100%, depending on the various sampling conditions; in particular, on whether the samples were taken upstream or downstream of the air cleaning systems. Relative humidity and temperature during the period of this series of samplings were between 60% and 80% and about 20°C, respectively. Significant differences were not found between the overall collection efficiencies obtained at the exit of the exhaust air cleaning system and at the stack.

At every stage of the filtration, iodine was not collected appreciably onto the HV-70 filter paper, so that it is concluded that the airborne iodine generated during processing is in the vapour phase and little, if any, iodine is associated with particles.

AIR CONTAMINATION OF WORKING AREAS

Service area

In the early stage of the iodine test production, air contamination by the leaked iodine occurred in the service area, despite a negative pressure differential of about 40 mm H_2O in each cell. The variations of concentrations

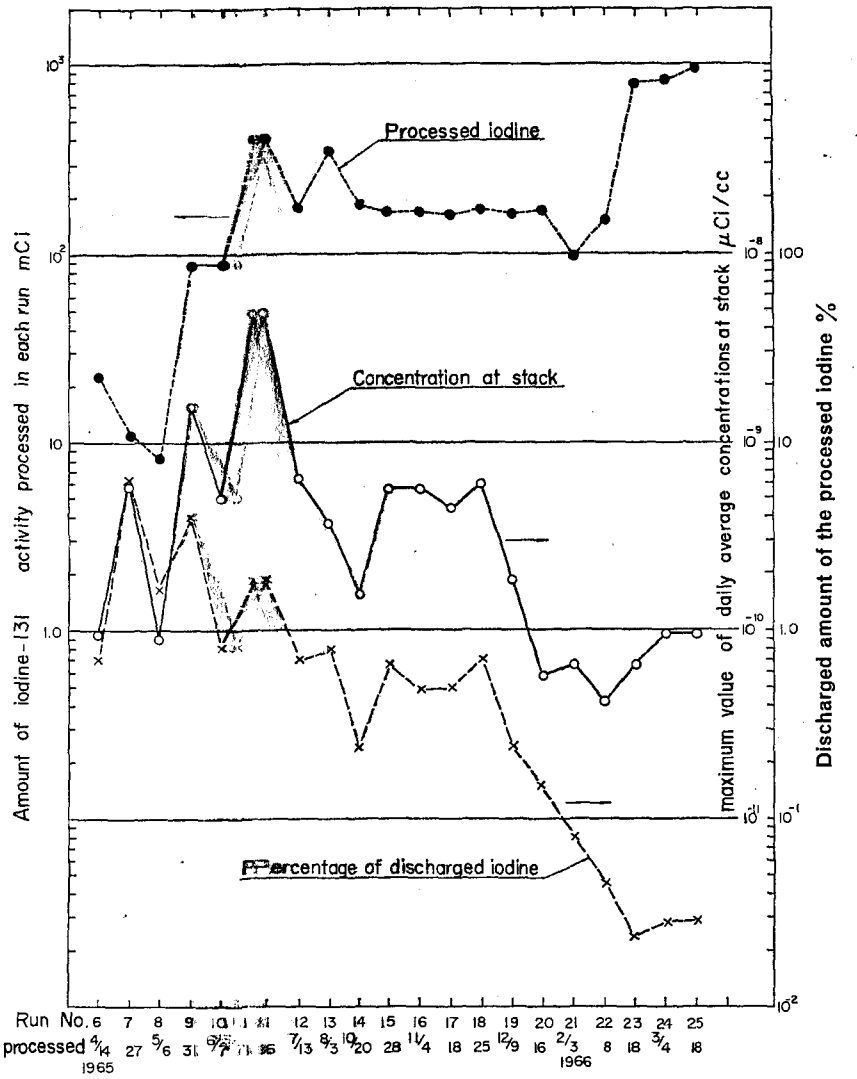

FIG. 8. Percentage of discharged iodine and maximum value of daily average concentrations at stack in relation to iodine processed in each run.

obtained at three sampling points behind the cells shown in Fig. 3 are illustrated in Fig. 10. The mode of variations is similar to that at the stack, but in Fig. 10 the first and second peak concentration appears about 10 hr and 1 day, respectively, later than those at the stack and the magnitude of the concentration is different at each sampling point. These indicate that the airborne iodine leaks from the distillation cell nearly proportionally to the amount generated, and gradually accumulates in the service area.

On the basis of such results, some attempts were made to prevent the leakage of the airborne iodine from the cells as follows: (1) the places where leakage was likely to occur, for example, joints of the cell air ventilation duct, openings of the cell attachment, etc., were sealed; and (2) the cell-ventilation air cleaning system

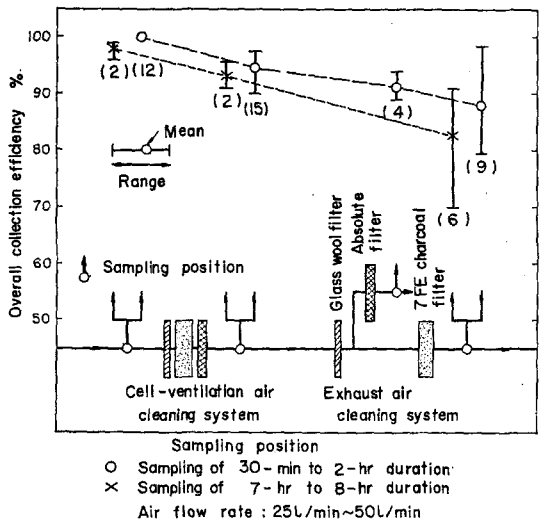

FIG. 9. Summary of collection efficiencies of the sampler at each stage of the filtration by air cleaning systems. Figures in brackets indicate number of measured samples.

was improved to maintain a negative pressure differential larger than 100 mm H_2O. In consequence, the air contamination of the service area decreased by about one order of magnitude or more, and at present the airborne iodine concentration is always kept below 5×10^{-11} μCi/cc during normal operation. An example of the air contamination after improving the air-tightness is shown in Fig. 10b. The mode of concentration variation in Fig. 10b is different from that in Fig. 10a and no correlation is present between the concentration variation at the stack and that in the service area. The air contamination in Fig. 10b might have been caused by the leakage of airborne iodine from a liquid waste bottle which was placed behind the cell access door to retain temporarily the irradiated telluric acid solution after the end of the processing.

Operation area

Airborne iodine monitoring is continuously performed in the operation area whenever operations are carried out. The results obtained in the operation area during the same run as in Fig. 10a are shown in Fig. 11. The concentration in the operation area reaches a maximum value of approximately 10^{-10} μCi/cc about 2 days after start of the processing and is about one tenth of the concentration in the service area. This air contamination mainly occurs by the diffusion of airborne iodine from the cells into the service area. After various measures for preventing the leakage were taken, the air contamination decreased to the minimum detectable limit (8×10^{-12} μCi/cc) during normal operation, except that slightly higher concentrations than the minimum detectable limit were found under incidental conditions for a day or so, two or three days after the distillation.

INTERNAL EXPOSURE OF THE OPERATING PERSONNEL

In order to examine the effectiveness of the air monitoring system in evaluating the inhalation hazard, the thyroid burden of the operating personnel was measured each time after the end of the processing using a whole body counter. The results measured for the period April 1965 to March 1966 are summarized in Fig. 12. The total number of individuals measured over the period was 69, in 28 of which thyroid uptakes were detected. The maximum of the thyroid burdens summed for each individual over the period was 4.3 m μCi, which gives an integrated thyroid dose of 28 mrem.

The amount of actual uptake in the thyroids, as determined by the whole body counter, is at most about 200 times and on the average about 20 times as large as the maximum probable uptakes calculated using both the daily average concentrations in the working areas and the working time. No significant correlation was found between the actual uptake and the calculated uptake, as shown in Fig. 13. This could be caused by the fact that such marked variations of concentration might exist in both time and space that the exposure cannot definitely be assessed with the daily average concentrations determined by the samplers at fixed points. In addition, human exposure due to the inhalation could be highly influenced by personal factors such as working habits, respiratory rate, etc.

To permit more precise assessment of the air contamination to which individuals are exposed, personal air samplers (using a charcoal filter paper and a charcoal cartridge at a flow rate

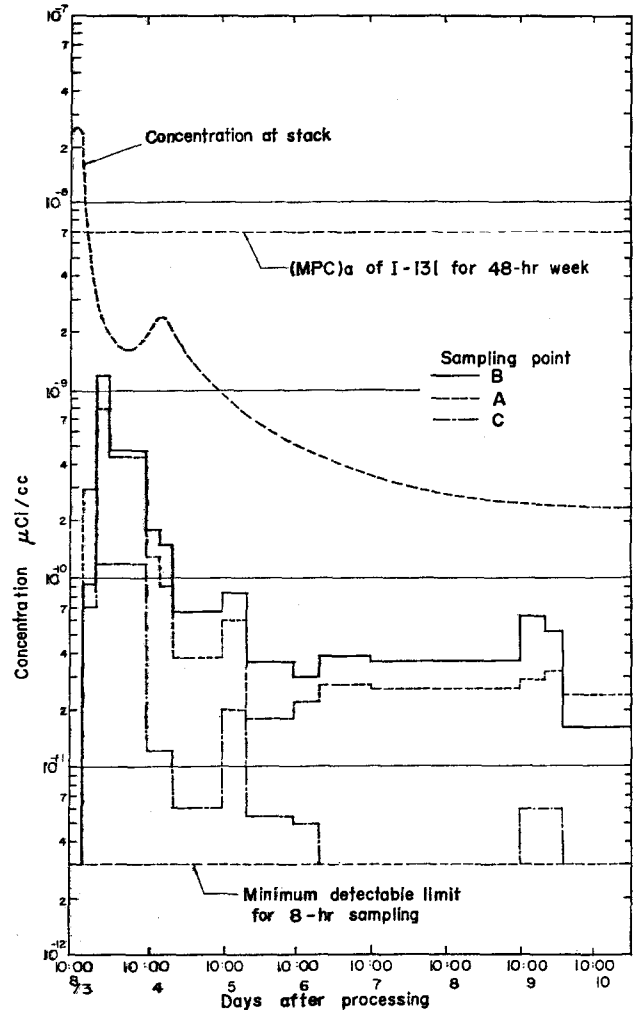

FIG. 10a. Variations of concentrations in the service area during and following the processing before improving an air-tightness of the cells. Air flow rate is 25 l./min.

of 10 l./min) are now employed. Preliminary results indicate a fairly good agreement between the activity on the charcoal paper, in which the collection efficiency is taken into consideration, and the actual thyroid burdens.

Further detailed investigations are planned to improve the existing air sampling system and to obtain reasonable correlations between the results of the samplers at fixed points, the results of the personal air sampler carried by operators, and the actual thyroid burdens.

CONCLUSIONS

The field test of the newly developed sampler conducted at the isotope test production plant shows that it can be satisfactorily employed for the purposes of routine monitoring within the error of $\pm$ 20%, and it is now widely applied to the airborne activity monitoring at JAERI.

Internal exposures of the operating personnel due to the inhalation of iodine-131 occurred during the test production. Although these exposures were not significant from the view-

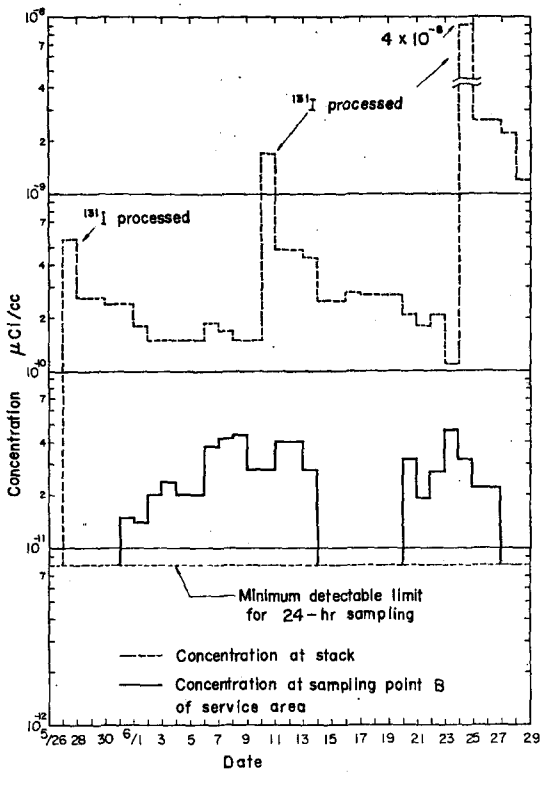

FIG. 10b. Variation of concentration in the service area after improving an air-tightness of the cells.

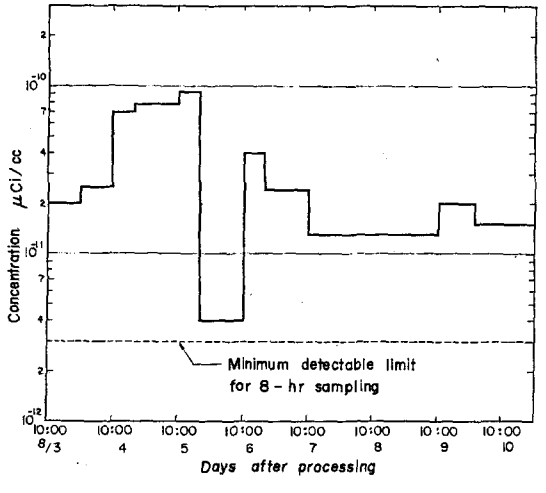

FIG. 11. Variation of concentration in the operation area in the same run as in Fig. 10a.

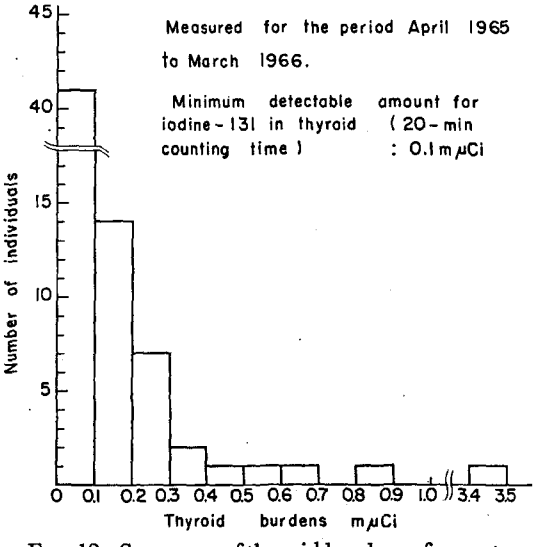

FIG. 12. Summary of thyroid burdens of operating personnel measured by a whole body counter. The total number of individuals measured over the period was 69, in 28 of which thyroid uptake was detected.

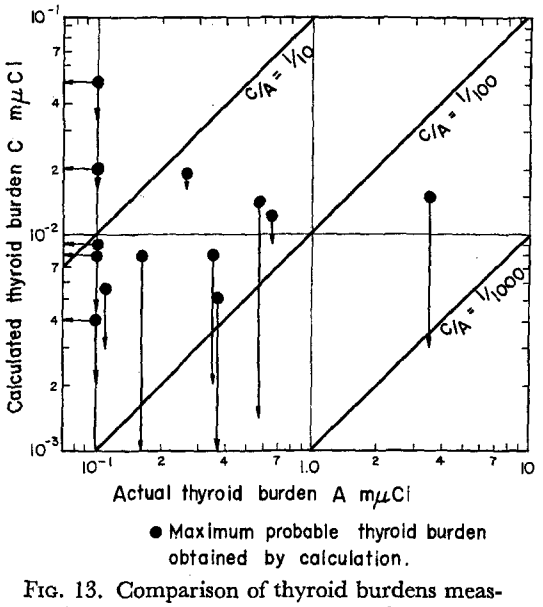

FIG. 13. Comparison of thyroid burdens measured by a whole body counter and those calculated using both the daily average concentration and the working time. Vertical arrow shows the extent of the uncertainty of the thyroid burden, which results from the concentrations of less than minimum detectable amounts in the working area. Horizontal arrow shows the thyroid burden of less than the minimum detectable amount of the whole body counter.

point of exposure control, many efforts were made to reduce both the airborne iodine generation and its leakage, which resulted in the remarkable reduction of the air contamination in the working areas. The amounts of iodine discharged through the stack were also reduced by about 2 orders of magnitude by installing a charcoal filter in the exhaust air cleaning system.

The monitoring system for the radioisotope test production plant will be applied in the more improved form to the new large-scale radioisotope production plant where the production of iodine-131 is planned at a cycle of 10 Ci/week.

ACKNOWLEDGEMENTS

The authors are indebted to many of their colleagues who took part in this series of airborne iodine monitoring and field test of the iodine sampler, and wish to express their appreciation to the staffs of Division of Radioisotope Production, JAERI, for their collaboration and assistance. The measurements by the whole body counter were carried out under the supervision of Dr. M. Fujita.

REFERENCES

1. J. K. SOLDAT. *J. Air Pollution Control Assoc.* **3,** 787 (1961).
2. J. D. MCCORMACK. ^{131}I sampling system efficiencies at Purex and Redox stacks. HW-73288 (1962).
3. J. D. MCCORMACK. Radioiodine sampling with activated charcoal cartridges. HW-77126 (1963).
4. C. F. FOELIX and L. GEMMEL. The use of activated charcoal iodine monitors during and following a release of fission product iodine. BNL-7522 (1964).
5. C. W. SILL and J. K. FLYGARE JR. *Health Phys.* **2,** 261 (1960).
6. H. J. ETTINGER and J. E. DUMMER, JR. Iodine-131 sampling with activated charcoal and charcoal impregnated filter paper. LA-3363 (1965).
7. H. J. ETTINGER. *Health Phys.* **12,** 305 (1966).
8. J. TADMOR. *Intern. J. Appl. Radiation and Isotope* **16,** 191 (1965).

THE SIGNIFICANCE OF RADIOACTIVE AEROSOL MEASUREMENTS MADE IN THE WORKING ENVIRONMENT

W. A. LANGMEAD and D. T. O'CONNOR
Radiological Protection Division, Authority Health and Safety Branch, UKAEA, Harwell, Didcot, Berks., U.K.

Abstract—The objectives of radioactive aerosol measurements in the working environment are reviewed; it is emphasized that a clear distinction must be maintained between (i) sampling to determine personal exposure—both chronic and acute intakes; (ii) sampling to determine general contamination levels in the working environment; and (iii) early warning sampling using alarm devices to detect important increases in the level of air contamination in the working area.

The suitability of personal air samplers for the measurement of personal exposure is discussed, in particular the relevance of short term or even individual exposure measurements. In many areas upper limits to average personal exposure can be estimated satisfactorily from continuously operated static samplers. In such cases it is necessary to make assumptions about the relationship between the long-term average air contamination as measured by such static samplers and average personal exposure as measured by personal air samplers.

Published mean values of the ratio of results obtained with personal air samplers and static air samplers are reviewed and shown to vary widely depending on the nature of the aerosol and the working environment, and the relative positions of the instruments. It is concluded that in the absence of evidence to the contrary, a factor of 0.1 should be applied to the ICRP maximum permissible concentrations to convert them to criteria against which the long-term average of the results from static air samplers may be used to demonstrate compliance.

Measurements of the particle size distributions of aerosols encountered in establishments of the Atomic Energy Authority are discussed and the application of this data to allow modified values of ICRP maximum permissible concentrations to be employed. These modified values involve a factor derived from the difference between the lung retention of the fraction of the sample assumed to be respirable and that of the ICRP Standard Lung Model. The further modifications to the current ICRP values of $(\text{m.p.c.})_a$ permitted by the lung model proposed by the ICRP Task Group on Lung Dynamics are briefly considered in relation to the particular aerosols discussed.

THE MONITORING OF RADIOACTIVE NOBLE GASES IN AIR

W. F. MERRITT

Environmental Research Branch, Biology and Health Physics Division, Atomic Energy of Canada Limited, Chalk River, Ontario, Canada

Abstract—The radioactive noble gas content of 400-litre air samples collected in meteorological balloons was measured by γ-ray spectrometry. Particulates and iodines were removed by a filter and a bed of activated charcoal in the sample line. The balloons were placed over a 3 in. × 3 in. NaI (Tl) crystal in a large lead shield (30 in. × 30 in. × 30 in.) with 4 in. of shielding on all sides. The apparatus was calibrated with gas samples that had been assayed by absolute counting techniques. Argon-41 was calibrated against cobalt-60 in a high pressure 4π ionization chamber. Xenon-133 and xenon-135 were separated from irradiated xenon on a mass separator and assayed by internal gas proportional counting. The counting efficiency of the crystal with varying gas volumes was measured and optimum conditions selected. Efficiencies varied from 0.1% for argon-41 to 0.4% for xenon-135. Sensitivities were in the range of femtocuries (10^{-15}) per cm^3 and in all cases were two orders of magnitude less than the MPC_a as set by the ICRP.

ÉTUDE DE L'EFFICACITÉ DE VÊTEMENTS DE PROTECTION EN UTILISANT LE TRITIUM COMME TRACEUR

F. BILLARD et A. CHARAMATHIEU
Service Technique d'Études de Protection, CEA, Centre d'Études Nucléaires, Fontenay-aux-Roses, France

Résumé—En vue de déterminer, lors d'une intervention dans un local contaminé par du tritium, le type de scaphandre devant être utilisé pour obtenir une protection optimale, le taux de renouvellement dans ce scaphandre et, le cas échéant, la durée de l'intervention, nous avons étudié le comportement des différents scaphandres existant en France, dans des atmosphères dont la concentration en tritium était variable.

Les manipulations ont porté sur six types de scaphandres. Des mannequins portant les scaphandres étaient disposés dans un caisson étanche et alimentés en air frais à des débits variant de 5 à 30 l/min. Sur chaque scaphandre on avait placé un point de prélèvement situé au niveau de la tête; pour les vêtements en deux parties on avait un autre point de prélèvement à hauteur de la ceinture.

Les premiers essais ont rapidement démontré que les vêtements de protection en deux ou trois pièces ne sont pas très efficaces, l'activité spécifique à l'intérieur de ces vêtements dépassant respectivement dans les meilleures conditions, c'est-à-dire avec un débit de ventilation maximum, 1/1000 et 1/600 de l'activité spécifique dans la pièce (soit une efficacité de 1000 et de 600). Les vêtements d'une seule pièce assurent une protection supérieure d'au moins un facteur 3.

Les meilleurs résultats ont été obtenus avec le scaphandre Scalhène dans lequel l'activité spécifique a toujours été inférieure, dans les conditions normales de ventilation, à l'activité minimale mesurable correspondant au bruit de fond des chambres d'ionisation utilisées pour la mesure, ce qui implique une efficacité d'au moins 16.000.

Toutefois, l'expérimentation ayant été effectuée sur des scaphandres habillant des mannequins, les effets de soufflet provoqués par les mouvements d'un manipulateur étaient éliminés. Or, ces effets pourraient accroître dans de grandes proportions l'activité spécifique dans les scaphandres. Un essai a donc été effectué avec le scaphandre Scalhène porté par un opérateur: l'activité spécifique dans le scaphandre est encore restée inférieure à la valeur minimale mesurable, si bien que l'on peut affirmer que son efficacité est toujours supérieure à 16.000.

Cette étude semble montrer que plus que la nature des matériaux plastiques constituant les parois du scaphandre, son étanchéité d'une part, le débit et la répartition de la ventilation interne d'autre part, conditionnent son efficacité. Il en résulte que la sélection opérée au moyen de tritium est valable pour d'autre produits contaminants.

DISCUSSION

J. SHAPIRO (*U.S.A.*):

Would Dr. McCaslin please supply additional information on his prong reading method with regard to ease of reading, training required, time to read a film, accuracy and sensitivity.

J. B. MCCASLIN:

Although we realize that a certain amount of subjectivity may be involved in identification of nuclear tracks, I would like to add to what has been said that Wade Patterson and Ronald Omberg recently compared cosmic ray spectra and the spectra of radiation existing near the Bevatron with both the threshold detector techniques and with the technique of using gray prongs from nuclear stars. The spectra shapes showed good agreement using these independent techniques.

G. A. SVENSSON (*Sweden*):

Do you have any comment on the competing reactions when using the Be-reaction in a high-energy bremsstrahlung radiation field?

J. B. MCCASLIN:

We realize of course that these reactions can occur; however, we have not done any work along these lines.

E. W. JACKSON (*U.K.*):

In the case of radiation which is escaping in the form of narrow beams, it seems possible for workers to receive significant doses without any recorded dose appearing on their film badges. Can the author say whether he has met this problem at CERN and what steps are taken to obtain an accurate assessment of the dosages received?

W. J. MEININGER (*Netherlands*):

In Fig. 1 you showed a plan of CERN, showing two regions for radiation control. How do you prevent non-radiological workers walking into the radiological areas?

J. DUTRANNOIS:

All areas where dose-rates higher than 2.5 mrem/hr exist are restricted areas which are under supervision; they are enclosed by shielding and fences and access is through interlocked doors. An access permit is required for entering these areas, which prevents access by non-radiation workers.

L. DE FRANCESCHI (*Italy*):

I would like to ask Mr. Dutrannois what is done at CERN in the very frequent case of a dose below the sensitivity of the personnel dosimeter (gamma and neutron). Do they put in the personal record the value "zero" or, instead, the accepted value of the lower limit of dosimeter detection (for instance 10 mR or so)?

J. DUTRANNOIS:

The lower limits of sensitivity are fixed at 10 mrem for the γ-films, and at 15 mrem for the neutron films. Doses lower than these limits are taken as zero. Even in the case of a weekly film distribution, the maximum error will be only of the order of 0.5 rem per year.

J. M. REES (*U.K.*):

I should like to ask Mr. Dutrannois what is considered the maximum acceptable dose rate at places where maintenance work has to be done on the accelerator.

J. DUTRANNOIS:

The maximum permitted dose level in an area where work has to be carried out is the one existing on the spot, as the work has to be done. In practice this corresponds to 6 to 8 rem/hr. When it is possible, some cooling time is allowed. In such places of course the work is done under the close and direct supervision of Health Physics, and the dose distributed between the maximum practicable number of people.

T. A. STEELE (*U.S.A.*):

Do you have radiation areas in which there are neutrons with energies between 0.1 eV and 0.4 MeV and, if so, how do you monitor personnel for neutrons in this energy region?

J. DUTRANNOIS:

For neutrons in the range of 0.1 eV to 0.4 MeV we have no means of measuring the dose in our personnel

monitoring system so we neglect it. Statistically this is unimportant and is probably compensated for by double counting of some other component of the dose.

A. RINDI (*CERN*):

Nella 11ª riga a partire dal fondo del riassunto si deve leggere ^{7}Be invece di ^{7}B.

A. P. HULL (*U.S.A.*):

Are these areas in which the radioactive gases are produced off-gassed, and if so are the total amounts involved sufficient to cause any environmental problems?

A. RINDI:

Gli isotopi a vita media molto corta (inferiore a qualche minuto) non rappresentano un rischio importante dato che l'intervallo di tempo fra l'arresto dell'acceleratore e il momento in cui il personale può penetrare all'interno è tale da permettere il decadimento di questi isotopi.

P. HUBLET (*Belgium*):

J'aimerais savoir s'il y a de la radio-activité induite dans la terre qui recouvre les accélérateurs. Si la réponse est affirmative, quels sont les problèmes éventuels de santé publique qui se posent?

J. BAARLI:

We have made measurements at CERN of the radioactivity of shielding and earth close to the accelerators. There is induced radioactivity with concentrations decreasing away from the machines. The concentrations seem, however, to be of little concern at present but will certainly have to be considered for accelerators with increasing intensities or energies.

L. DE FRANCESCHI (*Italy*):

I would like to hear from Dr. Rindi which technique was employed in measuring the air contamination. In particular how do they measure the percentage concentration of the different contaminants. Also, if they tried to find the form in which the isotopes are present (except A^{41} of course).

Inoltre, tornando indietro alla domanda di un delegato riguardo i neutroni intermedi eventualmente presenti e non registrati, mi pare che il Dr. Dutrannois abbia detto che attraverso misure eseguite dal Dr. Nachtigall è risultato che la percentuale della dose neutronica dovuta ai neutroni della zona termica, diciamo, e fino a 0.5 MeV, è trascurabile.

Ora a me sembra, ma potrei sbagliare, che invec il Dr. Nachtigall abbia proprio trovato in molti casi un'alta percentuale di neutroni ntermedi; anzi, se ben ricordo, ne ha fatto addirittura oggetto di una comunicazione al recente congresso di Vienna.

A. RINDI:

Il monitoraggio dei gas è stato fatto soltanto in aria ed è stato usato un "portable gas monitor" AL53C. E' un apparecchio a camera di ionizzazione a flusso, munita di un filtro assoluto prima della camera di ionizzazione, quindi gli isotopi radioattivi presi in considerazione sono soltanto quelli gassosi. La determinazione degli isotopi presenti nelle misure è stata fatta per separazione geometrica della curva di decadimento. Per l'altra domanda risponderà il dott. Baarli.

J. BAARLI (*CERN*):

I could make a brief comment on the intermediate neutrons, i.e. neutrons from thermal up to 0.5 MeV.

Outside the shielding of high-energy accelerators, all kinds and energies of particles up to the maximum energy of the accelerator might exist. At the present time no suitable instrument has been made for a direct evaluation of the radiation hazard, i.e. dose in rem. This information is therefore obtained indirectly by a set of instruments which has been selected at CERN for the purpose. The set is based on commercially available instruments which measure in principle:

(1) thermal neutron dose,
(2) fast neutron dose,
(3) dose from high-energy radiation (strong nuclear interactions),
(4) dose from gammas and the ionization.

When using this set, allowance for the epithermal neutrons has been made in the measurements of the fast neutron dose and in the fact that the system measures the dose from high-energy radiation twice, i.e. by the ionization (4) and by the dose from the observation of strong nuclear interactions (3). A separate measurement of the intermediate neutrons is of no particular interest for the dose assessment for protection purposes. The measurement of intermediate neutrons might however be of interest as such, but this problem as well as the problem of measuring, e.g. thermal neutrons or any other particular component near high-energy accelerators separately, is complicated by the presence of all other radiation types and energies.

M. PELLICCIONI (*Italy*):

Abbiamo trattato principalmente tutti i problemi di radioprotezione inerenti la prossima entrata in funzione dell'acceleratore lineare da 40 kW.

In particolare abbiamo calcolato quali devono

essere gli spessori degli schermi lungo l'acceleratore, intorno ai bersagli e intorno al pozzo di spegnimento. Sono stati poi stimati i livelli di radiazione dovuti all'attivazione del ferro e del rame della guida d'onda e alla produzione di gas tossici (O_3 e NO_2) e radioattivi (N^{13}, O^{15}, Cl^{38}) nell'aria del tunnel dell'acceleratore.

Parte dei risultati sono stati già pubblicati in note interne dei Laboratori Nazionali di Frascati.

R. LEIMGRUBER (*Switzerland*):

Wurden Messungen darüber gemacht, ob ein Iodfilter nach der einmaligen Beladung mit Iod und der nachfolgenden Spülung mit Luft das gesammelte Iod wieder abgegeben hat oder nicht? Was für Raumabluft-Iodfilter werden verwendet, und welchen Retentionsfaktor haben diese für die verschiedenen Iodkomponenten?

Y. YOSHIDA:

1. The overall collection efficiency of the iodine sampler was determined by using one or two reference cold traps which were connected to the sampler in series and consisted of the glass wool and the activated granular charcoal (Barnabey Cheney −10, 130 g used) maintained at temperature of less than −50 °C with dry ice immersed in ethanol. The activities collected in each component of the sampler were measured every 30 min or 8 hr, respectively, depending on short period or long period sampling. From the distribution of iodine deposited in the components, the removal of iodine can be checked.

2. Concerning filter papers, for aerosol sampling HV-70 (cellulose asbestos) filter paper is used. For iodine sampling, charcoal impregnated filter paper which consisted of carbon particles (diameter = $\sim 2\mu$) imbedded between two cellulose filter papers, manufactured by Toyo Roshi Co. Ltd. in Japan was used.

P. COURVOISIER (*Switzerland*):

1. Is the factor of 0.1, suggested in the abstract as a conversion factor for maximum permissible concentrations according to ICRP tables, a gross mean value or some limit?

2. Is there any trend in the ratios between personal and static air samplers showing differences between different types of work done, such as laboratory work, workshop activities, or work in a reactor hall?

W. A. LANGMEAD:

In answer to question 1 dealing with the use of a factor of 0.1 referred to in the abstract and at the invitation of the Chairman to comment further on the work described in the abstract, I will make the following comments.

Mr. Hermiston, from the U.K. Atomic Energy Establishment of Windscale, discussed yesterday some measurements of plutonium aerosols made with personal air samplers (P.A.S.) and with static air samplers (S.A.S.) and referred to the values of the ratio P.A.S. reading/S.A.S. reading obtained on single occasions and average values of the ratio obtained over long periods of time. The Authority Health and Safety Branch has been studying these and other results obtained at various establishments of the Authority and have confirmed that the statistical distribution of both P.A.S. readings and S.A.S. readings are usually log-normal and also values of the ratio referred to above are distributed log-normally in many situations. The average long-term value of the ratio depends not only on the type of aerosol but also on the relative positioning of the two instruments, the type of work undertaken and the manner in which the contamination is released. Low level chronic contamination often gives values of the ratio around 2–3 whereas contamination arising locally from the activities of the worker gives values from about 3–30. Only in circumstances where it has not been possible to undertake a programme of operational research to determine the appropriate value of the factor is it suggested that a factor of 10 for this ratio be assumed (corresponding to a fraction of 1/10 to be applied to ICRP $(mpc)_a$ values) in the belief that such a value will not be in error by more than a factor of 3.

The paper also describes measurements of particle size distributions of aerosols encountered at various establishments using the Centripeter designed and described by Sherwood (AERE, Harwell, U.K.). This instrument enables 4 ranges of aerodynamic particle size to be separated and the activity of the four filter papers corresponding to particles $< 1.4\ \mu$, 1.4–4 μ, 4–14 μ, and $> 14\ \mu$ determined. In this way one can determine whether the particle size distribution is log-normal, and the value of A.M.A.D. and geometric standard deviation found which largely determine the physical characteristics of the aerosol. Using the lung model proposed by the Task Group on Lung Dynamics of Committee II of ICRP, one can determine the percentage of the activity breathed which is retained in the deep lung.

In general this percentage is less than the $12\frac{1}{2}\%$ predicted by the current ICRP lung model, the respirable fraction of the aerosols encountered in the Authority ranging from 35–75%. It is emphasized that these values are provisional.

B. W. EMMERSON (*U.K.*):

Has the portable air sampler been used for the measurement of airborne I^{131} using a charcoal loaded

filter paper? If so, how do results from these measurements compare with results taken with a static air sampler within the same area, and what factor would be recommended?

W. A. LANGMEAD:

In answer to the question about the use of personal air samplers for measuring radio-iodine, I want to say that measurements of this kind had been made using special filter papers but I cannot recall the details.

L. DE FRANCESCHI (*Italy*):

I apologize Mr. Chairman if my comments cover a subject which has already been raised by others. First of all it seems that the comparison of personal and static device data is very difficult, in particular because of the different volumes of air sampled which makes the statistics much poorer for personal devices. It would also be interesting to know if the larger values are always on the same side. As far as the factor 1/10 is concerned, I think that if we begin to correct our measurements with factors, any time we don't like them it may mislead us.

S. O. W. BERGSTROM (*Sweden*):

In connection with Pu work at AB Atomenergi, Studsvik Research Station we analysed these problems and found that the larger air volumes and the possibility of applying alpha spectrometry made static air samplers superior to personal ones by a very large factor—larger than the ratio 3 to 30 found by the author for the ratio between measured concentrations of personal and static samplers respectively.

As one usually investigates all significant levels of air contamination, would it not be unnecessary to make corrections to the ICRP long term average MPC values as body burden measurements will anyhow be the real criterion for actual exposure. Personal air samplers are very awkward to carry and we have preferred fixed samplers at the glove-boxes. In both these cases, do you think there is a possibility that entrainment of activity with the sampler, air current towards the worker might actually increase the exposure?

W. A. LANGMEAD:

In answer to a question as to whether the air flow through the personal air sampler was likely to interfere with the aerosol concentration in the breathing zone, I would say that this is unlikely in view of the low flow-rate (2 l./min) and experiments carried out at AERE Harwell, U.K. have shown reasonable agreement between P.A.S. results and simultaneous measurements of the contamination in air actually breathed achieved by fitting a special filter to a respirator, the air flow being provided by the wearer's breathing.

W. A. LANGMEAD:

In answer to a further remark that the results of excreta measurements are more reliable than estimates of activity breathed as a measure of body burden, I agree that this is generally so but that the P.A.S., coupled with particle size determinations, is likely to give good results for lung burden and lung dose and should be considered a satisfactory alternative or auxiliary method for this purpose.

D. K. CRAIG (*South Africa*):

Mr. Chairman, I think that this is a very important matter. It must be emphasized that an 0.3 μ diameter particle of plutonium metal (density ~19 g/cc) behaves like an aerodynamic equivalent unit density sphere of about 6 μ diameter, plutonium oxide (density ~11.2 g/cc) like about a 3 μ diameter unit density sphere. Presumably, the man, and therefore the personal sampler, is quite close to the source of the airborne plutonium. The static sampler is quite far away. Therefore, differential setting of the larger particles is bound to give significant differences between the concentrations detected by the personal and static samplers. However, this does not give us much information about the relative hazard of the aerosol. I think that it is important that we should use as personal samplers some size selective sampling device that will give us an idea of the aerodynamic size distribution of the plutonium and, therefore, the likely hazard in terms of the amount of Pu likely to reach the functional areas of the lung. I think that the implementation of such consideration would help to resolve a lot of the questions raised by Dr. Langmead.

W. A. LANGMEAD:

In answer to a further question from Dr. Craig, I would like to repeat that the determination of the factor referred to in the abstract is the result of measurements made over an extended period of time and that the figure of 0.1 was quoted as a rule of thumb guide which is not likely to be very much in error. It is very much better to apply such a factor to static air sample results than to trust such readings unmodified by any factor. In general S.A.S. readings underestimate the breathing air concentration of contaminants by × 10.

L. FITOUSSI (*France*):

Je voudrais demander au Dr. Langmead les dispositions qui sont normalement prises lorsque des travaux doivent être effectués en présence d'une

contamination atmosphérique. En général les moyens de protection, c'est-à-dire vêtements, appareils, respiratoires, etc., sont choisis en fonction des niveaux de contamination atteints.

Le Dr. Langmead peut-il nous donner quelques informations sur ce sujet en particulier lorsque l'on a affaire à une contamination atmosphérique par du plutonium ou des radionucléides à activité massique faible?

W. A. LANGMEAD:

The methods of protection available for the worker when it is necessary for him to work for lengthy periods in a contaminated atmosphere depend very much on the circumstances and the breathing air activity concentration. In the decontamination of heavily contaminated items, full pressurized suit facilities including clean breathing air supply would be provided. In transient situations where the activity concentration in the air temporarily exceeds the $(\text{m.p.c.})_a$, respirators or even half-face masks would probably be adequate depending on the number of $(\text{m.p.c.})_a \times$ hours involved in the work.

However, for the handling of large quantities of plutonium, increasingly we are separating the working-faces of the glove boxes involved from the areas where maintenance of equipment in the boxes is undertaken. Contamination of the workers' breathing air then becomes a transient incident, due usually to glove puncturing, which can be rapidly dealt with, the air in the working area returning quickly to normal.

THE MEASUREMENT AND MANAGEMENT OF INSOLUBLE PLUTONIUM–AMERICIUM INHALATION IN MAN*

A. BRODSKY, J. A. SAYEG, N. WALD and R. WECHSLER
Graduate School of Public Health, University of Pittsburgh, Pittsburgh, Pennsylvania, 15213, U.S.A.
and
Radiation, Medicine Department, Presbyterian University Hospital, Pittsburgh, Pennsylvania, 15213, U.S.A.
and
ROGER CALDWELL
NUMEC, Inc., Apollo, Pennsylvania, U.S.A.

Abstract—A drybox explosion on January 17, 1966, exposed three individuals to inhalation of dust containing a mixture of ^{239}Pu and ^{241}Am. Preliminary measurements at the University of Pittsburgh whole body counter 27 hr after the incident, using a 1 mm thick, 2 in. D, NaI detector indicated a possible lung burden as high as 0.4 μCi ^{239}Pu in one of the individuals. Although a considerable fraction of the contamination was believed to be ^{241}Am, upper-limit estimates of ^{239}Pu in the lung were still as high as 0.24 μCi on day 4 (post-exposure), so the decision was made to administer 1 g/day DTPA intravenously for the next three days. On day 5, a hundredfold increase appeared in the count-rate and changes occurred in the spectral shapes indicating a sudden appearance of new surface contamination on the anterior chest. This activity, as well as its probable source (another spot of contamination found on the forehead) was removed. Subsequent spectral shapes indicated that further measurements were indicative of lung radioactivity. Isotopic analyses of contamination and air samples showed that the major fraction of the activity was ^{241}Am. Interim estimates of lung burden were then: 7×10^{-3} μCi of ^{241}Am on day 4; 4×10^{-3} μCi on day 11; 6×10^{-4} μCi on day 28; and 4×10^{-4} μCi on day 57. These values are consistent with the elimination of about 36,600 d/min of ^{241}Am and 54 d/min of ^{239}Pu in the first fecal sample. Urine excretion rates, initially less than 0.4 dpm/24 hr, increased 50–100 times between days 5–8, suggesting the efficacy of DTPA in removing insoluble ^{241}Am from the lung.†

I. INTRODUCTION

In this paper, measurements and final evaluations of internal and external ^{239}Pu and ^{241}Am on a glovebox operator following a contamination-releasing explosion will be summarized, showing how a single 2 in. D $\times$ 1 mm sodium-iodide detector may be used together with other bioassay and survey data in the medical management of inhalation accidents involving X-ray emitting nuclides. Also, the possible effi-

* Supported in part by a grant from the Health Research and Services Foundation, Pittsburgh, Pennsylvania. An interim report of this work was presented at the annual meeting of the Health Physics Society in Houston, Texas, June 1966.

† There was an error in the abstract in the *Health Physics* journal. The surprising aspect of this case was that the DTPA seemed to remove what initially behaved like "insoluble" AmO_2.

cacy of DTPA administration in removing inhaled plutonium and americium oxides is indicated.

II. DESCRIPTION OF THE INCIDENT

At 2:05 p.m., Monday, January 17, 1966, an explosion occurred in a glovebox when a technician attempted to ignite a propane torch. The torch had apparently leaked after a new cylinder was attached. The explosion blew out the gloves and knocked the operator to the floor. Within seconds the operator proceeded to the change room and within one minute the plant evacuation alarm was sounded.

Hot gases from the open glove ports had singed the operator's eyebrows and produced minor first degree facial burns. He was also contaminated over his face, hair and chest with alpha activity up to several hundred thousand disintegrations per minute per 100 cm^2. Nose swipes read 100,000 counts/min for the right nostril. The glovebox operator showered until all external alpha contamination had been removed, except for one spot reading 1200 counts/min on the right front chest. His nasal contamination was reduced below 1000 counts/min per smear by irrigating with water. Urine samples were collected from all persons involved in the incident and fecal samples were also collected from those who entered the area immediately after the explosion.

Air samples indicated alpha air concentrations of up to $1.1 \times 10^{-7}\mu Ci/cc$ in the room where the accident had occurred, averaged over 10–20 min after the accident. Floor contamination levels in the vicinity of the incident were up to 300,000 counts/min per 100 cm^2, and contamination was spread throughout the entire plant. However, the glovebox operator involved had the highest contamination and was the only one who was found later to have measurable internal activity. Thus only his measurements will be summarized here.

III. EVALUATION AND MEDICAL

On the day after the accident, the company health physicist learned that our new whole body counter facility* had just obtained a thin-window 2 in. D × 1 mm NaI detector.

The equipment was immediately set up and the exposed technician was brought in for his first interim examination 18 hr after the incident. In Fig. 1 the technician is shown lying on a cloth cot, with the 1 mm NaI crystal detector

* See J. O. MEHL and K. R. BECK (Editors), *Directory of Whole-Body Radioactivity Monitors*, IAEA, 1964. In the first case study from the whole body counter, the authors would like to acknowledge the contributions of their former associate, Dr. Francis J. Bradley, toward the design and specifications of the facility.

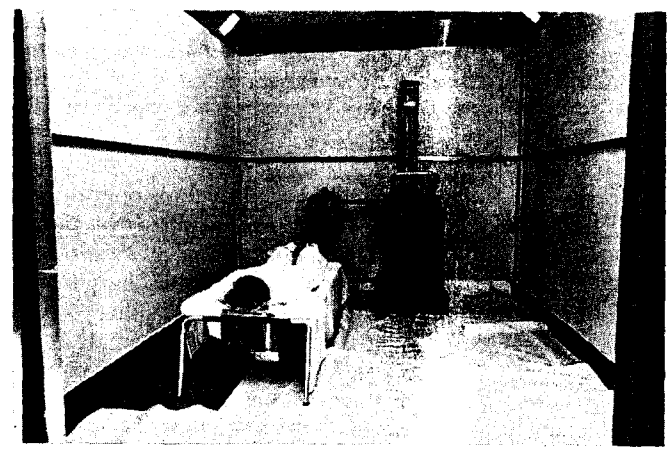

FIG. 1. View of simple apparatus used for emergency detection, 2 in. D × 1 mm NaI crystal with 0.005 in. Al window beneath cloth cot.

placed about 2 cm underneath his chest. This detector was purchased from Harshaw with a 0.005 in. aluminium window, which transmits about 96% of 17 keV photons. This detector is similar to that originally developed by Roesch and Baum for wound monitoring.[1] Twenty minute counts at a given position were repeatable within a factor of two. Many 20-min counts were subsequently taken near different body positions, and spectral shapes and intensities were utilized together with geometry considerations to discriminate between internal and external radioactivity and its location in the body. Only a brief illustration of the measurements, lines of reasoning, and resulting medical actions will be given here.

All spectra were recorded on a Northern Scientific Company 256-channel analyzer and a teletype printer, with all settings remaining fixed during the series of examinations. Only half the memory was used for each count so that spectral shapes could be inter-compared on a log scale. This turned out to be a valuable procedure in the detective work that followed. With so many variables to consider during such an emergency, it is most important to fix those parameters that can be fixed and constantly inter-compare data with given standards. In this way, confusion and inadvertent errors may be minimized.

All spectra connected with the evaluations were photographed with a polaroid camera and kept in a notebook in order of date.

Figure 2 shows a comparison of the chest spectra of the exposed technician (on the right) with that of one of the unexposed technicians (on the left) as first observed 18 hr after the accident. Due to time considerations in the early period of the emergency, the gain was fixed to that of the preceding measurement with the 17 keV peak (of ^{239}Pu or ^{241}Am) in only channel 3 and the 60 keV peak of ^{241}Am in channels 21–25. This turned out to be a fortunate operational decision since the printer began to print out zeros above channel 30 several days after the accident. Although a more expanded spectra would have been clearer, the highest count of the 17 keV peak remained consistently in channel 3 for an unattenuated source during the critical weeks of measurement. Thus, ratios of counts in channels 21–25 could be used to study body absorption. The low relative height of the 17 keV peak, as in Fig. 2, compared to that of a smear of contamination from the incident was initially indicative of a possible internal burden of plutonium or americium.

At the time of the first measurement 18 hr after the accident, standard solutions of plutonium and americium were not yet prepared. Thus, a preliminary estimate was made of the maximum possible internal lung burden, as-

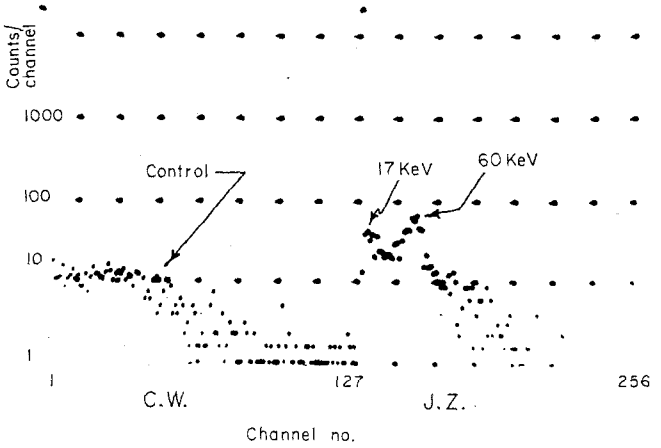

FIG. 2. Comparison of spectra of uncontaminated employee ("control" indicated on left) with spectrum of exposed technician 18 hr post-accident (right). Vertical counts channel scale is logarithmic.

Table 1. *Excretion Data Versus Time: Urine Data*

Date	Total activities in sample*	
	dpm ^{238}Pu	dpm ^{241}Am
1/18 (1st void)	0.05 ± 0.05	0.3 ± 0.2
1/18 (24 hr)	0.3 ± 0.2	0.5 ± 0.3
1/20 (24 hr)	1.33 ± 0.16	0.6 ± 0.3
1/21 (24 hr)	0.29 ± 0.06	Lost Sample
1/22 (*Preinfusion*)		0.08 ± 0.08
1/22 (*Post DTPA* 1)	2.6 ± 0.33	4.4 ± 0.2
1/23 (*Post DTPA* 2)	1.55 ± 0.31	31.4 ± 2.6
1/24 (*Post DTPA* 3)	2.37 ± 0.24	28.5 ± 2.8
1/25 (24 hr)	1.92 ± 0.13	7.5 ± 0.8
1/26 (24 hr)	2.6 ± 0.7	36.7 ± 2.3
1/27 (24 hr)	2.2 ± 0.2	25.4 ± 1.5
1/28 (24 hr)	1.29 ± 0.16	17.6 ± 1.2
1/29 (24 hr)	0.94 ± 0.12	10.1 ± 0.5
1/30 (24 hr)	0.8 ± 0.1	17.4 ± 0.8
2/8 (24 hr)	1.1 ± 0.1	0.5 ± 0.23
2/9 (24 hr)	0.84 ± 0.15	4.9 ± 0.4
2/14 (24 hr)	0.29 ± 0.12	1.3 ± 0.1
3/20 (24 hr)	0.09 ± 0.08	10.9 ± 0.9

Fecal Data.

Date	dpm ^{238}Pu	dpm ^{241}Am
1/19 (83.7 g)	57 ± 6	36,600 ± 1,100
1/21 (84.1 g)	1.9 ± 0.8	8.8 ± 1.5
1/22	0.8 ± 0.9	2.8 ± 1.3
1/23	2.1 ± 0.9	16.9 ± 1.7
1/24	2.2 ± 0.9	15.3 ± 1.6
1/26	2.3 ± 0.5	26.6 ± 2.2
1/27		18.6 ± 1.6
1/29		15.1 ± 1.6
1/30		11.3 ± 1.5
2/8	0.48 ± 0.15	1.5 ± 0.2
2/9	2.7 ± 0.7	12.8 ± 1.1
2/14	0.5 ± 1.1	4.7 ± 0.6
3/20	2.6 ± 0.7	1.5 ± 0.3

* Attempts were made to obtain 24-hr samples from the subject, but collection may be uncertain in some cases; also collections were separated between DTPA infusions in order to determine the effects of each treatment.

sumed to be ^{239}Pu, on the basis of the assumption that about 4% of the alphas from ^{239}Pu are accompanied by ^{235}U L X-rays in the 17 keV region. Using the reported attenuation of 17 keV X-rays in the tissue of dogs,[2] considering the half-value layers of about 0.6 cm from 17 keV X-rays in soft tissue and 0.03 cm in bone,[3] and a conservative factor of 3 to correct for rib absorption, it was estimated at 18 hr after the accident that the maximum possible lung burden of the exposed technician could be as high as 0.4 μCi—about 10 times the amount that could be permitted to solubilize and enter the bone. The detection limit for ^{239}Pu with a 20-min count was estimated to be 0.03 μCi, with a 5% chance of not detecting this amount if present in the lungs. This is only about twice the detection limit of Swinth, Griffin, and Park[2] of 0.016 μCi in dogs using a 52-detector arrangement for total body counting. Since the single detector may be placed closer to a particular organ containing the activity, the use of more and more detectors may reach a point of diminishing returns when activity is located in a small region of the body.

Since the probable contamination was believed on the day after the incident to be insoluble plutonium oxide, it was decided to establish the fecal and urinary excretion for a few days and take further counts before deciding whether to administer DTPA. It was believed that any remaining plutonium in the lung at 18 hr would be solubilized by the body to a negligible degree in a few days, and that any soluble portion of the plutonium had probably already been transported to bone and could be partly removed by DTPA at a later time.[4, 5] The fecal and urinary excretion data may be followed in Table 1 and an abstract of the chest count data with the 2 in. D × 1 mm NaI detector is presented in Table 2. Counts over other areas of the body were also used in establishing the locations of internal and external contamination.

By day 4 post-accident, standard solutions were prepared containing 1 μCi of ^{239}Pu and 0.044 μCi of ^{241}Am in each of three solution volumes: 100 cc, 500 cc, and 1000 cc. The 1000 cc solution was used to simulate the lung spectrum and X-ray emission for comparison with the technician. The other solution gave some idea of the change in spectral shape with varying degrees of self-absorption, for use in discriminating between surface and internal contamination. The actual percentage of ^{241}Am in the contamination was initially believed to be smaller than this. However, the high ^{241}Am content of the fecal samples had indicated by day 4 that ^{241}Am, which had previously been handled in the same glovebox, might actually be the major fraction of the contamination unless the body was preferentially eliminating the ^{241}Am. (A paper in this conference[6] indicates that such preferential elimination may actually occur under some circumstances.) Thus,

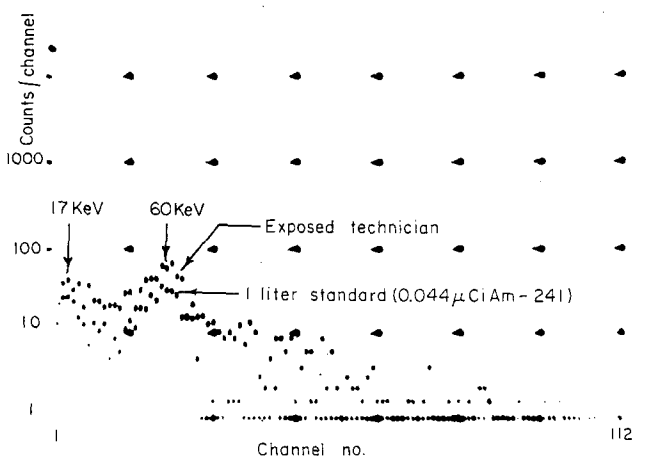

FIG. 3. Comparison of spectrum of exposed technician 4 days post-accident with spectrum of 1 μCi ^{239}Pu and 0.044 μCi ^{241}Am in 1 l. solution in polyethylene. Control counts of normal subject have not been subtracted from the technician's spectrum.

Table 2. Summary of Chest Count Data from Whole Body Counter

Date	Detector position	Net counts above control[a] per 20 minutes		Estimated maximum quantity of ^{241}Am in lung (μCi)
		17 keV peak	60 keV peak	
1/18/66 (1 day post-incident)	1 in. below right front chest	239	427	0.021 μCi ^{241}Am or 0.46 μCi ^{239}Pu*
1/21/66 (4 days post-incident)	Right front chest	118	253	0.012 μCi ^{241}Am or 0.27 μCi ^{239}Pu*
	Right front chest repeat	28	126	0.006 μCi ^{241}Am
	Right back chest	13	56	0.003
	Left front chest	32	114	0.006
1/22/66 (5 days post-incident) (DTPA treatment at noon)	Right front chest, 5:20 pm (*Note*: High 17/60-keV peak ratios and comparison of front and back counts indicated the sudden appearance of contamination in chest region.)	17,464	8,472	†
	Right front chest, 5:55 pm	22,731	13,704	†
	Left front chest (*Note*: Contamination removed with undershirt, patient showered.)	3,810	5,679	†
	Right front chest, 10:00 pm	249	372	0.018
1/23/66 (6 days post-incident) (DTPA treatment at noon)	Right front chest	91	230	‡
	Left front chest	24	50	
	Left back chest	56	148	
	Right back chest	60	104	
	Right front chest *Note:* Repeated after shower, spot of head contamination removed.)	83	140	0·007
1/24/66 (7 days post-incident) (DTPA treatment at noon)	Right front chest	11	52	0.003
		8	17	< 0.002
1/28/66 (11 days post-incident)	Average of 4 chest positions	30	82	0.007
2/8/66 (22 days post-incident)	Average of 4 chest positions	6	20	< 0.002
2/14/66 (28 days post-incident)	Average of 4 chest positions	9	12	< 0.002

* Early interpretations assumed ^{239}Pu predominant and used a conservative factor of 3 to correct for rib absorption.

† Surface contamination.

‡ These counts were influenced partly by contamination found on the forehead.

(a) Control counts of 26 per 20 min in the 17-keV region and 69 per 20 min in the 60-keV region were subtracted from each 20 min patient count.

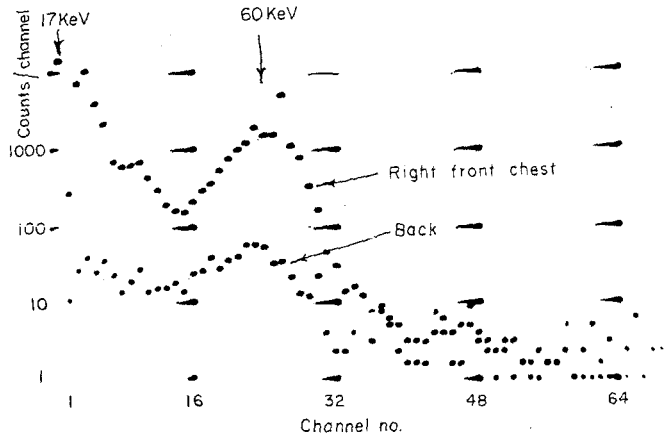

FIG. 4. Spectra of contamination discovered on chest, day 5 post-accident as viewed by crystal from front right chest (top) and through back (bottom). Oscilloscope *X*-axis was expanded, but analyzer gain was the same as in Figs. 2 and 3.

the presence of a known amount of ^{241}Am in the standard was desirable.

Consequently, estimates of lung burden based on assumed ^{239}Pu were made using only channels 2–4 in the region of the 17 keV peak. Estimates of ^{241}Am were made using only the 60 keV peak in the region of channels 21–25 (see Figs. 2–6). Of course, ^{241}Am also yields *L* X-rays (0.12 of 13.96 keV, 0.13 of 17.76 keV, and 0.03 of 20.80 keV per disintegration) as well as gamma-rays (0.36 of 59.57 keV and 0.025 of 26.36 keV per disintegration),[7] so it was recognized that if an appreciable quantity of ^{241}Am were present, the ^{239}Pu burden could be grossly overestimated. Later radiochemical analyses of air samples and contamination showed that more than 85 per cent of the activity was ^{241}Am, so evaluations of ^{239}Pu given in Table 2 are given only to illustrate the sequence of events that determined courses of action. Figures 2–6, as well as spectra of the contamination, also confirm that any additional ^{239}Pu represented in the 17 keV peak can be considered to contribute only a fraction of the

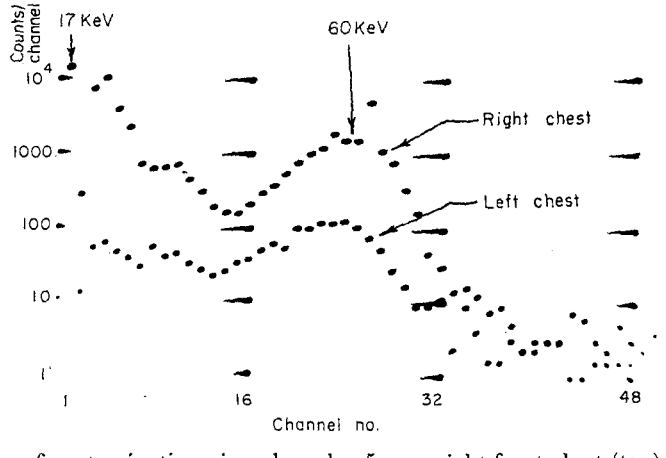

FIG. 5. Spectra of contamination viewed on day 5 near right front chest (top) and left front chest (bottom).

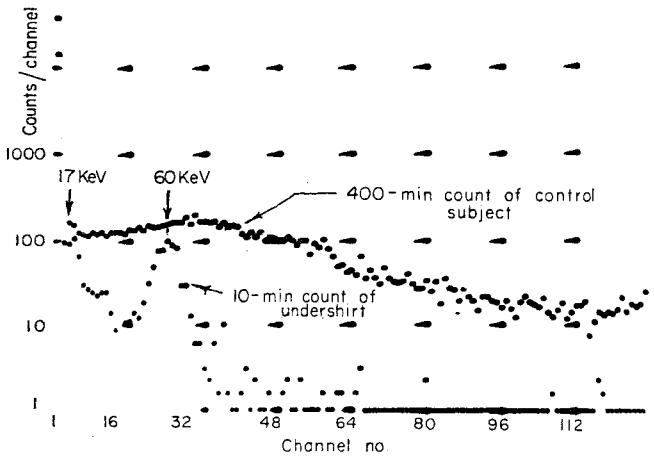

FIG. 6. Spectra of contaminated undershirt (bottom—10-min count) and unexposed subject (top—400 min-count).

exposure, since the permissible burdens of ^{239}Pu and ^{241}Am are about the same, and the proportion of $^{241}Am/^{239}Pu$ may be expected to grow with time.[8]

On Friday, January 21 (day 4 post-incident), spectra were obtained similar in shape to that observed 18 hr post-incident, but somewhat lower in intensity (Table 2). Figure 3 shows one of the chest spectra taken on day 4 compared to the spectrum of the standard solution that was obtained by that day. The 1 l. standard contained 1 μCi ^{239}Pu and 0.044 μCi ^{241}Am. By 4 days post-incident, information from fecal analyses had indicated that the dust might be predominantly ^{241}Am; yet the low 17 keV/60 keV peak ratio compared to that of the smear indicated a probable internal burden greater than 10% of the MPBB even for ^{241}Am. Also, fecal excretion after the first day had decreased to very low levels. So the decision was made to administer 1 g DTPA intravenously on each of days 5, 6, and 7, and to follow the lung burden and excretion data daily to determine whether fecal and/or urinary levels would increase and whether the lung burden would subsequently decrease.

Suddenly, after the first DTPA treatment on day 5, an increase by up to a factor of 1000 was noted in the count-rate over the right chest area. Figure 4 shows the spectrum viewed with the crystal near the front right chest (top), and viewed through the back (bottom), with the horizontal oscillope scale expanded. The relatively high 17/60 keV peak ratio from the front of the chest (see Fig. 4) and the much lower intensity viewed through the back, indicated the presence of a new speck of contamination on the chest.

Figure 5 shows a spectrum near the right front chest (top) compared to that near the left front chest (bottom), localizing the contamination to the right front chest area. Late on the 5th day, the technician's undershirt was carefully removed and placed in a plastic bag. Then his chest was washed, the wash-rag was saved in a plastic bag, and the technician was sent in for another shower.

In Fig. 6, a spectrum of the undershirt counted for 10 min (bottom) is shown together with the spectrum of an unexposed individual counted for 400 min. The spectrum from the undershirt, which offered little absorption of the 17 keV peak, again shows a high 17 keV/60 keV peak ratio.

Since the undershirt was contaminated, and the wash-rag was found uncontaminated, it was deduced that the observed contamination had suddenly appeared on the undershirt when it was pulled over the head that morning. On the 6th day, further alpha monitoring with an Eberline PAC-3A found some residual contamination of about 1000 dpm on the forehead,

indicating the probable source of the contamination found on the undershirt the previous day. After further showering the count near the head was reduced somewhat but not enough to indicate from geometry considerations that the contamination, while on the head, had appreciably affected lung measurements before day 5. Further chest spectra were consistent in shape and intensity, as viewed from front and back, and indicated true lung burdens.

After isotopic analyses confirmed that the contamination was more than 85% ^{241}Am, evaluations of lung burden using the 60 keV peak then ranged from 0.021 μCi ^{241}Am after 1 day to less than 0.002 μCi by day 7. In these evaluations only a factor of 2 was used to correct for rib absorption since experiments with a human skeleton showed this would be sufficiently conservative to account for the range of factors observed.*

Table 1 shows the high initial fecal excretion of 36,000 dpm ^{241}Am (0.016 μCi) and 57 $\pm$ 6 dpm ^{239}Pu on the first day, with a negligible amount initially in urine. The fecal excretion dropped sharply on the 2nd and 3rd days and then both the fecal and urine excretion increased sharply following the DTPA administration. This striking effect of the DTPA was somewhat surprising since the inhaled material was mostly americium and plutonium oxides. No mathematical models can be fitted precisely to the data since the body processes were complicated by the DTPA administration, which apparently assisted in the rapid reduction of the internal portion of the contamination to below the sensitivity of the counter. (Table 2). Of course, there was no opportunity for a control experiment to determine whether the lung burden would have decreased even without DTPA administration. The primary medical consideration was to minimize the risk to the technician.

The initial amount of fecal excretion (0.016 μCi), and the remaining lung burden of 0.02 μCi after day 1 (Table 2) are considered within the range of ICRP models. This lends further confidence that the evaluated burdens in Table 2 are of the correct order of magnitude. The technician was followed for 4 months with no further appearance of detectable ^{241}Am.

IV. CONCLUSIONS

The following main points were emphasized in the above incident:

1. Although not conclusive, the correlation with time between the increase in excretion rates and the rapid disappearance of the lung burden following DTPA administration, suggests that DTPA may hasten the removal of even insoluble oxides of plutonium and americium from the human lung, although removal rates cannot be specified accurately from the data of this case.

2. A number of principles of emergency management of inhalation accidents were emphasized in this incident, including:

(a) Necessity for direct supervision of all measurements and actions at the whole body counter.
(b) Recording of all data and events with time and date as they occur.
(c) Necessity to keep exposed subject properly informed and briefed to develop an attitude of co-operation and trust, while avoiding alarming statements or divulging premature evaluations to unauthorized persons.
(d) Necessity to assign tasks quickly to all staff; everyone wants to help in an emergency, and their help must be constructive.

3. Multiple measurements and examination of spectral shapes with a 2 in. D $\times$ 1 mm NaI detector can be helpful in the detection of ^{241}Am or ^{239}Pu in the human lung, and in discriminating between internal and external body contamination. A 20-min count with the detector within a few centimeters of the chest can detect more than approximately 0.002 μCi ^{241}Am or 0.03 μCi ^{239}Pu. A 200-min count (or ten 20-min counts, which give the same statistical precision but better information on time dependence and fluctuations of measurement) can detect about 0.01 μCi ^{239}Pu or 0.0007 μCi ^{241}Am at the 5% level of significance, as defined by Roesch and Baum.[1]

* The authors are indebted to Mr. Andrew Bukovitz for carrying out the measurements.

ACKNOWLEDGEMENTS

The authors acknowledge the assistance of Mr. Robert Goempel, Mr. William Moore, Dr. Plinio Rey, and Mr. William C. Judd in setting up equipment and helping with the measurements during this incident.

REFERENCES

1. W. C. Roesch and J. W. Baum. Detection of Plutonium in Wounds. Paper P/756. *Proc. 2nd U.N. Conference on the Peaceful Uses of Atomic Energy*, Geneva, 1958.
2. K. L. Swinth, B. I. Griffin and J. F. Park. Whole body counting of plutonium in dogs. Preprint from Battelle-Northwest Laboratories, Richland, Washington, 1965.
3. W. C. Roesch and H. E. Palmer. *Health Physics* **8,** 773 (1962).
4. W. D. Norwood. Therapeutic removals of plutonium in humans. *Health Physics* **8,** 747–750 (1962).
5. W. V. Baumgartner, H. V. Larson, G. H. Crook, M.D. and C. E. Newton, Jr. The treatment and evaluation of internal deposition from a plutonium wound. Preprint from Battelle-Northwest Laboratories, Richland, Washington, 1965.
6. W. J. Bair and J. F. Park. Comparative disposition of four types of plutonium dioxides inhaled by dogs. This volume.
7. H. R. Bowman, E. K. Hyde, S. G. Thompson and R. C. Jared. *Science* **151,** 563 (1966).
8. C. M. Unruh. The radiological physics of plutonium. HW-SA-2740. Presented at the American Nuclear Society National Topical Meeting, Richland, Washington, September 13 and 14, 1962.

EARLY ASSESSMENT OF THE SERIOUSNESS OF LUNG CONTAMINATION BY INSOLUBLE ALPHA AND LOW ENERGY BETA EMITTING MATERIALS AFTER INHALATION EXPOSURE

B. A. J. LISTER
Health Physics & Medical Division,
Atomic Energy Research Establishment,
Harwell, Didcot, Berks, England

Abstract—After inhalation of gamma- and high energy beta-emitting materials, the lung content can be measured by direct *in vivo* counting methods. For materials with less penetrating radiation this approach is not possible (except perhaps to give an upper limit) and indirect information, such as that from measurements on excreta and examination of air sample papers, must be used to make an assessment of lung content.

This paper reviews the usefulness of such indirect information and suggests ways in which it can be used to arrive at the best estimate of lung burden. Data from some relevant inhalation incidents illustrate the points made.

AFTER inhalation of airborne radioactive contamination, the fate of the radionuclides concerned will be determined by the physical and chemical forms in which they occur in the air. Their depth of penetration into the respiratory system and their site of deposition will be influenced mainly by particle size, shape and density, and partly by their chemical reactivity. Transfer from the respiratory system and subsequent metabolism will be determined by chemical form and particle characteristics.

In their 1959 report[1] Committee II of I.C.R.P. described a simple model for the behaviour of particulates in the respiratory tract. In this model, for compounds other than those which are readily soluble, it is supposed that of the material inhaled, 25% is exhaled and 50% is deposited in the upper respiratory passages and subsequently swallowed; of the remaining 25% deposited in the lungs, half is eliminated and swallowed within the first 24 hr, the other half being retained in the lungs with a long half time of removal.

In 1964 Committee II established a Task Group to review this lung model. In their report[2] this Task Group has developed a deposition model which depends on dust sampling data and which describes deposition in terms of three anatomical compartments—the nasopharynx, the trachea and bronchial tree and the pulmonary compartment. The clearance of dust deposited in each compartment is dealt with "quantitatively, kinetically and by pathways" and an attempt is made to classify chemical compounds according to their retention in the respiratory system.

This report clearly represents a major advance in our understanding of the behaviour of particulates in the lung and will lead to a new appraisal of maximum permissible levels of airborne contamination. For the operational health physicist, however, the important question is whether the new model gives him an improved weapon for attacking one of his major problems, how to make an early assessment of the seriousness of lung contamination after a suspected inhalation exposure.

The general methods available to the health physicist are:

(i) Direct measurement of activity in the lung by *in vivo* counting techniques.

(ii) Interpretation of measurements of the rates of excretion of the radionuclides concerned.
(iii) Interpretation of other indirect information.

This paper reviews the usefulness of various approaches for insoluble materials emitting radiation of low penetrating power and suggests methods which have been found useful in practice.

IN VIVO MEASUREMENTS

For many gamma and beta-emitting radionuclides it is possible to make *in vivo* measurements of the body content at levels far below the maximum permissible.[3, 4] For those radionuclides which emit alpha and low energy beta radiation, such direct measurement is either impossible or extremely difficult. For example, only now is it becoming possible, with extreme sophistication of instrumentation, to make *in vivo* measurements of ^{239}Pu in the lung at a level approximating to the maximum permissible lung burden (16 nCi).[5, 6]

URINARY EXCRETION

Measurements of urinary excretion are used in most establishments handling large amounts of unsealed radioactive materials as a method of assessing internal contamination. Their quantitative, or perhaps even qualitative, usefulness for assessing the body content of "insoluble" materials must be seriously questioned.[4, 7, 8]

For some elements, for example strontium,[7] neither the chemical form nor the method of intake seem markedly to affect the urinary excretion pattern which is similar after, for example, inhalation of the soluble chloride and the insoluble carbonate. Experience has shown, however, that for many elements it is quite possible for the lung content of an insoluble material to be considerable without significant activity appearing in urine.[8, 9] In such cases, application of relationships worked out to relate the rate of urinary excretion to the body content of soluble material can be wholly misleading. Although it may be possible to relate the excretion in urine to lung retention many months or years after intake (e.g. for plutonium oxide[10]), the use of such relationships cannot be expected to give any useful information on lung retention of insoluble material at a time when therapeutic action is being considered.

FAECAL EXCRETION

More valuable information on lung retention of insoluble materials can be obtained from measurements of the activity excreted in faeces, but quantitative interpretation is complicated by reason of variations in excretion pattern with particle size of the inhaled material.[9]

In most cases of accidental inhalation, faecal excretion follows the general pattern shown in Fig. 1. The excretion rate rises to a maximum on the second or third day after intake and then falls away to reach a lower, relatively constant level after some 10–12 days which is maintained for perhaps more than 100 days after the intake. The ratio of the peak excretion rate to the "plateau" excretion rate apparently varies with particle size of the inhaled material, the fall being dramatic over several orders of magnitude after inhalation of large particles and less marked for particles of small diameter.

The simple I.C.R.P. lung model suggests that the amount of insoluble material transferred to the GI tract ($62\frac{1}{2}\%$) is five times that retained in the lung ($12\frac{1}{2}\%$). By application of this model, faecal excretion measurements can be related to the amount retained in the lung, since the total amount of radionuclide excreted in faeces during the first few days after inhalation probably represents all that was deposited in the upper respiratory tract. If particle size information is available, a more refined approach can be made using the lung dynamics model proposed by the I.C.R.P. Committee II Task Group.

Sometimes (fortunately rarely) the incident resulting in the intake is not immediately recognized. In such a case the early faecal excretion data are not available and only the longer term "plateau" excretion rate can be determined. To obtain useful data at this interval after the intake when faecal excretion is at a relatively low level, the individual must be removed from active work for at least a week prior to the start of the sampling programme, thus eliminating the possibility of high results being due to a recent small acute

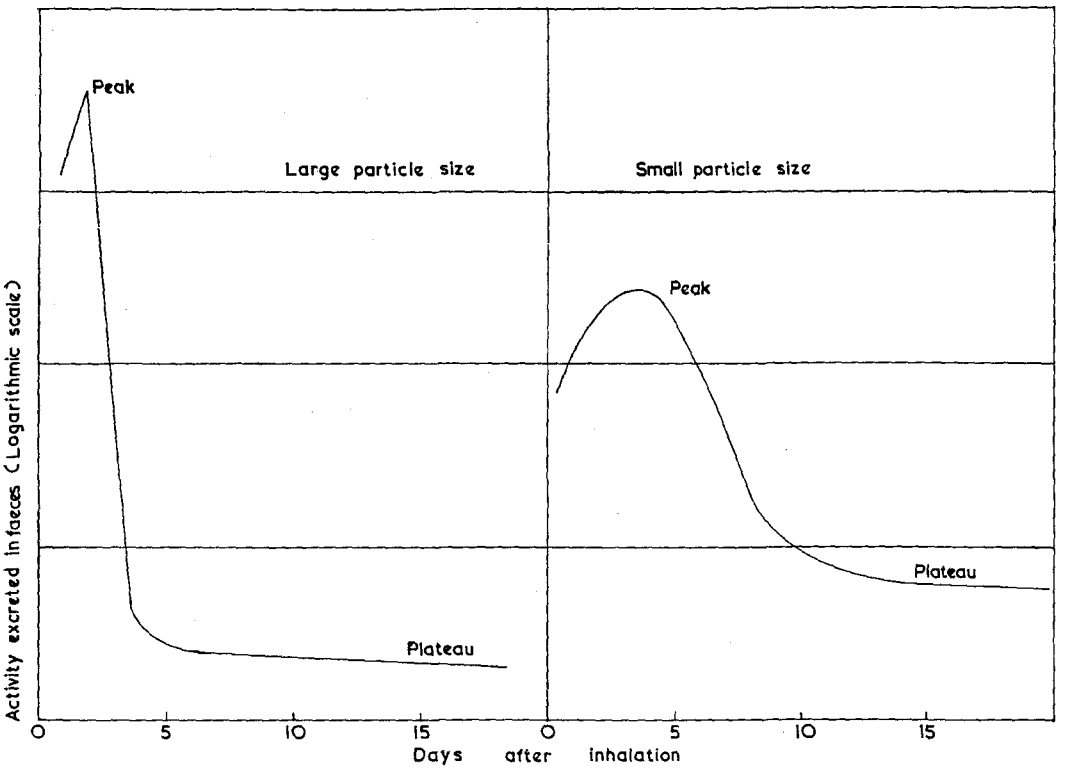

FIG. 1. Faecal excretion patterns following inhalation of insoluble material.

intake. The "plateau" level can be determined by a series of samples.

Such "plateau" data can only be useful in evaluating lung content if some relationship can be assumed between the "plateau" level and the early (cumulative four day) faecal excretion. Cases where the necessary full data are available are unfortunately rare, but examination of a few well documented cases at the Harwell and Aldermaston establishments allows some hope that this plateau value might give a "feel" for the seriousness of lung content. The relevant data for these cases are given in Table 1. (Although in column 2 and throughout this paper reference is made to the first four day faecal excretion, in cases where the first four samples cover a longer period, this longer period is inferred.)

In only nine of the eleven cases in Table 1 does the data allow a reasonably firm figure to be given for the ratio in the last column. In these cases, which cover a wide range of particle sizes, all the ratios fall between 10^2 and 10^4. Combination of this range with the I.C.R.P. simple lung model would suggest a range of 20–2000 for the ratio of the long-term retention (R) to the average daily low level faecal excretion (F_p) between about 10 and 100 days after the exposure.

If the I.C.R.P. Task Group constants are accepted, i.e. that two thirds of the material leaving the lung with a long half time is cleared via the gastro-intestinal tract, then the ratio, $R/F_p \times 2/3$ can be taken as the inverse of the average daily rate of removal from the lung (λ in the expression $\lambda t^{1/2} = 0{\cdot}693$). The ratios observed in the cases in Table 1 correspond to biological half times in the lung of from 9 days to $2\frac{1}{2}$ years. Most cases of inhalation exposure to insoluble materials in which clearance from the lung has been measured *in vivo* come within this range, as does the value adopted by the

Table 1. Faecal Excretion Data from Inhalation Cases

Case	Approximate faecal excretion in first 4 days ($\Sigma_0^4 F$) (pCi)	Average daily faecal excretion in "plateau" region (F_p) (pCi)	Ratio ($\Sigma_0^4 F/F_p$)
A	8×10^3	1	8×10^3
B	10^3	0·5	2×10^3
C	10^2	0·5	2×10^2
D	10^2	0·5	2×10^2
E	50	0·5	10^2
F	5×10^4	8	6×10^3
G	8×10^5	2×10^2	4×10^3
H	$>6 \times 10^3$	3	$>2 \times 10^3$
I	$> 10^2$	1	$> 10^2$
J*	2×10^3	12	10^2
K*	7×10^2	8	10^2

* Very small particle size.

I.C.R.P. Task Group, 360 days, corresponding to an R/F_p ratio of 780.

Although use of this range for R/F_p or any selected value within it, can only give a very approximate indication of lung retention, it might be helpful as a guide to the seriousness of lung contamination.

ANALYSIS OF NOSE BLOW SAMPLES

For many years the analysis of nasal swabs has been used to indicate whether or not significant amounts of radioactive material have been inhaled. Over the past two or three years at Harwell, on occasions when there has been a known or suspected release of insoluble airborne radioactive material, each person concerned in such an incident has been asked, as soon as possible after recognition of the incident and after washing his hands, to blow his nose into a paper tissue. The tissue is then rapidly assessed in the bioassay laboratory by wet ashing followed by direct counting. (This procedure has now been adopted in other laboratories in the United Kingdom and elsewhere.[11]) Whenever possible, on the detection of activity on nose-blow samples, faecal voidings over the first four days (or the first four voidings if this covers a longer period) have been collected and assayed, and the results compared with the results from the nose-blow samples. Combined results from plutonium laboratories at Harwell and A.E.E. Winfrith, shown in Fig. 2, show a strong positive correlation.

The few occasions on which significant levels of activity were detected in nose-blow samples although the subsequent faecal excretion was very low, can be explained if the aerosols involved in these exposures were of large particle size, so that virtually complete deposition occurred in the nose and nasal passages. (The I.C.R.P. Task Group model suggests 90% deposition in the naso-pharyngeal compartment for particles of 10μ equivalent diameter and 99% deposition at 30μ). Under these circumstances, clearance via the gastro-intestinal tract may have been negligible. The median of the observed ratios of the cumulative activity excreted in faeces during the first four days to that in the nose-blow sample is almost exactly unity and this ratio is illustrated by the continuous line in Fig. 3. The broken lines enclose 90% of all the points and indicate that, by assuming a ratio unity, one can normally predict early faecal excretion from the activity in the nose-blow sample within a factor of 20. Such variation is not inconsistent with calculations based on deposition and clearance figures given by the I.C.R.P. Committee II Task Group, if limits

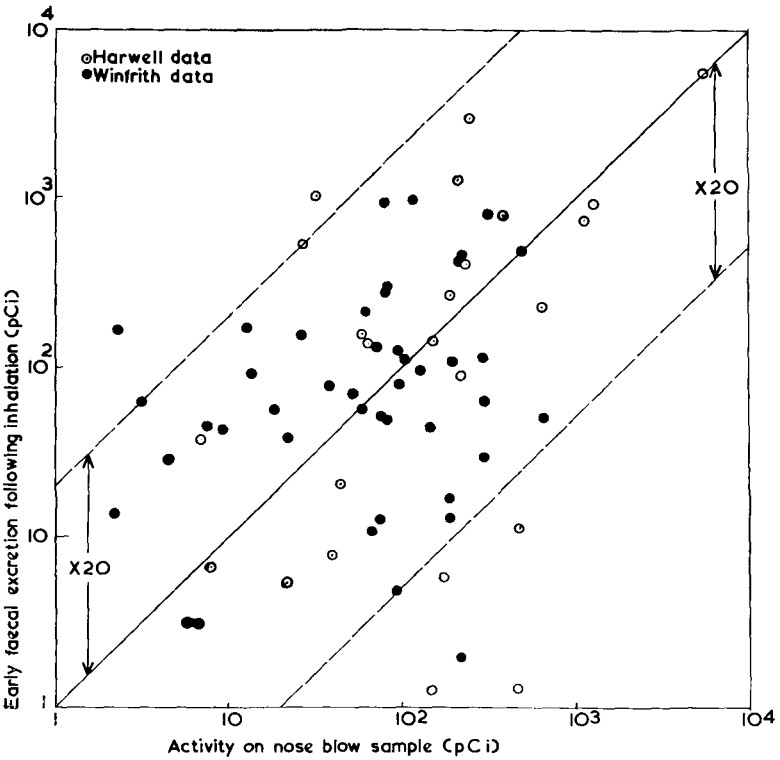

FIG. 2. Comparison of alpha activity in noseblow sample and in subsequent faecal samples (generally four days).

are assumed for nasal clearance when collecting the nose blow sample.

It is of value to consider in detail the case of ^{239}Pu. For the maximum permissible lung burden of 16 nCi, the I.C.R.P. simple lung model implies an original deposition of 96 nCi and early faecal excretion of 80 nCi. If this latter figure is taken as an "action" level, then an "investigation" level of one-tenth of this, i.e. 8 nCi, may be set for faecal excretion of plutonium corresponding to 8 nCi for the nose-blow sample.

This lung model does not take into account differences in particle size of the inhaled material. As the particle size decreases, the retained lung burden will constitute a higher proportion of the total deposition and vice versa. The I.C.R.P. Task Group suggests that for particles of 0.1μ equivalent diameter, deposition in the pulmonary compartment is as high as 50%, resulting in long-term retention of 30%, and for particles of 20μ diameter only 5%, with retention 3%. To take this uncertainty into account when, as is usual, the particle characteristics of the inhaled material are unknown, a safety factor must be introduced. Presumably the incidents giving rise to the results plotted in Fig. 2 must have involved a wide range of particle sizes as well as wide variations both in nose-blow "techniques" and delays after inhalation before the sample was taken. In spite of this, with two exceptions all the points indicate a ratio of less than 20 for faecal excretion to nose-blow content. With the introduction of a safety factor of 20, the investigation level for the nose-blow sample is reduced to 400 pCi. It is suggested that if a nose-blow sample exceeds this level, subsequent faecal samples should be collected to obtain further evidence of the degree of internal contamination.

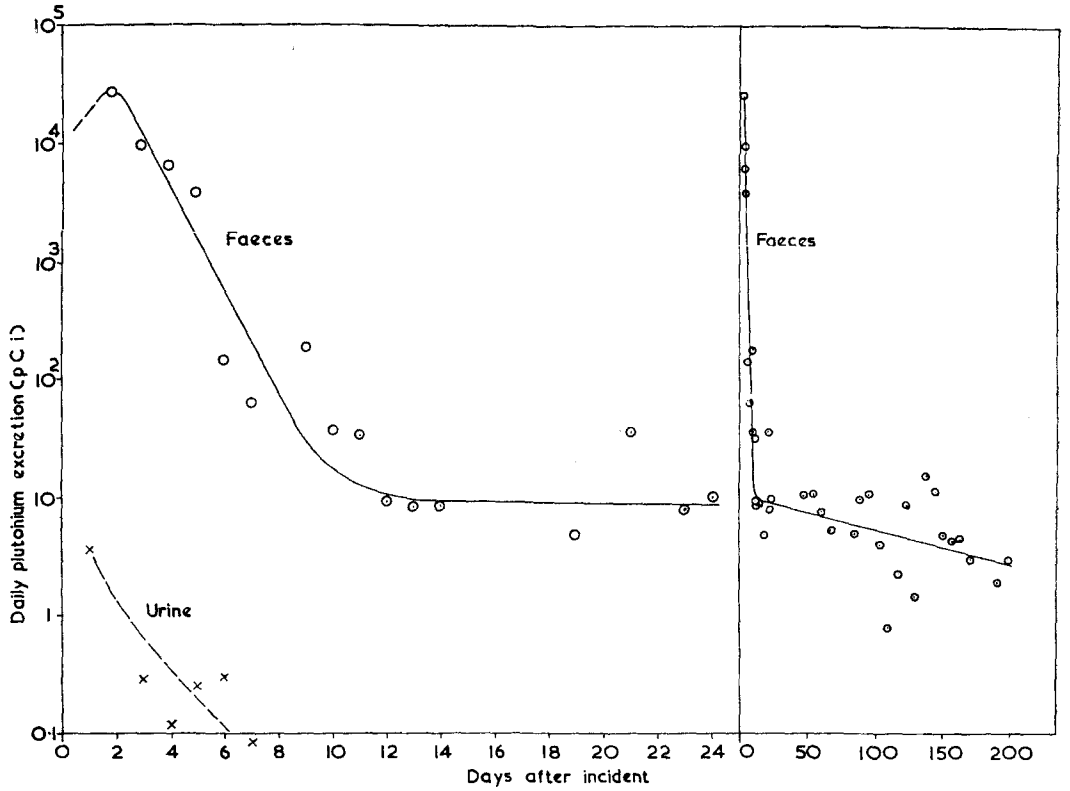

FIG. 3. Excretion data following plutonium inhalation (case F).

If the particle size is extremely small or if a person breathes through the mouth, either from habit, or because of a cold, very little of the material inhaled may be deposited in the nose. A negative result from a nose-blow sample taken following a known incident which has been confirmed by environmental monitoring will not therefore necessarily rule out the need for further biological sampling. The decision will depend on the severity of the incident as indicated by the other evidence. However, if a nose-blow result is less than 400 pCi and there is no other firm evidence of a significant release, there is little justification for requesting faecal samples, as the retained lung burden will almost certainly be less than 10% of the maximum permissible value. At Harwell an investigation level of 250 pCi has resulted in an important reduction in the number of faecal samples analysed. As with all biological sampling great care must be taken to prevent spurious contamination of samples. In the case of nose-blow samples skin contamination around the area of the nose is a danger and some of the low ratios found between activity in faecal and nose-blow samples may be due to this cause. In some cases it has been found that a second nose-blow sample contains significant activity although in most cases the bulk of the removable activity can be cleared with one blow.

The above discussion relates to airborne plutonium contamination, but the same argument can be applied to any material recognized as insoluble in the lung environment.

THE ASSESSMENT OF LUNG BURDEN AFTER INHALATION

It is quite clear that no one piece of information alone can be expected to give a good assessment of the retained lung burden within a few

days after an accident. Information of the following type may be relevant in assisting the health physicist in his evaluation of such exposures:

(i) *In vivo* measurement.
(ii) Analysis of urine (of little value).
(iii) Analysis of the early faecal excretion.
(iv) Analysis of late ($>$ 10 days) faecal excretion.
(v) Analysis of nose-blow samples.
(vi) Particle size analysis of air samples.
(vii) Other relevant evidence.

The way such information can be used in practice is exemplified by an incident which occurred at Harwell in which a man was exposed for a short period to high levels of airborne contamination, confirmed by spectrometry measurements to be mostly ^{239}Pu. *In vivo* measurements on the second day after the incident failed to detect any plutonium contamination in the lung, thus giving an *upper limit of 30 nCi* (the limit of sensitivity at that time) or about twice the maximum permissible lung burden.

Examination of personal and other air samples by counting and stripping film autoradiography[12] and of samples collected on a cascade centripeter[13] indicated that the man was exposed to about 6×10^4 mpc hours of plutonium airborne contamination and that he had inhaled 135 nCi of plutonium on particles of activity median equivalent diameter 5μ. Direct application of the I.C.R.P. simple lung model suggests a retained lung burden of 12·5% of the inhaled amount, i.e. of *17 nCi*. A detailed analysis of the particle size data obtained and application of the I.C.R.P. Task Group lung model suggested that the initial pulmonary deposition was 11·6% of that inhaled, i.e. 16 nCi of which 60% (*10 nCi*) would be retained with a half time of about a year.

Since the airborne contamination was not detected until routine counting of air samples at the end of the day, a nose-blow sample was not taken until some hours after the release of activity. Its plutonium content (43 pCi) was therefore of little use in assessing lung content.

The plutonium content of urine samples dropped rapidly (see Fig. 3) from about 3·6 pCi on the first day of the exposure to below the detectable level (0·02 pCi) after 12 days. This urinary excretion may have been due to uptake from the lung or from the gastro-intestinal tract and no valid use can be made of these figures.

Faecal samples showed a plutonium content of 26 nCi on the second day, the subsequent daily excretion falling rapidly (see Fig. 3) for a few days until, after day 12, there was a relatively constant daily faecal excretion of plutonium falling only from 10 pCi to 3 pCi by day 200. From the second to the fifth day after the intake 46 nCi were excreted in faeces. Although the voiding on the day following the incident was not collected, experience suggests that excretion in the first 24 hr is unlikely to exceed half the peak value on the following day. This assumption leads to a cumulative first five day excretion of $\sim$60 nCi, corresponding, according to the I.C.R.P. simple lung model, to a long-term retention of $\sim$ *12 nCi*.

This figure is based on a very much simplified lung model. In this incident the known particle size distribution of the inhaled cloud combined with the I.C.R.P. Task Group lung model indicates initial deposition in the pulmonary compartment of 11·6% of that inhaled (implying 7% long-term retention), of 76% in the nasopharynx and of 8% in the tracheal-bronchial region. It is reasonable to assume in the existing circumstances that all plutonium deposited in the tracheobronchial and nasopharyngeal compartments (84%) appeared in faeces in the first few days. This, together with 40% of that initially deposited in the pulmonary region, i.e. a total of 89%, corresponds to the measured faecal excretion of 60 nCi. The long term retention of 7% therefore corresponds to *4·7 nCi*.

Although more directly relevant data is available in this case, it is interesting to note that use of the ratio of 20–2000 for early cumulative excretion to daily "plateau" excretion leads to the suggestion that the long-term lung retention is *between 0·16 and 16 nCi*. Use of the I.C.R.P. Task Group figures for rate of clearance from the lung together with the "plateau" excretion level suggests a retention ($F_p \times 780$) of *6·2 nCi*.

Thus values have been obtained (see Table 2) ranging from 0·16 to 17 nCi with a definite upper limit of 30 nCi and a decision has to be made as to which of the approaches used is

Table 2. Analysis of Data for Cases of Inhalation of "Insoluble" Plutonium

Approach	Retained lung content (nCi)
1. *In vivo* measurement	<30
2. I.C.R.P. (1959) lung model	17
3. Air sample data + T.G.* lung model	10
4. Nose blows	—
5. Urine analysis	—
6. Early faecal analysis + I.C.R.P. (1959) lung model	12
7. Early faecal analysis + T.G.* lung model	4·7
8. Faecal "plateau" excretion + T.G.* clearance data	6·2
9. Faecal "plateau" excretion + Table 1 data	0·16–16

* I.C.R.P. Committee II Task Group on lung dynamics.

more valid in this particular case. Since the faecal excretion and particle size characteristics of the airborne contamination are known with certainty it is felt that the assessment using these data gives the best chance of approaching the truth. The individual was therefore accredited with an initial retained lung burden of 5 nCi of ^{239}Pu. In this case we were fortunate in possessing useful air sample data; usually such data are not available and the answer must be arrived at on less secure grounds.

Some of the approaches described in this paper are purely empirical and have no pretence of precision; neither can they give any information on the systemic burden. But in giving a guide as to the seriousness of the lung content they can assist medical officers and health physicists in their early treatment of the exposed person.

ACKNOWLEDGEMENTS

As well as data obtained in our bioassay laboratory at Harwell, data have been used from laboratories at Winfrith and Aldermaston. I thank the Directors of these establishments for permission to include these data in this paper.

REFERENCES

1. *Recommendations of the International Commission on Radiological Protection.* Report of Committee II on Permissible Dose for Internal Radiation. I.C.R.P. Publication 2, Pergamon Press (1959).
2. Deposition and retention models for internal dosimetry of the human respiratory tract. *Health Physics* **12,** 173 (1966).
3. J. G. MEHL and J. RUNDO. *Health Physics* **9,** 607 (1963).
4. J. SEDLET, W. D. FAIRMAN and J. J. ROBINSON. *Personnel Dosimetry for Radiation Accidents,* p. 395, I.A.E.A. Vienna (1965).
5. R. EHRET, H. KIEFER, R. MAUSHART and G. MOHRLE. Assessment of radioactivity in man. *Proc. Karlsruhe Symposium,* Vol. 1, p. 141. I.A.E.A. Vienna (1964).
6. B. TAYLOR and J. RUNDO. Unpublished work.
7. B. A. J. LISTER. *Diagnosis and Treatment of Radioactive Poisoning,* p. 23. I.A.E.A. Vienna (1963).
8. C. W. SILL. Assessment of radioactivity in man. *Proc. Karlsruhe Symposium,* Vol. 1, p. 217. I.A.E.A. Vienna (1964).
9. J. D. EAKINS and A. MORGAN. Ibid. p. 231.
10. S. A. BEACH and G. W. DOLPHIN. Ibid. Vol. 2, p. 603.
11. N. VALENTIN. BLG 371 (CEN Bruxelles) (1966).
12. D. C. STEVENS. *Ann. Occup. Hyg.* **6,** 31 (1963).
13. R. F. HOUNAM and R. J. SHERWOOD. *Am. Ind. Hyg. Ass. J.* **26,** 122 (1965).

THE UPTAKE, RETENTION AND EXCRETION OF INHALED EUROPIUM OXIDE IN TWO HEALTHY ADULT MALES

P. L. ZIEMER, R. E. GEORGE* and W. V. KESSLER

Bionucleonics Department,
School of Pharmacy and Pharmacal Sciences,
Purdue University, Lafayette, Indiana

Abstract—Body burdens and activity excreted were repeatedly measured following an accidental europium oxide inhalation by two adult males at Purdue University. Isotopic composition of the europium involved was determined to be 93.4% ^{156}Eu, 3.25% ^{155}Eu, 2.9% ^{154}Eu and 0.35% ^{152}Eu. Initial body burdens were found to be 55 μCi and 38 μCi of the mixed europium isotopes. Retention following the early rapid elimination processes was described by a power function: $R(t) = At^{-n}$. One subject cleared 80% of his initial respiratory tract burden during the first day; the second cleared 89% of his burden. Based on the recent lung model of the ICRP, integral lung doses for the two subjects were calculated to be 6.8 rad and 2.2 rad; lower large intestine doses resulting from early rapid clearance were 3.1 and 2.2 rad.

INTRODUCTION

On December 28, 1966, two members of the Purdue University Physics Department were exposed to a high level of airborne radioactivity for a short period of time. The inhalation occurred when a quartz ampoule, which contained reactor-produced europium isotopes in the form of insoluble europium oxide, ruptured. The material had been prepared by exposing 98.7% enriched ^{153}Eu oxide for 24 days to a flux of 2×10^{14} neutrons/cm^2/sec. The resulting activity, although initially stated by the supplier to contain 40 mCi of ^{154}Eu and 2 mCi ^{152}Eu, was later determined to contain 950 mCi ^{156}Eu, 23 mCi ^{155}Eu, 29 mCi ^{154}Eu, and 1.2 mCi ^{152}Eu.

Emergency procedures were carried out by Health Physics personnel, and the exposed individuals, after being externally decontaminated, were immediately placed under medical observation. Preliminary estimations of their body burdens were made with a medical scanning unit utilizing a sodium iodide crystal detector. Collection of urine and feces was also initiated to assist in determining body burdens.

By day three following the incident, the body burdens in the two individuals were reduced sufficiently to allow whole body counting to be initiated in the Purdue University, 4-pi, large volume, liquid scintillation counter, SINCO-P. This counter has been described in detail in the literature.[1]

Since very little has been reported in the literature on the behavior of europium compounds in biological systems, the measurements have served to characterize an excretion model for inhaled insoluble europium oxide. These data may further assist in the characterizing of the retention and excretion of other rare earth compounds in the body.

METHODS AND MATERIALS

The exposed subjects were counted three times a week for the first two weeks, then twice a week through the month of February. Weekly counts were then made for the next two months, bi-weekly counts were made during the month of

* Present address: Armed Forces Radiobiology Institute, Bethesda, Maryland.

May, and beginning in June counts were made once per month. Initially, the counting rates were such that only 2-min counting times were required. This was later increased to 4 and 6 min as body burdens decreased. Excreta were collected continuously for the first week following the exposure. Thereafter, single 24-hr urine and fecal samples were collected each week as regularly as the subjects' cooperation made possible. After the fourth month, collection was reduced to once per month.

Gamma spectroscopy was used to confirm the presence of ^{152}Eu and ^{154}Eu in the material inhaled by the exposed subjects. Spectra collected indicated that ^{156}Eu and ^{155}Eu were present in addition to ^{154}Eu and ^{152}Eu. The activity of the europium mixture at the time of the exposure was determined to be 93.5% ^{156}Eu, 3.25% ^{155}Eu, 2.9% ^{154}Eu, and 0.35% ^{152}Eu. Repeated counting of sources made possible calculation of the abundance of ^{156}Eu as it rapidly decayed out of the mixture. The relative activities of the other europium isotopes were found by examination of the mixture's gamma spectrum. To verify these observations, calculations were made to determine the expected yields of ^{156}Eu, ^{155}Eu, ^{154}Eu, and ^{152}Eu at the neutron flux, amount of target material, neutron cross sections, and irradiation time reported by the supplier. The results were in close agreement with the observed activities.

A single channel analyzer operated in the integral mode with the base discriminator set to pass pulses equivalent to about 100 keV or greater was used to collect the whole body counting data. Integral counting was selected because the gamma spectra of the euporium isotopes involved cover a broad range of energies from 19 keV to 2.19 MeV.

Counting standards were prepared from europium recovered from the scene of the incident. The absolute activity of the recovered europium standards was determined using 4-pi, gas flow, beta counting. Chest phantoms were prepared using 2-gallon polyethylene bottles filled with distilled water. Smaller phantoms were prepared for urine and fecal analyses.

Characterization of europium excretion was complicated by the presence of the four radioisotopes whose physical half-lives varied from 15 days to 16 years (Table 1). Nevertheless, an excretion model for inhaled europium oxide was developed after evaluating the data by two different methods. First, the fraction of the body burden excreted per day was obtained by determining both the body burden and the activity in the excreta for a given day. As a second method of evaluation, successive whole body counts were compared to normalized europium standard counts to find the fraction eliminated per unit time. Excretion models obtained by the two methods were in agreement. The fraction eliminated decreased with time and retention of inhaled europium oxide seemed to be best described by the power law: $R(t) = At^{-n}$, where $R(t)$ is the fraction of initial burden retained at time t, A is the fraction retained at unit time, and n is a constant.

Particle size distribution data were determined for unirradiated Eu_2O_3 from the same chemical batch used to prepare the europium involved in the exposure incident. A phase

Table 1. *Characteristics of europium isotopes*

Isotope	Physical half-life	Approximate number of gammas in spectrum	Range of gamma energies (MeV)	Thermal neutron cross-section (barns)
^{151}Eu	(stable)	—	—	5900
^{152}Eu	12.4 yr	22	0.122 to 1.41	5000
^{153}Eu	(stable)	—	—	320
^{154}Eu	16 yr	11	0.123 to 1.61	1400
^{155}Eu	1.8 yr	11	0.019 to 0.146	13000
^{156}Eu	15.2 days	27	0.60 to 2.19	

contrast microscope was used according to the methods of Drinker and Hatch.[2]

Radiation doses to lung, lower large intestine, and lymph tissue were then calculated in four ways:

1. Using the 1959 ICRP lung model.
2. Using the 1959 ICRP model modified to fit excretion data.
3. Using the recently proposed lung model of the ICRP task group.
4. Using the task group model modified to fit observed excretion data.

RESULTS

Whole body and excreta counting indicated that the initial internal body burdens of the two subjects, Z. G. and H. N., were 55 μCi and 38 μCi of mixed europium isotopes, respectively. Z. G. eliminated approximately 80% of his respiratory tract burden via the GI tract within the first 48 hr; H. N. cleared 89% of his burden within 48 hr by the same route. The retention equation fitting the data of Z. G. was found to be: $R(t) = 0.2t^{-0.09}$; for H. N.: $R(t) = 0.12t^{-0.1}$ although his data were far less consistent (see Figs. 1, 2, and 3). After the rapid early clearance mechanisms ceased to be effective, urine to fecal ratios of europium activity were equal to very nearly one.

Values of radiation doses to critical organs calculated for the 4 lung models are listed in Table 2.

The unirradiated sample of Eu_2O_3 was found to have a count median diameter and standard deviation of 0.54 μ and 2.0 μ respectively. The mass median aerodynamic diameter was calculated to be approximately 6.4 μ. Excretion data could be shown to agree with the recently proposed lung model if route (f), the rapid pulmonary compartment clearance rate, was assigned a half-time of 12 hr vs. the 24 hr time recommended by the ICRP task group.

DISCUSSION

The difference in retention observed in subjects Z. G. and H. N. may be explained as resulting from somewhat different exposure conditions. Z. G. remained in the vicinity of the spilled europium for an estimated 5 min, while H. N. left the area about 1 min after the incident occurred. Rapid settling of the larger Eu_2O_3 particles out of the breathing zone of the subjects may certainly have caused Z. G. to breath an aerosol of decreasing particle size, resulting in a higher percentage of pulmonary deposition. Since clearance mechanisms are far less rapid in the lungs than in the upper portions of the respiratory tract, retention at one day post exposure would be logically greater for Z. G.

Urine to fecal ratios of europium activity suggest that europium absorption was occurring in the lungs since the highly insoluble nature of

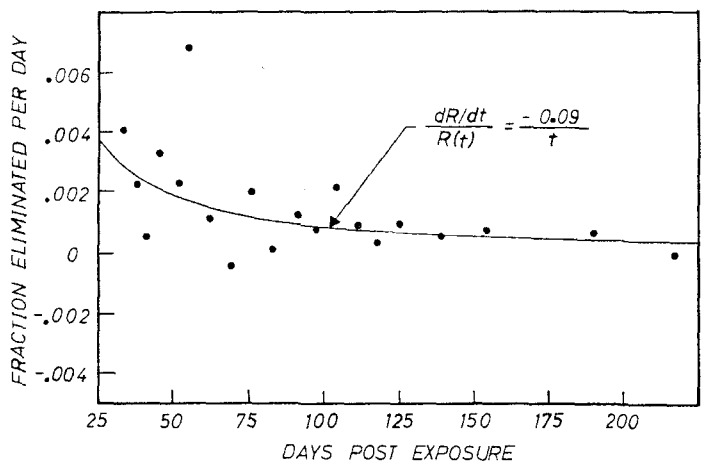

FIG. 1. Europium clearance determined from whole body measurements of Z. G. Curve represents power law retention where exponent for variable t is -0.09.

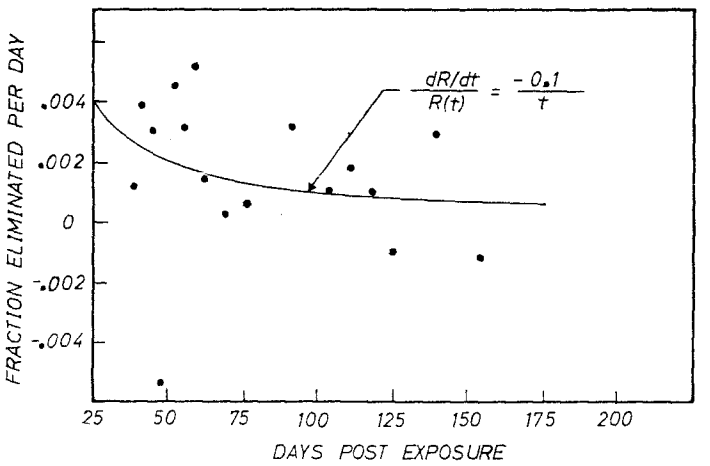

FIG. 2. Europium clearance determined from whole body measurements of H. N. Curve represents power law retention where exponent for the variable t is -0.10.

Table 2. Summary of Radiation Doses Calculated Using Various Lung Models

Subject	Organ	ICRP lung model–1959		ICRP Task Group lung model	
		Original	Modified to fit excretion data	Proposed	Modified to fit excretion data
Z. G.	lung*	4.4 rad	5.5 rad	8.7 rad	6.8 rad
	lower large intestine†	3.0	2.9	3.0	3.1
	lymph‡	—	—	10.0	—
H. N.	lung*	3.0	2.0	5.7	2.2
	lower large intestine†	2.1	2.2	2.1	2.2
	lymph‡	—	—	3.8	—

* Infinity dose; over 90% of lung dose absorbed within 4 years of exposure.
† Infinity dose; over 90% of lower large intestine dose absorbed within 3 days of exposure.
‡ 50-year dose to lymph tissue.

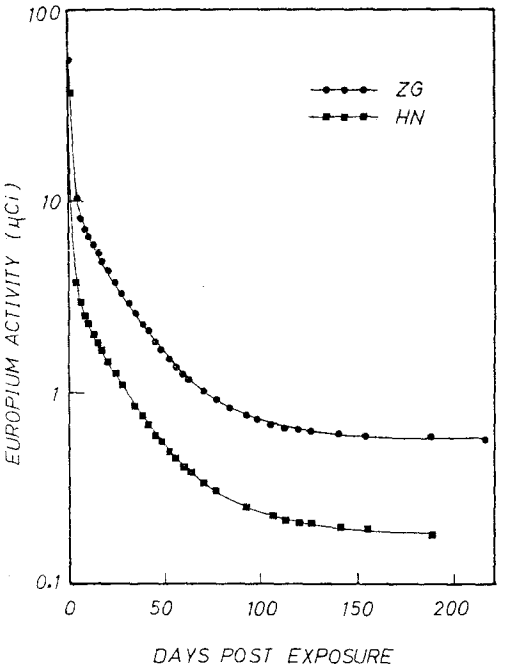

FIG. 3. Europium body burdens as determined by whole body counting in SINCO–P.

Eu_2O_3 would preclude a high percentage of absorption through the gut.

Use of the best present knowledge on respiratory tract clearance and other biological parameters of concern indicated that the lung and lower large intestine should still be considered the critical organs in the exposure incident. Had the mixture consisted only of long-lived isotopes of europium, lymph would have been the tissue of greatest concern.

The data also suggest a possibility of hold-up in the lungs in view of the fact that the retention power law overestimated excretion for the time period from 1 January 1966 through 24 January 1966. Hold-up of plutonium oxide in the lungs has been described by Langham.[5] Chemical similarities of actinides and lanthanides suggest that similar behavior on the part of europium oxide is a reasonable explanation.

REFERENCES

1. J. E. CHRISTIAN, W. V. KESSLER and P. L. ZIEMER. *Int. J. Applied Radiation and Isotopes* **13,** 557 (1962).
2. P. DRINKER and E. HATCH. *Industrial Dust*, 2nd ed., pp. 166–199. McGraw-Hill, New York, 1954.
3. *Recommendations of the International Commission on Radiological Protection*, Report of Committee II on Permissible Dose for Internal Radiation. ICRP Publication 2, Pergamon Press, New York, 1959.
4. P. E. MORROW. *Health Phys.* **12,** 173 (1966).
5. W. H. LANGHAM. *Assessment of Radioactivity in Man*, Vol. 2, pp. 565–581. International Atomic Energy Agency, Vienna, 1964.

INHALATION CASES OF ENRICHED INSOLUBLE URANIUM OXIDES*

NEIL B. SCHULTZ
Union Carbide Corporation,
Nuclear Division,
Oak Ridge Gaseous Diffusion Plant
Oak Ridge, Tennessee

Abstract—The retention and excretion of uranium by about 80 employees routinely assigned to calcining and fluorinating uranium-bearing materials enriched in the ^{235}U isotope have been closely followed for more than a year. *In vivo* measurements of body radioactivity were made by means of gamma spectrometry with two NaI scintillation detectors in an "iron-room" type, low background counter. Initial chest cavity burdens ranged from less than 0.006 μCi to about 0.050 μCi of enriched uranium, with only two cases having annual averages greater than 0.017 μCi. The effective half-lives for chest cavity retention of the three employees who were temporarily removed from uranium processing areas ranged from about 120 to 250 days. Urine samples collected over 24 hr were analyzed for uranium mass, alpha activity, and ^{235}U enrichment. Average ratios of chest cavity burden to urine excretion rate increased from about 550 to 1100 between the initial and final determinations. Fecal excretion rates averaged 40% to 180% of the uranium urinary excretion rates. Material balance calculations showed agreement ranging from 50% to 75% between total urinary–fecal excretion and reduction in chest cavity burden as shown by *in vivo* measurements. Pulmonary function tests of the employees revealed normal respiratory performance. Medical data, including chest X-rays, clinical urinalysis for albumin, and microscopic examination of urine for pathological cells and organisms, are normal in all cases. There is no evidence of personnel injury from these transient internal uranium depositions.

INTRODUCTION

During more than 20 years of operation of a uranium gaseous diffusion plant, appropriate environmental monitoring and operating controls have been maintained to limit exposure of employees to acceptable levels. For the past 5 years, *in vivo* gamma spectrometry measurements of the 186 keV gamma radiation associated with ^{235}U have been performed to supplement the urinalysis program for monitoring personnel involved in uranium processing. Over 90% of the personnel monitoring data reflect either less-than-detectable or negligible results, and present no problem in evaluating exposures. The retention and excretion of uranium by about 80 male employees routinely assigned to calcining and fluorinating uranium-bearing materials enriched in the ^{235}U isotope have been closely followed for the period of November 1964 through June 1966. The purpose of this paper is to record the results of this study, with data for 3 employees reported in detail.

SUMMARY

The operation of industrial-scale uranium recovery facilities at the Oak Ridge Gaseous Diffusion Plant by the Union Carbide Corporation, Nuclear Division, for the U.S. Atomic Energy Commission involves the calcining and fluorinating of uranium-bearing materials enriched in the ^{235}U and ^{234}U isotopes. Environmental air sampling and work surface

* This document is based on work performed at the Oak Ridge Gaseous Diffusion Plant, operated by Union Carbide Corporation, Nuclear Division, for the U.S. Atomic Energy Commission.

radio-activity surveys are conducted on a routine basis in all processing areas to evaluate internal exposure potential via inhalation. Personnel monitoring practices include urine analysis, fecal analysis, and *in vivo* gamma spectrum analysis programs. Urine and fecal samples, either single voiding or excreta collected over 24 hr, are analyzed for uranium mass alpha activity, and ^{235}U enrichment. *In vivo* measurements of body radioactivity were made by means of gamma spectrometry with 2 NaI scintillation detectors in an "iron-room" type, low background counter. The retention and excretion of uranium by about 80 male chemical operators and maintenance mechanics routinely assigned to calcining and fluorinating uranium-bearing materials enriched in the ^{235}U isotope have been studied during the period of November 1964 through June 1966. Only 8 detectable chest cavity burdens were recorded; of these, 3 had an annual average value less than 0.008 μCi of uranium; 3 averaged between 0.008 μCi and 0.017 μCi, and 2 averaged 0.028 μCi of uranium. The subjects of this report are the 2 latter cases and a third case in the 0.008 μCi to 0.017 μCi range, all of whom are male chemical operators and were temporarily transferred from uranium processing areas following the initial elevated urinalysis and *in vivo* measurements. The effective half-lives for chest cavity retention of these 3 employees ranged from about 120 to 250 days. Average ratios of chest cavity burden to urine excretion rates increased from about 550 to 1100 between the initial and final determinations. Fecal excretion rates averaged 40% to 180% of the uranium urinary excretion rates. Material balance calculations indicated that 50% to 75% of the reduction in chest cavity burden as shown by *in vivo* measurements are reflected in the total urinary-fecal excretion. Pulmonary function tests revealed normal respiratory performance, and medical data are within normal limits in all cases. There is no evidence of personnel injury from these transient internal uranium depositions.

BACKGROUND INFORMATION

Operations

Personnel in the study group were 80 employees assigned to the operations and maintenance activities in the enriched uranium recovery facility, involving the conversion of uranyl nitrate, $UO_2(NO_3)_2$, by calcining at about 750°C to urano-uranic oxide, U_3O_8, and the direct fluorination of the oxide to uranium hexafluoride, UF_6. These operations, conducted in closed systems, are located in relatively open areas of approximately 12,000 ft^2 and 3000 ft^2, respectively.

Environmental Monitoring

Established practices limit internal exposure to acceptable levels by appropriate environmental controls. To evaluate both the effectiveness of these controls and the internal exposure potential via inhalation, air sampling is conducted on a routine basis in all processing areas. In general, environmental air levels are well within the limits prescribed by the National Committee on Radiation Protection [1] and the International Commission on Radiological Protection. [2] Long-term or 8-hr shift-length samples are automatically collected, counted for alpha radioactivity concentration, and recorded by locally developed continuous air monitors. [3] During this study, 954 shift-length samples were collected, with an average concentration of 3.3×10^{-11} μCi/cc, and a maximum 8-hr value of 1.5×10^{-9} μCi/cc. Spot-air samples, taken over periods of 10 min or less in close proximity to equipment during maintenance or operation activities requiring momentary opening of the system to atmosphere, resulted in maximum air levels of 4.9×10^{-7} μCi/cc. Where the probability of relatively high air activity exists, the use of appropriate respiratory equipment is mandatory. Measurement of transferable uranium alpha activity on work surfaces provides a broad sampling base for estimating the potential personnel exposure. [4] Uranium alpha levels on floors and work surfaces averaged 1.1×10^{-5} μCi/cm^2, with a maximum value of only 4.5×10^{-5} μCi/cm^2, reflecting effective environmental control techniques.

Aerosol Characteristics

Evaluation of the potential hazard from inhaling radioactive airborne particulates requires not only monitoring of the concentration levels, but also careful consideration of the

physico-chemical characteristics of the particles, and the physiological characteristics of the human respiratory system. The two compounds of most likely exposure in these cases are urano-uranic oxide, U_3O_8, and uranium hexafluoride, UF_6. The oxides of uranium, generally listed as being insoluble in water, actually have widely varying solubilities (0–100%) in synthetic lung fluids,[5] with the U_3O_8 of interest in this study being about 16% soluble in test tube studies over a 4-month period. The uranium content of the powder is 84%, approximately 2/3 being hexavalent and 1/3 being tetravalent. This oxide powder has a surface area of 3.05 m^2/g and a density of 8.38 g/cc. A count median diameter of 1.0 $\pm$ 3.0 μ was determined from the photomicrograph shown in Fig. 1. The other potential exposure material, gaseous uranium hexafluoride, hydrolyzes if released to the atmosphere, with reaction products of hydrogen fluoride, HF, and uranyl fluoride, UO_2F_2. The particle size range of the highly soluble, short biological half-life UO_2F_2 aerosols varies widely from submicron to several microns in diameter, depending upon several factors, such as ambient temperature, relative humidity,

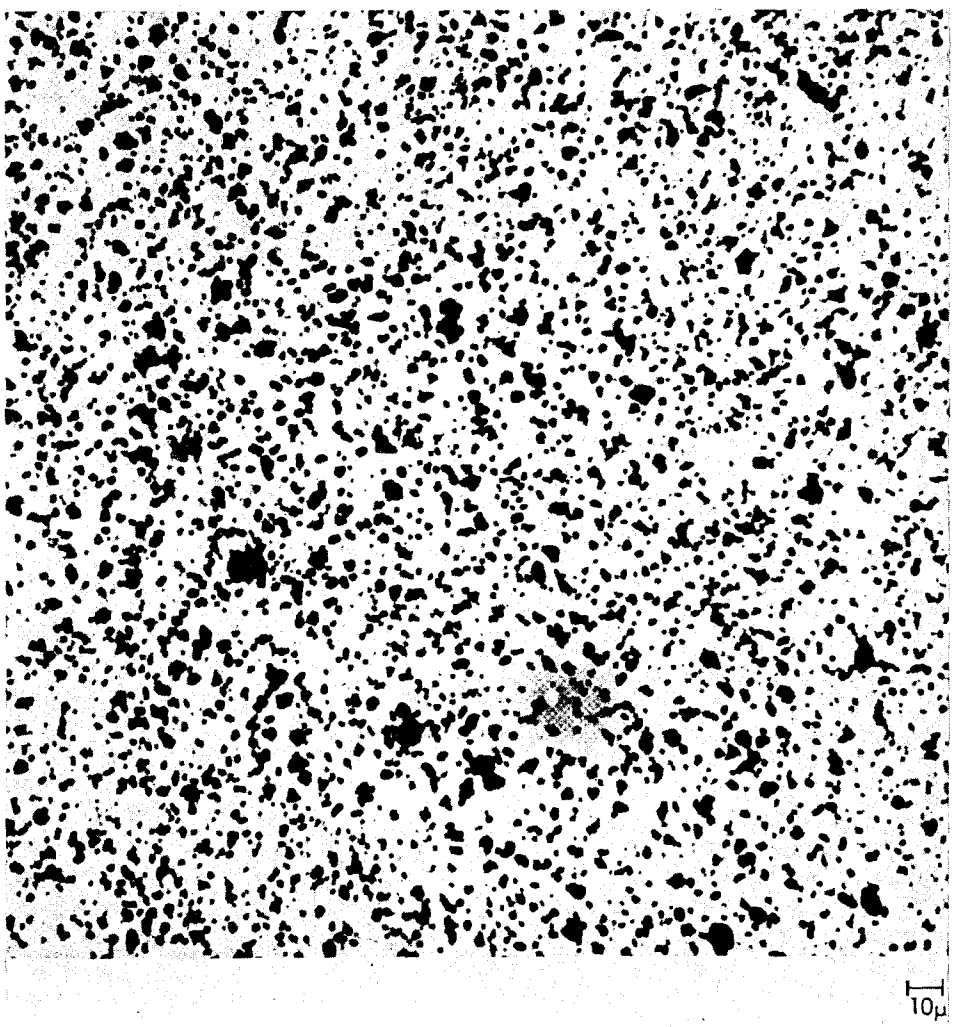

FIG. 1. Photomicrograph of U_3O_8 × 500 reduced to $\frac{8}{10}$.

and the concentration of the UF_6 at the time of the release.[4] During the study period, enrichments in the ^{235}U isotope ranged from about 10% to approximately 90%; for the 3 cases reported, the most likely enrichment of the exposure material was about 25% ^{235}U.

Personnel Monitoring

In order to evaluate the effectiveness of engineering design and operational practices, and to estimate the degree of internal exposure, personnel monitoring programs have been established. Monitoring of all personnel who work in uranium areas is accomplished by uranium urinalysis and *in vivo* gamma spectrum analysis. If either method points up potential exposure cases, fecal sampling as well as more frequent urinalysis and *in vivo* gamma spectrum analyses are used to more precisely evaluate the degree of exposure. The scheduled urinalysis sampling frequency is monthly for both the chemical operators and the maintenance mechanics, as well as the supervisory staff. These routine samples are obtained on a spot basis and are submitted after a 2- or 3-day work break, allowing time for the highly soluble uranium to be eliminated. When more frequent sampling is indicated, 24 hr urine and fecal voidings are submitted. In this study, when the employees were requested to provide such timed excretion samples, the importance was stressed to secure knowledgeable co-operation. Volumes of urine and masses of feces reported to be 24-hr samples averaged 1263 ml/day and 135 g/day, respectively, and are summarized in Table A5. Urine analyses are routinely made for both uranium mass and alpha activity, using the familiar laboratory procedures of (a) the fluorophotometric method for determining uranium mass, and (b) electroplating and counting for alpha activity. The ^{235}U enrichment is determined by surface ionization mass spectrometry.

The *in vivo* gamma spectrometry measurements of the 186 keV gamma radiation associated with ^{235}U reported in this study were made at the nearby Y-12 Plant, also operated by the Union Carbide Corporation, Nuclear Division, for the U.S. Atomic Energy Commission. Figure 2 is a photograph showing the positioning of the subject and the detectors.

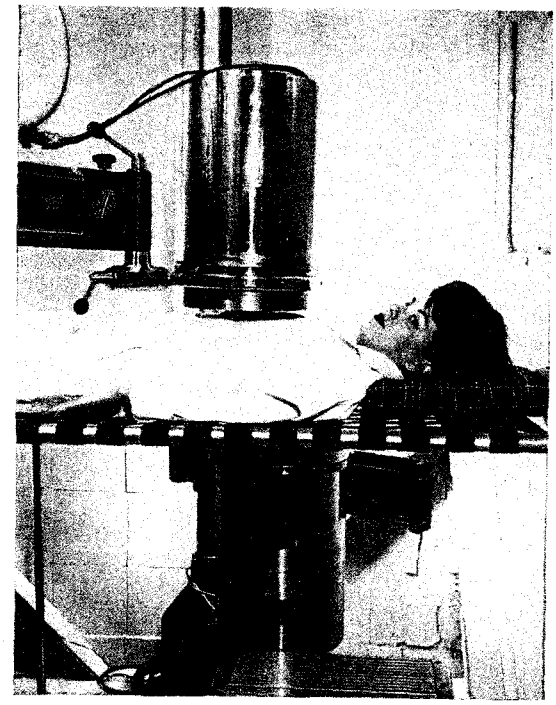

FIG. 2. *In vivo* gamma measurement—positioning of subject and detectors.

This gamma radioactivity measurement facility consists of the familiar low-background "iron-room" counting chamber, two 9-in. diameter by 4-in. thick thallium-activated sodium iodide crystals, and a 400-channel pulse height analyzer.[6] Quantities as low as 30% of the maximum permissible body burden of any of the isotopic enrichments investigated can be measured. For a wide sampling of employees representing the many crafts and skills working in a large gaseous diffusion plant, all chest cavity burdens, except as indicated in this report, averaged well below 0.008 μCi of uranium.

EVALUATION OF DATA

Medical Findings

Deposition, retention, and translocation of inhaled radioactive particles are related not only to their physical and chemical properties, but also to the physiologic and anatomic characteristics of the host. For example, cigarette smoke, a ciliostatic substance, might reduce the rate of mucus transport by over one-half,

and thus influence the respiratory system clearance, particularly during and shortly following the dust exposure.[7] Pulmonary function tests of the employees, two of whom are relatively heavy cigarette smokers, revealed normal respiratory performance. Medical data, including chest X-rays, clinical urinalysis for albumin, and microscopic examination of urine for pathological cells and organisms, are within normal limits in all cases.

In Vivo Gamma Measurements

Of the 80 employees considered in this study, 8 had detectable chest cavity burdens, 3 had an annual average value less than 0.008 μCi of uranium, 3 averaged between 0.008 μCi and 0.017 μCi of uranium, and 2 averaged 0.028 μCi. The subjects of this report are the 2 latter cases and a third case in the 0.008 μCi to 0.017 μCi range, all of whom are male chemical operators and were temporarily transferred from uranium processing areas following the initial elevated *in vivo* measurement. These data are detailed in Tables A1, A2, and A3 of the Appendix.

Excretion Data

The least square fit for excreta measurements on these employees predicted initial levels as high as 71 pCi/day in the urine and 593 pCi/day in the feces. The excretion pattern changes at a rate different from that of the chest burden, as shown in Figs. 3, 4, and 5.

Data Summary

For ease of interpretation, the tabulated data were fed to a computer program to determine the least square fit for the log of the measurement as a function of the number of days since the initial elevated *in vivo* measurement. The dates of the first elevated *in vivo* measurements are the time datum ($t = 0$) for the derived curves of uranium excretion and chest burden data for the 3 cases, shown, along with the exponential function-of-time formulae, in Figs. 3, 4,

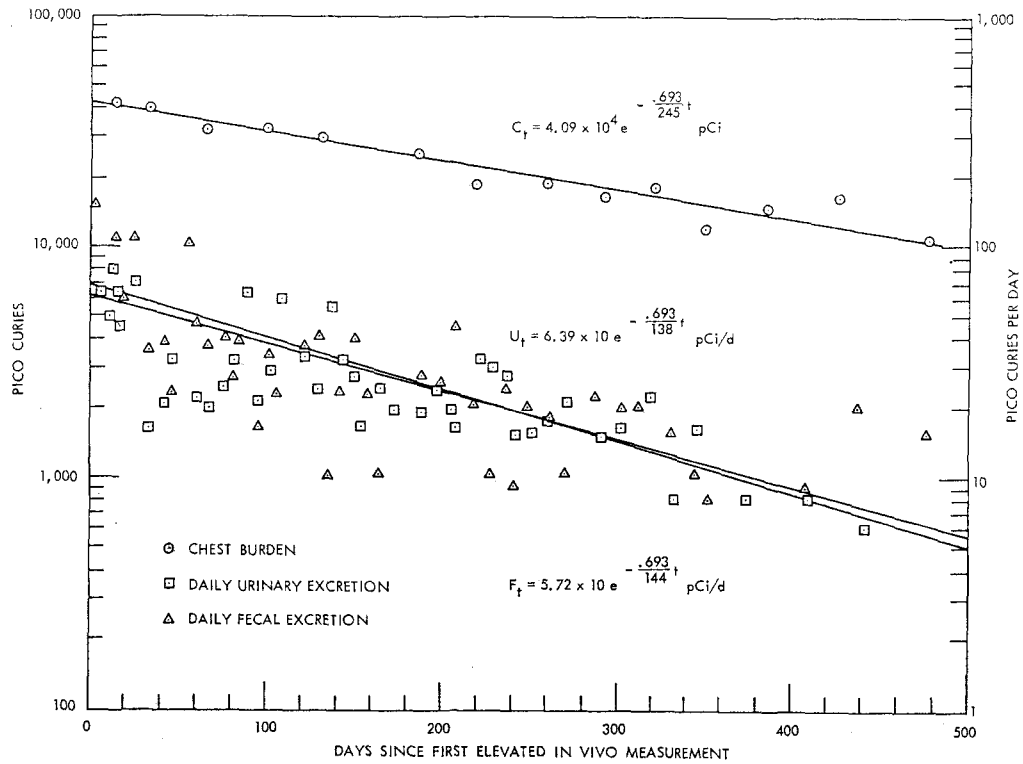

FIG. 3. Excretion and *in vivo* curves, case K-1.

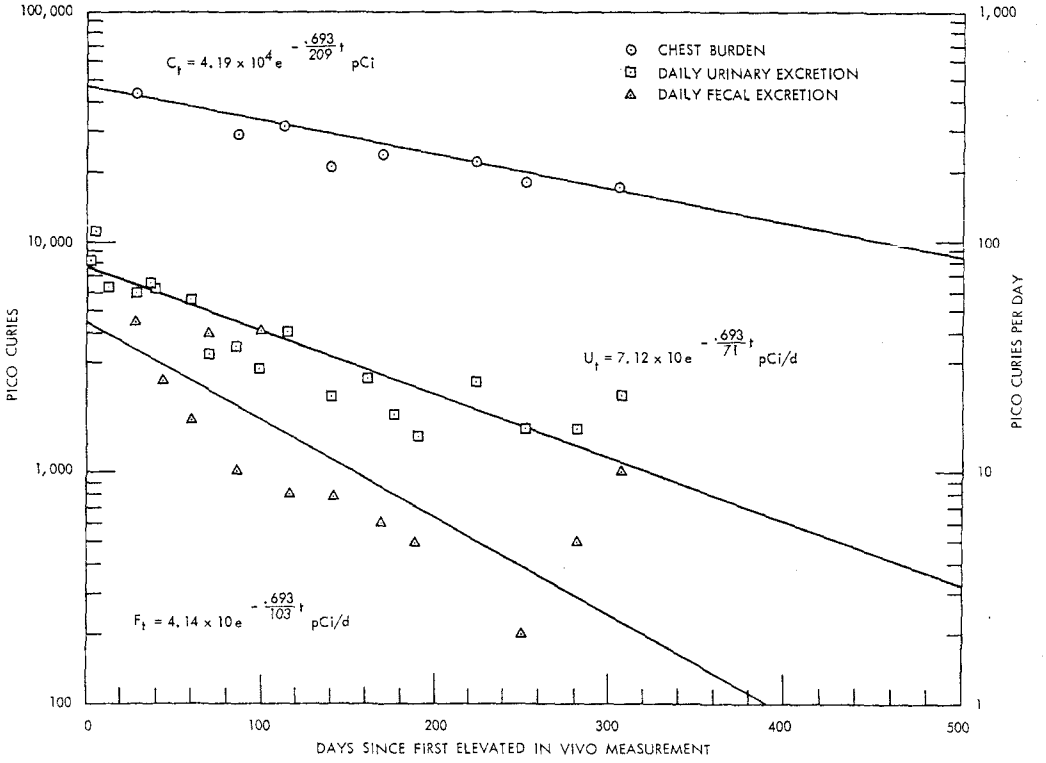

FIG. 4. Excretion and *in vivo* curves, case K-2.

and 5. Overall bioassay data averages for the 3 cases are summarized in Table 1. For the convenience of the reader, comparisons of excretion and *in vivo* data are listed for these and other cases [8–10] in Table A4.

The data suggest that the half-lives of insoluble or slightly soluble inhaled uranium in the chest cavity have long-lived components in these 3 cases ranging from about 120 to 250 days. The initial shorter half-life component of uranium excretion found in cases F-1[8] and UR-2[9] was seen in case K-3, but not in cases K-1 and K-2. Ratios of monthly averages of *in vivo* chest cavity burden and the quantity of uranium excreted daily in the urine varied from about 120 to 4130, averaging 1032, 904, and 357, respectively, for the 3 cases, suggesting the multiplication factor for estimating the quantity of uranium retained in the lung from the quantity of uranium excreted per day in the urine. For the 2 more similar cases, urinary excretion levels of 23 $\pm$ 17 pCi/day and 24 $\pm$ 15 pCi/day at 95% confidence levels would predict 0.017 μCi chest cavity burden of uranium. Fecal excretion was a significant mode of clearance in the 3 cases, averaging 92%, 44%, and 183%, respectively, of the urinary uranium elimination. These variances may be explained by such factors as differences in particle size, effective solubility, physiology of respiration, individual physical characteristics of the human anatomy governing dust deposition, and the elapsed time after exposure that fecal sampling started.

Material balances were calculated on the 3 cases for total excretion, and compared with the decrease shown by *in vivo* measurements. These data suggest that 50% to 75% of the chest burden decrease is accounted for through urinary and fecal excretion. A possible explanation is that a portion of the uranium retained in the lung is being transferred to another component,

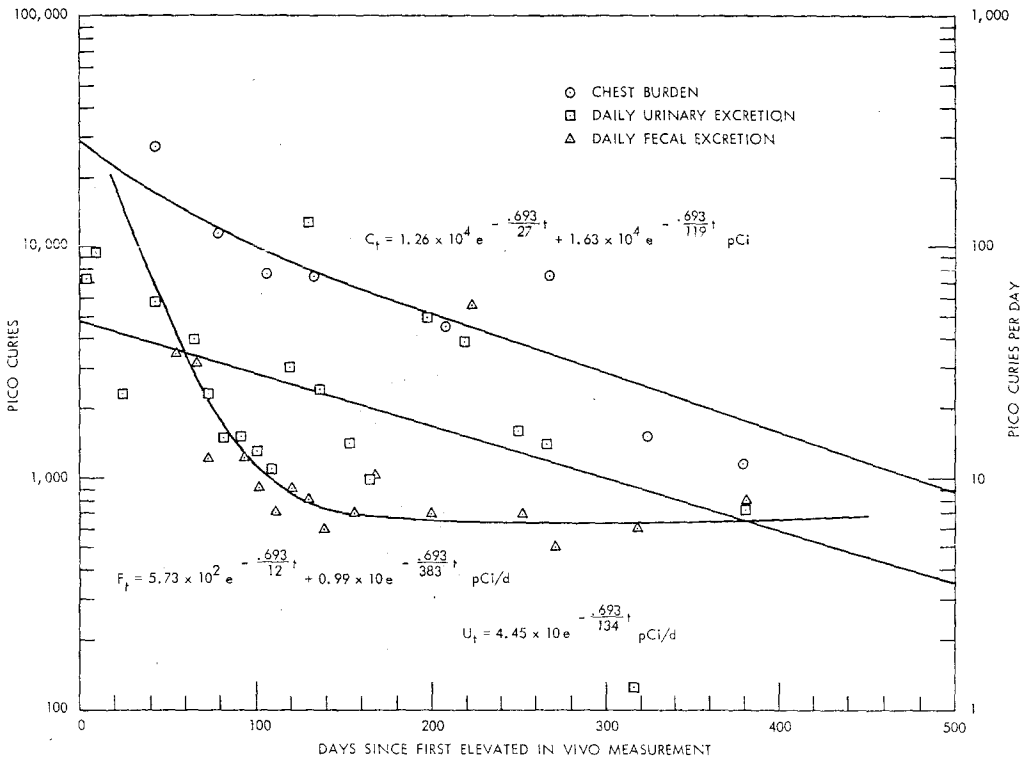

FIG. 5. Excretion and *in vivo* curves, case K-3.

Table 1. *Data Summary*

	Case K-1	Case K-2	Case K-3
Urinalysis			
Early excretion level (pCi/day)	64	71	45
Biological half-life (days)	138	103	134
Number of measurements	48	21	22
Fecal Analysis			
Early excretion level (pCi/day)	57	41	583
Biological half-life (days)	144	71	12,383
Number of measurements	43	17	18
Total Excretion			
Urine–fecal excretion (pCi)	22,000	13,000	20,000
In Vivo			
Early burden (pCi)	40,900	41,900	28,900
Biological half-life (days)	245	209	27,119
In vivo decrease (pCi)	29,000	26,000	29,000
Number of measurements	17	12	10
Ratio			
Fecal/urinary excretion	0.92	0.44	1.83
Total excretion/*in vivo* decrease	0.76	0.50	0.69

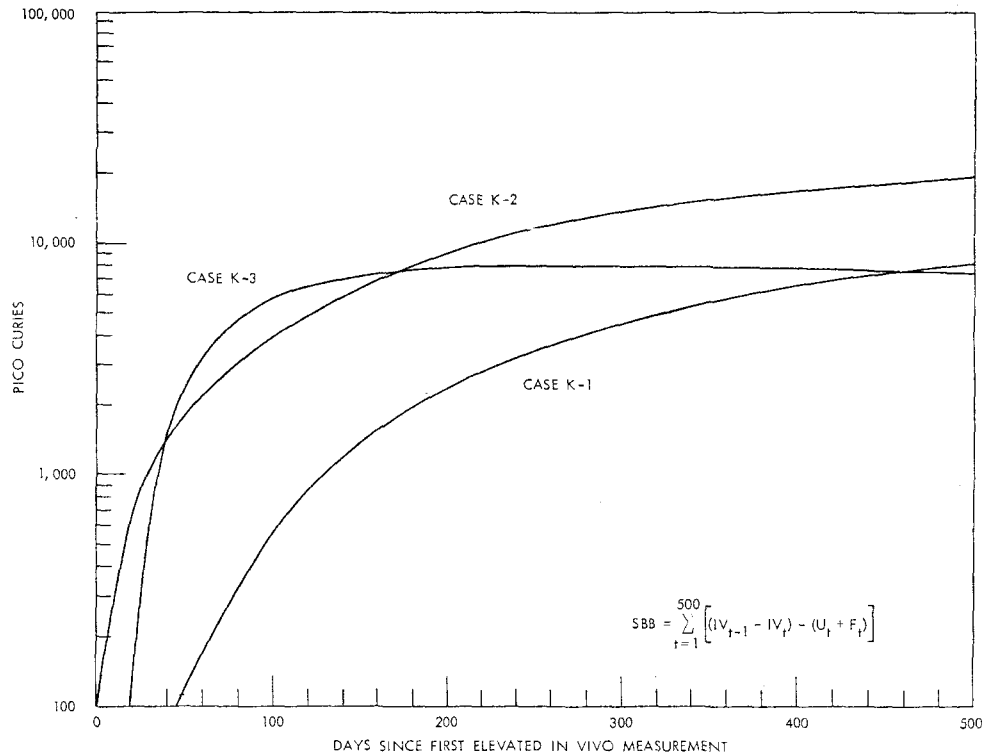

FIG. 6. Systemic burden build-up.

such as the bone or lymph nodes, where it is retained but is not detectable by *in vivo* gamma spectrometry. An estimate of the buildup of uranium in other body components was derived from a computer program which sums the differences between excretion and apparent elimination from the chest cavity. Plots of this buildup are shown in Fig. 6. As a point of reference, 50,000 pCi is the maximum permissible body burden (bone) for soluble, enriched uranium.

CONCLUSIONS

Three individuals with detectable quantities of enriched uranium in their chest cavities and excreting measurable quantities in their urine and feces were monitored for a period of over a year. The data are still being collected. For these cases, the following general conclusions are made:

1. Biological half-lives for insoluble uranium dust retained in the lung ranged from 120 to 250 days.
2. In the absence of current soluble uranium exposures, factors of about 1000 were reflected by the ratios of the chest burden and the daily urinary uranium excretion levels.
3. Fecal excretion is a significant mode of uranium elimination.
4. The apparent decrease of uranium in the chest is greater than the amount of uranium excreted, suggesting transfer of uranium from the chest cavity to another organ.
5. Systemic buildup for these lung burdens represents about 20 per cent of the maximum permissible body burden (bone) for soluble enriched uranium.
6. Urinalysis is of value in highlighting potential uranium exposure cases.
7. Urinalysis, fecal analysis, and *in vivo* gamma spectrometer measurements are

suggested for thorough evaluation of a significant uranium exposure.

8. Medical findings for these employees are within normal limits and there is no evidence of personnel injury from the transient internal uranium depositions.

ACKNOWLEDGEMENTS

The author gratefully acknowledges the valuable contributions of the following: the Y-12 Plant Radiation Safety Department, for providing the *in vivo* gamma radioactivity measurements; Dr. L. M. Scott, for his advice and assistance with data interpretation; ORGDP Production Division personnel for their cooperation in this study; and the subjects, for their good-natured acceptance of the sampling and counting procedures.

REFERENCES

1. Maximum Permissible Body Burdens and Maximum Permissible Concentrations in Radionuclides in Air and Water for Occupational Exposure. *National Bureau of Standards Handbook* 69 (1959).
2. Report of ICRP Committee II on Permissible Dose for Internal Radiation (1959) with Bibliography for Biological, Mathematical, and Physical Data. *Health Physics* **3,** 1 (1960).
3. W. O. GENTRY, R. SCHEDE and R. C. SMITH. Monitors for Alpha Air Contamination. Sixth Tripartite Instrumentation Conference at Chalk River. AECL-802, 94 (1959).
4. N. B. SCHULTZ and A. F. BECHER. Correlation of uranium alpha surface contamination, air-borne concentrations, and urinary excretion rates. *Health Physics* **9,** 901 (1963).
5. L. M. STECKEL and C. M. WEST. Characterization of Y-12 uranium process material correlated with *in vivo* experience. Y-1544 (1966).
6. P. C. MCREE, C. M. WEST and J. D. MCLENDON. Y-12 Radiation Safety Manual. Y-1401-Revised, 35 (1965).
7. Report of Task Group on Lung Dynamics, ICRP Committee II. *Health Physics* **12,** 173 (1966).
8. B. R. FISH. Inhalation of uranium aerosols by mouse, rat, dog and man. *Inhaled Particles and Vapors,* 151 (1961).
9. W. N. SAXBY, N. A. TAYLOR, J. GARLAND, J. DUNDO and D. NEWTON. A case of inhalation of enriched uranium dust. *Assessment of Radioactivity in Man* **2,** 535 (1964).
10. C. M. WEST and L. M. SCOTT. An evaluation of cases showing uranium chest burdens with long biological half-lives. *Health Physics,* in press (1966).

(*Appendix, Tables A1–A5, follow on pages 1214–17*).

APPENDIX

Table A1. *Excretion and* In Vivo *Data. Case K-1*

Date	*In vivo* (pCi)	Urine (pCi/day)	Feces (pCi/day)	Date	*In vivo* (pCi)	Urine (pCi/day)	Feces (pCi/day)
1/12/65	34,489	209	—	7/20/65	24,895	19	27
1/15/65	50,276	67	—	7/31/65	—	24	25
1/17/65	—	65	155				
1/18/65	—	25	—	8/9/65	—	16	42
1/24/65	—	49	—	8/20/65	17,730	—	—
1/27/65	41,209	82	—	8/22/65	—	32	20
1/28/65	—	64	109	8/29/65	—	30	10
1/31/65	—	45	59				
				9/5/65	—	27	24
2/7/65	—	73	109	9/12/65	—	15	9
2/15/65	—	16	35	9/19/65	—	15	20
2/16/65	39,549	—	—	9/28/65	18,337	—	—
2/23/65	—	21	37				
2/28/65	—	32	23	10/3/65	—	17	18
				10/10/65	—	21	20
3/7/65	—	8	94	10/29/65	—	16	22
3/14/65	—	22	45				
3/21/65	—	20	36	11/1/65	16,192	—	—
3/22/65	31,858	—	—	11/13/65	—	16	20
3/28/65	—	24	39	11/28/65	—	22	20
				11/30/65	17,609	—	—
4/4/65	—	32	26				
4/12/65	—	63	38	12/12/65	—	8	15
4/18/65	—	21	16	12/26/65	—	16	10
4/25/65	—	29	33	12/29/65	11,415	—	—
4/26/65	32,465	—	—				
				1/23/66	—	8	8
5/2/65	—	59	23				
5/16/65	—	33	37	2/4/66	14,370	—	—
5/23/65	—	24	40	2/27/66	—	8	9
5/25/65	28,700	—	—				
5/31/65	—	54	10	3/17/66	16,556	—	—
6/6/65	—	32	23	4/3/66	—	6	20
6/13/65	—	27	40				
6/20/65	—	16	22	5/8/66	10,160	10	15
6/27/65	—	24	10				
				6/15/66	5667	—	—
				6/19/66	—	8	17

Table A2. *Excretion and* In Vivo *Data. Case K-2*

Date	*In vivo* (pCi)	Urine (pCi/day)	Feces (pCi/day)
5/25/65	42,673	81	—
5/27/65	42,356	111	—
6/7/65	—	62	—
6/20/65	—	60	45
6/23/65	42,582	—	—
6/28/65	—	64	—
7/2/65	—	62	25
7/21/65	37,055	55	17
8/4/65	—	32	40
8/18/65	—	34	10
8/20/65	28,403	—	—
9/1/65	—	28	41
9/15/65	30,849	—	—
9/19/65	—	40	8
10/12/65	—	21	8
10/13/65	20,929	—	—
10/31/65	—	25	15
11/11/65	23,375	18	6
11/30/65	—	14	5
1/6/66	21,925	24	1
2/3/66	—	15	2
2/4/66	18,029	—	—
3/3/66	—	15	5
3/30/66	18,392	21	10
5/25/66	—	14	2
6/22/66	18,256	11	12

Table A3. *Excretion and* In Vivo *Data. Case K*-3

Date	*In vivo* (pCi)	Urine (pCi/day)	Feces (pCi/day)
1/11/65	24,868	74	—
1/19/65	—	94	—
2/4/65	—	23	—
2/23/65	27,610	59	—
3/4/65	—	33	34
3/14/65	—	40	31
3/23/65	—	23	12
3/29/65	11,227	—	—
4/1/65	—	15	15
4/11/65	—	15	12
4/19/65	—	13	9
4/29/65	7680	11	7
5/9/65	—	30	9
5/19/65	—	130	8
5/24/65	7424	—	—
5/27/65	—	24	6
6/14/65	—	14	7
6/24/65	—	10	10
7/28/65	—	52	7
8/10/65	4425	—	—
8/19/65	—	39	56
9/19/65	—	16	7
10/7/65	7460	—	—
10/10/65	—	14	5
11/25/65	—	3	6
12/2/65	1499	—	—
1/27/66	—	8	8
1/28/66	1134	—	—
6/16/66	4132	—	—

Table A4. *Comparison of Excretion and* In Vivo *Data.*

Case	Chest burden: Urine excretion (pCi/pCi per day)		Chest burden*: Total excretion (pCi/pCi per day)		Fecal excretion*: Urine excretion (pCi/pCi)	Chest burden drop*: Total excretion (pCi/pCi)
	Initial	Final	Initial	Final		
1	270	610	—	—	0.1	0.9
UR-2	2200	3100	200	1200	1.1	2.6
Y-1	1700	2200	1200	1400	0.5	1.6
Y-2	1600	3800	900	1800	0.9	1.1
Y-3	1100	1600	520	540	1.6	0.9
Y-4	2100	4900	1300	1800	1.0	0.7
Y-5	3200	5700	920	1300	3.3	0.7
K-1	780	980	370	560	0.9	0.8
K-2	660	1100	440	840	0.4	0.5
K-3	550	160†	370	110†	1.8	0.7

* Over the period covered by fecal analyses.
† Chest burden less than 6000 pCi enriched uranium.

Table A5. *Excretion Quantities*

Case Number	Urine (volume)				Feces (mass)			
	No. samples	(ml/day)			No. samples	(g/day)		
		Min.	Avg.	Max.		Min.	Avg.	Max.
K-1	39	610	1325	1900	39	51	181	362
K-2	14	860	1369	1700	14	18	54	126
K-3	18	440	1023	1540	18	48	92	186
Total	71	440	1263	1900	71	18	135	362

DISCUSSION

W. N. SAXBY (*U.K.*):

1. Were measurements carried out in other parts of the trunk?

2. Were any further D.T.P.A. treatments carried out after the first series?

3. Is there any later data on the faecal and urinary output and in particular of their ratio?

A. BRODSKY:

1. Yes, as also mentioned in the printed version of this paper, measurements were taken near many body positions to determine the locations of internal and external contamination. However, the detailed data are voluminous, so only a sample of the more important chest measurements are to be published here.

2. Of course, it would have been of scientific interest to give further administration and follow subsequent excretions, even after the lung burden was below detectable limits. However, the medical members of this team felt that DTPA was not without its risks and thus further administrations could not be justified after the lung burden was well within safe limits.

3. Faecal excretion dropped to very low values within a few weeks after the DTPA administration. About 5 months after the accident, the employee changed jobs and we no longer have access to this data. However, the lungs and other parts of the body were counted through May, 1966, and no appreciable indication of contamination reappeared after the period covered by Table 2 of this paper.

J. R. HORAN (*U.S.A.*):

In the calibration of your phantom did you employ radioactive material from the incident itself, such as the radioactive particle recovered from the operator's undershirt?

A. BRODSKY:

Not directly, since insufficient material was available. However, samples of the contamination were examined with respect to the relative attenuation of the 17 and 60 keV peaks in water, and the information was utilized in analyzing the results obtained with the more intense 1 liter standard. Since ultimately only the 60 keV peak was used to obtain Am^{241} burdens, this procedure was satisfactory.

F. BERTHOLD (*Germany*):

For the assessment of plutonium incorporated in lungs using external detectors, Kiefer, Maushart and co-workers have described a system using a triple large area flow-counter allowing both energy and range discrimination. Their results were better than with any practical scintillation counter system.

With an improved version of this instrument it is possible to resolve the different Pu-X-ray lines. Using the relative line-intensities of the *in vivo* spectrum, a calculation of the depth from which the radiation originated and the absolute activity incorporated is possible. The detection limits are about 0.01 μCi incorporated Pu.

B. A. J. LISTER:

I am, of course, aware of the work of Maushart and the parallel work of Rundo at Harwell. The present limit of detection by direct measurement is about three-quarters of the maximum permissible lung burden. Probably with even greater sophistication of instrumentation this will be reduced—but I am not sure that the reduction will ever be considerable. We still have a great interest in assuming lung burdens well below this level and we shall still need the alternative approaches.

D. K. CRAIG (*South Africa*):

Dr. Lister, you several times mentioned that analyses of particle size were carried out. Could you please give us some idea as to the range of the observed particle size distributions involved?

B. A. J. LISTER:

Yes, I can certainly give you the range of particle sizes found in practice. The largest particles are several hundred microns and the smallest are much smaller than a tenth of a micron. We can find almost any size you care to mention.

Hub. WIJKER (*Netherlands*):

Showing his second slide, the speaker remarked that 15% of the material was soluble. Can the speaker give his opinion on how to define soluble? Soluble in body fluids or an equivalent of it? If so, what equivalent? Have other parameters to be included in the definition, e.g. the speed with which the

material dissolves, which in itself may be a function of particle shape and size?

N. B. SCHULTZ:

The solubility studies are described in detail in ref. 5 of our paper: L. M. STECKEL and C. M. WEST, Characterization of Y-12 uranium process material correlated with *in vivo* experience. Y-1544 (1966).

W. N. SAXBY (*U.K.*):

In the U.K. we have had experiences similar to those reported by Mr. Schultz. The cases he quotes are the result of incidents resulting in largish single exposures. The case he attributes to the study by my co-workers and myself (Saxby *et al.*, IAEA Symposium, Heidelberg 1964, IAEA, Vienna 1964) was also probably from a single incident. Routine monitoring of enriched uranium workers is carried out, for reasons of practicability by urinalysis—it is convenient to have a quickly useable factor to convert daily urinary output of uranium to uranium in the chest—not as an absolute measure but as a guide to further investigation. In my earlier paper (see above) a factor of 500 was suggested. Recent work with chronically exposed workers and the data quoted by Schultz to-day suggest that this figure should be reconsidered, and replaced by a factor of 1000. Mr. Wijker who preceded me asked for further information on the difficulty of deciding on the solubility of the uranium. This subject is discussed at some length by the ICRP Task Group on Lung Dynamics and their report is in the February 1966 *Health Physics* (ICRP Task Group on Lung Dynamics, *Health Physics*, Feb. 1966, Pergamon Press, Oxford, 1966). The use of the terms "soluble" and "insoluble" is perhaps unfortunate, as the phenomena observed are not solely dependent on chemical solubility as it is normally defined—chemical form and solubility, valence states, physical form and dimensions, previous heat treatment, and metabolic processes, and biological factors in the body all affect the material's subsequent movements. It would be more readily understandable to talk, not of a material being "soluble" or "insoluble", but of it being "readily transferable" within the body, "mildly transferable" or "easily transferable".

N. B. SCHULTZ:

Thank you for your comments, with which we concur.

J. CHALABREYSSE (*France*):

Sur la base de son expérience personnelle et dans le cas particulier de l'uranium, je voudrais demander à l'orateur si d'une part il est d'accord avec les conclusions du Groupe de Travail de l'ICRP concernant le schéma pulmonaire de rétention et d'épuration des particules inhalées et si d'autre part il peut préciser les différentes fractions s'épurant par voie sanguine, donc s'excrétant dans les urines, puis par voie digestive, donc s'éliminant dans les fèces, et enfin par voie lymphatique, donc susceptibles de rester fixées définitivement dans les ganglions.

N. B. SCHULTZ:

The recent Task Group report appears to incorporate the latest research and carefully weighed opinions of our scientific community.

DESCRIPTION ET ANALYSE DE L'ACCIDENT DE CRITICITÉ SURVENU AU RÉACTEUR VENUS À MOL EN DATE DU 30 DÉCEMBRE 1965

G. PENELLE
C.E.N., Mol, Belgique

Résumé—Le trente décembre 1965, un agent technique attaché au réacteur Venus du CEN à MOL a été fortement irradié lors d'une manipulation de barres neutrophages effectuée sur le noyau de ce réacteur.

Le réacteur Venus (*V*ulcain *E*xperimental *NU*clear *S*tudy) constitue le modèle nucléaire du réacteur Vulcain; il sert à déterminer les principales caractéristiques physiques de ce réacteur.

Une description brève des installations du réacteur Venus, nécessaire à la bonne compréhension des circonstances de l'accident, est présentée dans la communication.

L'accident s'est produit lorsque l'agent a voulu extraire une barre neutrophage du noyau du réacteur; il a appliqué d'une façon erronée un ordre d'opération qui, lui-même, n'était pas conforme aux consignes régissant l'exploitation du réacteur.

La communication expose l'enchaînement des circonstances et la séquence des manœuvres qui ont conduit à l'accident. L'analyse de cette séquence est faite du point de vue du bilan réactif.

L'arrêt du réacteur a résulté de la retombée de la barre manipulée par l'agent; le dépassement de niveaux de rayonnement prédéterminés a, en outre, provoqué la vidange automatique de la cuve du réacteur.

La séquence des événements qui ont suivi l'emballement nucléaire est décrite. Après l'accident, un examen de l'état du réacteur a été effectué; les conclusions en sont fournies.

De nombreuses études ont également porté sur les doses reçues par l'agent accidenté et sur les aspects physiques de l'accident. Les études de dosimétrie sont traitées dans une autre communication (Parmentier et Boulenger).

En ce qui concerne les aspects physiques, la présente communication résume les résultats des études portant sur la cinétique, l'énergie dégagée pendant l'emballement, la nature des rayonnements émis.

Enfin, les conclusions principales sont tirées de cet accident.

L'INSTALLATION critique Venus (*V*ulcain *E*xperimental *NU*clear *S*tudy) a été mise en service à Mol dans le courant de l'année 1964; sa réalisation visait à déterminer les caractéristiques du noyau à spectre variable qui, dans le cadre du projet Vulcain, devait être utilisé dans le réacteur BR 3/VN, à Mol, et, éventuellement, dans le réacteur Vulcain Mark I.

Conformément à cette spécification, l'installation a été utilisée de manière intensive au cours des années 1964 et 1965 et plus de mille approches critiques avaient été effectuées en fin d'année 1965. Le programme expérimental prévu était près de s'achever lorsqu'un accident de criticité survint le 30 décembre 1965.

Afin de faciliter la compréhension des circonstances qui ont amené et accompagné l'accident, il est utile de décrire d'abord succinctement l'installation.

DESCRIPTION DE L'INSTALLATION

D'une manière schématique, elle comprend une casemate blindée dans laquelle se trouve le réacteur; un local contient la casemate, la salle de contrôle du réacteur, un bureau et un laboratoire (fig. 1).

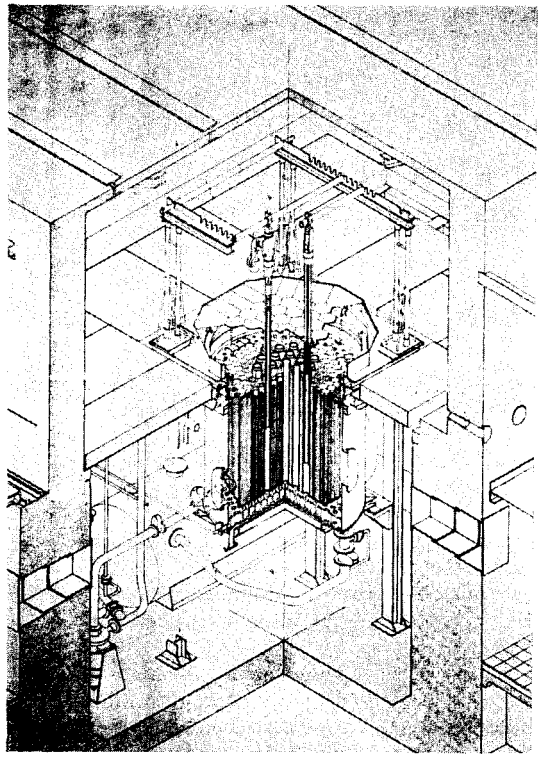

FIG. 1. Vue explosée du réacteur.

La casemate a des parois en béton lourd; elle est fermée par une porte coulissante également faite en béton lourd. Elle comporte un niveau de travail auquel on accède de l'extérieur par des escaliers conduisant près de la porte de béton. Ce niveau de travail présente une superficie de 4 m × 5,5 m et, en sa partie centrale, il est découpé de manière à donner accès à la partie supérieure de la cuve du réacteur, dressée verticalement sous le niveau de travail. Cette cuve d'acier inoxydable est cylindrique; son diamètre est de 1,6 m et elle est haute de 1,73 m. Elle contient le noyau du réacteur, c'est-à-dire des assemblages combustibles, des assemblages modérateurs, des assemblages réflecteurs, des barres de sécurité et de régulation, le tout immergé dans un mélange d'eau lourde et d'eau légère. Le combustible se présente sous forme de tubes d'acier inoxydable remplis de pastilles de dioxyde d'uranium enrichi à 7%; trente-sept de ces crayons forment un assemblage combustible, dont l'enveloppe extérieure est un boîtier hexagonal d'acier inoxydable, percé de trous. Une particularité, qui aura son importance dans les doses délivrées lors de l'accident, réside dans la présence d'un bouchon d'acier inoxydable au sommet de chaque crayon combustible et de six grilles d'acier inoxydable dans les assemblages combustibles qui ont pour but de centrer les trente-sept crayons combustibles. Le noyau contient 73 assemblages combustibles.

Les assemblages modérateurs contiennent les barres de sécurité et de régulation. Dixhuit assemblages modérateurs sont distribués au sein des assemblages combustibles.

Les barres de contrôle comprennent huit barres de sécurité et deux barres de régulation. Les barres de sécurité (barres S) sont suspendues par câbles à une superstructure métallique qui surplombe le réacteur à l'intérieur de la casemate; en cas de signal d'arrêt d'urgence, des embrayages électromagnétiques libèrent automatiquement le système de suspension des barres de sécurité, ce qui provoque la chute de ces dernières dans le noyau. Par contre, les deux barres de régulation (barres R) sont mues par l'intermédiaire d'un dispositif à vis sans fin qui ne permet pas de les larguer. Le déplacement des barres de sécurité et des barres de régulation est commandé à distance à partir de la salle de contrôle. Outre les barres de contrôle à commande motorisée, il existe des barres que l'on insère ou que l'on retire sur place à la main (barres M); ces barres sont au nombre de huit. Les diverses barres de contrôle constituent des unités indépendantes qui peuvent être placées dans n'importe quel assemblage modérateur.

Des circuits hydrauliques comprenant les réservoirs et pompes indispensables, ainsi qu'un déminéraliseur sont situés dans la casemate sous le niveau de travail. Celui-ci est matérialisé par un poutrellage sur lequel sont posées des dalles de béton.

DESCRIPTION DE L'ACCIDENT

Le programme expérimental qui était en cours le 30 décembre 1965 avait pour but la détermination de la valeur réactive des barres absorbantes par l'observation de la corrélation entre le déplacement du niveau du modérateur et le déplacement de groupes de barres, le réacteur restant critique (fig. 2). Le niveau du modéra-

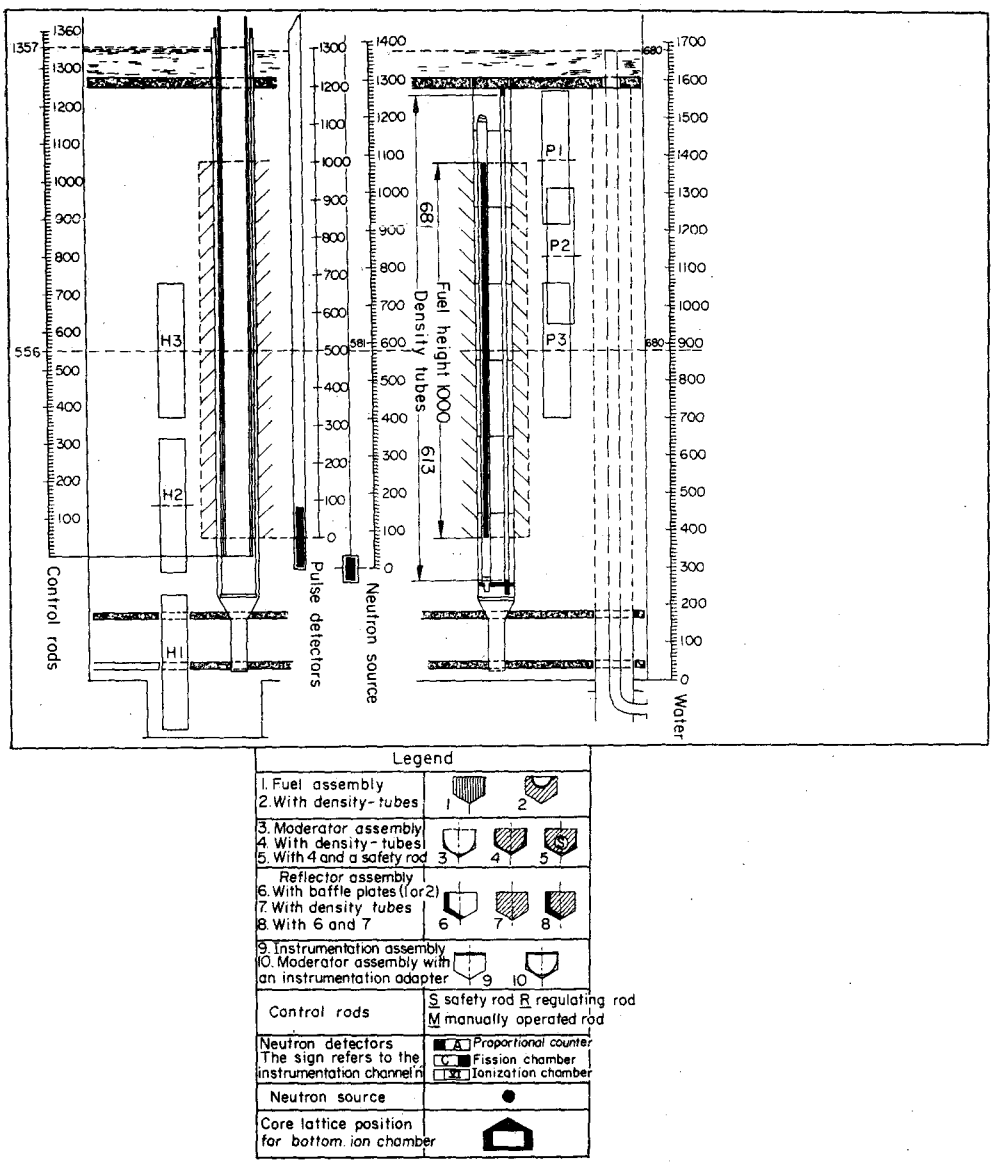

FIG. 2. Section verticale du noyau.

teur pouvait varier entre une valeur minimum correspondant à l'atteinte de l'état critique toutes barres extraites, c'est-à-dire avec 24 cm de combustible immergé, et le niveau nominal correspondant à 30 cm d'eau au-dessus de l'extrémité supérieure du combustible. Le 30 décembre 1965, le modérateur contenait 70% d'eau légère et 30% d'eau lourde en volume; le travail en cours visait à rechercher une configuration de $(18 - x)$ barres absorbantes complètement insérées avec x barres partiellement ou complètement extraites, qui devait permettre d'atteindre l'état critique avec le modérateur au niveau nominal.

Le dernier essai effectué était caractérisé par les conditions suivantes (fig. 3): 7 barres de sécurité et 7 barres manuelles complètement enfoncées; une barre de sécurité (S_2), une barre de régulation (R_2), une barre manuelle (M, correspondant à l'emplacement IO) complètement extraites; une barre de régulation (R_1) à la cote 553,I mm. Dans ces conditions, l'état critique avait été observé à deux reprises, la dernière de ces deux observations ayant été faite à 12 h 45 alors que la casemate était inoccupée et fermée conformément aux règles régissant l'exploitation du réacteur. A 12 h 47, le chef d'équipe qui venait d'être rejoint par l'ingénieur de conduite dans la salle de contrôle quitta l'installation pour aller déjeuner; il fut remplacé par le pilote et l'ingénieur de conduite mit le réacteur à l'arrêt par largage de la barre S_2 et insertion des deux barres R; toutefois, l'ingénieur de conduite interrompit presqu'immédiatement cette insertion pour exposer au pilote, qui venait de reprendre son service, quelle allait être la séquence des opérations.

Cette séquence comportait une modification de la configuration des barres insérées pour en réaliser une autre mieux adaptée à l'objectif poursuivi; il s'agissait:

1. de larguer la barre S_2, ce qui était fait à ce moment
2. et 3. d'insérer complètement les barres R_1 et R_2, ce qui avait été entamé puis interrompu
4. d'insérer une barre manuelle dans la position IO
5. de retirer une barre manuelle de la position G 330,
6 et 7. de monter les barres S_4 et S_5.

Après cet exposé, l'ingénieur de conduite donna l'ordre au pilote de reprendre la manœuvre d'insertion des barres R_1 et R_2 qu'il avait lui-même entamée, et entreprit de rédiger dans le cahier d'ordres deux ordres écrits relatifs aux points 4 et 5 de la séquence, c'est-à-dire à l'insertion d'une barre manuelle dans la position IO suivie du retrait d'une barre manuelle de la position G 330. L'ingénieur de conduite alla remettre ces instructions écrites à l'agent chargé des manipulations qui se trouvait dans un local voisin et revint à la salle de contrôle. L'agent chargé des manipulations se dirigea alors vers la casemate, porteur des ordres qu'il venait de recevoir, en ouvrit la porte, chaussa des souliers spéciaux et pénétra dans la casemate. Les constatations faites sur place après l'accident et les déclarations des divers intéressés permettent de reconstituer comme suit le comportement de l'agent dans la casemate. Tout d'abord, il se mit à l'œuvre sans attendre l'autorisation de la salle de contrôle qui est reliée à la casemate par parlophone; or, à ce moment, si l'introduction de la barre R_1 était complète, il n'en allait pas de même pour la barre R_2 dont l'enfoncement n'était que très partiel. Ensuite, il entreprit l'exécution des ordres dans un ordre inverse de l'ordre défini, c'est-à-dire qu'il commença à retirer la barre manuelle localisée en G 330 avant d'insérer une barre manuelle en IO. Le réacteur était donc sous-critique de la valeur des barres S_2 et R_1, lorsque l'agent entreprit de retirer la barre située en G 330, alors qu'il aurait dû l'être de la valeur des barres S_2, R_1, R_2 et M en IO. La barre manuelle située en G 330 fut soulevée par l'agent sur une distance telle que la libération de réactivité associée à ce déplacement devint supérieure à l'antiréactivité totale des barres S_2 et R_1. Le réacteur divergea brutalement et l'agent qui était fortement penché sur le noyau pour exécuter sa manœuvre vit une luminosité soudaine dans le réacteur. Il lâcha alors la barre manuelle qui retomba dans le noyau et il sortit très rapidement de la casemate tandis que les alarmes sonores et visuelles signalaient à l'ingénieur de conduite et au pilote présents dans la salle de contrôle qu'un évènement anormal venait de se produire. Il était environ 12 h 52. L'ingénieur de conduite ordonna l'évacuation de ses deux subordonnés, s'assura de l'arrêt du réacteur, actionna les alarmes audibles dans les locaux voisins, referma la porte de la casemate puis évacua les lieux. Tandis que l'accidenté était pris en charge par le département "Médical" du C.E.N. un agent du département "Mesure et Contrôle des Radiations" constatait que les taux de dose de rayonnement dans la salle de contrôle du réacteur et dans les locaux voisins étaient de l'ordre du niveau de tolérance.

La porte de la casemate fut alors cadenassée pour en interdire l'accès avant que l'autorisation officielle en soit donnée. Cette autorisation

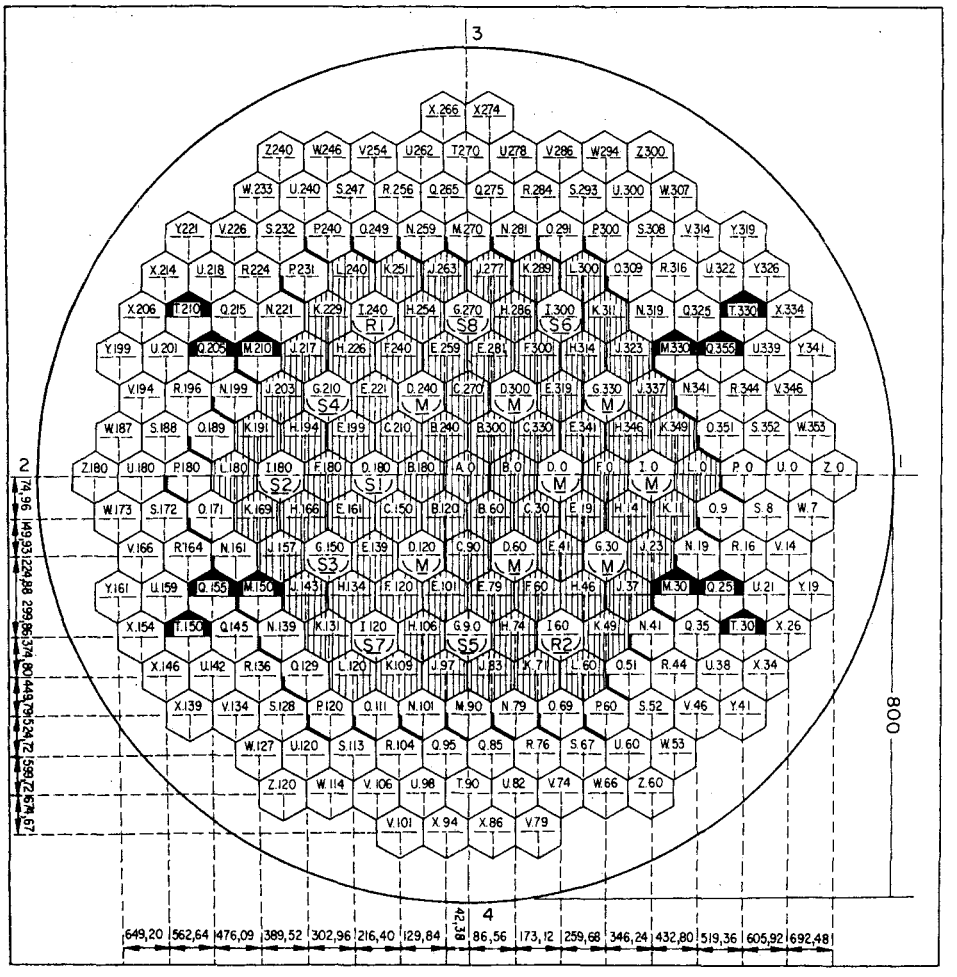

FIG. 3. Repérage des emplacements du noyau.

Radius	Dimension	Nombre	Radius	Dimension	Nombre
A	0	1	N	458,02	12
B	86,56	6	O	481,94	12
C	149,93	6	P	519,36	6
D	173,12	6	Q	526,53	12
E	229,01	12	R	540,57	12
F	259,68	6	S	567.61	12
G	299,86	6	T	599,72	6
H	312,09	12	U	605,92	18
I	346,24	6	V	624,18	12
J	377,31	12	W	653,51	12
K	396,67	12	X	676,05	12
L	432,80	6	Y	687,05	10
M	449,79	6	Z	692,48	6

intervint le 31 décembre 1965 en début d'après-midi; après que l'absence de contamination dans l'atmosphère de la casemate eut été vérifiée, il fut procédé à l'ouverture de la porte de la casemate en présence des autorités du C.E.N. et de l'Inspection technique du Travail. Le niveau de rayonnement autorisait l'approche du réacteur et l'on put faire les constatations suivantes: les ordres écrits remis par l'ingénieur de conduite à l'accidenté se trouvaient à proximité du réacteur; le tube modérateur IO ne contenait pas de barre manuelle et celle-ci se trouvait couchée sur une table d'entreposage située dans la casemate; le tube modérateur G 330 contenait toujours la barre manuelle présente lors des observations de l'état critique antérieur à l'accident; par contre, cette barre était désaccouplée de sa pièce d'accrochage. Toutes les autres barres étaient à l'enfoncement prévu, sauf la barre de régulation R_2 dont l'enfoncement était très partiel; aucune déformation mécanique des éléments constitutifs du réacteur n'était apparente; la cuve du réacteur était vide d'eau, ce qui s'explique par l'intervention du dispositif de vidange automatique lors de l'emballement nucléaire.

Ce sont ces premières constatations qui ont permis de comprendre les causes de l'accident et d'entreprendre des investigations plus approfondies.

ANALYSE DES CIRCONSTANCES DE L'ACCIDENT

Il apparaît tout d'abord que si les ordres avaient été rédigés dans une séquence logique, ils n'avaient pourtant pas tenu compte d'une règle générale, édictée dans le rapport de sécurité du réacteur, suivant laquelle le déchargement d'une barre de contrôle ne pouvait se faire qu'avec la cuve du réacteur vide d'eau. Cette vidange se justifiait en outre du fait de la condition imposée pour les manipulations sur réacteur à l'arrêt avec la cuve remplie d'eau, et qui était d'avoir trois barres de sécurité relevées pendant ce type d'opération; cette condition ne pouvait être remplie avec la configuration réalisée au moment de l'accident. La coïncidence de cette erreur de conduite et de l'erreur de manipulation commise par l'agent accidenté qui a retiré une barre manuelle avant d'en introduire une autre, exécutant ainsi les ordres reçus dans un ordre inversé, fut la cause de l'accident.

Une analyse de résultats obtenus expérimentalement quelques jours après l'accident permet d'atteindre cette conclusion. Tout d'abord, il est évident que si la cuve avait été vidée du mélange d'eau lourde et d'eau légère qu'elle contenait avant d'entreprendre la modification projetée de la configuration des barres de contrôle, aucun accident n'aurait pu résulter d'une erreur de manipulation affectant un noyau de réacteur placé dans l'air. La reconstitution expérimentale a en outre montré que si la séquence des manipulations ordonnées avait été exécutée dans l'ordre prévu, aucune atteinte d'état critique ne serait survenue, même en tenant compte de ce que la barre R_2 n'était pas insérée au moment où l'exécution de la séquence fut entreprise (fig. 4). Il est apparu expérimentalement que la séquence des manœuvres conçues par l'ingénieur de conduite aurait eu les conséquences suivantes du point de vue du bilan réactif: partant de l'état critique avec 14 barres complètement insérées et la barre R_1 partiellement insérée, le réacteur serait parvenu à k eff = 0,986 après l'exécution des opérations 1, 2 et 3, c'est-à-dire après l'insertion complète des barres S_2, R_1 et R_2; l'introduction d'une barre manuelle M en 10 aurait encore réduit k eff à 0,980; enfin, le retrait de la barre M localisée en G 330 aurait relevé k eff à la valeur de 0,990; si la barre R_2 était restée complètement extraite au moment du début des manipulations sur le noyau, comme ce fut approximativement le cas, la valeur de k eff à cet instant eût été de 0,993 au lieu de 0,986; l'introduction d'une barre M en IO l'eût fait descendre à 0,986 puis le retrait d'une barre M de G 330 l'eût ramené à 0,996. Le défaut d'introduction de R_2 n'eût donc pas provoqué d'accident si la séquence des manipulations avait été exécutée dans l'ordre correct.

L'insertion complète de R_2 n'eût pas davantage empêché l'atteinte de l'état critique provoquée par l'exécution des manipulations telle qu'elle a été effectuée en réalité. Comme indiqué précédemment, le défaut d'insertion avait amené le k eff du réacteur à la valeur de 0,993 au moment du début des manipulations de barres manuelles; le retrait de la barre M localisée en G 330 a alors provoqué le passage à

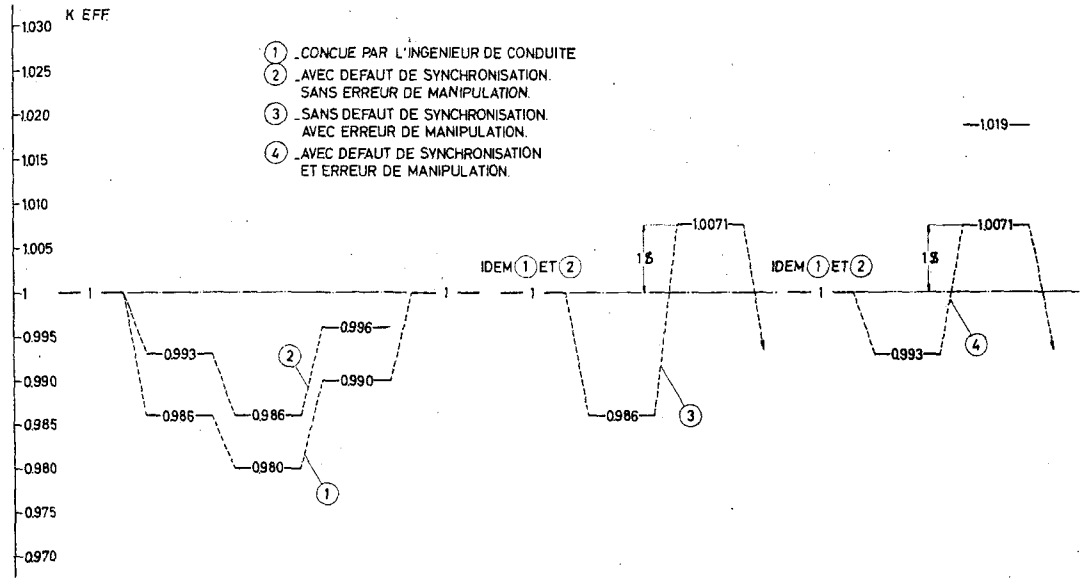

FIG. 4. Suite des états réactifs.

l'état critique; poussé à sa limite il eût amené k eff à la valeur 1,019; si R_2 avait été correctement introduite, l'extraction complète de la barre M placée en G 330 eût fait passer k eff de 0,986 à 1,013, c'est-à-dire de toute façon dans un état prompt critique.

À ce jour, on ne sait pas de façon certaine quelles ont été les circonstances précises dans lesquelles l'emballement nucléaire est survenu et s'est étouffé; en particulier, on ignore à quelle vitesse la barre a été extraite, à quel niveau elle a été arrêtée dans son mouvement ascendant, pendant combien de temps ce mouvement a été interrompu, selon quelle loi la chute de la barre s'est faite. De façon correspondante, on ignore la loi d'injection de réactivité lors de l'extraction de la barre manuelle et la loi d'insertion d'antiréactivité résultant: de la chute de cette même barre, de l'insertion progressive de la barre R_2, de l'effet de température, de la vidange automatique de la cuve. Des études sur calculateur analogique devraient permettre de préciser ces paramètres en utilisant comme grandeurs de référence les activations du combustible et des matériaux ainsi que les doses reçues par l'accidenté. Ces études ont toutefois été considérées comme ayant une importance secondaire par rapport aux études visant à calculer les doses reçues par l'accidenté aux différents endroits du corps; les résultats de ces évaluations devaient en effet conditionner le traitement médical appliqué. Ces études de dosimétrie ayant été effectuées de manière intensive n'ont pas permis d'entreprendre simultanément les études dynamiques de l'accident; cette lacune doit être comblée dans les mois qui viennent.

ÉTAT DU MATÉRIEL APRÈS L'ACCIDENT

Après l'accident, l'installation a fait l'objet d'un examen rapide en vue de déterminer ses possibilités d'utilisation future. Il est tout d'abord apparu qu'aucune contamination n'était détectable dans l'atmosphère de la casemate, sur les surfaces de celle-ci, dans le modérateur, sur les crayons combustibles; certaines déformations ont pu être mises en évidence sur des crayons prélevés dans la région la plus irradiée du noyau. La dose gamma maximum au contact des assemblages ne dépassait pas 9R/h, 5 jours après l'accident. Rien dans ces observations n'a fait apparaître que le combustible serait devenu impropre à une utilisation dans des expériences critiques, aussi a-t-il été réutilisé dans la suite du programme.

Les mécanismes des barres de contrôle, les

circuits de commande, les chaînes de sécurité et les chaînes de mesure de Contrôle Santé se trouvaient tous en état de marche. Au point de vue matériel, on peut donc dire que l'emballement nucléaire n'a provoqué aucun dégât appréciable, ce qui s'explique d'ailleurs par la quantité relativement faible d'énergie dégagée par l'accident; les estimations actuelles fixent à cette quantité d'énergie un ordre de grandeur de 15 Mws. De plus, la résistance mécanique des gaines d'acier inoxydable des crayons combustibles a fortement limité les conséquences des sollicitations mécaniques et thermiques que ces crayons ont subies.

Ce maintien en état de fonctionnement de l'installation malgré l'accident s'est révélé très important car il a permis d'entreprendre sans délai des irradiations de mannequins garnis de dosimètres dans le but de préciser les doses qu'avait reçues l'accidenté aux diverses parties du corps; ces données constituèrent un élément très important dans les appréciations des médecins traitants; la communication de Parmentier et Boulenger d'une part, la communication des Drs Jammet et Faes d'autre part, le montrent à suffisance.

CONCLUSION

En conclusion, cet accident de criticité a résulté de la coïncidence d'une erreur de conduite et d'une erreur de manipulation et s'est accompagné d'un défaut de synchronisation dans l'exécution des opérations. Ce défaut n'a pas eu d'incidence sur le déroulement de l'accident qui a mis une nouvelle fois en évidence l'importance du facteur humain en matière de sécurité car il s'est produit à la suite de défaillances purement humaines.

REMERCIEMENTS

En terminant, je souhaiterais remercier MM Motte, Debrue, ainsi que leurs collaborateurs du CEN, grâce auxquels de nombreuses informations figurant dans cette communication ont pu être réunies.

PROBLÈMES DE DOSIMÉTRIE LORS DE L'ACCIDENT DE CRITICITÉ SURVENU AU RÉACTEUR VENUS À MOL, EN DATE DU 30 DÉCEMBRE 1965

N. C. PARMENTIER
Commissariat à l'Énergie Atomique, Département de la Protection Sanitaire

R. BOULENGER
Centre d'Études Nucléaires de Mol, Département "Mesure et Contrôle des Radiations"

et

G. PORTAL
Commissariat à l'Energie Atomique, Service Technique d'Études de Protection

Résumé—Les mesures de dosimétrie externe qui ont pu être faites dans les heures qui ont suivi l'accident survenu à une personne à Mol, le 30 décembre 1965, sont décrites ainsi que leur résultat.

Les circonstances de cet accident sont analysées dans le papier de G. Penelle au même Congrès.

Vu les doses importantes, 550 R de rayonnement gamma au film-dosimètre porté à hauteur de poitrine par l'irradié, celui-ci a été confié le jour même au Dr. Jammet à Paris.

À la demande du Dr Jammet et avec l'aide de l'équipe de dosimétrie de son département au CEA diverses irradiations de mannequins RANDO et REMAB, munis de dosimètres externes et internes, ont été faites tant pour guider les soins à donner à l'irradié que pour permettre la comparaison des effets biologiques.

Les méthodes de dosimétrie gamma et neutrons utilisées sont indiquées ainsi que leur résultat.

L'irradiation présentait deux particularités:

(1) inhomogénéité, vu la proximité de la source, ce qui imposait la connaissance des doses aux différentes régions du corps;

(2) instantanéité, ce qui rendait possible une reconstitution relativement précise avec fantômes.

I. HISTORIQUE

M. G. Penelle vient de nous décrire l'accident survenu à Mol le 30 décembre 1965. Nous allons vous montrer les problèmes de dosimétrie qui se sont posés et nos essais pour les résoudre. Il nous a semblé plus vivant de vous présenter les évènements dosimétriques tels qu'ils se sont succédés dans le temps. C'est pourquoi, nous vous indiquerons en premier, les aspects "contrôle des radiations" qui ont eu lieu immédiatement après l'accident.

Vers 13 h le "contrôle radiations" est appelé. Un opérateur (F. J.) se trouvant dans la casemate et devant exécuter des opérations manuelles de barres de contrôle a observé une divergence (lumière de l'effet de Cerenkov) et est sorti précipitamment de la casemate.

Les détecteurs de flux de neutrons ont déclenché:

—les alarmes,

—le largage des barres de sécurité—ce largage n'a pu avoir lieu les barres étant déjà en position basse,

—la vidange du modérateur.

Cette vidange est malheureusement lente vis-à-vis de la descente des barres de sécurité.

Deux personnes se trouvaient au pupitre de contrôle à l'extérieur de la casemate.

Après vidange du modérateur, nous nous sommes assurés que plus aucune divergence n'est possible. La casemate est fermée.

Parallèlement aux mesures à faire sur les trois personnes et leurs dosimètres, la non-contamination de l'installation et de son environnement est vérifiée (mesure de frottis et des poussières de l'air prélevées sur filtres).

Ultérieurement un échantillon du modérateur sera contrôlé par spectrométrie gamma; des mesures de frottis sont faites à l'intérieur de la casemate y compris sur le gainage des éléments de combustible. Aucune contamination n'a pu être détectée. Les trois personnes sont conduites immédiatement au bâtiment "Médical Contrôle des Radiations". Chacune portait un film-dosimètre (voir annexe No. 1) muni de détecteurs par activation et un stylo-dosimètre pour faibles doses gamma ou X (0 à 200 mR). Le film-dosimètre (pastille d'indium) de l'opérateur (F. J.) indique une forte activation, son stylo-dosimètre est déchargé, son corps et ses vêtements présentent une activation facilement décelable avec les détecteurs de contamination bêta, gamma. Après une douche et un changement de vêtement pour diminuer l'influence d'une contamination éventuelle, la personne est mesurée au "body counter" et on observe une activité de 8,5 μCi en ^{24}Na. Aucune contamination par produits de fission n'est mesurable. La personne est mise au repos dans un lit.

Les stylos-dosimètres des deux autres personnes indiquent des irradiations gamma de 60 et 32 mR; leur mesure au "body counter" n'indique aucune activation mesurable en ^{24}Na, ni aucune contamination. Vers 15 h les films-dosimètres sont développés et mesurés; malheureusement dans la précipitation du moment, le bain de développement ne contenait pas d'étalons de doses élevées.

En se référant aux étalons de doses élevées de la semaine précédente, la dose gamma est au maximum de 700 R.

Une série de films sont irradiés avec une source de ^{60}Co pendant la nuit du 30 au 31 décembre; leur développement indique une bonne identité de noircissement avec celui obtenu la veille dans le domaine des faibles doses et permet de déduire une dose de 550 R gamma, d'après le nouvel étalonnage.

La différence de noircissement sous cadmium et sous étain est trop faible pour estimer une dose de neutrons thermiques.

Les détecteurs par activation permettent suivant J. A. Dennis, l'évaluation des doses neutrons suivantes:

—la pastille de soufre activée en phosphore 32 par la réaction ^{32}S (n, p) ^{32}P donne 600 dés./min. g de soufre, soit 55 rads de neutrons de fission,

—la pastille d'or, sous cadmium, activée en ^{198}Au par la réaction ^{197}Au (n, γ) ^{198}Au donne 1,47 dés./min.g soit 1 rad de neutrons intermédiaires,

—les pastilles d'or, externes (moins l'activité d'or sous cadmium) donnent 5,1 10^5 dés./min.g, soit 0,6 rad de neutrons thermiques.

La mesure du ^{32}P dans les cheveux de l'intéressé donne pour deux échantillons, 320 à 380 dés./min.g soufre, soit 29,4 et 35 rads de neutrons de fission, en supposant une teneur en soufre de 5% du poids des cheveux.

L'importance de l'irradiation et les vomissements du sujet nous amènent à consulter le Dr Jammet le jour même à 16 h. Le Dr Jammet indique immédiatement au médecin du C.E.N. de MOL les premières mesures à prendre. L'irradié est transporté à Zaventem dans la soirée, de là par avion militaire, au Bourget où il est pris en charge par le Dr Jammet. Donc, à cette date, les premières mesures de dosimétrie permettent de déduire que la dose gamma reçue à hauteur de poitrine (endroit du film-dosimètre) est importante et comprise entre 500 et 700 R (avec comme valeur la plus probable 550 R), que la dose due aux neutrons de fission est environ 10 fois plus faible que la dose gamma et que les doses dues aux neutrons épithermiques et thermiques sont négligeables.

Entre le 31 décembre et le 5 janvier, plusieurs faits ont été étudiés, d'une part à MOL, d'autre part à PARIS.

L'interrogatoire de l'accidenté permet déjà d'avoir une idée des conditions d'irradiation, ce qui nous a conduits à faire une série de photographies (fig. 1) auprès du réacteur, avec un opérateur exécutant la même manœuvre.

FIG. 1. Photographie d'une personne pendant la reconstitution: position qui se rapproche le plus de celle de l'accidenté.

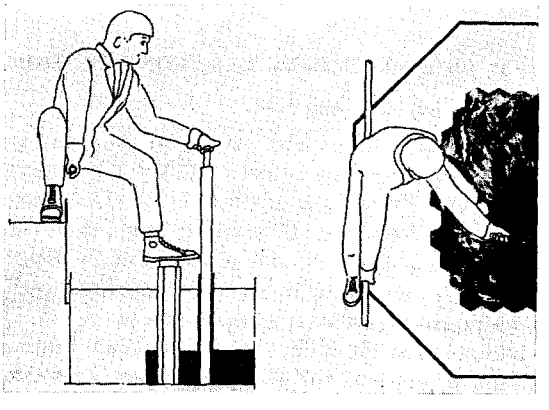

FIG. 2. Schéma de profil et positionnement de l'irradié.

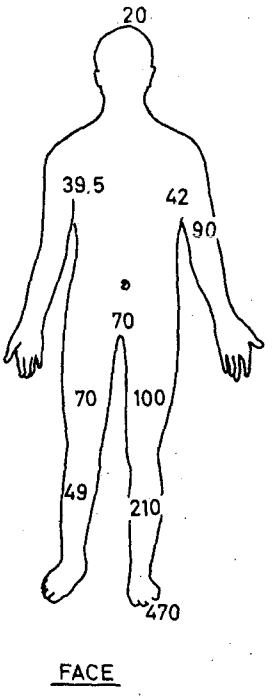

FIG. 3. Doses neutrons de fission en rad. d'après la mesure des phanères.

Ces photographies montrées à l'accidenté nous ont permis de déterminer sa position la plus probable (fig. 2).

Les mesures d'activation du soufre dans les phanères faites au laboratoire d'analyses et de mesures radiobiologiques du D.P.S. mettent en évidence une importante hétérogénéité de l'irradiation comme vous le montre la figure No. 3.

De plus, la mesure d'activation du sodium-24 refaite dans ce laboratoire confirme la mesure initiale faite à MOL.

Le 5 janvier, une réunion groupant l'équipe médicale et les spécialistes en dosimétrie du D.P.S. et du C.E.N. MOL permet de faire un bilan clinique et dosimétrique, d'où ressort la nécessité de pratiquer le plus rapidement possible une reconstitution de l'accident en utilisant un mannequin.

Sur quels paramètres connus, peut se baser cette reconstitution?

—D'abord, l'irradiation est due en majeure

partie à des rayonnements gamma dont la répartition énergétique s'étale jusque 8 MeV. Ces gamma sont dus aux réactions n, γ, particulièrement importantes par suite de l'utilisation de gainage et de matériaux de support en acier inoxydable et inconel. La composante neutronique, constituée essentiellement de neutrons rapides, représente 10% de la dose gamma.

—De plus, cette irradiation a lieu en un temps très bref. Les graphiques des enregistreurs des détecteurs de flux ne permettent pas de préciser ce temps par suite des constantes d'intégration des circuits de mesure. Il est donc logique de supposer l'opérateur pratiquement immobile pendant la courte durée de l'irradiation.

—Enfin, la position de l'accidenté, relativement bien reconstituée, implique une répartition très hétérogène de l'énergie absorbée dans l'organisme.

Le 7 janvier, soit une semaine après l'accident, les premiers essais de mise en place et l'irradiation d'un mannequin muni de dosimètres gamma et neutrons ont lieu. Le but principal de ces essais est de retrouver les rapports entre les activités en différents points du corps, telles qu'elles sont établies par la mesure des phanères de l'accidenté.

Le 8 janvier, une fois la position reconstituée, un premier mannequin, muni de dosimètres externes pour gamma et pour neutrons, et de dosimètres internes gamma, est irradié. Les premiers résultats sont fournis le 10 janvier à l'équipe médicale. La précision des mesures en gamma peut être estimée à 20%. Elles soulignent trois points importants du point de vue médical:

—la colonne vertébrale dans la partie cervicale et dorsale haute a reçu des doses supérieures à 200 rads mais inférieures à 270 rads gamma, donc à 300 rads au total,

—le bassin a subi une forte irradiation, environ 4 fois supérieure à celle de la zone précédente,

—le pied gauche a subi une irradiation très élevée de 4000 à 5000 rads.

Une ponction de moelle osseuse au niveau de la septième vertèbre cervicale confirme la dose relativement faible reçue à ce niveau.

Le 8 février, plus d'un mois après l'accident, devant l'évolution des lésions radiologiques au niveau du pied gauche, une irradiation d'un fantôme de pied est faite pour mesurer les doses internes, surtout au niveau du squelette.

Enfin, en mars 1966, une deuxième (mesure gamma), puis une troisième (mesure neutrons) reconstitution avec mannequin, ont lieu pour mesurer avec plus de précision la répartition des doses absorbées en utilisant 300 points de mesure dans le mannequin pour la dosimétrie gamma et 3 fois 70 points pour la dosimétrie neutrons. Il est bien évident que ces différentes expériences mettant en jeu des moyens importants n'ont pu être réalisées que par une collaboration étroite de différents groupes de travail:

—le Département "Mesure et Contrôle des Radiations" et le Service d'Études des Réacteurs de MOL qui ont assuré l'organisation pratique des reconstitutions ainsi que la dosimétrie neutrons et gamma externe par films et par dosimètres "Manufacture Belge de Lampes et de Matériel Électronique",

—Le Groupe Dosimétrie Biologique du Département de la Protection Sanitaire qui a assuré la dosimétrie gamma interne,

—le Service Technique d'Études de Protection qui a participé à la dosimétrie gamma externe par films, et interne par fluorure de lithium.

Nous n'exposerons pas en détail les résultats des différentes irradiations et ne parlerons que des résultats obtenus après confrontation des expériences successives.

II. PRÉPARATION DE LA RECONSTITUTION

II. 1. *Choix du mannequin*

En réalité, nous n'avons qu'un type de mannequin à notre disposition le "RANDO" fabriqué par ALDERSON aux États-Unis. Ce mannequin est constitué de matière équivalente aux tissus mous vis à vis des rayonnements électromagnétiques. Il comporte un squelette réel et des poumons en matière équivalente (fig. 4). La composition en différents éléments est résumée dans le tableau suivant (fig. 6) où les valeurs sont exprimées en pourcentage par rapport au poids.

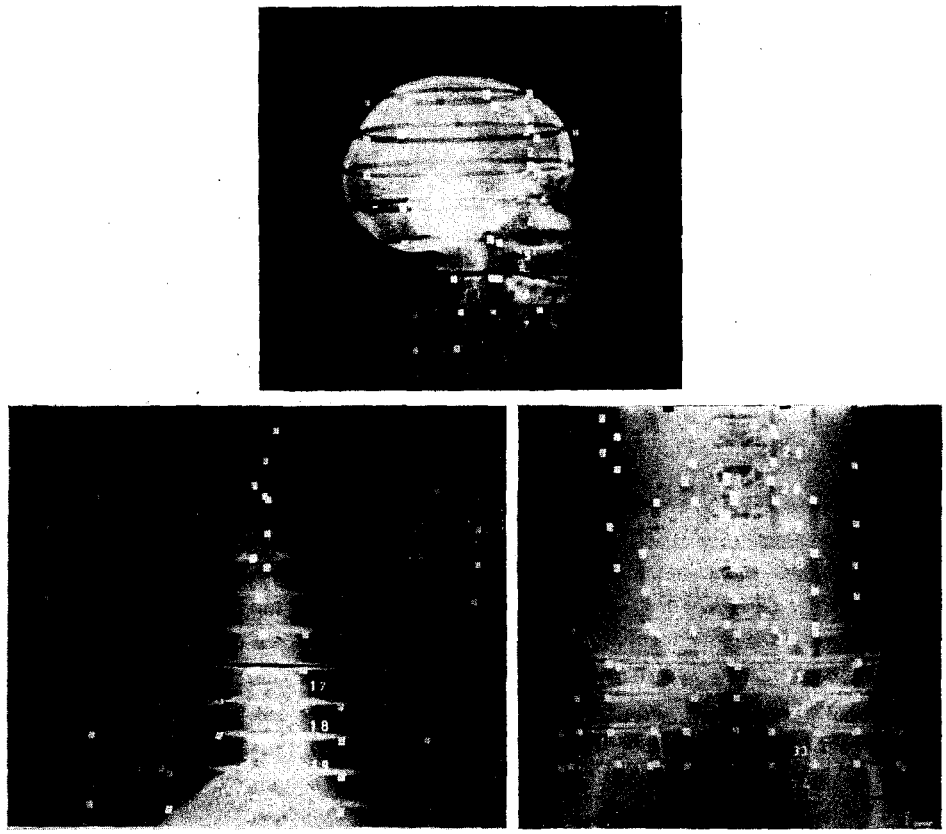

FIG. 4. Radiographies du mannequin "Rando" avec positionnement des détecteurs internes.

	Masse volumique	Nombre d'électrons par g. (Effet Compton)	$\tau\bar{Z}$ (Effet photoélectrique)	$\pi\bar{Z}$ (Création de paires)
Eau	1	$3{,}34.10^{23}$	7,42	6,6
Muscle	1	$3{,}32.10^{23}$	7,50	6,54
Rando	0,995	$3{,}30.10^{23}$	7,43	5,96

FIG. 5. Comparaison de la matière Rando au muscles humain et à l'eau (Equivalence pour les rayonnements électromagnétiques).

Éléments	Rando	Muscle
Hydrogène	9,687%	10,2%
Carbone	65,406%	12,3%
Oxygène	20,146%	77,29%
Azote	2,240%	3,5%
Chlore	2,270%	—
Antimoine	0,069%	
Calcium		0,007%
Potassium		0,3%
Soufre		0,5%
Phosphore		0,2%
Magnésium		0,02%
Sodium		0,08%

FIG. 6. Composition comparée "Rando" – Muscle (% par rapport au poids)

II. 2. *Choix des dosimètres*

II. 2.1. *Dosimétrie gamma.* Deux types de dosimètres gamma ont été utilisés:

—des dosimètres photographiques, du type des badges utilisés en protection, modèle PS1 du CEA[2] et du CEN/Mol, dont l'étalonnage est identique,

—les dosimètres thermoluminescents d'une part, des stylos "M.B.L.E." au fluorure de calcium en externe et surtout des poudres de fluorure de lithium du type 7 (fig. 7) qui permettent seules un nombre important de points de mesure en dosimétrie interne.

Nous vous décrirons surtout la méthode utilisant le fluorure de lithium qui présente les avantages suivants:

—faible encombrement,

—indépendance en fonction de l'énergie des rayonnements électromagnétiques (fig. 8 tirée des réf. 3 et 4). Il est, en effet, indépendant entre 100 keV et 30 MeV mais surestime la dose de 20% pour les rayonnements d'énergie inférieure à 100 keV.

—le fluorure de lithium de type 7 est pratiquement insensible aux neutrons rapides.

Par contre, nous ne pouvons l'utiliser, du moins en ce qui concerne la qualité en notre possession qu'entre 1 rad et 500 rads. Il semble, en effet, exister plusieurs plages de linéarité pour une gamme de doses étendue. Enfin, nous ne ferons que donner ici les conditions de lecture utilisées au laboratoire sans les discuter. L'information obtenue par irradiation du fluorure de lithium est lue au moins 48 heures après l'irradiation au moyen d'un appareil Conrad modifié au laboratoire tant au niveau alimentation haute tension qu'au niveau de la chaîne de lecture. En cours d'étalonnage, la poudre est lue par échantillon de 30mg et le lecteur réglé pour avoir 1 rad par "digit"; dans ces conditions, en particulier, utilisation toujours de la même plaquette, l'écart quadratique moyen est de 5%. Précisons que l'étalonnage est fait par comparaison avec une chambre

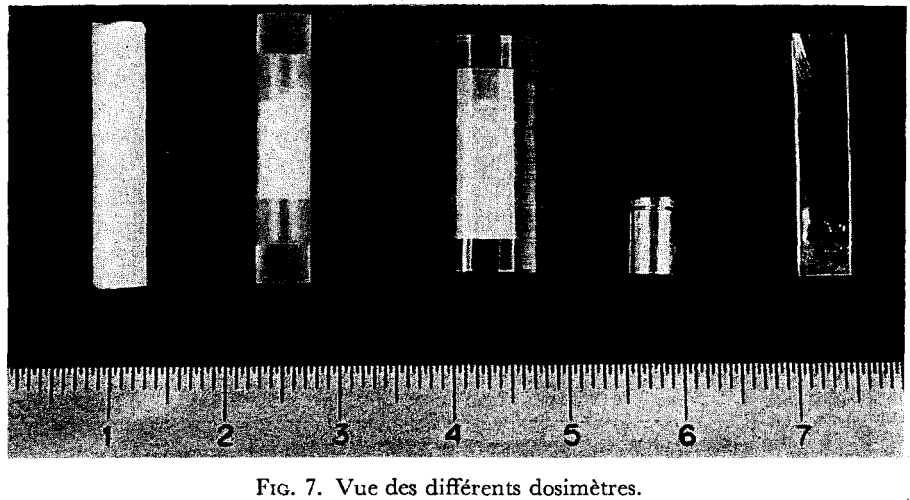

FIG. 7. Vue des différents dosimètres.

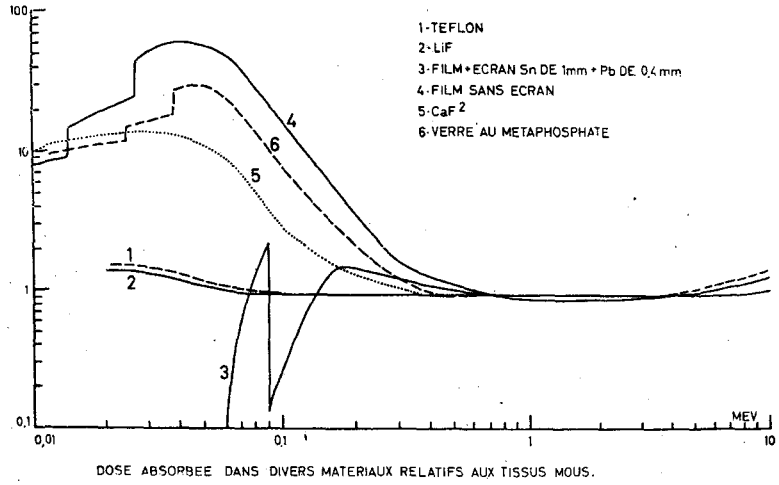

FIG. 8. Courbe de réponse gamma en fonction de l'énergie pour différents dosimètres.

d'ionisation à paroi équivalent air placée en condition d'équilibre électronique dans un faisceau d'une source de ^{60}Co collimatée. Les lectures sont traduites en énergie absorbée en tenant compte du rapport des coefficients d'absorption énergétiques comparés de l'air et du F Li pour un rayonnement γ de 1,25 MeV.

Les lectures pour les manipulations sont faites dans les mêmes conditions. Les containers utilisés pour la reconstitution, de petits cylindres de polyéthylène, contiennent 120 mg de cristaux, permettant ainsi quatre lectures par dosimètre. Dans ces conditions, la précision n'est plus que 10% (utilisation de plaquettes différentes).

II. 2.2. *Dosimétrie neutrons:— Neutrons intermédiaires.* Des détecteurs d'or placés dans un boîtier de cadmium ont été utilisés. Vu le peu de place disponible (trous de 5mm de diamètre dans le mannequin) une épaisseur d'or de 1 mm a été enployée afin d'augmenter la masse du détecteur, le diamètre étant limité à 3 mm.

D'autre part, pour avoir une indication de l'anisotropie du flux ainsi que pour diminuer l'influence de celle-ci, la pastille d'or a été entourée de deux autres pastilles identiques. Seule la pastille centrale a été systématiquement mesurée.

Lors de la mesure, il existe un effet d'autoabsorption important dans le détecteur d'or entraînant un comptage plus efficace des bords de la pastille affectés par l'anisotropie du flux. Afin de diminuer cet effet lors du comptage, le détecteur est inséré dans une pastille de métal non irradié de Z voisin de celui de l'or.

Nous avons utilisé une pastille de Pb de 1 mm d'épaisseur et de 12 mm de diamètre.

Les mesures ont été effectuées dans 4 cristaux NaI à puits de $1\frac{3}{4}'' \times 2''$ connectés à un sélecteur 400 canaux. La durée de mesure était de 20 minutes par échantillon. La surface du pic était obtenue par intégration numérique.

—Neutrons thermiques. Des détecteurs d'or de 4,5 mm × 20 × 0,1 mm ont été placés dans des trous voisins de ceux occupés par les détecteurs sous cadmium.

—Calibration des détecteurs d'or sous cadmium. Nous nous sommes référés aux détecteurs d'or minces de dimensions généralement utilisées soit des pastilles de 8 mm de diamètre et de 0,127 mm d'épaisseur. D'après Baumann[5] on sait que:

$$\frac{(RCd - I)_0}{(RCd - I)x} = 0{,}227 \text{ pour } x = 0{,}127 \text{ mm}$$

Des détecteurs épais blindés par Au et Cd ont été irradiés en même temps que des détecteurs minces dans un convoyeur de BR 1 et dans une pile étalon. On a obtenu:

$$(N/m) \text{ épais.}/(N/m) \text{ mince} = \alpha = 0{,}267$$

N/m étant le taux de comptage sous le pic par

gramme d'or. On pourra donc passer du résultat N/m mesuré au résultat équivalent avec détecteurs minces en le multipliant par I/α.

—*Calcul du flux de neutrons d'énergies intermédiaires.* On a:

$$\text{Øé}_{pi} \cdot t = \frac{1}{\alpha}\left(\frac{N}{m}\right) 1\text{ mm} \cdot \frac{M_A}{N_A} \cdot \frac{1}{R} \cdot \frac{T}{0{,}693} \cdot \frac{I}{IR} \cdot \frac{(RCd - I)x}{(RCd - I)_0}$$

où $\text{Øé}_{pi} \cdot t$ = flux intégré par intervalle logarithmique d'énergie (si $t \ll T$).

M_A = masse atomique,

N_A = nombre d'Avogadro,

R = rendement du dispositif de comptage,

T = demi-vie du radio-élément formé,

IR = intégrale de résonnance = 1556 barns,

RCd = rapport cadmium,

x = épaisseur de détecteur (0,127 mm).

On suppose que le spectre est de forme $\frac{1}{E}$ et que les limites d'énergie sont 0,12 eV et 1 MeV.

d'où

$$\frac{dE}{E} = 15{,}9.$$

Le flux épithermique total sera égal à 15,9 fois le flux obtenu ci-dessus.

On a pris d'autre part la valeur indiquée par J. A. Dennis: 1 rad "surface absorbed dose" = $2{,}81\ 10^9$ n/cm².

—*Calcul du flux thermique.* On a:

$$\text{Ø}_{th} \cdot t = \frac{N}{m} \cdot \frac{M_A}{N_A} \cdot \frac{1}{R} \cdot \frac{T}{0{,}693} \cdot \frac{1}{\sigma_{th}} \cdot \left(1 - \frac{1}{RCd}\right) \cdot \frac{1}{F}$$

où F = facteur de dépression de flux = 0,9,

σ_{th} = 98,8 barns

Pour déterminer RCd on se basera sur le résultat d'un détecteur or 1 mm sous Cd de position voisine. On a:

$$(N/m)_{0{,}1\ mm} = (N/m)_{1\ mm} \cdot 1/\alpha'$$

où $$\alpha' = \alpha \frac{(RCd - I)_{0{,}1\ mm}}{(RCd - I)_{0{,}127\ mm}} = 0{,}267 \cdot \frac{0{,}227}{0{,}250} = 0{,}242$$

d'où $$RCd = \frac{0{,}242\ (N/m)_{0{,}1\ mm}}{(N/m)_{1\ mm}}$$

On a pris d'autre part la valeur indiquée par J. A. Dennis: 1 rad "surface absorbed dose" = $1{,}59\ 10^{10}$ n/cm².

—*Neutrons de fission.* Les détecteurs de neutrons de fission sont des cylindres de soufre de 5 mm de diamètre et de 25 mm de long. Leur activité en ^{32}P a été mesurée aux compteurs GM après séparation chimique.[6] La dose en rads, due aux neutrons de fission est calculée en supposant, suivant J. A. Dennis, que 1 rad correspond à 10,9 dés./min. et g de soufre. Ces différents détecteurs sont montrés sur la fig. 7.

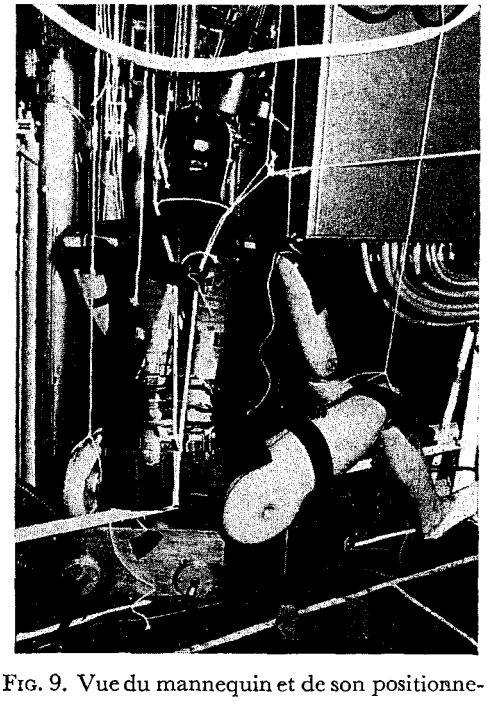

FIG. 9. Vue du mannequin et de son positionnement à Venus.

II. 3. *Reconstitution de la position*

Elle a reposé essentiellement sur trois données:

—l'interrogatoire de l'accidenté: il a eu lieu en deux temps, d'abord un simple interrogatoire qui a permis de faire des essais de position par des agents de tailles voisines avec prises de photographies, puis l'agent a précisé sa position en choisissant les clichés qui lui semblaient les plus proches de ses souvenirs et en les corrigeant;

—la hauteur de la barre de contrôle au moment de la criticité prompte qui a pu être évaluée; l'accidenté la tenait de sa main gauche dont la position est ainsi déterminée;

—enfin, les mesures de l'activité des phanères prélevées en différents points du corps qui nous ont donné des rapports entre l'irradiation de différents points du corps: tête, pubis, membres, en particulier. Les figures 9, 10 et 11 vous montrent le mannequin et son positionnement à Venus lors des différentes reconstitutions.

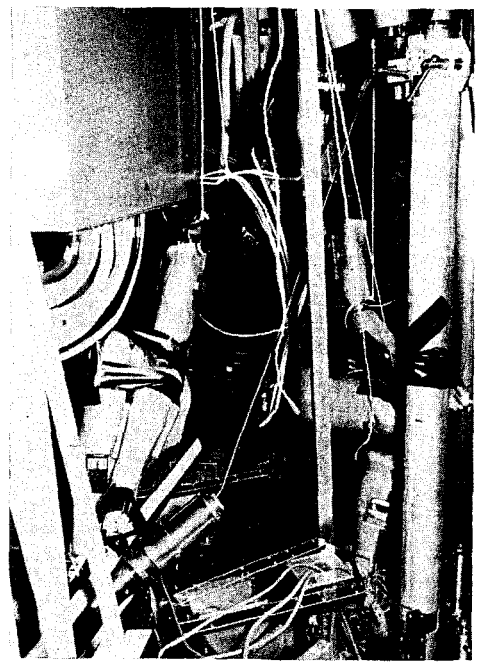

FIG. 11. Vue du mannequin et de son positionnement à Venus.

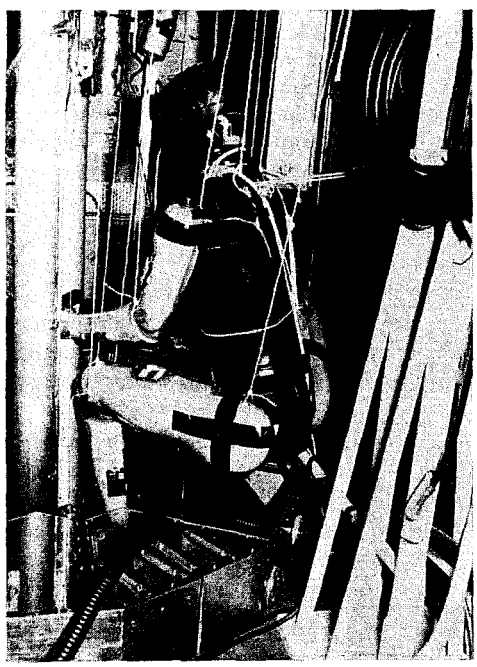

FIG. 10. Vue du mannequin et de son positionnement à Venus.

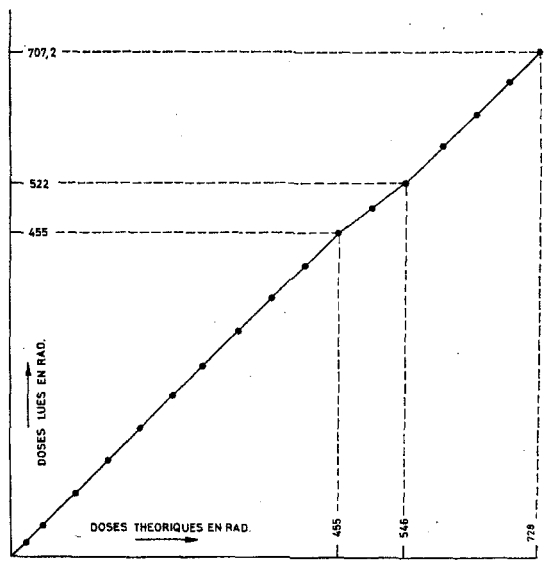

FIG. 12. Courbe d'étalonnage du fluorure de lithium.

II. 4.—*Choix de la dose et valeur de celle-ci lors des reconstitutions.* Les critères de choix ont été les suivants:

—la dose devait être suffisante pour assurer un taux de comptage raisonnable du ^{32}P des bâtonnets de soufre;

—la dose gamma aux différents points du mannequin devait être comprise dans la plage de linéarité du fluorure de lithium (entre 1 R et 500 R; fig. 12).

—la dose ne devait pas être trop importante pour éviter une activité gênante du combustible du réacteur lors de ses manipulations ultérieures.

La reconstitution ne pouvait donc se faire que par des irradiations à flux raisonnable, dans le cœur du réacteur: 10^9 neutrons/cm² sec. au maximum; toutefois cette approximation n'était pas mauvaise, la contribution des doses gamma des produits de fission étant estimée à 14% des doses de gamma prompts de fission et de capture pour une irradiation de deux heures. Le temps d'irradiation choisi est de 2 heures (dose de l'ordre de 500 R au pied gauche).

Le facteur entre l'irradiation lors de l'accident et celle obtenue lors de la reconstitution a été déterminé par plusieurs calculs: d'une part le rapport des doses gamma enregistrées par les films-dosimètres de l'accidenté et du mannequin, soit 7,35, d'autre part, le rapport d'activité en lanthane-140 entre un barreau de combustible prélevé après l'accident et un nouveau barreau utilisé lors des reconstitutions. Ce rapport est de $7{,}2 \pm 0{,}2$.

La concordance de ces deux valeurs nous semble justifier la validité des mesures faites.

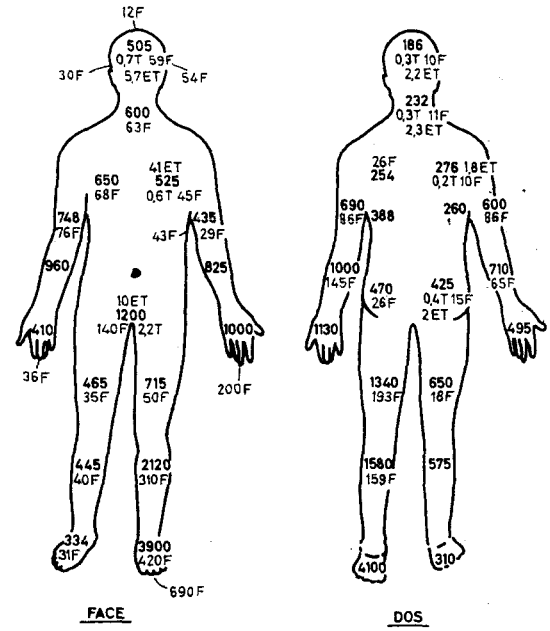

FIG. 13. Doses externes exprimées en rads (γ-pas d'indication—T—neutrons thermiques ET neutrons épithermiques—F neutrons de fission). Sur ce cliché, le degré d'hétérogénéité est déjà mis en évidence—la dose gamma, de même que la dose neutrons est de 2,37 fois plus grande au pubis qu'au front sans parler de la surexposition importante du membre inférieur gauche où les doses γ et neutrons atteignent respectivement 3.900 et 420 rads.

III. EXPOSÉ DES RÉSULTATS

Il est pratiquement impossible de donner les résultats de tous les points de mesure. Voici, d'abord, les résultats des mesures externes (fig. 13):

Nous allons montrer quelques exemples de mesures au niveau de quelques coupes (figs. 14, 15, 16, 17, 18); puis nous tenterons de résumer les données pour l'organisme entier (figs. 19 et 20).

Comme vous le montrent ces 5 exemples, il nous a paru difficile de chiffrer, de manière simple, l'irradiation subie par l'accidente. Il est possible de résumer nos résultats de deux manières:

—d'une part, en traçant les isodoses dans deux plans intéressants: le plan sagittal médian et le plan frontal médian,

—d'autre part, en estimant les doses aux différents organes.

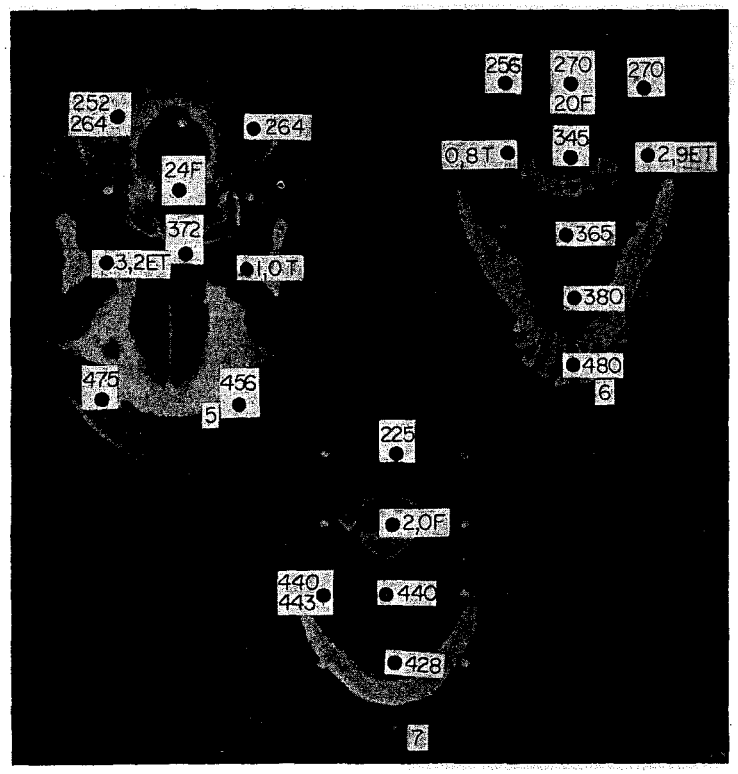

FIG. 14. Cette figure nous montre un exemple des doses mesurées dans 3 tranches situées respectivement au niveau du trou occipital et au niveau du maxillaire inférieur. Elle montre des doses absorbées variant entre 252 et 345 rads au niveau des premières vertèbres cervicales pour des doses atteignant 400 et plus au niveau du maxillaire inférieur. Soulignons tout de suite que la position de la tête est la plus sujette à caution, le degré de flexion étant impossible à préciser.

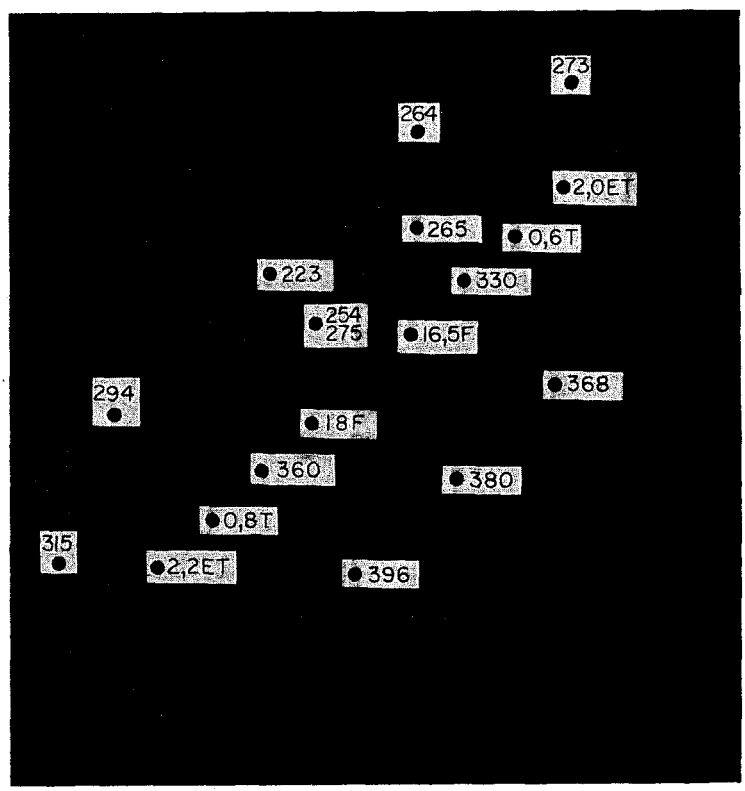

FIG. 15. Cette tranche se situe au niveau de la première vertèbre dorsale et de l'acromion. Elle permet de voir que la dose absorbée dans le corps vertébral, riche en moelle, est de 275 rads, atteignant 400 environ à la face antérieure du thorax. Déjà apparaît sur cette coupe, la diminution de l'énergie absorbée, d'une part d'avant en arrière, d'autre part de droite à gauche.

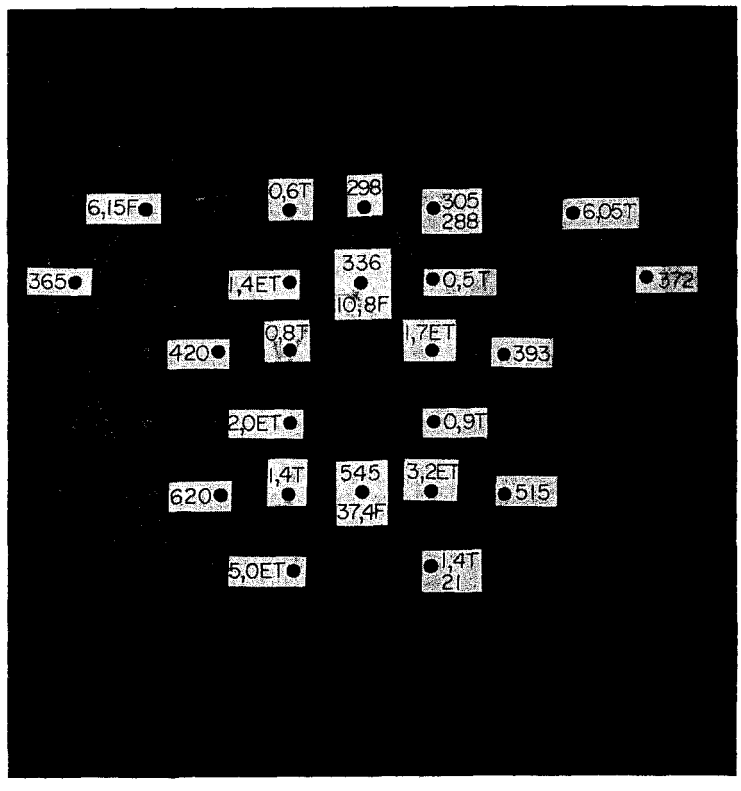

FIG. 16. Ici, la coupe passant par la 10 ème vertèbre dorsale, intéresse la région diaphragmatique. Les doses absorbées varient ici entre 620 et 515 dans la région antérieure, et 300 au niveau du corps vertébral. C'est sur cette tranche que l'on peut admettre qu'il existe une thermalisation des neutrons rapides; le rapport entre rapides et thermiques est plus faible que pour les mesures faites en externes.

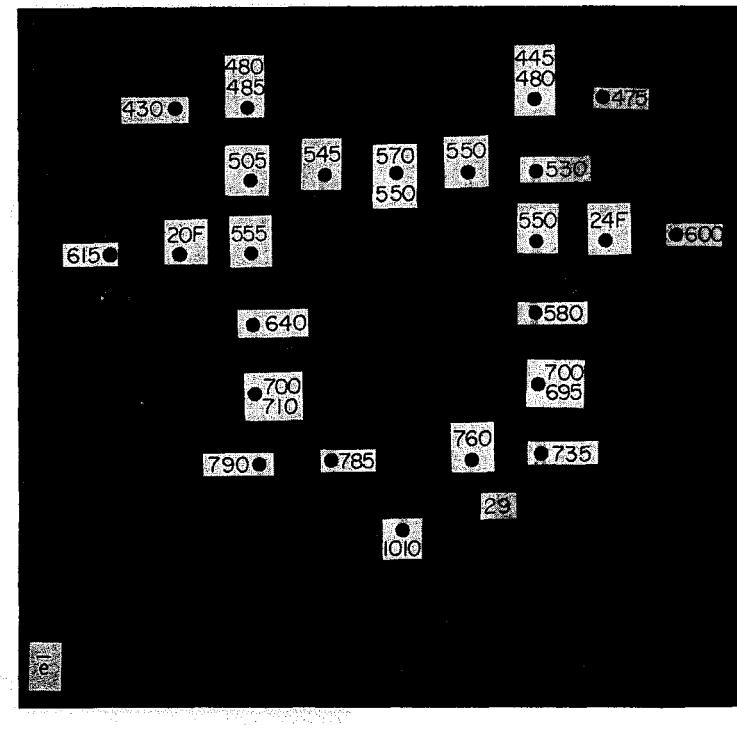

FIG. 17. Cette coupe passe par la dernière vertèbre lombaire et les crêtes iliaques. Cette région du bassin a été irradiée déjà de manière importante, avec un gradient de dose plus marqué d'avant en arrière, atteignant un facteur 2 (de 500 à 1000 rads), tandis que la dissymétrie latérale disparaît, ce qui se conçoit parfaitement, si l'on se rapelle la position du fantôme. Enfin, ici, le rapport dose neutrons rapides/dose gamma, qui était de 1/10 à la surface, n'est plus que de 1/25, traduisant très certainement la thermalisation neutronique.

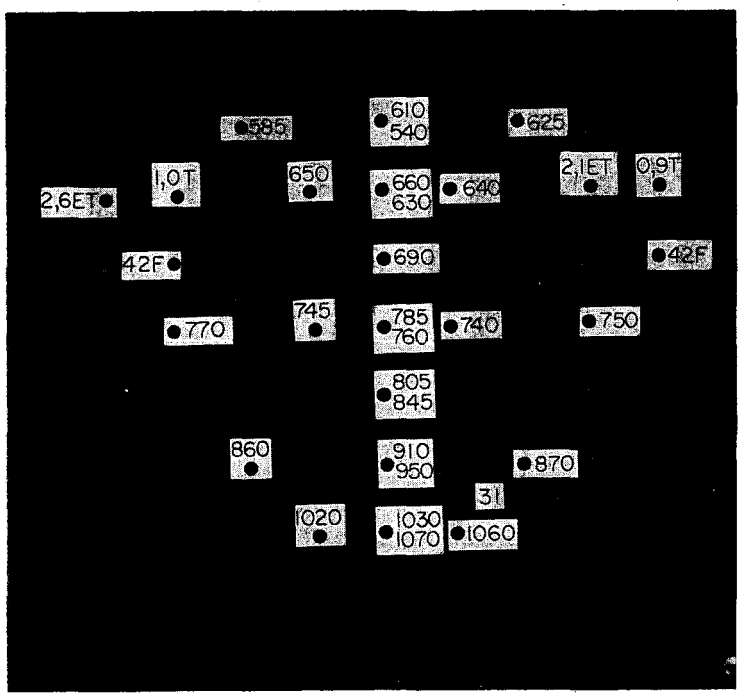

FIG. 18. Ce dernier exemple de tranche du fantôme montre l'irradiation importante subie par le bassin: pratiquement, plus de 600 rads dans toute la ceinture pelvienne, qui représente une quantité importante, de moelle osseuse, et des doses absorbées supérieures à 1.000 rads dans la région antérieure.

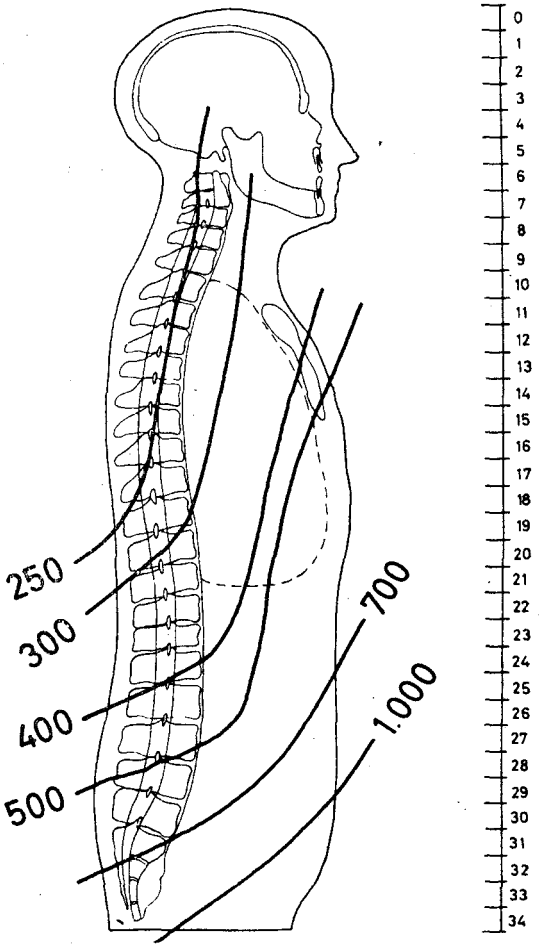

FIG. 19. Isodoses dans le plan sagittal médian. Elles mettent en évidence: (1) que les vertèbres cervicales et les 8 premières dorsales sont dans une zone irradiée à moins de 300 rads; (2) que l'abdomen a reçu de 500 à 800 rads; (3) que le rachis lombaire et le sacrum ont reçu plus de 500 rads.

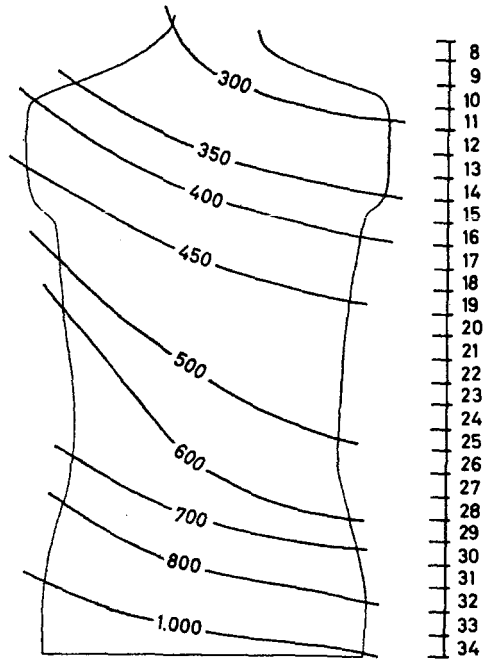

FIG. 20. Isodoses dans le plan frontal médian. L'intérêt de ces isodoses réside surtout dans l'irradiation de l'abdomen qui est très importante. Elles montrent, de plus, la dissymétrie liée à la position du thorax (flexion et rotation interne de l'épaule droite).

Intervalle de doses	Pourcentage total de moelle osseuse représentée	Zone medullaire intéressée
250 à 300	16	Partie postérieure du crâne Humérus Vertèbres cervicales de C_3 à C_7 et dorsales D_1 à D_7.
300 à 350	17	Partie antérieure du crâne. Omoplate et clavicule gauches. Régions postérieures des côtes. Vertèbres cervicales C_1 et C_2 et dorsales de D_8 à D_{10}.
350 à 400	11	Omoplate et clavicule droites. Vertèbres dorsales D_{11} et D_{12}
400 à 500	8	Maxillaire inférieur et sternum. Région antérieure des 6 premières côtes. Vertèbres lombaires L_1 et L_2.
500 à 1000	48	Région antérieure des 6 dernières côtes. Vertèbres lombaires L_3 à L_5. Sacrum et ceinture pelvienne.

FIG. 21. Doses absorbees au niveau de différents territoires médullaires

Organe	Dose Gamma (en rad)	Dose Neutrons (en rad)	Dose totale arrondie au nombre supérieur (en rad)
Cerveau	180 à 270	18 à 27	200 à 300
Cœur	360 à 400	36 à 40	400 à 450
Rate	360	36	400
Foie	360 à 450	36 à 45	400 à 500
Tractus digestif:			
Grêle	500 à 730	50 à 73	550 à 800
Colon ascendant caecum	640	64	700
angle droit	450	45	500
Colon transverse	400 à 450	40 à 45	450 à 500
Sigmoïde	550 à 820	55 à 82	600 à 900
Rectum	680 à 770	68 à 77	750 à 850
Reins	360 à 450	36 à 45	400 à 500
Vessie	730 à 930	73 à 93	800 à 1000
Glandes endocrimes:			
Hypophyse	300	30	330
Thyroïde	270	27	300
Surrénales	320 à 360	32 à 36	350 à 400
Gonades	1000	100	> 1100

FIG. 22. Doses absorbées au niveau de différents organes.

Ces doses absorbées au niveau des différents organes peuvent être calculées de manière relativement précise pour les territoires médullaires (fig. 21), mais beaucoup plus approximative pour les autres organes dont la localisation anatomique n'est pas reproduite sur le fantôme (fig. 22).

Enfin, voici les résultats obtenus lors de l'irradiation d'une reproduction du pied gauche. Le mannequin a été fabriqué en MixD avec squelette traité incorporé. Les mesures ont été faites en externe et en interne par du fluorure de lithium pour la dosimétrie gamma et par des détecteurs au soufre pour la dosimétrie des neutrons rapides. Cette reproduction a été posée à l'endroit exact où se trouvait le pied gauche de l'accidenté et a été irradiée à la même dose que lors des précédentes reconstitutions. Nous avons pensé intéressant de vous donner les doses mesurées au niveau du pied en les superposant aux lésions observées (figs. 23, 24 et 25).

Nous avons également reporté les doses absorbées gamma sur les radiographies osseuses du pied (fig. 26).

IV. CONCLUSIONS

Pour conclure cet exposé, il faut tout d'abord rappeler que cette étude dosimétrique a été menée pour résoudre les problèmes posés par l'évolution clinique de la maladie. L'utilisation des dosimètres au fluorure de lithium, quelles que soient les critiques que l'on puisse leur faire, se justifiait par la possibilité d'obtenir rapidement un grand nombre de mesures ponctuelles, par leur qualité d'équivalence aux tissus mous et leur indépendance en fonction de l'énergie. Les résultats ont montré la grande hétérogénéité de la répartition de l'énergie absorbée et la certitude qu'il existait des territoires médullaires encore fonctionnels. Cette donnée a été la base de l'action thérapeutique car dans ce cas, la dose moyenne absorbée n'avait qu'une signification biologique limitée.

De plus, quelques remarques peuvent être faites:

—avec l'apparition des nouveaux matériaux de gainage, la composante γ de la dose devient prédominante, en cas d'accident. Peut-être

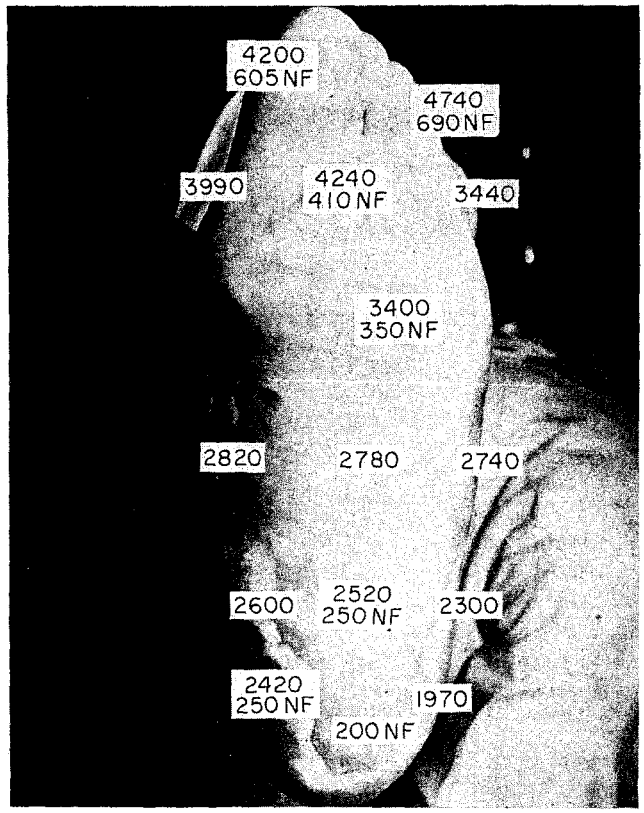

FIG. 23. Doses externes sur la plante du pied Cette photographie montre la plante du pied où les doses atteignent 4700 rads γ et 700 en neutrons rapides au niveau des orteils, zone la plus atteinte.

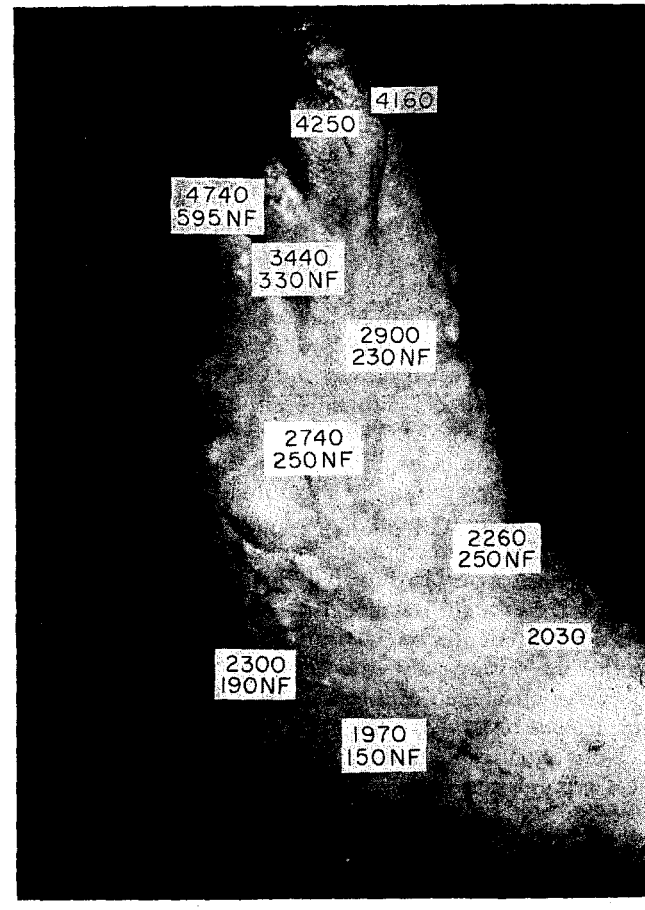

FIG. 24. Cette photographie montre la face supérieure du pied où les doses très importantes sont également au niveau de la zone dont les lésions sont les plus importantes, c'est-à-dire les orteils, alors que les doses de 2000 à 2700 rads γ auxquelles il faut toujours rajouter 10% des doses en neutrons rapides, se trouvent au niveau des zones où apparaissent des bourgeons de réépithélialisation, la photographie du pied ayant été faite 2 mois environ après l'accident.

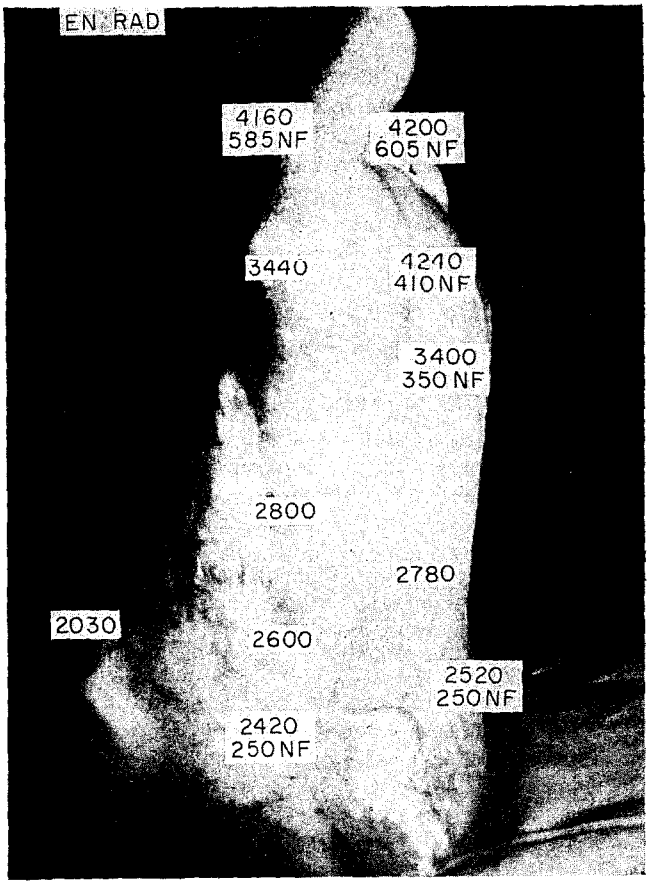

FIG. 25. Cette photographie montre le bord interne du pied où se retrouvent les mêmes phénomènes.

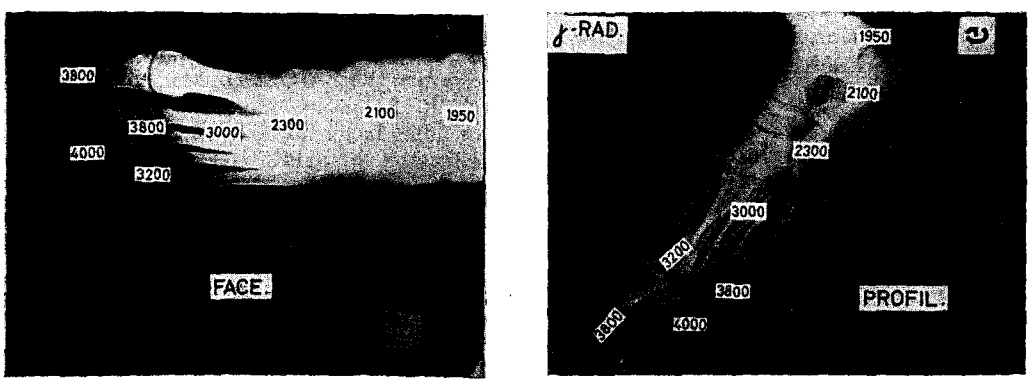

FIG. 26. Doses gamma internes du pied sur radiographie. Voici les doses mesurées dans le fantôme du pied aux différents étages osseux; elles varient de 3.800 et 4.000 rads, au niveau des orteils et 2.000 au niveau de la cheville.

serait-il utile alors de doubler le badge classique par d'autres détecteurs γ;

—du point de vue clinique et thérapeutique, il est important de pouvoir estimer le degré d'hétérogénéité de l'irradiation: il serait donc intéressant d'équiper les ceintures de sécurité en dosimètres γ;

—enfin, si l'on veut procéder à une reconstitution immédiate après l'accident, il faut disposer des fantômes, de l'instrumentation de dosimétrie nécessaire et d'une équipe rodée à leur emploi.

REMERCIEMENTS

Nous nous permettons de remercier ici les si nombreuses personnes qui nous ont aidés sans compter à l'exécution de ces mesures et les personnes et organismes qui nous ont prêté le matériel qui nous manquait (nous pensons tout particulièrement au Service de Radiobiologie de l'Université de Liège, à l'Unité de Radiophysique de l'Institut Gustave Roussy, à l'Institut voor Toepassing van Atoomenergie in de Landbouw te Wageningen et à la Manufacture Belge de Lampes et de Matériel Électronique.

ANNEXE No. 1

(m) *FILM-DOSIMÈTRE C.E.N.*

Le film-dosimètre C.E.N. est muni de deux films Gevaert D_2 et D_{10} permettant la mesure des doses de quelques mR à 1 millier de R. Ces films sont placés dans un boîtier de matière plastique. Ce boîtier contient 4 jeux d'écrans:

1—écrans γ-X: plomb 220 mg/cm², étain 110 mg/cm², aluminium 27 mg/cm²

2—écrans n thermiques: plomb 220 mg/cm², cadmium 1100 mg/cm², aluminium 27 mg/cm².

3—écrans X mous et β: plastique 300 mg/cm²

4—écrans β: plastique 100 mg/cm².

L'identification des films est assurée par marquage aux rayons X de 10 keV au moyen de chiffres de plomb incorporés au boîtier, la partie utile du dosimètre étant protégée.

La seule particularité de ce dosimètre est de contenir des languettes de films non enveloppés dans du papier étanche à la lumière, cette étanchéité étant assurée par le boîtier de polypropylène chargé. L'absence d'enveloppe de papier permet une manipulation plus rapide en chambre noire.

La mesure des doses neutrons dues aux accidents de criticité est faite grâce à trois détecteurs par activation semblables à ceux utilisés à l'A.E.R.E.

—une pastille de soufre de 1 g

—un jeu de 3 pastilles d'or de 4 mm de diamètre et de 0,1 mm d'épaisseur; la pastille centrale est insérée entre 2 écrans de cadmium de 0,7 mm d'épaisseur.

—une pastille d'indium pour la détection rapide des irradiés.

RÉFÉRENCES

1. J. A. Dennis. Neutron dosimetry using activation techniques. (A.E.R.E.) Les techniques de la dosimétrie individuelle des radiations externes. ENEA OECD, Madrid, 1963.
2. G. Soudain et G. Portal. Caractéristiques d'un dosimètre individuel à fonction multiple. Note CEA 603.
3. G. Portal. Bague dosimètre au fluorure de lithium thermoluminescent. Congrès international sur la Radioprotection dans l'utilisation des radioéléments, Paris, 13–15 déc. 1965.
4. H. Joffre. Considération sur les problèmes de la dosimétrie individuelle des radiations β, γ et X. (Centre d'Etudes Nucléaires de Saclay.) Les techniques de la dosimétrie individuelle des radiations externes. ENEA/OECD. Madrid, 1963.
5. N. P. Baumann. Resonance integrals and self shielding factors for detector foils. DP-817 (1963).
6. Petersen, Mitchell et Langham. Estimation of fast neutron doses in man by ^{32}S (n, p) ^{32}P reaction in body hair. *Health Physics* **6**, 1–5 (1961).

OBSERVATION CLINIQUE ET TRAITEMENT D'UN CAS D'IRRADIATION GLOBALE ACCIDENTELLE

H. P. JAMMET, R. GONGORA, R. LE GO, G. MARBLÉ et M. FAES

Fondation Curie, Service de Radiopathologie
Commissariat à l'Énergie Atomique, Département de la Protection Sanitaire
Centre d'Études Nucléaires de Mol, Service Médical

Résumé—Il s'agit d'un accident radiologique survenu récemment auprès d'un réacteur nucléaire et dont les aspects relatifs à la sûreté et à la dosimétrie font l'objet d'une communication de Boulenger et Parmentier.

L'irradiation subie se caractérise par sa soudaineté, son importance et son hétérogénéité. Il en est résulté un syndrome général d'irradiation totale et un syndrome local de surexposition d'un membre inférieur.

Le syndrome général a comporté une phase initiale de choc important avec vomissements, polynucléose et dégradation métabolique; une phase de latence de trois semaines au cours de laquelle la gravité de l'atteinte a pu être mise en évidence par l'effondrement des fonctions hématopoïétiques; une phase de crise de quatre semaines caractérisée par un état fébrile hectique, une aplasie médullaire totale, des manifestations toxémiques graves; une phase de récupération spectaculaire des fonctions hématopoïétique; une phase de convalescence prolongée. Les examens hématologiques concernant les érythrocytes, les réticulocytes, les neutrocytes, les lymphocytes, les thrombocytes, la trombo-élastographie et les médullogrammes, ainsi que les examens cytogénétiques concernant les chromosomes ont permis d'effecteur une évaluation clinique de la dose globale résultante.

Le syndrome local de surexposition d'un membre inférieur a évolué, après une phase de latence de 10 jours, comme une radio-lésion extrêmement grave avec les manifestations cutanées conjonctives, vasculaires, nerveuses et osseuses auxquelles on pouvait s'attendre.

Le traitement a consisté, pour le syndrome général, en isolement total contrôlé bactériologiquement, en prévention antihémorragique, en administration d'antibiotiques adéquats, en un soutien dietétique, en transfusions érythrocytaires. Le traitement du syndrome local se poursuit encore avec isolement bactériologique, pommades vivifiantes et padutine.

INTRODUCTION

Le 30 Décembre 1965, au Centre d'Études Nucléaires de Mol en Belgique, un accident survenait auprès de l'assemblage critique "Venus".

Dans la communication de M. Penelle, les circonstances de cet évènement ont été exposées. Cet accident a eu pour conséquence une irradiation humaine globale par un flash de rayons γ et de neutrons.

Immédiatement après l'accident, dès qu'ont été connus les premiers résultats dosimétriques, la victime était adressée au Service de Radiopathologie de la Fondation Curie à Paris où elle parvenait le jour même. Durant les 120 jours de son hospitalisation à l'Hôpital Curie, ont été effectués les études dosimétriques, les investigations cliniques et biologiques et les actes thérapeutiques nécessaires. Le Service de Radiopathologie a été conseillé, dans cette tâche, par un Collège de Consultants: les travaux effectués ont nécessité la collaboration d'équipes spécialisées appartenant aux Laboratoires de la Fondation Curie, au Centre d'Études Nucléaires de Fontenay-aux-Roses et au Centre d'Études Nucléaires de Mol.

Les données relatives aux études dosimétriques ont été exposées dans la communication de N. Parmentier, R. Boulenger et G. Portal.

Dans la présente communication, sont développées l'observation clinique, l'évolution biologique et la conduite thérapeutique. Pour des raisons de commodité de présentation, elles portent d'abord sur le syndrome d'irradiation globale aiguë. Par ailleurs, il n'était pas possible d'exposer la totalité des faits observés et des actes effectués. Sur les milliers d'examens pratiqués, un choix a été fait portant essentiellement sur certains aspects des investigations hématologiques, biochimiques et cytogénétiques. De même, ont été spécialement retenus les essais d'interprétation en dosimétrie médullaire qui ont conditionné la conduite thérapeutique.

À la sortie de la Fondation Curie, la guérison du syndrome d'irradiation globale aiguë était acquise, mais il restait à poursuivre le traitement du syndrome de surexposition locale du membre inférieur gauche. Le malade a été alors transféré dans le Service de Chirurgie du Prof. Morelle aux cliniques universitaires de Louvain. Pour des raisons de présentation, sont donc groupées, en fin d'exposé, l'évolution clinique et la conduite thérapeutique relatives aux radiolésions du membre inférieur gauche.

I. OBSERVATIONS CLINIQUES

1. *Évolution clinique*

L'évolution clinique a été dominée:

—au cours des 7 premières semaines, par le *syndrome hématologique* et son retentissement sur l'état général.

—ensuite, par le syndrome d'irradiation du *pied* et de la *jambe* gauches.

1.1. *Le syndrome général* présente quatre phases distinctes parfaitement objectivées par la courbe de température (Fig. 1):

—une phase de choc initial,

—une phase de latence clinique,

—une phase critique,

—une phase de rémission des signes généraux, au cours de laquelle le problème local passe au premier plan.

1.1. 1. *Phase de choc initial.* Dès la 2ème heure, le sujet a présenté des nausées et des vomissements: les nausées ont persisté quelques heures. À ce stade, le sujet était pâle, anxieux, adynamique, avec une température à 39°C, un pouls à 90 et une tension artérielle à 11-7. Cette phase a duré 24 heures.

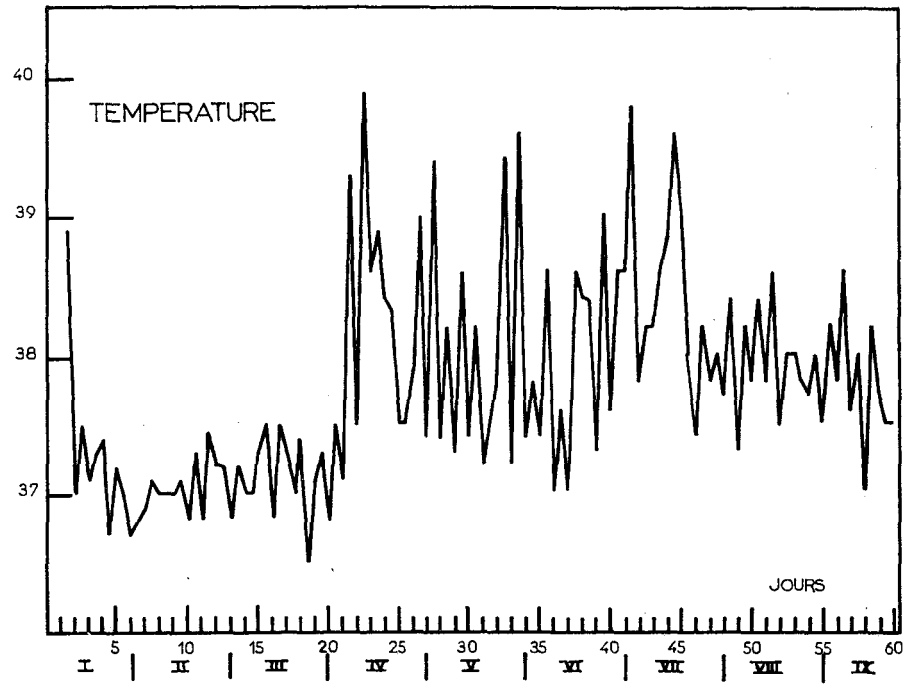

FIG. 1. Courbe thermique (cf. § I-II).

1.1. 2. *Phase de latence clinique.* Elle s'est maintenue durant 3 semaines. Dès le 2ème jour:

—amélioration de l'état général et de l'asthénie,

—régression des signes neuro-végétatifs et digestifs.

—retour de la température à la normale.

1.1. 3. *Phase critique.* Elle débute le 21ème jour: la fièvre s'allume. L'hyperthermie va comporter 2 périodes:

—l'apparition de l'hyperthermie coïncide avec la phase critique hématologique;

—mais l'hyperthermie va durer bien au-delà de la restauration hématologique, qui intervient à la 5ème semaine, alors que la fièvre se maintient jusqu'à la 7ème semaine.

Les symptômes généraux éclatent brusquement le 21ème jour dans l'après-midi, par une montée thermique à 40°C avec asthénie, prostration, obnubilation—des céphalées frontales violentes. Le pouls est à 100—la TA à 12-8. Dès lors la courbe thermique présente durant 24 jours de grandes oscillations entre 37° et 40°C.

1.1. 4. *Phase de rémission thermique.* Elle débute au 45ème jour et, durant la 7ème semaine, la température décroche, sans atteindre toutefois la normale: un état sub-fébrile entre 37,5°C et 38,5°C se maintient encore au cours des semaines suivantes. Le tableau clinique est alors dominé par les lésions locales, du pied et de la jambe gauches.

1.2. *Les manifestations cutanées* présentent plusieurs caractéristiques: la peau a été irradiée dans sa totalité, mais inégalement; aussi la chronologie d'apparition et l'intensité des lésions, reflètent l'hétérogénéïté des doses reçues par la peau.

1.2. 1. *L'érythème* débute au 7ème jour au niveau du pied et de la jambe puis s'intensifie. Le 11ème jour, il apparaît au niveau du scrotum où il s'accentue et s'accompagne le 13ème jour d'une ulcération, qui régressera le 18ème jour.

1.2. 2. *L'épilation* débute le 13ème jour par la jambe et le pubis. Elle s'étend, au cours de la 3ème semaine, à l'abdomen et au thorax, puis au crâne où elle intéresse les régions fronto-temporo-pariétales, avec une nette prédominance du côté gauche.

Enfin, à la face, l'épilation touche la lèvre supérieure, le menton et les joues. La région occipitale de la tête est respectée. Le maximum d'épilation est atteint à la 4ème semaine.

1.2. 3. *La reprise d'activité du système pileux* se manifeste à partir de la 5ème semaine, au niveau de la face, avec un décalage d'une semaine entre la joue gauche et la joue droite.

Les cheveux recommencent également à pousser. L'épilation est restée persistante au niveau du pied et de la jambe, jusqu'au genou. Les caractéristiques de cette reprise sont les suivantes:

—la repousse des poils et des cheveux est plus rapide qu'avant l'accident;

—ils repoussent plus durs et plus pigmentés;

—la surface de pilosité est augmentée, en particulier au niveau des joues, où elle remonte très haut sur les pommettes.

2. *Évolution hématologique*

2.1. *Remarques d'ordre général*:

2.1. 1. Les courbes d'évolution hématologique chez cet accidenté présentent un intérêt tout particulier, en ce sens qu'elles n'ont été influencées par aucun apport extérieur transfusionnel durant les 30 premiers jours. Elles représentent donc une évolution hématologique "*à l'état pur*" après irradiation totale.

2.1. 2. Nous avons établi ces courbes en *coordionnées semi-logarithmiques*, qui rendent compte immédiatement des pentes évolutives.

2.1. 3. Toutes les courbes de cellules sanguines expriment, non des pourcentages, mais des *nombres absolus par millimètre cube* de sang.

2.2. *Taux absolu des lymphocytes* (Fig. 2). Ce taux est surtout intéressant au cours des 2 ou 3 premiers jours: le taux minimal a été atteint à la 48ème heure; il a été de 130 lymphocytes par mm^3. La comparaison avec les courbes d'autres accidentés (Fig. 3) montre que la pente est plus forte que chez les irradiés de Vinca, sauf chez l'un d'eux. Elle est toutefois moins forte que celles des trois cas mortels de Los Alamos, qui avaient reçu des doses considérables.

2.3. *Taux absolu des granulocytes neutrophiles* (Fig. 4):

2.3. 1. Cette courbe met en évidence:

—un pic initial à 12.500 à la 6ème heure, pour 16.500 granulocytes totaux;

—une première chute rapide vers 800 au 8ème jour (norme: 4000–6000) suivie d'une remontée abortive à 1750;

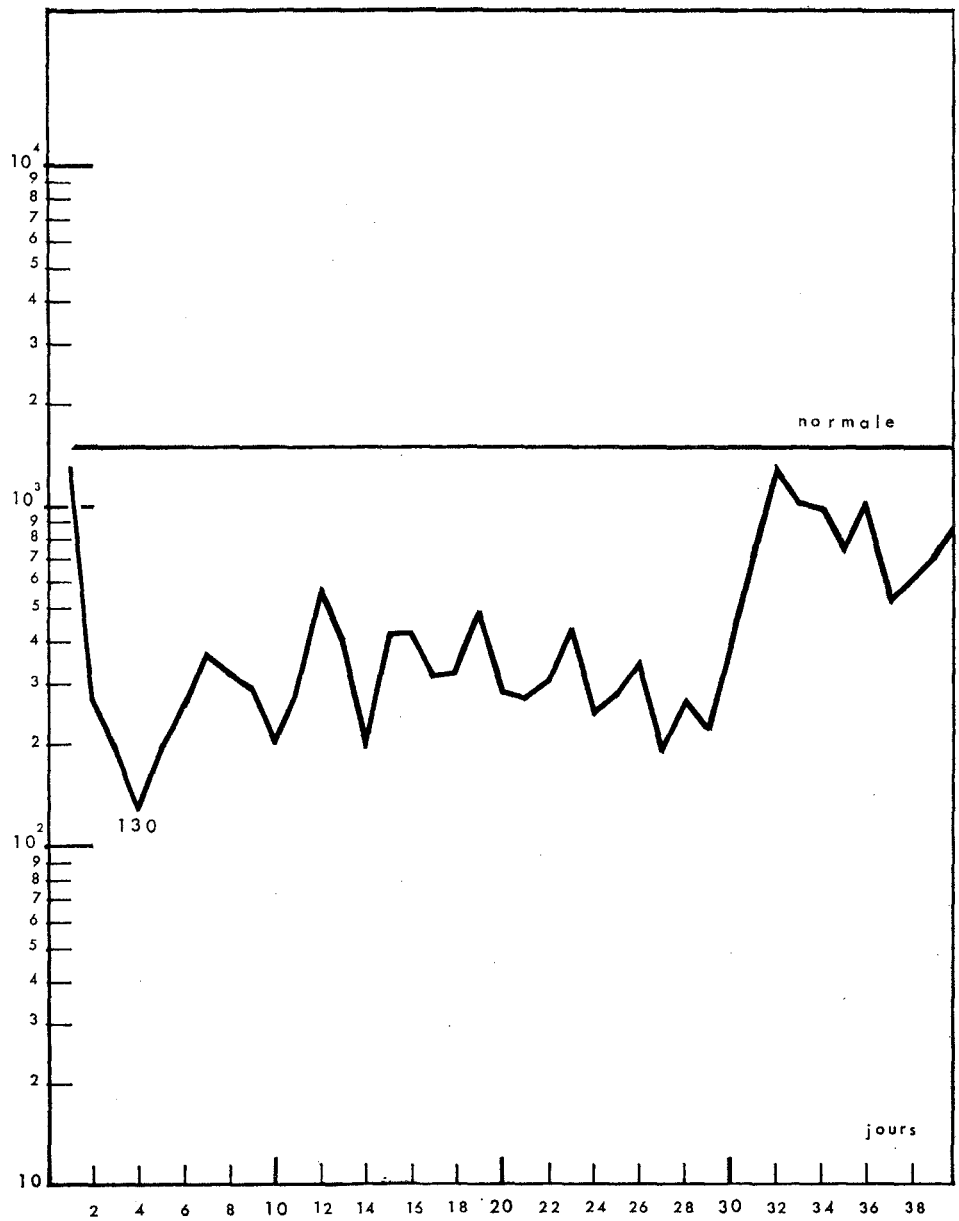

FIG. 2. Évolution des lymphocytes en nombre absolu par mm³ (échelle semi-log).

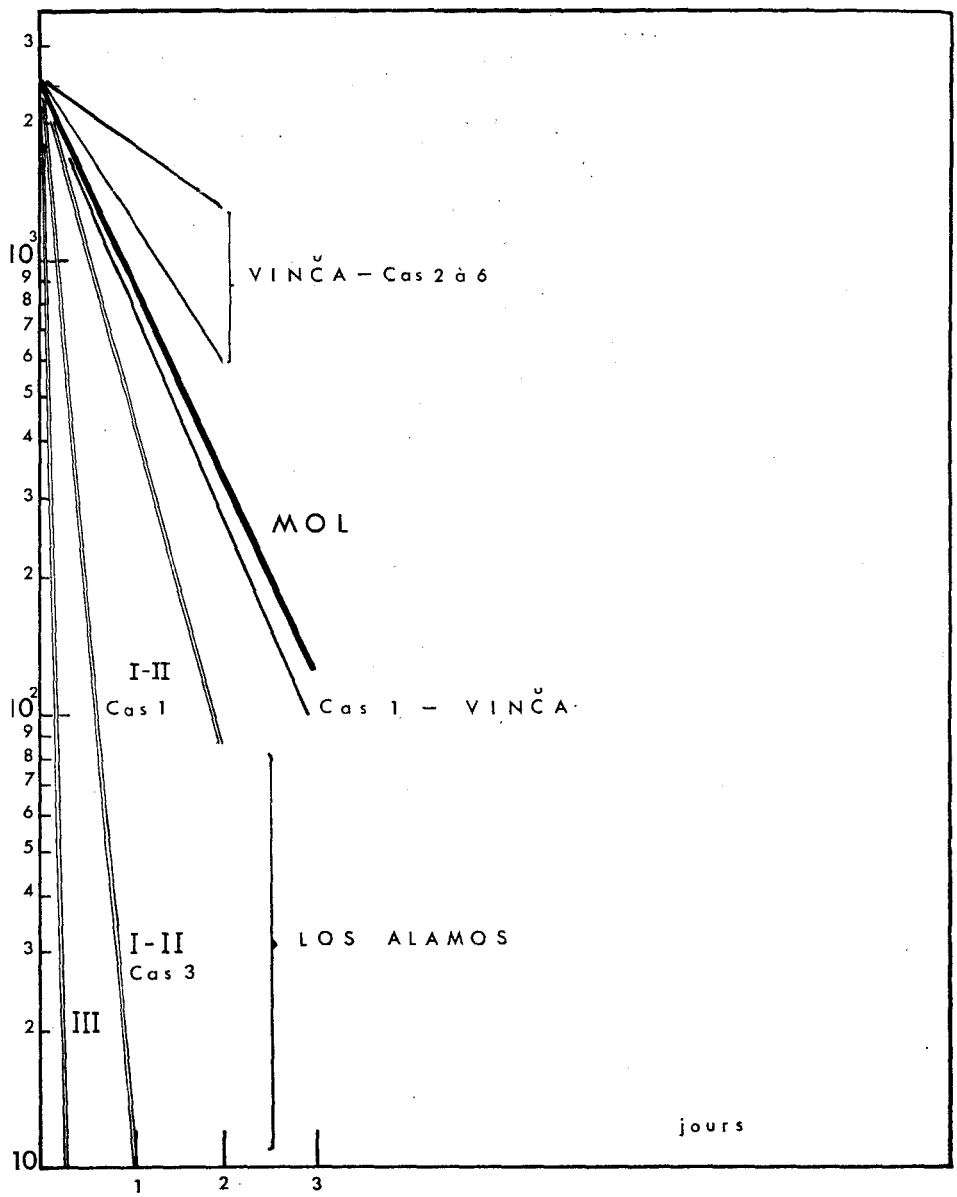

FIG. 3. Comparaison entre les chutes initiales des lymphocytes observées, aux cours des trois premiers jours, sur plusieurs accidents.

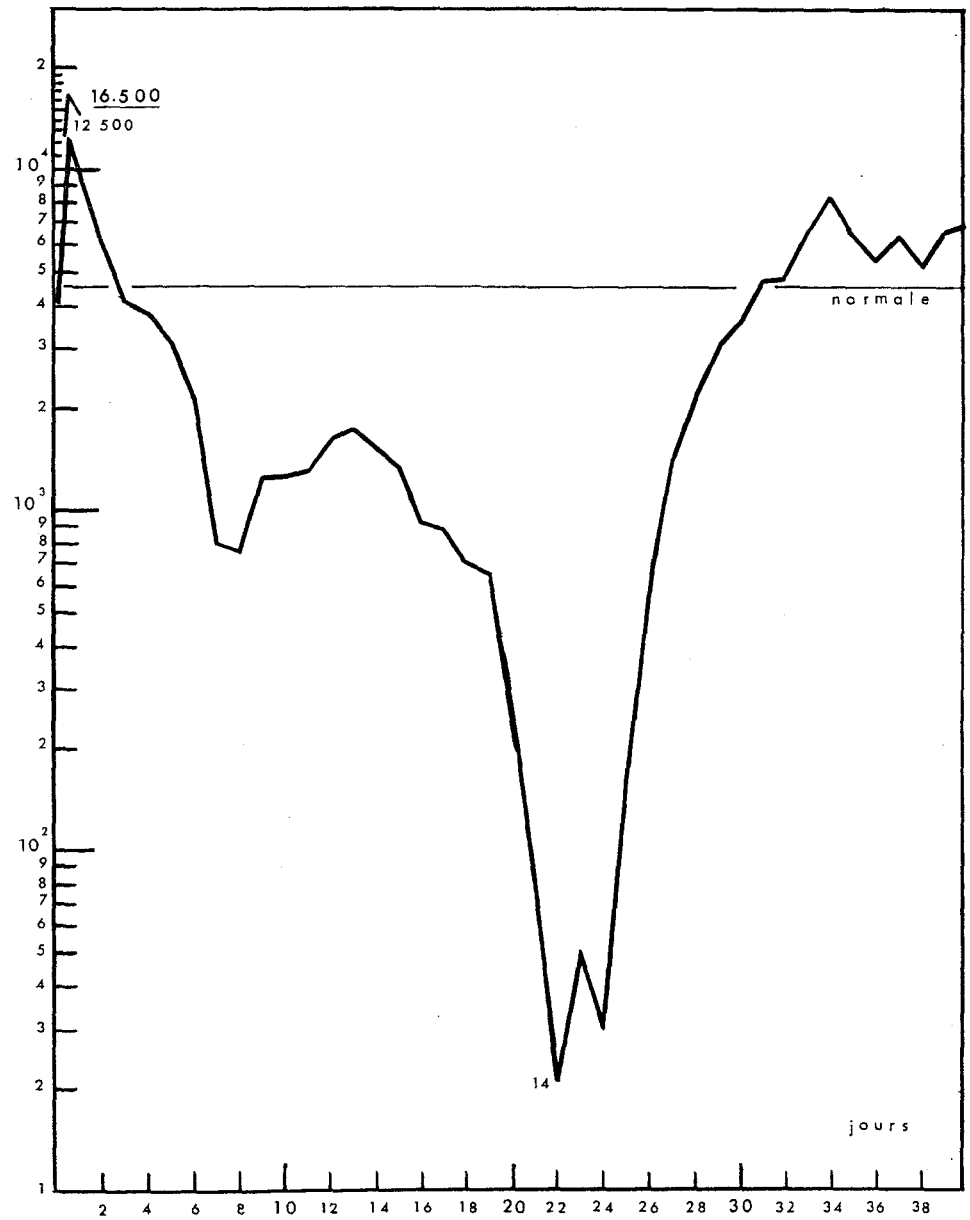

FIG. 4. Évolution des granulocytes neutrophiles en nombre absolu par mm³. Le pic initial est à 12.500. (On a figuré, à 16.500 le pic des granulocytes totaux). Noter la chute rapide interrompue par une reprise abortive du 8ème au 18ème jour, l'effondrement à 14 par mm³ au 22ème jour, la reprise rapide au 24ème jour.

—ensuite se situe la période la plus critique de l'évolution, depuis le 15ème jour jusqu'au 25ème jour. Le taux des granulocytes s'effondre, pour atteindre au 21ème jour, le chiffre catastrophique de 14 *par mm*³. Enfin, la restauration débute au 22ème jour et rétablit des taux voisins de la normale dès le 30–32ème jour.

2.3. 2. *Comparaisons*:

—le pic initial à 16.500 se situe au-dessous des pics observés à Los Alamos (28.000 et 20.000) et au-dessus de tous les autres pics accidentels observés, notamment à Vinca (10.000–12.000);

—la pente de chute peut être comparée seulement avec celles de Vinca, les accidentés de Los Alamos étant décédés dès les premiers jours. Elle se situe au-dessous de tous ces accidentés y compris le cas létal (Fig. 5).

2.4. *L'évolution de la lignée rouge* (Fig. 6) ne met pas en évidence de variations considérables, dans ce pool cellulaire d'énorme inertie. Encore faut-il prendre en considération les très nombreux prélèvements qui, sur l'ensemble du séjour du malade, se chiffrent à près de 1 litre de sang.

2.4. 1. *La courbe des réticulocytes* est plus parlante (Fig. 6); elle présente le même type évolutif que celle des granulocytes, avec la remontée rapide au 25ème jour.

2.5. Nous avons effectué au 7ème jour une *épreuve d'incorporation du fer-59 dans les érythrocytes*, en injectant 1 micro-Curie de radio-fer. Normalement, la moelle osseuse restitue environ 80% de l'activité injectée, en 6 à 7 jours, dans les globules rouges nouvellement produits. La courbe de l'accidenté nous a montré une restitution d'environ 17% de la quantité injectée, au 12ème jour après l'injection, c'est-à-dire au moment où débutait la période de restauration médullaire (Fig. 7).

On a établi également la courbe du *Fer-59 fécal*, en tant que détecteur possible de microhémorragies intestinales: nous pouvions détecter par l'activité du Fer, une hémorragie de 50 centimètres cubes environ. Il n'en a rien été: aucun pic n'a été décelé sur la courbe du Fer fécal.

2.6. *La courbe des thrombocytes* (Fig. 8.) suit une descente progressive, *sans reprise*, et qui atteint le minimum de 15.000 par mm³ au 21–22ème jour (au lieu des 200.000 normaux).

2.7. Nous avons étudié la *coagulation sanguine*, par la méthode globale de *thrombo-élastographie* (Figs. 9 et 10). Les constantes longitudinales (r, k, $r+k$), se sont allongées au cours de la période critique. Les constantes transversales (Am, Em) ont suivi assez fidèlement l'évolution de la courbe des thrombocytes. À noter que Am commence à se relever 1 ou 2 jours avant la courbe des plaquettes et qu'elle marque un "rebound" post-critique. Ces deux phénomènes peuvent s'expliquer par l'apparition d'une génération plaquettaire extrêmement jeune, au moment de la reprise de l'hématopoïèse. Leur hyperactivité fonctionnelle a marqué son empreinte sur la courbe du thrombo-élastogramme.

2.8. *L'évolution de la myélémie* est un point à l'étude duquel nous nous sommes attachés particulièrement. Nous avons noté, en effet, la présence d'un pourcentage important de cellules de la moelle, dans le sang périphérique. Nous en avons tiré les chiffres absolus par mm³. Ils sont ici exprimés (Fig. 11) dans un code personnel, semi-logarithmique, dans lequel on a superposé les différentes cellules de la *lignée myéloïde*. On trouve de bas en haut: les cellules les plus jeunes (pro-myélocytes) et successivement, les moins jeunes (myélocytes, puis métamyélocytes).

On constate que l'enveloppe de cet histogramme reproduit fidèlement l'allure évolutive que l'on a vue sur les granulocytes neutrophiles. On y retrouve: la remontée abortive initiale—la chute à zéro du 20 au 23ème jour puis l'inondation du sang périphérique par des cellules jeunes de la moelle, puisque par exemple au 27ème jour, *la moitié* des cellules granuleuses présentes dans le sang sont des myélocytes de la moelle.

2.9. Toujours sur les étalements de sang—et plus particulièrement sur les concentration leucocytaires préparées pour le comptage des lymphocytes binucléés-nous avons rencontré de *nombreuses figures de mitoses*. Tous les stades de la mitose ont été observés (prophase—métaphase—anaphase—télophase). Certaines éaient anormales, avec de petits fragments de chromatine isolés.

2.10. Nous avons établi presque chaque jour, sur 10.000 lymphocytes normaux, le *taux des lymphocytes binucléés*. Ce taux s'est élevé franchement, à partir du 15ème jour. Il atteint un plateau à 40 p. 10.000 qui s'est maintenu durant 20 jours autour de cette valeur, pour diminuer

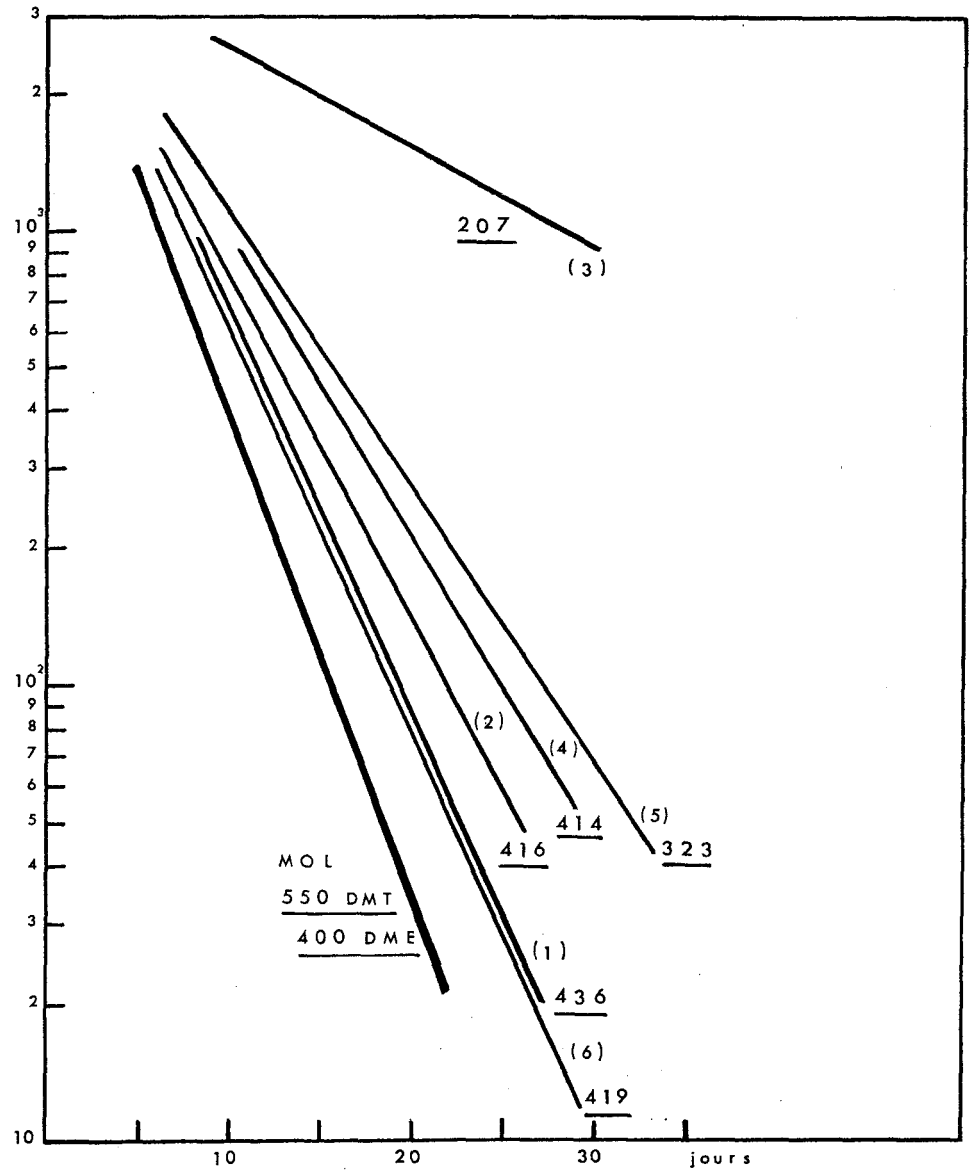

FIG. 5. Comparaison entre les "pentes de chute" des granulocytes neutrophiles. On a tenu compte d'un même chiffre de départ au jour zéro. On a figuré le taux minimal, au jour où il a été atteint. La chute observée à MOL se situe au-dessous de tous les accidents connus ayant survécu jusqu'au 20ème jour.

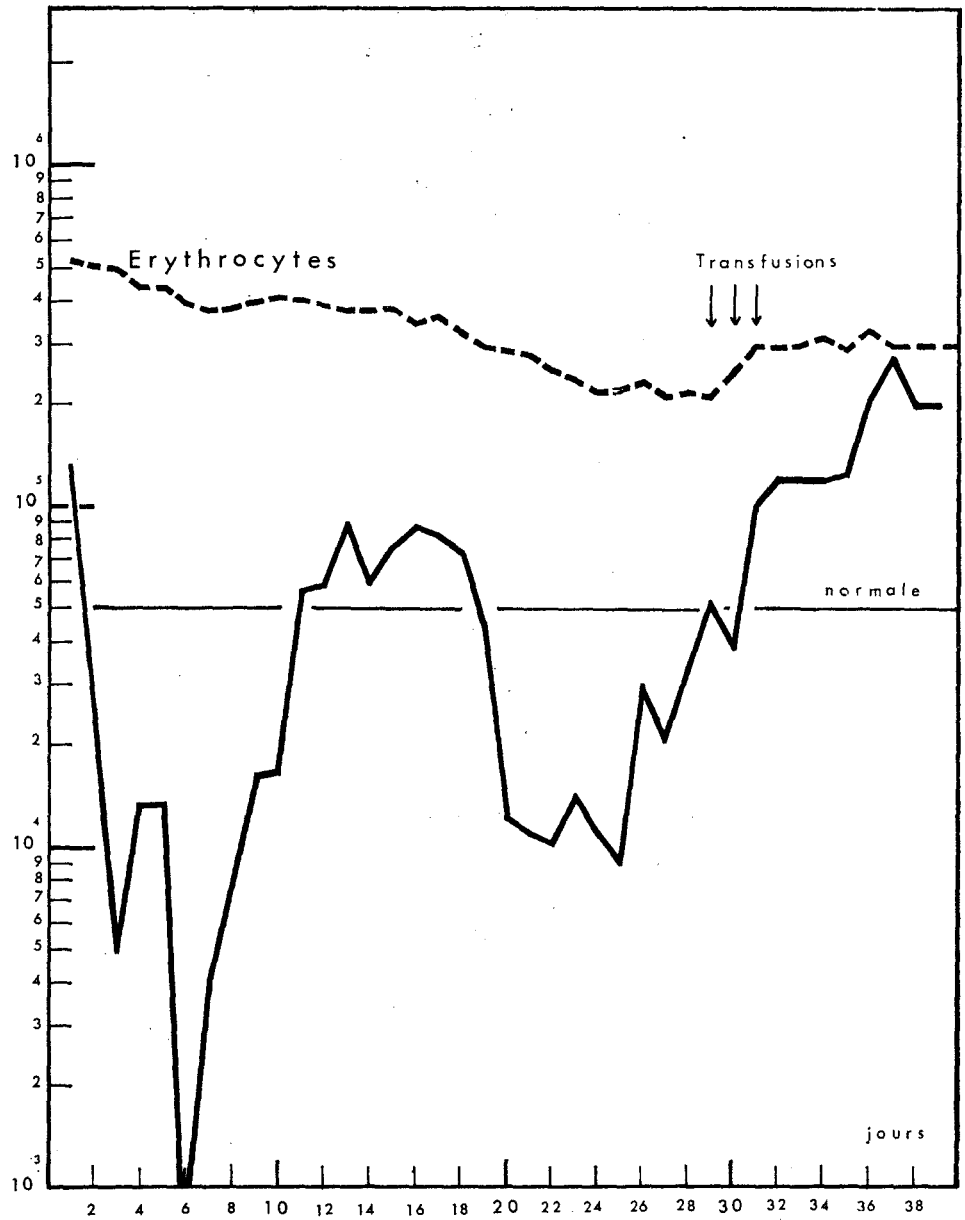

FIG. 6. Évolution de la lignée rouger en nombre absolu par mm³. On a figuré la courbe des érythrocytes (pointillé) : sa décroissance est progressive et de pente faible; il faut y faire intervenir les nombreux prélève-ments nécessités par les examens biologiques. La courbe des réticulocytes (trait plein) est parlante. On y trouve : la chute initiale très brusque, la reprise abortive, la restauration à partir de 25ème jour.

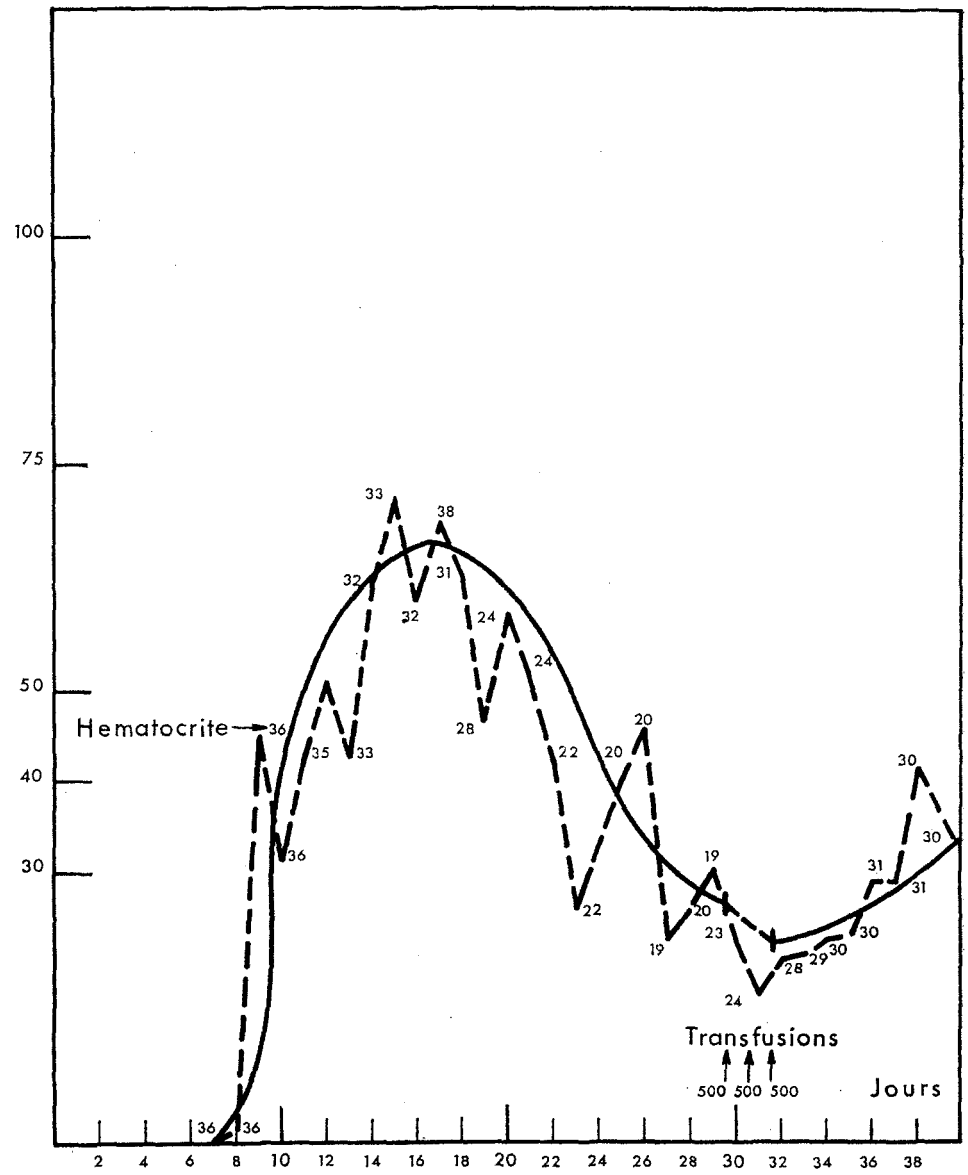

FIG. 7. Épreuve d'incorporation du ^{59}Fe après injection intraveineuse de 1 μ Ci de ^{59}Fe, faite au jour J+7. L'activité érythrocytaire, exprimée en pCi/ml d'érythrocytes, monte seulement à 17% de l'activité injectée, en 10 jours.

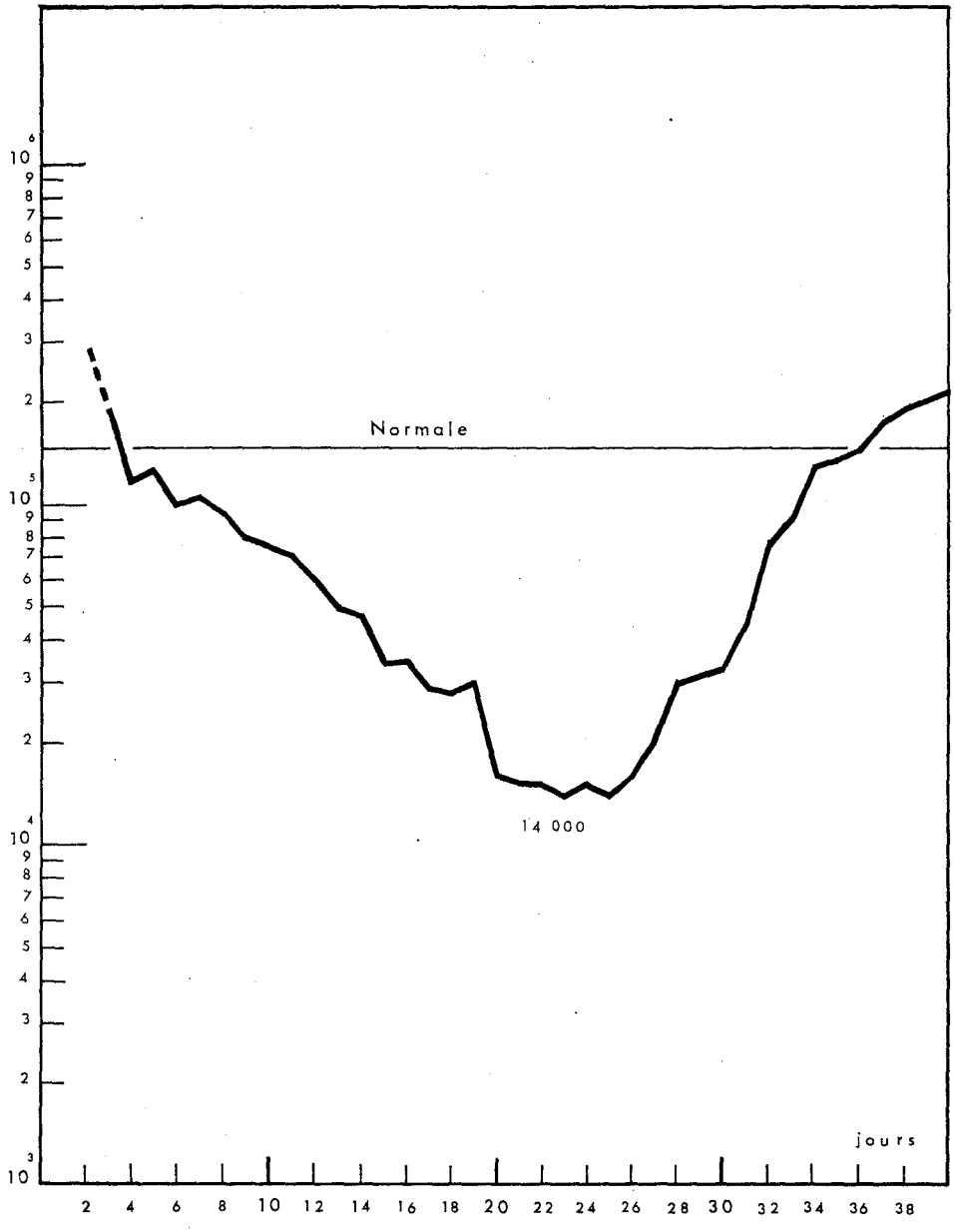

FIG. 8. Évolution des thrombocytes, en chiffre absolu par mm³. Taux minimal atteint: 14.000/mm³ entre J+20 et J+25.

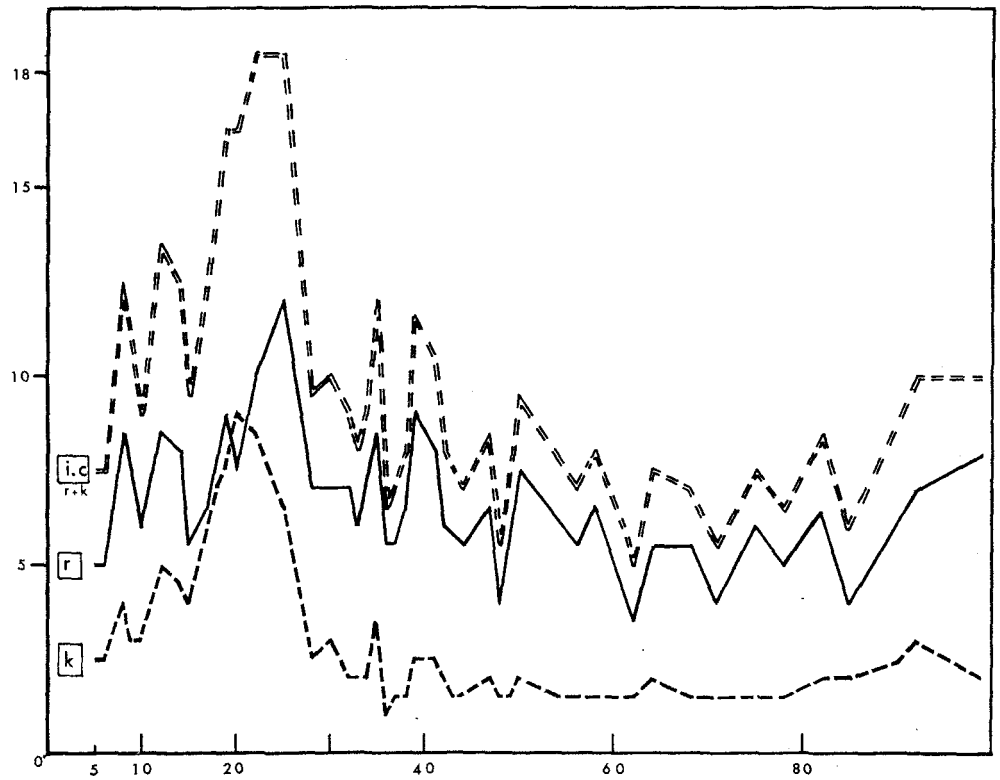

FIG. 9. Évolution des constantes thrombo-dynamographiques: constantes longitudinales: r, k, $r + k$.

ensuite, mais en restant toujours au-dessus des taux normaux de 1 à 4 p. 10.000 (Fig. 12). La courbe en pointillé montre l'évolution des lymphocytes banaux, ceci à une toute autre échelle. Ces lymphocytes binucléés ont donné de très belles images. Beaucoup d'entre eux étaient porteurs de fragments nucléaires (caryomères).

Nous avons également observé une plasmocytose réactionnelle importante, avec souvent des plasmocytes binucléés ou tri-nucléés.

2.11. *L'index mitotique de la moelle osseuse* a été établi sur des ponctions en série. L'index de la lignée rouge présente son pic au 20ème jour. L'index de la lignée granuleuse montre un pic un peu plus tardif, au 30ème jour (Fig. 13).

2.12. *Analyses chromosomiques.* Nous avons procédé chez cet irradié, à des analyses chromosomiques, par étude de caryotypes montés, provenant de cultures de sang prélevé le 4ème jour après l'irradiation. Le but était d'obtenir, si possible, un pourcentage des lésions chromosomiques observables. Mais rappelons qu'au 4ème jour de l'évolution, il y avait dans le sang seulement 130 lymphocytes par mm³. Le nombre de métaphases exploitables a donc été seulement de 24.

Sur ces caryogrammes, on a observé tous les types de lésions: délétions, translocations, anneaux, dicentriques. (Figs. 14–16). Certaines de ces cellules étaient porteuses à la fois de 2 anomalies: le pourcentage global des lésions a donc été relativement élevé. Le tableau en est donné (Tableau 1).

Il faut en retenir les chiffres, exprimés en "nombre de coups", obtenus:

—pour les dicentriques: 125;

—pour les cassures (sans les translocations): 253.

Ces chiffres pouvaient, en effet, être comparés avec les chiffres obtenus par Kelly et Brown au cours de leurs expériences faites sur du sang

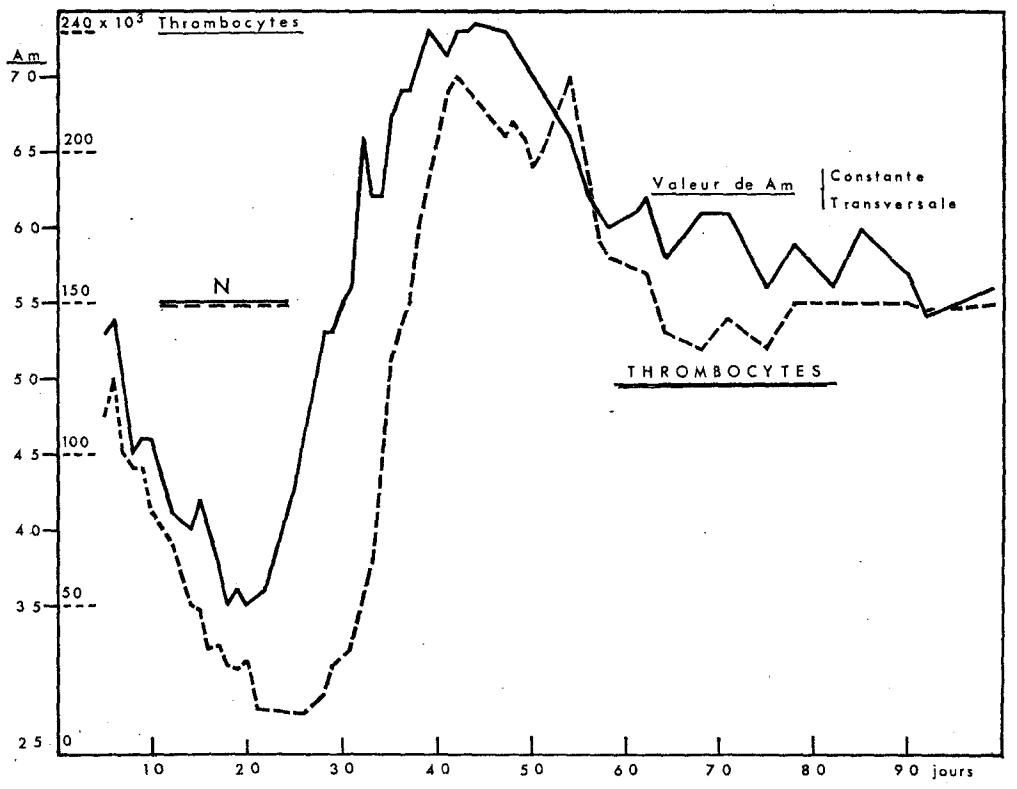

FIG. 10. Évolution des constantes thrombo-dynamographiques: constante transversale Am, (trait plein) comparée avec la courbe des thrombocytes (pointillé)

irradié *in vitro*. Établissant une courbe dose-effet d'après leurs données expérimentales, nous y avons reporté les valeurs que nous obtenions pour l'irradié:

—sur la courbe des dicentriques, notre point se situe à la dose de 500 *R* (Fig. 17);

—sur la courbe des cassures (sans les translocations) notre point se situe à 470 *R* (Fig. 18).

Il faut noter que cette dernière courbe, établie d'après Kelly et Brown, c'est-à-dire par l'examen direct au microscope sans monter les caryotypes, comporte une sous-estimation certaine des doses. On peut donc dire que, sur la base de l'estimation de l'analyse chromosomique, on pouvait situer approximativement le niveau de dose, aux environs de 500 *rads*. Cette notion sera retrouvée à propos de la dosimétrie médullaire.

3. *Évolution biochimique*

Différents paramètres biochimiques ont été étudiés au niveau du sang et des urines.

3.1. *Variations sanguines.* Mise à part la glycémie, les variations sanguines ont été de faible amplitude.

3.1. 1. Le taux d'*urée sanguine* est resté dans les limites normales.

3.1. 2. Les *électrolytes plasmatiques* (sodium, potassium, chlore) ont été suivis quotidiennement. On a observé seulement une légère diminution du sodium dans les premiers jours (120 mEq/litre).

3.1. 3. La courbe (Fig. 19) traduisant les variations de la *glycémie* présente plusieurs oscillations:

—hyperglycémie à 1,54 g/l, le premier jour;

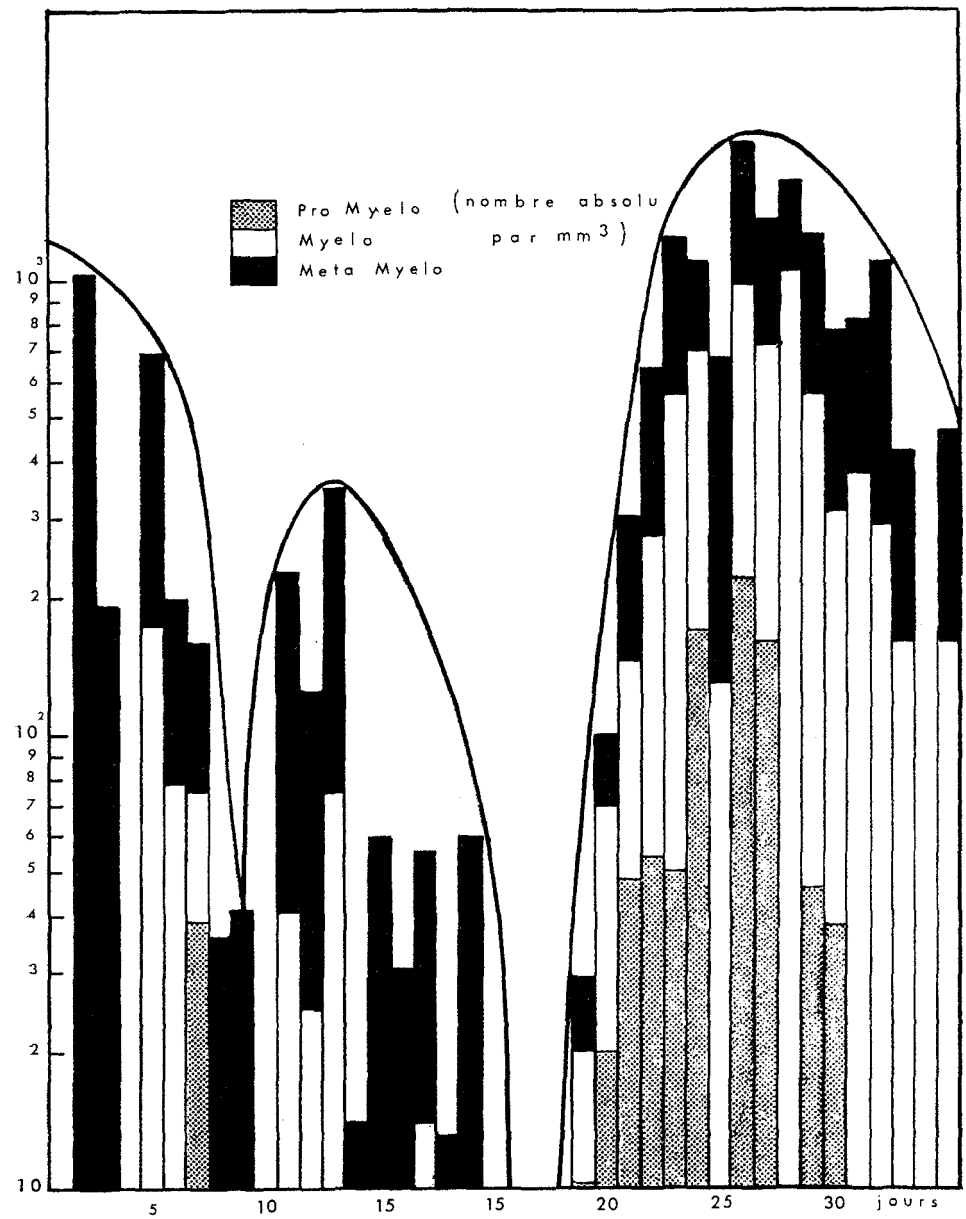

FIG. 11. Évolution de la myélémie. Chaque élément de la lignée myéloïde est figuré par un rectangle dont la longueur est proportionnelle à son chiffre absolu par mm³ de sang périphérique: en gris = promyélocytes; en blanc = myélocytes; en noir = métamyélocytes. L'enveloppe de l'histogramme reproduit la même évolution que la courbe des granulocytes neutrophiles.

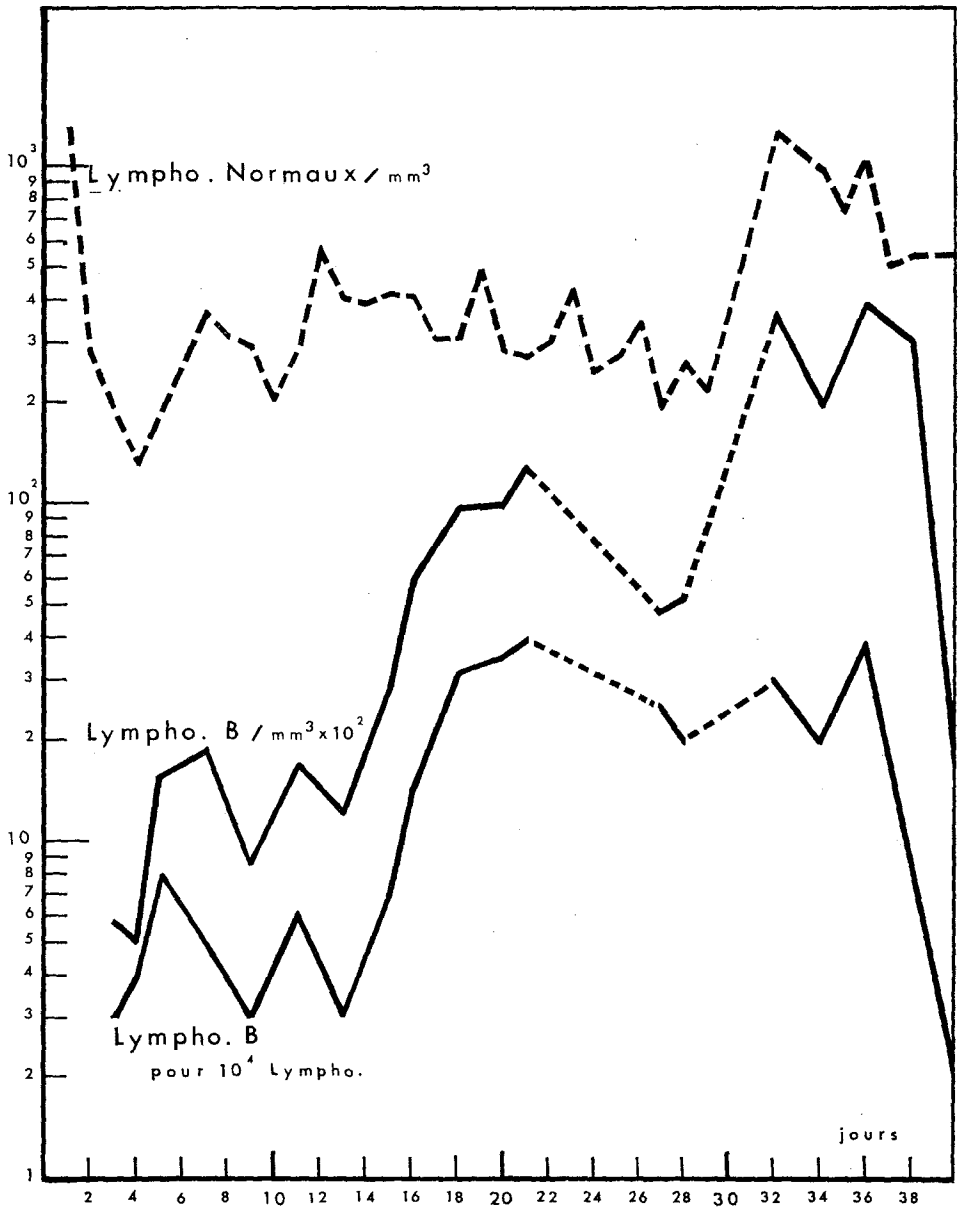

FIG. 12. Évolution des lymphocytes binucléés. Le taux en a été établi par comptage sur 10.000 lymphocytes normaux (courbe inférieure trait plein). Le nombre absolu par mm^3 est exprimé dans la courbe supérieure en trait plein ($\times 10^2$). La courbe en pointillé représente les lymphocytes banals.

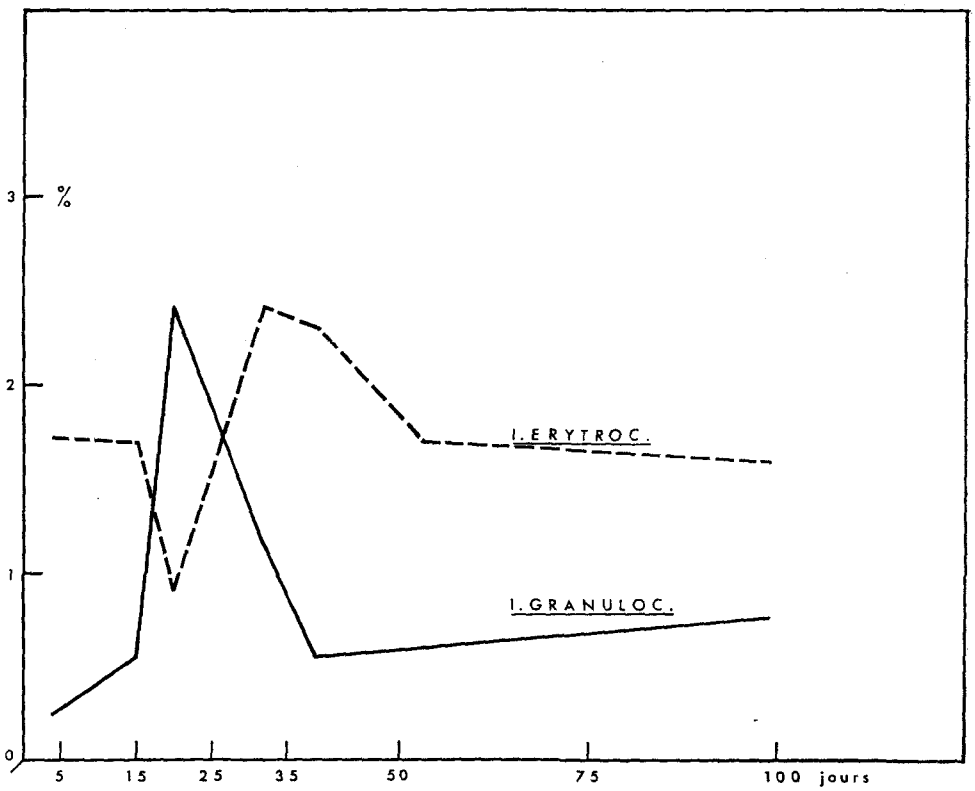

FIG. 13. Index mitotique de la moelle osseuse.

FIGS. 14–16. Quelques types de lésions chromosomiques observées:

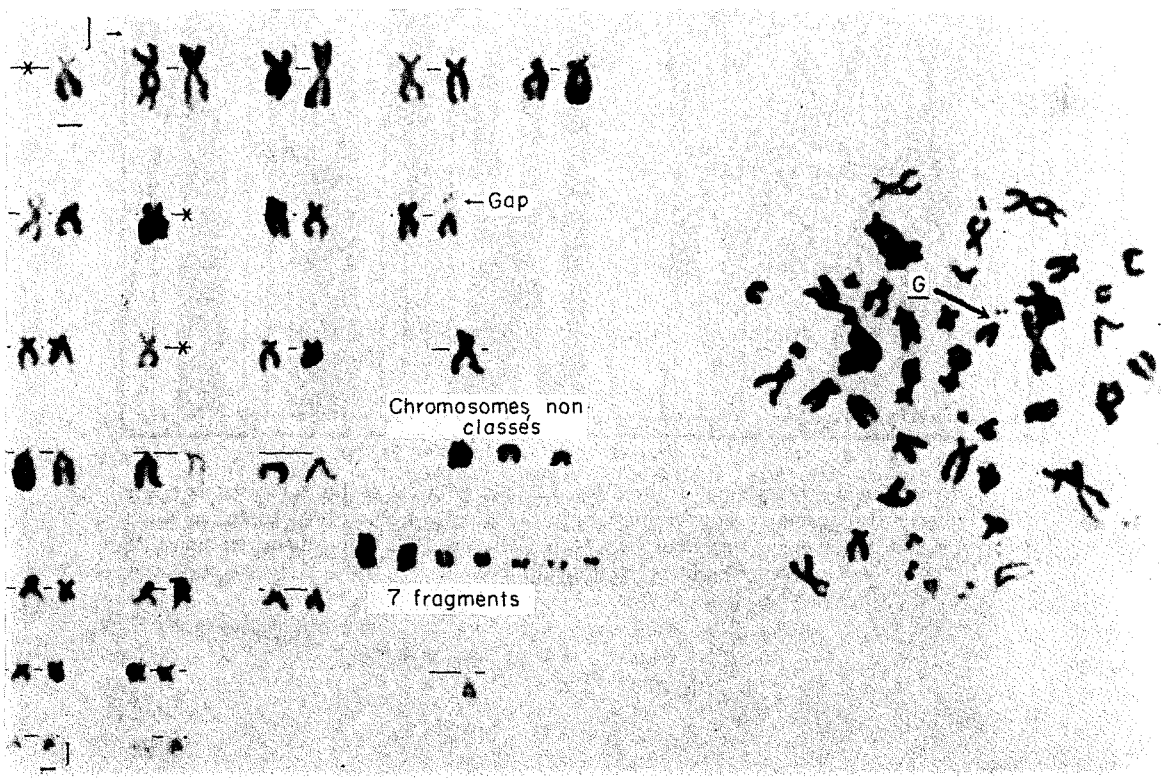

FIG. 14. Cellule avec 7 cassures (fragments).

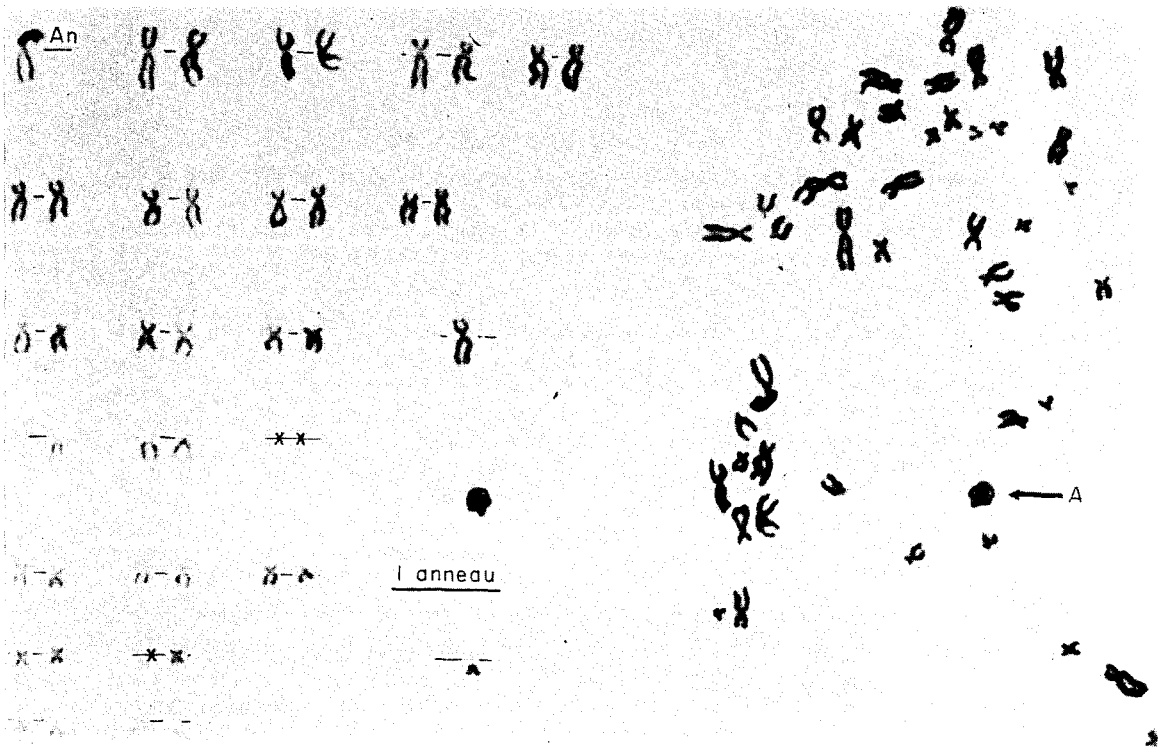

FIG. 15. Cellule avec 1 anneau (2 cassures).

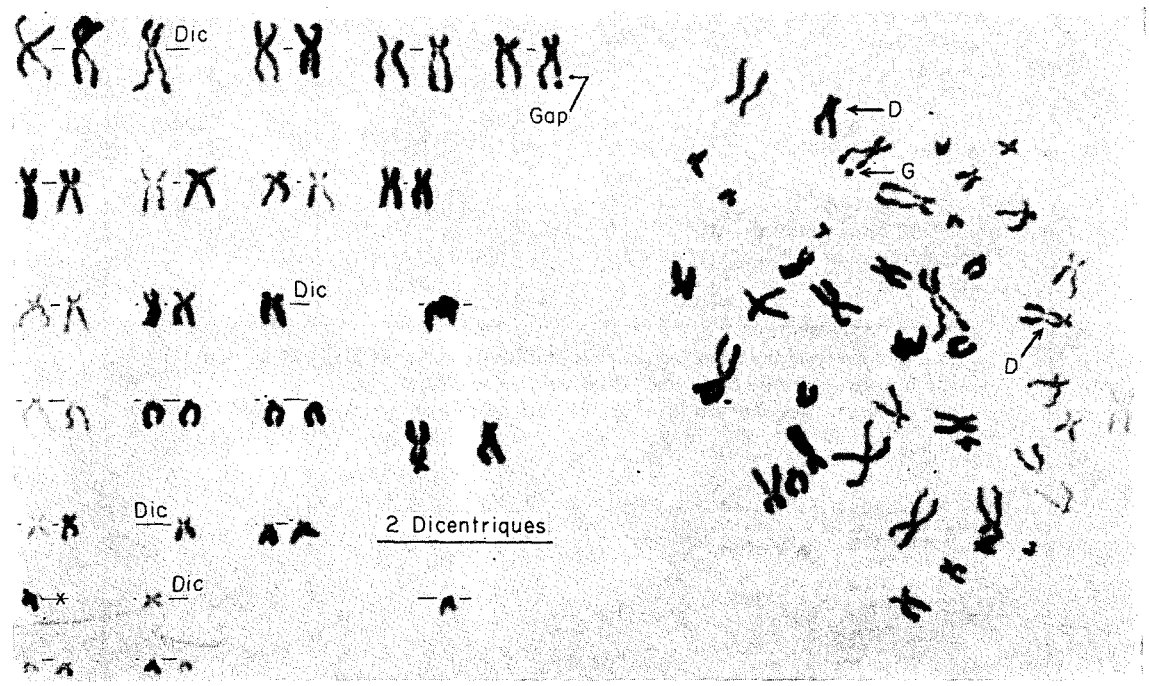

FIG. 16. Cellule avec 2 dicentriques (4 cassures).

Tableau 1. *Tableau des résultats de l'analyse chromosomique, faite sur culture de sang de 72 heures, prélevé au tour J + 4. Pourcentage établis sur 24 cellules.*
Noter: (1°) *le nombre des dicentriques* (125); (2°) *le nombre des cassures* (*sans translocations*) (253); (3°) *le nombre des cassures* (*translocations comprises*) (277)

Caryotypes	Observés	Pourcentage
Examinés	24	
Normaux	1	4
Normaux, avec cassure d'isochromatide	1	4
Normaux, avec hypoploïdie	1	4
Avec hyperploïdie	0	0
Avec aberrations, type chromosome	21	84

Aberrations	Observées	Exprimées en p. 100 cellules	Exprimées en nb. de coups p. 100 cellules
Délétions	6	25	25
Fragments	8	33	33
Cassures de chromosomes	15,5	62,5	62,5
Dicentriques	15	62,5	125
Anneaux	1	4	8
			253
Translocations	2	12	24
			277
Anomalies de chromatide	0	0	
Hypoploïdie dans cellules anormales	9	37,5	

Points correspondants sur les courbes établies *in vitro* par Kelly et Brown;
— sur la courbe des dicentriques: Dose estimée = 520 R;
— sur la courbe des cassures (sans translocations): Dose estimée = 470 R.

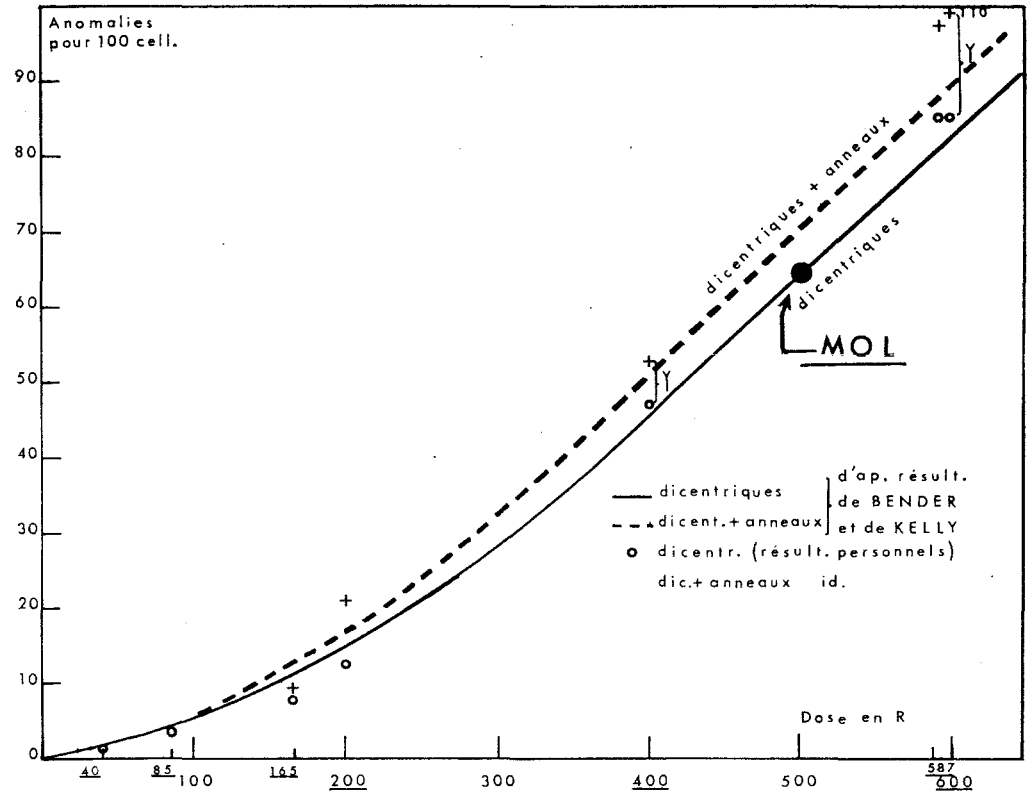

FIGS. 17–18. Reportés sur des courbes de relation dose-effet après irradiation *in vitro*, les chiffres précédents donnent les doses estimées de 520 R (courbe des dicentriques) (fig. 17), 470 R (courbe des cassures, translocations exclues) (fig. 18).

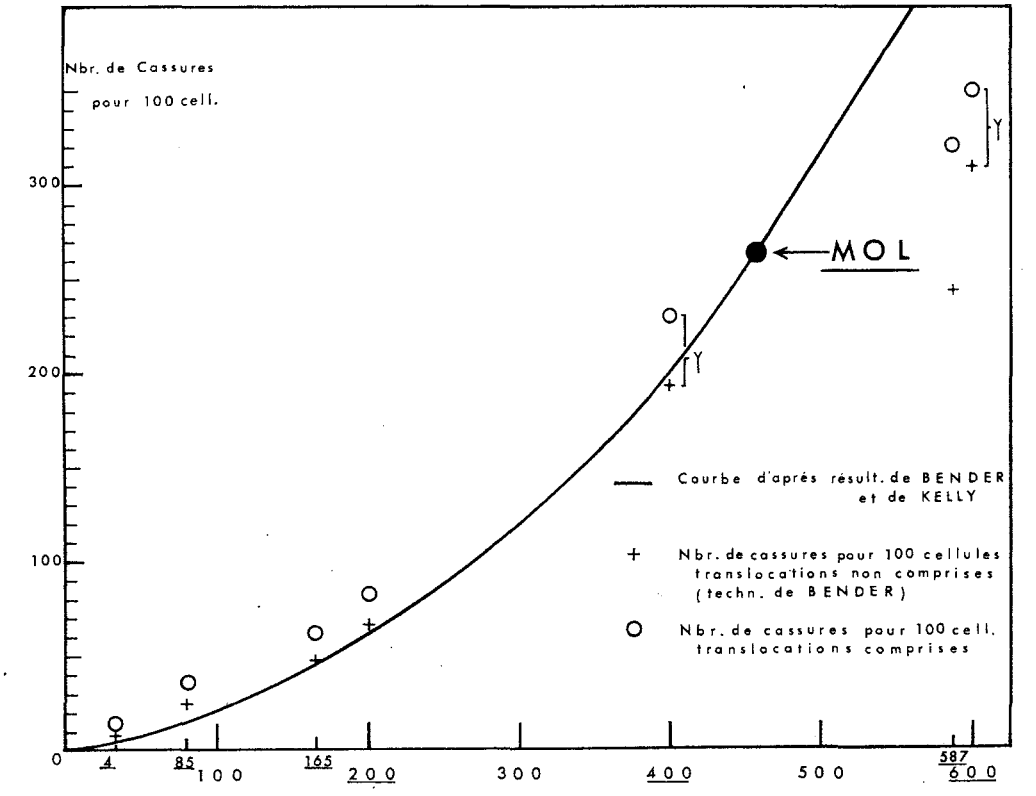

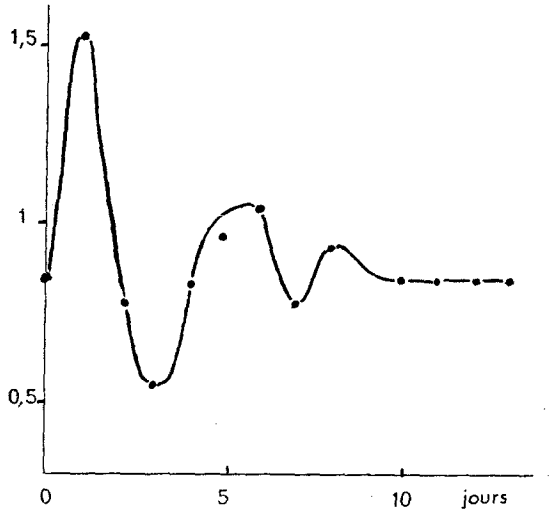

FIG. 19. Évolution de la glycémie.

—suivie d'hypoglycémie à 0,50, le troisième jour;

—et retour à la normale à la fin de la première semaine.

3.1. 4. Les *protéines totales plasmatiques* ont diminué:

—de 82 g/l le premier jour;

—à 63 g/l le 12ème jour.

L'analyse électrophorétique des fractions protéiques (Fig. 20) montre que cette diminution porte surtout sur les Albumines. On notera le pic du 30ème jour, dû aux transfusions.

3.2. *Variations de l'excrétion urinaire:*

3.2. 1. *Les électrolytes urinaires* ont été suivis pendant trois mois. L'excrétion du *potassium* présente trois pics (Fig. 21): le premier jour, ainsi que les 15ème et 21ème jours. L'excrétion du *sodium* (Fig. 22) est nettement diminuée d'abord pendant les quatre premiers jours—puis du 18ème au 30ème jour. La variation du *chlore* est analogue à celle du sodium.

3.2. 2. Les *17-cétostéroïdes totaux* ont été dosés pendant 45 jours (Fig. 23). L'excrétion a été supérieure à la normale le premier jour (16,6 mg/24 h). Puis on observe une diminution franche à 2,4 le 5ème jour et un taux qui reste bas par la suite.

3.2. 3. *L'urée urinaire* n'a pas subi de variations sensibles. L'excrétion d'*acide urique* est nette-

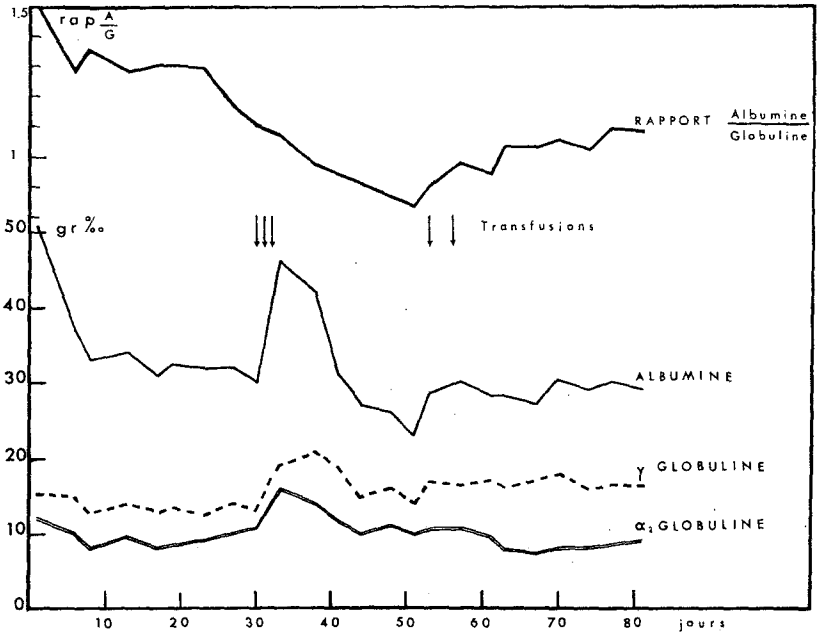

FIG. 20. Évolution des protéines sériques: électrophorèse sur acétate de cellulose.

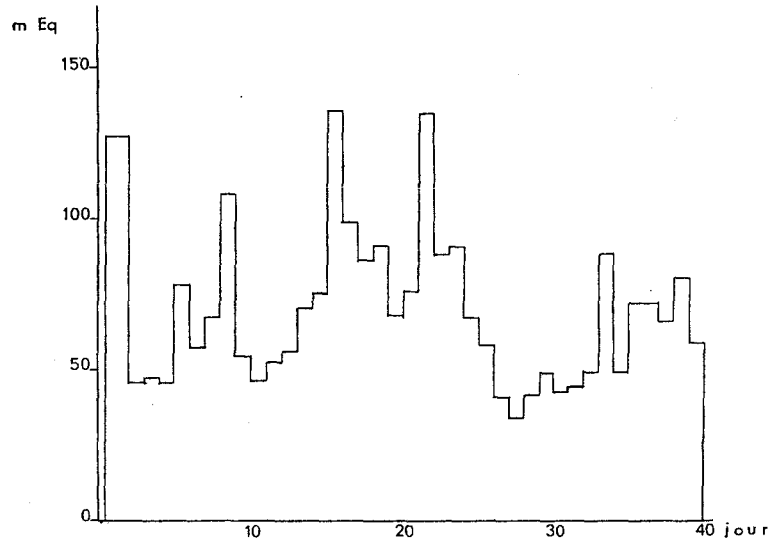

FIG. 21. Excrétion urinaire du potassium.

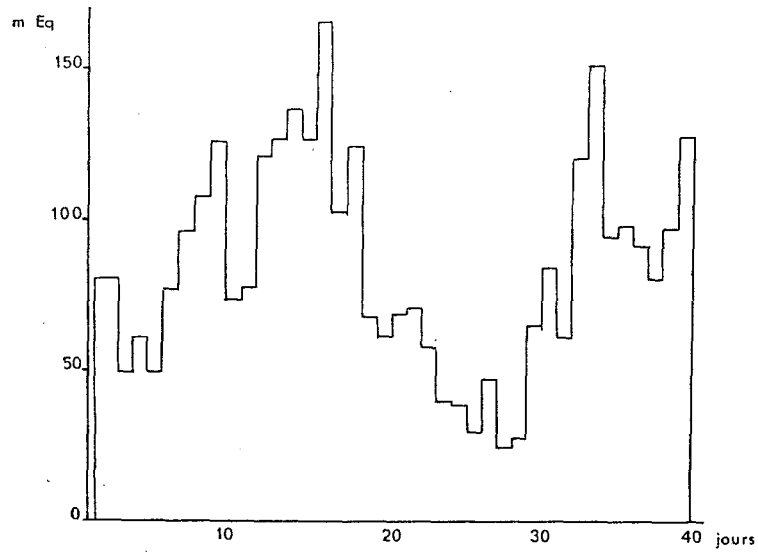

FIG. 22. Excrétion urinaire du sodium.

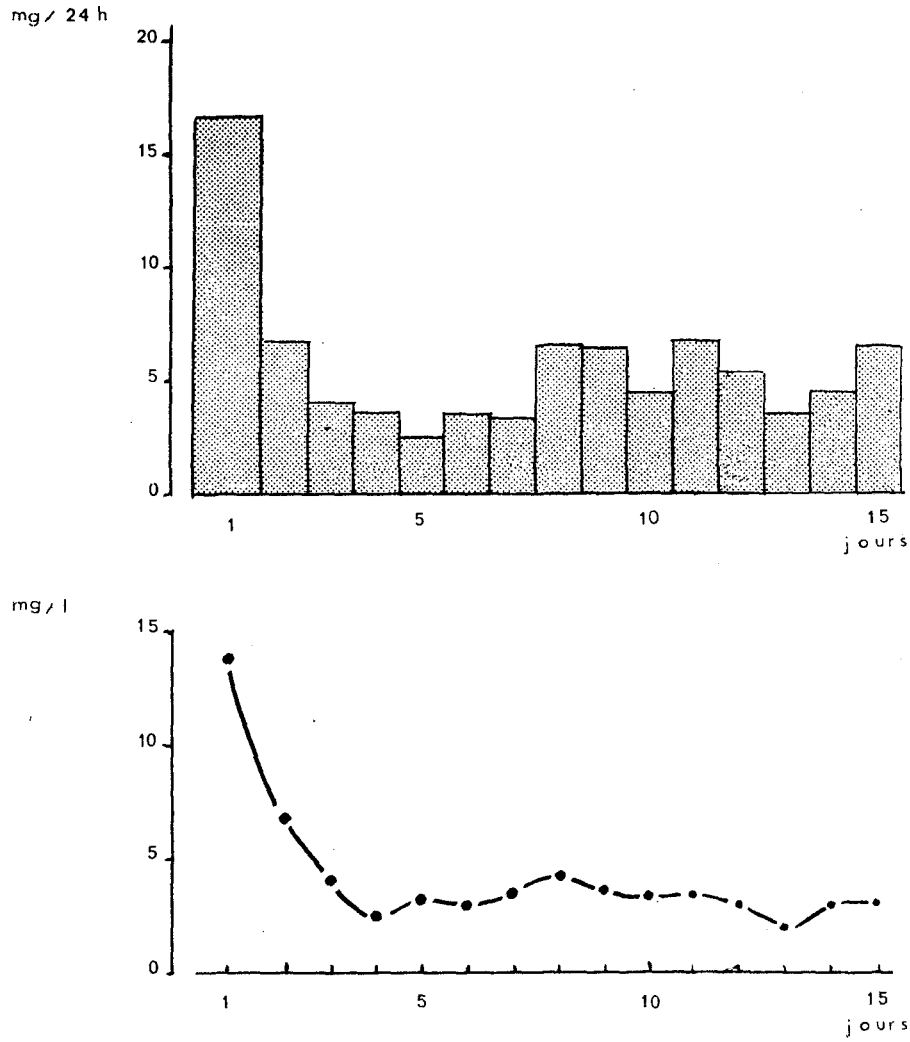

FIG. 23. Excrétion urinaire des 17 cétostéroïdes.

ment augmentée au 21ème jour, au moment de la phase critique.

3.2. 4. *Créatine–créatinine* ont été suivies pendant 45 jours; l'excrétion de *créatine* a été augmentée, avec deux pics: l'un du 5ème au 8ème jour, l'autre vers le 12–13ème jour. La méthode de dosage utilisée (méthode de Jaffe après hydrolyse acide) n'a pas permis de saisir les fluctuations faibles de la créatinine: seules les valeurs de pointe ont été décelées (Fig. 24).

3.2. 5. *Les acides aminés urinaires* ont été évalués quantitativement par analyse chromatographique sur colonne échangeuse d'ions et réaction à la ninhydrine, selon la méthode de Moore et Stein. Vingt-deux composés aminés ont été évalués quantitativement, mais la *Proline* et *l'hydroxyproline*, en quantités trop faibles, n'ont pu être évaluées.

Les *acides aminés totaux urinaires* augmentent nettement (Fig. 25) vers un maximum de 2,7 g/24 h, le 4ème jour. Il en est de même de

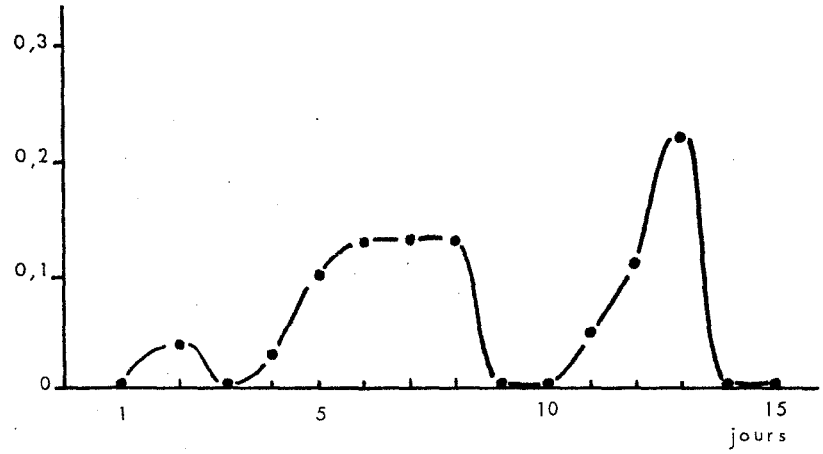

FIG. 24. Excrétion urinaire de la créatinine et de la créatine, exprimée sous forme de rapport créatine/créatinine.

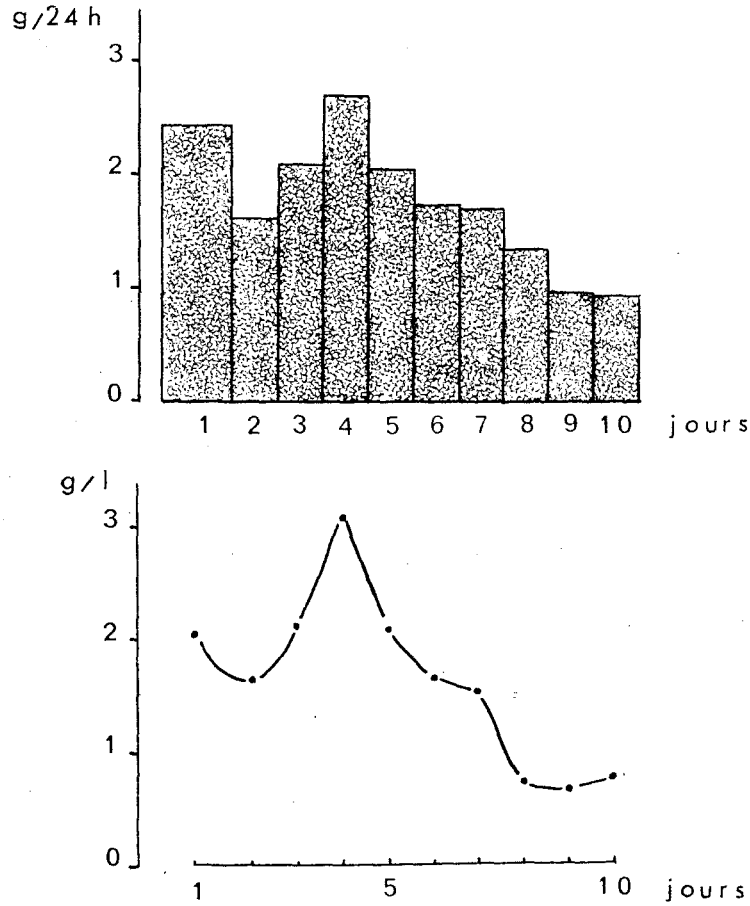

FIG. 25. Excrétion urinaire des acides aminés totaux.

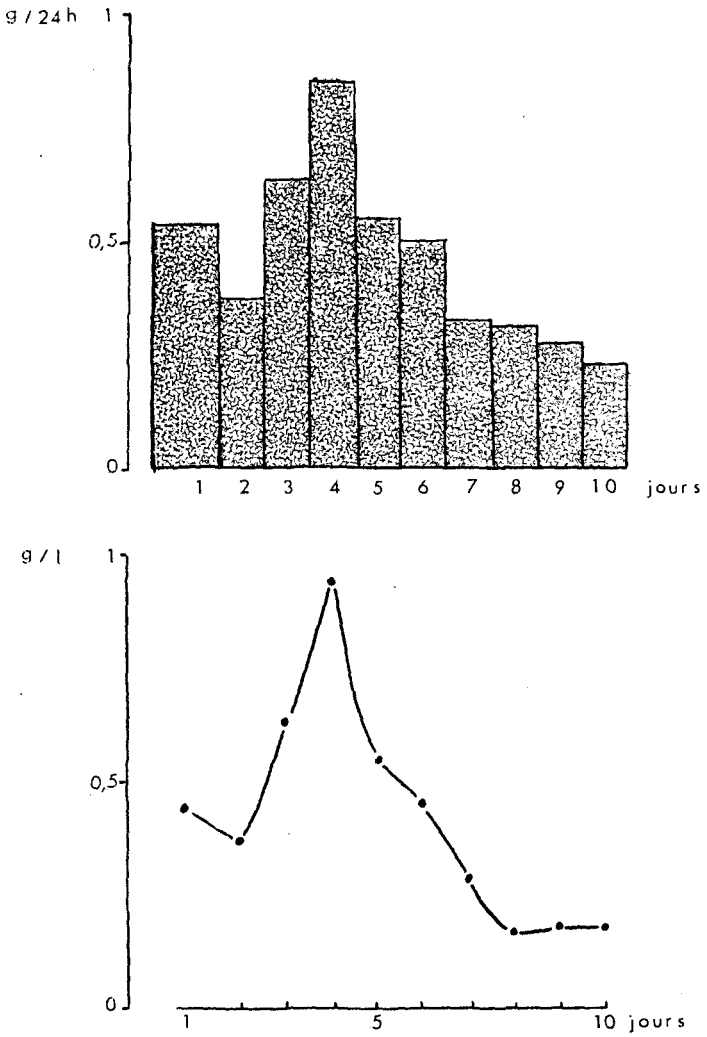

FIG. 26. Excrétion urinaire du glycocolle.

l'excrétion du *glycocolle* (Fig. 26) qui représente environ, en masse, le tiers des amino-acides excrétés le 4ème jour (850 mg/24 h.).

De même pour la *taurine:* maximum à 380 mg/24 h., le 5ème jour: (Fig. 27)

—l'*acide glutamique*: maximum 77 mg/24 h, le 2ème jour;

—l'*acide aspartique*: maximum 187 mg/24 h, le 7ème jour;

—la *cystine*: maximum 115 mg/24 h, le premier jour;

—la *lysine*;

—le *tryptophane*;

—l'*acide β-amino-isobutyrique* (Fig. 28): maximum 41 mg/24 h, le 4ème jour.

À l'inverse on observe une chute nette de l'excrétion urinaire de la *sérine*, à partir du 2ème jour (Fig. 29):

premier jour: 81,5 mg/24 h
2ème jour: 11 mg/24 h
3ème jour: 6,2 mg/24 h
4ème jour: 4,3 mg/24 h.

La courbe d'excrétion de la *thréonine* est similaire.

3.2. 6. Quant à l'alanine, l'acide cysteïque, la tyrosine, la phenulalanine, et l'arginine, les vari-

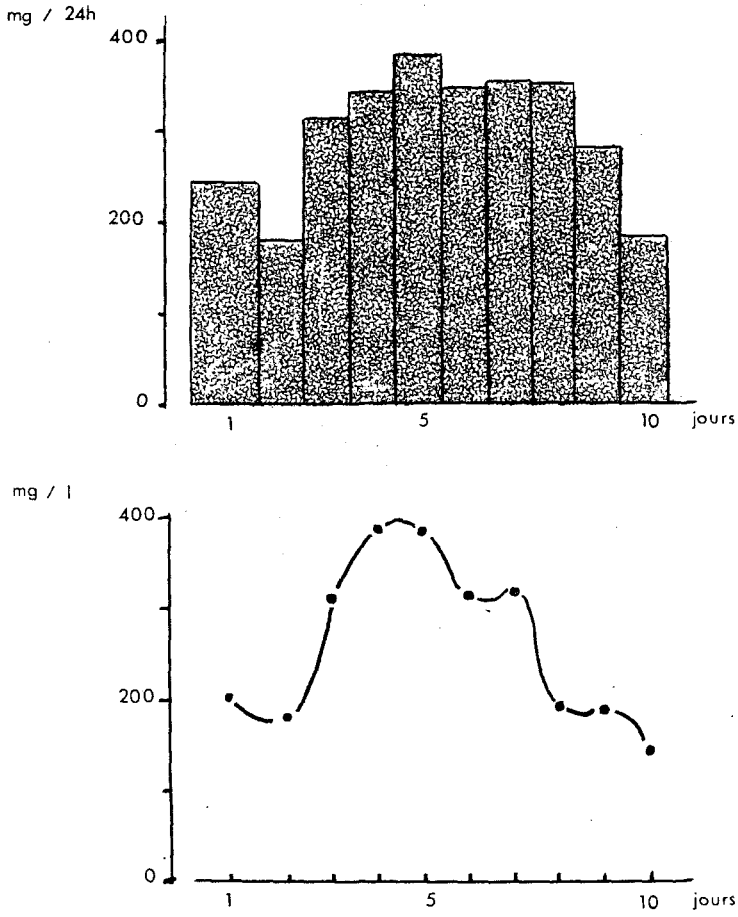

FIG. 27. Excrétion urinaire de la taurine.

ations de leurs taux d'excrétions restent dans les limites normales.

4. *Étude de la moelle osseuse—Cytologie et dosimétrie*

4.1. Nous avons fait chez cet irradié un grand nombre d'examens de la moelle osseuse, par des ponctions exécutées en des points divers. Voici comment les choses se sont présentées.

4.1. 1. *Le premier jour*, on ne disposait que d'une notion dosimétrique assez globale: irradiation aux environs de 550 rads, dose estimée d'après le film badge, porté par le sujet à la poche poitrine. La première ponction a donc été une *ponction sternale*, au jour J+1 et elle a montré une moelle très pauvre.

4.1. 2. *Les jours suivants*, on sut que l'irradiation était inhomogène, que le sujet était placé très obliquement, à cheval sur la margelle en béton du réacteur. On a fait des ponctions symétriques, aux extrémités d'un diamètre du bassin: l'une à l'épine iliaque antérieure gauche (située au-dessus du réacteur), l'autre à l'épine iliaque postérieure droite, qui était censée avoir être protégée.

L'examen de ces deux moelles, au jour J+4, a montré une cellularité aussi pauvre que précédemment. Ensuite, on a pensé que le membre inferieur droit, qui était replié sur la margelle de béton, avait peut-être été protégé. Et l'on a fait une ponction du tibia, à son épiphyse supérieure et une ponction de calcaneum. L'une

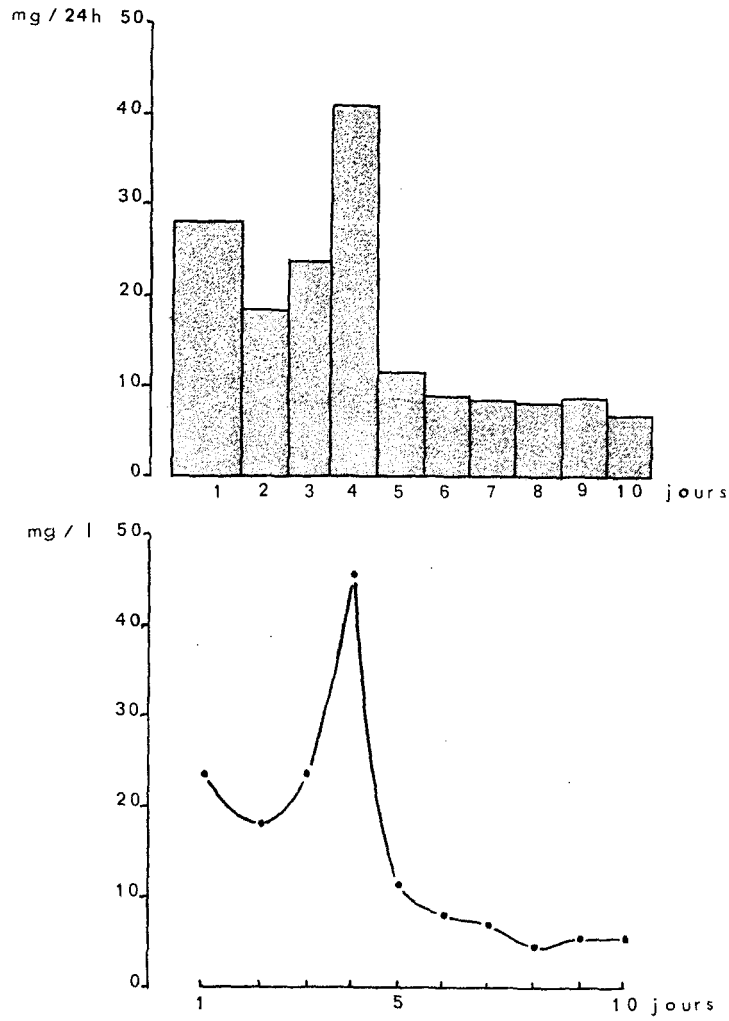

FIG. 28. Excrétion urinaire de l'acide β-aminoisobutyrique (BAIBA).

comme l'autre ont montré une moelle déserte, au jour J+7.

4.1. 3. C'est alors que les notions de dosimétrie se sont affinées, grâce à la reconstitution d'accident, faite sur le fantôme en matériau synthétique tissu-équivalent. L'enorme inhomogénéité des doses est apparue clairement sur les résultats numériques de la dosimétrie interne.

Nous avons donc utilisé tous les résultats numériques de cette dosimétrie et commencé par établir les *ZONES ISODOSES* correspondant à chacune des tranches du fantôme. Puis nous avons fait construire une copie en plexiglas de chacune de ces tranches, et nous y avons figuré les zones isodoses, dans un code de hachures colorées: (noir = au-dessous de 1000 rads; hachures rouges = 800–1000, etc.).

En réassemblant ces tranches, porteuses de notre code, dans la même géométrie que le fantôme, nous obtenions un "Bonhomme de verre", (Fig. 30) qui donnait une représentation dosimétrique spatiale tri-dimensionnelle.

4.1. 4. En effet, le problème de l'estimation du dommage, qui nous était posé par les médecins traitants—et tout le problème thérapeutique

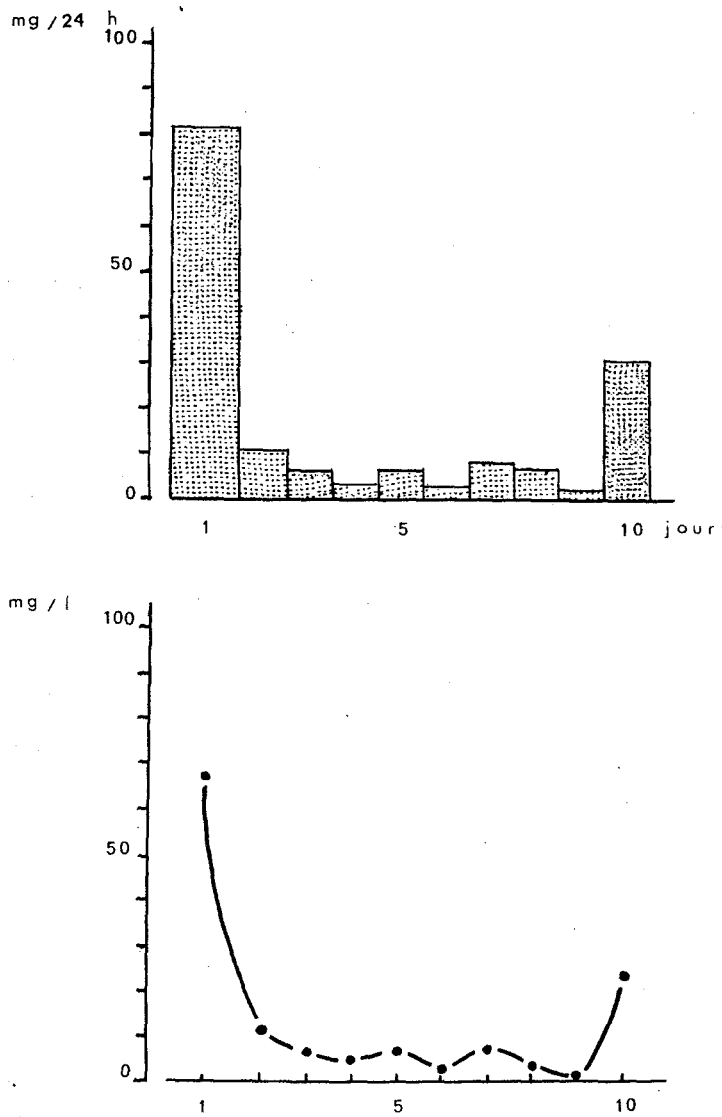

FIG. 29. Excrétion urinaire de la sérine.

qui en découlait—était de savoir quelles étaient les doses et comment elles étaient réparties: problème physique.

Mais aussi: *où* il pouvait subsister un peu de moelle ayant reçu moins que la DL-50—qui serait donc susceptible de restaurer, par duplications successives, la population normale de cellules-souches.

Et ceci étant établi, *combien* il restait, non pas de moelle, mais de *cellules-souches* survivantes et viables: problème biologique.

Nous avons donc tenté, par nos moyens disponibles, de donner une réponse à ces deux problèmes biologiques: où et combien?

4.2. *Recherche de la présence de moelle active:*

4.2. 1. Le bonhomme de verre nous montrait que toute la partie antérieure du bassin (celle qui comporte les zones noires et rouges) était

FIG. 30. "Bonhomme de verre". Technique de représentation spatiale des isodoses. (Dr. Le Go)

certainement atteinte de façon considérable et qu'il n'y avait pas à espérer trouver de moelle intacte à ce niveau, ni au niveau de la région lombaire; que les régions supérieures du tronc étaient dans des zones moins sombres, notamment le dos supérieur, et que la région postérieure de la tête, ainsi que le cervix, étaient en zone claire: inférieure à 300 rads.

4.2. 2. C'est pourquoi l'étude ultérieure de la moelle osseuse au 15ème jour, a été faite par trois ponctions: au niveau de sternum—au niveau de l'épine iliaque postérieure droite—et la troisème au niveau de l'apophyse épineuse de la *sixième vertèbre cervicale.* La ponction sternale était déserte. La ponction illiaque était déserte. La ponction de la vertèbre C^6, montrait une moelle riche, au 15ème jour. Cette moelle présentait en particulier un rapport érythro-myéloïde égal à 1,9. Et les cellules-souches y étaient présentes:

cellules réticulaires	2%
hémo-histioblastes	2,2%
hémo-cytoblastes	1,8%

soit *6% de cellules-souches.*

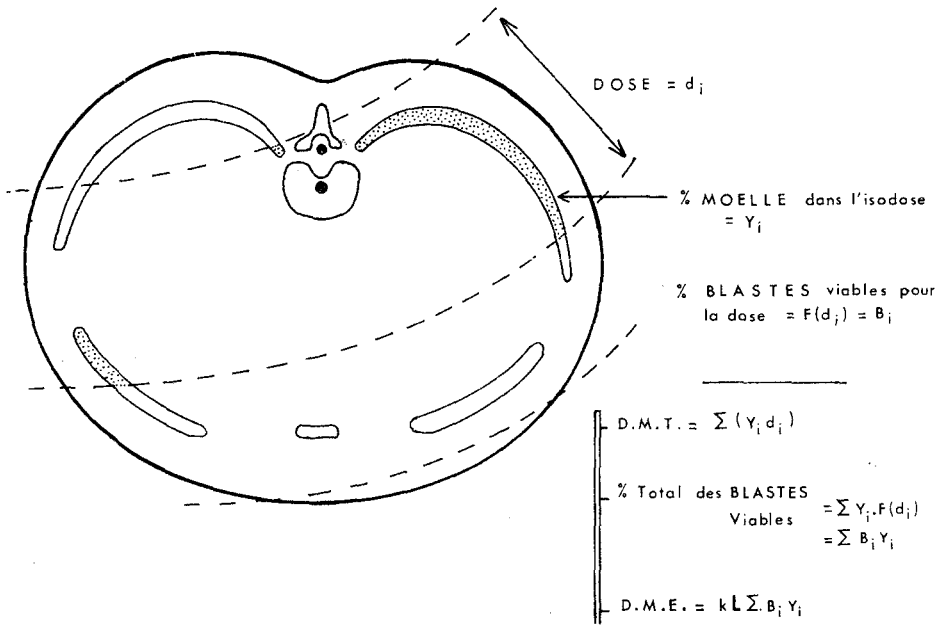

FIG. 31. Mode d'établissement de la dose médullaire théorique (DMT) et de la dose médullaire équivalente (DME).

Nous savions donc *où* il restait des cellules souches viables. Il fallait estimer *combien*—et en déduire les chances que l'irradié avait peut-être, de survie par ses *propres moyens hématologiques*.

4.3. *Estimation du taux de cellules-souches viables*:

4.3. 1. Nous ne pouvons nous étendre ici sur les calculs entrepris, qui font l'objet d'un travail en cours de rédaction. Disons seulement que nous avons repris notre fantôme isodose. Sur chacune des coupes, nous avons estimé le pourcentage de moelle présent dans chaque zone isodose figurée sur la coupe. Puis nous avons pondéré chacun de ces pourcentages locaux, par le chiffre de la dose correspondante (Fig. 31). La sommation de ces résultats élémentaires donne une dose moyenne intégrée à l'ensemble de la moelle, qui est une estimation purement physique de l'énergie transmise à la moelle et que nous avons appelée la *dose médullaire théorique*. Nous l'avons trouvée égale à 550 rads.

Puis nous avons transposé le problème sur le plan biologique. Nous avons calculé pour chaque dose, le pourcentage de cellules-souches viables, en nous référant aux courbes de Lajtha. Et nous avons pondéré par cette valeur, chacun des pourcentages de moelle locale, trouvés précédemment (Fig. 32). La sommation de ces résultats partiels nous a donné un taux de cellules-souches survivantes égal à 3 p. 1000. Ce taux de survie est réalisé, en irradiation homogène, par une *dose de 400 rads environ*. C'est cette dose que nous appelons *dose médullaire équivalente*.

Que représentent ces deux notions?

4.3. 2. La *dose médullaire théorique* est une valeur physique qui représente le transfert d'énergie à la moelle. La valeur de 550 rads permet donc d'imaginer quelle aurait été l'évolution de l'irradié, si le transfert d'énergie avait été homogène. D'où le terme de dose médullaire théorique (Fig. 33).

4.3. 3. La *dose médullaire équivalente* prend en considération le dépeuplement local de la moelle en fonction de la dose. C'est donc, par définition, la dose qui, si elle est reçue de façon homogène, laisse le même pourcentage de cellules-souches survivantes. En conséquence, cette valeur a donc toutes les chances d'être représentative de l'évolution hématologique dans le cas étudié (Fig. 34).

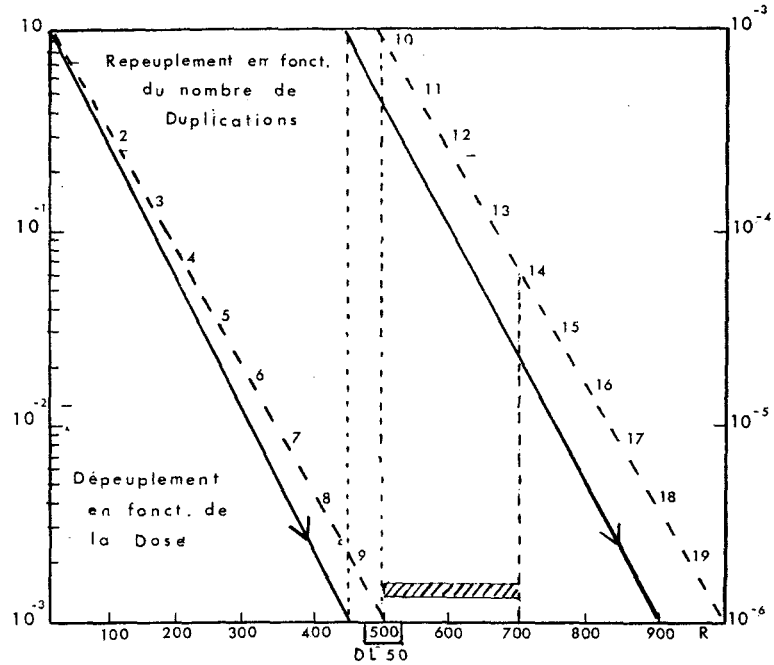

FIG. 32. Courbe de dépeuplement des cellules-souches de la moelle osseuse, en fonction de la dose, établie d'après les données publiées par Lajtha.

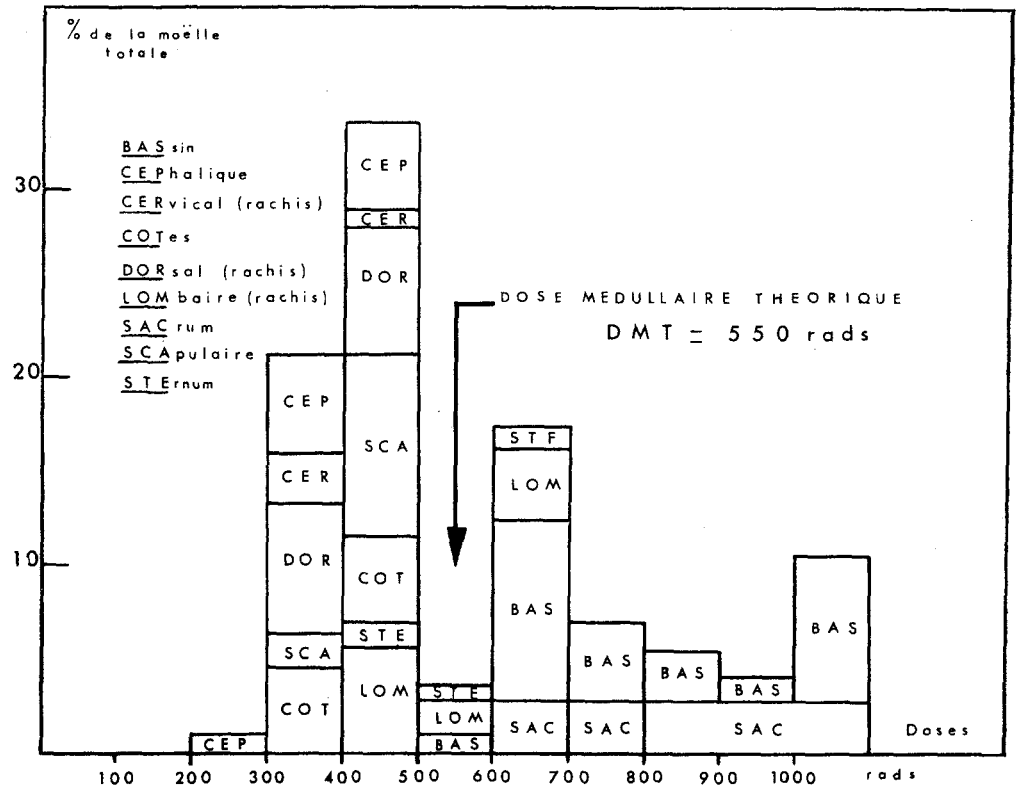

FIG. 33. Histogramme montrant la répartition des doses reçues par la moelle osseuse des différentes régions squelettiques. La dose médullaire théorique est figurée par une flèche.

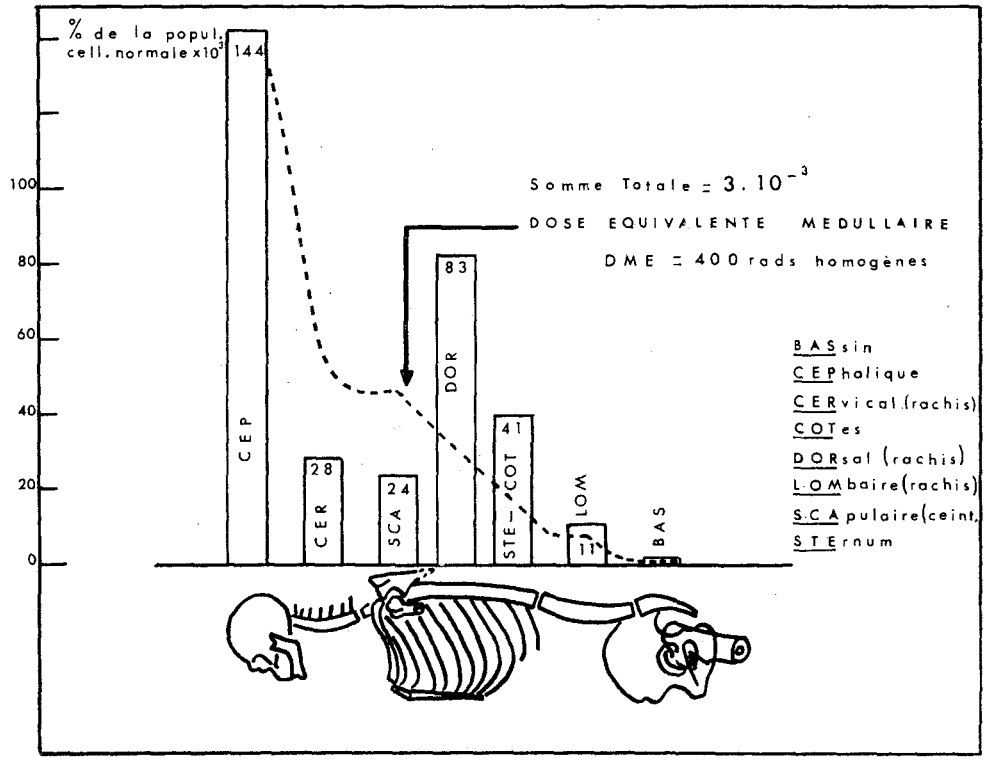

FIG. 34. Histogramme montrant la répartition des cellules-souches restées viables, dans la moelle osseuse. Les chiffres portés en haut des rectangles expriment le pourcentage de la population totale des blastes restant présents dans la région considérée ($\times 10^3$). Exemple: dans la région céphalique, se trouvait 1,44 p 1000 de la population des blastes. La proportion totale des blastes survivants est de 3 pour 1000.

4.4. *Estimation des chances de survie spontanée:*

4.4. 1. Si l'on traduit en termes de chances de survie les deux doses calculées précédemment: DMT et DME, on constate que (Fig. 35):

—pour 550 rads, les chances de survie sont inférieures à 10%;

—pour 400 rads, elles sont de l'ordre de 45%.

On peut donc dire que la différence entre les deux chiffres de la DMT et de la DME exprime la différence évolutive entre une irradiation homogène et une irradiation très inhomogène, pour une même énergie transmise. Cette différence apporte, dans le cas particulier, un gain de 35% dans les chances de survie.

4.4. 2. Ce "glissement" a une importance pronostique considérable. Il fait passer l'irradié de la catégorie "survie virtuellement impossible", dans la catégorie "survie éventuellement possible".

4.5. Il faut maintenant tirer la philosophie de cette constatation. Le gain de 35% dans les chances de survie, n'a pas cependant été pour l'irradié, un gain net. Il faut le considérer comme un "prêt à long terme", sur le plan vital. Mais il s'est assorti d'un *AGIO* extrêmement lourd: *les lésions locales de surdosage* au niveau du membre inférieur, qui ont finalement nécessité l'amputation de ce membre.

En définitive, nous n'apportions donc, par cette tentative de dosimétrie médullaire, étayée cependant par la constatation d'une moelle active au niveau des vertèbres cervicales, que la notion de l'existence de "*chances de survie spontanée possible*".

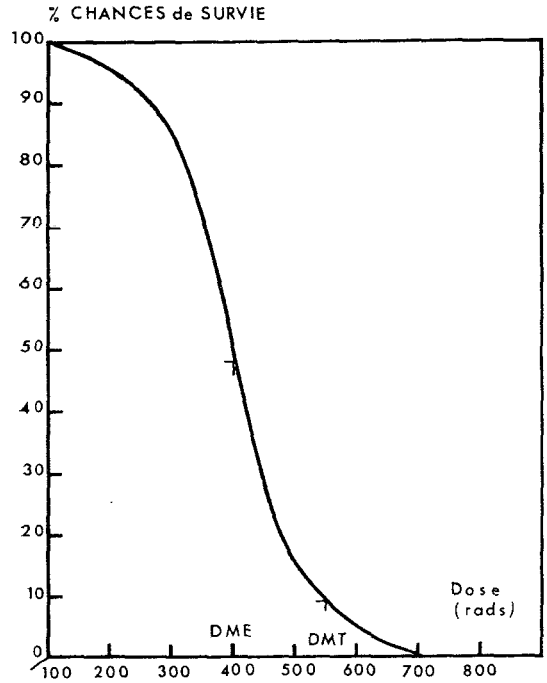

FIG. 35. Courbe de survie des populations, établie d'après les données de Leader, Williams et Smith.

Mais "survie possible" n'est pas "survie probable", encore moins "certaine". Restait donc le problème des décisions thérapeutiques qui fut loin d'être le moindre.

II. CONDUITE THÉRAPEUTIQUE

1 *Principes généraux*

Ainsi que cela a été exposé dans l'observation clinique, l'évolution générale du syndrome d'irradiation globale aiguë est caractérisée par quatre phases successives (Fig. 1):

—choc,
—latence,
—crise,
—rémission.

La conduite thérapeutique est fonction des manifestations apparaissant au cours de chacune de ces phases évolutives mais également des troubles inapparents qui nécessitent une mise en conditionnement.

À ces quatre phases correspondent schématiquement:

—un traitement anti-choc,
—un traitement prophylactique,
—un traitement héroïque,
—un traitement reconstitutif.

2. *Traitement au cours de la phase de choc*

Au cours des 24 premières heures, le choc initial s'est manifesté essentiellement par une phase fébrile avec déséquilibre neuro-végétatif à symptomatologie digestive.

Le traitement a consisté en repos absolu, diète légère et administration de médications neurosédatives de type largactil. Il faut tenir compte des propriétés myélotoxiques des médications chimiques.

Lorsque l'on fait l'inventaire des substances médicamenteuses, en particulier de nature synthétique présentant un caractère myélotoxique plus ou moins accentué, on constate qu'il existe finalement fort peu de médicaments utilisables. C'est ainsi que parmi les antalgiques, les antipyrétiques, les antibiotiques etc. . . . la plupart s'avèrent contre-indiqués.

3. *Traitement au cours de la phase de latence*

Le choc initial passé, s'est installée pour trois semaines une phase de latence clinique. Elle a été caractérisée par l'absence quasi complète de symptomatologie apparente et par une évolution implacable et silencieuse des radiolésions cutanées, hématologiques et viscérales.

À l'inverse de ce que l'on pourrait penser, cette période a été capitale pour les indications thérapeutiques, le traitement prophylactique et la préparation des traitements curatifs.

3.1. *Indications thérapeutiques.* La phase de latence, qui nous est heureusement accordée au cours du syndrome d'irradiation globale aiguë, doit être impérieusement mise à profit pour poser les indications thérapeutiques sur des bases dosimétriques et biologiques aussi complètes que possible.

C'est pendant ces 20 jours qu'ont été effectuées les études dosimétriques sur le patient lui-même et sur fantôme, au cours de la reconstitution de l'accident. Elles ont permis d'aboutir en temps voulu à deux constatations essentielles: l'hétérogénéité de l'irradiation et l'importance des doses absorbées au niveau des

différents organes. En outre, la méthode d'estimation de la dose médullaire théorique nous apermis de tabler sur une irradiation de l'ordre de 500 rads. Simultanément, les investigations hématologiques et biochimiques sont venues confirmer, jour après jour, le bien-fondé des estimations dosimétriques, en particulier la pente de la chute des lymphocytes. L'effondrement du nombre absolu des granulocytes et des thrombocytes a signifié que l'on se trouvait dans le domaine de la létalité. En outre, les ponctions médullaires pratiquées au sternum, aux ailes iliaques, au tibia, au calcaneum et aux vertèbres cervicales ont apporté la double preuve d'une irradiation massive de l'organisme et d'une irradiation moindre de l'extrémité céphalique.

Devant un tel bilan dosimétrique et biologique, il apparaîssait évident que le pronostic était extrêmement grave. D'une part, l'irradiation résultante dépassait les 500 rads, d'autre part, l'hétérogénéité de distribution contre-indiquait *a priori* des traitements héroïques tels que la transplantation médullaire. De ce fait, tout devait être mis en œuvre pour la prophylaxie de l'infection, de la dénutrition et de l'hémorragie. En outre, dès ce moment, toute prévision devait être faite pour mettre à disposition immédiate, des traitements hématologiques par transplantation ou par transfusion.

3.2. *Prophylaxie de l'infection.* Devant l'effondrement prévisible des défenses épithéliales, immunologiques et hématologiques de l'individu, tout devait être mis en œuvre pour le soustraire au risque d'infection exogène et pour limiter les risques d'infection endogène.

3.2. 1. *Prévention bactériologique.* La prévention bactériologique a été assurée simultanément par l'isolement absolu du malade et par des désinfections appropriées.

L'isolement du milieu extérieur a été poussé à son maximum, sous triple enceinte; l'installation comprenait:

—un antichambre maintenue stérile par antiseptiques et rayons ultra-violets,

—une chambre stérile à air comprimé et filtre.

À l'intérieur de cette chambre, un caisson en matière plastique, construit par la Section de Protection contre les Radiations de Fontenay-aux-Roses, et soumis à une légère surpression est muni d'un filtre, de gants de manipulation, d'un sas pour la nourriture et d'un sas pour l'accès du personnel médical. Tous les objets, médicaments et nourriture, pénétrant dans l'antichambre étaient préalablement stérilisés. Les visites étaient rigoureusement interdites, le personnel infirmier et médical pénétrant et séjournant le moins possible: de toute façon, il subissait une désinfection préalable, revêtait deux cagoules successives et pénétrait dans deux sas constitués par l'antichambre et le sas du caisson. En outre, la literie était stérile et les parois internes du caisson nettoyées chaque jour par antiseptiques.

Par ailleurs, le patient subissait, chaque jour, pendant au moins une heure, un nettoyage minutieux, par solution antiseptique, de la totalité de sa peau. Une attention toute particulière était apportée au nettoyage de la bouche, du nez, des yeux, des oreilles, du méat urinaire et de l'anus. De plus, des badigeonnages des cavités aéro-digestives supérieures étaient effectués chaque jour.

Un problème difficile à résoudre a été celui de la limitation de l'infection endogène. Dans ce but, a été prescrite l'administration systématique de mycostatine et de paromomycine en vue de juguler au moins partiellement la flore intestinale.

Sur le plan général, le traitement prophylactique a été complété par l'administration de gammaglobuline.

3.2. 2. *Surveillance bactériologique.* En vue de tester l'efficacité de la prévention bactériologique et de dépister des infections débutantes, une surveillance bactériologique extrêmement stricte a été appliquée représentant finalement plusieurs milliers d'examens. Tous les jours, l'atmosphère de l'antichambre, de la chambre stérile et du caisson d'isolement a été contrôlée au moyen de prélèvements sur boîtes de Petri ainsi que l'état des surfaces au moyen de frottis.

Ces contrôles quotidiens n'ont pas permis de déceler de pollution bactérienne appréciable.

Tous les jours, également, ont été contrôlés bactériologiquement des prélèvements cutanés et muqueux et ont été effectuées des urocultures et des coprocultures. Cette dernière a permis d'établir d'une façon précise la flore intestinale subsistante et d'effectuer les antibiogrammes correspondants.

Il convient de signaler que ces contrôles bactériologiques systématiques ont été complétés au moment de la phase critique par hémocultures et même par examens bactériologiques du liquide céphalorachidien. En outre, le personnel infirmier et médical a été soumis à des examens bactériologiques oropharyngés.

3.3. *Prophylaxie de la dénutrition.* Le syndrome d'irradiation globale aiguë s'accompagne d'une dénutrition importante. Il est nécessaire, dès la phase de latence, de mettre en œuvre un régime permettant de maintenir les équilibres thermiques et nutritifs et même de constituer des réserves en vue de la phase critique. En outre, une surveillance métabolique doit être exercée.

3.3. 1. *Diététique* (tableau 2). Dans le cas présent, l'apport calorique a été de 2000 à 3000 calories par jour. L'apport hydrique était de deux litres par jour. L'équilibre organique a été établi sur les bases d'un apport glucidique et protidique prépondérant et d'un apport lipidique restreint. L'équilibre minéral a été maintenu en fonction des résultats biochimiques.

Tableau 2. Prophylaxie de la dénutrition: diététique

Apport Calorique	2000 à 3000 Cal/j
Apport Hydrique	2 l/j
Apport Glucidique Apport Protidique Apport Lipidique	250 à 350 g/j 100 à 150 g/j 60 à 100 g/j
Apport Minéral	Fonction des concentrations sanguines
Apport Vitaminique	A, B_1, B_4, B_6, C, D, P, PP, K.

Une recharge vitamique complète a été constituée on administrant les vitamines A, B1, B4, B6, C, D, P, PP et K.

3.3. 2. *Surveillance métabolique.* Une surveillance métabolique systématique a été instituée. Elle comportait tout d'abord des test réguliers de digestibilité.

Ainsi que cela a été exposé dans l'observation clinique, l'étude des constantes biochimiques, sanguines et urinaires a été régulièrement effectuée en particulier en ce qui concerne le métabolisme protidique et minéral.

3.4. *Prophylaxie de l'hémorragie.* La prophylaxie de l'hémorragie réclame la mise en oeuvre d'abord d'une surveillance stricte, ensuite d'une prévention appropriée.

3.4. 1. *Survéillance de l'hemorragie.* La surveillance des signes hémorragiques a été mise en place dès la période de latence et poursuivie pendant toute la période critique. Elle comportait les examens cliniques habituels:

—dépistage de pétéchies cutanées ou muqueuses,

—signe du lacet,

—etc. . . .

Au niveau du tube digestif, l'examen systématique des selles par gammaspectrométrie permettait, après injection de Fer 59 de détecter des hémorragies de l'ordre de 50 cm^3.

L'examen cytologique urinaire a été réalisé quotidiennement. Enfin, ont été effectués sur él plan hématologique, des examens thromboél astographiques quotidiens, l'étude des divers facteurs de la coagulation et l'estimation de l'activité fonctionnelle des thrombocytes.

3.4. 2. *Prévention de l'hémorragie.* La prévention de l'hémorragie a comporté:

—une alimentation fluide dès que nécessaire,

—un surcharge en vitamines antihémorragiques,

—l'administration prophylactique d'acide ϵ—aminocaproïque.

3.5. *Prophylaxie de l'aplasie médullaire.* La prophylaxie de l'aplasie médullaire a été basée sur la surveillance hématologique et les prévisions thérapeutiques.

3.5. 1. *Surveillance hématologique.* La surveillance hématologique a été organisée de façon à fournir des informations complètes, fréquentes et contrôlées.

Ainsi que cela a été exposé dans l'observation clinique, l'évolution hématologique a été suivie en ce qui concerne les différentes lignées cellulaires sanguines, les différents territoires médullaires et par l'incorporation de Fer 59. La fréquence des examens a été au moins quotidienne et à certaines périodes multi-quotidiennes. Les examens ont été effectués simultanément dans

deux laboratoires différents et parfois dans trois afin d'exercer un contrôle strict. De toute façon, une planification très minutieuse des prélèvements sanguins et l'utilisation de micro-méthodes ont permis d'effectuer des milliers d'examens hématologiques et biochimiques avec une soustraction totale de 1 litre de sang en en deux mois.

3.5. 2. *Prévisions thérapeutiques.* Compte tenu du bilan dosimétrique et biologique, la phase de latence a été mise à profit pour la prévision des traitements hématologiques éventuels qu'il conviendrait d'instituer à la phase critique. Le premier souci a été d'effectuer le groupage sanguin du patient d'une façon extrêmement détaillée et dans deux laboratoires différents. Le phénotype a été établi concernant les systèmes A.B.O., MNS, P, RH, Kell, Lewis, Duffy, Kidd et Lutheran (Tableau 3). Toutes les démarches ont été effectuées auprès des organismes compétents pour faire effectuer dans les heures qui suivraient la demande, des différentes transfusions sanguines éventuelles. Pour le sang total, les donneurs aussi voisins que possible avaient été sélectionnés. En ce qui concerne l'obtention de concentrés d'érythrocytes, de thrombocytes et de granulocytes, la possibilité de l'obtention présentait un degré croissant de difficultés. En effet, sont nécessaires:

—pour les érythrocytes 4 donneurs,

—pour les thrombocytes 12 donneurs,

—pour les granulocytes 60 donneurs.

Ceci explique que certaines de ces transfusions particulières ne pouvaient être envisagées que sur des indications thérapeutiques impérieuses. Enfin, tout avait été prévu pour des greffes éventuelles de moelle osseuse. Étant donné que le patient appartenait à une famille nombreuse de 6 enfants, le groupage sanguin de ses ascendants et collatéraux a été effectué (tableau 3). Il a permis de mettre en évidence la possibilité d'utiliser, comme donneurs extrêmement voisins, le père et les deux frères. Quelques donneurs supplémentaires n'appartenant pas à la famille avaient été sélectionnés.

3.6. *Conditionnement psychique.* La phase de latence, sans être caractérisée par l'euphorie, peut être considérée comme n'entraînant aucune inquiétude chez le patient.

Par contre, dès les premières manifestations de la phase critique, on est en droit de s'attendre à un effondrement psychologique, compte tenu du caractère de l'affection. Aussi, le conditionnement psychique du malade a-t-il été préparé dès la phase de latence. On a tenu essentiellement à assurer sa distraction au moyen des émissions radiophoniques et de la télévision. La lecture a été proscrite du fait de l'impossibilité d'obtenir une stérilité convenable du document. En outre, le patient a pu converser à distance avec sa famille, ce qui a été, pour lui, un soutien moral considérable.

Tableau 3. *Groupage sanguin de la famille*

Date de naissance	Père 24.4.09	Mère 16.6.11	Sœur n°1 4.11.30	Sœur n°2 7.9. ?	Sœur n°3 7.10.35	Frère n°1 3.3.42	Frère n°2 30.4.47	Malade
Systemes								
A.B.O.	A_2	O	O	O	O	A_2	A_2	A_2
MNS	M/Ss	N/Ss	MN/Ss	MN/Ss	MN/Ss	MN/Ss	MN/Ss	MN/Ss
P	P_2	P_2	P_2	P_2	P_2	P_2	P_2	P_2
RH	CCD.ee	CcD.ee	CCD.ee	CcD.ee	CcD.ee	CdD.ee	CcD.ee	CCD.ee
Kell	K−	K−	K−	K−	K−	K−	K−	K−Kpa
Lewis	Le(a−b+)	Le(a−b+)	Le(a−b+)	Le(a−b+)	Le(a−b+)	Le(a−b+)	Le(a−b+)	Le(a−b+)
Duffy	Fy(a+)	Fy(a+)	Fy(a−)	Fy (a−)	Fy(a+)	Fy(a−)	Fy (a+)	Fy(a+)
Kidd	Jk(a−)	Jk(a+)	Jk(a−)	Jk(a−)	Jk (a−)	Jk(a+)	Jk(a+)	Jk(a+)
Lutheran	Lu(a−)	Lu(a−)	Lu(a−)	Lu(a−)	Lu(a−)	Lu(a−)	Lu(a−)	Lu(a−)

Prof. P. Moureau.

Les médications myélotoxiques n'ont, cependant, été utilisées qu'à la demande, à la phase critique.

3.7. *Télésurveillance continue.* La phase de latence a également été mise à profit pour mettre en place une télésurveillance continue. Celle-ci consistait dans la possibilité de conversations par interphone et de surveillance visuelle par télévision. Par ailleurs, pouvaient être enregistrés à distance:

—la température ambiante, la respiration, la température du malade, le pouls et la tension artérielle, l'électrocardiogramme et l'électroencéphalogramme.

Les examens radiographiques pouvaient être effectués dans l'antichambre au travers de la chambre et du caisson stériles. Enfin, la totalité des informations était répercutées à distance sous la surveillance jour et nuit du personnel infirmier. Le dispositif avait un système d'alarme préréglé sur des seuils concernant respectivement la température, le pouls et la respiration.

4. *Traitement au cours de la phase de crise*

4.1. *Principe d'action thérapeutique.* Au moment où la télésurveillance continue a donné l'alarme pour la première manifestation critique, les traitements prophylactiques envisagés jusqu'ici devaient faire place au traitement héroïque. Ceci devait permettre de compenser dans les meilleurs délais les différents troubles se manifestant. Mais, de toute façon, des questions extrêmement angoissantes d'indications thérapeutiques devaient se poser pendant les semaines de la phase de crise.

Le premier principe de notre action thérapeutique a été d'envisager le minimum d'interventions.

"Primum non nocere" dit le vieil adage médical mais, en outre, cette prudence thérapeutique devait également permettre a posteriori d'interpréter bien plus facilement l'évolution des phénomènes. Notre deuxième principe d'action thérapeutique a consisté à adapter d'une façon aussi étroite que possible le traitement aux manifestations. Il s'est donc agi, dans tous les cas, de traitements focalisés sur des objectifs extrêmement précis.

4.2. *Traitement du syndrome fébrile.* Le syndrome fébrile s'est manifesté brutalement au 21ème jour et a persisté sous forme d'une hyperthermie permanente entre 38 et 40°C pendant 4 semaines (Fig. 1). Il convient de rappeler que les deux premières semaines du syndrome fébrile ont coïncidé avec la crise hématologique alors que les deux dernières ont suivi la restauration hématologique.

Cette manifestation pose évidemment de nombreux problèmes pathogéniques concernant l'hyperthermie qui peut être d'origine infectieuse, toxique, métabolique, etc. . . . De fait, la distribution des doses reçues au niveau de la moelle et au niveau des viscères peut conduire à l'hypothèse que le syndrome fébrile a été en relation avec trois types de phénomènes:

—manifestations cataboliques générales,

—syndrome hématologique,

—syndrome viscéral.

En effet, les doses absorbées au niveau de la cavité abdominale sont de l'ordre de 600 à 800 rads et les portions terminales de l'intestin ont subi des irradiations dépassant 1000 rads. Bien que les hémocultures soient restées négatives et qu'aucune hémorragie intestinale n'ait été décelée, il est vraisemblable que des passages toxiques et bactériens se soient produits sans aboutir à un état septicémique. Ce sont ces considérations qui nous ont guidés dans les indications thérapeutiques pour le syndrome fébrile.

Les moyens de traitement utilisés ont consisté, tout d'abord, dans la réfrigération par abaissement de la température ambiante et par couverture de glace sur le patient. Nous n'avons utilisé ni les antipyrétiques, ni l'hibernation, les médications possibles présentant un caractère trop myélotoxiques. Les antalgiques et les tranquilisants ont été utilisés sous forme de valium et de palfium. Il n'y a pas eu d'administration de corticoïde. Le gros problème a été celui de l'utilisation des antibiotiques. Dès les manifestations fébriles initiales extrêmement violentes avec état comateux et malgré la réponse négative de trois hémocultures, en 6 heures, le traitement antibiotique a été institué.

Le choix des antibiotiques a été déterminé par les antibiogrammes utilisés sur la flore intestinale stabilisée (Tableau 4). Le spectre était couvert par l'emploi de colimycine et de virgimycine. Ces deux antibiotiques ont été administrés à

Tableau 4. *Traitement du syndrome infectieux*

Candida	*Mycostatine* +
Enterocoque	*Virgimycine* +
Staphylocoque	*Virgimycine* + Pristinamycine + Erythromycine + Terramycine + Spiramycine +
Citrobacter	*Colimycine* + Streptomycine + Gentamycine + Acide nalidixique (Negram) + Tetracycline + Chloramphénicol + Kanamycine −
E. Coli	*Colimycine* + Streptomycine − Gentamycine + Acide nalidixique (Negram) + Tetracycline − Chloramphénicol − Kanamycine −

Dr. Y. Chabbert.

doses massives et ce, pendant 4 semaines jusqu'à la fin du syndrome fébrile.

4.3. *Traitement du syndrome hématologique.*

4.3. 1. *Bases cliniques et dosimétriques.* Le syndrome hématologique a, de fait, débuté dès le jour de l'irradiation. Ses manifestations ont atteint un caractère éminemment critique à la fin de la troisième semaine et au début de la quatrième (cf. § 2). En ce qui concerne les granulocytes (Fig. 4):

—leur nombre absolu est resté inférieur à la normale du 3ème au 31ème jour,

—environ 1000 du 20ème au 25ème jour, avec un minimum de 14 mm³ au 21ème jour.

Les thrombocytes sont tombés (Fig. 8):

—au-dessous de 100.000 du 6ème au 33ème jour,

—au-dessous de 50.000 du 13ème au 31ème jour,

le minimum étant de 14.000 le 23ème jour.

À ces constatations cliniques, venaient s'ajouter les résultats dosimétriques. Ceux-ci se caractérisaient par une irradiation médullaire théorique de 550 rads et par une distribution hétérogène, avec un minimum de 2 à 300 rads au niveau de la tête, un maximum de plus de 4000 rads au niveau du pied gauche, et une irradiation pondérée prépondérante au niveau du bassin de 600 à 700 rads (cf. § 4.3).

4.3. 2. *Transplantation médullaire.* Sur les bases dosimétriques et cliniques précédentes, le problème essentiel qui se posait était celui d'une transplantation médullaire.

La dose médullaire théorique de 550 rads correspondait à une indication de greffe médullaire. Par contre, l'hétérogénéité de distribution et le sous-dosage relatif à moins de 300 rads de la moelle osseuse cervicale et céphalique contre-indiquaient, pour des raisons de conflit immunologique éventuel, la greffe médullaire.

Ce même sous-dosage laissait un léger espoir de restauration spontanée à partir des cellules souches survivant dans ces territoires. Aussi la décision a-t-elle été prise de prévoir une transplantation médullaire mais de ne l'effectuer que comme ultime ressource en cas de non restauration spontanée au cours de la 5ème semaine.

1.3. 3. *Transfusion sanguine.* Les indications de transfusion sanguine étaient conditionnées par la nécessité de conserver intactes les chances de succès d'une transplantation médullaire. De ce fait, devait être évitée, dans toute la mesure du possible, toute perturbation hématologique extérieure. Ceci a conduit à écarter les transfusions de sang total et à leur substituer, soit des injections de plasma, soit des transfusions de concentrés cellulaires. Les indications de transfusion de concentrés érythrocytaires étaient fondées sur l'apparition de signes d'anoxie cardiaque ou cérébrale.

Les indications de transfusion thrombocytaire reposaient sur l'apparition de signes manifestes d'hémorragie.

Les indications de transfusion de concentrés granulocytaires étaient liées à l'apparition d'un état septicémique impossible à juguler par les antibiotiques.

Seules, les transfusions de concentrés érythrocytaires ont dû être effectuées à l'apparition de signes manifestes d'anoxie cardiaque au cours de la 5ème semaine.

5. *Traitement au cours de la phase de rémission*

La phase de rémission a commencé la 3ème semaine, à la fin du syndrome fébrile. De fait, il ne s'est pas agi cliniquement d'un retour complet à la normale mais un état sub-fébrile aux environs de 38°C a persisté. Il était, selon toute vraisemblance, lié à l'évolution des radiolésions du pied et de la jambe gauches dont l'observation clinique et le traitement sont présentés ultérieurement (Section III).

Sur le plan général, la conduite thérapeutique, au cours de la phase de rémission a eu pour premier objectif de ramener le patient à des conditions normales d'existence. Elle a eu pour second objectif de le maintenir, toutefois, dans des conditions particulières du fait de l'évolution du syndrome d'irradiation locale du membre inférieur gauche.

C'est ainsi que le séjour sous triple enceinte a été maintenu pour assurer une asepsie complète des plaies cutanées.

Le retour à l'ambiance bactériologique normale ne s'est effectué que par paliers:

—sortie du caisson avec maintien en chambre stérile,

—sortie de la chambre stérile et,

—retour en Belgique.

Dans le domaine de la diététique, le régime alimentaire maintenu stérile pendant les phases de latence et de crise a cessé de l'être à la fin du 2ème mois; en même temps, un régime de suralimentation était instauré.

Le conditionnement psychique a été spontanément amélioré du fait de la prise de conscience par le patient de sa restauration générale. Toutefois, l'évolution douloureuse des radiolésions cutanées du membre inférieur gauche a nécessité la continuation du programme de distraction.

En outre, l'autorisation des visites familiales a été d'un appoint notable.

III. RADIOLÉSIONS DU MEMBRE INFÉRIEUR GAUCHE ÉTUDE CLINIQUE ET THÉRAPEUTIQUE

Lors de l'accident du 30 décembre 1965, la victime a subi une irradiation dont les exposés précédents ont précisé les circonstances et la dosimétrie.

Rappelons brièvement que les reconstitutions de l'accident ont révélé que la dose reçue part d'un maximum de 5.000 rads au niveau de l'avant pied et des orteils pour passer à 3.000 au niveau du torse, à 2.000 au niveau des chevilles, à 1.200 au niveau du pubis et décroître enfin en allant de bas en haut, d'avant en arrière et de gauche à droite pour atteindre 150 rads dans la région occipitale.

Il fallait s'attendre en conséquence à ce que le syndrome irradiatif général se complique à plus ou moins brève échéance d'une radionécrose très sévère au niveau du pied gauche.

Le patient a signalé qu'au moment de l'accident il a éprouvé très nettement une sensation de chaleur au niveau du pied et de la jambe gauches. Ce phénomène ne serait pas explicable uniquement par la température du réacteur, et en ce cas, il revêt un intérêt particulier en ce sens qu'il représente une sensation subjective directe du rayonnement.

1. *Evolution Clinique*

L'évolution totale du syndrome local a pris dans la phase aiguë que nous décrivons ici environ trente semaines.

L'érythème discret qui s'est montré vers la fin de la première semaine au niveau du pied et de la jambe s'accentue au cours de la seconde semaine en même temps qu'apparaissent l'épilation de la jambe et une première phlyctène au bord interne de la voûte plantaire.

Pendant la troisième semaine alors que les phlyctènes s'étendent depuis les orteils jusqu'aux malléoles on voit survenir l'œdème et les douleurs.

Au cours des semaines 4 et 5, les phlyctènes vont confluer, s'ouvrir en laissant échapper une sérosité claire et finalement se détacher pour laisser le derme à nu sur toute la face inférieure du pied jusqu'au talon.

La 6ème semaine est marquée par l'extension des phlyctènes à la face supérieure du pied dans son tiers antérieur; la chute des ongles 2 et 5 alors qu'une réépidermisation s'amorce au niveau des chevilles et de la voûte plantaire.

Les quatre semaines suivantes voient s'arrêter progressivement la réépithélisation pendant que les parties dénudées se couvrent d'une substance de consistance relativement résistante, de 1 à 2 mm d'épaisseur et d'aspect blanc laiteux qui se renouvelle aussitôt qu'on l'enlève. L'examen histologique de cette substance montre des tissus ayant subi une nécrose coagulante sans structure apparente, limitée en bordure par un exsudat formé de polynucléaires.

Vers la 11ème semaine, le tableau se présente comme suit: le pied est oedématié, recouvert sur la face inférieure et son tiers supéro-antérieur de la substance décrite plus haut qui englobe également les orteils. L'œdème de la jambe a régressé ainsi que l'érythème. A partir de ce moment, l'évolution torpide se poursuivra à un rythme ralenti pendant que les douleurs vont en progressant.

La sécrétion muqueuse recouvrant le pied, l'oedème du pied, de la jambe et de la cuisse et surtout la douleur évoluent par poussées successives de durée variable et d'intensité croissante.

Au cours de la 16ème semaine, le patient dont l'état général est très satisfaisant sera transféré dans le Service de Chirurgie du Professeur Morelle à l'Université de Louvain.

Pendant les semaines suivantes, l'œdème et l'érythème de la jambe et de la cuisse s'accentuent pendant que l'état du pied se dégrade progressivement présentant à côté d'hyperkératoses et de télangiectasies, de véritables zones de nécrose mettant à nu les articulations des orteils. Les douleurs sont difficiles à supporter malgré les analgésiques.

Une sympathectomie lombaire est effectuée au cours de la 24ème semaine. À la suite de cette intervention, la douleur semble changer d'aspect, devenant plus superficielle mais tout aussi aiguë. Par contre, l'œdème régresse rapidement tant au niveau de la jambe que de la cuisse, au point que la jambe gauche est nettement plus mince que la droite. Les tissus deviennent flaccides et pâles; quant aux lésions du pied, elles ne semblent pas être influencées par ce traitement.

Devant cette évolution torpide de la nécrose et la douleur insupportable au point que l'état général du malade recommence à décliner, il a fallu procéder à l'amputation au cours de la 25ème semaine.

L'état général semble avoir reçu un coup de fouet favorable après cette intervention. Au bout de deux semaines, les douleurs de projection ont pratiquement disparu; l'appétit et le sommeil reviennent et le malade reprend du poids très rapidement.

La plaie suinte pendant quelques jours; un liquide d'apparence purulente mais stérile à l'examen et à la culture s'écoule encore pendant 2 à 3 semaines. La remise en traction et l'administration de protéines humaines au cours de la semaine 28 remettent les choses dans l'ordre. Les injections de padutine sont arrêtées et au cours de la trentième semaine le malade rejoint son domicile après avoir déjà entamé sa rééducation motrice.

2. *Examens complémentaires*

2.1. *Examens radiographiques.* Les radiographies ont été faites à des intervalles réguliers. À la 6ème semaine, elles montrent un tissu osseux sans altération nette visible. À la 8ème semaine, on voit des décalcifications microgéodiques à l'extrêmité du pied gauche.

Les images prises ultérieurement montrent

l'aspect paradoxal d'une structure osseuse qui se détériore progressivement à droite alors qu'elle semble bien conservée à gauche.

M. Lacroix a interprété ces images comme celles d'un os sidéré n'ayant plus aucune vitalité et en tout cas aucun métabolisme calcique.

2.2. *Examens thermiques.* La thermographie effectuée au cours de la 1ère semaine n'a rien révélé de particulier si ce n'est peut être une légère hypothermie à gauche.

La thermométrie cutanée effectuée fin juin montre des valeurs égales à gauche et à droite sauf pour la zone du mollet et du coup de pied gauche où la température est inférieure de 2 à 3 degrés à celle de la région opposée.

2.3. *Examens électrologiques.* L'examen électromyographique effectué le 17 juin a montré à la contraction des tracés typiquement myogènes. Au repos, on détecte une activité de type neurogène. Les tracés myogènes ressemblent à ceux détectés dans les myodystrophies, notamment des potentiels finement dentelés à pointes brèves d'amplitude abaissée. Ceci correspond à une atteinte de la fibre musculaire même, en opposition avec les affections neurogènes où des unités entières sont éliminées. La détection de potentiels fibrillaires de type neurogène dans plusieurs muscles plaide pour une dénervation de plusieurs fibres musculaires. Le grand intérêt de cet examen a été de révéler en face des lésions nettes de la jambe un état fonctionnel relativement normal des muscles de la cuisse.

2.4. *Examens postopératoires.* Parmi les examens postopératoires, signalons que l'examen histologique se poursuit actuellement. Nous n'avons pas encore tous les renseignements dont nous souhaiterions disposer. Nous espérons pouvoir établir la corrélation entre la dose et les dégâts tissulaires.

Une artériographie pratiquée sur la pièce a montré que les artères principales étaient dégagées. Enfin, une étude approfondie des lésions osseuses est actuellement en cours dans le laboratoire du Prof. Lacroix à Louvain.

3. *Conduite thérapeutique*

3.1. *Informations de base.* La conduite thérapeutique a été dominée par les informations dosimétriques et l'évolution clinique.

Lorsqu'on a été informé après reconstitution de l'accident, des doses absorbées au niveau du pied et de la jambe, comprises entre 2.000 et 5.000 rads et leur répartition pratiquement homogène, il est apparu clairement que la probabilité de restauration spontanée au niveau du pied était quasi nulle et au niveau de la jambe fortement compromise.

L'évolution clinique est venue confirmer tout au long des semaines les prévisions basées sur la dosimétrie tant en ce qui concerne les lésions cutanées que les lésions profondes musculaires, vasculaires et osseuses. L'étude de la pièce opératoire est venue apporter une ultime information sur le bien-fondé des observations précédentes.

3.2. *Indications therapeutiques.* Les indications thérapeutiques ont été posées compte tenu des informations de base précédentes et dans un esprit éminemment conservatif.

Le premier objectif était la prophylaxie contre l'infection et toute agression externe, afin de permettre une observation des lésions cutanées aussi pure que possible et d'éviter toute complication, perturbation ou aggravation.

Le deuxième objectif était d'épuiser toutes les possibilités du traitement médical, en particulier par administration de produits nouveaux tels que la Padutine.

Le troisième objectif était de ne recourir aux interventions chirurgicales qu'en cas de nécessité et en commençant par les moins mutilantes, c'est ainsi que s'est successivement posée la question de la sympathectomie lombaire, des greffes cutanées, de l'amputation au niveau du pied, de la jambe et au niveau de la cuisse.

3.3. *Traitements effectués.* De fait, comme on s'y attendait, on a été contraint d'aboutir finalement à l'amputation haute au niveau de la cuisse.

Mais on n'a été conduit à celle-ci qu'après avoir épuisé toutes les autres possibilités thérapeutiques.

3.3. 1. *Traitement prophylactique.* Le traitement prophylactique a consisté essentiellement dans la prévention de l'infection. Celle-ci a été assurée par la mise du patient dans un caisson stérile même après la restauration du syndrome de l'irradiation globale aiguë.

Elle a été complétée par une toilette bi-quotidienne des lésions cutanées à l'aide de sérum physiologique de pulvérisation à la Néomycine et d'application de gaze imprégnée.

Un contrôle bactériologique systématique et quotidien a permis d'éviter toute pollution microbienne.

3.3. 2. *Traitement médical.* Le traitement médical a constitué en des injections de Padutine. Celles-ci ont débuté aussitôt après que le danger d'hémorragie dû au syndrome général ait semblé écarté et que la tension artérielle soit revenue à une valeur presque normale. Les injections ont été poursuivies même au-delà de l'amputation à titre préventif de l'altération du moignon. Si la padutine a obtenu des succès remarquables dans certaines radionécroses, il semble que ce soit dans des irradiations par rayonnements mous ou moyennement durs maintenant en profondeur le substratum relativement sain.

Dans le cas présent où l'extrémité inférieure du membre gauche a été prise en masse par des rayonnements pénétrants, son effet n'a pas eu la possibilité de se manifester.

Le deuxième aspect du traitement médical est celui du traitement de la douleur; malgré les antalgiques les plus puissants renouvelés jusqu'à 5 fois au cours d'une même nuit, il s'avérait impossible de supprimer une douleur qui compromettait l'appétit, le sommeil et même le repos, ayant pour corollaire une dégradation progressive de l'état général.

3.3. 3. *Traitement chirurgical.* Le premier traitement chirurgical qui s'est imposé a été celui de la douleur par sympathectomie lombaire. La sympathectomie a modifié l'aspect de la douleur. La douleur profonde paroxystique a fait place à une douleur plus superficielle, continue mais tout aussi aiguë. Par contre, l'érythème et l'œdème de la jambe et de la cuisse ont régressé en quelques jours montrant brusquement l'atrophie quasi totale des muscles de la jambe. Aussitôt après est apparue une escarre nécrotique au niveau du mollet, à l'endroit sur lequel reposait la jambe posée en porte-à-faux en raison des lésions du talon. Pour lutter contre les douleurs, il restait éventuellement à envisager la névrotomie qui laisse malheureusement souvent des séquelles sensitives et même motrices. Les greffes cutanées en vue de parfaire la restauration incomplète au niveau du pied ont été envisagées à un certain moment; elles n'ont pas été exécutées puisque le substratum ne permettait sûrement pas leur conservation et, peut-être, pas même leur prise.

La seule solution restait l'amputation. Vu la nécessité de pouvoir intervenir à une hauteur où le tissu de recouvrement permette d'envisager une cicatrisation normale, il a fallu fixer le niveau de section à mi-cuisse. Les examens cliniques et l'électromyographie ont permis de considérer cette zone qui a cependant reçu 1.500 rads environs, comme relativement normale du point de vue fonctionnel et tégumentaire. Les examens histologiques dont nous disposons actuellement ont confirmé le bien-fondé de cette hypothèse. La cicatrisation relativement ralentie de la plaie peut être due à l'oedème encore présent au moment de l'intervention. De plus, à ce moment, les protéines sanguines qui avaient cependant été relevées par plusieurs injections de protéines humaines atteignaient encore un niveau assez bas. Nous avons vu que l'administration de protéines humaines et la remise en traction ont été suivies d'une cicatrisation complète. Actuellement, le moignon est sain et l'état général semble excellent au point que le patient a même dépassé son poids normal avant l'accident et qu'il se déplace avec facilité à l'aide de béquilles en attendant de recevoir sa prothèse.

Cette conduite thérapeutique aboutissant à une amputation haute a été finalement parfaitement acceptée par le patient qui a compris que l'on avait auparavant épuisé toutes les autres possibilités de traitement.

CONCLUSION

L'observation clinique et le traitement de la personne ayant subi cette irradiation accidentelle, offrent un grand intérêt à de nombreux points de vue.

Dans le domaine de la dosimétrie, il a été possible, par des études poussées et par reconstitutions successives de l'accident, d'acquérir des notions précises sur les doses absorbées. La première constatation est celle de l'importance de l'irradiation globale de l'ordre de 500 rads en moyenne et de la sur-exposition locale du pied gauche atteignant 5.000 rads. Une deuxième constatation aussi importante est celle de l'hétérogénéité de distribution spatiale des doses absorbées allant de 200 à 300 rads à la tête à plus de 1.000 rads au pubis. Il en est

résulté la nécessité d'une interprétation dosimétrique biologique, en particulier en ce qui concerne la répartition des doses médullaires; ceci a conduit à l'estimation d'une dose médullaire théorique de 550 rads et d'une dose médullaire équivalente de 400 rads.

Dans le domaine des investigations cliniques et biologiques relatives au syndrome d'irradiation globale, plusieurs observations méritent mention. La phase de crise a été caractérisée par un syndrome fébrile dont la durée a largement dépassé la restauration hématologique et dont l'explication peut être trouvée soit dans un syndrome viscéral soit dans un syndrome toxi-infectieux. Le syndrome hématologique proprement dit a évolué de façon classique; il a pu être étudié dans toute sa pureté du fait de l'absence d'interférences thérapeutiques inadéquates. Sa gravité est apparue comme la plus sévère parmi les observations accidentelles humaines actuellement connues. Parmi les investigations pratiquées, celles qui ont présenté le plus d'intérêt pour l'étude clinique et la conduite thérapeutique ont été: les diverses numérations globulaires sanguines, les ponctions médullaires comparées en différents points du squelette et les transferts moelle-sang par myélémie. Les résultats des nombreux examens biochimiques ont montré l'intérêt que l'on peut attacher à l'élimination des acides aminés. Enfin, l'étude des caryotypes provenant de cultures de cellules sanguines, a mis en évidence de trēs nombreuses modifications chromosomiques; l'analyse quantitative des dicentriques et des cassures a permis d'aboutir, dans les deux cas, à une évaluation de la dose globale moyenne de l'ordre de 500 rads confirmant convenablement les autres données dosimétriques.

Dans le domaine de la conduite thérapeutique, ce cas d'irradiation accidentelle offrait un grand intérêt mais présentait de nombreuses difficultés. En ce qui concerne le syndrome d'irradiation globale aiguë, l'importance des doses reçues le situait dans l'éventail des irradiations létales avec chance de survie inférieure à 50%. L'hétérogénéité de distribution des doses absorbées contre-indiquait, sauf comme ultime recours, toute transplantation médullaire.

Le traitement a reposé, tout d'abord, sur une prophylaxie très minutieuse de la dénutrition, de l'infection et de l'hémorragie, mise en œuvre dès la phase de latence. Pendant la phase de crise, le syndrome fébrile a été traité par administration rationnelle d'antibiotiques. Les seules transfusions pratiquées ont été celles de concentrés d'érythrocytes au 30ème jour devant les signes d'anoxie cardiaque.

Le syndrome de surexposition locale du membre inférieur gauche a présenté plusieurs points d'intérêt. La prophylaxie de l'infection par isolement dans des conditions stériles rigoureuses a permis d'étudier parfaitement l'évolution des lésions cutanées. Le traitement médical à la padutine n'a pu aider à la restauration spontanée du fait de l'importance des doses reçues comprises entre 3.000 et 5.000 rads et du caractère massif de l'irradiation par des rayonnements très pénétrants. Il a été finalement nécessaire de se résoudre à pratiquer une amputation haute à la cuisse en présence de l'évolution nécrotique et des phénomènes douloureux.

Il est un enseignement de caractère général et non le moindre que l'on peut tirer de ce cas d'irradiation accidentelle. C'est l'intérêt de pouvoir effectuer, aussi variés et complets que possible, toutes les études dosimétriques, toutes les investigations cliniques et biologiques et tous les actes thérapeutiques; c'est également la nécessité de disposer d'une équipe cohérente et compétente s'appuyant sur des laboratoires hautement spécialisés. C'est finalement la démonstration de l'efficacité du travail d'équipe et de la collaboration inter-disciplinaire.

REMERCIEMENTS

Les auteurs adressent leurs plus vifs remerciements à toutes les personnes qui, sans compter leur temps, ont apporté leur aide précieuse:

—les laboratoires d'analyses médicales de la Fondation Curie,
—la Section de Protection contre les Radiations,
—le Groupement Technique, et
—les laboratoires du Département de Protection Sanitaire du Centre d'Études Nucléaires de Fontenay-aux-Roses;
—ainsi que tous les laboratoires médicaux ou hospitaliers, français ou étrangers.

DISCUSSION

A. DUNJIC (*Belgique*):

Quels ont été, à part le vomissement, les autres troubles digestifs présentés par la victime?

R. LE GO:

Il y a eu des nausées et vomissements au cours des premières heures de l'arrivée du malade à Paris. Les vomissements se sont calmés au bout de quelques heures. Les nausées ont persisté 24 heures. Puis tous les troubles digestifs se sont amendés définitivement. En particulier, il n'y a pas eu à déplorer d'hémorragie digestive, malgré les doses importantes (600–700 rads) reçues par la partie inférieure de l'abdomen.

M. GIUBILEO (*Euratom*):

Vorrei sapere se è stata studiata l'evoluzione della spermatogenesi ed eventualmente sono stati fatti rilievi di alterazioni cromosomiche delle cellule germinali.

H. JAMMET:

Examens spermatogénèses? Ils ont été faits et ont montré dès la deuxième semaine une disparition des spermatozoïdes. Il n'a pas été fait d'examens cytogénétiques des spermatozoïdes.

THE DETECTION AND MEASUREMENT OF PLUTONIUM CONTAMINATION IN WOUNDS

E. W. JONES and W. N. SAXBY
UKAEA, AWRE, Aldermaston

Abstract—Plutonium is extensively used in atomic research and industry and inevitably there occur wounds and injuries which contain plutonium. Because of its high toxicity it is important to identify, locate and measure any plutonium present. At levels which have medical significance, the quantities involved are minute, but there is sufficient emission of accompanying X- and gamma radiations to permit identification and assay by radiometric techniques.

X-rays in the band 13 to 20 keV, gamma rays of about 60 keV and gamma rays of about 384 keV can all be used for this work: the problems and the limitations associated with measurements in these three energy bands are discussed in the paper, including the usefulness of energy spectrometry to eliminate errors due to self absorption.

There are various instruments available, and usable, for radiometri determinations of plutonium in wounds. Several of these are described with their limitations and detection capabilities.

A case of a contaminated wound is quoted to illustrate some of the techniques and problems in the assessment of plutonium content. Some subsequent work undertaken to improve identification and measurement is also described.

A number of specific actions are suggested, which should be taken, following the occurrence of a wound to ensure that any plutonium present before and after medical treatment is correctly identified and measured.

1. INTRODUCTION

In working with plutonium and its compounds, one route by which radioactive material is accidentally introduced into the body is through minor wounds. These are usually small cuts, punctures and splinters in the hands, caused by objects sharp enough to penetrate through box gloves and through the skin. A few cases have been reported of more serious wounds resulting from accidents in plutonium workplaces. At the AWRE, persons working with radioactive materials are instructed to report all minor injuries which occur in controlled areas. Over a period of 18 months 225 injuries were reported. In 23 cases plutonium contamination was suspected and in 4 of these cases plutonium contamination was confirmed.

The available evidence appears to show that a small fraction of the plutonium injected as metal in minor injuries finds its way into the circulating body fluid within the first few days but most of the material remains at the site of the wound for a long time unless excised or sloughed off with scab.[1] It is generally considered desirable to remove as much as possible of the plutonium from superficial wounds in order to reduce the risk of dispersion in the body and to prevent high dose to local tissue. The maximum permissible body burden of ^{239}Pu when the bone is considered to be the critical organ is only 0·04 μCi (0·64 μg). A single piece of plutonium of this mass has a diameter of only about 40 μm.

There is thus a need to apply suitable radiation measuring techniques to:

(a) confirm and assess the initial contamination,
(b) locate the site of contamination accurately,
(c) demonstrate the success of surgical operations, and
(d) study the fate of any plutonium remaining at the wound site after surgical treatment.

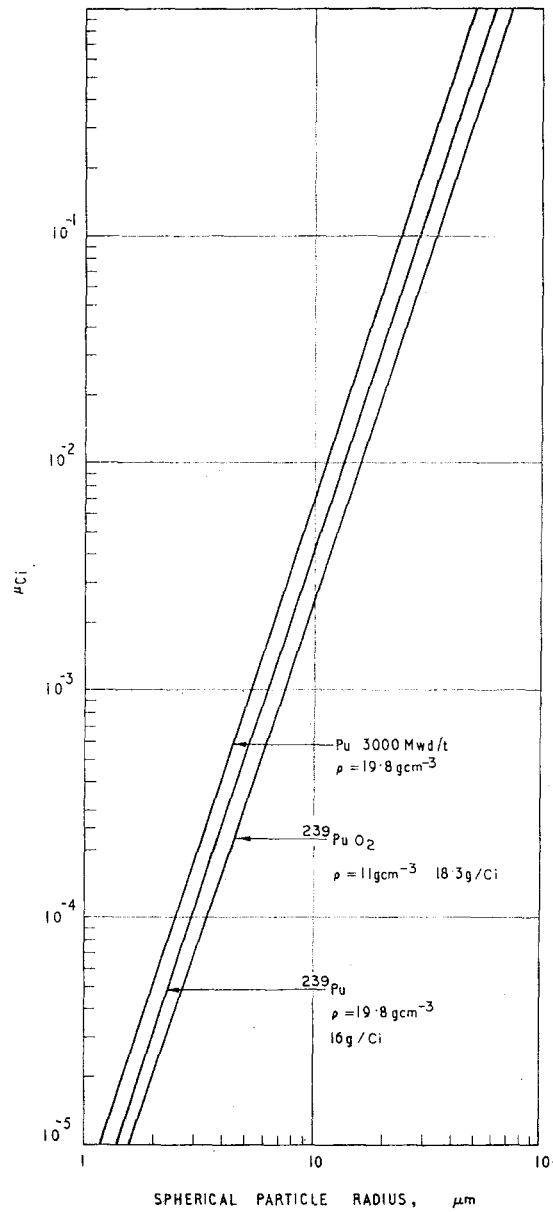

FIG. 1. The radioactivity of spherical particles.

2. MONITORING PRINCIPLES

Personal monitoring for plutonium contamination is usually carried out with a standard alpha particle detector but, owing to the short range of the alpha particles in tissue (about 40 μm), this method will not detect plutonium which has penetrated the outer skin layer or which is covered over with blood. If an alpha probe alone is used to check minor wounds after they have been washed, there is a distinct risk that persons will resume work while still carrying significant contamination below the skin. It has therefore become accepted practice to measure the uranium L X-ray emission at about 17 keV, which follows alpha decay in a small percentage of the disintegrations. Table 1 shows the principal energies and abundance of these emissions for disintegrations of plutonium isotopes and daughter products. The detectors employed are scintillation counters containing thin flat sodium iodide (Tl) crystals covered by aluminium or beryllium foils. These are discussed in more detail below.

Interpretation of the measurements at 17 keV may be complicated by absorption of the X-rays in overlying tissue, by self-absorption in particles of the contaminant, and by the presence of radio-nuclides other than ^{239}Pu which also emit both alpha-particles and X-rays. Tyler[2] has examined the problem of self-absorption for ^{239}Pu in the form of metal and certain compounds. He has shown that, because self-absorption of alpha particles is generally greater than self-absorption of 17 keV X-rays, monitoring with an X-ray probe does not underestimate the potential dose to tissue at the site of the wound but may lead to an underestimate of the amount of plutonium available for transfer to other parts of the body.

In addition to the uranium X-rays there are other penetrating radiations which may be emitted in sufficient quantity to yield useful information; notably the 60 keV gamma-rays of ^{241}Am (daughter of ^{241}Pu) and the 384 keV gamma-rays of ^{239}Pu. The latter are of very low abundance (0·0012%) but in the case of a very severely contaminated wound, could be used to determine an upper limit for the ^{239}Pu content, rapidly and with the minimum uncertainty of interpretation. The practical usefulness of measurements at the different energies is further discussed below.

3. THE TYPES OF MEASUREMENT REQUIRED

3.1. *Initial Monitoring*

Initial monitoring of suspected punctures and other very minor wounds is likely to be carried out, after washing, at the place of work or at the nearest health physics office, using a portable

Table 1. *Principal X- and γ-rays accompanying Disintegrations of Plutonium Isotopes.*

Isotope	Half-life (days)	α particles per sec per g of Pu isotope	No. of photons emitted per alpha particle emission					
			12–14 keV	17–18 keV	20–21 keV	52–65 keV	100 keV	384 keV
^{238}Pu	$3{\cdot}3 \times 10^{4}$	6×10^{11}		$13{\cdot}5 \times 10^{-2}$			$8{\cdot}4 \times 10^{-5}$	
^{239}Pu	$8{\cdot}9 \times 10^{6}$	$2{\cdot}25 \times 10^{9}$	$1{\cdot}3 \times 10^{-2}$	$1{\cdot}9 \times 10^{-2}$	$3{\cdot}15 \times 10^{-3}$	7×10^{-5}	$5{\cdot}2 \times 10^{-5}$	$1{\cdot}2 \times 10^{-5}$
^{240}Pu	$2{\cdot}4 \times 10^{6}$	$8{\cdot}3 \times 10^{9}$		11×10^{-2}				
^{241}Pu	$4{\cdot}8 \times 10$	$9{\cdot}6 \times 10^{7}$					·35	
^{237}U*	6·75		$3{\cdot}55 \times 10^{-2}$	$8{\cdot}15 \times 10^{-2}$	$2{\cdot}6 \times 10^{-2}$	·385	·56	
^{241}Am†	$1{\cdot}7 \times 10^{5}$	$5{\cdot}9 \times 10^{9}$	$14{\cdot}8 \times 10^{-2}$	$19{\cdot}7 \times 10^{-2}$	4×10^{-2}	·38	·315	

* The figures relate to the amount of ^{237}U in equilibrium with 1 g of ^{241}Pu and represent the number of photons per ^{241}Pu alpha emission.
† The figures relate to the amount of ^{241}Am present in 1 g of ^{241}Pu 1 year after separation.

or semi-portable instrument. It is important that contamination under the skin should not be missed at this stage so the monitoring must be performed carefully and slowly, since the count-rates for significant contamination are quite low and the X-ray probes have a sensitive area of only a few square centimetres. Certainty of detection is more important than precision of assessment at this stage and the lower limit of detection for ^{239}Pu ideally should be 0·005 μCi or less. It would assist in ensuring a really adequate check, if the whole hand could be monitored at once in an X-ray monitor for a fixed time interval in much the same way as with a normal α/β hand contamination monitor. No simple version of this appears to have been produced. A well-type phosphor large enough to monitor a whole finger has been tried, but so far, it has not been possible to make an inexpensive detector of this form sufficiently robust and sensitive for general use. Furthermore it would not cope with the small proportion of wounds which occur to the palm of the hand.

3.2. *Accurate Location of Contamination*

When a contaminated wound has been confirmed, it will be referred to the medical officer for treatment. A more precise measurement of the amount and location of the plutonium is now necessary. Accurate location by X-ray measurements is quite difficult because the count-rate per microcurie is very low and any degree of collimation of the detector reduces it still further. It has been found best to mount the detector in a stand about 5 mm above the wound at a point which gives the maximum count-rate and then slide straight-edged or iris-shaped absorbers over the skin, noting the points at which the count rate is sharply diminished.

3.3. *Precise Determination*

In the case of very superficial wounds there is generally no problem about excising the foreign matter. In a more serious case the medical officer may have to balance the desirability of removing all the material, against the possible damage to the individual as a result of surgical operation. In such a case he will require a fairly accurate estimation of the amount of plutonium involved. To achieve this, it is desirable to measure the spectrum of radiation emitted from the wound, and, if possible, obtain a sample of the relevant plutonium from which to prepare a reference source. The reference source should be a thinly deposited source suitable for alpha counting and alpha spectrometry in addition to gamma spectrometry. Corrections can then be made for the presence of isotopes other than ^{239}Pu and for self-absorption.

Any material which is excised from the wound is checked for activity using the X-ray detector. It may then be desirable to retain this material as an aid to further studies.

Finally when the wound has been treated, an attempt should be made to determine an upper limit for the residual contamination. Here again a knowledge of the radiation spectrum can assist towards obtaining a more accurate estimate.

4. INSTRUMENTS AVAILABLE FOR WOUND MONITORING

Several instruments suitable for the detection of X-rays from plutonium have been described.[3-5] The following have been used at the AWRE.

4.1. *Portable Contamination Monitor Type 1320X*

This employs a 55 mm diam. scintillation probe fitted with a sodium iodide phosphor 36 mm diam. × 1·0 mm thick under a 0·05 mm aluminium foil. The probe is coupled to a battery-powered portable ratemeter which, when used in the X-ray monitoring role, has an energy "window" extending from 11 keV to 23 keV approximately. The instrument is designed for general contamination survey duties in the field and has a background count-rate of about 20 counts/min when unshielded. It is used in laboratories for initial checks on suspected skin punctures. Under these conditions, the lower limit of detection is about 0·01 μCi ^{239}Pu. A similar probe gave a background of about 1 count/min in the AWRE low-background facility.[6]

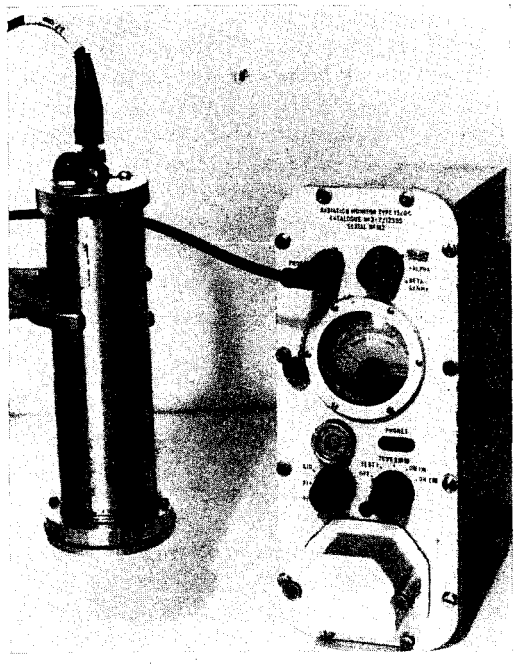

FIG. 2. Portable contamination monitor Type 1320 X.

4.2. *Plutonium Wound Monitor Type PNI 1080**

This instrument employs a 35 mm diam. probe fitted with a sodium iodide phosphor 10 mm diam. × 1·0 mm thick covered with a 0·05 mm aluminium foil. The small, mains-powered ratemeter incorporates an electro-mechanical register for use at low pulse-rates. The circuit has an energy "window" extending from 13 keV to 21 keV approximately. In normal laboratory environments the instrument has a background count-rate of about one count per minute and the lower limit of detection is about 0·005 μCi ^{239}Pu. It is used in our medical and health physics centres for measurement and accurate location of plutonium in wounds.

4.3. *Selective Gamma Monitor Type NIS 322 (Pu)*

In this instrument the scintillation detector, ratemeter and indicator are incorporated in a single pistol-grip unit which can be held comfortably in one hand. In its normal form it employs a phosphor 25 mm thick × 37 mm diam. and is "gated" to accept the 384 keV gamma-rays from ^{239}Pu. The lower limit of detection, in a normal environment is about 500 μCi (about 8 mg) at 5 cm from the end of the detector. Its role in wound monitoring

* Manufactured by Plessey Nucleonics Ltd., Northampton, England.

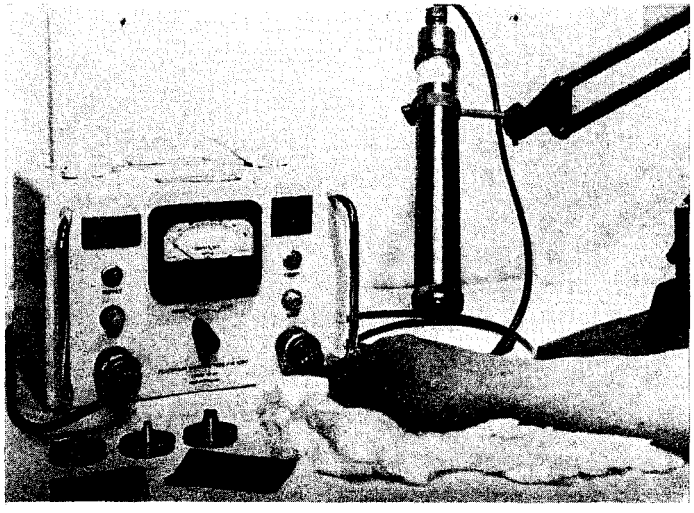

FIG. 3. Plutonium wound monitor Type PNI 1080.

would therefore be confined to a very serious accident where the amount of plutonium involved might imply considerable self-absorption of the low energy X-rays.

Better detection of the 384 keV radiation can be achieved with improved geometry. A 75 mm diam. crystal, having a central well and mounted in a 50 mm lead shield, enabled measurements to be made on a dummy finger, down to 2 μCi ^{239}Pu in a normal laboratory.

Because of the convenient shape and reliable operation of the Selective Gamma Monitor Type NIS 322, an experimental version of it has been constructed for measurements at low energy (Fig. 4). The dimensions of the scintillator and aluminium foil are the same as those of the Probe Type 1320X. The electronic circuit incorporates an energy window which can be switched to either of the ranges:

12 keV–22 keV (for uranium *L* X-rays)
or 48 keV–72 keV (for 60 keV emission from ^{241}Am).

It is hoped that this instrument will replace the Monitor Type 1320X for plutonium X-ray surveys.

4.4. *Use of Multi-channel Analysers*

If one of the thin-crystal scintillation probes is connected to a multi-channel analyser, the energy spectrum from about 12 keV to about 100 keV can be plotted for the radiation from the wound. The presence of ^{241}Am is then revealed by the peak at 60 keV. It may take about 20 min to obtain a useful spectrum so the subject must be positioned comfortably. It is useful to mount the scintillation probe in a simple lead castle into which the hand can be inserted conveniently or to carry out the measurement within a low background facility such as a whole-body counting room.

5. THE EFFECT OF ISOTOPES OTHER THAN ^{239}Pu

If the plutonium has undergone considerable reactor irradiation it will contain, in addition to ^{239}Pu, proportions of the alpha-emitters ^{238}Pu and ^{240}Pu and the beta emitter ^{241}Pu (half-life 13 years). After separation of pure plutonium from irradiated fuel, ^{237}U and ^{241}Am, the daughters of ^{241}Pu, will begin to grow. The short-lived ^{237}U (6·75 days) reaches equilibrium within a few weeks. ^{241}Am (458 years) will increase almost linearly with time for a few years after separation.

The presence of isotopes other than ^{239}Pu increases the alpha emission per gramme of material; however it increases even more the emission of low energy X-rays per gramme of material, so the significance of the X-ray measurements as an indicator of internal radiation hazard changes as high irradiation and long americium growth are attained. Table 2 shows that for plutonium which has undergone irradiation of 3,000 MWd/t followed by one year's

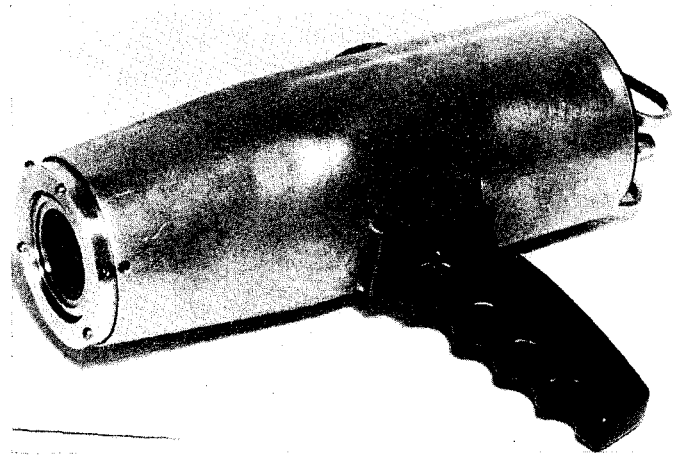

FIG. 4. Prototype of selective gamma monitor Type NIS 322 modified for X-ray monitoring.

Table 2. Emissions from 1 g of Plutonium 1 Year after Separation.

Irradiation / Isotope	500 MWd/t				3000 MWd/t				6000 MWd/t			
	Typical abundance w/o	α/s	*X-rays/s	60 keV γ/s	Typical abundance w/o	α/sec	*X-rays/s	60 keV γ/s	Typical abundance w/o	α/s	*X-rays/s	60 keV γ/s
^{238}Pu	0·0052	3.12×10^{7}	4.2×10^{6}		0·065	3.9×10^{8}	5.2×10^{7}		0·25	1.5×10^{8}	2.1×10^{8}	
^{239}Pu	96	2.15×10^{9}	6.8×10^{7}		82·6	1.86×10^{9}	5.85×10^{7}		69	1.55×10^{9}	4.9×10^{7}	
^{240}Pu	3·8	3.15×10^{8}	3.5×10^{7}		13·7	1.14×10^{9}	1.26×10^{8}		24·5	2.0×10^{8}	2.25×10^{8}	
^{241}Pu	0·22	2.1×10^{5}			3·3	3.15×10^{6}			5·6	5.3×10^{6}		
^{237}U			3.0×10^{4}	8.2×10^{4}			4.5×10^{5}	12.2×10^{5}			7.6×10^{5}	2.1×10^{6}
^{241}Am		1.3×10^{7}	5.2×10^{6}	5.0×10^{6}		1.94×10^{8}	7.7×10^{7}	7.4×10^{7}		3.3×10^{8}	1.32×10^{8}	1.27×10^{8}
Totals		2.5×10^{9}	1.1×10^{8}	5×10^{6}		3.58×10^{9}	3.14×10^{8}	7.5×10^{7}		5.38×10^{9}	6.16×10^{8}	1.3×10^{8}
Total X-rays/α		4.4×10^{-2}				8.75×10^{-2}				11.4×10^{-2}		
Total 60 keV/α		2×10^{-2}				2.1×10^{-2}				2.43×10^{-2}		

*12–21 keV photons.

growth of ^{241}Am, the X-ray measurements may overestimate the alpha hazard by a factor of 2 if the instrument were calibrated with low irradiation plutonium.

The effect of further increases in isotopic content can be determined from the information in Table 1.

6. THE EFFECT OF DEPTH OF PLUTONIUM IN THE WOUND

If the plutonium is injected well below the surface of the skin, the measurements will be affected by absorption of the radiation in the overlying tissue and by the increased distance between source and detector. For minor hand wounds these effects are unlikely to be significant. The X-rays with an average energy of 17 keV have a half-value thickness in tissue of about 7 mm while at 60 keV the half-value thickness is about 35 mm. The geometrical effect is greatest when the detector is placed very close to the skin. Figure 9 shows the effect of separating the source and detector by layers of approximately tissue-like material.

7. EFFECT OF SELF-ABSORPTION IN THE PARTICLES OF CONTAMINANT

Tyler has shown[2] that, if the activity in a wound is concentrated in a single spherical particle, self-absorption of the X-rays may be appreciable for total activities greater than about 10^{-4} μCi ^{239}Pu. When the total activity is about 1 μCi ^{239}Pu, self-absorption may lead to underestimation by an order of magnitude.

Similar calculations have been performed for the 60 keV emissions of ^{241}Am and show (Fig. 5) that self-absorption does not become significant until the single particle size corresponds to about 60 μm diameter (0·1 μCi ^{239}Pu). Hence, if the radiation spectrum from the wound can be plotted so as to include both the X-ray peak and a discernible 60 keV peak, the ratio of these peaks, for a given isotopic composition will indicate the amount of self-absorption. In practice the isotopic composition may not be known, but it may be possible to obtain a sample of the relevant material, from which to prepare a thin source of negligible self absorption. The ratio $\frac{17\text{ keV peak}}{60\text{ keV peak}}$ for the wound spectrum can then be compared with the same ratio for the thin source. Figure 6 shows how the ratio should theoretically be reduced with increasing particle size.

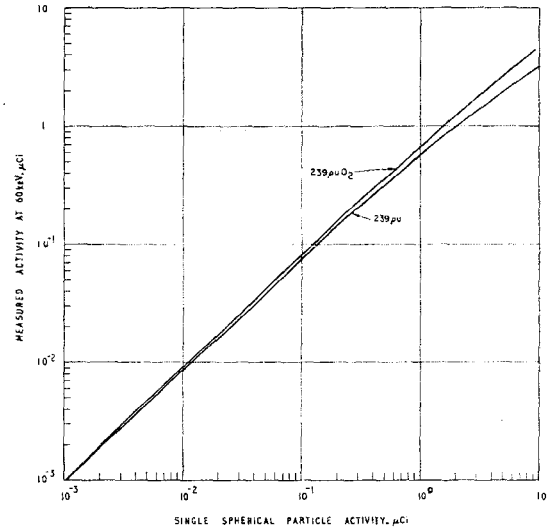

FIG. 5. Correction curves for self-absorption of 60 keV gamma radiation in spherical particles.

8. DESCRIPTION OF A CASE OF A CONTAMINATED WOUND

The following case history of a wound has been selected because it illustrates a number of the points made above.

8.1. *Initial Circumstances*

While manipulating plutonium metal with gloves the subject, "A", received a minor puncture wound close to the finger nail on the side of the middle finger, left hand. By error the hand was monitored only with an alpha probe. This gave a count rate of about 10 counts/s, which was reduced to less than 2 counts/s by washing. "A" then returned to work.

49 days later, on the evidence of urine analysis results, attention was drawn to "A" again and the finger was monitored using X-ray monitors Type PNI 1080 and Type 1320X, both calibrated against a standard plutonium source set in "Perspex". These measurements yielded an estimate of 1.6 μCi of plutonium alpha activity.

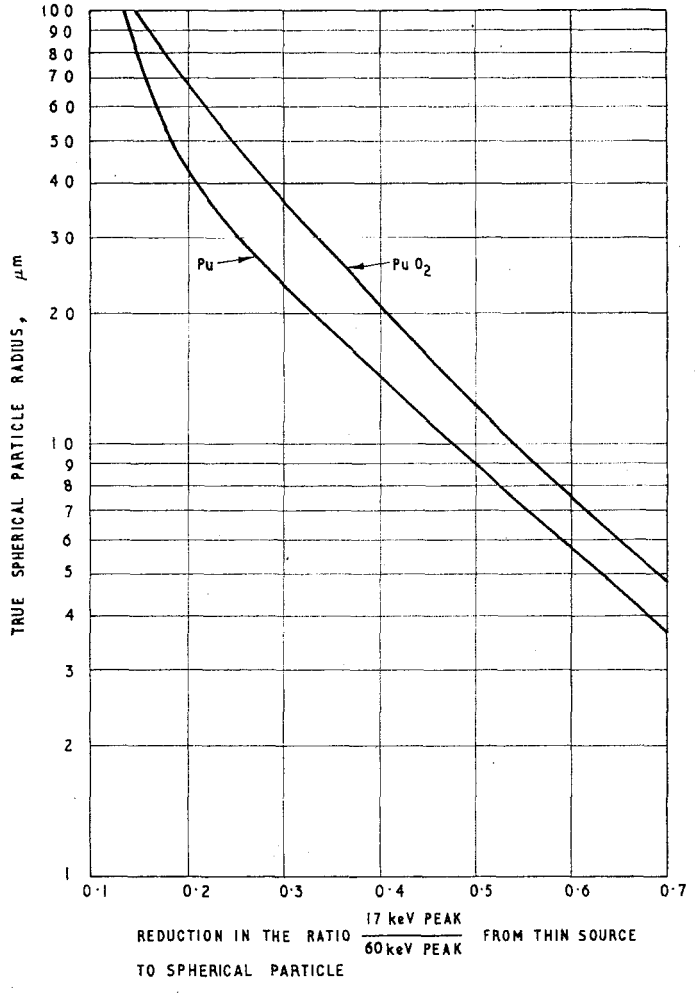

FIG. 6. Theoretical variation in the ratio $\frac{17 \text{ keV output}}{60 \text{ keV output}}$ with particle size.

The activity was then located as accurately as possible using the Monitor Type PNI 1080 with a number of masking devices, and the area was excised until monitoring showed that the contamination had been almost entirely removed.

As much as possible of the excised material, together with swabs, etc. was collected and analysed for plutonium. This measurement showed that at least 1·7 μCi of α activity had been removed from the wound. Monitoring the area of the wound then gave an estimated apparent residual alpha activity of about 0·005 μCi.

8.2. *Second Measurement*

After a further period of 10 months the finger was examined again, this time with a gamma spectrometer comprising a probe Type 1320X coupled to a multichannel analyser. The spectrum obtained is shown in Fig. 7. The ratio $\frac{17 \text{ keV peak}}{60 \text{ keV peak}}$ for this spectrum was very low

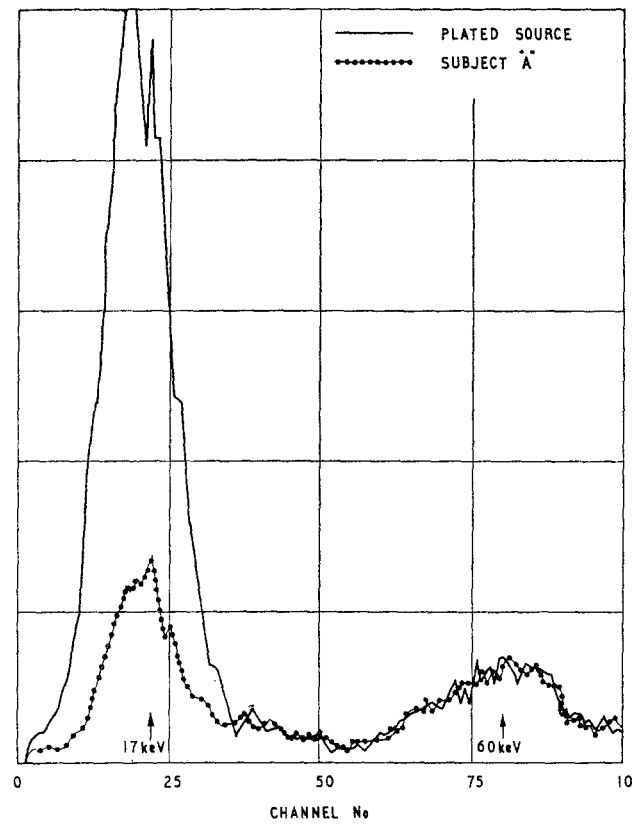

FIG. 7. Spectra from plutonium sources.

in comparison with that for a standard ^{239}Pu source which was used to set up the spectrometer and it was at first suspected that the plutonium in the wound must contain a high percentage of ^{241}Am. A thin electro-deposited source was therefore prepared from some of the material originally excised from "A"s finger. This source was calibrated in an alpha spectrometer giving an alpha activity of 0·023 μCi of which about 3% could be attributed to ^{241}Am. It was then used as a reference source for all future measurements on "A"s finger. The spectrum from the reference source is shown in Fig. 7. It has a much higher 17 keV peak. Comparison of the count-rates in the 17 keV X-ray region yielded an α activity in the finger of about 0·006 μCi, in good agreement with the original estimate. However a comparison at 60 keV indicated 0·022 μCi α activity in the finger. Applying Tyler's correction data for self-absorption in a single spherical particle of plutonium metal to the value at 17 keV, yields 0·020 μCi α activity in agreement with the 60 keV value. The estimate of alpha activity remaining at the wound site was therefore amended to 0·02 μCi approximately. This assessment made no allowance for the self absorption of 60 keV gamma rays nor for the possible effect of depth in the wound.

8.3. *Third Measurement*

The latest measurement on this subject was made 18 months after the original incident, using a similar probe coupled to a multi-channel analyser. Again the spectrum from the wound, after 20 min counting, showed 17 keV and 60 keV peaks and was compared with the spectrum from the reference source.

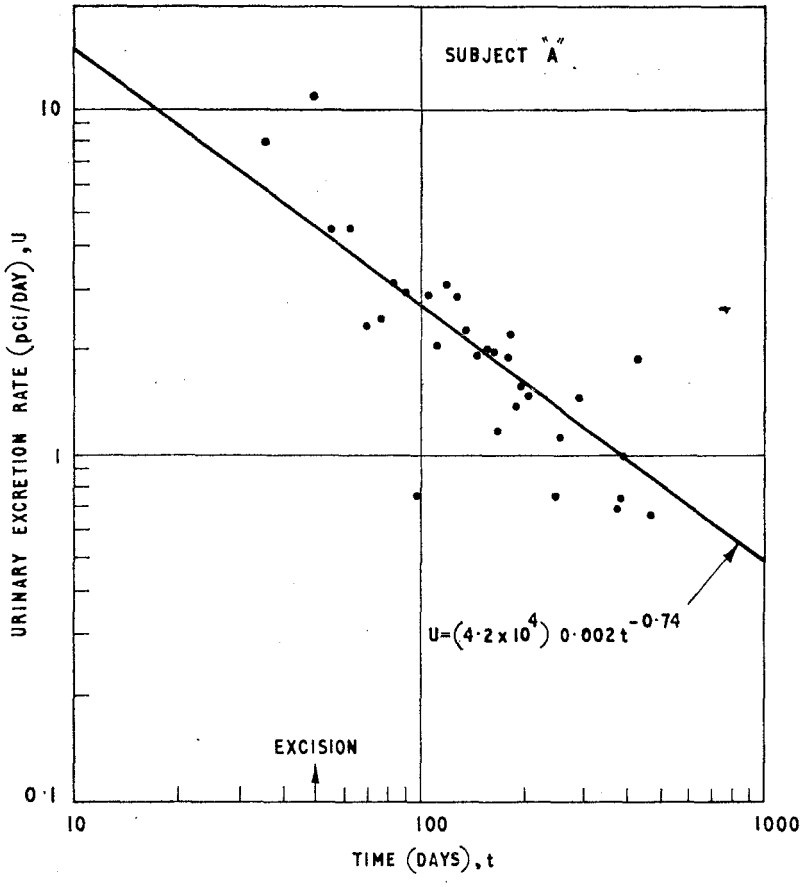

FIG. 8. Urinary excretion data for subject "A".

The total count at 17 keV corresponded to an apparent alpha activity of 0·004 μCi while that at 60 keV indicated 0·023 μCi.

The ratio $\frac{17\text{ keV}}{60\text{ keV}}$ was measured for each spectrum by integrating the total counts under the peaks. The values obtained were:

Electro-deposited reference source:

$$\frac{17\text{ keV peak}}{60\text{ keV peak}} = 6{\cdot}8$$

Wound contamination:

$$\frac{17\text{ keV peak}}{60\text{ keV peak}} = 1{\cdot}45.$$

This reduction in the ratio, if attributed solely to self-absorption in a particle of plutonium, corresponds to a particle radius of 30 μm (Fig. 6). However, such a particle would have an alpha activity of 0·12 μCi and would have given much higher total count-rates. Some of the reduction may be due to depth in the wound. In order to estimate this effect, spectra were plotted for the reference source covered by successive layers of tissue-equivalent plastic material. With 3 mm of plastic overlaying the source, the ratio $\frac{17\text{ keV peak}}{60\text{ keV peak}}$ was 4.9.

The reduction in ratio in going from the covered reference source to the actual wound now corresponds to a particle radius of 20 μm (0·035 μCi). The wound activity calculated from the total counts at 17 keV and corrected for self-absorption corresponds to a particle radius of 17·5 μm (0·024 μCi). The wound activity calculated from the total

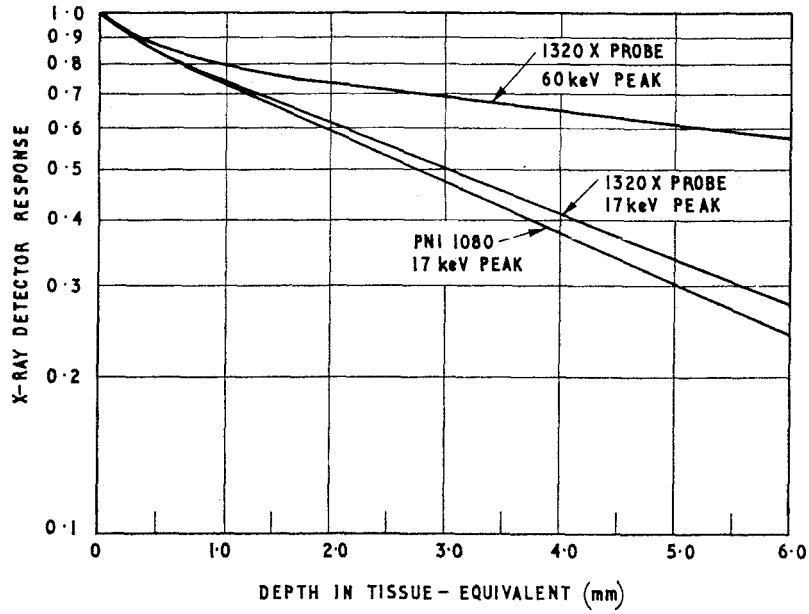

FIG. 9. Effect of depth in tissue on response of probes Type 1320X and PNI 1080 to radiation from thin source of plutonium.

counts at 60 keV and corrected for self-absorption corresponds to a particle radius of 18·5 μm (0·028 μCi). These are in fairly good agreement and it thus appears that the spectrum shapes and total counts are consistent with a plutonium particle of about 0·03 μCi alpha activity at a depth of about 3 mm below the surface.

9. GENERAL OBSERVATIONS CONCERNING THE ABOVE CASE

9.1. Monitoring with an alpha probe failed to detect the presence of plutonium in the finger. Simple monitoring with an X-ray probe after excision probably underestimated the residual activity by a factor of about 6.

9.2. The activity at the site of the wound does not appear to have changed significantly over a period of more than 1 year.

9.3. The results of urine analysis are shown in Fig. 8. They are consistent with the pattern suggested by Langham[8] for a plutonium injection of about 0·04 μCi into the system at about the time of the incident.

10. CONCLUSIONS

10.1. In the monitoring of wounds for plutonium contamination, using X-ray probes, errors can arise from self-absorption, from absorption in overlying tissue and from the presence of isotopes other than ^{239}Pu. These errors can be reduced if a thin reference source can be made from the same contaminating material and if both the wound and the reference source are examined using a low energy gamma spectrometer.

10.2. An actual case has illustrated the needs for reliable initial monitoring, for precise location and for accurate final assessment.

11. ACKNOWLEDGEMENTS

We are grateful for the help of Dr. J. B. Lynch, the Principal Medical Officer at Aldermaston, and of our colleagues Mr. J. A. Hole, Mr. N. T. Clarke, Mr. P. F. Beaver, Mr. N. Taylor and Mr. J. Coppard. We wish to thank the Director, AWRE for permission to publish the paper.

REFERENCES

1. W. H. LANGHAM. Physiology and toxicology of ^{239}Pu and its industrial medical control. *Health Physics* **2,** No. 2 (1959).
2. G. R. TYLER. Self-absorption of X-rays by plutonium particles, with special reference to wound monitoring. TRG Report 896 (D), Dounreay, 1965.
3. W. C. ROESCH and J. W. BAUM. Detection of plutonium in wounds. A/CONF 15/P/756 (1958).
4. H. J. GALE, L. H. J. PEAPLE and J. E. RICHARDS. A detector for the measurement of ^{239}Pu in wounds. AERE-M595, Harwell, 1960.
5. R. J. EPSTEIN and E. W. JOHANSON. Apparatus for monitoring ^{239}Pu in wounds. *Health Physics* **12,** No. 1 (1966).
6. D. RAMSDEN and D. WATT. In *High Sensitivity Counting Techniques*, Pergamon, Oxford, 1964.
7. N. A. TAYLOR. Private communication, AWRE, Aldermaston, 1966.
8. W. H. LANGHAM. In *The Measurement of Body Radio-activity. Brit. J. Radiol.* Suppl. 7 (1957).

THERAPEUTIC REDUCTION OF THYROIDAL IRRADIATION FROM ^{131}I BY THE USE OF POTASSIUM IODIDE AND THYROID STIMULATING HORMONE

MANFRED BLUM
Departments of Medicine and Environmental Medicine,
New York University Medical Center

and

MERRIL EISENBUD
Department of Environmental Medicine

Abstract—Experiments have been conducted in euthyroid adults for the formulation of procedures designed to reduce thyroidal radioiodine burdens in the event of iodine absorption due to accidental exposure.

The rate of reduction of thyroidal radioiodine concentration was measured by daily external scintillation counting twenty centimeters anterior to the neck in eight healthy adults who had received 10 μCi of ^{131}I for clinical purposes, the difference between neck and thigh activity reflecting thyroidal burdens. After the retention slope had become constant, the subjects were given KI 200 mg orally and/or thyroid stimulating hormone (TSH) 10 U intramuscularly.

In a typical subject the ^{131}I effective half-life ($T_{1/2}^{E}$) was 6.0 days during the control period, 5.5 days during 48 hr when two doses of TSH were given at 24 hr intervals, 2.6 days during 72 hr when KI and TSH were given daily, and 6.1 days during 72 hr when KI was given alone fourteen days after the use of TSH had been discontinued and the retention slope had returned to control levels. In the other subjects the range for the $T_{1/2}^{E}$ during the control, TSH and TSH/KI periods was 6.0 to 7.3, 5.3 to 5.8, and 1.7 to 2.6 days respectively.

The TSH/KI effect is of short duration as shown in one subject who received one dose of the combination. During each of the first three twenty-four hour periods the ^{131}I $T_{1/2}^{E}$ was 3.4, 5.6 and 5.7 days with a pre-treatment control of 6.3 days.

The indications are that TSH co-administered with KI may be effective in substantially reducing the dose commitment of the human thyroid from an absorbed dose of ^{131}I. Considerations about the safety of the regimen will be discussed.

BECAUSE iodine concentrates in the thyroid, the extensive use of ^{131}I for industrial, medical and research purposes as well as contamination of the environment with radioiodine released in nuclear weapons testing has led many to be concerned with the risk of human thyroid injury. Thyroid radioiodine burdens may occur in various segments of the population. Among these are nuclear industry employees, medical and other scientific personnel engaged in studies requiring the use of large amounts of radioactive iodine, patients, individuals exposed to fallout from nuclear weapons or accidents involving release of fresh fission products to the environment.[1] Thyroid nodules, hypothyroidism, and short stature have been observed in populations exposed to fallout and there may be a relationship between irradiation of the thyroid and the development of cancer in that organ.[2, 3]

Since the radioiodines are abundantly produced in fission and widely dispersed in the atmosphere, their release has caused local and widespread contamination and may constitute a major risk of the industrial use of nuclear energy.[4] The increasing interest in the commercial application of this source of power

requires the availability of methods designed to prevent thyroidal radioiodine accumulation and, in the event of absorption, to accelerate the excretion of this isotope. The prophylactic use of KI to block thyroidal iodine uptake has been suggested as a countermeasure for accidental exposure.[5-8] However, the drug does not facilitate discharge of the element already absorbed by the gland, and must be taken before exposure for maximal effect.[8] Therefore, should exposure to massive amounts of radioiodine occur, thyroidal burdens sufficient to cause irreversible damage may result.

In order to reduce thyroidal irradiation once radioiodine has concentrated in the gland, removal of the nuclide can be accomplished by altering thyroid metabolism so as to accelerate radioactive thyroxine secretion (see Fig. 1). This can be done by administering TSH, which stimulates both uptake by and discharge from the thyroid. Since reutilization of degraded radioiodine is enhanced by this agent, only a very slight reduction in thyroidal isotope burden will result. When iodide uptake is blocked, preventing recycling, TSH injection causes a much greater decrease in thyroidal ^{131}I.[10-14]

This study deals with acceleration of radioiodine release from the thyroid by administering potassium iodide and thyroid stimulating hormone.

METHOD

The rate of reduction of thyroidal radioiodine concentration was measured by daily external

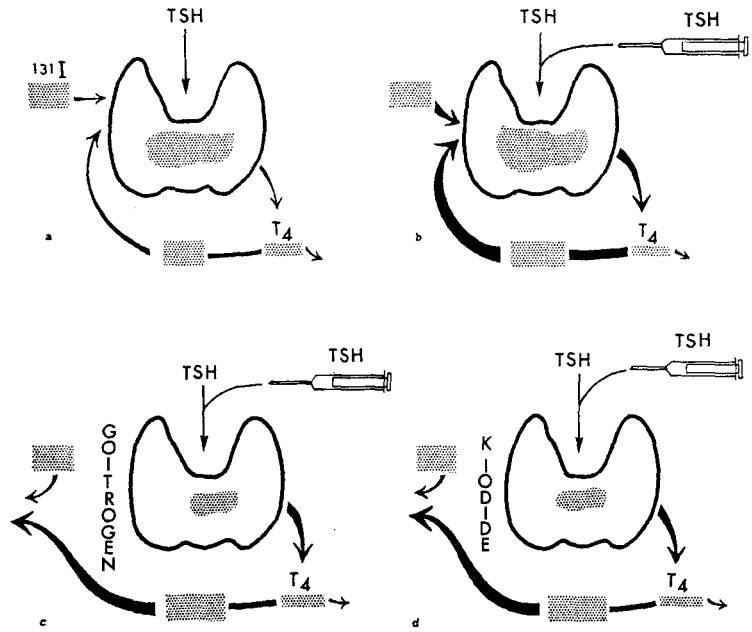

FIG. 1. Alteration of thyroid metabolism so as to reduce thyroidal iodine burdens. Stippling represents ^{131}I in its various forms. (a) Normal thyroidal ^{131}I metabolism. Radioiodine is sequestered by the thyroid and the synthesized isotope labeled hormone (T^4) is secreted; both of these steps are potentiated by TSH. The thyroid hormone is degraded and ^{131}I recycled or excreted. (b) Enhancement of thyroidal ^{131}I (hormonal) discharge by TSH. Radioiodine uptake is also potentiated and thyroid burdens do not change greatly. (c) Enhancement of thyroidal ^{131}I (hormonal) discharge by TSH while radioiodine uptake is inhibited by goitrogen (blockade of recycling). The thyroid burdens are reduced. (d) Enhancement of thyroidal ^{131}I (hormonal) discharge by TSH while radioiodine uptake is inhibited by potassium iodide (blockade of recycling). The thyroid burdens are reduced.

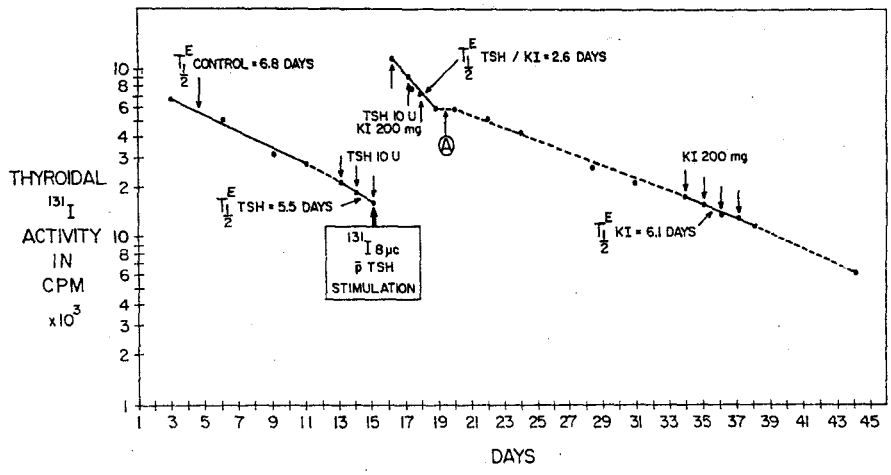

FIG. 2. Thyroidal ^{131}I retention in subject MH. The first part of the curve is the control period. TSH 10 U, IM were given daily on 10/4–10/6. On 10/6 ^{131}I 8 μCi PO was given as part of a TSH stimulation test performed to evaluate thyroidal responsiveness to exogenous TSH in a patient with the Basal Cell Nevus Syndrome. TSH 10 U IM daily together with KI 200 mg PO was administered on 10/7–10/9. "A" represents a period of retardation of the slope of the retention curve lasting about 1 day, 24 hours after discontinuation of KI/TSH. KI 200 mg PO was given daily on 10/25–10/28. The effective half-lives calculated by the method of least squares are indicated (for points on solid lines only).

scintillation counting 30 cm anterior to the neck in 10 adults who had received 10 μCi of ^{131}I for clinical purposes, and in whom standard clinical 3-day TSH stimulation tests had been ordered by their physicians to measure thyroid responsiveness to the tropin as part of their evaluation. All were euthyroid and 7 suffered from exogenous obesity and one each from papillary thyroid carcinoma, diabetes mellitus, and the basal-cell nevus syndrome. Radioactivity over the thigh was considered to be an index of neck extra-thyroidal iodide concentrations and was deducted from gross neck activity. The difference was taken to represent thyroid activity. After the thyroid retention curve slope, calculated by the method of least squares, had become constant, the subjects were given KI, 200 mg orally and/or Thyroid Stimulating Hormone (TSH, Thytropar, Armour) 10 units intramuscularly, and the slope of the retention curve was again determined.

RESULTS

Figure 2 shows the retention curve in a subject in whom the ^{131}I effective half-life ($T^{E}_{1/2}$) was 6.0 days during the control period, 5.5 days during the 48 hr when 3 doses of TSH were given at 24 hr intervals, 2.6 days during 72 hr when the KI/TSH regimen was given daily, and 6.1 days during 72 hr when the KI was given

Table 1. *Average* ($\pm$ *S.D.*) *Thyroidal* ^{131}I *Effective Half-life for Various Regimens*

Regimen	$T^{E}_{1/2} \pm$ S.D. in days	No. of subjects
Control	6.9 ± 0.7	8
TSH 10 U	5.3 ± 0.5	5
TSH 10 U + KI 200 mg	2.5 ± 0.7	8
KI 200 mg	6.5 ± 0.6	2

alone, 14 days after the use of KI/TSH had been discontinued. The PBI at this time no longer showed any evidence of inorganic iodide contamination (5.2 μg %), and the retention curve slope had returned toward control levels. In the other subjects (Table 1), the effective half-life ($T^{E}_{1/2}$) was 6.9 $\pm$ 0.7 days, during the control period, 5.3 $\pm$ 0.5 days when TSH alone was given, 2.5 $\pm$ 0.7 days when the KI/TSH combination was used, and 6.5 $\pm$ 0.6 days when the KI was given.

The duration of effect of one administration of the KI/TSH combination is about one day as is shown in Fig. 3. The $T^{E}_{1/2}$ was 2.7 days

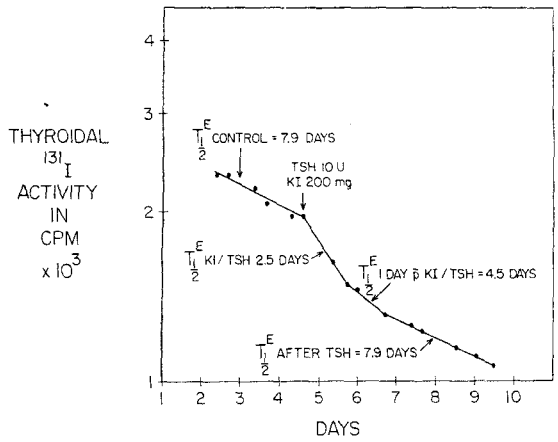

FIG. 3. Thyroidal ^{131}I retention in subject JP. On 5/14 TSH 10U, IM and KI 200 mg PO were given. The effective half-lives calculated by the method of least squares are indicated for each of four periods: (1) control; (2) 24 hr after TSH administration; (3) 24–48 hr after TSH administration; (4) 48–96 hr after TSH administration.

on the first day after KI/TSH administration, slowed to 4.5 days for the next 24 hr, and to 7.9 days for the subsequent 3 days. The pretreatment control was 7.9 days.

In several subjects there was evidence of retardation of thyroidal isotope discharge after the initial acceleration, as demonstrated in Fig. 2 (symbol A). This delay persisted no longer than 24 hr. Thyroidal discharge of ^{131}I was slightly accelerated when TSH alone was administered, and was not altered significantly by KI therapy.

No toxic reactions were observed in any of the subjects.

In order to evaluate the dose reduction using KI/TSH treatment for a single exposure, ^{131}I concentration as a function of time in the thyroid was assumed to follow single exponential functions having half times of 6.9 and 2.5 days respectively for periods of non-treatment and treatment; the dose contribution between the time of exposure and the maximum thyroid burden was negligible. The onset of thyroid radiation exposure was taken as the time o maximum burden.

Based on the above model, percent dose reduction was calculated considering various delay in initiating therapy and various durations o therapy. The data are given in Table 2.*

DISCUSSION

The feasibility of enhancing thyroidal radio iodine release was investigated in subjects wh received TSH to accelerate discharge and K to block ^{131}I recycling. Administration of 20

---

* Calculations were made using the followin formula for the infinity dose with treatment relativ to the infinity dose without treatment as a function o a delay interval and a treatment interval:

$$RD_{\infty}(\triangle t_o,\ \triangle t_T) = 1 - e^{-\Delta t_o/\tau_o} + \left[\frac{\tau_T}{\tau_o}\left(1 - e^{-\Delta_T/\tau_T}\right) + e^{-\Delta t_T/\tau_T}\right] e^{-\Delta t_o/\tau_o}$$

where

$^{\Delta}t_o$ = delay in initiating treatment,

$^{\Delta}t_T$ = duration of treatment,

$$\tau_o = \frac{{}_oT^{E}_{1/2}}{ln_2} = \text{effective mean life of } ^{131}\text{I in thyroid with no treatment,}$$

$$\tau_T = \frac{{}_\tau T^{E}_{1/2}}{ln_2} = \text{effective mean life of } ^{131}\text{I in thyro during treatment.}$$

The percent reduction in dose due to treatment is

$$100[1 - \mathrm{RD}_{\infty}(^{\Delta}t_o,\ ^{\Delta}t_T)].$$

Table 2 contains results of these calculatio assuming ${}_oT^{E}_{1/2}$ = 6.9 days and ${}_T T^{E}_{1/2}$ = 2.5 days.

Table 2. Percent Reduction in Thyroid Dose with KI/TSH Treatment

Delay in treatment (days)	Length of treatment (days)					
	0	1	3	5	7	14
0	0	15.4	36.0	47.8	54.6	62.8
1	0	13.9	32.6	43.2	49.4	56.8
2	0	12.6	29.5	39.1	44.8	51.3
4	0	10.3	24.1	32.0	36.5	42.0

mg KI was added to a standard 10 unit stimulation test regimen in the first subject, resulted in a reduction of the effective half-life of thyroidal ^{131}I from 6.2 to 1.9 days, and encouraged further study at the same dose levels. This preliminary report demonstrates that the effective half-life is changed negligibly by either TSH or KI alone, but is reduced more than 50% with the combined regimen. The acceleration of thyroidal radioiodine discharge in human subjects lasts 24 hr after a single administration of KI/TSH and repeated daily therapy is effective for at least 3 days (see Fig. 2). There seems to be a plateau of radioiodine discharge starting 24 hr after discontinuation of the regimen, lasting less than a day, followed by a return to the original rate of retention. This plateau has also been reported in studies measuring the effect of TSH on the secretion rate and may be due to inhibition of endogenous TSH production by the pharmacologic quantities of the tropin administered.[13] The irradiation dose to the thyroid would tend to be increased only slightly by this phenomenon. Our data demonstrate (see Table 2) that thyroidal irradiation is reduced by 15% when one dose of the drug combination is given promptly after radioiodine burdens have been established. Repeated daily KI/TSH administration is more effective in lowering the dose, daily therapy for 7 days resulting in a dose reduction of 55%. The regimen is less effective when one or more days have elapsed between concentration of radioiodine by the thyroid and administration of the drugs.

Studies in animals have demonstrated the efficiency of using goitrogens such as perchlorate, thicyanate and the thiourea compounds in combination with TSH in accelerating thyroidal radioiodine release.[10-15] The use of such a regimen in human subjects is undesirable, primarily because of the risk of toxic reactions provoked by these goitrogens.[16] On the other hand, short term use of KI as a blocking agent is innocuous,[17] and this compound, too, may be used to prevent radioiodine uptake and therefore, recycling. This combination, KI and TSH, has not been used previously for this purpose, the authors presume, because iodides retard the secretion rate rather than accelerate it and therefore might potentiate thyroid radiation doses.[12, 14, 18, 19]

The inhibitory effect of excess iodide on thyroid hormonal secretion has been demonstrated in several clinical and animal studies. However, this antagonistic effect may be relative, and probably depends on the conditions of the study. In one series of experiments,[19] retardation of hormone ^{131}I release was demonstrated in rats receiving 0.1–5 mg of propylthiouracil (PTU) for blockade but not in those animals pretreated with 30 mg. The retardation of release lasted for more than 40 hr, but was soon followed by resumption of normal discharge in spite of the administration of additional KI. In the same study, Yamata *et al.* showed in rats not prepared with PTU blockade that while 50 or 200 mg of KI was ineffective in altering the secretion rate of ^{131}I labelled hormone, 5 mg elicited a significant decrease in release rate in 3 of 8 animals. Large doses of KI were not effective in iodine-starved rats either. In analyzing this data, the authors reject the hypothesis that newly administered stable iodide is synthesized into thyroid hormone and thereby

decreases the specific activity of the gland and the amount of radioiodine released per unit time, assuming constancy of hormone secretion. Had dilution played a major role, large KI doses would have been more effective than small ones in antagonizing ^{131}I release, particularly in the iodine-starved animals. It is clear from these studies that iodide inhibits thyroidal radioiodine release in the rat only in selected conditions.

The risk of untoward reactions to short-term iodide administration is small; but it is possibly somewhat larger with TSH use. TSH has been implicated in thyroid carcinogenesis and certain thyroidal tumors are probably dependent upon this substance. The relative roles of the tropin and radioiodine in carcinogenesis are unclear. One study suggests that the administration of even 1 μCi of ^{131}I to Long-Evans rats may result in tumor development. Studies with these rats may clarify the incidence of tumor development in animals receiving ^{131}I alone as opposed to its occurrence in those treated with KI/TSH to reduce the glandular radioiodine burden. Although such data may not be completely applicable to the human circumstance, they could be valuable as an index of risks and should precede further human studies with the KI/TSH regimen.

With respect to irradiation injury producing hypothyroidism, dose reduction certainly may be expected to reduce this risk. It is premature to consider using this combination of drugs even in individuals who have absorbed large amounts of radioiodine. However, risk is a relative thing; a condition of huge thyroidal burdens may be envisioned, and in such a circumstance the thyroidal irradiation dose may be of sufficient magnitude to permit acceptance of a theoretical risk due to the countermeasure if it is highly effective in reducing irradiation. Daily treatment with KI/TSH for 7 days, promptly after the development of thyroid radioiodine burdens, decreases the effective half-life to 2.5 days during the time of treatment, resulting in a reduction in the dose to the thyroid of 55%. In the case of contamination with an initial burden of 1 Ci of ^{131}I in an average person (thyroid = 20 g, $T_{1/2}^{E}$ = 6.9 days, 24 hr thyroidal uptake 30%), the thyroidal dose without treatment would be about 5.2×10^6 rads, an amount sufficient to destroy the gland. After daily use of the countermeasure for 7 days, the dose would still be high enough for irreversible radiation injury (2.3×10^6 rad). With burdens in the 1–5 mCi range, the dose would be reduced to $2.3 \times 10^3 - 1.1 \times 10^4$ rad from $5.2 \times 10^3 - 2.6 \times 10^4$ rad. Since hypothyroidism has been reported to occur after at least $1–2 \times 10^4$ rad in most euthyroid individuals, using this drug regimen for ^{131}I burdens below 1 mCi is unnecessary and above 5 mCi unlikely to reduce the incidence of this disease. No information is available in people regarding alteration of tumor risk by lowering thyroidal radioiodine burdens in this range. Two concepts have been suggested: the first assumes that the risk of thyroid damage and tumor development is a dose related phenomenon; and the second that dangerous sequelae to thyroidal irradiation can only be avoided by completely destroying the gland after irradiation so as to prevent hyperplasia and neoplasia of tissue remnant. The latter approach is supported by the experimental finding of a higher incidence of tumor in rats given low doses of ^{131}I (1–4 μCi) than in those given larger ones (200–400 μCi).

Our study suggests that the administration of KI 200 mg and TSH 10 units daily may reduce the thyroidal irradiation dose and the risk of hypothyroidism after radioiodine exposure in selected circumstances; Table 2 indicates the percent reduction in thyroidal irradiation to be expected under various conditions of treatment. No information is offered about alteration of tumor incidence related to either irradiation or the use of the regimen.

This study has been limited to euthyroid patients who have required both radioiodine administration and standard clinical TSH stimulation tests for diagnostic purposes, but it is unlikely that the results are biased.

SUMMARY

Experiments were conducted to explore the feasibility of reducing thyroidal radioiodine burdens in order to decrease the radiation dose to the gland. These studies were done in euthyroid adults who required testing of their ^{131}I uptake and responsiveness to TSH. After completion of the clinical evaluation, thyroidal ^{131}I concentrating ability was arrested with KI,

hormone secretion was enhanced with TSH, and retention was observed. The rate of radioiodine discharge was doubled from the day the regimen was used and the calculated infinity radiation dose is reduced by 15 to 55% when the countermeasure is used for 1 or 7 days.

ACKNOWLEDGEMENTS

The authors wish to express their gratitude to Dr. Anthony Liuzzi for his general assistance and particularly for the mathematic and dosimetric formulations.

This investigation was supported by the Division of Radiological Health of the U.S. Public Health Service and is part of a core program supported by the U.S. Public Health Service, Bureau of State Services grant number ES 00014 and the National Cancer Institute grant number CA 06989.

REFERENCES

1. Proceedings of the Hanford Symposium on the Biology of Radioiodine. *Health Physics* **9** 1081–1426 (1963).
2. R. A. Conard, J. E. Rall and W. W. Sutow. Thyroid nodules as a late sequela of radioactive fallout. *New England J. Med.* **274,** 1391–1399 (1966).
3. S. Lindsay and I. L. Chaikoff. The effects of irradiation on the thyroid gland with particular reference to the induction of thyroid neoplasms. *Cancer Research* **24,** 1099–1107 (1964).
4. J. Z. Holland. Physical origin and dispersion of radioiodine. *Health Physics* **9,** 1095–1103 (1963).
5. C. A. Adams and J. A. Bonnell. Administration of stable iodide as a means of reducing thyroid irradiation resulting from inhalation of radioactive iodine. *Health Physics* **7,** 127–149 (1962).
6. E. E. Pochin and C. F. Barnaby. The effect of pharmacologic doses of non-radioactive iodide on the course of radioiodine uptake by the thyroid. *Health Physics* **7,** 125–126 (1962).
7. K. M. Saxena, E. M. Chapman and C. V. Pryles. Minimal dosage of iodide required to suppress uptake of iodine-131 by normal thyroid, *Science* **138,** 430–431 (1962).
8. M. Blum and M. Eisenbud. Prophylactic reduction of thyroidal irradiation from ^{131}I by the use of potassium iodide. Presented at the Eleventh Annual Meeting of the Health Physics Society, June 27–30, 1966, Houston, Texas.
9. R. E. Goldsmith, J. B. Stanburg and G. L. Brownell. The effect of thyrotropin on the release of hormone from the human thyroid. *J. Clin. Endocr.* **11,** 1079–1094 (1951).
10. R. Goldsmith, C. Herbert and G. Lutsch. The effect of iodide on the release of thyroid hormone in hyperthyroidism: Further observations. *J. Clin. Endocr.* **18,** 367–378 (1958).
11. R. S. Benua and M. B. Lipsett. The effect of iodide on the action of thyrotropin in the hypophysectomized patient. *J. Clin. Endocr.* **19,** 19–27 (1959).
12. M. A. Greer and L. J. DeGroot. The effect of stable iodide on thyroid secretion in man. *Metabolism* **6,** 682–696 (1956).
13. M. A. Greer and H. F. Skull. A quantitative study of the effect of thyrotropin upon the thyroidal secretion rate in euthyroid and thyrotoxic subjects. *J. Clin. Endocr.* **17,** 1030–1039 (1957).
14. D. H. Solomon. Factors affecting the fractional rate of release of radioiodine from the thyroid gland in man. *Metabolism* **5,** 667–681 (1956).
15. E. H. Graul, W. Stumpf and G. Frerichs. Experimental studies on the elimination of radioiodine from the body. *Health Physics* **9,** 1411–1418 (1963).
16. L. S. Goodman and A. Gilman. *The Pharmacological Basis of Therapeutics*, New York: The Macmillan Company, 1965, pp. 1489–1493.
17. *Loc. cit.*, pp. 812–813, 1494–1495.
18. C. J. Mercer, A. Sharard, C. J. M. Westernick and D. D. Adams. Slowing of thyroidal secretion rate by iodide in euthyroid people. *Lancet* **2,** 19–21 (1960).
19. T. Yamata, S. Iino and K. Shichijo. Inhibitory effect of excess iodide on thyroidal radioiodine return in the rat. *Endocrinology* **72,** 83–90 (1963).

THE DETECTION AND MEASUREMENT OF PLUTONIUM CONTAMINATION IN WOUNDS

E. W. JONES and W. N. SAXBY
UKAEA, AWRE, Aldermaston

Abstract—Plutonium is extensively used in atomic research and industry and inevitably there occur wounds and injuries which contain plutonium. Because of its high toxicity it is important to identify, locate and measure any plutonium present. At levels which have medical significance, the quantities involved are minute, but there is sufficient emission of accompanying X- and gamma radiations to permit identification and assay by radiometric techniques.

X-rays in the band 13 to 20 keV, gamma rays of about 60 keV and gamma rays of about 384 keV can all be used for this work: the problems and the limitations associated with measurements in these three energy bands are discussed in the paper, including the usefulness of energy spectrometry to eliminate errors due to self absorption.

There are various instruments available, and usable, for radiometri determinations of plutonium in wounds. Several of these are described with their limitations and detection capabilities.

A case of a contaminated wound is quoted to illustrate some of the techniques and problems in the assessment of plutonium content. Some subsequent work undertaken to improve identification and measurement is also described.

A number of specific actions are suggested, which should be taken, following the occurrence of a wound to ensure that any plutonium present before and after medical treatment is correctly identified and measured.

1. INTRODUCTION

In working with plutonium and its compounds, one route by which radioactive material is accidentally introduced into the body is through minor wounds. These are usually small cuts, punctures and splinters in the hands, caused by objects sharp enough to penetrate through box gloves and through the skin. A few cases have been reported of more serious wounds resulting from accidents in plutonium workplaces. At the AWRE, persons working with radioactive materials are instructed to report all minor injuries which occur in controlled areas. Over a period of 18 months 225 injuries were reported. In 23 cases plutonium contamination was suspected and in 4 of these cases plutonium contamination was confirmed.

The available evidence appears to show that a small fraction of the plutonium injected as metal in minor injuries finds its way into the circulating body fluid within the first few days but most of the material remains at the site of the wound for a long time unless excised or sloughed off with scab.[1] It is generally considered desirable to remove as much as possible of the plutonium from superficial wounds in order to reduce the risk of dispersion in the body and to prevent high dose to local tissue. The maximum permissible body burden of ^{239}Pu when the bone is considered to be the critical organ is only $0{\cdot}04$ μCi ($0{\cdot}64$ μg). A single piece of plutonium of this mass has a diameter of only about 40 μm.

There is thus a need to apply suitable radiation measuring techniques to:

(a) confirm and assess the initial contamination,
(b) locate the site of contamination accurately,
(c) demonstrate the success of surgical operations, and
(d) study the fate of any plutonium remaining at the wound site after surgical treatment.

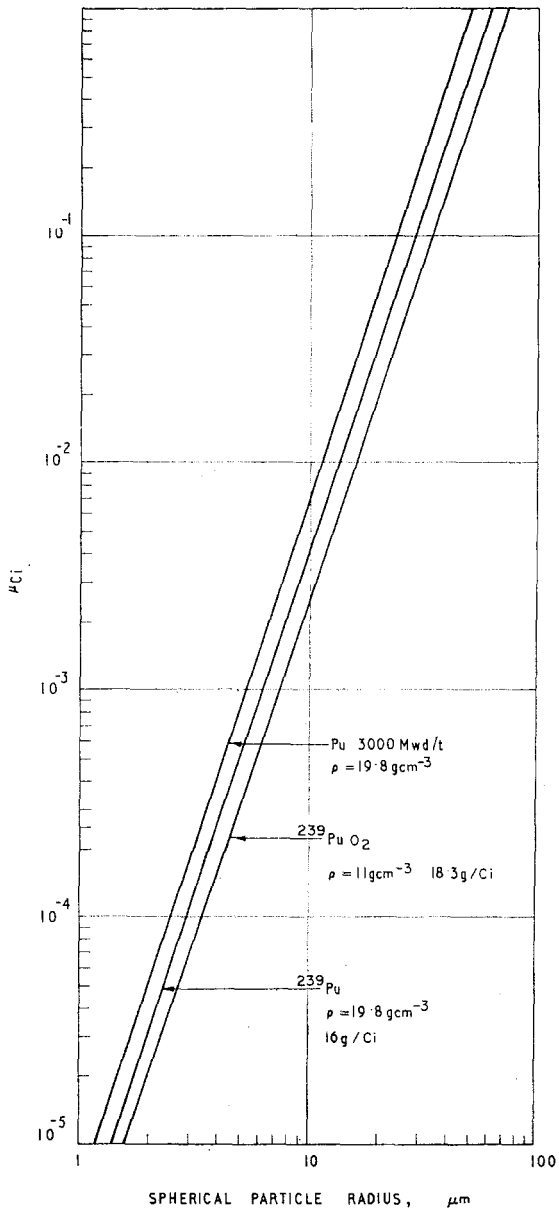

FIG. 1. The radioactivity of spherical particles.

2. MONITORING PRINCIPLES

Personal monitoring for plutonium contamination is usually carried out with a standard alpha particle detector but, owing to the short range of the alpha particles in tissue (about 40 μm), this method will not detect plutonium which has penetrated the outer skin layer or which is covered over with blood. If an alpha probe alone is used to check minor wounds after they have been washed, there is a distinct risk that persons will resume work while still carrying significant contamination below the skin. It has therefore become accepted practice to measure the uranium L X-ray emission at about 17 keV, which follows alpha decay in a small percentage of the disintegrations. Table 1 shows the principal energies and abundance of these emissions for disintegrations of plutonium isotopes and daughter products. The detectors employed are scintillation counters containing thin flat sodium iodide (Tl) crystals covered by aluminium or beryllium foils. These are discussed in more detail below.

Interpretation of the measurements at 17 keV may be complicated by absorption of the X-rays in overlying tissue, by self-absorption in particles of the contaminant, and by the presence of radio-nuclides other than ^{239}Pu which also emit both alpha-particles and X-rays. Tyler[2] has examined the problem of self-absorption for ^{239}Pu in the form of metal and certain compounds. He has shown that, because self-absorption of alpha particles is generally greater than self-absorption of 17 keV X-rays, monitoring with an X-ray probe does not underestimate the potential dose to tissue at the site of the wound but may lead to an underestimate of the amount of plutonium available for transfer to other parts of the body.

In addition to the uranium X-rays there are other penetrating radiations which may be emitted in sufficient quantity to yield useful information; notably the 60 keV gamma-rays of ^{241}Am (daughter of ^{241}Pu) and the 384 keV gamma-rays of ^{239}Pu. The latter are of very low abundance (0·0012%) but in the case of a very severely contaminated wound, could be used to determine an upper limit for the ^{239}Pu content, rapidly and with the minimum uncertainty of interpretation. The practical usefulness of measurements at the different energies is further discussed below.

3. THE TYPES OF MEASUREMENT REQUIRED

3.1. *Initial Monitoring*

Initial monitoring of suspected punctures and other very minor wounds is likely to be carried out, after washing, at the place of work or at the nearest health physics office, using a portable

Table 1. *Principal X- and γ-rays accompanying Disintegrations of Plutonium Isotopes.*

Isotope	Half-life (days)	α particles per sec per g of Pu isotope	No. of photons emitted per alpha particle emission					
			12–14 keV	17–18 keV	20–21 keV	52–65 keV	100 keV	384 keV
^{238}Pu	$3{\cdot}3 \times 10^{4}$	6×10^{11}		$13{\cdot}5 \times 10^{-2}$			$8{\cdot}4 \times 10^{-5}$	
^{239}Pu	$8{\cdot}9 \times 10^{6}$	$2{\cdot}25 \times 10^{9}$	$1{\cdot}3 \times 10^{-2}$	$1{\cdot}9 \times 10^{-2}$	$3{\cdot}15 \times 10^{-3}$	7×10^{-5}	$5{\cdot}2 \times 10^{-5}$	$1{\cdot}2 \times 10^{-5}$
^{240}Pu	$2{\cdot}4 \times 10^{6}$	$8{\cdot}3 \times 10^{9}$		11×10^{-2}				
^{241}Pu	$4{\cdot}8 \times 10$	$9{\cdot}6 \times 10^{7}$					·35	
^{237}U*	6·75		$3{\cdot}55 \times 10^{-2}$	$8{\cdot}15 \times 10^{-2}$	$2{\cdot}6 \times 10^{-2}$	·385	·56	
^{241}Am†	$1{\cdot}7 \times 10^{5}$	$5{\cdot}9 \times 10^{9}$	$14{\cdot}8 \times 10^{-2}$	$19{\cdot}7 \times 10^{-2}$	4×10^{-2}	·38	·315	

* The figures relate to the amount of ^{237}U in equilibrium with 1 g of ^{241}Pu and represent the number of photons per ^{241}Pu alpha emission.
† The figures relate to the amount of ^{241}Am present in 1 g of ^{241}Pu 1 year after separation.

or semi-portable instrument. It is important that contamination under the skin should not be missed at this stage so the monitoring must be performed carefully and slowly, since the count-rates for significant contamination are quite low and the X-ray probes have a sensitive area of only a few square centimetres. Certainty of detection is more important than precision of assessment at this stage and the lower limit of detection for ^{239}Pu ideally should be 0·005 μCi or less. It would assist in ensuring a really adequate check, if the whole hand could be monitored at once in an X-ray monitor for a fixed time interval in much the same way as with a normal α/β hand contamination monitor. No simple version of this appears to have been produced. A well-type phosphor large enough to monitor a whole finger has been tried, but so far, it has not been possible to make an inexpensive detector of this form sufficiently robust and sensitive for general use. Furthermore it would not cope with the small proportion of wounds which occur to the palm of the hand.

3.2. *Accurate Location of Contamination*

When a contaminated wound has been confirmed, it will be referred to the medical officer for treatment. A more precise measurement of the amount and location of the plutonium is now necessary. Accurate location by X-ray measurements is quite difficult because the count-rate per microcurie is very low and any degree of collimation of the detector reduces it still further. It has been found best to mount the detector in a stand about 5 mm above the wound at a point which gives the maximum count-rate and then slide straight-edged or iris-shaped absorbers over the skin, noting the points at which the count rate is sharply diminished.

3.3. *Precise Determination*

In the case of very superficial wounds there is generally no problem about excising the foreign matter. In a more serious case the medical officer may have to balance the desirability of removing all the material, against the possible damage to the individual as a result of surgical operation. In such a case he will require a fairly accurate estimation of the amount of plutonium involved. To achieve this, it is desirable to measure the spectrum of radiation emitted from the wound, and, if possible, obtain a sample of the relevant plutonium from which to prepare a reference source. The reference source should be a thinly deposited source suitable for alpha counting and alpha spectrometry in addition to gamma spectrometry. Corrections can then be made for the presence of isotopes other than ^{239}Pu and for self-absorption.

Any material which is excised from the wound is checked for activity using the X-ray detector. It may then be desirable to retain this material as an aid to further studies.

Finally when the wound has been treated, an attempt should be made to determine an upper limit for the residual contamination. Here again a knowledge of the radiation spectrum can assist towards obtaining a more accurate estimate.

4. INSTRUMENTS AVAILABLE FOR WOUND MONITORING

Several instruments suitable for the detection of X-rays from plutonium have been described.[3-5] The following have been used at the AWRE.

4.1. *Portable Contamination Monitor Type 1320X*

This employs a 55 mm diam. scintillation probe fitted with a sodium iodide phosphor 36 mm diam. × 1·0 mm thick under a 0·05 mm aluminium foil. The probe is coupled to a battery-powered portable ratemeter which, when used in the X-ray monitoring role, has an energy "window" extending from 11 keV to 23 keV approximately. The instrument is designed for general contamination survey duties in the field and has a background count-rate of about 20 counts/min when unshielded. It is used in laboratories for initial checks on suspected skin punctures. Under these conditions, the lower limit of detection is about 0·01 μCi ^{239}Pu. A similar probe gave a background of about 1 count/min in the AWRE low-background facility.[6]

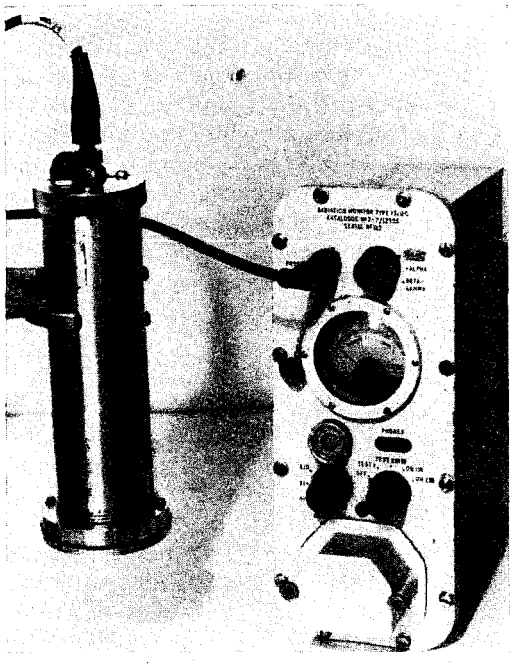

FIG. 2. Portable contamination monitor Type 1320 X.

4.2. *Plutonium Wound Monitor Type PNI 1080**

This instrument employs a 35 mm diam. probe fitted with a sodium iodide phosphor 10 mm diam. × 1·0 mm thick covered with a 0·05 mm aluminium foil. The small, mains-powered ratemeter incorporates an electro-mechanical register for use at low pulse-rates. The circuit has an energy "window" extending from 13 keV to 21 keV approximately. In normal laboratory environments the instrument has a background count-rate of about one count per minute and the lower limit of detection is about 0·005 μCi ^{239}Pu. It is used in our medical and health physics centres for measurement and accurate location of plutonium in wounds.

4.3. *Selective Gamma Monitor Type NIS 322 (Pu)*

In this instrument the scintillation detector, ratemeter and indicator are incorporated in a single pistol-grip unit which can be held comfortably in one hand. In its normal form it employs a phosphor 25 mm thick × 37 mm diam. and is "gated" to accept the 384 keV gamma-rays from ^{239}Pu. The lower limit of detection, in a normal environment is about 500 μCi (about 8 mg) at 5 cm from the end of the detector. Its role in wound monitoring

* Manufactured by Plessey Nucleonics Ltd., Northampton, England.

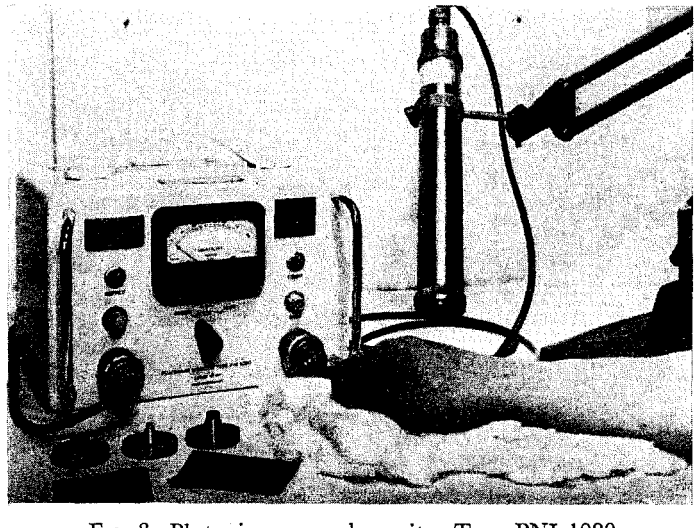

FIG. 3. Plutonium wound monitor Type PNI 1080.

would therefore be confined to a very serious accident where the amount of plutonium involved might imply considerable self-absorption of the low energy X-rays.

Better detection of the 384 keV radiation can be achieved with improved geometry. A 75 mm diam. crystal, having a central well and mounted in a 50 mm lead shield, enabled measurements to be made on a dummy finger, down to 2 μCi ^{239}Pu in a normal laboratory.

Because of the convenient shape and reliable operation of the Selective Gamma Monitor Type NIS 322, an experimental version of it has been constructed for measurements at low energy (Fig. 4). The dimensions of the scintillator and aluminium foil are the same as those of the Probe Type 1320X. The electronic circuit incorporates an energy window which can be switched to either of the ranges:

12 keV–22 keV (for uranium L X-rays)
or 48 keV–72 keV (for 60 keV emission from ^{241}Am).

It is hoped that this instrument will replace the Monitor Type 1320X for plutonium X-ray surveys.

4.4. *Use of Multi-channel Analysers*

If one of the thin-crystal scintillation probes is connected to a multi-channel analyser, the energy spectrum from about 12 keV to about 100 keV can be plotted for the radiation from the wound. The presence of ^{241}Am is then revealed by the peak at 60 keV. It may take about 20 min to obtain a useful spectrum so the subject must be positioned comfortably. It is useful to mount the scintillation probe in a simple lead castle into which the hand can be inserted conveniently or to carry out the measurement within a low background facility such as a whole-body counting room.

5. THE EFFECT OF ISOTOPES OTHER THAN ^{239}Pu

If the plutonium has undergone considerable reactor irradiation it will contain, in addition to ^{239}Pu, proportions of the alpha-emitters ^{238}Pu and ^{240}Pu and the beta emitter ^{241}Pu (half-life 13 years). After separation of pure plutonium from irradiated fuel, ^{237}U and ^{241}Am, the daughters of ^{241}Pu, will begin to grow. The short-lived ^{237}U (6·75 days) reaches equilibrium within a few weeks. ^{241}Am (458 years) will increase almost linearly with time for a few years after separation.

The presence of isotopes other than ^{239}Pu increases the alpha emission per gramme of material; however it increases even more the emission of low energy X-rays per gramme of material, so the significance of the X-ray measurements as an indicator of internal radiation hazard changes as high irradiation and long americium growth are attained. Table 2 shows that for plutonium which has undergone irradiation of 3,000 MWd/t followed by one year's

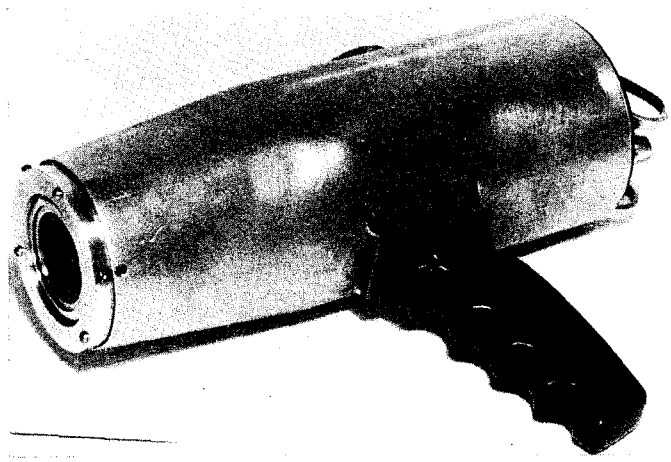

FIG. 4. Prototype of selective gamma monitor Type NIS 322 modified for X-ray monitoring.

Table 2. Emissions from 1 g of Plutonium 1 Year after Separation.

Irradiation / Isotope	500 MWd/t				3000 MWd/t				6000 MWd/t			
	Typical abundance w/o	α/s	*X-rays/s	60 keV γ/s	Typical abundance w/o	α/sec	*X-rays/s	60 keV γ/s	Typical abundance w/o	α/s	*X-rays/s	60 keV γ/s
^{238}Pu	0·0052	$3{\cdot}12 \times 10^{7}$	$4{\cdot}2 \times 10^{6}$		0·065	$3{\cdot}9 \times 10^{8}$	$5{\cdot}2 \times 10^{7}$		0·25	$1{\cdot}5 \times 10^{9}$	$2{\cdot}1 \times 10^{8}$	
^{239}Pu	96	$2{\cdot}15 \times 10^{9}$	$6{\cdot}8 \times 10^{7}$		82·6	$1{\cdot}86 \times 10^{9}$	$5{\cdot}85 \times 10^{7}$		69	$1{\cdot}55 \times 10^{9}$	$4{\cdot}9 \times 10^{7}$	
^{240}Pu	3·8	$3{\cdot}15 \times 10^{8}$	$3{\cdot}5 \times 10^{7}$		13·7	$1{\cdot}14 \times 10^{9}$	$1{\cdot}26 \times 10^{8}$		24·5	$2{\cdot}0 \times 10^{8}$	$2{\cdot}25 \times 10^{8}$	
^{241}Pu	0·22	$2{\cdot}1 \times 10^{5}$			3·3	$3{\cdot}15 \times 10^{6}$			5·6	$5{\cdot}3 \times 10^{6}$		
^{237}U			$3{\cdot}0 \times 10^{4}$	$8{\cdot}2 \times 10^{4}$			$4{\cdot}5 \times 10^{5}$	$12{\cdot}2 \times 10^{5}$			$7{\cdot}6 \times 10^{5}$	$2{\cdot}1 \times 10^{6}$
^{241}Am		$1{\cdot}3 \times 10^{7}$	$5{\cdot}2 \times 10^{6}$	$5{\cdot}0 \times 10^{6}$		$1{\cdot}94 \times 10^{8}$	$7{\cdot}7 \times 10^{7}$	$7{\cdot}4 \times 10^{7}$		$3{\cdot}3 \times 10^{8}$	$1{\cdot}32 \times 10^{8}$	$1{\cdot}27 \times 10^{8}$
Totals		$2{\cdot}5 \times 10^{9}$	$1{\cdot}1 \times 10^{8}$	5×10^{6}		$3{\cdot}58 \times 10^{9}$	$3{\cdot}14 \times 10^{8}$	$7{\cdot}5 \times 10^{7}$		$5{\cdot}38 \times 10^{9}$	$6{\cdot}16 \times 10^{8}$	$1{\cdot}3 \times 10^{8}$
Total X-rays/α		$4{\cdot}4 \times 10^{-2}$				$8{\cdot}75 \times 10^{-2}$				$11{\cdot}4 \times 10^{-2}$		
Total 60 keV/α		2×10^{-3}				$2{\cdot}1 \times 10^{-2}$				$2{\cdot}43 \times 10^{-2}$		

*12–21 keV photons.

growth of ^{241}Am, the X-ray measurements may overestimate the alpha hazard by a factor of 2 if the instrument were calibrated with low irradiation plutonium.

The effect of further increases in isotopic content can be determined from the information in Table 1.

6. THE EFFECT OF DEPTH OF PLUTONIUM IN THE WOUND

If the plutonium is injected well below the surface of the skin, the measurements will be affected by absorption of the radiation in the overlying tissue and by the increased distance between source and detector. For minor hand wounds these effects are unlikely to be significant. The X-rays with an average energy of 17 keV have a half-value thickness in tissue of about 7 mm while at 60 keV the half-value thickness is about 35 mm. The geometrical effect is greatest when the detector is placed very close to the skin. Figure 9 shows the effect of separating the source and detector by layers of approximately tissue-like material.

7. EFFECT OF SELF-ABSORPTION IN THE PARTICLES OF CONTAMINANT

Tyler has shown[2] that, if the activity in a wound is concentrated in a single spherical particle, self-absorption of the X-rays may be appreciable for total activities greater than about 10^{-4} μCi ^{239}Pu. When the total activity is about 1 μCi ^{239}Pu, self-absorption may lead to underestimation by an order of magnitude.

Similar calculations have been performed for the 60 keV emissions of ^{241}Am and show (Fig. 5) that self-absorption does not become significant until the single particle size corresponds to about 60 μm diameter (0·1 μCi ^{239}Pu). Hence, if the radiation spectrum from the wound can be plotted so as to include both the X-ray peak and a discernible 60 keV peak, the ratio of these peaks, for a given isotopic composition will indicate the amount of self-absorption. In practice the isotopic composition may not be known, but it may be possible to obtain a sample of the relevant material, from which to prepare a thin source of negligible self absorption. The ratio $\frac{17\text{ keV peak}}{60\text{ keV peak}}$ for the wound spectrum can then be compared with the same ratio for the thin source. Figure 6 shows how the ratio should theoretically be reduced with increasing particle size.

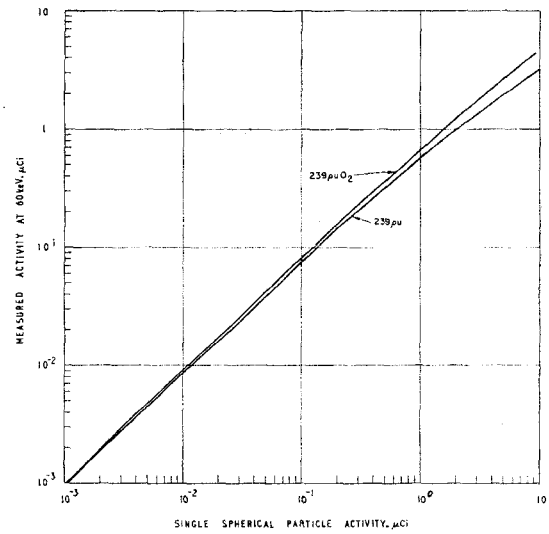

FIG. 5. Correction curves for self-absorption of 60 keV gamma radiation in spherical particles.

8. DESCRIPTION OF A CASE OF A CONTAMINATED WOUND

The following case history of a wound has been selected because it illustrates a number of the points made above.

8.1. *Initial Circumstances*

While manipulating plutonium metal with gloves the subject, "A", received a minor puncture wound close to the finger nail on the side of the middle finger, left hand. By error the hand was monitored only with an alpha probe. This gave a count rate of about 10 counts/s, which was reduced to less than 2 counts/s by washing. "A" then returned to work.

49 days later, on the evidence of urine analysis results, attention was drawn to "A" again and the finger was monitored using X-ray monitors Type PNI 1080 and Type 1320X, both calibrated against a standard plutonium source set in "Perspex". These measurements yielded an estimate of 1.6 μCi of plutonium alpha activity.

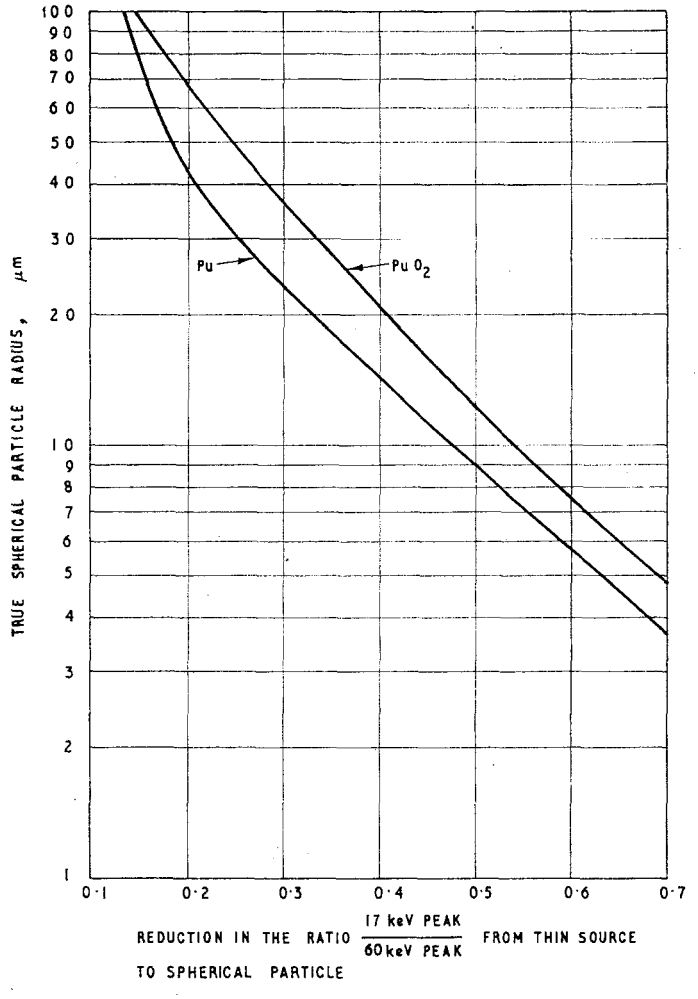

FIG. 6. Theoretical variation in the ratio $\frac{17 \text{ keV output}}{60 \text{ keV output}}$ with particle size.

The activity was then located as accurately as possible using the Monitor Type PNI 1080 with a number of masking devices, and the area was excised until monitoring showed that the contamination had been almost entirely removed.

As much as possible of the excised material, together with swabs, etc. was collected and analysed for plutonium. This measurement showed that at least 1·7 μCi of α activity had been removed from the wound. Monitoring the area of the wound then gave an estimated apparent residual alpha activity of about 0·005 μCi.

8.2. *Second Measurement*

After a further period of 10 months the finger was examined again, this time with a gamma spectrometer comprising a probe Type 1320X coupled to a multichannel analyser. The spectrum obtained is shown in Fig. 7. The ratio $\frac{17 \text{ keV peak}}{60 \text{ keV peak}}$ for this spectrum was very low

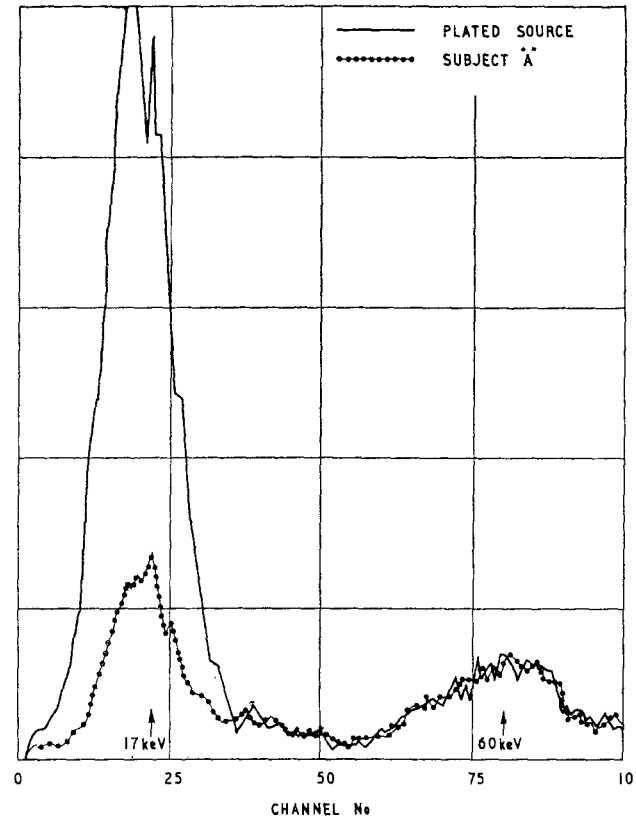

FIG. 7. Spectra from plutonium sources.

in comparison with that for a standard ^{239}Pu source which was used to set up the spectrometer and it was at first suspected that the plutonium in the wound must contain a high percentage of ^{241}Am. A thin electro-deposited source was therefore prepared from some of the material originally excised from "A"s finger. This source was calibrated in an alpha spectrometer giving an alpha activity of 0·023 μCi of which about 3% could be attributed to ^{241}Am. It was then used as a reference source for all future measurements on "A"s finger. The spectrum from the reference source is shown in Fig. 7. It has a much higher 17 keV peak. Comparison of the count-rates in the 17 keV X-ray region yielded an α activity in the finger of about 0·006 μCi, in good agreement with the original estimate. However a comparison at 60 keV indicated 0·022 μCi α activity in the finger. Applying Tyler's correction data for self-absorption in a single spherical particle of plutonium metal to the value at 17 keV, yields 0·020 μCi α activity in agreement with the 60 keV value. The estimate of alpha activity remaining at the wound site was therefore amended to 0·02 μCi approximately. This assessment made no allowance for the self absorption of 60 keV gamma rays nor for the possible effect of depth in the wound.

8.3. *Third Measurement*

The latest measurement on this subject was made 18 months after the original incident, using a similar probe coupled to a multi-channel analyser. Again the spectrum from the wound, after 20 min counting, showed 17 keV and 60 keV peaks and was compared with the spectrum from the reference source.

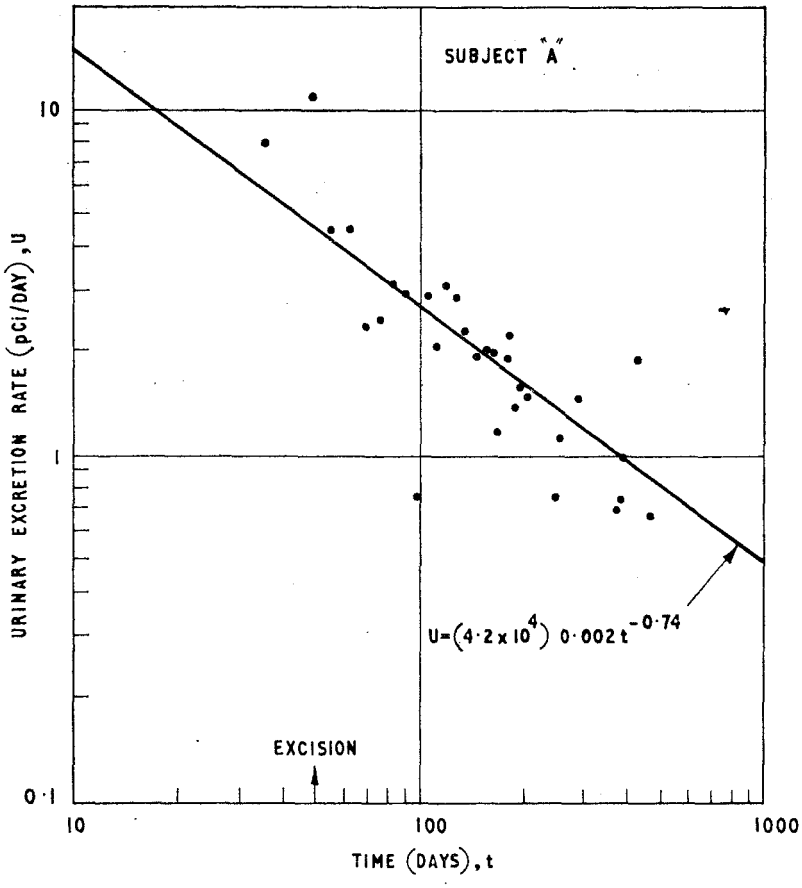

FIG. 8. Urinary excretion data for subject "A".

The total count at 17 keV corresponded to an apparent alpha activity of 0·004 μCi while that at 60 keV indicated 0·023 μCi.

The ratio $\frac{17\text{ keV}}{60\text{ keV}}$ was measured for each spectrum by integrating the total counts under the peaks. The values obtained were:

Electro-deposited reference source:

$$\frac{17\text{ keV peak}}{60\text{ keV peak}} = 6{\cdot}8$$

Wound contamination:

$$\frac{17\text{ keV peak}}{60\text{ keV peak}} = 1{\cdot}45.$$

This reduction in the ratio, if attributed solely to self-absorption in a particle of plutonium, corresponds to a particle radius of 30 μm (Fig. 6). However, such a particle would have an alpha activity of 0·12 μCi and would have given much higher total count-rates. Some of the reduction may be due to depth in the wound. In order to estimate this effect, spectra were plotted for the reference source covered by successive layers of tissue-equivalent plastic material. With 3 mm of plastic overlaying the source, the ratio $\frac{17\text{ keV peak}}{60\text{ keV peak}}$ was 4.9.

The reduction in ratio in going from the covered reference source to the actual wound now corresponds to a particle radius of 20 μm (0·035 μCi). The wound activity calculated from the total counts at 17 keV and corrected for self-absorption corresponds to a particle radius of 17·5 μm (0·024 μCi). The wound activity calculated from the total

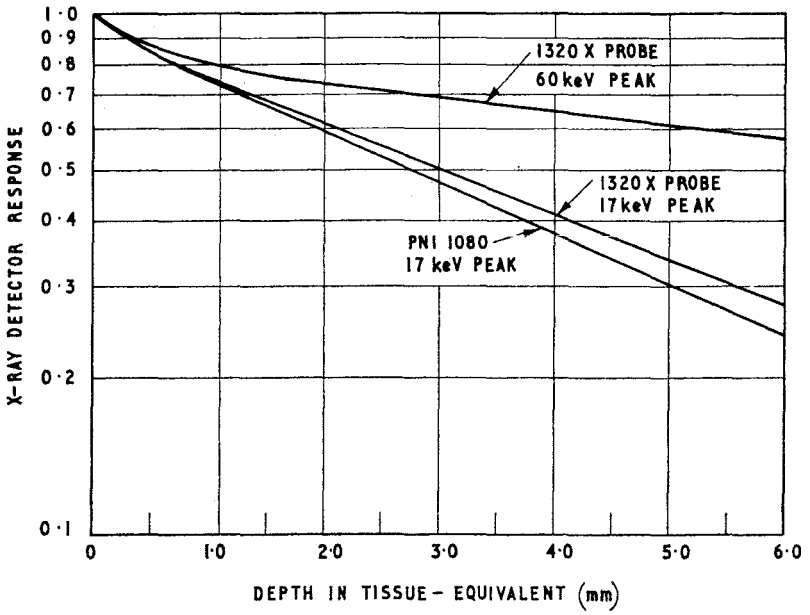

FIG. 9. Effect of depth in tissue on response of probes Type 1320X and PNI 1080 to radiation from thin source of plutonium.

counts at 60 keV and corrected for self-absorption corresponds to a particle radius of 18·5 μm (0·028 μCi). These are in fairly good agreement and it thus appears that the spectrum shapes and total counts are consistent with a plutonium particle of about 0·03 μCi alpha activity at a depth of about 3 mm below the surface.

9. GENERAL OBSERVATIONS CONCERNING THE ABOVE CASE

9.1. Monitoring with an alpha probe failed to detect the presence of plutonium in the finger. Simple monitoring with an X-ray probe after excision probably underestimated the residual activity by a factor of about 6.

9.2. The activity at the site of the wound does not appear to have changed significantly over a period of more than 1 year.

9.3. The results of urine analysis are shown in Fig. 8. They are consistent with the pattern suggested by Langham[8] for a plutonium injection of about 0·04 μCi into the system at about the time of the incident.

10. CONCLUSIONS

10.1. In the monitoring of wounds for plutonium contamination, using X-ray probes, errors can arise from self-absorption, from absorption in overlying tissue and from the presence of isotopes other than ^{239}Pu. These errors can be reduced if a thin reference source can be made from the same contaminating material and if both the wound and the reference source are examined using a low energy gamma spectrometer.

10.2. An actual case has illustrated the needs for reliable initial monitoring, for precise location and for accurate final assessment.

11. ACKNOWLEDGEMENTS

We are grateful for the help of Dr. J. B. Lynch, the Principal Medical Officer at Aldermaston, and of our colleagues Mr. J. A. Hole, Mr. N. T. Clarke, Mr. P. F. Beaver, Mr. N. Taylor and Mr. J. Coppard. We wish to thank the Director, AWRE for permission to publish the paper.

REFERENCES

1. W. H. LANGHAM. Physiology and toxicology of ^{239}Pu and its industrial medical control. *Health Physics* **2,** No. 2 (1959).
2. G. R. TYLER. Self-absorption of X-rays by plutonium particles, with special reference to wound monitoring. TRG Report 896 (D), Dounreay, 1965.
3. W. C. ROESCH and J. W. BAUM. Detection of plutonium in wounds. A/CONF 15/P/756 (1958).
4. H. J. GALE, L. H. J. PEAPLE and J. E. RICHARDS. A detector for the measurement of ^{239}Pu in wounds. AERE-M595, Harwell, 1960.
5. R. J. EPSTEIN and E. W. JOHANSON. Apparatus for monitoring ^{239}Pu in wounds. *Health Physics* **12,** No. 1 (1966).
6. D. RAMSDEN and D. WATT. In *High Sensitivity Counting Techniques*, Pergamon, Oxford, 1964.
7. N. A. TAYLOR. Private communication, AWRE, Aldermaston, 1966.
8. W. H. LANGHAM. In *The Measurement of Body Radio-activity. Brit. J. Radiol.* Suppl. 7 (1957).

PHARMACEUTICAL AND RADIATION HYGIENE PROBLEMS IN RELATION TO RADIOPHARMACEUTICALS

KNUD KRISTENSEN
The National Health Service of Denmark,
Department of Radiation Hygiene and Radiation Hygiene Laboratory,
Copenhagen

Abstract—Preparation, distribution, storage, and use of radioactive pharmaceuticals involves a number of pharmaceutical and radiation hygiene problems. In recent years these have been emphasized by the rapidly increasing use of this type of drug.

A study of radiation hygiene and pharmaceutical aspects of radiopharmaceuticals has underlined the possible conflict between radiation-hygiene and pharmaceutical viewpoints.

A close cooperation between experts representing radiation hygiene and pharmacy is therefore considered of utmost importance. In view of the rapid development of nuclear medicine it is likewise of great importance to furnish an up-to-date service for the clinician from both these fields.

In Denmark it has been proposed that we establish a Pharmaceutical Isotope Laboratory ("Isotope Pharmacy"), which should assume the responsibility that all radiopharmaceuticals are of satisfactory quality, e.g. by purchasing, controlling and distributing radioactive drugs.

INTRODUCTION

Radioactive pharmaceuticals are playing an increasingly important role in recent years. Since the introduction of isotopes as tracers in humans in the thirties and up to the sixties, only radiochemicals have been used in medicine. During the sixties, however, a new approach has started and greater attention is being paid to pharmaceutical problems since these substances in fact are drugs, regardless of whether they are used for diagnostic or therapeutic purposes. Recently, an entire symposium was devoted to problems of radioactive pharmaceuticals.[1]

Radioactive substances are not the answer to Galen's request for "one drug for each disease", nor to the alchemist's search for "the philosopher's stone", but they have assumed a very great importance in medicine and are about to find their permanent place in the new medical field, nuclear medicine.

PRODUCTION AND USE

In the United States the increase in sales of radiopharmaceuticals by 20 to 30% per year illustrates the rapid increase in their use.[1] At the end of 1965 the National Health Service of Denmark had given permission to 45 hospital laboratories for the diagnostic use of labelled substances. The corresponding figure was 19 in 1960. In contrast, the number of places with permission to make therapeutic use of such substances is almost unchanged in the same period (about 10 departments). The application of radioactive pharmaceuticals has rapidly increased. For instance during 1964 and 1965, the number of purchases has increased by 13% and 44%, respectively, in comparison to 1963. In 1965 the number was about 1800.[2] Preparations for diagnostic use shows the greatest increase which is especially marked for the more complex labelled compounds. In 1965 Silver[3] lists about 80 different radioactive pharmaceuticals for diagnostic and 12 for therapeutic use. Among the new preparations are substances which have not previously been used as drugs in non-radioactive form.

The trend appears to be, on the one hand, towards the very short lived isotopes and, on

the other hand, towards biologically important isotopes such as carbon-14 and tritium with a long half-life.

The number of producers of radioactive substances has almost doubled in the period 1959–64 according to the International Atomic Energy Agency.[4-6] Another important development is the production of radioactive substances for application in humans at drughouses or isotope plants which have special sections devoted to the manufacture of this type of substances and which employ pharmacists. This is an important step from radiochemicals towards radiopharmaceuticals.

Distribution, storage, and use of radiopharmaceuticals involves many problems. Some of these are the same as for ordinary drugs but many are due to the radioactivity of the product. It is impossible in this short communication to touch upon all these aspects but I shall try to outline some radiation hygiene and pharmaceutical problems as seen from the point of view of safety.

RADIATION HYGIENE PROBLEMS

From the "radiation hygiene point of view" the ideal radiopharmaceutical is one which will lead to a maximum of information with a minimum of radiation dose to the patient, the personnel, and the environment. From a pharmaceutical point of view it is a substance that is non-toxic, stable and in ready-for-use form. The radiation dose to the patient can be reduced by using isotopes with a short physical and/or biological half-life and by using compounds of a high organ specificity, and finally, using isotopes emitting gamma-rays of a suitable energy. Of course it is important that the preparations are not contaminated with radioisotopes or radiochemical impurities. Last but not least it is of importance to use adequate instrumentation and techniques.

External doses to the staff can be reduced by using compounds ready for use, preferably in dose units, so that little manipulation is needed, and furthermore by avoiding hard beta- or gamma-emitters. The risk of internal contamination can be reduced by using compounds that are not volatile, and do not require complicated manipulations.

PHARMACEUTICAL PROBLEMS

In relation to radiation hygiene one has to consider problems which are relevant both for the patient, for staff members, and for the environment. In regard to pharmaceutical problems, as a rule only protection of the patient is involved.

First of all the preparation must be suitable as a drug which means that it is of low toxicity and high efficiency. It must be free from radiochemical impurities, chemical impurities, and pharmaceutical or biological impurities. It should be available in a suitable formulation in a form ready for use. It is highly desirable to apply "stable" compounds, thus allowing sufficient time for synthesis and control by the producer.

CONTROL AND DISTRIBUTION

The importance of stringent drug control is stressed in all parts of the world. In Denmark control of all pharmaceuticals is compulsory but at the present time there is no check of radiopharmaceuticals from a drug safety point of view.

It is normally impossible to employ the conventional control and distribution system as used for ordinary drugs, in any case the system used in Denmark is not suitable. Since most radiopharmaceuticals cannot be stored for a long time the preparations must be made in small batches which means that daily or weekly production and frequent distribution is required. Another problem is the use of very short lived substances which may have to be separated from a mother substance shortly before use. An example is the use of technetium-99m separated from molybdenum-99. Here we have the pharmaceutical problem of formulation of the preparation. There is little time for control of the preparation's sterility or the presence of pyrogens. The problem is further complicated if the consumer wishes to prepare labelled substances with such short lived isotopes in his own laboratory.

In recent years, consumers have voiced concern about the quality of radiopharmaceuticals and expressed a demand for more purified substances. It is very difficult to express in general terms which degree of purity one should claim in radiopharmaceuticals. Each substance

must be considered separately in relation to the purpose for which it is intended. In my opinion it is much more important to know the exact composition of the preparation than to know that it is 99% pure. In some cases it may indeed be preferable to use a substance with 10% of a known impurity than a substance that is 99% pure, with an unknown impurity 1%.

In Denmark a physician is free to administer to his patient on his own responsibility whatever compound he may find suitable for the treatment. In practice he may rely on the advice of the pharmacist regarding the properties of drugs. Also with radiopharmaceuticals, there is a need for guidance as regards radiation hygiene and pharmacy.

Concerning the radiation hygiene and pharmaceutical problems and how to solve them, there is a latent conflict between the radiation hygiene point of view—short lived substances—and the pharmaceutical point of view—long lived "stable" substances. This fact emphasizes the need for close co-operation between the pharmacist and the health physicist. It is very important that both play a part in the service for the clinician in his treatment of the patients.

"ISOTOPE-PHARMACY"

In Denmark, it has been proposed to solve some of the problems in connection with radioactive pharmaceuticals by establishing a Pharmaceutical Isotope Laboratory ("Isotope Pharmacy").[2] This laboratory should supply Danish hospitals with radioactive drugs and at the same time serve as adviser with regard to quality, properties, storage, etc. The Pharmaceutical Isotope Laboratory should also advise the physicians concerning quality, properties, storage, etc., of radiopharmaceuticals, and develop as well as publish guides and instructions for the control of radioactive drugs. Furthermore, the supply of radioactive drugs throughout the country should be organized in such a way that the total cost will be at a minimum. An additional important responsibility of such a laboratory should be to act as an adviser to the public health authorities and to be able to solve special problems arising in the clinics. In my opinion it is of utmost importance to have a laboratory where experience with and knowledge of relevant problems concerning radiopharmaceuticals is available and can be placed at the disposal of the clinician. The Pharmaceutical Isotope Laboratory should maintain close collaboration with the National Health Service Laboratories for Drug Control and for Radiation Hygiene and with the Isotope Laboratory at the Atomic Energy Commissions Research Establishment at Risö. The collaboration with the last mentioned is of special interest on account of the laboratory's production of isotopes.

The establishment of such a laboratory in Denmark, with five million people, will not render redundant the pharmaceutical and radiation hygiene experts at the bigger hospitals where research with radiopharmaceuticals is going on. It is primarily intended to serve those hospitals where one cannot have resident pharmaceutical and radiation hygiene experts available. At the bigger hospitals problems may be solved in close cooperation between the "central pharmaceutical isotope laboratory" and the health physicist and pharmacist at the hospital.

REFERENCES

1. *Radioactive pharmaceuticals.* Conf-651111, Oak Ridge, 1966.
2. K. KRISTENSEN. *Dansk Tidskrift Farmaci, Copenhagen* **40,** 171 (1966).
3. S. SILVER. *Nucleonics* **23,** 106 (1965).
4. I.A.E.A. *International Directory of Radioisotopes,* 1st ed. Vienna, 1959.
5. I.A.E.A. *International Directory of Radioisotopes,* 2nd ed. Vienna, 1963.
6. I.A.E.A. *International Directory of Isotopes,* 3rd ed. Vienna, 1964.

ON THE EXTENT OF X-RAY EXAMINATIONS IN FINLAND

AULIS ISOLA
Institute of Radiation Physics, Helsinki

Abstract—The annual genetically significant dose of the Finnish population from 2,716,900 X-ray examinations and 80,000 dental exposures carried out in 1963 has been calculated to be 16.8 mrem. The male, female, and foetal contributions to this dose were respectively 4.2 mrem, 8.7 mrem, and 3.9 mrem. The high female contribution observed here is largely due to pelvimetry, hysterosalpingography, obstetrical abdomen, and lower gastrointestinal tract procedures, for which the male contribution only amounts to 5.6% although these examinations account for 42.5% of the total genetic dose. Scrutiny of the contributions of various examinations to the total genetic dose reveals that abdomen and lower gastrointestinal tract account for 26.1% of this dose. Chest surveys cause 6.9% of the genetic dose. This remarkably high proportion is largely due to the fact that approximately 11% of the Finnish population undergoes this survey annually. Although the frequency of mass miniature radiography was very high, about three persons out of ten undergoing this survey annually, its contribution to the genetic dose was found to be not more than 0.9%.

INTRODUCTION

Investigations carried out in the late 1950's in different countries showed that the diagnostic use of X-rays is responsible for the major human-induced exposures of populations. The aim of this work [1] was to find out the radiation burden of the Finnish population due to diagnostic roentgen exposure. This burden is generally expressed in the form of the annual genetically significant dose. This dose formulated by the ICRP/ICRU Joint Study Group [2] is the average of individual gonad doses, each weighted for the expected number of children conceived subsequent to exposure. The fraction of annual genetically significant dose for both sexes caused by class j exposure in age class k can be expressed, for the present purpose, as follows:

$$D^*_{jk} = \frac{N^*_{jk}}{N} \frac{w^*_{jk}}{w} d^*_{jk} \cdot$$

where N^*_{jk} = annual number of individuals of age class k, subjected to class j.

N = the total number of individuals in the population,

w^*_{jk} = future number of children expected by an exposed individual of age class k subsequent to a class j exposure,

w = mean child expectancy of the population,

d^*_{jk} = gonad dose per class j exposure of an individual of age class k, and

the asterisk denotes the sex. The classification of examination followed that given in United Nations report No. 17 (A3838) [3] and has been reproduced in Table 1. During analysis of the data some slight inaccuracies in the classification list became apparent. Especially the lumbosacral, lumbar spine, and dorsal spine had been mutually confused as had also the chest and thorax. However, the classification was satisfactory in general.

MATERIAL AND METHODS

Data collection

All X-ray examinations carried out during one month in 1964 in all medical institutions, hospitals and private physician's offices were recorded according to object of examination, age,

Table 1. *Gonad Doses in Different Age and Examination Classes (mrem)*

	Males		Females	
	<15 yr	⩾15 yr	<15 yr	⩾15 yr
1. Hip and femur (upper third)	90	590	48	20
2. Femur (middle and lower third)	11	92	8	13
3. Pelvic region	139	278	20	80
4. Lumbosacral	7	145	84	260
5. Lumbar spine	191	199	120	727
6. Dorsal spine	108	154	76	113
7. Urography	44	322	468	273
8. Retrograde pyelography	111	153	216	1247
9. Urethrocystography	259	1346	850	850
10. Pelvimetry			520	520
11. Hysterosalpingography			760	760
12. Obstetrical abdomen				113
13. Abdomen (pancreas, spleen, liver)	42	44	720	787
14. Lower gastrointestinal tract (small intestine, appendix, colon)	650	102	1735	1140
15. Upper gastrointestinal tract (pharnyx, oesophagus)	7	25	102	93
16. Cholecystography	7	39	136	136
17. Chest (heart, aorta, lungs)	22	13	8	20
18. Thorax (sternum, ribs, shoulder, clavicle)	40	16	12	20
19. Upper extremities	9	15	8	13
20. Lower leg and foot	16	29	32	13
21. Head and cervical spine	19	16	4	27
22. Fluoroscopy	7	18	56	93
23. Mass miniature radiography	0.2	0.2	0.2	0.9
24. Dental	0.25	0.25	0.05	0.05

and sex. Furthermore, the best possible estimate was requested of the number of examinations carried out in 1963. The total number of mass miniature radiographies (1,205,000) was obtained from the Annual Report of Activities of the Finnish National Anti-Tuberculosis Association,[4] and the number of dental exposures (80,000) was estimated on the basis of the film consumption.

The uncertainty in estimation of the genetic dose is probably mostly due to the uncertainties involved in the measurement of gonad doses. These may be greatly different in different hospitals. In order to gain an idea of this variation, gonad doses were measured in different hospitals. About 2100 fluoro-glass dosimeters were dispatched to 124 hospitals chosen in advance, to be used for measurements of the gonad exposure received by patients undergoing roentgen examination.

Requisite data concerning the structure and birth rates of the population were derived from the *Statistical Yearbook of Finland*[5] and from the archives of the Finnish Central Statistical Office. The number of the Finnish population at the time of the study was about 4,523,300.

Relative Frequency of Examinations

During the control period, 143,320 examinations classified according to object of examination, age and sex were recorded. The resultant chart was utilized in determining the distribution of 2,716,900 examinations carried out in 1963, with respect to various age and examination groups. As regards the distribution of dental examinations, the assumption was made that the share of females was 60% and that of males 40%. The age classes chosen were: under 15 years, 15–19 years, 20–30 years, 31–44 years, and over 44 years. The relative number of examinations N^*_{jk}/N was calculated separately for both sexes and for different age groups.

Child Expectancy

From the birth rates and the probability of death as stated in the *Statistical Yearbook*, the mean child expectancy w was calculated to be 1.316. Assuming that the examination performed has no connection with the patient's child expectancy, the w^*_{jk}/w ratios were calculated for different age and examination classes.

As to foetal exposure, pelvimetry and obstetrical abdomen excluded, it was inferred, taking into account the number of live births, the mean pregnancy time and the number of fertile women, that 6% of the women examined were pregnant.

Gonad Doses

As mentioned before, fluoro-glass dosimeters were used for measurements of gonad doses. In some examination classes the sensitivity of the glass pieces was insufficient. In such instances ionization chamber measurements were performed. Glass pieces were used for measurement

Table 2. Annual Genetically Significant Doses (mrem)

Examination class	Males	Females	Foetal	Total	% of total
1	0.439	0.085	0.005	0.529	3.1
2	0.097	0.007	0.002	0.106	0.6
3	0.370	0.070	0.024	0.464	2.8
4	0.131	0.164	0.068	0.363	2.2
5	0.404	1.079	0.363	1.846	11.0
6	0.295	0.178	0.070	0.543	3.2
7	0.232	0.525	0.078	0.835	5.9
8	0.010	0.126	0.039	0.175	1.0
9	0.104	0.209	0.045	0.358	2.1
10		0.607	1.031	1.638	9.8
11		0.438	0.066	0.504	3.0
12		0.216	0.395	0.611	3.6
13	0.129	1.624	0.719	2.472	14.7
14	0.269	1.199	0.453	1.921	11.4
15	0.012	0.055	0.025	0.092	0.6
16	0.032	0.296	0.130	0.458	2.7
17	0.519	0.531	0.116	1.166	6.9
18	0.146	0.080	0.023	0.249	1.5
19	0.172	0.072	0.012	0.256	1.5
20	0.413	0.180	0.018	0.611	3.6
21	0.258	0.173	0.037	0.468	2.8
22	0.172	0.666	0.149	0.987	5.9
23	0.027	0.106	0.014	0.147	0.9
24	<0.002	<0.001	<0.001	0.003	0.01
Total	4.233	8.687	3.883	16.803	
%	25.2	51.7	23.1		

of skin doses on the testicles and on the back near the ovaries. These doses were used as such as gonad doses for men. In order to work out the female gonad doses from the skin exposures, each examination class was treated separately, employing phantom measurements and considering the position of the ovaries in relative to the primary radiation. In fixing the tissue absorption, the values of Trout *et al.*[6] were used in some cases.

Calibration of the glass pieces was accomplished by using an average kV value in each examination class and assuming the total filtration in all machines to be 2 mm of aluminium, in agreement with Finnish radiation protection regulations.

The gonad doses used in the calculations have been presented in Table 1. Only average doses have been given, although it should be noted that great deviations occur in every examination class.

CONCLUSIONS

The annual genetically significant dose received by the Finnish population from exposure to diagnostic X-rays is found to be 16.8 mrem. In Table 2 the composition of this dose is presented in greater detail. The male, female, and foetal contributions to the genetic dose were 4.2 mrem (25.2%), 8.7 mrem (51.7%), and 3.9 mrem (23.1%), respectively. The high female contribution observed here is largely due to pelvimetry, hysterosalpingography, obstetrical abdomen, abdomen, and gastrointestinal tract procedures, in respect of which the male contribution only amounts to 5.6% although these examinations account for 42.5% of the total genetic dose.

Scrutiny of the contributions of various examinations to the total genetic dose reveals that abdomen and lower gastrointestinal tract account for 26.1% of this dose. Chest surveys cause 6.9% of the genetic dose. This remarkably high proportion is largely due to the fact that approximately 11% of the Finnish population undergoes this survey annually. Although the annual frequency of mass miniature radiography was very high, about three persons out of ten, the contribution of this survey to the genetic dose was found to be not more than 0.9%.

ACKNOWLEDGEMENTS

I wish to express my thanks to the Central Medical Board of Finland, under the supervision of which this work was carried out. Particular gratitude is due to my colleague Mr. O. Ojala for valuable co-operation at all stages of the work. My English manuscript was revised by Mr. U. Attila.

REFERENCES

1. Aulis Isola and Olli Ojala. The genetically significant dose from roentgen examinations in Finland in 1963. *Excerptum Acta Radiologica Supplementum* **254** (1966).
2. International Commission of Radiological Protection and International Commission of Radiological Units and Measurements, Joint Study Group Report of Exposure of Man to Ionizing Radiation arising from Medical Procedures. *Physics in Medicine and Biology*, **2** 107 (1957).
3. Report of the United Nations Scientific Committee on the Effects of Atomic Radiation, United Nations, New York, 1958.
4. Report of Activities of the Finnish National Anti-Tuberculosis Association (1963).
5. *Statistical Yearbook of Finland,* New Series, 59yt (1963).
6. E. D. Trout, J. P. Kelley and G. A. Chathey. The use of filters to control radiation exposure to the patient in diagnostic roentgenology. *Am. J. Roentgenol.* **67** 946 (1952).

PHYSIOLOGICAL CONDITIONS IN PRESSURIZED SUITS: EVALUATION AND CONTROL OF THERMAL STRESS

R. P. ROWLANDS
United Kingdom Atomic Energy Authority,
Authority Health and Safety Branch,
Radiological Protection Division, Harwell, Berkshire, England

Abstract—The thermal conditions experienced by the wearer of a pressurized suit are described by an "index of thermal stress". The value of this index depends on the temperature, humidity and flow rate of the breathing air supplied to the suit, the man's metabolic heat production which depends on his rate of energy expenditure, and the thermal conditions of the workplace outside the pressurized suit. Formulae are given which relate these parameters so that the index can be evaluated for a given pressurized suit operation. A third formula is given which predicts likely sweat rates.

Other physiological responses such as body temperature and heart rate are related to the value of the index of thermal stress. It is convenient to group values of the index into four zones, representing conditions which are physiologically comfortable, tolerable, barely tolerable or intolerable. Control charts, based on the formulae, enable breathing air supply rates to be decided for these conditions after objective consideration of operational factors such as the duration and nature of the work task, the need for rest pauses and thermal conditions in the pressurized suit facility. The thermal stress on the man is thereby controlled and his physiological responses kept within acceptable limits.

INTRODUCTION

Men work in heavily contaminated areas safely protected from the inhalation or absorption of radioactive materials by wearing pressurized suits.[1] Accepting that the suits are designed and operated to provide sufficient air to the breathing zone to avoid any excessive re-inhalation of carbon dioxide the main physiological stress is due to heat. In performing muscular work the suit wearer generates heat which must be dissipated rapidly enough for him to attain thermal equilibrium at an acceptable body temperature. Heat is removed from the man's surface by the air circulating through the suit, via convective cooling and the evaporation of sweat. Further heat exchanges take place between the outside surface of the suit and the workplace.

Continued exposure to heat stress, even at levels below those which are directly harmful, can bring about a deterioration in human performance[2-4] including declining vigilance and the loss of manual dexterity. In view of the radiological protection reasons for using pressurized suits, the physiological responses of the wearer are of considerable importance.

EVALUATION OF THERMAL STRESS

A programme of experiments has been carried out investigating the basic principles of the thermal situation for men working in pressurized suits. The objective was to determine air supply rates for physiologically safe conditions. The results of the investigation are presented in this paper while a full account is reported elsewhere.[5] A pressurized suit can be regarded as a small peculiarly shaped room, which is flexible and mobile, inside which the man is dressed in ordinary clothing. The level of thermal stress to which he is exposed depends

on the temperature and humidity of the air within the suit. These air conditions are influenced by:

(i) the temperature, humidity and volume flow rate of the breathing air supplied to the suit,
(ii) the rate at which heat is produced by the man, and
(iii) the rate at which heat is transferred from the suit to the workplace.

This is illustrated schematically in Fig. 1. The thermal situation can be described as relationship between five variables, $x_1, \ldots, x_5$. Formulae which quantify the relationship were derived from the results of our experiments.[5]

The level of thermal stress is given by:

$$x_5 = 0{\cdot}903(x_1 + 1)^{0{\cdot}79} + 0{\cdot}045(x_2 + 1)^{0{\cdot}87} - 0{\cdot}0027(x_3 + 1)^{1{\cdot}41} + 7{\cdot}02(x_4 - 2)^{-1{\cdot}46} + 14{\cdot}66 \qquad (1)$$

The variable x_5 is called the index of thermal stress. It takes account of the temperature and humidity of the air within the suit, the environment to which the man is directly exposed.

$$x_5 = 0{\cdot}15\ \mathrm{DB} + 0{\cdot}85\ \mathrm{WB}$$

where DB and WB are dry bulb and wet bulb air temperatures, respectively, in degrees Centigrade.

The temperature and humidity of the breathing air supplied to the suit are represented by the variable x_1 which is a weighted mean of dry bulb and wet bulb air temperatures, similar to x_5.

The variable x_2 is the man's rate of production of metabolic heat expressed in kilocalories per hour. Normally with muscular work 80% of the gross energy expenditure appears as heat.[6] The relation between different grades of muscular work and ranges of energy expenditure, as well as the variation of energy expenditure with body weight for particular work tasks, has been discussed by Brown and Crowden[7] and Passmore and Durnin.[8] In general, for the average man wearing one of the U.K.A.E.A. standard pressurized suits, work tasks can be categorized in the manner shown in Table 1.

The actual rate of energy expenditure of a man performing a particular work task can be obtained from measurements of his rates of oxygen consumption and carbon dioxide production.[9] A pressurized suit is a sealed system so that analysis of the inlet and exhaust air with measurement of the air flow rate provides the necessary data. With routine pressurized suit operations, however, the man's metabolic heat output (80% of his energy expenditure) can be estimated from considering the type of work carried out. For guidance, examples of tasks[10]

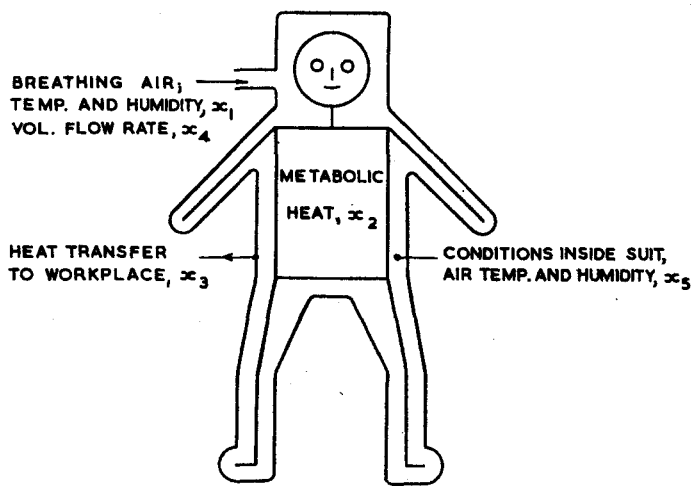

FIG. 1. Schematic diagram of the thermal situation.

Table 1. *Ranges of Energy Expenditure and Metabolic Heat Outputs corresponding to Different Grades of Muscular Work for U.K.A.E.A. Standard Pressurized Suits*

Nature of external work task	Rubber pressurized suit		PVC pressurized suit	
	Energy expenditure (kcal/hr)	Metabolic heat (kcal/hr)	Energy expenditure (kcal/hr)	Metabolic heat (kcal/hr)
Light	150–225	120–180	125–190	100–150
Moderate	225–375	180–300	190–310	150–250
Heavy	375–600	300–480	310–500	250–400

Note: The higher rates of energy expenditure with the rubber suit compared to those with the PVC suit are a reflection of the increased effort required with the former to perform the same external work task, probably due to the heavier weight of the suit.

corresponding to the three work categories listed in Table 1 are given in Table 2.

The variable x_3 is the rate of transfer of heat, in kilocalories per hour, between the outside surface of the pressurized suit and the workplace. Two avenues of heat transfer are considered significant, convection (symbol C) and radiation (symbol R).

$$x_3 = C + R$$

The heat transferred by convection[11] is given by

$$C = 0{\cdot}5\ V^{0{\cdot}5}\ A_s(t_s - t_a) \qquad (2)$$

where C is the rate of heat transfer, in kcal/hr,
V is the speed of movement of the air in the workplace, in ft/min,
t_s is the mean temperature, in °C, of the outside surface of the pressurized suit,
t_a is the temperature of the workplace air, in °C,
A_s is the surface area of the pressurized suit, in m².

The radiant heat transfer[11] is given by

$$R = 5{\cdot}7\ A_s\ (t_s - t_g) \qquad (3)$$

where R is the rate of heat transfer, in kcal/hr,
A_s and t_s are as defined above,
and t_g is the globe[12] temperature of the workplace, in °C.

Table 2. *Examples of Tasks corresponding to Three Work Categories*

Work category	Task
Light	Standing with moderate arm and leg movements, e.g. instrument maintenance, etc.
Moderate	Intermittent walking with moderate lifting and pushing, e.g. mechanical maintenance, operating machines, decontaminating surfaces, etc.
Heavy	Continuous walking with heavy lifting and pushing, e.g. erecting shielding, dismantling heavy machines, manhandling heavy weights, pick and shovel work, etc.

There was little movement of the laboratory air during the programme of experiments,[5] conditions which are reasonably representative of actual pressurized suit facilities. In the experiments the subjects, dressed in pressurized suits, walked on a treadmill which was a motor driven conveyor belt. A value of 150 ft/min is assigned to the parameter V on the basis of the findings of Nelson *et al.*[13] that movement of the arms and legs while walking results in an increase in the apparent air movement which amounts to 150 ft/min over the environmental air speed.

To evaluate C and R, and hence x_3, the value of t_s is required. The results of the experiments[5] were used to derive a second formula from which the value of t_s is obtained.

$$t_s = 0{\cdot}298\ t_a + 0{\cdot}298\ t_g + 0{\cdot}302\ t_{skin} + 0{\cdot}102\ t_i \qquad (4)$$

where t_s, t_a and t_g are as defined above,

t_{skin} is the mean temperature of the man's skin, in °C,

t_i is the temperature of the breathing air supply at the point of entry to the suit, in °C.

The experiments[5] showed that the value of t_{skin} is approximately related to the value of x_5, the index of thermal stress, in the manner shown in Table 3.

Table 3. Relation between Mean Skin Temperature and the Value of the Index of Thermal Stress

Index of thermal stress (x_5)	Mean skin temp. (°C)
Below 25.5	34.0
Between 25.5 and 27.5	34.5
Above 27.5	35.0

The procedure to determine the value of t_s is first to assume a skin temperature of 34°C. The resulting value of t_s obtained from equation (4) is used in the evaluation of x_5. If this value of x_5 exceeds 25·5 it is necessary to repeat the calculation using the appropriate value of t_{skin} taken from Table 3.

The variable x_4 is the volume flow rate of the breathing air supplied to the suit expressed in cubic feet per minute normalized to 15°C, 760 mm Hg.

PHYSIOLOGICAL RESPONSES

A third formula was derived from data from the programme of experiments[5] which enables the man's rate of sweating to be calculated.

$$W = 1{\cdot}486\ (100 - a)(b - a) \qquad (5)$$

where W is the man's rate of loss of weight through sweating, in g/hr,

a is the water vapour content of the breathing air supply in vol. %,

b is the water vapour content of the outlet air from the pressurized suit, in vol. %, derived from the assumption that the air emerges saturated with water vapour and at a temperature, in °C, numerically equal to the value of x_5, the index of thermal stress.

Equation (5) gives the man's sweat rate but this does not necessarily mean that all the sweat is evaporated. The proportion of the sweat which is evaporated and removed from the suit as water vapour in the exhaust air depends on the detailed design of the suit, in particular the method used to circulate the air inside the suit. It also depends on the breathing air flow rate; at low air flow rates some liquid sweat remains inside the suit. Both the U.K.A.E.A. standard pressurized suits use the internal ventilation system which is the most effective for the removal of evaporated sweat out of four different types of pressurized suit which were investigated.

The value of one of the man's responses to thermal stress, i.e. sweat rate, is obtained from equation (5). Investigations into the responses of man exposed to heat stress[11] have shown that different levels of thermal stress can be grouped into four broad zones representing different severities of stress. Likely values of the other physiological responses, body temperature and heart rate, are obtained from consideration of these zones into which the values of the index of thermal stress, x_5, are grouped.

(i) *Comfortable:* $25{\cdot}5°C > x_5 > 15°C$.
The zone of thermal comfort.

(ii) *Tolerable:* $27{\cdot}5°C > x_5 > 25{\cdot}5°C$.
The zone of modest discomfort which most

men can endure, body temperatures tend to equilibrate around 37·8°C (100°F) and heart rates may rise to about 140 beats/min.

(iii) *Barely tolerable:* $31 \cdot 0°C > x_5 > 27 \cdot 5°C$.

The upper limit for sustained work, the zone in which some men may find conditions beyond endurance; body temperatures may not equilibrate so that time of exposure control would be prudent. A suggested basis is: Time of exposure = three-quarters of the average time for body temperatures to reach 39.2°C (102.5°F). It is possible that heart rates may approach 180 beats/min.

(iv) *Intolerable:* $x_5 > 31.0°C$.

Thermal conditions under which men are unable to achieve bodily thermal equilibrium and therefore cannot be expected to work for more than short periods. Heat collapse is likely if exposure is prolonged.

ACCURACY OF THE FORMULAE

In the programme of experiments[5] the values of x_5, t_s and W were measured, thus comparisons between measured values and the values predicted by the formulae, equations (1), (4) and (5) respectively, enable the 95% limits of confidence to be evaluated; these are given in Table 4.

Table 4. Accuracy of the Formulae.

Equation	Variable	95% confidence limits
1	x_5	± 1·73°C
4	t_s	± 0.85°C
5	W	± 93 g/hr

OPERATIONAL CONTROL

Equations (1), . . . , (5), together with consideration of the zones of values of the index of thermal stress and their corresponding physiological responses, provide the means of assuring physiologically safe conditions for men engaged in pressurized suit operations. For a particular operation the following information would be available:

(i) the temperature and humidity of the breathing air supply,

(ii) the nature of the work task,

(iii) the thermal conditions prevailing in the workplace and the type of pressurized suit used, and

(iv) the available rates of supply of breathing air.

The formulae are used to draw up control charts which enable the man in charge to decide the appropriate rate of supply of breathing air. Control charts can be prepared for a wide variety of conditions. As examples, two types of chart are shown in Figs. 2 and 3; both rest on the physical conditions listed below which are reasonably representative of those prevailing in pressurized suit facilities in the U.K.A.E.A.

(a) The air and globe temperatures in the pressurized suit facility are the same, i.e. there is no radiant heat load. The rate of movement of the air in the facility is low.

(b) The temperature of the breathing air supply, at the point of entry to the suit, is the same as the temperatures of the workplace. This allows complete heat equilibration between the air supply pipe and the pressurized suit facility which it traverses. The water vapour content of the breathing air is 0.46 vol. %; at 20°C and 760 mm Hg this corresponds to a relative humidity of 20%.

Figure 2, which applies for the U.K.A.E.A. standard rubber pressurized suit at breathing air and workplace temperatures of 20°C, shows the relation between the index of thermal stress and the man's rate of energy expenditure for air supply rates ranging from 3 to 10 ft³/min; sweat rates are also shown. The values of the index of thermal stress and the sweat rate increase as the work load becomes heavier and decrease as more breathing air is supplied. As an example of reading the chart, 4 ft³/min of breathing air are required to provide thermal comfort at an energy expenditure of 375 kcal/hr (moderate to heavy work). Under these conditions the man's body temperature would tend to equilibrate below 37.8°C (100°F) and his rate of sweating would be about 400 g/hr. There would be no need to limit time of exposure from a heat stress point of view. Continuous heavy work at an energy expenditure of 500

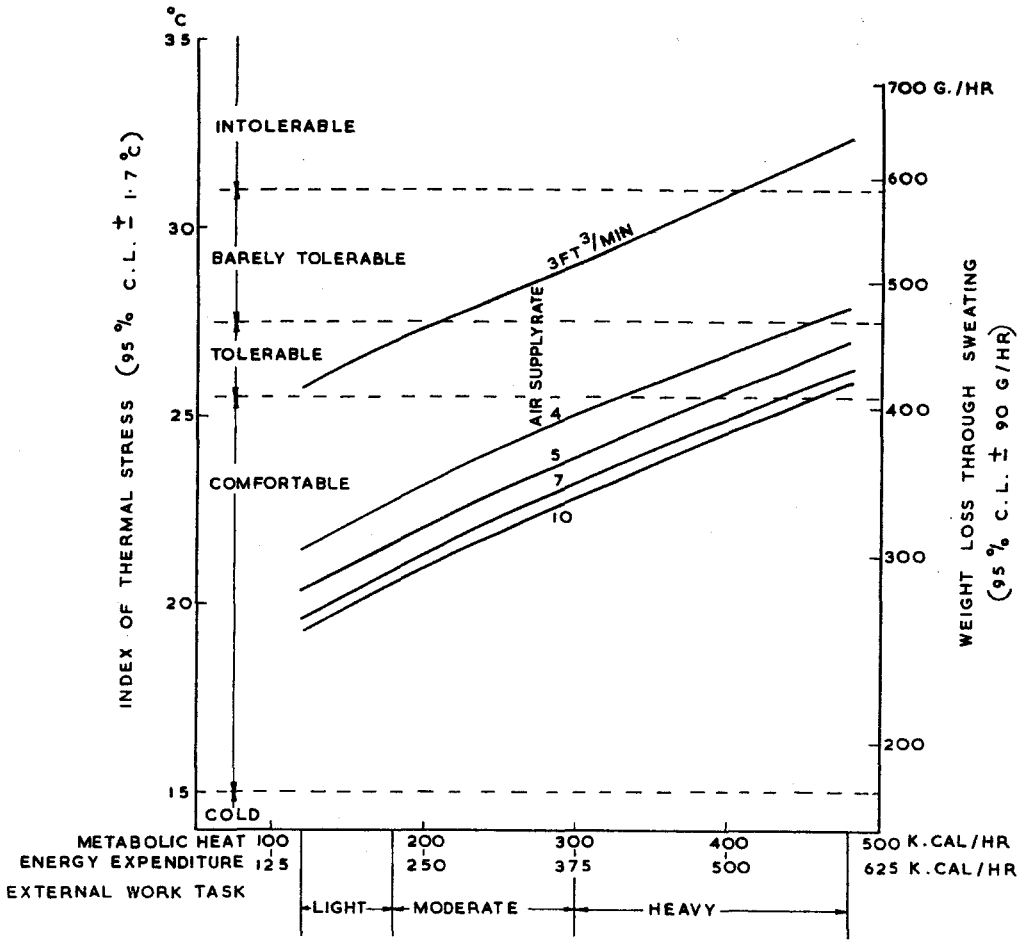

FIG. 2. Control chart for constant temperatures and varying work load.

STANDARD RUBBER PRESSURIZED SUIT
BREATHING AIR. TEMP. 20°C, WATER VAPOUR CONTENT 0·46 VOL. %
WORKPLACE. AIR AND GLOBE TEMP. 20°C

kcal/hr, however, would require 7 ft³/min of breathing air to ensure thermal comfort. Should it be necessary to conserve breathing air supplies, the introduction of rest pauses reduces the mean rate of energy expenditure and consequently the required air supply rate. Thermal equilibrium of the body is achieved fairly slowly thus the rest pauses could be spaced at intervals of about 20 min.

The control chart shown in Fig. 3 applies for the U.K.A.E.A. standard PVC pressurized suit. This chart is prepared for a constant rate of energy expenditure of 310 kcal/hr which corresponds to moderate to heavy work for the average man wearing this suit. This rate of energy expenditure is typical for many pressurized suit operations. The chart enables air supply rates to be chosen for comfort over a range of breathing air and workplace temperatures (at a particular value the three tempera-

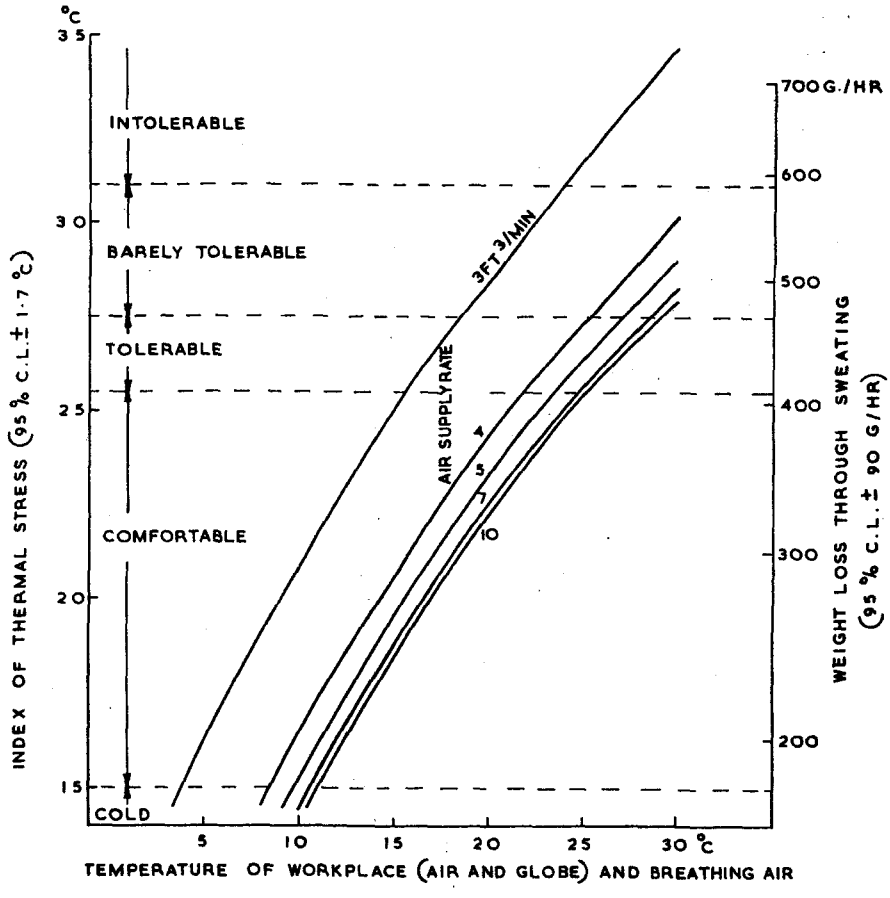

FIG. 3. Control chart for a constant work load and varying temperatures.

STANDARD P.V.C. PRESSURIZED SUIT.
ENERGY EXPENDITURE. 310 K.CAL/HR (MODERATE TO HEAVY WORK)
BREATHING AIR. WATER VAPOUR CONTENT 0·48 VOL. %

tures are the same). At 14°C an air supply rate of 3 ft³/min provides conditions in the zone of thermal comfort, while at 24°C some 10ft³/min of air would be required. Above 24°C the level of thermal stress increases with increasing temperature. Further action such as drying the breathing air and cooling it, possibly by using a vortex tube,[14] would reduce the level of thermal stress at these higher workplace temperatures.

In the above examples of the use of control hcarts the aim has been to produce a value for the index of thermal stress which lies in the zone of thermal comfort. Some physical conditions may preclude this aim. In this case judgement of the acceptable stress coupled with duration of exposure can be made by referring to the other zones of thermal stress and their corresponding physiological responses.

Figures 2 and 3 show that the relation between the value of the index of thermal stress and the air supply rate is such that a change from 3 to 4 ft³/min produces a larger decrement in the value of the index than does a change from 7 to 10

ft³/min. Above 10 ft³/min the reduction in the value of the index is marginal so that there is little to be gained from using air supply rates above 10 ft³/min.

CONCLUSION

The use of control charts, based on formulae derived from a programme of experiments, enables the level of thermal stress imposed on the wearer of a pressurized suit to be evaluated in quantitative terms for given operational conditions. The levels of thermal stress can be divided into four broad zones of increasing severity. Likely values of the physiological responses, body temperature and heart rate are given corresponding to each zone; the value of the man's sweat rate can be obtained from another formula. Thus control of pressurized suit operations can be exercised in a practical way and if ideal conditions cannot be achieved the degree of physiological strain can be estimated in advance and the workload planned accordingly.

REFERENCES

1. R. P. Rowlands. A catalogue of available whole body protective clothing. UKAEA document AHSB(RP)R.9, H.M.S.O., London, 1961.
2. N. H. Mackworth. Researches on the measurement of human performance. M.R.C. Special Report Series No. 268, H.M.S.O., London, 1950.
3. R. K. Macpherson. Physiological responses to hot environments. M.R.C. Special Report Series No. 298, H.M.S.O., London, 1960.
4. L. Brouha. *Physiology in Industry*. Pergamon Press, 1960.
5. R. P. Rowlands. Physiologically safe working conditions for men wearing pressurized suits. UKAEA document AHSB(RP)R.70, 1966.
6. R. H. Fox. Thermal comfort in industry. *Ergonomics for Industry* 8. Ministry of Technology, London, 1965.
7. J. R. Brown and G. P. Crowden. Energy expenditure ranges and muscular work grades. *Brit. J. Industr. Med.* **20,** 277 (1963).
8. R. Passmore and J. V. G. A. Durnin. Human energy expenditure. *Physiol. Review* **35,** 801 (1955).
9. C. G. Douglas and J. C. Priestley. *Human Physiology*. Clarendon Press, Oxford, 3rd edition, 1952.
10. H. S. Belding and T. F. Hatch. Index for evaluating heat stress in terms of resulting physiological strains. *Trans. Amer. Soc. Heating and Air-conditioning Engineers* **62,** 213 (1956).
11. C. S. Leithead and A. R. Lind. *Heat Stress and Heat Disorders*. Cassell, London, 1964.
12. H. M. Vernon. The measurement of radiant heat in relation to human comfort. *J. Industr. Hyg.* **14,** 95 (1932).
13. N. Nelson, L. W. Eichna, S. M. Horvath, W. B. Shelley and T. F. Hatch. Thermal exchanges of man at high temperatures. *Amer. J. Physiol.* **151,** 626 (1947).
14. James F. Ham. Use of a vortex tube in safety clothing. *Arch. Envir. Hlth.* **10,** 619 (1965).

DISCUSSION

E. W. JACKSON (*U.K.*):

In some circumstances it may not be possible to administer potassium iodide before intake of radioiodine. If potassium iodide is taken orally in such cases, after intake of I^{131}, would you expect any worthwhile degree of removal of radioiodide from the thyroid?

M. BLUM:

If potassium iodide is given after exposure to radioiodine there is blockade of further iodine incorporation by the thyroid but we found no evidence of any discharge of contained radioiodine.

P. C. JOHNSON (*U.S.A.*):

When endogenous thyroid production decreases as a result of the goiterogen, TSH production by the pituitary will increase, releasing radioactive T4 and T3 by resorption of colloid. The concurrent administration of iodide would dilute the uptake of radioactive iodide produced by the increase in TSH activity. Perhaps a combination of all three—goiterogen, iodide, and TSH—might be most effective in reducing the radiation dose. Certainly the goiterogen would prevent synthesis of organic iodide which has a longer biologic half time than does iodide in the absence of thyroid function.

P. C. JOHNSON (*U.S.A.*):

One note of caution. We find about a 5% toxic reaction to KI and TSH. The iodide produces skin reactions in large doses. TSH produces anaphylactic reactions.

Have you tried a combination of a goiterogen, e.g. propylthiouracil, to stimulate endogenous TSH and potassium iodide to prevent recirculation of the iodide?

In spite of the possible hazards, I would agree with the author that this would be a practical method for reducing radiation exposure. He is to be complimented on a well performed study.

M. BLUM:

Concerning the incidence of skin reactions, we did not have any. However, a small incidence of ioderma might be worthwhile if the regimen is sufficiently useful in reducing the thyroid radiation dose. This certainly is not a terrible reaction. Furthermore, I think this figure of 5% is greater than my clinical experience with iodine would suggest. The extensive use of iodides in clinical medicine is relatively free of toxicity, with the exception of allergy and ioderma, which are not too common. As for the allergic reaction to TSH, providing the individual has not received the drug previously, I think it is fairly safe to say that he will not have an allergic reaction until antibody levels develop, which will take about two weeks. We think that if this regimen has any place at all, probably a seven-day course should not be exceeded.

We would be reluctant to use a goiterogen such as propylthiouracil to block thyroxin production, thereby stimulating secretion of endogenous TSH, because this is a slow process and one associated with risk of serious bone marrow toxicity. TSH injection in combination with oral potassium iodide works promptly and is relatively safe.

G. COWPER (*Canada*):

Would the authors recommend the use of this therapy in cases where acute exposure leading to an infinity dose of 3 rem had occurred?

M. BLUM:

I do not believe I would under those circumstances. Probably the only case in which this procedure may have any role at all is in the 1 to 5 mCi range.

I think I should point out that we do not know what would happen if we were to give different proportions of KI/TSH. There is some evidence in rats that the ratio of the two may be critical. I would not undertake to determine a dose response curve with humans; we do not know what the effect of TSH on the tumour incidence is, for instance. Some caution is necessary in the use of this agent.

S. LIN (*Italy*):

Io mi rallegro per l'interessante relazione del dott. Blum e vorrei riferire sulla esperienza che abbiamo noi avuto nel nostro laboratorio, nel quale impieghiamo correntemente il test di Querido-Stambury che serve per differenziare gli ipotiroidismi primari dai secondari. Noi abbiamo impiegato il medesimo sistema del dott. Blum un anno fa circa per ridurre la dose nei bambini. Quando noi facciamo delle capitazioni tiroidee, abbiamo appunto impiegato il

metodo del TSH e dello iodio nei bambini e abbiamo avuto dei risultati analoghi, cioè abbiamo una riduzione immediata della dose in tiroide. Però d'altra parte abbiamo avuto anche una serie di inconvenienti con l'impiego del TSH. Abbiamo per esempio descritto un caso di una grave tiroidite insorta dopo somministrazione di 2 dosi di 10 unità, u.s.p., di TSH. E soprattutto abbiamo osservato che queste reazioni si manifestano quando l'individuo ha avuto degli episodi anche lievi di tiroidite nel passato, oppure in individui che avevano delle malattie del mesenchima, tipo reumatismo articolare. In un caso abbiamo avuto delle reazioni piuttosto serie in una persona affetta precedentemente da una forma tubercolare. Impressione nostra è che l'impiego di una dose singola di TSH di 10 unità non dia mai disturbi, ma se noi continuiamo la somministrazione per 2 o 3 giorni, molte volte le persone, i pazienti ci riferiscono di dolori al collo, certe volte abbiamo febbre anche abbastanza alta, uno stato di malessere continuato, e perciò io credo che sia necessario avere un po' di attenzione in questi casi, a meno che noi non riusciamo ad avere a disposizione dei preparati di TSH altamente purificati, che al momento attuale non sono in commercio.

M. BLUM:

Thank you for your remarks. I would like to ask you what type of TSH you used. Did you use the Armour "Thytropar"?

S. LIN:

No.

M. BLUM:

We use Armour Thytropar which is fairly pure. I must say that in the clinical experience of the Isotope Service of the New York University Hospital, where we do approximately 10 TSH stimulation tests a year, and at the Bellevue Hospital where we do several more than that number (we give ten units of TSH for this clinical circumstance daily for 3 days), we also see tenderness of the thyroid which disappears very quickly after we discontinue the use of TSH. We have never seen fever with it. There have been a few allergic reactions in people who had a repeated dose of TSH several weeks later. Now, in the translation it was said that you called this "inflammation". I am not sure that this is exactly the word you meant. Did you mean thyroiditis?

I do not believe this is a thyroiditis as such. I think that more likely it is just an enlargement of the gland, engorgement, with a stretching of the capsule.

A. LAFONTAINE (*Belgium*):

Aux aspects fort intéressants du problème des "radiomédicaments" qui viennent d'être évoqués par M. Kristensen, je voudrais ajouter deux considérations:

1. Les radiomédicaments ne doivent pas être envisagés seulement sous l'angle de leur protection, de leur distribution, et de leur conservation (qui échappent aux circuits pharmaceutiques normaux), mais doivent également n'être confiés qu'à des cliniciens compétents qui sauront utiliser ces produits à bon escient sans danger pour leurs patients, le public, le personnel et eux-mêmes.

2. Les radiomédicaments doivent répondre aux exigences de la physique et de la chimie nucléaires mais doivent aussi être controlés sous l'angle conventionnel (stérilité, pyrogénicité, toxicité, identité, conformité).

A. LAFONTAINE (*Belgium*):

Pourrais je demander à l'orateur si l'examen de masse au point de vue pulmonaire se justifie à un rythme annuel? En d'autres termes si les bénéfices que l'on peut retirer d'un tel examen systématique l'emportent sur les risques potentiels?

A. ISOLA:

If I understood correctly, there is no reason, in the light of this study, to decrease the extent of chest surveys from the point of view of radiation protection.

ÉTUDE SYSTÉMATIQUE DE LA RADIO-ACTIVITÉ D'UN BASSIN FLUVIAL ORGANISÉE SUR UN PLAN INTERNATIONAL

P. RECHT et M. COLLET
Communauté Européenne de l'Énergie Atomique,
Direction de la Protection Sanitaire

Résumé—Afin de mettre au point l'étude systématique de la radio-activité de l'ensemble d'un bassin fluvial, la Commission de l'Euratom—Direction de la Protection Sanitaire—a procédé au cours des dernières années à une étude très complète des méthodes et moyens propres à obtenir les résultats les plus représentatifs possibles en ce qui concerne la pollution radio-active des cours d'eau situés sur l'ensemble d'un bassin fluvial.

Pour ce faire, après avoir établi un programme détaillé de recherches, le bassin du Rhin a été retenu à la fois comme intéressant le plus grand nombre possible d'États de la Communauté et en raison de son étendue qui permet de prendre en considération des éléments géologiques, climatiques, industriels et sociaux très diversifiés.

Après avoir effectué l'étude générale de la radio-activité des boues situées sur le fond du fleuve et de ses affluents principaux et en de très nombreux points, il a été procédé à une étude détaillée de la radioactivité des eaux, des matières en suspension et des boues d'une façon permanente pendant une année complète; ensuite, pour 42 points choisis de manière appropriée, on a procédé à l'étude de la capacité de fixation des boues à l'égard de divers radio-éléments. Cette étude sur les boues globales a fait apparaître la nécessité de rechercher ces mêmes capacités de fixation pour les diverses fractions de la boue à l'égard des mêmes radio-éléments.

Les recherches systématiques du radium et du strontium ont été également effectuées sur tout le cours du bassin, aussi bien dans les eaux que dans les différents composants des boues fluviales.

Parallèlement à cette étude systématique, qui s'est poursuivie pendant plusieurs années, il a été procédé à une étude générale théorique très importante qui a contribué à une meilleure connaissance des facteurs naturels et artificiels susceptibles d'influencer la contamination du bassin rhénan.

Enfin, toutes les données concernant les précipitations et les retombées radio-actives sur le bassin rhénan, ont été rassemblées afin d'établir un bilan aussi exact que possible pour la période de 1962 à 1965, au cours de laquelle l'étude s'est déroulée.

Les mesures et déterminations sont terminées depuis le premier mars 1966. Il reste à regrouper et à analyser les nombreuses données recueillies et à les présenter dans un document d'ensemble.

De toute manière, il apparaît dès à présent que les principes et les méthodes adoptés ont permis d'aboutir à des résultats valables et pourraient être appliqués à l'étude d'autres bassins fluviaux.

A. INTRODUCTION

Le programme d'étude présenté dans cet exposé a été mis au point et réalisé par la Commission de la Communauté Européenne de l'Énergie Atomique, en collaboration avec les autorités nationales, à partir de 1962.

Il a poursuivi les objectifs suivants:

1. Accomplissement des obligations du Traité de Rome, qui a confié à l'Euratom un rôle de coordination et de promotion dans le domaine de la protection sanitaire en vue de réaliser dans les 6 Pays de la Communauté (Allemagne, Belgique, France, Italie, Luxembourg, Pays-Bas), une politique sanitaire commune de radioprotection.

Certains articles du Traité prescrivent notamment aux États membres d'établir les installations nécessaires pour effectuer le contrôle de la radio-activité ambiante et d'en communiquer les résultats aux services de la Commission.

Le contrôle effectué par les autorités responsables des Pays membres sur les eaux de surface porte en général sur la mesure de l'activité bêta totale; il est parfois étendu à la mesure des autres rayonnements ou à celle de quelques rayonnements particuliers naturels ou artificiels. Depuis 1959, la Direction de la Protection Sanitaire de l'Euratom suit l'évolution de la radio-activité des eaux de surface; elle coordonne et harmonise les méthodes ou techniques employées dans la surveillance routinière de la radioactivité.

2. Établissement d'une base de référence précise en fonction de laquelle les rejets d'effluents radio-actifs pourraient être autorisés et leurs risques sanitaires appréciés d'une manière objective.

Le Traité créant l'Euratom oblige en effet les États membres à envoyer à la Commission les données générales de tous les projets de rejets d'effluents radio-actifs. Un avis est remis aux autorités nationales sur le risque de pollution radio-active que présenteraient ces rejets pour l'eau, le sol et l'air d'un état voisin. En appliquant ces dispositions du Traité, le problème de la sommation des pollutions a été également considéré par la Commission de l'Euratom; à cet égard, les fleuves internationaux présentent un intérêt tout particulier.

3. Réalisation d'une étude à caractère scientifique et technique permettant non seulement d'éprouver les techniques de prélèvements et de mesures existantes, mais aussi de mettre au point des méthodes nouvelles. Le programme a été établi en commun par la Commission de l'Euratom et les autorités sanitaires des Pays membres et a précisé les principes et les méthodes qui devaient conduire à mettre en œuvre une étude systématique portant sur un bassin fluvial, considéré dans son ensemble.

Le bassin du Rhin a été retenu, parce qu'il intéressait 4 États de la Communauté (Allemagne, France, Luxembourg, Pays-Bas) et parce qu'en raison de son étendue, son étude aurait permis de prendre en considération des facteurs géologiques, climatologiques, industriels et sociaux très diversifiés.

Le programme envisagé comprenait *cinq parties essentielles*:

(1°) Une étude générale des caractéristiques géographiques, géologiques, économiques, industrielles et humaines du bassin rhénan.

(2°) Une première série de mesures faites en de nombreux points de prélèvements et portant sur les sédiments, avec recherche des activités alpha, bêta, gamma et l'établissement du spectre.

(3°) Une seconde série de mesures, mensuelles, pendant 12 mois, en des points sélectionnés en fonction des résultats de la première série et portant cette fois sur les radio-activités des eaux, matières en suspension et des sédiments.

(4°) Une étude particulière sur les facteurs de concentration dans les sédiments, en prenant en considération les fractions telles que sable, argil eet matières organiques.

(5°) Une étude particulière portant sur le Radium 226 et le Strontium 90 dans les eaux et les sédiments.

Il nous a paru intéressant, dans le cadre de cette première conférence internationale de radioprotection, de présenter les grandes lignes de l'organisation qui a présidé à la conduite de ce programme et de donner quelques résultats de mesures de radio-activité, étant entendu qu'une publication d'ensemble est en cours de rédaction.

L'intention de la Commission est de diffuser largement cette publication et nous souhaitons

qu'au-delà des informations directes apportées sur la radio-activité du bassin du Rhin, elle puisse faire bénéficier les spécialistes du contrôle des eaux de l'expérience acquise au cours des travaux menés depuis plusieurs années, avec une parfaite coordination au sein de la Communauté Européenne de l'Énergie Atomique.

Deux exposés seront également présentés au cours de cette session et apporteront des précisions complémentaires: le premier, sur l'étude de la radio-activité des différents milieux présents dans les cours d'eau du bassin du Rhin, le second, sur les facteurs de concentration des radio-éléments dans les sédiments du fleuve et de ses affluents.

B. ORGANISATION DE L'ÉTUDE ET PREMIERS RÉSULTATS

(1) *Étude générale des caractéristiques du bassin du Rhin*

Dans le présent rapport, il ne sera pas fait mention de cette étude; nous rappelons uniquement que le cours du Rhin a une longueur approximative de 1500 km; la surface du bassin rhénan est de 24.000 km². La population vivant sur cette surface est d'environ 20 millions d'habitants.

(2) *Étude des sédiments du lit du fleuve et de ses affluents principaux*

Il s'agit d'une série de mesures faites en de nombreux points de prélèvements, distribués sur une longueur totale de 2367 km et intéressant le Rhin et ses principaux affluents.

Les fleuves et rivières furent divisés en 25 secteurs dans lesquels 592 points de prélèvements avaient été déterminés. En 532 points, il a été trouvé des échantillons de boue ou sédiments. Ceux-ci, après avoir subi des préparations minutieusement mises au point, furent analysés, mesurés et répertoriés. Les résultats furent ensuite regroupés par secteurs pour procéder à une première étude globale et déterminer les emplacements à choisir pour les mesures ultérieures.

Cette étude fut commencée en octobre 1962. Les prélèvements furent effectués, à l'aide d'un grappin "Bergman", pendant une période de deux mois.

Les valeurs moyennes et maximales suivantes ont été obtenues pour l'ensemble des 532 échantillons mesurés dans les cours d'eau du bassin du Rhin (*en pCi/g de matières sèches*) (voir Tableau 1.) Le spectre gamma a été déterminé afin d'identifier les émetteurs gamma présents dans chaque sédiment prélevé.

(3) *Étude de la radio-activité des eaux, des matières en suspension et des sédiments*

3.1. *Organisation et préparation des prélèvements.*

Sur la base des informations apportées par la deuxième partie du programme, 42 points de prélèvements ont été sélectionnés comme présentant un intérêt particulier (présence permanente de boue, proximité d'un centre nucléaire ou d'une grande ville, contrôle d'un affluent en fonction de sa nature hydrogéologique, présence remarquable ou plus élevée d'une radio-activité particulière, intérêt géographique, etc.).

Tableau 1.

	pCi/g	alpha	bêta (y compris K^{40})	gamma
Rhin 271 prélèvements	Moyenne	32	52	23
	Maximum	58	140	65
Affluents 261 prélèvements	Moyenne	24	45	23
	Maximum	78(278)	131	141

Ces 42 points ont été répartis comme suit:

—19 points sur le cours du Rhin proprement dit,

—11 points sur la totalité du bassin de la Moselle (7 pour La Moselle, 2 pour la Sûre, 1 pour la Meurthe, 1 pour la Sarre),

—12 points répartis sur les six affluents principaux du Rhin.

En ces 42 points, on a procédé à des échantillonnages d'eaux, de matières en suspension et sédiments pendant des intervalles de temps déterminé. La fréquence de prélèvement a été fixée à un mois. Des casiers spéciaux ont été mis au point et utilisés pour ces prélèvements.

3.2. *Résultats des mesures de radio-activité.*

3.2. 1. *Radio-activité des sédiments.* 4.032 mesures ont été effectuées pour donner, point par point, et mois par mois, les valeurs des activités totales alpha, bêta, gamma et les valeurs dues au:

$Ce^{141} + Ce^{144}$
$Ru^{103} + Ru^{106}$
Cs^{137}
$Nb^{95} + Zr^{95}$
K^{40}

Les divers constituants des sédiments (sable, argile, matières organiques) ont été séparés et mesurés afin de connaître pour chaque point, les activités qui leur étaient particulières. Des moyennes générales ont été calculées pour l'ensemble du bassin qui permettent de comparer la répartition des différentes activités entre les divers constituants.

3.2. 2. *Radio-activité des eaux.* 2.016 mesures ont été effectuées sur les eaux filtrées pour donner les valeurs des activités globales alpha, bêta, gamma, exprimées en pCi/l.

3.2. 3. *Radio-activité des matières en suspension.* Les échantillons des matières en suspension dans les eaux ont été également mesurés et exprimés en pCi/g de matières sèches et également en pCi/l d'eau avant filtration.

3.024 résultats ont été obtenus et analysés.

3.2. 4. *Valeurs moyennes des résultats pour l'ensemble du bassin du Rhin.* Le tableau ci-dessous donne quelques valeurs moyennes de résultats en ce qui concerne les sédiments, les eaux et les matières en suspension. Il convient de noter que la dispersion des résultats obtenus autour des valeurs moyennes est variable selon les rayonnements et les milieux étudiés: elle est excellente pour les activités bêta des sédiments et de l'eau. En ce qui concerne l'activité alpha et l'activité gamma de l'eau et des matières en suspension, la dispersion est plus importante en raison notamment des faibles activités rencontrées dans ces milieux, ce qui a diminué la précision des mesures effectuées. La dispersion la plus importante se recontre en ce qui concerne les matières en suspension, car il s'agit de collectes sur filtre avec un poids souvent très faible de substance recueillie (voir Tableau 2).

(4) *Étude des facteurs de concentration dans les sédiments*

La quatrième partie du programme a été consacrée à la recherche des facteurs de concentration dans les sédiments et leurs consti-

Tableau 2

Milieux étudiés	alpha	bêta	gamma	
Sédiments	21,9	73,9(*)	25,0	en pCi/g de matières sèches
Eaux	0,9	10,9(†)	8,6	en pCi/l
Matières en suspension	0,25	2,5	3,3	en pCi/l

* La valeur moyenne pour l'ensemble du bassin en ce qui concerne l'activité due au K^{40} est de 10,5 pCi/g de matières sèches pour la période considérée (octobre 1963—septembre 1964).

† La valeur moyenne pour l'ensemble du bassin en ce qui concerne l'activité due au K^{40} est de 5,5 pCi/l pour la période considérée (octobre 1963—septembre 1964).

tuants (argile, sable, matières organiques) à l'égard de six éléments: iode, phosphore, ruthénium, cérium, césium et strontium.

Le facteur de concentration peut être défini comme le rapport à l'équilibre de l'activité de l'élément par gramme de sédiment à l'activité de ce même élément par ml de liquide (au contact).

3.024 mesures ont été effectuées pour les études mensuelles relatives aux sédiments à l'égard des six éléments de base en 42 points de référence.

1.813 mesures ont été effectuées pour les études mensuelles relatives aux composants des sédiments (argile, sable, matières organiques) à l'égard des six éléments de base et en 15 points de référence.

Des informations et des détails sur cette partie du programme seront apportés au cours de l'exposé suivant.

CONCLUSIONS

Il est encore prématuré de tirer des conclusions définitives à l'étude qui a été entreprise, mais on peut, dès à présent, formuler quelques remarques d'ordre général dont certaines confirment ce que nous savions déjà au sujet de la radio-activité des eaux:

—la radio-activité évolue dans le temps et l'espace, c'était prévisible, mais cette évolution est moins importante qu'on pouvait le croire, en examinant l'ensemble des résultats pour un fleuve aussi long et aux caractéristiques aussi variées. En fait, la radio-activité reste relativement homogène aussi bien quand on compare les résultats provenant de nombreux points de prélèvements que l'évolution de la radio-activité dans le temps en chacun des points examinés. En première analyse, les écarts constatés sont peu importants et négligeables du point de vue sanitaire;

—les mesures effectuées n'ont pas permis de mettre en évidence des rejets industriels avec radio-isotopes artificiels, malgré un nombre très élevé de points de prélèvements et d'échantillonnages;

—les sédiments représentent des intégrateurs et des indicateurs utiles de la radio-activité et la recherche de facteurs de concentration présente incontestablement un intérêt du point de vue sanitaire;

—l'expérience acquise au cours de l'étude a déjà été mise à profit par certains organismes nationaux qui ont pour mission habituelle d'effectuer des mesures de la radio-activité des cours d'eau. C'est ainsi, par exemple, que les systèmes de prélèvements en continu des sédiments déposés sont utilisés en des lieux qui nécessitent une surveillance spéciale. Il arrive même qu'ils soient substitués aux systèmes antérieurement utilisés, lorsqu'il devient nécessaire de rechercher outre les activités globales, les activités dues à des radio-éléments particuliers.

FLUSS-SCHLAMM ALS SAMMLER FÜR RADIOAKTIVE STOFFE

M. COLLET*, R. MAUSHART† und P. SPAANDER‡

Zusammenfassung—Im Rahmen der Untersuchungen über die Radioaktivität des Rheineinzugsgebietes sollte auch das Fixationsvermögen von Fluss-Schlamm für radioaktive Stoffe bestimmt werden, um aus den Ergebnissen Schlüsse auf die Ablagerung von Spaltprodukten und anderer radioaktiver Isotope im Flussbett ziehen zu können.

Zu diesem Zweck ist im Labor für die Elemente Ce, Cs, J, P, Ru und Sr der Verteilungskoeffizient C_p zwischen Fluss-Schlamm und Fluss-Wasser, d.h. das Verhältnis der absorbierten Menge des untersuchten Elements je Gramm Schlamm zur Konzentration des gleichen Elementes in dem im Gleichgewichtszustand mit dem Schlamm befindlichen Wasser, bestimmt worden. Als Markierungsisotope fanden ^{141}Ce, ^{137}Cs, ^{131}I, ^{32}P, ^{103}Ru und ^{89}Sr Verwendung.

Insgesamt sind 756 Einzelproben aufgearbeitet und untersucht worden, davon während eines Jahres monatlich je 42 Gesamtschlammproben und während eines weiteren halben Jahres monatlich je 14 Schlammproben, die mit einem Zentrifugierverfahren in die drei Fraktionen Sand, Ton und organisches Material aufgetrennt worden waren, um Aufschluss über die Wirkung der einzelnen Bestandteile des Schlamms zu erhalten.

Die Methoden werden geschildert, die Ergebnisse mitgeteilt und das so gefundene Anlagerungsvermögen des Schlamms zu der im Schlamm tatsächlich vorhandenen Aktivität der einzelnen Fallout-Nuklide in Beziehung gesetzt.

1. EINFÜHRUNG

Im Rahmen des Euratom-Forschungsvorhabens "Untersuchung der Radioaktivität des Einzugsgebietes des Rheins" sollte auch das Fixationsvermögen von Fluß-Schlamm für radioaktive Stoffe bestimmt werden, um aus den Ergebnissen Schlüsse auf die Ablagerung von Spaltprodukten und anderer radioaktiver Isotope im Flußbett ziehen zu können.

Zu diesem Zweck ist im Labor für die Elemente Ce, Cs, J, P, Ru und Sr der Verteilungskoeffizient C_p zwischen Fluß-Schlamm und Flußwasser, d.h. das Verhältnis der absorbierten Menge des untersuchten Elements je Gramm Schlamm zur Konzentration des gleichen Elementes in dem im Gleichgewichtszustand mit dem Schlamm befindlichen Wasser bestimmt worden. Als Markierungsisotope fanden ^{141}Ce, ^{137}Cs, ^{131}J, ^{32}P, ^{103}Ru und ^{89}Sr Verwendung.

Insgesamt sind 756 Einzelproben aufgearbeitet und untersucht worden, davon während eines Jahres (Oktober 1963 bis September 1964) monatlich je 42 Gesamtschlammproben und während eines weiteren halben Jahres (April 1965 bis Oktober 1965) monatlich je 14 Schlammproben, die mit einem Zentrifugierverfahren in die drei Fraktionen Sand, Ton und organisches Material aufgetrennt worden waren, um Aufschluß über die Wirkung der einzelnen Bestandteile des Schlamms zu erhalten.

Im folgenden sollen die dazu verwendeten Methoden beschrieben und die Ergebnisse zusammengefaßt werden. Nähere Angaben über die Art und die Orte der Probenahmen sowie die Ergebnisse im einzelnen finden sich in dem zusammenfassenden Euratom-Bericht, der in Kürze veröffentlicht wird.

* Direction de la Protection Sanitaire, Communauté Européenne de l'Énergie Atomique, 51, Rue Belliard, Bruxelles.

† Kernforschungszentrum Karlsruhe, Strahlenmessdienst, 75 Karlsruhe, Postfach 947.

‡ Rijks Instituut voor de Volksgezondheid, Utrecht, Sterrenbos 1.

FLUSS-SCHLAMM ALS SAMMLER FÜR RADIOAKTIVE STOFFE

M. COLLET*, R. MAUSHART† und P. SPAANDER‡

Zusammenfassung—Im Rahmen der Untersuchungen über die Radioaktivität des Rheineinzugsgebietes sollte auch das Fixationsvermögen von Fluss-Schlamm für radioaktive Stoffe bestimmt werden, um aus den Ergebnissen Schlüsse auf die Ablagerung von Spaltprodukten und anderer radioaktiver Isotope im Flussbett ziehen zu können.

Zu diesem Zweck ist im Labor für die Elemente Ce, Cs, J, P, Ru und Sr der Verteilungskoeffizient C_p zwischen Fluss-Schlamm und Fluss-Wasser, d.h. das Verhältnis der absorbierten Menge des untersuchten Elements je Gramm Schlamm zur Konzentration des gleichen Elementes in dem im Gleichgewichtszustand mit dem Schlamm befindlichen Wasser, bestimmt worden. Als Markierungsisotope fanden ^{141}Ce, ^{137}Cs, ^{131}I, ^{32}P, ^{103}Ru und ^{89}Sr Verwendung.

Insgesamt sind 756 Einzelproben aufgearbeitet und untersucht worden, davon während eines Jahres monatlich je 42 Gesamtschlammproben und während eines weiteren halben Jahres monatlich je 14 Schlammproben, die mit einem Zentrifugierverfahren in die drei Fraktionen Sand, Ton und organisches Material aufgetrennt worden waren, um Aufschluss über die Wirkung der einzelnen Bestandteile des Schlamms zu erhalten.

Die Methoden werden geschildert, die Ergebnisse mitgeteilt und das so gefundene Anlagerungsvermögen des Schlamms zu der im Schlamm tatsächlich vorhandenen Aktivität der einzelnen Fallout-Nuklide in Beziehung gesetzt.

1. EINFÜHRUNG

Im Rahmen des Euratom-Forschungsvorhabens "Untersuchung der Radioaktivität des Einzugsgebietes des Rheins" sollte auch das Fixationsvermögen von Fluß-Schlamm für radioaktive Stoffe bestimmt werden, um aus den Ergebnissen Schlüsse auf die Ablagerung von Spaltprodukten und anderer radioaktiver Isotope im Flußbett ziehen zu können.

Zu diesem Zweck ist im Labor für die Elemente Ce, Cs, J, P, Ru und Sr der Verteilungskoeffizient C_p zwischen Fluß-Schlamm und Flußwasser, d.h. das Verhältnis der absorbierten Menge des untersuchten Elements je Gramm Schlamm zur Konzentration des gleichen Elementes in dem im Gleichgewichtszustand mit dem Schlamm befindlichen Wasser bestimmt worden. Als Markierungsisotope fanden ^{141}Ce, ^{137}Cs, ^{131}J, ^{32}P, ^{103}Ru und ^{89}Sr Verwendung.

Insgesamt sind 756 Einzelproben aufgearbeitet und untersucht worden, davon während eines Jahres (Oktober 1963 bis September 1964) monatlich je 42 Gesamtschlammproben und während eines weiteren halben Jahres (April 1965 bis Oktober 1965) monatlich je 14 Schlammproben, die mit einem Zentrifugierverfahren in die drei Fraktionen Sand, Ton und organisches Material aufgetrennt worden waren, um Aufschluß über die Wirkung der einzelnen Bestandteile des Schlamms zu erhalten.

Im folgenden sollen die dazu verwendeten Methoden beschrieben und die Ergebnisse zusammengefaßt werden. Nähere Angaben über die Art und die Orte der Probenahmen sowie die Ergebnisse im einzelnen finden sich in dem zusammenfassenden Euratom-Bericht, der in Kürze veröffentlicht wird.

* Direction de la Protection Sanitaire, Communauté Européenne de l'Énergie Atomique, 51, Rue Belliard, Bruxelles.

† Kernforschungszentrum Karlsruhe, Strahlenmessdienst, 75 Karlsruhe, Postfach 947.

‡ Rijks Instituut voor de Volksgezondheid, Utrecht, Sterrenbos 1.

2. MESSMETHODEN

2.1. *Messung des Verteilungskoeffizienten*

2.1.1. *Verwendete radioaktive Nuklide.* Die Untersuchungen des Fixierungsvermögens der Schlammproben wurden mit folgenden Isotopen durchgeführt:

^{141}Ce	($CeCl_3$)
^{137}Cs	($CsCl$)
^{131}J	(Naj)
^{32}P	(Na_3PO_4)
^{103}Ru	($RuCl_3$)
^{89}Sr	($SrCl_2$)

In Klammern ist die in den Versuchen benutzte chemische Verbindung angegeben.

Von jedem dieser Isotope wurde durch Zusatz von inaktivem Material gleicher chemischer Zusammensetzung oder eines Salzes, welches das betreffende Element in der gleichen Wertigkeitsstufe enthält, eine Stammlösung hergestellt. In der Stammlösung lag das jeweils interessierende Element in einer Konzentration von 10^{-4} Gramm-Atomen pro ml vor. Die Aktivität der Stammlösungen betrug ca. 0,1 μCi/ml.

2.1.2. *Probenvorbereitung.* Zur Bestimmung des Verteilungskoeffizienten C_p, d.h. des Verhältnisses der absorbierten Menge des untersuchten Elementes je Gramm Schlamm zur Konzentration des gleichen Elementes in dem im Gleichgewichtszustand mit dem Schlamm befindlichen Wasser, wurden 15 ml Schlamm in einer 250 ml Kunststofflasche mit 100 ml Flußwasser und 1 ml der Stammlösung vermischt. Der Schlammanteil entstammte in jedem Falle einer zuvor durch Rühren gut homogenisierten Schlammprobe. Bei dem zugesetzten Wasser handelte es sich um Flußwasser, das an der gleichen Probeentnahmestelle wie der Schlamm am Ende der jeweils vierwöchigen Sammelperiode entnommen worden war. Die Kunststofflaschen wurden mit einem Schraubdeckel dicht verschlossen, 3 min geschüttelt und dann 48 Stunden stehen gelassen.

Bei den Elementen Cäsium, Jod, Ruthen und Strontium wurde zu jeder Meßreihe bestehend aus 22 Proben eine Blindprobe mit destilliertem Wasser angesetzt. Bei Cer und Phosphor war es wegen der Bildung von Niederschlägen notwendig, zu jeder Probe eine Blindprobe mit Flußwasser anzusetzen, um eine Verfälschung des Verteilungskoeffizienten durch die Fällung zu vermeiden. Eine zu jeder Meßreihe zusätzlich angesetzte Blindprobe mit destilliertem Wasser erlaubte die getrennte Bestimmung des Fällungsfaktors. Die Blindproben wurden genau wie die Proben mit Schlammzusatz behandelt.

Nach einer Standzeit von 48 Stunden hatte sich der Schlamm in jedem Falle so gut abgesetzt, daß aus der überstehenden Lösung 10 ml mit einer Pipette abgezogen werden konnten. Bei der Untersuchung von Cäsium, Strontium, Phosphor und Cer wurden die entnommenen 10 ml Flüssigkeit unter einem Infrarotstrahler verdampft, während bei den leichtflüchtigen Elementen Jod und Ruthen in Reagenzgläser abgefüllt wurde.

Zur Bestimmung des Trockengewichtes des den Proben zugesetzten Schlamms von 15 cm³ wurde der durch Rühren homogenisierte Schlamm von 15 cm³ entnommen und auf einem zuvor gewogenen Filter *ca.* 2 Stunden getrocknet.

2.1.3. *Messung.* Die in Weißblechschalen von 20 cm Durchmesser eingebrachten Meßpräparate der Cäsium-, Phosphor-, Cer- und Strontium-Proben wurden in einem Großflächenproportionalzählrohr ausgemessen. Der Zählerwirkungsgrad betrug bei Eichung mit der β-Strahlung des ^{40}K 66%, der Nulleffekt 150 Imp/min. Gemessen wurde jeweils 10 min.

Die in Reagenzgläser abgefüllten Proben von Jod und Ruthen wurden in einem Szintillationszähler mit Bohrlochkristall ausgemessen. Der verwendete NaJ-Kristall (Durchmesser 60 mm, Höhe 60 mm, Bohrlochdurchmesser 18 mm, Bohrlochtiefe 45 mm) saß auf einem Photomultiplier Typ DuMont 6363. Kristall und Photomultiplier waren zusammen mit einem Vorverstärker in einer zylindrischen Bleiabschirmung von 100 mm Höhe untergebracht. Gezählt wurden die γ-Impulse unter der jeweils intensivsten γ-Linie.

2.1.4. *Berechnung des Verteilungskoeffizienten.* Aus den gemessenen Impulszahlen wurde der Verteilungskoeffizient C_p nach folgender Formel berechnet

$$C_p = \frac{(A_1 - A_0)/a}{A_1/V} \frac{\text{ml}}{\text{g}}$$

Dabei bedeutet

A_0 Impulsrate der Blindprobe,
A_1 Impulsrate der Meßprobe,

a Trockengewicht des zugesetzten Schlamms,
V Volumen der mit dem Schlamm im Gleichgewichtszustand befindlichen Lösung.

Das Volumen V setzt sich zusammen aus dem Volumen des mit dem feuchten Schlamm zugegebenen Wassers, dem Volumen des zugesetzten Flußwassers (100 ml) und dem Volumen der zugesetzten Stammlösung (1 ml).

2.2. *Auftrennung des Schlamms in seine Bestandteile*

Die Auftrennung des Schlamms in seine Hauptbestandteile Sand, organische und anorganische nicht sandhaltige Stoffe erfolgte durch Zentrifugieren. Zu diesem Zweck wurden die vier Liter Schlamm in einem Behälter durch Rühren homogenisiert, danach gleichmäßig auf die acht Becher der Zentrifuge (Fa. Stock, Marburg) verteilt und 5 Minuten zur Abtrennung des Flußwassers bei 2200 g zentrifugiert. Das Flußwasser wurde verworfen.

Zur Abtrennung des Sandes, der Fraktion a, füllte man die den Schlamm enthaltenden Becher mit etwa 200 cm^3 destilliertem Wasser auf und verrührte den Inhalt zu einer homogenen Masse. Es wurde kurzzeitig bis 50 g zentrifugiert und die auf der Oberfläche schwimmende Schicht, die Ausgangssubstanz für die Fraktion b (nicht sandige anorganische Stoffe) sorgfältig dekantiert. Der Rückstand wurde viermal mit destilliertem Wasser gewaschen. Zur Abtrennung des Waschwassers zentrifugierte man kurzzeitig bis 50 g. Nach den ersten beiden Washcvorgängen gab man das Wasser zur dekantierten Substanz, danach wurde das Waschwasser verworfen. Der Rückstand blieb in der Zentrifuge und wurde 5 min lang bei 2200 g getrocknet. Er bildete die Fraktion a (Sand).

Um den anorganischen, nicht sandhaltigen Anteil des Schlamms abzusondern, verteilte man die abdekantierte Schicht der Fraktion a auf die acht Zentrifugenbecher und ließ die Zentrifuge eine Minute lang bei 500 g laufen. Die überstehende Schicht wurde als Ausgangssubstanz für die Fraktion c, organische Stoffe des Schlamms, sorgfältig abgegossen. Der Rückstand wurde mit destilliertem Wasser aufgerührt und eine Minute lang bei 1000 g zentrifugiert. Das Wasser wurde entfernt, der Rückstand 5 min lang bei 2200 g zur Trocknung zentrifugiert und als Fraktion b (nicht sandhaltige anorganische Stoffe) weiter verwendet.

Die Ausgangssubstanz für die Fraktion c verteilte man auf vier Becher der Zentrifuge und ließ sie 5 min lang bei 2200 g laufen. Den Rückstand wusch man einmal mit destilliertem Wasser und trocknete ihn durch 5 min dauerndes Zentrifugieren bei 2200 g. Der Rückstand bildete Fraktion c (organische Stoffe).

Zur Messung der prozentualen Gewichtsverteilung der drei Schlammfraktionen wurde die Schlammenge gewogen. Danach bestimmte man das Gewicht von 15 cm^3 Substanz jeder Fraktion vor dem Trocknen und nach der Trocknung im Trockenschrank. Daraus ließ sich das Verhältnis Naßgewicht zu Trockengewicht und die prozentuale Gewichtsverteilung berechnen.

2.3. *Korngrößenanalyse*

In einer gesonderten Untersuchung[1] versuchte man einen Überblick zu bekommen, wie die Korngrößenverteilung innerhalb der einzelnen Fraktionen aussieht und wie gleichmäßig das Zentrifugierverfahren bei verschieden beschaffenen Schlämmen arbeitet.

Die Kornverteilung wurde anhand einer Siebanalyse gewonnen und der Anteil organischer Substanz durch eine Oxydation mit H_2O_2 bestimmt. Durch die Korngröße sind die Begriffe Sand, Schluff und Rohton eindeutig bestimmt. Aus der gemessenen Korngrößenverteilung lassen sich die Anteile dieser drei Stoffe in den Schlammfraktionen a, b, c, die durch Zentrifugieren gewonnen wurden, genau angeben. Ein Beispiel zeigt die Abb. 1, in der die Korngrößenverteilung innerhalb der drei Fraktionen für eine Schlammprobe dargestellt ist. Die Meßwerte der Korngrößenverteilung sind in der Tabelle 1 zusammengestellt.

Anhand der Proben, die mit der Siebanalyse untersucht worden sind, kann man sagen, daß die Trennung durch Zentrifugieren keine eindeutige Aussagemöglichkeit über die Zusammensetzung der Fraktion liefert. So besteht die Fraktion a keineswegs immer aus Sand, sondern es gibt Proben, die weitgehend aus Schluff bestehen. Der Gehalt an organischer Substanz steigt von der Fraktion a zur Fraktion c an,

Tabelle 1. *Zusammensetzung der durch Zentrifugieren gewonnenen Fraktionen von Rheinschlamm.*

Probe Nr.	Original-Rheinschlamm (Gesamttrockengewicht = 100%; Gesamt-β-Aktivität = 100%)																	
	Fraktion a						Fraktion b						Fraktion c					
	1	2	3	4	5	6	1	2	3	4	5	6	1	2	3	4	5	6
		Anteil am Gewicht der Fraktion a in %						Anteil am Gewicht der Fraktion b in %						Anteil am Gewicht der Fraktion c in %				
	Trockengewicht in %	Sand	Schluff	Rohton	Organisch.	β-Aktivität in %	Trockengewicht in %	Sand	Schluff	Rohton	Organisch.	β-Aktivität in %	Trockengewicht in %	Sand	Schluff	Rohton	Organisch.	β-Aktivität in %
1	90,0	77	23	0	0,6	75,0	9,5	1	89	10	0	22,7	0,5	—	—	—	—	2,3
2	16,0	24	71	5	1,5	9,7	74,0	6	78	16	3,8	70,6	10,0	—	—	—	—	19,7
3	61,0	79	17	4	0,6	39,6	35,0	7	84	9	0,5	52,3	4,0	—	—	—	—	8,1
4	22,0	32	62	6	1,0	13,6	60,0	0	78	22	2,8	55,4	18,0	8	2,8	64	6,0	31,0
5	51,0	85	15	0	0,5	34,3	40,0	24	62	14	3,0	48,2	9,0	2	40	58	5,0	17,5
6	13,5	—	—	—	—	7,6	68,5	5	85	10	3,0	62,0	18,0	6	47	47	4,5	30,4
7	9,0	—	—	—	—	4,5	73,5	18	65	17	2,0	69,3	17,5	0	48	52	4,3	26,2
8	16,0	—	—	—	1,9	8,7	70,0	7	81	12	1,0	65,5	14,0	0	57	43	2,5	25,8

Spalte 1: Anteil des Trockengewichtes der jeweiligen Fraktion am Gesamttrockengewicht des Schlamms in Prozent.
Spalte 2–4: Trockengewichtsanteile von Sand, Schluff und Rohton, bestimmt nach dem Siebverfahren und Trockengewicht der jeweiligen Fraktion in % (ohne organische Substanz).
Spalte 5: Trockengewichtsanteil der organischen Substanz mit H_2O_2 aus den jeweiligen Fraktionen.
Spalte 6: Anteil der β-Aktivität der jeweiligen Fraktionen an der Gesamtaktivität des Schlamms in %.

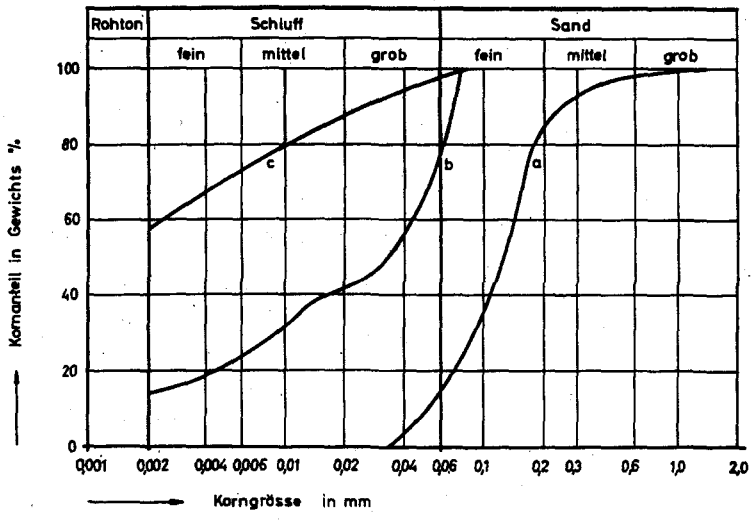

ABB. 1. Kornverteilung in den Fraktionen a, b und c.

doch enthält auch die Fraktion c nur einen geringen Anteil an organischen Stoffen, maximal 6%.

Dennoch hat die Aktivitätsbestimmung der einzelnen Schlammfraktionen ergeben, daß die spezifische Aktivität sich innerhalb einer Fraktion von Probe zu Probe trotz stark schwankender Korngrößenverteilung nur wenig unterscheidet. Das bedeutet, daß das Zentrifugierverfahren zur Aktivitäts- und Anlagerungskoeffizientbestimmung ausreicht, da die Korngrößenverteilung innerhalb einer Fraktion offenbar nur geringen Einfluß auf die spezifische Aktivität hat. Viel entscheidender ist der Anteil an organischem Material. Es wäre deshalb wünschenswert, eine Methode zur reproduzierbaren Abtrennung der organischen Bestandteile zu finden, deren Substanzmenge bisher zwar festgestellt, aber nicht getrennt auf Radioaktivität und Fixierungsvermögen untersucht werden kann.

3. DISKUSSION DER ERGEBNISSE

3.1. *Gesamt-Schlamm*

Als wichtigstes Ergebnis der Untersuchungen kann festgestellt werden, daß Cer weitaus am stärksten vom Schlamm angelagert wird. Es folgen, mit immer noch sehr starker Anlagerung, Ruthen und Phosphor. Cäsium und Strontium werden mittelstark fixiert, während Jod fast überhaupt nicht angelagert wird. Die für Phosphor ermittelten Werte schwanken stark, und zwar sowohl von Monat zu Monat für die gleiche Entnahmestelle, als auch von Entnahmepunkt zu Entnahmepunkt im jeweiligen Jahresmittel. Das ist jedoch nicht besonders erstaunlich, wenn man die Gegebenheiten des Phosphor-Metabolismus bei den pflanzlichen und tierischen Organismen im Schlamm in Betracht zieht.

Die über alle Entnahmestellen gemittelten Monatswerte sind in Abb. 2 aufgetragen. In diesem zeitlichen Verlauf sind, obwohl infolge der nicht unerheblichen Schwankungen eine detaillierte Analyse kaum möglich scheint, doch zwei deutlich voneinander verschiedene Gruppen zu betrachten. Die Elemente Jod, Cäsium und Strontium, die insgesamt eine geringe Anlagerung zeigen, weisen in den Wintermonaten ein Minimum des Verteilungskoeffizienten und die Tendenz zu einem Frühjahrsmaximum auf. Die Elemente Phosphor, Ruthen und Cer mit einem insgesamt hohen Anlagerungsvermögen haben dagegen ein Wintermaximum des Verteilungskoeffizienten und ein Minimum im Frühjahr und Frühsommer. Das Verhalten während der Sommer- und Herbstmonate ist jedoch bei allen Elementen sehr

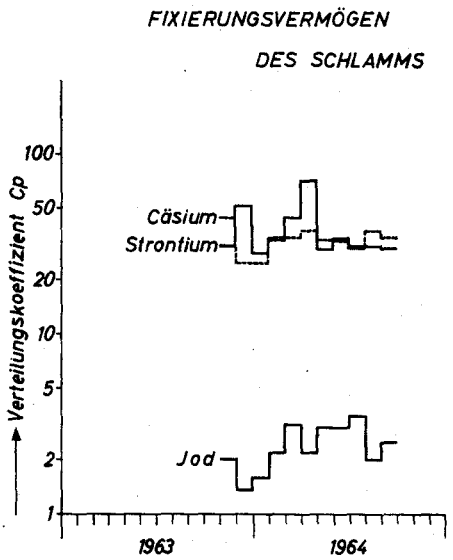

Abb. 2a. Jahresgang des Anlagerungsvermögens für Jod, Strontium und Cäsium.

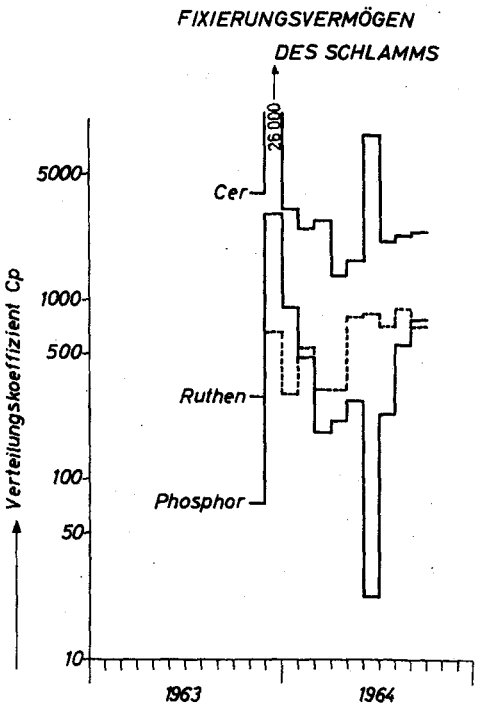

Abb. 2b. Jahresgang des Anlagerungsvermögens für Phosphor, Ruthen und Cerium.

unterschiedlich. Ob es sich bei den beschriebenen Erscheinungen um typische Verhaltensweisen der einzelnen Elemente handelt oder ob diese nur während eines einzigen Jahreszyklus durchgeführten Messungen zufällige Ergebnisse aufweisen, könnte nur durch weitere mehrjährige Untersuchungen geklärt werden.

Die in den einzelnen Schlämmen gemessene Radioaktivität steht nicht in einer erkennbaren zeitlich konstanten Beziehung zum Anlagerungsvermögen. Das ist auch nicht zu erwarten, da sowohl die spezifische Aktivität des Flußwassers als auch das Anlagerungsvermögen starken, aber voneinander unabhängigen zeitlichen Schwankungen unterworfen sind. Dagegen läßt sich innerhalb einzelner Flußgebiete im zeitlichen Mittel ein Zusammenhang zwischen Aktivität und Anlagerungsvermögen erkennen.

Tabelle 2. Verteilungskoeffizienten der einzelnen Schlammanteile für die untersuchten Elemente.

(*Mittelwerte aus jeweils etwa 90 Einzelwerten.*)

Element	Sand	Lehm	Organ. Material
Cer	836	751	747
Ruthen	214	301	627
Jod	1,0	2,0	5,2
Phosphor	200	149	438
Cäsium	32	45	80
Strontium	21	31	75

Zum Beispiel findet man in den Schlämmen der Ruhr eine besonders hohe Fallout-Aktivität und ebenso ein stark erhöhtes Anlagerungsvermögen.

3.2. *Schlammfraktionen*

In Tabelle 2 sind die Mittelwerte der Verteilungskoeffizienten für die untersuchten 6 Elemente in den einzelnen Schlammfraktionen wiedergegeben. Jede Zahl der Tabelle repräsentiert einen Mittelwert aus jeweils rund 90 Einzelwerten. Mit Ausnahme des Ceriums, das ein sehr hohes, aber etwa gleichbleibendes Anlagerungsvermögen zeigt, und des Phosphors, bei dem der Wert für Lehm relativ zu niedrig liegt, nimmt bei den untersuchten Elementen das Anlagerungsvermögen von der Sand- zur Lehm-Fraktion um etwa den Faktor 1,5, von der Lehm- zur organischen Fraktion um etwa den Faktor 2 zu. Daraus ist zu schließen, daß einerseits die vergrößerte Gesamtoberfläche der feinkörnigen Fraktion, andererseits aber mehr noch der Gehalt an organischen Bestandteilen die Anlagerung der Radioelemente begünstigen.

LITERATUR

1. R. MAUSHART and M. WINTER. *DIRECT INFORMATION*, 17/65. Braun Verlag, Karlsruhe.

LA RADIO-ACTIVITÉ DES EAUX, DES MATIÈRES EN SUSPENSION ET DES BOUES DANS LES COURS D'EAU DU BASSIN DU RHIN (MÉTHODES ET RÉSULTATS)

P. KAYSER
Service de Radioprotection, Direction de la Santé Publique, Luxembourg (Luxembourg)

B. JUGUET
Section Radioactivé, Laboratoire d'Hygiène de la Ville de Paris (France)

et

M. COLLET
Direction Protection Sanitaire, Euratom, Bruxelles (Euratom).

Résumé—L'étude de la radio-activité du bassin du Rhin, menée conjointement par des laboratoires des différents pays de la Communauté Européenne, fut executée selon des méthodes de prélèvement et de mesure uniformes ou harmonisées, afin d'arriver à des résultats comparables.

On a à la fois, déterminé les activités alpha, bêta et gamma globales des eaux, des matières en suspension et des sédiments du Rhin et de ses affluents et les radio-éléments particuliers, comme le ^{90}Sr, le ^{226}Ra, le ^{141}Ce–^{144}Ce, le ^{103}Ru–^{106}Ru, le ^{137}Cs, le ^{95}Nb–^{95}Zr et le ^{40}K.

Dans cet exposé seront décrites les méthodes de prélèvement et de mesure ayant servi à cette étude commune.

Un aperçu des résultats obtenus sera présenté, suivi de commentaires sur l'évolution de l'activité au cours du temps et sur les activités enregistrées en fonction des différents points de prélèvements.

Des conclusions seront tirées à la lumière des résultats obtenus.

REMOVING RADIOACTIVITY FROM MILK

JAMES G. TERRILL, Jr., RONALD E. BALES and JOHN L. S. HICKEY
U.S. Department of Health, Education and Welfare, Public Health Service,
National Center for Radiological Health, Washington, D.C.

Abstract—The need for measures to reduce public exposure to environmental radiological contamination from accidents and fallout has led to a program of research, development, field testing, and operations by the Public Health Service in the United States over a period of several years. This effort has now been focused to form a consistent pattern under the guidance of the Federal Radiation Council. Laboratory, field sampling, and evaluation experiments related to radioactive iodine will be presented. The data from various research investigations useful to operating agencies in the benefit-risk decisions will be described. The research, development, and large-scale testing of methods for concurrently removing anions and cations from milk during processing will be described including presentation of data from both laboratory and large-scale experiments. Cost data related to some large-scale experiences will be given where it would be useful for comparative purposes. Presently, for example, the work indicates that a ^{90}Sr removal process alone will add approximately 2 cents per quart to the cost of milk. Indicators of possible ways to reduce this cost by combining control procedures, such as for ^{131}I and ^{90}Sr, will be given. The administrative procedures used to initiate each phase of the laboratory research, development, and field evaluations of these systems will be described.

INTRODUCTION

Historically, the Public Health Service has had the principal Federal responsibility for protecting the public from health hazards in the United States. In the radiological health field, the Public Health Service has adopted a two-prong approach; first, to determine where the radiation health hazards exist, and second, to do something to eliminate them. This approach might be termed one of "surveillance plus action". This program is carried out by the National Center for Radiological Health of the Public Health Service.

To demonstrate how this approach works, let me refer to Fig. 1 which is derived from the U.S. Federal Radiation Council chart showing several important paths of ingestion of radioactive material in man. It is not the intention to cover the entire National Center for Radiological Health program, but to briefly describe the range of our surveillance-plus-action approach and then focus on how this approach was carried out in the development of practical methods for protection of the public from radiation exposure through milk.

You will note in Fig. 1 that tobacco and water have been added to the Federal Radiation Council chart as being part of the chain of human ingestion. Under the "surveillance" portion of our program, the Center now monitors the amount of radioactive traffic along several of these paths through extensive networks. The Center monitors the amount of radioactivity in the atmosphere and the extent to which it is deposited on the earth's surface. The amounts of radioactivity in water, milk, and food are also regularly determined. This information is summarized and made available to the profession and the public regularly through Radiological Health Data and Reports, a publication of the National Center for Radiological Health. [1]

This surveillance is essential in that it indicates existing potential problem areas of environmental radiation exposure and guides the direction of our "action" program. Some of our

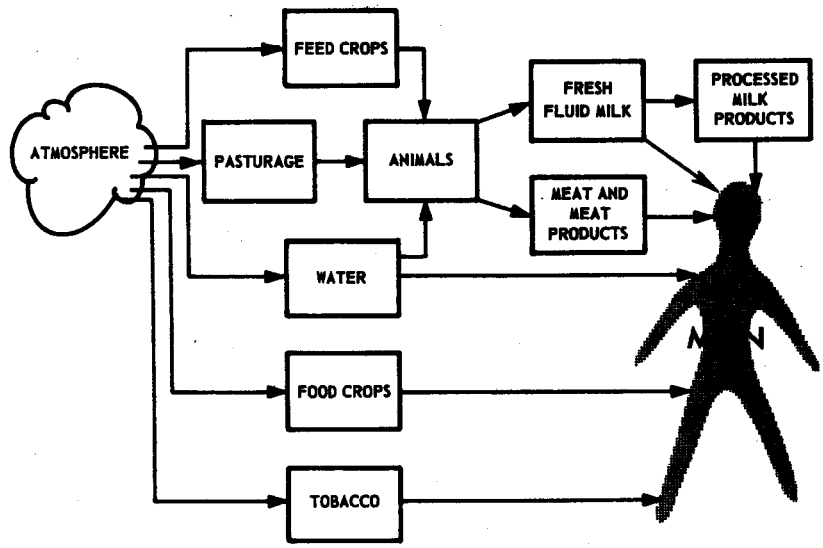

FIG. 1. Important paths of ingestion of radioactive materials in man.

action consists of notification of states or industry of the data observed. A system through which surveillance networks can be used to implement the Protective Action Guide applicable to ^{131}I recommended by the Federal Radiation Council has been described earlier.[2] This system can be applied on a regional, state, milk shed or individual farm basis. Other actions consist of research on ways to break this transmission chain at several points. For example, the Center is now doing research aimed at controlling uptake of radionuclides from the soil into feed crops. It is also investigating methods for removal of radioisotopes from tobacco, and has two projects under way to determine practical methods for reducing the uptake of radionuclides in meat and milk from animals which eat feed containing high levels of radioactivity.

One of the major efforts over the years has been directed at the problem of radioactivity in fresh milk as a result of fallout. This paper will describe this research and development in some detail. In the United States, the persons responsible for weapons development began in the early 1950's to be concerned about the projected increase in strontium–calcium ratios in the environment and to a degree based their testing plans on learning more about this factor with the aim of reducing the amount of strontium released to the environment. The Public Health Service began in 1954 to analyze selected U.S. milk supplies for certain radioisotopes. By 1958, the levels of ^{90}Sr observed in this milk indicated that the maximum permissible concentration (MPC) which existed at that time for milk might be exceeded in some locales in the United States. At this time, the consensus of testimony before Congressional hearings on fallout in milk was that the MPC should be between 33 and 150 PCi/l., with the most commonly discussed figure at 73 PCi/l.

Because of the long half-life of ^{90}Sr and its biological similarity to calcium, it is generally regarded to be one of the principal fission products which may affect the health of humans. Since milk is such a basic food and is the main source of calcium for most western countries, it therefore has received principal attention as a health hazard.

Several laboratories have done work which indicated that an ion-exchange process could be developed for removing ^{90}Sr from milk. As early as 1954 the University of California investigated radiostrontium removal from milk by ion-exchange under contract with the U.S. Atomic Energy Commission. There were also the studies of Migicovsky[3] of the Canadian

Department of Agriculture, studies by the British Atomic Energy Research Establishment,[4] the work sponsored by the Atomic Energy Commission of the University of Tennessee[5, 6] and studies by the Public Health Service in Cincinnati.

ORGANIZATION OF RESEARCH AND DEVELOPMENT

There was thus at this time (1958) strong indications that a practical process for removing ^{90}Sr from milk could be developed. Since no private milk producer could have been expected to underwrite the necessary research, the three government agencies most vitally concerned (the Atomic Energy Commission, the Department of Agriculture and the Public Health Service) entered into a cooperative agreement to underwrite jointly the cost of a program to develop a feasible process for removing ^{90}Sr from milk. The program, financed equally by the three agencies, was carried out in the Agricultural Research Service's Eastern Utilization Research and Development Division in Beltsville, Maryland. Representatives of the cooperating agencies established two criteria for the process: first, it had to remove substantial quantities of ^{90}Sr from fresh milk, and second, it had to do so without impairing the milk. Laboratory scale research was carried out by the Agricultural Research Service and the Public Health Service, and on the basis of these tests a pilot plant was constructed to test the practicability of the process before taking the final step upward to the construction of a commercial scale milk plant.

In September 1959, at the suggestion of the Public Health Service, a joint advisory committee for overall planning was established with membership from the three U.S. agencies and advice from the Canadian Department of Agriculture. This group acted as a steering committee guiding the direction of the research work.

COMMERCIAL SCALE FIXED-BED CATION REMOVAL

In September 1962 this committee recommended that the agencies develop a commercial scale plant for radionuclide removal from milk. This recommendation was based on the laboratory and pilot plant work to date[7-9] which indicated success in the treatment of milk in the pilot plant without impairment of nutritional or organoleptic qualities.

In October 1962 the Public Health Service and the Department of Agriculture jointly agreed to finance investigations on the commercial feasibility of the pilot plant process. As a result of this agreement, a contract was let in June 1963, equally financed by both agencies, with the Producers Creamery Company of Springfield, Missouri for the construction, operation, and evaluation of a full-scale ion-exchange plant capable of treating 100,000 lb of milk per 8-hr day. It should be noted that the Atomic Energy Commission did not participate in this phase of the project, as the Commission believed it was not within its province to carry their support past the research into the practical application stage.

As an aside, I would like to point out that at this time, mid-1962, the ^{90}Sr levels in the U.S. milk supply were near the low end of the range considered by the Federal Radiation Council to be an acceptable intake for a lifetime. Although these levels were expected to remain low for the foreseeable future, from a long-range viewpoint it appeared, and still appears, that we should be in a position to safeguard such a vital food as milk in the event of any emergency. The possible seriousness of widespread contamination of the U.S. milk supply is indicated by the fact that over four million liters of fresh milk are consumed daily by infants less than two years old, the age group which is considered to be critical from the standpoint of radionuclide intake. This is based on a population of eight million in this age group with an average consumption of 500 ml of fresh milk per day.[10] It should be noted that fresh milk consumption by individual infants may approach 1000 ml per day, but because a large number consume no fresh milk, the average intake is lower.

In the contract with Producers Creamery Company, the development of the mechanical design was left in the hands of the Company. The ultimate objective of this contract was to produce practical working drawings which could be duplicated by the milk industry in the construction of other large scale plants for removal of radionuclides from milk if necessary. The

contract included requirements for the performance of tests to determine the percent removal of ^{90}Sr and the effect of the treatment on the milk from the standpoint of sanitary, organoleptic, and nutritional quality.

Within a year after letting of this contract, the full-scale plant (shown in Fig. 3) had been completed and on June 24, 1964, the first full-scale treatment of 107,000 lb of fresh whole milk was successfully carried out in 12 hr and 10 min.

The environmental level of ^{90}Sr in the raw milk was 38.4 PCi/l. Samples of the treated milk taken at intervals indicated that the treatment process reduced the ^{90}Sr levels to between 1 and 3.2 PCi/l., a removal of greater than 90%. Subsequently, on September 16, 1964, and on February 25, 1965, full-scale milk treatment operations were carried out with similar results.

This series of tests successfully demonstrated the commercial feasibility of the process. The plant removed more than 90% of the environmental levels of ^{90}Sr with no increase in microbial population, a very slight decrease in flavor score, and only minor compositional changes.[11, 12] The cost of processing was estimated to be 1.7 to 2.3 cents per quart of milk.[11]

The first full-scale test (June 24, 1964) was observed by the joint advisory committee, with representatives of the Public Health Service, the Agricultural Research Service and the Canadian Department of Agriculture present. A meeting of this group immediately following the tests laid the groundwork for expanding this commercial process to include a unit for the removal of radioactive anions, particularly ^{131}I, from milk.

LABORATORY SCALE FIXED-BED ANION-CATION REMOVAL

In the early days of nuclear testing, radioiodine had been overlooked as a hazard in milk, because of the difficulty in measuring it and also because of the short half-life. As a result of weapons testing in 1961 and 1962 it had been observed that the quantities of ^{131}I in milk in the United States reached relatively high levels, as shown in Fig. 2. When these results were associated with the doses of radioiodine considered safe for lifetime intake, it

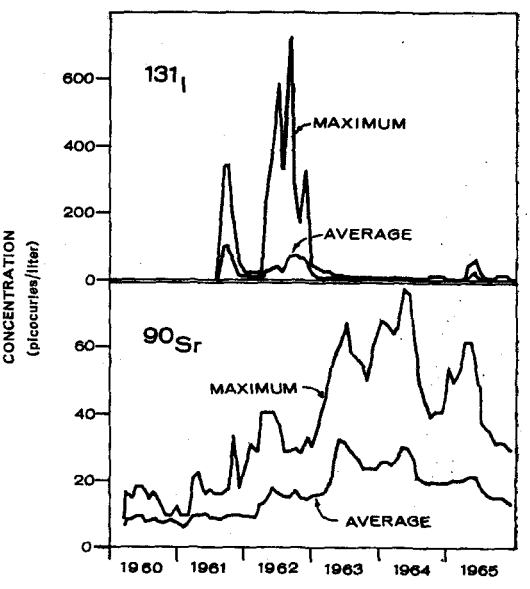

FIG. 2. ^{131}I and ^{90}Sr concentrations in milk. From U.S.P.H.S. pasteurized milk network.

became apparent that the dose of radioiodine to the susceptible population group might, in some geographic areas, exceed the radiation protection guide which had been established by the Federal Radiation Council for "normal peacetime operations". Thereafter, radioiodine was recognized to be a nuclide of major concern in milk. Public Health Service action included development of techniques for rapid measurement of radioiodine and investigation of ways to break the transmission chain (again referring to Fig. 1) between the contaminated feed and the milk-producing cattle. The Division of Radiological Health established a dairy farm near the nuclear test site in the State of Nevada to evaluate whether iodine levels in milk, following radioiodine release, could be kept low by various means, including substituting uncontaminated feed for pasturage on which local dairy cattle ordinarily grazed. As a result of these studies, whenever this technique has been used, the results were much as the earlier studies had predicted. It is therefore considered to be a practical method in localized areas for preventing radioiodine contamination of milk in a

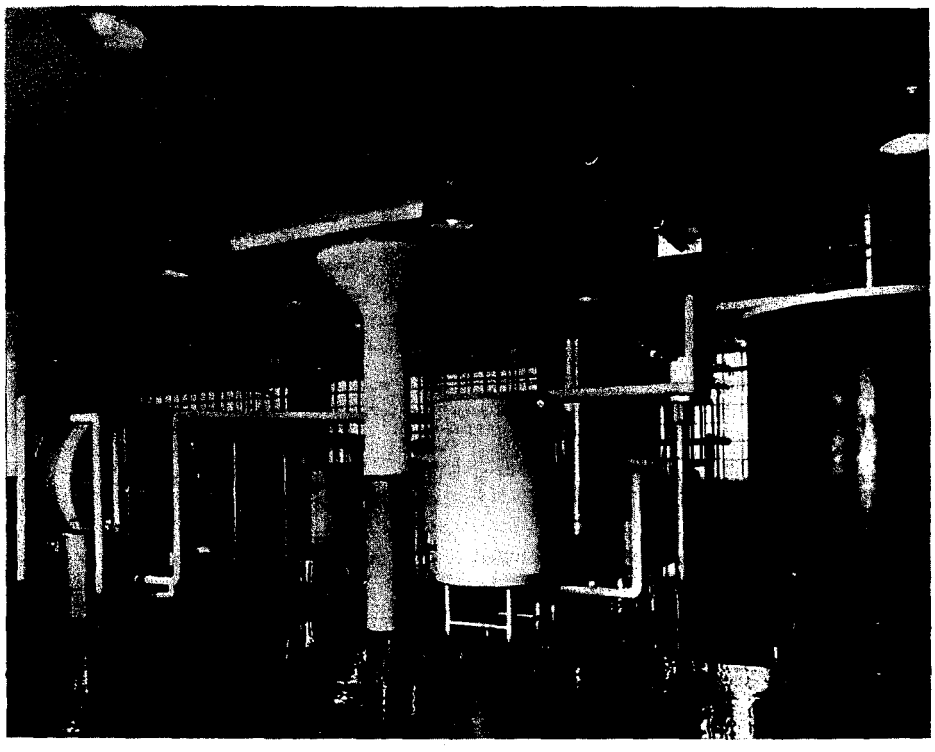

FIG. 3. Commercial scale fixed-bed plant for removing ^{90}Sr from fresh milk.

country such as the United States, where a rapid monitoring system for radioiodine exists.

Even with the development of this method for reducing transmission of radioiodine from atmosphere to man, the Public Health Service had encouraged laboratory scale studies to develop methods for removal of anionic radionuclides, principally ^{131}I, from milk by ion-exchange. Murthy *et al.*[13, 14] had obtained 90% ^{131}I removal from fluid whole milk labeled *in vivo*, and removal of over 95% of ^{131}I from milk labeled *in vitro* by passage through Dowex 2-X8 resin. The flavor of the treated milk was comparable to that of untreated milk, and the anionic composition of the milk was not altered significantly.

By 1964, it was felt that a practical method for removing ^{131}I from milk could be developed on the basis of the laboratory work. Under sponsorship of the Public Health Service and the Department of Agriculture, a contract was let with the same commercial milk processor to design and build a full-scale system to remove ^{131}I from milk which would be compatible with the cation removal process, and to incorporate it into the existing full-scale plant. The contract also included full-scale testing of the enlarged plant to confirm the feasibility of the combined strontium–iodine removal process. The progress and results of this endeavor are reported here in some detail, as the final tests were only recently completed.

Prior to design and construction of the full-scale anion removal unit, further laboratory tests were performed by the contractor. The laboratory-scale system consisted of an anion-exchange column of 200 ml Dowex 2-X8 resin followed by a cation-exchange column of 920 ml amberlite IR 120 resin. The flow diagram of this system is shown in Fig. 4. The treatment is similar to that previously described[8, 11] except that treatment for anion removal precedes the cation removal process. Following passage through the anion column, milk was acidified

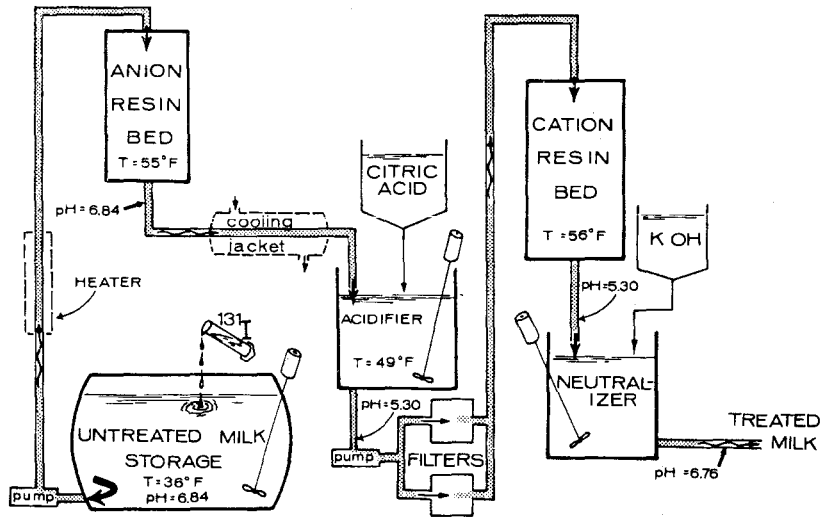

FIG. 4. Laboratory scale cation-anion bed system, with typical pH and temperature.

to pH 5.3 with 20% citric acid solution and filtered before passage through the cation removal column. The pH was then adjusted to 6.8 with 2M KOH (about 15 ml/l. of milk).

Anion removal preceded cation removal because the regenerant salts for the anion resin bed had been proportioned on the basis of the ionic content of normal raw milk. Since cation treatment increases the potassium and citrate content in the milk, treatment for anion removal subsequent to cation removal would have required further laboratory development on regenerant salt proportioning and delayed the program. It may be practical to have cation treatment precede anion treatment.

Four trial runs were made with this system. In each run, 35 l. of grade A whole raw milk were processed at a flow rate equivalent to 16,200 lb/hr in the full-scale cation-removal plant.

The milk was labeled with from 4000 to 48,000 PCi/l. of ^{131}I, as the environmental level was too low to be readily detectable. A small quantity of sodium sulfite (50 μg) was added to the ^{131}I tracer solution to prevent iodide oxidation. The environmental level of ^{90}Sr in the milk was approximately 30 PCi/l.

The laboratory-scale plant performed satisfactorily. In the final trial run, ^{131}I was reduced 97.1% (from 3970 to 115 PCi/l.), and ^{90}Sr was reduced 84.5% (from 30.7 to 4.7 PCi/l.). ^{90}Sr removal was less than expected on the basis of past experience. However, because of the limited accuracy in ^{90}Sr analysis at such low levels and the demonstrated ability of the full-scale plant to remove over 90% of ^{90}Sr, it was decided that further laboratory testing of cation removal was not necessary.

The organoleptic quality of the processed milk (which had been pasteurized) was compared with that of the raw milk and also with pasteurized homogenized milk purchased locally. The processed milk showed a slight but insignificant change in flavor.

Chemical analyses of the raw and processed milk showed no significant changes due to processing other than the expected increase in the citrate and potassium from the acidification and neutralization processes.

Of some concern was the formation of a visible precipitate in samples of processed milk after standing overnight. Solubility index determinations were made on various fractions of processed milk from one trial in an effort to determine the seriousness of the problem. On the basis of these tests, it was concluded that this was due to inadequate mixing of the acid and neutralizer with the milk, and that rapid mixing

of both citric acid and potassium hydroxide is necessary to insure stability of the milk.

From the results of the laboratory tests, it was concluded that, assuming good control of acid-base mixing, the commercial scale combined process would produce a commercially acceptable homogenized milk. Design of the anion resin unit therefore proceeded on the basis of the laboratory findings.

COMMERCIAL SCALE FIXED-BED ANION-CATION REMOVAL

The full-scale ^{90}Sr removal plant has been described previously.[11, 12] The flow diagram in Fig. 5 shows where the anion resin column was inserted in the system. The anion column (Fig. 6) is a mild carbon steel cylinder 26 in. in diameter and 100 in. long with an inner lining

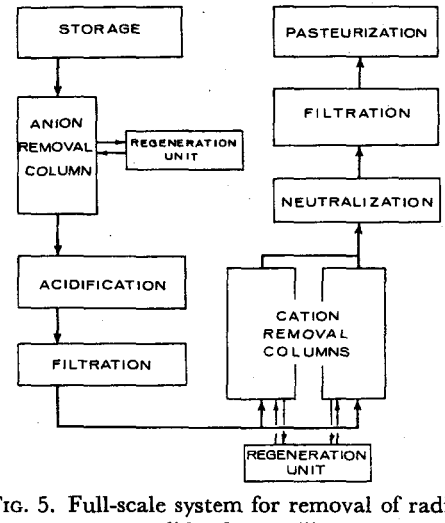

FIG. 5. Full-scale system for removal of radionuclides from milk.

of $\frac{1}{4}$ in. thick, high density polyethylene. The cylinder contains 284 l. of Dowex 2-X8 resin. The resin is supported on a sixty-mesh woven nylon screen resting on a 5 in. bed of graded glass beads $\frac{1}{2}$ to 1 in. in diameter. As in the remainder of the plant, all materials, chemicals and resins used in the anion unit in contact with milk had been previously approved by the U.S. Food and Drug Administration for use in food processing.

Three full-scale plant tests of the system were made in May and June 1966, with 100,000 lb of fresh milk processed in each test.[15] In the first test (May 18, 1966) the milk was labeled *in vitro* with 1880 PCi/l. of ^{131}I. Processing reduced this to 87 PCi/l., a removal of 95.4%. Radiation levels outside the anion column reached 0.1 mr/hr on the surface of the column at a point opposite the surface of the resin. The treated milk lost some flavor; however, this was noticed principally in the first 15,000 lb of milk, and thus the flavor loss was related to the start up of the process.

The second test run was made June 8, 1966. The milk was labeled *in vitro* with 2000 PCi/l. of ^{131}I and 3000 PCi/l. of ^{85}Sr, as environmental levels of both ^{131}I and ^{90}Sr in the raw milk were too low for accurate determination of the efficiency of radionuclide removal. The milk was processed at the rate of 19,300 lb/hr, approximately 50% above the design flow rate of the cation column and 20% above the design flow rate of the anion column.

The final test run was made June 22, 1966. Milk was labeled *in vitro* with 4760 PCi/l. of ^{131}I and 4225 PCi/l. of ^{85}Sr, and processed at approximately 20,000 lb/hr. The results of the last two test runs are shown in Tables 1 through 4.

As shown in Table 1, the process removed over 99% of the ^{131}I and over 91% of the ^{85}Sr. The strontium removal efficiency decreased toward the end of each run, falling below 90% removal after treatment of 25 resin bed-volumes (rbv) of milk at a flow rate of 0.11 rbv/min. This decrease is thought to be due to the high flow rate as reported by Walter.[16] It may be necessary to use a larger amount of cation resin to maintain satisfactory strontium removal at high flow rates.

Analysis of the milk processed on June 8, 1966, by gamma spectroscopy also showed that treatment reduced the environmental (*in vivo*) levels of ^{140}Ba by 88% and ^{137}Cs by 71%.

Chemical analyses of the milk processed on June 8, 1966, are given in Table 2. The increases in citrate and potassium are due to chemicals added in the acidification and neutralization processes. The differences in the other chemical ions in the raw and processed milk are inherent in the process, as the quantities of regenerant

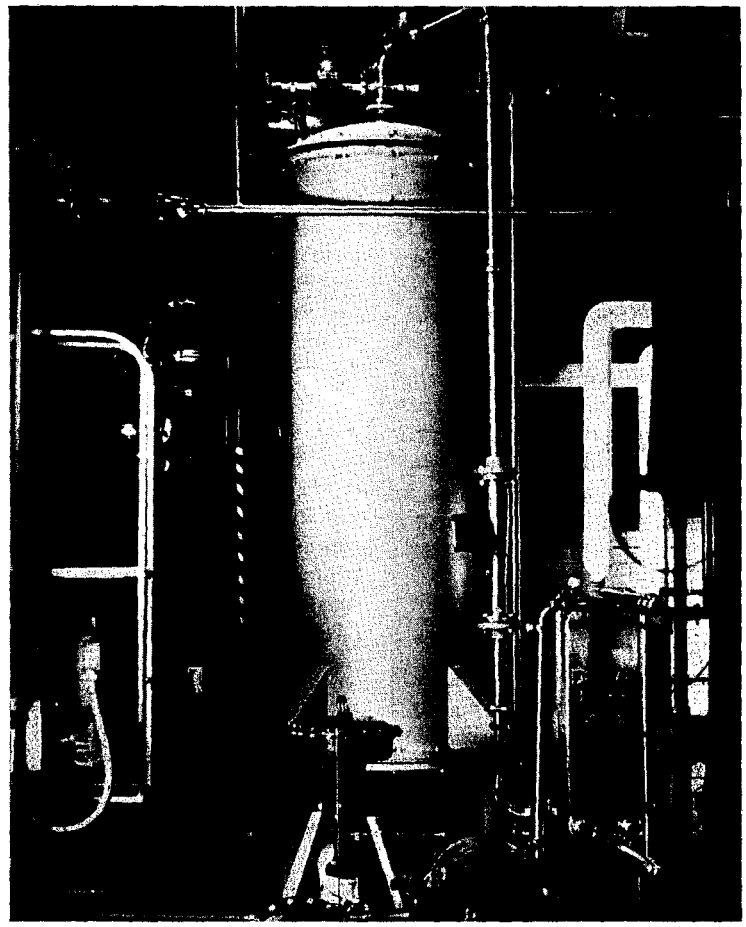

FIG. 6. Commercial scale resin bed for removing ^{131}I from milk.

salts are based on an "average" milk, which may differ from the milk processed on any single day. These differences between the raw and processed milk are not considered significant.

The dilution of the milk due to processing was calculated on the basis of the change in total solids and fat content of the milk during processing. These values are shown in Table 2. Approximately 2.5 to 3% of this is due to water added in the acidification and neutralization processes. The remainder, particularly the excessive dilution in the first 3000 lb of milk processed, is due to the fact that the system is full of water when processing begins and there is considerable mixing at the water-milk interface. As a result, the first portion of milk processed is quite heavily diluted. Chemical analyses of the milk treated on June 22, 1966, were comparable to those of the milk treated on June 8, 1966.

Flavor tests were made on the raw and processed milk to determine the effects of treatment on the organoleptic quality of the milk. Results are shown in Table 3. The first 1000 lb of milk treated on June 8, 1966, was not acceptable in flavor, and contained a taste described as "astringent". This taste, associated with starting plant operation, had been observed before and is tentatively attributed to the anion resin regeneration and storage procedure. Laboratory tests have shown that storage of the anion resin in 2 M HCl deteriorates the resin. Storage at a higher pH (2.0) is indicated to minimize resin deterioration.

Table 1. Removal of ^{131}I and ^{85}Sr from Fresh Milk

Pounds of milk processed	^{131}I				^{85}Sr			
	June 8, 1966		June 22, 1966		June 8, 1966		June 22, 1966	
	pCi/l.	% removed	pCi/l.	% removed	pCi/l.	% removed	pCi/l.	% removed
Tank No. 1* 0	2220	—	4760	—	3030	—	4225	—
Tank No. 2* 0	2070	—	—	—	2680	—	—	—
15,000	34	98.5	43	99.1	20	99.3	378	99.2
30,000	21	99.0	38	99.2	25	99.2	356	91.6
45,000	28	98.7	56	98.8	95	96.9	337	92.0
60,000	32	98.5	52	98.9	108	96.0	298	93.0
75,000	30	98.6	59	98.8	269	90.0	412	90.3
90,000	40	98.0	85	98.2	414	84.6	568	86.6
Composite sample of 100,000 lb of processed milk	15	99.3	43	99.1	70	97.5	357	91.6

* The first 50,000 lb of milk treated was from Tank No. 1 and the remainder was from Tank No. 2.

Table 2. Composition of Milk Processed June 8, 1966

Pounds of milk processed		Solids %	Fats %	Ash %	Na ppm	K ppm	Ca ppm	Mg ppm	Citrate ppm	Chloride ppm	Phos. ppm	Sol. Index
(Raw)	0	12.43	3.59	0.73	457	1725	1217	112	1840	984	653	0.04
	3000	10.84	3.04	0.73	488	2488	994	241	4000	465	533	—
	9000	12.02	3.33	0.81	431	2625	1108	245	4140	666	586	—
	15,000	12.12	3.41	0.78	401	2275	1157	263	3400	858	583	—
	45,000	12.18	3.38	0.84	451	3075	1117	147	3600	954	595	0.04
	60,000	12.25	3.40	0.89	487	3200	1163	99	3840	954	600	—
	75,000	12.21	3.40	0.87	438	2825	1124	134	3520	968	598	—
	90,000	12.22	3.41	0.86	443	2850	1185	119	3320	982	595	0.04
(Composite)	100,000	12.06	3.37	0.83	490	2725	1155	145	3640	908	550	0.05

% Dilution of milk from processing calculated from change in	Solids %	Fats %
First 3000 lb	17.8	18.1
Next 6000 lb	6.3	7.8
Next 80,000 lb	4.3	5.6
(Composite) 100,000 lb	5.5	6.5

Table 3. Evaluation of Flavor in Processed Milk

Pounds of milk processed	Flavor score*					
	Raw milk		Effluent from anion column		Fully processed pasteurized milk	
	June 8	June 22	June 8	June 22	June 8	June 22
0	37.4	soured	—	—	—	—
1,000			—	37.2	33.6	35.3
9,000			36.1	36.7	—	36.8
15,000			—	36.6	35.3	36.7
22,000			36.1	—	—	—
26,000			—	—	35.6	—
30,000			—	36.8	36.2	35.8
38,000			36.4	—	—	—
60,000			—	36.3	36.0	36.3
61,000			36.4	—	—	—
90,000			—	36.7	36.2	36.4
95,000			36.3	—	—	—
Composite of 100,000			—	—	35.9	36.3

* American Dairy Science Association standard flavor test; perfect score is 40; acceptable score for pasteurized commercial market milk is 35.

The flavor score of the last 70,000 lb of processed milk was higher than that of the composite sample, indicating that the initial volume of unacceptable milk affected the quality of the entire 100,000 lb of milk.

To minimize the taste problem, the anion resin was stored at pH 2.0 between June 8 and June 22, 1966. This procedure, plus discarding the first 1000 lb of milk treated on June 22, 1966, was believed to be responsible for the improved flavor scores in the milk treated on June 22 (see Table 3).

The results of microbiological examination of the milk processed on May 18 and June 8, 1966, are shown in Table 4. The high coliform counts are attributed to contamination after pasteurization due to immediate storage of the finished milk in the raw milk tank which had not been adequately cleaned. The microbiological examination indicates no significant defects in the processing system itself from the sanitation viewpoint. Bacteriological examination of the milk processed on June 22, 1966, confirm these results.

The use of the woven mesh screen and the glass bead bed in the anion column has caused some concern from the sanitation viewpoint, but no bacteriological growth in this space could be detected from the test results.

In summary, the full-scale plant effectively reduced the levels of ^{131}I and ^{85}Sr in fresh fluid milk without any serious changes in organoleptic, chemical or microbial quality of the milk, and without significant operational problems.

The cost of chemicals for regenerating the anion unit in the full-scale tests was approximately 1.5 cents per quart of milk (¢/qt). Cost of plant operation for strontium removal was 1.7 to 2.3 ¢/qt, including approximately 0.6 ¢/qt for chemicals.[11] Since the addition of the anion column did not increase labor or other costs appreciably, it appears that the combined process adds approximately 3.2 to 3.8 ¢/qt to the cost of milk.

The use of processes involving additives to food shipped interstate commerce requires approval by the U.S. Food and Drug Administration. Therefore, extensive testing of the

Table 4. Microbiological Analysis of Raw and Processed Milk

Sample	Micro-organisms per ml			
	Std. plate count	Psychrophilic	Coliform	Staph.
Test of May 18, 1966				
Raw	137,000	51,000	—	—
Processed and pasteurized	3 500	—	980	0
Test of June 8, 1966				
Raw	9,100,000	10,900,000	—	—
Processed and pasteurized	15,800	—	2260	0
Public Health Service *Recommended Standards**				
Raw	100,000	—	—	—
Pasteurized	20,000	—	10	—

* Grade A Pasteurized Milk Ordinance—1965 recommendations of the United States Public Health Service, PHS Publication No. 229, pp. 39–40, Washington, D.C. (1965).

wholesomeness and nutritional and toxicological quality of the treated milk was necessary to provide the FDA with sufficient data for evaluation of the process as a basis for approval.

In addition to the tests reported above, further chemical and vitamin analysis is being done on the raw and processed milk. Chemical determinations include analysis for crude protein, acidity, ash, iron, copper, iodine, silicone, cobalt, zinc, aluminum, manganese, and molybdenum. Vitamin assays include determination of thiamine (bound and unbound), riboflavin, vitamins A, B_6 and B_{12}, folic acid, ascorbic acid, pantothenic acid, niacin, biotin, and a wide spectrum of fatty acids. Biological and chemical analysis of protein quality will also be carried out.

To evaluate the nutritional quality of the processed milk, baby rats will be maintained 10–12 weeks in seven groups which will receive diets prepared with dried processed or raw (control) milk. Baby pigs (one day old and ten days old) will be maintained until 8 weeks of age on diets prepared from dried processed milk. Feeding studies may also be done with other species of animals.

To provide the materials for this test program, 3000 lb each of the processed and raw milk from the June 8, 1966, test run have been dried and sealed in containers in a nitrogen atmosphere. The testing will be conducted at the PHS Radiological Research Laboratory in Rockville, Maryland.

LABORATORY SCALE MOVING-BED ANION-CATION REMOVAL

The Department of Agriculture and the Public Health Service have been encouraged to conduct research and development for practical methods for removing radionuclides from milk using processes developed in the scientific and industrial community at large, as well as those developed in their own laboratories. One of these which has shown promise is the Higgins continuous ion-exchange contactor.* In this process (see Fig. 7) an ion-exchange resin bed moves counter-current to the flow of milk

* Manufactured by Chemical Separations Corporation, Oak Ridge, Tennessee.

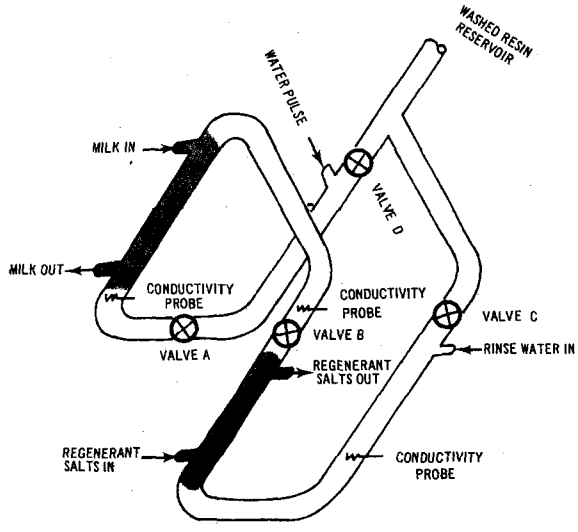

FIG. 7. Flow diagram of moving bed ion-exchange system.

through a closed system, and is regenerated in another section of the system.

Edmondson,[17] using an early model of the system, obtained 90% removal of ^{85}Sr from milk acidified to pH 5.3 and over 90% removal of ^{134}Cs. Edmondson also treated milk for concurrent cation-anion removal by passing acidified milk through a fixed cation resin bed and then through an anion resin in the contactor. The anion resin was charged for simultaneous ^{131}I removal and neutralization of the milk. Removal of 86 to 91% of the ^{131}I was achieved. Although problems were encountered in these investigations with pH control, milk flavor, and regeneration of the anion resin, the results obtained were sufficiently encouraging to warrant further study of the process.

PILOT SCALE MOVING-BED ANION-CATION REMOVAL

In 1964, the Public Health Service and the Department of Agriculture jointly sponsored construction of a moving bed ion-exchange milk treatment plant, based on the Higgins patent.[18] The public's rights to patents resulting from work sponsored by these agencies have been protected under the provisions of the Atomic Energy Act.

Since the process had not been used to treat milk on a large scale, extensive laboratory work was necessary before the plant was designed. Investigations by the Public Health Service[19] formed the basis for the design of the pilot plant. These studies established flow rate, the depth/diameter ratio of the ion-exchange unit necessary for adequate treatment, and identified the need for continual cooling of the milk and adjacent sections of the loop during processing to prevent microbial growth.

The plant (shown in Fig. 8) has a capacity of 7000 lb of milk per 8 hr and consists of two continuous ion-exchange contactors, one for removal of radioactive cations and one for removal of radioactive anions. The resins are the same type used in the full-scale fixed-bed plant. The plant is self-contained (except for power supply) and is designed for mounting on a

FIG. 8. Pilot plant moving bed ion-exchange system.

standard 40 ft × 8 ft truck trailer to make it readily transportable.

This process is still in the experimental stage, and has a large degree of flexibility designed into it, particularly in the operation of the anion bed. The anion removal portion was originally conceived to be a moving resin bed. However, system testing will be done initially with a small anion fixed-bed column, since the high efficiency and large capacity of the anion resin indicates this to be the most simple and adequate operating design for anion removal. Dual anion columns are provided to achieve continuous operation.

The pilot plant is scheduled to be operated at the Public Health Service laboratory in Montgomery, Alabama to evaluate its effectiveness. The plant testing program will include evaluation for efficiency of radionuclide removal, product acceptability (in terms of taste, odor and appearance), product alteration, and sanitary quality. As the operation becomes refined, nutritional testing and/or chemical analyses of the treated milk are planned, using methods similar to those used in evaluating the product from the full-scale fixed-bed plant.

SUMMARY

Although the environmental levels of ^{90}Sr and ^{131}I and other radionuclides in milk are presently well within acceptable limits,[20] it is prudent to have a system capable of treating milk for the removal of these radionuclides in the event of gross environmental contamination to a milk producing area.

In the case of acute contamination of milk with radioiodine, action must be taken promptly to effectively reduce the radiation dose to humans. If a week elapses before controls are initiated, more than half of the human dose will already have been received. With this in mind, the moving-bed unit has been designed and constructed for placement on a standard truck trailer, to determine whether such a mobile unit would be practical. If so, it is estimated that the strategic location of six to twelve full-scale standby mobile treatment units would make it possible to place a unit in operation in any milk shed in the United States within 24 hr should an emergency arise. Because even the large-scale units are limited in capacity, they would be adequate only in the event of radiological contamination covering a limited area. Obviously, an effective surveillance system is required in order to know when to initiate and terminate these control actions.

A major use of the two existing plants in the near future is in the development and refinement of lower-cost treatment techniques or treatment of milk massively contaminated. They may also be used for training and for demonstrating the processes.

It is emphasized, however, that the objective in developing these processing plants is to provide the capability to treat fresh whole milk for immediate human consumption. To this end, formal approval of the U.S. Food and Drug Administration has been requested to use the full-scale combined anion-cation fixed-bed unit for this purpose on an emergency basis, and extensive testing has been undertaken to insure the wholesomeness of the product. Similar approval will be sought for the moving-bed plant at the appropriate stage in its development.

REFERENCES

1. Radiological Health Data and Reports. Published monthly by Public Health Service, National Center for Radiological Health, Washington, D.C., 1960.
2. J. G. TERRILL, JR. Public health radiation surveillance. *Health Physics* **11,** 917 (1965).
3. B. B. MIGICOVSKY. Removal of strontium and cesium from milk. *Can. J. Biochem. Physiol.* **37,** 1287 (1959).
4. P. COSSLETT and R. E. WATTS. The removal of radioactive iodine and strontium from milk by ion exchange. Atomic Energy Research Establishment, Publication AERE-R 2881 (1959).
5. D. G. EASTERLY, B. J. DEMOTT and R. G. CRAGLE. Removal of Sr^{89} and Ca^{45} from milk with ion exchange resins (Abstract). *J. Dairy Science* **42,** 897 (1959).
6. D. G. EASTERLY, B. J. DEMOTT and R. G. CRAGLE. Strontium in milk, I and II. *J. Dairy Science* **43,** 137 and 146 (1960).
7. G. K. MURTHY, E. B. MASUROVSKY, J. E. CAMPBELL and L. F. EDMONDSON. Method for removing cationic radionuclides from milk. *J. Dairy Science* **44,** 2158 (1961).
8. L. F. EDMONDSON, H. E. WALTER, A. M. SADLER, F. P. HANRAHAN, D. G. EASTERLY, J. Y. HARRIS, D. H. KEEFER and A. R. LANDGREBE. Removing radiostrontium from milk—current status of a pilot plant process. *J. Dairy Science* **45,** 800 (1962).

9. R. E. ISAACKS, D. G. HAZZARD, J. BARTH, J. P. WALKER, J. H. FOOKS and L. F. EDMONDSON. Nutritional evaluation of milk processed for removal of cationic radionuclides, II. Feeding Studies. *J. Agr. and Food Chem.* (in press).
10. T. F. MCCRAW. The half-time of cesium-137 in man. *Radiological Health Data and Reports* **6,** 711 (1965).
11. B. HEINEMANN and E. J. BALDI. Large scale fixed bed ion-exchange system for removing strontium-90 from fluid milk. Presented at American Dairy Science Association, June 1965; *J. Dairy Science* (in press).
12. J. H. FOOKS, J. G. TERRILL, JR., B. H. HEINEMANN, E. J. BALDI and H. E. WALTER. Evaluation of full-scale strontium removal system for fluid milk. Presented at Health Physics Society, June 1965; *Health Physics* **13** (3), 279 (1967).
13. G. K. MURTHY, J. E. GILCHRIST and J. E. CAMPBELL. Method for removing iodine^{131} from milk. *J. Dairy Science* **45,** 1066 (1962).
14. G. K. MURTHY and J. E. CAMPBELL. Removal of radionuclides from milk. *J. Dairy Science* **47,** 1188 (1964).
15. Contractors final report. PHS contract p. 86–65–127, Producers Creamery Co., Springfield, Mo., Clearing house for Federal Scientific and Technical Information PB 175709.
16. H. E. WALTER. Pilot-plant and commercial scale development of process for removal of radionuclides from milk. Presented at joint Food and Agriculture Organization—International Atomic Energy Agency Seminar, Vienna, Austria (July, 1966).
17. L. F. EDMONDSON. Ion exchange processes for removing radioactive contamination from milk. *J. Dairy Science* **47,** 1201 (1964).
18. I. R. HIGGINS. Radioactive decontamination of milk, U.S. Patent No. 3, 194, 663 (July 13, 1965).
19. G. K. MURTHY, S. Cox and L. KAYLOR. Removal of radionuclides from milk. Unpublished monthly reports of Milk and Food Research Program, Public Health Service, Cincinnati, Ohio (1964–1966).
20. Application of radionuclide concentrations in pasteurized milk to intake guides, September 1964–August 1965. Radiological Health Data and Reports 6, 688 (1965).

RELEASE OF RADIOACTIVITY FROM NUCLEAR CRATERING EXPERIMENTS*

JOHN A. MISKEL
Lawrence Radiation Laboratory, University of California,
Livermore, California

Abstract—Within the current technology, the use of nuclear explosives for excavation purposes results in the release of radioactivity to the atmosphere. The fraction of the total amount of a given species produced and released to the atmosphere depends on the chemical properties of the species and on the nature of the cratering process.

Data obtained from several nuclear cratering experiments indicate that the fractions of the more volatile species released are relatively insensitive to the cratering phenomenology, whereas the fraction of the refractory species released are highly dependent on it. The controlling factor for the refractory species appears to be the filtering action of the earthmound raised in the initial stages of the crater formation. Two different cratering processes have been studied experimentally. In one, an erosional crater was formed which resulted in essentially no filtering of the debris during the release; in the other, two craters were formed, one with "normal" filtering and one with a much thicker filter bed than optimum. The results of these experiments are presented to document the effect of the filter action on the various radionuclides.

The hazard evaluation for engineering programs involving nuclear excavations can be divided into two parts: first, the close-in area which is of interest with respect to the time-delay of further work on the engineering project; and second, the long-range distribution of the radioactive materials with respect to the entry of radiation into the outside world.

Data from the excavation experiments to date indicate that the close-in fallout is dependent primarily on the chemical species involved; the long-range concentrations appear to be independent of the detailed nature of the source, but depend primarily on the atmospheric dissipative processes once the early fallout has occurred.

INTRODUCTION

A knowledge of the behaviour (and ultimate fate) of the radioactive products produced by a nuclear explosion is essential for the planning of programs involving applications of nuclear explosives. For cratering applications where some of the radioactivity is released to the atmosphere, it is important to have a predictive capability with regard to the amounts released and their probable distribution.

Since an important part of the Plowshare (Civil and Industrial Uses of Nuclear Explosives) Program is concerned with the applications of nuclear cratering phenomena, considerable attention has been given to the design and execution of experiments to obtain data on the release and distribution of radioactivity during crater production. In early 1961 a series of experiments (Project YoYo) was performed in which small craters were produced with buried, 100 g charges of high explosive containing a radioactive tracer. Measurements were made to determine the fraction of the activity that remained in the crater as a function of the depth of the explosive. [1]

Although it was apparent from these experiments that the greater the depth of burial the greater the fraction of the activity that remained in the crater, many detailed questions about the process were left unanswered.

Since the resumption of nuclear testing in the fall of 1961, several cratering experiments have been performed with nuclear explosives; data

* This work was performed under the auspices of the U.S. Atomic Energy Commission.

on the release of radioactive species in these experiments are presented here.

CRATERING EXPERIMENTS

Three cratering experiments have been performed in hard rock at the Atomic Energy Commission's Nevada Test Site; the radioactivity distributions from these experiments have been examined in detail.

A useful parameter for comparing cratering phenomena resulting from explosives with different energy releases is the "scaled depth of burial". The scaled depth is obtained by dividing the actual depth by $W^{1/3.4}$, where W is the "yield" or energy release of the explosive.* The use of scaled depth of burial to describe the emplacement of an excavation explosive essentially removes the dependence of crater dimensions on the yield of the explosive.

Two of the events described here were at a scaled depth of 56.4 m/(kt)$^{1/3.4}$. The other was at a scaled depth of 43.3 m/(kt)$^{1/3.4}$. A description of the resultant craters is given later in the paper.

Measurements were made of the concentrations of various radioactive species in the close-in fallout and in the radioactive cloud. These data were then used to estimate the amount of a given nuclide that was released to the atmosphere. The amount of each isotope released was assumed to be equal to the sum of the total amount of that species in the fallout pattern and in the cloud. The total activity in the cloud was obtained from the earliest cloud sample (in all cases less than 15 min after detonation). This assumes that only a negligible amount of the activity in the cloud at this time results in fallout within the measured pattern. For example, in the Danny Boy experiment, 12% of the ^{137}Cs formed was in the cloud at 8 minutes and 1% in the fallout pattern. Therefore, it was assumed that 13% of the ^{137}Cs was released to the environment.[2]

To determine the total activity of a given nuclide in the fallout pattern it is necessary to measure its activity per unit area (as a function of position in the pattern) and then to integrate the activity over the pattern. The assumption of the effective area of the fallout collector and the relationship between field measurements (which delineate the pattern) and the amount of a specific nuclide present introduce considerable error into the absolute values obtained. Similarly, for the cloud samples the estimation of the total cloud volume at the time of sampling and of the fraction of the cloud sampled also make uncertain the absolute amounts of any given species present. However, the relative amounts of the various nuclides present in a given sample are much more precisely known.

The amount of any given species released to the atmosphere in a cratering experiment is dependent on the chemical nature of the isotope. In examining the radioactivities released in these cratering experiments, an attempt was made to choose nuclides that would be representative of each of the three classes of chemical species: refractory, volatile and intermediate.*

CRATER PRODUCTION PHENOMENOLOGY

An understanding of the mechanism of crater production by buried explosives is useful in discussing the behaviour of the radioactive species produced by the explosive. For this reason a brief outline of the phenomenology is given here.

When a nuclear explosive, buried at the proper depth for crater production, is detonated the following sequence of action leading to a crater occurs: (1) The medium surrounding the explosive is vaporized, melted, and fractured (Fig. 1, A); (2) a shock wave proceeds radially outward from the high-pressure cavity region (Fig. 1, B); (3) when the shock wave reaches the surface, the cavity grows preferentially in that direction (Fig. 1, C); (4) the surface material is accelerated, rising as a dome-like structure and the gaseous materials within the cavity

* The energy release of nuclear explosives is frequently expressed as "kilotons-equivalent" (or just "kilotons") where 1 kiloton is defined as 10^{12} cal and is approximately equivalent in energy release to 10^9 g of TNT.

* The designation "refractory, volatile or intermediate" refers to the chemical species present at the time of venting and condensation.[3] Thus strontium, although chemically a refractory substance, when produced as ^{89}Sr by the fission process is primarily bromine and krypton at early times, and its behaviour with respect to venting and condensation is considered typical of volatile elements.

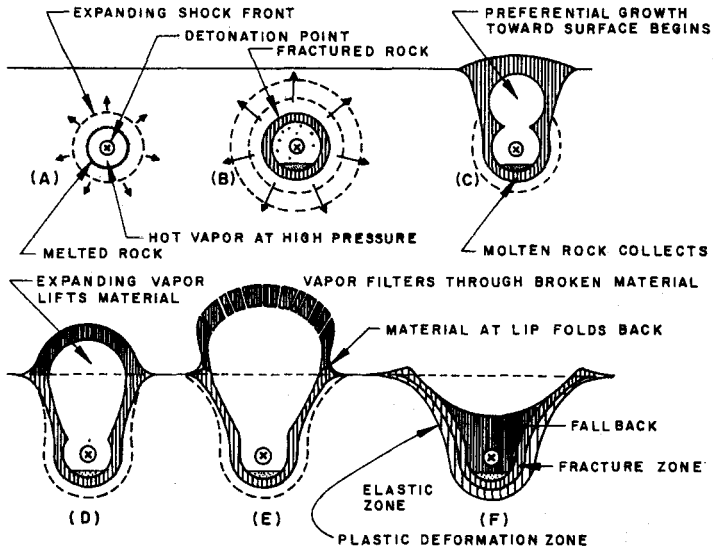

FIG. 1. Crater formation phases.

may be released through cracks and pores in the dome (Figs. 1, D, 1, E); (5) some of the material is thrown outside the resulting crater and the remainder falls back and reduces the crater depth (Fig. 1, F).

For Danny Boy, the above description is fairly accurate. For Sulky, the same description applies but the depth of burial was such that essentially all the material fell back into the crater area and the net result was a small mound with a depression in its center (but still above the initial ground surface level) rather than a crater. Thus in Sulky, the effective thickness of the filter bed through which the radioactive materials were released was greater than for Danny Boy.

In Palanquin, the material and method used to stem the emplacement hole apparently represented a weak spot in the medium. On detonation of the device this stemming material was ejected and the high-temperature, high-pressure gases were released through this void, resulting in an erosional crater somewhat analogous to a volcano in action. Thus, the filtration of the released material was greatly reduced in this case.

DISCUSSION OF RESULTS

To establish a basis for comparing the releases from the various experiments, the total amount of each isotope released in a given experiment was normalized to unit fission yield and compared with other isotopes of the same class (i.e. volatile, refractory, or intermediate). The average values for each class can then be compared.

Table 1 gives, for each experiment, the relative releases of the various activities, normalized to ^{147}Nd and grouped according to class.

Table 1 shows a decided variation in the ratios of the volatile species to the refractory species for the three experiments. If for each experiment, the average value* of the amount of activity released for the volatiles is calculated and compared with the average value for the refractories the differences are more clearly seen. These averages are given in Table 2.

The intermediate species exhibit no clear cut trend. This is not unexpected since ^{136}Cs is a "shielded nuclide" (and thus its behaviour

* For the volatile species the values being averaged differ by as much as a factor of 10. Although the average value therefore has very little precision, the differences observed are large enough to justify this treatment. In the case of the refractories, except for Sulky, the spread is considerably less. Again, for Sulky, the magnitude of the difference between volatile and refactory is well outside the uncertainty in the average.

*Table 1. Relative Amounts of Nuclides Released**

Nuclide	Class	Danny Boy†	Sulky‡	Palanquin**
^{89}Sr	Volatile	60	1×10^5	2
^{137}Cs	Volatile	10	7×10^4	0.4
^{140}Ba	Volatile	6	1×10^4	0.5
^{136}Cs	Intermediate	50	—	20
^{141}Ce	Intermediate	2	700	0.6
^{95}Zr	Refractory	0.5	—	0.5
^{99}Mo	Refractory	0.4	0.3	0.4
^{144}Ce	Refractory	0.6	60	0.5
^{147}Nd	Refractory	1.0	1.0	1.0

* Normalized to unit fission yield and to ^{147}Nd.
† Scaled depth: 43.3 m/(kt)$^{1/3.4}$ normal crater.
‡ Scaled depth: 56.4 m(kt)$^{1/3.4}$ "negative" crater.
** Scaled depth: 56.4 m/(kt)$^{1/3.4}$ erosional crater.

Table 2. Average Relative Release Values for Volatiles and Refractories

Class	Danny Boy	Sulky	Palanquin
Volatile	25	6×10^4	1
Refractory	0.6	20	0.6

depends only on the physical-chemical properties of cesium) whereas ^{141}Ce is derived by β^- decay from several different elements* and is therefore much more sensitive to the time-temperature-environmental history of the cratering and venting process.

It is obvious from Table 2 that the main difference between Palanquin and Danny Boy (or Sulky) is the ratio of the releases of volatile to refractory species. In the "well-behaved" cratering events, the refractory species are reduced with respect to the volatiles by at least an order of magnitude, whereas in the volcanic-type release the refractories and the volatiles are essentially released to the same degree. It is reasonable to conclude that this difference is primarily due to the filtering action of the earth mound in the true cratering events.

* The mass 141 chain for thermal fission of ^{235}U is as follows:

$$^{141}Xe \xrightarrow{1.7s} {}^{141}Cs \xrightarrow{25s} {}^{141}Ba \xrightarrow{18m} {}^{141}La \xrightarrow{3.9h}$$
(1.3) (4.6) (6.3)

$$^{141}Ca \xrightarrow{33d} {}^{141}Pr$$

(The numbers in parenthesis are the cumulative chain yields to that point).

CONCLUSION

In normal crater formation the raised earth "dome" acts as an efficient filter medium for the refractory species. The volatile species are affected to only a minor degree. Proper choice of depth of burial for a nuclear explosive may result in a large reduction in the release of the more refractory radioactivities.

REFERENCES

1. M. Linder, K. V. Marsh, J. A. Miskel and R. J. Nagle. University of California, Lawrence Radiation Laboratory, Livermore. UCRL-6998 (1962).
2. N. A. Bonner and J. A. Miskel. *Science* **150,** 495 (1965).
3. J. A. Miskel. U.S. Atomic Energy Commission Document TID-7695 (1964), pp. 153–158.

ON DEPTH-DOSE DISTRIBUTIONS FOR FALLOUT AND SIMULATED FALLOUT FIELDS

R. L. FRENCH
Radiation Research Associates, Inc.,
1506 W. Terrell Ave.,
Fort Worth, Texas 76104,
U.S.A.

and

C. W. GARRETT
Armed Forces Radiobiology Research Institute,
Defense Atomic Support Agency,
Bethesda, Maryland 20034,
U.S.A.

Abstract—Gamma-ray depth-dose patterns in a phantom exposed to fallout were calculated by the Monte Carlo method. The phantom consisted of a tissue equivalent vertical right cylinder 60 cm in height and 30 cm in diameter. The center of the phantom was 111.8 cm above a smooth ground surface uniformly contaminated with ^{235}U fission products. The energy and angular distribution of the gamma rays incident upon the phantom were taken from a previous Monte Carlo study.

The depth-dose patterns were found to be relatively insensitive to fallout age over the period investigated (1 hr to 9 days). The dose rate at the center of the phantom is approximately 65% of the free-field dose rate, while that at the lateral surface is approximately 80%. Except near the extremities, the dose rate along the vertical axis of the phantom varies at approximately the same rate with height above ground as does the free-field dose rate. Approximately one-half of the dose rate at the center of the phantom is from photons which have suffered previous collisions in the phantom.

The depth-dose patterns were also calculated for two arrangements of artificial sources which, although not duplicating the fallout energy spectra, were intended to simulate fallout biological effects. The patterns produced by revolving the phantom on its vertical axis while exposed to a point ^{60}Co source at a horizontal distance of 61 m are similar to those from the fallout, except for internal positions near the bottom of the phantom. A special arrangement of ^{60}Co, ^{137}Cs and ^{144}Ce sources produced substantially the same depth-dose patterns throughout the phantom as did the fallout.

INTRODUCTION

The possible exposure of populations to radioactive fallout has motivated numerous studies of the characteristics of the radiation environment produced by fallout.[1-4] Most of these studies have been concerned with the free-field dose rates and the energy and angular spectra of the gamma-ray flux at a reference height of approximately one meter above a contaminated ground surface. The present study is concerned with calculating the distribution of the gamma-ray dose within a phantom representative of a body exposed to fallout. Because the radiobiologist in investigating the effects of radiation upon biological systems must often perform experiments in simulated radiation fields, the study included depth-dose distributions produced by simulated fallout radiation fields.

A Monte Carlo approach was selected for performing the depth-dose calculations because

it allows a more accurate treatment of the radiation environment and of the geometry of the phantom than do the more rigorous analytic methods for solving the radiation transport problem. However, to provide guidance for the Monte Carlo calculations and to establish the validity of a simpler method, calculations were also performed using exponential attenuation and infinite medium dose buildup factors.

PHANTOM

The phantom consisted of a tissue equivalent vertical right cylinder 60 cm in height and 30 cm in diameter. The center of the phantom was 111.8 cm above the ground surface. For tissue equivalence, the phantom was composed of a homogeneous mixture of the elements indicated in Table 1.

RADIATION ENVIRONMENTS

The fallout radiation environments for which depth-dose distributions in the phantom were calculated were those previously computed by Monte Carlo techniques for a position 0.914 m (3 ft) above fallout with ages of 1.12 hr, 23.8 hr, 4.57 days and 9.82 days uniformly deposited on a smooth ground surface.[3] The fallout was assumed to consist of non-volatile ^{235}U fission products with gamma-ray energy spectra as given by Nelms and Cooper.[5] The simulated fallout radiation environments were those produced by a point isotropic ^{60}Co source (~1.25 MeV) at a horizontal separation distance of 61 m (200 ft), and by a special arrangement of ^{60}Co, ^{137}Cs (~0.67 MeV), and ^{144}Ce (~0.10 MeV) sources known as the AFRRI Compact Simulator.[6]

The geometries of the various radiation sources to which the phantom was exposed are illustrated in Fig. 1. The separation distance of the ^{60}Co point source was selected to give the best approximation of the energy and angular distribution from an infinite plane fallout source.

The AFRRI Compact Simulator, which is a conceptual design, consists of a uniform disc source located on the ground surface, a ring source above the perimeter of the disc source, and a slab of water of equal radius positioned above and concentric with the disc and ring sources. The ring source serves as a virtual source for that portion of an infinite plane source not represented by the disc source while the water serves as a scattering medium for gamma-rays from both the disc and ring source to simulate skyshine from an infinite plane source. The relative concentrations of the ^{60}Co, ^{137}Cs and ^{144}Ce in the disc and ring sources and the thickness of the water slab were selected to give the best approximation of the energy and angular distributions 0.914 m above a 1.12-hr fallout source.

The previous Monte Carlo calculations of the gamma-ray environments produced by the above sources give the total photon flux at the receiver in each of eighteen 10-degree intervals on polar angle, θ, and in each of ten energy groups: 0.04–0.06, 0.06–0.10, 0.10–0.18, 0.18–0.30, 0.30–0.50, 0.50–0.75, 0.75–1.00, 1.00–1.50, 1.50–2.50, and 2.50–3.50 MeV.[3, 6] The fluxes are, for all sources, integrated over azimuthal angle, ø. Thus, the environment computed for the ^{60}Co point source is that which would be experienced by revolving the subject about its vertical axis during exposure.

The characteristics of the fallout and simulated fallout radiation environments are illus-

Table 1. Composition of Tissue Equivalent Phantom

Element	% by weight	Partial density (g cm^{-3})	Atomic concentration (atoms cm^{-3})
Carbon	15.6	0.1585	7.944×10^{21}
Hydrogen	9.8	0.0996	5.948×10^{22}
Oxygen	71.0	0.7214	2.714×10^{22}
Nitrogen	3.6	0.0366	1.573×10^{21}
Total	100.0	1.0161	9.614×10^{22}

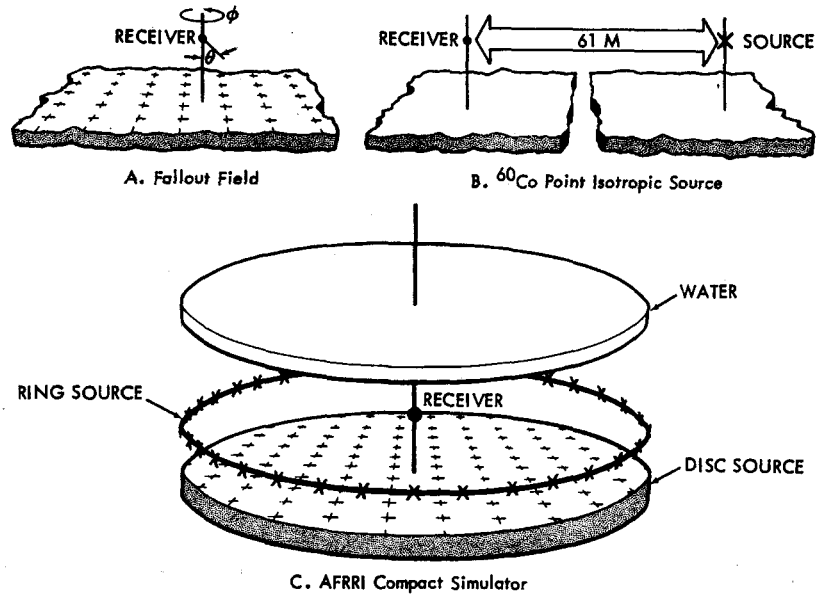

FIG. 1. Source geometries used in free-field radiation environment calculations.

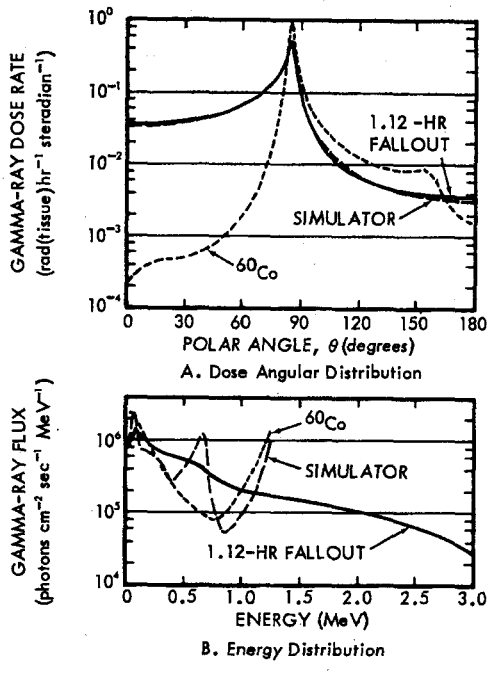

FIG. 2. Gamma-ray energy and angular distributions from 1.12-hr fallout, ^{60}Co point source and AFRRI Compact Simulator (normalized to unit dose rate).

trated in Fig. 2. The angular distributions of the total dose rate, given in the upper part of the figure, have the same gross shape for $\theta > 80$ degrees; but below 80 degrees, the ^{60}Co point source dose angular distribution bears no resemblance to that from fallout. Neither the AFRRI Compact Simulator nor the ^{60}Co point source provides a good simulation of the energy spectra as may be seen in the lower part of the figure.

CALCULATIONAL METHODS

In order to compute the distribution of the gamma-ray dose in the phantom it is necessary to consider the gamma-rays incident over its entire surface and their transport until they are absorbed in, or escape from, the phantom. Actually, photons which escape the phantom may be scattered back into it, but this effect is very small and its neglect is consistent with the neglect of perturbation by the phantom in performing the free-field calculations. In performing the radiation transport calculations, the energy dependent photon flux must be determined at a suitable number of positions in the phantom to allow, after conversion to dose, construction of dose or dose fraction profiles.

The Monte Carlo procedure which was used to perform the transport calculations is a multipurpose code known as COHORT.[7] Its description here will be limited to those features actually used in this study. Basically, the procedure allows photons to be randomly sampled from arbitrary source probability distributions in energy, angle and space. Individual photons are then traced through a random walk generated by sampling from collision probability distributions and angular scattering distributions for the particular materials being penetrated. The collision probability distributions are generated from consideration of the cross sections for Compton scattering, pair production, and absorption. Absorption is not allowed to occur. Instead, the photon weight is reduced upon each interaction by the probability that that particular interaction was an absorption. The angular scattering distributions are generated from the well-known Klein–Nishina formula. Each photon history is terminated upon reaching a specified minimum energy, a specified maximum number of collisions, or escaping from the defined geometry.

An adequate number of photon histories must be traced to assure a representative sampling from the source distributions and a representative distribution of photon interactions. In the process of tracing photon histories, the location of each interaction and the resultant photon energy and direction are recorded on tape. The resultant "collision tape" may then be analyzed to determine the photon track length in arbitrarily specified volume regions. Photon fluxes are obtained by dividing by the volume of the region. Finally, flux-to-dose conversion factors[8] are applied and a summation made over photon energy.

Ideally, the volume regions would be of infinitesimal size to obtain the highest resolution of the spatial dependence of the dose. If valid results are to be obtained, however, each region must be finite and large enough for each to intercept a statistically significant number of photons. Figure 3 shows the volume regions into which the phantom was divided for the COHORT Monte Carlo calculations. The volume regions are concentrated along the horizontal midplane and the vertical axis since it was desired to compute the radial and axial

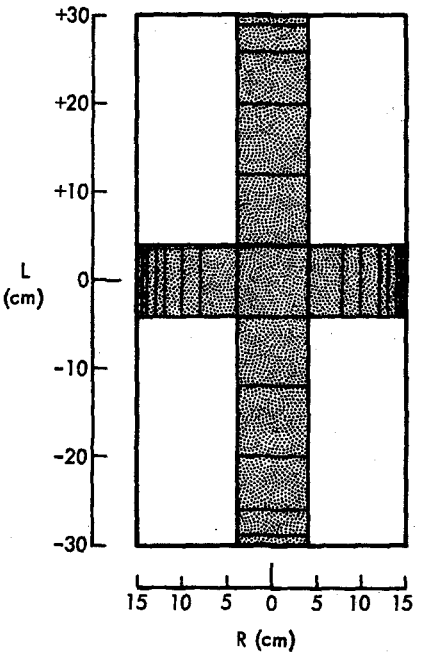

FIG. 3. Division of phantom into volume regions for Monte Carlo calculations.

distributions of the dose. The dimensions of the volume elements are smallest near the phantom surface where the largest dose gradients were expected.

The source probability distributions on energy and angle were developed directly from the flux tables from the free-field radiation environment calculations. It was assumed that the energy and angular distribution did not vary with height above ground over the length of the phantom. However, the variation of the total incident flux with height was considered too great to be neglected. Special calculations of the total flux above a 1.25-MeV plane isotropic source showed that it varied by 12% over the height of the phantom. In the depth-dose calculations it was assumed that the incident flux from all of the sources except the ^{60}Co point source had a similar height dependence.

In performing the Monte Carlo calculations, each photon was allowed to undergo 15 collisions or be degraded in energy to less than 0.04 MeV before termination. However, it was found that approximately 96% of all photon

histories were terminated by escape from the phantom. Only 3% and 1% were terminated by minimum energy and maximum number of collisions, respectively. An average of only 3.8 collisions were suffered by each photon before its history was terminated.

Exploratory calculations led to the selection of 10,000 photon histories as the minimum problem size to give acceptable statistical accuracy. To further improve the statistical accuracy, four different computer runs using different random number sequences were made for each problem. The final results for most positions in the phantom had standard deviations of less than 5%. No biasing of any type was used in the Monte Carlo calculations.

Prior to the Monte Carlo calculations, exploratory calculations were performed using a simple analytic approach based on exponential attenuation and infinite water medium dose buildup factors[9] for point isotropic sources. For the dose rate at a particular position in the phantom, this type of calculation may be described by the equation

$$D = \sum_{\varphi} \sum_{\theta} \sum_{E} B_E (\mu_E t_{\theta,\varphi}) F_{E,\theta,\varphi} G_E e^{-\mu_E t_{\theta,\varphi}}$$

where μ_E is the linear attenuation coefficient of water for photons of energy E,

$t_{\theta,\varphi}$ is the distance from the dose point to the phantom surface in direction θ and $\varnothing$,

$B_E(\mu_E t_{\theta,\varphi})$ is the dose buildup factor for penetration of $\mu_E t_{\theta,\varphi}$ mean free paths of water by photons of energy E,

$F_{E,\theta,\varphi}$ is the free-field flux with energy E from directions θ and $\varnothing$, and

G_E is the flux-to-dose conversion factor for photons of energy E.

In order to express the depth-dose distribution in terms of dose fractions, both the Monte Carlo and the analytic results were divided by the free-field dose rate 0.914 m above the ground.

RESULTS AND DISCUSSION

Monte Carlo calculations were performed for 1.12-hr fallout, 23.8-hr fallout, the ^{60}Co point source, and the AFRRI Compact Simulator. The results are summarized in Table 2. Analytic calculations were performed for 4.57-day and 9.82-day fallout in addition to the above sources. The results of the various calculations were analyzed to determine:

1. The general characteristics of the depth-dose distributions in the phantom.
2. The sensitivity of the distributions to fallout age.
3. The extent to which the simulated fallout fields reproduce the fallout depth-dose distributions.
4. The validity of the simplified analytic calculations.

The case of principal interest is the 1.12-hr fallout field since this particular age of fallout has been studied extensively.[2, 3, 6] Figure 4 compares the Monte Carlo and analytic calculations for this case. A total of 44,000 photon histories divided into four machine runs were used in the Monte Carlo calculations. The data points shown in the figure are the average of the four runs and the bars indicate the standard deviation as determined from the results of the individual runs. The standard deviations on the radial distribution are seen to be quite small ($\sim$2 to 8%). Owing to the use of much smaller volume regions, the standard deviations on the axial distribution are larger near the bottom and the top of the phantom.

The Monte Carlo results indicate a dish-shaped radial distribution with 81% of the free-field dose near (0.5 cm) the lateral surface of the phantom as compared to 66% at the center. For $-20 < L < +20$ cm, the axial distribution is approximately a straight line which closely follows the height-above-ground dependence of the free-field dose rate.

The fine structure near the upper and lower extremities of the phantom can probably be attributed to the combined effect of the boundaries and of the characteristics of the radiation field. The radiation environment to which the phantom is exposed is so strongly peaked near the horizon ($\theta = 90°$) that most of the flux incident upon the bottom and top is at large angles with respect to the normal to these surfaces. Thus, the uncollided component from

Table 2. Depth-dose Distributions in Phantom based on Monte Carlo Calculations (fraction of free-field dose)

Position L or R (cm)	Source			
	1.12-hr fallout	23.8-hr fallout	AFRRI Compact Simulator	^{60}Co point source
		Radial Distribution		
2.83	0.6571	0.6848	0.6418	0.6684
6.67	0.6701	0.6673	0.6600	0.6828
9.06	0.6955	0.6782	0.6806	0.6997
11.04	0.7126	0.7173	0.7190	0.7236
12.51	0.7621	0.7173	0.7676	0.7540
13.51	0.7687	0.7405	0.7597	0.7584
14.26	0.7967	0.7500	0.7724	0.7717
14.75	0.8114	0.7844	0.7812	0.7740
		Axial Distribution		
−29.5	0.9357	0.9023	0.9132	0.5350
−27.5	0.6744	0.6436	0.6937	0.5976
−23.0	0.7210	0.6836	0.6832	0.6333
−16.0	0.6860	0.6443	0.6393	0.6500
− 8.0	0.6926	0.6452	0.6380	0.6809
0	0.6571	0.6848	0.6418	0.6684
8.0	0.6382	0.6500	0.5818	0.6611
16.0	0.6360	0.6042	0.5859	0.6437
23.0	0.5673	0.5754	0.5615	0.6549
27.5	0.5305	0.5253	0.4873	0.5782
29.5	0.5848	0.4809	0.4618	0.6591

the incident flux is highly attenuated in penetrating to positions near the ends of the phantom, giving rise to the relatively strong negative gradient just inside the surface. At the same time, the scattered dose from the much larger number of photons incident upon the sides of the phantom would be expected to decrease near the end surfaces.

The analytic results differ from the Monte Carlo results in two respects:

1. They tend to give slightly higher (~8%) dose fractions in the central regions of the phantom.
2. They do not exhibit the fine structure near the upper and lower extremities.

It was expected that the analytic calculations would generally overpredict the dose fractions owing to the use of infinite medium buildup factors. It is perhaps surprising that the overprediction was no larger since the Monte Carlo calculations indicated that the average photon undergoes only 3.8 collisions before escaping from the phantom. Since the analytic calculations indicated that approximately 50% of the dose near the center of the phantom is from uncollided photons, a component which should contain little error, the 8% difference in the total dose fractions noted above may be attributed to the scattered component alone. This corresponds to an overestimate of approximately 16% in the scattered component of the analytic calculations.

In the analytic results it may be presumed that the absence of fine structure near the upper and lower extremities is a consequence of using infinite medium buildup factors. The excellent agreement between the analytic and Monte Carlo radial distributions near the lateral surfaces is fortuitous; the analytic calculations

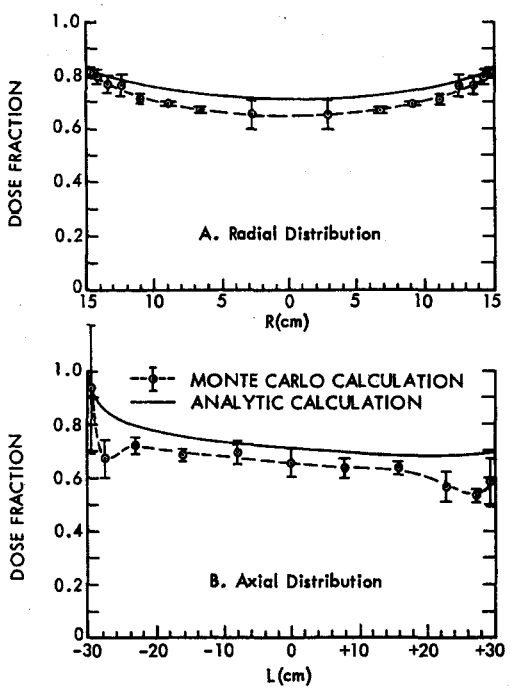

FIG. 4. Depth-dose distribution in phantom exposed to 1.12-hr fallout field.

underpredict the dose fraction in these positions, relative to the central positions, because they do not include reflection of photons from deeper within the phantom.

Figure 5 shows the Monte Carlo calculated depth-dose distributions for the phantom exposed to 23.8-hr fallout. A smoothed curve approximation of the Monte Carlo results for 1.12-hr fallout is included for comparison. The 23.8-hr results, which are based on 40,000 photon histories, tend to be slightly lower near the phantom surfaces and higher near the center than did those for the 1.12-hr fallout. However, it must be concluded that within the statistical accuracy of the results, the two ages of fallout produce essentially identical depth-dose distributions in the phantom. This conclusion is supported by the analytic results (not shown) which differed by not more than approximately 1% at any point in the phantom from those computed for the 1.12-hr fallout.

Originally it was planned to perform Monte Carlo calculations for two additional ages of fallout: 4.57 and 9.82 days. These ages were not considered in the final calculations because their energy spectra do not differ from that of 1.12-hr fallout as much as does that of 23.8-hr fallout, which was found to produce essentially the same depth-dose distributions as 1.12-hr fallout. Moreover, analytic calculations performed for the two additional ages of fallout are within approximately 1% of those for the earlier ages.

The depth-dose distributions produced by a 1.12-hr fallout field simulated by the AFRRI Compact Simulator are compared with those from 1.12-hr fallout in Fig. 6. The radial distribution from the simulator is similar to that for the actual 1.12-hr fallout. The axial distribution is also similar but is slightly lower than that from the fallout. The simulator results shown in Fig. 6 are based on Monte Carlo calculations using 40,000 photon histories. The depth-dose distributions for the AFRRI Compact Simulator computed with the simple analytic method were found to be within 2% of the analytic results for the 1.12-hr fallout.

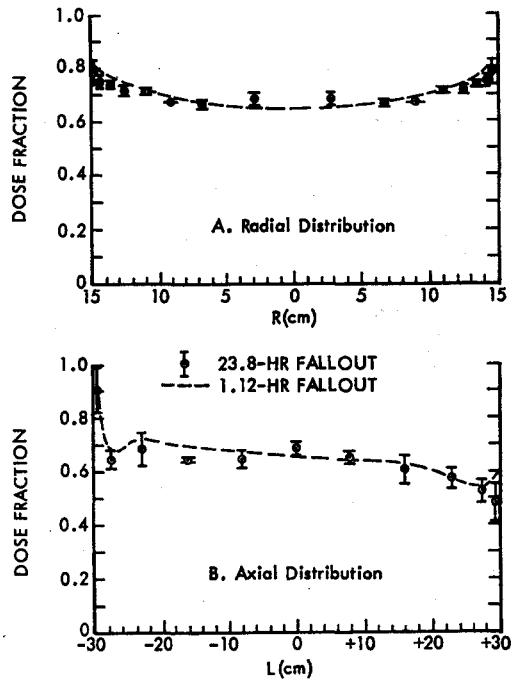

FIG. 5. Comparison of depth-dose distributions for 23.8-hr and 1.12-hr fallout.

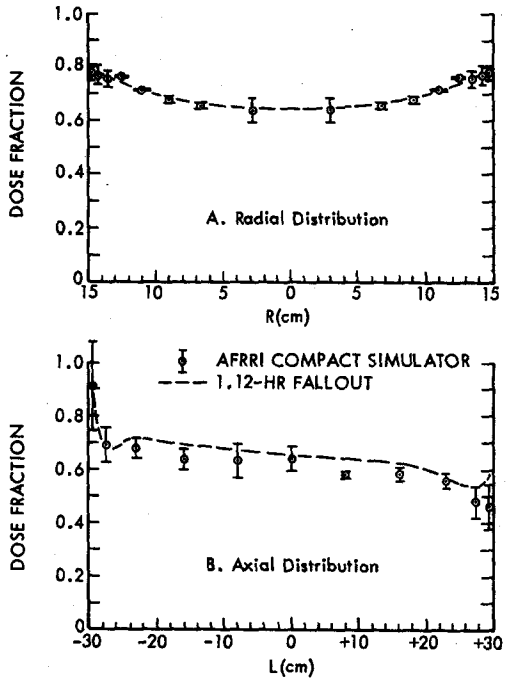

FIG. 6. Comparison of depth-dose distributions for AFRRI Compact Simulator and 1.12-hr fallout.

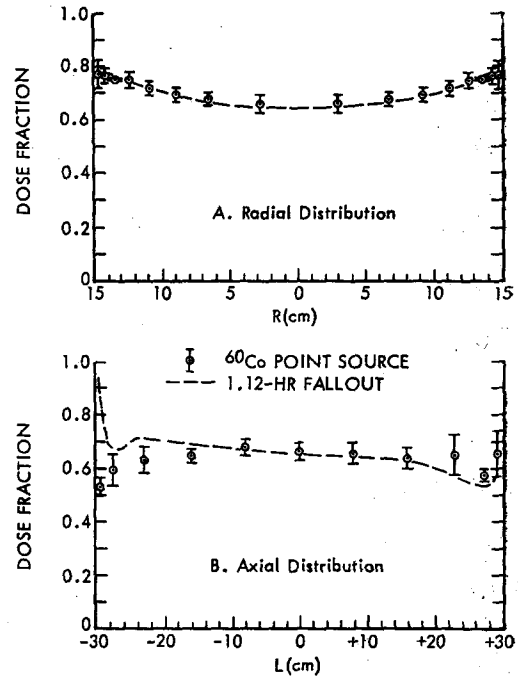

FIG. 7. Comparison of depth-dose distributions for ^{60}Co point source and 1.12-hr fallout.

Figure 7 compares the depth-dose distributions produced by the ^{60}Co point source at a horizontal separation distance of 61 m from the phantom with those produced by 1.12-hr fallout. The radial distribution from the ^{60}Co point source agrees very well in both shape and magnitude with that from the fallout. The axial distribution for the ^{60}Co is also similar to that from the fallout for $-20 < L < +20$ cm. The ^{60}Co dose fraction is lower near the bottom of the phantom because the bottom surface is not exposed to a strong uncollided component as is the case with fallout. However, this difference is probably of trivial significance since the concept of a cylindrical phantom is least valid near the axial extremities. Forty thousand photon histories were used for the ^{60}Co Monte Carlo calculations. Analytic calculations for the ^{60}Co agreed with the Monte Carlo calculations to about the same extent as they did for the other sources.

Although the depth-dose distributions from fallout are simulated reasonably well except near

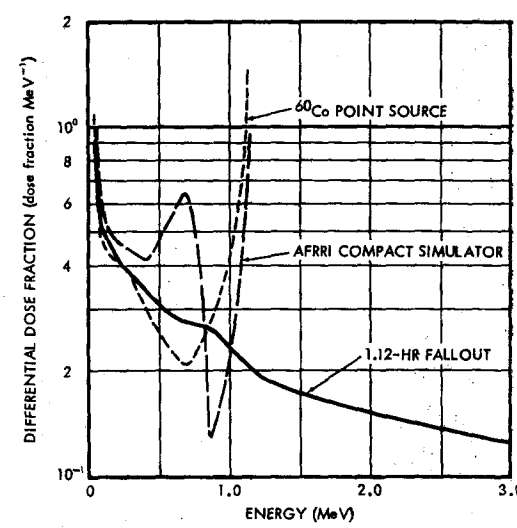

FIG. 8. Differential energy distribution of dose fraction at center of phantom.

the axial extremities by both the AFRRI Compact Simulator and by the ^{60}Co point source at a horizontal separation distance of 61 m, it does not necessarily suffice to simulate the depth-dose distributions alone. The energy distribution of the dose at a given point is also of interest. Figure 8 compares the differential energy spectrum of the dose fraction at the center of the phantom based on the Monte Carlo calculations for the 1.12-hr fallout, the AFRRI Compact Simulator, and the ^{60}Co point source. The two simulated dose spectra are vastly different from that produced by fallout at energies above 1 MeV, and they show only a gross similarity below 1 MeV.

CONCLUSIONS

This investigation has shown that the depth-dose distribution in a phantom exposed to a fallout field is quite insensitive to the age of the fallout. In the horizontal midplane the dose ranges from approximately 65% of the free-field dose at the center of the phantom to approximately 80% at the lateral surfaces. The dose fraction along the vertical axis of the phantom varies at approximately the same rate with height above ground as does the free-field dose rate except near the extremities where boundary effects and the characteristics of the radiation field combine to produce strong dose gradients.

A simple arrangement consisting of a single ^{60}Co point source and a sophisticated arrangement of combined ^{60}Co, ^{137}Cs and ^{144}Ce sources were both found to produce depth-dose distributions over the important regions of the phantom which were very similar to those from the fallout although the energy spectra are quite different. Depth-dose distributions calculated with a simple exponential attenuation and infinite medium buildup factor approach show the same general trends as the more sophisticated Monte Carlo calculations, but are approximately 8% higher in the central portions of the phantom and do not have the same behavior near the boundaries.

ACKNOWLEDGEMENTS

The authors are indebted to L. Olmedo, J. H. Price and K. W. Tompkins, all of Radiation Research Associates, for their assistance with various phases of the calculations. A special acknowledgement is due Col. James T. Brennan, formerly director of the Armed Forces Radiobiology Research Institute, for suggesting the investigation.

REFERENCES

1. R. L. Mather, R. F. Johnson and F. M. Tomnovec. *Health Physics* **8,** 245 (1962).
2. L. V. Spencer. Structure shielding against fallout radiation from nuclear weapons. NBS Monograph 42 (1962).
3. R. L. French. *Health Physics* **11,** 369 (1965).
4. C. M. Huddleston, Q. G. Klingler, Z. G. Burson and R. M. Kinkaid. *Health Physics* **11,** 537 (1965).
5. A. T. Nelms and J. W. Cooper. *Health Physics* **1,** 427 (1959).
6. R. L. French. A comparative study of radioactive source arrangements for simulating fallout gamma radiation fields. RRA-T45 (1964).
7. D. G. Collins and M. B. Wells. COHORT, a Monte Carlo program for calculation of radiation heating and transport. RRA-T62, Vols. I–IV (1966).
8. B. J. Henderson. Conversion of neutron or gamma ray flux to absorbed dose rate. XDC 59–8–179 (1959).
9. H. Goldstein and J. E. Wilkins, Jr. Calculations of the penetration of gamma rays. NYO-3075 (1954).

EFFET DE PROXIMITÉ DU RELIEF SUR LE TAUX DE RETOMBÉES RADIO-ACTIVES

NGUYEN BA CUONG, G. LAMBERT et B. ARDOUIN
Service d'Électronique Physique, CEA, Centre d'Études Nucléaires, Saclay, France

Résumé—Certaines stations françaises et italiennes de collection des retombées radioactives situées directement au pied des Alpes présentent des résultats près de deux fois supérieurs à ceux qui sont enregistrés dans les stations de plaine, situés à même latitude (45°N) et même altitude (0–200 m).

Les différences de pluviométrie ne semblent pas pouvoir rendre compte de cet effet, qui ne peut non plus être attribué à la situation continentale des stations alpines car de telles différences ne se retrouvent pas aux latitudes plus septentrionales exemptes de grands massifs montagneux. On montrera que cet effet peut être attribué aux phénomènes orographiques affectant seulement les stations situées sur le versant exposé au vent et on examinera les différentes hypothèses qui peuvent expliquer que les pluies plus abondantes qui en découlent sont néanmoins d'avantage contaminées par les débris radio-actifs, aussi bien d'origine stratosphérique que troposphérique.

DIE EIGENAKTIVITÄT VON BLEI

WALTER A. KOLB
Physikalisch-Technische Bundesanstalt,
Braunschweig und Berlin,
33 Braunschweig, BRD

Zusammenfassung—Angesichts der zunehmenden Bedeutung von Abschirmmaterial niedriger Eigenaktivität wurden einige Untersuchungen an Blei ausgeführt. Dabei sollten hauptsächlich zwei Fragen geklärt werden:

1. Der Ursprung des ^{210}Pb-Gehalts des handelsüblichen Bleis.
2. Die Möglichkeit, Blei niedriger Eigenaktivität herzustellen.

Im einzelnen wurden folgende Meßreihen durchgeführt:

(a) Messung der β-Impulsrate gepreßter Erzkonzentratproben aus verschiedenen Ländern und Untersuchung daraus hergestellter Metallschmelzen,
(b) Laufende Messung an Werkbleiproben aus dem Schachtofen über einen Zeitraum von mehreren Wochen,
(c) Messung von Bleiproben aus dem einzelnen Raffinationsstufen,
(d) Untersuchung über den Einfluß von Bleischrott und Zuschlagstoffen.

Die Ergebnisse zeigen, daß es prinzipiell möglich ist, durch Auswahl geeigneter Erzsorten Blei sehr geringer Eigenaktivität herzustellen. Bei handelsüblichem Blei rührt ein Teil der Aktivität von stets mitverhüttetem Bleischrott und anderen Zuschlagsstoffen her, so daß das Verhüttungsverfahren eine ausschlaggebende Rolle spielen dürfte. So wurden die günstigsten Resultate bei schwedischem Elektroofenblei gefunden, obwohl das verhüttete Erz keine besonders geringe Eigenaktivität aufwies. Abschließend wird die an Bleiproben üblicherweise gemessene β-Impulsrate mit der für die Praxis wichtigen γ-Impulsrate einer Bleiabschirmung verglichen.

In den letzten Jahren ist der Bedarf an Meßeinrichtungen zur Bestimmung sehr niedriger Aktivitäten sprunghaft angestiegen. Während sich die Anwendung derartiger Geräte noch in den 50er Jahren im allgemeinen auf die Kernphysik und die Altersbestimmung beschränkte, finden sich heute "low-level"-Zähler in zahlreichen Laboratorien, die sich z.B. mit Strahlenschutz (Untersuchung der Umweltaktivität), medizinischer Diagnostik, Hydrologie, Biologie, Geologie oder Meteoritenkunde beschäftigen. Die Weiterentwicklung der Meßtechnik konzentriert sich dabei vor allem auf die Reduzierung des Nulleffektes, der im wesentlichen von der kosmischen Strahlung, der Umgebungsstrahlung und der Eigenaktivität der verwendeten Bauelemente des Detektors und der Abschirmung abhängt. Wegen seiner hohen Dichte und Ordnungszahl sowie seines günstigen Preises ist zur Abschirmung der Umgebungsstrahlung, die den größten Beitrag zum Nulleffekt liefert, Blei besonders gut geeignet, sofern seine Eigenaktivität vernachlässigbar klein ist.

Schon seit langem ist allerdings bekannt, daß diese Voraussetzung im allgemeinen nicht erfüllt ist. Außer den vier stabilen Bleiisotopen kann das natürliche Blei ^{210}Pb—das RaD aus der ^{238}U-Zerfallsreihe—enthalten. Die sehr weiche β- und γ-Strahlung dieses Nuklids, trägt nur wenig zum Nulleffekt bei, umsomehr aber sein Folgeprodukt ^{210}Bi (Ra-E, $T_{1/2} = 5$ d), dessen energiereiche β-Strahlung (1,17 MeV) im Blei Bremsstrahlung und charakteristische Röntgenstrahlung erzeugt. Da die Halbwertszeit des ^{210}Pb 22a beträgt, hat man in den Fällen, in denen nur relativ geringe Mengen zur Abschirmung benötigt wurden, altes Blei verwendet, dessen ^{210}Pb-Gehalt abgeklungen war.[1, 2] Zeitweise stehen auch größere Mengen aus

Bergungen gesunkener Segelschiffe zur Verfügung.[3]

Daß man sich nicht nur auf das Alter allein verlassen kann, mögen indes Messungen zeigen, deren Ergebnisse in Tabelle 1 wiedergegeben sind. Aus dem Blei eines alten Daches wurde eine Scheibe von 50 mm Ø herausgedreht und in einem β-Antikoinzidenz-Zähler (Tracerlab CE-14, 2 "Ø) gemessen.

Es zeigt sich deutlich, daß die Wetterseite eine Kontamination aufweist, die anscheinend durch ^{210}Pb-Anreicherung aus dem Niederschlag hervorgerufen wurde. Nach dem Umschmelzen solchen Altbleies braucht deshalb, wie weitere Messungen gezeigt haben, die Aktivität keineswegs vernachlässigbar klein zu sein. Auf die gleiche Weise dürften auch die relativ hohen Eigenaktivitäten von Altblei zu erklären sein, die Grinberg und Le Gallic[4] gefunden haben.

Für die Abschirmung größerer Räume, wie sie z.B. für in vivo Untersuchungen am Menschen erforderlich sind, werden heute meistens Stahlabschirmungen verwendet, die aus "Vor-Atomzeitalter-Stahl" hergestellt sind. Neuer Stahl ist mehr oder weniger durch Co-60 oder auch durch Ru-103 und Ru-106[3] kontaminiert, das aus Präparaten stammt, die zur Kontrolle des Abbrands in das Hochofenfutter eingebaut werden. Selbst Stahl aus Hochöfen, deren Futter keine radioaktiven Präparate enthält, ist durch den verarbeiteten Schrott nicht frei von solchen radioaktiven Verunreinigungen.

Da sowohl die Beschaffung von genügend altem Blei (vor allem bei größeren Mengen) als auch von Vorkriegsstahl mit Schwierigkeiten und z.T. auch erheblichen Kosten verbunden ist, haben wir die Eigenaktivität von Blei systematisch untersucht und dabei die Frage geprüft, inwieweit es möglich ist, Blei mit niedriger Eigenaktivität herzustellen.

BLEIERZE UND ERZKONZENTRATE

Alle oben zitierten Autoren beschränken sich, wie auch Paakkola und Steinert,[5] auf die Untersuchung einzelner Metallproben bestimmter Lieferanten. Eigene Messungen hatten gezeigt, daß die Eigenaktivität von Bleiproben desselben Herstellers sehr unterschiedlich sein kann. Dies ist nicht verwunderlich, wenn man bedenkt, daß von vielen Bleihütten Erze sehr verschiedenen Ursprungs verhüttet werden. Aus diesem Grunde erschien es notwendig, zunächst Untersuchungen an Bleierzen und Erzkonzentraten vorzunehmen. Zu diesem Zweck wurden jeweils zwei pulverisierte repräsentative Proben des Materials, das vorwiegend als Erzkonzenr trat vorlag, mit etwas Wachs zu Scheiben von 38 mm Durchmesser gepreßt. Die Dicke der Scheiben betrug mindestens 5 mm. Diese Scheiben wurden in dem bereits erwähnten Antikoinzidenzzähler gemessen. Der Durchmesser des Zählrohrfensters betrug 2", seine Flächendichte 0,9 mg/cm^2, der Nulleffekt lag zwischen 1,2 und 1,5 Imp/min und wurde laufend kontrolliert. Für jedes Material lagen Analysenwerte für Pb, Bi, Au, Cu, As, Zn, Sb, SiO_2, Fe, S und Ag vor. Die gemessenen Impulsraten wurden auf 100% normiert. Diese Werte sind in Tabelle 2 zusammengestellt.

Aus Tabelle 2 ergibt sich, daß die marokkanischen Erzkonzentrate Alzi und Ain Arkos eine relativ hohe, die peruanischen Erzkonzentrate Palca, Venturosa und Santa Rita eine relativ niedrige Eigenaktivität aufweisen. Die Aktivität eines in Tabelle 2 nicht aufgeführten nigerianischen Erzes lag unter der Nachweisgrenze.

Tabelle 1. *Oberflächenkontamination zweier Bleiblechproben von einem alten Dach*

Bezeichnung der Proben	Impulsrate/Fläche min^{-1}/dm^2		
	Wetterseite	Rückseite	nach Oberflächenbearbeitung
Nr. 6	43	7,1	1,0
Nr. 8	45	6,1	< 1

Tabelle 2. Auf die Fläche bezogene Impulsraten von gepreßten Erz- und Erzkonzentratproben aus verschiedenen Ländern; die angegebenen Werte sind auf einen Bleigehalt von 100% normiert

Material Nr.	Bezeichnung	Impulsrate/Fläche (min^{-1}/dm^2)	
		Probe 1	Probe 2
Peru			
671	Palca	5,3	7,1
1030	—	89	87
1424	Santa Rita	9.7	11,5
880	Raura	86	78
51	Milpo	64	63
673	Huampar	19	21
19	Rio Pallanga	71	71
1504	Venturosa	4,4	7,1
20	Condoroma	55	51
599	—*	68	78
Marokko			
377	—*	25	27
1571	Alzi	293	255
1572	Ain Arkos	242	248
236	Aouli	28	29
Schweden			
33	Vassbo	12	11
1550	Stora Kopparberg	78	84
34	Saxberget	59	59
35	Stollberg	30	35
340	Garpenberg	89	86
Bolivien			
164	—*	138	155
Deutschland			
1	Bollerich	65	—
2	EB Grund	19	—
3	Rammelsberg	30	—
Polen	Durchschnittsproben	13	14

* Bei diesen Proben handelt es sich um Erze, bei allen anderen um Konzentrate.

Der Faktor zwischen den Extremwerten der Tabelle 2 ist > 50. Eine Korrelation zwischen der Eigenaktivität und bestimmten Spurenelementen, für die Analysenwerte vorlagen, konnte nicht festgestellt werden. Von der Sorte Palca wurden darüber hinaus verschiedene Lieferungen aus den Jahren 1964 und 1965 untersucht: von sieben Lieferungen zeigten sechs Nettoimpulsraten von weniger als 0,5 min^{-1}/dm^2; lediglich bei einer betrug die Nettoimpulsrate 76 min^{-1}/dm^2. Hierbei liegt der Verdacht nahe, daß es sich um eine falsche Lieferangabe handelt, was nach Auskunft des Hüttenwerkes nicht ausgeschlossen ist.

LABORATORIUMSSCHMELZEN

Von einigen der in Tabelle 2 aufgeführten Erzkonzentraten wurden im Hüttenlaboratorium metallische Schmelzen hergestellt und daraus etwa 3 mm dicke Scheiben von 50 mm

Durchmesser gedreht. Diese Scheiben wurden ebenfalls im Antikoinzidenzzähler gemessen. Aus den in Tabelle 3 zusammengestellten Ergebnissen ist ersichtlich, daß die auf die Flächeneinheit bezogenen Impulsraten nur jeweils 10 bis 20% der an den Erzproben gemessenen betragen. Der größte Teil der im Erz enthaltenen radioaktiven Verunreinigungen wird demnach von der Schlacke aufgenommen.

Radiochemische Analysen an einigen Metallproben bestätigen, daß in überwiegendem Maße ^{210}Pb und seine Folgeprodukte für die Eigenaktivität verantwortlich sind [1-3] und ergaben einen Umrechnungsfaktor von 0,2 (pCi/g)/(min^{-1}/dm^2) $\pm$ 25% für die Bestimmung der spezifischen Aktivität aus der auf die Flächeneinheit bezogenen Impulsrate.

PROBEN AUS DEM HÜTTENWERK (SCHACHTOFENVERFAHREN)

Die Untersuchung von Laboratoriumsschmelzen hat gezeigt, daß es durchaus möglich ist, bei Auswahl geeigneter Erzsorten Blei mit der gewünschten niedrigen Eigenaktivität herzustellen. Technologisch treten in dieser Hinsicht jedoch einige Schwierigkeiten auf. Deshalb wurde zunächst die Möglichkeit geprüft, inwieweit man durch laufende Analyse des Werkbleis aus dem Schachtofen geeignete Chargen auswählen kann. Abb. 1 zeigt die über einem Zeitraum von mehreren Wochen an Proben aus dem Schachtofen gemessenen Impulsraten.

Die laufende Registrierung zeigt, daß von einem Tag zum anderen erhebliche Schwankungen auftreten können, deren Ursachen bisher nicht geklärt sind, da sie von zu vielen Faktoren abhängen können. Aus der Häufigkeitsverteilung ergibt sich eine mittlere Impulsrate von 16 min^{-1}/dm^2. 76% der Proben weisen eine Impulsrate zwischen 10 und 20 min^{-1}/dm^2 auf. Die Eigenaktivität ist also um eine Größenordnung höher als die ausgesuchter Laborschmelzen. Im Verlauf der Weiterverarbeitung (Entkupferung, Antimon-Raffination, Entsilberung und Entzinkung) zeigten sich keine signifikanten Änderungen der Eigenaktivität mehr, weshalb auf die Tabellierung der Ergebnisse von drei Meßreihen an dieser Stelle verzichtet werden kann. Im Gegensatz hierzu fanden Grinberg und Le Gallic [4] nach der Antimon-Raffination eine starke Reduzierung der Eigenaktivität. Sofern ihre Messungen kurze Zeit nach der Raffination vorgenommen wurden, ließe sich dieser Effekt durch die Mitabtrennung des ^{210}Bi erklären, das sich chemisch ähnlich wie Antimon verhält. (Unsere Proben wurden zu einem Zeitpunkt gemessen, nachdem sich ^{210}Bi im Gleichgewicht mit ^{210}Pb befinden mußte.)

Bei der Auswertung der am Schachtofenblei erhaltenen Meßergebnisse (Abb. 1) fällt die relativ hohe maximale Impulsrate von 36 min^{-1}/dm^2 auf. Die an der Laboratoriumsschmelze "Ain Arkos" (nach Tabelle 1 eines der Erzkonzentrate mit sehr hoher Aktivität) gemessene Impulsrate betrug dagegen nur 24 min^{-1}/dm^2. Die Aktivität des Schachtofenbleis kann demnach nicht allein aus den verarbeiteten Erzkonzentraten stammen. Wir haben deshalb je 10 Einzelproben von Akkumulatoren- und sonstigem Bleischrott, der den Erzkonzentraten zugemischt wird, sowie eine größere Anzahl

Tabelle 3. *Vergleich zwischen der Eigenaktivität verschiedener Erzproben und daraus erschmolzener Metallproben*

Probe	Nr.	Impulsrate/Fläche (min^{-1}/dm^2)		
		Erzkonzentrat*	Laborschmelze	Hüttenschmelze
Vassbo	33	12	2,1	—
Palca	671	6,2	0,5	4,5
Venturosa	1504	5,8	0,5	—
Ain Arkos	1572	245	24	—
Polen	—	14	1,3	—

* Impulsrate auf 100% Pb-Gehalt normiert.

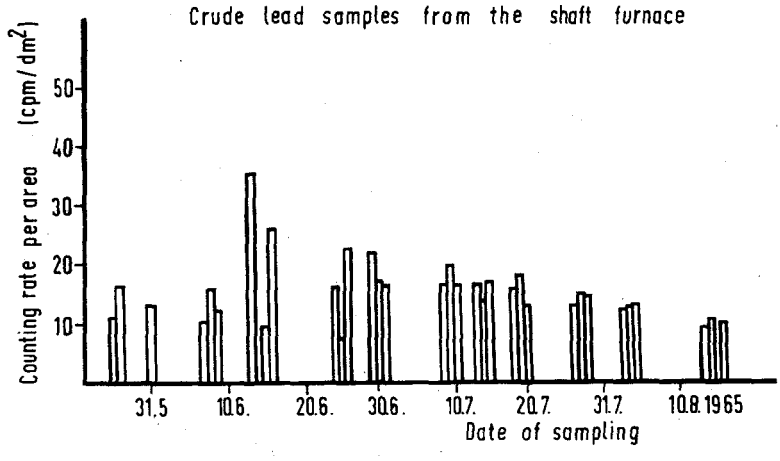

ABB. 1. An Werkbleiproben gemessene Impulsraten, auf der Abszisse ist das Datum der Entnahme aus dem Schachtofen aufgetragen.

von Proben verschiedener Zuschlagsstoffe untersucht und die gemessenen Impulsraten in Tabelle 4 zusammengestellt. Die Proben lagen als gegossene bzw. gepreßte Scheiben vor.

Die vorstehenden Meßergebnisse sollen lediglich zeigen, daß vor allem durch Schrottblei die Eigenaktivität des Hüttenbleis nicht unwesentlich erhöht werden kann. Für die an den Zuschlagsstoffen gemessenen Impulsraten können neben den ^{238}U-Folgeprodukten auch ^{40}K und die ^{232}Th-Folgeprodukte verantwortlich sein. Da eine quantitative Untersuchung wegen des häufigen Wechsels der Erzsorten bei kontinuierlichem Betrieb und der damit verbundenen Mischvorgänge im Schachtofen kaum möglich erscheint, wurde auf weitere Analysen verzichtet.

Schließlich sollte noch erwähnt werden, daß das als Nebenprodukt in der Zinkhütte gewonnene Blei eine besonders hohe Eigenaktivität aufwies. An zwei Proben aus dem Seigerofen der Feinzink-Anlage wurde eine Impulsrate von 280 bzw. 340 min^{-1}/dm^2 gemessen.

PROBEN AUS ANDEREN VERHÜTTUNGSVERFAHREN

Ähnliche Ergebnisse zeigten Messungen an Durchschnitts-Proben aus zwei anderen deutschen Bleihütten. In beiden Fällen war die

Tabelle 4. Auf die Fläche bezogene Impulsraten von Bleischrott und verschiedenen Zuschlagsstoffen

Material	Probenanzahl	Impulsrate/Fläche min^{-1}/dm^2
Akkublei	10	57 bis 140
sonstiger Bleischrott	10	40 bis 110
Eisenkonzentrate	3	120 bis 170
Kupfereisenstein	7	28 bis 38
Kalksteingrus	9	46 bis 66
Sand	2	50 und 61
Schlacken-Granalien	8	97 bis 110
Koks	2	37 und 46

Eigenaktivität des Hüttenbleis im Vergleich zur Aktivität der verarbeiteten Erzkonzentrate unerwartet hoch. Auch ein Versuch, aus dem aktivitätsarmen Erzkonzentrat "Palca" in einem kleinen Hüttenofen nach dem Tarnowitzverfahren ein reines Erzblei zu gewinnen, führte nicht zu dem erwarteten Ergebnis (siehe Tabelle 3, Spalte 5). Die Aktivität dieser Sonderschmelze war um eine Größenordnung höher als die der entsprechenden Laborschmelze. So lag es dann nahe, nach einem saubereren Verfahren zu suchen, wozu sich die in Nordschweden übliche Verhüttung im Elektroofen[6] anbot. Bereits 1962 hatten wir an einer schwedischen Bleiprobe eine Impulsrate von 2,6 min^{-1}/dm^2 gemessen. Auch Proben aus den folgenden Jahren zeigten ähnlich niedrige Werte. Die Impulsraten von 5 Proben einer Charge "B 65" lagen zwischen 1,4 und 2,4 min^{-1}/dm^2. Vergleicht man hiermit die auf 100% Pb-Gehalt normierte Impulsrate einer Probe des zugehörigen Erzkonzentrats "Laisvall 1965" mit 40 min^{-1}/dm^2 so erkennt man, daß das andersartige Verhüttungsverfahren offenbar der Grund für die hinsichtlich der Eigenaktivität gute Qualität dieses Bleis sein muß.* Andererseits dürfte nach Tabelle 2 eine weitere Reduzierung der Eigenaktivität zu erreichen sein, wenn das Erzkonzentrat der Grube Vassbo (12 min^{-1}/dm^2) nach diesem Verfahren verarbeitet würde.

PRAKTISCHE AUSWIRKUNGEN

Abschließend soll noch kurz die Frage behandelt werden, welche Anforderungen hinsichtlich der Eigenaktivität einer Bleiabschirmung für empfindliche Strahlungsdetektoren gestellt werden müssen. In Abb. 2 sind zwei Nulleffekts-Spektren eines Szintillationszählers mit einem NaJ(Tl)-Bohrloch-Kristall (Durchmesser 10 cm, Höhe 10 cm, mit 5 cm dickem NaJ-Absorberlichtleiter) wiedergegeben. Im Inneren eines 15 cm dicken Eisengehäuses† befindet sich noch eine 4 mm dicke zylindrische

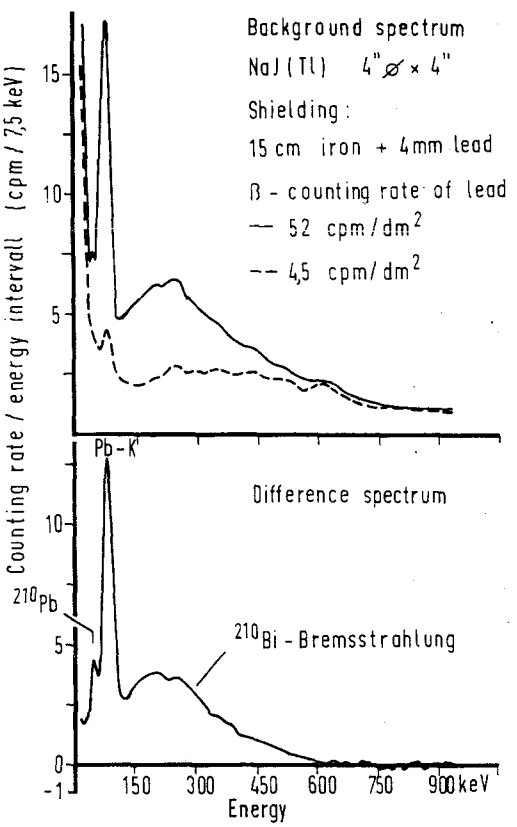

ABB. 2. oben: Nulleffekt eines Szintillationsspektrometers, Kristall: NaJ(Tl) 4" Ø × 4"; Abschirmung 15 cm Stahl + 4 mm Blei; ß-Impulsrate des Bleis: ausgezogene Kurve 52 min^{-1}/dm^2, gestrichelte Kurve 4,5 min^{-1}/dm^2 unten: Durch Differenzbildung ergibt sich im wesentlichen das Spektrum der Eigenstrahlung der Abschirmung mit der höheren Eigenaktivität.

Bleiabschirmung (Durchmesser etwa 11 cm, Höhe 20 cm), die in einem Fall aus handelsüblichem Blei mittlerer Eigenaktivität (10 pCi/g), im anderen Fall aus einer Sonderschmelze des peruanischen Erzkonzentrats "Palca" (0,9 pCi/g) hergestellt war.

Die Wahl des aktivitätsarmen Bleis hat eine Reduzierung des Nulleffekts in den Energiebereichen 60–105 keV, 40–500 keV und 40–960 keV auf 31%, 45% bzw. 56% bei der vorliegenden Anordnung zur Folge. Die auf die Fläche bezogene β-Impulsrate des Palca-Bleis ist in Tabelle 3 mit 4,5 min^{-1}/dm^2

* Wie wir inzwischen erfahren haben, werden außer 10% Kalkstein und 1% Koks keine anderen Stoffe, insbesondere auch kein Bleischrott dem Bleikonzentrat zugesetzt[7].

† hergestellt aus handelsüblichem Flachstahl, der geringfügig mit ^{60}Co kontaminiert ist.

angegeben. Dieser Wert, der einer spezifischen Aktivität von etwa 1 pCi/g entspricht, sollte bei Bleiabschirmungen für empfindliche Detektoren keinesfalls überschritten werden.

Das in Abb. 2 außerdem dargestellte Differenz-Spektrum, das näherungsweise als das Spektrum der Eigenstrahlung des handelsüblichen Bleis mittlerer Aktivität angesehen werden kann, stimmt gut mit dem von R. I. Weller und Mitarbeitern[3] erstmals veröffentlichten überein und zeigt darüber hinaus die 47 keV-γ-Strahlung des ^{210}Pb.

Zum Schluß danke ich den Herren Hüttendirektoren Knackstedt, Goslar und Schünemann, Nordenham sowie Herrn Professor Feiser, Oker und Herrn Dr. Kraume, Goslar für anregende Diskussionen. Besonderen Dank schulde ich Herrn Dr. Siegert, Nordenham, der wesentlichen Anteil am Zustandekommen dieser Arbeit hatte und dazu weit über 100 Proben zur Verfügung stellte.

LITERATUR

1. H. L. DE VRIES und G. W. BARDENSEN. *Physica* **19,** *Isotope* **12,** 987 (1953).
2. G. W. BARENDSEN. Ouderdomsbespaling met radioactive kool stof. Diss. Groningen, 1955.
3. R. I. WELLER, E. C. ANDERSON und J. L. BARKER, JR. *Nature* **206,** 1211 (1965).
4. B. GRINBERG und Y. LE GALLIC. *Int. J. appl. Radiat. Isotopes* **12,** 104 (1961).
5. O. PAAKKOLA und H.-J. STEINERT. *Atompraxis* **9,** 232 (1963).
6. H. I. ELVANDER. The Boliden lead process. Symposium on Pyrometallurgical Processes in Nonferrous Metallurgy. Pittsburgh, 1965.
7. S. WALLDÉN. Bolidens Gruvaktiebolaget, Skelleftehamn, Private Mitteilung.

MONITORING FOR LEAD CONTAMINATION

R. I. WELLER
Department of Physics, Franklin and Marshall College, Lancaster, Pennsylvania, U.S.A.

Abstract—One of the first accomplishments of the Sub-committee on Low-Level Contamination of Materials and Reagents of the National Research Council, National Academy of Sciences, has been a study of the radioactive contamination of commercial lead. Twelve lead samples, ten from current commercial production and two "aged" specimens, showed a wide range of contamination levels. Yet, several of the commercial samples were comparable to the best aged leads available for low-level gamma shielding. The contaminant was identified as ^{210}Pb. Good correlation was observed in the measurements at three laboratories. The radioactive contamination in lead is caused by ^{210}Pb which occurs in lead derived from ores geologically associated with uranium. Since the decay products have a high ratio of alpha to gamma radiation and since alpha counting is considerably less complex than gamma counting, the alpha technique is definitely indicated. ^{210}Pb concentrations of 1 to 100 pCi/g could be measured by means of the ^{210}Po daughter. Therefore, lead samples may be monitored by alpha counting. A similar rationale is applicable to the beta radiation from ^{210}Pb and its daughters. Therefore, beta counting must be considered as an alternate possible monitoring technique. Commercially available alpha and beta counters and techniques have been investigated to determine which of these would be applicable to a monitoring system, what counting times are required and what methods are most suitable. Apparatus on hand has been tested, and some apparatus was borrowed and purchased for evaluation. The results indicate that standard commercial equipment will provide adequate monitoring for lead contamination and so make practical the supply and acquisition of very-low activity lead.

*Research sponsored by the U.S. Atomic Energy Commission.

DISCUSSION

F. DUHAMEL (*France*):

La Commission dont vous avez parlé et qui est chargée d'étudier la pollution du Rhin a-t-elle la possibilité de s'adjoindre un représentant d'un pays fortement intéressé à la pollution du Rhin et qui n'est pas membre de l'Euratom?

P. RECHT:

Rien ne s'oppose à ce qu'un représentant d'un autre pays que l'Euratom puisse participer aux travaux et à l'étude. D'ailleurs, dès le début des études, les autorités suisses ont été informées et certaines opérations de prélèvement et de mesures ont été accomplies en étroite collaboration avec la Suisse.

H. JACOBS (*Germany*):

Herr Dr. Maushart, Sie wiesen hin auf die Bedeutung der organischen Bestandteile im Schlamm in Bezug auf die Anlagerung der von Ihnen untersuchten Nuklide. Gibt es Korrelationen zwischen den Verteilungskoeffizienten und den Vegetationsperioden.

R. MAUSHART (*Germany*):

Wir haben einen Jahresgang des Verteilungskoeffizienten beobachtet. Ob er charakteristisch ist, lässt sich jedoch mit Sicherheit erst auf Grund von Messungen sagen, die sich über mehre Jahre erstrecken.

G. BAGLIANO (*Italy*):

Pourriez-vous nous donner une idée sur la dispersion des résultats que vous avez obtenus?

P. KAYSER:

La dispersion des résultats de tous les points de prélèvement du bassin du Rhin était assez faible. En d'autres termes, les variations des résultats dans le temps, pour un même point de prélèvement, étaient du même ordre de grandeur que les variations dans l'espace.

Ch. TRITREMMEL (*Austria*):

Im Reaktorzentrum Seibersdorf in Österreich wurden ebenfalls Schlammuntersuchungen im Vorfluter in Zusammenarbeit mit der IAEA-Wien durchgeführt. Dabei wurde eine wesentlich unterschiedliche Ablagerung von Radionukliden im Schlamm vom normalen Flussboden und vom Boden im Bereich von Wehranlagen gefunden. Besonders war dies beim Radionuklid Cs^{137} der Fall.

Frage: Wurden bei den Untersuchungen im Rhein auch Schlämme im Bereich von Wehranlagen untersucht und unterschiedliche Ablagerungsmengen von Radionukliden festgestellt?

P. KAYSER:

Les résultats des mesures ont montré que les activités étaient généralement plus élevées en amont des barrages, bien que du point de vue sanitaire ces différences fussent peu significatives.

P. M. BIRD (*Canada*):

Could Mr. Terrill give us any indication of the cost per quart if this process is applied to smaller volumes than indicated in his presentation?

J. G. TERRILL:

It is our current belief that within the range of sizes that we are studying, namely, from 10,000 lb. to 100,000 per 8-hr day, that the cost would not vary greatly per unit weight of milk. However, if the plants would be much smaller, we believe it would be more expensive to maintain the equipment in working order with the type of technical help required for its proper operation. We would not expect the cost to decrease greatly per unit weight of milk for larger plants because much of the cost is related to the materials used in the regeneration processes.

P. SPAANDER (*Netherlands*):

I should like to ask two questions:

1. How did you succeed in keeping the calcium in the milk while removing the strontium from it?

2. How can it be explained that there were coliform organisms in the milk after pasteurization and after treating in such an excellent installation as you described?

J. G. TERRILL:

1. For the pH which removes a maximum amount of strontium-90 consistent with maintenance of milk in its normal form, it was necessary to develop a

regeneration solution which would assure an equilibrium with respect to the major milk cations. The factors affecting the optimum composition and a procedure for selecting the relative proportion of each salt are given in A. R. Landgrebe, L. F. Edmonson, and F. W. Douglas, Jr.: "Optimum Ration of Cations on Nuclear Sulfuric Acid Resin for Minimum Change in Composition of Resin-Treated Milk", *Journal of Dairy Science* (March 1963); and A. R. Landgrebe, L. F. Edmonson, and F. W. Douglas, Jr.: "The determination of the Apparent Equilibrium Constants of the Exchange Reactions of Sodium, Potassium, Calcium, and Magnesium with Amberlite IR-120", *Journal of Agricultural and Food Chemistry* **11** (March 1963).

2. Pasteurized milk with or without strontium removal treatment is milk from which the pathogens have been removed. Normal pasteurized milk in the United States still may contain *E. coli* and other non-pathogenic bacteria up to the levels indicated for the grades indicated as quoted from the Milk Ordinance and Code of the Public Health Service: "In all cases the milk shall show efficient pasteurization as evidenced by satisfactory phosphatase test, and at no time after pasteurization and before delivery shall the milk have a bacterial plate count exceeding 30,000 per milliliter, or a coliform count exceeding 10 per milliliter, as determined in accordance with section 6: Provided, that the raw milk at no time between dumping and pasteurization shall have bacterial plate count or direct microscopic clump count exceeding 400,000 per milliliter".

J. SHAPIRO (*U.S.A.*):

Do you have any hot particle problems from this cratering experiment; i.e. particles that could produce injury if inhaled or retained on the skin?

R. L. KATHREN:

There should be no internal hazard created by the release of "hot" particles. I would expect such particles to be relatively large and therefore well above the respirable range; moreover, if any, these would tend to settle rapidly and close to or within the crater. Normal health physics practice on re-entry is adequate.

Y. FEIGE (*Israel*):

Did you consider depth distribution of fall-out in the ground, or assume a surface plane source?

R. L. FRENCH:

If I understand your question, the answer would be that we assumed the ground surface to be perfectly smooth. We did not consider ground roughness effects.

D. BLANC (*France*):

Le sujet me semble extrêmement important, et je regrette vivement le manque de temps. Je voudrais poser deux questions:

1. Quels radio-éléments ont été utilisés dans ces mesures?

2. Quelle a été la durée des mesures, et quelle valeur statistique possèdent-elles?

NGUYEN BA CUONG:

Nous avons étudié la radio-activité de l'eau de pluie:

— en β totale en France
— et en Sr^{90} aux États-Unis
pendant les périodes suivantes:
— pour la France:
de Mars 1962 à Mai 1963
de Janvier 1964 à Juin 1965
— pour les États-Unis:
de Septembre 1961 à Août 1963
de Septembre 1963 à Juin 1965

K. ŻARNOWIECKI (*Poland*):

Haben Sie Aktivitätsdifferenzen im Blei verschiedener Reinheitsgrade bemerkt?

W. KOLB (*Germany*):

Wir haben Hüttenweichblei, Feinblei und andere handelsübliche Qualitäten aus verschiedenen Hütten untersucht und keine Abhängigkeit der Aktivität vom Reinheitsgrad gefunden. Dies ist auch nicht anders zu erwarten, solange für die Aktivität überwiegend ein Bleiisotop verantwortlich ist.

THE 1965 RECOMMENDATIONS OF ICRP

F. D. SOWBY
International Commission on Radiological Protection,
Sutton, Surrey, U.K. (ICRP)

Abstract—In 1965 the ICRP adopted the text of an entirely revised edition of its basic recommendations; this has recently been published as ICRP Publication 9.* The new recommendations are intended to replace those published in 1959, which were amended and revised in 1962. While the new publication results from an extensive review that the Commission has been carrying out during the past three years, most of the basic principles previously formulated by the Commission remain essentially unchanged; the new recommendations are intended as a clarification of the fundamental bases of radiation protection. Some of the more important modifications that have been introduced will be discussed, including the following: the concept of the dose limit (or maximum permissible dose) in relation to an acceptable risk; the distinction between dose limits for controlled situations and action levels for unforeseen and unplanned conditions; new emphasis on a year as the period over which the dose limit is assessed; the new recommendation for the raising of the amount permitted in a quarter of a year to one-half of the annual limit; doses to be permitted for planned special exposures; dose limits for members of the public, and the concept of the critical group; accidental and emergency exposure of radiation workers and of the public; categories of exposure—adults exposed in the course of their work, and members of the public.

*Recommendations of the International Commission on Radiological Protection. ICRP Publication 9, Pergamon Press (1966).

A QUANTITATIVE ESTIMATION OF THE HAZARDS INVOLVED IN WORK WITH RADIONUCLIDES

TH. FRANKE, G. HERRMANN and W. HUNZINGER
Health and Safety Division,
European Company for the Chemical Processing of
Irradiated Fuels (Eurochemic), Mol, Belgium

Abstract—The damage caused to the critical organ by accidentally incorporated radionuclides is taken as a quantitative measure of the hazard associated with those radionuclides. If the damage itself is assumed to be proportional to the dose equivalent, then the hazard is the product of: (1) the total amount of radioactivity handled, (2) the dose equivalent to the critical organ after a single intake of one unit of radioactivity and (3) the incorporated fraction of the total activity handled.

The first two factors require no particular discussion. For the third factor it is assumed that the accidental intake is by inhalation. Because a derivation of a quantitative figure for this factor is not possible, a statistical investigation of accidents that have already occurred has been started. The accidental inhalations have been classified according to different characteristics of the operations: type of ventilation, physical state, temperature, etc. The preliminary results show that it is possible to obtain average figures for the inhaled fraction of the total activity handled during specified operations. The figures lie almost within one order of magnitude and are independent of the type of accident. The knowledge of these figures permits either the hazard or the maximum permissible quantities of radioactive material to be handled to be derived quantitatively.

INTRODUCTION

Everybody handling radioactive material, particularly unsealed sources, is interested in knowing the risk involved in an operation. The Health Physicist who is asked for advice is given the task of somehow correlating all circumstances of the operation with the possibility of injuring, disabling or shortening the life of the operator. His advice should be in practical terms, for instance by stating an upper limit of activity to be handled during a specified operation, or by recommending that the procedure should be carried out in a glove box instead of a fume cupboard, or by recommending that respirators should be worn, and so on.

Well-known figures for maximum permissible concentrations or body burdens,[1] for radiotoxicity classes,[2] for permissible dose equivalents, etc. might greatly encourage the Health Physicist in his attempt to solve this problem. But in fact, the tide of figures, proposals, and recommendations, which do not give all the information required, is greatly discouraging. Two publications, one by Duhamel *et al.*[3] and one by Morgan *et al.*[4] however, define a hazard figure and calculate it for all radionuclides. With the aid of these figures the hazard involved in a particular operation can be deduced relative to the hazard in a similar operation employing a different amount of another nuclide. It is evident that these tables of the relative hazard of radionuclides solve the problem only partly.

Apparently, the most advanced solution is given by the International Atomic Energy Agency (IAEA),[5] recommending maximum activities of radionuclides to be handled in different types of laboratories, subdividing all radionuclides into four classes of radiotoxicity, and differentiating between five types of operation. Considering for instance the maximum permissible concentrations of all radionuclides in air, which cover a range of 8 orders of magnitude, it is surprising to see that, according to the IAEA, the maximum recommended amount of a

slightly radiotoxic nuclide to be handled in a particular laboratory is only 1000 times more than the maximum recommended amount of a very highly radiotoxic nuclide. The scale of toxicity is not as wide as the range of maximum permissible concentrations in air or of body burdens.

DEFINITION OF THE HAZARD

Generally speaking, the hazard resulting from work with radioactive material can be considered in two different ways: first, the hazard resulting from exposure to radiation during the normal course of the operation, and secondly, the hazard resulting from an accidental exposure if the operation does not follow its expected course. An efficient service of Applied Health Physics ensures that during normal operation neither the external nor the internal radiation exposure of an operator will exceed the permissible levels, and therefore that the dose equivalent received will "carry, in the light of present knowledge, a negligible probability of severe somatic or genetic injuries".[1] The usual radiation dosimetry and survey provide sufficient data for any corrective action necessary if there is unexpectedly high exposure during normal operation.

Accidental exposures, however, should also be considered in such a way that all necessary measures are taken in advance to keep the hazard within limits. We restrict the meaning of the word "hazard" to the probability of injury to the operator if an accident happens and, in this paper, to the somatic and genetic injury resulting from accidental internal exposure to radioactive materials. We do not intend "hazard" to mean the probability of an accident happening. In this connection, however, it is important to consider the average number of accidents that an operator will experience during his life. Over many years of operation of nuclear establishments in the United States,[6] Australia[7] and Sweden[8] the accident frequency is no higher than 2 incidents involving radiation or radioactive materials per million working hours. Comparing this figure with the approximately 0.1 million hours worked by an operator during his life, it follows that only every fifth radiation worker has a chance of being involved in an incident, and that the probability of a radiation worker having two work accidents is negligible. For the purpose of calculating maximum amounts of radioactive material to be handled, one can therefore adopt an exposure of 25 rem as acceptable in any accident.[1]

Evaluation of the hazard should be based on the largest hazard associated with operations involving radioactive materials, i.e. the hazard from a single intake by inhalation. In fact, most accidental exposures reported so far have been due to inhalation of airborne radioactive material. Other accidental incorporations of radioactive material, such as those through wounds, will be considered in a later paper according to the same principles as those applied to accidental inhalations. Provided that the amount of the radionuclide accidentally inhaled and its chemical and physical form are known, the dose equivalent to the critical organ can be derived at once. For instance, it can be taken directly from the tables published by Dolphin *et al.*,[9] who calculated the dose equivalents delivered to the critical organs during 50 years after a single intake.

Derivation of the dose equivalent to the critical organ as a result of an accidental inhalation is most important, because it gives a direct measure, in terms of rem, of the consequences of the accident as far as internal radiation exposure is concerned, and hence gives a direct measure of the hazard. Thus, this figure for the hazard has a meaning, which is easily defined. It has a unit and a dimension. It follows that the hazard from a particular operation with radionuclides is the product of three factors:

—total amount of activity handled (Ci),
—dose equivalent to the critical organ after a single intake of a unit of activity (rem/Ci),
—inhaled fraction of total activity handled, IFTAH (dimensionless).

The last of the three factors, that fraction of the total activity handled which is finally inhaled accidentally, is obviously the most difficult one to assess.

INHALED FRACTION OF THE TOTAL ACTIVITY HANDLED

In general, the inhaled fraction of the total activity handled depends on a great number of circumstances which can be called the

characteristics of an operation. These characteristics of an operation include:

—the fraction of radioactive material present which becomes accidentally airborne,
—the volume of breathing air polluted accidentally, and the extent of the pollution,
—the ventilation rate of the area where the accident occurs,
—the length of exposure of the operator affected, and,
—the effectiveness of any protective measures, such as respirators worn at the time of the accident.

The knowledge of these factors together with the breathing rate of the operator is sufficient for a figure to be derived quantitatively for the inhaled fraction of total activity handled during the operation under consideration.

The last three factors just mentioned—ventilation rate, length of exposure, and filter efficiency—are assessed, or assumed, in a quite straightforward way. The first two factors, however, depend on a great number of circumstances, including dilution of the activity handled with inactive material, chemical form and physical properties of the radioactive compound, temperature, and so on, all of which can be defined for any particular operation. In addition, the type of accident, which is by definition unpredictable, might substantially influence the magnitude of the first two factors. An explosion or other violent reaction accompanied by the production of large volumes of gases might well lead to a heavier air pollution than even a large spill.

By carefully considering all these parameters and trying to make no unjustified assumptions, it has not been possible to derive quantitatively a figure for the inhaled fraction of the activity handled, even for the most simple operation imaginable.

Therefore, a statistical investigation of accidents which occurred in laboratories and which resulted in detectable amounts of radionuclides being inhaled has been started. From these accidental inhalations, the inhaled fraction of the total activity handled has been classified according to combinations of two out of six characteristics of the operation which led to the accident. Concerning the containment, a distinction has been made between glove boxes, ventilated areas, and areas not artificially ventilated. Concerning the physical form of the radionuclide present, the distinction is only between solid material and aqueous solutions, both at ambient temperature. A last characteristic is given by elevated temperatures like those involved in distillations, brazing, etc. The preliminary results from 16 cases are shown in Table 1.

From this table, only rough quantitative conclusions can be drawn about the order of magnitude of the inhaled fraction of radionuclides. It is to be hoped that more accidents which have already happened will be reported in sufficient detail for them to contribute to the statistics. When more cases are known the types of operation distinguished in the table might, of course, be classified in more detail. For instance, operations in ventilated areas could be subdivided into those carried out on laboratory benches and those carried out in fume cupboards; the ventilation rates of these two working places normally differ by two orders of magnitude. A special type of operation involving inflammable material might also be included, and so forth, if it appears that the results of accidents warrant the distinction.

CONCLUSIONS

There is only one conclusion one can draw from the present figures, that this approach to hazard evaluation looks encouraging. We believe that in continuing to collect the relevant data of accidents which have occurred in radiation laboratories, and to classify them as in the above table but with much more closely defined conditions, one would arrive at an average figure for the inhaled fraction for each closely defined type of operation. It should be noted that this average figure will be independent of the type of accident, and will have a variance. This variance will depend on the relative frequency with which the different types of accidents have happened during operations in these closely defined conditions and on their consequences. Predictions based on these results cannot apply to operations widely different from those covered by the statistics, even though they may come within the specified conditions.

The practical use of these figures can be best

Table 1. Inhaled Fraction of Total Activity Handled (IFTAH) for Accidents Involving some Types of Operation

	Glove boxes	Ventilated areas	Non-vent. areas
Solid compound Ambient temp.	1×10^{-7} (1)* 1×10^{-8} (2)	3×10^{-8} (3) 2×10^{-7} (4) 4×10^{-7} (5) 2×10^{-7} (15) 1×10^{-6} (19)	7×10^{-7} (7) 2×10^{-6} (20)
Aqueous sol. Ambient temp.		5×10^{-7} (6) 4×10^{-7} (8) 2×10^{-8} (9)	
Elevated temperatures		7×10^{-6} (10) 1×10^{-5} (11) 3×10^{-6} (12) 2×10^{-6} (13) 1×10^{-5} (16)	

* Numbers in brackets denote number of accident (see appendix).

explained by an example. Assume that the statistics yield a figure of $(1 \pm 0.5) \times 10^{-7}$ for the inhaled fraction in accidents during operations involving aqueous solutions at ambient temperature in a ventilated area. Assume further that such an operation is carried out with 10 mCi of ^{90}Sr, for which the dose equivalent to the critical organ has a value of 3.8×10^{7} rem/Ci. Multiplying these three figures, as explained above, yields a hazard for this operation of

$$H = (4 \pm 2) \times 10^{-2} \text{ rem}$$

This figure means that as a result of any accident during an operation in these conditions the operator's skeleton would probably receive a dose equivalent of 40 ± 20 mrem.

Similarly the opposite question of the maximum working limit of activity to be handled can be answered. Assuming the same type of operation and allowing for an accidental dose equivalent of 25 rem in the following 50 years, it follows that the maximum amount to be handled should be smaller than 6 Ci ^{90}Sr.

It is obvious that this type of analysis does not produce figures for the probability of an accident occurring, but it can predict the consequences in terms of dose equivalent. This information should not be neglected—if it is available.

REFERENCES

1. Recommendations of the International Commission on Radiological Protection. Publications 2 and 6, Pergamon Press, New York, 1959 and 1964.
2. A Basic Toxicity Classification of Radionuclides. Technical Reports Series No. 15, International Atomic Energy Agency, Vienna, 1963.
3. F. Duhamel, J. M. Lavie and L. Titoussi. *Proc. Second United Nations International Conference on the Peaceful Uses of Atomic Energy*, Vol. 23 (1958).
4. K. Z. Morgan, W. S. Snyder and M. R. Ford. *Health Physics* **10,** 151 (1964).
5. Safe Handling of Radioisotopes. Safety Series No. 1, International Atomic Energy Agency, Vienna, 1958.
6. Operational Accidents and Radiation Exposure Accidents, USAEC, 1965.
7. A. D. Thomas. Personal communication.

8. STIG O. W. BERGSTRÖM. Personal communication.
9. G. W. DOLPHIN, A. FAIRNBAIRN and T. MURPHY. AHSB (RP) R20 (1962).
10. USAEC. *Serious Accidents*, Issue No. 242 (1965).
11. I. D. EAKINS and A. MORGAN. Symposium on Assessment of Radioactive Body Burdens in Man. International Atomic Energy Agency, 1964.
12. H. R. DONTH and R. MAUSHART. *Health Physics* **12,** 106 (1966).
13. J. RUNDO and K. WILLIAMS. *Brit. J. Radiology* **XXXIV,** 734 (1961).
14. F. J. BRADLEY, N. WALD and R. L. WECHSLER. Loc. cit. (11).
15. I. O. SNIHS. Personal communication.
16. Massachusetts Institute of Technology. Progress Report, 1961.
17. L. D. MARINELLI, W. P. NORRIS, P. E. GUSTAFSON and T. W. SPECKMAN. *Radiology* **61,** 903 (1953).
18. F. P. COWAN, L. B. FARABEE and R. A. LOVE. *Am. J. Roentgenology* **67,** 805 (1952).

(Appendix follows on page 1406)

APPENDIX

Characteristics of Operations and Activity Accidentally Inhaled

Case	Radio-nuclide	Activity handled	Operation	Place	Protective measures	Description of accident	Activity incorporated	Reference
1	^{238}Pu	28 Ci	no operation	glove box	half-mask respirators	explosion of glove box	3×10^{-8} Ci	10
2	^{239}Pu	100 Ci		glove box		explosion of glove box	1×10^{-6} Ci	11
3	^{239}Pu metal	6×10^{-3} Ci	cryogenic operation	laboratory		explosion of container	2×10^{-10} Ci	11
4	^{137}Cs powder	3 Ci	unpacking	laboratory		broken container	5×10^{-7} Ci	12
5	^{90}Sr $SrCO_3$ powder	0.95 Ci		laboratory		rupture of a window	4×10^{-7} Ci	13
6	FP solution	0.1 Ci		laboratory		rupture of container	5×10^{-8} Ci	12
7	^{90}Sr $SrTiO_3$ powder	7 Ci	unpacking	room without ventilation		broken container	5×10^{-6} Ci	14
8	$^{95}Zr/Nb$	2×10^{-2} Ci	unspecified chemical work	laboratory		spilling	8×10^{-9} Ci	12
9	^{90}Sr solution	3 Ci		laboratory		spilling	5×10^{-8} Ci	12
10	FP solution	1×10^{-2} Ci	distillation	laboratory		splashes	7×10^{-8} Ci	12
11	FP solution	5×10^{-4} Ci	distillation	laboratory		splashes	5×10^{-9} Ci	12
12	^{106}Ru solution	3×10^{-3} Ci	evaporation	laboratory			1×10^{-8} Ci	12
13	^{137}Cs solid	5×10^{-2} Ci	brazing (900°C)	laboratory			1×10^{-7} Ci	12
14*	^{192}Ir metal	10 Ci	sawing of source capsule	laboratory		accidentally sawed into Ir	$0.3-1.0 \times 10^{-6}$ Ci	12
15	^{233}Pa	6.6 Ci	unpacking	laboratory		rupt. container	10^{-6} Ci	15
16	^{152}Eu powder	10^{-3} Ci	heating	hood		spill of powder	10^{-8} Ci	16
17*	^{226}Ra $RaSO_4$	50 mCi				ruptured capsule	$1-3 \times 10^{-7}$ Ci	17
18*	^{90}Sr chloride solution	10^{-3} Ci	preparation of source from aqueous solution	laboratory		faulty experimental technique	5×10^{-9} Ci	18
19	^{137}Cs	0.35 Ci	handling of contam. container	storage room		inadvertent uptake	3×10^{-7} Ci	8
20	^{82}Br NH_4Br	1 Ci	tracer (powder) studies in sea	open air		broken container	$1-3 \times 10^{-6}$ Ci	8

* Not included in Table 1, because the characteristics of the operation are uncertain.

CLASSIFICATION DES RADIONUCLÉIDES DU POINT DE VUE DE LEUR TOXICITÉ RELATIVE

P. GAIRON et Y. FEIGE
Soreq Nuclear Research Centre,
Yavne, Israel

Résumé—Toute classification des nucléides radio-actifs non-scellés d'après leur toxicité relative, dépend des unités employées. En plus de l'activité (exprimée en μC), le poids (en μg) et le nombre d'atomes radio-actifs (N) ont servi de critères pour évaluer la toxicité relative des isotopes radio-actifs. Certains auteurs sont arrivés à des formules permettant de calculer les concentrations maximales admissibles dans l'air (CMA_a) en se servant de l'activité spécifique ($\mu C/\mu g$) comme fonction poids afin de refléter dans une certaine mesure aussi bien les classifications suivant l'activité que celles d'après le poids.

Nous proposons afin d'établir les quantités maximales admissibles dans le corps, un tableau classant les radionucléides d'après la comparaison de ces deux classifications. Ce tableau superpose un code de hachure à une représentation graphique à deux dimensions; les deux classifications sont ainsi maintenues intactes, tout en mettant en relief les restrictions pratiques rencontrées en utilisant l'une ou l'autre exclusivement.

Toute représentation bidimensionnelle est encore incomplète et d'autres classifications peuvent être déduites selon le couple de paramètres que l'on choisit parmi les quatre ou plus qui apparaissent dans la formule de nocivité. Un avantage de notre méthode réside dans la possibilité d'en étendre l'application à d'autres composés toxiques, même non radio-actifs, et de permettre ainsi d'évaluer quantitativement les risques quand il y a danger simultané de contamination radio-active et chimique.

INTRODUCTION

Plusieurs critères ont été proposés pour classifier les radionucléides du point de vue de leur toxicité relative. Aucune de ces classifications n'a été universellement acceptée.[1]

Pour déterminer le danger relatif des sources radio-actives non-scellées et évaluer les "Quantités Maximales Admissibles" dans le corps on a le choix entre trois systèmes d'unités: l'activité (en μC), le poids (en μg) ou le nombre d'atomes radio-actifs. Les classifications qui en résultent, présentent des intérêts différents: la classification d'après l'activité est généralement préférée et c'est elle, la plupart du temps, qui est présentée dans les tableaux[2, 3]; la classification d'après le poids a son importance pratique dans les laboratoires de radiochimie et la classification d'après le nombre d'atomes radio-actifs peut avoir un certain intérêt pour les personnes travaillant aux accélérateurs et à la production d'isotopes.

Le système d'unité choisi peut avoir une influence sur la place relative des radionucléides dans la classification. Les classifications d'après le poids et le nombre d'atomes radio-actifs étant semblables, il faut comparer l'une de celles-ci avec la classification suivant l'activité pour obtenir une information plus complète sur les dangers relatifs présentés par les radionucléides.

Dans le présent travail nous avons choisi de comparer la classification d'après le poids et la classification d'après l'activité. Nous proposons un tableau qui réunit les mérites des deux classifications et en même temps, révèle les restrictions pratiques rencontrées dans l'utilisation de l'une ou l'autre exclusivement.[4, 5] De plus, il est possible d'inclure dans ce tableau des éléments stables toxiques, permettant ainsi d'évaluer quantitativement les risques d'intoxication quand des produits radio-actifs et des poisons chimiques sont présents simultanément.

MÉTHODE DE CLASSIFICATION

Les Quantités Maximales Admissibles (QMA) pour les 225 isotopes présentés dans le rapport du deuxième Comité de l'*ICRP*[6] ont été calculées en μC, en μg et en nombre d'atomes (tableau 1 de (4)). Ces valeurs s'étendent de 0,05 μC à 1000 μC pour l'activité, de 10^{-10} μg à 10^{12} μg pour le poids, et de 10^{6} à 10^{28} atomes radio-actifs. Chacun de ces intervalles est divisé en 6 groupes de la manière suivante: pour l'activité les groupes vont en croissant par facteurs de 10 et pour le poids et le nombre d'atomes, par facteurs de 1000 (tableau 1).

Tableau 1. *Limites des groupes de toxicité pour les valeurs des QMA.*

Numéro de groupe	Limites en μC	Limites en μg	Limites en nombre d'atomes
1	$\leqslant 0.1$	$\leqslant 10^{-6}$	$\leqslant 10^{10}$
2	0.2–1	$2 \times 10^{-6} - 10^{-3}$	$2 \times 10^{10} - 10^{13}$
3	2–10	$2 \times 10^{-3} - 1$	$2 \times 10^{13} - 10^{16}$
4	20–100	$2 - 10^{3}$	$2 \times 10^{16} - 10^{19}$
5	200–1000	$2 \times 10^{3} - 10^{6}$	$2 \times 10^{19} - 10^{22}$
>5		$>2 \times 10^{6}$	$>2 \times 10^{22}$

En représentant les QMA de chaque radionucléide par les numéros des groupes dans lesquels ils se trouvent pour chaque classification, on forme un tableau à 3 colonnes (tableau 1 de (4)) où 90% des radionucléides ont le même numéro de groupe dans les classifications suivant le poids et le nombre d'atomes, (les 10% qui restent ont des numéros de groupe voisins, près de la limite qui sépare des groupes adjacents), alors que la classification suivant l'activité, est essentiellement différente. Ceci tient à ce qu'il faut tenir compte de paramètres indépendants tels que la période, la sélectivité biologique, etc. Les radionucléides et leurs numéros de groupe suivant le poids et l'activité sont donnés dans le tableau 2.

Le tableau 3 représente une grille où les radionucléides seront placés d'après leurs numéros de groupes. Dans cette grille on peut distinguer trois catégories de radionucléides:

1. Ceux qui se trouvent sur la diagonale et pour lesquels les numéros des deux groupes sont identiques.

2. Ceux qui se trouvent au-dessus de la diagonale et pour lesquels le numéro du groupe-poids est inférieur à celui du groupe-activité, c'est-à-dire qu'ils apparaîtront dans un groupe plus restrictif quand ils sont classés suivant le poids.

3. Ceux qui se trouvent en-dessous de la diagonale et qui apparaîtront dans un groupe plus restrictif quand ils sont classés suivant l'activité.

Un code de hachure permet la distinction entre les groupes et entre les classifications (fig. 1). Chaque rectangle de la grille a été hachuré d'après le plus petit des deux numéros de groupe. La hachure désigne ainsi le groupe dans la classification la plus restrictive. Cette conception est préférée, en général, dans les recommandations de Physique de Santé (fig. 2).

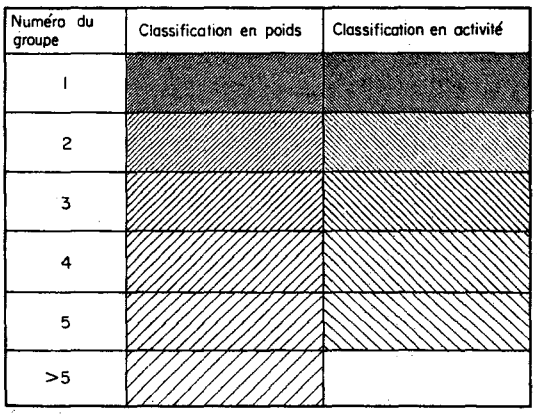

FIG. 1. Code de hachure pour groupes de toxicité.

Tableau 2.

Groupes de toxicité des radionucléides pour les QMA

Nucléide	Symbole & poids atomique		Groupe de toxicité	
			Classification en Poids	Activité
Actinium	Ac	227	2	1
		228	1	1
Americium	Am	241	3	1
		243	3	1
Antimoine	Sb	122	2	4
		124	2	3
		125	3	4
Argent	Ag	105	2	4
		110m	3	3
		111	2	4
Arsenic	As	73	3	5
		74	2	4
		76	2	4
		77	2	4
Astatine	At	211	1	1
Barium	Ba	131	2	4
		140	2	3
Berkélium	Bk	249	2	2
Berylium	Be	7	2	5
Bismuth	Bi	206	2	2
		207	3	3
		210	1	1
		212	1	1
Brome	Br	82	2	3
Cadmium	Cd	109	3	4
		115m	2	3
		115	2	3
Calcium	Ca	45	2	4
		47	2	3
Californium	Cf	249	3	1
		250	2	1
		252	2	1
Carbone	C	14	4	5
Cerium	Ce	141	2	4
		143	2	3
		144	2	3
Césium	Cs	131	3	5
		134m	2	4
		134	3	4
		135	5	5
		136	2	4
		137	3	4
Chlore	Cl	36	5	4
		38	1	3
Chrome	Cr	51	3	5
Cobalt	Co	57	3	5
		58m	2	5
		58	2	4
		60	3	3
Cuivre	Cu	64	2	3
Curium	Cm	242	2	1
		243	3	1
		244	2	1
		245	3	1
		246	3	1
Dysprosium	Dy	165	1	3
		166	2	3
Erbium	Er	169	2	4
		171	2	3
Etain	Su	113	3	4
		125	2	3
Europium(h)	Eu(h)	152	2	3
(y)	(y)	152	3	4
		154	3	3
		155	3	4
Fer	Fe	55	3	5
		59	2	4
Fluor	F	18	1	4
Gadolinium	Gd	153	3	4
		159	2	4
Gallium	Ga	72	1	3
Germanium	Ge	71	2	4
Hafnium	Hf	181	2	3
Holmium	Ho	166	2	3
Hydrogéne	H	3	3	5
Indium	In	113m	1	4
		114m	2	3
		115m	2	4
		115	>5	4
Iode	I	126	2	2
		129	5	3
		131	2	2
		132	1	2
		133	1	2
		134	1	2
		135	1	2
Iridium	Ir	190	2	4
		192	2	3
		194	2	3
Lanthane	La	140	2	3

Tableau 2 (*suite*).

Nucléide	Symbole & poids atomique		Groupe de toxicité	
			Classification en Poids	Activité
Lutetium	Lu	177	2	4
Manganèse	Mn	52	2	3
		54	3	4
		56	1	3
Mercure	Hg	197m	2	3
		197	2	4
		203	2	3
Molybdène	Mo	99	2	3
Neodyme	Nd	144	>5	1
		147	2	3
		149	1	3
Neptunium	Np	237	4	1
		239	2	4
Nickel	Ni	59	5	5
		63	4	5
		65	1	3
Niobium (Columbium)	Nb	93m	3	5
		95	2	4
		97	1	3
Or	Au	196	2	4
		198	2	4
		199	2	4
Osmium	Os	185	2	3
		191m	2	4
		191	2	4
		193	2	3
Palladium	Pd	103	2	4
		109	2	3
Phosphore	P	32	2	3
Platine	Pt	191	2	3
		193m	2	4
		197m	1	3
		197	2	3
Plomb	Pb	203	2	4
		210	3	2
		212	1	1
Plutonium	Pu	238	3	1
		239	3	1
		240	3	1
		241	3	2
		242	4	1
Polonium	Po	210	2	1
Potassium	K	42	1	3
Praseo-dyme	Pr	142	2	3
		143	2	4
Prométheum	Pm	147	3	4
		149	2	4

Nucléide	Symbole & poids atomique		Groupe de toxicité	
			Classification en Poids	Activité
Protacti-nium	Pa	230	2	1
		231	3	1
		233	2	4
Radium	Ra	223	1	1
		224	1	1
		226	3	1
		228	2	1
Rhénium	Re	183	3	4
		186	2	4
		187	>5	5
		188	2	3
Rhodium	Rh	103m	2	5
		105	2	4
Rubidium	Rb	86	2	4
		87	>5	5
Ruthénium	Ru	97	2	4
		103	2	4
		105	1	3
		106	2	3
Samarium	Sm	147	>5	1
		151	4	4
		153	2	4
Scandium	Sc	46	2	3
		47	2	4
		48	2	3
Sélènium	Se	75	3	4
Silicium	Si	31	1	3
Sodium	Na	22	2	3
		24	1	3
Soufre	S	35	3	4
Strontium	Sr	85m	1	4
		85	3	4
		89	2	3
		90	3	3
		91	1	3
		92	1	3
Tantale	Ta	182	2	3
Technètium	Tc	96m	1	4
		96	2	3
		97m	2	4
		97	5	4
		99m	2	5
		99	4	3
Tellure	Te	125m	2	4
		127m	2	3
		127	2	4
		129m	2	3

Tableau 2 (*suite*)

Nucléide	Symbole & poids atomique		Groupe de toxicité: Classification en Poids	Groupe de toxicité: Classification en Activité
Tellure (*suite*)	Te	129	1	3
		131m	2	3
		132	2	3
Terbium	Tb	160	2	4
Thallium	Tl	200	2	4
		201	2	4
		202	2	4
		204	3	3
Thorium	Th	227	1	1
		228	2	1
		230	4	1
		231	2	4
		232	5	1
		234	2	3
		Nat. Th	5	1
Thulium	Tm	170	2	3
		171	3	4
Tungstène	W	181	3	4
		185	3	4
		187	2	4
Uranium	U	230	1	1
		232	2	1
		233	4	1
		234	4	1
		235	5	1
		236	4	1
		238	5	1
		Nat. U	5	1
Vanadium	V	48	2	3
Ytterbium	Yb	175	2	4
Yttrium	Y	90	2	3
		91m	1	3
		91	2	3
		92	1	3
		93	1	3
Zinc	Zn	65	3	4
		69m	1	2
		69	1	2
Zirconium	Zr	93	5	4
		95	2	4
		97	2	3

Il peut cependant y avoir un intérêt pratique à envisager la classification qui suggère un degré de danger moindre, sans cependant perdre de vue la conception précédente. C'est ainsi que dans la figure 3 les deux classifications apparaissent simultanément; toutefois la prépondérance est donnée au groupe le moins restrictif. La figure 3 est en fait, une superposition de deux tableaux: l'un, appelé "Classification en Poids" comporte, dans les Regions I et II, les radionucléides qui étaient dans la figure 2, au-dessous de la diagonale et sur celle-ci; l'autre, appelé "Classification en Activité", comporte dans les Régions III et II, les radionucléides qui étaient dans la figure 2, au-dessus de la diagonale et sur celle-ci. La Région II, identique dans ces deux tableaux, sert d'axe à la superposition.

Les rectangles hachurés de la figure 2 sont incorporés dans la figure 3 dans la région caractérisée par le plus grand de leur deux numéros de groupe. Le code de hachures est appliqué de manière à dévoiler instantanément les niveaux de danger dans les deux classifications: la hachure extérieure au rectangle indique les conditions les moins restrictives; la hachure à l'intérieur du rectangle rappelle les conditions les plus restrictives et la classification.

Pour comparer des radionucléides qui se trouvent dans les Régions I et III il faut les transposer dans la Région qui nous intéresse. Cela se fait en déterminant la ligne dont la hachure correspond à celle du rectangle à transposer.

La figure 3 peut être généralisée afin d'inclure des éléments stables mais toxiques chimiquement. Dans le tableau 4 les QMA de quelques éléments stables toxiques ont été calculées, à partir de leur concentrations maximales admissibles dans l'air,[7] à l'aide de la formule suivante:

$$W = \frac{(CMA)_a \times (T_{biol.}) \times (f_a)}{10^{-4} \times (f_2)}$$

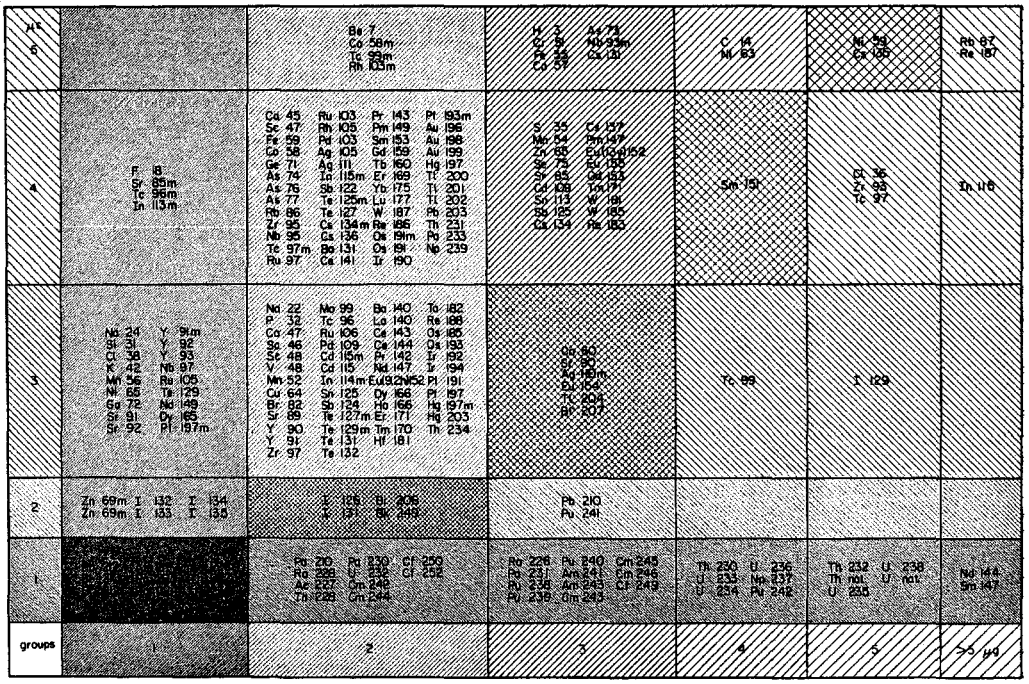

FIG. 2. Représentation à deux dimensions de la toxicité des radionucléides.

Tableau 3. Grille donnant les numéros des groupes de toxicité

μC						
5	(1,5)	(2,5)	(3,5)	(4,5)	(5,5)	(>5,5)
4	(1,4)	(2,4)	(3,4)	(4,4)	(5,4)	(>5,4)
3	(1,3)	(2,3)	(3,3)	(4,3)	(5,3)	(>5,3)
2	(1,2)	(2,2)	(3,2)	(4,2)	(5,2)	(>5,2)
1	(1,1)	(2,1)	(3,1)	(4,1)	(5,1)	(>5,1)
groupes	1	2	3	4	5	>5 μg

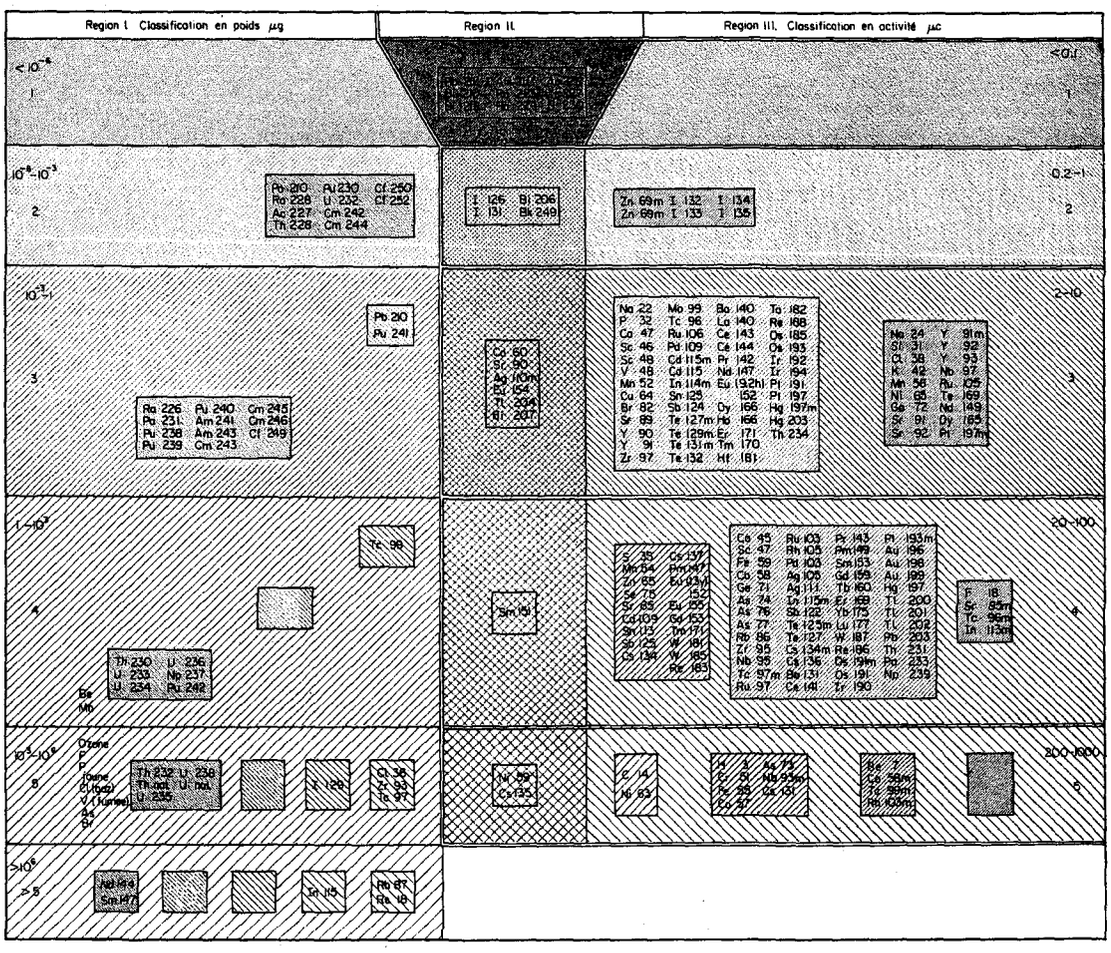

FIG. 3. Tableau composé pour toxicité relative des radionucléides.

où W est la QMA exprimée en μg, $T_{biol.}$ la période biologique en jours, $(CMA)_a$ la concentration maximale admissible dans l'air en mg/m^3, f_a la fraction de radionucléide dans l'organe critique par rapport à la quantité absorbée dans les poumons, et f_2 la fraction de radionucléide dans l'organe critique par rapport à la quantité présente dans tout le corps. Ces éléments ont été incorporés dans la figure 3 sur les lignes correspondant à leur QMA dans la Région I (Classification en Poids).

DISCUSSION

La figure 3 a été composée pour classer et comparer les radionucléides, en même temps que pour permettre une évaluation grossière du danger qu'ils représentent. Les niveaux de danger ont été établis en fonction des quantités maximales admissibles dans le corps plutôt qu'en fonction des concentrations maximales admissibles dans l'air, vu que ces dernières sont susceptibles de changer avec le progrès de nos connaissances et avec les conditions de travail. Les facteurs secondaires, comme la grosseur des particules, le temps de travail, et l'habileté personnelle des employés, sont à prendre en considération et peuvent faire varier dans de grandes proportions les quantités que l'on peut manipuler.

Les radionucléides pour lesquels les QMA dépassent 1000 μC ne sont soumis à aucune limitation. Dans la figure 3, la ligne du groupe

Tableau 4. Numéros de groupes de toxicité en poids de quelques éléments toxiques stables à partir de leur $(CMA)_a$

Élément	CMA_a*	$\frac{T_b \times f_a}{f_2}$	W (mg)	Numéro du groupe de toxicité dans la classification en poids
Be	0.002	45	0.9	4
Ozone	0.2	10.5	21	5
F	0.2	606	1212	5
P_{jaune}	0.1	162	162	5
Cl (gaz)	3	21	630	5
V (fumée)	0.1	11	11	5
Mn	0.002	5.1	0.1	4
As	0.5	75.5	380	5
Br	7	6	420	5
Cd	0.1	50	50	5
Sb	0.5	10.3	51.5	5
Te	0.1	5.7	5.7	5
I (gaz)	1	104	1040	5
Hg	0.1	6.3	6.3	5
Pb	0.1	423	423	5

* Valeurs tiriées de Moeschlin[7].

> 5 est vide. On peut en conséquence, renoncer à limiter les radionucléides du groupe > 5 de la "Classification en Poids", bien que certains d'entre eux auraient appartenu à des groupes plus élevés dans la classification en activité. Des habitudes correctes de travail suffiront à éviter la pénétration dans le sang de 1g de radionucléide. Ceci concerne les radionucléides suivants: ^{144}Nd, ^{147}Sm, ^{115}In, ^{87}Rb, et ^{187}Re. D'un autre point de vue, il est convenu de ne pas limiter l'utilisation des radionucléides dont l'activité spécifique est inférieure à 0,002 μC/g (le double de l'activité spécifique du Potassium naturel). En ce qui concerne la contamination interne, le seuil peut être élevé à 0,1 μC/g, ce qui supprime les limitations sur les radionucléides suivants: ^{87}Rb, ^{115}In, ^{129}I, ^{144}Nd, ^{147}Sm, ^{187}Re, ^{237}Th, Th nat., ^{238}U, U nat., c'est-à-dire, tous les radionucléides du groupe > 5 dont il a été question plus haut, ainsi que quelques émetteurs-α à longue période du groupe 5 de la "Classification en Poids".

Certains auteurs préfèrent déterminer le danger de sources radio-actives non-scellées sous forme de concentrations maximales admissibles dans l'air ou dans l'eau. Des tables de CMA_a ont été établies par Duhamel et Lavie[8] et ont été présentées sous forme graphique. Leur fonction de danger

$$H = \frac{1}{\sqrt{(CMA)_g \times (CMA)_c}}$$

peut être mise sous la forme

$$H = \frac{\sqrt{(C/g)}}{(CMA)_c}$$

C/g étant l'activité spécifique, ce qui fait apparaître l'activité spécifique comme facteur de correction dans la formule de danger classique $H = \frac{1}{(CMA)_c}$. Cette correction a pour effet d'accroître l'influence de l'activité spécifique, paramètre qui n'est représenté dans la formule classique que par l'intermédiaire de la période effective dans l'expression de la (CMA) d'après le développement suivant:

$$(CMA)_a = \frac{10^{-7}\, q f_2}{T f_a} \quad \text{en } \mu C/cm^3$$

la période effective:

$$T = \frac{T_b \times T_r}{T_b \div T_r} = \frac{T_b}{1 \div T_b/T_r}$$

En conclusion, il n'est pas surprenant qu'une représentation à deux dimensions d'une relation qui contient au moins quatre paramètres indépendants, soit incomplète, et que les résultats dépendent des deux paramètres choisis parmi les quatre. Malgré les intérêts pratiques de chacune de ces représentations, aucune ne peut être considérée comme idéale et définitive. Une classification plane ne peut être tout au plus qu'une projection dans un sous-espace à deux dimensions d'une fonction qui serait univalente dans un espace à cinq dimensions. Notre représentation est une tentative pour obtenir une dimension supplémentaire à l'aide du partage du tableau en deux régions et de la superposition des hachures.

RÉFÉRENCES

1. H. JAMMET et G. VACCA. *Proc. 2nd U.N. International Conference on Peaceful Uses of Atomic Energy.* Geneva, 1958, Vol. **23,** p. 346.
2. *Safe Handling of Radioisotopes.* IAEA Vienne Safety Series No. 1, 1958.
3. *NBS Handbooks. U.S.* Department of Commerce No. 69, 1959.
4. Y. FEIGE et P. GAIRON. Classifications of radionuclides according to maximum permissible body burdens. Israel AEC Report IA-821 (1963).
5. Y. FEIGE et P. GAIRON. Relative toxicity of radionuclides. Israel AEC Report IA-989 (1965).
6. Report of ICRP Committee II on Permissible Dose for Internal Radiation. *Health Physics,* **3** (1960).
7. S. MOESCHLIN. *Klinik und Therapie der Vergiftungen.* G. Thieme, Stuttgart, 1959, pp. 19–24.
8. F. DUHAMEL et J. M. LAVIE. La Limitation des Quantités de Substances Radio-actives Manipulées ou Transportées. *Health Physics,* **10,** No. 7, 453 (1964).
9. K. Z. MORGAN, W. S. SNYDER et M. R. FORD. Relative hazard of the various radioactive materials. *Health Physics,* **10,** No. 3, 151 (1964).
10. K. Z. MORGAN. Recommendations of Publication 6 of the ICRP Nuclear Safety, **6,** 20 (1964).

la période radio-active:

$$T_r = \frac{1.308 \times 10^8}{A \times (C/g)}$$

d'où

$$(CMA)_a = \frac{10^{-7} \times q \times f_2}{f_a \times T_b} \times \left[1 \div \frac{A \times T_b \times (C/g)}{1.308 \times 10^8} \right] \text{ en } \mu C/cm^3$$

La formule de Duhamel et Lavie donne une évaluation plus basse du degré de danger des radionucléides à longue période (ce qui est en accord avec l'expérience); par contre, l'évaluation du degré de danger des radionucléides à courte période croît systématiquement avec l'activité spécifique.

Morgan *et al.*[9] ont introduit des facteurs limitants comme la concentration de poussière dans l'air, la grosseur des particules, des facteurs de dilutions, etc. . . . Leur fonction de danger comporte une fonction poids à borne supérieure égale à 10 fois la limite du Radium 226 pris comme unité de danger.

$$H = \frac{2{,}92 \times 10^{-11} \Phi\,(C/g)}{(CMA)_C}$$

où Φ est défini comme suit:

$$\Phi\,(C/g) = \begin{cases} C/g, & \text{quand } (C/g) \leqslant 10 \\ 10, & \text{quand } (C/g) > 10 \end{cases}$$

(On pourrait l'exprimer sous une forme continue à un ordre de grandeur près de la manière suivante: $\Phi\,(C/g) = \dfrac{10}{1 \div 10(g/C)}$.)

Morgan obtient ainsi une évaluation encore plus basse du degré de danger des radionucléides à période longue sans cependant élever l'évaluation du degré de danger des radionucléides à période courte.

Morgan *et al.*[10] et Duhamel et Lavie ont obtenu des résultats semblables pour les radionucléides à activité spécifique comprise entre 10^{-2} et $10^4 C/g$. A l'extérieur de cet intervalle, les radionucléides à longue période ($C/g < 10^{-2}$) et à courte période ($C/g > 10^4$) sont classés moins dangereux dans la classification de Morgan, ce qui, dans la plupart des cas, est en accord avec l'expérience.

Notre classification conduit à des résultats comparables. Nous obtenons un abaissement dans l'évaluation du degré de danger à l'aide du réarrangement de ceux des radionucléides pour lesquels la classification en poids conduit à un degré de toxicité plus bas que la classification en activité. Ceci concerne en premier lieu les radionucléides à période longue et à activité spécifique inférieure à 10^{-2} C/g dont il a été question plus haut à propos de la classification de Morgan.

Cette méthode conserve sans altération, les classifications d'après le poids et l'activité, sans nécessiter un réarrangement mathématique.

Il est intéressant de rappeler que les quantités maximales admissibles pour les différents radionucléides sont, par définition, les valeurs qui, d'après nos connaissances actuelles équivalent à un danger d'égale contamination. Ces valeurs sont sensées représenter la toxicité relative des isotopes. En se servant de ces valeurs pour évaluer le danger de contamination on est en fait en train de remonter à la formule dont elles ont été dérivées. La quantité maximale admissible est donnée par

$$q = \frac{2{,}8 \times 10^{-3}\, m\, R}{f_2\, [\Sigma\, EF(RBE)_n]} \quad \text{en } \mu C,$$

ou par $W = \dfrac{q \times A \times T_r}{1.308 \times 10^8}$ en μg, d'où

$$W = \frac{2.8 \times 10^{-3}\, m\, R\, A\, T_r}{f_2\, [\Sigma\, EF(RBE)n]\ 1.308 \times 10^8}$$

Pour déterminer le danger relatif d'après l'activité $\dfrac{1}{q}$ la connaissance de plusieurs paramètres indépendants est nécessaire:

R = la dose admissible dans les tissus (100 mrem pour tout le corps ou 300 à 600 mrem suivant la sensibilité radio-active de l'organe critique),

m/f_2 = la concentration dans l'organe critique,

$[\Sigma\, EF(RBE)n]$ = l'énergie effective.

Le danger relatif d'après le poids introduit, en plus, le poids atomique de l'élément ainsi que sa période radio-active.

ESTIMATION OF RADIATION PROTECTION GUIDES: INTERSPECIES CORRELATIONS*

C. R. RICHMOND and J. E. FURCHNER
Los Alamos Scientific Laboratory,
University of California,
Los Alamos, New Mexico

Abstract—Values recommended for maximum permissible concentration (MPC) of radionuclides in air and water and for retention by the body and its component tissues are commonly based on data obtained from acute tracer studies in rodents. Conceptually, however, conditions of chronic exposure for human subjects are embodied in MPC calculations. Unfortunately, studies on retention of many radionuclides by human subjects are impossible or impracticable, even though the development of ultrasensitive human counters represents a significant contribution to the problem. Metabolically speaking, a 70-kg mouse or rat is sometimes regarded as a standard man.

One approach to resolving this problem is to find interspecies correlations in radionuclide metabolism and ways of extrapolating to MPC values for man. During continuous ingestion of a constant amount of a material, an equilibrium level may be reached within the body. This level is predictable from acute administration studies. The integral of the effective retention function (limits of zero to infinity) is proportional to equilibrium level and has dimensions of multiples of the daily intake. The integral is also proportional to radiation dose.

Interspecies correlations of the form $E = aX^b$, which relate equilibrium levels (E) obtained for mice, rats, dogs, monkeys, and men to grams body weight (X), have been developed for tritium water (HTO), ^{22}Na, ^{54}Mn, ^{65}Zn, ^{86}Rb, ^{131}I, and ^{137}Cs. The proportionality constant b differs for each element. In each case, values obtained directly from human studies agree well with values for man derived from the correlation. Equilibrium levels as a function of body surface, body weight, and metabolic rate using the power function (with and without the log transform) and a first-degree polynomial were also considered as models. The polynomial relating equilibrium level to body surface best describes cesium metabolism and accounts for shorter turnover times observed in children.

INTRODUCTION

Radiation protection guides for human beings are sometimes based on data obtained not from man but from laboratory animals. The proper choice of species or, more properly, the applicability of data obtained from one animal to man is sometimes referred to as the "species problem". At least two avenues of investigation related to the field of radiation protection are concerned with this problem. The first is that of determining reparable and irreparable damage components following radiation exposure. The rate at which damage is repaired varies among species and tends to decrease as body weight increases.[1] The second, which we will consider in this paper, is that of estimating maximum permissible concentrations (MPC's) for various radionuclides.

One biological parameter used in calculating MPC values is the effective residence time for a specific radionuclide within the body or within a specific organ. More precisely, we want to know how much of a material will be present within the system when equilibrium conditions are reached between intake and excretion. Equilibrium levels are estimated from measurements of effective turnover of the

* Work performed under the auspices of the U.S. Atomic Energy Commission.

element in question by using radionuclides or from a knowledge of the relation between daily intake (or output) and total body content of the stable species of the element.[2] Ideally, the necessary experimental data should be obtained from man, but this is not always practicable or prudent. Alternatively, metabolic correlations among mammalian species that relate the equilibrium body burden to some physiological parameter such as body weight can be used as a first approximation when human data are inadequate or totally lacking.[3-7] For convenience, the adaptation of the interspecies correlation, as used in this paper, to the ICRP method of calculating MPC values is presented in an appendix.

This report summarizes interspecies correlations established at our Laboratory for tritium, sodium, rubidium, cesium, zinc, iodine, and manganese. We also present several physiological parameters other than body weight as the basis of relating equilibrium burdens interspecifically. Factors that can shift the position of a given species within the correlation are also discussed.

METHODS AND MATERIALS

The laboratory animals used in the studies reported here were RF strain mice, Sprague-Dawley strain rats, beagle hounds, and macaque monkeys. Female mice were used because of fighting among males; otherwise, attempts were made to use only male animals. The dogs and mice were selected from animals bred at our Laboratory; rats and monkeys were secured from commercial suppliers. Only mature animals in apparent good health were used. Rodents were approximately 90 days old before use. Dogs and monkeys must be 1½ to 2 years old. Two difficulties with rats are that growth continues and weight increases throughout the experimental period, and there is a high incidence of respiratory difficulty. We are now in the process of replacing the albino rat with a longer-lived rodent (*Mystromys albicaudatus*) that seems to be quite free from respiratory problems and that shows only a small weight change with age.

Commercial diets are used for all animals. Because the data reported here were collected over several years, several suppliers have been used. All species but monkeys are currently fed diets from a single supplier.* The animals are fed the rations *ad libitum* without dietary supplements. Water is always available.

Tritium water (HTO) was given orally (dog and man) or parenterally (mouse, rat, rabbit, monkey, and horse). For each species the volume of water containing the tritium was small compared to the volume of the body water reservoir. The total radiation dose delivered to the human subjects was of the order of 200 mrad, assuming homogeneous distribution of tritium throughout the body and using the observed effective half-life. At 2, 3, and 4 hr after administration and at appropriate subsequent times, the concentration of HTO was measured in pure water obtained from the blood of each species but man. Urine was the source of body fluid for human subjects.

At each blood sampling time, 20 μl of blood were drawn into a Sahli hemoglobin pipette from a small incision in the tail vein of rodents or from the marginal ear vein of rabbits and were immediately mixed with 1 ml of normal saline. After mixing and centrifugation, 0.5 ml of clear supernatant was pipetted into 24 ml of scintillator solution. One-ml aliquots of pure water were obtained from blood samples removed from dogs, monkeys, and horses and from urine samples voided by the human subjects by using a vacuum distillation procedure modified after Cooper *et al.*[8] To avoid any possible isotope fractionation effects, each sample was distilled to dryness. All samples were stored at 4°C for 1 hr prior to tritium assay in a scintillation detector. Composition of the scintillator solution and details of the assay are given elsewhere.[9] The tritium activity of each sample obtained from whole blood (mice, rats, and rabbits) was converted to μCi/ml body water by multiplying by an appropriate dilution factor and correcting for the water content of blood at termination of the experiment. Blood water was measured in samples of whole blood dried to constant weight at 100°C.

In the other experiments reported here, gamma-emitting radionuclides were administered and assayed by means of whole-body (*in vivo*) counting techniques. Both the whole-body

* Wayne, Chicago, Illinois.

counting procedures for the 4π steradian geometry detectors (liquid scintillator variety) and the automatic data reduction and analytical methods have been reported in detail.[10, 11] Use of large-volume detectors reduces errors arising from translocation of the radionuclide within the animal during the experiment. For the gamma-emitting nuclides considered in this paper, the individual doses per animal were of the order of 1 μCi or less.

RESULTS AND DISCUSSION

Tritiated water (HTO)

Retention of HTO (per ml body water) was described for each species by a simple exponential function,

$$R_t = a \exp(-kt), \quad (1)$$

in which a is the initial concentration of HTO in the body water, k is the rate constant in reciprocal days, and t is days. The rate constant is related to biological half-life (T_b) and average residence time (τ) for a hydrogen atom within the body by the following:

$$k = \frac{\ln 2}{T_b} = \frac{1}{\tau}. \quad (2)$$

Values of T_b ranged from average values of 1.1 days for mice to 9.5 days for human subjects. These data were presented in detail elsewhere.[4]

Figure 1 shows an interspecific correlation between log of daily water loss and log of body weight for seven species. Average daily water turnover was calculated from k and body water reservoir volume (W) for the individual animals comprising the sample. W was determined by the dilution principle using the intercept a of eq. (1) as the equilibrium specific activity of ^3H in body water during early mixing.

One can calculate total daily water turnover from a knowledge of the size and turnover of the exchangeable water pool. The derivative of the retention function, which corresponds to excretion rate, is:

$$-\frac{dR_t}{dt} = a\,(k) \exp(-kt). \quad (3)$$

If the volume of the body water pool (W) is substituted for the tritium concentration in eq. (3), one can then determine the instantaneous

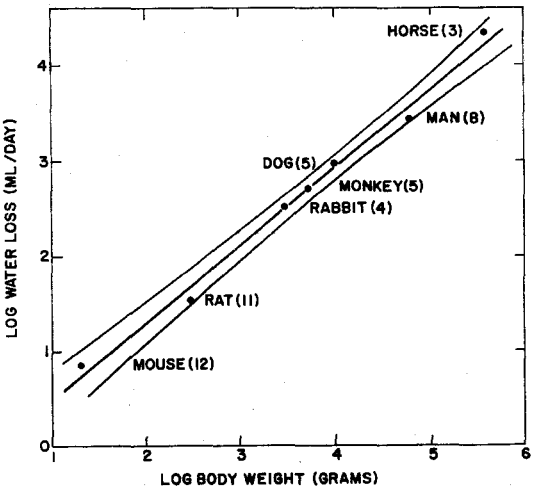

FIG. 1. Interspecies correlation between log daily water loss and log body weight (in g) for 7 mammalian species. The regression equation is: log water loss = $-0.4188 + 0.8180 \log X$.

rate of water loss by setting t equal to zero as follows:

$$-\frac{dR_t}{dt} = W \cdot (k). \quad (4)$$

The regression line, which was fit by the least-squares method, and the 95% confidence limits are given. The correlation coefficient (r) between the variables is 0.993. The regression equation is:

$$\log \text{water loss} = -0.4188 + 0.8180 \log X, \quad (5)$$

and the standard error of the slope constant (S_b) is $\pm$ 0.0129. A value of $\pm$ 0.122 was obtained for the standard error of estimate (S_e) for the regression line.

It is clear from the value of parameters r, S_e, and S_b that a high degree of confidence may be placed on the regression equation relating body water turnover to body weight. The value of the slope constant indicates that body water turnover is proportional to the 0.82 power of body weight. Relative to body weight, larger mammals have a slower turnover of body water than smaller ones.

Figure 2 shows the equilibrium factor (E) for tritium water as a parabolic function of

body weight (in g) for 12 mice, 12 rats, 4 rabbits, 5 dogs, 5 monkeys, and 8 human subjects. Age, sex, body weight, and equilibrium factor are given in Table 1 for each human subject. Using a parabolic model (i.e. $y = ax^b$), the best computer fit to the 46 data points is:

$$E = 1.24\ X^{0.2057}. \quad (6)$$

As indicated by the exponent, E increases not in direct proportion to body weight but as the 0.2057 power of body weight. As shown in the appendix, E is equal to the mean residence time for the atom within the body. Thus, because retention of tritium water by the body is a monotonic process (for all practical purposes), the ordinate values in Fig. 2 are equivalent to mean residence times, $\left(\frac{T_b}{\ln 2}\right)$. Values of E tend to increase with age as well as with body weight for the human subjects. All 3 subjects aged 16 or younger fall below the curve. Of the 5 adults, all but 1 fall above the curve. If we solve eq. (6) for 7×10^4 g, we obtain a value of 12.35 for E, which corresponds to a T_b value of 8.6 days. From data given in Table 1 we can calculate a mean T_b value of 8.4 days for all 8 subjects. For the 5 adults, with an average body weight of 6.7×10^4 g, the average experimentally determined T_b was 9.5 days.

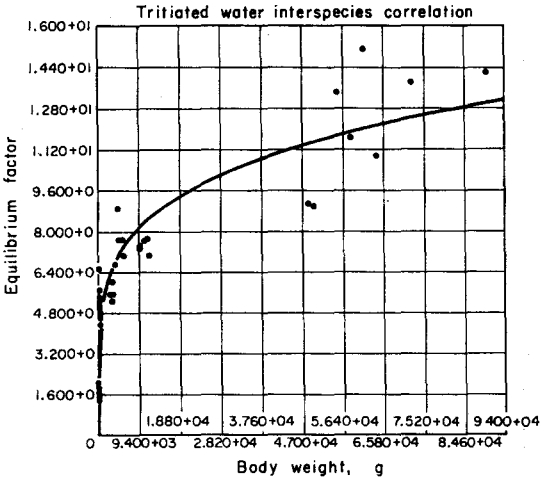

FIG. 2. Interspecies correlation between equilibrium factor (E) and body weight (in g) for mice, rats, rabbits, monkeys, dogs, and men given tritium water. The regression equation is: $E = 1.24\ X^{0.2057}$.

Figure 3 shows equilibrium values obtained from the individual animals plotted as a function of body surface. The best computer fit to the data points is:

$$E = 10.42\ X^{0.2818}. \quad (7)$$

As in eq. (6), no logarithmic transformation of the variables was made prior to fitting the data. Equilibrium factor E is proportional to body surface (in m^2) raised to the 0.28 power. The intercept (10.42) is the value of E when body surface is 1 m^2. However, as can be seen in Fig. 3, when body surface becomes very small, E

Table 1. Age, Sex, Weight, and Equilibrium Factor (E) for Human Subjects given Tritium Water by Mouth

Subject No.	Sex	Age (yr)	Weight (kg)	E*
1	M	43	72.3	13.82
2	M	14	64.1	10.94
3	M	10	49.5	8.93
4	M	24	61.2	15.12
5	M	23	89.8	14.11
6	F	16	48.2	9.07
7	F	36	58.2	11.66
8	F	45	55.0	13.39

* Multiples of the daily intake.

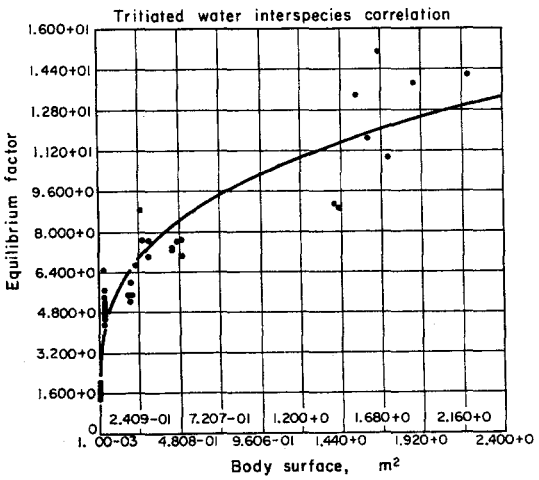

FIG. 3. Interspecies correlation between equilibrium factor (E) and body surface (in m^2) for mice, rats, rabbits, monkeys, dogs, and men given tritium water. The regression equation is: $E = 10.42\ X^{0.2818}$.

approaches zero. An interspecific relation derived by von Schelling[12] was used to convert body weight to body surface.

Equilibrium factors shown in Figs. 2 and 3 were also fit as a function of several physiological parameters in the normal plane using a first-degree polynomial. The computer-obtained regression equations that correlate E with body weight, body surface, and metabolic rate are given in Table 2. Body surface and metabolic rate were calculated from the body weight of each animal using the equations of von Schelling[12] and Brody.[13]

The average $(MPC)_w$ value for continuous intake, calculated from equilibrium factors obtained from the eight human subjects (Table 1), was 8×10^{-2} μCi ^3H/ml, as compared with a value of 5×10^{-2} now listed by the ICRP.[2] If one substitutes a value of 7×10^4 g in the interspecies correlation based on grams body weight (eq. 6), the resultant equilibrium factor (E) is 11.15. The value of $(MPC)_w$ is then calculated by substituting E in the equation,

$$(MPC)_w = \frac{q}{E \cdot S}, \tag{8}$$

where q is 2×10^3 μCi and S is 2200 ml/day (see eqs. (A1) to (A4) in the appendix).

If human data were not available, the interspecies correlation and subsequent $(MPC)_w$ estimation would be based on the data obtained solely from laboratory animals. Table 3 gives regression equations for E as a function of body weight and body surface with and without data from the human subjects. All values of E and $(MPC)_w$ are reasonably similar. Data extrapolated from animals to man yield essentially the same values of E and $(MPC)_w$ as those obtained from the correlation that includes the human data.

Cesium

Figure 4 shows the interspecies relation between E and body weight (in g) for 74 animals (21 mice, 35 rats, 4 monkeys, 7 dogs, and 7 human subjects) given radiocesium. Table 4 gives age, weight, and equilibrium factor for

Table 2. Interspecies Correlation between Equilibrium Factor (E) and Several Physiological Parameters for Mice, Rats, Rabbits, Dogs, Monkeys, and Men given Tritiated Water by Mouth

Independent variable (X)	Interspecies correlation	Correlation coefficient
Body weight (g)	$4.30 + 0.00013\ X$	0.574
Body surface (m^2)	$3.91 + 5.22\ X$	0.679
Metabolic rate (cal/day)	$3.92 + 0.006\ X$	0.677

Table 3. Comparison of Equilibrium Factor (E) and $(MPC)_w$ Values for Tritium Water in Man using Interspecies Correlations of the Form $E = aX^b$ with and without Data from Human Subjects

Independent variable (X)	Interspecies correlation	E*	$(MPC)_w$ (μCi/ml)
Body weight (g)†	$1.24\ X^{0.2057}$	11.15	8.1×10^{-2}
Body weight (g)‡	$1.43\ X^{0.1861}$	11.40	7.9×10^{-2}
Body surface (m^2)†	$10.42\ X^{0.2818}$	12.31	7.4×10^{-2}
Body surface (m^2)‡	$9.75\ X^{0.2549}$	11.32	8.0×10^{-2}
ICRP[2]	—	—	5.0×10^{-2}
From 7 human subjects**	—	—	8.0×10^{-2}

* Value of interspecies correlation calculated for a person with a body weight of 7×10^4 g or a body surface of 1.8 m^2.
† Man included in the derivation of the interspecies correlation.
‡ Man omitted from the derivation of the interspecies correlation.
** Using observed turnover values in equation used by the ICRP.[2]
See eq. (A1) in the appendix.

each male subject. The best computer fit to the data given in Fig. 4 is:

$$E = 0.23\ X^{0.5914}. \quad (9)$$

Thus, E varies as the 0.5914 power of body weight. The exponent indicates a closer proportionality between E and body weight for cesium than in the case of tritium water (eq. 6). Equation (9) also predicts a value of 0.23 for E when body weight is 1 g. No logarithmic transformation of the variables was made prior to fitting the data.

Table 4. Age, Weight, and Equilibrium Factor (E) for Male Human Subjects given Radiocesium by Mouth

Subject No.	Age (yr)	Weight (kg)	E*
1	33	81.8	133.30
2	35	77.3	164.60
3	37	57.0	144.09
4	27	68.2	187.26
5	28	75.4	191.05
6	34	70.3	217.98
7	53	61.2	161.96

*Multiples of the daily intake.

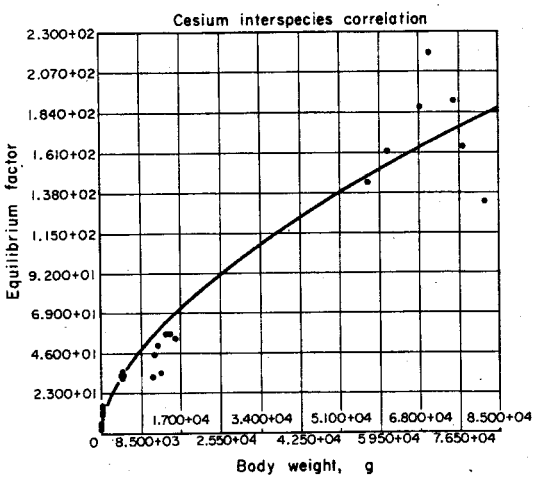

FIG. 4. Interspecies correlation between equilibrium factor (E) and body weight (in g) for mice, rats, monkeys, dogs, and men given radioactive cesium. The regression equation is: $E = 0.23\ X^{0.5914}$.

Figure 5 shows the interspecies relation between E and body surface (in m^2) for the same animals. In this case, the best computer-derived regression equation is:

$$E = 97.35\ X^{0.8618}. \quad (10)$$

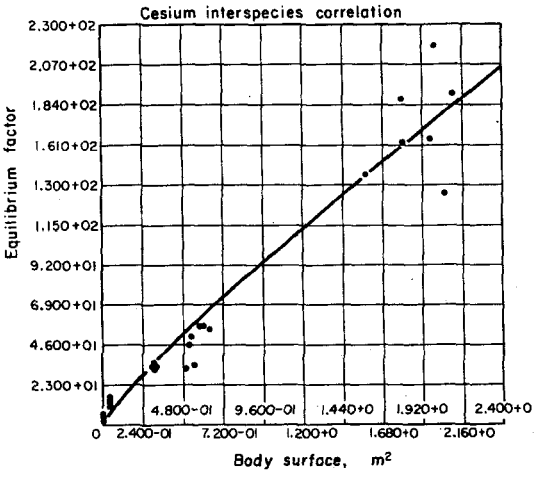

FIG. 5. Interspecies correlation between equilibrium factor (E) and body surface (in m^2) for mice, rats, monkeys, dogs, and men given radioactive cesium. The regression equation is: $E = 97.34\ X^{0.8518}$.

The coefficient indicates a value of 97.35 for E when body surface is unity. Figure 5 shows, however, that for body surfaces approaching zero, E approaches zero.

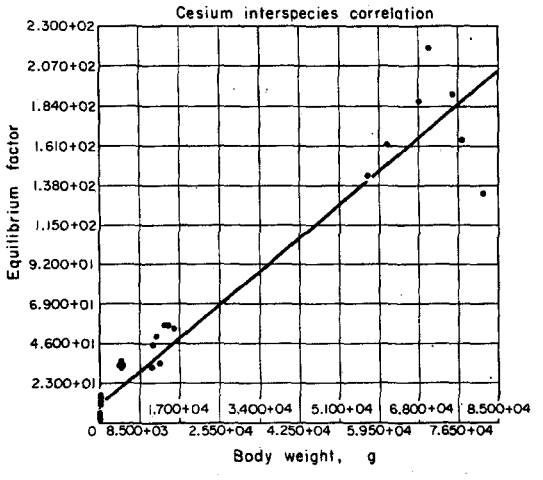

FIG. 6. Interspecies correlation between equilibrium factor (E) and body weight (in g) for mice, rats, monkeys, dogs, and men given radioactive cesium. The regression equation is: $E = 10.88 + 0.0023\ X$.

The cesium data were also fit using a first-degree polynomial. Figure 6 shows the interspecies correlation between E and grams body weight. The best computer-derived fit is:

$$E = 10.88 + 0.0023\ X, \qquad (11)$$

with a correlation coefficient of 0.962.

If E is fit as a function of body surface (Fig. 7), the best regression equation is:

$$E = 6.64 + 85.59\ X, \qquad (12)$$

with a correlation coefficient of 0.981.

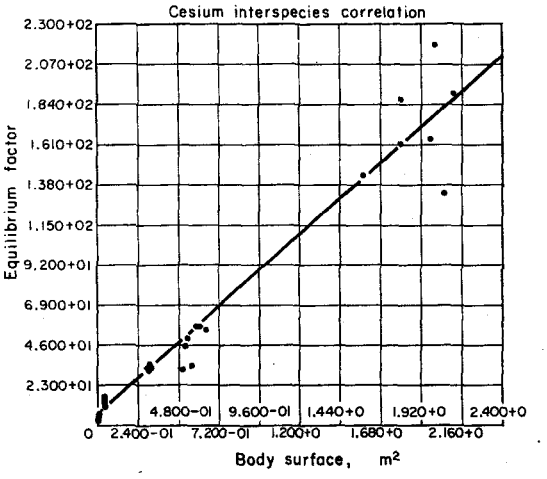

FIG. 7. Interspecies correlation between equilibrium factor (E) and body surface (in m^2) for mice, rats, monkeys, dogs, and men given radioactive cesium. The regression equation is: $E = 6.64 + 85.59\ X$.

Table 5 compares $(MPC)_w$ values obtained from the 7 human subjects with the value currently listed by the ICRP.[2] The average value obtained from our sample is about one-third that recommended by the ICRP. Values for $(MPC)_w$, calculated from interspecies correlations shown by Figs. 4 through 7, are in each case 0.8×10^{-4} μCi ^{137}Cs/ml. Values of 7×10^4 g, or 1.8 m^2, are used in solving the regression equations for E. The value of $(MPC)_w$ is then calculated by substituting E in eq. (8) (see also eqs. (A1) to (A4) in appendix). The respective values of q and S are 30 μCi and 2200 ml/day.

Table 5. Maximum Permissible Concentration of ^{137}Cs in Water $[(MPC)_w]$ for Continuous Exposure when the Whole Body is considered as the Critical Organ

Source of value	$(MPC)_w$* (μCi/ml)
ICRP[2]	2.0×10^{-4}
Subject 1	0.9×10^{-4}
Subject 2	0.7×10^{-4}
Subject 3	0.8×10^{-4}
Subject 4	0.6×10^{-4}
Subject 5	0.7×10^{-4}
Subject 6	0.6×10^{-4}
Subject 7	0.8×10^{-4}
Average T for 7 subjects	0.7×10^{-4}

$$*(MPC)_w = \frac{3.15 \times 10^{-4}\, q \cdot f_s}{T \cdot f_w[1 - \exp(-0.693t/T)]},$$

where q equals 30 μCi, f_s and f_w both equal 1, t equals 50 yr, and effective half-life (T) is determined individually for each subject.

Table 6 shows values of E and $(MPC)_w$ calculated for a standard man (i.e. 7×10^4 g or 1.8 m^2) from interspecies correlations. When man is not included in the correlation, an equilibrium level of 87 or 83 is calculated, depending on the choice of body weight or surface as the independent variable. When man is included in the data used to calculate the correlation, the calculated equilibrium levels are higher by about a factor of 2, and the resulting $(MPC)_w$ values are reduced by a factor of 2. Extrapolation to man results in underestimating E and overestimating $(MPC)_w$. When a first-degree polynomial is used (Table 7), extrapolation to man on the basis of body weight results in an overestimation of E; the reverse is true when body surface is used as the independent variable. Good agreement exists between interspecies correlations based on body surface in Table 7, whether human data are included ($E = 161$) or excluded ($E = 142$). The average value for E obtained from the 7 human retention studies is 171.

For predictive purposes, the interspecies correlation of the form $E = a + bX$, where X is body surface in m^2, yields equilibrium values for man that agree best with human experimental data.

Figure 8 shows the interspecies relation between E and basal metabolic rate for the radiocesium data. The best computer fit to the data is:

$$E = 0.44\, X^{0.8062}, \qquad (13)$$

in which X is calories/day. The basal metabolic rate was calculated from each animal's body weight according to Brody.[18] The relation between E and specific metabolic rate (calories/g body weight · day) is given in Fig. 9. The computer-derived equation,

$$E = 48.37\, X^{-2.2233}, \qquad (14)$$

Table 6. Comparison of Equilibrium Factor (E) and $(MPC)_w$ Values for ^{137}Cs in Man using Interspecies Correlations of the Form $E = aX^b$ with and without Data from Human Subjects

Independent variable (X)	Interspecies correlation	E*	$(MPC)_w$ (μCi/ml)
Body weight (g)†	$0.23\, X^{0.5914}$	167	0.8×10^{-4}
Body weight (g)‡	$1.66\, X^{0.3550}$	87	1.6×10^{-4}
Body surface (m^2)†	$97.35\, X^{0.8518}$	161	0.8×10^{-4}
Body surface (m^2)‡	$63.81\, X^{0.5100}$	83	1.6×10^{-4}

* Value of interspecies correlation calculated for a person with a body weight of 7×10^4 g or a body surface of 1.8 m^2.
† Man included in the derivation of the interspecies correlation.
‡ Man omitted from the derivation of the interspecies correlation.

Table 7. Comparison of Equilibrium Factor (E) and $(MPC)_w$ Values for ^{137}Cs in Man using Interspecies Correlation of the form $E = a + bX$ with and without Data from Human Subjects

Independent variable (X)	Interspecies correlation	E*	$(MPC)_w$ (μCi/ml)
Body weight (g)†	$10.88 + 0.0023\ X$	172	0.8×10^{-4}
Body weight (g)‡	$9.37 + 0.0031\ X$	226	0.6×10^{-4}
Body surface (m^2)†	$6.64 + 85.59\ X$	161	0.9×10^{-4}
Body surface (m^2)‡	$7.47 + 74.84\ X$	142	1.0×10^{-4}

* Value of interspecies correlation calculated for a person with a body weight of 7×10^4 g or a body surface of 1.8 m^2.
† Man included in the derivation of the interspecies correlation.
‡ Man omitted in the derivation of the interspecies correlation.

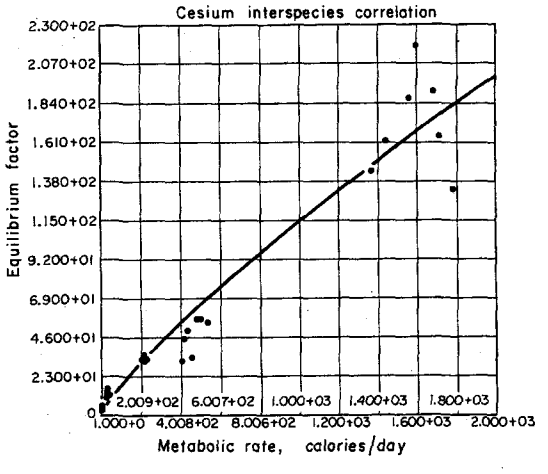

FIG. 8. Interspecies correlation between equilibrium factor (E) and metabolic rate (in calories/day) for mice, rats, monkeys, dogs, and men given radiocesium. The regression equation is: $E = 0.44\ X^{0.8062}$.

indicates that E decreases as specific metabolic rate increases. Smaller animals produce more calories/g body weight · day as the result of a higher metabolic rate. Therefore, at least for many elements which are not deposited in nonlabile pools such as bone matrix, equilibrium levels are at least partially determined by metabolic rate. Higher metabolic rates result in faster biological turnover and in lower equilibrium burdens. Consequently, one would predict faster turnover of these materials in the young of one species as compared with adults with lower metabolic rates. Recent studies indicate that this is true for cesium.[14, 15] The Federal Radiation Council uses a value of 30 days as the biological half-life of ^{137}Cs in infants.[16]

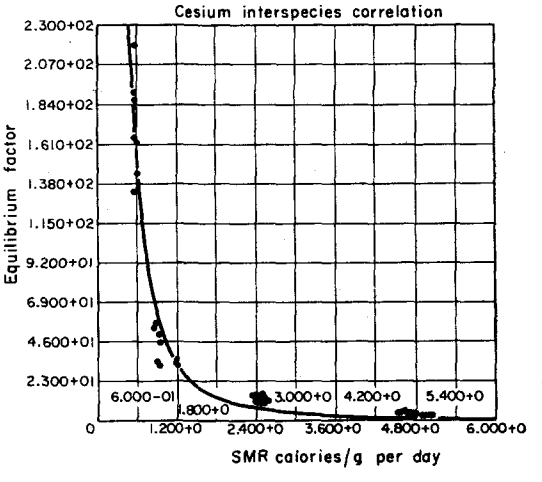

FIG. 9. Interspecies correlation between equilibrium factor (E) and specific metabolic rate (in calories/day/g) for mice, rats, monkeys, dogs, and men given radiocesium. The regression equation is: $E = 48.37\ X^{-2.2233}$.

At this point we should examine some of the factors that can alter the position of a species within the correlation. First, any agent that affects metabolic rate may influence the turnover and change the equilibrium factor. Included in this category are environmental temperature, age, and certain drugs. A second factor is diet. Simple exchange of the tracer with its stable form or with a physiologically similar element appears to govern turnover for some elements. Increasing water intake, therefore, will accelerate tritium turnover. Also, increasing the intake of potassium will accelerate the loss of cesium, which has similar physiochemical properties. A third factor is that of

Zinc

Zinc, unlike tritium and cesium, is not completely absorbed from the gastrointestinal tract. Figure 10 shows the interspecies correlation relating log E to log body weight (in g) for ^{65}Zn given orally to 12 mice, 6 rats, 3 dogs, and 4 human subjects. The regression line calculated from the average E value for the mice, rats, and dogs is:

$$\log E = 0.1903 + 0.3833 \log X. \quad (15)$$

The rather large range for the human data is due mainly to differences in gastrointestinal absorption rather than to differences in turn-

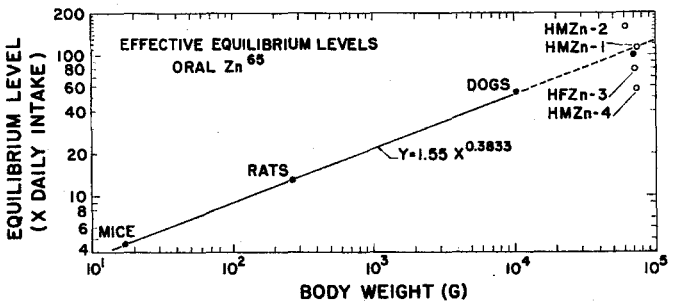

FIG. 10. Interspecies correlation between equilibrium factor (E) and body weight (in g) for mice, rats, dogs, and men given ^{65}Zn. The regression equation is: $\log E = 0.1903 + 0.3833 \log W$.

specific binding agents. For example, certain natural foodstuffs act as ion exchangers in the lumen of the gut, thereby preventing initial absorption or recycling across the gut wall.[17, 18] Specific ion binding within the gut is the basis of recent work in which ferric ferrocyanide was used to reduce radiocesium burdens in animals and man.[19-21] The equilibrium level can be reduced by 60% in the rat by ferric ferrocyanide feeding.[20]

The fibrous, potassium-rich food consumed by cows probably acts to accelerate cesium turnover. It is known that the biological half-life for cesium in cows[22] and in goats,[23] both ruminants, is shorter than would be expected on a body weight basis. In both species fecal loss exceeds urinary loss for cesium; the reverse is true for nonruminant mammals.

over. The effective retention parameters obtained for the human subjects were used to calculate $(MPC)_w$ values for continuous occupational exposure using the basic equation from the ICRP Report of Subcommittee II (eq. A1). Values of 60 μCi and unity were used for q and f_2, respectively. The effective half-life of the last component of the retention function was used for T, and its intercept was used for f_w. Values for the 4 subjects were 2.4, 1.7, 3.4, and 4.7 $\times 10^{-4}$ μCi ^{65}Zn/ml. Although zinc is concentrated largely in bone, the range of its hard electromagnetic radiation makes assumption of the whole body as the critical organ reasonable. An $(MPC)_w$ value of 2.4 $\times 10^{-4}$ μCi/ml was calculated for ^{65}Zn using values of 60 μCi for q, 112 for E, and 2200 ml for S. Details of this work are available.[5]

Iodine

The interspecific correlations for orally ingested iodine are given in Fig. 11 for biological retention of non-radioactive iodine and for effective retention of ^{131}I. It is apparent that biological retention data afford a more accurate extrapolation to measured human values than effective retention. If equilibrium levels are, in fact, a function of metabolic rates, the relation between biological equilibrium levels and body weights follows. Short-lived isotopes tend to decrease the value of the slope constants of the interspecies relation derived from biological retention data. Nevertheless, it is the effective retention that is of interest in estimating MPC values for any particular radionuclide. Extrapolation of the ^{131}I effective retention data to 7×10^4 g body weight gave a value of 4.7 for E, whereas human retention data gave a value of 2.4. If the human data are used to establish the interspecific relation, then the value for E for 7×10^4 g is 3.4.

These values of E are derived from whole-body retention data. Although the thyroid is the critical organ for ^{131}I, whole-body retention is paralleled by thyroid retention and may be used as an approximation of thyroid retention. $(MPC)_w$ may then be calculated from

$$(MPC)_w = \frac{q f_2}{f_w E S}, \tag{16}$$

where E and S have the same meaning as in eq. (8), f_2 is the fraction in the organ of reference of that in the total body, and f_w is the fraction of that ingested that is retained in the critical organ: 0.2 and 0.3, respectively.[2] The value of q is 0.7.[2] Values for $(MPC)_w$ were 4.5×10^{-5}, 6.3×10^{-5}, and 8.8×10^{-5} μCi ^{131}I/ml, respectively, when E values of 4.7, 3.4, and 2.4 are used in eq. (16). The value now listed by the ICRP, 2.0×10^{-5}, agrees best with that obtained from the interspecies extrapolation to man given in Fig. 11. These data are available in more detail.[6]

Manganese

The relation between body weight and E for 12 mice, 9 rats, 3 monkeys, and 4 dogs is shown in Fig. 12. The data were derived from

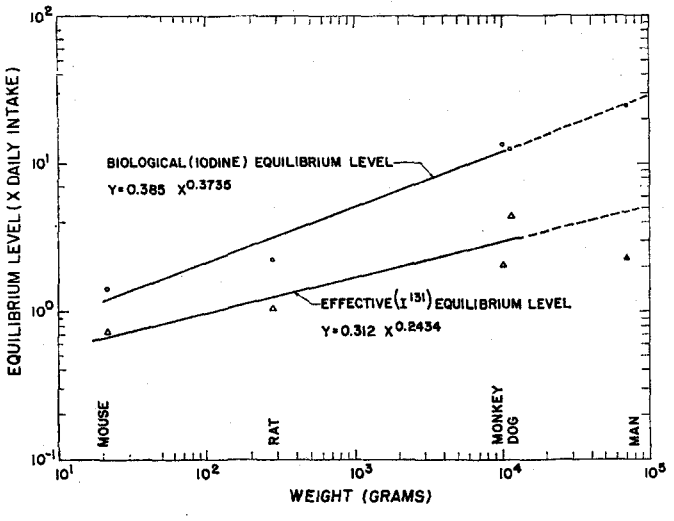

FIG. 11. Interspecies correlation between equilibrium factor (E) and body weight (in g) for mice, rats, monkeys, dogs, and men given ^{131}I. The regression equations are:

$$\log E = -0.4145 + 0.2434 \log X \text{ (for } ^{131}I)$$

and

$$\log E = -0.5059 + 0.3735 \log X \text{ (for stable iodine).}$$

whole-body retention measurements following a single oral dose of ^{54}Mn. Details of this work appear elsewhere.[7] Extrapolation of the data shown in Fig. 12 to 7×10^4 g body weight gives a value of 2.8 as an estimate of E for man. The value for q, when the whole body is considered to be the critical organ, is 40 μCi.[2] Using 2200 ml as the daily water intake (S) and substituting both values in eq. (8), a value of 6×10^{-3} μCi/ml as the $(MPC)_w$ for continuous intake of ^{54}Mn is obtained. This agrees well

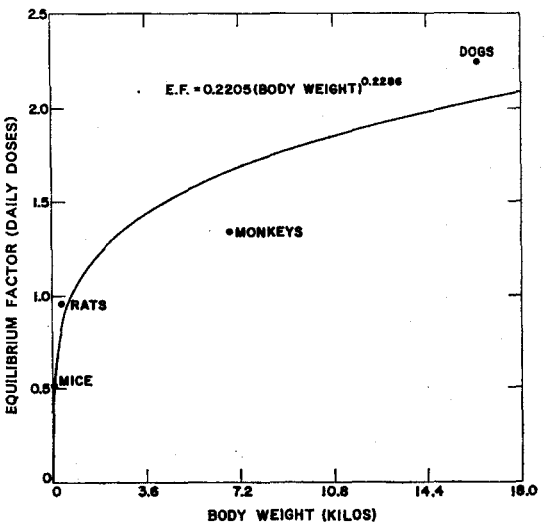

FIG. 12. Interspecies correlation between equilibrium factor (E) and body weight (in kg) for mice, rats, monkeys, and dogs given ^{54}Mn. The regression equation is:

$$E = 0.22 + 0.2286 \log W.$$

with the value of 8×10^{-3} currently listed by the ICRP.[2]

Sodium

The interspecies relation between the log of biological half-life and log of body surface (in m^2) for 12 mice, 6 rats, 4 dogs, 4 monkeys, and 3 human subjects was reported in 1958.[3] This method of presenting the data was complicated by the presence of three components in the curve describing retention by the whole body. Later,[24] $\log E$ was related to grams body weight by the following equation:

$$\log E = 0.1139 + 0.2400 \log X. \quad (17)$$

The value of E, calculated from the human data, was 17.85. From eq. (17) a value of 18.91 can be calculated for a 7×10^4-g man. The calculated MPC value using E values of either 17.85 or 18.91 is approximately 2.6×10^{-4} μCi ^{22}Na/ml, and agrees well with the 4.0×10^{-4} currently listed by the ICRP[2] for the whole body.

Rubidium

Preliminary results for ^{86}Rb were given elsewhere.[24] In general, E increased as body weight increased in a manner similar to that observed for cesium.

Strontium

Analysis of our experimental data for ^{85}Sr and ^{90}Sr given to five mammalian species is incomplete. However, the reader is directed to recent work by Fujita and Iwamoto[25] in which long-term retention of strontium in humans is predicted from small-animal experimental data. These authors, who also noted species similarities in retention patterns, suggest that retention patterns obtained from small animals are "epitomes" of human retention patterns.

USE OF HUMAN DATA IN CALCULATING MPC VALUES

Liden,[26] in a summary of cesium metabolism, noted that biological half-lives reported from Finland, Sweden, and Russia are clustered in the 50- to 80-day range, while values from England fall into the 80- to 110-day range and German values average 140 days. The scatter of values reported from the United States is large, but most fall into the 100- to 130-day range. Liden speculates that perhaps real differences in cesium metabolism exist for people living and working in various parts of the world as the result of differences in climate, dietary habits, working habits, etc. For example, Eskimos in the Anaktuvuk Pass, Alaska area, have resting metabolic rates (room air 35°C) that average about 35% higher than non-Eskimos.[27] The results of this paper indicate that the observed variation may be at least in part due to differences in metabolic rate. These

observations suggest a consideration of *which* human data, if available, should be used to calculate radiation protection guides such as MPC values. Perhaps extrapolations to man on the basis of interspecies correlations can also supply estimates of variability one might expect to find for human subjects because of variables such as metabolic rate.

SUMMARY

Whole-body retention data obtained from mice, rats, monkeys, dogs, and in some cases men were used to calculate equilibrium factors (E) for continuous intake of tritium water (HTO) ^{137}Cs, ^{65}Zn, ^{131}I, ^{54}Mn, ^{22}Na, and ^{86}Rb. This was done by integrating the effective retention functions obtained experimentally between the limits of zero and infinity. The values of E for the different species were then fit as a function of grams body weight, m^2 body surface, or metabolic rate in calories/day. Maximum permissible concentrations for continuous intake $(MPC)_w$ were then calculated using the proper value for man in the interspecies correlation.

For tritium water and radiocesium, both of which distribute throughout the entire body, $(MPC)_w$ values calculated from the interspecies correlations agreed extremely well with data obtained directly from human subjects. A comparison of linear and parabolic models was also made for HTO and radiocesium. Either model gave good fits to the experimental data. For predictive purposes, however, the parbolic model is best for HTO data and the linear model is best for radiocesium data. Metabolic rate provides the best independent variable for correlations for both HTO and radiocesium.

Interspecies correlations are also given in varying detail for ^{65}Zn, ^{131}I, ^{54}Mn, ^{22}Na, and ^{86}Rb. Zinc and iodine are good examples for materials which do not distribute throughout the entire body. The parabolic model, with log transformation of the variables, was used. In each case, predicted values of E for man agreed well with observed or reported values.

The partial dependence of turnover and, therefore, E on metabolic rate helps to explain shorter turnover times observed for radiocesium in children as compared with adults, as well as suggested latitudinal differences in reported turnover times.

REFERENCES

1. S. M. Michaelson and L. T. Odland. *Radiation Res.* **16,** 281 (1962).
2. International Committee on Radiation Protection. Report of Committee II on Permissible Dose for Internal Radiation (1959). *Health Phys.* **3** (1960).
3. C. R. Richmond. *Los Alamos Scientific Laboratory Report* LA-2207 (1958).
4. C. R. Richmond, W. H. Langham and T. T. Trujillo. *J. Cell. Comp. Physiol.* **59,** 45 (1962).
5. C. R. Richmond, J. E. Furchner, G. A. Trafton and W. H. Langham. *Health Phys.* **8,** 481 (1962).
6. J. E. Furchner and C. R. Richmond. *Health Phys.* **9,** 277 (1963).
7. J. E. Furchner, C. R. Richmond and G. A. Drake. *Health Phys.* **12,** 1415 (1966).
8. J. A. D. Cooper, N. S. Radin and C. Borden. *J. Lab. Clin. Med.* **52,** 129 (1958).
9. W. H. Langham, W. J. Eversole, F. N. Hayes and T. T. Trujillo. *J. Lab. Clin. Med.* **47,** 819 (1956).
10. C. R. Richmond, J. E. Furchner, P. N. Dean and P. McWilliams. *Health Phys.* **10,** 3 (1964).
11. P. N. Dean and C. R. Richmond. *Radioisotope Sample Measurement and Techniques in Medicine and Biology*, pp. 139–168. IAEA, Vienna, 1966.
12. H. von Schelling. *Ann. N.Y. Acad. Sci.* **56,** 1143 (1954).
13. S. Brody. *Bioenergetics and Growth.* Reinhold, New York (1945).
14. J. K. Miettinen, A. Jokelainen, P. Roine, K. Liden and Y. Naversen. *Ann. Acad. Sci. Fennicae.* Ser. AII, Chemica No. 120 (1963).
15. L. G. Bengtsson, Y. Naversen and K. G. Svensson. *Assessment of Radioactivity in Man*, Vol. II, pp. 21–32. IAEA, Vienna (1964).
16. Federal Radiation Council. *Background Material for the Development of Radiation Protection Standards*, p. 26, Report No. 7, Government Printing Office, Washington, D.C. (1965).
17. F. R. Mraz and H. Patrick. *Proc. Soc. Exp. Biol. Med.* **94,** 409 (1957).
18. F. R. Mraz and H. Patrick. *J. Nutrition* **61,** 535 (1957).
19. V. Nigrovic. *Int. J. Radiation Biol.* **7,** 307 (1965).
20. C. R. Richmond and D. E. Bunde. *Proc. Soc. Exp. Biol. Med.* **121,** 664 (1966).
21. K. Madshus, A. Stromme, F. Bohne and V. Nigrovic. *Int. J. Radiation Biol.* **10,** 519 (1966).
22. S. L. Hood and C. L. Comar. *Arch. Biochem. Biophys.* **25,** 423 (1953).
23. R. H. Wasserman, C. L. Comar and A. R. Twardock. *Int. J. Radiation Biol.* **4,** 299 (1962).
24. C. R. Richmond. *Los Alamos Scientific Laboratory Report* LAMS-2445, pp. 71–79 (1960).

25. M. FUJITA and J. IWAMOTO. *Health Phys.* **11,** 271 (1965).
26. K. LIDEN. *Assessment of Radioactivity in Man,* Vol. II, pp. 33–40. IAEA, Vienna, 1964.
27. D. W. RENNIE, B. G. COVINO, M. R. BLAIR and K. RODAHL. *J. Appl. Physiol.* **17,** 326 (1962).
28. C. R. RICHMOND, J. E. FURCHNER and G. A. TRAFTON. *Health Phys.* **7,** 219 (1962).

APPENDIX

An equilibrium level will be established within an organism for any physiologically soluble element that is ingested at a constant rate for a sufficiently long time. This point of metabolic homeostasis is one at which the RBE dose rate to the critical organ* reaches a maximum value for that particular radionuclide intake level. Prior to reaching equilibrium, daily intake of the radionuclide exceeds daily output; after reaching equilibrium, intake and output are essentially equal. The time required to reach equilibrium is determined by the parameters that describe retention of the radionuclide by the organism. Therefore, the maximum permissible body burden (q) is that quantity of a radionuclide that will deliver the permissible RBE dose rate to the critical organ. Likewise, a maximum permissible concentration (MPC) for an ingested radionuclide is the amount per day that will result in the critical organ receiving the permissible RBE dose rate when equilibrium conditions are reached.

If we know values for q and for effective half-life (T), then MPC of a radionuclide in water (for a 40-hr work week) can be estimated as follows:

$$(MPC)_w = \frac{9.2 \times 10^{-4}\, q\, f_2}{T f_w\, [1 - \exp - (0.693t/T)]}, \quad \text{(A1)}$$

as given in eq. (8) of ref. 2. The quantities f_w and f_2 are fractionation constants which become unity if, for simplicity, we consider the whole body as being the critical organ. The numerical constant in the numerator is obtained by dividing ln 2 by 750 (the latter assumed to represent the effective daily water intake). Thus, the step preceding eq. (8), in the derivation of the MPC equation,[2] is:

$$(MPC)_w = \frac{0.693\, q\, f_2}{T \cdot S \cdot f_w\, [1 - \exp - (0.693t/T)]}. \quad \text{(A2)}$$

For continuous exposure, the daily intake (S) is 2200 ml and the numerical constant in eq. (A1) becomes 3.15×10^{-4}.

At equilibrium, for cases where the whole body is the critical organ, eq. (A1) reduces to:

$$(MPC)_w = \frac{0.693\, q}{T \cdot S\, [1 - 0]}. \quad \text{(A3)}$$

At this point, we can substitute a factor (equilibrium factor E) for $T/0.693$ in eq. (A3):

$$(MPC)_w = \frac{q}{E \cdot S}. \quad \text{(A4)}$$

Re-arrangement of eq. (A4) is as follows:

$$q = (MPC)_w \cdot E \cdot S, \quad \text{(A5)}$$

which indicates that the maximum permissible body burden (q) is equal to the product of the maximum permissible radionuclide concentration (μCi/ml), the volume ingested daily (ml/day), and an equilibrium factor. For eq. (A5) to be dimensionally correct, E must have dimensions of days. E can be obtained by integrating between the limits of zero and infinity, the effective retention function (R_t) which describes retention by human subjects following a single intake of the radionuclide:

$$E = \int_0^\infty (R_t)\, dt. \quad \text{(A6)}$$

Reference 28 describes this step in more detail.

The equilibrium factor is proportional to the area bounded by the retention function and has the dimension of dependent variable times days. E can also be estimated for humans by extrapolating similar values obtained from laboratory animals on the basis of some physiological parameter such as body weight or surface.

The equilibrium factor is calculated for single administration tracer experiments as follows. Let us assume a single daily intake (I) of a radionuclide that is subsequently lost from the body in an exponential manner governed by the rate constant k. Then retention at any time (R_t) is:

$$R_t = I \exp(-kt), \quad \text{(A7)}$$

* As defined in ref. 2.

and, by integration,

$$\int_1^2 (R_t)\,dt = I\int_1^2 \exp(-kt)\,dt$$

$$= -\frac{I}{k}\left[e^{-kt_2} - e^{-kt_1}\right]$$

$$= \frac{I}{k}\left[e^{-kt_1} - e^{-kt_2}\right].$$

If limits 1 and 2 are zero and infinity, respectively,

$$\int_0^\infty (R_t)\,dt = \frac{I}{k}[1 - 0]. \qquad \text{(A8)}$$

Because the mean residence time (τ) for the average atom is the reciprocal of the rate constant, eq. (A8) becomes:

$$\int_0^\infty (R_t)\,dt = I\tau = E. \qquad \text{(A9)}$$

Thus, the dimensions of E become days if I is considered one daily intake. Therefore, the equilibrium factor (E) as substituted in eq. (A4), is the mean time that the atoms under study remain within the body.

Equation (A4) is not limited to conditions where the whole body is considered to be the critical organ. However, it is imperative to use an equilibrium factor that relates to the same critical organ as does q (see ref. 28 for more detail).

PROBLÈMES POSÉS PAR LA FIXATION DE NIVEAUX DE CONTAMINATION ADMISSIBLES POUR DES COMPOSÉS ORGANIQUES MARQUÉS. ESSAI D'ÉVALUATION POUR LA THYMIDINE TRITIÉE ET LA MÉTHIONINE TRITIÉE

P. G. BEAU

Département de la Protection Sanitaire, CEA, Centre d'Études Nucléaires, Fontenay-aux-Roses (France).

Résumé—La surveillance dans les locaux où sont préparées ou utilisées des molécules marquées repose habituellement sur des normes établies pour l'élément marqueur. Il est bien connu qu'une telle pratique représente une approximation grossière qui *a priori* doit parfois sous-estimer le risque.

De nombreux composés marqués au tritium étant préparés, il nous a paru utile d'essayer de fonder ces normes sur le métabolisme de la molécule.

Nous avons tenté de faire une telle évaluation pour deux molécules biologiques: la thymidine tritiée et la méthionine tritiée.

THE FEDERAL RADIATION COUNCIL: ITS RESPONSIBILITIES AND ACTIVITIES

C. C. PALMITER
Federal Radiation Council,
Washington, D.C.

Abstract—Prior to 1959 there was no official agency within the Executive Branch of the United States Government assigned the responsibility for the formulation of radiation protection standards or guidance for all Federal agencies. Each agency was free to formulate whatever standards it deemed appropriate within the bounds of its radiation protection responsibilities. Consequently, the programs and responsibilities of many agencies and departments tended to impinge and overlap. Radiation protection regulations and practices generally were based on the recommendations of the National Committee (now Council) on Radiation Protection and Measurements (NCRP). Although the NCRP was a leading authority in this field and was in part sponsored by the U.S. National Bureau of Standards, it was not an official agency of the government.

At the direction of the President of the United States, a study was carried out on the radiation protection activities within the Federal Government. As a result it was decided that basic radiation protection standards and guidance involved health, economic, social and ethical considerations of such a nature that the person or persons making the decision represented by that guidance should be publicly accountable. Consideration was given to vesting that function in one of the several agencies with radiation protection responsibilities. However, none was found with the necessary breadth of responsibility or jurisdiction to establish such policies for the entire Federal Government. Consequently, the President approved the recommendation that he be advised by a Federal Radiation Council on radiation matters directly or indirectly affecting health, including guidance for Federal agencies in the establishment and execution of programs of cooperation with the individual states comprising the nation.

The author describes some of the problems and some of the benefits that have developed from the creation of the Federal Radiation Council which serves as a forum where all considerations can be brought together to establish and recommend to the President a national policy on radiation protection.

THE development and implementation of radiation protection standards may differ from one nation to another. The form and content of these standards depend to a large extent upon the specific needs of the nation, its involvement in the uses of atomic energy, and the various agencies within that nation that have radiation protection responsibilities.

Prior to 1959 there was no official agency within the Executive Branch of the United States Government assigned the responsibility for the formation of radiation protection standards or guidance for all Federal agencies. Each agency was free to formulate whatever standards it deemed appropriate within the bounds of its radiation protection responsibilities. Consequently the programs and responsibilities of many agencies and departments tended to impinge and overlap. Radiation protection regulations and practices generally were based on the recommendations of the National Committee (now Council) on Radiation Protection and Measurements (NCRP). Although the NCRP was a leading authority in this field and was in part sponsored by the U.S. National Bureau of Standards, it was not an official agency of the government.

In 1959, at the direction of the President of the United States, a study was carried out on the radiation protection activities within the

Federal Government. As a result it was decided that basic radiation protection standards and guidance involved health, economic, social and ethical considerations of such a nature that the person or persons making the decision represented by that guidance should be publicly accountable. Consideration was given to vesting that function in one of the several agencies with radiation protection responsibilities: however, none was found with the necessary breadth of responsibility or jurisdiction to establish such policies for the entire Federal Government. Consequently, the President approved the recommendations that he be advised by a Federal Radiation Council on radiation matters directly or indirectly affecting health, including guidance for Federal agencies in the establishment and execution of programs of cooperation with the individual states comprising the nation.

The Council consists of the heads of those Federal agencies having major responsibilities in atomic energy and radiological health activities. They are the Secretaries of Health, Education, and Welfare; Defense; Labor; Commerce; Agriculture; and the Chairman of the Atomic Energy Commission. The Special Assistant to the President for Science and Technology participates in the deliberations of the Council and also acts as its advisor. Staff work of the Council is carried on by a professional staff responsible for developing recommendations and proposals for consideration by the Council. In addition, the Council is required by law to consult with the National Academy of Sciences, the NCRP, and qualified experts in the field of biology and medicine and in the field of health physics.

The Federal Radiation Council is concerned primarily with the development of national policy in the field of radiation protection. Implementation of this policy requires cooperation between various Federal agencies and their counterparts at other levels of government. The Council is interested in developing a general framework within which such cooperation can be carried out. It does not issue or approve regulatory rules. These are issued by the Federal agencies according to their statutory authority within the policy framework recommended by the Council and approved by the President.

The President has approved twenty-one recommendations developed by the Federal Radiation Council, and the Council has published reports concerning the recommendations; it also has prepared reports on other aspects of radiation which are summarized here.

Report No. 1 provided a general philosophy of radiation protection for Federal agencies, introduced the term Radiation Protection Guide (RPG), and provided numerical values for the guides for the whole body and certain organs of radiation workers and for the whole body of individuals in the general population as well as an average population gonadal dose. These guides were generally compatible with similar values recommended by the NCRP and ICRP.

Report No. 2 extended the basic RPG's for normal peacetime operations, as issued in Report No. 1, to include specific numerical guides for organ doses to the thyroid, bone, and bone marrow for the general public. It also recommended that the radiological health activities of Federal agencies, in connection with environmental contamination by radioactive materials, be based on a graded series of appropriate actions related to ranges of intake of radioactive materials by exposed population groups.

Reports 3, 4, and 6 were concerned with inventories of radionuclides in the environment resulting from the testing of nuclear devices and levels of population exposures. The reports concluded that the health risks from radioactivity in foods were too small to justify protective actions to limit intake of radionuclides by diet modifications, or by altering the normal distribution and use of food, particularly milk and dairy products.

In reports 5 and 7 the Council provided Protective Action Guides (PAG) for accidental exposures of the population from iodine-131, strontium-89, strontium-90, and cesium-137. The PAG is defined as "the projected absorbed dose to individuals in the general population which warrants protective action following a contaminating event". The projected dose is the dose that would be received in the future by individuals in the population group from the contaminating event if no protective action is taken. A protective action is an action or measure taken to avoid most of the exposure to radiation that would occur from future

ingestion of foods contaminated with radioactive materials, and is appropriate when the health benefits associated with the reduction in exposure to be achieved are sufficient to offset the undesirable features of the protective actions.

The brevity of this summary has not allowed me to discuss in detail the socioeconomic or political implications which are evident in the Council's recommendations. The responsibility for establishing radiation protection guidance depends on so many factors that it has been said it is remarkable that any appropriate guides can be formulated under the complex conditions of our society.

In this regard, I would like to respond to Professor W. V. Mayneord in his Rock Carling Fellowship Monograph of 1964, "Radiation and Health". I consider his monograph to be an exceptional contribution to the field of radiation protection. The point raised concerns part of the definition of the Radiation Protection Guide, which is defined as "the radiation dose which should not be exceeded without careful consideration of the reasons for doing so; every effort should be made to encourage the maintenance of radiation doses as far below this guide as practicable". Professor Mayneord asks: "Who is going to do the considering, and what reasons might be advanced?"

In the United States the Federal Radiation Council serves as a forum where all considerations can be brought together to establish and recommend to the President a national policy on radiation protection. On the basis of conservative assumptions, radiation protection standards must be established by a process of balancing biological risk and the benefits derived from those activities related to sources of radiation. Such a balance cannot be made on the basis of a precise mathematical formula; it must be a matter of informed judgment on such factors as health and safety, feasibility of action, economic impact, the needs of the people, and the reasons for accepting exposure to radiation. The problem then is to find the best possible compromise between these conflicting considerations in order to develop the most appropriate guides possible.

Under these assumptions there can be no single "permissible" or "acceptable" level of exposure, without regard to the reasons for permitting the exposure. The radiation dose to the population which is appropriate to the benefits derived will vary widely depending upon the importance of the reasons for exposing the population to a radiation dose. For example, once weapons testing in the atmosphere has taken place, the dose to be permitted in lieu of such alternatives as depriving the population of essential foodstuffs might also be quite different from levels used in the planning phases for normal peacetime operations. As another example, for radiation workers emergency situations will almost certainly arise which make exposures in excess of those applicable to normal operations acceptable.

I must agree with Professor Mayneord that there have been social confusion and alarm when, at brief intervals, concentrations of radioactive materials in the environment have resulted in radiation doses approximating those of our RPG's and that the advice of Proverbs XI: 14, "In the multitude of counsellors there is safety," may apply to safety of the counsellors too; however, I suggest we consider an additional thought from Proverbs XV: 22, "Without counsel plans go wrong, but with many advisers they succeed."

It is not an easy task to determine the benefits and risks in the field of radiation protection. It takes careful consideration of more than pure scientific information. To this end, I feel as Professor Mayneord does: I hope we are not misunderstood, and that we in the United States, as well as various national and international bodies, may all act as advisers and counsellors so that our mission for radiation safety may succeed throughout the world.

PRACTICAL PROBLEMS IN THE APPLICATION OF RADIATION PROTECTION STANDARDS IN THE FIELD OF PUBLIC HEALTH

HANSON BLATZ*
New York University Medical Center,
New York City Office of Radiation Control,
325 Broadway,
New York, New York 10007

Abstract—The growth of the nuclear age has been rapid, and enlightenment about the biological effects of radiation has followed. To protect ourselves, a wide variety of standards, recommendations, guides, laws and regulations has evolved. They were naturally first developed by those using radionuclides and machines producing ionizing radiation. They were then the only persons with knowledge of such matters.

Now that public health agencies are rightfully assuming more of the responsibility for this new and growing public health problem, they find that they have inherited many established standards and rules formulated by authors who lacked experience in public health administration. Standards and rules are often inconsistent with public health tradition (which in some respects may not be bad), and in many cases difficult if not impossible to administer adequately within the framework of most public health agency resources and personnel.

UNTIL about ten years ago, the hazard of radiation exposure was considered primarily in terms of occupational exposure. It is true that some efforts were made to minimize the exposure of patients during the medical application of radiation, but it was largely by miscellaneous committee recommendations which could be followed on a voluntary basis by those who were interested.

Although radioactive fallout from nuclear weapons has been recognized since 1945, it was not until about 1955 that it received widespread consideration as a possible public health problem. The anxiety, expressed by many, stimulated studies by several national and international committees[1] of the total population radiation exposure from various sources and also of the known biological effects of radiation. All of the reports indicated that the greatest and probably the most rapidly growing public health problem involving radiation was associated with the medical use of X-rays. Although the health and safety aspects of all atomic energy activities were being most vigorously regulated, little official recognition was being given at that time to the non-atomic energy applications of radiation, notably in the fields of medicine and academic research.

Because of public concern about fallout and a sharply increased interest in X-ray exposures, public health agencies began to enter the field of radiation protection. In attempting to establish workable standards that could be enforced, and to keep them reasonably consistent with existing recognized standards of good practice, they found themselves faced with an inconsistent dichotomy of standards. In the atomic energy field, they inherited a set of meticulously detailed radiation regulations designed to be enforced by a system (as described by Recht[2]) employing "almost military discipline . . . and a tight and efficient system of surveillance". In the non-atomic energy uses of radiation, there

* Assoc. Professor of Environmental Medicine, New York University Medical Center—Director, Office of Radiation Control, New York City Department of Health.

existed a set of loosely worded committee recommendations intended for voluntary compliance. In fact, the authors of some such recommendations reminded us in the preface of the report that the recommendations were not intended to be used as official regulations. On the other hand, they were the only existing standards suitable for adoption and were widely accepted. It is interesting to note that although the authors of both the atomic energy regulations and the more general radiation recommendations and standards have included many leading scientists in the field of radiation, few contributors appear to have had experience in the field of public health. It is perhaps for that reason, among others, that many standards and procedures established for the protection of the public against radiation exposure are quite incompatible with most other public health practices developed as a result of a century of experience.

When we compare the health hazards of chronic exposure to radiation with those of many other agents, we see that there are close similarities. In the case of radiation, we are concerned primarily with carcinogenic, genetic and non-specific aging effects. As in the case of many other health hazards, we consider them in terms of occupational exposure, residential risks (such as air, water and food pollution) and possible accidents.

Although we are much better informed about the effects of radiation, probably because of a stimulated public interest, we do know much about other agents having similar effects.[3] Tars and oils, carbon tetrachloride and benzol are known to be carcinogenic. Many pesticides and food additives are also suspect. The use of estrogenic hormones to improve the quality of domestic fowl for human consumption has been restricted because of the carcinogenic potential.

Many chemical agents have been found to cause genetic mutations. They include formaldehyde, epoxides, phenol, mustard gas, caffeine, ethyl alcohol and theobromine (found in cocoa). It is true that the genetic effects of chemicals on mammals are not as well understood as in the case of radiation. A relative lack of public and consequently official interest has inhibited extensive research.

It has become obvious that public health agencies should assume the responsibility for protecting the public against the hazards of radiation sources not otherwise under the control of atomic energy agencies. In certain cases, where atomic energy radiation problems have clearly entered the domain of public health, e.g. the possible contamination of water, food or air from fallout, radioactive wastes or nuclear accidents, health agencies should assume complete control of the public health aspects if they are prepared to do so. A strong case has been made for the transfer of all health protection responsibilities from atomic energy agencies, because of a possible conflict of interest. Such agencies have a mandate to promote the use of nuclear energy and its byproducts. It has been argued that the determination of any necessary public health protection restrictions on nuclear development and use should not be the responsibility of the same agency promoting its development and use. In practice, however, it is observed that any imbalance that may exist between efforts to promote atomic energy and efforts by the same agencies to protect the public appear to indicate a degree of overregulation, when compared to society's efforts to protect the public against comparable health hazards. This may result from a sensitive awareness by atomic energy agencies of the conflict, and a desire to avoid possible criticism of not protecting the public adequately.

The great amount of detail in most atomic energy health and safety regulations is well known to most of this audience. It covers a variety of units of measurement and dose expression, various permissible levels of radiation and dose rates for different classes of individuals and in different areas, details of radiation surveys, personnel monitoring, record keeping, reporting, caution signs and labels, employee instructions and notices, storage, waste disposal, contamination control, transportation and many other matters. The meticulous detail with which our U.S. atomic energy rules have been developed can be indicated by the fact that the printed rules covering routine matters of radiological health, exclusive of such special items as criticality hazards, or reactor design and siting, constitutes a substantially greater volume of printed matter than our entire New York City Health Code which was developed to protect

eight million people against every health hazard known to man, including radiation.

There is no intention of criticizing the careful development of refined and detailed standards. It should be pointed out, however, that when each detail is considered to be a legally enforceable regulation subject to inspection, record keeping and enforced correction, the burden upon both the regulatory agency and those regulated becomes very great. From what is known of efforts to control atomic energy related radiation hazards in other countries, the U.S. practice is not unique, as Dr. Recht has inferred in the paper previously cited.

If we now consider the existing standards and rules for the use of X-ray equipment, we observe that they appear to have been intended primarily for large well-staffed hospital X-ray departments. The I.C.R.P. X-ray report [4] has several recommendations employing references to the "head of the department" and "the expert knowledge of the staff". Experience in our country and in many developing countries shows that most medical X-ray equipment is located in physicians' offices or small clinics and hospitals not staffed with the highly trained radiologists and physicists upon whom many existing protective recommendations depend for their administration. It is in such small installations where the greatest deficiencies in equipment and use are usually found.

If radiation and radioactive contamination are considered a public health problem, which now seems to be a generally accepted premise, it seems obvious that the ultimate control and the establishment of control principles should be the responsibility of public health agencies. The World Health Organization has made a strong plea to that end. [5] It appears that this policy has not been followed previously because persons with training and experience in atomic energy, radiation and radiation effects were not available to health agencies. In many countries, health responsibility was given to atomic energy agencies by statute, probably because health agencies were not prepared to assume the responsibility.

For most radiation protection workers, whose experience has usually been limited either to atomic energy programs or to large medical center radiation control programs, a brief outline of the manner in which public health agencies usually operate to control health hazards is in order. In most establishments subject to public health inspection, the staff and employees are likely to be well trained in the appropriate technology, whether it be food processing or restaurant management. They usually know little however about the technical aspects of health protection. Health agencies usually have a program director in each special field who is a highly trained expert in his particular health speciality. Although the field workers who are in constant communication with the establishments under control are usually highly skilled technicians in the processes they survey and in the health standards they employ, they are not usually investigative scientists.

For these reasons public health standards must be as simple as possible and clearly expressed in a manner that will permit uniform interpretation and administration, without undue hardship to anyone and with little risk of a lapse in effectiveness. In other words, the precise determination of whether any individual has or has not been exposed in violation of a code should not constitute a scientific research project as is often the case for some existing radiation protection rules. This obviously requires a certain degree of compromise with the precise scientific evidence, by the establishment of arbitrary measurable working limits. Experience has proven this to be necessary in virtually every other health or safety regulation that exists, whether it pertain to foods, drugs, fire prevention or motor vehicle safety. The alternative requires a staff of investigative scientists that appears to have formed in some atomic energy regulatory programs.

To cite examples, several typical principles of radiation protection that present formidable problems, when a public health agency tries to adopt them for use are:

1. *Permissible Doses*

Most standards are written in terms of a specified cumulative radiation dose to a particular organ or system of organs (viz., the gonads or the blood forming system). This is quite scientific and very precise, but it would be much like specifying that food should contain

no more lead contamination than would result in a concentration of over 100 μg of lead per gram in the consumer's kidneys. It requires an experienced investigator to determine whether such criteria have been met.

Dunster[6] has described the I.C.R.P. permissible dose recommendations[7] as "indispensable, infallible and to some extent incomprehensible". If Dunster, who is one of our most distinguished and experienced scientists in the field of radiation protection, finds them somewhat incomprehensible, it is not difficult to understand the uncertainty with which a public health worker faces this new problem.

2. *Occupational Category*

In the I.C.R.P. Standards, a distinction is made between the maximum permissible doses of occupationally exposed persons (5 rem/year) and other workers in the vicinity of controlled areas (1.5 rem/year). In the United States N.C.R.P. Standards, the same general distinction is made, except that those in the environs are not described as workers and their dose is limited to 0.5 rem/year. In fact, the occupational limit is not actually 5 rem/year but follows the relationship of $5(N\text{-}18)$ based upon past exposure history.

No valid argument can be presented to refute the reasoning nor scientific justification for arriving at various grades of permissible doses. The uncertainties in the biological data upon which the limits are based, however, and the errors inherent in field measurements, as well as in the translation from radiation measurement to critical organ dose are all great. The proliferating uncertainties regarding the actual critical organ doses usually far exceed the numerical distinctions employed in classifying workers and others into permissible dose categories differing by factors of only 3 or 10.

3. *X-Ray Installation Shielding Recommendations*

This category, both the international recommendations[7] and our own national recommendations in the United States provide for considerable speculation about the manner in which any particular piece of X-ray equipment is to be used and its adjacent spaces occupied. Assumptions must be made of the expected operating kilovoltage and workload, the directions in which the beam is likely to be pointed, the degree of occupancy of any adjacent space and also the occupational category of persons likely to be there. Strangely enough, certain recommendations appear to permit a considerably higher exposure of persons not classified as radiation workers than those who are considered occupationally exposed. For example, rest and lounge rooms to be used by occupationally exposed personnel must be shielded to a greater degree than similar rooms to be used by personnel not classified as occupationally exposed to radiation.

A distinction is made between persons in controlled areas and persons outside of controlled areas, with a difference in permissible exposure by a factor of either three or ten, depending upon whether those persons are considered workers or not. Experience in atomic energy establishments has shown that it is feasible in such places to designate areas where certain persons may or may not be permitted access. A tight system of security with guards at every point of entrance often permits the close surveillance of such matters. In a busy hospital X-ray department or in the offices of a physician, at least from our observations in the United States, it is most difficult to delineate areas that might be controlled or uncontrolled and to restrict radiation workers, clerical and administrative workers, patients, and patients' escorts, and to distinguish between those who should be permitted to enter controlled areas and those who must be excluded. In the case of our own atomic energy establishments, the guard at the entrance requires that any person authorized to enter wear a personnel monitoring dosimeter, with the user's name and identification recorded. In the case of most medical installations this is quite impractical.

It would seem that in medical installations, where there is likely to be considerable uncertainty about each person's radiation exposure category and also a lack of control of the movement of individuals, there is the least justification for the current speculation about radiation levels that may be permitted to exist in any room.

A reasonable evaluation of the relative degree of radiation protection according to each individual's permissible dose is troublesome. The

employment of personnel monitoring devices is convenient only for regular employees. In the case of diagnostic X-rays, measurements are particularly subject to error because of energy and geometry reasons.

It is suggested that the structural shielding designs be based upon the maximum workload of the machine and that the X-ray beam be mechanically restricted to a few needed directions as it is now done for teletherapy machines. All adjacent areas could easily and adequately be shielded for any degree of occupancy by any category of person. The added shielding cost would be slight by comparison with the high cost of modern X-ray installations. The degree of certainty about radiation exposures would be vastly improved.

4. *Control of the Size and Direction of Diagnostic X-Ray Beams*

If we consider published reports of population exposure to man-made radiation, it is evident that medical patients receive most of it. When we study technical reasons for excessive or unnecessary exposure, one category is widely agreed upon to exceed all others in magnitude of excessive population dose. It comprises X-rays that strike a patient's body but serve no diagnostic purpose. In other words, the exposure resulting from failure to collimate the X-ray beam down to at least the size of the film being used, constitutes the greatest amount of useless human exposure to man-made radiation.

In spite of the prime importance of this problem, health agencies that seek to solve it are virtually powerless to do so under today's standards. In the case of most other technical or scientific apparatus, where it is necessary to direct a beam of any kind at a target, mechanical means are invariably built into the apparatus. For the purpose of deliberately aiming an X-ray beam of high intensity at a human target, most X-ray equipment lacks even a simple aiming device. The beam size is therefore usually enlarged to about three to five times the necessary size in order that the film not be missed because of poor aiming. Most collimators produce a round beam, whereas they should at least be rectangular to match the film or preferably be shaped exactly to fit the organ or area being examined. Modern technology, if properly applied, could certainly attain that goal.

When we, in public health agencies, observe the manner in which radiation protection is usually administered in national atomic energy programs, we know that we could not expect to devote the time of such highly trained specialists to the detailed investigation of possible sources of radiation hazards without a substantial change in health agency customs and policies. When we analyze the problem further, it appears that a considerable amount of effort is often devoted to the collecting, recording and analyzing of data that might better be classified as scientific research or legal documentation rather than public health administration.

Many other public health enforcement activities consist of observing that someone is doing something wrong, instructing him to do it differently and, for serious offenses, noting what action was taken. The notation is for the purpose of learning about habitual offenders.

There is some difference of opinion about the trend away from this simple straightforward approach in many regulatory activities today. In the opinion of some it is to be deplored. There are officers whose function it is to insure that a certain level of efficiency is maintained, but to be able to prepare their evaluations, they must be supplied with statistics. The number of inspections per man-day, the number and classification of corrected deficiencies per inspection, etc., must be collected and tabulated. The result is a significant increase in the required record keeping. Meticulous records are also kept to furnish evidence of compliance or non-compliance in case of controversy. The overall need for the legal enforcement of health regulations is quite rare and the needed records for those few cases can be accumulated after efforts at persuasion have failed.

SUMMARY

To summarize, the following conclusions and recommendations are made:

1. The protection of the public against radioactive contamination and radiation exposure is basically a public health problem and should be administered by public health agencies

as soon as they are prepared to assume the responsibility.

2. The standards and rules regarding radiation protection should be coordinated and simplified so that they be made more compatible with existing public health practices. In regulations, greater emphasis should be placed on arbitrary permissible environmental radiation levels rather than on accumulated doses to various human organs of different categories of persons, since the latter is virtually impossible to measure routinely with an acceptable degree of accuracy.

Much of the detail embodied in atomic energy oriented radiation regulations should be eliminated. A considerable part of the detail appears to have been introduced for legal record keeping reasons, to provide evidence of compliance or non-compliance. Some records seem to be employed for scientific data collecting reasons. If employers wish such records for their own needs, they may be accumulated, but only those actually necessary to demonstrate a reasonable degree of current compliance should be mandatory.

4. For medical X-ray installations, simpler, uniform and more readily checked standards should be set, particularly for structural shielding and to guarantee adequate beam collimation, the two demonstrated sources of most excessive or uncertain exposure.

REFERENCES

1. (a) The Hazards to Man of Nuclear and Allied Radiations—A Report to the (British) Medical Research Council. H.M.S.O. London, 1956.
(b) The Biological Effects of Atomic Radiation—Summary Reports, (U.S.) National Academy of Sciences—National Research Council, Washington D.C. 1956.
(c) Report of the United Nations Scientific Committee on the Effects of Atomic Radiation, U.N., New York (1958).
2. P. Recht. Regulations governing ionizing radiations. *Health Physics* **12,** 1, 65 (1966).
3. Radiation Hazards in Perspective, World Health Organization Technical Report No. 248, W.H.O., Geneva (1962).
4. Recommendations of the International Commission on Radiological Protection. Report of Committee III on Protection against X-rays up to Energies of 3 MeV and Beta and Gamma-Rays from Sealed Sources, I.C.R.P. Publication 3, Pergamon Press, Oxford (1960).
5. Public Health Responsibilities in Radiation Protection, World Health Organization Technical Report No. 254, W.H.O., Geneva (1963).
6. H. J. Dunster. Some problems in the application of I.C.R.P. maximum permissible levels for occupational exposure. *Health Physics* **12,** 1, 77 (1966).
7. Recommendations of the International Commission on Radiological Protection, I.C.R.P. Publication 6, Pergamon Press, Oxford (1964).

À PROPOS DE L'ARGUMENTATION DE L'ÉTABLISSEMENT DES NORMES DES GAZ RADIO-ACTIFS INERTES

N. G. GOUSSEV, O. A. KOTCHETKOV, L. M. MIKHAILOV, A. D. TOURKINE, E. S. TROUKHMANOVA et V. P. PHILIPOVITCH

Institut de Biophysique du Ministère de la Santé Publique de l'URSS.

Résumé—Jusqu' à présent on a défini les normes des gaz radio-actifs inertes (GRI) du type des isotopes Ar, Kr, Xe en établissant leurs concentrations maximum admissibles (CMA) dans l'air des locaux de travail et dans l'atmosphère des localités. Conformément aux recommendations de la CIPR (Commission Internationale de Protection contre les Radiations[1]) la CMA est déterminée dans ce cas selon la dose de radiation β, γ externe qu'une personne recevrait si elle était éntourée par un nuage hémisphérique infini de GRI.

On montre dans ce rapport que, dans le cas du rejet des GRI par le tube de ventilation dans la direction de propagation du panache, il n'y a pas de concordance stricte entre la concentration des gaz inertes dans la couche d'air au niveau de la terre et la dose calculée de radiation γ externe. C'est pourquoi l'établissement des normes des isotopes Ar, Kr et Xe dans l'air atmosphérique doit se faire non pas d'après la CMA, mais d'après la dose annuelle de radiation γ externe produite par le panache des gaz radio-actifs à la surface de la terre. Dans ce cas, le rejet maximum admissible I,Ci/unite de temps, représente la grandeur principale contrôlable.

Dans l'air des locaux de travail l'établissement des normes est fait d'après la CMA mais, dans les formules de calcul, il est nécessaire de prendre en considération les limites de volume des salles et le fait que le danger d'irradiation, pratiquement, se détermine complètement par le champ de radiation de particules β et d'électrons de conversion.

Dans ce rapport sont présentés les résultats de calcul et les résultats expérimentaux d'une étude concernant les questions d'établissement des normes des GRI (gaz radio-actifs inertes).

1. RELATION ENTRE LA DOSE À LA SURFACE DU SOL ET LE REJET DES GRI

On sait que la dose de radiation externe provenant des GRI* dépasse considérablement la dose de radiation interne correspondante, au cas où la personne irradiée se trouve dans une salle de volume limité.

Si des GRI se trouvent dans l'air atmosphérique leur effet d'irradiation se détermine essentiellement par la dose de radiation γ externe, créée par le panache de gaz radio-actifs à la surface de la terre; la contribution des radiations β est négligeable. Dans ce paragraphe, on présente les données expérimentales et théoriques concernant la relation entre la dose de radiation γ externe à la surface de la terre et la grandeur mesurant le rejet des GRI.

1. *Relation théorique entre la dose à la surface du sol et le rejet des GRI*

Considérons la source d'éjection des GRI, ayant la forme d'un tube, de hauteur H_{eff}, dont la base se trouve au centre du système rectangulaire de coordonnées (x, y, z).

Nous prenons pour direction positive de l'axe x la projection de l'axe du panache sur la surface de la terre, c'est-à-dire sur le plan xy (fig. 1).

L'intensité moyenne de la dose $\overline{\mathcal{P}}(\rho)$ de rayons γ créée par le panache de GRI à la distance ρ de la source de rejets, étant supposé un

* On considère toujours les isotopes Ar, Kr, Xe.

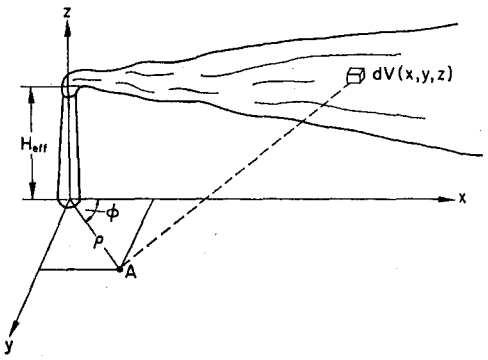

FIG. 1. Géometrie de la source de radiations.

mouvement uniforme du panache le long de l'azimut ϕ, peut être calculée par la relation

$$\overline{\mathscr{P}}(\rho) = \frac{\int_0^{2\pi} \mathscr{P}(\rho, \phi) d\phi}{\int_0^{2\pi} d\phi} =$$

$$\frac{\kappa_\gamma, i}{2\pi} \int_0^{2\pi} d\phi \int_0^{\infty} dx \int_{-\infty}^{\infty} dy \int_0^{\infty} \frac{Q(x, y, z)\, e^{-\mu_i r} B(\mu_i r, E_i, Z) dz,}{r^2} \quad (1)$$

avec: κ_γ = constante γ de l'isotope donné, rad × cm²/heure × Ci;[2]

μ = coefficient linéaire d'atténuation des rayons γ dans l'air;

$r = \sqrt{(x - \rho\cos\phi)^2 + (y - p\cos\phi)^2 + (z - z_0)^2}$

distance entre l'élément de volume du panache dv et le point où se fait la détection de la dose;

$B(\mu r, E, Z)$ = "build-up factor", c.-à-d.—facteur d'accumulation de dose de rayons γ dans l'air. Dans les calculs, il est représenté par la somme de deux fonctions exponentielles $B(\mu r, E, Z) = Ae^{-\alpha_1 \mu r} + (1 - A)e^{-\alpha_2 \mu r}$;

$Q(x, y, z)$ = fonction décrivant la distribution des GRI dans le volume du panache.

Alors la formule pour la détermination de la dose annuelle moyenne de radiation γ à la surface du sol $\overline{\mathscr{D}}(\rho)$ sera

$$\overline{\mathscr{D}}(\rho) = \frac{\overline{\mathscr{P}}(\rho)\mathscr{T}\alpha t}{\mathscr{T}_0} \text{ rad/an} \quad (2)$$

$\overline{\mathscr{P}}(\rho)$ = intensité de la dose déterminée par la formule (1), en R/heure;

$\mathscr{T}$ = intensité de la source d'éjection, Ci/sec; éjection normée: $\mathscr{T}_0$ = 1Ci/sec;

α = part de vent-heures pour le rhumb considéré;

t = quantité totale de vent-heures pour les 8 rhumbs, en heures/an.

Pour faire les calculs on a pris le type de fonction $Q(x, y, z)$ de la partition de la concentration des GRI dans le volume du panache conformément à l'ouvrage de D. L. Laikhtmann[3]

$$Q(x, y, z) = \frac{\mathscr{T}_0 e^{-\frac{y^2}{2(0{,}2\,x^{0{,}9})^2}} (Z\,H_{eff})^{\frac{\varepsilon}{2}} Z^{1-\varepsilon}}{\sqrt{2\pi}(0{,}2\,x^{0{,}9})^2 (1 + m + \epsilon)\kappa_1 x} \times I_B - \frac{\epsilon}{m + \epsilon + 1}$$

$$\left[\frac{(Z\,H_{eff})^{\frac{(1+m+\varepsilon)}{2}}}{x\,\frac{(1+m+\epsilon)^2}{2} \cdot \frac{\kappa_1}{u_1} Z^{m+\varepsilon-1}}\right] \times$$

$$\times \exp\left[-\frac{Z^{1+m+\varepsilon} + H_{eff}{}^{1+m+\varepsilon}}{x\,(1+m+\epsilon)^2 \frac{\kappa_1}{u_1} Z^{m+\varepsilon-1}}\right] \quad (3)$$

Avec: $\mathscr{T}_0$ = 1 Ci/sec—intensité d'éjection normée;

u_1 = vitesse de vent au niveau fixé Z, m/sec ($1\,m \leqslant Z \leqslant 7$m);

κ_1 = coefficient d'échange vertical turbulent au niveau Z;

H_{eff} = hauteur effective du tube,

m = paramètre caractérisant le profil de la vitesse de vent (il dépend de la stratification de l'atmosphère et des rugosités de la surface sous-jacente);

ϵ = paramètre caractérisant la stratification de l'atmosphère. $\mathcal{J}l$ représente la fonction de la différence des températures ($\triangle t$) et de la vitesse du vent (U_1) au niveau fixé Z_1 ($\epsilon = 0$ à l'équilibre indifférent,—$0{,}3 < \epsilon < -0{,}1$ à la stratification instable et $0{,}1 < \epsilon < 0{,}3$—à la stratification stable); $I_B - \dfrac{\epsilon}{m + \epsilon - 1}$ [- - - -] intégrale de Bessel.

À l'aide des formules (1–3) on a calculé les doses annuelles de radiation γ à la surface de la terre pour des hauteurs définies du tube de ventilation et les différentes conditions météorologiques.

Les résultats des calculs et les données expérimentales sont indiqués sur les figures 2 et 3.

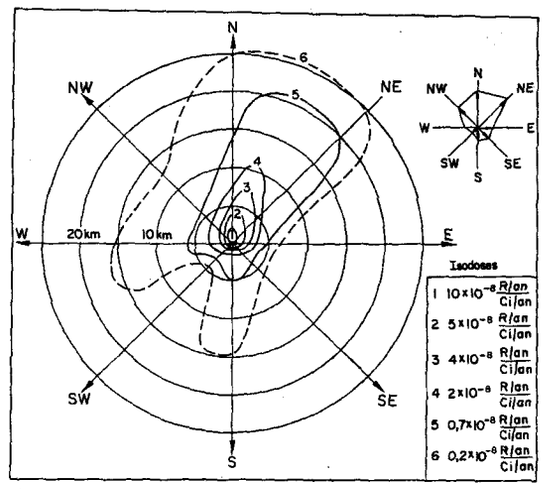

FIG. 2. Distribution expérimentale (normalisée) des isodoses.

1.2. *Corrélations expérimentales entre la dose de radiation α et le rejet des GRI*

Les mesures ont été effectuées dans les conditions naturelles pendant les années 1963 à 1965. Comme source d'éjection continue de Ar^{41} on utilisait un tube de hauteur $H_{eff} = 91$ m. Quelques centaines de dosimètres intégrateurs construits à base de verres thermoluminescents étaient placés dans les différentes directions à des distances de la source allant jusqu'à 20 km. Les dosimètres étaient installés à des hauteurs de 1 à 3 m au-dessus du sol. Chaque exposition durait un an et on a fait des observations pendant deux années. L'erreur dans la détermination de la dose était de l'ordre $\pm$ 20%.

En même temps on menait les observations concernant l'éjection des GRI et les conditions météorologiques. Pour la détermination du fond de radio-activité naturelle, des détecteurs de rayonnement étaient installés à des distances de 40 à 70 km de la source de rejet.

Les résultats expérimentaux avec les données

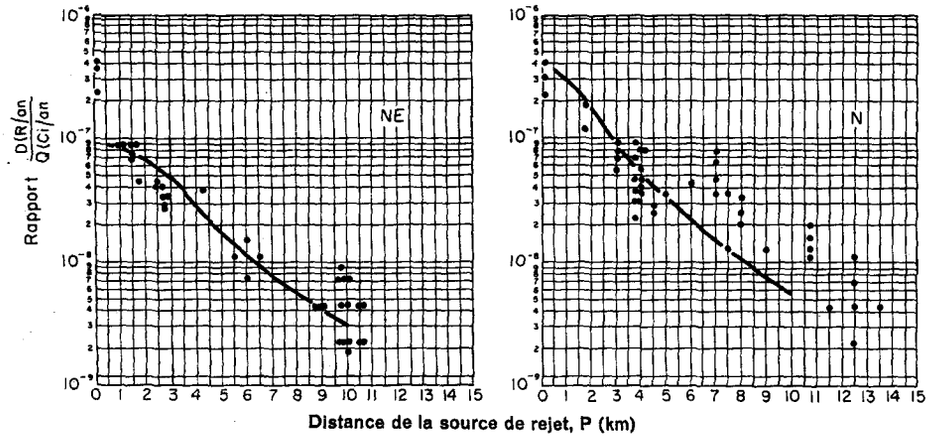

FIG. 3. Relation normalisée entre la dose $D(P, \mathcal{T})$ et la distance, $\dfrac{R/an}{Ci/an}$. — calcul; . points experimentaux.

de calcul pour deux aires de vent, sont présentés sur les figures 2 et 3. Sur la figure 3 la distance de la source de rejet ρ km, est portée le long de l'axe des abscisses, et la grandeur normée de la dose $D\ (\rho, \mathscr{J}_0) = D_1$, rad/an/$\mathscr{J}_0$, Ci/an—le long de l'axe des ordonnées.

La figure 3 montre un bon accord des données expérimentales et des résultats des calculs faits pour les conditions météorologiques réelles. La pire divergence atteint $\pm$ 70%. Cette divergence provient des erreurs de détermination de la grandeur totalisant les rejets ($\pm$ 30%), des erreurs de mesure sur la dose à la surface du sol ($\pm$ 20%) et des erreurs de détermination des paramètres météorologiques $\pm$ 20%.

La figure 3 montre que la courbe de changement de la dose avec la distance a un caractère harmonique: la dose de radiation γ s'atténue graduellement avec l'augmentation de la distance.

On sait que la valeur de la concentration des gaz (ainsi que des aérosols) au niveau du sol suit une autre loi: la courbe de dépendance de la concentration des GRI au niveau du sol avec la distance a son maximum à la distance de 4 à 40 fois la longueur du tube. Cette circonstance indique qu'on doit faire le pronostic du facteur principal de l'action radio-active des GRI non selon la concentration au niveau du sol, mais à partir de la dose de radiation γ externe à la surface de la terre; cette dosees détermine à son tour par trois paramètres principaux: éjection, distance et conditions météorologiques. Ces données créent en principe la possibilité de déterminer la valeur d'éjection maximum admissible $\mathscr{J}$ avec la quelle la dose maximum admissible sur la localité sera obtenue à la distance ρ de la source.

2. RELATION ENTRE LA DOSE D'IRRADIATION DU CORPS ENTIER ET LA CONCENTRATION DES GRI DANS L'ATMOSPHÈRE DES LOCAUX DE TRAVAIL

Dans les recommandations de la CIPR[1] le calcul des CMA des gaz radio-actifs inertes dans l'atmosphère de locaux de travail est fait de la même façon que le calcul pour l'air atmosphérique, c.-à-d. selon les formules valables pour un nuage étendu infini et sans tenir compte de l'absorption des particules β dans les couches tégumentaires des organes critiques.

Dans ce paragraphe, on présenté les résultats expérimentaux et théoriques concernant la détermination de la relation entre la dose profonde et la CMA des GRI. Ces expériences et calculs ont été réalisés en tenant compte des différences existant entre les doses maximum admissibles de certains organes critiques particuliers, de l'existence d'une couche protectrice (tégumentaire) dans chacun d'eux, de la limitation du volume des salles impliquant que l'équilibre des rayonnements n'est pas réalisé pour les photons γ, ni même pour les particules β.

2.1. *Relation théorique entre la dose profonde dans le tissu et la concentration des GRI dans l'atmosphère des locaux de travail*

Il est rationnel de considérer le volume émetteur (local de travail) comme un hémisphère absorbant de rayon R_0, à la base duquel se trouve, au centre un objet exposé à l'irradiation. Il faut envisager séparément la dose de radiation γ externe et la dose de radiation β. La dose de radiation γ ($\mathscr{D}_\gamma$), dans le centre de l'hémisphère, se détermine par une intégration étendue à tout le volume de l'hémisphère de rayon R_0 selon une concentration des GRI de Q, mCi/cm³

$$\mathscr{D}_\gamma = 2\pi Q t \sum \frac{K_{\gamma, i}}{\mu_i}(1 - e^{-\mu_i R}), \qquad (4)$$

avec: $K_{\gamma, i}$ = constante différentielle γ pour l'énergie E_i, de l'isotope donné, rad × cm²/heure. mCi;[2]
μ_i = coefficient linéaire d'atténuation des photons γ dans l'air, cm^{-1};
t = temps.

On peut négliger la distribution des doses profondes dans les premières couches ainsi que la différence en valeurs numériques de "R" et "rad" dans les tissus biologiques.

On sait que la distribution en profondeur des doses absorbées de particules β issues d'une source uniforme infiniment épaisse est bien décrite par la formule de Löwinger.[4] Pourtant on rencontre souvent en pratique des cas où les conditions de l'équilibre radio-actif pour les particules β ne sont pas réalisées. Dans ces cas le calcul des doses profondes de particules β avec un spectre continu de radiations peut être réalisé par l'intégration de la fonction de dose

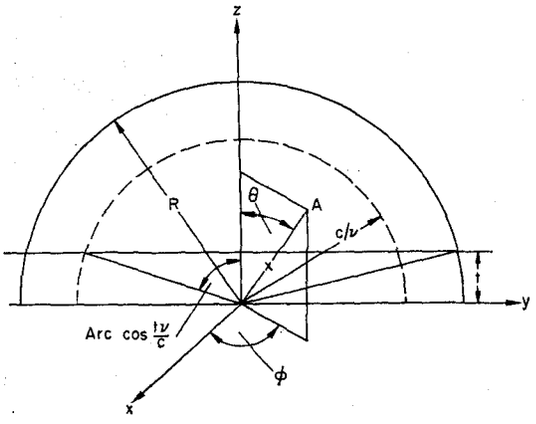

FIG. 4. Coordonnées pour le calcul de la dose absorbée de particules β dans les tissus biologiques.

d'une source ponctuelle, étendue à tout le volume de l'hémisphère, lequel est équivalent au volume de la salle.

La formule de départ pour le calcul de la dose absorbée par une particule β, $\mathscr{D}_\beta$, sera

$$\mathscr{D}_{\beta_1}(t) = \frac{\tau\kappa}{\rho_b}\int_0^{2\pi} d\phi \int_0^{\arccos \frac{vt}{c}} \sin\zeta d\zeta \int_{t\sec\zeta}^{c/v} \frac{1}{(\nu\kappa)^2}\left[1 - \frac{v\kappa}{c}e^{1-\frac{v\kappa}{c}}\right] c\kappa^2 d\kappa + \int_0^{2\pi} d\phi \int_0^{\arccos t/R} \sin\zeta d\zeta \int_{t\sec\zeta}^{R} \frac{1}{(v\kappa)} e^{1-v\kappa} x^2\, dx, \tag{5}$$

Les paramètres géométriques ϕ, ζ et R sont indiqués par la fig. 4, le paramètre (R) contenant le rayon de l'hémisphère et l'épaisseur d'absorbeur t, mg/cm²; ρ_b = densité de tissu biologique, g/cm³; les coefficients τ, κ, c, ν, x sont définis conformément à l'ouvrage de Löwinger.[4]

On a écrit la formule (5) en supposant que les matières de la source et de l'absorbeur sont identiques. Pour tenir compte de la différence des densités et des pouvoir d'arrêt de l'air et du tissu nous introduisons la notion de relation équivalente:

$$R_{eqv} = \left[\frac{t}{\rho_b} + \frac{R - t\ L_b}{\rho_a\quad L_a}\right], \tag{6}$$

où l'épaisseur de tissu t et le rayon $R = R_0 + t$ sont exprimés en g/cm², les densités de tissu biologique (ρ_b) et d'air (ρ_a) en g/cm³ et les parcours maximum des particules β dans le tissu biologique (L_b) et dans l'air (L_a) en cm.

En faisant l'intégration de la relation (5) avec utilisation de la formule (6) et en introduisant les facteurs de conversion nécessaires nous obtenons la formule définitive liant $\mathscr{D}_\beta$ (rad/sec) avec la concentration Q des GRI dans l'air:

$$\mathscr{D}_\beta = Q\,\bar{E}\,\eta\left\{c^2\left[3 - e^{1-\frac{vt}{c}} - \frac{\nu t}{c}\left(2 + \ln\frac{c}{\nu t}\right)\right] + e^{1-v(t+u)}(1 + \nu u)\right\}, \tag{7}$$

avec: $\mathscr{D}_\beta$ = intensité de la dose absorbée à la profondeur t, rad/sec;
Q = concentration du gaz radio-actif inerte, mCi/cm³;
$\bar{E}$ = énergie moyenne des particules β, Mev/désintégration;

et $u = (R - t)\,\frac{\rho_b L_b}{\rho_a L_a}$;

$$\eta = \frac{3{,}7.10^7\ \frac{\text{désintégration}}{\text{sec. mCi}}\ 1{,}6.10^{-6}\ \frac{\text{erg}}{\text{Mev}}}{2.100\ \frac{\text{erg}}{\text{g. rad}}\ 1{,}293.10^{-3}\ \frac{\text{g}}{\text{cm}^3}} = 230\ \frac{\text{rad. cm}^3\text{, désintégr.}}{\text{sec. mCi. Mev}}$$

Le terme $\left[3 - e^{1-\frac{vt}{c}} - \frac{\nu t}{c}\left(2 + \ln\frac{c}{\nu t}\right)\right] = 0$,

si $t \geqslant \frac{c}{\nu}$

La formule (7) ne permet pas de calculer la dose produite par des électrons de conversion. À cause de cela, pour une espèce donnée de

radiation, nous utiliserons les résultats des travaux de Radzievski et Osanov[6] qui ont montré qu'en présence d'une source infiniment épaisse se trouvant au contact d'un fantôme plat équivalent au tissu, la distribution en profondeur des doses absorbées produites par des électrons peut être calculée par la formule suivante:

$$\mathscr{P}_{e^-}(t) \cong \int_{(E)} \frac{E}{R(E)} \left[1 - \bar{\rho}(E)\right] N(E) \left[1 - \frac{t}{R(E)}\right] dE, \qquad (8)$$

où $N(E) = S(E)^{-1} \int_{E}^{E_{max}} n(E)\, dE$

est appelé "spectre passant", c.-à-d. densité de flux d'électrons atteignant la surface du fantôme équivalent au tissu;

$R(E)$ = parcours des électrons à l'énergie E dans la matière du fantôme;
$\bar{\rho}(E)$ = facteur énergétique de retro-diffusion (dans les milieux à faible numéro atomique du type de tissu biologique: $\bar{\rho}(E) \ll 1$);
$S(E)$ = dE/dx—pouvoir d'arrêt des électrons dans l'air;
$n(E)$ = spectre énergétique des électrons émis par unité de volume (ou de masse) de la source.

La formule (8) a été appliquée pour le calcul des doses profondes d'électrons de conversion avec $n(E) \sim \delta(E - E_0)$ ou fonction delta, E_0 étant l'énergie des électrons de conversion.

Les moyens décrits ci-dessus ont été utilisés pour le calcul des doses absorbées produites par des particules β des électrons de conversion et des photons γ pour des groupes différents d'organes critiques, γ compris:

—la couche basale d'épiderme de peau $t = 7$ mg/cm²
—le tissu musculaire et graisseux $t = 100$ mg/cm²
—le cristallin $t = 300$ mg/cm².

Les résultats des calculs et les données expérimentales sont indiqués sur la figure 5.

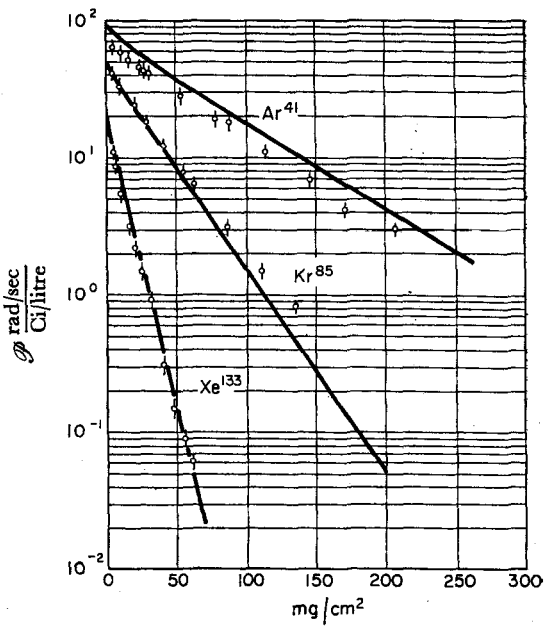

FIG. 5. Variation de doses profondes avec le profondeur. — calcul; . points expérimentaux.

2.2. *Contrôle expérimental de la distribution des doses profondes dans le fantôme*

En vue de contrôler la distribution des doses profondes de particules β et d'électrons de conversion nous avons effectué deux séries d'expérience.

Les essais de la première série concernaient la distribution des doses profondes créées par Ar^{41}, Kr^{85} et Xe^{133} dans une chambre hermétique de dimensions 240 × 240 × 200 cm. La concentration des gaz radio-actifs et l'uniformité de leur distribution dans le volume étaient contrôlées par un radiomètre pour gaz radioactifs. Une chambre d'ionisation à géométrie plane (fig. 6) servait de détecteur. Cette chambre d'ionisation placée au centre du fond inférieur de la chambre hermétique avait un volume de 1 litre et l'épaisseur de la couche d'air était de 2 cm. Nous avons utilisé comme absorbeurs équivalents au tissu, des filtres de polyéthylène d'épaisseur différente (dans la première série d'expérience) et du papier paraffiné (dans la seconde).

La seconde série expérimentale a été effectuée avec des émetteurs de faible énergie en particules β (C^{14}) et en électrons de conversion

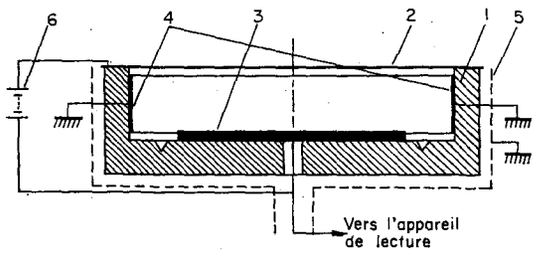

FIG. 6. chambre d'ionisation pour la mesure des doses profondes de particules β.
1, armature de la chambre; 2, pellicule de terlon metallisée, d'épaisseur 3,5 mg/cm²; 3, électrode collectrice; 4, depôt de carbone pour l'aplanissement du champ électrique dans le volume utile de la chambre; 5, écran métallique; 6, source de haute tension (300 V.)

(Xe^{131m}). Les mesures ont été réalisées par le même détecteur dans une chambre hémisphérique de diamètre 70 cm.

Les résultats des expériences et des calculs concernant la distribution des doses profondes sont présentés sur la figure 5, où le long de l'axe des abscisses est portée l'épaisseur de l'absorbeur t, mg/cm², et le long de l'axe des ordonnées l'intensité de la dose $\mathscr{P}(t)$, rad/sec, normalisée par rapport à la concentration de gaz dans un volume radiant, Q, curie/l.

La précision des données expérimentales est égale à $\pm$ 10 à 15%. Sur la figure 5 on peut voir un bon accord des résultats de l'expérience et du calcul. Les résultats présentés ci dessus nous donnent la possibilité de trouver un rapport entre une dose maximum admissible (DMA) pour chacun des organes critiques et les grandeurs correspondantes des concentrations maximum admissibles (CMA) des GRI dans l'atmosphère des locaux de travail.

Les résultats de ce calcul pour une salle hémisphérique de rayon R_0 = 5m. sont donnés dans le tableau 1 où se trouvent aussi les CMA recommandées par la CIPR.[1]

Le tableau 1 montre que les valeurs des CMA, calculées dans le présent travail surpassent de 10 à 50 fois celles recommandées par la CIPR. Il est nécessaire de noter que dans tous les cas cités on a trouvé comme organe critique la couche basale de l'épiderme de la peau (DMA = 0,6 rem/semaine), la contribution principale à la dose (plus de 90%) étant conditionnée par les particules β tandis que la contribution des photons γ est petite.

CONCLUSIONS

1. Pour l'établissement des normes des GRI dans l'atmosphère on doit se baser non sur les CMA au sol, mais sur la dose d'exposition créée par un panache de gaz radio-actifs à la surface de la terre en prenant en considération la hauteur du tube de rejet, la rose des vents et les autres paramètres météorologiques. On doit choisir une direction de plus grande répétition des vents. Un facteur contrôlable est l'éjection maximum admissible des GRI par le tube de ventilation $\mathscr{S}$, Ci/an.

2. La courbe des doses en fonction de la distance, $\mathscr{D}(\rho)$, n'a pas de maximum et par

Tableau 1. *CNA des gaz radio-actifs inerts dans l'atmosphère de locaux travail Q, Ci/l.*

Isotopes	CMA, Ci/l		Rapport des CMA Auteurs	Isotopes	CMA, Ci/l		Rapport des CMA Auteurs
	Auteurs	CIPR	CIPR		Auteurs	CIPR	CIPR
AR^{41}	5.10^{-9}	2.10^{-9}	25	Kr^{90}	1.10^{-8}	—	—
Kr^{77}	1.10^{-8}	—	—	Kr^{91}	1.10^{-8}	—	—
Kr^{85m}	1.10^{-7}	6.10^{-9}	16	Xe^{131m}	4.10^{-7}	2.10^{-8}	20
Kr^{85}	1.10^{-7}	1.10^{-8}	10	Xe^{133}	5.10^{-7}	1.10^{-8}	50
Kr^{87}	1.10^{-8}	1.10^{-9}	10	Xe^{135}	8.10^{-8}	4.10^{-9}	20
Kr^{88}	6.10^{-8}	—	—	Xe^{137}	6.10^{-9}	—	—
Kr^{89}	1.10^{-8}	—	—	Xe^{138}	2.10^{-8}	—	—

conséquent les formules connues de calcul des concentrations des GRI à la surface du sol en fonction de la distance (où ce maximum existe à une distance de 4 à 50 fois la hauteur du tube de rejet) ne peuvent pas être utilisées comme critère de sécurité radiologique.

3. Les résultats de calcul obtenues dans ce rapport coïncident bien avec ceux de l'expérience: l'erreur d'évaluation de dose sur une localité se trouve dans les limites de $\pm$ 60 á 70% en prenant en considération les erreurs causées par tous les facteurs y compris ceux de la météorologie.

4. L'éjection maximum admissible $\mathscr{I}$, Ci/an, peut être déterminée par la relation suivante:

$$\mathscr{I}, \text{ Ci/an} = \xi \, \text{DMA},$$

où DMA est une dose maximum admissible, établie pour un groupe de population en question, rad/an;

$\xi = \dfrac{\mathscr{I}(\rho), \text{ Ci/an}}{\mathscr{D}_0(\rho), \text{ rad/an}}$ est un facteur de normalisation, qu'on peut trouver pratiquement ou théoriquement par une courbe du type exposé à la figure 3.

Dans ce rapport, nous avons obtenu les valeurs suivantes d'éjections maximum admissibles de Ar^{41} pour une hauteur efficace de tube de ventilation, $H_{eff} = 91$ m, DMA = 0,17 rad/an et la distance $\rho = 1500$ m (voir la table ci-dessous).

L'éjection maximum admissible des autres gaz radioactifs inertes sera déterminée par la différence du rendement et de l'énergie des radiations γ en comparaison avec Ar^{41}. Pour les autres hauteuts (H) du tube de ventilation, qui différent de la valeur prise dans ce rapport notamment $H_{exp} = 91$ m, l'éjection maximum admissible, $\mathscr{I}$, peut être calculée par la relation suivante:

$$\mathscr{I} = \mathscr{I}_{exp} H^2/H^2_{exp}.$$

5. Les résultats du calcul des doses profondes d'une source infinie (où il y a équilibre de rayonnement de particules β) coïncident bien avec ceux de l'expérience. La divergence est $\pm$ 15 à 20%. Sil n'y a pas d'équilibre de rayonnement c.-à-d. si la dimension des salles de travail est inférieure à 2 ou 3 longueurs de libre parcours de particules, la formule (7) n'est plus exacte.

La distribution en profondeur dans le cas des électrons de conversion obéit à la formule (8).

6. Le calcul des CMA des GRI dans l'atmosphère des locaux de travail doit être effectué en tenant compte des DMA pour les organes critiques particuliers, de l'absorption des particules β par les tissus superficiels, et de la géometrie du volume radiant. Les calculs et les expériences présentés dans ce rapport indiquent que les CMA des GRI dans l'air des locaux de travail peuvent surpasser de 10 à 50 fois les CMA recommandées par la CIPR.[1]

7. Le principe que nous avons utilisé ici pour établir les normes des GRI dans l'atmosphère ainsi que dans l'atmosphère des locaux de travail, peut être utilisé aussi pour certains isotopes radio-actifs tels que C^{11}, O^{15}, O^{19}, N^{13} et quelques autres.

RÉFÉRENCES

1. Report of Committee 11 International Commission on Radiological Protection on Permissible Dose for International Radiation. *Health Physics*, **3** (1960).
2. N. G. Goussev *et al.* *Isotopes radio-actifs émetteurs de rayonnement.* Atomisdat, 1964.
3. D. L. Laikhtmann *et al.* Principes de statistique de conditions météorologiques pour servir aux projets de l'industrie—Dans le recueil. *Problèmes de diffusion turbulente dans les basses couches de l'atmosphère* VIP 15M, 1963.
4. R. Lövinger. In *Radiation Dosimetry*, ed. G. L. Hine and G. L. Brownell, N.Y. 1956, ch. 16.

Rhmb	U, m/sec	α	η, Ci/rad	$\mathscr{I}$, Ci/an	$\bar{\mathscr{I}}$, Ci/jour
N	2,7	0,155 (15,5%)	$6{,}7.10^6$	$1{,}2.10^6$	3300
NO	3,5	1,175 (17,5%)	$1{,}1.10^7$	$1{,}9.10^6$	5200

5. A. M. KONIENKO *et al.* Distribution de la dose loin de l'axe d'un disque plat émetteur β—Dans le recueil. *Techniques de mesure des preparations radioactives.* Atomisdat, 1962, pp. 110–115.

6. G. B. RADZIEVSKI et D. P. OSANOV. Distribution en profondeur de l'énergie absorbée à partir d'électrons non monoénergétiques—Dans le recueil. *Problèmes de dosimétrie et de protection contre les radiations.* Atomisdat, 1964, pp. 125–139.

DISCUSSION

D. NACHTIGALL (*Euratom*):

Ich möchte Herrn Sowby bitten, den Punkt 16 auf Seite 4 der ICRP-Publication 9 zu interpretieren. Dieser Punkt enthält die Empfehlung, bei Bestrahlung der Augen einen modifizierenden Faktor einzuführen, der beispielsweise für schnelle Neutronen 3 und für thermische Neutronen etwas kleiner als 2 wäre. Das würde bedeuten, dass die maximal zulässigen Flussdichten für Neutronen um diese Faktoren verringert würden. Dieses wiederum hätte weitreichende Folgen für die Messung des Neutronendosisäquivalentes mit den sogenannten rem-countern.

F. D. SOWBY:

The method of interpolation has been left open to allow the maximum degree of flexibility for the design of instruments.

Hub. WIJKER (*Netherlands*):

Are the limits recommended for planned special exposures also meant for rescue operations where human lives are involved?

F. D. SOWBY:

The Commission's recommendation (in paragraph 100) is that for life-saving procedures; it will not be possible to specify dose limits, since the acceptability of the dose will depend on the importance of the objective.

Hub. WIJKER:

It may be important to consider whether the decision to surpass the limit has to be taken by the man who will do the rescue, or can he be ordered? And the limit to which it can be surpassed (75 R or so?).

F. DUHAMEL (*France*):

Au sujet des facteurs à prendre en considération pour l'évaluation des dangers des radio-éléments, je suis d'accord avec M. Hunzinger mais, concernant le cas particulier de laboratoires possédant une excellente surveillance continue, je voudrais faire une remarque. Depuis la publication de nos travaux signalés par M. Feige nous nous sommes intéressés spécialement à ce cas particulier et notre conclusion—encore tout à fait provisoire—est que l'on pourrait mesurer le danger physique relatif des radio-éléments, par le rapport de la quantité minimum détectable dans le corps humain grâce aux moyens couramment utilisés, à la quantité maximum admissible correspondante.

A. BRODSKY (*U.S.A.*):

Although the scheme for classification of radioactivity incorporating the specific activity of the pure nuclide as a factor may be interesting and have special applications, it can be very misleading to classify the inherent radiotoxicities by these methods for general purposes. In most practical cases, the specific activity of the pure nuclide is so high that probabilities of intake would be independent of the specific nuclide mass, but would instead depend on the various factors given by Dr. Hunzinger. This is an extremely important matter, so I would like to refer you to my detailed discussion in an article in the *American Industrial Hygiene Association Journal*, May 1966, and in recent comments to a committee of the American Standards Association under Dr. Dade Moeller-whose committee is giving this subject a serious re, evaluation. The approach by Dr. Hunzinger and his colleagues toward collecting estimates of fractions of material inhaled in accidents is most worthwhile, and I wonder if he can continue on a worldwide basis. It would be particularly worthwhile if Dr. Hunzinger's group could send questionnaires to the people knowledgeable in the details of each accidental release as it occurs to ensure the gathering of *all* the pertinent data needed to determine likely probabilities of intake, such as total quantity involved in the accident, total quantity escaping enclosures or vessels involved, and best estimates of air concentrations and total quantities inhaled.

W. HUNZINGER:

We would welcome any reports of radiation incidents to be brought to our knowledge. The information required should include:

— Amount and nuclide handled;
— Characteristics of the operation carried out (ventilation, containment, temperature, chemical and physical form of the material handled);
— Short description of the incident;
— Amount of nuclide accidentally inhaled.

J. POMAROLA (*France*):

Nous n'avons pas assez de temps pour discuter de la probabilité pour qu'une personne soit impliquée dans un incident et je pourrai peut-être en discuter ensuite avec le Dr. Hunzinger s'il le veut bien. Mais je désire lui poser la question suivante: Les évaluations des quantités inhalées, au cours des incidents, sont-elles obtenues à partir des prélèvements atmosphériques ou bien des prélèvements biologiques ou bien encore à partir de ces deux moyens simultanément?

W. HUNZINGER:

The evaluation of the activity inhaled was carried out by whole body counting in most of the cases.

B. A. J. LISTER (*U.K.*):

I should like to refer to a programme of experiments which we are carrying out at Harwell in which accidents are simulated in glove-boxes and fume cupboards containing plutonium oxide or fluorescent powder. The fractions of the material inhaled have been assessed using personal air samplers worn by the operators who were, of course, wearing respiratory protection.

The fraction inhaled depends of course on the type of accident and often dramatically on the precise position of the operators, but the figures found in the Harwell experiments are in quite good agreement with those presented by Dr. Hunzinger.

F. W. SPIERS (*U.K.*):

Has Dr. Richmond attempted to fit data in the biological half-times of Cs^{137} in children and infants to his inter-species data? We have some recent data, for example, on biological half-times in infants from birth to six months which give values of 10 to 14 days for Cs^{137}, compared with values of about 7 days for potassium.

C. R. RICHMOND:

Data reported from several sources concerning retention of cesium by infants and children do indeed tend to follow the correlations shown for both body weight and body surface. As regards your statement on the trabeculation of dog bone, I agree entirely. However, the purpose of the interspecies correlation is to attempt to relate the differences which are seen interspecifically by some formulation which can be used to extrapolate to human values. The point, however, is an excellent one.

L. FITOUSSI (*France*):

Avec votre permission, M. Le Président, je voudrais demander à M. Beau de bien vouloir faire quelques commentaires au sujet de son rapport présenté en titre. En particulier j'aimerais connaître les résultats de son évaluation concernant les niveaux de contamination admissible pour les deux composées organiques citées dans le résumé de son rapport: la thymidine et la méthionine tritiée.

P. G. BEAU:

Nous avons calculé deux niveaux de contamination interne par inhalation et par ingestion pour la méthionine tritiée à l'aide d'un modèle simplifié du métabolisme de cette molécule, car ce dernier est très complexe (c'est le cas de la majorité des molécules marquées). Nous obtenons des normes plus sévères que celles employées actuellement pour l'eau tritiée (cf. abstract). En ce qui concerne la thymidine tritiée, on ne connaît chez l'homme, d'une manière *quantitative*, que les produits finaux du métabolisme (HTO et BAIBA) et les étapes intermédiaires au niveau cellulaire, dans les organes, sont mal connues, d'où la difficulté d'établir une norme d'organe.

Hub. WIJKER (*Netherlands*):

A comment on the point raised in the discussion concerning specific activity. For some years we have used three different specific activities in our laboratory:

σ_n = activity per gram of nuclide (also referred to as pure specific activity);

σ_e = activity per gram of element (elemental specific activity);

σ_m = activity per gram of material in which the nuclide is homogeneously or nearly homogeneously distributed, e.g. per gram of solvent (material specific activity).

(Reported to the Nederlandse Vereniging voor Stralingshygiene on its session of February 1962.)

E. W. JACKSON (*U.K.*):

If I understand the speaker, he is recommending that dose received should be used as a criterion and not the downwind concentration of released radioactive gas. Is not, however, this dose proportional to this concentration and since in practice, in the field, it is the concentration that is measured, would it not be easier to multiply these concentration values by a constant? Also regarding the extensive mathematical work that has been done by the author, could I ask whether this theoretical work carries the subject much further than has been done by Pasquill in the U.K.?

N. G. GOUSSEV:

First I shall answer the question on the inert radioactive gases in the atmospheric air. As I have already

mentioned, the character of the curve of gamma irradiation dose as a function of distance from the source differs essentially from the curve of the downwind concentration dependence upon distance. For instance if the plume of radioactive gases goes high up or to one side of the detection point, the downwind concentration would be equal to zero, yet the gamma irradiation dose can be considerable.

Therefore a constant coefficient to be used for the transition from concentration to dose does not exist, although it is possible that such a correlation exists at great distances from the source (more than two kilometers). It exists also for closed spaces—in working establishments. Let us note that in this case the radiation hazard of inert radioactive gases is determined by the external β-radiation dose on skin. The contribution of the gamma irradiation dose may not be taken into account if the concentrations do not exceed permissible values.

In all cases, rooms in working establishments as well as an open locality, the external irradiation dose exceeds considerably the internal irradiation dose caused by radioactive gases, this difference may be more than 100.

As to the works of Pasquill concerning the atmospheric diffusion, I believe they may be used for calculating γ-irradiation doses from radioactive gases at a point in space.

A. P. HULL (*U.S.A.*):

By way of documenting the speaker's remarks with regard to the relative importance of gamma and beta radiations from plumes containing inert radioactive gases, I should like to indicate some of our data at Brookhaven National Laboratory. The Brookhaven Graphite Research Reactor emits 20,000 Ci per day of Ar^{41} from a 100 m stack. At 0.5 km from the stack a ground level monitoring station in a prevailing downwind direction indicates an average dose of about 5 mR/wk, although the instrumentation indicates the plume is seldom at ground level this close to the stack. At slightly more than 1.0 km, near the predicted point of ground level maximum concentration, the dose attributable to Ar^{41} is about 1.5 mR/wk. At 2.5 km it is about 0.75 mR/wk. We have recently installed a station at 6 km for another purpose, but will be measuring the Ar^{41} at this location also.

N. G. GOUSSEV:

Your investigations, Dr. Hull, are very interesting and it would be useful to compare them with the results of our work. We have conducted our experiment during a period of two years, using a large number of thermoluminescent dosimeters with the exposure duration of one year. Your measurements seem to involve a shorter period of time—they rather characterize the dose rate for one week. The extrapolation to the integral annual dose may thus lead to great errors because of the difference in meteorological conditions. In comparing the experiments with the theoretical data it must be noted that both O. G. Sutton's formula and D. L. Leichtmann's one (the latter is used in our work) cannot give the correct response about the law of dose distribution as a function of distance from source.

These formulae give the value of the downwind concentration of a radioactive gas at a given site; in this case, as it is known, the curve of the dependence of downwind concentration on distance to the stack shows a peak. The height of this peak and its distance from the source depend on the stack height and meteorological conditions. In the experiments concerning measurements of the integral dose such a peak was not observed—the dose declines gradually as a function of distance. Thus the gamma-ray integral dose on a locality is not always proportional to the downwind concentration.

DOSE DISTRIBUTION FUNCTIONS FOR NEUTRONS AND GAMMA-RAYS IN ANTHROPOMORPHOUS AND RADIOBIOLOGICAL PHANTOMS*

T. D. JONES, J. A. AUXIER, J. W. POSTON and D. R. JOHNSON
Health Physics Division,
Oak Ridge National Laboratory,
Oak Ridge, Tennessee

Abstract—A right circular cylinder, 30 cm in diameter and 60 cm in height, was assumed to be composed of standard soft tissue, and dose as a function of penetration depth was computed for plane beams of incident neutrons. Data are presented for monoenergetic neutrons of various energies up to 14.0 MeV as well as for the neutron spectrum from the Health Physics Research Reactor (HPRR). The calculations were of a Monte Carlo nature using a slightly revised version of Snyder's linear energy transfer (LET) code.[1] New LET curves were obtained for C, N, O, B, Be, protons, tritons, and alpha particles, and recently obtained values of cross sections for these same elements were used with the code.[2] Many previous theoretical treatments of similar problems tended to ignore inelastic scattering reactions due to (1) the complexity of coding, (2) the difficulty of obtaining appropriate inelastic cross sections, and (3) inadequate "fast memory" capacity of many computational machines. Results of these calculations were compared with (1) those for the infinite slab 30 cm thick in the National Bureau of Standards (NBS) Handbook 63, (2) those obtained for a burro cadaver exposed to the neutron spectrum from the HPRR,[3] and (3) those presented by Auxier *et al.*,[4] in their description of a belt containing various radiation detection devices to be used in the determination of the orientation of persons exposed to unscheduled criticality excursions.

THE Monte Carlo Linear Energy Transfer (LET) code used by Snyder in previous work [1, 5] has been modified and extended so that a more realistic treatment of various exposure situations is now possible. New stopping-power data[6] have been obtained for ions of C, N, O, B, Be, protons, tritons, and alpha particles, and are shown in Fig. 1. These curves are similar to those previously used by Snyder[1] for ions of C, N, O, and protons, except the low energy tail is now assumed to fall as the inverse power of velocity rather than the inverse power of energy. The code has been extended to include neutron inelastic scattering reactions in which the emitted neutron is assumed to come off isotropically in the center of mass system. For elastic scattering, preliminary calculations were made for incident neutron energies of 7 and 14 MeV. An energy cutoff of 2.5 MeV was used to determine the maximum influence of the assumption that all reactions were of an isotropic nature. The phantom is shown at the bottom of Table 1, and the results of the calculations are as shown in the table. Although the errors due to the assumption of isotropy are well within the bounds of the values of the coefficients of variation given in columns 4 and 6, the calculations, for the elastic case, were made without this simplifying assumption. Cross-sections used in the code were presented by Auxier (a complete discussion of the 33 nuclear cross-sections would be much too extensive for this paper) in his paper entitled "Neutron Cross-Sections and Reaction Products for H, C, N, and O for the Energy Range from Thermal to 15 MeV", and calculations were made for various

* Research sponsored by the U.S. Atomic Energy Commission under contract with the Union Carbide Corporation.

Table 1. Results of an Isotropic Treatment of Anisotropic Reactions in a Slab Phantom

Energy (MeV)	Slab no.	Isotropic $\left(\frac{\times 10^{-8}\text{ rad}}{\text{neutron cm}^2}\right)$	C. of V. (%)	Anisotropic $\left(\frac{\times 10^{-8}\text{ rad}}{\text{neutron cm}^2}\right)$	C. of V. (%)	Error (1-iso./aniso.) × 100 (%)
7 (2.5 cutoff)	1	0.456	6.8	0.448	6.2	− 1.8
	2	0.253	7.1	0.249	10.4	− 1.7
	3	0.120	10.8	0.126	15.9	+ 4.8
	4	0.054	12.0	0.059	17.0	+ 9.5
14 (2.5 cutoff)	1	0.526	7.2	0.457	6.4	−11.5
	2	0.336	8.3	0.323	9.9	− 4.1
	3	0.192	11.5	0.196	10.2	+ 2.3
	4	0.099	17.4	0.115	11.3	+14.2
14 (no energy cutoff)	1	0.562	6.2	0.484	6.2	−16.1
	2	0.329	11.5	0.332	7.2	+ 0.8
	3	0.203	9.8	0.214	8.9	+ 5.2
	4	0.106	11.3	0.137	19.7	+22.6

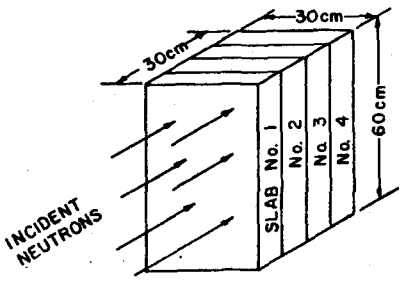

SLAB PHANTOM

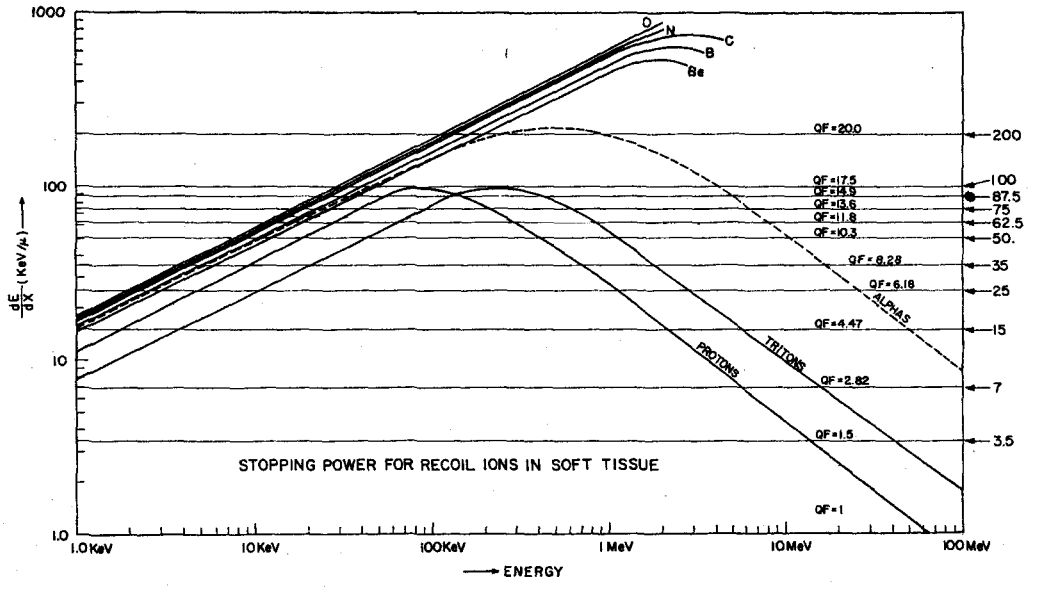

FIG. 1. Stopping power for recoil ions in soft tissue.

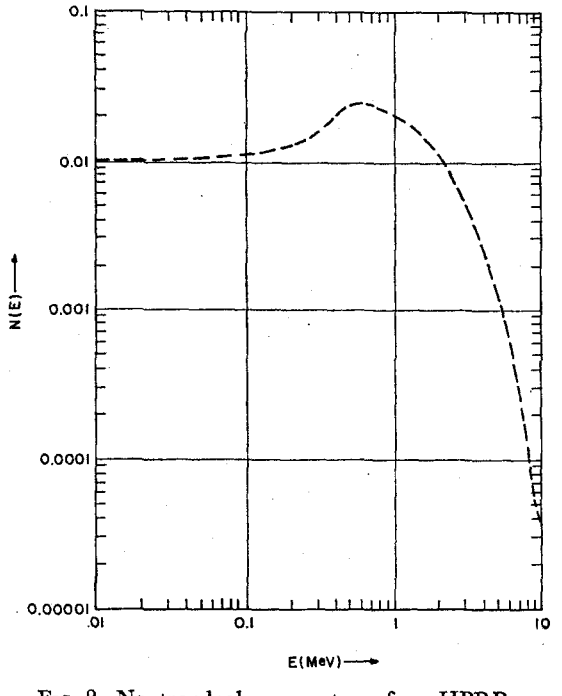

FIG. 2. Neutron leakage spectrum from HPRR.

monoenergetic neutron beams as well as the Health Physics Research Reactor (HPRR) neutron spectrum.[7, 8] The HPRR is an unshielded critical assembly of enriched ^{235}U[9] producing neutrons having the spectral distribution shown in Fig. 2. The exposure situation was assumed to be a plane parallel beam of neutrons incident unilaterally on the cylindrical phantom shown in Fig. 3. The cylinder was assumed to be 15 cm in radius and 60 cm high, composed of H,

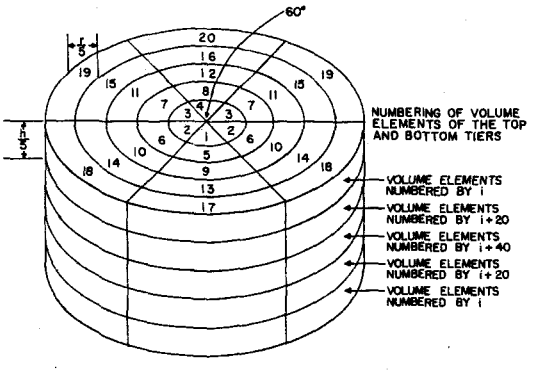

FIG. 3. Numbering of volume elements in the cylindrical phantom.

C, N, and O in the proportions found in standard, soft tissue.[10] The cylinder was subdivided into 150 volume elements, but due to geometrical symmetry, only 60 different elemental exposures were possible.

Table 2 shows the list of reactions that may occur in the phantom and the contribution averaged over the entire phantom from each of the various reactions. From this it is evident that many of the 33 possible reactions could have been ignored since they contribute an almost insignificant amount to the total dose. The reactions are listed in three groups. The reactions in the first group, numbers 1 through 4, are those of elastic scattering of neutrons by the nuclei in the medium. The second group, numbers 5 through 16, is that of the inelastic type in which a nucleus absorbs a neutron and is raised to an excited state and emits a neutron or two, in the case of the C(n, $2n'$) reaction, and one or more gamma-rays. The third group is that of the absorption type, in which a neutron is captured by a nucleus and one or more charged particles are emitted with or without accompanying gamma-rays.

The absorbed dose as a function of penetration depth, due to neutron reactions exclusive of the neutron-produced gamma dose, and the dose as a function of penetration depth, due to neutron-produced gamma-rays, for representative energies are shown in Fig. 4. For instance, the n and γ curves for a specific energy could be summed to obtain the total dose for a particular exposure situation.

Dose equivalent as a function of penetration depth is shown in Fig. 5 and was obtained through the use of ICRP-recommended quality factors[11] shown in the inset of this figure. The absorbed dose was separated into 12 LET intervals, and quality factors denoted by the arrows, representing the mean quality factor for that particular interval, were used to compute the dose-equivalent curves shown in this figure. The coefficients of variation for both the

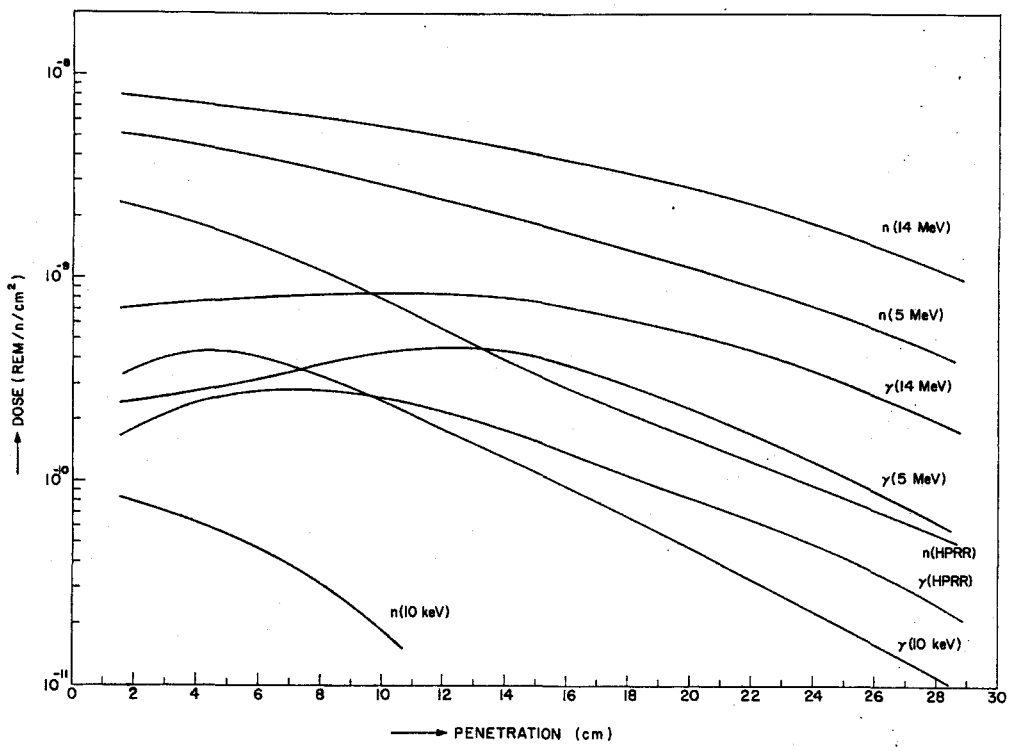

FIG. 4. Absorbed dose as a function of penetration depth in a cylindrical phantom (30 cm × 60 cm).

Table 2. Contributions to Dose Averaged over a Cylindrical Phantom from Reactions in Tissue

	Reaction	HPRR†	5 MeV†	7 MeV†	10 MeV†	14 MeV†
1.	H (n, n) H	6.9232	22.44	28.26	33.58	34.10
2.	C (n, n) C	0.1780	0.57	0.59	0.63	0.60
3.	N (n, n) N	0.0146	0.06	0.06	0.06	0.06
4.	O (n, n) O	0.4228	1.36	1.97	1.50	1.44
5.	C (n, n') *C; *C $\rightarrow$ C + γ_1; $\gamma_1 = 1.75$ MeV				0.05	0.03
6.	C (n, n') *C; *C $\rightarrow$ C + γ_2; $\gamma_2 = 4.43$ MeV	0.0099	0.03	0.26	0.59	0.69
7.	C (n, n') *C; *C $\rightarrow$ C + γ_3; $\gamma_3 = 6.8$ MeV	0.0001				0.14
8.	N (n, n') *N; *N $\rightarrow$ N + γ_1; $\gamma_1 = 1.63$ MeV	0.0004				0.01
9.	N (n, n') *N; *N $\rightarrow$ N + γ_2; $\gamma_2 = 2.31$ MeV	0.0002			0.02	0.03
10.	N (n, n') *N; *N $\rightarrow$ N + γ_3; $\gamma_3 = 5.1$ MeV	0.0001			0.03	0.02
11.	N (n, n') *N; *N $\rightarrow$ N + γ_4; $\gamma_4 = 10.0$ MeV					0.03
12.	N (n, n') *N; *N $\rightarrow$ N + γ_5; $\gamma_5 = 11.0$ MeV					0.03
13.	O (n, n') *O; *O $\rightarrow$ O + γ_1; $\gamma_1 = 6.1$ MeV	0.0083		0.14	1.36	1.54
14.	O (n, n') *O; *O $\rightarrow$ O + γ_2; $\gamma_2 = 7.12$ MeV	0.0036			0.30	0.38
15.	O (n, n') *O; *O $\rightarrow$ O + γ_3; $\gamma_3 = 3.8$ MeV					1.58
16.	O (n, n') *O; *O $\rightarrow$ O + γ_4; $\gamma_4 = 4.8$ MeV					0.77
17.	C (n, a_2) *Be; *Be $\rightarrow$ Be + n; Be $\rightarrow 2a$					0.58
18.	C (n, n') *C; *C $\rightarrow$ Be + a					0.51
19.	N $(n, 2N)$ N					0.01
20.	H (n, γ) H	1.7250	1.64	1.41	1.21	0.89
21.	C (n, a_0) Be	0.0006			0.11	0.36
22.	N (n, a_0) B	0.0127	0.10	0.06	0.10	0.11
23.	O (n, a_0) C	0.0284	0.55	0.69	0.73	1.11
24.	C (n, a_1) *Be; *Be $\rightarrow$ Be + γ; $\gamma = 1.75$ MeV	0.0001				0.05
25.	N (n, a_1) *B; *B $\rightarrow$ B + γ_1; $\gamma_1 = 2.1$ MeV	0.0006	0.01	0.01	0.02	0.04
26.	N (n, a_2) *B; *B $\rightarrow$ B + γ_2; $\gamma_2 = 4.5$ MeV	0.0001		0.01	0.02	0.05
27.	N (n, a_3) *B; *B $\rightarrow$ B + γ_3; $\gamma_3 = 5.0$ MeV	0.0004			0.04	0.06
28.	O (n, a_1) *C; *C $\rightarrow$ C + γ_1; $\gamma_1 = 3.1$ MeV	0.0014			0.11	1.03
29.	O (n, a_2) *C; *C $\rightarrow$ C + γ_2; $\gamma_2 = 3.8$ MeV	0.0009			0.22	2.46
30.	O (n, a_3) *C; *C $\rightarrow$ C + γ_3; $\gamma_3 = 7.0$ MeV					1.00
31.	N (n, p) *C	0.1495	0.19	0.22	0.22	0.18
32.	O (n, p) *N; *N $\rightarrow$ N + γ; $\gamma = 6.1$ MeV					0.51
33.	N (n, t) C			0.01	0.01	0.02
	Total doses	9.4809	26.95	33.69	40.91	50.42

† $\times 10^{-10}$ rad/neutron/cm^2.

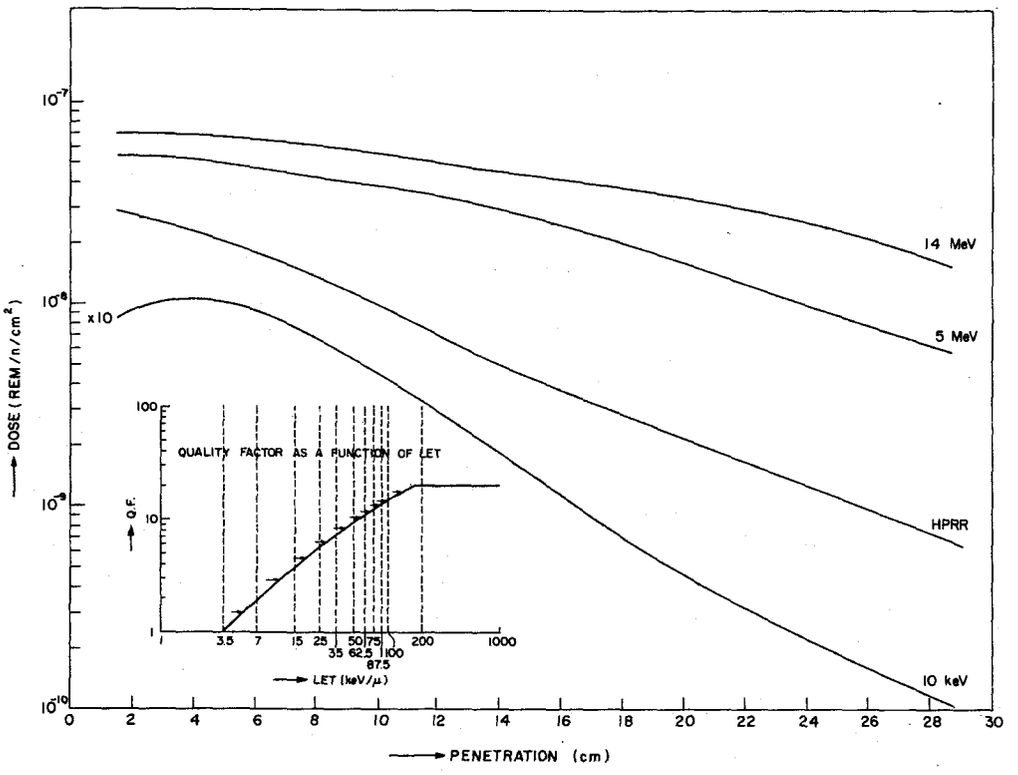

FIG. 5. Dose equivalent as a function of penetration depth in a cylindrical phantom (30 cm × 60 cm).

rad and rem dose curves range from about 7% at the front where the volume elements are large to 22% at the center where they were much smaller to about 17% at the rear where the volume elements are large, but the statistical parameters are influenced by the exponential nature of the attenuation of neutrons. For the spectrum from the HPRR, the coefficients of variation range from 5% at the front to 40% at the center and rear. The determinant factor here is the statistical nature of the energy of the incident neutrons.

Figure 6 shows dose as a function of LET for incident neutrons of energies 2.5, 5, and 14 MeV at penetration depths of 1.5, 13.5, and 28.5 cm. This illustrates the changing LET spectrum with both penetration depth and energy. For example, the LET spectral distribution of dose for 5 MeV neutrons at a penetration depth of 1.5 cm is not very unlike that for 14 MeV neutrons at a penetration depth

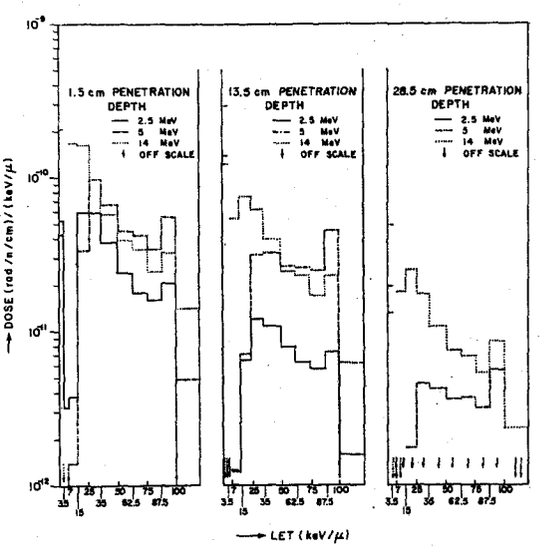

FIG. 6. Dose as a function of LET.

of 13.5 cm. Calculations of the above type have been completed for incident neutrons of representative energies between thermal and 14 MeV.

REFERENCES

1. W. S. SNYDER. The LET distribution of dose in some tissue cylinders, *Biological Effects of Neutron and Proton Irradiations*, Vol. 1, p. 3, IAEA, Vienna, 1964.
2. J. A. AUXIER and M. D. BROWN. Neutron cross-sections and reaction products for H, C, N, and O for the energy range from thermal to 15 MeV. This volume.
3. J. W. POSTON and D. R. JOHNSON. Oak Ridge National Laboratory. Personal communication, 1966.
4. J. A. AUXIER, F. W. SANDERS and P. N. HENSLEY. *Health Phys.* **5,** 226 (1961).
5. W. S. SNYDER. Distribution of dose and dose equivalent resulting from broad-beam irradiation of a man-sized cylindrical phantom by monoenergetic neutrons. Health Physics Society Meeting, Los Angeles, 1964.
6. D. R. DAVY. Oak Ridge National Laboratory. Personal communication, 1966.
7. Health Physics Division Annual Progress Report for Period Ending July 31, 1965. Oak Ridge National Laboratory Report ORNL-3849.
8. Health Physics Division Annual Progress Report for Period Ending July 31, 1964. Oak Ridge National Laboratory Report ORNL-3697.
9. J. A. AUXIER. *Health Phys.* **11,** 89–93 (1965).
10. Measurement of absorbed dose of neutrons, and of mixtures of neutrons and gamma rays. *Nat. Bur. Stand. Handbook* **75** (1961).
11. *Recommendations of the International Commission on Radiological Protection*, ICRP Publication 4, Report of Committee IV (1953–1959), Pergamon Press, 1964.

EFFECTS OF PHANTOM GEOMETRY ON DOSE DISTRIBUTION*

JACOB NEUFELD, V. E. ANDERSON, HARVEL WRIGHT, W. S. SNYDER and J. E. TURNER
Health Physics Division, Oak Ridge National Laboratory,
Oak Ridge, Tennessee

Abstract—Calculations have been made of the spatial distribution of dose and dose equivalent due to protons of energies 250 MeV and 400 MeV incident on a tissue phantom which has dimensions approximating those of a human torso and has the form of a right elliptical cylinder with a height of 70 cm and with semiaxes of the elliptical base as 20 cm and 10 cm. The results obtained have been compared with the corresponding data previously obtained for a tissue slab having thickness of 30 cm. It is shown that within the limits of accuracy due to statistical fluctuations the distribution of dose and dose equivalent are not substantially different in a cylindrical phantom from the corresponding values in a slab phantom.

THIS is a continuation of a recently reported study dealing with the estimates of dose and dose equivalent due to the exposure to high-energy nucleons. This study undertaken by the Neutron Physics and Health Physics Divisions of the Oak Ridge National Laboratory is based on Monte Carlo techniques and deals with the statistical behavior of physical interactions which result from the penetration of high-energy nucleons into an appropriate phantom having the same elemental composition as tissue.[1-3] These interactions include both elastic and inelastic collisions and also take into account the contribution of cascade particles, nuclear recoils, and nuclear evaporation products ranging in complexity from nucleons to alpha particles. A relatively detailed outline of the physical aspects of the problem is given in refs. 1 and 2. The principal quantities which are determined on the basis of these interactions are the absorbed dose D which represents the amount of energy absorbed per unit mass of tissue expressed in rads and the dose equivalent DE which gives a measure of the biological hazard from the standpoint of radiation protection expressed in rems. The generally accepted procedure for determining the dose equivalent is based on the consideration of linear energy transfer (LET) at the points at which the energy deposition takes place and of the appropriate weighting factors (QF) which are applied to the corresponding LET values. These weighting factors have been determined from the QF-LET relationship based on routine occupational exposure.[4]

The distribution of dose within a large phantom is generally not uniform and it depends to a large extent on the conditions of irradiation and on the geometry of the phantom. It is our object here to determine for high energy incident protons the effect of the phantom geometry under some simplified and idealized assumptions concerning the condition of irradiation. In previous investigations it was assumed that a body can be approximated by a 30-cm thick slab of tissue. The preliminary data presented in this report are based on a more realistic model which approximates the dimensions of a human torso. The two cases considered in this report deal with the incidence of monoenergetic proton beams having energies 250 and 400 MeV.

The phantom used in the present calculations is assumed to be composed of hydrogen, carbon, nitrogen, and oxygen in approximately the proportion by weight of standard man (density of about 1 g/cm^3) and has the form of a right

* Research sponsored by the U.S. Atomic Energy Commission under contract with Union Carbide Corporation.

elliptical cylinder with a height of 70 cm and with semiaxes of the elliptical base as 20 cm and 10 cm (see Figs. 1a and 1b). These dimensions are approximately the same as the ones selected by Hayes and Brucer.[5] For dose analyses the phantom was divided into four regions by three planes perpendicular to the axis of the cylinder, 6 axial planes, and 2 surfaces each of which forms an elliptical cylinder co-axial with the axis of the phantom. The subdivisions of the phantom are indicated in Figs. 1a and 1b. Because of certain symmetries

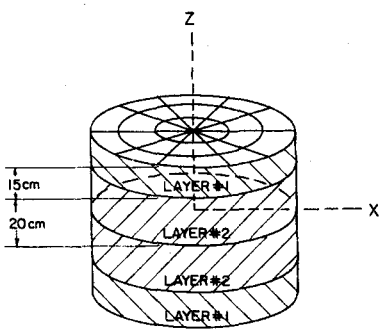

FIG. 1a. Tissue phantom, perspective view.

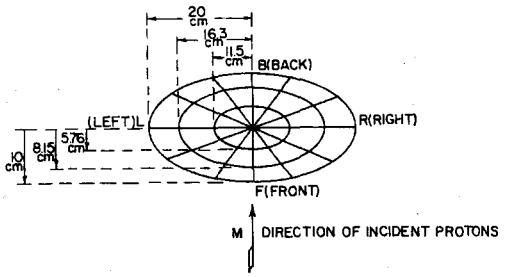

FIG. 1b. Ellipse formed by the intersection of the cylinder and a plane perpendicular to its axis.

resulting from conditions of exposure, certain volume elements within the phantom receive the same dose to within statistical fluctuations. The energy deposited in such volume elements was combined to give greater statistical accuracy to the resulting estimates of dose.

It was assumed that protons are incident in a direction perpendicular to both the axis of the cylindrical phantom and to the major axis LR of the ellipse shown in Fig. 1b. This ellipse is formed by the intersection of the cylinder with a plane perpendicular to the axis. The direction of incidence of the protons is indicated by an arrow M.

The results of the calculations for incident protons having energies 250 and 400 MeV are shown in Figs. 2 through 5. At each energy 10,000

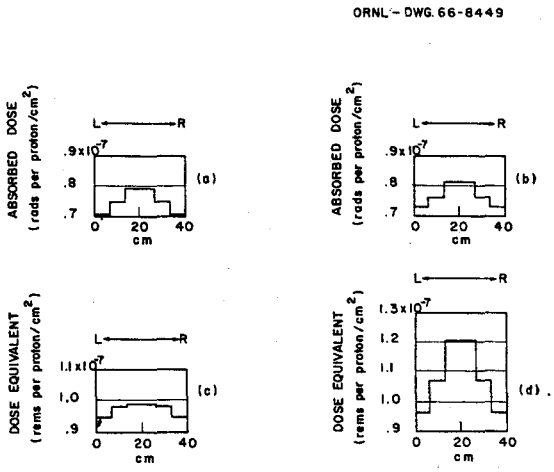

FIG. 2. Distribution of absorbed dose (D) and of dose equivalent (DE) along the traverse LR ("left–right") for a unidirectional 250-MeV proton beam; (a) distribution of D in layer No. 1; (b) distribution of D in layer No. 2; (c) distribution of DE in layer No. 1; (d) distribution of DE in layer No. 2.

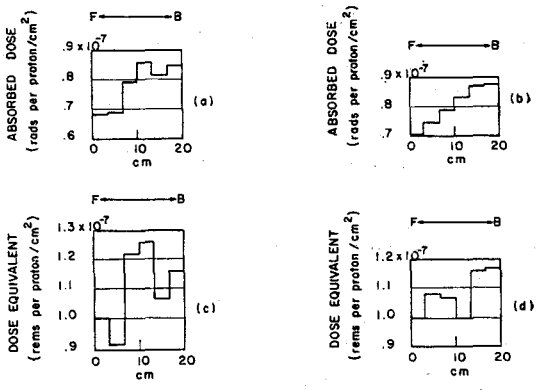

FIG. 3. Distribution of absorbed dose (D) and of dose equivalent (DE) along the traverse FB ("front–back") for a unidirectional 250-MeV proton flux; (a) distribution of D in layer No. 1; (b) distribution of D in layer No. 2; (c) distribution of DE in layer No. 1; (d) distribution of DE in layer No. 2.

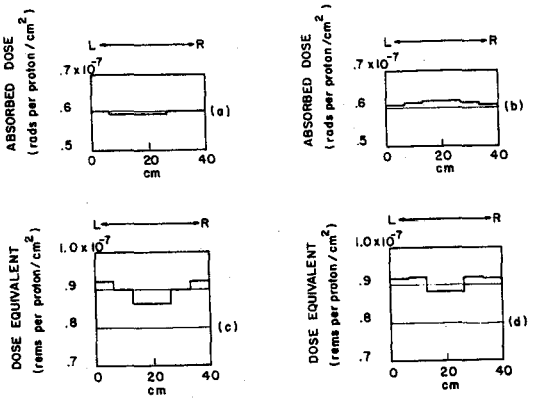

FIG. 4. Distribution of absorbed dose (D) and of dose equivalent (DE) along the traverse LR ("left–right") for a unidirectional 400-MeV proton beam; (a) distribution of D in layer No. 1; (b) distribution of D in layer No. 2; (c) distribution of DE in layer No. 1; (d) distribution of DE in layer No. 2.

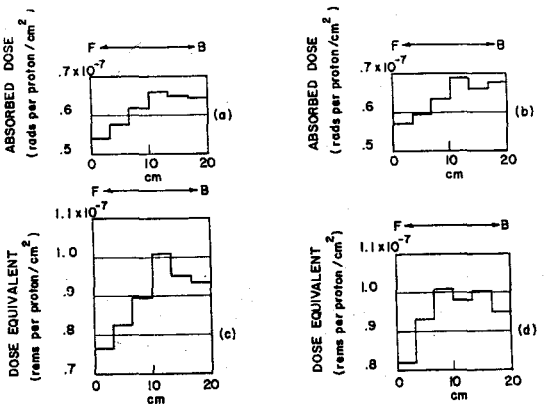

FIG. 5. Distribution of absorbed dose (D) and of dose equivalent (DE) along the traverse FB ("front–back") for a unidirectional 400-MeV proton flux; (a) distribution of D in layer No. 1; (b) distribution of D in layer No. 2; (c) distribution of DE in layer No. 1; (d) distribution of DE in layer No. 2.

incident protons were used, and the fate of each and its secondaries was determined on the basis of Monte Carlo techniques, and particle histories analogous to those of the infinite slab were generated in the phantom. The values of dose and dose equivalent are represented graphically along two traverses in the layers No. 1 and No. 2. One of these traverses is aligned along the axis FB ("front to back") and the other runs diagonally along the axis LR ("left to right"). The position of the traverses and of the layers No. 1 and No. 2 are indicated in Figs. 1a and 1b.

The values of dose and dose equivalent presented in Figs. 2 to 5 have been compared with the corresponding values previously obtained[1] for a 30-cm thick tissue slab. One can easily see the occurrence of the "build-up" factor in the dose distribution, both in the cylindrical and in the slab phantoms. In both cases the dose gradually increases in the direction of the proton beam, and has the lowest value in the region of the incidence of the beam. The build-up-factor is due to the generation of secondary protons and heavier particles at each point of interaction and to the corresponding energy degradation which accounts for the increase in both LET and QF values.

The characteristic increase of the dose with the depth is shown in the graphs of Figs. 3 and 5 which show the distribution of dose and dose equivalent along the FB traverse for layers No. 1 and No. 2.

In order to compare the build-up effects in both phantoms we shall define a "build-up index" K_D for the dose (D) distribution and a "build-up index" K_{DE} for the distribution of the dose equivalent (DE), respectively, as follows:

$$K_D = \frac{\text{dose at the depth of 20 cm}}{\text{dose in the region of incidence}}$$

and

$$K_{DE} = \frac{\text{dose equivalent at the depth of 20 cm}}{\text{dose equivalent in the region of incidence}}.$$

Table 1 contains data which permit one to compare the values of dose and dose equivalent at the corresponding points in both phantoms and also give the values of the build-up indexes for various energies of the incident proton beams. It is apparent that K_D and K_{DE} decrease with the increase of proton energy and show in both phantoms substantially the same values for protons of corresponding energy values. Because the statistical fluctuations are so large, one cannot make any precise interpretation. (These fluctuations are particularly evident in Fig. 3.) The above results show,

Table 1

	Tissue slab	Cylindrical phantom (traverse FB in layer 2)
(A) Dose in the region of incidence of the beam	0.84×10^{-7} for 200 MeV 0.65×10^{-7} for 300 MeV 0.58×10^{-7} for 400 MeV	0.71×10^{-7} for 250 MeV 0.57×10^{-7} for 400 MeV
(B) Dose at the depth of 20 cm	1.2×10^{-7} for 200 MeV 0.78×10^{-7} for 300 MeV 0.7×10^{-7} for 400 MeV	0.88×10^{-7} for 250 MeV 0.67×10^{-7} for 400 MeV
Build-up index K_D	1.43 for 200 MeV 1.20 for 300 MeV 1.21 for 400 MeV	1.24 for 250 MeV 1.18 for 400 MeV
(A) Dose equivalent in the region of incidence of the beam (in rem)	1.1×10^{-7} for 200 MeV 0.9×10^{-7} for 300 MeV 0.9×10^{-7} for 400 MeV	1.00×10^{-7} for 250 MeV 0.83×10^{-7} for 400 MeV
(B) Dose equivalent at the depth of 20 cm	1.15×10^{-7} for 200 MeV 1.01×10^{-7} for 300 MeV 1×10^{-7} for 400 MeV	1.17×10^{-7} for 250 MeV 1.01×10^{-7} for 400 MeV
Build-up index K_{DE}	1.36 for 200 MeV 1.12 for 300 MeV	1.17 for 250 MeV 1.22 for 400 MeV

however, that within the limits of accuracy due to statistical fluctuations the calculated dose distributions in the direction of incident beams do not differ substantially in the two phantoms considered.

The code for performing the above calculations has been designed to determine the estimates of dose in a region of any size or any location within the cylindrical phantom and to determine the dose deposited in critical organs of the human body under various conditions of high-energy exposure.

REFERENCES

1. J. E. Turner, C. D. Zerby, R. L. Woodyard, Harvel Wright, W. E. Kinney, W. S. Snyder, and Jacob Neufeld. Calculation of radiation dose from protons to 400 MeV. *Health Phys.* **16,** 783 (1964).
2. C. D. Zerby and W. E. Kinney. Calculated tissue current-to-dose conversion factors for nucleons below 400 MeV. *Nuclear Instrs. and Methods* **36,** 125 (1965).
3. Jacob Neufeld, W. S. Snyder, J. E. Turner and Harvel Wright. Calculation of radiation dose protons and neutrons to 400 MeV. *Health Phys.* **12,** 227 (1966).
4. Recommendations of the International Commission on Radiological Protection, ICRP Publication 9, p. 3, Pergamon Press, Oxford (1965).
5. R. L. Hayes and M. Brucer. Compartmentalized phantoms for the standard man, adolescent, and child. *Intern. J. Appl. Rad. Isotopes* **9,** 113–118 (1960).

DISTRIBUTION OF DOSE IN THE BODY FROM A SOURCE OF GAMMA RAYS DISTRIBUTED UNIFORMLY IN AN ORGAN*

H. L. FISHER, Jr.† and W. S. SNYDER
Health Physics Division,
Oak Ridge National Laboratory,
Oak Ridge, Tennessee, U.S.A.

Abstract—When a gamma emitter is present in an organ of the body, only a fraction of the emitted gamma energy is absorbed in that organ. Many evaluations of the absorbed fraction have been published, mostly for highly idealized and perhaps oversimplified cases. The use of an effective radius and a spherical geometry is one instance of such drastic simplification. Although an exact theory of gamma photon interaction with matter is known in detail, application of this theory is usually difficult since an enormous amount of mathematical computation is involved. However, by use of a high-speed digital computer these calculations become feasible. A Monte-Carlo-type calculation has been used to estimate the dose in 22 organs and 100 subregions of an adult human phantom for four initial gamma energies. This report is divided into three sections; in section one is a description of the phantom, in section two are some details of the Monte Carlo method used, and in section three are the dose estimates from a gamma source distributed uniformly in (1) the total body and (2) the skeleton.

I. THE PHANTOM

Shown in Fig. 1 is the phantom and subregions in which dose was determined. The dimensions of the phantom were chosen after consideration of the average size and weight of humans[1-3] and the phantoms designed by Hayes and Brucer.[4] In order to describe the various regions, a coordinate system is needed. As shown in the figure, the origin of the rectangular coordinate system is located at the center of the base of the trunk. The positive z-axis extends vertically through the head, the left side of the phantom will be taken along the positive x-axis, and the rear will be taken along the positive y-axis. All units of length are given in centimeters.

Using the coordinate system in Fig. 1, the body of the phantom may be described as follows. The trunk is an elliptical cylinder given by

$$\left(\frac{x}{20}\right)^2 + \left(\frac{y}{10}\right)^2 \leqslant 1$$

$$0 \leqslant z \leqslant 70.$$

The head is also an elliptical cylinder

$$\left(\frac{x}{7}\right)^2 + \left(\frac{y}{10}\right)^2 \leqslant 1$$

$$70 < z \leqslant 94.$$

The legs are considered together to be a truncated elliptical cone

$$\left(\frac{x}{20}\right)^2 + \left(\frac{y}{10}\right)^2 \leqslant \left(\frac{100 + z}{100}\right)^2$$

$$-80 \leqslant z < 0.$$

It is now a simple matter for the computer to take any point (x, y, z), substitute it into these inequalities, note whether the inequalities are satisfied, and thereby determine whether this

* Research sponsored by the U.S. Atomic Energy Commission under contract with Union Carbide Corporation.

† On loan from the USPHS.

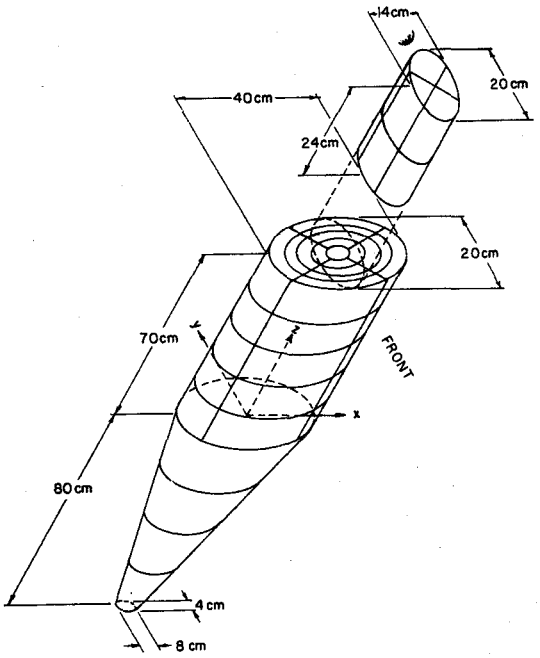

FIG. 1. The human phantom.

point is inside or outside the phantom and whether it is in the head, trunk, or legs of the phantom. Except for the head, this phantom is convex. Account has been taken of the photons which transverse the void between trunk and head.

The arbitrary subregions into which the phantom was sectioned and in which dose was determined are outlined in Fig. 1. The legs were cut into four layers by equidistant horizontal planes; the trunk was divided into five layers by equidistant horizontal planes. Two vertical planes, intersecting at right angles along the central axis of the trunk and having an angle of 45 degrees from either the x- or y-axis, cut these layers. The final volume element is obtained by four vertical, concentric, elliptical cutting cylinders. The major axes of these elliptical cylinders are 4, 8, 12, and 16 cm, and the minor axes are 2, 4, 6, and 8 cm. The innermost elliptical cylinder was not cut by the vertical planes. The head was sectioned into two layers equal in thickness and was cut by the same two vertical planes which cut the trunk. Although dose was determined in these arbitrary regions, the results are not presented in this report since the principal purpose is to give organ doses. However, results from the arbitrary regions permit an approximation of the variation of dose throughout the phantom. In particular, if an organ is very small, e.g. ovary, thyroid, pituitary, etc., the dose estimate may be statistically unreliable on a given calculation, and one may use instead an average dose over one of these layer regions.

Mathematical descriptions of the organs were formulated after consideration of the descriptive and schematic material from several general anatomy references.[5, 6] The scaled cross sections of the human body by Eycleshymer and Schoemaker[7] were helpful in locating the positions at which to place the organs as well as aiding in the construction of the organs. The representations of the organs by the mathematical equations given herein are only approximate, and many other geometrically simple approximations might be used. The goal in constructing these mathematical organs was to obtain the approximate size and shape of an average organ through the use of a few simple mathematical equations. If the size and shape approximate those of the real organ, the dose estimate should be correspondingly accurate. To minimize running time and, therefore, cost, the formulas used should be as simple as possible.

The composition of the phantom is tissue[8] of density 1 g/cm^3. There is no low density area for the lung nor is there a high density region with modified mass absorption coefficient for bone. However, for gamma energies between 0.2 and 4 MeV, the mass absorption coefficients for bone and soft tissue are essentially the same within several percent. Below 0.2 MeV the photoelectric cross section for bone rises much more rapidly than that for soft tissue. This is one of the major limitations of the present approach. The volume in cubic centimeters of most mathematical organs will be equal to the weight of an average organ in grams. This is not true for the lungs or for regions of bone. The linear dimensions of all organs including lungs and bones have been used as the primary basis for developing the mathematical equations.

In Fig. 2 is an anterior view of some of the larger organs and their positions in the phantom. In the following account, a brief description of each mathematical organ will be given followed

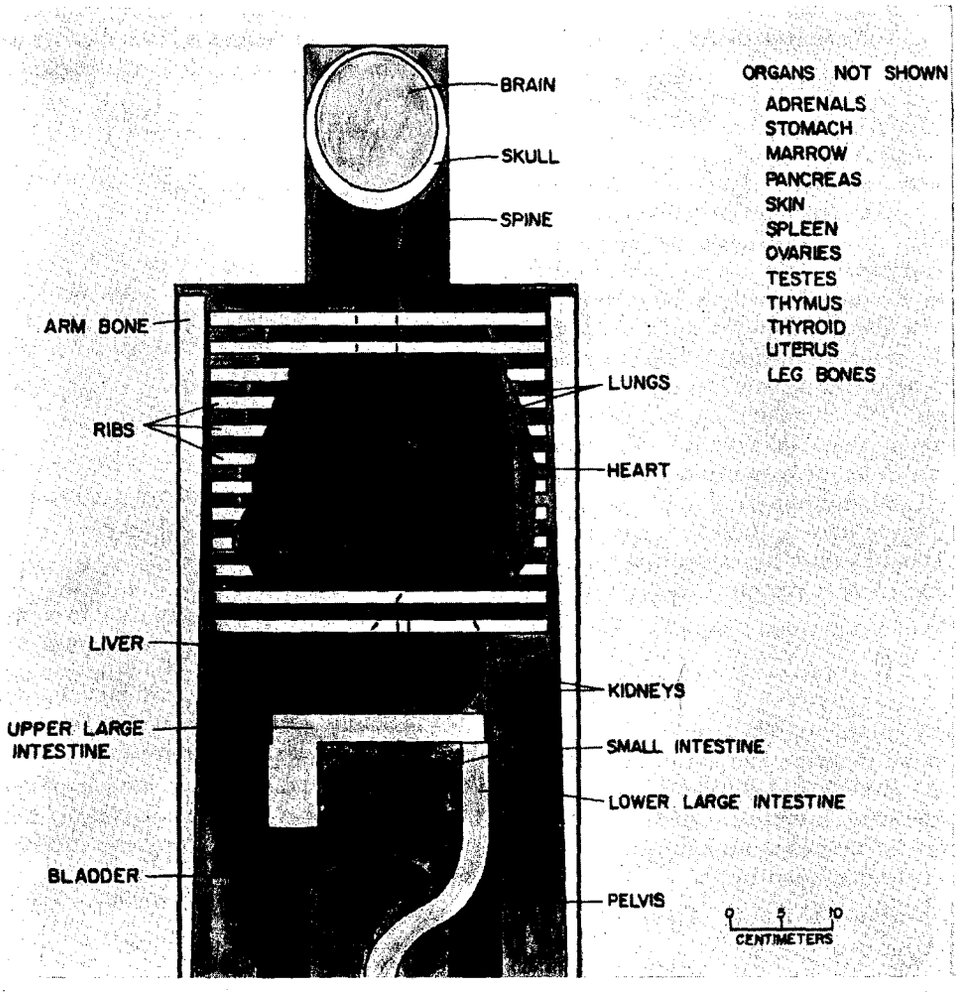

FIG. 2. Anterior view of the principal organs in the head and trunk of the phantom.

by the mathematical inequalities which must be satisfied for the point (x, y, z), in the coordinate system of Fig. 1, to be in the organ. The volumes which are given were determined by integration.

The volumes of the head, trunk, legs, and total body are 5278 cm³, 43,982 cm³, 20,776 cm³, and 70,036 cm³, respectively. When there are left and right organs, the equations for only one, the left, will be given. The equations for the other may be obtained by replacing x by $-x$ in the inequalities.

Adrenals. Each adrenal is half an ellipsoid sitting atop a kidney. The left adrenal is given by

$$\left(\frac{x-4.5}{1.5}\right)^2+\left(\frac{y-6.5}{0.5}\right)^2+\left(\frac{z-38}{5}\right)^2\leqslant 1$$

$$z\geqslant 38.$$

The volume of both adrenals is 15.71 cm³.

Bladder (urinary). The bladder plus contents when moderately full is an ellipsoid given by

$$\left(\frac{x}{6}\right)^2+\left(\frac{y+4.5}{4.5}\right)^2+\left(\frac{z-8}{4.5}\right)^2\leqslant 1.$$

The volume is 508.9 cm³.

Brain. The brain is an ellipsoid given by

$$\left(\frac{x}{6}\right)^2 + \left(\frac{y}{9}\right)^2 + \left(\frac{z - 86.5}{6.5}\right)^2 \leqslant 1.$$

The volume is 1470 cm³.

Gastrointestinal tract. The form of the gastrointestinal (GI) tract given here represents the mass of the tract itself plus the 24-hr average mass of contents. This is a particularly difficult organ to fix since its volume and location are subject to change between individuals as well as in the same individual. The intestines are taken to be in the somewhat-idealized standard positions. The stomach is the most difficult to represent since its volume will change by nearly an order of magnitude several times in 24 hr. The constant-sized and fixed-position stomach given here is, therefore, not very realistic but should suffice for estimating an approximate dose in that region. The stomach is an ellipsoid,

$$\left(\frac{x - 8}{4}\right)^2 + \left(\frac{y + 4}{3}\right)^2 + \left(\frac{z - 35}{8}\right)^2 \leq 1,$$

and has a volume of 402.1 cm³.

The small intestine has not been constructed in detail. Instead the volume occupied by the coils of the small intestine is used. This volume, which lies in the pelvic region, is a section of a circular cylinder given by

$$x^2 + (y + 3.8)^2 \leqslant (11.3)^2$$
$$-7 \leqslant y \leqslant 3$$
$$17 \leqslant z \leqslant 27.$$

Exclude large intestine volume.

The upper large intestine is simulated by two cylinders, one cylinder with its axis vertical representing the ascending colon and an elliptical cylinder with its axis horizontal representing the transverse colon. The upper large intestine is the region satisfying

1. $(x + 8.5)^2 + (y + 4.5)^2 \leqslant (2.5)^2$
   $15.4 \leqslant z \leqslant 24$

or

2. $\left(\frac{y + 4.5}{2.5}\right)^2 + \left(\frac{z - 25.5}{1.5}\right)^2 \leqslant 1$
   $-10.5 \leqq x \leqq 10.5,$

and its volume is 416.3 cm³.

The lower large intestine is composed of an elliptical cylinder and an S-shaped figure formed from half of a torus. It is the region satisfying

1. $\left(\frac{x - 9.5}{1.6}\right)^2 + \left(\frac{y + 4.3}{2}\right)^2 \leqslant 1$
   $13.4 \leqq z \leqq 24$

or

2. $0 \leqslant z \leqslant 13.4$
   $\left(\sqrt{E^2 + (z - 6.7 + 6.7\,m)^2} - 6.7\right)^2 + F^2 \leqslant (1.6)^2$

where $E = (x - 4.75)\,0.7090 - (y - 0.4252)\,0.7053$

$F = (x - 4.75)\,0.7053 + (y - 0.4252)\,0.7090$

$m = 1$ if $E \geqslant 0$

$m = -1$ if $E < 0$

and has a volume of 275.8 cm³.

Heart. The heart is half an ellipsoid caped by a hemisphere which is cut by a plane. A rotation and translation are then effected. The heart,

$$x_1 = 0.6943\,(x + 1) - 0.3237\,(y + 3) - 0.6428\,(z - 51)$$

$$y_1 = 0.4226\,(x + 1) + 0.9063\,(y + 3)$$

$$z_1 = 0.5826\,(x + 1) - 0.2717\,(y + 3) + 0.7660\,(z - 51)$$

$$\left(\frac{x_1}{8}\right)^2 + \left(\frac{y_1}{5}\right)^2 + \left(\frac{z_1}{5}\right)^2 \leqslant 1$$

$$x_1^2 + y_1^2 + z_1^2 \leqslant (5)^2 \text{ if } x_1 < 0$$

$$\frac{x_1}{3} + \frac{z_1}{5} \geqslant -1 \text{ if } x_1 < 0,$$

has a volume of 603.1 cm³.

Kidneys. Each kidney is an ellipsoid cut by a plane. The left kidney is given by

$$\left(\frac{x - 6}{4.5}\right)^2 + \left(\frac{y - 6}{1.5}\right)^2 + \left(\frac{z - 32.5}{5.5}\right)^2 \leqslant 1$$

$$x \geqslant 3.$$

The volume of both kidneys is 288.0 cm³.

Liver. The region of the liver is defined by an elliptical cylinder cut by a plane as follows:

$$\left(\frac{x}{16.5}\right)^2 + \left(\frac{y}{8}\right)^2 \leqslant 1$$

$$\frac{x}{35} + \frac{y}{45} - \frac{z}{43} \leqslant -1$$

$$27 \leqslant z \leqslant 43.$$

Its volume is 1614 cm³.

Lungs. Each lung is half an ellipsoid with a section in front removed. The defining inequalities for the left lung are

$$\left(\frac{x-8.5}{5}\right)^2 + \left(\frac{y}{7.5}\right)^2 + \left(\frac{z-43.5}{24}\right)^2 \leqslant 1$$

$$z \geqslant 43.5$$

$$\left(\frac{x-2.5}{5}\right)^2 + \left(\frac{y}{7.5}\right)^2 + \left(\frac{z-43.5}{24}\right)^2 \geqslant 1$$

if $y < 0$.

The volume of both lungs is 3378 cm³.

Ovary. Each ovary is an ellipsoid. The left ovary is given by

$$(x-6)^2 + \left(\frac{y}{0.5}\right)^2 + \left(\frac{z-15}{2}\right)^2 \leqslant 1.$$

The volume of both ovaries is 8.378 cm³.

Pancreas. The pancreas is half an ellipsoid with a section removed. It is defined by

$$\left(\frac{x}{15}\right)^2 + y^2 + \left(\frac{z-37}{3}\right)^2 \leqslant 1$$

$$x \geqslant 0$$

$$z \geqslant 37 \text{ if } x > 3$$

and has a volume of 61.07 cm³.

Skeleton. The skeleton consists of six parts—the leg bones, the arm bones, the pelvis, the spine, the skull, and the ribs. Each piece will be described separately. Each arm bone is the frustrum of an elliptical cone. The left one is defined by

$$\left(\frac{\frac{1.4}{138}(z-69) + (x-18.4)}{1.4}\right)^2 + \left(\frac{y}{2.7}\right)^2 \leqslant \left(\frac{138+(z-69)}{138}\right)$$

$$0 \leqslant z \leqslant 69.$$

The volume of both arm bones is 956.0 cm³.

The pelvis is a volume between two nonconcentric circular cylinders described by

$$x^2 + (y+3)^2 \leqslant (12)^2$$

$$x^2 + (y+3.8)^2 \geqslant (11.3)^2$$

$$y + 3 \geqslant 0$$

$$0 \leqslant z \leqslant 22$$

$$y \leqslant 5 \text{ if } z \leqslant 14.$$

Its volume is 606.1 cm³.

The spine is an elliptical cylinder given by

$$\left(\frac{x}{2}\right)^2 + \left(\frac{y-5.5}{2.5}\right)^2 \leqslant 1$$

$$22 \leqslant z \leqslant 78.5$$

and has a volume of 887.5 cm³.

The rib volume is that region between two concentric, right, vertical, elliptical cylinders. This region is sliced by a series of equispaced horizontal planes into slabs, every other slice being a rib. The statements that must be satisfied are

$$\left(\frac{x}{17}\right)^2 + \left(\frac{y}{9.8}\right)^2 \leqslant 1$$

$$\left(\frac{x}{16.5}\right)^2 + \left(\frac{y}{9.3}\right)^2 \geqslant 1$$

$$35.1 \leqslant z \leqslant 67.3$$

$$\text{Integer}\left(\frac{z-35.1}{1.4}\right) \text{ is even.}$$

The total rib volume is 694.0 cm³.

Each leg bone is the frustrum of a circular cone. The left one is

$$\left(x - 10 - \frac{8}{79.8}z\right)^2 + y^2 < \left(3.5 + \frac{2.5}{79.8}z\right)^2$$

$$-79.8 \leqq z \leqq 0.$$

The volume of both is 2799 cm³.

The skull is the volume between two nonconcentric ellipsoids defined by

$$\left(\frac{x}{6}\right)^2 + \left(\frac{y}{9}\right)^2 + \left(\frac{z-86.5}{6.5}\right)^2 \geqslant 1$$

$$\left(\frac{x}{6.8}\right)^2 + \left(\frac{y}{9.8}\right)^2 + \left(\frac{z-85.5}{8.3}\right)^2 \leqslant 1$$

and has a volume of 846.6 cm³.

Dose to the entire skeleton is determined by adding together the energies deposited in each part of the skeleton and dividing by the volume of the skeleton as follows. Let E_i be the energy in MeV deposited in region i having a volume V_i. Then the dose in rads to n such regions is

$$D_N = 1.6 \times 10^{-8} \frac{\sum_{i=1}^{n} E_i}{\sum_{i=1}^{n} V_i}.$$

The proportion of marrow in each bone of the skeleton has been given by Mechanik.[9] Using average values for this proportion, f_i, and assuming that the marrow in each region receives the average dose received by that region, the marrow dose is

$$D_N = 1.6 \times 10^{-8} \frac{\sum_{i=1}^{n} f_i E_i}{\sum_{i=1}^{n} f_i V_i}.$$

The proportions, f_i, are skull 0.2, spine 0.5, leg bones 0.4, arm bones 0.3, rib 0.4, and pelvis 0.45.

Skin. The so-called skin of the phantom was constructed to give the dose at the surface. This region is a layer about 0.2-cm thick just inside the surface of the phantom. For a point to be located in skin, it must be in one of the following six subregions:

1. $z \geqslant 93.8$
2. $70 < z < 93.8$

$$\left(\frac{x}{6.8}\right)^3 + \left(\frac{y}{9.8}\right)^2 \geqslant 1$$

3. $z \geqslant 69.8$

$$\left(\frac{x}{6.8}\right)^2 + \left(\frac{y}{9.8}\right)^2 \geqslant 1$$

4. $0 < z < 69.8$

$$\left(\frac{x}{19.8}\right)^2 + \left(\frac{y}{9.8}\right)^2 \geqslant 1$$

5. $z \leqslant -79.8$
6. $-79.8 < z \leqslant 0$

$$\left(\frac{x}{19.796}\right)^2 + \left(\frac{y}{9.799}\right)^2 \geqslant \left(\frac{98.485 + z}{98.485}\right)^2.$$

The total volume of skin is 2677 cm³.

Spleen. The spleen is defined by the ellipsoid

$$\left(\frac{x-11}{3.5}\right)^2 + \left(\frac{y-3}{2}\right)^2 + \left(\frac{z-37}{6}\right)^2 \leqslant 1$$

and has a volume of 175.9 cm³.

Testes. The left testis, an ellipsoid, is given by

$$\left(\frac{x-1.3}{1.3}\right)^2 + \left(\frac{y+2.2}{1.5}\right)^2 + \left(\frac{z+2.3}{2.3}\right)^2 \leqslant 1.$$

The volume of both testes is 37.57 cm³.

Thymus. The thymus is formed by the ellipsoid

$$\left(\frac{x+2}{3}\right)^2 + \left(\frac{y+6}{0.5}\right)^2 + \left(\frac{z-60.5}{4}\right)^2 \leqslant 1$$

and has a volume of 25.13 cm³.

Thyroid. The lobes of the thyroid lie between two concentric cylinders and are formed by a cutting surface. The inequalities for this organ are

$$x^2 + (y+6)^2 \leqslant (2.2)^2$$

$$x^2 + (y+6)^2 \geqslant (1)^2$$

$$y + 6 \leqslant 0$$

$$70 \leqslant z \leqslant 75$$

$$\Big((y+6) - 1 \times 1\Big)^2 \geqslant 2\Big(x^2 + (y \times 6)^2\Big) T^2$$

where

$$T = \frac{2(\sqrt{2}-2)}{5}(z-70) + 1$$

$$\text{for } 0 \leqslant z - 70 \leqslant \frac{5}{4}$$

$$T = \frac{2\,(2-\sqrt{2})}{15}(z-70) + \frac{2\sqrt{2}-1}{3}$$

$$\text{for } \frac{5}{4} < z - 70 \leqslant 5.$$

The volume is 19.89 cm³.

Uterus. The uterus is an ellipsoid cut by a plane and is given by

$$\left(\frac{x}{2.5}\right)^2 + \left(\frac{y+2}{5}\right)^2 + \left(\frac{z-14}{1.5}\right)^2 \leqslant 1$$

$$y \geqslant -4.5.$$

It has a volume of 66.27 cm³.

A computer code has been written which takes a point (x, y, z) and applies the tests for each organ sequentially. For points distributed uniformly in the entire phantom, a Control Data 1604 computer using this code can classify the points as to their organ location at an average rate of about 10,000 per minute.

II. A MONTE CARLO METHOD

A Monte-Carlo-type method of estimating dose was used. This method requires that the history of a photon be mathematically determined by selecting interaction sites and types of interactions in an unbiased manner. Through probabilistic rules, the energy deposition of the photon at an interaction site is recorded. After a large number of such simulated photon histories have been calculated, the average energy deposition per photon in a region is then estimated and the dose per photon may be calculated. This code is similar to the one used by Ellett, Callahan, and Brownell,[10] but the phantom used here is different. The gamma-ray attenuation coefficients for the medium were taken from Grodstein.[11]

After specifying the location of the source region, photons are randomly selected uniformly in that region. Then the direction of flight for each photon is selected randomly. The flight distance to the first interaction site is determined randomly using the cross section of the medium at the energy of the photon. After selecting a new flight direction emanating from this interaction site probabilistically from the Klein–Nishina distribution, the energy deposition at this site can be determined. The process of photon flight is now repeated but with a decreased energy. Let $n-1$, n, and $n+1$ be consecutive interaction sites for a photon. The mathematical photon is characterized by eight independent quantities—x, y, and z, the coordinates of the present interaction site; a and b, the direction cosines specifying the direction of flight to the next interaction site; L, the length of the photon's flight path to the next interaction site; E, the energy of the photon during its flight; and W, the weight of the photon during its flight. The weight of a mathematical photon takes on all values from zero to one. It is set equal to one for a photon just started from the source and is reduced after each interaction. This fictitious quantity, the weight of a photon, is introduced to obtain better statistics for a given number of source photons in an absorbing media. Suppose a photon, $P_{n-1} = P(x_{n-1}, y_{n-1}, z_{n-1}, a_{n-1}, b_{n-1}, L_{n-1}, E_{n-1}, W_{n-1})$, is in flight between points $n-1$ and n. One now desires to know the energy deposition at point n and the location of the point $n+1$ which may be found if we find P_n and use it in conjunction with P_{n-1}. The coordinates x_n, y_n, and z_n may be found by applying algebraic geometry using x_{n-1}, y_{n-1}, z_{n-1}, a_{n-1}, b_{n-1}, and L_{n-1}. The new direction of flight, a_n, and b_n, is determined by using E_{n-1} and the Klein–Nishina gamma, photon-scattering distribution. The new energy E_n is calculated from the angle of scatter which involves a_{n-1}, b_{n-1}, a_n, and b_n. Length L_n is calculated as follows:

$$L_n = \frac{-1}{\sigma(E_n)} \ln N$$

where $\sigma(E_n)$ is the attenuation cross section of the medium, and N is a random number chosen uniformly on $0 \leqslant N \leqslant 1$. The weight W_n is given by

$$W_n = W_{n-1} \frac{\sigma_c(E_n)}{\sigma(E_n)}$$

where $\sigma_c(E_n)$ is the cross section for the Compton process. The energy deposition at point n is

$$E\triangle_n = W_{n-1} \frac{\sigma_p(E_{n-1})}{\sigma(E_{n-1})} E_{n-1} + \frac{\sigma_c(E_{n-1})}{\sigma(E_{n-1})} (E_{n-1} - E_n) + \frac{\sigma_{pp}(E_{n-1})}{\sigma(E_{n-1})} (E_{n-1} - 2e)$$

where $\sigma_p(E_n)$, $\sigma_c(E_n)$, and $\sigma_{pp}(E_n)$ are the cross sections for the photoelectric, Compton, and pair production processes, respectively, and e is the rest mass of an electron in energy units. The total flight history of a photon may end in one of three ways. It may end by escaping from the phantom, or when its energy falls below 2 keV, or when its weight falls below 10^{-5}.

The uncertainty due to statistical variation from a finite sample size of source photons may be calculated. Although there may be many regions in which dose and its standard deviation are to be determined, the following account will be concerned with only one region.

Let ${}_iE\triangle_n$ be the energy deposited in the region on the nth interaction of the ith source photon. The total energy deposited by the ith photon or on the ith history to the region will be

$$iE\triangle = \sum_{n=1}^{m_i} {}_iE\triangle_n$$

where m_i is the number of interactions occurring in the ith history before termination of the photon. The average energy deposited per photon in the region is merely

$$\bar{E} = \frac{1}{M}\sum_{i=1}^{M} {}_iE\triangle$$

where M source photons were begun. Let σ be the standard deviation of $\bar{E}$. Then for the region

$$\sigma^2 = \frac{1}{M-1}\sum_{i=1}^{M} ({}_iE\triangle - \bar{E})^2.$$

Dose and its standard deviation will be proportional to $\frac{\bar{E}}{W}$ and $\frac{\sigma}{W}$ where W is the mass of the region.

Other than the obvious inaccuracies that the shape of the phantom only roughly approximates the shape of the human body and that the phantom remains in a fixed standing position and is in free space from which no backscatter occurs, there is one restriction that should be emphasized. This phantom is homogeneous throughout. There is no low density area for the lungs, nor is there a high density and modified cross sectional area for bone. To take these into account would involve a rewriting of the entire code and the use of different cross sections for these regions. These complex regions probably would increase the running time considerably. For gamma energies above 0.2 MeV, the cross sections for bone are like those for tissue within several percent. Below 0.2 MeV, bone has a much larger photoelectric cross section than that of soft tissue, and interpretation of results for these low-energy X- or gamma photons must be made with care.

III. GAMMA DOSE TO ORGANS

(a) *Whole Body Source*

A source of gamma photons uniformly distributed in the phantom was programmed for the computer. The first objective was to estimate the fraction of the emitted energy that would be absorbed in the phantom. Determination of dose to individual organs will be given later. Photons were given an initial energy E_0 and the energy they imparted in the phantom was recorded. This procedure was followed for seven different initial energies—0.02, 0.05, 0.2, 0.5, 1.0, 2.0, and 4.0 MeV. There were 1000 photons generated at each energy.

The fractional energy absorption by the total body, which is defined as the ratio of the energy emitted per photon to the average energy absorbed by the total body per photon, was determined from the Monte Carlo data. These results are given in Fig. 3. One standard deviation for our data points is less than 1.6% of the mean. An interpolating curve passing through the data points permits the estimation of the fractional

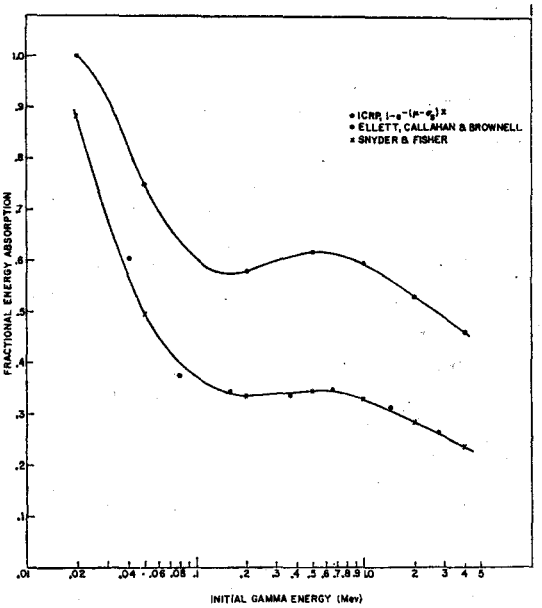

FIG. 3. Fractional gamma energy absorption by the total body.

energy absorption at other energies. A large number of gamma-emitting radionuclides produce gamma photons with energies in the range 0.1 to 1 MeV, and for such photons the total body fraction absorption is about 35%. At higher energies, the mean free path is larger, permitting a larger percentage of such photons to escape from the phantom and resulting in a lower fractional absorption. Toward lower photon energies, the photo-electric cross section rises steeply, producing an increasing fractional absorption which reaches about 90% at 0.02 MeV.

Also shown in Fig. 3 are the Monte Carlo results of Ellett, Callahan, and Brownell[12] for a source uniformly distributed in an ellipsoid. Although their phantom was an ellipsoid, its mass was nearly the same as the mass of the phantom used here, and the fractional absorptions are very similar to those predicted in this paper. The upper curve in Fig. 3 gives the fractional energy absorption predicted from the ICRP first-collision formula. In deriving this formula, three major assumptions were made. First, the organ or body is assumed to be spherical. Second, the entire organ or body burden is located at the center of the sphere. Third, a first-collision-dose calculation is then effected to obtain the formula giving the fractional energy absorption

$$AF = 1 - e^{-(\mu - \sigma_s) r}$$

where r is the radius of the sphere (effective radius),
μ is the total gamma cross section at E_0,
σ_s is the Compton scattering cross section at E_0.

It is evident from Fig. 3 that the ICRP formula gives a conservative estimate of the fractional absorption since the Monte Carlo results are seen to be about 55% of those of the ICRP method at intermediate gamma energies.

With the source again uniformly distributed in the phantom, dose to 22 organs was determined. To obtain estimates of dose to individual organs with, at most, 10% statistics required the generation of a larger number of source photons than had been generated in the first case. This was done for initial photon energies of 0.05, 0.2, 0.5, and 1.0 MeV. The number of source photons produced at each energy was 20,000, 30,000, 30,000, and 40,000 photons, respectively.

These results are presented graphically in Figs. 4–7 to permit interpolation. The source

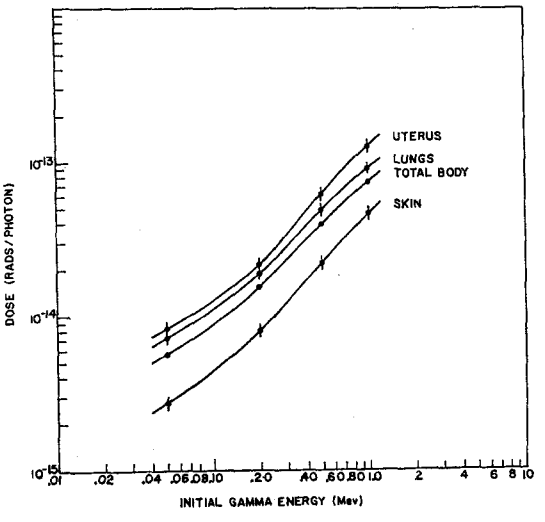

FIG. 4. Gamma dose from a source uniformly distributed in the body.

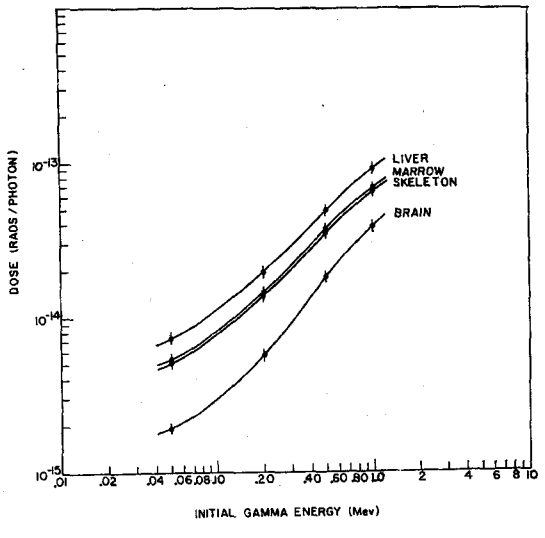

FIG. 5. Gamma dose from a source uniformly distributed in the body.

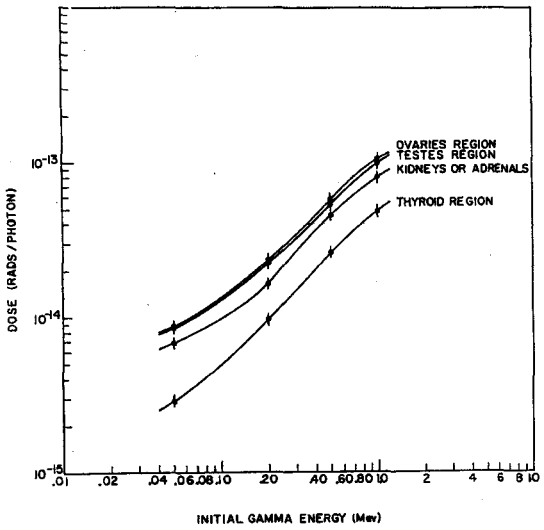

FIG. 6. Gamma dose from a source uniformly distributed in the body.

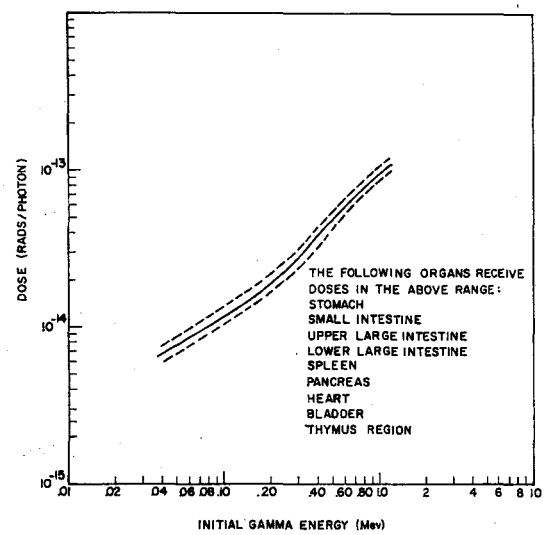

FIG. 7. Gamma dose from a source uniformly distributed in the body.

is distributed uniformly in the entire phantom, and the dose to various organs in rad/photon emitted by the source is given on the ordinate. The bars on the Monte Carlo data points represent one standard deviation on either side of the mean as estimated from the Monte Carlo calculation. When no bars are given, one sigma is less than 2%.

Organs located near the center of the phantom, such as the uterus and ovaries, receive a dose of about 1.5 times that of the total body. Most of the organs, however, receive a dose of 1.2 to 1.4 times that of the total body. Of the phantom's organs, the brain receives the lowest dose, 0.45 times that of the total body. This is followed closely by skin with 0.55 times the body average.

Even with 40,000 initial photons, some organs do not receive a sufficient number of photon collisions to determine the dose received to within 10%. This may be due to the small size of the organ or to its distance from many source photons. An alternative to producing more source photons is to increase the volume in which dose is estimated. This latter procedure was followed. When the standard deviation of dose exceeded 10%, the dose in the arbitrary region(s) (Fig. 1) encompassing the organ was taken as the best available estimate of dose received by that organ. When this procedure was necessary, these dose estimates shown in the graphs bear the name of the organ followed by the word "region".

The doses received by the group of organs listed in Fig. 7 varied little from each other. Rather than give the doses to each organ individually, the doses received by these organs will lie in the range between the dashed curves in Fig. 7.

It is possible to examine the doses received by the organs for very low-energy photons analytically, bypassing the Monte Carlo procedure. At low photon energies, the total cross section is composed almost entirely of that contributed by the photoelectric effect. In addition, the numerical value of this cross section becomes very large, resulting in a small range of the gamma photons before absorption.

If there is a homogeneous medium, infinite in extent, containing a source uniformly distributed throughout which is emitting gamma photons isotropically of energy E_0 MeV at the rate of N_0 per unit time per unit volume, then under steady-state conditions the energy emitted per unit time per unit volume will be equal to the energy absorbed per unit time per unit volume.

The dose rate in rads per unit time in any region is then

$$D = \frac{N_0 E_0}{\rho} 1.6 \times 10^{-6} \frac{\text{erg}}{\text{MeV}} \frac{\text{g rad}}{100 \text{ erg}}$$
$$= 1.6 \times 10^{-8} \frac{N_0 E_0}{\rho}$$

where ρ is the density of the medium in g/cm^3. Suppose now that instead of an infinite medium, there is a finite volume of mass W_T grams. Also, suppose that the mean range of the photon is small compared to the dimensions of the volume so that the result discussed above applies far from the surfaces in the interior with only a small error. If the source produces photons homogeneously distributed in this medium at the rate of n photons per unit time, then the normalized dose in rads/photon for any interior volume which is far from the boundary of the phantom as compared with the mean free path of the photon is

$$D_p = \frac{D}{n} = 1.6 \times 10^{-8} \frac{N_0 E_0}{n\rho} = 1.6 \times 10^{-8} \frac{E_0}{W_T}.$$

In the case of a gamma source in the total body, the dose to interior organs should asymptotically approach

$$D_p \text{ (rad/photon)} = 2.28 \times 10^{-13} E_0 \text{ (MeV)}$$

as the mean free path approaches zero. At 0.01 MeV and below, the mean free path of photons in tissue is less than 1/4 cm, and this formula should yield a more reliable result than could be obtained by Monte Carlo even with large photon sample sizes.

The above does not apply to organs located near the surface. Even in this case, however, one may obtain information as to the surface dose by examining a special case. Suppose that a medium, infinite in extent, is cut by a plane and one-half of the medium is removed. The dose rate at the newly formed surface will be one-half of the equilibrium dose rate in the infinite media by symmetry. The normalized dose at such a surface of a large finite volume is, therefore,

$$D_{ps} = 0.8 \times 10^{-8} \frac{E_0}{W_T}.$$

Although the phantom has no such plane surface, the radius of curvature of the elliptical cylinder of the trunk is large compared to the mean free path of low-energy gamma photons. An approximate surface dose for a source distributed uniformly in the total body is, therefore,

$$D_{ps} \text{ (rad/photon)} = 1.14 \times 10^{-13} E_0 \text{ (MeV)}$$
$$E_0 \leqslant 0.01 \text{ MeV}.$$

These limiting dose rates appear consistent with the Monte Carlo calculations at 0.02 MeV. The organs inside the rib cage of the trunk received doses within 10% of the predicted equilibrium dose, 4.56×10^{-15} rad/photon, while the skin of the trunk received a dose within 10% of the equilibrium surface dose.

(b) *Skeletal Source*

A source of gamma photons uniformly distributed in the skeletal region of the phantom was also simulated on the computer. This program was carried out for five gamma energies—0.2, 0.5, 1.0, 2.0, and 4.0 MeV.

The fractional energy absorption by the skeleton is given in Fig. 8. The standard deviation of the data points is less than 2.5% of the mean. Although there is some variation of the absorbed fraction from 0.2 to 1.0 MeV, as shown in Fig. 8, an approximate value of 8% could be used over this energy range with little error. The Monte Carlo estimates given here are about a factor of two lower than those given by the first-collision, effective radius method of the ICRP.

In the energy range under consideration, 0.2 to 4.0 MeV, the gamma cross sections for tissue are very similar to those for bone within several percent. Therefore, there should be little error introduced by the use of a tissue phantom, except for the fact that bone is a denser material than tissue.

The photoelectric cross section for bone rises steeply with decreasing gamma energy, and although the skeleton is not a compact organ, gamma-ray absorption will be essentially complete at 0.01 MeV and below since the mean free path of these photons will be less than 0.05 cm. In order to obtain a rough estimate for the fractional energy absorption for photons with energies between 0.01 and 0.2 MeV, the entire phantom was considered to be bone. The

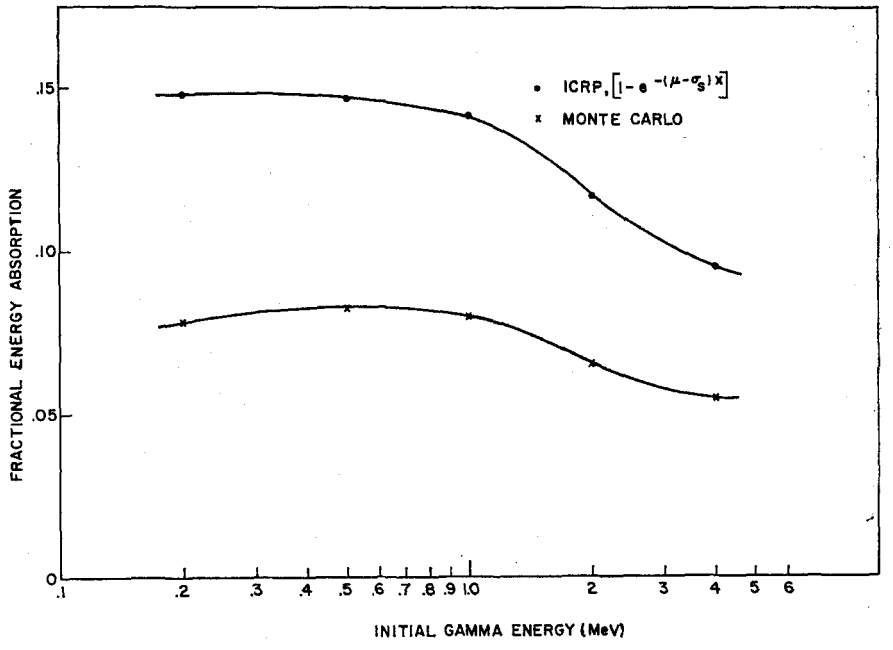

FIG. 8. Fractional gamma energy absorption by the skeleton.

material in the entire phantom was given the cross section for bone. With the source in bone, the fractional absorption should be more nearly correct for the skeleton than that obtained by using the tissue phantom. However, these results will still be lower than the true values by an undetermined amount for the following reasons. Photons that remain in the skeleton of the phantom will contribute the same amount of energy that a real photon would. However, once a photon escapes from the phantom's skeleton, it will still find itself in a strongly absorbing medium and, therefore, have a smaller probability of returning to the skeleton than a photon would have if it escaped from skeleton into tissue. A somewhat smaller estimate of the absorbed fraction for the skeleton is obtained, therefore, with the bone phantom at low energies than occurs in the actual situation. With the bone phantom, the fractional energy absorption for the skeleton was 0.81 at 0.02 MeV and 0.41 at 0.05 MeV.

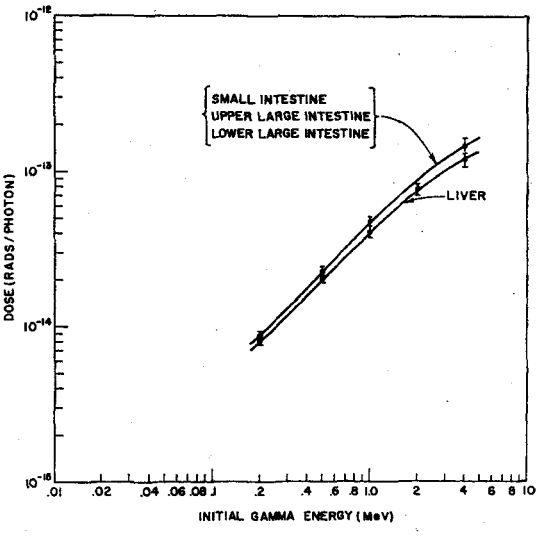

FIG. 9. Dose from a source uniformly distributed in the skeleton.

The dose rate to other organs using the skeletal source and tissue phantom and for energies between 0.2 and 4.0 MeV is given in Figs. 9–12. The notation on these graphs is the same as that described for the total body source. As expected, the skeleton was the organ with the highest dose. Marrow appears to receive a slightly greater dose than the skeleton but

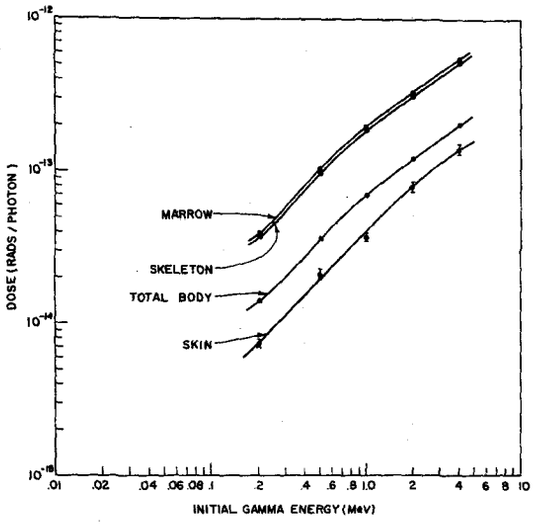

FIG. 10. Dose from a source uniformly distributed in the skeleton.

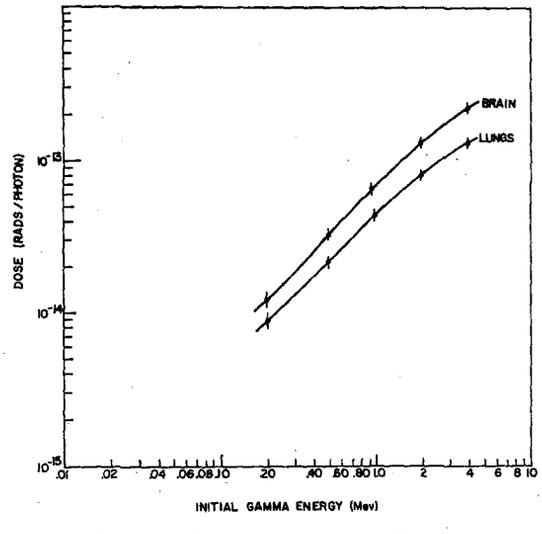

FIG. 11. Dose from a source uniformly distributed in the skeleton.

not significantly so. This is because the bones which receive the higher doses happen to contain a greater portion of the marrow. There are compensating factors which would tend to lower the marrow dose, but they are not represented in the model. Marrow is not so uniformly distributed in bone as has been assumed in the model. For a radionuclide that localizes in bone, the marrow should not contain as great a concentration as the bone. This is not the case with the model. Consideration of these factors as well as the Monte Carlo results leads one to believe that the average marrow and average skeletal gamma doses are not very different. The dose estimates to many of the organs or regions were very similar and are not shown separately. The doses received by organs listed in the group called range I in Fig. 12 received doses between the lower and middle curve in the graph. Similar remarks apply to the organs of range II.

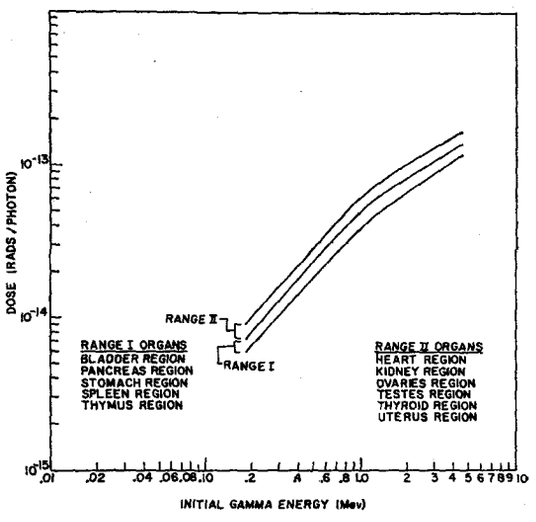

FIG. 12. Dose from a source uniformly distributed in the skeleton.

For energies below 0.01 MeV where absorption is nearly complete, the skeleton would receive a dose in rads per photon of about $1.6 \times 10^{-12} E_0$ where E_0 is the initial gamma energy in MeV. An estimate of dose to the various bones of the skeleton also was obtained from the Monte Carlo code. The part of the skeleton receiving the highest dose was the leg bone, while that receiving the lowest was rib. For energies between 0.2 and 4.0 MeV, the ratio of the dose in rad/photon of a skeletal

part to that of the entire skeleton was formed. These ratios are approximately as follows:

1.	Leg Bones/Skeleton	$\approx$	1.4
2.	Spine/Skeleton	$\approx$	1.2
3.	Pelvis/Skeleton	$\approx$	0.8
4.	Arm Bones/Skeleton	$\approx$	0.8
5.	Skull/Skeleton	$\approx$	0.6
6.	Ribs/Skeleton	$\approx$	0.5

IV. CONCLUSION

It appears that a Monte Carlo method of estimating organ doses is feasible under certain conditions. Anatomical differences such as variation of body and organ size have been neglected. Doses have been determined to fixed organ-similar regions of a homogeneous tissue phantom. This gives results that may be extrapolated to many real situations. This paper has examined the dose to organs from gamma sources located in the total body and in the skeleton, although external as well as various other internal sources may be used in conjunction with the Monte Carlo code and phantom.

V. ACKNOWLEDGEMENTS

Appreciation is expressed to A. M. Craig, G. G. Warner, and R. T. Boughner of the ORNL Mathematics Division for the programming and computer operations.

REFERENCES

1. P. L. ALTMAN and D. S. DITTMER. Growth including reproduction and morphological development. *Biological Handbook*, Fed. Am. Soc. Exptl. Biol. Washington, 1962.
2. W. M. KROGMAN. Growth of man, in *Tabulae Biologicae*, Vol. XX, pp. 712–15, ed. by H. Denzer *et al.*, Den Haag, 1941.
3. Report of ICRP Task Group on the Revision of Standard Man, in preparation.
4. R. L. HAYES and M. BRUCER. *Intern. J. Applied Rad. Isotopes* **9,** 111 (1960).
5. H. GRAY. *Anatomy of the Human Body.* Lea and Febriger, Philadelphia, 1942.
6. W. J. HAMILTON. *Textbook of Human Anatomy.* Macmillan and Co., London, 1957.
7. A. C. EYCLESHYMER and D. M. SCHOEMAKER. *A Cross-Section Anatomy.* D. Appleton-Century Co., New York, 1911.
8. *Protection Against Neutron Radiation up to* 30 *Million Electron Volts.* NBS Handbook 63, U.S. Dept. of Commerce, 1957.
9. N. MECHANIK. Untersuchungen uber des Gewicht des Knochenmarkes des Merschen. *Zeit fur anat. u. Entwicklungagesch* **79**(1) (1926).
10. W. H. ELLETT, A. B. CALLAHAN and G. L. BROWNELL. *Brit. J. Radiol.* **37**(433), 45 (1964).
11. G. W. GRODSTEIN. X-ray attenuation coefficients for 10 kev to 100 Mev. NBS Circular 583, 1957; and R. T. MCGINNIS. Supplement to NBS Circular 583, 1959.
12. W. H. ELLETT, A. B. CALLAHAN, and G. L. BROWNELL. *Brit. J. Radiol.* **38,** 541–4 (1965).

CALCULATION OF RADIATION DOSE DUE TO HIGH-ENERGY PROTONS*

HARVEL WRIGHT, E. E. BRANSTETTER, JACOB NEUFELD, J. E. TURNER and W. S. SNYDER

Health Physics Division, Oak Ridge National Laboratory,
Oak Ridge, Tennessee

Abstract—The work reported here represents some of the results obtained in a continuing program of the study of the dosimetry of high-energy protons and neutrons. Studies in high-energy proton dosimetry are of interest in assessing the potential radiation hazards for manned space flight and are also of interest for radiological protection in the vicinity of high-energy accelerators and for biological irradiation experiments.

The present calculations consider the dose deposited in tissue by protons with energies from 400 MeV to 2 GeV. Some of the results dealing with the dose due to protons with energies up to 400 MeV have been reported previously.[1,2] For proton energies below 400 MeV, the production of pions in the cascade process was not sufficiently common to be considered significant. However, in the present calculations it is necessary to take pions into account.

The basic quantity of interest in dosimetry is the absorbed dose, defined in units of the rad where 1 rad is equal to 100 ergs/gram. In order to calculate the dose equivalent, one specifies a quality factor (QF) which is often related to the values of linear energy transfer (LET) at which the energy deposition takes place. This QF–LET relationship is then used to determine the dose equivalent.

The tissue phantom is the same as used previously and has the form of a slab 30 cm thick and infinite in lateral extent. The protons are assumed to be normally incident on one surface of the tissue slab. The slab is divided into 30 sub-slabs, each of which is 1 cm thick and the dose and dose equivalent in each of the sub-slabs is calculated.

The Monte Carlo technique has been used in writing a code for the CDC-1604 computer to obtain the present estimates of absorbed dose and dose equivalent. The calculations have been simplified considerably by using a simpler model for the nuclear interactions than was used in the calculations up to 400 MeV. The straight-ahead approximation is used in this report (i.e. the nucleons emitted in the cascade process are assumed to have the same direction as the incident nucleon which initiates the cascade). The validity of the straight-ahead approximation has been considered at 400 MeV by Alsmiller *et al.*[3] and found to give good agreement with more refined methods. It is expected that the straight-ahead approximation is even better at higher energies. Much of the statistical information concerning products of the cascade such as the average number and energy distribution of emitted protons, neutrons, and pions, excitation of the residual nucleus, etc. is obtained from Metropolis *et al.* [4] The details of the calculations will be described further in Part II of this investigation. As new statistical information becomes available, it can easily be incorporated into the program. The estimates of dose equivalent are made on the basis of the QF–LET relationship endorsed by the International Commission on Radiological Protection (ICRP) for long-term occupational exposure.

The information regarding nuclear interactions that is currently available is very incomplete and it has been necessary to make several assumptions and compromises due to the lack of sufficient experimental data. Therefore, the results presented here are preliminary and are expected to be refined when new data are available. The program runs rapidly and can process 1000 incident particles in approximately 3 min on the CDC-1604 computer.

* Research sponsored by the U.S. Atomic Energy Commission under contract with Union Carbide Corporation.

DESCRIPTION OF THE CALCULATIONS

(a) *Slowing down of protons and pions*

The slowing down of protons and pions is calculated by means of the stopping power formula,[5]

$$-\frac{dE}{dx}=\frac{4\pi e^4}{mv^2}\sum_i N_i Z_i\left\{In\frac{2mv^2}{I_i(1-\beta^2)}-\beta^2\right\}. \quad (1)$$

In this expression, e and m are the electron charge and mass, respectively; v is the proton or pion velocity; $\beta = v/c$ where c is the velocity of light; N_i is the number of atoms with atomic number Z_i per cm^3; and I_i is the mean excitation energy of atoms of type i. The tissue phantom considered in these calculations is assumed to be a 30-cm thick homogeneous infinite slab composed of hydrogen, carbon, nitrogen, and oxygen in the same proportions as they occur in a standard man.[6]

Equation (1) is used to calculate the slowing down of a proton or pion until the energy reaches 1 MeV at which point the proton or pion is assumed to be absorbed locally and thus the 1 MeV of energy is deposited at that point.

(b) *Transport of particles*

An incident proton is allowed to enter and slow down through the tissue slab and a distance to a collision point is selected using geometric cross-sections for carbon, nitrogen, and oxygen and using the cross section for hydrogen given in fig. 1 of Metropolis.[4] If the distance to the point of the collision is greater than the thickness of the tissue slab, then eq. (1) is used to allow the proton to slow down until it either escapes from the tissue phantom or its energy reaches 1 MeV at which point the 1 MeV of energy is assumed to be absorbed locally. If the distance to the collision point is less than the thickness of the tissue phantom, then eq. (1) is used to allow the proton to slow down until its energy is 50 MeV or until it reaches the collision point. (It is assumed that no nuclear collisions occur for energies below 50 MeV and, therefore, if the energy reaches 50 MeV before it reaches the collision site, it is allowed to slow down to 1 MeV.) The energy of the proton at the collision point is thus determined. The type of tissue element with which the collision occurs is then determined on the basis of the relative contribution to the total cross-section that is made by each element for the energy that the particle has at the collision site.

(c) *Cascade process*

If the collision is determined to be with hydrogen, then the information given in table II of Metropolis *et al.* is used to determine whether zero, one, or two pions are produced. If one or more pions are produced, then the kinetic energy and charge of each pion is selected from information given by Melissinos *et al.*[7] and by Bugg *et al.*[8] The kinetic energy plus the rest energy of the pions is then subtracted from the energy of the incident nucleon and half of the remaining energy is assigned to each of the two nucleons. Each of these two nucleons is assumed to travel in the same direction as the incident nucleon.

If the collision is determined to be with an element other than hydrogen, fig. 5 of Metropolis *et al.* is used to determine whether zero, one, or two pions are produced. If one or more pions are produced, a charge and kinetic energy is assigned to each pion from information given in tables XI and IX of Metropolis *et al.* The information for aluminum in fig. 4 and table VIII of Metropolis *et al.* is then used to select the number of cascade protons and neutrons which result from the nuclear interaction. The kinetic energy of each of these particles is then assigned by using figs. 12 and 13 of Metropolis *et al.* Each of the nucleons thus produced are assumed to travel in the same direction as the nucleon which initiated the cascade.

(d) *Excitation of the residual nucleus*

The excitation energy of the residual nucleus is selected from fig. 14 of Metropolis *et al.* Experience with the calculations of the evaporation process[9] used in the calculations of dose due to protons and neutrons with energies up to 400 MeV[1, 2] has shown that approximately one-half of the excitation energy is absorbed in the tissue as dose with a quality factor of approximately 8. The excitation energy will be somewhat higher at higher incident energies, but it is expected that the fraction of the energy deposited will be approximately the same.

Therefore, one-half of the excitation energy is deposited locally with a quality factor of 8.

(e) *Energy deposited by pions*

Pions produced in the cascade process are treated in the following manner.[10] The π^0 decays almost immediately into two photons and is not assumed to contribute to dose. A π^- or π^+ pion is assumed to lose energy by ionization according to formula (1) until it escapes from the tissue phantom or its energy reaches 1 MeV where the remaining 1 MeV is deposited locally. The π^- is usually absorbed by a nucleus giving rise to two 70-MeV nucleons within the nucleus. One-half of the rest energy of the pion is deposited locally with a quality factor of one at the point where the π^- stops. The π^+ decays into a 4-MeV μ^+ and a neutrino. The μ^+ then decays into a positron and two neutrinos. The average energy of the positron is assumed to be 45 MeV.[11] In these preliminary calculations when a π^+ stops, 50 MeV of energy with a quality factor of 1 is deposited locally.

A history is calculated for each nucleon produced in the cascade process. The incident nucleon is absorbed in the nucleus and since its identity is then lost it is considered as one of the cascade products. Each cascade nucleon is considered to be born at the point of the collision, a flight distance to a collision site is chosen, and the process described above is followed. After the history of each of the cascade nucleons has been calculated, another incident proton is started and the process is repeated.

Dose equivalent has also been estimated. For this purpose the energy deposited in the tissue during the slowing-down process has been recorded separately for various ranges of linear energy transfer (LET). The quality factor assigned to each range of LET in this investigation is based on the recommendations of the National Committee on Radiation Protection and Measurements (NCRP) for application to cases of long-term occupational exposure.[12]

The absorbed energy in each of the chosen ranges of LET has been recorded separately and quality factors other than those used here could be substituted for the purpose of a specific application such as, for example, a manned space flight to the moon. The particular quality factors used here for the LET ranges 35 or less, 35–70, 70–230, 230–530, and 530–1750 are, respectively, 1, 1.35, 3.04, 7.15, and 11.39.

RESULTS

The calculations have been performed for protons with the five incident energies 400, 600, 1000, 1500, and 2000 MeV. For each of these energies a total of 10,000 incident protons were used and the absorbed dose and dose equivalent were calculated. The results thus obtained are presented in Figs. 1 through 5. Each of these

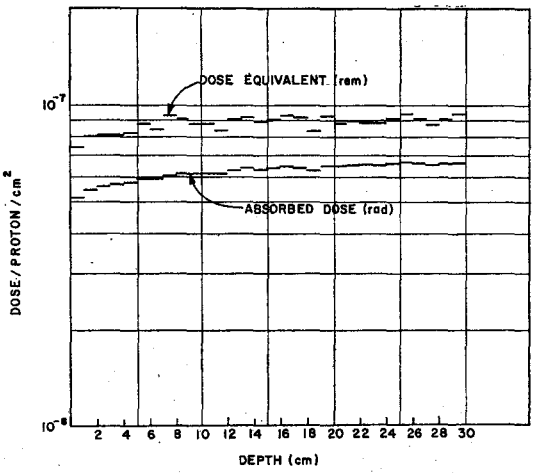

FIG. 1. Dose from 400-MeV protons incident normally on 30-cm tissue slab.

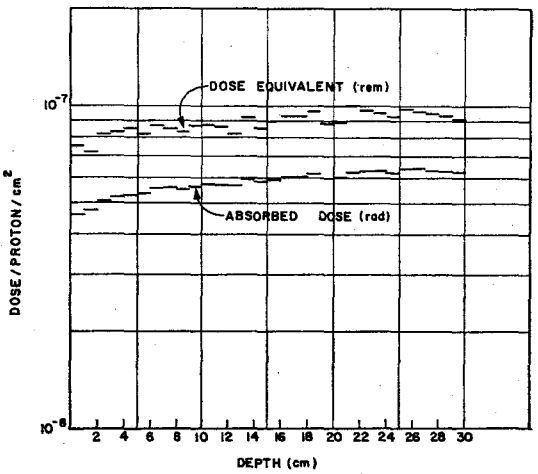

FIG. 2. Dose from 600-MeV protons incident normally on 30-cm tissue slab.

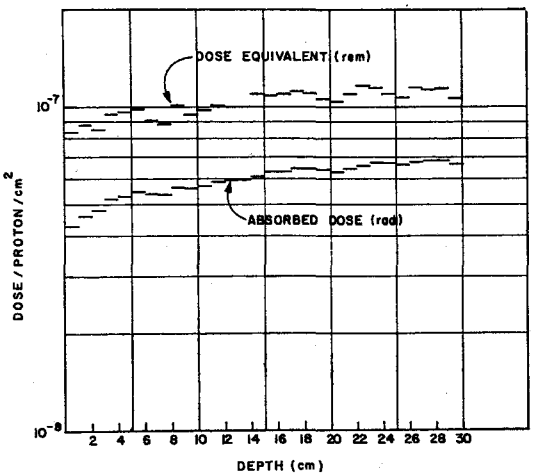

FIG. 3. Dose from 1000-MeV protons incident normally on 30-cm tissue slab.

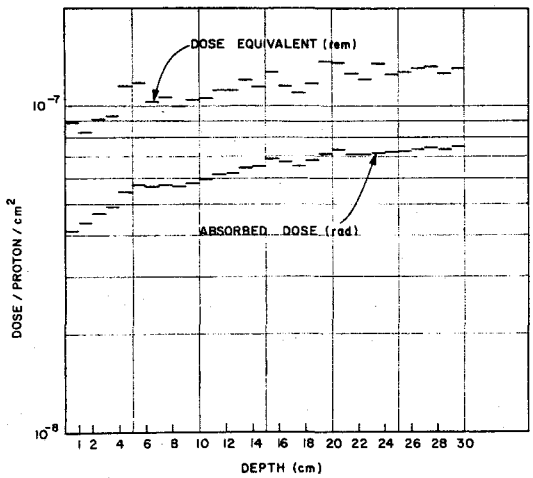

FIG. 4. Dose from 1500-MeV protons incident normally on 30-cm tissue slab.

figures shows the absorbed dose and dose equivalent plotted as a function of depth within the tissue slab.

It is noted that both absorbed dose and dose equivalent increase with depth within the tissue phantom. There is a rapid buildup of absorbed dose within the first few centimeters and then a more gradual increase throughout the remainder of the slab. The absorbed dose increases about 30% in the first 5 cm and then

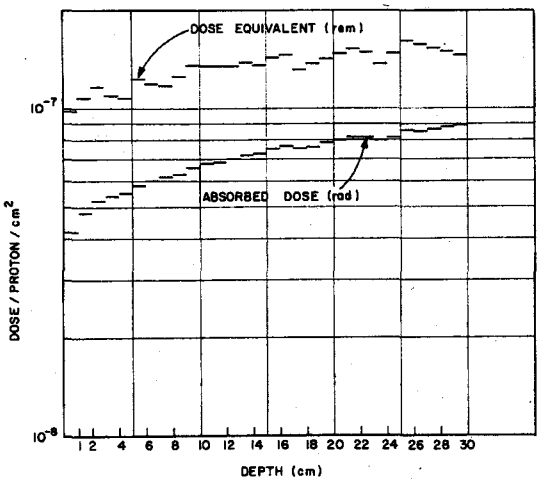

FIG. 5. Dose from 2000-MeV protons incident normally on 30-cm tissue slab.

gradually increases another 30 to 40% in the remaining 25 cm, reaching its largest value near the back of the tissue slab. The dose near the back of the tissue slab for 2000-MeV incident protons is approximately 30% more than that from 400-MeV protons. The increase in dose results from the contribution of secondary particles. The number of secondary particles given off during a cascade caused by a high-energy proton increases with the energy of the proton causing the cascade. Also, the excitation energy increases with the incident particle energy.

Figure 6 gives a breakdown of the absorbed dose for 2000-MeV incident protons into components due to ionization by primary protons, ionization by secondary protons, excitation, ionization by pions, and dose deposited by pions that stop. Near the surface the most important contribution to dose results from ionization by primary protons while near the back of the slab the most important contribution results from ionization by secondary protons. Figure 7 gives a corresponding breakdown of dose equivalent. The largest contribution to dose equivalent results from the excitation energy.

It is of interest to compare the results given here with the results given in the report of Committee IV (1953–1959) of the International Commission on Radiological Protection.[13] The

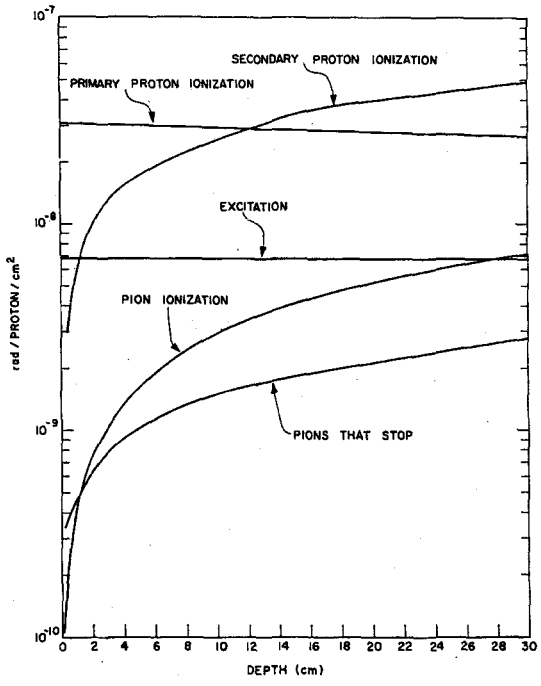

FIG. 6. Breakdown of absorbed dose into various components from 2000-MeV protons incident normally on a 30-cm tissue slab.

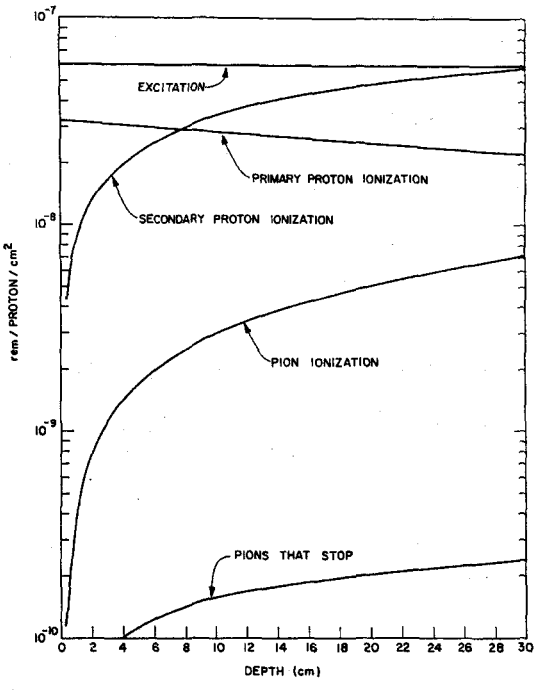

FIG. 7. Breakdown of dose equivalent into various components from 2000-MeV protons incident normally on a 30-cm tissue slab.

estimates of Committee IV, based on the work of Neary and Mulvey,[14] indicate that the dose equivalent for 1000-MeV incident protons is almost twice the value of dose equivalent for 400-MeV incident protons, whereas the results obtained here indicate an increase of only approximately 20%. However, the model used here differs substantially from that used by Neary and Mulvey. For example, Neary and Mulvey assumed the incident beam to be in equilibrium with secondaries produced as a result of passage through a shield. This would tend to result in a more rapid rate of increase of absorbed dose with increasing incident energy.

It is also of interest to compare the results obtained here with the results from the more detailed calculations that were reported by Turner *et al.*[1] It is seen by comparing fig. 13 of Turner *et al.* with Fig. 1 of this study that at 400 MeV the absorbed dose agrees within only a few percent and the dose equivalent obtained by Turner *et al.* is approximately 10 to 15% higher than that obtained here. In view of the approximation made here in this less detailed calculation the agreement is considered to be quite good.

REFERENCES

1. J. E. TURNER, C. D. ZERBY, R. L. WOODYARD, H. A. WRIGHT, W. E. KINNEY, W. S. SNYDER and J. NEUFELD. *Health Physics* **10,** 783 (1964).
2. JACOB NEUFELD, W. S. SNYDER, J. E. TURNER and HARVEL WRIGHT. *Health Physics* **12,** 227 (1966).
3. R. G. ALSMILLER, JR., D. C. IRVING, W. E. KINNEY and H. S. MORAN. *Proc. Second Symposium on Protection Against Radiations in Space,* Gatlinburg, 1964. NASA SP-71, p. 177 (1965).
4. N. METROPOLIS, K. BIVINS, M. STORM, J. M. MILLER, G. FRIEDLANDER and ANTHONY TURKEVICH. *Phys. Rev.* **110,** 204 (1958).
5. Cf. U. FANO. *Ann. Rev. Nucl. Sci.* **13,** 1 (1963).
6. Protection against neutron radiation up to 30 MeV. *National Bureau of Standards Handbook* 63, p. 8 (1957).
7. A. C. MELISSINOS, T. YAMANOUCHI, G. G. FAZIO, S. J. LINDENBAUM and L. C. L. YUAN. *Phys. Rev.* **128,** 2372 (1962).

8. D. V. Bugg, A. J. Oxley, J. A. Zoll, J. G. Rushbrooke, V. E. Barnes, J. B. Kinson, W. P. Dodd, G. A. Doran and L. Riddiford. *Phys. Rev.* **133,** B1017 (1964).
9. L. Dresner. EVAP—a Fortran program for calculating the evaporation of various particles from excited compound nuclei. Oak Ridge National Laboratory Report ORNL CF-61-12-30 (1961).
10. J. E. Turner. *Proc. USAEC First Symposium on Accelerator Radiation Dosimetry and Experience,* Conf. 651109, U.S. Dept. of Commerce, p. 346 (1965).
11. T. D. Lee and C. S. Wu. *Ann. Rev. Nucl. Sci.* **15,** 381 (1965).
12. Recommendations of the International Commission on Radiological Protection, ICRP Publication 9, p. 3. Pergamon Press, Oxford, 1966.
13. Recommendations of the International Commission on Radiological Protection. Report of Committee IV (1953–1959) on Protection against Electromagnetic Radiation above 3 MeV and Electrons, Neutrons and Protons, ICRP Publication 4, p. 3. Pergamon Press, Oxford, 1964.
14. G. J. Neary and J. Mulvey. Maximum Permissible fluxes of High-Energy Neutrons and Protons in the Range 40 to 100 MeV, Report of the Medical Research Council, Radiological Research Unit, AERE, Harwell, 1957, unpublished.

BERECHNUNG DER TIEFENDOSISVERTEILUNG VON BETA-STRAHLEN

A. WENSEL und S. WITTIG
Institut für Kernphysik der Universität, Frankfurt/Main (F.D.R.)

Zusammenfassung—Mit einem Monte-Carlo-Verfahren wurde die Tiefendosisverteilung von Elektronen im Gewebe untersucht. Die Elektronenbahnen wurden mit Hilfe der Vielfachstreutheorie berechnet. Besonderer Wert wurde auf die Behandlung des Stragglings beim Energieverlust durch Ionisation gelegt. Das Verfahren berücksichtigt auch Bremsstrahlungsverluste.

Aus der Energieabgabe der Elektronen längs ihrer Bahnen im Gewebe lässt sich die Dosis in Abhängigkeit von der Eindringtiefe ermitteln.

Die Rechnungen wurden sowohl für monoenergetische Elektronen mit verschiedenen Anfangsenergien und Einfallsrichtungen durchgeführt als auch für β-Spektren von einigen häufig benutzten Radio-Isotopen. Die Dosisverteilungen im letztgenannten Fall wurden für verschiedene Geometrien der Quelle und des absorbierenden Materials bestimmt. Die Energiespektren von β-Strahlen beim Durchgang durch Gewebe werden angegeben. Die Ergebnisse werden mit Messungen und Theorien verschiedener Autoren verglichen.

Bei der Berechnung von β-Dosen für Strahlenschutzzwecke wird im allgemeinen die mittlere Energie des β-Spektrums zugrunde gelegt. Die Berechtigung dieser Annahme wird für eine spezielle geometrische Anordnung diskutiert.

DISCUSSION

D. NACHTIGALL (*Euratom*):

Haben sie bei ihren Berechnungen Spallationsprozesse in Rechnung gesetzt und wie kann, in diesen Fällen, bei denen in sehr kleinen Volumina sehr viel Energie freigesetzt wird, das LET-Konzept angewendet werden?

J. NEUFELD:

We have not taken into account spallation processes. Dr. Nachtigall brought out the question whether in some interaction the concept of LET loses its significance and this would be the approach which will be considered. So we should consider spallation processes and also the recoil of heavy ions, like nitrogen, oxygen, and carbon, which produce a total destruction of a cell. We have the case described by Tobias as "spikes". We have not taken these into consideration. They may be of some account at higher energies; for the time being we have not taken them into consideration. We have not taken into consideration also the non-ionizing collisions which are due to the recoil of these heavy ions which cause directly molecular destructions. This tissue destruction does not pass through the process of ionization and excitation.

G. JOYET (*Switzerland*):

Vos calculs très importants et actuellement très utiles sont basés sur une composition homogène de l'organisme en H, C, N et O. N'estimez-vous pas nécessaire de considérer également à l'avenir une composition atomique différentiée de certains tissus ou organes critiques comme les ovaires, les testicules, les os, la moelle et le cristallin?

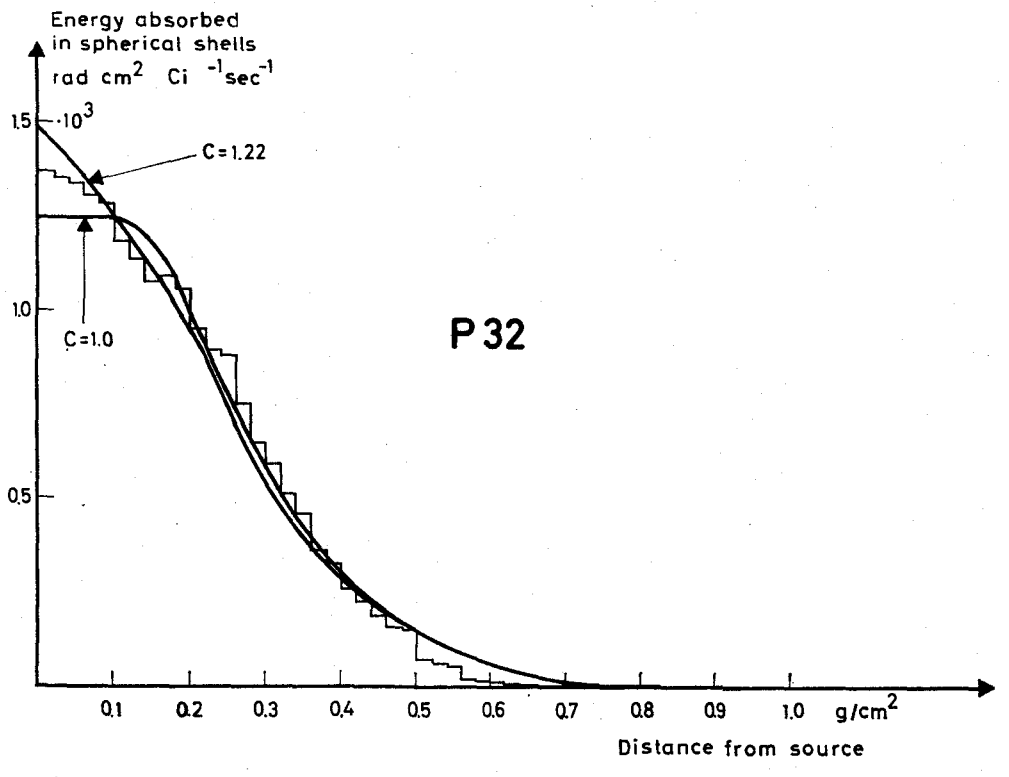

Absorbierte Energie in konzentrischen Kugelschalen um eine isotrope Punktquelle von P 32 in weichem Gewebe. Das Histogramm stellt die Ergebnisse der Monte-Carlo-Rechnung dar (2000 Elektronen). Die ausgezogenen Linien geben die Lövingersche Theorie wieder.

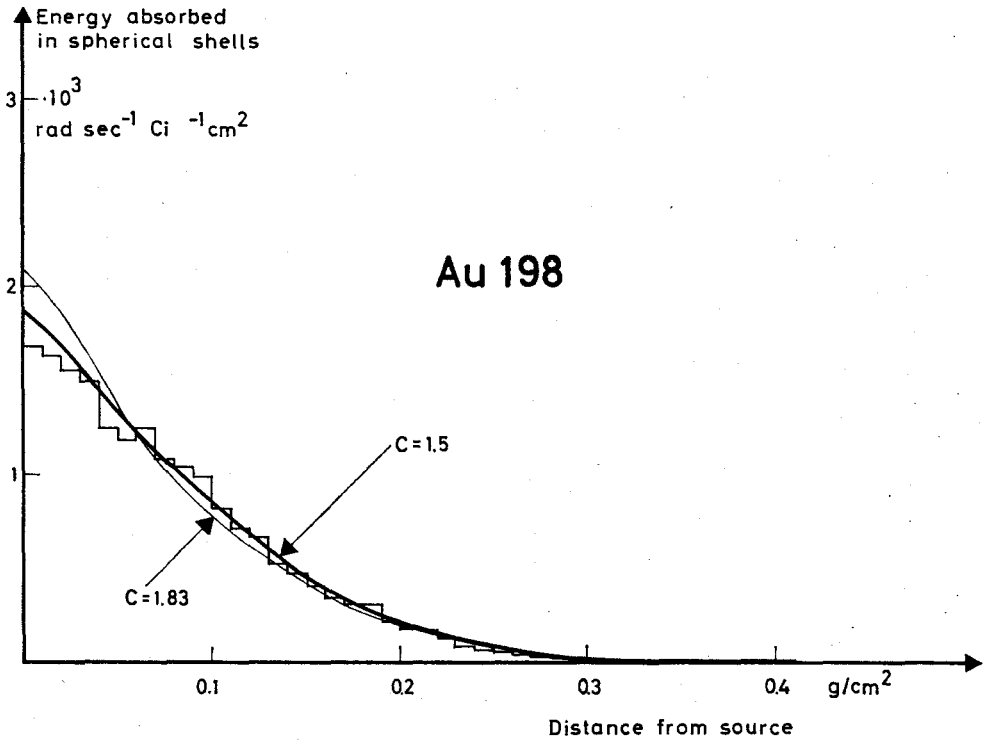

Absorbierte Energie in konzentrischen Kugelschalen um eine isotrope Punktquelle von Au 198 in weichem Gewebe. Das Histogramm stellt die Ergebnisse der Monte-Carlo-Rechnung dar (1000 Elektronen). Die ausgezogenen Linien geben die Lövingersche Theorie wieder.

J. NEUFELD:

Our program includes this study. We will take into account both different compositions of different elements in various organs and also, what is important, the position of the most sensitive organs, for instance the eye, and the calculations are in progress at the present time.

W. A. LANGMEAD (*U.K.*):

I should be glad if Dr. Wensel could indicate how his results compare with those of other authors, notably Dr. Bob Loevinger.

A. WENSEL (*Germany*):

Die Übereinstimmung der mit der Monte Carlo Methode berechneten Tiefendosisverteilung mit den Ergebnissen der Theorie von Lövinger ist sehr gut. Die Rechnungen wurden für P^{32} und Au^{198} durchgeführt und die Ergebnisse in den beiden folgenden Abbildungen zusammengestellt; c ist einer der empirischen Faktoren der Lövingerschen Theorie, für den in der Literatur unterschiedliche Werte für Gewebe angegeben sind.

P. N. KRISHNAMOORTHY (*India*):

In the abstract of his paper Dr. Wensel refers to the average energy of β-spectra used in health physics calculations. Would he care to make any remarks on the subject?

A. WENSEL (*Germany*):

Das bezieht sich darauf, dass bei der Lövingerschen Theorie eine mittlere Energie verwendet wird und die Form des Betaspektrums nicht berücksichtigt ist. Das Ergebnis unserer Arbeit geht dahin, dass trotz dieser sehr vereinfachenden Annahmen die Betadosistiefenverteilung durch die Lövingersche Theorie sehr gut wiedergegeben wird.

P. N. KRISHNAMOORTHY (*India*):

We have made detailed computations on the average energies of β-spectra, particularly the forbidden spectra. We have found that, depending on the order of forbiddenness, the average energies vary significantly from the average energy values currently in use.

DECONTAMINATION OF FISSION PRODUCTS ON HUMAN SKIN AND HAIR

YASUSHI NISHIWAKI and HAJIME NISHIOKA
Department of Radiation Protection and Health Physics,
Research Laboratory of Nuclear Reactor,
Tokyo Institute of Technology, Tokyo, Japan

Abstract—The contamination and decontamination of human skin and hair may be influenced not only by the colloidal adsorption on the surface or absorption of radioactive substances into human tissue, but also by various physical, chemical and biological factors which make a reproducible decontamination experiment difficult. Therefore, in order to compare the efficiencies of various decontaminating agents we have employed a special device with which the conditions of decontamination could be kept more or less constant.

In these experiments, water, citric acid and the powerful chelating agents EDTA and DTPA were used for the purpose of decontamination of fission-products on a non-living, human skin sample and on hair. The decontaminated percentage (D_t), expressed in total gross activities, and the change of the decontaminated radioactivities per unit volume of eluting solution were measured.

Judged on the basis of the decontaminated percentage (D_t), the chelating agents were similarly effective in decontaminating the samples of human skin as with those of human hair. The radioactivities rapidly removed in the initial eluting solution seemed to indicate that there was a component that can be easily decontaminated with the chelating agents.

The persistently remaining activity appearing in the eluting solution after elution with 300–400 ml seemed to indicate that some of the strongly fixed or reacted component might have been gradually eluted out with the chelating agents. The decontaminated percentage (D_n) of each nuclide as estimated by the analysis of the γ-spectrum is given to show an order of magnitude.

The similarity in the mode of decontamination between the samples of human skin and those of hair may indicate, at least partly, the possibility of the existence of a competing effect of chelating agents against some of the reactions between metals in fission-products and proteins, for instance, keratin, collagen and so on which exist commonly in both samples.

Although it is anticipated that the use of chelating agents may enhance the absorption of some radioactive nuclides through the skin, if the solution containing the chelating agents were used for the decontamination of skin and hair in the form of a shower or by running water over the contaminated skin or hair to minimize the skin absorption, it may be extremely useful in some cases.

INTRODUCTION

With the increasing use of radioactive materials, the chances of radioactive contamination of the human body through the direct contact of the skin and the hair with radioactive substances may also increase. Since George *et al.*[1] reported the radioautographic studies on Pu-contaminated pig skin in 1956 and Khodyreva *et al.*[2] studied the internal permeability and transport into blood of Ra deposited on rabbit skin in 1959, many workers have studied radioactive contamination of the skin. As examples of using human skin as the experimental material, there have been such studies as the theoretical analysis of the behavior of Pu on the skin of the hand by Lister *et al.*[3] in 1963, the research on internal permeation of ^{22}Na and ^{131}I by Van Dilla *et al.*[4] in 1961, and the experiment of permeability of ^{90}Sr by Il'in[5] in 1960, and so on.[6-15]

These studies on skin contamination by various authors have been made with special attention to permeability or absorption of the radioactive ion into skin tissue. Therefore, it is natural that the studies of decontamination have also been done in relation to the skin permeability of the radioactive ion, for instance, as a function of the depth below the skin surface.

On the other hand, it has been observed that some of the biochemical substances existing in skin tissue, keratin or collagen, etc. may easily form a stable compound with metal ions.[16, 17] Therefore, it seems likely that the mechanism of contamination by radioactive metals on skin surface may be influenced not only by the phenomena of absorption or permeation of radioactive substances into tissue, but also by the colloidal adsorption and some reaction of the contaminant with the local tissue. In developing the method of decontamination of skin, we may have to take into consideration such a possibility.

In case of the contamination and decontamination of hair, there have been not so many studies in the past. However, this is an important problem, in view of the relatively large frequency of hair contamination. In this case also, the possible reaction between the radioactive contaminant and the biochemical substances in the hair such as protein, etc., may play an important role.

Judging from these points of views, it may be an effective decontamination method to use powerful chelating agents[18, 19] which have comparatively high abilities of chelate formation with a metal ion and compete with the conjugation between radioactive ions and protein, etc.

This study, although it is in a preliminary stage, was undertaken to estimate the chemical or biochemical significance of chelating agents at the time of decontamination of human skin and hair. With these purposes in mind, some chelating agents, citric acid, EDTA and DTPA which have various stability constants, were used for this decontamination experiment.

MATERIAL AND METHOD

1. *Human Skin Sample*

Sample materials used in this experiment were the human skin supplied by the Tokyo Metropolitan Medical Examiner's Office. The skin of size about 3 × 15 cm with subcutaneous fat was cut from the central part of the breast of a Japanese adult at about 10 hr after accidental death. At about 1 hr after sampling, the fat was removed and the skin was cut into squares, 3 × 3 cm. No pathological change was observed macroscopically at this stage. The skin sample was spread on a glass plate (4 × 4 cm) and fixed at four corners by Scotch tape, the back side of the skin facing the glass plate. As pretreatment, the skin surface, after having been slightly wiped with absorbent cotton soaked in 0.01 wt% DBS (dodecyl benzene sulfonate) solution, was cleaned several times with absorbent cotton soaked in water and then the excess moisture was absorbed off lightly by blotting with filter paper. The skin sample was contaminated with fission products solution (adjusted to pH 6.8 about 100 days after production) by micropipette and dried for one hour at room temperature. Gross activities T_0 of the contaminated samples were measured prior to decontamination by GM counter (SA-230, Kobe Kogyo). After the contaminated samples were

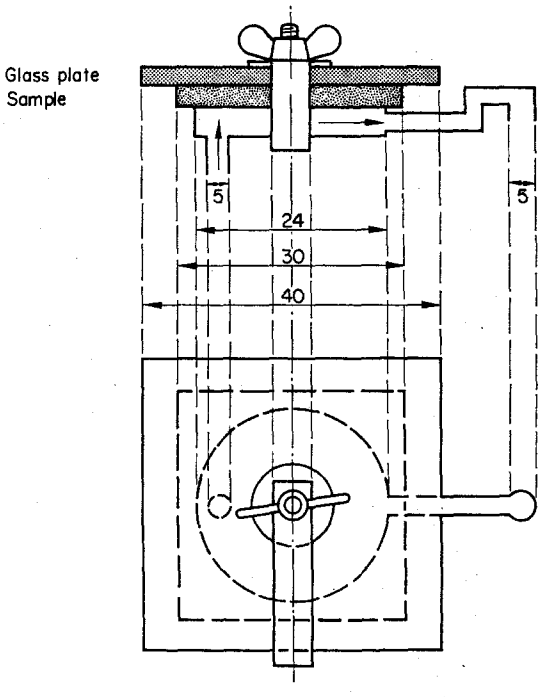

FIG. 1. Experimental apparatus for decontamination of fission products on human skin (mm).

set in the experimental apparatus as shown in Fig. 1, the skin was decontaminated by flowing water, citric acid, EDTA or DTPA solution (0.01 m/l.)[20, 21] at the rate of 6 ml/min, and 1 ml of the eluting solution was collected successively at intervals into sample cells. The radioactivities of these samples after drying on a hot plate were measured by use of a 2π gas flow, low background GM counter (SC-5, Aloka). The temperature of the flowing solution was about 20°C. After having flowed a total volume of 1 l. of decontaminating water or the solutions, these sample materials were taken out from the apparatus. After drying the sample, the gross activities T_1 of the sample after decontamination were measured. The γ-ray spectra of these contaminated samples were also taken before and after decontamination with a 256 channel pulse height analyser. For this analysis a NaI (Tl) crystal of diameter 3 in. and length 3 in. was used. The distance between samples and detector was about 5 mm.

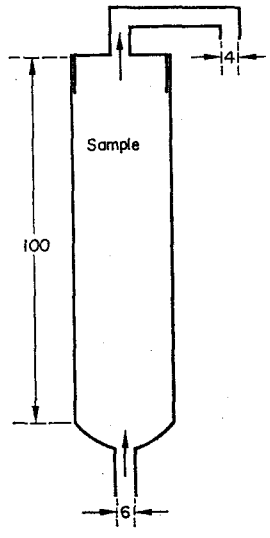

FIG. 2. Experimental apparatus for decontamination of fission products on hair (mm).

2. *Human Hair Sample*

Sample materials used were hair of several Japanese men 18–22 years old which were collected at a barber shop. They had a diameter of about 0.1–0.2 mm and length about 8–15 cm. As pretreatment, the samples were immersed and stirred in 0.01 wt% DBS solution for 30 min in order to remove the adsorbed dust, organic substances, etc. After washing with 5 l. of water, the samples were dried at room temperature on filter paper for about 2 hr. Then, 4 g of these sample materials were put in a gauze bag of diameter about 2.5 cm and length about 10 cm. These bags, containing 4 g, were immersed in the solution of fission products in the same way as in experiment 1, so that the solution contacted the sample hair homogeneously. After having been taken out from the solution of fission products, these samples were dried for 4 hr at room temperature on filter paper. After measuring the gross activities T_0 of the contaminated samples prior to decontamination, they were set in a cylindrical column made of glass as shown in Fig. 2. The contaminated samples were decontaminated by flowing water and decontaminating solution through the column and the radioactivity eluted into water or into the solution of citric acid, EDTA or DTPA was measured as in experiment 1. After measuring the gross activities T_1 of the sample after decontamination, the samples in the bag were transferred into the tube made by polystyrol with the same size as the column and the γ-ray spectrum was taken. When measuring the γ-ray spectrum, the detector was placed as close to the side of the polystyrol tube as possible.

RESULTS

From the gross activities T_0 and T_1, decontaminated per cents, D_t, of the samples of human skin and hair were calculated. The results are shown in Table 1. D_t was calculated by the following equation.

$$D_t = \left(1 - \frac{T_1}{T_0}\right) \times 100$$

Figure 3 for human skin and Fig. 4 for hair show the relation of the gross activity cpm/ml and the volume of the eluting solution. One ml was sampled at the beginning of the elution and thereafter 1 ml every 10 ml of elution up to the initial 100 ml; from 100 ml to 500 ml of elution, 1 ml every 20 ml; from 500 to 1000 ml of elution, 1 ml every 50 ml; Each aliquot of the sampled solution was measured for gross activity. In Fig. 5 for human skin and in Fig. 6 for hair,

Table 1. Gross Activities of Fission Products before and after decontamination of Contaminated Human Skin and Hair and Decontaminated Percentage (D_t)

	Decontamination agents	Before decontamination T_0 (cpm)	After decontamination T_1 (cpm)	Decontaminated percentage D_t $\left(1-\frac{T_1}{T_0}\right)\times 100$
Skin	Water	8.36×10^3	7.96×10^3	5
	Citric acid	7.96×10^3	5.14×10^3	35
	EDTA	8.60×10^3	2.91×10^3	66
	DTPA	8.94×10^3	3.67×10^3	59
Hair	Water	1.22×10^4	1.18×10^4	3
	Citric acid	1.08×10^4	6.50×10^3	40
	EDTA	1.14×10^4	3.95×10^3	74
	DTPA	1.22×10^4	4.25×10^3	65

γ-ray spectra of the contaminated sample prior to decontamination and that of the samples after decontamination by water, citric acid, EDTA or DTPA solution are shown as an example. The data concerning the possible radionuclides corresponding to the clear peaks in these spectra are shown in Table 2. The possible corresponding nuclides are ^{141}Ce, ^{144}Ce, ^{103}Ru, ^{95}Zr, ^{95}Nb, ^{91}Y and ^{140}La as listed in Table 2.

The peak area of each corresponding nuclide

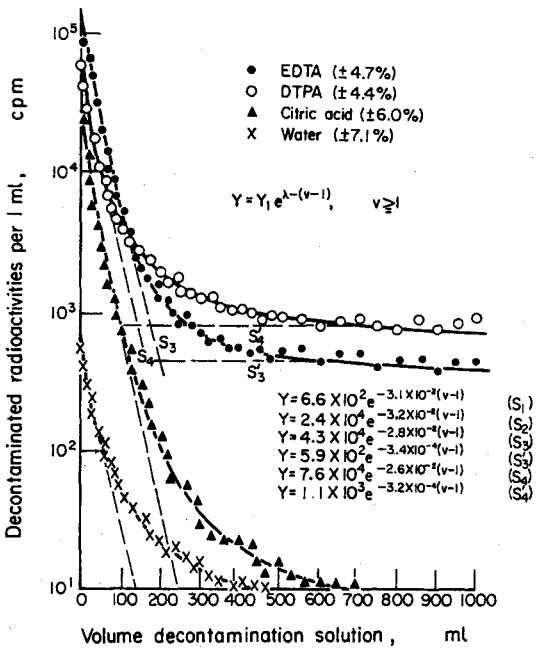

FIG. 3. Decontamination rate of fission products on human skin.

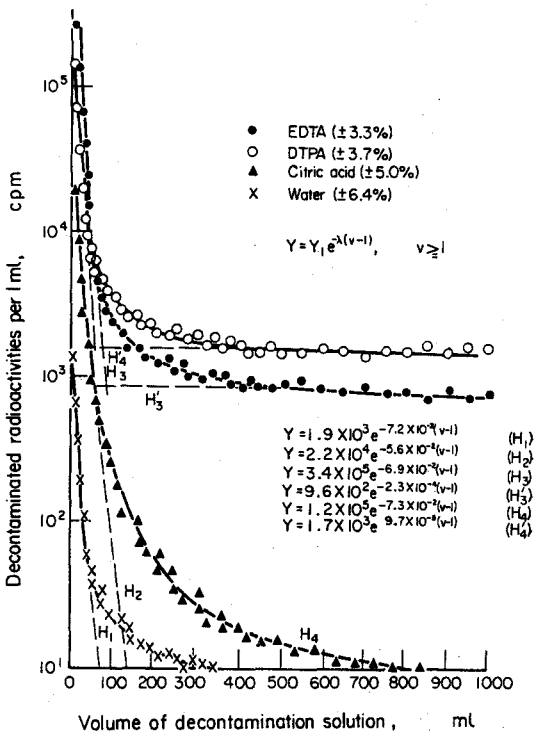

FIG. 4. Decontamination rate of fission products on hair.

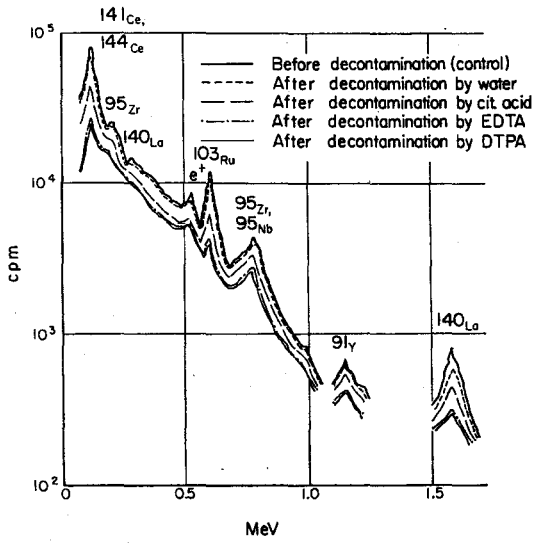

FIG. 5. γ-ray spectra before and after decontamination of skin contaminated with fission products.

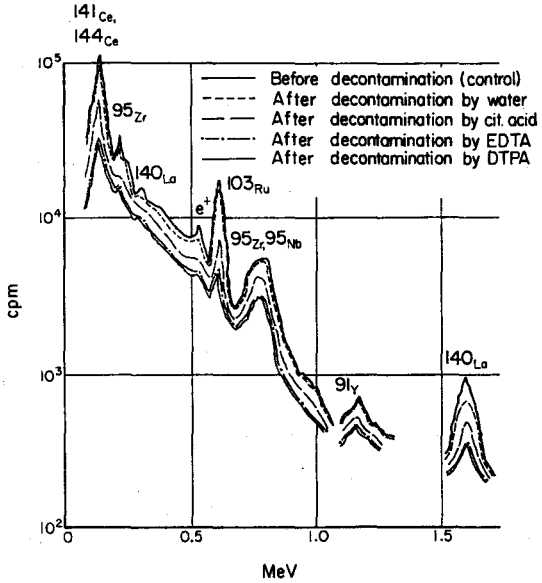

FIG. 6. γ-ray spectra before and after decontamination of hair contaminated with fission products.

was obtained by Covell's method,[232] and the decontaminated percentage D_n of each nuclide calculated from the peak area count N_0 and N_1 are shown in Table 3[23] for human skin and in Table 4 for hair. D_n was calculated as follows,

$$D_n = \left(1 - \frac{N_1}{N_0}\right) \times 100$$

where N_0 is the activity of the contaminated sample prior to decontamination and N_1 that of the sample after decontamination.

DISCUSSION

For the effective decontamination of the radioactive contamination on human skin and hair,

Table 2. γ-Spectrum Assaying Data for Fission Products used in these Experiments

Spectrum peak (MeV)	Corresponding nuclide	γ-ray energy (MeV)	Abundance in fission products at 150 days[22]	Traced peak
0.13	^{144}Ce ^{141}Ce	0.134 0.145	0.97 0.45	O
0.22	^{95}Zr	0.235	1.55	
0.33	^{140}La	0.328	f	
0.51	e^+	0.51		
0.62	^{103}Ru	0.61	0.55	O
0.75	^{95}Zr ^{95}Nb	0.725 0.75 0.768	1.55 2.40	O
1.15	^{91}Y	1.19	1.25	O
1.61	^{140}La	1.60	f	O

f: a trace amount.

Table 3. Decontaminated Percentage of Each Traced Nuclide in Fission Products on Skin

Traced nuclide	Decontamination agents	Decontaminated percentage D_n* $\left(1+\frac{N_1}{N_0}\right)\times 100$
^{141}Ce, ^{144}Ce	Water	2
	Citric acid	28
	EDTA	47
	DTPA	48
^{103}Ru	Water	10
	Citric acid	34
	EDTA	46
	DTPA	46
^{95}Zr, ^{95}Nb	Water	4
	Citric acid	22
	EDTA	45
	DTPA	39
^{91}Y	Water	5
	Citric acid	25
	EDTA	52
	DTPA	44
^{104}La	Water	24
	Citric acid	40
	EDTA	57
	DTPA	60

* These figures should be interpreted to show only an order of magnitude estimate, because of the difficulty of exactly reproducible experiments.

it may be necessary to clarify the contamination mechanism on these surfaces.

In the actual contamination of mixed fission products it is very difficult to understand the mechanism because of the multiple complex factors involved in contamination and reproducible experiments are usually very difficult. Therefore, in order to compare the efficiences of various decontaminating agents we have employed a special device so that the conditions of decontamination could be kept more or less constant, as shown in Figs. 1 and 2.

Judging from our experimental results, the percentage of free contamination that can be removed easily even by water alone seems to be quite large. Therefore, in our cases of the contamination of biological surfaces, the percentage of fixed or reacted contamination appeared to be relatively small, although there may be some biologically reactive substances included in the skin tissues. However, depending upon the mode of contamination and the physical-chemical state of the contaminant, the reacted contamination may not be considered negligible. Especially, in case of heavy contamination, even though the percentage of the fixed or reacted contamination is small, the residual fixed contamination that cannot be easily

Table 4. Decontaminated Percentage of Each Traced Nuclide in Fission Products on Hair

Traced nuclide	Decontamination agents	Decontaminated percentage D_n* $\left(1+\frac{N_1}{N_0}\right)\times 100$
^{141}Ce, ^{144}Ce	Water	4
	Citric acid	31
	EDTA	45
	DTPA	52
^{103}Ru	Water	9
	Citric acid	35
	EDTA	51
	DTPA	52
^{65}Zr, ^{95}Nb	Water	1
	Citric acid	24
	EDTA	43
	DTPA	42
^{91}Y	Water	2
	Citric acid	26
	EDTA	53
	DTPA	46
^{103}La	Water	26
	Citric acid	46
	EDTA	55
	DTPA	59

* These figures should be interpreted to show only an order of magnitude estimate, because of the difficulty of exactly reproducible experiments.

removed by water alone may play an important role.

In these experiments, a fission product mixture, which is one of the most important contaminants at the time of a reactor accident, was used. On the other hand, as the materials to be contaminated, human skin and hair were used.

Table 1 shows the gross activity of the fission product mixture on human skin and hair before and after decontamination as well as the decontamination percentage. As can be seen in Table 1 the difference of decontamination effect between water, citric acid and the strong chelating agents (EDTA, DTPA) was clearly observed. The highest decontamination effect was observed with EDTA and DTPA and the lowest with water alone. Citric acid showed an intermediate efficiency. These tendencies were observed both for human skin and human hair. These differences in the decontamination efficiency may be ascribed to the difference in the stability constant of the decontaminating agents with some of the metal ions in the fission product mixture. The strong chelating agents such as EDTA and DTPA with a high stability constant may remove some of the metal ions of the fission products competitively from some of the

less reactive biological substances with a smaller stability constant included in the skin and hair tissues. The eluted radioactivity per unit volume of elution as a function of the volume of eluting decontamination solution is shown in Fig. 3 for human skin and in Fig. 4 for human hair on a semi-logarithmic scale. Although these experiments were conducted at the elution rate of 6 ml/min and at room temperature (about 20°C), it is very likely that the results may be influenced by the flow rate and the composition of the decontaminating solutions, the temperature at the time of decontamination and other various physical, chemical and biological factors which may affect the state of contamination. As can be seen in these figures, tangent lines were drawn along the linear part of the decontamination rate curves on the semi-logarithmic plot. These lines are designated as S_1, S_2, S_3, S_3', S_4 and S_4' in case of human skin and by H_1, H_2, H_3, H_3', H_4, and H_4' in case of human hair. They may be approximately expressed by the following empirical formula,

$$Y = Y_1 e^{-\lambda(v-1)}, \qquad (v \geq 1)$$

where Y is the decontaminated activity per unit volume (1 ml) of decontaminating solution, Y_1 the initial decontaminated activity into the initial unit volume (1 ml) of decontaminating solution, v the volume of eluting decontamination solution expressed in ml, and λ the decontamination constant.

The values of the initial decontaminated activity Y_1 and the decontamination constant λ are listed in Table 5. As can be seen in the table, the values of the decontamination rate constant λ for the initial part of the decontamination are almost the same. They are roughly about 0.03 in the case of human skin and about 0.06–0.07 in the case of human hair under the conditions of our experiment. However, considerable differences were observed in the initial decontaminated activity Y_1 for water alone and for the different chelating agents. In the case of human skin, the decontamination rate constant λ after about 300 ml of elution with EDTA and DTPA is observed to decrease down to about 1/100 as compared with the initial part, while in the case of human hair the value of λ after about 200 ml of elution with EDTA and DTPA decreases down to about 1/300–1/700. Although the initial decontaminated activity is much higher with citric acid than with water alone, the overall shapes of the decontamination rate curves are similar for both citric acid and water alone, and are quite different from those of EDTA and DTPA. In case of citric acid and water alone, the decontaminated radioactivity

Table 5. The Values of the Initial Decontaminated Activity Y_1 and the Decontamination Constant λ ($Y = Y_1 e^{-\lambda(v-1)}$).

Samples	Decontamination agents	Y_1	λ
Human skin	Water (S_1)	6.6×10^2	3.1×10^{-2}
	Citric acid (S_2)	2.4×10^4	3.2×10^{-2}
	EDTA (S_3)	4.3×10^4	2.8×10^{-2}
	(S_3')	5.9×10^2	3.4×10^{-4}
	DTPA (S_4)	7.6×10^4	2.6×10^{-2}
	(S_4')	1.1×10^3	3.2×10^{-4}
Human hair	Water (H_1)	1.9×10^3	7.2×10^{-2}
	Citric acid (H_2)	2.2×10^4	5.6×10^{-2}
	EDTA (H_3)	3.4×10^5	6.9×10^{-3}
	(H_3')	9.6×10^2	2.3×10^{-4}
	DTPA (H_4)	1.2×10^5	7.3×10^{-3}
	(H_4')	1.7×10^3	9.7×10^{-5}

per unit volume of elution decreased down close to the natural background level after about 200–300 ml of elution, which seems to indicate that no more appreciable decontamination is available thereafter. The stability constants of citric acid are lower than that of EDTA and DTPA for most of the metals. In case of the strong chelating agents EDTA and DTPA with high stability constants with some of the metals, although the rate of decontamination decreases greatly after about 200–300 ml of elution as can be seen in the decrease of λ, the elution of a considerable activity was observed to continue until the total volume (1000 ml) of decontaminating solution available for our experiments was used.

Some of the γ-ray spectra of fission products taken before and after decontamination are shown in Fig. 5 for human skin and in Fig. 6 for hair. In these spectra the peaks corresponding to the nuclides ^{144}Ce, ^{141}Ce, ^{95}Zr, ^{140}La, ^{90}Y, ^{103}Ru were traced as shown in Table 2. The peak areas of the peaks corresponding to the traced nuclides were calculated by Covell's method and the decontaminated percentage of each corresponding nuclide was estimated. These values are shown in Table 3 for human skin and in Table 4 for hair. Although they should be interpreted to show only an order of magnitude, it is clear that the decontamination effect of the chelating agents is remarkably better than that of the water alone.

However, because of the possible existence of various decay chains in the fission product mixture, in order to obtain more precise results a more detailed time analysis of the γ-spectra and radiochemical analysis may be necessary. In our experiment, we have taken several γ-spectra, but in cases where there is a possibility of the parent and daughter nuclides separating out, we must be extremely cautious about the interpretation of the γ-spectra.

Although some minor differences were observed in the decontamination effect on human skin and hair, overall similarity was observed in the effects and modes of decontamination for skin and hair under the conditions of our experiments. In either case, the strong chelating agents EDTA and DTPA with high stability constants with metal ions seem to be effective decontaminating agents for fission product mixture.

If the solution containing the chelating agents were used for the decontamination of skin surfaces in the form of a stagnant bath, it may be anticipated that the chelating agents may enhance the absorption of some radioactive nuclides through the skin surfaces.

However, if the chelating agents were used for the decontamination of skin and hair in the form of a shower or by running water over skin and hair to minimize the skin absorption, it may be extremely useful in some cases of skin and hair contamination.

REFERENCES

1. L. A. George, Jr., N. L. Dockum and L. K. Bustad. Decontamination of pig skin contaminated with a plutonium solution. Hanford Report HW-44526, 1956.
2. M. A. Khodyreva. The permeability of radium bromide through intact skin. *Med. Radiol.* **4,** 77–81 (1959).
3. B. A. J. Lister, A. Morgan and R. S. Sherwood. Excretion of plutonium following accidental skin contamination. *Health Physics* **9,** 80–915 (1963).
4. M. A. Van Dilla, C. R. Richmond and J. E. Furchner. Cutaneous absorption by human subjects. 1. Studies with sodium-24 and iodine-131. LAMS-2526, 1961.
5. L. A. Il'in. Contamination of the skin by radioactive substances and comparative effectiveness of certain methods of purification. *Gigiena Truda i Professional Zabolezaniya* **4,** 28–32 (1960).
6. W. J. Friedman. Decontamination of synthetic radioactive fallout from the intact human skin. *Am. Ind. Hyg. Ass. J.* **19,** 15–19 (1958).
7. J. Nosek and V. Chmelar. On the present possibilities of washing radioactive substances off the skin of living animals. *Health Physics* **2,** 306–307 (1960).
8. M. H. Weeks and W. D. Oakley. Biology research—annual report for 1953–1954. Hanford Report HW-30437: 102–110, 1954. Ibid. HW-35917: 59–64, 1955.
9. L. A. George, Jr., N. L. Dockum and L. A. Bustad. Biology research—annual report for 1956. Ibid. HW-47500: 147–156, 1956.
10. W. D. Oakley and R. C. Thompson. Biology research—annual report for 1955. Ibid. HW-41500: 106–122, 1955.
11. F. P. Hungate and E. G. Swedea. Biology research—annual report for 1961. Ibid. HW-69500: 111–135, 1961.
12. R. H. Wilson and W. B. Silker. Plutonium contaminated injury case study and associated

use of Na_2 EDTA as a decontamination agent. Ibid. HW-55309: 5–6, 1960.
13. Y. Nosek and V. Khmelarzh. Skin disactivation in contamination with radioactive substances. *Med. Radiol.* **4,** 74–76 (1959).
14. J. Toulet and J. Tabernat. Contribution to the study of processes for external decontamination experimentation with a new product in the case of radioactive contamination of the teguments. *Arch. Maladies Profess. Med. Travail et Securite Sociale* **20,** 272–282 (1959).
15. M. H. Faes. Skin decontamination in presence of thallium-204. *Nature* **194,** 1188–1189 (1962).
16. I. M. Klotz. The conjugation between protein and micromolecule ion or micromolecule compound. *Protein Chemistry* **4,** 15–63 (1956).
17. H. Noda. Collagen. *Protein Chemistry* **4,** 65–125 (1956).
18. A. E. Martell and M. Calvin. *Chemistry of the Metal Chelate Compounds,* p. 454, Prentice Hall, New York, (1952).
19. Y. Nishiwaki and H. Nishioka. The method of decontamination of radioactive surface contamination (The effect of surfactants and chelating agents). *Bull. of Tokyo Institute of Technology* **54,** 131–136 (1963).
20. Y. Nishiwaki and H. Nishioka. On the removal of the radioactive surface contaminations. Ibid. **61,** 13–28 (1964).
21. H. Nishioka. The mechanism of radioactive surface contamination and decontaminating agents **1,** II. *Industrial Environmental Engineering* **30,** 2–9 (1964). Ibid. **31,** 1–8 (1964).
22. H. F. Hunter and N. E. Ballou. Fission-products decay rates. *Nucleonics* **9,** C.2–C.7 (1951).
23. D. F. Covell. Determination of gamma-ray abundance directly from the total absorption peak. *Anal. Chem.* **31,** 1785–1790 (1959).

DÉCONTAMINATION DE LA PEAU CONTAMINÉE EXPÉRIMENTALEMENT PAR LE MÉLANGE DE PRODUITS DE FISSION ET PAR LE FALL-OUT SYNTHÉTIQUE

J. S. STAJIĆ, D. B. STOJANOVIĆ et A. V. MILOVANOVIĆ*
Institut des Sciences Nucléaires "Boris Kidrič", Vinča,
Service de Protection Médicale

Résumé—On a examiné l'efficacité de la radiodécontamination de la peau des animaux d'expérience contaminée par des mélanges de produits de fission à longues périodes dissous sous forme de nitrate et par des mélanges de produits de fission à période moyenne dissous sous forme de chlorure. On a testé: (a) les décontaminants solubles dans l'eau de robinet, (b) les décontaminants solubles dans l'eau de mer, (c) les décontaminants classiques dont l'utilisation est précédée de l'application d'une crème protectrice, et (d) les matières destinées à la décontamination sans utilisation d'eau. Les résultats obtenus indiquent que la plupart de ces matières peuvent éliminer efficacement de la peau les mélanges liquides de produits de fission (audessus de 95% après quatre traitements). Des résultats similaires, même peut-être meilleurs, ont été obtenus quand le contaminant était une retombée synthétique (poussière radio-active artificielle marquée à ^{141}Ce). On a examiné aussi l'efficacité de la décontamination de la peau poilue, contaminée par des contaminants liquides. L'effet obtenu était relativement satisfaisant.

INTRODUCTION

La radiodécontamination de la peau s'effectue pour prévenir l'apparition de radiodermite provoquée par les rayons bêta du contaminant, pour éviter la contamination interne (transcutanée ou perorale) et pour diminuer l'exposition de l'organisme aux rayonnements gamma, émis par les particules du contaminant.

Le choix des méthodes et des moyens de décontamination est conditionné par plusieurs facteurs (nature du contaminant, sa composition chimique, intégrité et état physiologique de la peau, qualité et quantité de poils, espèce et quantité de décontaminant disponible, nombre de sujets à traiter, etc.). Un bon décontaminant doit être efficace sans provoquer de lésions cutanées et sans faciliter la résorption transcutanée du contaminant. Puis, il doit être bon marché, facile à manipuler et disponible en quantité suffisantes. La plupart des auteurs qui ont étudié le probléme de la radiodécontamination de la peau.[1-7] sont d'accord pour constater que les savons et les détergents sont les meilleures parmi les matières destinées à la décontamination.

Dans presque tous les essais effectués jusqu'à présent, les contaminants ont été des radionucléides particuliers, tandis que les décontaminants ont été solubles dans l'eau de robinet[1-3, 5-7]. Ces expériences ont été faites sur la peau épilée ou non poilue. Cependant, dans certaines situations (par exemple après des accidents aux installations nucléaires, après des tests thermonucléaires, etc.), les contaminants sont des mélanges de produits de fission à l'état liquide ou pulvérulent. C'est dans ces circonstances qu'un grand nombre d'individus pourraient être contaminés, dont la décontamination exigerait d'énormes quantités d'eau, qui, à ce moment, devient rare. Enfin, ce ne sont pas seulement les parties du corps sans poils, mais aussi celles qui en sont couvertes, qui risquent d'être contaminées. C'est pourquoi nous avons effectué une série d'expériences destinées à décontaminer la peau animale contaminée par un mélange de produits de fission dissous, ou par une retombée

* Assistant technique: Z. B. Ralević.

synthétique. Parmi les matières de décontamination, nous avons choisi celles que nous avons toujours sous la main en quantités suffisantes et celles qui peuvent être facilement improvisées. Étant donné que dans certaines régions, l'eau douce est un article d'approvisionnement critique, par exemple au bord de la mer ou dans les îles, nous nous sommes proposé d'étudier les qualités de décontamination de l'eau de mer et les détergents qui y sont solubles. Les expériences ont été faites sur la peau poilue et sur la peau épilée.

MATÉRIEL ET MÉTHODE

L'efficacité de la décontamination a été examiné sur 440 Albino rats des deux sexes (pesant 200 g environ), en fonction des facteurs suivants: composition chimique et espèce du contaminant; espèce du décontaminant; absence ou présence de poils; nombre de traitements de la peau. Les animaux sont classés en trois groupes. Le contaminant du 1er groupe était un mélange de produits de fission à longue période, dissous sous forme de nitrate ($^{90}Sr + {}^{137}Cs + {}^{144}Ce$).† Le contaminant du 2ème groupe était un mélange de produits de fission à période moyenne, dissous sous forme de chlorure ($^{89}Sr + {}^{141}Ce$)‡ et celui de 3ème groupe était une retombée synthétique marqué à ^{141}Ce (poussière radioactive artificielle dont les particules ont de 65 à 150 μ de diamètre).‡

Les décontaminants utilisés sont les suivants: (a) eau de robinet, (b) décontaminants solubles dans l'eau de robinet (savon liquide et eau; solution aqueuse à 1% de détergent "Nila"), (c) eau de mer, (d) détergents solubles dans l'eau de mer (solution à 3% de "Radion extra" et de "Albus special"), (e) décontaminants solubles dans l'eau de robinet dont l'utilisation est précédée par l'application de la crème protectrice "Octa", (f) matières de décontamination sans utiliser d'eau (pâte No. 1: farine de maïs avec de l'eau additionnée jusqu'à l'obtention de consistance de la pâte; pâte No. 2: mélange à quantité égale de farine de maïs et de détergent "Nila" avec adjonction d'eau jusqu'à l'obtention de la consistance de la pâte; pâte No. 3: mélange à 64% de kaoline, à 15% de savon liquide, à 3% de Na_2CO_3 et à 18% d'eau de robinet; matière No. 4: savon liquide sans utilisation d'eau).

Pour vérifier l'efficacité des décontaminants examinés on en a fait la comparaison avec le mélange de la solution à 3% de détergent "Nila" et à 2% de complexon Na_2EDTA. Ce mélange est cité dans la littérature comme un des décontaminants les plus efficaces,[1, 2, 7] bien qu'il facilite, d'après quelques auteurs, la résorption transcutanée du contaminant.[6]

Le pH de tous les contaminants variait de 5,5 à 8,5. Les décontaminants examinés ont été testés sur la peau épilée, tandis que ceux de groupes (a), (b), (c) et (d), (détersifs solubles dans l'eau de robinet et dans l'eau de mer)—sur la peau poilue. La décontamination a toujours commencé 30 minutes après le début de la contamination.

Technique de travail. Chaque animal a été narcotisé avant l'expérience, par la solution à 25% d'uréthane injecté s.c. (dose de 0,7 ml/100 g de poids). Après avoir fixé l'animal sur une table d'opération, on lui a coupé soigneusement les poils de la région abdominale. Les poils n'ont pas été coupé dans le cas des expériences relatives à la peau poilue. La zone à contaminer a été marquée à l'aide d'un sceau coloré rond de 3 cm de diamètre (surface de 7 cm² environ). Une goutte de solution contaminante est portée par une pipette au centre de la zone marquée et puis répartie par une petite spatule en verre sur toute la surface marquée. L'activité de la goutte était de 1,5 à 2,0 μCi et le pH du contaminant était réglé à 5,0 (c'est le pH de la peau des animaux d'expérience). Dans le cas d'une retombée utilisée comme contaminant, la contamination a été faite par la pulvérisation au moyen d'une boîte dont le couvercle était perforé de façon que la densité de contamination était 1,5 mg/cm² et l'activité de toute la surface—2 μCi. L'activité initiale de la peau (A_i) a été mesurée immédiatement avant la décontamination, au moyen du compteur GM adopté pour les animaux d'expérience. La décontamination ensuite effectuée comportait quatre traitements de la peau. Dans le cas des décontaminants liquides, chaque traitement comprenait trois lavages au tampon de coton imbibé de solution décontaminante, suivi de

† Produit au centre de Saclay, près de Paris.

‡ Produit à l'institut nucléaire, "Boris Kidrič", Vinča.

l'essuyage par un tampon sec. Si les expériences comportaient l'application d'une crème protectrice, il est à noter que la crème devrait être appliquée uniformement sur la peau marquée, immédiatement avant la contamination (0,5 g de la crème environ à 7 cm² de surface). La décontamination par des pâtes sans utiliser de l'eau a été faite de la manière suivante: le décontaminant est appliqué sur la surface de la peau contaminée lors de chaque traitement (1 g à 7 cm² de surface) et au bout de 30 à 40 secondes, les complexes formés sont éliminés en essuyant la peau avec trois tampons de coton. La décontamination par le savon liquide a été faite de la même manière que celle par d'autres décontaminants liquides, mais sans utiliser d'eau.

Après chaque traitement l'activité finale (A_f) de la peau a été mesurée et l'efficacité de la décontamination (E_d) a été calculée selon la formule suivante:

$$E_d = \frac{(A_i - A_f) \cdot 100}{A_i}$$

RÉSULTATS ET DISCUSSION

Le tableau 1 et la figure 1 présentent l'efficacité de la décontamination de la peau épilée. L'analyse des résultats indique qu'il est plus difficile d'éliminer de la peau la solution de nitrate que la solution de chlorure. Il a été constaté aussi qu'il est plus difficile d'éliminer de la peau ces deux solutions que la poussière radio-active artificielle. Il semble que les possibilités de décontamination differentes des solutions de nitrate et de chlorure sont dues à leurs composants anioniques (NO_3^-, Cl^-). Cela à été prouvé aussi par les expériences de décontamination effectuées antérieurement sur la peau contaminée par des radionucléides particuliers.[7] Il a été révélé alors aussi que les nitrates sont plus difficilement décontaminables que les chlorures et que les composants cathioniques n'y jouent aucune rôle.

D'autre part, la poussière radio-active artificielle peut être éliminée de la peau plus facilement que les contaminants liquides parce que le mode de fixation des particules de poussière sur la peau est mécanique et physique (maintien sous les poils, dans les pores et rides (plis) de la peau, absorption et adhérence), tandis que les contaminants liquides sont liés au support surtout chimiquement (échange d'ions, réaction avec des constituants de la peau, etc.).

En général, les effets de décontamination de toutes les matières essayées sur la peau épilée ont été très bons, pour n'importe quelle espèce et n'importe quel état, parce que après le 4ème traitement l'activité était toujours diminuée de plus de 95% (à l'exception de la décontamination de la solution de nitrate par l'eau de robinet

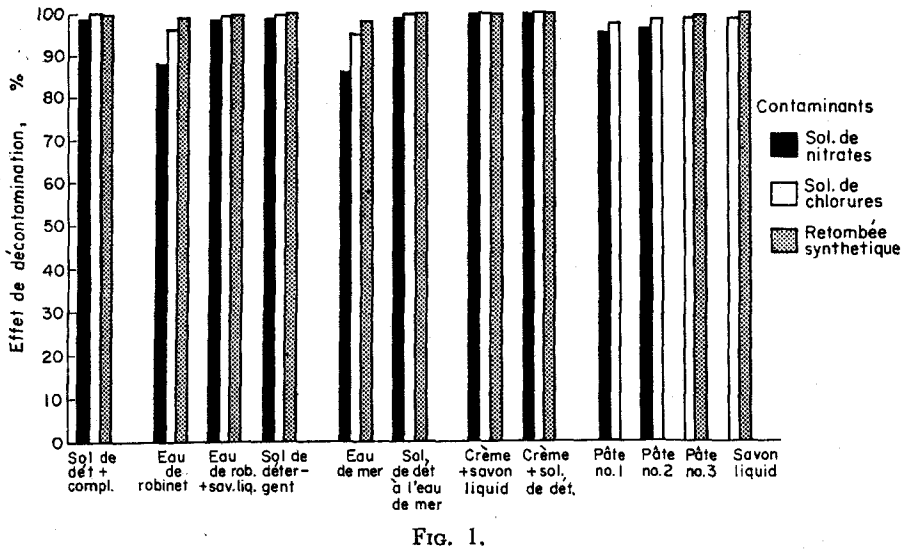

FIG. 1.

Tableau 1. *Décontamination de la peau contaminée expérimentalement par des produits de fission et par une retombée synthétique.*

Décontaminant	Contaminant								
	Solution de produits de fission sous forme de nitrates (Sr^{90} + Cs^{137} + Ce^{144})			Solution de produits de fission sous forme de chlorures (Sr^{89} + Ce^{141})			Poudre: Fall-out synthétique		
	Effet de décontamination (E_o) après								
	Nombre d'anim	un traitement	quatre traitements	Nombre d'anim	un traitement	quatre traitements	Nombre d'anim	un traitement	quatre traitements
Décontaminants solubles à l'eau de robinet									
3% sol. détergent + 2% sol. de complexon	10	95,2	98,7	10	99,4	100,0	10	99,3	99,8
Eau de robinet	10	77,6	88,4	10	94,8	96,7	10	96,7	98,8
Eau de robinet + savon liquide	10	95,7	98,4	10	98,4	99,5	10	99,4	99,8
1% sol. de détergent	10	95,7	98,6	10	99,0	99,5	10	99,3	99,9
Décontaminants solubles à l'eau de mer									
Eau de mer	10	77,7	86,1	10	90,4	95,0	10	94,0	98,0
3% sol. de détergent à l'eau de mer	10	92,6	98,7	10	98,6	99,8	10	98,3	99,8
Crème protectrice + lavage									
Crème + eau de robinet + savon liquide	10	99,3	99,7	10	98,7	99,8	10	98,7	99,7
Crème + eau de robinet + 1% sol. de détergent	10	98,7	99,8	10	99,1	99,9	10	99,3	99,8
Décontaminants sans utilisation de l'eau									
Pâte No. 1	10	78,9	94,7	10	85,8	97,3	—	—	—
Pâte No. 2	10	85,6	96,4	10	91,4	98,1	—	—	—
Pâte No. 3	10	90,5	98,4	—	—	—	10	95,6	98,9
Savon liquid	10	94,8	98,2	—	—	—	10	98,5	99,6

ou l'eau de mer). Il est à souligner que l'eau de mer et les détergents qui y sont solubles présentent de très bonnes qualités et peuvent être comparés aux meilleurs décontaminants connus. Un excellent effet des pâtes de décontamination et surtout du savon liquide (qui était le plus efficace parmi tous les décontaminants testés sans utilisation d'eau), a attiré aussi notre attention.

Les expériences de décontamination de la peau poilue sont présentées dans le tableau 3 et la figure 3. Il est évident que le savon liquide et un détergent en combinaison avec de l'eau de robinet, ainsi que les détergents solubles

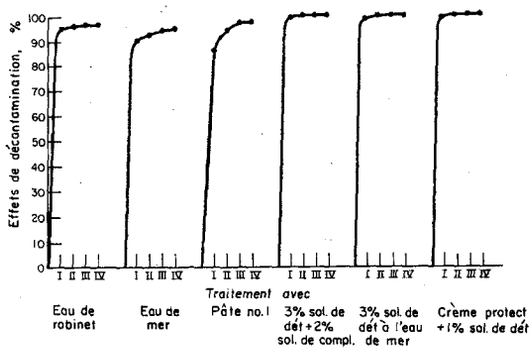

FIG. 2.

dans l'eau de mer, présentent un effet de décontamination moins bon après le 4ème traitement de la peau poilue que de celle épilée. Cependant, dans ce cas les effets de décontamination ont été aussi supérieurs à 92%, ce qui est à souligner.

Presque tous les décontaminants essayés présentent statistiquement, comme il est montré aux tableaux 2 et 4, une efficacité de décontamination significativement plus faible ($P = 0{,}01 - 0{,}001$ et $P = < 0{,}001$) que le mélange de détergent et de complexe dissous. Cependant, du point de vue pratique, ces differences étant limitées le plus souvent à 0,1–1,0% (pour la peau épilée), n'ont pas d'importance surtout quand la contamination initiale n'est pas trop élevée.

Dans tous les essais il a été prouvé le fait bien connu, que le 1er traitement élimine le plus grand pourcentage du contaminant (figs.

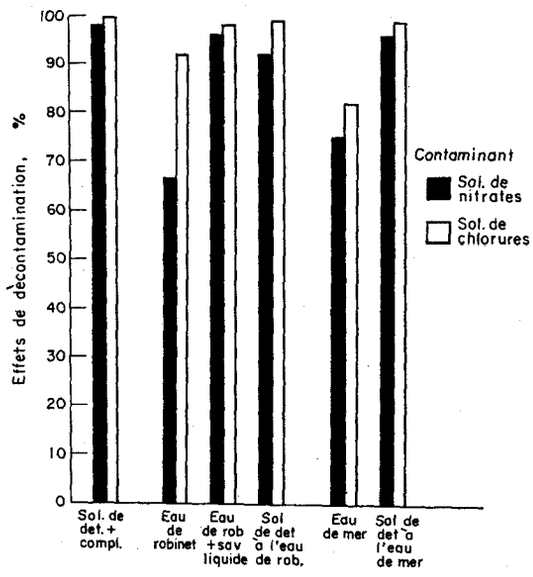

FIG. 3.

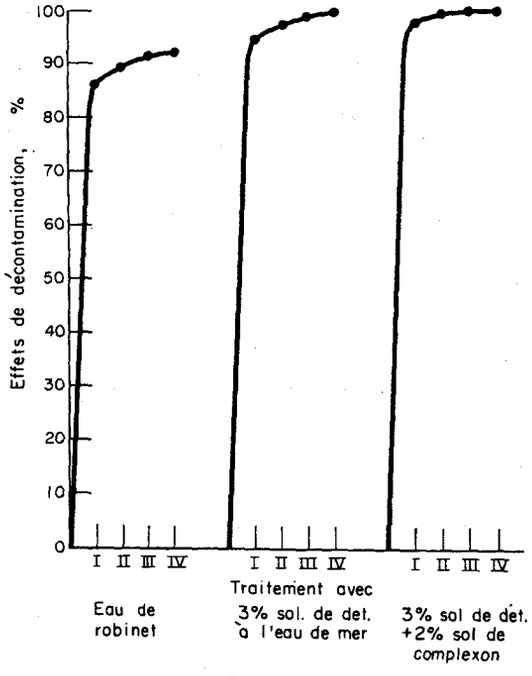

FIG. 4.

Tableau. 2. Décontamination de la peau contaminée expérimentalement par des produits de fission et par une retombée synthétique.

Décontaminant	Contaminant: Solution de produits de fission sous forme de nitrates (Sr^{90} + Cs^{137} + Ce^{144})				Solution de produits de fission sous forme de chlorures (Sr^{89} + Ce^{141})				Poudre: Fall-out synthétique			
	Effet de décontamination après 4 traitements											
	Nombre d'animaux	E_o	Efficacité par rapport à E_o de sol. dét. + complexon t	P	Nombre d'animaux	E_o	Efficacité par rapport à E_o de sol. dét. + complexon t	P	Nombre d'animaux	E_o	Efficacité par rapport à E_o de sol. dét. + complexon t	P
Décontaminants solubles à l'eau de robinet												
3% sol. de détergent + 2% sol. de complexon	10	98,7 ± 0,54			10	100,0 ± 0,06			10	99,8 ± 0,12		
Eau de robinet	10	88,4 ± 2,09	14,3	<0,001	10	96,7 ± 2,45	4,0	<0,001	10	98,8 ± 0,60	5,0	<0,001
Eau de robinet + savon liquide	10	98,4 ± 1,27	0,66	>0,5	10	99,5 ± 0,17	8,3	<0,001	10	99,8 ± 0,10		—
1% sol. de détergent	10	98,6 ± 0,36	0,55	>0,6	10	99,5 ± 0,18	7,9	<0,001	10	99,9 ± 0,09		—
Décontaminants solubles à l'eau de mer												
Eau de mer	10	86,1 ± 2,43	15,3	<0,001	10	95,0 ± 1,45	10,4	<0,001	10	98,0 ± 0,57	9,0	<0,001
3% sol. de détergent à l'eau de mer	10	98,7 ± 0,48		—	10	99,8 ± 0,05	7,5	<0,001	10	99,8 ± 0,15		—
Crème protectrice + lavage												
Crème + eau de robinet + savon liquide	10	99,7 ± 0,14		—	10	99,8 ± 0,07	6,3	<0,001	10	99,7 ± 0,17	1,4	>0,1
Creme + 1% sol. de détergent	10	99,8 ± 0,01		—	10	99,9 ± 0,05	3,7	<0,01	10	99,8 ± 0,16		—
Décontaminants sans utilisation d'eau												
Pâte No. 1	10	94,7 ± 1,02	10,5	<0,001	10	97,3 ± 0,90	9,0	<0,001		—		—
Pâte No. 2	10	96,4 ± 0,68	8,0	<0,001	10	98,1 ± 1,37	4,1	<0,001		—		—
Pâte No. 3	10	98,4 ± 0,66	1,07	>0,2		—		—	10	98,9 ± 0,52	5,0	<0,001
Savon liquide	10	98,2 ± 0,50	2,0	>0,05		—		—	10	99,6 ± 0,20	2,6	>0,01

Tableau 3. *Décontamination de la peau contaminée experimentalement par des produits de fission et par une retombée synthétique.*

Décontaminant	Contaminant					
	Solution de produits de fission sous forme de nitrates (Sr^{90} + Cs^{137} + Ce^{144})			Solution de produits de fission sous forme de chlorures (Sr^{89} + Ce^{141})		
	Effet de décontamination après					
	Nombre d'anim.	un traitement	quatre traitements	Nombre d'anim.	un traitement	quatreu traitements
Décontaminants solubles à l'eau de robinet						
3% détergent + 2% complexon	10	85,8	97,8	10	97,5	99,6
Eau de robinet	10	57,9	66,7	10	85,8	92,0
Eau de robinet + savon liquide	10	82,1	95,9	10	93,0	97,9
1% sol. de détergent à l'eau de robinet	10	77,0	92,0	10	96,3	98,7
Décontaminants solubles à l'eau de mer						
Eau de mer	10	64,7	75,0	10	70,8	82,1
3% sol. de détergent à l'eau de mer	10	84,8	96,0	10	94,7	98,7

2 et 4). L'efficacité de chaque traitement suivant est plus faible que celle du traitement précédent. Par conséquent, quand il s'agit de décontaminants très efficaces, tels que le savon liquide et les solutions de détergents, il n'y a pas pratiquement de différence entre le troisième et le quatrième traitement.

Enfin, il est à souligner que les décontaminants essayés n'ont pas provoqué de lésions macroscopiques sur la peau traitée.

CONCLUSIONS

1. Tous les décontaminants essayés ont présenté une efficacité satisfaisante lors de la décontamination de la peau épilée, contaminée par des mélanges de produits de fission dissous et par une retombée synthétique.

2. Il est à noter surtout l'effet de décontamination de l'eau de mer et des détergents qui y sont solubles, ainsi que l'effet de décontamination de matières sans utilisation d'eau.

3. Lors de la décontamination de la peau poilue, les décontaminants essayés ont présenté une efficacité plus faible que dans le cas de décontamination de la peau épilée, mais les résultats obtenus sont relativement satisfaisants.

4. L'effet de décontamination est le meilleur lors du 1er traitement, puis il diminue brusquement. Il n'y a pas pratiquement de différence entre E_d du troisième et E_d du quatrième traitement.

Tableau. 4. Décontamination de la peau contaminée expérimentalement par des produits de fission et par une retombée synthétique.

Décontaminant	Contaminant							
	Solution de produits de fission sous forme de nitrates (Sr^{90} + Cs^{137} + Ce^{144})				Solution de produits de fission sous forme de chlorures (Sr^{89} + Ce^{141})			
	Effet de décontamination après 4 traitements							
	Nombre d'anim.	E_o	Efficacité par rapport à E_o de sol. déterg. + complexon		Nombre d'anim.	E_o	Efficacité par rapport à E_o de sol. déterg. + complexon	
			t	P			t	P
Décontaminants solubles à l'eau de robinet								
3% détergent + 2% complexon	10	97,8 ± 0,72			10	99,6 ± 0,20		
Eau de robinet	10	66,7 ± 7,42	12,4	<0,001	10	92,0 ± 1,78	12,6	<0,001
Eau de robinet + savon liquide	10	95,9 ± 1,06	4,4	<0,001	10	97,9 ± 0,36	13,0	<0,001
1% sol. de détergent à l'eau de robinet	10	92,0 ± 1,15	13,2	<0,001	10	98,7 ± 0,66	3,8	<0,01
Décontaminants solubles à l'eau de mer								
Eau de mer	10	75,0 ± 5,86	11,5	<0,001	10	82,1 ± 3,89	16,1	<0,001
3% sol. de détergent à l'eau de mer	10	96,0 ± 1,07	4,5	<0,001	10	98,7 ± 0,30	7,5	<0,001

RÉFÉRENCES

1. W. J. FRIEDMAN. *Am. Ind. Hyg. J.* **19,** 15 (1958).
2. P. GENAUD. *Rev. du Corps de Santé Mil.* **11,** 3 (1955).
3. B. M. ZLOBINSKI. *Bezopasnost rabot s radioaktivnimi veščestvami.* Medgiz, Moskva, 1961.
4. R. A. CONARD. Symposium on the Shorter-Term Biological Hazards of a Fallout Field. AEC, Washington, 1956.
5. R. H. BLACK. *Am. Ind. Hyg. J.* **21,** 162 (1960).
6. H. FOREMAN. *Proc. Symposium on Diagnosis and Treatment of Radioactive Poisoning,* IAEC, Vienna, 1963.
7. B. PENDIĆ, K. MILIVOJEVIĆ et D. STOJANOVIĆ. Referat na II medjuinstitutskom sastanku službi zaštite od zračenja SKNE, Rovinj, 1964.
8. J. STAJIĆ, D. STOJANOVIĆ et A. MILOVANOVIĆ. Referat na II medjuinstitutskom sastanku službi zaštite od zračenja SKNE. Rovinj, 1964.

CONTAMINATION INTERNE AU ^{137}Cs PAR VOIE TRANSCUTANÉE ET EFFET DES MOYENS DE DÉCONTAMINATION ET DE PROTECTION SUR LA RÉSORPTION TRANSCUTANÉE DE CE RADIONUCLIDE

B. PENDIĆ et K. MILIVOJEVIĆ

Service de Protection Médicale, Institut des Sciences Nucléaires B. Kidrič, Vinča (Yugoslavia)

Résumé—Dans le cas d'une contamination externe, souvent causée par un accident radiologique, en outre de l'effet nuisible local sur la peau dû aux rayonnements ionisants, il apparaît un autre problème concernant la contamination interne par voie transcutanée, due à la résorption des radionuclides.

En étudiant la dynamique de pénétration du radionuclide ^{137}Cs à travers la peau non abîmée mais dégraissée chez des rats Albino, on a constaté que la résorption par voie transcutanée de cet élément est très rapide et que ses traces dans le sang peuvent être enrégistrées quelques minutes après la contamination de la peau. La quantité pénétrant dans l'organisme par voie transcutanée sur une surface de quelques cm^2, au cours d'une période assez courte (jusqu'à 6 h), est relativement remarquable, atteignant une valeur de 3% de la quantité appliquée de $^{137}CsCl$ dans la solution aqueuse. On a constaté aussi une distribution diffuse dans l'organisme avec une accumulation maximale dans les reins, les muscles (surtout dans le muscle cardiaque) et dans le foie.

Tenant compte de la résorption par voie transcutanée rapide, il est nécessaire de faire une décontamination urgente et efficace de la peau. Il a été montré que les moyens de décontamination simples et usuels—détergents par exemple—utilisés dans les procédés de décontamination standard, ainsi que le décontaminant spécialement préparé MO 8.385, provoquent l'augmentation de la pénétration du césium radio-actif par voie transcutanée.

Il a été montré par les expériences destinées à vérifier les effets de l'application préventive des crèmes protectrices, préparées à la base des graisses naturelles et du silicon, que ces crèmes ont un effet non seulement sur la vitesse et l'efficacité de la décontamination, mais sont en plus susceptibles de diminuer remarquablement et même d'inhiber complètement la résorption transcutanée.

Les résultats obtenus au cours des expériences confirment que la peau ne devrait pas être négligée en tant qu'une voies éventuelles de contamination interne.

A FOLLOW-UP OF 1000 THOROTRAST CASES IN DENMARK

MOGENS FABER
The Finsen Laboratory,
Finseninstitutet og Radiumstationen, Copenhagen, Denmark

Abstract—A series of Thorotrast injected patients has been followed in Denmark since 1949. The series now numbers 1000 patients of which 510 are still alive. The follow-up is performed through hospital contacts and is activated by notice of death. Some patients have been seen but only as a neurosurgical follow-up. All patients have had a neurosurgical carotid arteriography. Record of death is verified from the physicians, hospital records and autopsy records.

The most common cause of death is of course the neurosurgical diseases of which some 300 have died. Non-malignant diseases of other organs have been the cause of death in 150 cases, and 40 cases of malignant diseases have been observed. Among the non-malignant diseases there has been observed a number of bone-marrow discrasias of non-leukaemic type but amazingly few signs of serious hepatic disorder.

The total number of malignant diseases is very close to the one expected from cancer statistics in Denmark. However, 4 haemangioendotheliomas and 8 leukaemias have been met with, both a definite increase above expectation. The number of primary hepatic tumors are also slightly above expectation. The significance of these results will be discussed in relation to other comparable materials.

SINCE Thorotrast was introduced into clinical medicine in 1930 a very large but unknown number of patients have been injected with this radioactive contrast medium. It is still being produced and publications on the use of Thorotrast appear every year. In Denmark it was used from 1935 until 1946, when it was discontinued with the reappearance of iodine containing contrast media after the war. Thorotrast was used practically only for arteriography in neurosurgical departments and accordingly the series will only consist of patients with the classical deposits in liver and spleen as it is seen after intravenous injections. After a thorough search of hospital records we have now collected 1000 injected patients and of these some 500 are still alive. The doses used were relatively small. 75% of the injected patients had doses below 20 ml.

The status of the series is illustrated in Fig. 1 where the living patients are registered according to time of observation and the dead according to the time of death after injection. The very large number of deaths just after the injection is of course due to the neurosurgical disease for which the contrast medium was injected.

This group of patients has now been followed for more than 15 years. The follow-up has in general been performed without contact with the patients, through hospital records when known, through folk registries, etc. Although a system has been set up which should detect all dead patients it has been necessary to check at intervals on the status of the patients surviving at that time. In the following discussion I shall concentrate on some of the diseases which might be considered as being due to the presence of Thorotrast.

The presence of a radioactive substance will immediately give rise to the question whether this group of patients shows an increase in the incidence of malignant tumors, and if so where the tumors are to be found. Figure 2 shows the expected cumulative incidence of cancer in a population of the size of the Danish Thorotrast series calculated on the basis of tables published from the Danish Cancer Registry in relation to the known number of cancers occurring up till

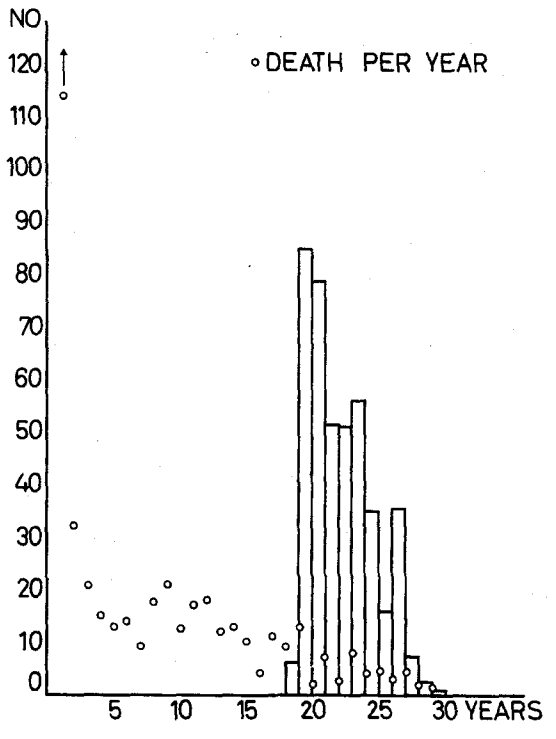

FIG. 1. The dead and the surviving Danish Thorotrast patients in relation to time of injection.

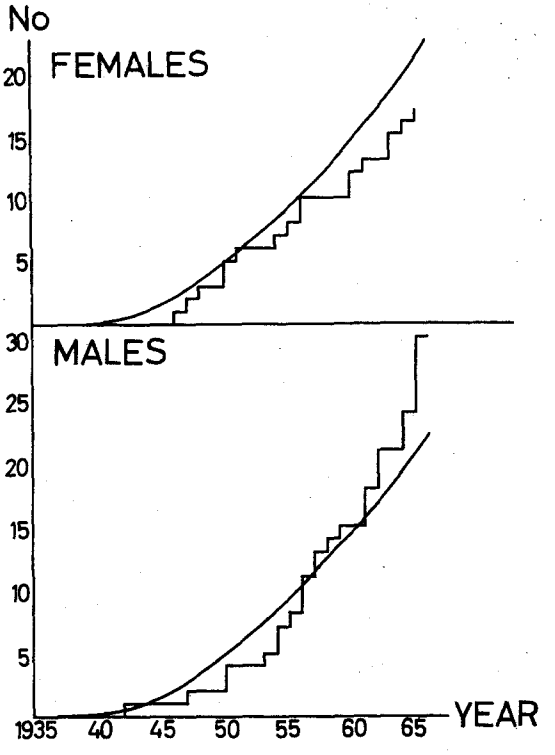

FIG. 2. The observed cumulative cancer mortality in relation to the expected, calculated on cancer registry data.

January 1, 1966. It can be seen that the two curves follow each other fairly closely during most of the follow-up period. Not until the last year or two has any sign of an increase in the general cancer incidence been observed, and so far this increase is of no statistical significance.

If we, however, leave the total incidence of cancer and look for tumors which might be due to Thorotrast, it has to be noted that the number of haemangioendotheliomas of the liver is now increasing. During the last years four cases of haemangioendothelioma, the classical Thorotrast tumor, have appeared among the Danish Thorotrast patients. This increase which occurred after many years of observation of an apparently symptomless group is of very great interest, and can with present knowledge be discussed from two points of view.

The first question is whether the occurrence of haemangioendothelioma in man can be shown in any way to be dependent on the dose of Thorotrast injected. Unfortunately only in very few of the published cases are both dose and latency period known. Only two large series can be used for this purpose, our own group of four cases among 1000 injected persons and the fourteen histologically verified Portugese cases published by da Silva Horta[1] from a group of 1800 cases. To these can be added seven isolated cases from the literature. As can be seen from the figure it is very difficult to claim that there is a relationship between the dose injected in ml Thorotrast and the time at which the tumor appears.

The next question is whether it is possible to evaluate now the risk of the future appearance of haemangioendotheliomas in a series of Thorotrast injected persons. At present 41 cases of haemangioendothelioma of the liver have been published, where time of injection and time of

Table 1. *Cancer in Thorotrast Group*

	No.			Latency period month
	Males	Females	All	
Stomach	2	1	3	237–286–291
Small intestine	1	—	1	19
Colon A. Rectum	2	2	4	103–196–263–290
Pancreas	1	—	1	277
Liver	6	3	9	221*–225–226–250–257* –266–312–321*–331*
Lung	8	—	8	121–123–156–158–162 –247–254–319
Uterus	—	3	3	55–79–176
Leukaemia	5	3	8	106–122–170–205–234 –258–261–302
Others	6	5	11	30–59–63–67–87–88– 123–137–157–211–233

death from the tumor is known. We have tabulated these cases and the result can be seen in Fig. 4. In this connection it must be remembered that the longest observation period of these patients under all circumstances must be below the 35 years that have elapsed since Moniz[3] in 1930 started injecting Thorotrast into patients. The first 4–5 years after the introduction of the procedure it was mainly used in Portugal, and other countries did not join the Thorotrast users until somewhat later. It is quite evident from the figure that the maximum incidence of haemangioendotheliomas in relation to the time after injection of Thorotrast has not yet been reached. This perhaps can not be considered to be unexpected if we compare with the observation of Goolden and collaborators[3] on the latency period for pharynx malignancies after therapeutic irradiation of the thyroid where the maximum incidence of radiation cancer appears after 30 years. This, however, is a short time irradiation with no exposure to ionizing radiation afterwards. It is difficult to compare these conditions with the chronic irradiation in the Thorotrast patients, when furthermore the dose delivered is smallest in the initial period after injection. The minimum figures for the incidence of haemangioendothelioma in Thorotrast cases must so far be taken from the Portugese series where evidence for haemangioendothelioma is present in 26 cases among 1800 intravenously injected patients.

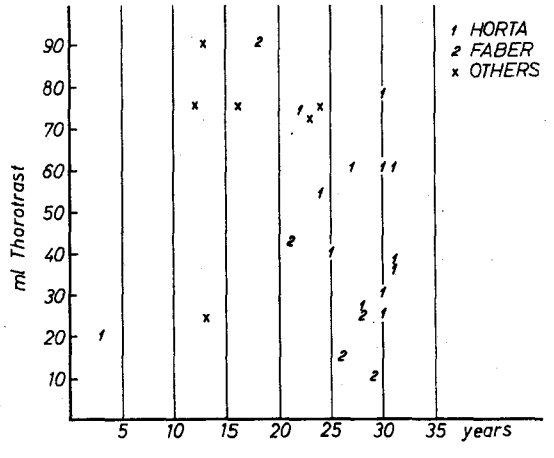

FIG. 3. The relationship between time of death of verified haemangioendotheliomas and dose of Thorotrast injected. Own and other published data.

The two series are, however, not quite comparable because some of the Portugese patients were injected up to 5 years before the first Danish patients, while a large group was injected simultaneously or later. It is, however, known (Silva

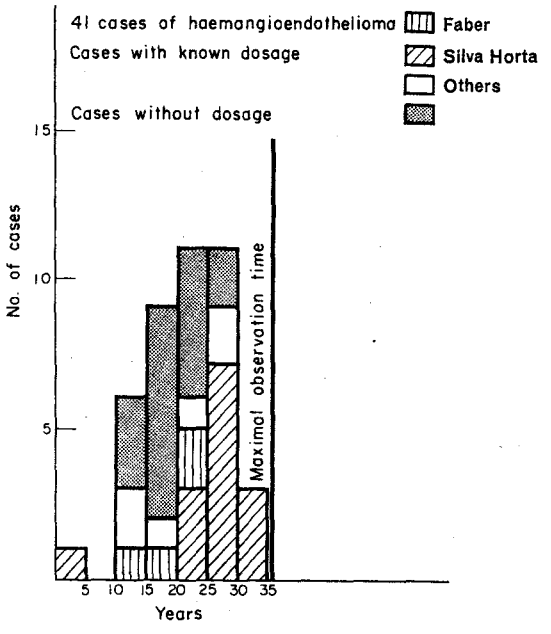

FIG. 4. Latency period in Thorotrast induced haemangioendotheliomas. Own and other published data.

Horta) that approximately one-third of the Portugese patients were injected before the Danish neurosurgeons started using large amounts of Thorotrast and when the latency period of the haemangioendotheliomas from Fig. 4 is taken into consideration, then it must be from this group that most of the tumor cases stem.

The evaluation of a minimum figure should then be possible. A direct calculation would suggest 10–14 new cases in the Danish group during the next 10 years. If this result has to be corrected for the difference in date of injection it may be too low by a factor of 2–3. The influence of a difference in injected doses resulting in a difference in radiation dose is so far unknown, but it may decrease the expected incidence due to the larger doses injected in Portugal.

It is evident that this calculation would gain considerably if the two series could be treated as one, and attempts are being made at present to realize such a pooling. With the increase in knowledge of dosimetry and other necessary parameters it appears possible that the Thorotrast injected person may supplement our knowledge on the effect of chronic irradiation in man and one must hope that a sufficiently large number of well-planned epidemiological studies can be initiated to collect this valuable material before it is too late.

REFERENCES

1. J. DA SILVA HORTA. *Ann. N.Y. Acad. Sci.* (in press).
2. I. MONIZ. *L'angiographie cerebral.* Paris, Masson, 1934.
3. A. W. G. GOOLDEN and R. L. MORGAN. Radiation cancer of the pharynx. *Acta. Radiol.* (*Therap.*) **3,** 353 (1965).

UNRESOLVED PROBLEMS ASSOCIATED WITH EVALUATION OF TISSUE DOSE FOR THE THOROTRAST PATIENT GROUP*

JOHN B. HURSH

Department of Radiation Biology and Biophysics, University of Rochester School of Medicine and Dentistry, Rochester, New York

Abstract—With the intent of enabling a more precise specification of radiation dose to Thorotrast-injected patients, a study has been made of the physico-chemical properties of Thorotrast solutions. This study has focussed on the tendency of ^{232}Th daughters to adsorb on glass of the vials in which Thorotrast is dispensed by the manufacturer. It has been found that 50 to 90% of ^{228}Ra and ^{228}Th daughters adsorb when ultracentrifugation experiments show them to exist as polymers in the solution. It has not been possible to relate the tendency to form aggregates to pH, age of the solution, or concentration of the daughters. It is shown by calculation that the maximum uncertainty of radiation dose (15-year interval of exposure) may be as much as 50 per cent due to inability to specify the daughter content of the injected Thorotrast.

INTRODUCTION

Thorotrast is an aqueous suspension of thorium dioxide widely used by radiologists as an X-ray opaque medium during the period 1930 to 1945. Since then its use has been greatly curtailed because of a significant incidence of injection site sequelae and because of the recognition of potential late radiation injury to the injected patient. The existence of a sizeable group[1] of living subjects who have borne a low level radioactive burden for 20–35 years creates a challenge for the radiation biologists to relate the late injury effects with the radiation dose. In contrast to the radium dial painter group who acquired their burden by occupational exposure, this group of Thorotrast patients present three unique advantages. The range of thorium burdens is relatively small since standard volumes of Thorotrast were customarily used for a particular diagnostic procedure. Secondly, in many cases, the amount of Thorotrast used and date of injection can be obtained from the hospital records. Thirdly, the radiation exposure is presumptively an exposure of the reticulo-endothelial system, expanding the information gained from the radium group, for which the skeleton was the radiation target. To oppose to these advantages radiation dose calculation for Thorotrast subjects presents some special problems. These problems may be considered as: (1) specification of the ^{232}Th daughter-product content of the injected suspension; (2) determination of self-absorption of alpha emissions in the Thorotrast particles, particularly since large aggregates tend to form in the reticulo-endothelial system; and (3) the study of the fate and body distribution of the long-lived thorium daughters. Since categories 2 and 3 have been considered elsewhere,[1, 2] the present paper will report experimental data bearing on the first problem area. Several investigators have noted[3, 4] the tendency for the long-lived daughters ^{228}Ra and ^{228}Th (Fig. 1) to adsorb on the glass walls of the vial supplied by the manufacturer. Accordingly, even though the volume of Thorotrast injected may be known, the daughter content may be uncertain. The retrospective reconstruction of the total radiation dose sustained

* This report is based on the work performed under contract with the U.S. Atomic Energy Commission at the University of Rochester, Atomic Energy Project, Rochester, New York.

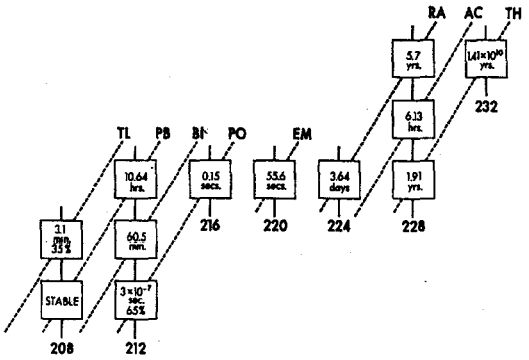

FIG. 1. Thorium decay scheme.

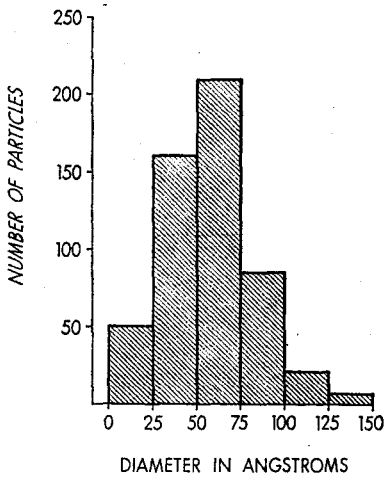

FIG. 2. Data obtained from electron microscope study of Thorotrast particle size.

is therefore subject to error. In the following we shall consider the physico-chemical properties of Thorotrast as related to thorium daughter behavior and shall inquire as to whether a likely daughter-product content of the injected material can be discovered.

GENERAL PROPERTIES

Thorotrast is a brownish colored, opaque, freely flowing suspension labeled as containing "24% to 26% stabilized colloidal Thorium Dioxide; 25% aqueous Dextrin; 0.15% Methyl Parasept as preservative". On each bottle an expiration date (month, day, and year) appears, set ahead five years from date of packaging into vials. This practice is probably[5] not related to expected instability of the suspension due to aging but more likely associated with the increased radioactivity of the material as the long-lived daughter ^{228}Ra increases with time after the chemical separation of thorium.

Rundo[6] quotes Johansen as authority for the statement that Thorotrast produced in the United States contains 0.22 g ^{232}Th per ml and, in Germany, 0.195 g ^{232}Th per ml. Analysis by us of Thorotrast manufactured in the United States yielded 0.22—0.23 g ^{232}Th per ml. The specific gravity is found to be 1.3 g ml. The size of the suspended thorium dioxide particles has been measured by use of an electron microscope in this laboratory[7] and by others.[8] The data obtained by us is plotted in Fig. 2. The photographs used for the particle measurement show them as roughly spherical in shape. The average diameter is 55 $\pm$ 25A°.

DAUGHTER PRODUCT CONTENT OF THOROTRAST VIALS AS PREPARED FOR USE

It is usually assumed that thorium-bearing ore contains the thorium daughters in equilibrium by virtue of its age. The chemical separation of thorium in the refining process segregates ^{232}Th and ^{228}Th from the long-lived ^{228}Ra and, less significantly, from the remaining short-lived daughters. The change in ^{228}Th and ^{228}Ra content of the thorium salt subsequent to chemical separation can be predicted by reference to details of the decay chain (see Fig. 1) and application of the Bateman equations yielding the result shown in Fig. 3.

If a single chemical separation is postulated and if no preferential loss of ^{232}Th, ^{228}Ra, or ^{228}Th occurs during processing of the thorium salt, it would be expected that Thorotrast as prepared for use would have parent-daughter relationships according to Fig. 3.

Three lots of Thorotrast available to us have been analyzed for daughter content using gamma spectrographic measurement techniques. Lot A subsequently referred to as "fresh" Thorotrast included six vials measured four months after packaging; Lot B and Lot C, subsequently referred to as "aged" Thorotrast, included 3 and 4 vials respectively and were measured 5.25 and 5.75 years after packaging. The average value and standard deviation is plotted

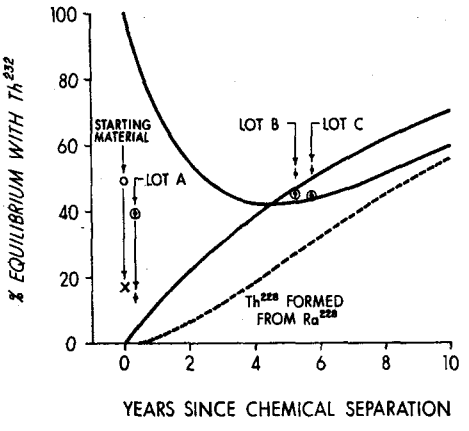

FIG. 3. Calculated curves to show growth of ^{228}Th (concave curve) and ^{228}Ra (convex curve) in a closed system, assuming that at $t = 0$, ^{228}Th is at 100% activity equilibrium with ^{232}Th and ^{228}Ra is zero.

in Fig. 3 with the abscissa taken as the packaging to measurement time interval.

All three sets of points indicate that the last chemical separation took place some time before product packaging and, indeed, the description of the manufacturing process[9] indicates that this interval is no less than 6 months and may be in excess of a year, depending on the age of the thorium oxalate used as a starting material. However, even if each set of points is shifted to the right so that the ^{228}Ra value falls on the predicted line, the ^{228}Th activity for the "fresh" Thorotrast is only about 50% of that predicted. This is interpreted to indicate that during the processing of the ore and the preparation of thorium oxalate several chemical separations took place over a period of some years, and that at each separation radium was removed so that the period of growth yielding the measured ^{228}Ra activity is much shorter than the time during which the ^{228}Th, initially at equilibrium in the ore, has decayed. Qualitative evidence to support this comes from an analysis of a sample of thorium oxalate used as starting material by the Testagar Company, producers of Thorotrast. The ^{228}Ra and ^{228}Th values for the oxalate are included in Fig. 3, and show a similar ^{228}Th deficiency.

EFFECT OF THOROTRAST TRANSFER ON DAUGHTER-PRODUCT CONTENT

The next set of experiments was to transfer the Thorotrast from its original container to a vial of identical size and shape. The empty vial as well as the vial containing the transferred material was measured by gamma spectroscopic techniques at appropriate times so that the transferred amounts of the various daughters could be determined. The results appear in Table 1 and indicate the completely different behavior of the daughters in the fresh and aged lot. Only about 1% of the daughters remained in the original vial for the fresh lot. A substantial fraction of this must have been Thorotrast solution incompletely drained from the vessel walls. For the aged lot 63 and 88% of the ^{228}Ra and 55 to 78% of the ^{228}Th remained adsorbed on the walls of the original vial. Radium-224 was estimated in each case and showed insignificant variations from ^{228}Th.

DAUGHTER CONTENT OF ULTRACENTRIFUGE FRACTIONS

Several experiments were performed in which 4 ml portions of the fresh and the aged Thorotrast were simultaneously centrifuged at 40,000 rpm for times from 3 to 5 hr at a force of from 84,000 to 175,000 g (depending on position in the centrifuge tube). The results obtained from a typical experiment (3 hr centrifugation) are shown in Fig. 4. The fractions A, B, C, and D were removed with the least possible disturbance of the contents and represent the top quarter, the second quarter, the third quarter, and bottom quarter of the centrifuged Thorotrast. They were then analyzed by gamma spectroscopy. It may be seen that fractions A, B, and C show no significant difference in concentration of ^{228}Ra and ^{224}Ra for the fresh Thorotrast. Fraction D shows an increase in concentration for ^{228}Ra and for ^{224}Ra of 65 and 12% respectively. The ^{228}Th presents a different picture and to a first approximation, appears to be distributed according to the ThO_2 content of the fractions. This is reasonable on the likely grounds that a major fraction of the ^{228}Th is in the form of the oxide and a relatively small amount (see Fig. 3) has been generated by ^{228}Ra decay taking place after the Thorotrast was sealed in the vial.

Table 1. *Daughters Adsorbed as Found by Transfer of Fresh* (*Vial Nos.* 2–6) *and Aged* (*Vial Nos.* 13, 14, *and* 15) *Lots of Thorotrast from Original Vials*

Vial No.	^{228}Ra content μCi			^{228}Th content μCi		
	Before transfer	After transfer	% Left	Before transfer	After transfer	% Left
2	0.0406	0.0005	1.2	0.112	0.0013	1.1
3	0.0398	0.0005	1.2	0.111	0.0014	1.2
4	0.0428	0.0006	1.3	0.117	0.0015	1.3
5	0.0402	0.0005	1.2	0.113	0.0015	1.3
6	0.0440	0.0004	1.0	0.119	0.0014	1.2
13	0.139	0.0880	63	0.122	0.0672	55
14	0.153	0.1330	87	0.138	0.108	78
15	0.144	0.1252	87	0.129	0.101	78

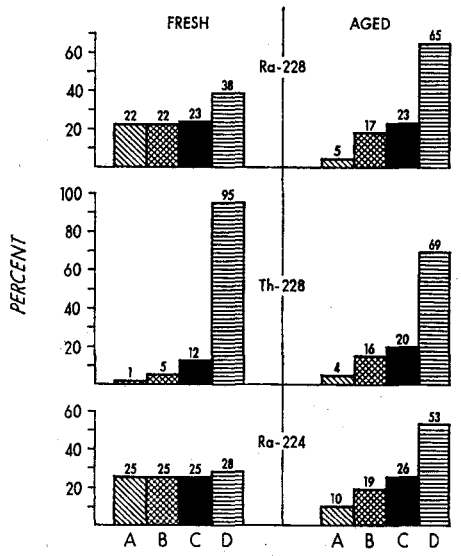

FIG. 4. Comparison of sedimentation in the fresh and aged lots of Thorotrast. Percent of thorium daughter per milliliter in ultra centrifuge fractions of increasing density gradient from A to D.

The fractional distribution of the aged Thorotrast shows a grossly similar pattern for all three daughters, indicating a considerable amount of sedimentation. The amount in each fraction appears to be nearly the same for ^{228}Ra and ^{228}Th whereas ^{224}Ra shows a somewhat greater concentration in the "lighter" fractions.

DISCUSSION

Taken together the transfer experiments and the ultracentrifuge experiments suggest that if the thorium daughters exist as small entities, probably in ionic form, they do not adsorb to the glass walls, whereas if they exist as polymers, they have a marked tendency to adsorb to glass. A similar tendency of polonium to adsorb on walls of the container has been related to the formation of polymers.[10] Although this situation is by no means well understood in physico-chemical terms, one may speculate that the low velocities and the tendency to become insoluble of the larger aggregates would predispose toward adsorption on glass. Any theory, and none will be presented here, would need to include an explanation of why the daughter aggregates do not adsorb on the Thorotrast particles themselves.

The question of more concern to the immediate study is, "Why do aggregates form in one Thorotrast suspension and not in the other?" The experience of investigators injecting animals with radium, as well as the studies with polonium,[10] is that adsorption occurs when the pH of the solution is near neutrality. We were not able to establish that the pH of the "fresh" versus "aged" lot varied in a significant way.

Eleven vials of the fresh lot measured from pH 6.03 to 6.22 whereas 3 vials of the aged lot measured from 6.02 to 6.40. No drift was noticed during measurement. If the result of the polonium study can be extrapolated to the present investigation, it might be supposed that, in terms of pH, conditions were suitable for formation of polymers in both "fresh" and "aged" lots.

Other conditions favoring the formation of aggregates would be the presence of foreign particles, concentration of daughters, and "age" of suspension. Our limited study does not permit identification of any of these factors as critical in producing the differences noted. An interpretation on grounds of relative "age" is not convincing since the important distinction would be expected to be on a time scale of days or weeks rather than years.

In summary we must present the conclusion that if the daughters exist in the Thorotrast suspension as aggregates, adsorption to the glass walls will occur, but that the critical condition bringing about aggregation in one lot and not in another lot remains unidentified.

PERTINENCE OF THIS STUDY TO DOSE CALCULATION

On the basis of these studies and other measurements an arbitrary opinion is presented that for the Thorotrast subject group the injected material contained ^{228}Ra in amounts from 2.5% to 35% of radioactive equilibrium with ^{232}Th and that the corresponding values for ^{228}Th were 15 to 40%. It is hoped that further study may improve on these estimates.

In order to justify such further effort, it is appropriate to consider what fraction of a total 15-year dose can be attributed to the injected ^{228}Ra and ^{228}Th daughters as contrasted with the fraction produced by daughters formed *in vivo*. The results of such a calculation are shown in Fig. 5 and the area for each curve (integrated from zero time to 15 years) is noted. In the simplified model used for calculation it is assumed that the ^{228}Th burden will be a sufficient measure of relative dose rate. The extreme values of ^{228}Ra at 35% and ^{228}Th at 40% have been used for the injected levels. It has been assumed that the excretion of ^{228}Ra will occur at 0.35% per day for the period 0 to 700 days and at 0.1% per day for 700 days to 15 years after injection.[11] It is further assumed that the excretion of ^{228}Th is zero[12] at all times. A calculation done in this way stipulates that about one-third of the dose can come from the injected daughters. It should be understood that this is believed to be a maximum, and it is acknowledged that use of other plausible assumptions about daughter excretion rate and/or calculation for a longer exposure period would yield a lower estimate.

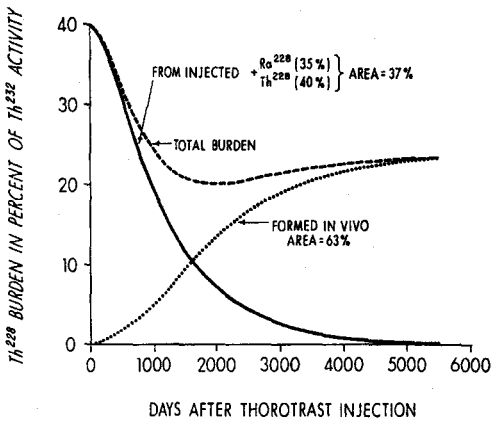

FIG. 5. Calculated curves of the ^{228}Th *in vivo* burden assuming injected amounts of ^{228}Th and ^{228}Ra are as stipulated.

May I conclude this paper with an endorsement of the theme of Dr. Robert Dudley's presentation of Thorotrast dosimetry at the New York Academy of Science,[1] i.e. "Thorotrast dosimetry is complicated," and add the footnote that the thorium daughters begin to misbehave before they get out of the bottle.

REFERENCES

1. Conference on Distribution, Retention, and Late Effects of Thorium Dioxide. April 20–22, 1966, New York Academy of Science, New York.
2. J. ROTBLAT and G. B. WARD. *Nature* **72,** 769 (1953).
3. J. RUNDO. *Phys. Med. Biol.* **1,** 138 (1956).
4. J. B. HURSH, L. T. STEADMAN, W. B. LOONEY and M. COLODZIN. *Acta Radiol.* **47,** 481 (1957).
5. R. H. CARRIGAN. Chief Chemist, Testagar Company, Detroit, Michigan. Personal communications.

6. J. RUNDO, A. H. WARD and P. G. JENSEN. *Phys. Med. Biol.* **3,** 101 (1958).
7. J. B. HURSH. Unpublished data.
8. J. C. HAMPTON. The distribution of colloidal thorium dioxide in mouse liver after intravenous injection. Presented orally at New York Academy of Science conference listed as Ref. 1.
9. R. H. CARRIGAN. Manufacture of thorium dioxide suspension, thorotrast. Presented orally at New York Academy of Science conference listed as Ref. 1.
10. R. G. THOMAS and J. N. STANNARD. *Radiation Res. Suppl.* **5,** 23 (1964).
11. J. B. HURSH. *Brit. J. Radiol.* **38,** 776 (1965).
12. J. B. HURSH. Loss of thorium and its daughter by thorium dioxide patients. Presented orally at New York Academy of Science conference listed as Ref. 1.

EXPOSITION CHRONIQUE D'UN GROUPE D'OUVRIERS AUX PEINTURES LUMINEUSES RADIO-ACTIVES. CONTRIBUTION À L'ÉTUDE DES EFFETS BIOLOGIQUES

V. TOMIN, M. TRAJKOVIĆ, D. VELJKOVIĆ, D. JANKOVIĆ, Z. UBOVIĆ, B. PENDIĆ, Dj. BEK-UZAROV et Z. DJUKIĆ

Service de Protection Médicale, Institut des Sciences Nucléaires B. Kidrič, Vinča (Yugoslavia)

Résumé—Un groupe d'ouvriers ayant travaillé au cours d'une longue période avec des peintures lumineuses radio-actives ont subi un examen médical au Service de Protection Médicale de l'Institut des Sciences Nucléaires "Boris Kidrič", Vinča. Compte tenu des conditions de travail, une contamination interne aux matières radio-actives a été possible.

Des examens cliniques et de laboratoires ont été faits sur les ouvriers cités ci-dessus afin de révéler si une contamination interne a eu lieu et de constater des altérations éventuelles y relatives.

Les résultats de ces examens (analyses radiotoxicologiques de l'urine, mesure de la radioactivité totale du corps, radiographie du squelette et autres) ont confirmé l'existence d'une contamination interne provoquée chez des ouvriers, qui, d'après l'anamnèse, ont été embauchés depuis longtemps au travail mentionné. Des altérations hématologiques dans le sang périphérique, décelées chez ces ouvriers, suggèrent une corrélation causale entre leur apparition et le temps d'exposition, ce qui nous renseigne, ainsi que d'autres constatations, sur le degré des contaminations internes dans l'organisme.

DISCUSSION

J. W. Ch. VAN STEEDEN (*Netherlands*):

Ich möchte Herr Nishiwaki fragen, in wie weit seine Ergebnisse Beziehung auf lebendes Gewebe haben.

Y. NISHIWAKI:

The sampling material used in these experiments was human skin, supplied by the Tokyo Metropolitan Medical Examiner's Office. Therefore, the skin was not living. The skin, of the size of about 3 by 15 cm with subcutaneous fat, was cut off from the central part of the breast of the adult at about 10 hr after accidental death and therefore under the conditions of the experiment we cannot expect any metabolic action.

Hub. WIJKER (*Netherlands*):

What was the time lapse between contamination and the start of decontamination? Has the speaker some idea whether the contamination penetrated the skin and, if so, if it diffused back during the decontamination procedure.

Y. NISHIWAKI:

We have conducted these experiments about 1 hr after contamination of the skin surface and we have not tested to what extent contaminants were absorbed in the tissues. But we have conducted previous experiments on which we already reported during the Gatlinburg Conference. These experiments were done with other biological material and in this case we think that some of the absorbed nuclides may come out if we wash thoroughly with a running chelating solution. However, we had considerable differences in this type of experiment because the results may differ depending on the conditions of the decontamination. If these conditions are different, we cannot compare in a fair way the effectiveness of the different decontaminating materials. This is very difficult. Therefore we have designed the elaborate equipment to set these conditions at the time of the decontamination, so that experiments can be compared one to the other.

E. W. JACKSON (*U.K.*):

The curves you put on the screen, showing spectral distribution before and after decontamination showed a uniform degree of removal for each gamma energy and yet the experiments in which separate nuclides were used showed a diversity of removal values. Are these two findings wholly consistent? Another point, could I have details of the pH of the contaminant used? As it is well known, to dissolve some of the fission elements requires strong acids. Did you apply strong acid solutions to the skin in this work?

I would also like to ask whether any fundamental study has been considered to determine the mode of attachment of some of the nuclides in a more simple form. Some years ago I did some laboratory experiments in which I determined the zeta potential at a solid-liquid boundary and I found that the degree of absorption, that is, the tightness in which nuclides were held, could be related to the zeta potential. I wonder if any work of this kind has been undertaken.

Y. NISHIWAKI:

The data appeared to be rather uniform, but the corresponding nuclides were estimated by Covell's method and after the estimation the results are indicated in the last slide which was shown at the end of my speech.

The pH of the solution was about 6.8. We wanted to conduct many series of experiments, but we had considerable difficulties in obtaining the skin material, so this may be considered only the beginning of the experiments. However, not to damage the surface of the skin, in this first series of experiments we tried to use solutions rather close to neutral. Therefore the pH which was measured before the start of the experiments was 6.8. Also about the zeta potential, we did not measure it, but we should like to obtain your paper, if this is possible later. Thank you very much for your remarks.

J. SHAPIRO (*U.S.A.*):

My question is actually addressed to either of the two speakers or to the audience. Some radiochemists I know when they have to decontaminate their fingers will use a skin stripping by using successive applications of adhesive to peel off the skin, of course not going to the base and removing the skin completely, but removing quite a bit. Or they use sand paper as a file to scrape away the contamination. I wonder whether the speakers have any comment on this method.

[*Dr. Stajić not having understood the question, Dr. Shapiro repeats as follows.*]

In discussing decontamination with radiochemists,

I found one, perhaps a very practical-minded individual, who got some cesium on his skin and he strips the top layers of his skin with successive applications of adhesive, just a few layers in order not to take the skin off, but enough to remove the surface activity; for the same purpose he used sand paper as a file, which is a dry method, a dry method without worry. Now, my question is, to the speakers who have used other methods, have they any comments on this approach?

Hub. WIJKER:

The following information can be given concerning the peeling-off procedure for skin decontamination. This procedure has advantages if spreading of the contaminant by using solvents should be avoided. In the Kema labs there has not been need to use this procedure but in other labs in Holland some experience has been gained. Destruction of the granular layer has to be avoided (stratum granulorum) as this layer works as a barrier against penetration in many cases. More details can be found in my papers presented at the Euratom Symposia at Munich (1962) and Nice (1966).

J. STAJIĆ:

Nous avons protégé la peau de nos mains par la crème protectrice "Octa" et par des gants en caoutchouc.

P. M. BIRD (*Canada*):

I would like to ask either of the speakers if they have any experience of using ultrasonic techniques for removal of contamination from the hands.

J. STAJIĆ:

Non, nous n'avons pas essayé de méthode ultrasonique.

N. VALENTIN (*Belgium*):

L'auteur peut-il indiquer:

1. Si des études de dynamique de pénétration ont été faites avec d'autres composés chimiques du Cs^{137} que le chlorure, et dans ce cas, si des différences notables dans la vitesse de résorption transcutanée ont été constatées.

2. Quelle était, dans le cas du chlorure de Cs^{137}, l'acidité de la solution et s'il existe une relation entre l'acidité et la vitesse de résorption transcutanée.

B. PENDIĆ:

1. On a fait aussi des expériences avec une solution de nitrate. Nous avons observé que la pénétration de cette solution est moins grande que celle de la solution de chlorure.

2. On a expérimenté dans le travail présentement rapporté, seulement avec des solutions dont l'acidité était de 0, 1 N HCl.

K. KOREN (*Norway*):

I would like to ask Prof. Faber whether he has tried to evaluate the yearly absorbed dose to the liver from a given amount of injected thorotrast?

M. FABER:

Due to the inhomogeneous distribution of Thorotrast the dosimetry is difficult. Mean doses to organs have been calculated, but the significance of these figures is still undecided in relation to cancenogenesis.

F. WACHSMANN (*Germany*):

Da keine Angaben über die Höhe der lokalen Dosen nach der Anwendung von Thorotrast gemacht wurden, möchte ich angeben, dass ich mich erinnere von lokalen Dosen gehört zu haben, die hin zu 50 bis 100000 rad gehen! Halten Sie—Herr Faber—diese hohen Dosen für möglich?

M. FABER:

The dose around particles is not as high as suggested by the Chairman, but even so is not negligible.

H. KRIEGEL (*Germany*):

In neuerer Zeit sind verschiedentlich Mitteilungen über Schädigungen nach Anwendung von Peteosthor bei Kindern erschienen. Ich möchte Herrn Dr. Faber fragen, ob er darüber Erfahrungen besitzt.

M. FABER:

Peteosthor is a colloid preparation containing ^{224}Ra. It was used for bone diseases and tuberculosis. A certain number of bone tumours and leukemias have occurred in this group. It is known that German groups are tracing these children in order to evaluate the dose response relations.

RAPPORTEUR PAPER

OPERATIONAL HEALTH PHYSICS

J. PRADEL
Commisariat à l'Energie Atomique, Paris

LA SÉCURITÉ des installations atomiques est, pour une grande part, fondée sur l'efficacité des dispositifs d'épuration de l'air. Or, l'efficacité de ces dispositifs peut se trouver réduite, parfois dans de très grandes proportions, pour des causes multiples telles que éléments défectueux, montage incorrect, détériorations consécutives au colmatage, empoisonnement par des vapeurs, vieillissement des matériaux. . . .

Il apparaît donc nécessaire:

—d'assurer le contrôle systématique des dispositifs installés,

—d'éliminer les éléments défectueux avant leur mise en place,

—de contrôler les éléments eux-mêmes,

—de contrôler également le medium filtrant.

MM. Billard et Brion préconisent une procédure détaillée pour l'exécution de ces contrôles.

Ils indiquent les caractéristiques contrôlées et les essais correspondants pour les filtres à aérosols à base de papier plissé et les pièges à iode, à base de charbon actif.

En ce qui concerne les filtres, seul le contrôle de l'efficacité est délicat et pour les filtres à haute efficacité, couramment utilisés, il importe de choisir une méthode à la fois sensible et fidèle parmi les nombreuses qui existent: méthode au bleu de méthylène, méthode de la flamme de sodium, méthode au DOP polydispersé, méthode au DOP monodispersé, etc. . . C'est vers la méthode à l'uranine étudiée par L. Silvermann et K. T. Whitby et dont la caractéristique principale est une grande sensibilité que s'orientent MM. Billard et Brion.

Un aérosol liquide est produit par pulvérisation d'une solution aqueuse d'uranine à 1%. Les gouttelettes de diamètre supérieur à 2 μ sont arrêtées dans un impacteur. Après évaporation dans un tube chauffant et dilution avec de l'air sec, on obtient un aérosol solide dont le diamètre maximum est voisin de 0,5 μ. On effectue des prélèvements en amont et en aval du filtre en essai sur des filtres qui sont ensuite lavés. Les solutions de lavage sont mesurées par fluorimétrie. La sensiblité de la méthode est telle qu'on obtient une mesure du prélèvement aval égale à deux fois le "bruit de fond" pour un volume d'air prélevé de un mètre cube derrière un filtre d'efficacité 10.000 avec, en amont, une concentration en aérosol solide de 4 γ/m^3 seulement.

Parmi les autres caractéristiques vérifiées sur les éléments filtrants, citons: la capacité de colmatage, l'ininflammabilité, l'inaltérabilité à l'eau, la tenue à la température, la résistance mécanique.

Le contrôle des pièges à iode est, comme pour les filtres à aérosols, divisé en trois parties:

—contrôle du matériau adsorbant, c'est-à-dire du charbon actif,

—contrôle de l'élément adsorbant,

—contrôle du piège installé sur le site.

Parmi les caractéristiques vérifiées sur le charbon: densité, humidité, granulométrie, perte de charge, friabilité, pH, température d'inflammation, l'efficacité à l'iode est évidemment la caractéristique essentielle. Pour les contrôles d'efficacité, le mode de génération d'iode 131 doit être soigneusement étudié. Les auteurs préconisent de faire passer de l'iode 127 sous forme vapeur mélangée à l'air sur un dépôt d'iodure 131 par échange isotopique à température ambiante.

Des expérimentateurs anglais et américains ayant démontré l'existence de la forme iodure de méthyle et la possibilité de la piéger au moyen de charbon imprégné, il apparaît nécessaire à MM. Billard et Brion de contrôler à l'iodure de méthyle de tels charbons. L'iodure de méthyle gazeux marqué à l'iode 131 est produit suivant un procédé utilisé par Collins, puis envoyé pour l'essai dans un circuit d'air conditionné à 90%

d'humidité. Les pièges de référence sont constitués de couches de charbon de houille activé imprégné à 5% de triéthylènediamine.

En dehors des examens de conformité concernant les dimensions, les dispositifs garantissant le maintien du tassement, la protection, les joints, etc. . . . , on vérifie les caractéristiques suivantes sur les éléments adsorbants:

—perte de charge

—efficacité à l'iode

—résistance aux chocs et vibrations.

Le contrôle in situ à l'iode moléculaire est effectué par les auteurs suivant la méthode déjà décrite pour le charbon actif. Ils utilisent une source d'iode portative de 3 Curies.

L'expérience prouve qu'il est nécessaire de contrôler assez fréquemment—plusieurs fois par an—les pièges à iode installés sur un circuit en fonctionnement permanent. En effet, l'efficacité du charbon actif vis-à-vis de l'iode est affectée par des vapeurs diverses, en particulier par celles émises par les peintures. Pour réduire la fréquence des essais in situ, toujours onéreux et souvent gênants pour l'exploitation, MM. Billard et Brion font installer, en dérivation sur le piège principal, un ou deux petits pièges témoins qu'il est facile de retirer de temps à autre pour un contrôle d'efficacité au laboratoire.

MM. Hans Flyger et H. C. Rosenbaum se sont eux essentiellement penchés sur le probléme des tests de filtres in situ. Ils comparent le test proposé avec utilisation d'un aérosol provenant d'une solution au sulfate de lithium à 2%, aux tests classiques avec le bleu de méthylène ou le chlorure de sodium associé à la photométrie de flamme. Les avantages suivants sont obtenus avec la méthode préconisée:

Il n'est plus nécessaire comme dans le cas du chlorure de sodium d'obtenir une génération très stable puisque l'on n'effectue plus un étalonnage par prélèvement amont de courte durée.

Il n'est pas nécessaire également d'avoir une liaison entre les points de prélèvement amont et aval, et de posséder un photomètre spécialement adapté et non commercialisé.

Le test proposé consiste à utiliser un générateur comme dans la méthode à l'uranine décrite précédemment, type Collison, pour obtenir un aérosol sec de 0,6 μ de diamètre en moyenne et à effectuer des prélèvements amont et aval sur membrane filtrante. Un traitement approprié de ces membranes en phase liquide permet de doser le lithium contenu dans la solution par photométrie de flamme. On préfère le lithium au sodium car il est beaucoup moins répandu dans la nature, et bien que la sensibilité de la méthode soit 10 fois moindre théoriquement, elle se révèle pratiquement supérieure. Il ne faut pas oublier, en effet, que l'on peut avoir jusqu'à 20 mg/m^3 de ClNa dans l'air au voisinage des mers.

Signalons pour le traitement des filtres de prélèvement que, après l'attaque nitrique, l'adjonction d'acétone associée à une filtration permet aux auteurs d'obtenir par photométrie une réponse linéaire en fonction de la concentration et une meilleure sensibilité. On peut alors mesurer 2.10^{-4} γ/ml soit une quantité de sulfate de lithium de 7.10^{-3} γ par prélèvement.

Pour comparer les diverses méthodes, MM. Flyger et Rosenbaum ont testé sur banc d'essai 3 types de filtres avec la méthode au sodium activé, associée à une mesure de la radioactivité du prélèvement, avec celle au lithium et aussi avec le compteur de Pollak qui permet le dénombrement des noyaux de condensation naturellement présents ou créés artificiellement. Ils ont obtenu des résultats comparables pour les deux premiers tests, mais avec le troisième ont observé une pénétration plus grande.

Un contrôle in situ sur la ventilation du réacteur DR3 à Riso a été effectué. Le débit de cette installation est de 6000 m^3/h avec des gaines de 1 m^2 de surface. Les premiers essais ont donné les résultats suivants pour la perméabilité: 0,69–0,70–0,10 et 0,60. La dispersion s'explique par la non observation de règles fondamentales pour obtenir une bonne génération et de bons prélèvements. En respectant les règles préconisées récemment par Smith: distance de l'ordre de 30 diamètres entre l'injection et le point de prélèvement amont avec interposition souhaitable d'écrans ou de coudes, et distance identique entre filtre et prélèvement aval, on a obtenu les valeurs stables suivantes:

0,06 avec le lithium en accord avec le test au ClNa

0,12 avec le compteur de Pollak.

Au cours d'un autre essai avec un autre filtre placé en parallèle, on a également obtenu des résultats analogues.

Il existe donc un test commode au lithium qui peut être remplacé pour des débits élevés par un test basé sur le comptage des noyaux de condensation avec le compteur de Pollak avec ou sans enrichissement de l'air en noyaux.

Etudiant à l'échelon du laboratoire le piégeage de l'iode radioactif dans l'air, MM. Hacke et Jacobi, décrivent un cycle d'expérimentation effectué en vue de déterminer la perméabilité vis-à-vis des différentes formes d'iode radioactif de filtres à fibres, de pièges en charbon activé et de filtres combinés.

(1) Dans une première série d'expériences, quatre membranes filtrantes en série suivies d'un piège en charbon activé sont traversées par un courant d'air, à la température de 20–22°C, à 35–45% d'hygrométrie et contaminé à l'iode 132.

Les efficacités mesurées, rapport de l'activité dans le piège à l'activité totale dans l'air filtré, sont respectivement pour les quatre membranes de 55–11–10–6 et de 15% pour le charbon.

Ces essais montrent que, après le premier filtre, la perméabilité varie exponentiellement en fonction du nombre de filtres en série et que l'on est en présence de deux formes physiques d'iode:

—une forme arrêtée par les filtres

—une forme mal arrêtée par les filtres qui auraient une efficacité de l'ordre de 26% vis-à-vis de celle-ci.

La forme arrêtée serait de l'iode fixé sur les aérosols et représenterait 40% de l'activité de l'iode présent dans l'air.

(2) Des expériences identiques ont été effectuées avec quatre cartouches garnies de charbon activé, en série, suivies d'une seule membrane filtrante.

Les efficacités mesurées sont respectivement de 92,2–0,19–0,14 et 0–12 pour le charbon et de 0,35% pour le filtre. Après le premier piège, la perméabilité varie exponentiellement.

On a encore dans ce cas:

—une forme d'iode bien arrêtée représentant 99% de l'activité totale comprenant de l'iode à l'état élémentaire et de l'iode fixé sur les aérosols,

—une forme d'iode mal arrêtée, que l'on peut évaluer en moyenne dans les conditions d'essais à 1% et qui est probablement composée d'iodures organiques, principalement d'iodure de méthyle, et d'iode adsorbé sur des aérosols fins mal arrêtés par les pièges en charbon. L'efficacité des charbons vis-à-vis de ces formes est en moyenne de 24%.

(3) Enfin, dans une troisième série d'expérience, les auteurs ont examiné la perméabilité de trois filtres combinés, constitués par une membrane et un piège en charbon, placés en série.

Là encore, ils constatent que la perméabilité après le premier filtre varie exponentiellement et ils en déduisent que si l'efficacité totale du premier est de 99,9%, celle des suivants n'est plus que de 43%. La forme vapeur mal piégée serait principalement l'iodure de méthyle et représente, 0,1% de l'activité totale.

En conclusion, les auteurs estiment que dans les conditions de leur expérimentation, l'iode présent dans l'air se trouve sous trois formes:

(1°) une forme fixée sur les aérosols, presque totalement arrêtée par les filtres fibreux et partiellement dans le charbon activé, et représentant 40% de l'activité totale,

(2°) une forme vapeur, à l'état élément, arrêtée presque totalement par le charbon activé et partiellement par les membranes et représentant 60% de l'activité,

(3°) une forme vapeur à l'état combiné (iodure de méthyle principalement) arrêtée à 40–50% par le charbon activé et représentant 0,1% de l'activité.

Ces proportions sont des résultats moyens qui sont appelés à varier en fonction de la concentration de l'air en iode et de l'humidité relative. On a, en particulier, pour l'iodure de méthyle les perméabilités suivantes:

—0,3% pour 10^{-5} Ci/m³ d'I_{132} et

—0,003% pour 10^{-3} Ci/m³ d'I_{132}

Les auteurs rappellent enfin que l'humidité fait croître la valeur de la composante mal filtrée et que des charbons imprégnés spécialement permettent d'avoir une efficacité de 99% pour l'iodure de méthyle.

MM. Yoshida, K. Kitano, M. Murata s'intéressent à la comparaison des mediums filtrants.

Ils examinent les différentes caractéristiques: efficacité, perte de charge, pénétration de différents filtres, soit japonais, soit étrangers, utilisés par la Japan Atomic Energy Research

Institute. L'aérosol test utilisé est le dépôt actif du thoron et le filtre de référence la membrane millipore AA. La granulométrie de l'aérosol a été effectuée par microscopie électronique, et a montré que la presque totalité des particules avait un diamètre inférieur à 0,1 μ.

La mesure de l'efficacité des filtres est effectuée en comparant la radioactivité collectée sur une première membranne millipore, placée derrière le filtre à étudier, à celle collectée sur une seconde placée en parallèle.

Le diamètre des filtres étudiés est de 40 mm et les vitesses de passage de 32–48 et 64 mètres/minute.

Pour les filtres cellulosiques, les auteurs ont constaté une augmentation de l'efficacité en fonction de la vitesse de passage en bon accord avec les résultats déjà publiés dans ce domaine.

Pour mesurer la pénétration, deux méthodes sont utilisées:

—La première basée sur l'évaluation des pertes $\alpha\beta$ dues à la pénétration de l'aérosol,

—La deuxième basée sur la mesure de la résolution d'un pic α obtenu par spectrométrie.

La membrane millipore AA est prise en référence en considérant qu'il n'y a pas pénétration de l'aérosol à l'intérieur du filtre.

Avec la méthode de la perte de comptage, la radioactivité α ou β est tout d'abord déterminée sur le filtre et sur la membrane de référence. Un comptage γ (pic 0,239 MeV du ThC) est ensuite effectué. Le rapport des valeurs $\frac{\alpha}{\gamma}$ ou $\frac{\beta}{\gamma}$ pour le filtre étudié et pour la membrane donne une efficacité relative de collection en surface.

L'efficacité de collection en surface varie de 0,12 à 0,95 pour le comptage α et de 0,36 à 0,89 pour le comptage β pour les différents filtres étudiés sans que l'on ait constaté de différences significatives lorsque l'on opère à des vitesses de 32, puis 64 m/mn.

Pour la méthode de la résolution d'un pic α, les auteurs utilisent le pic α de 8,77 MeV du ThC' et font la mesure à l'aide d'un détecteur à jonctions associé à un spectromètre multicanaux.

Les résultats obtenus indiquent une amélioration de la résolution en fonction de la vitesse. Ces résultats semblent s'accorder avec la loi théorique qui prévoit une augmentation de la contribution de l'effet d'impact aux grandes vitesses.

La résolution pour la membrane prise comme référence étant de 8%, les résolutions pour les autres filtres varient de 16 à 46%.

De ces résultats, il ressort que parmi les filtres essayés ceux qui arrêtent le mieux l'aérosol en surface sont les filtres de fibres de verre Gelman E et GB 100 et le filtre japonais HE 40.

Un tableau récapitulatif compare les résultats obtenus pour ces filtres par divers auteurs avec différents aérosols et il n'y apparaît pas de différence significative.

Quant à MM. K. G. Vohra et P. V. N. Nair, ils s'intéressent, eux, à l'élimination des poussières par une utilisation judicieuse des dispositifs d'épuration. Ils remarquent que les particules radioactives dans l'air qui présentent une nocivité importante d'après le nouveau modèle pulmonaire préconisé par l'I.C.R.P., sont essentiellement submicroniques et que la rétention de ces particules par des filtres absolus est en général très coûteuse. Aussi proposent-ils l'utilisation d'un précipitateur électrostatique mobile à haute efficacité qui permet la filtration d'un grand volume d'air par recyclage. Les caractéristiques principales de cet appareil particulièrement adapté à l'épuration d'air peu chargé en poussière, comme cela est le cas des zones de travail, sont:

—perte de charge faible pour un grand volume d'air traité,

—efficacité particulièrement élevée pour les particules submicroniques,

—puissance d'aspiration moins élevée de plusieurs ordres de grandeur que pour les filtres mécaniques,

—mobilité du filtre.

Le système de filtration comprend un préfiltre en Dacron, un ioniseur et un collecteur, et un ventilateur.

Pour un débit de 100 m³/mn, il a les dimensions suivantes:

—largeur et profondeur 85 cm

—hauteur 180 cm

Les auteurs fournissent un certain nombre de résultats expérimentaux.

(a) Tout d'abord, ils ont étudié la décontamination d'une enceinte polluée avec du dépôt actif du thoron.

Pendant la génération de thoron, une fois l'équilibre atteint, le précipitateur est mis en

marche. Après 50 minutes, l'activité de la pièce, d'un volume de 80 m³, est inférieure au mouvement propre.

(b) Ensuite ils ont étudié la rétention des produits de filiation du ^{88}Kr et ^{138}Xe présents dans le hall de la pile piscine Apsara.

Le volume du hall étant de 280 m³, un volume d'air équivalent est filtré en deux minutes environ et la décontamination de la pièce est obtenue après 4 à 5 renouvellements.

(c) De même, la décontamination d'un atelier de broyage de thorium où les thorium B et C sont à l'équilibre est obtenue après 30 à 40 minutes au bout desquelles il ne reste qu'une activité négligeable.

Les auteurs concluent que cet appareil est parfaitement adapté à l'épuration de volumes importants d'air avec recyclage, qu'on peut atteindre des taux de renouvellement de l'ordre de un par minute sans encombrement excessif de l'installation, et qu'une telle technique permet d'envisager d'effectuer à l'air libre certains travaux normalement effectués en boîtes à gants.

J'ai terminé la présentation des travaux décrits dans ces cinq documents où des résultats très complets ont été obtenus par les auteurs dans le domaine de l'épuration de l'air, domaine fort important pour la radioprotection.

Vous avez pu constater que des méthodes précises et relativement faciles à mettre en oeuvre existent maintenant pour effectuer les différents contrôles nécessaires à toutes les étapes de la construction de l'installation et de l'exploitation d'un dispositif d'épuration. L'utilisation de ces tests nous a montré à nous-mêmes l'existence de défauts fréquents et d'origines très diverses et l'expérience ainsi acquise nous amène à insister très fortement pour que les procédures de contrôle, maintenant faciles à élaborer, le soient rigoureusement. La sécurité des installations sera ainsi accrue d'une façon considérable et ce à peu de frais.

Dans le domaine de l'épuration de l'iode, les problèmes sont maintenant assez bien résolus et l'on doit étudier s'il est judicieux de remplacer les charbons actifs par des charbons spécialement imprégnés pour arrêter l'iodure de méthyle tout en tenant compte du prix élevé de ces charbons.

Enfin, je partage le point de vue de MM. Vohra et Nair qui préconisent l'utilisation de recyclage dans les ventilations. Ces recyclages d'un air conditionné doivent entraîner des diminutions importantes dans le coût des ventilations; la solution qu'ils préconisent avec de très forts débits mérite d'être envisagée et il faut retenir la possibilité de faire ainsi certaines manipulations en supprimant les enceintes étanches.

De façon générale, la connaissance plus profonde des performances des dispositifs d'épuration doit nous amener à leur meilleure définition dans chaque cas particulier ce qui doit contribuer non seulement à l'augmentation de la sûreté mais aussi à la diminution du coût des installations.

CONTRÔLE DES INSTALLATIONS D'ÉPURATION DE L'AIR—ESSAIS DE CONFORMITÉ DES ÉLÉMENTS—TESTS *IN SITU*

FRANÇOIS BILLARD et JACQUES BRION
Service Technique d'Études de Protection, Aérosols et Mines

Résumé—La sûreté de fonctionnement des installations d'épuration de l'air est fonction des contrôles auxquels ces installations sont soumises.

Si les tests in situ sont les plus importants puisqu'ils constituent le contrôle final de l'installation terminée, les essais de conformité des éléments constitutifs sont également nécessaires. Ils permettent l'élimination d'éléments défectueux avant leur mise en place, la discrimination des défauts du montage de ceux de l'élément et sont en outre plus sensibles. De même, le contrôle des matériaux constitutifs de l'élément s'avère fort utile.

On décrit les différents contrôles, d'une part, pour les filtres à aérosols, d'autre part, pour les pièges à iode.

Les caractéristiques vérifiées sont: nature des matériaux, dimensions des éléments, efficacité, perte de charge, résistance mécanique, inflammabilité, tenue à l'humidité, tenue à la température, résistance au détassement des pièges à iode, friabilité du matériau adsorbant, etc.

En ce qui concerne les installations de piégeage d'iode, il est prévu un contrôle de pièges témoins fonctionnant en parallèle avec le piège principal. Ce contrôle, simple, permet de réduire la fréquence des tests in situ, en particulier lorsqu'il s'agit de déceler un empoisonnement éventuel par des vapeurs organiques.

INTRODUCTION

La sécurité des installations atomiques vis-à-vis de l'environnement est, pour une grande part, fondée sur l'efficacité des dispositifs d'épuration de l'air. Or, l'efficacité de ces dispositifs peut se trouver réduite, parfois dans de grandes proportions, par des causes multiples: éléments défectueux, montage incorrect, détériorations consécutives au colmatage, empoisonnement par des vapeurs, vieillissement des matériaux, etc. . . . Il apparaît donc nécessaire d'assurer le contrôle systématique des dispositifs installés.

En outre, afin d'éliminer les éléments défectueux avant leur montage, et de distinguer les défauts de l'élément de ceux du montage, tout en améliorant la sensibilité des mesures, on est amené à contrôler les éléments eux-mêmes.

Enfin, pour des raisons homologues, il est souhaitable de contrôler le principal constituant de l'élément.

Pour fixer la procédure selon laquelle ce contrôle est effectué, il faut donc établir trois documents ou ensembles de documents:

(1°) Un document général précisant les modalités du contrôle: les essais imposés, le stade de la fabrication ou de la livraison auquel ils sont pratiqués, le pourcentage d'éléments sur lequel ils portent, les sanctions prévues en fonction des résultats, etc. . . .

(2°) Des fiches techniques qui décrivent chaque essai d'une façon détaillée.

(3°) Un cahier des charges et spécifications techniques qui précise, pour une commande donnée, les caractéristiques exigées et leurs tolérances.

Seules, les descriptions techniques du contrôle seront développées ici. Les deux seuls types de dispositifs épurateurs considérés sont les filtres à aérosols à base de papier plissé et les pièges à iode, à base de charbon actif.

1. CÔNTROLE DES FILTRES

Ainsi qu'il a déjà été mentionné, le contrôle est divisé en trois parties:

—contrôle du papier filtrant,

—contrôle de l'élément filtrant,

—contrôle du filtre complet installé sur le site.

1.1. *Contrôle du Papier Filtrant.*

Les constructeurs de filtres français effectuent un contrôle systématique de leur papier filtrant. Le contrôle du C.E.A. a pour but de vérifier ce contrôle des constructeurs. A cet effet, on prélève des échantillons de papier sur des bobines déjà contrôlées et on vérifie les caractéristiques suivantes:

—le grammage ou poids superficiel,
—la résistance à la traction,
—la perte de charge,
—l'efficacité.

1.1. 1. *Grammage.* La mesure du grammage ou masse de l'unité de surface de papier filtrant, couramment exprimé en grammes par mètre carré, est effectuée par simple pesée d'échantillons de papier. Toutefois, ces échantillons doivent être découpés avec suffisamment de précision et il peut être nécessaire de les conditionner en humidité. Tout dépend de la tolérance accordée et de l'influence de l'humidité. Un exemple chiffré permet d'exposer plus clairement la relation entre les différents facteurs:

Soit un papier de grammage moyen égal à 100 g/m², avec une tolérance normale de fabrication de $\pm$ 7 g/m². Si l'on choisit des échantillons carrés de 100 mm de côté, il est illusoire de chercher à les découper à mieux de 0,5 mm près, ce qui correspond à une précision superficielle de 1%. Il est logique d'admettre la même tolérance pour l'influence de l'humidité. Sur cette base, avec des papiers peu hygroscopiques, le conditionnement en humidité peut être évité. Si la pesée est effectuée avec cette même précision de 1%, la précision globale del a mesure sera de 3% et il faudra porter la tolérance à 10% pour l'acceptation des résultats, pour une tolérance réelle de fabrication comprise entre 7 et 13%.

Pour réduire la marge d'incertitude, il faut augmenter la dimension des échantillons et les conditionner en humidité. Cependant, comme il n'est pas essentiel de vérifier la caractéristique considérée avec une grande précision, on pourra généralement éviter le conditionnement.

1.1. 2. *Résistance à la traction* La méthode proposée pour la mesure de la résistance à la traction d'un papier filtrant s'inspire de la norme AFNOR concernant les essais de traction des papiers en général. On opère sur des éprouvettes de 15 mm de largeur et de 100 à 200 mm de longueur. L'essai de traction est effectué sur une petite machine spéciale qui indique la charge de rupture et l'allongement de l'éprouvette. Une série d'éprouvettes est découpée dans la direction de déroulement du papier, une autre série est découpée dans la direction perpendiculaire.

1.1. 3. *Perte de charge.* Le circuit de mesure de la perte de charge d'un papier filtrant est constitué d'une trompe à air à col sonique qui assure un débit constant à travers un porte-filtre muni de prises de pression. Ce porte-filtre ne contient pas de grille ni de joint, afin que la surface effective de papier filtrant soit connue avec précision. L'air est préalablement filtré pour éviter tout colmatage. La vitesse de passage de l'air au niveau de l'échantillon est voisine de la vitesse nominale en utilisation industrielle, soit 1 cm/s.

Un deuxième circuit semblable au premier, mais fonctionnant à une vitesse dix fois plus grande, permet une mesure plus précise, particulièrement sur les papiers à faible perte de charge.

1.1. 4. *Efficacité.* Il existe de nombreuses méthodes pour la détermination de l'efficacité des filtres à air: méthode au bleu de méthylène, méthode de la flamme de sodium, méthode au DOP polydispersé, méthode au DOP monodispersé, etc. . . . Afin d'obtenir des résultats comparables, la méthode adoptée doit être applicable aussi bien au contrôle du papier filtrant qu'à celui du filtre installé sur le site. Cette condition exclut la méthode au DOP monodispersé, qui nécessite une installation trop importante pour les essais in situ. La méthode au DOP polydispersé présente l'inconvénient de nécessiter une forte concentration en amont du filtre, qui entraîne un colmatage non négligeable et est une cause de mauvaise reproductibilité des mesures par suite des phénomènes de coalescence, d'importance variable avec la disposition du circuit contrôlé. Nous nous orientons vers la méthode à l'aérosol d'uranine étudiée par L. Silverman[1] et K. T. Whitby,[2, 3] dont la caractéristique principale est une grande sensibilité et dont le principe est décrit ci-après.

Un aérosol liquide est produit par pulvérisation

d'une solution aqueuse d'uranine à 1%. Les gouttelettes de diamètre supérieur à 2 μ sont arrêtées dans un impacteur. Après évaporation dans un tube chauffant et dilution avec de l'air sec, on obtient un aérosol solide dont le diamètre maxima est voisin de 0,5 μ. On effectue des prélèvements en amont et en aval du filtre en essai sur des filtres qui sont ensuite lavés. Les solutions de lavage sont mesurées par fluorimétrie.

La sensibilité de la méthode est telle qu'on obtient une mesure du prélèvement aval égale à deux fois "le bruit de fond" pour un volume d'air prélevé de un mètre cube derrière un filtre d'efficacité 10 000 (99,99%), avec, en amont, une concentration en aérosol solide de 4 $\mu g/m^3$ seulement, soit une émission en aérosol liquide équivalent à 0,4 mg/m^3.

1.2. *Contrôle des Éléments Filtrants*

Le contrôle des éléments filtrants comprend la vérification des caractéristiques suivantes:

—pour mémoire, caractéristiques dimensionnelles et aspect général (dimensions du cadre, nombre de plis, aspect du joint, du papier, protections, etc. . . .),
—perte de charge,
—colmatage,
—inflammabilité,
—inaltérabilité à l'eau,
—tenue à la température,
—résistance mécanique,
—efficacité.

Un élément filtrant peut être utilisé dans une gamme de débits assez large. Or, les résultats de certains essais sont fonction du régime adopté. On a donc choisi un débit de référence, ou débit nominal, proportionnel au volume de l'élément. En effet, l'étude économique d'une installation de filtration tient compte, d'une part des frais d'investissement, d'autre part, des frais d'entretien. Si l'élément filtrant est utilisé à un fort débit unitaire, l'encombrement de l'installation est moindre, donc les frais d'investissement sont moindres, mais en contrepartie, les frais d'entretien sont augmentés car les éléments doivent être remplacés plus fréquemment. Il est donc logique de rapporter le débit unitaire de référence au volume de l'élément.

Cependant, l'encombrement d'une installation de filtration n'est pas proportionnel à l'encombrement des éléments lorsque ceux-ci sont de profondeurs très différentes, car le volume des amenées et des départs d'air est indépendant de cette profondeur. La proportionnalité du débit de référence au volume de l'élément n'est donc valable que pour des éléments de profondeurs comparables.

Pour le plus petit élément couramment utilisé en France, ce débit nominal est pris égal à 100 m^3/h. La valeur correspondante pour l'élément de 600 × 600 × 300 mm est de 1 400 m^3/h.

1.2. 1. *Perte de charge.* La mesure de la perte de charge d'un élément filtrant ne présente pas de difficulté particulière. Il faut toutefois s'assurer que le circuit d'essai lui-même ne présente aucune perte de charge sensible en l'absence de filtre.

1.2. 2. *Colmatage.* La durée de vie d'un filtre est généralement limitée par son colmatage, c'est-à-dire par l'augmentation de sa perte de charge, au fur et à mesure de l'accumulation des poussières. L'expérience prouve que, dans les mêmes conditions d'empoussiérage, cet accroissement est très variable d'un type de filtre à un autre et dépend au premier chef de la vitesse de l'air à travers le papier filtre et, donc, de la surface de papier disponible dans un volume donné, et aussi du mode de plissage du papier.

La caractéristique de colmatage d'un filtre est déterminée en faisant fonctionner ce filtre dans des conditions voisines des conditions d'utilisation, c'est-à-dire en atmosphère naturelle. La perte de charge est périodiquement relevée, en même temps que l'empoussiérage atmosphérique. Il est ainsi possible d'établir la courbe de colmatage du filtre. Le défaut de la méthode est sa lenteur et nous cherchons à définir une méthode artificielle de colmatage accéléré qui soit représentative du colmatage naturel.

1.2. 3. *Ininflammabilité.* L'ininflammabilité des filtres à air ne se définit pas aisément et on est conduit à considérer différents comportements possibles des filtres au contact d'une flamme.[4] On aboutit ainsi à la classification suivante:

Classe A: filtres ne propageant pas la flamme ou la combustion d'un élément à l'autre.

Classe B: filtres ne propageant pas la flamme

ou la combustion au sein du médium filtrant, ne relâchant pas de débris incandescents et ne dégageant pas de fumée abondante.

Classe C: filtres de la classe B ne relâchant pas les poussières stockées.

Classe D: filtres de la classe C conservant une efficacité suffisante, à préciser dans chaque cas en fonction des conditions particulières d'emploi notamment de la présence éventuelle de poussières pyrophoriques.

Classe O: filtres éminemment inflammables.

Le principe de l'essai d'un filtre en vue de son classement est le suivant:

Le filtre est monté sur un circuit permettant son fonctionnement au débit nominal. Pendant une minute, on amène au contact du filtre la flamme d'un brûleur à gaz, définie en dimensions et en température et on note les effets observés. On effectue plusieurs essais en différents points du filtre, notamment au centre et à proximité du cadre; l'épreuve est répétée à très faible débit d'air, car on a constaté que certains éléments propagent la flamme à très faible débit alors qu'il n'y a aucune propagation au débit nominal.

L'abondance des fumées éventuellement produites est repérée au moyen d'un photomètre à aérosols. La baisse d'efficacité éventuelle est mesurée au moyen du même appareil par une mesure avant et après l'épreuve avec un aérosol produit par un fumigène.

1.2. 4. *Inaltérabilité à l'eau.* Un filtre peut, dans certaines conditions, être soumis à l'action d'aérosols liquides. Il est intéressant de connaître et de contrôler la tenue du filtre dans ces conditions. On peut craindre, en dehors du colmatage inévitable mais provisoire, une altération permanente des caractéristiques d'efficacité, de perte de charge et de résistance mécanique, par suite d'une modification de la texture du papier.

La méthode utilisée consiste à immerger avec précautions dans un bac rempli d'eau l'élément à contrôler. On évite notamment toute différence importante de pression de part et d'autre du médium filtrant. Après un séjour d'une heure dans l'eau, le filtre est retiré du bac avec les mêmes précautions. Après séchage naturel jusqu'à équilibre avec l'atmosphère ambiante, on détermine les nouvelles valeurs d'efficacité, de perte de charge et de résistance mécanique. Cette méthode peut paraître sévère; nous l'avons choisie pour sa facilité de définition et de mise en œuvre.

1.2. 5. *Tenue à la température.* Pour vérifier la tenue d'un filtre à la température, on le soumet à une épreuve simplifiée. Alors que le principe de l'épreuve conforme à l'utilisation réelle serait de faire fonctionner le filtre à la température prévue, pendant une longue période, par exemple un mois, l'épreuve simplifiée consiste à placer le filtre dans une étuve, sans circulation d'air, pendant 24 heures, à une température supérieure à la température limite pour un fonctionnement permanent.

On établit la corrélation entre la température d'épreuve et la température limite de fonctionnement permanent au moyen d'essais comparatifs préliminaires dans une étuve et sur un circuit à haute température.

1.2. 6. *Résistance mécanique.* Il est intéressant de contrôler la résistance mécanique des filtres à air, c'est-à-dire la pression différentielle maximum qu'ils peuvent supporter avant rupture ou déformation notable, puisque cette caractéristique permet de préjuger de leur comportement en cas de surpression accidentelle, dans un hall de réacteur par exemple.

Pour ce contrôle, l'élément filtrant est monté sur un circuit permettant de le faire fonctionner à un débit régulièrement croissant, depuis la valeur nominale jusqu'à une valeur 40 fois supérieure. On enregistre la courbe de la perte de charge en fonction du débit grâce à des manomètres à traduction éléctrique. Dans ces conditions, toute déformation du filtre et a fortiori, sa rupture, se traduit par une variation brusque de la pente de la courbe. Les coordonnées correspondantes sont les valeurs limites de perte de charge et de débit. Comme la perte de charge mesurée dans ces conditions extrêmes est plus influencée par les caractéristiques dynamiques de l'écoulement que par la résistance aéraulique du médium filtrant lui-même, on choisit d'exprimer la résistance mécanique de l'élément par la valeur du débit limite.

1.3. *Contrôle des Installations de Filtration In Situ*

Le contrôle des installations de filtration sur le site se réduit à la vérification de la perte de charge et de l'efficacité.

La méthode de contrôle de l'efficacité à l'uranine est tout à fait adaptée du fait de sa grande sensibilité. On élimine ainsi toute possibilité de colmatage même après de nombreux essais (concentration amont: quelques microgrammes par mètre cube; cf. essais des papiers filtrants) et il est possible de contrôler des installations importantes, de plusieurs centaines de milliers de mètres cubes par heure, à partir d'un seul générateur portatif. Cependant, la mesure est rarement faite dans d'aussi bonnes conditions que pour les éléments filtrants, par suite des difficultés généralement rencontrées pour le choix des points d'introduction et de prélèvement d'aérosol.

2. CONTRÔLE DES PIÈGES À IODE

Comme pour les filtres à aérosols, le contrôle est divisé en trois parties:

—contrôle du matériau adsorbant, c'est-à-dire du charbon actif,
—contrôle de l'élément adsorbant,
—contrôle du piège installé sur le site.

2.1. *Contrôle du Charbon Actif*

Contrairement à ce qui se passe pour les filtres, qui sont d'utilisation courante dans l'industrie, le charbon actif destiné à la confection de pièges à iode est commandé pour une utilisation spécifique. Mais sa fabrication ne peut être entreprise que pour des quantités minimums supérieures à celle nécessaire à l'équipement d'une installation. Le charbon est donc commandé et contrôlé séparément par lots.

Les caractéristiques vérifiées sont:

—la densité,
—l'humidité,
—la granulométrie,
—la perte de charge,
—la friabilité,
—le pH,
—l'indice d'adsorption de benzène,
—la teneur en corps volatils et en imprégnants éventuels,
—la température d'inflammation,
—l'efficacité à l'iode moléculaire,
—l'efficacité à l'iodure de méthyle.

2.1. 1. *Densité.* Le charbon actif est vendu au poids. Mais pour le remplissage d'un piège, c'est le volume qui est défini. La relation entre ces grandeurs est la densité. Il est donc important de la contrôler.

La détermination d'une densité implique la mesure d'un volume. Or, le volume occupé par un matériau granuleux est essentiellement fonction de son tassement. Il faut donc définir celui-ci le mieux possible en précisant les caractéristiques du dispositif adopté et son utilisation.

2.1. 2. *Humidité.* La densité d'un charbon actif est essentiellement variable avec la proportion d'humidité adsorbée. On vérifie que cette proportion est inférieure à une valeur limite afin que le prix du charbon ne puisse être artificiellement faussé.

2.1. 3. *Granulométrie.* La granulométrie d'un charbon actif est une caractéristique fondamendale pour son efficacité vis-à-vis de l'iode.[5] Par ailleurs, la proportion de grains fins doit être aussi faible que possible pour éviter le colmatage du tamis qui maintient le charbon et un éventuel détassement par élimination d'une partie du matériau.

La granulométrie d'un charbon actif est classiquement établie au moyen d'un jeu de passoires. On adopte un dispositif vibrateur mécanique qu'il est plus facile de définir qu'une méthode manuelle, toujours subjective.

2.1. 4. *Perte de charge.* La mesure de la perte de charge d'un charbon ne présente pas de difficulté particulière. Il est toutefois préférable de définir le matériel utilisé, en particulier le dispositif pour tasser le charbon, le porte-charbon, l'épaisseur de couche et la vitesse de passage de l'air.

Les valeurs adoptées sont:

—diamètre du porte-charbon: 60 mm,
—épaisseur de couche: 50 mm,
—vitesse de l'air: 30 cm/s.

2.1. 5. *Friabilité.* La friabilité d'un charbon actif est une caractéristique de résistance mécanique à considérer. En effet, les éléments remplis d'un charbon friable supportent mal un transport ou des manutentions sans précautions speciales. Les grains s'effritent et il y a production de grains plus fins, avec risque de détassement et de colmatage du tamis qui maintient le charbon. De même, en cours de fonctionnement sur un circuit d'air, les vibrations éventuelles peuvent produire les mêmes effets.

Il importe donc de fixer une valeur limite de la

friabilité admissible, et de définir sa mesure. Le principe de la mesure est le suivant: dans un cylindre perforé, on introduit une quantité déterminée de charbon et une masselotte cylindrique. On fait tourner le cylindre à la vitesse de 100 t/mn pendant 10 minutes. La poussière de charbon produite est recueillie à travers les perforations du cylindre. L'indice de friabilité du charbon est égal à mille fois le rapport du poids de poussière recueillie au poids de charbon introduit. Par exemple, si 5 grammes de charbon donnent un gramme de poussière, l'indice de friabilité correspondant est égal à 200.

2.1. 6. *pH.* Le pH du charbon actif est contrôlé dans le but d'éliminer le risque de corrosion de l'élément.

Le principe de la mesure du pH d'un charbon actif est le suivant: on met à digérer pendant deux heures un échantillon de charbon dans de l'eau distillée dans la proportion de 10 g de charbon pour 100 cm^3 d'eau. Après filtration, on mesure le pH de l'eau. Par convention, ce pH est considéré comme étant celui du charbon.

2.1. 7. *Indice d'adsorption de benzène.* L'indice d'adsorption de benzène caractérise le degré d'activation du charbon dont dépend en partie l'efficacité à l'iode. Pour la déterminer, on amène un échantillon de charbon en équilibre avec de l'air sec à 18°C contenant du benzène à 10% de sa pression saturante. Le pourcentage en poids de benzène est, par définition, l'indice d'adsorption de benzène du charbon considéré.

2.1. 8. *Teneur en corps imprégnants volatils.* On a observé l'action désastreuse de certaines vapeurs facilement condensables sur l'efficacité du charbon actif vis-à-vis de l'iode. Il peut être utile de vérifier que le charbon destiné au remplissage de pièges n'en contient pas. Pour ce faire, on fait traverser par de l'azote à température progressivement croissante jusqu'à 300° un échantillon de charbon placé dans un tube laboratoire calorifugé. On recueille le condensat, qui peut être éventuellement analysé et on détermine par pesée la perte de poids de l'échantillon.

2.1. 9. *Température d'inflammation.* En cas d'accident de réacteur, les effluents gazeux à épurer avant rejet sont souvent portés à haute température. Il est donc important de connaître et de vérifier la température d'inflammation du charbon. À cette fin, on utilise le dispositif décrit au paragraphe précédent. L'azote est remplacé par de l'air, ou du gaz carbonique, et on enregistre les températures en amont et en aval du charbon en augmentant progressivement le chauffage. L'ignition se traduit par un changement de pente de la courbe d'enregistrement de la température aval.

2.1. 10. *Efficacité à l'iode.* L'efficacité à l'iode d'un charbon actif destiné à la fabrication de pièges à iode est évidemment la caractéristique essentielle.

La méthode de génération d'iode 131 telle qu'elle a déjà été exposée[5] a subi quelques modifications. Initialement, un dépôt sec diodure alcalin marqué à l'iode 131 était oxydé par de l'air sec à haute température (600 à 800°C).[6] Mais, à cette température, se formait probablement un composé gazeux instable de silice et d'iode qui perturbait les mesures. En outre, la génération de fortes concentrations d'iode était limitée par la volatilisation partielle de l'iodure, entraînant par condensation la formation de dépôts gênants et d'aérosols indésirables. Dans le nouveau procédé, on n'introduit plus l'iode 127 sous forme d'iodure, mais sous forme vapeur mélangée à l'air de balayage. On obtient ainsi une libération d'iode 131 par échange isotopique à la température ambiante.

Le charbon à contrôler est tassé dans un porte-charbon comme pour la mesure de la perte de charge. Les prélèvements amont et aval sont effectués à travers des porte-charbons semblables, dont on mesure la radio-activité du contenu, ainsi qu'il a déjà été décrit dans les documents précités.

2.1. 11. *Efficacité à l'iodure de méthyle.* Des expérimentateurs anglais et americains[7-15] ayant démontré l'existence de la forme iodure de méthyle et la possibilité de la piéger au moyen de charbon imprégné, il apparaît nécessaire de contrôler à l'iodure de méthyle de tels charbons.

Dans l'appareillage en cours de réalisation, l'iodure de méthyle gazeux marqué à l'iode 131 est produit par réaction du sulfate de méthyle sur l'iodure de potassium[16] suivant un procédé utilisé par Collins. L'iodure de méthyle est alors stocké dans des ampoules en verre et ultérieurement envoyé pour l'essai dans un circuit d'air conditionné à 90% d'humidité. La durée d'émission d'iodure de méthyle est de

quinze minutes et la durée totale de l'essai de quatre heures. Les pièges de référence sont constitués de couches de charbon de houille activé imprégné à 5% de triéthylènediamine.

2.2. *Contrôle des Éléments Adsorbants*

Pour la fabrication des éléments adsorbants, la quantité nécessaire de charbon actif est prélevée dans le lot déjà réceptionné, pour être livrée au constructeur.

Après fabrication, un pourcentage d'éléments adsorbants, variable avec l'importance du lot, est alors prélevé pour contrôle.

En dehors des examens de conformité concernant les dimensions, les dispositifs garantissant le maintien du tassement, la protection, les joints, etc. . . ., on vérifie les caractéristiques suivantes:

—perte de charge,
—efficacité à l'iode,
—résistance aux chocs et vibrations.

La mesure de l'efficacité à l'iodure de méthyle n'apparaît pas strictement nécessaire, puisque la mesure de l'efficacité à l'iode suffit en principe à établir que la mise en œuvre du charbon actif, déjà essayé à l'iodure de méthyle, a été correctement effectuée. Nous estimons donc pouvoir nous en dispenser, ce qui évite l'installation d'un dispositif de conditionnement à forte humidité sur le banc d'essai à grand débit utilisé.

2.2. 1. *Perte de charge.* La mesure de la perte de charge d'un élément adsorbant ne présente aucune difficulté. Elle est déterminée pour une vitesse moyenne de passage de l'air à travers la couche de charbon de 30 cm/s.

2.2. 2. *Efficacité à l'iode.* L'efficacité à l'iode des éléments adsorbants est contrôlée suivant la méthode appliquée au contrôle de l'efficacité du matériau adsorbant.

2.2. 3. *Résistance aux chocs et aux vibrations.* L'efficacité d'un piège est liée à la qualité du tassement du charbon. Il est important que ce tassement se maintienne en dépit des chocs durant la manutention ou des vibrations éventuelles en cours de fonctionnement. Le constructeur des pièges prévoit généralement divers dispositifs pour garantir la conservation du tassement et éviter la formation de passages préférentiels. Pour éprouver l'efficacité de ces dispositifs, on soumet l'élément à contrôler aux chocs d'une machine vibrante en répétant l'essai pour différentes positions. On vérifie ensuite l'efficacité à l'iode.

2.3. *Contrôle sur le Site des Installations de Piégeage d'iode*

Le contrôle des pièges à iode installés se réduit à la vérification de l'efficacité à l'iode moléculaire, puisque la mesure de l'efficacité à l'iodure de méthyle serait peu significative en raison de l'impossibilité pratique de conditionner à forte humidité l'air traversant le piège à contrôler.

Le contrôle in situ à l'iode moléculaire est effectué suivant la méthode déjà décrite pour le charbon actif;[6] on utilise une source d'iode portative de volume et de poids très réduits par rapport au premier modèle. Cette nouvelle source est beaucoup plus robuste et peut supporter des chocs importants sans que son étanchéité vis-à-vis de l'extérieur soit rompue. Elle est constituée d'une ampoule de verre munie de deux sorties avec robinets, l'une des sorties aboutissant à un tube plongeur. Cette ampoule est maintenue par l'intermédiaire d'un moulage en mousse de polyuréthane, à l'intérieur d'un château de plomb étanche. Les sorties et les commandes des robinets sont protégées par des bouchons étanches pendant le transport. Le chargement s'obtient par introduction d'une solution d'iodure de sodium, ensuite réduite à un extrait sec par distillation sous vide. La capacité de cette source est de 3 curies. Pour obtenir ultérieurement la génération d'iode 131, on balaie l'ampoule avec de l'air sec chargé d'iode 127 à la température ambiante. Pour assurer dans le circuit d'air de l'installation à contrôler une concentration en iode total représentative d'un accident, on place un générateur supplémentaire d'iode 127 en amont du générateur d'iode radio-actif.

L'expérience prouve qu'il est nécessaire de contrôler assez fréquemment—plusieurs fois par an—les pièges à iode installés sur un circuit en fonctionnement permanent. En effet, l'efficacité du charbon actif vis-à-vis de l'iode est affectée par des vapeurs diverses, en particulier par celles émises par les peintures. Pour réduire la fréquence des essais in situ, toujours onéreux

et souvent gênants pour l'exploitation du réacteur, on installe, en dérivation sur le piège principal, un ou deux petits pièges témoins qu'il est facile de retirer de temps à autre pour un contrôle d'efficacité au laboratoire. On prévoit une marge de sécurité entre la baisse d'efficacité du piège principal et celle du témoin en réduisant l'épaisseur de la couche de charbon de ce dernier. Cet artifice permet en outre d'établir la circulation à travers le piège témoin et son circuit de raccordement, comprenant un débitmètre et une vanne de réglage, par la seule pression différentielle du piège principal.

CONCLUSION

Si les méthodes succinctement décrites de contrôle des filtres et des pièges à iode ne peuvent être élaborées et améliorées au fur et à mesure de l'évolution des techniques que par un laboratoire du C.E.A., au fait des problèmes d'épuration de l'air, il a paru cependant important que la mise en œuvre du contrôle soit confiée à un organisme dont l'indépendance vis-à-vis du C.E.A. comme des constructeurs, ne puisse être mise en doute.

Cependant, en raison des fortes activités d'iode manipulées, une exception a dû être faite pour les contrôles in situ des pièges à iode, qui seront confiés aux services de radioprotection des centres nucléaires. Pour tous les autres contrôles, le Centre d'Études de Prévention, auquel nous nous sommes adressés, a acquis la formation nécessaire, si bien que l'on peut espérer leur systématisation prochaine au C.E.A.

RÉFÉRENCES

1. Burgess, Silverman et Stein. A new technique for evaluating respirator performance. *A.I.H.A.J.* **22,** No. 6 (1961).
2. K. T. Whitby et C. M. Peterson. Electrical neutralization and particle size measurement of dye aerosols. *Ind. and Engry. Chem. Fund.* **4,** 66.
3. K. T. Whitby, D. A. Lundgren et C. M. Peterson. Homogeneous aerosol generators. *Int. J. Air Water Poll.* **9,** 263–277 (1965).
4. Critères de comportement au feu des filtres à air C.E.A., Service Technique d'Études de Protection, 16 mai 1966.
5. F. Billard, G. Chevalier et J. Pradel. Résultats obtenus dans la recherche des caractéristiques de piégeage de l'iode 131 par les charbons actifs. Colloque International sur la Pollution Radioactive des Milieux Gazeux, Saclay, novembre 1963.
6. J. Pradel, G. Chevalier, F. Billard et J. Miribel. Méthode d'essai des pièges à iode équipant les circuits de ventilation des réacteurs. Congrès Health Physics Society, New York, 1963. Note CEA No. 455, 1963.
7. D. H. Atkins et A. E. J. Eggleton. Iodine compounds formed on release of carrier-free iodine 131. AERE-M-1211, 1963.
8. A. C. Chamberlain. Physical chemistry of iodine and removal of iodine from gas streams. Report of Aerosol Group, part 1, AERE-R-4286, 1963.
9. G. W. Parker, G. E. Creek, W. J. Martin et C. J. Barton. Fission product retention in reactor confinement systems—Efficiency of the ORR confinement system. ORNL-3591, 1964.
10. R. D. Collins et J. J. Hillary. Some experiments relating to the behavior of gasborne iodine. Int. Symp. on Fission Products Release and Transport, Oak Ridge, avril 1965.
11. D. A. Collins, R. Taylor et L. R. Taylor. The removal of methyl iodide from reactor effluent gases. Int. Symp. on Fission Products Release and Transport, Oak Ridge, avril 1965.
12. R. E. Adams et W. E. Browning, Jr. Removal of iodine compounds from air systems by activated charcoal. Int. Symp. on Fission Products Release and Transport, Oak Ridge, avril 1965.
13. D. A. Collins, R. Taylor et W. D. Yuille. Sampling and characterization techniques used in the study of iodine release from irradiated fuel elements. Int. Symp. on Fission Products Release and Transport, Oak Ridge, avril 1965.
14. A. W. Castleman, Jr., I. N. Tang et H. R. Munkelwitz. Chemical state of iodine released from irradiated fuel into steam. Int. Symp. on Fission Products Release and Transport, Oak Ridge, avril 1965.
15. W. E. Browning, Jr., R. E. Adams, R. D. Ackley, M. E. Davis et J. E. Attrill. Identity, character and chemical behavior of vapor forms of radioiodine. Int. Symp. on Fission Products Release and Transport, Oak Ridge, avril 1965.
16. H. R. Diffey, C. H. Rumary, M. J. S. Smith et R. A. Stinchcombe. Iodine clean-up in a steam suppression system—Appendix. Int. Symp. on Fission Products Release and Transport, Oak Ridge, avril 1965.

ON-SITE TESTING OF FILTERS WITH SPECIAL REFERENCE TO SOLID AEROSOLS

HANS FLYGER and H. C. ROSENBAUM
Research Establishment Risö, Danish Atomic Energy Commission

Abstract—A lithium flame photometer test is proposed for on-site testing of filter installations. The lithium test is intercalibrated with the standard Sodium Flame Test. The spraying time needed to introduce the lithium salt into a ventilation system is considered inconvenient for systems handling more than 10^6 m³/hr. For such systems photoelectric particle counters can be used with the dust naturally present in the local atmosphere. Where the dust level is too low, Aitken nuclei can easily be artificially generated in sufficient amounts. The relation between filter evaluation by such particle counting and by lithium measurements is established.

INTRODUCTION

The on-site testing of installed filters presents problems which are generally absent from the techniques involved in the laboratory testing of filter elements.

In the laboratory a small filter element or system can be treated as a single unit and the test set-up arranged so that the efficiency of the unit appears in the results as the ratio between truly representative samples of particle concentrations taken before and after the test unit.

In on-site testing, the physical layout might make it impossible to carry out determinations equivalent to those on the laboratory scale. Usually large filter banks are dealt with, containing one or more dust filters and the same number of absolute filters. These filter banks are installed to accommodate one or more large ventilation channels servicing an entire building section. The air flow in these channels is of the order of thousands to tens of thousands of cubic metres per hour.

It is the intention here to discuss some of the laboratory methods available for measuring the effectiveness of filters and to show how one of these methods can be adapted to accommodate the on-site evaluation of filter installations.

DISCUSSION OF SOME STANDARD LABORATORY FILTER TESTS IN RELATION TO ON-SITE TESTING

An estimation of the performance of a highly efficient filter is made on the basis of an experiment in which a cloud of particles in the micron range, moving at a certain velocity, is passed through the filter. The ratio between the concentrations of particles in the air before and after the filter is then determined.

The experimental techniques discussed here involve the use of an inhomogeneous test cloud consisting of solid particles with an approximate mean size of about 0.5 micron. Examples of the employment of an inhomogeneous test cloud are the two British Standard tests, the Methylene Blue Test[1] and the later developed Sodium Flame Test.[2] Both tests involve an atomizer which delivers a spray from a solution of methylene blue or sodium chloride. The spray is dried in an evaporation tube, thus forming a particulate cloud with particles of about 0.5 micron.

A common feature of the Methylene Blue and the Sodium Flame Test is that the attainment of reliable results depends on a most careful control of the atomizer air-flow system.

In the Methylene Blue Test a subjective comparison is made of the stain intensities on two filter papers sampling the air on either side of the test filter. The air sample from before the filter is obtained within a few seconds by means of a small hand pump, while the collection of an air sample from behind the filter takes about half an hour for highly efficient test filters. For a test filter with a penetrability of 0.2% the unfiltered volume of methylene-blue cloud may have to be about 12 ml (drawn evenly with a

hand pump) as compared with 60 l. of the filtered cloud, so that the two stain intensities lie close together for reliable comparison. In a comparable situation the lithium-flame test requires one or two litres as a sufficient sample. The lithium test[3] is furthermore free of subjective approximations, and the lithium amounts sampled before and after the test filter are measured quite independently of each other.

The Sodium Flame Test requires an even more carefully controlled atomizer air-flow system as no air sample is taken before the filter, the efficiency of the latter being evaluated only by measurement of the concentration of sodium in the air after the filter. The measurement is made by means of a specially designed flame photometer that can analyse a continuous air stream. The instrument has to be calibrated every time it is to be used, by allowing a diluted sample of the unfiltered test gas to enter the flame. In an on-site test, the required calibration equipment, which may involve the use of two flow meters and a mixing bottle for each decade by which the unfiltered test gas is diluted, is very inconvenient. In some, not uncommon, cases the section before a filter bank is in fact isolated from the effluent side by the wall in which the filter bank has been installed. In such cases it may prove impossible to connect the calibration equipment to the flame apparatus.

To avoid such difficulties, an essential specification for onsite equipment is that the sampling units before and after the test filter must be independent of each other. The equipment for the lithium flame test fulfils this demand and avoids the tedious task of repeated calibration of an air-flow system.

The hardware required for the construction of the sodium flame photometer is not among standard production items and must therefore be produced by each individual laboratory from the Porton specifications.[4] Any type of high quality flame photometer may be used for the lithium test.

The application of the lithium flame test on-site will be discussed later in connection with a practical example.

The basic scheme of the lithium flame photometer test is briefly as follows:

A 2% aqueous solution of Li_2SO_4 is atomized by a Collison atomizer (see Fig. 1). The spray is diluted with prefiltered dry air in an evaporation tube, which thus yields a diluted particulate

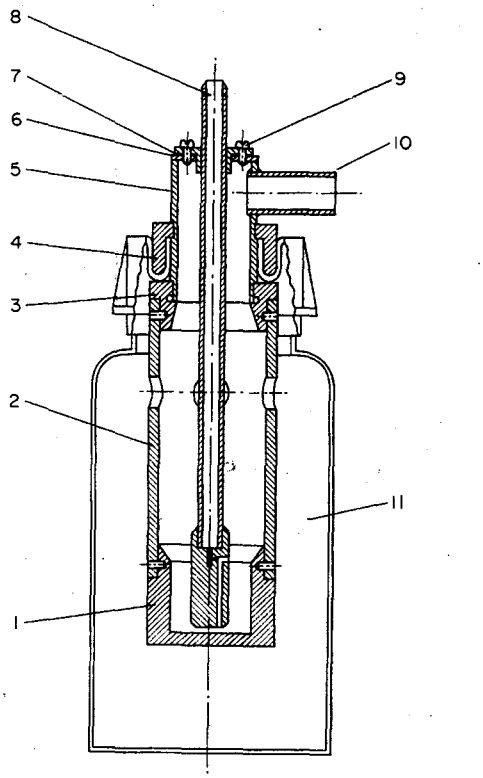

FIG. 1. Modified Collison atomizer. This design allows the atomizer to be used for small quantities of radioactive solutions. The cap construction ensures complete tightness of the system.

stream of Li_2SO_4 crystals. The stream enters a mixing chamber where a few litres per minute is tapped and passed through a membrane filter. A portion, or all, of the remaining flow is passed through the filter to be tested. The effluent air enters a second mixing chamber identical with the first, and an appropriate amount of the flow is tapped and passed through a second membrane filter. The membrane filters are then processed

chemically, and two solutions are produced in which concentrations of lithium as low as 0.0002 γ/ml can be detected with a sensitive flame photometer.

The ratio between the lithium contents of the two solutions is then, after compensation for differences of air volumes sampled, a measure of the effectiveness of the test filter.

Lithium has been chosen as a tracer substance although a flame photometer is about ten times as sensitive to sodium as to lithium, because of the relative rarity of lithium in laboratory surroundings and the ease with which it is measured on a flame photometer because of the lack of interference from other alkali metals present.[5] In coastal areas, concentrations of NaCl in the air[6] of up to 20,000 μg NaCl per m^3 have been measured.

A set of membrane filters rubbed over various surfaces at this laboratory were processed for lithium determinations on a photometer capable of detecting 0.0002 γ Li/ml in the 5 ml solution used. In no case was any lithium found.

The inapplicability of sodium as a tracer component is further emphasized by the variations in the amounts of sodium found on fresh membrane filters. An amount of sodium large enough to allow us to neglect the variation in the sodium content of the filters should be sampled from the air after the filter to be tested, which means in practice that sodium would be much less sensitive than lithium as a tracer component.

The mean size by mass of the Li_2SO_4 particles was not measured, but the atomizers employed in all the experiments deliver NaCl particles of a mean size by mass of 0.6 micron from a 2%NaCl solution.

Electron microscopy reveals that Li_2SO_4 crystals appear as elongated rhombic forms unlike the cubic NaCl crystals from a Sodium Flame Test cloud.

As the original atomizer made from the Porton specifications was of steel, it was reconstructed in a hard plastic to avoid corrosion. At the same time the container was changed, the glass jar originally used being replaced by a plastic bottle to avoid the difficulties of tightening the screw-lid. For radioactive tracer experiments, in which the amount of radioactivity applied in the atomizer should not exceed that necessary for the experiment, a special beaker was attached to the bottom of the impaction shield. In this case the holes in the impaction shield should be closed to avoid waste of liquid.

CALIBRATION OF THE LITHIUM TEST WITH THE SODIUM FLAME TEST AND POLLAK COUNTERS

In order to determine what differences a filter might display between a sodium chloride cloud and a lithium sulfate cloud, a series of investigations was made. The importance of such inter-calibration is apparent as the Sodium Flame Test is a standard test widely used by filter manufacturers.

The inter-calibration was carried out by spraying 2% solutions of Li_2SO_4 and NaCl into the open end of a cylindrical duct of diameter 8 cm leading to the test filter. From the latter the duct continued to a larger one through which a ventilation fan drew the air. The air flow through the test filter was measured by a flow meter of the rotameter type and controlled by adjusting a valve opening into the large duct.

The cylindrical duct from inlet to test filter was about 8 metres long and contained two baffle plates. It had a sharp bend two metres from the test filter.

A before-filter tap-hole was situated after the bend and an after-filter tap-hole about 8 m from the test filter, after a baffle plate.

The atomizer was of the type shown in Fig. 4. An aluminium pot contains three atomizers of the collision type, made from the Porton specifications. The atomizers are interconnected by a distributor plate allowing a general feed of compressed air to them of about 7 atm. In order to obtain an efficient impingement of the atomized liquid, the atomizers are surrounded by a special baffle-plate arrangement allowing an equally efficient impingement of the droplets from all sides. Fast evaporation of the droplets and an improved yield of lithium crystals are obtained by the addition of an air flow through a range of small holes placed along the circumference of the aluminium pot. The extra air is distributed through the holes by means of a circular tube welded to the outside of the pot.

The total output from the atomizer pot was measured at about 8 ml liquid/min. With a compressed-air flow at 7 atm and an auxiliary

evaporation air flow of about 100 l./min the consumption of compressed air is 252 l. air (760 mm Hg)/min.

The NaCl solution was spiked with ^{24}Na so that the test-filter penetration could be measured directly by counting the activities sampled from the air before and after the filter.

The lithium measurements were made by the method mentioned previously. The details of this method are described in the following section.

The test filters comprised the types 33, 44, 55 manufactured by the British filter manufacturing company Vokes Ltd. The manufacturer's penetration ratings for the filter in the above order were 25%, 2% and 0.05%. The filters were tested at a flow rate of 850 litres per minute.

In addition to these tests the natural particles found in the building were used to test the filters. The before and after particle concentrations were determined by means of two Pollak counters[7] operating from the two tap-holes. The penetration of these natural aerosols is shown together with the results of the intercalibration. The reason for using the Pollak counters is to demonstrate the relation between the mass penetration of the lithium and sodium salts and the particle-number penetration of the natural aerosol.

In cases where the natural particles found in the air are present in concentrations too low to be measured accurately after passage through a highly efficient filter, particles can be generated artificially by inflating a large rubber balloon with air containing particles from a heated filament over which a boat of TUFNOL is suspended. Within a short time a large reservoir can be loaded with a very high particle concentration.

The particles generated in this way have a diameter of about 10^{-5} cm provided that during the heating process, the air around the Tufnol boat is only circulated by the free convection from the heat developed. If forced convection is applied, the diameter of the particles may fall in the range of 10^{-6} to 10^{-7} cm.

A test with a 66 type filter (manufacturer's rating 0.1% penetration) displays the so-called pinhole effect, see Fig. 2. The effect, when present, can easily be demonstrated by means of a

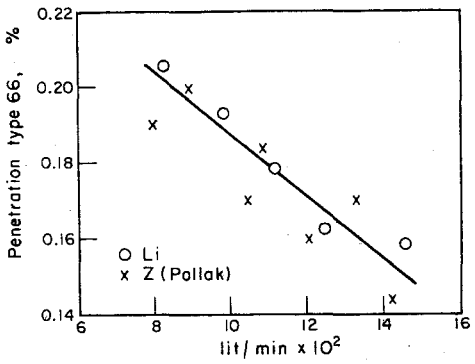

FIG. 2. Plot of results from tests with filter 66.

Pollak counter as well as by a lithium test as the penetration appears to decrease with increasing air speed through the filter. The pinhole effect may dominate the performance of a filter.

Whether there were actual pinholes in the filter material or pinhole leaks due to damage or faulty installation, was not determined. It can only be said that the unit did not function according to the manufacturer's specifications.

PREPARATION OF THE FLAME-PHOTOMETER SOLUTIONS FOR THE DETERMINATION OF LITHIUM ON MEMBRANE FILTERS

A Göttingen membrane filter type MF of 50 mm diam. can be dissolved under gentle heating in 1 ml conc. HNO_3. If this solution is diluted with H_2O to 5 ml, a Zeiss flame photometer (type PF 5) is able to detect the presence of 0.003 γ/ml Li. It has been found that the response of the photometer to these solutions is not linear in the range 0.003 γ/ml Li to 0.03 γ/ml Li. Further, the responses are quite unstable.

In order to increase the sensitivity of the photometer readings, the addition of 1 part of acetone to 4 parts of the final solution was tried.

A membrane filter was dissolved in 1 ml concentrated HNO_3 in a 5 ml measuring flask by heating gently over a bunsen flame and shaking. After cooling to room temperature 1 ml of distilled water was added, and the solution was again allowed to cool to room temperature. The following quantities of a 3 γ Li/ml solution were added to the measuring flasks: 5, 10, 20, 25, and 50 μl, giving standard solutions of

0.003, 0.006, 0.012, 0.015, and 0.03 γ Li/ml. 1 ml of acetone was added producing a white precipitate. Distilled H_2O was added up to the 5 ml mark, and the flask was shaken thoroughly. After filtration through a Whatman glass-fibre filter the clean effluent was set aside in another 5 ml measuring flask. On account of the constant formation of gas from this solution it is advisable to leave the flasks only lightly covered.

In the determination of the amount of lithium adsorbed on a membrane filter, a total solution of 5 ml (minimum) is used to allow a reasonable measuring time of up to 45 sec. One must be particularly careful with these small amounts to measure the 1 ml of acetone accurately.

It was noted that even after 7 days the solutions, standing in open measuring flasks, did not show any change in their concentration of lithium. In order to ascertain whether any of the lithium was lost in the precipitate, another calibration series was made in which the aliquots of 3 γ Li/ml sol. were added in the final step after filtration.

The measurements on the flame photometer are shown in Fig. 3. In addition to these tests, one was performed in which the photometer was set at its maximum sensitivity and the null solution adjusted to zero on the scale. In this case the 0.003 γ Li/ml sol. read 25 units on the scale. If the instrument is assumed to respond approximately linearly to these solutions at this setting, then a solution containing about 0.0002 γ Li/ml would give a scale deflection of more than one unit.

All the above readings were quite stable and easily reproducible.

DISCUSSION OF AND CONCLUSIONS FROM INTER-CALIBRATION TEST

Some initial experiments were performed in which the test filter was omitted to ensure that losses to the walls and baffle plates did not affect the Li and Na contents in the air samples from the different tap-holes. It was found that the Li and Na contents of the air samples were within the measuring accuracy of the gasometers.

The Li and Na calibration experiments for the two filter types 55 and 44 (see Figs. 5 and 6), while very consistent individually revealed a qualitative shift in the Li–Na ratio of penetrability of the two filters. The shift was somewhat surprising and could not be explained by means

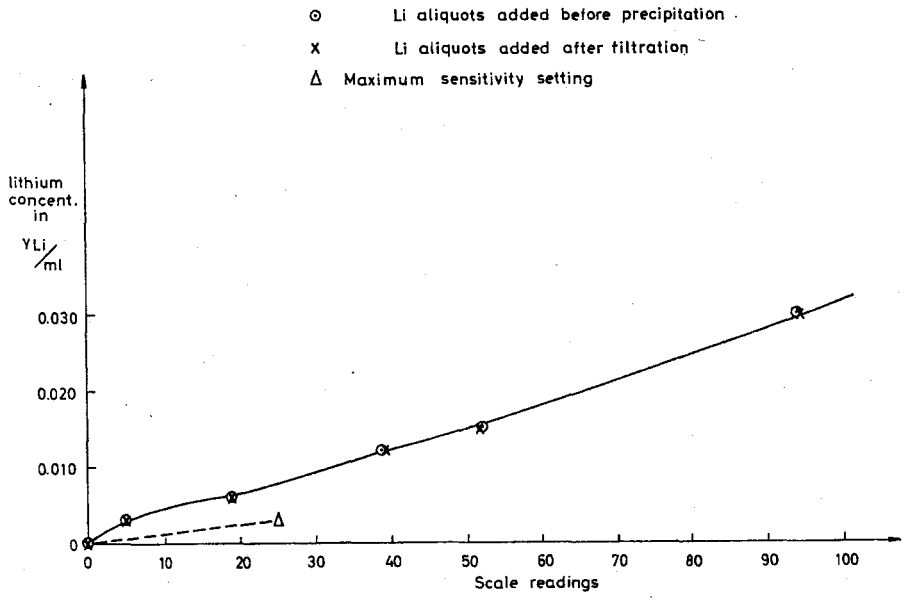

FIG. 3. Calibration curves for Zeiss PF5 flame photometer: air pressure = later; acetylene pressure = 90 mm W.

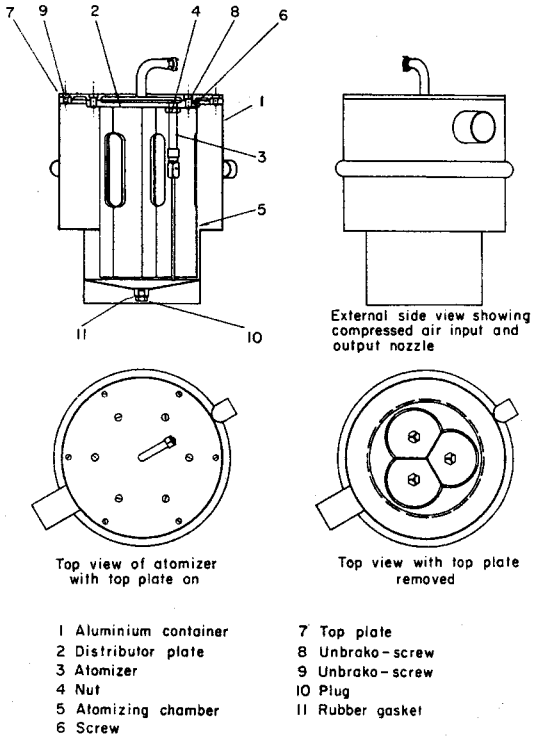

FIG. 4. Portable atomizer for on-site testing. The three atomizer elements included are equivalent in structure to the elements used in the Collison Atomizer shown in Fig. 1.

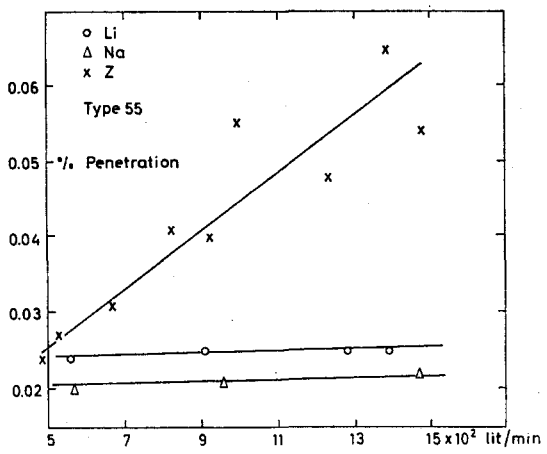

FIG. 5. Plot of results from tests with filter 55.

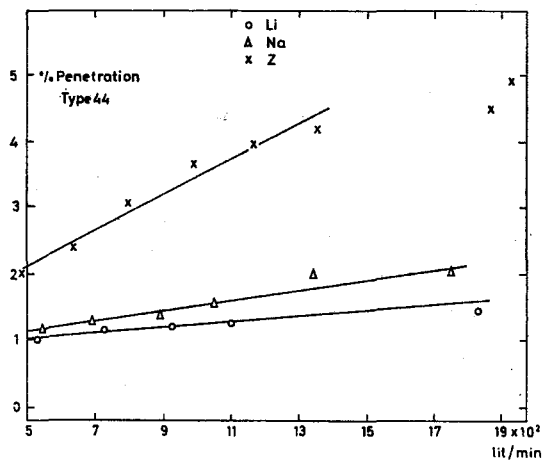

FIG. 6. Plot of results from tests with filter 44.

of the filtration theory. The filters were consequently reinstalled, and the calibration experiments were repeated. Figures 8 and 9 display the results. Comparing the results from Fig. 5 with those from Fig. 8 and the results from Fig. 6 with those from Fig. 9, we notice the same qualitative shift in the Li–Na ratio of penetrability, but in this particular case it is not related

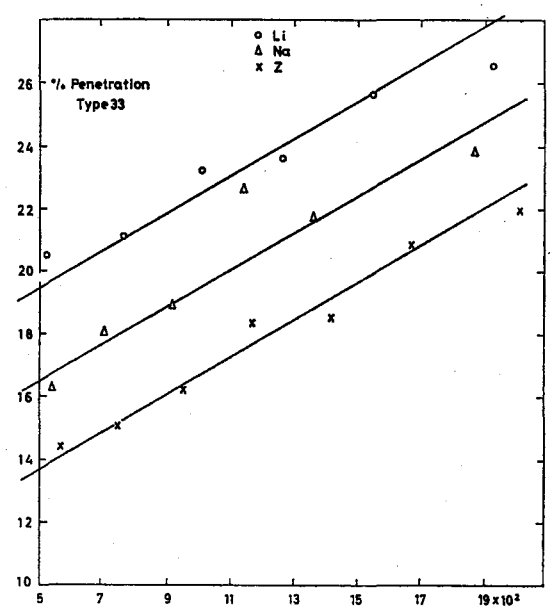

FIG. 7. Plot of results from tests with filter 33.

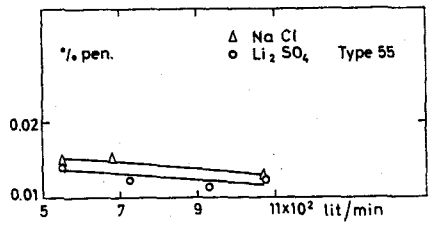

FIG. 8. Repetition of tests with filter 55 after removal and reinstallation.

to a shift in filter type, but connected with the same individual filter.

The observed difference may have been caused by using two different G.M. counters, depending upon the activity to be measured. Therefore, a new series of similar experiments with the same 44-filter was performed in which all the counting was done on a single scintillation counter. The shifts between the effectivity curves from test to test for both sodium and lithium were found to be the same as those observed previously. Therefore it was concluded that the counting technique was not a cause of this apparent shifting.

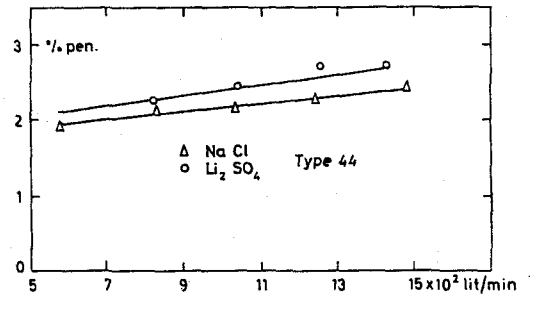

FIG. 9. Repetition of tests with filter 44 after removal and reinstallation.

There were two other possibilities that might each lead to such variations.

(1) If a variation in the atomizer mechanism were responsible for the shifts then one could hope to observe such variations by taking effectivity measurements before and after stopping and starting the atomizer again.

(2) If there is an intrinsic variation in the filter itself from test to test then one could try to produce such variations by varying the air-flow through the filter from extreme to extreme and seeing if a given effectivity determination taken before and after these impressed flow changes holds the same value.

It was shown that no significant shifts were present due to either cause but that there was a shift when the air flow was completely stopped then started again. For the 44 type filter, there was a change from a penetrability of 4.85% to a penetrability of 4.50%, at a flow of 1000 l/min.

Two experiments were performed to confirm this phenomena.

A test cloud of ^{24}Na spiked NaCl was used with the 44-filter. Points on each curve were determined as the air flow was increased from zero to maximum and back to zero again. The shift between the two curves shown in Fig. 10 indicates the existence of the start phenomenon.

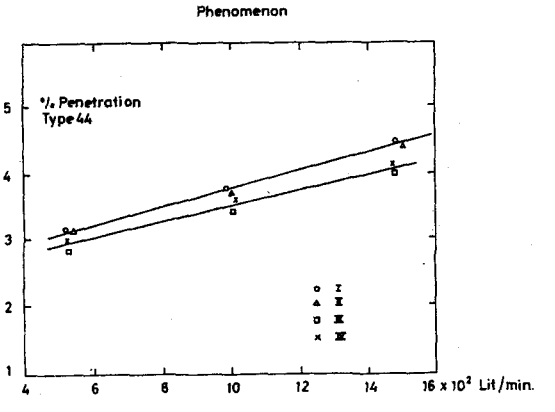

FIG. 10. Repetition of tests with filter 44 demonstrating the start phenomenon.

Therefore, according to our measurements a given filter of the type 33, 44 or 55 displays a start phenomenon that dominates any discrimination of these filters between Li_2SO_4 and NaCl particles. The Li_2SO_4 test is therefore practically equivalent to the NaCl test.

The Pollak counter curves, on the other hand, are consistent relative to the lithium and sodium curves as shown.

DISCUSSION OF AN EXAMPLE OF AN ON-SITE TEST

An example of a large installed filter system is that cleansing the air of the reactor building DR 3 at Risö.

The installation consists of a single ventilation channel, cross-section about 1 m^2, in which the flow is 6000 m^3/hr. In this duct a primary dust filter and an absolute filter are installed. The under-pressure in the channel is about 80 mm H_2O before the primary filter and about 150 mm H_2O after the absolute filter.

At a point about six metres from the face of the primary filter a cloud of droplets atomized from a 2% Li_2SO_4 aqueous solution is sprayed into a tap-hole. At a point between the primary and the absolute filter another tap-hole is connected to a piston pump which draws about 20 l./min from the channel air through a membrane filter. Further downstream, about ten channel diameters from the end face of the absolute filter and round a gradual right-angle bend in the channel, a final tap-hole draws 20 l./min of air through a membrane filter.

The flow of sampled air is monitored by two flow meters of the float type, and the air volumes are measured by two gasometers. The atomizer used was of the type shown in Fig. 4. Four runs were performed, and the results were as follows: trial 1: 0.69%, trial 2: 0.70%, trial 3: 0.10%, and trial 4: 0.60% penetration.

According to recent determinations,[8] thorough mixing in such a duct is assumed for points lying more than 30 channel diameters downstream of a source of contamination or the effluent face of a filter, and then only if there is some baffle arrangement within this length. If the duct has one or more bends within the region from the point of injection of the aerosol to the final hole, these bends might, if sufficiently acute, be effective as baffle surfaces. If sampling points exist which satisfy these criteria and are accessible, the above procedure can yield a measurement of the efficiency of the filter bank as a whole.

A second on-site test that fulfilled the above requirements was therefore carried out on the same filter at the DR 3 reactor. In this case, the aerosol, a ^{24}Na spiked 2% NaCl solution from a modified Collison atomizer delivery 15 ml/hr was introduced into one of the inlets of a ventilation duct in the reactor hall itself. The tap-hole for the before filter was situated just before the primary filter face and the after tap-hole about 15 m downstream of the absolute filter; the length of duct in between had four sharp bends. The measured penetration was 0.06%.

A total of 10 mCi ^{24}Na was sprayed into the ventilating system in order to ensure good after-filter measurements. The spraying time was 6 hr. The same DR 3 filter bank could have been evaluated by means of a 2% Li_2SO_4 solution atomized by the portable atomizing unit capable of delivering 8 ml solution per min. The total number of litres to be sampled by the after filter in order to ensure a good flame photometer reading was calculated at about 80.

The above test using ^{24}Na was performed on an auxiliary filter unit situated in parallel to the first, the penetration was 0.10%.

A test was then performed with the Pollak counters, using the natural aerosol. The first filter displayed a particle-number penetration of 0.12%, twice that of the NaCl cloud. The auxiliary filter displayed a particle-number penetration of 0.25%, 2½ times that of the NaCl cloud.

CONCLUDING REMARKS

The question arises as to the significance of the efficiency measured by these methods. It is not the inherent penetrability of the adsorbing material that is of principal interest since it is always specified by the manufacturer. What concerns us here is the performance of the installed units, since such a determination can reveal a malfunction in the filter bank, e.g. a badly installed or damaged filter.

When the results of an on-site lithium test indicate that the manufacturer's specifications are not fulfilled by the installation as a whole, one knows exactly the extent of the failure because the lithium test is directly comparable with the Sodium Flame Test used by the manufacturer. Thus one is in a position to quantitatively evaluate the performance of a filter installation by direct comparison with the figures offered by the manufacturer as to the expected performance of the unit. In other words, the lithium on-site test represents an easy way of comparing the actual efficiency of a filter installation in operation with the efficiency attainable according to the manufacturer's test.

The spraying time needed to introduce sufficient amounts of lithium salts into a ventilation system sets a practical upper limit to the utilization of a lithium salt as a tracer in very high capacity systems. For example, in a ventilating system through which the flow is 100,000 m³/hr and whose filter bank shows a penetration of 0.01%, it would be necessary to sample about 8000 l. on the after filter. This figure is based upon the output of the portable atomizer unit mentioned previously. The time of sampling based upon a sampling rate of 20–50 l./min through a 5 cm diameter membrane filter would be from 7 to 3 hr.

For these very high capacity systems the use of Pollak counters measuring the natural particles found before and after the filter bank is a reliable indication of the integrity of the filter bank. Allowance must be made for the difference between the effectiveness of a filter bank as determined by Pollak counting and the effectiveness as an expression of mass concentrations before and after the filter bank. This difference is demonstrated and established by the inter-calibration curves (Figs. 5–9). These curves are valid only for filters in which the pinhole effect is not significant.

In cases where it is possible to vary the air flow through a filter bank and thus demonstrate the existence of a pinhole effect by Pollak counting, the effectiveness thus obtained converges with the effectiveness as measured by the lithium and sodium methods (Fig. 2).

It might be desirable to determine the exact location of a pinhole defect (if it cannot be tolerated from a safety point of view). This can be done by scanning the back surface of each filter with a flexible probe introduced through a hole in the conduit wall. The air injected into this probe, e.g. by means of an ejector, is passed directly into a flame, and the intensity of the lithium line is registered on a photometer. In this way a continuous profile of the lithium in the effluent air is obtained. In this procedure the lithium concentrations due to a leak are very high, and thus it suffices to use a cheap and simple flame-photometer device. Such a system has been constructed (Fig. 11) by modifying a cheap, commercially available flame photometer (Evans Electroselium Ltd.). At the most sensitive setting a scale deflection of 10 units ($\sim$ 1.5 cm) is obtained from a channel concentration of 1.2×10^{-2} γ Li/l. air.

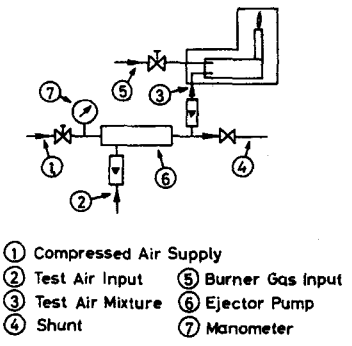

FIG. 11. Flow diagram of the modified EEL flame photometer.

ACKNOWLEDGEMENTS

We wish to thank P. O. Heidemann for his help in planning and drawing the atomizer assemblies shown in Figs. 1 and 4.

REFERENCES

1. Methylene Blue Particulate Test for Respirator Filters. British Standard No. 2577 (1955).
2. Sodium Flame Particulate Test. Chemical Defence Experimental Establishment, Porton Down, Salisbury, Wilts, England. Porton Specification No. 1632 A.
3. H. FLYGER and H. C. ROSENBAUM. A lithium flame photometer test for highly efficient filters. *J. Am. Ind. Hyg. Ass.* **26** (1965).
4. Drawing No. 6536, Sodium Flame Test Equipment. Chemical Defence Experimental Establishment, Porton Down, Salisbury, Wilts.
5. T. F. BOROVIK-ROMANOVA. Mutual influence of alkali metals in their determination by flame photometry. *Bull. Acad. Sci. USSR* No. 7,955 (1962).
6. R. M. MOYERMAN and K. E. SHULER. The concentration of contaminant alkali salts in ground-level air. *Science* **118,** 512 (1953).
7. A. L. METNIEKS and L. W. POLLAK. Instruction for the use of photoelectric condensation nucleus counters. *Geophys. Bull.* **16** (1959).
8. S. E. SMITH and P. A. WHITE. Design of radioactive filtration systems. *Nucl. Eng.* June (1962).

COMPARISON OF PERFORMANCE CHARACTERISTICS OF SOME FILTERS USING THORON DAUGHTERS AS RADIOACTIVE AEROSOL

YOSHIKAZU YOSHIDA, KYOSHIRO KITANO, MIKIO MURATA
Division of Health Physics and Safety, Japan Atomic Energy Research Institute,
Tokai-mura, Ibaraki-ken, Japan
and
SEIZABURO MORIYASU
Nuclear Power Department, Kansai Electric Power Company,
3–5 Nakanoshima, Kita-ku, Osaka-shi, Japan

Abstract—The important characteristics of air sampling filters are collection efficiency, flow resistance and surface collection efficiency. A comparison was made for these performance characteristics between the filters used at present in JAERI for air sampling (mostly imported) and those (made in trial) by a Japanese manufacturer. Collection efficiency, and surface collection efficiency and also alpha energy resolution were tested using the Millipore AA filter as a reference filter and thoron decay daughters as a test aerosol; the significant particles were less than 0.1 micron in diameter.

In the cellulose filters tested, Toyo No. 5A and Toyo No. 1 showed nearly the same performance characteristics as Whatman 41, and the collection efficiencies of these three types of filters were over 90% at face velocities larger than 64 meters per minute.

In the cellulose asbestos filters tested, for alpha air sampling Toyo HE-40 proved superior to HV-70. This filter has a collection efficiency greater than 99.5%, and about the same surface collection efficiency as the glass fiber filter Gelman E, generally used for alpha air sampling. On the basis of these tests, it was decided to use the cellulose asbestos filter Toyo HE-40 for alpha air sampling in JAERI.

1. INTRODUCTION

The important characteristics of air sampling filters are collection efficiency, air flow resistance and surface collection efficiency. The last one is more important for alpha air sampling, because direct alpha counting is only effective for particles collected on or near the filter surface. A comparison was made for these performance characteristics between the filters used at present in JAERI for air sampling (mostly imported) and those proposed for use (mostly made in trial by a Japanese manufacturer).

Collection efficiency, surface collection efficiency, and also alpha energy resolution were tested using the Millipore AA filter as a reference filter and thoron decay daughters as a test aerosol; the significant particles were less than 0.1 micron in diameter.

It is recognized that Millipore AA does not collect all particles in the size range of natural activity,[1] whereas it is reported that Millipore AA has an efficiency over 99.9% for D.O.P. particles 0.3 micron in diameter,[2, 3] and for uranine particles both 0.27 micron and 0.025 micron in diameter.[4]

The present report describes the testing procedure and the results obtained. The data obtained were compared on relative, rather than absolute, values.

2. FILTERS TESTED AND RADIOACTIVE AEROSOL USED

The characteristics of filters used at present and proposed for use in air sampling in JAERI are shown in Table 1. The pore sizes tabulated for the filters, except Millipore AA, were

Table 1. *Filter Tested*

Filter and type	Thickness mm	Weight mg/cm²	Tensile strength kg/cm	Pore size μ	Fiber diameter μ
Cellulose					
Whatman 41	0.22	12.1	1.40	38	25
Toyo No. 1	0.21	11.6	2.60	25	25
Toyo No. 5A	0.23	12.1	1.13	30	25
Cellulose asbestos					
HV-70 9 mil	0.39	16.6	2.66	30	25
Toyo HE-10	1.11	41.5	1.13	36	25
Toyo HE-13	0.97	36.2	1.40	44	25
Toyo HE-40	0.42	13.5	3.07	32	25
Glass Fiber					
Gelman E	0.29	9.7	0.55	8.9	0.4
Toyo GA-100	0.30	10.0	0.08	12	0.6
Toyo GA-200	0.75	31.0	0.16	12	0.6
Toyo GB-100	0.41	14.8	0.08	8	0.3
Toyo GH-100	0.36	17.2	0.33	12	0.6
Membrane					
Millipore AA	0.17	4.2	0.33	0.80	—

obtained using the so-called bubble test* based on capillarity, which measures the maximum value. Millipore AA was found to have a pore size of 2.5 microns when measured by this method.

Thoron decay daughters were used as the test aerosol; the decay series is shown in Fig. 1. The size distribution for the series of particles

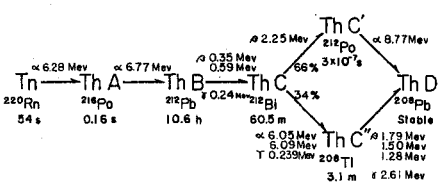

FIG. 1. Thoron decay series.

* The data were presented by the research group of Toyo Roshi Co., Ltd.

was measured using an electron microscope, after collecting the particles on a collodion film. This method was used because measurements made first by the cascade impactor method indicated most of the particles to be smaller than 0.3 micron in diameter. The results of electron microscope measurements showed that most of the particles were smaller than 0.1 micron in size. Consequently, the size distribution for the test aerosol was considered as approximately the same as, or a little larger than, the size range of the natural radioactive aerosol in the atmosphere—0.015–0.5 micron in size range.[5]

3. TEST PROCEDURE AND RESULTS

3.1. *Collection Efficiency*

The experimental apparatus used is shown in Fig. 2. Two air samplers, with a Millipore AA filter as the reference collector, were used

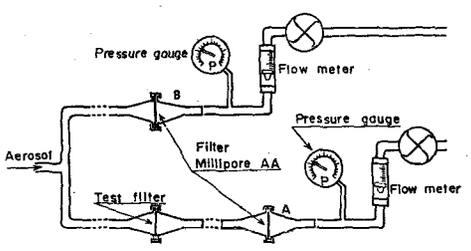

FIG. 2. Experimental apparatus.

simultaneously at the same flow rate. The reference filter (A) collected the aerosol penetrating the test filter, and the other, (B), collected the aerosol directly.

The collection efficiency ϵ was determined from the following equation;

$$\epsilon = (1 - \eta) \times 100\ (\%), \quad \eta = n_A/n_B,$$

where n_A = gross alpha count rate for the particles collected on the reference filter (A),

n_B = gross alpha count rate for the particles collected on the reference filter (B).

The sampling periods varied from about 10 to 30 min, depending on the concentration of airborne activity, which was of the order of 10^{-8} μCi/cc during the test. As a rule, the sampling time was determined by the times required for the counting rate of the reference filter (B) to be more than 2000 cpm. The effective diameters of the filters were 40 mm, and the face velocities tested were 32, 48 and 64 m/min. Gelman E was selected as the reference filter at the face velocities of 48 and 64 m/min. This was because Millipore AA could not be used at higher velocities due to a shortage of the pumping power. The collection efficiency of Gelman E was considered to be over 99%, compared with Millipore AA, from the results obtained in the measurements described below and by others.[2, 3]

The results, obtained for the cellulose filters, are shown in Fig. 3, in which it is seen that the collection efficiency will increase with the face velocity, as described in other reports.[2-4] The average values of collection efficiencies for the filters tested are summarized in Table 2, together with other performance data. From the collection efficiency data in Table 2, it is seen that Toyo HE-10 and HE-40 are not inferior to HV-70 of the cellulose asbestos filters.

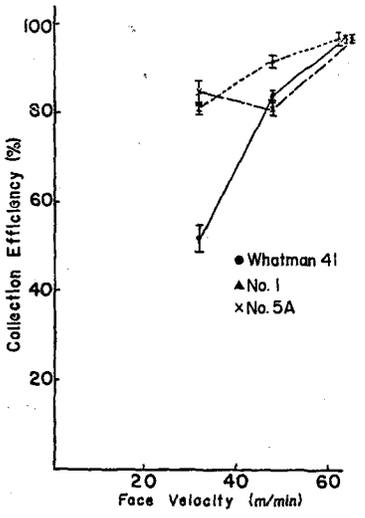

FIG. 3. Collection efficiency of cellulose filters.

3.2. *Surface Collection Efficiency*

In order to compare surface collection, two different techniques are usually used: one[6] is to measure the counting loss due to the burial of radioactive particles in the filter material, and the other[7] is to measure the alpha energy resolution of particles collected on the filter material. In the present experiment, both techniques were used for comparing surface collection efficiency for the thoron decay daughters. For the Millipore AA filter used as a reference filter, the alpha counting loss due to burial can be neglected because of the filter thickness (4 mg/cm^2 in weight) and the superiority in surface collection efficiency; that is, the surface collection efficiency is considered to be approximately one.

(a) *Comparison of counting loss due to burial.* In order to compare the surface collection efficiency of test filters with that of Millipore AA, the

ratios were determined by the following equation:

$$F_i^x = \frac{N_i^x / N_\gamma^x}{N_i^{AA} / N_\gamma^{AA}},$$

where F_i^x $(i = \alpha, \beta)$ = relative surface collection efficiency for alpha or beta activity, respectively,

N_i^x $(i = \alpha, \beta)$ = counting rate of the alpha or beta emitters, respectively, collected on the filters denoted by x,

N_γ^x = net count rate of the 0.239-MeV ThC gamma, which is that within the channel width of a half maximum in the gamma pulse height spectrum.

Filters were counted using the following detectors: a ZnS(Ag) scintillation counter for alphas, a G.M. counter for betas, and a NaI scintillation counter with pulse height analyzer for gammas. The measurements were made at the face velocities of 32 and 64 m/min, but no significant difference was observed in the ratios at the two velocities. The average values for the face velocity of 32 m/min are shown in Table 2.

(b) *Alpha energy resolution.* Measurements were made of the thoron daughters collected on the filters at both a face velocity of 32 m/min, and at the maximum face velocity available by the 2 h.p. vacuum pump, which is used for air sampling in JAERI. The energy resolution (%) for 8.77 MeV ThC′ alphas was determined, using a solid-state (silicon p-n junction) detector and multichannel PHA, at room temperature (20°C) and without a collimator. Under these conditions the energy resolution was 6.0% for a ^{239}Pu ($E_\alpha = 5.15$ MeV) source, thinly deposited on a metal disk.

The alpha spectra for HE-40 are shown in Fig. 4. The energy resolution data obtained are shown in the right columns of Table 2, in which it can be seen that the energy resolution improves with increase of the face velocity. These results agree with theory because the contribution of impaction to the collection is larger at higher velocities.

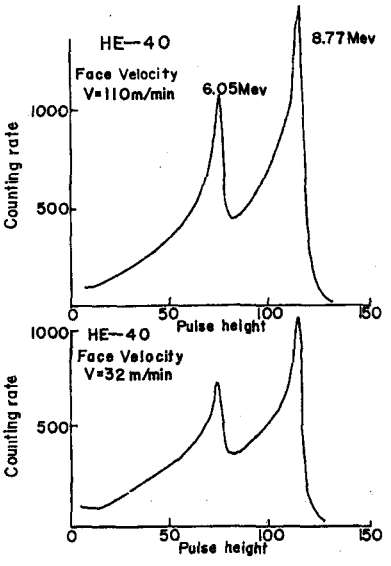

FIG. 4. Alpha spectra of Tn daughters collected on HE-40 filter.

From the data on surface collection efficiency and alpha energy resolution in Table 2, it can be seen that the glass fiber filters Gelman E and GB-100, and the cellulose asbestos filter HE-40 are superior in surface collection efficiency to the others, excepting Millipore AA.

3.3. *Air Flow Resistance*

The relationship between the air flow rate and pressure drop was measured on the test filters for an effective filter diameter of 50 mm. The results obtained for the celullose filters are shown in Fig. 5. The glass fiber filters GB-100 and GH-100 were mechanically so weak that they broke at higher velocities. The face velocities for the test filters at the pressure drops 200 and 300 mm Hg are shown in Table 2.

Table 2. Summary of Characteristics of the Filter Tested

Filter and Type		Face velocity (m/min)		Collection efficiency (%)			Surface collection efficiency		Alpha energy resolution at 8.77 MeV	
		Pressure drop		Face velocity			α	β		
		mm/Hg 200	mm/Hg 300	m/min 32	m/min 48	m/min 64	m/min 32	m/min 32	m/min 32	max face velocity
Cellulose	Whatman 41	△ 92 × 120	△ 120 × 180	52	84	97	0.67	0.73	37	(%) 28 (95 m/min)
	Toyo No. 1	80	100	81	92	97	0.36	0.49	45	26 (80 m/min)
	Toyo No. 5A	100	140	85	81	97	0.63	0.81	38	26 (87 m/min)
Cellulose asbestos	HV-70	100	150	99	98	98	0.61	0.76	28	18 (130 m/min)
	Toyo HE-10	100	140	99.7	99.7	99.7	0.55	0.74	46	24 (100 m/min)
	Toyo HE-13	200	—	79	92	89	0.12	0.36	30	31 (160 m/min)
	Toyo HE-40	100	140	99.7	99.9	99.6	0.81	0.86	16	13 (110 m/min)
Glass fiber	Gelman E	130	180	99.7	(99.9)	—	0.91	0.89	19	13 (96 m/min)
	Toyo GA-200	150	190	98	97	99	0.53	0.86	32	24 (96 m/min)
	Toyo GB-100	160	—	99	(99.9)	99.95	0.95	0.69	20	13 (80 m/min)
	Toyo GH-100	200	—	79	85	93	0.55	0.86	28	18 (80 m/min)
Membrane	Millipore AA	—	—	99.95	—	—	1.0	1.0	8.4	8.4 (34 m/min)

△ and × show that the weight of the filter paper is 19 and 17 mg/cm^2, respectively.

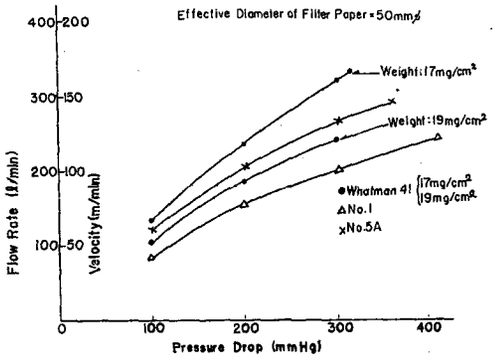

FIG. 5. Pressure drop vs. flow rate of cellulose filters.

4. DISCUSSION

4.1. *Comparison of the Results With Those by Others*

The collection efficiency of filters depends a great deal on the characteristics and size distribution of the particles. In Table 3, the data obtained by other workers[3, 4, 6] are compared with the data obtained by the authors. It appears that no significant difference can be observed among the given data.

The surface collection efficiencies measured by others[6, 8] are compared with the authors' data in Table 4, where the values by C. L. Lindeken[6] were measured relative to Millipore AA. In Table 4, it can be seen that the data agree on a relative basis with respect to filter material.

Table 3. Collection Efficiency of Filter for Various Aerosols

Filter	Particle		Collection efficiency			Reference
	Material	Diameter μ	m/min 15 %	m/min 30 %	m/min 60 %	
Whatman 41	D.O.P.	0.3	72	84	98	3
	Uranine	0.025	82.0	75.0	82.0	4
	Uranine	0.27	87.2	91.0	94.5	4
	Natural activity	—	52	68	78	6
	Natural activity	—	—	69.0	86.1	3
	Tn daughters	<0.1	—	52	97	
Toyo No. 5A	D.O.P.	0.3	68	76	86	3
	Natural activity	—	—	—	—	6
	Natural activity	—	—	77.8	91.6	3
	Tn daughters	<0.1	—	85	97	
HV-70	D.O.P.	0.3	98.2	99.2	99.8	3
	Uranine	0.025	95.2	97.6	98.9	4
	Uranine	0.27	98.2	97.2	96.5	4
	Natural activity	—	—	—	98	6
	Natural activity	—	—	98.4	99.8	3
	Tn daughters	<0.1	—	99	98	
Toyo HE-40	D.O.P.	0.3	99.93	99.98	99.996	3
	Natural activity	—	—	—	—	6
	Natural activity	—	—	100.1	99.3	3
	Tn daughters	<0.1	—	99.7	99.7	
Gelman E	D.O.P.	0.3	99.964	99.970	99.986	3
	Natural activity	—	—	—	98	6
	Natural activity	—	—	99.8	99.5	3
	Tn daughters	<0.1	—	99.7	—	

Table 4. Comparison of Surface Collection Efficiency of Filters

Filter	Surface collection efficiency		
	Uranium compound[6]	Natural activity[6]	Tn daughters
Whatman 41	~70	38	67
HV-70		80	61
Gelman E		89	91

4.2. *Reliability of the Data*

The data obtained for the collection efficiency and the surface collection efficiency, relative to Millipore AA, were not very accurate. However, from the comparisons given above and because of the rather good performance of Millipore AA as a reference filter, the data obtained could furnish information of considerable value.

5. SUMMARY

The important performance characteristics of filters were measured, mainly relative to Millipore AA. The results obtained are summarized in Table 2, in which it is seen that the data obtained agree well with those by others.

Of the cellulose filters tested, Toyo No. 5A and No. 1 showed similar performances to Whatman 41, and the collection efficiencies of these three filters were over 90% for thoron daughters at face velocities larger than 64m/min. However, these filters are not suitable for alpha air sampling because of poor surface collection efficiency.

The collection efficiencies of the cellulose asbestos filters, excepting Toyo HE-13, were over 98% at the face velocities tested. Toyo HE-40 proved to be superior to HV-70 in alpha air sampling because this filter has a large collection efficiency and about the same surface collection efficiency as the glass fiber filter, Gelman E.

Of the glass fiber filters, Toyo GB-100 showed a similar performance to Gelman E which is usually used for alpha air sampling due to its good performance. This filter, made in trial, cannot be used for routine air sampling because of mechanical weakness.

Finally, it may be considered that for air sampling, the cellulose filter Toyo No. 5A and No. 1 can be used instead of Whatman 41, and the cellulose asbestos filter Toyo HE-40 can be used instead of HV-70 and Gelman E. That is, Toyo HE-40 is found to be sufficiently usable for alpha air sampling.

6. ACKNOWLEDGEMENTS

The authors would like to express their thanks to Dr. N. Makino and Mr. S. Fukuda for their encouragement and helpful suggestions, and to Mr. M. Oshino for his kind arrangements and helpful suggestions in using a solid state detector. Thanks are also given to the research group of Toyo Roshi Co. Ltd. who presented the data concerning the physical characteristics of the filters.

REFERENCES

1. J. J. Fitzgerald and C. C. Detwiler. *A.M.A. Arch. Ind. Health* **15,** 3 (1957).
2. W. J. Smith and N. F. Suprenant. *Proc. ASTM* **53,** 1122 (1953).
3. L. B. Lockhart and R. L. Patterson. NRL-6054 (1964).
4. S. Posner. TID-7627 (1961).
5. G. Schuman. *J. Geophy. Res.* **68,** 3867 (1963).
6. C. L. Lindeken. *Am. Ind. Hyg. Assoc. J.* **22,** 232 (1961).
7. C. L. Lindeken, F. K. Petrock, W. A. Phillips and R. D. Taylor. *Health Phys.* **10,** 495 (1964).
8. J. S. Alercio and J. H. Harley. *Nucleonics* **10,** 87 (1952).

A NEW APPROACH TO THE REDUCTION OF INHALATION DOSE IN WORKING AREAS USING MOBILE ELECTROSTATIC PRECIPITATORS

K. G. VOHRA and P. V. N. NAIR
Bhabha Atomic Research Centre, Bombay, India

Abstract—A system for the rapid continuous decontamination of air has been investigated for reducing the inhalation dose in working areas where continuous small releases of radioactive contaminants in the air are unavoidable due to the nature of the operations involved. Continuous replacement of conditioned air used in such areas with the atmospheric air is generally not feasible due to large differences between the temperature of the conditioned air and the atmospheric air. Consequently recirculation has to be employed. Recirculation through the filters in the air conditioning system generally does not remove a large fraction of the submicron particles which are mainly responsible for the dose to the lung. The system described in this paper is based on a mobile electrostatic precipitator which can remove the particulate matter from the air down to the submicron size range at large flow rates. A description of the electrostatic precipitator used for continuous decontamination of the air, and studies carried out with the system in a test room and in typical working areas are presented.

1. INTRODUCTION

Inhalation dose in nuclear energy operations and handling and processing of radioactive materials is mainly caused by the deposition of submicron sized radioactive particles in the lower respiratory system. The total bulk of solid matter responsible for this dose is generally very small. Therefore, the problem of filtration of radioactive particulate matter from the air in nuclear energy plants and laboratories has to be treated differently from the problem of normal air cleaning, where large dust loads have to be handled. This is particularly so because these areas are normally fed with dust free conditioned air and the problem is essentially that of removal of radioactive and other particulate matter generated within the plant or laboratory. The radiotoxic particulate matter in the air is generally in the form of submicron particles. To remove such particles from the air effectively it is necessary to have a special filtering system. Mechanical filtration with absolute filters for efficient removal of these particles generally gives large pressure drops across the filters and it is very expensive to treat large volumes of air with such filters in most working areas.

In this paper we have described a recirculating system for high efficiency filtration of large volumes of air in working areas by electrostatic precipitation. The important features of this system are, (a) large volumes of air can be cleaned without excessive pressure drop across the filtering system, (b) filtering efficiency is particularly high for submicron particles in which we are mainly interested, (c) running power required is less than that for mechanical filters by more than an order of magnitude, (d) the filtering system can be made mobile and (e) the normal conditioned air supplied to the laboratory is adequate for the filtering system.

2. INHALATION DOSE AND AIR ACTIVITY

The concept of inhalation dose has been recently reconsidered by the ICRP on the basis of a new lung model.[1] This model recognises the importance of particle size distribution and takes into consideration the mass median diameter of the particles for pulmonary deposition mainly responsible for dose to the lung. The highly retained dust particles with mass median diameters in the range of 0.1 to 1 micron give pulmonary deposition of 20 to 50% of that inhaled (although pulmonary deposition for

particles below 0.1 micron is higher, their diffusion coefficients are so large that they are retained in the upper respiratory tract). Considerable reduction in the dose to the lung could therefore be achieved by the removal of submicron particles.

The fraction of the inhaled particles deposited in the lung can be reduced by 3 to 4 orders of magnitude by the removal of submicron particles from the air with an efficiency of 99.99% and higher. A recirculating filtering system can attain a very high efficiency for the removal of submicron aerosols from the air in working areas. Therefore in the present paper we have laid emphasis on this system of air cleaning for achieving very large decontamination factors.

In a recirculating system the rate of decrease in the concentration of particulate matter in the air would depend on the total volume of the room and the volume of air decontaminated per unit time. If C_0 is the initial concentration and C' the concentration after time t, the reduction factor is given by

$$\frac{C_0}{C'} = e^{kt}$$

where k is the constant (i.e. fraction removed per unit time) given by

$$k = \frac{v \text{ (volume filtered per unit time)} \times \text{efficiency}}{V \text{ (volume of the room)}}$$

The efficiency term would account for filtering efficiency and the efficiency of mixing in the room.

If there is a constant supply of the radioactive aerosol in a room at a rate of N particles per unit time, the following equations give the number of particles N' in the room at any time t after the start of the filter

$$\frac{dN'}{dt} = N - kN'$$

$$N' = \frac{N}{k}(1 - e^{-kt})$$

For t much larger than the decontamination half time $(0.693/k)$, $N' = \frac{N}{k}$. The reduced concentration C' is given by

$$C' = \frac{N'}{V} = \frac{N}{V} \cdot \frac{1}{k}$$

This shows that the concentration of aerosols can be maintained at the supply level as k approaches unity, and the build up of radioactive atoms attached to aerosols is prevented. In the case of radioactive aerosol contamination in the air the supply level is generally small and the build up of activity in the air with time is an important consideration.

3. DESCRIPTION OF THE FILTERING SYSTEM

The filtering system which is based on the conventional two stage electrostatic precipitator has been designed to meet the special requirements of working areas where the normal dust load is small and the supply of conditioned air has to be conserved. The special design features are, (a) free flowing decontaminated air at the breathing level, (b) low consumption of corona power, (c) extremely small production of ozone, (d) large collecting surface to handle significant loads of submicron particles and (e) high efficiency for submicron particles.

Figure 1 gives the schematic illustrating the main components of the precipitator. The overall dimensions of the unit are 34 × 34 × 72 in. (high). The clean air outlet is provided on all four sides of the cabinet with the main flow at a height of 3.5 ft from the ground. A 24 in. propeller fan is used for drawing the air through the filtering system located on the top of the cabinet as illustrated in the sketch in Fig. 1. The integrated flow rate at the outlet is 3500 ft³/min.

The dimensions of the precipitator inlet are 31 × 31 in. The ionizer consists of 30 parallel wires. The collection surface is provided partly by the perforated plates on either side of the ionizer and partly by 30 parallel collecting plates placed after the ionizer. The charging and collecting potentials are adjusted to give nearly 100% efficiency for submicron particles. The high voltage supply consisting of a voltage tripler is placed in the bottom compartment of the cabinet. The ionizer and collecting plate assemblies are made readily removable for cleaning.

A dacron fibre pre-filter is placed at the inlet

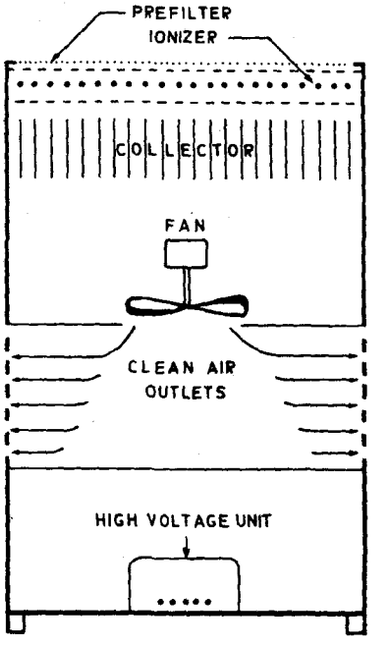

FIG. 1. Schematic illustrating the main components of the precipitator.

to remove fibrous material and large particles from the air. The present filtering unit was fabricated as a "test model" for initial studies.

4. EXPERIMENTS

(a) *Studies in the test room with a thoron generator*

The first study with the filtering system was made in a small test room having a total volume of about 2000 ft³. This room was fitted with a normal air conditioning unit which maintained the temperature in the room at 25°C. Thoron gas was generated in the room from a thoron generator consisting of a specially designed bubbler containing thorium nitrate solution. A continuous air monitor with a moving filter paper and a strip chart recorder was installed in the test room to record the levels of thoron daughter activity continuously. The initial equilibrium concentration of thoron daughter activity with the bubbler was attained in about 3–4 hr. After the equilibrium was attained, thoron daughter activity showed almost a steady level with the thoron generator in operation. The electrostatic filter was then switched on. The airborne activity in the room decreased with time with the electrostatic filter in operation and with the thoron generator continuously running. After the filter was in operation for about 50 min, the airborne activity in the room shown by the continuous air monitor was even lower than the normal background air activity in the room.

(b) *Studies at the laboratory room attached to Apsara Hall*

The airborne radioactivity in the swimming pool reactor area is mainly due to ^{88}Kr and ^{138}Xe daughters, present during the normal operation.[2, 3] For our studies we selected a large enclosed laboratory room attached to the main hall of the swimming pool reactor Apsara at Trombay. A moving filter-paper type of continuous air monitor was first placed in the room to find the normal level of activity with the reactor in operation. This showed an initial build-up of activity on the filter paper (paper speed 2 in./hr) for about 20 min, before attaining a steady value. When the electrostatic filter was started in the room the airborne activity started decreasing and came down to the normal background value (the reactor was running at its normal power). Figure 2 shows the decrease in activity caused by the electrostatic filter. The room volume is about 7000 ft³ and a

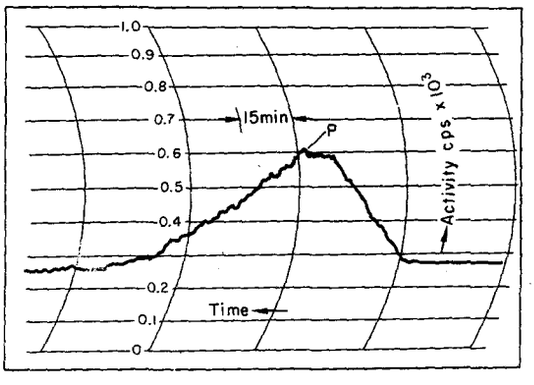

FIG. 2. Continuous air monitor trace showing decontamination of the air attained with the electrostatic filter operated in the laboratory room in the Apsara Reactor Building. Filter started at point *P*.

volume of air equivalent to the volume of the room passed through the filter in about 2 min. Although complete decontamination of the room air would be expected after 4 to 5 air passages through the recirculating filter, the longer time shown by the air monitor was due to the movement of the filter paper being slower compared to the speed of decontamination.

In both of the above experiments an additional indication of the cleanliness of decontaminated rooms was provided by the appearance of a completely unstained filter paper in the air monitor after the precipitator had run long enough to give a few air circulations through the filter.

(c) *Studies at the Thorium Plant at Trombay*

The packing room attached to the crushing room of the Thorium Plant at Trombay was selected for studies on decontamination of the air in a plant area. This room is fed by a supply line of conditioned air at a small flow-rate and is kept closed to prevent direct spray of thorium nitrate from the crushing room. The room had an equilibrium concentration of thorium (B+C). The continuous air monitor showed a steady level after nearly 25 min. of operation. Figure 3 shows a typical trace indicating a decrease in activity with operation of the electrostatic filter. It is interesting to note that in spite of high initial levels of activity, the degree of decontamination was so large that the air monitor showed negligible air activity after the initial operation of the filter for 30–40 min (as in the previous case, actual time of decontamination would be smaller). Nearly all the particulate airborne activity in the room was due to build-up of thorium (B+C) which could be controlled by rapid decontamination of the air.

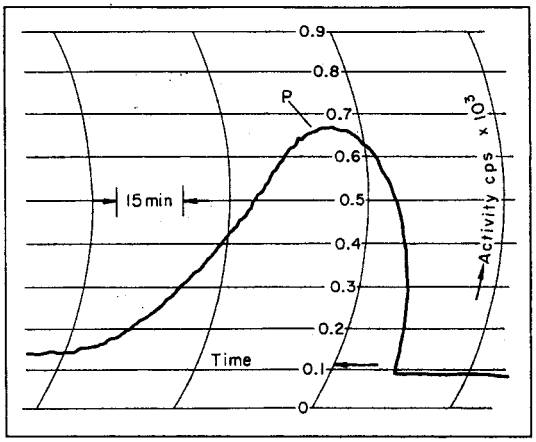

FIG. 3. Continuous air monitor trace showing decontamination of the air attained with the electrostatic filter installed in the packing room of the Thorium Plant. Filter started at point *P* (Equilibrium case).

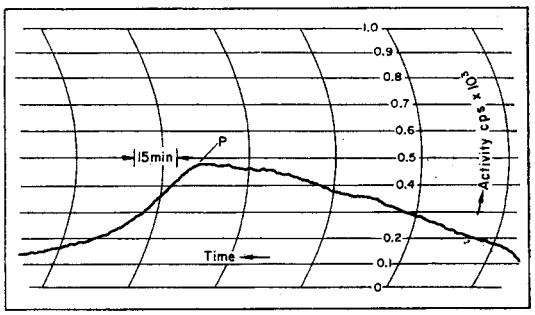

FIG. 4. Continuous air monitor trace showing decontamination of the air attained with the electrostatic filter operated in the packing room of the Thorium Plant. Filter started at point *P* (Non-equilibrium case).

Figure 4 gives the trace from the continuous air monitor showing the building-up of air activity in the room when the electrostatic filter was switched off. The filter was restarted at time corresponding to point *P* in the figure, and the trace also shows the decrease in air activity. The longer time of build-up in this case was due to growth of thorium-B and thorium-C in the room air (from the decay of thoron continuously produced in the room).

5. DISCUSSION

On the basis of the experiments carried out with the present system we can define the situations in nuclear energy operations where electrostatic filters of the present design can be applied with great advantage. Our suggested approach using mobile electrostatic filters has taken into consideration the adverse experiences

of installed electrostatic filters[4] where the initial costs and maintenance problems have been the limiting factors and absolute filters with asbestos and glass fibre have been extensively used.

The working areas involving small unavoidable releases of radioactive materials in the form of fine particles from the processes can be ideally protected by using the suggested recirculating type of electrostatic filters. Although the normal concentration of contaminants in the air in these areas may be less than the maximum permissible concentration in the air by one or two orders of magnitude, it may be desirable to reduce the inhalation dose for maintaining higher standards of radiation hygiene in these areas.

A recirculating electrostatic filter, installed in an air-conditioned room, passing one volume of the room air through it per minute is equivalent in performance to the supply of one air change in the room per minute through absolute filters and conditioning unit. Whereas for most working areas the latter would be prohibitively expensive in initial cost and running expenditure, the former could be installed at moderate initial investment and very small running expenditure.

From the limited operational experience, the suggested areas for use of the proposed filtering system are the working areas in uranium and thorium processing plants where major contamination is due to radon and thoron daughter products, working areas in the swimming pool type of reactors where the contamination is caused by the daughter products of gaseous fission products ^{88}Kr and ^{138}Xe, chemical laboratories attached to isotope production plants and chemical control laboratories attached to fuel processing plants where the hazard is primarily due to airborne plutonium.

Several minor radiochemical operations normally carried out in glove boxes can be carried out more freely in open laboratories with the protection from air contamination provided by mobile electrostatic filters. This would increase the production efficiency considerably. This filtering system would be particularly useful in sterile areas for the preparation of labelled compounds for medical uses.

The obvious limitation to the suggested system for use in areas of higher contamination is the build-up of radioactivity on the collecting plates giving rise to higher radiation dose in the vicinity of the filtering unit. For this purpose it is proposed to incorporate a gamma radiation dosimeter in the filtering unit to provide a warning of the need for decontamination of the filter plates.

Further investigations on the applications of the proposed filtering system are in progress.

REFERENCES

1. ICRP Task Group on Lung Dynamics. Report to Committee II. *Health Physics*, **12,** 173 (1966).
2. K. G. Vohra. Release of fission gases in reactor coolants under normal operations. *Proc. Third International Conference on Peaceful Uses of Atomic Energy*, Vol. 13, p. 439, Geneva, August 31–September 9, 1964.
3. R. Berner, W. Hunzinger and T. Hurlimann. Air pollution observed at Saphir. *Proc. Symposium on Health Physics in Nuclear Installations*, page 247, Riso, 1959.
4. L. Silverman. Economic aspects of air and gas cleaning for nuclear energy processes. *Proc. I.A.E.A. Conference on Disposal of Radioactive Wastes*, Vol. 1, p. 139, Monaco, 16–21 November, 1959.

ABSCHEIDUNG VON RADIOAKTIVEM JOD IN ATEMFILTERN

J. HACKE und W. JACOBI
Hahn-Meitner-Institut für Kernforschung Berlin, Abteilung Strahlenphysik,
Berlin 39, Glienicker Straße 100, Germany

Zusammenfassung—Die Abscheidung von Radiojod im Atemfilter und seinen beiden Bestandteilen (Faser- und Aktivkohlefilter) wurde mit Hilfe der Mehrfiltermethode untersucht. Mit dieser Methode konnten die verschieden filterbaren Jodkomponenten in der Luft getrennt und ihre Anteile bestimmt werden. Elementares Jod und an Aerosolteilchen angelagertes Jod werden im Filter nahezu vollständig zurückgehalten. Für eine dritte schwache Jodkomponente, bei der es sich wahrscheinlich vorwiegend um Methyljodid handelt, ist das Filter relativ durchlässig. Der Anteil dieser Komponente nahm umgekehrt proportional der J-Konzentration in der Luft ab und betrug bei einer spezifischen J^{132}-Aktivität der Luft von etwa 10^{-4} Ci/m³ etwa 0,03%; dem entsprach eine Gesamt-Jod-Durchlässigkeit des Atemfilters von 0,02%. Die Eignung des Geräts für den beabsichtigen Verwendungszweck wird diskutiert.

1. EINLEITUNG

Bei einem Reaktorunfall spielt bezüglich der Gefährdung von Menschen das freigesetzte Jod eine entscheidende Rolle. Während alle anderen Spaltprodukte von Schwebstoffiltern nahezu vollständig zurückgehalten werden, gelingt dies bei Jod nur sehr unvollständig. In den letzten Jahren wurden deshalb zahlreiche Untersuchungen über die Freisetzung von Jod aus Kernbrennstoffen und sein physikalisch-chemisches Verhalten in verschiedenen Gasatmosphären bei Unfallbedingungen (1–12), sowie über Verfahren der Jodfilterung (13–22) durchgeführt. Das Ziel dieser Untersuchungen war die Entwicklung geeigneter Jodfilter für die Abluft von Reaktoranlagen zum Schutze der benachbarten Bevölkerung bei Reaktorunfällen. Um auch das Reaktorpersonal bei einem Unfall wirksam vor der Inhalation von Spaltprodukten zu schützen, wurde von der Auergesellschaft mbH Berlin ein als "Reaktorfluchtgerät" bezeichnetes Atemgerät entwickelt, das aus einem Mundstück in Verbindung mit einem kombinierten Schwebstoff–Aktivkohle–Atemfilter besteht. Die Abteilung Strahlenphysik am Hahn–Meitner–Institut für Kernforschung Berlin wurde von der Auergesellschaft beauftragt, Messungen des Abscheidewirkungsgrades dieses Atemfilters für Radiojod durchzuführen.

2. VERSUCHSANORDNUNG UND VERSUCHSDURCHFÜHRUNG

Die Versuche wurden mit dem Jodisotop ^{132}J (Halbwertszeit $t_{1/2} = 2{,}26$ h) durchgeführt, das als Tochtersubstanz von ^{132}Te gewonnen wurde.

Abb. 1 zeigt eine schematische Darstellung der Versuchsanordnung. Die aus dem Jodgenerator entweichende J-haltige Luft durchströmte zunächst ein Glaswattefilter, um den Luftstrom von Wassertröpfchen zu befreien und wurde dann am Eingang einer zylindrischen Mischkammer einem Luftstrom von normaler, ungefilterter Zimmerluft zugesetzt (Temperatur 20–22°C, relative Feuchte 35–45%). Der gesamte Luftdurchsatz durch die Mischkammer betrug (entsprechend der mittleren Atemleistung des Menschen) $v = 30$ l/min. Am Ausgang der Mischkammer befand sich die Filteranordnung, die aus mehreren—mindestens drei—in Reihe geschalteten Filtern der zu prüfenden Filterart bestand.

Die Sammelzeit betrug bei den Versuchen 1 h. Danach wurden die relativen Aktivitäten

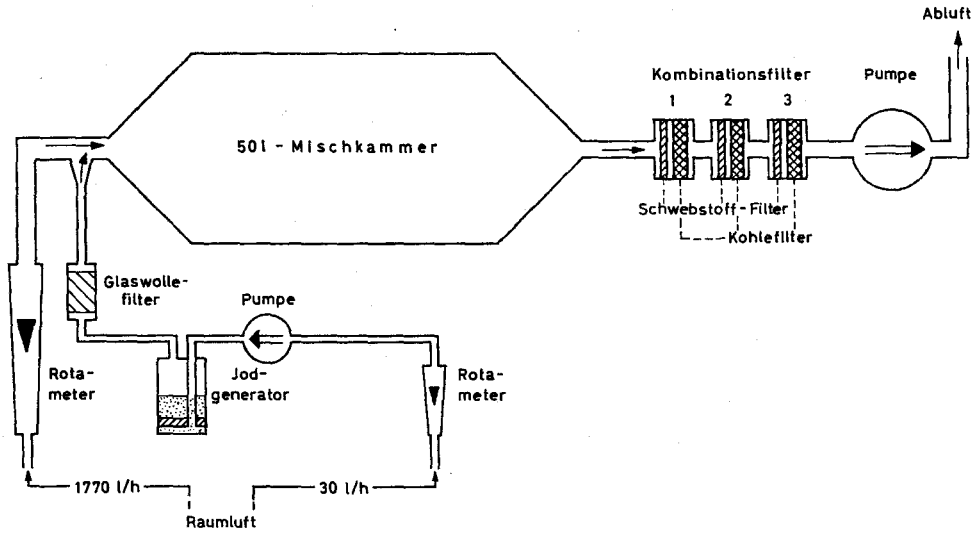

ABB. 1. Filterprüfanlage (schematische Darstellung).

der einzelnen hintereinandergeschalteten Filter mit einem γ-Szintillationsspektrometer bei konstanter Meßgeometrie gemessen.

Die Bestimmung des Abscheidewirkungsgrads der Filter erfolgte nach der bei Schwebstoffiltern üblichen Mehrfiltermethode, wobei bei jedem Versuch 3–4 Filter in Reihe in den Luftstrom geschaltet wurden. Die gemessenen relativen Aktivitäten A_1, A_2, A_3 und A_4 des 1., 2., 3. und 4. Filters in der Reihe wurden in halblogarithmischer Darstellung in Abhängigkeit von der Nummer n des Filters in der Filterreihe aufgetragen.

Die Versuche zeigten (vgl. Abschnitt 3), daß die Filteraktivität hinter dem 1. Filter innerhalb der Fehlergrenzen exponentiell mit n abfällt, d.h. das Verhältnis

$$q = \frac{A_n + 1}{A_n} \qquad (n \geq 2)$$

ist bei jedem Versuch konstant. q wurde aus der mittleren Neigung der Exponentialkurve im Bereich $n = 2 - 4$ bestimmt. Die gesamte filterbare Aktivität L_0 der angesaugten Luft folgt somit zu

$$L_0 = A_1 + A_2 + A_3 + A_4 \cdot (1 + \sum_{i=1}^{\infty} q^i)$$

$$= A_1 + A_2 + A_3 + A_4 \cdot \frac{1}{1-q}$$

Das Verhältnis A_n/L_0 gibt den relativen Anteil der Luftaktivität an, der im n Filter der Filterreihe zurückbleibt. Die Durchlässigkeit $D(n)$ einer Filterreihe aus n Filtern beträgt demnach:

$$D(n) = 1 - \sum_{i=1}^{n} \frac{A_i}{L_0}$$

Für das 1. Filter der Filterreihe ist somit der Abscheidewirkungsgrad $\eta_1 = A_1/L_0$ und die Durchlässigkeit $D_1 = 1 - \eta_1$.

3. VERSUCHSERGEBNISSE UND DISKUSSION

Es wurden drei Versuchsreihen durchgeführt. Bei der ersten Versuchsreihe wurden jeweils 3 Kombinationsfilter, wie sie in den Reaktorfluchtgeräten verwendet werden, hintereinandergeschaltet. Jedes Kombinationsfilter enthielt ein Schwebstoff- und ein Kohlefilter. Bei der zweiten Versuchsreihe wurde das Kohlefilter entfernt, um den Wirkungsgrad des Schwebstoffilters allein zu prüfen. Bei diesen Versuchen wurden jeweils 4 Schwebstoffilter hintereinandergeschaltet; dahinter wurde als 5. Filter noch ein Kohlefilter gesetzt, um den

durch die Schwebstoffilter durchgehenden Jodanteil zu erfassen. Bei der dritten Versuchsreihe wurde umgekehrt wie bei der zweiten Versuchsreihe verfahren. Aus den Kombinationsfiltern wurden in diesem Fall die Schwebstoffilter entfernt, um die Abscheidung im Kohlefilter allein zu bestimmen. Es wurden jeweils 4 Kohlefilter hintereinandergeschaltet; dahinter befand sich ein Schwebstoffilter, um den von den Kohlefiltern durchgelassenen Jodanteil zu erfassen.

Die spezifische ^{132}J-Aktivität der am 1. Filter anströmenden Luft hing von dem Alter des Te-J-Präparates ab und variierte bei den Versuchsreihen von 10^{-3} — 10^{-5} Ci/m^3, was einer Jod-Konzentration von 10^{-10} — 10^{-12} g/m^3 in der Luft entspricht.

Im folgenden sind die Ergebnisse der einzelnen Versuchsreihen zusammengestellt.

3.1. *Jodabscheidung in Schwebstoffiltern*

In Tabelle 1 ist die gemessene ^{132}J-Aktivität A_1, A_2, A_3, A_4 des 1., 2., 3. und 4. Schwebstoffilters im Verhältnis zur gesamten ^{132}J-Aktivität L_0 der angesaugten Luft angegeben, außerdem ist das entsprechende Verhältnis für das nachgeschaltete Kohlefilter angegeben. Das Verhältnis A_1/L_0 ist somit gleich dem Abscheidewirkungsgrad für ein einzelnes Schwebstoffilter. Die Zahlen sind Mittelwerte aus 5 Versuchen.

Von der anströmenden ^{132}J-Aktivität der Luft werden also im Mittel im

1. Schwebstoffilter 55%
   (Schwankungsbereich 28–76%)
2. Schwebstoffilter 11%
   (Schwankungsbereich 7–14%)
3. Schwebstoffilter 10%
   (Schwankungsbereich 5–21%)
4. Schwebstoffilter 6,5%
   (Schwankungsbereich 3–12%)

zurückgehalten.

In Abb. 2 ist die Durchlässigkeit in Abhängigkeit von der Zahl der hintereinandergeschalteten Schwebstoffilter aufgetragen. Hinter dem 1.

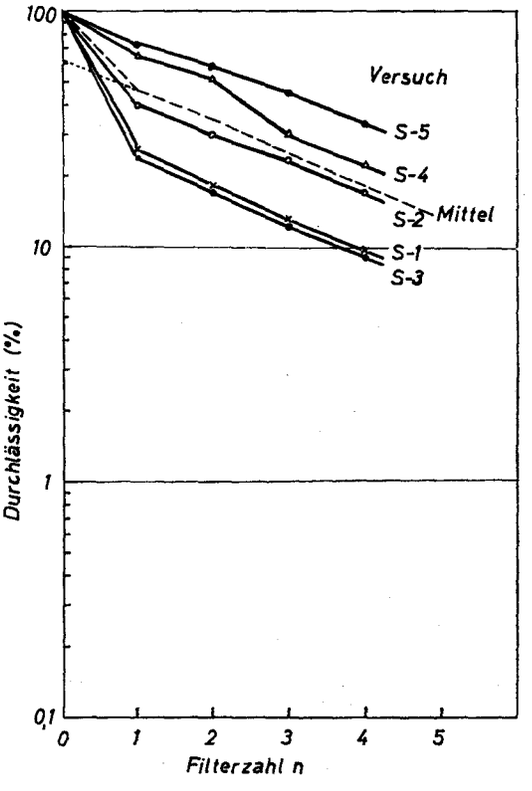

ABB. 2. ^{132}J-Durchlässigkeit in Abhängigkeit von der Zahl der hintereinandergeschalteten Schwebstoffilter.

Tabelle 1. *Relative ^{132}J-Aktivität* A *von* 4 *hintereinandergeschalteten Schwebstoffiltern und einem nachgeschalteten Kohlefilter (bezogen auf die Aktivität* L_0 *der angesaugten Luft vor der Filteranordnung)*

Schwebstoffilter				Kohlefilter
A_1/L_0	A_2/L_0	A_3/L_0	A_4/L_0	A_5/L_0
0,546	0,108	0,103	0,065	0,147

Filter fällt die Durchlässigkeit annähernd exponentiell ab, wobei die Durchlässigkeitskurven bei allen Versuchen annähernd parallel verlaufen. Aus Abb. 2 folgt, daß im Hinblick auf die Filterung von Jod durch Schwebstoffilter 2 Komponenten unterschieden werden können:

(1.) Eine gut filterbare Komponente, die praktisch vollständig im 1. Schwebstoffilter zurückgehalten wird.

(2.) Eine schlecht filterbare Komponente, welcher der langsame exponentielle Abfall der Durchlässigkeitskurve hinter dem 1. Filter zuzuschreiben ist. Der Abscheidewirkungsgrad der Schwebstoffilter für diese Komponente beträgt im Mittel 26% (Schwankungsbereich 16–31%).

Eine Extrapolation der Durchlässigkeitskurven gegen $n = 0$ ergibt, daß auf die erste Komponente im Mittel 40% (Schwankungsbereich 15–70%), auf die 2. schlecht filterbare Komponente im Mittel 60% (Schwankungsbereich 30–85%) der Jodaktivität in der angesaugten Luft entfallen. Da der Abscheidewirkungsgrad der Schwebstoffilter für Aerosole nahezu 100% beträgt, ist die gut filterbare Jodkomponente offensichtlich dem an Aerosolteilchen angelagerten Jod zuzuschreiben.

Aus Abb. 2 folgt jedoch, daß selbst 4 hintereinandergeschaltete Schwebstoffilter noch im Mittel 18% (Schwankungsbereich 9–33%) der schlecht filterbaren Jodkomponente durchlassen. Dieser Wert stimmt innerhalb der Fehlergrenzen überein mit der relativen Jodaktivität auf dem nachgeschalteten Kohlefilter (vgl. Tab. 1). Daraus folgt, daß es sich bei der durch Schwebstoffilter schlecht filterbaren Jodkomponente vorwiegend um gasförmiges, an der Aktivkohle gut adsorbierbares Jod handelt. Andererseits zeigt dieses Ergebnis, daß Schwebstoffilter auch eine recht beträchtliche Abscheidefähigkeit für gasförmiges Jod besitzen. Die Unterschiede in dem Abscheidewirkungsgrad bzw. der Durchlässigkeit der 1. Schwebstoffilter werden offensichtlich durch die unterschiedlichen Anteile beider Jodkomponenten in der anströmenden Luft bei den einzelnen Versuchen verursacht.

3.2. *Jodabscheidung in Aktivkohlefiltern*

In Tabelle 2 ist die gemessene ^{132}J-Aktivität A_1, A_2, A_3, A_4 des 1., 2., 3. und 4. Kohlefilters im Verhältnis zur gesamten ^{132}J-Aktivität L_0 der angesaugten Luft angegeben; die letzte Spalte zeigt das entsprechende Verhältnis für das nachgeschaltete Schwebstoffilter. Das Verhältnis A_1/L_0 gibt somit den Abscheidewirkungsgrad eines einzelnen Kohlefilters für Radiojod ohne vorherige Schwebstoffilterung an. Die Zahlen sind Mittelwerte aus 6 Versuchen.

Von der anströmenden ^{132}J-Aktivität der Luft werden also im Mittel im

1. Kohlefilter 99,2%
   (Schwankungsbereich 98,0–99,97%)
2. Kohlefilter 0,19%
   (Schwankungsbereich 0,004– 0,42%)
3. Kohlefilter 0,14%
   (Schwankungsbereich 0,008– 0,34%)
4. Kohlefilter 0,12%
   (Schwankungsbereich 0,004– 0,29%)

zurückgehalten.

Abb. 3 zeigt die Jod-Durchlässigkeit in Abhängigkeit von der Zahl der hintereinandergeschalteten Aktivkohlefilter. Wie bei den Versuchen mit Schwebstoffiltern kann auch hier aus dem Kurvenverlauf auf die Existenz von 2 Jodkomponenten geschlossen werden, einer gut filterbaren Komponente, die praktisch vollständig bereits im 1. Filter zurückgehalten

Tabelle 2. Relative ^{132}J-Aktivität A von 4 hintereinandergeschalteten Aktivkohlefiltern und einem nachgeschalteten Schwebstoffilter (bezogen auf die Aktivität L_0 der angesaugten Luft)

Kohlefilter				Schwebstoffilter
A_1/L_0	A_2/L_0	A_3/L_0	A_4/L_0	A_5/L_0
0,99185	0,00186	0,00137	0,00119	0,00350

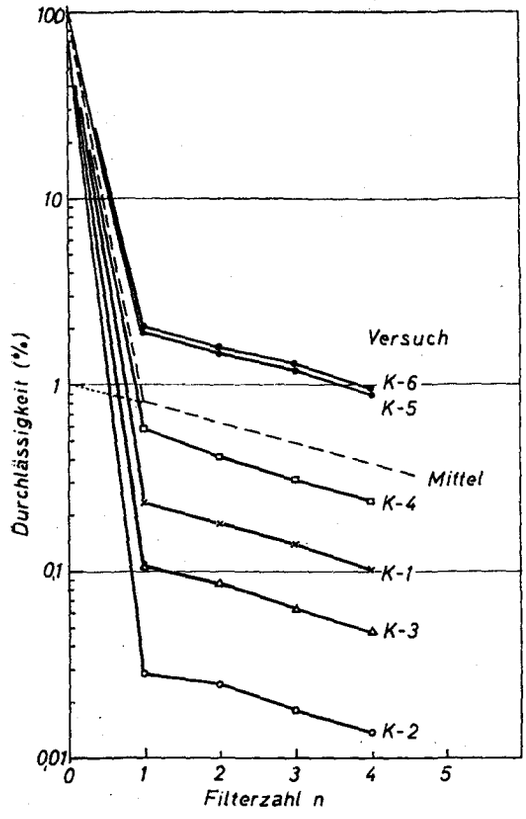

ABB. 3. ^{132}J-Durchlässigkeit in Abhängigkeit von der Zahl der hintereinandergeschalteten Kohlefilter.

wird, und einer demgegenüber schlecht filterbaren Komponente, der der langsame exponentielle Abfall hinter dem 1. Filter zuzuschreiben ist. Der Abscheidewirkungsgrad eines einzelnen Kohlefilters für letztere Komponente beträgt im Mittel 24% (Schwankungsbereich 16–35%). Extrapoliert man auch hier wieder die Durchlässigkeitskurve dieser Komponente gegen $n = 0$ (s. Abb. 3), so ergibt sich ihr Anteil an der gesamten Jodaktivität der anströmenden Luft vor dem 1. Filter im Mittel zu 1% (Schwankungsbereich 0,05–3%). Im Mittel entfallen also 99% der Jodaktivität auf die gut filterbare Komponente (Schwankungsbereich 97–99,9%).

Bei der Deutung der gemessenen Durchlässigkeitskurven für die Aktivkohlefilter ist zu berücksichtigen, daß derartige Filter für Aerosole—im Gegensatz zu den verwendeten Schwebstoffiltern—nur einen begrenzten und von der Teilchengröße abhängigen Wirkungsgrad haben. Auf Grund der Erfahrungen über die Abscheidung von Aerosolen in Faser-, Poren- und Kornfiltern ist zu erwarten, daß in einem derartigen Kohlefilter sowohl der feindisperse Aerosolanteil durch Diffusion als auch der grobdisperse Aerosolanteil infolge der Massenträgheit der Teilchen weitgehend zurückgehalten werden und das Minimum der Abscheidung in dem dazwischen liegenden Teilchengrößenbereich liegt.

Daraus folgt für die Jodfilterung im Kohlefilter, daß die beobachtete gut filterbare Komponente sich aus gasförmigem, gut adsorbierbarem Jod—es handelt sich hierbei wahrscheinlich in erster Linie um elementares Jod—und aus dem an das grob- bzw. feindisperse Aerosol angelagerten Jod zusammensetzt. Dementsprechend enthält die zweite, relativ schlecht filterbare Komponente das vorwiegend an das mitteldisperse Aerosol angelagerte Jod sowie gasförmiges, aber an Aktivkohle schlecht adsorbierbares Jod (letzteres liegt wahrscheinlich vorwiegend in Form von Methyljodid vor).

Die Ergebnisse vermögen auch bereits Aufschluß darüber zu geben, ob bei der zweiten, durch das Kohlefilter schlecht filterbaren Komponente die gasförmige oder die Aerosolkomponente des Jods überwiegt. Ein Vergleich der von 4 hintereinandergeschalteten Kohlefiltern durchgelassenen Jodaktivität (Abb. 3) mit der im nachgeschalteten Schwebstoffilter abgeschiedenen Aktivität (A_5/L_0 in Tab. 2) zeigt, daß bei allen Versuchen diese Werte annähernd gleich sind. Betrachtet man z.B. die Mittelwerte, so beträgt nach Abb. 3 die von 4 Kohlefiltern noch durchgelassene relative Aktivität 0,37% (Schwankungsbereich 0,013–0,95%) und nach Tab. 2 die relative Aktivität des nachgeschalteten Schwebstoffilters 0,35% (Schwankungsbereich 0,01—0,98%). Aus dieser Übereinstimmung folgt, daß die vom Kohlefilter schlecht zurückgehaltene Jodkomponente, auf die im Mittel 1% der Jodaktivität in der Luft entfällt, zum größten Teil am Aerosol angelagert sein muß.

3.3. *Jodabscheidung in Kombinationsfiltern*

Es wurden sechs Versuche mit Kombinationsfiltern ohne Jodvorbeladung und ein Versuch

mit Kombinationsfiltern, die vor Versuchsbeginn mit 20 g inaktivem Jod vorbeladen worden waren, durchgeführt. Bei allen Versuchen waren jeweils drei Kombinationsfilter hintereinandergeschaltet.

Aus den Versuchsergebnissen folgt, daß bei den vorliegenden Versuchsbedingungen die Durchlässigkeit eines einzelnen Kombinationsfilters 0,002–0,2% beträgt. Sie liegt im Mittel etwa eine Größenordnung niedriger als die Durchlässigkeit des Kohlefilters (vgl. 3.2.). Dies ist auf Grund der Messungen bei den Kohlefiltern zu erwarten, aus denen hervorging, daß diese Filter für einen Teil der Schwebstoffkomponente relativ durchlässig sind. Bei dem Kombinationsfilter wird dieser Anteil durch das vorgeschaltete Schwebstoffilter praktisch effektiv zurückgehalten.

Auffallend ist der relativ große Schwankungsbereich der Durchlässigkeitswerte, der weder durch Meßfehler noch durch fabrikationstechnisch bedingte Unterschiede der Filter verursacht wird.

Aufschluß über die Ursache ergibt die in Abb. 4 dargestellte Abhängigkeit der Durchlässigkeit von der Zahl der hintereinandergeschalteten Kombinationsfilter. Danach muß auch bei den Kombinationsfiltern wieder zwischen einer gut und schlecht filterbaren Komponente unterschieden werden, wobei der Abscheidewirkungsgrad für letztere Komponente bei allen Versuchen etwa gleich blieb und im Mittel 43% (Schwankungsbereich 30–50%) betrug. Durch Extrapolation der Durchlässigkeitskurve für diese 2. Komponente ergibt sich für $n = 0$ der relative Aktivitätsanteil dieser Jodkomponente an der gesamten Jodaktivität der angesaugten Luft. Dieser Anteil schwankt offensichtlich zwischen 0,005% und 0,4% und beträgt im Mittel 0,08%.

Daraus ergibt sich, daß die beobachteten Schwankungen der Durchlässigkeit des Kombinationsfilters auf den unterschiedlichen Anteil der schlecht filterbaren Jodkomponente in der anströmenden Luft bei den einzelnen Versuchen zurückzuführen sind. Nach Untersuchungen von Eggleton *et al.*,[19] Collins *et al.*,[17] Adams *et al.*,[18] Parker *et al.*[11] und Parsley *et al.*[12] handelt es sich bei dieser Komponente wahrscheinlich um gasförmiges Jod in Form von Aklyljodiden, und zwar vor-

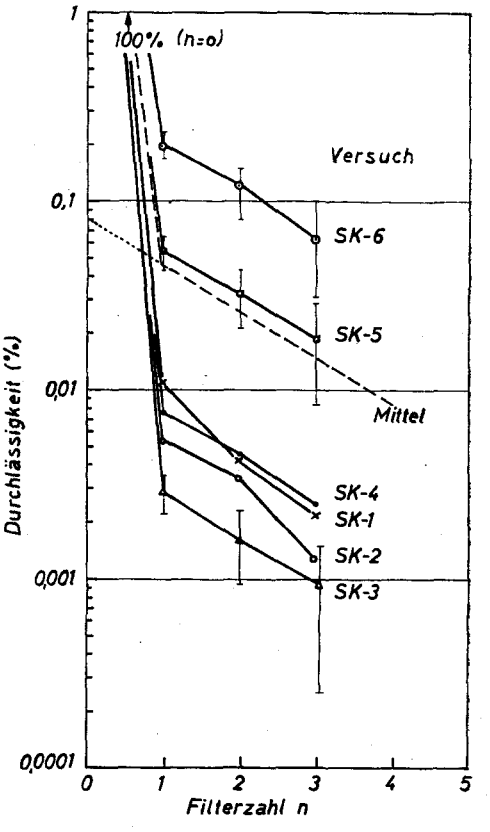

ABB. 4. ^{132}J-Durchlässigkeit in Abhängigkeit von der Zahl der hintereinandergeschalteten Kombinationsfilter.

wiegend um Methyljodid. Im folgenden wird daher diese Komponente als Methyljodid bezeichnet.

Untersuchungen von Collins *et al.*[3] sowie von Billard *et al.*[20, 21] über die ^{131}J-Durchlässigkeit von Aktivkohle bei Jodkonzentrationen von 10^{-9} — 10^{-3} g J/m³ Luft lassen die Tendenz erkennen, daß die Durchlässigkeit mit zunehmender Jodkonzentration abnimmt. Die vorliegenden Messungen an Kombinationsfiltern ergeben den gleichen Zusammenhang. Abb. 5 zeigt die aus den Messungen resultierende Abhängigkeit der ^{132}J-Durchlässigkeit des 1. Filters von der Filter- bzw. Luftaktivität L_o. Letztere ist proportional der spezifischen ^{132}J-Aktivität der anströmenden Luft; unter den vorliegenden Meßbedingungen entspricht einer Luftaktivität L_o von 10^6 ipm eine mittlere spe-

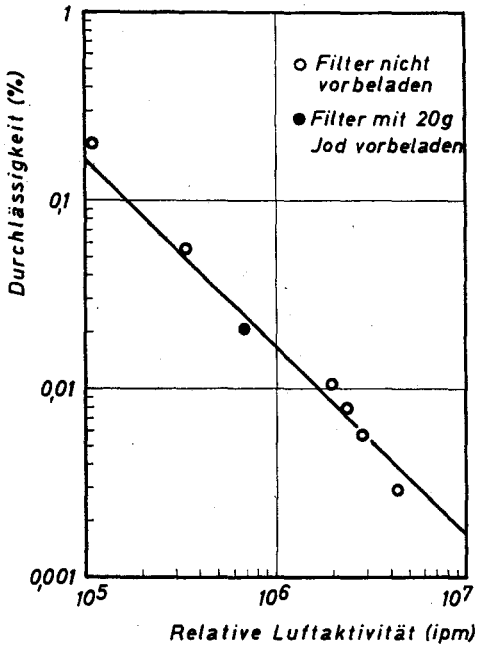

ABB. 5. Abhängigkeit der ^{132}J-Durchlässigkeit eines Kombinationsfilters von der spezifischen Jodaktivität der Luft.

zifische ^{132}J-Aktivität der Luft von 10^{-4} Ci/m³. Die vorliegenden Messungen erfassen somit einen Konzentrationsbereich von 10^{-3} — 10^{-5} Ci/m³ bzw. 10^{-10} — 10^{-12} g Jod/m³ Luft.

Aus Abb. 5 geht hervor, daß in diesem Bereich die J-Durchlässigkeit des Kombinationsfilters umgekehrt proportional der Jodkonzentration in der Luft ist. Dieser Zusammenhang wird nicht durch eine Änderung der Filtereigenschaften mit der Jodkonzentration verursacht. Die mit Hilfe der angewandten Mehrfiltermethode mögliche Analyse der Durchlässigkeitskurven (Abb. 4) zeigt vielmehr eindeutig, daß die Konzentration der schlecht filterbaren Methyljodid-Komponente umgekehrt proportional mit der Jodkonzentration der Luft abnimmt.

Eine Vorbeladung der Kombinationsfilter mit 20 g inaktivem Jod hatte keinen erkennbaren Einfluß auf die Durchlässigkeit für Radiojod. Aus Abb. 5 geht hervor, daß die in diesem Fall gemessene Durchlässigkeit von 0,02% mit dem für unbeladene Filter zu erwartenden Wert übereinstimmt. Eine Abnahme der Filterwirksamkeit infolge Erschöpfung des Aktivkohlefilters tritt daher offensichtlich erst bei Jodmengen ein, die weit oberhalb der für den beabsichtigten Verwendungszweck des Reaktorfluchtgeräts in Frage kommenden Jodkonzentrationen liegen.

4. SCHLUSSFOLGERUNGEN

Aus den durchgeführten Untersuchungen über die Abscheidung von Radiojod in den Atemfiltern ergeben sich zusammenfassend nachstehende Schlußfolgerungen:

1. Hinsichtlich der Abscheidung des Radiojods können auf Grund der vorliegenden Versuche folgende Komponenten unterschieden werden:

(a) Gasförmiges Jod, das von Aktivkohle gut adsorbiert wird; hierbei dürfte es sich vorwiegend um elementares Jod handeln.
(b) Jod, das vom Schwebstoffilter des Atemfilters effektiv zurückgehalten wird; hierbei handelt es sich um an Aerosolteilchen angelagertes Jod.
(c) Jod, das weder im Schwebstoff- noch im Aktivkohlefilter gut zurückgehalten wird; bei dieser Komponente liegt das Jod gasförmig, und zwar wahrscheinlich in Form von organischen Jodverbindungen, hauptsächlich als Methyljodid, vor.

2. Die zur Prüfung der Wirksamkeit der Filter für Radiojod angewandte Mehrfiltermethode ermöglicht in einfacher Weise die Trennung dieser Komponenten und die Bestimmung ihrer relativen Anteile in der zu filternden Luft. Bei den vorliegenden Versuchsbedingungen entfielen von der Jodaktivität in der anströmenden Luft im Mittel etwa 60% auf elementares Jod, etwa 40% auf das am Aerosol gebundene Jod und nur etwa 0,1% auf die Methyljodidkomponente.

3. Das Schwebstoffilter des Atemfilters hält das am Aerosol angelagerte Jod vollständig zurück, während sein Abscheidewirkungsgrad für elementares Jod im Mittel nur 26% (Schwankungsbereich 16–31%) beträgt. Der hindurchgehende Restanteil des elementaren Jods wird im nachgeschalteten Aktivkohlefilter vollständig zurückgehalten. Das Atemfilter ist somit ein

sehr effektives Filter sowohl für elementares Jod als auch für das am Aerosol angelagerte Jod. Die Verteilung der Aktivität auf das Schwebstoff- und Kohlefilter hängt von den Anteilen beider Komponenten in der ausströmenden Luft ab. Unter Berücksichtigung der oben angegebenen mittleren Anteile wird im Schwebstoffilter etwa 55% und im Kohlefilter etwa 45% der Aktivität zurückgehalten.

4. Der Abscheidewirkungsgrad des Atemfilters für die Methyljodidkomponente beträgt im Mittel 43% (Schwankungsbereich 30–50%). Die Durchlässigkeit des Atemfilters für Radiojod wird daher nahezu ausschließlich durch den Anteil der Methyljodidkomponente in der anströmenden Luft bestimmt. Dieser Anteil nahm unter den vorliegenden Versuchsbedingungen umgekehrt proportional der Jodkonzentration in der Luft ab. Er betrug bei einer spezifischen ^{132}J-Aktivität der Luft von 10^{-5} Ci/m^3 etwa 0,3%, bei 10^{-3} Ci/m^3 etwa 0,003%. Dementsprechend sank die Joddurchlässigkeit des Atemfilters von etwa 0,2% bei 10^{-5} Ci/m^3 auf etwa 0,002% bei 10^{-3} Ci/m^3 ab.

5. Eine Vorbeladung des Atemfilters mit 20 g inaktivem Jod hatte keine Änderung der Durchlässigkeit für Radiojod zur Folge.

6. Die Versuche wurden bei einer relativen Luftfeuchtigkeit von 35–45% durchgeführt; bei 90% Feuchte ist mit einer Erhöhung der Joddurchlässigkeit um etwa den Faktor 3 zu rechnen (vgl.[20, 21]), die in erster Linie durch die Zunahme des Anteils der Methyljodidkomponente in der Luft mit steigender Feuchte bedingt ist.

Die Ergebnisse zeigen, daß das vorliegende Atemfilter für die Methyljodidkomponente weitgehend durchlässig ist. Nach Abschluß dieser Messungen veröffentlichte Untersuchungen von Collins[22] sowie am Oak Ridge National Laboratory[23] haben ergeben, daß die Durchlässigkeit von Aktivkohle für Methyljodid durch geeignete Imprägnierung, z.B. mit inaktivem Jod, Brom, einigen Jod- bzw. Bromsalzen sowie mit Triäthylendiamen auf unter 1% reduziert werden kann. Bei dem beschriebenen Atemfiltergerät ist eine entsprechende Imprägnierung der Aktivkohle beabsichtigt, da die jetzige Imprägnierung mit Schwermetallen offensichtlich ohne Einfluß auf die Methyljodidkomponente ist.

ANERKENNUNG

Für die wirksame Unterstützung dieser Untersuchungen sind wir der Auergesellschaft zu Dank verpflichtet. Dieser Dank gebührt insbesondere den Herren Dr. Lemcke und Dr. Brauer von der Entwicklungsabteilung dieser Firma, die zahlreiche wertvolle Anregungen zur Durchführung dieser Untersuchungen und bei der Diskussion ihrer Ergebnisse gegeben haben. Für die Durchführung der Messungen danken wir Fräulein K. Tramme und Fräulein T. Kiehne.

LITERATUR

1. W. J. Megaw und E. G. May. The behaviour of iodine released in reactor containers. *React. Science and Technology* **16,** 427 (1962).
2. A. C. Chamberlain, A. E. J. Eggleton, W. J. Megaw und J. B. Morris. Physical chemistry of iodine and removal of iodine from gas streams. *React. Science and Technology* **17,** 519 (1963).
3. R. D. Collins und A. E. J. Eggleton. Control of gas-borne activity arising from reactor faults. *Proc. 3rd U.N. Conf. on the Peaceful Uses of Atomic Energy.* Gen. 1964.
4. A. W. Castleman, Jr., I. N. Tang und H. R. Munkelwitz. Chemical reactions and transport behavior of fission-product iodine. Int. Symp. on Fission Product Release and Transport under Accident Conditions, Oak Ridge, April 1965; Conf-650407, S.325.
5. W. S. Clough, L. B. Cousins und A. E. J. Eggleton. Radioiodine absorption on particulate matter. Int. Symp. on Fission Product Release and Transport under Accident Conditions, Oak Ridge, April 1965; Conf-650407, S.242.
6. R. D. Collins und J. J. Hillary. Some experiments relating to the behavior of gasborne iodine. Int. Symp. on Fission Product Release and Transport under Accident Conditions, Oak Ridge, April 1965; Conf-650407, S.830.
7. M. E. Davis, W. E. Browning, Jr., G. W. Parker, G. E. Creek und L. F. Parsley. The deposition of fission product iodine on structural surfaces. Int. Symp. on Fission Product Release and Transport under Accident Conditions, Oak Ridge, April 1965; Conf-640407, S.730.
8. H. R. Diffey, C. H. Rumary, M. J. S. Smith und R. A. Stinchcombe. Iodine clean-up in a steam suppression system. Int. Symp. on Fission Product Release and Transport under Accident Conditions, Oak Ridge, April 1965; Conf-650407, S.776.
9. C. E. Miller, Jr., W. E. Browning, Jr., R. P. Shields und B. F. Roberts. In-pile fission

product release experiments: Atmospheric effects. Int. Symp. on Fission Product Release and Transport under Accident Conditions, Oak Ridge, April 1965; Conf-650407, S.276.
10. J. B. MORRIS und B. NICHOLLS. The deposition of iodine vapour on surfaces. Int. Symp. on Fission Product Release and Transport under Accident Conditions, Oak Ridge, April 1965; Conf-650407, S.142.
11. G. W. PARKER, W. J. MARTIN, G. E. CREEK und C. J. BARTON. Behaviour of radioiodine in the containment mockup facility. Int. Symp. on Fission Product Release and Transport under Accident Conditions, Oak Ridge, April 1965; Conf-650407, S.212.
12. L. F. PARSLEY, L. F. FRANZEN, P. P. HOLZ, T. H. ROW und J. L. WANTLAND. Behaviour of iodine in the nuclear safety pilot plant model containment vessel. Int. Symp. on Fission Product Release and Transport under Accident Conditions, Oak Ridge, April 1965; Conf-650407, S.196.
13. A. C. CHAMBERLAIN, A. E. J. EGGLETON, W. J. MEGAW und J. B. MORRIS. Removal of radioactive odine vapour from air. AERE-R 3412 (1960).
14. W. E. BROWNING. Removal of radio-iodine from gases. *Nucl. Safety* **4,** 83 (1962).
15. F. G. MAY und J. B. MORRIS. Performance of the BEPO scrubber for iodine removal. AERE-M 1163 (1963).
16. J. B. MORRIS und C. H. RUMARY. Tests on absorbers for iodine at low concentrations. AERE-R 4219 (1963).
17. D. A. COLLINS, R. TAYLOR und L. R. TAYLOR. The removal of methyl iodide from reactor effluent gases. Int. Symp. on Fission Product Release and Transport under Accident Conditions, Oak Ridge, April 1965; Conf-650407, S.853.
18. R. E. ADAMS und W. E. BROWNING, JR. Removal of iodine and volatile iodine compounds from air systems by activated charcoal. Int. Symp. on Fission Product Release and Transport under Accident Conditions, Oak Ridge, April 1965; Conf-650407, S.869
19. A. E. J. EGGLETON und D. H. F. ATKINS. The identification of trace quantities of radioactive iodine compounds by gas-chromatography and effusion methods. *Radiochimica Acta* **3,** 151 (1964).
20. F. BILLARD, J. CARON, G. CHEVALIER und J. V. D. MEERSCH. The influences of physical parameters on the adsorption of iodine-131 by activated charcoals. Int. Symp. on Fission Product Release and Transport under Accident Conditions, Oak Ridge, April 1965; Conf-650407, S.814.
21. F. BILLARD, G. CHEVALIER und J. PRADEL. Résultats obtenus dans la recherche des caractéristiques de piégeage de l'iode-131 par les charbons actifs. La Pollution Radioactive des Milieux Gazeux; Presses Universitaires de France, Paris 1965, S.347-353.
22. R. D. COLLINS. Trapping radioiodine. *Nucleonics* **23,** No. 9, 7 (1965).
23. Oak Ridge National Laboratory. Nuclear Safety Program. Semiannual Progress Report for Period Ending Dec. 31, 1965. ORNL-3915.

A HOSPITAL RADIUM ACCIDENT

OLE BERG, KNUD KRISTENSEN, P. GRANDE and C. B. MADSEN
The Radiation Hygiene Laboratory, The National Health Service, Copenhagen, and Radiophysical Laboratory, Radium Center, Århus, Denmark

Abstract—Uncontrolled spread of radium from a damaged radium tube resulted in extensive building contamination. There was no serious contamination of personnel. Decontamination work and the measurement of internal contamination of personnel is described.

ON THE 24th of November 1964, damage was discovered to one of the tubes in the radium safe in the Radiumstation's operating theatre in Århus. The Radiophysical Laboratory established that there was a hole in one end of the tube and that the inner cell containing the radium sulphate powder had disappeared. Measurements showed contamination in the room containing the combined radium safe and radium bench, indicating that the missing cell was not intact.

The accident was assumed to have happened on 20th of November, 4 days before its discovery, since the type of tube concerned was last used on that day, though it cannot be completely excluded that it happened even earlier.

The damaged 10 mg radium tube was of the type RAC9, manufactured by the Radiochemical Centre, Amersham. This type is designed for calibration purposes and is not so strongly made as those normally used for clinical purposes.

The tube was sent to the Radiochemical Centre for examination and it appears from the metallurgical laboratory's report that the tube had no manufacturing faults and that the most probable cause of failure was that the tube had suffered mechanical damage such as a blow or by bending.

It has not been possible to explain satisfactorily how the damage could have happened, but the possibility cannot be entirely excluded that the tube was cut open in the radium safe as the drawer containing it was moved in or out.

EXTENT OF CONTAMINATION

Mapping of the contamination was done by personnel from the Radiophysical Laboratory, and from the Radiation Hygiene Laboratory. Measurements were made with a portable battery-powered α-monitor and a gamma scintillation monitor.

Measurable contamination was confined to the surgical department and to the hospital laundry, where it was probably carried in cloths used for wiping down the radium bench before the accident was discovered.

In the surgical department, the radium room was highly contaminated. The greatest activity was measured on the radium bench around the part of the safe where the leaky tube had been kept. The contamination level of the floor in the radium room which, like the rest of the department, is terrazzo-covered, was higher than 10^{-4} μCi/cm^2, the limit of permissible α-contamination (MPL) in an "active area" according to British recommendations (1957).

Floor contamination was measured over all the actual walking space in the department, but nowhere else was it more than 10^{-4} μCi/cm$_2$. Besides the floor, there was detectable contamination of porous surfaces, such as the joints between wall tiles. The rubber soles of the staff's wooden shoes were also found to be contaminated.

In the laundry, the waste ducts of the two laundering units were contaminated. The sides and bottoms of these ducts had a calcareous deposit (from the washing water) in which appreciable quantities of activity had been found (estimated quantity about 1.5 mg).

Among the finished articles on the laundry shelves there was a pile of hand towels with measurable but insignificant activity. A bag

of unwashed articles from the surgical department was also weakly contaminated.

The staff of the surgical department and the laundry sorting departments were examined for surface contamination with an α-monitor the day after the discovery of the accident. Of the first group, all but one had contaminated fingers, but none exceeded the maximum permissible level for "parts of the body", i.e. 10^{-5} μCi/cm^2 according to the British recommendations (1957).[1] There was no sign of contamination among the laundry staff.

None of the clothes and personal effects of the surgical department and laundry staff were found contaminated.

A rough estimate of the amount of activity found by the contamination survey can be given as follows:

Table 1.

Place	Estimated amount of Ra (mg)
Laundry drainage ducts	1·5
Remainder in tube	1
Wall and floor in radium room	0·25
Radium safe and bench	0·2
Floor of rest of surgical dept.	0·05
Total found	3 mg

When evaluating the amount of radium on contaminated surfaces it was assumed that one half of the radon had escaped.

This corresponds to about 30% of the original activity. Most of the missing 70% presumably has gone out through the laundry sewer, as indicated by the large quantity found in the waste ducts. The radium cell, which was never found, may have been picked up in a cleaning cloth and carried to the laundry with much of its original contents. This would explain the comparatively small contamination of places apart from the radium room.

After the mapping out of the contamination, it was necessary to prevent its further spread and to check the surgical department staff for internal contamination. These operations were carried out by the Radiophysical Laboratory and the Radiation Hygiene Laboratory respectively.

DECONTAMINATION

Decontamination of the laundry drainage ducts was begun the day after the discovery. The ducts were filled with 0·1 N sodium hydroxide containing 1% EDTA-3 Na. The solution remained for 15 hr, after which the ducts were rinsed out. After this there was no detectable α-activity.

The decontamination of the radium safe and room proceeded as follows: All radium appliances were cleaned with a mixture of nitric and sulphuric acids and taken to another safe. The safe and all walls and furniture were covered with a layer of plastic strip-coat. When dry, this was stripped off and removed 90% of the activity with it. The safe needed several applications and the drawers had to be removed for cleaning. Rubber gloves, face masks and special overalls were used in the beginning but precautions were relaxed as the contamination was reduced. A few parts of the safe could not be sufficiently cleaned in this way so the paint had to be dissolved and scraped off.

While the walls and safe were being cleaned the floor was covered with thick plastic sheeting. The cleaning of the floor was left to the end so as not to recontaminate it while the other parts of the room were being cleaned. From the experience with the walls, it had been hoped that the strip-coat would remove the activity from the floor, but it was soon apparent that the method would not work on terrazzo, so the surface had to be ground off, using wet grinding to avoid dust. Afterwards the room and safe were painted.

The lower contamination in the corridor outside the radium room was removed by similar methods.

During decontamination the activity was followed with an α-monitor. When all was finished in January 1965, the average surface contamination was 5% of the MPL.

The activity has decreased continuously throughout 1965, presumably because of daily cleaning. After 20 months only a few places with uneven surfaces showed activity approximately 2% of the MPL.

All waste was collected in bags and buried in a deep hole on the hospital grounds.

CONTROL OF INTERNAL CONTAMINATION OF PERSONNEL

Urine samples collected from the surgical department staff during the first week after the discovery showed definite signs of activity in 8 of 13 persons. More samples were taken 8 weeks later, this time also from the Radiophysical Laboratory, but no more cases were discovered. Urine measurements were chosen for sorting the exposed personnel because this was a simple and sufficiently sensitive method.

The two apparently most contaminated persons were further examined by whole-body, faeces and urine sample counting 2, 6, 12 and 19 months after the accident. At the time of the 12 months whole-body count, exhaled radon-222 was measured, with a view to determining accurately ^{226}Ra body burden.

Methods:

Urine Sample Measurements

12-hour urine samples were collected away from the premises in polythene bottles containing 10 ml of 10% nitric acid. A longer collection time might have been desirable and was in fact used for the three latest measurements, but would have entailed collection at the hospital, with possible contamination of the samples. A method given by Harley in a WHO-report[2] was used. Two independent analyses of each sample were made. 10 mg of barium-carrier were added and samples were counted in a windowless flow counter with a background of about 0·2 cpm. Counting efficiency was 82% as determined by a standard radium solution (IAEA, Vienna). Radium was identified by counting samples at different intervals after preparation and thereby noting the increase of daughter products.

Faeces Sample Measurements

About 30 g from a 24 hr faeces sample was ashed by a combination of wet combustion and incineration at 900°C. The ash was then treated with hydrofluoric acid and dissolved in concentrated sulphuric acid. 20 mg of barium-carrier were used.

Whole Body Measurements

Whole body measurements of the γ-emission from Ra-C (^{214}Bi) were used to determine that part of the body ^{226}Ra content, which is in equilibrium with the retained ^{222}Rn. The total body burden is obtained by adding that quantity of ^{226}Ra, which is in physical equilibrium with the exhaled ^{222}Rn.

Whole body measurements were made at Lund University with a 8 × 4 in. sodium iodide crystal in both scanning bed and chair arrangements.[3]

Determination of exhaled radon was made at Statens strålskyddsinstitutt Stockholm.[4]

RESULTS

The results of the urine measurements for the two persons (P. and M.) who were followed further are given in Table 2.

It should be emphasized that the figures refer only to amounts excreted in 24 hr and that the relevant metabolic periods can differ from 24 hr. The actual uncertainty is therefore greater than that given in the table, which only includes counting errors. Faeces results are given in Table 3.

None of the results indicated contamination during collection or preparation.

There are few reports on excretion of radium

Table 2. Urinary Excretion, pCi ^{226}Ra/24 hr

Time after accident, months	0·3	1	6	11	12	20
P.	9·5 ± 1·0	2·4 ± 0·3	1·4 ± 0·1	0·3 ± 0·1	0·4 ± 0·1	0·3 ± 0·1
M.	7·4 ± 0·5	1·2 ± 0·1	0·5 ± 0·1	<0·1	0·3 ± 0·1	0·4 ± 0·1

Table 3. Faecal Excretion, pCi ^{226}Ra/24 hr

Time after accident, months	11	12	20
P.	20 ± 2	3 ± 1	10 ± 2
M.	1 ± 1	3 ± 1	4 ± 1

in urine after intake of radium sulphate. Marinelli[5] has followed a few cases but gives little information specifically on urinary excretion. On the other hand, Norris *el al.*[6] have good information on radium chloride. Basing our calculations on this work, P. and M. should have body burdens 2 months after the accident of about 20 and 8 nCi respectively (MPBB = 100 nCi). This first estimate of internal contamination should, of course, be taken with all possible reservations.

Whole body measurements were made on P. and M. at Lund University after 2, 6, 12 and 19 months. A third person from the staff with a small radium excretion in urine compared with P and M. was also measured on the first occasion. The values found are given in Table 4.

The values for 1 month and 6 months were obtained from measurements using chair geometry which is more sensitive to an inhomogenous distribution of ^{214}Bi in the body than the more accurate scanning-bed geometry used in the two last measurements.

Exhaled Radon

Determination of radon exhaled by P. and M. was made after 12 months. The calculated amount of ^{226}Ra in physical equilibrium with the observed rate of exhaled ^{222}Rn, was for P. 4·3 ± 1·1 nCi and for M. 2·7 ± 1·1 nCi.

Total Body Burden

From the whole body measurements 12 months after the accident and exhaled radon measurements, the total body burdens of ^{226}Ra of P. and M. can be determined as:

1 year after the accident

P.: 8·4 + 4·3 = 12·7 ~ 13 nCi (± 2 nCi)
M.: 2·1 + 2·7 = 4·8 ~ 5 nCi (± 2 nCi)

From these figures the retention of ^{222}Rn can be calculated to be P.: 66 + 13% and M.: 44 + 27%.

DISCUSSION

The retention values found for ^{222}Rn are relatively high compared with the figure of 30% normally used. This might be due to external contamination contributing to the whole body measurement, but Marinelli[5] has also found comparable values in some cases of $RaSO_4$ inhalation.

Figure 1 shows results from case P. Total body burden is calculated from a Rn retention value of 66%. The function described by Norris *et al.*[6] is given for comparison and a rather good agreement is found.

The urinary excretion rate is also given in the figure. We found a slower urinary excretion rate than Norris. This may easily be explained by $RaSO_4$ being a very insoluble compound.

Table 4. Body Content, nCi ^{214}Bi

Time after accident, months	1	6	12	19
P.	18	10·6	8·4 ± 1·0	4·4 ± 1·0
M.	4·6	3·4	2·1 ± 1·0	1·1 ± 1·0
R.	3		(not measured)	

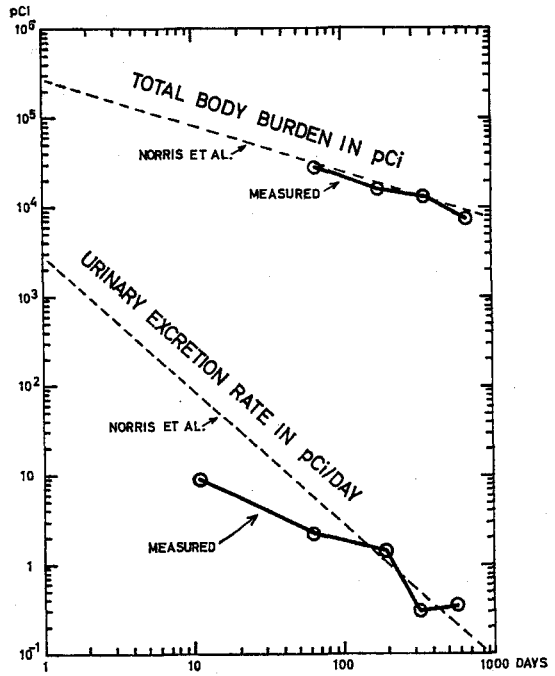

FIG. 1. ^{226}Ra body burden and urinary excretion rate (case P).

Unfortunately faeces samples were not obtained until the last three measurements, so no conclusion could be drawn about what percentage of the total excretion was represented by the urine measurements.

CONCLUSION

1. From the available measurements it can safely be concluded that none of the 20 persons investigated after the accident has acquired a lasting ^{226}Ra body burden of more than one-tenth of the maximum permissible according to the ICRP, i.e. 0·1 μCi.

2. The accident shows how important it is for a radium clinic to have some system of control that can detect leaky radium appliances in time. A simple and inexpensive solution is the daily use of a reliable handy α-monitor with low β- and γ-sensitivity.

In Denmark, as a direct result of the accident just described, the Radiation Hygiene Laboratory has now ordered all users of radium to make such a daily check.

ACKNOWLEDGEMENTS

Whole body measurements were made at the Radiation Physics Department, University of Lund, by G. K. Svensson (M.Sc.) and G. Bengtsson (M.Sc.). Measurements of exhaled radon were made at Statens Strålskyddsinstitut in Stockholm by Jan-Olof Snihs (M.Sc.).

The authors would like to express their gratitude for this valuable assistance and also to thank Miss Bente Nielsen for her conscientious performance of the chemical analyses.

REFERENCES

1. Code of Practice for the Protection of Persons Exposed to Ionising Radiations. London, 1957.
2. Methods of Radiochemical Analysis. WHO Techn. Report Series No. 173. Rome, 1959, p. 81.
3. International Atomic Energy Agency: Directory of Whole Body Counters. Vienna, 1965.
4. JAN OLOF SNIHS. *Arkiv för Fysik* **25** 65–85 (1963).
5. L. D. MARINELLI, W. P. NORRIS, P. F. GUSTAFSON and T. W. SPECKMAN. Transport of radium sulfate from the lung and its elimination from the human body following single accidental exposures. *Radiology* **61,** 903 (1953).
6. W. P. NORRIS, T. W. SPECKMANN and P. F. GUSTAFSON. Studies of the metabolism of radium in man. *Am. J. Roent.* **73,** 785 (1955).

FAILURE OF RADIUM NEEDLE LEAK TESTING PROCEDURES

E. W. MASON
Argonne Cancer Research Hospital,* Chicago, Illinois
and M. L. ROZENFELD
Department of Radiology and Argonne Cancer Research Hospital,* University of Chicago, Illinois (U.S.A.)

Abstract—The extreme personnel health hazard due to radium contamination associated with the use of radium needles and tubes in the medical profession was recognized several decades ago. Chief among the concerns was, and remains, the need to detect those needles which are likely to leak radium. The most widely used procedures rely on the collection of radon gas, a daughter product of radium, which emanates from openings too small for radium salt to pass through. Such tests are frequently required by law at six-month intervals. Results of such tests can be misleading unless the exposure of the needles or tubes to liquids is known. Liquids which are likely to have been in contact with radium needles and tubes include washing and sterilizing solutions. In this paper, long term observations of radon leak rate modification by liquids are presented for about a dozen radium needles and tubes. Other methods for predicting needle and tube failure are discussed including subjection to elevated temperatures under controlled conditions.

* Operated by the University of Chicago for the United States Atomic Energy Commission.

RADIATION SAFETY HAZARD OF CHLORMERODRIN

PHILIP C. JOHNSON, LEO WADE
Radioisotope Department, Methodist Hospital, and Department of Medicine,
Baylor University College of Medicine, Texas Medical Center, Houston, Texas 77025

and O. L. PIRTLE
Hastings Radiochemical Works, Highway 35, Houston, Texas

Abstract—Elemental mercury is a well known occupational hazard which vaporizes slowly at room temperature permitting inhalation of toxic quantities. Not usually appreciated is the tendency of organic compounds containing radioactive mercury to release mercury vapor in amounts large enough to cause significant radioactive contamination of laboratory areas and to pose a possible radiation hazard to employees working in these areas. This is a particular hazard in medical radioisotope laboratories where chlormerodrin, ^{203}Hg, is used in large quantities for scanning of the brain and kidneys.

At room temperatures, release of mercury occurs continuously from commercial solutions of radioactive chlormerodrin prepared for human use. While the release rate is variable from bottle to bottle, we have found multi-injection bottles containing 5–15 mCi of chlormerodrin which release, even before the top has been punctured by a needle, 22.5 $\mu\mu$Ci ^{203}Hg/24 hr. Release was measured by placing a beaker of trichloracetic acid into a closed jar containing a vial of radioactive chlormerodrin. Release of mercury vapor could be increased by alkalinization. Vaporization was decreased by acidification and the addition of weak protein solutions to the bottle of chlormerodrin. Areas in which this compound are used or prepared show significant contamination with mercury not only in areas accessible to liquid spillage but also in exhaust ducts and on ceilings.

Because of its long half-time, progressive build-up of ^{203}Hg was found to occur in our radioisotope laboratory. This occurs particularly on containers used to store chlormerodrin bottles and in the storage hood. The high absorption of mercury into glassware sets the stage for later release of mercury from bottles during storage for radioactive decay. The methods we developed for controlling this hazard will be discussed.

In a recent discussion of the properties of ^{203}Hg labeled Chlormerodrin, it was suggested by one of us that the use of this compound might result in the contamination of radioisotope laboratories because of the ease with which elemental mercury and certain mercury compounds vaporize if exposed to the atmosphere.[1-3] We thought it might be advisable to determine whether ^{203}Hg Chlormerodrin would volatize and whether this could result in a radiation health hazard. This seemed particularly pertinent because of the long physical half-life of ^{203}Hg and because of the long biological half-lives of mercury compounds.

Our investigation showed that pharmaceutically prepared solutions of ^{203}Hg Chlormerodrin do volatize at room temperature. We believe this explains our finding radioactive mercury as a contaminant on the outside of bottles containing millicurie amounts of Chlormerodrin.

METHOD

In this study bottles of ^{203}Hg Chlormerodrin were used as soon as they were delivered. With the exception of one local company, these bottles were sent by air express, leaving the manufacturing plant about 18 hours before being tested. Chlormerodrin from various United States suppliers was used. Several of the studies were done using Chlormerodrin obtained from firm A because their bottles had the highest amount of contamination and because they were our primary supplier of Chlormerodrin at the time of these tests. In addition, the

Chlormerodrin bottles of firms B, C, D, and E were used. Hereafter, each company product will be referred to by these letters to indicate common origin of some of the samples.

Each Chlormerodrin stock bottle was removed from the outer cardboard protective container and was immediately placed in a 400-ml glass beaker which contained an open-topped glass vial into which 1 ml of 15% trichloracetic acid solution had been pipetted. The beaker was sealed with Parafilm M* and masking tape. The beaker remained at room temperature in subdued light or darkness. After 24 hr, 0.5 ml of the trichloracetic acid solution was removed and its gamma activity was determined in a scintillation well counter by its pulse height analyzer. Enough counts were accumulated to obtain a 5% average statistical counting error. ^{203}Hg was proved to be the only contaminant by the use of spectrum analysis with a 400-channel analyzer and by the estimation of the rate of decay. In the laboratory in which these studies were performed, ^{131}I is the only other radioisotope which is used in large enough quantities to make it a potential contaminant.

Another phase of the study consisted of testing the effect of pH on the release of ^{203}Hg from Chlormerodrin. One-millicurie amounts of ^{203}Hg Chlormerodrin (A) were injected into each of three 30-ml, multi-injection, rubber-stoppered vials (sodium chloride injection, U.S.P.—Cutter Labs., Berkeley, Calif.). The pH of the normal saline had been adjusted with NaOH and HCl to pH 2, 7, and 10. These bottles were placed in 400-ml beakers with vials of TCA solution in the manner already described. After 24 hr the gamma activity of the TCA solution was determined.

* Marathon Division, American Can Company, Neenah, Wisconsin.

RESULTS

Table 1 shows the mercury contamination found from the bottles obtained from the various suppliers of radioactive pharmaceuticals. Each determination represents a separate shipment. This table also contains the results obtained during a period between February and June 1966.

During that time, two of the suppliers learned of our study and we discussed the amounts of contamination with them. Evidently the contamination is difficult to remove since both suppliers continued to have mercury contamination on the outside of their bottles four months later. One supplier (B) furnished us a single shipment of ^{203}Hg Chlormerodrin which did not

Table 1.

Supplier	mCi in stock bottle	% trapped × 10^5
A	5.15	46.8
A	10.30	22.4
A	5.15	17.3
B	3.00	12.2
A	5.15	9.2
E	15.00	0.2
D	5.00	0.1
C	5.00	0.1
4 months later		
B	5.00	8.7
A	5.00	13.5
5 months later		
B	5.00	0.1

contain contamination. After questioning this supplier, we learned that these bottles had been washed with acid prior to shipment.

To determine if acid washing the bottles was a practical way to prevent this problem, one of two bottles which were received at the same time from a single manufacturer was washed with 0.1 N HCl. Both bottles had been shipped by air express in the same cardboard container. Bottle 1 was placed in a beaker as it was received from the manufacturer. Bottle 2 was immersed once in 0.1 N HCl and placed in a separate beaker. The trichloracetic acid placed in the beaker with bottle 1 contained 455 mμCi. The trichloracetic acid placed in the beaker with bottle 2 contained 5 mμCi of ^{203}Hg, and the wash water from the bottle contained 625 mμCi of ^{203}Hg. This was good evidence that most of the contamination existed on the outside of the bottle since these bottles had never been opened.

The results of the effect of pH on the release of ^{203}Hg from Chlormerodrin are shown in Table 2.

Table 2.

pH	% × 10^5
7	0.12
2	0.07
10	0.43

The highest amount of mercury was released at a pH of 10. Neohydrin is known to be soluble in alkali and stable at pH 10.[4] Therefore the released radioactive mercury is probably not Chlormerodrin but elemental mercury. The release of ^{203}Hg from these bottles would indicate that the release of mercury vapor is not prevented by the rubber stopper of the multi-injection vials used here.

DISCUSSION

It has been known since antiquity that mercury compounds vaporize producing industrial poisonings.[5] Both elemental mercury and mercuric chloride are known to vaporize slowly at room temperatures. Mercurous chloride, in the presence of light, will be converted to mercuric chloride and elemental mercury. Thus, all valence states of mercury are potentially volatile.[2] We have found no literature evidence that Chlormerodrin will volatize at room temperature. Radioactive neohydrin has been reported to be stable up to 60 days.[4] However, the study which reported this was not designed to detect the small amounts of volatilization found here. It has been our experience that alkali added to Chlormerodrin will at times produce a black precipitate characteristic of elemental mercury.[6] Commercial preparation of radioactive Chlormerodrin consists of refluxing mercuric acetate, sodium acetate, and allyurea in a methanol solution. The addition of sodium chloride causes the precipitation of the Chlormerodrin. An alternate route of production might be by an isotope exchange method. Both techniques are ordinarily followed by chromatography to produce a pure Chlormerodrin. It is likely that the manufacturing process eliminates free mercury from the final product. However, during each of these steps volatilization of the radioactive mercury is potentially possible. This might result in contamination of the equipment, bottles, etc. in the near vicinity.

The results of the study reported here suggest that solutions of Chlormerodrin release mercury vapors in small amounts. This was shown by the presence of mercury in the trichloracetic acid solution when it was placed in a beaker which also contained a rubber stoppered container in which a dilute solution of chlormerodrin had been placed. It would seem that the mercury vapor is capable of passing around the rubber stopper and into the air contained within the beaker. Volatilization during shipment with subsequent contamination of the bottle would explain the results obtained here. It is possible that the bottles were shipped by the manufacturer without contamination.

Thus it is not surprising that bottles containing radioactive Chlormerodrin are contaminated with mercury on the outside surface when they are received from the manufacturer. We have found some degree of contamination on the bottles of all suppliers tested. The degree of contamination is greater with some suppliers than with others which may relate to the volume of Chlormerodrin produced by each and to

differences in manufacturing techniques. The long half-life of ^{203}Hg makes it probable that manufacturers store the Chlormerodrin for periods prior to shipment. During this time cross contamination among bottles could occur.

Acid washing of the outside of these bottles seems to be an adequate method for removing most of this surface contamination. It does not prevent further volatilization of the mercury, however, and the results show that prolonged storage of Chlormerodrin would probably result in further release of radioactive mercury vapors.

The amounts of mercury contamination found in our tests are not very great and probably do not present a radiation health hazard by themselves. However, the long half-life of ^{203}Hg would allow gradually increasing levels to accumulate in the laboratory. The released mercury vapor is in constant equilibrium with the air breathed by the personnel allowing continuous inhalation of radioactive mercury. Even though large amounts of ^{203}Hg have been used in this laboratory over the past two years, no personnel have been found who have detectable amounts of ^{203}Hg in their urine or in the kidney area. Thus to date, this has not proven to be a radiation safety hazard to our personnel.

SUMMARY

1. Chlormerodrin manufactured with ^{203}Hg volatilizes in the concentrations used by pharmaceutical manufacturers.

2. This tendency to volatize causes contamination of the outside of containers even though these containers are sealed.

3. Acid washing of the bottles removes much of this contamination.

REFERENCES

1. F. E. Noe. *New England J. Med.* **261,** 1003 (1959).
2. P. G. Stecher (Editor). *The Merck Index of Chemicals and Drugs.* Merck and Co., Inc., New Jersey, 1960.
3. P. A. Neal. *Am. J. Pub. Health* **28,** 907 (1938).
4. L. J. Anghileri. *J. Nuc. Med.* **4,** 410 (1963).
5. J. A. Turner. *Pub. Health Rep.* **39,** 329 (1924).
6. P. C. Johnson. Unpublished observations.

NEW TECHNIQUE FOR FULL RADIATION PROTECTION OF PERSONNEL IN TELECOBALT TREATMENTS

L. BOZÓKY
National Institute for Oncology, Budapest, Hungary

Abstract—The construction of a special cobalt unit designed for moving field therapy is described. The most important characteristic of the apparatus is that when switched off, at any point of the treatment head as well as the surrounding area, only natural background radiation is measurable. The apparatus can be safely operated even in the absence of electric current. Some results of the radiation protection measurements are discussed.

RADIATION protection in telecobalt treatment units, as in other fields, has undergone steady improvement. In the years 1930–40 physicians and radiographers were exposed to a significant whole body irradiation through the lead shields of X-ray tubes. Later, in order to reduce exposures, voltage was reduced between consecutive treatments, and today the X-ray apparatus is switched off during the adjustment of the patient. Therefore, the medical staff is not exposed to any radiation hazard at all.

With cobalt units, switching off the gamma-rays, like X-rays are switched off, is out of the question. Here attempts were made to keep down the intensities of exposure which sometimes reached multiples of 100 mR/hr by expensive improvements of the absorption of the shielding. The situation was aggravated by new cobalt units of greatly increased activity being put into operation.

With the cobalt units in general use the person dealing with the patient is exposed at an average distance of 1 m from the source to a whole body irradiation by the gamma-rays passing through the shielding. In addition, during the adjustment of the patient, hands and head are subjected to an exposure depending on the surface dose rate of the treatment head. International recommendations suggest average intensities of exposure at 1 m distance to be not more than 2 mR/hr, and for the surface not more than 10 mR/hr. It is, however, very difficult to keep to these levels and many treatment units fail to comply with these requirements.

In our Institute, work on the development of the best practical radiation protection systems has been going on for some thirty years. Following this tradition, we have endevoured to design a telecobalt unit which, similarly to an X-ray apparatus when switched off, gives the staff perfect radiation protection, and also provides improved radiation protection for the patient.

The first part of the problem was solved by the construction of the Gravicert equipment for fixed-field irradiations.[1-3] The apparatus was described at the IXth International Congress of Radiology in Munich in 1959.[4] In this paper we wish to discuss an improved version of the Gravicert system designed for moving field irradiation. It is a recently finished new design which we have called the Rotacert.[5]

The most important characteristic of the apparatus is that when switched off, at any point of the treatment head as well as in the surrounding area where the physician and radiographer are working only natural background radiation is measurable. The equipment offers full protection since when treatment has been finished, the radiation source goes automatically to the store in the wall. The lead, iron and concrete shielding permits a reduction of the intensity by 8 to 9 orders of magnitude by a most simple and relatively inexpensive means. As a consequence, when dimensioning the treatment head, only the radiation protection of the patient needs consideration. Due to the scattered radiation of the beam directed to the

patient, whole body irradiation is unavoidable, therefore to aim at maximum radiation protection by the shielding of the treatment head is unnecessary. As a rule, a reduction of the intensity in a ratio of 5000 to 1 is quite sufficient.

The cross-section of the apparatus is shown diagrammatically in Fig. 1. The treatment head is connected to the wall-store through a steel tube in which the capsule containing the radiation source slides between the treatment head and the store. To provide radiation protection for the patient, this steel tube is surrounded by an eccentrically located lead shield. Treatment head, wall-store and connecting steel tube form a single, rigid unit attached to a steel drum of 150 cm diameter. The drum is fitted into a circular orifice in the concrete wall of 110 cm thickness, in which, being balanced about its horizontal axis, it readily rotates.

Another feature of Rotacert is that the movement of the source from the wall container to the treatment head and back occurs by means of gravity, which is similar to radioactivity in being impossible to switch off and never fails. The apparatus can, therefore, be safely operated even after failure of the electricity supply. The capsule including the radiation source is moved back and forth by a steel cable fixed to a connecting rod. One end of the steel cable is loaded with weight No. 2, the other end with weight No. 1, somewhat heavier than No. 2 and detachable. When weight No. 1 is lifted either by a small motor or by a hand crank, the apparatus is cocked and, being operated with a push button, automatically sends the radiation source into the treatment head, or returns it to the wall-store. The button releases the locking of the lifted, heavier weight, the weight falls down and the steel cable connected to it moves the rod, which pushes the capsule into the head. At the same time it lifts the lighter weight, No. 2, fastened to the other end of the cable. The OFF button releases the connection of the heavier weight, No. 1 and so weight No. 2 pulls the capsule back into the wall-store.

In order to prevent unintentional irradiations the door of the treatment room is equipped with an automatic lock and pilot lamps. Should anything unusual occur, e.g. the patient happens to move, then photoelectric-cell controlled mechanical safety devices switch off the apparatus instantly.

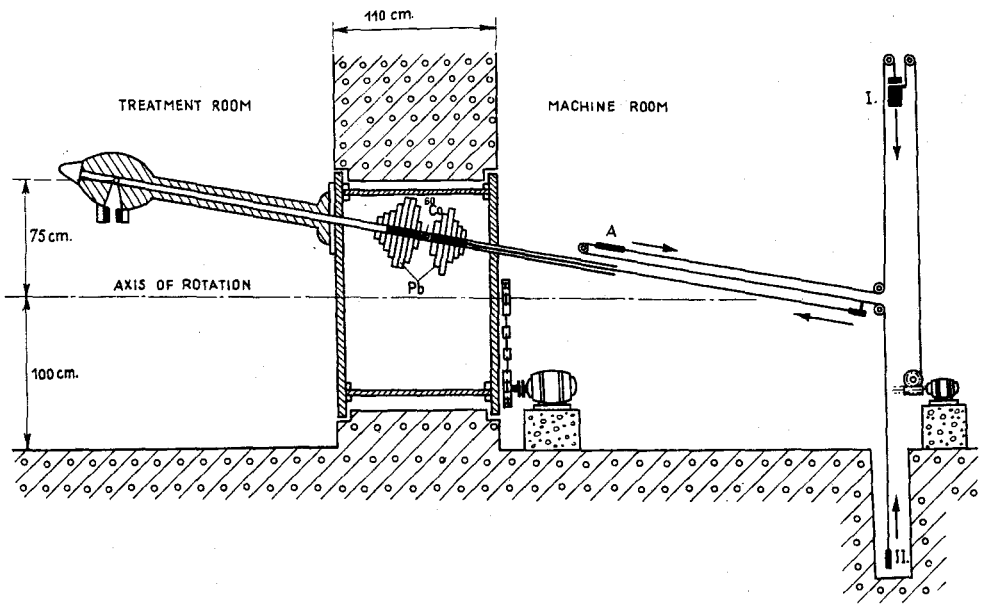

FIG. 1. Rotacert equipment. Schematic cross-section.

RADIATION PROTECTION MEASUREMENTS

Control measurements were made with a ^{60}Co source of 3000 Ci activity in the treatment room, gate, machine room and control room, as well as in the vicinity of the equipment and under it.

Measurements made while the apparatus was switched off have proved that at any point behind the head and near the supporting bar, as well as in the surrounding area where physician and assistant deal with the patient, the exposure rates are lower than 0·02 mR/hr which means that practically only natural background radiation is measurable. Only at the two corners of the wall containing the radiation source and in some parts of the treatment room above head height was ^{60}Co gamma-radiation of the same order of magnitude as the background measured.

With the apparatus switched to a maximum treatment field of 10 by 15 cm and with a tissue-equivalent scattering medium of 20 cm thickness, exposure rates were measured in the treatment room, gate, control room, and passages, at the points shown in Fig. 2. At the same places the exposure rates produced by the passing of the source through the supporting arm were measured. The results are listed in Table 1.

In addition to the above, the exposure rates of the primary gamma-radiation were checked in the rooms adjacent to and lying under the treatment room, at all points which in the course of the rotation of the source might possibly be subjected to direct gamma-radiation. At all points only natural background radiation could be measured.

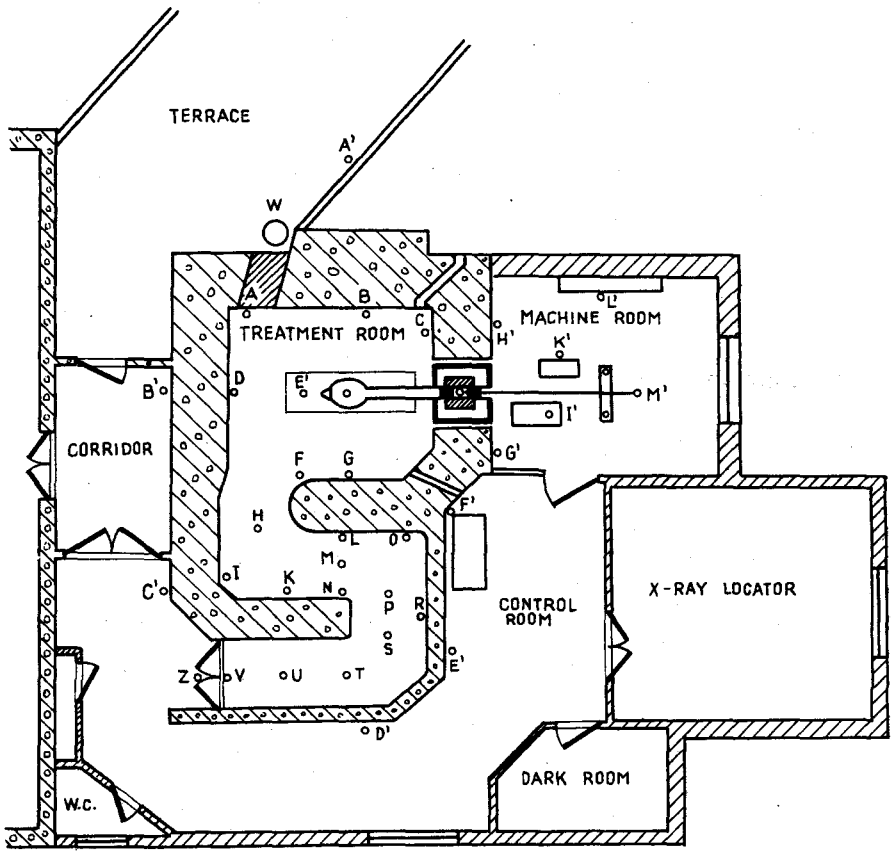

FIG. 2. Floor plan of the Rotacert telecobalt unit.

Table 1. *Results of Measurements at Points indicated in Fig.* 2.

Measuring points	mR/hr apparatus switched		mR for 1 transfer and return of source
	off	on	
A	background	360	2
B	,,	720	6
C	,,	650	17
D	,,	430	1
E	,,	1350	2
F	,,	520	3
G	,,	750	7
H	,,	42	—
I	,,	30	—
K	,,	18	—
L	,,	5	—
M	,,	10	—
N	,,	10	—
O	,,	1	—
P	,,	3·5	—
R	,,	3	—
S	,,	2·5	—
T	,,	0·3	—
U	,,	0·1	—
V	,,	0·06	—
A′	,,	background	—
B′	,,	,,	—
C′	,,	,,	—
D′	,,	,,	—
E′	,,	,,	—
F′	,,	,,	—
G′	0·03	,,	—
H′	0·03	,,	—
I′	0·15	,,	—
K′	0·08	,,	—
M′	0·06	,,	—

In the machine room several hundred measurements were made along the rotary drum and the radiation protection head as well as at other components of the equipment. Measurements were taken with the source in the wall store, in the treatment head and in mid-position in the arm. In contrast to the situation found in the treatment room, with the apparatus switched off, exposure rates in the machine room averaged 0·1 to 1·0 mR/hr. However, for periodical maintenance, these exposure rates may be cut down to the level of background radiation by shifting the source into the treatment head.

The whole-body exposure rates to which the patient is exposed in the course of the treatment were measured and the exposure for 1 transfer and return of the source was determined. According to the results, primary gamma-radiation passing through the shielding of the treatment head produces an exposure rate of 20 to 120 mR/min on the body of the patient, which corresponds to about 0·1% of the exposure rate of a treatment. The rate to which the patient

is subjected in the course of the transfer and return of the source is 5 to 20 mR, which, taking only 100 R exposures into consideration, means only 0·01%.

The foregoing proves that we have achieved our objective that with Rotacert medical and technical maintenance work can be done without the staff being exposed to radiation above natural background and that it ensures excellent radiation protection for the patient as well.

REFERENCES

1. L. Bozóky and I. Rodé. *Sugárzó Izotópok Hazai Felhasználása* I, 122 Budapest, 1958.
2. L. Bozóky. *Strahlentherapie* **112,** 629 (1960).
3. L. Bozóky. *Medicor News*, **3,** 16 (1962).
4. L. Bozóky. *Proc. IXth International Congress of Radiology*, Vol. II p. 975. Georg Thiem Verlag, Stuttgart, 1961.
5. L. Bozóky. *Proc. IInd Symposium on Health Physics*, p. 31. Pécs, Hungary, Budapest, 1966.

RADIATION SAFETY PROBLEMS CONNECTED WITH THE MEDICAL USE OF RADIOISOTOPES

R. J. CLOUTIER* and C. P. DALTON*
Oak Ridge Associated Universities, P.O. Box 117, Oak Ridge, Tennessee

Abstract—More than 3800 physicians and medical institutions in the United States use radioisotopes in diagnosis, therapy, and research. We review our work and others' on some of the connected radiation protection problems: techniques of administering radioactive drugs, control of radiation and contamination hazards to hospital personnel and visitors, criteria for release of radioactive patients from a hospital, autopsies of radioactive cadavers, and the radiation safety training of a hospital staff.

The problems are not completely solved. More thought, research, and communication among professional health physicists are needed to speed the work that remains to be done.

INTRODUCTION

The use of radioisotopes in medical diagnosis and therapy has developed rapidly in the United States since reactor-produced isotopes became available in the late 1940's. By 1966 about 3800 licenses permitting the medical use of radioactive material had been issued by the United States Atomic Energy Commission and the state governments that have assumed this responsibility. Approximately 1300 of these licenses have been issued to individual physicians, and about 2500 have been granted to medical institutions.[1] Since many physicians may use radioisotopes when an institution has a license, these are actually conservative estimates. About 90% of the licenses authorize diagnostic tests with radioisotopes; 50–60% control therapeutic uses; and slightly more than 1% permit use of radioactive materials in medical research.

Radium and X-rays are still the greatest sources of potential exposure to medical radiation workers and the public, but the medical uses of radioisotopes other than radium are increasing. Physicians use nearly 50 radioisotopes in more than 100 diagnostic tests and therapeutic procedures.[2] The recent introduction of radioisotope generators, an inexpensive and convenient source of short-lived isotopes, is likely to expand the variety.[3]

The USAEC regulations[4] and the recommendations of the ICRP,[5] IAEA,[6] and NCRP[7] establish general guidelines for a radiation safety program. The book *Safe Handling of Radioactive Isotopes in Medical Practice*,[8] the *Manual on Use of Radioisotopes in Hospitals*,[9] and a film *Radiation Protection in Nuclear Medicine*[10] can help the novice health physicist or physician who may be responsible for radiation protection in a hospital. They supply information about personnel monitoring programs, methods of receiving radioisotopes, keeping records, and low-level area monitoring.

Some radiation protection problems are special to medical installations and could well benefit from the increased attention of professional health physicists: methods of dispensing radiopharmaceuticals, confinement of contamination, patient and visitor control, autopsy of radioactive cadavers, and the radiation safety training of hospital personnel.

ADMINISTRATION OF RADIOPHARMACEUTICALS TO PATIENTS

1. *Oral Administration*

To reduce the risk of contamination and exposure to the physician, manufacturers usually place diagnostic doses of radioiodine (^{131}I) in a gelatin capsule for the patient to swallow. Therapeutic amounts are sometimes given in a capsule, but more often they are administered as a liquid. Glass[11] describes a shielded dispenser that eliminates most of the handling of radioiodine and allows the patient to take the isotope through a straw. Contamination and

* From the Medical Division, Oak Ridge Institute of Nuclear Studies, an operating unit of Oak Ridge Associated Universities, Inc., Oak Ridge, Tennessee, under contract with the United States Atomic Energy Commission.

radiation exposure are possible during administration of radioiodine, but the procedure is brief and simple—100-millicurie doses can be handled without significant hazard.

2. *Administration by Intravenous Injection*

At the ORINS Medical Division an intravenous drip of saline solution is established to prepare a patient for an injected radiopharmaceutical. Using a shielded syringe, Fig. 1, the physician injects the radioisotope into a rubber adaptor in the drip tube. This method has several advantages. The physician can take time to locate the patient's vein before he withdraws the radioactive material from its shielded container. Thus the doctor need not hunt for a vein while he is handling a radioactive syringe. His exposure and the chance of contamination are reduced. More importantly, extravasation of the radioisotope, which would result in a useless high exposure to a small part of the patient's body, is unlikely to occur.

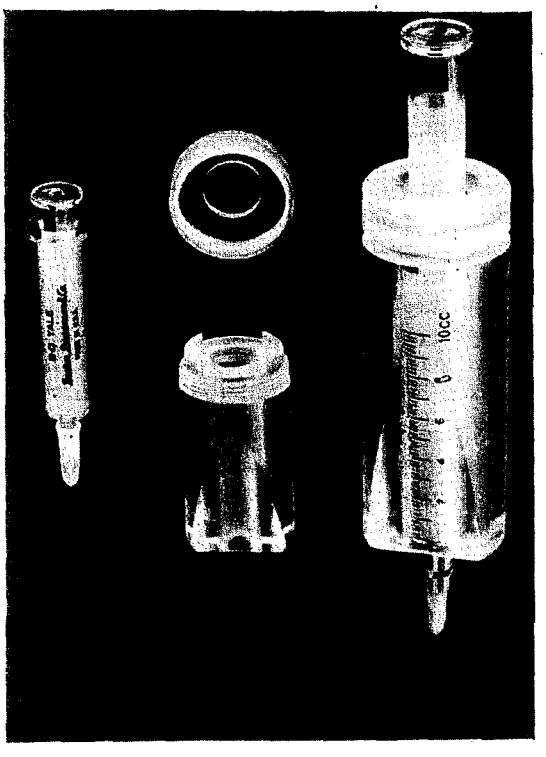

FIG. 1. Radioisotope syringes. The physician uses lucite shields to keep his hands at a distance from the radioactive syringe. The shields are beveled on one side for easier handling.

3. *Intracavitary Deposition*

One-hundred-millicurie amounts of colloidal ^{198}Au, or occasionally $Cr^{32}PO_4$ or ^{90}Y, are used for local irradiation of the pleural or peritoneal

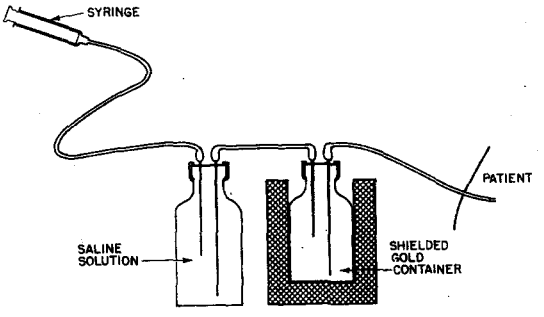

FIG. 2a. Apparatus for intracavitary administration of a radioisotope by pressure. Long-handled forceps are used to insert the needles connected to catheters into the rubber-membrane-top radioisotope container.

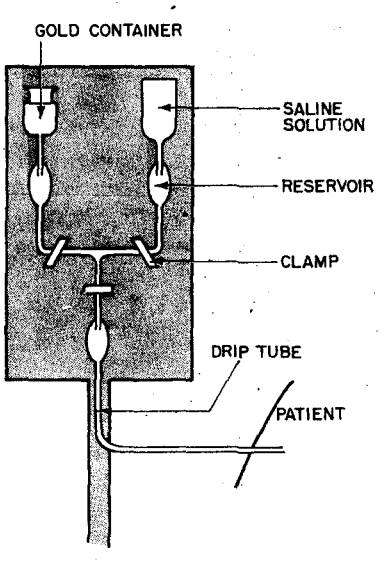

FIG. 2b. Apparatus for intracavitary administration of a radioisotope by gravity. A long-handled tool is used to remove the radioisotope from its transport container and to pour it into the container at the top of this apparatus. The clamps that regulate the rate of flow of radioisotope into the patient are adjusted with another long-handled tool.

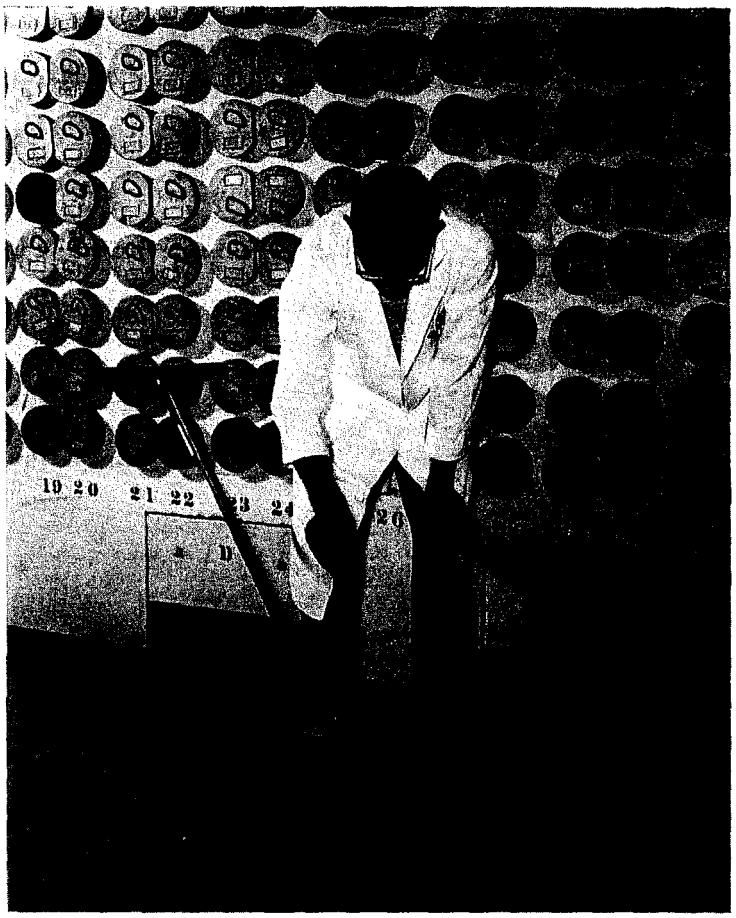

FIG. 3. Radioisotope caddy. This transport container reduces radiation levels and lessens the chance of contamination while radio-pharmaceuticals are transferred from the preparation area to the place where the patient will receive the isotope. Shielding is about $1\frac{1}{2}$ in. of lead.

cavity wall. Two methods of administration are diagrammed in Fig. 2, a and b; both rely on distance, efficient timing, and a small amount of shielding as protection factors.

The entrance to the patient's body cavity is made with a trocar, which is threaded with a catheter and then removed, leaving the catheter in place. After the doctor prepares the patient, a technician brings the radiogold to the treatment area, Fig. 3. The method shown in Fig. 2a places the radioisotope into the patient under pressure. When the plunger of the syringe is depressed, saline slowly forces the gold through the catheter into the patient. The likelihood of contamination is small since the system is closed. Colloidal ^{198}Au is a deep pink; the physician can easily see when all the isotope has entered the patient so that he can disconnect the administration apparatus. He then removes the catheter and closes the wound with a purse-string suture to best minimize leakage of the isotope.

4. *Sealed Implants*

Radiotherapists have tried many techniques and equipment designs for handling sealed sources in interstitial therapy,[12] most of them for intrauterine radium applicators. One of

the major hazards has been high exposure to the physician's hands while he is positioning a radioactive applicator, and this has been greatly reduced by "afterloading" techniques. A remote type of afterloading device using "cycling" sources is shown in Fig. 4.[13] After the unloaded applicator has been placed in position, the sources are pumped out of their shielded container through the plastic tubes into the patient. When the treatment is complete, the sources are remotely returned to their shield.

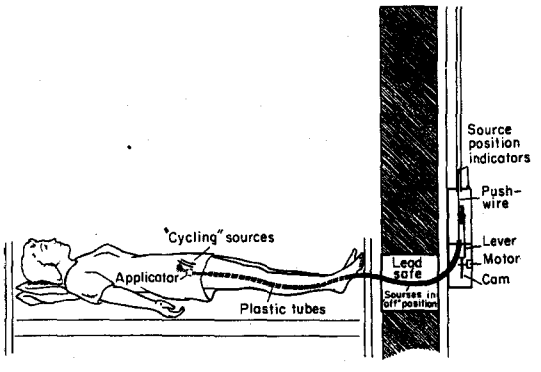

FIG. 4. Remote afterloading of uterus applicators with cycling sources. Reproduced from *Amer. J. Roentgenol.* **96,** 45 (1966) by permission of Charles C Thomas, publisher, and U. K. Henschke.

Another irradiation technique implants many small sealed sources in a tumor. The physician inserts small, hollow nylon tubes in the tumor and then quickly threads strings of iridium seeds through the tubes. The advantage of afterloading techniques is that the radiotherapist may take all the time he needs to position an empty applicator, and he does not need to install a radioactive applicator hastily to avoid exposing himself. At the end of the irradiation period he can quickly and easily remove the implanted sources.

Gold-198 metal is malleable, relatively inexpensive, easy to obtain and is often a substitute for radon seeds in interstitial therapy. Hodt, Sinclair, and Smithers[14] first described an automatic dispensing gun that promotes accurate placement of the gold grains and reduces exposure to the radiotherapist. Jones, Taylor and Stedeford[15] report modifications of the gun's magazine and barrel so that exposure to the person loading the gun is also decreased.

Exposure to a technician preparing radium needles for implant therapy can be reduced by the use of L-blocks, Fig. 5. Holes drilled in the base of the L-block permit insertion of the needle with only its eye above the block. A stiff wire helps to thread the needle and keep the technician's hands at a distance from the radium.

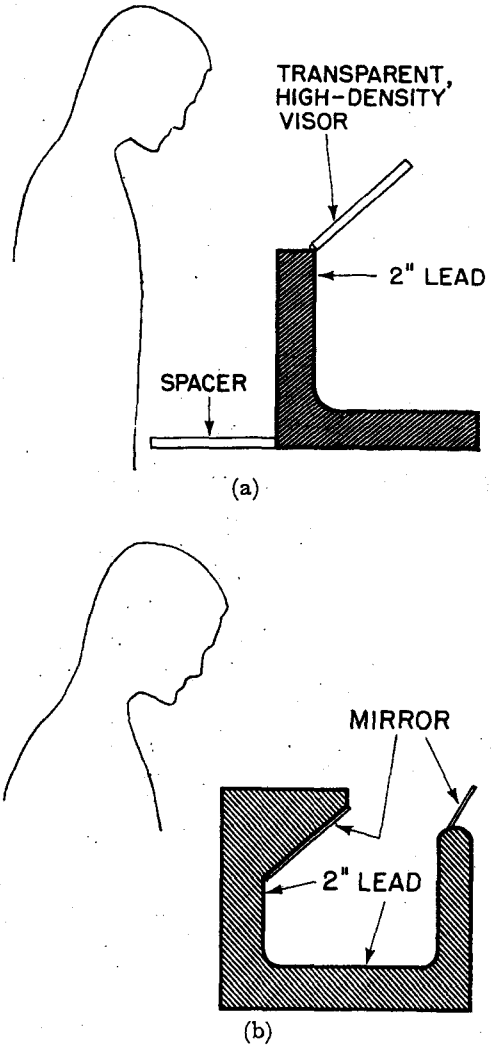

FIG. 5. Two types of L-blocks used to shield a technician working with radioactive materials. (b) used through courtesy of Applied Health Physics, Inc.

Spherical ^{60}Co beads are still often used for brachytherapy. Legal and Campbell[16] have designed an ingenious device for threading these beads that considerably reduces handling time and the potential of exposure. In the device (Fig. 6) the ^{60}Co spheres spin like tops and the thread holes assume a vertical position. The spheres are then dropped, threading themselves on a vertical stylus.

PATIENT CONTROL AND NURSING CARE

The restrictions required to control contamination and radiation hazards that follow the administration of a radiopharmaceutical to a patient depend upon the isotope, its amount, and its physical and chemical form.

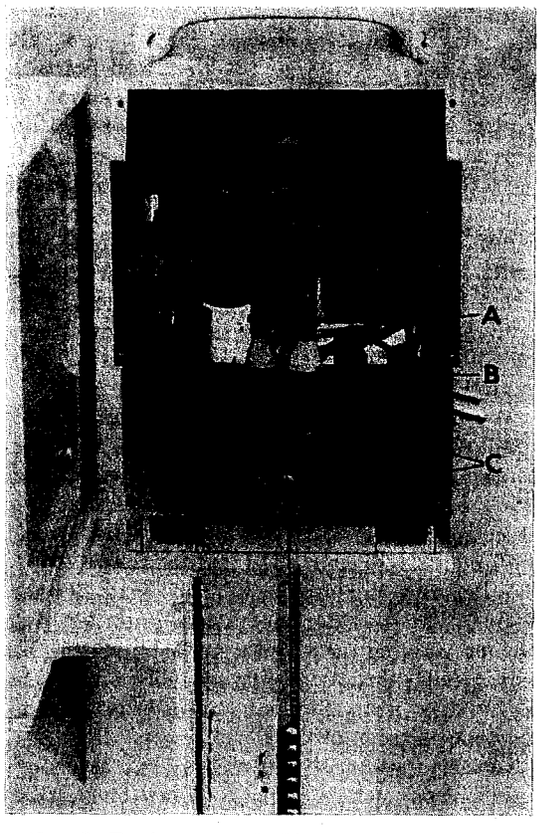

FIG. 6. Device to facilitate threading of ^{60}Co beads. A, spinning device; B, steel needle; C, solenoid-operated nylon jaws. Reproduced from *Radiology* **5,** 959 (1965) by permission of the Radiological Society of North America and E. M. Campbell.

In general, the hazard to hospital personnel from diagnostic amounts of radioisotopes is small. Nevertheless there is a potential contamination hazard to sensitive counting equipment so that care is still necessary.

1. *Radiation Hazards*

Patients who have received therapeutic radioisotopes pose a significant radiation hazard to hospital personnel and visitors. Table 1 lists approximate exposure rates at various distances from patients containing 100 mCi of ^{131}I, ^{198}Au, and ^{226}Ra. These radiation levels must be taken into account when assigning a nurse, room, and bed to a patient and when admitting visitors to see the patient. The best way to reduce the exposure to nurses is to adjust nursing procedures, train the nurses, and divide the work load among several so that the time each spends with the patient is a minimum. The isodose lines around a patient vary according to the location of the radioactive material in his body and the time elapsed since administration of the dose. Thus a patient's bed should be placed so that the higher radiation zones are near an outside wall or unoccupied area. Radiation exposure to visitors can be controlled by limiting the time they spend with a radioactive patient and by having them sit at a distance from the patient. At the ORINS Medical Division visitors are not permitted to remain in patient areas where the radiation levels exceed 2 mR/hr.

How long a patient remains a hazard to others depends upon the effective half-life of the radioisotope in his body. If a patient has been given 100 mCi of ^{131}I, the iodine may be eliminated from the body as rapidly as 60–90% in the first 24 hr. Patients given 3–10 mCi of ^{131}I for hyperthyroidism usually excrete only 20–30%. When colloidal ^{198}Au is in pleural or peritoneal cavities, the radiation levels around the patient will decrease with the half-life of the gold, 2.7 days, unless the physician removes the fluid from these cavities. The radiation hazard from long-lived, sealed implants such as radium or iridium will remain undiminished until the source is removed from the patient.

A radioactive patient's maximum body burden at the time of his discharge from the hospital is not regulated by United States law. For many years the USAEC has set 30 mCi as a condition

Table 1. Exposure Rates near Patient who has Received Therapeutic Doses of Radioactive Material

Distance from patient's midline (ft)	Exposure rate [17-20] from patient containing 100 mCi ^{131}I or 100 mCi ^{198}Au (mR/hr)	Exposure rate [19-21] from patient containing 100 mCi ^{226}Ra (mR/hr)
1	150	200–300
2	40	110
3 (approx. 1 m)	25	65
4	15	40
5	6	25
6 (approx. 2 m)	5	18
7	3	10
8	—	7

for licensing, but where possible this number should probably be revised downward. Sear[22] has reviewed the problem extensively and reached about the same conclusion. If a patient contains 30 mCi of ^{198}Au or ^{131}I (Table 1), the exposure rates may be as high as 50 mR/hr close to his body. He is potentially a hazard to children, pregnant women, and family members who might spend lengthy times near him. The ICRP[6] recommends the following release limits: 30 mCi ^{32}P, sealed ^{90}Y, or sealed ^{198}Au; 15 mCi ^{131}I; 12 mCi sealed ^{222}Rn; 10 mCi colloidal ^{90}Y or colloidal ^{198}Au. We have found that a practical limiting procedure has been to restrict patients to their hospital room until the exposure rate is approximately 2 mR/hr at one meter from the body. This corresponds to a body burden of less than 10 mCi of ^{198}Au or ^{131}I.

2. *Contamination Hazards*

The control required to prevent contamination after administering a radioisotope depends upon the isotope, its amount, and how the body handles it.

Significant contamination problems may arise in connection with the therapeutic use of ^{131}I since the patient may excrete much of the iodine in the urine within the first 24 hr after administration. Some hospitals use a simple, lightly shielded container for urine collection to reduce both contamination and radiation hazards. Iodine may also appear in saliva and perspiration, and nurses, aides, and orderlies should be aware of this when handling an iodine patient's linen and eating utensils.

Intracavitary colloidal ^{198}Au may not present the contamination problem that ^{131}I does because it is not metabolized. Leakage of gold from the patient can be controlled by a purse-string suture at the site of administration. Contamination is probable during a paracentesis, since the fluid withdrawn may contain 20–30% of the gold administered.[23]

We have found that a floor monitor, Fig. 7, enables rapid surveys of large areas to detect contamination arising from spilled radioactive urine or saliva. The instrument is capable of detecting contamination levels as low as 0.5 μCi and consists of two GM tubes connected in parallel and shielded by a 2-in. lead hemicylinder. The operator moves at slightly less than normal walking rates and uses earphones so that he may view the monitoring area. The meter can be removed from the floor monitor and connected to a portable probe for closer monitoring.

Contamination of bed clothes and linen can be expected when patients have been given radioisotopes that the body metabolizes, the contamination most frequently arising from patients with therapeutic amounts of ^{131}I. At ORINS we store contaminated linen in plastic bags to allow short-lived isotopes to decay, and after monitoring, we send the linen to a

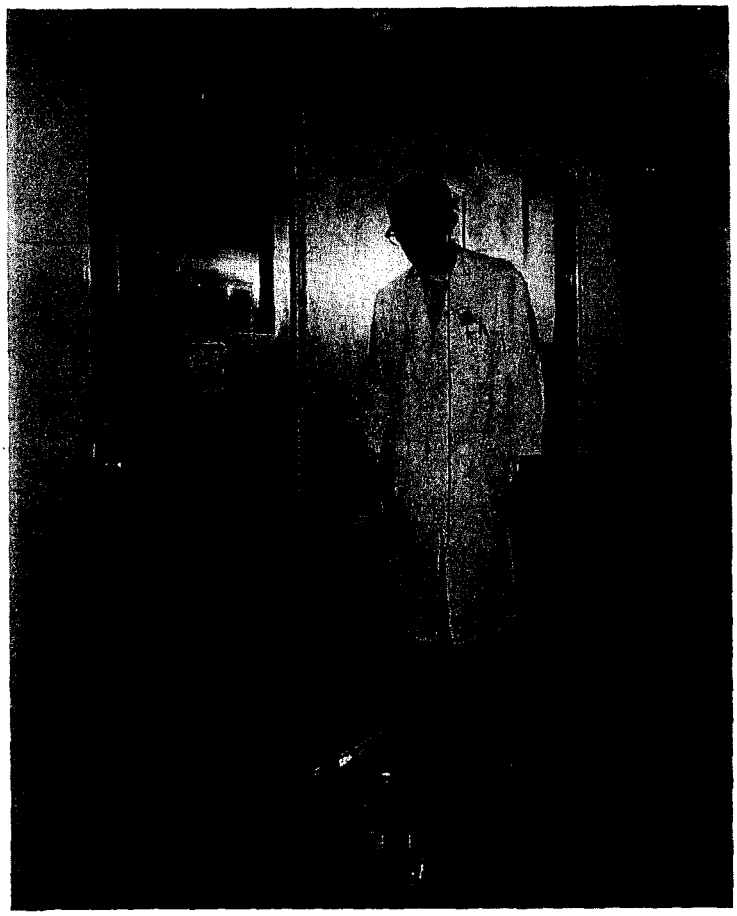

FIG. 7. A floor monitor for rapidly detecting low-level contamination.

commercial laundry if the contamination level is below 300 d/m/100 cm². Methods of handling contaminated laundry vary among hospitals and other industries as well, as noted by Harrington in his review article.[24]

Brown *et al.*[25] describe some generally effective methods of controlling hospital contamination in their report about the measures followed after administering 300–500 mCi of ^{35}S to patients. Sulfur-35 is a low-energy beta emitter that is difficult to monitor. The patients excreted the sulfur rapidly, and because it has an 87-day physical half-life, contamination was potentially a serious problem.

They administered the sulfur in the patient's room, or if biopsies were required, they gave the dose in the operating room. After administration they established a control point at the entrance to the patient's room where they confined him except for occasional tests necessary elsewhere. All hospital personnel wore protective gowns, gloves, and shoe covers, and after leaving the patient's room, they removed this clothing and were monitored. They further controlled contamination by using disposable equipment and by separately washing contaminated laundry. They found no contamination outside the patient's room and used standard cleaning techniques to eliminate the low-level contamination in the room.

The technique Hairr and Loughman[26] described for control of ^{90}Y contamination is unique.

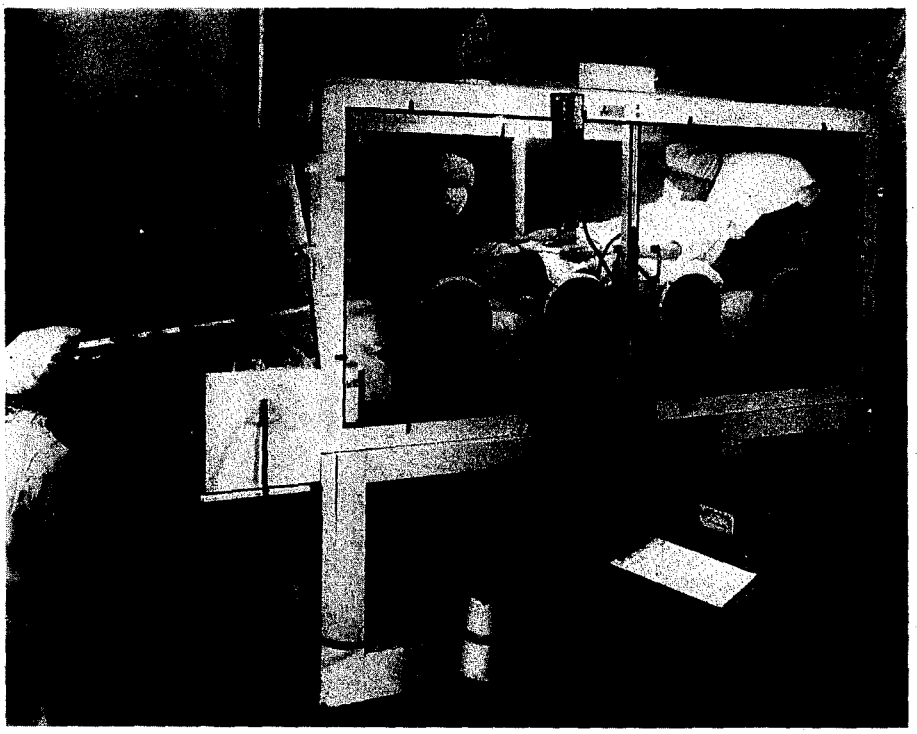

FIG. 8. Glove box used to contain a patient treated with 1.5 Ci of ^{90}Y-DTPA. Reproduced from *Health Physics* **9,** 987 (1963) by permission of the Health Physics Society and G. M. Hairr.

They maintained a patient for 24 hr in a 7- × 4- × 3-ft glove box, Fig. 8, after he was given 1.5 Ci of ^{90}Y-DTPA. Bag ports permitted minor surgery, physiologic monitoring, and collection of blood and urine samples. The box was kept at a slight negative pressure, and affluent and effluent air were passed through high-efficiency particulate filters. The glove box was constructed of plywood and lucite that reduced radiation levels from 20 rad/hr inside the box to 0.2–5 mrad/hr outside. Some additional shielding to reduce Bremsstrahlung levels was required near the areas where the ^{90}Y-DTPA concentrated. After they removed the patient from the glove box, they isolated him because of his vulnerability to infection. They restricted the number of personnel allowed in the patient's room and trained hospital staff members to change air filters, collect waste, assess contamination levels, and survey the patient.

AUTOPSY OF RADIOACTIVE BODIES

Most autopsies on radioactive cadavers are conducted the same as for nonradioactive bodies. Clinicians seldom prescribe therapeutic radioisotopes to terminal patients, and therefore most radioactive bodies contain less than one or two millicuries. Probably the best guide for pathologists and radiation safety personnel is NBS Handbook 65, *Safe Handling of Bodies Containing Radioactive Isotopes,*[27] which outlines general precautions.

Usually radioactive contamination will not be a primary problem during an autopsy since the precautions customarily taken to prevent the spread of bacterial infection simultaneously reduce the potential of radioactive contamination. A pathologist can easily adapt to the use of heavy gloves, long-handled tools, and plastic aprons and shoe covers because they are similar to his usual equipment. Contamination surveys

of the autopsy area and equipment conducted after the autopsy are usually adequate.

If the cadaver contains a radioisotope that concentrates in one or two specific organs, the autopsy procedure is modified so that these organs are among the first to be dissected and removed from the pathologist's working area. If body cavities contain residual radioisotope, the cavities are drained and the fluid is flushed into a closed system.

The NCRP[27] states that a body may be released directly to a funeral director for embalming if it contains less than 30 mCi, and further, that a crematorium may each year handle bodies containing a total of up to 200 mCi of ^{131}I and 2000 mCi of other radioisotopes (^{198}Au, ^{32}P, and ^{90}Y) without hazard to employees or the public. These limits have remained essentially unchanged since 1953, and probably they will not be exceeded or even met.

RADIATION SAFETY TRAINING FOR HOSPITAL PERSONNEL

1. *Physicians*

Training in nuclear medicine is available to physicians[28, 29] although the content and length of the training courses vary widely.[29] Most of these courses[30, 31] are designed to meet two goals: to satisfy the licensing requirements of the USAEC and state governments, and to promote professional competence in the use of radioactive drugs. The concern of the AEC and other licensing agencies is radiation protection, and the regulations state that the physician be "qualified by experience and training to use the material for the purpose requested in such manner as to protect health and minimize danger to life and property."[32] The extent of this training and experience is not specified. Understandably, the primary interest of the medical profession is the effective and competent use of radiopharmaceuticals. The American Medical Association and the Society of Nuclear Medicine have established committees to study the problem of professional standards in the use of radioactive drugs. The American Board of Radiology has a certification program that requires three months of training and satisfactory performance on an examination.

Although the guidelines are vague, the training for physicians is the most complete of any available to people in medical science. Most courses for physicians devote about a third of their time to basic material such as elementary nuclear physics, mathematics, instrumentation, and radiation safety. As a rule, physicians are interested in radiation safety to the extent of being able to satisfy the licensing requirements. They are interested in the "how-to-do-it" aspects of waste disposal, and they welcome information on maximum permissible exposures, monitoring equipment, exposure levels around radioactive patients, and so on. They need to be interested in such topics, for often in small hospitals a physician is responsible for the entire radiation safety program. On the other hand, developing more than a marginal concern about radiation protection is difficult, for a physician, reasonably enough, is more interested in the clinical aspects of radioactive materials. For this reason it is well to thoroughly integrate radiation safety practices into the physicians' clinical training so that radiation safety at least becomes a habit. It is surely a mistake to treat their training in radiation protection as a topic separate from the clinical use of radiopharmaceuticals.

2. *Nurses and Technologists*

Specialized training available for nurses in the care of radioactive patients is not well documented, but it is available. For example, the U.S. Public Health Service offers a one-week course, and Simon[33] describes a rather extensive four-month course for nurses in the U.S. Navy. This course devotes about 60 hours to lecture and laboratory sessions on radiation safety; 220 additional hours to mathematics, physics, biochemistry, and radiobiology; and the remainder of the 550-hour course to the study of clinical procedures.

More often nurses must be trained on the job. At the ORINS Medical Division the Radiation Safety Office provides about a half day of formal basic training for nurses new to the staff. During her work the nurse's training is directed by the nursing supervisor. Since the health physics staff participate in almost all the hospital procedures involving radioisotopes, they provide further instruction as needed. At frequent intervals review training sessions are presented for the entire nursing staff.

This training aims to provide the nurse with enough fundamental and practical knowledge so that she may safely and efficiently handle her nursing duties and at the same time minimize radiation exposure to herself and others. The training includes a brief description of the properties of different radiations, particularly the types that she will most often encounter. We emphasize ways of using time, distance, and shielding as protective devices. The "how" and "why" of monitoring and safety techniques are explained, and the nurses are taught to use laboratory monitors.

The American Society of Radiologic Technologists[34] has proposed an excellent minimum course of instruction leading to certification for both radioisotope and radiotherapy technologists. The Society suggests a 12-month, 300-hour course for each group, devoting about 100 hours to basic radiation physics, radiobiology, and radiological safety.

3. *Aides, Orderlies, Supporting Staff*

Since orderlies, aides, and many other hospital employees usually do not have specialized training, their instruction in radiation safety must be accomplished on the job. The training for ORINS hospital personnel is simple, practical, and directly related to their individual jobs. For example, we point out possible sites of contamination, such as linen, sample containers, and eating utensils, to the aides and orderlies who may handle these items. We instruct janitors in simple decontamination techniques. We teach all to use area monitors and to call upon radiation safety personnel for help when a mishap occurs or when they suspect contamination.

A CONCLUDING REMARK

Since radioisotopes became a medical tool, many ways have been found to reduce the attendant radiation exposure. Sometimes the innovations have been made by physicists; often they have been the work of physicians. Work still remains to be done. We hope our discussion will stimulate more thought, research, and communication among health physicists on medical radiation safety problems and standards.

REFERENCES

1. Daniel B. Howell. Personal communication. Isotopes Branch, Division of Materials Licensing, U.S. Atomic Energy Commission, August 10, 1966.
2. S. Silver. Uses of radioisotopes in medicine. *Nucleonics* **23** (8), 106–111 (1965).
3. M. Brucer. 118 Medical radioisotope cows. *Isotopes and Radiation Technology* **3**, 1–12 (1965).
4. Code of U.S. Federal Regulations. Title 10, Part 20: *Standards for Protection Against Radiation*; Part 35: *Human Uses of Byproduct Material.*
5. Recommendations of the International Commission on Radiological Protection, Report of Committee V, Handling and Disposal of Radioactive Materials in Hospitals and Medical Research Establishments. ICRP Publication 5, Pergamon Press (1964).
6. International Atomic Energy Agency, Vienna. Safety Series, No. 1: *Safe Handling of Radioisotopes* (1962); No. 2: *Safe Handling of Radioisotopes—Health Physics Addendum* (1960), No. 3: *Safe Handling of Radioisotopes—Medical Addendum* (1960); No. 13: *The Provision of Radiological Protection Services* (1965).
7. Recommendations of the National Committee on Radiological Protection and Measurements, National Bureau of Standards Handbooks, No. 73: *Protection Against Radiations from Sealed Gamma Sources* (1960); No. 76: *Medical X-ray Protection up to Three Million Volts* (1961); No. 92: *Safe Handling of Radioactive Materials* (1964). U.S. Government Printing Office, Washington, D.C.
8. E. H. Quimby. *Safe Handling of Radioactive Isotopes in Medical Practice.* The Macmillan Company, New York (1960).
9. American Hospital Association. *Manual on Use of Radioisotopes in Hospitals.* Chicago (1958).
10. Radiation Protection in Nuclear Medicine. A film produced by Fordel Films, New York, for the Bureau of Medicine and Surgery of the U.S. Navy (1961).
11. H. I. Glass. A radioiodine oral dose administration apparatus. *Lancet* **1**, 29–30 (January 5, 1963).
12. U. K. Henschke, B. S. Hilaris and G. D. Mahan. Afterloading in interstitial and intracavitary radiation therapy. *Amer. J. Roentgenol.* **90**, 386–395 (1963).
13. U. K. Henschke, B. S. Hilaris and G. D. Mahan. Intracavitary radiation therapy of cancer of the uterine cervix by remote afterloading with cycling sources. *Amer. J. Roentgenol.* **96**, 45–51 (1966).
14. H. J. Hodt, W. K. Sinclair and D. W. Smithers. A gun for interstitial implantation of radioactive gold grains. *Brit. J. Radiol.* **25**, 419–421 (1952).

15. C. H. JONES, K. W. TAYLOR and J. B. H. STEDEFORD. Modifications to the Royal Marsden Hospital gold grain implantation gun. *Brit. J. Radiol.* **38,** 622–624 (1965).
16. J. LEGAL and E. M. CAMPBELL. A device to facilitate threading of cobalt-60 beads. *Radiology* **85,** 959–961 (1965).
17. J. M. MORGAN and R. WIGH. Isointensity patterns from radioactive colloidal gold in serous cavities. *Amer. J. Roentgenol.* **89,** 567–569 (1963).
18. Calculated estimation by the authors.
19. C. E. NURNBERGER. Radiation exposure of nonradiologic hospital personnel during treatment of patients. *Amer. J. Roentgenol.* **83,** 507–513 (1960).
20. R. E. ELLIS. Problems in the Achievement of Optimal Radiation Levels in Hospital Practice. Symposium on Environmental Monitoring, Berkeley, Gloucestershire, England, October 3–4, 1963. CONF-365-9.
21. H. G. WANDEL. Isodose curves and radiation distribution about patients with intracavitary radium sources. *Amer. J. Roentgenol.* **87,** 500–503 (1962).
22. R. SEAR. Radiation hazards resulting from clinical use of radio-iodine. *Acta Radiologica Ther.* **2,** 263–272 (1964).
23. E. D. WITHERELL and R. F. COWING. Radiation protection problems associated with radioactive gold. USAEC Report, TID-20600 (May 7, 1964).
24. F. E. HARRINGTON. Operating practices in contaminated-clothing laundries. *Nuclear Safety* **4** (2), 96–99 (1962).
25. J. M. BROWN, JR., J. R. HOWLEY, Y. MCINTOSH, D. DRIVER and M. B. DICKINSON. Contamination problems associated with the administration of massive doses of sulfur-35 to patients. *Health Physics* **10,** 557–561 (1964).
26. G. M. HAIRR and W. D. LOUGHMAN. Health physics aspects of irradiation of large animals and human beings with curie quantities of internally administered isotopes. *Health Physics* **9,** 987–992 (1963).
27. Recommendations of the National Committee on Radiation Protection and Measurements, National Bureau of Standards Handbook No. 65: *Safe Handling of Bodies Containing Radioactive Isotopes* (A Guide for Surgeons, Pathologists, and Funeral Directors) (1958). U.S. Government Printing Office, Washington, D.C.
28. T. P. SEARS. Report of survey of teaching nuclear medicine. *J. Nucl. Med.* **5,** 400–403 (1964).
29. K. R. MCCORMACK. Training in nuclear medicine for radiology residents. *Radiology* **83,** 22–25 (1964).
30. R. M. KNISELEY. Training for clinical use of radioisotopes: qualification courses. *J. Nucl. Med.* **1,** 239–250 (1960).
31. J. STERNBERG. Nuclear medicine and medical education. *J. Nucl. Med.* **6,** 691–698 (1965).
32. Code of U.S. Federal Regulations. Title 10, Part 30, Section 30.33: General Requirements for Issuance of Specific Licenses.
33. L. SIMON. The nuclear age and nursing technology. *Military Medicine* **126,** 701–706 (1961).
34. The American Society of Radiologic Technologists. Proposed minimum radioisotope and radiotherapy curricula. *Radiologic Technology* **35,** 269–276 (1964).

REDUCTION OF UNNECESSARY EXPOSURE THROUGH LICENSING OF X-RAY TECHNICIANS

Saul J. HARRIS

National Center for Radiological Health, U.S. Public Health Service, New York, N.Y., U.S.A.

Abstract

I. *Introduction*

In 1964 the New York State legislature enacted, and the Governor signed into law, a bill establishing a licensing system for X-ray technicians for the purpose of reducing unnecessary radiation exposure during the use of medical X-ray. The law established a seven member Board of X-ray Technician Licensing including a health physicist, defined as "a person who is certified by the American Board of Health Physics, or the American Board of Radiology in Physics". The New York State Commissioner of Health appointed the author as the health physicist member for a four term commencing October 1964.

II. *Health department activities*

Recognizing the major interest of such licensing as being the promotion of public health, the law directs the State Health Department to administer the program. The agency responsible for this administration is the Bureau of X-ray technology in the Department of Health directed by Howard Goldman, a former X-ray technician and previously responsible for the radiological health control program associated with the medical and dental use of X-ray. Mr. Goldman serves as secretary of the Board. Dr. John Roach, a radiologist, was elected the first Chairman of the Board.

III. *Examination of applicants*

The law established three initial classifications of applicants: present practitioners having more than five years of practice, individuals with one to five years of service, and those with less than one year's experience and also set up a system of examinations for each group. In addition, the law authorized the Health Department to decide whether to license directly X-ray technicians who were registered with the American Registry of Radiation Technologists, an action followed after the Board recommended it at its first meeting. There was no automatic licensing of any "grandfathers" in the law. The over-five-year group was required to take a modest practical examination. The intermediate group was required to take a special written examination and oral exam. The beginning group was required to take a regular written examination. Included in the procedure was a system for review. Health physics questions were a major component in each examination.

IV. *X-ray technician schooling*

Although the New York State law reduces the number of hours of formal training required of X-ray technicians in state-approved schools, greater emphasis has been placed on radiation protection in the curriculum and in the operation of the schools. For example, the New York State program requires each school to have a staff radiation safety officer and must be in compliance with applicable state radiation regulations. More hours for radiation protection have been added to the basic curriculum. Standards of exposure for students are also stipulated.

V. *Conclusions*

The New York State program to license X-ray technicians provides a direct opportunity to improve radiation protection to patients as well as the technicians themselves during medical use of X-ray. Reduction of unnecessary exposure is consistent with obtaining the best possible radiograph through the employment of qualified personnel.

SOFT X-RAY SOURCES AS A MEANS OF REDUCING MEDICAL EXPOSURE TO RADIATION

D. C. LAWRENCE*
Hazleton Nuclear Science Corporation, Palo Alto, California, U.S.A.

Abstract—Medical use provides a major source of population radiation exposure. This includes exposure from the use of radium and other radioisotopes in the implant treatment of cancer. In such implants, the radio-therapist, patient, visitors, and attending staff, all typically receive some unwanted radiation.

A promising means of essentially eliminating such exposure is through the use of soft X-ray emitting radioisotopes as a replacement for radium and radon in brachytherapy. Particularly promising are the soft X-ray emitters cesium-131 and iodine-125, which emit monoenergetic 30 keV X-rays free of beta or higher energy gamma radiation. These radioisotopes, when properly encapsulated, provide a suitable substitute for use in radiotherapy. They have the marked advantage in that their radiation can be completely shielded by thin layers of heavy metals, yet they have a practical range in tissue. Physics, dosimetry, animal and clinical tests with human cancer patients have been initiated using commercially available miniature sources of ^{125}I and ^{131}Cs. Experience with these sources, called X-seeds, has now shown that they can be used to significantly reduce radiation exposure while at the same time they provide a substantially uniform tumor dose. In one instance, 970 mCi of ^{131}Cs were inserted in a leisurely series of animal implants, and, by the simple expedience of using a radiologist's lead apron, the radiotherapist kept his whole body dose under 1 mR and his hand dose under 10 mR. Recent progress and clinical experience with these sources will be described.

*Present address: Radiation Division, Varian Associates, Palo Alto, California (U.S.A.)

DISCUSSION

T. F. JOHNS (*U.K.*):

I was interested to hear that the Riso workers had failed to find agreement between the sodium flame test and the Pollak counter for determining the efficiency of filters. At Winfrith we have found remarkably good agreement between these two methods, and as a result we are now beginning to use the Pollak counter for the routine *in situ* testing of filters. This technique is so simple that we feel that this represents a real break-through in the business of *in situ* filter testing; other methods are difficult to perform, and as a result such measurements are frequently not made at all.

D. K. CRAIG (*South Africa*):

It depresses me to hear of filter testing procedures and filter efficiencies still reported with no reference to aerosol particle size distributions. Theoretically speaking, the physical properties of aerosols are such that one must obtain a minimum filtration efficiency for a given particle size. I know that there has been a lot of controversy about this, but, for aerodynamic equivalent unit density spheres, this minimum occurs at approximately 0.3μ diameter. If results different from this are reported, then an attempt should be made to advance a theoretical explanation for the difference (e.g. there will be a shift to smaller particle diameters in the minimum as the face velocity of air passing through the filters is increased). I disagree that the Pollack counter method can give an accurate measure of the minimum filter efficiency. I still believe that the best way to measure the efficiency of filters is to use 0.3 μ diameter spheres, such as are available from the D.O.P. generator. With the use of an 0.3μ diameter D.O.P. aerosol, one is not bothered by the varying filter efficiencies as a function of particle size. What one is measuring, then, is the minimum efficiency of the filter, the parameter in which I think we should be interested.

T. F. JOHNS:

No one was more surprised than we were when we found these two methods gave agreement. The explanation appears to be that one is not measuring true penetration, but merely finding how much aerosol passes through a small number of imperfections, the latter being so big that the apparent penetration is quite independent of particle size.

D. K. CRAIG:

In reply to Mr. Johns, what he is measuring is the efficiency of installation of the filter, not the filter efficiency, and I think that this point should be made clear when reporting filtration efficiency results.

T. F. JOHNS:

I quite agree, but I would point out that the whole purpose of *in situ* testing is to measure the effectiveness of the installation.

H. FLYGER (*Denmark*):

The photoelectric nuclei counters are not easily moved around for *in situ* testing of filters. The counters are heavy and the light source is easily put out of focus. The use of the lithium test is nevertheless very easy.

D. C. LAWRENCE (*U.S.A.*):

I would like to ask the authors if they can give further details on why they feel the testing of radon is not satisfactory for leak testing of radium needles and what it is they propose or suggest.

L. B. BEENTJES:

Possibly Mason refers to sealing of the Ra needles by water using the method of carbon in water. This was pointed out at the Health Physics meeting in Los Angeles in 1964.

K. KRISTENSEN (*Denmark*):

Have any measurements been made with regard to internal contamination of personnel?

PH. C. JOHNSON:

We have been unable to find Hg^{203} in the kidneys or urine of our laboratory personnel.

D. C. LAWRENCE (*U.S.A.*):

Were the commercial suppliers advised of the problem and if so what was their explanation of the apparent contamination?

PH. C. JOHNSON:

We notified the manufacturers. Their response was, essentially, to deny that it occurs. However, at least one supplier has begun to wash his bottles with acid prior to shipment.

D. C. LAWRENCE:

If the Chairman would permit, I would like for a minute to discuss another approach toward solving the problem of radiation exposure from interstitial therapy.

Essentially the problem which was outlined in the last paper is one of a radioactive patient after he has received interstitial therapy, and the patient must be handled with extreme care in order to prevent exposure of visitors, the person who has installed the radioisotope, and even the nursing staff.

Ideally what is desired is to install the radioisotope and have the radiation exposure uniformly distributed and yet remain within the tumour volume. One way of achieving this can be shown in Table I, which shows several radioisotopes now being used for radiotherapy, including Ir^{192}, Rn, and Au^{198}, the isotopes which were mentioned by the last author. If you look over to the last column, the shielding requirements as characterized by the lead half-value layers for Au^{198}, radon, and iridium range from 0.13 to 0.53 inches and they have a half-value layer in water of 7 to 9 centimeters. Now, if we look at the last three isotopes, I^{125}, Cs^{131} and Xe^{133}, you will note that these have varying half-lives from 5.3 days to 60 days and emit only soft X-rays. This results in the fact that a very small amount of lead can be used to shield these isotopes (Pb HVL = 0.001[11]) and yet they still have a reasonable range in tissues of 2 to 5 cm.

Table I. *Radioisotopes for Permanent Implants*

Radioisotope	Half-life	Gamma radiations	Other	Half-value layer Pb	Half-value layer H_2O (tissue)
Au^{198}	2.7 days	0.411 & 0.680 Mev	0.97 Mev β	0.13 inch	$\simeq$ 7 cm
Rn^{222}	3.8 days	0.24–2.43 Mev (many)	Alpha (2) & 0.65 Mev β	0.53 inch	$\simeq$ 9 cm
Ir^{192}	74.2 days	0.2–1.1 Mev (many)	0.54 & 0.67 Mev β	0.14 inch	$\simeq$ 7 cm
I^{125}	60 days	28 & 35 Kev	None	0.001 inch	$\simeq$ 2.1 cm
Cs^{131}	9.7 days	29.4 Kev	None	0.001 inch	$\simeq$ 2.1 cm
Xe^{133}	5.3 days	32 and 80 Kev	0.35 Mev β	$\simeq$0.01 inch	$\simeq$ 5 cm

We have approached the problem of radiation safety in interstitial implantation by incorporating these isotopes, primarily I^{125} and Cs^{131} in small seeds. By incorporating these isotopes in the small seeds, we noted the following advantages in interstitial therapy. First of all, by use of a radiologist's lead apron, we can eliminate the radiation exposure to the therapist. He can handle these isotopes using only a thin lead foil for radiation protection. Second, we have found an improved tumour dose distribution and therapeutic ratio over seeds of Au^{198} and Rn. Third, the reduction in exposure makes the implant therapy of very large tumours possible. We have also found it possible to protect healthy adjacent tissues by the use of thin metallic foils, particularly gold foils, which are non-toxic, and I^{125} seeds permit simple out-patient treatment, because the dose is retained within the tumour. It also makes possible the use of such isotope therapy in remote areas, because the sources can be carried safely by air in a very small lead container. The complete protection of the nurses and other patient associates also becomes a reality. The I^{125} seeds thus developed have now been used to treat over a dozen cancer patients. We have been able to see in actual practice all of the desired advantages, and we are going on with clinical testing.

This is just one way of solving the problem which was outlined in the last papers.

S. LIN (*Italy*):

Desidero ricordare un semplice dispositivo che viene impiegato nel nostro Laboratorio, costituito da un ago da anestesia tipo Olorson-Gohrd, il quale permette di iniettare il radionuclide, attraverso la piccolo camera chiusa da una membrana di gomma, dopo aver proceduto all'immissione dell'ago in vena.

Vorrei chiedere anche all'autore se ha esperienza del grado di contaminazione dell'aria ambientale, determinata dall'espirazione di pazienti sottoposti a terapia con alte dosi di radioiodio.

Vorrei infine richiamare l'attenzione su di una apparecchiatura costruita in Italia dalla SORIN-Saluggia, la quale permette non solo di eseguire a distanza l'infissione di sferule di materiale radioattivo, ma anche di contarne il numero per mezzo di n dispositivo elettromagnetico.

INDEX OF CONTRIBUTORS